F 1103

R

REFERÁLVA

ACADÉMIE DE LA RÉPUBLIQUE SOCIALISTE DE ROUMANIE

REVUE ROUMAINE DE CHIMIE

TOME 21
N° 1
Janvier 1976

RECHAX, **21**, *1*, 1 – 164 (1976)

EDITURA ACADEMIEI REPUBLICII SOCIALISTE ROMÂNIA

Rev. Roumaine Chim. **21**, *1*, p. 1 – 164 (1976), Bucarest

ACADÉMIE DE LA RÉPUBLIQUE SOCIALISTE DE ROUMANIE

COMITÉ DE RÉDACTION

Rédacteur en chef:

I. G. MURGULESCU, membre de l'Académie de la République Socialiste de Roumanie

Rédacteurs en chef adjoints:

A. T. BALABAN et V. EM. SAHINI, membres correspondants de l'Académie de la République Socialiste de Roumanie

Collège de rédaction:

EM. BRATU, ELENA CEAUŞESCU, ECATERINA CIORĂNESCU-NENITZESCU, C. DRĂGULESCU, RALUCA RIPAN, CR. SIMIONESCU, membres de l'Académie de la République Socialiste de Roumanie; P. SPACU, membre correspondant de l'Académie de la République Socialiste de Roumanie; MARGARETA AVRAM, D. I. MARCHIDAN, I. MOLDOVAN, G. NIAC et D. SĂNDULESCU

La Revue Roumaine de Chimie paraît 10 fois par an. Toute commande de l'étranger (fascicules ou abonnements) sera adressée à Intreprinderea ILEXIM, Serviciul Export-Import Carte/ Serviciul Export-Import Presă (Revues), P.O. BOX. 2001, 64-66, Calea Griviţei, Bucarest 12, Roumanie

Les manuscrits, les livres et les revues proposés en échange, ainsi que toute correspondance seront envoyés à la rédaction :

REVUE ROUMAINE DE CHIMIE

23, str. Dumbrava Roşie, Bucarest, Roumanie, téléphone 12 41 60

EDITURA ACADEMIEI REPUBLICII SOCIALISTE ROMÂNIA

125, Calea Victoriei, Bucarest, Roumanie, téléphone 50 76 80

MŰSZAKI KÖNYVTÁR ÉS DOKUMENTÁCIÓS KÖZPONT 1883 ORSZÁGOS

REVUE ROUMAINE DE CHIMIE

Tome 21, Nº 1 Janvier 1976

RODICA VÎLCU and ALEXANDRINA SIMION, Acoustic and volumetric properties of aqueous salt solutions 3–9

P. A. LAURENT et M. J. LAURENT-DUHAMEL, Sur une transformée simple de certains isothermes de démixtion ternaire 11–23

D. I. MARCHIDAN and LAURA VASU, Melting heats of alkali halide solid solutions 25–30

M. MARTÍN, V. MENÉNDEZ and J. M. FIGUERA, Equilibrium geometry and heat of formation of aliphatic diazocompounds, diazirines and related singlet carbenes. AMINDO/2 calculation 31–39

MARIA MAVRODIN-TĂRĂBÎC, IOANA ONACA et I. SOLACOLU, Contribution à l'étude de la réduction de l'oxygène sur les électrodes poreuses en argent. II. L'influence de la concentration de l'électrolyte sur les performances des électrodes 41–47

LOUIS FERRERO, SERGE GERIBALDI et MARCEL AZZARO, Essai de généralisation du phénomène de régiosélectivité dans la réduction des oximes par des agents aluminiques 49–58

IRINA CORNEA and VERA ICHIM, The efficiency of organic corrosion inhibitors in oil-field waters . . . . 59–64 Ref

Ž. D. JOVANOVIĆ et NADEŽDA N. JOVANOVIĆ, Texture des catalyseurs à base d'oxyde de zinc, cuivre et chrome pour la conversion de l'oxyde de carbone 65–72

I. V. NICOLESCU, M. SPINZI and D. CIOMÂRTAN, Relationships between properties and activity of alumo-chromia catalysts. I. Role of precursors in obtaining aluminium oxides 73–80

ELENA CATRINA, IR spectra of some chelates of thiazolidinic acids 81–87

M. ELIAN, M. BANCIU, LIGIA STĂNESCU and ECATERINA CIORĂNESCU, Thermal and photochemical rearrangements of dibenzobullvalene and related dibenzo-$(CH)_{10}$ hydrocarbons 89–99

ANISIA BOTA, A. T. BALABAN and F. CHIRALEU, Pyrylium salts formed by diacylation of olefins. XX. PMR spectra of 2,4,6-trimethyl-3-phenylpyrylium and -pyridinium salts 101–106

NICOLETA ŞTEFAN, I. G. DINULESCU and MARGARETA AVRAM, Investigations in the cyclobutane series. XXXVIII. Rearrangement of the dibenzo[*b*, *g*]bicyclo[4.2.0]octa-2,7-diene system 107–111

Rev. Roumaine Chim. **21**, *1*, p. 1–164 (1976), Bucarest

D. SUCIU and G. CSÁVÁSSY, Thiazole compounds. III. Kinetics of hydrolysis of some 2-aryl-4 and 5-diazo ketone derivatives 113–119

Ref L. KÉKEDY and IULIA KOVÁCS, Polarographic investigation of the decomposition of xanthates in acid medium 121–126

Ref H. WEXLER and V. BĂRBOIU, Contributions to the study of condensation reactions between cresols and isatin and its derivatives. I. A new molecular transposition 127–138

D. DONESCU, Kinetics of polymerization of 1,3-dioxepane with BF_3OEt_2 . . . 139–143

Ref SILVIA IOAN and I. BENEDEK, Study of N-vinylcarbazole ethyl methacrylate statistical copolymer by light scattering 145–154

DOINA GAVRILĂ, M. DIACONESCU and D. IORDACHE, Mechanical and electrical properties of irradiated polypropylene 155–160

COMPTES RENDUS 161–164

Revue Roumaine de Chimie 21, 1, 3-9 (1976)

ACOUSTIC AND VOLUMETRIC PROPERTIES OF AQUEOUS SALT SOLUTIONS

RODICA VÎLCU and ALEXANDRINA ŞIMION

Chair of Chemical Thermodynamics and Electrochemistry University
of Bucharest, Romania

Received 28 May, 1974

The densities and ultrasound velocities in ternary system K(Cl, Br) + H_2O and in binary solutions KCl + H_2O and KBr + H_2O were measured at the same molalities, at temperatures of 25, 35 and 45°. The adiabatic and isothermal compressibilities were computed as well as the internal pressures and the apparent molar volumes.

INTRODUCTION

In the development of the present-day theory of solutions, beside the study of the volume and thermal properties, the study of the acoustic properties was largely extended. The knowledge of these characteristics reveals the changes occurring as a consequence of the component interaction. [1, 2]

Several studies on velocity have shown that the non-linear curves of the velocity and of the adiabatic compressibility disclose not only the formation of the complexes but also the composition leading to the maximum formation of these complexes. [2]

The adiabatic compressibility that can be accurately studied by measurements with ultrasounds permits to estimate the variation of the free energy with the pressure. [3]

EXPERIMENTAL

Velocities were measured with a double-crystal interferometer, described in a previous paper. [4] Densities were determined by the picnometer method.

The errors of determination were 0.3% for velocity and 0.01% for density.

The determinations were made at temperatures of 25, 35 and 45°. The KCl and KBr used in the experiments were chemically pure and freshly recrystallized.

The water for the preparation of the solutions was twice distilled and degassed by boiling before use.

---

[1] D. O. Masson, *Phil. Mag.*, **7**, 218 (1929).

[2] S. S. Srivastava, S. Pracasli and S. Praclish, *Z. phys. Chem.*, (Leipzig) **201**, 91 (1952).

[3] S. Pracash and Y. D. Pandey, *Rev. Sci. Ind. Research*, **213**, 593 (1962).

[4] R. Vîlcu and A. Simion, *Rev. Roumaine Chim.*, (1975).

The mixtures were prepared at molal ratio 1 : 1, at concentration for which heat capacity values were available, by weighing the dry salt and dissolving it in the corresponding weight of water.

EXPERIMENTAL RESULTS AND DISCUSSION

Experimental data and those obtained for the estimated quantities are recorded in tables 1 — 7.

The adiabatic compressibility β_S, the isothermal compressibility β_T and the internal pressure, p_i, were computed by the following known relations

$$\beta_S = 1/c^2 \rho, \tag{1}$$

$$\beta_T = \beta_S + \alpha^2 \, TM/C_p\rho \tag{2}$$

$$p_i = \frac{T\alpha C_p Mc^2}{TV\alpha^2 Mc^2 + VC_p} \tag{3}$$

where

c is the ultrasound velocity

ρ is the density of the medium

α is the coefficient of isobaric expansion

T is the absolute temperature

M, V are the molar mass and volume.

The coefficient of expansion $\alpha = (\partial \ln \rho/\partial T)_p$, at 25° is estimated by relation

$$\alpha = \frac{V_{35} - V_{25}}{10V_{25}} \tag{4}$$

where V_{25}, V_{35} are the molar volumes at 25 and 35° respectively.

The values of heat capacities were borrowed from literature. [5]

The apparent molar volume, Φ_V, of binary solutions were computed with relation [6]

$$\Phi_V = \frac{1000}{m\,\rho\,\rho_0}(\rho_0 - \rho) + M_2/\rho \tag{5}$$

where

ρ_0 and ρ are the densities of water and of the solution, and m, M_2 are the molality and the molar masses.

In the ternary system [6]

$$\Phi_V = \frac{V - 55.51\overline{V_1^0}}{m_2 + m_3} \tag{6}$$

---

[5] M. S. Stakhanova, I. A. Epikhin and M. H. Karapetiant, *Zhur. fiz. Khim.*, **1963** 2750.

[6] H. S. Harned and B. Owen, "The Physical Chemistry of Electrolytic Solutions", 3rd. Ed., Reinhold publishing Corporation, New York, 1958, p. 358, 398.

and

$$\Phi_V = \frac{m_2\Phi_2 + m_3\Phi_3}{m_2 + m_3} \tag{7}$$

where

V is the volume of the solution containing 1000 g water

$\overline{V}_1^0$ is the molar volume of the pure water

m_2, m_3 are the molalities of the two electrolytes

Φ_2, Φ_3 are the apparent molar volumes of the electrolytes in the binary system, assuming that their ionic strength is equal to that corresponding to $m_2 + m_3$.

The maximum errors of determination with the above relations were : $\pm$ 0.6% for β_S, $\pm$ 0.7% for β_T, and $\pm$ 9% for p_i. For Φ_V the maximum error was $\pm$ 2% at $m = 0.5$, decreasing at greater molalities.

Density in all these systems increases with the concentration increase and diminishes with the temperature increase (table 1).

Table 1

Density ρ (g/cm³) in systems KCl+H₂O, KBr+H₂O and KCl+KBr+H₂O

KCl + H$_2$O				KBr + H$_2$O				KCl + KBr + H$_2$O			
m \ t	25	35	45	m \ t	25	35	45	m \ t	25	35	45
0.4970	1.0198	1.0164	1.0121	0.4998	1.0385	1.0348	1.0304	0.4984	1.0290	1.0255	1.0209
0.9929	1.0417	1.0380	1.0333	1.0017	1.0780	1.0739	1.0692	0.9973	1.0599	1.0562	1.0516
1.4954	1.0622	1.0586	1.0537	1.5002	1.1155	1.1111	1.1062	1.4955	1.0891	1.0851	1.0803
1.9922	1.0817	1.0778	1.0734	1.9936	1.1508	1.1463	1.1411	1.9999	1.1164	1.1115	1.1072
2.4897	1.1000	1.0959	1.0910	2.5017	1.1854	1.1805	1.1754	2.4957	1.1435	1.1386	1.1341
2.9829	1.1182	1.1140	1.1090	2.9967	1.2186	1.2134	1.2078	2.9898	1.1688	1.1639	1.1587
3.4958	1.1358	1.1314	1.1262	3.4950	1.2502	1.2444	1.2390	3.4954	1.1939	1.1891	1.1835
3.9737	1.1521	1.1472	1.1432	3.9920	1.2797	1.2739	1.2677	3.9828	1.2172	1.2117	1.2067
4.5056	1.1690	1.1644	1.1589	4.4793	1.3090	1.3032	1.2973	4.4924	1.2401	1.2345	1.2290

Actually, the solutions were all prepared at the same molality; molality m in the ternary system corresponds to

$$m = \frac{m_3 + m_2}{2}.$$

Up the to molal concentration 3.5, the density in the ternary system is practically equal to the average of the densities in the individual binary systems, at the same molality. At higher concentrations the density of the ternary system is greater than additively computed density, owing probably to the absence of the free water. [5] The ultrasound velocity increases with the temperature in the considered temperature interval and increases also with the solution concentration, which means that the compressibility decreases faster than the density increases with the concentration (tables 2, 3).

Table 2

Velocity, compressibility and internal pressure in system $KCl+H_2O$

m \ t	c ($m\,s^{-1}$)			$10^{12}\,\beta_S$ ($cm^2\,dyne^{-1}$)			$10^{12}\beta_T$ ($cm^2\,dyne^{-1}$)	p_i (atm)
	25	35	45	25	35	45	25	25
0.4970	1522	1544	1562	42.3	41.3	40.5	43.1	2308
0.9929	1548	1571	1586	40.1	39.0	38.5	41.0	2588
1.4954	1574	1586	1600	38.0	37.5	37.1	38.9	2607
1.9922	1585	1606	1618	37.0	35.9	35.6	38.2	3061
2.4897	1610	1625	1638	35.1	34.5	34.1	36.1	3082
2.9829	1622	1642	1646	34.0	33.3	33.2	35.1	3199
3.4958	1644	1663	1666	32.6	31.9	31.7	33.6	3422
3.9737	1650	1678	1684	31.9	31.0	30.8	32.8	3804
4.5056	1676	1692	1700	30.4	30.0	29.8	31.8	3776

Table 3

Velocity, compressibility and internal pressure in system $KBr + H_2O$

m \ t	c ($m\,s^{-1}$)			$10^{12}\beta_S$ ($cm^2 dyne^{-1}$)			$10^{12}\beta_T$ ($cm^2 dyne^{-1}$)	p_i (atm)
	25	35	45	25	35	45	25	25
0.4998	1511	1533	1545	42.2	41.1	40.6	42.4	2468
1.0017	1513	1535	1547	40.5	39.5	39.0	41.6	2753
1.5002	1526	1542	1555	38.4	37.8	37.4	39.6	2973
1.9936	1532	1551	1564	36.9	36.3	35.8	38.1	3056
2.5017	1540	1557	1565	35.6	34.9	34.7	36.9	3347
2.9967	1547	1562	1577	34.3	33.8	33.3	35.7	3565
3.4950	1548	1565	1578	33.4	32.8	32.4	35.1	3948
3.9920	1559	1569	1578	32.1	31.9	31.7	33.8	4008
4.4793	1620	1633	1640	31.2	30.9	30.8	32.8	4033

The ultrasound velocity in system $KCl + KBr + H_2O$ is practically equal to the average of the velocities of the two binary solutions at the same molality (table 4).

Table 4

Ultrasound velocity in system $KCl + KBr + H_2O$

m \ t	c ($m\,s^{-1}$)					
	exp.	adit.	exp.	adit.	exp.	adit.
	25		35	35	45	
0.4984	1517	1517	1538	1538	1550	1550
0.9973	1531	1530	1553	1566	1566	1566
1.4955	1546	1550	1566	1564	1582	1578
1.9929	1559	1558	1580	1578	1585	1590
2.4957	1570	1575	1590	1591	1602	1602
2.9898	1583	1584	1602	1602	1611	1612
3.4954	1597	1596	1614	1614	1620	1622
3.9828	1609	1604	1621	1621	1628	1623
4.4924	1618	1620	1627	1632	1635	1640

The adiabatic compressibility increases as the concentration of the solutions decreases because the primary effect of the dissolving process of an electrolyte is to diminish the compressibility of the solvent. This decrease is due to the electrostatic field influence of the ions upon the surrounding molecules which increases the total internal pressure so that the solution grows less compressible. Table 5 gives the compressibilities and internal pressures in the $KCl + KBr + H_2O$ system.

Table 5

Compressibility and internal pressure in system $KCl + KBr + H_2O$

m \ t	$10^{12} \beta_S$ (cm^2 dyne^{-1})			$10^{12} \beta_T$ (cm^2 dyne^{-1})	p_i (atm)
	25	35	45	25	25
0.4984	42.2	41.2	40.7	43.0	2359
0.9973	40.3	39.2	38.8	41.1	2534
1.4955	38.4	37.6	37.0	39.4	2863
1.9929	36.8	36.0	35.5	37.9	3418
2.4957	35.5	34.7	34.3	36.9	3469
2.9898	34.1	33.5	33.2	35.5	3458
3.4954	32.8	32.3	32.3	34.1	3515
3.9828	31.7	31.4	31.3	33.4	4037
4.4927	30.8	30.6	30.6	32.5	4149

The potential of an ion in the solution is expressed by equation

$$\psi_i = \pm \frac{z_i \varepsilon_i \varkappa}{D} \tag{8}$$

where

z_i is the ion valency

ε_i is the electric charge

D is the molecule permittivity

$$\varkappa = \left[\frac{4\pi \varepsilon^2 \Sigma\, n_i z_i^2}{DkT}\right]^{1/2},$$

n being the number of type i ions per mol, and $k = R/N$, the Boltzmann's constant.

From electrostatics, it is known that the pressure p between two charged particles undergoing a potential difference is given by

$$p = D\psi^2/8\pi = \frac{D(\mp z_i \varepsilon \varkappa/D)^2}{8\pi} = \frac{z_i^2 \varepsilon^2 \varkappa^2}{8\pi D}. \tag{9}$$

The diminution of the compressibility (water compressibility β_0 minus compressibility β of the solution) is due to this electrostatic pressure, i.e.

$$\beta_0 - \beta = \frac{z_i^2\, e^4}{2D^2kT}\, \Sigma n_i z_i^2. \qquad (10)$$

In the case of a monovalent electrolyte, $z_i = 1$ so that the above equation is reduced to

$$\mathrm{d}\beta = k'\, \Sigma n_i = k'(n_+ + n_-)$$

where k' is a constant corresponding to a particular temperature. It is to be remarked that the diminution of the water compressibility caused by an electrolyte at a particular temperature and concentration is a measure of the total number of the free ions. On the other hand, for electrolytes other than monovalent the diminution of compressibility is dependent on the therm $\Sigma n_i\, z_i^2$. It can then be told that the diminution of the compressibility is dependent on the ionic strength of the solution.

This assumption can be confirmed by our researches since the adiabatic compressibility has practically the same value in all three systems at a given particular temperature and concentration, the values of constant k' and of the ionic strength being the same, too.

By contrast with the organic liquids, the compressibility in water and aqueous solutions, up to a certain temperature, diminishes when temperature rises and then increases ; water presents a minimum of the compressibility at 64°. [7]

The temperature rise accompanies the break of the hydrogen bond and the diminution of the number of associated molecules which diminishes in turn the relaxational compressibility of the water. [8] This effect prevails over the increase of the usual or instantaneous compressibility, owing to the increase of the intermolecular distances up to the temperature corresponding to the minimum of compressibility (64°) which accounts for the decrease of the compressibility up to a certain temperature. [8]

The isothermal compressibility varies in the same manner as the adiabatical one.

The results obtained for the internal pressure at 25° shows somewhat higher values in the system $KBr + H_2O$ than $KCl + H_2O$ although ion Cl^- is smaller than ion Br^- ; this could be due to an additional interaction ion-dipole in system $KBr + H_2O$ or to the detachment of some associated water molecules in the presence of ions Br^-.

The internal pressure increases with the concentration of the solution.

The apparent molar volumes (tables 6, 7) grow with the temperature and with the concentration. In the case of the ternary system, the apparent molar volumes computed by equation (7) tally approximately with those computed by equation (6).

---

[7] J. Stuehr and E. Yeager, in "Physical Acoustics", Vol. 2, Part A, edited by Warren P. Masson, Academic Press, New York, 1964, p. 367.

[8] Otohiko Nomoto, *J. Phys. Soc., Japan*, **1956**, 1146.

Table 6

Apparent molar volumes Φ_V (ml/mol) in systems $KCl + H_2O$ and $KBr + H_2O$

m / t	$KCl + H_2O$			$KBr + H_2O$			
	25	35	45	m / t	25	35	45
0.4970	28.2	28.9	29.7	0.4998	34.6	35.8	36.6
0.9929	28.3	29.0	29.7	1.0017	35.2	36.2	36.8
1.4953	29.1	29.4	30.0	1.5002	35.7	36.5	37.1
1.9922	29.55	29.96	30.17	1.9936	36.23	36.83	37.31
2.4887	30.09	30.50	30.86	2.5017	36.73	37.33	37.65
2.9829	30.26	30.63	30.89	2.9967	36.83	37.42	37.82
3.4958	30.61	30.98	31.32	3.4950	37.10	37.75	38.03
3.9737	30.76	31.21	31.40	3.9920	37.52	38.08	38.51
4.5056	31.05	31.36	31.70	4.4793	37.57	38.90	38.37

Table 7

Apparent molar volumes Φ_V (ml/mol) in system $KCl + KBr + H_2O$

t	25		35		45	
m	ec. (6)	ec. (7)	ec. (6)	ec. (7)	ec. (6)	ec. (7)
0.4984	31.6	31.7	32.5	32.4	33.8	33.2
0.9973	31.8	31.8	32.3	32.6	32.9	32.2
1.4955	32.3	32.4	32.9	32.9	33.5	33.4
1.9929	32.89	32.89	33.73	33.39	33.84	33.74
2.4957	33.21	33.41	33.87	33.92	34.02	34.26
2.9898	33.55	33.55	34.09	34.03	34.43	34.37
3.4954	33.75	33.85	34.18	34.36	34.57	34.67
3.9828	34.01	34.14	34.54	34.65	34.74	34.86
4.4924	34.24	34.29	34.73	34.70	35.02	35.02

CONCLUSIONS

1) In the ternary system, the ultrasound velocity is practically equal to the average of the velocities in the binary solutions at the same molality.

2) The adiabatic and isothermal compressibilities are practically the same in the three systems, at the same ionic strength.

3) The internal pressure increases with the concentration being somewhat higher in system $KBr + H_2O$ than in system $KCl + H_2O$.

4) The apparent molar volumes in the ternary system, computed by formula of definition (6), agree with the apparent molar volumes additively computed.

Revue Roumaine de Chimie, **21**, *1*, 3–9 (1976).

Revue Roumaine de Chimie, 21, 1, 11–23 (1976)

Hommage à Raluca Ripan

SUR UNE TRANSFORMÉE SIMPLE DE CERTAINS ISOTHERMES DE DÉMIXTION TERNAIRE

P.A. LAURENT et M. J. LAURENT-DUHAMEL

Université de Pau (64010), France

Reçu le 25 décembre 1974

Si a, e, s, représentent respectivement les molécules d'éthanol, d'eau, et d'un solvant organique entièrement miscible à l'alcool et insoluble dans l'eau, la courbe de démixtion suit souvent une loi simple :

$$\log \frac{s}{a+e} = k \log \frac{a}{e} + \log M$$

où k est indépendant de la température, $\log M$ est une fonction linéaire de la température et du poids moléculaire de s.

La sensibilité de la fonction transformée est pratiquement la même que celle du triangle classique.

INTRODUCTION

Les systèmes de démixtion ternaire de constituants a, e, s peuvent être représentés par des fonctions qui, dans un système de coordonnées déterminé, sont de la forme :

$$\Phi(a, e, s) = 0$$

La nature de cette expression n'est pratiquement jamais connue et de fait, les résultats apparaissent dans la littérature sous forme :

— soit d'une courbe dont on ne peut tirer que des renseignements semi-quantitatifs,

— soit de tableaux de chiffres, ce qui entraîne de volumineux ouvrages de compilation.[1]

Tout serait beaucoup plus simple si l'on connaissait la fonction $\Phi(a, e, s) = 0$ ou, au moins, une expression analytique approchée.

Ce problème a préoccupé les chercheurs depuis très longtemps et il est assez facile de distinguer deux périodes majeures dans le passé :

Note : Pour les références se rapportant à des systèmes ternaires étudiés, il nous a paru utile de donner les références de la compilation de Steffen[1], Vol. II, en indiquant entre ( ) le numéro correspondant car les résultats des mémoires originaux y ont souvent été recalculés en % en poids.

---

[1] H. Stephen et T. Steffen, « Solubilities of Inorganic and Organic Compounds », Pergamon Press, Londres, 1964.

La première, s'arrêtant au début du siècle, comportant l'étude de nombreux systèmes avec diverses tentatives, parfois très ingénieuses, pour trouver une expression analytique simple. [2–8]

Puis, entre 1910 et 1940, relativement peu de travaux sont publiés. En 1940 et certainement comme conséquence de la guerre, un renouveau d'intérêt se manifeste. L'ensemble de ces travaux, qui est très considérable, n'a pas abouti non plus à une représentation simple, ni dans le cadre général, ni dans un cadre plus étroit de groupe de systèmes de démixtion analogue. [9–14]

Nous avons été amenés à nous intéresser à ce problème, non par spécialisation scientifique mais en raison des difficultés que présente la recherche en chimie organique dans des centres éloignés de France (Hanoï et Tananarive). [15,16]

Nos hypothèses de départ se sont situées dans deux domaines très différents :

1° La démixtion est un problème de molécules plutôt qu'un problème de quantités. Les variables devront donc être exprimées de préférence en molécules plutôt qu'en pourcentages en poids.

2° Des considérations mathématiques, pour lesquelles nous allons prendre un exemple concret :

Soit un mélange eau (*e* molécules), alcool (*a* molécules) dont le nombre total de molécules reste constant. A chaque mélange, pour obtenir une démixtion, il faut ajouter *b* molécules de benzène. On a ainsi pour

---

[2] C. Tuchschmidt et B. Follenius, *Ber. dtsch. Chem. Ges.*, **4**, 583 (1870).

[3] H. Pfeiffer, *Z. phys. Chem.*, **9**, 444 (1892).

[4] W. D. Bankroff, *Phys. Rev.*, 3, 21, 122, 131, 193, 205 (1895) formiate de butyle + 20° (3242) ; acétate de propyle + 20° (3241) ; propionate de propyle + 20° (3303) ; butyrate de méthyle + 20° (3238) ; butyrate d'éthyle + 20° (3301) ; butyrate de propyle + 20° (3359) ; isovalérate d'éthyle + 20° (3357) ; valérate de méthyle + 20° (3299) ; valérate d'éthyle + 20° (3356) ; monochloroacétate d'éthyle + 20° (3201) ; dichloroacétate d'éthyle + 20° (3197) ; trichloroacétate d'éthyle + 20° (3195).

[5] J. Waddel, *J. phys. Chem.*, **2**, 233 (1898).

[6] A. T. Lincoln, *J. phys. Chem.*, **8**, 248 (1904).

[7] J. M. Bemm, *J. phys. Chem.*, **9**, 531 (1905).

[8] W. D. Bonner, *J. phys. Chem.*, **14**, 738 (1910) *m*-xylène 0° (3377) ; heptane (3362) ; toluène 0° (3337) ; BrEt 0° (3164) ; BrPr 0° (3185) ; Br iso Bu 0° (3216) ; Br iso Am 0° (3243) ; Br Φ 0° (3261) ; dichlor-1,2 éthane 0° (3035) ; alcool benzylique 0° (3345) ; alcool isoamylique 0° (3254).

[9] I. Bachmann, *Ind. Ing. Chem.* (*Analyt. Ed.*), **12**, 38 (1940).

[10] A. V. Brancker, T. G. Hunter et A. W. Nash, *Ind. Eng. Chem. (Analyt. Ed.)*, **12**, 35 (1940).

[11] D. F. Othmer et P. E. Tobias, *Ind. Eng. Chem.*, **34**, 693 (1942).

[12] J. H. Hildebrand, « Solubility of Non Electrolyte », 2e édition, Reinhold, New York, 1936, p. 184.

[13] R. E. Treyball, *Ind. Eng. Chem.*, **36**, 875 (1944).

[14] J. A. Campbell, *Ind. Eng. Chem.*, **36**, 1158(1944).

[15] P. A. Laurent et M. J. Laurent-Duhamel, *Compt. rend.*, **234**, 2069 (1952) : *Bull. Soc. chim. France*, **1953** , 157, 161.

P. A. Laurent et J. P. Antunes Gomes, *Technica Lisboa*, **240**, 319 (1954).

[16] P. A. Laurent et M. J. Laurent-Duhamel, *Compt. rend.*, **265**, 333 (1967).

l'eau pure ($a = 0$) $b = 0$. Quand nous faisons tendre le mélange eau-alcool vers l'alcool pur, b tend vers l'infini (fig. 1*a*).
On aura ainsi une fonction :

$$b = f(a, e)$$

avec : $b = 0$ pour $a = 0$ (eau pure),
$b = \infty$ pour $e = 0$ (alcool pur).

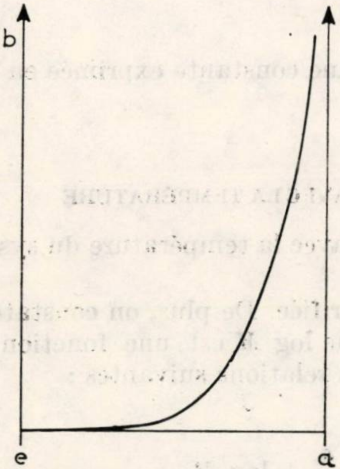

Fig. 1 *a*.

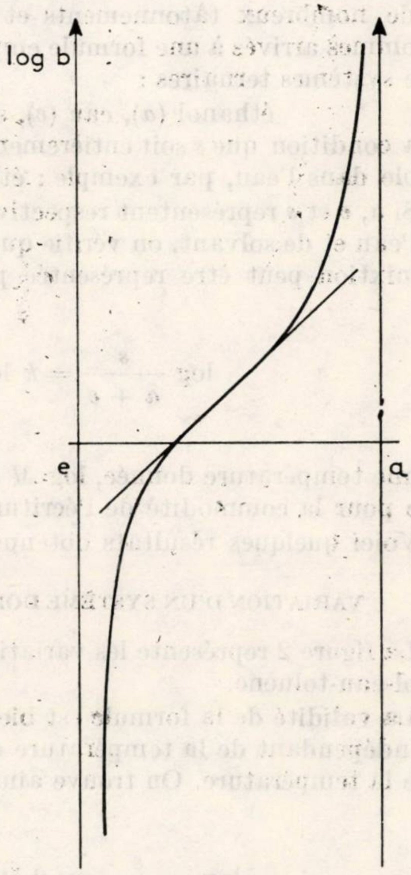

Fig. 1 *b*.

Si, au lieu de porter b en ordonnée, on porte $\log b$, on aura une nouvelle fonction :

$$\log b = \log f(a, e)$$

avec : $\log b = -\infty$ pour $a = 0$ (eau pure),
$\log b = +\infty$ pour $e = 0$ (alcool pur).

Entre ces deux extrêmités, une tangente d'inflexion peut être définie qui, sous une certaine approximation, pourra représenter valablement le phénomène dans un intervalle déterminé (fig. 1*b*).

Le problème consiste à trouver une fonction transformée de $b = f(a, e)$ telle que le contact avec la tangente d'inflexion soit d'ordre aussi élevé que possible.

Il résulte des considérations précédentes qu'il n'y a pas de solution unique mais tout un groupe de solutions.

Après de nombreux essais qui se sont soldés par des échecs, et à la suite de nombreux tâtonnements et d'ajustements souvent fastidieux, nous sommes arrivés à une formule empirique valable pour certains ensembles de systèmes ternaires :

éthanol (a), eau (e), solvants organiques (s)

sous la condition que s soit entièrement soluble dans l'alcool et totalement insoluble dans l'eau, par exemple : éthanol-eau-benzène.

Si a, e et s représentent respectivement le nombre de molécules d'alcool, d'eau et de solvant, on vérifie que dans un large intervalle, la courbe de démixtion peut être représentée par :

$$\log \frac{s}{a+e} = k \log \frac{a}{e} + \log M$$

où, à une température donnée, $\log M$ est une constante exprimée en logarithme pour la commodité de l'écriture.

Voici quelques résultats obtenus :

VARIATION D'UN SYSTÈME DONNÉ AVEC LA TEMPÉRATURE

La figure 2 représente les variations avec la température du système éthanol-eau-toluène.

La validité de la formule est bien vérifiée. De plus, on constate que k est indépendant de la température et que $\log M$ est une fonction linéaire de la température. On trouve ainsi les relations suivantes :

$$\log \frac{s}{a+e} = 2{,}58 \log \frac{a}{e} + \log M_t$$

avec :

$$\log M_t = \frac{1{,}14}{100}\, t + \bar{2}{,}84$$

A titre d'exemple, dans ce cas particulier, nous avons — à partir de la droite obtenue par la relation précédente — interpolé les valeurs (points ●) et reporté sur le même graphique les points expérimentaux (points ○) (fig. 3). Le résultat apparaît comme très satisfaisant.

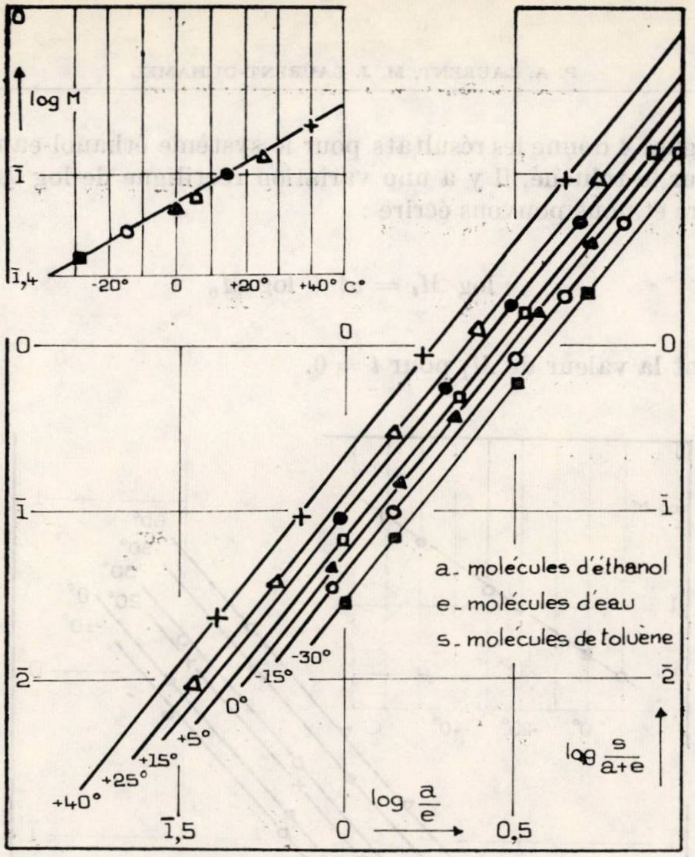
log M
Ī
Ī,4
-20°
0
+20°
+40° C°
0
0
0
Ī
Ī
2̄
2̄
a. molécules d'éthanol
e. molécules d'eau
s. molécules de toluène
-30°
-15°
0°
+5°
+15°
+25°
+40°
log $\frac{s}{a+e}$
log $\frac{a}{e}$
Ī,5
0
0,5

Fig. 2

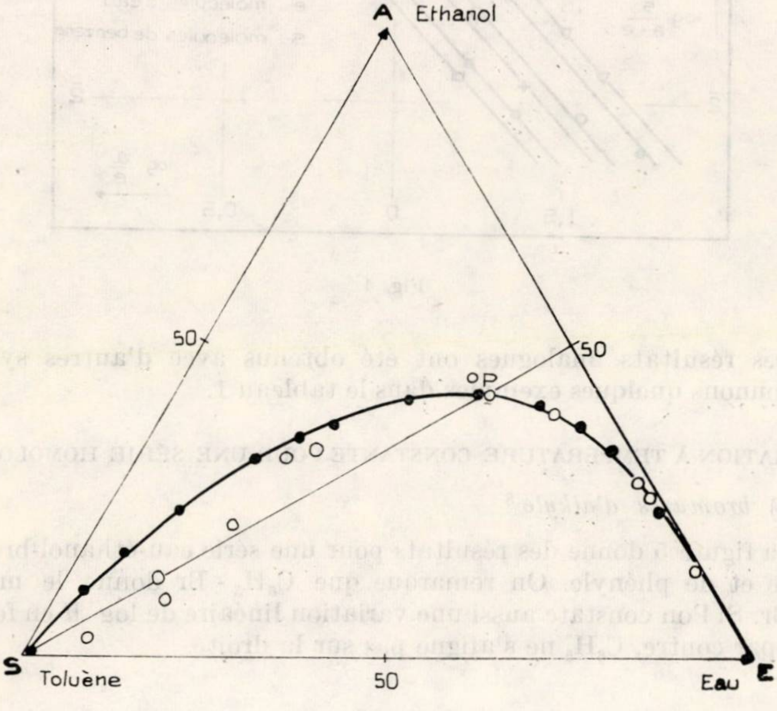
A Ethanol
50
50
P
S
Toluène
50
Eau
E

Fig. 3

La figure 4 donne les résultats pour le système éthanol-eau-benzène. Comme pour le toluène, il y a une variation rectiligne de log M_t avec la température et nous pouvons écrire :

$$\log M_t = \alpha t + \log M_0$$

M_0 étant la valeur de M_t pour $t = 0$.

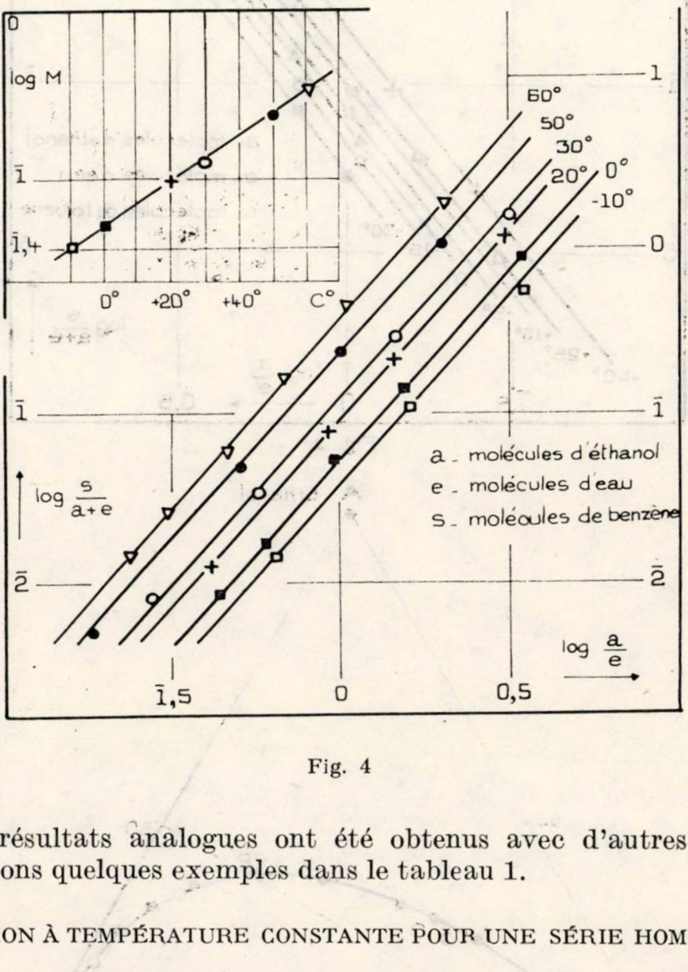

Fig. 4

Des résultats analogues ont été obtenus avec d'autres systèmes Nous donnons quelques exemples dans le tableau 1.

VARIATION À TEMPÉRATURE CONSTANTE POUR UNE SÉRIE HOMOLOGUE

a) *bromures d'alkyle* [8]

La figure 5 donne des résultats pour une série eau-éthanol-bromures d'alkyle et de phényle. On remarque que C_6H_5 - Br donne le même *k* que RBr. Si l'on constate aussi une variation linéaire de log *M* en fonction de C_n, par contre, C_6H_5 ne s'aligne pas sur la droite.

Tableau 1

Valeurs de k, α et log M_0 pour quelques systèmes ternaires

Systèmes eau et éthanol	Intervalle de température	Δt	k	log M_0	$\log M_t = \alpha t + \log M_0$	Références
benzène	$-10°$ à $+60°$	70°	2.23	$\bar{2},72$	$= \frac{1,60}{100} t + \bar{2},72$	14–19, 24–28
toluène	$-30°$ à $+40°$	70°	2,58	$\bar{2},84$	$= \frac{1,14}{100} t + \bar{2},83$	8,20–25
m-xylène	0° à $+50°$	50°	2,28	$\bar{2},42$	$= \frac{0,92}{100} t + \bar{2},42$	8,28,29
chloroforme	$+15°$ à $+65°$	50°	1,96	$\bar{1},14$	$= \frac{0,69}{100} t + \bar{1},14$	30
dichloro–1,2 éthane	0° à $+60°$	60°	2,28	$\bar{1},32$	$= \frac{0,97}{100} t + \bar{1},32$	8,31

[17] D. N. Tarasenkov et A. Paul'sen Ya, *Zhur. org. Khim.*, **7**, 2143 (1937), hexane (3316).

[18] J. Chang, J. Chung et R. W. Moulton, *Ind. Eng. Chem.*, **45**, 2350 (1953),isovalérate d'éthyle + 25° (3358).

[19] J. Barbaudy, *Rec. Trav. chim.*, **45**, 207 (1926) benzène +25° +60° (3274).

[20] D. N. Tarasenkov, Ye et N. Polozhentseva Ye, *Zhur. org. Khim.*, **84** (1932), toluène + 40° (3339).

[21] C. B. Kretschmer et R. Wiebe, *Ind. Eng. Chem.*, **37**, 1130 (1945), octane (3387).

[22] P. Mondain-Monval et J. Quiquares, *Compt. rend.*, **210**, 246 (1940), toluène + 25° (3342).

[23] H. Pfeiffer, *Z. phys. Chem.*, **9**, 444, 469 (1892), monochloracétate d'éthyle + 20° (3200) ; dichloracétate d'éthyle + 20° (3196) ; trichloracétate d'éthyle + 20° (3194) ; formiate de propyle + 20° (3211) ; formiate de butyle + 20° (3242) ; formiate d'amyle + 20° (3305) ; acétate de propyle + 20° (3241) ; acétate de butyle + 20° (3304) ; acétate d'amyle + 20° (3360) ; acétate d'isoamyle + 20° (3361) ; propionate de méthyle + 20° (3205) ; propionate d'éthyle + + 22° (3239) ; propionate de méthyle + 20° (3303) ; butyrate de méthyle + 20° (3237) ; isovalérate de méthyle + 20° (3300) ; isovalérate d'éthyle + 20° (3357) ; valériate d'éthyle + 20° (3356).

[24] F. Z. Wehrmann, *Elektrochem.*, **27**, 386 (1921), benzène −10°, 0°, +20°, +30° (3271).

[25] W. R. Ormandy et E. C. Craven, *J. Inst. Petrol. Techn.*, **7**, 325, 422 (1921), toluène −30°, −15°, 0°, +15° (3338).

[26] W. R. Ormandy et E. C. Craven, *J. Inst. Petrol. Techn.*, **8**, 181, 213 (1922), pentane (3247).

[27] J. L. Schweppe et J. R. Larah, *Ind. End. Chem.*, **46**, 2391 (1954), heptane (3364).

[28] A. Seidell et W. F. Linke, « Solubility of Inorganic Compounds », New York, 1950 ; benzène +20 +50° (3268) ; *méta*-xylène 0+50° (3378).

[29] E. Leikola, *Suomen Kem.*, **13 B**, 13 (1940), *méta*-xylène +20° (3379).

[30] N. Schoorl et A. Regen Boden, *Rec. Trav. chim.*, **41**, 1 (1922), chloroforme 0°+10°+ +15° +20° +25 +66° (2667).

[31] V. V. Udovenko et Log. Fatkulina, *Zhur. fiz. Khim.*, **26**, 892 (1952), dichloro-1,2 éthane +30° +40° +50° +60° (3036).

b) *esters* [23, 18]

Ils dépendent de deux facteurs : l'acide et l'alcool.

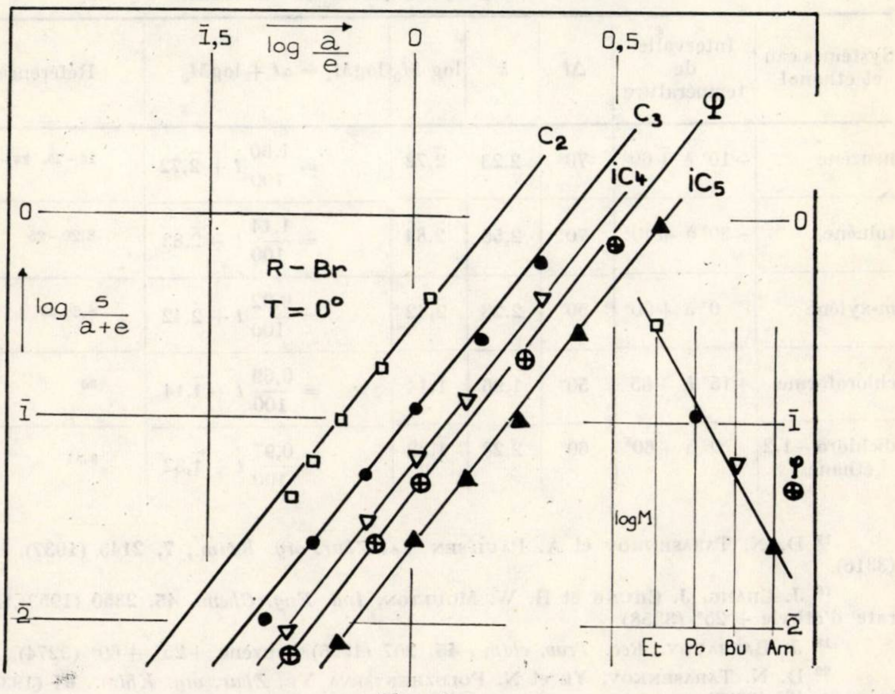

Fig. 5

VARIATIONS EN FONCTION DE L'ALCOOL

Pour un ester déterminé, la transformation de la courbe de démixtion est une droite ($k = 3$, 20). Pour différents esters d'un même acide avec des alcools différents, on obtient des droites parallèles ($k = 3{,}20$) et une variation linéaire de log M avec le poids moléculaire de l'alcool (fig. 6).

VARIATIONS EN FONCTION DE L'ACIDE

Quand, pour un même alcool, on faire varier l'acide, on s'attend à des résultats semblables mais on constate des différences assez nettes. Si l'on compare les esters d'un même alcool (les acides variant de l'acide formique à l'acide valérique), on obtient également des droites parallèles. La figure 6 donne des variations de log M en fonction du poids moléculaire de l'alcool pour différents acides (les points pour les acétates et les formiates de méthyle et d'éthyle sont extrapolés ; ces esters sont notablement solubles dans l'eau, ce qui est hors du cadre de l'hypothèse).

Quand on compare les variations de log M des esters d'un même alcool (ici les esters propyliques car la série est la plus complète), on constate en première approximation une décroissance, et en deuxième approximation une alternance des acides pairs et impairs. Nous avons essayé de retrouver cette alternance dans la solubilité des esters dans l'eau. Les résultats sont insuffisamment précis pour permettre une conclusion.

Des résultats analogues ont été obtenus pour la série éthanol-eau-chloracétates d'éthyle [4,23].

$$\log \frac{s}{a+e} = 2{,}44 \log \frac{a}{e} + \begin{array}{l} \bar{1}{,}70\ (CH_2Cl-COO-C_2H_5) \\ \bar{1}{,}30\ (CHCl_2-COO-C_2H_5) \\ \bar{2}{,}95\ (CCl_3\ -COO-C_2H_5) \end{array}$$

ALCANES [17,21,25–27]

Les résultats observés ci-dessus devraient se retrouver pour les alcanes (pentane à décane). En effet, ils répondent le mieux aux conditions de solubilité fixées au début : miscibilité totale à l'éthanol, insolubilité dans l'eau.

L'examen de nombreux systèmes éthanol-eau-alcane n'a cependant pas donné les résultats attendus. On obtient des droites mal définies dont les coefficients angulaires varient dans une même série homologue. Pour un même alcane, les variations avec la température ne sont pas cohérentes non plus.

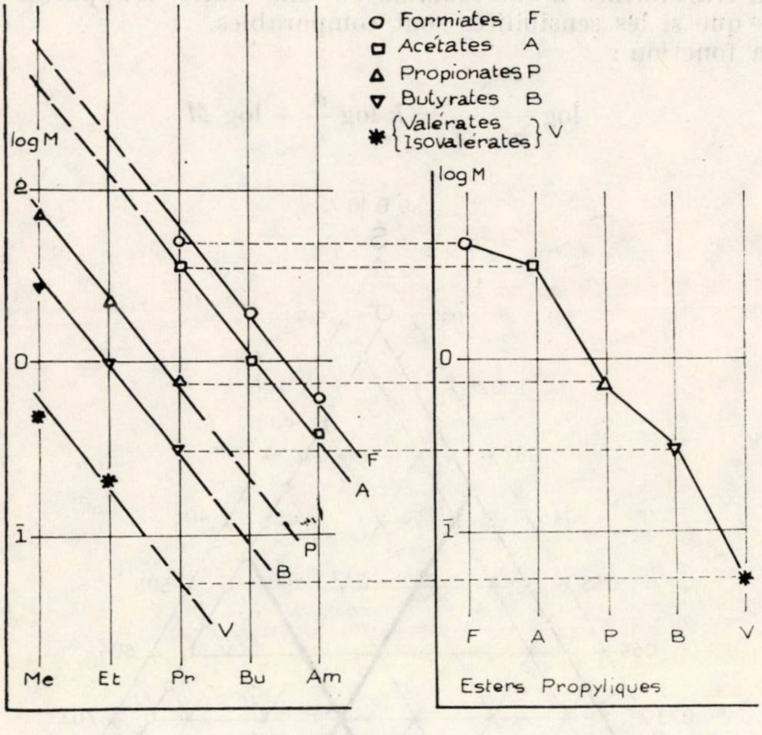

Fig. 6

L'hypothèse que les hydrocarbures ne soient pas purs ne doit sans doute pas être retenue quoique de nombreuses mesures soient assez anciennes. Nous n'avons pas trouvé de mesures faites avec des étalons du National Bureau of Standard.

AUTRES SYSTÈMES

Toujours sous la même hypothèse nous avons étudié un certain nombre de systèmes eau-solvant organique, avec le méthanol, le propanol ou l'isopropanol. Les résultats sont analogues à ceux qui sont exposés ci-dessus pour l'éthanol, sans qu'il soit toutefois actuellement possible de relier simplement ces groupes avec le groupe de l'éthanol.

Les systèmes comportant de l'acétone, du dioxanne, ou de la pyridine à la place de l'alcool, ne donnent pas de droite avec la formule indiquée.

SENSIBILITÉ DE LA TRANSFORMÉE

La transformée d'une fonction en une autre n'apparaît comme pratique que si les sensibilités sont comparables.

La fonction :

$$\log \frac{s}{a+e} = k \log \frac{a}{e} + \log M$$

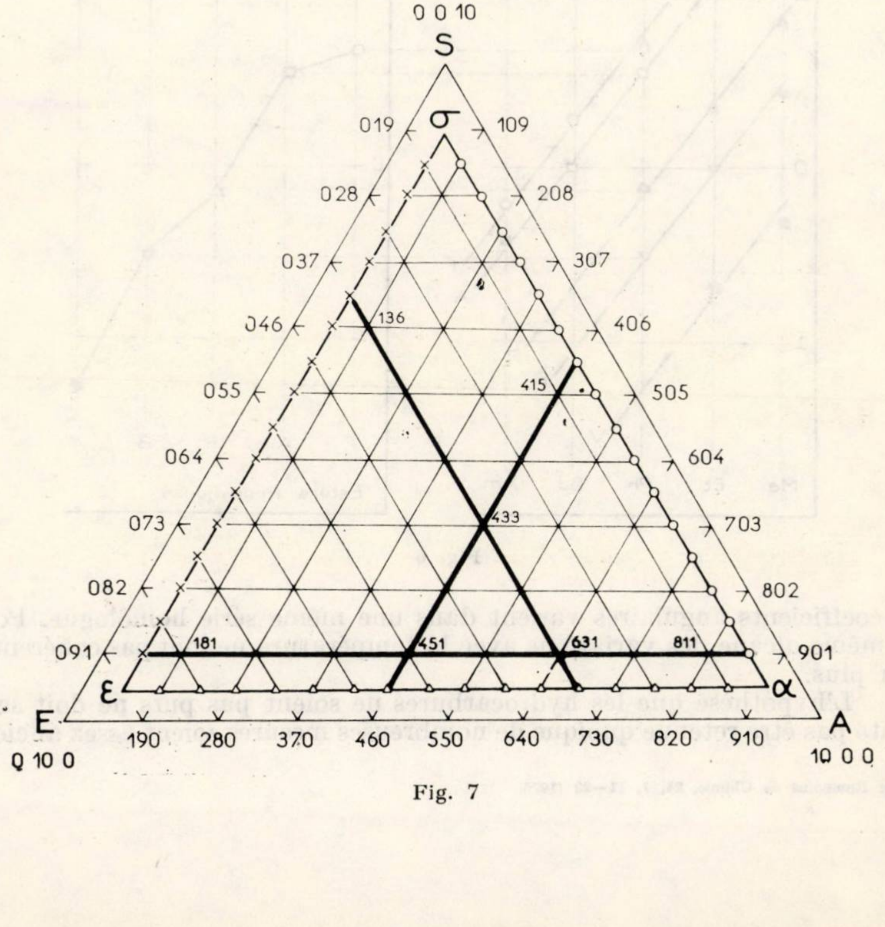
0 0 10
S
σ
019
109
028
208
037
307
046
136
406
055
415
505
064
604
433
073
703
082
802
091
181
451
631
811
901
ε
α
E
A
190
280
370
460
550
640
730
820
910
0 10 0
10 0 0

Fig. 7

n'est pas définie pour les valeurs nulles de *a*, *e*, *s*. Il en résulte que le triangle classique A E S (fig. 7) est transformé en un espace infini. Ce fait paraît enlever tout intérêt réel à la fonction transformée. Cependant, il est facile de voir qu'une très bonne approximation est réalisée.

Si dans le triangle classique A E S* (fig. 7) nous convenons que chaque point représente dix molécules (tout comme dans les représentations ordinaires chaque point représente 100 g de mélange ternaire), les sommets A E S sont représentés par :

	alcool	eau	solvant
A	10	0	0
E	0	10	0
S	0	0	10

et chaque point pourra être représenté par un ensemble de trois chiffres dont la somme devra être égale à 10.

En particulier, les points α, ε et σ seront représentés par :

	alcool	eau	solvant
α	9	0,5	0,5
ε	0,5	9,5	0,5
σ	0,5	0,5	9

Tous les points du triangle $\alpha\ \varepsilon\ \sigma$ sont représentés dans le triangle curviligne $\alpha\ \varepsilon\ \sigma$ de la fonction transformée (fig. 8) où nous portons en ordonnées log $\dfrac{s}{a+e}$ et en abscisses log $\dfrac{a}{e}$.

Considérons par exemple un ensemble de points représentés sur la figure 7 par la ligne :

460 Δ 451 433 415 ○ 406

La ligne transformée sur la figure 8 sera la courbe :

Δ 415 433 415 ○

les points 406 et 460 étant à l'infini.
Un raisonnement analogue montre que la ligne

901 ○ 811 631 451 181 X 091 (fig. 7)

---

* Nous avons représenté ce triangle avec le sommet *S* en haut pour faciliter la comparaison avec la figure 8.

est transformée en la droite horizontale

X 181 451 631 811 ○

de la figure 8. Les points 901 et 091 sont à l'infini. Même raisonnement pour :

037 X 136 433 431 Δ 730

de la figure 7 qui devient :

X 136 433 431 Δ

de la figure 8.

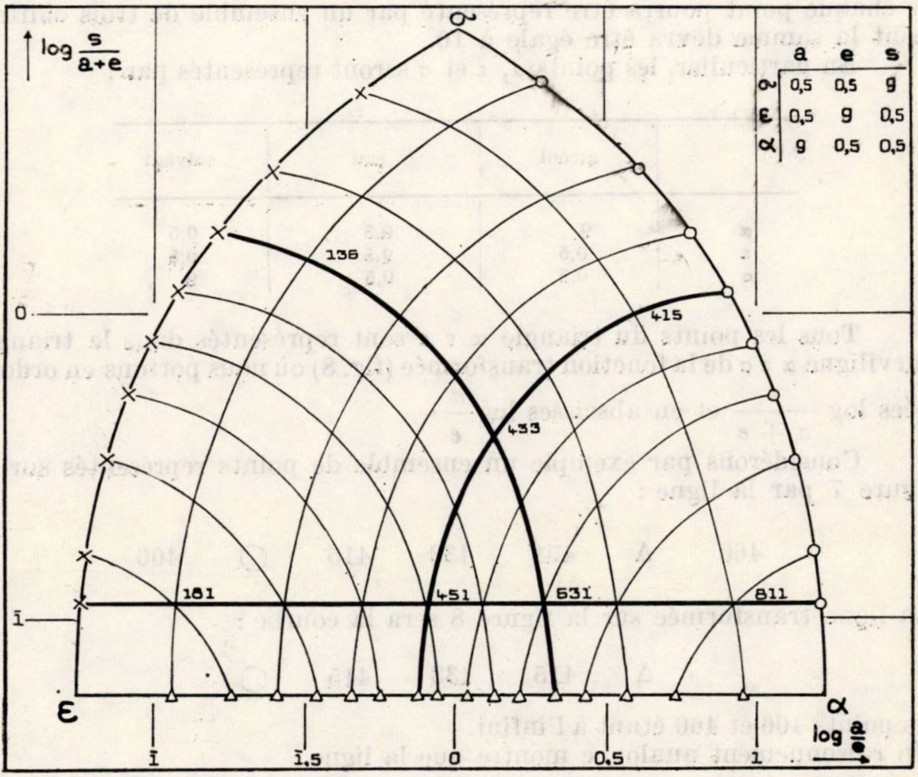
log $\frac{s}{a+e}$
σ
a e s
σ 0,5 0,5 9
ε 0,5 9 0,5
α 9 0,5 0,5
136
415
0
433
181
451
631
811
1̄
ε
α
log $\frac{a}{e}$
1̄
1̄,5
0
0,5
1

Fig. 8

Il s'ensuit que tous les points du triangle α ε σ de la figure 7 se trouvent dans le triangle curviligne α ε σ de la figure 8 et que seuls les points de la figure 7 compris entre le triangle A E S et le triangle α ε σ ne sont pas valablement représentés.

Plus subjectivement, nous donnons sur la figure 9 une courbe de démixtion en pourcentage en poids et en pourcentage en molécules, et la transformée. On s'aperçoit que les sensibilités sont tout à fait comparables.

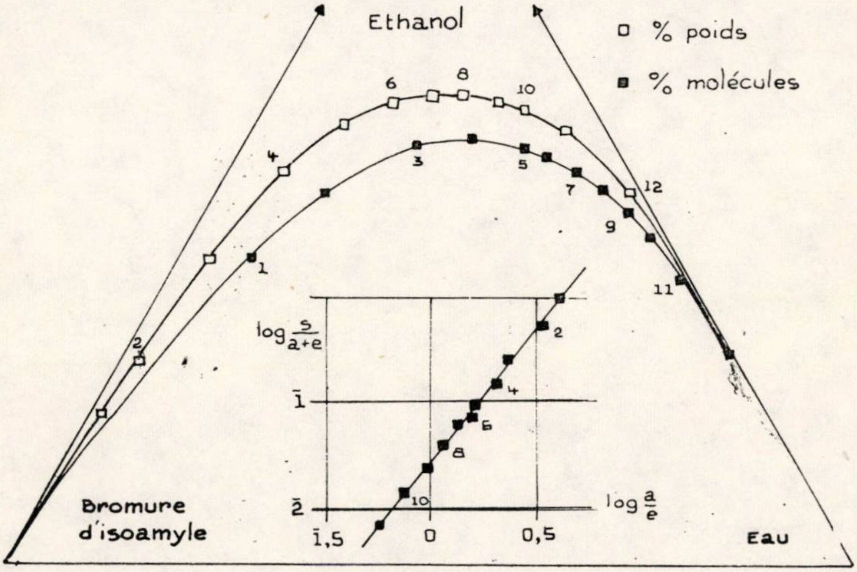

Fig. 9

CONCLUSION

La relation préconisée paraît être très satisfaisante pour les familles étudiées. Elle permet une interpolation excellente et une correction très valable des erreurs expérimentales.

Elle doit être considérée comme une forme simplifiée d'une relation beaucoup plus complexe qui serait justiciable d'une étude thermodynamique pour aller plus loin.

Revue Roumaine de Chimie, **21**, *1*, 25–30 (1976)

MELTING HEATS OF ALKALI HALIDE SOLID SOLUTIONS

D. I. MARCHIDAN and LAURA VASU

Centre of Physical Chemistry
Str. Galaţi 31, Bucharest, Romania

Received 17 Mai 1975

By means of a differential calorimetric method, the melting heats of the solid solutions in the following binary systems were obtained : $NaCl + KCl$; $NaBr + KBr$; $NaI + KI$. The results are correlated with the phase diagrams and other thermodynamic properties.

In this work, we have extended the differential calorimetric studies[1,2] on heats of melting to binary mixtures of alkali halides. The chosen systems : $NaCl + KCl$, $NaBr + KBr$, $NaI + KI$ form in solid state a continuous series of solutions[3,4] with minimum at molar fraction of the sodium salt equal to 0.5 for chlorides and bromides and 0.6 for iodides.

EXPERIMENTAL

A differential calorimeter for high temperatures was used ; the calorimeter block was made of refractory steel. Alumina was used as reference material. Both the sample and the alumina were contained in fused silica cells. The temperature difference between the cells was measured by means of 6 thermocouples, whose beads were symmetrically disposed on the bottom of the cells. Runs were carried out at a heating rate of 2.1°/min. The calorimeter was calibrated by a method already reported [1,2], using pure chemicals. To prepare the mixtures, the pure salts were dried and melted together in the respective acid atmosphere before introducing them into the cell.

For alkali halides, the Dworkin and Bredig's values[5] for the heats of melting are satisfying in the best way the sensitivity equation [2,6] of the calorimeter :

$$1/S = A + BT_m^3$$

S is sensitivity (mm²/joule), T_m—melting temperature and A, B—constants of the calorimeter

---

[1] D. I. MARCHIDAN and L. VASU, *Rev. Roumaine Chim.*, **17**, 1649 (1972).
[2] D. I. MARCHIDAN and L. VASU, *Rev. Roumaine Chim.*, **18**, 1295 (1973).
[3] N. K. VOSKRESENSKAYA, "Spravochnik po plavkosti sistem iz bezvodnykh neorganicheskikh solei", vol. 1, Izd. Nauka Moscow, 1961, p. 356–362, 334 and 393.
[4] P. V. CLARK, "Data cumulation : Fused salt mixtures : Eutectic compositions and melting points", Albuquerque, 1961, p. 66, 137 and 153.
[5] A. S. DWORKIN şi M. A. BREDIG, *J. Phys. Chem.*, **64**, 269 (1960).
[6] M. M. FAKTOR and R. HANKS, *Trans. Faraday Soc.*, **63**, 1122 (1967).

The values chosen for calibration are:
Sb (903 K; 19.89 kJ/mol); [7] CsCl (918 K; 20.235 kJ/mol); NaI(933 K; 23.575 kJ/mol); KI (954 K; 24.00 kJ/mol); RbCl (995 K; 23.70 kJ/mol); KBr (1007 K; 25.50 kJ/mol); NaBr (1020 K; 26.08kJ/mol); KCl (1043 K; 26.50 kJ/mol); NaCl (1073 K; 28.00 kJ/mol).

RESULTS AND DISCUSSION

By using the calibration curve the melting heats of the mixtures were obtained; the results are summarized in table 1.

Table 1

Heats of melting for the binary mixtures

System	x_{KCl}	ΔH_{exp} kJ/mol	$\Sigma x_i\, \Delta H_i$ kJ/mol	System	x_{KBr}	ΔH_{exp} kJ/mol	$\Sigma x_i\, \Delta H_i$ kJ/mol
NaCl–KCl	0.20	23.30	27.70	NaBr–KBr	0.25	22.61	25.94
	0.40	21.84	27.40		0.50	21.90	25.80
	0.50	21.53	27.25		0.75	22.10	25.65
	0.60	21.63	27.10		x_{KI}		
	0.80	23.72	26.80	NaI–KI	0.20	20.90	23.66
					0.40	19.65	23.74
					0.60	20.06	23.83
					0.80	20.70	23.92

The (Na — K) halide systems form in solid state a continuous series of solutions with minimum on the phase diagram.

For the compositions near the minimum, the values obtained for the heat of melting are the same, no matter how long ago the mixtures were prepared. For molar fractions far from minimum, the ΔH values for fresh mixtures (in the limit of a few days) are slightly smaller than that for older mixtures; the values reported here correspond to fresh mixtures.

As one can see from table 1, the melting heats for mixtures are smaller than those calculated additively from the melting heats of the components. As is to be expected, the difference is greater for compositions corresponding to minimum on the phase diagram.

For a binary solid solution AB, whose components (A and B) have no transition before melting, the heat of melting is obtained by means of a thermodynamic cycle:

$$\Delta H_{AB}(T_{AB}) = x_A\, \Delta H_A(T_{AB}) + x_B\, \Delta H_B(T_{AB}) - \Delta H_{ss}(T_{AB}) + \Delta H^L_{\mathrm{mix}}(T_{AB}) \quad (1)$$

---

[7] L. Malaspina, R. Gigli and V. Piacente, *Rev. Int Hautes Tempér. et Refract.*, **8**, 211 (1971).

where we have :

x_A, x_B — the molar fractions of the components ;

$\Delta H_A(T_{AB})$, $\Delta H_B(T_{AB})$ — the heats of melting of the components at the melting temperature of the mixture (T_{AB}) ;

$\Delta H_{ss}(T_{AB})$ — the heat of formation of the solid solution (*at* T_{AB});

$\Delta H^L_{mix}(T_{AB})$ — the heat of mixing in the liquid state (at T_{AB}).

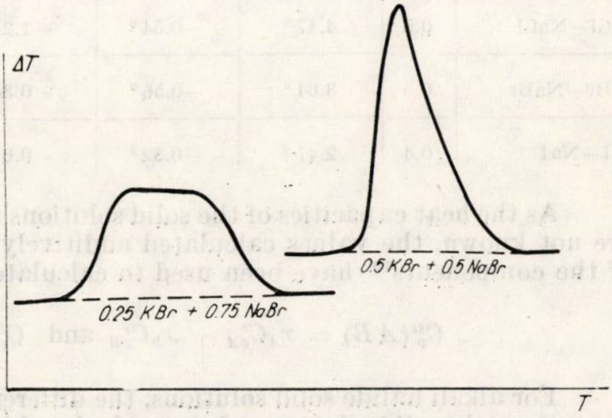

Fig. 1. — Shapes of different recorded $\Delta T - T$ curves.

As, in practice, all these heat effects are determined at other temperatures, an alternate expression to calculate $\Delta H_{AB}(T_{AB})$, taking into account only the known experimental values, would be :

$$\Delta H_{AB}(T_{AB}) = x_A \Delta H_A(T_{AB}) + x_B \Delta H_B(T_{AB}) + \Delta H^L_{mix}(T) - \Delta H^{298}_{ss} + \Delta H(C_p) \qquad (2)$$

$$(T > T_B > T_A > T_{AB})$$

T_A, T_B — are the melting temperatures of the pure components.

In this expression, as the values at higher temperatures are not known, the experimental values[8] ΔH_{ss} at 298 K were introduced. For binary mixtures of alkali halides, the heats of formation of the solutions are great (2.5 — 4.5 kJ/mol). The mixing heats in the liquid state have the order of 0.5 kJ/mol for these systems.

Further, a heat capacity correction $\Delta H(C_p)$ is necessary ; when the phase diagram presents a pronounced minimum the $\Delta H(C_p)$ contribution can be important.

In table 2, the experimental values of the heats of melting are compared with the values calculated by the Eq. (2), for compositions corresponding to minimum on the phase diagram, where the fluctuations of the experimental values are very small.

---

[8] M. V. Lister and N. F. Meyers, *J. Phys. Chem.*, **62**, 145 (1958).

Table 2

The calculated and the experimental heats of melting

System	x_{KX}	ΔH_{ss} kJ/mol	$\Delta H^L_{\text{mix}}(T)$ kJ/mol	$\Delta H(C_p)^{10}$ kJ/mol	ΔH_{calc} kJ/mol	ΔH_{exp} kJ/mol
KCl−NaCl	0.5	4.47 [8]	−0.54 [9]	−1.25	20.90	21.53
KBr−NaBr	0.5	3.64 [8]	−0.56 [9]	−0.34	21.23	21.90
KI−NaI	0.4	2.47 [8]	−0.52 [9]	−0.67	20.06	19.65

As the heat capacities of the solid solutions and of the liquid mixtures are not known, the values calculated additively from the heat capacities of the components[10] have been used to calculate $\Delta H(C_p)$:

$$C_p^{ss}(AB) = x_A C_{pA}^s + x_B C_{pB}^s \text{ and } C_{pA}^L + x_B C_{pB}^L.$$

For alkali halide solid solutions, the difference ΔC_p, between the heat capacity of the solid solution and that calculated from the values of the components cannot be too large. There are two contributions to this difference : ΔC_p^c — a configurational contribution and ΔC_p^v — a vibrational one. As the disorder is increasing at higher temperatures, the contribution of ΔC_p^c to ΔC_p is expected to decrease as the temperature is raising, but even at room temperature its value does not seem to exceed 2% from the total heat capacity . [11]

The ΔC_p^v contribution increases with increasing temperature. The quantities ΔC_p^c and ΔC_p^v vary in opposite directions as temperature is increasing, so that at higher temperature the ΔC_p value must be rather small.

Indeed, it is to be expected that $\Delta H_{ss}(T_{AB}) > \Delta H_{ss}^{298}$. The agreement between the calculated and the experimental values (see fig. 2 and table 2) shows that the temperature dependence of the heat of formation of the solid solution seems to be relatively small.

CONCLUSIONS

The experimental heats of melting for some alkali halide binary mixtures (solid solutions) were determined by using a differential calorimeter. The results confirm the idea that, for the studied systems, the heat capacities of the solid solutions can be well approximated by those calculated additively from the heat capacities of the components.

---

[9] L. S. Hersh and O. J. Kleppa, *J. Chem. Phys.*, **42**, 1309 (1965).

[10] "IANAF Thermochemical Tables" (ed. D. R. Stull), Dow Chemical Company, Midland, Mich., Aug. 1965, Nr. PB 168−370.

[11] V. Hovi, *Ann. Acad. Scient. Fennicae*, Ser. A_I **88**, **3**, 1 (1951).

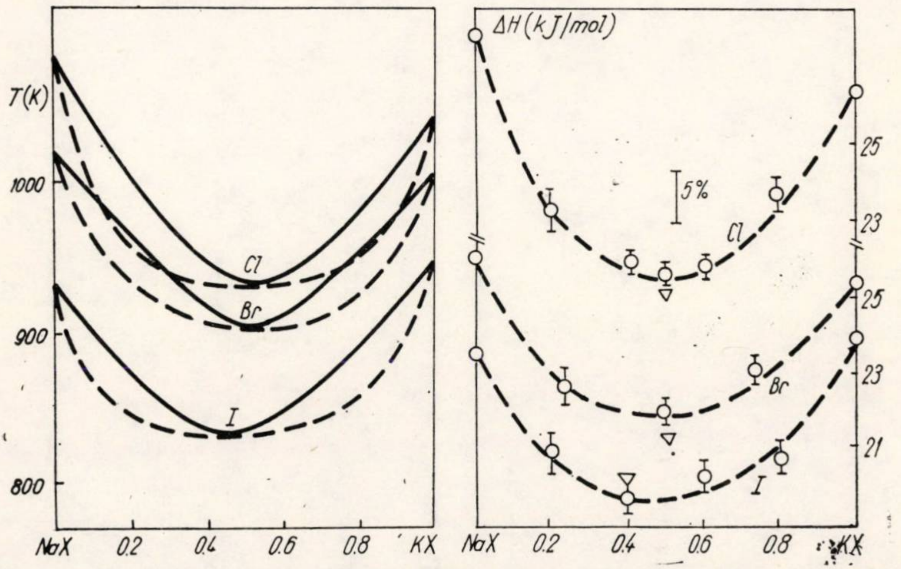

Fig. 2. — The phase diagrams and the melting heats — composition plots. ∇ — ΔH, calculated; ○ — ΔH, experimental.

As one can see from fig. 2, there is a direct correlation between the shape of the phase diagram and the shape of the curve heat of melting versus composition.

The magnitude of the heat of melting values for the mixtures and the shape of the recorded $\Delta T - T$ curves can indicate also the nature of the mixture. There are references, [12] for instance, indicating an eutectic in the NaCl — KCl system at atmospheric pressure (at equimolar composition). The agreement between the calculated values of the melting heats (by introducing the experimental value $\Delta H_{ss}^{298} = 4.47$ kJ/mol and the $\Delta H(C_p)$ correction) and the experimental ones supports a solid solution behaviour.

In addition, the shape of the recorded $\Delta T - T$ curve (which would be more sensitive to composition for an eutectic) also testifies a solid solution.

---

[12] D. S. Coleman and P. D. Lacy, *Mater. Res. Bull.*, **2**, 935 (1967).

Revue Roumaine de Chimie **21**, *1*, 31–39 (1976)

EQUILIBRIUM GEOMETRY AND HEAT OF FORMATION OF ALIPHATIC DIAZOCOMPOUNDS, DIAZIRINES AND RELATED SINGLET CARBENES. AMINDO/2 CALCULATION

M. MARTÍN, V. MENÉNDEZ and J. M. FIGUERA

Instituto de Quimica Física "Rocasolano", C.S.I.C., Serrano 119
Madrid — 6, Spain

Received 19 July 1974

Equilibrium geometry and heat of formation calculations of aliphatic diazocompounds up to diazo-*n*-butane, diazirine, its methyl substituted derivatives and the singlet carbenes related to these molecules have been performed by means of the semiempirical MINDO/2 method coupled with the STEPIT subroutine of minimum direct search. A good agreement of the evaluated geometrical parameters and the scarce experimental data is found. The heat of formation of diazomethane amounts to 80.2 kcal mol^{-1}, diazirine is evaluated as being less stable in 7 kcal mol^{-1}. The substantial decrease of the heat of formation caused by replacing an H atom by a methyl group is explained by the formation of a partial double bond. The results afford a self-consistent data set, not available previously for these molecules, which can be useful in thermochemical calculations.

INTRODUCTION

It is known [1, 2] that the first step of a number of thermal and photochemical reactions of diazocompounds and diazirines is the formation of a carbene.

An increased knowledge of molecular characteristics of these carbene precursors, such as electronic structure and geometry of the ground and excited states, heat of formation and bond energies will be helpful for the mechanistic understanding of the reactions leading to divalent carbon species.

Aromatic and aliphatic diazocompounds have been synthesized long time ago, in 1858 and 1883 by Griess and Curtins respectively, but diazines have been reported as late as 1961 [3, 4]. The linear arrangement of the C — — N — N group in diazocompounds, a puzzling problem for chemists during many years, has been established by physical methods, electron diffrac-

---

[1] W. Kirmse, "Carbene Chemistry" (2nd Edition), Academic Press, New York, 1971, p. 18, 35.

[2] J. M. Figuera, E. Fernández and M. J. Avila, *J. Phys. Chem.* **78** 1348 (1974).

[3] E. Schmitz and R. Ohne, *Tetrahedron Letters*, **1961**, 612.

[4] S. R. Paulsen, *Angew. Chem.*, **72**, 781 (1960).

tion [5] and microwave spectroscopy[6]; on the other hand, in diazirines this group builds a three-membered ring 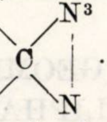 .

The heat of formation of the simplest aliphatic diazocompound, diazomethane, has been the subject of considerable controversy. Paulett and Ettinger [7] suggested the value of 49.3 kcal mol^{-1}, based on the results of electron impact experiments and assuming that the CH_2^+ ion was formed in its ground state. Bell analysed the above data [8], and bearing in mind the findings of Rabinovitch and Setser on diazomethane pyrolysis [9] proposed a value of 71 kcal mol^{-1}. Paulett and Ettinger [10] disagreed with this result and a new calculation afforded a higher value of 103 kcal mol^{-1} for the heat of formation of diazomethane. The kinetic data of Hassler and Setser [11] support a value higher than 68 kcal mol^{-1}.

Furthermore, Paulett and Ettinger evaluated the difference between the heat of formation of diazirine and diazomethane as 30 kcal mol $^{-1}$.

The situation as regards diazomethane being so confused, it follows the lack of consistent data for the heat of formation of the higher homologous in the series. A similar situation occurs for diazirines and aliphatic carbenes.

As an approach to this problem we have performed a set of consistent calculations of the heat of formation and ground state geometry of the aliphatic diazocompounds containing as many as 4 carbon atoms, diazirine and its methyl derivatives, as well as the singlet carbenes related to these molecules.

DESCRIPTION OF CALCULATIONS

The molecular energy may be written as $E = E(q_1, q_2 \cdots q_{3n-6})$ where the q_i are the position coordinates of the N atoms. We wish to find the geometrical configuration that corresponds to the minimum energy. The MINDO/2 method [12] has been used for the calculation of the energy and the minimum with respect to the position coordinates was located using the STEPIT subroutine. [13]

The MINDO/2 method has been selected because it has been proved reliable for the calculation of heats of formation and equilibrium geometries. *

The STEPIT subroutine is based on a procedure for direct search of minimum of a function of several variables for which derivatives are

---

* MINDO/2 method systematically overestimates CH bond length by 0.1 Å. The values reported in this work are corrected.

[5] H. Boersch, *Monatsh.*, **65**, 331 (1935).

[6] A. P. Cox, L. F. Thomas and J. Sheridan, *Nature*, **181**, 1000 (1958).

[7] G. S. Paulett and R. Ettinger, *J. Chem. Phys.*, **39**, 825 (1963). See also A. H. Laufer and H. Okabe, *J. Amer. Chem. Soc.*, **93**, 4137 (1971).

[8] J. A. Bell, *J. Chem. Phys.*, **41**, 2556 (1964).

[9] D. W. Setser and B. S. Rabinovitch, *Canad. J. Chem.*, **40**, 1425 (1962).

[10] G. S. Paulett and R. Ettinger, *J. Chem. Phys.*, **41**, 2557 (1964).

[11] J. C. Hassler and D. W. Setser, *J. Amer. Chem. Soc.*, **87**, 3793 (1965).

[12] M. J. S. Dewar and E. Haselbach, *J. Amer. Chem. Soc.*, **92**, 590 (1970).

[13] Q.C.P.E. 66, Bloomington, Indiana.

not available. As the computation time could be excessive, we have reduced the number of variables to those coordinates, which we call "actives", that we expect to influence the energy predominantly. The rest of the coordinates are fixed to their standard values.

The search of the function's minimum requires the evaluation of the function at a considerable number of points, 100 is a typical value in these calculations, depending on the number of active variables. A substantial decrease of the computing time (more than a half) is achieved if the eigenvectors of a MINDO calculation are saved and used as initial values in the following calculation. In this way SCF convergence requires only two or three iterations.

RESULTS AND DISCUSSION

DIAZOCOMPOUNDS

Calculations have been carried out for the first members of the aliphatic series. The active variables chosen are : CN, NN bond lengths and the $H\widehat{C}H$ and $H\widehat{C}N$ angles in the diazomethane molecule, one CH bond being replaced by the C_1C_5 bond (Fig. 1) as active variable in the alkyl substituted homologous.

Standard values for the geometrical parameters of the alkyl chain were used and no attempt was made to evaluate rotational barriers. The most stable chain configurations were selected with the help of molecular models. The results are shown in Fig. 1.

The calculated geometry of diazomethane is very close to the experimental ; also, its heat of formation agrees with the best experimental evidence.[9, 11]

Our calculation shows that diazoethane is substantially more stable than diazomethane (ΔH_f^0(diazomethane) — ΔH_f^0(diazoethane) $\approx$ 18 kcal mol^{-1}). The increased stability of diazo-*n*-propane and diazo-*n*-butane is less remarkable and is similar to the values predicted by additivity rules in hydrocarbons .[15] The source of this differential stabilization along the series is not obvious. The effect cannot be ascribed to changes in the geometrical structure (see Fig. 1) of the diazo group through the series, because it remains practically unchanged. Obviously this effect is not related either to the radical chain that is maintained at its standard bond lengths and angles. A possible source of the observed effect can be the $C_1 — C_5$ bond (Fig. 1).

It has been established [16] that the total overlap population as defined by Mulliken [17] is a measure of the energy of a bond. Our calculated values

---

[14] C. Bradley Moore and G. C. Pimental, *J. Chem. Phys.*, **40**, 329 (1964).

[15] Handbook of Chemistry and Physics (46th Edition), p. D-51. The Chemical Rubber Co. Cleveland, Ohio.

[16] S. Ehrenson and S. Seltzer, *Theor. Chim. Acta*, **20**, 17 (1971).

[17] R. S. Mulliken, *J. Chem. Phys.*, **23**, 1833 (1955).

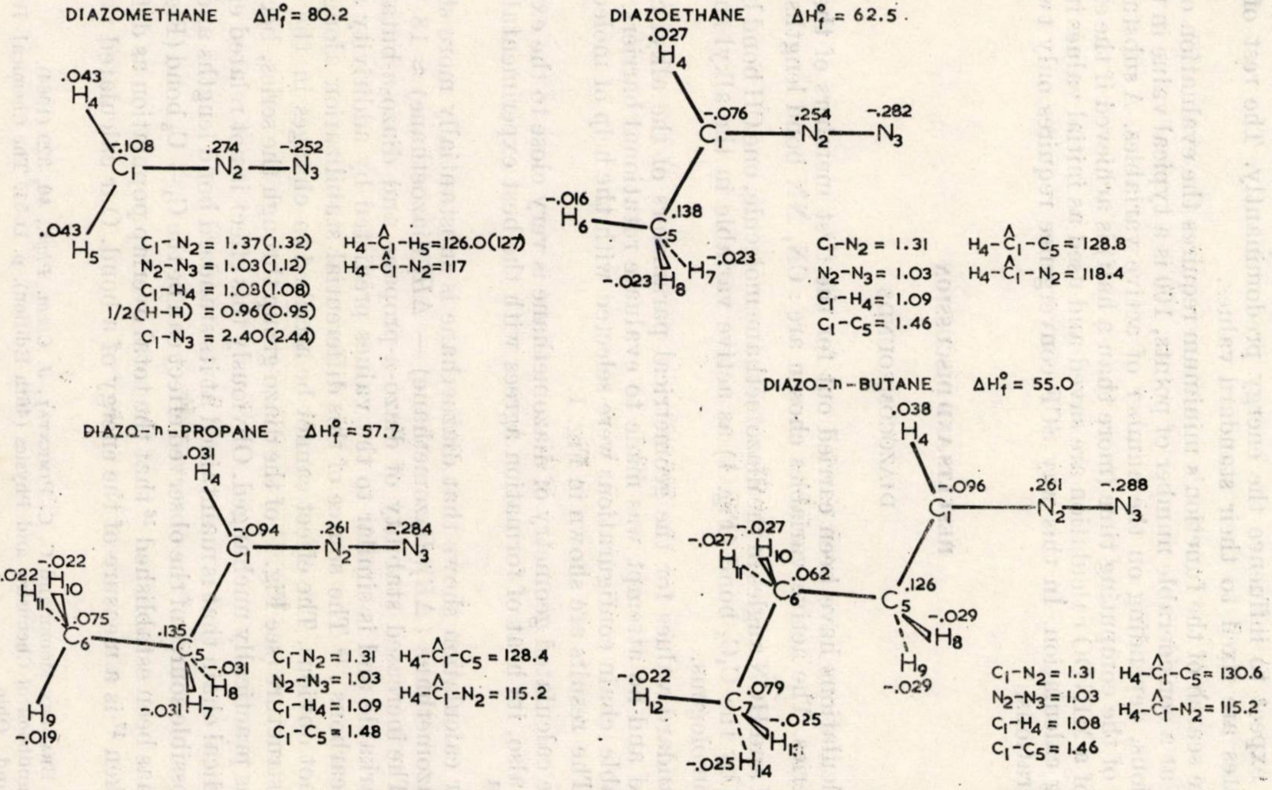
DIAZOMETHANE ΔH°f = 80.2
.043 H4
-.108 C1
.274 N2
-.252 N3
.043 H5
C1-N2 = 1.37(1.32)
N2-N3 = 1.03(1.12)
C1-H4 = 1.08(1.08)
1/2(H-H) = 0.96(0.95)
C1-N3 = 2.40(2.44)
H4-Ĉ1-H5 = 126.0(127)
H4-Ĉ1-N2 = 117
DIAZOETHANE ΔH°f = 62.5
.027 H4
-.076 C1
.254 N2
-.282 N3
-.016 H6
.138 C5
-.023 H7
-.023 H8
C1-N2 = 1.31
N2-N3 = 1.03
C1-H4 = 1.09
C1-C5 = 1.46
H4-Ĉ1-C5 = 128.8
H4-Ĉ1-N2 = 118.4
DIAZO-n-PROPANE ΔH°f = 57.7
.031 H4
-.094 C1
.261 N2
-.284 N3
-.022 H10
-.022 H11
.075 C6
.135 C5
-.031 H8
-.031 H7
H9 -.019
C1-N2 = 1.31
N2-N3 = 1.03
C1-H4 = 1.09
C1-C5 = 1.48
H4-Ĉ1-C5 = 128.4
H4-Ĉ1-N2 = 115.2
DIAZO-n-BUTANE ΔH°f = 55.0
.038 H4
-.096 C1
.261 N2
-.288 N3
-.027 H10
-.027 H11
.062 C6
.126 C5
-.029 H8
H9 -.029
-.022 H12
.079 C7
-.025 H13
-.025 H14
C1-N2 = 1.31
N2-N3 = 1.03
C1-H4 = 1.08
C1-C5 = 1.46
H4-Ĉ1-C5 = 130.6
H4-Ĉ1-N2 = 115.2

Fig. 1 — Heat of formation (kcal mol $^{-1}$), bond lengths (Å), angles (deg.) and net charges for aliphatic diazocompounds. Bracketed values are experimental [6,14].

of this index for the bond under consideration are ; 1.50 in diazoethane, and 1.48 in diazo-*n*-propane and diazo-*n*-butane. These values correspond to a partial double bond.

This double bond character could have been deduced from the calculated bond distances, that are intermediate between a single and double bond. Then, the remarkable stability of diazoethane is related to the presence of this partial double bond, further increase of the side chain does not alter significantly this bond and therefore the agreement of the stabilization effect with that predicted by additivity rules.

From the data in Figure 1 is apparent the great polarity of the NN and CN bonds.

The appearance of diazomethane HOMO is like that found by Hoffman in an EHT calculation of this molecule , [18] it is built up by the p_π orbitals, CN bonding and NN antibonding ; the first virtual MO, by contrast to EHT calculations, has the same symmetry (a'' in C_s group) and it is CN and NN antibonding.

This situation remains in the higher diazocompounds in accordance with the conservation of the geometrical parameters and formal charges in the CNN group.

Incidentally, it is remarkable the excellent agreement of ionization potentials, evaluated by means of the Koopman's theorem, of diazomethane and diazirine 8.9 and 10.15 eV with the experimental values, 9.03 and 9.00 eV [7,19] for diazomethane and 10.18 eV [7] for diazirine.

DIAZIRINES

Calculations have been performed for finding the equilibrium geometry of the diazirine molecule and its methyl derivatives. As active variables for the energy minimization the CN and CH bonds and NCN and HCH angles, in diazirine have been chosen. The CC (methyl group) bond has also been optimized in methyl substituted diazirines.

Figure 2 shows the results found for the heat of omratio n, geometrical parameters and net charges of these molecules.

It is clear from these results that the methyl group does not bring a substantial change of the ring geometry. This fact is supported by experimental data . [21]

The values found for the heat of formation of diazirines are similar to those of diazocompounds bearing the same number of carbon atoms (e. g. 80.2 kcal mol^{-1} for diazomethane and 78.3 kcal mol^{-1} for diazirine). These results of the heat of formation must be handled with some care.

---

[18] R. Hoffmann, *Tetrahedron*, **22**, 539 (1966).

[19] A. J. Merer, *Canad. J. Phys.*, **42**, 1242 (1964).

[20] L. Pierce and V. Dobnys, *J. Amer. Chem. Soc.*, **84**, 2651 (1962).

[21] J. E. Wobrab, L. H. Scharpen, D. P. Ames and J. A. Merrit, *J. Chem. Phys.*, **49**, 2405 (1968).

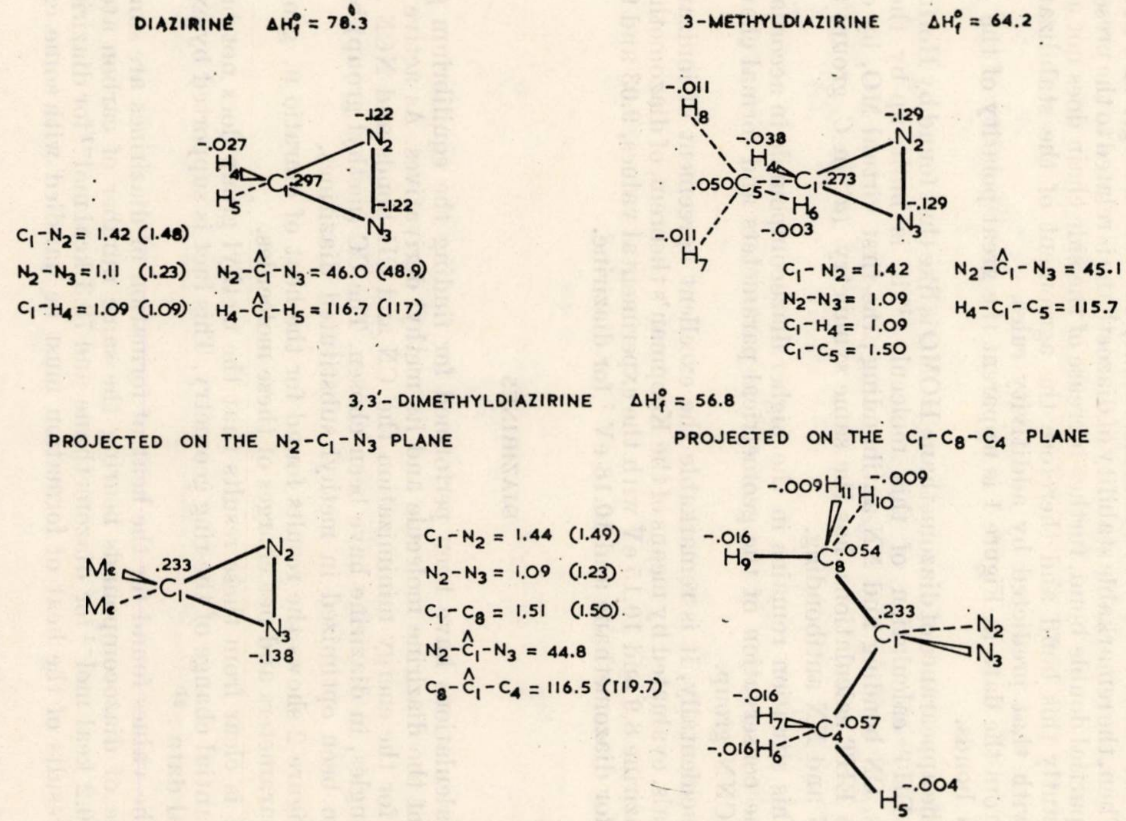

DIAZIRINE $\Delta H_f^\circ = 78.3$

$C_1-N_2 = 1.42$ (1.48)

$N_2-N_3 = 1.11$ (1.23)

$C_1-H_4 = 1.09$ (1.09)

$N_2-\hat{C}_1-N_3 = 46.0$ (48.9)

$H_4-\hat{C}_1-H_5 = 116.7$ (117)

3-METHYLDIAZIRINE $\Delta H_f^\circ = 64.2$

$C_1-N_2 = 1.42$

$N_2-N_3 = 1.09$

$C_1-H_4 = 1.09$

$C_1-C_5 = 1.50$

$N_2-\hat{C}_1-N_3 = 45.1$

$H_4-C_1-C_5 = 115.7$

3,3'-DIMETHYLDIAZIRINE $\Delta H_f^\circ = 56.8$

PROJECTED ON THE $N_2-C_1-N_3$ PLANE

PROJECTED ON THE $C_1-C_8-C_4$ PLANE

$C_1-N_2 = 1.44$ (1.49)

$N_2-N_3 = 1.09$ (1.23)

$C_1-C_8 = 1.51$ (1.50)

$N_2-\hat{C}_1-N_3 = 44.8$

$C_8-\hat{C}_1-C_4 = 116.5$ (119.7)

-.122
N2
-.027
H4
C1
.297
H5
N3
-.122
-.011
H8
-.129
N2
-.038
H4
.050
C5
C1
.273
H6
-.129
N3
-.011
H7
-.003
Me
.233
C1
Me
N2
N3
-.138
-.009
H11
H10
-.009
-.016
H9
C8
.054
.233
C1
N2
N3
-.016
H7
C4
.057
-.016
H6
-.004
H5

Fig. 2. — Heat of formation (kcal mol^{-1}), bond lengths (Å), angles (deg.) and net charges for diazirine and its methyl derivatives. Bracketed values are experimental for diazirine [20] and 3,3' dimethyldiazirine. [21]

It is well established that the MINDO/2 method overestimates the stability of small rings. *

Assuming that MINDO/2 makes a similar underestimation of strain energies of cyclopropane and diazirine, we found that the diazirine is 7 kcal mol $^{-1}$ less stable than diazomethane.

The effect of methyl groups upon the heat of formation can be explained in similar terms to those of the diazocompounds. It has been evaluated the total overlap population of the CC bond as 1.44 in the 3-methyldiazirine and 1.43 in 3,3′-dimethyldiazirine.

The difference between the electronic structure of CNN group in diazocompounds and their cyclic isomers is obvious. In diazirines the carbon atom bears a positive charge in contrast with the slightly negative charge in the linear arrangement, also the π system is less developed.

The HOMO and LUMO orbitals are similar to those found by EHT calculations. [18] The HOMO has σ symmetry, i. e. p_π orbitals do not participate, the reverse being true in the LUMO. [22]

CARBENES

Calculations have been performed for singlet carbenes related to the above diazocompounds and diazirines. The active variables used are the bond lengths C_1C_3, C_1H_2 and the angle $C_3C_1H_2$, $C_3C_1C_2$ in dimethylcarbene (See Fig. 3).

The heat of formation, equilibrium geometry and net charges are given in Figure 3. The data for methylcarbene and dimethylcarbene are close to those reported by Bodor and Dewar [23] and are included here for the sake of consistency and comparison purposes. It is noteworthy the stability of methylcarbene referred to that of methylene**(ΔH^0_f (methylene) — ΔH^0_f methylcarbene $\approx$ 24 kcal mol^{-1}). Recent thermochemical calculations [24] give ΔH^0_f (methylcarbene) $= 77$ kcal mol^{-1}in a reasonable agreement with the calculated value. Further increase of the length of the alkyl chain brings smaller charges in the heat of formation of higher carbenes.

Dewar [23] explains the stability of methylcarbene as due to a strong hyperconjugative interaction between the vacant p_z A. O. of the divalent carbon and the methyl group.

However, important stabilizations have been noticed in diazoethane and methyldiazirine, referred to diazomethane and diazirine respectively, where vacant p_zA.O.'s cannot be involved.

---

* MINDO/2 calculated heat of formation of cyclopropane is 3.8 kcal mol^{-1}, experimenta 12.7 kcal mol^{-1}. [12]

** The geometry of singlet methylene optimized by the same procedure.

[22] For a detailed description of the electronic structure of diazirine ring, see. "ab initio" calculations. E. Kochanski and J. M. Leh, *Theor. Chim. Acta*, **14**, 281 (1969), and R. B, Bonaccorsi, E. Scrocco and J. Tomasi, *J. Chem.Phys.*, **52**, 5270 (1970).

[23] N. Bodor and M. J. S. Dewar, *J. Amer. Chem. Soc.*, **94**, 9103 (1972), and N. Bodor, M. J. S. Dewar and J. S. Wasson, *ibid.* 9095 (1972).

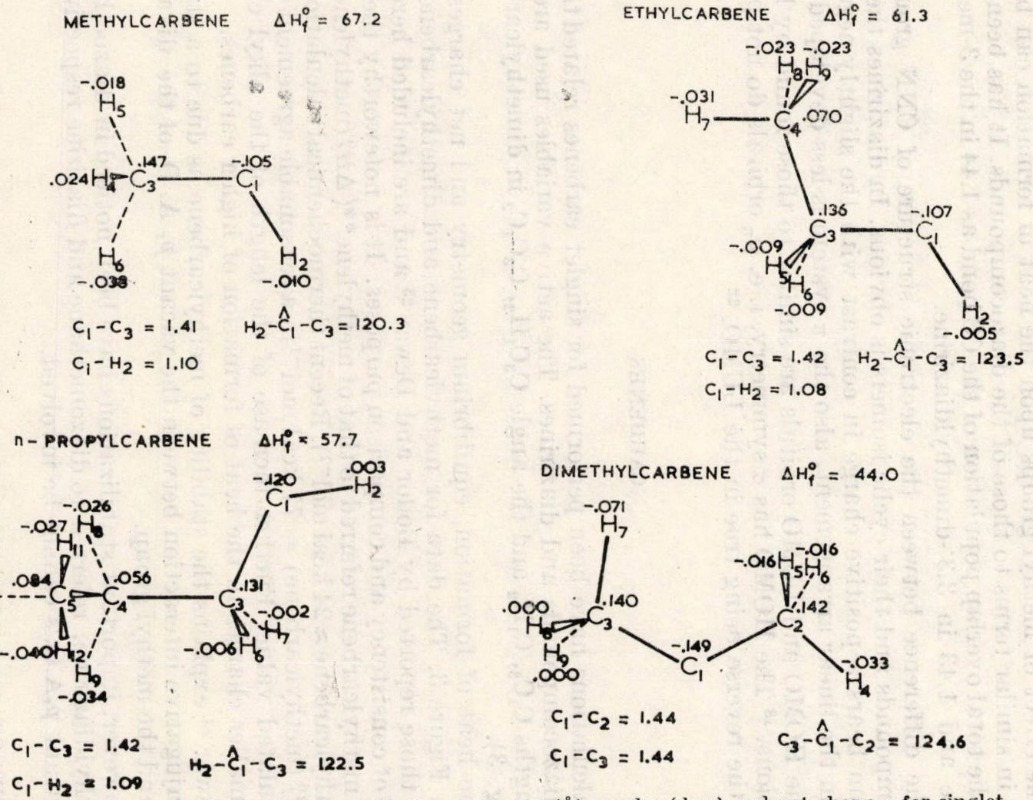
METHYLCARBENE
$\Delta H_f^\circ = 67.2$
H_5 -.018
H_4 .024
C_3 .147
C_1 -.105
H_6 -.038
H_2 -.010
$C_1-C_3 = 1.41$
$C_1-H_2 = 1.10$
$H_2-\hat{C}_1-C_3 = 120.3$
ETHYLCARBENE
$\Delta H_f^\circ = 61.3$
H_8 -.023
H_9 -.023
H_7 -.031
C_4 .070
C_3 .136
C_1 -.107
H_5 -.009
H_6 -.009
H_2 -.005
$C_1-C_3 = 1.42$
$C_1-H_2 = 1.08$
$H_2-\hat{C}_1-C_3 = 123.5$
n-PROPYLCARBENE
$\Delta H_f^\circ = 57.7$
C_1 -.120
H_2 .003
H_8 -.026
H_{11} -.027
H_{10} -.019
C_5 .084
C_4 .056
C_3 .131
H_7 -.002
H_6 -.006
H_{12} -.040
H_9 -.034
$C_1-C_3 = 1.42$
$C_1-H_2 = 1.09$
$H_2-\hat{C}_1-C_3 = 122.5$
DIMETHYLCARBENE
$\Delta H_f^\circ = 44.0$
H_7 -.071
H_8 .000
C_3 .140
H_9 .000
C_1 -.149
H_5 -.016
H_6 -.016
C_2 .142
H_4 -.033
$C_1-C_2 = 1.44$
$C_1-C_3 = 1.44$
$C_3-\hat{C}_1-C_2 = 124.6$

Fig. 3. — Heat of formation (kcal mol $^{-1}$), bond lengths (Å), angles (deg.) and net charges for singlet aliphatic carbenes.

Inspection of Table 1 shows a strong correlation between the methyl stabilizing effect (calculated as ΔH_f^0 (first term of a given series) — ΔH_f^0 (methyl substituted term)) and other magnitudes : overlap population, bond length, and charge released by the methyl group. It should be pointed out that no correlation with the charge of the methyl hydrogens is observed ; these hydrogens show a tendency to withdraw electrons in oposition to the net effect of the group. A close inspection of the mechanism of change donation shows a preponderance of donation through the π system. Then, the stabilization effect can be ascribed to the methyl donation of charge to the functional group. This donation allows to the bond involved a certain double bond character, that is reflected in a shorter bond length and an increasing stability of the molecule.

Table 1

Dependency of the methyl stabilizing effect with several parameters

Molecule	Methyl stabilizing[a] effect (kcal mol^{-1})	Overlap population	C — C bond length (Å)	Charge released by the methyl group	Sum of the methyl hydrogens formal charges
3-methyldiazirine	14.1	1.44	1.50	−0.025	−0.025
diazoethane	17.7	1.502	1.46	−0.076	−0.062
methylcarbene	24.0	1.652	1.41	−0.115	−0.032

a) Calculated as ΔH_f^0 (first term of a given series) − ΔH_f^0 (methyl substituted term).

ACKNOWLEDGEMENT. The listing of MINDO/2 program was kindly provided by Professor M.J.S. Dewar. Calculations wers performed at the Computer Center of Ministerio de Educación y Ciencia. One of us (M.M.) thanks Ministerio de Educación y Ciencia for a studentship.

---

[24] M. Pomerantz and R. H. Witherup, *J. Amer. Chem. Soc.*, **95**, 5977 (1973).

Revue Roumaine de Chimie, **21**, *1*, 41–47 (1976).

CONTRIBUTION À L'ÉTUDE DE LA RÉDUCTION DE L'OXYGÈNE SUR LES ÉLECTRODES POREUSES EN ARGENT. II[1]

L'INFLUENCE DE LA CONCENTRATION DE L'ÉLECTROLYTE SUR LES PERFORMANCES DES ÉLECTRODES

MARIA MAVRODIN-TĂRĂBÎC, IOANA ONACA et I. SOLACOLU
Centre de Chimie Physique, Bucarest, 31, str. Galaţi

Reçu le 12 mars 1974

On a déterminé l'influence de la variation de la concentration de l'électrolyte, entre 2N—9N, sur les performances des électrodes à gaz en argent du type DSK, dans la réaction de réduction de l'oxygène, à différentes températures comprises entre 25 et 65° et à différentes surpressions d'alimentation avec du gaz (200—600 mm Hg). L'étude a été effectuée par la technique potentiostatique et, en utilisant les courbes de polarisation $\eta - i$, on a tracé les courbes $\eta = f(c)$, qui démontrent l'effet de la variation de la concentration de l'électrolyte (dans le domaine étudié) sur la polarisation des électrodes à gaz en argent, à différentes densités apparentes du courant. On a établi le domaine de concentration de l'électrolyte (KOH), en fonction de la température de travail, dans lequel les électrodes présentent des polarisations réduites.

Dans un travail antérieur [1] on a démontré que les électrodes à gaz en argent présentent des performances supérieures dans la réaction de réduction de l'oxygène. Dans ce travail on a mis en évidence l'effet favorable de la structure du type DSK (« Doppel Skelet Katalyst ») sur les performances des électrodes, en concordance avec les données récentes publiées dans la littérature. [2–5]

On sait que, pour la réalisation des sources chimiques de courant caractérisées par des performances élevées (des piles à combustible ou des piles métal-air), en dehors de l'établissement des paramètres d'obtention des électrodes à gaz (pression, température et temps de frittage) qui conduisent à la réalisation d'une structure poreuse favorable au développement des processsus électrochimiques, un rôle très important revient à l'établissement des paramètres optimaux de fonctionnement des électrodes à gaz (température et concentration de l'électrolyte et surpression d'alimentation avec du gaz). Dans la littérature de spécialité il n'existe que peu de travaux [6,7] qui étudient l'effet de la variation des paramètres de fonctionnement sur les performances des électrodes à oxygène et ces travaux concernent seulement les électrodes en charbon.

---

[1] O. Radovici, M. Mavrodin-Tărăbîc, I. Onaca et I. Solacolu, *Rev. Roumaine Chim.*, **17**, 1153 (1972).

[2] J. Jausta, *Coll. Czech. Chem. Comm.*, **33**, 160 (1968).

[3] I. Lindholm, *J. Electrochem. Soc.*, **116**, 1150 (1969).

[4] Ling-Ying Ku et V. S. Bagotskii, *Electrokhimiya*, **3**, 1279 (1967).

[5] J. Mrha et J. Jindra, *Coll. Czech. Chem. Comm.*, **34**, 2465 (1969).

Dans un travail antérieur [8] on a démontré que, dans le cas des électrodes à gaz en nickel (dans la réaction de l'oxydation de l'hydrogène), il existe une corrélation étroite entre le système poreux de l'électrode, les paramètres de fonctionnement et les performances réalisées. En vue de l'établissement du régime de fonctionnement des électrodes à gaz en argent dans la réaction de réduction de l'oxygène, nous nous sommes proposé d'étudier l'influence de la concentration et de la température de l'électrolyte, de la surpression d'alimentation avec du gaz et de la densité du courant débité, sur la polarisation des électrodes du type DSK, réalisées dans notre laboratoire. Dans ce travail on présente les résultats obtenus dans l'étude de l'effet de la variation de la concentration de l'électrolyte.

1. PARTIE EXPÉRIMENTALE

1.1. RÉALISATION ET CARACTÉRISATION DES ÉLECTRODES

Les électrodes à gaz en argent du type DSK ont été réalisées par la compression, à $2{,}8.10^{8}$ N/m^2, d'un mélange homogène contenant 81,25% carbonate d'argent (dimension des particules <5 microns) et 18,75% bicarbonate d'ammonium (dimension des particules 20—40 microns). Les électrodes obtenues, de forme cylindrique, à un diamètre de 10 mm et] à une épaisseur de 3 mm, ont été frittées, pendant 15 minutes, à 375°, dans une atmosphère d'hydrogène. Le frittage a été réalisé dans un four électrique horizontal, en courant d'hydrogène, à un débit de 3 l/m. Le régime de frittage a été le suivant : le chauffage, avec une vitesse de 2 degrés par minute (paliers d'une heure à 100° et à 140°, pour éliminer l'eau et le poroformateur) et le refroidissement, avec une vitesse de 3 degrés par minute.

Les électrodes à gaz en argent ont été caractérisées au point de vue structural par l'examen microscopique, à l'aide d'un microscope métallographique de type MIM—7 et par la détermination de la porosité globale, en pesant les échantillons avant et après l'imprégnation avec du toluène. L'examen microscopique a mis en évidence la répartition uniforme des pores, grands et petits, dans la masse de l'électrode, la porosité globale étant de 30,5%.

1.2. LES MESURES ÉLECTROCHIMIQUES

L'étude de la réaction de réduction de l'oxygène sur les électrodes à gaz en argent a été effectuée par la technique potentiostatique, à l'aide d'un montage décrit dans un travail antérieur, [9] en utilisant un potentiostat de type CCF (précision ± 1 mV), un millivoltmètre électronique Radiometer 22 (précision ± 1 mV), un milliampermètre (classe de précision 0,2). Comme électrode auxiliaire on a utilisé une spirale de nickel de grande pureté (99,9%) et comme électrode de référence une électrode de calomel saturé. La cellule de travail (dimensions $120 \times 72 \times 56$ mm) a été confectionnée en polystyrène. L'alimentation des électrodes avec de l'oxygène à surpression constante, a été réalisée à l'aide d'une installation présentée dans un travail antérieur. [10]

---

[6] M. Marinescu, S. Doboș et I. Minea, *Studii și Cercetări Energetică Electrotehnică* **19**, 427 (1969).

[7] D. B. Lucesoli, Thèse, Univ. Paris, 1971, p. 71.

[8] I. Onaca, M. Mavrodin-Tărăbîc et I. Solacolu, *Rev. Roumaine Chim.*, **20**, 611 (1975).

[9] M. Mavrodin-Tărăbîc, I. Onaca et I. Solacolu, *Rev. Roumaine Chim.*, **18**, 1121 (1973).

[10] O. Radovici, M. Mavrodin-Tărăbîc, I. Onaca et I. Solacolu, *Rev. Roumaine Chim.*, **18**, 767 (1973).

Les courbes de polarisation $\eta - i$ ont été déterminées (en appliquant des niveaux de potentiel de 10 mV, à un intervalle de temps d'une minute), pour différentes surpressions de l'oxygène : 200, 300, 400,500 et 600 mm Hg. Les déterminations ont été effectuées à la température de 25°, 40°, 50° et 65°, maintenue constante à l'aide d'un ultrathermostate de type U — 10 (précision ± 0,1°). On a effectué des déterminations pour les concentrations de l'électrolyte (solution de KOH) de 2N, 3N, 4N, 5N, 6N, 7N, 8N et 9N. Pour préparer la solution de l'électrolyte on a utilisé du KOH Chemapol *p.a.*

2. RÉSULTATS ET DISCUSSION

L'effet de la variation de la concentration de l'électrolyte sur la polarisation des électrodes à gaz en argent, dans la réaction de réduction de l'oxygène, est illustré par la modification de l'aspect des courbes de polarisation. Pour mettre en évidence l'effet de la concentration de l'électrolyte sur les performances des électrodes, parmi les 160 conditions différentes dans lesquelles on a tracé les courbes de polarisation (la concentration a été variée entre 2N et 9N, les niveaux de concentration étant de 1 méquiv. cm^{-3}, la température a été de 25, 40, 50 et 65° et la surpression de l'oxygène a été variée dans le domaine 200—600 mm Hg, les niveaux de surpression étant de 100 mm Hg) on a considéré caractéristiques les courbes $\eta = f(i)$, tracées à 50° et à 400 mm Hg, à différentes concentrations comprises entre 3N et 7N (fig. 1).

L'augmentation de la concentration de l'électrolyte produit un déplacement de la polarisation des électrodes vers des valeurs plus petites. Dans les conditions de température et de surpression considérées, cet effet est plus accentué dans le domaine de 3N—5N.

Des courbes de polarisation $\eta = f(i)$, obtenues par la technique potentiostatique, on a déterminé les valeurs de la surtension caractéristique pour les densités apparentes de courant (rapportées à la surface extérieure de l'électrode à gaz) de 10, 20, 30, 40, 50, 60, 70, 80 et 90 mA/cm². A l'aide de ces valeurs on a tracé les courbes $\eta = f(c)$ présentées dans la figure 2 (température 50°, surpression de l'oxygène 400 mm Hg).

De l'examen de l'aspect de ces courbes on constate que, en ce qui concerne l'effet de la variation de la concentration de l'électrolyte sur la polarisation des électrodes à gaz étudiées, il existe, dans l'intervalle considéré (2N—9N), deux zones distinctes :

— dans le domaine 2N—5N, la surtension de l'électrode diminue sensiblement avec l'augmentation de la concentration de l'électrolyte, à toutes les valeurs des densités apparentes de courant, cet effet étant plus accentué à des concentrations plus réduites et à des densités de courant plus élevées. Ainsi, à une petite densité de courant (10 mA/cm²), la surtension décroît continuellement à partir de la valeur de 135 mV (2N) jusqu'à 57 mV (5N) ; à une densité de courant moyenne (40 mA/cm²), la surtension décroît à partir de 365 mV (2N) jusqu'à 170 mV (3N), 140 mV (4N) et 120 mV (5N) ; à de grandes densités de courant (90 mA/cm²), la surtension décroît à partir de 250 mV (4N) jusqu'à 200 mV (5N), dans le domaine 2N—4N, les valeurs de la surtension étant supérieures aux valeurs caractéristiques pour le fonctionnement de l'électrode à oxygène (450 mV) ;

— dans l'intervalle 5N — 9N, l'effet de l'augmentation de la concentration de l'électrolyte sur la polarisation des électrodes à gaz en argent étudiées est relativement moins prononcé. Ainsi, pour des densités apparentes de courant plus petites que 50 mA/cm², l'augmentation de la concentration de l'électrolyte n'influence pas, d'une manière significative, la valeur de la surtension de l'électrode ; à des densités de courant plus grandes, les surtensions diminuent à partir de la valeur de 150 mV (5N) jusqu'à 140 mV (9N), pour une densité de courant de 60 mA/cm² et à partir de 200 mV (5N) jusqu'à 190 mV (9N), pour une densité de courant de 90 mA/cm².

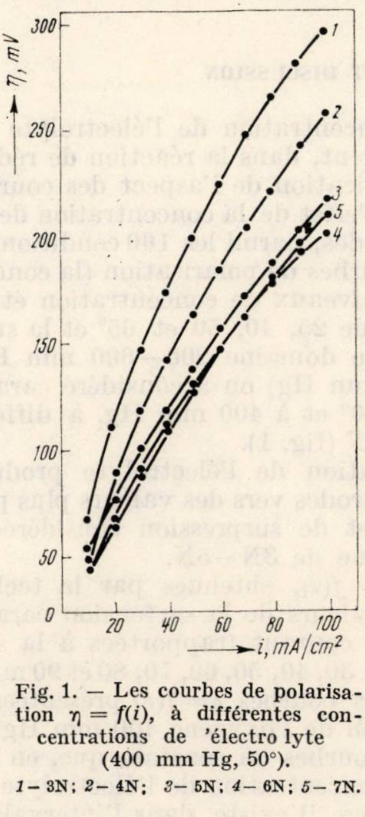

Fig. 1. — Les courbes de polarisation $\eta = f(i)$, à différentes concentrations de 'électro lyte (400 mm Hg, 50°).

1 – 3N; *2* – 4N; *3* – 5N; *4* – 6N; *5* – 7N.

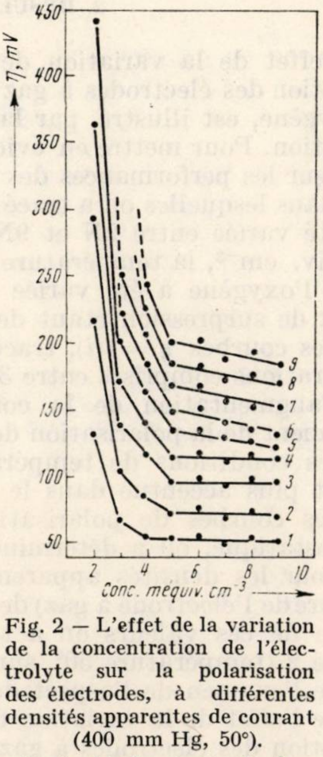

Fig. 2 — L'effet de la variation de la concentration de l'électrolyte sur la polarisation des électrodes, à différentes densités apparentes de courant (400 mm Hg, 50°).

1 – 10 mA/cm²; *2* – 20 mA/cm²;
3 – 30 mA/cm²; *4* – 40 mA/cm²;
5 – 50 mA/cm²; *6* – 60 mA/cm²;
7 – 70 mA/cm²; *8* – 80 mA/cm²;
9 – 90 mA/cm².

Tel qu'il résulte des données ci-dessus, la surtension de l'électrode diminue sensiblement avec l'augmentation de la concentration de l'électrolyte jusqu'à une certaine valeur (approx. 5N, à la température de 50° et à la surpression de l'oxygène de 400 mm Hg) ; l'augmentation de la concentration de l'électrolyte au-dessus de cette valeur ne diminue pas, pratiquement, la surtension de l'électrode à de petites densités apparentes de courant ou produit une faible diminution à des densités de courant moyennes et grandes.

L'augmentation de la concentration de l'électrolyte jusqu'à approximativement 5N – 6N influence favorablement sa conductibilité [11], effet qui domine l'effet défavorable sur la solubilité de l'oxygène,[12] ce qu'on peut constater de l'examen des courbes $\eta = f(c)$. A des concentrations plus élevées, les effets se compensent et l'augmentation de la concentration de l'électrolyte n'améliore pas les performances de l'électrode à gaz.

Pour illustrer l'effet de la variation de la concentration de l'électrolyte, à différentes valeurs de la surpression de l'oxygène (200–600mmHg), on a tracé les courbes $\eta = f(c)$ présentées dans la figure 3 (i = 70mA/cm³, etmpérature, 50°).

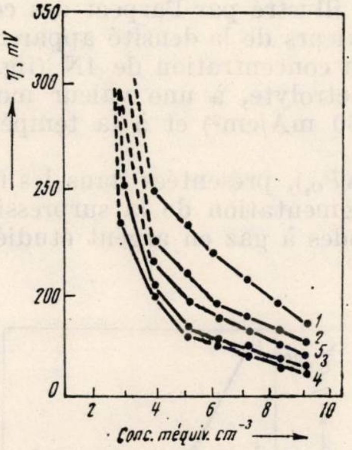

Fig. 3. — L'effet de la variation de la concentration de l'électrolyte sur la polarisation des électrodes, à différentes surpressions de l'oxygène (70 mA/cm², 50°).
1 – 200 mm Hg; *2* – 300 mm Hg; *3* – 400 mm Hg; *4* – 500 mm Hg; *5* – 600 mm Hg.

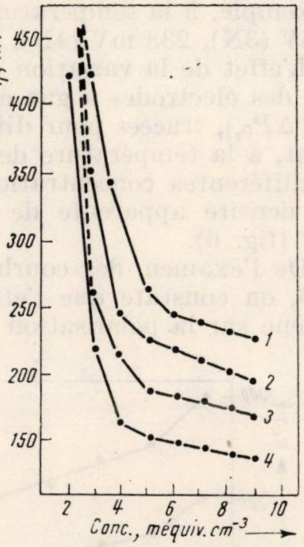

Fig. 4. — L'effet de la variation de la concentration de l'électrolyte sur la polarisation des électrodes, à différentes températures (70 mA/cm², 400 mm Hg).
1 – 25°; *2* – 40°; *3* – 50°; *4* – 65°.

De l'examen de ces courbes on constate que l'effet de la variation de la concentration de l'électrolyte est plus prononcé dans le domaine 2N–5N; par exemple, à ΔP_{O_2} = 400 mm Hg, la surtension diminue à partir de la valeur de 420 mV (2N) jusqu'à 240 mV (3N), 202 mV (4N) et 180 mV (5N). Dans le domaine 5N–9N, cet effet est, relativement, moins prononcé, surtout à des surpressions d'alimentation avec du gaz situées dans le domaine optimal (400–500 mm Hg) : ainsi, à la même valeur de la surpression (400 mm Hg), la surtension diminue seulement jusqu'à la valeur de 174 mV (9N).

---

[11] E. L. SIMONS, D. W. MCKEE et E. J. CAIRNS, « Comptes rendus des troisièmes journées d'étude des piles à combustible », Presses Académiques Européennes, Bruxelles, 1969, p. 132.

[12] A. SEIDELL, « Solubilities of Inorganic and Metal Organic Compounds », Ier vol., Van Nostrand Co., New York, 1953, p. 1352.

L'effet de la variation de la concentration de l'électrolyte sur la polarisation des électrodes à gaz en argent du type DSK, dans la réaction de réduction de l'oxygène, à différentes températures de l'électrolyte comprises entre 25 et 65°, est illustré par l'aspect des courbes $\eta = f(c)$ représentées dans la figure 4 ($i = 70$ mA/cm², surpression de l'oxygène 400 mmHg).

De l'examen des courbes présentées dans la figure 4, on constate aussi que ces effets sont plus prononcés dans le domaine 2N–5N (à des températures plus petites que 50°) ou 2N–4N (à la température de 65°). Par exemple, à la température de 40°, les valeurs de la surtension sont : 351 mV (3N), 238 mV (4N), 220 mV (5N), 198 mV (9N).

L'effet de la variation de la surpression de l'oxygène sur la polarisation des électrodes à gaz étudiées est illustré par l'aspect des courbes $\eta = f(\Delta P_{O_2})$, tracées pour différentes valeurs de la densité apparente de courant, à la température de 50° et à la concentration de 4N (fig. 5) et pour différentes concentrations de l'électrolyte, à une valeur moyenne de la densité apparente de courant (50 mA/cm²) et à la température de 50° (fig. 6).

De l'examen des courbes $\eta = f(\Delta P_{O_2})$, présentées dans les figures 5 et 6, on constate que l'effet de l'augmentation de la surpression de l'oxygène sur la polarisation des électrodes à gaz en argent étudiées est d'autant plus prononcé que la densité apparente de courant est plus élevée et que la concentration de l'électrolyte est moins grande. Cet effet est plus accentué dans le domaine 200–300 mm Hg et s'explique par l'augmentation de la zone triphasique de réaction (l'augmentation de la surface électrocatalytique active) et de la solubilité de l'oxygène dans l'électrolyte.

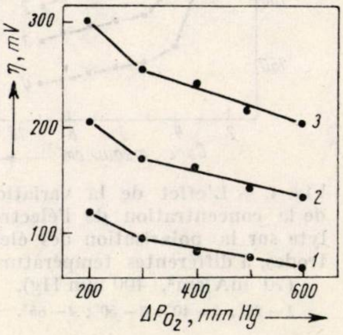

Fig. 5 – L'effet de la variation de la surpression de l'oxygène sur la polarisation des électrodes, à différentes densités apparentes de courant (KOH 4N, 50°).

1 – 20 mA/cm²; *2* – 50 mA/cm²; *3* – 90 mA/cm².

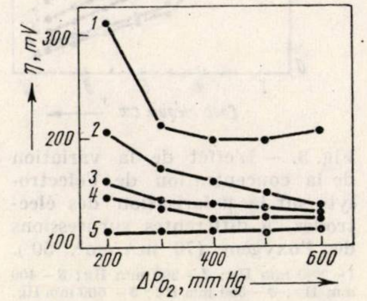

Fig. 6. – L'effet de la variation de la surpression de l'oxygène sur la polarisation des électrodes, à différentes concentrations de l'électrolyte (50 mA/cm², 50°).

1 – 3N; *2* – 4N; *3* – 6N; *4* – 7N; *5* – 9N.

3. CONCLUSIONS

1. L'étude de l'influence de l'augmentation de la concentration de l'électrolyte, dans le domaine compris entre 2N et 9N, sur la polarisation des électrodes à gaz en argent caractérisées par une structure du type DSK, dans la réaction de réduction de l'oxygène, a démontré qu'à toutes les valeurs de la température de travail (25—65°) et à toutes les surpressions d'alimentation avec du gaz (200—600 mm Hg), les performances des électrodes s'améliorent sensiblement jusqu'à une certaine valeur de la concentration de l'électrolyte (approx. 5N).

2. La diminution de la surtension des électrodes est d'autant plus prononcée que la concentration de l'électrolyte est plus réduite et que la densité apparente de courant est plus élevée.

3. A des concentrations plus grandes qu'approx. 5N, la surtension des électrodes reste pratiquement constante à de petites densités apparentes de courant et diminue, mais pas sensiblement, à des densités de courant moyennes ou grandes.

4. L'étude de l'influence de la variation de la surpression de l'oxygène, dans l'intervalle 200—600 mm Hg, a démontré que la surtension des électrodes à gaz en argent diminue avec l'augmentation de la surpression d'alimentation avec du gaz, cet effet étant d'autant plus prononcé que la densité apparente de courant est plus élevée et que la concentration de l'électrolyte est plus réduite.

Revue Roumaine de Chimie, **21**, *1*, 49 – 58 (1976)

ESSAI DE GÉNÉRALISATION DU PHÉNOMÈNE DE RÉGIOSÉLECTIVITÉ DANS LA RÉDUCTION DES OXIMES PAR DES AGENTS ALUMINIQUES

LOUIS FERRERO, SERGE GERIBALDI et MARCEL AZZARO

Laboratoire de Chimie Physique Organique, U.E.R.D.M. Université de NICE,
Campus Valrose 06034 NICE CEDEX

Reçu le 2 mai 1974

Les réductions de quelques cyclohexénones-oximes diversement alkylées ont été effectuées par l'hydrure d'aluminium lithium dans l'éther. L'analyse des composés formés permet de conclure à une régiosélectivité de la réduction, en fonction de la configuration *Z* ou *E* de l'oxime de départ. Une interprétation possible de ce phénomène est proposée.

INTRODUCTION

Au cours de nos travaux sur la préparation d'amines et d'aziridines par réduction d'oximes α, β-insaturées,[1,2] nous avons été amenés à considérer les mécanismes proposés à ce jour par de nombreux auteurs[3-5] et, en particulier, celui énoncé par Kotera[6] afin d'expliquer le phénomène de régiosélectivité observé pour les oximes saturées. Le problème abordé peut se résumer de la façon suivante : les réductions des oximes saturées par LAH sont menées le plus souvent dans l'éther diéthylique ou le tétrahydrofurane ; dans le premier cas, il est évident que la réduction ne peut conduire qu'à des amines primaires saturées quelle que soit la géométrie *Z* ou *E* de l'oxime (figure 1).

La problème de la régiosélectivité, c'est-à-dire la dépendance des produits formés avec la configuration *Z* ou *E* de l'oxime, s'est posé dans le second cas, quand l'utilisation du T.H.F., solvant plus basique que l'éther, est utilisé et conduit à la formation d'aziridines. Ce problème peut être illustré par quelques-uns des résultats obtenus par Kotera[6] (figure 2).

La fermeture du cycle aziridinique pouvant se faire sur le carbone primaire ou sur le carbone secondaire, ces résultats montrent que la forme *E*

---

[1] L. Ferrero, M. Decouzon et M. Azzaro, *Tetrahedron Letters*, **1973**, 4151.
[2] L. Ferrero, M. Rouillard, M. Decouzon et M. Azzaro, *Tetrahedron Letters*, **1974**, 131.
[3] K. Kitahonoki, Y. Takano et H. Takahashi, *Tetrahedron*, **24**, 4605 (1968).
[4] H. Tanida, T. Okada et K. Kotera, *Bull. Chem. Soc., Japan*, **46**, 934 (1973).
[5] J. R. Dimmock, W. A. Turner, P.J. Smith et R. G. Sutherland, *Canad. J. Chem.*, **51**, 427 (1973).
[6] K. Kotera et K. Kitahonoki, *Org. Prep. Proced.*, **1**, 305 (1969).

conduit préférentiellement à la cyclisation sur le carbone primaire et à l'amine et l'isomère *Z* sur le carbone secondaire proche de l'hydroxyle.

Les résultats sont tout aussi remarquables à partir d'une oxime ne permettant la formation que d'une seule aziridine, par exemple, quand

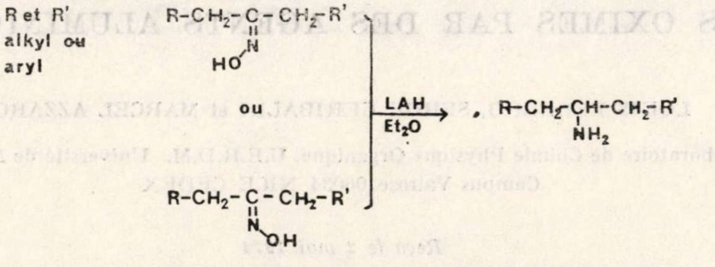
R et R' alkyl ou aryl
R-CH₂-C-CH₂-R'
HO N
ou
R-CH₂-C-CH₂-R'
N OH
LAH
Et₂O
R-CH₂-CH-CH₂-R'
NH₂

Fig. 1.—Réduction des oximes saturées par l'hydrure d'aluminium lithium dans l'éther.

l'un des carbones en α de la fonction oximino est un carbone tête de pont (figure 3).

Kotera[6] a donc été amené à expliquer cette régiosélectivité, en rapprochant ce type de réaction à deux autres déjà connus, à savoir l'action d'organomégnésiens sur les oximes [7] et le réarrangement de Neber[8]. En assimilant l'action de LAH à ces réactions, deux mécanismes pouvaient

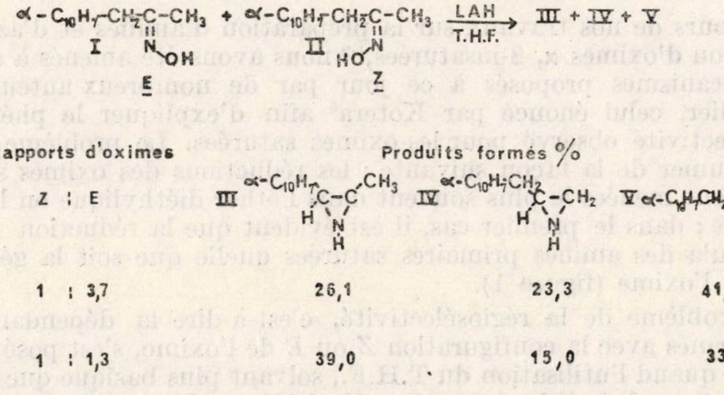
α-C₁₀H₇-CH₂-C-CH₃
I
N OH
E
+
α-C₁₀H₇-CH₂-C-CH₃
II
HO N
Z
LAH
T.H.F.
III + IV + V
Rapports d'oximes
Produits formés %
Z : E
III α-C₁₀H₇ C-C CH₃ H N H
IV α-C₁₀H₇CH₂ C-CH₂ H N H
V α-C₁₀H₇CH₂CHCH₃ NH₂
1 : 3,7
26,1
23,3
41,1
1 : 1,3
39,0
15,0
33,3

Fig. 2.—Réduction des α-naphtyl-1 propanone-2 oximes par l'hydrure d'aluminium lithium dans le tétrahydrofurane.

donc être proposés nécessitant tous deux l'élimination d'un proton en α de la fonction oximino, puis la formation directe d'azirine (1) ou le passage par un nitrène (2) évoluant ensuite vers l'azirine (figure 4).

Cependant, pour Kotera, ces deux mécanismes connus ne peuvent pas expliquer la régiosélectivité, dans la mesure où dans chacun d'eux, l'étape principale est l'élimination du proton en α, ce qui ne nécessite pas une géométrie syn (*Z*) pour se faire mais serait uniquement dépendante de l'acidité de ce proton. L'auteur a donc proposé un mécanisme un peu plus élaboré tenant compte de la régiosélectivité et consistant en un processus concerté intramoléculaire (figure 5).

---

[7] B. K. Campbell et K. N. Campbell, *J. Org. Chem.*, **9**, 179 (1944).

[8] H. O. House et W. F. Berkowitz, *J. Org. Chem.*, **28**, 2271 (1963).

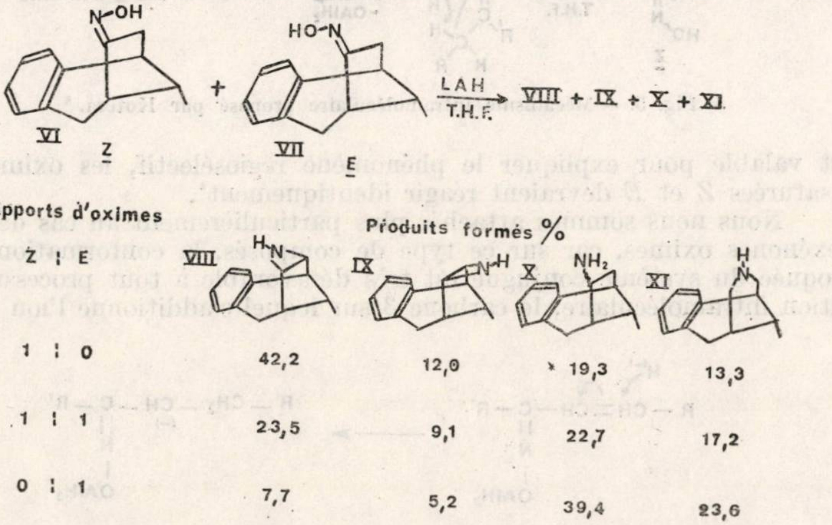

Z : E	VIII	IX	X	XI
1 : 0	42,2	12,0	19,3	13,3
1 : 1	23,5	9,1	22,7	17,2
0 : 1	7,7	5,2	39,4	23,6

Fig. 3. — Réductions des méthyl-8 endo benzo-2,3 bicyclo [3.2.1] octènone-6 oximes par l'hydrure d'aluminium lithium dans le tétrahydrofurane.

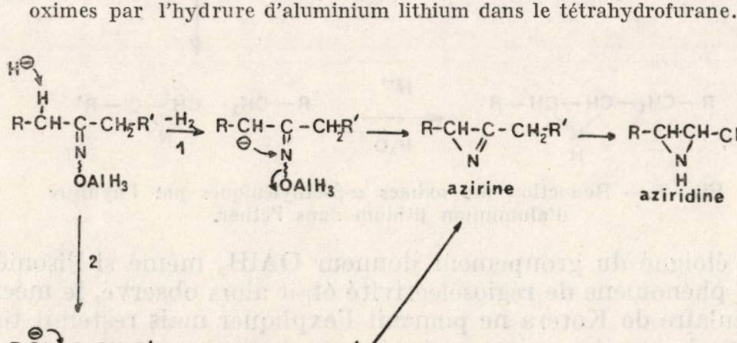

Fig. 4. — Mécanismes proposés pour la formation d'aziridine.

Ceci est parfaitement envisageable dans le cas des oximes saturées, où la formation du carbanion est due à l'arrachement d'un proton. Or, il existe un autre type de réaction susceptible d'induire aussi la cyclisation en aziridine, sans pour cela nécessiter la perte d'un proton, donc sans impliquer un mécanisme intramoléculaire : c'est la réduction par LAH des oximes α, β éthyléniques dans l'éther diéthylique, et qui peut être schématisée par la figure 6.

Il nous est donc apparu particulièrement intéressant de savoir s'il existe une régiosélectivité dans le cas des oximes α, β éthyléniques ; en effet, si seul le mécanisme intramoléculaire avec élimination d'un proton est valable pour expliquer le phénomène régiosélectif, les oximes α, β insaturées *Z* et *E* devraient réagir identiquement*.

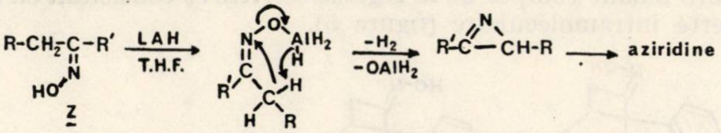

Fig. 5. — Mécanisme intramoléculaire proposé par Kotera.[6]

Nous nous sommes attachés plus particulièrement au cas des cyclohexénones oximes, car sur ce type de composés, la conformation *s-trans* bloquée du système conjugué est très défavorable à tout processus d'addition intramoléculaire, le carbone 3 sur lequel s'additionne l'ion hydrure étant très éloigné du groupement donneur OAlH$_3$ même si l'isomérie est syn. Si le phénomène de régiosélectivité était alors observé, le mécanisme intramoléculaire de Kotera ne pourrait l'expliquer mais resterait toutefois valable dans le cas des oximes saturées.

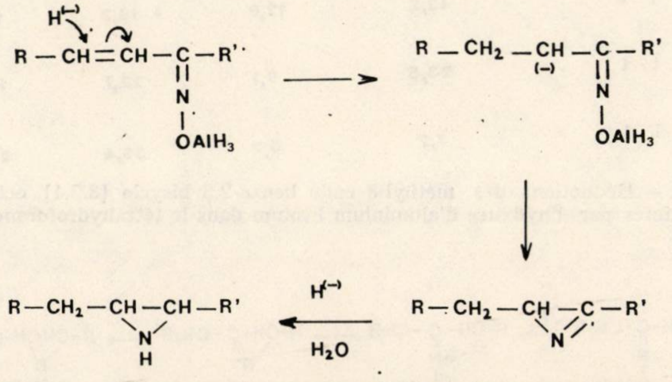

Fig. 6. — Réduction des oximes α-β-éthyléniques par l'hydrure d'aluminium lithium dans l'éther.

RÉSULTATS ET DISCUSSIONS

Trois types de cyclohéxénones oximes ont été choisis suivant leur critère configurationnel (figure 7) :

· isomérie *E* et *Z* possibles sur le même type d'oxime : isophorone oxime XII et méthyl-3 cyclohexène-2 one-1 oxime XIII ;

· isomérie *E* seule possible: carvone oxime XIV et méthyl-2 cyclohexène-2 one-1 oxime XV ;

· isomérie *Z* seule possible : pipéritone oxime XVI

---

* Même si l'oxime est anti (*E*), l'arrachement d'un proton sur le carbone saturé par un mécanisme intramoléculaire ou non est impossible puisque la réaction s'effectue dans l'éther.

Les résultats obtenus sont notés dans les tableaux 1, 2 et 3*.

Ainsi, nous pouvons constater que quelle que soit la substitution de l'oxime de départ, l'isomère *Z* conduit toujours préférentiellement à la formation d'aziridine, alors que la forme *E* semble favoriser l'obtention d'amines β-γ insaturées et parfois même, d'amines secondaires avec agrandissement de cycle. De plus, il nous faut prendre en considération le fait que, dans le cas des composés XII et XIII, l'isomère *E* ne réagit pas totalement (ceci est observé par analyse RMN du mélange réactionnel et par C.P.V.).

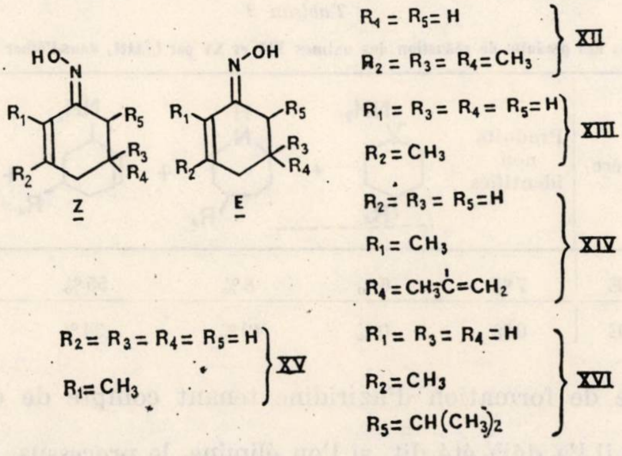
HO
N
N
OH
R1
R2
R3
R4
R5
Z
E
R4 = R5 = H
R2 = R3 = R4 = CH3
XII
R1 = R3 = R4 = R5 = H
R2 = CH3
XIII
R2 = R3 = R5 = H
R1 = CH3
R4 = CH3-C=CH2
XIV
R2 = R3 = R4 = R5 = H
R1 = CH3
XV
R1 = R3 = R4 = H
R2 = CH3
R5 = CH(CH3)2
XVI

Fig. 7. — Structures des cyclohexénones oximes utilisées.

Tableau 1

Pourcentages des produits de réduction des oximes XII et XIII par LiAlH$_4$ dans l'éther diéthylique

Oximes de départ	Rapport Z:E	Amines saturées	+ 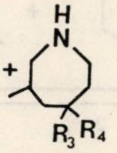	+ 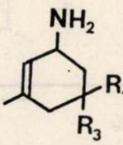 +	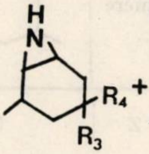 +	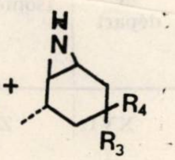
XII	1 : 1		6 %	40 %	24 %	30 %
	1 : 2		6 %	54 %	18 %	22 %
XIII	1 : 0	8 %	4 %	12 %	42 %	34 %
	1 : 2	13 %	16 %	31 %	21 %	19 %

H
N
R3
R4
NH2
R4
R3
H
N
R4
R3
H
N
R4
R3

* Les rapports des produits formés sont donnés en pourcentage et non pas en rendement des réactions. Ces pourcentages sont calculés à partir des aires intégrées des pics observés en C.P.V. et par analyses des spectres R.M.N. des mélanges réactionnels quand ceci est possible.

Ces résultats nous permettent donc de conclure que, même si un mécanisme intramoléculaire, avec élimination d'un proton, ne peut plus être envisagé, le phénomène de régiosélectivité se manifeste encore dans le cas des oximes α, β éthyléniques, ce qui nous a amené à tenter de préciser le mécanisme de formation d'aziridine tenant compte de cette régiosélectivité.

Tableau 2

Pourcentages des produits de réduction des oximes XIV et XV par $LiAlH_4$ dans l'éther diéthylique

Oximes de départ	Isomère	Produits non identifiés +	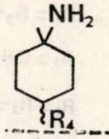 +	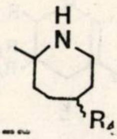 +	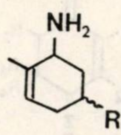 +	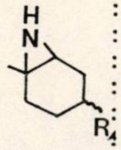
XIV	E	7%	6%	8%	55%	24%
XV	E	0%	0%	42%	34%	24%

Comme il l'a déjà été dit, si l'on élimine le processus d'élimination intramoléculaire, deux mécanismes peuvent être avancés. L'un d'eux nécessite le passage par un intermédiaire nitrène avant formation de l'azirine ; il peut être décrit en quatre étapes, comme le montre la figure 8.

Tableau 3

Pourcentages des produits de réduction de l'oxime XVI par $LiAlH_4$ dans l'éther diéthylique

Oximes de départ	Isomère	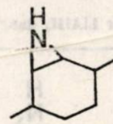 +	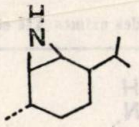 +	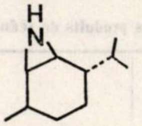 +	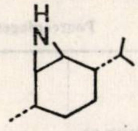
XVI	Z	34%	20%		46%

La première étape se fait avec rétention de configuration au niveau de la fonction oximino (ceci a été vérifié sur l'isophorone oxime XII). Le facteur stéréosélectif devrait donc intervenir dans la deuxième étape. Ce n'est pas le cas puisque, par définition, l'addition de l'ion hydrure et le transfert des liaisons Π vers l'azote se font dans le domaine Π de la molécule, alors que l'élimination du groupement $OAlH_3$ s'effectue dans le plan σ.

Dans ces conditions, il est vraisemblable que la position *Z* ou *E* du groupe partant n'a aucune influence sur la formation du nitrène. Ce mécanisme ne peut donc expliquer le phénomène de régiosélectivité. Il n'en va pas de même pour l'autre mécanisme avec formation directe d'azirine. En effet, dans ce processus, le transfert synchrone d'électrons ne se fait plus uniquement dans l'espace Π mais emprunte aussi le plan σ du système conjugué, pour former une liaison C-N à caractère σ (figure 9).

On peut alors concevoir une interaction responsable de la régiosélectivité. En effet, si nous considérons l'isomère *E*, la présence du doublet libre de l'azote dans le plan σ pourrait entraver le transfert des électrons de la liaison éthylénique du domaine Π à un domaine σ déjà riche en électrons. Inversement dans l'isomère *Z*, le transfert ne serait plus gêné par la présence du doublet libre de l'azote mais facilité du fait que dans le plan σ la liaison N-O est en instance de rupture et va créer une lacune électronique (figure 10).

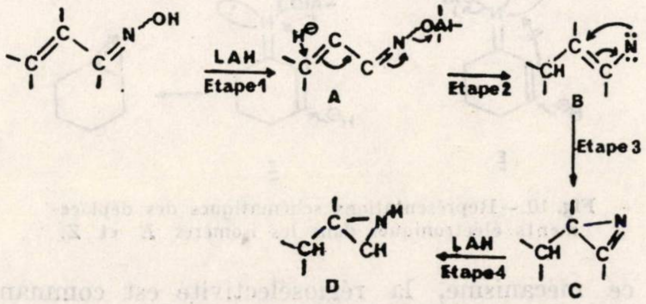

Fig. 8. — Premier mécanisme proposé avec formation d'un nitrène intermédiaire.

Si ce mécanisme a l'avantage de réfuter l'intermédiaire nitrène et d'expliquer à la fois la régiosélectivité et la plus grande réactivité de l'oxime *Z*, il semble, malgré tout, fort improbable car il procède par une *cis*-élimination bimoléculaire. De nombreux exemples de la littérature chimique montrent que la *cis*-élimination bimoléculaire est généralement défavorisée par rapport à la *trans*-élimination. Dans le cas contraire, les

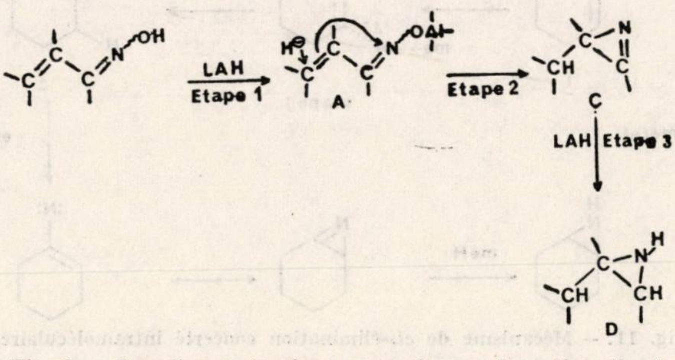

Fig. 9. — Deuxième mécanisme proposé avec formation directe d'azirine.

conceptions actuelles conduisent à envisager l'existence d'un processus intramoléculaire concerté.[9]

Cette dernière possibilité d'interprétation nous paraît donc être la plus valable pour expliquer le phénomène de régiosélectivité que nous avons observé. Le processus peut se concevoir à partir du chemin réactionnel suivant (figure 11).

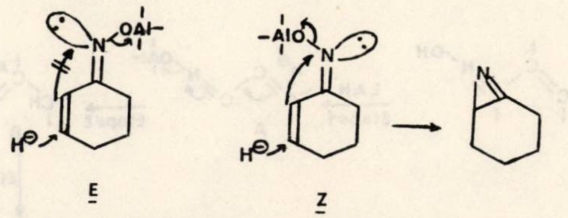

Fig. 10. — Représentations schématiques des déplacements électroniques dans les isomères *E* et *Z*.

Dans ce mécanisme, la régiosélectivité est commandée à la fois par les étapes 1 et 2. La délocalisation électronique du complexe métallique dans la forme *Z* favorise l'addition de la seconde molécule d'hydrure métallique. La seconde étape est la *cis*-élimination intramoléculaire avec participation du doublet libre de l'oxygène. Récemment, Landor et coll.[10] ont proposé pour cette *cis*-élimination un réarrangement sygmatropique (1 — 4), conduisant après formation d'un carbanion au nitrène, puis à l'azirine.

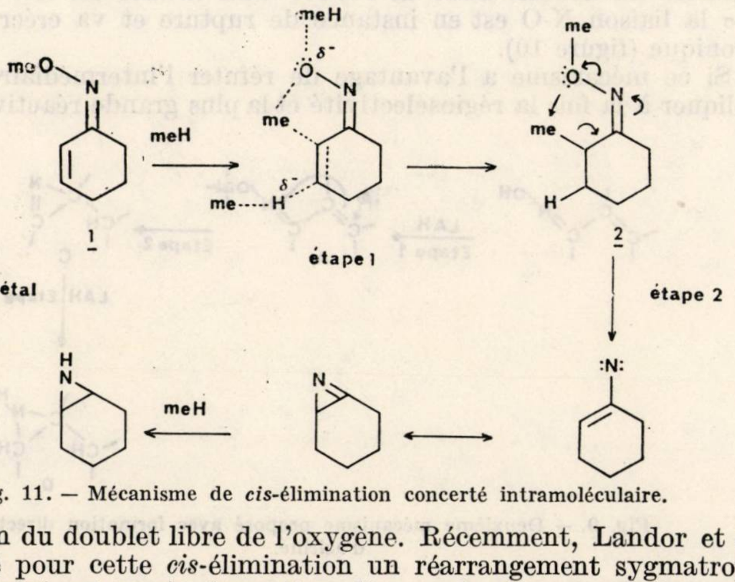

Fig. 11. — Mécanisme de *cis*-élimination concerté intramoléculaire.

---

[9] G. Guillaumet, V. Lemmel, G. Coudert et P. Caubere, *Tetrahedron*, **30**, 1289 (1974).

[10] S. R. Landor, O. O. Sonola et A.R. Tatchell, *J. Chem. Soc.*, *Perkin transactions I*, 1974, 1294.

Il est à remarquer que l'état de transition proposé pour mener à l'organo-métallique intermédiaire *2*, possède déjà la structure nécessaire au processus de *cis*-élimination.

Les étapes 1 et 2 peuvent donc être confondues, ce qui expliquerait le fait que nous n'avons jamais pu isoler d'oxime saturée résiduelle (hydrolyse de *2*).

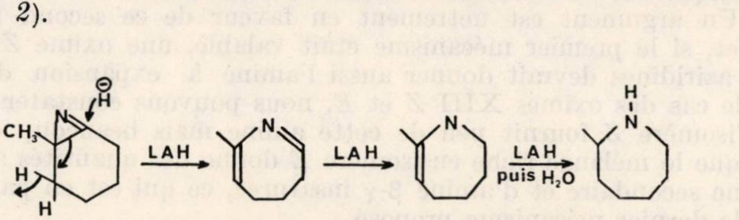

Fig. 12. — Premier mécanisme proposé pour la formation d'amine à agrandissement de cycle.[11]

Si cette interprétation par *cis*-élimination intramoléculaire ne semble souffrir d'aucune ambiguïté dans le cas des oximes XII et XVI qui ne conduisent qu'à des aziridines ou à des amines primaires, un problème se pose au niveau des composés XIII, XIV et surtout XV où une forte proportion d'amine à agrandissement de cycle est observée ; en effet, comme certains auteurs ont pu le suggérer,[11] cette amine pourrait provenir de la réduction de l'azirine intermédiaire et le phénomène de régiosélectivité serait à rejeter sur ces oximes (figure 12).

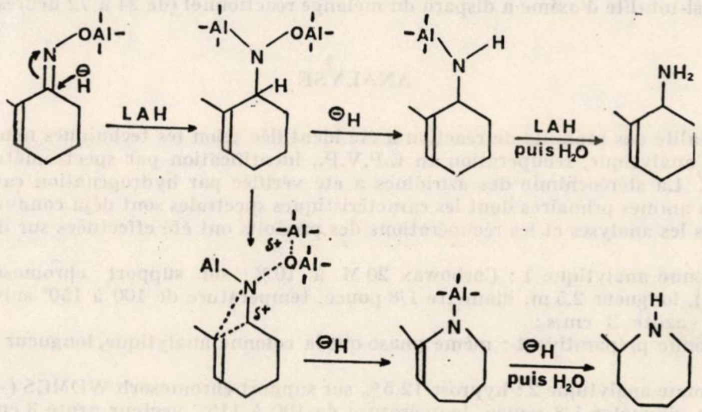

Fig. 13. — Deuxième mécanisme proposé pour la formation d'amine primaire insaturée et d'amine secondaire.[11]

Cependant, comme le font remarquer ces mêmes auteurs, une autre interprétation du phénomène est possible. Celle-ci a l'avantage de n'avoir aucun point commun avec la voie qui mène aux aziridines et implique, au contraire, la réduction initiale de la liaison C = N comme dans le cas de la formation d'amine β-γ éthylénique (figure 13).

---

[11] G. Ricart, D. Couturier et C. Glacet, *Compte rend., C*, **277**, 519 (1973).

Dans ce cas, la réduction serait orientée uniquement vers les amines primaires et secondaires, qui ne nécessitent pas une migration de la liaison éthylénique sur l'atome d'azote dans le stade initial de la réaction.

Un argument est nettement en faveur de ce second mécanisme; en effet, si le premier mécanisme était valable, une oxime *Z* conduisant à des aziridines devrait donner aussi l'amine à expansion de cycle, or, dans le cas des oximes XIII *Z* et *E*, nous pouvons constater (tableau 1) que l'isomère *Z* fournit peu de cette amine mais beaucoup d'aziridines, alors que le mélange riche en isomère *E* donne des quantités appréciables d'amine secondaire et d'amine β-γ insaturée, ce qui est en parfait accord avec le dernier mécanisme proposé.

PARTIE EXPÉRIMENTALE

Les caractéristiques structurales des composés synthétisés ont déjà été décrites en partie dans deux mémoires antérieurs[1,2]; Une étude détaillée de tous les produits formés fera l'objet d'une prochaine publication.

Toutes les oximes ont été synthétisées suivant les méthodes décrites par Sato et coll. [12] Les réductions ont été menées dans l'éther à reflux, avec des concentrations de 0,1 mole/litre et en utilisant cinq fois la quantité stœchiométrique de réducteur. Les réactions sont arrêtées quand la quasi-totalité d'oxime a disparu du mélange réactionnel (de 24 à 72 heures).

ANALYSE

La totalité des produits de réaction a été identifiée selon les techniques nouvelles : chromatographie analytique, récupération en C.P.V.P., identification par spectrométrie de masse, I.R., R.M.N. La stéréochimie des aziridines a été vérifiée par hydrogénation catalytique (Ni de Raney) en amines primaires dont les caractéristiques spectrales sont déjà connues.

Toutes les analyses et les récupérations des produits ont été effectuées sur deux types de colonne :

— colonne analytique 1 : Carbowax 20 M à 10% sur support chromosorb WDMCS (+6% KOH), longueur 2,5 m, diamètre 1/8 pouce, température de 100 à 150° suivant les dérivés, vecteur azote 3 cm/s ;

— colonne préparative 1 : même phase que la colonne analytique, longueur 4m, diamètre 3/8 pouce ;

— colonne analytique 2 : hyprose 12,5% sur support chromosorb WDMCS (+ 2% KOH), longueur 3 m, diamètre 1/8 pouce, température de 100 à 115°, vecteur azote 3 cm/s ;

— colonne préparative 2: même phase que la colonne analytique, longueur 2 m, diamètre 1 cm, vecteur azote 4 cm/s.

La pureté des oximes a été vérifiée à l'aide d'une colonne Carbowax 20 M à 10% sur support chromosorb WDMCS, longueur 1,60 m, diamètre 1/8 pouce, température 130°, vecteur azote 3 cm/s.

CONCLUSION

L'étude des mécanismes décrits à ce jour pour la réduction d'oximes et nos résultats obtenus à partir de cyclohexénones oximes *Z* et *E* nous ont permis de généraliser le phénomène de régiosélectivité et d'en proposer une explication plausible.

---

[12] T. Sato, H. Wakatsuka et K. Amano, *Tetrahedron*, **27**, 5831 (1971).

Revue Roumaine de Chimie, **21**, *1*, 59 – 64 (1976)

THE EFFICIENCY OF ORGANIC CORROSION INHIBITORS IN OIL-FIELD WATERS

IRINA CORNEA and VERA ICHIM

Institute of Physical Chemistry, Str. Galați 31, Bucharest, Romania

Received 13 June 1974

Electrochemical and immersion techniques were used to determine the inhibitive action of some organic inhibitors on the corrosion of a carbon steel. Attempts have been made to explain the differences arising from the two methods.

One of the most efficient methods of metallic surface protection against corrosion is addition of proper inhibitors to the corrosive medium. These inhibitors act, in the case of generalized corrosion process, either as physical or as chemical adsorbed films changing the electrochemical characteristic of the metal or functioning as a mechanical barrier.[1-3]

The nature of the inhibitor to be used, its efficiency in time and the mechanism of its action against corrosion of a metallic surface can be established by using two types of methods :

1. the loss of weight method;
2. the electrochemical methods.

The first one is easier to be applied, because it does not require a special equipment and can be used in quite different practical conditions. Its great disadvantage is that it does not provide any details about the mechanism of inhibition.

The electrochemical methods, even if they do not shorten the time of testing (as far as the time efficiency is concerned), they provide better results regarding the mechanism of inhibition.

The determination of time efficiency of an inhibitor by the weight losses technique requires the weighing of samples before and after immersion in testing medium and then the use of equation :

$$E\% = (G_0 - G_i)/G_0 \cdot 100 \tag{1}$$

where: E is the inhibitor efficiency ; G_0 is the corrosion rate in the absence of the inhibitor (g/m^2.d) ; G_i is the corrosion rate in the presence of the inhibitor (g/m^2.d).

---

[1] A. K. Dunlop, "4th Western States Corrosion Seminar", 1970, p. 9/1.
[2] W. Seiler, D. Oeder and H. Fischer, *Z. phys. Chem.* (*Leipzig*), **243**, 267 (1970).
[3] J. C. Răducanu and W. J. Lorenz, *Electrochim. Acta*, **16**, 995 (1971).

The determination of inhibitor efficiency by electrochemical methods requires that the polarization curves (intensio or potentiostatic) be recorded and the corrosion rate be calculated and then the following equation be used :

$$E\% = (i_0 - i_i)/i_0 . 100 \tag{2}$$

where : i_0 is the corrosion current in the absence of the inhibitor and i_i is the corrosion current in inhibitor-containing electrolyte.

The object of the present research is to make a comparison between the results obtained from electrochemical and weight losses techniques, applied in the study of a carbon steel (J-55) exposed to oil-field water inhibited with two organic inhibitors.

PROCEDURE

The chemical composition of steel used in this research is presented in table 1.

Table 1

The chemical composition of steel

steel	C	Mn	Si	P_{max}	S_{max}	Cr	Mo	V
J–55	0.43	0.85	0.27	0.025	0.019	—	—	—

The chemical composition of the electrolyte medium used can be seen in table 2.

Table 2

The chemical composition of the field oil water

Dissolved gases (mg/l)			Chemical composition (mg/l)					
O_2	H_2S	CO_2	$Ca(HCO_3)_2$	$Mg(HCO_3)_2$	NaCl	$CaSO_4$	$CaCl_2$	$MgCl_2$
2.5	4.0	52.8	400	—	44,800	500	3,600	1,000

The organic inhibitors used were of aminic type, IRI — 1150 and IP — 21.

The observations were carried out at 25, 50 and 80° for immersion times of 1,5,10, 20 and 30 days. At 80° measurements were taken in water containing crude oil.

Independent of the applied techniques, the tested steel was machined in a convenient form to be fixed in the electrochemical cell and for the immersion tests.

The electrochemical measurements were made by using the following set-up (figure 1):[4]

A current supply (B) in series with variable resistance (R) was used to apply different currents and potential variations were reported against the saturated calomel electrode used as reference.

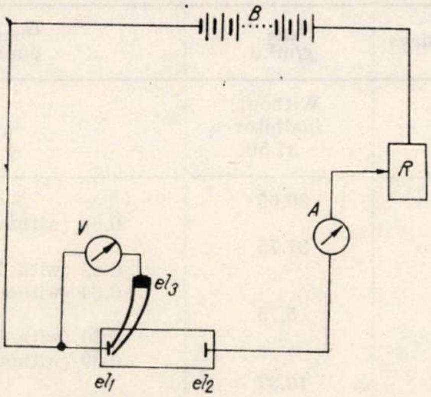

Fig.1 — Intensiostatic set-up.

In the immersion tests, the samples were exposed for the same period of time in the oil-field water with and without inhibitor.

For electrochemical measurements requiring longer exposure times, the samples were preimmersed only in inhibited water.

RESULTS AND DISCUSSION

The efficiencies obtained from immersion and electrochemical measurements of the tested carbon steel, at 25° in the presence of IRI-1150 inhibitor, are listed in table 3, and those carried out at 50°, in table 4.

It can be observed, from the above data, that there are quite big differences between the efficiencies resulting from the two applied techniques.

The differences can be explained as follows :

The determination of the metal lost was used to calculate the efficiencies of the immersion technique by using equation 1.

The efficiencies were estimated by weighing the corroded samples exposed for the same period in electrolyte with or without inhibitor addition.

In the case of electrochemical measurements, i_0 and i_i from equation (2) do not refer to the same exposure time, because negative efficiencies would result if the corrosion current is determined after 5 days exposure (for instance) in the presence and absence of the inhibitor. Thus, the obtained corrosion current in uninhibited water is less than that for inhibited environment. This finding may be due to the high resistance arising in the electrical circuit from the deposits of the corrosion products formed on the surface. For this reason in all calculations based on the corrosion currents, i_0 of uninhibited environment was determined without a former preimmersion.

---

[4] T. Erdey-Gruz, "Kinetics of Electrode Processes", Akad. Kiado, Budapest, 1972.

Table 3

The efficiencies obtained from immersion and electrochemical methods for carbon steel (J-55 type) at 25° in field oil water inhibited with IRI-1150

Time days	$G_{\text{elec.}}$ * g/m^2.d	$G_{\text{imm.}}$ g/m^2.d	$E_{\text{elec.}}$ %	$E_{\text{imm.}}$ %
0	Without inhibitor 37.50	—	—	—
0	30.65	—	18.7	—
1	31.75	0.69 (without IRI) 0.69 (with IRI)	15.3	—
5	5,75	0.34 (without IRI) 0.30 (with IRI)	84.6	11
10	10.37	0.30 (without IRI) 0.22 (with IRI)	72.4	26
20	3.75	0.30 (without IRI) 0.20 (with IRI)	90.0	33
30	3.75	0.30 (without IRI) 0.20 (with IRI)	90.0	33

* Estimated from corrosion currents by using Faraday equation.

Table 4

The efficiencies obtained from immersion and electrochemical methods for carbon steel (J-55 type) at 50° in field oil water inhibited with IRI-1150

Time days	G_{elec}+. g/m^2. d	G_{imm} g/m^2. d	$E_{\text{elec.}}$ %	E_{imm} %
0	Without inhibitor 60.00	—	—	—
0	45.00	—	25.00	—
1	56.25	0.82 (without IRI) 0.69 (with IRI)	16.25	15
5	36.25	0.65 (without IRI) 0.43 (with IRI)	39.50	33
10	32.00	1.00 (without IRI) 0.72 (with IRI)	46.60	28
20	32.00	1.44 (without IRI) 0.95 (with IRI)	46.60	34
30	32.00	1.47 (without IRI) 0.95 (with IRI)	46.60	35

* Estimated from corrosion currents by using Faraday equation

Thus, in the electrochemical measurements, the corrosion currents were deduced from the slope of cathodic curves, at the rest potential. These curves were recorded for preimmersed electrodes in the inhibited solution for a certain period, and i_i estimated, i_0 being established from the polarization curve without prior preimmersion.

As can be seen from table 3, a good agreement between the results of the two applied techniques is obtained only for 1 day exposure. A lack of agreement arises in all the other cases. The better results obtained electrochemically are not due to a higher degree of adsorption of the inhibitor, but on the contrary to the metal corrosion. The deposits of corrosion products on the surface cause very small i_i corrosion currents to be recorded and therefore a very high efficiency results.

The differences observed in E values at 25^0 show that this inhibitor (IRI-1150) has a reduced action, being adsorbed to a lower degree on the surface and thus permitting the development of the corrosion process.

A better agreement is obtained at 50^0. In this case $E_{\text{imm.}}$ is quite close to $E_{\text{elec.}}$ and thus it seems that at this temperature the inhibitor is adsorbed to a higher degree on the surface.

From both tables (3 and 4) it can be observed that the electrochemical rates of corrosion are about 10 times higher than the immersion rates. This is due to the fact that in electrochemical tests the electrolytes were stirred, while in the immersion tests stagnant conditions were used. The effect of stirring on the corrosion rates are reported by some other authors.[5,6]

Similar behaviours are observed in the case of IP-21 inhibitor. The calculated efficiencies $E_{\text{imm.}}$ and $E_{\text{elec.}}$ were more different, indicating even a smaller adsorption of this inhibitor on the metallic surface than in the case of IRI-1150 inhibitor.

In the presence of crude oil, the immersion measurements were taken for any quantities of the crude oil additions in the oil-field water.

However, the electrochemical measurements could be taken only until 10% crude oil additions. For more than 10% crude oil, the resistance of water becomes very high and the intensiostatic technique can no longer be applied as such.

The comparative results obtained on the J-55 steel in oil-field water containing less than 10% crude oil and IRI-1150 inhibitor, at 80^0 (in order that the crude oil viscosity be smaller) are presented in table 5.

The values of $E_{\text{imm.}}$ and $E_{\text{elec.}}$ are in a good agreement, because of the adherence of the crude oil to the metallic surface. However, the small values of obtained efficiencies prove that the addition of the inhibitor in this case is practically ineffective.

---

[5] F. Tödt, "Korrosion und Korrosion Schutz", Walter de Gruyter, Berlin, 1955.

[6] F. Ritter, ,,Korrosionstabellen Metalischer Werkstoffe", Wien, Springer Verlag, 952.

Table 5

The efficiencies obtained from immersion and electrochemical methods for carbon steel (J-55) type) at 80° in field oil water inhibited with IRI-1150 and crude oil addition)

Content of crude oil %		$G_{elec.}$ g/m². d	$G_{imm.}$ g/m². d	$E_{elec.}$ %	E_{imm} %
without IRI	with IRI				
0		21.6	51.50	44.5	56
	0	12.0	22.50		
1		17.0	2.40	52.9	54
	1	7.0	1.10		
5		19.0	2.57	42.1	69
	5	11.0	0.78		
10		17.5	4.47	60.0	75
	10	7.0	1.10		

CONCLUSIONS

The presented data have shown that under certain conditions the immersion and electrochemical techniques give concordant results.

The observed differences between the values of the time efficiencies of the inhibitors could be explained by the differences existing between the conditions of the application of the two techniques.

It seems that the intensiostatic technique is more convenient to be applied as far as the choice of an inhibitor for a certain medium is concerned.

From a practical point of view, the efficiency of a certain inhibitor should, however, be established by applying the immersion technique.

Revue Roumaine de Chimie, 21, 1, 65–72 (1976)

TEXTURE DES CATALYSEURS À BASE D'OXYDE DE ZINC, CUIVRE ET CHROME POUR LA CONVERSION DE L'OXYDE DE CARBONE

ŽARKO D. JOVANOVIĆ et NADEŽDA N. JOVANOVIĆ

Institut de Chimie, Technologie et Métallurgie, Département de la Catalyse, Belgrade

Reçu le 9 juillet 1974

Dans le cadre de la synthèse du catalyseur pour la conversion du monoxyde de carbone avec la vapeur d'eau on a étudié la texture des catalyseurs et son influence sur les propriétés des échantillons préparés. L'étude a compris la détermination de la surface spécifique, la porosité et la distribution du volume cumulatif des pores. Les promoteurs adjoints aux catalyseurs par un mélange mécanique n'avaient pas d'influence sur la texture des catalyseurs, tandis que le manganèse et l'aluminium incorporés par coprécipitation avec les oxydes de base produisaient un effet bien prononcé. L'étude de la texture des catalyseurs préparés a mis en évidence que le procédé établi de la synthèse et de la formation du catalyseur donne la possibilité de former une structure qui permet l'utilisation maximale du catalyseur dans la réaction de conversion de gaz à l'eau.

Pour le déroulement du procédé catalytique, ainsi que pour l'étude des conditions de l'application du catalyseur, la connaissance de la texture, de l'état de dispersion, de la grandeur et du relief de la surface du catalyseur ont une importance particulière.

Les catalyseurs pour la conversion de l'oxyde de carbone aux températures basses représentent une matière poreuse avec la surface interne bien développée, le degré d'utilisation de cette surface croissant rapidement avec la diminution du diamètre du grain et l'élargissement du diamètre des pores.[1]

Le catalyseur de type $ZnO-CuO-Cr_2O_3$ a été préparé dans notre laboratoire par coprécipitation. Un rapport optimal des oxydes a résulté d'une étude de variation de la composition, donnant après un traitement propre le catalyseur d'une activité bien prononcée. On a examiné l'influence sur l'activité catalytique des promoteurs introduits par un mélange mécanique des oxydes des métaux ou coprécipités avec les oxydes de base. L'étude a montré que l'introduction des promoteurs comme oxydes métalliques n'a pas une influence essentielle sur l'activité des catalyseurs. Cependant, les catalyseurs promus par coprécipitation des éléments de base avec le manganèse possèdent une grande activité, ainsi qu'une bonne stabilité thermique. L'aluminium, introduit par coprécipitation se comporte comme inhibiteur.[2] L'analyse des phases et l'analyse thermique

[1] F. P. Ivanovskii, G. E. Braude et T. A. Semenova, *Trudy GIAP*, 9, 195 (1959).

des échantillons sans promoteurs, ainsi que des catalyseurs promus, ont indiqué que la présence de la phase cristalline du zinc oxyde, ainsi que du cuivre métallique sont nécessaires pour une activité prononcée. La présence du spinelle du chromite de zinc n'a pas été constatée durant cette étude.[3–5]

Pour une analyse plus précise de l'influence de la texture sur les propriétés des catalyseurs préparés il a été nécessaire de déterminer la surface spécifique, la porosité totale et la distribution du volume des pores par diamètre pour les échantillons sans promoteurs et les catalyseurs avec les promoteurs introduits par un mélange mécanique ou par coprécipitation avec les oxydes de base.

La surface spécifique a été mesurée par la méthode de BET, à partir des isothermes d'adsorption du nitrogène à —196,5°, dans un appareil statique volumétrique. La porosité totale a été calculée à partir des densités réelles et apparentes, mesurées par la méthode picnométrique avec du benzène ou du mercure, respectivement. La distribution du volume des pores par diamètre a été déterminée à l'aide du porosimètre Aminco Winslow, modèle 5000 psi, pour l'intervalle des pores de 0,1 mm à 0,035 microns, tandis que la distribution des pores jusqu'à 350 Å a été mesurée selon la méthode de Cranstone et Inkley [6] à partir de l'isotherme d'adsorption pris à —196,5°.

La texture des catalyseurs sans promoteurs a été étudiée sur les échantillons avant et après la réduction qui se déroule au cours de l'activation des catalyseurs. Les résultats sont rassemblés dans le tableau 1. Les échantillons ont un rapport différent des oxydes de base, le contenu en cuivre augmentant de l'échantillon 1 à 5. Pour comparaison, les résultats de la mesure de l'activité catalytique y sont adjoints.

A partir des résultats obtenus on peut constater que les catalyseurs possèdent une grande porosité (~70%), les échantillons reduits étant, pour environ 7%, plus poreux qu'avant la réduction. En même temps, les surfaces spécifiques des catalyseurs diminuent après la réduction, devenant de l'ordre de 35 m²/g, ce qui est en concordance avec la relation entre ces deux propriétés des catalyseurs pour la conversion de l'oxyde de carbone.[7]

Les courbes différentielles de la distribution des pores par diamètre pour les catalyseurs avant la réduction (a) et les catalyseurs réduits (b) sont présentées sur la figure 1. Les échantillons avant réduction possèdent une distribution du rayon des pores homogène avec le maximum de volume au diamètre des pores de 1400 à 2000 Å. Cette uniformité indique que les échantillons ont été préparés et formés dans les conditions reproductibles. La pression de pastillage qui d'ailleurs peut influencer la texture des catalyseurs,[8] ne pouvait pas être régistrée dans nos conditions

---

[2] P. Putanov et Ž. Jovanović, *Bull. Soc. chim., Beograd*, **35**, 279 (1970).

[3] P. Putanov, Ž. Jovanović et Bj. Aleksić, *Bull. Soc. chim. Beograd*, **35**, 285 (1970).

[4] P. Putanov, Ž. Jovanović et R. Herak, *Hem. ind., Beograd*, **27**, 117 (1973).

[5] P. Putanov, Ž. Jovanović et R. Herak, *Rev. Roumaine Chim.*, **18**, 569 (1973).

[6] R. W. Cranston et F. A. Inkley, *Adv. Catalysis*, **9**, 143 (1957).

[7] P. Putanov, A. Terlecki, Ž. Jovanović et D. Karaulic, *Hem. ind., Beograd*, **20**, 319 (1966).

[8] D. S. Shishkov, *Doklady Bulg. Acad. Nauk*, **23**, 543 (1970).

de préparation, mais elle était tenue à peu près constante pour tous les échantillons.

La distribution du volume des pores s'élargit par réduction et le maximum se déplacen fonction des changements chimiques et de la transformation des phases. L'échantillon 5, avec la plus haute teneur en cuivre possède la plus large distribution. Cet échantillon a subi pendant la réduction les plus grandes transformations de phase par la formation des phases cristallines de l'oxyde de zinc et du cuivre métallique, ce qui est en concordance avec son activité catalytique (tableau 1).

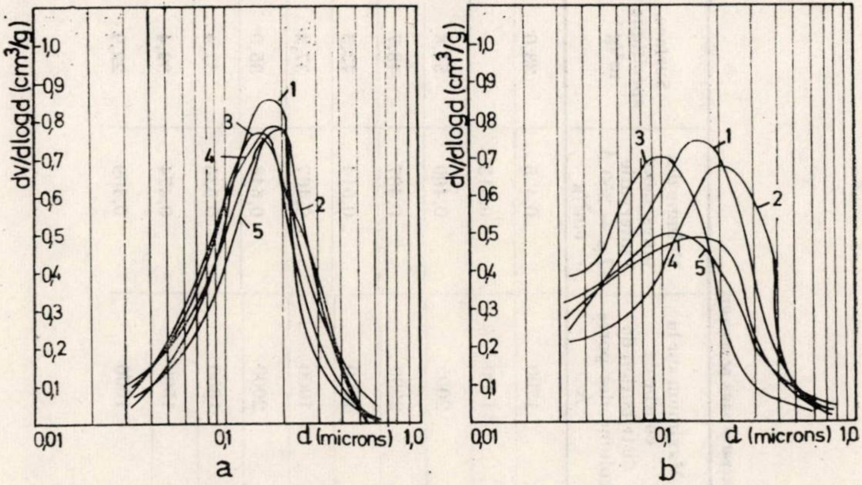

Fig. 1. — Courbe différentielle de la distribution de volume des pores par diamètre, pour les catalyseurs préparés sans promoteurs :

a, échantillons non réduits ; *b*, échantillons réduits ; (les numéros sur les courbes correspondent aus échantillons du tableau 1).

L'étude de l'influence sur la texture de catalyseur n° 6 des divers oxydes métalliques introduits comme promoteurs par mélange mécanique a été effectuée sur les échantillons avant et après la réduction. Les résultats rassemblés dans le tableau 2 montrent que l'addition des oxydes ne change pas essentiellement la texture, excepté le catalyseur n° 11 qui a été préparé avec l'oxyde de manganèse. La porosité de ce catalyseur n'a pas changé après la réduction, mais la surface spécifique est devenue plus basse que celle des autres catalyseurs promus, ainsi que du catalyseur n° 6. L'influence prononcée de l'oxyde de manganèse sur la texture des catalyseurs se manifeste aussi sur l'échantillon n° 14 auquel il est ajouté avec l'oxyde d'aluminium.

La texture des échantillons préparés par coprécipitation des promoteurs avec les oxydes de base a subi l'influence des additifs. Comme on peut voir du tableau 3, les catalyseurs promus par potassium, magnésium, calcium et manganèse n'ont pas subi un changement notable de porosité et de surface spécifique après la réduction, comparés au catalyseur n° 15

Tableau 1

Texture des catalyseurs $ZnO-CuO-Cr_2O_3$ préparés sans promoteurs

Catalyseur η^0		Densité réelle, g/cm³	Densité apparente g/cm³	Porosité totale %	Volume spécifique des pores cm³/g	Maximum sur la courbe de distribution de volume des pores Å	Volume des pores dans l'intervalle 77 μ — 350 Å cm³/g	Surface spécifique m²/g	Taux de conversion %
1	non réduit	3,61	1,41	61,0	0,433	1700	0,425	33,0	89,8
	réduit	4,81	1,58	67,5	0,425	1400	0,413		
2	non réduit	4,49	1,36	69,0	0,496	2000	0,400	54,8	95,2
	réduit	5,09	1,37	73,1	0,533	2000	0,487	48,7	
3	non réduit	4,05	1,31	67,7	0,514	1500	0,514	43,3	95,8
	réduit	5,14	1,24	67,6	0,612	1000	0,467	37,3	
4	non réduit	4,22	1,14	73,0	0,640	2000	0,648	35,0	98,0
	réduit	4,73	1,36	71,3	0,524	1800	0,536	37,9	
5	non réduit	4,30	1,40	67,5	0,482	1500	0,474	39,4	98,3
	réduit	4,68	1,30	72,0	0,554	1000	0,409	22,9	

Tableau 2

Texture des catalyseurs ZnO – CuO – Cr_2O_3 promus par un mélange mécanique d'oxydes des métaux

Catalyseur η^0		Promoteur	Densité réelle g/cm³	Densité apparente g/cm³	Porosité totale %	Volume spécifique des pores cm³/g	Surface spécifique m²/g	Taux de conversion %
6	non réduit	—	4,09	1,73	58,7	0,341	38,4	98,5
	réduit		4,61	1,66	64,0	0,385	35,4	
7	non réduit	MgO	4,39	1,42	67,7	0,477	37,6	97,8
	réduit		4,92	1,47	70,2	0,477	35,2	
8	non réduit	Al_2O_3	4,48	1,53	65,9	0,431	36,7	97,5
	réduit		4,56	1,43	68,6	0,480	33,9	
9	non réduit	CaO	4,63	1,63	64,8	0,399	35,9	97,7
	reduit		5,12	1,73	66,2	0,383	34,6	
10	non réduit	TiO_2	4,62	1,69	63,5	0,378	35,9	95,6
	réduit		4,59	1,58	65,6	0,415	31,9	
11	non réduit	MnO_2	5,00	1,62	68,0	0,420	16,8	97,5
	réduit		5,07	1,67	67,1	0,402	22,8	
12	non réduit	MgO Al_2O_3	4,52	1,78	60,7	0,342	37,6	98,2
	réduit		4,67	1,65	64,7	0,392	36,3	
13	non réduit	MgO, Al_2O_3 CaO	4,27	1,65	61,4	0,376	40,6	96,6
	réduit		4,64	1,71	63,2	0,370	38,1	
14	non réduit	MnO_2 Al_2O_3	4,20	1,47	65,0	0,436	26,0	97,5
	réduit		4,47	1,43	68,0	0,475	23,0	

Tableau 3

Texture des catalyseurs $ZnO - CuO - Cr_2O_3$ préparés par co-précipitation avec des promoteurs

Catalyseur n°		Promoteur	Densité réelle g/cm^3	Densité apparente g/cm^3	Porosité totale %	Volume spécifique des pores cm^3/g	Maximum sur la courbe de distribution de volume des pores Å	Volume des pores dans l'intervalle $77\mu - 350$Å cm^3/g	Surface spécifique m^2/g
15	non réduit	—	4,93	1,29	72,6	0,563	1500	0,493	35,1
	réduit		5,30	1,24	76,6	0,618	1500	0,416	27,4
16	non réduit	Mg	5,14	1,31	74,5	0,568	1500	0,500	37,0
	réduit		5,32	1,26	76,3	0,605	1500	0,512	26,7
17	non réduit	K	5,11	1,31	74,4	0,568	2000	0,447	33,6
	réduit		5,24	1,28	75,6	0,591	1900	0,480	24,4
18	non réduit	Ca	5,14	1,24	75,9	0,612	1000	0,496	38,9
	réduit		5,67	1,23	77,6	0,631	1000	0,512	28,6
19	non réduit	Al	4,48	1,13	74,8	0,662	1000	0,512	57,5
	réduit		3,83	1,22	68,5	0,561	1000	0,473	54,3
20	non réduit	Mn	4,95	1,63	66,7	0,409	1500	0,310	32,8
	réduit		5,06	1,55	69,5	0,448	600	0,287	30,0

préparé sans promoteurs. L'influence des promoteurs sur la distribution de volume cumulatif des pores est évidente (tableau 2), au point de vue de la formation des pores plus fins.

Comme on voit sur la figure 2, l'addition de manganèse a un effet prépondérant sur le changement de volume des pores. Les macropores ont disparu, et à partir de la différence de volume spécifique des pores et de volume des pores dans l'intervalle du rayon des pores de 70 microns à 350Å (limite de mesure du porosimètre), on peut constater que le catalyseur promu par manganèse possède 25% de volume de pore du diamètre moindre de 350 Å.

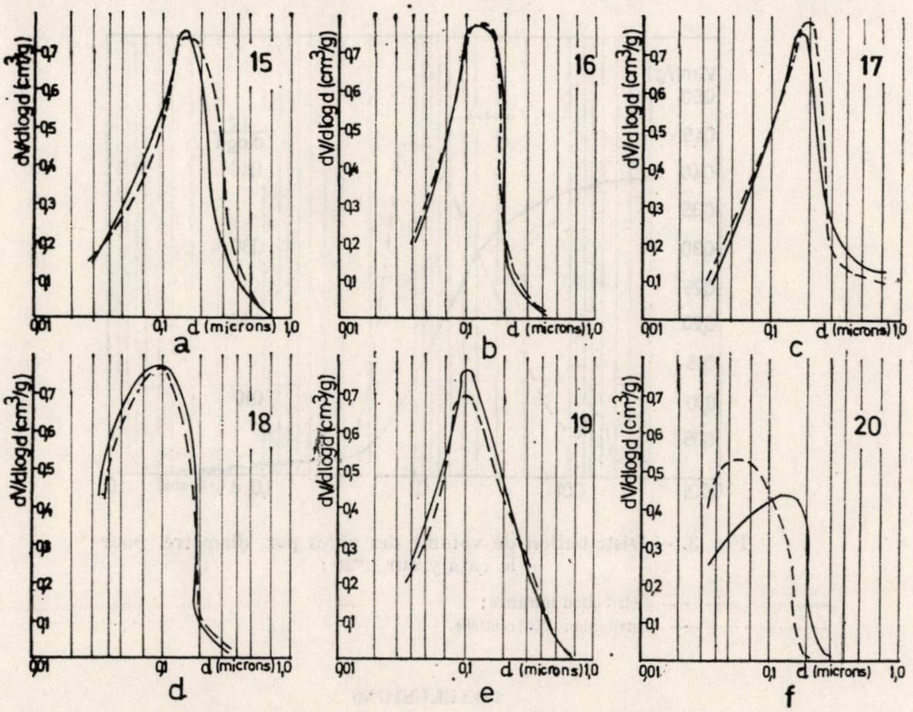

Fig. 2. — Courbe différentielle de la distribution de volume des pores par diamètre pour les catalyseurs préparés par coprécipitation avec les promoteurs :

——————— échantillons non réduits ;

— — — — — — échantillons réduits.

Pour l'étude de la distribution de volume cumulatif des pores du catalyseur n° 20 promu par manganèse dans l'intervalle de 15 Å à 70 microns, nous avons appliqué la méthode de condensation capillaire. Les distributions intégrale et différentielle du volume des pores par diamètre pour le catalyseur n° 20 sont représentées sur la figure 3. Le catalyseur possède une structure bidisperse avec un maximum mis en évidence à 1500 Å et l'autre à 65 Å, tandis que les pores du diamètre moindre que 50 Å pratiquement n'existent pas.

L'aluminium, comme promoteur adjoint par coprécipitation avec les oxydes de base, influence l'augmentation de volume cumulatif des pores, le déplacement de la distribution de volume des pores vers les pores plus fins et augmente remarquablement la surface spécifique du catalyseur (figure 2*e*).

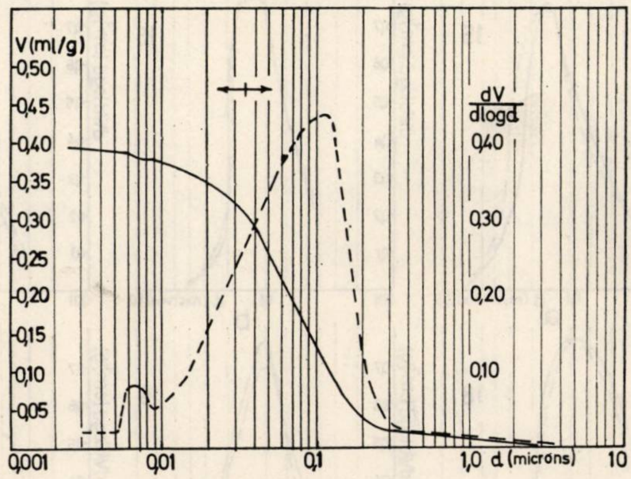

Fig. 3. — Distribution de volume des pores par diamètre pour le catalyseur n°20 :

———————— distribution intégrale;
– – – – – – – – distribution différentielle.

CONCLUSIONS

A partir des résultats obtenus par l'étude des catalyseurs préparés sans promoteurs, on peut conclure que le mode de préparation appliqué mène aux poudres homogènes, avec des particules à peu près uniformes, résultant des catalyseurs avec une structure des pores homogène, ce qui indique que les conditions de formation des catalyseurs étaient maintenues constantes.

Les promoteurs adjoints par un mélange mécanique aux catalyseurs préparés préalablement n'ont pas exercé un effet notable sur la texture des catalyseurs.

Parmi les échantillons avec les promoteurs adjoints par coprécipitation avec les oxydes de base l'influence du manganèse et de l'aluminium a été remarquée.

La diminution de la surface spécifique des échantillons réduits résulte de la transformation des phases au cours de la réduction.

Au point de vue des dimensions des molécules de l'oxyde de carbone et de la vapeur d'eau, on peut constater que la surface des catalyseurs préparés est complètement utilisée dans la réaction de conversion de l'oxyde de carbone. Les différentes activités des catalyseurs ne peuvent être attribuées qu'à la présence de différentes quantités de cuivre métallique.

Revue Roumaine de Chimie, 21, 1, 73–80 (1976)

RELATIONSHIPS BETWEEN PROPERTIES AND ACTIVITY OF ALUMO-CHROMIA CATALYSTS. I

ROLE OF PRECURSORS IN OBTAINING ALUMINIUM OXIDES

I. V. NICOLESCU*, M. SPINZI** and D. CIOMÂRTAN ***

* Faculty of Chemistry, Bucharest University, Spl. Independenței 89, Bucharest, Romania
** Institute for Nuclear Technology, P. O. Box 5204 Bucharest, Romania
*** Research and Design Institute for Glass and Fine Ceramics Technology, Bd. Ion Șulea 299, Bucharest

Received September 6, 1974

We have obtained a series of aluminium oxides different from structural and textural standpoint, by varying starting material and thermal treatment. We have emphasized the prevailing role of the raw material in determining the structural and textural character of the aluminium oxide.

INTRODUCTION

A large number of studies have been devoted to the problem of determining some criteria in selecting catalysts. Our researches have focussed on the interdependence between the constituents of the solid catalysts which have a direct bearing on their final activity.

One of our main objectives was to study the carrier contribution on the catalytic activity and the way in which it may be influenced during the elaboration process of the catalyst.

We directed our attention towards the $Al_2O_3-Cr_2O_3$ system since it is widely used in petrochemistry and it exhibits some characteristics that allow an independent investigation of the components by adequate physico-chemical techniques.

The present study is concerned with catalysts obtained by impregnation. In this case, as a carrier, the aluminium oxide represents the host-component, on the surface and inside the pores of which the active component deposits.

In order to investigate the manner in which the aluminium oxide texture and structure affect the deposited chromium oxide properties, we purpose to obtain controlled varieties of aluminium oxides and to define the importance of the raw material in the succession of the random parameters composing the biography of an oxide.

EXPERIMENTAL RESULTS AND DISCUSSION

1. PREPARATION OF ALUMINIUM OXIDE

We have investigated the role of the precursor and of the thermal treatment in conferring the structural and textural characteristics of the alumina, since these factors are considered to be of utmost importance in their obtention technology. There are a large number of comprehensive studies in this respect,[1–3] which consider the role of the precursor starting with the aluminium hydroxide phase, paying less attention to the influence exerted by the initial component nature.

The aluminium oxides have been obtained from the corresponding hydroxides resulting by precipitation of some solutions of potassium aluminate and aluminium nitrate. The transformation of hydroxides into oxide phase has been performed by a differentiated thermal treatment at 640°, 700°, 800° and 1100°, in a controlled atmosphere. The necessary precautions have been taken in order to obtain identical calcination conditions so that any modifications of each hydroxide should only depend upon the thermal treatment.

Following this line, four Al_2O_3 samples have been obtained for each hydroxide enabling us to follow the properties variation within each series having a common origin, as well as within parallel series under identical calcination conditions.

In order to have a better understanding of the text, we marked by different symbols the aluminium oxides samples prepared as indicated in table 1.

Table 1

Composition and symbols of samples

Symbol	Composition	Precursor
S_1	Aluminium hydroxide	$K_2Al_2O_4$
S_2	,,	$Al(NO_3)_3$
$S_{1.640}$	Aluminium oxide calcinated at 640°	S_1
$S_{1.700}$	,, at 700°	S_1
$S_{1.800}$	,, at 800°	S_1
$S_{1.1100}$	,, at 1100°	S_1
$S_{2.640}$	,, at 640°	S_2
$S_{2.700}$	,, at 700°	S_2
$S_{2.800}$	,, at 800°	S_2
$S_{2.1100}$	,, at 1100°	S_2

2. THERMAL ANALYSIS OF ALUMINIUM HYDROXIDES

The loss of water process undergone by the aluminium hydroxides due to their thermal treatment has been controlled by DTA and DTG. Powders with a 0.02 mm diameter and a heating rate of 10°/min have been employed.

The thermograms of the two hydroxides (fig. 1) point to certain differences even in this phase assigned by us to the influence of different ions pre-existing in the precipitation medium.

The process of loss of physisorbed water as well as of water of constitution may be considered as completed above a temperature of 500° for both hydroxides. However, the transformations of the two hydroxides occur in a differentiated manner within this temperature range. Thus,

---

[1] B. C. Lippens, Ph. D. Thesis, Techische Hogeschool, Delft, 1961.

[2] B. C. Lippens and C. Steggerda, in "Physical and Chemical Aspects of Adsorbents and Catalysts" Ed. B. G. Linsen, Academic Press, London, 1970.

[3] I. Ia Tiureaev, "Fizico-khimiceskie i tehnologiceskie osnovy polucenia divinila iz butana i butilena", Izd. Khim., Moscow, 1966, chapter 1.

at the end of the process the S_1 hydroxide loses 32.2% of its weight, whereas the S_2 hydroxide loses 55%; this points to the different water content as well as to the different water binding possibilities. If the process of losing physisorbed water, which represents the first peak on the DTG curve takes place at relatively close temperatures for both samples, the process of losing the water of constitution takes place at different temperatures and with different rates, the S_2 hydroxide undergoing some lattice changes during this process as it is indicated by the exothermal effects for 315° and 388°.

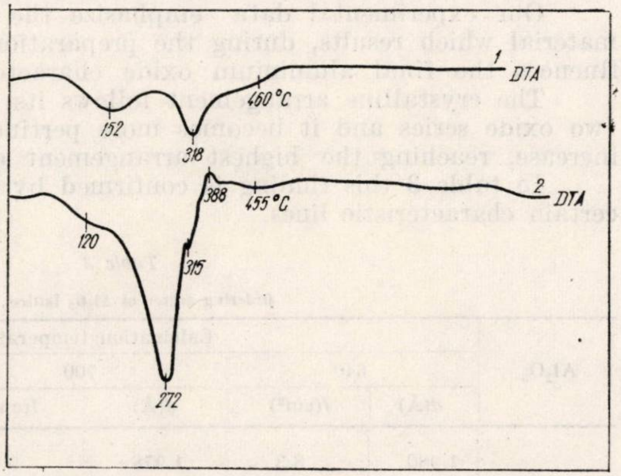

Fig. 1. — Thermograms of hydroxides S_1 and S_2.

Therefore, the thermal analysis points to a clearcut difference between the two initial hydroxides displaying different structures and binding strength for water molecules and for constituting hydroxyles.

3. X-RAY SPECTRA

The diffraction patterns have been obtained by the Debye-Sherrer method, employing the CuK_α radiation directed through a Ni filter.

The diffraction lines compared to the ASTM files pointed out a bayeritic structure for the S_1 and a pseudo-bohemitic structure for the S_2 aluminium hydroxide.

As it was expected, the differentiated thermal treatment applied to aluminium hydroxides led to the obtainment of different transition forms of Al_2O_3, as seen in table 2.

Table 2

Structural varieties of Al_2O_3

Calcination temp. °C	Structural varieties of Al_2O_3			
	640	700	800	1100
Al_2O_3(S_1 group)	$\gamma-Al_2O_3$	$\eta-Al_2O_3$	$\eta-Al_2O_3$	$\alpha, \theta, \delta-Al_2O_3$
Al_2O_3 (S_2 group)	$\Omega - Al_2O_3$	$\gamma-Al_2O_3$	$\eta-Al_2O_3$	$\alpha-Al_2O_3$

These data show that in most cases alumina with distorted spinelic tetragonal lattices have been obtained.[1,4,5] The structural varieties obtained within each alumina group point out that the thermal treatment calls for a certain structural organization. Even more worth noticing, when watching closely the development of the two groups for each calcination temperature, becomes the fact that the thermal treatment for identical environmental conditions is not sufficient for obtaining a certain structural variety. Therefore, in most cases, different structural varieties have been obtained under identical calcination circumstances.

Our experimental data emphasize the contribution of the raw material which results, during the preparation, into a matrix that influences the final aluminium oxide characteristics.

The crystalline arrangement follows its normal course within the two oxide series and it becomes more pertinent with the temperature increase, reaching the highest arrangement degree of 1100°.

In table 3 this finding is confirmed by the intensity variation of certain characteristic lines.

Table 3

Ordering degree of Al_2O_3 lattice

Al_2O_3	Calcination temperature °C					
	640		700		800	
	d(Å)	I(cm^2)	d(Å)	I(cm^2)	d(Å)	I(cm^2)
S_1 group	1.980	8.3	1.978	9.0	1.976	10.0
	1.386	10.5	1.395	12.0	1.394	17.5
S_2 group	1.860	2.3	1.990	3.5	1.990	9.0
	1.393	7.5	1.394	8.5	1.390	18.0

In general, spectra have presented more marked and better resolved intensities at the essential lines with the temperature rise and the diffuse lines have become clearer.

The mean diameters of the particles calculated by Sherrer's relation are presented in the same table, which offers a first rough information on the texture of these oxides and points to a variation ranging between 40–60 Å.

4. TEXTURAL ANALYSIS

Defining the texture as the total surface evaluation and the pore size distribution, Wheeler *et al.*[6,7] showed its special importance in the catalyst activity. The need of controlling these parameters even since the carrier preparation results from the above.

---

[4] C. Marcilly and B. Delmon, *Bull. Soc. chim. France*, **1970**, 446.

[5] C. Marcilly and B. Delmon, *J. Catalysis*, **24**, 336 (1972).

[6] A. Wheeler and S. E. Voltz, *Z. phys. Chem.* (*Frankfurt*), **5**, 100 (1955).

[7] C. P. Poole Jr. and S. Mac Iver, "Advances in Catalysis", Academic Press, New York, 1967, vol. 17, p. 233.

In determining the specific surface area and the microstructure we employed the adsorption nitrogen method at −196° and we used the mercury porosimetry method in determining the macrotexture. The main textural data are presented in table 4.

Table 4

Textural properties of Al_2O_3

Sample	Specific surface area (m²/g)	Volume of pores (cm³/g)		Average radius (Å)
		$\sum_{0}^{150} V_p$	$\sum_{150}^{75.000} V_p$	
$S_{1.640}$	192	0.481	0.301	50
$S_{1.700}$	175	0.425	0.273	49
$S_{1.800}$	168	0.471	0.217	55
$S_{1.1100}$	86	0.411	0.380	90
$S_{2.640}$	150	0.250	0.263	33
$S_{2.700}$	143	0.245	0.369	34
$S_{2.800}$	123	0.250	0.306	40
$S_{2.1100}$	70	0.267	0.301	75

In turn, the textural characteristics display certain differences that are due to both the precursor and the thermal treatment. Consequently, the alumina deriving from bayerite display a monodisperse structure of the pores at a temperature of 640° that becomes bidisperse with the increase of the calcination temperature, as it can be illustrated by the limit cases presented in Figs. 2 and 3. The oxides derived from pseudo-

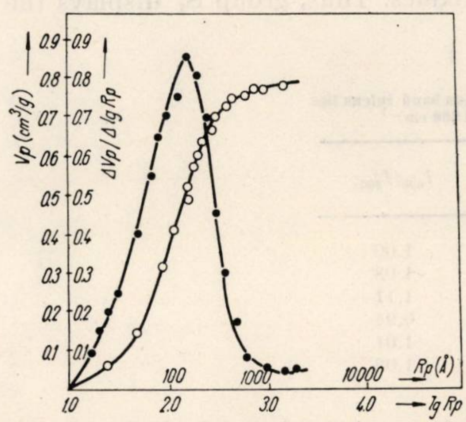

Fig. 2. — Volume distribution of pores as a function of pore size for $S_{1.640}$ aluminium oxide.

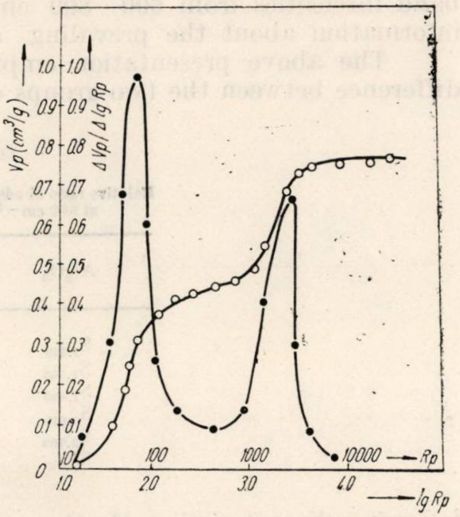

Fig. 3. — Volume distribution of pores as a function of pore size for $S_{1.1100}$ aluminium oxide.

bohemite show a bidisperse pore structure throughout the temperature range.

In both oxide series one could remark a shift of the most frequent radius towards higher values as the calcination temperature increases. Likewise, as it was expected, the calcination temperature increase brought about a diminution of the specific surface areas.

Differences exist, even in these cases, between the two groups and they must be due to their different origins, namely about 25% larger surfaces and up to 90% bigger micropore volumes for the S_1 group alumina against the S_2 group alumina.

5. IR SPECTROSCOPY

The IR absorption spectra obtained by transmission in KBr pellets have been recorded. They display sharp bands in the 1650 cm^{-1} range, that correspond to the deformation and stretching frequencies from the physisorbed molecular water spectrum.[8] The large absorption bands obtained for 3200—3700 cm^{-1} characteristic of the hydroxyl groups bound by hydrogen bridges mark a diminution of the hydroxyl groups with the calcination temperature, the effect being more pertinent for the S_2 group alumina.

The range corresponding to 400—900 cm^{-1} wavelengths provided us with information on the spinelic skeleton of the two alumina groups.[8,9] The fact that the absorption peaks occur in a range between 550—650 cm^{-1}, points out the presence of aluminium in the spinel condensed octahedra, between 700—800 cm^{-1} — in the spinel condensed tetrahedra and between 800—850 cm^{-1} — in the isolated tetrahedra. The relative ratio of band intensities from 600—800 cm^{-1} is presented in table 5, supplying information about the prevaling aluminium coordination form.

The above presentation emphasizes the existence of a structural difference between the two groups of oxides. Thus, group S_1 displays the following characteristics : the $S_{1.640}$ alumina contains ions relatively equally distributed in the spinelic tetrahedra and octahedra and the effect of the

Table 5

Relative ratio of adsorption band intensities at 600 cm^{-1} and 800 cm^{-1}

Al_2O_3	I_{600}/I_{800}
$S_{1.640}$	1.00
$S_{1.700}$	1.08
$S_{1.800}$	1.11
$S_{2.640}$	0.94
$S_{2.700}$	1.01
$S_{2.800}$	1.09

---

[8] J. B. Peri and R. B. Hannan, *J. Phys. Chem.*, **64**, 1526 (1960).

[9] A. J. Leonard, F. van Cavelaert, *J. Phys. Chem.*, **71**, 965 (1967).

temperature increase results in a transfer of aluminium into the octahedral holes, reflected by the superunitary value of the respective ratio.

In the S_2 series, the ratio becomes subunitary and the IR spectra show the prevalent presence of aluminium in the condensed tetrahedra and an adsorption maximum characteristic of aluminium found in the isolated tetrahedra, is found.

The temperature effect is the same as mentioned above, the octahedral coordinated aluminium prevailing only at 800°.

The indications from the IR spectra are convergent to those obtained by X-ray spectra supplying additional information on the superficial hydroxyls, too. These determinations point as well to certain differences between the aluminium oxide groups, as far as the free forces on the surface are concerned, by the preferential exposure of the 110, 111 or 100 planes. This indication is of a particular interest in interpreting the catalytic activity or the impregnation process.

CONCLUSIONS

The paper emphasizes the important contribution made by the raw material in defining the final characteristics of the aluminium oxide. All the transformation steps in the biography of the aluminium oxide largely depend on the nature of the respective raw material.

It was experimentally found that thermal treatment and the surrounding environments do not represent a sufficient condition in order to achieve the desired structure and texture.

Revue Roumaine de Chimie, 21, 1, 81–87 (1976)

IR SPECTRA OF SOME CHELATES OF THIAZOLIDINIC ACIDS

ELENA CATRINA

Institute of Agronomy, Department of Chemistry, Timişoara,
Spl. T. Vladimirescu 14-a, Romania

Received July 3, 1974

The ligands from the class of substituted thiazolidine-carboxylic acid for methyl and phenyl groups were obtained from cysteine, by condensation of aldehydes and ketones. The chelates of these ligands with 3d transitional metals; Mn, Fe, Co, Cu and Zn with a role of bioelements were synthetized. The IR spectra of the ligands and their chelates were recorded. The elemental analysis data and the characteristic absorption bands observed for these compounds verify the chemical structure proposed by us.

INTRODUCTION

In a previous work[1] we calculated the effective electronegativities of the constituent atoms of substituted thiazolidinic acids used as ligands with formula (I):

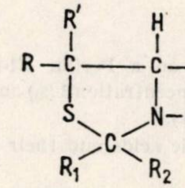

I a: R, R′, $R_1 = H$; $R_2 = CH_3$;
b: R, $R' = H$; R_1, $R_2 = CH_3$
c: R, R′, R_1, $R_2 = CH_3$
d: R, R′, $R_1 = H$; $R_2 = C_6H_5$

The conclusion of this work is that the oxygen atom of the carboxylic OH group and the iminic nitrogen atom are the most electronegative and that they are the best donor atoms for chelation in our compounds.

On that basis and using the analytical data for substituted chelate compounds of thiazolidinic acids we proposed the structural formulae

---

[1] E. Catrina, Z. Simon and Gh. Catrina. *Rev. Roumaine Chim.*, **20**, 651 (1975).

(II) and (III) a, b, c, d:

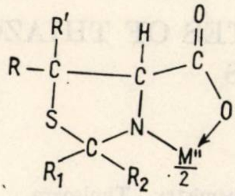

II (a, b, c, d)

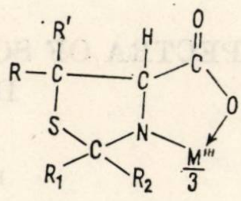

III (a, b, c, d)

a, b, c and d, are the same substituents as in formula (I).

$$M^{II} = Mn^{2+},\ Zn^{2+},\ Cu^{2+};\ M^{III} = Fe^{3+},\ Co^{3+}.$$

Since the investigated substances crystallize with two molecules of water, the following general formula could be assigned to them

$$(Tiac)_2 M^{II} \cdot 2H_2O; \qquad (Tiac)_3 M^{III} \cdot 2H_2O$$

where (Tiac) = thiazolidine-4-carboxylic acid.

In the present work the IR spectra of these compounds are studied. The spectra obtained by us for the chelates present essential changes related to the spectra of the original thiazolidinic acids used as ligands. The changes thus obtained prove that the carboxyl and imine groups of the thiazolidine carboxylic acids participate in the formation of the chelate-type bond.

EXPERIMENTAL

IR spectra were recorded in the 4000—400 cm^{-1} range, on a Perkin Elmer type 621 IR-spectrophotometer, samples were pressed in KBr pellets (concentration 1%) and on a Carl Zeiss—Jenna U. R.— 20 spectrophotometer (1 mg/300 mg KBr).

The IR spectra of the substituted thiazolidine-carboxylic acids and their chelates were recorded.

Preparation of ligands. The following four derivatives of the thiazolidine-4-carboxylic acid serve as starting substances for the synthesis of chelates ; 2-methyl-thiazolidine-4-carboxylic acid 2,2′-dimethyl-thiazolidine-4-carboxylic acid, 2-phenyl-thiyzolidine-4-carboxylic acid and 2,2′, 5,5′ tetramethyl-thiazolidine-4-carboxylic acid. The first three compounds were synthetized according to the methods of literature, [2−5] starting from cysteine chlorhydrate and its esthers by condensation with the corresponding aldehydes and ketones using as solvents water, ethanol

---

[2] A. H. Cook and J. M. Heilbron, "The Chemistry of Penicillin", Princeton Univ. Press, New Jersey, 1949, Chap. III.

[3] F. Michael and H. Emde, *Chem. Ber.*, **72 B**, 1229 (1967).

[4] F. E. King, J. W. Clarke and E. Wade, *J. Chem. Soc.*, **1957**, 880, 886.

[5] G. E. Woodward and E. F. Schroeder, *J. Amer. Chem. Soc.*, **59**, 1960 (1937).

or sometimes a completely anhydrous medium. The fourth compound was received from the Institute for Chemical and Pharmaceutical Research, Cluj.

Preparation of chelates. In the synthesis of the new compounds we used the pure ligands and the hydroxides of the above mentioned metals recently prepared, keeping an optimal chelating ratio between metal and ligand determining spectrophotometrically an optimal pH observing a temperature of 70 — 80°. We obtained crystallized products IIa Cu^{II} and IIIa, b, c, d, Co^{III} which were repeatedly washed with warm absolute ethanol, until the washing solutions did not contain metal ions any more, but IIa Zn^{II}, Mn^{II} and IIIa Fe^{III} products after the washing with ethanol; the purification is followed by recrystallization from water, due to the higher solubility of these compounds in water, and have been finally dried on P_2O_5. The metal chelates are crystallized products variously coloured, little soluble in water and insoluble in ethanol, acetone, chloroform, weak basic and acid reagents, soluble with decomposition in concentrated HCl and H_2SO_4. The elemental analysis of C, H and N were made by microcombustion. The sulphur and chlorine were determined after Schöniger method, Co^{III} was determined with nitrosonaphthol Zn^{II} and Cu^{II} after Spacu and Dick's method[6,7] as $[M^{II}Py_2(SCN)_2]$, Fe^{III} as Fe_2O_3 and Mn^{II} with oxichinoleine after Berg's method. [8] Analytical data for chelates are summarized in table 1 and lead to the structural formulae (II) and (III) (a, b, c, d).

Table 1

Analytical data of some substituted thiazolidinic-acid chelates (II), (III)

Chelate type	Colour	Mole weight	Elemental analysis			
			M	C	N	S
			Calcd. Found	Calcd. Found	Calcd. Found	Calcd. Found
IIIa $M^{III} = Cu^{III}$	dark-brown	532.94	11.05 11.25	33.77 34.00	7.88 7.92	18.01 18.15
IIa$M^{II} = Cu^{II}$	green-brown	391.57	16.49 16.30	30.65 30.89	7.15 7.35	16.62 16.22
IIa $M^{II} = Zn^{II}$	white	393.38	16.61 16.83	30.50 30.82	7.11 7.29	16.26 16.40
IIa$M^{II} = Mn^{II}$	beige	383.93	14.34 14.53	31.33 31.66	7.31 7.64	16.71 16.35
IIIa $M^{III} = Fe^{III}$	brown	525.84	10.53 10.24	33.97 34.18	7.92 8.15	18.11 18.29
IIIb $M^{III} = Co^{III}$	dark-brown	574.94	10.25 10.43	37.56 37.75	7.30 7.20	16.69 16.72
IIIc $M^{III} = Co^{III}$	”	661.94	8.94 8.35	43.70 43.50	6.37 6.59	14.56 14.34
IIId $M^{III} = Co^{III}$	”	718.94	8.19 8.30	50.07 49.85	5.84 5.70	13.35 13.29

---

[6] G. Spacu and J. Dick, *Z. analyt. Chem.*, **71**, 97 (1927).

[7] G. Spacu and J. Dick, *Bull. Soc. Sci. Cluj*, **4**, 177 (1928).

[8] C. G. Macarovici, "Elemente de analiză gravimetrică", Ed. Vrerea, Timişoara, 1944, p. 114.

RESULTS AND DISCUSSION

IR SPECTRA OF THE SUBSTITUTED THIAZOLIDINIC-ACIDS

An analysis of spectra reveals that the thiazolidinic acids synthetized by us present characteristic bands of this structure. IR spectra of these compounds exhibit important changes as related to the initial substances (cysteine, aldehydes and ketones) used in their synthesis and different of the unsubstituted thiazolidinic acid.[9,10,11] The frequencies of valence and deformation oscillation of the thiazolidinic acids are given in table 2.

Table 2

The IR spectra of the free ligands cm^{-1}

Ia	Ib	Ic	Id
640 (s)	640 (w)	650 (m)	540 (m)
			575 (m)
			690 (s)
750 (w)	750 (w)	750 (w)	700 (s)
780 (w)	770 (w)		800 (m)
840 (m)	840 (m)	840 (w)	840 (m)
870 (m)	865 (m)	860 (m)	
		870 (m)	
1050 (m)	1050 (m)	1050 (m)	
1070 (m	1060 (m)	1060 (m)	
1090 (m)			
1115 (m)	1105 (m)	1140 (m)	1140 (m)
1145 (m)	1140 (m)		1150 (m)
1180 (s)	1190 (s)	1180 (vs)	1180 (s)
1280 (m)	1200 (s)	1220 (m)	1250 (m)
	1270 (m)		1260 (m)
1355 (s)	1350 (m)		1325 (s)
1375 (s)		1380 (vs)	1380 (s)
1385 (s)		1390 (vs)	1400 (s)
1405 (s)	1405 (m)	1420 (vs)	1440 (m)
	1430 (m)	1440 (m)	1470 (m)
1575 (s)	1575 (w)	1520 (vs)	1580 (vs)
1620 (s)		1600 (s)	1640 (vs)
		1620 (m)	
1755 (vs)	1750 (vs)	1740 (vs)	1755 (vs)
1770 (vs)	1775 (vs)		
2620 (s)	2560 (w)	2500 (vs)	2700 (w)
2660 (s)	2640 (w)	2620 (vs)	
2700 (s)		2700 (vs)	
3000–2800 (vs) broad	3020–2900 (s) broad	3000–2880 (vs) broad	3050–2940 (s) broad
3440–3380 (vs) broad	3420–2900 (s) broad	3360–3350 (vs)	3480–3440 (s) broad

vs = very strong
s = strong
m = medium
w = weak

---

[9] L. J. Bellamy, "The Infrared Spectra of Complex Molecules", Methuen, London, 1968.

[10] P. Nanasi, E. Nanasi and P. Carletti, *Gazz. chim. Ital.*, **92**, 583 (1962).

[11] N. Otting and F. Drawert, *Chem. Ber.*, **88**, 1469 (1955).

The characteristic vibrations of water νH_2O and of the hydrogen bonds between COOH and NH groups, appear at 3440—3380 cm^{-1}. At 3000—2800 cm^{-1} there appears a broad and very intensive band characteristic of the NH valence vibrations. The intensive bands in the 2760—2530 cm^{-1} interval are due to the ionised dipolar structure ; these bands are placed in a relatively more free spectral range than are the other absorption bands, yet they do not appear in every case.[9] The νCO carboxylic valence vibrations yield very intensive characteristic bands in the 1770 cm^{-1} and 1755 cm^{-1} range. The deformation oscillations of water νOH and of iminic groups νNH, appear as a double absorption band at 1620 cm^{-1} (s) and 1575 cm^{-1} (s). The bands, due probably to the νC—N valence oscillations, appear at 1115 cm^{-1} and 1145 cm^{-1}, while those at 1180 cm^{-1}, 1050 cm^{-1}, 1070 cm^{-1}, 1030 cm^{-1}, are probably due to the skeleton oscillations also responsible for the group of bands from 870 cm^{-1}, 845 cm^{-1}, 780 cm^{-1}, 750 cm^{-1}. [12,13,14] The symmetric deformation oscillations of the CH_3-group appear at 1405 cm^{-1}, 1385 cm^{-1}, 1375 cm^{-1}, 1355 cm^{-1} and give intensive bands. The frequencies of valence oscillations of the —C—S— bond are situated at 640 cm^{-1}(s).[9,15] The aromatic skeleton is relevant in the spectrum of the 2-phenyl-thiazolidinic-4-carboxylic acid, characterized by the presence of a very intensive band at 1580 cm^{-1} and of the bands of a middle intensity at 1470 cm^{-1} and 1440 cm^{-1} due to the aromatic νCH vibrations, and the very intensive bands at 690—700 cm^{-1} of the aromatic γCH oscillations.[15]

STUDY OF IR SPECTRA OF THE CHELATE COMPOUNDS OF THIAZOLIDINE-4-CARBOXYLIC ACIDS WITH Mn^{2+}, Fe^{3+}, Co^{3+}, Cu^{2+}, Zn^{2+}

The frequencies of valence and deformation oscillations of the thiazolidine chelate compounds with metals are given in table 3. From the analysis of table 3 changes as related to spectra of the ligands are remarked, namely the absence of bands characteristic of the dipolar structure at 2700—2500 cm^{-1} (s), also the bands of oscillation frequencies of the carboxylic group at 1770 cm^{-1} (vs) and 1755 (vs) do no longer appear. The bands of valence oscillation νH_2O and of the hydrogen bonds from 3440—3380 cm^{-1} and that of νNH from 3000—2800 cm^{-1} (vs) are shifted towards smaller wavelengths of 3500—3200 cm^{-1}, with the appearance of a very wide and intensive single band in this range. There is also observed the modification of the double absorption band at 1620 cm^{-1} (s) and 1575 cm^{-1} (s) from the spectra of molecules of free acids ascribed to the deformation oscillation of both the water and NH group, and the formation of a broader and more intensive single band in this range between 1650—1550 cm^{-1} (vs). The skeleton vibrations appear very intense at

---

[12] J. R. Damm, G. L. Oliver and J. W. Gotes, *J. Amer. Chem. Soc.*, **79**, 1644, 1650 (1957).

[13] R. Mekcke, R. Mecke and A. Luttringhaus, *Chem. Ber.*, **90**, 975 (1957).

[14] G. B. B. M. Sutherland and S. E. Darmon, *Nature*, **164**, 440 (1949).

[15] A. R. Katritzky and A. P. Ambler, "Physical in Heterocyclic Chemistry", Vol. II, Academic Press New York, 1963.

Table 3

The IR spectra of the chelates cm^{-1} (II),(III)

IIa			IIIa		IIIb	IIIc	IIId
$M^{II} = Cu^{II}$	$M^{II} = Zn^{II}$	$M^{II} = Mn^{II}$	$M^{III} = Co^{III}$	$M^{III} = Fe^{III}$	$M^{III} = Co^{III}$		
470 (w)	470 (w)					470 (w)	425 (w)
670 (m)	680 (vs)	675 (s)	640 (vs)	670 (w)	640 (s)	680 (m)	600 (m)
							930 (m)
							980 (m)
1090 (s)	1020 (s)		1080 (vs)	1040 (m)	1020 (vs)	1080 (w)	1070 (s)
				1070 (m)			
				1080 (m)			
1140 (s)			1180 (vs)	1130 (m)	1140 (vs)	1140 (vs)	1160 (s)
				1190 (m)			
1350 (m)	1340 (s)	1360 (s)	1360 (s)	1340 (m)	1365 (m)	1350 (s)	1356 (vs)
				1375 (m)		1390 (s)	
1390 (s)	1420 (s)	1400 (s)	1420 (s)	1410 (s)	1420 (m)	1420 (s)	1440 (vs)
				1490 (s)	1500 (m)		1540 (vs)
1640–1630 (vs)	1640–1560 broad (vs)	1640–1560 broad (vs)	1640–1580 broad (vs)	1620–1580 broad (vs)	1640–1630 (s)	1620–1610 (s)	1620–1610 (s)
2390 (m)			2930 (vw)	2960 (m)	2930 (w)	2930 (s)	2940 (s)
3480–3260 broad (vs)	3500–3310 broad (vs)	3460–3340 broad (vs)	3540–3200 broad (vs)	3460–3340 broad (vs)	3500–3220 v. broad (vs)	3420–3180 broad (vs)	3470–3210 broad (vs)

vs = very strong
s = strong
m = medium
w = weak
v.w = very weak

1180 cm^{-1}, 1120 cm^{-1}, 1090 cm^{-1}, 1080 cm^{-1} like the group of bands in the 870–750 cm^{-1} (s) range, that indicate the presence of the thiazolidinic nucleus. The νC–S valence vibrations appear alike in the ligand's spectra as an intensive band at 640 cm^{-1}. A weak absorption band also appears at 470 cm^{-1}. In the literature [16–18] this weak absorption band is assigned to the formation of metal-ligand bond. The modifications that appear in the IR spectra of chelate compounds related to the free ligand indicate that in the formation of the chelates of the thiazolidinic acids with 3d transitional metals participate the NH group present in the thiazolidinic cycle and the COOH group, which according to literature [19] are donors of electrons and in our case are forming a five-membered chelate together with the metal ion.

---

[16] G. H. Barow, R. H. Krueger and F. Basolo, *J. Inorg. Nuclear Chem.*, **2**, 340 (1956).

[17] E. P. Bartin, I. Nacagawa, S. Mizushima, T. Y. Laue and J. V. Quagliano, *J. Amer. Chem. Soc.*, **80**, 525 (1958).

[18] K. Nakamoto, "Infrared Spectra of Inorganic and Coordination Compounds", Wiley, New York, 1965.

[19] P. Spacu and M. Brezeanu, "Chimia combinaţiilor complexe" Ed. didactică şi dedagogică, Bucharest, 1974.

Revue Roumaine de Chimie, 21, *1*, 89–99 (1976)

THERMAL AND PHOTOCHEMICAL REARRANGEMENTS OF DIBENZOBULLVALENE AND RELATED DIBENZO-$(CH)_{10}$ HYDROCARBONS[1]

M. ELIAN, M. BANCIU, LIGIA STĂNESCU and

ECATERINA CIORĂNESCU

Center of Organic Chemistry,
Spl. Independenţei, 202-B, Bucharest 15, Romania

Received May 22, 1974

The experimental procedure for synthesis of dibenzobullvalene (9) beginning with 5H-dibenzo[*a,d*]cycloheptene-5-acetic acid (5a) is described. Dehydration of dibenzotricyclic alcohol, 7, affords, beside 9, another dibenzo-$(CH)_{10}$ isomer 10, which could be also obtained by flow-pyrolysis of dibenzo-Nenitzescu's hydrocarbon 2. Pyrolysis of 9 has been found to lead to two other new dibenzo-$(CH)_{10}$ hydrocarbons, 11 and 12. In the pyrolyses of 10, 11 and 12 at higher temperatures benzo[*a*]anthracene (14) and chrysene (13) were identified. Proofs of structure for dibenzo-$(CH)_{10}$ hydrocarbons as well as the mechanisms of different valence isomerisations are discussed.

The investigations concerning the synthesis and chemistry of $(CH)_{10}$ valence isomers were greatly extended during the last years especially due to the various reaction paths available in this class of hydrocarbons. From 1960, when the first $(CH)_{10}$ hydrocarbon, tricyclo$[4.2.2.0^{2,5}]$ deca-3,7,9-triene (**1**)[2] (Nenitzescu's hydrocarbon *) was synthetized, and until now, 23 from the possible 93 valence isomers [3] of the annulene[10] were obtained. Recently, the research was extended to the benzo-$(CH)_{10}$ isomers by Vedejs,[4] Paquette[5] and Murata.[6]

---

* Name proposed by W. v. E. DOERING, *J. Amer. Chem. Soc.*, **88**, 2078 (1966).

[1] See preliminary communication: M. BANCIU, M. ELIAN, E. CIORĂNESCU and C. D. NENITZESCU, *Tetrahedron Letters*, **1972**, 2573.

[2] M. AVRAM, E. SLIAM and C. D. NENITZESCU, *Liebigs Ann. Chem.*, **636**, 184 (1960).

[3] A. T. BALABAN, *Rev. Roumaine Chim.*, **11**, 1097 (1966).

[4] (a) E. VEDEJS, *Tetrahedron Letters*, **1968**, 2633; (b) E. VEDEJS and T. SHEPHERD, *Tetrahedron Letters*, **1970**, 1863; (c) E. VEDEJS, R. A. SHEPHERD and R. P. STEINER, *J. Amer. Chem. Soc.*, **92**, 2158 (1970); (d) E. VEDEJS, *Tetrahedron Letters*, **1970**, 4963; (e) E. VEDEJS, M. F. SALOMON and P. D. WEEKS, *J. Amer. Chem. Soc.*, **95**, 6770 (1973); (f) E. VEDEJS and R. P. STEINER, *Chem. Comm.*, **1973**, 599; (g) E. VEDEJS and E.S.C. WU, *Tetrahedron Letters*, **1973**, 3793; (h) E. VEDEJS, *Chem. Comm.*, **1971**, 536; (i) E. VEDEJS, M. F. SALOMON and P. D. WEEKS, *J. Amer. Chem. Soc.*, **95**, 6770 (1973); (j) E. VEDEJS, R. P. STEINER and E.S.C. WU, *J. Amer. Chem. Soc.*, **96**, 4040 (1974).

[5] (a) L. A. PAQUETTE and J. C. STOWELL, *Tetrahedron Letters*, **1970**, 2259; (b) L. A. PAQUETTE and J. C. STOWELL, *J. Amer. Chem. Soc.*, **92**, 2584 (1970); (c) L. A. PAQUETTE, M. J. KUKLA and J. C. STOWELL, *J. Amer. Chem. Soc.*, **94**, 4920 (1972).

[6] (a) I. MURATA and Y. SUGIHAVA, *Tetrahedron Letters*, **1972**, 3785; (b) I. MURATA, Y. SUGIHAVA and N. UEDA, *Tetrahedron Letters*, **1973**, 1183.

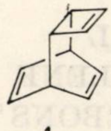

1

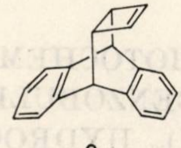

2

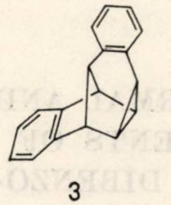

3

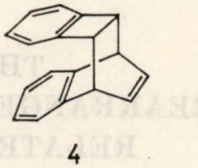

4

In this work we want to report about the synthesis and thermal and photochemical rearrangements of some dibenzo-$(CH)_{10}$ valence isomers. Before our preliminary paper [1] was published, only two dibenzo-$(CH)_{10}$ valence isomers, the hydrocarbons **2** [7] and **3** [8] were known ; recently the isomeric hydrocarbon **4** [9] was also obtained.

RESULTS

The synthesis of dibenzobullvalene (**9**) [1] (Scheme 1) was achieved starting from the known 5H-dibenzo[*a,d*]cycloheptene-5-acetic acid (**5a**).[10] The copper-catalyzed decomposition of the diazoketone **5c**, obtained from the acid chloride **5b**, gave the tricyclic ketone **6**. The alcohol **7**, resulted from the $LiAlH_4$-reduction of **6**, yielded the bicyclic bromoderivative **8** by treatment with PBr_3, and a 2 : 1 mixture of dibenzobullvalene (**9**) and the butadienic hydrocarbon **10** by dehydration with boric acid. Both **8** and **10** could be converted to dibenzobullvalene, the former by dehydrobromination with pyridine and the latter photochemically. The irradiation with UV light of the crude mixture obtained from the dehydration of the alcohol **7** is a convenient way for the synthesis of dibenzobullvalene.

Scheme 1

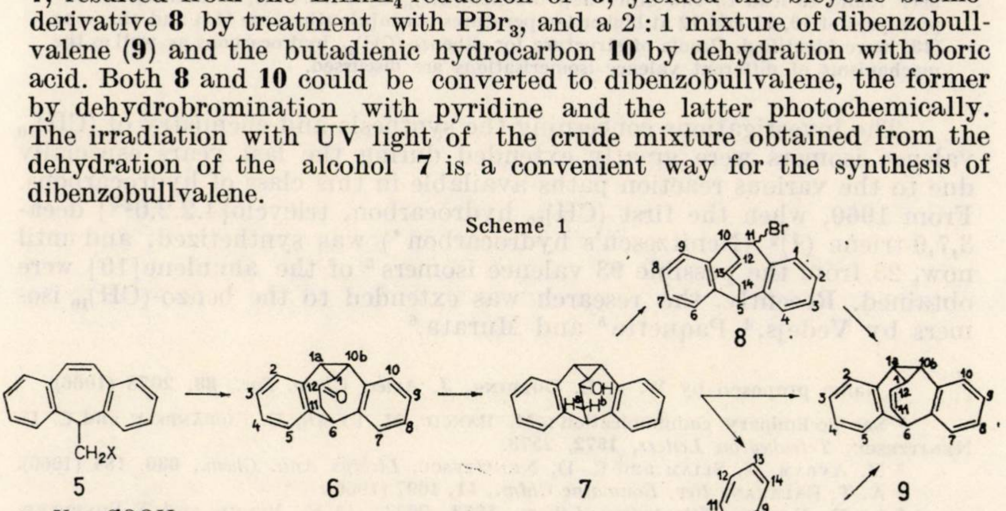

a ; X = COOH
b ; X = COCl
c ; X = $COCHN_2$

---

[7] M. Avram, I. G. Dinulescu and C. D. Nenitzescu, *Liebigs Ann. Chem.*, **691**, 9 (1966).

[8] M. Stiles, U. Burkhardt and G. Freund, *J. Org. Chem.*, **32**, 3718 (1967) ; L. Friedman, *J. Amer. Chem. Soc.*, **89**, 3071 (1967).

[9] I. G. Dinulescu, M. Pop, F. Chiraleu, M. Avram and C. D. Nenitzescu, *Rev. Roumaine Chim.*, **19**, 1197 (1974).

[10] C. van der Stelt, A. Haasjes, H. M. Tersteege and W. T. Nauta, *Rec. Trav. chim.*, **84**, 1466 (1965).

Thermal rearrangements of some dibenzo-(CH)$_{10}$ valence isomers. Three dibenzo-(CH)$_{10}$ valence isomers : dibenzobullvalene (**9**), the dibenzo-Nenitzescu's hydrocarbon (**2**) and the butadienic hydrocarbon **10** were flow-pyrolysed in inert gas at low pressure (5 torr) with a residence time of about one second. The results, obtained by v.p.c.-analysis, are given in figs. 1 and 2.

When dibenzobullvalene* was flow-pyrolysed over 400° (fig. 1) two new compounds **11** and **12** were formed, whose structures were deduced from the spectral evidence presented further. The conversion of dibenzobullvalene was almost complete at 550°, temperature at which the yields of both **11** and **12** reached a maximum. At still higher temperature, the reaction mixture contained more aromatic hydrocarbons.

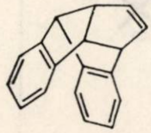
11

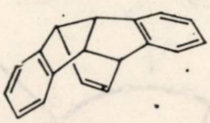
12

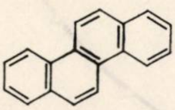
13

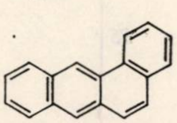
14

The major components of the aromatic fraction were crysene (**13**) and benzo[*a*]anthracene (**14**), identified by the characteristic UV spectra.

The major product of dibenzobullvalene pyrolysis at 550°, hydrocarbon **11** (m.p. 142–4°), was separated from the reaction mixture by recrystallization from ethanol. The minor constituent **12** (m.p. 99–100°) was obtained by preparative v. p. c. Both **11** and **12** when flow-pyrolyzed at 750° afforded as major products the aromatic hidrocarbons **13** and **14**.

The structures of hydrocarbons **11** and **12** were inferred from the following data. Both hydrocarbons correspond to $C_{18}H_{14}$, and the NMR spectra point to the existence of four aliphatic, two olefinic and eight aromatic protons. The two olefinic protons in **11** are not equivalent, as shown by the NMR spectrum ($\delta = 5.62$, *dd*, $J = 2.5$; 5.5 Hz and $\delta = 6.44$, *dd*, $J = 3.0$; 5.5 Hz) and the aliphatic ones are distributed into two multiplets at $\delta = 3.35$ (1H) and 3.6–4.0 (3H). The analysis of the coupling constants shows that hydrocarbon **11** contains the sequence $\rangle CH-CH=CH-CH\langle$ where the two olefinic protons are not equivalent. The examination of the structural formulas of all possible dibenzo-(CH)$_{10}$ valence isomers[11] which include this sequence leaves only the formulas **11**, **15** and **16**, after excluding the very unlikely structures and some structures corresponding to the known compounds. The structure **15** can be excluded due to the absence of signals in the range $\delta = 2-3$ ppm, and structure **16** by the inconsistent comparison of the spectrum

---

* A sample containing 86% **9** and 14% **10** was used. The thermal stability of hydrocarbon **10** between 400 and 600° was checked in a preliminary experiment.

[11] A. T. Balaban, *Rev. Roumaine Chim.*, **19**, 1185 (1974).

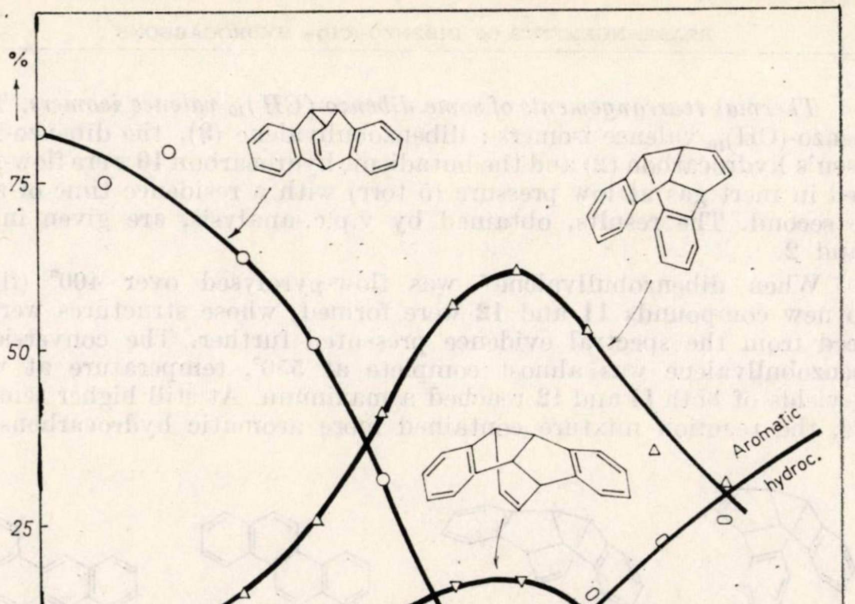

Fig. 1. — The composition of the pyrolysis products of dibenzobullvalene (9) as function of temperature (the differences up to 100 % are due to hydrocarbon 10 (14 %) as well as to the continuous decrease of yields at higher temperatures).

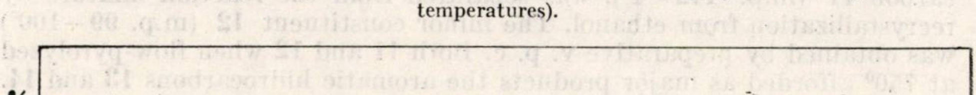

Fig. 2. — The composition of the pyrolysis products of dibenzo-Nenitzescu's hydrocarbon (2) (—) and 9,10-dihydro-9,10-[1,3]butadienoanthracene (10) (— — —).

with the NMR spectrum of some compounds with dibenzo[*b*,*g*]bicyclo [4.2.0] octane skeleton.[12]

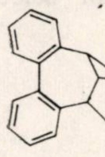

15

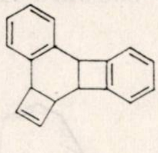

16

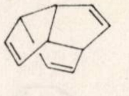

17

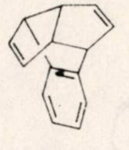

18

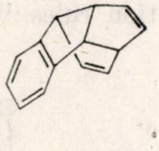

19

The NMR spectrum of the hydrocarbon **12**, consisting of three multiplets each corresponding to two protons at $\delta = 3.16$, 3.88 and 5.56 ppm, shows the high symmetry of this compound. The consistent comparisons of the spectrum with the NMR spectra of lumibullvalene **17**[13], monobenzoderivatives **18**[5c] and **19**[4c] and hydrocarbon **11**, indicates for the minor product obtained in the flow pyrolysis of dibenzobullvalene the structure **12**.

The flow-pyrolysis of hydrocarbon **2** over 450° shows the clear conversion into the butadienic hydrocarbon **10** (fig. 2). Over 650° the reaction mixture contains also the aromatic hydrocarbons **13** and **14**. As figure 2 shows, the aromatic hydrocarbons seem to be formed from **10** and not directly from **2**. The flow pyrolysis of the pure hydrocarbon **10** over 700° substantiates this hypothesis (the dotted line in fig. 2).

DISCUSSION

The thermal and photochemical transformations of dibenzo-$(CH)_{10}$ valence isomers **2**, **9**, **10**, **11** and **12** described in this paper are presented in scheme 2.

Scheme 2

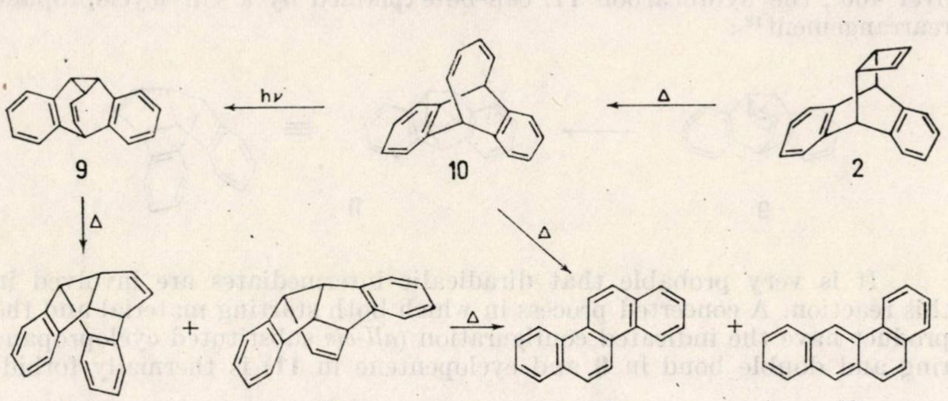

---

[12] N. Stefan, I. G Dinulescu, F. Chiraleu and M. Avram, *Rev. Roumaine Chim.*, **20**, 1473 (1975).

[13] M. Jones, *J. Amer. Chem. Soc.*, **89**, 4236 (1967); M. Jones, S. Reich and L. T. Scott, *ibid.*, **92**, 3122 (1970).

The photochemical rearrangement **10** → **9** is analogous to one known in the $(CH)_{10}$[14] and benzo-$(CH)_{10}$[4i] series and can be imagined as a concerted $[_{\sigma}2_s + _{\pi}2_s]$ process, allowed by the Woodward-Hoffmann selection rules :[15]

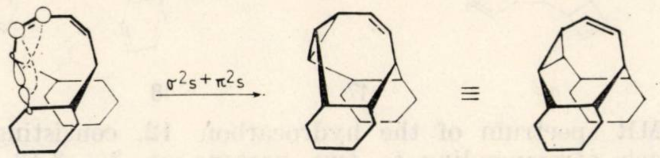

10 9

The irradiation of deuterated hydrocarbon **10** at C-12[16] gives dibenzobullvalene with the deuterium equally distributed between C-1 and C-12, in agreement with this mechanism. A di-π-methane mechanism, like the one proposed for the analogous rearrangement in the $(CH)_{10}$-series,[17] seems to be less probable in this case because the diradicalic intermediates would destroy the aromaticity of a benzene ring. Furthermore, one of the intermediates involved in the di-π-methane rearrangement would be the same as the diradical **20** (Scheme 3) which is very probably the precursor of hydrocarbon **11** ; this hydrocarbon does not appear during the photoisomerization of **10**. The experiment with the deuterated compound does not however exclude the di-π-methane mechanism.

The reverse rearrangement, **9** → **10**, could be realized with $PdCl_2 \cdot (PhCN)_2$, as reported in another paper.[16]

The occurrence of the main pyrolysis product of dibenzobullvalene over 400°, the hydrocarbon **11**, can be explained by a vinylcyclopropane rearrangement[18] :

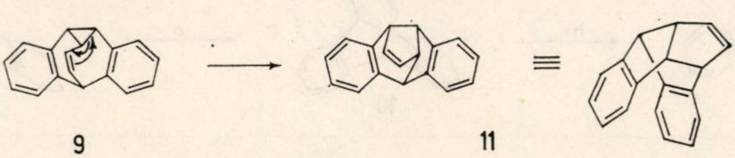

9 11

It is very probable that diradicalic intermediates are involved in this reaction. A concerted process in which both starting material and the product have the indicated configuration (*all-cis* substituted cyclopropane ring and double bond in **9** and cyclopentene in **11**) is thermally forbidden.[15] It is likely that the reaction proceeds in the following manner (Scheme 3):

---

[14] (a) W. v. E. Doering and J. W. Rosenthal, *Tetrahedron Letters*, **1967**, 349; (b) M. Jones and L. T. Scott, *J. Amer. Chem. Soc.*, **89**, 150 (1967).

[15] R. B. Woodward and R. Hoffmann "The Conservation of Orbital Symmetry", Academic Press, New York, 1970.

[16] M. Banciu, M. Elian, C. Drăghici and E. Ciorănescu, *Rev. Roumaine. Chim.*, **19**, 1179 (1974).

[17] H. E. Zimmerman and P. S. Mariano, *J. Amer. Chem. Soc.*, **91**, 1718 (1969).

[18] M. C. Flowers and H. M. Frey, *J. Chem. Soc.*, **1961**, 3547.

Scheme 3

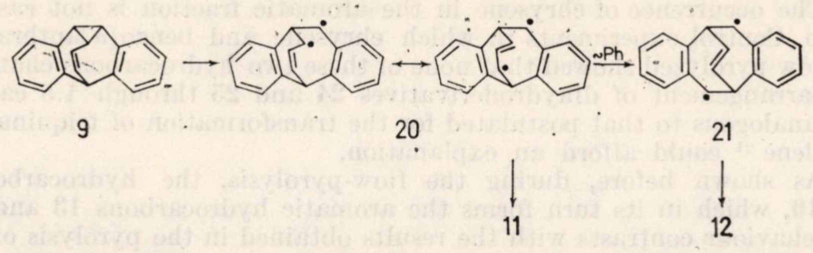

The minor product of dibenzobullvalene pyrolysis, the hydrocarbon **12**, could be formed from the same diradicalic intermediate **20** through a 1.2 phenyl shift.

The final products of dibenzobullvalene pyrolysis are aromatic hydrocarbons, mainly benzo[*a*]anthracene (**14**) and chrysene (**13**). The curves presented in fig. 1 together with control experiments showed that the aromatic hydrocarbons are formed from **11** and **12**. It is probable that the first products of this reactions are the dihydroderivatives, as for the $(CH)_{10}$[19] and benzo-$(CH)_{10}$[5c] valence isomers, and that the dihydroderivatives yield readily the aromatic hydrocarbons due to the high temperature used.

The transformation of hydrocarbon **12** into benzo[*a*]anthracene could be explained by an intermediate **22** analogous to the one proved in the degenerate rearrangement of lumibullvalene (**17**).[20] This intermediate could yield dibenzoannulene[10] (**23**), which in its turn can give the dihydroderivative **24** and then benzo[*a*]anthracene (**14**) (Scheme 4):

Scheme 4

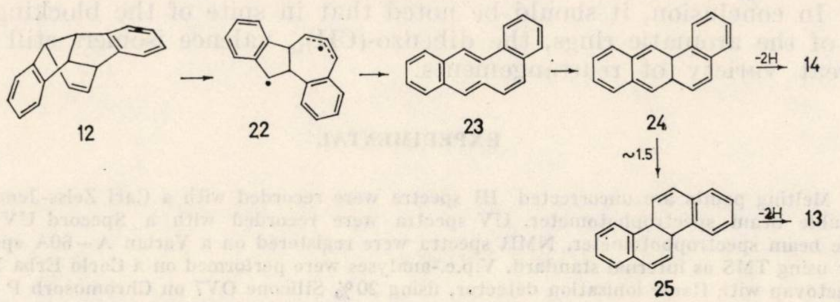

The formation of aromatic hydrocarbons from **11** could have as a first step the isomerization **11** → **12** through the sequence **11** → **20** → → **21** → **12** (Scheme 3). If this is true then the hydrocarbons **11** and **12** should interconvert into each other. The pyrolysis of pure hydrocarbon **11** gave indeed small quantities of **12** together with the aromatic hydrocarbons **13** and **14** and other unidentified compounds (the yield of **12** is 15% for a conversion of 26% at 550° and 12% for a conversion of 40% at 600°).

---

[19] W. v. E. Doering and J. W. Rosenthal, *J. Amer. Chem. Soc.*, **88**, 2078 (1966).
[20] L. A. Paquette and M. J. Kukla, *J. Amer. Chem. Soc.*, **94**, 6874 (1972).

The occurrence of chrysene in the aromatic fraction is not easy to explain. Control experiments in which chrysene and benzo[*a*]anthracene were flow-pyrolyzed showed that none of these two hydrocarbons changed. The rearrangement of dihydroderivatives **24** and **25** through 1.5 carbon shifts analogous to that postulated for the transformation of triquinacene in azulene [21] could afford an explanation.

As shown before, during the flow-pyrolysis, the hydrocarbon **2** gives **10**, which in its turn forms the aromatic hydrocarbons **13** and **14**. This behaviour contrasts with the results obtained in the pyrolysis of the corresponding cyclobutenic hydrocarbon without or with only one aromatic ring, where dihydronaphthalene or dihydrophenanthrene are obtained directly from the starting compound. [4,5]

The conversion of **2** into **10** is very probably a nonconcerted ring opening. However, the isomerization of the butadienic hydrocarbon **10** into a dihydroderivative **24** or **25** involved a deep skeletal reorganization. A possible reaction path consists of successive 1.3-shifts of the aromatic rings:

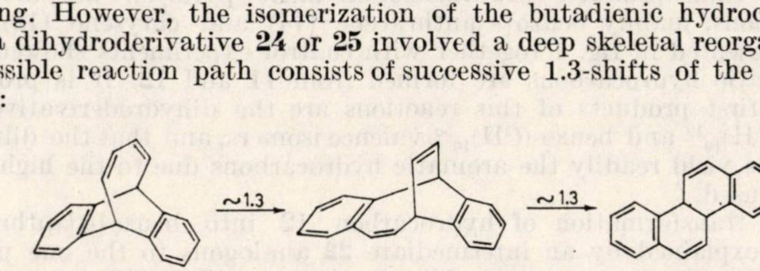

10 **26** **25**

A thermal rearrangement analogous to **26** → **25** is known in the benzo-$(CH)_{10}$ series.[5c]

In conclusion, it should be noted that in spite of the blocking action of the aromatic rings, the dibenzo-$(CH)_{10}$ valence isomers still give a great variety of rearrangements.

EXPERIMENTAL

Melting points are uncorrected. IR spectra were recorded with a Carl Zeiss-Jena UR 20 double beam spectrophotometer. UV spectra were recorded with a Specord UV—Vis double beam spectrophotometer. NMR spectra were registered on a Varian A—60A spectrometer using TMS as internal standard. V.p.c.-analyses were performed on a Carlo Erba Model D Fractovap with flame ionisation detector, using 20% Silicone OV7 on Chromosorb P (60—80 mesh) columns (1 m/2 mm diam.) at 220° with a nitrogen rate flow of 30 ml/min. V.p.c.-separations were performed on a Carlo Erba Model GV Fractovap using 10% Silicone OV7 on Anaprep (30—60 mesh) columns (2 m/10 mm diam.) at 200° with a hydrogen rate flow of 300 ml/min.

5H-*Dibenzo*[a,d]*cycloheptene-5-acetyl chloride* (**5b**), was obtained in 98% yield from the corresponding acid **5a**[10] on treatment with $SOCl_2$ in an analogous manner as described [10] for the saturated acid. *The acid chloride* **5b**, m.p. 160—162°. *Found*: C, 76.12; H, 5.15; Cl, 13.03. $C_{17}H_{13}OCl$ requires: C, 75.96; H, 4.88; Cl, 13.20. *IR spectrum* (CS_2; CCl_4; cm^{-1}): 689 s; 713 s; 740 m; 762 vs; 797 vs; 970 s; 1124 m; 1492 m; 1802 vs; 2930 w; 3024 m; 3050 w and 3074 w.

---

[21] L. T. Scott and G. K. Agopian, *J. Amer. Chem. Soc.*, **96**, 4325 (1974).

*5*H-*Dibenzo*[*a,d*]*cycloheptene-5-methyl-diazomethylketone* (**5c**). Over an ice-cooled stirred solution of acid chloride **5b** (10 g; 37.2 mmoles) in anhydrous ether (300 ml) triethylamine buffer (2 g; 19.6 mmoles) was added, then an ethereal solution of diazomethane (200 ml solution, obtained from 20 g nitrosomethylurea* was dropped during 1 hr. The reaction mixture was still stirred for 5 hrs then left overnight in a refrigerator. The hydrochloride of the amine was filtered and the yellow filtrate was evaporated *in vacuo* at room temp. The remaining yellow crystals of *diazoketone* **5c** (9.65 g; 95%) show a m.p. 107 – 110° (dec.). *Found* : N, 10.37. $C_{18}H_{14}N_2O$ requires: N, 10.22%. *IR spectrum* (CS_2; CCl_4; cm^{-1}): 689w; 716 s; 741 m; 762 vs; 794 vs; 1333 vs; 1364 vs; 1649 vs; 2108 vs; 3023 m and 3074 m.

1,1a, 6,10b-Tetrahydro-1,6-ethanodibenzo[a,e]*cyclopropa*[c]*cyclohepten-12-one* (**6**). Over a stirred warm (60°) solution of diazoketone **5c** (10 g; 36.3 mmoles) in anhydrous benzene (400 ml) copper bronze (4 g) was added in small portions during 3 hrs simultaneously rising the temperature at 80°. The reaction mixture was then refluxed for 3 hrs, after which time the evolution of N_2 ceased, filtered and then evaporated *in vacuo*. The dark-brown oily residue was left overnight, the partially crystallized mixture was filtered, the crystalls were washed with cold acetone, affording *the ketone* **6** (1.35 g; 15%) m.p. 227–228.5° (ethanol). *Found* : C, 87.68; H, 5.90; $C_{18}H_{14}O$ requires : C, 87.77; H, 5.73%. *IR spectrum* (KBr; cm^{-1}) : 688 w; 746 vs; 754 vs; 771 m; 786 m; 1496 s; 1671 vs; 2898 vw; 2914 w; 3024 w and 3071 w. *NMR spectrum* ($CDCl_3$; δ, ppm); 7.0–7.4 (m; 8H; H_{arom}); 3.88 (t, $J = 4.5$ Hz; 1H; H_6); 2.95 (apparently s; 3H; $H_{1,1a,10b}$); 2.82 (d; $J = 4.5$Hz; 2H; H_{11}).

The ketone **6** could also be obtained in the same yield working with CuCl instead of Cu and with cyclohexane instead of benzene.

1,1a,6,10b-Tetrahydro-1,6-ethanodibenzo[a,e]*cyclopropa*[c]*cyclohepten-12-ol* (**7**). Over a cooled suspension of $LiAlH_4$ (1.33 g; 35 mmoles) in anhydrous ether (50 ml) a suspension of finely powdered ketone **6** (4 g; 16.2 mmoles) in anhydrous ether (300 ml) was poured with stirring during 1 hr. The reaction mixture was stirred further for 4 hrs at room temp. then 2 hrs at reflux and left overnight. The usual working-up afforded *the alcohol* **7** (3.8g; 94%) m.p. 120–121° (methanol : water – 7 : 3). *Found* : C, 86.84; H, 6.60. $C_{18}H_{16}O$ requires : C, 87.06; H, 6.50. *IR spectrum* (CS_2; CCl_4; cm^{-1}) : 749 vs; 759 vs; 770 s; 1034 s; 1494 m; 2860 vw; 2922 m; 3024 m; 3069 w; 3300–3500 (broad) and 3615–3620 w. *NMR spectrum* ($CDCl_3$; δ, ppm) : 7.0–7.4 (m; 8H; H_{arom}); 4.35 (sextet, $J = 7$; 7; 3.5 Hz; 1H; H_{12}); 3.70 (q; $J = 3.5$; 5.5 Hz; 1H; H_6); 1.8–2.8 (m; 6H; $H_{1,\,1a,\,10b,\,11a,\,11b,\,OH}$); this multiplet was resolved using as shift reagent $Eu(DPM)_3$ in a complex/alcohol molar ratio of 0.307 : (δ ppm); 6.92 (H_{11b}); 6.30 (H_1); 5.58 (H_{11a}); 4.18 (H_{10b}) and 3.67 (H_{1a}).

*11-Bromo-10,11-dihydro-10,5-propeno-5*H-*dibenzo*[a,d]*cycloheptene* (**8**). Over a cooled solution of alcohol **7** (1.5 g; 6 mmoles) in anhydrous benzene (10 ml) 0.5 ml anhydrous pyridine was added, then a solution of PBr_3 (1.8 g; 0.65 ml; 6.6 mmoles) in anhydrous benzene (15 ml) was dropped with stirring during 1 hr. The reaction mixture was further stirred for 2 hrs at room temp., then 1 hr at 60° and left overnight. The cooled reaction mixture was decomposed with water, the organic layer was separated and the aqueous one ether-extracted. The combined organic layers were washed, dried and evaporated *in vacuo* affording the bromide **8** (1.4 g; 75%), m.p. 120° (*n*-hexane). *Found* : C, 69.49; H, 5.19; Br, 25.21. $C_{18}H_{15}Br$ requires : C, 69.45; H, 4.86; Br, 25.69%. *IR spectrum* (CS_2; CCl_4; cm^{-1}) : 628 s; 701 w; 734 vs; 751 m; 761 m; 1146 w; 1498 w; 2821 vw; 2900 w; 2916 w; 3023 m and 3072 w. *NMR spectrum* ($CDCl_3$; δ, ppm) : 6.9–7.6 (m; 8H; H_{arom}); 5.3–6.1 (m; 3H; $H_{1',13,11}$; d; $J = 4.5$ Hz at 5.79); 4.08 (t; $J = 4$; 4 Hz; 1H; H_5); 3.87 (q; $J = 4.5$; 8 Hz; 1H; H_{10}) and 2.0– 3.0 (m; 2H; H_{14}).

1,1a,6,10b-Tetrahydro-1,6-ethenodibenzo[a,e]*cyclopropa*[c]*cycloheptene* (*Dibenzobullvalene*) (**9**) *by dehydrobromination of bromide* **8**. A solution of bromide **8** (500 mg; 1.6 mmoles) in anhydrous pyridine (15 ml) was refluxed for 45 minutes, poured over crushed ice (15 g) and neutralized with conc. HCl. The solution was saturated with NaCl then thoroughly ether-extracted (3×30 ml). The combined organic layers were washed with satd. NaCl solution, dried and evaporated affording *dibenzobullvalene* (**9**) (55 mg; 15%), m.p. 108° (90% ethanol). *Found* : C, 93.57; H, 6.37. $C_{18}H_{14}$ requires : C, 93.87; H, 6.13% *IR spectrum* (CS_2; CCl_4; cm^{-1}) :

---

*1 ml solution contains 0.0189 g diazomethane, as indicated by benzoic acid titration.

726 vs; 741 vs; 750 vs; 771 vs; 899 s; 1461 m; 1494 vs; 2853 w; 2927 m; 2974 w; 3032 s and 3066 m. *NMR spectrum* ($CDCl_3$; δ ppm): 6.9–7.2 (m; 8H; H_{arom}); 5.5–6.1 (m; 2H; $H_{11,12}$); 3.68 (q; 1H; H_6); 2.20–2.85 ($A_2B(X)$-type spectrum; 3H; $H_{1,1a,10b}$). Except some enlargement of the signals, this spectrum remained unchanged on heating up to 200°.

Dibenzobullvalene (**9**) *and 9,10-dihydro-9,10-*[1,3]*butadieno-anthracene* (**10**) *by dehydration of alcohol* **7**. A finely powdered intimate mixture of alcohol **7** (250 mg; 1 mmole) and boric acid (200mg; 3.2 mmoles) was sublimated at 165–210°/1 mm Hg for 1 hr. The composition of the sublimated mixture (115 mg; 50%) determined by v.p.c.-analysis (or by NMR) was: 60–65% **9** and 25–35% **10**. After two recrystallizations (methanol, then ethanol) the pure *9,10-dihydro-9,10*[1,3]*butadienoanthracene* (**10**) (35 mg; 15%), m.p. 180–182° was obtained. *Found*: C, 93.58; H, 6.43. $C_{18}H_{14}$ requires: C, 93.87; H, 6.13%. *IR spectrum* (CS_2; CCl_4; cm^{-1}): 674 s; 738 vs; 836 m; 1454 w; 1481 m; 2920 w; 3023 m and 3070 w. *UV spectrum* (C_6H_{12}; $\lambda_{\max}^{\text{nm}}$; lgε): 252 (3.48); 264 (3.57); 273 (3.66); 284 (3.45). *NMR spectrum* ($CDCl_3$; δ, ppm): 7.0–7.3 (m; 8H; H_{arom}); 6.0–6.8 (m; 2H; $H_{11,14}$); 5.3–5.7 (m; 2H; $H_{12,13}$); 4.47 (d; $J = 9.5$ Hz; 2H; $H_{9,10}$).

By evaporation of mother-liquors from the recrystallization of **10**, a crude dibenzobullvalene (**9**) (80 mg) was obtained, which could be purified by column-chromatography on Al_2O_3 after photochemical conversion to **9** of the remaining **10** (see later).

Dibenzobullvalene (**9**) *by irradiation of hydrocarbon* **10**. A solution of hydrocarbon **10** (200 mg; 0.87 mmole) in anhydrous acetone (50 ml) was irradiated in argon atmosphere with a Hg-medium pressure UV lamp (130 W) through a Razotherm filter for 3–5 hrs. After evaporation *in vacuo* of the solution an oily residue (quantitative yield), which soon crystallized, was obtained. The v.p.c.-analysis of this crude mixture indicated 84–88% dibenzobullvalene (**9**), 10–14% diene **10**, besides many minor unidentified components. The pure dibenzobullvalene (**9**) could be obtained by column chromatography on neutral Al_2O_3 of the crude reaction mixture: on elution with petroleum ether (b.p. 30–40°), dibenzobullvalene (**9**) (140 mg; 70%) with m.p. 105–108° was first obtained, the last fractions being mixtures of **9** and **10**.

The same composition of the reaction mixture as mentioned above was determined by v.p.c.-analysis for the irradiation product of the crude mixture from the dehydration of the alcohol **7** with H_3BO_3 (see before). The last method is an easy and convenient preparation of dibenzobullvalene from alcohol **7**.

Pyrolyses of dibenzo-$(CH)_{10}$ *hydrocarbons.* All the pyrolyses were performed in a vertical quartz tube (10 mm diam.) packed with quartz chips for 200 mm. The heating was realized with an electrical oven, the temperatures being determined by means of a chromel-copel thermocouple. The pyrolyses were conducted at 5 mm Hg *vacuo* in an inert argon atmosphere, with contact times ⩽ 1 second. The pyrolysis products which crystallize in the lower cooled part of the quartz tube were dissolved in ether and v.p.c.-analysed. The results of the pyrolyses of **2**, **10** and **9** at different temperatures are represented in figs. 1 and 2. In the pyrolysis product of **11** at 750° aromatic hydrocarbons **13** and **14** represent 50%; beside these only minor components seemed to be formed. In the pyrolysis product of **12** at 750° aromatic hydrocarbons **13** and **14** were formed in about 30% yield. The major pyrolysis products of all dibenzo-$(CH)_{10}$ hydrocarbons at higher temperatures were benzo[*a*]anthracene (**14**) and chrysene (**13**) (see figs. 1 and 2). These compounds afford a single peak at v.p.c., but could be identified by comparison of the UV spectrum of some fractions separated through preparative v.p.c. with those of authentic samples (and mixtures).

Preparative pyrolysis of dibenzobullvalene. A sample of dibenzobullvalene (**9**) (200 mg; 0.87 mmole) was pyrolyzed at 550°/5 mm Hg and the crude product (140 mg; 70%) was recrystallized from ethanol affording *10,11-dihydro-11,5,10-*[1]*propen*[1]*-yl*[3]*-ylidene-5*H*-dibenzo* [a,d]*cycloheptene* (**11**) (70 mg; 35%) m.p 142–144°. *Found*: C, 93.94; H, 6.38. $C_{18}H_{14}$ requires: C, 93.87; H, 6.13%. *IR spectrum* (KBr; cm^{-1}): 721 s; 746 vs; 766 vs; 1471 m; 1485 m; 2931 m; 2959 m; 3026 w; 3040 vw and 3068 m. *UV spectrum* (C_6H_{12}; $\lambda_{\max}^{\text{nm}}$; lg ε): 263 (3.13); 272 (3.25) and 279 (3.22).

The mother liquors from the recrystallization of **11** were evaporated and subjected to v.p.c.-separation, when *4b, 4c, 8b, 8c-tetrahydro-4b,8b-ethenodibenzo*[a,e]*pentalene* (**12**) m.p. 99–100° was obtained. *Found*: C, 93.99; H, 6.37. $C_{18}H_{14}$ requires; C, 93.87; H, 6.13%. *IR spectrum* (CS_2; CCl_4; cm^{-1}): 701 vs; 753 vs; 802 s; 1467 s; 2954 s; 3023 s; 3045 s and 3068 s. *UV spectrum* (C_6H_{12}; $\lambda_{\max}^{\text{nm}}$; lg ε): 264.5 (3.37); 271 (3.47) and 278.5 (3.42).

Preparative pyrolysis of dibenzo-Nenitzescu's hydrocarbon (**2**). A sample of hydrocarbon **2**[7] (200 mg; 0.87 mmole) pyrolyzed at 625°/5 mm Hg, afforded a solid product (180 mg; 90%) which contained (v.p.c.-analysis) 86.5% butadienic hydrocarbon **10**, 1,5% starting hydrocarbon (**2**), 2.1 % chrysene and benzo[*a*]anthracene beside other unidentified components. The pure hydrocarbon **10** could be obtained by recrystallization from ethanol.

Catalytic amounts of $AgBF_4$ added to the starting hydrocarbon **2** allow conversions even at lower temperatures (500°), with very good yields of **10**. However, **2** could not be isomerised with $AgBF_4$ in refluxing acetone (15 hrs).

Acknowledgements. We wish to thank Miss E. Sliam and Mrs V. Daniel fo performing the elemental analyses and Mr. C. Drăghici for UV spectra.

Revue Roumaine de Chimie, **21**, *1*, 101–106 (1976)

PYRYLIUM SALTS FORMED BY DIACYLATION OF OLEFINS. XX[1]

PMR SPECTRA OF 2,4,6-TRIMETHYL-3-PHENYLPYRYLIUM AND -PYRIDINIUM SALTS

ANISIA BOTA[a], ALEXANDRU T. BALABAN[a,b] and FILIP CHIRALEU[c]

[a] Chair of Organic Chemistry, Chemical Institute, Bucharest, Romania
[b] To whom correspondence should be addressed at the Institute of Atomic Physics, P.O.B. 5206, Bucharest, Romania
[c] Organic Chemistry Research Centre, Bucharest, Romania

Received May 31, 1975

2-Methylpropenylbenzene yields on diacetylation with acetyl chloride and aluminium chloride mainly 2,6-dimethyl-4-benzylpyrylium, but yields with acetic anhydride and perchloride acid 2,4,6-trimethyl-3-phenylpyrylium. The NMR spectrum of the latter presents three distinct methyl peaks which were assigned taking into account the shielding due to the non-coplanar phenyl and the faster deuteration of the 4-methyl. The same considerations allowed the assignment of NMR peaks for the pyridine and pyridinium salts obtained from the latter pyrylium salt with ammonia, methylamine and aniline.

The formation of pyrylium salts by olefin diacylation was reviewed.[2,3] Propene is diacylated at both terminal carbons affording 2,6-disubstituted pyrylium salts,[4] whereas isobutene derivatives are diacylated at two carbons adjacent to the central carbon atom yielding corresponding 4-methylpyrylium salts.[5] Olefin rearrangements may take place under the acid reaction conditions employed.[6,7] In these conditions, it is not necessary to start from the preformed olefin but one may employ tertiary alcohols or halides which undergo at the same time dehydration or dehydrohalogenation, respectively. When the olefin or its possible rearrangement products are unsymmetrical, more than one pyrylium salts may be formed : it was observed[6] that the nature of the acylating agent, especially of the electrophilic catalyst, has a pronounced influence on the reaction course. Thus, for instance starting from 2-methyl-2-butene, t-pentyl alcohol or t-pentyl chloride, perchloric acid with acetic anhydride afford predominantly 2,3,4,6-tetramethylpyrylium with ca. 20% 2,6-dimethyl-4-ethylpyrylium, whereas aluminium chloride with acetyl chloride give only 2,6-dimethyl-4-ethylpyrylium.[6] This was interpreted as resulting from the fact that in the presence of the latter, stronger, catalyst, olefin rearrangements are very rapid and, therefore, only the more reactive 1,1-disubstituted ethylene (2-methyl-1-butene) reacts driving the equilibrium to completion, while in the former case the product derives mainly from the trisubstituted ethylene (2-methyl-2-butene) since the equilibration is not fast enough. Experiments with pure 1- and 2-methyl-2-butene substantiate this assumption.[7] So do also experiments with ^{14}C-labelled monoacylation products,[8,9] proving that olefin monoacylation is reversible.[10,11]

---

[1] Previous part, A. T. Balaban, *Rev. Roumaine Chim.*, **14**, 1331 (1969).

[2] A. T. Balaban and C. D. Nenitzescu, *Rev. Chim. Acad. R. P. Roumaine*, **6**, 269 (1961) in English; *Studii Cercet. Chim. Acad. R. P. România*, **9**, 251 (1961) in Romanian.

[3] A. T. Balaban, W. Schroth and G. Fischer, *Adv. Heterocyclic Chem.*, **10**, 241 (1969).

[4] A. T. Balaban, D. Fărcaşiu and C. D. Nenitzescu, *Tetrahedron*, **18**, 1075 (1962).

[5] A. T. Balaban and C. D. Nenitzescu, Org. Synth. Coll. Vol. 5, 1106; A. T. Balaban and A. J. Boulton, *ibid.*, 1112, 1114.

[6] A. T. Balaban and C. D. Nenitzescu, *J. Chem. Soc.*, **1961**, 3533; *Tetrahedron Letters*, **1960**, 7.

[7] P. F. G. Praill and A. L. Whittear, *J. Chem. Soc.*, **1961**, 3573.

Benzyldimethylcarbinol was prepared either from benzylmagnesium chloride and acetone, or from ethyl phenylacetate and methylmagnesium iodide. On dehydration with iodine it afforded 2-methylpropenylbenzene. Diacetylation of the olefin with acetyl chloride and aluminium chloride afforded 2,6-dimethyl-4-benzylpyrylium I, identified by conversion into the corresponding pyridine on treatment with ammonia and comparison with an authentic sample.[12] Diacetylation of the carbinol or olefin with acetic anhydride and perchloric acid afforded a different pyrylium perchlorate, which gave with ammonia a different pyridine.[12]

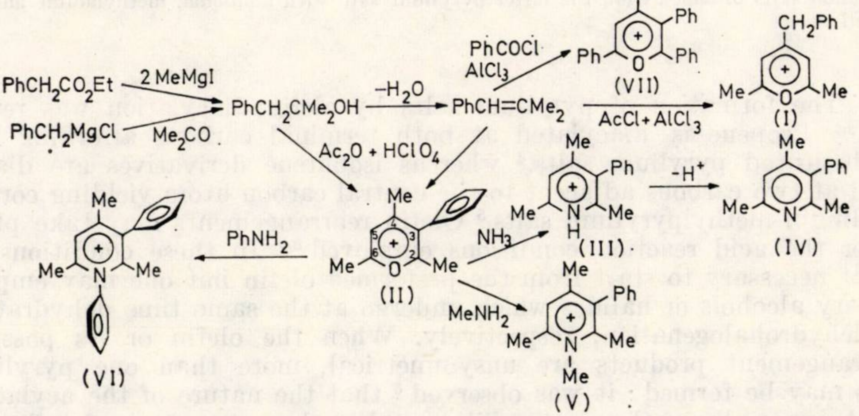

The NMR spectrum of this perchlorate in trifluoroacetic acid presents the phenyl multiplet at τ 2.2—2.9, the β-pyrylium proton at τ 2.19,

---

[8] M. Frangopol, A. Genunche, P. T. Frangopol and A. T. Balaban, *Tetrahedron*, **20**, 1881 (1964).

[9] D. Fărcașiu, A. T. Balaban and M. Gutman, *Rev. Roumaine Chim.*, **9**, 727 (1964).

[10] M. Frangopol, A. Genunche, N. Negoiță, P. T. Frangopol and A. T. Balaban, *Tetrahedron*, **23**, 841 (1967).

[11] A. T. Balaban, in "Omagiu pentru Prof. Raluca Ripan", Ed. Academiei, Bucharest, 1966, p. 103.

[12] A. T. Balaban, *Tetrahedron Letters*, **1963**, 91.

and three separate methyl peaks at τ 7.02, 7.26 and 7.48 in agreement with the proposed[12] structure, 2,4,6-trimethyl-3-phenylpyrylium (II). In order to assign the three peaks to the three methyl groups, we made use of the following previous observations :

(i) α-Standing methyl groups resonate at lower frequency than γ-methyl groups, e.g. for 2,4,6-trimethylpyrylium : α at 7.10 τ, γ at 7.26 τ (in liquid sulphur dioxide),[13] owing to the lower π-electron density in α than in γ.[14,15]

(ii) γ-Standing methyl groups are deuterated faster than α-methyl groups,[16,17] owing to the higher stability of the symmetrical γ-pyran intermediate as compared to the α-pyran.[14]

(iii) A phenyl substituent flanked by two methyl groups on the same aromatic nucleus shields these methyl groups : because of steric hindrance the two aryl groups cannot be coplanar and the ring current causes upfield shifts. Thus, in 2,4,6-trimetyl-1-phenylpyridinium perchlorate in liquid sulphur dioxide the α-methyl groups appeared at τ 7.61 ppm instead of 7.25 ppm as in 1,2,4,6-trimethypyridinium perchlorate ;[18] a separate X-ray structure determination confirmed[19] that the pyridinium and phenyl rings in the former salt formed a dihedral angle of 85°.

Observations (i) and (iii) made it plausible that the lowest-field peak of II at τ 7.02 was due to the 6-methyl, the next one at 7.26 to the 2-methyl, and the highest-field peak at τ 7.48 to the 4-methyl group. Indeed by heating on the steam bath for 10 minutes the perchlorate II in carboxyl-deuterated acetic acid and then precipitating the deuterated perchlorate with ether, the intensity of the peak at τ 7.48 is decreased relatively to the other two peaks. We assume that the faster deuteration of γ- than of α-methyl groups found in other pyrylium salts still holds for II, since the phenyl group cannot interact electronically with the pyrylium ring both because it is in β, and because the two rings are not coplanar ; a steric effect on the deprotonation of the methyl groups is not plausible.

Infrared data had indicated that the structure of the dibenzoylation product of 2-methylpropenylbenzene was 2,3,6-triphenyl-4-methylpyrylium (VII).[12] This assignment is now confirmed by the NMR spectrum in trifluoroacetic acid, which presents the phenyl multiplet at 1.7—2.8 τ, the β-pyrylium proton at τ 1.5, and a singlet due to the three γ-methyl protons at τ 7.30.

2,4,6-Trimethyl-3-phenylpyrylium perchlorate was conveited with ammonia into the corresponding pyridine, and with primary amines (methylamine, aniline) into 1-substituted pyridinium salts V and VI. The NMR spectra of the pyridine IV, its conjugate acid III, and methyl-

---

[13] A. T. Balaban, G. R. Bedford and A. R. Katritzky, *J. Chem. Soc.*, **1964**, 1646.

[14] C. C. Rențea, A. T. Balaban and Z. Simon, *Rev. Roumaine Chim.*, **11**, 1193 (1966).

[15] G. V. Boyd and A. T. Balaban, *Rev. Roumaine Chim.*, **14**, 1575 (1969).

[16] E. Gârd, I. Stănoiu, F. Chiraleu and A. T. Balaban, *Rev. Roumaine Chim.*, **18**, 257 (1973).

[17] E. Gârd, I. Vasilescu, G. D. Mateescu and A. T. Balaban, *J. Labelled Comp.*, **3**, 196 (1967).

[18] C. Toma and A. T. Balaban, *Tetrahedron*, Suppl. 7, 9 (1966).

[19] A. Camerman, L. H. Jensen and A. T. Balaban, *Acta Cryst.*, **25B**, 2623 (1969).

Table 1

^1H – NMR spectra in T-values

Compound	Solvent	5-H	2-Me	4-Me	6-Me	1-Me
I	TFA	2.25 [a]	7.12	5.64 [b]	7.12	—
II	TFA	2.19	7.26	7.48 [c]	7.02	—
III	CS_2	3.24	7.86	8.06 [c]	7.61	—
IV	TFA	— [d]	7.45	7.64	7.16	—
V	TFA	— [d]	7.40	7.68	7.10	5.80
VI	TFA	— [d]	7.79	7.56 [c]	7.49	—
VII	TFA	1.50	—	7.30	—	—

[a] 3,5-H_2 peaks; [b] Methylene group; [c] Checked by deuteration of the pyrylium salt which depresses this methyl peak; [d] Submerged under phenyl multiplet.

pyridinium derivative V are similar to that of the pyrylium salt : as seen in table 1, all corresponding peaks reveal the following deshielding order : pyridine — pyridinium — pyrylium. Although the first compound is neutral and the others cations, and despite the different solvents, this is the order of increasing electronegativity of the heteroatom. Whereas in the pyridine, the heteroaromatic β-proton appears at higher fields than the phenyl multiplet, and in the pyrylium salt at lower fields, in the pyridinium salts its position cannot be ascertained because it overlaps with the phenyl multiplet. In VI, the N-phenyl group introduces additional shieldings of the α-methyl groups as seen from table 1 : whereas the 4-methyl peak remains practically unchanged relatively to IV and V, peaks of 2- and 6-methyl groups are shifted upfield by ca. 0.4 ppm relatively to IV and V, and thus the 2-methyl peak shielded by the two perpendicular phenyl groups in positions 1 and 3 appears at 7.79 τ. This assignment was verified by reacting the partly 4-methyl-deuterated pyrylium salt with aniline, and seeing that the product has a less intense peak at τ 7.56 ppm relatively to the other methyl peaks.

EXPERIMENTAL PART

Benzyldimethylcarbinol was prepared by Grignard reaction, and had b.p. 95°/15 Torr, b.p. 75°/3 Torr, n_D^{20} 1.5165.[20–24]. Dehydration with iodine afforded 2-methylpropenylbenzene distilled at 180—190° and redistilled at 55°/3 Torr, n_D^{20} 1.5318.[20–23,25]

---

[20] R. H. Hall, R. G. Pyke and G. F. Wright, *J. Amer. Chem. Soc.*, **74**, 1597 (1952).

[21] H. C. Duffin, E. D. Hughes and C. K. Ingold, *J. Chem. Soc.*, **1959**, 2734.

[22] D. A. Shearer and G. F. Wright, *Canad. J. Chem.*, **33**, 1002 (1955).

[23] J. Farkas, P. Kourim and F. Sorm, *Chem. Listy*, **52**, 688 (1958).

[24] R. Heck and S. Winstein, *J. Amer. Chem. Soc.*, **79**, 3432 (1957).

[25] M. Voronkov, A. S. Brown and G. D. Karpenko, *Doklady. Akad. Nauk. S.S.S.R.*, **59**, 1437 (1948).

4-Benzyl-2,6-dimethylpyrylium. 2-Methylpropenylbenzene (1 mole) was introduced dropwise into a solution prepared in the cold from 5 moles acetyl chloride and 1.5 moles sublimed aluminium chloride. The mixture was stirred at room temperature for 4 hrs, left overnight, and hydrolyzed with ice. The aqueous layer was extracted twice with ether to remove the unsaturated ketones, concentrated in vacuum to half its volume, and treated with perchloric acid. The oily perchlorate gave after washing with ether an NMR spectrum indicating that it contains *ca.* 70% 4-benzyl-2,6-dimethylpyrylium and 30% 2,4,6-trimethyl-3-phenylpyrylium (see below).

4-Benzyl-2,6-dimethylpyridine was prepared from the above perchlorate and aqueous ammonia and ether. It was freed from by-products by dissolution in dil. hydrochloric acid, ether extraction and alkalinization of the aqueous layer, followed by vacuum distillation, b.p. 134°/4 Torr.[26,27]

Picrolonate, m.p. 195° (from ethanol), *Found* : C, 62.92; H, 5.02; N, 15.17. $C_{24}H_{23}N_5O_5$ requires C, 62.46; H, 5.02; N, 15.18%.

Picrate, m.p. 143° (from ethanol), gives no depression with an authentic sample kindly provided by prof. T. Kato.[26] *Found* : C, 56.46; H, 4.21; N, 12.89. *Calcd.* for $C_{20}H_{18}N_4O_7$, C, 56.33; H, 4.26; N, 13.14%. Literature m.p. 140–3°,[26] 142–3°.[27]

Chloroplatinate, m.p. 95° (from dil. hydrochloric acid), *Found* : C, 42.02; H, 4.15; Cl, 26.34; N, 3.69; Pt, 23.52. $C_{14}H_{16}NPt_{0,5}Cl_3$ requires : C, 41.79; H, 4.01; Cl, 26.45; N, 3.48; Pt, 24.27%

Methiodide, m.p. 163° (from ethanol-ether) *Found* : C, 53.34; H, 5.39; I, 36.73; N, 4.08. *Calcd.* for $C_{15}H_{18}IN$: C, 53.15; H, 5.35; I. 37.42; N, 4.12; literature [27] m.p. 151–2°.

2,4,6-Trimethyl-3-phenylpyrylium perchlorate. A mixture of 5 moles acetic anhydride and one mole of benzyldimethylcarbinol in a three-necked flask with dropping funnel, stirrer and reflux condenser, is treated dropwise with one mole of 70% perchloric acid without external cooling. The first drops of perchloric acid cause considerable heating, and the rate of introduction is controlled so that the mixture arrives at gentle refluxing (caution, otherwise the reaction becomes too rapid). Stirring is continued until the mixture cools at room temperature. An equal volume of ether is added, the lower black layer is separated and triturated several times with ether. An NMR spectrum shows that it contains *ca.* 96% trimethylphenylpyrylium and 4% 2,5-dimethylbenzylpyrylium perchlorate. It may be purified by recrystallization from water : m.p. 159°. Yield : 40%. *Found* : C, 56.48; H, 5.39; Cl, 12.17. $C_{14}H_{15}ClO_5$ requires : C, 56.28; H, 5.06; Cl, 11.87%.

Strong IR bands of the cation II (KBr pellet) : 1635, 1410, 1490, 1450, 1281, 1024, 995, 780, 715, 575 cm^{-1}.

If the carbinol is replaced by the olefin in the diacylation, the product is the same.

2,4,6-Trimethyl-3-phenylpyridine. The perchlorate was treated with aqueous ammonia and ether, and the pyridine was purified as above by extraction into dil. hydrochloric acid, and by distillation, b.p. 115°/3 Torr.

Picrolonate, m.p. 232° (from ethanol), *Found* : C, 62.61; H, 5.10; N, 14.98. $C_{24}H_{23}N_5O_5$ requires : C, 62.46; H, 5.02; N, 15.18%.

Picrate, m.p. 141° (from aq. ethanol), identical to that described earlier,[28] obtained on Friedel-Crafts acetylation of phenylacetone.

Chloroplatinate, m.p. dec. 248°, identical to that described earlier.[28]

Methiodide, m.p. 210° (from ethanol-ether), *Found* : C, 53.16; H, 5.25; N, 4.36; I, 37.22. $C_{15}H_{18}IN$ requires : C, 53.15; H, 5.35; N, 4.12; I, 37.42%.

1,2,4,6-Tetramethyl-3-phenylpyridinium perchlorate. A conc. ethanolic solution of the pyrylium perchlorate II was heated with an excess of aqueous methylamine, then acidified with perchloric acid. The precipitated perchlorate was recrystallized from water, m.p. 170°. *Found* : C, 58.10; H, 6.25; N, 4.39. $C_{15}H_{18}ClO_4$ requires : C, 57.79; N, 5.82, N, 4.49%. Strong IR bands of the cation (KBr pellet) : 1620, 1562, 1472, 1442, 1370, 1258, 1022, 921, 874, 801, 768, 709 cm^{-1}.

2,4,6-Trimethyl-1,3-diphenylpyridinium perchlorate. An ethanolic solution of the pyrylium perchlorate II was heated with a slight excess of aniline, then acidified with perchloric acid and chilled. The pyridinium perchlorate was recrystallized from aq. ethanol, m.p. 209°.

---

[26] T. Kato, *J. Pharm. Soc. Japan,* **75**, 1228, 1231 (1955).

[27] E. H. Huntress and E. N. Shaw, *J. Org. Chem.*, **13**, 674 (1958).

[28] A. T. Balaban, G. D. Mateescu and C. D. Nenitzescu, *Rev. Chim. Acad. R. P. Roumaine*, **6**, 295 (1961); *Studii și Cercetări Chim., Acad. R.P.R.*, **9**, 211 (1961).

Found : C, 64.15 ; H, 5.67 ; N, 3.68. $C_{20}H_{20}NClO_4$ requires : C, 64.25 ; H, 5.39 ; N, 3.72 %. Strong IR bands of the cation (in KBr) : 1622, 1585, 1550, 1488, 1472, 1452, 1439, 1030, 794, 780, 712 cm^{-1}.

2,3,6-Triphenyl-4-methylpyrylium perchlorate. To 4 moles benzoyl chloride, 1.5 moles aluminium chloride were added and stirred at room temperature, then 1 mole 2-methylpropenylbenzene was introduced dropwise at 25–30°. The solution was stirred for 4 hrs, left overnight, and hydrolyzed with ice and hydrochloric acid. The mixture was extracted with ether, and the aqueous layer was treated with perchloric acid. The precipitated yellow perchlorate had m.p. 255° (from acetic acid). *Found* : C, 68.44 ; H, 4.79 ; Cl, 8.30. $C_{24}H_{19}ClO_5$ requires : C, 68.17 ; H, 4.53 ; Cl, 8.38 %,

2,3,6-Triphenyl-4-methylpyridine. The above perchlorate was treated with ammonia and the pyridine was purified as above.

Picrate, m.p. 157° (from ethanol), *Found* : C, 65.56 ; H, 4.04 ; N, 10.21. $C_{30}H_{22}N_4O_7$ requires : C, 65.45 ; H, 4.12 ; N, 10.18 %.

Picrolonate, m.p. 144° (from ethanol), *Found* : C, 70.03 ; H, 4.67 ; N, 12.23. $C_{34}H_{27}N_5O_5$ requires : C, 69.73 ; H, 4.64 ; N, 11.96 %.

Acknowledgements. Elemental analyses were made by Elvira Şliam and Violeta Daniel ; Michel Dzabatou—Babeaux gave experimental assistance : thanks are expressed to them.

Revue Roumaine de Chimie, **21**, *1*, 107 – 111 (1976)

INVESTIGATIONS IN THE CYCLOBUTANE SERIES. XXXVIII[1]

REARRANGEMENT OF THE DIBENZO[*b*, *g*]BICYCLO-[4.2.0]OCTA-2,7-DIENE SYSTEM

NICOLETA ŞTEFAN, I. G. DINULESCU and MARGARETA AVRAM
Center of Organic Chemistry, Bucharest 15, Spl. Independenţei 202B, Romania

Received September 24, 1974

The rearrangement of compounds **3** and **4** with bicyclo[4.2.0]octadiene skeleton to compounds with bicyclo[3.2.1]octadiene skeleton (**5** and **6**) is reported. Stereochemical and mechanistic aspects are discussed.

It was previously shown [2,3] that the dibromide **1**, with dibenzo [*c*,*g*]bicyclo[4.2.0]octa-3,7-diene skeleton, bearing a bromine atom in the vicinity of the cyclobutene ring, rearranges, in the course of solvolyses, to compounds with dibenzo[*b*,*f*] bicyclo[3.2.1]octa-2,6-diene skeleton **2**.

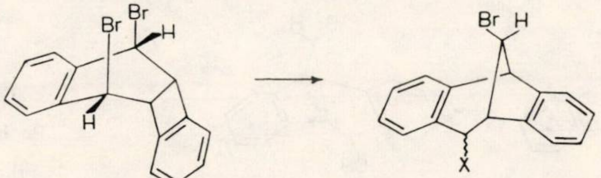

1

2

X=Br,OH,OCOCH$_3$

In a previous paper,[1] the synthesis of the bromo-acetoxy-derivative **3**, and of bromo-methoxy-derivative **4** with dibenzo [*b*,*g*] bicyclo-[4.2.0]octa-2,7-diene skeleton were reported.

As a continuation of this work, we investigated the behaviour of the angular derivatives with dibenzo[*b*,*g*]bicyclo[4.2.0]octa-2,7-diene skeleton, namely the bromo-methoxy compound **3** and the bromo-acetoxy one **4**, in reaction which generate a cationic center in the α-position to the cyclobutene ring.

By refluxing the bromo-acetoxy-derivative **3** with silver bromide in carbon tetrachloride, the bromo-acetoxy compound **5** with rearranged skeleton was obtained.

---

[1] Part XXXVII: N. Ştefan, I. G. Dinulescu, F. Chiraleu and M. Avram, *Rev. Roumaine Chem.*, **20**, 1473 (1975).

[2] I. G. Dinulescu, M. Avram, G. D. Mateescu and C. D. Nenitzescu, *Chem. and Ind.*, **1964**, 2023.

[3] I. G. Dinulescu, M. Avram, G. D. Mateescu and C. D. Nenitzescu, *Rev. Roumaine Chim.*, **9**, 351 (1964).

Under the same conditions, the bromo-methoxy-derivative **4** yielded **6**.

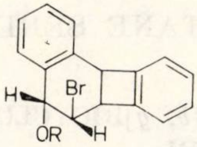

3, R=CH_3CO
4, R=CH_3

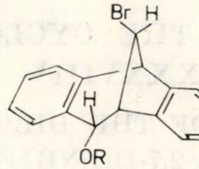

5, R=CH_3CO
6, R=CH_3

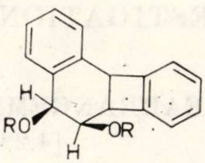

7, R=CH_3CO

On heating with silver acetate in acetic acid, **3** gave a mixture from which were isolated and identified : **5** with rearranged skeleton (25%), diacetoxy-derivative **7** (45%) and unreacted starting material **3** (25%).

The structure and configuration of the rearranged product **5** were assigned on the basis of spectral data and chemical reactions. Indeed, **5** gave by reduction with lithium-aluminium hydride the alcohol **8** from which, by oxidation with chromic acid, the bromo-ketone **9** was obtained. Ketone **9** was found to be identical with those previously obtained [2,3] by us by oxidation of the *exo*-hydroxy-derivative **11**.

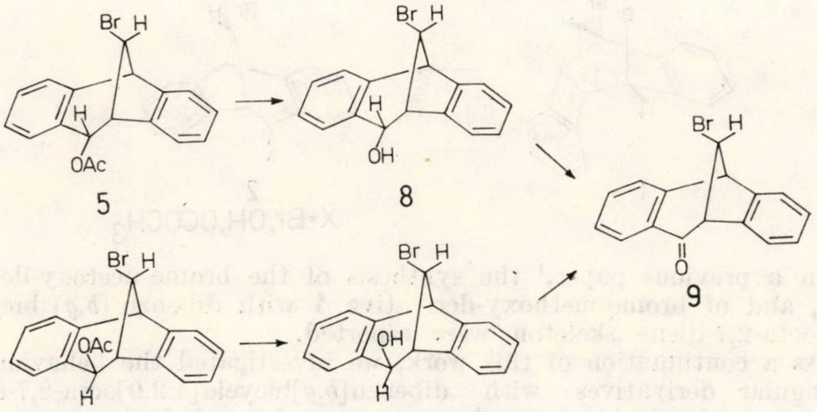

5 8 9 10 11

The following NMR data confirm the *endo* configuration of the acetoxy group in **5** and methoxy group in **6**.

The signals of the protons 1-H, 5-H and 8-H in **5** and **6** have virtually the same chemical shift. In accordance with literature data,[4,5,6]

[4] M. Avram, I. G. Dinulescu, C. D. Nenitzescu, R. A. Y. Jones, A. R. Katritzky and R. J. Wyatt, *Rev. Roumaine Chim.*, **18**, 441 (1973).

[5] A. R. Katritzky and J. B. Wallis, *Chem. and Ind.*, **1964**, 2025.

[6] S. J. Cristol, J. R. Mohrig and D. E. Plorde, *J. Org. Chem.*, **30**, 1965 (1956).

the signals for the bridgehead protons 1-H and 5-H appeared at δ 3.88–4.06 ppm. The coupling constant between 4-H and 5-H (doublets in both cases), characteristic of the stereochemistry of the substituent at 4-C, has a value of 5.5 Hz for **5** and 4.0 Hz for **6**, in accordance with an *exo*-orientation of the proton 4-H, and *endo*-configuration for the methoxy and acetoxy groups respectively. For the *exo*-acetoxy isomer **10**, this coupling has a value of 1.4 Hz.[5]

The NMR spectrum of the diacetoxy-derivative **7** indicated a *trans-diequatorial* conformation. Thus, large values of $J_{4\text{-}5}$ and $J_{5\text{-}6}$, which are expected for this conformer, are actually found (9.0 and 6.0 Hz, respectively). On the other hand, no shielding for the 4-acetoxy groups, as in **3** and **4**, are observed.

For the rearrangement of **3** and **4** to **5** and **6**, respectively, considering the established[1] diaxial conformation for *trans* oriented bromine and acetoxy or methoxy groups, it was assumed that the reaction takes place *via* the nonclassical phenonium ions **12** and **13**, resulted by participation of the 6-C/7-C bond, which is anticoplanar with the axial ionizing C-Br bond. This explains the stereospecificity of the final products, namely the *syn*-orientation of the 8-bromine in **5** and **6**. If the reaction took place within the ion-pair **14** or **15**, the intermediate ions **16** or **17** would have yielded, in addition to the *syn*-bromide, *anti*-8-bromo isomer **18**. This product was not actually detected.

The same ions can explain the formation of the diacetoxy-derivative **7**.

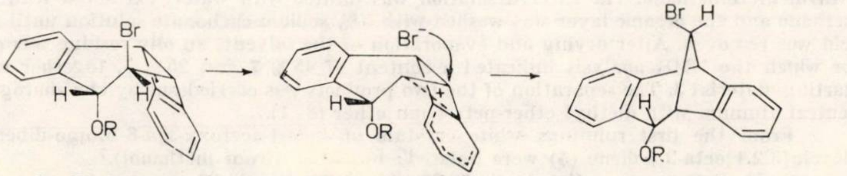

3, R=CH_3CO
4, R=CH_3

12, R=CH_3CO
13, R=CH_3

5, R=CH_3CO
6, R=CH_3

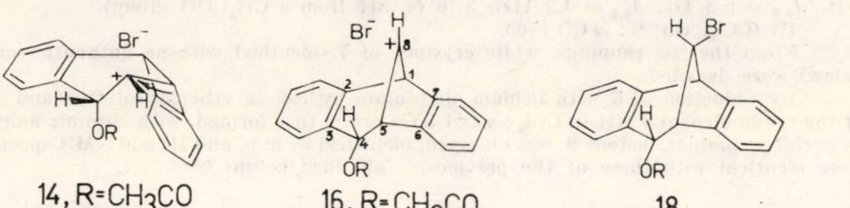

14, R=CH_3CO
15, R=CH_3

16, R=CH_3CO
17, R=CH_3

18

In polar media, which favour carbenium ions, intermediate ions like **14** or **15** cannot be ruled out of hand. The formation as main product of the *trans*-diacetoxy-derivative **7** could also be attributed to the sterical hindrance of the benzocyclobutene ring and to an equilibrium between the **7** *a,a* and **7** *e,e* conformers.

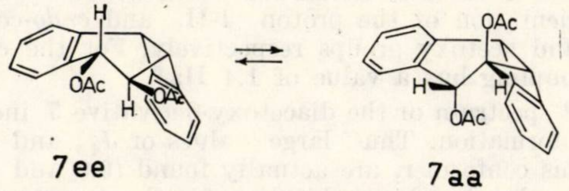

7ee **7aa**

The diacetoxy-derivative **7**, together with the rearranged compound **5**, were isolated when **3** was treated with silver propionate in acetic acid.

EXPERIMENTAL

Microanalyses were performed by Miss E. Şliam and Mrs. V. Daniel. IR spectra were recorded with a double beam UR 20 spectrophotometer. NMR spectra were determined with a Varian A-60A spectrometer (TMS internal standard).

REACTION OF BROMO-ACETOXY-DERIVATIVE 3 WITH SILVER ACETATE

A mixture of 0.5 g (1.4 mmoles) **3** and 0.5 g (2.9 mmoles) silver acetate in 20 ml anhydrous acetic acid was refluxed for 30 hours. The silver salts were filtered off and washed with dichloromethane. The filtered solution was diluted with water, extracted with dichloromethane and the organic layer was washed with 5% sodium carbonate solution until all acetic acid was removed. After drying and evaporation of the solvent, an oily residue was obtained, for which the NMR analysis indicated a content of 45% **7** and 25% **5**, together with 25% starting material **3**. The separation of the two products was carried out by chromatography on neutral alumina with diethyl ether-petroleum ether (8 : 1).

From the first runnings white crystals of *endo*-4-acetoxy-*syn*-8-bromo-dibenzo [*b,f*]-bicyclo[3.2.1]octa-2,6-diene (**5**) were isolated; m.p. 144° (from methanol).[7]

$C_{18}H_{15}BrO_2$ *Calcd.*: C, 62.98; H, 4.40; Br, 23.20
Found: C, 63.10; H,; 4.67 Br, 23.16.

NMR ($CDCl_3$, δ, ppm); 7.18 (s, 8H, aromatics), 6.43 (d, 1H, 4-H, $J_{4.5} = 5.5$ Hz), 4,91 (t, 1H, 8-H, $J_{1.8} = J_{5.8} = 4.2$ Hz), 4.06 (d, 1H, 1-H, $J_{1.8} = 4.2$ Hz), 3.93 (t, 1H, 5-H, $J_{4.5} = 5{,}5$ Hz, $J_{5.8} = 4.2$ Hz), 2.16 (s, 3H from a CH_3COO group).

IR (CCl_4, cm^{-1}): ν CO 1765.

From the last runnings, white crystals of **7** (identical with an authentic sample, see below) were isolated.

By reduction of **5** with lithium aluminium hydride in ethereal solution and oxidation of the crude alcohol **8** (IR in CCl_4; ν OH 3575 cm^{-1}) thus formed, with chromic anhydride — — pyridine complex, ketone **9** was obtained, identified by m.p. and IR and NMR spectra, which were identical with those of the previously obtained ketone.[2,3]

REACTION OF BROMO-ACETOXY-DERIVATIVE 3 WITH SILVER BROMIDE

A solution of 0.10 g (0.3 mmoles) **3** in 5 ml carbon tetrachloride was refluxed with 0.20 g anhydrous silver bromide (prepared from silver acetate and bromine, by a Hunsdiecker reaction), for 50 hrs. The filtered solution was then concentrated *in vacuo*, yielding 0.095 g oily residue, which was found (by NMR) to contain 95% **5** and 5% **7**.

[7] S. J. Cristol, E. P. Parungo, D. E. Plorde and K. Schwarzenbach, *J. Amer. Chem. Soc.*, **87**, 2879 (1965), indicated for **5** (prepared by another procedure) m. p. 114–116°.

REACTION OF BROMO-ACETOXY-DERIVATIVE **3** WITH SILVER PROPIONATE

A solution of 1.0 g (3 mmoles) **3** in 20 ml anhydrous acetic acid was refluxed with 1.5 g (8.3 mmoles) silver propionate for 30 hours. After working up as above, 0.97 g oily residue were obtained, in which a content of 18.5% **5** and 81.5% **7** was determined (by NMR spectra).

endo-4-*exo*-5-DIACETOXY-DIBENZO[*b*, *g*]BICYCLO[4.2.0]OCTA-2,7-DIENE (**7**)

A mixture of 0.85 g (2.5 mmoles) **3** and 1.0 g (10 mmoles) anhydrous potassium acetate in 20 ml acetic acid was refluxed for 60 hours. Water was added, the product was extracted with dichloromethane and the organic layer washed until neutral. After drying and evaporation of the solvent, the oily residue was chromatographied on Al_2O_3 column and eluted with ether; 0.5 g (53%) **7**, m.p. 99°, were obtained.

$C_{20}H_{18}O_4$ *Calcd.* : C, 74.51 ; H, 5.62

Found : C, 74.27 ; H, 5.90

NMR (CCl_4, δ, ppm) : 6.80—7.50 (m, 8H, aromatics), 5.62 (d, 1H, 4-H, $J_{4.5} = 9.0$ Hz), 5.21 (dd, 1H, 5-H, $J_{4.5} = 9.0$ Hz, $J_{5.6} = 6$ Hz), 4.69 (d, 1H, 1-H, $J_{1.6} = 5.0$ Hz), 4.27 (t, 1H, 6-H, $J_{1.6} = 5.0$ Hz), 2.06 and 2.09 (s, 6H from CH_3COO groups).

IR (CCl_4, cm^{-1}) : νCO 1730, 1740.

REACTION OF BROMO-METHOXY-DERIVATIVE **4** WITH SILVER ACETATE

A mixture of 0.45 g (1.4 mmoles) **4** and 0,5 g (2.9 mmoles) silver acetate in 20 ml anhydrous acetic acid was boiled for 30 hours. The filtered solution was diluted with water, extracted with dichloromethane and the organic layer was washed with 5% sodium carbonate solution. After drying and evaporation of the solvent, the oily residue was purified by chromatography (Al_2O_3/ether), yielding 0.20 g oily product, from which, by thin layer chromatography (Silicagel G after Stahl, eluent dichloromethane containing 5% acetone), pure *endo*-4-methoxy-*syn*-8-bromo-dibenzo[*b*, *f*]bicyclo[3.2.1]octa-2,6-diene (**6**) was obtained, m.p. 113°.

$C_{17}H_{15}BrO$ *Calcd.* : C, 64.76 ; H, 4.79 ; Br, 25.36

Found : C, 64.82 ; H, 5.06 ; Br, 25.05

NMR ($CDCl_3$, δ, ppm) ; 7.10—7.40 (m, 8H, aromatics), 4.95 (t, 1H, 8-H, $J_{1.8} = J_{5.8} = 4.2$ Hz), 4.86 (d, 1H, 4-H, $J_{4.5} = 4.0$ Hz), 4.00 (d, 1H, 1-H, $J_{1.8} = 4.2$ Hz), 3.88 (t, 1H, 5-H, $J_{4.5} = 4.0$ Hz, $J_{5.8} = 4.2$ Hz), 3.70 (s, 3H from a CH_3O group).

REACTION OF BROMO-METHOXY-DERIVATIVE **4** WITH SILVER BROMIDE

A solution of 0.25 g (0.8 mmoles) **4** in 10 ml carbon tetrachloride was refluxed with 0.30 g anhydrous silver bromide (prepared from silver acetate and bromine, by the Hunsdiecker reaction) for 50 hours. The filtered solution was then concentrated *in vacuo*, yielding 0.22 g, crude product, containing 40% **6**, together with 60% starting material **4**, as determined by means of NMR.

Revue Roumaine de Chimie, **21**, *1*, 113−119 (1976)

THIAZOLE COMPOUNDS. III[1]

KINETICS OF HYDROLYSIS OF SOME 2-ARYL-4-AND-5-DIAZO KETONE DERIVATIVES

D. SUCIU and G. CSÁVÁSSY

Oncological Institute, Cluj, Str. Republicii 34−36, Romania

Received June 24, 1974

The acid hydrolysis of substituted 2-aryl-4-and-5-diazo-acetylthiazoles takes place following an apparent first-order kinetics (mechanism A−2). At $\mathrm{pH} > 2$ there is, probably, no protonation of the thiazole ring and the 4-diazoacetyl derivatives have lower K_1 values than the corresponding 5-diazoacetyl compounds, whereas at $\mathrm{pH} \sim 1$ the hydrolysis of 4-diazoacetylthiazoles is enhanced. Substituents on the 2-aryl group affected the rate of hydrolysis by Hammett $|\rho|$ values of 0.2−0.3.

The chemical behaviour of substituted thiazoles is different according to the position of the substituent in molecule as a consequence of the unsymmetrical distribution of the charge density in the thiazole ring.[2] With respect to these, it was regarded as a matter of interest to investigate the kinetics of hydrolysis and the transmission of polar effects of some substituted 2-aryl-4 (I−V) and-5-diazoacetylthiazoles (VI−XI) (Table 1) which have been recently synthesized.[1,3]

The rate of hydrolysis was measured by monitoring the ultraviolet absorption of the diazo ketone derivatives. As can be seen from Table 1 the absorption bands of diazo ketones which appear in the near ultraviolet region are shifted to shorter wavelenghts after hydrolysis. The absorption maxima of α-hydroxyketones XII−XIV, which were isolated, are similar with those determined after the acid hydrolysis of the corresponding diazoacetyl derivatives VII−IX (Table 1).

The hydrolysis in perchloric acid [4,5] as well as the decomposition in acetic acid [6] of aromatic primary diazo ketones exhibits apparent first-order kinetics (mechanism A−2). On the other hand, the hydrolysis of secondary diazo ketones is

$$\mathrm{R-CO-CHN_2}\underset{\text{fast}}{\overset{\mathrm{H^+}}{\rightleftharpoons}}\mathrm{R-CO-CH_2-N_2}\underset{\text{slow}}{\overset{+\,\mathrm{H_2O}}{\rightleftharpoons}}\mathrm{R-CO-CH_2OH+N_2+H^+}$$

Mechanism A−2

characterized by a rate-determining protonation step (mechanism A−$\mathrm{S_E2}$) when the reaction constants are strictly dependent on both the

---

[1] Previous part: G. Csávássy and D. Suciu, *Liebigs Ann. Chem.* (in press).

[2] A. Pullman and M. J. Metzger, *Bull. Soc. chim. France*, **1948**, 1021.

[3] G. Csávássy and Z. Györfi, *Liebigs Ann. Chem.* **1974**, 1195.

[4] H. Dahn and H. Gold, *Helv. Chim. Acta*, **46**, 983 (1963).

[5] H. Dahn and M. Ballenegger, *Helv. Chim. Acta*, **52**, 2417 (1969).

[6] J. F. Lane and R. L. Feller, *J. Amer. Chem. Soc.*, **73**, 4230 (1951).

Table 1

Ultraviolet maxima of some thiazole compounds (I – XIV)

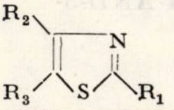

Compound	R_1	R_2	R_3	Dioxane 40%		0.1 N – $HClO_4$ solution[a]	
				λ max (nm)	log ε	λ max (nm)	log ε
I	C_6H_5	$CO-CHN_2$	H	300	4.44	280	4.25
II	$C_6H_4-CH_3(p)$	$CO-CHN_2$	H	302	4.42	287	4.18
III	$C_6H_4-OCH_3(p)$	$CO-CHN_2$	H	302	4.42	300	4.45
IV	$C_6H_4-Cl(p)$	$CO-CHN_2$	H	303	4.54	287	4.30
V	$C_6H_4-NO_2(p)$	$CO-CHN_2$	H	312	4.42	290	4.15
VI	C_6H_5	H	$CO-CHN_2$	335	4.56	318	4.36
VII	C_6H_5	CH_3	$CO-CHN_2$	335	4.56	319	4.38
VIII	$C_6H_4-CH_3(p)$	CH_3	$CO-CHN_2$	337	4.65	330	4.51
IX	$C_6H_4-OCH_3(p)$	CH_3	$CO-CHN_2$	352	4.44	343	4.35
X	$C_6H_4-Cl(p)$	CH_3	$CO-CHN_2$	337	4.50	325	4.34
XI	$C_6H_4-NO_2(p)$	CH_3	$CO-CHN_2$	352	4.47	340	4.30
XII	C_6H_5	CH_3	$CO-CH_2OH$	318	4.26		
XIII	$C_6H_4-CH_3(p)$	CH_3	$CO-CH_2OH$	330	4.37		
XIV	$C_6H_4-OCH_3(p)$	CH_3	$CO-CH_2OH$	343	4.38		

a 0.1 N – $HClO_4$ solution in dioxane 40%.

hydrogen ions concentration and the concentration of an acid HA present in the reaction mixture.[5,7] The data summarized in Table 2 show the dependence of the rate of hydrolysis of compounds I and VI on the hydrogen ions concentration. On the other hand, the reaction constants of I

Table 2

Rate constants of compounds I and VI at 45°

Compound	$HClO_4$[a]	$10^4 k_1 s^{-1}$
I	0.1 N	21.90 ± 0.25
	0.05 N	9.35 ± 0.12
	0.02 N	3.56 ± 0.02
	0.01 N	1.82 ± 0.17
VI	0.1 N	10.87 ± 0.08
	0.05 N	5.32 ± 0.16
	0.02 N	3.46 ± 0.09
	0.01 N	2.30 ± 0.11

a The HClO solutions were prepared in ethanol 40% ($\mu = 0.1$).

[7] H. Dahn, H. Gold, M. Ballenegger, K. Lenoi, G. Dietrich and R. Malherbe, *Helv. Chim. Acta*, **51**, 2065 (1968).

and VI (Table 3) are similar in both perchloric acid and dichloroacetate buffer of different concentrations when the hydrogen ions concentration is constant. These results indicate that the hydrolysis of I–XI takes place following the mechanism of the type A–2. [5]

Table 3

Hydrolysis of compounds I and VI in 0.1 M dichlor-acetic (HA) – sodium dichloroacetate (A^-) buffer,[a] $\mu = 0.1$, at 45°.

Compound	10^3 HA	10^3 A^-	10^2 $k_1 s^{-1}$
I	0[b]	0	1.82±0.17
	10.0	30.0	1.82±0.15
	17.5	52.5	1.78±0.10
	25.0	75.0	1.85±0.25
VI	0[b]	0	2.30±0.11
	10.0	30.0	2.26±0.31
	17.5	52.5	2.32±0.22
	25.0	75.0	2.31±0.13

a For the preparation of dichloroacetate buffer see the Experimental part.
b 0.01 N–$HClO_4$ solution prepared in ethanol 40% ($\mu = 0.1$), pH = 2.30 at 45°.

The data obtained for the activation parameters corresponding to the hydrolysis of I–V and VII–XI are included in Table 4. It is well known that $\Delta H^{\neq}$ or $\Delta E^{\neq}$ reflect the energy changes in the molecule caused by substitution and increase in a series of related compounds as the rate constants decrease.[8] However, such a correlation could not be observed for the derivatives presented in Table 4 as well as in the case of the hydrolysis of aromatic diazo ketones in acetic acid, which was previously reported by Lane and Feller.[6] Moreover, this correlation is lacking for the hydrolysis of substituted benzyl chlorides, [9] the substitution with pyridine of substituted benzyl bromides,[10] the hydrolysis and chlorine displacement with iodine of p-substituted aryl ß-chloroethyl-sulphides [11] and for the acid hydrolysis of substituted benzyl acetates,[12] in spite of the fact that the Hammett relation is applicable.[13] As an exception, in the case of the alkaline hydrolysis of substituted benzyl acetates [12] $\Delta E^{\neq}$ increases as K values decrease according to the effect of the substituent. In all reactions mentioned above the reaction center is located on a me-

---

[8] A. ALEMAGNA and T. BACCHETTI, P. BELTRAME, *Tetrahedron*, **24**, 3209 (1968).
[9] G. M. BENNETT and B. JONES, *J. Chem. Soc.*, **1935**, 1815.
[10] J. W. BAKER and W. S. NATHAN, *J. Chem. Soc.*, **1935**, 1840.
[11] G. BADDELEY and G. M. BENNETT, *J. Chem. Soc.*, **1933**, 261.
[12] E. TOMMILA and C. N. HINSHELWOOD, *J. Chem. Soc.*, **1938**, 1801.
[13] H. H. JAFFÉ, *Chem. Rev.*, **53**, 191 (1953).

Table 4

Hydrolysis of I–V and VII–XI in 0.1 N–HClO$_4$ solution (μ = 0.1) at different temperatures

Compound	$10^4 k_1 s^{-1}$				$\Delta F^{\neq}$ (25°) (kcal)	$\Delta H^{\neq}$ (kcal)	$\Delta S^{\neq}$ (25°) (e.u.)
	25°	35°	45°	50°			
I	2.24±0.07	6.31±0.09	21.90±0.25	34.70±0.67	22.38	20.29	− 7.00
II	2.40±0.003	6.76±0.14	24.05±0.33	37.20±2.10	22.36	20.34	− 6.77
III	2.51±0.005	7.60±0.10	25.71±0.81	39.80±0.45	22.34	20.14	− 7.37
IV	2.19±0.11	6.63±0.06	20.00±0.74	29.50±0.87	22.48	19.98	− 8.38
V	1.55±0.02	4.47±0.15	15.52±1.12	23.50±1.62	22.61	20.09	− 8.47
VII	1.20±0.05	3.89±0.03	11.00±0.08	18.20±0.54	22.77	19.47	−11.07
VIII	1.39±0.10	4.57±0.06	12.30±0.17	20.40±0.61	22.69	19.18	−11.76
IX	1.52±0.04	4.90±0.04	13.80±0.62	21.90±0.33	22.64	19.15	−11.71
X	1.02±0.008	3.24±0.10	9.14±0.44	15.50±0.31	22.79	19.52	−10.98
XI	0.708±0.09	2.40±0.02	6.31.±0.05	10.30±1.02	23.07	18.93	−13.91

thylene group, or according to the mechanism A–2 the rate-determining step of hydrolysis of diazo acetyl derivatives involves the elimination of the diazo group also bound to a methylene group. These data suggest that probably the interruption of conjugation by the methylene group is responsible for the absence of systematic changes in $\Delta H^{\neq}$ or $\Delta E^{\neq}$ values according to the modification of the rate constants. As a confirmation, the activation energies do not decrease as K values increase in the anionotropic rearrangement of substituted phenylpropenylcarbinols to the corresponding styrylmethylcarbinols.[14]

The data presented in Table 5 show that the Hammett relation [13] is applicable to the reaction of hydrolysis of II–V and VIII-XI. However, the theory [13] requires the decrease of $|\rho|$ values as the temperature increases, but this is only partially valid for our results. Similar deviations from the rule have been observed [13] for the acid hydrolysis of substituted benzyl acetates and phenoxyacetates[12] as well as for the reduction of substituted benzophenonehydrazones to the corresponding diphenylmethanes.[15]

As can be seen in the series of compounds I–V or VII–XI (Table 4) the reaction constants decrease as the electron withdrawing effect of the aryl-substituted group increases. In agreement with these, 2-aryl-4-diazo acetyl thiazoles have lower K_1 values in alcoholic 0.01 N−$HClO_4$ solution (pH = 2.3) than the corresponding 5-diazo acetyl thiazoles (Tables 2,3), because the charge density in the position 4 is lower than in position 5 of the thiazole ring.[2] Similar results were also obtained for the decomposition of I and VI in glacial acetic acid (Table 6). However, the situation changes at the hydrolysis in 0.05−0.1 N−$HClO_4$ solutions when 2-aryl-5-diazo acetyl thiazoles have lower K_1 values than the corresponding 4-diazo-acetyl thiazoles (Tables 2 and 4). According to these results, it seems that protonation of thiazole ring which probably[16] takes

---

[14] E. A. Braude and E. S. Stern, *J. Chem. Soc.*, **1947**, 1097.

[15] H. H. Szmant, H. F. Hernsberger, T. J. Butler and W. P. Barie, *J. Amer. Chem. Soc.*, **74**, 2724 (1952).

Table 5

Dependence of the rates of hydrolysis in 0.1 N $HClO_4$ solution ($\mu = 0.1$) of compounds II−V and VIII−XI on Hammett's parameters at different temperatures[a]

Compounds	$t°$	ρ	r
II−V	25	−0.186	0.92
	35	−0.209	0.98
	45	−0.208	0.99
	50	−0.219	0.99
VIII−XI	25	−0.244	0.84
	35	−0.300	0.90
	45	−0.319	0.99
	50	−0.308	0.96

[a] For the calculation of δ and r the rate constants K_1 of compounds II−V and VIII−XI included in table 3 were used.

Table 6

Hydrolysis of I and VI in acetic acid

Compound	$10^4 k_1 s^{-1}$ 40°	50°	60°	70°	$\Delta F^{\neq}$ (40°) (kcal)	$\Delta H^{\neq}$ (kcal)	$\Delta S^{\neq}$ (40°) (e.u.)
I	0.64±0.06	1.65±0.05	4.40±0.08	12.73±0.15	22.63	19.49	−10.0
VI	0.96±0.02	2.30±0.007	5.80±0.11	17.0±0.20	22.51	18.57	−12.6

---

[16] D. Suciu, *Rev. Roumaine Chim.*, **18**, 677 (1973).

place in 0.05 – 0.1 N – $HClO_4$ solutions accounts for a new distribution of the charge density in the thiazole ring in agreement with the K_1 values found at the hydrolysis of I – V and VI – XI (Tables 2 and 4).

From the data included in Table 7 it results that the transmission of polar effects according to the Hammett's law corresponds to $|\rho|$ values of about 0.29 for the hydrolysis of both 4- and 5-diazo-acetyl thiazoles in acetic acid. Similar $|\rho|$ values were determined at the hydrolysis in 0.1 N – $HClO_4$ solution of 5-diazo acetyl thiazoles (Table 5). However the $|\rho|$ values of about 0.20 obtained for 4-diazo-acetyly thiazoles (Table 5) show that protonation of the thiazole ring which very probably occurs in 0.1 N – $HClO_4$ solution significantly reduces the transmission of the polar effects in these compounds.

Table 7

Hydrolysis of compounds II – V and VIII – XI in acetic acid

Compound	$10^4 k_1 s^{-1}$ (60°)	ρ	r	Compound	$10^4 k_1 s^{-1}$ (50)°	ρ	r
II	4.90 ± 0.01	−0.286	0.988	VIII	2.60 ± 0.13	−2.299	0.995
III	5.12 ± 0.03			IX	2.93 ± 0.21		
IV	3.38 ± 0.09			X	1.95 ± 0.08		
V	2.58 ± 0.03			XI	1.40 ± 0.15		

EXPERIMENTAL

The compounds employed were partially synthesized as it has been previously described: I, VI – XI[2] and II – V.[3]

The compounds XII – XIV were synthesized by the acid hydrolysis of the corresponding diazo ketones VII – XI. A mixture of 0.0025 mole of the diazo ketone compound, 15 ml of ethanol and 20 ml of 0.1 N – H_2SO_4 solution was refluxed for 30 min., then charcoal was added and the reaction mixture was filtered. After neutralization with a solution of $NaCO_3H$ the precipitate was filtered and recrystallized from the suitable solvent. The analytical data of compounds XII – XIV are summarized in table 8.

Table 8

Analytical data of compounds XII – XIV

Compound	Molecular formula	m.p.° (solvent)	Yield %	Nitrogen %	
				Calcd.	*Found*
XII	$C_{12}H_{11}NO_2S$	112 – 114 (water)	72	6.00	6.12
XIII	$C_{13}H_{13}NO_2S$	131 – 133 (ethanol-water)	76	5.66	5.90
XIV	$C_{13}H_{13}NO_3S$	151 – 153 (ethanol-water)	74	5.31	5.72

The ultraviolet spectra were recorded with a VSU–2P (Carl Zeiss Jena) spectrophotometer. The kinetic measurements (Tables 2–7) were made in water-jacketed reaction vessels attached to temperature controlled bath. The $HClO_4$ solutions of different concentrations with a constant ionic strength of $\mu = 0.1$ (Tables 2,3) were prepared from a $HClO_4$ solution by dilution with $NaClO_4$ solution. The dichloracetate buffer (Table 3) was obtained from 12.895 g of dichloracetic acid and 3.00 g of NaOH diluted to 1000 ml with ethanol 40% ($\mu = 0.1$), pH = 2.35 at 45°. Glacial acetic acid (Tables 6,7) was purified as previously described.[17] Pseudo first-order rate constants (K_1) were obtained from the linear plots of $-\ln(D_t - D)$ *vs.* time, where D_t is the ultraviolet absorbance of the sample at the time t and D is the absorbance of the sample after the completion of hydrolysis. The mean of 3–6 determinations and the standard deviation are presented as K_1 values in Tables 2–7.

---

[17] * * * – "Organikum", VEB Deutscher Verlag der Wissenschaften, Berlin, 1967, p. 624.

Revue Roumaine de Chimie, **21**, *1*, 121–126 (1976)

POLAROGRAPHIC INVESTIGATION OF THE DECOMPOSITION OF XANTHATES IN ACID MEDIUM

LADISLAU KÉKEDY* and IULIA KOVÁCS**

* Department of Analytical Chemistry, "Babeş-Bolyai" University,
Str. Arany J., 11, Cluj-Napoca, Romania
** Medical and Pharmaceutical Institute, Str. Gh. Marinescu 38,
Tîrgu-Mureş, Romania

Received July 15, 1974

Decomposition rate constants in acid medium at pH = 4, and 25°, as well as the half-lives for a series of nine xanthates are reported, the investigations being made polarographically. Energies of activation of the decomposition have been obtained for potassium ethylxanthate (21.39±1.15 kcal/mol) and for potassium cyclohexylxanthate (24.32±3.77 kcal/mol) respectively. It has been found that in accordance with earlier observations the stability of fatty series xanthates in acid medium increases with the number of carbon atoms in the molecule.

The chemical stability of xanthates is of practical interest in the viscose rayon process, as well as in flotation procedure, where the xanthates are largely utilised as hydrophobizing agents. The acid-base catalysed decomposition studies are focussed mainly to the potassium ethylxanthate, being carried out spectrophotometrically.[1–3] Different acid and xanthate concentrations have been used and for explanation of the rate equations obtained, several mechanisms have been advanced. The main difficulty lies in the explanation of the decrease of the rate constant at high acidities.

Klein, Bosarge and Norman [2] postulated the existence of an ion – pair activated complex and protonated xanthic acid, along with xanthate ion and xanthic acid,to account for the decrease in the decomposition rate in highly acid solutions. According to Iwasaki and Cooke [3] the experimental data are consistent with the formation of a stable protonated xanthic acid, the decomposition being governed by the following equilibria:

$$\begin{array}{c} H^+ + X^- \overset{K_1}{\rightleftharpoons} HX + H^+ \overset{K_2}{\rightleftharpoons} H_2X^+ \\ \downarrow k_3 \\ ROH + CS_2 \end{array} \qquad (1)$$

---

[1] I. Iwasaki and S. R. B. Cooke, *J. Amer. Chem. Soc.*, **80**, 285 (1958).

[2] E. Klein, J. K. Bosarge and I. Norman, *J. Phys. Chem.*, **64**, 1666 (1960).

[3] I. Iwasaki and S. R. B. Cooke, *J. Phys. Chem.*, **68**, 2031 (1964).

Recent study on the polarography of a large number of xanthates[4] reveals the possibility of polarographic determination the concentration of xanthate, xanthic acid and the protonated xanthic acid, enabling the investigation of the above equilibria.

Decomposition rate constants for a series of xanthates are reported in this paper. Experimental conditions as well as the xanthates investigated are identical with those reported in our previous work.[4]

Denoting by C the total xanthate concentration, the rate of decomposition can be expressed [3] as :

$$\frac{-\,\mathrm{d}\ln C}{\mathrm{d}t} = \frac{k_3}{\dfrac{K_1}{/H^+/} + 1 + \dfrac{/H^+/}{K_2}} = k \tag{2}$$

If $/\mathrm{H}^+/ \ll K_1$, condition fulfilled in the 2.5 – 5 pH range, equation (2) can be approximated by

$$k = \frac{k_3}{K_1}/\mathrm{H}^+/ \tag{3}$$

or

$$\lg\ k = \lg \frac{k_3}{K_1}\ \mathrm{pH}$$

yielding a linear pH dependence of $\lg k$.

If $/\mathrm{H}^+/ \gg K_1$, condition fulfilled at $\mathrm{pH} < 1.7$; (2) simplifies to :

$$k = \frac{k_3}{1 + \dfrac{/\mathrm{H}^+/}{K_2}} \tag{4}$$

or

$$\frac{1}{k} = \frac{1}{k_3} + \frac{/\mathrm{H}^+/}{K_2 k_3}$$

k_3/K_1 can be determined from (3) and relation (4) allows to obtain k_3, permitting the calculation of K_1 and K_2.

The k values for the decomposition of ethylxanthate and cylcohexylxanthate, respectively, (Table 1) have been calculated from the data represented in Figs. 1 and 2. The data of Table 1 represent a linear relationship according to equation (3) ; the equation of regression line being

— for ethylxanthate :

$$\lg\ k = 2.54 \pm 0.12 - (1.09 \pm 0.03)\ \mathrm{pH} \tag{5}$$

---

[4] J. Kovács and L. Kékedy, Z. Anal. Chem. **274**, 24 (1975).

with

$$r = -0.9992 \text{ and } S_0 = \pm 0.035$$

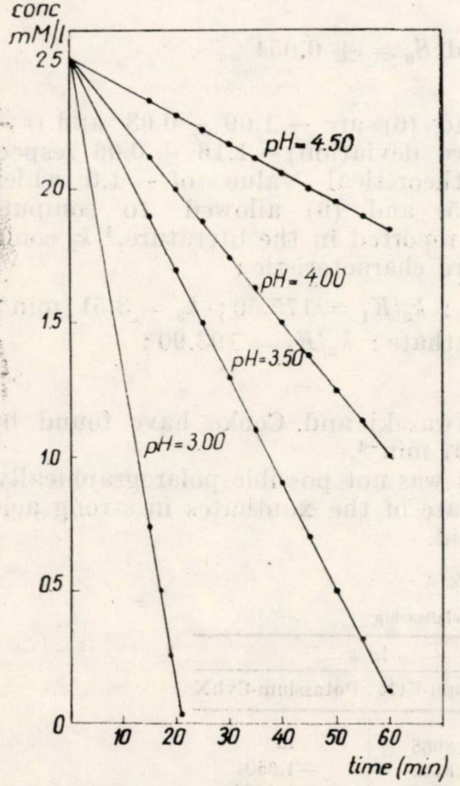

Fig. 1. — Decomposition of 2.5 mM potassium ethylxanthate in the pH range 3.00—4.50 at 25°.

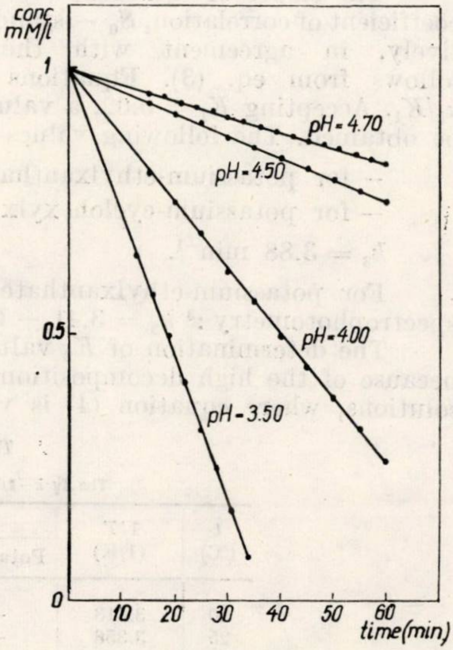

Fig. 2. — Decomposition of 1 mM potassium cyclohexylxanthate in the 3.50—4.70 pH range at 25°.

Table 1

The lg k values at 25° and different pH*

pH	lg k	
	Potassium-EtX	Potassium-CyhX
3.00	−0.6990	—
3.50	−1.2165	−1.1291
4.00	−1.8162	−1.6501
4.50	−2.2997	−2.3196
4.70	—	−2.4814

* Abbreviations: X = xanthate, Cyh = cyclohexyl and the remaining groups (Me Et, etc.) as in *Chem. Abstr.*

— and for the cyclohexylxanthate :

$$\lg k = 2.95 \pm 0.24 - (1.16 \pm 0.06)\ \mathrm{pH} \tag{6}$$

with

$$r = -\ 0.9975 \text{ and } S_0 = \pm\ 0.054$$

respectively.

The slopes of equations (5) and (6) are $-\ 1.09 \pm 0.03$ and (r — coefficient of correlation, S_0 — standard deviation) $-\ 1.16 \pm 0.06$ respectively, in agreement with the theoretical value of $-\ 1.0$ which follows from eq. (3). Equations (5) and (6) allowed to compute k_3/K_1. Accepting $K_1 = 0.02$, a value reported in the literature,[1] k_3 could be obtained. The following values are characteristic :

— for potassium-ethylxanthate : $k_3/K_1 = 175.50$; $k_3 = 3.51\ \mathrm{min}^{-1}$

— for potassium-cyclohexylxanthate : $k_3/K_1 = 193.90$;

$k_3 = 3.88\ \mathrm{min}^{-1}$.

For potassium-ethylxanthate Iwasaki and Cooke have found by spectrophotometry :[3] $k_3 = 3.41 \pm 0.01\ \mathrm{min}^{-1}$.

The determination of K_2 values was not possible polarographically, because of the high decomposition rate of the xanthates in strong acid solutions, where equation (4) is valid.

Table 2

The lg $k - 1/T$ relationship

t (°C)	$1/T$ (1/K)	lg k	
		Potassium-EtX	Potassium-CyhX
20	3.413	−1.8965	—
25	3.356	−1.8162	−1.6501
30	3.300	−1.6517	−1.4684
35	3.247	−1.5268	−1.4159
40	3.195	—	−1.1940

The energy of activation of the decomposition process was also evaluated from the $\lg k - 1/T$ relationship (Table 2). Statistical treatment of the data in Table 2 showed a linear relationship, the corresponding equations of regression being :

— for potassium-ethylxanthate

$$\lg k = 6.06 \pm 0.42 - (2337.7 \pm 126)\ 1/T \tag{7}$$

$$r = -\ 0.9995\ ;\quad S_0 = 0.02$$

— for potassium-cyclohexylxanthate

$$\lg\ k = 7.27 \pm 0.42 - (2657.3 \pm 412)\ 1/T \tag{8}$$

$$r = -\ 0.978\ ;\quad S_0 = \pm\ 0.05$$

From these equations the following energies of activation of the decomposition could be obtained :

– for potassium-ethylxanthate

$E^* = 21.39 \pm 1.15$ kcal/mol

– for potassium-cyclohexylxanthate

$E^* = 24.32 \pm 3.77$ kcal/mol

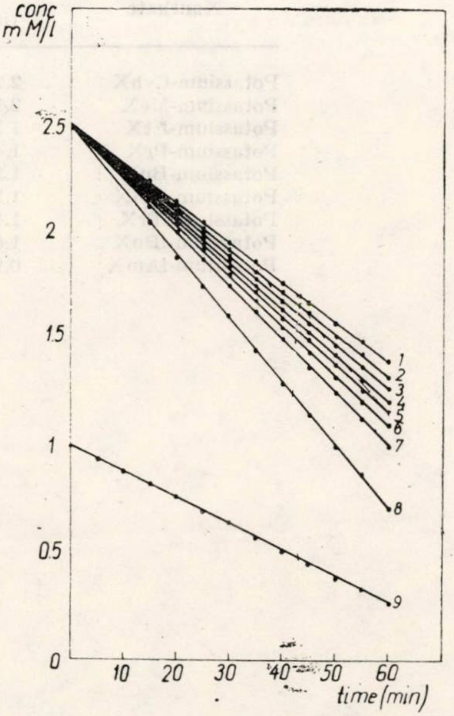

Fig. 3. – Decomposition curves of xanthates at pH = 4.00 and 25° as a function of the molecular weight.
1, Potassium i-AmX; *2*, Potassium-iBuX; *3*, Potassium-iPrX; *4*, Potassium-AmX; *5*, Potassium-BuX; *6*, Potassium-PrX; *7*, Potassium-EtX; *8*, Potassium-MeX; *9*, Potassium-CyhX *1 – 8*,: 2.5 mM; *9* 1.0 mM.

The rate of decomposition has been investigated also as a function of molecular weight of the xanthates, the measurements being made at pH = 4, and 25°. The decomposition curves obtained are represented in Fig. 3. The corresponding decomposition constants as well as the half-lives are listed in Table 3.

Inspection of Table 3 reveals that the stability of fatty series xanthates in acid medium increases with the increase of the number of carbon atoms in the molecule. This correlation has been reported by others too.[5,6] The $\tau_{1/2}$ value of 45 minutes (25°) found for potassium-ethylxanthate agrees well with that reported by Du Rietz[7] (55 minutes at 20°). The

---

[5] J. A. Kakovskii, *Tr. in-ta gornovo dela*, **3**, 25 (1956).

[6] P. N. Kovalenko, Z. J. Ivanova, V. K. Cebotarev and V. D. Dionisev, *Zhur. analit. Khim.*, **24**, 1810 (1969).

[7] C. Du Rietz, *Svensk. Kem. Tidskr.*, **69**, 310 (1957); *Chem. Abstr.* **52**, 7033 (1958).

increased stability of the higher members of the fatty acid xanthates series assures a higher actual xanthate concentration present in pulp solution, enhancing their collector properties for sulphide minerals.

Table 3

Decomposition constants and half-half-lives for different xanthates at pH = 4 and 25°C

Xanthate	k (minute^{-1})	$\tau_{1/2}$ (minute)
Potassium-CyhX	2.24×10^{-2}	31
Potassium-MeX	2.12×10^{-2}	33
Potassium-EtX	1.53×10^{-2}	45
Potassium-PrX	1.41×10^{-2}	49
Potassium-BuX	1.30×10^{-2}	53
Potassium-AmX	1.23×10^{-2}	56
Potassium-iPrX	1.14×10^{-2}	61
Potassium-iBuX	1.07×10^{-2}	65
Potassium-iAmX	0.97×10^{-2}	71

Revue Roumaine de Chimie, 21, 1, 127–138 (1976)

CONTRIBUTIONS TO THE STUDY OF CONDENSATION REACTIONS BETWEEN CRESOLS AND ISATIN AND ITS DERIVATIVES. I

A NEW MOLECULAR TRANSPOSITION

H. WEXLER and V. BĂRBOIU
The "P. Poni" Institute of Macromolecular Chemistry,
Aleea Gr. Ghica Vodă, 41 A, Jassy, Romania

Received July 3, 1974

Condensation reactions between isatin and its derivatives and *m*- and *o*-cresols were carried out. It was observed that *m*-cresol leads to three 3,3-disubstituted oxindoles as a function of the reaction temperature: I — with the phenol rings differently bonded, one in the *para*-hydroxy position and the other in the *para*-methyl position, II — with the phenol rings similarly bonded, and namely in the *para*-methyl position, and III — with the phenol rings etherified. Compounds I are obtained between 25 and 65°, compounds II between 100 and 150° and compounds III between 200 and 240°, the sulphuric acid being used as a catalyst. It was found that compounds I, heated at temperatures higher than 100° are converted into compounds II, undergoing a transposition. On the other hand, compounds II become etherified, being converted into compounds III, at temperatures between 200 and 240° and in the presence of H_2SO_4. The structures of the three kinds of compounds were confirmed by chemical methods and mainly by h.r. proton NMR spectroscopy.

It is known that the reaction of phenol with isatin and its derivatives leads to *para*-substituted phenols. The reaction occurs in a wide temperature range (60 — 150°), the reaction time decreasing with the temperature.

According to a German patent, [1] the condensation of isatin with *m*-cresol, carried out in an acetic acid solution and in the presence of sulphuric acid at 65°, leads to the appearance of 3,3 — di(2′-methyl-4′-hydroxyphenyl)-oxyndole, i.e. a compound with both phenol rings substituted in the *para*-hydroxy position.

On the other hand, it was found that the condensation of *m*-cresol with phthalic anhydride [2] and acetone [3] leads to compounds with the phenol rings substituted in the *para*-methyl position.

Taking into account that both substituents are of the first order, it seems that the substitution of *m*-cresol may occur with the same probabiity in both *para*-hydroxy and *para*-methyl positions, unlike the case of

---

[1] I. G. FARBENINDUSTRIE, D.R.P. 488.760, 26/3, 1925; *Chem. Zentr.*, **I**, 1863 (1930).

[2] W. LAMBRECHT, *Ber. dtsch. chem. Ges.*, **42**, 3592 (1909).

[3] Soc. de Produits Chimiques Industriels. F.P. 1.057.249, 19/5, 1952; *Chem. Zentr.*, **1956**, 13261.

o- and *p*-cresols, where the substitution occurs only in the *para*-[4] and respectively *ortho*-hydroxy[5] positions. To contribute to the elucidation of such substitutions, we carried out a detailed study of the condensation reactions of cresols with isatin and its derivatives.

A. RESULTS AND DISCUSSION

THE CONDENSATION OF ISATIN AND ITS DERIVATIVES WITH *m*-CRESOL

Performing the condensation reaction of isatin with *m*-cresol similarly to the ref. 1, we obtained a compound with the characteristics indicated in that reference. However its NMR spectrum shows that it is not the 3,3-di (2′-methyl-4′-hydroxyphenyl)-oxyndole but the 3,3-(2′, 4″-dihydroxy-2″, 4′-dimethyldiphenyl)-oxindole (see fig. 1). Because the structure argumentation is given in section B, we only mention here that the methyl groups of this compound (denoted by I) are differently bonded at the fused ring and therefore the substitution of *m*-cresol occurs with the same probability in the *para*-methyl and *para*-hydroxy positions. In addition we observed that this compound is also formed at room temperature. Also, the solvent is not necessary if the reaction temperature is of 60–65°.

Carrying out the condensation reaction of isatin with *m*-cresol at a temperature between 140 and 150°, the appearance of a compound distinct from compound I was observed, being of low solubility in an 1% alkaline solution and showing a different melting point. Although both compounds were crystallized from acetic acid solutions, while compound I melts at 256–258°, the compound obtained at 140–150° (denoted by II) shows the following melting characteristic : it becomes liquid at 130–140°, resolidifies at 180° and melts at 238–240°. The thermogravimetric curve, elemental analysis and NMR and IR spectra indicate that compound II is crystallized together with one molecule of acetic acid and thus its melting characteristics might be explained by the removal of acetic acid in the temperature range from 130 to 180°.

The low solubility in an alkaline solution might be explained by a higher shielding of the hydroxyl groups, suggesting that the obtained compound is 3,3-(2′, 2″-dihydroxy-4′, 4″-dimethyl-diphenyl)-oxindole (see fig. 2), therefore a position isomer of compound I.

It was additionally observed that compound I, heated at about 140°, in *m*-cresol and in the presence of H_2SO_4, changes into compound II, therefore undergoes a molecular transposition. Specific of this transposition is the migration of a large substitute from the *para*-hydroxy position of *m*-cresol to the *para*-methyl position. The transposition reaction ends after a few minutes if the temperature is between 100 and 140°. It was also observed that compound II appears at room temperature, but the reaction time is of 8 – 10 hours. Thus it is to suppose that the change of compound I into compound II takes place even at room temperature, but evidently much slower.

---

[4] F. Hoffmann La Roche & Co. Akt. Ges. Basel Schweiz, D.R.P. 406.210, 26/6, 1923; *Chem. Zentr.*, **I**, 1246 (1925).

[5] H. Wexler and A. Caraculacu, *Anal. St. Univ. "Al. I. Cuza" Iași, Sect. I*, **13**, 71, (1967).

A transposition reported in the literature which is somehow similar to this is Iacobsen's transposition.[6] There, some nonvicinal polyalkyled or polyhalogenated derivatives of benzene change into vicinal compounds. Iacobsen suggested that sulphonic derivatives appear as intermediate compounds. It seems that such intermediaries are unlikely to appear in our reaction because the concentration of sulphuric acid does not show a significant influence.

Relative to the transposition mechanism, we think it would be similar to that of the condensation reaction of phenols with ketones : in the presence of the proton arising from the catalyst, the bond $C_3 - C_{1''}$ (seefig. 1) breaks, a carbonium cation appearing and one molecule of *m*-cresol being regenerated (see the chart).

Subsequently, the carbonium cation is connected to a molecule of *m*-cresol at the *para*-methyl position, and compound II appears.

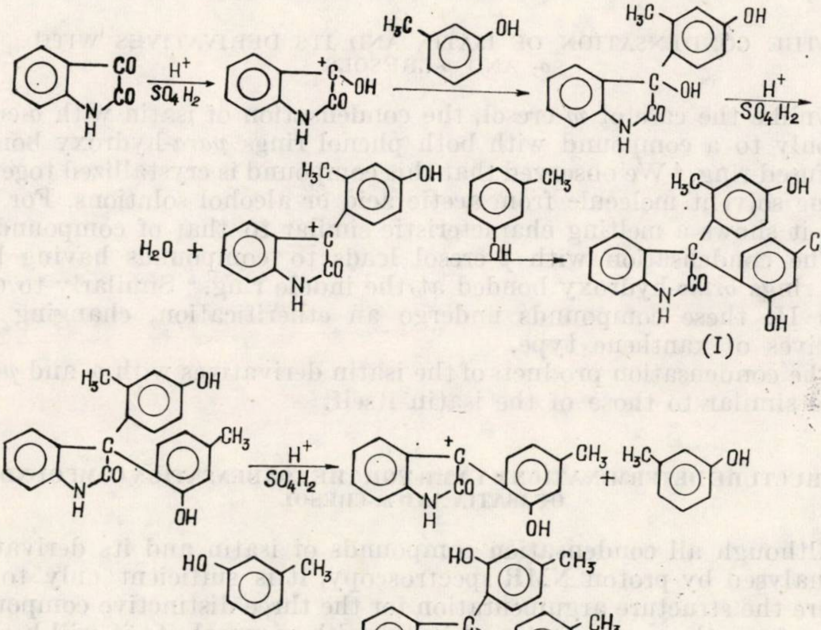

This molecular affinity of the carbonium cation would also explain the *para*-methyl substitution of one of the two phenol rings in compound I. It is probable that the *para*-hydroxy substituted phenol ring is firstly connected to C_3, and the *para*-methyl substituted phenol ring in a subsequent stage of reaction.

---

[6] O. Iacobsen, *Ber. dtsch. chem. Ges.*, **19**, 1209 (1886).

Revue Roumaine de Chimie, **21**, *1*, 127 – 138 (1976)

The possible two stage formation reaction of compound I was suggested by the reaction of phenol with benzylic acid.[7] Anyway, our attempt to obtain the compound with both phenol rings *para*-hydroxy bonded at the fused ring by decreasing the reaction temperature did not succeed; it was observed that compound I also appears at 20—25° and the reaction does not take place at lower temperatures.

The structure of compound II was chemically confirmed as follows: Heated at 200—240° in *m*-cresol and in the presence of sulphuric acid, compound II undergoes an internal etherification, changing into compound III (see fig. 3), which is a xanthene derivative. It is to mention that compound III, the name of which is 3,3-(4′, 4″-dimethyl-2′, 2″-oxydiphenylene)-oxindole, is similar to the compound arising from the condensation of isatin with *p*-cresol.

Relative to the methylated isatins, their condensation reactions with *m*-cresol also lead to compounds of the types I, II and III, the type being a function of the temperature and time of reaction.

THE CONDENSATION OF ISATIN AND ITS DERIVATIVES WITH *o*- AND *p*-CRESOLS

Unlike the case of *m*-cresol, the condensation of isatin with *o*-cresol leads only to a compound with both phenol rings *para*-hydroxy bonded at the fused ring.[4] We observed that this compound is crystallized together with one solvent molecule from acetic acid or alcohol solutions. For this reason, it shows a melting characteristic similar to that of compound II.

The condensation with *p*-cresol leads to compounds having both phenol rings *ortho*-hydroxy bonded at the indole ring.[5] Similarly to compounds II, these compounds undergo an etherification, changing into derivatives of xanthene type.

The condensation products of the isatin derivatives with *o*- and *p*-cresols are similar to those of the isatin itself.

B. STRUCTURE DETERMINATION BY NMR FOR THE CONDENSATION COMPOUNDS OF ISATIN AND *m*-CRESOL

Although all condensation compounds of isatin and its derivatives were analysed by proton NMR spectroscopy, it is sufficient only to expose here the structure argumentation for the three distinctive compounds resulting from the condensation of isatin with *m*-cresol. As it will be seen further on, a proeminent part in this argumentation has been played by the effects of methyl irradiation on the aromatic regions of spectra. The interpretation of these effects will be similar to that used in our study on the benzofuran acetylation.[8]

STRUCTURE OF COMPOUND I

According to the ref. [1], this compound is expected to be 3,3-di(2′-methyl-4′-hydroxyphenyl)-oxindole. But its NMR spectrum (fig. 1) shows that compound I, which has the two phenol rings differently bonded at the indole ring, appears. It is true that the spectrum in fig. 1 might also arise from an 1 : 1 mixture between the expected compound and the compound II, but this supposition is invalidated by both, the melting point, which is relatively sharp, and the paper chromatogram, which shows a unitary compound.

---

[7] B. ARVENTIEV, *Anal. St. Univ. "Al. I. Cuza", Iași*, **24**, 71 (1938).

[8] V. BĂRBOIU, H. WEXLER and B. ARVENTIEV, *Org. Mag. Res.*, **6**, 327 (1974).

There are two major spectral evidences supporting the structure I :

(1) Being evident that the two methyl groups of 3,3-di(2′-methyl-4′-hydroxyphenyl)-oxindole are chemically and magnetically equivalent, it is not explainable why the spectrum shows two distinct methyl signals, one at 1.84 ppm and another one at 2.22 ppm. Using the Heigh and Mallion's tables [9] to calculate the screening effects of the π electrons in the fused ring of compound I we really found that the protons of $Me_{2''}$ group are roughly 0.7 ppm more shielded than the protons of $Me_{4'}$, group and therefore the signal at 1.84 ppm belongs to the first kind of protons.

(2) The fact that the two hydroxy protons show extremely different chemical shifts, 9.32 and 8.20 ppm, is also favourable for the structure I. The difference of more than 1 ppm between their chemical shifts might be explained by the intramolecular hydrogen bonding between the hydrogen atom of $(OH)_{2'}$ group and the oxygen atom of carbonyl group in the position 2.

The signal of the proton NH was identified as being that at 10.05 ppm because it is sharpened when the nucleus ^{14}N is irradiated.

Another support for the structure I might result from the methyl decoupling effects in the aromatic region of the spectrum. Unfortunately, the aromatic protons of phenol rings are too little magnetically different to allow a clear interpretation of these double resonance effects. The signals affected by methyl irradiation are marked on fig. 1, and they show that the six aromatic protons of phenol rings absorb in the range from 6.50 to 6.65 ppm. In addition, they do not give rise to two identical ABC spectra, like in the case of 3,3-di (2′-methyl-4′-hydroxyphenyl)-oxindole, but rather to a superposition of two distinct ABC spectra.

STRUCTURE OF COMPOUND II

The spectrum in fig. 2 A belongs to the compound resulting by the condensation of isatin with *m*-cresol at 140 — 150°. One observes that there is only one methyl signal and thus the two methyl groups are magnetically equivalent. The position at 2.20 ppm for this signal suggests, by comparing with the position of $Me_{4'}$, of the compound I, that both phenol rings are *para*-methyl bonded at the fused ring.

There are two signals sensible at deuteration, one at 8.30 ppm, corresponding to 1 proton, and another one at 9.67 ppm, corresponding to 2 protons. The decoupling from ^{14}N affects a relative sharpening for the second signal and thus it arises from the proton NH and from one of the two OH protons. It is probable that the OH protons can be in two states,

---

[9] C. W. Haigh and R. B. Mallion, *Org. Mag. Res.*, *4*, 203 (1972).

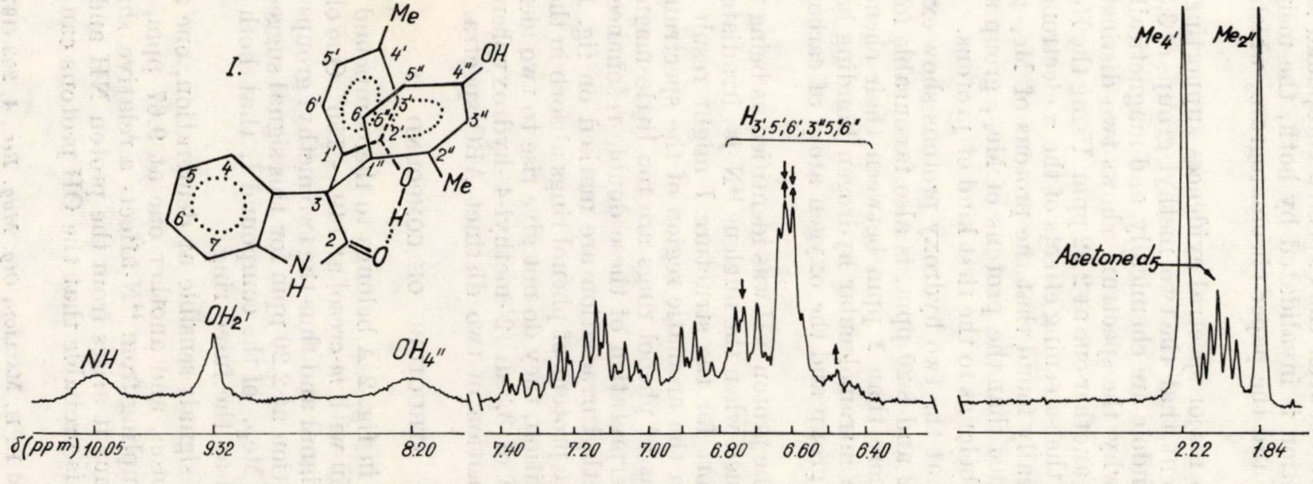

Fig. 1. — The proton NMR spectrum of the compound I. The signals affected by the irradiation on the signals Me$_{2''}$ and Me$_{4'}$ are marked by "↓" and "↑", respectively.

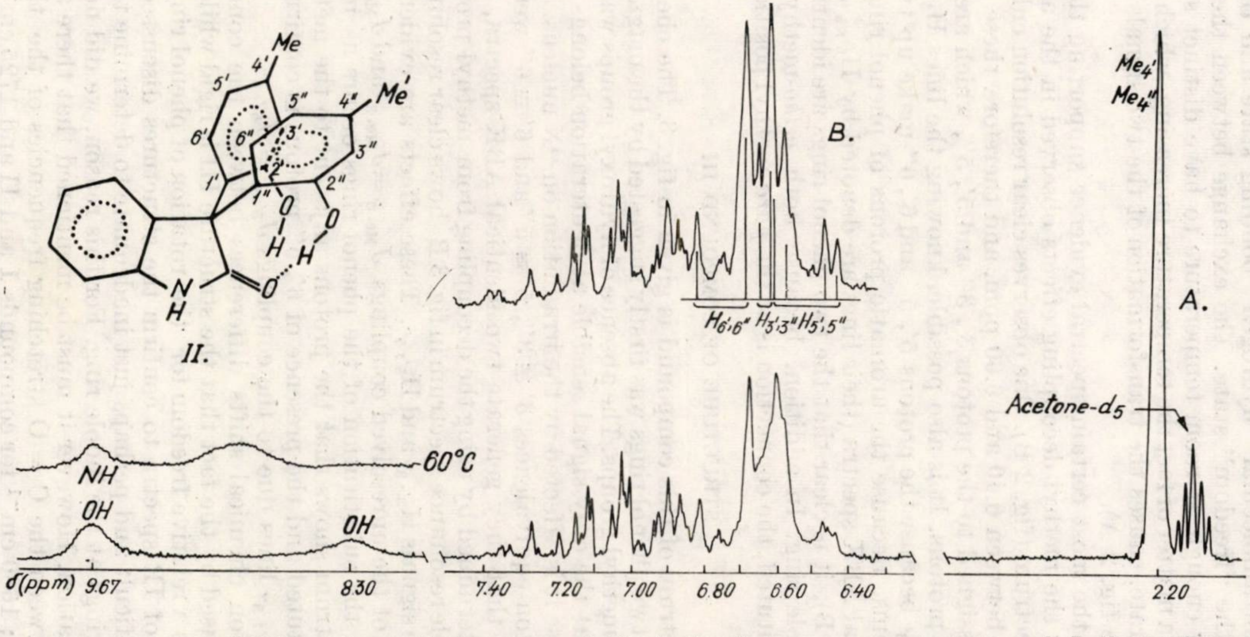

Fig. 2. — The proton NMR spectrum of the compound II: *A*, the single resonance spectrum, and *B*, the spectrum of aromatic protons decoupled from the methyl protons. The deuterable signals recorded at 60° are also shown.

so that when one is "hydrogen" bonded at the carbonyl group, the other is relatively "free", and reversely. One half of the signal at 9.67 ppm corresponds to the intramolecular "hydrogen" bonding state and the signal at 8.30 ppm to the "freedom" state. The exchange between these states is probably slow enough at room temperature to have distinct signals from each state. As a matter of fact the temperature increasing, which accelerates the exchange rate, causes the transformation of the two signals into a very broad one (see fig. 2 A).

Finally, the most certain spectral evidence supporting the structure II is given by the methyl decoupling effects observed in the aromatic region of the spectrum (fig. 2 B). One observes clear resolution enhancements for the signals between 6.40 and 6.60 ppm, and therefore these signals can be certainly assigned to the protons 3′, 3″ and 5′, 5″, which are most close to the methyl protons. It is also possible, knowing the lines $H_{5',\,5''}$, to find the lines $H_{6',\,6''}$ because the protons 5′, 5″ and 6′, 6″ make up two identical AB spin systems. Because the aromatic protons of phenol rings give rise to two identical ABK spectra (their lines are denoted by $H_{5',\,5''}$, $H_{6',\,6''}$ and $H_{3',3''}$ in fig. 2 B), it is clear that the two phenol rings are identically bonded at the indole ring. In addition, because both *ortho*-methyl positions are not substituted, the connection is at the *para*-methyl position.

STRUCTURE OF COMPOUND III

The spectrum of this compound is given in fig. 3. The chemical equivalence of the two phenol rings was firstly suggested by the magnetical equivalence of the methyl groups. The absence of hydroxyl groups was confirmed by the fact that the only signal sensible at deuteration belongs to the proton NH because it is affected by the irradiation on ^{14}N nucleus.

The proton equivalences $3' \equiv 3''$, $5' \equiv 5''$ and $6' \equiv 6''$ were confirmed by the fact that they generate two identical ABK spectra, the lines of which were determined by using the decoupling from methyl protons as follows. The double resonance spectrum in fig. 3 B shows clear resolution enhancements for the signals $H_{3',\,3''}$ and $H_{5',\,5''}$. These effects are evidently caused by the removal of the unresolved couplings $J_{Me.\,3'} = J_{Me.\,3''}$ and $J_{Me.\,5'} = J_{Me.\,5''}$. It results that the substitution of the phenol rings occurs as in fig. 3 because the spectrum shows that the protons adjacent to the methyl groups are not substituted and the presence of 6′, 6″ protons is confirmed by the splitting of $H_{5',\,5''}$ lines due to the couplings $J_{5'.\,6'} = J_{5''.\,6''}$.

The proton chemical shifts differences between the compounds II and III are caused by the fact that the structure III is rigid while the structure II permits a relative freedom for the rotation of phenol rings.

The use of IR spectra to confirm the structures discussed before is much more difficult and perhaps just inadequate to determine the bonding of the phenol rings at the indole ring. For this reason, we did not insist on their interpretation. However it must be mentioned that there are evident differences between the C = O stretching frequencies of the three types of compounds; 1680 cm^{-1} for compounds I and II and 1725 cm^{-1} for compound III. These differences are caused by the presence of intramolecular hydrogen bondings in the first kind of compounds only.

The appearance of a strong absorption band at 1260 cm^{-1} in the spectra of III compounds confirms that they are of the xanthene type.

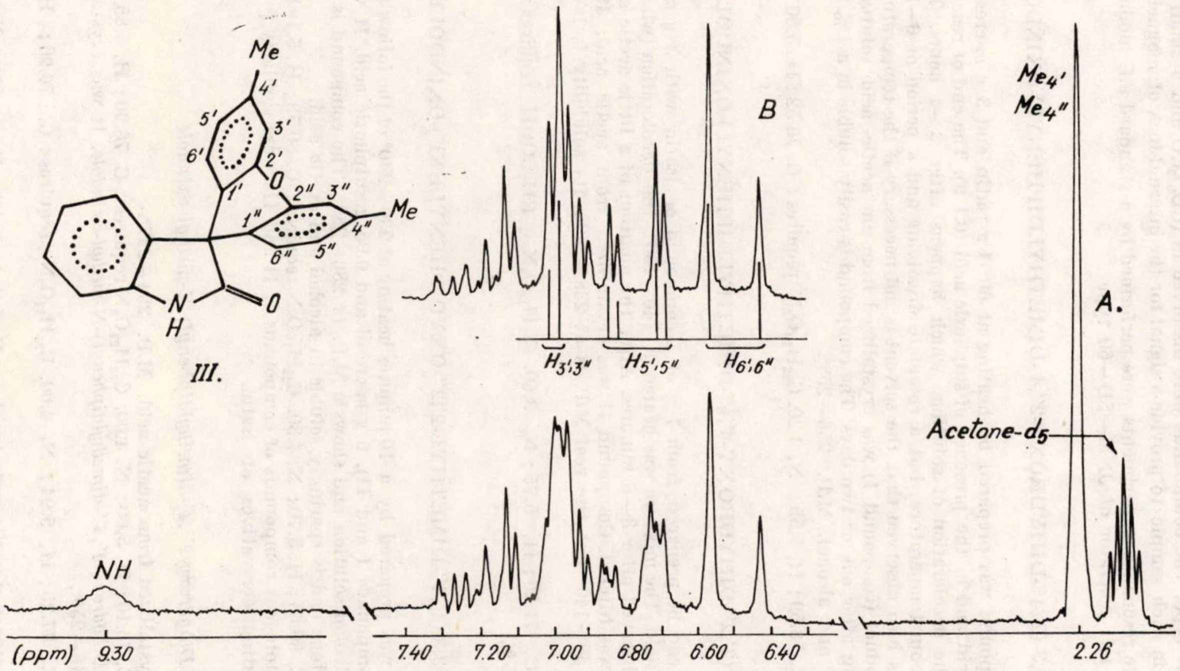

Fig. 3. — The proton NMR spectrum of the compound III : *A*, the single resonance spectrum, and *B*, the spectrum of aromatic protons decoupled from the methyl protons.

EXPERIMENTAL

All NMR spectra were obtained at room temperature on a 60 MHz spectrometer of JNM—C—60 HL type. The compounds were dissolved in $(CD_3)_2CO$ and a small quantity of TMS was added in each sample to provide a signal for the internal lock of magnetic field.

The double resonance experiments were performed by a standard a.f. modulation technique using an a.f. generator of JNM—SD—60 type.

I. 3,3-(2′,4″-DIHYDROXY-2″,4′-DIMETHYLDIPHENYL)-OXINDOLE

This compound was prepared by heating at 60° 1 g isatin and 3 g *m*-cresol dissolved in 5 ml acetic acid and in the presence of sulphuric acid (0.1 g). The end of reaction can be recognized by the decoloration of solution, which happens after 3—4 hours. The reaction also occurs at room temperature, but a complete dissolving and a period of 6—8 hours are necessary. It was also observed that the solvent is not necessary if the temperature is of 60°. The reaction product (compound I) was crystallized from an acetic acid solution, the first crystals appearing after one or two days. The compound is easily soluble in a 1% NaOH solution, acetic acid and alcohol. M.P. 256—258°.

(*Found* : C, 76.59 ; H, 5.55 ; N, 4.20. $C_{22}H_{19}O_3N$ requires : C, 76.52 ; H, 5.50 ; N, 4.05%)

II. 3,3-(2′,2″-DIHYDROXY-4′,4″-DIMETHYLDIPHENYL)-OXINDOLE

This compound can be prepared from 1 g of I compound or isatin with 3 g *m*-cresol and 0.05 g sulphuric acid. The mixture was heated at 140—150°, the decoloration (when the isatin is used) being observed after 3—5 minutes. After the addition of a little acetic acid, the resulting mixture was filtered. Compound II was crystallized from acetic acid. It shows an nitial M.P. at 130—140° but the real M.P. is at 238—240°. Its solubility is low in an 1% alkaline solution.

(*Found*: C, 71.20 ; H, 5.75 ; N, 3.60. $C_{22}H_{19}O_3N + CH_3COOH$ requires : C, 71.11 ; H, 5.67 ; N, 3.45%)

III. 3,3-(4′,4″-DIMETHYL-2′,2″-OXYDIPHENYLENE)-OXINDOLE

This compound was prepared by a 10 minutes heating at 230—240° of the following mixture : 1 g isatin (or compounds I and II), 6 g *m*-cresol and 0.05 g sulphuric acid. It was crystallized from an alcohol solution and shows a M.P. of 286—289°. The compound is not soluble in alkaline solutions and is sparingly soluble in alcohol and acetic acid.

(*Found* : C, 80.65 ; H, 5.70 ; N, 4.30. $C_{22}H_{17}O_2N$ requires : C, 80.73 ; H, 5.19 ; N, 4.28%)

Some homologous compounds of compounds I, II and III were similarly prepared, but using corresponding derivatives of isatin.

3,3-(2′-4″-Dihydroxy-2″,4′-dimethyldiphenyl)-N-methyl-oxindole

It was crystallized from acetic acid. M.P. 294—297°.

(*Found* : C, 76.10 ; H, 5.60 ; N. 4.00. $C_{23}H_{21}O_3N$ requires : C, 76.90 ; H, 5.85 ; N, 3.90%)

3,3-(2′,2″-Dihydroxy-4′,4″-dimethyldiphenyl)-N-methyl-oxindole. It was crystallized from alcohol. M.P. 248—250°.

(*Found* : C, 77.25 ; H, 5.94 ; N, 4.00. $C_{23}H_{21}O_3N$ requires : C, 76.90 ; H, 5.85 ; N, 3.90%)

3,3-(4′,4″-Dimethyl-2′,2″-oxydiphenylene)-N-methyloxindole. It was crystallized from alcohol. M.P. 200°.

(*Found* : C, 80.87 ; H, 5.27 ; N, 4.00. $C_{23}H_{19}O_2N$ requires : C, 80.90 ; H, 5.57 ; N, 4.10%)

3,3-(2′,4″-Dihydroxy-2″,4′-dimethyldiphenyl)-7-methyloxindole. It was crystallized from acetic acid. M.P. 262°.

(*Found* : C, 76.84 ; H, 5.96 ; N, 3.67. $C_{23}H_{21}O_3N$ requires : C, 76.90 ; H, 5.85 ; N, 3.90%)

3,3-(2′,2″-Dihydroxy-4′,4″-dimethyldiphenyl)-7-methyloxindole. It was crystallized from alcohol. M.P. 290°.

(*Found* : C, 76.40 ; H, 6.50 ; N, 3.85. $C_{23}H_{21}O_3N$ requires : C, 76.90 ; H, 5.85 ; N, 3.90%)

3,3-(4′,4″-Dimethyl-2′,2″-oxydiphenylene)-7-methyloxindole. It was crystallized from alcohol. M.P. 266–269°.

(*Found* : C, 80.97 ; H, 5.25 ; N, 4.30. $C_{23}H_{19}O_2N$ requires : C, 80.90 ; H, 5.57 ; N, 4.10%)

3,3-(2′,4″-Dihydroxy-2″,4′-dimethyldiphenyl)-5,7-dimethyloxindole. It was crystallized from acetic acid. M.P. 273–275°.

(*Found* : C, 77.10 ; H, 5.83 ; N, 3.67. $C_{24}H_{23}O_3N$ requires : C, 77.21 ; H, 6.16 ; N, 3.75%)

3,3-(2′,2″-Dihydroxy-4′,4″-dimethyldiphenyl)-5,7-dimethyloxindole. This compound can be obtained by the transposition of the last compound at 100–110°. It was crystallized from acetic acid. M.P. 228–229°.

(*Found* : C, 77.30 ; H, 6.50 ; N, 3.80. $C_{24}H_{23}O_3N$ requires : C, 77.21 ; H, 6.16 ; N, 3.75%)

3,3-(4′,4″-Dimethyl-2′,2″-oxydiphenylene)-5,7-dimethyloxindole. It was crystallized from alcohol M.P. 330°.

(*Found* : C, 81.19 ; H, 6.21 ; N, 3.80. $C_{24}H_{21}O_2N$ requires : C, 81.12 ; H, 5.90 ; N, 3.90%)

The condensation reaction of *o*-cresol with isatin and its derivatives was also performed in the sulphuric acid presence. The resulting products can be easily extract after the decoloration of solution but it is indicated to add a little acetic acid.

3,3-(3′,3″-Dimethyl-4′,4″-dihydroxydiphenyl)-oxindole. It was crystallized from acetic acid. Apparent M.P. 145–155°. Real M.P. 245°.

(*Found* : C, 71.20 ; H, 5.80 ; N, 3.50. $C_{22}H_{19}O_3N + CH_3COOH$ requires : C, 71.11 ; H, 5.67 ; N, 3.45%)

3,3-(3′,3″-Dimethyl-4′,4″-dihydroxydiphenyl)-7-methyloxindole. It was crystallized from acetic acid. M.P. 262–265°.

(*Found* : C, 77.00 ; H, 5.90 ; N, 4.00. $C_{23}H_{21}O_3N$ requires : C, 76.90 ; H, 5.85 ; N, 3.90%)

3,3-(3′,3″-Dimethyl-4′,4″-dihydroxydiphenyl)-N-ethyloxindole. It was crystallized from acetic acid. M.P. 200–203°.

(*Found* : C, 77.50 ; H, 6.30 ; N, 3.80. $C_{24}H_{23}O_3N$ requires : C, 77.21 ; H, 6.16 ; N, 3.75%)

3,3-(3′,3″-Dimethyl-4′,4″-dihydroxydiphenyl)-5,7-dimethyloxindole. It was crystallized from acetic acid. M.P. 255–258°.

(*Found* : C, 77.40 ; H, 6.20 ; N, 3.90. $C_{24}H_{23}O_3N$ requires : C, 77.21 ; H, 6.16 ; N, 3.75%)

The condensation reaction of *p*-cresol with isatin and its derivatives can lead to two kinds of compounds. The compounds with the both phenol rings substituted in the *ortho*-hydroxy position were obtained as follows : 1g of *p*-cresol with 3g of isatin derivative were melted together by 60–80°, then it was added 0.05 g of sulphuric acid and heated by 140°. The alcohol was used to solve the resulting mixture and the crystallization was made from alcohol or acetic acid. The compounds of xanthene type were similarly obtained as the compound III.

3,3-(2′,2″-dihydroxy-5′,5″-dimethyldiphenyl)-oxindole and *3,3-(2′,2″-dihydroxy-5′,5″-dimethyldiphenyl)-N-methyloxindole* are described elsewhere[5].

3,3-(5′,5″-Dimethyl-2′,2″-oxydiphenylene)-oxindole. It was crystallized from dioxan. M.P. 323–325°.

(*Found* : C, 80.55 ; H, 5.70 ; N, 4.60. $C_{22}H_{17}O_2N$ requires : C, 80.73 ; H, 5.19 ; N, 4.26%)

3,3-(5′,5″-Dimethyl-2′,2″-oxydiphenylene)-N-methyloxindole. It was crystallized from alcohol. M.P. 209–212°.

(*Found* : C, 80.49 ; H, 5.78 ; N, 4.20. $C_{23}H_{19}O_2N$ requires : C, 80.90 ; H, 5.57 ; N, 4.10%

3,3-(2′,2″-Dihydroxy-5′,5″-dimethyldiphenyl)-N-ethyloxindole. It was crystallized from acetic acid. M.P. 244°.

(*Found* : C, 77.60 ; H, 5.70 ; N, 3.80. $C_{24}H_{23}O_3N$ requires : C, 77.21 ; H, 6.16 ; N, 3.73%)

3,3-(5′,5″-Dimethyl-2′,2″-oxydiphenylene),N-ethyloxindole. It was crystallized from alcohol. M.P. 197°.

(*Found* : C, 81.64 ; H, 6.30 ; N, 4.00. $C_{24}H_{21}O_2N$ requires : C, 81.12 ; H, 5.90 ; N, 3.90 %)

3,3-(2′,2″-Dihydroxy-5′,5″-dimethyldiphenyl)-7-methyloxindole. It was crystallized from acetic acid. M.P. 287—289°.

(*Found* : C, 77.20 ; H, 5.80 ; N, 4.00. $C_{23}H_{21}O_3N$ requires : C, 76.90 ; H, 5.85 ; N, 3.90 %)

3,3-(5′,5″-Dimethyl-2′,2″-oxydiphenylene)-7-methyloxindole. It was crystallized from alcohol. M.P. 273—275°.

(*Found* : C, 80.60 ; H, 5.30 ; N, 4.00. $C_{23}H_{19}O_2N$ requires : C, 80.90 ; H, 5.57 ; N, 4.10 %)

3,3-(2′,2″-Dihydroxy-5′,5″-dimethyldiphenyl)-5,7-dimethyloxindole. It was crystallized from acetic acid. M.P. 283°.

(*Found* : C, 76.80 ; H, 6.40 ; N, 3.80. $C_{24}H_{23}O_3N$ requires : C, 77.21 ; H, 6.16 ; N, 3.75 %)

3,3-(5′,5″-Dimethyl-2′,2″-oxydiphenylene)-5,7-dimethyloxindole. It was crystallized from alcohol. M.P. 322°.

(*Found* : C, 81.45 ; H, 5.80 ; N, 4.00. $C_{24}H_{21}O_2N$ requires : C, 81.12 ; H, 5.90 ; N, 3.90 %

Revue Roumaine de Chimie, **21**, *1*, 139–143 (1976)

KINETICS OF POLYMERIZATION OF 1,3-DIOXEPANE WITH BF_3OEt_2

DAN DONESCU

Institute of Macromolecular Chemistry "P. Poni", Department
"Polymerization Processes", Bucharest IX, str. Dumbrava Roşie 18, Romania

Received May 28, 1974

Studies are made on the kinetics of 1,3-dioxepane (DH) polymerization in the presence of BF_3OEt_2 as catalyst. In the presence of this catalyst the initial polymerization rate is proportional with the value of expression : $[M]_0\{[M]_0-[M]_e\}$. As in the case of polymerization with the catalytic system $AlEt_3+H_2O$ results obtained are verified by a kinetic scheme which takes into consideration in the initial period of the polymerization the existence of the transfer of active centers to monomer and in the final period to polymer. The catalytic activity of BF_3OEt_2 is greater than that of $AlEt_3+$ $+H_2O$, a fact which is demonstrated both by the much higher polymerization rate of DH in the presence of the former catalyst and by the higher values of transfer constants.

1. INTRODUCTION

We have previously studied the kinetics of homopolymerization of DH [1] and of its copolymerization with epichlorohydrin (ECH), [2] in the presence of the catalytic system $AlEt_3 + H_2O$. The kinetic data obtained and the variation of the intrinsic viscosities have demonstrated the existence in the cationic homopolymerization of this monomer, of secondary transfer reactions of active centers to monomer and to polymer, reactions also mentioned for polymerization reactions of other cyclic formals. [3]

In order to establish the influence of the catalyst on the complicated process of cationic homopolymerization of DH we have undertaken to study in this paper the kinetics of this process catalysed by BF_3OEt_2.

2. EXPERIMENTAL

The working procedure was similar to that mentioned in another paper.[2] Polymerization temperature was always 30°.

BF_3OEt_2 was purified by vacuum distillation. It was used in polymerization as benzene solution prepared under purified argon atmosphere and dosed in thin wall glass balls closed by flame. The concentration used was $3.2\cdot10^{-2}$ mol/l.

---

[1] D. Donescu, *Makromol. Chem.*, **175**, 2355 (1974).
[2] D. Donescu, *Rev Roumaine Chim.*, **20**, 1491 (1975).
[3] D. Donescu, *Materiale Plastice*, **11**, 394 (1974).

3. RESULTS

The polymerization of DH under the experimental conditions of this procedure takes place similar to that occurring in the presence of the catalytic system $AlEt_3 + H_2O$ yet much faster. In the case of low monomer concentrations, polymerization starts after an induction period having a much shorter duration than in the case of catalysis with $AlEt_3 + H_2O$.

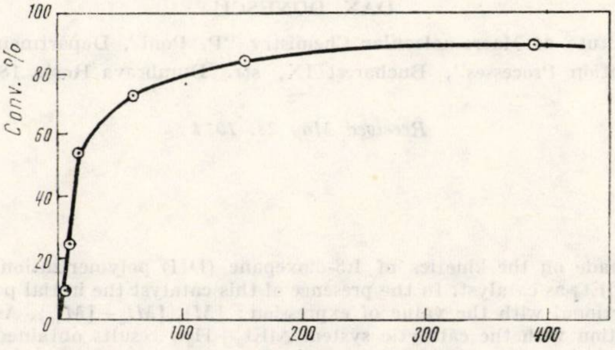

Fig. 1. — Time-conversion curve in polymerization of $DH(|DH|_0 = 6.1$ mol/l).

Another similarity with previously presented data [1] is also observed n relation to the manner in which the intrinsic viscosity varies during polymerization (see Fig. 2). In this case too, the value of the intrinsic viscosity is observed to decrease in the slow polymerization period and this decrease keeps taking place even after the equilibrium conversion has been attained.

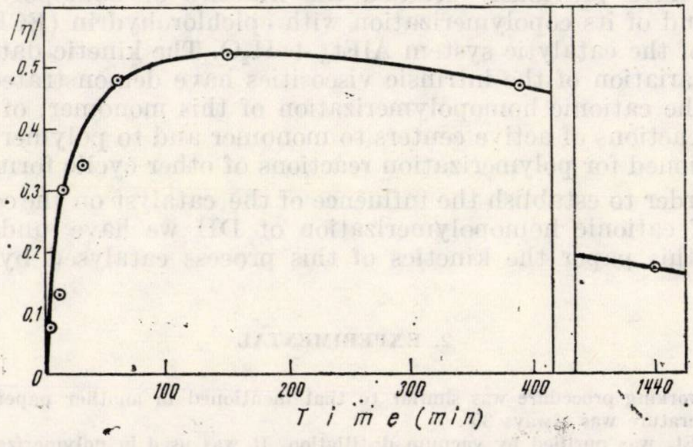

Fig. 2. — Variation of intrinsic viscosity in polymerization of DH (reaction conditions are the same as in Fig. 1).

When the catalyst BF_3OEt_2 is used, the value of intrinsic viscosities are much smaller than those obtained with $AlEt_3 + H_2O$ a fact which shows an increased efficiency of the first catalyst.

What distinguishes the two cataylsts is the manner in which the initial polymerization rate depends on the monomer concentration (see Fig. 3).

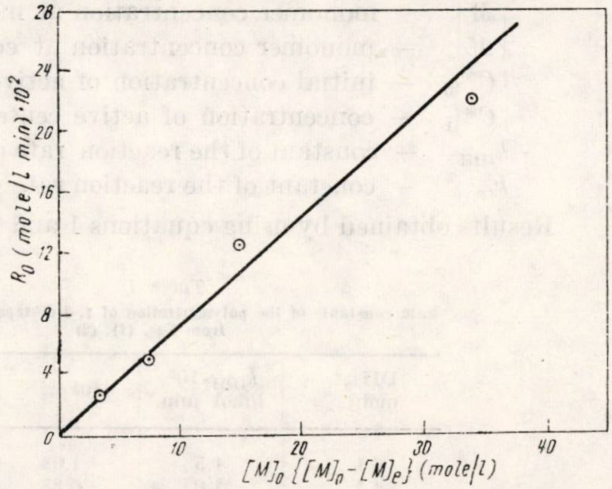

Fig. 3. — Dependence of initial rate, R_0, of polymerization of DH on $|DH|_0$.

In contrast to the catalytic system $AlEt_3+H_2O$, in the case of BF_3OEt_2 catalyst the initial rate depends on the expression $|M|_0\{|M|_0-|M|_e\}$. In the case of catalysis with BF_3OEt_2 additions of ECH in catalytic concentrations failed to have promoting effect. Yet, the rate of consumption of DH rises with ECH additions in concentrations of a similar order of magnitude to the concentration of the former, a fact which tallied with the results obtained by Okada *et al.*[4]

4. DISCUSSION

The above data have shown that when using BF_3OEt_2 and $AlEt_3+H_2O$ as catalysts, polymerization and variation of the intrinsic viscosity in time develops in a similar manner. Owing to this fact, experimental data obtained are verified by the previously suggested kinetic scheme[1] which consider in the first polymerization period the disappearance of active centers by transfer to monomer and in the second, by transfer to polymer.

Verification of the results and determination of the transfer constant was made by means of the same relations :[1]
For the rapid stage

$$\ln\left(-\frac{\mathrm{d}\ln\{|M|-|M|_e\}}{\mathrm{d}t}\right)=\ln k_p|C^*|_0-k_{t\mathrm{DH}}\int_0^t\{|M|-|M|_e\}\,\mathrm{d}t \qquad (1)$$

For the slow stage

$$\ln\left(-\frac{\mathrm{d}\ln\{|M|-|M|_e\}}{\mathrm{d}t}\right)=\ln k_p|C^*|_1-k_{tp}\int_{t_2}^{t_1}\{|M|_0-|M|\}\,\mathrm{d}t \qquad (2)$$

---

[4] M. Okada, S. Kozawa and Y. Yamashita, *Makromol. Chem.*, **127**, 271 (1969).

where:

$|M|_0$ — initial monomer concentration

$|M|$ — monomer concentration at moment t

$|M|_e$ — monomer concentration at equilibrium

$|C^*|_0$ — initial concentration of active centers

$|C^*|_1$ — concentration of active centers at moment t_1

$k_{t\mathrm{DH}}$ — constant of the reaction rate of the transfer to monomer

k_{tp} — constant of the reaction rate of the transfer to polymer

Results obtained by using equations 1 and 2 are presented in table 1.

Table 1

Rate constants of the polymerization of 1, 3-dioxepane with BF_3OEt_2 from Eqs. (1), (2)

$\lvert DH\rvert_0$ mol/l	$k_{t\mathrm{DH}}\cdot 10^2$ l/mol min.	$\ln k_p k_i$	$k_{tp}\cdot 10^3$ l/mol min.
6.1	1.5	1.09	2.0
4.1	1.0	0.88	1.0
3.0	1.2	0.89	1.8
2.1	0.95	0.93	—

A very good verification of the kinetic scheme is also observed when using BF_3OEt_2 as catalyst.

Owing to much higher rates obtained in this case compared to the catalytic system $AlEt_3+H_2O$, the values of rate constants of transfer reactions are much higher. However, in both cases the same ratio is maintained between the value of $k_{t\mathrm{DH}}$ and k_{tp}, a perfectly explicable fact since it depends on the nature of transfer agent, the monomer and the polymer.

Using the results included in Fig. 3 one may write the following relation:

$$|C^*|_0 = k_i |M|_0 |BF_3OEt_2|_0 \tag{3}$$

A linear dependence is observed also in this case between the value of the induction period and expression $\{|M|_0 - |M|_e\}/R_0$, which is inversely proportional with $|C^*|_0$ (see Fig. 4).

A comparison between expression 3 and the corresponding expression established for catalyst $AlEt_3 + H_2O$ shows that the formation of active centers changes when changing the catalyst, as a result of the change in the secondary reactions preceding their formation.[5,6]

The fact that transfer reaction to monomer occurs in the presence of BF_3OEt_2 is also demonstrated by the results obtained by Yamashita *et al.*[7] By treating the reaction products between complex BF_3.1,3-dioxolane and 1,3-dioxolane with sodium methoxide it was possible to identify β-methoxyethyl formate, a product occurring as a result of hydride ion transfer from formal.[7]

---

[5] St. Penczek and P. Kubisha, *Makromol. Chem.*, **165**, 121 (1973).

[6] P. Kubisha and St. Penczek, *Makromol. Chem.*, **144**, 169 (1971).

[7] Y. Yamashita, M. Okada and K. Suyama, *Makromol. Chem.*, **111**, 277 (1968).

The verification of the kinetic scheme suggested by us is an additional evidence of the important role played by secondary reactions in the polymerization of cyclic formals.

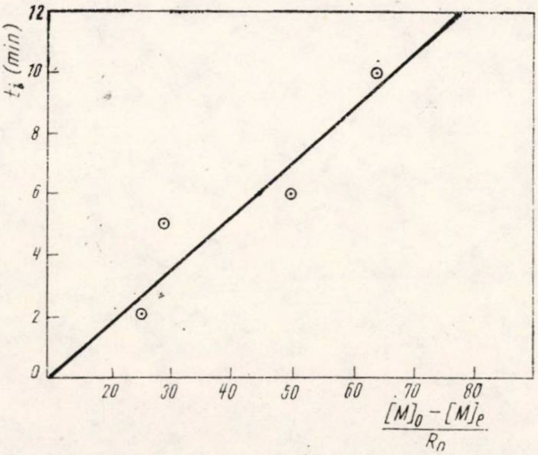

Fig. 4. — Correlation between the length of the induction period, t_i, and $\{|M|_0 - |M|_e\}/R_0$. (reaction conditions are the same as in Fig. 3).

For the polymerization of DH with BF_3OEt_2, the value of the activation energy is 11.1 kcal/mol, which is inferior to that determined for the catalytic system $AlEt_3 + H_2O$.[2] This difference shows a more marked readiness in the formation of active centers for the catalyst used in this work.

Revue Roumaine de Chimie, **21**, *1*, 145–154 (1976)

STUDY OF N-VINYLCARBAZOLE ETHYL METHACRYLATE STATISTICAL COPOLYMER BY LIGHT SCATTERING

SILVIA IOAN and I. BENEDEK

"Petru Poni" Institute of Macromolecular Chemistry,
Aleea Gr. Ghica Vodă 41 A, Jassy, Romania

Received July 9, 1974

The present paper deals with the investigation of the random N-vinylcarbazole-ethyl methacrylate copolymer by light scattering. The main structural characteristics, i.e. gravimetric average molecular weight (M_w), the second virial coefficient (A_2), the heterogeneity parameters P and Q, and the sterical factor (σ) have been investigated. Some information regarding the compatibility of the system has been obtained. The experimental viscometry data confirmed the results obtained by the light scattering method.

The viscometry and light scattering methods used in this paper gave valuable information regarding the structural features and the compatibility of polymers.

The system chosen,i. e. N-vinylcarbazole (NVC)-ethyl methacrylate (EMA) is particularly difficult owing to the strong electrostatic forces of EMA (from CO ester group) and bulky substituents that stiffen the NVC backbone. For this copolymer of different compositions the heterogeneity by molecular weight and composition has been investigated (table 2) and the parameters that characterize the dimension of the macromolecule, sequence distribution and compatibility of the system (figs. 4 – 7, copolymers 6, 7, 8 and 9) have been determined.

EXPERIMENTAL

1. SYNTHESIS OF POLYMERS

Poly(N-vinylcarbazole) (PNVC), poly(ethyl methacrylate) (PEMA), and NVC–EMA copolymers were synthesized by radicalic polymerization of the corresponding monomers in benzene solution at 70° using benzoyl peroxide as initiator. The polymers were precipitated in n-octan, washed and reprecipitated 3–4 times in ethyl ether and methanol, respectively in order to remove the unreacted monomer and homopolymers (in the case of the copolymer).

In order to obtain some indices regarding the polymer sequences, the reactivity ratios were determined at 75° in benzene using the same initiator (benzoyl peroxide). For these determinations the composition data obtained by interferometry and elementary analysis were used (table 1).

The polymerizations from table 1 were carried out for yields smaller than 4–5%. The reactivity ratios were calculated using the Finemann-Ross method.[1] The copolymerization data were plotted by the least square method using a 9100 A Hewlett-Peackard calculator. The following values were determined for NVC (1) and EMA (2):

---

[1] M. Finemann and S. D. Ross, *J. Polymer Sci.*, **5**, 259 (1950).

$$r_1 = 0.132$$
$$r_2 = 1.486$$
$$R = 0.993$$

where r_1 and r_2 are the reactivity ratios and R the correlation factor.

Table 1

Composition data of the calculation of reactivity ratios. M_1 and M_2 – feed concentrations for NVC and EMA, respectively. dM_1 and dM_2 – molar composition (instantaneous) of the copolymer for a time period dt

M_1 %(w/w)	dM_1 % ml	M_2 % (w/w)	dM_2 % ml
91.97	78.89	8.03	21.11
87.97	61.78	12.04	38.22
83.50	67.25	16.49	42.75
75.84	48.09	24.06	51.91
67.92	43.09	32.08	56.91

Because of the lack of data for this system, the reactivity ratios for the copolymerization of NVC (1) with methyl methacrylate (2), (MMA), are given[2] for the sake of comparison:

$$r_1 = 0.20 \pm 0.03$$
$$r_2 = 2.03 \pm 0.03$$

As one may expect it can be seen that both systems have a similar behaviour in copolymerization, their reactivity ratics being of the same magnitude order. However, there is a rather large difference between the reactivity ratios of NVC and EMA but their values are small. This finding allows us to say that the monomers have a strong copolymerization tendency. Consequently, a random structure may be admitted for a copolymer in which EMA blocks may eventually appear. Moreover, because of the fact that $r_1 r_2 < 1$ for both systems but much smaller for NVC—EMA system, the alternation tendency is enhanced for this copolymer.

2. INCREMENTS OF THE REFRACTION INDICES

The increments of the refractive indices for copolymers 1—5 were determined with Zeiss interferometer and the experimental data were verified with the additivity law:

$$\nu = x\nu_A + (1 - x)\nu_B \tag{1}$$

where ν, ν_A, and ν_B are the increments of the refraction indices of the copolymer, homopolymer A and homopolymer B, respectively, and x and $(1 - x)$ are the weight fraction of the components A and B.

The experiments were carried out at 23° using brombenzene (BB), toluene (T), benzene (B) and dioxane (D) as solvents. The results are given in fig. 1.

For copolymers 6—9 having 67% NVC(w/w), the interferometric data were used for copolymer composition determination and the results were confirmed by elementary analysis. Thus, for these copolymers in benzene = 0.155 ml/g corresponding to a content of 66.5% NVC (w/w).

---

[2] L. Y. Young, *J. Polymer Sci.*, **54**, 446 (1961).

3. LIGHT SCATTERING

The light scattering measurements were made using a P.C.L. Peaker device at 23°. The used wavelength was of 4360 Å in the angular domain comprised between 40° and 140°. The samples were purified by filtration under pressure on filters of G-5 porosity. The weight mean molecular mass and the second virial coefficient were determined from the Zimm plot. Fig. 2. respresents a typical Zimm plot for a copolymer sample of 55.03 % NVC (w/w) in benzene.

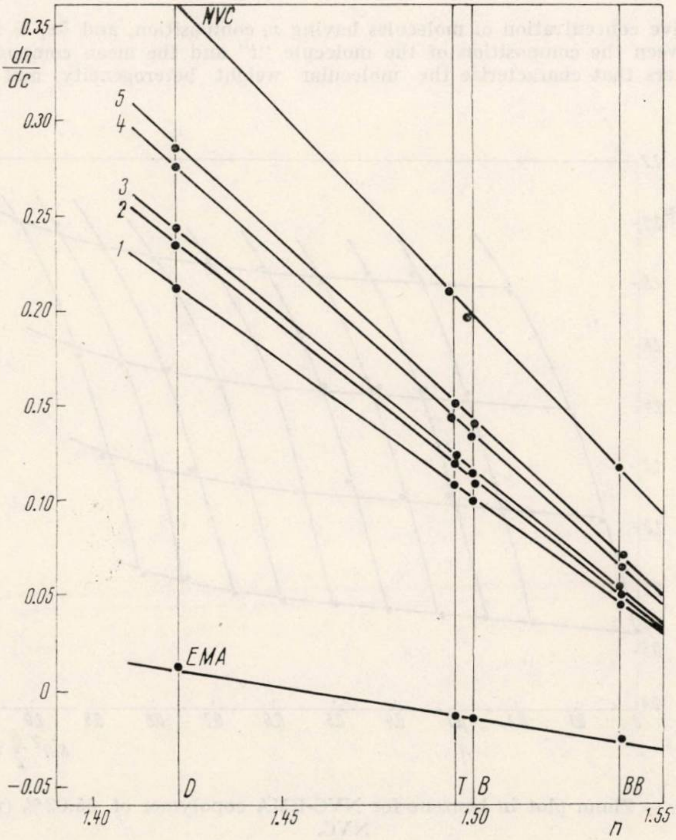

Fig. 1. — Increments of the refraction index of different composition NVC-EMA copolymers as a function of the refraction index of the solvents used.

The real weight mean molecular mass, M_w, was determined from the apparent molecular mass, M_{ap}, in BB, T, B and D using the equation[3]:

$$M_{ap} = M_w + 2P\left(\frac{\nu_A - \nu_B}{\nu}\right) + Q\left(\frac{\nu_A - \nu_B}{\nu}\right)^2 \tag{2}$$

[3] W. Bushuc and H. Benoit, *Canad. J. Chem.*, **36**, 1616 (1958).

where

$$P = \sum_i \gamma_i \, M_i \, \delta x_i \, ; \quad Q = \sum_i \gamma_i \, M_i \, \delta x_i^2$$

γ_i is the relative concentration of molecules having x_i composition, and $\delta x_i = x_i - x$ is the difference between the composition of the molecule "i" and the mean composition. P and Q are parameters that characterize the molecular weight heterogeneity and composition heterogeneity. A M_{ap} which varies with the refraction index of the solvent is plotted *versus* $\frac{\nu_A - \nu_B}{\nu}$ and a parabola is obtained. From this plot M_w, P and Q may be estimated. Generally P and Q may vary in the following limits:

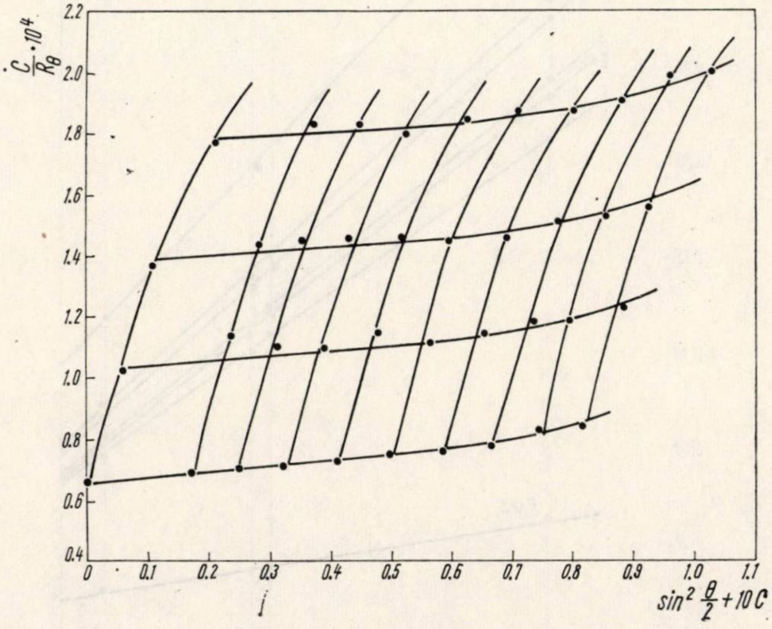

Fig. 2. — Zimm plot in benzene for NVC-EMA copolymer of 55.03 % (w/w) NVC.

$$xM_W \leqslant P \leqslant (1 - x)M_W$$

$$0 \leqslant Q \leqslant (1 - x(1 - x))\, M_W$$

If the copolymer is monodisperse by molecular mass or if the composition distribution of the chain is independent of molecular mass, then $P = 0$ and Q may take values between 0 and $x(1 - x)M_w$. If the copolymer is monodisperse by composition then the molecular mass will not depend on the refraction index of the solvent and $M_{ap} = M_w$.

Based on this study the heterogeneities of the NVC—EMA copolymer of different compositions were calculated.

4. VISCOMETRY MEASUREMENT

Viscometric measurements were carried out in benzene at 23° using an Ubbelohde viscometer. In this way the intrinsic viscosity as a function of composition (table 2) and molecular mass (fig. 7) was determined.

RESULTS AND DISCUSSIONS

1. HETEROGENEITY BY MOLECULAR MASS AND COMPOSITION

In order to obtain some information regarding heterogeneity of the NVC—EMA copolymer of different compositions (i.e. the copolymers 1— 5), M_{ap} in the four different solvents has been determined (i. e. BB, T, B and D) and its variation with the value of the refraction index has been observed. The plot of the relation $M_{ap} = f\left(\frac{\nu_A - \nu_B}{\nu}\right)$ given in fig. 3 allowed the calculation of the real weight mean molecular mass as well as of the parameters characterizing the heterogeneity.

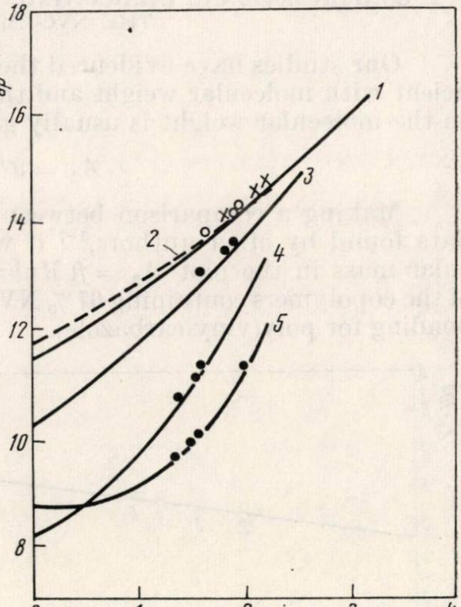

Fig. 3. — $M_{ap} = f\left(\frac{\nu_A - \nu_B}{\nu}\right)$ for copolymers of different compositions.

The parabolae of fig. 3 are the first indication for the heterogeneity of the investigated NVC — EMA copolymers of different compositions. This fact is confirmed by the large variation of M_{ap} in different solvents.

The parameters obtained from fig. 3, i.e. M_w, P and Q, are listed in table 2.

Table 2

Light scattering structural characteristics of the NVC–EMA copolymer of different compositions

N° Copol.	NVC % (w/w)	M_w real $\times 10^{-5}$	$[\eta]$ dl/g	$P \times 10^{-5}$	$Q \times 10^{-5}$	A_2(B) $\times 10^4$	A_2 (BB) $\times 10^4$
1	55.03	1.14150	0.575	0.06884	0.00581	7.90	9.89
2	60.90	1.16639	0.360	0.06191	0.00533	8.48	20.60
3	63.75	1.02290	0.325	0.08157	0.00815	10.55	26.30
4	72.13	0.81935	0.179	0.03485	0.07548	16.00	55.04
5	77.71	0.85764	0.150	0.02919	0.09727	18.30	103.20

One may see in table 2 that Q increases with the increase of the NVC content in the copolymer. This means that composition heterogeneity increases. The real molecular mass is influenced by the copolymer composition and decreases with the increase of NVC content in the copolymer. The fact that the values obtained for P are different from zero allows us to say that copolymers are heterogeneous by the molecular mass too.

2. CONFORMATIONAL CHARACTERISTICS AND THE INCOMPATIBILITY OF THE NVC-EMA COPOLYMER

Our studies have evidenced the variation of the second virial coefficient with molecular weight and the solvent used. The dependence of A_2 on the molecular weight is usually given by the equation [4] :

$$A_2 = a/M^{1/2} + b \qquad (3)$$

Making a comparison between our data for copolymers 6 – 9 and data found by other authors,[5–7] it was observed that for the same molecular mass in the plot $A_2 = f(M^{-1/2})$ (fig. 4), the second virial coefficient of the copolymers containing 67 % NVC (w/w) is greater than the value corresponding for poly(vinylcarbazole).

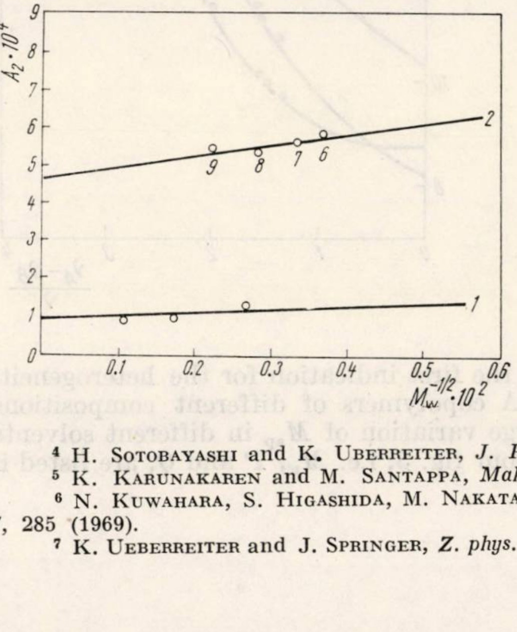

Fig. 4. – $A_2 = f(M^{-1/2})$ for PNVC (curve *1*) and NVC-EMA copolymer of 67% (w/w) NVC different molecular masses (copolymers 6–9, curve *2*), benzene, 25°.

---

[4] H. Sotobayashi and K. Uberreiter, *J. Polymer Sci.*, *A*-2, **2**, 1667 (1964).

[5] K. Karunakaren and M. Santappa, *Makromol. Chem.*, **111**, 20 (1968).

[6] N. Kuwahara, S. Higashida, M. Nakata and M. Kaneka, *J. Polymer Sci.*, *A*-2 **7**, 285 (1969).

[7] K. Ueberreiter and J. Springer, *Z. phys. Chem.* (*Frankfurt*), **36**, 299 (1963).

Like in the case of other random copolymers [8,9] we may say that the values of A_2 obtained by light scattering measurements change with the composition (table 2) and are higher than that of the constituent polymers [57]. At the same time the variation of A_2 as a function of the solvent nature may be noted. Thus, in the case of our copolymers of different compositions the highest values for A_2 in comparison with other solvents used were obtained for brombenzene. This means that for this solvent the interactions of polymer-solvent type are the highest and increase with the increase of NVC content in the copolymer. Considering the strong polar nature of brombenzene and that of NVC this phenomenon is quite expected.

Using the dependence of A_2 *vs.* M, as it is given by the combination of Casassa-Markowitz [10] expression (regarding A_2) with Fixman theory [11] (referring to the expansion coefficient caused by the excluded volume) one may write :

$$A_2 M^{1/2} = \psi_\infty A^3 + 0.631 \psi_\infty B M^{1/2} \tag{4}$$

where $\psi_\infty = 1.518 \times 10^{23}$ being constant, and B is a parameter characterizing the polymer solventinteractions, and $A = (<L^2>_0/M)^{1/2}$, ($<L^2>_0$ is the square mean distance between the ends of the polymer chain in the unperturbed state). From eq. 4 the parameters A and B may be determined (fig. 5).

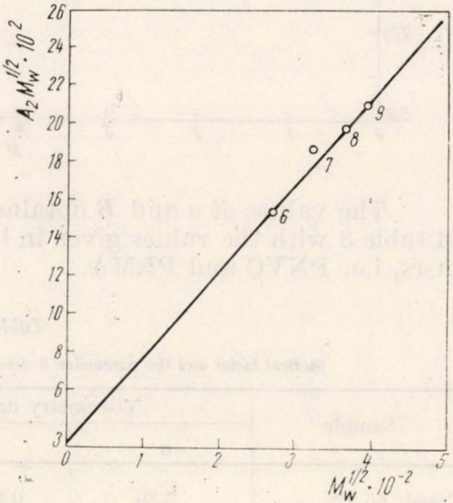

Fig. 5. – $A_2 M^{1/2} = f(M^{1/2})$ for copolymers 6–9, benzene, 25°.

If A is known, one may calculate the sterical factor $\sigma = <L^2>_0/<L^2>_{of}$ where $<L^2>_{of}$ is the square mean distance between the ends of the chain in which a free rotation around C – C bonds is allowed. Supposing that

---

[8] Y. Shimura, *J. Polymer Sci.*, *A-2*, **4**, 423 (1966).

[9] W. Wunderlich, *J. Polymer Sci.*, *C*, **39**, 145 (1972).

[10] E. F. Casassa and H. Markowitz, *J. Chem. Phys.*, **29**, 493 (1958).

[11] M. Fixman, *J. Chem. Phys.*, **23**, 1656 (1955).

$(<L^2>_{of}/P)^{1/2}$ is independent of the substituent [8,12] it has been found that $(<L^2>_{of}/M)^{1/2} = 237 \times 10^{-11})$ and that the value of the sterical factor is 2.80.

The parameters A and B were also determined from viscometric data applying the Stockmayer-Fixman equation : [13]

$$[\eta]M^{-1/2} = \Phi A^3 + 0.51\ B\,\Phi\,M^{1/2} \tag{5}$$

where A and B have the same meaning as in eq. 4 and Φ is a universal constant, $\Phi = 2.87 \times 10^{13}$.

The variation $[\eta]M^{-1/2} = f(M^{1/2})$ from which the sterical factor and parameter B were calculated is plotted in fig. 6.

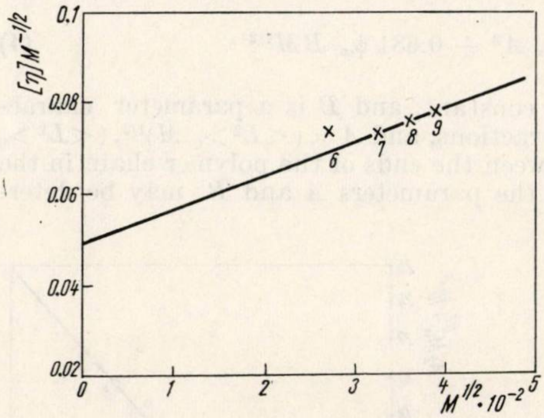

Fig. 6. — $[\eta]\ M^{-1/2} = f(M^{1/2})$ for copolymers 6−9, benzene, 25°.

The values of σ and B obtained by these two methods are compared in table 3 with the values given in literature [5-7] for constituent homopolymers, i.e. PNVC and PEMA.

Table 3

Sterical factor and the parameter *B* determiend by viscometry and light scattering

Sample	Viscometry data		Light scattering data		Ref.
	σ	B	σ	B	
Copol. 66.5 % (w/w) NVC	2.80	0.512×10^{-27}	2.77	4.31×10^{-27}	—
NVC	2.85	0.177×10^{-27}	—	0.175×10^{-27}	7,8
EMA	1.31−1.58	—	1.58	0.161×10^{-27}	6

It is well known that for a flexible chain in unperturbed state the sterical factor (which is a measure for the hindrance of the free rotation around the simple C — C bond) depends on the molar volume of the sub-

---

[12] P. J. Flory "Principles of Polymer Chemistry", Cornell Univ. Press, Ithaca, New York, 1953.

[13] W. H. Stockmayer and M. Fixman, *J. Polymer Sci.*, *C*-1, *1*, 137 (1963).

stituents from the main chains as well as on the short distance interactions between the units of the random copolymer in solution. These interactions are represented by the characteristics of the polar groups, i.e. by the dipolar moments of substituents. Due to the fact that NVC has very bulky substituents that stiffen the chain and that in EMA there are electrostatic interactions between the ester carbonyl, in the copolymerization process the presence of bulky substituents in the copolymer will reduce the electrostatic interactions between ester carbonyls. It may be affirmed that the electrostatic interactions in the copolymer are strongly dependent on the distribution of NVC sequences, i.e. copolymer composition. Consequently, for a composition of 67 (w/w) NVC, the sterical factor is close to that corresponding to NVC but quite different from that of EMA. At the same time the copolymer chain exhibits a low flexibility and a high repulsion between the lateral groups.

The investigation of the copolymers showed that the parameter B was not an additive result derived from homopolymer values multiplied by the actual weight components. Approximately the following equation may be written for random copolymers : [14–16]

$$B = xB_1 + (1 - x)B_2 + 2x(1 - x)B_{12} \tag{6}$$

where B_1 and B_2 are the values of the parameters characterizing the polymer solvent interaction that corresponds to constituent homopolymers and B_{12} is a measure for the interactions occurring between monomer units 1 and 2 from copolymer.

The positive value obtained for B_{12}, i.e., $B_{12} = 9.3 \times 10^{-27}$ is a consequence of the incompatibility of the NVC–EMA system of high chemical heterogeneity.

For the copolymers 6 – 9 of 67% (w/w) NVC in benzene at 25° the following type of Mark-Houving equation has been found :

$$[\eta] = 1.3335 \times 10^{-2} \, M_w^{0.657} \tag{7}$$

For the same temperature the following relation was reported [7] for the PNVC-benzene system :

$$[\eta] = 3.350 \times 10^{-2} \, M_w^{0.58} \tag{8}$$

The variation of the intrinsic viscosity *versus* the weight mean molecular mass both for this copolymer and PNVC is plotted in fig. 7. One may see that for the same experimental conditions the intrinsic viscosity of the copolymer is lower than that corresponding to NVC. This fact

---

[14] W. H. Stockmayer, L. D. Moore, M. Fixman and B. N. Epstein, *J. Polymer Sci.*, **17**, 517 (1955).

[15] T. Kataka, Y. Murakami and H. Inagaki, *J. Phys. Chem.*, **72**, 829 (1968).

[16] T. Kataka, H. Ohnuma and H. Inagaki, *Bull. Inst. Chem. Res., Kyoto, Univ.*, **46**, 107 (1968).

should contradict the random character of the random copolymer chain if the second virial coefficient is taken into consideration.

Having in mind that A_2 characterizes the intramolecular and intermolecular interactions, and $[\eta]$ characterizes the intramolecular interactions, then A_2 and $[\eta]$ have different sensitivities intramolecular precipitation effects, i.e. chain splitting effects. Our experimental results show that A_2 is more sensitive to configuration changes than $[\eta]$. The influence of bulky lateral groups of NVC on chain extension is thus evidenced.

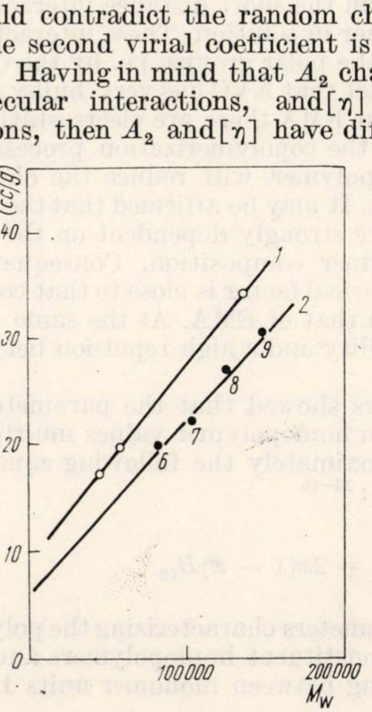

Fig. 7. — $[\eta] = f(M)$ for PNVC (curve *1*) and copolymers 6—9 (curev *2*), benzene. 25°

These results allow us to state that in an unperturbed state the NVC-EMA copolymer is more extended than the constituent homopolymers. Thus, the random character of the chain distribution of monomers is proved.

CONCLUSIONS

The random NVC—EMA copolymer of different compositions has been investigated and compositional and molecular mass heterogeneities have been evidenced.

The random character of the chain of NVC — EMA copolymer of 67 % (w/w) NVC has been proved and the fact that in an unperturbed state the copolymer chain is more extended than that of the constituent homopolymers has been found. The strong influence exerted by the bulky lateral groups of NVC on the configuration, respectively on the flexibility of the copolymer chain, has also been pointed out.

The positive value obtained for the parameter of interaction between the two monomer units from copolymer B_{12} allows us to say that the NVC—EMA system is incompatible. This is not an unexpected conclusion for systems having a high chemical heterogeneity.

The authors would like to thank Prof. Margareta Giurgea for discussion and helpful indications.

Revue Roumaine de Chimie, 21, *1*, 155–160 (1976)

MECHANICAL AND ELECTRICAL PROPERTIES OF IRRADIATED POLYPROPYLENE

DOINA GAVRILĂ*, M. DIACONESCU** and D. IORDACHE*
* Department of Physics, Polytechnic Institute of Bucharest,
Splaiul Independenţei, 313
** Electrical Engineering and Research Institute, Bucharest,
Bd. T. Vladimirescu 45–47

Received July 10, 1974

The variation of Young's modulus, the breaking elongation, the limiting tensile strength are studied and the reticulation efficiency is deduced from the results. The influence of γ radiation on the electric properties (surface and volume resistivity, dielectric rigidity, permittivity and loss angle tangent) is determined and several correlations are established between these quantities and the polymer structure as determined by infrared spectroscopy.

The interest aroused by the action of ionizing radiations on polypropylene derives from the fact that its behaviour under the action of the ionizing radiations is intermediate between polyethylene where the reticulation prevails and polyisobutylene where only a degradation occurs. Moreover, it is interesting because it can be obtained in various stereospecific forms at various degrees of crystallinity.

On the other hand, its uncommon qualities as a dielectric and the extremely small modification of its electric properties raised the problem of its application under strong radiation fields.

Some of the early data on propylene behaviour under the action of high energy radiations were supplied in 1965 by Rexer and Wuckel,[1] who indicated the manner in which its mechanical properties vary. Recent results obtained by Matveev, Vaisberg and Carpov[2] within wide limits of the radiation dose mention the loss increase in irradiated polypropylene at room temperature with γ radiation at $\sim 10^{10}$ Hz frequency.

The researches effected by Keyser and Williams[3] in 1969 and by Keyser[4] in 1970 revealed the presence of the physically captured electrons in the irradiated polypropylene.

---

[1] E. Rexer and L. Wuckel, "Chemische Veränderungen von Stoffen durch energiereiche Strahlung", VEB Deutscher Verlag für Grundstoffindustrie, Leipzig, 1965, p. 198.

[2] V. C. Matveev, S. E. Vaisberg and V. L. Carpov, *Vysokomol. Soedineniya*, **11**, 2666 (1969).

[3] R. M. Keyser and F. Williams, *J. Phys. Chem.*, **73**, 1623 (1969).

[4] M. Dole, "Radiation Chemistry of Polymeric Systems", vol. 2, New Academic Press, New York, 1972, p. 35.

As to the mechanism of the reticulation or degradation due to radiations the literature proposes several different free radicals, although on the other hand no general agreement has been reached thereupon. The problem was recently discussed by Rånby and Carstensen[5] and it seems that the spectra of electronic spin resonance are due in this case to a structure of several radicals.

EXPERIMENTAL RESULTS

The researches made by our group were concerned with the study of certain mechanical and electrical properties of polypropylene as a function of the γ irradiation dose at a uniform sample thickness and at various frequencies of the field applied. The samples were taken from granules by pressure at high temperature, their dimension was 150/150 mm and their thickness 2 mm.

The γ irradiations were made in the air, in two types of equipments: 1) an irradiation equipment of the mobile source type with remote control, made by IFA, with Co^{60} with an initial activity of 480 Cu and an increased specific activity and 2) an irradiation equipment of the fixed source type with a 0.7 l (volume) irradiation chamber, of Gammator M38—2 model, made by the Radiation Machinery Corporation.

Three of the principal properties are modified by irradiation : Young's modulus of elasticity, the breaking elongation and the limiting tensile strength. The experimental values of the modulus of elasticity behaviour as a function of the radiation dose are given for the isotactic polypropylene in figure 1.

Except for the case of small doses, the dependence of the modulus of elasticity on the irradiation dose is linear and coincides with the theoretical one established by Charlesby on the basis of the tetrahedral form model proposed for the three-dimensional polymers by Flory and Rehner.[6] The theoretical formula established by Charlesby is :

$$E = 3\,\rho R T\, q_0\, w^{-1}(r - r_0) \tag{1}$$

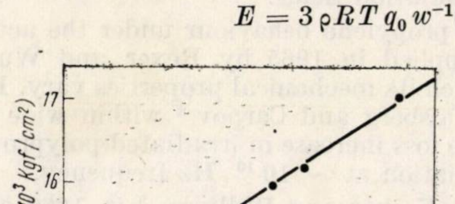

Fig. 1. — Variation of Joung's modulus as a function of the radiation dose at the 24° temperature.

---

[5] B. RÅBY, and P. CARSTENSEN, *Adv. Chem. Ser.*, **66**, 256 (1967).

[6] A. CHARLESBY, "Atomic Radiation and Polymers. International Series of Monographs on Radiation Effects in Materials", vol. 1, Pergamon Press, Oxford, 1960.

where :

ρ is the polymer density
q_0 is the initial density of reticulation
w is the average molecular weight of a polymer molecule
r is the dose of irradiation in Mrad
r_0 is the correction imposed by the initial molecular weight.

It can be assumed that the actual deviation from the linear dependence of curve $E(r)$ in the case of small doses is due to the terminal bonds.

The empirical formula proposed by us of the form :

$$E = 14.25 \cdot 10^3 + 0.022 \text{ r} \cdot 10^3 \tag{2}$$

with E expressed in kgf/cm^2.

Comparing this relation with Carlesby's theoretical formula[6] :

$$E = 6.24 \cdot 10^{-6} \rho R T r G \tag{3}$$

where G is the reticulation efficiency, there results $G = 0.1$, which means a low reticulation efficiency.

Figure 2 represents the dependence of tension f as a function of the deformation factor $\left(\alpha - \dfrac{1}{\alpha^2}\right)$, where α is the ratio of the sample length drawn along the direction force, to its initial length ; this dependence was established for the non-irradiated sample as well as for the irradiated one with 28 Mrad.

It is to be remarked that the dependence of these quantities is proportional up to great elongations which agrees with the theoretical dependence established in the case of three dimensional polymers : [6]

$$f = \frac{\rho RT}{M_c}\left(\alpha - \frac{1}{\alpha^2}\right) \tag{4}$$

where M_c is the average molecular mass between reticulations.

The fact that at great elongations relation (4) does not apply any more, could be due to the following causes : crystallinity or the limiting length of the chain between knots which diminishes the deformation with regard to the given tension.

It can also be assumed that the disagreement between the theoretical linear dependence and the actual experimental dependence could be due to the fact that the theory admits the validity of the Gaussian expression in the case of a function of probability though this only applies to the case of small tensions.

Figure 3 represents the results of the dependence of the breaking elongation (%) as a function of the radiation dose at temperature 24°, which showes its continuous and asymptotic decrease towards a constant value.

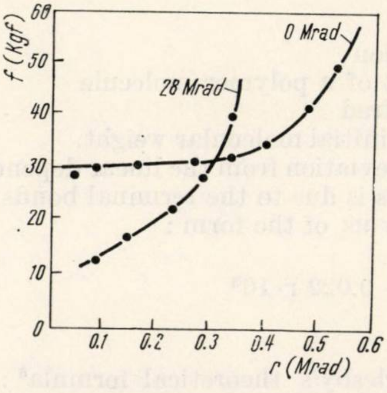

Fig. 2. — Experimental curve tension-deformation factor in the case of 0 and 28 Mrad doses.

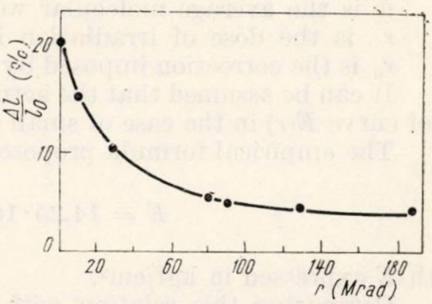

Fig. 3. — Dependence of the breaking elongation as a function of the radiation dose at the 24° temperature.

Moreover, we can see the decrease of the tensile breaking strength as a function of the radiation dose, as is also given in table 1.

It is well known that the electric conductivity of polymers increases when they are exposed to high energy ionizing radiations, which is due to the free charges : ions, electrons and holes, produced by irradiation.[7]

The primary effect of the high energy radiations is the production of photo and Compton electrons.

Table 1

Dependence of the tensile breaking strength as a function of the radiation dose

r (Mrad)	0	28	80	90
σ (Kgf/cm^2)	370	300	170	180

It is considered that the most important results are due to the degradation processes produced by the radiations and reflected by the changes in dielectric conductivity and polarization of the materials.

Polypropylene is a very valuable material as a dielectric. On the other hand, its electric properties hardly change under the action of radiations.

Hereafter we are interested in the irreversible changes of the polypropylene electric properties under the action of the radiations, appearing at high doses (generally over 10 Mrad) and persisting after the cessation of the irradiation. [7]

The increase of the polypropylene conductivity as a consequence of the degradation phenomena can be deduced from the decrease of the volume resistivity ρ_v and of the surface resistivity ρ_s. In figure 4, we see that both ρ_v and ρ_s display a large decrease up to doses of about 100 Mrad beyond which they remain practically constant.

---

[7] P. Hedvig, "Proceeding Tihany Symposium Radiation Chemistry 2nd", Akademiai Kiado, Budapest, 1967.

Besides, we see that the decrease of the surface resistivity ρ_s is larger ; this can be attributed to the much stronger processes of degradation on the polymer surface owing to the action of the external factors (humidity, impurities, oxygen).

Owing to the increase in the number of charge carriers, the diminution of the dielectric rigidity due to the irradiation is to be expected and indeed a similar diminution can be observed in the case of the resistivities (fig. 5).

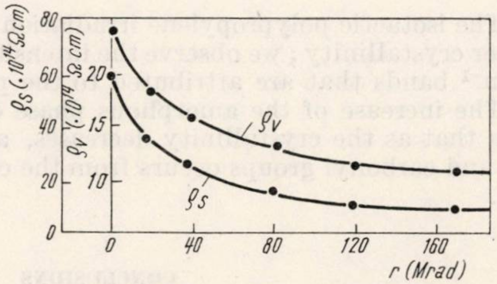

Fig. 4. — Dependence of the volume resistivity ρ_v and of surface resistivity ρ_s upon the radiation dose.

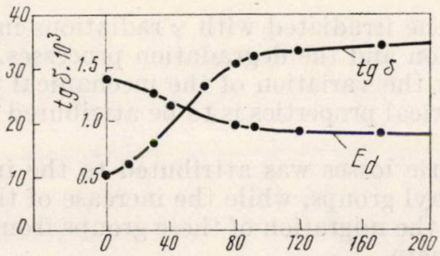

Fig. 5. — Experimental curves : loss angle tangent and dielectric rigidity as a function of the radiation dose.

In the same figure 5, we find the results of the dependence of tg δ at 50 Hz as a function of the radiation dose and observe its fast increase up to doses of about 80 Mrad with a tendency to a subsequent stabilization. The dependence of the concentration of the carbonyl groups—determined by infrared spectroscopy (in the 1770 cm^{-1} band) — as a function of the radiation dose presents approximately the same form. The data thus obtained show that the increase of the tg δ values under irradiation in the open air can be attributed to the formation of strongly polar carbonyl groups.

This result agrees with the experimental results obtained by Matveev, Vaisberg and Carpov. [2] By irradiating in vacuum the polyethylene, a polymer similar to polypropylene, they observed no change either of the losses or of the infrared spectrum in the above-mentioned area. The dielectric permittivity of the material is unchanged by the irradiation.

The measurements made at various frequencies : 50 Hz, 10^6 Hz and 10^{10} Hz showed that the dielectric permittivity does not vary (table 2).

Table 2

Dependence of the dielectric permittivity on the radiation dose at various frequencies

Dose (Mrad) Frequency (Hz)	0	28	80	170
50	2.20	2.21	2.21	2.20
10^6	2.20	2.18	2.18	2.20
10^{10}	2.30	2.24	2.25	2.30

The isotactic polypropylene irradiation leads to the diminution of the polymer crystallinity; we observe the intensity decrease of the 997, 841 and 809 cm^{-1} bands that are attributed to the polymer crystallinity.

The increase of the amorphous phase contents can lead to the conclusion that as the crystallinity decreases, a migration process of the radicals and carbonyl groups occurs from the crystalline into the amorphous phase.

CONCLUSIONS

The isotactic polypropylene irradiated with γ radiations in the open air displays both the reticulation and the degradation processes. The reticulation can be emphasized by the variation of the mechanical properties while the variation of the electrical properties is to be attributed to the degradation phenomena.

The increase of the electric losses was attributed to the increase of the concentration of the carbonyl groups, while the increase of the electric conductivity was attributed to the migration of these groups from the crystalline into the amorphous domain.

The low efficiency of the reticulation is due in this case to the oxygen presence during the irradiation in the open air.

Acknowledgements. We wish to thank the personnel associated with the University of Bucharest, Radioactive Isotope Laboratory, and especially Dr. J. Păun for his assistance with irradiations. We are also grateful to Dr. J. Păun for his suggestions.

Revue Roumaine de Chimie, **21**, *1*, 161 – 164 (1976)

COMPTES RENDUS

"Structure and bonding." vol. 19, Springer Verlag, Berlin, Heidelberg, New York, 1974, 165 p.

The 19th volume of the series covers various topics concerning the chemical bonding in solids. The first chapter "Covalency, interatomic distances and magnetic properties in halides and chalcogenides" deals with relationships between covalency, interatomic distances and magnetic properties in halides and chalcogenides. The authors, R. D. Shannon and H. Vincent, point out some recent systematic discrepancies found in tetrahedral oxyanion distances and in the unit cell volumes of certain series of fluoride compounds. The anomalies cited are the V—O distances in Ca_2Vo_4, shorter than those predicted by the effective ionic radii, the greater unit cell volume of the Ni compound than of the Mg compound in the isostructural series of rutiles (MF_2, M = Ni, Mg, Co, Fe and Mn) and perovskites ($CsMF_3$), the smaller interatomic distances and unit cell dimensions of the Fe compounds than those of the Mg compounds in M_2GeS_4 (M = Fe or Mg) in contradiction to their ionic radii in oxides (Fe^{2+} high-spin 0.78Å Mg^{2+} 0.72 Å).

In order to explain these apparent discrepancies, a "covalency contraction" parameter R_v is defined, as the ratio of the unit cell volume of a transition metal compound M_mX_n to the unit cell volume of Mg_mX_n. This parameter indicates the change of the distance of a covalent bond M—X relative to the distance of the less covalent bond Mg—X. It is found to be proportional to the electronegativity of X and thus inversely proportional to the degree of covalence of the M—X bond. It is shown how systematic decreases in the ratio R_v (therefore, in the distances M—X) accompany changes in the electronegativity differences between M and X. Thus it is apparent how varying degrees of covalence of the M—X bond can explain these anomalies in the relative unit cells of Mg^{2+}, Fe^{2+}, Ni^{2+}, Co^{2+}, Mn^{2+}, Zn^{2+}, Cd^{2+}, Ca^{2+} and In^{3+} compounds. A direct relationship between R_v and the reduction in the magnetic moment for Mn^{2+}, Co^{2+} and Ni^{2+} compounds and between R_v and the Mössbauer isomer shift in Fe^{2+} compounds are also presented. Consequently, a consistent relationship between covalency, interatomic distance and magnetic properties of the transition metal ions, Mn^{2+}, Fe^{2+}, Co^{2+}, and Ni^{2+} is evidenced.

The work includes an important chapter "The valence concept" carried out by A. Kjekshus and T. Rakke dealing with some aspects of the chemical bonding referred to the classic concept of valence. They frequently use a mathematical formalism in order to facilitate precise statements and semi-empirical rules relating the composition, structure, etc. of a given compound to the valence states and features of the electron configurations of the anionic and cationic constituents with the purpose of systematization and prediction.

Among the rules mentioned above, the generalized (8-N) rule is formulated for the anionic as well as for the cationic constituents of the molecular system. In order to obtain supplementary information, the principles on which the concept of bonding rests, are examined. On focussing the attention on the electrons, the electron-pair bond as fundamental principle is adopted and electron-pair formalism is derived. Although adequate in special cases, some unsatisfactory implications arise from the application of the electron-pair idea. In these cases (i.e. for the macromolecular inorganic compounds) and also in a number of cases where this formalism may be adequate, another bonding principle appears to be fulfilled. Based on this principle, an additional counting procedure, the neutral-bonded formalism, generalized from quantum chemical treatment of very simple systems, is constructed.

A following chapter "The marcasite type structure", written also by A. Kjekshus and T. Rakke, the same authors like for the previous chapter, deals with geometrical considerations on the marcasite type structure. Two somewhat interrelated models (the pair-reorientation model and the expansion model) were previously discussed by one of the authors. A critical reexamination of the pair-reorientation model leads out a number of interesting points of view here presented in the sections : geometrical relations between the types FeS_{2-p} and FeS_{2-m}, quasi-hexagonal close-packing of $X(X_2)$ in the FeS_{2-m} type relations between the structure types FeS_{2-p}, random FeS_{2-p}, $Fe-S_{2-m}$, CaC_2 and NaCN.

In the last chapter "Electronic spectra of hexafluorocomplexes", G. C. Allen and K. D. Warren survey the spectra of the hexafluorocomplexes of the 4d and 5d elements in conjunction with those of the anions of the 3d series reviewed in a previous paper and conclude : a) for a given d^n configuration the ligand field splitting parameter Dq increases in the sense $3d < 4d < 5d$, so that the spin-allowed $d-d$ transitions occur at higher energies in the second and third series, b) the one-ion values of the interelectronic repulsion parameter B and c) the values of β the covalent involvement of the ligands, decrease in the sense $3d > 4d > 5d$. The passage from the 3d to 4d and 5d series is also characterized by an increase in the stability of the higher oxidation states and by the most significant feature, the considerable greater magnitude of the spin-orbit coupling constant within the first transition series.

Throughout the volume, the effort for assigning a physical meaning to the mathematical concepts used is obvious and in important cases the calculated data are correlated with those determined experimentally. Each article ends with an up-to-date bibliography so that the whole work is valuable for the chemists interested in the subject.

Florica Popea

J. O'M. BOCKRIS and D. DRAZIĆ, "Electro-Chemical Science", Taylor & Francis Ltd., LONDON, 1972, viii + 300 p.

The book presents for the first time the "Electro-Chemical Science" expounding on the most important findings in the domain, e.g. electrolytic metal production and refinding, obtaining of drinking water from salted water by electrodialysis, synthesis of nylon by an electrochemical process, transmission of pictures from space vehicules using electric cells, etc.

In comparison with the old electrochemistry by Volmer, Gurney, Butler and Frumkin published in 1930, the present electrochemistry made a huge leap both in the area of energy production from chemical derivatives without atmospheric pollution, or of cooperation with nuclear science in order to give in future the electrical energy necessary to all human activities.

Some of the major problems facing electrochemistry today are : 1) In biology, the encephalographic waves which indicate the potential differences between different parts of the brain as related to our psychological state. However, the origin of these oscillations is less understood in psychological terms but it seems that they originate in an electrochemical way. 2) Electroanalytical chemistry is a new branch of electrochemistry, well-developed today, strongly associated with chemistry, biology, metallurgy, engineering, etc. More than half of the chemical analyses are now based on electrochemical methods. 3) Nuclear reactions will supply large amounts of electrical energy the distribution of which will be achieved either through metallic conductors or superconducting materials. While, today, latest materials work at very low temperatures, room temperature devices are discussed. Another proposed way is to use the electrical energy supplied by a nuclear power station in order to produce hydrogen by water electrolysis. The hydrogen thus obtained is to be distributed to consumers and used as such. The transport of electrical energy through metallic conductors could be in this way avoided and the cost reduced to half.

The electrochemical science is ever more based on the technologies of the future when the atomic reactor or solar batteries will be the real energy sources.

The book contains eleven chapters : in the first chapter the main directions of the application of electrochemistry are presented and some considerations are made regarding the future development of this new science. The second chapter deals with the structure of the double electric layer, the double layer surrounding colloidal particles, etc. The charge transfer with its aspects viz. velocity of electrochemical reactions, overpotential, multistep reactions, pseudo-equilibrium, etc., form the topics of the third chapter. Transport processes and the action of electrochemical cells, i.e. transport in solution, the limiting current, polarography and transport difficulties in real electrochemical systems are discussed in the fourth chapter. The fifth chapter deals with electrocatalysis and electrosynthesis and a series of examples are also given. The next chapter deals with electrogrowth and electrodepositation. By electrogrowth one means crystal formation under the influence of an electric field. Direct conversion of chemical energy to electrical energy is reported in the seventh chapter. A series of methods of obtaining energy are given and the efficiency of electrochemical energy conversion is discussed. Some solutions to calculate the power produced by an electrical reaction and the necessity for porous electrodes are also considered. In addition, the uses of fuel cells which are feasible now in widely different domains, e.g. space power, railway traction, naval propulsion, biological and recreational applications, etc., are briefly presented. The eighth chapter shows electrochemical storage of electrical energy and unsolved related problems. In the next chapter, problems of stability, corrosion, passivation and the electrical criterion of hydrogen damage in metals are discussed. The tenth chapter presents topics in electrobiophysics : the cell and its potential, the Hodgkin-Huxley theory, some aspects of biochemical energy conversion and oscillatory phenomena in biological systems. The last chapter makes an overview of the whole book and presents future prospects of the environment unpolluted by power generation based on electrical technologies.

An index and a large number of tables and figures facilitate the reading.

The book is useful for chemists and is highly recommended to everybody active in the theoretical and applied field of electrochemistry.

Ioan Petrariu

ALEC WILLIAMS, *"Furans Synthesis and Applications"* Noyes Data Corporation, N.J., S.U.A., 1973, x + 303 p.

The book of Alec Williams, which in fact is volume 18 of Chemical Technology Review (series published by NDC) represents a very useful work especially for people dealing with synthesis and applications of furan and related derivatives. It gives a detailed description of technologies in this field and is based mostly on the American patents that appeared in the sixties and seventies to 1973.

In comparison with the usual way of presenting literature data specific to one domain, i.e. to process data published in journals and patents, the present book tried, in a original and successful way, to systematize and cover the huge amount of material on furan technologies existing in American patents.

Noyes Data Corporation used the latest techniques in order to eliminate the bibliographic gaps which usually appear due to the time passed since the manuscript is ready for publication and the time when the book is published (i.e., periods related to culling, printing, binding, etc.).

Noyed Data Corporation avoids these difficulties publishing in a new and concise style a series of monographs related to the most important subjects in chemical technology, e.g. fatty acids, metallocene technology, organic peroxide technology, organoboron technology, etc.

In 1780 furoic acid was obtained by dry distillation of mucic acid. While furfural was isolated in 1832, furan itself was not known at that time and was synthetized much later (i.e. 1870) by heating barium furoate with soda lime.

Furfural, one of the most important derivatives related to furan, was produced in industrial amounts only after 1920 when considerable activity was devoted to finding an outlet for various grains and husks. Thus it was found that the treatment of husks with an aqueous mineral acid produced furfural and industrial processing development and application technologies have been accelerated since then. Two dihydrofurans are accessible, namely, 2,3 dihydrofuran and 2,5 dihydrofuran, but perhaps tetrahydrofuran is most commonly known due to its being used as a high boiling solvent for high molecular weight polyvinyl chloride and polyvinylidene chloride in the preparation of printing inks, lacquers, adhesives and other oating compositions. Tetrahydrofuran is also used in Grignard and lithium aluminum hydride reactions; it is also widely employed as an intermediate leading to polytetramethylene ether glycol which is then in polyurethane technology.

From condensed furans, composed of a furanic and benzenic ring, there is benzofuran (sometimes referred to as coumarone) much used in pharmaceutical, insecticidal and photochromic applications.

The book is divided into five chapters which in their turn are subdivided into two to five sections.

The first chapter deals with furan and its substituted derivatives such as furonitrile, dicyanofuran, tetracyanofuran, aliphatic furanic acids, tetraphenylfuran, dimethylfuran, etc. The second chapter discusses technologies of tetrahydrofurans. Recent methods of obtaining tetrahydrofuran and its main substituted derivatives are given, nitroalkyl, trinitromethyl, isocyanates, acetonyl etc., as well as polycyanotetrahydrofuran. The copolymers obtained from tetrahydrofuran and unsaturated epoxy compounds are also discussed, e.g., copolymers with, allyl-2,3-epoxypropyl ether (allyl glycidyl ether), allyl-3,4-epoxybutyl ether, 5-phenyl-3,4-epoxy-1-pentene, etc. A section is then devoted to complexes obtained by solvatation of triaryl chromium derivatives in tetrahydrofuran (THF); e.g. (C_6H_5) $(C_6H_5)_3Cr.(THF)_3.3MgBrCl$ $(THF)_3$ as well as the alike structures. The second chapter concludes with some recipes to obtain stabilizers for tetrahydrofuran and similar cyclic ethers in order to avoid the formation of oxides and peroxides during storage. The next chapter refers to benzo and dibenzofuran. A series of methods to obtain these derivatives are presented such as catalytic dehydrocyclization of substituted phenols and catalytic oxidative dehydrocyclization of substituted aromatics as well as the pharmacological activity of substituted benzofurans.

Because of the photochromy exhibited by some substituted benzofurans these are used as such or in combination with other materials in systems in which photochromy is requested.

Thus, among various and numerous applications the following ones should be mentioned: photocopying and photographying processes, memory devices, windows with variable transparency, jewelry, photochromatic copying paper sheets, etc.

The class of dihydrobenzofuran and the pharmacological and insecticidal properties of dihydrobenzofurans are presented in the fourth chapter. The next chapter contains data on dihydrofurans and related compounds which are starting materials for insecticides, or are used in the food industry (furanone) or as fungicides (griseofulvins).

The book is recommended to organic chemists and engineers in the chemical, textile and pharmaceutical industries. This is a real help to those active in theoretical and applied furan chemistry.

The book contains an index of companies interested in synthesis and reevalution of furan and related derivatives, as well as a patent index and inventors index for patents cited in the book.

Ioan Petrariu

NOTE POUR LES AUTEURS

La *Revue Roumaine de Chimie* publie des articles en anglais, français, russe, allemand ou espagnol. Les auteurs sont priés d'envoyer des articles, notes, communications et comptes rendus inédits.

Les manuscrits seront dactylographiés à deux intervalles. Les tableaux seront dactylographiés sur des feuilles séparées, de même que la légende des figures. Les diagrammes seront tracés à l'encre de Chine sur papier calque. Les tableaux et les figures seront numérotés par des chiffres arabes, en nombre strictement nécessaire. Prière de ne pas inscrire les mêmes données dans les tableaux et les figures. Les formules chimiques seront incluses dans le texte ; en outre, elles seront transcrites sur des feuilles séparées. Les auteurs sont priés d'indiquer les caractères italiques (en soulignant les lettres au crayon), ainsi que tout autre caractère spécial. L'ordre des références bibliographiques sera celui de leur mention dans le texte ; le nom de l'auteur sera précédé de l'initiale du prénom ; les publications périodiques seront présentées suivant les prescriptions internationales. Les références seront ajoutées à la fin de l'article ; elles paraîtront comme des notes, au bas de la page. Le texte sera précédé d'un résumé comprenant 15 lignes au maximum.

L'entière responsabilité du contenu des articles appartient aux auteurs. On publie des articles dus aux collaborateurs roumains ou étrangers.

PRINTED IN ROMANIA

TRAVAUX PARUS AUX ÉDITIONS DE L'ACADÉMIE DE LA RÉPUBLIQUE SOCIALISTE DE ROUMANIE

FRANCISC A. GOTHARD, **Echilibre lichid-vapori. vol. I. Baze teoretice** (Equilibres liquide-vapeurs. Ier vol. Bases théoriques et méthodes de calcul), 1975, 262p., 28 lei

I. ZUGRĂVESCU, MAGDA PETROVANU, **Chimia N-Ilidelor** (La Chimie des N-Ylures), 1974, 347 p., 19 lei.

MARGARETA AVRAM, **Antidăunători** (Pesticides), 1974, 494 p., 41 lei.

CR. SIMIONESCU, VIORICA RUSAN, N. POPA, **Chimia algelor marine** (La Chimie des algues marines), 1974, 211 p., 18 lei.

MARIA FITI, **Dozimetria chimică a radiaţiilor ionizante** (La dosimétrie chimique des radiations ionisantes), 1973, 240 p., 13,60 lei.

MIHAI FLORESCU, **Eficienţa economică a cercetării ştiinţifice** (L'efficience économique de la recherche scientifique), 1972, 115 p., 15 lei.

GEORGETA LĂZĂRESCU, **Sistematizarea informaţiilor în Chimia organică** (La systématisation des informations dans la chimie organique), 1972, 252 p., 10,50 lei.

P. BALTĂ et E. BALTĂ, **Introducere în chimia fizică a stării vitroase** (Introduction à la chimie physique de l'état vitreux), 1971, 240 p., 15,50 lei.

LYDIA-MARIA VAICUM, **Biodegrabilitatea detergenţilor** (La biodégrabilité des détergents), 1971, 254 p., 16 lei.

TIBERIU NĂŞCUŢIU, **Metode radiometrice de analiză** (Méthodes radiométriques d'analyse), 1971, 346 p., 19,50 lei.

I. ZUGRĂVESCU et L. STOICESCU-CRIVETZ, **Polimeri heterociclici** (Polymères hétérocycliques), 1971, 190 p., 9,50 lei.

CRISTOFOR SIMIONESCU et C. V. UGLEA, **Fracţionarea compuşilor macromoleculari** (Fractionnement des composés macromoléculaires), 1962, 292 p., 18,50 lei.

I. MAXIM, **Materiale nucleare** (Matériaux nucléaires), 1969, 444 p., 30 lei.

CRISTOFOR SIMIONESCU et CLEOPATRA VASILIU-OPREA, **Mecanochimia compuşilor macromoleculari** (La mécanochimie des composés macromoléculaires), 1967, 344 p., 23,50 lei.

CORNEL BODEA et collab., **Tratat de biochimie vegetală**, partea I, **Fitochimie** (Traité de biochimie végétale, Ier partie Phytochimie), Ier vol. 1964, 747 p. + 4 annexes + 2 pl., 41 lei; IIe vol., 1965, 1262 p., 1 pl., 56 lei; IIIe vol., 1967, 773 p., 35 lei.

I.P.I. 564

43 426

Lei 25. —

F 1103

R

ACADÉMIE DE LA RÉPUBLIQUE SOCIALISTE DE ROUMANIE

REFERÁLVA

REVUE ROUMAINE DE CHIMIE

TOME 21
N° 2
Février 1976

RECHAX, **21**, *2*, 165–318 (1976)

EDITURA ACADEMIEI REPUBLICII SOCIALISTE ROMÂNIA

Rev. Roumaine Chim. **21**, *2*, p. 165–318 (1976), Bucureşti

ACADÉMIE DE LA RÉPUBLIQUE SOCIALISTE DE ROUMANIE

COMITÉ DE RÉDACTION

Rédacteur en chef:

I. G. MURGULESCU, membre de l'Académie de la République Socialiste de Roumanie

Rédacteurs en chef adjoints:

A. T. BALABAN et V. EM. SAHINI, membres correspondants de l'Académie de la République Socialiste de Roumanie

Collège de rédaction:

EM. BRATU, ELENA CEAUŞESCU, ECATERINA CIORĂNESCU-NENITZESCU, C. DRĂGULESCU, RALUCA RIPAN, CR. SIMIONESCU, membres de l'Académie de la République Socialiste de Roumanie; P. SPACU, membre correspondant de l'Académie de la République Socialiste de Roumanie; MARGARETA AVRAM, D. I. MARCHIDAN, I. MOLDOVAN, G. NIAC et D. SĂNDULESCU

La Revue Roumaine de Chimie paraît 10 fois par an. Toute commande de l'étranger pour les travaux parus aux Editions de l'Académie de la République Socialiste de Roumanie sera adressée à ILEXIM, Serviciul Export—Import Carte (Livres)/Serviciul Export-Import Presă (Revues), P. O. B. 2001, télex 011226 64—66, Calea Griviţei, Bucarest 12, Roumanie

Les manuscrits, les livres et les revues proposés en échange, ainsi que toute correspondance seront envoyés à la rédaction :

REVUE ROUMAINE DE CHIMIE
23, str. Dumbrava Roşie, Bucarest, Roumanie, téléphone 124160

EDITURA ACADEMIEI REPUBLICII SOCIALISTE ROMÂNIA
125, Calea Victoriei, Bucarest, Roumanie, téléphone 50 76 80

ORSZÁGOS MŰSZAKI KÖNYVTÁR ÉS DOKUMENTÁCIÓS KÖZPONT 1883

REVUE ROUMAINE DE CHIMIE

Tome 21, N° 2 Février 1976

Nécrologie 167–168

I. G. MURGULESCU and EUGENIA IVANA, The absorption spectrum of PbI_2 in vapour phase 169–175

RODICA VÎLCU et ALEXANDRINA SIMION, Grandeurs d'excès par des mesures acoustiques, dans les systèmes binaires de liquides 177–186

D. FĂTU and E. SEGAL, Decomposition kinetics of copper tetra-ammine sulphate monohydrate 187–191

VASILE MACOVEI, Spectral solvent effects in aromatic compounds solutions. II. The solvent effects on the position and intensity of chlorobenzene band, at 2600 Å 193–205

R IOANA ONACA, MARIA MAVRODIN-TĂRĂBÎC et I. SOLACOLU, L'étude de la réduction de l'oxygène sur les électrodes poreuses en argent. III. L'effet de la température de l'électrolyte sur les performances des électrodes. Energies apparentes d'activation . . . . 207–216 Ref

R. F. HAJJAR, Correlation between energies of vaporization, molecular parameters and critical temperatures and pressures 217–222

H. H. EMONS und G. BRÄUTIGAM, Physikalish-chemische Eigenschaften von Schmelzgemischen aus Calciumchlorid und Cäsiumchlorid 223–228

R A. G. GALINOS et P. B. ISSOPOULOS, Préparation d'antimoine colloïdal de haute pureté. . . . . 229–230 Cf

R C. LUCA and ANGELA POPA, Utilization of the urea-polyvinyl chloride adducts in the polyvinyl chloride fractionation . . . . 231–235 Ref

R S. P. WALVEKAR, A. B. HALGERI, S. RAMANNA and T. N. SRINIVA SAN, Thermal effect on surface acidity and catalytic activity of $ZrO_2-Al_2O_3$ and ZrO_2-SiO_2 catalysts . . . . 237–240 Ref

A. T. BALABAN, Mass spectrum of 3,7-di-t-butyl-5-methyl-4*H*-1,2-diazepine : possible steric inhibition of dinitrogen expulsion 241–249

CORNELIA UNCUŢA and A. T. BALABAN, Reaction of pyrylium salts with nucleophiles. XI. Chemical shift non-equivalence of isopropyl in atropisomeric 1-aryl-2-isopropyl-4,6-dimethylpyridinium salts 251–255

F. URSEANU, C. TĂRĂBĂŞANU-MIHĂILĂ and L. FLORU, New disperse dyes with naphth[2,3-c] acridan[5,6-de]pyrimidin-5,11-dione structure 257–262

M. H. YOUSSEF, A. G. EL-KASSAS, M. I. RUSHDY and I. K. ABDOU, Aromatic hydrocarbons from high boiling petroleum distillates 263–267

R D. FELDMAN, MARIA CIUGUREANU and MARTHA CIUBOTARIU, Some data on the compatibility of polyacrylonitrile with other polymers . . . . 269–275 Ref

Rev. Roumaine Chim. **21**, *2*, p. 165–318 (1976), Bucarest

D. DONESCU, Kinetic studies on the copolymerization of 1,3-dioxepane with epichlorohydrin initiated with BF_3OEt_2 277–283

N. BÎLBĂ et V. ABABI, La synthèse des zéolithes du système $Na_2O-Al_2O_3-SiO_2-H_2O$, de type A et faujasitique 285–291

R. MIHAIL, C. SINGER und C. IONESCU, Ein Modell für die Verweilzeitverteilung der dispersen Phase in einem Gas-Flüssig oder Flüssig-Flüssig System 293–304

R ELENA HOPÎRTEAN and EUGENIA ŞTEFĂNIGĂ, Membrane-electrodes of the metallic wire-plastic membrane type. III. Membrane-electrodes for organic cations . . . . 305–312 Ref

COMPTES RENDUS 313–318

RALUCA RIPAN

Academician Raluca Ripan, President of the Cluj-Napoca Branch of the Academy of the Socialist Republic of Romania, well-known personality in the field of science and of higher education in our country died on December 5 after a short but painful suffering.

Born in the region of Moldavia on June 27, 1894, she completed her academic studies in Jassy and was transferred to the University of Cluj, in 1920. After obtaining the degree of doctor in chemistry she developed there a fruitful didactic and scientific activity for over five decades, educating the students in the spirit of professional conscience and of patriotism and training numerous generations of specialists in the field of inorganic and analytical chemistry.

The long and fruitful didactic activity carried on as a professor, Dean of the Faculty of Chemistry and Rector of the University of Cluj-Napoca, devoted to the progress of higher education has brought her the recognition and esteem of students and of the teaching staff.

Ever since the beginning of her career, Raluca Ripan has proved to be exceptionally gifted for research work. Her desire to understand and to know was combined with a remarkable know-how. Always based on a thorough documentation in the problems under study, she would enthusiastically accept the new, boldly attacking the topical themes, applying modern research methods and imagining and adopting with confidence the new concepts in the interpretation of results.

In the field of scientific research, Acad. Raluca Ripan has created a new school and new directions in inorganic chemistry.

Working in the laboratory day by day, organizing, conducting and guiding strong research teams both at her chair and at the Institute of Chemistry in Cluj-Napoca, Acad. Raluca Ripan has developed a prodigious scientific activity materialized in nearly 300 original works which cover a series of essential problems of inorganic chemistry of a theoretical and practical importance.

Among them we cite in the first place the research in the field of polyelectrolytes and of complex compounds. Her studies on iso- and heteropolyacids of silicon, phosphorus, boron, molybden, wolfram and their salts relative to constitution, basicity and reactivity have been highly appreciated by specialists in our country and abroad.

Apart from elucidating numerous theoretical aspects, Acad. Raluca Ripan has paid special attention to the practical application of the results of investigations. This involves primarily the separation, concentration or analysis of numerous, rare and disperse elements found in the subsoil of our country and also the establishment of certain technological processes, emphasizing the talents of the true scientist who has known how to orient research and creativity towards the development of science in an indissoluble relation with industrial production.

For her rich scientific activity, Raluca Ripan was elected member of the Academy of the Socialist Republic of Romania in 1942 and she was awarded the State Prize and the title of Honoured scientist.

The scientific work of Acad. Raluca Ripan has enjoyed an international appreciation, a fact illustrated by her election as a honorary member of the Society of Chemical Engineering of France and as a doctor honoris causa of the University of Torun, Poland.

The didactic and scientific activity of Acad. Raluca Ripan was harmoniously combined with a many-sided social-political activity by which she has proved the same commitment and perseverance.

A member of the Romanian Communist Party since the year 1946, Raluca Ripan was a patriotic scientist, constantly present in the public life. Thus she carried out a rich activity as a deputy in the Great National Assembly, in several legislatures, as a member in the National Council for Science and Technology, in the National Council for the Safeguarding of Peace, in the Women National Council. This multiple activity of Acad. Raluca Ripan in the field of science and of education, in the public life, has found a high recognition in the title of hero of socialist work, in the orders and medals conferred on her by our State.

By the death of Acad. Raluca Ripan the cultural and scientific life in our country loses one of its most brilliant representatives. Her personality will remain an example of tireless scientific creativity and of high patriotism for the future generations.

Revue Roumaine de Chimie, **21**, 2, 169–175 (1976)

THE ABSORPTION SPECTRUM OF PbI_2 IN VAPOUR PHASE

I. G. MURGULESCU and EUGENIA IVANA

The Center of Physical Chemistry, Bucharest
Str. Galați 31, Romania

Received July 14, 1975

The absorption spectra were studied, both in visible light and in the UV, for gaseous PbI_2 in the 439–506° temperature range. The absorption spectrum was attributed to PbI_2 species. The vaporization heat was calculated for PbI_2.

1. INTRODUCTION

The study of electronic absorption spectra of gaseous $PbCl_2$ and $PbBr_2$[1] revealed a simple composition of vapours of the respective substances. The absorption spectra were attributed to $PbCl_2$ and $PbBr_2$ molecules.

These facts concerning the composition of $PbCl_2$ and $PbBr_2$ were confirmed by the results obtained through the determination of vapour pressure[2] and by mass spectrometry.[3,4]

Concerning the composition of PbI_2 vapours, Akishin[5] has shown that the possibility cannot be excluded that, besides the PbI_2 species, the biatomic molecule of PbI also exists. Klemperer[6] employed mass spectrometry for the study of the geometry of PbX_2 molecules in vapour phase, and reported on the presence of PbI in the vapour of lead iodide.

Berkovitz[7] has shown that PbI_2 vapours are constituted only from the PbI_2 monomer. Many attempts to reduce PbI_2 with a view to obtaining PbI were unsuccessful.

Fisk and others,[8] made photoionisation studies of PbI_2 vapours at high temperatures and concluded that the ions identified by them resulted only from the photolysis of PbI_2 molecules, and not from PbI that would result from the direct reaction of thermal dissociation :

---

[1] I. G. Murgulescu and E. Ivana, *Rev. Roumaine Chim.*, **18**, 1667 (1973).

[2] a I. L. Barton and H. Bloom, *J. Phys. Chem.*, **60**, 1413 (1956) ; b H. Bloom and J.O'M Bookris, *J. Amer. Chem. Soc.*, **80**, 2044 (1958). c L. C. George, R. M. Doerr and A. Visnapuu, *J. Chem. Eng. Data*, **14**, 23 (1969).

[3] H. Bloom, S. R. Richards and D. J. Williams, *Austral. J. Chem.*, **25**, 2077 (1972).

[4] H. Bloom and J. W. Hastie, *Austral. J. Chem.*, **21**, 583 (1968).

[5] P. A. Akishin, V. P. Spiridonov and A. N. Khodcenko, *Zhur. fiz. Khim.*, **32**, 1679 (1958).

[6] A. Buchler, J. L. Stanffer and W. Klemperer, *J. Amer. Chem. Soc.*, **86**, 4544 (1964).

[7] J. Berkowitz, "Advances in High Temperature Chemistry", vol. 3, Academic Press, London, 1971, p. 149.

[8] G. A. Fisk, B. H. Mahan and E. K. Parks, *J. Chem. Phys.*, **47**, 2649 (1967).

$$PbI_2 \rightarrow PbI + I \qquad (1)$$

Computations of equilibrium constants for this reaction, employing the tabulated [9] bond energies, and making reasonable suppositions concerning the PbX_2 geometry, indicate a ratio PbI/PbI_2 of 4.10^{-5}, in the working conditions of the authors.

In the present study we have investigated the absorption spectra of PbI_2 in the UV and the visible (500—600 nm) ranges, in the 439—506° temperature interval.

2. EXPERIMENTAL

PbI_2, twice recrystallized from hot water, was dried in vacuum for 10 hours. For a better purification PbI_2 was vapourized in vacuum.

Cylindrical quartz cells with optical surfaces were employed, whose length varied between 2 and 4.4 cm.

In our experiments the samples were irradiated continuously with radiations in the ranges 54.000—28.000 cm^{-1} and 25.000—14.000 cm^{-1}, respectively.

3. RESULTS AND DISCUSSIONS

In figures 1 and 2 the absorption spectrum of PbI_2 vapours in the UV and in the visible ranges is presented.

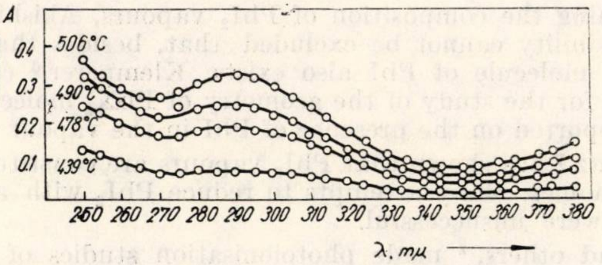

Fig. 1. — UV absorption spectrum of gaseous PbI_2.

In the fields investigated the spectrum presented continuous absorptions with maximae at 2.900 and at 5.150 Å. No vibrational structures were obtained for these continuous absorptions.

The concentration of PbI_2 vapours was calculated knowing the dependence of vapour pressure on temperature.[10] We have considered that the PbI_2 vapours behave like an ideal gas.

---

[9] C. E. MOORE, "Atomic Energy Levels", Natl. Bur. Std. (U.S.) Circ. No. 567, 3 (1958).

[10] O. KUBASCHEWSKI and E. U. EVANS, "La thermochimie en metallurgie" Ed. Gauthier-Villars, Paris, 1964, p. 311.

The linear variation of the absorption with concentration shows that the Beer's law applies for the computation of molecular absorption constants (figures 3 and 4) :

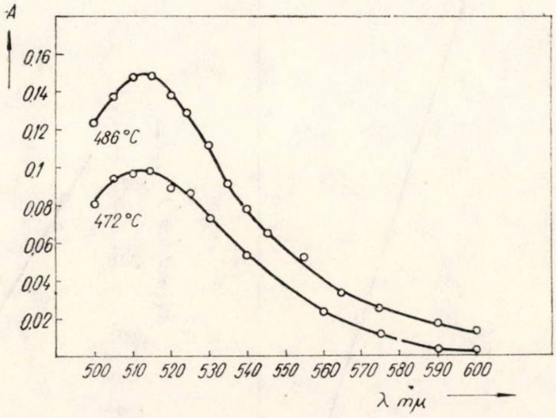

Fig. 2. — Absorption spectrum of gauseos PbI_2 in visible.

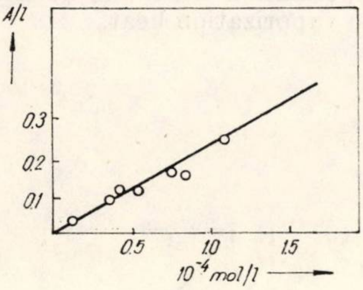

Fig. 3. — Dependence of gaseous PbI_2 absorption on concentration (in the UV range).

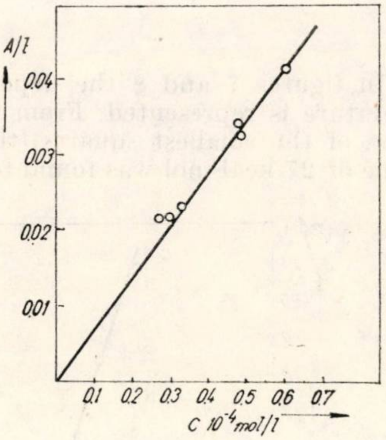

Fig. 4. — Dependence of gaseous PbI_2 absorption on concentration (in the visible range).

The temperature dependence of the molecular absorption constants, corresponding to the two absorption maxima is presented in figures 5 and 6 :

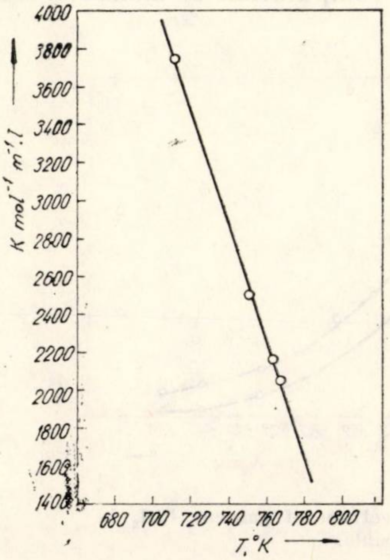

Fig. 5. — Dependence of the molecular absorption constant of gaseous PbI_2 on the temperature (in the UV range).

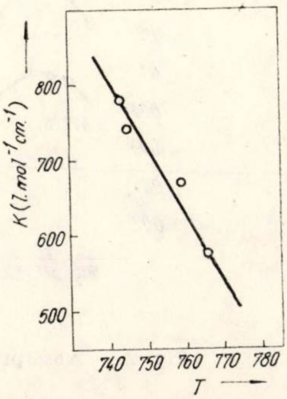

Fig. 6. — Dependence of the molecular absorption constant of gaseous PbI_2 on the temperature (in the visible range).

In figures 7 and 8 the dependence of lg $[(A/1) . T]$ on the inverse temperature is represented. From the slope (computed according to the method of the smallest squares) the vaporization heat was determined. A value of 27 kcal/mol was found for the vaporization heat.

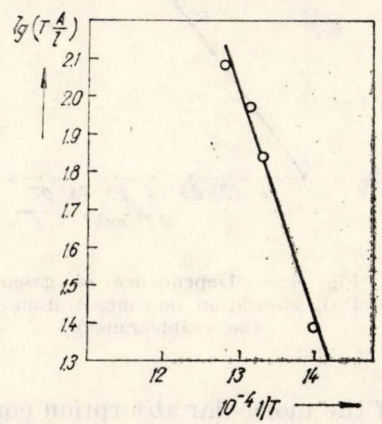

Fig. 7. — Dependence on temperature of the absorption of gaseous PbI_2 for $\lambda = 290$ nm.

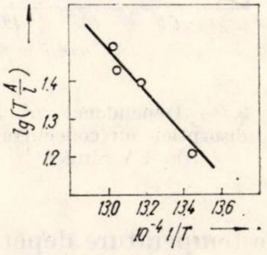

Fig. 8. — Dependence on temperature of the absorption of gaseous PbI_2 for $\lambda = 515$ nm.

As appears from figures 1 and 2, the absorption increases with temperature, as long as the vapours are in equilibrium with the fluid phase. The absence of the vibrational structure of the two maxima could be caused by two phenomena that may occur at the same time.

In the first place, due to high temperature, absorptions from superior vibrational levels can determine considerable superposition.

On the other hand, the continuous absorption observed could result from the superposition of absorption bands of the species that can exist in the PbI_2 vapours. These species can be the following ones : PbI_2, $(PbI_2)_2$, PbI, Pb, I. The last three species result from thermal dissociation and/or photo-dissociation reactions, phenomena that are characteristic for the lead halides.[11-18]

The study concerning the composition of PbI_2 vapours, performed with the aid of mass spectrometry,[7] showed that the ratio between the dimer and the monomer is of 1/2000 ($5 \cdot 10^{-4}$).

Taking into consideration the low concentration of PbI_2 in the vapours, the contribution of the dimer to the absorption is negligible.

Through photo-ionization studies of PbI_2 vapours it was found that the ratio PbI/PbI_2 is $\sim 4.10^{-5}$. In our working conditions, even if the concentration of PbI — resulting, for instance, through reaction (1) — is high, it would break down (reaction 2) because of the small dissociation energies [19] (1.98 eV) :

$$PbI \rightleftarrows Pb_{(g)} + I_{(g)} \tag{2}$$

The lead atoms appear in the system, either as a product of reaction (2) and/or as a product of the thermal dissociation reaction (3) of lead iodide :

$$PbI_2 \rightleftarrows Pb_{(g)} + I_{2(g)} \tag{3}$$

The contribution of lead vapours to the measured absorptions (figures 1 and 2) can be neglected if we take into account the extremely low absorption of lead vapours in equilibrium with fluid lead. Thus, for temperatures between 540° and 640° the absorption of lead vapours is only slightly above the limits of experimental error.[1]

In the 250—300 nm range, the absorption of I_2 vapours is low.

Thus, the constant of molecular absorption [20] at $\lambda = 290$ nm for the temperature of 420° is 11 $l.mol^{-1}.cm^{-1}$.

---

[11] A. Kaldor and D. A. Somorjai, *J. Phys. Chem.*, **70**, 3538 (1966).

[12] D. I. Morentz, R. A. M. Scott and J. J. Shortland, *J. Phys. Chem. Solids*, **33**, 1235 (1972).

[13] C. Renz, *J. anorg. Chem.*, **116**, 62 (1921).

[14] W. C. Tennent, *J. Phys. Chem.*, **70**, 3523 (1966).

[15] K. J. De Vries and J . H. von Santen, *Physica*, **30**, 2051 (1964).

[16] J. F. Verwey, *J. Phys. and Chem. Solids*, **31**, 163 (1970).

[17] M. R. Tubbs, *Proc. Roy. Soc.*, **280**, 566 (1964).

[18] R. I. Dawood, A. J. Forty and M. R. Tubbs, *Proc. Roy. Soc.*, **284**, 272 (1965).

[19] K. Wieland and R. Newburgh, *Helv. Phys.*, **25**, 87 (1952).

[20] A. A. Passchier, and N. W. Gregory, *J. Phys. Chem.*, **72**, 2697 (1968).

The absorption spectrum of I_2 in visible has several peaks of absorption.[21]

Knözinger and Dobelstein have shown that the spectrum of I_2 vapours in the 500–600 nm range is characterized by a low absorption with maxima at $\lambda = 530$ nm and 580 nm.

As appears from the data presented above, the contribution of Pb and of I_2 vapours, respectively, to absorption (for small absorption constants) is low, but it is manifested in the computation of molecular constants of absorption of PbI_2 vapours. Thus, the decrease of absorption constants (figures 5 and 6), computed according to the Lambert-Beer law in relation with the rise of the temperature, is particularly high. The phenomenon is believed by us to be due, in part at least, to the thermal dissociation of PbI_2 (see reaction 3), which has not been considered in the computation of the concentrations.

If α is the degree of dissociation, and K_0 is the constant of true absorption, the Lambert-Beer law (for a determined wavelength) can be written as follows:

$$A = K_0 (l - \alpha) C_0 \tag{I}$$

where: C_0 is the concentration (in mol/l);
l is the length of the cell.

If the dissociation is not taken into consideration, then equation (I) will be written as follows:

$$A = KC_0 \tag{II}$$

The absorption constant K, computed from equation (II) is represented in figures 5 and 6.

From equations (I) and (II) it results:

$$\alpha = 1 - \frac{K}{K_0} \tag{III}$$

The true absorption constant K_0 can be estimated through the extrapolation of experimental constants at a temperature at which dissociation does not occur.

We have chosen the melting temperature of lead iodide as extrapolation temperature because we suppose that, in the given conditions, the thermal dissociation is negligible.

By the extrapolation of experimental values of K at $\lambda = 290$ nm and $\lambda = 515$ nm, the values for K_0 are 4550 $l.mol^{-1}.cm^{-1}$ and 1298 $l.mol^{-1}.cm^{-1}$, respectively.

---

[21] K. Knözinger and Kl. Dabelstein, Beckman Report 1+2/74, p. 1.

Table 1 contains the values of the degree of dissociation computed according to equation (III). Also in Table 1 are included the recalculated K values, taking into consideration the dissociation. Obtained in this way K shows a considerable lower variation with temperature.

The degree of dissociation cannot be used in the computation of the equilibrium constant because the extrapolation for the obtention of K_0 values is rather arbitrary.

Table 1

Degree of dissociation of PbI_2 calculated according to equation (III)

	$\lambda = 290$ nm				$\lambda = 515$ nm			
T	712	751	763	767	743	745	759	766
α	0.19	0.46	0.53	0.54	0.40	0.43	0.47	0.54
K*	4545	4620	4500	4482	1297	1286	1265	1232

* expressed in $l.mol^{-1}.cm^{-1}$.

We admit that absorption (figures 1 and 2) is due to PbI_2 species, with very small contributions by lead and I_2 vapours.

The attribution of the spectrum observed to PbI_2 species is based on the following facts :

— the vaporization heat calculated for wavelengths corresponding to the two maxima absorption peaks ($\lambda = 290$ nm and 515 nm) has the same value and is 27 kcal/mol, as well as the calorimetric-determined value;

— the vapours are in equilibrium with the fluid phase;

— the PbI species have only a slight absorption in the visible region in the 450—480 nm range,[22] an absorption that was not observed.

---

[22] R.W.B. Pearse and A. G. Gaydon, "The Identification of Molecular Spectra". Chapman and Hall, London, 1963, p. 259.

Revue Roumaine de Chimie. 21, 2, 177–186 (1976)

GRANDEURS D'EXCÈS PAR DES MESURES ACOUSTIQUES, DANS LES SYSTÈMES BINAIRES DE LIQUIDES

RODICA VÎLCU et ALEXANDRINA SIMION
Université de Bucarest, Chaire de Thermodynamique Chimique,
Bucarest, 13, B-dul Republicii

Reçu le 22 juin 1974

On a mesuré les densités et la vitesse des ultrasons aux températures de 25, 35, 45, 50° et la capacité thermique à 25°, dans le système alcool méthylique + benzène, ainsi que la vitesse des ultrasons à 20, 40, 60°, dans l'alcool éthylique + tétrachlorure de carbone. On a calculé plusieurs grandeurs en utilisant des données de densité, vitesse et capacité thermique : volume d'excès, compressibilité adiabatique d'excès, compressibilité isotherme, pression interne. Des calculs similaires ont été effectués concernant le système alcool méthylique + eau, avec, en outre, la compressibilité isotherme d'excès, au moyen des données des vitesses et des densités fournies par la littérature.

INTRODUCTION

La mesure de la vitesse des ultrasons, en corrélation avec d'autres grandeurs de l'état liquide, permet de calculer quelques grandeurs importantes, difficiles à déterminer par voie expérimentale.

Ainsi, la méthode acoustique apparait comme une méthode fondamentale et simple pour la détermination de la capacité thermique des liquides.

Deux méthodes indépendantes [1] sont utilisées pour le calcul de la capacité thermique à volume constant : acoustique et thermodynamique.

La méthode acoustique consiste, essentiellement, à représenter la compressibilité adiabatique β_S à l'aide de la formule hydrodynamique de la vitesse des ultrasons,

$$c^2 = 1/\rho\beta_S \tag{1}$$

qui fournit :

$$C_p/C_v = c^2\,\rho\beta_T \tag{2}$$

où :

C_p, C_v — les capacités thermiques à pression et à volume constants
c — la vitesse des ultrasons
ρ — la densité du milieu
β_T — le coefficient de compressibilité isotherme

---

[1] V. E. Nozdrev, « Primenenie Ultraakustiki v moleculiarnoi fizike », Gosudarstvenoe izdat. fiz. mat. literatury, Moscou, 1958, p. 300.

Dans la méthode thermodynamique, la formule est :

$$C_p - C_v = \frac{T\,(\partial V/\partial T)_p^2}{(\partial V/\partial p)_T} \tag{3}$$

A condition que les capacités thermiques à pression constante soient fournies par des mesures calorimétriques, les deux formules conduisent à des résultats concordants. Clausius, en calculant par voie thermodynamique le rapport C_p/C_v pour l'eau, a trouvé la valeur 1. Ceci a fait croire que le rapport C_p/C_v est pratiquement égal à 1 pour tous les liquides, bien que, en réalité, les rapports C_p/C_v d'un grand nombre de liquides se rapprochent plutôt des valeurs trouvées pour le gaz.[2]

Si l'on tient compte de la relation thermodynamique de la compressibilité isotherme

$$\beta_T = \beta_S + \frac{\alpha^2 T M}{\rho C_p} \tag{4}$$

on voit que pour faire le calcul complet de la capacité thermique à volume constant par ces formules, il est nécessaire de connaître le coefficient de dilatation thermique, aussi bien que la capacité thermique, C_p. La méthode est possible lorsque les données sur la capacité thermique à pression constante sont fournies par des mesures calorimétriques.

Remarquons qu'il est possible de calculer au moyen de données acoustiques, des densités, des coefficients de dilatation thermique et de la compressibilité isotherme, les grandeurs suivantes : C_p/C_v, C_v et C_p. Inversement, si l'on connaît C_p par des données calorimétriques, on pourra calculer, par la relation (4), le coefficient de compressibilité isotherme.

Hildebrand et Scott,[3] en partant de quelques relations thermodynamiques, ont établi la formule suivante qui donne la variation du volume dans le cas des mélanges :

$$V^E = V^M = \beta_T^0\, V^0(\partial E/\partial V_0)_T - (\partial E_0/\partial V_0)_T \tag{5}$$

où :

β_T^0 — la compressibilité isotherme idéale
V_0 — le volume idéal
E — l'énergie interne

La relation (5) jointe à l'expression de la pression interne

$$p_i = (\partial E/\partial V)_T = -p + T\alpha/\beta_T \tag{6}$$

---

[2] E. B. Freyer, J. C. Hubbard et D. H. Andrews, *J. Amer. Chem. Soc.*, **51**, 759 (1929).

[3] J. H. Hildebrand et R. L. Scott, « Solubility of nonelectrolytes », Reinhold, New York, 1950, p. 136.

pourra être exprimée approximativement[4] par

$$V^E = \beta_T^0 V_0 \left[(T\alpha/\beta_T) - (T\alpha_0/\beta_T^0) \right] \tag{7}$$

Van der Waals[5] a trouvé que, si le volume d'excès à pression constante, V^E, est négatif, la variation de l'énergie de mélange à volume constant, E^M peut être exprimée par

$$E^M = H^E - T\,\alpha_0\, V^E/\beta_T^0 \tag{8}$$

où H^E désigne l'enthalpie d'excès.

PARTIE EXPÉRIMENTALE

Les liquides ont été purifiés selon les méthodes décrites par Vogel.[6]

Les densités ont été déterminées par la méthode picnométrique à une erreur maximale de 0,01 % et les vitesses des ultrasons au moyen d'un interféromètre à double cristal, décrit dans un travail antérieur,[7] à une erreur maximale de 0,3 %.

Les capacités thermiques ont été déterminées à l'aide d'un calorimètre adiabatique de construction propre, similaire à celui présenté dans le travail de Vîlcu et Irinei.[8]

Pour avoir la valeur exacte de la variation de température Δt, on s'est servi d'une correction graphique.[9]

Le calorimètre permet d'obtenir la capacité thermique à une précision de 0,5 %.

RÉSULTATS EXPÉRIMENTAUX ET DISCUSSIONS

On a étudié les systèmes : benzène + alcool méthylique et eau + alcool méthylique.

Dans le tableau 1, on trouve les valeurs de la densité et dans les figures 1 et 2, les variations de la vitesse des ultrasons et de la compressibilité adiabatique, avec la fraction molaire de l'alcool, pour le système alcool méthylique + benzène.

Tableau 1

Densités du système benzène + alcool méthylique

x_{CH_3OH}	(g cm^{-3})			
	25°	35°	45°	50°
0,0000	0,8731	0,8625	0,8515	0,8464
0,2189	0,8631	0,8524	0,8414	0,8363
0,3589	0,8559	0,8452	0,8347	0,8289
0,6329	0,8358	0,8250	0,8146	0,8096
0,7955	0,8183	0,8082	0,7986	0,7932
1,0000	0,7865	0,7770	0,7680	0,7634

---

[4] S. Sternberg et V. Vasilescu, *J. Chem. Thermodynamics*, **1**, 195 (1969).

[5] J. H. Van der Waals, *Trans. Faraday Soc.*, **52**, 916 (1956).

[6] A. I. Vogel, « A Textbook of Practical Organic Chemistry Including Qualitative Organic Analysis », 2e Ed. Longmans Green, Londres, 1951, p. 169, 172.

[7] R. Vîlcu et A. Simion, *Rev. Roumaine Chim.* (sous presse).

[8] R. Vîlcu et F. Irinei, *Anal. Univ. București, Seria St. Nat.*, **42**, 87 (1963).

[9] R. Vîlcu, E. Tomuș, I. Găinar et F. Irinei, « Lucrări practice de Termodinamică Chimică », Centrul de multiplicare al Universității din București, 1972, p. 102.

Les courbes de la vitesse présentent une légère convexité vers le haut à cause de la déviation du comportement idéal.

Les capacités thermiques, à 25°, déterminées par le calorimètre sont inscrites au tableau 3. Avec leur aide, on a calculé les valeurs des coefficients de compressibilité isotherme par la formule (4), ainsi que les valeurs des coefficients de dilatation, par la formule :

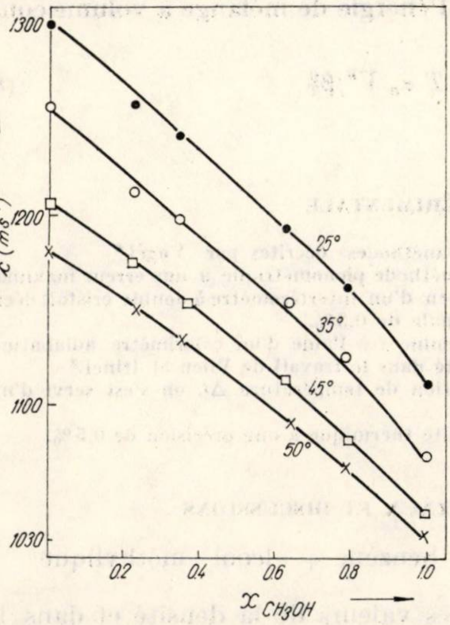

Fig. 1. — Variation de la vitesse des ultrasons avec la composition et la température, dans le système benzène + alcool méthylique.

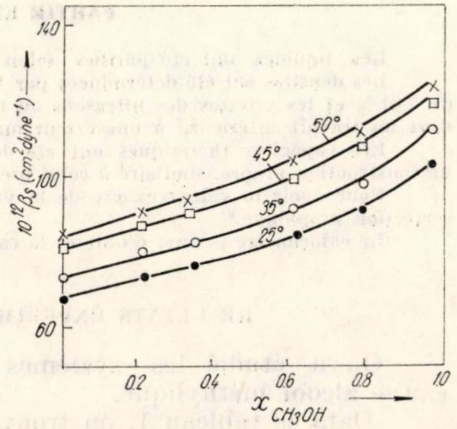

Fig. 2. — Variation de la compressibilité adiabatique avec la composition et la température, dans le système benzène + alcool méthylique.

$$\alpha = \frac{V_2 - V_1}{V_1\ \Delta t} = \frac{V_{35} - V_{25}}{10\ \ \ V_{25}}$$

où V_1 et V_2 désignent le volume molaire, à 25 et 35°.

Tableau 2

Grandeurs thermodynamiques, à 25°, dans le système benzène + alcool méthylique

x_{CH_3OH}	0,0000	0,2189	0,3589	0,6329	0,7955	1,0000
C_P (J.mol^{-1})	133,67	129,32	129,85	114,29	103,21	84,19
$10^{12}\ \beta_T$(cm^2 dyne^{-1})	98	102	103	110	115	125
	1,44	1,39	1,36	1,30	1,27	1,21
C_v (J.mol^{-1} k^{-1})	92,57	92,97	95,20	87,7	81,14	69,63
E^M (J.mol^{-1})		195	177	132	78	
H^E(J.mol^{-1})		163	165	115	68	

Tableau 3

Grandeurs thermodynamiques, à 20°, dans le système eau + alcool méthylique

x_{CH_3OH}	0,0000	0,058	0,1233	0,1942	0,2727	0,3600	0,4576	0,5676	0,6923	0,8350	1,0000
$10^{12}\beta_T$(cm$^2\cdot$dyne^{-1})	46,6	46,9	44,0	48,0	48,3	54,1	61,3	70,8	83,7	99,6	123,0
C_v (J.mol^{-1}K^{-1})	74,53	73,09	78,46	78,40	76,76	74,72	72,57	70,75	69,87	68,21	65,81
$10^{12}\beta_S^E$ (cm^2. dyne^{-1})	0,00	−9,35	−16,72	−23,27	−26,84	−28,30	−28,04	−25,91	−20,31	−12,44	0,00
$10^{12}\beta_{T_s}^{E'}$(cm^2. dyne^{-1})	0,00	−9,1	−20,9	−28,4	−33,2	−35,1	−35,2	−32,8	−26,77	−17,2	0,00
V^E (cm^{3}mol^{-1})	0,00	−0,35	−0,35	−0,61	−0,79	−0,92	−0,99	−0,97	−0,83	−0,52	0,00

En outre, on a calculé le coefficient $\gamma = \beta_T/\beta_S$, ainsi que la capacité thermique à volume constant, C_v.

L'énergie de mélange à volume constant, E^M, a été calculée par l'équation (8) avec les volumes d'excès déduits des densités et par les valeurs expérimentales de H^E fournies par la littérature.[10]

Le tableau 3 fournit des grandeurs similaires pour le système alcool méthylique + eau, à 20°. Les valeurs des densités et de la vitesse des ultrasons ont été empruntées au travail de Nozdrev [10] et celles des capacités thermiques aux Tables critiques internationales.[11]

Dans le système eau + alcool méthylique, les compressibilités adiabatiques d'excès β_S^E et isothermes d'excès, β_T^E, sont négatives et grandes et varient de la même façon que les volumes d'excès.

Les volumes d'excès et les compressibilités isothermes d'excès présentent des maxima à $x_2 = 0{,}4576$.

Le tableau 4 fournit les volumes de mélange calculés au moyen des densités, comparativement aux volumes de mélange calculés par l'équation (7).

Tableau 4

Volumes d'excès dans les systèmes : benzène + alcool méthylique et eau + alcool méthylique

benzène + alcool méthylique			eau + alcool méthylique		
x_{CH_3OH}	$V^E(\mathrm{cm^3.mol^{-1}})$		x_{CH_3OH}	$V^E(\mathrm{cm^3.mol^{-1}})$	
0,0000	0,00	0,000	0,0000	0,00	0,00
0,2189	−0,09	−0,95	0,1233	−0,35	−1,01
0,3589	−0,03	−1,10	0,1942	−0,61	−2,27
0,6329	−0,05	−1,34	0,2727	−0,79	−3,39
0,7955	−0,03	−0,83	0,3600	−0,93	−4,01
1,0000	0,00	0,00	0,4576	−0,99	−4,07
			0,5676	−0,97	−3,82
			0,6923	−0,83	−2,73
			0,8350	−0,53	−1,48
			1,0000	0,00	0,00

Les volumes d'excès déduits des densités — du système benzène + alcool méthylique sont très petits et décroissent en valeur absolue à mesure que la température augmente.

Les volumes d'excès du système eau + alcool méthylique sont grands et négatifs.

Les volumes d'excès calculés par l'équation (7) sont également négatifs, mais on remarque une faible concordance avec les volumes expérimentaux, qui est d'autant plus marquée que le volume d'excès est moindre.

Ceci est probablement dû à l'approximation

$$(\partial E/\partial V_0)_T = (\partial E/\partial V)_T = T\alpha/\beta_T$$

---

[10] « International Critical Tables of Numerical Data, Physics, Cehmistry and Technology », V^e. vol., Mc. Grow—Hill Book Company, Inc., 1929, p. 116.

[11] A. G. Williamson et R. L. Scott, *J. Phys. Chem.*, **64**, 440 (1960).

Les pressions internes dans les deux systèmes, calculées par la formule (6), sont enregistrées dans le tableau 5.

Tableau 5

Pression interne dans les systèmes benzène + alcool méthylique et eau + alcool méthylique

Benzène + alcool méthylique		Eau + alcool méthylique	
x_{CH_3OH}	p_i (atm) 25°	x_{CH_3OH}	p_i (atm) 20°
0,0000	3740	0,0000	1641
0,2189	3668	0,1233	2972
0,3589	3661	0,1942	3778
0,6329	3524	0,2727	4252
0,7955	3238	0,3600	4352
1,0000	2919	0,4576	4202
		0,5676	3978
		0,6923	3591
		0,8350	3228
		1,0000	2923

La pression interne dans le benzène est plus élevée que dans l'eau et l'alcool, ce qui est explicable si l'on tient compte du fait que la pression interne est due aux forces de dispersion ; or, dans les composants associés des types de l'eau et de l'alcool ce sont des liaisons hydrogène qui prédominent, les forces de dispersion n'apparaissant qu'entre les agrégats de molécules.

Dans le système eau + alcool méthylique, la pression interne varie dans le même sens que le volume de mélange et la compressibilité d'excès atteint un maximum ; après cela elle commence à diminuer jusqu'à sa valeur dans l'alcool.

Dans la littérature,[12] on voit que la différence $E_V - p_i V$, (où E_V désigne l'énergie de vaporisation), pourrait bien être une mesure de l'énergie d'association.

Le calcul des erreurs maximales des grandeurs ci-dessus, en tenant compte des erreurs expérimentales a fourni les valeurs suivantes : ± 6% pour β_S, ± 2,3% pour β_T, ± 6,5% pour p_i et 3% pour γ — dans le système alcool méthylique + benzène — et 1,5% pour β_T, 8,5% pour p_i et 2% pour γ, dans le système alcool méthylique + eau.

Le système tétrachlorure de carbone + alcool méthylique

Les figures 3 et 4 donnent les variations de la vitesse des ultrasons et de la compressibilité adiabatique, avec la fraction molaire de tétrachlorure de carbone.

---

[12] E. B. BAGLEY et H. H. WOOD, *Polymer Eng. Sci.*, **6**, 141 (1966) ; I. A. WIEHE et E. B. BAGLEY, *Amer. Inst. Chem. Engineers J.*, **1967**, 836.

La compressibilité adiabatique a été calculée au moyen des densités empruntées à la littérature.[13]

Le tableau 6 contient les valeurs calculées des compressibilités d'excès et des volumes d'excès.

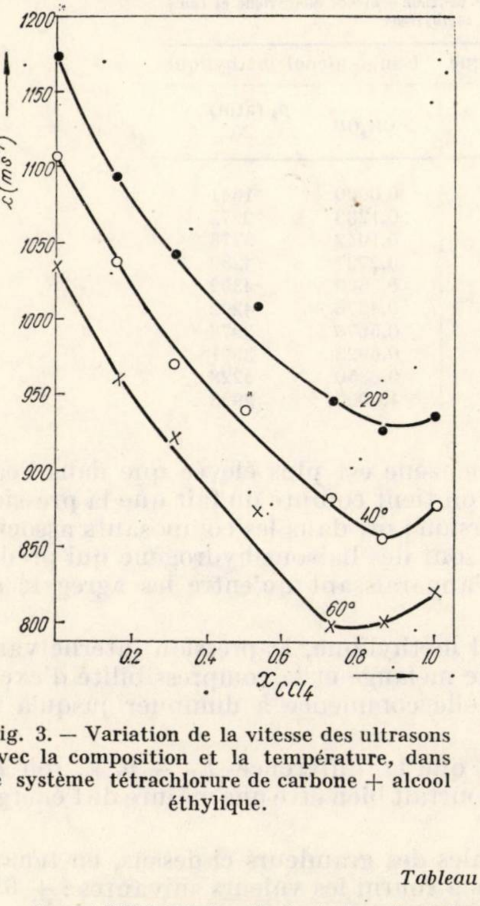

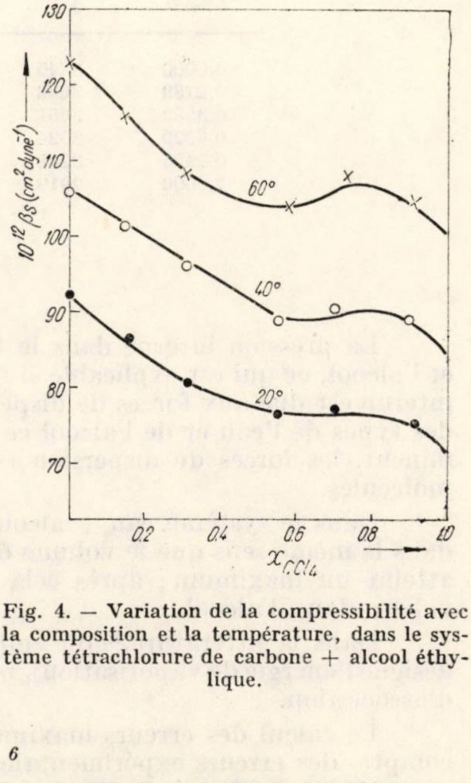

Fig. 3. — Variation de la vitesse des ultrasons avec la composition et la température, dans le système tétrachlorure de carbone + alcool éthylique.

Fig. 4. — Variation de la compressibilité avec la composition et la température, dans le système tétrachlorure de carbone + alcool éthylique.

Tableau 6

Compressibilité adiabatique d'excès et volume d'excès dans le système tétrachlorure de carbone + alcool éthylique

t	V^E (cm^3 mol^{-1})			$10^{12}\,\beta_S^E$ (cm^2 dyne^{-1})		
$x_{C_2H_5OH}$	20	40	60	20	40	60
0,141	−0,03	0,00	0,04	2,6	3,6	4,2
0,271	0,20	0,23	0,27	6,5	2,7	8,5
0,467	0,12	0,10	0,20	−3,8	−4,4	−6,3
0,690	−0,06	0,04	0,12	−2,4	−2,3	−3,6
0,838	−0,19	−0,18	−0,14	−0,5	−0,5	−1,1

---

[13] B. I. Konobeev et V. V. Liapin, *Zhur, priklad. Khim.*, **43**, 803 (1970).

La figure 4 met en évidence que la vitesse des ultrasons présente aux faibles concentrations d'alcool un maximum qui se déplace vers les concentrations plus fortes à mesure que la température augmente. Les vitesses des ultrasons dans ce système, à d'autres températures et concentrations, ont été déterminées par Sette[14].

Une interprétation de l'existence du minimum sur la courbe de la vitesse pourrait être offerte en partant de la relation (1), laquelle, différenciée par rapport à la concentration $\tilde{c}$, donne :

$$(\partial c/\partial \tilde{c})_t = -\frac{c}{2}\left[\frac{1}{\beta_S}(\partial \beta_S/\partial \tilde{c})_t + \frac{1}{\rho}(\partial \rho/\partial \tilde{c})_t\right]$$

Le sens de la variation de la vitesse avec la concentration sera déterminé par le signe et la valeur des deux termes du second membre de l'équation.

Le terme $\frac{1}{\rho}(\partial \rho/\partial c)_t < 0$, tandis que $\frac{1}{\beta_S}(\partial \beta_S/\partial \tilde{c})_t \gtrless 0$, selon le domaine de concentration choisi, ce qui signifie qu'une diminution de la vitesse avec la concentration est conditionnée par les deux inégalités suivantes :

$$\frac{1}{\beta_S}(\partial \beta_S/\partial \tilde{c})_t > 0$$

et

$$\left|\frac{1}{\beta_S}\left(\frac{\partial \beta_S}{\partial \tilde{c}}\right)_t\right| > \left|\frac{1}{\rho}\left(\frac{\partial \rho}{\partial \tilde{c}}\right)_t\right|$$

Aux concentrations correspondant au minimum, le signe opposé et la valeur égale des deux termes conduit à l'annulation de la dérivée, donc à un minimum de la vitesse. Aux concentrations plus fortes, la contribution des deux termes est contraire et la valeur $\partial c/\partial \tilde{c}$ représente alors un accroissement de la vitesse avec la concentration.

Les compressibilités adiabatiques d'excès (tableau 5) varient à peu près de la même façon que les volumes d'excès.

Rowlinson [15] a montré que les propriétés d'un mélange d'un liquide associé avec un liquide non polaire sont avant tout, une chaleur d'excès positive avec un maximum dans le cas du mélange pauvre en composant polaire, une enthalpie d'excès négative avec un minimum dans le cas du mélange riche en composant polaire et une énergie libre d'excès qui est grande, positive et quasi symétrique à la composition.

La chaleur positive d'excès est en moyenne une mesure du nombre de liaisons hydrogène ou d'autres interactions électrostatiques locales, qui sont rompues lors de la formation du mélange.

---

[14] D. Sette, *Niovo Cim. Suppl.* **7**, 140 (1951).

[15] J. S. Rowlinson, « Liquids and Liquids Mixtures », Butterworths, Scientific Publications, Londres, 1959, p. 180.

Cette chaleur est moindre dans les mélanges riches en alcool, par exemple, puisque l'addition d'une petite quantité d'un diluant inerte ne brise que peu de liaisons. La grande partie du diluant se trouve probablement englobée parmi les molécules d'alcool liées aux agrégats.

Cette possibilité expliquerait pourquoi, à ces concentrations, les volumes d'excès et, par conséquent, les compressibilités adiabatiques d'excès également, sont négatifs. La chaleur de mélange est plus grande dans le cas des mélanges pauvres en alcool puisque l'addition d'une petite quantité d'alcool à une grande quantité de liquide non polaire doit briser toutes les liaisons de l'hydrogène. L'augmentation de volume pourrait donc être déterminée par la désassociation de l'alcool.

Revue Roumaine de Chimie, **21**, *2*, 187–191 (1976)

DECOMPOSITION KINETICS OF COPPER TETRA-AMMINE SULPHATE MONOHYDRATE

D. FĂTU and E. SEGAL
Chair of Physical Chemistry and Electrochemical Technology,
Polytechnic Institute of Bucharest

Received October 5, 1974

The results obtained in the kinetic analysis of the decomposition of copper tetra-ammine sulphate monohydrate in connection with various experimental factors are presented.

INTRODUCTION

Following the research concerning the kinetics of thermal decomposition of complexes,[1] in this paper are presented the results obtained by investigating the thermal behaviour of copper tetra-ammine sulphate monohydrate. This compound has been chosen because of the few literature data known about its thermal stability,[2] as well as to complete a previous isothermal kinetic study of its first steps of decomposition.[3] On the other hand, the research in the field of nonisothermal kinetics raised some problems about the reliability of the kinetic parameters values, as it is known that these values, in determined conditions, change with the heating rate, the sample surrounding atmosphere and the sample weight.[4,5] To select most reliable values of the kinetic parameters, we considered useful to investigate the influence of all these factors on the reaction rate.

EXPERIMENTAL

We used copper tetra-ammine sulphate, synthesized and analysed according to the methods described in the literature.[6] The crystals have been crushed and sieved, retaining only the granules between 0.1 and 0.09 mm diameter.

---

[1] I. G. Murgulescu, D. Fătu and E. Segal, *J. Thermal Anal.* **1**, 97 (1969).

[2] E. Renker, *Bull. Soc. chim. France*, **1973**, 1992; E. Renker and P. Vallet, *Compt. rend.*, **204**, 1337 (1973); M. M. T. Anous, *Rec. Trav. chim.*, **78**, 97 (1959); T. Flora, *Magyar Kém. Folyóirat*, **68**, 156 (1962).

[3] I. G. Murgulescu and E. Segal, *Rev. Chim. Acad. R.P.R.* **8**, 51 (1963).

[4] D. Schultze, *J. Thermal Anal.*, **5**, 353 (1973).

[5] J. Simon, *J. Thermal Anal.*, **5**, 271 (1973).

[6] J. Paulik and F. Paulik, *Talanta*, **17**, 1224 (1970).

The heating curves necessary for the kinetic analysis have been simultaneously recorded by means of a MOM, Paulik-Paulik-Erdey type derivatograph.

For the kinetic analysis of the experimental data, we used the Coats-Redfern [7] method, as well as a method based on a hyperbolic heating program.[8]

RESULTS AND DISCUSSION

While in nonisothermal conditions, the curves corresponding to the release of the water molecule and of the first two ammonia molecules overlap considerably,[6] rendering more difficult the kinetic analysis, a previous isothermal investigation [3] of the decomposition allowed us to separate these two processes according to the following reactions :

$$[Cu(NH_3)_4]SO_4.H_2O(s) \rightarrow [Cu(NH_3)_4]SO_4(s) + H_2O(g) \qquad \text{I}$$

$$[Cu(NH_3)_4]SO_4(s) \rightarrow [Cu(NH_3)_2]SO_4(s) + 2NH_3(g) \qquad \text{II}$$

The release of the last two ammonia molecules can be analysed in nonisothermal conditions and takes place in the following stages :

$$[Cu(NH_3)_2]SO_4(s) \rightarrow [Cu(NH_3)]SO_4(s) + NH_3(g) \qquad \text{III}$$

$$[Cu(NH_3)]SO_4(s) \rightarrow CuSO_4(s) + NH_3(g) \qquad \text{IV}$$

According to the data of J. Paulik and F. Paulik, in the last step (IV), a small amount of sulphur trioxide also evolves. Our data reproduce the above-mentioned ones, but only for fresh samples. Using old samples (several days after the compound was prepared), the last two ammonia molecules evolve according to reactions III and IV, without any sulphur trioxide release (figure 1). Such curves were used for the kinetic analysis of the reactions III and IV.

Taking into account the previously mentioned difficulty of performing a kinetic analysis of reactions I and II, in nonisothermal conditions, in order to obtain a complete kinetic description of the decomposition, we shall use the results of an isothermal kinetic study [3] which lead to :

— for reaction I

$n = 0$, $E = 15.900$ cal/mole, $Z = 3.82 \cdot 10^4$ g.s^{-1}

— for reaction II

$n = 0$, $E = 19.900$ cal/mole, $Z = 2.90 \cdot 10^6$ g.s.$^{-1}$

where n means the reaction order, E — the activation energy and Z the preexponential factor.

---

[7] A. W. Coats and J. P. Redfern, *Nature*, **21**, 68 (1964).

[8] D. Fătu and E. Segal, *Rev. Roumaine Chim.*, **16**, 343 (1971).

The nonisothermal kinetic analysis of reactions III and IV leads to a reaction order of the same value, $n = 2/3$, which indicates a contracting sphere mechanism.

In table 1 are presented the kinetic parameters values for different heating rates. The rate constant values are sensitive to the shift of the heating rate values from 11.6°/min to 5,3-min. Between 5.3°/min and 2.5°/min, the rate constant remains practically unchanged. Thus, the heating of the samples whose rates are less than 5.3°/min, does not have any influence on the decomposition rates and provides reliable kinetic data. In this last range of heating rates, the values of the activation energy and the preexponential factor exhibit a compensation effect.

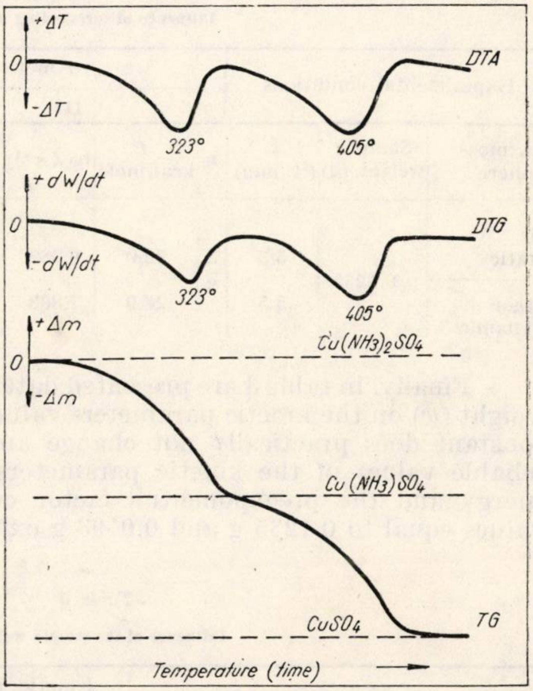

Fig. 1. — Thermogram for the decomposition of $[Cu(NH_3)_2]SO_4$ $w = 0.3004$ g; $\beta = 5.3$°/min; air).

Table 1

Influence of heating rate (β)

Experimental conditions			Kinetic parameters of reactions							
			III				IV			
Atmosphere	Sample weight (g)	β (°C/min)	n	E kcal/mole	lg $(Z.s^{-1})$	lg $(k.s^{-1})$ (553°K)	n	E kcal/mole	lg$(Z.s^{-1})$	lg$(k-s^{-1})$ (655°K)
air		2.5	$\frac{2}{3}$	19.5	4.959	$\bar{3}.251$	$\frac{2}{3}$	42.5	11.903	$\bar{3}.721$
static	0.1235	5.3		32.0	9.898	$\bar{3}.249$		60.2	17.724	3.635
		11.6		32.4	9.609	$\bar{4}.80$		59.3	16.676	4.887

The data about the influence of the surrounding atmosphere on the kinetic parameters of reactions III and IV are given in table 2. The rate constant is practically the same, but the data exhibit also a compensation effect.

Table 2

Influence of surrounding atmosphere

Experimental conditions			Kinetic parameters of reactions							
			III				IV			
Atmosphere	Sample weight (g)	β (°C/min)	n	E kcal/mole	lg($Z.s^{-1}$)	lg($k.s^{-1}$) (553°K)	n	E kcal/mole	lg($Z.s^{-1}$)	lg($k.s^{-1}$) (655°K)
air static	0.1235	5.3	$\frac{2}{3}$	32.0	9.989	$\bar{3}.249$	$\frac{2}{3}$	60.2	17.724	$\bar{3}.635$
argon dynamic		5.5		26.9	7.863	$\bar{3}.212$		58.22	17.209	$\bar{3}.820$

Finally, in table 3 are presented data about the influence of the sample weight (w) on the kinetic parameters values. Below $w = 0.1235$ g, the rate constant does practically not change and the kinetic analysis leads to reliable values of the kinetic parameters. The values of the activation energy and the preexponential factor corresponding to sample weight values equal to 0.1235 g and 0.0593 g exhibit also a compensation effect.

Table 3

Influence of the sample weight

Experimental conditions			Kinetic parameters of reactions							
			III				IV			
Atmosphere	Sample weight (g)	β (°C/min)	n	E kcal/mole	lg($Z.s^{-1}$)	lg($k.s^{-1}$) (553°K)	n	E kcal/mole	g($Z.s^{-1}$)	lg($k.s^{-1}$) (655°K)
Air static	0.0593	5.3	$\frac{2}{3}$	14.5	2.976	$\bar{3}.265$	$\frac{2}{3}$	36.6	10.095	$\bar{3}.881$
	0.1235			32.0	9.898	$\bar{3}.2439$		60.2	17.724	$\bar{3}.635$
	0.3004			35.3	10.922	$\bar{4}.970$		60.5	17.434	$\bar{3}.245$

The observed phenomena could be explained by assuming that the investigated compound is characterized by a Maxwell distribution of the centres responsible for the chemical activity in the decomposition reaction. The compensation effect observed when the heating rate is lowered from 5.3°/min to 2.5°/min could be considered as due to the gases accumulation over the sample, thus blocking the active centres at higher heating rates. The blocking action could be realised either by adsorption, or by reverse reaction. At lower heating rates, the blocking of the few (low value of Z) active (low value of E) centres is reduced.

The influence of the surrounding atmosphere could be explained in the same way, taking into account the fact that, in static atmosphere, the less active centres are responsible for the reaction.

The compensation effect put into evidence by changing the sample weight could be explained in a similar way. According to the general above-mentioned assumption, the smaller partial pressure value of the resulting gas over the sample, when using small sample weights, allows the higher activity centres to be expressed in the kinetic parameters values.

CONCLUSIONS

1. The thermal decomposition of the old samples of powdered copper tetra-ammine sulphate takes place without release of sulphur trioxide.
2. The kinetic parameters of water and ammonia release were determined.
3. The optimum conditions to evaluate the kinetic parameters were established.
4. A plausible explanation of the influence of different experimental factors on the reaction rate was presented.

Revue Roumaine de Chimie, **21**, 2, 193–205 (1976)

SPECTRAL SOLVENT EFFECTS IN AROMATIC COMPOUNDS SOLUTIONS. II*

THE SOLVENT EFFECTS ON THE POSITION AND INTENSITY OF CHLOROBENZENE BAND, AT 2600 Å

VASILE MACOVEI
Physical Chemistry Laboratory, University of Jassy, Calea 23 August, 11, Romania

Received May 28, 1974

The knowledge of the molecular chlorobenzene properties may be improved by studying the solvent influence on the electronic spectra of this molecule. Thus, the present paper aims at contributing to the elucidation of the factors determining the spectrum shift and the intensity increase of the spectral band under the solvents action. It also follows the dipole moment evaluation in the excited state for the interpretation of the spectral changes.

I. INTRODUCTION

Little is reported about the solvent influence on the chlorobenzene spectrum in the literature. Thus, Ugande,[1] based on the previous investigations[2–7] and his own observations involving the iodobenzene spectrum in cyclohexane, alcohol, and water, claims that the spectrum of the monosubstituted benzene with electron donor groups shifts toward the blue with increasing solvent polarity. The investigation of the chlorobenzene spectrum in six solvents[8] led to a relation of linearity between the spectrum displacement in solution and the refractive index function $f(n^2) = (n^2 - 1)/(2n^2 + 1)$ of the solvent. The same correlation was reached by comparing the spectral band positions of chlorobenzene in various solvents with spectral positions of the liquid chlorobenzene,[9] at 36,760 and 37,760 cm^{-1}, correctly using the refractive indices of the 26 used solvents (measured, with some exceptions, at $\lambda = 2500$Å). We used the refractive indices measured on the yellow natrium light.[10] Earlier, Lamotte *et al*[11] have correlated graphically the experimental and theoretical results regarding the chlorobenzene spectral shifts under the solvents influence.

---

* Pat I see ref. 10.

[1] H. E. Ungnade, *J. Amer. Chem. Soc.*, **75**, 432 (1953).
[2] L. Doub and J. M. Vandenbelt, *J. Amer. Chem. Soc.*, **69**, 2714 (1947).
[3] K. Bowden and E. A. Braude, *J. Chem. Soc.*, **1952**, 1068.
[4] W. W. Robertson and F. A. Matsen, *J. Amer. Chem. Soc.*, **72**, 5252 (1950).
[5] H. Conrath-Billroth, *Z. phys. Chem.*, **B 25**, 139 (1934).
[6] R. A. Drurie, T. Iredale, and J. M. S. Jarvie, *J. Chem. Soc.*, **1950**, 1182.
[7] F. Smith and L. M. Turton, *J. Chem. Soc.*, **1951**, 1702.
[8] N. S. Bayliss and L. Hulme, *Austral. J. Chem.*, **6**, 257 (1953).
[9] O. V. Sverdlova, *Opt. i Spektrosk.*, **6**, 349 (1959).
[10] V. Macovei, Rev. Roum. Chim., **20**, 1413 (1975).
[11] M. Lamotte, G. A. Gerhold, and J. Joussot-Dubien, *J. Chim. phys.*, **67**, 2006 (1970)

Thus, it is necessary to carry out a more detailed investigation of the chlorobenzene spectrum behaviour under the solvents action to draw some general conclusions concerning the interaction with the solvent.

II. RESULTS AND DISCUSSION

The spectral behaviour of the substituted benzene is similar with that of the original compound. The substitution of a hydrogen atom in benzene by a chlorine atom slightly modifies the spectrum, but displaces its origin in passing from gas to solution.[12] In the ultraviolet spectral range, the spectra of monosubstituted benzenes consist of two bands[2,3,13] of which that on the visible side is theoretically and experimentally better known,[14] and called "secondary band".[2] The complex band, located approximately at 2000 Å, is called "primary band". Usually, there is a deep absorption minimum between these two bands. If the interaction between the benzene ring and the substituent is strong, a new band appears, called "conjugation band" ("*K*" band).[3,15] It is easy to practically examine the "secondary band", originating in the $^1A_{1g} \rightarrow {}^1B_{2u}$ forbidden transition of benzene and becoming the allowed transition $^1A_1 \rightarrow {}^1B_1$ in the monosubstituted benzene derivatives, on the basis of their C_{2v} symmetry in the ground and excited states,[16] hence through the perturbation of the D_{6h} symmetry of benzene.[17] This transformation is theoretically established,[18] and it is shown practically that the band shifts on the benzene substitution, as it happens with all benzene bands.[2,19-21] But there still exist disagreements in the assignment of the electronic transitions of the monosubstituted benzene, as it results from the experimental[2-4, 22-26] and theoretical[19,21,27-33] works.

---

[12] N. Fuson, C. Garrigou-Lagrange, and M. L. Josien, *Spectrochim. Acta,* **16**, 106 (1960).

[13] M. Ballester and J. Castaner, *J. Amer. Chem. Soc.*, **82**, 4259 (1960).

[14] M. Ballester, J. Palan, and J. Riera, *J. Quant. Spectrosc. Radiant Transfer*, **4**, 819 (1964).

[15] A. Mangini, A. Trombetti, and C. Zauli, *J. Chem. Soc.*, **B 2**, **1967**, 153.

[16] P. C. Upadhya, G. D. Baruah, K. N. Upadhya, and D. K. Rai, *Isr. J. Chem.*, **9**, 7 (1971).

[17] H. H. Jaffé and M. Orchin, "Theory and Applications of Ultraviolet Spectroscopy", Wiley, New York, 1964.

[18] F. A. Matsen, *J. Amer. Chem. Soc.*, **72**, 5243 (1950).

[19] L. Doub and J. M. Vandenbelt, *J. Amer. Chem. Soc.*, **71**, 2414 (1949).

[20] L. Doub and J. M. Vandenbelt, *J. Amer. Chem. Soc.*, **77**, 4535 (1955).

[21] P. E. Stevenson, *J. Mol. Spectroscopy*, **15**, 220 (1965).

[22] W. W. Robertson and F. A. Matsen, *J. Amer. Chem. Soc.*, **72**, 5248 (1950).

[23] W. W. Robertson and F. A. Matsen, *J. Amer. Chem. Soc.*, **72**, 5250 (1950).

[24] J. F. Music and F. A. Matsen, *J. Amer. Chem. Soc.*, **72**, 5252 (1950).

[25] W. W. Robertson, J. F. Music, and F. A. Matsen, *J. Amer. Chem. Soc.*, **72**, 5260 (1950).

[26] A. E. Lutskii, *Zhur. obshchei Khim.*, **33**, 1601 (1963).

[27] J. R. Platt, *J. Chem. Phys.*, **19**, 101 (1951).

[28] A. Mangini and R. Paserii, *J. Chem. Soc.*, **1952**, 1168.

[29] A. Mangini and C. Zauli, *J. Chem. Soc.*, **1956**, 4960.

[30] J. Petruska, *J. Chem. Phys.*, **34**, 1111 (1961).

[31] L. Goodman and H. Shull, *J. Chem. Phys.*, **23**, 33 (1955).

[32] L. Goodman, I. G. Ross, and H. Shull, *J. Chem. Phys.*, **26**, 474 (1957).

[33] L. Goodman and H. Shull, *J. Chem. Phys.*, **27**, 1388 (1957).

In the $^1A_1 \rightarrow {}^1B_1$ ($\pi \rightarrow \pi^*$) transition of the monosubstituted benzenes the vibrations the benzene ring are efficient,[16] namely the C—C vibrations are prominent. The results in figure 1 for the chlorobenzene spectrum confirm the spectral shifts in some solvents, as compared with the vapour spectrum,[12] and the C—C vibrations prominence. The numbers in figure 1 correspond to the solvents in table 1, notation used throughout the paper. The vibrational component (0, 0) is distincly detached from the remainder spectrum, on the long waves side, and with a remarkable intensity, being no longer forbidden by the symmetry. The spectrum shifts in the same direction, but the shift amount differs in various solvents. The vibrational structure is blurred, as compared with that of the benzene.[10] The examination of a component from the fine structure in the $^1A_1 \rightarrow {}^1B_1$ transition represents the spectrum behaviour as a whole, regarding the displacement on the solvent action.[10] The position of the (0, 0) vibrational component is determined in the vapour spectrum with a precision of several cm^{-1}, and approximately with 30 cm^{-1} in the solution

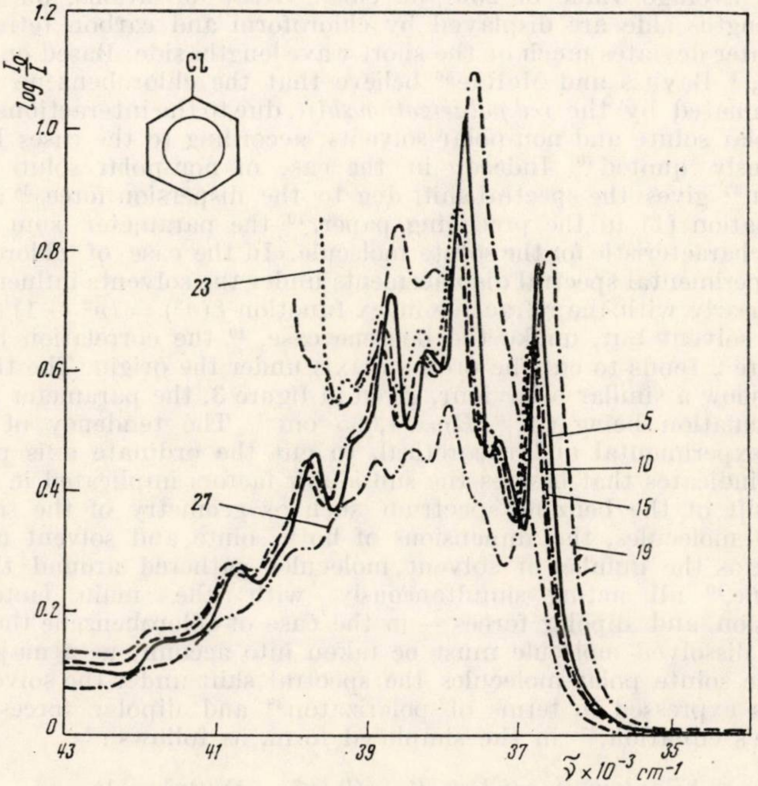

Fig. 1. — The chlorobenzene spectrum in solvents: 5. *n*-Heptane; 10. Ethanol; 15. Ethyl ether; 19. Carbon tetrachloride; 23. Ethyl acetate; 27. Water.

spectrum.[34] Therefore, the position of this component under the solvents influence has been examined. In the vapour spectrum[35] the position of the (0, 0) vibrational component is at 37,052 cm^{-1}. The majority of shift values, $\Delta\tilde{\nu}(\mathrm{cm}^{-1})$, under the solvents action are grouped around the overall average value of 256 ± 50 cm^{-1}. Great deviations, on the long wavelengths side are displayed by chloroform and carbon tetrachloride, and water deviates much on the short wave lengths side. Based on previous results, [8] Bayliss and McRae[36] believe that the chlorobenzene spectrum is dominated by the *red polarization shift*, due to the interactions between non-polar solute and non-polar solvents, according to the cases I and II, previously quoted[10]. Indeed, in the case of non-polar solute McRae's relation[37] gives the spectral shift due to the dispersion forces[38] according to equation (1) in the preceding paper,[10] the parameter sum $(A + B)$ being characteristic for the solute molecule. In the case of chlorobenzene, the experimental spectral displacements under the solvents influence correlate linearly with the refractive index function $f(n^2) = (n^2 - 1)/(2n^2 + 1)$ of the solvent but, unlike the benzene case, [10] the correlation line given in figure 2 tends to cut the ordinate axis under the origin. The theoretical shifts show a similar behaviour, given in figure 3, the parameter sum used in calculation being $(A + B) = 1{,}065$ cm^{-1}. The tendency of the two lines, experimental and theoretical, to cut the ordinate axis under the origin indicates that besides the subsidiary factors implicated in the spectral shift of the benzene spectrum such as geometry of the solute and solvent molecules, the dimensions of both solute and solvent molecules, as well as the number of solvent molecules gathered around the solute molecule,[10] all acting simultaneously with the main factors — the dispersion and dipolar forces — in the case of chlorobenzene the polarity of the dissolved molecule must be taken into account as a major factor. For the solute polar molecules the spectral shift under the solvent influence is expressed in terms of polarizaton[38] and dipolar forces by the McRae's equation,[37] in the simplified form, as follows:

$$\begin{aligned}\Delta\tilde{\nu}_{\mathrm{abs.}}(\mathrm{cm}^{-1}) &= (A + B + C)\,(n^2 - 1)/(2n^2 + 1)\\ &\quad + E\,[(D - 1)/(D + 2) - (n^2 - 1)/(n^2 + 2)] \qquad (1)\\ &\quad + F\,[(D - 1)/(D + 2) - (n^2 - 1)/(n^2 + 2)]^2\end{aligned}$$

where n is the refractive index and D is the dielectric constant of the solvent; the parameters $(A + B + C)$, E and F are characteristic constants of the dissolved molecule, and their values* were calculated by the least-squares method. [39] The calculated values of the parameters are: $(A + B + C) = 1{,}436 \cdot 63$ cm^{-1}, $E = 83 \cdot 40$ cm^{-1}, and $F = -247 \cdot 33$ cm^{-1}. The theoretical displacements, calculated by means of the relation (1), given

---

* The calculation program was established at the Territorial Center of Electronic Calculus, Jassy.

[34] J. PETRUSKA, *J. Chem. Phys.*, **34**, 1120 (1961).

[35] H. SPONER and S. H. WOLLAM, *J. Chem. Phys.*, **9**, 816 (1941).

[36] N. S. BAYLISS and E. G. MCRAE, *J. Phys. Chem.*, **58**, 1002 (1964).

[37] E. G. MCRAE, *J. Phys. Chem.*, **61**, 562 (1957).

[38] F. LONDON, *Z. Physik*, **63**, 245 (1930).

[39] D. YORK, *Canad. J. Phys.*, **44**, 1079 (1966).

Fig. 2. — The experimental shift dependence of the chlorobenzene absorption band on the $(n^2 - 1)/(2n^2 + 1)$ function of solvent.

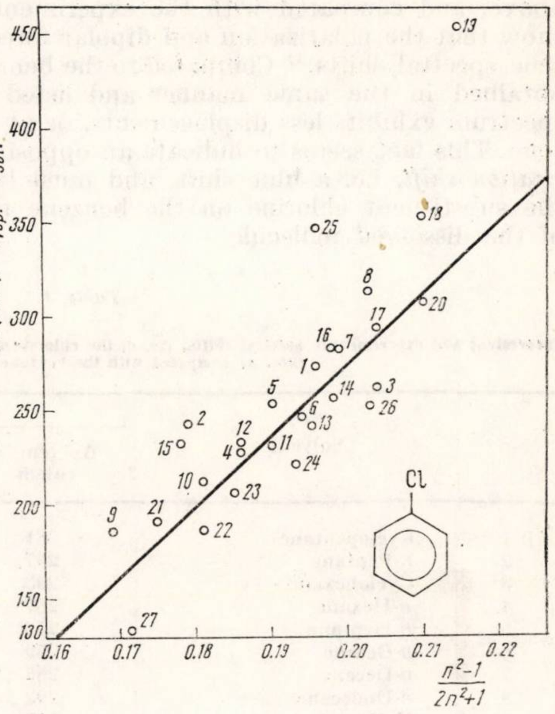

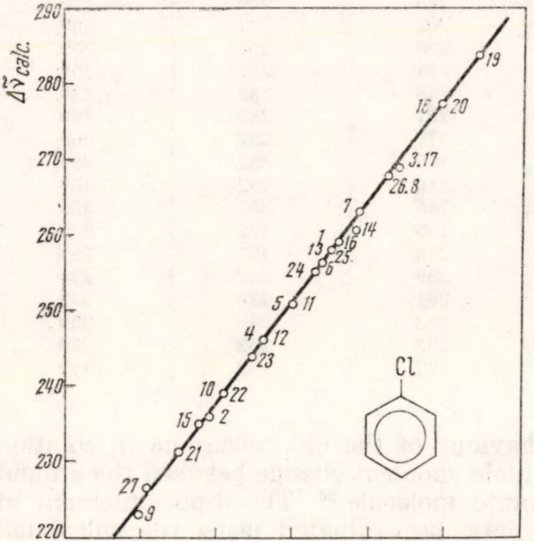

Fig. 3. — The theoretical shift dependence of the chlorobenzene absorption band on the $(n^2 - 1)/(2n^2 + 1)$ function of solvent.

above, and compared with the experimental values, as seen in table 1, show that the polarization and dipolar forces contribute to the chlorobenzene spectral shifts.[37] Compared to the benzene spectral shifts in solution,[10] obtained in the same manner and listed in table 1, the chlorobenzene spectrum exhibits less displacements, or at most equal with those of benzene. This fact seems to indicate an opposite phenomenon to the *red polarization shift*, i.e. a blue shift, and must be related with the presence of the substituent chlorine on the benzene ring, that is with the polarity of the dissolved molecule.

Table 1

Theoretical and experimental spectral shifts, $\Delta\tilde{\nu}$, of the chlorobenzene band at 2600 Å, under the solvent influence, as compared with the benzene spectral shifts

N°	Solvent	C_6H_5Cl		C_6H_6
		$\Delta\tilde{\nu}$ (cm^{-1}) calcd	$\Delta\tilde{\nu}$ (cm^{-1}) Experim.	$\Delta\tilde{\nu}$ (cm^{-1}) Experim.
1	Cyclopentane	281	272	279
2	*n*-Pentane	257	242	259
3	Cyclohexane	293	262	259
4	*n*-Hexane	267	227	259
5	*n*-Heptane	273	252	279
6	*n*-Octane	279	247	259
7	*n*-Decane	286	282	259
8	*n*-Dodecane	292	312	279
9	Methanol	149	187	219
10	Ethanol	205	212	259
11	1-Propanol	225	232	259
12	2-Propanol	202	232	259
13	1-Butanol	238	242	259
14	3-Methyl-1-butanol	231	257	259
15	Ethyl ether	258	232	239
16	Isoamyl ether	291	282	299
17	Methylene chloride	277	292	359
18	Chloroform	305	352	399
19	Carbon tetrachloride	310	452	459
20	1,2-Dichloroethane	283	307	359
21	Acetonitrile	185	192	239
22	Methyl acetate	248	187	259
23	Ethyl acetate	259	207	239
24	Butyl acetate	261	222	239
25	*n*-Amyl acetate	283	345	259
26	1,4-Dioxane	293	252	299
27	Water	167	132	179

To clarify the spectral behaviour of the chlorobenzene in solution one must take into account the dipole moment change between the ground and the excited states of the solute molecule.[36] The dipole moment of the chlorobenzene excited state may be evaluated using the calculated value of the parameter E and its explicit form from the equation of McRae,[37] that is:

$$E = (2/hc)[M_{00}(M_{00} - M_{ii})/a^3] \tag{2}$$

where h is the Planch constant; c is the light speed; M_{00} and M_{ii} are, respectively, the dipole moments in the ground and excited states, and a is the solvent cavity radius. The dipole moment of the ground state, M_{00}, is 1.56 D for the liquid chlorobenzene[40] and 1.72 D for the gaseous chlorobenzene.[40] The average value of the solvent cavity radius, a, is calculated for the spherical molecular model, asuming that it is equal with the mean radius of the molecule in the liquid state, or in pure crystal,[11] according to the expression:

$$a^3 = 3M/4\pi N\rho \qquad (3)$$

where M is the molecular weight; N is Avogadro's number, and ρ is the material density. Using the known values[41] of M and ρ (at 20°) for the chlorobenzene, one calculates: a^3 (Å^3) = 40.35. The introduction of the M_{00} and a^3 values in the equation (2) of this paper leads to the M_{ii} values listed in table 2. Regardless of M_{00} value for the liquid or gaseous chlorobenzene, the M_{ii} value is, in both cases, smaller. A similar result was previously obtained using a slightly different method.[11] The explanation of the dipole moment decrease in the excited state of the chlorobenzene is as follows: two Kékulé structures, (I) and (II), may be formulated for the chlorobenzene, each of them with a dipole moment of 2.13 D, mostly located in the C—Cl bond, the positive charge being on the carbon, and the negative charge on the chlorine atom; there are small moments in the C—H bonds, and secondary, reduced moments in the benzene ring.[42]

Table 2

The evaluated dipole moment of chlorobenzene, M_{ii}, in the excited state

a^3(Å^3)	$M_{00}(D)$	$M_{ii}(D)$	Literature data $M_{ii}(D)$
40.35	liquid 1.56[40] gas 1.72[40]	1.346 1.526	1.519[11]

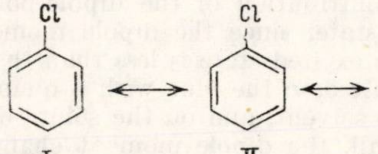

I II

---

[40] O. A. Osipov, V. J. Minkin, and A. D. Garnovskii, "Spravochinik po Dipolnym Momentam", Izd. Vysshaya Shkola, Moskva, 1971.

[41] A. Weissberger, E. S. Proskauer, J. A. Riddick, and E. E. Toops, Jr., "Technique of Organic Chemistry. Vol. VII, Organic Solvents," 2nd ed., Interscience, New York, 1955.

[42] C. P. Smith, "Dielectric Behaviour and Structure", McGraw-Hill, New York, 1955.

In each of the structures (I) and (II) the resonance results from contribution of the structures C—Cl and C^+Cl^-. In terms of the resonance theory there are in addition three less stables structures,[43,44] which have a small, yet appreciable contribution to the molecular structure, namely the (III), (IV), and (V) structures. These structures appear by the migration of an

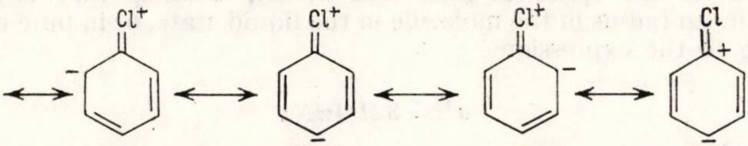
(III) (IV) (V) (VI)

electron pair from the chlorine atom, leaving thereon a positive charge, to the C—Cl bond, causing an electronic displacement in the benzene ring, with the formation of a negative charge on an *ortho* or *para* carbon. As the structures (III)—(V) have dipole moments opposite in direction to the moments of the structures (I) and (II), the dipole moment of the molecule will be diminished below that resulting only from the Kékulé structures. A series of theoretical papers [45–47] show that in the case of the halogen-substituent presence on the benzene ring the substituent withdraws σ electrons and donates π electrons. The calculated charge distribution in the fluorobenzene case [47] agrees with valence structures (I)—(V) to which the structure (VI) is added. From the calculations [45–47] there results that the dipole moment of C—Halogen bond opposes the mesomeric component. If we assume the preferential stabilization of the polar structures in the excited state[1] the dipole moment decrease of chlorobenzene is explained, and the hyperconjugation phenomenon is experimentally proved, confirming the previous result.[11]

Now, the spectral shift is easily interpreted according to the Franck-Condon principle.[36] In non-polar solvents, the orientation strain is not acting. The solvation energy is caused by the dispersion and dipole-polarization forces. The contribution of the dipole-polarization forces diminishes in the excited state, since the dipole moment decreases, and the solvation energy of the excited state is less than that of the ground state, the spectrum being shifted to the blue with a quantity depending on the refractive index of the solvent, and on the solute dipole moment change. The effect will be small, the dipole moment change being insignificant. The total displacement is on the red, dominated by the polarization shift. The vibrational structure of the spectrum is maintained. Thus, the chlorobenzene spectrum in solution of non-polar solvents behaves corresponding to the case III-*a* in the Bayliss-McRae's theory.[36] In polar solvent, the solvation energy is determined by the dipole-dipole forces, the solvent cavity being oriented. In the non-equilibrium Franck-Condon state the decrease of the dipole moment of the solute causes the reduction of the

---

[43] L. E. Sutton, *Proc. Roy. Soc. (London)*, **133 A**, 688 (1931).

[44] L. E. Sutton, *Trans. Faraday Soc.*, **30**, 789 (1934).

[45] J. A. Pople and M. S. Gordon, *J. Amer. Chem. Soc.*, **89**, 4253 (1967).

[46] W. J. Hehre and J. A. Pople, *J. Amer. Chem. Soc.*, **92**, 2191 (1970).

[47] W. J. Hehre, L. Radom, and J. A. Pople, *J. Amer. Chem. Soc.*, **94**, 1496 (1972).

orientation strain of the solvent cavity, i.e. a smaller solvation energy of the excited equilibrium state than that of the ground state. The spectrum will be displaced on the blue. The decrease of the dipole moment causes an insignificant reduction of the orientation strain and, consequently, the vibrational structure is preserved to a large extent. The total spectral displacement, originating in the dominant polarization shift and in the blue shift, is on the red. Thus, the chlorobenzene spectrum in polar solvents behaves according to the case IV-*a* in the Bayliss-McRae's theory.[36]

It was shown[10] that the intensities of the spectral bands increase in solution, compared to their values in the vapour spectrum. The comparison may be made using *the molar extinction coefficients*,[48] ε_ν, given in equation (2) of the previous paper[10] (very useful in the fine vibrational structure analysis), or employing *the oscillator strengths*,[49] f, involving the

Table 3

Position and intensity of chlorobenzene band at 2600 Å in various solvents, compared with literature data

N°	Solvent	$\tilde{\nu}_{max}$ (cm^{-1})	λ_{max} (Å)	ε_{max} (l·mol^{-1}·cm^{-1})	$f\cdot 10^3$
1	Cyclopentane	37,750	—	263.0	2.81
2	*n*-Pentane	37,780	—	258.2	2.74
3	Cyclohexane	37,775	2649	266.7	2.99
		—	2648[8]	283.0[8]	3.00[8]
4	*n*-Hexane	37,790	2646	249.2	2.68
		—	2646[8]	277.0[8]	2.80[8]
5	*n*-Heptane	37,770	2648	256.2	2.75
		—	2610[50]	270.0[50]	—
6	*n*-Octane	37,780	—	250.0	2.77
7	*n*-Decane	37,740	—	259.5	2.86
8	*n*-Dodecane	37,700	—	261.5	2.85
9	Methanol	37,840	—	200.0	2.57
10	Ethanol	37,820	—	207.5	2.62
11	1-Propanol	37,805	—	240.0	2.80
12	2-Propanol	37,785	—	251.2	2.87
13	1-Butanol	37,785	—	224.2	2.65
14	3-Methyl-1-butanol	37,770	—	248.2	2.76
15	Ethyl ether	37,740	—	211.7	2.54
16	Isoamyl ether	37,740	—	258.7	—
17	Methylene chloride	37,725	—	210.0	—
18	Chloroform	37,680	2654	211.5	2.64
		—	2651[8]	—	—
19	Carbon tetrachloride	37,370	2678	274.5	—
		—	2657[8]	296.0[8]	
20	1,2-Dichloroethane	37,725	—	210.7	2.68
21	Acetonitrile	39,315	—	281.0	—
22	Methyl acetate	37,860	—	225.0	2.34
23	Ethyl acetate	37,820	—	220.0	—
24	Butyl acetate	37,820	—	225.2	—
25	*n*-Amyl acetate	37,700	—	217.5	—
26	1,4-Dioxane	37,780	—	213.2	2.84
27	Water	37,925	—	—	—

---

[48] H. H. WILLARD, L. L. MERRITT, JR., and J. A. DEAN, "Instrumental Methods of Analysis," 3rd ed., D. Van Nostrand, Princeton, 1960.

expression of ***the integrated*** (***absolute***) ***intensities***, as it is seen in equation (4) of the previous paper.[10] We have evaluated the quantities ε_ν (corresponding to the $\tilde{\nu}_{\max.}$ frequencies), and f for the chlorobenzene spectra, and their values are listed in table 3. The examination of the data in table 3 shows that our values are comparable with the few data in the literature[8,50] (the references in brackets), and justifies their consideration when examining the chlorobenzene spectrum behaviour on the solvent action. One of the factors which contributes to the intensity increase in solution is the appearance of new vibrational components, forbidden in the vapour spectrum and becoming allowed in the solution spectrum by the solute-solvent interaction. For the chlorobenzene solutions it was considered[51] that the best results of the spectrum vibrational analysis have been obtained.[8] However, the comparison of the present data with those previously reported[8] (table 4) shows that our results significantly contribute to better reveal the new components in the vibrational structure. Thus, the ε_ν values are more accurate than those reported by others.[8] The quantities ε_ν are sensitive to the slit width in the case of a well-resolved vibrational structure as it is in the chlorobenzene spectrum. In the preceding study[8] the slit width was maintained constant in each measurements series of the solute in a series of solvents; in the present work the slit width has changed automatically, according to a program dependent on the wave number, so that the spectral band width is less than 30 cm^{-1} on the whole range used.

We notice that the chlorobenzene spectrum in carbon tetrachloride, as well as the benzene spectrum,[10] displays a significant displacement, as compared to its position in vapour state and in the remainder solvents, and also a substantial increase of the ε_ν value. These peculiarities may be explained by the formation of a weak complex between chlorobenzene and carbon tetrachloride, in the same way as in the benzene case,[10] because the chlorine atom increases the charge density in the aromatic ring, that is its electron donor capacity. This assertion is supported by the investigation of mesitylene[52] and hexamethylbenzene[53] in carbon tetrachloride solutions showing an increase of the complex strength with the augmentation of the donor ability of the aromatic ring. Thus, the carbon tetrachloride behaves as an electron acceptor. In the chlorobenzene case the π-bond may form between the benzene ring, with an increased electron density from the substituent, and the 3*d* vacant level of the chlorine atom in carbon tetrachloride.[54] The unusual red displacement may be explained by the packing strain action in the excited state in which the complex molecule is much bigger, compared with the solute molecule.[10] The solvation energy will be greater than the solvation energy of the ground state, and the spectrum is red shifted.

[49] R. S. Mulliken, *J. Chem. Phys.*, **7**, 14 (1939).

[50] P. P. Shoryghin, V. A. Petukhov, and A. H. Khomenko, *Zhur. fiz. Khim.*, *42*, 1057 (1968).

[51] N. S. Bayliss and N. W. Cant, *Spectrochim. Acta*, **18**, 1287 (1962).

[52] R. Anderson and J. M. Prausnitz, *J. Chem. Phys.*, **39**, 1225 (1963).

[53] R. F. Weimer and J. M. Prausnitz, *J. Chem. Phys.*, **42**, 3643 (1965).

[54] J. R. Goates, R. J. Sullivan, and J. B. Ott, *J. Phys. Chem.*, **63**, 589 (1954).

Table 4

Vibrational analysis of chlorobenzene transition at 2600 Å. The $\tilde{\nu}$ (cm^{-1})–and ε-values* (in brackets) in some solvents, compared with the data from reference[8]

The present work $\tilde{\nu}$	ε	Reference[8] $\tilde{\nu}$	ε
		CYCLOHEXANE	
41,745	(41.25)	shoulder	
41,065 inflex.	(50.00)		
40,725	(73.25)	40,720	(78.00)
40,130 should.	(82.50)		
39,750	(125.00)	39,740	(133.00)
39,190	(135.00)	39,140	(174.00)
38,740	(192.50)	38,760	(207.00)
38,250	(187.50)	38,240	(187.00)
37,755	(266.75)	37,770	(283.00)
37,320	(131.25)	37,340	(141.00)
37,205 inflex.	(117.50)		
36,790	(205.25)	36,800	(221.00)
		n-HEXANE	
41,680 should.	(38.25)	shoulder	
41,120 inflex.	(45.00)		
40,750	(67.50)	~40,820	(74.00)
40,150	(75.75)		
39,780	(112.50)	39,780	(126.00)
39,245 should.	(122.50)	~39,200	(138.00)
38,780	(178.00)	38,760	(200.00)
38,275	(156.75)	38,240	(175.00)
37,790	(249.25)	37,790	(277.00)
37,360	(118.75)	37,380	(137.00)
37,190 inflex.	(103.75)		
36,825	(193.25)	36,830	(215.00)
		ETHANOL	
41,780 should.	(38.25)	shoulder	
40,770	(65.75)	~40,860	(74.00)
40,150	(80.50)		
39,775	(106.75)	39,840	(125.00)
39,260	(121.75)	39,200 should.	(~144.00)
38,820	(158.75)	38,840	(184.00)
38,280	(153.75)	38,300	(179.00)
37,820	(207.50)	37,840	(231.00)
37,400 should.	(119.50)	37,420	(137.00)
36,840	(150.00)	36,870	(172.00)

Table 4 (continued)

		CHLOROFORM		
40,630	(69.50)			
39,665	(109.25)	39,740		—
39,130	(127.50)		shoulder	
38,650	(163.75)	38,700		—
38,180	(161.25)	38,220		—
37,680	(211.50)	37,720		—
37,320 inflex.	(140.00)		shoulder	
36,700	(151.75)	36,730		—
		CARBON TETRACHLORIDE		
?		39,680		(157.00)
39,180	(115.50)	~39,120	should.	(~161.00)
38,825	(150.75)	38,650		(223.00)
38,320	(210.50)	38,180		(205.00)
37,845	(191.75)	37,630		(296.00)
37,340	(274.50)			
36,965 inflex.	(175.75)		shoulder	
36,600	(200.00)	36,640		(219.00)
		WATER		
41,820	(29.50)		shoulder	
40,840	(50.00)	~40,790		(~65.00)
39,905	(80.00)	39,920		(103.00)
39,370 should.	(97.50)	~39,290	should.	(~126.00)
38,900	(114.50)	38,910		(149.00)
38,400	(119.25)	38,400		(157.00)
37,925	(138.00)	37,920		(185.00)
37,480 should.	(93.75)	~37,520	should.	(~127.00)
36,920	(95.25)	36,950		(128.00)

* The $\tilde{\nu}$ and $\in_{\nu}$ values are only approximately for shoulders and inflexions.

We have seen[10] that the spectral intensity in solution as against its value in the vapour spectrum changes by a factor given in the ratio $f_{\text{exp.sol.}}/f_{\text{exp.vap.}}$, f being the corresponding *oscillator strength.* But Chako[55] and Bakhshiev *et al.*,[56–58] have formulated, on classical bases, the theoretical increase factor of the spectral intensity in solution as β, given in equation (5) of the previous paper ;[10] also, Abe[59] has established, on quantum bases, the increase factor as β', given in relation (6) of the quoted paper.[10] Using $f_{\text{exp.vap.}} = 1.800$ of the chlorobenzene[60] and our $f_{\text{exp.sol.}}$ from table 3, we listed in table 5 the ratio values $f_{\text{exp.sol.}}/f_{\text{exp.vap.}}$, to be com-

---

[55] N. Q. Chako, *J. Chem. Phys.*, **2**, 644 (1934).
[56] O. P. Girin and N. G. Bakhshiev, *Uspekhi Fiz. Nauk.*, **79**, 235 (1963).
[57] N. S. Libov, N. G. Bakhshiev, and O. P. Girin, *Opt. i Spektrosk.* **16**, 1016 (1964).
[58] N. G. Bakhshiev, *Opt. i Spektrosk.*, **24**, 896 (1968).
[59] T. Abe, *Bull. Chem. Soc. Japan*, **43**, 625 (1970).
[60] H. Sponer, *J. Chem. Phys.*, **22**, 234 (1954).

Table 5

Comparison of experimental and theoretical intensities of the 2600 Å chlorbenzene band

Solvent	$\frac{f_{exp.\,sol.}}{f_{exp.\,vap.}}$	β	β′
Cyclopentane	1.561	1.248	1.419
n-Pentane	1.522	1.208	1.382
Cyclohexane	1.661	1.267	1.437
n-Hexane	1.489	1.223	1.397
n-Heptane	1.528	1.233	1.408
n-Octane	1.539	1.242	1.415
n-Decane	1.589	1.255	1.420
n-Dodecane	1.583	1.264	1.431
Methanol	1.428	1.186	1.392
Ethanol	1.455	1.211	1.385
1-Propanol	1.555	1.231	1.406
2-Propanol	1.594	1.223	1.397
1-Butanol	1.472	1,243	1.417
3-Methyl-1-butanol	1.533	1.251	1.425
Ethyl ether	1.411	1.205	1.387
Chloroform	1.467	1.285	1.449
1,2-Dichloroethane	1.489	1.286	1.453
Methyl acetate	1.300	1.212	1.387
Dioxan	1.578	1.264	1.436

pared with the theoretical evaluated ratios β and β′. We notice that, generally, the spectral band intensity increase under the solvents influence, but the Chako-Bakhshiev increase factor, β, is much smaller than the experimental ratio value of the oscillator strengths. This fact indicates that along the dispersion forces some others causes may contribute to the intensity growth. Although closer to the ratio $f_{exp.sol.}/f_{exp.vap.}$, the Abe increase factor, β′, remains lower, even if the refractive index function is improved (see Ref.[10]) by the multiplication with the ratio of the transition frequencies $\tilde{\nu}_{0i}/\tilde{\nu}^0_{0i}$. Since the chlorobenzene molecule is polar the dipolar forces contribute to the intensity increase, but their action is not taken into account by the theoretical expressions.[55–58] The sizes of the solute and solvent molecules may have a role, as well as their geometrical shapes, but no such factors are theoretically considered. The obliteration of the rotational structure in solution is added to the above factors because the solute molecule surrounded by the solvent molecules rotates freely no more.[17]

III. EXPERIMENTAL

The chlorobenzene and solvents purification was done as previously described,[18] the purity criteria being the same. The refractive indices, *n*, the dielectric constants, *D*, and the boiling points (*b.p.*) were given in the preceding paper.[10] The solutions were prepared in the same conditions as reported,[10] but the concentrations ranged between 0.04 and 0.002 M. The spectra were recorded with the previously described apparatus, in the same conditions.[10] The position of each absorption peak and the spectral intensities are averages of at least three recordings. The integrated intensities were determined by cutting up and weighing, the limits of the integration being from the onset of spectral band, on the small wave numbers side, to the deepest minimum, on the great wave numbers side.

Revue Roumaine de Chimie, **21**, *2*, 193–205 (1976)

Revue Roumaine de Chimie, **21**, *2*, 207–216 (1976)

L'ÉTUDE DE LA RÉDUCTION DE L'OXYGÈNE SUR LES ÉLECTRODES POREUSES EN ARGENT. III[1]

L'EFFET DE LA TEMPÉRATURE DE L'ÉLECTROLYTE SUR LES PERFORMANCES DES ÉLECTRODES. ÉNERGIES APPARENTES D'ACTIVATION

IOANA ONACA, MARIA MAVRODIN-TĂRĂBÎC et I. SOLACOLU
Centre de Chimie Physique, Bucarest, 31, str. Galaţi

Reçu le 28 mai 1974

On a étudié l'effet de la variation de la température de l'électrolyte (dans le domaine compris entre 15–65°) sur les performances des électrodes à gaz en argent du type DSK. Des courbes de polarisation $\eta - i$, déterminées par la technique potentiostatique, à différentes concentrations de l'électrolyte (2N – 9N) et surpressions d'alimentation avec de l'oxygène (200–600 mm Hg), on a extrait les valeurs des surtensions qui correspondent aux densités du courant comprises entre 10 et 100 mA/cm^2 et on a tracé les courbes $\eta = f(t)$. On a déterminé les valeurs des courants d'échange apparents et des énergies apparentes d'activation pour différentes concentrations de l'électrolyte et surpressions d'alimentation avec du gaz. À l'aide des données obtenues on a établi le régime de fonctionnement des électrodes de ce type.

Dans un travail antérieur[1] on a étudié l'effet de la concentration de l'électrolyte sur les performances réalisées dans la réaction de réduction de l'oxygène par une série d'électrodes à gaz en argent caractérisées par une structure du type DSK (« Doppel Skelet Katalyst »). Dans ce travail nous nous sommes proposé de déterminer l'influence de la température de l'électrolyte, en vue d'établir le domaine de fonctionnement des électrodes – cathodes pour les piles à combustibles hydrogène-oxygène ou pour les piles du type métal-air.

1. PARTIE EXPÉRIMENTALE

La réalisation et la caractérisation structurale des électrodes à gaz en argent du type DSK ont été présentées dans un travail antérieur.[1]

L'étude de la réaction de réduction de l'oxygène a été effectuée par la technique potentiostatique, à l'aide d'un montage décrit dans un travail antérieur.[2]

Les déterminations ont été effectuées en utilisant comme électrolyte des solutions de KOH, de concentration 2N, 3N, 4N, 5N, 6N, 7N, 8N et 9N. La température de travail (15, 20, 25, 30, 35, 40, 45, 50, 55, 60 et 65°) a été maintenue constante à l'aide d'un ultrathermostate de type U-10 (précision $\pm 0,1°$). Les électrodes ont été alimentées avec de l'oxygène, à des surpressions de 200, 300, 400, 500 et 600 mm Hg, à l'aide d'une installation décrite dans un travail antérieur.[3]

---

[1] M. Mavrodin-Tărăbîc, I. Onaca et I. Solacolu, *Rev. Roumaine Chim.* (sous presse).
[2] M. Mavrodin-Tărăbîc, I. Onaca et I. Solacolu, *Rev. Roumaine Chim.*, **18**, 1121 (1973)

2. RÉSULTATS ET DISCUSSIONS

2.1. *Effet de la température de l'électrolyte et de la surpression de l'oxygène*

Pour illustrer l'effet de la variation de la température de l'électrolyte sur la polarisation des électrodes à gaz en argent étudiées, parmi ces 400 conditions différentes pour lesquelles on a tracé les courbes de polarisation $\eta = f(i)$ (la température a été variée dans le domaine 15—65°, les niveaux de température étant de 5°, la concentration dans le domaine 2N—9N, les niveaux de concentration étant de 1 méquiv. cm^{-3}, et la surpression de l'oxygène dans le domaine de 200—600 mm Hg, les niveaux de surpression étant de 100 mm Hg), on a considéré comme caractéristiques les courbes tracées à la concentration KOH 6N et à la surpression de l'oxygène de 400 mm Hg, à différentes températures comprises entre 15 et 65° (fig. 1).

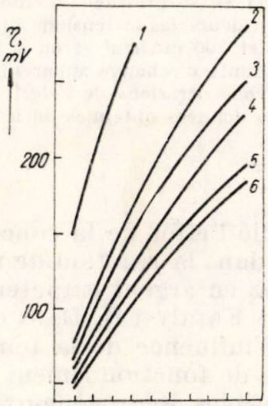

Fig. 1.—Courbes de polarisation $\eta = f(i)$, à de différentes températures de l'électrolyte (400 mm Hg, KOH 6N).
1 – 15°; *2* – 25°; *3* – 35°; *4* – 45°; *5* – 55°; *6* – 65°.

L'augmentation de la température de l'électrolyte produit un déplacement de la polarisation des électrodes vers des valeurs plus petites. Dans les conditions de concentration et de surpression considérées, cet effet est plus prononcé dans le domaine de 15—55°.

Des courbes de polarisation $\eta = f(i)$, caractéristiques pour la réaction de réduction de l'oxygène sur les électrodes à gaz en argent du type DSK, obtenues par la technique potentiostatique, dans différentes conditions de concentration, de température et de surpression d'alimentation avec du gaz, on a extrait les valeurs de la surtension caractéristique pour les densités apparentes de courant de 10, 20, 30, 40, 50, 60, 70, 80, 90 et 100 mA/cm². A l'aide de ces valeurs on a tracé les courbes $\eta = f(t)$ présentées dans la figure 2 (concentration de KOH 6N, $\Delta P_{O_2} = 400$ mm Hg).

---

[3] O. RADOVICI, M. MAVRODIN-TĂRĂBÎC, I. ONACA et I. SOLACOLU, *Rev. Roumaine Chim.*, **18**, 667 (1973).

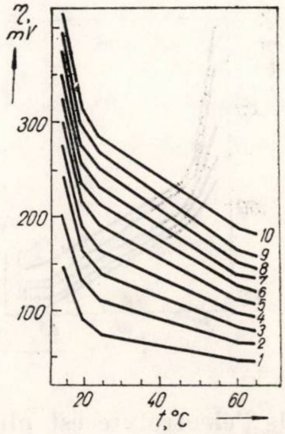

Fig. 2. — Effet de la variation de la température de l'électrolyte sur la polarisation des électrodes à de différentes densités apparentes de courant (400 mm Hg, KOH 6N).,
1 – 10 mA/cm²; *2* – 20 mA/cm²; *3* – 30 mA/cm²; *4* – 40 mA/cm²; *5* – 50 mA/cm²; *6* – 60 mA/cm²; *7* – 70 mA/cm²; *8* – 80 mA/cm²; *9* – 90 mA/cm²; *10* – 100 mA/cm².

De l'examen des courbes $\eta = f(t)$, présentées dans la figure 2, on peut constater que l'augmentation de la température de l'électrolyte a un effet favorable sur la polarisation des électrodes. Cet effet est plus prononcé à des densités apparentes de courant plus élevées et à des températures plus basses. Ainsi, dans les conditions de concentration et de surpression considérées, les valeurs de la surtension pour les températures de 20, 35, 50 et 65°, sont :

— à 10 mA/cm² : 92, 63, 57 et, respectivement, 46 mV ;
— à 40 mA/cm² : 189, 146, 121 et, respectivement, 93 mV ;
— à 100 mA/cm² : 314, 203, 220 et, respectivement, 171 mV.

Pour illustrer l'effet de la variation de la température de l'électrolyte sur la polarisation des électrodes en argent étudiées, à différentes valeurs de la surpression d'alimentation avec de l'oxygène (200–600 mm Hg), on a tracé les courbes $\eta = f(t)$, présentées dans la figure 3 ($i = 50$ mA/cm², concentration de KOH, 8N).

On constate que l'effet de la variation de la température est très prononcé dans le domaine 15–25°, à toutes les valeurs de la surpression de l'oxygène. Dans le domaine 25–60° cet effet est plus modéré ; l'augmentation de la température au-dessus de 60° n'a pas un effet significatif (on constate que le domaine optimal de la surpression des électrodes correspond aux valeurs de 400–500 mm Hg.) A une valeur de la surpression située à proximité de la valeur optimale (400 mm Hg), les valeurs de la surtension des électrodes étudiées sont : 225 mV (15°), 195 mV (20°), 170 mV (25°), 103 mV (60°) et 102 mV (65°).

L'effet de la variation de la température de l'électrolyte sur la polarisation des électrodes à gaz en argent, à différentes concentrations comprises entre 4 N et 9N, est illustré par l'aspect des courbes $\eta = f(t)$, représentées dans la figure 4 ($i = 50$ mA/cm², $\Delta P_{O_2} = 400$ mm Hg).

De l'examen de l'aspect de ces courbes on constate que l'effet de la variation de la température est d'autant plus prononcé que la concentration de l'électrolyte est plus réduite. A une concentration proche de la concentration optimale (6N) on constate qu'il existe deux domaines de température : jusqu'à 35° l'effet est plus prononcé, tandis qu'à des températures plus élevées, cet effet diminue.

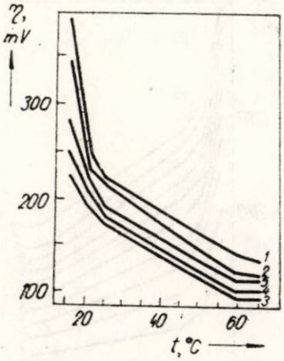

Fig. 3. — Effet de la variation de la température de l'électrolyte sur la polarisation des électrodes, à de différentes surpressions de l'oxygène (50 mA/cm², KOH 8N).

1 — 200 mm Hg ; *2* — 300 mm Hg ; *3* — 400 mm Hg ; *4* — 500 mm Hg ; *5* — 600 mm Hg.

Ce comportement des électrodes à gaz étudiées s'explique par l'effet différent de la variation de la température et de la concentration de l'électrolyte (dans le domaine étudié) sur la conductibilité de l'électrolyte,[4] la solubilité de l'oxygène dans l'électrolyte[5] et la diffusion des espèces réactives et des produits de réaction vers et à partir de la zone triphasique de réaction : la conductibilité de l'électrolyte augmente avec la température dans tout l'intervalle étudié et avec la concentration jusqu'à approximativement 6N ; la solubilité de l'oxygène dans l'électrolyte

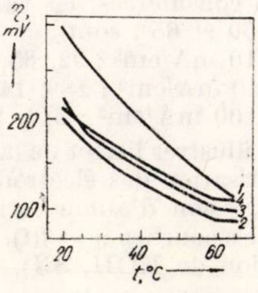

Fig. 4. — Effet de la variation de la température de l'électrolyte sur la polarisation des électrodes, à de différentes concentrations de l'électrolyte (50 mA/cm², 400 mm Hg).

1 — 4N ; *2* — 6N ; *3* — 8N ; *4* — 9N.

---

[4] N. L. Simons, D. W. McKee et E. J. Cairns, « Comptes Rendus des Troisièmes Journées d'étude des piles à combustible », Presses Académiques Européennes, Bruxelles, 1969, p. 132.

[5] A. Seidell, « Solubilities of Inorganic and Metal Organic Compounds », Ier vol., Van Nostrand, New York, 1953, p. 1352.

diminue avec l'augmentation de la température (spécialement vers la limite supérieure du domaine) et avec l'augmentation de la concentration de l'électrolyte, surtout à des concentrations moins grandes.[6] L'augmentation de la température a un effet favorable sur la diffusion des espèces réactives et des produits de réaction, tandis que l'augmentation de la concentration de l'électrolyte rend plus difficile l'évacuation des produits de réaction.

La réduction de l'oxygène sur les électrodes en argent, dans les solutions alcalines concentrées, n'a pas lieu dans une étape

$$O_2 + H_2O + 4e^- \rightleftarrows 4\,OH^-$$

parce que l'argent, à la différence de quelques autres métaux catalytiques (Pt, Pd), ne se caractérise pas par une adsorption dissociative de l'oxygène ($O_{2(gaz)} \rightarrow 2\,O_{(ads)}$) qui favorise la réduction de l'oxygène dans une seule étape. Des études récentes [7–10] ont démontré que cette réaction a lieu par un processus intermédiaire de formation des ions HO_2^-

$$O_2 + H_2\,O + 2e^- \rightleftarrows HO_2^- + OH^-$$

qui se décomposent :

$$HO_2^- \rightleftarrows OH^- + \frac{1}{2}\,O_2$$

Cette étape détermine la vitesse de la réduction et la valeur du potentiel de l'électrode dépend du rapport des concentrations des espèces ioniques OH^- et HO_2^- se trouvant dans la zone de réaction.[11] Il est évident que l'augmentation de la concentration de l'électrolyte déplace l'équilibre dans le sens défavorable.

L'effet de l'augmentation de la température de l'électrolyte sur la polarisation des électrodes à gaz en argent est moins évident à des densités apparentes du courant moins élevées parce que, dans ces conditions, les polarisations de résistance ohmique et de concentration interviennent d'une manière moins importante dans la polarisation globale de l'électrode à gaz. Les courbes $\eta = f(t)$, à de petites densités apparentes du courant, présentent un palier à des températures plus grandes que 40°, grâce à l'effet de la diminution de la solubilité de l'oxygène dans l'électrolyte.

L'effet de la variation de la surpression d'alimentation avec de l'oxygène, dans le domaine de 200–600 mm Hg, sur la polarisation des électrodes à gaz en argent du type DSK et la corrélation entre cet effet et l'effet de l'augmentation de la température de l'électrolyte, dans l'intervalle considéré, sont illustrés par l'aspect des courbes $\eta = f(\Delta P_{O_2})$, tracées à une concentration de KOH 4N et à une densité apparente de courant de 90 mA/cm², pour de différentes températures de l'électrolyte (fig. 5).

---

[6] D. B. Lucesoli, Thèse, Univ. Paris, 1971, p. 71.

[7] S. Beer, *J. Electrochem. Soc.*, **112**, 1133 (1965).

[8] T. Hurlen et I.L. Sandler, *Electrochim. Acta*, **11**, 1273 (1966).

[9] K. Miska, *Electrochim. Acta*, **12**, 1273 (1967).

[10] U. Evans, *Nature*, **1968**, 602.

[11] W. Mitchell, « Fuel Cells », Academic Press, New York, 1963, p. 122.

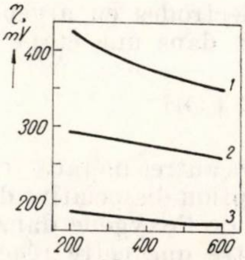

Fig. 5. — Effet de la variation de la surpression de l'oxygène sur la polarisation des électrodes, à de différentes températures de l'électrolyte (90 mA/cm², KOH 4N).

1– 40° ; *2*– 50° ; *3*– 60°.

Ainsi qu'il résulte des courbes $\eta = f(\Delta P_{O_2})$, présentées dans la figure 5, l'effet de l'augmentation de la surpression de l'oxygène sur la polarisation des électrodes à gaz en argent étudiées est d'autant plus évident que la température est plus basse. Cet effet est plus prononcé dans le domaine de 200 à 400 mm Hg.

2.2. *Les énergies apparentes d'activation*

Pour déterminer les valeurs des énergies apparentes d'activation, caractéristiques pour la réaction de réduction de l'oxygène en milieu alcalin sur les électrodes à gaz en argent du type DSK, on a tracé les courbes $\eta = f(\log i)$ pour les températures de 20, 25, 30, 35, 40, 45, 50, 55, 60 et de 65°, à de différentes concentrations de l'électrolyte (3N–8N) et surpressions d'alimentation avec du gaz (300–500 mm Hg). En extrapolant les portions linéaires de ces courbes on a déterminé les densités apparentes du courant d'échange ($\log i_0$), dont les valeurs sont présentées dans le tableau 1.

De l'examen des données présentées dans le tableau 1, il résulte que la valeur des courants d'échange augmente avec l'augmentation de la température et de la concentration de l'électrolyte, en concordance avec les données présentées à 2.1. et dans un travail antérieur,[1] en mettant en évidence l'effet favorable de l'augmentation de la température et de la concentration de l'électrolyte sur les performances des électrodes à gaz en argent de ce type.

Les valeurs des énergies apparentes d'activation (E_{ap}) ont été déterminées à l'aide de la relation [12]

$$\frac{\partial \ln i_0}{\partial 1/T} = -\frac{E_{ap}}{R}$$

---

[12] G. Kortüm, « Treatise on Electrochemistry », Elsevier, Amsterdam, 1965, p. 471.

Tableau 1

Valeurs des courants d'échange apparents (mA/cm^2) caractéristiques pour la réduction du l'oxygène sur les électrodes poreuses en argent du type DSK

Température de travail, K	3N			4N			5N			6N			7N			8N		
	300 mm Hg	400 mm Hg	500 mm Hg	300 mm Hg	400 mm Hg	500 mm Hg	300 mm Hg	400 mm Hg	500 mm Hg	300 mm Hg	400 mm Hg	500 mm Hg	300 mm Hg	400 mm Hg	500 mm Hg	300 mm Hg	400 mm Hg	500 mm Hg
293	−0,35	−0,18	−0,32	−0,05		−0,12	0,14	0,11	0,02	0,24	0,04	0,18	0,02	0,13	0,11	0,20	0,20	0,33
298	−0,30	−0,15	−0,25	0	−0,08	−0,06	0,37	0,18	0,09	0,34	0,21	0,26	0,20	0,30	0,45	0,30	0,32	0,48
303	−0,16	−0,03	−0,18	0,05	−0,1	−0,04	0,41	0,21	0,04	0,41	0,24	0,33	0,31	0,30	0,48	0,35	0,40	0,70
308	−0,08	0,05	−0,02	0,5	0,05	0,19	0,55	0,39	0,08	0,51	0,31	0,38	0,48	0,33	0,52	0,41	0,52	0,88
313	0	0,1	0,2	0,26	0,15	0,31	0,58	0,47	0,38	0,59	0,33	—	0,52	0,38	0,55	0,52	0,65	0,91
318	0,21	0,23	0,46	0,41	0,36	0,58	0,68	0,57	0,60	0,63	0,35	0,40	0,65	0,48	0,63	0,64	0,74	0,97
323	0,32	0,29	0,56	0,54	0,56	0,71	0,73	0,70	0,65	0,66	0,39	0,46	0,68	0,55	0,71	0,70	0,77	1
328	0,43	0,43	0,61	0,56	0,63	0,70	0,76	0,73	0,71	0,74	0,45	0,51	0,73	0,62	0,71	0,80	0,92	1,02
333	0,55	0,44	0,69	0,65	0,66	0,75	0,77	0,76	0,72	0,84	0,47	0,62	0,74	0,60	0,70	0,84	1,0	1,1
338	0,67	0,71	0,75	0,78	0,70	0,84	0,75	0,74	0,69	0,80	0,45	0,63	0,72	—	0,66	0,78	—	—

en utilisant les courbes log $i_0 = f(1/T)$. Les valeurs obtenues, pour les différentes valeurs de la concentration de l'électrolyte et de la surpression d'alimentation avec de l'oxygène, sont présentées dans le tableau 2.

Tableau 2

Energies apparentes d'activation (kcal/mole), caractéristiques pour la réduction de l'oxygène sur les électrodes à gaz en argent, à de différentes concentrations de l'électrolyte et surpressions d'alimentation avec du gaz

	300 mm Hg	400 mm Hg	500 mm Hg
3N	10,5	10,8	10,2
4N	9,3	9,6	9,2
5N	6,9	7,4	7,1
6N	4,4	4,0	4,5
7N	5,0	4,5	4,4
8N	5,9	5,6	6,2

Les énergies apparentes d'activation diminuent avec l'augmentation de la concentration de l'électrolyte et présentent des valeurs minimales dans le domaine 6N–8N. Les valeurs d'approximativement 4–6 kcal. mole^{-1}, caractéristiques pour la réaction de réduction de l'oxygène sur les électrodes à gaz en argent étudiées, dans le domaine de 6N–8N, démontrent que, dans ces conditions (caractéristiques pour les piles à combustible et les piles métal-air), le processus d'électrode est contrôlé par l'étape de diffusion, en concordance avec les données présentées dans la littérature de spécialité [13] et avec celles déterminée par Lucesoli [6] sur les électrodes à gaz en charbon.

2.3. *Détermination du régime de fonctionnement*

Les résultats que nous avons obtenus dans l'étude de l'effet de la variation de la concentration (2N–9N), de la température de l'électrolyte (15–65°) et de la surpression d'alimentation avec de l'oxygène (200–600 mm Hg) sur les performances des électrodes à gaz en argent du type DSK dans la réaction de réduction de l'oxygène, ont démontré que, pour établir le domaine de fonctionnement, il faut tenir compte de la valeur de la densité apparente du courant que l'électrode à gaz (cathode dans la pile à combustible ou dans la pile du type métal-air) va fournir dans le circuit extérieur.

En fonction du but proposé, les piles à combustible peuvent fonctionner en différents domaines de la densité du courant. Ainsi, dans le cas des installations fixes, de grand gabarit (grande puissance installée), chaque cellule peut fonctionner à de petites densités apparentes du courant, dans des conditions proches de la réversibilité, avec de grands avantages économiques résultant des rendements supérieurs réalisés dans la conversion en énergie électrique de l'énergie chimique du combustible et de l'usure réduite des installations. Dans le cas des installations de puissance moyenne ou petite (sources mobiles), pour lesquelles il est essentiel de réaliser un grand rapport kW/kg ou kW/m^3, donc une puissance maximale dans le circuit extérieur, chaque cellule va fonctionner à une densité apparente du courant moyenne, à laquelle la puissance fournie est maximale. Évidemment, dans certaines conditions, il est nécessaire que ces installations fonctionnent aussi, pour un intervalle de temps relativement court, à de grandes densités apparentes du courant.

---

[13] S. Glasstone, K. J. Laidlen et H. Eyring, « The Theory of Rate Processes », McGraw-Hill, New York, 1941, p. 582.

En fonction de la densité apparente du courant proposée, le domaine de fonctionnement des électrodes à gaz en argent est différent. Pour les petites densités apparentes (dans le cas des électrodes que nous avons étudiées, 10 mA/cm^2), les données obtenues démontrent que l'augmentation de la surpression d'alimentation avec de l'oxygène au-dessus de la valeur de 300 mm Hg ne conduit pas à l'amélioration des performances des électrodes à gaz (l'augmentation de la surpression d'alimentation avec du gaz au-dessus d'une certaine limite qui dépend du système poreux de l'électrode produit, inévitablement, dans les systèmes ouverts, des pertes de gaz par bullage). Dans ces conditions, le domaine de fonctionnement des électrodes est le suivant : la concentration de l'électrolyte 4N – 6N et la température 30 – 40°. Dans le cas des densités apparentes du courant moyennes (50 mA/cm^2), les valeurs sont, respectivement : $\Delta P_{O_2} = 400$ mm Hg, la concentration de l'électrolyte 5N – 6N et la température 40 – 60°. Dans le cas des densités apparentes du courant grandes (90 – 100 mA/cm^2), les valeurs sont : $\Delta P_{O_2} = 500$ mm Hg, la concentration de l'électrolyte 5N – 7N et la température à la limite supérieure du domaine étudié (65°).

Des données présentées ci-dessus, il résulte que les électrodes étudiées fonctionnent, à de petites densités apparentes du courant, sous le contrôle de la dissolution de l'oxygène, tandis qu'à de grandes densités apparentes du courant, sous le contrôle de la conductibilité de l'électrolyte.

3. CONCLUSIONS

1. L'étude de l'influence de la température de l'électrolyte, dans le domaine compris entre 15 et 65°, sur les performances des électrodes à gaz en argent du type DSK, a mis en évidence l'effet favorable de l'augmentation de la température, d'autant plus accentué que la densité apparente du courant est plus élevée et que la température est plus basse.

2. L'étude de l'effet de la variation de la surpression d'alimentation avec de l'oxygène, dans le domaine compris entre 200 et 600 mm Hg, a démontré que les performances des électrodes s'améliorent sensiblement par suite de l'augmentation de la surpression jusqu'à une certaine valeur qui dépend de la température et de la concentration de l'électrolyte et aussi de la densité apparente du courant.

3. Les valeurs des énergies apparentes d'activation, caractéristiques pour la réaction de réduction de l'oxygène sur les électrodes à gaz en argent étudiées, en milieu de KOH, baissent par suite de l'augmentation de la concentration de l'électrolyte. Les valeurs minimales, de 4 – 6 kcal/

mole, caractéristiques pour le domaine de concentration dans lequel fonctionnent les électrodes dans les piles à combustible ou dans les piles du type métal-air (6N—8N), indiquent que, dans ces conditions, le processus d'électrode est contrôlé par l'étape de diffusion.

4. Les études effectuées ont mis en évidence l'étroite corrélation qui existe entre la densité apparente du courant et les paramètres de fonctionnement de l'électrode (la température et la concentration de l'électrolyte et la surpression d'alimentation avec de l'oxygène).

5. Le régime de fonctionnement des électrodes étudiées est le suivant :

— pour les petites densités apparentes du courant (10 mA/cm²), $\Delta P_{O_2} = 300$ mm Hg, la concentration de KOH = 4N—6N et la température = 30—40° ;

— pour les densités apparentes du courant moyennes (approx. 50 mA/cm²), $\Delta P_{O_2} = 400$ mm Hg, la concentration = 5N — 6N et la température = 40—60° ;

— pour les grandes densités apparentes du courant (90—100 mA/cm²), $\Delta P_{O_2} = 500$ mm Hg, la concentration = 5N—7N et la température = 50—65°.

Revue Roumaine de Chimie, **21**, 2, 217–222 (1976)

CORRELATION BETWEEN ENERGIES OF VAPORIZATION, MOLECULAR PARAMETERS AND CRITICAL TEMPERATURES AND PRESSURES

RAJA F. HAJJAR
Natural Science Division, Beirut University College, P.O.Box 4080 $\underline{1}$
Beirut, Lebanon

Received September 3, 1974

Equations correlating the energies of vaporization ΔE_v, the molar density change $\Delta \rho_v$, the Lennard-Jones molecular parameters ε_0 and b_0 and the critical temperatures and pressures have been derived. These equations have been tested on a number of compounds using both viscosity and second virial coefficient data. Plots of $\Delta E_v/\Delta \rho_v$ *vs* $b_0\ \varepsilon/k$ for twenty eight compounds indicate linear relationships with slopes close to the theoretically predicted value of -5.35 cal/deg mole. Correlation between $\Delta E_v/\Delta p_v$ and T_c^2/P_c has also been demonstrated for these compounds.

INTRODUCTION

It is of theoretical as well as practical interest to develop connecting relationships between thermodynamic functions, molecular parameters and critical constants. Two such relationships have been developed in this paper using Mei's potential function.

At low pressures a gas may be adequately represented by a system of rigid particles each possessing a potential field acting between itself and neighbouring bodies. The properties of such a gas may be interpreted in terms of molecular dimensions and specific interaction potentials.

GENERAL THEORY

For a classical molecule there is no change in translational, vibrational or rotational energies for a constant temperature process such as vaporization. The energy accompanying vaporization of a liquid is therefore almost entirely potential, assuming that the configuration energy in the liquid is identical to that of the vapour.

For a particular molecule p, the number of molecules in a shell of thickness dr and at a distance r from p is $4\ \pi c r^2 \mathrm{d}r$ where c is the molecular concentration. The potential energy between molecule p and any other molecule in the system is assumed to be a function of r and some energy parameter ε, which is characteristic of the particular chemical species, designated by $\Phi\ (r)$. Hence the total potential energy between molecule p and all other molecules in the system is

$$\text{p.e.} = 4\pi c \int_{\sigma}^{\infty} \Phi\ (r)\ r^2\ dr, \tag{1}$$

where the lower limit is taken as one collission diameter, σ. The designation of this lower limit assumes that the centers of relatively very few molecules are closer than one collision diameter, i.e. the molecules are assumed to be hard spheres.[1]

The potential function $\Phi(r)$ will be assumed to be given by Mie's equation [2]

$$\Phi\ (r) = \frac{\varepsilon}{n-m}\left(\frac{n^n}{n^m}\right)^{\frac{1}{n-m}}\left[\left(\frac{\sigma}{r}\right)^n - \left(\frac{\sigma}{r}\right)^m\right], \tag{2}$$

where $n > m > 3$. When n and m are set equal to 12 and 6 respectively, Equation 2 reduces to the familiar Lennard-Jones $12-6$ potential. When Equation 2 is substituted into Equation 1 and integrated, the result is

$$\text{p.e.} = -4\pi\ c\ J\ \varepsilon\sigma^3 \tag{3}$$

in units of energy per pair of molecules. Here J is the dimensionless number

$$J = \frac{(n^n/m^m)^{\frac{1}{n-m}}}{(3-n)(3-m)}. \tag{4}$$

For the Lennard-Jones $12-6$ potential $J = 8/9$.

The total potential energy, P.E., is then given by

$$\text{P.E.} = -4\pi\ c\ J\ \varepsilon\ \sigma^3 \frac{N\ (N-1)}{2} = -4\pi c J \varepsilon \sigma^3\ \frac{N^2}{2}, \tag{5}$$

where N is the number of particles in volume V and $N(N-1)/2$ is the number of pairs of molecules in the system. Since c is the molecular concentration N/V, then

$$\text{P.E.} = -2\pi\ N^3\ J \varepsilon \sigma^3 \left(\frac{1}{V}\right). \tag{6}$$

---

[1] H. L. Frisch and E. Helfand, *J. Chem. Phys.*, **32**, 269 (1960). They determined that the necessary and sufficient condition for a single maximum and no minimum of the second virial coefficient $B\ (T)$, is for $\int_{\sigma}^{\infty} \Phi\ (r)\ r^2\ dr > 0$ if $\Phi\ (r) < 0$, i.e. $\Phi = \infty$ for $r < \sigma$.

[2] E. A. Moelwyn-Hughes, "Physical Chemistry", Chapter VII, 2nd edition, Pergamon Press, Oxford, 1965.

For vaporization of a liquid

$$\Delta \text{P.E.} = \Delta E_v = -2\pi N^3 J \varepsilon \sigma^3 \left(\frac{1}{V_{\text{liq}}} - \frac{1}{V_{\text{vap}}}\right). \qquad (7)$$

Here both ε and σ^3 are in molecular units. Equation 7 may be expressed in molar units as

$$\Delta E_v = -2\,\pi\, N\, J \varepsilon\, \sigma^3\, \Delta \rho_v, \qquad (8)$$

where the molar density $\rho = \frac{1}{V}$. Let $b_0 = \frac{2}{3}\,\pi\,\sigma^3$ so that

$$\frac{\Delta E_v}{\Delta\,\rho_v} = -3\, b_0\, N\, J\varepsilon \qquad (9)$$

and hence

$$\left(\frac{\Delta E_v}{\Delta\,\rho_v}\right)\Big/\, b_0 \left(\frac{\varepsilon}{k}\right) = -3J\,N\,k = -3\,JR = -5.35 \text{cal/deg mol}. \quad (10)$$

Equation 8 above links the ratio of the energy of vaporization to the density change upon vaporization and the Lennard-Jones constants ε and σ. This general procedure may also be used with other models. The limitation of these results is the assumption made above that the intermolecular interactions in the gaseous phase are negligible as compared with the more dominant interactions in the liquid phase. This of course may not be true for liquid-gaseous systems near their boiling points.

The quantity $\Delta E_v / \Delta_v$ may be expressed as a function of the critical temperature, T_c, and the critical pressure, P_c. From Equation 9

$$\Delta E_v / \Delta \rho_v = \text{const}\,(b_0\,\varepsilon) = \text{const}\,(\sigma^3\,\varepsilon).$$

Since V_c is proportional to σ^3 and T_c is proportional to ε and also since the critical compressibility $z_c = P_c\,V_c\,/RT_c$ is constant, then

$$\Delta E_v / \Delta \rho_v = \text{const}\,(T_c^2 / P_c). \qquad (11)$$

RESULTS SND DISCUSSION

Table 1 shows values of $\Delta E_v / \Delta\,\rho_v$, $b_0\,\varepsilon/k$ and T_c^2/P_c for a number of compounds including hydrocarbons, halogen substituted hydrocarbons

Table 1

Values of $\Delta E_v/\Delta\rho_v$, $b_0\varepsilon/k$ and T_c^2/P_c for various compounds

Compound	$-\Delta E_v/\Delta\rho_v$ liter calorie/(mol)^2 (a)	$b_0\,\varepsilon/k$, liter degree/mol from viscosity data (b)	$b_0\,\varepsilon/k$, liter degree/mol from B(T) data (c)	T_c^2/P_c (deg)^2/atm. (d)
methane	75	10.0		794
ethane	190	25.1		1,910
propane	291	41.5		3,163
n-butane	461	64.7		5,046
i-butane	424	60.1		4,481
n-pentane	657	83.6	207	6,705
n-hexane	910	107.6	284	8,748
n-heptane	1,132		389	10,881
n-octane	1,379	167.0		13,170
cyclohexane	789	92.4	224	7,602
benzene	622	81.3	180	6,614
toluene	905			8,476
chlorobenzene	921			8,967
methyl chloride	249	41.5		2,634
carbon tetrachloride	673	83.9		6,877
methanol	330	29.5		3,347
ethanol	544	43.6		4,224
propanol	750			5,765
butanol	933			6,484
methyl formate	379			4,010
propyl acetate	964			9,174
ethyl ether	599			6,143
carbon dioxide	126	15.6	21	1,268
carbon disulfide	351	53.9	105	3,925
acetone	519		160	5,495
water	174			1,923
ethylene oxide	275			3,085
perfluoro *n*-heptane	1,870		673	14,090
perfluoro- methyl cyclohexane	1,420		520	9,866
perfluoro 2-butyl tetrahydrofuran	1,872		710	14,740
perfluoro *n*-butane	815			6,495
methylene chloride	400	55.3		
chloroform	518	66.1		

(a) Data calculated from thermodynamic properties, vapor pressures and density data using the Clapeyron equation. See reference 3.

(b) Data calculated from J. O. Hirchfelder, C. F. Curtiss and R.B. Bird, "Molecular Theory of Gases and Liquids" John Wiley and Sons, Inc., New York, 1964. See reference 3.

(c) Data of G. F. Leverett and W. B. Kay. See reference 3.

(d) Calculated from N. A. Lang (Editor), "Handbook of Chemistry", Handbook Publishers, Sandusky, Ohio (1959).

and alcohols. Values of $\Delta E_v/\Delta\rho_v$ were calculated by Leverett and Kay[3] using the Clapeyron equation. Values of $b_0\,\varepsilon/k$ were calculated from data of Hirchfelder *et al.*[3,4] using viscosity and second virial coefficient $B(T)$ data in the temperature range 0 to 200°.

The constant slopes of Figures 1 and 2 confirm the validity of Equations 9 and 10. The proportionality between $\Delta E_v/\Delta\rho_v$ and $b_0\varepsilon/k$ depends on the experimental method used to determine the parameters b_0 and ε.

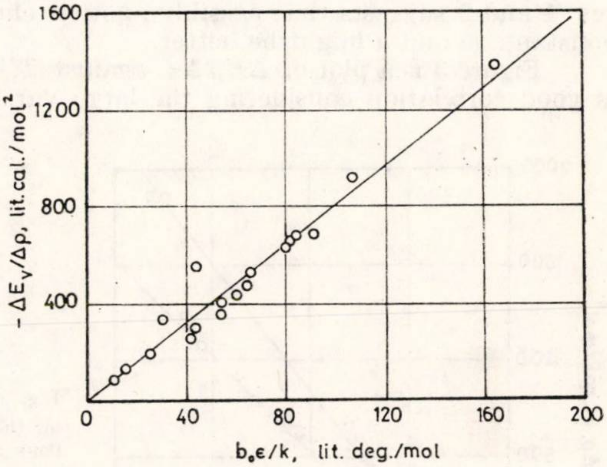

Fig. 1. — A plot of $(\Delta E_v/\Delta\rho)$ *vs* $(b_0\,\varepsilon/k)$ using the viscosity data of Table 1.

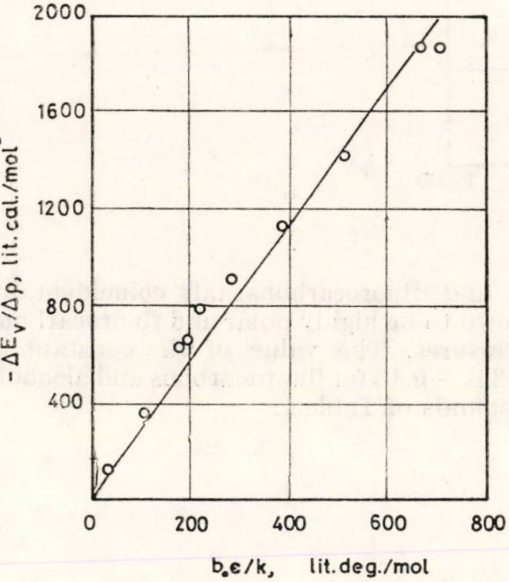

Fig. 2. — A plot of $(\Delta E_v/\Delta\rho)$ *vs* $(b_0\,\varepsilon/k)$ using the second virial coefficients, $B(T)$, of Table 1.

---

[3] G. F. Leverett, Ph. D. Dissertation, Ohio State University, Columbus, Ohio, 1959.

[4] J. O. Hirchfelder, C. F. Curtiss and R. B. Bird, "Molecular Theory of Gases and Liquids", John Wiley and Sons, Inc., New York, 1964.

Viscosity data give a slope of approximately -8 cal/deg mol while second virial coefficient data give a slope of approximately -3 cal/deg mol. The theoretical slope of -5.35 cal/deg mol as required by Equation 10 is of the same order of magnitude and is approximately the mean of these two values. The smaller slopes obtained by using the Lennard-Jones force constants b_0 and ε, obtained from second virial coefficients $B(T)$, indicate stronger intermolecular forces predicted by this method than from that using viscosity data. Lack of agreement between the correlations of Figures 1 and 2 suggests that possibly another choise for the Lennard-Jones constants m and n might be better.

Figure 3 is a plot of $\Delta E_v / \Delta \rho_v$ against T_c^2/P_c. It indicates that there is good correlation considering the large variation in the nature of the compounds considered. Alcohols and fluorocarbons fall coincidentally on a separate line; alcohols are known to be highly polar and fluorocarbons have an unusually low critical pressures. The value of the constant in Equation 11 obtained from Figure 3 is -0.13 for fluorocarbons and alcohols and -0.10 of the rest of the compounds of Table 1.

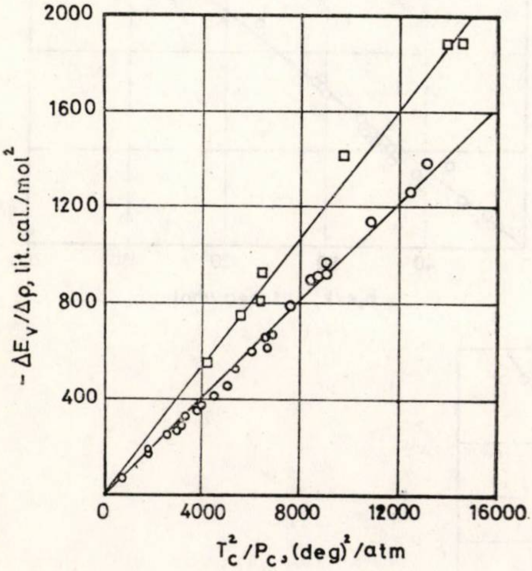

Fig. 3.— A plot of (T_c^2/P_c) vs $(\Delta E_v/\Delta \rho)$ for the compounds of table □ Fluorocarbons and alcohols; ○ The rest of the compounds of table 1.

Revue Roumaine de Chimie, **21**, *2*, 223–228 (1976)

PHYSIKALISCH-CHEMISCHE EIGENSCHAFTEN VON SCHMELZGEMISCHEN AUS CALCIUMCHLORID UND CÄSIUMCHLORID

HANS-HEINZ EMONS und GUNTER BRÄUTIGAM
Technische Hochschule ,,Carl Schorlemmer" Leuna-Merseburg, Sektion Verfahrenschemie,
Anorganisch-technische Chemie DDR – 42 Merseburg, Geusaer Straße

Eingegangen am 24. September 1974

Aus *EMK*-Messungen an Zellen mit Überführung vom Typ

$$Cl_2,\ [C]\ CsCl\ //\ CsCl-CaCl_{2(x)}\ [C],\ Cl_2$$

werden die ,,inneren" Überführungszahlen und Ionenbeweglichkeiten im System $CaCl_2-CsCl$ bestimmt. Die Beweglichkeit der Calciumionen nimmt mit steigender Cäsiumchlordikonzentration in der Mischung ab. Die erhaltenen Ergebnisse werden im Zusammenhang mit anderen physikalisch-chemischen Parametern (elektrische Leitfähigkeit, Volumen, Mischungsenthalpie) diskutiert.

In früheren Arbeiten berichteten wir mit Ausnahme des Systems $CaCl_2-CsCl$ über die Bestimmung der *EMK* von Zellen mit Überführung in den Systemen $CaCl_2-MCl$, $SrCl_2-MCl$ und $BaCl_2-MCl$ ($MCl = LiCl$, $NaCl$, KCl, $RbCl$, $CsCl$) sowie die Berechnung von Überführungszahlen und Kationenbeweglichkeiten in diesen Mischungen.[1]

Aus diesen Untersuchungen ergab sich, daß für ein gegebenes Erdalkalimetallion die Ionenbeweglichkeit mit steigender Alkalimetallionenkonzentration (Ausnahme $LiCl-MCl_2$) und mit wachsendem Radius der Alkalimetallionen abnimmt. Der Anteil der Alkalimetallionen an der Überführung erhöht sich nach $Li < Na < K < Rb$.

Mit Abnahme der Ladungsdichte an den Erdalkalimetallionen und der damit verbundenen Abschwächung der lokalen Wechselwirkung Kation – Anion nimmt die Ionenbeweglichkeit der Erdalkalimetallionen in der Reihenfolge $Ca < Sr < Ba$ zu.

Im folgenden wird über die Bestimmung der *EMK* von Zellen mit Überführung und die Berechnung der Überführungszahlen und Kationenbeweglichkeiten im System $CaCl_2-CsCl$ berichtet. Die Ergebnisse werden in Verbindung mit anderen thermodynamischen und Transporteigenschaften diskutiert.

---

[1] H.-H. Emons, G. Bräutigam u. H. Wader, *Z. anorg. Chem.*, **403**, 97 (1974).
G. Roewer u. H.-H. Emons. *Z. anorg. Chem.* **370**, 119 (1969).
H.-H. Emons, ,,Third International Conference on chemical Thermodynamics", Baden/Vienna, Vol. IV, 1973, 157–164.
H.-H. Emons, G. Bräutigam u. R. Scheunpflug, *Z. anorg. Chem.*, **411**, 118 (1975).

EXPERIMENTELLES UND ERGEBNISSE

Für die experimentelle Bestimmung der *EMK* an Zellen mit Überführung vom Typ

$$\mathrm{Cl_2,\ [C]\ CsCl\ //\ CsCl-CaCl_{2(x)}[C],\ Cl_2}$$

wurde die von uns früher verwendete Meßapparatur geringfügig modifiziert[1].

Der Fehler in den *EMK*-Werten betrug ± 1 *mV*.

Tabelle 1 enthält die experimentellen Daten; die numerisch ausgeglichene Kurve zeigt Abb. 1.

Tabelle 1

EMK **der Kette** $\mathrm{Cl_2}$**,** **[C]** $\mathrm{CsCl/CsCl-CaCl_{2(x)}}$ **[C],** $\mathrm{Cl_2}$ **bei 960°**

$x_{\mathrm{CaCl_2}}$	$EMK(mV)$	$x_{\mathrm{CaCl_2}}$	$EMK\ (mV)$
0,10	10,3	0,49	73,1
0,11	12,0	0,51	75,3
0,19	26,1	0,59	89,1
0,25	33,2	0,63	93,4
0,28	35,8	0,72	101,8
0,31	43,3	0,77	106,3
0,33	50,3	0,91	113,0
0,43	66,0	1,00	113,0

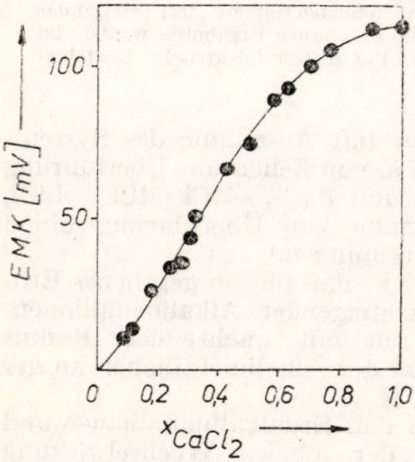

Abb. 1. — *EMK*-Werte der Kette $\mathrm{Cl_2}$, [C] / CsCl // $\mathrm{CaCl_{2(x)}}$[C] $\mathrm{Cl_2}$ bei 960°

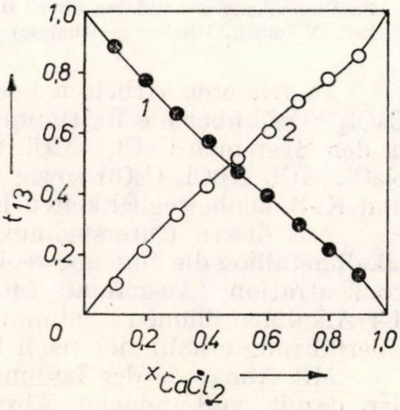

Abb. 2. — „Innere" Überführungszahlen t_{13} im System $\mathrm{CaCl_2}$–CsCl bei 970° (1 = = CsCl; 2 = $\mathrm{CaCl_2}$).

Analog zu Behl und Egan [2] erfolgte die Berechnung der inneren Überführungszahlen (Abb. 2) nach der Gleichung

$$t_{13} = \frac{2E'.F(1 - x_{\mathrm{CsCl}})}{2{,}303\, RT(2 - x_{\mathrm{CsCl}})} + \frac{x_{\mathrm{CsCl}}}{2 - x_{\mathrm{CsCl}}} \tag{1}$$

mit $E' \equiv \left(\dfrac{\partial E}{\partial \lg a_{\mathrm{CsCl}}} \right)$

---

[2] W. K. Behl u. J. J. Egan, *J. Phys. Chem.*, **71**, 1764 (1967).

Die Berechnung der ,,relativen“ Kationenbeweglichkeiten erfolgte nach der Beziehung

$$b_{i3} = \frac{t_{i3} . \Lambda}{X_{i3} . F} \tag{2}$$

$E = EMK$
x = Molenbruch
t_{i3} = innere Überführungszahl
Λ = Äquivalentleitfähigkeit
b_{i3} = ,,relative“ Kationenbeweglichkeit
X_{i3} = Äquivalentbruch

Zur Bestimmung von E' wählten wir eine numerische Auswertung nach der Beziehung

$$EMK = \mathrm{EMK}_{(x_{\mathrm{CsCl_2}}=1)}[1 - \exp. (-b \lg a_{\mathrm{CsCl}})], \tag{3}$$

wobei E' durch Differentiation dieser Gleichung erhalten wird. Die Bestimmung der Konstanten erfolgt nach dem Fibunucci-Suchverfahren.
Für das System $CaCl_2 - CsCl$ ergibt sich folgende Funktion:

$$EMK = 114{,}9 \; [1 - \exp. (-0{,}790 \lg a_{\mathrm{CsCl}})]$$

Die zur Auswertung der Gleichungen 1 und 2 erforderlichen Aktivitätsdaten wurden aus Dampfdruckmessungen (Knudsen-Effusion), die Äquivalentleitfähigkeiten aus Dichte- und Leitfähigkeitsmessungen ermittelt.[3]

Tabelle 2

Aktivitäten, freie Exzeßenthalpie ΔG^E Überführungszahlen und Kationenbeweglichkeiten im System $CaCl_2 - CsCl$ bei 970°

$x_{\mathrm{CsCl_2}}$	a_{CsCl}	$a_{\mathrm{CsCl_2}}$	$t_{13\mathrm{CsCl}}$	$t_{23\mathrm{CaCl_2}}$	$10^4 b_{13\mathrm{CsCl}}$	$10^4 b_{23\mathrm{CaCl_2}}$	ΔG^E [cal]
0,1	0,666	0,001	0,893	0,107	10,9	5,8	−1695
0,2	0,428	0,020	0,785	0,215	9,6	5,1	−2356
0,3	0,254	0,100	0,675	0,325	8,1	4,5	−2556
0,4	0,174	0,205	0,578	0,422	7,6	4,2	−2483
0,5	0,124	0,312	0,487	0,512	7,6	4,0	−2296
0,6	0,080	0,446	0,400	0,600	8,1	4.0	−2022
0,7	0,042	0,632	0,308	0,692	9,3	4,5	−1635
0,8	0,024	0,759	0,228	0,772	11,4	5,2	−1147
0,9	0,010	0,881	0,146	0,854		6,2	− 612

Tabelle 2 enthält die berechneten Werte.

Für die Messungen wurde CsCl p. A. (Chemapol Prag) und $CaCl_2$ p. A. (Riedel de Haen, Selze – Hannover) verwendet.

Das umkristallisierte CsCl wurde bei 400° getrocknet; das entwässerte $CaCl_2$ vor dem Einsatz im trockenen HCl-Strom (700°) behandelt.

Die Analyse der Mischungen erfolgte durch komplexometrische Bestimmung der Calciumionen mit 0,05 m AEDTE-Lösung (Indikator Eriochromschwarz T) und argentometrischer Chlorid bestimmung nach Mohr.

---

[3] H.-H. Emons, G. Bräutigmam u. H. Vogt, *Z. anorg. Chem.*, **394**, 263 (1972); **394**, 279 (1972).
G. Bräutigam u. H. -H. Emons, *Z. anorg. Chem.*, **394**, 271 (1972).
H.-H. Emons u. L. Theisen, *Monatsh. Chem.*, **103**, 62 (1972).
H.-H. Emons, G. Bräutigam u. D. Kögler, *Z. Chem.*, **12**, 233 (1972).

DISKUSSION

Nach neueren Untersuchungen von Seifert[4] weist das Phasendiagramm „fest-flüssig" des Systems $CaCl_2-CsCl$ ein Dystektikum ($CsCaCl_3$) und zwei Peritektika der Zusammensetzung Cs_2CaCl_4 und $Cs_3Ca_2Cl_7$ auf (Abb. 3/1). Daraus ergibt sich die Frage, ob in diesem System infolge der starken lokalen Wechselwirkung der Calciumionen mit den Chloridionen bereits in der Schmelze Spezies der Form $[MCl_{2n}]^{n-}$ gebildet werden. Bredig[5] diskutierte die Bildung von Komplexionen in einigen binären Salzmischungen und schlußfolgert, daß noch kein sicherer experimenteller Beweis für das Aufreten von $[MX_3]^-$ bzw. $[MX_6]^{4-}$-Ionen in binären unsymmetrischen Halogenidschmelzen existiert.

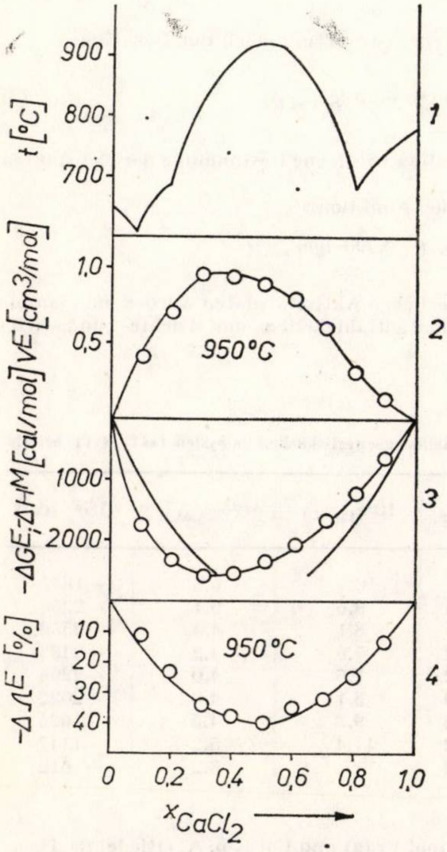

Abb. 3.—Thermodynamische und Transporteigenschaften im System $CaCl_2-CsCl$.

1 = Schmelzdiagramm[4] ; *2* = Exzeßvolumen[3] ; *3* = Mischungswärme[7] (900°) ; -o- Freie Exzeßenthalpie[3] (970°) ; *4* = Exzeßleitfähigkeiten[3].

Exakte kalorimetrische Messungen der Mischungsenthalpien in den Systemen $MgCl_2-MCl$; $NiCl_2-MCl$; $CoCl_2-MCl$; $FeCl_2-MCl$; $CdCl_2-MCl$ und $MnCl_2-MCl$ von Kleppa und Mitarbeitern[6] zeigen die Anwesenheit von $[MCl_4]^{2-}$-Komplexen an.

Aus kalorimetrischen Untersuchungen von Østvold[7] an Calciumchlorid-Alkalimetallchloridsystemen ergibt sich im System $CaCl_2-CsCl$ im Verlauf des Wechselwirkungsparameters $\Delta H^M/x\,(1-x)$ ein schwaches Minimum bei $x_{CaCl_2} = 0{,}5$. Dieses Minimum zeigt die Tendenz zur speziellen Stabilisierung der Schmelze an, ist jedoch zu schwach ausgeprägt, um daraus die Existenz von komplexen Ionen abzuleiten.

Unsere Bestimmungen der Aktivitäten und freien Exzeßenthalpie ΔG^E bestätigen diese Aussagen. Die ΔG^E-Werte sind weniger negativ als die ΔH^M-Werte, wobei das Minimum zu höheren Cäsiumchloridgehalten verschoben ist (Abb. 3/3).

---

[4] H.-J. Seifert u. U. Langenbach, *Z. anorg. Chem.*, **368**, 36 (1969).

[5] M. A. Bredig in „Molten Salts" Herausgeber: G. Mamantov, M. Dekker, New York, 1969, S. 55.

[6] O. J. Kleppa u. F. G. Mc Carthy, *J. Phys. Chem.*, **70**, 1249 (1966).
G. N. Papatheodorou u. O. J. Kleppa, *J. Inorg. Nuclear Chem.*, **32**, 889 (1970); **33**, 1249 (1971); *Inorg. Chem.*, **10**, 872 (1971).

[7] T. Østvold, „A Thermodynamic Study of Some Fused Salt Mixtures Containing Alkali and Alkaline Earth Chlorides, Bromides and Jodides", NTH Trondheim, Norway, 1971.

In diesem Bereich weisen die Exzeßvolumina ΔV^E ein Maximum auf (Abb. 3/2).

Die relativ starken Abweichungen der thermodynamischen Eigenschaften von der Idealität äußern sich deutlich im Verlauf der Transporteigenschaften.

Die molare elektrische Leitfähigkeit weicht bis zu 40% von der Idealitätsbeziehung von Markov[8] ab, wobei die Aktivierungsenergie der elektrischen Leitfähigkeit ein Maximum besitzt.[3] (Abb. 3/4)

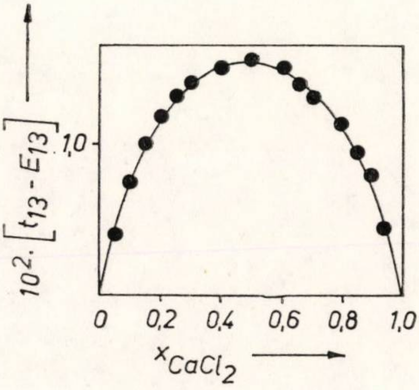

Abb. 4. — Funktion ($t_{13} - X_{13}$) (Exzeßüberführungszahlen) im System $CaCl_2-CsCl$ (970°).

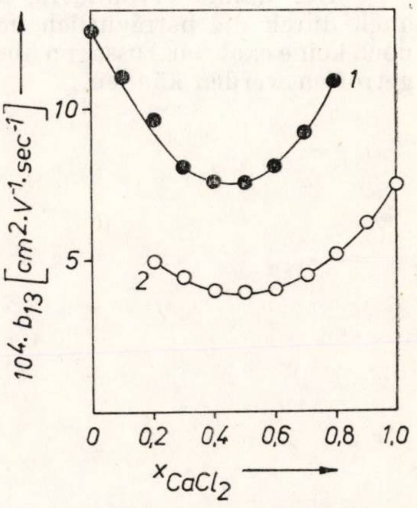

Abb. 5. — Kationenbeweglichkeiten im System $CaCl_2-CsCl$ bei 970° (1=CsCl; 2 = $CaCl_2$).

Bessere Aussagen über die Existenz komplexer Ionen liefern die Überführungszahlen und Kationenbeweglichkeiten.

Abb. 2 zeigt, daß die Calciumionen noch einen beträchtlichen Beitrag zum Transport liefern.

Bei gleicher Beweglichkeit der Calcium- und Cäsiumionen sollte der Betrag der Überführungszahlen im Schmelzgemisch dem jeweiligen Äquivalentbruch des Salzes entsprechen $t_{13} = X_{13}$.

Die positive Abweichung von der Funktion $t_{13} - X_{13}$ (Abb. 4) (Exzeßüberführung) resultiert aus der größeren Beweglichkeit des Cäsiumions gegenüber dem Calciumion.

Die Beweglichkeit der Calciumionen wird durch den Zusatz von Cäsiumchlorid auf Grund der Assoziation der Chloridionen an das Calciumion erniedrigt (Abb. 5). Das Minimum liegt im gleichen Konzentrationsbereich, in dem auch die thermodynamischen Eigenschaften die größten Abweichungen von der Idealität aufweisen.

---

[8] B. F. Markov u. L. A. Shumina, *Doklady Akad. Nauk S.S.S.R.*, **110**, 411 (1956); *Zhur. fiz. Khim.*, **31**, 1767 (1957).

Abb. 5 zeigt deutlich, daß auch in diesem Konzentrationsbereich die Calciumionen noch eine beträchtliche Beweglichkeit aufweisen und deshalb die Existenz stabiler komplexer Ionen im Sinne einer kinetischen Einheit wenig wahrscheinlich ist.

Die ermittelten thermodynamischen und Transporteigenschaften lassen sich zwangslos mit einer bevorzugten Assoziation der Calciumionen mit Chloridionen auf Grund der großen Unterschiede zwischen den Ionenpotentialen der Calcium- und Cäsiumionen erklären.

Der damit verbundene höhere Ordnungsgrad der Schmelze wird auch durch die beträchtlich negativen Entropiewerte [7] angezeigt, wobei noch keine exakten Aussagen über die Anordnung der Ionen in der Mischung getroffen werden können.

Revue Roumaine de Chimie, **21**, 2, 229 – 230 (1976)

PRÉPARATION D'ANTIMOINE COLLOÏDAL DE HAUTE PURETÉ

ANDRÉ G. GALINOS et PRODROME B. ISSOPOULOS
Laboratoire de Chimie Minérale, Université de Patras, Patras, Grèce
231, Rue Korinthou

Reçu le 9 octobre 1974

Il est montré que la réaction entre l'acide tétrachlorantimonique et l'α-pinène constitue une méthode rapide avec un rendement satisfaisant pour la préparation d'antimoine colloïdal de haute pureté.

La préparation d'antimoine colloïdal a déjà retenu l'attention de nombreux expérimentateurs et une série de méthodes pour cette préparation a été proposée.

Ces méthodes sont électrochimiques, mécaniques ou purement chimiques en fonction de la forme désirée d'antimoine colloïdal obtenu, c'est-à-dire si le produit se classe dans des catégories diverses comme Hydrosol, Aerosol ou Organosol.[1-9]

Malheureusement, bien que toutes les méthodes prescrites aient un rendement satisfaisant, elles ne donnent pas de l'antimoine colloïdal de haute pureté, qui est indispensable pour satisfaire les exigences de la technologie moderne.

La préparation d'antimoine colloïdal de haute pureté a été effectuée par nous par l'application de la méthode qui est prescrite dans cette Note.

PRINCIPE DE LA MÉTHODE

La méthode proposée est basée sur la réaction de l'acide tétrachlorantimonique $\{HSbCl_4 . 2Et_2O\}$ sur l'α-pinène. Cette réaction qui est exothermique nous a fourni une gamme de produits de polymérisation d'α-pinène, produits huileux ou cirés avec une réduction simultanée d'antimoine (III) à l'état d'antimoine métallique et d'antimoine colloïdal de haute pureté. Le rendement moyen de la méthode en antimoine colloïdal de haute pureté a été de presque 20%.

[1] W.A.D. Rudge, *Phil. Mag.*, **25**, 485 (1913).
[2] G. Wegelin, *Koll. Zeit.*, **14**, 66 (1914).
[3] V. I. Vaidyanathan, *Ind. J. Phys.*, **6**, 563 (1930).
[4] S. R. Rao, *Ind. J. Phys.*, **6**, 243 (1931).
[5] S. S. Bhatnager, M. R. Verma et M. Anwar-ul-Hag, *Koll. Zeit.*, **78**, 16 (1937).
[6] S. Miyamoto, *Koll. Zeit.*, **69**, 180 (1934).
[7] A. Gutbier et N. Kraütle, *Koll. Zeit.*, **20**, 195 (1917).
[8] A. Gutbier, B. Ottenstein et F. Allam, *Z. anorg. Chem.*, **164**, 292 (1927).
[9] A. Stock et W. Siebert, *Ber. dtsch. chem. Ges.*, **38**, 3844 (1905).

MÉTHODE DE PRÉPARATION

Les matières premières pour la préparation d'antimoine colloïdal de haute pureté sont l'α-pinène et l'acide tétrachlorantimonique.

L' α-pinène a été obtenu par plusieures distillations d'essence de térébenthine grecque, huile obtenue en distillant la résine de Pinus Halepensis.

L' α-pinène utilisé était la fraction de p. e. 155—157°, d_{15}^{15} =0,8351 dextrogyre, $\{a\}_D=$ $= 53° 7'$ qui était conservé sous une atmosphère d'azote pour éviter l'auto-oxydation par l'air et la formation des hyperoxydes.

L'acide tétrachlorantimonique a été préparé selon la méthode qui a été proposée par l'un de nous[10], tandis que tous les réactifs utilisés ont été de haute pureté et en plus toutes les manipulations ont été effectuées sous une boîte à gants.

Dans un ballon à trois tubulures comportant un agitateur, un thermomètre et un long tube à reflux on a introduit 83,5 g d' α-pinène et 10 ml $HSbCl_4.2Et_2O$ (p.s. = 1,35 g/ml) quantité correspondant à 7,51 g $SbCl_3$ ou à 4,00 g de Sb. La quantité de l'acide tétrachlorantimonique était 16,16% de la quantité d'α-pinène.

Le mélange a été légèrement chauffé et sous agitation dans un bain d'huile jusqu'à 40°. Le chauffage a été arrêté et une réaction exothermique accompagnée d'une élévation de la température du mélange jusqu'à 110° eut lieu. Cette température a été constante pendant 10 min à peu près et la couleur grise du mélange a changé en rougeâtre et enfin en brun.

A ce moment le mélange a été chauffé de nouveau à 130° quand une réaction exothermique violente s'est produite, accompagnée d'une élévation de la température à 180° et un dégagement de vapeurs qui avaient l'odeur de limonène.

La couleur de mélange a changé en noir, fait qui attestait la formation d'antimoine en état métallique et sous un partage fin.

En dissolvant le produit huileux de la réaction susnommée dans l'acétone une précipitation d'une poudre noire (antimoine métallique) a été observée et en même temps une solution colloïdale s'est formée dans l'acétone.

L'apparition du phénomène de Tyndall dans la solution acétonique avant la filtration plaide qu'elle était une solution colloïdale lyophobe.

Cette solution colloïdale a été filtrée par un filtre 4G et est restée invariable, tandis que l'antimoine colloïdal qui a été suspendu dans cette solution a été séparé quand la solution a été filtrée par un filtre de porcelaine (diamètre de pores : 100—200 mμ).

Ensuite a eu lieu l'analyse chimique instrumentale (analyse de traces) d'antimoine colloïdal séparé pour vérifier sa pureté. Les résultats obtenus sont consignés ci-dessous :

Fer (III)	2 p. p. m.
Plomb (II)	0,1 p. p. m.
Arsenic (III) et (V)	0,0, p. p. m.
Bismuth (III) et (V)	0,0 p. p. m.
Chlorures (Cl^-)	2,0 p. p. m.
Sulfates (SO_4^{2-})	1,0 p. p. m.

Si nous utilisons au lieu de $HSbCl_4.2Et_2O$ le $SbCl_3$ la préparation d'antimoine colloïdal est impossible et au lieu de l'antimoine colloïdal se forme un miroir constitué d'antimoine métallique.

---

[10] K. Askitopoulos, A. Galinos et I. M. Tsangaris, *Prakt. Akad. Athinon*, **32**, 388 (1957).

Revue Roumaine de Chimie, **21**, *2*, 231–235 (1976)

UTILIZATION OF THE UREA-POLYVINYL CHLORIDE ADDUCTS IN THE POLYVINYL CHLORIDE FRACTIONATION

CONSTANTIN LUCA and ANGELA POPA
Laboratory of Chemical Technology, "Al. I. Cuza" University, Calea 23 August 11
Jassy, Romania

Received September 3, 1974

In order to use the urea-polyvinyl chloride adducts in the fractionation of polyvinyl chloride, the conditions of their formation in solution and in urea packed columns were investigated. The adductive crystallization in solution, at the temperature of 20° for 24h, led to the formation of adducts with smaller terms of the homologous series, while the longer terms remained in solution. During fractionation through urea packed columns at the temperature of 20° for 48 h, the longer terms of the homologous series are distributed throughout the column in the decreasing order of their molecular weight, while the solution is improved with the smaller terms.

Based on the adductive crystallization phenomenon of the macromolecules inside the channels of the modified crystalline lattice of urea and thiourea,[1–4] a series of investigators have studied the possibility of the polymers fractionation in this way. Thus, Kern and Schmidt [5] have fractionated hexamethylenepolysuccinate using columns packed with urea and they think that their positive results are due to the formation of inclusion compounds. Also, Parrod, Kohler and Hild [6] in their studies on urea adducts with polyoxiethylenes, and Mayer [7] in his papers on urea adducts with linear aliphatic polyesters have shown the existence of a fractionating effect.

Since we wanted to verify if a similar effect takes place in the case of polyvinyl chloride, the present paper has studied the conditions of the urea-polyvinyl chloride adducts formation and their characterization with a view to establishing the possibilities of their utilization in the polyvinyl chloride fractionation.

---

[1] J. Parrod and A. Kohler, *Compt. rend.*, **246**, 1046 (1958).
[2] J. Parrod and A. Kohler, *Polymer Sci.*, **48**, 457 (1960).
[3] J.C. Rosso, F. Raffelini and M. Dubusc, *Compt. rend.*, **268**, 587 (1969).
[4] G. Hild, A. Kohler and J. Parrod, *Bull. Soc. chim. France*, **1966**, 2288.
[5] W. Kern and H. Schmidt, *Makromol. Chem.*, **16**, 74 (1955).
[6] A. Kohler, G. Hild and J. Parrod, *Compt. rend.*, **255**, 2763 (1962).
[7] R. Mayer, *Bull. Soc. chim. France*, **1966**, 2998.

EXPERIMENTAL

Samples of indigenous polyvinyl chloride, polymerized in suspension, were purified by extraction with a fifty-fifty mixture of petroleum ether and methanol for 8 h.

Urea was purified by repeated crystallization from methanol and its purity was verified by chemical and spectral analysis.

The urea-polyvinyl chloride adducts were prepared as follows: the solution of 5% polyvinyl chloride in cyclohexanone was treated with various amounts of powder urea at the temperature of 20°. After standing for 24 h, with interrupted stirring, the formed crystals were separated by vacuum filtration, washed with cyclohexanone and dried in air and in desiccator.

The adduct formation was verified by i. r. spectroscopy in a potassium bromide pellet, using a Unicam SP-100 spectrophotometer.

The polyvinyl chloride fractionation was carried out at a temperature of 20° by passing its cyclohexanone solution for 48 h with a flowrate of 4—6 cm^3/h,through a powder urea bed, placed into a celophane column with 80 cm in length and 1.5 cm in diameter. A solution of 2% polyvinyl chloride was used in cyclohexanone because the more concentrated solutions cannot pass through the column. Then, the columns were divided by cutting in an arbitrary number of equal segments and the obtained fractions were subjected to decomposition. The decomposition of the urea-polyvinyl chloride adducts was carried out by treating them with water at 50° when the polymer occurred as a very fine precipitate,which cooul however be separated by filtration. The purification of the separated polymer was done by washings with warm and cold water until its i. r. spectrum indicated no urea traces. For the fractions obtained as shown above, the viscosity was determined, using an Ubbelohde viscosimeter in cyclohexanone solution at the temperature of 25 ± 0.05°.

RESULTS AND DISCUSSION

Using the same quantity of polyvinyl chloride (40 cm^3 solution of 5% polyvinyl chloride in cyclohexanone) and different amounts of urea, the quantity of adducted polyvinyl chloride was found to vary according to the curve represented in fig. 1.

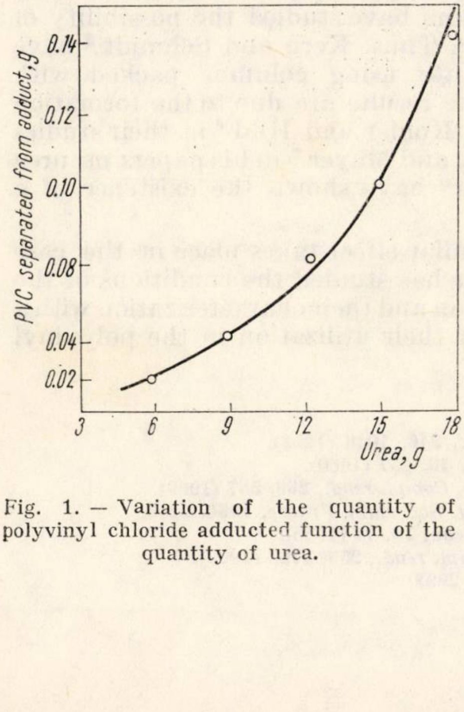

Fig. 1. — Variation of the quantity of polyvinyl chloride adducted function of the quantity of urea.

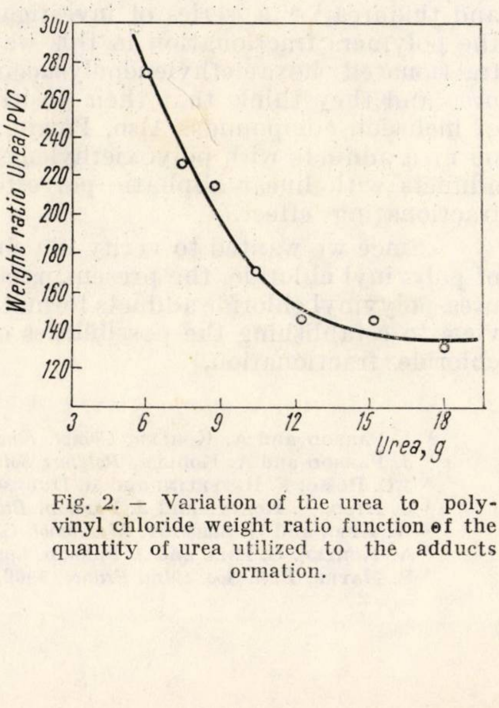

Fig. 2. — Variation of the urea to polyvinyl chloride weight ratio function of the quantity of urea utilized to the adducts ormation.

The urea/polyvinyl chloride, weight ratio, decreases with increasing of the quantity of urea up to a limit value (138.5), after which it remains constant (fig. 2); therefore, in the subsequent studies on fractionation, the weight ratio indicated above was utilized.

The i.r. spectra of the formed adducts are identical to each other, the characteristic frequencies compared to those of pure urea are summarized in table 1. From the data presented in table 1 it results that more significant differences between pure urea and urea-polyvinyl chloride adducts are situated in the range of the vibration frequencies of -NH_2 and $>$CO groups.

Table 1

The characteristic absorption frequencies (cm^{-1}) in the pure urea andinits addutes

Urea	Urea-polyvinyl chloride adducts	Nature of vibration
3475	3440	$\nu_{(NH)\ as.}$
3370	3330	$\nu_{(NH)\ s}$
1690	1685	$\nu_{C=O}$
	1670	
1640	1640 sh.	$\nu_{C=O} + \delta_{NH}$
1618	1605	
1475	1485	$\mathrm{C}\overline{\cdots}\mathrm{N}$
1155	1155	$\gamma_{NH_2}r$
1005	1011	ν_{CN}
790	795	$(CO + NH_{\omega})$

In the valence vibrations range of $-NH_2$ groups, the band corresponding to the antisymmetrical vibration which is at 3475 cm^{-1} for pure urea is displaced at 3440 cm^{-1} for adducts, and that corresponding to the symmetrical vibration situated at 3370 cm^{-1} for urea is displaced at 3330 cm^{-1} for adducts. This is a proof of the hydrogen bridges intensification, that has already been evidenced by the X-ray diffraction study.[8]

In the valence vibrations range of $>$CO groups, 3 bands occur for urea, at 1690, 1640 and 1618 cm^{-1}. For the adduct, in the range mentioned above, there occur 4 absorption bands at 1685, 1670, 1640_{sh} and 1605 cm^{-1}. The displacement of the ν_{CO} absorption band in urea from 1690 cm^{-1} towards low frequencies (1670 cm^{-1}) supports the hypothesis of the hydrogen bridges intensification in adducts. The fact that in the adducts spectra the absorption bands are found approximately at 1685 cm^{-1} and 1640 cm^{-1} (sh.) illustrates that not all groups in the molecular aggregate are affected by hydrogen bridges, and some of them are found in the same state as in pure urea. This shows that our products represent a mixture of urea and urea-polyvinyl chloride adducts. This fact justifies the magnitude of the urea-to-polyvinyl chloride weight ratio, which is much larger in comparison to that of urea with simple molecules.

---

[8] A. E. Smith, *Acta Cryst.*, **5**, 224 (1952).

The presence of polyvinyl chloride polymeric chains included in urea are shown in the i.r. spectra by some bands of their own spectra (the C—Cl bond at 655 cm^{-1}).

The spectra of the investigated adducts are similar to those of the urea-vinylic esters adducts with high fatty acids, the difference being that in the latter the absorption band corresponding to the $\nu_{NH}(s)$ vibration is displaced at 3240 cm [1-9].

The characteristics of polyvinyl chloride separated by adductive crystallization in solution compared with those of nonadducted polyvinyl chloride (that has remained in solution) are given in table 2.

Table 2

The characteristics of adducted polyvinyl chloride and of that remained in solution*

Urea, g	Solution of 5% polyvinyl chloride in cyclohexanone, cm^3	Adducted polyvinyl chloride				Polyvinyl chloride remained in solution			
		η_r	K_w	$[\eta]$	$M_w.10^{-3}$	η_r	K_w	$[\eta]$	$M_w.10^{-3}$
9	40	1.563	67.03	97	114	1.636	70.8	110	133
12	40	1.536	65.55	92.5	108	1.648	71.4	112	136
15	40	1.528	65.10	91	105	1.654	71.6	113.5	138
18	40	1.520	64.65	89	103	1.658	71.9	115	140

* The characteristics of the initial polyvinyl chloride are; $\eta_r = 1.622$; $K_w = 70.1$; $[\eta] = 104$; $\overline{M}_w 10^{-3} = 124$.

The values of K_w are estimated from the viscosimetrical data using Finkentscher's equation.[10]

$$\frac{\lg \eta_{rel.}}{C} = \frac{75\,K^2}{1 + 1.5KC} + K$$

where $\eta_{rel.}$ — relative viscosity of polymer solution;

C — concentration of polymer solution, 0.5 g/100 cm^3 solution;

K — value of $K_w \cdot 10^{-3}$

The values of $\overline{M}_w$ are computed by means of the relation found in literature [11] for the suspension polyvinyl chloride polymer-Geon.

$$[\eta]_{25^\circ} = 6.92 \cdot 10^{-3}\, \overline{M}_w^{0.82} \quad (cm^3/g)$$

where $[\eta]$ — intrinsic viscosity;

$\overline{M}_w$ — average gravimetric molecular weight.

The data presented in table 2 show that with the increase of urea quantity, for the same quantity of polyvinyl chloride, η_r, K_w, $[\eta]$, and

[9] A. Popa, C. Luca and I. Gabe, *Anal. Sti. Univ. "Al. I. Cuza" Iași*, Secț. I, **19**, 192 (1973).

[10] H. Fikentscher, *Cellulose Chem.*, **13**, 58 (1932).

[11] I. A. Schneider, C. Vasile and A. Onu, *Rev. Roumaine Chim.*, **15**, 1935 (1970).

$\bar{M}_w$ decrease for the adducted polyvinyl chloride and increase for the polyvinyl chloride that has remained in solution.

It follows that, under the operating conditions mentioned above, the lower terms of the homologous series do form urea-polyvinyl chloride adducts while the higher terms remain in solution.

The characteristics of the polyvinyl chloride fractions separated on column packed with powder urea are presented in table 3. From the data summarized in table 3 it results that, on the urea packed column, the polymer occupies continuously the entire column. The fractions with longer macromolecules are kept to the upper part of the column while the fractions with shorter macromolecules are kept to its inferior part. As it can be seen, the results obtained on urea packed columns are opposed to those obtained in solution. This can be interpreted by the fact that at the beginning, in solution, the shorter macromolecules, being more movable, form adducts and are then replaced by the longer macromolecules which are more strongly retained. Such a phenomenon takes time and may be due to a more energetic retention of the longer molecules inside the crystalline lattice.

Table 3

The characteristics of the polyvinylchloride fractionsseparated on the urea packed colums

Characteristics \ Fraction	1	2	3	4	5	Remains
η_r	1.752	1.706	1.659	1.628	1.563	1.589
K_w	76.1	74.1	71.9	70.4	67.0	68.4
$[\eta]$, cm^3/g	128	121	112	108	97	101
$\bar{M}_w \cdot 10^{-3}$	160	149	136	130	114	119

M_w decrease for the saturated polyvinyl chloride and increase for the polyvinyl chloride that is retained in solution.

It follows that, under the operating conditions mentioned above, the lower terms of the homologous series do form urea-polyvinyl chloride adducts while the higher terms remain in solution.

The characteristics of the polyvinyl chloride fractions separated on a column packed with powder urea are presented in table 3. From the data summarized in table 3 it results that, on the urea packed column, the [illegible]

Table 3

[illegible]

Fraction Characteristic	1	2	3	4	[illegible]
[illegible]	1.762	1.708	[illegible]	[illegible]	1.583
[illegible]	78.1	[illegible]	[illegible]	[illegible]	98
[illegible]	176	[illegible]	[illegible]	[illegible]	97
[illegible]	166	162	[illegible]	[illegible]	114

than separates continuously the entire column. The fractions with longer molecules [illegible] in the upper part of the column and [illegible] with shorter macromolecules [illegible] the lower part. As it can be seen, the results obtained on urea packed columns are opposed to those obtained in solution. This can be interpreted by the fact that at the beginning, in solution, the shorter macromolecules, being more mobile, [illegible] and are then replaced by the longer macromolecules which are more strongly [illegible]. This fact may be due to a more energetic retention of the longer molecules inside the crystal lattice.

Revue Roumaine de Chimie, **21**, *2*, 237 – 240 (1976)

THERMAL EFFECT ON SURFACE ACIDITY AND CATALYTIC ACTIVITY OF $ZrO_2 - Al_2O_3$ AND $ZrO_2 - SiO_2$ CATALYSTS

S. P. WALVEKAR, A. B. HALGERI, S. RAMANNA and T. N. SRINIVASAN
Department of Chemistry, Bangalore University, Bangalore – 560001,
India

Received August 5, 1974

Surface acidity and acid strength of $ZrO_2-Al_2O_3$ and ZrO_2-SiO_2 catalysts heated to various temperatures has been determined by the butylamine titration method. It is found that the amount of acid at all acid strengths increases with increasing temperature of heat treatment, reaches a maximum value around 500° and subsequently decreases. The acid sites with acid strengths of $pKa \leqq -3.0$ and $pKa \leqq -5.6$ appear on the surfaces of $ZrO_2-Al_2O_3$ and ZrO_2-SiO_2 catalysts, respectively. It has been observed that the catalytic activity of these mixed oxides for depolymerization of paraldehyde reaction correlates well with the acidities at $pKa \leqq -3.0$.

INTRODUCTION

Some mixed oxides like $SiO_2-Al_2O_3$, SiO_2-MgO, $Al_2O_3-B_2O_3$ and TiO_2-ZnO are known to exhibit high acidity, catalytic activity which are not found in the individual components.[1-2] These mixed oxides have been extensively used as catalysts for various acid catalysed reactions in petroleum chemistry. Recently many other mixed metal oxides were found to show significant surface acidity and catalytic activity.[3-7] However, not much work has been done on the effect of heat treatment on acidity and acid strength distribution of mixed oxides, hence we have initiated a systematic study on $ZrO_2-Al_2O_3$ and ZrO_2-SiO_2 catalysts. The present paper reports the thermal effect on acidic property and in the light of the observed surface acidic properties, the catalytic activity of these mixed oxides for the depolymerization of paraldehyde reaction has been studied.

---

[1] M. D. Navalikhina and E. I. Yaroslavtseva, *Kinetika i Kataliz*, **12**, 132 (1971).

[2] K. Tanabe, C. Ishiya, I. Matsuzaki and H. Hottori, *Bull. Chem. Soc. Japan*, **45**, 47 (1972).

[3] S. P. Walvekar and A. B. Halgeri, *J. Res. Inst. Catalysis, Hokkaido Univ.*, **20**, 219 (1972).

[4] S. P. Walvekar and A. B. Halgeri, *J. Indian Chem. Soc.*, **50**, 387 (1973).

[5] S. P. Walvekar and A. B. Halgeri, *J. Univ. Bombay*, **41**, 29 (1972).

[6] S. P. Walvekar and A. B. Halgeri, *Bull. Chem. Soc., Japan*, **47**, 1927 (1974).

[7] S. P. Walvekar and A. B. Halgeri, *Z. anorg. Chem.*, **400**, 83 (1973).

EXPERIMENTAL

Materials. Paraldehyde and pure quality benzene were dried over sodium, distilled and used in this investigation. All other chemicals were Analar quality reagents. The indicators were synthesized by known methods and used in this work.

Catalysts. The mixed metal oxides were prepared by the precipitation technique as described earlier.[6,7]

Measurement of surface area and acidic property. The surface area of $ZrO_2-Al_2O_3$ and ZrO_2-SiO_2 catalysts heat treated at various temperatures was determined by the liquid adsorption method using EGME technique of Heilman and Carter.[8] The acidity and acid strength of these mixed oxides have been determined by amine titration method[9] in benzene using a series of Hammet indicators with $pKa = +6.8$ to -5.6.

Kinetic measurement. The depolymerization of paraldehyde reaction was selected for the study of the catalytic activity of these catalysts. The technique adopted was essentially the same as described earlier by us.[3,6]

RESULTS AND DISCUSSION

The values of acidity at various acid strengths of $ZrO_2-Al_2O_3$ and ZrO_2-SiO_2 calcined at various temperatures are given in Tables 1 and 2 respectively. Mixed oxides which have been thermally treated at 120° do not have much acidic property and their acidity and acid strength distributions change remarkably with rise in temperature of heat treatment. It is observed from Table 1 that the acid sites stronger than $pKa = -3.0$ appear on the surface of $ZrO_2-Al_2O_3$ heat treated at temperatures between 260° and 800° and those at medium acid strengths of $pKa = 4.8 \sim 3.3$ appear on the surface at 120° to 1000°. In case of ZrO_2-SiO_2 (Table 2) the acidities and acid strengths stronger than $pKa = -3.0$ appear on the surface when heat treated at temperatures 100° to 1050° and the strong acid centres at $pKa \leqq -5.6$ appear on the surface heat treated at 500°.

Table 1

Acidity, acid strength distribution and catalytic activity of $ZrO_2-Al_2O_3$

Temperature of heat treatment °C	Surface area m^2/g	Acidity, mmoles/g				Depolymerisation of paraldehyde $k \times 10^3$ $min^{-2}g^{-1}$
		$pKa \leqq +6.8$	$pKa \leqq +4.8$	$pKa \leqq +3.3$	$pKa \leqq -3.0$	
120	158.9	0.40	0.26	0.12	—	—
260	122.5	0.48	0.38	0.20	0.025	—
380	122.8	0.52	0.45	0.33	0.08	8.26
500	98.88	0.58	0.52	0.38	0.16	21.68
610	92.04	0.50	0.48	0.31	0.12	17.92
720	81.42	0.44	0.40	0.26	0.08	9.84
800	55.76	0.38	0.32	0.14	0.04	4.76
1000	47.87	0.22	0.10	0.04	—	—

---

[8] M. D. Heilman and C. L. Carter, *J. Soil Sci.*, **100**, 409 (1965).

[9] O. Johnson, *J. Phys. Chem.*, **59**, 827 (1955).

Table 2

Acidity, acid strength distribution and catalytic activity of ZrO_2-SiO_2

Temperature of heat treatment °C	Surface area m²/g	Acidity, mmoles/g					Depolymerization of paraldehyde $k \times 10^3$ $min^{-1}g^{-1}$
		$pKa \leqq +6.8$	$pKa \leqq +4.8$	$pKa \leqq +3.3$	$pKa \leqq -3.0$	$pKa \leqslant -5.6$	
100	509.3	0.49	0.39	0.18	0.08	—	4.02
240	441.0	0.56	0.44	0.28	0.12	—	9.86
320	440.8	0.60	0.49	0.39	0.16	—	18.48
400	440.0	0.62	0.55	0.45	0.21	—	26.62
500	408.0	0.68	0.62	0.52	0.30	0.12	42.50
610	355.6	0.64	0.56	0.48	0.27	—	35.20
710	326.8	0.58	0.52	0.40	0.24	—	32.50
820	307.6	0.56	0.49	0.32	0.20	—	27.50
1050	98.63	0.52	0.41	0.20	0.092	—	7.20

It has been observed by Dzisko[10] in case of ZrO_2-SiO_2 catalyst that it has an acid strength of $pKa = -8.2$ on its surface. However, an acid strength of $pKa = -5.6$ on the surface of the ZrO_2-SiO_2 obtained in the present study indicates that a change in composition has affected the physico-chemical properties on the surface of this catalyst.

It is seen from the values in tables 1 and 2 that the amount of acid at all acid strengths initially increases with increasing temperature of heat-treatment, reaches a maximum at about 500° and subsequently decreases. This trend is probably due to the creation of new acid sites as a result of loss of water with the rise in the temperature of heat-treatment.[11] The creation of new acid sites continues up to a particular temperature of heat treatment, then it decreases with further rise in temperature because there is no more water to be lost. With further rise in temperature, structural changes take place on the surface which reduce the surface area which is evident from the values of surface area presented in Tables 1 and 2, and this accounts for the reduction in the surface acidity. This conclusion is in agreement with our earlier observation[12] in the case of some mixed oxides containing TiO_2.

CORRELATION OF ACIDIC PROPERTY WITH CATALYTIC ACTIVITY

The values of the first order rate constant K of the mixed oxide calcined at various temperatures for depolymerization of paraldehyde reaction are given in the last columns of Tables 1 and 2. It is observed that in all the cases the catalytic activity (first order rate constant k) exhibited a maximum against the temperature of heat-treatment of the catalyst. A reference to the rate constant values k indicates that there exists a correlationship between the acidity at pKa $\leqq -3.0$ and catalytic activity. In the case of $ZrO_2-Al_2O_3$, samples heat treated at 120°, 800° and 1000° have no strong acid sites at pKa $= -3.0$ but have a number of acid sites with an acid strength of pKa $\leqq +3.3$ and do not catalyse the depolymerization of paraldehyde. Therefore, it can be concluded that those relatively weak acid sites present are considered to be catalytically inactive. When samples of these catalysts with acid sites at pKa $= -3.0$ were poisoned by dicinnamal acetone (pKa $= -3.0$), they could not depolymerize paraldehyde. This lends support to the view that acid centres of pKa $= -3.0$ are catalytically active for depolymerization of paraldehyde. Our observation that acid centres of pKa $\leqq -3.0$ are necessary for this reaction implies selectivity in the use of acid centres of particular acid strength for particular reaction and this agrees with an earlier observation of ours [3,4,13] and also of Tanabe *et al.* [14] in the case of metal sulphates, in the study of depolymerization of paraldehyde.

---

[10] V. A. Dzisko, "Proceedings International Congress Catalysis", vol. 1, 3rd ed., Amsterdam, 1965, p. 422.

[11] S. G. Hindin and S. W. Weller, *J. Phys. Chem.*, **60**.

[12] S. P. Walvekar and A. B. Halgeri, *Indian J. Chem.*, **11**, 662 (1973).

Acknowledgements. **The authors wish to express their thanks to Professors M. Shadaksharaswamy and G.K.N. Reddy for providing research facilities.**

---

[13] S. P. Walvekar and A. B. Halgeri, *J. Indian Chem. Soc.*, **50**, 246 (1973).
[14] K. Tanabe and C. Mugiya, *J. Res. Inst. Catalysis, Hokkaido Univ.*, **19**, 29 (1971).

Revue Roumaine de Chimie, **21**, *2*, 241–249 (1976)

MASS SPECTRUM OF 3,7-DI-t-BUTYL-5-METHYL-4*H*-1,2-DIAZEPINE: POSSIBLE STERIC INHIBITION OF DINITROGEN EXPULSION

ALEXANDRU T. BALABAN
Chair of Organic Chemistry, The Polytechnic Institute of Bucharest, Romania (address for correspondence : Inst. of Atomic Physics, POB 5206, Bucharest)

Received August 21, 1975

Reaction of 2,6-di-t-butyl-4-methylpyrylium with hydrazine yields the title compound. Its IR, UV, NMR (^{1}H and ^{33}C) and MS spectra are described. In the fragmentation induced by electron impact, no dinitrogen molecule is split off (unlike related 1,2-diazepines) probably owing to a steric repulsion of the bulky t-butyl groups in the corresponding transition state.

INTRODUCTION

2,6-Disubstituted pyrylium salts react with hydrazine yielding either 4*H*-1,2-diazepines (in good yields from 2,4,6-triaryl-pyrylium salts [1,2] or 2,6-di-t-butyl-4-methylpyrylium salts), or N-amino-2,4,6-trialkyl-,[3] or 2,3,5,6-tetraalkylpyridinium salts [4] (the latter reaction, which affords an aromatic system, is preferred whenever the product is not sterically overcrowded, explaining thereby the different reaction course), or keto-substituted pyrazoline derivatives (with substituted hydrazines like phenylhydrazine, this is the main reaction).[1,5,6]

The facile synthesis of substituted 4*H*-1,2-diazepines prompted us to study more closely this class of compounds. We found [2] NMR evidence for the ring flip, and, in the mass spectra, a general fragmentation path under electron impact, namely expulsion of a dinitrogen molecule (this is a general feature of heterocycles with two vicinal nitrogen atoms, as pointed out in the bibliography of the preceding paper [2]).

The present paper presents an exception to this general pattern, which we presume to be of steric origin.

---

[1] A. T. Balaban, *Tetrahedron*, **26**, 739 (1970).

[2] O. Buchardt, C. L. Pedersen, U. Svanholm, A. Duffield and A. T. Balaban, *Acta Chem. Scand.*, **23**, 3125 (1969).

[3] G. N. Dorofeenko, A. N. Narkevich and Yu. A. Zhdanov, *Khim. Geterotsikl. Soed.*, **1970**, 1130.

[4] A. T. Balaban, *Rev. Roumaine Chim.*, **18**, 1609 (1973).

[5] A. T. Balaban, *Tetrahedron*, **24**, 5059 (1968).

[6] D. J. Harris, G. Y. P. Kan, V. Snieckus and E. Klingsberg, *Canad. J. Chem.*, **52**, 2798 (1974) ; V. Snieckus and G. Kan, *J.C.S. Chem. Commun.*, **1970**, 1208.

2,6-Di-t-butyl-4-methylpyrylium perchlorate (I) reacts smoothly with hydrazine affording in high yield 3,7-di-t-butyl-5-methyl-4*H*-1,2-diazepine (III). This structure is demonstrated by the spectral evidence below. To assist in the structural assignment, use was made of the facile deuteration of γ-methyl side chains in pyrylium salts (the α-benzylic hydrogens are deuterated more slowly, and β-benzylic ones not at all); [7,8] the deuterated pyrylium salt (II) was converted by hydrazine into the d_3-methyl diazepine (IV) with slight dedeuteration.

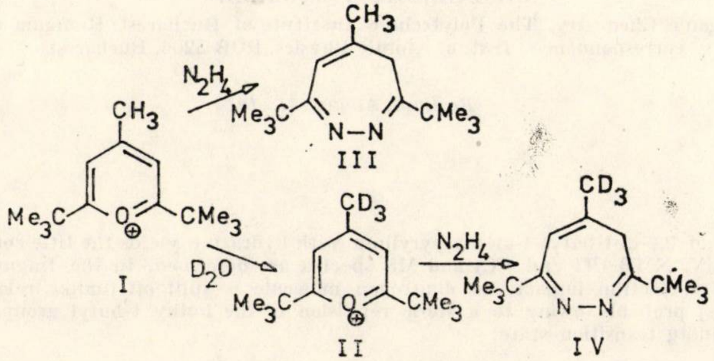

INFRARED ABSORPTION SPECTRUM

The pyrylium perchlorates I and II (in KBr pellets) present the normal[9] pyrylium bands at 1632 cm^{-1} (this strong band is a composite one, having shoulders at 1610 and 1641 cm^{-1}) and 1450 cm^{-1} together with ClO_4^- bands at 625 and 1100 cm^{-1}. On deuterating I, the following bands disappear: 1508, 1414,* 1230,* 930, 884, 570 cm^{-1}, and the following bands appear: 2180, 1492,** 943, 900, 828, 766,** 525cm^{-1}. The band at 2180 cm^{-1} is due to the CD stretching vibration, the other ones are deformation modes.

The infrared spectrum of III presents CH stretching vibrations at 2870, 2910, 2930, 2970 (strongest, composite band) and 3030 cm^{-1}. It has no absorption in the 1640—2000 cm^{-1} or 3050—3600 cm^{-1} ranges, excluding pyrazoline or pyridinium-betainic formulas. The double bond stretching band is a strong one at 1632 cm^{-1}. Bands which are present in the IR spectrum of III but absent from IV are at 1466, 1385, 1290, 1215, 939 and 871 cm^{-1}, whereas new bands appearing in III and absent from IV are at 2210, 2050 (CD stretching), 1055, 955, 890, 840 and 830 cm^{-1}.

---

* Reduced intensity.

** A very weak band existed also in I.

[7] E. GÂRD, A. VASILESCU, G. D. MATEESCU and A. T. BALABAN, *J. Labelled Comp.*, **3** 196 (1967).

[8] E. GÂRD, I. STANOIU, F. CHIRALEU and A. T. BALABAN, *Rev. Roumaine Chim.*, **18**, 257 (1973).

[9] A. T. BALABAN, G. MATEESCU and M. ELIAN, *Tetrahedron*, **18**, 1083 (1962).

ULTRAVIOLET ABSORPTION SPECTRUM

In ethanol, the diazepine III presents one absorption band at 237 nm, with an extinction coefficient of 6800.

^{1}H-NMR SPECTRA

In carbon tetrachloride, hexadeuteroacetone or deuterochloroform, accidental degeneracy of the t-butyl protons occurs, with one signal at 8.76 τ (18H).

The vinylic proton (*m*, τ 4.02) and methyl group (*d*, τ 7.91) have an allylic coupling of 1.5 Hz. The two methylene protons are not equivalent and appear as an AX quadruplet, one component of which overlaps with the methyl protons : τ 7.00 and 8.03, geminal coupling $J = 12.8$ Hz. The components of this quadruplet appear all to be split into doublets with a separation of 2.5 Hz, whose origin is probably due to allylic coupling. In $CDCl_3$ or CCl_4 the NMR spectrum is unchanged between −40 and +40°C.

In hexadeuterobenzene, the accidental degeneracy of the t-butyl groups is removed, and the two t-butyl groups appear as separate singlets at 8.76 and 8.87 τ. Some signals are shifted upfield : $-CH=4.24$ τ, CH_3 8.30 τ, methylene protons (AX quadruplet) at 7.34 and 8.00 τ.

It is likely that from the two C ^{4} -methylene protons, the one giving the higher field peak is *endo* above the conjugated triene system. The upfield shift produced by benzene relatively to the previous solvents is most strongly manifested for the methyl protons and for the *exo* methylene proton ; the vinylic proton and one t-butyl group have a smaller upfield shift, whereas the *endo* proton and the other t-butyl are not affected by benzene. Owing to the strong upfield shift of the methyl group in benzene, all four components of the AX multiplet are visible.

In order to ascertain the presence of the four components of the AX system formed by the geminal methylene protons in $CDCl_3$, the spectrum of IV was recorded : the formation of IV is however, always accompanied by a slight dedeuteration leaving a small residual methyl signal. Nevertheless, the vinylic proton becomes a broad singlet in this case, because the allylic coupling with the methyl deuterium atoms is too small to be observable.

In trifluoroacetic acid at room temperature the two t-butyl groups are distinct as in benzene, but all peaks appear at lower field than in deuterochloroform, probably owing to protonation : vinylic proton at 3.10 τ, methyl at 7.49 τ, t-butyl groups at 8.46 and 8.64 τ. Most conspicuous is the coalescence of the methylene protons into one singlet at 6.74 τ owing to ring flip as in other diazepines.

In a mixture of trifluoroacetic acid and chloroform, this peak is broadened at 0°, at −15° it is flattened out, and at −40° the methylene protons appear separated as in chloroform at room temperature. The lower energy barrier to ring flip in trifluoroacetic than in other solvents was noted first for triaryl-1,2-diazepines.[2] The separation between the two t-butyl peaks is smaller than in pure trifluoroacetic acid, and also the upfield shifts are smaller.

LIS PROTON NMR SPECTRA

On adding progressively $Eu(dpm)_3$ to a chloroform solution of the diazepine, all peaks undergo downfield shifts : one t-butyl group is deshielded faster than the other, so that the degeneracy is removed. The order of increasing relative deshielding is : tBu, Me, tBu, low-field sat. CH, =CH, high-field sat. CH. A comparison with the effect of benzene reveals that $Eu(dpm)_3$ and benzene have almost opposite effects : benzene does not shield the high-field (*endo*) sat. CH which is most strongly shielded by $Eu(dpm)_3$, whereas the low field sat. CH (*exo*) and methyl protons, are most strongly shielded by benzene and little deshielded by $Eu(dpm)_3$.

^{13} C-NMR SPECTRA

The ^{13}C-NMR spectra of the diazepine and its methyl-deuterated derivative were recorded in deuterochloroform at room temperature : here again, no evidence for ring flip was found at this temperature and in this solvent. The 3- and 7-t-butyl groups appear at 28.0 and 28.8 (methyl carbons) and 38.1 and 38.6 ppm (quaternary carbons). The methyl peak, which disappears on deuteration, is at 23.4 ppm, whereas the 4 and 6 carbon atom peaks appear at 34.0 and 117.7 ppm, respectively. The three quaternary unsaturated carbon atoms of the diazepine ring have very low intensity : one is visible in the spectra of both III and IV at 145.1 ppm but the other two are uncertain.

Since no other ^{13}C-NMR spectrum of such compounds has yet been reported, as far as we are aware, we recorded for comparison the ^{13}C-NMR spectrum of 3,5,7-triphenyl-4H-1,2-diazepine under the same conditions : the 4- and 6 carbons appear at 33.9 and 117.7 ppm, as in the alkyl-substituted derivative. The three quaternary unsaturated diazepine carbons appear at 145.1, 149.1 and 156.6 ppm. Phenyl carbons appear at 127.4, 127.8, 128.5 (broad), 129.0, 129.4, 129.8, 135.5, 137.6, 138.5 ppm : peaks 127.4 and 128.5 are more intense, peaks 129.4, 135.5, 137.6 and 138.5 less intense than the other ones.

MASS SPECTRA

Mass spectra of III and IV were recorded at 70 V (figure 1) and 20 V ionization potential. The most intense peaks are presented in table 1 with tentative assignments for their origin. These assignments are substantiated by the metastable peaks observed in the spectrum (table 2) and by the high-resolution mass spectrum (table 3) giving the molecular formulas of the most significant peaks. The fragmentations of the molecule under electron impact are summarized in figure 2 ; in this scheme, since the parent molecule does not have equivalent t-butyl groups, the t-butyl group undergoing fragmentation was arbitrarily selected.

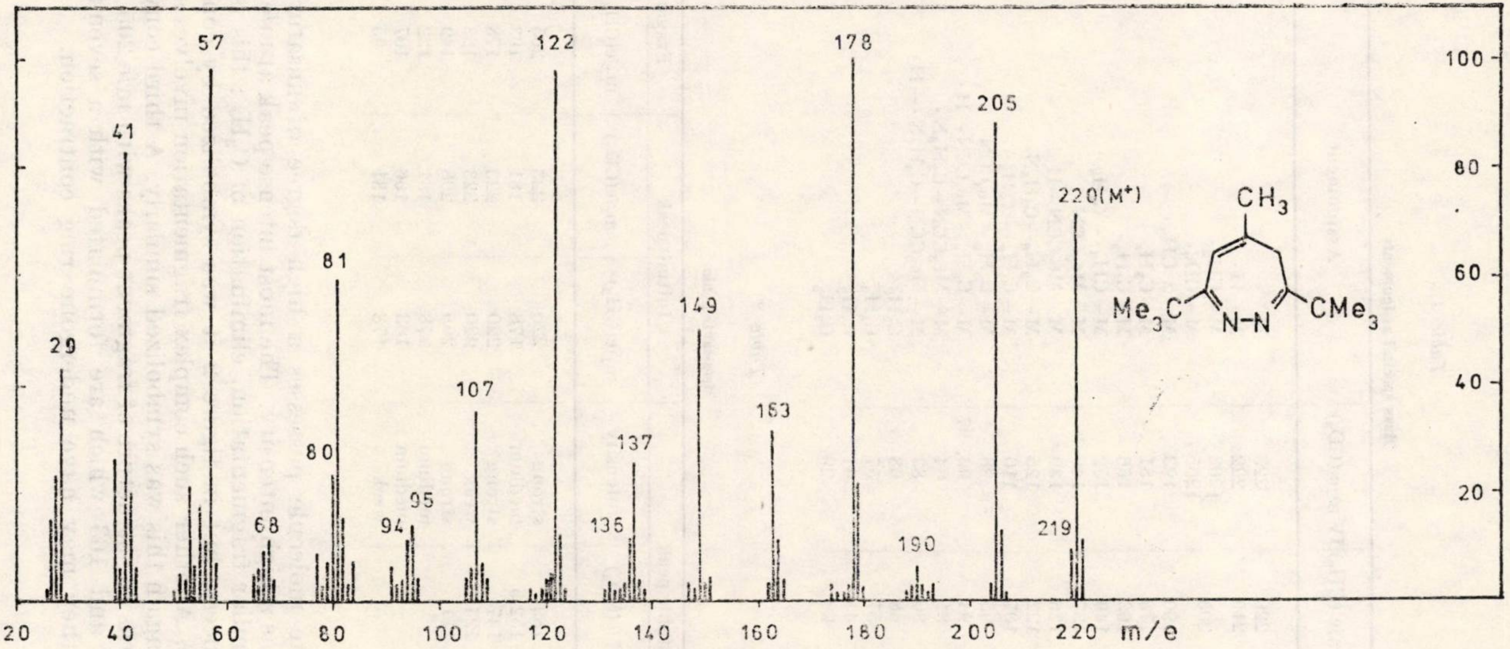

Fig. 1. — Mass spectrum of III at an ionization potential of 70 V.

Table 1

Mass spectral assignments

III m/e (CH_3)	IV m/e (CD_3)	Assignment
220	223	M
219	222	$M-H\cdot$
205	208	$M-CH_3\cdot$
	205	$M-CD_3\cdot$
190	193	$M-2\ CH_3\cdot$
178	181	$M-C_3H_6$
163	166	$M-C_4H_9\cdot$
149	152	$M-CH_3\cdot-C_4H_8$
137	140	$M-Me_3CCN$
136	139	$M-Me_3CCN-H\cdot$
122	125	$M-C_3H_6-C_3H_6N\cdot$
107	110	$M-C_4H_9\cdot-C_4H_8$
95	98	$M-C_3H_6-Me_3CCN$
94	96, 97	$M-C_3H_6-Me_3CCN-H\cdot$
81	84	$M-Me_3CCN-C_3H_6N\cdot$
80	83	$M-Me_3CCN-C_3H_6N\cdot-H\cdot$
68	68	$C_5H_8^+$
57	57	$C_4H_9^+$
41	41	$C_3H_5^+$
29	29	$C_2H_5^+$

Table 2

Metastable peaks

Metastable peak			Initial peak		Fragment peak	
m*/e(CH_3)	m*/e(CD_3)	Intensity	m_1/e(CH_3)	m_1/e(CD_3)	m_2/e(CH_3)	m_2/e(CD_3)
191.5	189	strong	220	223	205	205
149.5	152.5	medium	178	181	163	166
144	147	strong	220	223	178	181
121	124	weak	220	223	163	166
108.5	111	strong	205	208	149	152
83.5	—	medium	178	181	122	125
70	—	medium	163	166	107	110
51	—	weak	178	181	95	—

Since the molecule possesses a high degree of unsaturation, the parent peak has a high intensity. The most intense peak at m/e 178 arises by a very peculiar fragmentation, elimination of C_3H_6 : this is certainly a complex process, but in figure 2 it was symbolized by conversion of CMe_3 into Me. Another such complex fragmentation involves splitting of $C_3H_3N\cdot$, and again this was symbolized similarly. A third convention in figure 2 concerns the structure of fragment peaks with m/e 205 (left-hand formula), 178 and 163 which are formulated with a seven-membered ring, though they may have undergone ring contraction.

Table 3

High resolution mass spectra

Found m/e amu	Calc. m/e amu	Intens. %	Error. 10^3 amu	Formula
220.1920	220.1939	13.8	−1.99	$C_{14}H_{24}N_2$
205.1743	205.1705	78.3	+3.81	$C_{13}H_{21}N_2$
179.1530	179.1504	3.1	+2.64	$C_{10}{}^{13}CH_{18}N_2$
178.1468	178.1470	100.0	−0.15	$C_{11}H_{18}N_2$
163.1209	163.1235	2.1	−2.67	$C_{10}H_{15}N_2$
149.1084	149.1079	16.3	−0.54	$C_9H_{13}N_2$
122.0951	122.0970	30.1	−1.91	$C_8H_{12}N$
107.0608	107.0609	3.5	−0.17	$C_6H_7N_2$
95.0724	95.0735	6.7	−1.08	C_6H_9N

Doubly charged ions appear for all major odd-numbered peaks from Table 3 at 102.5, 81.5 and 74.5 a.m.u.

Previous studies [2] pointed out that 3,5,7-triaryl-4*H*-1,2-diazepines split off a methyl under electron impact, and a ring contraction to a 1,2-diazine was postulated to account for this fact. A similar process is shown in the upper right-hand side of figure 2. By studying the mass spectrum of IV, two peaks emerge in the 200−210 a.m.u. range, at m/e 205 and 208, revealing two different fragmentations of the molecular ion m/e 220 which splits either the 5-methyl, or gives the ring contraction : the former process gives a peak with m/e 205 both from III and for IV, the latter gives 205 from III and 208 from IV ; we assume different structures for the two fragment ions in figure 2.

A fragmentation which was predominant with 3,5,7-triaryl-4*H*-1,2-diazepines, and which here is less important, involves fragmentation with formation of a nitrile (m/e 220 → 137, 178 → 95).

Fragmentations involving formation of isobutene or t-butyl radicals are expected for t-butyl substituents (m/e 220 → 163 → 107, 205 → 149). Also, loss of a hydrogen atom (table 1) is a fairly common process. We assume that in the formation of peaks with m/e 219, 136, 94 and 80 the hydrogen is split from the CH_2 group. All these fragmentations are confirmed by weak metastable peaks. When the base peak m/e 178 splits a methyl group, it may yield the same structure for 163 as the direct process 220 → 163, or a different one; for simplicity, both structures were depicted as identical in figure 2.

The most conspicuous feature of the mass spectrum of III and IV is the absence of peaks corresponding to the formation of a nitrogen molecule, a process which is, however, common to all heterocyclic systems possessing two adjacent nitrogen atoms (literature cited in ref.[2]) and to the related 3,5,7-triaryl-4*H*-1,2-diazepines studied earlier.[2] By high-resolution mass spectroscopy it is certain (table 3) that the peak with m/e 190 still has the two nitrogens (it could have been formed by loss of $2H + N_2$). We assume that this is another consequence of the presence of two bulky t-butyl groups (along with diazepine formation

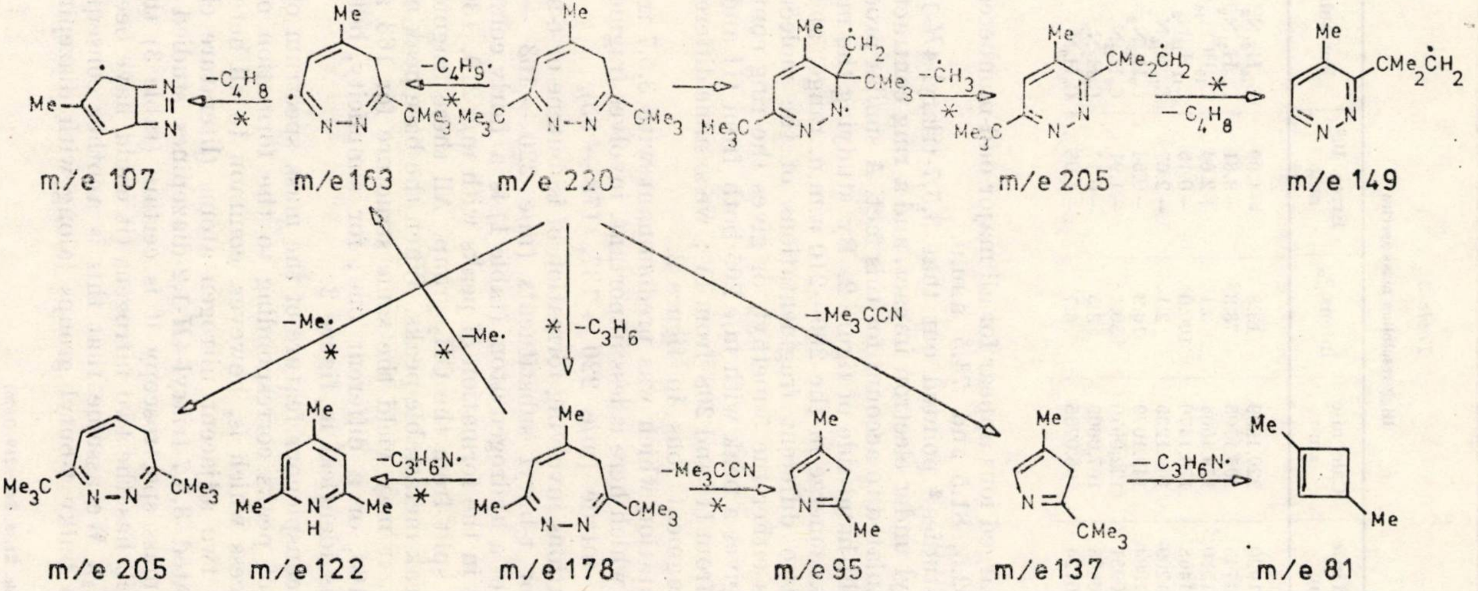
m/e 107
m/e 163
m/e 220
m/e 205
m/e 149
m/e 205
m/e 122
m/e 178
m/e 95
m/e 137
m/e 81
$-C_4H_8$
$-C_4H_9\cdot$
$-\dot{C}H_3$
$-C_4H_8$
$-Me\cdot$
$-Me\cdot$
$-C_3H_6$
$-Me_3CCN$
$-C_3H_6N\cdot$
$-Me_3CCN$
$-C_3H_6N\cdot$
Me
CMe_3
Me_3C
$CMe_2\dot{C}H_2$
N
H

Fig. 2. – Chart of the fragmentations observed in the mass spectrum of III. Hydrogen splittings are not included. All formulas represent positive ions or radical ions.

instead of N-aminopyridinium salt) : the transition state for the fragmentation of a nitrogen molecule must be energetically unfavourable owing to the overcrowding of the two t-butyl groups which become attached to adjacent carbons in the cyclopentadiene resulted from expulsion of dinitrogen. An alternative explanation is that, with t-butyl substituents, other fragmentations under electron impact are eased so much that loss of dinitrogen is no longer able to compete.

EXPERIMENTAL PART

2,6-Di-t-butyl-4-methylpyrylium perchlorate.[10] Into a mixture of pivaloyl chloride (2 moles) and tin tetrachloride (1 mole), one mole of t-butyl chloride was added and the homogeneous clear mixture was left at room temperature in a round bottom flask with a calcium chloride tube in a hood for 48 hours with occasional shaking. Hydrogen chloride is slowly evolved and the mixture darkens. Subsequently the mixture was heated for 3 hrs at 50°, cooled and hydrolyzed by pouring on ice (500 g), hydrochloric acid (20 ml) and ether (500 ml) with stirring. The ethereal layer was extracted six to eight times with portions of water (until no more pyrylium salt was extracted), and all aqueous layers were treated with perchloric acid which precipitated the perchlorate. This was filtered off and dried in the air. It may be recrystalized from acetic acid, but is sufficiently pure for the next step. Yield 30—35%.

3,7-Di-t-butyl-5-methyl-4H-1,2-diazepine. A suspension of the above perchlorate in ethanol or methanol is treated at 40—50° with excess hydrazine hydrate until in an exothermal reaction a clear solution results. Dilution with water yields white crystals of the 1,2-diazepine in 89% yield, m.p. 115° (from aq. methanol). Vpc evidences an impurity which has a higher retention time, and which is not removed by one recrystallization or vacuum sublimation; a pure product may either be obtained by preparative gas chromatography, or by slow cooling of a concentrated cyclohexane solution, which deposits large colourless prisms of III. Found: C, 75.5; H, 10.9; N, 12.4. $C_{14}H_{24}N_2$ requires: C, 76.3; H, 11.0; N, 12.7%. It may be sublimed without decomposition at reduced or normal pressure. Infrared absorption (KBr): 1632 vs, 1595 m, 1522 s, 1479 s, 1466 s, 1440 w, 1397 w, 1385 w, 1368 vs, 1327 s, 1290 vw, 1264 s, 1215 m, 1206 s, 1170 m, 1126 s, 1097 vs, 1049 m, 1012 m, 991 s, 939 s, 915 s, 871 s, 852 s, 816 w, 782 m, 698 m, 642 w, 550 vW, 530 m, 514 m, 483 w, 445 vw, 439 m, 510 w.

Deuteration of the methyl group. Redistilled acetic anhydride (1 mole) was refluxed for two hours with 1 mole deuterium oxide. This carboxyl-deuterated acetic acid was used for deuterating 2,6-di-t-butyl-4-methylpyrylium perchlorate by refluxation of the homogeneous solution for 20 minutes. After cooling and addition of ether, the deuterated perchlorate is filtered off and washed with ether. The perchlorate was converted as above into the 1,2-diazepine, avoiding heating (which favours dedeuteration).

Acknowledgements. Thanks are expressed to Alice Vasilescu and F. Chiraleu for the NMR spectra, to Elena Romas for IR spectra, to M. Paraschiv for the UV spectra, to Dr. A. J. Boulton (University of East Anglia, Norwich) and Prof. F. W. Mc Lafferty (Cornell University, Ithaca, N.Y.) for the low and high-resolution mass spectra, respectively, and to Dr. V. Wray (Ges. für Molekularbiologische Forschung, Stöckheim, W. Germany) for the ^{13}C-NMR spectra.

---

[10] A. T. Balaban and C. D. Nenitzescu, *Liebigs Ann. Chem.*, **625**, 74 (1959).

Revue Roumaine de Chimie, **21**, *2*, 251–255 (1976)

REACTION OF PYRYLIUM SALTS WITH NUCLEOPHILES. XI[1]

CHEMICAL SHIFT NON-EQUIVALENCE OF ISOPROPYL IN ATROPISOMERIC 1-ARYL-2-ISOPROPYL-4,6-DIMETHYL-PYRIDINIUM SALTS

CORNELIA UNCUŢA and A. T. BALABAN *

Institute of Atomic Physics, POB 5206, Bucharest, Romania

Received August 21, 1975

The ^{1}H-NMR spectra of 1-aryl-2-isopropyl-4,6-dimethyl-pyridinium perchlorates were investigated, the aryl group being phenyl, *o*-, *m*-,, and *p*-tolyl. Assignments of all peaks in the NMR spectra were made by partial methyl-deuteration. Magnetic nonequivalence of the diastereotopic methyls from the isopropyl group was observed at room temperature for the N-*o*-tolyl derivative, but not for the N-*m*-tolyl derivative even at −60°. Also, at temperatures +40 to −60° 2-ethyl-4,6-dimethyl-1-*o*-tolylpyridinium perchlorate does not present non-equivalence of the ethyl protons.

Atropisomerism in the biphenyl series is well documented,[2a] but much less for N-arylpyridinium salts.[2b] Since the reaction of pyrylium salts with arylamines affords pyridinium salts in high yield [3,4] and since pyrylium salts are easily available, [5] we investigated various such N-arylpyridinium salts (with suitable substituents, in order to be chiral, owing to restricted rotation).

The non-planarity of crystalline N-phenyl-2,4,6-trimethylpyrylium was evidenced by X-ray diffraction which revealed a dihedral angle of 83.5°;[6] even N-phenylpyridinium chloride hydrate has a non-coplanar cation in the crystal (unlike biphenyl) with an average dihedral angle of 47°, and a pairwise association of two cations in a head-to-tail arrangement, with the distance between parallel phenyl and pyridinium rings of approximately 3.5 Å.[7]

---

* To whom correspondence should be addressed.

[1] Preceding part in the series, A. T. BALABAN, *Rev. Roumaine Chim.*, **18**, 1609 (1973).

[2a] S. F. MASON, R. H. SEAL and D. R. ROBERTS, *Tetrahedron*, **30**, 167 (1974);

[2b] K. UNDHEIM and G. A. ULSAKER, *Acta Chem. Scand.*, **27**, 1059 (1973).

[3] K. DIMROTH and K. H. WOLF, in "Newer Methods of Preparative Organic Chemistry", **3**, 357 (1964); K. DIMROTH, *Angew. Chem.*, **72**, 331 (1960).

[4] C. TOMA and A. T. BALABAN, *Tetrahedron*, Suppl. 7, 9 (1966).

[5] A. T. BALABAN, W. SCHROTH and G. FISCHER in "Advances in Heterocyclic Chemistry", **10**, 241 (1969).

[6] A. CAMERMAN, L. H. JENSEN and A. T. BALABAN, *Acta Cryst.*, **25B**, 2623 (1969).

[7] To be published in collaboration with L. H. JENSEN.

To evidence the chirality, the most attractive method is the magnetic non-equivalence[8-10] of diastereotopic groups,[11] because this method does not involve resolution of enantiomers. Though this non-equivalence was observed for methylene groups of molecules with axial chirality like allenes [12] and biphenyls,[13-16] it was not reported until now for N-arylpyridinium salts.

1-Aryl-2-isopropyl- or -2-ethyl-4,6-dimethylpyridinium salts were selected owing to the following considerations :

(i) ease of preparation (see below);

(ii) presence of diastereotopic groups (isopropyl, ethyl);

(iii) bulkiness of substituents *ortho* to the phenyl-pyridinium bond, leading to a significant energy barrier to rotation.

PREPARATION

The precursor, 2-isopropyl-4,6-dimethylpyrylium perchlorate (I) was synthetized from mesityl oxide and isobutyryl chloride in the presence of aluminium chloride. An analogous acylation of the equilibrating mixture of the α, β- and β, γ-unsaturated ketone isomers with other acyl chlorides had been described earlier.[5,17,18] As known, [19,20] 4-methyl groups of pyrylium salts are rapidly deuterated in hot deuterium oxide whereas 2- and 6- alkyl groups are deuterated more slowly (this was explained by the higher stability of γ-methylenepyran than of α-methylenepyran intermediates). Therefore heating of this pyrylium salt in deuterium oxide solution for 20—30 minutes on the steam bath followed by cooling afforded a product whose 4-methyl group was deuterated to an extent of 40—50%, whereas the 2- and 6-alkyl groups were deuterated approx. 4—5% and the 3- or 5-hydrogens less than 1%.

Similarly, replacement of isobutyryl chloride in the above reaction by propionyl chloride afforded the known [17] 2-ethyl-4,6-dimethylpyrylium perchlorate.

Reaction of pyrylium perchlorates with primary aromatic amines (aniline, *o*-, *m*-, *p*-toluidine) afforded N-arylpyridinium perchlorates IIa-d when starting from I, and pyridinium salts IIId and IIIb when

---

[8] M. L. Martin and G. J. Martin, *Bull. Soc. Chim. France*, 2117 (1966).

[9] M. van Gorkom and G. E. Hall, *Quart. Rev.*, **22**, 14 (1968).

[10] T. H. Siddall and W . E. Stewart, in "Progress in NMR Spectroscopy", **5**, 33 (1969).

[11] K. Mislow and M. Raban, in "Topics in Stereochemistry", **1**, 1 (1967).

[12] M. L. Martin, R. Mantione and G. J. Martin, *Tetrahedron Letters*, **1965**, 3185.

[13] W. L. Meyer and R. B. Meyer, *J. Amer. Chem. Soc.*, **85**, 2170 (1963).

[14] K. Mislow, M.A.W. Glass, H. B. Hoffs, E. Simon and G. H. Wahl, *J. Amer. Chem. Soc.*, **86**, 1710 (1964); K. Mislow and M. A. W. Glass, *ibid.*, **83**, 2780 (1961).

[15] R. J. Kurland, M. B. Rubin and W. B. Wise, *J. Chem. Phys.*, **40**, 2426 (1964).

[16] M. Oki, H. Iwamura, and N. Haykawa, *Bull. Chem. Soc. Japan*, **37**, 1865 (1964).

[17] A. T. Balaban and C. D. Nenitzescu, *Liebigs Ann. Chem.*, **625**, 74 (1959).

[18] P. F. G. Praill and A. L. Whitear, *J. Chem. Soc.*, **1961**, 3573.

[19] E. Gârd, I. Stanoiu, F. Chiraleu and A. T. Balaban, *Rev. Roumaine Chim.*, **18**, 257 (1973).

[20] E. Gârd, A. Vasilescu, G. D. Mateescu and A. T. Balaban, *J. Labelled Comp.*, **3**, 196 (1967).

starting from 2-ethyl-4,6-dimethylpyrylium and *o*-toluidine and *p*-toluidine, respectively.

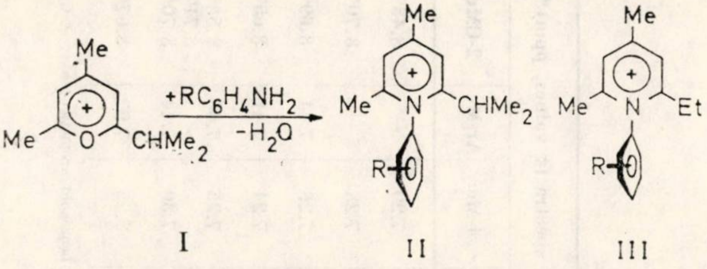

I II III

a, R=H; b, =*p*-Me; c, R=*m*-Me; d, R=*o*-Me

^{1}H-NMR SPECTRA

Proton magnetic resonance spectra were determined in trifluoroacetic acid solution (TFA), and table 1 presents the results as τ values relative to internal tetramethylsilane.

In agreement with previous data,[21] pyrylium salt I presents the 6-methyl peak at lower field than the 4-methyl peak , owing to the higher positive charge in α than in γ.[22] This was confirmed by the NMR spectrum of the partly deuterated pyrylium salt I, with the peak at 7.20 τ broadened and of lower intensity. The slight deuteration of the isopropyl group is accompanied by the appearance of a new peak due to $CDMe_2$ (between the doublet due to the $CHMe_2$ methyl protons) which reveals a triplet structure due to the small coupling with deuterium (ca. 0.5 Hz). The pyrylium protons in positions 3 and 5 appear accidentally at the same field.

In N-arylpyridinium salts, owing to the ring current and non-coplanarity of the phenyl and pyridinium rings, protons bonded to side-chain carbons *ortho* to the ring-ring bond are shielded and appear upfield with 0.5—0.6 ppm as shown by comparing the values for the 6-methyl group in I with those of II and III; protons bonded to the next carbons in the side-chain are shifted upfield only with 0.1—0.2 ppm, as revealed by comparing the values of 2-CMe protons for I with those for II and III. This shielding effect is also manifested *vice-versa* in the upfield shift of the *ortho*-toluidinic methyl proton in IId and IIId, relatively to IIb and IIc. The peak assignment was confirmed by recording also the NMR spectra of the pyridinium salts prepared from the partly (4-methyl)-deuterated pyrylium salt.

The achiral N-arylpyridinium salts IIa with N-phenyl, and IIb or IIIb with N-*p*-tolyl groups present, in accordance with expectations, only one kind of isopropyl for II or ethyl groups for III. On the other hand,

---

[21] A. T. Balaban, G. R. Bedford and A. R. Katritzky, *J. Chem. Soc.*, **1964**, 1646.
[22] G. V. Boyd and A. T. Balaban, *Rev. Roumaine Chim.*, **14**, 1575 (1969).

Table 1

Pyrylium and pyridinium perchlorates

Comp.	M.p.°C (uncorr.)	Formula	Anal. { calc. found				NMR spectra (τ values, ppm)[a]					
			C	H	Cl	N	2-CH	6-Me	4-Me	Ar-Me	2-CMe	3,5-H_2
I	124	$C_{10}H_{15}O^+ClO_4^-$	47.91	6.03	14.14	—	6.55[b]	7.03	7.20	—	8.48[c]	2.23
			47.56	6.18	13.81	—						
IIa	191	$C_{16}H_{20}N^+ClO_4^-$	58.99	6.19	10.88	4.30	7.10[b]	7.60	7.28	—	8.70[c]	[d]
			59.36	6.44	10.58	4.31						
IIb	152–154	$C_{17}H_{22}N^+ClO_4^-$	60.08	6.52	10.43	4.12	7.00[b]	7.62	7.26	7.44	8.69[c]	[d]
			60.12	6.73	10.71	4.01						
IIc	149–151	$C_{17}H_{22}N^+ClO_4^-$	60.08	6.52	10.43	4.12	7.05[b]	7.54	7.24	7.41	8.65[c]	[d]
			60.34	6.80	10.52	4.01						
IId	198–200	$C_{17}H_{22}N^+ClO_4^-$	60.08	6.52	10.43	4.12	7.15[b]	7.57	7.25	7.95	8.58[c]	[d]
	(dec.)		60.30	6.73	10.68	4.30					8.71[c]	
IIIb	125–127	$C_{16}H_{20}N^+ClO_4^-$	58.99	6.19	10.88	4.30	7.28[e]	7.56	7.30	7.44	8.70[f]	2.30
			59.51	6.75	10.40	3.95						
IIId	125–127	$C_{16}H_{20}N^+ClO_4^-$	58.99	6.19	10.88	4.30	7.34[e]	7.60	7.25	7.97	8.67[f]	[d]
			59.26	6.24	11.13	4.18						

[a] Room temperature, trifluoroacetic solution; [b] Septet with J = 7 Hz; [c] Doublet with J = 7 Hz; [d] Submerged under benzenoid aromatic peaks; [e] Quartet with J = 7.2 Hz; [f], Triplet with J = 7.2 Hz.

IId with an *o*-tolyl group affords at 40°—70° an NMR spectrum with two kinds of isopropyl groups : at 60 MHz the isopropyl methyls appear accidentally as a 1 : 2 : 1 triplet, but at 80 MHz they appear as two equal doublets. This proves that IId is a chiral molecule, since the diastereotopic methyls of the isopropyl group appear magnetically non-equivalent. However, the structurally chiral molecules IIc with an *m*-tolyl group, and IIId with an *o*-tolyl group, present at 38° NMR spectra with magnetically equivalent isopropyl and ethyl groups, respectively; this proves that the barrier to internal rotation in these latter compounds is lower than in IId and that at room temperature the rotation is faster than the NMR time scale. Indeed, the steric hindrance in IId is higher (*o* : *o*′ groups are Me, iPr; H, Me) than in IIc (Me, iPr; H, H) or in IIId (Me, Et; H, Me). At —60° (in deuterochloroform * IIc and IIId present broadened peaks for isopropyl or ethyl protons, respectively, but the rotation rate is still high enough to result in no extra splitting.

EXPERIMENTAL

2-Isopropyl-4,6-dimethylpyrylium perchlorate

Anhydrous aluminium chloride (31.4 g, 235 mmoles) was dissolved, under vigorous stirring, in 50 g (470 mmoles) isobutyryl chloride chilled in an ice-water bath. After complete dissolution, 23 g (235 mmoles) mesityl oxide was added dropwise with external cooling. The mixture was kept overnight at room temperature, then heated four hrs at 40—50°. The mixture was poured over 100 g of crushed ice, acidified with hydrochloric acid and extracted three times with ether. The aqueous solution, freed of ether traces by heating, was cooled and acidified with 12 ml 70% perchloric acid, when the pyrylium perchlorate precipitated. The product was filtered off, washed with a few ml of ice-water and dried. Yield : 12%. The salt was purified by recrystallization from water acidified with perchloric acid. Partial deuteration was effected by heating a saturated solution of the perchlorate in deuterium oxide at 100° (to which a small amount of P_2O_5 had been added) for 20—30 min, followed by cooling and filtration.

Preparation of the pyrydinium salts

The pyrydinium salts were obtained in the following general manner : 50 mmoles of pyrylium perchlorate were heated for 2—3 minutes in ethanolic solution with 100 mmoles of aromatic amine (aniline, *o*-, *m*-, and *p*-toluidine). The pyrydinium salt precipitated on addition of ether ; the product was filtered off, washed with ether and recrystallized from ethanol—ether.

NMR spectra were recorded with a Varian 60A and a Tesla 80 MHz instrument.

Thanks are expressed to A. Vasilescu, Dr. M. Elian and F. Chiraleu for the NMR spectra and to E. Sliam and V. Daniel for elemental analyses.

---

* The solubility of N-arylpyridinium salts in $CDCl_3$ is satisfactory. All alkyl proton peaks appear shifted upfield in deutero-chloroform with ca. 0.08 ppm relatively to solutions in trifluoroacetic acid.

IId with an o-tolyl group affords at 10°–70° an NMR spectrum with two bands of isopropyl groups; at 60 MHz the isopropyl methyls appear coincidentally as a 1 : 2 : 1 triplet, but at 80 MHz they appear as two equal doublets. This proves that IId is a chiral molecule, since the diastereotopic methyls of the isopropyl group appear magnetically non-equivalent. However, the structurally chiral molecules IIe with an m-tolyl group, and IIId with an o-tolyl group, present at 38° NMR spectra with magnetically equivalent isopropyl and ethyl groups, respectively; this proves that the barrier to internal rotation in these latter compounds is lower than in IId and that at room temperature the rotation is faster than the NMR time scale. Indeed, the steric hindrance in IId is higher (o,o' groups are Me, iPr; H, Me) than in IIe (Me, iPr; H, H) or in IIId (Me, Et; H, Me). At −68° (in deuterochloroform*) IIe and IIId present broadened peaks for isopropyl or ethyl protons, respectively, but the rotation rate is still high enough to result in the extra splitting.

EXPERIMENTAL

2-Isopropyl-4,6-dimethylpyrylium perchlorate

Anhydrous aluminium chloride (13.4 g, 100 mmoles) was dissolved under vigorous stirring, in 50 g (470 mmoles) isobutyryl chloride cooled in an ice-water bath. After complete dissolution, 25 g (255 mmoles) mesityl oxide were added dropwise with external cooling. The mixture was kept overnight at room temperature, then heated four hrs at 45–50°. The mixture was poured over 100 g of crushed ice acidified with hydrochloric acid and extracted three times with ether. The aqueous solution, freed of ether traces by heating, was cooled and acidified with 12 ml 70% perchloric acid, when the pyrylium perchlorate precipitated. The product was filtered off, washed with a few ml of ice-water and dried. Yield 12%. The salt was purified by recrystallisation from water acidified with perchloric acid. Partial deuteration was effected by heating a saturated solution of the perchlorate in deuterium oxide at 100° (to which a small amount of P_2O_5 had been added) for 20–30 min, followed by cooling and filtration.

Preparation of the pyridinium salts

The pyridinium salts were obtained in the following general manner: 50 mmoles of pyrylium perchlorate were heated for 2–3 minutes in ethanolic solution with 100 mmoles of aromatic amine (aniline, o-, m- and p-toluidine). The pyridinium salt precipitated on addition of ether; the product was filtered off, washed with ether and recrystallized from ethanol-ether.

NMR spectra were recorded with a Varian A60A and a Tesla BS 487 (80 MHz) instrument.

Thanks are expressed to A. Vasilescu, Dr. M. Elian and P. Cabuzu for the NMR spectra and to [illegible] and V. Daniel for elemental analyses.

---

* The solubility of N-arylpyridinium salts in $CDCl_3$ is satisfactory. All alkyl proton peaks appear shifted upfield in deuterochloroform with ca. 0.08 ppm relatively to solutions in trifluoroacetic acid.

Revue Roumaine de Chimie, **21**, 2, 257–262 (1976)

NEW DISPERSE DYES WITH NAPHTH[2,3-c]ACRIDAN [5,6-de]PYRIMIDIN-5,11-DIONE STRUCTURE

F. URSEANU, C. TĂRĂBĂŞANU-MIHĂILĂ and L. FLORU

Laboratory of Chemistry and Technology of Aromatic Intermediates and Dyes, Chemistry Institute, Calea Victoriei 149, Bucharest, Romania

Received December 16, 1974

Syntheses for the preparation of new disperse dyes with napht [2.3-c] acridan [5,6-de] pyrimidin-5,11-dione structure are described.

1. INTRODUCTION

A problem of great importance for the dye industry is to synthesize a large number of products, especially those of dark shades (violets, blues and greens), necessary to synthetic fibres dyeing; the new synthesized products must have better affinity to the dyied textile material and better fastness of the dyeings.

In the present work we undertook the synthesis of a series of new disperse dyes with naphth[2,3-c] acridan [5,6-de] pyrimidin-5,11-dione structure with the following general formula :

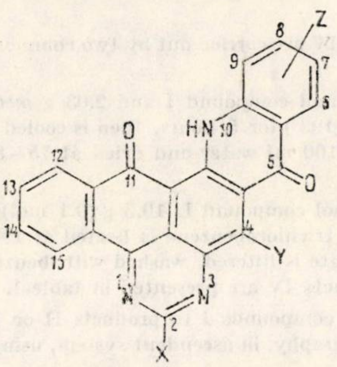

X=H	Y=H	Z=H	(II-1)	X=C_6H_5	Y=H	Z=H	(IV-1)
X=H	Y=OCH_3	Z=H	(II-2)	X=C_6H_5	Y=OCH_3	Z=H	(IV-2)
X=H	Y=$OCH_2CH_2OCH_3$	Z=H	(II-3)	X=C_6H_5	Y=$OCH_2CH_2OCH_3$	Z=H	(IV-3)
X=H	Y=H	Z=8–NO_2	(II-4)	X=C_6H_5	Y=H	Z=8-NO_2	(IV-4)
X=H	Y=OCH_3	Z=8–NO_2	(II-5)	X=C_6H_5	Y=OCH_3	Z=8-NO_2	(IV-5)
X=H	Y=H	Z=7–Br	(II-6)	X=C_6H_5	Y=H	Z=7-Br	(IV-6)
X=H	Y=$CONH_2$	Z=H	(II-7)	X=C_6H_5	Y=$CONH_2$	Z=H	(IV-7)

By using the above-shown substituents X, Y and Z on the mere naphth[2,3-c]acridan[5,6-de]pyrimidin-5,11-dione structure(II-1) we hoped to attain the modification of the tinctorial shades, to increase the affinity to the dyied synthetic fibres (OCH_3, $CONH_2$) and to improve the light (Br, NO_2), thermofixation (OCH_3, OCH_2CH_2 OCH_3) and wet treatments fastness.

2. SYNTHESIS OF NAPHTH [2,3-c] ACRIDAN [5,6-de] PYRIMIDIN-5,11-DIONE DERIVATIVES

Naphth[2,3-c]acridan[5,6-de]pyrimidin-5,11-dione dyes, in which X = H(II), have been synthesized according to a known literature method for anthra[1,9-de]pyrimidin-7-one,[1] namely by treating of miscellaneous substituted naphth[2,3-c]acridan-5,8,14-triones [2] I with formamide in the presence of *meta*-nitrobenzene-sulphonic acid (Ludigol); the reactions were carried out by refluxing in excess of formamide as solvent.

Naphth[2,3-c]acridan[5,6-de]pyrimidin-5,11,-dione dyes, in which X = C_6H_5 (IV), have been synthesized according to a literature method for miscellaneous anthrapyrimidines [3]; thus, the reactions were carried out by heating at 190° in trichlorobenzene of various substituted naphth[2,3-c]acridan-5,8-14-triones I with benzonitrile, in the presence of *para*-toluensulphonic acid.

3. EXPERIMENTAL

Syntheses of dyes II and IV are carried out by two common methods which are described in the following:

3.1. A mixture of 0.01 mol compound I and 2.03 g *meta*-nitro-benzenesulphonic acid in 30 ml formamide is refluxed (193°) for 5 hours, then is cooled at 10—15°; the formed precipitate is filtered, washed with 100 ml water and dried at 75—80°. The yields of products II are presented in Table 1.

3.2. A mixture of 0.01 mol compound I, 10.3 g (0.1 mol) benzonitrile and 1.72 g *para*-toluenesulphonic acid in 30 ml trichlorobenzene is heated at 190° for 6 hours, then is cooled at 10—15°; the formed precipitate is filtered, washed with benzene, ethanol, water and dried at 75—80°. The yields of products IV are presented in table 1.

Note. The conversion of compounds I to products II or III is controlled by means of Whatman n⁰ 1 paper chromatography, in ascendent system, using N.N-dimethylformamide as

---

[1] J. Reichel, ,,Tehnologia coloranţilor antrachinonici'', Ed. Academiei, Bucharest, 1961, p. 400.

[2] F. Urseanu, *Rev. Roumaine Chim.*, **18**, 1019 (1973).

[3] Badische Anilin und Sodafabrik, Brit. Pat., 1 061 117, Jan. 26, 1965; *J. Soc. Dyers and Colourists*, **85**, 244 (1967).

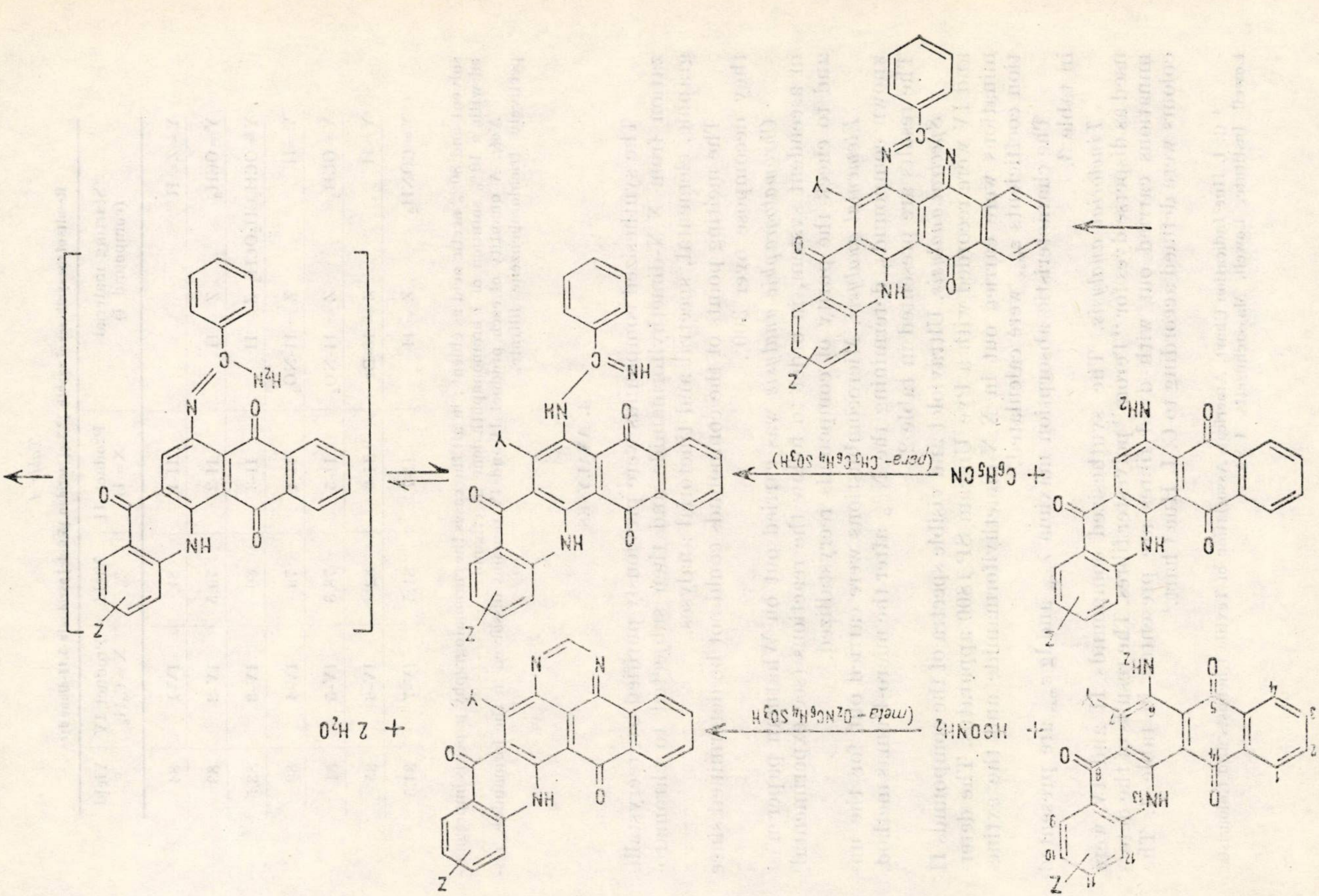+
HCONH2
(meta-O2NC6H4SO3H)
+ 2 H2O
+ C6H5CN
(para-CH3C6H4SO3H)
Z
Y
NH
NH2
O
1
2
3
4
5
6
7
8
9
10
11
12
13
14

Table 1

Results of the syntheses of naphth [2,3-c] acridan [5,6-de] pyridimin-5,11-dione dyes

Starting material (compound I)	Product II $X=H$	Yield %	Product IV $X=C_6H_6$	Yield %
$Y=Z=H$	**II-1**	81	**IV-1**	84
$Y=OCH_3$ $Z = H$	**II-2**	79,5	**IV-2**	83
$Y=OCH_2CH_2OCH_3$ $Z = H$	**II-3**	80	**IV-3**	83.5
$Y=H$ $Z = 11\text{-}NO_2$	**II-4**	79	**IV-4**	80
$Y=OCH_3$ $Z = 11\text{-}NO_2$	**II-5**	78,8	**IV-5**	81
$Y=H$ $Z = 10\text{-}Br$	**II-6**	82	**IV-6**	85
$Y=CONH_2$ $Z = H$	**II-7**	81,5	**IV-7**	84.5

solvent and 80% acetic acid as eluent; in all the cases the chromatography paper is impregnated with a 10% solution of 1-bromonaphthalene in ethanol.

Note. A quantity of each product II and IV remains dissolved in the formamide, respectively trichlorobenzene filtrate.

4. ANALYSES

The synthesized compounds were previously purified by recrystallization from N.N-dimethylformamide and then subjected to chromatographic, elemental, spectral and tinctorial analyses.

The melting points of the compounds could not be determined since they decompose over 300°.

Chromatographic analysis was carried out on Whatman paper n° 1 in ascendent system, in order to follow the reactions (see experimental) and to check the purity of compounds recrystallized.

Elemental analysis. Microcombustions were carried out for the unknown compounds, determining the N% after the micro-Dumas method. The results are presented in table 2.

Spectral analysis. Ultraviolet and visible spectra of the compounds II and IV were recorded with a Pye Unicam SP 1800 apparatus. The determinations were carried out in N.N-dimethylformamide and the extinction coefficients ε_{max} were calculated.

The characteristic absorption maxima λ_{max} and lg ε_{max} are presented in table 3.

Tinctorial analysis. The synthesized compounds II and IV were used as disperse dyes for "Terom" polyester fibres. The results of the determinations carried out with dyed fibres are presented in table 4. The colours were defined according to C. I. Hue Chart.[4]

---

[4] C. I. Hue Indication Chart, American Association of Textile Chemists and Colourists, Lowell Institute, Lowell, Massachusetts, USA.

Table 2

Results of the N% analysis

Compound	Empirical formula	N% *Calculated* *Found*	Compound	Empirical formula	N% *Calculated* *Found*
II-1	$C_{22}H_{11}N_3O_2$	12.03 12.15	IV-1	$C_{28}H_{15}N_3O_2$	9.88 9.55
II-3	$C_{22}H_{10}N_4O_4$	14.21 14.20	IV-2	$C_{28}H_{14}N_4O_4$	11.91 11.48

Table 3

Absorption maxima in ultraviolet and visible

Compound	DMF $\lambda_{max.}$ [nm]	lg $\varepsilon_{max.}$	Compound	DMF $\lambda_{max.}$ [nm]	lg $\varepsilon_{max.}$
II-1	270 472	3.802 3.417	IV-1	270 354 542	3.950 3.655 3.392
II-2	270 362 490 522	4.265 3.924 3.832 3.934	IV-2	270 361 480 548 596	4.101 4.064 3.606 3.711 3.509
II-3	270 366 462 550 590	4.167 3.662 3.477 3.568 3.732	IV-3	270 470	4.358 3.301
II-4	270 366 526	4.309 4.013 3.651	IV-4	270 604	3.929 3.341
II-5	270 366 526	4.146 3.643 3.204	IV-5	270 622	4.083 3.457
II-6	270 368 534 582 630	3.612 3.146 3.845 3.000 3.079	IV-6	278 352 462 594	4.190 3.939 3.571 3.942
II-7	270 365 494 526	4.123 3.820 3.608 3.651	IV-7	622 270	3.543 3.981

Table 4

Determination with dyed fibres

Compound	Colour	Fastness					
		Light	Cold water	Washing 40°	Perspiration		Rubbing
					acid pH=5.5	alkaline pH=8.8	
II-1	reddish orange 6–7	4–5	5/5/4-5	4-5/5/5	5/4-5/4-5	5/4-5/5	4–5
II-2	bluish violet 13–12	5	5/4-5/4-5	5/4-5/5	5/4-5/4	4/4-5/4-5	4–5
II-3	bluish violet 12–13	5	5/4-5/4-5	5/5/5	5/4/4	4-5/4-5/5	4–5
II-4	reddish violet 35	5	5/5/5	5/5/5	4-5/5/4-5	4-5/4-5/5	5
II-5	yellowish red (dull) 7	5	5/5/5	5/5/5	5/5/4-5	5/4-5/4-5	5
II-6	reddish blue 13	6	5/5/5	5/5/5	5/4-5/4-5	5/5/4-5	5
II-7	pink 49	6	5/4-5/5	5/5/5	5/4-5/5	4-5/5/4-5	5
IV-1	reddish blue (bright) 14–13	4–5	5/4-5/4	5/5/4-5	5/4-5/4-5	5/4/4	4–5
IV-2	bluish green 16–17	4–5	5/5/4-5	5/5/4-5	5/4-5/4	5/4-5/4	5
IV-3	bluish green 17–16	4–5	5/5/5	5/5/5	5/4-5/5	5/4-5/5	4–5
IV-4	bluish green 39	5–6	5/4-5/4-5	5/5/4-5	5/4-5/4-5	5/4-5/4-5	5
IV-5	bluish green (dull) 39–40	5	5/5/5	5/5/5	5/4-5/5	4-5/5/4-5	4–5
IV-6	blue 14	5–6	5/4-5/4-5	5/4-5/4-5	5/4-5/4-5	5/4/4-5	4–5
IV-7	bluish green 16	6	5/4-5/4-5	5/4-5/4-5	5/4-5/4-5	5/4-5/5	5

Generally, the dyeings are distinguished by a good affinity for polyesters fibres and good fastness to light and wet treatments.

The products **II-2**, **II-6**, **II-7**, **IV-1**, **IV-4**, **IV-6** and **IV-7** have the best qualities for applying to polyesters fibres dyeing.

Revue Roumaine de Chimie, 21, 2, 263–267 (1976)

AROMATIC HYDROCARBONS FROM HIGH BOILING PETROLEUM DISTILLATES

M. H. YOUSSEF, A. G. EL-KASSAS, M. I. RUSHDY and I. K. ABDOU
Petroleum Division, National Research Centre, Dokki, Cairo

Received September 24, 1974

The present work has been carried out to study the chemical nature of aromatic hydrocarbons from high boiling petroleum distillates of Egyptian crude oil. The distribution of naphthalene, 1 and 2-methylnaphthalene together with C_{12} and C_{13} naphthalene derivatives were determined in the 200°–285° boiling range fraction. A fairly detailed study of the different types of aromatic hydrocarbons in the fraction boiling above 300° was also performed.

INTRODUCTION

It has become increasingly important in the development of petroleum refining processes to learn more about the composition of high-boiling fractions. The philosophy is to increase knowledge of the constitution of crude oil and hence to help ensure that the best use is made of this valuable raw material.

Chromatographic analysis has been applied to the determination of the different types of aromatic hydrocarbons.[1] This technique used in conjunction with distillation and U. V. absorption spectrophotometric technique has been extended to obtain quantitative analysis for various aromatic hydrocarbon types or classes in high boiling petroleum fractions. It is also possible by the I. R. absorption to determine the degree of side-chain substitution on the aromatic nuclei.

The present study was undertaken to determine the composition of petroleum fractions boiling above 200°, with respect to aromatic hydrocarbons only.

EXPERIMENTAL

I. The fraction boiling range 200–300° was treated with sodium hydroxide solution, potassium permanganate solution and mercuric nitrate to eliminate acids and phenols, olefins and sulphur compounds, respectively. The treated fraction was further fractionated into four narrow boiling range cuts. These cuts were analyzed with the aid of ultraviolet spectrometry as given in Table 1. Measurements were carried out by Beckman Model Du-Spectrophotometer using iso-octane as a solvent.

---

[1] B. T. Brooks, S. S. Kurtz, C. E. Boord and L. Schmerling, "The Chemistry of Petroleum Hydrocarbons", Vol. I, Reinhold Publ. Corp., New York, 1954.

II. The fraction boiling above 300° was treated to isolate the oil. This is carried by elution with cyclohexane over alumina.[2] The oil obtained was subjected to two different methods.

1. The oil was distilled in vacuum. Two distillates boiling within the temperature ranges of 300—350° and 350—400° were collected. Each fraction was mixed with small amount of cyclohexane and passed through a small alumina column (30 × 1 cm), and eluted with cyclohexane. Up to 100 eluants were collected, each of about 4 mls. U.V. absorption spectra cf the eluants were measured using the same Beckman Du-Spectrophotometer, and compared with those of pure compounds.

Table 1

Ultraviolet measurements of 200°—285° fraction

Fraction	Boiling range °C	Absorption wavelength
1	200—248	311 mμ, 314 mμ & 319 mμ
2	248—265	280 mμ, 324 mμ
3	265—275	280 mμ, 324 mμ
4	275—285	280 mμ

2. The oil was separated into saturates, monocyclic aromatics, bicyclic aromatics and polycyclic aromatics by using the adsorption chromatographic technique proposed by Sergienco,[3] under the following conditions

Column length :	150 cm ;
Column diameter :	1.5 cm ;
Adsorbent :	Silica gel Davison (28—200 mesh) ;
Displacing reagent :	Hexane 60—70°, benzol, benzol-alcohol mixture (1 :1).

The I.R. absorption spectra of the different types of aromatic hydrocarbons were measured to determine the number of methyl and methylene groups per average mole. A double beam I.R. spectrophotometer Model IKC-14 was used.

RESULTS AND DISCUSSION

Bicyclic Aromatic Hydrocarbons in 200—285° fraction

Naphthalene, 1- and 2-methylnaphthalenes were determined quantitatively at 311 mμ, 314 and 319 mμ, respectively using the method proposed by Ayoub.[4] The results are presented in Table 2.

Infrared spectrophotometric determination of the number of methyl and methylene groups per average mole

The results of chromatographic separation of the oil fraction into monocyclic, bicyclic and polycyclic aromatics are shown in Table 3.

The 3 fractions (M.C.A., B.C.A. & P.C.A.) were examined with infrared rays for the determination of the number of methylene (NcH_2) and methyl (NcH_3) groups. From the spectra obtained for fractions in the range 2700—3200 cm^{-1}, the extinction of the methyl at 2958 cm^{-1} and methylene at 2927 cm^{-1} were determined using the base line technique. The use of relatively large interval of the spectrum was necessary for the exact determination of the base line. The solvent used was carbon tetrachloride which has practically no absorption in this region.

---

[2] A. A. Shalaby, M. Sc. Thesis, Ain Shams Univ., Cairo, 1964.

[3] S. R. Sergienko, A. A. Mikhnovskaya, *Doklady Akad Nauk S.S.S.R.*, **91**, 103 (1953); *Trudy Inst. Neft. AN. USSR, Moscow*, **10**, 139 (1947).

[4] S. M. Ayoub, M. I. Roushdy and I. K. Abdou, *J. Chem. U.A.R.*, **13**, 179 (1970).

Table 2

Distribution of naphthalene and its derivatives in 200° – 285° fraction

Fraction	Wt. %							
	Total aromatics	Naphthalene	1-methyl naph.	2-methyl naph.	Dimethyl naph.	Trimethyl naph.	Total bicyclic aromatics	Monocyclic aromatics
1	16.4	0.3	1.05	0.7	—	—	2.05	14.3
2	20.0	—	—	—	5.1	—	5.10	14.9
3	21.3	—	—	—	—	4.6	4.60	16.7
4	22.3	—	—	—	—	4.9	4.90	17.4

Table 3

Quantitative determination of aromatic types

Aromatic type		Wt. %
Monocyclic aromatics	(M.C.A.)	24.29
Bicyclic aromatics	(B.C.A.)	30.73
Polycyclic aromatics	(P.C.A.)	4.52
Saturates		40.66

The number of methyl and methylene groups were calculated using the method of Belafi, [5] with an accuracy of ± 0.5 for methyl group and ± 1 for methylene group. The results are shown in Table 4.

Table 4 also shows the percentage of aromatic carbon atoms/mole (C_A) of the different aromatic hydrocarbon types. Data in table 4 have been used to determine the degree of side-chain substitution on the aromatic nuclei.

Monocyclic aromatics: Since the six aromatic carbon atoms present in the molecule correspond to 13.7% ($\%C_A$), the total number of carbon

Table 4

Distribution of methyl and methylene groups

Aromatic type	%CA	NcH_2	NcH_3	$B. D^{\star}. = \frac{NcH_3-2}{NcH_2}$
M.C.A.	13.7	32.35	8.131	0.1895
B.C.A.	31.9	13.51	4.312	0.1711
P.C.A.	27.7	12.05	4.301	0.1901

---

[5] L. Belafi, *Mágyar Asnamy Olajes Folagns, iserleti intezet kozlemenegai*, **6**, 27 (1955).

atoms per mole is about 44. Meanwhile, according to the figures in table 4 the number of carbon atoms, in the aromatic ring, CH_2 and CH_3 groups are $6+32+8 = 46$. Therefore, it seems that the number of other types of carbon atoms (secondary or tertiary ones) must be as small as possible or even absent. As a result, nearly all the methyl groups are distributed in the largest possible number as short side chains attached to the aromatic ring.

Bicyclic aromatics : Since the ten carbon atoms of bicyclic aromatic represent 31.9%, the average number of carbon atoms per mole would be about 31.3. From the experimental figures in table 4 the different types of carbon atoms are :

Aromatic carbon atoms	10 ;
Average NO. of CH_3 groups	4.3 ;
Average No. of CH_2 groups	13.5 ;
Average *2ry* and *3ry* carbon	3.5.

It may be concluded, therefore, that the molecules are characterized by the presence of a small number of side chains attached to the ring structure. These side chains might be of ramified character .

Polycyclic aromatics : In polycyclic aromatic hydrocarbons, small number of alkyl side chains are similarly expected and could be calculated from table 4.

Identification of polycyclic aromatics in the 300—350° and 350°—400° fractions

A combination of liquid chromatography and ultraviolet absorption spectrophotometry has been developed by Wedgwood and Cooper.[6] This method is practically studied for the separation and identification of polynuclear aromatic hydrocarbons. It gives rapid results and enables the detection of trace quantities of several hydrocarbons (0.001 to 0.1 mg) in one sample.

Polycyclic aromatics in the 300°—350° fraction

The spectra of the different eluates show that 9,10-dihydroanthracene is poorly detected in the eluate No. 25 and increases gradually reaching its maximum concentration in eluate 30 as seen from its characteristic peaks at 263 mμ and 271 mμ.

All eluates coming after are nearly identical in their spectra showing the characteristic bands of alkylnaphthalenes. This may be due to the fact that the various alkylnaphthalene derivatives have closely identical spectrum characterised by their bands at about 275 mμ and 324 mμ.

Polycyclic aromatics in the 350°—400° fraction

The first polycyclic aromatic hydrocarbon separated by elution is 9,10-dihydroanthracene followed by alkylnaphthalenes with their characteristic absorption bands at approximately 326 mμ. 4-methylflourene with its bands at 265 mμ and 297 mμ is clearly detected. The polynuclear hydrocarbons obtained after fluorene are shown clearly to be phenanthrene followed by various types of its derivatives.

---

[6] P. Wedgwood and R. L. Cooper, *Chemistry and Industry*, **1**, 1066 (1951).

The characteristic peaks at 258 mμ and 299 mμ indicate the presence of 1,2-dihydropyrene. Finally, eluates containing hydrocarbon having the characteristic bands of 1,2-benzpyrene (289 mμ, 317 mμ and 332 mμ) are detected. These eluates are shown to attain the yellow coloured bands of benzpyrene. The movement of this coloured bands is usually useful for following the separation.

It could be seen that fraction 300°—350° contained mainly alkylnaphthalenes,while the main polycyclic aromatics in the heavier fraction (350°—400°) were found to be phenanthrene and its derivatives. Anthracene was not detected except in the form of 9,10-dihydroanthracene. This is in full agreement with observations given by other authors [7] for the majority of the crude oils analysed.

---

[7] B. T. Brooks, S. S. Kurtz, C. E. Boord and L. Schmerling, "The Chemistry of Petroleum Hydrocarbons", Vol. I, Reinhold Publ. Corp., New York, 1954, p. 30.

Revue Roumaine de Chimie. 21, 2, 263—267 (1976)

Revue Roumaine de Chimie, **21**, *2*, 269–275 (1976)

SOME DATA ON THE COMPATIBILITY OF POLYACRYLONITRILE WITH OTHER POLYMERS

D. FELDMAN, MARIA CIUGUREANU and MARTHA CIUBOTARIU
Macromolecular Chemistry Institute "P. Poni",
Aleea Gr. Ghica Vodă n⁰ 41 A, Jassy

Received August 5, 1974

The compatibility between polyacrylonitrile, poly(vinyl alcohol) and protein was studied. Using the viscometric method, the separation of phases and the microscopy, we established that they are incompatible. The blends of these pairs of polymers are spinnable and present better hygroscopicity and some tinctorial properties than polyacrylonitrile.

I. INTRODUCTION

In recent years the literature has pointed out studies regarding the blends of polymers, with a view to obtainin products with improved properties compared to initial polymers. The first obtained blends are mentioned in a British patent since 1912; Dow Chemical supplied on the world market a polystyrene with 5% butadiene-styrene copolymer with practical applicability.[1]

Most investigations into the field of the macromolecular blends are directed towards establishing the compatibility between polymers.

The increase of the number of macromolecular blends with practical applicability is much limited, because generally, homopolymers are incompatible and not soluble in common solvents. This gives inhomogeneous blends in which every component is maintained separately.

The literature shows that incompatibility of polymers is a general rule, while compatibility is an exception.

The first theoretical and kinetic studies about the compatibility of some polymers were approached by Flory,[2] Tompa [3] and recently by Bohn,[4] Fettes and Macleay.[5] In the other works concerned with establishing the compatibility, experimental methods like the determination of physico-mechanical indexes, the infrared spectroscopy, ultraviolet or visible one, the X-ray diffraction and the electronic microscopy were discussed in detail.[6–14]

---

[1] E. F. MATHEWS, Brit. Pat. **16**, 278, 6 June 1912; *Adv. Chem.*, **99**, 2 (1971).
[2] P. J. FLORY, "Principles of Polymers Chemistry", Cornell Univ. Press, Ithaca, New York, 1953.
[3] H. TOMPA, "Polymer Solutions", Butterworts, London, 1956.
[4] L. BOHN, *Kolloid-Z.Z. Polym.*, **55**, 213 (1966); *Rubber Chem. Technol.*, **41**, 495 (1968).
[5] E. M. FETTES and N. MACLAY., *J. Appl. Polym. Sci. Sym.*, **7**, 3 (1968).

The initial compatibility studies were effectuated especially on elastomers[15–18]; lately, the interest for realizing spinning polymer blends has increased.[19–20]

Riess and co-workers studied the possibility to realize the compatibility of polymers by using ternary systems with block copolymers.[21–23]

In this paper we study some spinning blends on the basis of polyacrylonitrile (PAN) with poly(vinyl alcohol) (PVA)and polyacrylonitrile with protein.

II. EXPERIMENTAL

A. PAN–PVA *blends*

PAN — was synthetized in the laboratory in an aqueous medium with redox initiators at a temperature of 60° and 180 minutes.

In this way a PAN was obtained with $[\eta] = 2.20$ in dimethyl sulphoxide (DMSO) ($n_D^{20} = 1.4764$) at a temperature of 20°.

PVA — from the Rîşnov factory has the following characteristics:

I saponify = 138.08 mg KOH/g
Ash, % = 1.5
K_w = 68.9
Insoluble in water, % = 16.02.

The study of the compatibility of PAN with PVA was effectuated by the method of the separation of phases and viscometrically, using mixtures in different ratios of the polymers at 2%, 3% and 5% concentration.

DMSO was used as solvent after purification by distillation in vacuum in a Vigreux column.

Using the method of separated phases one observed that regardless of the concentration or ratio between the two components while mixing the solutions, the system appears homogeneous and after some time, at room temperature, it does separate in two phases. It is remarked that the time necessary for this separation is longer, the smaller the concentration of the solutions, and as the amount of PVA in the blends is decreasing.

---

[6] S. S. Voyutsky, A. D. Zaionchkovsky and R. A. Reznikova., *Kolloid Zhur.*, **18**, 515 (1956).

[7] G. R. Williason and B. Wright, *J. Polymer Sci. Part A*, **3**, 3885 (1965).

[8] D. Feldman and M. Rusu, *European Polymer J.*, **6**, 627 (1970).

[9] D. Feldman and M. Rusu, *European Polymer J.*, **7**, 215 (1971).

[10] A. H. Schvartz and B. N. Dinzberg, "Sovmeshchenie caoutchonc s plastikami i sinteticheskimi smolami", Izdatelstvo khimia, Moskva, 1972, p. 7.

[11] C. Hugelin and A. Dondos, *Makromol. Chem.*, **126**, 206 (1969).

[12] C. Vasile, F. Sandru, I A. Schneider and N. Asandei, *Makromol. Chem.*, **110**, 20 (1967).

[13] V. I. Aleksenka, *Vysokomol. Soedineniya*, **2**, 1449 (1960).

[14] V. A. Kuleznev and K. M. Igosheva, *Vysokomol. Soedineniya*, **4**, 1858 (1962).

[15] G. M. Bartenev and G. S. Kongarov, *Vysokomol. Soedineniya*, **2**, 1692 (1960).

[16] V. I. Aleksenka and I. V. Mishustin, *Vysokomol. Soedineniya*, **1**, 1593 (1959).

[17] V. I. Aleksenka and I. V. Mishustin, *Kolloid Zhur.*, **18**, 257 (1956).

[18] H. Wolff, *Plaste und Kautschuk*, **4**, 244 (1957).

[19] W. Meibner, W. Berger and H. Hoffman, *Faserforschung und Textiltechnik*, **9**, 407 (1968).

[20] S. Hartig and W. Peters, *Faserforschung und Textiltechnik*, **23**, 447 (1972).

[21] J. Kohler, G. Riess and A. Banderet, *European Polymer J.*, **4**, 187 (1968).

[22] J. Kohler, G. Riess and A. Banderet, *European Polymer J.*, **4** 173 (1968).

[23] G. Riess, J. Kohler, C. Tournut and A. Banderet, *Plastiques*, **3**, 361 (1966).

The viscometric experiments (figs. 1 and 2) were effectuated with a Rotation-Viscometer Type RV (Medingen).

Figure 1 represents the variation of the dynamic viscosity depending on the solution composition and concentration (2%, 3% and 5%). The determinations were effectuated at a temperature of 20° and at a rate of shear $D\ (s^{-1}) = 1312$ and 243, respectively.

For higher concentrations (5%) the viscosity increases visibly according to curve (3) indicating the formation of aggregates which determine the viscosity increase. From these three diagrams (fig. 1) it appears that, regardless of the composition and concentration in DMSO, PAN and PVA are incompatible.

It is clear from figure 2, that at lower temperatures, departure from linearity of viscosity-composition curves is increased.

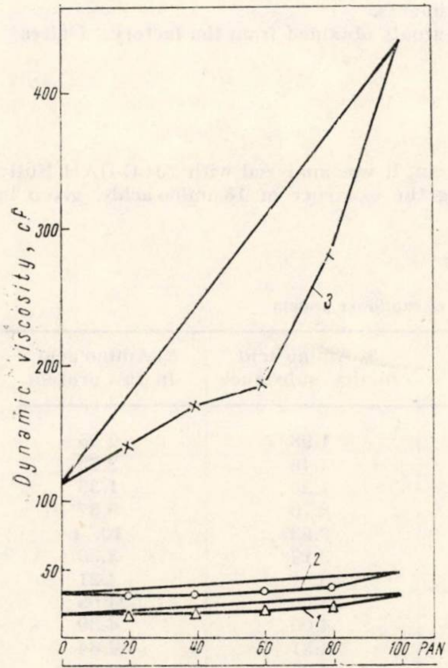

Fig. 1. — The variation of dynamic viscosity (cP) of solutions of PAN : PVA blends with composition of various concentrations.

1, Δ 2% concentration, $D = 1312\ s^{-1}$
2, ○ 3% concentration, $D = 1312\ s^{-1}$
3, × 5% concentration. $D = 245\ s^{-1}$

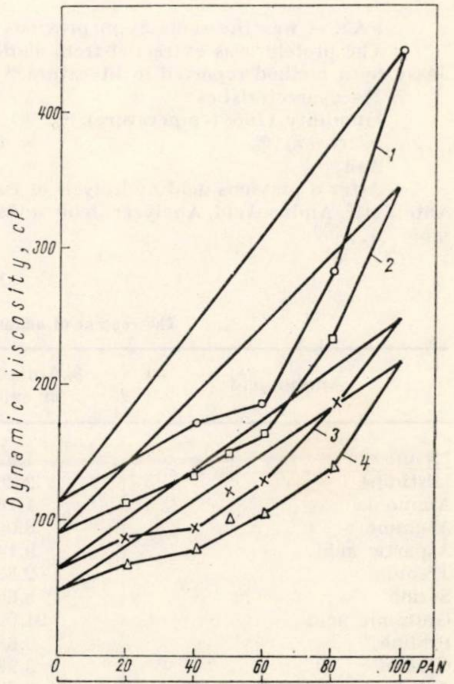

Fig. 2. — The variation of dynamic viscosity (cP) of solution of PAN : PVA blends with composition and temperature.

1, ○ 20° temperature
2, □ 30° temperature
3, × 40° temperature
4, Δ 50° temperature
$D = 243\ s^{-1}$

These diagrams attest the fact that in the range of experimented temperatures, these two polymers are incompatible.

To point out the inhomogeneous character of the PAN : PVA blend at different ratios of these two components, the optical microscopy was also used. An "Optical Microscope-MCL IOR" type was used. The investigations were effectuated on films obtained from DMSO solution-

Figures 3 and 4 give the most characteristic aspects of the above mentioned blends.

Figure 3 which represents the microscopic image of the PAN : PVA blend (80 : 20) has the aspect of the partially compatible system. Clear regions constituted from one polymer or another were not observed.

Inversing the ratio between components, it was observed (fig. 4) that the system is evidently incompatible.

The appearance of some characteristic formations of PAN in the matrix of the PVA is marked.

The data obtained by optical microscopy support the affirmation made about the system after viscometric and phase-separation studies.

B. PAN-*Protein blends*

PAN – was the same as in previous experiments.

The protein was extracted from sunflower groats obtained from the factory "Unirea", Jassy by a method reported in literature.[24]

Its characteristics :

Humidity (105° temperature), % = 7.85
Nitrogen, % = 12.30
Ash, % = 2.59

After a previous acid hydrolysis of the protein, it was analyzed with "JLC-GAH Fully Automatic Amino-Acid Analyzer-Jeol" evidencing the existence of 18 amino acids, given in table 1.

Table 1

The content of amino acids of sunflower protein

Amino acid	%Amino acid in sample	% Amino acid in dry substance	% Amino acid in raw protein
Lysine	1.92	1.98	2.25
Histidine	2.26	2.46	2.65
Ammonia	1.16	1.26	1.36
Arginine	8.00	8.70	9.37
Aspartic acid	9.14	9.93	10.71
Treonine	2.82	3.17	3.30
Serine	3.60	3.91	4.21
Glutamic acid	21.09	23.00	24.65
Proline	3.68	4.00	4.30
Glycine	3.96	4.31	4.64
Alanine	3.72	4.05	4.36
Cystine	0.60	0.65	0.70
Valine	4.70	5.10	5.50
Methionine	1.70	1.85	1.99
Izoleucine	4.03	4.38	4.72
Leucine	5.49	5.97	6.41
Tyrosine	2.40	2.61	2.81
Phenylalanine	4.76	5.18	5.58

Because among PAN solvents, the aqueous solution of 72% $ZnCl_2$ is a good solvent also for protein, all experiments regarding the binanary PAN : protein system were carried out in this solvent.

To obtain solutions (2%) of different ratios of the polymers the same procedure was applied as for the PAN : PVA system. A separation of the phases in time was also remarked. In addition to this, it was observed that protein itself without addition of PAN precipitates from solution after some time.

---

[24] Cr. Simionescu, V. Diaconescu, E. Calistru and D. Feldman, *Studii şi Cercetări Şt., Fil. Iaşi, Acad. R.P.R.*, **2** *3–4*, 227 (1951).

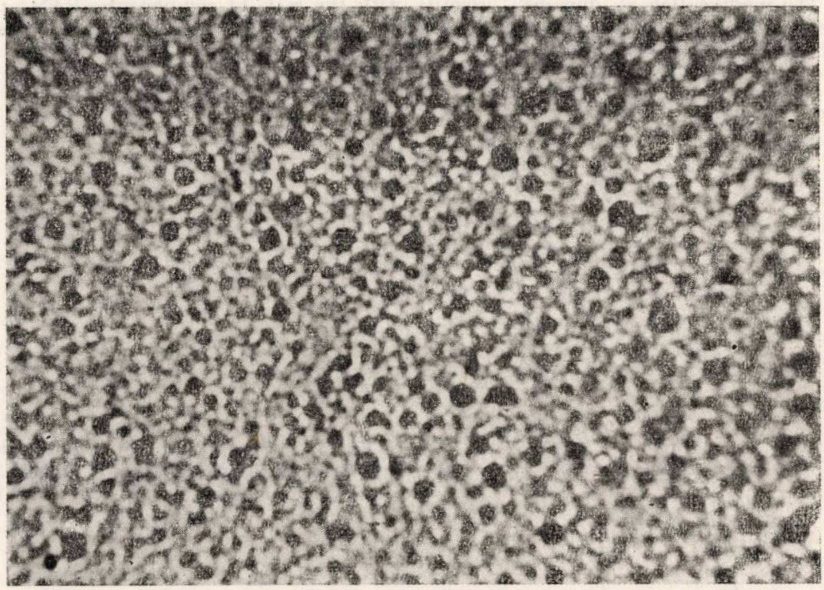

Fig. 3. – The microscopic image of PAN : PVA blend (80 : 20).

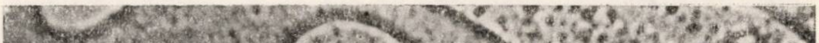

Fig. 4. – The microscopic image of PAN : PVA blend (20 : 80) .

The viscometric data (fig. 5) show that, as in the PAN : PVA blend, the PAN : protein system (in 72% $ZnCl_2$ aqueous solution) is incompatible.

The modification of dynamic viscosity with the ratio of components (PAN : protein) and the temperature, given in table 2, led to the conclusion that dynamic viscosity decreases with the increase of the amount of PAN.

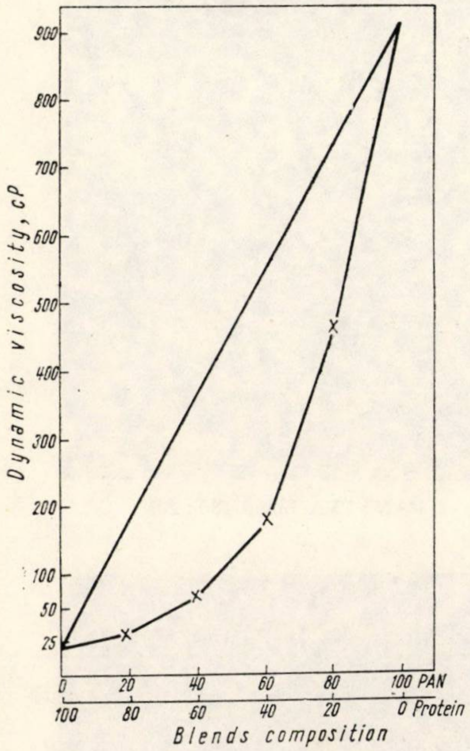

Fig. 5. — The variation of dynamic viscosity (cP) of solutions of PAN : Protein blends with composition at 2% concentration, in $ZnCl_2$ 72%.

Table 2

The variation of the dynamic viscosity (cP) against temperature and the composition of the PAN : Protein system (5% in the aqueous solution of 72% $ZnCl_2$)

PAN : Protein ratio	Temperature			
	20	30	40	50
0 : 100	55.8	40.5	26.1	18
40 : 60	1716	1276	880	616
50 : 50	2640	1892	1232	880
60 : 40	3520	2508	1804	1188
100 : 0	30141	19162	13484	9915

The variation of the viscosity is very accentuated, a fact which creates difficulties in the graphic presentation of the results.

Following in time the change of the dynamic viscosity of the solution (5%) of the blends PAN : protein, one observed (table 3) its sensible decrease. This fact is to be taken into account in the eventuality of some practical applications. Surely, this decrease is due especially to the degradation of the proteinic macromolecules.

Table 3

The variation of dynamic viscosity (cP) against time; PAN, protein and their mixture (5% concentration in aqueous solution of 72% $ZnCl_2$)

Polymer	Time h	η cP	Viscosity variation %
PAN	At the moment of mixing	11065	100
	After 24 hours	9737	87
	After 48 hours	7524	67
Protein	At the moment of mixing	66.6	100
	After 24 hours	59.4	89
	After 48 hours	46.8	70
PAN : Protein blend 1 : 1	At the moment of mixing	4866	100
	After 24 hours	2655	54
	After 48 hours	The viscosity decreases very much and cannot be determined	

C. *Properties of the blends achieved*

In the laboratory, the spinning behaviour of the solutions of these systems was verified; the hygroscopicity and the tinctorial properties of the blends precipitated from DMSO were determined.

It was remarked that the hygroscopicity of the PAN : PVA blend is 2% as against 0.84% for PAN; using the Red Reactiv B5A-reactiv, the PAN : PVA blend is more intensively coloured than PAN.

Regarding the other blend, since the PAN : protein system contains traces of $ZnCl_2$ it is much more difficult to determine the real hygroscopicity of the blend. The PAN : protein blend is coloured more intensively than PAN with an acid dyestuff (Xilol Red) and with a basic one (Methylen Blau).

III. CONCLUSIONS

1. The application of the separating phases and viscometric method to the solutions of the binary system, PAN : PVA and PAN : protein, demonstrates the incompatibility between these polymers.

This conclusion is also confirmed by the optical microscopy method which was applied to films obtained from these polymers.

2. Although the studied systems are incompatible, an increase of hygroscopicity and an improvement of the tinctorial properties of the blends against some dyestuffs are remarked.

Revue Roumaine de Chimie, **21**, *2*, 277–283 (1976)

KINETIC STUDIES ON THE COPOLYMERIZATION OF 1,3-DIOXEPANE WITH EPICHLOROHYDRIN INITIATED WITH BF_3OEt_2

DAN DONESCU
Institute of Macromolecular Chemistry "P. Poni", Department of "Polymerization Process",
str. Dumbrava Roșie 18, Bucharest IX, Romania

Received June 14, 1974

Studies have been made on the kinetics of the copolymerization of 1,3-dioxepane (DH) with epichlorohydrin (ECH) initiated by BF_3OEt_2. The results obtained show that the growth reaction occurs preponderantly by the interaction of each monomer with the growing macrocation whose last structural unit is ECH. Compared to homopolymerization the activation energy of the consumption reaction of DH decreases in copolymerization from 11.1 kcal/mol to 10.0 kcal/mol. The activation energy of the consumption reaction of ECH increases by copolymerization, compared to homopolymerization, from 0.6 kcal/mol to 9.6 kcal/mol. NMR spectra of copolymers show that the structural units of the comonomers are statistically distributed.

1. INTRODUCTION

In our previous papers referring to the homopolymerization of DH and its copolymerization with ECH in the presence of catalytic system $AlEt_3 + H_2O$ we have shown that during these processes there appear secondary transfer reactions of active site to monomer and polymer, and that ECH has a promoter role and copolymerizes with DH.[1,2] We have also shown that when BF_3OEt_2 is used as a catalyst, the kinetic schema verified for the catalytic system $AlEt_3 + H_2O$ are verified, but the reaction rates involved are much higher.[3]

Based on the results obtained, we considered necessary to study the copolymerization of DH in the presence of BF_3OEt_2 as catalyst and this has been accomplished in the present paper.

2. EXPERIMENTAL

The working procedure was described in the previous papers.[2,3]
The concentration of catalyst was $3.2.10^{-2}$ mol/l.

As in the case of the homopolymerization of DH,[3] monomer consumption rates are much higher in the case of catalysis with BF_3OEt_2 than with $AlEt_3 + H_2O$.[1,2] (see fig. 1).

---

[1] D. Donescu, *Makromol. Chem.*, **175**, 2355 (1974).
[2] D. Donescu, *Rev. Roumaine Chim.*, **20**, 1491 (1974).
[3] D. Donescu, *Rev. Roumaine Chim.*, in press.

Owing to the cationic character of active sites, when using the two above-mentioned catalysts the variation of monomer mole fraction in time is similar in both cases. Fig. 2 illustrates that, with BF_3OEt_2 as catalyst, the mole fraction of ECH consumed also decreases at the beginning of the process increasing thereafter as the concentration of DH decreases, and therefore the influence of depolymerization is large.

In order to establish the weight of the four elementary reactions which may occur in the copolymerization of the two monomers in the growing stage, we have studied the influence of comonomers concentrations on the rate of consumption reaction of each of them. It results from figs. 3 and 4 that the initial consumption rate of DH is directly proportional to its initial concentration (the equilibrium concentration was neglected), and to the concentration of ECH, that ECH is promoter also in BF_3OEt_3 catalysis.

Similar to the copolymerization in the presence of the catalytic system $AlEt_3 + H_2O$,[2] for a total constant monomer concentration, the initial consumption rate of PDH presents a maximum at a certain composition of monomer mixture (fig. 5). The position of this maximum demonstrates that the initial consumption rate of DH may be expressed by the equation :

$$\left\{-\frac{d|DH|}{dt}\right\}_0 = A + k_1 |ECH|_0 |DH|_0 \qquad (1)$$

$$A \ll k_1 |ECH|_0 \, |DH|_0$$

where : $|DH|_0$, $\{ECH\}_0$ — initial monomer concentrations

It is extremely interesting to note that, in contrast to DH, the manner in which the initial consumption rate of ECH is affected by its own concentration and by that of the comonomer remains identical for $AlEt_3 + H_2O$ and BF_3OEt_2. Based on the results presented in figs. 6 and 7 for the initial consumption rate of ECH the following empirical equation may be written :

$$\left\{-\frac{d|ECH|}{dt}\right\}_0 = k_2 |ECH|_0^2 \qquad (2)$$

The analysis of equations 1 and 2 leads to a conclusion similar to that formulated after studying the copolymerization of these monomers with $AlEt_3 + H_2O$:[2] the growth reaction occurs preponderantly by interaction with active sites having ECH as the last structural unit.

Differences appearing in the manner in which monomer concentrations influence the initial rate consumption of DH due to the substitution of the catalytic system $AlEt_3 + H_2O$ by BF_3OEt_2 (Eq. 1) are the reason for which no strong influence of the total concentration is observed any longer on the mole fraction of consumed monomers under the reaction conditions studied in this paper (see fig. 8).

In the case in which ECH is replaced by propylene oxide (PO), the copolymerization of DH no longer occurs in the case of the catalysis with BF_3OEt_2, either. In this new monomer system, cyclic ether is favoured relative to the cyclic formal, both from a kinetic and from a thermodynamic standpoint and this causes the consumption rate of PO to be very high, with DH being consumed after a sharp decrease in concentration of PO occurs, a phenomenon found also in the case of other monomers (tetrahydrofuran and 1,3-dioxolane).[4]

Another factor influencing the consumption rates of DH and ECH is the catalyst concentration (fig. 9). The manner in which this dependence is revealed shows that the number of active sites formed in the initial stage of the process is directly proportional dependent on catalyst concentration.

A study of the influence of temperature on the total consumption rates of the two comonomers shows similar characteristics to those mentioned in the case of catalysis with $AlEt_3 + H_2O$.[2] (Fig. 10). The activation energy of the consumption reaction of DH established for homopolymerization is 11.1 kcal/mol. This energy decreases in the copolymerization of DH to 10.0 kcal/mol. The activation energy of the consumption reaction of ECH is much more affected : it increases from 0.6 kcal/mol in homopolymerization to 9.6 kcal/mol in copolymerization. Thus, it has been noticed that, even in the presence of BF_3OEt_2, the activation energies of the two comonomers tend to draw closer by copolymerization.

[4] Y. Yamashita, S. Kozawa, K. Chika and M. Okada, *Makromol. Chem.*, **135**, 75(1970).

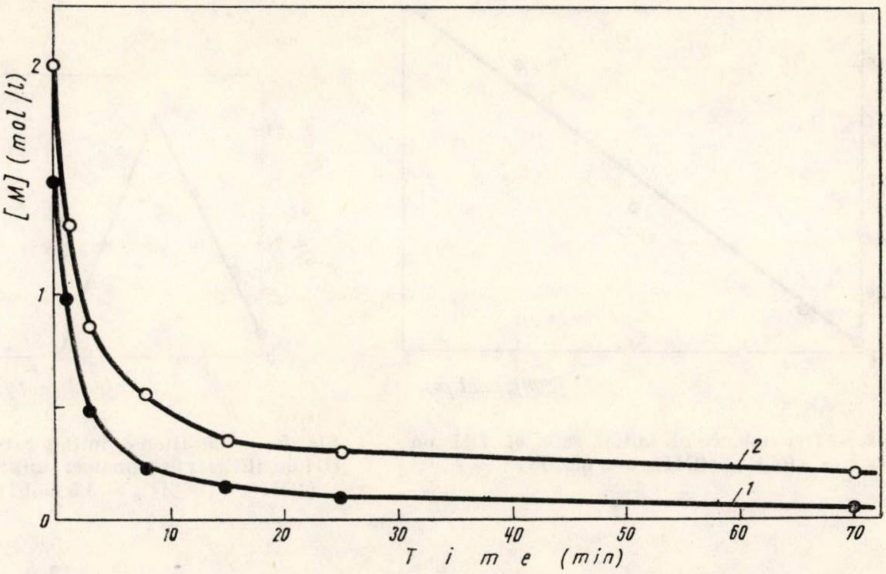

Fig. 1. — Variation of concentrations of DH(1) and ECH (2) with time. ($|DH|_0 = 1.5$ mol/l, $|ECH|_0 = 2$ mol/l)

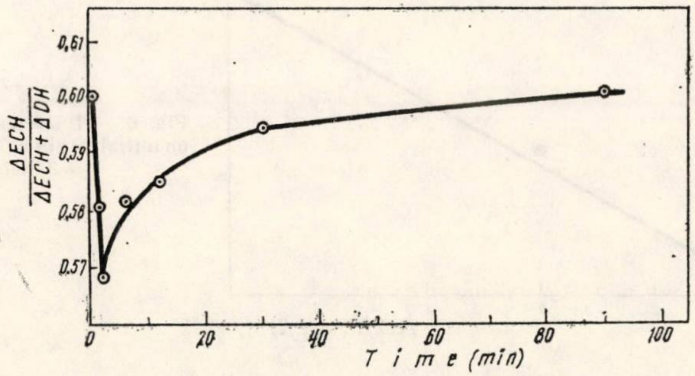

Fig. 2. — Variation of mole fraction of consumed ECH with time. ($|DH|_0 = 2$ mol/l, $|ECH|_0 = 4$ mol/l)

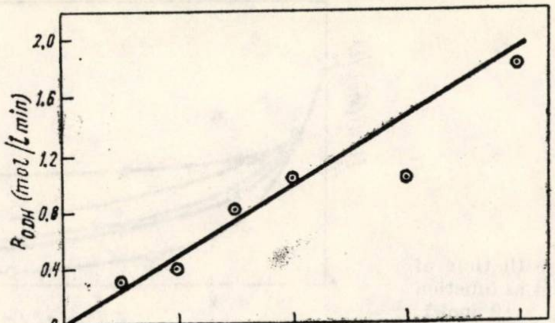

Fig. 3. — Dependence of initial rate of DH on $|DH|_0$. ($|ECH|_0 = 2$ mol/l)

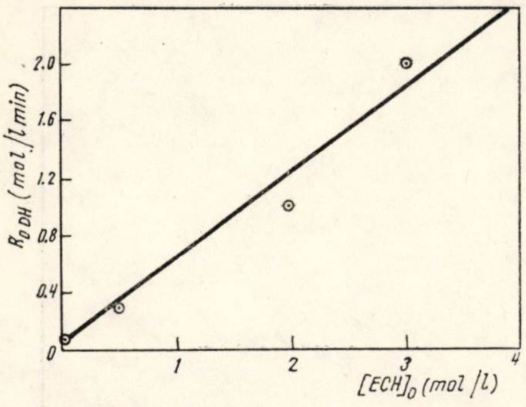

Fig. 4. — Dependence of initial rate of DH on $|ECH|_0 \cdot (|DH|_0 = 3$ mol/l)

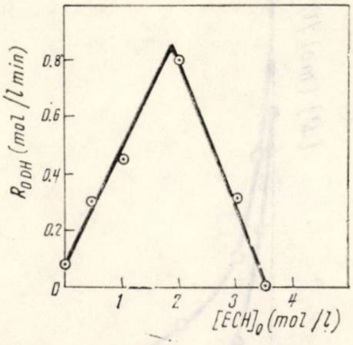

Fig. 5. — Variation of initial rate o DH on $|ECH|_0$ in monomer mixture ($|DH|_0 + |ECH|_0 = 3.5$ mol/l)

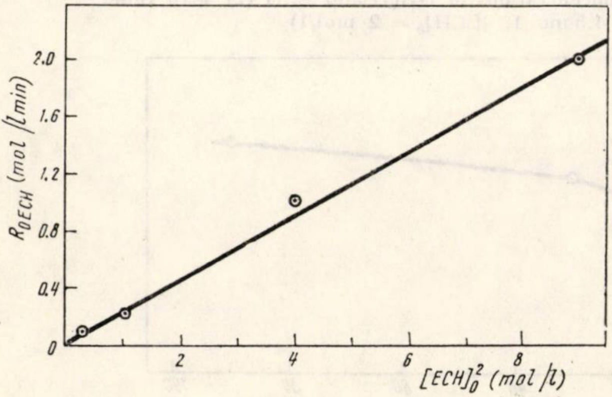

Fig. 6. — Influence of $|ECH|_0$ on initial rate of ECH$\cdot$($|DH|_0 =$ = 3 mol/l)

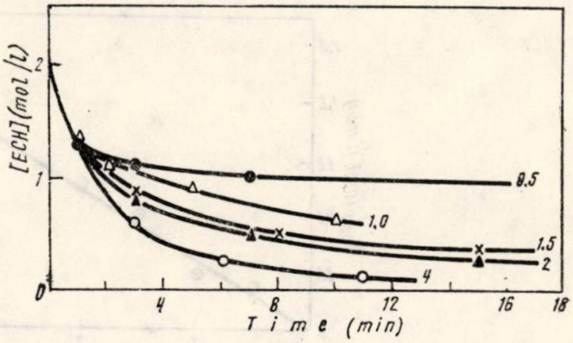

Fig. 7. — Variation with time of concentration of ECH as function of $|DH|_0 \cdot (|ECH|_0 = 2$ mol/l, $|DH|_0$ is mentioned on every curve)

Fig. 8. — Correlation between ECH relative activity and mole fraction of ECH in monomer mixture. ($|DH|_0 + |ECH|_0 = 3.5(0)$, 6.0(0) mol/l.

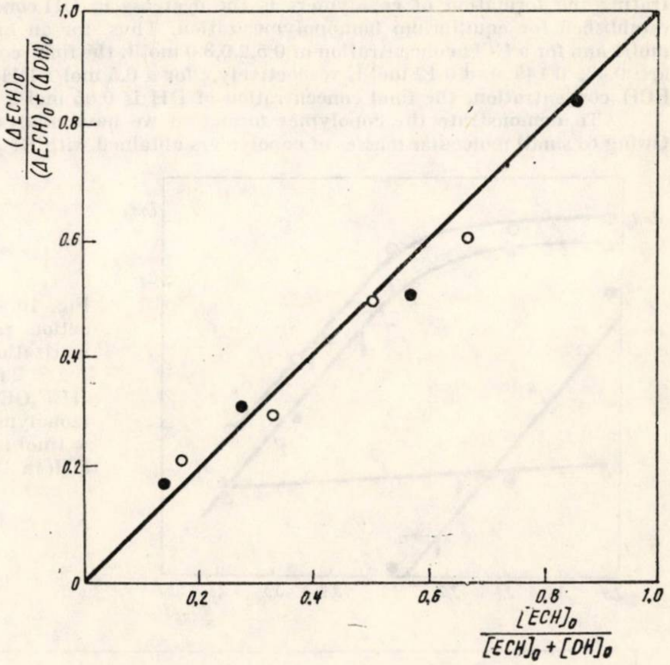

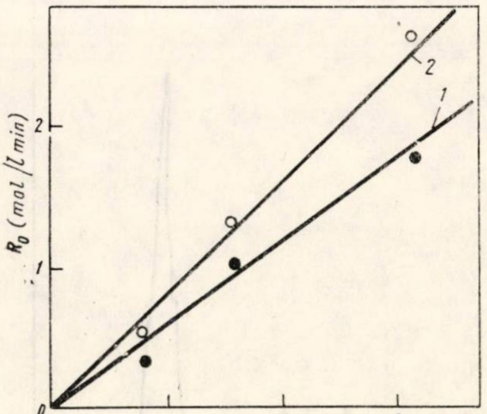

Fig. 9. — Variation of initial rates of ECH and DH on $|BF_3OEt_2|_0 \cdot (|DH|_0=2$ mol/l (1), $|ECH|_0 = 4$ mol/1/(2))

A comparison of the results obtained in the study of the copolymerization of DH with ECH in the presence of $AlEt_3 + H_2O$ and BF_3OEt_3 shows that the general characteristics are common to both catalytic systems. Using these results, it is possible to formulate also in the case of catalysis with BF_3OEt_2 kinetic arguments demonstrating the formation of copolymers. A first evidence of copolymer formation is the fact that ECH has a promoting role on the consumption reaction of DH, that the ring-opening reaction of the formal takes place by interaction with the growing macrocation having ECH as a last structural unit. Another argument demonstrating the formation of copolymers is the decrease in DH concentration below the values established for equilibrium homopolymerization. Thus, for an initial DH concentration of 3 mol/l and for a ECH concentration of 0.5,2.0,3.0 mol/l, the final concentrations of cyclic formal are 0.43, 0.145 and 0.12 mol/l, respectively, ; for a 0.5 mol/l DH concentration and a 2 mol/l ECH concentration, the final concentration of DH is 0.05 mol/l.

To demonstrate the copolymer formation we have analysed IR spectra of products. Owing to small molecular masses of copolymers obtained with BF_3OEt_2 (they appear under the

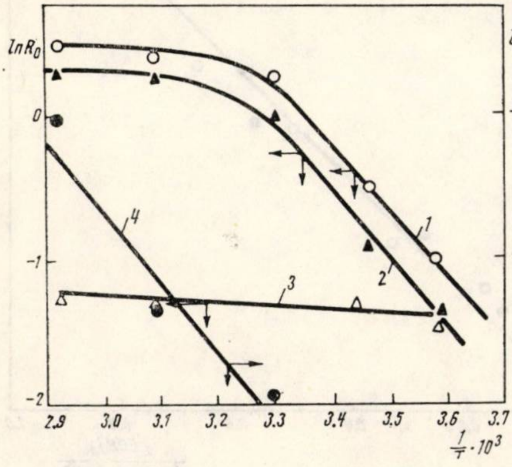

Fig. 10. — Relationship between reaction rate and temperature-copolymerization : ECH(1), DH(2)($|DH|_0 = 2$ mol/l, $|ECH|_0 = 4$ mol/l$\cdot$ $|BF_3OEt_2|_0 = 1.6.10^{-2}$ mol/l). -homopolymerization : ECH(3)($|ECH|_0 = 1$mol/l, $|BF_3OEt_2|_0 = 1\cdot 6\cdot 10^{-2}$mol/l), DH(4)($|DH|_0 = 3$mol/l, $|BF_3OEt_2|_0 = 3.2.10^{-2}$ mol/l).

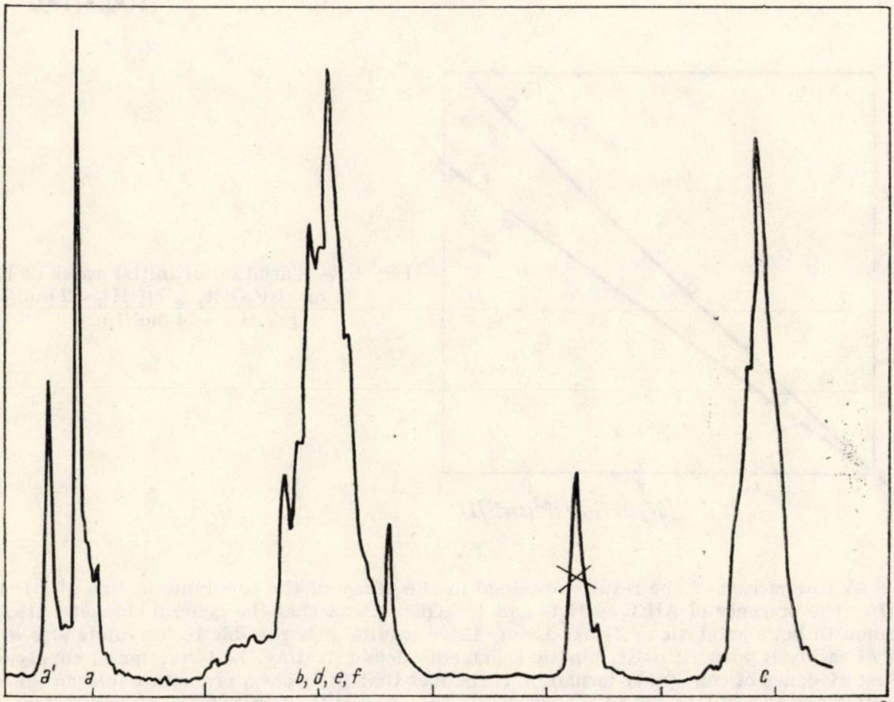

Fig. 11. — NMR spectrum of DH/ECH copolymer ($|DH|_0 = 4$ mol/l, $|ECH|_0 = 2$ mol/l, time reaction — 1 min.)

form of waxes) it is not possible to reveal their formation by selective dissolution and elementary analysis and IR spectra as in the case of catalysis with $AlEt_3 + H_2O$.[2] IR spectra of global reaction products present characteristic bonds of both monomers.

However, reduced molecular masses have permitted to determine the microstructure of copolymers by means of NMR spectra. The NMR spectrum of a DH/ECH copolymer is presented in fig. 11.

The protons in the sequence —AABBA-, for example, can be assigned as follows :

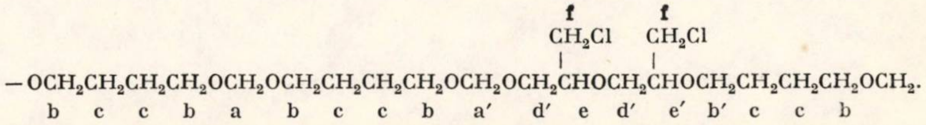

$$-\mathrm{O}\underset{b}{\mathrm{CH_2}}\underset{c}{\mathrm{CH_2}}\underset{c}{\mathrm{CH_2}}\underset{b}{\mathrm{CH_2}}\mathrm{O}\underset{a}{\mathrm{CH_2}}\mathrm{O}\underset{b}{\mathrm{CH_2}}\underset{c}{\mathrm{CH_2}}\underset{c}{\mathrm{CH_2}}\underset{b}{\mathrm{CH_2}}\mathrm{O}\underset{a'}{\mathrm{CH_2}}\mathrm{O}\underset{d'}{\mathrm{CH_2}}\underset{e}{\overset{\overset{f}{\mathrm{CH_2Cl}}}{\mathrm{CH}}}\mathrm{O}\underset{d'}{\mathrm{CH_2}}\underset{e'}{\overset{\overset{f}{\mathrm{CH_2Cl}}}{\mathrm{CH}}}\mathrm{O}\underset{b'}{\mathrm{CH_2}}\underset{c}{\mathrm{CH_2}}\underset{c}{\mathrm{CH_2}}\underset{b}{\mathrm{CH_2}}\mathrm{OCH_2}.$$

Protons corresponding to AB and BA diads are a′, b′, d′, e′. In the NMR spectrum of copolymer, only proton a′ have a distinct peak.

For the copolymer whose spectrum is exhibited in fig. 11, the composition may be calculated from the areas corresponding to protons c and b+d+e+f .

The run number[5] calculated for a statistical distribution is 43. From the calculation of the weight of AB diads corresponding to protons a′, the real run number is 41.2. A comparison of the above mentioned values demonstrates that the copolymers DH/ECH are random in sequence distribution.

---

[5] H. J. HARWOOD and W. M. RITCHEY, *J. Polymer Sci. -B*, **2**, 601 (1964).

Revue Roumaine de Chimie, **21**, *2*, 285−291 (1976)

LA SYNTHÈSE DES ZÉOLITHES DU SYSTÈME $Na_2O-Al_2O_3-SiO_2-H_2O$, DE TYPE A ET FAUJASITIQUE

N. BÎLBĂ et V. ABABI
Laboratoire de technologie chimique, Université « Al. I. Cuza » de Jassy-Roumanie, 11, str. 23 August

Reçu le 3 septembre 1974

On a établi les conditions pour l'obtention par voie hydrothermale des zéolithes de type A et faujasitique. La structure cristalline de toutes les zéolithes a été étudiée par diffraction de rayons X. Les résultats obtenus ont relevé que les principaux facteurs qui exercent une influence notable sur la structure et les propriétés des zéolithes sont la composition du mélange initial et la durée de la cristallisation.

I. INTRODUCTION

Les zéolithes sont des alumino-silicates cristallins, poreux, formés par les agrégats tridimensionnels de tétraèdres $[SiO_4]^{4-}$ et $[AlO_4]^{5-}$ contenant des cavités qui communiquent entre elles et avec l'extérieur par des pores qui ont des dimensions petites et constantes.

Dans les conditions habituelles, les cavités sont occupées par des molécules d'eau et par des cations métalliques, le nombre des derniers étant proportionnel au nombre des tétraèdres $[AlO_4]^{5-}$.

A cause de la liberté de mouvement des molécules d'eau et des cations à l'intérieur de la structure, les zéolithes peuvent se déshydrater et être soumises à l'échange réversible d'ions. Les dimensions des pores d'accès dans les cavités sont de l'ordre de grandeur moléculaire ce qui a déterminé l'utilisation des zéolithes à la séparation des mélanges de molécules, et pour cela la dénomination de celles-ci comme tamis moléculaires.

Par la synthèse hydrothermale, en utilisant comme matière première des substances qui contiennent de l'anhydride silicique, de l'oxyde d'aluminium et de l'hydroxyde de sodium, dans des conditions différentes de température on a obtenu la majorité des zéolithes naturelles connues et aussi de nouvelles zéolithes, non rencontrées dans la nature, et qui selon leurs propriétés et leur structure ont été dénommées par les lettres correspondantes : A, X, Y, L, R, S, B, D, H, J, M, P, T, U, Q, Z, Ω. ZK-4, ZK-5.[1-11]

---

[1] R. M. Barrer, *Trans. Brit. Ceram. Soc.*, **56**, 155 (1957).

[2] R. M. Barrer, J. M. Baynham, F. W. Bultitude et W. R. Meier, *J. Chem. Soc.*, **1959**, 195.

[3] A. G. Regis, L. B. Sand, C. Calmon et M. E. Gilwood, *J. Phys. Chem.*, **64**, 1567 (1960).

[4] S. P. Zhdanov, *Preprints of Chemical Industry Conference on Molecular Sieves*, Londres, 1967.

[5] L. J. Guth, P. Collin et R. Wey, *Bull. Soc. Fr. Mineral. Cristallogr.*, **93**, 59 (1970).

[6] C. Colella et R. Aiello, *Ann. Chim.*, (*Ital.*), **61**, 721 (1971).

[7] S. P. Zhdanov, *Adv. Chem. Ser.*, **101**, 20 (1971).

[8] F. Polak et A. Cichocki, *Zesz. Nauk. Univ. Jagiellon. Pr. Chem.*, **14**, 211 (1969) ; **15**, 281 (1970) ; **16**, 151 (1971) ; **18**, 327 (1973) ; **18**, 339 (1973).

[9] F. Polak et L. Wilkosz, *Przemysl Chem.*, **48**, 410 (1969).

[10] F. Polak, *Przemysl Chem.*, **51**, 295 (1972).

[11] W. Meise, F. E. Schwochov, *Adv. Chem. Ser.*, **121**, 169 (1973).

La géométrie des canaux à l'intérieur des zéolithes, et aussi le système des cavités, est caractéristique de chaque zéolithe,[12] mais la pénétration à l'intérieur des cavités est permise habituellement par des pores de 3–9 Å.

Parmi les zéolithes synthétiques qui possèdent des propriétés de tamis moléculaire se sont imposées dans la pratique tout particulièrement celles de type A pour les processus d'adsorption et de séparation, et celles de type faujasitique (X, Y) et mordénitique (M) pour les processus catalytiques.

Étant donné que dans le système quaternaire $Na_2O-Al_2O_3-SiO_2-H_2O$, par la modification des conditions on peut obtenir la majorité des zéolithes connues (dont un nombre réduit seulement présente un intérêt pratique) la connaissance de ces domaines dont la composition est favorable pour l'obtention des structures zéolithiques avec des propriétés supérieures est très importante. Le but de ce travail est l'étude du système $Na_2O-Al_2O_3-SiO_2-H_2O$ en vue d'établir les conditions optimales pour la synthèse des zéolithes de type A et faujasitique.

II. MÉTHODE EXPÉRIMENTALE

Les recherches expérimentales ont été rapportées à l'obtention et à la caractérisation du point de vue structurel et de la capacité d'adsorption des zéolithes de type A et faujasitique.

L'obtention des zéolithes a été réalisée par la méthode de synthèse hydrothermale, en utilisant des solutions de silicate, d'aluminate et d'hydroxyde de sodium. La solution de silicate de sodium a été préparée par la dissolution dans l'eau sous pression du silicate de sodium et par la dissolution du silicagel dans la solution d'hydroxyde de sodium, à chaud, tandis que la solution d'aluminate de sodium a été préparée par la dissolution de l'aluminium métallique, de l'alumine hydratée ou du sulfate d'aluminium en solution d'hydroxyde de sodium.

Dans les solutions ainsi préparées, on a déterminé la teneur en SiO_2 par voie gravimétrique, en Al_2O_3 par voie complexométrique et en Na_2O par voie photométrique.

Par le mélange de ces solutions en différentes proportions, à 25°, on obtient des gels qui,chauffés à 100° et après un certain intervalle de temps, cristallisent en donnant des cristaux de différentes formes et grandeurs.

III. RÉSULTATS

On a soumis à la cristallisation les mélanges dont la composition a été modifiée dans les limites très larges. Les valeurs des rapports molaires Na_2O/SiO_2, SiO_2/Al_2O_3 et H_2O/Na_2O ont été variées dans les limites suivantes : 0,09–2,64 ; 1,03–39,5 et respectivement 32–1080.

Des données expérimentales, il résulte qu'on a étudié un domaine très large de compositions, en obtenant finalement des zéolithes dont l'analyse par diffraction des rayons X a montré qu'elles se sont formées de structures de type NaA, NaP, NaX et NaY.

La représentation graphique des domaines de compositions favorables pour la formation des structures zéolithiques dans le cadre de ce système est faite en utilisant le diagramme tétraèdrique dont la base est constituée par un triangle [4] où aux sommets se trouvent les composantes SiO_2, Al_2O_3 et Na_2O ayant la concentration exprimée en pourcentages molaires, rapportés à la quantité totale de substance solide qui existe dans le mélange.

---

[12] D. W. Breck, *J. Chem. Educ.*, **41**, 678 (1964).

Avec les données expérimentales on a construit le diagramme triangulaire (fig. 1) dans lequel ont été délimités les domaines correspondant aux compositions favorables pour la formation des structures de tamis moléculaire NaA et faujasitique.

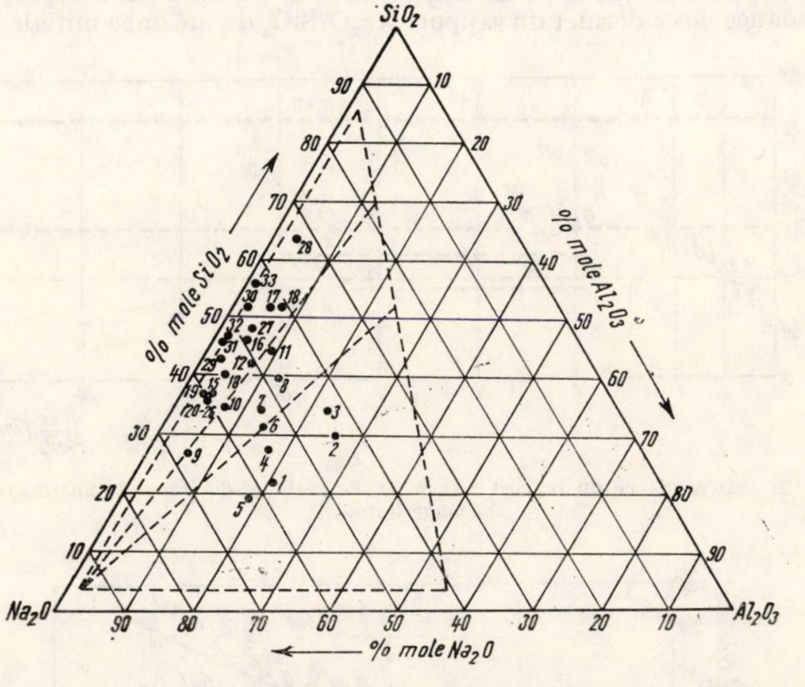

Fig. 1. — Domaines de compositions favorables pour la cristallisation des zéolithes de type A et faujasitique.

IV. INTERPRÉTATION DES RÉSULTATS

En étudiant la dépendance du processus de cristallisation de la nature des matières premières, de la composition initiale des solutions de contact, de la durée d'homogénéisation du gel à 25°, de la durée et de la vitesse d'agitation et aussi de la durée de cristallisation à 100° on a pu constater que le facteur déterminant dans l'obtention des zéolithes avec une structure caractéristique pour le type A et faujasitique, est la composition chimique du mélange initial.

L'expression quantitative de la composition chimique est faite sur la base des rapports molaires Na_2O/SiO_2, SiO_2/Al_2O_3 et H_2O/Na_2O entre lesquels il y a une forte dépendance.

On constate une dépendance visible entre la valeur du rapport SiO_2/Al_2O_3 et Na_2O/SiO_2 du mélange initial et le type structural de la zéolithe obtenue.

Ainsi, avec l'augmentation du rapport SiO_2/Al_2O_3, et avec la diminution du rapport Na_2O/SiO_2 de mélange initial, a lieu une augmentation du rapport SiO_2/Al_2O_3 dans le produit final, ainsi qu'une modification du type structural.

Dans la figure 2 on a représenté en coordonnées rectangulaires la variation du rapport SiO_2/Al_2O_3 de zéolithe en fonction de la valeur du même rapport de mélange initial, et dans la figure 3 on a représenté la dépendance de ce dernier du rapport Na_2O/SiO_2 du mélange initial.

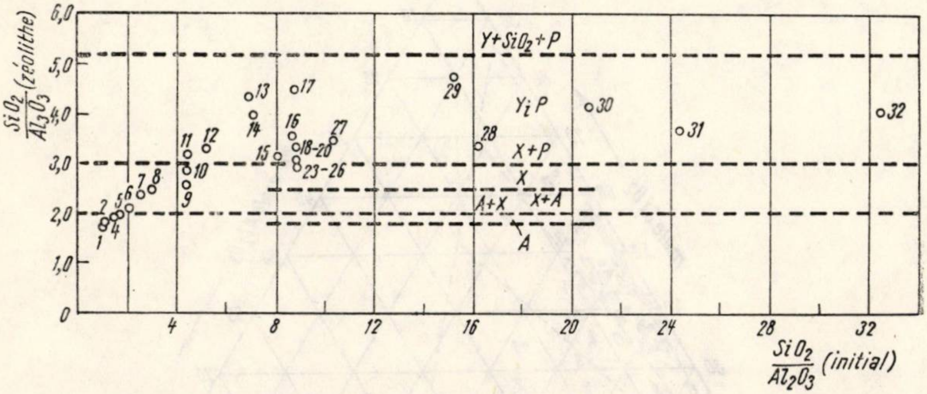

Fig. 2. — Dépendance du rapport SiO_2/Al_2O_3 de zéolithe du rapport SiO_2/Al_2O_3 du mélange initial.

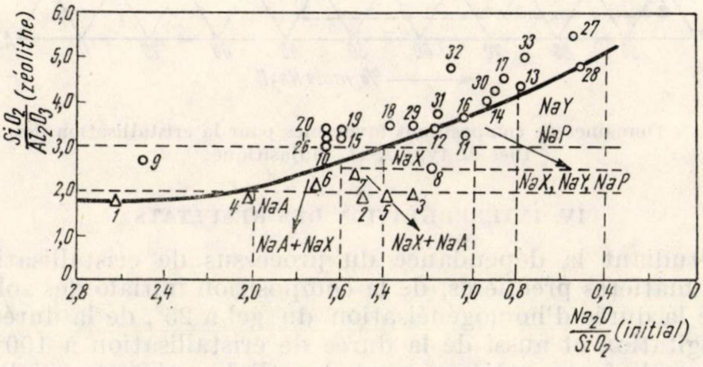

Fig. 3. — Dépendance du rapport SiO_2/Al_2O_3 de zéolithe du rapport Na_2O/SiO_2 du mélange initial.

Sur la base des données expérimentales, on peut formuler les conclusions suivantes :

— Les mélanges initiaux qui ont les rapports $SiO_2/Al_2O_3 < 2$ et $Na_2O/SiO_2 > 1{,}2$ conduisent toujours aux zéolithes de type NaA. Ces derniers ont le rapport molaire SiO_2/Al_2O_3 approximativement constant, la valeur de celui-ci étant comprise entre 1,80 et 1,96, ce qui confirme le fait déjà démontré que la zéolithe de type NaA a une structure tétraédrique Si—Al—O constante. La valeur admise de ce rapport est comprise entre 1,85 et 2,0 et correspond à un enchaînement parfait

—Si—O—Al—O—Si— dans lequel le rapport Si : Al = 1 : 1.[13] Par conséquent le tamis moléculaire de type A est obtenu seulment à partir de mélanges initiaux relativement riches en Al_2O_3 et qui représentent la limite de la possibilité d'enrichissement en Al_2O_3, puisque d'après la règle de Loewenstein, le nombre des tétraèdres ne peut être que plus petit ou tout au plus égal à celui des tétraèdres $[SiO_4]^{4-}$;

— Les mélanges initiaux qui ont le rapport $SiO_2/Al_2O_3 = 2{,}0-3{,}0$ et $Na_2O/SiO_2 = 2{,}0-1{,}6$ conduisent à un mélange des zéolithes, nommément zéolithe A contaminée par la zéolithe de type X ;

— Les mélanges initiaux avec le rapport $SiO_2/Al_2O_3 = 2{,}0-3{,}0$ et $Na_2O/SiO_2 = 1{,}6-1{,}4$ conduisent à un mélange des zéolithes, nommément zéolithe X contaminée par la zéolithe A ;

— Les mélanges initiaux avec le rapport $SiO_2/Al_2O_3 = 3{,}2-20$ et $Na_2O/SiO_2 = 1{,}6-1{,}0$ conduisent par la cristallisation aux zéolithes de type X dont le rapport SiO_2/Al_2O_3 a la valeur égale à $2{,}5 \pm 0{,}5$;

— Les mélanges initiaux avec le rapport $SiO_2/Al_2O_3 = 4{,}0-40$ et $Na_2O/SiO_2 = 0{,}9-0{,}4$ conduisent aux zéolithes de type Y dont le rapport SiO_2/Al_2O_3 est compris fréquemment entre 3,1 et 5,2. A côté des trois composantes qui participent à la composition de la structure zéolithique, dans le processus de cristallisation, participe aussi l'eau, dont le contenu exprimé par le rapport molaire H_2O/Na_2O exerce une influence notable sur le processus. La grandeur de ce rapport influe sur le temps nécessaire pour la cristallisation, sur le type structural du produit final et sur la forme et la grandeur des cristaux.

En général, aux petites valeurs du rapport, par exemple $H_2O/Na_2O < 10$, le processus de cristallisation est plus alourdi, mais aux grandes valeurs de celui-ci, $H_2O/Na_2O > 80$, on obtient habituellement des cristaux à des dimensions plus grandes et à une structure différente de celle du tamis moléculaire de type faujasitique.

Pour la synthèse des tamis moléculaires NaA, NaX, NaY les valeurs du rapport $H_2O/Na_2O = 30-80$ sont suffisantes.

Habituellement, la valeur du rapport H_2O/Na_2O est approximativement égale à 40.

Dans le domaine des zéolithes de type faujasitique on constate que l'augmentation du rapport SiO_2/Al_2O_3 dans la zéolithe a lieu en même temps que la croissance du même rapport du mélange initial. Il y a une liaison directe entre la valeur de ce rapport et celle du rapport Na_2O/SiO_2.

Ainsi, aux grandes valeurs du rapport Na_2O/SiO_2 si grand que soit la teneur en silicium, la zéolithe obtenue a le rapport SiO_2/Al_2O_3 approximativement égal à 3. Il en résulte ainsi qu'au cas d'une alcalinité augmentée a lieu l'élimination du silicium de gel formé et le passage de celui-ci dans le liquide intermicellaire.

Dans la figure 4 on a représenté la variation du rapport SiO_2/Al_2O_3 dans la zéolithe en fonction de l'alcalinité du milieu initial, en utilisant des mélanges avec un rapport SiO_2/Al_2O_3 constant.

---

[13] M. M. Dubinin, *Izvest. Akad. Nauk, S.S.S.R.*, **7**, 1183 (1961).

Pour l'explication de cette variation il faut prendre en considération les types de liaison possibles entre les tétraèdres $[SiO_4]^{4-}$ et $[AlO_4]^{5-}$.[14-16] Au cas de la formation des liaisons de type —Si—O—Si— on a pu constater que ceux-ci sont d'autant plus instables que l'alcalinité du milieu est plus grande, alors que les liaisons —Si—O—Al—O—Si— sont plus stables.

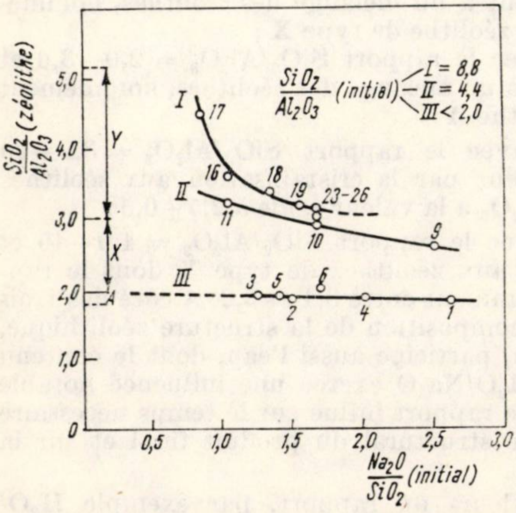

Fig. 4. — Dépendance entre l'alcalinité du milieu initial et la valeur du rapport SiO_2/Al_2O_3 dans le produit cristallisé.

Les milieux initiaux concentrés en hydroxyde alcalin favorisent l'obtention des zéolithes avec un rapport SiO_2/Al_2O_3 réduit.

Il en résulte que pour obtenir des zéolithes de type Y il est nécessaire d'utiliser des solutions dont l'alcalinité totale corresponde au rapport $Na_2O/SiO_2 = 1{,}0-0{,}4$.

Les compositions initiales qui se trouvent au voisinage des domaines caractéristiques pour une certaine structure conduisent habituellement à un mélange de ces deux produits (fig. 3), tandis que les compositions initiales situées vers le centre du domaine conduisent à des produits unitaires, avec un haut degré de cristallinité.

Le maintien des cristaux de zéolithe en contact avec la solution correspondant à l'équilibre de la cristallisation à 100° peut conduire à la modification de la structure et du degré de cristallinité.

Ainsi, dans le cas des zéolithes obtenues de compositions initiales voisines, le maintien des cristaux en contact avec la solution conduit à la modification de la structure (de la zéolithe X on passe légèrement à la zéolithe P), tandis qu'au cas de zéolithes obtenues à partir de compositions initiales trouvées vers le centre du domaine, le maintien de ceux-ci en contact avec la solution correspondante ne conduit pas à la modification

[14] B. D. Mc Nicol, G. T. Pott et K. R. Loos, *J. Phys. Chem.*, **76**, 3388 (1972).

[15] A. Culfaz et L. B. Sand, *Adv. Chem. Ser.*, **121**, 140 (1973).

[16] B. D. Mc. Nicol, G. T. Pott, K. R. Loos et N. Mulder, *Adv. Chem. Ser.*, **121**, 152 (1973).

de la structure, mais seulement du degré de cristallinité, en fonction de l'alcalinité du milieu.

La grandeur du domaine correspondant à la composition favorable pour la formation d'une structure peut être modifiée par la variation de la teneur en eau dans le mélange initial. En augmentant le rapport H_2O/Na_2O on constate une augmentation du domaine, mais cette croissance doit être mise en corrélation avec le contenu d'hydroxyde alcalin, sinon le gel colloïdal formé ne cristallise pas même après cinq jours.

V. CONCLUSION

En vue d'établir les conditions les plus favorables à la synthèse des zéolithes de type A et faujasitique, on a utilisé la méthode hydrothermale en variant : la composition des mélanges initiaux, la durée d'homogénéisation du gel et la durée de cristallisation à 100°. Les résultats expérimentaux ont conduit à la conclusion que le principal facteur qui exerce une influence notable sur la structure et les propriétés des zéolithes est la composition des mélanges initiaux. Pour l'obtention des zéolithes de type A il est nécessaire d'utiliser les mélanges initiaux dans lesquels $SiO_2/Al_2O_3 < 2$ et $Na_2O/SiO_2 > 1{,}2$.

Les zéolithes de type X s'obtiennent si l'on utilise des mélanges initiaux avec $SiO_2/Al_2O_3 = 3{,}2-20$ et $Na_2O/SiO_2 = 1{,}0-1{,}6$ et les zéolithes de type Y, si l'on utilise des mélanges avec $SiO_2/Al_2O_3 = 4{,}0-40$ et $Na_2O/SiO_2 = 0{,}4-0{,}9$. En utilisant les mélanges dont les valeurs des rapports entre les oxydes sont différentes, on obtient des mélanges des zéolithes.

On a aussi constaté que l'eau présente dans les mélanges initiaux exerce une influence visibile sur le processus de cristallisation et sur la structure des zéolithes.

Un rôle important dans la synthèse des zéolithes revient à l'alcalinité des mélanges exprimée par le rapport Na_2O/SiO_2. Pour obtenir des zéolithes de type Y il faut utiliser des mélanges initiaux dans lesquels la valeur du rapport Na_2O/SiO_2 varie entre 0,4 et 1,0.

Revue Roumaine de Chimie, **21**, *2*, 285–291 (1976)

Revue Roumaine de Chimie, **21**, *2*, 293 – 304 (1976)

EIN MODELL FÜR DIE VERWEILZEITVERTEILUNG DER DISPERSEN PHASE IN EINEM GAS-FLÜSSIG ODER FLÜSSIG-FLÜSSIG SYSTEM

R. MIHAIL, C. SINGER und C. IONESCU
Polytechnisches Institut, Bukarest, Cl. Griviţei nr. 132

Eingegangen am 24. September, 1974

Es wird ein stochastisches Modell vorgeschlagen in dem die Bahn eines Teilchens der dispersen Phase durch einen vereinfachten Weg ersetzt wird. Indem man eine Funktion definiert welche die Position eines Teilchens zu einem gewissen Zeitpunkt charakterisieren soll, das sich auf einer derartigen vereinfachten Bahn bewegt, werden Schlußfolgerungen über den Einfluß verschiedener Parameter auf die Verweilzeitenverteilungen der Teilchen der dispersen Phase gezogen.

1. EINLEITUNG

In einer früheren Arbeit[1] wurden einige stochastische Modelle beschrieben welche in letzter Zeit für das Simmulieren verschiedener Vorgänge benützt wurden. Bei dieser Gelegenheit ist ein allgemeines Schema nach dem stochastische Modelle aufgebaut werden, vorgeschlagen worden. Diese Arbeit gliedert sich in die Bemühungen des Erweiterns des Anwendungsbereiches dieser Art von Modellen ein, und befolgt im allgemeinen das in jenem Artikel beschriebene Schema.

2. ALLGEMEINE ÜBERLEGUNGEN

Man betrachte einen Blasensäulen-Reaktor. Die Blasen werden am unteren Teil der Säule eingespeist und verlassen den Reaktor am oberen Ende. Nimmt man einen konstanten Einspeisungsgasdurchsatz an so kann man, wie es übrigens auch aus[2] hervorgeht, am oberen Säulenende einen unregelmäßigen, im Laufe der Zeit sich zufällig ändernden, Gasdurchsatz bemerken. Diese Erscheinung ist auf das durch verschiedene Ursachen hervorgerufene Bremsen der Blasen zurückzuführen. Als Ursachen kann man die, durch Zusammenstoßen zwischen Blasen, konvektive Strömungen, einen Rührer oder die Existenz von verschiedenen Innenbauten, verursachten Abweichungen von einer senkrechten Bahn betrachten.

---

[1] R. MIHAIL und C. SINGER, *Studii Cercetări Chim. Acad. R. S. România*, **21**, 1207 (1973).
[2] H. HOFMANN, *Chem. Eng. Sci.* **14**, 193 (1961).

Im folgenden wird ein Modell vorgeschlagen, welches die Verweilzeitverteilung der Teilchen der dispersen Phase, die zufällig erscheinenden Abweichungen in Betracht ziehend, beschreiben soll.

Als Grundlage für diese Beschreibung dient ein Modell das in der Literatur[3] im Zusammenhang mit der Bewegung eines Gases in einem Festbettreaktor erschienen ist. In dem erwähnten Modell sind drei Bewegungszustände in Betracht gezogen worden, welche man spezifisch definiert. Der Übergang von einem Bewegungszustand zum anderen geschieht nur nach einer gewissen Zeitspanne, wodurch man die regelmäßige Struktur des festen Bettes in Erwägung zieht. In dem hier beschriebenen Fall wird angenommen, daß die Teilchen der dispersen Phase in zwei Bewegungszuständen existieren können, einem ungestörten und einem, in dem sie auf einer gewissen Höhe verweilen. Der Übergang von einem Zustand zum anderen findet nach zufällig langen Zeitspannen statt.

Man wird durch Störungen alle zufälligen Ursachen verstehen, welche die Bewegung der Teilchen der dispersen Phase bremsen. Es wird angenommen, daß jede Störung entweder ein plötzliches Stehenbleiben oder eine kurz andauernde Bewegung in einer horizontalen Ebene hervorruft. Im dem Augenblick, in dem der Einfluß der störenden Kraft verschwindet nimmt das Teilchen ebenso plötzlich die Bewegung in senkrechter Richtung wieder auf. Die wirkliche Bewegung der Teilchen wird also durch eine Bahn, die in Abb. 1 veranschaulicht wurde, annähernd beschrieben. Der so dargestellte Weg kommt der wirklichen Bahn der Teilchen in dem Falle nahe, in dem die Letzteren plötzlich von ihrem senkrechten Weg abgebracht werden. Die Darstellung ist jedoch, im Falle in dem die Teilchen wegen der Bewegungen der kontinuierlichen Phase auf ellyptischähnliche Bahnen gesetzt werden und so weiter aufsteigen, nicht ganz richtig. Dementsprechend wird sich das Modell in folgenden Lagen als richtig erweisen :

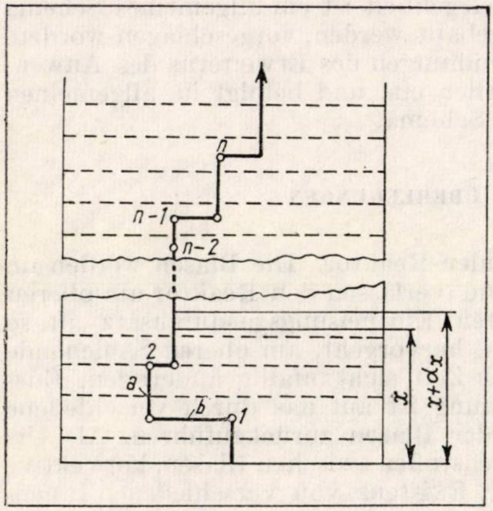

Abb. 1. — Die Bahn eines Teilchens so wie sie durch das Modell dargestellt ist ; a — Ungestörter Teil einer Strecke ; b — Gestörter Teil einer Strecke, 1,2, ..., $n-2$, $n-1$, n — Punkte an denen der gestörte Teil einer Strecke beginnt.

---

[3] H. Hoelscher und A. Schmalzer, *AIChE Journal*, **17**, 104 (1971).

a) Antreffen von Innenbauten welche plötzlich die senkrechte Bewegung der Teilchen bremsen;

b) Zusammenstöße zwischen Teilchen der dispersen Phase durch die es zu Abweichungen von dem senkrechten Weg kommt;

c) Bewegungen der kontinuierlichen Phase welche senkrecht zur Aufwärtsbewegung der Teilchen stehen (als Beispiel erwähne man horizontale Schwingungen die auf einer gewissen Höhe der Säule stattfinden); in diesem Fall ergibt das Modell um so bessere Ergebnisse, je weniger die Dichten der beiden Stoffe voneinander abweichen da so Richtungsänderungen stattfinden die den horizontalen näherkommen;

d) Antreffen eines Rührers; das Modell nähert sich in diesem Fall am besten der Wirklichkeit, wenn die Dichten der beiden Phasen möglichst verschieden sind, da sonst die Teilchen auf ellyptischen Bahnen aufsteigen.

DAS MATHEMATISCHE MODELL

Es wird durch $P_n(x, t)\,\mathrm{d}x$ die Wahrscheinlichkeit bezeichnet, daß ein Teilchen zwischen 0 und t bis zu einer Höhe zwischen x und $x + \mathrm{d}x$ sich bewegt und dabei n Mal in seiner Aufwärtsbewegung gestört wird.

$P_n(x, t)\,\mathrm{d}x$ wird sich also zwischen t und $t + \mathrm{d}t$ aus folgenden Gründen ändern:

a) das Teilchen befand sich zum Zeitpunkt t auf der Höhe $x - \beta \mathrm{d}t$ und steigt ungestört mit der Geschwindigkeit β im Zeitintervall $\mathrm{d}t$ bis zu einer Höhe x,

b) das Teilchen befand sich schon zum Zeitpunkt t auf einer Höhe zwischen x und $x + \mathrm{d}x$ doch wurde es hier im Zeitintervall $\mathrm{d}t$ das n-te Mal in seiner Aufwärtsbewegung gestört; durch $\pi\,(n-1, t|n, \mathrm{d}t)$ wird die Wahrscheinlichkeit der n-ten Störung des Teilchens im Zeitintervall $\mathrm{d}t$ bezeichnet, angenommen daß zwischen 0 und t schon $n-1$ Abweichungen von der senkrechten Bahn stattfanden. Es wird angenommen, daß folgende Beziehung besteht:

$$\pi\,(n - 1, t\,|\,n\,;\ \mathrm{d}t) = \mu\,\mathrm{d}t\,; \tag{1}$$

μ ist als eine Frequenz der Störungen zu betrachten, und hat als solche die Dimension t^{-1}. Gleichung (1) widerspiegelt also die Annahme, daß die Frequenz der Abweichungen unabhängig von den Modellveränderlichen ist;

c) das Teilchen befand sich zum Zeitpunkt t auf einer Höhe zwischen x und $x + \mathrm{d}x$ doch wurde es im Zeitintervall $\mathrm{d}t$ das $n+1$-ste Mal von der senkrechten Bahn abgewichen. Wenn die Bezeichnungen dieselben bleiben, so gilt, obige Charakterisierung von μ in Betracht ziehend die Beziehung:

$$\pi\,(n, t|n + 1\,;\ \mathrm{d}t) = \mu\,\mathrm{d}t \tag{2}$$

Die Größen β und μ gelten annäherungsweise als konstant. Es sind diesbezüglich folgende Bemerkungen zu machen.

a) Die Geschwindigkeit β hängt einerseits von Größen ab die das Teilchen charakterisieren, andererseits wird sie von den Bewegungen der kontinuierlichen Phase beeinflußt. Was die charakteristischen Größen des Teilchens anbelangt, so ändert sich β einerseits mit dem Radius der Teilchen, andererseits aber mit dem Leerraumanteil der dispersen Phase. Deswegen wird angenommen, daß die Wahrscheinlichkeit in Bezug auf eine Teilchenmenge definiert ist, deren Durchmesser sehr nahe beieinander liegen und daß der Leerraumanteil der dispersen Phase derselbe in der ganzen Säule ist. Eine Ausnahme bildet der Boden des Reaktors wo sich die Bedingungen ändern wie in (6) und den danach folgenden Bemerkungen gezeigt wird. Was die kontinuierliche Phase anbelangt, so wurde schon hervorgehoben, daß dieselbe sich entweder nicht bewegt, mit Ausnahme zufälliger horizontaler Schwingungen, oder einen kurz anhaltenden Einfluß auf das Teilchen ausübt. Wenn β konstant ist so kann man diesen Einfluß als unabhängig von x, t deuten.

b) μ als konstant zu betrachten ist nur annäherungsweise richtig, da warscheinlich die verschiedenen Störungsfaktoren mit ungleicher Frequenz die Bewegung der Teilchen beeinflussen. Deswegen muß angenommen werden, daß der Einfluß einer der oben erwähnten Faktoren viel stärker in Beziehung zu den andern ist. Es wird ferner der Einfluß der Zeit und der Höhe vernachlässigt.

Diese Bemerkungen beachtend, kann folgende Gleichung, die $P_n(x, t)$ erfüllen soll, geschrieben werden:

$$P_n(x, t + \mathrm{d}t)\,\mathrm{d}x = P_n(x - \beta\mathrm{d}t, t)\,\mathrm{d}x + \mu[P_{n-1}(x, t) - P_n(x, t)]\,\mathrm{d}x\mathrm{d}t \quad (3)$$

Wenn man in (3) $P_n(x, t)\,\mathrm{d}x$ auf beiden Seiten hinzuaddiert, und gleichzeitig laut obigen Bemerkungen in Betracht zieht, daß:

$$\mathrm{d}x = \beta\mathrm{d}t \quad (4)$$

so wird aus (3) ein System von partiellen Differentialgleichungen:

$$\frac{\partial P_n(x, t)}{\partial t} = -\beta\frac{\partial P_n(x, t)}{\partial x} + \mu[P_{n-1}(x, t) - P_n(x, t)] \quad (5)$$

Die gewählten Anfangs- und Grenzbedingungen, die das System erfüllen muß sind:

$$\left.\begin{aligned} P_n(x, 0) &= \delta_{no} \\ P_n(0, t) &= \frac{(\lambda t)^n\, e^{-\lambda t}}{n!}\,U(t) \end{aligned}\right\} \quad (6)$$

Man bezeichnet durch:

$$\delta_{no} = \begin{cases} 1 & n = 0 \\ 0 & n \neq 0 \end{cases}$$

$$U(t) = \begin{cases} 1 & t \geqslant 0 \\ 0 & t < 0 \end{cases}$$

Man kann aus der ersten Bedingung folgern, daß ein Teilchen, welches zum Zeitpunkt null sich auf irgend einer Höhe befände, ungestört seinen Weg fortsetzen würde. Gemäß der zweiten Bedingung ist einerseits die Wahrscheinlichkeit des Eintritts eines Teilchens ins System zwischen $t=0$ und t $U(t)$, andererseits aber, wird das Teilchen auf dem Boden der Säule wo es eingetreten ist, mit einer Wahrscheinlichkeit festgehalten, die jener eines Poissonschen Prozesses gleicht. Die Ursache der Abweichung des Teilchens die schon am Boden des Reaktors stattfindet, ist durch die Zusammenstöße mit andern Teilchen zu klären, die gleichzeitig ins System eingeschleußt wurden. Es wird somit eine der obigen Bemerkungen verdeutlicht laut der, die Störungsbedingungen am Boden der Säule sich von denen die im restlichen System stattfinden einigermaßen unterscheiden.

Mit den so gedeuteten Bedingungen kann man zur Lösung des Systems (5) übergehen.

Zunächst wird die Reihe von Verhältnisgleichungen :

$$\mathrm{d}t = \frac{\mathrm{d}x}{\beta} = \frac{\mathrm{d}P_n}{\mu[P_{n-1} - P_n]} \tag{7}$$

geschrieben. Aus der Gleichstellung der ersten zwei Verhältnisse kann man die Integralkurve :

$$t - x/\beta = C_1 \tag{8}$$

erhalten. Wenn man nun in (7) das erste und dritte Verhältnis gleichstellt so erhält man das Differentialgleichungssystem :

$$\frac{\mathrm{d}P_n}{\mathrm{d}t} = \mu(P_{n-1} - P_n) \tag{9}$$

Die Gleichungen (9) stellen einen Poissonprozeß dar. Wenn man also die erste Bedingung (6) in Betracht zieht, so kann man die Lösungen des Systems (9) in der Form von Integralkurven :

$$P_n(x, t) - \frac{(\mu t)^n e^{-\mu t}}{n!} = C_2 \tag{10}$$

darstellen. Die Bedingung $P_{-1}(x, t) = 0$, die aus physikalischen Gründen gestellt wird, ist in der Lösung (10) des Systems (9) beachtet worden. Damit die Lösungen des Systems (5) den Grenzbedingungen (6) genügen, untersuchen wir das Verhalten der Integralkurven (8) und (10) für $x = 0$:

$$t = C_1$$

$$\frac{(\lambda C_1)^n e^{-\lambda C_1}}{n!} U(C_1) - \frac{(\mu C_1)^n e^{-\mu C_1}}{n!} = C_2 \tag{11}$$

Wenn wir nun die Ausdrücke für C_1 aund C_2 aus (8) und (10) in (11) einfügen, so können die Lösungen von (5) in der Form:

$$P_n(x, t) = \frac{[\lambda(t - x/\beta)]^n e^{-\lambda(t-x/\beta)}}{n!} U(t - x/\beta) +$$

$$+ \frac{(\mu t)^n e^{-\mu t}}{n!} - \frac{[\mu(t - x/\beta)]^n e^{-\mu(t-x/\beta)}}{n!} \tag{12}$$

dargestellt werden.

Die durch (12) definierten Lösungen genügen sowohl der Normierungsbedingung:

$$\sum_{n=0}^{\infty} P_n(x, t) = 1 \tag{13}$$

als auch den Beziehungen (6).

Wenn man $t = x/\beta$ in (12) einsetzt so ist der Wert von $P_n(x)$:

$$P_n(x) = \frac{(\mu x/\beta)^n e^{-\mu x/\beta}}{n!}$$

x/β ist aber die für das Teilchen nötige Zeitspanne um ungestört das Niveau x zu erreichen. Folglich müßte $P_n(x, t) = 0$ insofern $n \neq 0$. Damit also die Lösung (12) physikalisch richtig sei, kann sie folgendermaßen dargestellt werden:

$$P_n(x, t) = \frac{[\lambda(t - x/\beta)]^n e^{\lambda-(t-x/\beta)}}{n!} U(t - x/\beta) +$$

$$+ \frac{(\mu t)^n e^{-\mu t}}{n!} U'(x/\beta) - \frac{[\mu(t - x/\beta)]^n e^{-\mu(t-x/\beta)}}{n!}$$

$$n \neq 0 \tag{14}$$

$$P_0(x, t) = e^{-\lambda(t-x/\beta)} + e^{-\mu t} - e^{-\mu(t-x/\beta)} \qquad t > x/\beta$$

$$P_0(x, t) = 1 \qquad t = x/\beta$$

In Gleichung (14) wurde durch $U'(x/\beta)$:

$$U'(x/\beta) = \begin{cases} 0 & t \leqslant x/\beta \\ 1 & t > x/\beta \end{cases}$$

bezeichnet.

Die Werte der Funktion $P_n(x, t)$, für verschiedene, n, x, t, μ, β, λ wurden mit Hilfe einer digitalen Rechenmaschine FELIX C256 bestimmt.

ANALYSE DER DURCH DAS MODELL BESCHRIEBENEN BEWEGUNG DER TEILCHEN

A. *Die Schwankungen der Wahrscheinlichkeit von* n *Abweichungen mit der Zeit*

In Abb. 2 wurden die Schwankungen der Funktion $P_3(x, t)$ mit der Zeit auf verschiedenen Höhen dargestellt. Aus der Abbildung ist das Ansteigen der Wahrscheinlichkeit mit der Höhe nach $\tau_{\min}(\tau_{\min} = x/\beta)$ ersichtlich. Angenommen, daß für zwei verschiedene Niveaus x_1 und x_2, $x_1/\beta - t_1$ gleich $x_2/\beta - t_2$ ist, so kann dieses Anwachsen auf den zweiten Ausdruck in der Summe (14) zurückgeführt werden, was zu bedeuten hat, daß die Wahrscheinlichkeit mehrerer Störungen (in diesem Fall drei) mit der Zeit wächst.

Wie aus der Abbildung hervorgeht, hat $P_3(x, t)$ mit wachsendem x auch in den gemeinsamen Zeitspannen t größere Werte. Um dies zu erklären, muß man in Betracht ziehen, daß $P_n(x, t)\,\mathrm{d}x$ auch den Bruchteil der Elemente der dispersen Phase verkörpert, welche zwischen $\tau = 0$ und $\tau = t$ auf einer Höhe, die sich zwischen x und $x + \mathrm{d}x$ befindet, aufzufinden sind, nachdem sie n Mal von der senkrechten Bahn abge-

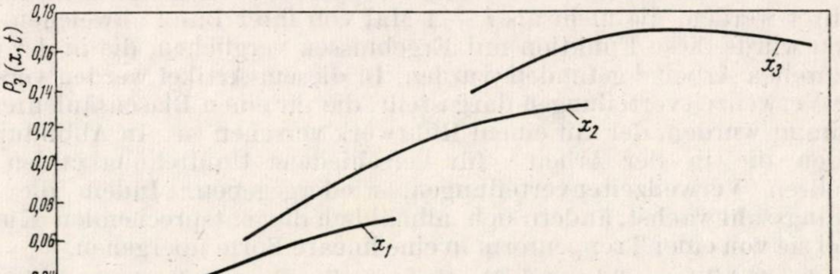

Abb. 2. – Die Schwankungen der Funktion $P_n(x, t)$ mit der Zeit für verschiedene Höhen, $n=3$, $\lambda=0{,}01\ \mathrm{s}^{-1}$, $\mu=0{,}003\ \mathrm{s}^{-1}$, $\beta=0{,}4$ cm/s, $x_1=10$ cm, $x_2=20$ cm, $x_3=30$ cm.

wichen sind. Auf einem niedrigeren Niveau ist die Anzahl der Teilchen mit demselben n kleiner, doch wächst dieselbe im Laufe des Aufsteigens, da je höher die Teilchen steigen, desto größer die Wahrscheinlichkeit ist einen Störungsfaktor anzutreffen, besonders für jene Teilchen die einen längeren Weg ungestört zurückgelegt haben.

Das Überlagern der beiden oben erwähnten Einflüsse erklärt das Verschieben des Maximums von Werten die weit entfernt von τ_{min} sind, auf der Kurve $x = 10$, in eine Gegend die relativ nahe zu τ_{min} ist für $x = 30$.

B. *Die Schwankungen der Wahrscheinlichkeit von mehr als* i *Abweichungen mit der Anzahl der Abweichungen, der Zeit und der Höhe*

Um Ergebnisse, die mit der Literatur vergleichbar sind, zu erhalten, wurde die Beziehung (13) in Betracht ziehend, die Funktion $F_i(x, t)$ definiert :

$$F_i(x, t) = 1 - \sum_{k=0}^{i} P_k(x, t) \tag{15}$$

$F_i(x, t)$ ist also die Wahrscheinlichkeit ein Teilchen, das mehr als $i+1$ Mal in seiner Aufwärtsbewegung gestört wurde, zwischen 0 und t auf einer Höhe zwischen x und $x + \mathrm{d}x$ anzutreffen. Wenn man nun annimmt, daß zwischen x und $x + \mathrm{d}x$ der Punkt ist in dem die Teilchen das System verlassen, so kann $F_i(x, t)$ als Verweilzeitenverteilung der Teilchen betrachtet werden, die mehr als $i + 1$ Mal von ihrer Bahn abweichen. Deswegen wurde diese Funktion mit Ergebnissen verglichen, die in der experimentellen Arbeit [4] gefunden wurden. In diesem Artikel werden verschiedene Verweilzeitverteilungen dargestellt, die für einen Blasensäulenreaktor bestimmt wurden, der mit einem Rührwerk versehen ist. In Abbildung 3a wurden die in der Arbeit [4] für verschiedene Umdrehungszahlen dargestellten Verweilzeitenverteilungen, wiedergegeben. Indem die Umdrehungszahl wächst, ändern sich allmählich die entsprechenden Kurven, wobei sie von einer Treppenform in eine lineare Form übergehen.

In Abbildung 3 b sind die Kurven F_0, F_1 und F_2 dargestellt. Man kann also, durch das Vergleichen der Kurven aus 3 a und 3 b folgern, daß durch das Anwachsen von i, Teilchenkollektive dargestellt werden, deren Verweilzeitverteilungen immer näher derjenigen, die in einem idealen Rührkesselreaktor herrscht, kommt. Also kann i als adimensionales Kriterium, für das im Reaktor herrschende Regime, benützt werden.

Wie aus dem Vergleich der Abbildungen hervorgeht, wird das Verhalten des Systems um so besser dargestellt, je weiter der betrachtete Zeitpunkt von τ_{min} ist. Die Anzahl der Teilchen andererseits, die nahe zu τ_{min} die Säule verlassen, ist um so kleiner, je größer i ist. Folglich wird das System durch das Modell um so genauer dargestellt je größer i ist.

---

[4] J. Hanhart, *Chem. Eng. Sci.*, **18**, 503 (1963).

Die Werte, die $F_0(x, t)$, die Wahrscheinlichkeit wenigstens einer Störung, im Laufe der Zeit annimmt, wurden für verschiedene Höhen in Tab. 1 geordnet. Durch Betrachten der Tabelle, kann man das Verkleinern des Zeitintervalls in dem die Funktion beachtlich schwankt mit Anwachsen der Höhe bemerken. Man könnte sich also vorstellen, daß auf einer sehr großen Höhe alle Teilchen die gleiche Verspätung aufweisen werden, was ein Treppenfunktionverlassen der Säule zur Folge hätte.

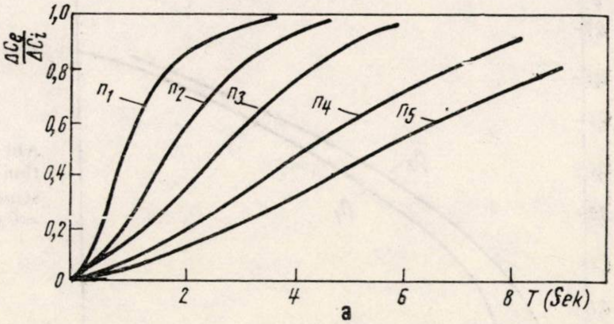

Abb. 3a. — Veränderungen der Verweilzeitverteilung mit der Umdrehungszahl sowie sie in Arbeit[4] erscheinen. Durchflußmenge des Gases $=3{,}2.10^{-3}\text{m}^3/\text{s}$; Durchmesser des Rührwerks $= 0{,}42$ m; Höhe $= 0{,}26$ m; $n_1 = 0{,}21$; $0{,}42$; $0{,}63$ Umdr./s $n_2 = 0{,}83$ Umdr./s; $n_3 = 1{,}04$ Umdr./s; $n_4 = 1{,}25$ Umdr./s $n_5 = 1{,}46$ Umdr./s

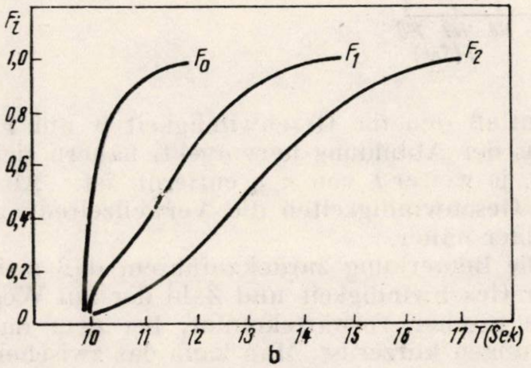

Abb. 3b. — Schwankungen der Funktion $F_i(x, t)$ mit der Zeit für verschiedene i. $\lambda = 0{,}8\ \text{s}^{-1}$; $\mu = 0{,}07\ \text{s}^{-1}$; $\beta = 1{,}0$ cm/s $x = 10$ cm.

Tabelle 1

Die Schwankungen der Funktion $F_0(x, t)$ mit der Zeit bei verschiedenen Höhen

$x = 0$		$x = 15$ cm		$x = 20$ cm	
F_0	T (Sek.)	F_0	T (Sek.)	F_0	T (Sek.)
0,185	10	0,214	30	0,278	40
0,369	20	0,363	40	0,425	50
0,454	30	0,492	50	0,540	60
0,548	40	0,605	60	0,646	70
0,673	50	0,681	70	0,724	80
0,695	60	0,754	80	0,789	90
0,755	70	0,806	90	0,835	100
0,793	80	0,857	100	0,877	110
0,827	90	0,893	110	0,915	120
		0,921	120	0,949	130

Diese Schwankungsart hat dieselben Ursachen wie jene die das Anwachsen der Funktion $P_n(x, t)$ mit x nach gleich langen Zeitspannen verursachen (siehe Abb. 2).

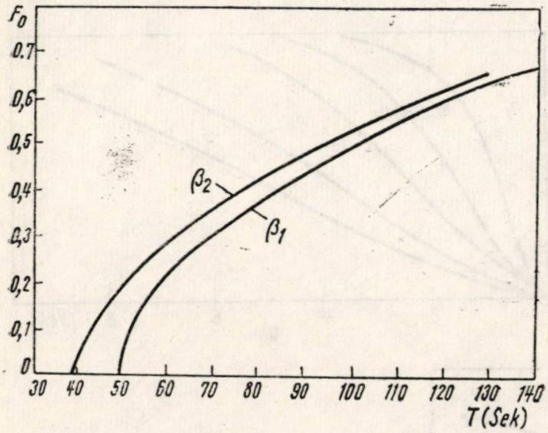

Abb. 4. — Schwankungen der Funktion $F_0(x, t)$ mit der Zeit für verschiedene β. $\lambda = 0{,}01\ \mathrm{s}^{-1}$; $\mu = 0{,}003\mathrm{s}^{-1}$; $x = 20$ cm; $\beta_1 = 0{,}4$ cm/s, $\beta_2 = 0{,}5$ cm/s.

In Abb. 4 wurde der Einfluß den die Geschwindigkeit β auf F_0 ausübt veranschaulicht. Wie aus der Abbildung hervorgeht, nähern sich die beiden Kurven um so mehr, je weiter t von $\tau_{\min}$ entfernt ist. Also kommen sich, für verschiedene Geschwindigkeiten die Verweilzeitenverteilungen im Laufe der Zeit immer näher.

Dieses Verhalten ist auf die Bemerkung zurückzuführen, daß zwischen zwei Teilchen mit gleicher Geschwindigkeit und Zahl der am Weg erlittenen Störungen, dasjenige rascher vorwärtskommt, bei dem das Zeitintervall zwischen zwei Störungen kürzer ist. Man kann das zwischen zwei Störungen vergangene Zeitintervall quantitativ abschätzen, wenn man diese Zeitspanne als zufällige Veränderliche betrachtet und ihre Verteilungsfunktion findet. Für einen Poisson Prozeß ist diese Verteilung in [5] definiert worden. In dem hier analysierten Fall wird diese Verteilung die Form:

$$S(\theta) = 1 - e^{-\mu\theta}\, U'(x/\beta) - e^{-\lambda(\theta - x/\beta)} - e^{-\mu(\theta - x/\beta)} \tag{16}$$

annehmen. Die ihr entsprechende Dichtefunktion ist für $\theta > x/\beta$ leicht ableitbar:

$$s(\theta) = \frac{\mathrm{d}S(\theta)}{\mathrm{d}\theta} = \mu e^{-\theta\mu} + \lambda e^{-\lambda(\theta - x/\beta)} - \mu e^{-\mu(\theta - x/\beta)} \tag{17}$$

Mit Hilfe von (17) kann man die mittlere Zeitspanne, die zwischen zwei Störungen vergeht, berechnen:

$$\mu = \int_{x/\beta}^{\infty} \theta s(\theta)\, \mathrm{d}\theta = \frac{1}{\lambda} - \frac{1}{\mu} + e^{-\mu x/\beta}(x/\beta + 1/\mu) \tag{18}$$

---

[5] GH. MIHOC, G. CIUCU und V. CRAIU, „Teoria probabilităţilor şi statistică matematică", Editura didactică şi pedagogică, Bucureşti, 1970, S. 529.

Die Ableitung von (18) in Bezug auf β ist:

$$\frac{\mathrm{d}M}{\mathrm{d}\beta} = e^{-\mu x/\beta}\,\mu x^2/\beta^3 \tag{19}$$

Da M proportional zu β ist, kann man wenigstens qualitativ das Annähern der beiden Kurven im Laufe der Zeit erklären.

In Tab. 2 wurde λ's Einfluß auf $F_2(x, t)$ dargestellt. Die direkte Proportionalität zwischen λ und $F_2(x, t)$ ist durch (18) erklärlich, da M kleiner wird wenn λ wächst und folglich das Niveau $x = 10$ in kürzerer Zeit erreichbar ist.

Tabelle 2

Die Schwankungen der Funktion $F_2(x, t)$ mit der Zeit für verschiedene Werte von λ

$\lambda = 0{,}85\ \mathrm{s}^{-1}$		$\lambda = 0{,}95\ \mathrm{s}^{-1}$		$\lambda = 1{,}05\ \mathrm{s}^{-1}$	
F_2	T	F_2	T	F_2	T
0,0	10	0,0	10	0,0	10
0,040	10,25	0,040	10,25	0,040	10,25
0,065	10,75	0,080	10,75	0,090	10,75
0,170	11,5	0,205	11,5	0,240	11,5
0,380	12,5	0,443	12,5	0,520	12,5
0,645	13,75	0,720	13,75	0,795	13,75
0,864	15,25	0,925	15,25	0,983	15,25

Der Einfluß des Parameters μ wurde in Abb. 5 dargestellt. Leitet man in (18) M in Bezug auf μ ab, so findet man:

$$\frac{\mathrm{d}M}{\mathrm{d}\mu} = 1/\mu^2 - e^{-\mu x/\beta}(x/\beta + 1/\mu + 1/\mu^2) \tag{20}$$

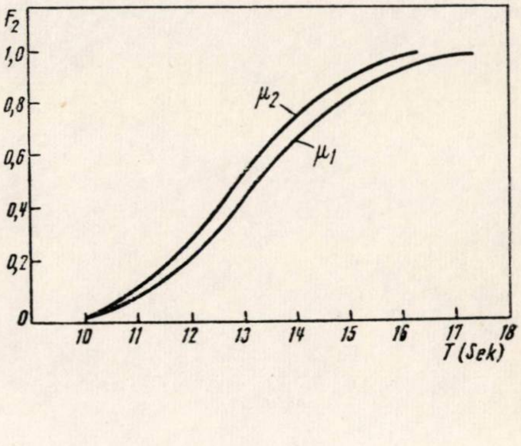

Abb. 5. — Schwankungen der Funktion $F_2(x, t)$ mit der Zeit für verschiedene μ. $\lambda = 0{,}08\ \mathrm{s}^{-1}$; $\beta = 1{,}0\ \mathrm{s}^{-1}$; $x = 10$ cm; $\mu_1 = 0{,}07\ \mathrm{s}^{-1}$; $\mu_2 = 0{,}09\ \mathrm{s}^{-1}$.

Wenn man die in der Abbildung angegebenen Bedingungen in Betracht zieht, so ist $\mathrm{d}M/\mathrm{d}\mu$ positiv, also ist das Anwachsen von $F_2(x, t)$ mit μ leicht erklärlich. Natürlich wird sich die Lage der zwei Kurven wechseln wenn die Bedingung :

$$\frac{\mu x}{\beta} > ln\left(\frac{\mu^2 x}{\beta} + \mu + 1\right) \tag{21}$$

nicht erfüllt ist.

SCHLUSSFOLGERUNGEN

Das hier vorgeschlagene Modell soll die Bewegung der Teilchen der dispersen Phase in einem reelen System nachahmen. Obwohl Vieles vereinfacht wurde, was sowohl die Grundideen, als auch das Wählen der Parameter betrifft, kann man trotzdem Ergebnisse erhalten, die wenigstens qualitativ den wirklichen nahekommen. Außerdem treten gewisse, den dispersen G-F und F-F Systemen, spezifische Eigenschaften auf, welche auch im Studium des Fließbettes erscheinen. Ein umfangreicheres Studium dieser Ähnlichkeiten wird den Inhalt einer anderen Arbeit bilden.

Revue Roumaine de Chimie, **21**, *2*, 305–312 (1976)

MEMBRANE-ELECTRODES OF THE METALLIC WIRE-PLASTIC MEMBRANE TYPE. III*

MEMBRANE-ELECTRODES FOR ORGANIC CATIONS

ELENA HOPÎRTEAN and EUGENIA ŞTEFĂNIGĂ
"Babeş-Bolyai" University, Department of Analytical Chemistry, Str. Arany János 11,
Cluj – Napoca, Romania

Received August 5, 1974

The paper studies the response of the membrane-electrode consisting of a Pt wire coated by a plastic membrane obtained from polyvinyl chloride with dibutylphtalate and K[BPh_4], towards organic cations as: alkaloids, vitamins, aminoacids. The electrode response is practical nernstian in the case of: quinine (the slope of electrode function being 55 mV in the concentration range $10^{-1} - 10^{-7}$ M), brucine (slope 54 mV in the concentration rage $10^{-1} - 3 \times 10^{-6}$ M) and cinchonine (slope 61 mV in the concentration range $10^{-1} - 10^{-5}$ M). High sensitivity of the electrode towards these alkaloids permits their potentiometric titration vith Na[BPh_4] down to a concentration of $10^{-4} - 10^{-5}$M. The electrode has also a good sensitivity towards other organic cations as: codeine, narcotine, papaverine, atropine, strychnine, antipyrine, pyramidon, B_1 and B_6 vitamins and may be used to determine these substances by potentiometric titration with Na[BPh_4].

1. INTRODUCTION

Membrane-electrodes known from the literature were used especially to determine inorganic ions: cations or anions. Few papers are dealing with organic cations. The first study on this subject,[1] published in 1970, investigated the electrodic behaviour of a plastic membrane, obtained from polyvinyl chloride and N, N′-dimethyloleamide or dioctylphthalate, towards some quaternary ammonium salts.

Since the tetraphenylborate anion is a reagent for many organic cations, being used in the determination of amines,[2–4] alkaloids,[5,6] and drugs,[7] it was used as electrode active component for some organic cations. Thus the electrode for choline, acetylcholine[8] and cholinesteraze[9], respectively, has been achieved on the basis of acetlylcholine *p*-chloro-

---

[*] Part. II. E. Hopîrtean and E. Ştefănigă, *Rev. Roumaine Chim.*, **20**, 863, (1975).

[1] T. Higuchi, G. R. Illian and J. L. Tossounian, *Analyt. Chem.*, **42**, 1674 (1970).

[2] F. E. Crane Jr., *Z. analyt. Chem.*, **157**, 40 (1957).

[3] F. E. Crane Jr., *Analyt. Chem.*, **30**, 1426 (1958).

[4] E. Smith, L. F. Wonell and J. E. Sinsheiner, *Analyt. Chem.*, **35**, 58 (1963).

[5] H. Wachsmuth and E. Mertens, *Z. analyt. Chem.*, **165**, 310 (1959).

[6] M. Bohtelsky and M. M. Cohen, *Analyt. Chim. Acta*, **22**, 328 (1960).

[7] H. Flaschka, A. Kolasek and A. M. Amin, *Z. analyt. Chem.*, **144**, 314 (1955).

[8] G. Baum, M. Lynn and F. B. Ward, *Analyt. Chim. Acta*, **65**, 385 (1973).

[9] G. Baum, F. B. Ward and S. Yaverbaum, *Clinica Chim. Acta*, **36**, 405 (1972).

tetraphenylborate. Scholer and Simon[10] have studied the behaviour of a liquid membrane-electrode with $Na[BPh_4]$ towards some inorganic (K^+, Na^+, Cs^+) and organic (quaternary ammonium salts and alkaloids) cations. Ishibashi and co-workers[11] have also realized a membrane-electrode sensitive to B_1 and B_6 vitamins, using tetraphenylborate as active electrode component. These authors, using as active electrode components : crystal violet,[12-14] *o*-phenantroline complexes,[13,14] dipicrylamine,[13] obtained sensitive electrodes towards several organic compounds, e.g. methacholine, neostigmine, *p*-aminosalicylic acid, malic acid, phthalic acid.

In a previous paper[14] the elaboration of membrane-electrode of Pt wire – plastic membrane type, with $K[BPh_4]$ as an active electrode component, has been described. The main characteristics of the electrode behaviour towards potassium[15] and ammonium[16] (electrode function, selectivity, response rate), have been established.

This paper has studied both the electrode response towards some organic cations and its performance as indicating electrodes in their potentiometric titration.

2. EXPERIMENTAL

2.1. *Apparatus and reagents*

The membrane-electrode was obtained[15] by coating the Pt wire with a plastic membrane formed of : PVC + dibutylphthalate + $K[BPh_4]$. The membrane-electrode potential was identified by the e.m.f. of the following electrolytic chain :

SCE ‖ salt bridge 10^{-1}M KNO_3—-agar-agar ‖ test solution | membrane-electrode

Potential measurements were performed at room temperature using a MV 11 pH-meter (accuracy ± 2 mV). Analytical grade reagents and commercial pharmaceutical products have been used.

2.2. *Results and discussion*

2.2.1 *Electrode functions.* The electrode functions have been established for the following alkaloids : quinine, cinchonine, brucine and codeine. Standard solutions have been prepared by successive dilutions of a stock solution of the soluble salt of the alkaloid (hydrochloride, nitrate).

---

[10] R. Scholer and W. Simon, *Helv. Chim. Acta*, **55**, 180 (1973).

[11] N. Ishibashi K. Kina and N. Mackawa, *Chem. Lett.*, **2**, 119 (1973) ; *Chem. Abstr.*, **78**, 156168 (1973).

[12] N. Ishibashi A. Jyo and M. Y. Morihisa, *Chem. Lett.*, **5**, 483 (1973) ; *Chem. Abstr.*, **79**, 73361 (1973).

[13] K. Kina, N. Mackawa and N. Ishibashi, *Bull. Chem. Soc. Jap.*, **46**, 2772 (1973).

[14] A. Jyo, M. Yonemistu and N. Ishibashi, *Bull. Chem. Soc. Jap.*, **46**, 3734 (1973).

[15] E. Hopîrtean, C. Liteanu and E. Ştefănigă, *Rev. Roumaine Chim.*, **19**, 1651 (1974).

[16] E. Hopîrtean and E. Ştefănigă, *Rev. Roumaine Chim.*, **20**, 863 (1975).

Electrode functions obtained for quinine and cinchonine are shown in fig. 1 and those for brucine and codeine in fig. 2.

For each alkaloid, the electrodic function obtained with standard solutions was completed in the low concentration range on the basis of the electrode response obtained in the potentiometric titration of the given alkaloid with $Na[BPh_4]$. For this purpose the equivalence potential was calculated [17] and by means of the electrode functions obtained in standard solutions, the corresponding *pC* value, respectively the solubility product of the tetraphenylborate of the respective organic cation, have been established. Further, by the solubility product obtained and accord-

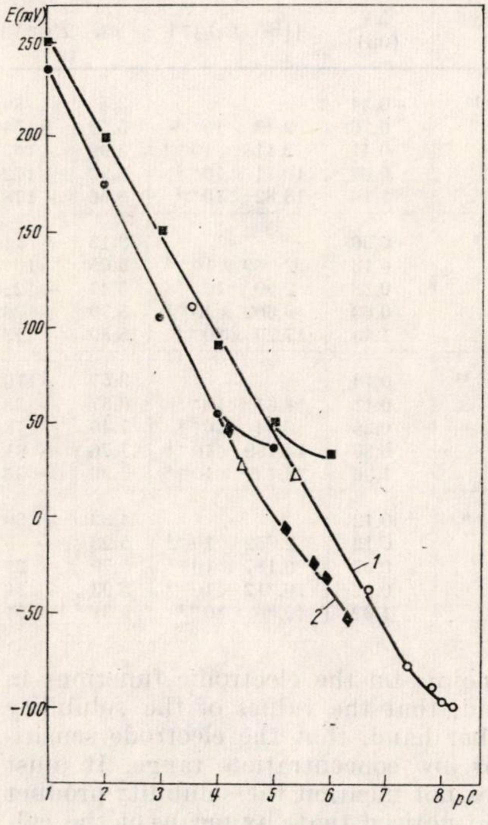

Fig. 1. — *E-pC* electrode functions.
1, quinine; *2*, cinchonine. —■—, —●— points obtained with standard solutions; —Δ— calculated point corresponding to the equivalence potential of the titration curve; —○—, —◆— points calculated from titration curves using the calculated value of the solubility product.

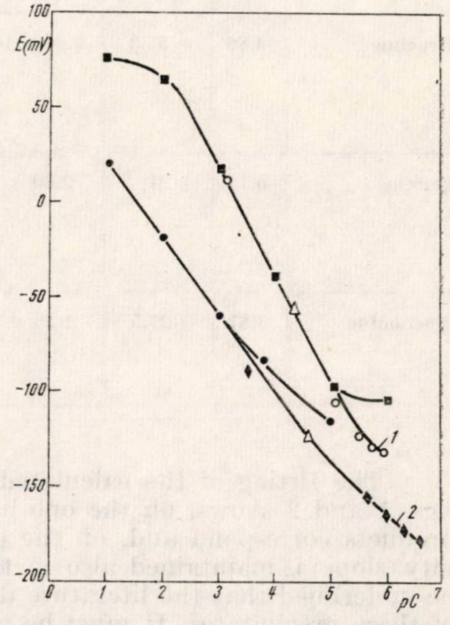

Fig. 2. — *E-pC* electrode functions.
1, brucine; *2*, codeine. —■—, —●— points obtained with standard solutions; —Δ— calculated point, corresponding to the equivalence potential of the titration curve; —○—, —◆— points calculated from titration curves using the calculated value of the solubility product.

---

[17] F. L. Hahn, *Z. analyt. Chem.*, **87**, 263 (1931).

ing to the titration stage, the pairs of values $E-pC$ have been calculated, as shown in table 1.

Table 1

Pairs of E-pC values calculated from the titration curve

Alkaloid	V_e (ml)	E_e(mV)	Solubility product	ΔV (ml)	$[[B(C_6C_5)_4]^-]$	pC	E(mV)
Codeine	7.34	-125	6.35×10^{-10}	-0.34	—	3.5	-89
				0.16	2.43×10^{-4}	5.59	-154
				0.41	3.118×10^{-4}	5.99	-165
				0.66	10.71×10^{-4}	6.20	-172
				1.16	18.82×10^{-4}	6.56	-178
Brucine	4.86	-57.3	1.99×10^{-9}	-0.36	—	3.13	$+11$
				0.13	2.069×10^{-4}	5.05	-107
				0.38	2.90×10^{-4}	5.47	-122
				0.63	9.602×10^{-4}	5.70	-126
				1.13	17.20×10^{-4}	5.80	-128
Quinine	5.14	$+21$	2.50×10^{-11}	-0.14	—	3.57	$+110$
				0.11	1.81×10^{-4}	6.87	-38
				0.36	5.94×10^{-4}	7.40	-78
				0.86	14.189×10^{-4}	7.76	-91
				1.36	22.439×10^{-4}	7.96	-96
Cinchonine	5.87	$+27.5$	1.25×10^{-9}	0.12	—	4.33	$+50$
				0.12	2.062×10^{-4}	5.23	-5
				0.37	6.187×10^{-4}	5.70	-21
				0.62	10.312×10^{-4}	5.93	-31
				1.62	49.80×10^{-4}	6.31	-51

The fitting of the calculated points on the electrodic functions in figs. 1 and 2 shows, on the one hand, that the values of the solubility products correspond and, on the other hand, that the electrode sensitivity (slope) is maintained also in this low concentration range. It must be underlined that the literature does not mention the solubility product of these precipitates. It must be also noticed that, by means of the calculated points, the lower limit of the concentration range in which a linear response may be obtained was extended from 10^{-5} M to 10^{-7}M for quinine and from 10^{-3} M to 10^{-5}M for codeine, respectively. Obviously, these results are closely correlated with the low values of the solubility products of these precipitates (Table 1) which permitted to obtain low concentrations in solution.

The slopes of the electrodic functions, including both the points obtained in standard solutions and those calculated from the titration curve, were calculated by the least squares method and are shown in table 2. Excepting codeine, the slopes of the electrodic functions correspond to the practical nernstian response.

The fact that the extension of the linear domain of the electrodic function occurred in the presence of Na^+ ions (resulting from the titrant) shows a high selectivity of the electrode towards the organic cations in the presence of Na^+ ions. The electrodic functions obtained in standard solutions of quinine, codeine, cinchonine and brucine in the presence of 10^{-2}M NaCl, confirm this fact. The slope of these functions is identical with that obtained in the absence of NaCl. The presence of bivalent cations (Ca^{2+}, Mg^{2+}) does not disturb the membrane electrode response towards organic cations.

Table 2

Slopes of the electrode function of some alkaloids

Alkaloid	Concentration interval (pC)	Slope (mV)
Quinine	1–7	55.4
Codeine	1–5.5	36.9
Cinchonine	1–5	61.4
Brucine	1–5.5	53.9

2.2.2. *Analytical use.* The tested organic compounds have been used as soluble salts (hydrochlorides, sulphates, nitrates), or have been dissolved in HCl to pH = 3.5.

The titration curves of the alkaloids : cinchonine, brucine, codeine, quinine and strychnine in concentration 10^{-2}M, with $\sim 5\times10^{-2}$M $Na[BPh_4]$ are shown in fig. 3.

Fig. 4 shows the titration curves of various quinine concentrations with $Na[BPh_4] \sim 5\times 10^{-2}$M. Similar titration curves have been obtained for codeine and brucine at various concentrations. The results for the determinations of quinine, codeine and brucine of various concentrations are given in table 3.

Table 3

Results of the determination of some alkaloids by the potentiometric titration with $Na[B(C_6H_5)_4]$

Alkaloid	V_{sample} (ml)	Alkaloid quantity Taken (g)	Alkaloid quantity Found (g)	Error (%)	$\Delta E_{\pm 2\%}$
Quinine	25	0.1112	0.1103	+0.8	132
	25	0.0120	0.0118	−1.6	37
	25	0.0014	0.00135	−3.5	5
	100	0.0014	0.00135	−3.5	3.5
Codeine	25	0.1260	0.1267	+0.4	44.5
	25	0.0118	0.0118	0	10
	25	0.0016	0.00159	−0.6	3
	100	0.0016	0.00154	−3.8	3.5
Brucine	25	0.0956	0.0945	−1.1	85
	25	0.0110	0.0107	−2.7	29
	25	0.0016	0.00165	+3.1	4
	100	0.0016	0.00165	+3.1	3

The determination errors were calculated referring to the weight of the sample. The alkaloid content of the sample was calculated by means of the Hahn-Weiler method[17] and of the Na[BPh$_4$] concentration determined by standardization with KCl (potentiometric titration using a K$^+$—sensitive membrane-electrode). The potential jump around the equivalence point was graphically determined for a ±2% error. The

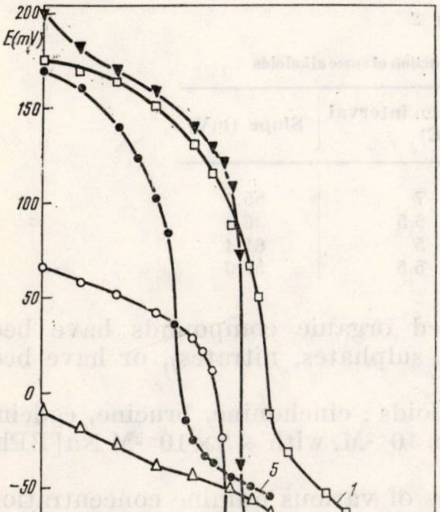

Fig. 3. — Titration curves of some alkaloids.
1 — cinchonine ; 2 — brucine ; 3 — quinine ; 4 — codeine ; 5 — strychnine.

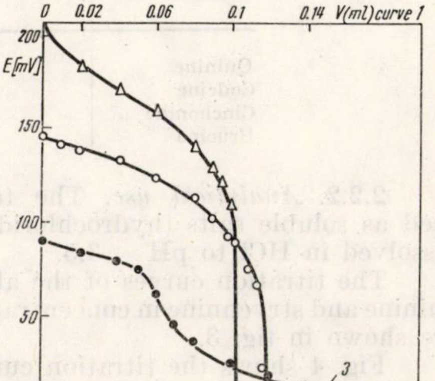

Fig. 4. — Potentiometric titration of quinine with Na[BPh$_4$] ~ 5 × 10^{-2}M at different concentrations.
1, $c = 10^{-2}$M ; 2, $c = 10^{-3}$M ; 3, $c = 10^{-4}$M.

samples titrated in 100 ml correspond to 13—16 μg alkaloid/ml, showing the high sensitivity of the membrane-electrode towards these alkaloids.

In figs. 5—7 the titration curves of narcotine, atropine, nicotine and of some other pharmaceutical products : procaine, antipyrine, pyramidon and vitamins B$_1$ and B$_6$, are given.

The potential jump around the equivalence point for a ±2% error, obtained in titrating these organic derivatives, are given in table 4.

Since, excepting cinchonine and strychnine, the determinations were performed on pharmaceutical products (tablets, vials) the accuracy could not be estimated. The high potential jump obtained in the titration of papaverine must be noticed.

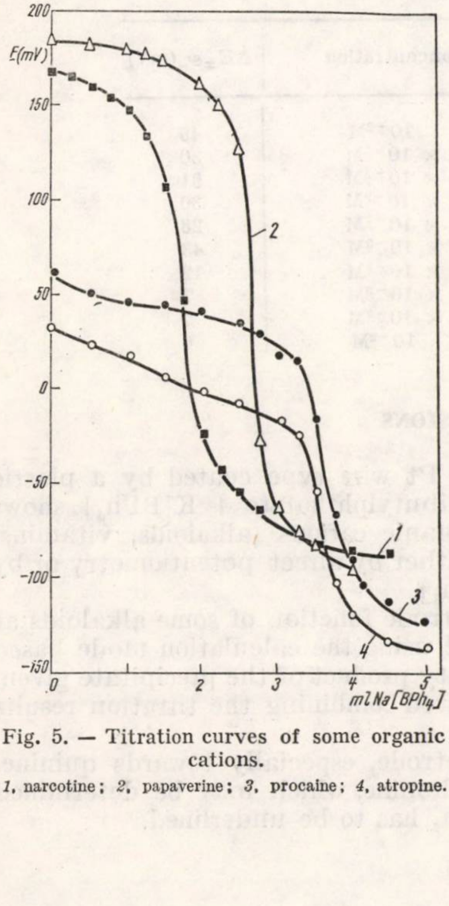

Fig. 5. — Titration curves of some organic cations.

1, narcotine; *2*, papaverine; *3*, procaine; *4*, atropine.

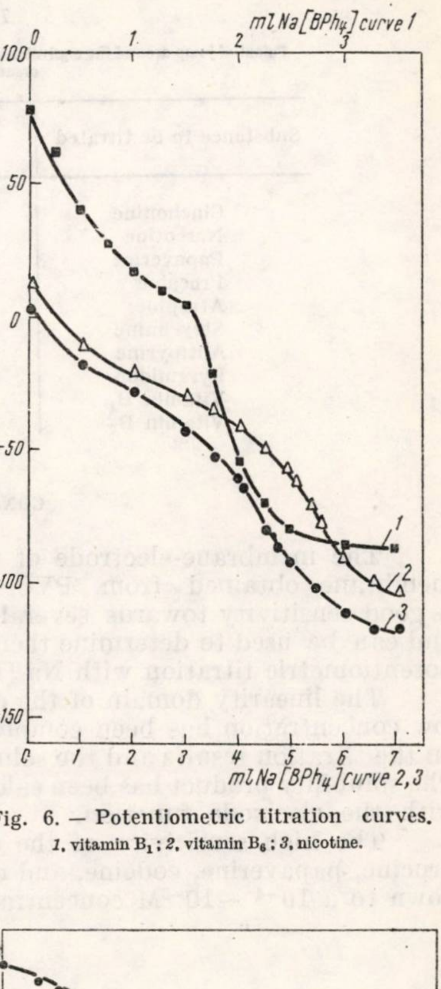

Fig. 6. — Potentiometric titration curves.

1, vitamin B_1; *2*, vitamin B_6; *3*, nicotine.

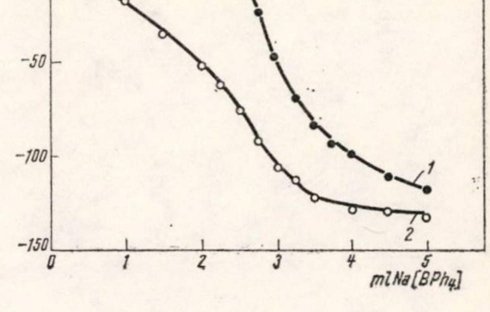

Fig. 7. — Potentiometric titration of antipyrine (curve *1*) and pyramidon (curve *2*), with $Na[BPh_4] \sim 5 \times 10^{-2}M$.

Table 4

Potential jump around the equivalence point at the potentiometric titration of some organic substances

Substance to be titrated	Concentration	$\Delta E_{\pm 2\%}$(mV)
Cinchonine	10^{-2}M	46
Narcotine	4×10^{-3}M	30
Papaverine	5×10^{-3}M	91
Procaine	7×10^{-3}M	30
Atropine	7×10^{-3}M	28
Strychnine	7×10^{-3}M	43
Antipyrine	5×10^{-3}M	12
Pyramidon	5×10^{-3}M	7
Vitamin B_1	5×10^{-3}M	7
Vitamin B_6	10^{-2}M	6

CONCLUSIONS

The membrane-electrode of the Pt wire type coated by a plastic membrane obtained from PVC + dibutylphthalate + $K[BPh_4]$ shows a good sensitivity towards several organic cations (alkaloids, vitamins) and can be used to determine them either by direct potentiometry or by potentiometric titration with $Na\,[BPh_4]$.

The linearity domain of the electrode function of some alkaloids at low concentration has been completed using the calculation mode based on the titration results and the solubility product of the precipitate given. The solubility product has been calculated combining the titration results with the electrode function.

The high sensitivity of the electrode, especially towards quinine, brucine, papaverine, codeine, and cinchonine, which may be determined down to a 10^{-4} -10^{-5}M concentration, has to be underlined.

Revue Roumaine de Chimie, 21, 2, 313–318 (1976)

COMPTES RENDUS

L. P. HAMMETT : *Physikalische organische Chemie* (Physical Organic Chemistry) Verlag Chemie, GmbH, Weinheim Bergstr., 1973, 413 pp.

The original work of the translated version "Physical Organic Chemistry. Reaction Rates, Equilibria and Mechanisms" was printed in 1970 by McGraw Hill, Inc. The translation is faithful to the original text of the second American edition. It has no additions or completions, but only a few footnotes of the translator. The previous edition, published 25 years ago corresponded to the early period of physical organic chemistry. However, since the subsequent breakthroughs have been so impressive what was known as mere assumptions at the time have become obvious facts at present. The great merit of Prof. L. P. Hammett, — considered nowadays as the father of physical organic chemistry and known in particular for the reactivity relations and the acidity functions which bear his name and are included in the essentials learned by students, — is to have processed these data in a unitary manner and to have included them into some theories and generalizations under the form of the second edition.

Similar to other scientific branches, physical and organic chemistry have had a parallel development for a long time, temporarily neglecting the phenomena which were common to the two disciplines. A considerable amount of facts, principles and theories have been accumulated over time and they have been grouped under the name of physical organic chemistry. This new discipline basically refers to the study of phenomena occurring in organic chemistry by means of quantitative mathematical methods. It can be stated without any exaggeration that the present articles in the field of speciality reflect ever more stringently the tendency to apply quantitative approaches in the evaluation of the relations between structure and reactivity and, particularly, in the study of reaction mechanisms, obtaining practical, immediate results for the basic problems of chemistry.

When revising the preceding edition, the author has ommitted the radicalic reactions and the theory of molecular orbitals, subjects which had already been treated independently in other books. The other chapters, dealing with rates, equilibria and reaction mechanisms referring to the heterolytic reactions in solutions have remained as such. The introduction comprises a few extremely convincing pages on the role and possibilities of the theory. The next chapters treat the following subjects:

— Thermodynamics of reactions in solution, including the chemical potential, the energy modification in a chemical reaction and the equilibrium state;

— Contribution of statistical mechanics to the study of transformations for ideal gases and for solutions, the modification of the enthalpy and of the potential energy;

— Kinetic data processing by establishing relations between the equilibrium and the rate of a reaction, the kinetics of reversible and irreversible reactions the reaction order, the investigation of the relative reactivity;

— Theory of the transition state for ideal and nonideal solutions, the mechanism of ionic reactions, the solvent participation in the reaction, the activation entropy, the catalysis;

— Some substitution reactions such as nucleophilic substitution reaction, solvolysis reactions and racemization, the role of solvents and of other substances, the electrophilic aromatic substitution;

— Salt effects, their influence on the activity coefficients and on the reaction rate under various conditions, ion pairs reactions, etc.

— Influence of the solvent on the reactivity, associations between ions and with different species, hydrogen bonding, ion solvation;

— Quantitative study of acids and of bases as a function of acidity ad their influence on various reactions, basicity and methods of determination, reactions in acidic and in basic media;

— Rate of reactions involving acids and bases, general catalysis by acids (including Lewis acids), bases, catalysis by solvents, catalytic effects in various reactions;

— Quantitative relations between structure and reactivity, including free energy linear relations, Hammett, Yukawa-Tsuno, Taft relations, steric effects;

— Influence of the structure on the enthalpy and entropy modifications isokinetic relations and their limits, influence of state parameters, other relations.

The readers of this book must have a background in physical and in organic chemistry. The book is intended both for students and for research-workers wishing to have a comprehensive outlook on the aspects relating to the mechanism of organic reactions which open up new and interesting avenues for the experimental research, by approximate or more accurate theories. The end of each chapter supplies the reader with a very selective bibliography which may help him study more thoroughly his subject of choice. Referring to basic principles, the book has not altered its utility. Other domains may possibly detach themselves and become independent in the future, as was the case in the interval between the Ist and IInd American editions. Finally, we must mention the fluent and very accurate German translation of Dr. P. Schmid which does not sound like a translation at all and also the exceptional graphical presentation of the book.

F. Cuiban

Structure and Bonding, vol. 23, Springer Verlag, Berlin, Heidelberg, New York, 1975, 193 pages.
Copper Proteins-Systems Containing the "Blue" Copper Center (J. A. Fee)

The article discusses the physical and chemical properties of proteins and enzymes containing copper under three distinct and unique forms : compounds with a "blue" center, or type I Cu^{2+} ; compounds with a "colourless" center or type $2Cu^{2+}$ typical of all oxidases which reduce the molecular oxygen to two water molecules ; and compounds with copper associated to the 330 nm absorption band, also typical of oxidases. The active centers and their bonds are described in particular, as they enable an interpretation of experimental data referring to the structure-function relations and the coordination manner. A particular attention is paid to studies on the kinetics and reaction mechanisms for copper oxidases. Among proteins containing one single "blue" active center, the article studies azurines, stellacyanine, umecyanine and plastocyanine. Further, the study deals with oxidases with several copper atoms such as laccases, ceruloplasmine and the oxidase of ascorbic acid. The article is concluded with general considerations on the three types of active centers bound to copper. Although the types of active centers may be satisfactorily delimited by their general physical and chemical features, their structure cannot yet be satisfactorily interpreted (227 references).

Mechanisms of Zinc Ion Catalysis in Small Molecules and Enzymes (M. F. Dunn)

The author undertakes to examine the role of the zinc ion in the homogeneous catalysis, in solution for complexes with small molecules and for the metalloenzymes with zinc. An attempt is particularly made to integrate the mechanistic physico-inorganic concepts deduced from kinetic, chemical and structural studies into the system with small molecules in the mechanism hypothesized for the enzymatic catalysis by zinc ion. The examples gathered from studies on small molecules suggest the assumption that the zinc ion behaves as an electrophile in aqueous solution. Data are selectively examined, considering only the advances made during the last 5—10 years. The information is grouped into 3 chapters containing : i. chemical and structural properties of zinc complexes (electronic structure, kinetics and mechanism of ligand substitution, comparison of Zn(II) with other divalent metallic ions) ; ii. Catalysis of zinc ion from studies on enzyme models (catalysis by Lewis acids, nucleophilic activation, case of nucleophilic attack by charge neutralization and by other effects) ; iii. Catalysis by metalloenzymes with zinc (chemical and structural properties of metalloenzymes with zinc, alcohol dehydrogenase in horse liver, human C carbon anhydrase, bovine A carboxipeptidase, thermolysine in the thermoproteolytic baccilus.

The examples of small molecules and of enzymes selected for this monograph provide an adequate outlook on the principles of zinc catalysis in the homogeneous catalysis in solution. The zinc ion may act as a Lewis acid catalyst only if the weak additional bonds are sufficient to bring the donor atom from the substrate inside the first coordination sphere of the metallic ion when the donor atom in the substrate is a relatively weak ligand such as for instance the carbonyl oxygens of an aldehyde or amide. In this situation, the summation of bond interactions between the substrate and the catalyst must be satisfactory to permit the substrate to compete with water in the coordination of the metal inner sphere. The assumption holds for small molecular systems and is compatible in principle even with some enzymatic systems. In other cases the zinc ion is involved in water activation for the nucleophilic attack such as on CO_2 in carbon anhydrase. The Lewis acid type catalysis seems to be differently involved in the mechanisms of enzymatic reactions even if the chemical conversion is the same. In some cases, e.g., with carboxipeptidase, the catalyst contributes to substrate activation. In contrast, in reactions catalysed by α-chemotripsine, catalysis is exerted by the activation of the nucleophilic attack of serine hydroxyl in the active center on the substrate (150 references).

Kinetics and Mechanism of Metalloporphyrin Formation
(W. Schneider)

The subject of this monograph considers the special position in the coordinative chemistry of hem and chlorophyll which are very stable complexes yet they are formed at much lower rates than the ordinary Fe and Mg complexes. More detailed studies have shown that the formation rates depend on the metallic ion, on the substituent of porphyrin nucleus, on the solvent and on the metal ion ligand. The article tries to reveal the nature of the dominant effects on the formation rates of metalloporphyrins in well-defined solutions, in order to draw some conclusions on the formation mechanism. After a series of general considerations, stress is laid on the results of formation kinetic studies in aqueous solution for Cu(II) Cu(I), Zn(II), Ni(II), Fe(II) and Fe(III) complexes and the saline effects. Kinetic studies in organic solvents are then presented (acetic acid ethanol dimethylsulphoxide) as well as the conclusions resulting thereof (65 references).

Hydrogen-Deuterium Exchange in Aromatic Compounds
(M. Orchin and D. M. Bollinger)

The hydrogen-deuterium exchange reactions have gained a particular importance in obtaining labelled compounds used as working tools in order to thoroughly elucidate the mechanisms of a large number of organic reactions. Studies deal either with the fate of deuterium atom during the reactions, which provide significant evidence on the mechanism, or with the measurement of the C—H bond splitting rate in comparison with the C—D bond splitting. If a kinetic isotopic effect is revealed, the C—H bond splitting is involved in the determining stage of the reaction rate. Useful information is concomitantly obtained on the properties of molecules in ground and in excited state. The article deals in particular with exchange reactions between hydrogen and deuterium in aromatic compounds . They are grouped in 5 chapters with the following coverage : the acid catalyzed exchange includes the electrophilic substitution mechanism (the kinetic isotopic effect as well as the Pi and sigma complexes), the protic acid catalysed exchange and the Lewis acid catalysed exchange. The base catalysed exchange includes the benzene intermediates and the arene-chromium and benzyl-chromium tricarbonyls. The *ortho* hydrogen exchanges in phosphine aromatic ligands of the complex metals and the catalysed exchange of platinum soluble catalysts are handled separately. The last chapter studies the selective hydrogenation-deyhydrogenation by means of di-cobalt-octacarbonyl (65 references).

F. Cuiban

T. BRAUN, G. GHERSINI. *Extraction chromatography*. Akadémiai Kiadó, 1975, 583 pages, 134 figures and 41 tables.

The monograph presents in collected and systematized form and comments upon the large amount of information concerning this relatively new field of reversed-phase partition chromatography.

The birth of extraction chromatography dates back to about 16 years ago, when S. Siekierski and J. W. Winchester independently reported their results. The data were obtained with chromatographic columns in separating inorganic substances, taking advantage of the selectivity features of organic compounds normally used as liquid-liquid extractants in reprocessing a spent nuclear fuel. A few isolated papers had appeared earlier, dealing with chelating compounds supported on different solid materials and used in columns for the separation of metals from aqueous solutions. Siekierski in particular has the merit of having recognized the possibilities of the method and having started a systematic demonstration of its versatility. Afterwards, many other research groups all over the world were attracted by the promising features of the new method that rapidly developed, so that a large number of original papers and a number of reviews have also appeared, covering some of the many aspects of the technique. Growing interest in extraction chromatography called for a work collecting and organizing the whole available information and discussing in detail the different aspects related to its theory and applications.

With this background and the authors interest and practical experience in the area of separation chemistry, the volume "Extraction chromatography" is aimed at filling such a gap. The book is the result of the collective work of many specialists, each being responsible for a chapter in which a definite aspect of the column extraction chromatography is thoroughly presented and discussed. The purpose of the monograph is to provide analytical chemists and radiochemists, especially those interested in separations, with a broad survey of the role that extraction chromatography can and should play in chemical analysis.

In the literature several different names have been proposed to define the separation of inorganic substances by means of chromatographic systems, involving an organic compound as the supported stationary phase and an aqueous solution as the eluent (mobile phase). The authors choose the term "extraction chromatography" first proposed by Hulet and used it throughout the book, because it effectively points out its strict linkage to liquid-liquid extraction.

The book succeeds in highlighting the complexity of the problem as it may be stated from its comprehensive contents and its systematic development.

The vast amount of widespread information has been systematized in 15 chapters. The theory and the experimental have been equally considered; a large number of tables and figures (41 tables and 134 figures) throughout the volume, but numbered in the chapter in which located, concentrate a wealth of data used by the authors.

The first two chapters concern with the theoretical aspects of extraction chromatography with particular attention paid to the correlation between extraction chromatography and liquid-liquid extraction, whereas chapter 3 is a guide to all technical aspects of the method.

The following two chapters (4th and 5th) describe the two most peculiar components of the technique (i.e. the organic stationary phase and its supporting material). Close related are the 11th and 13th chapters devoted to chelating compounds as stationary phase and to foamed materials as support.

The subject of chapter 6 is a survey of the available methods for the separation of elements with particular reference to radiochemical problems and the separation of closely similar elements arranged in groups of the periodic table.

The following chapters are devoted to special aspects in those fields of analytical chemistry, where extraction chromatography has proved particularly useful: separation of actinides (chapter 7); fundamental studies on the chemical behaviour of lanthanides and their separation (chapter 8); separation of fission products from one another, and from the bulk fissionable material (chapter 9); radiotoxicological determinations (chapter 10) and preconcentration of trace elements in various materials (chapter 12). In chapter 14 the usefulness of paper and thin-layer chromatographic data for planning column separation is discussed, and a general outline on the available laminar results is given. Finally, chapter 15 is a bibliographic study of the extraction chromatographic works that can be found in the literature until the end of the year 1972 and some of the papers published in 1973 (available at the data), covering both column and laminar systems, with particular attention to the former ones. The chapter encloses a very large tabular survey of experimental data on column extraction chromatographic investigations, as well as the stationary phases and support materials used in column extraction chromatography. The chapter encloses an author index and a corporate author index. The book ends with a thorough subject index.

Mention should be made of the excellent graphical conditions under which the book was printed. The topicality of the problem and data included in this work, the logical succession of the contents and the clarity of the exposition are attraction points for any specialist working in different fields such as analytical, environmental, organic and inorganic chemistry, biochemistry, physical chemistry, nuclear and isotope chemistry. It is also of great interest for students, postgraduate students, physicists and research workers in biology and medicine.

Florica Popea

D. DOBOS, Electrochemical data, Akadémiai Kiadó, Budapest, 1975, 340 pp.

The purpose of this book is to provide a source of rapid and comprehensive information for chemists and electrochemists engaged in universities, research field and industrial practice dealing with electrochemical problems during their day-to-day work.

The electrochemical data tabulated are given in the International System of Units (IS) and also in the more traditional units, in some cases.

The book contents is presented in VIII chapters.

The first chapter is in fact an introductory one, which contains a list of symbols, fundamental physical constants, atomic weights, electrochemical equations and formulae.

Chapter II contains conductivities, ionic mobilities, transport numbers, diffusion coefficients, thermodynamic data for ions in electrolyte solutions.

— Equivalent conductivities of solutions of inorganic electrolytes (arranged in alphabetical order dealing with metallic ions) at 18°, for different solvents, like : water, liquid SO_2, methanol and ethanol, the tabulated conductivities of pure solutions, molten salts and some binary systems of molten salts are given for different temperatures. Not too large spaces are used for conductivities of pure and mixed organic liquids.

— Anion transport numbers in aqueous solutions of alkali salts in pure electrolytes or in molten salts are given at 18° and 25°.

Chapter III encloses equilibrium values, activity coefficients, solubility products and r_H values.

— The dissociation constants of organic and inorganic acids and bases are separately tabulated.

— For some organic and inorganic compounds there are tables of their degrees of electrolytic dissociation at 25°.

— Mean activity coefficients values of different inorganic salts (arranged in alphabetical order dealing with metallic ions) in aqueous electrolytes or in mixt solvents are given for majority at 25° and for few of them at different temperatures.

— A very little number of tables with solubility products of slightly soluble electrolytes are mentioned.

— For redox systems there are a few tables with r_H values of some redox systems at 30° and the conversion of r_H to E (pH = 7).

In chapter IV are included : indicators, measurements of pH, buffer solutions, approximate values of pH for different materials, standard mixtures for dielectrometric investigations.

Indicators, transition pH range of indicators and colour change of mixed indicators are located at the beginning of this chapter following redox potentials, redox indicators for ordinary substances and some redox resins. Recipes for preparing buffer solutions for any pH-values are given. Tables with pH-values of different materials, like biological fluids and foodstuffs are mentioned.

In respect with the permittivity constants there are presented the relative permittivities of pure liquids and standard mixtures like acetone — benzene and water — acetone at 25° and at 400 MHz.

Chapter V comprises electrode potential, electromotive forces, diffusion potentials, zero charge potentials, galvanic cells and accumulators.

Standard electrode potentials of metals in aqueous solution, aprotic solvents, mixed solvents and their pure molten halides are given. All potential values, like Ag/AgCl ; Hg/Hg_2Cl_2 ; Hg/Hg_2SO_4 ; Pb — $Hg/PbSO_4$, are given with respect to Standard Hydrogen Electrode (SHE).

Electromotive forces of the Weston normal cell and of the Clark standard cell are tabulated at different temperatures. The same electromotive forces of chemical and galvanic cells with fused salts at various temperatures are presented.

Diffusion potentials are tabulated at either the boundary of the same aqueous electrolyte solution of different concentrations, or at the boundary of different aqueous electrolyte solutions of the same concentration.

Zero charge potentials of mercury *vs.* Normal Calomel Electrode (NCE) in aqueous electrolyte solution at room temperature are presented. There are mentioned zero charge potentials of liquid metals in fused KCl—LiCl eutectic mixture.

Electrochemical data dealing with electrolytes, electrodes and other accumulators characteristics are tabulated for three accumulator kinds : Pb — accumulators ; Ag — accumulators and Ni—Fe accumulators.

Chapter VI contains coulometry, electrogravimetry, deposition potentials, decomposition potentials, polarographic half-wave potentials.

For polarographic studies there are presented half-wave potentials of organic and inorganic substances.

Chapter VII includes electrokinetic data and isoelectric points.

Electrophoretic migration rate of suspended particles of some materials and their electrokinetic potentials in water and in organic liquids are presented.

For some proteins and amino acids in aqueous solution at 25° the isoelectric points, pH-values and dissociation constants are tabulated.

Chapter VIII, the last one, contains some important books on electrochemistry and related topics dealing with theoretical electrochemistry, electrochemical methods of analysis and instrumentation, electroplating, corrosion, batteries, accumulators, fuel cells.

The value of the book presented lies not only in the great number of electrochemical data, but especially in their logical arrangement. At the end of each chapter there are some numerical techniques for handling the electrochemical data contained, that will greatly contribute to the successful work of many students, chemists and electrochemists in academic and industrial environments.

Qualities of contents and graphic presentation both make the book a very useful reference source for electrochemists.

Iuliana Vartires

NOTE POUR LES AUTEURS

La *Revue Roumaine de Chimie* publie des articles en anglais, français, russe, allemand ou espagnol. Les auteurs sont priés d'envoyer des articles, notes, communications et comptes rendus inédits.

Les manuscrits seront dactylographiés à deux intervalles. Les tableaux seront dactylographiés sur des feuilles séparées, de même que la légende des figures. Les diagrammes seront tracés à l'encre de Chine sur papier calque. Les tableaux et les figures seront numérotés par des chiffres arabes, en nombre strictement nécessaire. Prière de ne pas inscrire les mêmes données dans les tableaux et les figures. Les formules chimiques seront incluses dans le texte ; en outre, elles seront transcrites sur des feuilles séparées. Les auteurs sont priés d'indiquer les caractères italiques (en soulignant les lettres au crayon), ainsi que tout autre caractère spécial. L'ordre des références bibliographiques sera celui de leur mention dans le texte ; le nom de l'auteur sera précédé de l'initiale du prénom ; les publications périodiques seront présentées suivant les prescriptions internationales. Les références seront ajoutées à la fin de l'article ; elles paraîtront comme des notes, au bas de la page. Le texte sera précédé d'un résumé comprenant 15 lignes au maximum.

L'entière responsabilité du contenu des articles appartient aux auteurs. On publie des articles dus aux collaborateurs roumains ou étrangers.

PRINTED IN ROMANIA

01. IUN. 1975

TRAVAUX PARUS AUX ÉDITIONS DE L'ACADÉMIE DE LA RÉPUBLIQUE SOCIALISTE DE ROUMANIE

CONST. GH. MACAROVICI et D. MACAROVICI, **Chimia oxizilor dubli şi utilizările lor** (La Chimie des oxydes doubles et leur utilisation), 1975, 195 p., 13 lei.

FRANCISC A. GOTHARD, **Echilibre lichid-vapori. Ier vol. Baze teoretice şi metode de calcul** (Equilibres liquide-vapeurs. Ier vol. Bases théoriques et méthodes de calcul), 1975, 262 p., 28 lei.

ELENA CEAUŞESCU, **Research work on syntheses and characterization of macromolecular compounds. Contributions**, 1974, 251 p., 20 lei.

I. ZUGRĂVESCU et MAGDA PETROVEANU, **Chimia *N*-Ilidelor** (La chimie des N-Ylures), 1974, 347 p., 19 lei.

MARGARETA AVRAM, **Antidăunători** (Pesticides), 1974, 494 p., 41 lei.

CR. SIMIONESCU, VIORICA RUSAN et N. POPA, **Chimia algelor marine** (La Chimie des algues marines), 1974, 211 p., 18 lei.

CRISTOFOR SIMIONESCU, MARGARETA GRIGORAŞ, AGATA CERNĂTESCU-ASANDEI et GHEORGHE ROZMARIN, **Chimia lemnului din România — plopul şi salcia** (La chimie du bois en Roumanie—le peuplier et le saule), 1973, 228 p., 28 lei.

TIBERIU NĂŞCUŢIU, **Metode radiochimice de analiză** (Méthodes radiochimiques d'analyse), 1973, 384 p., 23 lei.

MARIA FITI, **Dozimetria chimică a radiaţiilor ionizante** (La dosimétrie chimique des radiations ionisantes), 1973, 240 p., 13,60 lei.

MIHAI FLORESCU, **Eficienţa economică a cercetării ştiinţifice** (L'efficience économique de la recherche scientifique), 1972, 115 p., 15 lei.

GEORGETA LĂZĂRESCU, **Sistematizarea informaţiilor în Chimia organică** (La systématisation des informations dans la Chimie organique), 1972, 252 p., 10,50 lei.

P. BALTĂ et E. BALTĂ, **Introducere în chimia fizică a stării vitroase** (Introduction à la chimie physique de l'état vitreux), 1971, 240 p., 15,50 lei.

LYDIA-MARIA VAICUM, **Biodegradabilitatea detergenţilor** (La biodégradabilité des détergents), 1971, 254 p., 15 lei.

I. ZUGRĂVESCU et L. STOICESCU-CRIVETZ, **Polimeri heterociclici** (Polymères hétérocycliques), 1971, 190 p., 9,50 lei.

CRISTOFOR SIMIONESCU et C. UGLEA, **Fracţionarea compuşilor macromoleculari** (Fractionnement des composés macromoléculaires), 1962, 292 p., 18,50 lei.

I. MAXIM, **Materiale nucleare** (Matériaux nucléaires), 1969, 444 p., 30 lei.

CRISTOFOR SIMIONESCU et CLEOPATRA VASILIU-OPREA, **Mecanochimia compuşilor macromoleculari** (La mécanochimie des composés macromoléculaires), 1967, 344 p., 23,50 lei.

I. P. I. — c. 614

43426

Lei 25. —

F 1103

ACADÉMIE DE LA RÉPUBLIQUE SOCIALISTE DE ROUMANIE

R

REFERÁLVA

REVUE ROUMAINE DE CHIMIE

TOME 21
Nº 3
Mars 1976

RECHAX, **21**, *3*, 319–462 (1976)

EDITURA ACADEMIEI REPUBLICII SOCIALISTE ROMÂNIA

Rev. Roumaine Chim. **21**, *3*, p. 319–482 (1976), Bucarest

U

ACADÉMIE DE LA RÉPUBLIQUE SOCIALISTE DE ROUMANIE

COMITÉ DE RÉDACTION

Rédacteur en chef :

I. G. MURGULESCU, membre de l'Académie de la République Socialiste de Roumanie

Rédacteurs en chef adjoints :

A. T. BALABAN et V. EM. SAHINI, membres correspondants de l'Académie de la République Socialiste de Roumanie

Collège de rédaction :

EM. BRATU, ELENA CEAUŞESCU, ECATERINA CIORĂNESCU-NENITZESCU, C. DRĂGULESCU, RALUCA RIPAN, CR. SIMIONESCU, membres de l'Académie de la République Socialiste de Roumanie; P. SPACU, membre correspondant de l'Académie de la République Socialiste de Roumanie; MARGARETA AVRAM, D. I. MARCHIDAN, I. MOLDOVAN, G. NIAC et D. SĂNDULESCU

La Revue Roumaine de Chimie paraît 10 fois par an. Toute commande de l'étranger pour les travaux parus aux Editions de l'Académie de la République Socialiste de Roumanie sera adressée à ILEXIM, Serviciul Export-Import Carte (Livres)/ Serviciul Export-Import Presă (Revues), 64–66, Calea Griviţei P.O.B. 2001. télex 011226. Bucarest, Roumanie

Les manuscrits, les livres et les revues proposés en échange, ainsi que toute correspondance seront envoyés à la rédaction :

REVUE ROUMAINE DE CHIMIE

23, str. Dumbrava Roşie, Bucarest, Roumanie, téléphone 12 41 60

EDITURA ACADEMIEI REPUBLICII SOCIALISTE ROMÂNIA
125, Calea Victoriei, Bucarest, Roumanie, téléphone 50 76 80

REVUE ROUMAINE DE CHIMIE

Tome 21, N° 3 Mars 1976

V. E. SAHINI and LILIANA TELEA, Molecular interactions in anisidine isomers. I. Dipole moments 321–325

RODICA BELDIE, A. BUTUCELEA and V. E. SAHINI, The carbon-carbon stretching frequency in ethane, ethane-d_6 and ethane-t_6 327–331

RODICA VÎLCU, EDDA CONSTANTZA DE MADRIÑAN and FLORICA IRINEI, Thermodynamic properties of electrolyte solutions. V. Differential cryoscopy in $NaCl + CuCl_2 + H_2O$ and $KCl + CuCl_2 + H_2O$ ternary systems and in associated binaries 333–341

RODICA VÎLCU and ZOICA CENUȘE, Activity coefficients and hydrogen bond energy from calorimetric measurements 343–350

Б.Н. ОЩЕРИН, Взаимосвязь поверхстного натяжения, сжимаемости и ближнего порядка расплавов вблизи точки плавления. I. Щелочно-галоидные соли и полупроводники 351–354

R. NUȚIU, Z. SIMON and C. DRUGĂRIN, Molecular orbital study of 2-thio-5-nitro-barbituric acid 355–358

LUDMILA POPESCU, Influence of the cell diaphragm on the electromotive force of concentration cells with transport in molten salts 359–365

ANCA GHEORGHIU, D. FĂTU and E. SEGAL, Critical considerations on the nonisothermal methods for the evaluation of the kinetic parameters of endothermal decompositions in solid-gas systems. Nickel acetate tetrahydrate dehydration 367–372

MARIA MAVRODIN-TĂRĂBÎC, IOANA ONACA et I. SOLACOLU, Contribution à l'étude de la source chimique de courant $Zn/MeOH/O_2$. III. La détermination des paramètres optimaux de fonctionnement pour une pile à cathode en argent 373–383

GH. MARCU and MARIANA RUSU, Heteropolytungstates with U(IV) as central atom. I. Photocolorimetrical study of the formation of heteropolycombination UL_2 where $L = PW_{11}O_{39}^{7-}$ and $P_2W_{21}O_{71}^{6-}$ 385–390

CECILIA CONSTANTINESCU und GH. C. CONSTANTINESCU, Einfluss von Methoxyl-Substituent auf die Reaktion zwischen $[TlBr_4]^-$ und Malachitgrün 391–400

Revue Roumaine de Chimie **21**, *3*, 319–482 (1976), Bucarest

P. B. ISSOPOULOS, Complex chelate compounds of Mo(VI) and W(VI) iso- and heteropolyanions with Chrome Azurol S. I. Complex chelate compounds of Mo(VI) and W(VI) isopolyanions 401–406

MARIA BREZEANU and IOANA JITARU, Coordination compounds with iron-tin bonds. 407–412

FLORICA POPEA, CRISTINETA MĂRCULESCU and ZAMFIRA TOMA, Contributions to the coordination chemistry of phthalic acid derivatives. I. Condensation products of phthalic anhydride with *m*-phenylenediamine as coordination ligands for copper. 413–421

CANDIANO LEONTE and ION ZUGRĂVESCU, The reaction of pyridinium-cyano-carbalkoxy-methylids with α-nitroso-β-naphthol, a route to naphthoxazinones 423–426

F. URSEANU and L. FLORU, Bromamine acid — anthraquinonic intermediate used in dyes syntheses 427–445

M. IOVU and ECATERINA VOINA, Mixed aromatic esters of phosphoric acid 447–453

M. VLASSA, Exo- and endohormones. I. Application of the ketoxime activation to the synthesis of the melanocyte inhibiting factor 455–459

ELENA ANTONESCU and ECATERINA VASILESCU, The corrosion of some steels in synthetic river waters, in heat transfer conditions 461–467

P. BALTĂ and C. SPURCACIU, Study of the formation and homogenization processes of the melts by means of EMF measurements 469–480

COMPTES RENDUS 481–482

ORSZÁGOS MŰSZAKI KÖNYVTÁR ÉS DOKUMENTÁCIÓS KÖZPONT 1883

Revue Roumaine de Chimie, **21**, *3*, 321–325 (1976)

MOLECULAR INTERACTIONS IN ANISIDINE ISOMERS. I

DIPOLE MOMENTS

V. E. SAHINI and LILIANA TELEA

Institute of Physical Chemistry, Str. Galaţi 31, Bucharest, Romania

Received September 13, 1975

Dipole moments in ground state prove the existence of an appreciable amount of weak intramolecular hydrogen bonds in *ortho*-anisidine, which becomes stronger in the first excited state. "Active" solvents may partly destroy the chelate forming specific association with anisidine.

INTRODUCTION

Mesomeric effects require both methoxy- and phenyl-radicals to be coplanar in anisidine, two configurations being possible for *ortho*- and *meta*-isomers [1]:

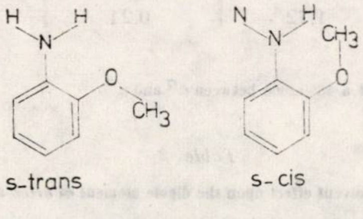

Fig. 1. — Hydrogen bond in *ortho*-*anisidine*.

The intramolecular hydrogen bond, which is formed in *s-trans ortho*-anisidine between the electron repulsive substituents, is weak. In contradiction with I. R. data in CCl_4,[2] dipole moment measurements, carried out in decaline,[3] indicate the presence of an appreciable amount of *s-trans ortho*-anisidine, the break of intramolecular bond becoming quite obvious at 140° only.

The aim of the present paper is to study the formation of the intramolecular hydrogen bond taking into account the competitive process of intermolecular association, namely the solvent effect upon the dipole moment and the electronic spectrum.

---

[1] H. Lumbroso and G. Palamidessi, *Bull. Soc. chim. France*, **1965**, 3150.

[2] P. J. Krueger, *Tetrahedron*, **26**, 4753 (1970); *Canad. J. Chem.*, **41**, 363 (1963).

[3] A. E. Lutskii and V. A. Grajan, *Zhur. strukt. Khim.*, **8**, 490 (1967).

EXPERIMENTAL

B.D.H. anisidine isomers were purified by distillation at low pressure. The solvents, spectrochemical grade, were dried and distilled before use.[4] The dipole moments have been measured at 25° using the Guggenheim method.[5] Spectra have been recorded by means of a UNICAM SP 800 spectrophotometer in 9 aprotic solvents: *n*-hexane, *n*-heptane, isooctans, cyclohexane, methylcyclohexane, benzene, chlorobenzene, carbon tetrachloride, dioxane. Solvent shift plots have been drawn using the least square method.

RESULTS AND DISCUSSION

The dipole moments data obtained for the ground state of anisidine isomers are listed in tables 1 and 2.

Table 1

Ground state dipole moments

Compound	Experimental dipole moment in C_6H_6 (D)	$\Delta\mu$* (D)	Calculated dipole moment *cis* (D)		*trans*
aniline	1.48–1.53[6,7]	0.25–0.28[6,7]	—	1.55 **	—
o-anisidine	1.42	0.20	3	—	1.28
m-anisidine	1.84	—	2.28	—	1.54
p-anisidine	1.72	0.24	—	1.79	—

* $\Delta\mu = \mu^{\text{dioxane}} - \mu^{\text{benzene}}$

** calculated taking into account a 43° angle between μ^{σ} and μ^{π}.

Table 2

The solvent effect upon the dipole moment of *ortho*-anisidine

Solvent	*n*-hexane	CCl_4	C_6H_6	dioxane
μ^{exp} (D)	1.35	1.39	1.42	1.62
$\varkappa_H^*$	0.70	0.68	0.67	0.55

* calculated according to the relation:[8]

$$\mu^2_{\text{exp.}} = \chi_H \mu^2_{trans} + (1 - \chi_H)\,\mu^2_{cis}$$

---

[4] A. Weissberger and A. Proskauer, "Technique of Organic Chemistry (Organic Solvents)", vol. 7, Interscience, New York, 1965, p. 308–413.

[5] E. A. Guggenheim, *Trans. Faraday Soc.*, **45**, 74 (1949).

[6] A. E. Lutskii and B. V. Kondratiev, *Zhur. fiz. Khim.*, **33**, 2017 (1959).

[7] C. W. N. Cumper and A. Singleton, *J. Chem. Soc. B*, **1967**, 1096.

[8] N. Vatanabe, S. Mizushima and Y. Morino, *Sci. Papers, Inst. Phys. Chem. Res. (Tokyo)*, **39**, 401 (1942).

The intramolecular hydrogen bond leads to a significant decrease in the dipole moment of the *ortho* isomer as compared with that of the *para* isomer. The values of the dipole moments obtained on the basis of the π and σ moments of the molecule (the former calculated by the H.M.O. method,[9] the latter using the σ bond moments [10] and compared with the experimental ones, indicate for the *ortho*-anisidine the presence of an appreciable quantity of *s-trans* conformer in the molecule. For the *meta* isomer, a similar evaluation of the dipole moment shows that both the *trans* and *cis* forms have an almost equal share in the molecule. The quantity of chelated isomer in the *ortho*-anisidine molecule decreases when instead of an "inert" solvent (*n*-hexane), an "active" solvent (dioxane) is used. The positive dioxane effect of *ortho*-anisidine, comparable with that of the *para* isomer, is an evidence of the instability of the five-membered cycle formed by the intramolecular hydrogen bond.

The intramolecular charge transfer between the substituent and the aromatic hydrocarbon represents the most important influence to which the dipole moments and the electronic spectra of aromatic derivatives are submitted. In general, electronic migration is larger in an excited state and the differences between the dipole moments in the excited and ground states ($\Delta\vec{\mu}$) are mainly an effect of this growth.[11] In the first excited state the charge density and the double bond order of the anisidine isomers show an increase in the charge transfer from the nitrogen towards the cycle (table 3) and the hydrogen bond is expected to strengthen.

Table 3

Variation of charge density on the aminic nitrogen in the electronic transition

Isomer	q_N		p_{CN}	
	Ground state	First excited state	Ground state	First excited state
o-anisidine*	1.904	1.654	0.307	0.513
m-anisidine	1.917	1.747	0.291	0.446
p-anisidine	1.922	1.747	0.280	0.467

* chelated isomer

---

[9] A. Streitwieser Jr., "M. O. Theory for Organic Chemists", Wiley, New York, 1962, p. 135.

[10] C. P. Smith, *J. Chem. Phys.*, **4,** 209 (1937).

[11] N. Mataga, *Bull. Chem. Soc. Japan*, **36,** 654 (1963).

As a consequence to the increase of intramolecular interaction in excited state, the solvent induced band shifts in electronic spectra of *ortho*-anisidine are much diminished as compared to the other two isomers. For a polar solute molecule, the energy of the absorption maximum varies linearly with the dielectric constant of the solvent.[12,13]

We have used the following relation :[14]

$$Y(ij) = \frac{2D + (\Delta\vec{\mu})^2}{h\,c\,a_0^3} + \frac{2(\Delta\vec{\mu}\cdot\vec{\mu}_g)}{h\,c\,a_0^3}\,X(ij)$$

where

$$Y(ij) = \frac{\tilde{\nu}_j - \tilde{\nu}_i}{Q_i - Q_j} \qquad X(ij) = \frac{S_i - S_j}{Q_i - Q_j}$$

$$Q_i = \frac{n_i^2 - 1}{2n_i^2 + 1} \qquad S_i = \frac{\varepsilon_i - 1}{2\,\varepsilon_i + 1}$$

“n_i” and “ε_i” being the refractive index and the dielectric constant of the “i^{th}” solvent respectively, a_0 the radius of the spherical cavity occupied by the molecule (with the ground state permanent dipole moment $\mu_g \neq 0$) calculated from the Onsanger's classical model, the factor D is determined by the solute but its detailed expression needs not be taken into account.[14]

Such plots of $\tilde{\nu}$ against $f(\varepsilon)$ are shown in fig. 2 for the three isomeric anisidines. For the aprotic solvents, selected in order to avoid specific interactions as much as possible, there is a linear dependence of the absorption maximum on the dielectric constant of the solvent for the three anisidine isomers. The positive value of the slope shows an increase of the dipole moment in excited state, much diminished for the *ortho* isomer, where the short distance between the substituents produces an increased intramolecular interaction.

A great deviation from the above mentioned linearity appears in the case of dioxane, giving a further proof of the specific anisidine-dioxane interaction. The intramolecular association with dioxane can be explained taking into account :

a) the change in the electronic density at the nitrogen during the electronic transition leading to a different proton-donor ability of the NH_2 group, and

---

[12] M. B. Ledger and P. Suppan, *Spectrochim. Acta*, **23A**, 641 (1967) ; **30A**, 1939 (1974).

[13] P. Suppan, *J. Chem. Soc. A*, **1968**, 3125.

[14] G. O. Varma and E. J. Groenen, *Rec. Trav. chim.*, **91**, 296 (1972).

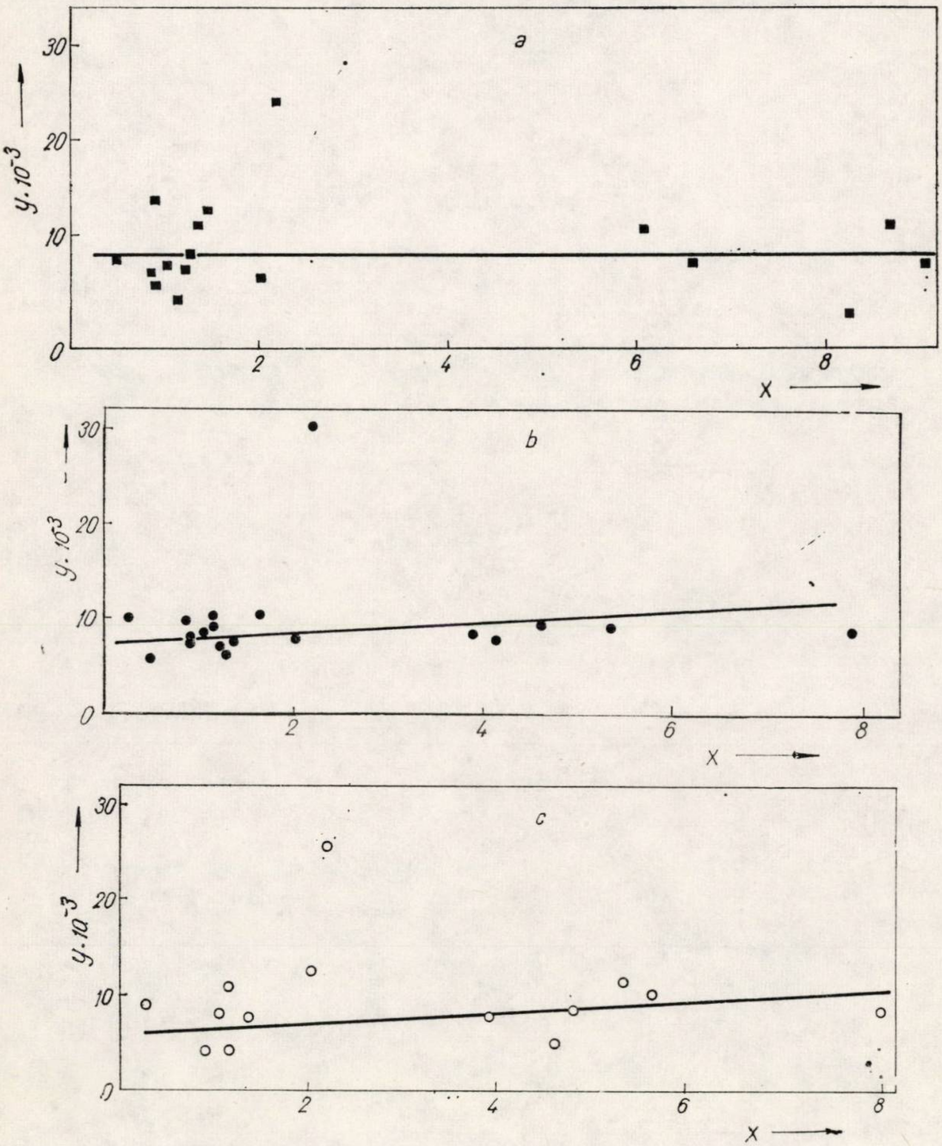

Fig. 2. — Solvent shifts for the first band of anisidine: *a*, *ortho*-anisidine; *b*, *meta*-anisidine; *c*, *para*-anisidine.

b) the increase of the nitrogen lone pair interaction with the aromatic π electrons (i.e. the decrease of N electronegativity) when intermolecular hydrogen bonds are formed.

Revue Roumaine de Chimie, 21, 3, 327–331 (1976)

THE CARBON-CARBON STRETCHING FREQUENCY IN ETHANE, ETHANE-d_6 AND ETHANE-t_6

RODICA BELDIE, A. BUTUCELEA and V. E. SAHINI
Center of Physical Chemistry, Str. Galaţi 31, Bucharest 9, Romania

Received August 7, 1975

An explanation of the observed magnitude inversion of the $\nu_1(A_{1g})$ and $\nu_3(A_{1g})$ vibrational frequencies in passing from ethane to hexahaloethanes is given, based on a study of ethane, ethane-d_6 and ethane-t_6.

The vibrational spectra of ethane-type compounds show that whereas for C_2H_6 the C–C stretching frequency ν_1 is smaller than the CH_3 deformation frequency ν_3, for C_2F_6 and the other hexahaloethanes, C_2Cl_6 and C_2Br_6, the reverse is true. For C_2D_6, a normal coordinate analysis[1] has revealed that both A_{1g} frequencies ν_1 and ν_3 have a predominant C–C stretching character. Since C_2D_6 lies between C_2H_6 and C_2F_6 in so far as the atom mass attached to carbon is concerned, we supposed the mentioned inversion to be mainly a mass effect.

A good testing molecule, placed in this respect between C_2D_6 and C_2F_6, would be hexatritiumethane (C_2T_6). For this compound, the vibrational frequencies necessary to carry out a normal coordinate treatment are, to our knowledge, not known. However, using force constant values obtained[1] for its isotopic molecules, C_2H_6 and C_2D_6, we were able to obtain the calculated frequencies of this compound and the corresponding assignments (table 1).

The ν_1 frequency value of C_2T_6, calculated by this method is larger than ν_3, as for C_2F_6, i.e. the inversion must have taken place somewhere between C_2H_6 and C_2T_6. Taking advantage of the fact that any hypothetical C_2Y_6 molecule having the Y atomic mass m_Y between 1 and 3 a.m.u. could be regarded as an isotopic molecule of C_2H_6, we chose four such molecules with $m_Y = 1.33$, 1.57, 1.83 and 2.5 a.m.u. Using the same method as for C_2T_6 (the programs BGLZ and LSMB written by Shimanouchi *et al.*[2]), we carried out the normal coordinate analyses for these hypothetical molecules. The ν_1 and ν_3 frequencies calculated for these

---

[1] R. Beldie, A. Butucelea, V. E. Sahini and M. K. DeArmond, *Rev. Roumaine Chim.*, to be published.

[2] T. Shimanouchi, "Normal Coordinate Treatment of Polyatomic Molecules", Tokyo University, Tokyo, 1968.

C_2Y_6 molecules are given in table 2, together with the potential energy distributions among symmetry coordinates (PES) and among force constants (PEF) as defined in reference 2.

Table 1

Calculated vibrational frequencies of ethane-t_6 (cm^{-1})

Species	Mode	Frequency	Assignment^a
A_{1g}	ν_1	1116	νCC
	ν_2	1724	$\nu_s CT_3$
	ν_3	890	$\delta_s CT_3$
A_{1u}	ν_4	168	τCT_3CT_3
A_{2u}	ν_5	1751	$\nu_s CT_3$
	ν_6	927	$\delta_s CT_3$
E_g	ν_7	1902	$\nu_a CT_3$
	ν_8	880	$\delta_a CT_3$
	ν_9	749	ρCCT_3
E_u	ν_{10}	1905	$\nu_a CT_3$
	ν_{11}	884	$\delta_a CT_3$
	ν_{12}	552	ρCCT_3

a Abbreviations: νCC = C–C stretching; $\nu_{s(a)}CT_3$ = symmetric (asymmetric) CT_3 stretching; $\delta_{s(a)}CT_3$ = symmetric (asymmetric) CT_3 deformation; τCT_3CT_3 = torsion; ρ CCT_3 = C–CT_3 rocking.

Table 2

Assignment of ν_1 and ν_3 frequencies based on the potential energy distributions (PES and PEF)^{1,2} for C_2Y_6 molecules

Mode	m_Y	Y	Calcd. freq. (cm^{-1})	PES^a				PEF (%)^b					
				S_1	S_2	S_3	S'_3	K_{CC}	K_{CY}	H_{CCY}	H_{YCY}	F_{CY}	F_{YY}
ν_1	1.0	H	1003	*1.0*	0.0	0.0	0.0	54	1	1	1	43	0
	1.33	—	949	*1.0*	0.0	0.1	0.1	40	1	6	6	46	1
	1.57	—	903	*1.0*	0.0	0.3	0.2	31	1	10	11	46	1
	1.83	—	1173	*1.0*	0.0	0.6	0.4	41	0	24	26	7	2
	2.0	D	1161	*1.0*	0.0	0.5	0.4	44	0	22	24	8	2
	2.5	—	1134	*1.0*	0.0	0.4	0.3	49	0	18	20	11	2
	3.0	T	1116	*1.0*	0.0	0.3	0.2	51	1	16	17	13	2
	18.99	F	1417	*1.0*	0.1	0.1	0.1	62	10	1	8	17	3
ν_3	1.0	H	1359	0.3	0.0	*1.0*	0.7	11	0	36	40	8	3
	1.33	—	1244	0.8	0.0	*1.0*	0.7	25	0	32	35	5	3
	1.57	—	1201	*1.0*	0.0	0.8	0.6	34	0	28	30	6	2
	1.83	—	855	*1.0*	0.0	0.6	0.4	24	1	14	15	45	1
	2.0	D	825	*1.0*	0.0	0.7	0.5	21	1	15	17	44	1
	2.5	—	750	0.8	0.0	*1.0*	0.7	15	1	19	21	42	2
	3.0	T	690	0.6	0.0	*1.0*	0.7	12	1	21	23	40	2
	18.99	F	570	0.0	0.0	0.7	*1.0*	0	1	1	30	47	21

a Potential energy distribution among internal symmetry coordinates S_i for modes of A_{1g} species; S_1 = C–C stretching; $S_2 = CY_3$ symmetric stretching; S_3, S'_3 = CY_3 symmetric deformation.

b Potential energy distribution for Urey-Bradley force constants.

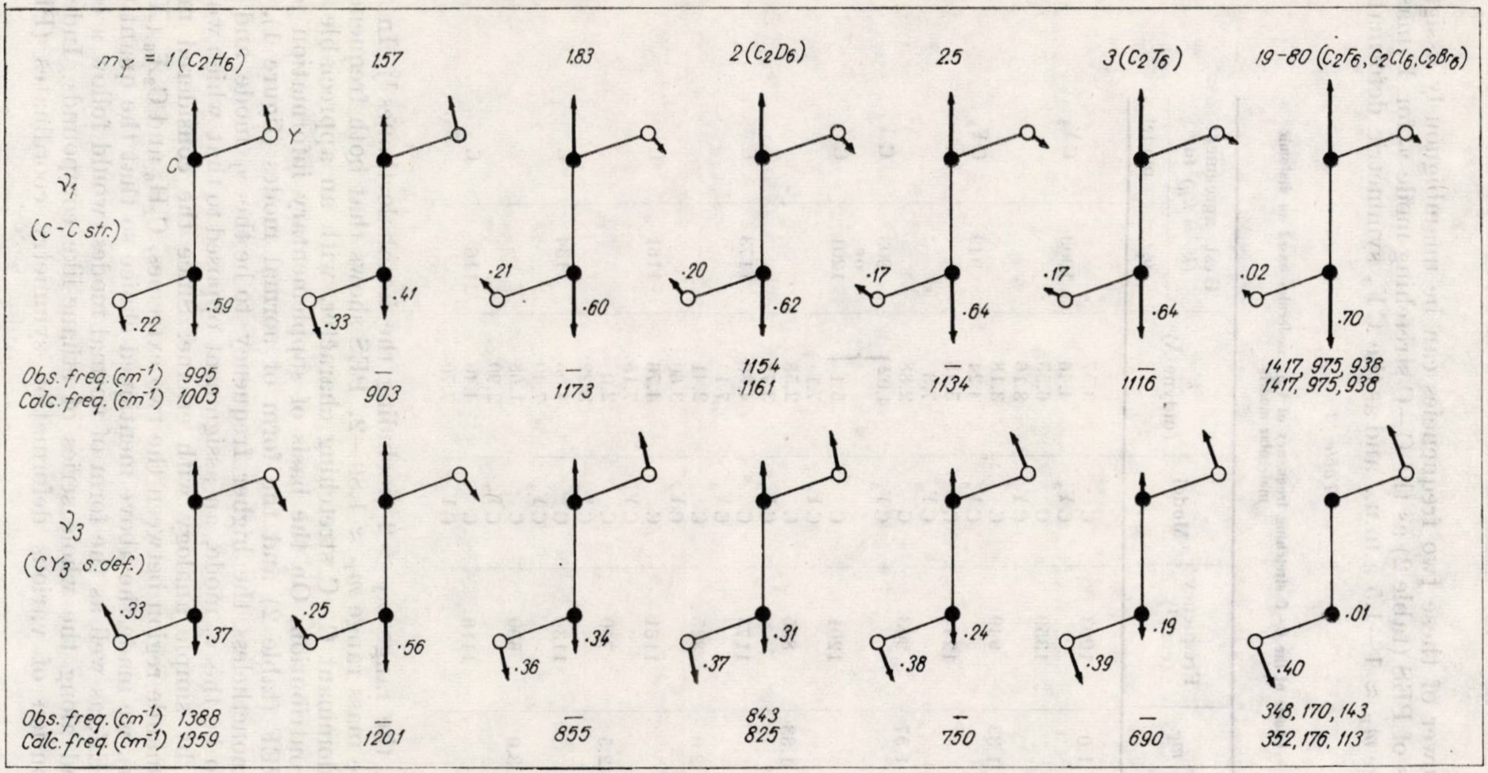
m_Y = 1 (C_2H_6)
1.57
1.83
2 (C_2D_6)
2.5
3 (C_2T_6)
19-80 (C_2F_6, C_2Cl_6, C_2Br_6)
ν_1
(C-C str.)
C
Y
.22 .59
.33 .41
.21 .60
.20 .62
.17 .64
.17 .64
.02 .70
Obs. freq. (cm^{-1}) 995 — — 1154 — — 1417, 975, 938
Calc. freq. (cm^{-1}) 1003 903 1173 1161 1134 1116 1417, 975, 938
ν_3
(CY_3 s.def.)
.33 .37
.25 .56
.36 .34
.37 .31
.38 .24
.39 .19
.40 .01
Obs. freq. (cm^{-1}) 1388 — — 843 — — 348, 170, 143
Calc. freq. (cm^{-1}) 1359 1201 855 825 750 690 352, 176, 113

Fig. 1. — Form of the A_{1g} normal modes ν_1 and ν_3 of C_2Y_6 staggered molecules. The arrows represent the relative nuclear displacements, with values written alongside for various real or hypothetical molecules with different Y atom mass m_Y. For the sake of simplicity a single plane containing the C—C bond and two opposite C—Y bonds is drawn.

The lower of these two frequencies can be unambiguously assigned on the basis of PES (table 2) as the C—C stretching mode ν_1 for Y masses in the range $m_Y \approx 1-1.5$ a.m.u., and as the CY_3 symmetric deformation

Table 3

Choice of the C—C stretching frequency of C_2Y_6 molecules based on diatomic molecular models

m_Y	Frequency (cm^{-1})	Model	k' (mdyne/Å)	Best agreement ($k' = k_R$) for	
				ν_1	model
1.0	1003	C	3.57		
		CY_3	4.46	1003	CY_3
	1359	C	6.53		
		CY_3	8.16		
1.33	949	C	3.18		
		CY_3	4.24	949	CY_3
	1244	C	5.48		
		CY_3	7.3		
1.57	903	C	2.88		
		CY_3	4.02 }	903	CY_3
				or	
	1201	C	5.1 }	1201	C
		CY_3	7.1		
1.83	855	C	2.58		
		CY_3	3.78		
	1173	C	4.86	1173	C
		CY_3	7.1		
2.0	825	C	2.41		
		CY_3	3.60		
	1161	C	4.76	1161	C
		CY_3	7.15		
2.5	750	C	2.0		
		CY_3	3.22		
	1134	C	4.55	1134	C
		CY_3	7.40		
3.0	690	C	1.68		
		CY_3	2.90		
	1116	C	4.40	1116	C
		CY_3	7.70		

mode ν_3 in the range $m_Y > 2$ (including the hexahaloethanes [1]). In the intermediate mass range $m_Y \approx 1.80-2$, PES shows that both frequencies have a predominant C—C stretching character, with an appreciable deformation contribution. On the basis of supplementary information provided by PEF (table 2) and the form of normal modes (figure 1), we considered nonetheless the higher frequency to be the ν_1 mode and the lower one to be the ν_3 mode, an assignment opposed to that which would be reached by simple analogy with ethane. Since the considered mass region is a middle region between the two extremes, C_2H_6 and C_2X_6 ($X =$ $=$ F, Cl, Br), we made the above mentioned choice so that the quantities PES and PEF, as well as the form of normal modes, would follow a consistent trend along the whole series of ethane-like compounds. Indeed, the contribution of various deformation symmetry coordinates (PES) or C—C stretching and angle bending force constants (PEF) to the ν_1 and ν_3 modes show either a maximum or a minimum around $m_Y = 1.80$ a.m.u., situated in this middle mass region.

The main trend in the form of the ν_1 and ν_3 modes is a drastic decrease of the vibration amplitude of atom Y or C, respectively (figure 1), reaching zero values for hexahaloethanes. Thus, if for C_2H_6 the C—C stretching is the result of the relative motion of the two $-CH_3$ groups, for hexahaloethanes it is due to the high-amplitude relative motion of the carbon atoms only. Therefore, two diatomic molecular models would have to be considered in order to estimate the C—C stretching force constant k' from the frequency chosen as ν_1, using the classic relation $k' = 4\pi^2c^2\ \nu^2\mu$ applied to a diatomic model with the reduced mass μ : (*i*) a *CY_3 model* with $\mu = (m_C + 3m_Y)/2$, and (*ii*) a *C model* with $\mu = m_C/2$. The agreement between the k' value thus obtained and the GVFF C—C stretching force constant k_R obtained from the normal coordinate analysis of C_2H_6, $k_R = 4.56$ mdyne/Å [1,3] could be used as a criterion for the right assignment of one of the two A_{1g} frequencies under discussion to the ν_1 C—C stretching mode. In table 3 the k' values obtained for both frequencies with the two models are listed. The last column indicates, for each molecule, the frequency and the model which led to the best fit between k' and k_R. The assignment given in table 2 is thus confirmed, i.e. that for $m_Y < 1.80$ the lower, and for $m_Y \geqslant 1.80$ the higher, of the two A_{1g} frequencies must be assigned to the C—C stretching mode ν_1.

---

[3] I. Nakagawa and T. Shimanouchi, *J. Mol. Spectroscopy*, **39**, 255 (1971).

Revue Roumaine de Chimie, **21**, *3*, 333–341 (1976)

THERMODYNAMIC PROPERTIES OF ELECTROLYTE SOLUTIONS. V

DIFFERENTIAL CRYOSCOPY IN $NaCl+CuCl_2+H_2O$ AND $KCl+CuCl_2+H_2O$ TERNARY SYSTEMS AND IN ASSOCIATED BINARIES

RODICA VÎLCU*, EDDA CONSTANTZA DE MADRIÑAN** and FLORICA IRINEI*
* Institute of Chemistry, Department of Physical Chemistry, Bucharest, Romania
** "Carton de Columbia" Paper and Pulp Works Cali-Columbia

Received December 26, 1974

The present paper enlarges on the conclusions reached in the study of halogen solutions of alkali metals and mixtures of uni-bivalent electrolytes, and at the same time, contributes to the investigation of systems with absorption spectrometry in the ultraviolet and visible range. This contribution is aimed both at confirming the results yielded by the above methods and at carrying on an in-depth study of the nature of the effects of ionic interaction alteration in ternary systems as against associated binaries expressed in the values of solutions additivity deviated thermodynamic magnitudes.

INTRODUCTION

Assessing the nature of ionic interactions in electrolyte solutions just as establishing their thermodynamic particularities, is a basic element in defining these systems. Previous works [1] report on the thermodynamic properties of some electrolyte ternary aqueous solutions obtained by associating cryoscopic, calorimetric and refractometric measurements with a view to obtaining as complete as possible information on ionic and ion-solvent interactions.

Such interactions were expressed in excess thermodynamic magnitudes and activity coefficients closely related to systems aditivity deviation functions for uni-univalent electrolyte mixtures with common anion.

Taking up again some of the formulations of the best represented deviated magnitudes in electrolyte solutions, these could be expressed through a deviation function δ as follows:

$$\log(\gamma_2)_{23} = \log\gamma_2 - \alpha_{23}\, m_3 \qquad (1)$$

$$\log(\gamma_3)_{23} = \log\gamma_3 - \alpha_{32}\, m_2$$

---

[1] R. Vîlcu and F. Irinei, *Bull. Soc. chim. belges*, **81**, 479 (1972).

where $(\gamma_2)_{23}$ and $(\delta_3)_{23}$ are the activity coefficient of electrolytes 2 and 3, respectively in the ternary system, γ_2 and γ_3 the activity coefficients of electrolytes in the binary systems.

Harned's coefficients are defined by the relations :

$$\alpha_{23} = \frac{\log \delta}{2m_2\, m_3} + \frac{\Phi_3 - \Phi_2}{2.303\,(m_2 + m_3)}$$

$$\alpha_{32} = \frac{\log \delta}{2m_2\, m_3} - \frac{\Phi_3 - \Phi_2}{2.303\,(m_2 + m_3)} \tag{2}$$

where Φ is the osmotic coefficient of the solvent in the respective electrolyte solutions.

Gibbs free excess energy gives the electrolyte mixture solutions deviation from ideality by the relation

$$G^E = -\,2.303\ RT \log\, \delta \tag{3}$$

A unitary thermodynamic treatment of the electrolyte mixture justifies the form of Lewis and Randall's equations for the activity coefficients calculated from the coligative properties of the systems

$$\log \gamma_{23} = \log\,(\gamma_{23})_0 - \int_{m_0}^{m} j\cdot \mathrm{d} \log m - \frac{j - j_0}{2.303} + \frac{0.00025}{\nu} \int_{\vartheta(m_0)}^{\vartheta(m)} \frac{\vartheta}{m}\, \mathrm{d}\vartheta \tag{4}$$

EXPERIMENTAL RESULTS

The activity coefficients calculated from cryoscopic data for the $NaCl + H_2O$; $KCl + H_2O$ and $CuCl_2 + H_2O$ binary systems studied are given in tables 1, 2 and 3.

Table 1

Thermodynamic magnitudes of $NaCl+H_2O$ system components as yiel ded by cryoscopic data

m	ϑ	j	Φ	a_1	$\int_{m_0}^{m} \frac{j}{m}\, \mathrm{d}m$	$\int_{\vartheta_0}^{\vartheta} \frac{\vartheta}{m}\, \mathrm{d}\vartheta$	γ_2
0.5000	1.6936	0.0885	0.9115	0.9837	0.1949	0.6001	0.6378
1.0000	3.3960	0.0861	0.9138	0.9676	0.0657	5.7738	0.5996
1.5000	5.1399	0.0778	0.9221	0.9512	0.0345	5.9494	0.5852
2.0000	7.0311	0.0539	0.9460	0.9339	0.0197	6.5642	0.5887
2.5000	9.0000	0.0312	0.9687	0.9160	0.0098	7.0049	0.5975
3.0000	11.2400	0.0082	1.0082	0.8961	0.0024	8.2283	0.6216

$m_0 = 0.1000$
${}_0 = 0.3419$
$\log(\gamma_2)_0 = -\,0.1074$

Table 2

Thermodynamic magnitudes of $KCl + H_2O$ system components as yielded by cryoscopic data

m	ϑ	j	Φ	a_1	$\int_{m_0}^{m} \frac{j}{m}\,dm$	$\int_{\vartheta_0}^{\vartheta} \frac{\vartheta}{m}\,d\vartheta$	γ_2
0.5000	1.6469	0.1136	0.8863	0.9842	0.2194	4.3717	0.6028
1.0000	3.2500	0.1254	0.8745	0.9689	0.0881	5.2451	0.5463
1.5000	4.8499	0.1298	0.8701	0.9539	0.05299	5.1866	0.5167
2.0000	6.5715	0.1157	0.8842	0.9382	0.03612	5.6113	0.5061
2.5000	8.3189	0.1050	0.8949	0.9223	0.02497	5.7601	0.4998
3.0000	10.0742	0.0963	0.9036	0.9065	0.01853	5.8823	0.4957

$m_0 = 0.1000$
$\vartheta_0 = 0.3393$
$\log(\gamma_2)_0 = 0.1135$

Table 3

Thermodynamic magnitudes of $CuCl_2 + H_2O$ system components as yielded by cryoscopic data

m	ϑ	j	Φ	a_1	$\int_{m_0}^{m} \frac{j}{m}\,dm$	$\int_{0} \frac{\vartheta}{m}\,d\vartheta$	γ_2
0.5000	2.4850	0.1083	0.8916	0.9761	0.3533	9.7477	0.3760
1.0000	5.6900	0.0208	1.0208	0.9462	0.0489	17.0826	0.4087
1.5000	8.9266	0.0676	1.0676	0.9168	0.0164	18.8387	0.4370
2.0000	12.4832	0.1197	1.1197	0.8853	0.0262	21.6829	0.4746
2.5000	16.0832	0.1541	1.1541	0.8546	0.0304	22.8149	0.5086
3.0000	19.8332	0.1860	1.1860	0.8235	0.0309	24.4582	0.5441

$m_0 = 0.1000$
$\vartheta_0 = 0.4710$
$\log(\gamma_2)_0 = -0.2924$

From extreme dilutions we assumed the limit values m_0 ϑ_0 and γ_0 given by Scatchard and Prentiss [2] for the $NaCl + H_2O$; $KCl + H_2O$ systems and Robinson and Stokes[3] for the $CuCl_2 + H_2O$ system.

Variation with the concentration of NaCl, KCl, $CuCl_2$ activity coefficients in binary aqueous solutions at the solution freezing temperature is shown in fig. 1.

Fig. 2 shows the activity coefficients of the solvent in the three binary systems in terms of concentration.

The values of the activity coefficients specific to the solvent in the $NaCl + H_2O$ and $CuCl_2 + H_2O$ systems are subunitary almost over the whole range of concentrations, a fact that places (Na^+) and (Cu^{2+}) ions into the same hydration group. On the other hand, the presence of K^+

---

[2] G. Scatchard and S. S. Prantiss, *J. Amer. Chem. Soc.*, **55**, 4855 (1933).

[3] R. A. Robinson and R. H. Stokes, *Trans. Faraday Soc.*, **36**, 733 (1940).

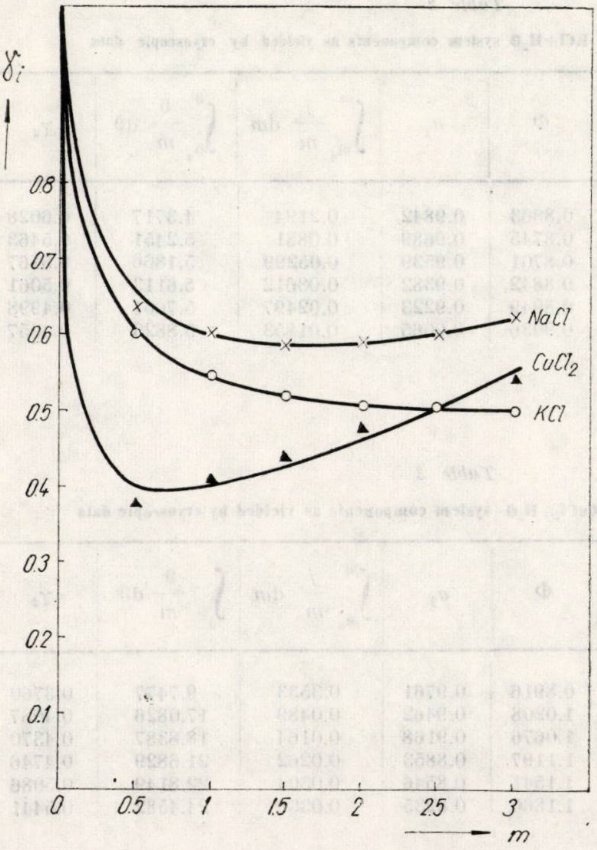

Fig. 1.— Variation of electrolyte activity coefficients in binary solutions.

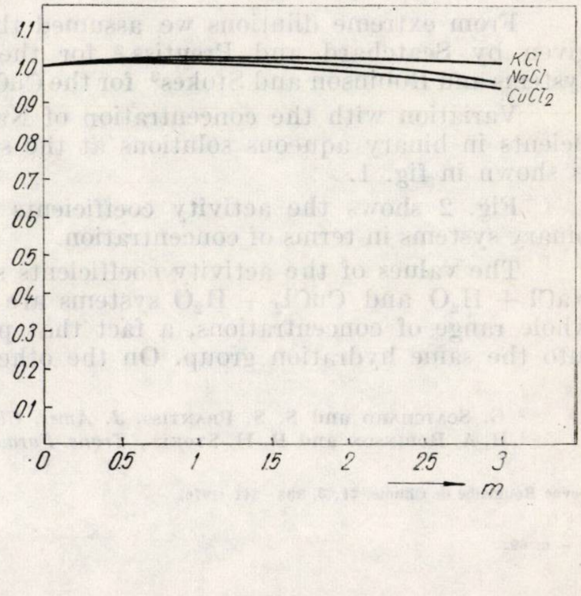

Fig. 2. — Variation of solvent activity coefficients in binary solutions.

ion results in positive values for the activity coefficient of the solvent in the $KCl + H_2O$ system. Hence, Na^+ and Cu^{2+} ions behave similarly and this fully agrees with the conclusions reached with regard to the variation with the concentration of soluted electrolyte activity coefficients.

Tables 4 and 5 indicate the thermodynamic magnitudes specific to the components of the two $NaCl + CuCl_2 + H_2O$ and $KCl + CuCl_2 + H_2O$ ternary systems.

Table 4

Thermodynamic magnitudes of $(NaCl+CuCl_2)+H_2O$ systems as yielded by cryoscopic data

m	ϑ	j	Φ	$\int_{m_0}^{m} \frac{j}{m} dm$	$\int_{\vartheta_0}^{\vartheta} \frac{\vartheta}{m} d\vartheta$	γ_{23}
0.5000	2.2433	0.0341	0.9659	0.2484	7.8707	0.54820
1.0000	4.4533	0.0412	0.9587	0.0273	9.8785	0.5308
1.5000	6.8600	0.0154	0.9845	0.0128	10.8622	0.5391
2.0000	9.5166	0.0244	1.0244	0.0005	12.3952	0.5628
2.5000	12.3833	0.0664	1.0664	0.0097	13.9201	0.5946
3.0000	15.2833	0.0967	1.0967	0.0147	14.5692	0.6241

$m_0 = 0.1000$
$\vartheta_0 = 0.4099$
$\log(\gamma_2)_0 = -0.1901$

Table 5

Thermodynamic magnitudes of $(KCl+CuCl_2)+H_2O$ system compounds as yielded by cryoscopic data

m	ϑ	j	Φ	$\int_{m_0}^{m} \frac{j}{m} dm$	$\int_{\vartheta_0}^{\vartheta} \frac{\vartheta}{m} d\vartheta$	γ_{23}
0.5000	1.9533	0.1589	0.8410	0.3056	6.1719	0.4546
1.0000	4.0533	0.1274	0.8726	0.1113	8.3578	0.4206
1.5000	6.2866	0.0977	0.9023	0.0481	9.2060	0.4137
2.0000	8.5166	0.0832	0.9167	0.0267	9.4210	0.4096
2.5000	10.9833	0.0542	0.9458	0.0158	10.6705	0.4161
3.0000	13.4333	0.0360	0.9639	0.0084	10.8671	0.4212

$m_0 = 0.1000$
$\vartheta_0 = 0.4087$
$\log(\gamma_{23})_0 = -0.1938$

Figure 3 illustrates the variation with concentration of the activity coefficients of $NaCl + CuCl_2$ and, respectively, $KCl + CuCl_2$ equimolar mixtures.

The values of the electrolyte mixtures activity coefficients differ widely from the activity calculated values represented by discontinuous plots. The difference grows with the concentration being much higher than in uni-univalent electrolyte mixtures.

Harned's coefficients calculated from cryoscopic data by means of relation (2) are listed in table 6.

Table 6

Harned coefficients of ternary system components

m	System			
	$NaCl + CuCl_2 + H_2O$		$KCl + CuCl_2 + H_2O$	
	α_{23}	α_{32}	α_{23}	α_{32}
0.5000	−0.2045	−0.1872	0.0826	0.0780
1.0000	−0.0140	−0.1059	0.1647	0.0377
1.5000	0.0262	−0.1002	0.1659	−0.0056
2.0000	0.048819	−0.1027	0.1802	−0.02434
2.5000	0.05423	−0.1068	0.1793	−0.0458
3.0000	0.0567	−0.0976	0.1833	−0.0619

Table 7 and figure 4 give the values of electrolyte individual activity coefficients in the two ternary systems.

Table 7

Individual activity coefficients of mixture electrolytes

m	System			
	$NaCl + CuCl_2 + H_2O$		$KCl + CuCl_2 + H_2O$	
	$(\gamma_2)_{23}$	$(\gamma_3)_{23}$	$(\gamma_2)_{23}$	$(\gamma_3)_{23}$
0.5000	0.7212	0.4169	0.5728	3.3601
1.0000	0.6096	0.4626	0.4523	0.3914
1.5000	0.5759	0.5009	0.4075	0.4207
2.0000	0.5747	0.5510	0.3342	0.5266
2.5000	0.5876	0.6018	0.3624	0.4778
3.0000	0.6101	0.6383	0.3657	0.5322

One can notice with non-symmetric electrolyte mixtures that the regularity of electrolyte activity coefficients in a ternary mixture and in the associated binaries is preserved, too.

Table 8 shows the values of Gibbs free excess energy at solution freezing temperatures.

Table 8

Free excess energy of ternary systems

m	$\Delta m G^E$	
	$NaCl - CuCl_2 - H_2O$	$KCl - CuCl_2 - H_2O$
0.5000	30.35	− 12.46
1.0000	37.18	− 62.33
1.5000	50.73	−110.08
2.0000	65.74	−118.80
2.5000	97.95	−250.18
3.0000	108.51	−324.42

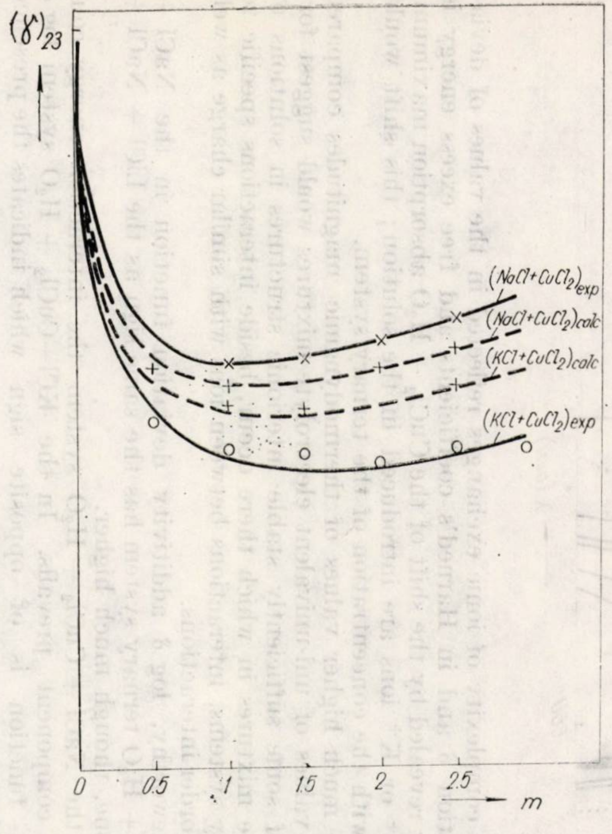

Fig. 3. — Variation with the concentration of electrolyte equimolar mixture activity coefficients.

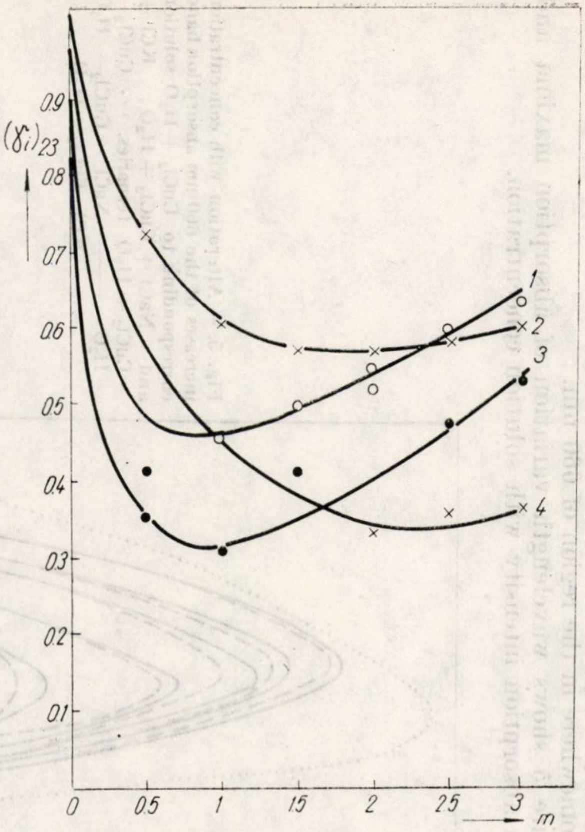

Fig. 4. — Variation of electrolyte individual activity coefficients in the respective ternary systems.
1. $(CuCl_2)_{(NaCl+CuCl_2+H_2O)}$; *2.* $(NaCl)_{(NaCl+CuCl_2+H_2O)}$;
3. $(CuCl_2)_{(KCl+CuCl_2+H_2O)}$ *4.* $(KCl)_{(KCl+CuCl_2+H_2O)}$.

A study by absorption spectroscopy revealed the electronic spectrum of $CuCl_2 + H_2O$; $NaCl + CuCl_2 + H_2O$ and $KCl + CuCl_2 + H_2O$ systems somewhere in the region of 660 nm.

Figure 5 shows wavelength variation of absorption maxima and maximum absorption intensity with solution concentration.

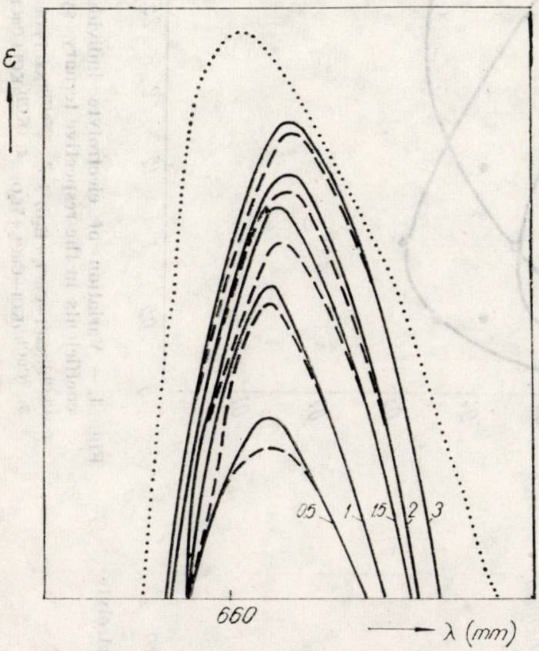

Fig. 5. — Alteration with concentration increases of the 660 nm absorption band corresponding to $CuCl_2 + H_2O$ solution and $NaCl + CuCl_2 + H_2O$; $KCl + CuCl_2 + H_2O$ ternaries. ··· $CuCl_2 - H_2O$ ——— $NaCl - CuCl_2 - H_2O$ – – – $KCl - CuCl_2 - H_2O$

The complexity of ionic exchanges reflected in the values of deviation function δ and in Harned's coefficients and free excess energy is spectrally revealed by the shift of the $CuCl_2 + H_2O$ absorption maximum, when Na^+ or K^+ ions are introduced in the solution; this shift would increase with the concentration of the ternary system.

The much higher values of thermodynamic magnitudes compared to the values of uni-univalent electrolyte mixtures would suggest formation of some sufficiently stable interionic structures in solutions of electrolyte mixtures in which there occur, beside interactions specific to the binary systems, interactions between ions with similar charge as well as higher order interactions.

Noteworthy, log δ additivity deviation function in the $NaCl + CuCl_2 + H_2O$ ternary system has the same sign as the $LiCl + NaCl + H_2O$ one, though much higher.

In the $NaCl + CuCl_2 + H_2O$ system the interaction energy coulumbian component prevails. In the $KCl + CuCl_2 + H_2O$ system log δ deviation function is of opposite sign which indicates the presence of the polarization component.

The strong influence exerted by Cu^{2+} ion on Na^+ and K^+ ions could be also evidenced by Harned's coefficients. Thus, in the presence of $CuCl_2$, both NaCl and KCl record positive Harned coefficients, and their absolute value is much higher than in the $NaCl + KCl + H_2O$ system, where α_{NaCl} is negative and α_{KCl} positive.

The much greater difference between $(\gamma_i)_{23}$ and γ_i in $NaCl + CuCl_2 + H_2O$ and $KCl + CuCl_2 + H_2O$ ternary mixtures as against $NaCl + KCl + H_2O$ indicates the presence of either some complex ions involving higher order ion — ion interactions or alterations of ion-dipole interactions.

Hindman[4] has stated, based on nuclear magnetic resonance measurements, that most of the univalent ions in aqueous solutions disaggregate the structure of water whereas polyvalent ions polarize the molecules of water.

The high values of Gibbs free excess energy emphasize some additional interactions in ternary mixtures against the respective binaries.

Spectroscopic data attest the formation of ionic complexes, i.e. the presence of higher-order interactions.

Concluding, one may say that extending the regularities established for univalent electrolyte solutions to univalent electrolyte mixture solutions leads to some values for characteristic thermodynamic variables, whose significance is correct as has been also proved experimentally.

---

[4] J. C. Hindman, *J. Chem. Phys.*, **36**, 1000 (1962).

Revue Roumaine de Chimie, **21**, *3*, 343–350 (1976)

ACTIVITY COEFFICIENTS AND HYDROGEN BOND ENERGY FROM CALORIMETRIC MEASUREMENTS

RODICA VÎLCU and ZOICA CENUȘE

Chair of Chemical Thermodynamics and Electrochemistry,
Bucharest University, Bd. Republicii 13, Romania

Received July 13, 1974

Mixing enthalpies were measured at 25, 40 and 55° in the isobutyl alcohol-benzene system. The activity coefficients and hydrogen bond energy were calculated using the group solution method.

1. INTRODUCTION

The Gibbs-Helmholz correlation comprises two aspects:

$$\frac{\partial}{\partial T}\left[\frac{G^E}{T}\right]_{P,X} = -\frac{H^E}{T^2} \tag{1}$$

On the one hand, the possibility of estimating from laboriously obtained isothermal liquid-vapour equilibrium at several levels of temperature, i.e. from activity coefficients, hence from Gibbs excess free energy, G^E.

On the other hand, the possibility of estimating activity coefficients from calorimetric measurements of the excess enthalpies readily accessible.

Numerous attempts have been made with remarkable results, in particular for binary hydrocarbon systems. We may quote the works of Fried and Lieberman[1] and Gothard.[2]

For other mixtures, however, which disagree with Scatchard-Hildebrand's theory of regular solutions, the determination of the activity coefficients from excess enthalpies can be achieved proceeding from the hypothesis that caloric excess capacities show a linear variation with temperature

$$\bar{c}_i - c_i^0 = a_i + b_i T \tag{2}$$

where a_i, b_i are not dependent upon the pressure in the field of mean pressures.

---

[1] R. Liebermann and V. Fried, *Ind. Eng. Chem. (Fundamentals)*, **11**, 350 354 (1972).
[2] F. Gothard. *Communication at the Bucharest Polytechnic Institute*, (1970).

Equation (1) may be written as:

$$\frac{\partial}{\partial T}\left[-RT^2\frac{\partial \ln \gamma_i}{\partial T}\right]_{P,X} = \frac{\partial}{\partial T}[\bar{H}_i - H_i^0] = \bar{c}_i - c_i^0 = a_i + b_i T \tag{3}$$

which by integration becomes:

$$\ln \gamma_i = A_1 + \frac{A_2}{T} + A_3 \ln T + A_4 T + \ldots \tag{4}$$

where A_1, A_2 are functions of pressure and composition.

If vapour pressure of the more volatile pure component is chosen as reference state, constants, which do not depend on pressure, may be introduced and relation (4) becomes:

$$\ln \gamma_1 = \sum_{n=1}^{N}\left[D_{n,1} + \frac{D_{n,2}}{T} + D_{n,3}\ln T + \sum_{m=4}^{M} D_{n,m}\, T^{m-3}\right]_{x_2} n+1 \tag{5}$$

$$\ln \gamma_2 = \sum_{n\neq 1}^{N}\left[D_{n,1} + \frac{D_{n,2}}{T} + D_{n,3}\ln T + \sum_{m=4}^{M} D_{n,m}\, T^{m-3}\right]\left[X_2^{n+1} - \left(\frac{n+1}{n}\right)_{x_2}^{n} + \frac{1}{n}\right] \tag{6}$$

Consequently, we are able to evaluate activity coefficients from excess enthalpy measurements.

Furthermore, we can obtain also parameters from Van Laar, Margules, Wilson correlative equations of activity coefficients. These parameters represent the logarithm of the activity coefficients at infinite dilution, γ_i^0 and, consequently, equation (1) may be written:

$$\left[\frac{\partial \ln \gamma_i^0}{\partial T}\right]_{P,x} = -\frac{H_i^{E0}}{RT^2} \tag{7}$$

If we assume a linear variation of the excess enthalpy at infinite dilution, with temperature, then:

$$H_i^{E0} = a_i + b_i T \tag{8}$$

hence

$$\mathrm{d}\ln \gamma_i^0 = -\frac{a_i}{RT^2}\,\mathrm{d}T - \frac{b_i T}{RT^2}\,\mathrm{d}T \tag{9}$$

which by integration becomes:

$$\log \gamma^0_i = \frac{a_i}{2.3\,RT} - \frac{b_i}{R}\log T + c_i \tag{10}$$

where a_i, b_i may be determined from excess enthalpy calorimetric measurements at infinite dilution at two levels of temperature, and where c_i

is an integral constant obtained from a particular value, γ_i^0, hence from an isothermal liquid-vapour equilibrium at a given experimental temperature.

Van Laar, Margules, Wohl, Scatchard-Hamer, Wilson equations, where, the parameters of equation (10) are introduced, contain a number of four constants added to the correlative equations of activity coefficients; a_i and b_i constants, two for every component of the system, are calculated from the variation of the molar excess enthalpies at infinite dilution as a function of temperature by means of equations:

Van Laar $$H^E = \frac{H_1^{E0} \cdot H_2^{E0}}{x_1 H_1^{E0} + x_2 H_2^{E0}} \tag{11}$$

Margules $$H^E = x_1 x_2 [x_1 H_2^{E0} + x_2 H_1^{E0}] \tag{12}$$

Wilson $$H^E = x_1 \left(\frac{x_2 \Lambda_{12}}{x_1 + x_2 \Lambda_{12}}\right)(\lambda_{12} - \lambda_{11}) + x_2 \left(\frac{x_1 \Lambda_{21}}{x_2 + x_1 \Lambda_{21}}\right)(\lambda_{21} - \lambda_{22}) \tag{13}$$

2. EXPERIMENTAL RESULTS AND DISSCUSION

We proposed to calculate the activity coefficients from excess enthalpies and to estimate the hydrogen bond energy.

Measurements at three temperatures were made, at 25, 40 and 55° in a isothermal calorimeter which, in principle, employs mercury to isolate the spaces containing the two separate components.

The measurements of the thermic effects were registered by a Fe-constantan-thermocouple at a scale galvanometer of a 10^{-10} A/mm/m sensibility and which by means of a 21,000 ohms resistance operated as a voltmeter.

To calibrate the calorimeter the 1.4-dioxan-cyclohexane [3] system was used and for the verification of the apparatus the tertiary butyl-alcohol system was employed.[4]

The experimental excess enthalpies are indicated in table 1 and in figure 1 down to an accuracy of ±2%.

Table 2 and figure 2 indicate the values of the excess enthalpies by extrapolating $H^E/x_1 x_2$ as a function of composition.

With particular values of A_{ij}, previously determined at 55 [5] we obtain the following values of the activity coefficients at infinite dilution, by means of equation (10).

---

[3] A. W. Andrews, *J. Chem. Thermodynamics*, **3**, 519 (1971).

[4] K. Sosknowska Kehiaian, *Bull. Acad. polon. sci. Ser. Sci. chim.*, **13**, 649 (1965).

[5] R. Vîlcu şi Z. Cenuşe, *Rev. Roumaine Chim*, **18**, 377 (1973).

To interprete the experimental curves of H^E we use the concept of partial molar magnitude at infinite dilution which gives us information about the hydrogen bond energy and also, about other specific interactions.

Table 1

Experimental excess enthalpies in the isobutyl alcohol-benzene system

	25		40		55	
	x_2	H^E (J/mol)	x_2	H^E (J/mol)	x_2	H^E (J/mol)
1	0.1022	1153.4	0.0939	1260.4	0.0982	1750.5
2	0.2039	1526.7	0.1893	1833.0	0.1967	2240.3
3	0.3052	1513.2	0.2856	1860.4	0.2957	2260.2
4	0.4059	1330.6	0.3838	1800.6	0.3951	2130.4
5	0.5061	1140.0	0.4830	1599.5	0.2949	2025.5
6	0.6059	1053.4	0.5836	1440.2	0.5951	1710.0
7	0.7051	780.5	0.6855	1130.9	0.6957	1485.3
8	0.8039	533.3	0.7889	830.7	0.7967	1110.0
9	0.9022	480.5	0.8937	430.3	0.8981	617.8

Generally, the excess enthalpy of a binary system formed by one associated component and a non-polar one is made up of three contributions :

- the rupture of hydrogen bonds
- dispersion effect
- other specific forces

Assuming these contributions to be independent of each other, we can write

$$H^E = h^E_{HB} + h^E_{\text{disp}} + h^E_{\text{sp}} \tag{14}$$

and if the non-polar component is a saturated hydrocarbon, whose structures is similar to that of the associated component, this equation can be reduced to the simpler form :

$$H^E = h^E_{HB} \tag{15}$$

Table 2

Excess enthalpies values at the infinite dilution

Temperature	25	40	55
$H_1^{E^0}$ (kJ)	7	8.2	9.3
$H_2^{E^0}$ (kJ)	16	17.6	19.5

Table 3

The constants of the isobutyl alcohol-benzene system

Constants	25−55	25	40	55
a_1	−5472			
b_1	24			
a_2	−6124			
b_2	33			
c_1	0.5604			
c_2	0.6229			
A_{12}		0.0735	0.5267	1.0530
A_{21}		0.1001	0.3153	1.3524

Fig. 1. — Experimental excess enthalpies (J/mol) in the isobutyl alcohol-benzene system.

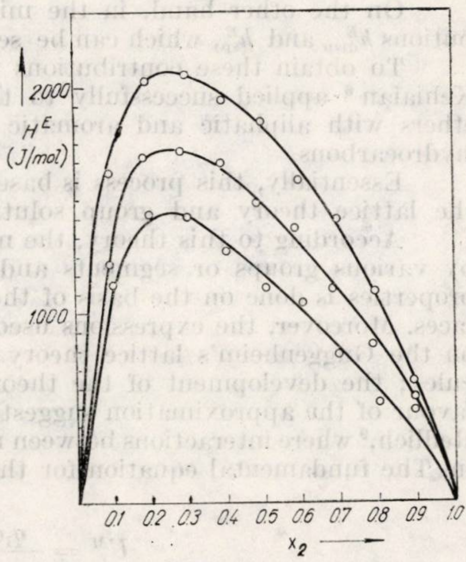

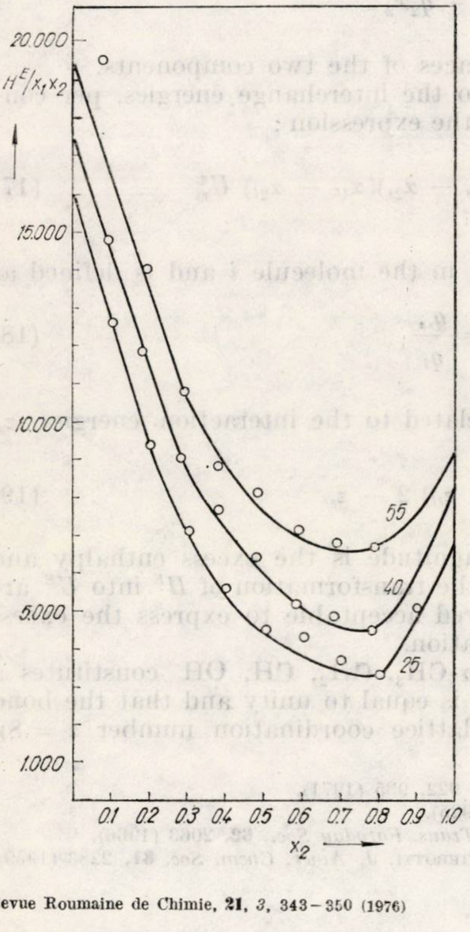

Fig. 2. — Excess enthalpies (kJ/mol) at the infinite dilution.

On the other hand, in the mixtures with benzene we find contributions h^E_{disp} and h^E_{sp}, which can be separated only if we know one of them.

To obtain these contributions we have used the method which H. Kehiaian[6] applied successfully to the study of aliphatic and aromatic ethers with aliphatic and aromatic ethers and aliphatic and aromatic hydrocarbons.

Essentially, this process is based on more or less refined versions of the lattice theory and group solution theory.

According to this theory, the molecules can be considered as formed by various groups or segments and the analysis of the thermodynamic properties is done on the basis of the interactions between molecular surfaces. Moreover, the expressions used in this process are based essentially on the Guggenheim's lattice theory for mixtures of heterogeneous molecules; the development of the theory puts aside the lattice pattern in favour of the approximation suggested by Langmur,[7-8] and developed by Redlich,[9] where interactions between molecular contact surfaces are brought in. The fundamental equation for this treatment is:

$$U_v^M = \frac{q_1 q_2 x_1 x_2}{q_1 x_1 + q_2 x_2} U^* \tag{16}$$

where q_1 and q_2 are the contact surfaces of the two components.

The parameter U^* is related to the interchange energies, per conventional unit area and per mole by the expression:

$$U^* = -\frac{1}{2} \sum_s \sum_t (\alpha_{1s} - \alpha_{2s})(\alpha_{1t} - \alpha_{2t})\, U^*_{st} \tag{17}$$

where α_{is} is the fraction of species s in the molecule i and is defined as

$$\alpha_{is} = \frac{q_{is}}{q_i} \tag{18}$$

The interchange energies, U^*_{st}, are related to the interaction energies ε_{st} in the following way:

$$U^*_{st} = (\varepsilon_{ss} + \varepsilon_{tt})/2 - \varepsilon_{st} \tag{19}$$

As the direct experimental magnitude is the excess enthalpy and since the data necessary to perform the transformation of H^E into U^E are frequently unavailable, it is considered acceptable to express the excess enthalpy by means of a similar equation.

It is assumed that each group CH_3, CH_2, CH, OH constitutes a segment whose area in isolated state is equal to unity and that the bond area is 0.125 (corresponding to a lattice coordination number $z = 8$).

---

[6] K. W. KEHIAIAN, *J. Chim. phys.* **68,** 922, 935 (1971).

[7] I. LANGMUIR, *Colloid Symp.*, **37,** (1925).

[8] K. W. MORCOM and D. N. TRAVERS, *Trans. Faraday Soc.*, **62,** 2063 (1966).

[9] O. REDLICH, E. L. DERR and A. J. PIEROTTI, *J. Amer. Chem. Soc.* **81,** 2283 (1959).

The areas and surface fractions used are shown in tables 4 and 5 where α_{ia}, α_{ib}, α_{iOH} are the surface fractions of aliphatic, aromatic and hydroxylic species, respectively.

Table 4

Group contact areas $q(z = 8)$

Group	CH_3	CH_2	CH	OH	C_6H_6
q_G	0.875	0.750	0.625	0.875	3.8

The area of benzene is the one given by Kehiaian, obtained from the maximum position of the H^E-composition curves corresponding to the binary mixtures of both components with aliphatic hydrocarbons.

Table 5

Areas and fraction of areas

Compound	q_i	aliphatic	aromatic	hydroxyl
iso $C_4H_{10}O$	4	0	1	0
C_6H_6	3.8	0.78125	0	0.21875

Likewise, the values for the interchange enthalpies obtained from the maximum height of the same curves are $h^*_{ab} = 830$ J/mol.

So, for isobutyl-alcohol-benzene contacts equation (17), applied to excess enthalpies, leads to :

$$h^* = -[(\alpha_{1a} - \alpha_{2a})(\alpha_{1b} - \alpha_{2b})]h^*_{ab} = 648{,}4375 \text{ J/mol} \qquad (20)$$

We suppose that, at experimental temperatures, the structure of the alcohol will be sufficiently rigid to inhibit aliphatic-aliphatic contacts, which could exist in a less ordered structure.

In consequence, the rupture of hydrogen bonds will be accompanied by a compensating exothermic effect.

On raising the temperature, the structure of the alcohol loses rigidity and the experimental curves will then be more representative of the hydrogen bond.

Inserting these values in the equation equivalent to (15) for excess enthalpies, we obtain contribution of the dispersion effects due to isobutyl alcohol-benzene contacts :

$$h^E_{\text{disp}} = q_1 q_2 \frac{x_1 x_2}{q_1 x_1 + q_2 x_2} h^*_{ab} \qquad (21)$$

which are indicated in table 6 and in figure 3.

From extrapolation at infinite dilution we have:

$$H^{E0}_{\mathrm{disp}} = 2.550\ \mathrm{J/mol}.$$

We have tried to obtain, then, the value of the energy of the hydrogen bond by an indirect route.

Table 6

Dispersive excess enthalpies at 25

x_2	0.1022	0.2039	0.3052	0.4059	0.5061	0.6059	0.7051	0.8039	0.9022
h^E_{disp}	236.81	416.69	54.133	612.41	631.51	600.19	52.000	392.74	218485

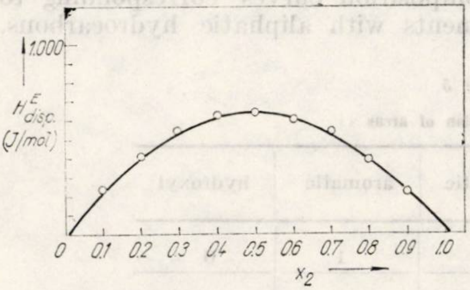

Fig. 3. — Dispersive excess enthalpies (J/mol).

Assuming that the specific interactions OH$-\pi$ have the same value, with isobutyl alcohol as with other alcohols[10] we shall calculate the value for the isobutyl alcohol-benzene system, using data obtained by Van Ness for partial molar excess enthalpy of straight-chain aliphatic alcohols at infinite dilution in benzene -7.1kJ which is an average value.

We have calculated the energy of the hydrogen bond on the basis of the experimental curve for isobutyl alcohol-benzene at 25° by equation (14). Considering that:

$$\bar{H}^{E0}_2 = 16\ \mathrm{kJ},\ h^{E0}_{\mathrm{disp}} = 2.55\ \mathrm{kJ},\ h^{E0}_{\mathrm{sp}} = -7.1\ \mathrm{kJ}$$

we obtain for the energy of the hydrogen bond in isobutyl alcohol-benzene system, the value

$$\bar{h}^{E0}_{HB} = 20.45\ \mathrm{kJ} = 4.9\ \mathrm{kcal}.$$

which agrees with the values of Pimentel[11] (3.2$-$7.0 kcal/mol) and with the Van Ness's values[12] of about 4.2 kcal/mol for alcohols.

---

[10] C. C. S. Van Ness, *J. Chem. Eng. Data*, **10,** 168 (1965).

[11] G. C. Pimental "The Hydrogen Bond", W. H. Freeman and Company, San Francisco, 1960, p. 216.

[12] C. C. S. Van Ness, *Trans. Faraday. Soc.* **58,** 879 (1962).

Revue Roumaine de Chimie, **21**, *3*, 351–354 (1976)

ВЗАИМОСВЯЗЬ ПОВЕРХНОСТНОГО НАТЯЖЕНИЯ, СЖИМАЕМОСТИ И БЛИЖНЕГО ПОРЯДКА РАСПЛАВОВ ВБЛИЗИ ТОЧКИ ПЛАВЛЕНИЯ

I. ЩЕЛОЧНО-ГАЛОИДНЫЕ СОЛИ И ПОЛУПРОВОДНИКИ

Б. Н. ОЩЕРИН

Технологический институт имени Ленсовета, Ленинград 198013

Получена 3 апреля 1975 г.

The application of previously reported for crystalls[1] interdependence of surface energies, bulk modulus and local order in form of the melting point is discussed. The cases are analysed in which the structure factors in (1) greatly change at the transition "solids-melts": alkali halides (type NaCl-sphalerite); Ge (diamond type-b.c.c.).Attention is paid of the possibility of gaining additional information about the properties of melts at the melting point from eg. (1). For example, while using comparatively easily defined values such as the ultrasonic velocity and surface tension one can receive information of the local order.

1. Взаимосвязь поверхностной энергии, модуля сжимаемости и структуры кристаллов установлена структурно-термодинамической теорией, развитой в работах.[1,2] Новизна подхода состоит в том, что « толщина » поверхности одноатомного слоя определяется толщиной поверхностных избытков $h_{(hkl)}$, ограниченных со стороны кристалла поверхностью раздела и со стороны вакуума радиусом действия поля избыточных величин. Численное значение $h_{(hkl)}$ находится из предположения, что h — — высота части атомного шара в поверхности (шарового сегмента), которая принадлежит поверхности. (Первое такое определение $h_{(hkl)}$ дано в[3]).

$$h_{(hkl)} = \left(1 - \cos\left\{\frac{\Delta z}{z}(\mathrm{hkl})\,180\right\}\right) r.$$

Энергия в поверхности (hkl) с минимумом энергии или плоскости скола определена как работа образования единицы новой поверхности[1,2]

$$\Sigma_{(hkl)} = \frac{3}{8}\cdot\left(1 - \cos\left\{\frac{\Delta z}{z}(\mathrm{hkl})\,180\right\}\right) rK_s = A_1 rK_s = A_2 aK_s \qquad (1)$$

---

[1] N. B. Oshcherin, *Phys. stat. sol.* (a) **22**, K227 (1974).

[2] Б.Н. Ощерин, ЖФХ, **44**, 547 (1970); **45**, 992 (1971); **47**, 2447 (1973; **47**, 2448 (1973); **48**, 483 (1974).

[3] B. N. Oshcherin, *Phys. stat. sol.*, **6**, K157 (1964).

($\Delta z/z$(hkl) — относительное число недостающих соседей у атома в первой координационной сфере поверхности (hkl) с координационным числом z: a — постоянная решетка; r — половина кратчайшего межатомного расстояния; K_s — модульсжимаемости).

Равенство (1) описывает поверхностную энергию кристаллов полупроводников со структурами алмаза, сфалерита и NaCI; щелочно-галоидных солей и окислов типа NaCI и CsCI; фторидов и окислов типа CaF_2, металлов; фаз внедрения.[1,2] В данном сообщении оно обсуждается в приложении к расплавам.

2. Расплав вблизи точки плавления характеризуется ближним порядком и равенство (1) может быть использовано, если принять, что его поверхность имеет минимум энергии соответствующий поверхности (hkl) кристалла той же структуры. Нами рассмотрены случаи, когда при плавлении структурные рассчетные коэффициенты в (1) изменяются существенно (табл. 1). Экспериментальные данные о поверхностном натяжении в расплавах щелочно-галоидных солей описываются равенством (1), если, в соответствии с работой,[4] принять ближний порядок структуры сфалерита (табл. 2). Это согласуется с работой,[5] где установлено появление вблизи плавления щелочно-галоидных кристаллов тетраэдрических квазикомплексов. В табл. 3 проведено сопоставление для кристаллов тех же веществ величин расчитанных нами и С.Н. Задумкиным.

Таблица 1

Расчетные коэффициенты в равенстве (1)

Структура	(hkl)	$\Delta z/z$(hkl)		A_1	$A_2 \times 10^2$
		A*)	B*)		
ГЦК	(111)	3/12	—	0,1098	3,90
ГП	(101)	3/12	—	0,1098	—
ОЦК	(110)	2/8	—	0,1098	4,76
Алмазня и сфалерита	(111)	1/4	1/4	0,1098	2,37
Тип NaCI	(100)	1/6	1/6	0,0502	1,325
Тип CaF_2	(110) (111)	2/8	1/4	1,098	2,37

*) Подрешетки А и В динарного соединения.

В расплаве тетраэдрических полупроводников предполагают ближний порядок структур типа ОЦК или NaCI.[7,8] Наши расчеты (табл. 4), подтверждают ОЦК структуру расплавов элементарных полупроводников. Из опыта[9] $K_s = 4{,}0.10^{10}$ дин/см^2 Ge и $3{,}57.10^{10}$ дин/см^2 Si. Численное согласие расчетов для Si достигается, если предположить $\Delta z/z$ Si

---

[4] A. D. Pelton, *Nature. phys. sci.*, **229**, 57 (1971).

[5] М.В. Смирнов, М.М. Василевская и Г.В. Буров, в сб. « Кристаллизация и фазовые превращения », изд. « Наука и техника », Минск, 1971, стр. 27.

[6] G. Janz, "Molten Salts Handbook", A. P., New York, 1967.

[7] H. Krebs, "Grundzüge der anorganische Kristallchemie", F. Enke Verlag, Stuttgard, 1968, s.195.

[8] В.М. Глазов, С.Н. Чижевская и Н.Н. Глаголева, «Жидкие полупроводники», изд. « Наука », Москва, 1967.

[9] В.В. Байдов и М.Б. Гитис, *Физика и техн. полупроводников*, **4**, 967 (1970).

Таблица 2

Сгущение энергии и энтропии в поверхности расплавов солей вблизи плавления (опытные данные взяты из[6])

Расплав	$K_s 10^{10}$ дин см^{-2}	$\beta\, 10^{-4}$ град^{-1}	$\Sigma_{(110)}$ эрг см^{-2} расчет по (I)	$\Sigma_{\text{пл.}}$ дин см^{-1} опыт	$d\Sigma/dT$ расчет по (3)	$d\Sigma/dT$ из опыта
LiF	(18,50)	2,79	—	250	0,116	0,109
LiCl	5,65	2,96	113	137	0,068	0,069
LiBr	5,24		111		—	
NaF	(13,0)	2,91	—	202	0,097	0,082
NaCl	4,79	3,65	104	116	0,071	0,095
NaBr	3,82	3,62	88	99	0,060	0,061
NaI	3,45	3,63	85	88	0,057	0,090
KF	(7,9)	3,53	—	142	0,083	0,075
KCl	3,76	3,98	93	99	0,066	0,073
KBr	3,23	4,06	82	89	0,060	0,072
KI	2,99	4,07	81	79	0,054	0,087
RbF	(6,7)	—	—	131	—	0,102
RbCl	(4,5)	4,13	—	99	0,062	0,058
RbBr	(3,9)	4,12	—	91	0,062	0,058
RbI	(3,4)	—	—	83	—	—
CsF	(5,3)	—	—	107	—	—
CsCl	3,49	4,04	95	90	0,861	0,081
CsBr	2,89	4,04	81	85	0,058	0,061
CsI	(2,9)	—	—	75	—	—

Таблица 3

Поверхностная энергия кристаллов щелочно-галоидных солей со структурой NaCl

Кристалл	a, A	$K_s\, 10^{11}$ дин $\text{см}^{-2\cdot 12}$	$\Sigma_{(100)}$, эрг/см^2 по (1)	$\Sigma_{(100)}$, эрг/см^2 по работе[11]
LiF	4,017	6,98	321	205
LiCl	5,129	3,15	214	212
LiBr	5,490	2,56	186	200
LiI	6,000	1,88	149,5	176
NaF	4,620	4,85	297	205
NaCl	5,628	2,36	175	184
NaBr	5,961	1,99	157	173
NaI	6,462	1,61	138	155
KF	5,34	3,17	224	206
KCl	6,278	1,74	144	155
KBr	6,586	1,55	135	146
KI	7,052	1,24	116	132
RbF	5,64	2,44	182	197
RbCl	6,54	1,64	142	150
RbBr	6,854	1,38	125	140
RbI	7,326	1,075	104,5	122

---

[10] Ю.Г. Полтавцев и Т. В. Ремизович, *Неорганические материалы*, **9**, 894 (1973).

[11] С.Н. Задумкин и А.И. Темроков, *Изв. высш. уч. зав.*, *Физика*, **11**, 44 (1968).

[12] O. Anderson, in : "Physical Acoustics", Ed. W. P. Mason, vol. 3, part B, Academic Press, New York, 1965, p. 46.

[13] В.Б. Лазарев и М.Я. Дашевский, *Изв. АН. СССР*, *серия химическая*, **1965**, 170.

иным чем у Ge, что согласуется с особенностью изменения плотности Si при плавлении. Для расплавов GaP и CuCI следует ожидать структуру типа NaCI. Для остальных (табл. 4) вероятна более плотная упаковка, т.к. расчетные K_s расплава выше K_s кристалла. Это согласуется с найденным[10] для InSb $z = 7{,}7$.

2.1. Температурный коэффициент поверхностного натяжения можно получить дифференцируя равенство (1):

$$d\Sigma/dT(\mathrm{hkl}) = -\Sigma_{(\mathrm{hkl})}\left(\frac{1}{K_s}\cdot\frac{dK_s}{dT} + \frac{1}{3}\cdot\beta\right) \tag{2}$$

где β — коэффициент объемного термического расширения. Принимая, что[16] $\dfrac{1}{K_s}\cdot\dfrac{dK_s}{dT} = -2\beta\gamma$, где γ — постоянная Грюнейзена; для расплавов γ не имеет физического смысла и $\gamma = 1$. Тогда, из (2) получаем

$$d\Sigma/dT = -\Sigma_{(\mathrm{hkl})}\,\beta\left(\frac{6\gamma - 1}{3}\right) = -\frac{5}{3}\,\Sigma_{(\mathrm{hkl})}\cdot\beta \tag{3}$$

В табл. 3 расчетные величины сопоставлены с опытными.

3. Обсужденная выше взаимосвязь (1) описывает имеющиеся для некоторых расплавов данные о ближнем порядке, модуле адиабатической сжимаемости и поверхностном натяжении и может способствовать получению дополнительной информации о свойствах расплавов. Например, по сравнительно легко определяемым K_s и Σ можно получить информацию о ближнем порядке.

Таблица 4

Модули сжимаемости расплавов некоторых полупроводников: расчет из равенства (1)

Расплав	Структура	(hkl)	2r, Å	$\Sigma_{пл}$ дин см$^{-1}$	$K_s\,10^{10}$ дин см$^{-2}$ расплав (расчет)	$K_s\,10^{10}$ дин см$^{-2}$ кристалл (298° К)
Si	ОЦК	(110)	2,40	720[13]	5,45	9,78
Ge	ОЦК	(110)	2,70	609[13]	4,17	7,54
	NaCl	(100)	2,83		8,7	7,54
AlSb	NaCl	(100)	2,7	480[14]	7,06	5,92
GaSb	NaCl	(100)	2,65	454[14]	6,85	5,64
InSb	NaCl	(100)	3,15	432[14]	5,46	4,33
GaP	NaCl	(100)	2,4	420±20[15]	6,9	8,71
CuCl	NaCl	(100)	2,35	92[6]	1,46	4,4

Исходя из тождества ближнего порядка нитратов в кристалле и расплаве[17] по K_s и Σ расплавов можно определить эмпирически $\Delta z/z$ и затем по K_s для кристаллов рассчитать $\Sigma^{\min}_{(\mathrm{hkl})}$ кристалла.

---

[14] В.Б. Лазарев и М.Я. Давшевский, *Неорганические материалы*, **3**, 561 (1967).

[15] Л. Ильин, В. Сорокин и Д. Яськов, *Неорганические материалы*, **5**, 1365 (1969).

[16] R. C. Tripathi and C. Bhandari, *Physica*, **45**, 332 (1969).

[17] А.К. Дорош и Б.А. Орлов, Тезисы докладов, пятое Всесоюзное совещание по электрохимии, том I, АН. СССР, Москва, 1974, стр. 45.

Revue Roumaine de Chimie, **21**, *3*, 355–358 (1976)

MOLECULAR ORBITAL STUDY OF 2-THIO-5-NITRO-BARBITURIC ACID

R. NUŢIU, Z. SIMON and C. DRUGĂRIN

University of Timişoara, Department of Chemistry, Bd. V. Pârvan 4, Romania

Received October 4, 1974

Hückel molecular orbital calculations are performed for the different possible tautomers of 2-thio-5-nitro-barbituric acid and its anions. The results are used to evaluate the relative stabilities of these tautomeric structures and spectral transitions. Molecular diagrams are given for the most stable tautomers of the non-ionized acid and of its anions.

In a previous note,[1] 2-thio-5-nitro-barbituric acid was characterized by several spectral and analytical methods. The spectral study indicates that the anhydrous form is 6-keto-4-hydroxy-2-thio-1,2,3,6-hexahydropyrimidine while the hydrated form is the anion of the 4,6-diketo-2-mercapto-1,4,5,6-tetrahydropyrimidin-5-nitronic-acid. In this note Hückel molecular orbital calculations are performed for the possible tautomeric structures of this acid and of its anions. The relative stabilities of the tautomers are calculated as well as the first transitions in the electronic spectra for the different ions.

The tautomeric structures considered are listed in table 1. The numbering of atoms in the study was done as indicated on structure (II).

The α and β parameters for the heteroatoms are selected according to Streitwieser's[2] recommendations and were used in our previous notes[3,4]; some new parameters used here are listed in table 2. The nitro group was considered as heteroatom with one free orbital.

The energies of the first transitions in the electronic spectra were put equal to the energy difference between the lowest empty (ε_{LE}) and highest occupied (ε_{HO}) molecular orbitals.

The evaluation of relative stabilities for the tautomeric structure was performed as in our previous notes,[3,4] but the figure $\beta = -16.5$ kcal/mole was used for resonance energy calculations and for the lactamic tautomeric structures an extra stabilization of -10 kcal per lactamic group was considered relative to the lactimic one, according to evaluations of Branch and Calvin.[5]

---

[1] R. Nuţiu, I. Sebe and Maria Nuţiu, *Rev. Roumaine Chim.*, **19**, 679 (1974).

[2] A. Streitwiesser, Jr., "Molecular Orbital Theory for Organic Chemists", John Wiley, New York, 1961, chap. 5, & 2.

[3] Z. Simon, Fr. Mihai and R. Nuţiu, *Rev. Roumaine Chim.*, **13**, 147 (1968).

[4] R. Nuţiu and Z. Simon, *Rev. Roumaine Chim.*, **14**, 311 (1969).

[5] cited by I. M. Klotz and T. Askounis, *J. Amer. Chem. Soc.*, **69**, 801 (1974).

Table 1

Tautomeric structures of 2-thio-5-nitro-barbituric acid and of its anions

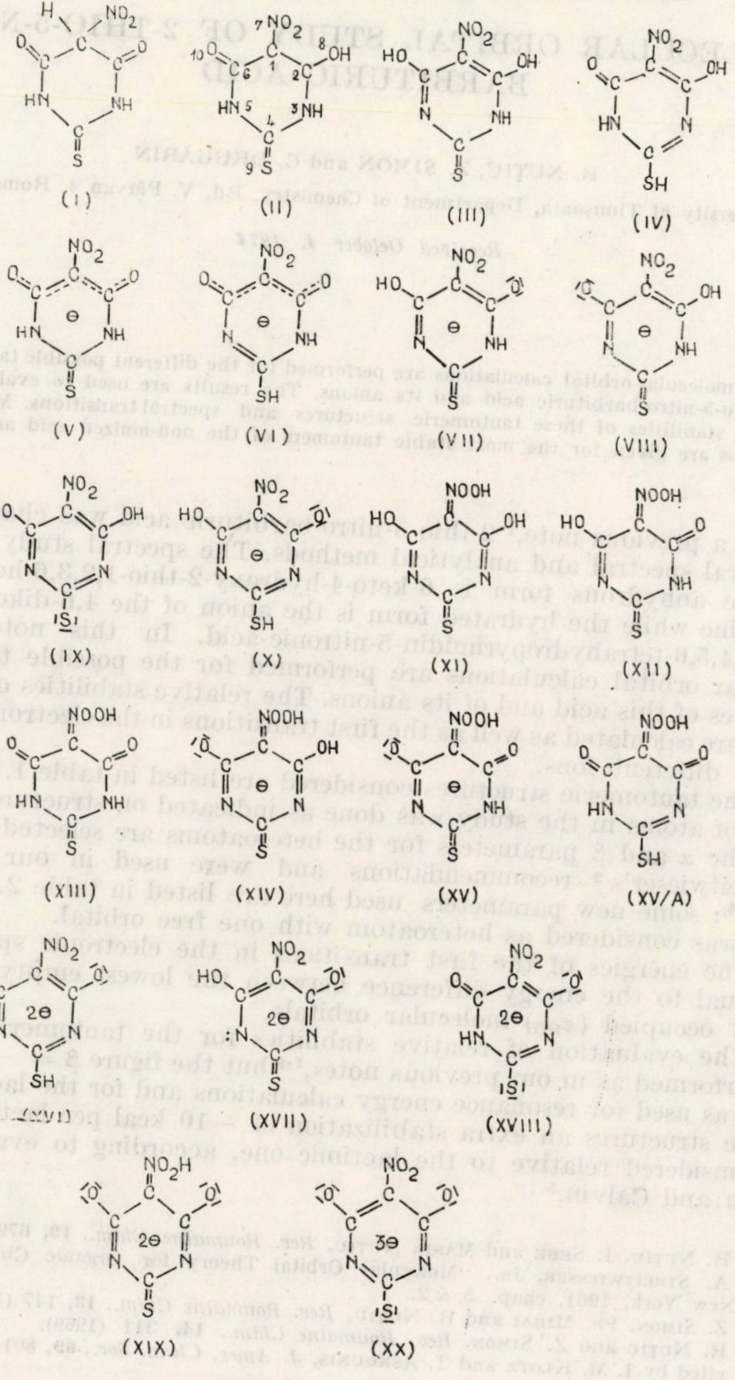
(I)
(II)
(III)
(IV)
(V)
(VI)
(VII)
(VIII)
(IX)
(X)
(XI)
(XII)
(XIII)
(XIV)
(XV)
(XV/A)
(XVI)
(XVII)
(XVIII)
(XIX)
(XX)

Table 2

Hückel parameters used in calculations

Coulomb integrals	Exchange integrals
$\alpha_{-\ddot{S}-} = \alpha + \beta$	$\beta_{CS} = 0.6\,\beta$
$\alpha_{=S} = \alpha = \alpha_{-S}{}^{\theta}$	

Table 3 lists the total energies (E) in kcal/mole units, resonance energies (R) β-units, the energies of highest occupied (ε_{HO}) and lowest empty (ε_{LE}) molecular orbitals, the double bond order (π) of the $C-NO_2$ bond and the π-electronic charge of the nitro group (q). The A, B, C and D energies of table 3 are reference energies for the undissociated acid and the various anions, as in previous notes.[3,4]

As indicated in table 3, the tautomer (II) should be the most stable undissociated tautomeric structure in agreement with the results of previous IR studies [1] for unhydrated crystals of our acid. For the monoanion, tautomers (V), (VI) and (X) have almost equal calculated total energies. The IR spectrum of hydrated crystals, in which 2-thio-5-nitro-barbituric acid should be found as monoanion, indicates the tautomer (VI) as the real one, but the other two can not be excluded. For the dianion, tautomer (XVI) is indicated as the most stable one, while for the trianion a single tautomer, (XX), is possible.

Table 3

Total energies, E_{tot}, resonance stabilization, R, and other Hückel parameters

Structure	$E_{tot.}$ (kcal/mole)	R (β units)	$\frac{\varepsilon_{HO}-\alpha}{\beta}$	$\frac{\varepsilon_{LE}-\alpha}{\beta}$	π	q
I	A −87.1	2.156	+0.275	−0.665	0.000	0.000
II	A −73.1	3.256	+0.229	−0.431	0.558	0.301
III	A −74.2	3.068	+0.171	−0.408	0.534	0.306
IV	A −84.5	3.145	+0.824	−0.393	0.534	0.263
V	B −86.0	3.189	+0.229	−0.444	0.560	0.302
VI	B −84.1	3.065	+0.849	−0.404	0.529	0.256
VII	B −78.3	3.318	+0.170	−0.427	0.557	0.324
VIII	B −77.9	3.295	+0.164	−0.421	0.545	0.308
IX	B −73.0	3.000	+0.837	−0.364	0.487	0.228
X	B −88.8	3.958	+0.815	−0.575	0.440	0.176
XI	A −56.4	3.413	+0.496	−0.011	0.527	1.694
XI/A	A −62.7	3.200	+0.956	+0.162	0.856	1.232
XII	A −72.6	3.488	+0.429	+0.005	0.580	1.622
XIII	A −83.5	3.543	+0.359	+0.040	0.671	1.496
XIV	B −63.0	3.614	+0.453	−0.017	0.533	1.682
XV	B −70.9	3.691	+0.385	−0.001	0.590	1.605
XV/A	A −66.1	3.401	+0.941	+0.141	0.851	1.248
XVI	C −80.4	3.448	+0.828	−0.405	0.531	0.260
XVII	C −53.2	1.438	+0.122	−0.427	0.562	0.344
XVIII	C −60.1	1.619	+0.164	−0.466	0.593	0.346
XIX	C −43.3	2.623	+0.414	−0.024	0.542	1.668
XX	D −50.8	1.657	+0.120	−0.447	0.578	0.350

The percentage of *aci*-nitro limit structure considered equal to the π-bond order of the $C-NO_2$ bond, is according to table 3, 56% for the nonionised structure (II), 56% for the monoanionic structure (V), 53%

for (VI). For the dianionic structure (XVI), this percentage is 53%, for the trianionic one, (XX), 58%.

The first (the longest wavelength) transition in the uv spectra of the undissociated acid, monoanion and trianion are listed in table 4, together with the $\varepsilon_{LE} - \varepsilon_{HO}$ figures. The bathochromic effect observed on going from the monoanion to the trianion is correctly predicted by the HMO calculation if tautomer (V) is the real one for the monoanion.

Table 4

First calculated and experimental UV transition

Structure	Transition	
	$\varepsilon_{LE} - \varepsilon_{HO}$	Expr. λ_{max} (nm)
II undissociated acid	0.660β	245
V	0.673β	
VI monoanion	1.340β	337
X	1.380β	
XVI dianion	1.233β	—
XX trianion	0.567β	354

The molecular diagrams for structures (II), (V), (XVI) and (XX) which represent the real structures of 2-thio-5-nitro-barbituric acid and its anions are given in figure 1.

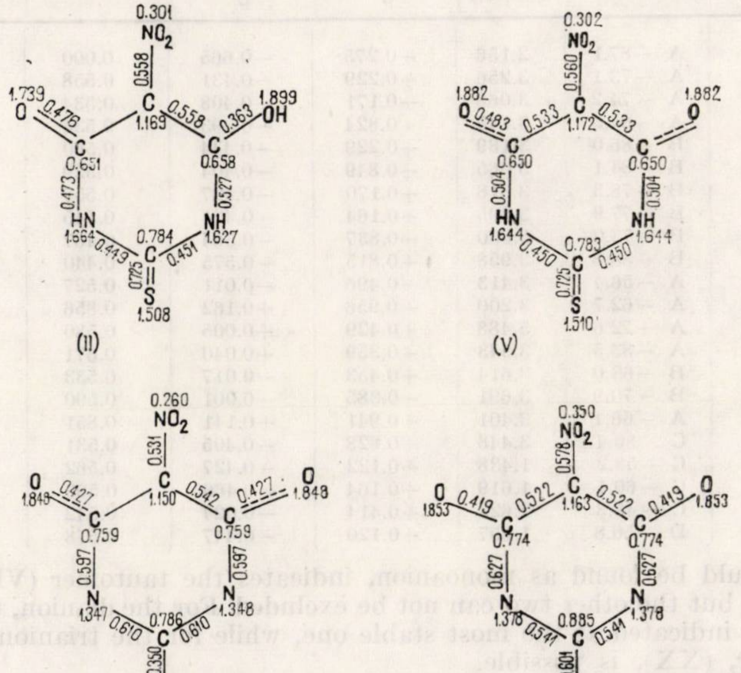
0.301
NO2
0.558
1.739
O
0.476
C
1.169
0.558
0.363
1.899
OH
C
0.651
C
0.658
0.473
0.327
HN
1.664
NH
1.627
0.449
0.784
C
0.451
0.725
S
1.508
(II)
0.302
NO2
0.560
1.882
O
0.483
0.533
C
1.172
0.533
1.882
O
C
0.650
C
0.650
0.504
0.504
HN
1.644
NH
1.644
0.450
0.783
0.450
C
0.725
S
1.510
(V)
0.260
NO2
0.531
O
1.848
0.427
C
1.150
0.542
0.427
O
1.848
C
0.759
C
0.759
0.597
0.597
N
1.347
N
1.348
0.610
0.786
0.610
C
0.350
SH
1.893
(XVI)
0.350
NO2
0.578
O
1.853
0.419
0.522
C
1.163
0.522
0.419
O
1.853
C
0.774
C
0.774
0.627
0.627
N
1.378
N
1.378
0.541
0.885
0.541
C
0.604
S
1.592
(XX)

Fig. 1. — Molecular diagram for tautomeric structures (II), (V), (XVI) and (XX), corresponding to the (probable) real structures of 2-thio-5-nitro-barbituric acid and of its anions.

Revue Roumaine de Chimie, **21**, *3*, 359 – 365 (1976)

INFLUENCE OF THE CELL DIAPHRAGM ON THE ELECTROMOTIVE FORCE OF CONCENTRATION CELLS WITH TRANSPORT IN MOLTEN SALTS

LUDMILA POPESCU

Center of Physical Chemistry, Str. Galați 31, Bucharest 13, Romania

Received June 19, 1974

The concentration cell with transport of the type:

$$\mathrm{Ag(s)}\left|\begin{array}{c|c} \mathrm{AgCl}(l),\ x^{\mathrm{I}}_{\mathrm{AgCl}} & \mathrm{AgCl}(l),\ x^{\mathrm{II}}_{\mathrm{AgCl}} \\ \mathrm{KCl}(l),\ x^{\mathrm{I}}_{\mathrm{KCl}} & \mathrm{KCl}(l),\ x^{\mathrm{II}}_{\mathrm{KCl}} \end{array}\right|\mathrm{Ag}(s)$$

has been studied; use has been made of quartz diaphragms of different porosities and asbestos diaphragms. The e.m.f. values thus obtained were compared to those of the cell without diaphragm and the experimental conditions in which these agree were established.

The problem of achieving the liquid junction is certainly the most important experimental problem in the study of concentration cells.

The junction must be achieved through a diaphragm of a sufficiently low porosity so as to prevent the diffusion of the salts (which would lead to concentration variations in the two compartments) from occurring yet sufficiently high to allow a good contact between the two compartments. An unsuitably chosen diaphragm brings about time variations of the e.m.f., the electrical resistance of the cell becomes very high and the contact between the salts is not achieved rapidly enough.

In the case of a free junction, without any diaphragm, we must also avoid the mixing and diffusion of the salts in the two compartments and the junction must be so as to yield an e.m.f. stable in time and reproducible.

Different ways of achieving the junction were advanced which observe these conditions. They are listed in table 1.[1-38]

---

[1] C. Gordon, *Z. phys. Chem.*, **28**, 302 (1899).

[2] J. Terpiłowski and J. Josiak, *Roczniki Chem.*, **38**, 97(1964) ; **39**, 805 (1965) ; **39**, 1777 (1965) ; **40**, 1833 (1966).

[3] M. S. Zahariewskii and T. V. Permiakova, *Zhur. obshchei. Khim.*, **26**, 2947 (1956).

[4] J. Richter and E. Amkreutz, *Z. Naturforsch.*, **27 a**, 280 (1972).

[5] I. G. Murgulescu and D. I. Marchidan, *Rev. Chim. Acad. RPR*, **3**, 69 (1958) ; *ibid.*, **5**, 17, 299 (1960) ; *Zhur. fiz. Khim.*, **34**, 2534 (1960).

[6] I. G. Murgulescu and L. Popescu, *Rev. Roumaine Chim.*, **18**, 737 (1973).

[7] J. Terpiłowski, J. Josiak and A. Wojakowska, *Roczniki Chem.*, **42**, 219 (1968) ; J. Josiak, *Roczniki Chem.*, **44**, 35 (1970) ; ibid. **44**, 1875 (1970) ; ibid. **46**, 1029 (1972) ; J. Terpiłowski and A. Wojakowska, *Roczniki Chem.*, **46**, 1971 (1972).

[8] R. W. Laity and A. S. Tenney, *J. Phys. Chem.*, **74**, 3112 (1970).

[9] R. W. Laity, *J. Amer. Chem. Soc.*, **79**, 1849 (1957).

[10] K. H. Stern, *J. Electrochem. Soc.*, **112**, 1049 (1965).

[11] H. Bloom and A. J. Easteal, *Austral. J. Chem.*, **18**, 2039 (1965) ; *ibid.*, **19**, 1577 (1966) ; *ibid.*, **19**, 1779 (1966) ; *ibid.*, **21**, 2649 (1968) ; *ibid.*, **21**, 2793 (1968).
A. J. Easteal and S. J. Heron, *Austral. J. Chem.*, **22**, 681 (1969).

[12] H. A. Øye, *Acta Chem. Scand.*, **18**, 361 (1964).

[13] P. Mirabel and J. Guion, *Compt. rend.*, **269 C**, 516 (1969) ; P. Mirabel, *Compt. rend.* **269 C**, 1348 (1969) ; P. Mirabel, Thesis, Strasbourg (1968).

[14] K. A. Romberger and J. Braunstein, *Inorg. Chem.*, **9**, 1273 (1970) ; K. A. Romberger, J. Braunstein and R. Thoma, *J. Phys. Chem.*, **76**, 1154 (1972).

[15] G. Grube and E. A. Rau, *Z. Electrochem.*, **40**, 352 (1934).

[16] H. Townsend and P. Duby, *J. Electrochem. Soc.*, **115**, 605 (1968) ; *ibid.*, **117**, 1126 (1970).

[17] K. H. Stern and J. A. Stiff, *J. Electrochem. Soc.*, **111**, 893 (1963).

[18] F. R. Duke and H. M. Garfinkel, *J. Phys. Chem.*, **65**, 461 (1961) ; *ibid.*, **65**, 1627 (1961) ; *ibid.*, **65**, 1629 (1961).

[19] A. A. Kolotii and Iu. K. Delimarskii, *Zhur. neorg. Khim.*, **8**, 163 (1963) ; A. A. Kolotii, *Ukrain. khim. Zhur.*, **38**, 323 (1972).

[20] S. N. Flengas and T. R. Ingraham, *Canad. J. Chem.*, **35**, 1139 (1957) ; *J. Electrochem. Soc.*, **106**, 714 (1959).

[21] C. Sinistri, *Ricerca sci.*, **1**, 56 (1961).

[22] M. Bakès and J. Guion, *Compt. rend.*, **258 C**, 1223 (1964) ; M. Bakès, Thesis, Strasbourg (1965) ; M. Bakès, *Ber. Bunsengesellschaft Phys. Chem.*, **70**, 581 (1966) ; J. Guion, Thesis, Strasbourg (1964) ; J. Guion, *Compt. rend.*, **261 C**, 3371 (1965) ; *ibid.* **261 C**, 4079 (1965) ; *ibid* **262 C**, 11 (1966) ; *ibid.* **262 C**, 169 (1966).

[23] M. Blander, F. F. Blankenship and R. F. Newton, *J. Phys. Chem.*, **63**, 1259 (1959).

[24] J. Braunstein and M. Blander, *J. Phys. Chem.*, **64**, 10 (1964) ; H. Braunstein, J. Braunstein, and P. T. Hardesty, *J. Phys. Chem.*, **77**, 1907 (1973) ; C. Vallet and J. Braunstein *J. Phys. Chem.*, **77**, 2672 (1973).

[25] H. Słaby, *Roczniki Chem.*, **48**, 915 (1974).

[26] E. Kundys, *Roczniki Chem.*, **48**, 201 (1974).

[27] K. Okajima and H. Sakao, *Trans. Japan Inst. Mell.*, **10**, 403 (1969).

[28] A. A. Kolotii, *Zhur. fiz. Khim.*, **30**, 508 (1956) ; *Ukrain. khim. Zhur.*, **24**, 572 (1958) ; *ibid.*, **38**, 1107 (1972) ; Iu. K. Delimarskii and A. A. Kolotii, *Ukrain. khim. Zhur.*, **24**, 146 (1958).

[29] O. Sackur, *Z. phys. Chem.*, **83**, 297 (1913).

[30] H. J. Blikslager, *Rec. Trav. chim.*, **46**, 305 (1927).

[31] Z. Moser and K. Fitzner, *J. Electrochem. Soc.*, **120**, 914 (1973).

[32] W. K. Behl and J. J. Egan, *J. Phys. Chem.*, **71**, 1764 (1967).

[33] G. Roewer and H. H. Emons, *Z. anorg. Chem.*, **370**, 119 (1969) ; *ibid* **370**, 128 (1969) ; *ibid.*, **394**, 279 (1972) ; H. H. Emons, G. Bräutigam and H. Wader, *Z. anorg. Chem.*, **403**, 97 (1974) ; H. H. Emons, Third Conf. on Chem. Thermodynamics, Baden (1973).

[34] M. Okada and K. Kawamura, *Denki Kagaku.*, **38**, 812 (1971).

[35] B. F. Markov, *Zhur. fiz. Khim.*, **23**, 1464 (1949).

[36] K. H. Stern, *J. Phys. Chem.*, **63**, 741 (1959).

[37] H. Flood, T. Førland and K. Motzfeldt, *Acta Chem. Scand.*, **6**, 257 (1952).

[38] F. R. Clayton, G. Mamantov and D. L. Manning, *High Temp. Sci.*, **5**, 358 (1973).

Table 1

Types of junctions in concentrations cells with molten salts

Type of diaphragm	Authors
Cells without diaphragm	
Junction achieved by two glass capillaries or tubes	Gordon,[1] Terpiłowski, Josiak ;[2] Zaharievskii, Permiakova ;[3] Richter, Amkreutz.[4]
Junction achieved by a doubly bent capillary	Murgulescu, Marchidan ;[5] Murgulescu, Popescu.[6]
Junction achieved by a singly bent capillary	Terpiłowski *et al.* ;[7] Laity, Tenney.[8]
Cells with diaphragm	
Fritted quartz	Laity ;[9] Stern ;[10] Bloom, Easteal ;[11] Øye ;[12] Mirabel, Guion ;[13] Romberger, Braunstein.[14]
Fritted glass	Grube, Rau ;[15] Townsend, Duby ;[16] Stern, Stiff ;[17] Duke, Garfinkel.[18]
Asbestos	Kolotii, Delimarskii ;[19] Flengas, Ingraham ;[20] Sinistri ;[21] Bakès, Guion ;[22] Blander et al. ;[23] Braunstein *et al.* ;[24] Slaby ;[25] Kundys ;[26] Okajima, Sakao.[27]
Corundum tube or crucible	Kalotii, Delimarskii.[28]
Porous crucible	Sackur.[29]
Alundum	Blikslager ;[30] Moser, Fitzner.[31]
Alumina (powder)	Behl, Egan ;[32] Emons *et al.* ;[33] Okada, Kawamura.[34]
Ceramic (powder)	Markov.[35]
Graphite (spectral)	Stern.[36]
Magnesium oxide	Flood *et al.*[37]
Lanthanum trifluoride (single crystal)	Mamantov *et al.*[38]

Lately there have appeared in the literature a series of papers showing that the separation diaphragm between the two compartments of the cell, both for concentration cells [19] and when studying the transport phenomena [39,40] is not simply an inert matter separating the compartments, but the e.m.f. value and the value of the transport numbers depend as much on the nature of the diaphragm as on its degree of porosity.

---

[39] R. J. Labrie and V. A. Lamb, *J. Electrochem. Soc.*, **110**, 810 (1963).
[40] R. W. Laity and C. A. Sjöblom, *J. Phys. Chem.*, **71**, 4157 (1967).

Moreover, certain authors[41] have shown that when measuring electrical conductance, the electrical resistance differs very much from the transparent silica to the mat one, when they are immersed into a molten salt.

To study the influence of the diaphragm on the e.m.f. of the concentration cells we have used, in the present paper, cells with two types of diaphragms : cells with quartz diaphragms of various porosities and with an asbestos diaphragm (in powder form).

The e.m.f. values obtained in the cells with the two types of diaphragms were then compared to those obtained in cells without diaphragm, determined by us in a former paper.[6]

EXPERIMENTAL

The cells used in the present paper were of quartz.

The cell without diaphragm, with a doubly bent capillary (1 mm internal diameter), is described elsewhere.[6] The experimental technique is described in the same paper.

The cell with a quartz diaphragm is shown in figure 1.

The diaphragms used were of pure fritted silica disks (Quartex, France) with a fine porosity ($\varnothing = 5-15\mu$) of a 18 mm in diameter and 2.5 mm thick.

The fritted silica disks were welded at the bottom of tube *B*.

We have found out experimentally that the unprocessed quartz diaphragms, with a $5-15\mu$ porosity, allowed the mixing of the melts used (AgCl + KCl) and, consequently, these frits have previously been heated by flame to reduce their porosity.

The compactness of each frit was characterized by measurements of the cell's electrical resistance, (R_{cell}), in diluted HCl solutions.

In a cell with pure salt (AgCl), or a cell with the same mixture in both compartments ($x^{\text{I}}_{\text{AgCl}} = x^{\text{II}}_{\text{AgCl}} = 0.5$), we have measured the asymmetry potential of the cell, which was found to be negligible.

The cell with asbestos diaphragm is shown in figure 2.

The diaphragm was achieved by means of an asbestos plug inserted at the end of the doubly bent capillary *C*, welded to the tube *B*.

The asbestos used was reagent grade (in fibre form), previously heated up to 800° to remove any water traces. The asbestos powder thus obtained was previously wetted with the mixture that was to be introduced into the tube *B* (the higher density mixture, that is $x^{\text{I}}_{\text{AgCl}} > x^{\text{II}}_{\text{AgCl}}$, has always been placed into the tube *B*).

With asbestos diaphragms, special care had to be taken to avoid the formation of gas bubbles in the capillary, which could have interrupted the contact between the two compartments.

When using a too compact asbestos diaphragm we have also observed the interruption of the contact between the two compartments.

It was found necessary that the levels of mixtures in the two compartments should always be equal. We have, therefore, calculated, in advance, the volume of the melts which were to be examined.

The cell with a doubly bent capillary, at whose end an asbestos plug was inserted, offers the advantage of an easier handling in comparison to the U-shaped cells, used in certain experiments with concentration cells. Moreover, the doubly bent capillary itself avoids the mixing of the contacting salts.

The e.m.f. was measured by means of a "Solartron" digital voltmeter of high input resistance ($2 \times 10^{10}\ \Omega$).

The preparation and purification of salts are described elsewhere.[6]

---

[41] J. A. A. KETELAAR and P. P. E. MAENAUT, *Electrochim. Acta*, **17**, 2195 (1972).

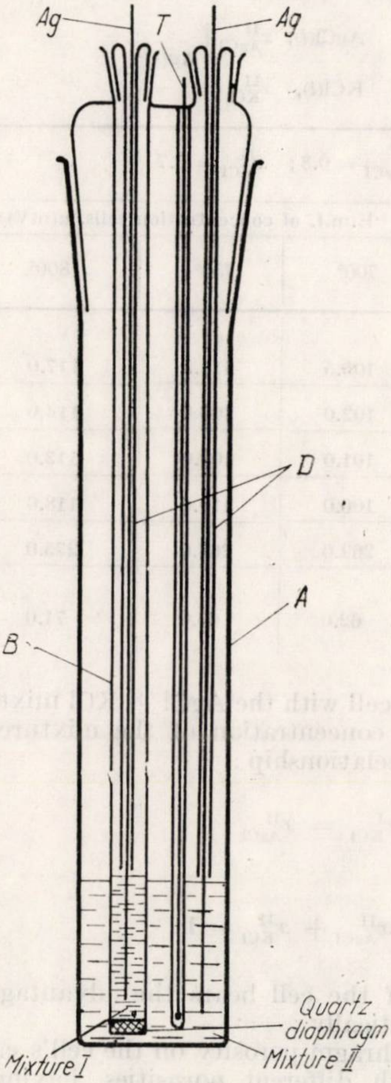
Ag
T
Ag
D
A
B
Quartz diaphragm
Mixture I
Mixture II

Fig. 1. — Cell with quartz diaphragm.

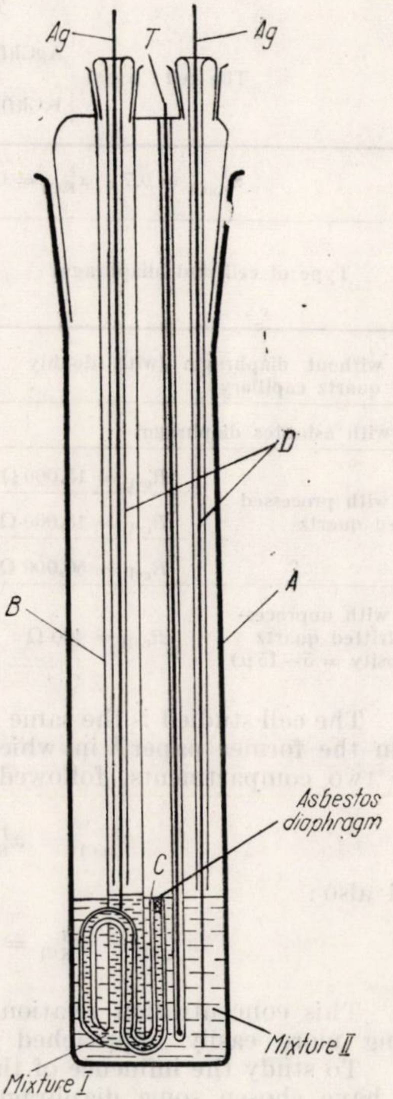
Ag
T
Ag
D
A
B
Asbestos diaphragm
C
Mixture II
Mixture I

Fig. 2. — Cell with asbestos diaphragm.

RESULTS AND DISCUSSION

Table 2 gives the e.m.f. values, ε of the concentration cell with AgCl + KCl mixture both for cells with a fritted quartz diaphragm of different porosities and for cells with asbestos diaphragm, within the temperature interval 700°—800°.

Table 2

$$\text{The cell: } \mathrm{Ag}(s) \left| \begin{array}{l} \mathrm{AgCl}(l),\ x^{\mathrm{I}}_{\mathrm{AgCl}} \\ \mathrm{KCl}(l),\ x^{\mathrm{I}}_{\mathrm{KCl}} \end{array} \right\| \begin{array}{l} \mathrm{AgCl}(l),\ x^{\mathrm{II}}_{\mathrm{AgCl}} \\ \mathrm{KCl}(l),\ x^{\mathrm{II}}_{\mathrm{KCl}} \end{array} \Bigg| \mathrm{Ag}(s)$$

$x^{\mathrm{I}}_{\mathrm{AgCl}} = 0.7;\ x^{\mathrm{I}}_{\mathrm{KCl}} = 0.3;\ x^{\mathrm{II}}_{\mathrm{AgCl}} = 0.3;\ x^{\mathrm{II}}_{\mathrm{KCl}} = 0.7$

Type of cell and diaphragm		E.m.f. of concentration cells, ε(mV)		
		700°	750°	800°
Cell without diaphragm (with doubly bent quartz capillary)		105.5	111.5	117.0
Cell with asbestos diaphragm		102.0	108.0	114.0
Cell with processed fritted quartz	$R_{\mathrm{cell}} = 15{,}000\ \Omega$	101.0	108.0	113.0
	$R_{\mathrm{cell}} = 18{,}000\ \Omega$	106.0	111.0	118.0
	$R_{\mathrm{cell}} = 50{,}000\ \Omega$	262.0	268.0	275.0
Cell with unprocessed fritted quartz (porosity = 5–15 μ)	$R_{\mathrm{cell}} = 400\ \Omega$	62.0	65.0	71.0

The cell studied is the same as the cell with the AgCl + KCl mixture, from the former paper,[6] in which the concentration of the mixture, in the two compartments, followed the relationship:

$$x^{\mathrm{I}}_{\mathrm{AgCl}} = x^{\mathrm{II}}_{\mathrm{KCl}}; \quad x^{\mathrm{I}}_{\mathrm{KCl}} = x^{\mathrm{II}}_{\mathrm{AgCl}}$$

and also:

$$x^{\mathrm{I}}_{\mathrm{AgCl}} + x^{\mathrm{I}}_{\mathrm{KCl}} = 1; \quad x^{\mathrm{II}}_{\mathrm{AgCl}} + x^{\mathrm{II}}_{\mathrm{KCl}} = 1$$

This concentration relationship of the cell bears the advantage of being more easily approached theoretically.

To study the influence of the diaphragm porosity on the cell's e.m.f. we have chosen some diaphragms with different porosities, having as comparison criterion the e.m.f. of the cell without diaphragm, with the same mixture at the same temperatures.

We notice in table 2 that we obtain e.m.f. values near to the e.m.f. values of the cell without diaphragm only for cells with moderately closed quartz diaphragm ($R_{\mathrm{cell}} = 15{,}000-18{,}000\ \Omega$).

The too "open" diaphragm ($R_{\mathrm{cell}} = 400-500\ \Omega$), that is cells that have not undergone the flame processing or are only slightly closed, as well as those that are too "closed" ($R_{\mathrm{cell}} = 50{,}000\ \Omega$), give erroneous e.m.f. values. We have found out experimentally that in these cases the e.m.f. varies in time but does not reach the e.m.f. value of the cell without diaphragm, even after 24 hours.

Only in the medium-porosity cells ($R_{\text{cell}} = 18{,}000\ \Omega$) have we obtained steady and reproducible e.m.f.'s.

With the asbestos diaphragm cells we have also obtained e.m.f. values close to those obtained with cell without diaphragm (free junction).

As resulted from experimental data, we obtain real e.m.f. values only for certain porosities of the fritted quartz diaphragm, that are to be established by comparison with the e.m.f. value obtained with cell without diaphragm.

Only the e.m.f. stability and reproducibility cannot be determining criteria in choosing a certain type of diaphragm. The wrong diaphragm may consistently alter the e.m.f. value and implicitely the value of the diffusion potential which is part of the e.m.f. of the concentration cell with transport; the diffusion potential may in some cases have very small values (only a few mV), as was shown in the formerly mentioned paper.[6]

The experimental results obtained in the present paper prove that the most suitable for this kind of measurements are the free junction cells or those with an asbestos diaphragm. To avoid the influence of some external factors, difficult to control, it is advisable to choose free junction cells.

Revue Roumaine de Chimie, 21, 3, 367–372 (1976)

CRITICAL CONSIDERATIONS ON THE NONISOTHERMAL METHODS FOR THE EVALUATION OF THE KINETIC PARAMETERS OF ENDOTHERMAL DECOMPOSITIONS IN SOLID-GAS SYSTEMS

NICKEL ACETATE TETRAHYDRATE DEHYDRATION

ANCA GHEORGHIU, D. FĂTU and E. SEGAL

Chair of Physical Chemistry and Electrochemical Technology, Polytechnic Institute of Bucharest, Bd. Republicii 13, Bucharest, Romania

Received March 15, 1975

The results of a kinetic comparative study of the methods used to determine the kinetic parameters values for nonisothermal decomposition reactions are presented. As a test reaction, nickel acetate tetrahydrate dehydration has been chosen.

INTRODUCTION

In the last decades, the nonisothermal methods used to determine the kinetic parameters values of the heterogeneous reactions, particularly of the decomposition reactions, have largely developed.

The use of the nonisothermal methods is justified by the advantages they present, such as the rapidity and the possibility to investigate the whole succession of the phenomena unfolded over a large range of temperatures.

Simultaneously with the elaboration of some proper methods for the evaluation of the kinetic parameters values under nonisothermal conditions and the accumulation of an important volume of experimental work, some disadvantages of these methods in comparison with the classical isothermal ones have been put into evidence.

Consequently, some critical points of view on the proceedings for the kinetic parameters determination of the heterogeneous reactions under nonisothermal conditions have been expressed.

Thus, the use of the nonisothermal methods raises not only some problems connected with the general errors which affect the thermogravimetry and the differential thermal analysis,[1,2] but also basical problems.

---

[1] I. G. MURGULESCU and E. SEGAL, *Studii şi Cercetări Chim. – Acad. R.P.R.* **15**, 261, (1967).

[2] D. FĂTU, Thesis, Department of Chem., Univ. Bucharest, (1972).

According to Mac Callum and Tanner,[3] the rate equation :

$$d\alpha/dt = Z \exp(-E/RT)\, f(\alpha), \tag{1}$$

in which α stands for the conversion degree, the other constants being all known, fits only for isothermal kinetics.

To describe the processes which take place under nonisothermal conditions, the rate equation should contain another term $(\partial\alpha/\partial T)_t\, dT/dt$. But the whole nonisothermal kinetics is based on the validity of the equation (1).

As a result of the progressive heating of the system submitted to the kinetic analysis, the conversion degree values could be shifted with respect to the equilibrium ones.[4]

The problem to be solved consists in the extent to which these "false equilibria" do not affect the kinetic parameters values determined by the use of the heating curves.

Other problems were raised of which we mention :

— the activated character validity of the decomposition and its adequate kinetic description, using Arrhenius'equation ;[5]

— the extent to which heat and mass transfer phenomena influence the kinetic parameters values.[6]

Without going into details concerning the different points of view about the critical analysis of the nonisothermal kinetics,[4,7,8] we mention only the general conclusion according to which the nonisothermal proceedings maintain their validity, the experimentalist being able to check the accuracy of the results taking into account the available criteria.

Considering the above mentioned facts, we add the researches of Simon[9] and Fătu and Segal[10] concerning the influence of the different experimental factors on the kinetic parameters of calcium oxalate monohydrate dehydration, as well as of the decomposition of copper tetraammine sulphate monohydrate. In the same framework is also enlisted this paper in which we try to present a critical analysis of some nonisothermal methods frequently used in the kinetic analysis of the heterogeneous decompositions.

As a test reaction, nickel acetate tetrahydrate dehydration has been chosen. We have selected this substance, as the dehydration process occurs in only one step, expressed in TG and DTG curves without any discontinuity.

---

[3] J. R. Mac Callum and J. Tanner, *Nature*, **225**, 1127 (1970).

[4] J. Sestak, "Thermal Analysis. Proceedings of the Third International Conference on Thermal Analysis", Davos, vol. 2, Birkhäuser Verlag, Basel, 1972 p. 3.

[5] J. Sestak, P. Holba and J. Kratochvil, "Gheteroghenniie khimicheskie reactsii", Minsk, 1975 (in print).

[6] A. L. Draper and I. K. Sveum, *Thermochimica Acta*, **1**, 345 (1970).

[7] D. Schultze, *J. Thermal Anal.*, **5**, 353 (1973).

[8] R. M. Felder and P. Stahel, *Nature*, **228**, 1085 (1970).

[9] J. Simon, *J. Thermal Anal.*, **5**, 271 (1973).

[10] D. Fătu and E. Segal, *Rev. Roumaine Chim.*, **21**, 000 (1976).

EXPERIMENTAL

Nickel acetate tetrahydrate Riedel pure was used. The substance has been ground and sieved, retaining the granules between 0.1 and 0.09 mm diameter.

The thermogravimetric TG, the derivative thermogravimetric DTG, the temperature *T* and the differential thermal analysis DTA curves have been simultaneously recorded by means of a MOM Budapest Paulik-Paulik-Erdey type derivatograph, using different values of the heating rate.

The experiments have been performed both in static atmosphere and in a 5l/h nitrogen flow.

RESULTS AND DISCUSSION

The derivatogram corresponding to a heating rate of nickel acetate tetrahydrate dehydration of 10°/min is given in figure 1.

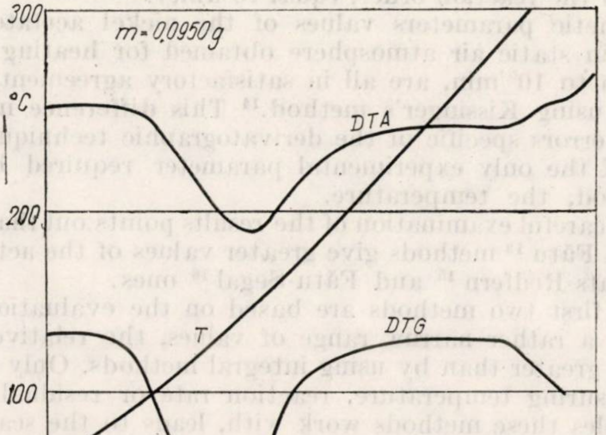

Fig. 1.—Derivatogram of $Ni(CH_3COO)_2.4\,H_2O$ dehydration.

The continuous aspect of the heating curves, which are well fit for a kinetic analysis, should be noticed.

A preliminary examination of the slightly asymmetrical shape of the DTG and DTA curves based on Kissinger's criterion, [11] suggests a near unity value of the reaction order.

The kinetic analysis of nickel acetate tetrahydrate dehydration involved two "Δ" methods, a thermogravimetric one, according to Freeman-Carroll,[12] and a differential one, according to Fătu;[13] a differential thermogravimetric method, according to Kissinger,[14] and two integral thermogravimetric methods, according to Coats-Redfern[15] and Fătu-Segal.[16]

The results obtained are given in table 1:

From table 1, it is easy to see that all the methods used led to the same value of the reaction order, equal to unity.

The kinetic parameters values of the nickel acetate tetrahydrate dehydration in static air atmosphere obtained for heating rates varying from 2.5°/min to 10°/min, are all in satisfactory agreement, except those obtained by using Kissinger's method.[14] This difference may be due to the inherent errors specific of the derivatographic technique which affect the values of the only experimental parameter required by the Kissinger's [14] method, the temperature.

A more careful examination of the results points out that the Freeman-Carroll [12] and Fătu [13] methods give greater values of the activation energy than the Coats-Redfern [15] and Fătu-Segal [16] ones.

As the first two methods are based on the evaluation of the finite difference on a rather narrow range of values, the relative scattering of the results is greater than by using integral methods. Only one important error in measuring temperature, reaction rate or residual area of DTA curve, variables these methods work with, leads to the scattering of two points on the recorded diagrams for the determination of the reaction order and activation energy. That is the reason why the slope and the intercept have been evaluated by the last mean squares method.

The "Δ" type methods used are nevertheless advantageous, as they allow to get the value of the reaction order using only one derivatogram.

Once the reaction order value known, the use of Coats-Redfern [15] and Fătu-Segal [16] methods led to more accurate activation energy values. These methods allow the evaluation of the preexponential factor Z, too.

The constancy of the determined values of the kinetic parameters in static air atmosphere, with respect to the heating rate changes, indicates neither heat nor mass transfers limitations, as well as no important shifts from equilibrium.

Dealing with the influence of the surrounding atmosphere, we mention that the activation energy value in inert gas flow is inferior to those obtained in static air atmoshpere. The lower values of the preexponential

---

[11] H. E. Kissinger, *Analyt. Chem.*, **29**, 1602 (1957).

[12] E. S. Freeman and B. Carroll, *J. Phys. Chem.*, **62**, 394 (1958).

[13] D. Fătu, *J. Thermal Anal.*, **1**, 285 (1969).

[14] H. E. Kissinger, *J. Res. Nat. Bur. Stand.*, **57**, 217 (1956).

[15] A. W. Coats and J. P. Redfern, *Nature*, **20**, 88 (1964).

[16] D. Fătu and E. Segal, *Rev. Roumaine Chim.*, **16**, 343 (1971).

Table 1

Kinetic parameters values of the reaction $Ni(CH_3COO)_2\ 4H_2O(s) \longrightarrow Ni(CH_3COO)_2(s) + 4H_2O(g)$

Method				
Freeman-Carroll (TG and DTG)	Fătu (DTA)	Kissinger (DTG)	Coats-Redfern (TG)	Hyperbolic heating Fătu – Segal
$m = 0.0950$ g $\beta = 10°$/min $n = 1$ $E = 33,85$ kcal/mole	$m = 0.050$ g $\beta = 10°$/min $n = 1$ $E = 34.05$ kcal/mole $Z = 1.89 \cdot 10^{16} s^{-1}$	$m = 0.0950$ g $m = 0.1023$ g $m = 0.1058$ g $m = 0.1009$ g $m = 0.1037$ g $\beta = 10°$/min $\beta = 5.3°$/min $\beta = 2.5°$/min $\beta = 1.25°$/min $\beta = 0.6°$/min $n = 1$ $E = 22.9$ kcal/mole	$m = 0.0950$ g $\beta = 10°$/min $n = 1$ $E = 30.49$ kcal/mole $Z = 9.19 \cdot 10^{14} s^{-1}$	$m = 0.1016$ g $b = 0.87 \cdot 10^{-6} (°Ks)^{-1}$ $n = 1$ $E = 25.8$ kcal/mole $Z = 5.2 \cdot 10^{12} s^{-1}$
$m = 0.1058$ g $\beta = 2.5°$/min $n = 1$ $E = 35.56$ kcal/mole			$m = 0.1058$ g $\beta = 2.5°$/min $n = 1$ $E = 29.42$ kcal/mole $Z = 1.9 \cdot 10^{14} s^{-1}$	
$m = 0.0539$ g $\beta = 5.3°$/min $n = 1$ $E = 32.16$ kcal/mole			$m = 0.0539$ g $\beta = 5.3°$/min $n = 1$ $E = 27.45$ kcal/mole $Z = 2.03 \cdot 10^{13} s^{-1}$	
			$m = 0.1023$ g (inert gas flow) $\beta = 5.3°$/min $n = 1$ $E = 20.2$ kcal/mole $Z = 6.22 \cdot 10_8 s^{-1}$	

factor compensate the decrease of the activation energy, so that the dehydration rate does not shift (the kinetic constants of the dehydration process, both in static air atmosphere and in inert gas flow for the same temperature value, have been estimated). To explain this compensation effect, we presume that the release of water vapours in an inert gas flow unblocks the superficial sites with greater reactivity. Presuming the existence of a distribution of the activation energy values, the number of the more active sites is smaller, so it is understandable why the preexponential factor value obtained under inert gas flow is lower, compared to the value of the same factor obtained in a static air atmosphere. Similar effects of compensation were put into evidence in the kinetic study of copper tetra-ammine sulphate monohydrate decomposition, [10] too.

As it can be seen from table 1, the kinetic parameters values are quite insensitive to the changes of the sample weight from 0.1000 g to 0.0500g, too. In this way, it is also confirmed that in the sample weight range used, the reaction occurs under kinetic regime.

The lack of mass and heat transfer limitation is also confirmed by the preexponential factor values obtained under static air atmosphere which, in the limits of experimental errors, agrees satisfactorily with the expected value, based on the transition states theory.[17]

CONCLUSIONS

1. A kinetic nonisothermal investigation of nickel acetate tetrahydrate dehydration has been performed, in order to analyse critically the methods frequently used for the evaluation of the kinetic parameters values.

2. The determined kinetic parameters values are all in satisfactory agreement, except those obtained by using Kissinger's method.

3. The kinetic parameters values are insensitive to heating rates changes from 2.5°/min to 10°/min.

4. A compensation effect has been put into evidence with respect to the changes of the surrounding atmosphere of the sample.

5. The kinetic parameters values are also insensitive to the changes of the sample weight.

---

[17] K. Laidler, "Chemical Kinetics", McGraw Hill, London, 1966, p. 166.

Revue Roumaine de Chimie, 21, 3, 373–383

CONTRIBUTION À L'ÉTUDE DE LA SOURCE CHIMIQUE DE COURANT $Zn/MeOH/O_2$. III[1]

LA DÉTERMINATION DES PARAMÈTRES OPTIMAUX DE FONCTIONNEMENT POUR UNE PILE À CATHODE EN ARGENT

MARIA MAVRODIN-TĂRĂBÎC, IOANA ONACA et I. SOLACOLU
Centre de Chimie Physique, Bucarest, 31, str. Galaţi

Reçu le 25 juin 1974

En vue de la détermination du régime optimal de fonctionnement d'une pile Zn-oxygène à cathode en argent, on a tracé les courbes de décharge sur résistance variable, dans de différentes conditions de concentration (5N – 7N), de température (50 – 70°) et de surpression d'alimentation avec du gaz (400 – 500 mm Hg). Des données obtenues on a calculé les valeurs des pertes par polarisation, les rendements moyens de conversion, les densités apparentes de courant et les puissances maximales et on a testé, par l'analyse dispersionnelle, la signification de l'influence de la variation des paramètres étudiés. Vu que le caractère de la variation de la surpression, dans le domaine étudié, est non significatif, on a effectué un calcul d'optimisation du processus, à partir d'un programme de $3^2 = 9$ expériences, qui a permis la détermination des valeurs optimales de la concentration et de la température.

Dans un travail antérieur [1] on a étudié l'effet de la variation des paramètres de fonctionnement, la concentration (2N – 7N) et la température (20 – 70°) de l'électrolyte, la surpression de l'oxygène (300 – 600 mm Hg), sur les performances d'une source chimique de courant de type $Zn/KOH/O_2$ à cathode en argent (électrode à gaz du type DSK). Cette étude a mis en évidence l'effet favorable de l'augmentation de la concentration, jusqu'à la valeur de 6N, de la surpression, jusqu'à approximativement 400 mm Hg et de la température, dans tout le domaine étudié et nous a permis de déterminer un domaine dans lequel la source chimique de courant présente des performances élevées (5N – 7N ; 50 – 70° ; 400 – 500 mm Hg). Les données obtenues ont mis en évidence la complexité de cet effet et le caractère interdépendant des effets singuliers et ont démontré que, pour la détermination des valeurs optimales des paramètres étudiés, il est nécessaire d'effectuer une étude mathématique d'optimisation, à partir d'un programme d'expériences factorielles.

---

[1] M. Mavrodin-Tărăbîc, I. Onaca et I. Solacolu, *Rev. Roumaine Chim.* (sous presse).

Vu que le modèle mathématique d'optimisation à trois facteurs (concentration, température, surpression) présente des difficultés particulières, les données expérimentales concernant l'effet de la variation des paramètres de fonctionnement sur les caractéristiques électriques et sur les performances réalisées par la source chimique de courant ont été soumises à une analyse dispersionnelle en vue d'éliminer les paramètres, dont la variation n'a pas d'effet significatif. L'effet de la variation de la surpression d'alimentation avec du gaz étant non significatif, on a effectué l'optimisation du processus à partir d'un modèle mathématique à deux facteurs et trois niveaux (les données ont été obtenues dans un programme de $3^2 = 9$ expériences).

1. PARTIE EXPÉRIMENTALE

Pour réaliser, dans le laboratoire, la source chimique de courant

$$(-)\ \mathrm{Zn/KOH/O_2(Ag)}\ (+)$$

on a utilisé : pour l'anode — des plaques de zinc de pureté 99,9 %, pour la cathode — des électrodes à gaz en argent du type DSK, dont l'obtention et la caractérisation ont été présentées dans un travail antérieur [1].

On a tracé les courbes de décharge, sur résistance variable $E - i$, à l'aide d'un montage décrit dans un travail antérieur,[2] en utilisant un millivoltmètre électronique de type Universal-Röhrenvoltmeter 187a (précision $\pm$ 2 mV), un milliampèremètre de type DU 20 (précision $\pm$ 1 %) et une boîte à résistances de type VEB Messtechnik (précision $\pm$ 0,1Ω).

Les données expérimentales ont été obtenues pour des concentrations de l'électrolyte de 5N, 6N et 7N, des températures de 50, 60 et 70° et des surpressions d'alimentation avec de l'oxygène de 400 et de 500 mm Hg. Les paramètres de fonctionnement ont été maintenus constants dans les limites : $\pm$ 0,005 méquiv. $\mathrm{cm^{-3}}$, $\pm 0{,}1^\circ$ et, respectivement, $\pm$2 mm Hg.

2. RÉSULTATS ET DISCUSSIONS

Les données obtenues par l'interprétation des courbes de décharge $E - i$, tracées pour de différentes conditions de concentration, température et surpression, sont présentées dans le tableau 1. Les données thermodynamiques caractéristiques pour la réaction qui est à la base du fonctionnement de la pile $\mathrm{Zn} + \frac{1}{2}\ \mathrm{O_2} + 2\ \mathrm{OH^-} \rightleftarrows \mathrm{ZnO_2^{2-}} + \mathrm{H_2O}$, ainsi que le calcul des caractéristiques électriques ont été présentés dans un travail antérieur.[2]

---

[2] O. Radovici, M. Mavrodin-Tărăbîc, I. Onaca et I. Solacolu, *Rev. Roumaine Chim.*, **18**, 767 (1973).

Tableau 1

Performances de la source chimique Zn-oxygène, à de différentes conditions de concentration, température et surpression de l'oxygène

Conditions de travail			Tension idéale	Tension réelle	Pente de la zone de fonctionnement	Pertes par polarisation	Densité de courant moyenne	Puissance maximale	Rendement de conversion moyen
conc.	temp.	ΔP_{O_2}	E_i	E_r	R	σ	i_m	$P_{\max}$	η_m
mé-quiv. cm^{-3}	°C	mm Hg	V	V	ohm	%	mA/cm²	mW/cm²	%
5	50	400	1,69	1,385	4,27	15,2	162,2	112,3	34,2
				1,400	4,38	14,5	159,8	111,9	34,6
	60		1,70	1,455	3,56	12,1	204,4	148,7	35,6
				1,460	3,54	11,9	206,2	150,5	35,7
	70		1,71	1,470	3,55	11,7	207,2	152,3	35,6
				1,460	3,60	12,2	202,8	148,1	35,3
6	50		1,69	1,475	4,48	10,7	164,6	121,4	36,4
				1,485	4,47	10,2	166,1	123,3	36,7
	60		1,70	1,490	3,63	10,4	205,2	152,9	36,4
				1,480	3,57	10,9	207,3	153,4	36,2
	70		1,71	1,500	3,58	10,3	209,5	157,1	36,3
				1,525	3,68	9,1	207,2	158,0	36,8
7	50		1,69	1,410	4,00	13,9	176,3	124,3	34,8
				1,425	4,10	13,2	173,8	123,8	35,2
	60		1,70	1,445	3,60	12,6	200,7	145,0	35,8
				1,460	3,61	11,9	202,2	147,6	35,4
	70		1,71	1,470	3,51	11,7	209,4	153,9	35,7
				1,460	3,41	12,2	214,1	156,3	35,3
5	50	500	1,69	1,425	4,56	13,2	156,3	111,3	35,2
				1,430	4,56	13,0	156,8	112,1	35,3
	60		1,70	1,465	3,69	11,6	198,5	145,4	35,8
				1,470	3,65	11,4	201,4	148,0	35,9
	70		1,71	1,530	3,71	8,8	206,2	157,7	37,0
				1,520	3,69	9,3	206,0	157,3	36,8
6	50		1,69	1,470	4,46	11,0	164,8	121,1	36,3
				1,500	4,58	9,5	163,7	122,8	37,0
	60		1,70	1,515	3,83	9,2	197,8	149,8	37,0
				1,505	3,75	9,6	200,8	151,0	36,8
	70		1,71	1,530	3,72	8,8	205,6	157,3	37,0
				1,535	3,74	8,6	205,2	157,5	37,1
7	50		1,69	1,480	4,56	10,5	162,3	120,1	36,5
				1,420	4,29	13,4	165,5	117,5	35,1
	60		1,70	1,390	3,79	15,3	183,4	127,5	34,0
				1,445	4,02	12,6	179,7	129,9	35,3
	70		1,71	1,450	3,40	13,7	213,4	154,7	35,1
				1,470	3,54	11,7	207,6	152,6	35,6

2.1. L'ANALYSE DISPERSIONNELLE DE L'EFFET DE LA VARIATION DES PARAMÈTRES DE FONCTIONNEMENT

Étant donné le caractère complexe de l'effet des paramètres de fonctionnement sur les performances de la source chimique de courant Zn-oxygène et l'interdépendance des effets singuliers, il a été nécessaire d'effectuer une analyse dispersionnelle des données obtenues par l'interprétation des courbes de décharge $E - i$. Cette méthode statistique d'interprétation des données expérimentales nous a permis de séparer et de tester les effets dus à la variation des paramètres et d'éliminer les paramètres de fonctionnement dont la variation n'a pas d'effet significatif. Les effets, une fois identifiés, ont été testés en comparant les dispersions dues aux facteurs variables avec la dispersion due aux facteurs aléatoires.

Pour l'analyse dispersionnelle [3] des données expérimentales, on a choisi un modèle mathématique à trois facteurs (surpression, température et concentration — A, B et, respectivement, C) et avec deux, trois et, respectivement, trois niveaux. Les valeurs des niveaux (400 et 500 mm Hg ; 50, 60 et 70° ; 5N, 6N et 7N) sont caractéristiques pour tout le domaine dans lequel la source chimique de courant présente des performances élevées.[1]

Étant donné le caractère difficile de l'analyse dispersionnelle pour un modèle à trois facteurs, le tableau d'analyse a été décomposé dans des tableaux partiels à deux facteurs (surpression-température, surpression-concentration et température-concentration), en éliminant un facteur du tableau initial.[4] On a calculé, pour chaque tableau, les sommes des carrés (S) pour les effets principaux et pour les effets d'interaction. A l'aide de ces sommes et en tenant compte du nombre des degrés de liberté (ν) caractéristique pour chaque facteur, on a calculé les dispersions (s) pour les effets individuels et d'interaction du second ordre. En vue de la détermination du caractère significatif de l'effet de la variation des paramètres de fonctionnement sur les performances de la source chimique de courant Zn-oxygène, on a effectué, à partir de ces dispersions, le test Fischer-Snedecor (F) et on a comparé les valeurs de F avec les valeurs critiques (F_α), correspondant à un seuil de signification $\alpha = 0{,}05$. Les résultats obtenus sont présentés dans le tableau 2.

De l'examen des données présentées dans le tableau d'analyse dispersionnelle il résulte que, pour toutes les caractéristiques électriques considérées (σ, η_m, i_m, $P_{\max}$), l'effet de la variation du facteur A (la surpression d'alimentation avec de l'oxygène) et des interactions de second ordre AB (surpression-température) et AC (surpression-concentration) n'est pas significatif (les valeurs de F calculées sont plus petites que les valeurs critiques F_α). L'analyse dispersionnelle des données expérimentales a mis en évidence le caractère significatif de la variation de la concentration de l'électrolyte (C) et de l'interaction température-concentration (BC) sur les pertes par polarisation (σ) et sur le rendement moyen de conversion (η_m), ainsi que de la variation de la température (B), de la concentration (C) et de l'interaction température-concentration (BC) sur la densité apparente de courant (i_m) et sur la puissance maximale ($P_{\max}$). La dispersion, relativement petite, due aux facteurs aléatoires (la dispersion résiduelle s_r) indique une précision satisfaisante des données expérimentales et que l'interaction de troisième ordre (ABC) est non significative.

---

[3] A. GLÜCK, « Metode matematice în industria chimică », Ed. tehnică, Bucarest, 1971, p. 86.

[4] G. E. P. BOX et N. R. DRAPER, « Evolutionary Operation », Wiley, New York, 1969, p. 63.

Tableau 2

Analyse dispersionnelle des effets de la variation des paramètres de fonctionnement

Caractéristique électrique considérée	Source de dispersion	Somme des carrés	Degrés de liberté	Dispersion	F	F_α	
σ	A	2,5688	1	2,5688	3,01	7,71	
	B	8,5972	2	4,2986	5,03	6,94	
	C	27,6057	2	13,8029	16,16	6,94	*
	AB	1,3007	2	0,6504	0,76	6,94	
	AC	3,0004	2	1,5002	1,76	6,94	
	BC	5,7056	4	1,4264	1,67	6,39	
	S_r	3,4156	4	0,8539			
η_m	A	0,6689	1	0,6689	3,24	7,71	
	B	0,9102	2	0,4551	2,21	6,94	
	C	6,1726	2	3,0863	14,97	6,94	*
	AB	0,4077	2	0,2038	1,01	6,94	
	AC	0,7226	2	0,3613	1,75	6,94	
	BC	1,2424	4	0,6212	3,01	6,39	
	S_r	0,8124	4	0,2062			
i_m	A	56,92	1	56,92	6,18	7,71	
	B	6337,24	2	3168,62	344,04	6,94	*
	C	19,06	2	9,53	1,03	6,94	
	AB	71,16	2	35,58	3,86	6,94	
	AC	56,16	2	28,08	3,05	6,94	
	BC	297,79	4	74,45	8,08	6,39	*
	S_r	37,92	4	9,21			
$P_{\max}$	A	30,42	1	30,42	3,93	7,71	
	B	4368,42	2	2184,21	282,19	6,94	*
	C	140,56	2	70,28	9,08	6,94	*
	AB	70,51	2	35,25	4,56	6,94	
	AC	72,27	2	36,14	4,67	6,94	
	BC	224,87	4	56,22	7,26	6,39	*
	S_r	30,95	4	7,74			

En vue de l'établissement du domaine de concentration-température qui doit être exploré pour optimiser le processus, on a élaboré un tableau dont il résulte l'effet de la variation des paramètres significatifs sur les caractéristiques électriques de la pile Zn-oxygène (les valeurs présentées dans ce tableau représentent la valeur moyenne des données correspondant aux surpressions de 400 et de 500 mm Hg). Pour pouvoir tirer des conclusions sur l'effet des paramètres étudiés on a calculé l'intervalle de confiance dans lequel s'inscrivent les différences existentes entre deux données du tableau d'interaction ; on a utilisé la formule

$$\mathrm{d} \pm t_\alpha \sqrt{s_r} \sqrt{\frac{1}{n_1}+\frac{1}{n_2}}$$

dans laquelle t_α représente les valeurs critiques de la distribution Student, correspondant à un seuil de signification $\alpha = 0{,}05$, s_r la dispersion résiduelle et $n_1 = n_2$, le nombre d'expériences qui ont servi pour obtenir la valeur moyenne considérée. Les résultats obtenus sont présentés dans le tableau 3.

Tableau 3

Effet d'interaction concentration-température sur les performances de la source chimique Zn-oxygène
(ΔP_{O_2} = 400 – 500 mmHg)

		5N		6N		7N	
Pertes par polarisation σ, % d ± 2,4	50°	14,8 13,1	13,95	10,5 10,2	10,35	13,6 12,0	12,8
	60°	12,0 11,5	11,75	10,6 9,4	10,0	12,2 13,9	13,05
	70°	12,0 9,0	10,5	9,7 8,7	9,2	12,0 12,7	12,35
Rendement de conversion moyen η_m, % d ± 1,2	50°	34,4 35,2	34,8	36,5 36,7	36,6	35,0 35,8	35,4
	60°	35,6 35,9	35,75	36,3 36,9	36,6	35,6 34,6	35,1
	70°	35,5 36,9	36,2	36,6 37,1	36,85	35,5 35,3	35,4
d.c. apparente moyenne i_m, mA/cm² d ± 8,4	50°	161 156,5	158,75	165,3 164,3	164,8	175 163,9	169,45
	60°	205,3 200	202,65	206,2 199,2	202,7	201,4 181,5	191,45
	70°	205 206,1	205,55	208,3 205,4	206,85	211,7 210,5	211,1
Puissance maximale P_{max} mW/cm² d ± 7,7	50°	112,1 111,7	111,9	122,3 122	122,15	121,4 118,8	121,4
	60°	149,6 146,7	148,15	153,1 150,4	151,75	146,3 128,7	137,5
	70°	150,2 157,5	153,85	157,5 157,4	157,45	155,1 153,6	154,35

De l'examen des données présentées dans le tableau d'interaction il résulte que :

— L'augmentation de la concentration de l'électrolyte à partir de la valeur de 5N jusqu' à 6N produit une diminution des pertes par polarisation, significative à la température de 50° ; l'augmentation de la concentration à partir de la valeur de 6N jusqu'à 7N a un effet négatif, dans tout le domaine de température étudié. La variation de la température de l'électrolyte n'a pas d'effet significatif sur les pertes par polarisation, dans le domaine de concentration considéré.

— L'augmentation de la concentration de l'électrolyte à partir de la valeur de 5N jusqu'à 6N a un effet favorable sur le rendement moyen de conversion, significatif à la température de 50° ; la variation de la concentration à partir de 6N jusqu'à 7N a un effet défavorable, significatif dans tout le domaine de température étudié. La variation de la température de l'électrolyte n'a pas d'effet significatif.

— L'augmentation de la température de l'électrolyte à partir de la valeur de 50° jusqu'à 60° a un effet favorable sur la densité apparente de courant, significatif dans tout le domaine de concentration étudié. L'effet de l'augmentation de la température à partir de 60° jusqu'à 70° n'est pas significatif. La variation de la concentration de l'électrolyte n'a pas d'effet significatif dans tout le domaine de température étudié.

— L'augmentation de la température de l'électrolyte, à partir de la valeur de 50° jusqu'à 70°, a un effet favorable sur la puissance maximale de la source chimique de courant Zn-oxygène étudiée, significatif dans tout le domaine de concentration considéré. L'augmentation de la concentration de l'électrolyte à partir de la valeur de 5N jusqu'à 6N a un effet favorable, significatif à la température de 50° ; l'augmentation de la concentration à partir de 6N jusqu'à 7N a un effet défavorable sur la puissance maximale de la pile.

Ainsi qu'on peut voir des données présentées ci-dessus, l'analyse dispersionnelle nous a permis de séparer les paramètres dont l'effet sur les performances de la source chimique de courant est significatif (concentration, température) ; ces conclusions sont nécessaires dans l'étude effectuée pour optimiser le processus.

2.2. L'ÉTABLISSEMENT DES PARAMÈTRES OPTIMAUX DE FONCTIONNEMENT

Conformément aux méthodes modernes d'interprétation des données expérimentales,[5,6] après avoir localisé un domaine dans le voisinage duquel les performances sont maximales, il faut explorer cette zone, en vue de déterminer les paramètres optimaux du processus. La méthode consiste dans l'établissement, à partir d'un programme d'expériences

---

[5] G. E. P. Box, L. R. Connor, R. W. Consins, O. L. Davies, F. R. Himsworth et G. P. Sillitto, « The Design and Analysis of Industrial Experiments », ed. O. L. Davies, Oliver and Boyd for Imperial Chemical Industries Ltd., Londres, 1963, p. 247.

[6] A. G. Worthing et J. Geffner, « Treatment of Experimental Data », Wiley, Londres, 1955, p. 91.

factorielles, des fonctions de régression qui décrivent, d'une manière satisfaisante, les relations qui existent entre les variables dans le voisinage des conditions qui correspondent aux performances maximales et dans l'exploration locale de la surface de réponse.

Les fonctions qui décrivent les relations qui existent entre les variables indépendantes significatives — la température (x_1) et la concentration (x_2) — et les variables dépendantes (y) — les pertes par polarisation, le rendement moyen de conversion, la densité apparente de courant, la puissance maximale — sont du type

$$y = b_0 + b_1x_1 + b_2x_2 + b_{12}x_1x_2 + b_{11}x_1^2 + b_{22}x_2^2$$

Le calcul des valeurs des coefficients des fonctions de régression ($b_0 \ldots b_{22}$) a été effectué par la méthode des moindres carrés,[5] à partir des données obtenues dans un programme d'expériences factorielles (un système ortogonal de $3^2 = 9$ expériences, symétrique par rapport à un point central, dont les coordonnées ont été établies par l'analyse dispersionnelle — 6N, 60°).

On a considéré que les distances de déplacement (la différence qui existe entre les valeurs des paramètres), de 1 méquiv. cm^{-3} et de 10°, sont caractéristiques pour l'effet de la variation des paramètres significatifs. Les valeurs codifiées des variables indépendantes correspondent à : $-1 = 50°$; $0 = 60°$; $1 = 70°$ (pour x_1) et $-1 = 5\text{N}$; $0 = 6\text{N}$; $1 = 7\text{N}$ (pour x_2).

Pour vérifier la validité des fonctions de régression, établies pour chaque caractéristique électrique considérée, on a calculé les valeurs y_{calc}, pour chaque combinaison température-concentration et on a testé l'écart des valeurs observées par rapport aux valeurs calculées (on a vérifié le caractère linéaire des fonctions de régression). Dans ce but on a calculé la dispersion due à la régression (s_1^2), la dispersion due aux erreurs expérimentales (s_r^2) et la valeur du facteur $F(s_1^2/s_r^2)$, qui a été comparée avec les valeurs critiques F_α, correspondant à un seuil de signification $\alpha = 0{,}01$.

En annulant les dérivées partielles des fonctions de régression, par rapport aux variables indépendantes, on a obtenu, pour chaque caractéristique électrique considérée, un système à deux équations linéaires, dont la solution a conduit à l'établissement des valeurs optimales des variables indépendantes, auxquelles les performances sont maximales.

Les résultats obtenus dans les calculs d'optimisation sont présentés dans le tableau 4.

De l'examen des données présentées dans le tableau 4, on constate que, pour toutes les caractéristiques électriques considérées, les valeurs de F sont plus petites que les valeurs critiques F_α, ce qui nous a permis d'accepter l'hypothèse de zéro et de tirer la conclusion que les fonctions de régression établies décrivent d'une manière satisfaisante, les relations qui existent entre les variables dans le domaine optimal de fonctionnement.

A l'aide de ces fonctions de régression on a tracé les courbes de réponse dans le plan des paramètres significatifs, pour les pertes par pola-

Tableau 4

Fonctions de régression pour les caractéristiques électriques de la pile Zn-oxygène (ΔP_{O_2} = 400–500 mm Hg)

	N°	x_1	x_2	y_1	y_2	$\bar{y}$		y_{calc}		
σ	1	−1	−1	14,8	13,1	13,95		12,75		
	2	0	−1	12,0	11,5	11,75	b_0 = 9,95	11,4		
	3	1	−1	12,0	9,0	10,5	b_1 = − 0,834	9,7	s_1^2 = 3,54	89,9°
	4	−1	0	10,5	10,2	10,35	b_2 = 0,333	10,9		4,38N
	5	0	0	10,6	9,4	10,0	b_{12} = 0,75	10,0	s_r^2 = 0,666	
	6	1	0	9,7	8,7	9,2	b_{11} = 0,01	9,9	F = 5,30	7,5%
	7	−1	1	13,6	12,0	12,8	b_{22} = 1,56	12,0		
	8	0	1	12,2	13,9	13,05		11,9	F_α = 6,99	
	9	1	1	12,0	12,7	12,35		11,9		
η_m	1	−1	−1	34,4	35,2	34,8		34,9		
	2	0	−1	35,6	35,9	35,75	b_0 = 36,63	35,5		
	3	1	−1	35,5	36,9	36,2	b_1 = 0,277	36,8	s_1^2 = 0,71	55,4°
	4	−1	0	36,5	36,7	36,6	b_2 = − 0,128	36,7		6,08N
	5	0	0	36,3	36,9	36,6	b_{12} = − 0,67	36,6	s_r^2 = 0,16	
	6	1	0	36,6	37,1	36,85	b_{11} = 0,3	37,2	F = 4,44	36,7%
	7	−1	1	35,0	35,8	35,4	b_{22} = − 1,225	36,0		
	8	0	1	35,6	34,6	35,1		35,3	F_α = 6,99	
	9	1	1	35,5	35,3	35,4		35,4		
i_m	1	−1	−1	161,0	156,5	158,75		161,7		
	2	0	−1	205,3	200,0	202,65	b_0 = 199,96	197,6		
	3	1	−1	205,0	206,1	205,55	b_1 = 21,75	207,8	s_1^2 = 93,1	68,5°
	4	−1	0	165,3	164,3	164,8	b_2 = 0,842	165,4		5,92N
	5	0	0	206,2	199,2	202,7	b_{12} = − 1,287	200,0	s_r^2 = 19,01	
	6	1	0	208,3	205,4	206,85	b_{11} = − 12,783	208,9	F = 4,89	210,1
	7	−1	1	175,0	163,9	169,45	b_{22} = − 1,558	166,0		mA/cm²
	8	0	1	201,4	181,5	191,45		199,25	F_α = 6,99	
	9	1	1	211,7	210,5	211,1		207,0		
P_{max}	1	−1	−1	112,1	111,7	111,9		111,1		
	2	0	−1	149,6	146,7	148,15	b_0 = 152,14	144,3		
	3	1	−1	150,2	157,5	153,85	b_1 = 18,675	153,5	s_1^2 = 62,04	66,5°
	4	−1	0	122,3	122,0	122,15	b_2 = 0,725	122,4		5,99N
	5	0	0	153,1	150,4	151,75	b_{12} = − 1,5	152,1	s_r^2 = 11,35	
	6	1	0	157,5	157,4	157,45	b_{11} = − 15,033	157,8	F = 5,47	157,9
	7	−1	1	124,0	118,8	121,4	b_{22} = − 5,092	119,6		mW/cm²
	8	0	1	146,3	128,7	137,5		145,8	F_α = 6,99	
	9	1	1	155,1	153,6	154,35		151,9		

risation, le rendement moyen de conversion, la densité apparente de courant et la puissance maximale (fig. 1).

De l'examen des courbes présentées dans la figure 1, on constate que les centres des courbes de réponse P_{max} et i_m se trouvent tout proche (5,99N – 66,5° et, respectivement, 5,92N – 68,5°). Le déplacement de ces maxima n'est pas significatif (pour les coordonnées du P_{max}, $i_m > 200$ mA/cm² et, l'intervalle de confiance pour la densité apparente de courant étant de ±8,4 mA/cm², la différence peut être considérée non significative).

Le centre des courbes de réponse η_m est déplacé vers des températures plus petites (6,08N–55,4°) et ce déplacement présente un caractère significatif parce que les coordonnées de ce point correspondent à des densités apparentes de courant $i_m < 195$ mA/cm².

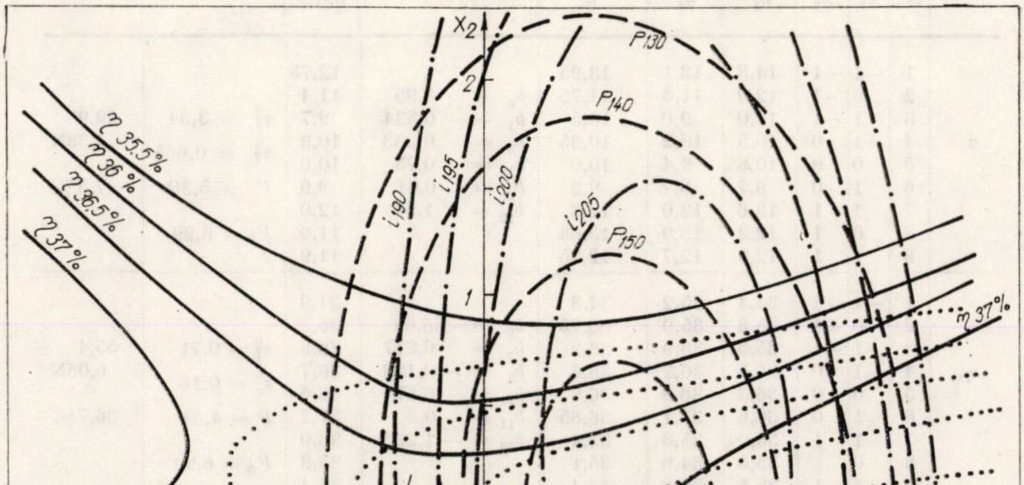

Fig. 1. — Courbes de réponse, caractéristiques pour les performances électriques de la source chimique Zn-oxygène étudiée ($\Delta P_{O_2} = 400-500$ mm Hg).

Le centre des courbes de réponse σ est déplacé vers des températures plus élevées ; évidemment ce domaine de fonctionnement ne présente pas d'intérêt pratique à cause des difficultés d'exploitation (l'augmentation de la pression de vapeurs de l'électrolyte, les pertes élevées de chaleur, la corrosion puissante en milieu de KOH, le gabarit de l'installation, etc.). Les valeurs comprises entre 9 et 9,5%, pour les pertes par polarisation, correspondant aux coordonnées des centres des courbes de réponse $P_{\max}$ et i_m, peuvent être considérées suffisamment réduites.

Pour les coordonnées du maximum de la puissance et de la densité apparente de courant la valeur du rendement moyen de conversion est plus grande que 36,5%, valeur proche de celle qui correspond aux coordonnées de 6,08N – 55,4° (36,7%), ce qui nous a conduit à la conclusion que le domaine optimal du fonctionnement de la pile correspond à la zone se trouvant dans le voisinage du maximum de la densité apparente de courant et de la puissance (la différence entre les valeurs du rendement moyen de conversion est plus petite que l'intervalle de confiance, $\pm 1,2\%$).

Ces données nous ont permis d'établir les paramètres optimaux de fonctionnement de la source chimique de courant Zn-oxygène, à cathode en argent (pour le domaine $\Delta P_{o_2} = 400-500$ mm Hg) aux valeurs suivantes : concentration de KOH, approximativement 6N, température, 67 – 68°. Dans ces conditions, la pile étudiée réalise un rendement moyen de conversion d'environ 36,5%, les pertes par polarisation étant d'approximativement 9,5% ; la densité apparente de courant est d'environ 210 mA/cm^2 et la puissance maximale de 157 mW/cm^2.

3. CONCLUSIONS

1. On a testé, par l'analyse dispersionnelle, l'effet de la variation de la concentration (5N – 7N), de la température (50 – 70°) et de la surpression de l'oxygène (400 et 500 mm Hg), sur les performances d'une source chimique Zn/KOH/O_2 à cathode en argent. On a constaté que la variation de la surpression de l'oxygène n'a pas d'effet significatif, dans le domaine considéré ; la variation de la concentration de l'électrolyte présente un effet significatif sur les pertes par polarisation et sur le rendement moyen de conversion réalisé par la source chimique de courant ; la variation de la température, de la concentration et de l'interaction température-concentration présente un effet significatif sur la densité apparente de courant et sur la puissance maximale de la pile.

2. A partir des données obtenues dans un programme orthogonal de $3^2 = 9$ expériences, symétrique par rapport à un point central défini par les coordonnées 6N – 60° (unités de déplacement de 1 méquiv. cm^{-3} et, respectivement, de 10°), on a établi les fonctions de réponse du type $y = b_0 + b_1x_1 + b_2x_2 + b_{12}x_1x_2 + b_{11}x_1^2 + b_{22}x_2^2$, pour chaque caractéristique électrique considérée (pertes par polarisation, rendement moyen de conversion, densité apparente de courant, puissance maximale).

3. A l'aide de ces fonctions de régression on a tracé les courbes de réponse, dans le plan des paramètres significatifs et, par l'interprétation de ces courbes, on a établi les valeurs optimales pour la concentration et la température de l'électrolyte (à une surpression de l'oxygène dans le domaine 400 – 500 mm Hg) : 6N et 67 – 68°. Dans ces conditions, les performances de la pile sont : pertes par polarisation 9 – 9,5%, rendement moyen de conversion 36,5%, densité apparente de courant 210 mA/cm^2 et puissance maximale 157 mW/cm^2.

Revue Roumaine de Chimie, **21**, 3, 373 – 383 (1976)

Revue Roumaine de Chimie, **21**, *3*, 385−390 (1976)

HETEROPOLYTUNGSTATES WITH U(IV) AS CENTRAL ATOM. I

PHOTOCOLORIMETRICAL STUDY OF THE FORMATION OF HETEROPOLYCOMBINATION UL_2 WHERE $L = PW_{11}O_{39}^{7-}$ AND $P_2W_{21}O_{71}^{6-}$

GH. MARCU and MARIANA RUSU
Chemistry Laboratory of Radioactive Elements,
University "Babeş-Bolyai", str. Arany Janos nº 11, Cluj, Romania

Received July 15, 1974

The U(IV) ion has a rapid reaction with the unsaturated heteropolyanions, forming UL_2 complexes where $L = PW_{11}O_{29}^{7-}$ and $P_2W_{17}O_{61}^{10-}$. The conditions of forming in solution were measured for the heteropolyanions of the type UL_2, where $L = PW_{11}O_{39}^{7-}$ and $P_2W_{21}O_{71}^{6-}$ depending on concentration, pH, temperature and time, using the method of molar ratios applied in photocolorimetry.

1. GENERALITIES

It is well known that the "unsaturated" heteropolyanions of the type $PW_{11}O_{39}^{7-}$, $SiW_{11}O_{39}^{8-}$ and $P_2W_{17}O_{61}^{10-}$ are reacting with various cations M^{2+}, M^{3+} and M^{4+} forming mixed heteropolyanions of type ML,[1-6] where $L = SiW_{11}O_{39}^{8-}$, $PW_{11}O_{39}^{7-}$ and $P_2W_{17}O_{61}^{10-}$.

The ions of lanthanides and actinides are rapidly reacting with the "unsaturated" heteropolyanions, forming mixed heteropolycompounds of type ML_2, where $L = PW_{11}O_{39}^{7-}$ and $P_2W_{17}O_{61}^{10-}$ which are resulting from the incomplete degradation of heteropolyanions of type 12 and 18 at a pH situated in the near proximity of neutrality.[7]

In the chemical literature mixed heteropolyanions of the type ML_2 of lanthanides and actinides were reported only in the last years.[8-10]

---

[1] C. M. Tourne and G. F. Tourne, *Compt. rend.*, **266**, 702 (1968).
[2] C. M. Tourne and G. F. Tourne, *Compt. rend.*, **266**, 1363 (1968).
[3] T. J. R. Weakley and S. A. Malik, *J. Inorg. Nuclear Chem.*, **29**, 2935 (1967).
[4] S. A. Malik and T. J. R. Weakley, *Chem. Comm.*, **1094**, (1967).
[5] C. M. Tourne and G. F. Tourne, *Bull. Soc. chim. France*, **1969**, 1124.
[6] L. C. W. Baker and T. P. McCutcheon, *J. Amer. Chem. Soc.*, **78**, 4503 (1956).
[7] P. Souchay, *Ann. Chim.* (*France*), **20**, 73 (1967).
[8] R. D. Peacock and T. J. R. Weakley, *J. Chem. Soc.* (*A*)., **1971**, 1836.
[9] A. V. Botar and T. J. R. Weakley, *Rev. Roumaine Chim.*, **18**, 1155 (1973).
[10] Gh. Marcu, M. Rusu and A. V. Botar, *Rev. Roumaine Chim.*, **19**, 827 (1974).

During the present work the conditions of forming in solution were measured, for the heteropolyanions of type UL_2 where $L = PW_{11}O_{39}^{7-}$ and $P_2W_{21}P_{71}^{6-}$, depending on concentration, pH, temperature and time, using the method of molar ratios applied in photocolorimetry.[11-17]

2. EXPERIMENTAL PART

If to a solution of the potassium salt of heteropolyanions $PW_{11}O_{39}^{7-}$ a solution which contains the U(IV) ion is added, an intense modification of colour may be qualitatively observed, the reaction takes place rapidly, even during the mixing of the reaction partners, according to equation (1)

$$2\,K_7PW_{11}O_{39} + U(SO_4)_2 = K_{10}[U(PW_{11}O_{39})_2] + 2K_2SO_4 \qquad (1)$$

To establish the forming conditions of heteropolycompounds $K_{10}[U(PW_{11}O_{39})_2]$ and $K_8[U(P_2W_{21}O_{71})_2]$ trials were made on solutions of different concentrations of 10^{-2}—$5 \cdot 10^{-3}$M.

To establish the optimal pH value of the formation in solution of the considered heteropolyanion, a series of 16 samples containing the two components were prepared, $K_7PW_{11}O_{39}$ with the concentration $5 \cdot 10^{-3}$M and $U(SO_4)_2$ with the concentration $5 \cdot 10^{-2}$M, where the tungsten was measured by precipitation with cinchonine and ignition to WO_3[18] and the uranyl ion was measured by spectrophotocolorimetrical dosage with Arsenazo III at 665 nm, using cuvettes of 1 cm,[19] with molar ratio of 2 : 1 at the following pH values : 0.5 ; 1 ; 1.5 ; 2 ; 2.5 ; 3 ; 3.5 ; 4 ; 4.5 ; 5 ; 5.5 ; 6 ; 6.5 ; 7 ; 7.5 and 8 the extinction of these solutions being measured an hour after their preparation.

The extinctions were measured with a photocolorimeter of ΦEK—KM type, using blue filter and cuvette of 1 cm the values of pH being measured with a pH-meter MV—11 with glass electrode.

The experimental results are indicated on curve *1* in figure 1.

The forming of heteropolycombinations $K_{10}[U(PW_{11}O_{39})_2]$ and $K_8[U(P_2W_{21}O_{71})_2]$ depending on temperature was photocolorimetrically studied as well; by heating the above mentioned samples, for 10 minutes at 70°. The samples were allowed to cool and the pH and extinctions values were measured.

The results of measuring are indicated on curve 2 in figure 1.

Further the forming of heteropolyanions $K_{10}[U(PW_{11}O_{39})_2]$ and $K_8[U(P_2W_{21}O_{71})_2]$ depending on pH was studied for the following time period : an hour after preparing the solutions, after 1 day, 2 days, 3 days and 7 days. The obtained results are indicated in figure 2, curves *1—6*.

The stoichiometry of chemical forming reactions of the potassium salt of $[U(PW_{11}O_{39})_2]^{10-}$ was established using the method of photocolorimetrical titration. For this purpose a series of 16 samples containing the two components ($K_7PW_{11}O_{39}$ with $T_W = 0.008505$ and $U(SO_4)_2$ with $T_U = 0.001570$) was prepared in different molar ratios. The pH of samples was adjusted to 4.5 using 0.1 M KOH and 0.1 M HCl then their extinctions were measured. The experimental results are indicated in figure 3.

The stoichiometry of the forming reaction of the heteropolyanion $[U(P_2W_{21}O_{71})_2]^{8-}$ was also established using in this case the method of photocolorimetrical titration.

For this purpose, a series of 16 samples containing the two components $K_7PW_{11}O_{39}$ with $T_W - 0.007804$ and $U(SO_4)_2$ with $T_U - 0.001575$ in different molar ratios were prepared

---

[11] S. A. Meyer Jr. and G. H. Ayres, *J. Amer. Chem. Soc.*, **77**, 2671 (1955).

[12] P. Courtin, F. Chaveau and P. Souchay, *Compt. rend.*, **258**, 1247 (1964).

[13] P. Courtin. *Bull. Soc. chim. France*, **1970**, 4799.

[14] P. Souchay and P. Courtin, *Compt. rend.*, **270**, 1714 (1970).

[15] A. F. Babko and Yu. F. Shkaravski, *Zhur. neorg. Khim.*, **7**, 1565 (1962).

[16] Yu. F. Shkaravski, *Zhur. neorg. Khim.*, **10**, 1179 (1965).

[17] Yu. F. Shkaravski, *Zhur. neorg. Khim.*, **8**, 2668 (1963).

[18] I. A. Vogel, "Text Book of Quantitative Inorganic Analysis", 2nd ed., London 1951, p. 418.

[19] B. S. Savvin, *Talanta*, **8**, 673 (1961).

Fig. 1. — Extinction variation of $5 \cdot 10^{-3}$ M $K_7PW_{11}O_{39}$ and $5 \cdot 10^{-2}$M $U(SO_4)_2$ solution mixtures, with a molar ratio of 2:1 depending on pH (curve *1*) and temperature (curve *2*).

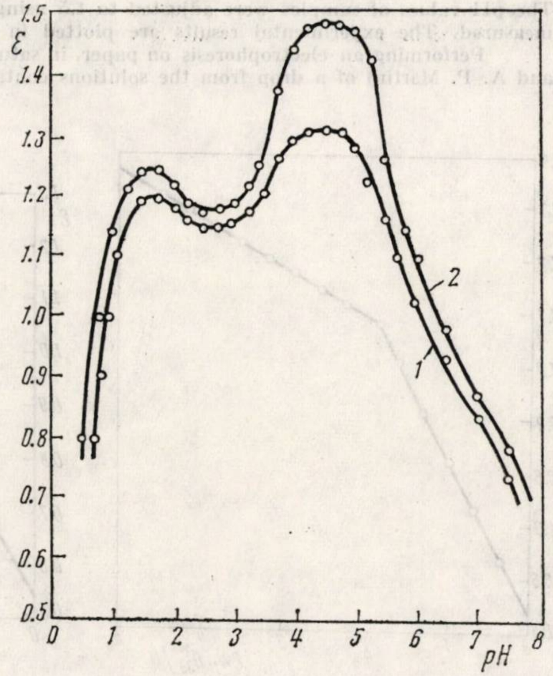

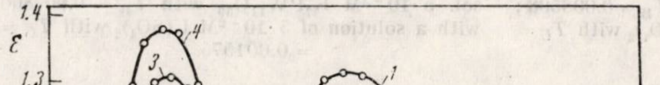

Fig. 2. Extinction variation of $5 \cdot 10^{-3}$M $K_7PW_{11}O_{39}$ and $5 \cdot 10^{-2}$M $U(SO_4)_2$ solution mixtures with a combination ratio of 2:1 with pH depending on time. *1*, one hour after the preparing of solutions; *2*, after 6 hours; *3*, after one day; *4*, after 2 days; *5*, after 3 days; *6*, after 7 days.

The pH values of samples were adjusted to 1.5 using 0.1 M HCl, then the extinctions were measured. The experimental results are plotted in figure 4.

Performing an electrophoresis on paper, in saturated NaCl (according to A. H. Gordon and A. P. Martin) of a drop from the solutions containing the two components ($K_7PW_{11}O_{39}$ and $U(SO_4)_2$) at pH = 4.5 and 1.5, two different electrograms were obtained, which are indicated in figure 5.

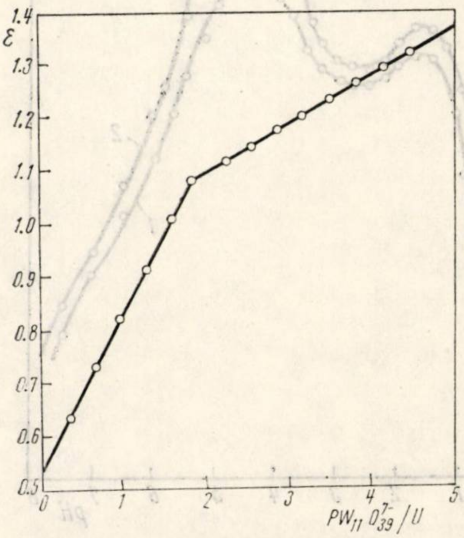

Fig. 3. Photocolorimetrical titration of 25 ml sol. $5 \cdot 10^{-3}$M $K_7PW_{11}O_{39}$ with $T_W = 0.008508$; with a solution $5 \cdot 10^{-2}$M $U(SO_4)_2$ with $T_U = 0.001575$.

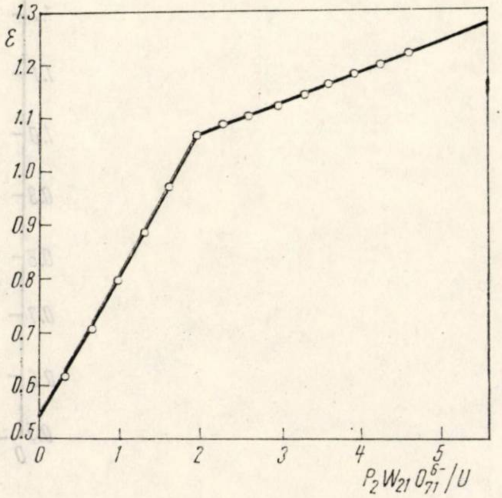

Fig. 4. Photocolorimetrical titration of 25 ml sol. $5 \cdot 10^{-3}$M $K_7PW_{11}O_{39}$ with $T_W = 0.007800$ with a solution of $5 \cdot 10^{-2}$M $U(SO_4)_2$ with $T_U = 0.001575$.

On the first electrogram only one spot appeared due to the heteropolycompound. This was identified by its own colour.

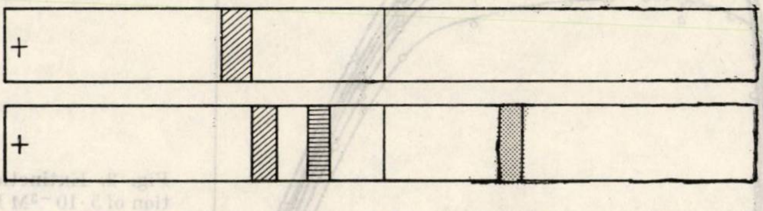

Fig. 5. The electrochromatograms obtained using electrochromatography in saturated NaCl of the following solution mixtures:

1) $K_7PW_{11}O_{39}$ + U(IV) with pH = 4.5
2) $K_7PW_{11}O_{39}$ + U(IV) with pH = 1.5

The second electrogram reveals three spots: one corresponding to the heteropolycompound identified by its own colour, the second due to $H_3PW_{12}O_{40}$ identified by reduction with UV radiations to "tungsten blue" and the third, which is caused by the uncomplexated U(IV) ion, identified by spraying the electrochromatogram with $K_4[Fe(CN)_6]$.

3. RESULTS AND DISCUSSION

The forming conditions in solution of the heteropolyanions $K_{10}[U(PW_{11}O_{39})_2]$ (I) and $K_8[U(P_2W_{21}O_{71})_2]$ (II) depending on concentration, pH, temperature and time were studied, using the method of molar ratios applied to photocolorimetry. The extinctions in solutions of different concentrations were measured and the optimal value of concentration for the measuring of extinction was established, as being comprised between $5 \cdot 10^{-3}$M and $5 \cdot 10^{-2}$M.

To establish the optimal pH of forming in solution of the heteropolyanions I and II, the extinction of samples in solution was plotted graphically, depending on pH. Figure 1 on which the experimental values of extinction, depending on pH, are plotted shows that the maximal extinction corresponding to the domain of maximal stability of the heteropolycompound (I) is comprised between pH = 4 and pH = 5.

The presence of another extinction peak was pointed out corresponding to the domain of pH = 1—2. This fact demonstrates the presence of a second compound in the studied pH domain, a fact that may be explained by a degradation in acidic medium of the heteropolycompounds containing P of series 11,[20] according to the equation:

$$3[U(PW_{11}O_{39})_2]^{10-} + 84\,H^+ = PW_{12}O_{40}^{3-} + \\ + [U(P_2W_{21}O_{71})_2]^{8-} + 2U^{4+} + 42\,H_2O \qquad (2)$$

This new heteropolycompound in solution recognized by the present authors, using the photocolorimetrical method, was synthesized and analysed, the above given formulation being established with certainty.

Studying the variation of extinctions with pH, depending on temperature (curve 2, figure 1) we established the positive influence of temperature on the formation of the heteropolycompound $[U(PW_{11}O_{39})_2]^{10-}$ the forming of heteropolycompound $[U(P_2W_{21}O_{71})_2]^{8-}$ being less influenced; the stability pH domain of the studied heteropolycompounds being at the same time extended.

Curves *1—6* (figure 3) indicate that time has no positive influence on the heteropolyanion forming $[U(PW_{11}O_{39})_2]^{10-}$ the extinction already decreased 6 hours after preparing the solutions, which demonstrates the poor stability in solution of this heteropolyanion. With regard to the heteropolycompound $[U(P_2W_{21}O_{71})_2]^{8-}$, time influences positively its forming, the extinction increases with time (curves *2* and *3*) attaining the maximal value after two days (curve *4*) and then, from the third day on (curve *5*), the extinction decreases, after *7* days the obtained curves present the character of curve *6*, the extinction decreases very much, degradation products appearing in samples, both in alkaline and acidic medium.

A study of the photocolorimetrical curves (figures 3 and 4) indicating the variations of extinction depending on the molar ratio, L : U, where $L = PW_{11}O_{39}^{7-}$ and $P_2W_{21}O_{71}^{6-}$, shows that these curves are formed of two half-lines, which are crossing each other at a molar ratio value equal to two.

---

[20] P. Souchay, "Ions Mineraux Condensés", Masson et Cie Editeurs, Paris, 1969, p. 98.

CONCLUSIONS

1. Using photocolorimetrical studies, the forming in solutions of heteropolyanions of the type $[U(PW_{11}O_{39})_2]^{10-}$ and $[U(P_2W_{21}O_{71})_2]^{8-}$ was established.

2. The forming of these heteropolyanions is depending on concentration, pH, temperature and time. The optimal pH value for the forming of the compound $[U(PW_{11}O_{39})_2]^{10-}$ is 4.5 and for the $[U(P_2W_{21}O_{71})_2]^{8-}$ it is 1.5.

3. From photocolorimetrical titration the combination ratio of L : U was established, which in both cases has a 2 value.

4. The temperature influences positively the forming of $[U(PW_{11}O_{39})_2]^{10-}$ compound and has a less positive influence on the forming of $[U(P_2W_{21}O_{71})_2]^{8-}$ compound.

5. The time influences negatively the forming of $(U(PW_{11}O_{39})_2]^{10-}$ compound, due to the equilibrium process, which takes place in solution, what indicates the little stability of this compound. The more stable compound $[U(P_2W_{21}O_{71})_2]^{8-}$ is formed in time by the acid degradation of $[U(PW_{11}O_{39})_2]^{10-}$ compound.

Revue Roumaine de Chimie, **21**, *3*, 391 – 400 (1976)

EINFLUSS VON METHOXYL-SUBSTITUENT AUF DIE REAKTION ZWISCHEN [TlBr$_4$]$^-$ UND MALACHITGRÜN

CECILIA CONSTANTINESCU und GH. C. CONSTANTINESCU
Polytechnische Hochschule ,,Gh. Gheorghiu-Dej"
Bukarest, Splaiul Independenţei 213

Eingegangen am 15. Juni 1974

In der vorliegenden Arbeit wurden die optimalen Reaktionsbedingungen zwischen den basischen Farbstoffen *ortho*-Anisgrün bzw. *para*-Anisgrün und Komplexanionen von Thallium (III) studiert. Die gewonnenen Farbstoffe wurden zum Studium der Reaktion mit TlBr$_4^-$ benutzt und festgestellt, daß sie wasserunlösliche aber benzollösliche Verbindungen bilden, welche dann in Benzol extrahiert werden. Die organischen Extrakte wurden dann spektrophotometrisch und konduktometrisch untersucht. Außerdem wurden die Verbindungen ausgefällt und einer Elementaranalyse bzw. IR Spektralanalyse unterworfen. Die Ergebnisse stimmten überein. Die studierte Reaktion ist für die spektrophotometrische Analyse des Thalliums geeignet.

In einigen vorherigen Arbeiten wurden die Reaktionen zwischen den Thalliumkomplexionen und basischen Farbstoffen der triphenylmethanischen Klasse spektrophotometrisch studiert.[1–3]

Der Mechanismus ähnlicher Reaktionen wurde zuerst von Onishi [4] bestimmt und besteht in der Bildung in wäßrigen Medien der komplexen hallogeno-metallischen Säuren : HMX_4 ; H_2MX_5 ; H_3MX_6 ; die durch die Bindung des komplexen Anions MX^{n-}_{3+n} am Farbstoffskation gefolgt wird.

In dieser Arbeit werden die Synthese der basischen Farbstoffe *ortho*- und *para*-Anisgrün, die Ergebnisse der Forschungen bezüglich der Bildungsreaktion der ionischen Assoziation zwischen dem komplexen Anion TlBr$_4^-$ und der Kationen der Farbstoffe sowie auch die Struktur und einige Eigenschaften der erhaltenen Verbindungen dargestellt.

VERSUCHSTEIL

SYNTHESE DER FARBSTOFFE

Ortho-und *para*-Anisgrün wurden durch Anwendung der geeigneten Methode zur Erhaltung des triphenylmethanischen Farbstoffes Malachitgrün synthetisiert [5] d.h. durch die Kon-

---

[1] C. Constantinescu und S. Fişel, *Rev. Roumaine Chim.*, **19**, 329 (1974).

[2] C. Constantinescu, *Rev. Chim.* (*Bucureşti*), **23**, 495 (1972).

[3] C. Constantinescu und S. Fişel, *Rev. Roumaine Chim.*, **19**, 509 (1974).

[4] M. Onishi und E. B. Sandell, *Analyt. Chim. Acta*, **24**, 413 (1961).

[5] H. Sanielevici und C. Floru, ,,Sinteza intermediarilor aromatici şi a coloranţilor", Ed. II, Ed. didactică şi pedagogică Bukarest, 1971 p. 277.

densierung der *ortho-* und *para*-metoxybenzaldehyde (Anisaldehyde) mit Dimethylanilin. Die durch Erhitzung auf dem Wasserbad erhaltene dickflüssige Masse ist mit Wasserdampf angetrieben. Der zurückgebliebene Rückstand ist in Äthylalkohol aufgelöst, woraus die Leukobasis wieder ausgefällt wird. Durch Oxydation der Leukobasis mit Bleidioxyd erhält man das entsprechende Carbinol oder Pseudobase, welches mit Chlorwasserstoff die Kombination mit folgender Struktur bildet :

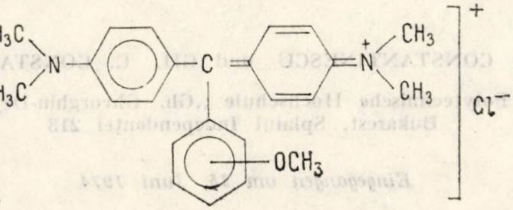

$-OCH_3$ in *Orto* oder *Para*stellung

Die Farbstoffe werden weiterhin in verkürzter Form bezeichnet : $[oR^+]Cl^-$; $[pR^+]Cl^-$

Die Reinigung erfolgte durch wiederholte Umkristallisation, wonach die Reinheit durch die Kaliumdichromatmethode bestimmt wurde.[6]

REAGENZIEN UND LÖSUNGEN

— Die wäßrige Lösung des Tl(III) war durch die Auflösung des Thallium (I) Nitrats, Zufügung von konzentriertem Bromwasserstoff, und Oxydierung mit Bromwasser hergestellt. Nach der Entfernung des Bromwasserstoffs durch Verdampfen wird eine Eichlösung vorbereitet, die 204 μg Tl/cm^3 enthält. Der Titer der Thalliumlösung wurde durch Fällung in Form von Thalliumjodid bestimmt.[7] Die in dieser Arbeit benutzten Lösungen wurden durch angemessene Verdünnungen vorbereitet.

— Man verwendet $1 \cdot 10^{-3}$ M Lösung bezogen auf die 100%ige Reinheit von *ortho-* und *para*-Anisgrün ;

— 64% ige Bromwasserstoff

— Benzol p.a.

— Lösungen verschiedener Kationen unter Form von Nitraten, Sulfaten und/oder Chloriden.

EXTRAKTION DES KOMPLEXES

Die $1 \cdot 10^{-5}$M Lösung von Tl(III) in Volumina von 0,1—2 cm^3 wird in einem Scheidetrichter oder Meßkolben von 50 cm^3 mit 64% igem Bromwassertoff (1 cm^3) und 1.10^{-3}M Reagenzlösung geführt. Man füllt destilliertes Wasser bis zum Volumen von 10 cm^3, fügt 10 cm^3 organisches Lösungsmittel hinzu und schüttelt 2 Minuten lang. In ähnlicher Weise wird auch die Blindprobe vorbereitet. Man mißt die Extinktionen der gefärbten organischen Phase bei den entsprechenden Wellenlängen in 1 cm dicken Küvetten.

DIE SYNTHESE DER KOMPLEXE

Um das Kombinationsverhältnis in festem Zustand des thallischen Anions mit den untersuchten Reagenzien festzulegen, wurden 0,25 g *ortho-* oder *para*-Anisgrün in 25 cm^3 Wasser gelöst und mit 0,25 g in 1 cm³ gelöster Tl(III) gemischt. Es erscheint ein blauer Niederschlag, der durch Filtrierung unter Vakuum getrennt und mit Wasser gewaschen wurde. Die Verbindungen wurden bezüglich des Gehalts an Thallium durch die Fällungsmethode (in Form von Thalliumjodid [7] an Stickstoff nach Pregel und an Brom nach Schöniger [8] analysiert. Die erhaltenen Ergebnisse sind in Tabelle 1 eingetragen, woraus hervorgeht, daß das Kombinationsverhältnis Metall-Farbstoff 1 : 1 ist.

---

[6] R. P. LESTONSKII und IO. I. VAINSTEIN „Tekhnicheskii analiz. v proizvodstve promezhjutochinykh productiv i crasitelei Gosudarstvenoe nauchino tekhnichescoe izdatelstvo khimichescoi literatury", Moskva, 1958.

[7] N. H. FURMAN, „Standard Methods of Chemical Analysis, Ed. VI, Van Nostrand", New York, 1963, p. 1051.

Tabelle 1

Die Elementaranalyse der Komplexe

Verbindung	Thallium		Stickstoff		Brom	
	Berechnet %	Gefunden %	Ber. %	Gef. %	Ber. %	Gef. %
$o-R^+ TlBr_4^-$	23,12	23,02	3,16	3,10	36,0	35,40
$p-R^+ TlBr_4^-$	23,12	22,90	3,16	3,08	36,0	35,33

ERGEBNISSE UND DISKUSSIONEN

Die Wahl des Lösungsmittels. Es wurden folgende Lösungsmittel erprobt: Benzol, Toluol, Chloroform, Aceton, Zyklohexanol, Benzol gemischt mit Methylethylceton und Benzol gemischt mit Äther. Man stellt fest, daß die Benzolmischung mit kleinen Mengen von Methylethylceton zur größten Extinktion führten, gefolgt von reinem Benzol. Da die Benzol-Methylethylceton Mischung auch eine Menge freien Farbstoff mitextrahiert, wurde in unseren Forschungen nur das Benzol als Lösungsmittel für beide Komplexverbindungen verwendet.

VERTEILUNGSKONSTANTE

Um die Verteilungskonstante des Metalls zwischen der wäßrigen und der organischen Phase festzustellen, kam eine spektrophotometrische Methode zur Anwendung.[9] Die Komplexverbindung wurde unter den optimalen Reaktionsbedingungen hergestellt und in Benzol extrahiert. Die beiden Phasen wurden getrennt, dann mit konzentrierter Schwefelsäure und Wasserstoffperoxyd behandelt. Die gelösten Tl (III) wurden in beiden Fällen durch Methylviolett nach Voskressenskaia [10] in Gegenwart von Bromwasserstoff bestimmt. Die erhaltenen Ergebnisse sind in Tabelle 2 nachgetragen. Die Verteilungskonstante

$$q = \frac{\mu\text{g Tl/cm}^3 \text{ organische Phase}}{\mu\text{g Tl/cm}^3 \text{ wäßrige Phase}}$$

---

[8] I. S. Lealicov, „Metode fizico-chimice de analiză", Ed. didactică şi pedagogică, Bukarest, 1963, p. 339.

[9] S. Fişel, „Chimia analitică cantitativă" Bukarest, 1973, p. 294.

[10] N. T. Voscresenscaia, *Zhur. anal. Khim.*, **11**, 585 (1956).

und die prozentuale Extraktion berechnet man nach:

$$\%E = \frac{100\ q}{q + \frac{V_{H_2O}}{V_{Benzol}}}$$

Tabelle 2

Der Verteilungskoeffizient

Verbindung	µg Tl/cm³		q	E%
	Zugegeben	in der Wasserphase geblieben		
$o-R^+\ TlBr_4^-$	2	0,2	0	90,0
$p-R^+\ TlBr_4^-$	2	0,3	5,66	85,0

Eine bessere Extraktion stellt man bei der Verwendung von *o*-Anisgrün fest. Es ist zu erwähnen, daß die mit *orto*-Anisgrün hergestellten Komplexverbindungen außerordentlich stabil sind (die Stabilität der organischen Phase in Kontakt mit der wäßrigen geht über 50 Stunden), die mit *para*-Anisgrün aber nur 2 Stunden.

Die größere Beständigkeit und Extraktibiltät der $(o-R^+;\ TlBr_4^-)$ im Vergleich zu $(p-R^+;\ TlBr_4^-)$ könnte auf dem von elektronenabstoßenden in *orto*-Stellung befundenden Substituenten hervorgerufenen größeren Effekt über die Unkoplanarität der Farbstoffsmoleküle hingedeutet werden. Ob dies als allgemeine Regel gilt, ist mit anderen Substituenten bzw. anderen Komplexanionen nachzuweisen.

ABSORBTIONSSPEKTREN IM SICHTBAREN BEREICH

Bei Bestimmung der elektronischen Absorbtionsspektren der wäßrigen Lösungen von *ortho*-Anisgrün (Abbildung 1) als Kurve C_1 und von *para*-Anisgrün als Kurve C_3 wird festgestellt, daß die beiden Spektren ein Absorptionsmaximum bei $\lambda_{max} = 606$ nm haben. Gleichzeitig ist zu erwähnen, daß das Absorptionsmaximum für Malachitgrün bei 620 nm ist, was mit der Feststellung von Dewar [11] übereinstimmt u.z., daß die elektronenabstoßenden Substituenten einen hypsochromischen Effekt zur Folge haben. Die mit Tl(III) in 10 cm³ Benzol erhaltenen Verbindungen haben ein Absorptionsmaximum bei $\lambda_{max} = 615$ nm sowohl für das *ortho*-Anisgrün (C_2) als auch für *para*-Anisgrün (C_4). Wir erwähnen, daß die Benzolextrakte der Kontrollproben ohne Gehalt an Tl(III) bei dem verwendeten pH-Wert überhaupt keine Färbung ergeben. Aus Abbildung 1 ist ersichtlich, daß die Maxima der Absorptionsbänder der Komplexe mit

---

[11] M. J. S. Dewar, *J. Chem. Soc.*, **1950**, 2327; **1954**, 2134.

Tl batochrom verschoben sind, im Verhältnis zu den Farbstoffspektren, Verschiebung, die der Bildung von Komplexen mit Ladungsübertragung vom Typus $\sigma-\pi$ zugeschrieben werden kann.

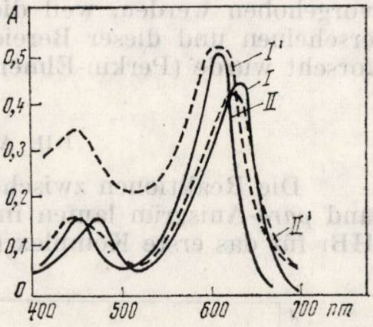

Abb. 1. — Elektronische Absorptionsspektren : I' — Farbstoff *orto*-Anisgrün ; I — Komplexverbindung mit *orto*-Anisgrün ; II' — Farbstoff *para*-Anisgrün, II — Komplexverbindung mit *para*-Anisgrün.

DIE IR ABSORPTIONSSPEKTREN

Diese Spektren werden in einem Bereich von 400—4 000 cm^{-1} erforscht. Bei Vergleichung der IR Spektren der freien Verbinder mit denen der entpsrechenden Thalliumkomplexverbindungen wurde festgestellt, daß die Lagen und die Größen der Vibrationsbänder nach der Reaktion sich nicht verändert haben, ein Hinweis dafür, daß sich die Komplexe mit Ladungsübertragung bildeten. Die charakteristischen Vibrationen der

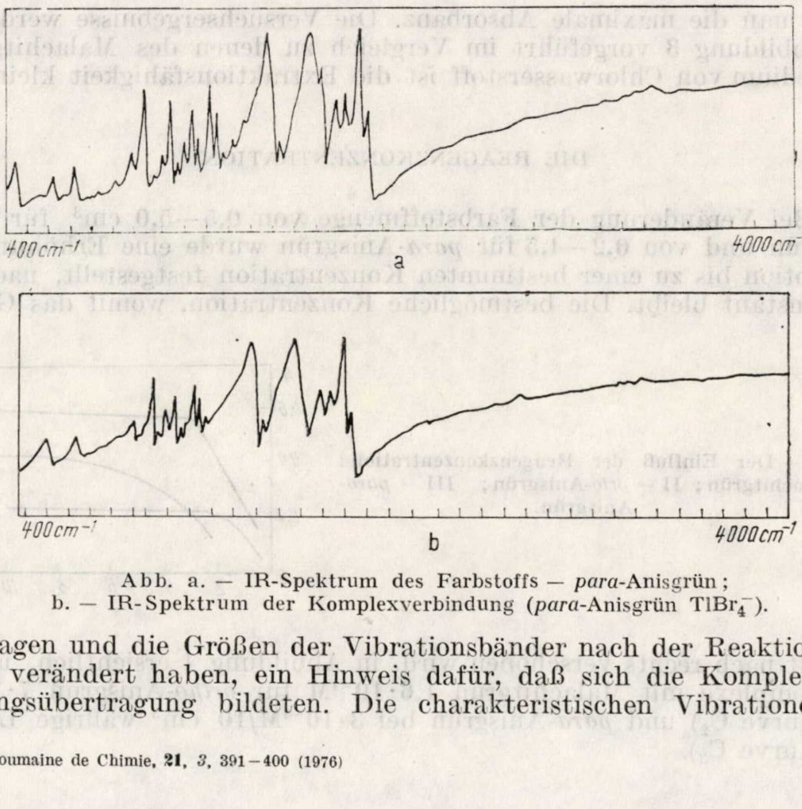

Abb. a. — IR-Spektrum des Farbstoffs — *para*-Anisgrün ;
b. — IR-Spektrum der Komplexverbindung (*para*-Anisgrün $TlBr_4^-$).

Verbindungen C—N (1 400 cm^{-1}), C—C (1 600 cm^{-1}), C—H (1 000 cm^{-1}) in den Spektren der Komplexen sind gewöhnlich etwas verschoben gegen kleinere Frequenzen wegen der Ausdehnung dieser Verbindungen nach der Komplexierung. Die Verbindungen mit Thallium konnten nicht hervorgehoben werden, weil die betreffenden Vibrationen unter 400 cm^{-1} erscheinen und dieser Bereich nicht mit dem verwendeten Apparat erforscht wurde (Perkin-Elmer 337).

DIE AZIDITÄT DER LÖSUNG

Die Reaktionen zwischen Thallium (III) und den Reagenzien *ortho-* und *para*-Anisgrün laufen im Milieu von Bromwasserstoff ab. Bei 2,8 N HBr für das erste Komplex (C_1) und 5,5 N HBr für den das zweite (C_2), erhält man die maximale Absorbanz. Die Versuchsergebnisse werden in der Abbildung 3 vorgeführt im Vergleich zu denen des Malachitgrüns. Im Medium von Chlorwasserstoff ist die Extraktionsfähigkeit klein.

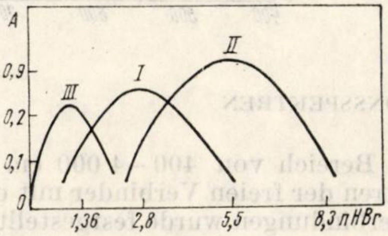

Abb. 3. — Der Einfluß der Lösungsazidität. I — Komplexverbindung mit *orto*-Anisgrün; II — Komplexverbindung mit *para*-Anisgrün. III — Komplexverbindung mit Richtmaß.

DIE REAGENZKONZENTRATION

Bei Veränderung der Farbstoffmenge von 0,5—5,0 cm^3 für *ortho*-Anisgrün und von 0,2—4,5 für *para*-Anisgrün wurde eine Erhöhung der Absorbtion bis zu einer bestimmten Konzentration festgestellt, nach der sie konstant bleibt. Die bestmögliche Konzentration, womit das Gleichgewicht nach rechts verschoben wird, in Abbildung 4 ersichtlich, ist für die Komplexe mit Malachitgrün $1{,}6 \cdot 10^{-4}$M für *ortho*-Anisgrün $7 \cdot 10^{-4}$M (die Kurve C_2) und *para*-Anisgrün bei $3 \cdot 10^{-4}$M/10 cm^3 wäßrige Lösung (die Kurve C_3).

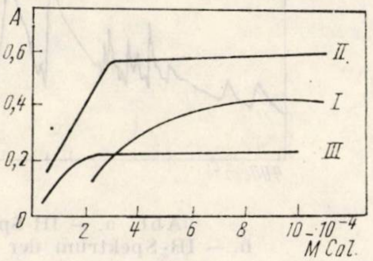

Abb. 4. — Der Einfluß der Reagenzkonzentration: I — Malachitgrün; II — *orto*-Anisgrün; III — *para*-Anisgrün.

DIE EICHKURVE

Das Studium der Absorptionsvariation in Abhängigkeit von der Konzentration von Thallium (III) hat gezeigt, daß das Bouguer-Lambert-Beer'sche Gesetz zwischen folgenden Grenzen als wahr erwiesen ist (Tabelle 3, Abbildung 5). Die Beständigkeit der komplexen Kombinationen beträgt

1/2 Stunde für Malachitgrün
2 Stunden für *para*-Anisgrüm
48 Stunden für *ortho*-Anisgrün

Tabelle 3

Die Grenzen des Lambert-Beer'schen Gesetzes

Verbindung	μg Tl/cm³	ε
o–$R^+ TlBr_4^-$	0,2–2	19.600
p–$R^+ TlBr_4^-$	0,2–2	23.000

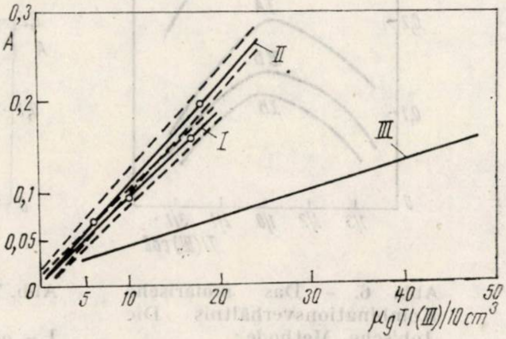

Abb. 5. — Die Eichkurve.
I — Malachitgrün ; II — *orto*-Anisgrün ; III — *para*-Anisgrün.

Die Eichungsgeraden wurden durch Verbesserung der Versuchsdaten mit Hilfe der Methode der kleinsten Quadrate erhalten. Durch die statistische Bearbeitung der Ergebnisse (Wahrscheinlichkeit 0,95) wird ersichtlich, daß die relative Abweichung für beide Methoden zwischen ± 3,2% wechselt.

DAS STUDIUM DER ZUSAMMENSETZUNG GEBILDETER KOMPLEXVERBINDUNGEN

Für die Bestimmung des Kombinationsverhältnisses Metall-Farbstoff in der organischen Lösung kamen die Methode Job [12] und die Methode des molaren Verhältnisses[13], zur Anwendung. Die erhaltenen Ergebnisse bei der Durchführung der Methode Job sind in der Abbildung 6 wiedergegeben, bei Benutzung zweier Paare von Isomolarlösungen : $1 \cdot 10^{-3}$M die Kurve C_1 und C_4 und $5 \cdot 10^{-4}$M die Kurven C_2, C_3. Bei der Methode des molaren Verhältnisses ist die Konzentration des Metalls konstant geblieben und die Konzentration des Farbstoffs verändert

---

[12] P. Job und Justus v Liebigs, *Ann. Chim. (France)*, **9**, 113 (1928).
[13] J. H. Yoe und H. E. Harvey, *J. Amer. Chem. Soc.*, **70**, 648 (1948).

(Abbildung 7 die Kurven C_1 und C_2). Beide Lösungen hatten gleiche Konzentration u.z. $1 \cdot 10^{-4}$M.

Die angewandten Methoden führten zum selben Ergebnis u.z. daß: das Kombinationsverhältnis Metall/Farbstoff für beide Verbindungen 1 : 1 ist. Dieses Ergebnis war zu erwarten, weil die Reaktionen im pH-Bereich durchgeführt wurden, in dem der Farbstoff hauptsächlich als Kation in monomerer Form vorliegt

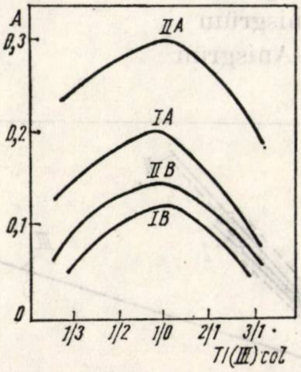

Abb. 6. — Das molarische Kombinationsverhältnis Die Job'sche Methode: IA; IB — *orto*-Anisgrün; IIA; IIB — *para*-Anisgrün.

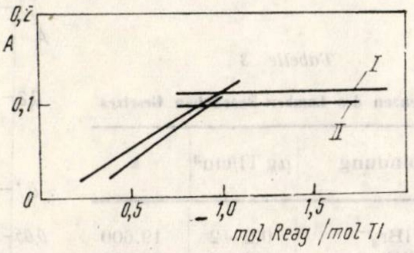

Abb. 7. — Das molarische Kombinationsverhältnis I — *orto*-Anisgrün; II — *para*-Anisgrün.

DIE BILDUNGSKONSTANTE DER KOMPLEXVERBINDUNGEN

Aus der graphischen Darstellung des molaren Verhältnisses (Abbildung 7) wurde die Bildungskonstante [13] K_f errechnet und es wurde für das zwichen Tl(III) und *ortho*-Anisgrün gebildete Komplex, $K = 2{,}0 \cdot 10^6$ gefunden und für Tl(III)-*para*-Anisgrün $K = 1{,}2 \cdot 10^7$.

Die erhaltenen Ergebnisse zeigen, daß sich durch Fällung hauptsächlich Komplexe vom Typus $R^+ \, [TlBr_4]^-$ bildeten. In Lösung wegen der Übermenge an Bromwasserstoff könnten folgende Gleichgewichte erscheinen:

$$TlBr_3 + HBr \rightleftarrows H[TlBr_4]$$

$$H[TlBr_4]^- + HBr \rightleftarrows H_2[TlBr_5]$$

$$H_2[TlBr_5]^- + HBr \rightleftarrows H_3[TlBr_6]$$

Unter den obenerwähnten Bedingungen herrscht das Bromkomplex $H[TlBr_4]^-$ vor, aus welchem Grund sich die ionische Assoziation bildet:

$$R^+Cl^- + H[TlBr_4]^- \rightleftarrows [R]^+[TlBr_4]^- + HCl$$

Es ist aber möglich, daß in der Lösung auch andere in Gleichgewicht bleibende Arten existieren wie:

$$R_2^+ \, [TlBr_5]^{2-}; \; R_3^+ \, [TlBr_6]^{3-}.$$

Der Einfluß fremder Ionen

Es wurden die Interferenz jener Ionen geprüft, die gewöhnlich in verschiedenen Materialien Thallium begleiten, so wie : Indium, Gallium, Eisen, Antimonium, Vanadium, Gold und Germanium. Die Reaktion ist vom Wachsen der Absorption in folgender Reihenfolge gestört :

$$Au(III) > Fe(III > In(III).$$

DER THERMISCHE ABBAU

Der thermooxydative Abbau von reinen Farbstoffen und deren mit $TlBr_4$-hergestellten Komplexverbindungen erfolgte thermogravimetrisch [7] in einem Temperaturintervall von 20–900° mit einem Gerät von Typ MOM Budapest, Erwärmungsgeschwindigkeit 9°/min in 100 min. In Abbildung 8 geben wir als Beispiel die Derivatogrammen vom Farbstoff *orto*-Anisgrün und deren Komplexverbindung mit $TlBr_4$ wieder.

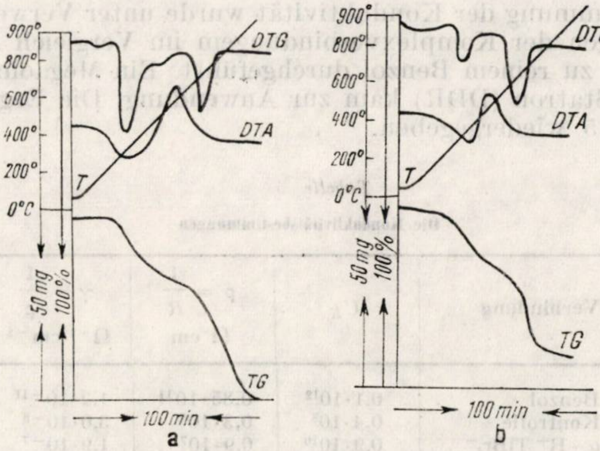

Abb. 8. — Die Derivatogrammen.

a — Der Farbstoff *orto*-Anisgrün ; *b* — Die Komplexverbindung *orto*-Anisgrün$^+$ $TlBr_4^-$.

Der Farbstoff ist bis 620° in vier Stufen abgebaut. Die DTA-Kurve gibt uns Informationen über den thermischen Effekt jeder Abbaustufe. Die ersten drei Stufen zeigen einen schwachen endothermischen Effekt und die vierte Stufe von 460–620°, einen ausgeprägten exothermischen Effekt, als Folge der Oxydation von Abbauproduktionen.

Der Abbau von Komplexverbindung zeigt ein ähnliches Verhalten aber mit anderen Gewichtverlusten für jede Stufe (Abbildung 8, Tabelle 4).

Bis 480° zeigt die Verbindung einen sehr schwachen Abbau und ab 480° zeigt die Entwicklung einen exothermischen Effekt, welcher zu

Thallium führt. Die Komplexverbindung ist temperaturbeständiger als der Farbstoff. Der Rückstand, in Gewichtsprozenten zu Einwaage, stimmt mit der berechneten Zusammensetzung der Elementaranalyse überein. Bis cca. 160° können die Verluste von 4% als Wasserverlust betrachtet werden.

Tabelle 4

Die Stufen des thermischen Abbaues

Verbindung	I. Stufe °C	II. Stufe °C	III. Stufe °C	IV. Stufe °C
($o-R^+ TlBr^-_4$)	45–160	160–240	240–460	460–620
($p-R^+ TlBr^-_4$)	45–180	180–350	350–585	–

KONDUKTIVITÄTSBESTIMMUNGEN

Die Bestimmung der Konduktivität wurde unter Verwendung organischer Lösungen der Komplexverbindungem im Vergleich zu der Kontrollprobe und zu reinem Benzol durchgeführt. Ein Megaohmmeter vom Typ Tetralin Statron (DDR) kam zur Anwendung. Die Ergebnisse sind in der Tabelle 5 wiedergegeben.

Tabelle 5

Die Konduktivitätsbestimmungen

Verbindung	U_K	$\rho = \frac{1}{R}$ Ω cm	$\gamma = \frac{1}{\rho}$ Ω^{-1} cm^{-1}
Benzol	$0{,}1 \cdot 10^{12}$	$0{,}85 \cdot 10^{11}$	$1{,}2 \cdot 10^{-11}$
Kontrolle	$0{,}4 \cdot 10^{8}$	$0{,}3 \cdot 10^{8}$	$3{,}0 \cdot 10^{-8}$
$o-R^+ TlBr_4^-$	$0{,}9 \cdot 10^{10}$	$0{,}9 \cdot 10^{7}$	$1{,}9 \cdot 10^{-7}$
$p-R^+ TlBr_4^-$	$0{,}7 \cdot 10^{10}$	$0{,}7 \cdot 10^{7}$	$1{,}5 \cdot 10^{-7}$

Der Konduktivitätsunterschied zwischen Benzol und der Kontrollprobe wird wohl der Gegenwart von in Benzol gelöstem Wasser und Säuremengen, als Folge der Mischung beider Phasen zugeschrieben. Im Vergleich zur Kontrolle steigt die Konduktivität der gelösten Komplexverbindungen etwa mit einer Größenordung, was auf eine gewisse Ionisierung hindeutet. Als Ursache vermuten wir auch das in Benzol gelöste Wasser.

Revue Roumaine de Chimie, **21**, *3*, 401–406 (1976)

COMPLEX CHELATE COMPOUNDS OF Mo(VI) AND W(VI) ISO- AND HETEROPOLYANIONS WITH CHROME AZUROL S. I

COMPLEX CHELATE COMPOUNDS OF Mo(VI) AND W(VI) ISOPOLYANIONS

P. B. ISSOPOULOS*

Department of Inorganic Chemistry, University of Patras, Patras, Greece, and
Institut für Anorganische Chemie der Universität Würzburg, Würzburg-BRD

Received October 19, 1974

The present work refers to the formation of complex chelate compounds of Mo(VI) and W(VI) isopolyanions with Chrome Azurol S. Their formation and composition is shown to depend on the pH of the reaction mixture. The compounds thus formed and their composition are studied spectrophotometrically by the method of continuous variations.

INTRODUCTION

The trisodium salt of 3″-sulpho-2″, 6″-dichloro-4′-hydroxy-3,3′-dimethylfuchsono-5,5′-dicarboxylic acid, known as Chrome Azurol S(C.I. N° 43825), has been employed for a long time and by many investigators as a ligand for the preparation of a large number of chelate compounds with typical metals or transition elements.

We have prepared recently such compounds of Chrome Azurol S (CAS) with metals as : indium (III), vanadium (III), copper (II) and iron (III) for the purpose of either studying the conditions of their structure or using these compounds for the determination of metal ions.[1–4]

A literature research revealed that no study has been undertaken on the reaction of CAS with Mo(VI) and (W(VI) iso- or heteropolyanions, except an analytical work for the determination of Mo(V) in which mention is made of the action of CAS on tungsten.[5]

---

[*] Author's present address : Department of Inorganic Chemistry, University of Patras, Patras, Greece.

[1] P. B. Issopoulos and A. Galinos, *Analusis*, **2**, 672 (1973).
[2] P. B. Issopoulos, *Ann. Chim.* (*France*), **9**, 157 (1974).
[3] P. B. Issopoulos, *Ann. Chim.* (*France*), **10**, 17 (1975).
[4] P. B. Issopoulos and A. Galinos, *Chim. Chron.*, in press.
[5] Y. Horiuchi and H. Nishida, *Bunseki Kagaku*, **18**, 1092 (1969).

In the present work the formation of the complex compounds between the isopolyanions $\{Mo_7O_{24}\}^{6-}$ and $\{HW_6O_{21}\}^{5-}$ and CAS is described, as well as the influence of pH on their formation. Also a study of the composition of these compounds by the method of continuous variations (Job's method) [6] is included.

EXPERIMENTAL PART

INSTRUMENTS

- Spectrophotometer Optica CF4R
- Spectrophotometer Hitachi-Perkin-Elmer 139
- Quartz cells, 10.0 mm
- pH-meter, Radiometer 22, with glass and calomel electrodes
- Thermostat, Ultrathermostat NBS (Gebrüder Haake K.G.).

REAGENTS

— Ammonium heptamolybdate	*p.a.*	Merck
— Ammonium tungstate	R	Carlo Erbe
— Chrome Azurol S		Merck
— Perchloric acid	"Suprapur"	Merck
— Sodium hydroxide	"Suprapur"	Merck
— Sodium nitrate	"Suprapur"	Merck

SOLUTIONS

Standard ammonium heptamolybdate (*AHM*) *solution.* An amount of 123.6 mg of $(NH_4)_6MO_7O_{24} \cdot 4H_2O$ is weighed accurately and transferred quantitatively in a 100 ml volumetric flask, where it is dissolved and diluted with doubly distilled water up to the mark. The resulting solution has a concentration in AHM of 1×10^{-3}M.

Standard ammonium tungstate (*AW*) *solution.* This solution is prepared by dissolving and diluting with doubly distilled water to a final volume of 100 ml, 313.4 mg of $(NH_4)_{10}W_{12}O_{41} \cdot 5H_2O$. The final concentration of the solution in AW is 1×10^{-3} M.

Standard Chrome Azurol S (*CAS*) *solution.* An amount of 60.6 mg. of Chrome Azurol S is weighed accurately and transferred quantitatively in a 100 ml volumetric flask, where it is dissolved and diluted with doubly distilled water. The resulting solution has a concentration, in CAS, 1×10^{-3} M.

- Perchloric acid solution 0.1N.
- Sodium hydroxyde solution 0.1N.
- Sodium nitrate solution 0.1N.

FORMATION OF THE COMPLEX CHELATE COMPOUND $\{MO_7O_{24}\}^{6-}$—CAS. INFLUENCE OF THE pH UPON THE FORMATION OF THE COMPOUND

In a series of solutions of $NaNO_3$ 0.1N, each 250 ml, the pH is regulated by the addition of $HClO_4$ 0.1N or NaOH 0.1N so that the final solutions have the following pH values: 3.10, 4.25, 5.20, 6.10, 7.50, 8.95, 9.70, 10.50 and 11.20.

In a 100 ml volumetric flask about 75 ml of $NaNO_3$ 0.1N, with constant pH regulated as described above are placed, and to this 0.1 ml of standard AHM solution and 2.0 ml of standard CAS solution are added. The content of the flask is mixed and the solution is completed to a final volume of 100 ml with $NaNO_3$ 0.1N of the same pH.

In the same way a blank solution of $NaNO_3$ 0.1N of the same pH is prepared. The process is obviously repeated for the whole series of the remaining nine (9) of the $NaNO_3$ 0.1N solutions of constant pH values.

---

[6] P. Job, *Ann. Chim.* (*France*), **9**, 113 (1928).

The solutions allowed to stand for 30 min in the dark and then spectrophotometric measurements of each solution are taken in the visibile region of the spectrum with the blank solution of the same pH as a reference.

The solutions of pH 3.10, 4.25, and 9.70, 10.50, 11.20 show no absorption throughout the whole visible region while the solutions of pH 5.20, 6.10, 7.50 and 8.95 gave absorbance measurements from which the curves of fig. 1 are traced.

FORMATION OF THE COMPLEX CHELATE COMPOUND $\{HW_6O_{21}\}^{5-}$—CAS. INFLUENCE OF THE pH ON THE FORMATION OF THE COMPOUND

Solutions of constant ionic strength corresponding to that of the $NaNO_3$ 0.1N solution and for pH of 5.00, 6.10 and 7.00 are prepared by the aforementioned method.

In each one of these, final volume 100 ml, 1.0 ml of standard AW solution and 2.0 ml of standard CAS solution are added.

Likewise, blank solutions of corresponding pH values are prepared. The solutions are allowed to stand for 30 min in the dark and their spectrophotometric measurements are taken in the visible region. From the values of the measured absorption the curves of fig. 2 are traced.

From the curves of fig. 1 it is clearly seen that, as a function of the pH of the solution, the wavelength $\lambda = 510$ nm, where the maximum absorption is observed, remains constant, while the value of $\log I_0/I$ changes, which is illustrated by the curve shown in fig. 3.

From fig. 3 it can be seen that the maximum absorption is exhibited by the pH 6.10 solution and, consequently, this is the optimum pH for the formation of the complex species.

From the curves of fig. 2 it can be seen, that depending upon the pH, the curves exhibit different maxima. Thus, at pH 6.10 the maximum appears at $\lambda = 510$ nm, while at pH 5.00 and 7.00 this appears at $\lambda = 550$ nm and $\lambda = 540$ nm, respectively.

This change of maximum absorption as a function of pH suggests a probable change in the nature or structure of the absorbing species, which was confirmed, as described below, by the method of continuous variations.

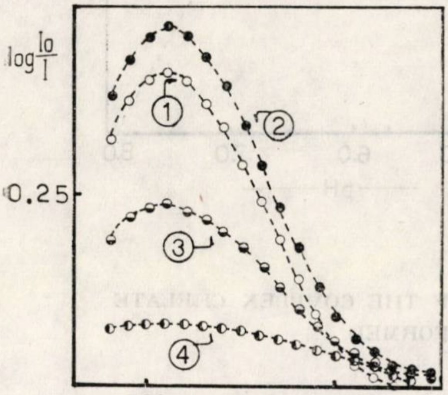

Fig. 1. — Influence of the pH upon the formation of the complex chelate compound $\{Mo_7O_{24}\}^{6-}$—CAS. *1*, pH : 5.20 ; *2*, pH : 6.10 ; *3*, pH : 7.50 ; *4*, pH : 8.95.

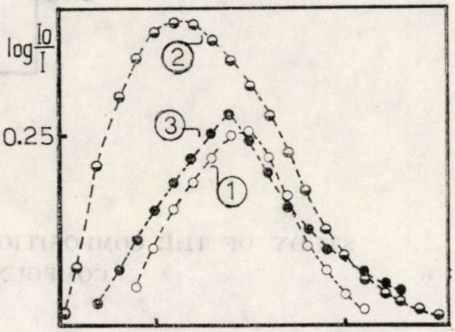

Fig. 2. — Influence of the pH upon the formation of the complex chelate compound $\{HW_6O_{21}\}^{5-}$—CAS. *1*, pH : 5.00 ; *2*, pH : 6.10 ; *3*, pH : 7.00.

Finally, the change of the log I_0/I value as a function of pH is also observed in the curves of fig. 2, the maximum value occurring at a pH 6.10. The observed change is illustrated in fig. 4.

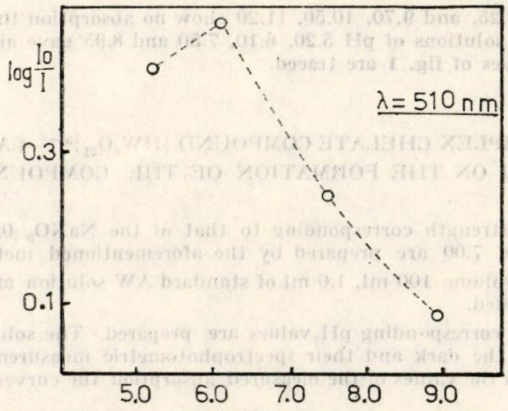

Fig. 3. — Variation of log I_0/I values against pH.

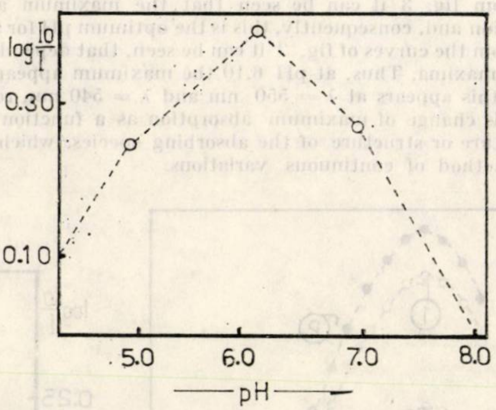

Fig. 4. — Variation of log I_0/I values against pH.

STUDY OF THE COMPOSITION OF THE COMPLEX CHELATE COMPOUNDS FORMED

The study of the composition of the complex compounds formed in the $\{Mo_7O_{24}\}^{6-}$-CAS and $\{HW_6O_{21}\}^{5-}$—CAS systems was carried out by the method of continuous variations (Job's method).

This method was employed in a solution of constant pH, the constant ionic strength corresponding to that of the $NaNO_3$ 0.1N solution and under constant temperature (25°C ± 0.1).

From these measurements the curves of figs. 5, 6, 7 and 8 were traced. These curves yield information on the composition of these complex chelate compounds. All the data collected from this work appear systematically in table 1.

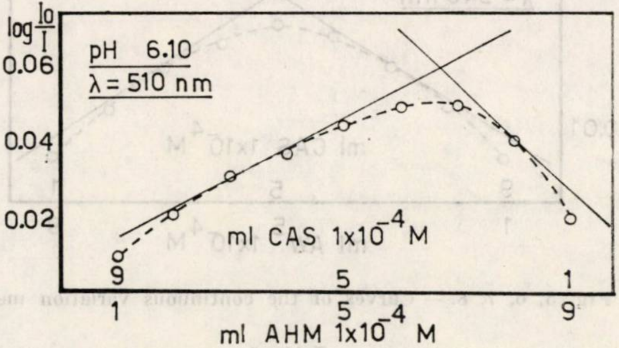

Fig. 5

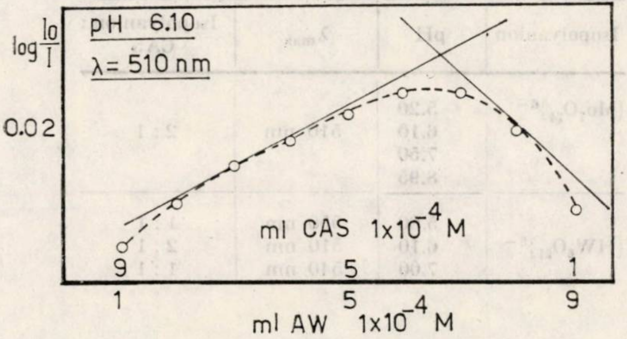

Fig. 6

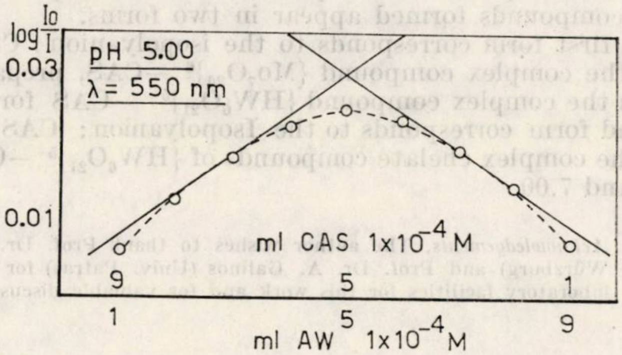

Fig. 7

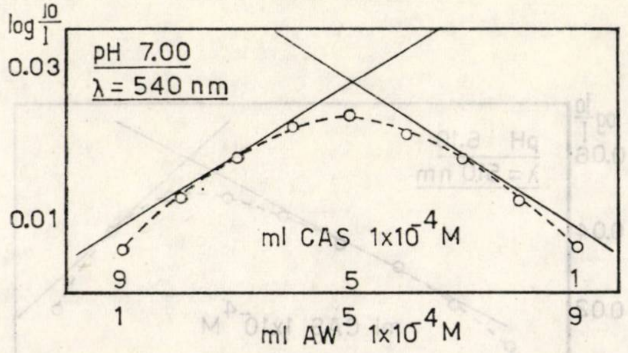

Fig. 8

Fig. 5, 6, 7, 8. — Curves of the continuous variation method.

Table 1

The composition and λ_{max} of the complex chelate compounds as a function of pH

Isopolyanion	pH	λ_{max}	Isopolyanion : CAS
$\{Mo_7O_{24}\}^{6-}$	5.20 6.10 7.50 8.95	510 nm	2 : 1
$\{HW_6O_{21}\}^{5-}$	5.00 6.10 7.00	550 nm 510 nm 540 nm	1 : 1 2 : 1 1 : 1

RESULTS

As shown by the results presented in the experimental part, the complex compounds formed appear in two forms.

The first form corresponds to the isopolyanion : CAS (2 : 1) which includes the complex compound $\{Mo_7O_{24}\}^{6-}$—CAS, prepared at any pH, as well as the complex compound $\{HW_6O_{21}\}^{5-}$ —CAS formed at pH 6.10. The second form corresponds to the Isopolyanion: CAS (1:1) to which belongs the complex chelate compounds of $\{HW_6O_{21}\}^{5-}$—CAS formed at a pH 5.00 and 7.00.

Acknowledgements. The author wishes to thank Prof. Dr. M. Schmidt (Univ. Würzburg) and Prof. Dr. A. Galinos (Univ. Patras) for arranging necessary laboratory facilities for this work and for valuable discussions.

Revue Roumaine de Chimie, **21**, *3*, 407–412 (1976)

COORDINATION COMPOUNDS WITH IRON-TIN BONDS

MARIA BREZEANU and IOANA JITARU
University of Bucharest, Inorganic Chemistry Laboratory,
Splaiul Independenţei 87, Bucharest, Romania

Received November 1, 1974

Two series of Fe(II) and Fe(III) compounds were synthesized in the system $FeCl_3$—$SnCl_2$—choline chloride, as well as a series of oxygen adducts of Fe(II) compounds which correspond to the following general formulas: $(\text{choline})_2\,[Fe(SnCl_3)_nCl_{4-n}]$ $(n = 1{,}2)$, $(\text{choline})\,[Fe(SnCl_3)_nCl_{4-n}] (n = 1{,}2)$ and $(\text{choline})_2[Fe(SnCl_3)_n\,Cl_{4-n}(O_2)]$ $(n=1{,}2)$. The resulted compounds were characterized by elemental chemical analysis, electronic spectra, molecular electric conductivity determinations and thermodifferential analysis.

In a previous paper[1] we have shown the results obtained in the synthesis and the characterization of some polynuclear complex compounds of Cu(I) of the form $(\text{choline})_3[Cu(SnCl_3)_nCl_{4-n}] (n = 1, 2, 3, 4)$. These compounds are characterized by the property of reversibly fixing the molecular oxygen.

Since the achievement of such oxygen carrying systems depends both on the nature of ligands and of the central metallic ion, we have considered of interest to study other compounds in which the central ion presents the property of existing in several states.

In this sense, the present paper exhibits the results obtained in the study of the system $FeCl_3$ - $SnCl_3$-choline chloride which has permitted us to characterize three series of complex compounds which correspond to the following general formulas:

$$(\text{choline})_2[Fe(SnCl_3)_nCl_{4-n}]\ (n = 1, 2),\ (\text{choline})[Fe(SnCl_3)_nCl_{4-n}(O_2)]$$

$$(n = 1, 2)\ \text{and}\ (\text{choline})[Fe(SnCl_3)_nCl_{4-n}]\ (n = 1, 2).$$

The compounds obtained were characterized by elemental chemical analysis, electronic spectra, molecular electric conductivity determinations and thermodifferential analysis.

---

[1] M. Brezeanu and I. Jitaru, *Rev. Roumaine Chim.*, **17**, 1857 (1972).

RESULTS AND DISCUSSION

The synthesis of these compounds was made in an alcoholic solution of hydrochloric acid at $FeCl_3 : SnCl_2$ ratios varying from 1 : 1 to 1 : 10.

The compounds immediately separated from the solution in which they had formed present a light yellow colour; they contain Fe(II) and correspond to the following general formula $(choline)_2[Fe(SnCl_3)_nCl_{4-n}]$ $(n = 1,2)$.

If the separation from the solution takes place after a few days and not immediately, we shall obtain — as a function of the $FeCl_3 : SnCl_2$ ratio used — two Fe(III) compounds having a yellow colour and corresponding to the general formula $(choline)\ [Fe(SnCl_3)_nCl_{4-n}](n = 1, 2)$.

It is of interest to mention that the maximum number of $SnCl_3$ ligands fixed in these compounds is two, even if the synthesis has been conducted in the presence of a high excess of $SnCl_2$.

The Fe(II) compounds have the property of intensifying their colour merely by being exposed to the air and this modification is accompanied by an increase in weight which corresponds to one O_2 molecule per iron atom.

Similar to the case of Cu(I) complex compounds, it has been observed that in Fe(II) compounds, the ease of the O_2 fixation from the air varies as a function of the composition of the respective compounds, namely, it decreases with the increase in the number of the present $SnCl_3$ ligands. Such a behaviour may have a similar explanation to that given for the analogous complex compounds of Cu(I).[1]

Electronic spectra. The electronic spectra of the complex compounds of Fe(II), Fe(III) and of the oxygen adducts of the Fe(II) compounds were interpreted in terms of establishing the most probable stereochemistry of these compounds.

The electronic spectra of the two Fe(II) compounds, $(choline)_2$ $[Fe(SnCl_3)_nCl_{4-n}](n = 1, 2)$, have the same general aspect: a highly intense band with charge transfer below 400 nm and an absorption beginning towards the near infrared range beyond 1100 nm. The presence of a large split band in the near infrared attributed to the transition $^5T_2 \leftarrow {}^5E$ pleads for a tetrahedral configuration as being the most probable [2] (fig. 1).

The electronic spectra of oxygen adducts (fig. 1) are very similar to those of unoxygenated compounds.

The electronic spectra of Fe(III) compounds $(choline)[Fe(SnCl_3)_nCl_{4-n}]$ $(n = 1, 2)$ which resemble very much to each other may be satisfactorily interpreted on the base of a tetrahedral configuration, the weak band at approximatively 800 nm being attributed to the spin forbidden transition $^4E \leftarrow {}^6A_1$. The relatively intense band in the ultraviolet range, below 400 nm, is most probably a charge transfer band $L \rightarrow M$[3] (fig. 2).

Molecular conductivities. The formulation assigned to these compounds in terms of their nature as electrolytes, was confirmed by the determination of their molecular electric conductivities. From the data

---

[2] P. Day and C. K. Jorgensen, *J. Chem. Soc.*, **1964**, 6226.

[3] B. J. Hathaway and D. G. Holah, *J. Chem. Soc.*, **1964**, 2400.

Fig. 1. — Electronic spectra of complex compounds:

1. $(\text{choline})_2[\text{Fe}(\text{SnCl}_3)\text{Cl}_3]$; 2. $(\text{choline})_2[\text{Fe}(\text{SnCl}_3)_2\text{Cl}_2]$; 3. $(\text{choline})_2[\text{Fe}(\text{SnCl}_3)\text{Cl}_3(\text{O}_2)]$; 4. $(\text{choline})_2[\text{Fe}(\text{SnCl}_3)_2\text{Cl}_2(\text{O}_2)]$

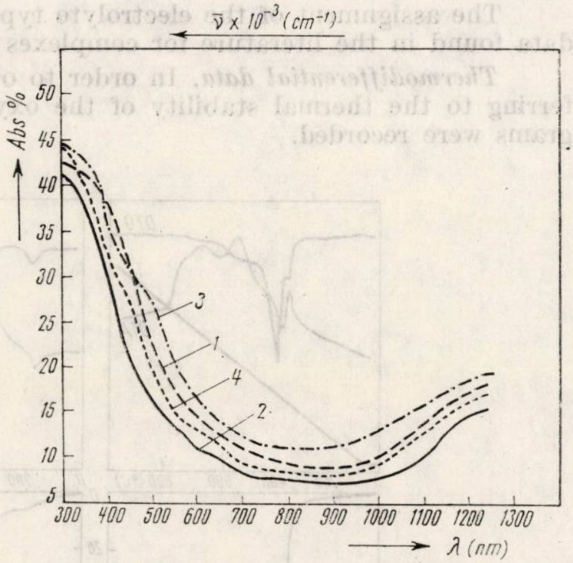

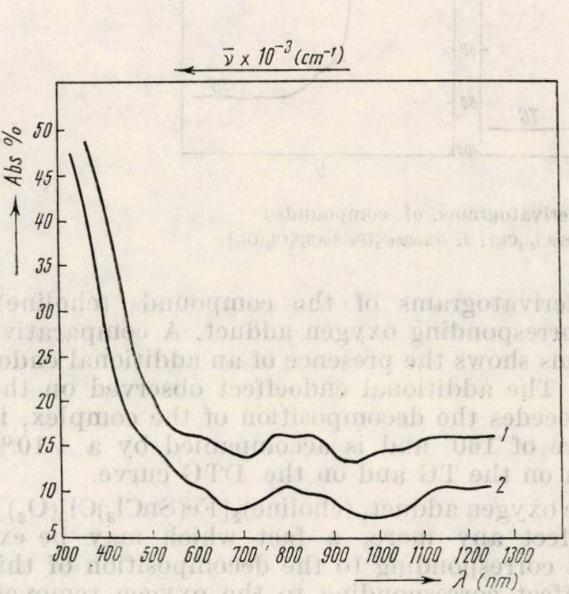

Fig. 2. — Electronic spectra of complex compounds:

1. $(\text{choline})[\text{Fe}(\text{SnCl}_3)\text{Cl}_3]$;
2. $(\text{choline})[\text{Fe}(\text{SnCl}_3)_2\text{Cl}_2]$

listed in table 2 we observe that the Fe(II) compounds and their oxygen adducts are 1 : 2 electrolytes and the Fe(III) compounds are 1 : 1 electrolytes.

The assignment of the electrolyte type was made according to the data found in the literature for complexes with $SnCl_3$ ligands.[4-6]

Thermodifferential data. In order to obtain more accurate data referring to the thermal stability of the oxygen adducts, their derivatograms were recorded.

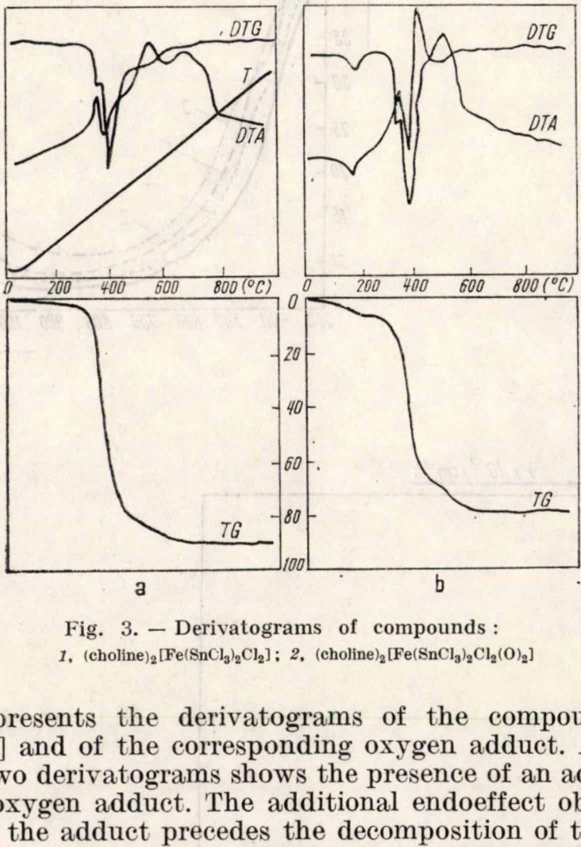

Fig. 3. — Derivatograms of compounds :
1, $(choline)_2[Fe(SnCl_3)_2Cl_2]$; *2*, $(choline)_2[Fe(SnCl_3)_2Cl_2(O)_2]$

Fig. 3 presents the derivatograms of the compounds $(choline)_2[Fe(SnCl_3)_2Cl_2]$ and of the corresponding oxygen adduct. A comparative study of the two derivatograms shows the presence of an additional endoeffect in the oxygen adduct. The additional endoeffect observed on the DTA curve of the adduct precedes the decomposition of the complex, it corresponds to a temperature of 160° and is accompanied by a 4.10% loss in weight, observed both on the TG and on the DTG curve.

The derivatogram of the oxygen adduct, $(choline)_2[Fe(SnCl_3)Cl_3(O_2)]$, presents no distinct endoeffect any more, a fact which may be explained in that the exoeffect corresponding to the decomposition of this compound covers the endoeffect corresponding to the oxygen removal.

---

[4] I. F. Jonug, R. D. Gillord and G. Willkinson, *J. Chem. Soc. (A).*, **1964,** 5176.

[5] D. J. Phillips and S. Y. Zyree, *J. Amer. Chem. Soc.*, **83,** 1806 (1961).

[6] J. V. Quagliano, J. Fujita, G. Franz, D. J. Phillips, J. A. Walmsle and S. Y. Tyree, *J. Amer. Chem. Soc.*, **83,** 3370 (1961).

Such a behaviour confirms the assumptions referring to the fact that the stability of oxygen adducts increases with the increase of the number of $SnCl_3$ ligands.

EXPERIMENTAL DATA

I. SYNTHESIS OF COMPLEXES

To an alcoholic solution obtained by dissolving 0.25 g $FeCl_3 \cdot 2\ H_2O$ in 5 ml ethanol, there were added 1 ml concentrated HCl, 0.36 g solid $SnCl_2.2\ H_2O$ (0.72 g $SnCl_2.2\ H_2O$ respectively) and 0.96 g choline chloride dissolved in a minimum quantity of ethanol (molar ratio Fe : Sn : choline = 1 : 1 : 4 and 1 : 2 : 4, respectively). White-yellowish coloured compounds are formed, which are allowed to stand in solution for 24 hours and are then filtered, washed with ethanol and air-dried. The white-yellowish compounds $(choline)_2[Fe(SnCl_3)_n\ Cl_{4-n}]$ ($n = 1, 2$) change in the air, after a few hours (for $n = 1$) and after a few days, respectively (for $n = 2$) into yellow compounds, the change being accompanied by an increase in weight of 5.13, 3.92% respectively. Compounds of the type $(choline)[Fe(SnCl_3)_nCl_{4-n}]$($n = 1,2$) were obtained by maintaining compounds $(choline)_2[Fe(SnCl_3)_nCl_{4-n}]$ ($n = 1,2$) in an alcoholic solution for 1–2 weeks. The yellow compounds thus obtained are filtered and thoroughly air-dried.

The analytical data corresponding to the three main types of compounds are listed in table 1.

Table 1

Data of the elemental chemical analysis

Compound	Fe %		Sn %		Cl %		N %	
	Calcd.	*Found*	*Calcd.*	*Found*	*Calcd.*	*Found*	*Calcd.*	*Found*
$(choline)_2[Fe(SnCl_3)Cl_3]$	9.41	8.90	20.00	19.85	35.51	35.29	4.71	4.90
$(choline)_2[Fe(SnCl_3)_2Cl_2]$	7.13	6.85	30.32	29.75	36.21	36.10	3.58	3.75
$(choline)_2[Fe(SnCl_3)Cl_3(O_2)]$	8.95	8.80	18.78	18.50	33.85	33.62	4.45	4.60
$(choline)_2[Fe(SnCl_3)_2Cl_2(O_2)]$	6.82	6.70	29.35	29.20	35.30	35.10	3.10	3.35
$(choline)[Fe(SnCl_3)Cl_3]$	11.41	10.95	24.26	24.10	41.40	41.40	3.30	3.30
$(choline)[Fe(SnCl_3)_2Cl_2]$	8.25	7.90	34.30	34.55	41.80	41.65	2.35	2.45

II. ELECTRONIC SPECTRA

The electronic spectra were recorded at room temperature using a VSU 1 Zeiss-Jena spectrophotometer and magnesium oxide as reference material.

Table 2

Molecular electric conductivities of the compounds studied

Compound	Electric conductivity (solvent DMF)	Type of electrolyte
(choline)$_2$[Fe(SnCl$_3$)Cl$_3$]	130.5	1 : 2
(choline)$_2$[Fe(SnCl$_3$)$_2$Cl$_2$]	132.6	1 : 2
(choline)$_2$[Fe(SnCl$_3$)Cl$_3$(O$_2$)]	128.5	1 : 2
(choline)$_2$[Fe(SnCl$_3$)$_2$Cl$_2$(O$_2$)]	130.2	1 : 2
(choline)[Fe(SnCl$_3$)Cl$_3$]	81.5	1 : 1
(choline) [Fe(SnCl$_3$)$_2$Cl$_2$]	80.5	1 : 1

III. MOLECULAR ELECTRIC CONDUCTIVITY MEASUREMENTS

Molecular conductivity measurements were made on solutions having 10^{-3}M dimethylformamide concentration at a temperature of 25° using a Conductometer II (Czechoslovakia) with a constant $K = 0.52$.

IV. THERMAL ANALYSIS

The derivatograms were recorded by a F. Paulik, J. Paulik, L. Erdey derivatograph with concomitant registering of T, TG, DTG and DTA curves. The curves were recorded in air, using a sensitivity of the weighing system of 100 mg, a heating velocity of 5°/min, calcined Al$_2$O$_3$ as a standard.

Revue Roumaine de Chimie, **21**, *3*, 413–421 (1976)

CONTRIBUTIONS TO THE COORDINATION CHEMISTRY OF PHTHALIC ACID DERIVATIVES. I*

CONDENSATION PRODUCTS OF PHTHALIC ANHYDRIDE WITH *m*-PHENYLENEDIAMINE AS COORDINATION LIGANDS FOR COPPER

FLORICA POPEA, CRISTINETA MĂRCULESCU and ZAMFIRA TOMA
Center of Physical Chemistry Bucharest, Dumbrava Roșie, 23, Romania

Received October 10, 1974

The condensation reaction of phthalic anhydride with *m*-phenylenediamine was studied in different conditions and for various reactant ratios. The resulting products were characterized by physico-chemical methods, in view of their application as ligands in the coordination chemistry. New copper (II) complexes were synthesized and studied with the purpose to elucidate the mechanism of the condensation reaction.

Bistizycki,[1] Anderlini,[2] Meyer,[3] Thiele and Falk,[4] Ruppe and Thiess [5] have studied the reaction of aromatic diamines with phthalic acid derivatives as early as by the end of the last century.

Bidermann[6] dealt with the action of phthalic anhydride upon the aromatic diamines and evidenced the formation of mono- and diphthalyl *m*-phenylenediamine. Among the condensation products of the diamines with phthalic anhydride, Maier [7] obtained phenylene phthalimides and phenylenediphthalimides with *m*-phenylenediamine, only in the presence of sodium acetate. With an excess of phthalic anhydride and in the absence of sodium acetate, the formation of a product of acidic character was found.

More recently, the condensation of aromatic diamines with dicarboxylic acids derivatives was studied in order to obtain macromolecular compounds with multiple uses or macrocyclic compounds, basic components of some natural products with biological importance.

---

* Presented at the IV th Conference in General and applied Physical Chemistry, Bucharest — September 1974.

[1] R. Bistizycki, *Berl. Ber.*, **23**, 1042 (1890); **24**, 629 (1891); **25**, 1084 (1892).
[2] F. Anderlini, *Berl. Ber.*, **26**, 600 (1893).
[3] R. Meyer, *Liebigs Ann. Chem.*, **41**, 327 (1903).
[4] J. Thiele and K. G. Falk, *Liebigs. Ann. Chem.*, **349**, 115 (1906).
[5] H. Ruppe and K. G. Thiess, *Berl. Ber.*, **42**, 4287 (1909).
[6] R. Biedermann, *Chem. Ber.*, **10**, 1160 (1907).
[7] J. Maier, *Liebigs Ann. Chem.*, **327**, 17 (1903).

In this regard, the condensation of phthalic anhydride with *m*-phenylenediamine, under various conditions, the physical and chemical behaviour of the resulted compounds, as well as their reactivity towards the copper ion, are presented.

In the condensation of phthalic anhydride with *m*-phenylenediamine different compounds are formed depending on the ratio of the reactants, the medium and the time of reaction.

The reaction proceeds as in scheme 1.

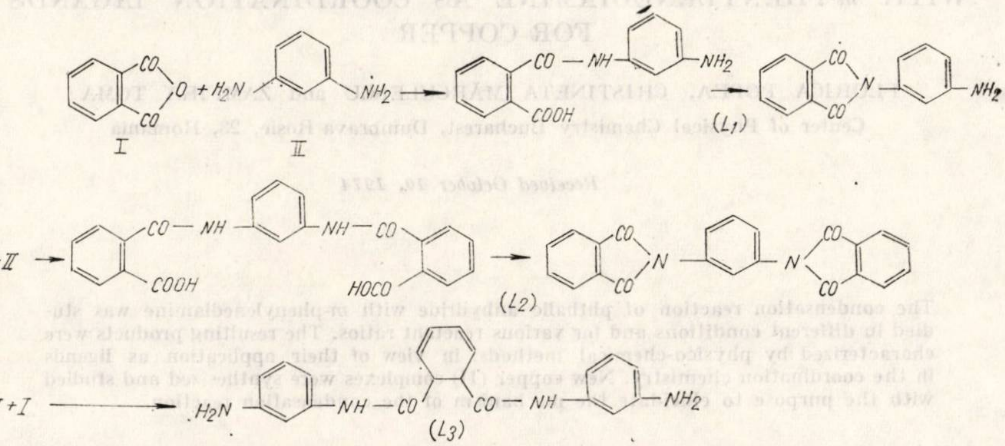

EXPERIMENTAL

Starting materials. The compounds were prepared using phthalic anhydride purified by recrystallization from ethanol and *m*-phenylenediamine by recrystallization from benzene in the presence of active charcoal.

Analyses. The elemental analyses for C, H, N were made by microcombustion and Cu by the G. Spacu analytical micromethod.

Measurements. The melting points were determined with a Boetius heating plate and were not corrected.

The electrical conductivities were measured with a OK-102/1 Model Conductivity bridge in DMF solution.

The electronic reflectance spectra were recorded at room temperature on a VSU−1 C. Zeiss-Jena spectrophotometer, in the 260−1200 nm range, using the standard reflectance attachment and magnesium oxide as reference.

The IR spectra were recorded using KBr pellets on a UR 10 C. Zeiss-Jena spectrophotometer, in the 400−3500 cm^{-1} range.

N-(*m*-PHENYLENEDIAMINE) PHTHALIMIDE (L_1)

a. *m*-phenylenediamine (0.01 mol) was dissolved in chloroform and this was followed by gradual addition under stirring, during 30 minutes, of a 0.01 mol phthalic anhydride solution in chloroform. The reaction mixture was stirred at room temperature for 15 hours, whereupon the white product formed was filtered, washed with warm chloroform and dried in vaccum over P_4O_{10}.

b. A phthalic anhydride solution in DMF was added dropwise to a DMF solution of *m*-phenylenediamine (molar ratio 1 : 1). The reaction mixture was stirred at room temperature for 4 hours and allowed to stand overnight. Anhydrous diethyl ether was added to the resulting dark brown oil, after cooling in an ice bath. The process was repeated several times and the grey powder obtained was filtered and washed with ether. The product was purified by washing repeatedly with hot $CHCl_3$. $L_1 \cdot \frac{1}{2}$ $CHCl_3$ (m.p. = 142–144°); *Found* : C, 58.70; N, 9.87%; $C_{29}H_{21}N_4O_4Cl_3$ *Required* : C, 58.39; N, 9.39%.

N,N-*m*-PHENYLENE-DIPHTHALIMIDE (L_2)

A mixture of *m*-phenylenediamine and phthalic anhydride (molar ratio 1 : 4) was heated to open flame in a flat-bottom flask. The excess of phthalic anhydride with the water vapour formed in the reaction was distilled and removed by sublimation. When the vapour evolution has ceased, the melt solidified, passing into a transparent brownish mass, which was slightly chilled. This mass was treated with glacial acetic acid and then brought to boiling. The warm product was filtered, a large part remaining undissolved. The solid substance was washed with boiling ethanol and filtered; a crystalline white-beige product was obtained. From the initial filtrate, a part of the dissolved product was extracted with ethanol. The purification was achieved by repeated washing with ethanol, then with chloroform and by drying *in vacuo* over P_4O_{10}.

$L_2-C_{22}H_{12}N_2O_4$ (m.p. 308–310°). *Found* : C, 72.13; N, 8.03%; *Required* : C, 71.70; N, 7.60%

PHTHALOYL DI-*m*-PHENYLENEDIAMINE (L_3)

A phthalic anhydride suspension in $CHCl_3$ was gradually added (25°) to a cool chloroform solution of *m*-phenylenediamine (molar ratio : *m*-phenylenediamine/phthalic anhydride 4 : 1). The reaction mixture was stirred for 6 hours; during this time a slightly beige-yellowish precipitate was formed. It was rapidly filtered, washed with cold chloroform and dried *in vacuo* over P_4O_{10}.

$L_3 \cdot \frac{1}{2}$ $CHCl_3$. *Found* : C, 60.41; N, 13.52% $C_{41}H_{37}N_8O_4Cl_3$ *Required* : C, 60.67; N, 13.81%

$CuL_1(OCOCH_3)_2$

1.04 g ligand (L_1) suspended in $CHCl_3$ was refluxed and treated dropwise with 0.90 g. copper(II) acetate solution in a mixture of chloroform and ethanol. The volume of chloroform did not exceed 100 ml and the ethanol was about 45% of the $CHCl_3$ amount necessary to dissolve the copper salt. After refluxing for 8–9 hours the green-khaky product obtained was purified by washing with warm chloroform and ethanol and dried *in vacuo* over P_4O_{10}. (m.p. = 340°). *Found* : C, 51.15; Cu, 15.52; N, 6.64%. $C_{18}H_{16}O_6N_2Cu$. *Required* : C, 51.49; Cu, 15.48; N, 6.67%

COPPER PHTHALIMIDE $Cu(ft)_2$

An aqueous solution of 5 g potassium phthalimide was added to the equivalent amount of $CuSO_4.5H_2O$ (aqueous solution). A blue-violet precipitate was formed immediately; on heating the mixture turned intense blue. After cooling it was filtered and dried over P_4O_{10}.

$CU(ft)_2(mfa)$

1 g copper(II) phthalimide in 15 ml acetone was refluxed for 5 hours, with a slight excess of *m*-phenylenediamine. The resulting dark brown mass was allowed to crystallize overnight, it was then filtered, washed with acetone and dried over P_4O_{10}.

RESULTS AND DISCUSSIONS

In the condensation of phthalic anhydride with *m*-phenylenediamine different compounds are formed because of the presence, in each reactant molecule, of 2 groups capable to react simultaneously or stepwise and depending on the ratio in which they are present in the reaction medium. Varying the phthalic anhydride/*m*-phenylenediamine ratio (1 : 1, 2 : 1, 4 : 1 or 1 : 2 and 1 : 4 respectively), the compounds L_1, L_2, L_3 in the amide or imide forms are obtained.

The compound L_1 results for 1 : 1 and 1 : 2 ratios, while L_2 and L_3 are obtained for the 4 : 1 and 1 : 4 ratios, respectively. For the 2 : 1 ratio, the same L_2 compound as for the 4 : 1 ratio is obtained but with a very low yield and impurified with *m*-phenylenediamine, whereas for the 4 : 1 anhydride/amine ratio, besides L_2, a small amount of the L_1 compound is also separated.

The L_3 compound is very difficult to isolate, resulting only at low temperature (below 5°) in chloroform medium; it turns into a resinous dark coloured product on processing at higher temperature.

It can be safely concluded that a large excess of phthalic anhydride is necessary in order to obtain the L_2 compound, whereas the formation of the L_3 compound requires, besides low temperature, an excess of amine. The reaction proceeds in chloroform and ethanol for L_1 and L_3 and in the melt for L_2.

L_1 and L_2 are white crystalline compounds, with a slight yellowish colour probably due to the *m*-phenylenediamine, which although purified before use, darkens on subsequent processing.

L_1 and L_3 are sparingly soluble in the usual solvents (ethanol, acetone, chloroform, etc.), L_3 is more soluble in DMF and DMSO than in the solvents mentioned above.

By titration with an N/200 KOH solution, the presence of a COOH group in L_1 and its absence in L_2 is evidenced. Thus, the amidic form for L_1 and the imidic form for L_2, can be certainly ascribed. The determination of the % total base content allows to evidence two free NH_2 groups in the L_3 compound.

In order to characterize the L_1 and L_3 compounds obtained, their ability to react with transition metals salts, respectively with copper acetate, was investigated.

By refluxing L_1 with copper acetate in chloroform and ethanol, during 8 hours, a compound of the general formula $CuL_1(OCOCH_3)_2$ is isolated and easily purified.

The L_2 compound does not react with copper acetate, even after a much longer time and the reactants (L_2 and $Cu(OCOCH_3)_2$ can be separated almost pure from the reaction medium. This dissimilar behaviour of the two compounds L_1 and L_2 confirms the results obtained by titration with an n/200 KOH solution, which evidenced the presence of one COOH group in L_1 and the absence of the free COOH groups in the L_2 compounds (diphthalimide derivative).

Under the same conditions, the reaction of the L_3 compound with copper acetate results in an impure and nonunitary compound, probably due to the marked tendency of *m*-phenylenediamine to resinify even at normal temperature and in open air.

Due to the failure of the L_2 ligand to react with $Cu(OCOCH_3)_2$ and considering the structure of the $CuL_1(OCOCH_3)_2$ and L_2 compounds, a convenient synthetic route for $CuL_1(OCOCH_3)_2$ was designed involving the use of the phthalimidic group in reaction as copper phthalimidate (in view of the well-known high reactivity of the phthalimidate ion with respect to the amino groups). Thus, in acetone medium, under reflux, a compound of general formula $Cu(ft)_2(am)_{1(2)}$ mentioned in the literature, was obtained. (am = aliphatic amine, α, α′-dipyridil or *o*-phenantroline).[8]

Both $CuL_1(OCOCH_3)_2$ and $Cu(ft)_2$ (mfa) are microcrystalline powders, intensely dark brown coloured, air — stable in solid state, soluble in DMF, DMSO but sparingly soluble in ether, ethanol and chloroform.

The electric conductivity in DMF at 25°, for the last two compounds is 18 and, respectively, 20 $ohm^2cm^{-1}mol^{2}$ suggesting that they are non-electrolytes. Consistent with literature [9] data, these values seem to indicate the coordination of the phthalimidate ion together with the amine.

Subsequently, based on the information provided by the literature as well as on the electronic and IR spectra, the coordination possibility, either through nitrogen or through carbonyl oxygen will be further discussed.

ELECTRONIC SPECTRA

The reflectance spectra of L_1, L_2, L_3 (table 1) reveal in the UV range an absorption band at 270—290 nm, a region in which an absorption band at 292 nm and at 289 nm for phthalimide and, respectively, for *m*-phenylenediamine are mentioned.[10]

Table 1

Electronic spectra

Compounds	250—360 nm	360—600 nm	600—1200 nm
L_1	275—280	—	—
L_2	290—300	—	—
L_3	285—290	—	—
$CuL_1(OCOCH_3)_2$	285	390	675
$Cu(ft)_2(mfa)$	290	—	690

---

[8] G. Narain, *Indian J. Chem.*, **4**, 248 (1966).

[9] P. Shukla, M. P. Khane and L. N. Srivastava, *J. prakt. Chem.*, **29**, 38 (1965).

[10] L. Lang "Absorption Spectra in the Ultraviolet and Visible Region", v. 11, Akademiai Kiadó, Budapest, 1968.

Besides, two additional bands, for phthalimide at 216 and 238 nm and for *m*-phenylenediamine at 211 and 238 nm, are known. The absorption bands of the L_1, L_2, L_3 compounds in this region cannot be discussed in view of the low sensitivity under 250 nm of the equipment used in these measurements.

The UV spectrum of the $CuL_1(OCOCH_3)_2$ compound exhibits an absorption band at 285 nm, characteristic of the ligand L_1 (275–280 nm) shifted by coordination.

The UV spectrum of the $Cu(ft)_2(mfa)$ compound in DMF solution shows a band at 290 nm, characteristic of the ligand.

The $CuL_1(OCOCH_3)_2$ compound shows in the visible range an absorption band at 390 nm, which may be assigned to a metal-ligand charge transfer and an absorption band at 675 nm.

This last band as well as the band at 690 nm present in the spectrum of the $Cu(ft)_2(mfa)$ compound are lying in the 600–900 nm region characteristic of the $Cu(ft)_2$ complexes with amines.[11]

Grant and Kollrack[12] tried to correlate the position of the absorption band with the ligand configuration. They concluded that the copper phthalimidate complexes have *trans* configuration because of the presence in their absorption spectrum of a maximum at 665 nm in formamide solution. But Bjerrum[11] ascribes an absorption maximum at 670 nm to the *cis* isomer and an absorption maximum at 620 nm to the *trans* isomer. The Bjerrum's value of 620 nm for the *trans* isomer is obtained in aqueous solution, while the above value of 665 nm, for the same isomer, is in formamide. The high polarity of formamide is likely to cause the shift of the absorption maximum from 620 nm (aqueous solution) to 665 nm (formamide solution). This is analogous with the $[Cu(NH_3)_4]^{2+}$ spectrum which shows an absorption maximum at 590 nm in aqueous solution and at 620 nm in formamide solution.

INFRARED SPECTRA

The IR spectra of L_1, L_2, L_3 as well as spectra of phthalic anhydride and of *m*-phenylenediamine are comparatively presented in table 2.

The spectra exhibit a series of characteristic bands very slightly shifted from one compound to another. Thus, the bands at 655 (630, 655) cm^{-1}, 715 (730, 725) cm^{-1} assigned to the vibrations of the amide or imide CO group are found displaced with respect to the bands at 635 and 720 cm^{-1} of the phthalic anhydride spectrum.

The symmetric frequencies vibration occurring at 1375 and 1480 cm^{-1} in the phthalic anhydride spectrum are found more or less shifted in the L_1, L_2, L_3 spectra at 1380 (1390, 1395) cm^{-1} and 1450 (1475, 1460) cm^{-1} and are situated at 1440–1395 cm^{-1} in the stretching vibration range of the carbonyl group in the carboxylic acids.

---

[11] L. N. SRIVASTAVA, P. R. SHUKLA and M. P. KHARE, *Z. phys. Chem. (Leipzig)*, **234**, 159 (1967).

[12] D. M. GRANT and R. KOLLRACK, *J. Inorg. Nuclear Chem.*, **23**, 25 (1961).

Table 2

Infrared spectra

Phthalic anhydride	*m*-phenylene diamine	L_1	L_2	L_3	Assignments
430	—	—	—	430	
540	525	525	540	535	1,3-disubstituted benzene ring
635	—	655	630	655	secondary amide
680	690	695—705	690—695	685	disubst. aromat. compounds
720	—	715	730	725	bonded secondary amide
—	790	790	795	790	substituted aromatic amines
810	—	—	805	—	
845	850	—	870	—	
920	—	880—912	895	895	CH group
—	960	970	945—980	—	
1015	1000	—	1020	1000	*m*-disubstituted compounds
1080	1080	1080	1080	1085	*m*-disubstituted compounds
1120	—	1150	1125	1120	C—O—stretching in phthalates
1180	1170—80	1175	1160—90	1165	
1225	1210	—	1215	—	
1265	—	1280	1240—65	—	C—O—stretching in phthalates
1345	1330	1345	1305	1300	C—N vibr. in aromat. amines
1375	—	1385	1390	1395	symmetric vibrations COO^-
1480	—	1450	1475	1460	symmetric vibrations COO^-
—	1515	1510	1515	—	band amide II
1620	1620	1630	1615	1620	asymmetric vibrations O—C—O—
1710	—	1725	1710	1725	
—	—	—	1730	—	asym. CO from cyclic imides
1780	—	—	1780—1800	1780	CO val. vibr. in cyclic anhyd.
—	—	2920	2850—2980	2900	chelate compounds
—	3345	3300	—	3380	NH frequencies
—	3425	—	—	3480	,, ,,

While the carbonyl antisymmetric vibration is evidenced in the L_1, L_2, L_3 spectra at 1630 (1615, 1620) cm^{-1} and in the phthalic anhydride at 1620 cm^{-1}, the carbonyl frequency vibration in the cyclic imide (1730 cm^{-1}) is observed out only in the L_2 compound spectrum. Also, the carbonyl stretching vibration of cyclic anhydrides, at 1780 cm^{-1} in the phthalic anhydride, keeps the same place in the L_2 and L_3 spectra, but fails to appear in the L_1 spectrum.

The absorption bands at 525 (540, 535) cm^{-1}, 790 (795, 790) cm^{-1} and 1080 (1080, 1085) cm^{-1} in the spectra of L_1, L_2, L_3 show the presence of the *m*-disubstituted aromatic ring in these compounds. The same bands are also exhibited by the *m*-phenylenediamine spectrum at 525, 790 and 1080 cm^{-1}, respectively.

In the NH frequencies vibration range (3050—3500 cm^{-1}) the L_2 spectrum is completely free of any absorption bands, but an absorption band at 3300 cm^{-1} for L_1, 2 absorption bands for L_3 (3380 and 3480 cm^{-1}) as well as for *m*-phenylenediamine (3345 and 3425 cm^{-1}) are present in their respective spectra. In this range the primary amines exhibit 2 absorption bands and the secondary amines a single band while the tertiary amines with the deprotonated nitrogen do not exhibit any absorption This fact may explain the lack of any absorption band in the spectrum of the L_2 compound, with only tertiary nitrogen in the molecule.

The spectra of the compounds L_1 and $CuL_1(CH_3COO)_2$ are presented comparatively in table 3. Some L_1 characteristic bands are modified or shifted and others were completely absent in the $CuL_1(CH_3COO)_2$ spectra, probably due to coordination. Thus, the band at 1650 cm^{-1} from L_1 is found as a shoulder, at 1675 cm^{-1}, in $CuL_1(CH_3COO)_2$, while the bands at 1150, 1385, 1725 cm^{-1} from L_1 disappear in the coordination compound as well as those at 3080 and 3175 cm^{-1} in the range of the NH frequency vibration : in both products there remains only the band at 3300 cm^{-1} which is characteristic of the primary amines.

Table 3

Infrared spectra

L_1	$CuL_1(CH_3COO)_2$
—	470
525	—
590	600
—	660
695–705	690–700
715	720
760	755
790	795
880–910	860–890
970	980
1080	1090
1150	—
1175	1175
1280	1280
1345	1330
1385	—
1450	1420–60
1510	1510
1570	1560
1630	1625
1650	1675
1725	—
3080	—
3175	—
3300	3300

Table 4

Infrared spectra

Phthalimide	Cu phthalimide	Cu(ft)$_2$(mfa)
645	645	—
715	710	725
790	—	800
815	850	860
1055	1055	
1070	1085	—
1140	1140	1130
1185	1185	1185
1310	1310	1315
1380	1380	1385
1465	1465	1480–90
1605	1605	1610
1745	1725	1730
1770	1765	1770
3180	3140	3225
—	—	3375

In table 4 the IR absorption bands of the Cu(ft)$_2$(mfa) compound in the 400–3500 cm^{-1} range are compared with those reported in the literature [9] for phthalimide and copper phthalimide Cu(ft)$_2$.

In these compounds, the bands due to the vibrations of the NH and CO groups, respectively, are important for suggesting the type of coordination.

The three compounds exhibit an intense band above 3100 cm^{-1}, characteristic of the NH vibration, present at 3180 cm^{-1} in phthalimide, at 3140 cm^{-1} in Cu(ft)$_2$, and at 3225 cm^{-1} in Cu(ft)$_2$(mfa). In the latter compound an additional strong band appears at 3375 cm^{-1}, also assigned to the NH vibration (this occurs at 3414 and 3400 cm^{-1} in NH_3 and aliphatic amines, respectively). This negative frequency shift is probably due to the coordination of the amine to the copper atom. The resulting Me—N strong covalent bond weakens the NH bond and decreases with the increase of the amine molecular weight. It seems possible to explain these facts through combined effects : the weakening of the Me—N covalent bonding at the same time with the molecular weight and also through the α-mass effect.[13]

The strong bands at 1315 and 1385 cm^{-1} in the $Cu(ft)_2(mfa)$ spectrum confirm the presence of the free NH group in both compounds unlike the $Cu(ft)_2$ spectrum, where the same bands are weak.

The carbonyl group is evidenced by two absorption bands at 1770 and 1730 cm^{-1}, the first shaped only as a shoulder, the last broadened and intense. Both are slightly shifted with respect to the phthalimide (1770 and 1745 cm^{-1}) and $Cu(ft)_2$ (1765 and 1725 cm^{-1}) bands, in the proximity of the two ranges (1770—1720 cm^{-1} and 1710—1670 cm^{-1}) characteristic of the compounds containing the structural elements CONHCO and CONH in the molecule.

On the basis of IR spectral data, Borisevich and Hovratovich[14] conclude that in phthalimide and phthalimide derivatives, the carbonyl groups are involved in intramolecular hydrogen bonding with the imido group, but the position of the carbonyl absorption band remains unaffected.

The examination of the IR spectra leads to the conclusion that the carbonyl group as well as the imido nitrogen may be involved in coordination. But in agreement with Lewis concepts[15] the coordination *via* the nitrogen atom seems to be more probable due to its negative charge, and more prone to coordination, than the oxygen of the carbonyl group.

Besides, the IR spectra of the compounds with the imido nitrogen close to the carbonyl group, do not provide the necessary support to conclude on the exact manner of coordination; a modification in the imido nitrogen, directly linked to the carbonyl group, will affect the neighbouring groups, even if they are not involved in coordination.

---

[13] R. N. Johns, N. E. Farbers and W. A. Mieller, *Canad. J. Chem.*, **35**, 504 (1957).

[14] N. A. Borisevich and N. N. Hovratovich, *Zhur. priklad. Spektrosk.*, **7**, 538 (1967).

[15] J. C. Bailar, "Chemistry of Coordination Compounds", Reinhold, New York, 1956, p. 180.

Revue Roumaine de Chimie, **21**, *3*, 423–426 (1976)

THE REACTION OF PYRIDINIUM-CYANO-CARBALKOXY-METHYLIDS WITH α-NITROSO-β-NAPHTHOL, A ROUTE TO NAPHTHOXAZINONES

CANDIANO LEONTE and ION ZUGRĂVESCU
Department of Organic Chemistry, Polytechnic Institute, Calea 23 August 11, Jassy, Romania

Received February 6, 1975

In the reaction of pyridinium-cyano-carbalkoxy-methylids with α-nitroso-β-naphthol, the corresponding nitrones appear only as intermediates, leading, by an intramolecular *trans*-esterification process, to 3H-(naphtho-[1,2-e]-1,4-oxazine)-2-cyano-3-one-1-oxide.

The formation of nitrones from pyridinium ylids and such nitrosoaromatic compounds as nitrosobenzene or *p*-nitroso-N-dimethylaniline is one of the most interesting reactions of pyridinium ylids,[1] being intensely applied in the synthesis of various carbonyl compounds.

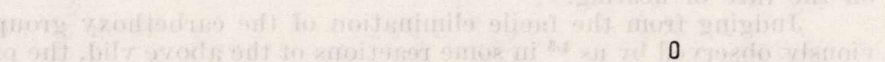

$$C_5H_5\overset{+}{N}-\overset{-}{\underset{..}{C}}\begin{smallmatrix}R_1\\R_2\end{smallmatrix} + O=N-C_6H_4-R_3\,(p) \xrightarrow[-C_5H_5N]{} (p)\,R_3-C_6H_4-\overset{\overset{O}{\uparrow}}{N}=C\begin{smallmatrix}R_1\\R_2\end{smallmatrix}$$

I II III

a. $R_3 = H$
b. $R_3 = N(CH_3)_2$

As concerns the reaction between pyridinium ylids and α-nitroso-β-naphthol, this was investigated, to our knowledge, in one work only.[2] The ylids studied in this respect were of type (I) ($R_1 = H$, $R_2 = C_6H_4Br$ (*p*) and $R_1 = H$, $R_2 = CSSR'$) and the reaction in which the corresponding nitrones appear only as intermediates leads, by two different ways of cyclization, to (IV, $R_2 = C_6H_4Br(p)$)(H_2O elimination) and (V) (R′SH elimination), respectively.

---

[1] F. Kröhnke, *Angew. Chem.*, **75**, 317 (1963).
[2] K. Gerlach and F. Kröhnke, *Chem. Ber.*, **95**, 1124 (1962).

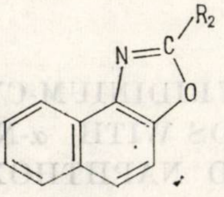

IV

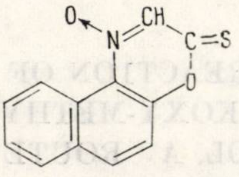

V

It was of interest to investigate the behaviour in the reaction with α-nitroso-β-naphthol of pyridinium-cyano-carbethoxy-methylid (I, $R_1 = CN$, $R_2 = COOC_2H_5$),[3] an ylid whose reactivity was previously studied by us in some other respects.[4,5] In a preliminary attempt, this ylid was found to be, in spite of the advanced delocalization of the negative charge afforded by the two powerful electron-withdrawing substituents, nucleophilic enough to react with *p*-nitroso-N-dimethylaniline, yielding the corresponding cetonitrone (III, $R_1 = CN$, $R_2 = COOC_2H_5$, $R_3 = N(CH_3)_2$), m.p. 137–138°. An analogous nitrone (III, $R_1 = CN$, $R_2 = CONH_2$, $R_3 = N(CH_3)_2$), m.p. 214–215° (decomp.), has also been obtained from the pyridinium-cyano-carbamyl-methylid (I, $R_1 = CN$, $R_2 = CONH_2$).[4] In contrast, no reaction between the *symmetrical* pyridinium-dicarbethoxy- or pyridinium-dicyano-methylid (I, $R_1 = R_2 = COOC_2H_5$ and $R_1 = R_2 = CN$) and *p*-nitroso-N-dimethylaniline was observed.

In the reaction of the pyridinium-cyano-carbethoxy-methylid with α-nitroso-β-naphthol (effected in various solvents at room temperature) pyridine was ejected, and a solid product, in the form of bright mustard-coloured crystals (from methylene chloride – carbon tetrachloride), has been isolated. They have a variable m.p., 219–232° (decomp.), depending on the rate of heating.

Judging from the facile elimination of the carbethoxy group, previously observed by us [4,5] in some reactions of the above ylid, the product was expected to have a naphthoxazolic structure of type (IV, $R_2 = CN$), with a molecular formula $C_{12}H_6N_2O$, formed by the loss of H_2O and $COOC_2H_5$ from the intermediate hypothetical nitrone (VI). Instead, a molecular formula $C_{13}H_6N_2O_3$ (MW = 238) was found for the reaction product, corresponding to a simple stoichiometry*, as follows :

$$\underset{\text{ylid}}{C_{10}H_{10}N_2O_2} + \underset{\text{nitrosonaphthol}}{C_{10}H_7NO_2} = \underset{\text{product}}{C_{13}H_6N_2O_3} + \underset{\text{pyridine}}{C_5H_5N} + \underset{\text{ethanol}}{C_2H_6O}$$

Thus it was conceivable to assume that the structure of the product is (VII), 3H-‹naphtho-[1,2-e]-1,4-oxazone›-2-cyano-3-one-1-oxide, analogous to (V), resulting from the cyclization of the hypothetical intermediary nitrone (VI) by an unusual intramolecular *trans*-esterification.

---

* MW (determined by the cryoscopic method in camphor) = 239. From the analytical data, a close molecular formula $C_{13}H_8N_2O_3$, corresponding to a less plausible reductive process, has also been considered, but this formula is not in agreement with the NMR spectrum of the product.

[3] F. Kröhnke, *Ber. dtsch. chem. Ges.*, **72**, 83 (1939).

[4] C. Leonte and I. Zugrăvescu, *Tetrahedron Letters*, **20**, 2027 (1972).

[5] C. Leonte and I. Zugrăvescu, *Tetrahedron Letters*, **20**, 2029 (1972).

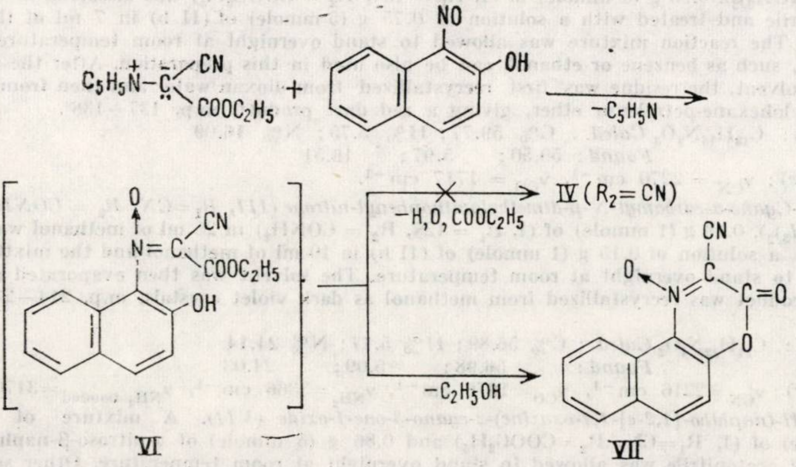

The following facts are in accordance with this structure :

a) The compound was shown to be identical (melting point and IR spectrum) with the product isolated from the analogous reaction between pyridinium-cyano-carbomethoxy-methylid (I, R_1 = CN, R_2 = $COOCH_3$) and α-nitroso-β-naphthol (with C_5H_5N and CH_3OH elimination).

b) In the IR spectrum (KBr) the CO group appears as doublet (as in some α, β-unsaturated δ-lactones) at 1743, 1728 cm^{-1}; the CN group is also present at 2280 cm^{-1} (low intensity). Neither OH (naphthol) nor NH (of a possible amidic group) absorptions are present.

c) In the NMR spectrum only aromatic protons are observed; they appear as multiplets at δ = 8.5 and δ = 8.0 ppm. The relative intensities of the two signals are 1.5, corresponding to the six aromatic protons of the substituted naphtalene nucleus.

Mechanistically, the trans-esterification process is probably favoured by the increased positivation of the carbonyl carbon atom in the intermediate nitrone; it may also be assumed that the naphthol group reacts in a more nucleophilic form, as naphtholate.

In thermodynamic terms, the easy formation of (VII) may be attributed to the resonance stabilization of the resulting cyclic system, as follows :

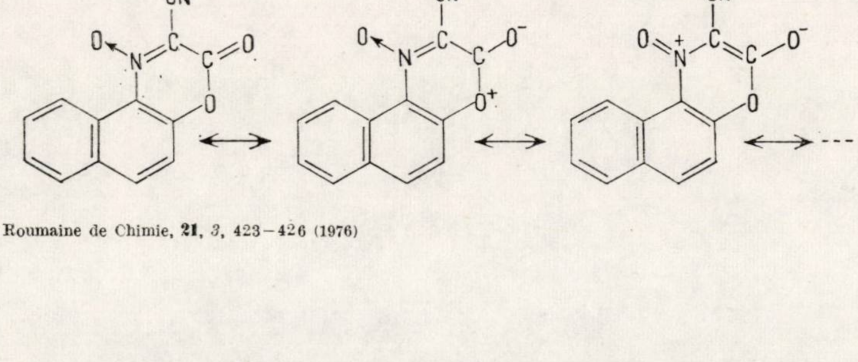

EXPERIMENTAL

α-Cyano-α-carbethoxy-N-p-dimethylaminophenyl-nitrone (*III*, $R_1 = CN$, $R_2 = COOC_2H_5$ $R_3 = N(CH_3)_2$). 0.95 g (5 mmole) of (I, R_1 = CN, R_2 = $COOC_2H_5$) was dissolved in 7 mol of acetonitrile and treated with a solution of 0.75 g (5 mmole) of (II b) in 7 ml of the same solvent. The reaction mixture was allowed to stand overnight at room temperature. Other solvents, such as benzene or ethanol, can be also used in this preparation. After the removal of the solvent, the residue was first recrystallized from dioxan/water and then from chloroform/cyclohexane-petroleum ether, giving a red dust product, m.p. 137–138°.

Analysis : $C_{13}H_{15}N_3O_3$ *Calcd.* : C% 59.77 ; H% 5.75 ; N% 16.09
Found : 59.50 ; 5.97 ; 16.51

IR (KBr) : $\nu_{CN} = 2270\ cm^{-1}$, $\nu_{CO} = 1717\ cm^{-1}$.

α-Cyano-α-carbamyl-N-p-dimethylaminophenyl-nitrone (*III*, $R_1 = CN$, $R_2 = CONH_2$, $R_3 = N(CH_3)_2$). 0.16 g (1 mmole) of (I, R_1 = CN, R_2 = $CONH_2$) in 25 ml of methanol was treated with a solution of 0.15 g (1 mmole) of (II b) in 10 ml of methanol and the mixture was allowed to stand overnight at room temperature. The solvent was then evaporated and the crude product was recrystallized from methanol as dark violet crystals, m.p. 214–215° (decomp.).

Analysis : $C_{11}H_{12}N_4O_2$ *Calcd.* : C% 56.89 ; H% 5.17 ; N% 24.14
Found : 56.98 ; 5.09 ; 24.03

IR (KBr) : $\nu_{CN}=2216\ cm^{-1}$, $\nu_{CO}=1676\ cm^{-1}$, $\nu_{NH_2}=3366\ cm^{-1}$, $\nu_{NH_2\ bonded}=3170\ cm^{-1}$.

3H-(naphtho-[1,2-e]-1,4-oxazine)-2-cyano-3-one-1-oxide (*VII*). A mixture of 0.95 g (5 mmole) of (I, R_1=CN, R_2=$COOC_2H_5$) and 0.86 g (5 mmole) of α-nitroso-β-naphthol in 60 ml of acetonitrile was allowed to stand overnight at room temperature. Other solvents, like ethanol (45 ml) or dimethylformamide (6ml), can also be used. After the removal of the solvent, the dark residue was triturated with an ethanol-ether mixture, filtered and washed with ether. The crude product (0.53 g 44.5%) was recrystallized from CH_2Cl_2/CCl_4 as bright mustard-coloured crystals with a variable m.p., 219–232° (decomp.), depending on the rate of heating. Other solvents, such as dimethylformamide/ethanol, acetone/ethanol or chloroform/ethanol, can also be used for recrystallization.

From (I, R_1 = CN, R_2 = $COOCH_3$)[4] (2 mmole) and (II b) (2 mmole) in acetonitrile (25 ml) or dimethylformamide (3 ml), the same product has been obtained (mixed m.p. unchanged).

MW (cryoscopic in camphor) = 239 (*Calcd.* : 238).

Analysis : $C_{13}H_6N_2O_3$ *Calcd.* : C% 65.55 ; H% 2.52 ; N% 11.76
Found : 65.63 ; 2.60 ; 11.81
65.52 ; 2.84 ; 11.77
65.71 ; 2.89 ; 11.43

(*Calcd.* for $C_{14}H_8N_2O_3$: C% (65.00 ; H% 3.33 ; N% 11.67).

IR (KBr) : $\nu_{CN}= 2280\ cm^{-1}$, ν_{CO} (doublet)=1743, 1728 cm^{-1}. NMR (in HMPT and pyridine) : multiplets in aromatic region at δ = 8.0 and 8.5 ppm.

Revue Roumaine de Chimie, 21, 3, 427–445 (1976)

BROMAMINE ACID–ANTHRAQUINONIC INTERMEDIATE USED IN DYES SYNTHESES

F. URSEANU and L. FLORU

Laboratory of Chemistry and Technology of Aromatic Intermediates and Dyes,
Chemistry Institute, Calea Victoriei 149, Bucharest, Romania

Received November 17, 1973
Completed March 14, 1975

The paper presents the methods used to obtain the bromamine acid, its properties and different types of synthesized dyes, taking into account their tinctorial characteristics.

1. INTRODUCTION

It is extremely important for the technology of different anthraquinone dyes to elaborate a varied number of anthraquinone intermediates which may represent the starting material for their synthesis. Thus, the literature[1] presents numerous substituted anthraquinone intermediates containing amino, hydroxy, nitro, halogen, carboxy and sulphonic groups.

Patented in 1911, the 1-amino-4-bromoanthraquinone-2-sulphonic acid (bromamine acid[2]) became soon one of the most important anthraquinone intermediates, due to the great number of dyes that may be obtained from it, by relatively simple means.

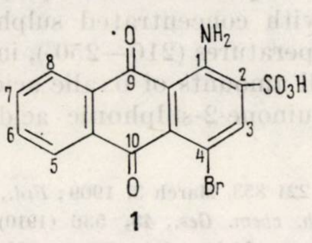

1

The great number of dyes deriving from the bromamine acid is due first to the relatively facile substitution of bromine by various amines under the conditions of Ullmann reaction, [3-6] and secondly to the numerous possibilities of replacement of the sulphonic group after the replacement of bromine. Numerous dyes, belonging to different classes have thus been synthesized : acid, vat, substantive, disperse, cationic and reactive dyes which will be further presented.

---

[1] J. Reichel, "Tehnologia coloranţilor antrachinonici", Ed. Academiei, Bucharest, 1961, p. 70, 148, 228.

[2] Badische Anilin und Sodafabrik, Ger. Pat. 263 395, Jan. 13, 1911; *Frd.*, **11**, 555.

2. PREPARATION OF BROMAMINE ACID

There are two important phases in the process of obtaining the bromamine acid : the sulphonation of the 1-aminoanthraquinone and the bromination of the 1-aminoanthraquinone-2-sulphonic acid :

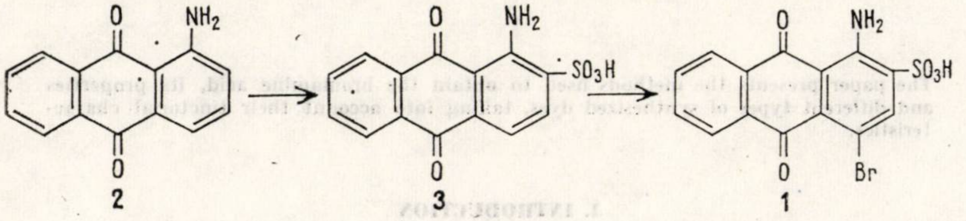

2.1. SULPHONATION

The literature indicates two possibilities for the sulphonation of 1-aminoanthraquinone to 1-aminoanthraquinone-2-sulphonic acid : with oleum or with chlorosulphonic acid ; for both methods many variants are described all of them leading to high yields and preventing the formation of secondary products (disulphonic acids, hydroxyderivatives, etc.).

The sulphonation with concentrated sulphonic acid [7,8] by baking is carried out at high temperatures (210—250°), in the presence of an inert gas ; the addition of small amounts of oxalic acid [9] leads to an increased yield of 1-aminoanthraquinone-2-sulphonic acid.

---

[3] F. ULLMANN, Ger. Pat. 221 853, March 3, 1909 ; *Frd.*, **10,** 703.

[4] F. ULLMANN, *Ber. dtsch. chem. Ges.*, **43,** 536 (1910).

[5] F. ULLMANN and M. SONNE, *Liebigs Ann. Chem.*, **380,** 336 (1911).

[6] F. ULLMANN and P. OCHSNER, *Liebigs Ann. Chem.*, **381,** 1 (1911).

[7] A. DAVIDSON, W. W. THATUM and G. E. WATTS, Brit. Pat. 299 279, May 30, 1928 ; *Chem. Zentr.*, **1929 I,** 1615.

[8] Imperial Chemical Industrie Ltd., Fr. Pat. 662 908, Oct. 25, 1928 ; *Chem. Abstr.*, **24,** 379 (1930).

[9] A. DAVIDSON, W. W. THATUM and G. E. WATTS, Brit. Pat. 311 977, July 2, 1928 ; *Chem. Abstr.*, **24,** 865 (1930).

Many patents[10–15] indicate the possibility to sulphonate 1-aminoanthraquinone with oleum in sulphuric acid in the presence of sodium or potassium sulphate or bisulphate; the sulphonation temperature may vary between 120° and 250°. More recent works[16] show that the boric acid has a favourable catalytic effect on the sulphonation of 1-aminoanthraquinone in position 2; thus, by the sulphonation of 1-aminoanthraquinone at 100–130°, with 65% oleum, in the presence of boric acid, 1-aminoanthraquinone-2-sulphonic acid is obtained in 90% yield.

Sulphonation with chlorosulphonic acid is also described in some patents.[17–19] In several variants the sulphonation is carried out in inert solvents having high boiling points, such as nitrobenzene, tetrachloroethane, *ortho*-dichlorobenzene, trichlorobenzene, etc., at temperatures varying between 90–120°, with a small excess of chlorosulphonic acid; in some cases[20–23] tertiary bases (quinoline, pyridine, dimenthylaminociclohexane) are added. According to literature indications,[24,25] the sulphonation of 1-aminoanthraquinone is best done in nitrobenzene, at 120–

---

[10] I. F. Farbenindustrie Akt.-Ges., Ger. Pat. 484 997, April 24, 1927; *Chem. Abstr.*, **24,** 1 124 (1930).

[11] Chemische Fabrik vorm Sandoz, Ger. Pat. 530 135, March 12, 1930; *Chem. Abstr.*, **25,** 5 178 (1931).

[12] I. G. Farbenindustrie Akt.-Ges., Brit. Pat. 289 097, April 23, 1928; *Chem. Zentr.*, **1929 II,** 2 373.

[13] Imperial Chemical Industrie Ltd., U.S. Pat. 1 873 300, Aug. 23, 1930; *Chem. Abstr.*, **26,** 5 971 (1932).

[14] Chemische Fabrik vorm Sandoz, Fr. Pat. 712 221, Feb. 26, 1931; *Chem. Abstr.*, **26,** 1 942 (1932).

[15] G. W. Seymour, V. S. Salvin and M. E. Meville, U. S. Pat. 2 413 790, Jan. 7, 1947; Chem. Abstr., 41, 2 445 (1947).

[16] L. Hruska, T. Pfliger and H. Taeublova, Ceh. Pat. 105 953, Dec. 15, 1962; *Chem. Abstr.*, **60,** 2 874 (1964).

[17] H. R. Lee and D. X. Klein, U.S. Pat. 2 135 346, Nov. 1, 1938; *Chem. Abstr.*, **33,** 1 155 (1939).

[18] J. Ogilvie and R. C. Hoare, U. S. Pat. 2 251 688, Aug. 5, 1940; *Chem. Abstr.*, **35,** 6 979 (1941).

[19] J. Ogilvie, U. S. Pat. 2 360 010, Oct. 10, 1944; *Chem. Abstr.*, **39,** 946 (1945).

[20] Gesellschaft für Chemische Industrie in Basel, Swiss Pat. 270 049, Nov. 1, 1950; *Chem. Abstr.*, **46,** 1 046 (1952).

[21] Gesellschaft für Chemische Industrie in Basel, Swiss Pat. 272 150, Feb. 16, 1951; *Chem. Abstr.*, **46,** 3 083 (1952).

[22] P. Grossmann, U. S. Pat, 2 581 016, Jan. 1, 1952; *Chem. Abstr.*, **46,** 9 608 (1952).

[23] Gesellschaft für Chemische Industrie in Basel, Brit. Pat. 664 839, Jan. 16, 1952; *Chem. Abstr.*, **47,** 615 (1953).

[24] FIAT Final Rep., nr. 1 313, vol. 2, p. 214, 202, 232, 213, 233, 237, 230, 228, 238, 239, 143.

[25] G. Stanislaw and S. Stanislaw, Pol. Pat. 45 480, Feb. 28, 1962; *Ref. Zhur. Khim.*, **1963** (2), H 69.

140°, with a small excess of chlorosulphonic acid ; nitrobenzene is finally removed by distillation at low pressure.

From an industrial point of view, both methods, with oleum in the presence of alkaline sulphates and with chlorosulphonic acid în inert solvents with high boiling points, are interesting.

The former method is technically more facile, involving no special apparatus ; it is easy to pass to the bromination phase by diluting the sulphonic mass with water and ice, even without separating 1—aminoanthraquinone-2-sulphonic acid, but large amounts of oleum and sodium sulphate are consumed.

The latter method does not require an excess of reactants, but special equipment is necessary because of corrosion and inflammability danger, as well as for the final separation of the solvent by distillation at low pressure, followed by its purification for reutilization.

The yields obtained by both methods vary between 90—95%.

2.2. BROMINATION

The literature indicates [15,24,26,27] that an aqueous solution of sodium 1-aminoanthraquinone-2-sulphonate is treated with bromine (in small excess) and hydrochloric acid solution, at temperatures between 0—3°. 1-Amino-2,4-dibromoanthraquinone is formed as secondary product, which is separated from the bromamine acid by filtration ; finally, it is isolated by adding sodium chloride followed by filtration and drying. The yields are nearly 90%.

In our laboratory bromamine acid was synthesized [28] by sulphonation of 1-aminoanthraquinone with oleum in sulphuric acid, followed by the bromination in cold aqueous solution of the 1-aminoanthraquinone-2-sulphonic acid formed, the total yield varying between 80—83%. Bromamine acid was also synthesized by sulphonating 1-aminoanthraquinone with chlorosulphonic acid in nitrobenzene, followed by bromination of the reaction mixture poured over water and ice ; finally, nitrobenzene was separated and purified by distillation for reutilization, while to the aqueous layer sodium chloride was added in order to precipitate the bromamine

---

[26] British Celanese Ltd., Brit. Pat. 659 684, Oct. 14, 1951 ; *Chem. Abstr.*, **46**, 10 207 (1952).

[27] British Celanese Ltd., Brit. Pat. 598 797, Feb. 26, 1948 ; *Chem. Abstr.*, **42**, 7 992 (1948).

[28] H. Sanielevici, J. Reichel and L. Floru, *Rev. Chim.* (*Bucureşti*), **20** (12), 717 (1969).

acid as sodium salt. The total yield in the latter case is better (90–91%), and the experimental results were used as a basis for the manufacturing process of bromamine acid in the chemical plant "Colorom" – Codlea, Braşov.

3. THE PROPERTIES OF BROMAMINE ACID

1-Amino-4-bromoanthraquinone-2-sulphonic acid is used as sodium salt. It has the form of fine, red-yellowish crystals, readily soluble in water at 60–70°.

We shall further present some chemical properties of bromamine acid, as they are presented in literature.

Bromamine acid has an amino group with low basicity due to the influence of the electron-attractive sulphonic group in position 2 and of the carbonyl group in position 9 of the anthraquinonic moiety; hence, reactions like alkylation, acylation, diazotisation are carried out under energetic conditions; thus, diazotisation with nitrous acid, which is also a method of analysing bromamine acid,[29] is carried out in a mixture of concentrated sulphonic acid and glacial acetic acid. The sulphonic group, which ensures the solubility in water of the bromamine acid, can be replaced only under drastic conditions. Heating at 180° in concentrated sulphuric acid, in the presence of mercury sulphate, leads thus to 1-amino-4-bromoanthraquinone.[30,31]

The bromine of bromamine acid may be replaced relatively easily, due to the activating effect of the neighbouring carbonyl group in position 10 and of the sulphonic acid group. Thus, by heating with sulphuric acid and boric acid,[32] or by heating with an aqueous solution of sodium hydroxide,[28] 1-amino-4-hydroxy-anthraquinone-2-sulphonic acid is formed.

By refluxing the bromamine acid with mercaptoethanol [33] in alkaline aqueous solution both the sulphonic group and the bromine are replaced, 1-amino-2,4-bis(hydroxyethylthio) anthraquinone being obtained; it is assumed that bromine is first replaced, then the sulphonic group.

By heating bromamine acid with aqueuos solutions of alkaline sulphides, two molecules become linked by a sulphur bridge, bromine being replaced.[34] Treatment with ammonia [35] leads to 1,4-diaminoanthraquinone-2-sulphonic acid, while treatment with various amines, under the conditions of the Ullmann reaction,[3–6] leads to 4-N-substituted derivatives (many of them used as acid blue dyes [1,36,37] for wool, as it will be further shown). It is worth noting that after bromine is replaced with the amino group, the sulphonic group may be easily replaced [28] by various groups: alkoxy [24,38,39], cyano, [29,38,40] hydrogen. [28,38,41,42] The resulting products may be used as disperse dyes for synthetic fibres.

---

[29] H. Sanielevici and L. Floru, "Sinteza intermediarilor aromatici şi a coloranţilor", Ed. didactică şi pedagogică, Bucharest, 1971, p. 388, 308.

[30] Badische Anilin und Sodafabrik, Ger. Pat. 265 727, Feb. 17, 1911; *Frd.*, **11**, 556.

[31] Badische Anilin und Sodafabrik, Ger. Pat. 266 563, Oct. 8, 1911; *Frd.*, **11**, 557.

[32] Chemische Fabrik vorm Sandoz, Brit. Pat. 754 902, Aug. 5, 1956; *Chem. Abstr.*, **51**, 12 146 (1957).

[33] V. S. Salvin and E. F. Landau, U. S. Pat. 2 640 059, Iuly 20, 1949; *Chem. Abstr.*, **48**, 5 223 (1954).

4. DYES OBTAINED BY MEANS OF BROMAMINE ACID

4.1. ACID DYES

As it was previously shown, the bromamine acid reacts with amines $R-NH_2$ **4** in aqueous medium, under the conditions of the Ullmann reaction: [3–6] heating in the presence of alkaline carbonates acetates or hydroxides which neutralize the hydrobromic acid formed during the reaction and copper powder (or copper sulphate, chloride, acetate) as catalyst; the resulting products **5** are dyes soluble in water, used to dye wool, natural silk, leather, in blue or bluish-green shades; some of them may also dye polyamide fibres.

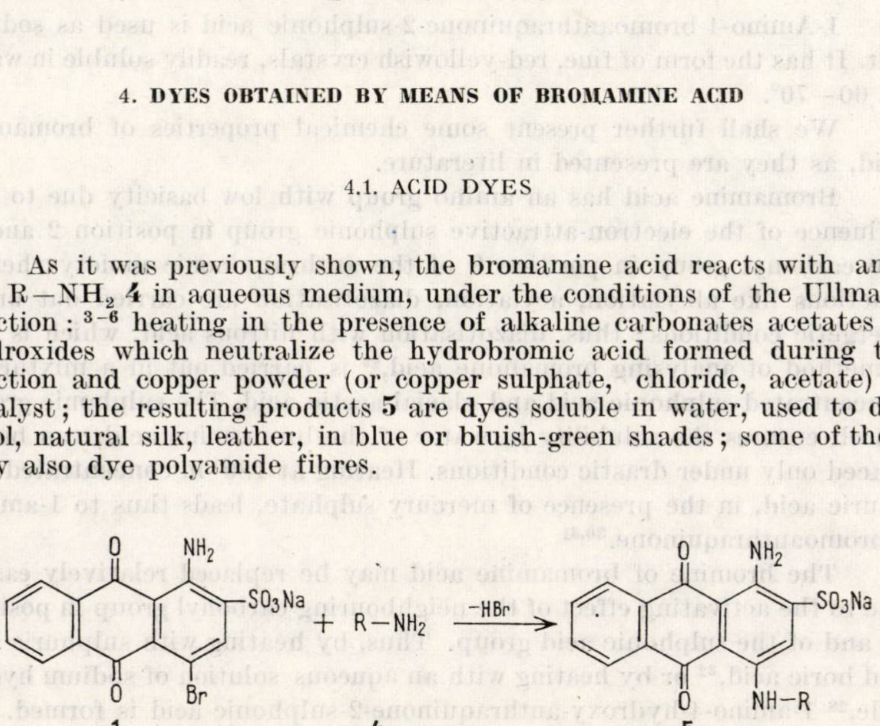

1 **4** **5**

Numeorus dyes with general formula **5** have been synthesized, differing by the radical R; they are presented in Table 1.

[34] H. Krzikalla şi H. Pohlemann, D.B. Pat. 956 263, Jan. 9, 1955; *Chem. Zentr.*, **1957,** 12 311.

[35] K. Maier, D.A.S. 1 142 174, Nov. 17, 1959; *Chem. Zentr.*, **27,** 257 (1964).

[36] I. M. Kogan, "Khimia Krasitelei", gosudarstvenoe nauchino-tekhnichescoe izdatelstvo Kimichescoi literatur, Moskva, 1956, p. 525.

[37] E. N. Abrahart, "Dyes and their Intermediates", Pergamon Press Ltd., Headington Hill Hall, Oxford, 1968, p. 168.

[38] F. Urseanu, C. Drăghici, R. Vintilă and E. Sliam, *Rev. Roumaine Chim.*, **18,** 1 019 (1973).

[39] F. Urseanu, M. Gheorghiu and L. Indrei, *Rev. Chim.* (*Bucureşti*), **24,** 165 (1973).

[40] BIOS Final Rep., nr. 1 484, p. 56, 41, 30.

[41] Badische Anilin und Sodafabrik, Ger. Pat. 287 615, Jun. 11, 1914; *Frd.*, **12**, 478.

[42] R. N. Heslop, F. Irving and A. Livingston, Brit. Pat. 586 999, April 10, 1947; *Chem. Abstr.*, **42**, 4 761 (1948).

Table 1

Anthraquinone acid dyes (obtained from bromamine acid)

Dye with general formula **5**, in which *R* =	References	Dye with general formula **5**, in which R =	References
0	1	0	1
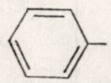	**24,40** **43,44**	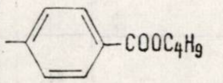	**49**
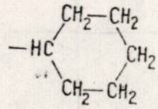	**24,40** **45**	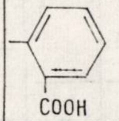	**38,50**
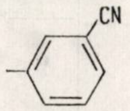	**24,46**	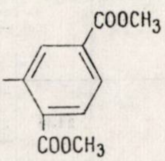	**47,51**
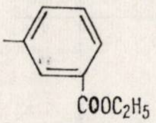	**24,47**	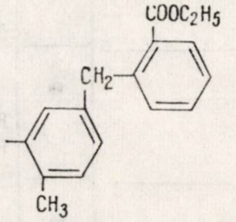	**24,47** **52**
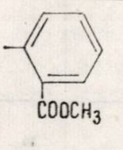	**48**		

Note. The dyes obtained from the reaction of diamines with two bromamine acid molecules are also included in the table.

[43] Aktiengesellschaft für Anilinfabrikation, Ger. Pat. 280 646, July 15, 1913; *Frd.*, **12**, 453.

[44] Farbenfabriken Bayer Co., Ger. Pat. 288 878, May 2, 1914; *Frd.*, **12**, 453.

[45] K. Weinand, Ger. Pat. 456 114, Nov. 24, 1925; *Frd.*, **16**, 1 304.

[46] K. Weinand, Ger. Pat. 511 043, Feb. 26, 1929; *Frd.*, **17**, 1 194.

[47] G. Kränzlein and F. Diefenbach, Ger. Pat. 555 966, April 5, 1930; *Frd.*, **19**, 1909.

[48] I. G. Farbenindustrie Akt.-Ges., Pat. Brit. 355 810, May 29, 1930; *Chem. Abstr.*, **26**, 6 155 (1932).

[49] FIAT Final Rep. nr. 1 313, vol. 3, p. 60, 62–65.

[50] R. Vintilă and F. Urseanu, *Industria Textilă*, **24**, 37 (1973).

[51] G. Kränzlein and E. Diefenbach, Ger. Pat. 558 491, Dec. 25, 1930; *Chem. Abstr.*, **27**, 607 (1933).

[52] G. Kränzlein and E. Diefenbach, Ger. Pat. 553 001, Feb. 7, 1930; *Frd.*, **19**, 1 987.

Table 1 (continued)

Dye with general formula **5**, in which R =	References	Dye with general formula **5**, in which R=	References
0	1	0	1
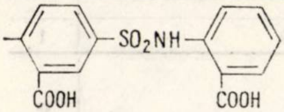	53	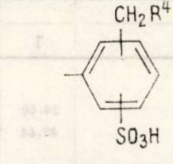 $R^4 = N(CH_3)_2$, piperidinyl, morpholinyl, pirotrolinyl	49
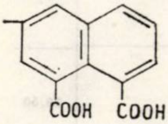	54		
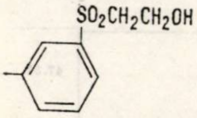	55	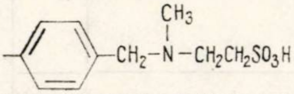	49
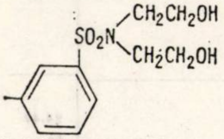	24,56 57	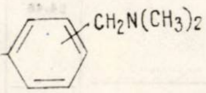	49
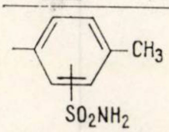	58	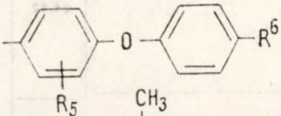 $R^5 = SO_3H, SO_2-\overset{CH_3}{\overset{\vert}{N}}-CH_2CH_2SO_3H$ $R^6 = H, C(CH_3)_3$	49
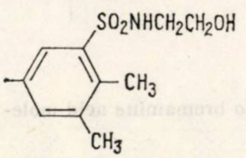	59	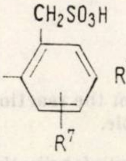 R^7 = alkyl, alkoxy, halogen	49
$R^3 = H, CH_3$ 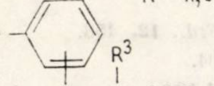	49	$CH_2OCH_2CH_2OH$	

---

[53] C. G. Vogt, U.S. Pat. 2 453 104, Nov. 2, 1948; *Chem. Abstr.*, **43**, 7 709 (1943).

[54] W. Zerweck and E. Heinrich, Ger. Pat. 824 815, Dec. 15, 1951; *Chem. Abstr.*, **49**, 626 (1955).

[55] J. Heyna, E. Schinzel and W. Noll, D.B. Pat. 1 154 892, Aug. 8, 1959; *Ref. Zhvr. Khim.*, **1965** (4), H 120.

[56] General Aniline Works, U. S. Pat. 2029 059, April 5, 1935; *Chem. Abstr.*, **30**, 2013(1936).

[57] E. Diefenbach and E. Fischer Swiss Pat. 182 721, April 10, 1935; *Chem. Zentr.*, **1936 II**, 4 164.

[58] Badische Anilin und Sodafabrik A.-G., Brit. Pat. 1 141 659, Dec. 15, 1966; *Chem. Abstr.*, **70**, 79 078 h (1969).

[59] J. R. Geigy A.-G., Brit. Pat. 1 167 664, April 5, 1967; *Chem. Abstr.*, **72**, 56 696 k (1970).

Table 1 (continued)

De with general formula **5**, in which R=	Refe-rences	Dye with general formula **5**, in which R=	Refe-rences
0	1	0	1
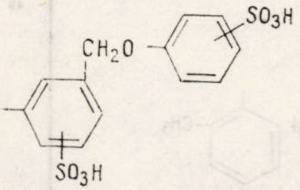	49	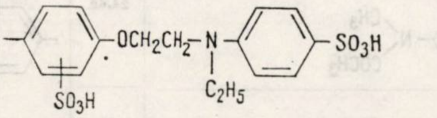	
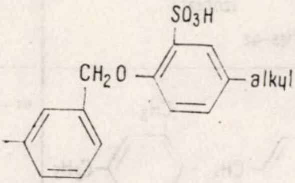		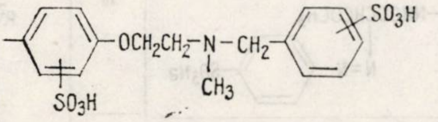	
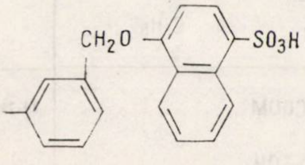		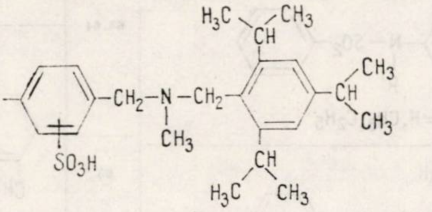	
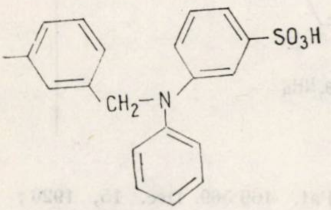		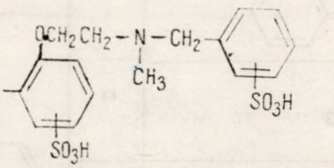	
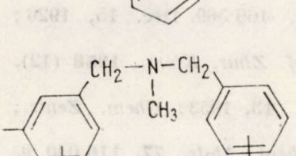		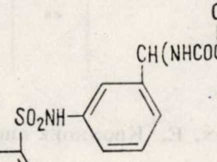	60
		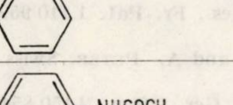	24,43 61

---

[60] B. N. Parsons and T. J. Smith, Brit. Pat. 1 300 742, Feb. 10, 1969; *Chem. Abstr.*, **78**, 73 643 g (1973).

[61] Farbenfabriken Bayer A.-G., Ger. Pat., 933 353, Sept. 22, 1955; *Chem. Abstr.*, **50**, 2 983 (1956).

Table 1 (continued)

Dye with general formula **5**, in which R =	References	Dye with general formula **5**, in which R =	References
0	1	0	1
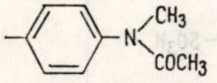	24,62	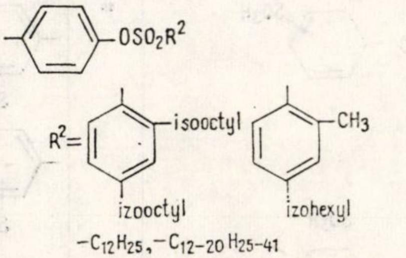 OSO2R2 R2= isooctyl izooctyl CH3 izohexyl -C12H25, -C12-20 H25-41	49
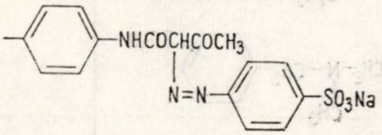 NHCOCHCOCH3 N=N SO3Na	49		
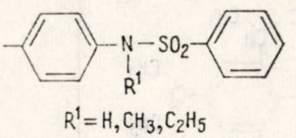 N-SO2 R1 R1 = H, CH3, C2H5	63,64	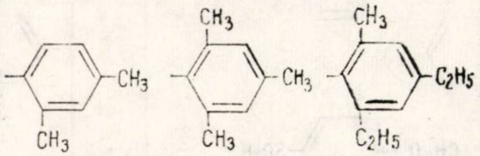 CH3 CH3 CH3 CH3 CH3 CH3 C2H5 C2H5	67–71
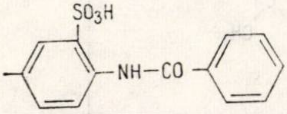	65	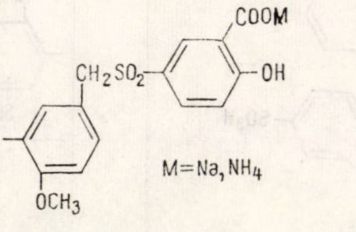 COOM CH2SO2 OH OCH3 M=Na, NH4	24,72
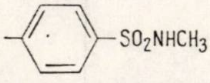	64		
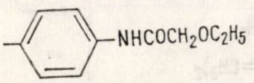 NHCOCH2OC2H5	66		

---

[62] G. Kränzlein, E. Kronholz and F. Römer, Ger. Pat. 469 569, Dec. 15, 1926; *Frd.*, **16**, 1 306.

[63] Sandoz Akt.-Ges., Fr. Pat. 1 110 959, Feb. 2, 1956; *Ref. Zhur. Khim.*, **1958** (12), 40 663.

[64] J. Günthard and A. Peter, Swiss Pat. 315 562, Feb. 13, 1953; *Chem. Zentr.*, **1957**, 11 728.

[65] J. F. Feeman, Ger. Offen. 2 150 854, Oct. 12, 1970; *Chem. Abstr.*, **77**, 116 040 g, (1972).

[66] Sandoz Ltd., Brit. Pat. 799 732, Aug. 13, 1958; *Chem. Abstr.*, **53**, 3 175 (1959).

[67] Sandoz Ltd., Swiss Pat. 255 968, Feb. 1, 1949; *Chem. Abstr.*, **45**, 3 162 (1951).

[68] Sandoz Ltd., Swiss Pat. 261 859, Sept. 1, 1949; *Chem. Abstr.*, **44**, 7 543 (1950).

[69] S. Hotta and T. Akamatsu, Jap. Pat. 71 41 232, Nov. 14, 1967; *Chem. Abstr.*, **76**, 128 819 k (1972).

[70] M. Tobita, T. T. Chang and I. Tanabe, Jap. Pat. 72 36 855, Sept. 30, 1968; *Chem. Abstr.*, **78**, 59 784 x (1973).

[71] J. Guenthard, Fr. Pat. 1509 724, Feb. 2, 1966; *Chem. Abstr.*, **70**, 79 158 j (1969).

[72] I. G. Farbenindustrie Akt.-Ges., Ger. Pat. 632 376, Aug. 7, 1936; *Chem. Abstr.*, **30**, 7 863 (1936).

Table 1 (continued)

Dye with general formula **5**, in which R=	References	Dye with general formula **5**, in which R =	References
0	1	0	1
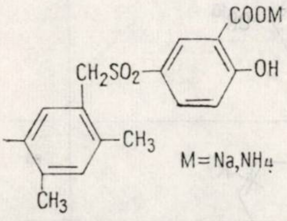 $M = Na, NH_4$	24,72	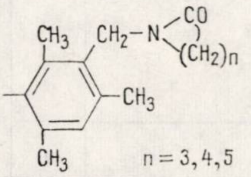 $n = 3, 4, 5$	75
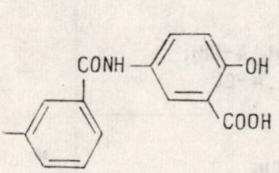	24,72	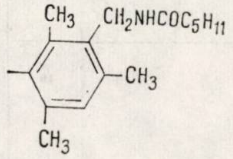	76
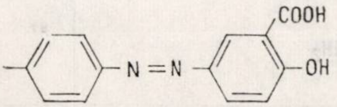	73	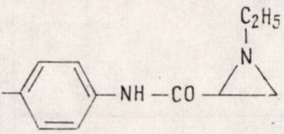	77
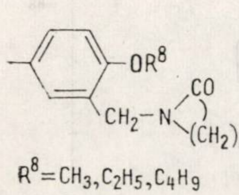 $R^8 = CH_3, C_2H_5, C_4H_9$ $n = 5-11$	74	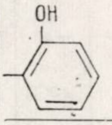	78
		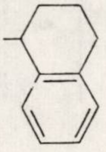	79

---

[73] Imperial Chemical Industrie Ltd., Brit. Pat. 478 665, July 22, 1936; *Chem. Zentr.*, **1938 I,** 4 723.

[74] H. Machaatzke, Brit. Pat. 1 190 543, Ian. 26, 1968; *Chem. Abstr.*, **73,** 36 567 m (1970).

[75] H. Kemmoci, T. Kanda and T. Akamatsu, Jap. Pat. 71 32 594, Aug. 3, 1968; *Chem. Abstr.*, **76,** 60 942 u (1972).

[76] H. Kemmoci, T. Kanda and T. Akamatsu, Jap. Pat. 72 14 354, Feb. 14, 1968; *Chem. Abstr.*, **77,** 90 069 w (1972).

[77] D. Maeusezahl and A. Wohlkoening, Ger. Offen. 2 155 464, Nov. 12, 1970; *Chem. Abstr.*, **77,** 103 288 u (1972).

[78] K. Weinand, Ger. Pat. 534 935, Feb. 9, 1930; *Chem. Abstr.*, **26,** 1 452 (1932).

[79] Sandoz Ltd., Brit. Pat. 602 419, May 26 1948; *Chem. Abstr.*, **42,** 7 990 (1948).

Table 1 (continued)

Dye with general formula **5**, in which R=	References	Dye with general formula **5**, in which R=	References
0	1	0	1
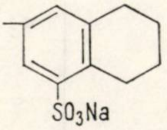	80	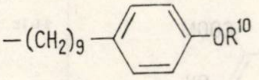 R^{10}= alkyl	84
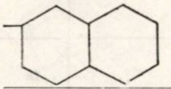	81	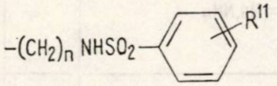 n = 3, 4, 6 R^{11} = H, 4-$NHCOCH_3$, 4-CH_3, 3-SO_2NHCH_3, 4-Cl	85
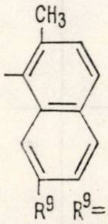 R^9 = H, CH_3	49	—$CH_2CH_2CH_2NHCH_2CH_2CH_3$	86
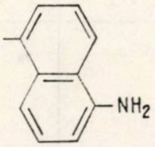	82	—$C_3H_6NHC_3H_6NH_2$	87
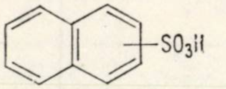	83	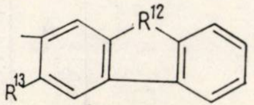 R^{12} = O, NH R^{13} = H, OCH_3	88

---

[80] I. G. Farbenindustrie Akt.-Ges., Brit. Pat. 355 697, April, 26, 1930; *Chem. Abstr.*, **26,** 6 155 (1932).

[81] Sandoz Ltd., Swiss Pat. 269 049, Oct. 2, 1950; *Chem. Abstr.*, **45,** 5 416 (1951).

[82] G. Kalischer and E. Honold, Ger. Pat. 534 932, July 18, 1929; *Chem. Abstr.*, **26,** 1 452 (1932).

[83] S. Inoue and V. Hirosawa, Jap. Pat. 71 33 236, Oct. 20, 1967; *Chem. Abstr.*, **76,** 60 946 s (1972).

[84] A. J. Kizber, I. M. Bilik and K. V. Kornyushina, U.R.S.S. Pat. 106 778, Aug. 25; 1957; *Chem. Abstr.*, 52, 3 351 (1958).

[85] Z. Jankowski and A. Wawrzyniak, Pol. Pat. 61 945, Nov. 11, 1967; *Chem. Abstr.*, **77,** 7 296 z (1972).

[86] M. Z. Bil and W. H. Brunner, U. S. Pat. 3 168 441, July 31, 1961; *Ref. Zhur. Khim.*, **1966** (13), H 214.

[87] Clairol Inc., Brit. Pat. 969 377, July 31, 1961; *Chem. Abstr.*, **61,** 15 928 (1964).

[88] J. G. Kern, U.S. Pat. 2 407 704, Sept. 17, 1946; *Chem. Abstr.*, **41,** 1 458 (1947),

Table 1 (continued)

Dye with general formula 5, in which R =	References	Dye with general formula 5, in which R =	References
0	1	0	1
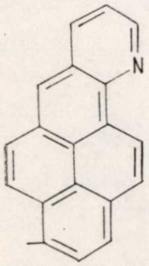	49	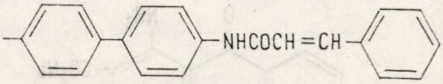	93
		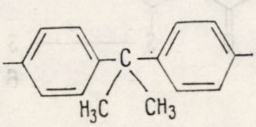	24,94
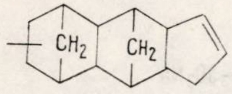	89	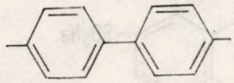	95
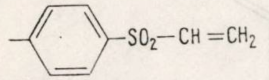	90	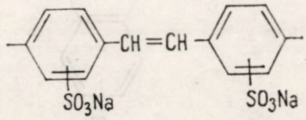	96
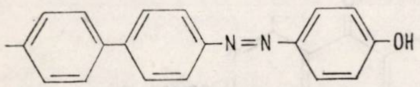	91		
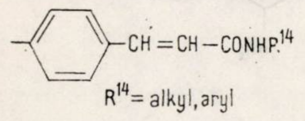	92	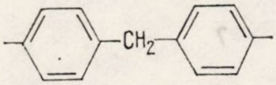	97

---

[89] Badische Anilin und Sodafabrik, Brit. Pat. 1 142 027, Iun. 10 1965; *J. Soc. Dyers and Collourists*, **85,** 169 (1969).

[90] Farbwerke Hoechst Akt.-Ges., vormals Meister Lucius Brüning, Swis Pat. 301 821, July 16, 1951; *Chem. Zentr.*, **1955,** 10 387.

[91] I. G. Farbenindustrie Akt.-Ges., Fr. Pat. 811 890, April 24, 1937; *Chem. Abstr.*, **32,** 792 (1938).

[92] I. G. Farbenindustrie Akt.-Ges., Fr. Pat. 756 131, May 26, 1933; *Chem. Zentr.*, **1934 I,** 1721.

[93] Soc. pour l'ind. chim. à Bâle, Fr. Pat. 804 457, Oct. 24, 1936; *Chem. Abstr.*, **31,** 3 703 (1937).

[94] K. Weinand, Ger. Pat. 644 408, April 30, 1937; *Chem. Abstr.*, **31,** 5 593 (1937).

[95] Chemische Fabrik vorm Sandoz, Fr. Pat. 785 494, Feb. 11, 1935; *Chem. Zentr.*, **1936 I,** 651.

[96] C. G. Vogt, U.S. Pat. 2 476 642, Iuly 19, 1949; *Chem Abstr.*, **43,** 9 467 (1949).

[97] Chemische Fabrik vorm Sandoz, Fr. Pat. 777 164, Aug. 13, 1934; *Chem. Zentr.*, **1935 II,** 1 968.

Acid dyes may also be obtained from bromamine acid by other reactions, e.g. by treatment with sodium trisulphides [98] the blue dye **6** results, which contains a bridge of three sulphur atoms connecting the two rests of bromamine acid, while by condensation with tionaphtholes [99] violet dyes **7** are formed; by heating bromamine acid in aqueous acid medium with copper powder or copper oxide the blue dye **8** results, 4,4′-diamino-1,1′-dianthraquinonyl-3,3′-disulphonic acid (sodium salt).[100]

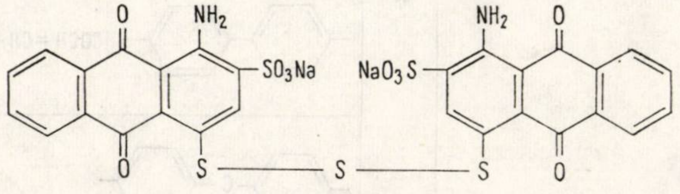

6

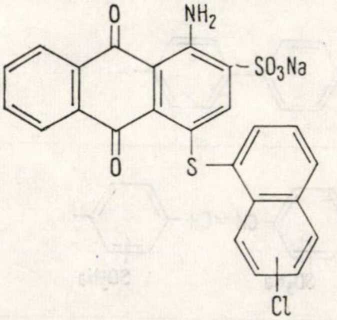

7

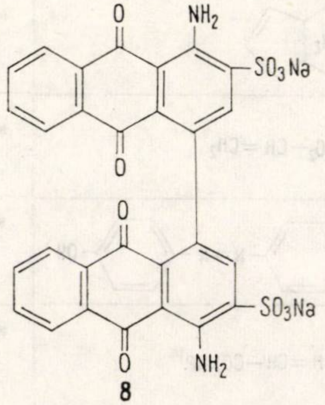

8

4.2. OTHER DYES OBTAINED STARTING FROM BROMAMINE ACID

Numerous other types of dyes have been synthesized using bromamine acid as starting material; the first stage is the reaction with various amines, leading to products **5**, most of them used as acid dyes, as shown above (Table 1). Further examples of dyes of various tinctorial properties are presented, together with the literature corresponding to the respective class.

---

[98] Badische Anilin und Sodafabrik, Ger. Pat. 956 267, Jan. 17, 1957; *Chem. Abstr.*, **53**, 3 715 (1959).

[99] F. Osterloch, Ger. Pat. 892 042, Oct. 5, 1953; *Chem. Abstr.*, **52**, 11 432 (1958).

[100] Ciba Ltd., Brit. Pat. 926 514, May 5, 1960; *Chem. Zentr.*, **31**, 2 449 (1964).

4.2.1. Vat dyes[3-6,24,38,41,42,101-105]

In this category there are included the dyes with naphth[2,3-c] acridan-5,8,14-trione* structure of the general formula **12**, which are obtained[1] by the condensation of bromamine acid **1** with anthranilic acid (substituted or unsubstituted), followed by the acridonic ring closure by heating with concentrated sulphuric acid, oleum of low concentration or chlorosulphonic acid of the resulted 4-amino-1-anilinoanthraquinone-3-sulphonic-2′-carboxylic acids (**10**), simultaneously with the elimination of the sulphonic group. Syntheses[8] have been realized in which the sulphonic group in the compound **10** was previously eliminated by refluxing in aqueous solution with glucose and sodium hydroxide and then acridonic ring closure in the intermediate 4-amino-1-anilinoanthraquinone-2′-carboxylic acids (**11**) was carried out in chlorosulphonic acid. The amino group may be further modified by treatment with various aroyl chloride (**13**) in an inert organic solvent with high boiling point (*ortho*-dichlorobenzene, nitrobenzene) resulting N-aroyl dyes with the general formula **14**.

The dyes *12* and *14* dye the cotton in blue and greenish blue (in the alkaline tube of NaOH + $Na_2S_2O_4$) being higly resistant to light and hypochlorite. They show, however, a certain sensibility to the alkaline solutions; the reduction in tube is, therefore, performed at temperatures between 20–25°, under moderate alkaline conditions, according to the variant of cold dyeing.

4.2.2. Disperse dyes[24,28,29,38,40,106-108]

To synthesize some disperse dyes with the general formula **15**, used for dying synthetic fibres, one starts from the condensation products **5**, to which the solubilizing sulphonic groups are substituted with hydrogen,[28, 38,41,42] alkoxy [24,38,39] or cyano groups (subsequently, the latter are transformed by hydrolysis with aqueous solution of sulphuric acid

---

* According to the old terminology : anthraquinoneacridone dyes.

[101] I. G. Farbenindustrie Akt.-Ges., Ger. Pat. 531 013, Dec. 13, 1931; *Frd.*, **18**, 1 312.

[102] I. G. Farbenindustrie Akt.-Ges., Ger. Pat. 693 610, June 20, 1940; *Chem. Abstr.*, **35**, 4 968 (1941).

[103] I. G. Farbenindustrie Akt.-Ges., Brit. Pat. 495 375, May 5, 1937; *Chem. Abstr.*, **33**, 3 170 (1939).

[104] B. S. Ioshi, B. D. Tilak and K. Venkataraman, *Proc. Indian Acad. Sci.*, **32 A**, 201 (1950).

[105] Farbenfabriken Bayer A.-G., Brit. Pat. 775 802, May 29, 1957; *Chem. Abstr.*, **51**, 15 142 (1957).

[106] V. Karthaschoff and G. Farine, *Helv. Chim. Acta*, **11**, 820 (1920); Chem. Zentr., **1929 I**, 1 272.

[107] F. Urseanu, C. Tărăbăşanu-Mihăilă, L. Floru and V. Zdrenţu, *Rev. Chim. (Bucureşti)*, **25**, 873 (1974).

[108] F. Urseanu, C. Tărăbăşanu-Mihăilă, L. Negoiţă and V. Zdrenţu, *Rev. Roumaine Chim.*, **20**, 791 (1975).

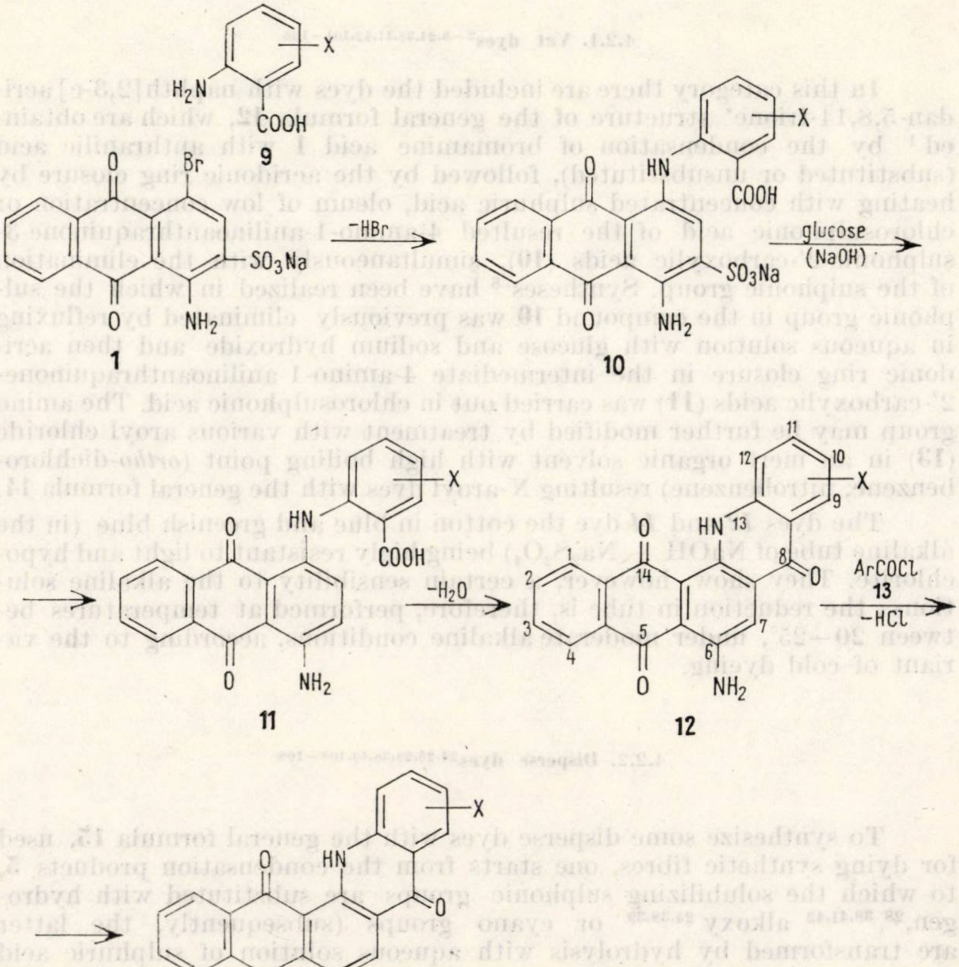
X
H$_2$N
COOH
9
Br
SO$_3$Na
NH$_2$
1
−HBr
HN
10
glucose
(NaOH)
11
−H$_2$O
12
ArCOCl
13
−HCl
NHCOAr
14

X — 10-Cl ; 11-Cl ; 10,12-dichlorine ; 10-Br ; 10-CF_3 ; 11-CF_3 ; 12-CF_3 ; 9-CF_3 ; 11-SO_2 CH_3 ; 10-F ; 10,12-dibromine.

Ar — COC_6H_5 ; CO(2′-Cl)C_6H_4 ; CO(3′-Cl)C_6H_4 ; CO(4′-Cl)C_6H_4 ; CO(3′-F) ; CO(3′-CH_3) C_6H_4.

into the carbamoyl group $CONH_2$)[29,38,40] ; these substituents favour the affinity to the dyed textile material and improve the tinctorial properties of the dyeings obtained.

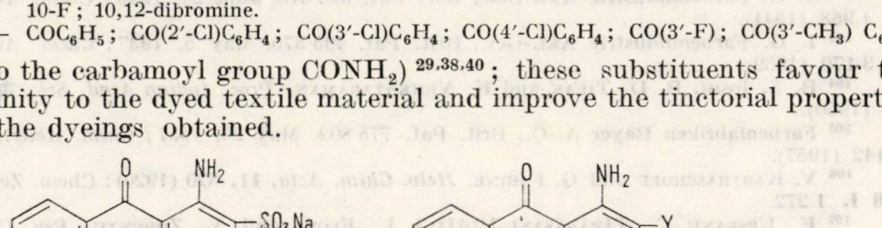
SO$_3$Na
NH$_2$
NH−R
5
Y
Y=H, OAlkyl,
CN(→CONH$_2$)
15

The replacing of the sulphonic group by hydrogen is performed by treating compounds **5** with sodium hydrosulphite or glucose and sodium hydroxide, by an alkoxy group by treatment with alcohol and potassium hydroxide and by a cyano group by treatment with sodium or potassium cyanide.

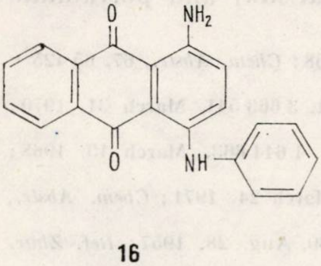

16

Disperse Blue 19
(C.I. 61 110)

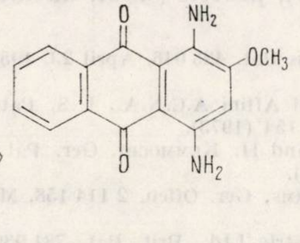
O
NH2
OCH3
O
NH2

17

Disperse Red 11
(C.I. 62 015)

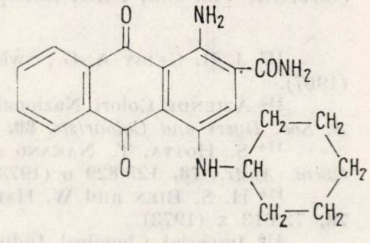
O
NH2
CONH2
CH2—CH2
O
NH—CH
CH2
CH2—CH2

18

Disperse Blue 6
(C.I. 62 050)

4.2.3. Cationic dyes[28,108–111]

Cationic dyes used for dyeing polyacrylonitrile fibres are obtained by condensing bromamine acid with various aminoheterocycles which may quaternize at the tertiary nitrogen by alkylation with dimethylsulphate; intermediately, before quaternization, the sulphonic group in the anthraquinonic rest is replaced, e.g. for the synthesis of the **22** cationic dye, for which 3-amino-1,2,4-triazole (**19**) was used for condensation with bromamine acid.

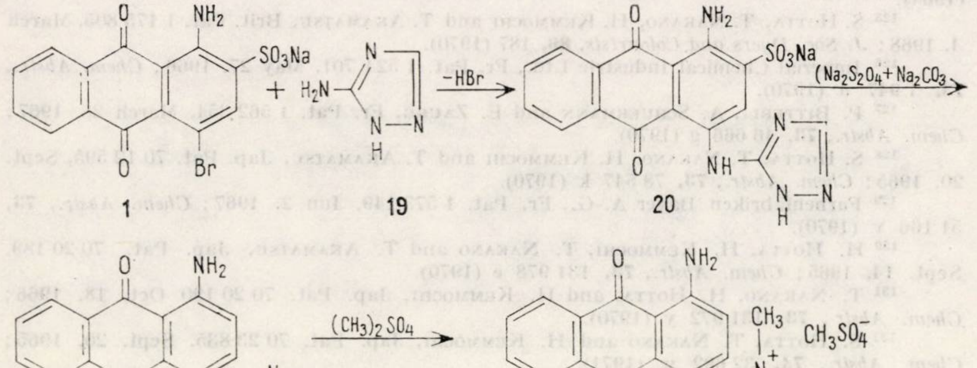
O
NH2
SO3Na
O
Br
1
+ H2N
N
N—N
H
19
–HBr
O
NH2
SO3Na
(Na2S2O4+Na2CO3)
O
NH
N
N—N
H
20
O
NH2
O
NH
N
N—N
H
21
(CH3)2SO4
O
NH2
CH3
CH3SO4−
N+
O
NH
N—N
H
22

---

* Colour Index, vol. 3. The Society of Dyers and Colourists. The American Association of Textile Chemists and Colourists. Lowell Technological Institute. Lowell Mass. USA 1956.

[109] H. Sanielevici, F. Brodmann, S. Rosenberg and C. Stuleanu, Brit. Pat. 1 104 053, Feb. 13, 1967 ; **68,** 106 077 z (1968).

[110] F. Urseanu, R. Vintilă and M. Preoteasa, *Rev. Chim.* (Bucureşti), **26,** 105 (1975).

[111] F. Urseanu and L. Floru, *Rev. Chim.* (*Bucureşti*), **26,** 453 (1975).

4.2.4. Reactive dyes[112–143]

During the last few years numerous syntheses of reactive dyes were carried out. These are modern products used successfully to dye cellulosic (cotton, viscose, flax, hemp), proteic (wool, natural silk) and polyamidic

---

[112] J. R. Geigy A.-G., Swiss Pat. 423 046, April 23, 1958; *Chem. Abstr.*, 67, 65 425 v (1967).

[113] Aziende Colori Nazionali Affini A.C.N.A., U.S. Pat. 3 663 541, March 31, 1970; *J. Soc. Dyers and Colourists*, **89**, 154 (1973).

[114] S. Hotta, T. Nakano and H. Kemmochi, Ger. Pat. 1 644 663, March 13, 1968; *Chem. Abstr.*, **78**, 125 829 u (1973).

[115] H. S. Bien and W. Harms, Ger. Offen. 2 114 158, March 24, 1971; *Chem. Abstr.*, **78**, 73 613 x (1973).

[116] Imperial Chemical Industrie Ltd., Brit. Pat. 781 930, Aug. 28, 1957; *Ref. Zhur. Khim.*, **1959** (20), 72 240.

[117] Imperial Chemical Industrie Ltd., Brit. Pat. 803 473, Oct. 29, 1958; *Ref. Zhur. Khim.*, **1960** (4), 14 564.

[118] A. Schwezer, Swiss Pat. 410 230, April 10, 1959; *Chem. Abstr.*, **66**, 38 867 p (1967).

[119] J. R. Geigy A.-G., Swiss Pat. 427 083, April 30, 1959; *Chem. Abstr.*, **67**, 101 009 y (1967).

[120] K. Matsui and E. Kobayashi, Jap. Pat. 68 08 942, March 13, 1964; *Chem. Abstr.*, **69**, 37 106 q (1968).

[121] Imperial Chemical Industrie Ltd., Fr. Pat. 1 495 035, Aug. 23, 1965; *Chem. Abstr.*, **70**, 12 667 f (1969).

[122] H. Iida and M. Tsukada, Kogyo Kogaku Zasshi, 21 (12), 2033 (1968); *Chem. Abstr.*, **71**, 4 488 (1969).

[123] Imperial Chemical Industrie Ltd., Brit. Pat. 1 120 392, Feb. 16, 1965; *Chem. Abstr.*, 70, 97 948 w (1969).

[124] H. S. Bien și F. Baumann, Fr. Pat. 1 277 113, Jan. 2, 1961; *Chem. Zentr.*, 31, 2 440 (1964).

[125] S. Hotta, T. Nakano, H. Kemmochi and T. Akamatsu, Brit. Pat. 1 175 805, March 4, 1968; *J. Soc. Dyers and Colourists*, **86**, 187 (1970).

[126] Imperial Chemical Industrie Ltd., Fr. Pat. 1 524 701, May 27, 1966; *Chem. Abstr.*, **73**, 1 947 u (1970).

[127] P. Bitterli, A. Schuermann and E. Zaugg, Fr. Pat. 1 562 354, March 23, 1967; *Chem. Abstr.*, **73**, 46 666 g (1970).

[128] S. Hotta, T. Nakano, H. Kemmochi and T. Akamatsu, Jap. Pat. 70 12 595, Sept. 20, 1965; *Chem. Abstr.*, **73**, 78 547 k (1970).

[129] Farbenfabriken Bayer A.-G., Fr. Pat. 1 573 149, Iun 2, 1967; *Chem. Abstr.*, **73**, 51 166 v (1970).

[130] H. Hotta, H. Kemmochi, T. Nakano and T. Akamatsu, Jap. Pat. 70 20 189, Sept. 14, 1965; *Chem. Abstr.*, **73**, 131 978 e (1970).

[131] T. Nakano, H. Hotta, and H. Kemmochi, Jap. Pat. 70 20 190 Oct. 18, 1966; *Chem. Abstr.*, **73**, 131 972 y (1970).

[132] S. Hotta, T. Nakano and H. Kemmochi, Jap. Pat. 70 23 835, Sept. 20, 1965; *Chem. Abstr.*, **74**, 32 692 w (1971).

[133] F. Meininger and H. Springer, Ger. Offen. 1 953 600, Oct. 24, 1969; *Chem. Abstr.*, **75**, 50 409 j (1971).

[134] S. Hotta, H. Kemmochi and T. Akamatsu, Jap. Pat. 71 14 837, Sept 3, 1968; *Chem. Abstr.*, **75**, 65 291 p (1971).

[135] H. Kemmochi, S. Hotta and T. Akamatsu, Jap. Pat. 71 33 234, Feb. 13, 1967; *Chem. Abstr.*, **76**, 73 746 c (1972).

[136] T. J. Smith, Ger. Offen. 2 149 532, Oct. 11, 1970; *Chem. Abstr.*, **77**, 76 673 g (1972).

[137] Aziende Colori Nazionali Affini A.C.N.A., Italia Pat. 795 216, April 20, 1963; Chem. Abstr., **77**, 50 143 j (1972).

[138] M. Asahi, F. Fujii and T. Nakahara, Jap. Pat. 71 36 515, May 21, 1968; *Chem. Abstr.*, **77**, 103 307 z (1972).

[139] K. Shigemasa and G. Sato, Ger. Offen. 2 140 069; Aug. 10, 1971; *Chem. Abstr.*, **78**, 137 950 q (1973).

fibres (nylon, perlon), which are remarkable for the fastening on the textile material, namely by covalent (esteric, etheric, tioetheric, amidic) bonds formed between the dye and the textile fibre.

Basically, a reactive dye is made up of a dyeing part, that may be a rest of an azoic, anthraquinonic, phtalocyaninic, etc. product, a part which comprises the reactive group which forms the covalent bond with the fibre by substitution or addition (triazinic rest with a labile chlorine atom, the rest of a vinyl reactive system, etc.) and solubilizing groups (SO_3H, COOH) which ensure the dissolving of the product in water.

The reactive dyes with anthraquinone structure, obtained on the basis of bromamine acid, are generally prepared by condensing the latter with an aromatic diamine (*para*-phenylenediamine [142]) or with a sulphonic acid derived from it (*para*-phenylenediamino-sulphonic acid, *meta*-phenylenediaminosulphonic acid [143]).

5. CONCLUSIONS

The paper shows that the bromamine acid is important both for the obtention of acid anthraquinonic dyes and the synthesis of a large number of dyes belonging to other tinctorial classes (vat, disperse, cationic, reactive dyes) using as intermediates its acid dyes derivatives.

---

[140] O. Manabe, T. Kamei and H. Fujii, Jap. Pat. 72 36 837, March 24, 1969; Chem. Abstr., **78**, 45 042 s (1973).

[141] M. Asahi and T. Watanabe, Jap. Pat. 72 23 708; Aug. 7, 1968; *Chem. Abstr.*, **78**, 59 786 z (1973).

[142] W. Woytkiewicz, Pol. Pat. 48 011, March 7, 1964; *Ref. Zhur. Khim.* 1964, (23), H 241.

[143] Badische Anilin und Sodafabrik, D.A.S. 1 109 920, Oct. 31, 1957; *Chem. Zentr.*, **1963**, 5 260.

Revue Roumaine de Chimie, **21**, 3, 447–453 (1976)

MIXED AROMATIC ESTERS OF PHOSPHORIC ACID

M. IOVU and ECATERINA VOINA

Faculty of Pharmacy, Traian Vuia 6, Bucharest, Romania

Received September 27, 1973

Completed March 15, 1975

Mixed aromatic esters treated in the present note are added to the aromatic esters of phosphoric and phosphorous acids previously synthesized. Synthesized esters have the general formula $(Ar-O-)_2PO-O-C_6H_4-Ph$ or $Ar-O-PO(-O-C_6H_4-Ph)_2$ in which Ar is a benzene nucleus substituted by one or two methyl radicals. The new mixed esters of phosphoric acid are characterized by their physical properties.

In a previously published work[1] we presented the results of the synthesis of corresponding tris (*p*-cyclohexyl-phenyl) phosphite and phosphate, new esters of the phosphorous and phosphoric acids.

In a previous work [2] we described new phosphorous esters of the general formula $(Ar-CH_2-Ar'-O-)_3P$, in which the radical Ar′ can be substituted by one or two methyl radicals, as well as the corresponding phosphoric esters of the general formula $(Ar-CH_2-Ar'-O-)_3PO$.

The mixed aromatic esters having the general formula $(Ar-O)_2-PO-O-C_6H_4-Ph$ and $Ar-O-PO(-O-C_6H_4-Ph)_2$, in which Ar is a benzene nucleus substituted by one or two methyl radicals, have not yet been synthesized. However, the two corresponding compounds in which Ar is a phenyl radical,[3] have been synthesized.

In the present note we present the results of the synthesis of the above mentioned esters by using as raw material *o*-, *m*- and *p*-cresol, 3,4-dimethylphenol, 2,5-dimethylphenol and 3,5-dimethylphenol and 4-hydroxybiphenyl.

For the synthesis of phosphoric esters having the general formula $(Ar-O)_2-PO-O-C_6H_4-Ph$, we used two synthetic approaches :

a. Dicresyl or dixylenyl chlorine anhydride of phosphoric acid was obtained by the reaction of the corresponding cresol or xylenol with phosphorus oxychloride.

$$2ArOH + POCl_3 \rightarrow (ArO)_2POCl + HCl$$

---

[1] M. Iovu, E. Voina and N. Miclovici, *Anal. Sti. Univ. Buc.*, **19,** 101 (1970).

[2] M. Iovu, E. Voina and M. Bossanyi, *Rev. Chim. (Buc.)*, **00,** 000 (1975).

[3] B. M. Ludin, A. A. Maksimov, I. P. Kolenko and G. A. Semerneva, *Trudy Inst. khim. Akad. Nauk S.S.S.R. Ural'skii Filial*, **13,** 103 (1966) ; *Chem. Abstr.*, **62,** 59205 (1968).

and the condensation of purified chlorine anhydride through distillation, with 4-hydroxybiphenyl.

$$(Ar-O)_2POCl + Ph-C_6H_4-OH \rightarrow (Ar-O-)_2PO-C_6H_4-Ph + HCl$$

This approach has also been used by Lundin and his co-workers [3] for the synthesis of phosphate biphenyl.

b. 4-Biphenyl chlorine anhydride of phosphoric acid was obtained through the reaction of 4-hydroxybiphenyl with phosphorus oxychloride.

$$Ph-C_6H_4-OH + POCl_3 \rightarrow Ph-C_6H_4-O-POCl_2 + HCl$$

The condensation of 4-biphenylchlorine anhydride with a cresol or xylenol has not been mentioned in the literature, as for example :

$$Ph-C_6H_4-O-POCl_2 + 2ArOH \rightarrow (Ar-O-)_2-PO-O-C_6H_4-Ph$$

For the synthesis of phosphoric esters of the general formula $Ar-O-PO-(O-C_6H_4-Ph)_2$, monocresyl or monoxylenyl dichlorine anhydride phosphoric acid was first obtained

$$ArOH + POCl_3 \rightarrow Ar-O-POCl_2 + HCl$$

which was then condensed with 4-hydroxybiphenyl :

$$Ar-O-POCl_2 + 2HO-C_6H_4-Ph \rightarrow Ar-PO(-O-C_6H_4-Ph)_2 + 2HCl$$

The reaction of cresol, xylenol or 4-hydroxybiphenyl with phosphorous oxychloride was achieved in the presence of sodium chloride as a catalyst as suggested by Katiskina and Krofp,[4] in view of obtaining chloranhydrides and esters of arylphosphoric acids.

Monochlor and dichlor condensations of phosphoric ester anhydrides with the corresponding phenols were effected in the presence of triethylamine in a benzene solvent.

RESULTS AND DISCUSSION

Table 1 contains the formulas of the fourteen mixed aromatic phosphoric esters. The results of the elementary phosphorous anaylsis, the melting temperatures of solid products of the densities or the refractive indices for liquid products are also listed.

Examining the table one can find that all mixed phosphoric esters having only one biphenoxidic radical, the rest of them being cresoxidic or xylenoxidic, are oleaginous liquids which cannot be distilled due to their heavy molecular weights.

---

[4] V. V. Katishina and M. Ia Kroff, *Zhur. obshchei Khim.*, **26**, 3060 (1956).

Table 1

Esters of the phosphoric acid

		Formula	P % Calcu-lated	P % *Found*	D_4^{25}	n_D^{25}	Melting point °C	Yield %
1	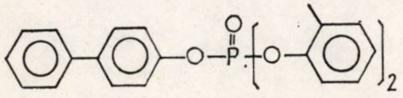	$C_{26}H_{23}PO_4$	7.20	7.34 ; 7.30	1.2370	1.59		91.43
2	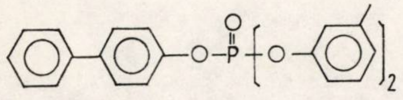	$C_{26}H_{23}PO_4$	7.20	7.25 ; 7.28			65	94.30
3	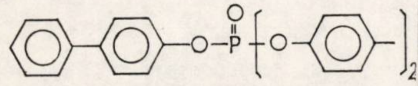	$C_{26}H_{23}PO_4$	7.20	7.28 ; 7.32			84−85	93.20
4	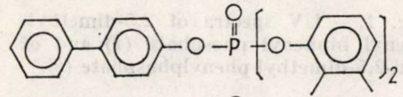	$C_{28}H_{27}PO_4$	6.78	6.84 ; 6.86	1.3135	1.5905		80.00
5	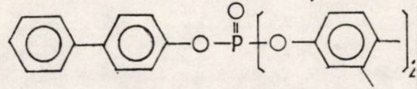	$C_{28}H_{27}PO_4$	6.78	6.70 ; 6.72			66	91.70
6	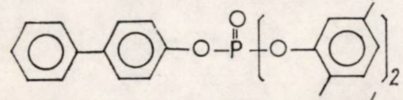	$C_{28}H_{27}PO_4$	6.78	6.78 ; 6.80	1.1954	1.5858		84.33
7	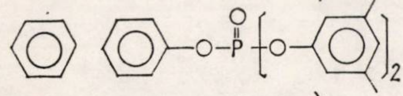	$C_{28}H_{27}PO_4$	6.78	6.84 ; 6.86	1.2236	1.5862		92.00
8	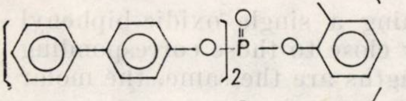	$C_{31}H_{25}PO_4$	6.29	6.20 ; 6.15	1.2011	1.6175		95.07
9	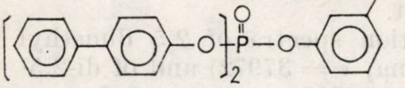	$C_{31}H_{25}PO_4$	6.29	6.30 ; 6.38			99−100	94.57
10	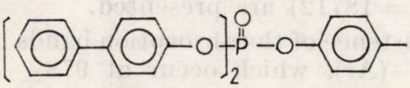	$C_{31}H_{25}PO_4$	6.29	6.21 ; 6.24				95.61
11	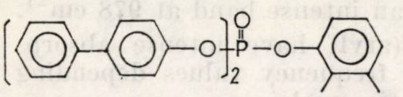	$C_{32}H_{27}PO_4$	5.92	5.95 ; 5.98	1.2054	1.6204	66−67	90.81
12	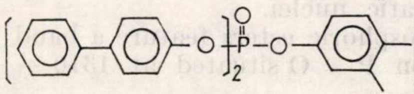	$C_{32}H_{27}PO_4$	5.92	5.95 ; 5.93			101	93.91
13	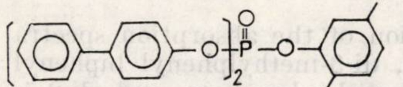	$C_{32}H_{27}PO_4$	5.92	6.10 ; 6.02			84	94.62
14	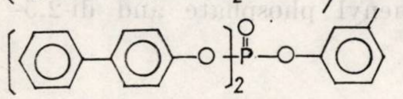	$C_{32}H_{27}PO_4$	5.92	6.08 ; 6.10			83	95.35

The mixed phosphoric esters containing two oxidic biphenyl radicals are solid.

The UV spectral analysis of all synthesized mixed esters shows the existence of a single absorption (maximum) which is mostly found at 251 mμ.

The value of the absorption (maximum) of mixed esters is identical to that of biphenyl (251 mμ).

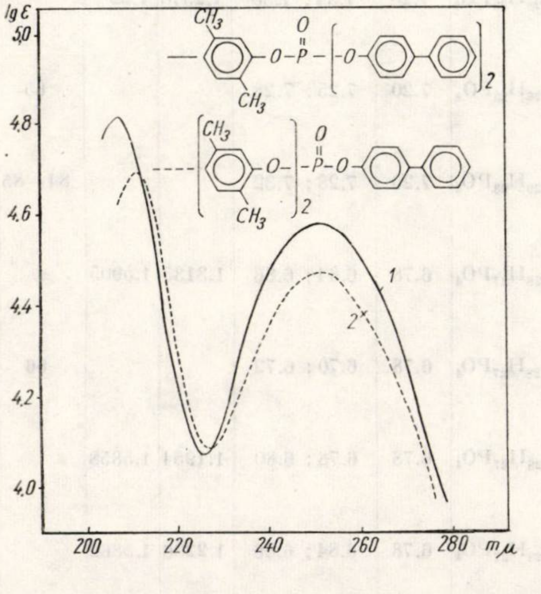

Fig. 1. — UV spectra of 2,5-dimethylphenyl biphenyl phosphate (*1*) and of di-2,5-dimethyl phenylphosphate (*2*).

The mixed phosphoric esters containing a single oxidic-biphenyl rest shows an UV absorption spectrum very close to those corresponding to two biphenyloxidic radicals. The wavelengths are the same, the molar extinction coefficients are slightly different.

By way of exemplifying the absorption spectra of 2,5 dimethyl phenyl, of dibiphenyl phosphate ($\lambda = 251$ mμ, $\varepsilon = 37972$) and of di-2,5-dimethylphenylphosphate ($\lambda = 251$ mμ, $\varepsilon = 18712$) are presented.

The IR spectral analysis reveals the existence of the absorption bands characteristic of valence vibrations P—O—(Ar), which occur at 978 ± 10 cm^{-1}, most of the new esters having an intense band at 978 cm^{-1}.

The stretching vibrations (P)—O—C(aryl) have intense absorption bands between 1210—1110 cm^{-1}, the frequency values depending on the position of the radical in the aromatic nuclei.

Likewise all synthesized aromatic phosphoric esters feature a band characteristic for the elongation vibration P = O situated at 1310 — —1290 cm^{-1}.

Fig. 2 contains only an exemplification of the absorption spectra of 3 methyl-phenyl di-biphenyl phosphate, di-3-methylphenyl biphenyl phosphate, of 2,5-dimethyl-phenyl di-biphenyl phosphate and di-2,5-dimethyl-phenyl biphenyl phosphate.

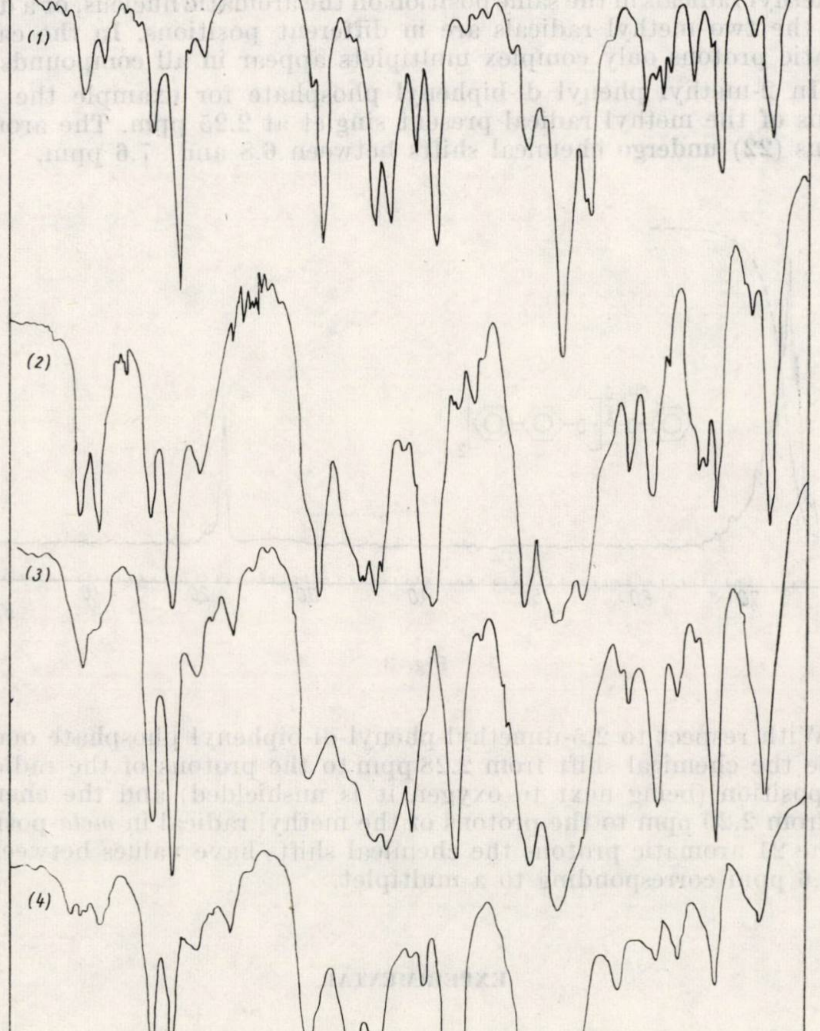

Fig. 2. — IR spectra of 3-methylphenyl di-biphenyl phosphate (*1*), di-3-methylphenyl biphenyl phosphate (*2*) of 2,5-dimethylphenyl di-biphenyl phosphate (*3*) and di-2,5-dimethyl-phenyl phosphate (*4*).

For the protons of methyl radicals the nuclear magnetic resonance spectra present either a singlet, when there is only one methyl radical or two methyl radicals in the same position on the aromatic nucleus, or a dublet when the two methyl radicals are in different positions. In the case of aromatic protons only complex multiplets appear in all compounds.

In 2-methyl phenyl di-biphenyl phosphate for example the three protons of the methyl radical present singlet at 2.25 ppm. The aromatic protons (22) undergo chemical shifts between 6.8 and 7.6 ppm.

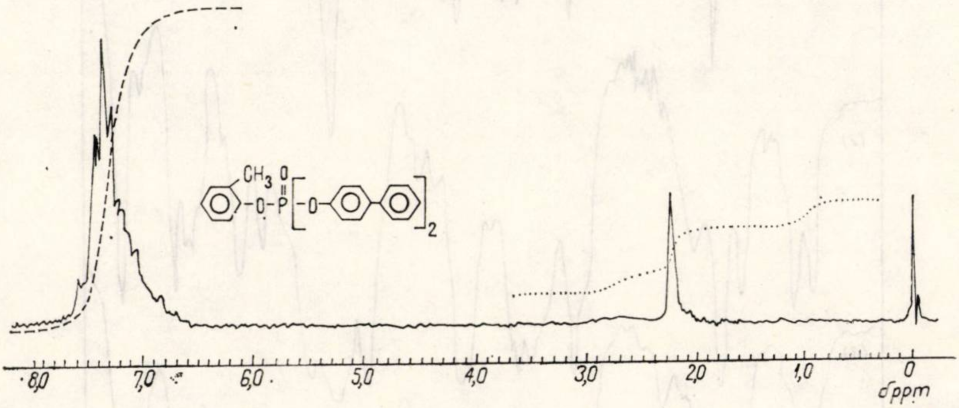

Fig. 3

With respect to 2,5-dimethyl-phenyl-di-biphenyl phosphate one can ascribe the chemical shift from 2.28 ppm to the protons of the radical in *ortho*-position (being next to oxygen it is unshielded) and the chemical shift from 2.20 ppm to the protons of the methyl radical in *meta*-position. For the 21 aromatic protons the chemical shifts have values between 6.8 and 7.6 ppm corresponding to a multiplet.

EXPERIMENTAL

The cresols, xylenols, 4-hydroxybiphenyl and phosphorous oxychloride used as starting material were pure commercial products.

1. SYNTHESIS OF 4-METHYL-PHENYL PHOSPHORIC DICHLORANHYDRIDE

27 g 4-Methylphenol (1/4 mole) 51 g (0.33 mole), phosphorous oxychloride, and 1 g NaCl as a catalyst were introduced in a 100 ml flask equipped with a reflux cooler and a device for dehydrochlorination. After heating the reaction mixture for a period of 24 hours at low reflux, the excess of phosphorous oxychloride and 2-methyl-phenyl-dichloranhydride (at 130 – 140° and 14 mm Hg) were distilled in vacuum obtaining 63 g product (yield 96.43 %). 2-Methylphenyl dichloranhydride is an oil-like liquid ; $n_D^{25} = 1.5314$; $d_{25}^{4} = 1.3388$; P % determined 13.66 ; 13.65 as to 13.76 calculated.

2. SYNTHESIS OF DI(2,5-DIMETHYL)PHENYL PHOSPHORIC CHLORIDE-ANHYDRIDE

81.49 (2/3 mole) 2,5-Dimethylphenol, 51.85 g (1/3 mole) phosphorous oxychloride (molar ratio 2 : 1) and 1 g NaCl were mixed in a unit similar to that used for synthesis n° 1. The mixture reaction was heated till the chloride hydride ceased to be released (48 hours). By vacuum distillation (200—250°/3 mm Hg) 115 g di(2,5-dimethylphenyl)chloranhydride were obtained (yield 86,60%). $n_D^{25} = 1.5680$; $d_{25}^{4} = 1.3380$; P% = 9.61 ; 9.64 as to 9.54 calculated.

3. SYNTHESIS OF 4-METHYL-PHENYL-DI-BIPHENYL PHOSPHATE

2 g 4-methyl-phenyl phosphoric dichlor anhydride, 3.02 g 4-hydroxydiphenyl, 1.8 g triethylamine, and 10 ml benzene as a solvent were introduced in a 50 ml round-bottomed flask equipped with a reflux cooler and a tube with calcium chloride. The molar ratio 1 : 2 : 2. After heating the mixture reaction for a period of 8 hours, the cooled reaction product was filtered by means of a G_4 crucible. 4.8 g of solid product was obtained and it was recrystallized in a mixture of gasoline and benzene (3 : 1). Yield 95.61%. The physical constants of the product are given in table 1.

4. SYNTHESIS OF DI(4-METHYL-PHENYL) BIPHENYL PHOSPHATE

2 g biphenyl phosphoric dichlor anhydride, 1.5 g *p*-cresol, 1.40 g triethylamine, and 10 ml benzene were introduced in a unit similar to that used for synthesis n° 3. The operation was identical to synthesis n° 3.3.27 g(yield 93.20%) of solid product was obtained. The physical constants are given in table 1.

The synthesis of the other mixed phosphoric aromatic esters was obtained under similar conditions.

The IR spectra were recorded by means of a Unicam SP 200 G apparatus in pellet or in film.

The RMN spectra were obtained with Varian A-60-A apparatus using the tetramethyl silane as an internal standard and the carbon tetrachloride as a solvent.

Revue Roumaine de Chimie, **21**, *3*, 455–459 (1976)

EXO- AND ENDOHORMONES. I

APPLICATION OF THE KETOXIME ACTIVATION TO THE SYNTHESIS OF THE MELANOCYTE INHIBITING FACTOR

M. VLASSA

Laboratory of Natural Products, Institute of Chemistry, Cluj-Napoca Str. Donath 65–103

Received July 22, 1974

Esters of Z-L-proline or Z-L-prolyl-L-leucine with simple ketoximes (acetoxime or cyclohexanonoxime) were employed in the synthesis of the title compound.

The release of melanocyte hormone is inhibited by a factor (MIF) discovered first in human hypothalamus [1,2] and later in bovine ones [3] and whose surprisingly simple structure was found to be L—Pro—L—Leu—Gly amide*. Its formation in organisms is due to the degradation of oxytocine under the action of microsomal exopeptidase.[4]

Friedmann *et al.*[5] reported the first direct neurochemical evidence that MIF exerts a stimulating effect on the central synthesis of neurotransmitter dopamine, suggesting a possible anti-Parkinsonian and antidepressant activity.

In the synthetic routes to MIF so far reported the following carboxyl activation methods were employed: mixed anhydride,[6–8] azide[8], carbodiimide,[9] *p*-nitrophenyl [10] or 4-nitroguaiacyl [11] esters. For masking the amino group carbobenzoxy [6-8,10,11] or *o*-nitrophenylsulfenyl [9] groups were used.

---

* The following abbrevations are used: AE = 1-ethoxycarbonyl-propen-2-yl; BA = 1-benzoyl-propen-2-yl; DCHA = dicyclohexylamine; DCC = dicyclohexylcarbodiimide; DCU = dicyclohexylurea; THF = tetrahydrofuran; TEA = triethylamine; TFA = trifluoroacetic acid; Z = carbobenzoxy.

The symbols used for amino acids derivatives correspond to the recommendations of IUPAC—IUB Commission on Biochemical Nomenclature, published in *J. Biol. Chem.*, **247,** 125 (1972).

[1] A. J. Kostin and A. V. Scalley, *Gen. Comp. Endocrinol.*, **7,** 452 (1966).

[2] S. Talaisnik and M. E. Tamalis, *Endocrinol.*, **81,** 819 (1967).

[3] M. E. Clis, S. Talaisnik, and R. Walter, *Proc. Nat. Acad. Sci. U.S.*, **68,** 1428(1971).

[4] R. M. G. Nair, A. J. Kostin and A. V. Schally, *Biochem. Biophys. Res. Commun.*, **43,** 1376 (1971).

[5] E. Friedman, J. Friedman and S. Gershan, *Science*, **182,** 831 (1973).

[6] M. Zaoral and J. Rudinger, *Coll. Czech. Chem. Comm.*, **20,** 1183 (1955).

[7] W. D. Cash, *J. Org. Chem.*, **26,** 2136 (1961).

[8] R. A. Boissonnas, S. Guttman, P. A. Ioguenad and J. P. Walter, *Helv. Chim. Acta*, **28,** 1491 (1955).

[9] K. Poduska, Czech., 124, 953, 15 Nov. 1967; *Chem. Abstr.*, **69,** 107079 (1968).

[10] M. Bodanszky and V. du Vigneud, *J. Amer. Chem. Soc.*, **81,** 5688 (1959).

[11] K. Bankowski, A. W. Lipkowski and S. Prabarek, *Roczniki Chem.*, **48,** 715 (1974).

Masahiko's investigations [12] concerning the acylation reactions of simple ketoximes with N-protected amino acids and his suggestion to employ these esters in peptide synthesis prompted us to check new alternatives to the above mentioned methods of preparing MIF.

In our hands, the starting N-protected amino acid I (Chart I) gave readily under the action of acetoxime and cyclohexanonoxime, respectively, in the presence of dicyclohexylcarbodiimide, the corresponding esters IIa, b, which without isolation were treated with the methyl ester of L-leucine (III). The dipeptide IV was formed in both cases in high yield. The same activation procedure, also with good results, was used in the convertion of the dipeptide V into the tripeptide VII, through the agency of the ketoxime esters VIa, b. No efficiency differences between the two activating agents were observed.

The alkaline hydrolysis of the methyl ester IV to the corresponding acid V was performed with nearly quantitative yield. Another improvement consisted of the preparation of amide VIII in the presence of catalytical amounts of diethylene glycol[13]; this shortened the reaction time and increased considerably the yield, giving an end product pure enough to be processed further on without purification.

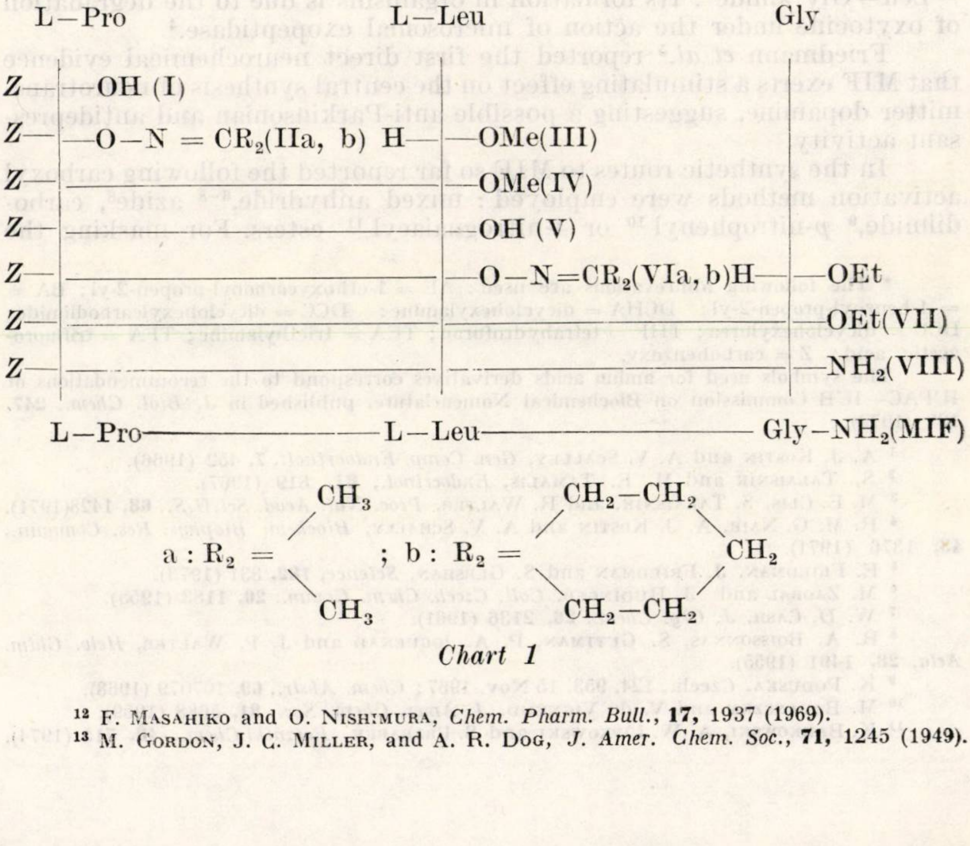

Chart 1

---

[12] F. Masahiko and O. Nishimura, *Chem. Pharm. Bull.*, **17**, 1937 (1969).

[13] M. Gordon, J. C. Miller, and A. R. Dog, *J. Amer. Chem. Soc.*, **71**, 1245 (1949).

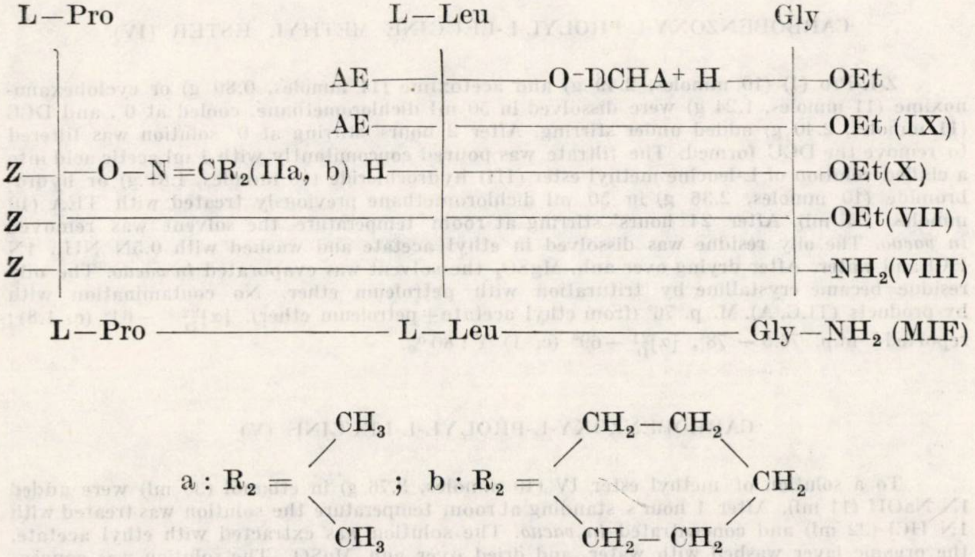

Chart 2

The removal of the carbobenzoxy group from compound VIII to give L−Pro−L−Leu−Gly−NH_2(MIF) took place under the action of trifluoroacetic acid. This reaction was so far performed by catalytic hydrogenation [6] or with hydrobromic acid.[6,8]

In another approach (Chart 2), the N-protected tripeptide ethyl ester VII was prepared from the ketoxime esters IIa, b and the dipeptide ethyl ester hydrochloride X. The latter could be obtained only when AE was used as protecting group. Attempts to prepare compound IX starting with BA−L−Leu [14,15] failed, since the protecting group could not be removed from BA−L−Leu−GlyOEt under the usual conditions. This agrees to the findings of other authors [16] who faced the same difficulties with this protecting group in similar cases.

EXPERIMENTAL

The melting points were taken on a Mikroheitztisch Boetius. Rotations were determined in ethanol solutions. For TLC two solvent systems were used : A. ethyl acetate + benzene 7 : 3, B. isopropanol + ammonia + water 8.5 : 0.75 : 0.75 ; indicators : phosphomolybdenic acid or ninhydrin.

---

[14] G. L. Southard, G. S. Brooke and J. M. Petlee, *Tetrahedron*, **27**, 1359 (1971).

[15] A. Balogh, D. Breazu, E. Vargha, F. Gönczy and L. Beu, *Rev. Roumaine Chim.*, **15**, 1375 (1970).

[16] E. Vargha, A. Balogh, F. Gönczy, D. Breazu and L. Beu, *Rev. Roumaine Chim.*, **18**, 1627 (1973).

CARBOBENZOXY-L-PROLYL-L-LEUCINE METHYL ESTER (IV)

Z-L-Pro (I) (10 mmoles, 2.49 g) and acetoxime (11 mmoles, 0.80 g) or cyclohexanonoxime (11 mmoles, 1.24 g) were dissolved in 50 ml dichloromethane, cooled at 0°, and DCC (11 mmoles, 2.40 g) added under stirring. After 2 hours' stirring at 0° solution was filtered to remove the DCU formed. The filtrate was poured concomitantly with 1 ml acetic acid into a chilled solution of L-leucine methyl ester (III) hydrochloride (10 mmoles, 1.81 g) or hydrobromide (10 mmoles, 2.36 g) in 50 ml dichloromethane previously treated with TEA (10 mmoles, 1.4 ml). After 24 hours' stirring at room temperature the solvent was removed *in vacuo*. The oily residue was dissolved in ethyl acetate and washed with 0.5N NH_3, 1N HCl and water. After drying over anh. $MgSO_4$ the solvent was evaporated *in vacuo*. The oily residue became crystalline by trituration with petroleum ether. No contamination with by-products (TLC, A). M. p. 76° (from ethyl acetate+petroleum ether), $[\alpha]_D^{22.5}$ $-64°$ (c. 1.8); reported[7] m.p. 76.5 – 78°, $[\alpha]_D^{21}$ $-69°$ (c. 1) Y : 80%.

CARBOBENZOXY-L-PROLYL-L-LEUCINE (V)

To a solution of methyl ester IV (10 mmoles, 3.76 g) in ethanol (30 ml) were added 1N NaOH (11 ml). After 1 hour's standing at room temperature the solution was treated with 1N HCl (22 ml) and concentrated *in vacuo*. The solution was extracted with ethyl acetate, the organic layer washed with water, and dried over anh. $MgSO_4$. The solution was concentrated *in vacuo*, diluted with petroleum ether, and the colourless precipitate collected. No contamination with by-products (TLC, B). Y : 90%. M.p. 141–143° (from ethyl acetate + petroleum ether), $[\alpha]_D^{21.5}$$-55°$ (c. 1.9); reported[7] m.p. 138.5–139.5°, $[\alpha]_D^{22}$$-55.5°$ (c. 1).

CARBOBENZOXY-L-PROLYL-L-LEUCYL-GLYCINE ETHYL ESTER (VII)

a. Starting with compound V (10 mmoles, 3.62 g) the ketoxime esters VIa, b were prepared as described above. The solution containing the activated dipeptide was poured, concomitantly with 1 ml acetic acid, into a chilled dichloromethane (50 ml) solution of freshly distilled glycine ethyl ester (10 mmoles, 1.03 g). Working as usual the end product VII was obtained in the form of a colourless crystalline precipitate. M.p. 152–153° (from aqueous ethanol), $[\alpha]_D^{21}$$-78°$ (c. 2.8). Y : 80%.

b. The solution containing one of the ketoxime esters IIa, b (10 mmoles) prepared as described above, was poured, concomitantly with 1 ml acetic acid, into a dichloromethane solution (50 ml) of L-Leu-GlyOEt(X) hydrochloride (10 mmoles, 2.42 g) or hydrobromide (10 mmoles, 2.86 g) previously treated with TEA (10 mmoles, 1.4 ml). Working as for compound IV, the end product VII was obtained. Y : 86% M.p. 150–151° (from aqueous ethanol) $[\alpha]_D^{21}$$-77°$ (c.3); reported,[6,7,9,10,17,18] m.p. 150–151°, 150–152°, 151–152°, 149–150°, 148–, –149°, $[\alpha]_D^{21-25.3}$$-79.8°$, $-81.2°$, $-83,2°$, $-82.6°$ (c. 2.5–2.7).

CARBOBENZOXY-L-PROLYL-L-LEUCYL-GLYCINE AMIDE (VIII)

Compound VII (2 mmoles, 0.78 g) was dissolved in 9N ammoniacal methanol (100 ml) and diethyleneglycol (0.2 g) was added. After 4 hours' standing at room temperature the reaction mixture was evaporated to dryness *in vacuo*. The oily residue was triturated with water and the colourless precipitate collected. M.p. 162–164° (from water), $[\alpha]_D^{21}$$-72°$ (c. 2.5); reported[6-8,10,17] m.p. 162–163°, 161–163°, 163°, 162–164°, 163–163.5°, $[\alpha]_D^{22,20}$$-73.3°$, $-71.9°$ (c. 2.95, 2.50). Y : 90%.

---

[17] Ch. Ressler and V. du Vigneud, *J. Amer. Chem. Soc.*, **76**, 3107 (1954).

[18] E. M. Goodman and K. C. Stueben, *J. Amer. Chem. Soc.*, **81**, 3980(1959).

L-PROLYL-L-LEUCYL-GLYCINE AMIDE (MIF)

Compound VIII (1 mmole, 0.40 g) was dissolved in 1 ml TFA and treated with anisole (0.25 ml). The solution was boiled for 1 hour, the solvent removed *in vacuo*, the residue triturated with ether and dissolved in water. The solution was stirred for 2 hours with an anionite (Amberlite IR 4B or IRA 410). After filtration the solution was evaporated to dryness *in vacuo*. The residue was triturated with ethyl acetate, the precipitate collected and dried *in vacuo*. M.p. 120–122°; reported[6,8,9] m.p. 122–123°, 120°, 122–124°. Y : 86%. Anal. *Found* : N, 19.35 ; *Calcd.* for $C_{13}H_{24}O_3N_4 \cdot 1/2\, H_2O$: N, 19.11.

N-(1-ETOXYCARBONYL-PROPEN-2-YL)-L-LEUCYL-GLYCINE ETHYL ESTER (IX)

a. A suspension of $AE\text{-}L\text{-}Leu\text{-}O^-Na^+$[15] (40 mmoles, 10.50 g) in THF (150 ml) was cooled to about −10° and treated with N-methyl-morpholine (1–2 drops). The stirred mixture was treated with pivaloyl chloride (5.76 ml) for 2–5 minutes, and the stirring continued for 15 minutes. Glycine ethyl ester hydrochloride (47 mmoles, 6.55 g) and TEA (6.55 ml) were added under stirring. The mixture was stirred at the same temperature for 1 hour and subsequently at room temperature for 2 hours. A saturated sodium bicarbonate solution (50 ml) was added and the organic layer removed *in vacuo*. The oily residue was extracted with ethyl acetate, washed with water, dried over anh. $MgSO_4$, and the solvent evaporated *in vacuo*. The oily residue became crystalline after standing for several days at room temperature. Y : 95%. TLC (A) showed no contamination with by-products. M.p. 69–71° (from ethyl acetate + petroleum ether), $[\alpha]_D^{21} + 105°$ (c. 0.8).

b. To a cold solution of $AE\text{-}L\text{-}Leu\text{-}O^-DCHA \cdot H^+$[15] (10 mmoles, 4.25 g) dissolved in THF (100 ml), N-methyl-morpholine (1–2 drops) and ethyl chloroformate (10 mmoles, 1 ml) were added. After 15 minutes the DCHA hydrochloride precipitate was filtered and a solution prepared from glycine ethyl ester hydrochloride (10 mmoles, 1.40 g) and TEA (10 mmoles, 1.4 ml) in dichloromethane (15 ml) was added into the cold filtrate (−10°) under stirring. The mixture was stirred at this temperature for an additional 1/2 hour and kept overnight at room temperature. The mixture was worked as described above for IXa. Y : 70%. M.p. 69–71°, $[\alpha]_D^{21} + 105°$ (c. 0.8). Anal. *Found* : C, 59.18 ; H, 8.73 ; N, 7.10. *Calcd.* for $C_{16}H_{29}N_2O_5$: C, 59.28 H, 8.68 ; N, 7.10.

L-LEUCYL-GLYCINE ETHYL ESTER (X) HYDROCHLORIDE

Compound IX (10 mmoles, 3.34 g) was dissolved in ethanol (50 ml) and acidified with ethanolic hydrochloric acid. The mixture was kept overnight at room temperature. The solvent was removed *in vacuo* and the oily residue which showed no crystallization tendency was washed with anh. ether. TLC (B) indicated the absence of by-products. Y : 80%.

L-LEUCYL-GLYCINE ETHYL ESTER(X) HYDROCHLORIDE

The removal of AE group was brought about with a hydrobromic acid in acetic acid solution (30%) under the above described method.

N-(1-BENZOYL-PROPEN-2-YL)-L-LEUCYL-GLYCINE ETHYL ESTER

A solution of $BA\text{–}L\text{–}Leu\text{–}O^-DCHA \cdot H^+$[14,15] (10 mmoles, 3.60 g) in THF (100 ml) was cooled at −10° and treated with N-methyl-morpholine (1–2 drops) and ethyl chloroformate (10 mmoles, 1 ml). After 15 minutes the DCHA hydrochloride was filtered and a solution prepared from glycine ethyl ester hydrochloride (10 mmoles, 1.40 g) and TEA (10 mmoles, 1.40 ml) in dichloromethane (15 ml) was added into the mixed anhydride solution, at −10°, under stirring. Working up as for IX a white precipitate was obtained. Y : 60%. M.p. 106–108° (from ethyl acetate + petroleum ether), $[\alpha]_D^{22} + 248°$ (c. 0.9) Anal. *Found* : C, 66.77 : H, 7.85 ; N, 7.95. *Calcd.* for $C_{20}H_{28}N_2O_4$: C, 66.66 ; H, 7.77 ; N, 7.77.

Revue Roumaine de Chimie, **21**, *3*, 461–467 (1976)

THE CORROSION OF SOME STEELS IN SYNTHETIC RIVER WATERS, IN HEAT TRANSFER CONDITIONS

ELENA ANTONESCU and ECATERINA VASILESCU
Institute of Physical Chemistry, Str. Galaţi 31, Bucharest, Romania

Received May 27, 1974

The corrosion of a carbon steel and two austenitic stainless steels was studied in heat transfer conditions. The metallic specimens were heated at 100° and the medium conditions (temperature and content in chloride ions of the electrolyte) were varied. It was concluded that the rate of corrosion of the two austenitic stainless steels increases as temperature and chloride ions content increases; and that at the upper limits, pitting is present. Similar but stronger increases in the corrosion rates are found for carbon steel, excepting pitting.

The corrosion of pure metals and alloys in the electrolyte solutions at high temperature as well as in heat transfer conditions puts up some special problems, as a result of electrolytic composition changes[1] and the deposition of corrosion products on the metallic surfaces.[2]

These deposits on the surface should be the cause of the existing disagreement between the results obtained in heat transfer by different authors working in identical conditions.[3]

An increase in the temperature is accompanied by an increase in the corrosion range and by a reduction in the degree of passivity of the metals.[4,5]

This work is concerned with the effect of heat transfer on the corrosion of two austenitic stainless steels and a carbon steel in synthetic river waters having different temperatures.

EXPERIMENTAL

The compositions of the metals examined are listed in table 1.

Table 1
The compositions of the steels tested

Type of steel	% content								
	C	S	P	Mn	Si	Cr	Ni	Mo	Ti
18Cr–10Ni	0.10	—	—	2.00	1.00	18.0	10.0	—	⩾5C
18Cr–12Ni–2Mo	0.10	—	—	2.00	1.00	17.5	11.5	2.25	⩾5C
carbon steel	0.18	0.022	0.025	0.35	0.03	—	—	—	—

---

[1] H. H. Uhlig, "Corrosion Handbook", ed. John Wiley, New York, 1948, p. 128.

[2] Report, *Br. Corros. J.*, **2**, 4 (1967).

[3] D. T. Porter, M. Donimirska and R. Wall, *Corrosion Sci.*, **8**, 833 (1968).

[4] H. F. Townsend, *Corrosion Sci.*, **10**, 343 (1970).

[5] M. Pourbaix, *Corrosion*, **25**, 267 (1969).

The steels were machined as cylindrical electrodes, equipped with an attached resistance to be heated at 100°, continuously controlled with a Fe-constantan thermocouple.

For the electrochemical measurements, the electrodes were mechanically polished, degreased in boiling benzene for 5 minutes and then pickled either in $HNO_3 + HF + H_2O$, at 90°, for 10 minutes in the case of stainless steels, or in 5 % HNO_3, at 80°, for 2 minutes in the case of carbon steel.

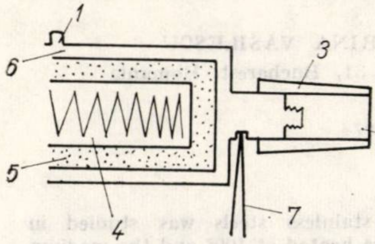

Fig. 1. — Specimen heater.

1, electrical contact; *2*, working electrode; *3*, teflon gasket; *4*, electrical resistance; *5*, insulator; *6*, brass furnace; *7*, thermocouple.

The synthetic river waters were prepared from reagent chemicals and double distilled water. Their compositions are shown in table 2.

A double-walled glass cell was used for polarization measurements. The anodic and cathodic compartments were separated by fritted glass. An auxiliary platinum electrode was provided for polarization. The potentials were reported to the saturated calomel electrode used as reference electrode.

Table 2

The compositions of synthetic waters (mgl)

		Type of water	
Type of ions	31.51	163	250
Ca^{2+}	52.10	89.40	89.40
Mg^{2+}	4.60	15.50	15.50
Na^+	20.94	68.40	228.00
K^+	3.58	5.43	5.43
SO_4^{2-}	49.27	67.30	67.30
Cl^-	31.51	163.79	500.00
HCO_3^-	134.54	159.21	159.21

The electrode assembly was tightly pressed on a teflon gasket and then fixed in a special inlet of the electrochemical cell.

The electrochemical measurements were taken by applying the potentiostatic step-by-step technique (50mV/5 minutes) from a Wenking potentiostate. The resulting currents were measured on an outside instrument.

The measurements were carried out by keeping the metallic specimen at 100° and varying the temperature of the electrolyte from 25, 40, 60 to 80°.

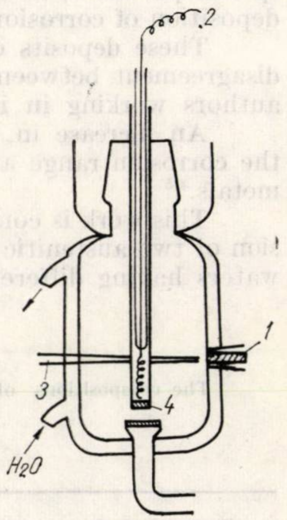

Fig. 2. — The electrochemical polarization cell:

1, working electrode; *2*, auxiliary platinum electrode; *3*, Luggin capillary; *4*, fritted glass.

The obtained anodic and cathodic polarization curves have permitted to appreciate the nature of the rate determining process, the rates of corrosion and critical pitting potentials [6] (when present).

---

[6] J. Horvath and H. H. Uhlig, *J. Electrochem. Soc.*, **99**, 212 (1962).

RESULTS

1. STAINLESS STEELS

As can be seen from figure 3, the corrosion process of stainless steels in studied conditions is under an anodic control. In these circumstances, the rate of corrosion (in the pitting absence) was estimated from the next equation :

$$G = A/z.\ 1/F.i.t$$

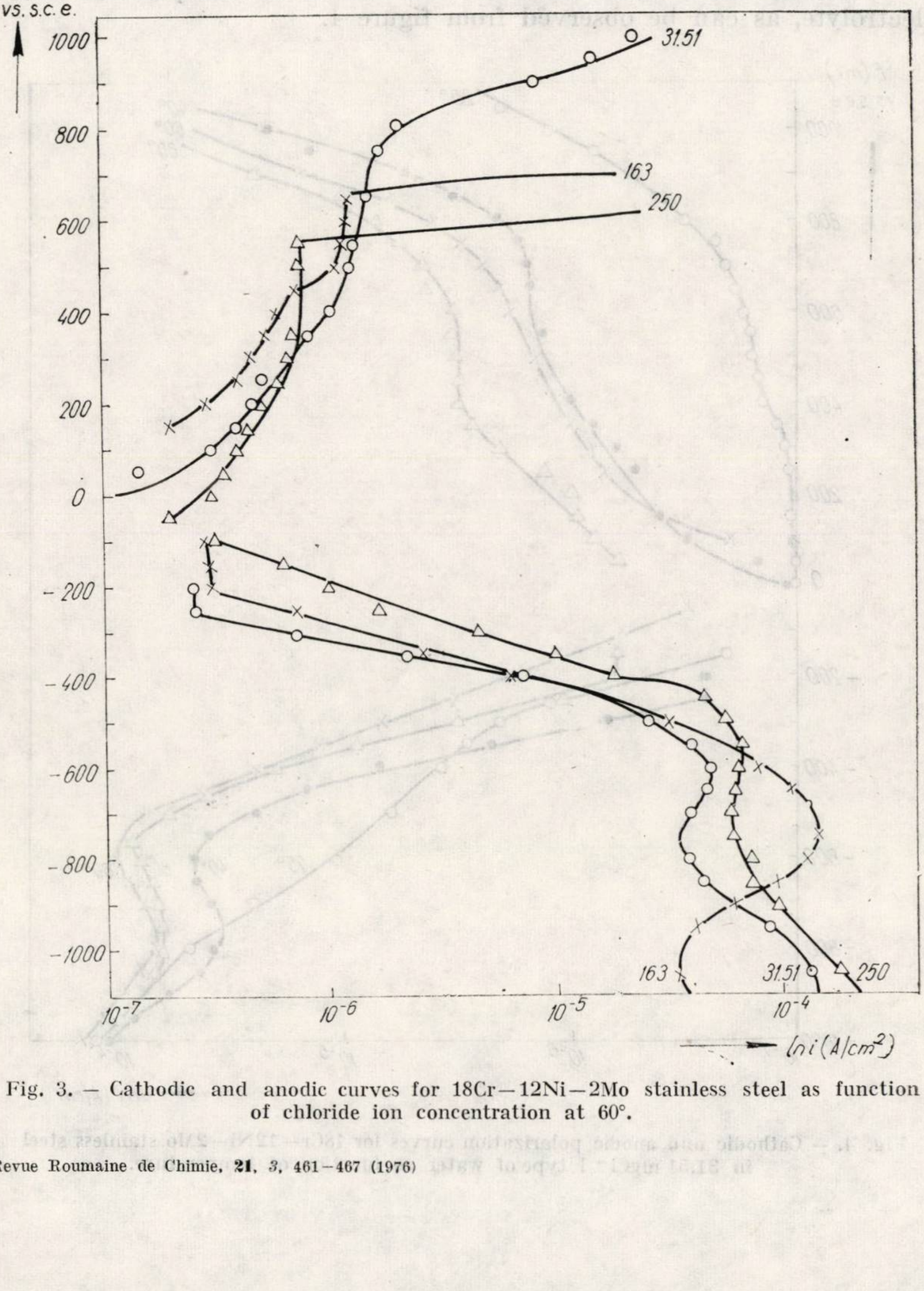

Fig. 3. – Cathodic and anodic curves for 18Cr–12Ni–2Mo stainless steel as function of chloride ion concentration at 60°.

where : A is the iron atomic weight ($= 55.85$), z is the iron valency ($+2$), F is the Faraday constant, t is time in seconds and i is current density (considered as the avarage value of passivity current).

Both types of stainless steels present a wide range of passivity, 18Cr—12Ni—2Mo steel showing, however, smaller passivity currents than 18Cr—10Ni steel (maybe due to the higher nickel content).

As can be seem from figure 3, the passivity currents (thus the rates of corrosion) increase with chloride ions content in the waters.

Similar effects result from the variation of the temperature of the electrolyte, as can be observed from figure 4.

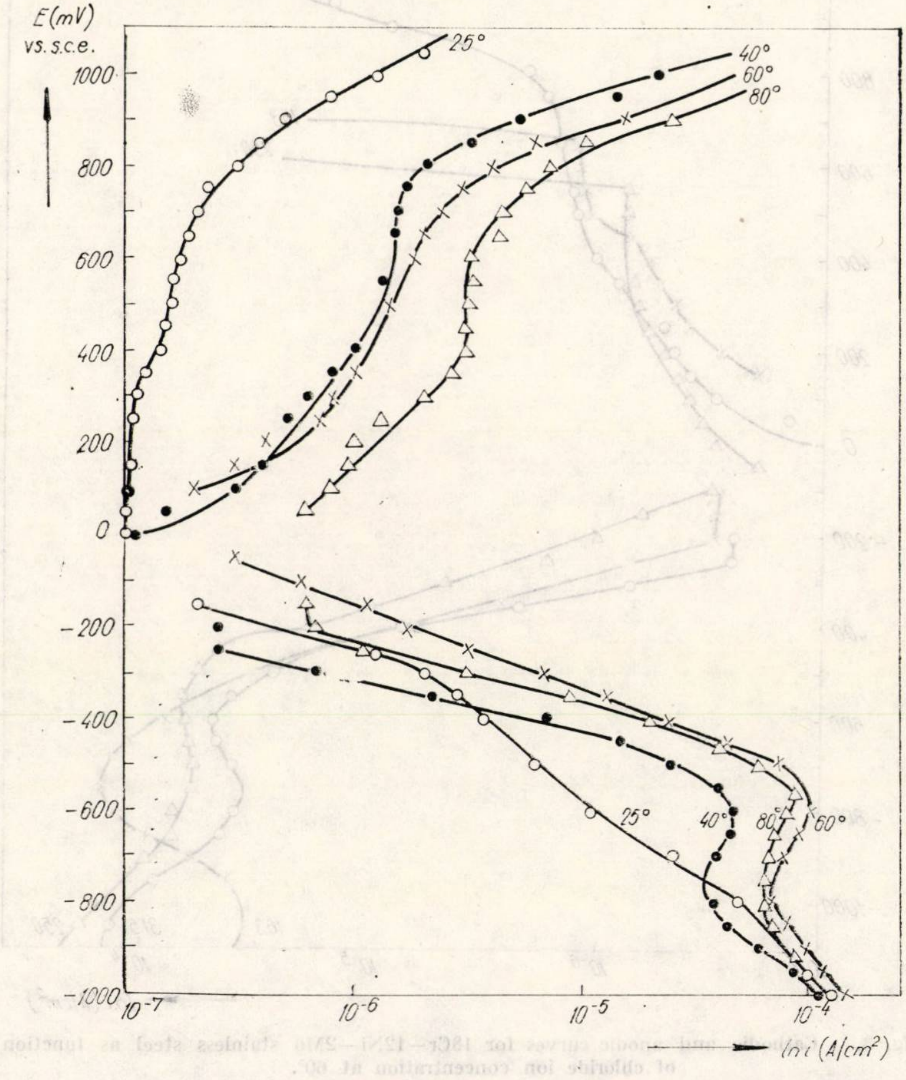

Fig. 4. — Cathodic and anodic polarization curves for 18Cr—12Ni—2Mo stainless steel in 31.51 mgCl$^-$/l type of water as function of temperature.

The dependence of the corrosion rates on the synthetic waters composition and temperature for the two stainless steels is listed in table 3.

The above figures (3 and 4) show that at higher temperatures and chloride ions contents, both stainless steels are susceptible to pitting corrosion.

Table 3

The values of the corrosion rates (mdd) of austenitic stainless steels 18Cr−10Ni and 18Cr−12Ni−2Mo in heat transfer conditions

Steel temperature	Type of steel	Water temperature	Type of water 31.51	163	250
100°	18Cr−10Ni	25°	0.35	0.39	0.49
		40°	1.64	0.74	0.60
		60°	1.89	1.12	*
		80°	2.19	*	*
	18Cr−12Ni−2Mo	25°	0.22	0.30	0.82
		40°	0.36	0.40	1.50
		60°	0.63	0.90	*
		80°	1.00	1.12	*

* pitting.

The critical pitting potentials determined with ±50mV accuracy are presented in table 4.

Table 4

The critical pitting potentials (mV) of 18Cr−10Ni and 18Cr−12Ni−2Mo stainless steels in heat transfer conditions

Steel temperature	Type of steel	Water temperature	Type of water 31.51	163	205
100°	18Cr−10Ni	25°	—	—	—
		40°	—	—	—
		60°	—	—	+450
		80°	—	+250	+150
	18Cr−12Ni−2Mo	25°	—	—	—
		40°	—	—	—
		60°	—	—	+550
		80°	—	—	+450

The analogous results obtained by Ciolac and Radovici[7] by working in the same medium conditions and on the same metals, but in the absence of heat transfer, show that the heat transfer does not affect the corrosion process of stainless steel.

---

[7] O. Radovici and S. Ciolac, *Rev. Roumaine Chim.*, **19**, (1974).

2. CARBON STEEL

The dependence of the anodic and cathodic curves of carbon steel function on the temperature is presented in figure 5.

In this case and in all the others, the corrosion process is under the cathodic control of oxygen diffusion. The rates of corrosion were thus estimated from the values of the limiting diffusion currents and are listed in table 5.

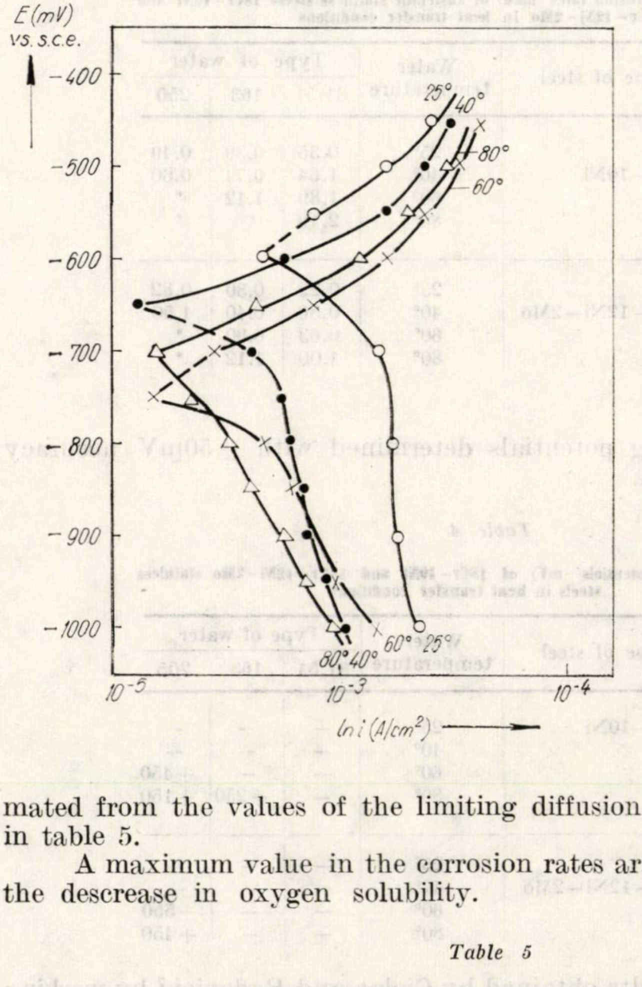

Fig. 5. — Cathodic and anodic polarization curves for carbon steel as function of temperature of a 250 mgCl$^-$/l type of water.

A maximum value in the corrosion rates arises at 40°, as a result of the descrease in oxygen solubility.

Table 5

The corrosion rates (mdd) of carbon steel in heat transfer conditions

Steel temperature	Water temperature	Type of water		
		31.51	163	250
100°	25°	411	350	461
	40°	474	450	500
	60°	301	250	374
	80°	159.7	214	250

The rate of carbon steel corrosion in heat transfer conditions is almost 8 times higher than in its absence.

CONCLUSIONS

The obtained results prove that the rates of corrosion of austenitic stainless steels increase with electrolyte temperature and its chloride ions content and that they are susceptible to pitting corrosion for upper limits of these parameters. It appears that 18Cr–12Ni–2Mo stainless steel is more resistant to the local attack than 18Cr–10Ni stainless steel.

As to carbon steel, its corrosion rate is very much affected by the heat transfer, showing a maximum at 40° electrolyte temperature.

Revue Roumaine de Chimie, **21**, *3*, 461–467 (1976)

Revue Roumaine de Chimie, **21**, *3*, 469–480 (1976)

STUDY OF THE FORMATION AND HOMOGENIZATION PROCESSES OF THE MELTS BY MEANS OF EMF MEASUREMENTS

P. BALTĂ and C. SPURCACIU

Laboratory for Glass Technology, Polytechnic Institute, Str. Polizu 1, Bucharest, Romania

Received November 13, 1973

Completed May 8, 1975

EMF measurements on the $(O_2)Pt/melt/Pt(O_2)$ chain in the melts belonging to the $PbO-B_2O_3$ system by means of an installation of own design, have proved the possibility to trace the homogenization process by diffusion. According to theoretical provisions it has also been demonstrated that this method can point out phenomena related to formation-melting and clearing-homogenization processes as well as structural and phase changes in vitrogenous melts of the micro- and macroimmiscibility type and also dwell on conversions at superliquidus temperatures. The authors also deal with the probable mechanisms of the electrode processes and with the residual potential.

The state of the melt prior to formation is one of the factors determining the qualities of the final glass product. The technological practice requires, therefore, a certain degree of homogeneity of the melt as a measure of its quality. This is usually statically and statistically tested by physical measurements based on the connection : chemical homogeneity — physical homogeneity — isotropy. The procedure entails some drawbacks. Usually the properties measured in view of determining the homogeneity are of a macroscopic level (density, refraction index a.s.o.) also the theoretical considerations and recent experimental data [1] certify the dependence of the properties on the microscopic state of the system with respect to the constitution (at molecular level), distribution of present polymers, degree of the advance of the chemical structural equilibrium, a.s.o. Another disadvantage refers to the procedure ; although the evolution of the tested system (state of the melt) is a dynamical one, the measurements are carried out statically on samples from the final product. Thus, under real conditions the information obtained is not representative enough and otherwise the process-monitoring decisions are possibly made with a certain delay which make them sometime inefficient in due time.

---

[1] P. BALTĂ and E. BALTĂ, "Introducere in chimia fizică a stării vitroase", Ed. Academiei, Bucharest, 1971.

The authors have, therefore, aimed at devising a method which should provide the greatest amount of immediate and efficient information on the processes occurring in the furnace melt.

One of the methods, also tested by some researchers [2-4], able to meet such requirements is that based on EMF measurements in the $(O_2)Pt/melt/Pt(O_2)$ electrochemical chain.

The available data as well as some own results[5] point to certain still unclarified theoretical and experimental aspects. At the same time as regards the study of some phenomena such as melting, clearing, immiscibility the possibilities provided by the method are not yet wholly turned to account.

Some of these aspects have been studied in the laboratory for Glass Technology of the Polytechnic Institute of Bucharest, some of the results being presented below.

THEORETICAL BASIS

Considering a cell of the $(O_2)Pt/melt/Pt(O_2)$ type (fig. 1) in conditions of equal partial pressure of the gaseous oxygen at the two electrodes, for the case when in the melt homogenization takes place only by diffusion, we are facing the particular case of a concentration cell with transport. For thermodynamic reasons, the EMF of such a cell will be proportional with the difference of the chemical potentials of the participants in the elec-

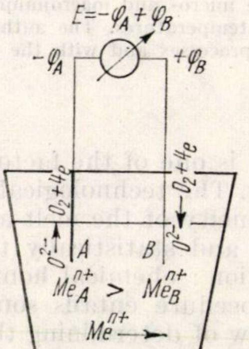

Fig. 1. — Concentration cell with oxide melts.

---

[2] E. S. Ahlestin and A. F. Borisov, *Trudi Gorsk. Polit. Inst. im. A. A. Jdanova*, **21**, 50 (1965).

[3] I. V. Timoșenko and A. F. Borisov, *ibid.*, **23**, 75 (1965).

[4] Z. P. Voronkova, *ibid.*, **23**, 4, 16 (1967).

[5] S. Solacolu, P. Baltă, C. Spurcaciu and G. Jitianu, "The Following of Structural Changes of Glasses by Means of EMF Measurements", Communicated at the 2nd National Conference of Pure and Applied Physical Chemistry, Bucharest, Sept. 1970.

trode reaction in the two melts:

$$E = -\varphi_A + \varphi_B = \frac{1}{ne}(\mu_A - \mu_B) \qquad (1)$$

Introducing the standard values and activities, we get:

$$\mu = \mu_0 + RT \ln a$$

$$E = \frac{RT}{nF}\ln(a_{O^{2-}})_A/(a_{O^{2-}})_B \qquad (2)$$

Considering the activities of the cations (essential carriers) equal to their concentrations, the diffusion (contact) potential is given by

$$E_{\text{diff}} = -\,RT/nF \int_{C_{Me_B^{n+}}}^{C_{Me_A^{n+}}} \mathrm{dln}\ C_{Me^{n+}} \qquad (3)$$

for the experimental case under considerations its value being low (practically within experimental errors[6]) the integration limits in the expression (3) being very close.

Thus, in the absence of other processes except (simple) diffusion, the EMF of the cell can reflect the homogeneization process, the progressive decrease of the E value (eq. 2) (in isothermal – isobar conditions) signifying homogenization.

Besides diffusion, structural changes also take place in the melt leading to the change of the diffusion unity structure and of the chemical potentials of the participants in the electrode processes (the cations and oxygen ions as polymer anions). On the other hand, a change in the structure of the double electric layer is to be expected in the sense of a qualitative and quantitative variation of the adsorbed dipoles. Under these circumstances, the system in fig. 1 should be more correctly considered as a structure-concentration cell whose EMF is given by:

$$E = -\,\varphi_A + \varphi_B = 1/ne\int_{C_A}^{C_B} \partial\mu/\partial e \ \mathrm{d}c \qquad (4)$$

An essential part is played by the platinum electrodes which have been specifically studied by a number of researchers. In the oxidic melts the platinum electrode behaves as a platinum oxygenated electrode, of the first kind[7], reversible [8–11] with different constructive and functional variants.

---

[6] I. A. EFTIUHINA, N. G. KORSICOVA and L. L. KUNIN, in "Svoistva i struktura slocovih rasplavov", Izd. Nauka, Moskova, 1970, p. 107.

If such two electrodes, identical from all points of view, are placed in oxidic melts a difference of the potential will appear between them if the state of the melt (concentration, temperature, structure, etc.) around the two electrodes is not identical. The electrode process determining the potential of the oxygenated platinum electrode is considered as described by the reaction :

$$O_2 + 4e^- \rightleftarrows 2O^{2-} \qquad (5)$$

Recent experimental data [12] as well as the results of the present work show that such representation of the process would be too simple, given the very complex structure of oxidic melts. This should provide some features characteristic of their electrochemical behaviour.[5] According to Dertev,[12] the value of the electrode potential has to be determined by the adsorption density of the reacting ions, by their size and their dipole moment, and so on. Since these characteristics are closely related to the structural state of the melt in the context of the present conceptions,[1] the scheme described by equation (5) and advanced by Minenko [9] was supplemented by us in the light of the aforesaid.

The mechanism of the processes that take place at electrodes can be plotted by the sequence of the following subprocesses :

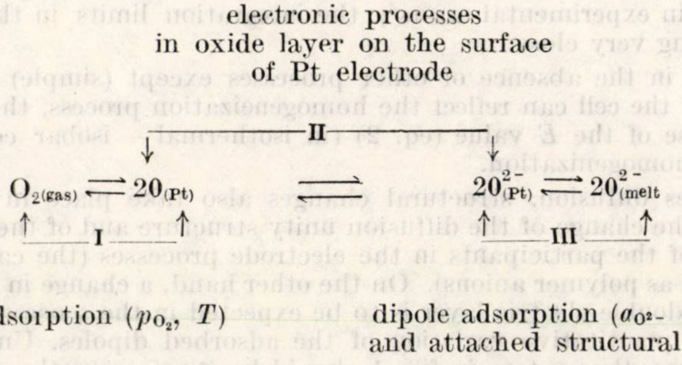
electronic processes
in oxide layer on the surface
of Pt electrode
II
I
III
adsorption (p_{O_2}, T)
dipole adsorption ($a_{O^{2-}}$ of the melt
and attached structural variables)

$$O_{2(gas)} \rightleftarrows 2O_{(Pt)} \rightleftarrows 2O^{2-}_{(Pt)} \rightleftarrows 2O^{2-}_{(melt)} \qquad (6)$$

where the prevailing phenomena of the sub-processes with their related variable have been also considered.

For the vitreous oxidic structures, considered as integrated systems of heterocatenary polymers,[1] the activity of the oxygen ions is a characteristic magnitude both for the structural state at a given moment and the dynamics of structural changes under the action of various fields (as thermal, electrical, mechanical, etc). Thus, the advance degree of the chemical-structural equilibrium in the melts can be described by the dynamics of the equilibrium :

---

[7] C. Deportes and M. Darcy, *Silic. Ind.*, **6**, 499 (1961).

[8] A. S. Esicov and N. F. Smakota, *Zhur. neorg. Khim.*, **6**, 1206 (1968).

[9] V. I. Minenko, S. M. Petrov and N. S. Ivanova, *Zhur. fiz. Khim.*, **35**, 1534 (1961).

[10] G. I. Beliaev, A. S. Esicov and N. F. Smakota, *Zhur. neorg. Khim.*, **10**, 2194 (1966).

[11] A. Pons and A. Parent, *Verres et Refr.*, **23**, 324 (1969).

[12] N. K. Dertev and Z. P. Voronkova, in "Stekloobraznoie sostoianie", Izd. Nauka, Leningrad, 1971, p. 361.

$$O^{2-} + O^{\circ} \rightleftharpoons 2O^{-} \qquad (7)$$

On the other hand, the transport processes and the various phase and structural transformations (crystallization-devitrification, macro- and micro- liquation, configurational and conformational changes in the chains of polymers, etc), in the absence of chemical reactions may be represented by equations which reveal the dynamics of the energetic states of the bridging and non-bridging oxygen ions of the type :

$$O^{\circ} \rightleftharpoons O^{-} \qquad (8)$$

$$O^{-}_{(\varepsilon_1)} \rightleftharpoons O^{-}_{(\varepsilon_2)} \qquad (9)$$

ε_1 and ε_2—representing two different energetical states of the non-bridging oxygen ion.

The investigation possibilities of the electrochemical methods are plainly evinced by considering the electrode processes (eq. 6) corroborated with the dynamics of the oxygen ions in the above mentioned processes.

EXPERIMENTAL

Taking into account the proposed objectives, melts of the B_2O_3-PbO system have been selected. On the one hand, given the light fusibility of the components in the system, the study at temperatures over T_{liq} becomes possible under good working conditions for the oxygenated platinum electrode ($T \leqslant 1000-1100°$). On the other hand, this system is characterized by the presence of various phenomena : eutectical meltings, stable phase separation phenomena (macroliquation) and metastable-subliquidus (microliquation). Finally, the system is interesting for the technology of enamelings, of electro-vacuum and optical glasses.

Three compositions have been studied, respectively (wt %) : 98 % B_2O_3 – 2 % PbO (98 B) in the range of metastable separation,[13] 65 % B_2O_3 – 35 % PbO (65 B) situated in the immiscibility range in liquid phase[14] and 12 % B_2O_3–88 % PbO, (12B) the composition of the eutectic of the sub-system $4PbO \cdot B_2O_3 - 2\ PbO \cdot B_2O_3$.[15]

As raw materials we used : PbO *p.a.* (Budochemia) and B_2O_3 glass prepared by melting H_3BO_3 *p.a.* (Reactivul) in a platinum crucible. This solution was preferred in view of avoiding the shortcomings brought about by the dehydration of H_3BO_3 on melting.

The B_2O_3 previously prepared glass was brought to a 0.3–0.4 mm fineness; the mixture was dry dosed and homogenized in ether medium to ensure an advanced homogeneity and to avoid B_2O_3 hydration. To ensure a constant level for the melt in the crucible (7 mm) and a constant plunging of the electrodes (4 mm) for various measurements, constant volumes of the mixture (5 cm³) were introduced into the platinum crucible.

---

[13] E. Zarzycki and F. Naudin, *Phys. Chem. Glasses*, **8**, 11 (1967).

[14] D. J. Liedberg, C. G. Ruderer and C. G. Bergeron, *J. Amer. Ceram. Soc.*, **48**, 440 (1965).

[15] H. Rawson, in "Inorganic Glass-Forming Systems", Academic Press, London, 1967, p. 104.

Measurements have been carried out with an installation of own design consisting mainly of a measuring probe, electrical furnace and electrical set-up for the EMF measuring by the compensation method (fig. 2). Constructive characteristics and experimental precautions allowed a reproducibility of data of ±1–3%, the lower values corresponding to more basic compositions.

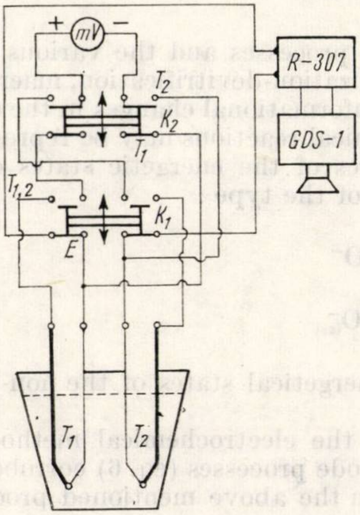

Fig. 2. — Measuring circuit. T_1, T_2 — thermocouple Pt—Pt 10 Rh and position in circuit; E — cell's electromotive force; mV — milivoltmeter; K_1, K_2 — switches; R—307 — potentiometer; GDS—1 — galvanometer.

RESULTS AND DISCUSSION

The analysis of the results point to a number of phenomena described in what follows.

An initial zone called reaction-melting zone, which corresponds to the domain around the liquids temperature of the respective compositions, could be evidenced.

For the three experimental compositions the EMF variation *versus* temperature in this initial zone is shown in fig. 3.

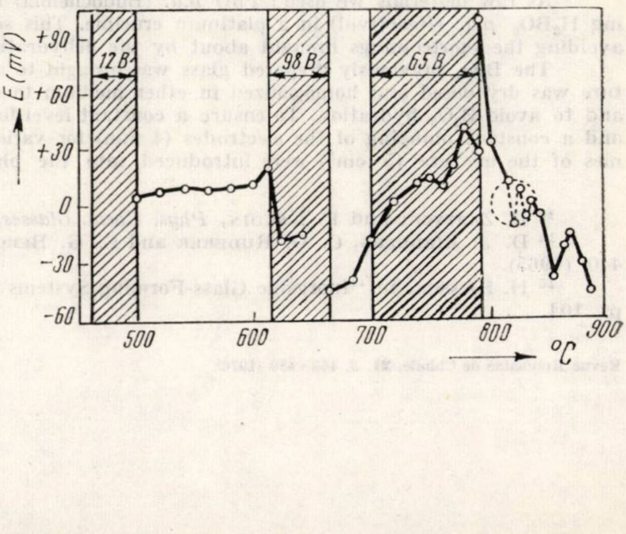

Fig. 3. — Reaction-melting zones for three compositions.

This zone is characterized by rapid variations of the signs and the values of EMF and, therefore, the actual values could not be measured, as order of magnitude these being of hundreds and tens of mV. The visual inspection of the state system in this period (which was allowed by the installation) revealed the presence of a melt film along the wall of the crucible, the aspect of the mixture in its central zone being typical for a melting stage at its beginning.

This behaviour must be considered in accordance with the mechanism of the electrode processes (eq. 6) and the dynamics of the reaction equilibrium in the melting-reaction conditions. The frequent variation of the EMF signs and values (eq. 2) implies strong variation of the activity of the oxygen ions and implicitly modifications in the adsorbed double electric layer. It is quite significant that the moment of establishing some measurable values practically coincides with the moment of total melting (PbO solid phase disappears), stated by macroscopic observation.

Thus, the EMF onset is depending on the attainment of a state corresponding to a sufficient mobility of the structural formations participating in the electrode processes, the total melting pointing out the beginning of the processes in liquid phase (homogeneous phase system). The behaviour in the melting-reaction stage is kinetically and phenomenologically interrelated, the sign with which the EMF settles in the homogeneous regime (macroscopical) is not law- abidingly governed and has a statistical random character, the same as the variation of the composition, of the oxygen ions activity around the two electrodes, respectively.

Although the interpretations referring to the phenomena characterizing the reaction-melting zone, not yet studied so far, have qualitative character, they point altogether to the possibility of this method to evidence these phenomena, a fact quite interesting for the melting technology practice.

The evolution of EMF in isothermal and dynamic regime (heating, cooling, reheating with a 2°/min rate) differs qualitatively for the three compositions under study, as one can suppose according to their different position in the equilibrium diagram. Thus, for the eutectical composition for which the melt is already at 500° (temperature of the eutectic) very fluid, perfectly clear (with no bubbles), the stabilization of the EMF values at this temperature is rapid and the homogenization follows a curve with the shape typical of diffusion processes (fig. 4, a_1).

The value of plus 5 mV is reached in about 50 min from the beginning of the isothermal regime remaining practically unchanged thereafter.

As already known, both the diffusion coefficient, the essential variable of the homogenization process and the fluidity which is connected to the diffusion through the Stokes-Einstein law, increase exponentially with the temperature; as a consequence, at 650° the homogenization is much more rapid and the value of -3 mV is reached in 12 minutes. During the second heating run for both temperatures we find for the EMF values close to those obtained in the first heating run and these values remain constant (fig. 4, curves a_3 and a_4).

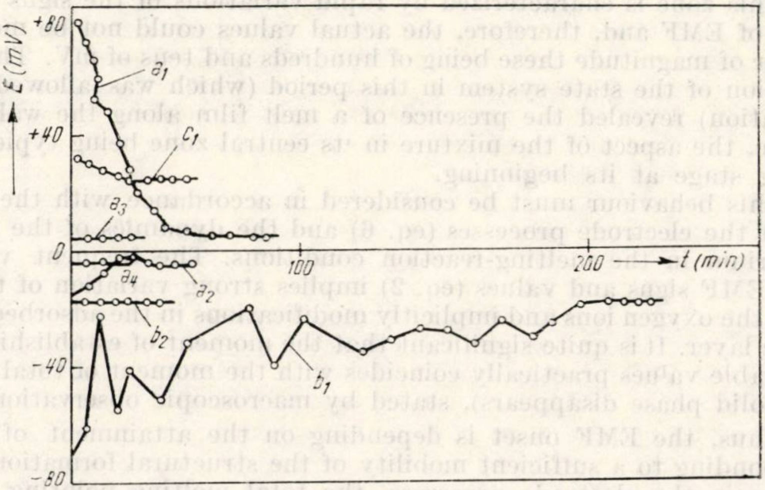

Fig. 4. — Variation of EMF in isothermal regime. $a_1 - T = 500°$ heating first run 12—B ; $a_2 - T = 650°$, heating first run 12—B ; $a_3 - T = 500°$, heating second run 12—B ; $a_4 - T = 650°$, heating second run 12—B ; $b_1 - T = 880°$, heating first run 65—B ; $b_2 - T = 880°$ — heating second run 65—B ; $c_1 - T = 780°$, heating first run, 98—B ; after melting at 1300°.

When bubbles are present in the melt, both the curves for isothermal regime and those for dynamic regime (having the temperature as variable) bear a peculiar aspect. For example, in fig. 4 — curve b_1 ; the EMF variation *versus* time is shown at 880° for the 65 B melt. In the case of the 98 B composition which is very viscous and with many bubbles having diameters between 0.5 and 4 mm, within the whole temperature range under consideration measurements could be performed only after the sample probe had been heated to 1300° for 2 hours in a silite furnace. Subsequently, the measurements in isothermal regime have also evidenced the homogenization process (fig. 4, c_1).

The presence of bubbles and of the clearing process influences the structure of the double electric layer and the electrode processes, especially the process which implies the presence of molecular oxygen, e.g. the adsorption $O_2 \rightleftarrows 2O(Pt)$ (eq. 6), which depends on the moment values of the oxygen partial pressure.

Curve b_1 in fig. 4 shows that the present method is suitable to trace the clearing process. The high and frequent variations of EMF are due to the gas bubbles which get together and then leave the electrodes. When bubbles evolving stops, the rapid variation of EMF also stops and tends to a constant value hereupon called "residual potential". The value of the residual potential — 19.5 mV for the 65 B sample at 880° is reached 25 minutes after the disappearance of bubbles, respectively 210 minutes after the setting up of the isothermal regime.

In the series of the measurements in dynamic regime for the three compositions we demonstrated that this method allows to evidence also other phenomena similar to those mentioned here-above.

Thus, in the case of eutectical composition a discontinuity in the 620–630° zone was noticed, located by 120–130° over the eutectical temperature. The existence of this discontinuity is positive and it is present in all the three series of determinations (fig. 5).

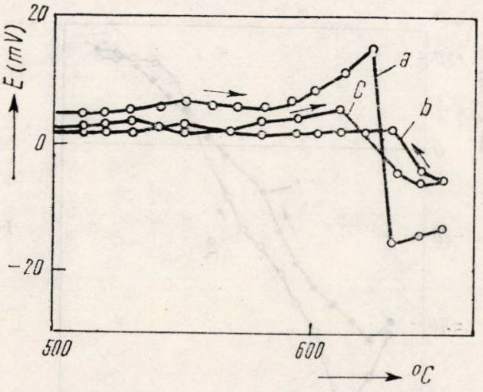

Fig. 5. — EMF *vs.* temperature for the 12–B sample. a) heating first run; b) cooling first run; c) heating second run.

All three curves (*a*, *b*, *c*) are characterized by a variation of $E =$ = constant type up to a temperature for which the EMF values start to increase slightly, preparing the jump from 610–630°. The higher value of EMF in the case of "a" curve is likely to be a consequence of the less homogeneous character of the melt corresponding to the first heating.

The existence of structural changes in melts at temperatures higher than the liquidus curve experimentally proved for silicate melts,[1] seems to be more probable for the eutectical melts which are featured by advanced destruction and disorder structures and, accordingly, by an increased mobility of the structural elements.[6] It is interesting to note that in the present case, the value of 620° coincides with the temperature at which, according to De Luca *et al.*[16] a change takes place in the mechanism of electrical conductivity in the lead-borate melts in this zone. By assuming for the compositions with over 20% mole PbO the structure proposed by Bray,[17] a modification of the ligand-bidentate structure might very likely take place at this temperature by the opening of the cage type $B_4O_7^{2-}$ cycles.

For 65 B sample it was found out that in the case of first heating (fig.3), a run of the EMF values takes place around 820°. Since after clearing, the heating and cooling curves give the same polarity modifications at practically the same temperature (fig. 6, obviously the phenomena which take place in the melt at this temperature are not related to the presence of bubbles but are proper to the melt. The significance of this experimental conclusion must be looked for in the coincidence between the 820°—830° value and that of the intersection between the temperature tie line and the immiscibility gap for the 65 B composition.

---

[16] J. P. De Lucca and C. Bergeron, *J. Amer. Ceram. Soc.*, **54**, 191 (1971).
[17] P. J. Bray and M. Leventhal, *Phys. Chem. Glasses*, **4**, 47 (1963).

However, the presence of the phenomena related to separation is felt especially in the case of the 65 B and 89 B compositions by the hysteresis aspects of the EMF *versus* temperature curves which corresponds to some successive heatings and coolings in identical conditions (figs. 6 and 7). This aspects is typical for the passing of this system to some non-equilibrium states undoubtedly related to the kinetics of the separation processes. For the 98 B sample it is worth mentioning that the position of the maximum on the heating curve (fig. 7) as well as of the inflection point for the reheating curve correspond to a temperature of about 700°, i.e. the intersection of the tie line with the immscibility gap.

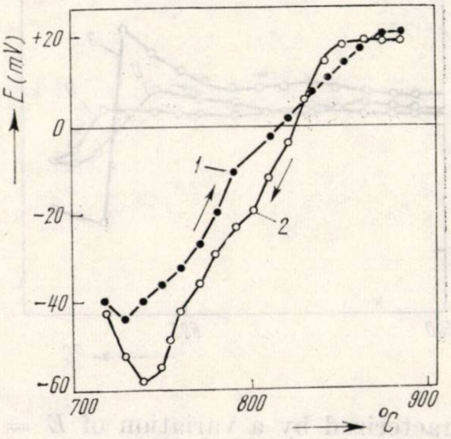

Fig. 6. — EMF *vs.* temperature for 65—B sample *1*, heating; *2*, cooling.

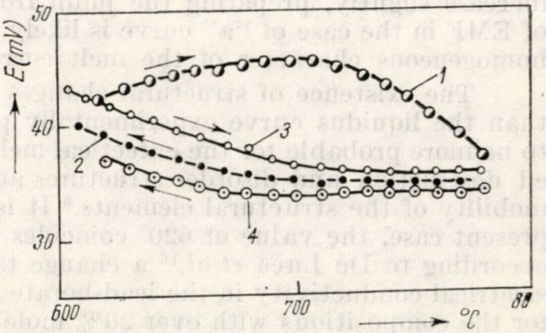

Fig. 7. — EMF *vs.* temperature for 98—B sample. *1*, heating first run; *2*, cooling first run; *3*, heating second run; *4*, cooling second run.

The shape of the curve corresponding to the first heating run suggests a disordering process for the range up to 700° when the slope of the curve is positive ($dE/dT = \Delta S > 0$) a process which is followed as one can see by a homogenization process characterizing supercritical temperatures.

It is finally necessary to refer mainly to the so-called residual potential.

For the testing and calibration of the symmetry of thermocouples and implicitly of the platinum electrodes (fig.2) an oxidic salt of ionic type, KNO_3 was selected on purpose and at the same time the behaviour of the cell $(O_2)Pt/KNO_3/Pt(O_2)$ during the heating and in isothermal regime has been studied. It was found that in this case the homogenization of the melt takes place suddenly the very moment of the melting as expected, and what is very important, the residual potential is absent, the EMF value vanishing right after the melting. However, for the present installation all the precautions have been taken in order to remove the "experimental" causes which might bring about false potential differences, including the possibility of controlling the thermal symmetry of the electrochemical system (fig. 2) at any time.

Thus, the "asymmetry" of the electrodes which determines the existence of the residual potential is assumedly assigned to the peculiarities of the melts under study. Most likely the melt film adherent to the surface of the electrodes differs to a certain extent as regards the compositions and the structure. Such differences in certain portions of the melt might occur either in the initial phase of the melting process or as a consequence of the beginning of the separation process.

The above hypothesis is supported by the fact that the sign of the measured EMF (of the residual potential) varies randomly (see again fig. 4 — curves "a") and the value of the residual potential depends on the composition, as it results from fig. 8. The adherence and the stability of the electrodes films are particularly good under our working conditions.

Attempts for a better outline of the above hypothesis is the authors, steady concern. However, due to this phenomenon, valuable information can be obviously obtained regarding the structural peculiarities of the melts under study.

Fig. 8. — Residual EMF *vs* the concentration of B_2O_3.

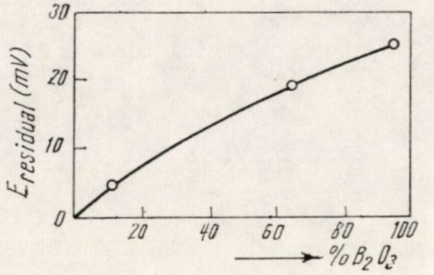

CONCLUSIONS

The results prove that by using a couple of identically oxygenated platinum electrodes interesting information may be obtained regarding the processes that take place during the elaboration of an oxidic melt.

— In a first phase we may follow the period when the reactions leading to the formation of the melt take place, characterized by disorderly EMF variations which cannot be measured.

— Clearing of the melt is characterized by high amplitude and random EMF variations.

— The homogenization is characterized by the asymptotical decrease in its absolute value of EMF, up to a limit called residual potential.

— EMF measurements supply data regarding the range of temperatures in which the processes under study take place and in isothermal conditions, regarding their kinetics.

— Some inflexions, which have been noticed, can be correlated with structural changes in the melts, namely : configurational changes, phase and microphase separations, etc.

Revue Roumaine de Chimie, 21, 3, 481–482 (1976)

COMPTES RENDUS

"Mössbauer Spectroscopy" edited by V. Gonser (Topics in Applied Physics, vol. 5), Springer-Verlag, Berlin—Heidelberg—New York, 1975, 241 pp.

The six chapters of this monograph and their authors are the following: From a strange effect to Mössbauer spectroscopy (V. Gonser), Mössbauer spectroscopy in chemistry (P. Güttlich), Mössbauer spectroscopy in magnetism: characterization of magnetically-ordered compounds (R. W. Grant), Mössbauer spectroscopy in biology (G. E. Johnson), Mössbauer spectroscopy in lunar geology and mineralogy (S. S. Hafner), Mössbauer spectroscopy in physical metallurgy (F. E. Fujita).

Though this is a monograph appearing in a collection on applied physics, several chapters are of considerable interest to the chemists involved in the study of transition-metal compounds. Written by scientists from W. Germany, USA, England and Japan in a very readable form, this monograph is neither a compilation of data, nor a textbook on the theory and practice of Mössbauer spectroscopy, but rather a consistent collection of chapters dealing with various aspects of the field.

The first chapter combines an authoritative account of the basic laws and facts on Mössbauer spectra with an agreable and highly readable style. The second chapter overlaps in its introduction with some information already provided in the first chapter, but its main sections describe briefly various chemical applications of Mössbauer spectroscopy. Though perhaps too brief (it only has 81 references), this chapter summarizes all main uses to which Mössbauer spectra can be put. The chapter on biological applications deals exclusively with iron proteins and provides a review of recent uses of this technique, most of the 29 references being dated 1970—1974. The chapter on applications in lunar geology and mineralogy also deals mainly with the favoured Mössbauer isotope, ^{57}Fe (which, by the way, is written as Fe^{57} contrary to IUPAC recommandations) and constitutes a fascinating lecture. A definite trend to increase the use of Mössbauer spectroscopy in iron metallurgy is noted in the last chapter.

The monograph has a subject index and each chapter contains references to further reading. The printing is excellent.

The book is recommended to chemists and physicists interested in the applications o Mössbauer spectroscopy.

A. T. Balaban

E. Buncel, "Carbanions: Mechanistic and Isotopic Aspects", Elsevier Sci. Publ. Comp., Amsterdam, Oxford, New York, 1975, 270 p.

The 9th volume of the series of monographs on "Reaction Mechanisms in Organic Chemistry", edited by C. Earborn and N. B. Chapman is devoted to carbanions. This chapter of organic chemistry has been particularly developed in the last 25 years owing to theoretical research on the chemical bond and to preparative works. In many laboratory reactions and in industrial processes, carbanions are found both as defined chemical species, which can be isolated, and as in short-life intermediates, in extremely reduced concentrations, with practical applications, in the most diverse domains: from plastics and synthetic rubber to the most sophisticated chemicals on the fine organic synthesis industry.

The work was devised as an introduction to the chemistry of carbanions, including an investigation of their structure and reaction mechanisms and being accessible to any reader having a basic background of organic chemistry. A broad outlook on the subject has prompted the author to make a large number of analogies and interferences with other domains of organic chemistry even if they are not related to carbanions, in order to provide a comprehensive insight into the problem. Reference is often made to isotope-based studies which are more convincing and precise methods in establishing the reaction mechanisms. The monograph places a special emphasis on the general principles and fundamental experimental facts, revealing the general properties and the regularities critically examined by a modern approach to the latest breakthroughs in this field.

The adoption of such a point of view with the elimination of a descriptive section on the reactions of carbanions has contributed to a better systematization of data ending up with a very clear presentation. It is worth mentioning the logical succession of the content which handles at the beginning the structural aspects of various types of carbanions and, then, the transpositions of carbanions with their governing laws, concluding with carbanions in the reactions of organometallic compounds. The coverage of the seven chapters of the monograph is the following:

1. *Carbon acids and carbanions*. The basic structural and electronic principles of carbanions species derived from their acid precursors are discussed and a critical appraisal is made on the methods for the determination of *pKa* and their limitations.

2. *Stereochemistry of carbanionic, processes*. The stereochemical aspects of carbanions are first examined, considering them as isolated (hypothetical) species, free of any influence on the part of the solvent medium or of the ionic partner, passing then to real systems involving solvation and phenomena relating to ion pairs. Problems regarding the chirality of carbanions adjacent to sulphur and phosphorus are also included.

3. *Carbanions and tautomerism*. The prototropy of various systems and particularly of keto-enolic ones is examined from the point of view of carbanionic intermediates (enolate ions) compared to acid catalyzed equilibria. Other studied equilibria refer to nitro-*aci*-nitro, unsaturated derivatives, methylene-azomethine, nitriles, etc.

4. *Classical and nonclassical carbanions* include the principles of nonclassical interactions in carbanionic and related systems.

5. *Enolate and homoenolate rearrangements*. Some carbanions transpositions are selected (Favorskii, transposition of α-epoxy-ketones, etc.) and particularly that of carbanions occurring by means of enolate and homoenolate ions.

6. *Orbital symmetry control in carbanion rearrangements* deals with the analysis of electrocyclic carbanionic transpositions relative to those occurring by carbonium ions and of sigmatropic transpositions with migration of hydrogen or of some alkyl or aryl groups.

7. *Carbanions in reactions of organometallic compounds* deals in particular with aspects of the chemistry of compounds with nontransitional metals treated from the point of view of carbanionic processes in an attempt to point to the large perspective and to the variety of structural and mechanistic aspects of the problem such as for instance the alkaline splitting of the organic compounds of silicium, stanium or germanium.

Each chapter includes a large number of bibliographical points carefully selected which cover the literature of the year 1973 inclusively.

The Indexes of subjects and of authors facilitate the study of the themes by those interested in them. The monograph is addressed to students, to postgraduate students preparing their doctoral thesis, to researchers and specialists in industry who work in the field of organic products. They will find useful and interesting data to complete their knowledge on carbanions, which have been seldom treated in monographs (D. J. Cram, Fundamentals of Carbanion Chemistry, Academic Press, New York 1965; M. Schlosser Struktur un Reaktivität polarer Organometalle, Springer Verlag, Berlin, Heidelberg 1973).

F. Cuiban

NOTE POUR LES AUTEURS

La *Revue Roumaine de Chimie* publie des articles en anglais, français, russe, allemand ou espagnol. Les auteurs sont priés d'envoyer des articles, notes, communications et comptes rendus inédits.

Les manuscrits seront dactylographiés à deux intervalles. Les tableaux seront dactylographiés sur feuilles séparées, de même que la légende des figures. Les diagrammes seront tracés à l'encre de Chine sur papier calque. Les tableaux et les figures seront numérotés par des chiffres arabes, en nombre strictement nécessaire. Prière de ne pas inscrire les mêmes données dans les tableaux et les figures. Les formules chimiques seront incluses dans le texte ; en outre, elles seront transcrites sur des feuilles séparées. Les auteurs sont priés d'indiquer les caractères italiques (en soulignant les lettres au crayon), ainsi que tout autre caractère spécial. L'ordre des références bibliographiques sera celui de leur mention dans le texte ; le nom de l'auteur sera précédé de l'initiale du prénom ; les publications périodiques seront présentées suivant les prescriptions internationales. Les références seront ajoutées à la fin de l'article ; elles paraîtront comme des notes, au bas de la page. Le texte sera précédé d'un résumé comprenant 15 lignes au maximum.

L'entière responsabilité du contenu des articles appartient aux auteurs. On publie des articles dus aux collaborateurs roumains ou étrangers.

PRINTED IN ROMANIA

TRAVAUX PARUS AUX ÉDITIONS DE L'ACADÉMIE DE LA RÉPUBLIQUE SOCIALISTE DE ROUMANIE

FRANCISC A. GOTHARD, **Echilibre lichid-vapori vol. I. Baze teoretice şi metode de calcul** (Equilibres liquide-vapeurs. Ier vol. Bases théoriques et méthodes de calcul), 1975, 262 p., 28 lei.

ELENA CEAUŞESCU, **Research work on synthesis and characterisation of macromolecular compounds. Contributions**, 1974, 251 p., 20 lei.

CONST. GH. MACAROVICI et D. MACAROVICI, **Chimia oxizilor dubli şi utilizările lor** (La Chimie des oxydes doubles et leur utilisation), 1975, 195 p., 13 lei.

I. ZUGRĂVESCU et MAGDA PETROVANU, **Chimia N-Ilidelor** (La chimie des N-Ylures), 1974, 347 p., 19 lei.

MARGARETA AVRAM, **Antidăunători** (Pesticides), 1974, 494 p., 41 lei.

CR. SIMIONESCU, VIORICA RUSAN et N. POPA, **Chimia algelor marine** (La chimie des algues marines), 1974, 211 p., 18 lei.

CRISTOFOR SIMIONESCU, MARGARETA GRIGORAŞ, AGATA CERNĂTESCU-ASANDEI et GHEORGHE ROZMARIN, **Chimia lemnului din România — plopul şi salcia** (La chimie du bois en Roumanie — le peuplier et le saule), 1973, 228 p., 28 lei.

TIBERIU NĂŞCUŢIU, **Metode radiochimice de analiză** (Méthodes radiochimiques d'analyse), 1973, 384 p., 23 lei.

MARIA FITI, **Dozimetria chimică a radiaţiilor ionizante** (La dosimétrie chimique des radiations ionisantes), 1973, 240 p., 13,60 lei.

MIHAI FLORESCU, **Eficienţa economică a cercetării ştiinţifice** (L'efficience économique de la recherche scientifique), 1972, 115 p., 15 lei.

GEORGETA LĂZĂRESCU, **Sistematizarea informaţiilor în Chimia organică** (La systématisation des informations dans la Chimie organique), 1972, 252 p., 10,15 lei.

P. BALTĂ et E. BALTĂ, **Introducere în chimia fizică a stării vitroase** (Introduction à la chimie physique de l'état vitreux), 1971, 240 p., 15,50 lei.

LYDIA-MARIA VAICUM, **Biodegrabilitatea detergenţilor** (La biodégrabilité des détergents), 1971, 254 p., 16 lei.

I. ZUGRĂVESCU et L. STOICESCU-CRIVETZ, **Polimeri heterociclici** (Polymères hétérocycliques), 1971, 190 p., 9,50 lei.

I. MAXIM, **Materiale nucleare** (Matériaux nucléaires), 1969, 444 p., 30 lei.

CRISTOFOR SIMIONESCU et CLEOPATRA VASILIU-OPREA, **Mecanochimia compuşilor macromoleculari** (La mécanochimie des composés macromoléculaires), 1967, 344 p., 23,50 lei.

1976 AUG 2 3

I. P. I. – c. 692

43 426

Lei 25. —

F1103

R
REFERINȚA

ACADÉMIE DE LA RÉPUBLIQUE SOCIALISTE DE ROUMANIE

70

REVUE ROUMAINE DE CHIMIE

TOME 21
N° 4
Avril 1976

RECHAX, **21**, *4*, 483–642 (1976)

EDITURA ACADEMIEI REPUBLICII SOCIALISTE ROMÂNIA

Rev. Roumaine Chim. **21**, *4*, p. 483–642 (1976), Bucarest

U

ACADÉMIE DE LA RÉPUBLIQUE SOCIALISTE DE ROUMANIE

COMITÉ DE RÉDACTION

Rédacteur en chef:

I. G. MURGULESCU, membre de l'Académie de la République Socialiste de Roumanie

Rédacteurs en chef adjoints:

A. T. BALABAN et V. EM. SAHINI, membres correspondants de l'Académie de la République Socialiste de Roumanie

Collège de rédaction:

EM. BRATU, ELENA CEAUŞESCU, ECATERINA CIORĂNESCU-NENITZESCU, C. DRĂGULESCU, RALUCA RIPAN, CR. SIMIONESCU, membres de l'Académie de la République Socialiste de Roumanie; P. SPACU, membre correspondant de l'Académie de la République Socialiste de Roumanie; MARGARETA AVRAM, D. I. MARCHIDAN, I. MOLDOVAN, G. NIAC et D. SĂNDULESCU

La Revue Roumaine de Chimie paraît 10 fois par an. Toute commande de l'étranger (fascicules ou abonnements) sera adressée à ILEXIM—Serviciul Export-Import Carte (Livres)/Serviciul Export-Import Presă (Revues), 64—66, Calea Griviţei, P.O.B. 2001, télex 011226, Bucarest, Roumanie

Les manuscrits, les livres et les revues proposés en échange, ainsi que toute correspondance seront envoyés à la rédaction:

REVUE ROUMAINE DE CHIMIE

23, str. Dumbrava Roşie, Bucarest, Roumanie, téléphone 12 41 60

EDITURA ACADEMIEI REPUBLICII SOCIALISTE ROMÂNIA

125, Calea Victoriei, Bucarest, Roumanie, téléphone 50 76 80

ORSZÁGOS MŰSZAKI KÖNYVTÁR ÉS DOKUMENTÁCIÓS KÖZPONT
8884

REVUE ROUMAINE DE CHIMIE

Tome 21, N° 4 Avril 1976

I. BACIU, MIHAELA HILLEBRAND, V. EM. SAHINI and ELENA VOLANSCHI, ESR spectra of nitrodibenzo-*p*-dioxin radicalic species . . . 485–489

RODICA VÎLCU, FLORICA IRINEI and ELENA TATU, Extension of some regularities of ternary electrolytic aqueous solutions in ionic liquids . . . 491–494

LETIŢIA TOPOR and IVONA MOLDOVEANU, Thermodynamic properties of $NaCl-CaCl_2$ and $KCl-CaCl_2$ molten systems 495–501

MIHAELA CONSTANTINESCU, E. SEGAL and M. VASS, Field effect investigation of adsorption on semiconductor films 503–508

IOANA GROZA et D. I. MARCHIDAN, L'énergie accumulée par la déformation plastique à froid des laitons binaires et alliés 509–515

S. PETRESCU, S. STERNBERG, I. GALASIU et VALERIA PETRESCU, Application du modèle du pore partiellement rempli dans le processus d'adsorption électrochimique sur les électrodes halogène-charbon actif dans les sels fondus 517–529

I. SOLACOLU, MARIA MAVRODIN-TĂRĂBÎC et IOANA ONACA, L'étude de la réduction de l'oxygène sur les électrodes poreuses en argent. IV. L'effet de la variation des paramètres de fonctionnement sur la polarisation des électrodes à de différentes densités de courant 531–543

S. SOLACOLU, MARINA BULZAN and E. SEGAL, Studies on the formation kinetics of barium hexaferrite $BaO.6Fe_2O_3$ in the binary system $BaO-Fe_2O_3$ 545–548

R MARIA ENCULESCU, Influence of titanium dioxide on the structure and on the properties of mineralogical compounds in white Portland cements . . . 549–562

N. DUŞOIU, Anisotropie diélectrique de certains blocs en carton et en papier dans le domaine des micro-ondes 563–570

CECILIA CONSTANTINESCU und GH. CONSTANTINESCU, Einfluss der Substituenten auf die analytischen Eigenschaften von organischen Reagenzien in der Reaktion mit $[TlBr_4]^-$ 571–583

R P. B. ISSOPOULOS, Complex chelate compounds of iso- and heteropolyanions of Mo(VI) and W(VI) with Chrome Azurol S. II. Complex chelate compounds of heteropolyanions of Mo(VI) and W(VI) 585–588

R GH. MARCU and LETIŢIA GHIZDAVU, New mixed heteropolycompounds: tungstoniobiosilicates 589–594

Rev. Roumaine Chim. **21**, *4*, p. 483–642 (1976), Bucarest

A. SPILIADIS, POMPILIA GHEORGHE, HEDWIGA SZÖGY and ANGELA SĂVULESCU, Dyes for synthetic fibers. IX. Disperse azo-dyes for polyester fibers 595–620
VALER FĂRCĂŞAN and STELIAN FLOREA, Benzofuro-benzothiazoles. V. 2-Amino- and 2-mercapto-benzofuro-benzothiazoles 621–625
ALEXANDRA GOCAN and F. HODOŞAN, Exo- and endohormones. III. New derivatives of synthetic ecdysone analogues and related compounds 627–629
STELIANA MAXIM and M. DIMA, Viscosimetric study of the poly(4-vinylpyridine) salts with the halogen(alkyl)aryloxyalkyl carboxylic acids 631–635
COMPTES RENDUS 637–641

ORSZÁGOS MŰSZAKI KÖNYVTÁR ÉS DOKUMENTÁCIÓS KÖZPONT
1883

THE FIFTH NATIONAL CONFERENCE OF PURE AND APPLIED PHYSICAL CHEMISTRY

The Centre of Physical Chemistry of the Central Institute for Chemical Research will organize The Fifth National Conference of Pure and Applied Physical Chemistry in Bucharest, 1–4 September 1976.

The main objective of the Conference is to contribute to the mutual knowledge of the new original results obtained by people working in the research institutes, universities and chemical engineering.

The Conference aims at an exchange of experience between the Romanian and foreign scientists dealing with various aspects of physical chemistry research.

The Conference will be organized in sections covering the topics listed below:

1. Quantum chemistry; theory of the chemical bond; molecular structure; reactivity.
2. States of the matter; transport phenomena; colloids; chemical kinetics; photochemistry; radiochemistry.
3. Chemisorption; homogeneous and heterogeneous catalysis; catalytic reactions.
4. Chemical thermodynamics; thermochemistry; statistical thermodynamics; thermodynamics of metallurgical processes; thermodynamics of irreversible processes.
5. Electrochemistry; solutions of electrolytes; ionic liquids (molten salts); electrode processes; electrometallurgy; corrosion and anticorrosion protection.
6. Chemical engineering; mass and heat transfer; effect of surface phenomena; kinetics of unit processes; modelling, optimization and automation of processes in chemical industry.
7. Physico-chemical analysis; automation of physico-chemical analysis and control.

Only unpublished original papers may be submitted. The time allowed for a lecture is 15 minutes, including discussions. The registration fee is 75 lei and it includes the Conference materials.

The official language of the Conference is Romanian; the foreign participants may deliver their papers in English, Russian, French, Spanish or German. No simultaneous translation will be provided, but all the papers will have their abstracts translated in one of the above mentioned languages.

In order to obtain supplementary details as well as for inquiries, please contact the Organizing Committee: *Centrul de Chimie Fizică, Str. Galaţi 31, sector 2, 7000 Bucureşti–I. Cable: CHIMFIZ, Bucureşti, ROMANIA.*

THE FIFTH NATIONAL CONFERENCE OF PURE AND APPLIED PHYSICAL CHEMISTRY

The Centre of Physical Chemistry of the Central Institute for Chemical Research will organize The Fifth National Conference of Pure and Applied Physical Chemistry in Bucharest, 1 — 4 September 1986.

The main objectives of the Conference is to contribute to the mutual knowledge of the new original results obtained by people working in the research institutes, universities and chemical engineering.

The Conference aims at an exchange of experience between the Romanian and foreign scientists dealing with various aspects of physical chemistry research.

The Conference will be organized in sections covering the topics listed below:

1. Quantum chemistry; theory of the chemical bond; molecular structure; reactivity.
2. States of the matter; transport phenomena; colloids; chemical kinetics; photochemistry; radiochemistry.
3. Chemisorption; homogeneous and heterogeneous catalysis; catalytic reactions.
4. Chemical thermodynamics; thermochemistry; statistical thermodynamics; thermodynamics of metallurgical processes; thermodynamics of irreversible processes.
5. Electrochemistry; solutions of electrolytes; ionic liquids (molten salts); electrode processes; electrometallurgy; corrosion and anticorrosion protection.
6. Chemical engineering: mass and heat transfer; effect of surface phenomena; kinetics of unit processes; modelling, optimization and automation of processes in chemical industry.
7. Physicochemical analysis; automation of physico-chemical analysis and control.

Only unpublished original papers may be submitted. The time allowed for a lecture is 15 minutes, including discussions. The registration fee is 75 lei and it includes the Conference materials.

The official language of the Conference is Romanian; the foreign participants may deliver their papers in English, Russian, French, Spanish or German. No simultaneous translation will be provided, but all the papers will have their abstracts translated in one of the above mentioned languages.

In order to obtain supplementary details as well as for inquiries, please contact the Organizing Committee: *Centrul de Chimie Fizică, Str. Galați 37, sector 2, 7000 București — Cable: CHIMFIZ, București, ROMANIA.*

Revue Roumaine de Chimie, 21, 4, 485 – 489 (1976)

ESR SPECTRA OF NITRODIBENZO-*p*-DIOXIN RADICALIC SPECIES

I. BACIU, MIHAELA HILLEBRAND, V. EM. SAHINI and ELENA VOLANSCHI
Department of Physical Chemistry, Polytechnic Institute, Bucharest, B-dul Republicii 13, Romania

Received August 1, 1975

ESR spectra of the anion- and cation-radicals provided by 2-nitrodibenzo-*p*-dioxin are reported and discussed. The hyperfine splitting constants are well accounted by Hückel and McLachlan calculations.

The role of the nitro substituent in conferring an acceptor character to well-known donor heterocycles, like phenothiazine and phenoxatellurine, was recently reported. [1,2] It was stated that the presence of such an electronegative group does not prevent the oxidation to cation-radicals but allows the formation of negative radicalic species. Continuing these studies, the behaviour of a related compound, 2-nitrodibenzo-*p*-dioxin in oxido-reduction processes is now investigated.

EXPERIMENTAL

2-Nitrodibenzo-*p*-dioxin was prepared as indicated in literature.[3] The anion-radical was generated by electrochemical reduction in dimethylformamide (DMF), or dimethylsulphoxide (DMSO) using a technique previously described.[4] Tetra-*n*-butylammonium perchlorate 0.1M was used as supporting electrolyte. The cation-radicals were prepared by dissolution in concentrated sulphuric acid in the presence of small amounts of other oxidants (H_2O_2 or $NaNO_3$). To improve the solubility of the compound and to decrease the viscosity of the sulphuric acid, organic solvents like acetonitrile or nitromethane were added.

The ESR spectra were recorded on a JES–3B spectrometer in the X-band frequency, using peroxylamminedisulphonate as standard ($a_N = 13G$).

M.O. CALCULATIONS

The M.O. calculations were carried out within the framework of Hückel and McLachlan approximations. The nitro group parameters were those suggested by Rieger and Fraenkel[5] and those for oxygen were already tested in the study of other dibenzo-*p*-dioxin cation-radicals.[6]

---

[1] M. Hillebrand and M. Răileanu, *Rev. Roumaine Chim.*, **19**, 1227 (1974).

[2] A. Gioabă, V. Sahini and E. Volanschi, *J. C. S. Perkin II*, in press.

[3] M. Tomita, *J. Pharm. Soc. Japan*, **55**, 1060 (1936).

[4] A. Maki and D. M. Geske, *J. Amer. Chem. Soc.*, **82**, 2671 (1960).

[5] P. H. Rieger and G. K. Fraenkel, *J. Chem. Phys.*, **39**, 609 (1963).

[6] P. D. Sullivan and J. R. Bolton, *J. Magnetic Res.*, **1**, 356 (1968).

RESULTS AND DISCUSSION

The ESR spectrum of the anion-radical obtained from 2-nitrodibenzo-*p*-dioxin in DMSO is presented in fig. 1 and is interpreted with the splitting constants contained in table 1.

Table 1

Experimental (E) and calculated* (C) hyperfine splittings (G)

Ion-radical		a_1^{**}	NO$_2$ a_2(N)	a_3	a_4	a_6	a_7	a_8	a_9
2-nitrodibenzo-*p*-dioxin anion-radical	E	3.58	9.54	3.58	1.19	<0.30	<0.30	<0.30	<0.30
	C	3.13	12.14	3.13	1.18	0.03	0.02	0.05	0.02
2-nitrodibenzo-*p*-dioxin cation-radical	E	<0.15	0.30	0.90	0.30	0.30	3.45	3.14	0.30
	C	0.14	0.51	1.68	0.47	0.51	2.59	2.41	0.37
2,(8)-dinitrodibenzo-*p*-dioxin cation-radical	E	0.29	0.44	1.79	0.81	0.81	1.79	0.44	0.29
	C	0.25	0.57	2.12	0.58	0.58	2.12	0.57	0.25

* $a_H = /27/ \rho_C^{\pi}\ a_N = 99.0\,\rho_N^{\pi} - 2\times 35.8\,\rho_{O(NO_2)}^{\pi}$

$h_0 = 2.00;\ h_N = 2.20;\ h_0(NO_2) = 1.40$

$k_{CO} = 0.71;\ k_{CN} = 1.00;\ k_{NO(NO_2)} = 1.67$

** Numbering as indicated in Chemical Abstract

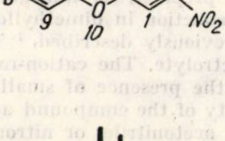

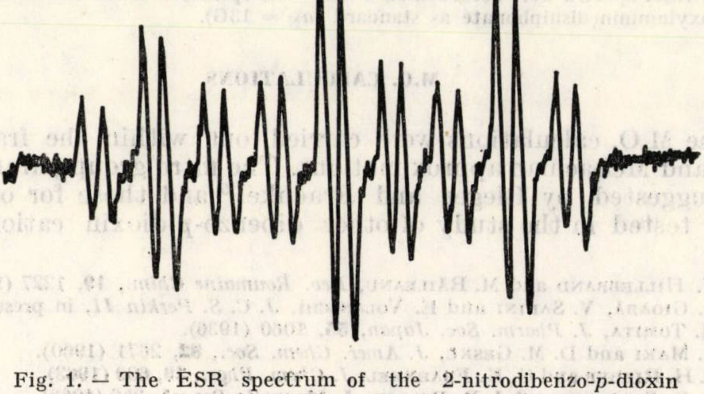

Fig. 1. — The ESR spectrum of the 2-nitrodibenzo-*p*-dioxin anion-radical electrochemically generated in DMSO.

Examining the results, the great constant of the nitrogen atom points out a high degree of localization of the odd electron on the nitro group. As the "hfs" constants are similar to those reported for several *p*-substituted nitrobenzene, [5] we assign the 3.58 G splittings to positions 1,3 (*ortho* to the nitro group) and that of 1.18 G to position 4. The splittings of the second ring are unresolved in the recorded spectrum, being smaller than the line-width.

The behaviour of 2-nitrodibenzo-*p*-dioxin is rather similar to that of 3,4-substituted nitrobenzene with little perturbing substituents. An analogous situation was encountered for 2-nitrophenoxatellurine, but not for 2-nitrophenothiazine-5-oxide when the two 1,3 protons become inequivalent. Therefore, it may be stated that in the anion-radicals of these mononitroderivatives the dominant role is exerted by the nitro group, the heteroatoms of the central ring influencing only the distribution of the spin density in the nitro-containing ring : their presence is not sufficient as to ensure the delocalization of the odd electron on the whole molecule. The difference between the pairs of heteroatoms is more evidenced by the study of the dinitroderivatives, as was performed for 2,8-dinitrophenoxatellurine and 3,7-dinitrophenothiazine-5-oxide. The presence of the oxygen atom maintained the localization of the odd electron on the nitro-containing ring, while the N—SO pair provides an extended conjugation on both rings.

As expected from previous data, the dissolution of 2-nitro-dibenzo-p-dioxin in sulphuric acid with small amounts of $NaNO_3$ leads to the cation-radical, whose ESR spectrum is presented in fig. 2.

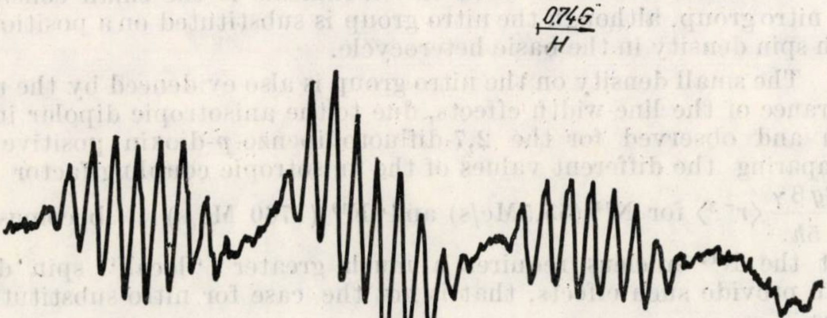

Fig. 2. — The ESR spectrum of the 2-nitrodibenzo-*p*-dioxin cation-radical in H_2SO_4.

In the presence of more $NaNO_3$ and especially when the sulphuric acid was diluted with CH_3NO_2, another radical species appears, with the ESR spectrum of fig. 3.

As Tomita and Ueda [7] discussed the possibility for such derivatives to undergo in these conditions a nitration reaction, we assigned this second spectrum to the dinitrodibenzo-*p*-dioxin cation-radicals. The "hfs" for both ions are also listed in table 1. In agreement with the positions of the greatest spin densities in the dibenzo-*p*-dioxin ions, we assigned

---

[7] M. TOMITA and S. UEDA, *Chem. Pharm. Bull.*, **12**, 33 (1964).

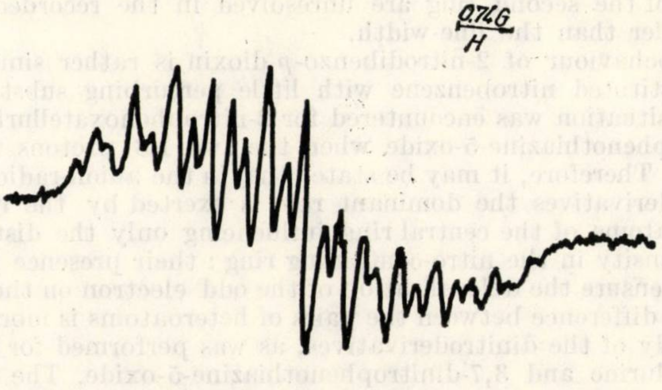

Fig. 3. – The ESR spectrum of the dinitrodibenzo-*p*-dioxin cation-radical in $H_2SO_4-CH_3NO_2$ solution.

the three significant splittings in the spectrum of the mono-nitro cation-radical to positions 3,7 and 8.

The main feature of both cation-radicals is the small constant of the nitro group, although the nitro group is substituted on a position with high spin density in the basic heterocycle.

The small density on the nitro group is also evidenced by the nonappearance of the line-width effects, due to the anisotropic dipolar interaction and observed for the 2,7-difluorodibenzo-*p*-dioxin positive ion. [8] Comparing the different values of the anisotropic coupling factor $B_0 = \frac{2g\beta\gamma}{5h}\langle r^{-3}\rangle$ for N^{14} (55.5Mc/s) and F^{19} (1760 Mc/s) it becomes clear that the N^{14} nucleus requires a much greater "local" spin density as to provide such effects, that is not the case for nitro-substituted cations.

The presence of a second nitro group determines also a reduction of the total width of the spectrum. The observations made on the nitro group effect on the ESR spectra of cation-radicals agree with those discussed for nitrophenothiazines. The lack of other data concerning nitrosubstituted cation-radicals prevents us to make a more extended comparison about the nitro behaviour in positive ions, but our experimental results outline the concurrent effect between the heterocyclic moiety and the nitro group : the spin density pattern is determined by the first in the cations and by the second in the anion-radicals.

---

[8] I. Baciu, M. Hillebrand and V. Sahini, *J. C. S. Perkin II*, **1974**, 986.

The M.O. calculations performed describe well the main features of the experimental data and the agreement of the calculated and experimental hyperfine proton splittings supports the assignment given in table 1. The most interesting result of the spin density calculations is the dependence of the $a_N^{NO_2}$ constant on the charge of the radical species, that is a much greater value for the anion- than for the cation-radical (12.40G *vs cca.* 0.51G). This may be explained by the different form obtained for the odd electron orbital in the two ions : in the cation-radicals the orbital containing the odd electron maintains the same features as in the unsubstituted ion, while in the anion-radical it is mainly localized on the nitro group.

Revue Roumaine de Chimie, **21**, *4*, 491–494 (1976)

EXTENSION OF SOME REGULARITIES OF TERNARY ELECTROLYTIC AQUEOUS SOLUTIONS IN IONIC LIQUIDS

RODICA VÎLCU, FLORICA IRINEI and ELENA TATU

Chemistry Institute Bucharest, Chair of Physical Chemistry, Bdul. Republicii nº 13

Received December 26, 1974

This paper reports on the correlation achieved among the functions of deviation from the ideality of the components of some ionic liquids and it brings as a new element in the literature the extension of Harned's laws regarding the ternary solutions of electrolytes in water. The melted three-salts systems are exemplified by $LiNO_3 + NaNO_3 + KNO_3$.

The thermodynamic characterization of the melted salts, isolated or in mixtures, is to a large extent a consequence of the transposition of the results obtained in the study of aqueous solutions.

Therefore, equation

$$\log (\gamma_i)_t = \log (\gamma_i)_b - \alpha_i m(1 - y_i), \tag{1}$$

where $(\gamma_i)_t$ is the activity coefficient of the i-th electrolyte in the ternary mixture, and $(\gamma_i)_b$ is the activity coefficient of the i-th electrolyte in the binary system, specific of aqueous solutions, can be used in the case of melted-salts mixtures when the activity coefficients contribution is considered additive for a component in the two binary systems. From this it results that

$$\log (\gamma_i)_t = \frac{1}{2} [\log (\gamma_i)_{b_1} + \log (\gamma_i)_{b_2}] - \alpha_i m(1 - y_i) \tag{2}$$

The coefficients α_i, called Harned's coefficients characterize the behaviour of an electrolyte in the ternary system when all the other components are present in the mixture.

Harned's coefficients, expressing the deviation from the ideal behaviour, can be associated with the excess free energy by the relation [1]

$$\Delta_m G^E = -2,303\ RT \left(\prod_{i=1}^{n} m_i \right) \left(\sum_{i=1}^{n} \alpha_i \right) \tag{3}$$

---

[1] R. Vîlcu and Fl. Irinei, *St. şi Cerc. Chim. Acad. Bucureşti*, **20** (1972).

Equation (3) permits the calculation of the thermodynamic excess magnitudes in the specific conditions of the parameters at the solid-liquid equilibrium state.

The present work is an analysis of the thermodynamic behaviour of the components of a ternary system, namely $LiNO_3 + NaNO_3 + KNO_3$ with respect to the binary associates $(Li + Na)NO_3$; $(Li + K)NO_3$; $(Na + K)NO_3$, by using cryoscopic methods, which permit a much more accurate evaluation of the compounds activities, on the basis of the following equation

$$\ln a_T = \frac{\Delta H_\theta}{R}\left(\frac{1}{T} - \frac{1}{\theta}\right) + \frac{\Delta C_p}{R}\left(\ln\frac{\theta}{T} - \frac{\theta - T}{T}\right) \tag{4}$$

For the systems under study, the contribution of the second term in equation (4) to the activity magnitude is too small and it can be neglected.

The cryoscopic effects were determined by the method of cooling curves,[2] and the temperature was measured with a Pt — Pt/Rh thermocouple attached to an electronic millivoltmeter. Since the data found in the literature for the systems under research focus on the establishment of the melting diagrams rather than on thermodynamic calculations, we have considered useful the accurate experimental establishment of the cryoscopic depressions.

The thermodynamic activities of the binary systems components calculated from the cryoscopic data are presented in table 1.

Table 1

Thermodynamic activities of the binary systems components

	$LiNO_3 + KNO_3$				$LiNO_3 + NaNO_3$				$NaNO_3 + KNO_3$			
	$LiNO_3$		KNO_3		$LiNO_3$		$NaNO_3$		$NaNO_3$		KNO_3	
x	T(K)	a_{873}	T(K)	a_{873}	T(K)	a_{873}	T(K)	a_{873}	T(K)	a_{873}	T(K)	a_{873}
1	525	1	610	1	525	1	581	1	581	1	610	1
0.9	517	0.906	569	0.887	517	0.922	561	0.897	564	0.908	584	0.916
0.8	497	0.755	533	0.778	501	0.769	545	0.811	545	0.811	559	0.816
0.7	477	0.607	477	0.639	489	0.663	529	0.720	527	0.720	533	0.739
0.6	453	0.477	405	0.488	473	0.557	509	0.626	508	0.624	507	0.646
0.5	426	0.350					485	0.521	494	0.543		

The melting temperature and heat for the pure components, necessary for calculating the thermodynamic activities have been taken from the bibliographic references [3]

$\theta_{LiNO_3} = 526$ K $\Delta^t H_{LiNO_3} = 6400$ cal

$\theta_{NaNO_3} = 579.1$ K $\Delta^t H_{NaNO_3} = 3600$ cal

$\theta_{KNO_3} = 607.4$ K $\Delta^t H_{KNO_3} = 2300$ cal

---

[2] S. Sternberg and L. Bejan, *Rev. Roumaine Chim.*, **13**, 1555 (1968).

[3] M. Blander, "Molten Salt Chemistry", Wiley, New York, 1964.

Using the least squares method with the experimental data the following expressions of the thermodynamic activities as a function of the temperature were obtained :

$$\log a_{\mathrm{KNO_3}} = -1136\ T^{-1} - 2.685 \log T + 9.337$$

$$\log a_{\mathrm{NaNO_3}} = -1206\ T^{-1} - 1.756 \log T + 6.932$$

From the values of the activity coefficients it is possible to calculate the excess partial molar free energies for the binary systems components, with the help of the relation

$$\bar{G}_i^E = RT \ln \gamma_i$$

The computed values for those excess partial molar free energies are tabulated in table 2.

Table 2

Excess partial molar free energies of binary systems components

	$LiNO_3 + KNO_3$		$LiNO_3 + NaNO_3$		$NaNO_3 + KNO_3$	
X	$G^E_{\mathrm{LiNO_3}}$	$G^E_{\mathrm{KNO_3}}$	$G^E_{\mathrm{LiNO_3}}$	$G^E_{\mathrm{NaNO_3}}$	$G^E_{\mathrm{NaNO_3}}$	$G^E_{\mathrm{KNO_3}}$
0.9	53.50	− 25.23	41.70	− 4.10	16.32	27.80
0.8	− 9.80	− 46.37	− 67.07	−25.03	25.03	67.01
0.7	−242.86	−156.52	− 92.47	49.90	49.99	94.78
0.6	−393.02	−354.05	−126.86	70.24	71.85	128.74
0.5	−614.79			72.17	144.60	

The activities of the components for the ternary systems are presented in table 3.

Table 3

Thermodynamic activities of the ternary systems components

	$LiNO_3 + (NaNO_3 + KNO_3)$		$NaNO_3 + (LiNO_3 + KNO_3)$		$KNO_3 + (LiNO_3 + NaNO_3)$	
x	$LiNO_3$		$NaNO_3$		KNO_3	
	$T(K)$	a_{873}	$T(K)$	a_{873}	$T(K)$	a_{873}
1	525	1	581	1	610	1
0.9	519	0.921	566	0.919	581	0.907
0.8	503	0.783	560	0.860	551	0.813
0.7	486	0.651	539	0.747	515	0.703
0.6	471	0.548	518	0.654	475	0.594
0.5	461	0.462	498	0.555	439	0.490

All the values for the thermodynamic activities have been recalculated for $T = 873$ K using relation

$$\ln\,(\gamma_i)_{T_2} = \frac{T_1}{T_2}\ln\,(\gamma_i)_{T_1}$$

Table 4 contains the values of the excess partial molar free energies for the ternary systems components.

Table 4

Excess partial molar free energies for the ternary systems components

x	$G^E_{LiNO_3}$	$G^E_{NaNO_3}$	$G^E_{KNO_3}$
0.9	44.87	36.02	14.30
0.8	− 35.30	126.50	28.10
0.7	−123.02	128.50	7.96
0.6	−156.01	147.01	−21.89
0.5	−134.20	181.50	−33.43

By correlating the activity coefficients values of the electrolytes in the ternary systems with those of the binary systems according to the relations of the Harned type equations, the $[\alpha\, m]$ products values shown in table 5 were found.

Table 5

Harned's coefficients of electrolytes in the ternary systems

$LiNO_3 + (NaNO_3 + KNO_3)$		$NaNO_3 + (LiNO_3 + KNO_3)$		$KNO_3 + (LiNO_3 + NaNO_3)$	
x_{LiNO_3}	m	x_{NaNO_3}	m	x_{KNO_3}	m
0.9	−0.0144	0.9	−0.8768	0.9	−0.0327
0.8	−0.0595	0.8	−0.1275	0.8	−0.0223
0.7	−0.0374	0.7	−0.0664	0.7	−0.0487
0.6	−0.0715	0.6	−0.0455	0.6	−0.0573

The results underline the contribution of the polarization component to the interaction energy.

Thus, for mixtures containing $LiNO_3$ in excess, with respect to the remaining two components, the product $[\alpha\, m]$ is greater than for the mixtures containing the other two components in excess.

Therefore, there is respected the proportionality between $[\alpha\ m]$ and Δr, necessary to evidence the polarization force.

With the help of equation (3) the value for $\Delta mG^E = -318.4$ cal/mol has been obtained for the ternary mixture $LiNO_3 + NaNO_3 + KNO_3$ at $x_1 = 0.5$, $x_2 = x_3 = 0.25$.

Kleppa[4] has obtained for the same system, on the basis of some relations specific of the regular solutions, $\Delta\, mH^E = -320$ cal/mol, which is very close to our value for $\Delta\, mG^E$ confirming, the regular behaviour of the system considered as well as the accuracy of the relations used.

---

[4] O. J. Kleppa and L. S. Hersh, *J. Chem. Phys.*, **34**, 351 (1961).

Revue Roumaine de Chimie, **21**, *4*, 495–501 (1976)

THERMODYNAMIC PROPERTIES OF $NaCl-CaCl_2$ AND $KCL-CaCl_2$ MOLTEN SYSTEMS

LETIŢIA TOPOR and IVONA MOLDOVEANU
Centre of Physical Chemistry str. Galaţi 31, Bucharest, Romania

Received February 4, 1975

The thermodynamic activities in molten $NaCl-CaCl_2$ and $KCl-CaCl_2$ systems, as a composition function, from vapour pressure measurements at 1373 K and 1423 K have been obtained. The partial molar free energies, the excess partial molar free energies and the partial molar entropies have been calculated. From the variation of these thermodynamic data as a composition function, the tendency for association and the possibility of a local order has been deduced.

INTRODUCTION

Charge-unsymmetrical fused salt systems have been investigated by different methods. The thermodynamic properties of the $NaCl-CaCl_2$ system have been obtained by electromotive force measurements for concentration [1-3] and formation [4] cells, by cryoscopic [5,6] and calorimetric [7] methods. The $KCl-CaCl_2$ system has been investigated by electromotive force for concentration cells, [1,2,8] calorimetric [7,9] and vapour pressure measurements. [10] Vapour pressure measurements yielded only the information concerning the composition of vapour phase. The corresponding thermodynamic data have not been calculated.

The electromotive force technique has mainly used the concentration cells with an alkali ion conducting glass, separating the two half cells. In these cells the transport number for alkali ions is very close to the unity and the chemical work connected with the junction potential was negligible. The special glass membrane acts as an alkali electrode. The accuracy of these measurements is dependent on the transport properties of the glass membrane and on the vapour pressure of the salts.

---

[1] T. Østvold, *High. Temp. Sci.*, **4**, 51 (1972).

[2] J. J. Egan and J. Bracher, *J. Chem. Thermodynamics*, **6**, 9 (1974).

[3] T. Østvold, *Acta Chem. Scand.*, **20**, 2320 (1966).

[4] V. Ya. Denischenko and A. G. Marachevski, *Zhur. priklad. Khim.*, **9**, 2110 (1971).

[5] S. Sternberg and I. Adorianm, *Rev. Roumaine Chim.*, **7**, 1317 (1962).

[6] S. Fukushima, R. Oyamada and H. Hagiwara, *J. Electrochem. Soc. Japan*, **33**, 43 (1965).

[7] T. Østvold, *J. Phys. Chem.*, **76**, 1616 (1972).

[8] G. D. Robbins, T. Førland and T. Østvold, *Acta Chem. Scand.*, **22**, 3002 (1968).

[9] B. F. Markov and T. A. Tisura, *Ukrain. khim. Zhur.*, **39**, 757 (1973).

[10] S. A. Frid, O. G. Poliachenov and I. G. Novicov, *Zhur. neorg. Khim.*, **9**, 1017 (1964).

The salts having a high vapour pressure will evaporate during the experiment and the binary mixture composition will change.

We have determined the thermodynamic properties of NaCl $-$ $CaCl_2$ and KCl$-$ $CaCl_2$ molten systems at 1373 K and 1423 K from vapour pressure measurements. The vapour pressure value obtained by Rodebush-Dixon method is given by the pressure of the molten alkali halide, because the vapour pressure for the alkaline earth halide in these conditions is negligible.

EXPERIMENTAL

The quasi-static Rodebush-Dixon apparatus and the required procedure have been described previously.[11] The quartz cell was modified because the two arms had the inner diameter too small for introducing quantitatively the weighted mixture. The new cell (fig. 1) had an arm with a larger inner diameter (about 10 mm) in order to allow the introduction on powdered mixtures. After filling the cell, the larger arm was reduced for experimental measurements by introduction of a quartz rod, provided with a ground joint, to connect the cell to the apparatus.

The NaCl and KCl analytical reagents grade Merck and $CaCl_2$ Chemapol-Czechoslovakia were used. The salts were purified by repeted crystallizations. $CaCl_2$ was dehydrated by fusing the salt in Ar stream. The solidification was made by dropping the molten $CaCl_2$ in liquid CCl_4. NaCl and KCl were dried by gradually heating to 300° under vacuum. The salts were then fused under a constant flow of HCl. All weighings of the samples and the filling of the cell were carried out in a drybox. The different compositions were obtained by the addition of a small quantity of NaCl or KCl at the initial mixture. The small samples were then taken out after measurements and the exact composition determined by potentiometrical titration of the total chlorine ions and complexometrical titration of calcium ions with Complexon III.

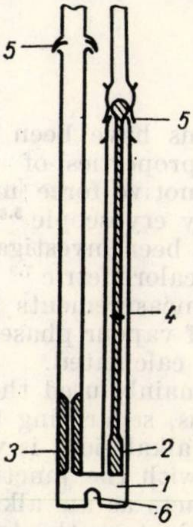

Fig. 1. — The cell :
1, molten salts ; *2*, the quartz rod ; *3*, the quartz capillary ; *4*, the arm with the larger inner diameter ; *5*, the grounded joint ; *6*, the thermocouple tube.

The pressure values were measured with a mercury manometer, using a Griffen & George Limited catethometer with a precision of 0,01 mm. The temperature was measured with Pt$-$PtRh thermocouple and maintained constant within ± 1° by a thermoregulator system.

---

[11] I. G. Murgulescu and L. Topor, *Rev. Roumaine Chim.*, **11**, 1353 (1966).

RESULTS AND DISCUSSION

We have determined the vapour pressure of NaCl and KCl in the molten mixture $NaCl - CaCl_2$ and $KCl - CaCl_2$ at 1373 K and 1423 K. The activities of NaCl and KCl in the mixture were calculated from the vapour pressures of alkali halide in the molten mixtures and that of pure molten alkali halides obtained previously.[12] The activity coefficients at different mole fractions were obtained. The activity coefficients of molten $CaCl_2$ in both mixtures were obtained by graphical integration of Gibbs-Duhem equation. The partial molar free enthalpies of mixing ($\overline{\Delta G_i}$) and the excess partial molar free enthalpies ($\overline{\Delta G_i^E}$) were deduced from the activities and activities coefficients. The partial molar enthalpies of mixing of the alkali halides were calculated from the integral enthalpies of mixing equation by derivation. The equation for the integral enthalpy of mixing in $NaCl - CaCl_2$, $KCl - CaCl_2$ systems is of the type :[13]

$$\Delta H^M = x_1 x_2 (a + b x_2)$$

where a is -4.482 kcal/mole, b is 1.602 kcal/mole for $NaCl - CaCl_2$ system and -10.447 kcal/mole, 3.257 kcal/mole for $KCl - CaCl_2$ respectively and x_2 is the mole fraction of the $CaCl_2$ in the mixture. The partial molar enthalpies of mixing were obtained from the equation :

$$\overline{\Delta H}_{NaCl(KCl)} = (a - b)\, x_2^2 + 2\, b x_2^3$$

The author[13] did not give any indication regarding the temperature dependence of the integral enthalpies of mixing for $NaCl - CaCl_2$ and $KCl - CaCl_2$ systems. The partial molar entropies were calculated from partial molar enthalpies and partial molar free enthalpies. The vapour pressure values of NaCl and KCl in $NaCl - CaCl_2$ and $KCl - CaCl_2$ systems at 1373 K, 1423 K at different molar fractions are presented in table 1 and 2.

Figures 2–7 present the variation of the activities, the coefficients of activity, the excess free enthalpies of the system and the partial molar entropies vs. composition. In figures 2 and 4 are compared the activities obtained from vapour pressure measurements with that obtained from e.m.f.[2] and cryoscopic[14] methods. The agreement between the values obtained by different methods is satisfactory.

The activities and the coefficients of activity show negative deviations from ideality for both systems (fig. 2–5) and are greater in the $KCl - CaCl_2$ system. The excess free enthalpies are negative for the

---

[12] L. Topor, *J. Chem. Thermodynamics*, **4**, 739 (1972).

[13] T. Østvold, *J. Phys. Chem.*, **76**, 1616 (1972).

[14] A. M. Pitschugin, "Spravochnik po plavkosti sistem iz bezvodnych neorganicheskich solezhj", Izdatel'stvo Akademii Nauk S.S.S.R., Moskva 1964 from G. Roewer and H. H. Emons, *Z. anorg. Chem.*, **370**, 114 (1969).

Table 1

Vapour pressures of NaCl (p_{NaCl}) in molten NaCl − $CaCl_2$ system at different mole fractions of NaCl (X_{NaCl})

X_{NaCl}	p_{NaCl} (mm Hg) T = 1373 K	p_{NaCl} (mm Hg) T = 1423 K
0.13	1.46	2.90
0.29	3.77	7.32
0.42	7.37	13.79
0.53	11.35	18.37
0.61	14.30	24.79
0.69	17.47	30.08
0.78	20.92	36.05
0.84	24.48	41.10
0.86	25.71	43.18
0.88	27.19	46.08
0.90	28.43	47.70
0.91	28.87	48.91
1.00	32.07*	56.34*

* − vapour pressure of pure NaCl previously obtained.[12]

Table 2

Vapour pressures of KCl (p_{KCl}) in molten KCl − $CaCl_2$ system at different mole fractions of KCl (X_{KCl})

X_{KCl}	p_{KCl} (mmHg) T = 1373 K	p_{KCl} (mmHg) T = 1423 K
0.22	2.19	5.26
0.32	—	9.50
0.37	5.30	—
0.43	8.00	16.09
0.47	10.09	18.60
0.60	17.57	32.26
0.70	25.02	43.61
0.79	32.63	53.33
0.83	34.93	58.49
0.90	43.34	72.00
1.00	54.52*	87.80*

* − vapour pressure of pure KCl previously obtained[12]

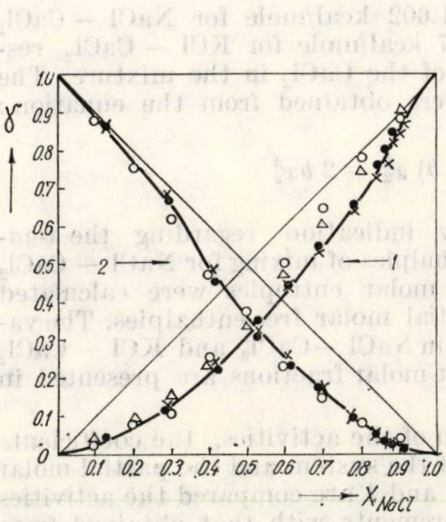

Fig. 2. — The activities of NaCl and $CaCl_2$ in molten NaCl−$CaCl_2$ system:

1 − a_{NaCl}; 2 − a_{CaCl_2}; ● − our values at 1373 K; × − our values at 1423 K; △ − J. J. Egan and J. Bracker at 1098 K; ○ − A. M. Pitshugin at 1083 K.

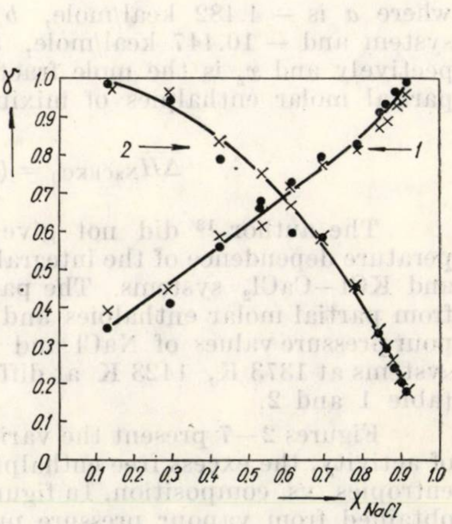

Fig. 3.— The activity coefficients of NaCl and $CaCl_2$ in molten NaCl−$CaCl_2$ system:

1 − γ_{NaCl}; 2 − γ_{CaCl_2}; ● − our values at 1373 K; × − our values at 1423 K.

two systems (fig. 6) being more negative for KCl − $CaCl_2$ system. The partial molar free enthalpies and the excess partial molar free enthalpies are negative and are presented in table 3,4.

The partial molar entropies (fig. 7) in the NaCl − $CaCl_2$ melt are closer to the ideal Temkin entropies (dotted lines) while in the KCl − $CaCl_2$ system they show larger deviations from ideality.

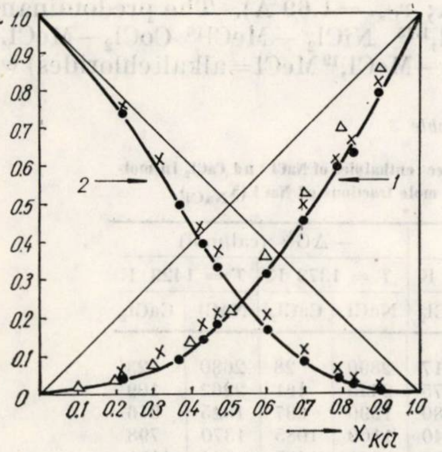

Fig. 4. — The activities of KCl and $CaCl_2$ in molten KCl — $CaCl_2$ system: $1 - a_{KCl}$; $2 - a_{CaCl_2}$; ● – our values at 1373 K; × – our value at 1423K; △ – J. J. Egan and J. Bracker at 1058 K.

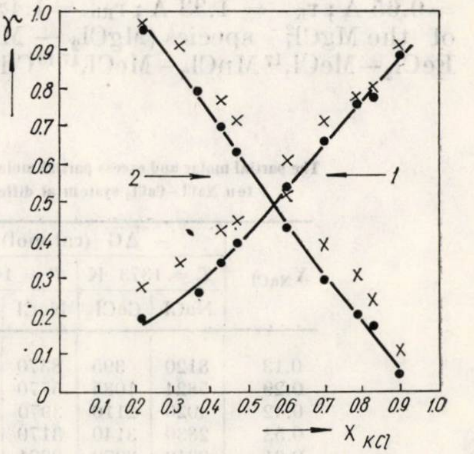

Fig. 5. — The activity coefficients of KCl and $CaCl_2$ in molten KCl–$CaCl_2$ system: $1 - \gamma_{KCl}$; $2 - \gamma_{CaCl_2}$; ● – our values at 1373 K; × – our values at 1423 K.

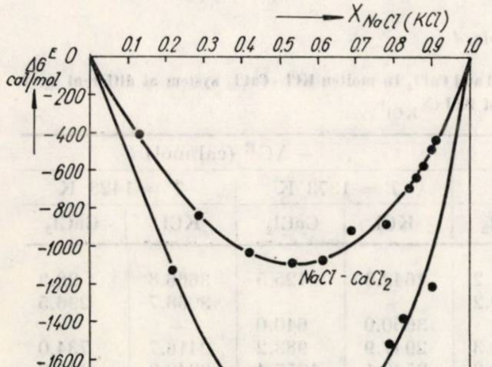

Fig. 6. — The excess free enthalpies for molten NaCl–$CaCl_2$ and KCl–$CaCl_2$ systems at 1373 K.

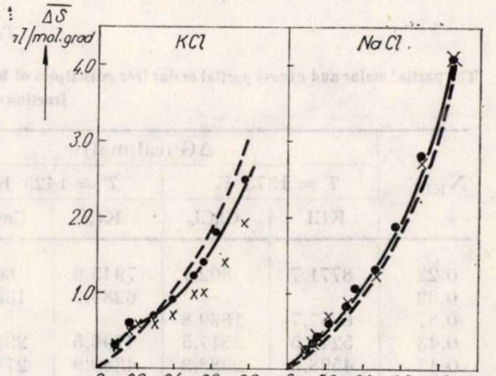

Fig. 7. — The partial molar entropies of alkali halides in molten NaCl–$CaCl_2$ and KCl–$CaCl_2$ systems:
● – $\Delta\bar{S}$ KCl (NaCl) at 1373 K; × – $\Delta\bar{S}$ KCl (NaCl) at 1423 K; —$\Delta\bar{S}^{id}$ KCl (NaCl)

In the charge-unsymmetrical salt mixtures the smaller cations with higher charge will attract the anions stronger than the larger cations with lower charge. For example in the system $MgCl_2$ — MeCl (Me = K, Rb, Cs) the Cl^- anions will associate preferentialy with Mg^{2+} (r^{2+}_{Mg} =

$=0.65$ Å ; $r_{K^+} = 1.33$ Å ; $r_{Rb^+}=1.48$ Å; $r_{Cs^+}=1.69$ Å). The predominance of the $MgCl_4^{2-}$ species ($MgCl_2 - MeCl$,[1,15] $NiCl_2 - MeCl$[16] $CoCl_2 - MeCl$,[17] $FeCl_2 - MeCl$,[17] $MnCl_2 - MeCl$,[17,18] $CdCl_2 - MeCl$,[19] $MeCl$ = alkali chlorides) was indicated in some unsymmetrical systems. In mixtures containing calcium and alkali ions the tendency for association between the anions and the divalent cation is much lower than, for example, for the magnesium chloride mixtures. The polarizing strength of the calcium ion is lower than of the

Table 3

The partial molar and excess partial molar free enthalpies of NaCl and $CaCl_2$ in molten $NaCl-CaCl_2$ system at different mole fractions of NaCl (X_{NaCl})

X_{NaCl}	$-\overline{\Delta G}$ (cal/mol)				$-\overline{\Delta G^E}$ (cal/mol)			
	$T = 1373$ K		$T = 1423$ K		$T = 1373$ K		$T = 1423$ K	
	NaCl	$CaCl_2$	NaCl	$CaCl_2$	NaCl	$CaCl_2$	NaCl	$CaCl_2$
0.13	8120	395	8370	417	2890	28	2680	23
0.29	5824	1085	5770	1075	2445	161	2262	109
0.42	4020	2110	3970	2080	1590	637	1525	516
0.53	2830	3140	3170	2840	1100	1085	1370	798
0.61	2210	3970	2321	3800	861	1405	924	1131
0.69	1660	4660	1775	4840	650	1465	724	1515
0.79	1165	6260	1291	6520	511	2141	560	2235
0.84	738	8110	883	8280	263	2975	399	3070
0.86	605	8700	752	9000	194	3340	326	3430
0.88	547	9620	568	9800	102	3950	206	3690
0.90	451	10600	474	10800	44	4300	174	4270
0.91	287	11210	400	11560	30	4620	133	4740

Table 4

The partial molar and excess partial molar free enthalpies of KCl and $CaCl_2$ in molten $KCl-CaCl_2$ system at different mol fractions of KCl (X_{KCl})

X_{KCl}	$-\overline{\Delta G}$ (cal/mol)				$-\overline{\Delta G^E}$ (cal/mol)			
	$T = 1373$ K		$T = 1423$ K		$T = 1373$ K		$T = 1423$ K	
	KCl	$CaCl_2$	KCl	$CaCl_2$	KCl	$CaCl_2$	KCl	$CaCl_2$
0.22	8771.7	802.1	7945.9	801.2	4642.9	125.5	3666.8	98.3
0.32	—	—	6285.9	1359.2	—	—	3068.7	296.5
0.37	6357.7	1899.8	—	—	3650.0	640.0	—	—
0.43	5243.5	2517.5	4796.5	2325.3	2947.9	983.2	2416.7	734.0
0.47	4598.3	2988.3	4380.9	2740.2	2545.1	1257.4	2248.9	945.2
0.60	3088.0	4561.7	2831.0	4434.8	1699.4	2309.1	1386.8	1848.6
0.70	2122.0	6623.1	1974.6	6084.0	1148.9	3338.1	967.3	2671.6
0.79	1401.1	8574.6	1409.9	7808.2	758.6	4323.3	745.5	3372.3
0.83	1211.9	9555.7	1148.0	8953.3	705.1	4756.2	623.2	3960.8
0.90	625.1	14438.4	560.5	12737.3	339.1	8088.1	263.2	6235.7

---

[15] O. J. Kleppa and F. G. J. Mc Carty, *J. Phys. Chem.*, **68**, 3846 (1964).

[16] G. N. Papatheodorou and O. J. Kleppa, *J. Inorg. Nuclear Chem.*, **32**, 889 (1970).

[17] G. N. Papatheodorou and O. J. Kleppa, *J. Inorg. Nuclear Chem.*, **33**, 1249 (1971).

[18] T. Østvold, *Acta Chem. Scand.*, **26**, 2788 (1972).

[19] G. N. Papatheodorau and O. J. Kleppa, *J. Inorg. Chem.*, **10**, 872 (1971).

magnesium ion. The presence of "complex species" in the $CaCl_2$ — alkali halides mixtures, has not been proved either from e.m.f. or from calorimetrical or other studies. The negative deviations of thermodynamic properties obtained in the $CaCl_2$ — MeCl (Me = Na, K) can be explained supposing a higher configurational order than a random mixture. This configurational order may be due to the preferential association of Cl^- with the Ca^{2+} having higher charge densities than the alkali ions. The tendency for a stronger Ca^{2+} — Cl^- association is increasing with increase of the alkali ion radius because the differences of the charge densities are larger and the cation — cation repulsion is lower.

The transference number and ionic mobility studies for the $CaCl_2$— MeCl (Me = Na, K) [20,21] and $MgCl_2$ — KCl[21] systems, show an agreement with the hypothesis of a preferential association of Ca^{2+} — Cl^-, indicating a relatively larger mobility of alkali ions than that of the alkaline earthe and magnesium ions.

---

[20] G. ROEWER and H. H. EMONS, *Z. anorg. Chem.*, **370**, 119, 128 (1969).

[21] W. K. BEHL and J. J. EGAN, *J. Phys. Chem.*, **6**, 1764 (1967).

Revue Roumaine de Chimie, **21**, *4*, 503–508 (1976)

FIELD EFFECT INVESTIGATION OF ADSORPTION ON SEMICONDUCTOR FILMS

MIHAELA CONSTANTINESCU, E. SEGAL and M. VASS

Institute of Physical Chemistry Bucharest, Str. Dumbrava Roşie 23 – Romania

Received May 8, 1975

D. c. field effect method was used in an investigation of oxygen adsorption on zinc oxide thin films. The enhanced adsorption of the oxygen due to the application of a negative potential on the field plate was irreversible. To explain the experimental results, a model based on the potential values changes at the two interfaces of the semiconductor was given.

The field effect consists in the change of the surface parameters due to the application of a capacitive electrical field normal on the surface. The field induced charge distributes itself on the surface states and in the space charge region. As a result of the field strength values changes, the height of the potential barrier and its connected value of the Fermi level are also changed.

The measurements were generally made either on the surface conductivity, or on the capacity associated to the surface layer, both properties being directly related to the change of the surface induced charge due to the application of different field strength values.

The influence of the applied field on the chemosorptive and catalytic properties of semiconducting oxides was theoretically predicted in the framework of the electronic theory of chemisorption and catalysis.[1,2]

For zinc oxide thin films, the theory was reported in literature to be checked up for the adsorption of oxygen [3] and dehydrogenation of ethanol.[4] The measurements were made on a plane condenser model, including a field plate parallely placed with the investigated surface in the very working cell.

---

[1] F. F. Volkenstein and V. S. Sandomirski, *Doklady Akad. Nauk S.S.S.R.*, **118**, 980 (1958).

[2] V. G. Baru and F. F. Volkenstein, *Doklady Akad. Nauk S.S.S.R.*, **167**, 1314 (1966).

[3] S. A. Hoenig and G. R. Lane, *Surface Sci.*, **11**, 163 (1968).

[4] D. P. Mc Arthur, H. Bliss and J. B. Butt, *J. Catalysis*, **28**, 183 (1973).

EXPERIMENTAL

To avoid the errors introduced by the possible adsorption on the field plate, a working cell based on a cylindrical condenser model[5] with the field plate on the outer wall was used. The electrical conductivity as a measured parameter was chosen.

The field plate consists of a thin gold film deposited on the outer wall of a glass tube. The wall was 1 mm thick (figure 1). The other plate consists of the zinc oxide film deposited on the tube inner wall, equiped with two platinum contacts for conductibility measurements,

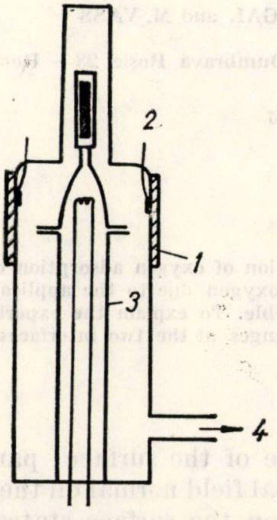

Fig. 1. — The working cell; *1*, field plate; *2*, conductibility measuring electrodes; *3*, system for film deposition; *4*, to high vacuum device.

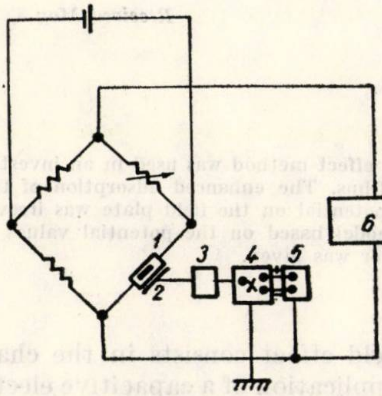

Fig. 2. — The sketch of the electrical circuit used for field effect measurements; *1*, zinc oxide film; *2*, field plate; *3*, voltmeter; *4*, switch for sign change of the applied voltage; *5*, high voltage generator; *6*, recorder.

The measured capacity value of such condenser was 8.1 pF. The working cell was connected to the high vacuum system.

The method used to obtain the zinc oxide films was described in an earlier paper.[6] The film thickness used was of 3000Å.

The electrical circuit used for the measurements, based mainly on the Low method[7] is shown in figure 2.

The electrical circuit used included two units, one for measurements of the electrical resistance values, provided with a d.c. bridge and a recorder, the other for application of different positive and negative voltages on the field plate. The voltage range was of 1000—5000V.

All the measurements were performed at room temperature.

To investigate the field effect influence on the chemisorptive properties of zinc oxide thin films with respect to oxygen, two kinds of experiments were performed:

1. On the fresh outgased film, a given amount of oxygen was introduced ($P = 10^{-4}$ Torr). After the electrical resistance change reached its stationary value, oxygen was pumped out. During the pumping time, no variation of the electrical resistance value was recorded. After the above mentioned treatment of the film, positive and negative voltages on the field plate were applied in steps from 1000 V to 5000V, each step changing the voltage value with

---

[5] N. P. Keier, E. P. Mikheeva and L. M. Usoltseva, *Kinetika i Kataliz*, **11**, 1009 (1970).

[6] M. Constantinescu and E. Segal, *Rev. Roumaine Chim.*, **12**, 75 (1967).

[7] G. E. Low, *Proc. Phys. Soc. B*, **69**, 133 (1956).

1000V. Every step lasted 10 minutes. The electrical resistance values were recorded during this period as well as during the relaxation period after the voltage was switched off.
2. After keeping the zinc oxide film in oxygen atmosphere for 36 hours, the positive and negative field effect, as well as the relaxation, were recorded.

RESULTS

Positive values of the voltage induced a decrease of the film electrical resistance. Negative values of the voltage gave an opposite effect.

The results were sensitive to the different values of the oxygen pressure, only for negative voltages, the relative change of the electrical resistance increasing with oxygen pressure. The results were graphically illustrated in figure 3.

Figure 4 shows that after switching off the positive voltages, the film electrical resistance increases until it returns to its original value, the phenomenon being completely reversible.

The slopes of the straight lines obtained when applying negative voltages, for different values of the oxygen pressure, were different.

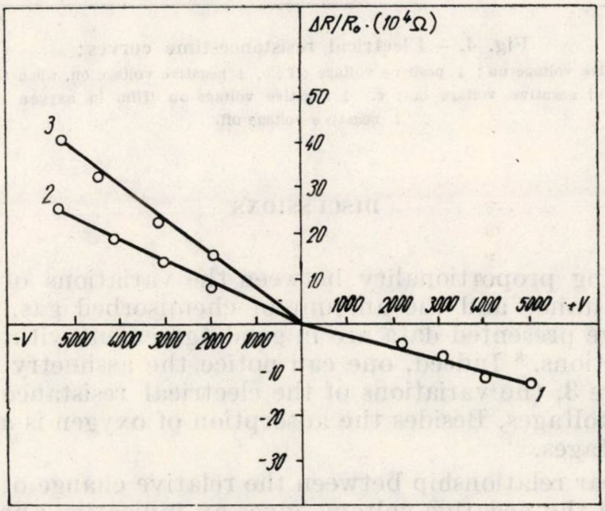

Fig. 3.—Relative changes of the electrical resistance of zinc oxide film with respect to the applied voltage;
1, positive voltage; *2*, negative voltage when the film is in vacuum; *3*, negative voltage with the film in oxygen atmosphere.

After switching off the negative voltages, the film electrical resistance, although decreasing, does not reach its original value, that is the relaxation is irreversible. The final values of the film electrical resistance, reached after switching off the negative voltage, are higher for higher values of the oxygen pressure.

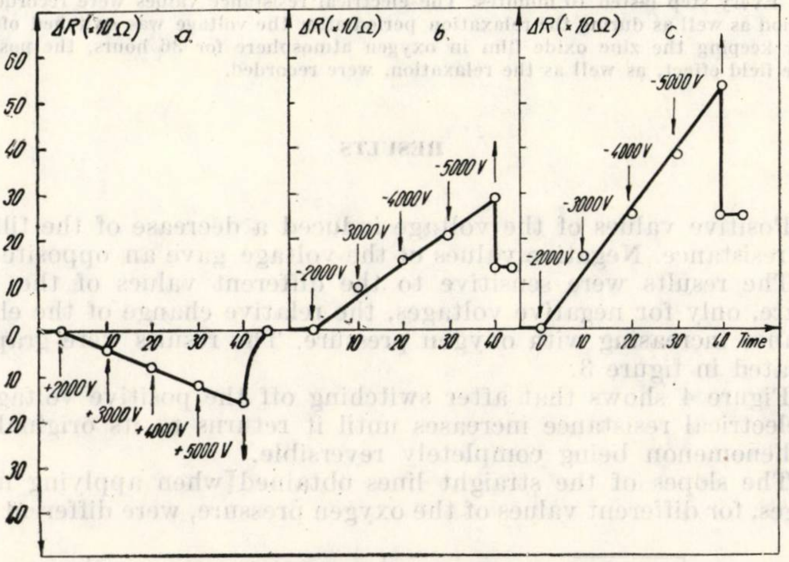

Fig. 4. — Electrical resistance-time curves;
a, ↑ positive voltage on; ↓ positive voltage off; b, ↓ negative voltage on, when the film is in vacuum; ↑ negative voltage off; c, ↓ negative voltage on (film in oxygen atmosphere); ↑ negative voltage off.

DISCUSSIONS

Presuming proportionality between the variations of the recorded electrical resistance and the amount of chemisorbed gas, we can state that the above presented data are in good agreement with the electronic theory predictions.[8] Indeed, one can notice the assimetry of the curves given in figure 3, the variations of the electrical resistance being higher for negative voltages. Besides the adsorption of oxygen is accelerated by negative voltages.

The linear relationship between the relative change of the electrical resistance and the negative voltage, gives an indication about a quasihomogeneous behaviour of the surface. The chemisorption of oxygen seems to be sensitive only to the field strength and not to the surface coverage.

The carriers concentration n_0 can be evaluated from the initial value of the electrical resistance, by using the relationship:

$$n_0 = \sigma_0/q\mu_e = L/a\,q\,\mu_e R_0 \qquad (1)$$

where: L is the film length, q—the elementary electrical charge, μ_e—the electrons mobility, σ_0 — the film conductibility and a — the cross section of the film. According to the literature data,[9] $\mu_e = 1$ cm^2/VS and thus $n_0 = 2 \cdot 10^7$ cm^{-3}.

---

[8] F. F. VOLKENSTEIN, "Fiziko khimia poverkhnosti poluprovodnikov" Izd. Nauka, Moskva, 1973, p. 196.

The Debye length can be calculated with the formula :[10]

$$1 = \sqrt{\frac{x\,kT}{8\pi\, q^2 n_0}} \qquad (2)$$

where : x is the dielectric constant of the semiconductor, k – the Boltzmann constant and T – the temperature.

In the present case, we obtain : $1 = 5{,}5.10^{-5}$ cm, which is of the same order of magnitude as the film thickness.

For a capacitive field, the thickness of the space charge region z_s can be calculated with the formula :[10]

$$z_s = \frac{\varepsilon_0\, V_0}{z_0\, n_0\, q} \qquad (3)$$

where ε_0 is the dielectric constant of the glass, and z_0 is the thickness of the glass.

For $V_0 = 5.10^3$ V, $z_s = 3.10^3$ Å, a value which also corresponds to the thickness of the film.

The above presented results can be understood in terms of our proposed model, based mainly on the potentials changes at the two interfaces : semiconductor-dielectric and semiconductor-gas.

The adsorption of an acceptor gas induces a potential barrier and a positive charge region at the semiconductor-gas interface. The bands

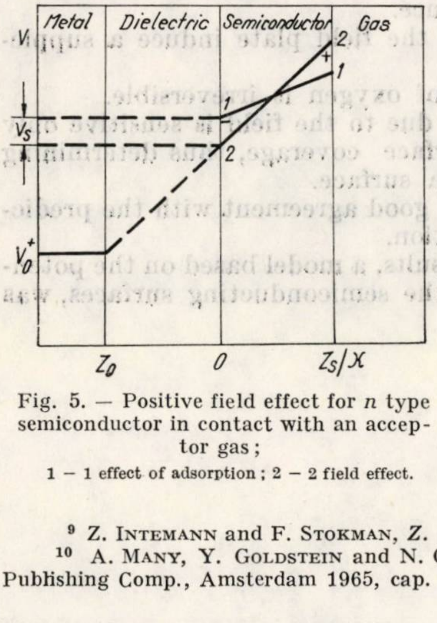

Fig. 5. — Positive field effect for n type semiconductor in contact with an acceptor gas ;

1 – 1 effect of adsorption ; 2 – 2 field effect.

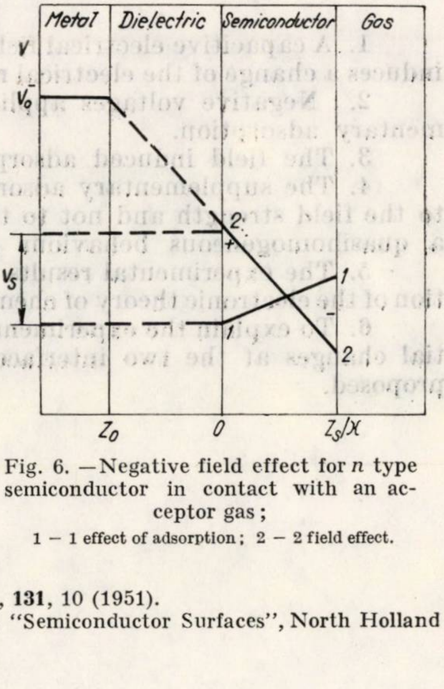

Fig. 6. — Negative field effect for n type semiconductor in contact with an acceptor gas ;

1 – 1 effect of adsorption ; 2 – 2 field effect.

---

[9] Z. Intemann and F. Stokman, *Z. Physik.*, **131**, 10 (1951).

[10] A. Many, Y. Goldstein and N. Grover, "Semiconductor Surfaces", North Holland Publishing Comp., Amsterdam 1965, cap. 6–8.

at the surface become up curved and the position of the Fermi level is down shifted, as shown in figures 5 and 6 by the line 1—1.

A positive potential applied on the field plate induces a negative space charge at the interface semiconductor-dielectric, with down curvature of the bands (fig. 5). At the interface semiconductor-gas, supplementary positive charges were induced, which increase the potential barrier. Moreover, the induced positive charge can be localised on the levels due to the acceptor adsorbed particles and thus either desorb or partially discharge the charged forms of chemisorption.

A negative field on the field plate (fig. 6), induces a positive space charge at the semiconductor-dielectric interface and an up curvature of the bands.

At the interface semiconductor-gas, negative charges are accumulated, which shift down the bands and the potential barrier, thus enhancing the adsorption of the acceptor gas. The adsorbed amounts are higher, the higher the applied voltages applied on the field plate are. The supplementary adsorption is sensitive only to the field strength and not to the surface coverage, in the investigated voltage range.

The proposed model can be applied only for films whose thickness is thinner than the Debye length or the value of z_s, because only in this case the change in the bands curvature at the interface semiconductor-dielectric has an influence on the potential barrier at the interface semiconductor-gas.

CONCLUSIONS

1. A capacitive electrical field, normal on the zinc oxide film surface, induces a change of the electrical resistance.

2. Negative voltages applied on the field plate induce a supplementary adsorption.

3. The field induced adsorption of oxygen is irreversible.

4. The supplementary adsorption due to the field is sensitive only to the field strength and not to the surface coverage, thus determining a quasihomogeneous behaviour of the surface.

5. The experimental results are in good agreement with the prediction of the electronic theory of chemisorption.

6. To explain the experimental results, a model based on the potential changes at the two interfaces of the semiconducting surfaces, was proposed.

Revue Roumaine de Chimie, **21**, *4*, 509 – 515 (1976)

L'ÉNERGIE ACCUMULÉE PAR LA DÉFORMATION PLASTIQUE À FROID DES LAITONS BINAIRES ET ALLIÉS

IOANA GROZA* et D.I. MARCHIDAN**

*Institut Polytechnique, Splaiul Independenţei 313, Bucarest
** Centre de Chimie Physique, str. Galaţi 31, Bucarest

Reçu le 28 décembre 1974

On a fait des mesurages d'énergie accumulée dans les laitons déformés 10 – 93%. Sur la base de l'analyse de la grandeur des effets thermiques et du rapport Q_r/Q (effet thermique de restauration/effet thermique total) on fait des appréciations sur les mécanismes de dislocation de la déformation plastique et sur l'influence des éléments de l'alliage sur ceux-ci.

L'emmagasinage d'une partie de l'énergie dépensée pour la déformation par l'accumulation des défauts dans le réseau cristallin est une caractéristique importante du processus de déformation plastique à froid des matériaux métalliques. La déformation modifie l'énergie libre du métal – la mesure de l'instabilité produite par la déformation – mais la quantité qu'on mesure est l'énergie interne car la variation d'entropie associée aux défauts de réseau est négligeable. Les valeurs de l'énergie accumulée expriment le degré d'imperfection du réseau du matériel déformé permettant ainsi l'explication de la variation des propriétés par l'écrouissage, aussi bien que l'obtention des informations sur le mécanisme de déformation plastique.

La méthode de mesurage de l'énergie accumulée – semblable au DTA[1-8] – comporte le chauffage de l'échantillon à mesurer à une certaine vitesse constante et l'enregistrement de la différence de température ΔT entre les deux épreuves. Cette différence de température est déterminée par l'élimination de l'énergie de l'échantillon écrouissé par des mécanismes de réarrangement et d'annihilation des défauts de réseau.

---

[1] J. L. White et K. Koyama, *Rev. Sci. Instrum.*, **34**, 1104 (1963).

[2] P. D. Garn, « Thermoanalytical Methods of Investigation », Academic Press, New-York, 1965.

[3] L. L. Chin et N. J. Grant, *Powder Metallurgy*, **10**, 344 (1967).

[4] D. I. Marchidan et C. Telea, *Rev. Roumaine Chim.*, **13**, 1291 (1968).

[5] F. H. Cocks, *Trans. ASM*, **62**, 802 (1969).

[6] H. Toshya et M. Shigern, *Trans. Jap. Inst. Met.*, **11**, 200 (1970).

[7] H. Luethyh, C. Isler et P. Tissot, *Helv. Chim. Acta*, **54**, 2194 (1971).

[8] F. H. Cocks, « Second International Conference Strenth Metalls Alloys », 1970, p. 2, 631.

PARTIE EXPÉRIMENTALE

MATÉRIAUX ÉTUDIÉS

Les mesurages d'énergie accumulée ont été réalisés sur des laitons monophasiques α élaborés dans une atmosphère d'argon. On situe les laitons binaires à environ 30% Zn et les laitons alliés contiennent en outre des proportions variables de Ti, Mn, Fe et Ni, de manière à ce que leur structure ne soit pas modifiée. Les opérations préliminaires pour l'obtention des échantillons-forgeage, recuit d'homogénéisation, laminage à froid, recuit de recristallisation- ont assuré la même grosseur initiale des grains pour tous les matériaux analysés (60 μm). La déformation finale à froid a été réalisée par laminage en sens unique avec un spectre large de taux de réduction entre 10 et 93%.

APPAREILLAGE UTILISÉ

L'appareillage utilisé consiste en un calorimètre différentiel proprement dit, un système de programmation de la température et un système d'enregistrement de la courbe différentielle en fonction de température ($\Delta T - T$).

En vue d'optimiser l'uniformité de la température, le bloc calorimétrique a été construit en aluminium avec deux cavités symétriquement disposés par rapport à l'axe, dans lesquelles on a introduit des creusets en aluminium avec des quantités approximativement égales de matériel à analyser et de matériel étalon (fig. 1).

Comme matériel étalon on a choisi toujours un laiton monophasique recuit afin qu'il ne présente pas de modifications structurelles pendant l'intervalle de température mesurée (20—500°). Pour un meilleur contact des épreuves avec les thermocouples, les creusets s'appuisent directement sur la soudure chaude située au centre de la base du creuset spécialement façonnée. En vue de l'accroissement de la sensibilité et de l'amplification de la valeur de la différence de température enregistrée, le montage différentiel des thermocouples a compris une inscription de 4 par 4 thermocouples chromel-copel disposés symétriquement sous chaque creuset (fig. 1, détail A).

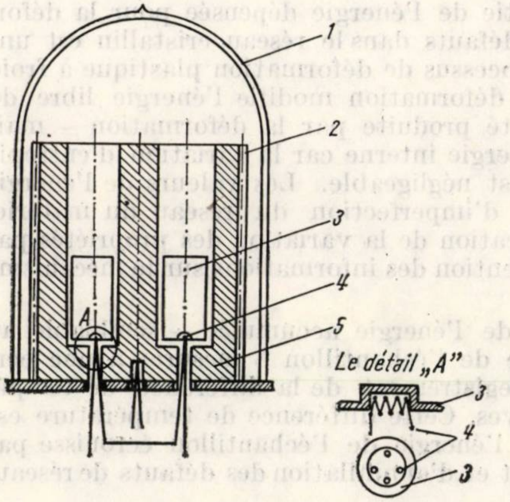

Fig. 1. — Schéma de la cellule calorimétrique.

1, récipient Dewar; *2*, résistances de chauffage; *3*, creusets en aluminium; *4*, thermocouples; *5* corps du calorimètre.

Conformément aux recommandations de la littérature, [3,9–11] la vitesse uniforme de chauffage adoptée a été de 2,7°/mn et elle a été réalisée à l'aide d'un autotransformateur pour

---

[9] D. Michell, *Phil. Mag.*, **1**, 584 (1956).

[10] L. M. Clarebrough, M. E. Hargreaves et M. H. Loretto, *Proc. Roy. Soc.*, **A 260**, 500 (1961).

lequel on a établi au préalable un régime de variation de la tension. Pour tracer la courbe différentielle $\Delta T = f(T)$ on a utilisé un enregistreur $X-Y$ type « Luxytrace » pourvu de deux galvanomètres sensibles antichocs et antivibrations. Une attention toute particulière, à la détermination du régime de chauffage, fut accordée à l'obtention d'une ligne de base aussi lisse que possible.

On a démontré théoriquement et expérimentalement que la sensibilité d'un tel calorimètre différentiel varie inversement à la troisième puissance de la température absolue.[12] Etant donné que le domaine de travail a été compris entre 20 et 500°, pour l'étalonnage du calorimètre on a utilisé la chaleur dégagée par la transformation de phase du KNO_3 à 127° et la chaleur latente de fusion du plomb à 327°. Les quantités de substance utilisées à l'étalonnage ont été choisies de manière que les effets thermiques donnés soient comparables aux quantités d'énergie accumulée. On a effectué un nombre suffisant de déterminations pour établir la sensibilité de l'appareil, de sorte que l'erreur de déterminations soit $\leqslant 8\%$, erreur située à la limite inférieure des valeurs citées dans la littérature.[13–17] L'évaluation des surfaces sous les courbes expérimentales mesurées avec un planimetre Coradi à une erreur de 2% a été effectuée de manière différenciée pour les deux intervalles de température pendant lesquels ont été établies les sensibilités.

RÉSULTATS ET DISCUSSIONS

L'aspect des courbes de dégagement de l'énergie accumulée par les laitons binaires et alliés déformés plastiquement et chauffés dans l'intervalle 20–500° met en évidence deux zones principales d'élimination de l'énergie situées entre 100 et 250° et entre 280 et 430° (fig. 2). La largeur des domaines de dégagement de la chaleur accumulée peut être expliquée par les non-uniformités introduites par le procédé utilisé pour la déformation – le laminage.

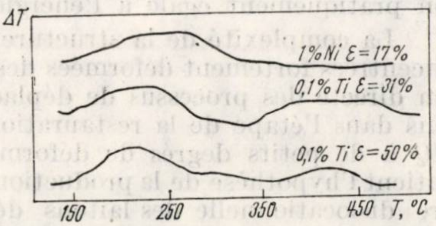

Fig. 2. — Aspect des courbes de dégagement de l'énergie accumulée en laitons plastiquement déformés.

La position et les dimensions des pointes de dégagement de la chaleur accumulée correspondant aux deux processus principaux – la restauration et la recristallisation – peuvent être caractérisés par les valeurs du rapport Q_r/Q (Q_r – la chaleur dégagée la restauration, Q – la chaleur totale dégagée) présentés dans le tableau 1 pour les laitons

---

[11] L. M. Clarebrough, M. E. Hargreaves et M. H. Loretto, *Proc. Roy. Soc.*, **A 257**, 363 (1960).

[12] M. M. Faktor et R. Hanks, *Trans. Faraday Soc.*, **63**, 1122 (1967).

[13] R. L. Segall, P. G. Partridge et P. B. Hirsch, *Phil. Mag.*, **6**, 1493 (1961).

[14] L. M. Clarebrough, M. H. Loretto et M. E. Hargreaves, « Vozvrat i recristalizatia metallov », Metallurghia, Moscou, 1966, p. 69.

[15] A. Wolfender et A. S. Appleton, *Rev. Sci. Instrum.*, **38**, 826 (1967).

[16] H. Wollenberger, *Phys. Stat. Sol.*, **2**, 511 (1970).

[17] A. L. Titchener et M. B. Bever, « Progress in Metall Physics », vol. 7, Pergamon Press, p. 247.

binaires et alliés en fonction du taux de réduction. A certaines exceptions près on peut remarquer que les plus grandes valeurs du rapport Q_r/Q se situent au niveau des petits taux de déformation. L'alliage avec le titane modifie assez peu les valeurs du rapport Q_r/Q comparées aux laitons binaires mais l'alliage avec le nickel et le manganèse produit une augmentation considérable de la valeur du rapport. Ainsi dans les laitons alliés avec 4% Ni déformés 17% presque toute l'énergie accumulée est éliminée pendant la restauration ($Q_r/Q = 0{,}97$) et pour le laiton avec 1% Mn le rapport Q_r/Q arrive à égalité avec l'unité.

L'interprétation du mécanisme d'élimination de l'énergie durant la restauration est très complexe parce qu'on doit tenir compte tant des défauts introduits par la déformation que des interactions multiples qui interviennent dans les solutions solides concentrées.

Bien que jusqu'à présent les recherches au microscope électronique n'aient pas réussi à mettre en évidence les changements intervenus dans la distribution ou dans la densité des dislocations au moment de la restauration des matériaux déformés, pourtant, d'après la quantité d'énergie dégagée pendant cette étape, on peut supposer que les groupes de dislocations à grande énergie subissent des processus de déplacement et d'annihilation. Les seules observations sur l'élimination des boucles de dislocation durant la restauration ont été effectuées par Segall et d'autres [13] dans le cuivre pur soumis à un petit nombre de cycles de fatigue. Dans ce cas simple du cuivre pur peu déformé les calculs effectués ont prouvé que l'énergie consommée pour l'annihilation des boucles correspond à l'énergie dégagée par chauffage au cours de l'étape de restauration pratiquement égale à l'énergie totale dégagée.

La complexité de la structure dislocationnelle des solutions solides concentrées fortement déformées des laitons étudiés a empêché l'observation directe des processus de déplacement et d'annihilation des dislocations dans l'étape de la restauration, mais la grande valeur du rapport Q_r/Q à de petits degrés de déformation expérimentalement remarquée soutient l'hypothèse de la production de tels phénomènes. Le type de structure dislocationnelle des laitons déformés — des agglomérations planes de dislocations, conditionnées par l'énergie diminuée des défauts d'empilement — suppose la possibilité du dégagement d'énergie à la restauration et par la reconstruction et le relâchement des petites groupes d'agglomérations planes de dislocations. Ainsi les valeurs plus élevées de l'énergie totale dégagée et du rapport Q_r/Q dans les laitons alliés avec le nickel et le manganèse sont mises en corrélation d'une manière satisfaisante avec les valeurs diminuées de l'énergie des défauts d'empilement de ces laitons par rapport aux laitons binaires.[18] Ces valeurs attestent la stabilisation des groupements plans de dislocations à grandes énergies dans les laitons alliés avec le nickel et le manganèse grâce aux interactions puissantes dislocations — atomes dissous. Cette stabilisation de la configuration de dislocation conduit à l'alourdissement du mouvement des dislocations pour la formation des germes de recristallisation et pour l'aggrandissement des grains, fait qui explique la hausse des températures de recristallisation des laitons alliés et les plus grandes

---

[18] I. Groza, *Metalurgia*, 1975 (à paraître).

Tableau 1

L'énergie totale dégagée, l'énergie dégagée au cours de la restauration et de la recristallisations des laitons binaires et alliées déformées

Matériel	Elément d'alliage %	Taux de réduction %	Chaleur accumulée, 10^3 J/Kg			$\frac{Q_r}{Q}$
			Totale Q	à la restauration, Q_r	à la recristallisation	
Laiton binaire	—	33	5,4132	3,8996	1,5136	0,72
		53	5,8830	1,6190	4,2639	0,27
		68	5,2131	3,5448	1,6683	0,67
		80	5,8353	2,8454	2,9898	0,48
		87	7,5445	5,5603	2,0142	0,73
		92	6,7933	3,7237	3,0695	0,54
Laiton allié avec du nickel	1	19	5,1390	3,8067	1,3323	0,74
		48	7,3400	5,2783	2,0616	0,72
		79	7,5158	5,2304	2,2854	0,70
		93	7,7620	5,1897	2,5523	0,67
	2	40	7,8493	5,3113	2,5379	0,67
		80	8,0392	4,6593	3,3799	0,58
		87	5,9273	3,1270	2,8003	0,53
		93	7,3021	3,5793	3,7728	0,48
	4	17	3,0295	2,9679	0,0616	0,97
		49	4,6065	3,2169	1,3887	0,70
		63	8,1312	3,7912	4,3400	0,46
		87	10,4172	8,6745	1,7427	0,83
		93	12,2816	9,5560	2,7256	0,79
	8	16*	4,8581	2,8337	2,0244	0,58
		35	5,8916	5,4172	0,4743	0,91
		53	6,3109	3,9170	2,3839	0,62
		80	6,9551	5,4776	1,4775	0,78
		86	7,4422	5,4268	2,0154	0,72
		93	6,5647	4,1109	2,4338	0,62
Laiton allié avec du manganèse	1	31	6,1605	6,1605	—	1,00
		66	9,2439	5,3123	3,9315	0,57
		93	8,2495	4,0022	4,2473	0,48
	4	18	3,7595	1,5088	2,2506	0,40
		45	6,4448	4,2374	2,2074	0,66
		64	7,5508	2,7677	4,7831	0,37
Laiton allié avec du titane	0,01	11	4,2541	1,6793	2,5747	0,39
		34	8,9689	5,3274	3,6414	0,59
		80	13,0324	12,4375	0,5948	0,95
		87	8,6235	2,6085	6,0149	0,30
		91	16,7609	12,0537	4,7071	0,71
	0,1	31	9,5782	4,4102	5,1680	0,46
		50	4,4805	2,6130	1,8675	0,58
		66	10,8221	5,2983	5,5238	0,49
		84	15,2332	6,0051	9,2281	0,40

*) On constate une absorption d'énergie à ~ 170° de 0,112.10^3 J/Kg.

quantités d'énergie dégagée au chauffage. Ce sont les suppléments de titane qui ont l'influence la plus prononcée sur les valeurs d'énergie accumulée par déformation, mais, dans ce cas-là, il faut prendre en considération aussi la contribution des particules de composés de titane observés dans la microstructure (fig. 3).

A la détermination de la valeur de l'énergie accumulée par les laitons déformés, on peut apprécier que le rôle de la configuration des dislocations est plus important que la densité de celles-ci soutenue par certains chercheurs.[19] On a calculé de la sorte le rapport entre les énergies dégagées dans les laitons alliés et les laitons binaires à l'aide de la formule donnée par Pedchenko et Karassev[20] qui tient compte de la distribution des dislocations dans les boucles Frank et dans les tetraèdres des défauts d'empilement :

$$E = \frac{1}{(c+A)\beta^2}\left\{e^{-\beta\rho}\left[a\beta\rho^2 + (\beta\rho+1)\left(1\text{n}\,\rho + \frac{2A}{\beta} + c\right) + 1\right] - E_1(\beta, \rho)\right\}$$

où A est un coefficient dépendent des dimensions du tetraèdre (L), $c = 1\text{n}(4L/b) + B$, $b = a/\sqrt{2}$, (a — le paramètre du réseau), ρ — la densité des dislocations, β, B — des constantes. On observe que le rapport des énergies calculées de cette manière coïncide, de manière satisfaisante, avec la valeur de ce rapport déterminée expérimentalement (tableau 2) confirmant le rôle de la configuration des défauts dans la détermination de la quantité d'énergie accumulée par la déformation.

Tableau 2

Les rapports $Q_{\text{alliées}}/Q_{\text{binaire}}$ calculés et expérimentales des laitons alliées

Matériel	Taux de déformation %	Le rapport $Q_{\text{alliés}}/Q_{\text{binaire}}$	
		calculé	expérimentale
Laiton allié avec 8% Ni	34	1,06	1,06
Laiton allié avec 1% Mn	34	1,04	1,14
Laiton allié avec 8% Ni	80	1,11	1,19
Laiton allié avec 1% Ni	80	1,02	1,29
Laiton allié avec 8% Ni	87	0,96	0,98

L'ordre à petites distances présent dans les laitons binaires et alliés constitue un autre phénomène dont l'incidence ne saurait être négligée dans l'évaluation de l'énergie accumulée par déformation. Mais les calculs de Clarebrough[21] ont prouvé qu'après des traitements thermiques prolongés de recuit, l'énergie dépensée pour détruire l'ordre représente seulement 14% de l'énergie théoriquement nécessaire pour l'installation d'un ordre à petites distances et donc les traitements mêmes de recuit ne mènent

---

[19] D. L. Holt, *Acta Met.*, **13**, 39 (1965).

[20] K. S. Pedcenko, et V. S. Karassev, *Phys. Stat. Sol.* (*a*), **2**, 263 (1970).

[21] L. M. Clarebrough, M. E. Hargreaves et M. H. Loretto, *Proc. Roy. Soc.*, **A 257**, 338 (1960).

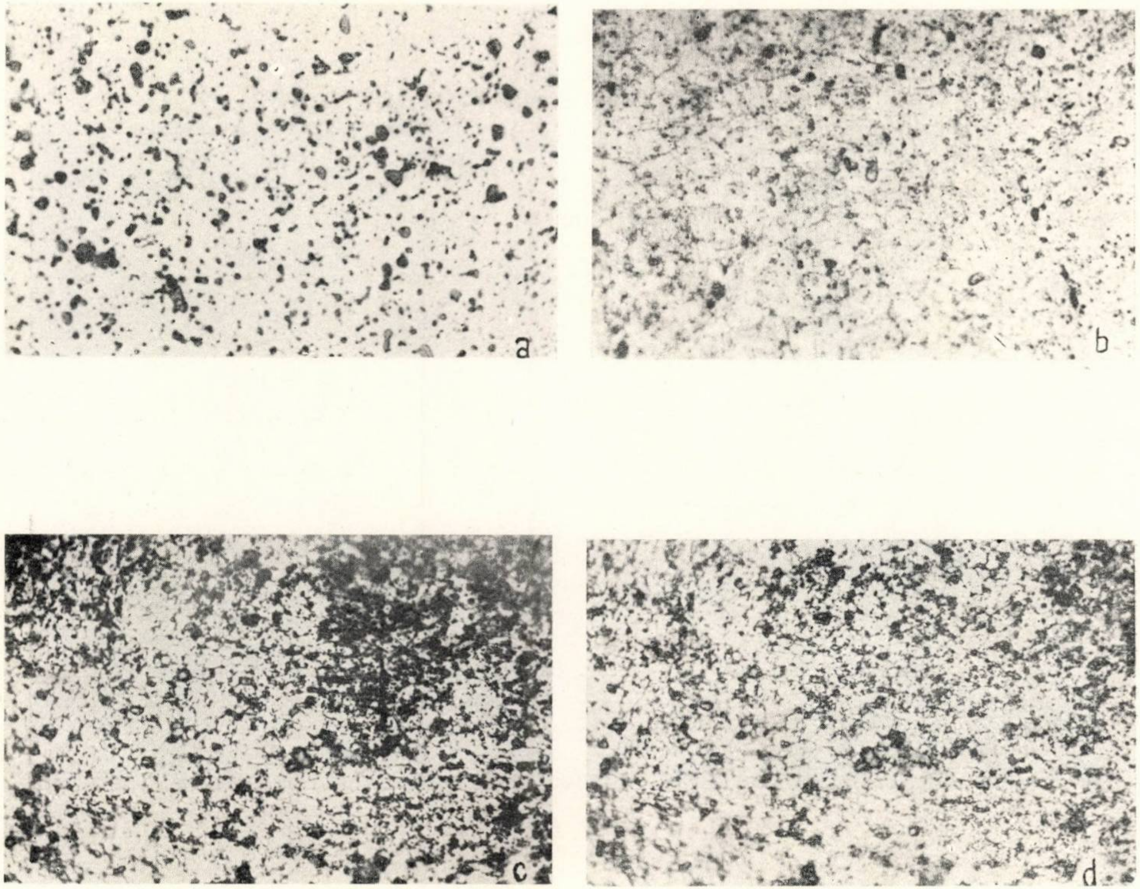

Fig. 3. — Microstructures du laiton allié avec 0,1% Ti. Attaque : tiosulfate de sodium ;
a, non déformé ; *b*, déformé 20% ; *c*, déformé 31% ; *d*, déformé 66% ; 400: 1.

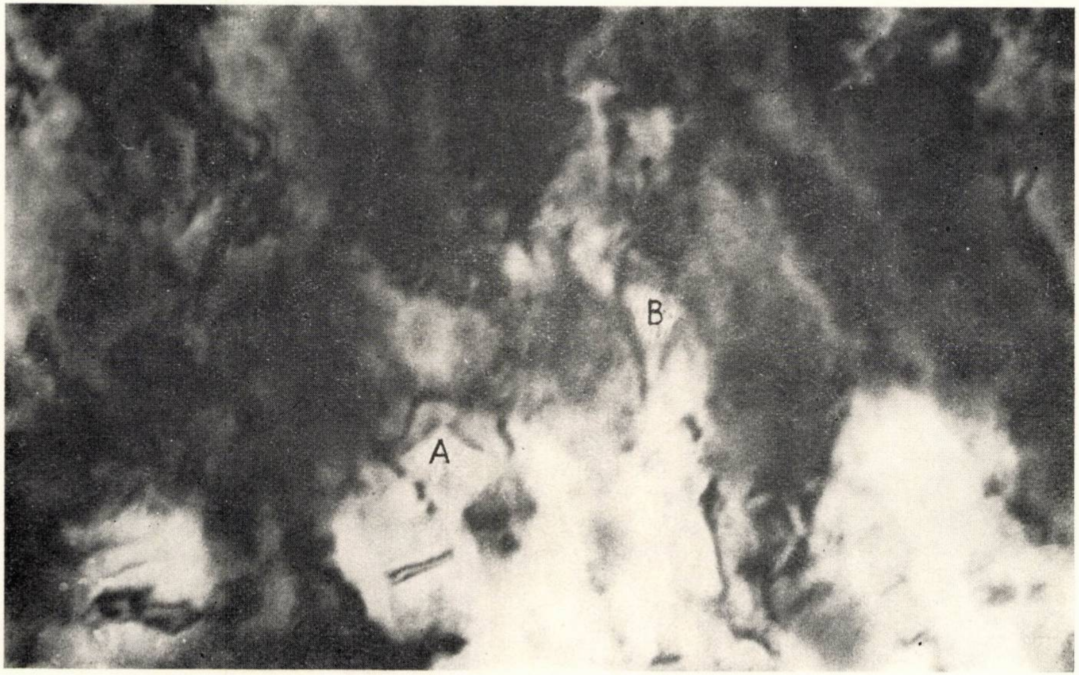

Fig. 4. — La micrographie électronique du laiton binaire déformé 20%. 35 000 :1.

qu'à l'installation d'une fraction de l'arrangement possible. En ce cas-là il faut envisager la redistribution des atomes de zinc dans les atmosphères de dislocation — les atmosphères Suzuki-mises en évidence dans les laitons étudiés par les observations qualitatives à l'aide du microscope électronique (les zones A – fig. 4).

CONCLUSIONS

En conclusion, nous soulignons le rôle des déterminations d'énergie accumulée par la déformation, en vue d'établir le mécanisme de dislocation de déformation dans les laitons binaires et alliés par la mise en évidence de l'importance de la configuration de dislocation dans les matériaux déformés et des processus de déplacement, redistribution et annihilation de dislocations pendant l'étape de restauration.

Revue Roumaine de Chimie, **21**, *4*, 509–515 (1976)

Revue Roumaine de Chimie, **21**, *4*, 517–529 (1976)

APPLICATION DU MODÈLE DU PORE PARTIELLEMENT REMPLI DANS LE PROCESSUS D'ADSORPTION ÉLECTROCHIMIQUE SUR LES ÉLECTRODES HALOGÈNE-CHARBON ACTIF DANS LES SELS FONDUS

S. PETRESCU*, S. STERNBERG*, I. GALASIU ** et VALERIA PETRESCU**
* Institut Polytechnique, 1, str. Polizu, Bucarest
** Centre de Chimie physique, 31, str. Galatzi, Bucarest

Reçu le 14 janvier 1975

On calcule les dimensions caractéristiques au modèle du pore partiellement rempli (courant de diffusion, longueur du pore et épaisseur de la couche de diffusion) pour les électrodes halogène-charbon actif dans les sels fondus. On fait une étude comparative pour les électrodes formées et non formées.

Dans l'étude expérimentale [1,2] de l'adsorption électrochimique sur l'électrode halogène-charbon actif dans les sels fondus on a constaté l'existence d'un potentiel rémanent (à la suite d'un processus de polarisation cathodique). L'existence de ce potentiel rémanent nous a suggéré la présence d'une polarisation de concentration dans les pores du charbon actif durant la décharge, phénomène mis en évidence à l'aide des courbes de relaxation présentées pour le cas du chlore dans un travail antérieur[3]. Dans le travail mentionné on est arrivé à la conclusion que le modèle du pore partiellement rempli explique le mieux tant du point de vue qualitatif que quantitatif le phénomène de la polarisation de concentration (comparativement au modèle du film mince et de la diffusion dans la couche adsorbée). En traitant avec ce modèle les données fournies par les courbes de relaxation on a obtenu des informations sur le mécanisme de déroulement du processus de polarisation cathodique pour le chlore, tout en réussissant à estimer l'ordre de dimension de la longueur du pore et de l'épaisseur de la couche de diffusion dans l'électrolyte présente dans les pores. En même temps on a mis en évidence un phénomène de déplacement de l'électrolyte vers l'intérieur des pores, à la place du chlore qui diffuse par l'électrolyte pendant la polarisation cathodique.

Dans le présent travail on se propose d'analyser les objectifs suivants :

a) Si le modèle du pore partiellement rempli s'applique aussi dans le cas des électrodes brome-charbon et iode-charbon actif et com-

---

[1] S. Sternberg et I. Galasiu, *Rev. Roumaine Chim.*, **15**, 1169 (1970).
[2] S. Sternberg et V. Petrescu, *Rev. Roumaine Chim.*, **19**, 25 (1974).
[3] S. Petrescu, S. Sternberg et V. Petrescu, *Rev. Roumaine Chim.*, **18**, 1715 (1973)

ment se comportent ces électrodes envers l'électrode chlore-charbon actif du point de vue de la polarisation de concentration qui existe dans les pores.

b) Le comportement de l'électrode halogène (chlore, brome, iode) charbon actif durant la formation. Formation qui consiste dans le traitement de l'électrode par des polarisations anodiques et cathodiques successives qui assurent la pénétration de l'électrolyte dans les pores, opération qu'on effectue jusqu'à la garantie de la reproductibilité de la quantité d'halogène adsorbée.

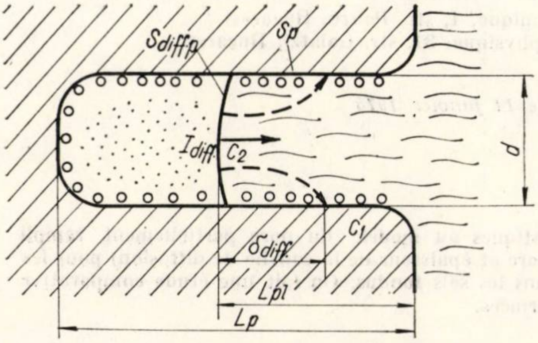

Fig. 1. — Section d'un pore de charbon actif partiellement rempli d'électrolyte.

Dans la figure 1 on présente la section d'un pore de charbon actif rempli partiellement d'électrolyte. Conformément au modèle du pore partiellement rempli durant le processus de polarisation cathodique, la concentration du chlore de la surface mouillée du pore diminue à cause de la réaction électrochimique du chlore qui quitte la surface active passant dans l'électrolyte à l'état d'ion. A la suite de cette réduction de concentration il apparaît dans la couche du liquide un gradient de concentration qui détermine une diffusion du chlore dans la couche de diffusion de l'épaisseur $\delta_{\text{diff.}}$ (épaisseur moyenne de diffusion). En appliquant la loi I de Fick à ce modèle on est arrivé à l'expression [3] suivante pour le produit $\delta_{\text{diff.}} L_p$ (L_p — longueur du pore)

$$\delta_{\text{diff.}} L_p = \frac{\mathrm{NFD}}{8} \cdot \frac{dS\Delta C_{\max}}{I_{\text{diff. moyen}}} \qquad (1)$$

où

n, F = ont les significations connues

D = coefficient de diffusion de l'halogène dans l'électrolyte

d = diamètre du pore

S = surface totale active du charbon (mouillée et non mouillée)

$\Delta C_{\max}$ = différence maximale de concentration de l'halogène dans la couche de diffusion

$I_{\text{diffusion moyen}}$ = flux moyen de diffusion qui apparaît à cause de la présence du gradient de concentration dans l'électrolyte. On le calcule à l'aide des courbes de relaxation et de la courbe $\varphi - Q$ avec la relation

$$I_{\text{diffusion moyene}} = \frac{\Delta Q_{\text{relaxation}}}{2t_{\text{relaxation}}} \tag{2}$$

$\Delta\, Q_{\text{relaxation}}$ = représente la variation de la quantité de chlore adsorbée correspondant à la variation du potentiel $\Delta\, \varphi_{\text{relaxation}}$ durant la relaxation

$$\Delta\, \varphi_{\text{relaxation}} = \varphi_{\text{relaxation}} - \varphi_1$$

où

φ_1 = le potentiel au commencement de la courbe de relaxation

$\varphi_{\text{relaxation}}$ = le potentiel atteint durant le temsp $t_{\text{relaxation}}$

Pour $\Delta C_{\text{maximal}}$ on a trouvé l'expression

$$\Delta C_{\text{maximal}} = K(Q_0 - t_a \cdot I_{\text{diffusion moyen}} - Q_1) \tag{3}$$

où

t_a = temps de la polarisation cathodique qui précède la courbe de relaxation

Q_0 = quantité d'halogène qui se trouve sur l'électrode au moment où commence la polarisation cathodique

Q_1 = quantité d'halogène sur l'électrode au moment où finit la polarisation cathodique et commence la relaxation (on la prend de la courbe $\varphi - Q$)

$$K = \frac{C_{\text{rev}}}{Q_{\text{rev}}} \tag{4}$$

où

C_{rev} = concentration de l'halogène en électrolyte à la pression d'une atmosphère correspondant au potentiel réversible φ_{rev}

Q_{rev} = quantité d'halogène adsorbée, correspondant au potentiel réversible (on la prend de la courbe $\varphi - Q$)

a) APPLICATION DU MODÈLE DU PORE PARTIELLEMENT REMPLI AUX ÉLECTRODES FORMÉES BROME-CHARBON ACTIF ET IODE-CHARBON ACTIF

On a effectué pour le brome et l'iode (tout comme pour le chlore) une polarisation cathodique à plusieurs échelons, dans les eutectiques fondus KBr + AgBr et respectivement KI + AgI, en attendant le temps de relaxation, on a obtenu les courbes de relaxation présentées dans les figures 2 et 3.

Tant pour le brome que pour l'iode, l'hypothèse de la diffusion du brome, et respectivement de l'iode dans l'électrolyte pénétré dans les pores du charbon actif est confirmée du point de vue qualitatif par l'allure des courbes de relaxation obtenues.

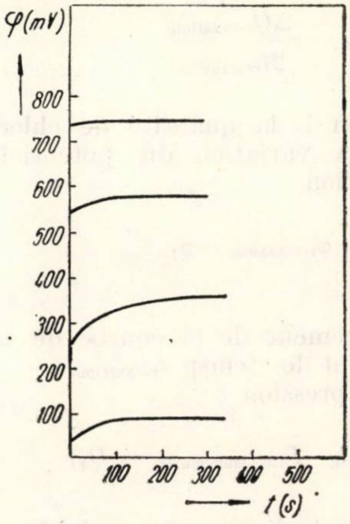

Fig. 2. — Courbes de relaxation pour l'électrode brome-charbon actif formée.

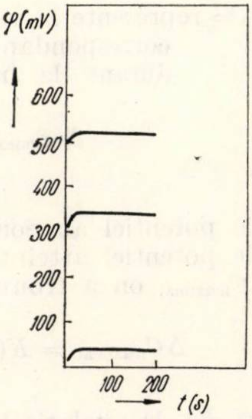

Fig. 3. — Courbes de relaxation pour l'électrode iode-charbon actif formée.

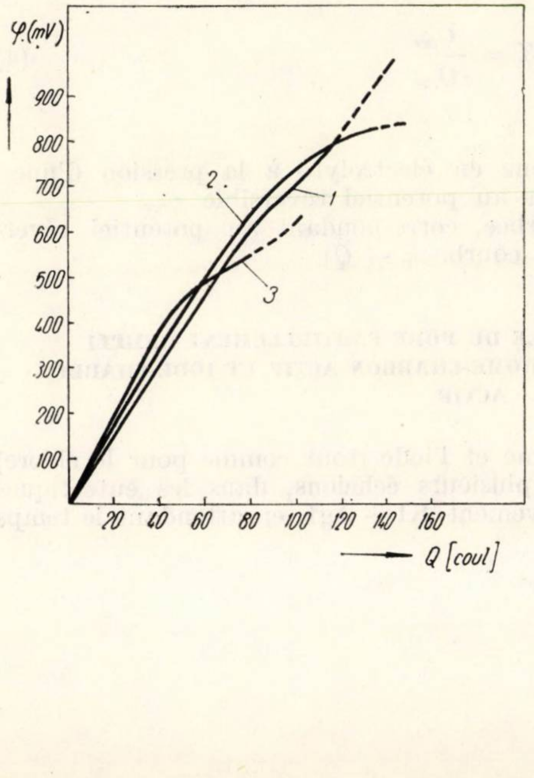

Fig. 4. — Courbes $\varphi - Q$ pour les électrodes chlore-charbon actif (1), brome-charbon actif (2) et iode-charbon actif (3).

Les courbes de polarisation cathodique qui ont précédé les courbes de relaxation ont eu la même durée (5 minutes) à un courant $I_d = 0{,}1$ A. La température a été la même, 400°.

Avec les valeurs des φ_1 et φ_{relax} on a déterminé des courbes $\varphi - Q$ (figure 4) les valeurs du Q_1 (les quantités de brome et respectivement d'iode qui se trouvent sur l'électrode au potentiel respectif) notées dans les tableaux 1 et 2. Des courbes de relaxation (figures 2 et 3) on a estimé le temps de relaxation, t_{relax}. Avec la relation (2) on a calculé les valeurs de $I_{\text{diffusion moyenne}}$, notées aussi dans les tableaux 1 et 2.

Tableau 1

Application du modèle du pore partiellement rempli sur l'électrode brome-charbon actif, formée et non formée

N° courbe de relaxation	φ [mV]	Q_φ [coul]	$\Delta Q_{\text{relaxation}}$ [coul]	$t_{\text{relaxation}}$ [sec]	$I_{\text{diff.moyenne}}$ [A]
L'électrode brome-charbon actif formée					
0	825	129	—	—	—
1	$\varphi_{\text{relax}} = 745$ $\varphi_1 = 735$	100 98	2	40	0,025
2	$\varphi_{\text{relax}} = 580$ $\varphi_1 = 545$	71 66	5	92	0,0272
3	$\varphi_{\text{relax}} = 355$ $\varphi_1 = 255$	43 30	13	200	0,0325 *
4	$\varphi_{\text{relax}} = 85$ $\varphi_1 = 40$	11 5	6	100	0,03
L'électrode brom-charbon actif en formation					
0	745	100			
1	$\varphi_{\text{relax}} = 700$ $\varphi_1 = 682$	90 86	4	40	0,05
3	$\varphi_{\text{relax}} = 673$ $\varphi_1 = 574$	85 70	15	30	0,25
5	$\varphi_{\text{relax}} = 645$ $\varphi_1 = 465$	80 56	24	60	0,2
7	$\varphi_{\text{relax}} = 609$ $\varphi_1 = 294$	75 35	40	150	0,133
9	$\varphi_{\text{relax}} = 536$ $\varphi_1 = 140$	65 18	47	290	0,081

De la relation (3) on a calculé le rapport $\Delta C_{\max}/K$ pour les courbes de relaxation. Les valeurs obtenues sont données dans les tableaux 3 et 4.

Tableau 2

Application du modèle du pore partiellement rempli sur l'électrode iode-charbon actif formée et en formation

Nº courbe de relaxation	φ [mV]	Q_φ [coul]	ΔQ_{relax} [coul]	t_{relax} [s]	$I_{\text{diff.moyenne}}$ [A]
	l'électrode formée				
0	585	88	—	—	—
1	$\varphi_{\text{relax}} = 518$ $\varphi_1 = 495$	70 64	6	30	0,1
2	$\varphi_{\text{relax}} = 342$ $\varphi_1 = 311$	35 32	3	20	0,07
3	$\varphi_{\text{relax}} = 40$ $\varphi_1 = 10$	6 2	4	40	0,05
	l'électrode en formation				
0	565	83			
1	$\varphi_{\text{relax}} = 493$ $\varphi_1 = 461$	62 54	8	20	0,2
2	$\varphi_{\text{relax}} = 350$ $\varphi_1 = 295$	36 29	7	50	0,07
3	$\varphi_{\text{relax}} = 75$ $\varphi_1 = 45$	9 6	3	30	0,05

Tableau 3

Le calcul du produit $\delta_{\text{diff.}}\,L_p$ pour l'électrode brome-charbon actif formée et en formation

Nº courbe de relaxation	$\frac{\Delta C_{\max}}{K}$ [coul]	$\Delta C_{\max}$	$\delta_{\text{diff.}}\,L_p$ [cm²]
	l'électrode brome-charbon actif formée		
1	23,50	$1{,}575 \cdot 10^{-6}$	$1{,}520 \cdot 10^{-4}$
2	25,84	$1{,}730 \cdot 10^{-6}$	$1{,}536 \cdot 10^{-4}$
3	31,25	$2{,}090 \cdot 10^{-6}$	$1{,}550 \cdot 10^{-4}$
4	29,00	$1{,}940 \cdot 10^{-6}$	$1{,}560 \cdot 10^{-4}$
	l'électrode brome-charbon actif en formation		
1	11	$7{,}36 \cdot 10^{-7}$	$3{,}55 \cdot 10^{-5}$
3	14,5	$9{,}7 \cdot 10^{-7}$	$0{,}935 \cdot 10^{-5}$
5	15	$10 \cdot 10^{-7}$	$1{,}205 \cdot 10^{-5}$
7	35,02	$23{,}5 \cdot 10^{-7}$	$4{,}25 \cdot 10^{-5}$
9	45,14	$30{,}2 \cdot 10^{-7}$	$9 \cdot 10^{-5}$

Tableau 4

Le calcul du produit $\delta_{diff.} L_p$ pour l'électrode iode-charbon actif formée et en formation

N° courbe de relaxation	$\frac{\Delta C_{max}}{K}$ [coul]	ΔC_{max}	$\delta_{diff} L_p$ [cm²]
	l'électrode formée		
1	3	$3 \cdot 10^{-7}$	$0{,}723 \cdot 10^{-5}$
2	16	$16 \cdot 10^{-7}$	$5{,}12 \cdot 10^{-5}$
3	18	$18 \cdot 10^{-7}$	$8{,}65 \cdot 10^{-5}$
	l'électrode en formation		
1	8	$8 \cdot 10^{-7}$	$0{,}964 \cdot 10^{-5}$
2	12	$12 \cdot 10^{-7}$	$4{,}14 \cdot 10^{-5}$
3	15	$15 \cdot 10^{-7}$	$7{,}7 \cdot 10^{-5}$

Avec la relation (1) on a aussi calculé le produit $\delta_{diff} \cdot L_p$ pour les courbes de relaxation, les valeurs obtenues sont notées dans les tableaux 3 et 4.

Dans le calcul nous avons employé les valeurs suivantes prises de la littérature[4-6] : $S = 10^5$ cm²; $C_{rev} = 10^{-5}$ moles/cm²; $D = 10^{-5}$ cm²/s ; d $= 10^{-4}$ cm.

Pour la longueur du pore[3], à l'hypothèse que $\delta_{diff} = L_p/4$ il résulte :

$$L_p = 2\sqrt{\delta_{diff} \cdot L_p} \tag{5}$$

alors

$$\delta_{diff} = \frac{(\delta_{diff} \cdot L_p)_1}{L_{p_1}} \tag{6}$$

Les valeurs de $\delta_{diffusion}$ pour les courbes de relaxation du brome, et respectivement de l'iode sont déterminées et on obtient une valeur constante[3] pour L_p (par exemple la valeur du L_p pour la première courbe de relaxation).

On constate du tableau 5 que $I_{diffusion\ moyenne}$, L_p et δ_{diff} ont des valeurs du même ordre de dimension pour l'électrode halogène-charbon actif formée, ce qui constitue une confirmation du modèle du pore partiellement rempli.

Dans le cas du brome on ne constate qu'une augmentation petite de δ_{diff} (pour le chlore cette augmentation était plus prononcée) ce qui correspond à un déplacement réduit de l'électrolyte vers l'intérieur des pores. C'est ce qui explique pourquoi le potentiel rémanent et la correc-

---

[4] S. Sternberg et I. Galasiu, *Rev. Roumaine Chim.*, **17** 1697 (1972).

[5] G. Mamantov, « Molten Salts », ed. Marcel Dekker, New York, 1969, p. 5—15.

[6] D. A. J. Swinkels, *J. Electrochem Soc.*, **113**, 16 (1966).

Tableau 5

Valeurs comparatives L_p, δ_{diff}, α au cas des électrodes halogène (chlore, brome, iode)-charbon actif, formées et non formées

N° de la courbe de relaxation	$I_{\text{diff.moyenne}}$	L_p	$\delta_{\text{diff.}}$	α	N° de la courbe de relaxation	$I_{\text{diff.moyenne}}$	L_p	$\delta_{\text{diff.}}$	α
				l'électrode chlore-charbon actif					
		formée					*non formée*		
1	0,028	$1{,}41\cdot10^{-2}$	$0{,}353\cdot10^{-2}$	1	1	0,0458	$0{,}672\cdot10^{-2}$	$0{,}168\cdot10^{-2}$	1
2	0,0267	$1{,}54\cdot10^{-2}$	$0{,}422\cdot10^{-2}$	1,196	2	0,0516	$0{,}84\cdot10^{-2}$	$0{,}263\cdot10^{-2}$	1,56
3	0,0214	$1{,}79\cdot10^{-2}$	$0{,}57\cdot10^{-2}$	1,615	3	0,0345	$1{,}06\cdot10^{-2}$	$0{,}42\cdot10^{-2}$	2,5
4	0,0327	$0{,}95\cdot10^{-2}$	$0{,}666\cdot10^{-2}$	1,885					
				l'électrode brome-charbon actif					
		formée					*non formée*		
1	0,025	$2{,}468\cdot10^{-2}$	$0{,}616\cdot10^{-2}$	1	3	0,05	$0{,}612\cdot10^{-2}$	$0{,}0492\cdot10^{-2}$	1
2	0,0272	$2{,}48\cdot10^{-2}$	$0{,}621\cdot10^{-2}$	1,006	5	0,25	$0{,}696\cdot10^{-2}$	$0{,}0633\cdot10^{-2}$	1,285
3	0,0325	$2{,}492\cdot10^{-2}$	$0{,}628\cdot10^{-2}$	1,02	7	0,133	$1{,}304\cdot10^{-2}$	$0{,}224\cdot10^{-2}$	4,55
4	0,03	$2{,}5\cdot10^{-2}$	$0{,}632\cdot10^{-2}$	1,025	9	0,081	$1{,}9\cdot10^{-2}$	$0{,}473\cdot10^{-2}$	9,67
				l'électrode iode-charbon actif					
		formée					*non formée*		
1	0,1	$5{,}4\cdot10^{-3}$	$0{,}134\cdot10^{-2}$	1	1	0,2	$6{,}22\cdot10^{-3}$	$1{,}555\cdot10^{-2}$	1
2	0,07	$14{,}3\cdot10^{-3}$	$0{,}358\cdot10^{-2}$	2,67	2	0,07	$12{,}8\cdot10^{-3}$	$0{,}323\cdot10^{-2}$	2,08
3	0,05	$18{,}6\cdot10^{-3}$	$0{,}465\cdot10^{-2}$	3,47	3	0,05	$17{,}6\cdot10^{-3}$	$0{,}437\cdot10^{-2}$	2,82

tion de rémanence sont plus réduits pour le brome que pour le chlore. En d'autres termes, à l'électrode brome-charbon actif, la pénétration de l'électrolyte dans les pores est plus profonde, et « le sac » de gaz est moins riche en brome , fait qui est mis aussi en évidence par les valeurs plus grandes du δ_{diff} l'ordre de dimension restant le même.

Des informations relatives sur le degré de pénétration de l'électrolyte dans les pores durant la polarisation cathodique nous offrent le coefficient de déplacement α défini par le rapport [3] :

$$\alpha = \frac{\delta_{\mathrm{diff}_i}}{\delta_{\mathrm{diff}_1}} \tag{7}$$

où
$i = 2, 3, 4 =$ nombre de la courbe de relaxation.

On constate (le tableau 5) que pour le brome ce coefficient de déplacement a des valeurs bien rapprochées de l'unité (entre 1 et 1,025), tandis que pour le chlore elles varient de 1 à 1,885. Le comportement de l'électrode iode-charbon actif sera discuté ci-dessous.

b) APPLICATION DU MODÈLE DU PORE PARTIELLEMENT REMPLI SUR LES ÉLECTRODES CHLORE, BROME-CHARBON ACTIF EN FORMATION

Vu que le modèle présenté offre des informations sur le déplacement de l'électrolyte dans les pores, par l'intermédiaire du coefficient de déplacement α on pourrait l'employer aussi pour obtenir des informations similaires durant la formation de l'électrode.

La constatation expérimentale de la croissance de la quantité d'halogène adsorbé durant la formation [4] rend évidente l'hypothèse de la pénétration graduelle (après chaque polarisation anodique et cathodique) de l'électrolyte dans les pores du charbon durant la formation. On considère comme déjà formé l'électrode halogène-charbon actif quand la quantité d'halogène adsorbé se reproduit aux courbes successives de polarisation anodique et cathodique.

Il était normal que l'application du modèle sur une électrode en formation conduise à des valeurs plus petites du δ_{diff} par rapport à celles d'une électrode formée ce qui mettrait en évidence le phénomène de déplacement de l'électrolyte dans les pores durant la formation.

Du point de vue du modèle, on considère l'électrode formée quand le processus de mouillage de la surface active du charbon avec de l'électrolyte atteint une limite. La présence des courbes de relaxation à l'électrode formée relève le fait que quoique le liquide ait atteint la limite de pénétration dans les pores du charbon des « sacs » de gaz restent encore dont la grandeur dépend de la nature de l'halogène et de la tension superficielle de l'électrolyte. Comme nous l'avons déjà montré [4], il est possible que la tension superficielle de l'électrolyte influence le degré de sa pénétration dans les pores. C'est ainsi qu'on attend que le sac de gaz de chlore soit plus grand que celui de brome et donc le phénomène de rémanence soit plus prononcé pour le chlore.

On a enregistré les courbes de relaxation pour le chlore dans l'eutectique AgCl + KCl et pour le brome dans l'eutectique AgBr + KBr sur

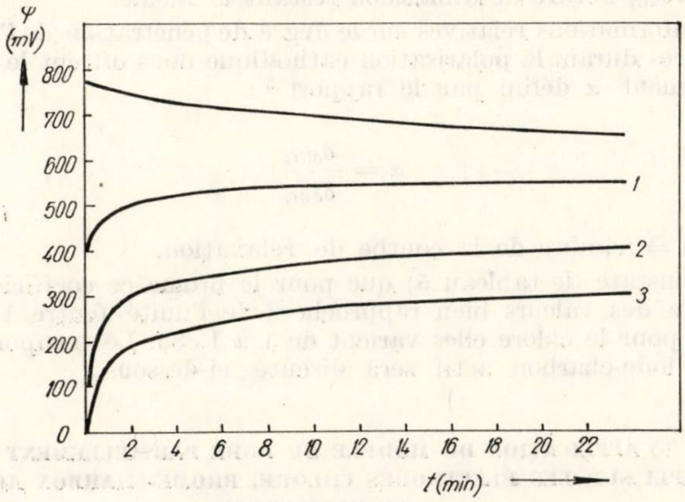

Fig. 5. — Courbes de relaxation pour l'électrode chlore-charbon actif non formée.

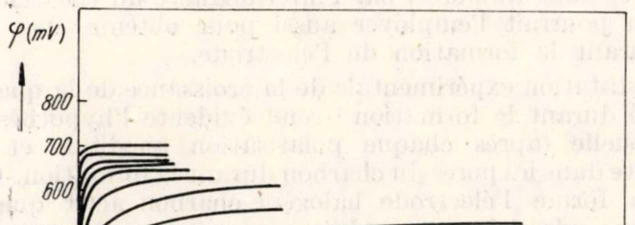

Fig. 6. — Courbes de relaxation pour l'électrode brome-charbon actif non formée.

une électrode en formation, à $t = 400°$ de la même manière que celle présentée antérieurement pour l'électrode formée. On voit les résultats dans les figures 5 et 6. A cause du fait que la formation de l'électrode brome-charbon actif se fait plus rapidement que celle de l'électrode chlore-charbon actif, la durée des courbes de polarisation cathodique qui ont précédé les courbes de relaxation, au cas du brome, a été prise 1 minute par rapport aux 5 minutes au cas du chlore. L'intensité du courant à la charge et à la décharge a été la même : 0,1 A. La courbe $\varphi - Q$ pour le chlore est donnée dans la figure 4. On a calculé les grandeurs caractéristiques au modèle ($I_{\text{diffusion moyenne}}$, L_p, $\delta_{\text{diffusion}}$, α) et les valeurs résultées ont été notées dans le tableau 5.

On peut obtenir des informations sur le déplacement de l'électrolyte dans les pores de la valeur du coefficient de déplacement α, lequel, tant pour le chlore que pour le brome, aux électrodes en formation est plus grand qu'aux électrodes formées. C'est ainsi qu'à l'électrode chlore-charbon actif en formation α varie de 1 à 2,5 et pour la même électrode formée, α varie de 1 au 1,885, ce qui indique un déplacement plus grand de l'électrolyte dans les pores durant la formation. Même après la formation de l'électrode α reste supraunitaire ce qui s'explique par la présence du sac de gaz dans les pores. Au cas du brome les valeurs de l'α pour l'électrode en formation sont nettement supérieures à celles de l'électrode formée (9,67 par rapport à 1,025). On constate une grande mobilité de l'électrolyte à cause de sa tension superficielle plus réduite ce qui mène à un « remplissement » plus rapide et plus complet des pores par rapport à celui du chlore, et ayant pour conséquence à la fin de la formation des sacs de gaz plus petits que ceux du chlore. C'est pourquoi, le phénomène de rémanence au brome est plus diminué, les courbes de relaxation sont plus aplaties, le déplacement de l'électrolyte durant la polarisation cathodique pour l'électrode formée étant de beaucoup plus réduit.

Quant aux valeurs de L_p et $\delta_{\text{diffusion}}$ aux électrodes en formation, elles ont le même ordre de grandeur pour les deux cas, mais plus petites que celles de l'électrode formée, ce qui confirme l'idée que durant la formation une pénétration de plus en plus profonde de l'électrolyte a lieu dans les pores.

c) COMPORTEMENT DE L'ÉLECTRODE D'IODE-CHARBON ACTIF

L'électrode d'iode-charbon actif se comporte un peu différemment des deux autres électrodes (chlore, brome-charbon actif).

En comparant les grandeurs caractéristiques du modèle du pore rempli partiellement présentées dans le tableau 5, on constate les traits caractéristiques suivants dans le comportement de l'électrode d'iode-charbon actif :

Le courant de diffusion I_{diff} est relativement grand, tant pour l'électrode en formation que pour l'électrode formée. Dans la première courbe de relaxation la valeur du courant de diffusion dépasse 0,1 A, c'est-à-dire elle dépasse la valeur de l'intensité du courant avec lequel on a effectué la polarisation cathodique antérieure à la relaxation.

Dans le modèle [3] on a fait l'hypothèse que le courant de diffusion I_{diff} est engendré par le gradient de concentration qui apparaît dans les pores durant la polarisation cathodique d'intensité I_d. Par conséquent, la cause qui détermine l'apparition du courant de diffusion est à la fin le courant de décharge I_d qui précède la relaxation. Il est normal que I_{diff} soit plus réduit, au moins égal à I_d. Il résulte que l'hypothèse de la distribution linéaire de la concentration de l'iode dans le pore, hypothèse qui est à la base du calcul de I_{diff} fait par la relation (2), est peu probable pour la première courbe de relaxation. L'allure des courbes de relaxation suggère l'idée que dans le cas de l'iode la distribution de la concentration dans les pores du charbon actif doit avoir la forme représentée dans la figure 7, car de telles distributions conduisent à des temps de relaxation réduits (pour l'iode et non pour le chlore et le brome). C'est pourquoi dans le calcul $\Delta C_{\max}/K$ (tableau 4) pour la première courbe de relaxation on a considéré $I_{\text{diff}} < 0{,}1$ A et précisement égal à I_{diff} de la deuxième courbe de relaxation (on a considéré qu'à mesure que I_{diff} diminue, il s'approche de plus en plus des valeurs réelles).

Si l'on admet aussi que pour l'iode la valeur de α donne une orientation sur le déplacement de l'électrolyte dans les pores durant la polarisation cathodique, on arrive à la conclusion que ce déplacement est très prononcé au début du processus (α augmente de 1 à 3,47) après quoi il devient plus réduit (tableau 5). Cela s'explique par une condensation capillaire dans un «sachet de liquide». Ce qui est aussi en concordance avec les valeurs relativement grandes de I_{diff} (tableau 2). L'allure de la courbe $\varphi - Q$ (figure 4) pour l'électrode d'iode-charbon actif présente aux grands potentiels une tendance d'aplatissement. Cela constitue un argument de plus à la faveur de l'hypothèse énoncée plus haut. Une discussion plus en détail sur cette hypothèse a été faite dans un travail antérieur.[7] Comparant les valeurs de $\delta_{\text{diffusion}}$ (tableau 5) pour l'électrode d'iode-charbon actif formée et non formée on observe qu'aux courbes de relaxation 2 et 3 elles sont plus grandes à l'électrode formée, ce qui constitue une indication sur la pénétration plus profonde de l'élec-

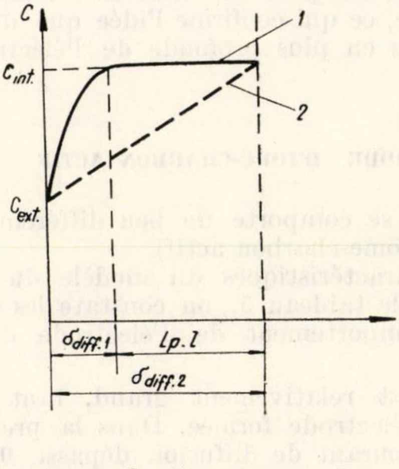

Fig. 7. — Hypothèse sur la distribution de concentration de l'iode dans les pores(1) comparativement à la distribution linéaire plausible pour le chlore et le brome (2). $\delta_{\text{diff.}1}$ — épaisseur de la couche de diffusion à l'hypothèse de la distribution non linéaire. $\delta_{\text{diff.}2}$ – épaisseur de la couche de diffusion à l'hypothèse de la distribution linéaire. $L_{p,1}$ — longueur « du sachet d'iode condensé ».

---

[7] S. Sternberg et I. Galasiu, *Rev. Roumaine Chim.*, **19**, 967 (1974).

trolyte dans le pore de l'électrode formée (situation analogue à celle du chlore et du brome).

Dans la première courbe de relaxation, la situation est inverse, ce qui s'explique par l'existence d'un sachet d'iode liquide plus grand dans le cas de l'électrode formée (qui déplace l'électrolyte vers l'extérieur du pore, tout en diminuant δ_{diff}). La petite valeur de δ_{diff_1} à l'égard de celle de $\delta_{\mathrm{diff}_{2,3}}$ mène, en conséquence, a de plus grandes valeurs de α pour l'électrode formée par rapport à celle non formée. Cela signifie, d'ailleurs, un déplacement prononcé de l'électrolyte durant le processus de décharge, tout en occupant la place restée libre à la suite de la diffusion de l'iode du sachet de liquide. L'intensité du courant de diffusion I_{diff} étant relativement grande dans ces conditions, au bout du processus de polarisation cathodique le sachet de liquide qui est pratiquement vidé fait que le potentiel rémanent soit négligéable.

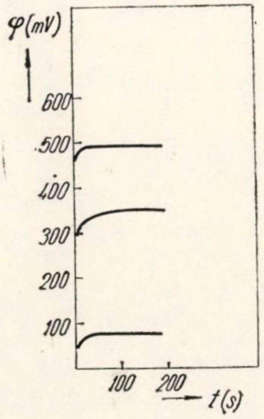

Fig. 8. — Courbes de relaxation pour l'électrode iode — charbon actif non formée.

Ainsi que nous l'avons montré [4], à la différence des électrodes chlore, brome-charbon actif, la formation de l'électrode d'iode est extrêmement rapide, ce que l'on constate tout en comparant les courbes de relaxation pour l'électrode d'iode formée et pour celui employée la première fois (figures 3 et 8). On constate des allures parfaitement analogues. De plus, les données résultées du traitement du modèle du pore partiellement rempli pour l'électrode d'iode confirme très bien cette idée par les valeurs très rapprochées des L_p, δ_{diff} et celles de α (tableau 5) pour les deux électrodes (formée et non formée).

Par les informations fournies sur la longueur du pore, l'épaisseur de la couche de diffusion et sur le déplacement de l'électrolyte dans les pores, tant pour l'électrode en formation que pour celle formée, le modèle du pore partiellement rempli constitue un instrument de calcul utile dans l'étude du processus d'adsorption électrochimique sur l'électrode halogène-charbon actif.

Revue Roumaine de Chimie, 21, 4, 517–529 (1976

Revue Roumaine de Chimie, **21**, *4*, 531–543 (1976)

L'ÉTUDE DE LA RÉDUCTION DE L'OXYGÈNE SUR LES ÉLECTRODES POREUSES EN ARGENT. IV

L'EFFET DE LA VARIATION DES PARAMÈTRES DE FONCTIONNEMENT SUR LA POLARISATION DES ÉLECTRODES À DE DIFFÉRENTES DENSITÉS DE COURANT

I. SOLACOLU, MARIA MAVRODIN-TĂRĂBÎC et IOANA ONACA
Centre de Chimie Physique, Bucarest, 31, str. Galați

Reçu le 5 juin 1974

En vue d'établir le régime optimal de fonctionnement des électrodes à gaz en argent dans la réaction de réduction de l'oxygène en milieu de KOH, on a testé, par l'analyse dispersionnelle, la signification de l'influence de la température et de la concentration de l'électrolyte, ainsi que de la surpression de l'alimentation avec du gaz, en utilisant les données expérimentales obtenues, par la technique potentiostatique, dans un travail antérieur, pour de différentes valeurs de la densité apparente de courant (10, 30, 50, 70 et 90 mA cm^2). On a constaté que l'effet de la variation de la surpression de l'oxygène, entre les limites de 400–500 mm Hg, n'est pas significatif, tandis que l'effet de la variation de la concentration (4N–7N) et de la température de l'électrolyte (45–65°), de même que l'effet de leur interaction, sur la polarisation des électrodes, est significatif. Par l'analyse de l'intervalle de confiance de l'effet d'interaction concentration-température et, par un calcul d'optimisation du processus, on a établi les paramètres optimaux de fonctionnement des électrodes étudiées.

En vue d'établir les conditions optimales de fonctionnement (surtensions minimales) des électrodes à gaz en argent, caractérisées par une structure bidispersée du type DSK (« Doppel Skelet Katalyst ») — cathodes pour les piles à combustible, dans des travaux antérieurs [1,2] nous avons étudié l'effet de la température (dans le domaine 15–65°) et de la concentration de l'électrolyte (2N–9N), de même que de la surpression d'alimentation avec du gaz (200–600 mm Hg), sur la polarisation des électrodes, à de différentes valeurs de la densité apparente de courant (10–100 mA/cm^2). L'étude expérimentale et les valeurs des énergies apparentes d'activation calculées ont démontré qu'il existe entre les paramètres de fonctionnement, les performances et le système poreux des électrodes, une interdépendance étroite et nous ont permis d'établir le domaine intéressant pour le fonctionnement des électrodes de ce type : 400–500 mm Hg, 4N–7N et 45–65°.

Etant donné le caractère complexe de l'interdépendance qui existe entre les paramètres de fonctionnement et l'effet de ces paramètres

---

[1] I. Onaca, M. Mavrodin-Tărăbîc et I. Solacolu, *Rev. Roumaine Chim.* **20**, 209 (1975).
[2] M. Mavrodin-Tărăbîc, I. Onaca et I. Solacolu, *Rev. Roumaine Chim.* **20**, 915 (1975).

sur la polarisation des électrodes à gaz en argent, nos études antérieures nous ont uniquement permis, par l'interprétation des courbes $\eta = f(\Delta P)$, $\eta = f(c)$ et $\eta = f(t)$, de déterminer un domaine de fonctionnement et non pas d'établir exactement les valeurs optimales des paramètres. Ces résultats sont en concordance avec les résultats obtenus dans le cas des autres types d'électrodes à gaz. [3-6]

Pour déterminer les valeurs optimales des paramètres de fonctionnemment, à de différentes densités de courant, nous avons appelé à l'analyse dispersionnelle des données expérimentales obtenues par la technique potentiostatique. Cette méthode moderne d'interprétation statistique nous a permis de séparer et de tester les effets produits par la variation des paramètres, ainsi que d'éliminer du champ d'observation les paramètres dont la variation n'est pas significative. Une fois identifiés, les effets ont été testés en comparant les dispersions produites par les facteurs variables avec la dispersion produite par les facteurs aléatoires qui influencent le processus étudié. De même, l'établissement du caractère non significatif de l'effet de la variation d'un de ces paramètres considérés (dans le cas étudié, la surpression d'alimentation avec de l'oxygène) nous a permis de séparer l'effet de la variation des deux paramètres (la température et la concentration de l'électrolyte), dont l'effet est significatif, de l'effet des facteurs aléatoires.

Nous avons choisi un modèle mathématique à trois facteurs (la surpression d'alimentation avec du gaz, la concentration et la température de l'électrolyte) et deux, trois et, respectivement, quatre ou trois niveaux. L'analyse dispersionnelle a été effectuée pour cinq densités apparentes de courant (10, 30, 50, 70 et 90 mA/cm^2), caractéristiques pour l'entier domaine de fonctionnement des électrodes de ce type dans les piles à combustible.

L'analyse de l'intervalle de confiance dans lequel s'inscrit l'effet de l'interaction des deux paramètres significatifs (la concentration et la température de l'électrolyte) nous a permis d'établir les prémisses pour le calcul d'optimisation du processus par des expériences factorielles.

1. PARTIE EXPÉRIMENTALE

La réalisation et la caractérisation structurale des électrodes à gaz en argent du type DSK ont été présentées dans un travail antérieur. [2] L'étude de l'effet des paramètres de fonctionnement (la concentration et la température de l'électrolyte, la surpression d'alimentation avec de l'oxygène) sur les caractéristiques de polarisation des électrodes à gaz a été effectuée par la technique potentiostatique, en appliquant des niveaux de potentiel de 10 mV, à l'intervalle d'une minute. La concentration de l'électrolyte (KOH) a été variée entre 4N et 7N (niveaux de concentration de 1 m équiv. cm^{-3}) et la température entre 45 et 65° (niveaux de température de 5°). Pour maintenir la température constante ($\pm 0{,}1°$), on a utilisé un ultrathermostat de type U—10. La surpression d'alimentation avec de l'oxygène (400 et 500 mm Hg) a été maintenue constante ($\pm$ 2 mm Hg) à l'aide d'une installation présentée dans un travail antérieur. [7]

---

[3] M. Marinescu, S. Dobos et I. Minea, *Studii şi Cercetări Energetică Electrotehnică*, **19**, 427 (1969).

[4] D. B. Lucesoli, Thèse, Univ. Paris, 1971, p. 71.

[5] J. Lindholm, *J. Electrochem. Soc.*, **116**, 1150 (1969).

[6] J. Mrha et J. Jindra, *Coll. Czech. Chem. Comm.*, **34**, 2465 (1969).

[7] O. Radovici, M. Mavrodin-Tărăbîc, I. Onaca et I. Solacolu, *Rev. Roumaine Chim.*, **18**, 767 (1973).

2. RÉSULTATS ET DISCUSSIONS

2.1. L'ANALYSE DISPERSIONNELLE DE L'EFFET DE LA VARIATION DES PARAMÈTRES DE FONCTIONNEMENT

Des courbes de polarisation η-i, caractéristiques pour la réaction de réduction de l'oxygène sur les électrodes à gaz en argent du type DSK, tracées par la technique potentiostatique dans de différentes conditions de concentration, de température et de surpression d'alimentation avec de l'oxygène, on a extrait les valeurs de la surtension caractéristiques pour les densités apparentes de courant de 10, 30, 50, 70 et de 90 mA/cm² (tableau 1). Pour l'analyse dispersionnelle des données expérimentales on a utilisé un modèle mathématique à trois facteurs (A, B, C) et plusieurs niveaux : deux niveaux pour le facteur A, trois pour le facteur B et trois ou quatre pour le facteur C. (A = la surpression d'alimentation avec du gaz, B = la concentration et C = la température de l'électrolyte.) Les valeurs des paramètres (les niveaux) ont été établies, en conformité avec les études antérieures, [1,2] afin qu'elles soient caractéristiques pour chaque densité apparente de courant.

Tableau 1

Les valeurs de la surtension (mV), caractéristiques pour la réduction de l'oxygène sur les électrodes à gaz en argent, à de différentes températures, concentrations de l'électrolyte (KOH), surpressions d'alimentation avec du gaz et densités de courant

		400 mm Hg				500 mm Hg			
		4N	5N	6N	7N	4N	5N	6N	7N
10 mA/cm²	45°	59	53	63		69	52	63	
	50°	55	45	57		51	45	56	
	55°	53	47	50		50	44	52	
	60°	47	43	46		43	43	44	
30 mA/cm²	50°		90	97	90		89	94	90
	55°		87	88	96		85	89	92
	60°		83	81	97		82	80	98
	65°		87	78	99		86	79	99
50 mA/cm²	50°		130	133	125		127	129	123
	55°		123	118	126		120	119	120
	60°		118	109	124		113	108	126
	65°		117	107	123		116	108	122
70 mA/cm²	50°		162	171	157		161	167	154
	55°		155	149	151		153	149	145
	60°		150	137	151		143	136	151
	65°		146	132	145		144	132	143
90 mA/cm²	55°		186	178	177		182	178	168
	60°		180	164	177		172	163	174
	65°		174	158	166		171	155	163

Étant donné qu'un modèle à trois facteurs est difficile à résoudre, ce tableau a été décomposé dans des tableaux à deux facteurs[8] (en éliminant un facteur du tableau initial) et pour chaque tableau on a calculé les sommes des carrés pour les effets principaux et pour les effets

Tableau 2

Analyse des dispersions

Densité de courant	Source de dispersion	Somme des carrés	Degrés de liberté	Dispersion	$F_{\text{calc}} = s/s_r$	$F\alpha$	Obs.
10 mA/cm²	S_A	54	1	54	4,61	5,99	
	S_B	62	2	31	2,65	5,14	
	S_C	592	3	197,3	16,86	4,76	*
	S_{AB}	90	2	45	3,85	5,14	
	S_{AC}	56	3	18,7	1,59	4,76	
	S_{BC}	146	6	24,3	2,08	4,28	
	S_r	70	6	11,7			
30 mA/cm²	S_A	4	1	4	2,18	5,99	
	S_B	451	2	225,5	133,22	5,14	*
	S_C	78	3	29,3	16,01	4,76	*
	S_{AB}	0	2	0	—		
	D_{AC}	3	3	1	0,55	5,99	
	S_{BC}	433	6	72,1	39,40	4,28	*
	S_r	11	6	1,83			
50 mA/cm²	S_A	19	1	19	5,43	5,99	
	S_B	211	2	105,5	30,14	5,14	*
	S_C	575	3	191,6	54,74	4,76	*
	S_{AB}	6	2	3	0,86	5,14	
	S_{AC}	8	3	2,7	0,74	4,76	
	S_{BC}	363	6	61	17,43	4,28	*
	S_r	21	6	3,5			
70 mA/cm²	S_A	60	1	60	4,88	5,99	
	S_B	170	2	85	6,91	5,14	*
	S_C	1344	3	448	36,42	4,76	*
	S_{AB}	0	2	0	—		
	S_{AC}	18	3	6	0,49	4,76	
	S_{BC}	378	6	63	5,12	4,28	*
	S_r	74	6	12,3			
90 mA/cm²	S_A	63	1	63	2,11	7,71	
	S_B	400	2	200	6,71	6,94	
	S_C	560	2	280	9,39	6,94	*
	S_{AB}	14	2	7	0,23	6,94	
	S_{AC}	3	2	1,5	0,05	6,94	
	S_{BC}	89	4	22,2	0,74	6,39	
	S_r	119	4	29,8			

* L'effet est significatif.

---

[8] G. E. P. Box et N. R. Draper, « Evolutionary Operation », Wiley, New York, 1969, p. 63.

d'intéraction (S). [9,10] À l'aide de ces sommes et en tenant compte du nombre des degrés de liberté (ν), caractéristique pour chaque facteur, on a calculé les dispersions (s) pour les effets individuels et d'interaction du second ordre. A l'aide des dispersions ainsi calculées, on a effectué le test Fischer-Snedecor (F_{calc}) qui indique, par comparaison avec les valeurs critiques (F_α) qui correspondent à un seuil de signification $\alpha = 0{,}10$, le caractère significatif de l'effet de la variation des paramètres sur la polarisation des électrodes.

De l'examen des données présentées dans le tableau d'analyse dispersionnelle (le tableau 2) il résulte qu'à toutes les valeurs de la densité apparente de courant, les valeurs calculées pour F sont, pour l'effet de la variation du facteur A (la surpression d'alimentation avec de l'oxygène) et des interactions AB et AC, moins grandes que les valeurs trouvées dans le tableau de la distribution $F\alpha$, pour le même nombre de degrés de liberté qui a servi au calcul des dispersions (s). Dans ce cas on accepte l'hypothèse de zéro et on tire la conclusion que la variation (dans le domaine de 400 –500 mm Hg) du paramètre considéré (et ses interactions) n'influence pas, d'une manière significative, les valeurs de la surtension des électrodes à gaz en argent, les écarts étant produits par des facteurs aléatoires.

De l'examen des données obtenues par l'analyse dispersionnelle, il résulte qu'à de différentes valeurs de la densité apparente de courant, sur la polarisation des électrodes à gaz en argent, présente un effet significatif la variation des facteurs suivants :

— à 10 mA/cm², la température de l'électrolyte (C) ;

— à 30 mA/cm², la concentration (B) et la température de l'électrolyte (C), ainsi que leur interaction (BC) ;

— à 50 mA/cm², la concentration (B) et la température de l'électrolyte (C), ainsi que leur interaction (BC) ;

— à 70 mA/cm², la concentration (B) et la température de l'électrolyte (C), ainsi que leur interaction (BC) ;

— à 90 mA/cm², la température de l'électrolyte (C).

La dispersion, relativement petite, produite par les facteurs aléatoires (s_r) indique que, en général, les expériences ont eu lieu dans des conditions satisfaisantes et que l'interaction du troisième ordre (ABC) est non significative.

2.2. LES CONDITIONS OPTIMALES DE FONCTIONNEMENT

En utilisant les résultats obtenus par l'analyse dispersionnelle des données de polarisation concernant l'effet de la variation des paramètres

---

[9] G.E.P. Box, L. R. Connor, W. R. Consins, O. L. Davies, F. R. Himsworth et G. P. Sillitto, « The Design and Analysis of Industrial Experiments », ed. O. L. Davies, Oliver and Boyd, London, 1963, p. 247.

[10] A. Glück, « Metode matematice în industria chimică », Ed. tehnică, Bucarest, 1971, p. 86.

de fonctionnement sur la polarisation des électrodes à gaz en argent du type DSK, dans la réaction de réduction de l'oxygène en milieu de KOH, on a rédigé, pour chaque valeur de la densité apparente de courant, un tableau dont il résulte l'influence de la variation des facteurs significatifs sur la polarisation des électrodes. Vu que les conclusions sur l'effet des paramètres étudiés ne peuvent être tirées que par l'analyse de l'intervalle de confiance dans lequel les différences entre deux données présentées dans les tableaux d'interaction s'inscrivent, on a calculé, pour chaque densité apparente de courant, l'intervalle de confiance caractéristique, à l'aide de la relation

$$\mathrm{d} \pm t_\alpha \sqrt{s_r} \sqrt{\frac{1}{n_1} + \frac{1}{n_2}}$$

dans laquelle t_α représente la valeur critique de la distribution Student, correspondant à un certain seuil de signification ($\alpha = 0{,}10$) et à un certain nombre de degrés de liberté, s_r la valeur de la dispersion résiduelle et $n_1 = n_2$, le nombre d'expériences pour lequel on a calculé la valeur moyenne.

L'effet de la variation de la température et de la concentration de l'électrolyte sur la polarisation des électrodes à gaz en argent, à une densité apparente de courant de 10 mA/cm², est illustré par les données présentées dans le tableau 3. (Les valeurs de la surtension correspondent à $\Delta P_{O_2} = 400$ et 500 mm Hg.)

La valeur calculée pour l'intervalle de confiance est : d ± 6,5.

On constate que l'augmentation de la température de l'électrolyte a comme résultat la diminution de la polarisation des électrodes dans tout l'intervalle considéré (45 – 60°), cette diminution étant significative entre 45 et 50°, pour les concentrations de 4N, 5N et de 6N. L'augmentation de la concentration de l'électrolyte à partir de 4N jusqu'à 5N a un effet favorable sur le processus d'électrode, tandis que le changement

Tableau 3

Valeurs de la surtension de l'électrode à gaz (mV), à de différentes températures et concentrations de l'électrolyte (KOH), pour une densité de courant de 10 mA/cm²

	45°	50°	55°	60°
4N	$\left.\begin{matrix}59\\69\end{matrix}\right\}64$	$\left.\begin{matrix}55\\51\end{matrix}\right\}53$	$\left.\begin{matrix}53\\50\end{matrix}\right\}51{,}5$	$\left.\begin{matrix}47\\43\end{matrix}\right\}45$
5N	$\left.\begin{matrix}53\\52\end{matrix}\right\}52{,}5$	$\left.\begin{matrix}45\\45\end{matrix}\right\}45$	$\left.\begin{matrix}47\\44\end{matrix}\right\}45{,}5$	$\left.\begin{matrix}43\\43\end{matrix}\right\}43$
6N	$\left.\begin{matrix}63\\69\end{matrix}\right\}66$	$\left.\begin{matrix}57\\56\end{matrix}\right\}56{,}5$	$\left.\begin{matrix}50\\52\end{matrix}\right\}51$	$\left.\begin{matrix}46\\44\end{matrix}\right\}45$

de la concentration de 5N à 6N conduit à l'augmentation de la polarisation des électrodes, effet qui est significatif à la température de 50°.

Des données du tableau 3, il résulte que les surtensions minimales correspondent à la concentration de 5N et à la température de 50°. De même, à l'établissement du régime de fonctionnement de la pile à combustible on peut tenir compte aussi de la possibilité 4N — 60°. (On peut choisir entre ces solutions en fonction des résultats obtenus par l'étude du transfert de chaleur, de la résistance à la corrosion, etc.)

L'effet de la variation de la température et de la concentration de l'électrolyte sur la polarisation des électrodes à gaz, à une densité apparente de courant de 30 mA/cm^2, est illustré par les valeurs des surtensions présentées dans le tableau 4.

La valeur calculée pour l'intervalle de confiance est de d ± 2,6.

À la concentration de 5N, la variation de la température de l'électrolyte, de la valeur de 50 à 60°, a un effet favorable sur le processus d'électrode, tandis que le changement de la température à 65° a comme résultat l'augmentation de la polarisation des électrodes à gaz. A la concentration de 6N, l'effet favorable de l'augmentation de la température est significatif seulement jusqu'à 60°, la diminution de la polarisation des électrodes à partir de la valeur de 80,5 mV (60°) jusqu'à 78,5 mV (65°) étant non significative. À la concentration de 7N, l'augmentation de la température a un effet défavorable sur le développement de la réaction de réduction de l'oxygène. L'augmentation de la concentration de l'électrolyte, à partir de la valeur de 6N jusqu'à 7N, a un effet défavorable, significatif à 55° ; à 60°, l'effet de la variation de la concentration de l'électrolyte entre 5N et 6N n'est pas significatif, tandis que la variation de la concentration de la valeur de 6N à 7N produit une augmentation de la polarisation des électrodes. À la température de 65°, on constate des surtensions réduites à la concentration de 6N.

Tableau 4.

Valeurs de la surtension de l'électrode à gaz (mV), à de différentes températures et concentrations de l'électrolyte (KOH), pour une densité de courant de 30 mA/cm^2

<table>
<tr><th></th><th colspan="2">50°</th><th colspan="2">55°</th><th colspan="2">60°</th><th colspan="2">65°</th></tr>
<tr><td rowspan="2">5N</td><td>90</td><td rowspan="2">89,5</td><td>87</td><td rowspan="2">86</td><td>83</td><td rowspan="2">82,5</td><td>87</td><td rowspan="2">86,5</td></tr>
<tr><td>89</td><td>85</td><td>82</td><td>86</td></tr>
<tr><td rowspan="2">6N</td><td>97</td><td rowspan="2">95,5</td><td>88</td><td rowspan="2">88,5</td><td>81</td><td rowspan="2">80,5</td><td>78</td><td rowspan="2">78,5</td></tr>
<tr><td>94</td><td>89</td><td>80</td><td>79</td></tr>
<tr><td rowspan="2">7N</td><td>90</td><td rowspan="2">90</td><td>96</td><td rowspan="2">94</td><td>97</td><td rowspan="2">97,5</td><td>99</td><td rowspan="2">99</td></tr>
<tr><td>90</td><td>92</td><td>98</td><td>99</td></tr>
</table>

Les données de polarisation présentées dans le tableau 4 recommandent, pour une densité apparente de courant de 30 mA/cm^2, l'exploration du domaine dans le voisinage des conditions : la concentration de l'électrolyte, 5N et la température, 60°. Il faut tenir compte aussi de la possibilité 6N — 65°, cette solution présentant l'avantage de la diminution de la surtension de 4 mV, mais à l'établissement du régime optimal il faut tenir compte aussi d'autres facteurs (pertes de chaleur, résistance à la corrosion, etc.).

Tableau 5

Valeurs de la surtension de l'électrode à gaz (mV), à de différentes températures et concentrations de l'électrolyte (KOH), pour une densité de courant de 50 mA/cm²

	50°	55°	60°	65°
5N	$\left.\begin{matrix}130\\127\end{matrix}\right\}128,5$	$\left.\begin{matrix}123\\120\end{matrix}\right\}121,5$	$\left.\begin{matrix}118\\113\end{matrix}\right\}115,5$	$\left.\begin{matrix}117\\116\end{matrix}\right\}116,5$
6N	$\left.\begin{matrix}133\\129\end{matrix}\right\}131$	$\left.\begin{matrix}118\\119\end{matrix}\right\}118,5$	$\left.\begin{matrix}109\\108\end{matrix}\right\}108,5$	$\left.\begin{matrix}107\\108\end{matrix}\right\}107,5$
7N	$\left.\begin{matrix}125\\123\end{matrix}\right\}124$	$\left.\begin{matrix}126\\120\end{matrix}\right\}123$	$\left.\begin{matrix}124\\126\end{matrix}\right\}125$	$\left.\begin{matrix}123\\122\end{matrix}\right\}122,5$

L'effet de la variation de la concentration et de la température de l'électrolyte sur la polarisation des électrodes à gaz en argent, à une densité apparente de courant de 50 mA/cm², est présenté dans le tableau 5.

La valeur calculée pour l'intervalle de confiance est de $d \pm 3{,}6$.

De l'examen des données présentées dans le tableau 5, on constate, qu'à la concentration de 7N, la variation de la température de l'électrolyte, dans le domaine 50 — 65°, n'a pas un effet significatif sur la polarisation des électrodes. A la concentration de 5N et de 6N, l'augmentation de la température de l'électrolyte a une effet favorable sur le processus d'électrode. À la température de 60° et de 65°, l'augmentation de la concentration a un effet favorable, significatif entre 5N et 6N et non significatif entre 6N et 7N.

Les données du tableau 5 recommandent l'exploration du domaine situé dans le voisinage des valeurs : la concentration de l'électrolyte, 6N et la température, 60 — 65°.

L'effet de la variation de la température et de la concentration de l'électrolyte sur la polarisation des électrodes à gaz étudiées, à la densité apparente de courant de 70 mA/cm², est illustré par les données présentées dans le tableau 6.

La valeur calculée pour l'intervalle de confiance est de $d \pm 6{,}8$.

La variation de la température de l'électrolyte, dans le domaine étudié, a un effet favorable sur le processus d'électrode. La variation de la concentration de l'électrolyte n'a pas un effet significatif à la température de 50° et de 55°. À la température de 60 et de 65°, on constate des surtensions réduites à la concentration de 6N. Les données de polarisation, présentées dans le tableau 6, recommandent l'exploration du domaine défini par la concentration de KOH 6N et par la température de 60—65°.

L'effet de la variation de la température et de la concentration de l'électrolyte sur la polarisation des électrodes à gaz en argent, à une densité apparente de courant de 90 mA/cm², est illustré par les données présentées dans le tableau 7.

Tableau 6

Valeurs de la surtension de l'électrode à gaz (mV), à de différentes températures et concentrations de l'électrolyte (KOH), pour une densité de courant de 70 mA/cm²

	50°		55°		60°		65°	
5N	162 161	161,5	155 153	154	150 143	146,5	146 144	145
6N	171 167	169	149 149	149	137 136	136,5	132 132	132
7N	157 154	155,5	151 145	148	151 151	151	145 143	144

Tableau 7

Valeurs de la surtension de l'électrode à gaz (mV), à de différentes températures et concentrations de l'électrolyte (KOH), pour une densité de courant de 90 mA/cm²

	55°		60°		65°	
5N	186 182	184	180 172	176	174 171	172,5
6N	178 178	178	164 163	163,5	158 155	156,5
7N	177 168	172,5	177 174	175,5	166 163	164,5

La valeur calculée pour l'intervalle de confiance est de d ± 11,7.

La variation de la température de l'électrolyte, dans le domaine de 55 — 65°, n'a pas un effet significatif sur le processus d'électrode, à la concentration de 5N et de 7N, tandis qu'à la concentration de 6N l'augmentation de la température a un effet favorable, dans tout le domaine étudié. L'augmentation de la concentration de l'électrolyte, de la valeur de 5N à 6N, a un effet favorable, significatif à la température de 60 et de 65°.

Des données présentées ci-dessus et en analysant l'intervalle de confiance dans lequel s'inscrivent les différences existantes entre deux surtensions se trouvant dans les tableaux d'interaction, il résulte que les domaines qui doivent être explorés en vue de l'optimisation du processus (la détermination des valeurs optimales des paramètres de fonctionnement) sont les suivantes : pour 10 mA/cm^2, 5 N — 50° ; pour 30 mA/cm^2, 5N — 60° ; pour 50 mA/cm^2, 6N — 60–65° ; pour 70 mA/cm^2, 6N — 60 — 65° ; pour 90 mA/cm^2, 6N — 60–65°.

La valeur de la concentration optimale, d'approximativement 6N, (à des densités de courant grandes et moyennes) est en concordance avec les valeurs minimales des énergies apparentes d'activation, caractéristiques pour la réaction de réduction de l'oxygène sur les électrodes étudiées, en milieu de KOH. [1]

Des données présentées ci-dessus il résulte que l'utilisation de la méthode d'analyse dispersionnelle à l'étude de l'effet de la variation des paramètres de fonctionnement (la température et la concentration de l'électrolyte, la surpression d'alimentation avec du gaz) sur la polarisation des électrodes à gaz en argent du type DSK, dans la réaction de réduction de l'oxygène en milieu alcalin, nous a permis d'éliminer les facteurs non significatifs (dans ce cas, la variation de la surpression d'alimentation avec de l'oxygène entre 400 et 500 mm Hg), ainsi que de déterminer, pour de différentes valeurs de la densité apparente de courant, les domaines qui doivent être explorés en vue de l'optimisation du processus. Évidemment, pour la détermination rigoureuse du régime optimal de fonctionnement des électrodes à gaz (surtensions minimales), il est nécessaire d'effectuer une étude mathématique d'optimisation du processus.

Les méthodes modernes d'interprétation des données expérimentales prévoient, [8,9] après la localisation du domaine situé dans le voisinage des conditions qui assurent l'obtention des performances maximales, par une des méthodes connues (dans ce cas, par l'analyse dispersionnelle), l'exploration rigoureuse de ce domaine, en vue de la détermination des paramètres optimaux du processus. La méthode consiste dans la détermination d'une fonction de régression qui décrit, avec une approximation satisfaisante, les relations qui existent entre les variables dans le voisinage des conditions qui correspondent aux performances optimales (à l'aide des résultats obtenus dans un programme d'expériences factorielles) et l'exploration locale de la surface de réponse.

La fonction objectif qui décrit la relation entre les variables indépendantes significatives — la concentration (x_1) et la température de l'électrolyte (x_2) — et la variable dépendante — la surtension des électrodes à gaz, à une certaine valeur de la densité apparente de courant (y), est de type

$$y = b_0 + b_1x_1 + b_2x_2 + b_{12}x_1x_2 + b_{11}x_1^2 + b_{22}x_2^2$$

Le calcul des valeurs des coefficients de la fonction de régression ($b_0 \ldots b_{22}$) a été effectué par la méthode des moindres carrés, en utilisant les résultats d'un programme expérimental qui comprend un système ortogonal de $3^2 = 9$ expériences, symétrique par rapport à un point central, dont les paramètres (concentration-température) ont été établis par l'analyse dispersionnelle. Dans tous les cas, la différence entre les valeurs des paramètres (les distances de déplacement) ont été : pour la concentration, 1m équiv. cm^{-3} et pour la température, 5°.

Pour vérifier la validité de la fonction de régression on a testé l'écart des valeurs observées de la surtension par rapport aux valeurs calculées. Dans ce but, on a utilisé le procédé, connu dans l'analyse dispersionnelle, de calcul de la dispersion due à la régression.

$$s_1^2 = \frac{k \sum_{i=1}^{n} (\bar{y}_i - y'_i)^2}{n - r}$$

(relation dans laquelle n représente le nombre des expériences considérées, r le nombre des constantes dans l'équation de régression, k le nombre des expériences effectuées dans des conditions identiques, y_i les valeurs moyennes des données observées et y'_i les valeurs calculées à l'aide de la fonction de régression) et la dispersion due aux erreurs expérimentales

$$s_r^2 = \frac{\sum_{i=1}^{n} (y_i - \bar{y}_i)^2}{n(k - 1)}$$

(relation dans laquelle y_i représente les valeurs de la surtension déterminées par voie expérimentale). À l'aide de ces dispersions, on a effectué le test Fischer-Snedecor (F) et on a comparé les valeurs de F calculé avec les valeurs critiques (F_α) correspondant à un seuil de signification $\alpha = 0{,}1$ et pour un nombre de degrés de liberté $\nu_1 = n - r$ et $\nu_2 = n\ (k - 1)$.[10] Les résultats obtenus sont présentés dans le tableau 8.

Tableau 8

Les valeurs des coefficients et la validité des fonctions de régression à de différents densités de courant

Densité de courant mA/cm²	Valeurs des constantes de la fonction de regression						S_1^2	S_r^2	F	Fα
	b_0	b_1	b_2	b_{12}	b_{11}	b_{22}				
10	45,334	0,833	−2,075	−0,617	9,333	3,501	58,44	4,91	11,92	27,34
30	81,666	5,917	−0,750	1,125	8,417	1,917	42,20	1,63	25,94	27,34
50	110,221	2,833	−2,750	1,125	9,166	1,917	25,62	2,19	11,70	27,34
70	138,721	−0,417	−5,0	1,250	8,917	0,666	45,66	1,72	26,39	27,34
90	165,770	−3,417	−6,833	0,875	8,417	0,501	57,42	5,72	10,04	27,34

De l'examen des données présentées dans le tableau 8, on constate qu'à toutes les valeurs considérées pour la densité apparente de courant, les valeurs de F sont plus petites que les valeurs critiques $F\alpha$, ce qui nous a permis d'accepter l'hypothèse de zéro et de tirer la conclusion que les fonctions de régression établies décrivent, d'une maniére satisfaisante, les relations qui existent entre les variables dans le domaine situé dans le voisinage des performances maximales.

En vue de déterminer les valeurs des paramètres (concentration-température) pour lesquelles la fonction de régression devient minimale, il faut annuler les dérivés partielles par rapport à x_1 et x_2

$$\frac{\partial y}{\partial x_1} = 0 \text{ et } \frac{\partial y}{\partial x_2} = 0$$

On obtient un système à deux équations dont la solution conduit à la détermination des valeurs optimales de la concentration (x_1) et de la température de l'électrolyte (x_2), valeurs pour lesquelles les électrodes à gaz en argent étudiées présentent des surtensions minimales dans la réaction de réduction de l'oxygène (le tableau 9).

Afin d'expliquer la variation de la valeur optimale des paramètres de fonctionnement (concentration, température), il faut tenir compte de :

— l'effet de cette variation sur la solubilité de l'oxygène et sur la conductibilité de l'électrolyte[11–15];

— la participation différente des polarisations d'activation, de concentration et de résistance ohmique à la polarisation totale de l'électrode, en fonction de la densité de courant.

Tableau 9

Les conditions optimales de fonctionnement des électrodes à gaz en argent étudiées et les valeurs correspondentes des surtensions, à de différentes densités de courant

Densité de courant mA/cm^2	Concentration méquiv. cm^{-3}	Température °C	Surtension mV
10	4,96	51,5	44,7
30	5,62	61,5	77,9
50	5,80	64,1	106,7
70	5,75	78,9	128,8
90	5,68	94,8	147,2

La solubilité de l'oxygène diminue avec l'augmentation de la température et de la concentration de l'électrolyte ; la conductibilité augmente continuellement avec la température et jusqu'à approx. 6N, avec la concentration de l'électrolyte. A de petites densités de courant (10 mA/cm^2) ces effets se compensent,[1] fait qui est aussi illustré par les valeurs optimales de la température (51,5°) et de la concentration (5N KOH). À des densités

---

[11] International Critical Tables, vol. VI, 1929, p. 230.

[12] A. N. Campbell, E.M. Kartzmark, D. Bisset et M. E. Bednas, *Canad. J. Chem.*, **31**, 303 (1953).

[13] J.E. Roughton, *J. Appl. Chem.*, **1**, S141 (1951).

[14] B. B. Owen et F. H. Sweeton, *J. Amer. Chem. Soc.*, **63**, 2811 (1941).

[15] L. G. Austin, «Handbook of Fuel Cell Technology», ed. C. Berger, Prentice-Hall, New York, 1968, p. 48.

de courant élevées, la polarisation ohmique devient, de plus en plus, plus grande, ce qui a comme résultat le déplacement important de la température optimale vers des valeurs plus grandes (tableau 9), tandis que la valeur optimale de la concentration de l'électrolyte reste presque constante dans l'intervalle 5N—5,8N KOH.

Évidemment, à l'établissement de la température de l'électrolyte il faut tenir compte aussi d'une série de facteurs (pertes de chaleur, corrosion, dimensions de l'installation, etc.) qui limitent l'augmentation de la température au-dessus d'une certaine valeur.

3. CONCLUSIONS

1. L'analyse dispersionnelle des données de polarisation (obtenues par la technique potentiostatique), caractéristiques pour la réaction de réduction de l'oxygène sur les électrodes à gaz en argent du type DSK, en milieu de KOH, a mis en évidence l'effet non significatif de la variation de la surpression d'alimentation avec du gaz dans le domaine 400 — 500 mmHg, ainsi que de son interaction du second ordre (surpression-température et surpression-concentration), sur la polarisation des électrodes, dans tout l'intervalle de concentration (4N—7N) et de température (45—65°) considéré.

2. Aux densités apparentes de courant de 10 et 90 mA/cm^2, l'effet de la variation de la température de l'électrolyte sur la polarisation des électrodes à gaz est significatif, tandis qu'aux densités apparentes de courant de 30, de 50 et de 70 mA/cm^2 se sont les effets de la variation de la concentration de l'électrolyte et de l'interaction du second ordre température-concentration qui deviennent aussi significatifs.

3. L'analyse dispersionnelle des données de polarisation nous a permis d'établir (pour chaque valeur de la densité apparente de courant), un domaine de concentration-température, dans lequel les électrodes à gaz en argent étudiées présentent des surtensions minimales dans la réaction de réduction de l'oxygène.

4. Par un calcul mathématique d'optimisation du processus, on a établi (pour chaque densité apparente de courant) les fonctions de régression qui décrivent les relations qui existent entre la surtension de l'électrode à gaz et la concentration et la température de l'électrolyte et, par l'exploration locale de la surface de réponse, on a déterminé les valeurs optimales des paramètres de fonctionnement: 10 mA/cm^2, 4,96N et 51,5°; 30 mA/cm^2, 5,62N et 61,5°; 50 mA/cm^2, 5,80 N et 64,1°; 70 mA/cm^2, 5,75N et 78,9°; 90 mA/cm^2, 5,68N et 94,8° ($\Delta P_{O_2} = 400 - 500$ mm Hg).

Revue Roumaine de Chimie, **21**, *4*, 545–548 (1976)

STUDIES ON THE FORMATION KINETICS OF BARIUM HEXAFERRITE $BaO.6Fe_2O_3$ IN THE BINARY SYSTEM $BaO-Fe_2O_3$

S. SOLACOLU, MARINA BULZAN and E. SEGAL

Center of Physical Chemistry, Bucharest,
Str. Dumbrava Roşie, 23, Romania

Received March 3, 1975

The results of a nonisothermal kinetic study of the solid phase reaction between barium carbonate and ferric oxide ($\alpha - Fe_2O_3$) when barium hexaferrite is formed, are presented.

1. INTRODUCTION

The binary system $BaO-Fe_2O_3$ is well-known, and much research work is dedicated to its study, among which the most recent paper is due to Goto and Takada.[1]

This system belongs to the extensively studied $BaO-Me^{II}O-Fe_2O_3$ type, where $Me^{II}=Zn$, Co, Cu, Ni, Mg, Fe^{2+} or Mn^{2+} which has a great practical importance, because the ternary compounds of this kind are the hexagonal ferrites.[2] The system $BaO-Fe_2O_3$ is interesting due to the practical importance of the barium hexaferrite $BaO.6Fe_2O_3$ as a permanent magnet.[3] The thermal phase diagram reveals the existence of two other compounds, whose formulae are $2BaO.Fe_2O_3$ and $BaO.Fe_2O_3$.[1] They crystallize on the cubic and orthorhombic system respectively; barium hexaferrite crystallizes on the hexagonal system, in the structure of magnetoplumbite type ($PbO.6Fe_2O_3$).[4]

The formation kinetics of this compound has been studied using different methods, and there exist some viewpoints on the possible intermediary compounds.[5–7] This paper presents the results of the nonisothermal kinetic study of the interaction in mixtures of powdered barium carbonate and ferric oxide, that lead to the formation of barium hexaferrite in the solid phase.

---

[1] Y. Goto and T. Takada, *J. Amer. Ceram. Soc.*, **43**, 150 (1960).

[2] I. Gordon, R. I. Harvey and R. A. Braden, *J. Amer. Ceram. Soc.*, **15**, 297 (1962).

[3] J. J. Went, G. W. Rathenau, E. W. Gorter and G. W. van Oosterhant, *Philips Tech. Rev.*, **13**, 194 (1951–52).

[4] V. Adelsköld, *Arkiv. Kemi. Mineral. Geol.*, **12 A**, 1 (1938).

[5] M. Erchak Jr., I. Fankuchen an R. Ward, *J. Amer. Chem. Soc.*, **68**, 2085 (1946).

[6] J. Suchet, *Bull. Soc. franç. Ceram.*, **33**, 33 (1956).

[7] G. C. Bye and C. R. Howard, *J. Appl. Chem. Biotechnol.*, **21**, 319 (1971).

2. EXPERIMENTAL

The reagents used have been $BaCO_3$ (UCB) and Fe_2O_3 (Reanal), analytical grade.

A powdered mixture of the desired stoichiometry was obtained by dry homogenization.

The heating curves were obtained on a derivatograph MOM-Budapest, Paulik-Paulik Erdey type, with variable heating rates up to 1000°.

The barium hexaferrite formation was confirmed by X-ray analysis, using the Debye-Scherrer method, on a TUR M−60 apparatus, with the $Mo_{k\alpha}$ radiation.

3. RESULTS AND DISCUSSION

Progressive heating of barium carbonate (fig. 1) results in the occurrence, at 810°, of a transition from rhombic to hexagonal system, and at 960°, of a transition from hexagonal to cubic system. [8] Continuing the rising of temperature in the range 1000−1175°, the decomposition of barium carbonate occurs. Differential thermal analysis of ferric oxide (fig. 1) reveals the endothermic effect at 675°, due to the magnetic phase transition which is, more exactly, the sum of the two transitions, corresponding to the Curie point and Néel point. [9]

In fig. 2 one can see that, in the case of the mixture we prepared, barium carbonate transition at 800° and also the transition of the ferric oxide at 675° are again found.

As in the temperature range corresponding to the phase transformations the mobility of lattice elements is markedly increased and the evolution of carbon dioxide in the range 670−880° (fig. 2) is shifted towards lower temperatures as in the case of pure barium carbonate, this phenomenon could be regarded as a consequence of the Hedwall effect [10]. Carbon dioxide evolution is accompanied by the formation of barium hexaferrite $BaO.6Fe_2O_3$ during a solid phase reaction.

The kinetic analysis of the reaction was made by working the experimental results with the aid of Freeman-Caroll and Coats-Redfern methods, for heating rates between 2.1−10°/min. The experimentally determined value of the reaction order equals the unity, and one could conclude from here that the limiting step is the evolution of carbon dioxide. Bye and Howard, [7] studying the same system under isothermal conditions, came to a similar conclusion.

The experimentally determined activation energy and pre-exponential factor values are independent of the heating rate, thus indicating that the reaction occurs in the kinetic regime. Table 1 gives the mean values of the activation energy and pre-exponential factor, computed according to the two above mentioned methods.

---

[8] E. K. Keler and A. K. Kuznetsov, *Zhur. priklad. Khim.*, **34**. 2146 (1961).

[9] R.C. Mackenzie, "Differential Thermal Analysis", Academic Press, London, 1970, p. 274.

[10] J. A. Hedvall and L. Leffter, Z. *anorg. Chem.*, **234**, 235 (1937).

From the kinetic viewpoint, the Hedvall effect is pointed out examining the activation energy value, which is smaller than the value of 62 kcal/mole[11] obtained in the case of pure barium carbonate decomposition.

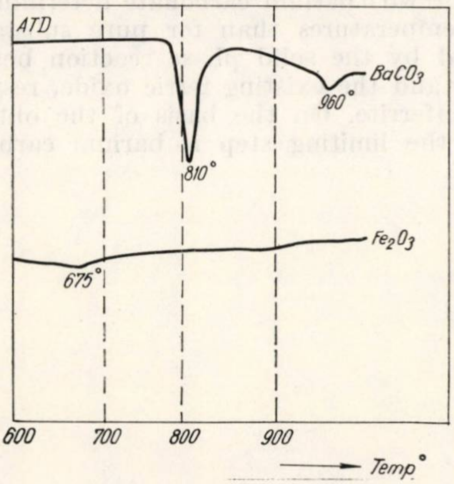

Fig. 1. — Differential thermal analysis; curves of pure $BaCO_3$ and Fe_2O_3.

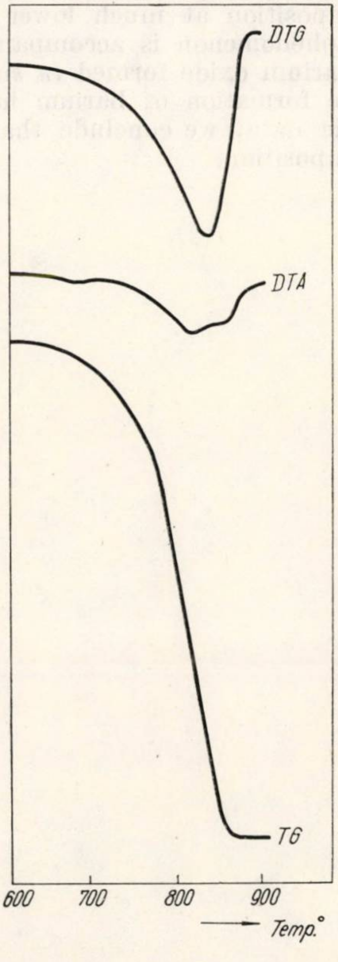

Fig. 2. — Differential thermal analysis and differential thermal gravimetric analysis; curves of the $BaO.6Fe_2O_3$ mixture.

Table 1

Values of the kinetic parameters of the reaction $BaCo_3(s) + 6Fe_2O_3(s) \rightarrow BaO.6Fe_2O_3(s) + CO_2(s)$

Freeman-Caroll method	Coats-Redfern method
$n = 1$ $E_a = 44.5$ kcal/mole $A = 8 \cdot 10^5 \cdot s^{-1}$	$n = 1$ $E_a = 48$ kcal/mole $A = 4.6 \cdot 10^6 \cdot s^{-1}$

---

[11] F. B. Burriel-Marti and M. E. Garcia-Clavel, "Proceedings of the First International Conference on Thermal Analysis", Aberdeen, Scotland, MacMillan & Co. Ltd., London, 1965, p. 110.

Revue Roumaine de Chimie, 21, 4, 545–548 (1976)

4. CONCLUSIONS

The interaction of ferric oxide with barium carbonate determines its decomposition at much lower temperatures than for pure substances. This phenomenon is accompanied by the solid phase reaction between the barium oxide formed *in situ* and the existing ferric oxide, resulting in the formation of barium hexaferrite. On the basis of the obtained kinetic data, we conclude that the limiting step is barium carbonate decomposition.

Revue Roumaine de Chimie, **21**, *4*, 549–562 (1976)

INFLUENCE OF TITANIUM DIOXIDE ON THE STRUCTURE AND ON THE PROPERTIES OF MINERALOGICAL COMPOUNDS IN WHITE PORTLAND CEMENTS

MARIA ENCULESCU
FOREXIM, Calea Victoriei, 111, Bucharest, Romania

Received: February 12, 1975

The paper discusses the influence of titanium dioxide on the formation and stabilization of the principal mineralogical compounds of white Portland cement clinkers. The solubilization limits, the formulas of solid solutions of calcium silicates and their structural modifications by exceeding the solid solution limit are outlined. Likewise, the paper presents the influence exerted by titanium dioxide on mechanical resistances and on the whiteness degree of the principal mineralogical compounds of white Portland cement.

1. CONSIDERATIONS ON THE STRUCTURE OF TRICALCIUM SILICATE

Alit is the highly important principal phase in white and coloured Portland cement clinkers, which has formed the subject of many investigations in our country too. [1–11] As mentioned in earlier papers [1,7–10] the irregular coordination of calcium ions and the adjacent cavities of such ions confer good binding properties on tricalcium silicate.

In alit, Ni^{2+}, Cu^{2+}, Zn^{2+} divalent ions replace divalent Ca^{2+}. On the other hand, these ions are too bulky to substitute silicon in the tetrahedral lattice.

---

[1] M. Enculescu, Doctorial thesis, Polytechnic Institute, Bucharest, 1972.

[2] Kondo Yoshida, "C. A. I. Review on the 17th General Meetings", Jap., May, 1963 p. 31–32.

[3] I. F. Ponomarev, A. N. Gracian and N. V. Rotichi, *Izvest. V.U.Z.V.O. S.S.S.E., Khim. i khim. Tekhnol.*, **11**, 317 (1968).

[4] M. M. Sycheev, V. I. Korneev and N. F. Fedorov, "Izdateli literatura po stroitelnyie", Leningrad, 1965.

[5] I. M. Erşhov, *Zhur priklad. Khim.*, **41**, 1196 (1968).

[6] O. Yanuaquis, I. Yamaquelic and T. Ono, *Bull. Soc. Franc. Mineral. Crist.*, **5**, 271 (1962).

[7] M. Enculescu, *Studii şi Cercetări Chim., Acad. Bucureşti*, **27**, 12 (1973).

[8] M. Enculescu, *Rev. Roumaine Chim.*, **19**, 1491 (1974).

[9] M. Enculescu and E. Marton, *Rev. Construcţii şi Materiale de Construcţii*, **6**, 321 (1967); **3**, 145 (1968).

[10] M. Enculescu, *BIDT pt. Materiale de Construcţii*, **6**, 11 (1971); **4**, 9 (1972).

[11] I. Teoreanu, M. Enculescu and E. Marton, "Cimenturi albe şi colorate". Ed. tehnică, Bucharest, 1969.

Due to Ti^{4+} valence and to its high polarization power, it is likely to substitute Si^{4+}. Kondo and Yoshida[2] show the possibility of substituting Si by Ti. Ponomarev, Gracian and Rotici [3] have studied the influence of transitional elements on white cement colouring; they mention that due to its strong bonding energy with oxygen, Ti^{4+} tends to be placed in the tetrahedral lattice.

Our own investigations [1,7–10] have established that even in small quantities TiO_2, Na_2O; SO_3 etc., influence the physico-chemical process in the burning process of white and coloured Portland clinker, sensibly lowering the eutectics of the basic system. Thus, coloured cement clinkers must be located in complex polynar systems. In achieving coloured clinkers, account was taken of the formation of an increased amount of C_3S and C_2S in α or β form.

2. INFLUENCE OF TITANIUM DIOXIDE ON THE FORMATION OF TRICALCIUM SILICATE

Tricalcium silicate was synthetized with TiO_2 microadditions in a proportion of 0.5–8% TiO_2 by repeated burning at 1500°.

The determination of free CaO after synthesis gave the following values:

	after 2 burnings	after 3 burnings
$C_3S + 0.5\%$ TiO_2	4.45	2.99
$C_3S + 2.0\%$ TiO_2	2.75	—
$C_3S + 4.0\%$ TiO_2	1.68	—
$C_3S + 8.0\%$ TiO_2	1.39	0.68

The diffractometric analysis of $3CaO.SiO_2$ synthesized samples with various TiO_2 properties shows the principal identification of characteristic lines for $3CaO.SiO_2$, with an intensity corresponding to a percentage of over 90%, which proves the synthesis in good conditions as resulted from table 1.

Samples with the strongest lines, hence a high $3CaO.SiO_2$ content, were those with 4% TiO_2. Therefore, the limit of TiO_2 solid solution in $3CaO.SiO_2$ is 4%.

Based on the above mentioned studies, it may be concluded that TiO_2 is included in the lattice of tricalcium silicate and that the solid solution limit is 1–2%.

Solid solutions of $3CaO.SiO_2$ with TiO_2 may be described by formula: $[Ca_{3-x}.Ti_x]\ [Si_{1-y}.Ti_y].O_{5-z}$ in which $0 \leqslant x = y \leqslant 0.02 \ldots 0.04$ and $z = x + 2y - \frac{u}{2}(x + y)$, u being the valence of the metallic content.

Sychev and Korneev [4] found that in the presence of TiO_2, on cooling clinkers corresponding to tricalcium silicate, the latter is powdered. The reason is not related to β conversion into $\gamma - 2CaO.SiO_2$. The authors have shown that powdering will take place by introducing

Table 1

Diffractograms of 3 CaO.SiO$_2$ and 2CaO.SiO$_2$ with TiO$_2$

C_3S	x 3.03	x 2.77	x 2.76	x 2,61	y 2.18	y 1.76	z 1.62	z 1.59	z 1.44				
$C_3S + 0.5\%\ TiO_2$	x 3.0558	x 2.7945	x 2.7609	x 2.6196	y 2.1892	y 1.7697	y 1.6407	y 1.5499	y 1.4955	z 1.9960	z 1.9473		
$C_3S + 2.0\%\ TiO_2$	x 3.0558	x 2.7945	x 2.7444	x 2.6196	y 2.9955	y 2,1994	y 1.7697	z 1.6407	z 1.5499	z 1.4955			
$C_3S + 4.0\%\ TiO_2$	x 3.0558	x 2.7945	x 2.7444	x 2.6196	y 2.1994	y 1.7697	z 1.9473	z 1.6681	z 1.5546	z 1.4955			
$C_3S + 8.0\%\ TiO_2$	x 3.0354	x 2.7945	x 2.7444	x 2.6196	y 2.9760	y 2.1994	y 1.7697	y 1.6407	y 1.5452	y 1,4955	z 2.3422	z 1.9473	z 1.9087
$C_3S + 3\%\ TiO_2 +$ $+ 0.5\%\ B_2O_3$.	x 2 7945	x 2.7444	y 2.6345	y 2.1994	z 3.0558	z 2.8822	z 2.4402	z 2.4024	z 2.2850	z 2.0298	z 1.9877	z 1.9087	z 1.7958 1.6300z
$C_3S + 0.6\%\ TiO_2$	x 3.0153	x 2.7609	x 4.3497	y 3.8906	y 1.9163	y 1.8804	y 1.8091	z 4.1106	z 2.5474	z 2.4661	z 2.3422	z 2.2860	2.1994 z z 2.0298

x = parameter "d" in Å, with large intensity.
y = parameter "d" in Å, with middle intensity.
z = parameter "d" in Å, with small intensity.

1–2% TiO_2 into tricalcium silicate charge and by burning the mixture at 1400–1500°.

Powdering at a higher percentage that 3% TiO_2 is particularly intense. Free CaO was not found in the samples synthetized.

The petrographic study has revealed an increase of n_p and n_g protection indices as against pure $3CaO.SiO_2$. Variable alit amounts were found. The increase in alit refraction indices is related to the formation of TiO_2 solid solution in C_3S, also found by Erşov. [1,5] Apart from the phase identified as alit, another phase was found to appear, which can be neither $3CaO.SiO_2$ nor $\beta 2CaO.SiO_2$. Similarly, it can be neither calcium titanosilicate nor calcium titanate. It could be assumed that some calcium silicates lower in CaO may have formed; also, based on classical considerations, the existence of free CaO may be suggested but the fact has not been confirmed. Thus, it was assumed that in the case of the absence of free CaO, less basic compounds may possibly form.

The powdering phenomenon is related to the polymorphism of the phase being formed together with alit in $3CaO.SiO_2$ clinker, which is accompanied by a reduction in specific weight.

A study of thermograms of tricalcium silicate with various TiO_2 proportions has shown that by introducing TiO_2, $3CaO.SiO_2$ has passed into alit with one single endothermal effect whose displacement increases with the rise of TiO_2 content from 900° to 850°.

Another effect is found at 1180–1200°, whose intensity increases proportionally with the increase of TiO_2 content. It induces a reduction of the mechanical resistances of samples, so that at 10% TiO_2 content, the samples have not binding properties any more.

The increase in mechanical resistances is related to the high activity of TiO_2 solid solution in C_3S; after surpassing the $3CaO.SiO_2$ solid solution with maximum 3% TiO_2 addition, white cement clinkers have poor or even null hydraulic properties.

3. CONSIDERATIONS ON THE STRUCTURE OF CALCIUM ORTHOSILICATE

Calcium orthosilicate is the second principal mineralogic compound in white Portland clinkers.

Calcium orthosilicate has several polymorphic forms which have formed the subject of many investigations. [1-19] Among all polymorphic

---

[12] I. TEOREANU, M. ENCULESCU and T. ROŞESCU, *Rev. des Matériaux de Constuction*, **655**, 103 (1971).

[13] I. TEOREANU, M. ENCULESCU and T. ROŞESCU, *Rev. Roumaine Chim.*, **16**, 1091 (1971).

[14] H. HORNAIN, "Sur la répartition des éléments de transition et leur influence sur quelques propriétés du clinker et du ciment", Service Physique du CERILM– I.L.D./2080, 1971.

[15] E. N. MASLYI, "Alit i belit v portland sementov klinkere", Izdatelnyi Literatury stroitelnye Politekhn. Inst. im. S. M. Kirova – Tomsk, 1971.

[16] M. REGOURD, "Symposium International de la Chimie du ciment", Tokyo, 6–11 Oct., 1968.

[17] A. DIETZEL and L. TSCHEISCHWILI, *Ber. dtsch. Keram. Ges.*, **30**, 151 (1953).

[18] L. REVAY, *Epitoanyag*, **3**, 100 (1968).

[19] E. WOERMANN, W. EYSEL and TH. HAHN, *Zement, Kalk, Gips*, **6**, 1 (1968).

forms α, α', β and γ the most important polymorphic form is $\beta-2CaO.SiO_2$ form.

Yannaquis, Yamaguchi, Ono, Kawamura and Soda[1,6] have analysed the pure β C_2S phase defined by the monocyclic lattice parameters: $a = 5.48$ Å; $b = 6.76$ Å; $c = 9.28$ Å; $\beta = 94°33'$.

The structure of $\beta-2CaO.SiO_2$ microcrystals stabilized with 0.5% B_2O_3 is monoclinic; it is constructed starting from independent $[SiO_4]^{4-}$ tetrahedra and from two species of calcium atoms.

The structure can be defined by columns of alternative tetrahedra and Ca atoms bonded by 4 Ca atoms (CaII) placed in the cavities between tetrahedra.

3.1. INFLUENCE OF TITANIUM DIOXIDE ON THE FORMATION OF DICALCIUM ORTHOSILICATE

The synthesis of dicalcium orthosilicate with various proportions of titanium dioxide was performed by repeated burning at 1400°.

Diffractometric analyses made on calcium orthosilicate samples synthesized with various % TiO_2 percentages have evidenced the characteristic lines of $2CaO.SiO_2$ form at $d = 2.77$ Å; $d = 2.74$ Å; $d = 2.61$ Å; $d = 2.19$ Å as well as other lines as resulted.

When 3% TiO_2 and 0.5% B_2O_3 are introduced, form $\beta-2CaO.SiO_2$ is stabilized, as seen in diffractograms of table 1.

In the case boric anhydride is not introduced into the mixture of calcium orthosilicate and TiO_2, not $\beta-2CaO.SiO_2$ but rather $\gamma-2CaO.SiO_2$ will form with characteristic lines at $d = 3.01$ Å, $d = 2.74$ Å and $d = 1.91$ Å and also other lines with lower intensities, yet characteristic of form $\gamma-2CaO.SiO_2$, as seen in table 1. This is evidenced by the appearance of high-intensity lines characteristic of forms $\beta-2CaO.SiO_2$ at $d = 2.79$ Å; $d=2.74$ Å; $d = 2.63$ Å and $d = 2.19$ Å. Fig. 1 exhibits microphotographs of $\beta-2CaO.SiO_2$ samples with 0.6% TiO_2 and 3% TiO_2 stabilized with 0.5% B_2O_3.

Diffractograms of $2CaO.SiO_2$ with various TiO_2 proportions without B_2O_3 addition show the obtention of the form $\beta-2CaO.SiO_2$ with characteristic lines at $d = 3.01$ Å; $d = 2.76$ Å and $d = 1.92$ Å, rather than the obtention of the γ-form.

An optical microscope was used to analyse this sections (10–20 micrometers) with 0.6% and 3% TiO_2 stabilized with 0.5% B_2O_3. It was observed that dicalcium orthosilicate under β-form appears as round crystals. Their relief is strong, with medium birefringence, the polarization colours are yellow or even orange and they have multiple polysynthetical twin-crystals.

Microphotographs made for synthesized $\beta-C_2S$ samples reveal a certain decrease in the size of calcium orthosilicate crystals proportionally with the rise in oxides content of transitional elements. The influence exerted by TiO_2 microadditions on the $\beta-C_2S$ texture also determines an improved resistance. According to Dietzel and Tscheischwili's hypothesis[12] the substances which may stabilize the $\beta-C_2S$ lattice introduce into the lattice either ions bigger than Ca^{2+}, or ions which form anionic complexes smaller than the $[SiO_4]^{4-}$ group.

Based on the above facts and considering the sizes of Mn^{4+}, Co^{2+}, Ti^{2+}, Cu^{2+} and Ni^{2+} ions, fig. 1, it results that MnO_2, Co_3O_4 and NiO fail to stabilize β C_2S. The β C_2S stabilization by 0.4 and 0.6 % Co_3O_4 additions may be explained by its possible physical action, similar to that observed in the case o molybdenum and zirconium oxides.

By incorporating various extraneous atoms, the $2CaO.SiO_2$ structural formulas correspond to : $Ca_2[Me_x^{3+} \cdot Si_{1-x}]\, O_{4-\frac{x}{2}}$ with $Me = B^{3+}$; $0 \leqslant x \leqslant 0.10$ $Me = Fe^{3+}$; $0 \leqslant x \leqslant 0.02$ $Me = Al^{3+}$; $0 \leqslant x \leqslant 0.06$ $Me = Ti$; $0 \leqslant x \leqslant 0.060 \ldots 0.012$

In the case of silicon substitution :

$$Ca_2[Co_x \cdot Si_{1-x}]O_{4-\frac{x}{2}} \text{ for } Co^{2+} ;\ 0 \leqslant x \leqslant 0.006$$

$$Ca_2[Ni_xSi_{1-x}]O_{4-\frac{x}{2}} \text{ for } Ni^{2+} ;\ 0 \leqslant x \leqslant 0.012$$

In case of calcium substitution :

$$Ca_{2-x} \cdot Ti_x \cdot SiO_{4-\frac{x}{2}} \quad 0 \leqslant x \leqslant 0.006 - 0.012$$

$$Ca_{2-x} \cdot Co_x \cdot SiO_{4-\frac{x}{2}} ;\ 0 \leqslant x \leqslant 0.012 \quad Ca_{2-x} \cdot Ni_x \cdot SiO_{4-\frac{x}{2}} ;\ 0 \leqslant x \leqslant 0.012$$

In the case of the simultaneous substitution of Ca^{2+} and Si^{4+}, the structural formula becomes :

$$Ca_{2-x}\left\{\begin{matrix} Ti \\ \\ Co \\ \\ Ni \end{matrix}\right. - Si_{1-x}\left\{\begin{matrix} Ti \\ \\ Co \\ \\ Ni \end{matrix}\right\} O_{4-\frac{x}{2}} \text{ for } Co^{2+} ;\ 0 \leqslant x \leqslant 0.006 \text{ for } Ni^{2+} ;\ 0 \leqslant$$
$\leqslant x \leqslant 0.012$ for Ti^{2+} ; $0 \leqslant x \leqslant 0.012$

3.2. INFLUENCE OF TiO_2 ON CALCIUM ORTHOSILICATE BY MEANS OF DIFFERENTIAL THERMAL ANALYSIS AND OF THERMOGRAVIMETRIC ANALYSIS AND BY HIGH-TEMPERATURE OPTICAL MICROSCOPY

The differential thermal analysis has revealed the fact that in $\beta-2CaO \cdot SiO_2$ sample with 0.6 % TiO_2 addition, strong peaks appear at 325° and 405° which represent silicagel dehydration, a peak at 600° and strong peaks at 850° and 925° characteristic of $CaCO_3$ decarbonation. The TGA curve, fig. 2, indicates mass transformations occurring at such temperatures. In the $\beta-2CaO.SiO_2$ sample with 3 % TiO_2 addition stabilized with 0.5 % B_2O_3 we observe characteristic peaks of silicagel dehydration. A peak also appears at 910° including also the peak at 870°, due to larger TiO_2 quantities, evidencing the decarbonation effect and the beginning of $\beta-2CaO \cdot SiO_2$ formation process. At 985° we also

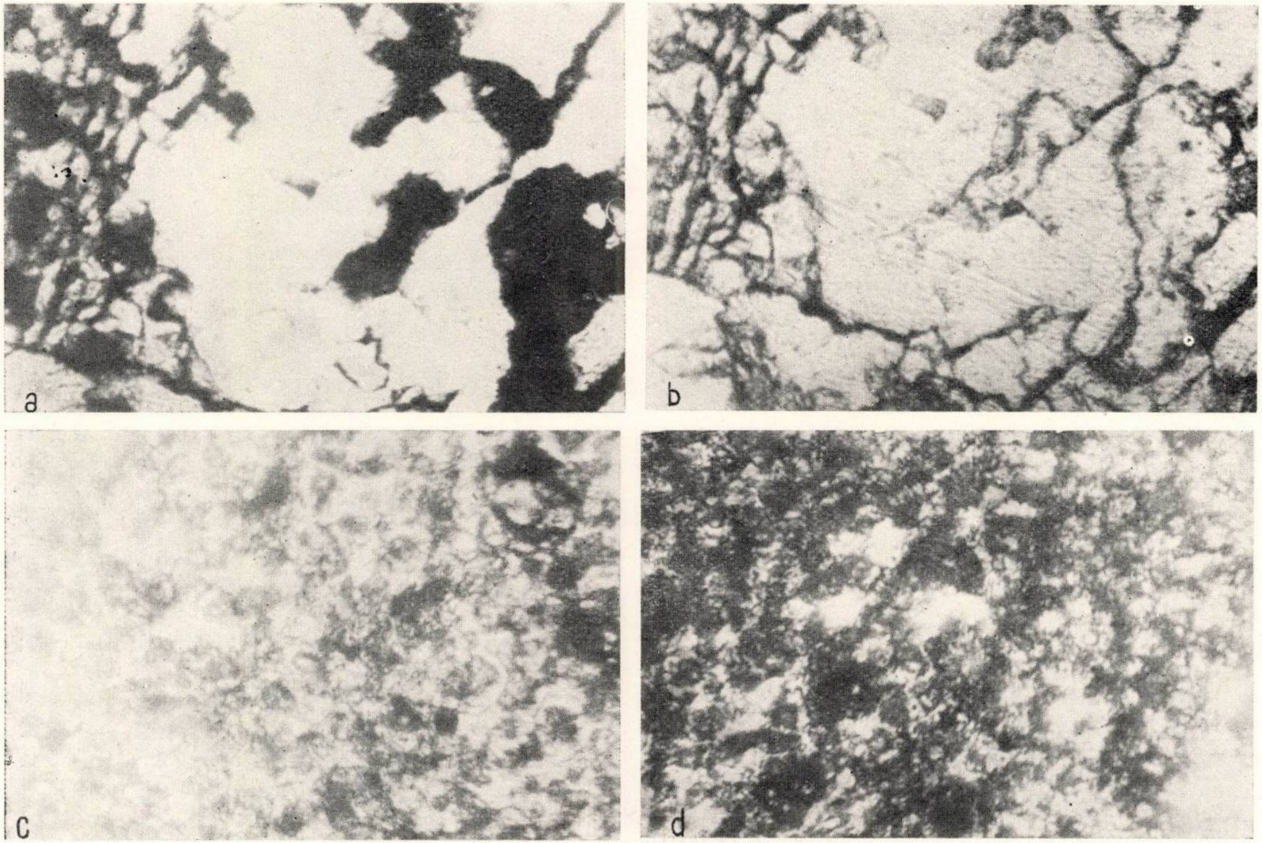

Fig. 1 — *a*) Microphotograph of dicalcium silicate with addition of 0.6 % TiO_2 and 0.5 % B_2O_3. Thin section, nicols X, 20 × 30 ; *b*) Microphotograph of dicalcium silicate with addition of 0.6 % TiO_2 and 0.5 % B_2O_3. Thin section, parallel nicols 20 × 10 ; *c*) Microphotograph of dicalcium silicate with addition of 3 % TiO_2 and 0.5 % B_2O_3. Thin section, nicols X, 20 × 15 ; *d*) Microphotograph of dicalcium silicate with addition of 3 % TiO_2+0.5 % B_2O_3. Thin section, parallel nicols— 30 × 10.

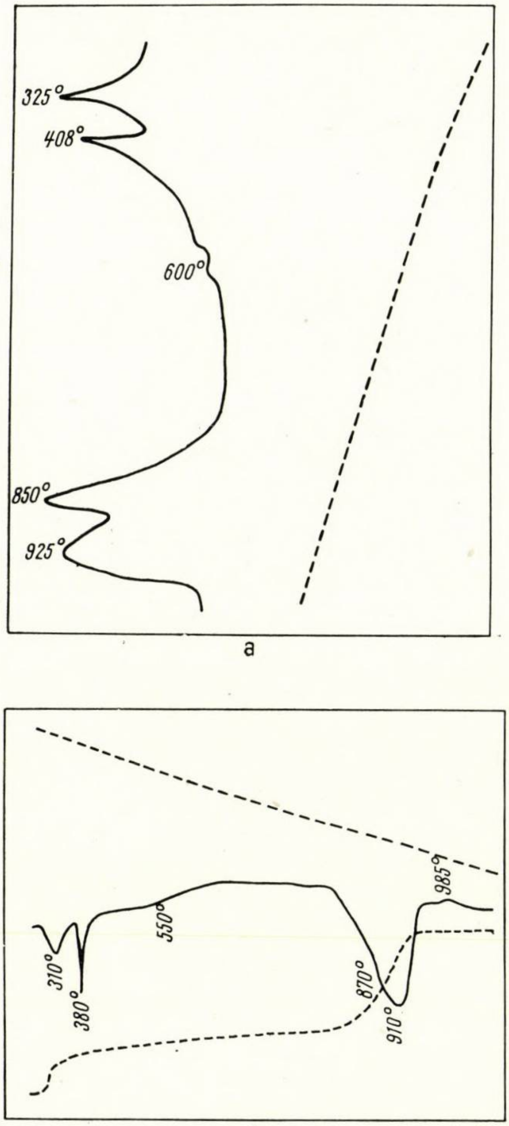

Fig. 2 — *a*) Differential thermal analysis and gravimetric thermal analysis of dicalcium silicate with addition of 0.6 % TiO_2 and 0.5 % B_2O_3 ; *b*) Differential thermal analysis and gravimetric thermal analysis fo dicalcium silicate with addition of 3 % TiO_2 and 0,5 % B_2O_3.

find a low-intensity peak at 985°. Analyses by means of high-temperature microscope have been carried out in correlation with the results obtained by DTA and thermogravimetric analyses.

Thus, the stabilizing role of $\beta-2CaO\cdot SiO_2$ form was evidenced by means of various TiO_2 proportions.

The results listed in fig. 3 show a volume variation towards lower temperatures relative to the volume variation of pure standard

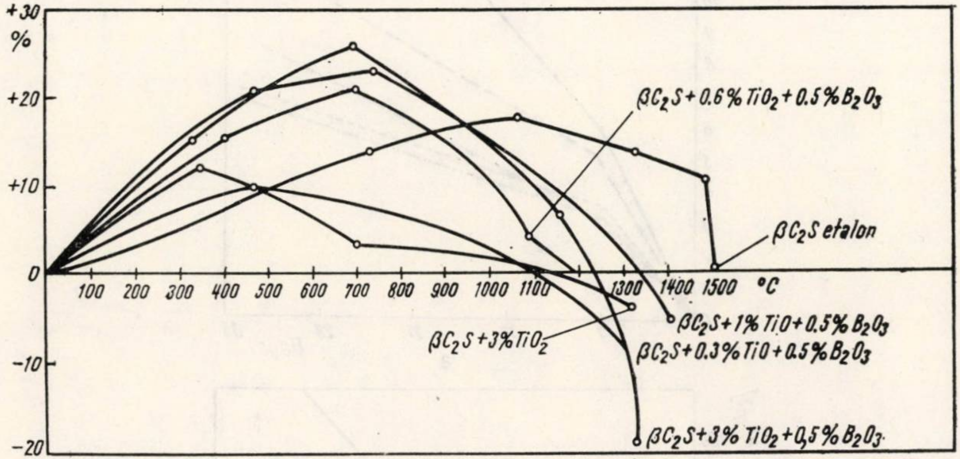

Fig. 3. — Volume variation of β $2CaO.SiO_2$ samples with various TiO_2 additions.

$\beta-2CaO\cdot SiO_2$ sample; e.g. in samples of $\beta-2CaO\cdot SiO_2 + TiO_2$ – 460° – –730° – $\beta-2CaO\cdot SiO_2$ + 3 % TiO_2 – 340° as against 920 – 1060° for pure standard $\beta-2CaO\cdot SiO_2$.

The results given in diagram 11 show the fusing-accelerating agent role of the samples liquid phase appearance with low TiO_2 amounts. Compared to the temperature at which the liquid phase of $\beta-2CaO\cdot SiO_2$ standard sample appears, i.e. 1450°, samples with 0.3 % TiO_2 have 1380°, hence $\Delta = 80°$; with 0.6 % TiO_2, 1350°, hence $\Delta = 100°$; with 1.0 % TiO_2 – 1250°, hence $\Delta = 200°$ and in a sample with 3.0 % TiO_2 – 1260°, hence $\Delta = 210°$.

This demonstrates that over 1 % TiO_2 the TiO_2 fusing agent role is constant.

The 3 % TiO_2 addition has the role of fusing agent of $\beta-2CaO\cdot SiO_2$ sample, reducing the temperature of the liquid phase appearance by 200°.

3.3. HYDRATION OF CALCIUM ORTHOSILICATE WITH VARIOUS PERCENTAGES OF TiO_2 ADDITION

Based on the studies carried out, it was established that TiO_2 introduced into calcium orthosilicate fails to act as a stabilizer of

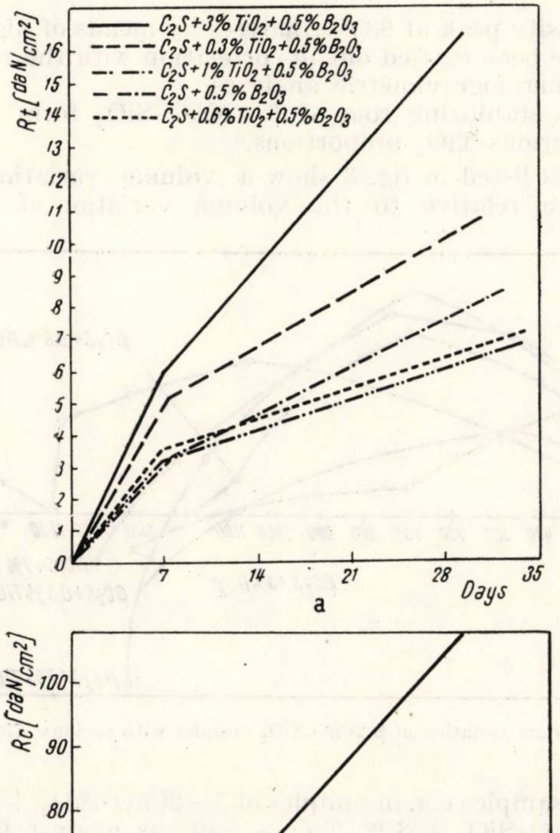

Fig. 4. — *a*) Tensile strengths of dicalcium silicate samples with various TiO_2 additions; *b*) Strengths of compression of dicalcium silicate samples with various TiO_2.

$\beta-2CaO \cdot SiO_2$ form, leading only to $\gamma-2CaO \cdot SiO_2$ form which fails to have hydraulic properties.

However, if 0.5 % B_2O_3 is introduced together with TiO_2 micro-additions, one obtains $\beta-2CaO \cdot SiO_2$ form whose hydraulic properties are proportional with the percentage of TiO_2 addition. The results listed in table 2 and fig. 4 demonstrate the above statements.

Table 2

Mechanical resistances determined by Kühl microsounds

Synthesized samples	Mechanical resistances			
	Compression daN/cm²		Tensile daN/cm²	
	7 days	28 days	7 days	28 days
$2CaO \cdot SiO_2 + 0.3\% \ TiO_2 + 0.5\% \ B_2O_3$	33.00	46.50	3.32	6.25
$2CaO \cdot SiO_2 + 0.6\% \ TiO_2 + 0.5\% \ B_2O_3$	34.00	51.00	3.60	6.46
$2CaO \cdot SiO_2 + 1.0\% \ TiO_2 + 0.5\% \ B_2O_3$	39.00	54.00	5.10	10.20
$2CaO \cdot SiO_2 + 3.0\% \ TiO_2 + 0.5\% \ B_2O_3$	57.60	106.60	6.10	16.00

Considering the mechanical resistances obtained with $\beta-2CaO \cdot SiO_2$ samples stabilized with boric anhydride and with oxides of transitional elements, it is possible to make up an efficiency scale of oxides of transitional elements on $\beta-2CaO \cdot SiO_2$ hydraulic properties :

$$Ti > Cu > Co > Ni > Mn$$

4. NUCLEAR PARAMAGNETIC RESONANCE APPLIED TO THE STUDY OF TiO_2 INFLUENCE ON CALCIUM ORTHOSILICATE

Investigations based on the EPR method, fig. 5, have shown that all clinkers present a spectrum with a well-shaped resonance line, characteristic of Fe^{3+} in tetrahedral coordination, with an effective magnetic moment at $g = 4.26$.

The spectrum intensity of a clinker with TiO_2 addition is lower than in a clinker containing only MnO_2 and Fe_2O_3. This indicates that in the former clinker, the content of paramagnetic Fe^{3+} particles in tetrahedral coordination is lower than in the latter clinker. It has been stated that in Ti^{4+} presence, part of Fe^{3+} passes into an octahedral coordination. This leads to a sensible increase in the whiteness degree of clinker.

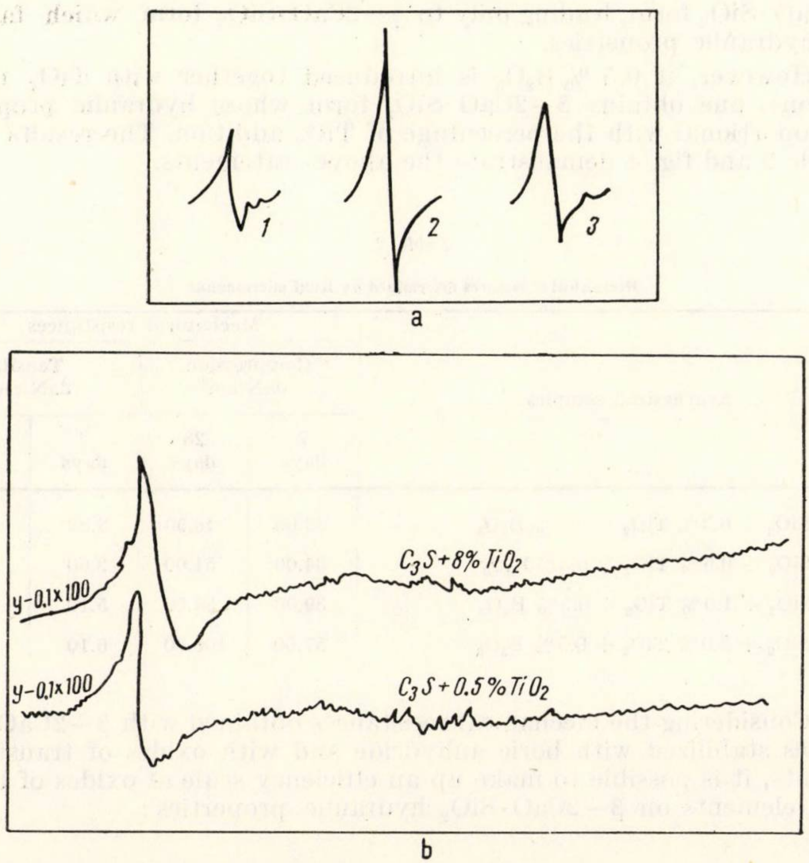

Fig. 5. — *a*) Nuclear paramagnetic resonance spectra of clinkers with addition: *1*, clinker with 0.2 % Fe_2O_3 addition; *2*, clinker with 0.2 % Fe_2O_3 and 0.5 % Mn_2O_3 addition; *3*, clinker with 0.2 % Fe_2O_3 and 0.05 % Mn_2O_3 addition; *b*) Electronic paramagnetic resonance of samples of $3CaO \cdot SiO_2$ with 0.5 % TiO_2 and 8 % TiO_2 addition.

5. THE LIGANDS THEORY APPLIED TO THE STUDY OF TiO_2 INFLUENCE ON CALCIUM ORTHOSILICATE

The ligands theory helps to explain the stability of the structures adopted to various compounds, of some cations with partly occupied "d" covers. This explains why in ferric spinel (Fe_3O_4) bivalent ions are characterized by an octahedral coordination whereas Mn_3O_4, the octahedral arrangement is characteristic of trivalent ions (Mn^{3+}); the octahedral crystalline field stabilize Mn^{3+} and Fe^{2+} rather than Mn^{2+} and Fe^{3+}.

Substances with differing structures are compared in practice. For instance, while TiO_2 lattice is of a simple N—P resonance with dominant polar bonds, the SiO_2 lattice is of a complex N—P resonance with coupled complex groups; neither are TiO_2 and SiO_2 interionic distances similar, the former having a greater importance.

Mention is made of the influence of the coordination number, a fact explained by the interrelation of ions in the lattice, which is stronger when the coordination number is larger. Substances characterized by larger interionic distances than similar ones, may be as hard as the latter due to the higher coordination number. For instance TiO_2 is characterized by the coordination number 6 and has 2.06 Å interionic distances.

6. INFLUENCE of TiO_2 ON THE WHITENESS DEGREE OF PORTLAND CLINKERS

In previous works$^{1-8}$ it was specified that a correlation exists between the calcium orthosilicate coloration and the introduced dyeing oxide, mainly depending on the nature of the chromophore ion, on its valence, on its coordination and on the solubilization degree of ions of transitional elements in the dicalcium silicate lattice. Ions of transitional elements have free permissive energetical levels on which optically activated electrons may pass, thus presenting a high colouring capacity.

It was found that the higher the bonding energy between the dyeing ion and oxygen, the more reduced is the reflection coefficient and the stronger is the coloration. Therefore, for the same ion, in the case the coordination number is more reduced, the bonding energy with oxygen will be thus stronger. Ions of transitional metals : Fe, Mn, Co, Cr, Cu, Ni, Ti have a marked polarization power. The polarization power of a cation is the higher the smaller is its volume and the higher is its charge. As the effect of polarization is a restriction of ionic rays, it favours a lower coordination.

Therefore, it can be concluded that for the same ion of transitional element, coloration will be more intense when the valence is higher.

Based on previous considerations and considering the fact that in tetrahedral coordination the bonding energy value of cobalt with oxygen is higher than that existing between manganese and oxygen, manganese may be looked upon as a less strong chromophore.

In the case of the two oxides MnO_2 and Co_3O_4, experimental data obtained and exhibited in table 3 confirm this conclusion. It results from table 4 that for equivalent addition values of dyeing oxide, the reflection coefficient for synthetic C_2S with cobalto-cobaltic oxide is more reduced.

Likewise with regard to other oxides, Ni^{2+}, Cu^{2+} and Ti^{4+} nickel oxide is found to have a higher coloration power than copper oxide and the latter has a higher $\beta-C_2S$ coloration power than titanium dioxide.

Thus, a law is confirmed by which the ion possessing the highest bonding energy favours the decrease of reflection coefficients. As was expected, the coloration intensity and the wavelength rise with the percentage of the dyeing oxide added; however, it must be kept in mind that from a certain quantity on, the added oxide has a less important influence upon the colour of dicalcium silicate. This finding may be explained by the fact that the principal effect related to C_2S colour is presented by the ion included in the dicalcium silicate lattice.

The results listed in table 2 indicate a TiO_2 decolourizing effect related to its bonding energy with oxygen. The decolourizing effect is particularly found in 0.6 % TiO_2 samples.

In our previous works we have shown the influence of compounds of oxides of transitional elements on the properties of white Portland cement.

The polarization capacity of a ion increases with the coordination reduction. The stability of the coordination figure in compounds is determined by the bonding energy between the respective atom and the surrounding atoms coordinating it.

The bonding energy values for transitional elements in cation-oxygen coordination are shown in table 3.

Table 3

The bonding energy values for transitionalelements in cation-oxygen coordination

Element	Bonding energy in eV	
	octahedral coordination	tetrahedral coordination
TI(IV)	0.55	0.88
V(III)	0.35	1.44
Cr(III)	0.37	2.00
Mn(III)	0.37	0.56
Fe(III)	0.36	0.62
Co(II)	0.20	0.93
Ni(II)	0.22	0.48

The bonding energy between ions with tetrahedral coordination is higher. If we analyse the diffusive reflection dependence on the coordination of the ion introduced, the reflection coefficient is higher as the bonding energy of the transitional elements Cr, Co, with surrounding ions increases and it results in a marked decrease of the whiteness degree. In combination with several components containing 3 or several elements at the same time, it sensibly influences the positive charges of such atoms. This phenomenon is based on the tendency to obtain maximum bonding energies between positive and negative atoms, i.e. the tendency to obtain a maximum energetic effect during the formation process of compounds.

The ions of transitional elements will tend to obtain tetrahedral positions since they have a high bonding energy and will influence coordination as a whole.

The ion possessing the higher bonding energy largely favours the decrease of the cement reflection coefficient.

It was experimentally found that by introducing a 0.05 % TiO_2 microaddition into raw materials for white cement, the whiteness degree will be improved, hence the reflection coefficient will rise by 4.5 — 5.5 %.

The rise of the reflection coefficient in clinkers with TiO_2 additions is more reduced than in clinkers with manganese and iron oxide. Since

Table 4

Reflection coefficients of $2CaO.SiO_2$ with TiO_2 addition

Compound	ρwhite ρw	ρ red ρr	ρgreen ρg	ρ blue ρb	$x_L = \frac{\rho_r}{\rho_b+\rho_r+\rho_g}$	$y_L = \frac{\rho_g}{\rho_b+\rho_r+\rho_g}$	Saturation %	Colour according to C.I.E. chromicity diagram
C_2S + 0.5% B_2O_3	83.6	74.8	85.8	74.8	0.318	0.365	12	standard white
C_2S + 0.3% TiO_2 + 0.5% B_2O_3	82.3	73.2	84.4	73.9	0.317	0.364	13	idem
C_2S + 0.6% TiO_2 + 0.5% B_2O_3	87.8	76.2	91.2	90.0	0.296	0.355	17	idem
C_2S + 1% TiO_2 + 0.5% B_2O_3	86.2	77.7	87.8	78.1	0.319	0.364	18	idem
C_2S + 3% TiO_2 + 0.5% B_2O_3	65.5	54.6	68.2	61.9	0.295	0.269	20	standard white towards pink
C_2S	93.6	79.2	96.0	97.5	0.294	0.352	15	standard white
C_2S+ 0.3% TiO_2	87.4	76.35	90.5	91.6	0.295	0.350	16	idem
C_2S + 0.6% TiO_2	77.4	69.5	81.8	77.1	0.304	0.354	17	idem
C_2S + 1% TiO_2	84.4	76.1	87.9	86.0	0.305	0.351	18	idem
C_2S + 3% TiO_2	45.5	37.4	48.0	52.8	0.270	0.354	15	standard white towards pink

Ti^{4+} has a high bonding energy with oxygen it will assume a tetrahedral coordination when introducing titanium dioxide into clinkers and will favour Fe^{3+} and Mn^{3+} ordering in octahedral positions.

7. CONCLUSIONS

Various investigations have helped to establish the solid solution limit of titanium dioxide in calcium orthosilicate and in tricalcium silicate.

The solubilization degree of Ti^{4+} ion, the inclusion modality into the lattice, the bonding energy with oxygen, the coordination number and the correlation with silicates basicity and the effect upon the whiteness degree of dicalcium silicate and of tricalcium silicate have a particular importance.

Mechanical resistances were found to be improved by adding small TiO_2 quantities up to the solid solution limit. By surpassing this limit, both dicalcium and tricalcium silicate are decomposed and mechanical resistances diminish as a function of the TiO_2 introduced.

---

[20] M. Enculescu and E. Marton, Rom. Brevet 51751, 1967.

[21] M. Enculescu, I. Ionescu and E. Marton, Rom. Brevet 51805, 1967.

[22] M. Enculescu and E. Marton, Rom. Brevet, 51468, 1966.

[23] I. Teoreanu and M. Enculescu, Rom. Brevet, 64952, 1971.

Revue Roumaine de Chimie, **21**, *4*, 563–570 (1976)

ANISOTROPIE DIÉLECTRIQUE DE CERTAINS BLOCS EN CARTON ET EN PAPIER DANS LE DOMAINE DES MICRO-ONDES

N. DUŞOIU
Centre de Chimie-Physique, 31, str. Galaţi, Bucarest, Roumanie

Reçu le 28 septembre 1974

On a déterminé les composantes de dispersion et d'absorption électriques pour différents échantillons en carton et en papier sur deux directions perpendiculaires par rapport au champ électrique. On a étudié la dépendance de l'humidification de la biréfringence et du dichroïsme des micro-ondes ($\beta = \varepsilon'_{//} - \varepsilon'_{\perp}$ et $\delta = \varepsilon''_{//} - \varepsilon''_{\perp}$) et du contenu de fibre pure de l'échantillon. Les lois de dépendance sont linéaires dans le domaine 0,1 – 0,5 cm^3 H_2O/cm^3 échantillon.

1. INTRODUCTION

Les études d'anisotropie diélectrique des matériaux à structure fibreuse, dans le domaine des micro-ondes, ont été initiées dans le cadre du laboratoire d'optique ultra-hertzienne de l'Université de Bordeaux par Servant.[1-8] De ces mesurages on obtient des informations sur la constante diélectrique complexe $\varepsilon = \varepsilon' - \delta\varepsilon''$, donc simultanément sur la dispersion et l'absorption électriques.

Les blocs en carton et en papier se comportent, du point de vue électrique comme un cristal anisotrope uniaxe. Ce comportement est dû au fait que les fibres en cellulose sont toutes couchées dans le même plan (leurs directions sont en général quelconques), par le processus de feutrage. Les fibres forment dans le plan de la feuille un ensemble de révolution autour d'un axe de symétrie perpendiculaire au plan de la feuille. Cela conduit à l'apparition de deux permittivités caractéristiques (principales) de la substance, comme on voit dans la fig. 1.

---

[1] R. Servant, *Bulletin Ampère*, fasc. spécial, 1960, **9**, p. 35.

[2] R. Servant et J. W. Weavers, *Compt. rend., Soc., Française de Physique*, **35**, 955 (1960).

[3] R. Servant et C. Demau, *Compt. rend.*, **254**, 656 (1962).

[4] R. Servant et C. Demau, *J. Phys. Rad.*, **23**, 948 (1962).

[5] R. Servant, *J. Phys.*, **24**, 405 (1963).

[6] R. Servant et A. Charru, « Proceedings of the 12th Colloque Ampère – Bordeaux 1963 », ed. R. Servant and A. Charru, Bordeaux, North-Holland Publishing Comp., Amsterdam, 1964, p. 476.

[7] R. Servant, « Extrait des Proces-Verbaux de la Société de Sciences Physiques et Naturelles de Bordeaux », 14 déc. 1961.

[8] R. Servant et C. Faure, *Compt. rend.*, **253**, 841 (1961).

Les mesurages expérimentaux ont confirmé l'identité des valeurs pour les positions 1 et 1' et une grande différence par rapport à la position 2.

En dernière analyse, les études d'anisotropie de la constante diélectrique complexe, sur des matériaux à structure fibreuse, représentent une transposition des phénomènes optiques très connus de « biréfringence » et de « dichroïsme » dans le domaine des micro-ondes, ce qui offre des informations similaires sur la structure des échantillons étudiés. Grâce à leur opacité ces substances ne permettent pas de telles études dans le domaine de l'optique.

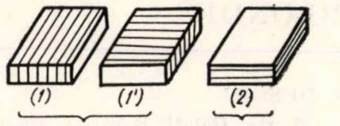

Fig. 1. — Position de l'échantillon par rapport à la direction du champ électrique.

Dans le présent travail on expose les résultats obtenus sur certains échantillons en carton et en papier, de fabrication roumaine. Les résultats expérimentaux ont mis en lumière une étroite dépendance de l'anisotropie diélectrique de la teneur en eau de l'échantillon.

La technique expérimentale utilisée est semblable à celle décrite par Servant[7] en un banc de mesure de micro-ondes pour la band de 3 cm (Tesla. R.S.C.). Le calcul des composantes de la constante diélectrique complexe a été fait à l'aide des mêmes diagrammes indiqués dans.[7]

2. RÉSULTATS EXPÉRIMENTAUX

Les principales caractéristiques des échantillons étudiés sont présentées dans le tableau 1.

Tableau 1

Principales caractéristiques des échantillons étudiés

N° de échantillon	Provenance	Épaisseur mm	Densité Humidification normale g/cm³	Densité Desséché g/cm³	Humidification naturelle %
1	Carton — C.H.H. Brăila	0,78	0,564	0,513	7,2
2	Carton — P. Neamţ	0,7	0,679	0,654	5
3	Mie carton triplex C.C.H. — Suceava	0,33	0,567	0,525	7,3
4	Papier Kraft C.C.H. — Suceava	0,13	0,623	0,583	6,5
5	Papier Kraft C.C.H. — Suceava	0,12	0,625	0,584	6,5
6	Papier Kraft C.C.H. — Suceava	0,1	0,620	0,578	6,7

Le tableau 2 contient les valeurs mesurées des composantes $\varepsilon'_{//}$, $\varepsilon'_{\perp}$, $\varepsilon''_{//}$ et $\varepsilon''_{\perp}$, pour les six échantillons numérotés en ordre dans le tableau 1, à humidification normale. Dans le même tableau sont donnés aussi les résultats des mesurages sur les échantillons desséchés. Le dessèchement a été fait dans l'étuve à 100° durant 3 heures.

Tableau 2

Les composantes des constantes diélectriques mesurées

Échantillon	$\varepsilon'_{//}$		$\varepsilon'_{\perp}$		$\varepsilon''_{//}$		$\varepsilon''_{\perp}$	
	desséché	normal	desséché	normal	desséché	normal	desséché	normal
1	2,46	3,02	2,17	2,64	0,29	0,73	0,15	0,49
2	1,99	2,35	1,78	2,01	0,30	0,47	0,18	0,29
3	2,30	2,85	1,99	2,35	0,35	0,70	0,17	0,35
4	1,81	2,34	1,41	1,76	0,08	0,42	0	0,05
5	1,78	2,32	1,37	1,73	0,05	0,32	0	0,04
6	1,75	2,35	1,32	1,75	0,10	0,35	0	0,04

Les échantillons étudiés ont été obtenus de l'« Institut de Projections et Recherches pour la Cellulose et le Papier » —Bucarest. Du point de vue de la composition, entre les échantillons 1,2 et 3 il a existé la différence suivante : échantillon N° 1 — 93% matériel fibreux, échantillon N°2 — 87% matériel fibreux et échantillon N° 3 — 100% matériel fibreux.

Si l'on définit « improprement » la biréfringence « β » et le dichroïsme « δ », de micro-ondes, ainsi :

$$\beta = \varepsilon'_{//} - \varepsilon'_{\perp}$$
$$\delta = \varepsilon''_{//} - \varepsilon''_{\perp} \qquad (I)$$

alors les données expérimentales indiquent pour le papier et le carton une biréfringence double par rapport au spath d'Islande dans le domaine visible. De même, elles présentent un fort dichroïsme rectiligne, dû à l'absorption inégale sur les deux directions // et ⊥. Ce phénomène est analogue à celui présenté par la tourmaligne, et dû, principalement, à la présence de l'eau. Par desséchage, le dichroïsme diminue jusqu'à sa disparition et la biréfringence diminue de façon appréciable. L'eau engendre une anisotropie supplémentaire car elle se répartit uniformément sur un support anisotrope constitué par les fibres de cellulose. Les mesurages effectués ne mettent pas en évidence des différences significatives entre les blocs en carton et ceux en papier, quoique par feuillets, le nombre des plans parallèles préférentiels pour fixer l'eau, croît.

L'observation ci-dessus conduit à la conclusion que la présence de l'eau influence la biréfringence et le dichroïsme dû à sa fixation sur les fibres cellulosiques et donc la constante diélectrique de l'eau fixée, jusqu'à une certaine limite l'humidification, doit être très différente par rapport à la valeur 80.

Supposant que les molécules d'eau sont distribuées uniformément dans la masse de l'échantillon, pour calculer la constante diélectrique de l'eau, on peut appliquer une formule simple, pour des mélanges binaires, de la forme :

$$\varepsilon_h = \varepsilon + m(\varepsilon_{(H_2O)} - 1)$$

$$\varepsilon'_h = \varepsilon' + m(\varepsilon'_{(H_2O)} - 1) \qquad (II)$$

$$\varepsilon''_h = \varepsilon'' + m(\varepsilon''_{(H_2O)})$$

où ε représente la constante diélectrique relative de l'échantillon désséché, ε_h celle de l'échantillon à l'humidification considérée, $\varepsilon_{(H_2O)}$ — la constante diélectrique de l'eau et m le degré d'humidification.

À l'aide de la formule (II) ont été calculées les constantes diélectriques de l'eau contenue dans les échantillons, à l'humidification normale, indiquée dans le tableau 1. Les résultats obtenus sont présentés dans le tableau 3, pour les quatre composantes.

Tableau 3

La constante diélectrique de l'eau dans un échantillon à humidification normale

Échantillon	$\varepsilon'_{(H_2O)_{//}}$	$\varepsilon'_{(H_2O)_{\perp}}$	$\varepsilon''_{(H_2O)_{//}}$	$\varepsilon''_{(H_2O)_{\perp}}$
1	14,7	12,5	10,8	2,7
2	11,6	8	5	3,2
3	14,2	9,6	8,4	4,3
4	14,2	9,7	9	1,2
5	14,3	9,3	6,6	0,97
6	15,4	11,3	6	0,9

Les données du tableau 3 suggèrent qu'une grande partie des dipôles de l'eau sont bloqués par fixation rigide sur les fibres cellulosiques, probablement par un mécanisme de liaison hydrogène. Ce serait l'eau « liée », qui se fixe à l'intérieur des cristaux et engendre le gonflement intraréticulaire des fibres. Par contre, l'eau libre engendre le gonflement extraréticulaire, étant partiellement fixée à la surface des fibres.

3. DÉPENDANCE DE L'ANISOTROPIE DE L'HUMIDIFICATION

La différence entre les valeurs de « β » et « δ » (tableau 2), pour les échantillons desséchés et à une humidification normale, a suggéré la réalisation d'une étude de la dépendance $\beta(C)$ et $\delta(C)$, C étant la quantité d'eau contenue dans l'échantillon. Une étude similaire a été faite aussi par Servant,[8] pour les blocs d'amiante. La teneur en eau introduite dans l'échantillon a varié entre les limites 0 — 0,5 cm^3 H_2O/cm^3 échantillon. Les valeurs des composantes de dispersion $\varepsilon'_{//}$ et $\varepsilon'_{\perp}$, pour les échantillons 2 et 3 sont présentées dans la fig. 2.

Les courbes expérimentales indiquent un accroissement appréciable des différences $\varepsilon'_{//} - \varepsilon'_{\perp}$, pour les deux échantillons. Dans la fig. 3

sont représentés les résultats expérimentaux pour les composantes d'absorption $\varepsilon''_{//}$ et $\varepsilon''_{\perp}$.

Dans ce cas aussi on remarque un accroissement de la différence de l'absorption sur les deux directions perpendiculaires, en même temps que l'accroissement du degré d'humidification.

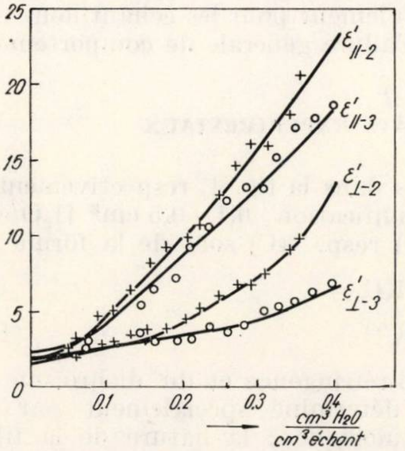

Fig. 2. — Dépendance de l'humidification des composantes de dispersion $\varepsilon'_{//}$ et $\varepsilon''_{\perp}$, pour les échantillons n°s 2 et 3.

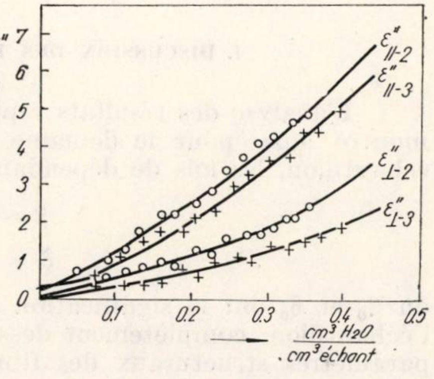

Fig. 3. — Dépendance de l'humidification des composantes d'absorption $\varepsilon''_{//}$ et $\varepsilon''_{\perp}$, pour les échantillons n°s 2 et 3.

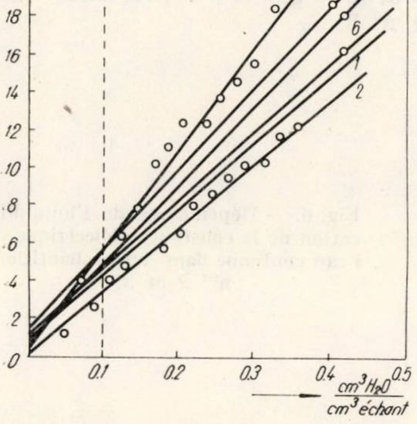

Fig. 4. — Dépendance de l'humidification de la biréfringence pour les six échantillons du tableau 1.

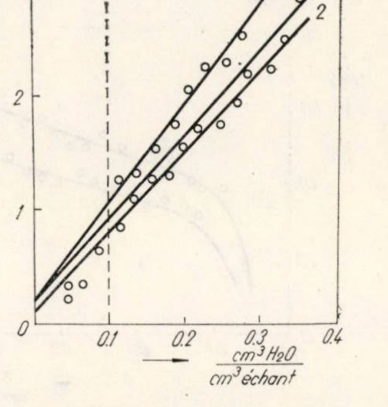

Fig. 5. — Dépendance de l'humidification du dichroïsme pour les échantillons n°s 1, 2 et 3.

Dans la fig. 4 et la fig. 5 sont représentées directement les grandeurs $\beta(C)$ et $\delta(C)$ pour le domaine d'humidification $0-0{,}5$ cm^{3}H$_2$O/cm^3 échantillon.

Les résultats expérimentaux mettent en évidence une dépendance linéaire de la biréfringence et du dichroïsme de micro-ondes de la quantité d'eau introduite dans l'échantillon. Dans les figures sont complètement représentés les points expérimentaux seulement pour les échantillons n° 2 et n° 3, pour faciliter l'observation de l'allure générale de comportement.

4. DISCUSSION DES RÉSULTATS EXPÉRIMENTAUX

L'analyse des résultats représentés dans la fig. 4, respectivement 5, montre que pour le domaine d'humidification $0{,}1-0{,}5$ cm^3 H$_2$O/cm^3 échantillon, les lois de dépendance $\beta(C)$ resp. $\delta(C)$ sont de la forme :

$$\beta = \beta_0 + KC$$
$$\delta = \delta_0 + K'C \qquad \text{(III)}$$

où β_0 et δ_0 ont la signification de la biréfringence et du dichroïsme de l'échantillon complètement desséchés déterminé spécialement par les paramètres structuraux des fibres cellulosiques : la nature de la fibre (sulfité, sulfaté, etc), la longueur de la fibre, le degré de feutrage et d'orientation dans le même plan, l'influence des matériaux annexes ; les constantes de proportionnalité *K* et *K'* sont dépendantes, en principal, du contenu spécifique de fibre pure de l'échantillon et du mécanisme de fixation de l'eau sur les fibres cellulosiques. On remarque que ces lois de dépendance sont valables seulement pour le domaine d'humidification mentionné, car dans l'immédiat voisinage de la valeur 0,5 cm^{3}H$_2$O/cm^3 échantillon on doit s'attendre à l'apparition d'un phénomène de saturation, fait illustré aussi par l'allure de la courbe $\varepsilon'_{(H_2O)}$ (C) représentée dans la figure 6 pour les échantillons n° 2 et n° 3.

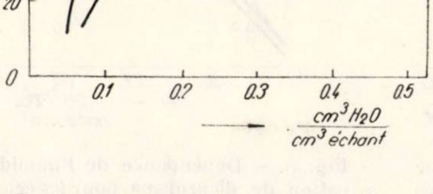

Fig. 6. — Dépendance de l'humidification de la constante diélectrique de l'eau contenue dans les échantillons n°s 2 et 3.

On remarque la tendance d'accroissement de la grandeur $\varepsilon'_{(H_2O)}$ avec la quantité d'eau introduite dans l'échantillon et le rapprochement vers la valeur 80, qui représente la constante diélectrique de l'eau libre.

L'allure des courbes représentées dans les figures 4 et 5 suggère l'observation qu'entre les pentes des droites et la quantité de matériel fibreux de l'échantillon (le contenu de fibre pure) il existe certaines relations de dépendance. La représentation graphique de la valeur des pentes par rapport à la quantité de matériel fibreux sur cm,^{3} pour les échantillons 1, 2 et N° 3 montre l'existence d'une dépendence approximativement linéaire, de la forme :

$$\begin{aligned} \beta &= \beta_{ad} + \beta_{sp} M \\ \delta &= \delta_{ad} + \delta_{sp} M \end{aligned} \qquad \text{(IV)}$$

où M représente la densité de la fibre pure ; β_{ad} et δ_{ad} représentent la biréfringence et le dichroïsme engendrés par les matériaux annexes : remplissage, imprégnation, encollage, colorants, etc. et les facteurs de proportionnalité β_{sp} et δ_{sp} sont déterminés par : le degré d'humidification de l'échantillon, les mécanismes de frottement de l'eau sur les fibres cellulosiques et par la nature des fibres cellulosiques.

Une complète confirmation de ces lois de dépendance peut être obtenue si l'on fait des déterminations sur un plus grand nombre de cartons et de papiers, àvec le contenu de fibre variant entre 75% et 100% (le domaine usuel) ; sur des fibres de nature différente, ainsi qu'une étude plus détaillée sur l'influence des matériaux annexes sur la biréfringence et du dichroïsme.

5. CONCLUSIONS

1° Les blocs en carton et en papier présentent une forte anisotropie diélectrique dans le domaine des micro-ondes.

2° La biréfringence et le dichroïsme de micro-ondes dépendent linéairement de la teneur en eau de l'échantillon et de la quantité de fibre pure.

3° La constante diélectrique de l'eau d'humidification varie dans la quantité d'eau de l'échantillon qui croît vers la valeur 80.

4° Les déterminations d'anisotropie diélectrique des cartons et papiers présentent un intérêt pratique, car elles conduisent à la détermination de quatre grandeurs caractéristiques : $\varepsilon'_{//}$, $\varepsilon'_{\perp}$, $\varepsilon''_{//}$ et $\varepsilon''_{\perp}$. Ces grandeurs offrent des informations sur l'uniformité de la densité de l'échantillon par la détermination des invariants de Gladstone $\frac{\varepsilon_{//} - 1}{d}$ et $\frac{\varepsilon_{\perp} - 1}{d}$, « d » étant la densité de l'échantillon. Les invariants de Gladstone, valables dans une première approximation, pour tous les matériaux à structure fibreuse, constituent aussi des corrélations simples entre les constantes diélectriques et la densité.

5° L'influence de l'humidification sur la biréfringence et le dichroïsme peut constituer le principe physique d'une méthode usuelle de contrôle de l'humidification et du grammage dans le processus de fabrication.

6° Les résultats expérimentaux confirment l'hypothèse de Wooster[9] conformément à laquelle l'eau se fixe sur les fibres de cellulose le long des fibres, en augmentant la densité linéaire des fibres ce qui conduit au croissement de la polarisation sur la direction longitudinale par rapport à la direction transversale. L'accroissement de l'anisotropie diélectrique avec le contenu d'eau est déterminée seulement par l'eau fixée sur les fibres cellulosiques. Cela permet de réaliser une discrimination entre l'eau libre et l'eau fixée.

---

[9] W. A. Wooster, « Etude des molécules d'eau dans les solides, par les électromagnétiques », Editions du C.N.R.S., Paris, 1953, p. 24.

Revue Roumaine de Chimie, **21**, *4*, 571–583 (1976)

EINFLUSS DER SUBSTITUENTEN AUF DIE ANALYTISCHEN EIGENSCHAFTEN VON ORGANISCHEN REAGENZIEN IN DER REAKTION MIT $[TlBr_4]^-$

CECILIA CONSTANTINESCU und GH. CONSTANTINESCU
Polytechnische Hochschule Bukarest, str. Polizu, N^r. 1

Eingegangen am 18. Juli 1974

In der vorliegenden Arbeit wurden die Reaktionen zwischen dem Komplexanion $[TlBr_4]^-$ und dem mit kondensierten Ringen substituierten Farbstoff Malachitgrün studiert. Die Farbstoffe sind aus der tryphenylmetanischen Klasse Derivaten des Malachitgrüns. Sie bilden mit $[TlBr_4]^-$ im sauren Milieu unlösliche Verbindungen, die dann der Elementar- bzw. IR-Spektralanalyse unterworfen werden. Da diese Verbindungen sich in organischen Lösungsmitteln auflösen, lassen sie sich aus der wäßrigen Phase durch Benzol extrahieren. Die organischen Extrakte besitzen bestimmte optische und elektrische Eigenschaften, die zur Anwendung der Reaktionen zu Thallium-Bestimmung führen können.

Der Komplexanion $[TlBr_4]^-$ besitzt eine große Fähigkeit, sich mit organischen Reagenzien unter Bildung von in Wasser unlöslichen in organischen Lösungsmitteln aber löslichen Verbindungen umzusetzen.

Der Mechanismus solcher Reaktionen besteht in der Bildung in wäßrigen Lösungen der komplexen hallogeno-metallischen Säuren, die durch die Bindung des Komplexen Anions am Farbstoffkation gefolgt wird. Die vom Typ der ionischen Assoziation gebildeten Verbindungen sind leicht löslich in organischen Lösungsmitteln. [1]

Unsere Anstrengungen sind in die Richtung der Darstellung neuer Verbindungen orientiert worden; gleichzeitig ist der Einfluß der kondensierten Ringen im unsubstituierten Ring des Farbstoffes Malachitgrün verfolgt d.h. durch die Erhöhung der Basizität von Farbstoffen hervorgerufene Reaktionsfähigkeit und deren Einfluß auf die Empfindlichkeit und Selektivität der Reaktionen.

---

[1] M. Onishi und E. B. Sandell, *Analyt. Chim. Acta*, **24**, 413 (1961).

VERSUCHSTEIL

Die verwendeten Farbstoffe sind:

Malachitgrün

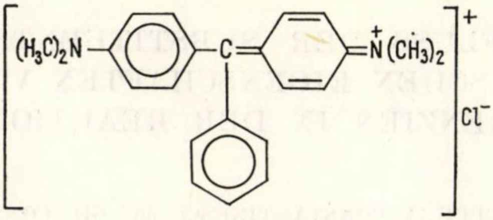

Tetralingrün

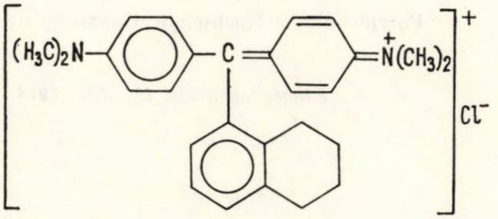

Naphtalingrün

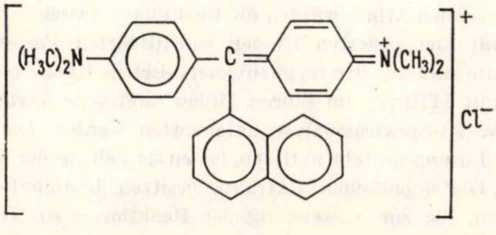

Victoria reinblau BO

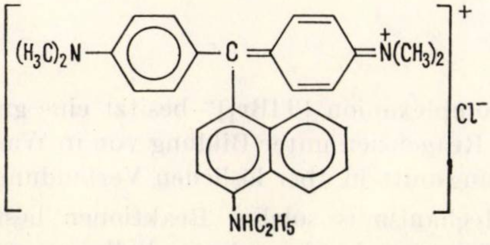

In der Molekel von Malachitgrün wurde der Benzolring durch Tetralin, Naphtalin bzw. Äthylaminonaphtalin ersetzt, welcher mit einer Erhöhung der Basizität von Farbstoffen verbunden ist. Die Reaktivität des Komplexanions $[TlBr_4]^-$ ist stark von den im aromatischen Ring des Malachitgrüns befindenden Substituenten beeinflußt, je höher die Basizität des Farbstoffes ist, desto größer ist die Reaktionsfähigkeit und die Empfindlichkeit der Reaktion. Unsere Forschungsergebnisse stimmten mit den theoretischen Voraussetzungen sehr gut überein. Die Reaktion des $[TlBr_4]^-$ - Anions mit Viktoria reinblau BO führt zu einem molarischen Extinktionskoeffizient $\varepsilon = 110\,000$, zu einer großen Stabilität und Selektivität.

Die Farbstoffe Tetralingrün, Naphtalingrün wurden nach [2] dargestellt. Zusammen mit Viktoria reinblau BO (Geigy) wurden sie durch wiederholte Umkristallisation aus Äthylalkohol gereinigt, wonach die Reinheit durch die Kaliumdichromatmethode bestimmt wurde. [3] Die

---

[2] C. Albu und C. Bălaiţa, *Rev. Chim. şi fiz.* (*Roumanie*) ser. A. 2. **12,** 447 (1965).

[3] R. P. Lestowski und Io. I. Vainstein, „Tekhnicheskii analiz v proizvodstvo premezhutochinikh productov i crasitelei Gosudarstvenoe nauchino tekhnichescoe izdatelstvo khimichescoi literatury", Ed. Moskva, 1958.

Papierchromatogrammen zeigten einheitliche Zusammensetzung. Die Reinigung der Farbstoffe erfolgte durch wiederholte Umkristallisation aus Äthylalkohol wonach die Reinheit durch die Kaliumdichromatmethode bestimmt wurde.[3] Die Papierchromatogrammen mit dem Äthylalkohol Wasser 1:1 zeigten einheitliche Zusammensetzung.

REAGENZIEN

Die verwendeten Farbstoffe sind leicht wasserlöslich und besitzen einen großen Lichtwiderstand:

a) Die Wasserlösungen der Farbstoffe Tetralingrün, Naphtalingrün und Viktoria reinblau BO hatten folgende Konzentrationen: $2\cdot10^{-3}$M, $1\cdot10^{-2}$ M und $1\cdot10^{-4}$ M.

b) Die Wasserlösung des Tl(III) wurde aus Thallium (I)-Nitrat durch Oxydierung mit Bromwasserstoff gewonnen. Der Titer wurde durch die grawimetrische Methode als Jodid[4] festgestellt. Durch Verdünnungen erhält man Lösungen von $1\cdot10^{-4}$ und $1\cdot10^{-5}$ M.

c) Bromwasserstoff 64%ig.

d) Benzol p.a.

e) Methyläthylceton

DIE EXTRAKTION DER KOMPLEXE

Die $1\cdot10^{-3}$M und $1\cdot10^{-4}$ M Lösungen von Tl(III) in Volumina von 0,1—5 ccm. wurden in einen Scheidetrichter von 50 ccm mit 64%igem Bromwasserstoff (1 ccm), destilliertes Wasser und $1\cdot10^{-2}$ oder $1\cdot10^{-3}$M Reagenzlösung bis zum Volumen von 10 ccm geführt. Man fügt 10 ccm organisches Lösungsmittel hinzu und schüttelt 2 Minuten lang am Schüttelapparat. In ähnlicher Weise werden auch die Kontrollproben vorbereitet. Man mißt die Extinktionen der gefärbten organischen Phase bei den entsprechenden Wellenlängen in 1 cm dicken Küvetten. Es ist zu erwähnen, daß das Lösungsmittel im Fall des Farbstoffes Viktoria reinblau BO[5-7] keinen freien Farbstoff mit extrahiert.

DIE SYNTHESE DER KOMPLEXE

Um das Kombinationsverhältnis im festen Zustand des thalischen Komplexanions mit dem Viktoria reinblau BO festzulegen, wurden 0,25 g $H[TlBr_4]$ gelöst in 1 ccm Wasser und Bromwasserstoff bis zu der optimalischen Normalität und mit etwa 0,35 g in 10 ccm gelöstem Farbstoff gemischt. Es erscheint ein blauer Niederschlag, der durch Filtrierung unter Vakuum getrennt und mit Wasser gewaschen wurde. Die Verbindungen wurden bezüglich des Gehaltes an Thallium[4] an Stickstoff und an Brom analysiert. Die erhaltenen Ergebnisse sind in Tabelle 1 eingetragen, woraus hervorgeht, daß das molarische Kombinationsverhältnis Metall-Farbstoff 1:1, ist.

Tabelle 1

Die Elementaranalyse

Verbindung	Gefunden			Berechnet		
	Tl%	N%	Br%	Tl%	N%	Br%
$(R^+ ; TlBr_4^-)$	13,32	5,09	25,31	13,07	5,37	25,59

---

[4] N. H. FURMAN, „Standard Methods of Chemical Analysis", Ed. VI, Van Nostrand, New York, 1962—1963, p. 1051.

[5] C. CONSTANTINESCU, *Rev. Chim. (Bucureşti)*, **24**, 565 (1973).

[6] C. CONSTANTINESCU, *Bul. Inst. Politeh. Iaşi (Chimie)*, **25**, 2 (1974).

[7] C. CONSTANTINESCU, *Anal. Sti. Univ. „Al. I. Cuza" Iaşi*, **19**, 47 (1973).

ERGEBNISSE UND DISKUSSIONEN

In der Lösung wurde zuerst der Verteilungskoeffizient zwischen den beiden Phasen (wäßrige und organische) bestimmt, dann wurden die Bildungsgleichgewichte und die Einflußfaktoren studiert: Lösungsmittel, Lösungsazidität, Konzentration der Reagenzien. Die Verbindungen wurden dann charakterisiert, was die Zusammensetzung, die Struktur und die Instabilitätskonstante betrifft.

DIE WAHL DES LÖSUNGSMITTELS

Es wurden folgende Lösungsmittel erprobt: Benzol, Toluol, Chloroform und Gemische von Benzol mit kleinen Mengen von Aceton, Cyklohexanon, Methyläthylceton, Alkohole oder Äther, die sich in ähnlichen Arbeiten wirksam zeigten. Die Ergebnisse sind in Tabelle 2 eingetragen. In unseren Forschungen wurden dann Gemische von Benzol mit Methyläthylceton verwendet. Die Kontrollproben waren farblos nur im Fall des Viktoria reinblau BO.[5-7] Um die einheitliche Zusammensetzung der Farbstoffe zu überprüfen wurden Papierchromatogramme durchgeführt.[8]

Tabelle 2

Absorptionsmaxima der organischen Lösungen von Komplexen

Lösungsmittel	Komplex Tl(III)-T-Grün	Komplex Tl(III)-N-G	Komplex Tl(III)-V.BO
	$A^{620}_{1\,cm}$	$A^{630}_{1\,cm}$	$A^{625}_{1\,cm}$
Benzol	0,308	0,485	0,170
Toluol	0,285	0,480	0,110
Cloroform	0,05	0,045	0,04
Cyclohexanol	0,07	0,07	0,06
Benzol + metylätylceton 2:1	0,350	0,50	0,650
Idem 6:1	0,280	0,208	0,760
Benzol + Äthylalkohol 2:1	0,110	0,138	0,140

ABSORPTIONSSPEKTREN IM SICHTBAREN BEREICH

Bei Bestimmung der elektronischen Absorptionsspektren von wäßrigen Lösungen (Abbildung 1) wird festgestellt, daß die Spektren von den Verbindungen mit Tl(III) batochromische Verschiebungen der elektronischen Absorptionsmaxima im Vergleich zu den wäßrigen Lösungen der freien Verbinder aufweisen. Diese Verschiebung kann der Bildung von Komplexen mit Ladungsübertragung von Typ $\sigma-\pi$ zugeschrieben werden. Die Wellenlängen der Absorptionsmaxima sind in der Tabelle 3 wiedergegeben.

---

[8] W. L. Poter, *Analyt. Chem.*, **23**, 412 (1951).

Man kann einen hypsochromischen Effekt der Absorptionsmaxima von den verwendeten Farbstoffen im Vergleich zu dem von Malachitgrün feststellen.

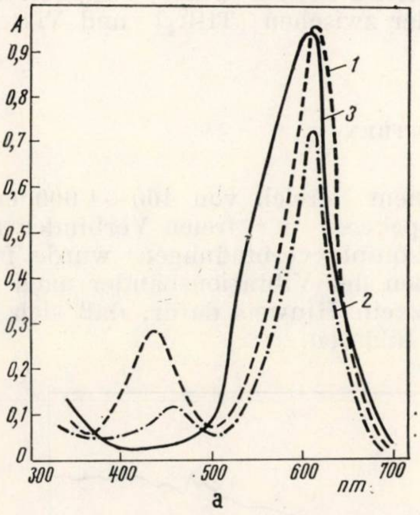

Abb. 1a. — Die elektronischen Absorptionsspektren der Farbstoffe:

C_1 – Tetralingrün, C_2 – Naphtalingrün, C_3 – Victoria reinblau BO.

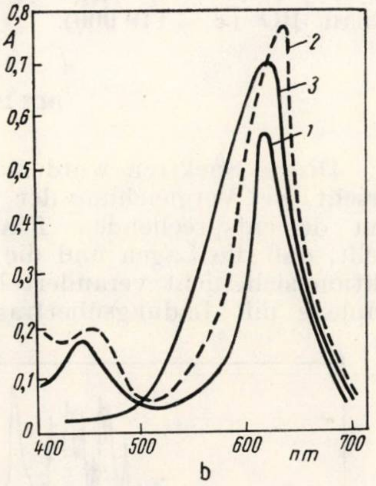

Abb. 1b. — Die elektronischen Absorptionsspektren der Komplexverbindungen:

C_1 – (Tetralingrün$^+$: TlBr$_4^-$); C_2 – (Naphtalingrün$^+$; TlBr$_4^-$) ; (Victoria reinblau BO+ ; TlBr$_4^-$).

Tabelle 3

Die Werte der Absorptionsmaxima λ_{max} (nm)

Farbstoff	λ_{max}	Lösungsmittel	Komplex	λ_{max}	Lösungsmittel
Malachitgrün (MG)	620	Wasser	—		
Tetralingrün (TG)	606	Wasser	Tl(III)–T.G	620	B + mec 2 :1
Naphtalingrün (NG)	615	Wasser	Tl(III)–N.G	630	B + mec 2 :1
Victoria reinblau (V.BO)	610	Wasser	Tl(III)–V.BO	625	B + mec 6 :1

Die drei Farbstoffe weisen Absorptionsmaxima zwischen 606–615 nm und die mit [TlBr$_4$]$^-$ entsprechenden dargestellten Verbindungen zwischen 620–630 nm auf. Das Ersetzen eines Benzolrings (Phenyl) durch einen hydrogenierten Rest (Tetralinkern) führt zu einem vernachlässigsten des auf den Chinonring hervorgerufenen Effekts. Der auxochromische Einfluß der Gruppen Tetralin, Naphtalin und Äthylaminonaphtalin ist um so stärker, je basischer die Gruppe ist. Diese Erläuterungen (also das Fehlen von den π-Elektronen zu der Tetralin-Gruppe) erklären die niedrige Empfindlichkeit der Reaktion zwischen $[TlBr_4]^-$ und Tetralingrün ($\varepsilon = 43\,000$) im Vergleich zu der zwischen $[TlBr_4]^-$ und Viktoria reinblau BO ($\varepsilon = 110\,000$).

DIE IR-SPEKTREN

Disese Spektren wurden in einem Bereich von 400 – 4 000 cm^{-1} erforscht. Bei Vergleichung der IR-Spektren der freien Verbinder mit denen der entsprechenden Thalliumkomplexverbindungen wurde festgestellt, daß die Lagen und die Größen der Vibrationsbänder nach der Reaktion sich nicht verändert haben, ein Hinweis dafür, daß sich die Komplexe mit Ladungsübertragung bildeten.

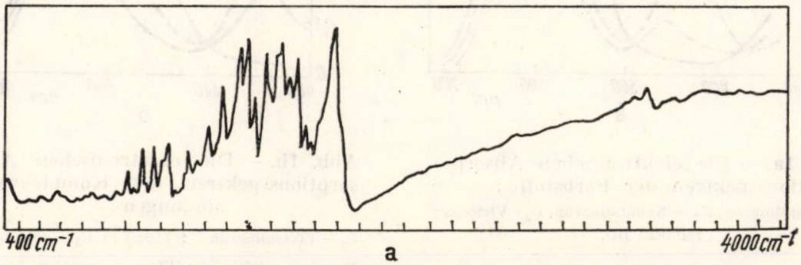

Abb. 2a. – IR-Spektrum des Farbstoffs Victoria reinblau BO.

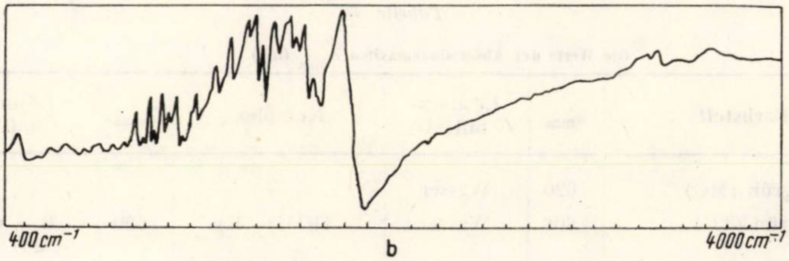

Abb. 2b. – Ir-Spektrum der Komplexverbindung Victoria reinblau $BO^+; TlBr_4^-$).

DIE LÖSUNGSAZIDITÄT

Für die Wahl optimaler Konzentration der Wasserstoffionen, wofür die maximale Extraktibilität der Komplexe festgestellt wird, ist die Fähigkeit der Hallogenowasserstoffsäuren mit Tl(III) Hallogenokomplexsäure zu bilden, in Betracht gezogen.

$$[TlI_4]^- > [TlBr_4]^- > [TlCl_4]^-$$

Da Tl(III) im Gegenwart von Hl zu Tl(I) reduziert wird, ist diese Säure für unsere Zwecke unanwendbar. Die Bildungskonstante des $[TlCl_4]^-$-Anions ist kleiner.[9] Es folgt also, daß in solchen Reaktionen die geeigneteste Säure die Bromwassserstoffsäure ist.

Die Kurven der Abbildung 3 zeigen, daß die Empfindlichkeit der Reaktion größer ist, wenn der optimale Aziditätsintervall länger ist.

DIE REAGENZKONZENTRATION

Bei Veränderung der Farbstoffmenge von 0,5—5,0 ccm Lsg $.1.10^{-3}$M (um das eingestellte Gleichgewicht zu verschieben) wurde eine Erhöhung der Extinktion bis zu einer bestimmten Konzentration festgestellt, nach der sie konstant bleiben. Die bestmögliche Konzentrationen für jeden Farbstoff sind in Abbildung 4 ersichtlich.

DAS STUDIUM DER ZUSAMMENSETZUNG IN ORGANISCHER LÖSUNG GEBILDETEN KOMPLEXVERBINDUNGEN

Für die Bestimmung des Kombinationsverhältnisses Metall-Farbstoff in der organischen Lösung kam die Methode Job[10] zur Anwendung. Die erhaltenen Ergebnisse sind in der Abbildung 5 dargestellt.

Das Kombinationsverhältnis für die ersten zwei Verbindungen ist 1 : 1 und für die Verbindung (Viktoria reinblau $BO^+[TlBr_4]^-$) nähert sich zu 2 : 1. Es scheint, daß in der wäßrigen Lösung zu starken Aziditäten auch $[TlBr_5]^{2-}$ gebildet worden sei :

$$TlBr_3 + HBr \rightleftharpoons H\,[TlB_4]^-$$

$$H[TlBr_4] + HBr \rightleftharpoons H_2[TlBr_5]^{2-}$$

$$H_2\,[TlBr_5] + R^+Cl^- \rightleftharpoons R_2^+[TlBr_5]^{2-} + HCl$$

Das Kombinationsverhältnis Metall-Farbstoff im festen Zustand ist 1 :1 (s. die Elementaranalyse und der thermische Abbau).

DER VERTEILUNGSKOEFFIZIENT

Um den Verteilungskoeffizient des Metalls zwischen den beiden Phasen festzulegen, kam eine spektrophotometrische Methode zur An-

---

[9] L. Johansson, *Acta Chem. Scand.*, **20**, 79 (1966).

[10] P. Job, *Ann. Chim.* (*France*), **9**, 113 (1928).

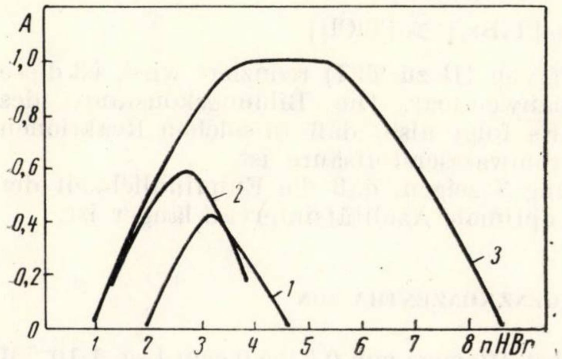

Abb. 3. — Einfluß der Lösungsazidität:
C_1 – Tl(III) – Tetralingrün; C_2 – Tl(III) – Naphtalingrün; C_3 – Tl(III) – Victoria reinblau BO.

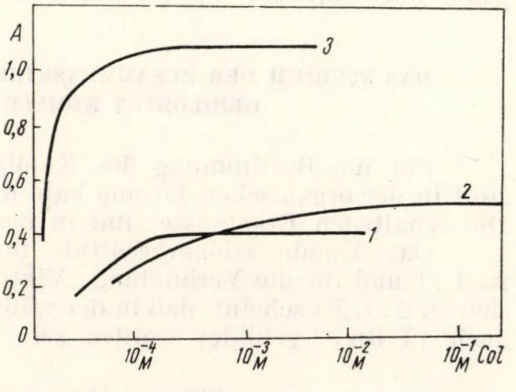

Abb. 4. — Einfluß der Farbstoffkonzentration:
C_1 – Tetralingrün; C_2 – Naphtalingrün; C_3 – Victoria reinblau BO.

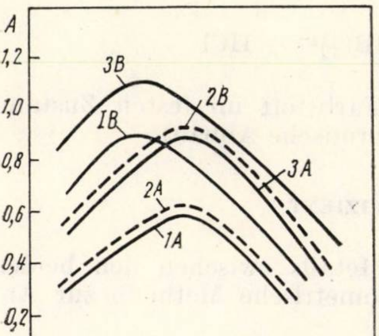

Abb. 5. — Die Bestimmung des Kombinationsverhältnisses nach der Job'schen Methode
1_A – Tl(III) – Tetralingrün $6\cdot10^{-4}$M
1_B – Tl(III) – Tetralingrün $1\cdot10^{-3}$M
2_A – Tl(III) – Naphtalingrün $1\cdot10^{-4}$M
2_B – Tl(III) – Naphtalingrün $4\cdot10^{-4}$M
3_A – Tl(III) – Victoria reinblau BO $5\cdot10^{-5}$M
3_B – Tl(III) – Victoria reinblau BO $1\cdot10^{-4}$M

wendung[11]. Die Komplexverbindungen wurden unter optimalen Bedingungen hergestellt und in Lösungsmitteln extrahiert. Die beiden Phasen wurden getrennt, dann jede mit konzentrierter Schwefelsäure und Wasserstoffperoxyd behandelt. Die auf diese Weise gelösten Thalliummengen wurden in beiden Fällen durch Methylviolet[12] in Gegenwart von Bromwasserstoff bestimmt. Die Ergebnisse sind in der Tabelle 4 eingetragen.

Tabelle 4

Der Verteilungkoeffizient

Verbindung	μg Tl/cm^3 Tallium zugegeben	Geblieben in der Wasserlösung	q	% E
Tl(III) – V.BO	2,0	0,1	19,0	98,0
Tl(III) – N.G	2,0	0,3	5,66	85,0

Der Verteillungskoeffizient ist das Verhältnis zwischen der Thalliumkonzentration in der organischen und in der wäßrigen Phase :

$$q = \frac{\mu\text{gTl/ccm organ. Phase}}{\mu\text{g Tl/ccm wässrg. Phase}}$$

und die prozentuale Extraktibilität ist :

$$\%E = \frac{100\, q}{q + \dfrac{V_{H_2O}}{V_{\text{Lösungsmittel}}}}$$

Aus Tabelle 4 ist ersichtlich, daß man eine praktisch vollkommene Extraktibilität im Fall des Farbstoffes Viktoria reinblau BO fand.

DIE BILDUNGSKONSTANTE

Um die Annäherung der Instabilitätskonstante für die Komplexe festzustellen, wurden Paare von unisomolarischen Lösungen nach der Job'schen Methode für biphasische Systheme angewendet.[13]

Die experimentell erzielten Ergebnisse sind in der Abbildung 6 wiedergegeben; die X-Werte aus der Abbildung 6 wurden in die Formel eingetragen:

---

[11] S. Fisel, „Chimia analitică calitativă", Ed. didactică şi pedagogică, Bukurest, 1973, p. 294.

[12] N. T. Voscresenscaia, *Zhur analit. Khim.*, **11**, 585 (1956).

[13] J. H. Joe und A. E. Harvey, *J. Amer. Chem. Soc.*, **70**, 648 (1948).

$$K_i = \frac{G[(1+p)(x-1)]^2}{(p-1)(1-2x)}$$

wo p ist:

$$p = \frac{G' \text{ (molarische Konzentration des Farbstoffes)}}{G \text{ (molarische Konzentration des Metalls)}}$$

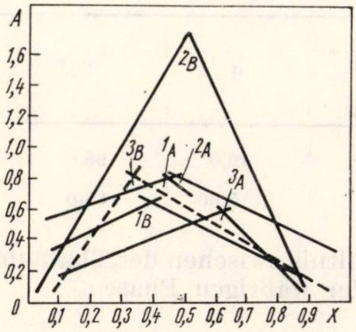

Abb. 6. — Die Bestimmung des x-Wertes für die Annäherung der Instabilitätskonstante. Die Methode Job
$1_A - 1_B$ — Tl(III) — Tetralingrün
$2_A - 2_B$ — Tl(III) — Naphtalingrün
$3_A - 3_B$ — Tl(III) — Victoria reinblau BO

In der Tabelle 5 sind die Werte der Instabilitätskonstanten vorgeführt. Die Verbindung (Victoria reinblau $BO^+[TlBr_4]^-$) ist wohl die stabilste.

Tabelle 5

Die Instabilitätskonstanten

N°	molarische Konzentration		$p = \frac{G'}{G}$	X_{max}	K_i	$K_f = \frac{1}{K_i}$
	Tl(III)	Farbstoff				
1_A	$2\cdot10^{-4}$	TG : $1\cdot10^{-3}$	5,0	0,40	$4{,}9\cdot10^{-4}$	$7\cdot10^4$
1_B	$4\cdot10^{-4}$	$1\cdot10^{-3}$	2,5	0,45	$9{,}1\cdot10^{-4}$	
2_A	$1\cdot10^{-4}$	NG : $4\cdot10^{-4}$	4	0,35	$6{,}25\cdot10^{-5}$	$8{,}4\cdot10^5$
2_B	$1\cdot10^{-4}$	$1\cdot10^{-3}$	10	0,49	$1{,}07\cdot10^{-6}$	
3_A	$2{,}5\cdot10^{-5}$	V.BO : $5\cdot10^{-5}$	2	0,62	$5{,}8\cdot10^{-5}$	$1{,}2\cdot10^6$
3_B	$5\cdot10^{-5}$	$1\cdot10^{-4}$	2	0,52	$9{,}8\cdot10^{-5}$	

DERIVATOGRAPHISCHE ANALYSE

Um die Zusammensetzung und das Verhalten der Verbindungen während des thermischen Abbaues zu verfolgen, führten wir eine Destruktion in einem Temperaturintervall von 20—900° mit einem Gerät von Typ MOM Budapest, Erwärmungsgeschwindigkeit 9° min in 100 min. durch

(Abbildungen 7a und 7b). Bis 180° ist ein Verlust von cca 4% festzustellen, welcher als Wasser betrachtet werden kann. Über 640° bleibt nur Thallyumtrioxyd. Der Rückstand, in Gewichtsprozenten zu Einwaage, zeigt ein molarisches Kombinationsverhältnis Metall-Farbstoff von 1 : 1, welches mit der Elementaranalyse übereinstimmt. Es wurden auch die exothermischen und endothermischen Effekte studiert (Abbildungen 7a und 7b die Kurven DTA). Der Abbau ist schwach endothermisch in den ersten zwei Stufen und stark exothermisch in der dritten Stufe, auf Grund der Verbrennungsprodukte

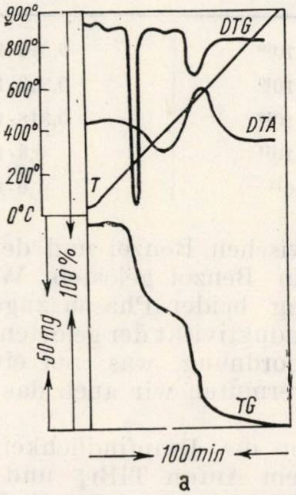

Abb. 7a. — Das Derivatogramm des Farbstoffs Victoria reinblau BO.

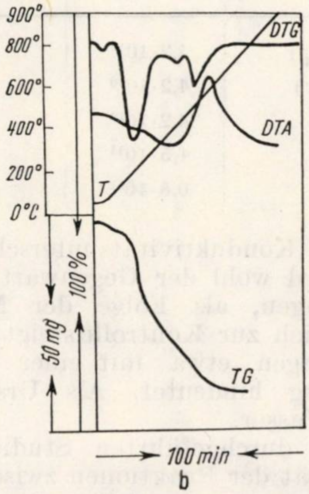

Abb. 7b. — Das Derivatogramm der Komplexverbindung (Victoria reinblau BO^+ ; $TlBr_4^-$).

Tabelle 6

Die Abbaustufen

Verbbdg.	1.St.	Verluste	2.St.	Verluste	3.St.	Verluste	4. St.	Verluste
Victoria reinblau BO	35°–180°	3%	180°–320°	43%	320°–453°	9,4%	453°–650°	38%
Komplex : Tl(III)-Victoria reinblau BO	35°–180°	4%	180°–340°	42%	340°–640°	40%	—	—

KONDUKTIVITÄTSBESTIMMUNGEN

Die Bestimmung der Konduktivität wurde unter Verwendung organischer Lösungen der Komplexverbindungen im Vergleich zu der

Kontrollprobe und zu reinem Benzol durchgeführt.[14] Ein Megaohmmeter vom Typ Tetralin Statron (DDR) kam zur Anwendung. Die Ergebnisse sind in der Tabelle 7 wiedergegeben.

Tabelle 7

Die Konduktivitätsbestimmungen

Verbindung	U_K	Resistivität $\rho = \frac{1}{R}$ (Ω.cm)	Konduktivität $\gamma = \frac{1}{\rho}$ ($\Omega^{-1}\,cm^{-1}$)
(R_1^+ ; $TlBr_4^-$)	$4{,}2\cdot10^{10}$	$3{,}15\cdot10^{10}$	$0{,}318\cdot10^{-10}$
(R_2^+ ; $TlBr_4^-$)	$4{,}2\cdot10^{10}$	$3{,}15\cdot10^{10}$	$0{,}318\cdot10^{-10}$
(R_3 ; $TlBr_4^-$)	$4{,}2\cdot10^{10}$	$3{,}15\cdot10^{10}$	$0{,}318\cdot10^{-10}$
Benzol	$1{,}5\cdot10^{11}$	$1{,}25\cdot10^{11}$	$0{,}8\cdot10^{-11}$
Kontrolle	$0{,}8\cdot10^{11}$	$0{,}6\cdot10^{11}$	$1{,}6\cdot10^{-11}$

Der Konduktivitätsunterschied zwischen Benzol und der Kontrollprobe wird wohl der Gegenwart von in Benzol gelöstem Wasser und Säuremengen, als Folge der Mischung beider Phasen zugeschrieben. In vergleich zur Kontrolle steigt die Konduktivität der gelösten Komplexverbindungen etwa mit einer Größenordnung, was auf eine gewisse Ionisierung hindeutet. Als Ursache vermuten wir auch das in Benzol gelöste Wasser.

Die durchgeführten Studien über die Empfindlichkeit und die Selektivität der Reaktionen zwischen dem Anion $TlBr_4^-$ und die obengenannten Reagenzien führten zu der Schlußfolgerung, daß die Eigenschaften der dargestellten Komplexverbindungen sich für eine neue Bestimmungs methode des Thalliums eignen. In dieser Hinsicht wurde die Gültig-

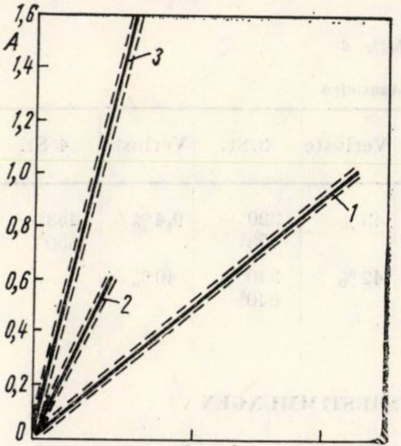

Abb. 8. — Die Eichungsgeraden
1. Tl(III) — Tetralingrün
2. Tl(III) — Naphtalingrün
3. Tl(III) — Victoria reinblau BO

---

[14] J. D. Phielipa, *J. Amer. Chem. Soc.*, **83**, 1806, 3370 (1961).

keit des Lambert-Beer'schen Gesetzes (Abbildung 8) studiert und die Ergebnisse statistisch bearbeitet[15].

Tabelle 8

Anwendungsbereich und die Empfindlichkeit der Reaktionen

Verbindung	Anwendungsbereich	ε	$t.s_m$	Stabilität
Tl-Tetralingrün	1–10,2 µg Tl/	43 100	±0,02	28 Stunden
Tl-Naphtalingrün	0,2–18,0 µg Tl/	81 400	±0,02	48 Stunden
Tl-Vikt. BO	0,2–30 µg Tl/	110 000	±0,004	96 Stunden

DER EINFLUSS FREMDER IONEN

Es wurde die Interferenz jener Ionen geprüft, die gewöhnlich in verschiedenen Materialien Thallium begleiten und ähnliche Verbindungen bilden, so wie Indium, Gallium, Eisen, Antimonium, Vanadium, Thallium, Germanium und Molibden. Die Reaktionen sind durch Wachsen der Absorption nur von Gold, Eisen und Indium in folgender Reihenfolge gestört :

Au(III) Fe(III) In(III)

Die Reaktion zwischen Viktoria reinblau BO und $TlBr_4^-$ ist für die Konzentration $1 \cdot 10^{-4}$ M von keinen Ionen gestört.

---

[15] M. Kozlicka, *Chem. Analit.*, **15**, 683 (1970).

Revue Roumaine de Chimie, **21**, *4*, 585–588 (1976)

COMPLEX CHELATE COMPOUNDS OF ISO- AND HETEROPOLYANIONS OF Mo(VI) AND W(VI) WITH CHROME AZUROL S. II[1]

COMPLEX CHELATE COMPOUNDS OF HETEROPOLYANIONS OF Mo(VI) AND W(VI)

P. B. ISSOPOULOS
Department of Inorganic Chemistry, University of Patras,
Patras — Greece

Received September 3, 1975

In the present paper the formation of the complex chelate compounds between the heteropolyanions $\{P(MO_3O_{10})_4\}^{3-}$ $\{P(W_3O_{10})_4\}^{3-}$ and $\{Si\,(W_3O_{10})_4\}^{4-}$ and CAS is described as well as the influence of pH on their formation.

In a previous work the formation of the complex chelate compounds of isopolyanions of Mo(VI) and W(VI) with Chrome Azurol S(CAS) was studied[1].

Also a determination of the form of these compounds by the method of continuous variations (Job's method) [2] is included.

EXPERIMENTAL

Visible spectra were determined on Optica CF4R or Hitachi-Perkin-Elmer 139 spectrophotometers. The pH's are measured with a Radiometer model 22 pH-meter equipped with glass-calomel electrodes.

All the measurements (spectra, pH) were carried out at a constant temperature, 25 ± ± 0. 1°C and an ionic strength $\mu = 0.1$ M ($NaNO_3$).

Standard molybdophosphoric acid solution. An amount of 182.5 mg of anhydrous molybdophosphoric acid *p.a.* is weighed accurately and transferred quantitatively in a 100 ml volumetric flask, where it is dissolved an diluted with doubly distilled water to volume.

The resulting solution has a concentration in molybdophosphoric acid (MPA) of $1 \times \times 10^{-3}$ M.

Standard tungstophosphoric acid solution. An amount of 288 mg of anhydrous tungstophosphoric acid *p.a.* is weighed accurately and treated as above. The resulting solutions has a concentration in tungstophosphoric acid (TPA) of 1×10^{-3} M.

Standard tungstosilicic acid solution. An amount of 287.8 mg of anhydrous tungstosilicic acid *p.a.* is weighed accurately and treated as above. The resulting solution has a concentration in tungstosilicic acid (TSA) of 1×10^{-3}M.

---

[1] Ière partie. P. B. Issopoulos, *Rev. Roumaine Chim.*, **21**, 000 (1976).

[2] P. Job, *Ann. Chim.* (*France*), **9**, 113 (1928).

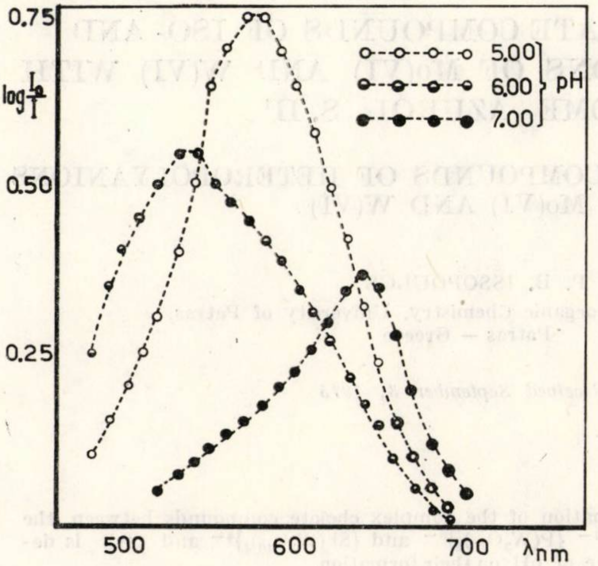

Fig. 1. — Influence of the pH upon the formation of complex chelate compounds of $\{P(Mo_3O_{10})_4\}^{3-}$ — CAS.

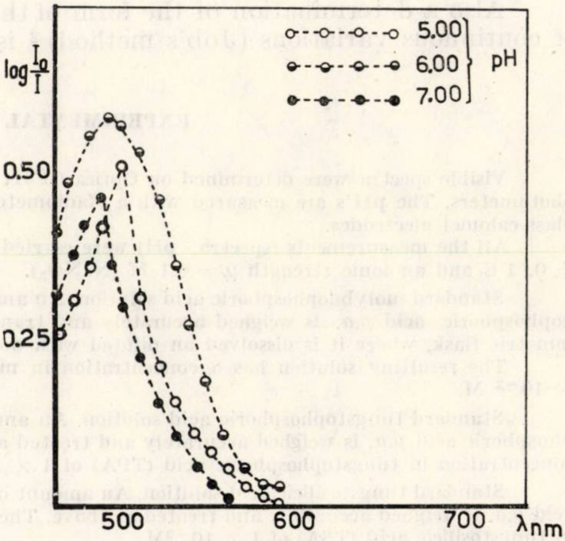

Fig. 2. — Influence of the pH upon the formation of complex chelate compound $\{P(W_3O_{10})_4\}^{3-}$ — CAS.

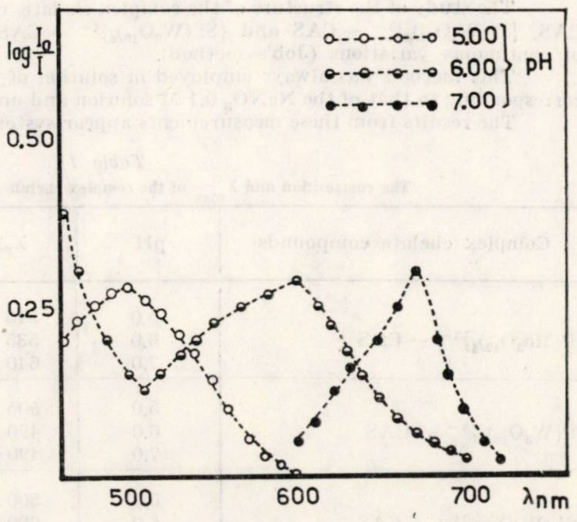

Fig. 3. — Influence of the pH upon the formation of complex chelate compounds of $\{Si(W_3O_{10})_4\}^{4-}$ — CAS.

Standard Chrome Azurol S solution. An amount of 60.6 mg of Chrome Azurol S (Merck N°2477)] is weighed accurately and treated as above. The resulting solution has a concentration in Chrome Azurol S (CAS) of 1×10^{-3}M.

The formation of the complex chelate compounds and the study of the influence of the pH on the formation of these compounds were carried out as follows:

In a series of solutions of $NaNO_3$ 0.1M, 500 ml each, the pH is regulated by the addition of $HClO_4$ 0.1 M or NaOH 0.1 M so that the final solutions have the following pH values: 3.0, 4.0, 5.0, 6.0, 7.0, 8.0, 9.0, 10.0 and 11.0.

In a 100 ml volumetric flask about 90 ml of $NaNO_3$ 0.1M are placed with constant pH regulated as described above and to this are added 1.0 ml of standard MPA solution and 2.0 ml of standard CAS solution.

The contents of the flask are mixed and the solution is made to a final volume of 100 ml with $NaNO_3$ 0.1 M of the same pH.

By the aforementioned method there are prepared solutions of constant ionic strength corresponding to that of $NaNO_3$ 0.1 M and for the same pH values. In each one of these, final volume 100 ml, 1.0 ml of standard TPA solution and 2.0 ml of standard CAS solution or 1.0 ml of standard TSA solution and 2.0 ml of standard CAS solution, are added.

In the same way blank solutions of corresponding ionic strength and pH values are prepared.

The solutions are allowed to stand for 30 min in the dark and then spectrophotometric measurements of each solution are taken in the visible region of the spectrum with the blank solution of the same pH as a reference.

The solutions of pH : 3.0, 4.0 and 8.0, 9.0, 10.0 and 11.0 showed no absorption throughout the whole visible region, while the solutions of pH : 5.0, 6.0 and 7.0 gave absorbance measurements from which the curves of figs. 1,2 and 3 are traced.

From fig. 1 it is seen that, as a function of pH, the curves exhibit different maxima. Thus, at pH 5.0 the maximum appears at $\lambda = 575$ nm, while at pH 6.0 and 7.0 this appears at $\lambda = 535$ nm and $\lambda = 640$ nm, respectively. From the curves of fig. 2 it is seen that at pH 5.0 the maximum appears at $\lambda = 505$ nm. At pH 6.0 and 7.0 the maximum appears at $\lambda = 490$ nm, while the value of $\log I_0/I$ changes.

From fig. 3 it is clearly seen that as a function of pH the curves exhibit different maxima. Thus, at pH 5.0 the maximum appears at $\lambda = 500$ nm, while at pH 6.0 and 7.0 this appears at $\lambda = 600$ nm and $\lambda = 670$ nm, respectively.

It was thought that the maximum absorption as a function of pH was due probably to a change of the nature or structure of the absorbing species.

The study of the structure of the complex chelate compounds formed $\{P(MO_3O_{10})_4\}^{3-}$ — CAS, $\{P(W_3O_{10})_4\}^{3-}$ — CAS and $\{Si(W_3O_{10})_4\}^{4-}$ — CAS was carried out by the method of continuous variations (Job's method).

This method was always employed in solution of constant pH, constant ionic strength corresponding to that of the $NaNO_3$ 0.1 M solution and under constant temperature 25 ± 0.1°C.

The results from these measurements appear systematically in table 1.

Table 1

The composition and λ_{max} of the complex chelate compounds as a function of pH

Complex chelate compounds	pH	λ_{max}	Heteropolyanion : CAS
$\{P(Mo_3O_{10})_4\}^{3-}$ — CAS	5.0 6.0 7.0	575 nm 535 nm 640 nm	1 :1 2 :1 1 :2
$\{P(W_3O_{10})_4\}^{3-}$ — CAS	5.0 6.0 7.0	505 nm 490 nm 490 nm	1 :1 1 :1 1 :1
$\{Si(W_3O_{10})_4\}^{4-}$ — CAS	5.0 6.0 7.0	500 nm 600 nm 670 nm	2 :1 1 :1 1 :2

DISCUSSION

From the data of table 1 it is concluded beyound doubt that the two complex chelate compounds, i.e. $\{P(Mo_3O_{10})_4\}^{3-}$ — CAS and $\{Si(W_3O_{10})_4\}^{4-}$ — CAS can appear, as a function of pH, in three possible forms, that is 1 :1, 1 :2 and 2 :1, each of which has its own absorption maximum.

The molar absorptivity of $\{P(Mo_3O_{10})_4\}^{3-}$ — CAS changes considerably as a function of the structure of the complex. Thus, the form 1 :1 has a value of $\varepsilon = 7.54 \times 10^4$, the form 2 :1 has $\varepsilon = 6.1 \times 10^4$ and the form 1 :2 has $\varepsilon = 3.7 \times 10^4$. The molar absorptivity in all three forms of $\{Si(W_3O_{10})_4\}^{4-}$ — CAS, i.e. 1:1, 2:1 and 1 :2 is about the same and has values of 2.7×10^4, 2.9×10^4 and 3.0×10^4, respectively. Finally the complex chelate compound, $\{P(W_3O_{10})_4\}^{3-}$ — CAS, appears only in one form, regardless of pH, the form 1 :1, which has an optimum pH of formation equal to 6.0 at which has $\varepsilon = 5.78 \times 10^4$ while, at pH 5.0 and 7.0 the value of ε decreases to 5.0×10^4 and 4.6×10^4, respectively.

These complex chelate compounds were shown experimentally to follow the Beer's law and can be used as a means of the quantitative determination of these heteropolyanions in the concentration range $10^{-5} - 2 \times 10^{-4}$ M per ml of the final solution used for spectrophotometric measurements. Interfering ions in the above determination are the same with those mentioned in our previous works on complex chelate compounds having the same ligand, that is, Chrome Azurol S. [1,2-8].

[3] P. B. Issopoulos and A. Galinos, *Analysis*, **2**, 672 (1973).

[4] P. B. Issopoulos and A. Galinos, *Chimika Chronika*, accepted for publication.

[5] P. B. Issopoulos, *Ann. Chim.* (*France*), **9**, 157 (1974).

[6] P. B. Issopoulos, *Technika Chronika*, **43** (12), 881 (1974).

[7] P. B. Issopoulos, *Ann. Chim.* (*France*), **10**, 17 (1975).

[8] P. B. Issopoulos, *Compt. rend.*, **280**, 1359 (1975).

Revue Roumaine de Chimie, 21, 4, 589–594 (1976)

NEW MIXED HETEROPOLYCOMPOUNDS: TUNGSTONIOBIOSILICATES

GH. MARCU and LETIȚIA GHIZDAVU
Chemistry Laboratory of Radioactive Elements, University "Babeş-Bolyai",
str. Arany Janos, No 11,
Cluj—Napoca, Romania

Received July 18, 1974

In this paper the synthesis of a new mixed heteropoly-acid : $H_6[SiW_{10}Nb_2O_{40}]$ and of its K^+, NH_4^+, Cs^+ and Tl^+ salts is reported. The structure in solution of the heteropolyacid was characterized through its electronic absorption spectrum and its polarogram, measuring of its basicity by conductometrical and potentiometrical titrations.

GENERALITIES

At the present state of development of the chemical research on heteropolycompounds, the synthesis of mixed combinations containing ligands of different nature, bonded to the central atom became a frequently used research tool. Not only the tungstate and molybdate radicals may act as ligands, but most of transitional elements, fact which demonstrated the overall generality of this class of compounds.

The heteropolycompounds of the elements from the Vth secondary group : V, Nb and Ta by which a more advanced substitution is possible, represent a special class of combinations. Although these heteropolycompounds exhibit very interesting properties which determine their use in the analytical chemistry, for the dosage of different elements and organical bases, so as their use as redoxites and ion exchangers, being used also as deshidratation and polymerisation catalists and inhibitors, for the recovery of fission products, also only a few papers were reported about these heteropolyacids, reason for which the present authors decide to extend their studies on some new mixed compounds, namely the tungstoniobiosilicates.

In the present paper, the synthesis of $H_6[SiW_{10}Nb_2O_{40}]$ and of its K^+, NH_4^+, Cs^+ and Tl^+ salts so as the establishment of their structure is described.

EXPERIMENTAL PART

The forming in solution of the anion decatungstodiniobiosilicic depending on concentration, pH, temperature and time [1] was spectrophotometrical studied and the optimal synthesis

---

[1] GH. MARCU and L. GHIZDAVU, *Stud. Univ. Babeş-Bolyai, Chem.*, 1974 (accepted for publication).

conditions were established as being: a molar ratio of W : Nb :Si = 10 :4 :3, pH = 2 and a temperature of 60°. Based on these results the synthesis of $H_6[SiW_{10}Nb_2O_{40}]$ was achieved from the following compounds: sodium tungstate, potassium niobate and sodium silicate, in the above indicated molar ratio, 10W :4Nb : 3Si, the pH = 2 being adjusted with H_2SO_4 2N and finally the mixture being heated to 60° during 2 hours.

The solution of potassium niobate was prepared by fusing Nb_2O_5 with KOH in excess and treating the melt according to method of [2], or treating metallical Nb with a hot concentrate KOH solution and removing the KOH in excess.

The sodium silicate was obtained dissolving SiO_2 in hot NaOH 25%, according to the method of [3].

The heteropolyacid was separated and purified by the method Drechsel of repeated extraction with ether in H_2SO_4 8N. The purity of the compound was controlled electophoretically using an instalation similar to that described by Consden, Gordon and Martin. [4] The study of electrocromatogram performed on a drop from the solution of the heteropolyacid, in NaCl 1 M, during 30 minutes at 2,5 mA and 580 V and the identification by exposing the cromatogram to a UV–lamp indicated the presence of only one spot with a mobility of:

$$u = + 2{,}66 \cdot 10^{-4}\ \mathrm{cm^2\ V^{-1}\ S^{-1}}$$

The chemical analysis of heteropolyacid imposed a detailed study of this system because the well known difficulty presented by the separation of tungstene from niobium. Many analytical methods were tried, the most adequate being the analysis of Si by volatilisation with HF[5] and dosage of W + Nb by precipiting as oxinates and ignition to oxides.[6,7] Separately the tungstene was measured spectrophotometrically as sodium tungstovanadophosphate. [8] The results of chemical analysis are indicated in table 1.

Table 1

Results of chemical analysis of the $H_6[SiW_{10}Nb_2O_{40}]$ solution

Compound	Molar concentration in solution			Si : Nb : W ratio	
	Si	Nb	W	from chemical analysis	from spectrophotometrical titration [1]
$H_6[SiW_{10}Nb_2O_{40}]$	5.5×10^{-3}	10.8×10^{-3}	5.6×10^{-2}	1 :1,96 :10.18	1. :2 :10

To measure the basicity of an acid, conductometrical titrations with Radelkis tip OK–102 and potentiometrical titration with NaOH using a pH – meter MV – 11 equiped with a glass electrode were performed. The basicity was controlled chemically too by the synthetising the K^+, NH_4^+, Cs^+ and Tl^+ salts of the heteropolyacid. These salts were generally obtained by the following method: to a freashly prepared and analyzed concentrated heteropolyacid solution, the calculated quantities of salts KCl, NH_4Cl, Cs_2SO_4 and $TlCH_3COO$ (aqueous solutions) were slowly added with continuous stirring, at the room temperature. After mixing, the solutions were a clear appearence (excepted the Tl^+salts), what demonstrated that they are pure, if not the respective salts of acids should be precipitated generating impurities more or less soluble (metatungstic acid and 12-tungstosilicic acid). After 2 folds recrystalisation from aqueous solution, in every case the pure salts are obtained as yellow bright crystals.

[2] M. Lehne and H. Goetz, *Bull. Soc. chim. France*, **1961**, 334.

[3] V. Chiola and C. D. Vanderpool (to Sylvania Electric Products Inc.) U.S. 3, 361, 518, 2 Jan. 1968; *Chem. Abstr.*, **68**, 61053v (1968).

[4] R. Consden, A. H. Gordon and A. P. Martin, *Biochem. J.*, **40**, 33 (1946).

[5] A. I. Kokorin and R. L. Dimant, *Zhur. obsehei Khim.*, **24**, 971 (1954).

[6] G. O. Müller, "Praktikum der Quantitativen Chemischen Analyse" S. Hirzel Verlag, Leipzig, 1959, p. 280.

[7] I. M. Kolthoff and P. J. Elving, "Treatise on Analytical Chemistry" Part II vol. 6, Interscience Publishers, New York–London, 1964, p. 285.

[8] B. Charreton, F. Chauveau, G. Bertho and P. Courtin, *Chem. analyt.*, **47**, 17 (1965).

Their chemical analysis was performed similarly as for the free acid in the case of W, Nb and Si. What concernes the dosage of cations, the following methods were used: K^+ and Cs^+ with tetra-phenylborate, [9,10], Tl as. TlI [11] and N by Dumas method. The content of water was thermogravimetrically measured. The results of chemical analysis are indicated in table 2.

Table 2

Chemical analysis of the K^+, NH_4^+, Cs^+ and Tl^+ salts of decatungstodiniobiosilicic acid

Compound		%							
		WO_3	Nb_2O_5	SiO_2	H_2O	K_2O	Cs_2O	Tl_2O	N
$K_6[SiW_{10}Nb_2O_{40}] \cdot 12\ H_2O$	calcd.	73.75	8.45	1.91	6.88	8.99			
	found.	74.02	8.40	1.89	6.86	8.91			
$(NH_4)_6[SiW_{10}Nb_2O_{40}] \cdot 4\ H_2O$	calcd.	80.71	9.25	2.10	2.50				2.92
	found.	80.81	9.08	2.05	2.48				2.86
$Cs_6[SiW_{10}Nb_2O_{40}] \cdot 4\ H_2O$	calcd.	65.09	7.46	1.69	2.02		23.74		
	found.	65.15	7.47	1.70	2.04		23.93		
$Tl_6[SiW_{10}Nb_2O_{40}] \cdot 6\ H_2O$	calcd.	57.57	6.60	1.49	2.68			31.64	
	found.	57.70	6.42	1.44	2.56			31.40	

The chemical character of solution was controlled by recording its spectrum in visible – ultraviolete domain with a spectrophotometer UV–VIS Zeiss and performing a polarographical analysis with a Radelkis analyser.

RESULTS AND DISCUSSIONS

The forming reaction of decatungstodiniobiosilicic anion may be expressed by the following equation:

$$SiO_3^{2-} + 10WO_4^{2-} + 2NbO_3^{-} + 18\ H^+ = [SiW_{10}Nb_2O_{40}]^{6-} + 9H_2O$$

The results of chemical analysis of the freshly prepared free heteropolyacid indicated in table 1 demonstrate that a combination with a ratio 10W :2Nb :Si was obtained, fact which was confirmed by spectrophotometrical titration too [1]. Although the decatungstodiniobiosilicic acid cannot be obtained in solid state, its solution is stable for a long time.

---

[9] M. Kohler, *Z. analyt. Chem.*, B, **138**, 9 (1953).

[10] G. Wittig and P. Raff, *Liebigs Ann. Chem.*, **573**, 195 (1950).

[11] I. M. Kolthoff and P. J. Elving, "Treatise on Analytical Chemistry" Part II vol. 2, Interscience Publishers, New York–London, 1962, p. 92.

The conductometrical curve of 10 ml from the solution of the heteropolyacid (Tw = 0,00392) with a solution of $TlCH_3COO$ ($T_{Tl}=0,02868$) is indicated in figure 1. A crossing point is obtained after a consuming 1,1 ml $TlCH_3COO$ what corresponds to a ratio of 10W : 6,19 Tl. During the titration the salt of the heteropolyacid is formed as a pale yellow precipitate according the following reaction at the equivalence point:

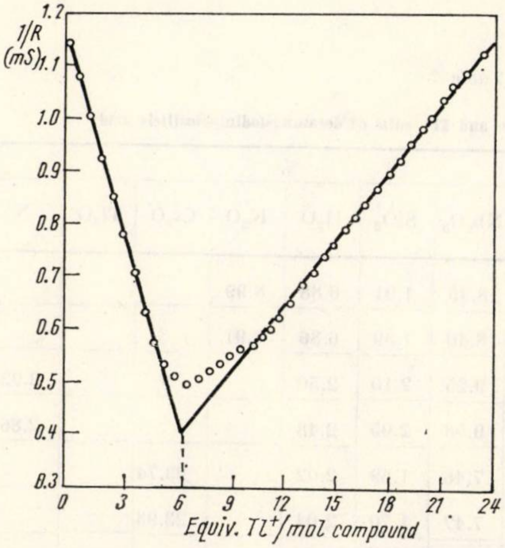

Fig. 1. — Conductometrical titrations curve of $H_6[SiW_{10}Nb_2O_{40}]$ with $TlCH_3COO$.

$$H_6[SiW_{10}Nb_2O_{40}] + 6\,TlCH_3COO = Tl_6[SiW_{10}Nb_2O_{40}] + 6\,CH_3COOH$$

Titrating the conductometrically 15 ml of heteropolyacid ($T_W = 0,00286$) with NaOH 10^{-1}N a crossing point is obtained at a consumption of 1,42 ml NaOH what corresponds to a ratio of 10 W : 6 Na (fig. 2).

The potentiometrical titration curve of the free heteropolyacid exhibits two points of inflexion (breaks in the curve) indicated in the figure 3.

The first point of inflexion corresponds to the neutralisation point of the H^+ ions (10W :6Na), the second point being correspondent to the total degradation of the heteropolyanion (10 W : 18NaOH) by the alkali. Because of the slowl proceeding of the anionical degradation to simple compounds at a temperature of 20°, a potentiometrical titration was performed on different samples, corresponding to each point of the curve, the pH being recorded 5 days after the preparing of the samples. The authors performed titration also the direct potentiometrical titration, but to realize the equilibres, after the adding of each NaOH portion, the samples were heated to 60° and cooled to room temperature.

The synthesis of the K^+, NH_4^+, Cs^+ and Tl^+ salts (see table 2) indicated also that the heteropolyanion exhibits a basicity of 6. As conclusion, the good correspondence between the theoretical basicity and the value measured by conductometrical and potentiometrical titrations (and controlled by synthesis and analysis of K^+, NH_4^+, Cs^+ and Tl^+ salts) was demonstrated.

If the heteropolyanion $[SiW_{10}Nb_2O_{40}]^{6-}$ exhibits a Keggin type structure, then its UV spectrum must have a peak at $\lambda \approx 260$ nm, which is the characteristic absobtions band of heteropolyanions 1:12

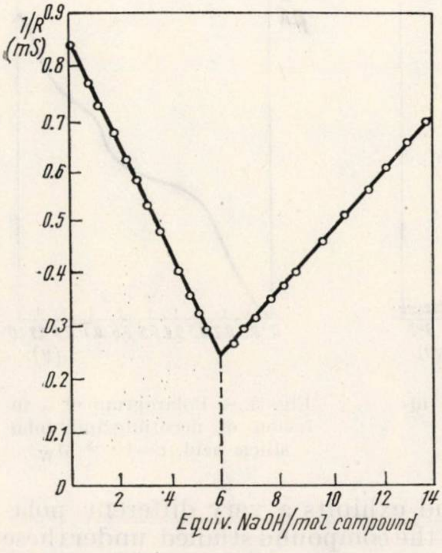

Fig. 2. — Conductometrical titrations curve of $H_6[SiW_{10}Nb_2O_{40}]$ with NaOH 10^{-1} N.

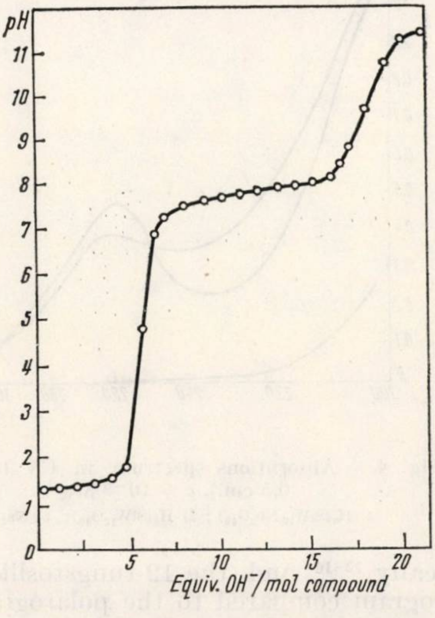

Fig. 3. — Potentiometrical titration of 15 ml $H_6[SiW_{10}Nb_2O_{40}]$ ($T_W = 0{,}00286$) with NaOH 10^{-1} N.

assigned to a charge transfer from the oxygen atoms of their structure to the tungsten atoms to a $p_\pi - d_\pi$ transfer[12] respectively. Indeed the visible — ultraviolet spectrum of a $H_6[SiW_{10}Nb_2O_{40}]$ solution, compared to the spectrum of $H_4[SiW_{12}O_{40}]$ solution (fig. 4) exhibits a more attenuated peak at $\lambda \approx 265$ nm, shifted to greater wave lengths as the value characteristic for the 12-tungstosilicic acid ($\lambda \approx 257$ nm). The shift of this band is depending on the strength of the $p_\pi - d_\pi$ — transfer. In our case, the shift of the peak to greater wave lengths is due to the weakening of the W — O bond from the octaeders nearer situated to the heteroatom Nb, which has less optical electronegativity as W, and so the formed Nb — O bonds are stronger.

Studying the polarographical reduction on dropping mercury electrode of the decatungstodiniobiosilicic acid having a concentration of 10^{-3} M in a solution of LiCl 1N in the 0— —1 V potential domain presented in the figure 5 it may be observed: that the polarogram exhibits two well defined steps at −0,15 V and −0,65 V.

---

[12] Hynso So and M. T. Pope, *Inorg. Chem.*, **11**, 1441 (1972).

These two steps are maintained also when the polarographical analysis is performed on the solution of the $K_6[SiW_{10}Nb_2O_{40}]$ salt. Because the anions : silicate, tungstate and niobiate were not reduced polarographically[13–16] and the 12-tungstosilicic acid exhibits a very different polarogram compared to the polarogram of the compound studied under these conditions, the present authors consider that these polarographical steps are characteristic for the $[SiW_{10}Nb_2O_{40}]^{-6}$ anion.

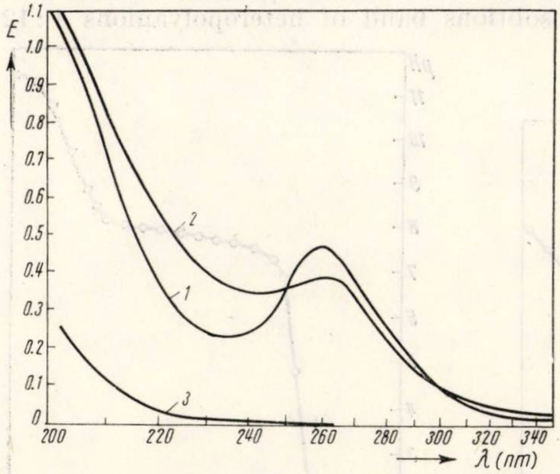

Fig. 4. — Absorbtions spectrum in UV (cuvette of 0,5 cm.), $c = 10^{-3}\ M_W$:
1) $H_6[SiW_{10}Nb_2O_{40}]$; 2) $H_4[SiW_{12}O_{40}]$; 3) Na_2WO_4.

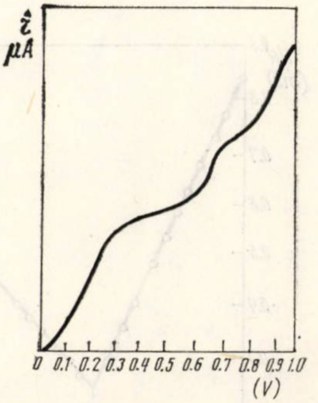

Fig. 5. — Polarogram of a solution of decatungstodiniobosilicic acid, $c = 10^{-3}\ M_W$.

CONCLUSIONS

The acid $H_6[SiW_{10}Nb_2O_{40}]$ was synthetised and its state in solution : composition, basicity and structure (through UV spectrum and polarographical reduction) was established.

The K^+, NH_4^+, Cs^+ and Tl^+salts of this heteropolyanion were synthetised, and the characterization of their solid state (X and IR spectres and thermal stability) will be described in a future paper.

[13] P. Souchay, *Talanta*, **12**, 1187 (1965).

[14] R. Ripan A. Duca and N. Calu, *Studii și Cercetări Chim. Fil. Cluj.*, **11**, 207 (1960).

[15] M. T. Pope and G. M. Varga Jr., *Inorg. Chem.*, **5**, 1249 (1966).

[16] G. Hervé, *Ann. Chim. (France)*, **6**, 219 (1971).

Revue Roumaine de Chimie, 21 4, 595–620 (1976)

DYES FOR SYNTHETIC FIBERS. IX[1]

DISPERSE AZO-DYES FOR POLYESTER FIBERS

A. SPILIADIS, POMPILIA GHEORGHE, HEDWIGA SZÖGY and
ANGELA SĂVULESCU

Chemical Research Institute, Spl. Independenţei 202, Bucharest, Romania

Received October 9, 1974

The work presents a series of aspects connected with the disperse dyes class that are used to dyeing synthetic fibers, especially polyester fibers. An analysis is made of the relation between the structure, absorption spectra and tinctorial properties (shade light-and thermofixation fastness, etc.) The principal classes of dyes, classified according to the chemical structure criterion, are reviewed with a view to pointing out the effect of the substituents for every class. The category of monoazo dyes without a heterocyclic ring includes especially the dyes with such groups as: nitro, halogeno, alkyl, cyano, etc. attached to the diazocomponent ring and such groups as: alkyl, cyanoalkyl, hydroxyalkyl, alkoxyalkyl, acetoxyalkyl, etc. existant in the coupling component. The category of monoazo dyes with a heterocyclic ring presents the dyes which are derived from thiophen, pyrazol and pyrazolone, thiazole, 2-aminobenzothiazole, pyridine and pyrimidine, indole, thiadiazole, 1, 3, 5—triazine and quinoline.

1. INTRODUCTION

Among the synthetic fibers the polyesters as such or in mixture require special qualities on the part of the disperse dyes. It is enough to recall the mandatary use of high temperature and pressures (wet Burlington beam process or dry thermosol proceses) the achievement of high dispersion degree and the use of "carriers" to increase the dye diffusion into the fiber, etc.

For these reasons, many of the called "acetate dyes" initially used to dye cellulose acetate fibers are unacceptable for the polyester, or generally for the dyeing of synthetic fibers.

In the United States, for example, although cotton holds the first place in the textile market according to Teintex,[2] the use of polyester fibers will increase by about 50% during 1974—1978 (4500 million lb in 1978). During the same interval, an increase of Nylon and acetate fibers about 30%, respectively 5%, is also stipulated. It is interesting to note that even a decrease in the use of cotton and wool is estimated. Regarding the use of disperse dyes an increase of about 36% is estimated for 1973— 1978.

---

[1] Part VIII A. Spiliadis, D. Breţcanu, R. Schip, V. Cornea, H. Szögy, A. Athanasiu, *Teintex-Revue gen. mat. col.*, **9**, 532 (1970).

[2] Cl. Delecluse, *Teintex — Revue gen. mat. col.*, **2**, 63 (1974).

This paper presents categories with or without a heterocyclic ring in the molecule, analysing different aspects such as : the relations between the structure and the colour of the dyes, the absorption spectra, the tinctorial performances, etc.

We would like to mention that the diazo and coupling compounds lead to dyes which are used to the dyeing of polyester fibers and often of other synthetic fibers.

2. GENERAL REMARKS ON THE RELATIONS BETWEEN STRUCTURE AND COLOUR OF THE DYES, TINCTORIAL PROPERTIES, FIBER, ETC. [3-6]

Taking into account the inductive effect (I) and the electromer or mesomer effects (E) transmitted through the C—C bonds, π-electron bonds, respectively the OH, O Alkyl, NH Alkyl, N(Alkyl)$_2$ groups have an electron-donating capacity (+E) higher than the electron-attracting capacity (—I).

So, this capacity should determine the decrease of light fastness (LF). For example, the N(Alkyl)$_2$ groups, more basic than the NH$_2$ group, present this LF decrease :

$4-NO_2$ — azobenzene — $4-NH_2$ . . . . LF 5—6

$4-NO_2$ — azobenzene — $2-N(CH_3)_2$ . . . LF 4—3

The groups with electron-accepting (—E) and electron-attracting (—I) capacity should produce an increase of LF determined by the decrease of the molecule polarity (e.g. NO_2, SO_2, NH_2, $CONH_2$, COOAlkyl).

The sublimation fastness values (SF) are particularly dependent on the dye vapour tension.[7-9] August's equation $\ln p = -\frac{E_s}{RT} + \text{const.}$ provides the vapour tension value (p), E_s being the interval sublimation heat (kcal/mol.grd), equal to the difference between the energy content of one mol. in solid, respectively gaseous state. This energy is necessary to overcome the binding forces in the transition from solid to gaseous state. [10]

The vapour tension is very likely influenced by the molecule polarity, besides other factors (molecule size and geometrical arrangement, temperature, time, auxiliary agent type. etc. [11]

A higher polarity (which means a lower vapour tension) should determine a higher SF and conversely.

---

[3] S. V. Sunthankar and V. Thanumoorthy, *Textile Res. J.*, **39**, 606 (1969).

[4] Ch. H. Giles, K. V. Datye, B. J. Hojiwala, N. B. Shah and D. Smith, *Textile Res. J.*, **36**, 587 (1966).

[5] H. G. Wippel, *Melliand Textilber.*, **50**, 1090 (1969).

[6] S. U. Sunthankar and V. Thanumoorthy, *Indian J. Chem.*, **8**, 599 (1970).

[7] K. V. Datye, S. C. Pitkar and V. M. Puzao, *Textilveredlung*, **5**, 262 (1973).

[8] C. J. Bent, T. D. Flynn and H. A. Summer, *J. Soc. Dyers and Colourists*, **12**, 606 (1969).

[9] R. T. Norris, *Textilveredlung*, **5**, 280 (1973).

[10] O. Stepanek, *Melliand Textilber.*, **6**, 707 (1970).

[11] H. U. von der Eltz, H. Selfert and W. Birke, *Chem. Fasern u. Textil Anwendungstechn.* **21**, 678 (1971).

So, it would follow that the electron donating (+E) or electron repellent (+E) groups, or the groups with $+E > -I$, should increase the sublimation (SF) and thermofixation fastness (TF) by the increase of the molecule polarity. A decrease of the LF should take place concomitantly.

Anyway, the fact must be specified that it is difficult or even very difficult to establish a precise and general available relation between the tinctorial fastnesses and the electronic arrangement.

Many factors contribute to the achievement of tinctorial performances and their way of interaction is very difficult and sometimes even impossible to specify.

Other aspects of the relations between structure and tinctorial fastnesses will be presented.

Regarding the fiber-dye interaction, for example, in the case of the disperse dyes migration (probably in the vapour phase), from the cellulose to the polyester fibres, the dyes with lower SF do not always present a diffusion rate appreciably higher than those with a high SF.[12]

On the other hand, the vapour tension as a decisive factor of the sublimation fastness must be regarded as related both to the partial vapour pressure of the pure dye and to the partial vapour pressure of its polymer solution.[13]

Although such groups as $N(C_2H_4OH)_2$; $N(C_2H_4OCOCH_3)$; $N(C_2H_4OC_2H_4CN)_2$, etc. found in the coupling component are electron-attracting, they do not always diminish the SF and TF (by the molecule polarity diminution) probably because of many reasons: on the one hand, the effect (−I) of the groups OH, $OCOCH_3$, OC_2H_4CN, etc. is much diminished by the length of the saturated chain; on the other hand, because of their structure, these groups increase the dyes solubility in the fiber and diminish the sublimation tendency, etc.

It is also difficult to account for nearly equal SF of the eight following disperse dyes.

(BCA = N-beta-cyanoethyl-N-beta-acetoxyethyl aniline)

1. Foronorange E–GFL (aniline → cresidine → phenol) 5
2. Foronorange RFL (aniline → 2,5-dimethoxy-aniline → phenol) 5
3. Palanilorange B (aniline → 1-naphthylamine → phenol) 4–5
4. Foronscharlach 3-GFL (2-chloro-4-nitro-aniline → BCA) 5
5. Forongelbbraun S-2RFL (2,6-dichloro-4-nitro-aniline → BCA) 5
6. Fornoscharlach GFL (2,4-dinitro-aniline → BCA) 5
7. Foronrot SFL (2-cyano-4-nitro-aniline → BCA) 5
8. Foronmarineblau S – 2 GL (6-chloro-2,4-dinitro-aniline → 1-methoxy– 4-N-acethylamino-2-N,N′-di-beta-acethyloxyethylamino-benzene) 4–5

---

[12] H. Gerber and F. Somm, *Tinctoria*, **9**, 315 (1972).

[13] W. Mc. Dowell, *Melliand Textilber.*, **11**, 1265 (1972).

The difficulty of finding the explanation to the fact that the SF values of these dyes are equal consists of the following :

— on the one hand, the last five dyes should have lower SF, according to the decrease of the molecule polarity, because of the electron-attracting groups ;

— on the other hand, the extension of the conjugated chain, by NO_2 groups, increases the whole electronic arrangement instability and the whole system becomes more unstable ; this should reduce the vapour tension and, therefore, increase the SF value ;

— the electronic system stability of the first three dyes should be lower ;

— the last five dyes should show a clearly higher polyester fiber solubility than the first three ;

— finally, the only doubtless fact is that, if other parametres (preponderantly the dye-fiber interaction) did not exist, the SF values should not be equal.

It follows that such groups as NO_2, CN, COOAlkyl directly attached to the diazo-or coupling-component ring can have a variable effect : a molecule polarity decrease (—I, —E effect), a polarity increase by the conjugated system extension (in the *ortho* and *para* position to the azo groups), an increase or a decrease of the solubility in fiber (the CN, COOAlkyl, etc. groups increase the solubility more than the NO_2 groups).

Thus, for certain dyes prepared from 2-chloro-4-nitroaniline and various pyrazolone derivatives, the TF on the polyester fiber increases in the following direction (this refers to the groups attached to the 5-pyrazolone ring)

$$3{-}CH_3 - < 1{,}3(C_6H_5)(CH_3) - < 1{,}3\,(C_6H_5)\,(COOCH_3) -$$

although the electronegativity increases in the same way (probably the solubility in fiber increases in the same way).

The dyes obtained from $2,4,1\text{-}(NO_2)_2C_6H_3NH_2$ or $2,4,1\text{-}(CN)\,(NO_2)C_6H_3NH_2$ and the same coupling component $C_6H_4N(C_2H_5)C_2H_4CN$ present light fastnesses of 2 and 5—6 respectively, although the NO_2 group electronegativity is about the same as that of the CN group.

The difference is probably due to the CN group, which seems to have a higher effect on the increased solubility in the fiber.

If the NO_2 group in the 2-position of the diazo compound is replaced by the CH_3 group (+I), the LF value increases from 2 to 4—5, although the molecule polarity grows.

At the same time, the TF values of the mentioned dyes do not correspond to their electronegativity ; thus, the dyes having in the 2-position of the diazo compound, the NO_2, CN, CH_3 groups present the following TF values : 3—4 ; 3—4 ; 2—3, although the probable polarization increase is $NO_2 \leqslant CN < CH_3$.

The same diazo compound $2,6,4,1{-}Cl_2(NO_2)C_6H_2NH_2$ coupled with different components presents an LF increase (on the polyester fiber) in the following way : $N{-}(C_2H_5)\,(C_2H_4OH) < N{-}(C_2H_4OH)\,(C_2H_4CN) < N{-}\,(C_2H_4CN)(C_2H_4OCOCH_3) \cong N{-}(C_2H_4CN)_2 \cong N{-}(C_2H_4OCOCH_3)_2 \cong N{-}(C_2H_4OC_2H_4COOCH_3)_2 \cong N{-}(C_2H_4OC_2H_4CN)_2$ which is in accordance with increase in electronegativity.

For the same dyes, the TF values decrease while the electronegativity increases, which is probably due to the increase in the solubility of the fibre too, caused by the replacement of the N–Alkyl groups by N-cyanoalkyl, N-acyloxyalkyl, N-cyanoalkyloxyalkyl, etc. groups.

In the case of the absorption spectrum, the influence of the electronic arrangement is more visible.

Thus, for the dyes obtained from the following diazo compounds: $C_6H_5NH_2$; 4,1-$(CN)C_6H_4NH_2$; 4,1-$(NO_2)C_6H_4NH_2$; 2,4,1-$(Cl)(NO_2)C_6H_3NH_2$; 2,4,1-$(NO_2)C_6H_3NH_2$; 2,4,6,1-$(NO_2)_2ClC_6H_2NH_2$; 2,4,6,1-$(NO_2)_3C_6H_2NH_2$ and the same coupling component, the maximum absorption increases in the enumeration sense.

The NO_2 groups with strong –I, –E effects produce a bathochromic effect because of the extension of the conjugation system (the NO_2 group being included in the conjugation system).

The situation is similar to the dyes obtained from certain heterocyclic amines, e.g. 6-methoxy-2-amino-benzothiazole (6–MABT).

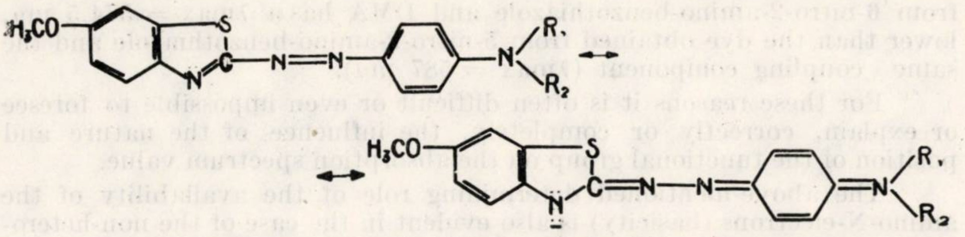

The bathochromic shift of the absorption spectrum is determined by the contribution of the dipolar structure to the ground state.

A higher contribution of the dipolar structure implies, generally speaking, a higher availability (basicity) of electrons of the amino-group, that leads to an increase in the heteroatom electrons density (basicity).

Finally, the nature of the R_1 and R_2 group determines, in particular, the higher or lesser amino-N-electron density (and, consequently, the heteroatom basicity).

For example, the 6-MABT diazotized and coupled with the components: $(C_6H_5)_2NCH_3$; $C_6H_5N(C_2H_4OH)_2$; $C_6H_5N(CH_3)_2$; $C_6H_5N(C_2H_5)_2$ leads to dyes (actually pigments) which present λ max increase in the order of their sequence. This increase is according to the amino-N-electrons availability, that is higher for $-N(CH_3)_2$ or $-N(C_2H_5)_2$ and lower for $-(C_6H_5)_2NCH_3$ (according to the $p-\pi$ conjugation and to the higher electron-repellent capacity of the alkyl groups).

The heteroatom basicity was studied by a comparative analysis of the N-quaternization reaction rates.

The dyes obtained from 2-amino-benzothiazole diazotized and coupled with N-beta-N-cyanoethyl-N-ethyl-aniline; N,N′-dimethyl-aniline (DMA); N,N-di-beta-hydroxyethyl-*m*-toluidine and 1-methoxy-4-N-acetylamino-2-(N-beta-cyanoethyl-N-beta-hydroxyethyl)-amino-benzene present a spectrum with wavelength lower than those of the dyes obtained from 2-amino-6-nitro-benzothiazole and the same coupling components, according to the previsions (conjugated chain extension by the presence of the nitro group).

The bathochromic shift of the spectrum, due to the conjugated chain extension (nitro group) is also certified in the case of dyes obtained by coupling DMA with 2-amino-benzothiazole (λmax = 509 mμ) or 6-nitro-2-amino-benzothiazole (λ max = 574.5 mμ) as well as in the case of dyes obtained from the same coupling component and the amines: 3-amino-benzo-isothiazole (λmax = 548 mμ) or 5-nitro-3-amino-benzo-isothiazole (λmax = 598 mμ).

A nearly equal spectrum (λmax = 556–566 mμ) of the dyes obtained from the DMA coupled with the amines: 4-chloro-; 5-chloro-; 6-chloro and 7-chloro-3-aminobenzoisothiazole is justified by the fact that chlorine has an electron-attracting capacity (–I) slightly higher than the electron-donating capacity (+E).[14]

But it is difficult to account for the fact that the dye obtained from 6-nitro-2-amino-benzothiazole and DMA has a λmax = 574.5 mμ, lower than the dye obtained from 5-nitro-2-amino-benzothiazole and the same coupling component (λmax = 587 mμ).

For these reasons it is often difficult or even impossible to foresee or explain, correctly or completely, the influence of the nature and position of the functional group on the absorption spectrum value.

The above-mentioned determining role of the availability of the amino-N-electrons (basicity) is also evident in the case of the non-heterocyclic dyes. In this case the availability of the electrons increases the polarity of the whole molecule.

For example, for the dyes obtained from 2,6,4,1-(Cl_2) $(NO_2)C_6H_4NH_2$ diazotized and coupled with $C_6H_5N-(C_2H_4OH)_2$; C_6H_5N-$(C_2H_4CN)_2$; $C_6H_5N-(C_2H_5)_2$, λ max increases according to the enumeration, concomitantly with the amino-N-basicity increase.

When the conjugation is interrupted, the bathochromic shift is diminished or even called off.

Thus 2,5,1-$(CH_3O)(NHCOCH_3)C_6H_3NH_2$ diazotized and coupled with 3-methyl-5-pyrazolone (MP) leads to a red shade, and with 1-phenyl-3-methyl-5-pyrazolone (FMP) presents a yellow-reddish shade;

4,1-$(NHCOCH_3)C_6H_4NH_2$ with MP leads to yellow-reddish; 4,1-$[N,N$-$(C_2H_5)_2]C_6H_4NH_2$ with MP to red; 2,4,1-(Cl) $(NO_2)C_6H_3NH_2$ with MP or with FMP leads to the yellow shade; 2,6,4,1-$(Cl)_2$ (NO_2) $C_6H_2NH_2$ with MP or with FMP leads also to the yellow and 6-MABT with MP leads to orange.

In such cases, the action of the nitro group consists only in the electronattracting effect on the electronic configuration of the whole dye molecule, without determining a conjugated chain extension. For this reason, a low spectrum hypsochromic shift can even occur by transition from pigment (without nitro group) to nitro pigment.

---

[14] H. G. Wippel, Melliand Textilber., **50**, 1090 (1969).

We go on by presenting the main publications on the dyes used in the dyeing of synthetic fibers (especially for polyester fibers).

To simplify, the following abbreviations are used: Alk = methyl or ethyl; Hlg = halogen; Ar = aryl; $X_1 = NHCOCH_3$; $X_2 =$ alcoxy; $X_3 = -O-\underset{\underset{O}{\|}}{C}-CH_3$; $X_4 = -C_2H_4CN$; $X_5 = C_2H_4OH$; $X_6 = -C_2H_4OCH_3$; $X_7 = -C_2H_4OCOCH_3$; TpA for 2-amino-thiophen; Pz for pyrazole; PzO for pyrazole-5-one; TzA for 2-amino-thiazole; ABz for 2-amino-benzothiazole; Py for pyridine; PyO for 2-pyridone; PyM for pyrimidine; TDz for thiadiazole.

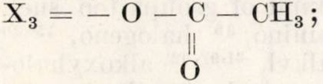

3. MONOAZO DYES WITHOUT HETEROCYCLIC RING

This class includes the dyes that require relatively simple processes of diazotization and coupling, but sometimes present special difficulties of a technological nature.

Generally, these dyes agree with this kind of formula:

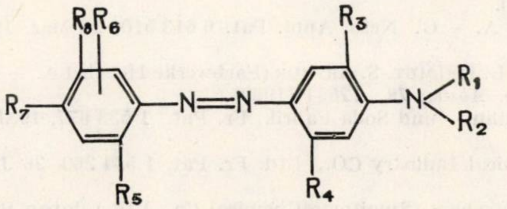

where: **R**$_1$ and **R**$_2$ = Alk; C_2H_4Cl; C_2H_4OH; C_2H_4CN; $C_2H_4OZ_1$ (Z_1 = Alk); C_2H_4CN; alkoxyalkyl; $C_2H_4OCOZ_2$ (Z_2 = H; Alk; Ar; alkoxyalkyl); $CH_2C_6H_4COOAlk$; $C_2H_4OCONHZ_3$ (Z_3 = H; Alk; Ar); $C_2H_4OCH_2CH_2SO_2C_2H_5$; $C_6H_4SO_2NHZ_4$ (Z_4 = H; Acetyl); $C_2H_4OCC_6H_3SO_2C_6H_5$; $CH_2CZ_5 = CH_2(Z_5 = H; \downarrow\uparrow Hlg)$; $(CH_2)_nC_2H_5(n = 1,2)$; $C_2H_4COC_2H_5$; $C_2H_4OC_2H_4OCOOCH_3$; $C_2H_4O_2COAlk$; $CH_2CH(OH)CH_2OZ_6(Z_6 = Alk; Ar)$; $CH_2CH(OZ_7)CH_2Cl(Z_7 = H; Acyl)$; $CH_2CH(OH)Z_8$ (Z_8 = Alk; Ar), etc.

R$_3$: H; Alk; X_1; X_2; Hlg; CN; NO_2, etc.

R$_4$: H; Hlg; Alk; OH; OAr; X_1; X_2; $NHCOCH = CH_2$; $NHCOCH_2OC_6H_5$; $OCH_2C_6H_5$; $OCOCH_3$, etc.

R$_5$, **R**$_6$, **R**$_7$: H; Hlg; Alk; CN; CF_3; NO_2; $COCH_3$; SO_2CH_3; CH_3; X_2; $SO_2NHC_2H_4Z_{10}(Z_{10} = OH, CN)$;
NHC_6H_4OAr; $C_6H_4CON(CH_3)_2$, etc.

R$_8$: H; Hlg; Alk; CN; CF_3; NO_2; $COCH_3$; SO_2CH_3. etc.

3.1. DIAZO-COMPONENTS

We go on by presenting aryl-amines with low or very low basicity that besides the nitro-group [15–35] have another kind of groups too such as: phenolic, [36,37] alkoxy, [38] alkoxy-phenyl-amino, [39] halogeno, [15–20,23,24,26–28,30,31,35,40–90] alkyl-halogeno, [61] trifluoro-alkyl, [31,91,92] alkoxyhalogeno, [93,94] carboxyalkyl, [46] acetiloxy,[36] cyano attached directly to the ring,[15,16,18,20,26,29,30,33,35,47,81,95–108] halogeno-cyano,[51,69,76,81,84,100,109–114] methyl-sulphonyl as such or with halogeno-groups, cyano, trifluoro-alkyl etc. [30,100,114–123]

[15] Ciba Ltd. Neth. Appl. Pat. 6 404 855 4 Nov. 1964; *Chem. Abstr.*, **62**, 13279 (1965).

[16] Ciba Ltd. Fr. Pat. 1 394 697, 2 Apr. 1965; *Chem. Abstr.*, **65**, 15550 (1966).

[17] Ferbwerke Hoechst A. G. Belg. Pat. 663 162, 28 Oct. 1965; *Chem. Abstr.*, **65**, 4002 (1966).

[18] P. W. Barker (Imperial Chemical Industries Ltd.) Brit. Pat. 988 629, 4 Apr. 1965; *Chem. Abstr.*, **63**, 3083 (1965).

[19] P. W. Barker, B. R. Fishwick, J. S. Hunter, H. R. Murton (Imperial Chemical Industries Ltd.) Brit. Pat. 993 162, 26 May 1965; *Chem. Abstr.*, **63**, 7 144 (1965).

[20] Ciba Ltd. Fr. Pat. 1 498 812, 20 Oct. 1967; *Chem. Abstr.*, **69**, 97 699 (1968).

[21] Cassella Farbwerke Mainkur A. — G. Belg. Pat. 672 259, 1 Mar. 1966; *Chem. Abstr.*, **65**, 12313 (1966).

[22] Badische Anilin— und Soda Fabrik A. — G. Belg. Pat. 642 241, 4 May, 1964; *Chem. Abstr.*, **65**, 710 (1965).

[23] J. R. Geigy A. — G. Neth. Appl. Pat. 6 613 510, 28 Mar. 1967; *Chem. Abstr.*, **67**, 109610 (1967).

[24] G. Helmut, L. Helmut, S. Arthur (Farbwerke Hoechst A. — G.) Ger. Pat. 1 276 255, 29 Aug. 1968; *Chem. Abstr.*, **70**, 12654 (1969).

[25] Badische Anilin — und Soda Fabrik Fr. Pat. 1 533 677, 19 Jul.1968; *Chem. Abstr.*, **71**, 71912 (1969).

[26] Mitsui Chemical Industry CO., Ltd. Fr. Pat. 1 534 269, 26 Jul. 1968; *Chem. Abstr.*, **72**, 4328 (1970).

[27] Enomoto Shigeham (Sumitomo Chemical Co., Ltd.) Japan Pat. 69 14, 714, 30 Jun. 1969; *Chem. Abstr.*, **72**, 45013 (1970).

[28] Nakagawa, Ryoichi (Daito Chemical Industry Co., Ltd.) Japan Pat. 69 30, 629, 9 Dec. 1969; *Chem. Abstr.*, **72**, 91 461 (1970).

[29] Farbwerke Hoechst A. — G., Fr. Pat. 1 533 014, 12 Jul. 1968; *Chem. Abstr.*, **72**, 101845 (1970).

[30] S. Koller (Geigy, J. R., A. — G.) Ger. Offen. Pat. 1 955 957, 27 May 1970; *Chem. Abstr.*, **73**, 67 662 (1970).

[31] R. Haehnle, E. Hayer (Farbwerke Hoechst A. — G.) Ger. Offen. Pat. 1 957 681, 8 Jun. 1971; *Chem. Abstr.*, **75**, 99250 (1971).

[32] E. Hahn, W. H. Guenter (Badische Anilin— und Soda Fabrik A. — G.) U.S. Pat. 3 642 767, 15 Feb. 1972; *Chem. Abstr.*, **77**, 128054 (1972).

[33] H. J. Angliker, R. Peter (Ciba — Geigy A. — G.) Ger. Offen. Pat. 2 154 916, 25 May 1972; *Chem. Abstr.*, **77**, 128037 (1972).

[34] F. Merlo, R. R. Battisti, D. Domenis (Montecatini Edison Sipih; ACNA — Aziende Colori Nationali Affini, A.p.A.) Ger. Offen. Pat. 2 159 574, 15 Jun. 1972; *Chem. Abstr.*, **77**, 128035 (1972).

[35] Aiga Hiroshi, Fujii Fumio, Mukui Ken (Mitsui Toatsu Chemical Co., Ltd.) Japan Kokai. Pat, 7225, 488, 20 Oct. 1972; *Chem. Abstr.*, **78**, 5978 (1973).

[36] Mitsui Chemical Industry Co., Ltd. Brit. Pat. 1 019, 9 Feb. 1966; *Chem. Abstr.*, **64**, 12848 (1966).

[37] Tsutomo Sasa, Matahiko Asani, Minoru Yamaguki (Mitsui Chemical Industry Co., Ltd.) Japan Pat. 14 396 (66) Aug. 11; *Chem Abstr.*, **66**, 11853 (1967).

[38] W. Groebke, C. Mueller, W. Wehrli (Sandoz Ltd.) Fr. Pat. 1 513 947, 16 Feb. 1968; *Chem. Abstr.*, **70**, 116219 (1969).

[39] Ciba Ltd. Brit. Pat. 1 134 374, 20 Nov. 1968; *Chem. Abstr.*, **70**, 69281 (1969).

[40] G. Lange, C. Schuster, I. Eisele, W. Federkiel (Badische Anilin— und Soda Fabrik A. — G.) Brit. Pat. 887 416, 17 Jan. 1962 ; *Chem. Abstr.*, **57**, 8699 (1962).

[41] J. D. Sterling Jr. (E.I. du Pont de Nemours et Co.) U.S. Pat. 3 081 295, 12 Mar. 1963 ; *Chem. Abstr.*, **59**, 8905 (1963).

[42] Farbwerke Hoechst A. — G. Belg Pat. 630 424, 21 Oct. 1963 ; *Chem. Abstr.*, **61**, 8445 (1964).

[43] Ciba Ltd. Belg. Pat. 626 734, 1 Jul. 1963 ; *Chem Abstr.*, **62**, 671 (1965).

[44] Imperial Chemical Industries Ltd. Belg. Pat. 637 800, 24 Mar. 1964 ; *Chem. Abstr.*, **62**, 13280 (1965).

[45] Imperial Chemical Industries Ltd. Neth. Appl. Pat. 6 505 844, 8 Nov. 1965 ; *Chem. Abstr.*, **64**, 14321 (1966).

[46] Imperial Chemical Industries Ltd. Neth. Appl. Pat. 6 511 146, 28 Feb. 1966 ; *Chem. Abstr.*, **65**, 5566 (1966).

[47] Farbenfabriken Bayer A. — G. Brit. Pat. 982 936, 10 Febr. 1965 ; *Chem. Abstr.*, **63**, 1918 (1965).

[48] E. Merian, O. Senn (Sandoz Ltd.) Ger. Pat. 1 219 608, 23 Jun. 1966 ; *Chem. Abstr.*, **65**, 12312 (1966).

[49] Farbwerke Hoechst A. — G. Belg. Pat. 634 029, 24 Dec. 1963 ; *Chem. Abstă.*, **61**, 5825 (164).

[50] E. Stead (Yorkshire Dyeware and Chemical Co. Ltd.) Brit. Pat. 985, 254, 3 Mar. 1965 ; *Chem. Abstr.*, **62**, 16417 (1965).

[51] Sandoz Ltd. Brit. Pat. 855 488, 30 Nov. 1960 ; *Chem. Abstr.*, **55**, 11871 (1961).

[52] P. Rhyner, K. Antz (Ciba Ltd.) U.S. Pat. 3 235 471, 13 Jun. 1967 ; *Chem. Abstr.*, **67**, 65392 (1967).

[53] W. Bossard, H. Wegmueller (T. R. Geigy A. — G.) Swiss Pat. 423 038, 29 Apr. *Chem. Abstr.*, **67**, 65409 (1967).

[54] Fukada Kazuo (Nippon Kayaku Co., Ltd.) Japan Pat. 6815, 310, 27 Jun. 1968 ; *Chem. Abstr.*, **69**, 107597 (1968).

[55] Matsumoto Jintano, Yamamoto Masashi (Nippon Kayaku Co., Ltd.) Japan Pat. 68 17, 304, 22 Jul, 1968 ; *Chem. Abstr.*, **69**, 107599 (1968).

[56] E. Stead, R. D. Beanlands (Yorkshire Dyeware and Chemical Co., Ltd.) Brit. Pat. 1 037 167, 27 Jul. 1966 ; *Chem. Abstr.*, **65**, 13850 (1966).

[57] B. R. Fishwick (Imperial Chemical Industries Ltd.) Brit. Pat. 1 053 830, 4 Jan. 1967 ; *Chem. Abstr.*, **66**, 66729 (1967).

[58] Hisashi Chiaki, Yoshia Kimura (Mitsubishi Chemical Industries) Japan Pat. 18, 838 ('66) Oct. 31 ; *Chem. Abstr.*, **66**, 38865 (1965).

[59] Farbwerke Hoechst A. — G. Fr. Pat. 1 413 474, 8 Oct. 1965 ; *Chem. Abstr.*, **69**, 37084 (1968).

[60] Sasa Tsutomu, Asahi Matahiko, Yamaguchi Minoru, Takizuka Hitoshi (Mitsui Chemical Ond. Co., Ltd.) Japan Pat. 6805, 672, 1 Mar. 1969 ; *Chem. Abstr.*, **69**, 37083 (1968).

[61] B. R. Fishwick, H. R. Murton (Imperial Chemical Ind., Ltd.) Ger. Pat. 1 291 035, 20 Mar. 1969 ; *Chem. Abstr.*, **71**, 51228 (1969).

[62] R. D. Beanlands, J. F. Dawson (Yorkshire Dyeware and Chemical Co. Ltd.) Brit. Pat. 1 148 672, 16 Apr. 1969 ; *Chem. Abstr.*, **71**, 71914 (1969).

[63] B. Altermatt, C. Ruedi (Sandoz Ltd.) Fr. Pat. 1 533 868, 19 Jul. 1968 ; *Chem. Abstr.*, **72**, 56679 (1970).

[64] W. Groebke (Sandoz Ltd.) Fr. Pat. 1 541 430, 4 Oct. 1968 ; *Chem. Abstr.*, **72**, 68196 (1970).

[65] R. Hahn, C. Mueller (Sandoz Ltd.) Ger. Offen. Pat. 1 920 359, 6 Nov. 1969 ; *Chem. Abstr.*, **72**, 80333 (1970).

[66] G. R. Genta (American Aniline Products, Inc.) U.S. Pat. 3 503 955, 31 Mar. 1970 ; *Chem. Abstr.*, **73**, 89142 (1970).

[67] S. Koller (Geigy, J. R., A. — G.) Ger. Offen. Pat. 2 011 051, 17 Sep. 1970 ; *Chem. Abstr.*, **74**, 4632 (1971).

[68] R. Hahn, C. Mueller (Sandoz Ltd.) Swiss Pat. 493 599, 31 Aug. 1970 ; *Chem. Abstr.*, **74**, 4645 (1971).

[69] Hattori Hiroshi, Tada Shoji, Kaida Etoshi (Nippon Kayaku Co., Ltd.) Japan Pat. 69 24, 710, 18 Oct. 1969 *Chem. Abstr.*, **74**, 65553 (1971).

[70] J. Meybeck (Sandoz Ltd.) Ger. Offen. Pat. 2, 035, 002, 28 Jan. 1971 ; *Chem. Abstr.*, **74**, 113218 (1971).

[71] Ono Shinjiro, Hattori Yutaka, Tada Shoji, Meguerita Nagatoshi (Nippon Kayaku Co., Ltd.) Japan Pat. 7038, 987, 8 Dec. 1970 ; *Chem. Abstr.*, **74**, 113209 (1971).

[72] R. Hahn, C. Mueller (Sandoz Ltd.) Ger. Pat. 1 920 358, 14 Jan. 1971 ; *Chem. Abstr.*, **74**, 113216 (1971).

[73] D. Cornelius, H. von Brachel, E. Hermann, O. Graewinger (Cassella Farbwerke Mainkur A. — G.) Ger. Offen. Pat. 1 943 057, 11 Mar. 1971 ; *Chem. Abstr.*, **74**, 143311 (1971).

[74] W. Groebke, R. Wirz (Sandoz Ltd.) Ger. Offen. Pat. 2 103 361, 19 Aug. 1971 ; *Chem. Abstr.*, **76**, 4896 (1972).

[75] Ono Nobujino, Hattori Hiroshi, Tada Shoji, Kaida Tsunetoshi (Nippon Kayaku Co., Ltd.) U.S. Pat. 3, 621, 009, 16 Nov. 1971 ; *Chem. Abstr.* **76**, 87150 (1972).

[76] W. Groebke (Sandoz Ltd.) Ger. Offen. Pat. 2 117 987, 28 Oct. 1971 ; *Chem. Abstr.*, **76**, 73728 (1972).

[77] W. Groebke (Sandoz Ltd.) Ger. Offen. Pat. 2 054 685, 4 Nov. 1971 ; *Chem. Abstr.*, **76**, 73731 (1972).

[78] M. A. Weaver, D. J. Wallace (Eastman Kodak Co.) U.S. Pat. 3 546 204, 8 Dec. 1970 ; *Chem. Abstr.*, **76**, 87148 (1972).

[79] F. Vyskocil, Czech. Pat. 138 970, 15 Nov. 1970 ; *Chem. Abstr.*, **76**, 114970 (1972).

[80] R. Brian Fishwick, A. Quayle (Imperial Chemical Industries Ltd.) Ger. Offen. Pat. 2 130 992, 30 Dec. 1971 ; *Chem. Abstr.*, **76**, 128975 (1972).

[81] Toda Shazi (Nippon Kayaku Co. Ltd.) Ger. Offen. Pat. 2 137 023, 27 Jan. 1972 ; *Chem Abstr.*, **76**, 155577 (1972).

[82] R. B. Fishwick (Imperial Chemical Industries Ltd.) U.S. Pat. 3 637 652, 25 Jan. 1972 ; *Chem. Abstr.*, **77**, 21554 (1972).

[83] R. Altermatt, C. Mueller (Sandoz Ltd.) Swiss Pat. 496 065, 30 Aug. 1970 ; *Chem. Abstr.*, **77**, 63334 (1972).

[84] G. Kilpper, J. H. Sturm, H. Jurgen, H. J. Quadbeck Seegar (Badische Anilin — und Soda Fabrik A. — G.) Ger. Offen. Pat. 2 054 882, 10 May 1972 ; *Chem. Abstr.*, **77**, 90043 (1972).

[85] J. Meybek (Sandoz Ltd.) S. African Pat. 7004 935, 17 Jan. 1972 ; *Chem. Abstr.*, **77** 128052 (1972).

[86] D. Brierley, M. Roche (Imperial Chemical Industries Ltd.) Ger. Offen. Pat. 2 159 305, 8 Jun. 1972 ; *Chem. Abstr.*, **77**, 128038 (1972).

[87] R. Schickfluss, N. Stteckelberg (Farbwerke Hoechst A. — G.) Ger. Offen. Pat. 2 107 798, 31 Aug. 1972 ; *Chem. Abstr.*, **78**, 5387 (1973).

[88] R. Hahn, C. Mueller (Sandoz Ltd.) U.S. Pat. 3 708 468, 2 Jan. 1973 ; *Chem. Abstr.*, **78**, 85914 (1973).

[89] Kurosawa Mitsuru, Imai Hidenori (Nippon Kayaku Co. Ltd.) Japan Pat. 72 33, 481, 25 Aug. 1972 ; *Chem. Abstr.*, **78**, 17610 (1973).

[90] O. Konrad (Farbwerke Hoechst A. — G.) Ger. Offen. Pat. 1 929 573, 7 Jan. 1971 ; *Chem. Abstr.*, **74**, 113223 (1971).

[91] E. Hahn, H. G. Wippel (Badische Anilin- und Soda Fabrik A. — G.) Belg. Pat. 641 495, 18 Jun. 1964 ; *Chem. Abstr.*, **62**, 16419 (1965).

[92] C. Mueller (Sandoz Ltd.) Swiss Pat. 468 444, 31 Mar. 1969 ; *Chem. Abstr.*, **71**, 71916 (1969).

[93] W. Groebke, C. Mueller, W. Wehrli (Sandoz Ltd.) Swiss Pat. 439 528, 29 Dec. 1967 ; *Chem. Abstr.*, **68**, 88183 (1968).

[94] W. Groebke, C. Mueller (Sandoz Ltd.) Swiss Pat. 455 090, 28 Jun. 1968 ; *Chem. Abstr.*, **70**, 5223 (1969).

[95] E. Merian, O. Senn (Sandoz Ltd.) Swiss Pat. 349 577, 15 Dec. 1960 ; *Chem. Abstr.*, **55**, 17023 (1961).

[96] Imperial Chemical Industries Ltd. Neth. Appl. Pat. 6 516 085, 25 Febr. 1966 ; *Chem. Abstr.*, **65**, 2381 (1966).

[97] M. Jirou, J. Leroy (Etablissements Kuhlmann) Fr. Pat. 1 458 333, 10 Nov. 1966 ; *Chem. Abstr.*, **67**, 3699 (1967).

[98] W. Groebke (Sandoz Ltd.) Fr. Pat. 1 539 436, 13 Sep. 1968 ; *Chem. Abstr.*, **66**, 76917 (1967).

[99] W. Kruckenberger (Farbenfabriken Bayer A. — G.) Brit. Pat. 1 122 169, 31 Jul. 1968 ; *Chem. Abstr.*, **69**, 107592 (1968).

[100] Imperial Chemical Industries Ltd. Belg. Pat. 637 801, 24 Mar. 1964 ; *Chem. Abstr.*, **62**, 7808 (1965).

[101] Farbwerke Hoechst A. — G. Neth. Appl. 6 610 136, 24 Jan. 1967 ; *Chem. Abstr.*, **67**, 74453 (1967).

Among the products without nitro-groups but with cyano-groups with strong electron-attracting capacity too, those which have only cyano-groups [124–127] or moreover alkyl-groups, [128]

---

[102] W. Kruckenberg (Farbenfabriken Bayer A. — G.) Brit. Pat. 1 137 037, 18 Dec. 1968; *Chem. Abstr.*, **70**, 69286 (1969).

[103] Imperial Chemical Ind. Ltd. Fr. Pat. 1 531 146, 28 Jun. 1968; *Chem. Abstr.*, **71**, 103163 (1969).

[104] Farbwerke Hoechst A. – G. Brit. Pat. 1 217 569, 31 Dec. 1970: *Chem. Abstr.*, **74**, 88650 (1971).

[105] J. H. Angliker (Ciba – Geigy A. — G.) Swiss Pat. 512 633, 29 Oct. 1971; *Chem. Abstr.*, **76**, 155584 (1972).

[106] R. Peter, J. Hans Angliker (Ciba-Geigy A. — G.) Ger. Offen. Pat. 2 136 062, 27 Jan. 1972; *Chem. Abstr.*, **77**, 501210 (1972).

[107] B. R. Fishwick, A. Quayle (Imperial Chemical Industries Ltd.) Ger. Offen. Pat. 2 210 143, 21 Sep. 1972; *Chem. Abstr.*, **78**, 5396 (1973).

[108] M. A. Weaver, C. Coates, Jr. Alvin (Eastman Kodak Co.) Ger. Offen. Pat. 2 231 952, 18 Jan. 1973; *Chem. Abstr.*, **78**, 99033 (1973).

[109] Imperial Chemical Industries Ltd. Belg. Pat. 637 801, 24 Mar. 1964; *Chem. Abstr.*, **62**, 7908 (1965).

[110] G. Lange, H. Wippel (Badische Anilin- und Soda Fabrik A. — G.) Fr. Pat. 1 478 973, 28 Apr. 1967; *Chem. Abstr.*, **67**, 118080 (1967).

[111] W. Kruckenberg (Farbenfabriken Bayer A. — G.) Ger. Pat. 1 232 292, 12 Jan. 1967; *Chem. Abstr.*, **66**, 76917 (1967).

[112] E. Merian, C. Mueller (Sandoz Ltd.) Brit. Pat. 971 167, 30 Sept. 1964; *Chem. Abstr.*, **63**, 4425 (1965).

[113] E. Merian, C. Mueller (Sandoz Ltd.) Swiss Pat. 459 399, 13 Sep. 1968; *Chem. Abstr.*, **70**, 88804 (1969).

[114] W. Groebke (Sandoz Ltd.) Ger. Offen. Pat. 2 227 081, 28 Dec. 1972; *Chem. Abstr.*, **78**, 99032 (1973).

[115] E. Merian, C. Mueller, G. Senn (Sandoz Ltd.) U.S. Pat. 2 967 858, 10 Jan. 1961; *Chem. Abstr.*, **55**, 8870 (1961).

[116] J. Meybeck, C. Mueller, F. Mueller (Sandoz Ltd.) Swiss Pat. 498 910, 31 Dec. 1970; *Chem. Abstr.*, **74**, 100585 (1971).

[117] R. Altermatt, C. Mueller (Sandoz A. — G.) Swiss Pat. 498, 907, 31 Dec. 1970; *Chem. Abstr.*, **74**, 113203 (1971).

[118] D. Cornelius, H. von Brachel (Cassella Farbwerke) Ger. Offen. Pat. 2 020 030, 11 Nov. 1971; *Chem. Abstr.*, **76**, 87135 (1972).

[119] G. Lange, H. G. Wippel (Badische Anilin- und Soda Fabrik A.— G.) Fr. Pat. 1 388 592, 5 Feb. 1965; *Chem. Abstr.*, **63**, 10098 (1965).

[120] E. Merian (Sandoz Ltd.) Ger. Pat. 929 568, 30 Jun. 1955; *Chem. Abstr.*, **52**, 6802 (1958).

[121] M. F. Santori (E. I. du Pont de Nemours Co.) Fr. Pat. 1 396 700, 23 Apr. 1965; *Chem. Abstr.*, **64**, 2200 (1966).

[122] W. Groebke, C. Mueller, R. Wirz (Sandoz (Ltd.) Fr. Pat. 1 505 707, 15 Dec. 1967; *Chem Abstr.*, **70**, 20982 (1969).

[123] D. Cornelius, H. von Brachel (Cassella Farbwerke Mainkur A. — G.) Ger. Offen. Pat. 2 024 699, 9 Dec. 1971; *Chem. Abstr.*, **76**, 101203 (1972).

[124] E. L. Johnson (Imperial Chemical Industries Ltd). Brit. Pat. 756 079, 29 Aug. 1956; *Chem. Abstr.*, **51**, 6168 (1957).

[125] Farbenfabriken Bayer A. — G. Brit. Pat. 1 024 485, 30 Mar. 1966; *Chem. Abstr.*, **65**, 2386 (1966).

[126] N. Kruckenberg (Farbenfabriken Bayer A. — G.) Brit. Pat. 933 160, 8 Aug. 1963; *Chem. Abstr.*, **62**, 7906 (1965).

[127] W. Kruckenberg (Farbenfabriken Bayer A. — G.) Ger. Pat. 1 276 843, 5 Sep. 1968; *Chem. Abstr.*, **70**, 38885 (1969).

[128] K. Komarowski, P. Kurtz, K. Key (Farbenfabriken Bayer A.—G.) Ger. Offen. Pat. 2 125 907, 14 Dec. 1972; *Chem. Abstr.*, **78**, 85904 (1973).

halogeno,[129–132] trifluoro-alkyl,[133] methylsulphonyl[16,134,135], etc. are quoted. Other publications mention some kinds of groups (without nitro- and cyano-groups) as : alkyl-sulformyl, [16,135–137] carboxyalkyl, [138–142] sulphonamide N-alkylate, [25,131,143–151] trifluoroalkyl, [124] styrene-groups [152], etc.

The aryl-amines, to which are attached only such groups with electron-repellent or-donating effect as halogeno and alkyl, [101,153] are scarcely found.

---

[129] W. Kruckenberg, K. Weiss (Farbenfabriken Bayer A. – G.) Ger. Pat. 1 218 090, 2 Jun. 1966 ; *Chem. Abstr.*, **65**, 9061 (1966).

[130] W. Kruckenberger (Farbenfabriken Bayer A. – G.) Brit. Pat. 1 119 326, 10 Jul. 1968 ; *Chem. Abstr.*, **69**, 87968 (1968).

[131] R. Altermatt, C. Mueller (Sandoz Ltd.) Swiss Pat. 465 089, 31 Dec. 1968 ; *Chem. Abstr.*, **71**, 51223 (1969).

[132] W. Kruckenberg (Farbenfabriken Bayer A. – G.) Ger. Pat. 1 719 073, 23 Sep. 1971 ; *Chem. Abstr.*, **76**, 47377 (1972).

[133] P. W. Barker, B. R. Fishwick, E. L. Johnson (Imperial Chemical Industries Ltd.) Brit. Pat. 872 204, 5 Jul. 1961 ; *Chem. Abstr.*, **57**, 993 (1962).

[134] E. Merian (Saul et Co.) U.S. Pat. 2 782 186, 19 Feb. 1967 ; *Chem. Abstr.*, **52**, 1626 (1958).

[135] R. Altermatt (Sandoz Ltd.) Cer. Offen. Pat. 1 935 482, 26 Feb. 1970 ; *Chem. Abstr.*, **73**, 89144 (1970).

[136] O. Senn, W. Wehrli (Sandoz Ltd.) Swiss Pat. 384 748, 26 Feb. 1965 ; *Chem. Abstr.*, **62**, 16419 (1965).

[137] O. Senn (Sandoz Ltd.) Swiss Pat. 472 483, 30 Jun. 1969 ; *Chem. Abstr.*, **72**, 22581 (1970).

[138] Badische Anilin- und Soda Fabrik A. – G. Neth Appl. 6 410 930, 22 Mar. 1965 ; *Chem. Abstr.*, **63**, 5791 (1965).

[139] G. Lange, H. G. Wippel (Badische Anilin- und Soda Fabrik A. – G.) Brit. Pat. 913 899, 28 Dec. 1962 ; *Chem. Abstr.*, **60**, 9393 (1964).

[140] Enomoto Shigeharu, Sueta Yoshihisa, Jitoshiro Atsumi (Sumitomo Chemical Co., Ltd.) Japan Pat. 70 37, 153, 25 Nov. 1970 ; *Chem. Abstr.*, **74**, 113210 (1972).

[141] E. Siegel, E. Klaike (Farbenfabriken Bayer A. – G.) Ger. Offen. Pat. 1 932 824, 4 Feb. 1971 ; *Chem. Abstr.*, **74**, 143313 (1971).

[142] S. Stefaniek (Zaklady Chemicznew W. Bydgoszczy) Pol. Pat. 62 943, 5 Jul. 1971 ; *Chem. Abstr.*, **77**, 7281 (1972).

[143] G. du Peloux, J. Leroy (Compagnie Française des Matières Colorantes) Fr. Pat. 1 258 328, 17 Jul. 1961 ; *Chem. Abstr.*, **56**, 13054 (1962).

[144] J. Voltz, W. Bossard (I. R. Geigy A. – G.) U.S. Pat. 3 321 459, 23 May, 1967 ; *Chem. Abstr.*, **67**, 65397 (1967).

[145] Sensu Hisashi ; Sato Yasuke (Mitsubishi Chemical Ind. Co., Ltd.) Japan Pat. 6805, 668, 1 Mar. 1968 ; *Chem. Abstr.*, **69**, 28573 (1968).

[146] P. Maderni, C. Mueller (Sandoz Ltd.) Swiss Pat. 465 093, 3 Dec. 1968 ; *Chem. Abstr.*, **71**, 51229 (1969).

[147] Altermatt, C. Mueller (Sandoz Ltd.) Swiss Pat. 465 089, 31 Dec. 1968 ; *Chem. Abstr.*, **71**, 82636 (1969).

[148] E. Siegel (Farbenfabriken Bayer A. – G.) Ger. Offen. Pat. 2 004 441, 5 Aug. 1971 ; *Chem. Abstr.*, **75**, 130769 (1971).

[149] E. Siegel (Farbenfabriken Bayer A. – G.) Ger. Offen. Pat. 2 044 442, Aug. 1971 ; *Chem. Abstr.*, 75, 130766 (1971).

[150] E. Siegel (Farbenfabriken Bayer A. – G.) Ger. Offen Pat. 2 064 595, 13 Jul. 1972 ; *Chem. Abstr.*, **77**, 166143 (1972).

[151] J. R. Pohe (Pont de Nemours E. I. and Co.) U.S. Pat. 3 707 533, 26 Dec. 1972 ; *Chem. Abstr.*, **78**, 73638 (1973).

[152] E. Siegel (Farbenfabriken Bayer A. – G.) Ger. Oifen. Pat. 2 053 711, 10 May 1972 ; *Chem. Abstr.*, **77**, 103283 (1972).

[153] Cassella Farbwerke Mainkur A. – G. Nath Appl. 6 516 268, 26 Jun. 1966 ; *Chem. Abstr.*, **65**, 17093 (1966).

3.2. COUPLING COMPONENTS

Coupling components have functional groups that, beside improving the tinctorial fastness, assure a higher solubility degree of the dye in the fiber. This last property is determined especially by the substituents of the amino-groups of the coupling component.

The literature mentions the presence, besides the amino-group, of another groups attached directly to the coupling component ring as alkyl, alkoxy, halogeno, acyl-amido, etc., or even such groups with strong electron-attracting capacity as trifluoro-methyl, nitro, etc.

We discuss further the large variety of the coupling components, pointing out especially more representative functional groups.

A first category includes only those products which have one diverse substituted amino-group, without other functional groups attached to the ring :

— $N(Alk)\,(X_4\,;\,X_7)$; [112,113,138]
— $N(Alk)X_4$; [123,138,144,145]
— $N(X_4)C_2H_4OAr$; [54,55]
— $N(X_4)\,(X_5\,;\,X_6\,;\,X_7)$; [20,40,48,139,153]
— $N(X_4)C_2H_4CO_2C_2H_4OCOAlk$;[96]
— $N(X_4)C_2H_4CONH_2$; [58,86]
— $N(X_4)C_2H_4O_2CNHAr$; [74,93]
— $N(X_4)C_2H_4CO_2Ar$; [151]
— $N(X_4)\,[CH_2CH\,(X_3)CH_2OAr]$; [30]
— $N(Alk)C_2H_4OCOCH_2CN$;[91]
— $N(Alk)C_2H_4O_2C\,C_3H_6SO_2Ar$; [21]
— $N(Alk)C_2H_4O\,C_2H_4SO_2Alk$; [47]
— $N(Alk)[CH_2CH(OH)CONH_2]$;[22]
— $N(Alk)C_2H_4OAr$; [70,85,90]
— $N(Alk)C_2H_4OCO_2CH_3$; [128]
— $N(Alk)CH_2C_6H_4SO_2NH_2$;[87]
— $NHCH_2C(CH_3)_2NO_2$;[31]
— $N(C_2H_4OC_2H_4CO_2Alk)_2$; [126]
— $N(Alk)\,CH_2CH{=}CHCH_2CN$;[34]
— $N(X_4)\,[CH_2C(Hlg) = CH_2]$;[101]
— $N(Alk)C_2H_4NHCOCH = CCl_2$.[137]

In the second category there are the products which contain, beside the diverse substituted amino-group, other functional groups attached to the ring as : alkyl, alkoxy, trifluoromethyl, halogeno, acyl, amino, methyl-sulfonyl, etc.

We present below only the amino-groups of these products with more representative substituents :

— $N(Alk)X_5$; [112,124]
— $N(Alk)C_3H_6OH$; [124]
— $N(X_4)X_5$, ; [37,134,138,145,146]
— $N(X_4\,;\,X_6)_2$; [16,27,43,72,94]
— $N(X_4)C_2H_4OC_2H_4OOCOAlk$ [130] ;
— $N(X_4)C_2H_4COOAlk$; [113,129,146]
— $N(Alk)X_4$; [45,51,95,98,115,120]
— $N(X_7)_2$; [36,122,127,140,146]
— $N(Alk)X_7$; [112]
— $N(Alk)CH_2Ar$; [35,150]
— $NH\,Ar$;[104]
— $N(X_5)_2$; [56]
— $NHCH(CH_3)CH_2COAlk$; [28]
— $N(X_2)X_4$; [41]
— $N(X_5\,;\,X_7)_2$; [18,145]
— $N(X_5)C_2H_4COAr$; [59]
— $N(C_2H_4O_2CC_2H_4\,COOAr)_2$; [106]
— $N(X_5)C_2H_4Ar$; [32]
— $N(C_2H_4OCONHAlk)_2$; [18]
— $N(X_4)C_2H_4O_2CCH(Cl)Ar$; [33]
— $(Alk)C_2H_4OC_2H_4OCOOAlk$;[99,102]
— $N(Alk)_2$; [28,92,97,108,114,116,131,135,141,142,147,148,154]

[154] C. Mueller (Sandoz Ltd.) Belg. Pat. 643 775, 1 Jun. 1964 ; *Chem. Abstr.*, **63**, 4429 (1965).

— $N(X_4)CH_2CHOHCH_2Cl$;[67]
— $N(C_2H_4O_2CCH_2OAr)_2$;[88]
— $N(X_4 ; X_7)C_2H_4OC_2H_4CN$;[15,16]
— $N(C_2H_4OCO_2CH_3)_2$;[125,132]
— $NHC_2H_4SO_2NH_2$;[25]
— $N(X_4)\ X_6$;[20] etc.

In the third category there are presented the products which contain, beside the diverse substituted amino-group, other two functional groups attached to the ring as: alkyl, alkoxy, halogeno, acyl-amino, carboxy-amido.

We present below only the amino-groups, with their more representative substituents:

— $N(X_5)X_7$;[44,65,66,98,100,107,110,133]
— $N(C_2H_4OC_2H_4CN)_2$;[44,45,52,111]
— $NHC_2H_4CO_2C_2H_4OAlk$;[46]
— $NHC_2H_4CO_2CH_3$;[24,76,111,118]
— $N(X_4 ; C_2H_4Cl)X_5$;[62,64]
— $NHCH_2CHOH\ CH_2O\ Ar$;[75]
— $N(X_4)\ CH_2CHOHCH_2OAlk$;[71]
— $NHC_2H_4OC_2H_4OAlk$;[89]
— $N(CH_2Ar)C_2H_4O_2C\ CH_3$;[23]
— $N(C_2H_4O_2C\ NH\ Ar)_2$;[60]
— $NHCH_2CHOHCH_2OAlk$;[26]
— $N(C_2H_4O_2CH)_2$;[63]
— $N(C_2H_4OCO_2CH_3)_2$;[79]
— $N(Alk)C_2H_4CO_2C_2\ H_4OAlk$;[80]
— $N(X_4)CH_2CH = CH_2$;[73]
— $N(X_7)_2$;[19,49,61,82,98,155]
— $N(Alk)_2$;[17,128]
— $N(C_2H_4O_2CCH_3)_2$;[38]
— $NH\ X_4$;[149]
— $NH\ Ar$;[84]
— $N(Alk)\ X_7$;[117]
— $NH[CH(CO_2C_7H_5)CH_2CO_2Alk]$,[77] etc.

Apart from the above, we would like to mention coupling components, namely the amino-derivatives of naphthaline [42,50,53,156–158] and the coupling components of hydroxy derivatives.[39,136,143,144,152,159]

3.3. GENERAL REMARKS ON THE CONDITIONS OF THE DYES SYNTHESIS AND FINISHING

As we also mentioned in our published work,[160] the usual diazo components are represented by amino-derivatives with low or very low basicity at amino-nitrogen. This calls for strong conditions of diazotization in which the reaction goes through the NO^+ ion.

As it was said, the usual coupling components contain groups that are likely to determine a higher solubility in the fiber, besides other influences.

The above traits, for both types of components, call for more special conditions of diazotization and coupling.

---

[155] B. R. Fishwick, H. R. Murton (Imperial Chemical Industries Ltd.) Belg. Pat. 631 100, 4 Nov. 1963; *Chem. Abstr.*, **61**, 1962 (1964).

[156] W. Bassard, H. Wegemueller (J. R. Geigy A. — G.) Swiss Pat. 395 387, 31 Dec. 1965; *Chem. Abstr.*, **64**, 14318 (1966).

[157] W. Groebke (Sandoz Ltd.) Ger. Pat. 2 116 315, 28 Oct. 1971; *Chem. Abstr.*, **76**, 73727 (1972).

[158] M. A. Weaver, Cl. A. Coates Jr., H. S. Pridgen (Eastman Kodak Co.) Ger. Offen. Pat. 1 963 590, 25 Jan. 1970; *Chem. Abstr.*, **73**, 100017 (1970).

[159] Badische Anilin—und Soda Fabrik A. — G. Fr. Demande Pat. 2 013 809, 10 Apr. 1970; *Chem. Abstr.*, **74**, 55120 (1970).

[160] A. Spiliadis, M. Hilzenrath, V. Cornea, E. Baltă, G. Molău, E. Teodorescu, L. Predescu, *Rev. Chim.* (*București*), **XVII**, 271 (1966).

We further present some of the more important problems, which have to be taken into account in both stages of study and industrial application:

— The diazotization of amines with low basicity (dinitroaniline, halogeno-nitro-aniline, cyano-nitro-aniline, etc. and heterocyclic amino-derivatives) must be effected in such conditions that the concentration of NO^+ ions be optimum in order to assure a maximum conversion.

— The diazo-compounds of low basicity amines have a high coupling capacity (the cationic character of the diazo-group is more amplified) but a great tendency towards decomposition.

Consequently, they must be utilized in conditions of a maximum stability (low temperature of the reaction and stockage, high concentration of the mineral acid, strong anhydrous medium of the reaction, etc.) For the same reason, a higher coupling rate then the degradation rate of diazo-group must be assured to the coupling.

— In the case of using some coupling components with acyloxyalkyl groups such as $-N(C_2H_4OCOCH_3)_2$ it is necessary to use the coupling conditions in which the hydrolysis of these groups is diminished to minimum or practically to zero. Thus, for example, the coupling of the diazo-salt of a halogeno-dinitro-amine (diazotized in nitrosyl-sulphuric acid) with a coupling component of the type $C_6H_5N(C_2H_4CN)C_2H_4OCOCH_3$, *in the absence of acetic acid and sodium acetate*, can conduct to an impurified product with the dye derived from halogeno-nitro-amine and $C_6H_5N(C_2H_4CN)C_2H_4OH$. This thing affects the tinctorial qualities of the dye.

— It must be taken into account that the structure of the coupling component can appreciably diminish the coupling rate, through steric hindering, in the case in which carrying out the diazo-component has a lower capacity of coupling. For example, we can cite the intermediate $1,4,2-(X_1)(X_2)C_6H_3[N(X_7)_2]$.

— The purity of dyes can determine the way of the intermediates synthesis. Thus, for example, 2-chloro-and a 6-dichloro-4-nitro-aniline must be made by other methods than direct chlorination. In this case, one obtains 2-chloro-4-nitro-aniline inpurified with 2,6-dichloro-4-nitro-aniline and 2,6-dichloro-4-nitro-aniline impurified with 2-chloro-4-nitro-aniline, etc.

The value of dyes also depends on the conditions in which the dyes, obtained by synthesis, are conditioned.

As it was already mentioned in our published work,[161–165] conditioning implies : *milling action* (in order achieve finishing at the

---

[161] A. Spiliadis, D. Brețcanu, V. Cornea, *Rev. Chim. (București)*, **XII**, 220 (1961).

[162] A. Spiliadis, D. Brețcanu, R. Schip, V. Cornea, E. Pamfil, *Rev. Chim. (București)*, **XIV**, 84 (1963).

[163] A. Spiliadis, D. Brețcanu, R. Schip, G. Molău, C. Eftimescu, E. Pamfil, *Rev. Chim. (București)*, **XIV**, 336 (1963).

[164] A. Spiliadis, D. Brețcanu, R. Schip, C. Eftimescu, G. Molău, *Rev. Chim. (București)*, **XV**, 345 (1964).

[165] E. B. Towne, Wm. H. Moore, J. B. Dickey (Eastman Kodak Co.), U.S. Pat. 2 825 726, 4 Mar. 1958; *Chem. Abstr.*, **52**, 9613 (1958).

desired size and of the suitable granulation curve), *drying* of the dispersed product in the atomizer, *stability of dispersion*, etc.

The selection of the conditioning method is determined by a complex of technical-economic factors. Thus, for example, there are disperse dyes which are not compatible with some dispersers.

Sometimes, the fine dispersed dyes can be obtained by synthesis; their separation from impurities must be made in the continuous centrifugal separator. There are also some disperse dyes that do not suffer the thermic shock of the drying in atomizer, etc.

4. MONOAZOIC DYES WITH HETEROCYCLIC RING

4.1. THIOPHEN DERIVATIVES

The dyes are generally characterized by weak tinctorial fastnesses, being indicated especially for the secondary acetate fibers, for which they manifest a remarkable affinity and equalization

In the case of the thiophen molecule, by the implication of the electron pair of nitro-heteroatom to the aromatic conjugation, the electron-density of heteroatom is much diminished, while the electron-density of carbon-atom increases.

This situation is well represented by the following structures :

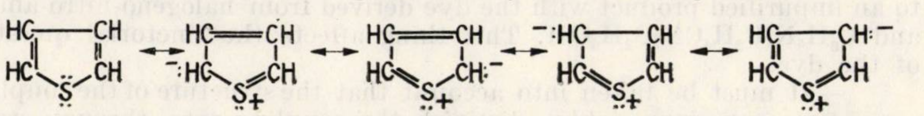

According to the above formulation, the thiophen is very sensitive to the electrophilic reagents.

It is also expected that the groups CH adjacent to the heteroatom (position alpha) will be richer in electrons, consequently more reactive than the CH more distant groups (position beta).

This also agrees with the facts observed. In the reaction of electrophilic substitution (for example coupling reactions) the alpha positions are occupied in the first place, if they are free. The literature indicates frequently, for the polyester fibers, the diazo compounds derived from 2-amino-thiophene, that contain in the 3-or(and) 5-position substituents of the type: nitro, acylmethylsulphonyl, sulphonamide, etc. [165–169] and coupling components of the type : cyclohexane-1,3-diones ;[165] 2,5,1-$(X_1)(X_2)$ C_6H_2 $[NH(C_2H_4COOAlk]$; [170] 1,2,3,4-tetrahydroquinoline; N-phenyl-morpholine. [166,167]

---

[166] E. B. Towne, Wm. H. Moore, J. B. Dickey (Eastman Kodak Co.) U.S. Pat. 2 827 450, 18 Mar. 1958 ; *Chem. Abstr.*, **52**, 17727 (1958).

[167] E. B. Towne, M. S. Bloom, J. B. Dickey (Eastman Kodak Co.) Brit. Pat. 774 611, 15 May 1957 ; *Chem. Abstr.*, **58**, 7607 (1959).

[168] Farbwerke Hoechst A. — G. Fr. Pat. 1 509 557, 12 Jan. 1968 ; *Chem. Abstr.*, **70**, 58910 (1969).

[169] H. Liechti (Ciba Ltd.) Swiss Pat. 455, 978, 15 Jul.1968 ; *Chem. Abstr.*, **69**, 107593 (1968).

[170] A. T. Costella, P. Smith (Imperial Chemical Industries Ltd.) Ger. Offen. Pat. 2 201 113, 3 Aug. 1972 ; *Chem. Abstr.*, **77**, 166148 (1972).

The stronger bathochromic effect is determined by the NO_2 group attached to the 3-position. For the dyes obtained from 5-(CH_3CO)-TpA or 3,5-(NO_2)(CH_3CO)-TpA and the same coupling component 3,1-(CH_3)C_6H_4[N(C_2H_5)CH_2CHOH CH_2OH] λmax has the values 520 mμ and 603 mμ, respectively.

The group 3 $-SO_2CH_3$ determines a weaker bathochromic effect than the NO_2 group. For the dyes synthetized from 3,5-(CH_3SO_2)$_2$-TpA or 3,5-(NO_2) (CH_3SO_2)-TpA and the same coupling component 3,1-(CH_3) C_6H_4 [N(C_2H_5) $CH_2CHOHCH_2OH$], λ max. has the values 570 mμ and 604 mμ, respectively.

Even the thiophen ring itself determines a bathochromic effect about 70 – 100 mμ. The dyes resulted from 5-(CH_3CO)-TpA or 4,1-(CH_3CO) $C_6H_4NH_2$ and the same coupling component 3,1-(CH_3)C_6H_4 [N(C_2H_5) $CH_2CHOHCH_2OH$] present λ max. values of 527 mμ and 452 mμ, respectively. Regarding the coupling component, the bathochromic effect for 3,1–(CH_3)C_6H_4 [N(C_2H_5)$CH_2CHOHCH_2OH$], for example, is less than that produced by the 2,5,1-(X_2) (X_1)C_6H_3 [N (X_7)$_2$] for the same diazo component 3,5-(NO_2)(CH_3CO)-TpA.

Tetrahydroquinoline increases the affinity. Generally, the tinctorial characteristics of this category of dyes do not justify the extension of their study on synthesis and application.

4.2. PYRAZOL AND PYRAZOL-5-ONE DERIVATIVES

In the pyrazolic derivatives series on can mention the pyrazol-compounds with SO_2Ar, SO_2Alk, COOAlk, etc. groups in the 1-and 3-positions[171,172] and frequently pyrazol-5-amine derivatives with one or two alkyl, alkoxy, benzyl, acetyloxyethyl, etc. groups, in the 1- or (and) 3-position. [173–181]

The 3,4,5-(CH_3)$_2$ Pz-NH_2 [175] derivative is utilized as a diazo component for various N,N-di-(beta-hydroxyethyl)-aniline derivatives. Various

---

[171] C. E. Lewis (American Cyanamid Co.) U.S. Pat. 3 198 783, 3 Aug. 1965; *Chem. Abstr.*, **63**, 11739 (1965).

[172] O. Senn (Sandoz Ltd.) Belg. Pat. 650 501, 30 Oct. 1964; *Chem. Abstr.*, **63**, 11738 (1965).

[173] J. R. Geigy A. – G. Neth. Appl. 6 409 878, 1 Mar. 1965; *Chem. Abstr.*, **63**, 3085 (1965).

[174] Farbenfabriken Bayer A. – G. Brit. Pat. 1 029 747, 18 May 1966; *Chem. Abstr.*, **65**, 15551 (1966).

[175] Farbenfabriken Bayer A. – G. Brit. Pat. 888 167, 24 Jan. 1962, *Chem. Abstr.*, **60**, 6957 (1964).

[176] W. Bossard, F. Favre (J. R. Geigy A. – G.) Brit. Pat. 955 085, 31 Jan. 1964; *Chem. Abstr.*, **61**, 5823 (1964).

[177] J. R. Geigy A. – G. Belg. Pat. 614 461, 27 Aug. 1962; *Chem. Abstr.*, **59**, 4074 (1963).

[178] W. Groebke (Sandoz Ltd.) Ger. Offen. Pat. 2 116 315, 28 Oct. 1972; *Chem. Abstr.*, **76**, 73727 (1972).

[179] H. J. Sturm, H. Armbrust, K. Mayer (Badische Anilin - und Soda Fabrik A. – G.) Ger. Offen Pat. 1 940 685, 18 Feb. 1971; *Chem. Abstr.*, **74**, 127530 (1971).

[180] H. J. Sturm, K. Mayer, G. Kilpper, H. Armburst (Badische Anilin- und Soda Fabrik A. – G.) Ger. Offen. Pat. 1 816 043, 25 Jun. 1970; *Chem. Abstr.*, **73**, 100013 (1970).

[181] Visvanathan Ramonathan (Ciba Ltd.) Swiss Pat. 439 526, 29 Dec. 1967; *Chem. Abstr.*, **68**, 88184(1968).

shades from yellow to red can be obtained with moderate tinctorial fastness.

The other derivatives [174,176,177] offer a better tinctorial fastness to light and thermofixation on the polyester fibers.

In the pyrazol-5-one derivatives series we can mention products with functional groups (alkyl, chlorophenyl, butyl, carboxyamide, etc.) in the 3 [182–185] or 1 [186] position and frequently disubstituted derivatives in the 1- and 3-position with the following radicals: alkyl, alkoxy, aryl, carboxy-alkyl, carboxy-amide, beta-hydroxyethyl-carboxy-amide, beta-cyano-ethyl-phenyl-N-methyl-sulphonamide, etc. [47,112,168,169,171,173,182–185,187–206]

---

[182] E. Merian, O. Senn (Sandoz Ltd.) U.S. Pat. 3 130 190, 21 Apr. 1964; *Chem. Abstr.*, **61**, 5825 (1964).

[183] L. N. Stanley, W. H. Armento, W. G. Huly U.S. Pat. 3 246 945, 19 Apr. 1966; *Chem. Abstr.*, **65**, 4002 (1966).

[184] Ciba Ltd. Fr. Pat. 1 539 515, 13 Sep. 1968; *Chem. Abstr.*, **73**, 100024 (1970).

[185] Senshu Hisashi, Sato Yosuke (Mitsubishi Chemical Ind. Co. Ltd.) Japan Pat. 68 05, 671, 1 Mar. 1968; *Chem. Abstr.*, **69**, 37087 (1968).

[186] Sumitani Mitsukuni Yehiro (Nippon Kayaku Co. Ltd.) Japan Pat. 70 08, 751, 30 Mar. 1970; *Chem. Abstr.*, **73**, 99996 (1970).

[187] H. Berrie, R. Windle (Imperial Chemical Ind. Ltd.) U.S. Pat. 3 325 469, 13 Jun. 1967; *Chem. Abstr.*, **67**, 65404 (1967).

[188] Farbenfabriken Bayer A. — G. Brit. 795 701, 28 May 1958; *Chem. Abstr.*, **52**, 19153(1958).

[189] R. Gangneux, J. de Blanc (Compagnie Française des Matières Colorantes) U.S. Pat. 3 012 843, 12 Dec. 1961; *Chem. Abstr.*, **56**, 14436 (1962).

[190] G. du Peloux, J. Leroy (Compagnie Française des Matières Colorantes) Fr. Pat. 1 255 348, 9 Jun. 1961; *Chem. Abstr.*, **56**, 14437 (1962).

[191] Hugo Illy (Ciba Ltd.) Swiss Pat. 373 496, 15 Jan. 1964; *Chem. Abstr.*, **61**, 12121 (1964).

[192] E. Merian, O. Senn (Sandoz Ltd.) Swiss Pat. 386 590, 15 Apr. 1965; *Chem. Abstr.*, **63**, 4425 (1965).

[193] Farbwerke Hoechst A. — G. Brit. Pat. 992 146, 19 May 1965; *Chem. Abstr.*, **63**, 4426 (1965).

[194] Imperial Chemical Industries Ltd. Neth. Appl. Pat. 6 411 226, 9 Apr. 1965; *Chem. Abstr.*, **63**, 5791 (1965).

[195] M. Kamel, M. A. Alam, M. Osman and F. Abdel Hay (Natl. Res. Center Textile Inst., Cairo) *Kolor Ert*, **5**, 137—42 (1967); *Chem. Abstr.*, **67**, 100980 (1967).

[196] V. Hladik (Inst. Treat. Paper, Ceska Trebova, Czech) *Wiss. Z. Tech.* Univ. Dresden, **20**, 715—18 (1971); *Chem. Abstr.*, **78**, 17587 (1973).

[197] G. Essbach, M. Zeiler, S. Schumann, W. Heyne, Ger. (East) 92 097, 20 Aug. 1972; *Chem. Abstr.*, **78**, 73639 (1973).

[198] J. M. L. Leroy, C. Bronard (Uzine Kuhlmann) U.S. Pat. 3 663 530, 16 May 1972; *Chem. Abstr.*, **77**, 166160 (1972).

[199] M. Wiessel, G. Wolfrum (Farbenfabriken Bayer A. — G.) Ger Offen. Pat. 2 064094, 6 Jul. 1972; *Chem. Abstr.*, **77**, 153905 (1972).

[200] H. von Brachel, E. Heinrich (Cassella Farbwerke Mainkur A. — G.) Ger. Offen. Pat. 2 009 277, 9 Sep. 1971; *Chem. Abstr.*, **76**, 47373 (1972).

[201] Farbenfabriken Bayer A. — G. Fr. Demande Pat. 2 015 686, 30 Apr. 1970; *Chem. Abstr.*, **74**, 65562 (1971).

[202] R. Alternatt, H. Burkhard, C. Mueller (Sandoz Ltd.) Swiss Pat. 484 989, 13 Mar. 1970; *Chem Abstr.*, **73**, 36542 (1970).

[203] W. Groebke, C. Mueller (Sandoz Ltd.) Swiss Pat. 448 326, 29 Mar. 1968; *Chem. Abstr.*, **69**, 37099 (1968).

[204] Obayashi Fujio Karasawa, Takashi Chinuki (Sumitomo Chemical Co., Ltd.) Japan Pat. 18 716 ('66), 28 Oct.; *Chem. Abstr.*, **66**, 105844 (1967).

[205] H. Burkhard, O. Senn (Sandoz Ltd.) Swiss Pat. 409, 191, 30 Sep. 1966; *Chem. Abstr.*, **66**, 19819 (1967).

[206] Farbenfabriken Bayer A. — G. Neth. Appl. Pat. 6 410 555, 15 Mar. 1965; *Chem. Abstr.*, **63**, 7144 (1965).

The diazo components used to obtain the pyrazolonic dyes are represented by aryl-amine with one, two or three functional groups of the type: alkyl [207]; nitro-alkoxy [168]; halogeno-nitro [47,171–173,178,180,182,186,192,199,201,202,205,208]; cyano-nitro with or without halogeno; [47,178–182] carboxy-alkyl; [182,188,201,209] alkoxy-dialkylsulphonamide; [190] etc. [169,173,182,184,185,187,194,203,209]

These products present an interrupted conjugation. For this reason, the series of shades is limited. The shades are generally brilliant, but the light, sublimation and thermofoxation-fastness are only satisfactory or even weak. Thus, for example, we can mention the dyes obtained from aniline, 4-anisidine or 4-methoxy-4′-amino-diphenyl-amine or 1-phenyl-3-methyl-PzO.

The presence of alkoxy, or halogeno and alkoxy groups, in the diphenyl-amine molecule seems to improve the fastness [183] such as 2,5-dimethoxy- or 2-methoxy-5-chloro-4′-amino-diphenyl-amine.

The N-alkyl-sulphonamide groups of the diazo compound determine higher fastness to light, sublimation, moist treatments and rubbing and satisfactory shades, such as the dye obtained from 2,5,1-(X_2) SO_2NH—$-C_4H_9)$ $C_6H_3NH_2$ and 1,3-(Ar) (CH_3)-PzO. [210]

The COOAlk group in the 3-position increases the affinity for the polyester fiber. [171,183,192,193,201,211]

The pyrazolonic disperse dyes having alkylable and quaternizable N-heteroatoms permit the combination of the disperse dyes technology with that of basic pyrazolonic dyes for polyacrylonitrile fibers.

4.3. THIAZOLE OR ISO-THIAZOLE DERIVATIVES

The thiazole or iso-thiazole derivatives, in contrast with the pyrazolonic derivatives, permit the obtaining of a larger colour scale with a better tinctorial fastness.

In the synthesis of these dyes, one can use diazocompounds represented by 2-amino-thiazole derivatives, which contain alkyl, [212] or nitro[12,45,54,126,212,213,214–223] groups in the 4- or 5-position, or other two combined groups in the 4- and 5-position such as trifluor-methyl-nitro, [224] methyl-sulfonyl-nitro [225,226] or alkyl-cyano. [227,228] It seldom works with unsubstituted 2-amino-thiazole. [229–231]

---

[207] BUDZIZ, Tomaszand Wajtkiewicz, *Wincenty Chem. Slosow, Ser. A.*, **12**, 77—113 (1968)

[208] H. G. HANKE, G. WOLFRUM, H. WUNDERLICH (Farbenfabriken Bayer A. — G.) Fr. Pat. 1 465 116, 6 Jan. 1967; *Chem. Abstr.*, **67**, 65402 (1967).

[209] H. BURKHARD, W. WEHRLI (Sandoz Ltd.) Swiss Pat. 418 495, 28 Feb. 1967; *Chem. Abstr.*, **67**, 12510 (1967).

[210] R. GANGNEUX, J. de BLANC (Compagnie Française des Matières Colorantes) Fr. Pat. 1 176 871, 27 Jun. 1957; *Chem Zentr.*, 1960, 7004.

[211] A. N. JOYCE (American Cyanamid Co.) U.S. Pat. 3 019 217, 30 Jan. 1962; *Chem. Abstr.*, **57**, 6073 (1962).

[212] D. J. WALLACE, M. A. WEAVER (Eastman Kodak Co.) U.S. Pat. 3 349 075, 24 Oct. 1967; *Chem. Abstr.*, **68**, 22710 (1968).

For isothiazole, the patent, [232] based on the diazotization and coupling of 4,3,5-(NO_2) (CH_3) (NH_2)-thiazole with N-alkyl-N-hydroxyalkyl-aniline derivatives, can also be mentioned.

Among the coupling components we can mention aryl-amines unsubstituted to the ring or aryl-amines that contain one or two other groups attached to the ring (alkyl, halogeno, acetyl-amino, etc.).

From the first group, we can mention the products with the amino-group substitued by $-(CH_3)$;[228] $(C_2H_4OCO_2CH_3)_2$; [213] $(C_2H_4SO_2NHCOCH_3)_2$, [218] etc. [54,220,233] and from the second group the aryl-amines having the amino-group substituted by the following substituents $-(C_2H_5)$; [215] $-C_2H_4CN$; [222] $-C_2H_4CONH_2$; [212] $-C_2H_4COOCH_3$; [45] etc.[214,217,221,229,231]

---

[213] W. Kruckenberg (Farbenfabriken Bayer A. — G.) Fr. Pat. 1 390 146, 19 Feb. 1965 ; *Chem. Abstr.*, **64**, 2200 (1966).

[214] R. Altermat, H. Wicki (Sandoz Ltd.) Fr. Addn. Pat. 93 514, 11 Apr. 1969 ; *Chem. Abstr.*, **72**, 122909 (1970).

[215] H. von Brachel, D. Cornelius (Cassella Farbwerke Mainkur A. — G.) Ger.Offen. Pat. 1 934 786, 12 Feb. 1970 ; *Chem. Abstr.*, **73**, 89146 (1970).

[216] M. A. Weaver, H. S. Pridge (Eastman Kodak Co.) U.S. 3 639 385, 1 Feb. 1972 ; *Chem. Abstr.*, **76**, 155583 (1972).

[217] M. A. Weaver (Eastman Kodak Co.) Ger. Offen. Pat. 2 231 951, 18 Jan. 1973 ; *Chem. Abstr.*, **78**, 99034 (1973).

[218] D. Guenther, H. Vollmann, W. Happe (Farbwerke Hoechst A. — G.) Ger. Offen. Pat. 1 917 891, 3 Dec. 1970 ; *Chem Abstr.*, **74**, 77386 (1971).

[219] W. Krukenberg (Farbenfabriken Bayer A. — G.) Brit. Pat. 933 160, 8 Aug. 1963 ; *Chem. Abstr.*, **62**, 7906 (1965).

[220] Cassella Farbwerke Mainkur A. — G. Fr. Pat. 1 497 263, 6 Oct. 1967 ; *Chem. Abstr.*, **69**, 37090 (1968).

[221] F. J. Dawson, E. Teale (Yorkshire Dyeware and Chemical Co. Ltd.) Brit. Pat. 1 237 017, 30 Jun. 1971 ; *Chem. Abstr.*, **75**, 110985 (1971).

[222] E. Hoyer, H. J. Schladetsch (Farbwerke Hoechst A. — G.) Ger. Offen. Pat. 1 963 009, 24 Jun. 1971 ; *Chem. Abstr.*, **75**, 119194 (1971).

[223] D. Guenther, H. Happe, E. Hoyer, H. Vollmann (Farbwerke Hoechst A. — G.) Ger. Offen. Pat. 1 941 375, 25 Feb. 1971 ; *Chem. Abstr.*, **75**, 78133 (1971).

[224] E.B. Towne, J. B. Dickey (Eastman Kodak Co.) U.S. Pat. 2 771 466, 20 Nov. 1956 ; *Chem. Abstr.*, **51**, 4719 (1957).

[225] E. B. Towne, J. B. Dickey, Melvin S. Bloom (Eastman Kodak Co.) U. S. Pat. 2 839 523, 17 Jun. 1958 ; *Chem. Abstr.*, **53**, 1752 (1959).

[226] E. B. Towne, J. B. Dickey, M. S. Bloom (Eastman Kodak Co.) U. S. Pat. 2 852504, 16 Sept. 1958 ; *Chem Abstr.*, **53**, 6627 (1959).

[227] K. Taube (Farbenfabriken Bayer A. — G.) Ger. Pat. 952 017, 7 Nov. 1956 ; *Chem. Abstr.*, **51**, 10068 (1957).

[228] A. T. Costello, S. C. Rennison, P. Smith (Imperial Chemical Industries Ltd.) Ger. Offen. Pat. 2 209 839, 14 Sep. 1972 ; *Chem. Abstr.*, **78**, 5390 (1973).

[229] Ciba Ltd. Brit. Pat. 883 342, 29 Nov. 1961 ; *Chem. Abstr.*, **57**, 4797 (1962).

[230] M. A. Weaver, H. S. Pridgen, C. A. Coates Jr. (Eastman Kodak Co.) U. S. Pat. 3 660 374, 2 May 1972 ; *Chem. Abstr.*, **77**, 76663 (1972).

[231] W. A. Max, J. M. Straley, W. H. Moore (Eastman Kodak Co.) Ger. Offen. Pat. 2 028 395, 23 Dec. 1970 ; *Chem. Abstr.*, **74**, 88653 (1971).

[232] R. H. Meen, W. H. Moore (Eastman Kodak Co.) U.S. Pat. 3 143 540, 4 Aug.1964 ; *Chem. Abstr.*, **62**, 670 (1965).

[233] D. Cornelius, H. W. von Brachel, O. Graewinger (Cassella Farbwerke Mainkur A.—G.) Brit. Pat. 1 067 040, 26 Apr. 1967 ; *Chem. Abstr.*, **67**, 22887 (1967).

Among the coupling components with a special structure but with a frequent utility, we can mention 1,2,3,4-tetrahydro-quinoline, N-phenylmorpholine [225] and 1,3-cyclohexandione. [226]

The group situated in the 4-position of the thiazolic ring seems to have a weaker bathochromic effect than those situated in the 5-position. The spectra of the dyes obtained from TzA derivatives substituted in the 4-position with $COOC_2H_5$, NO_2, CH_3SO_2 etc. groups and the coupling component 3,1-$(CH_3)C_6H_4$-$[N(C_2H_5)CH_2CHOHCH_2OH]$ are in the 8–10 mμ interval while for the same groups, situated in the 5-position, the interval of variation is about 60 mμ.

The groups with strong effect $-E$, $-I$ (NO_2; NH_2SO_2 etc.) increase very much the light fastness and decrease sublimation-fastness. The groups with $+I$ or $+E$ effect determine the increase of sublimation-fastness.

The thiazolic ring, itself, determines an appreciable bathochromic effect. The TzA coupled with 3,1-$(CH_3)C_6H_4$-$[N(C_2H_5)CH_2CHOHCH_2OH]$ has a λ max. = 500 mμ, while aniline with the same coupling component to a λ max = 417 mμ. Also, the dyes obtained from 5-(NO_2)-TzA and 4-nitro-aniline with the same coupling component have λ max= = 590 mμ and 492 mμ, respectively.

The group N-beta-hydroxyethyl-acyl (ex. acetyl) increases the sublimation and moist treatments fastness and also the affinity for the fiber.

The groups N-beta-cyanoalkyl or cyano-alkoxy-alkyl determine also an appreciable effect of increase of the fastness of affinity and shades vivacity, such as the dye 5-(NO_2)-Tza → $C_6H_5N(CH_3)$ $(C_2H_4OC_2H_4CN)$. [167]

The N-acyl-oxyalkyl, N-cyano-alkyl-oxyalkyl or N-gama, beta-dihydroxy-propyl groups have stronger effects of improvement than the N-alkyl, N-hydroxyalkyl, N-(alkyl)-(hydroxyalkyl) groups.

4.4. 2-AMINO-BENZOTHIAZOLE DERIVATIVES

The more arduous researches of this series are justified because good or very good fastness and a large colour scale can be obtained.

Beside the patents that present generally 2-amino-benzothiazole derivatives, [231,234–237] other derivatives can be mentioned, that have groups attached to the benzene ring such as methylsulphonyl [238–241];

---

[234] J. M. Straley, J. Sagal Jr. (Eastman Kodak Co.) U.S. Pat. 2 822 359, 4 Febr. 1958; *Chem. Abstr.*, **52**, 8569 (1958).

[235] J. M. Straley, J. G. Fischer (Eastman Kodak Co.) U.S. Pat. 2 857 373, 21 Oct. 1958; *Chem. Abstr.*, **53**, 5690 (1959).

[236] B. R. Fishwick (Imperial Chemical Industries Ltd.) Brit. Pat. 896 232, 16 May 1962; *Chem. Abstr.*, **58**, 605 (1963).

[237] Nishido Keuzo, Haruna Eijiro, Kumano Isao (Tokio Ind. Manuf. Co., Ltd.) Japan Pat. 72 33, 483 25 Aug. 1972; *Chem. Abstr.*, **78**, 17611 (1973).

[238] J. M. Straley, D. J. Wallace (Eastman Kodak Co.) U.S. Pat. 2 773 054, 4 Dec. 1956; *Chem. Abstr.*, **51**, 7026 (1957).

[239] S. Koller, D. Reinker, H. R. Schwander (Ciba-Geigy A. – G.) Ger. Offen. Pat. 2 101 912, 22 Jul. 1971; *Chem. Abstr.*, **75**, 141955 (1971).

[240] Kimura Yoshio, Kitawaki Hideo (Mitsubishi Chemical Industries Co., Ltd.) Japan Pat. 69 09, 758, 7 May 1969; *Chem. Abstr.*, **71**, 103161 (1969).

[241] R. Hahn, C. Mueller (Sandoz Ltd.) Fr. Pat. 1 536 737, 16 Aug. 1968; *Chem. Abstr*, **72**, 68199 (1970).

cyano ; [20,242,243] nitro ; [240,242,244–247] halogeno ; [240,248–252] etc. [121,253–257].

The coupling components are represented by the aryl-amines that contain substituents of the type beta-hydroxy-alkyl, beta-cyano-alkyl, beta-alkyl-hydroxyalkyl, etc. [121,229,237,240,241,245,246,248,249,251,252,255,258,259] alkylcarboxyalkyl[260]; acetoxyalkyl [236,243,250,254], etc. attached to the amino-group and groups attached to the ring of type alkoxy, halogen, etc.

The light fastness and the affinity for the fiber are increased by the hydroxyalkyl-6-sulphonyl groups, attached to the diazo compounds and by the N-beta-cyanoalkyl, N-beta-acetoxyethyl presented on the coupling component. [261]

We must mention, in this category, the dye obtained from 6,5-(CH_3SO_2) (CH_3)-ABz and 3,1-$(CH_3)C_6H_4$ $[N(X_4 ; X_7 ; C_2H_4COOCH_3)_2]$.[259]

The NO_2 groups attached to the benzene ring and the acyloxyalkyl groups attached to the aminic nitrogen, determine higher fastness than those offered by the N-alkyl or beta-hydroxyalkyl groups.

The $NHCOCH_3$ group of the coupling-component increases the thermofixation-fastness, [236,243,254,255] such as to the dye 6-(NO_2)-ABz → → 3,1-$(X_1)C_6H_4[N(X_7)_2]$.

---

[242] M. A. Weaver, J. M. Straley, J. F. Dale (Eastman Kodak Co.) U.S. Pat. 3 385 842, 28 May, 1968 ; *Chem. Abstr.*, **69**, 44560 (1968).

[243] Ciba Ltd. Fr. Pat. 1 571 625, 14 Jun. 1967 ; *Chem. Abstr.*, **73**, 46622 (1970).

[244] J. W. Dehn Jr., R. A. Pizzarello, E. Eltonhead (Interchimical Corp.) U.S. Pat. 3 090 789, 21 May 1963 ; *Chem. Abstr.*, **59**, 5291 (1963).

[245] Matsumoto Jintaro, Hosoi Hiroomi (Nippon Kayaku Co. Ltd.) Japan Pat. 69 13, 389, 16 Jun. 1969 ; *Chem. Abstr.*, **72**, 33233 (1970).

[246] K. Artz (Ciba-Geigy A. — G.) Ger. Offen. Pat. 2 139 449, 10 Feb. 1972 ; Chem. Abstr., **77**, 7289 (1972).

[247] N. B. Desai, W. Jenny (Ciba-Geigy A. — G.) Ger. Offen. Pat. 2 104 563, 12 Aug. 1971 ; *Chem. Abstr.*, **75**, 141958 (1971).

[248] Sumitani Mitsukuni, Kajikawa Akira (Nippon Kayaku Co. Ltd.) Japan Pat. 69 30, 628, 9 Dec. 1969 ; *Chem. Abstr.*, **72**, (1970).

[249] Sumitani Mitsukumi, Kajigawa Akira (Nippon Kayaku Co. Ltd.) Japan Pat. 70 08, 750, 30 Mar. 1970 ; *Chem. Abstr.*, **73**, 100015 (1970).

[250] A. Rhodes (Martin-Marieta Corp.) Ger. Offen. Pat. 2, 111,784, 23 Sep. 1971 ; *Chem. Abstr.*, **76**, 60918 (1972).

[251] R. Sommer, G. Holfrum, H. Wunderlich (Farbenfabriken Bayer A. — G.) Ger. Offen. Pat. 2 053 079, 4 May 1972 ; *Chem. Abstr.*, **77**, 15902 (1972).

[252] A. T. Peters, *J. Soc. Dyers and Colourists*, **85**, 507—509 (1969) ; *Chem. Abstr.*, **72**, 44990 (1970).

[253] W. Bossard, F. Favre (J. R. Geigy A. — G.) Swiss Pat. 373 842, 31 Jan. 1964 ; *Chem. Abstr.*, **61**, 5823 (1964).

[254] H. Wunderlich (Farbenfabriken Bayer A. — G.) Belg. Pat. 667 856 ; *Chem. Abstr.*, **65**, 15549 (1966).

[255] M. F. Santori (Du Pont de Nemours, E. I.) U.S. Pat. 3 405 118, 3 Oct. 1968 ; *Chem. Abstr.*, **70**, 30034 (1969).

[256] Kimura Yoshio, Kitawaki, Hideo (Mitsubishi Chemical Industries Co., Ltd.) Japan Pat. 69 30 627, 9 Dec. 1969 ; *Chem. Abstr.*, **72**, 112786 (1970).

[257] Badische Anilin-und Soda Fabrik A. — G. Brit. Pat. 1 222 849, 17 Feb. 1971 ; *Chem. Abstr.*, **74**, 127536 (1971).

[258] J. Gamaj, H. Seibisz (Institut Przemaslu Organicznego) Pol. Pat. 54, 341, 15 Feb. 1968 ; *Chem. Abstr.*, **70**, 107511 (1969).

[259] R.K.K. Fourness (Yorkshire Dyeware Chemical Co., Ltd.), Brit. Pat. 944 250, 11 Dec. 1963 ; *Chem. Abstr.*, **61**, 5824 (1964).

[260] A. H. Berrie, N. Hughes, E. Young (Imperial Chemical Industries) Ger. Offen. Pat. 2 130 991, 30 Dec. 1971 ; *Chem. Abstr.*, **76**, 128794 (1972).

[261] B. R. Fishwick (Imperial Chemical Ind. Ltd.) Brit. Pat. 953 887, 2 Apr. 1964 ; *Chem. Abstr.*, **61**, 5825 (1964).

The dyes obtained from 6,4-(X_2) (NO_2)-ABz and the components of the type C_6H_5N $(Alk)_2$ or $C_6H_5N(C_2H_4OH)_2$ or $(C_6H_5)_2N-CH_3$ presents a weak fastness and a reduced affinity for the polyester fiber except the dye 6-(X_2)ABz → 2,5,1-(X_2) (CH_3)$C_6H_3NH_2$, that presents good fastness to light (5), sublimation (4) and thermofixation (4–5).

The NO_2 group in the 6-position of the benzene ring has an appreciable bathochromic effect, because of the extension of the conjugation system.

The substitution by the halogen in any of the four positions of the benzene ring produces a bathochromic effect.

It has been found, in the series of halogenated benzothyazolic dyes, that those which contain halogen-atoms in the 4-position present high SF values and low LF values on the polyester fibers. They also present a greater stability on the acetate fiber, probably determined by the connections between the hydroxy-groups and the nitrogen-heteroatom.[252]

4.5. PYRIDINE AND PYRIDONE-2-DERIVATIVES

The dyes of this class are characterized by good and very good tinctorial properties. They are used to the dyeing and printing of the polyester fibers in yellow shades.

We present below some general considerations about the behaviour of pyridine and its derivatives in the electrophilic substitution reactions, which also include the coupling reaction.

The electrophilic substitution reactions of these derivatives develop considerably weaker than in the benzene series.

The cause of this difference consists of a higher electronegativity of the nitrogen-atom. This determines a general decrease of the ring electron density and a selective decrease of the ring electron density in the alfa, alfa prime and gama positions.

The electron distribution in the pyridine molecule may be represented by the following structures :

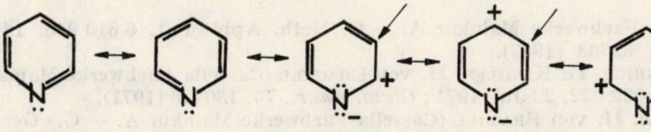

The electrophilic substitution reactions take place in the beta-position richer in electrons than the others (alfa and gama positions).

In the electrophilic substitution reactions the pyridine derivatives are actionless. This behaviour is accentuated by the strong acid medium in which pyridine is present as pyridinium ion (by fixation of the proton to the heteroatom).

The electron-attracting effect of the positive charged nitrogen-atom on the entire pyridine molecule is also increased.

This is the reality in the coupling reaction (strong acid medium).

The utilisation of the pyridine derivatives as coupling components may be illustrated by the following examples : 2,6,3,4-$(OH)_2$ $(CONH_2)$ (Alk)-Py [262–264]; 1,3,4,6-(Ar)(CN)(Alk)(OH)-PyO [265]; 1,3,4,6-[Alk ; $N(Alk)_2$] (CN) (Alk ; p-$CH_3C_6H_4$) (OH)-PyO. [266–268]

The diazo-components are represented by heterocyclic amino-derivatives of the 2-amino-thiazole type, [266] or by aryl-amines substituted in the ring by the —Hlg, —NO_2, C_6H_5NHCOO— etc. groups. [263,266,269–271]

4.6. PYRIMIDINE DERIVATIVES

Unlike the pyridine derivatives, the pyrimidine derivatives permit to obtain dyes with a larger colour scale (from yellow to red) and a good tinctorial fastness (to the light sublimation, perspiration, etc.) and also utilizable in the field of triacetate fiber.

The electronegative character of the nitrogen-atoms determines a general decrease of the electron density to the entire ring and a selective decrease of the electron density in the 2-, 4-, 6-position, according to the structures :

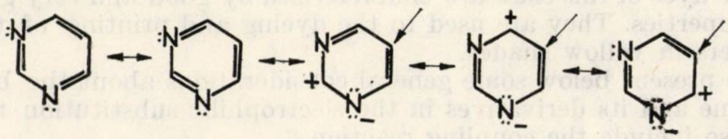

Because of the diminished electron density of the ring, the electrophilic substitution develops more difficulty being possible only in the 5-position, the greatest electronegative charge.

The aromatic character of the pyrimidine and its substitutes to the ring with alkyl, aryl, halogeno and nitro groups decreases gradually, when we introduce OH or NH_2 groups in the 2-,4- and 6-position of the ring.

Also, while the pyrimidine and its derivatives with alkyl, halogeno, nitro groups are very fast to the electrophilic substitution, the derivatives

---

[262] Cassella Farbwerke Mainkur A. — G. Neth. Appl. Pat. 6 610 943, 14 Feb. 1967; *Chem. Abstr.*, **67**, 65393 (1967).

[263] E. Heinrich, H. Kindler, H. von Brachel (Cassella Farbwerke Mainkur A. — G.) Ger. Offen. Pat. 2 022 022, 22 Jul. 1971 ; *Chem. Abstr.*, **75**, 130776 (1971).

[264] Heinrich, H. von Brachel (Cassella Farbwerke Mainkur A. — G.) Ger. Offen. Pat. 2 001 821, 22 Jul. 1971 ; *Chem. Abstr.*, **75**, 130775 (1971).

[265] A. H. Berrie, N. Hughes (Imperial Chemical Industries Ltd.) Ger. Offen. Pat. 1 932 806, 19 Feb. 1970 ; *Chem. Abstr.*, **73**, 46639 (1970).

[266] H. Burkhard, R. Entschel, W. Steinemann (Sandoz Ltd.) Ger. Offen. Pat. 1 901 711, 9 Apr. 1970 ; *Chem. Abstr.*, **73**, 16264 (1970).

[267] J. Ribka, E. Heinrich (Cassella Farbwerke Mainkur A. — G.) Ger. Offen. Pat. 2 120 095, 2 Nov. 1972 ; *Chem Abstr.*, **78**, 45034 (1973).

[268] H. von Brachel, B. Heinrich, H. Kindler (Cassella Farbwerke Mainkur A. — G.) Ger. Qffen. Pat. 2 015 172,21 Oct. 1971 ; *Chem. Abstr.*, **76**, 87 133 (1972).

[269] A. H. Berrie, N. Hughes (Imperial Chemical Industries Ltd.) Brit. Pat. 1 256 340, 8 Dec. 1971 ; *Chem. Abstr.*, **76**, 101205 (1972).

[270] H. Burkhard, F. Mueller, U. Zirngibl (Sandoz Ltd.) Ger. Offen. Pat. 2 149 137, 6 Apr. 1972 ; *Chem. Abstr.*, **77**, 63336 (1972).

[271] H. Burkhard, F. Mueller, U. Zirngibl (Sandoz Ltd.) Ger. Offen. Pat. 2 150 226, 20 Apr. 1972 ; *Chem. Abstr.*, **77**, 90039 (1972).

with OH, NH_2, NH-Alk are even sensible to the weak electrophilic reagent. They react in the 5-position.

We further mention some compounds of this class which are utilized like coupling components : 2,6-(NHAlk) (AlkO ; ArO)-PyM [272] ; 2,6,4-(NH_2 ; NHAlk)$_2$(NHAr ; NHAlk)-PyM [273,274] ; 2,4,6-(NHAr) ($NHCH_3$; NHAr) ($NHCH_2CH_2OH$)-PyM. [275]

It is possible to use, as diazo compound, aryl-amines, with the following groups attached to the ring (the NH_2-group occupies the 1-position) : 2,4-(NO_2)$_2$-arylamine. [274]

4.7. INDOLE DERIVATIVES

Indole derivatives dye the polyester fibers and, sometimes, the triacetate and polyamide in the yellow to orange shade.

The indole reacts easily with electrophilic reagents (for example in the coupling reaction).

The substitution occurs usually in the beta-position, because of the specific conjugation effect to this product, that can be represented by the following structures :

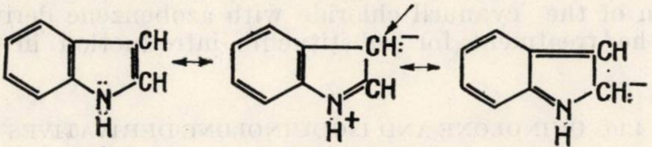

I II III

Evidently the structure II is favoured in comparison with the structure III because III involves the benzene ring into an ortho-quinoide form.

A part of the conjugation energy is consumed for the formation of this structure. For this reason the greatest electron density is in the beta-position.

In the case the beta-position is occupied, the electrophilic substitution reaction takes place in the alfa-position, as in the undermentioned examples, where the different indole derivatives are used as coupling components : alfa-(Ar)-indole[276,277]; alfa-(Alk)-indole.[278,279] As diazo components the following are used : 2,4(5),1-($COOC_2H_4OCH_3$) (H ; NO_2)$-C_6H_2-NH_2$.[276,277]

---

[272] H. Ackermann, W. Bossard, J. Holtz, H. Wegmueller (Geigy J. R., A. – G.) Swiss Pat. 475 311, 29 Aug. 1969 ; *Chem. Abstr.*, **72**, 101844 (1970).

[273] H. Ackermann, W. Bossard, J. Holtz, H. Wegmueller (Geigy J. R., A. – G.) Swiss Pat. 473 190, 15 Jul. 1969 ; *Chem Abstr.*, **72**, 13802 (1970).

[274] Geigy J. R., A. – G., Brit. Pat. 1 109 628, Apr. 1968 ; *Chem. Abstr.*, **69**, 28577 (1968).

[275] H. Ackermann, W. Bossard, J. Volz, H. Wegmueller (Geigy J. R., A. – G.) Swiss Pat. 476 075, 15 Sep. 1969 ; *Chem. Abstr.*, **76**, 26395 (1972).

[276] J. Dehnert, G. Gnad (Badische Anilin-und Soda Fabrik A. – G.) U.S. Pat. 3 557 080, 19 Jan. 1971 ; *Chem. Abstr.*, **74**, 113211 (1971).

[277] Badische Anilin- und Soda Fabrik A.—G. Brit. Pat. 1 224 919, 10 Mar. 1971 ; *Chem. Abstr.*, **77**, 128060 (1972).

[278] Badische Anilin- und Soda Fabrik A. – G. Fr. Pat. 1 582 470, 26 Sep. 1969 ; *Chem. Abstr.*, **73**, 67672 (1970).

[279] Johanes Dehnert (Badische Anilin- und Soda Fabrik A. – G.) Brit. Pat. 1 224 919, 18 Aug. 1965 ; *Chem. Abstr.*, **63**, 18313 (1965).

4.8. THIADIAZOLE DERIVATIVES

The dyes of this class dye sometimes the polyester fibers and polyamide fibers in red light fast shades.

Among the thiadiazol derivatives (NH_2-group occupies the 5-position), 2-(SC_2H_5)-1,3,4-TDz [280]; 2-(C_6H_5)-1,3,4-TDz [281]; 3-($CH_3OOCC_2H_4S$)-1,2,4 TDz [282] can be cited as diazo compounds used.

As coupling components, the following are used: 2,5,1-$(CH_3)(X_1)C_6H_3[NHCH(CH_3)C_2H_5]$ [280]; $C_6H_5[N\ (CH_2Ar)C_2H_4COOC_2H_5]$ [282]; 2,5-$(X_1)C_6H_4\ [N(X_5\ ;\ X_7)\ C_6H_{11}]$. [281]

1,3,5-TRIAZINE DERIVATIVES

The 1,3,5-triazine derivatives dye in yellow to orange shades the polyester and polyamide fibers.

The use of these derivatives as coupling components is illustrated by the example: 2,4,1-(CN) (Cl)$C_6H_3NH_2 \rightarrow$ 4-[C_6H_5(Alk) $C_2H_4N(Alk)_2$]-2,6-$(OCH_3)_2$-triazine-1,3,5. [283]

The dyes of this class are obtained, besides other methods, by the condensation of the cyanuril chloride with azobenzene derivatives, followed by the treatment for substituents introduction in the triazine ring. [284]

4.10. QUINOLONE AND ISOQUINOLONE DERIVATIVES

The dyes from quinolone derivatives dye the polyester and sometimes polyamide fibers in yellow to violet shades with good light fastness. There can be cited: 3,1-$(SO_2CH = CHCl)C_6H_4NH_2 \rightarrow$ 1,4-$(CH_3)(OH)$-quinolone [142]; 2,4,1-$(CN)(NO_2)C_6H_3NH_2 \rightarrow$ 8-(ArNH)-quinolone-2 [90]; 2,1-$(NO_2)\ C_6H_4NH_2 \rightarrow$ 2,3-(Alk) (OH)-isoquinolone. [260]

---

[280] M. A. Weaver, D. J. Wallace (Eastmann Kodak Co.) U.S. Pat. 3 657 215, 18 Apr. 1972; *Chem. Abstr.*, **77**, 50128 (1972).

[281] Badische Anilin- und Soda Fabrik A. – G. Fr. Demande 2 019 449, 2 Aug. 1970; *Chem. Abstr.*, **75**, 7441 (1971).

[282] E. Hahn, H. G. Wippel (Badische Anilin- und Soda Fabrik A.– G.) U. S. Pat. 3 621 007, 16 Nov. 1971; *Chem. Abstr.*, **76**, 87151 (1972).

[283] H. J. Angliker, R. Peter (Ciba-Geigy A. – G.) Ger. Offen. Pat. 2 135 216, 20 Jan. 1972; *Chem. Abstr.*, **77**, 72809 (1972).

[284] E. Siegel, H. Horstmann (Farbenfabriken Bayer A. – G.) Ger. Offen. Pat. 2 017 907, 28 Oct. 1971; *Chem. Abstr.*, **76**, 73726 (1972).

Revue Roumaine de Chimie, **21**, *4*, 621–625 (1976)

BENZOFURO-BENZOTHIAZOLES. V[1]

2-AMINO- AND 2-MERCAPTO-BENZOFURO-BENZOTHIAZOLES

VALER FĂRCĂŞAN and STELIAN FLOREA
Department of Chemistry "Babeş-Bolyai" University
Str. Arany Janos 11, Cluj-Napoca, Romania

Received September 27, 1974

The obtainment of the 2-amino-benzofuro-benzothiazoles I and VII from IV and VII was reported, and the linear structure of I is demonstrated by using physical methods. By reacting 3-amino-dibenzofuran (III) with carbon disulphide and sulphur, the 2-mercapto-benzofuro-benzothiazole (IX) and the 2(3-dibenzofurylamino)-benzofuro (2,3–f) benzothiazole (X) were prepared.

An objective of our researches in the benzofuro-benzothiazole series is the study of the interaction between nucleus and substituents. For such purposes the 2-amino and 2-mercapto-derivatives are very suited, owing to the known tautomerism of the 2-substituted thiazoles.[2]

This paper reports the attempts to obtain 2-amino- and 2-mercapto-benzofuro-benzothiazoles.

The 2-amino-benzofuro (2,3-f) benzothiazole (I) was first prepared by Gilman et al[3] via the corresponding o-thiocyanatamine (II), but no proof of linear structure was offered for this compound. We obtained I following the same way but another reagent. Namely, the 3-amino-dibenzofuran (III) was treated with cupric thiocyanate and the reaction product cyclised in the presence of hydrochloric acid. After repeated recrystallizations we isolated I with the reported m.p.,[3] but the yields were very low.

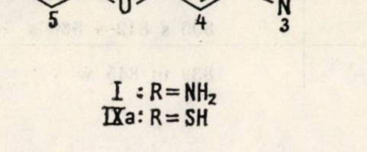

I : $R = NH_2$
IXa: $R = SH$

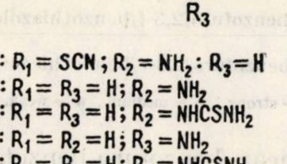

II: $R_1 = SCN$; $R_2 = NH_2$; $R_3 = H$
III: $R_1 = R_3 = H$; $R_2 = NH_2$
IV: $R_1 = R_3 = H$; $R_2 = NHCSNH_2$
V: $R_1 = R_2 = H$; $R_3 = NH_2$
VI: $R_1 = R_2 = H$; $R_3 = NHCSNH_2$

---

[1] Part IV, V. FĂRCĂŞAN and S. FLOREA, *Stud. Univ. Babeş-Bolyai*, *Chem.* **18**, 143 (1973).

[2] J. M. SPRAGUE and A. H. LAND "Heterocyclic Compounds", vol. 5, Edited by R. C. Elderfield, New York, 1957, p. 562 and 572.

[3] H. GILMAN, P. T. PARKER, J. C. BAILIE and G. E. BROWN, *J. Amer. Chem. Soc.*, **61**, 2836 (1939); *Chem. Zentr.*, **1940**, 539.

A more successful route to I proved to be the conversion of III into 3-N-dibenzofuryl-thiourea (IV) and ring closure by bromine in chloroform, i.e. the general Hugerschoff synthesis[4] for 2-amino arylthiazoles.

This technique has also been used by us to obtain from 4-aminodibenzofuran (V) via 4-N-dibenzofuryl-thiourea (VI), the 2-amino-benzofuro(2,3-e)benzothiazole (VII).

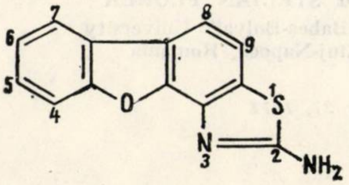

VII

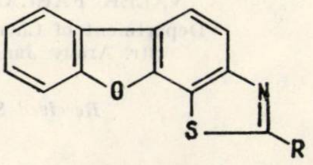

VIII: R=NH₂
IXb: R=SH

If for substance VII the structure is indubitable, in compound I it claims to be demonstrated. Indeed in the reaction sequences leading to I not exclusively the 2-position but also the 4 one can be involved; thus, beside a linear (I) an angular (VIII) benzofuro-benzothiazole may also be formed.

The linear structure of I isolated by us is supported by the following data:

By comparing the IR spectra of I and VII (see table 1) it can be observed that, unlike 2-amino-benzofuro(2,3-e)benzothiazole (VII) with angular structure, substance I exhibits a band in the 860–900 cm^{-1} region. It is known[5–7] that polycyclic derivatives containing a tetrasubstituted benzene ring, show absorbtions in the above mentioned range, if the two hydrogens are para with respect to each other as in the case of a linear benzofuro-benzothiazole. The NMR spectrum of I exhibits singlets which may be assigned to protons 9 and 4(δ = 7.68 and 8.41 ppm),

Table 1

IR spectra of I and VII in the range 800–900 cm^{-1}

Compound	1/λ cm^{-1}
2-Amino-benzofuro/2,3-f/benzothiazole (I)	805 s 842 s 860 s
2-Amino-benzofuro/2,3-e/benzothiazole (VII)	833 m 845 w

s = strong, m = medium, w = weak.

---

[4] A. Hugerschoff, *Ber. dtsch. chem. Ges.*, **34**, 3130 (1901); **36**, 3121 (1903).

[5] P. Bassignana, C. Cogrossi and M. Gandino, *Ann. Chim. (Ital.)*, **53**, 747 (1963).

[6] S. G. Fridman and D. K. Golub, *Khim. Geterotsikl. Soedin. Akad. Nauk Latv. SSR*, **1966**, 247.

[7] V. Fărcăşan and S. Florea, *J. prakt. Chem.*, **312**, 1007 (1970).

while in the spectrum of VII the protons 9 and 8 are represented by doublets ($\delta = 7 \cdot 75$ and $7 \cdot 86$ ppm).

Generally, linear polycyclic aromatic compounds absorb at longer wavelengths than the corresponding angular one.[8] A similar difference emerges if the UV spectra of 2-amino-benzofuro(2,3-f)-benzothiazole (I) and 2-amino-benzofuro(2,3-e)benzothiazole (VII) are compared (see experimental section).

By reacting 3-amino-dibenzofuran (III) with carbon disulphide and sulphur under pressure at 220°, two reaction products were isolated. The former, soluble in sodium hydroxide, is a 2-mercapto-benzofuro-benzothiazole (IX) as shown by the mass spectrum and the elemental analysis. III being unsymetrical, on cyclisation it is expected to yield IX_a or IX_b. The unsharp m.p. as well as the feature of the NMR spectrum of IX, if compared with those of compounds I and VII, pointed out the presence of both IX_a and IX_b, IX_a being the major compound. The detalied analysis of the NMR spectra of substances I, VII and IX will be the topic of a future paper. Attempts to resolve the isomers failed. The second substance isolated from the crude reaction product is a 2-(3-dibenzofuryl-amino)-benzofuro-benzothiazole (X). The obtention of X is supported by the elemental analysis, the mass spectrum and the literature data[9,10] which record the formation of an analogous compound, the 2-phenyl-amino-benzothiazole (XI), if aniline was reacted with carbon disulphide and sulphur. Taking into account the behaviours of X, it may be consi-

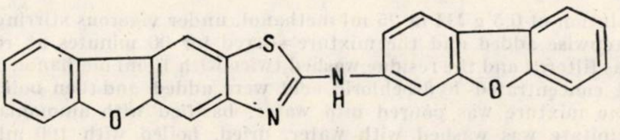

Xa

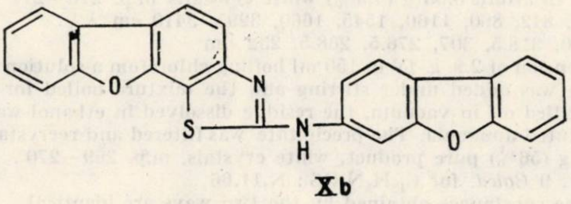

Xb

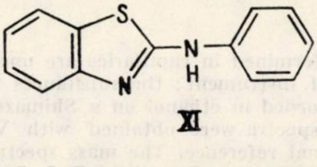

XI

---

[8] R. S. SILVERSTEIN and G. C. BASSLER, "Spectrometric Identification of Organic Compounds", John Wiley, New-York, 1967, p. 165.

[9] T. KIMIJIMA and S. MIYAMA. *J. Soc. Chem. Ind. Japan*, **46**, 264 (1943) ; *Chem. Abstr.*, **43**, 2021 e (1949).

[10] V. A. IVANOVA and N. SHEBUEV, *Zhur, priklad. Khim.*, **30**, 447 (1957).

dered as a pure substance and from the two possible structures (X_a and X_b) we assume X_a to be the most likely.

If the reaction yielding IX and X is carried out under milder conditions, X becomes the main product.

EXPERIMENTAL*

3-N-DIBENZOFURYL-THIOUREA (IV)

From III,[11] under the conditions described in [12] M.p. 220–222°.

4-N-DIBENZOFURYL-THIOUREA (VI)

The 4-aminodibenzofuran hydrochloride (XI), [13] 2.3 g, was added to a solution of 1 g ammonium thiocyanate in 4 ml water and heated for 10 hours on a steam-bath. Then the solvent was evaporated and the residue warmed for the next 15 hours on the steam-bath. The crude product, 2.3 g (90.5 %), was recrystallized from methanol-water. White-light yellow crystals, m.p. 197—198°.

Found : C, 64.6 ; H, 4.2 ; N, 11.4. Calculated for $C_{13}H_{10}N_2OS$:
C, 64.46 ; H, 4.13 ; N, 11.57

2-AMINO-BENZOFURO (2,3-f) BENZOTHIAZOLE (I)

a) To a solution of 0.5 g III in 25 ml methanol, under vigorous stirring, 2 g cupric thiocyanate were stepwise added and the mixture stirred for 90 minutes at room temperature. Afterwards it was filtered and the residue washed twice with 10 ml methanol. To the methanolic solution 3.5 ml concentrated hydrochloric acid were added and then boiled for one hour. After cooling the mixture was poured into water, basified with ammonia and directly filtered. The precipitate was washed with water, dried, boiled with 100 ml benzene and hot filtered. The solution was concentrated to 15—20 ml, cooled and the precipitate, 0.2 g, filtered. This product was extracted twice with 10 ml boiling benzene and the residue recrystallized from 25 ml benzene to afford 0.03 g (4.5 %) white crystalls m.p. 270–271° (lit. [3] 270°).

IR : 745, 805, 842, 860, 1160, 1545, 1660, 3295, 3410 cm^{-1}

UV : λ_{max} 330, 318.5, 307, 276.5, 268.5, 232 nm

b). To a suspension of 2.9 g IV in 150 ml boiling chlorofom a solution of 0.8 ml bromine in 15 ml chloroform was added under stirring and the mixture boiled for another 3 hours. The solvent was distilled off in vacuum, the residue dissolved in ethanol-water and the solution basified with diluted ammonia. The precipitate was filtered and recrystallized from amyl-alcohol yielding 1.6 g (56 %) pure product, white crystals, m.p. 269–270°.

Found : N, 11. 9 *Calcd.* for $C_{13}H_8N_2OS$: N,11.66
The IR spectra of the substances obtained by the two ways are identical.

---

* The melting points determined in capillaries are uncorrected. The IR spectra were recorded on a Perkin-Elmer 521 instrument ; the substances were prepared as KBr pellets. The electronic spectra were recorded in ethanol on a Shimazu Bausch & Lomb Spectronic 200 UV instrument. The NMR spectra were obtained with Varian HR-SC-220 spectrometer in DMF-d_7, TMS as internal reference. The mass spectra were recorded on a Varian MAT-CH 7 mass spectrometer. The source temperature was 220° and ionizing energy 70 eV.

[11] V. FĂRCĂȘAN, S. FLOREA and R. BEJU, *Stud. Univ. Babeș-Bolyai, Chem.*, **15**, 63 (1970).

[12] V. GRINSTEINS and G. CEMA, *Latvijas PSR Zinatum Akad. Vestis. Khim. Ser.*, **1962**, 247.

[13] H. GILMAN and R. K. INGHAM, *J. Amer. Chem. Soc.*, **75**, 4843 (1953).

2-AMINO-BENZOFURO (2,3-e) BENZOTHIAZOLE (VII)

From 0.6 g VI under the conditions given by the preparation of I, 0.55 g (92%) crude VII were obtained. After recrystallization from ethanol-water, the pure substance, white crystals, melts at 282–283°.

IR : 730, 740, 833, 920, 1183, 1430, 1530, 1615, 3075, 3270, 3440 cm^{-1}.

UV : λ_{max} 315, 292.5, 273, 254, 221 nm.

Found : C, 64.8 ; H, 3.3 ; N, 11.6. *Calcd.* for $C_{13}H_8N_2OS$:
C, 65.00 ; H, 3.33 ; N, 11.66

2-MERCAPTO-BENZOFURO-BENZOTHIAZOLE (IX)

A mixture of 2.7 g III, 0.5 g suplhur and 10 ml carbon disulphide was heated for 6 hours at 220° in an autoclave. After cooling the crude product was extracted with 10% sodium hydroxide at 60–70°. The alcaline solution was acidified with diluted hydrochloric acid, the precipitate filtred, dried, macerated with carbon disulphide to remove the unreacted sulphur and then dissolved in acetone. The acetonic solution was passed through an alumina column and then eluted with the same solvent. The acetone was removed and the residue, 0.95 g (25%), was recrystallized from xylene. M.p.> 240° is not sharp.

Found : C, 60.6 ; H, 2.7 ; N, 5.3. *Calcd.* for $C_{13}H_7NOS_2$:
C, 60.70 ; H, 2.72 ; N, 5.44

In the portion which is not soluble in 10% sodium hydroxide X was identified.

2-(3-DIBENZOFURYLAMINO) BENZOFURO (2,3-f) BENZOTHIAZOLE (X)

a) A mixture of 2.7 g III, 0.5 g sulphur and 10 ml carbon disulphide was heated at 220° for 90 minutes in an autoclave. The reaction product was extracted with 10% sodium hydroxide at 60–70° to remove IX, the residue washed with water, macerated with carbon disulphide and filtered. The solid, 2.15 g (36%), was recrystallized from aniline. M.p.275–276° M. W. 406

Found : C, 74.0 ; H, 3.3 ; N, 7.2. *Calcd.* for $C_{25}H_{14}N_2O_2S$:
C, 73.89 ; H, 3.44 ; N,6.89.

From the alcaline solution after acidifying 0.3 g (7.9%) crude IX were obtained.

b) A mixture of 0.85 g IV 0.12 g sulphur and 2.5 ml carbon disulphide was heated for 4 hours at 235° in a sealed tube. The reaction product was treated as described above to yield 0.55 g crude X and 0.15 g crude IX. After recrystalization X and IX show the m.p. 276° and > 240° respectively.

Acknowledgements. The authors are grateful to Prof. Dr. H. Kaiser ("Institut für Spektrochemie" Dortmund) for providing facilities to work and to Dr. Wendisch (Bayer Leverkusen) for the facilities for the recording of the NMR spectra at 220 MHz. One of us (S.F.) thanks DAAD foundation for financial support

Revue Roumaine de Chimie, **21**, *4*, 627–629 (1976)

EXO- AND ENDOHORMONES. III[1]

NEW DERIVATIVES OF SYNTHETIC ECDYSONE ANALOGUES AND RELATED COMPOUNDS

ALEXANDRA GOCAN and F. HODOŞAN
Laboratory of Natural Products, Institute of Chemistry, Cluj-Napoca, Str. Donath 65

Received May 22 1975

Nitrate esters of hydroxysteroids related to ecdysone were prepared.

When converted into the corresponding nitrate esters, hydroxysteroids with hormonal activity in mammalia undergo changes of their biological profile [2]. In order to elucidate whether such changes occur also in insects, we prepared nitrate esters deriving from a series of compounds related to ecdysone.

2β, 3β — Dihydroxy — 6 — oxo — 5α — cholestane 2 — acetate (I) gave by alkaline hydrolysis the allomeric dihydroxyderivatives II a, b [3] which could be converted under the action of acetyl nitrate prepared *in situ* into the corresponding dinitrates III a, b. IR spectral data of these compounds support the previously reported observation [4] that vicinal dinitrates with synclinal conformation exhibit an upward shift of the antisymmetric NO_2 stretching band in this way appearing at about 1650 cm^{-1}.

O—Nitration of compound I gave the acetate-mononitrate IV which could be subsequently converted under mild alkaline conditions into the hydroxy-mononitrate pair Va, b. The configuration at C—5 was established by conversion of compound Va into the dinitrate IIIa.

When treated with potassium hydroxide in boiling methanol compound IV gave the cyclo-steroid VI identical with that reported by V. Cerny et al. [5] (elemental analysis, IR, NMR, ORD [6]). Its formation is due to the ability of $C-O-NO_2$ group to undergo either O—N or C—O cleavage depending on reaction condition and/or structural factors. In the case reported here, the nitrate group behaves like a tosyloxy group, consequently the formation of compound VI can be represented as in Scheme 1. The enol-anion derived from the starting ketone under the action of the base acts as an internal nucleophile displacing the nitrato group and forming a 3α, 5α — bond. We suggest that the more rapidly liberated 2β — hydroxy group provides intramolecular catalysis by hydrogen bonding to the ether-oxygen of the nitrato group*.

---

[1] Part II: M. Vlassa, *Rev. Roumaine Chim.*, **21**, (1976).

[2] F. Hodoşan, O. Mantsch, I. Jude, D. Breazu, B. Cuparencu, and N. Sterescu, *Arzneim. — Forsch.*, **19**, 684 (1969).

[3] M. J. Thompson, W. E. Robbins, J. N. Kaplanis, C. F. Cohen, and S. M. Lancaster, *Steroids*, **16**, 85 (1970).

[4] F. Hodoşan and I. Jude, *Spectrochim. Acta*, **23A**, 461 (1967).

[5] V. Černy, A. Kasal, and F. Šorm, *Coll. Czech. Chem. Comm.*, **35**, 1235 (1970).

[6] C. Djerassi and W. Colsson, *J. Amer. Chem. Soc.*, **78**, 3761 (1956).

Finally, by selective O-nitration of 2β, 3β, 14α — trihydroxy—6—oxo—5β—cholest—7—ene (VII)[3] we prepared the corresponding 2,3—dinitrate VIII.

The results of the bioassays which are in progress will be published elsewhere.

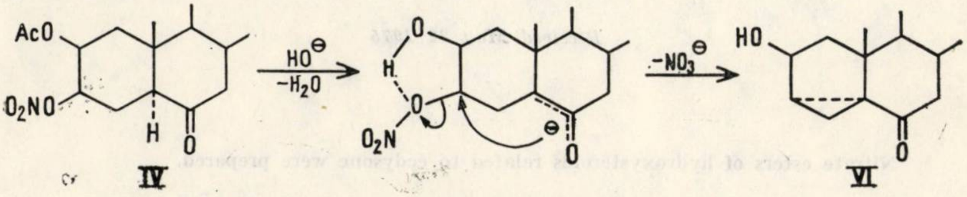

Scheme 1

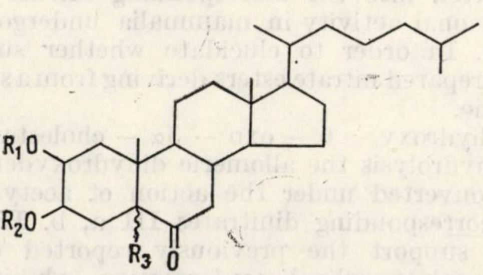

I. $R_1 = Ac$; $R_2 = H$; $R_3 = \alpha - H$
IIa. $R_1 = R_2 = H$; $R_3 = \alpha - H$
IIb. $R_1 = R_2 = H$; $R_3 = \beta - H$
IIIa. $R_1 = R_2 = NO_2$; $R_3 = \alpha - H$
IIIb. $R_1 = R_2 = NO_2$; $R_3 = \beta - H$
IV. $R_1 = Ac$; $R_2 = NO_2$; $R_3 = \alpha - H$
Va. $R_1 = H$; $R_2 = NO_2$; $R_3 = \alpha - H$
Vb. $R_1 = H$; $R_2 = NO_2$; $R_3 = \beta - H$

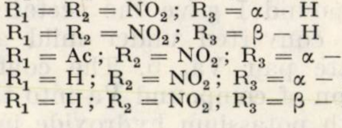

VII. R = H
VIII. $R = NO_2$

---

* An interaction between the hydroxyl-hydrogen and the negative end of the $-N^+O_2^-$ dipole is also imaginable.

EXPERIMENTAL

Melting points were taken on a "Mikroheitiztsch Boetius". IR spectra were recorded using a Zeiss UR–10 spectrophotometer.

O–Nitrations were performed according to I. Tănăsescu and co-workers.[7]

2β, 3β-Dihydroxy-6-oxo-5α-cholestane dinitrate (IIIa)

Starting with compound IIa (0.6.g). Mp 152–155° (methanol). Y :0.45 g. IR (CCl_4) : 850, 870, 1270, 1289, 1655, 1720 cm^{-1}. Anal. *Found* : C, 63.65 ; H, 8.72 ; *Calcd.* for $C_{27}H_{44}N_2O_7$: C, 63.75 ; H, 8.72

2β,3β-Dihydroxy-6-oxo-5β-cholestane dinitrate (IIIb)

Starting with compound IIb (0.6 g). Mp 113–115° (methanol). Y : 0.5 g. IR (CCl_4) : 855, 1272, 1289, 1655, 1712 cm^{-1}.
Anal. *Found* : C, 63.73 ; H, 8.75 ; *Calcd.* for $C_{27}H_{44}N_2O_7$: C, 63.75 ; H, 8.72

2β, 3β-Dihydroxy-6-oxo-5α-cholestane 2-acetate 3-nitrate (IV)

Starting with compound I (6 g). Mp 142–144° (methanol).
Y : 4.6 g. IR (CCl_4) : 865, 1285, 1640, 1710, 1740 cm^{-1}.
Anal. *Found* : C, 69.05 ; H, 9.51 ; N, 3.02 ; *Calcd.* for $C_{29}H_{47}NO_6$: C, 68.88 ; H, 9.37 ; N, 2.77

2β, 3β-Dihydroxy-6-oxo-5α-cholestane 3-nitrate (Va) and 2β, 3β-Dihydroxy-6-oxo-5β-cholestane 3-nitrate (Vb)

Compound IV (1.25 g) was stirred with 0.625 g of potassium carbonate in 125 ml of methanol for 4 hours. After standing overnight and processing as usual, the crude product was separated on plates coated with silica gel G, in benzene – ether 10 : 1 ($R_fVa > R_fVb$).

Compound Va, mp 185–190° (methanol). Y : 0.4 g. IR ($HCCl_3$) : 865, 1285, 1640, 1712, 3430 cm^{-1}. Anal. Found : C, 69.88 ; H, 9.96 ; Calcd. for $C_{27}H_{45}NO_5$: C, 69.94 ; H, 9.78.

Compound Vb, mp 203–207° (methanol). Y : 0.15 g. IR ($HCCl_3$) : 860, 1285, 1640, 1705, 3400 cm^{-1}.

Anal. *Found* : C, 69.92 ; H, 9.67 ; *Calcd.* for $C_{27}H_{45}NO_5$: C, 69.94 ; H, 9.78

2β-Hidroxy-6-oxo-3α, 5α-cyclo-cholestane (VI)

Compound IV (1 g) was refluxed for 2 hours with 5% methanolic potassium hydroxide (15 ml). After usual processing and recrystallization from heptan, mp 176–178° (Lit.[5] mp 184–185°). Y : 0.3 g. IR (KBr) : 1080, 1298, 1680, 3360 cm^{-1}. ORD (methanol) : λ_{min} 306, λ_0 292, λ_{max} 262 nm.
Anal. *Found* : C, 81.19 ; H, 11.24 ; *Calcd.* for $C_{27}H_{44}O$: C, 80. 94

VI–Acetate, mp 136–139° (methanol) (Lit.[5] mp 139–140°). IR (CCl_4) : 1015, 1070, 1220, 1250,1695, 1740 cm^{-1}) NMR ($DCCl_3$, δ) : 0.700 (CH_3–18), 0.822 (CH_3–26,27), 0.909 (CH_3–21), 1.013 (CH_3–19), 5.270 (–CH–O–) ppm.

Anal. *Found* : C, 78.36 ; H, 10.58 ; *Calcd.* for $C_{29}H_{46}O_3$: C, 78.68 ; H, 10.47

2β, 3β, 14α-Trihydroxy-6-oxo-5β-cholest-7-ene 2,3-dinitrate (VIII)

Starting with compound VII[3] (50 mg). Mp 145–147°(heptan-ether). Y : 17mg. IR (CCl_4) : 855, 1272, 1289, 1655, 1673, 3430 cm^{-1}.

Anal. *Found* : C, 62.28 ; H, 7.49 ; *Calcd.* for $C_{27}H_{37}N_2O_8$: C, 62.65 ; H, 7.20

---

[7] I. TĂNĂSESCU, I. GANEA, F. HODOȘAN, and M. TERDIC, *Rev. Chim. Acad. R.P.R.*, **4**, 189 (1959).

Revue Roumaine de Chimie, **21**, *4*, 631–635 (1976)

VISCOSIMETRIC STUDY OF THE POLY (4-VINYLPYRIDINE) SALTS WITH THE HALOGEN (ALKYL)ARYLOXYALKYL CARBOXYLIC ACIDS

STELIANA MAXIM and M. DIMA
Institute of Macromolecular Chemistry "P. Poni"
Aleea Grigore Ghica Vodă 41-A, Iassy, Romania

Received February 16, 1974

The influence of the halogen(alkyl)aryloxyalkyl carboxylic acid radical, chemically bound to the poly(4-vinyl pyridine) chain, on the reduced viscosity of macromolecular salts solutions is studied.

The conformation of the macromolecular chain is influenced by its structure as well as by the intra- and inter-molecular interactions of the chain segments.[1,2]

In the case of macromolecules bearing electric charges the conformation of the macromolecular chain also depends on its electrostatic potential.[3–7]

The ionization of the polyelectrolytes increases very much the viscosity of their solutions, and this is due in part to the unfolding of the macromolecular coil owing to the interaction of the charges attached to the macromolecular chain[8,9] and in part to the decrease of the screening of the fixed charges on the chain by the electrostatically attracted counterions and by the fact that meanwhile the extension of the macromolecular chain[10] takes place.

The nature of the coions and counterions present in a polyelectrolyte's solution affects the inter- and intramolecular electrostatic interactions and thereby changes the hydrodynamic volume of the macromolecular chain.[7,9,11–14]

[1] P. J. Flory and T. G. Fox, *J. Amer. Chem. Soc.*, **73**, 1904 (1951).

[2] T. G. Fox and P. J. Flory, *J. Amer. Chem. Soc.*, **73**, 1909 (1951).

[3] J. B. Donnet and P. Morquier, *J. Polymer Sci.*, **23**, 601 (1957).

[4] H. Eisenberg, *J. Polymer Sci.*, **23**, 579 (1957).

[5] D. O. Iordan, T. Kurucsev and R. L. Darscus, *Polymer*, **6**, 303 (1965).

[6] P. Holt and B. Tamami, *Makromol. Chem.*, **155**, 55 (1972).

[7] B. B. Mukherjec and M. N. Das, *J. Indian Chem. Soc.*, **34**, 701 (1957).

[8] Encyclopedia Polymer Science Technic, Vol. 14, Interscience, London 1971, p. 717.

[9] A. Katchalsky and D. Spitnik, *J. Polymer Sci.*, **2**, 432, 487 (1947).

[10] M. Nagasawa "Polyelectrolyte Solutions", Academic Press, London, 1961, p. 208.

[11] R. M. Fuoss and U. P. Strauss, *J. Polymer Sci.*, **3**, 602 (1948).

[12] R. L. Darscus, D. O. Iordan, T. Kuruscev and M. L. Martin, *J. Polymer Sci.*, **3**, 1941 (1965).

[13] A. Komo and M. Kaneko, *Makromol. Chem.*, **138**, 189 (1970).

[14] H. P. Gregor, D. H. Gold and M. Frederik, *J. Polymer Sci.*, **23**, 467 (1957).

In the present paper the authors aim to study the influence of the halogen(alkyl)aryloxyalkyl carboxylic (counterions) acids chemically bound to the macromolecular chain of the poly (4—vinyl pyridine), on the reduced viscosity of the poly (4—vinyl pyridinium) salts solutions of the above mentioned acids.

MATERIALS AND METHODS

— poly (4-vinyl pyridinium chloride) (PVP.HCl) *p.a.*
— poly (4-vinyl pyridine) (P.V.P) *p.a.*
— 2,4-dichlorophenoxyacetic acid (2,4—D) *p.a.*
— *p*-chlorophenoxiacetic acid (C.F.A.) *p.a.*
— 2,4,5-trichlorophenoxyacetic acid (2,4,5—T) *p.a.*
— 2,4,5-trichloro-α-phenoxypropionic acid (2,4,5—T.P.) *p.a.*
— 2-methyl-4-chlorophenoxiacetic acid (MCP) *p.a.*
— 2-methyl-4-chlorophenoxybutyric acid (MCPB) *p.a.*

The viscosimetric measurements were carried out by means of an Ubbelohde viscometer, capillary I($K = 0.00999$). For P.V.P. HCl water was used as solvent, and for PVP and its salts with the above mentioned acids, DMSO.

RESULTS AND DISCUSSIONS

Figure 1 shows the variation of the reduced viscosity $\left(\frac{\eta_{sp}}{c}\right)$ of the aqueous solution of PVP HCl, versus its concentration.

Naturally there is no linear relationship between these two parameters, owing to the fact that concurrently with the dilution, the macromolecular coil is extended [7,10] as a result of the decrease of the screening of the fixed charges on the chain, owing to the counterions in the neighborhood and simultaneously to its decrease, the intramolecular repulsion forces increase.

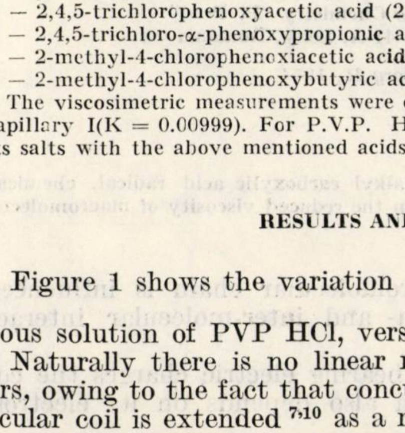

Fig. 1. — $\left(\frac{\eta_{sp}}{c}\right)$ dependence on the concentration of the poly (4-vinyl pyridinium chloride) aqueous solution.

Figure 2 shows the dependence of the reduced viscosity on the concentration of the PVP solutions (figure 2, curve 6) and of its salts with some halogenaryloxyalkyl carboxylic acids in DMSO (figure 2, curves 1–5). One notices that the solutions of these macromolecular salts with relatively small (α) transformation degrees (fig. 2, curves 3 and 4) shows a linear dependence of these parameters. The transformation degree (α) defines the number of structural units transformed into macromolecular salt on 100 vinyl pyridinic units taken into account.

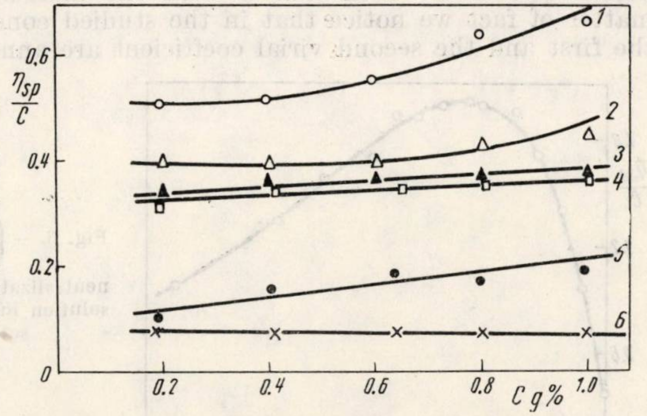

Fig. 2. – $\left(\frac{\eta_{sp}}{c}\right)$ dependence on the concentration, of the transformation degree (α) and the nature of the acid. Solvent D M S O, 25%.
1, α = 81.03 ; acid 2,4 – D ; *2*, α = =78.8 ; acid 2,4,5 – T ; *3*, α = 8.43 ; acid 2,4,5 – T ; *4*, α = 11.48 ; acid 2,4,5 – T ; *5*, α = 66.3 ; acid 2,4,5 – T.P. ; *6*, P.V.P.

This behaviour of the macromolecular salts of the halogenaryloxyalkyl carboxylic acids with a low transformation degrees may be assigned to two factors, namely : the ionization of these salts is feeble in DMSO [7] while the acid radical with which the reaction took place, being voluminous and having a strongly hydrophobic character, could determine the formation of some hydrophobe bonds with the macromolecular chain, which would result in a similar behaviour with that of the polysoaps. [8]

In the case of macromolecular salts with high (α) transformation degrees (fig. 2, curves 1 and 2), the linear dependence of the reduced viscosity on concentration is observed only for diluted solutions (0.1–0.3%). With the increase of the concentration, a non-linear increase of the reduced viscosity takes place. This behaviour is assigned to the steric repulses which appear between the acid radicals chemically bound to the macromolecular chain, and must by needs set themselves very near to one another, with the increase of the concentration.

By taking into account the structural peculiarity of the 2,4–D and 2, 4, 5–T acids, it would be natural that in the case of the last one (fig. 2, curve 2), the steric repulsion forces being stronger, the value of the reduced viscosity should be higher. The differences between the experimental values of the reduced viscosity, X, represented by curves 1 and 2 (fig. 2) are due to the fact that these samples have different (α) transformation degrees.

In the case of solution in DMSO of the poly (4–vinyl pyridinium salt) of the 2, 4, 5–trichlor–α–phenoxypropionic acid, no variation of the reduced viscosity in the studied concentration domain is observed (fig. 2, curve 5). This brings us to the assumption that in the concentration field extending from 0.1 to 1.0 g% for this macromolecular salt, no intra-

and intermolecular repulsion forces appear between the acid radicals bound to the polymer chain. This is probably due to the fact that the methyl in α position of the hydrocarbonate chain brings about a strong association of the acid radical with the macromolecular chain. As a matter of fact we notice that in the studied conditions (curve 5, fig. 2) the first and the second virial coefficient are annulled and therefore the macromolecular chain of the poly (4—vinyl pyridinium— 2, 4, 5—trichlor —α—phenoxypropionate) is in the shape of a statistic coil.[15,16]

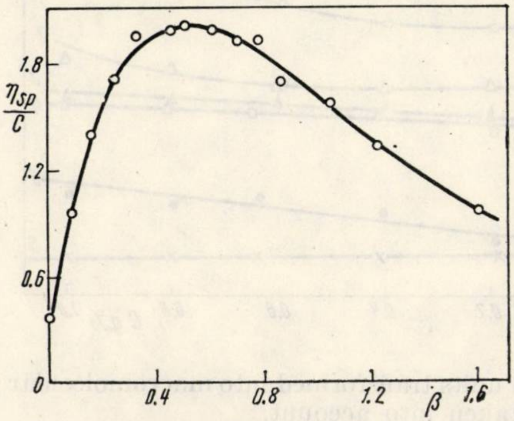

Fig. 3. — $\left(\frac{\eta_{sp}}{c}\right)$ dependence on the neutralization degree (β) of the P V P solution in D M S O with an aqueous solution M/1 of HCl, 25°.

For the PVP solution in DMSO (fig. 2, curve 6) we notice that the dependence of the reduced viscosity on the concentration shows a slow increase with the increase of the concentration.

Figure 3 gives the dependence of the reduced viscosity on the neutralization degree β (calculated from the number of 1 M acid solution ml consumed) for the PVP solution in DMSO. On the curve we notice a maximum of the reduced viscosity at $\beta = 0.5$, after which a decrease of the same takes place with the neutralization degree.

Concurrently with the progress of the neutralization reaction there takes place a creation of positive charges on the macromolecular chain, which brings about its extension,[13,14] owing to the intramolecular repulsion between the charges of the same sign found on the PVP chain, and in consequence an increase of the reduced viscosity takes place. It is admitted that the macromolecule reaches a maximum rigidity[1] at $\beta = 0.5$.

In the field of low neutralization degrees (β between 0 and 0.5) the number of charges on the chain being small, we may assume that they don't influence one another and therefore the ionogen groups on the chain are dissociated in a higher proportion.[10] Concurrently to the neutralization degree, and hence to the number of reacted groups, a decrease of the reduced viscosity takes place, probably due to the decrease of the dissociation degree of the macromolecular salt[10] and therefore of the electrostatic interactions which would determine the extension of the macromolecule.

---

[15] P. C. Deb and S. R. Chatterijee, *J. Indian Chem. Soc.*, **46**, 468 (1969).

[16] J. R. Patel and R. D. Patel, *Makromol. Chem.*, **120**, 103 (1968).

In the case of neutralizing the PVP solutions in DMSO with the halogen (alkyl) aryloxyalkyl carboxylic acids (fig. 4), we notice a different dependence of the reduced viscosity on the degree of neutralization. Thus, up to $\beta = 0.5$ the increase of the reduced viscosity may be also assigned to the repulsion between the charges created on the chain, concurrently with the protonization of the pyridinic nitrogen of the macromolecule, with the protons of the above mentioned acids. The further increase of the reduced viscosity's value, concurrently with the increase of the value of β, may be assigned to the steric repulsions between the acid radicals attached to the macromolecular chain, determining its new rigid form.

The nature of the acid radical by means of which the neutralization was carried out, has a bearing on the dependency of the two studied parameters. Concurrently to the increase of the number of substitutes of the aromatic cycle of the acid radical, the steric repulsion forces increase and meanwhile the value of the reduced viscosity increases (fig. 4, curves 1, 2 and 5). The bigger the number of carbon atoms separating the substitute phenoxyl radical from the carboxylic group, hence the feebler the acid the more will the value of the reduced viscosity decrease, owing to decrease of, the dissociation degree of its macromolecular salt (fig. 4, curve 1 and 4).

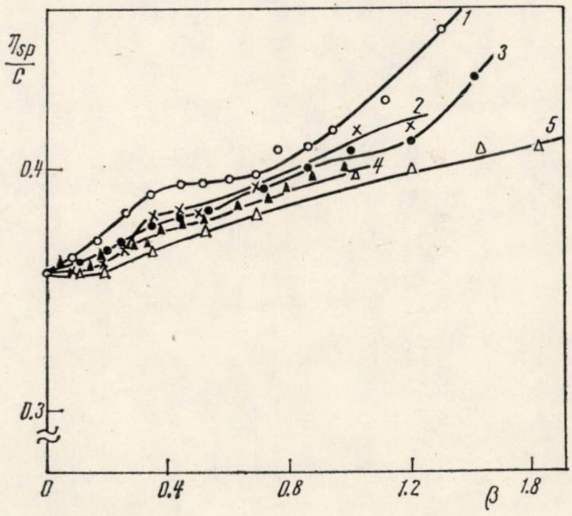

Fig. 4. — $\left(\frac{\eta_{sp}}{c}\right)$ dependence on the neutralization degree (β) of the M/10 P V P solutions in D M S O with M/1 D M S O solutions of following acids;
1, 2,4,5−T acid; *2*, MCP acid ; *3*, 2,4,5 − T P acid; *4*, MCPB acid ; *5*, CFA acid; temperature 25°.

CONCLUSIONS

1. The influence of the neutralization degree β on the reduced viscosity of the poly (4—vinyl pyridinium) salts of the halogen (alkyl) aryloxyalkyl carboxylic acids was studied.

2. The influence of the nature of the counterion chemically bound in the PVP macromolecule, on the reduced viscosity of its salts with the above mentionned acids was pointed out.

3. The influence of the degree of transformation (α) on the dependence of the reduced viscosity on the concentration of the macromolecular salts of the halogen (alkyl) oxyaryl carboxylic acids was emphasized

Revue Roumaine de Chimie, 21, 4, 637–641 (1976)

COMPTES RENDUS

P. LASZLO, «Leçons de Chimie. I, La liaison chimique; II, Les états de la matière; III, La réaction chimique», Hermann, Paris, 1974, 3×180 p.

On parle beaucoup ces dernières années de l'intégration de l'enseignement : d'une part il s'agit de rapprocher l'enseignement de la recherche scientifique et de l'activité de production; d'autre part, il s'agit d'une autre façon d'enseigner les disciplines traditionnelles, en les rapprochant les unes des autres par dessus des barrières traditionnelles. En ce qui concerne la chimie, les barrières entre la chimie inorganique, la chimie organique et la chimie physique ne permettaient qu'une lente diffusion des idées d'une discipline à l'autre, surtout chez les étudiants. Même chez les chercheurs, l'affranchissement de ces barrières a nécessité un effort conscient et a déterminé la création des branches fleurissantes de la recherche actuelle telles que la chimie organique physique, la chimie organométallique ou la radiochimie, c'est-à-dire des domaines de frontière.

L'ouvrage de Pierre Laszlo, professeur à l'Université de Liège, a réalisé d'une manière excellente une telle présentation intégrée de la chimie générale, physique, inorganique, organique et biologique pour l'usage des étudiants dans les années préparatoires aux grandes écoles ou dans les premières années des universités, aux professeurs du secondaire et aux chercheurs qui souhaitent une vision fraîche et innovatrice de l'enseignement chimique.

Le premier volume traite de la structure de l'atome, les principes de la mécanique quantique, la liaison chimique, les molécules diatomiques homo- et hétéronucléaires, et les molécules polyatomiques. On fait appel à des connaissances fort simples de mathématique et de physique, mais tout de même on aboutit à passer en revue la majorité des notions de base de la chimie physique. Pour les molécules polyatomiques on fait appel aux règles de Gillespie qui explique leur géométrie, et non pas à l'hybridation. Sur la base des nombres quantiques on discute la classification périodique des éléments. Les fonctions d'ordre sont présentées en détail assez poussé.

Le second volume passe en revue la thermodynamique chimique, les lois de la phase liquide, solide et gazeuse, et des changements d'état. On discute les propriétés électriques des cristaux et des solutions, l'hydration des ions, la structure des protéines en solution aqueuse et divers autres sujets dérivés, comme par exemple « l'eau polymérique » qui s'est avérée une « bulle crevée ».

Le troisième volume présente les énergies de liaison influencées par les distances internucléaires et par les différences d'électronégativité, les acides et bases selon Brönsted et Lewis, l'oxydo-réduction, les mécanismes réactionnels, la cinétique chimique, et l'évolution chimique depuis la formation des noyaux atomiques jusqu'aux protéines.

Ce qui rend la lecture agréable est le style léger, les digressions à point (telles que la discussion de la méthode scientifique à propos de la pollution atmosphérique et du parfum d'ananas; ou bien les crèmes solaires à propos des réactions photochimiques; même les titres de ces digressions sont entraînants, par exemple « Tartiner, un plaisir dangereux? »; « Une réaction périodique dans le temps et dans l'espace »).

La plupart de ces digressions, ainsi que de nombreux passages du texte, sont illustrés avec humour par Savignac, ce qui rend ces volumes particulièrement attractifs (parfois les illustrations sont assez piquantes, comme celle du second volume à propos de la liaison hydrogène et du code génétique).

Revenant aux choses sérieuses, l'esprit pédagogique de l'auteur se révèle dans les excercices à réponses multiples qui accompagnent chaque chapitre (dont la solution se trouve à la fin de chaque volume), dans les appendices qui accompagnent chaque volume (incluant le système international d'unités qui est utilisé dans tout l'ouvrage, poids atomiques, facteurs de conversion d'unités, nomenclature organique, énergies de liaison, glossaire, etc.), et indices de sujets et de formules.

La présentation graphique est attrayante. Il y a peu de fautes de typographie, qui vont probablement être corrigées dans une prochaine édition : seulement une erreur vaut la peine d'être mentionnée car elle se répète, comme tous les appendices, à chaque volume, notamment la définition des diastéréomères dans le glossaire : l'allène et le cyclopropène ne sont pas de tels isomères, mais des isomères de constitution.

Le but de l'ouvrage est le mieux présenté par l'auteur lui-même dans les paragraphes suivants de la préface :

"Il est paradoxal qu'il existe et que l'on enseigne une biologie moléculaire, dérivée pour une large part de la chimie, alors que la chimie continue d'être enseignée comme du temps d'Ostwald ou de Grignard : il faut restituer à la chimie la vigueur de son tempérament moléculaire.

En préparant ce cours de chimie moderne, j'ai voulu intégrer à mon enseignement mon expérience de chercheur, et l'ouvrir sur les conquêtes récentes les plus importantes. J'ai résolu de passer outre à la distinction néfaste et périmée entre chimie inorganique, chimie organique, et chimie biologique : les exemples sont empruntés indifféremment à un secteur ou à l'autre.

Certes, la chimie n'est pas encore parvenue au stade où on pourrait l'enseigner de manière strictement axiomatique et déductive. Une méthode inductive a davantage d'attrait pour les étudiants de première année des universités et grandes écoles auxquels ce livre est destiné. On a conservé la plus grande rigueur dans l'exposé tout en refusant de s'encombrer d'un important appareil mathématique. On a utilisé au maximum les ressources didactiques de l'image ; de nombreux problèmes viennent préciser les ponts délicats, relier l'une à l'autre les différentes parties du cours, ou proposer plusieurs types d'explications".

Il est probable que tous les chimistes ne seront pas d'accord qu'il est « inutile et même dangereux d'introduire des formalismes arbitraires tels que l'électronégativité * ou la notion d'hybridation », ou bien de « distinguer entre différents types de liaisons chimiques », pour citer encore quelques phrases de la préface. On tend d'habitude à adopter une attitude plus prudente, c'est-à-dire à laisser le temps trier les théories. Cependant la vitesse avec laquelle la science progresse de nos jours, ne permet plus cette expectative, et l'ouvrage du professeur Laszlo représente une expérience audacieuse, qui s'éloigne de la ligne traditionnelle.

N'aurait-il fait que cet essai et il mériterait en être fier, mais de plus il a réussi à présenter de façon cohérente, instructive et attrayante une introduction à la chimie pour une large audience.

A. T. Balaban

L. ERDEY and G. SVEHLO, "Ascorbinometric titrations", Akademiai Kiado, Budapest, 1973, 183 p.

The term "ascorbinometric titrations" has been created by one of the authors who was the first to suggest the use of ascorbic acid as a titrant due to its properties of strongly reducing agent. It must be emphasized from the very beginning that the main contribution in advocating the use of vitamin C as described in the monograph, belongs to the authors and is based on their own works.

By systematizing and presenting these data the authors are permanently focusing on the applicative aspect of the method.

Based in particular on the data reported in the literature, the introductory chapter describes the physico-chemical and especially the oxido-reducing properties of the system ascorbic acid-dehydroascorbic acid. The 2nd chapter exclusively refers to the preparation, titre establishment and preservation of standardized ascorbic acid solutions which are known to decompose quite readily, particularly in the presence of oxygen and of heavy metals. The next chapter presents the general methods for establishing the equivalence point during titrations. Both visual indicators and the current instrumental methods (potentiometric, amperometric, etc.) used to establish the final point in titration are thus described. The last two chapters provide different examples for the use of ascorbic acid as a direct or indirect titrant. Among the direct methods, mention is made of dosages of some classical oxidizers (halogens, ferricyanides, chlorates, bromates, iodates, etc.) and of heavy metals (mercury, silver, copper, gold, iron, thalium, vanadium). With regard to the indirect methods, the use of ascorbic acid in iodometry is illustrated as well as the methods relying on the titration of some oxidisers such as ferricyanides, iron III and thalium III. The monograph is completed by a list of

---

* Celle-ci est tout de même discutée dans le premier volume (les echelles de Pauling et de Mulliken).

bibliographical references, an index of authors and an index of subjects. All these data including the accurate description of analytical titration methods help those interested in the field to reproduce and to use ascorbic acid as a titrant. In this way, the objective proposed by the authors, to provide support in promoting this method, has been accomplished.

As approximately 60 out of a total of 170 bibliographical points may be considered to refer to treatises, monographs or subjects with no direct relevance to the use of ascorbic acid as a titrant, it results that most points relate to the original works of the authors. The only problem arising is the extent to which the analysts would prefer the ascorbinometric methods to the classical ones, taking into account the fact that these classical methods will be applied for the standardization of solutions and the difficulties of having stable ascorbic acid solutions available cannot be disregarded.

F. Cuiban

"Topics in Current Chemistry", Fortsch. Chem. Forsch., **57**, 1975, "Cyclic Compounds", Springer Verlag, Berlin — Heidelberg — New York 1975, 143 p.

The first review of the book, "Structure and Reactivity of Cyclopropenones and Triafulvenes", is written by Professor Theophil Eicher and Dipl. Chem. Joseph L. Weber from Institut für Organische Chemie und Biochemie der Universität Hamburg. In 109 pages the authors offer the readers a complete and up-to-date (303 references up to August 1974) presentation of the very interesting and largely developed field of cyclopropenones and triafulvenes. The material is divided into five main parts: Introduction; Synthesis of Cyclopropenones and Triafulvenes; Structural Criteria for Cyclopropenones and Triafulvenes; Reactions of Cyclopropenones and their Heteroanalogs and Reactions of Triafulvenes.

The clear presentation of the very well organized material is a characteristic feature of the review. One may mention, for example, the attractive description of the general methods for synthesis of cyclopropenones (carbene method, trichlorocyclopropenium cation method and dibromoketone method), accompanied by numerous schemes and tables. The chapter dedicated to structural criteria deals with the difficult task of generalizing the present data (which are sometimes contradictory) on cyclopropenones and triafulvenes, on the basis of dipole moments, microvawe spectra, IR-, UV- and NMR-spectra (^{1}H, ^{13}C, ^{19}F), mass spectra as well as MO calculations. The chapter dealing with reactivity may impress the reader with the large possibilities of the various types of reactions involving these simple and small molecules, e.g.: thermolysis and photolysis, oxidations and reductions, reactions with electrophiles and nucleophiles, reactions with systems containing multiple bonds, reactions with 1,3-dipoles as well as interactions with metal compounds.

The second review, "The higher Annulenones", is written by Melvin V. Sargent and Terrence M. Cresp from the University of Western Australia, Nedlands. The authors have succeeded in presenting briefly (32 pages with 65 references) the interesting and often intriguing field of higher annulenones. The domain of annulenes, linked to the names of three pioneer workers: F. Sondheimer, E. Vogel and V. Boekelheide, has emerged from the modern developments of the theory of aromaticity. In connection with annulenes, the higher annulenones are now under extensive investigation.

Many organic synthetists are probably wondering why tropone ([7] annulenone) is, still, the largest annulenone known. There appears to be no answer as yet, although it is now clear that the higher annulenones indicate an enhanced susceptibility to structural perturbations. Two such structural perturbations have until now proved their value, namely bridging of the molecule with methylene (or heteroatom) units and the presence of acetylene bonds in the molecule. Consequently, these two types of annulenones are discussed in the article. Beside introduction and conclusions the laconic headings of the chapters are: $4n + 3 (n = 2)$; $4n + 1 (n = 3)$; $4n + 3 (n = 3)$; $4n + 1 (n = 4)$; $4n + 3 (n = 4)$; $4n + 1 (n = 5)$ and Annulenediones.

The most important problem developed in every chapter is the diatropicity or paratropicity of the described annulenones, such as they appear from NMR spectra. From this point of view different diatropic (aromatic) annulenones are described, *e.g.*: bridged [11] annulenones, tetradehydro [15] annulenones, oxygen-bridged [19] annulenones as well as some paratropic annulenones as: dimethyl-bis-dehydro [13] annulenone, dehydro [17] annulenones, oxygen-bridged [21] annulenone. In every case the synthetic routes are described in detail. The reader will thus follow the specific reactions used in this field. For example, the importance of oxidative couplings of terminal acetylenes (after Eglington, Glaser or Hay procedures) is stressed. Other reactions often used in the series are the Wittig reaction and Vogel's sequence for the synthesis of bridged annulenes and derivatives.

The scarcely investigated chemistry of the annulenones is also described. The most studied annulenones are the Vogel's bridged [11] annulenones and annulenediones. Some interesting characterictics of the class such as: substitution and cinesubstitution, Diels-Alder reaction, conversion into anions or cations, etc. are mentioned.

At the end of the review some unsolved problems of the domain are underlined, *e.g.*: the limiting ring size for diatropicity and paratropicity, a correct theoretical treatment of higher annulenones, the conversion of dehydroannulenones into annulenones.

In conclusion, volume **57** from Fortsch. Chem. Forsch. offers a very interesting and valuable presentation of two important and modern fields of organic chemistry.

Mircea Banciu

FRANCIS S. GALASSO: "Structure, Properties and Preparation of Perovskite. Type Compounds", Int. Series of Monographs in Solid State Physics, vol, 5, Pergamon Press, Oxford, 1969, 207 p.

Compounds having a perovskite-type structure have aroused the interest of researchers since 1945 due to the simultaneous discovery in several countries of $BaTiO_3$ exceptional ferroelectric properties. This event was the starting point of systematic investigations into the structure and the properties of compounds with the general formula ABO_3.

F. S. Galasso belongs to a working team at United Aircraft Research Laboratories which has carried out extensive studies on the preparation, structure and properties of mixed $AB'B''O_3$ compounds of a perovskite type.

In this monograph, the author provides detailed information on about 500 perovskite type compounds.

After a short introduction (ch. 1), chapter 2 describes the perovskite type structure, a classification of simple and of mixed compounds according to cations valency states and to the departure from stoichiometry. Further considerations are presented with regard to Madelung energies corresponding to some cubic and tetragonal perovskite structures.

Chapter 3 focuses on X-ray diffraction and on EPR studies providing tables with crystallographic data of compounds, which are highly important being comprehensive and systematized according to cations valency states.

Further chapters 4—9 describe the properties of perovskite-type compounds i.e.: electric conductivity, ferroelectricity, ferromagnetism, optical and catalytic properties, melting points, heats of formation, thermal dilatation and mechanical properties.

Chapter 10 describes the methods of preparation of perovskite-type oxidic compounds as a function of the ordering degree: polycrystalline materials, thin films and monocrystals.

Chapter 11 deals with the preparation, structure and properties of perovskite-type non oxidic phases.

All the chapters provide ample bibliographical references. An index of compounds presented in the monograph is included at the end.

The work meets high scientific standards and stands out due to a remarkable conciseness and at the same time to its accessibility, being useful to scientific researchers involved in the study and the development of ferroelectric materials, to those working for obtaining their doctoral degree and to junior students at the faculties of chemistry and of physics.

Eva Bărbulescu

« Le 5ème Colloque Franco-Polonais sur la Catalyse »

Le 5ème Colloque Franco—Polonais sur la Catalyse a eu lieu dans la vieille ville de Torun, en Pologne, dans la période du 8 au 14 septembre 1975.

La participation nombreuse, tant du côté polonais, que du côté français (environ 120 personnes), a réuni des spécialistes de la catalyse,travaillant dans l'enseignement, dans la recherche, dans l'industrie.

Les 49 travaux inscrits ont été divisés suivant leur spécifique, ainsi :

I. Résonance électrono-paramagnétique (EPR)
II. Structure de molécules. Réactivité
III. Chimie quantique
IV. Spectroscopie infrarouge (IR)
V. Spectroscopie LEED — AUGER
VI. Spectroscopie électronique (ESCA)
VII. Divers

Parmi les 8 travaux inscrits dans la première section, on remarque la préoccupation pour l'étude des zéolithes (4 travaux), la RPE étant utilisée pour la mise en évidence de la formation, de la mobilité des espèces adsorbées sur les catalyseurs (Z. Dudzik, M. Bliska-Ziólek, A. Bielanski et J. M. Lagan, S. Krzyzanowski et H. Hoser, J. C. Védrine et J. Massardier).

Dans le groupe des 5 travaux de la Section « Structure de molécules. Réactivité » on examine les étapes intermédiaires ou les mécanismes de différentes réactions (oxydation homogène des hydrocarbures — W.K. Rybac et J. J. Ziolkowski, hydrogénation sélective — Z. Dudzik M. Gasiorek et Z. Szuba, hydrogénolyse d'hydrocarbures aliphatiques — G. Leclercq, L. Leclercq et R. Maurel, etc.).

Dans un domaine qui se développe, celui de la chimie quantique en catalyse, on assiste à la présentation de trois études, à l'occasion de ce colloque.

Les travaux tentent d'appliquer les méthodes de la chimie quantique à la description des phénomènes observés dans la catalyse hétérogène (J. Haber et coll., de Montgolfier et coll., W. Grabowski et coll.).

Les préoccupations des spécialistes de l'infrarouge sont aussi orientées vers l'étude des zéolithes et la mise en évidence des propriétés acides (Bielanski et coll., M. F. Guilleux et D. Delafosse, P. Pichat et D. Barthomeuf, J. Fraissard et coll., etc.).

D'autres études, comme celles des catalyseurs métalliques ont été faites par I. Ratajczykowa et par M. Primet.

La spectroscopie Auger et Leed permet de suivre des interactions superficielles entre les métaux et l'hydrogène et les hydrocarbures (communication de W. Palczewska et coll.), d'examiner la diffusion du souffre vers la surface des métaux, sous l'influence de l'hydrogène (comm. de I. Szymerska et M. Lipski), ou bien d'étudier l'adsorption sur certaines faces d'un métal (communication de J. C. Bertolini et G. Dalmai-Imelik).

Cinq travaux indiquent l'utilisation de l'ESCA à l'étude des catalyseurs à base de molybdène (J. Haber et coll.), de molybdène — cobalt (P. Canneson, G. Delvaux et P. Grange), de nickel (J.C. Vedrine et coll.), de cobalt (J. P. Bonnelle et coll).

Dans la VIIème et dernière section on a groupé divers travaux, qu'on ne pouvait encadrer dans les chapitres précédents.

On peut signaler ainsi la communication sur le phénomène de spillover, dans le cas des catalyseurs Pt ou Ni, avec l'alumine (S. J. Teichner et coll.,) l'utilisation de la spectroscopie Mössbauer à des recherches en catalyse (P.Bussière et coll.), différentes études d'adsorption et de thermodésorption (système zéolithe-ammoniac et zéolithe-butènes — A. Baranski et coll., adsorption du benzène sur Ni Raney) — G. A. Martin et coll., adsorption des xylènes sur des zéolithes — M. Milevski et J. M. Berak, etc.).

Réunion devenue traditionnelle, le 5ème Colloque Franco-Polonais sur la Catalyse a démontré son utilité. Manifestation scientifique bi-latérale, tenue tous les deux ans, en Pologne ou en France, elle permet aux spécialistes de la catalyse des deux pays de présenter leurs derniers travaux, de s'intéresser aux résultats de leurs collègues, de visiter des laboratoires, d'échanger des idées.

Maria Gruia

TRAVAUX PARUS AUX ÉDITIONS DE L'ACADÉMIE DE LA RÉPUBLIQUE SOCIALISTE DE ROUMANIE

I. GĂLĂŢEANU, **Radiochimia aplicată. Metode şi probleme** (La radiochimie appliquée. Méthodes et problèmes), 1976, 305 p., 19 lei.

FRANCISC A. GOTHARD, **Echilibre lichid-vapori. I. Baze teoretice şi metode de calcul** (Equilibres liquide-vapeurs. I. Bases théoriques et méthodes de calcul), 1975, 263 p., 2 pl., 28 lei.

CONST. GH. MACAROVICI, D. MACAROVICI, **Chimia oxizilor dubli şi utilizările lor** (La chimie des oxydes doubles et leur utilisation), 1975, 195 p., 13 lei.

M. AVRAM, **Antidăunători** (Pesticides), 1974, 496 p., 41 lei.

ELENA CEAUŞESCU, **Research work on synthesis and characterization of macromolecular compounds. Contributions**, 1974, 251 p., 20 lei.

DUMITRU COSTACHE, **Analiza chimică prin metoda cinetică** (L'Analyse chimique par la méthode cinétique), 1974, 276 p., 15,50 lei.

G. A. RĂDULESCU, **Proprietăţile ţiţeiurilor româneşti** (Les propriétés des pétroles roumains), 1974, 267 p., 2 pl. 18 lei.

CR. SIMIONESCU, VIORICA RUSAN, V. POPA, **Chimia algelor marine** (La chimie des algues marines), 1974, 212 p., 1 pl., 18 lei.

I. ZUGRĂVESCU, MAGDA PETROVANU, **Chimia n-ilidelor** (La chimie des n-Ilures), 1974, 348 p., 19 lei.

MARIA FITI, **Dozimetria chimică a radiaţiilor ionizante** (La dosimétrie chimique des radiations ionisantes), 1973, 240 p., 13,50 lei.

TIBERIU NĂŞCUŢIU, **Metode radiochimice de analiză** (Méthodes radiochimiques d'analyse), 1973, 384 p., 23 lei.

CRISTOFOR SIMIONESCU, MARGARETA GRIGORAŞ, AGATA CERNĂTESCU-ASANDEI, ROZMARIN GHEORGHE, **Chimia lemnului în România. Plopul şi salcia** (La Chimie du bois en Roumanie. Le peuplier et le saule), 1973, 299 p., 13 pl., 26 lei.

MIHAI FLORESCU, **Eficienţa economică a cercetării ştiinţifice** (L'efficience économique de la recherche scientifique), 1972, 115 p., 15 lei.

1977 JAN 06

I. P. I. — c. 1018

43426

Lei 25. —

F1103

ACADÉMIE DE LA RÉPUBLIQUE SOCIALISTE DE ROUMANIE

REFERÁLVA

REVUE ROUMAINE DE CHIMIE

TOME 21
N° 5
Mai 1976

RECHAX, **21**, *5*, 643–802 (1976)

EDITURA ACADEMIEI REPUBLICII SOCIALISTE ROMÂNIA

Rev. Roumaine Chim. **21**, *5*, p. 643–802 (1976), Bucarest

ACADÉMIE DE LA RÉPUBLIQUE SOCIALISTE DE ROUMANIE

COMITÉ DE RÉDACTION

Rédacteur en chef:

I. G. MURGULESCU, membre de l'Académie de la République Socialiste de Roumanie

Rédacteurs en chef adjoints:

A. T. BALABAN et V. EM. SAHINI, membres correspondants de l'Académie de la République Socialiste de Roumanie

Collège de rédaction:

EM. BRATU, ELENA CEAUŞESCU, ECATERINA CIORĂNESCU-NENITZESCU, C. DRĂGULESCU, RALUCA RIPAN, CR. SIMIONESCU, membres de l'Académie de la République Socialiste de Roumanie; P. SPACU, membre correspondant de l'Académie de la République Socialiste de Roumanie; MARGARETA AVRAM, D. I. MARCHIDAN, I. MOLDOVAN, G. NIAC et D. SĂNDULESCU

La Revue Roumaine de Chimie paraît 10 fois par an. Toute commande de l'étranger (fascicules ou abonnements) sera adressée à ILEXIM, Serviciul Export-Import Carte (Livres) / Serviciul Export-Import Presă (Revues) POB 2001, télex 011226, 64—66, Calea Griviţei, Bucarest 12, Roumanie

Les manuscrits, les livres et les revues proposés en échange, ainsi que toute correspondance, seront envoyés à la rédaction:

REVUE ROUMAINE DE CHIMIE
23, str. Dumbrava Roşie, Bucarest, Roumanie, téléphone 12 41 60

EDITURA ACADEMIEI REPUBLICII SOCIALISTE ROMÂNIA
125, Calea Victoriei, Bucarest, Roumanie, téléphone 50 76 80

REVUE ROUMAINE
DE
CHIMIE

Tome 21, No 5 Mai 1976

ORSZÁGOS MŰSZAKI KÖNYVTÁR ÉS DOKUMENTÁCIÓS KÖZPONT 1883

V. E. SAHINI and LILIANA TELEA, Molecular interactions in anisidine isomers. II. Electronic spectra 645–649

MARINA BULZAN and E. SEGAL, The influence of Fe_2O_3 on the thermal stability of $BaCO_3$. 651–653

S. STERNBERG and LUCIA BEJAN, Thermodynamic properties of AgI + + NaI + KI fused salt ternary system by formation cell method . . . 655–660

D. I. MARCHIDAN and LIANA PANDELE, Study of the isomorphic transitions of some iron oxides 661–666

M. VLAD and E. SEGAL, On the stochastic analysis of the reaction networks. I. 667–676

M. VLAD, On the frequency of reaction events in a system with first order reaction network 677–681

OPESCU and L. KÉKEDY, Experimental approach to the characterization of pretreated electrode surfaces. VI. Chronopotentiometric study of differently pretreated gold electrodes 683–694

MARIA MAVRODIN-TĂRĂBÎC, IOANA ONACA and I. SOLACOLU, Mathematical model in the range 50–70° and 5N–7N KOH for a hydrogen-oxygen fuel cell. 695–702

А. А. ВОЛКОВ, З. Е. АКСЕНОВА, Е. С. ФИЛАТОВ, Ан. Н. НЕСМЕЯНОВ, Поведение церия (III) в водно-метанольных растворах 703–706

CONSTANŢA GHEORGHIU and CRISTINETA MĂRCULESCU, Contribution to the coordination chemistry of *s*-triazines. I. Coeordination compounds of copper with thioammeline derivatives 707–715

MAGDA PETROVANU, MAI VAN TRI et VIRGIL BĂRBOIU, Pyridazinium-ylures. I. Addition du 3-(*p*-cumyl)-pyridazinium-phénacylure et du 3-(*p*-cumyl)-pyridazinium-(*p*-nitro)-phénacylure sur les alcynes activés 717–725

A. C. RĂZUŞ, ZS. ARVAY, ANA HANEŞ and ALICE MARIE GLATZ, Aluminium chloride catalyzed reactions of unsaturated acids with benzene. VIII. Participation of carboxyl group in the reaction of cyclopentylideneacetic, 1- and 2-cyclopentenylacetic acids with benzene 727–731

A. GIOABĂ, O. MAIOR and MARIA MITRAN, Reaction of tellurium tetrachloride with 4-fluoro-4′-methyldiphenyl ether 733–738

A. GIOABĂ, MARILENA NEDEA and O. MAIOR, Chemistry of phenoxatellurine. Action of tellurium tetrachloride on 4-halodiphenyl ethers 739–744

O. MAIOR and N. RĂŞANU, Syntheses based on thieno[2,3-b]-benzothiachromone 745–747

J. V. KNOP, N. TRINAJSTIĆ, and A. SABLJIĆ, Topological studies of fused tricyclic and tetracyclic molecules having planar conjugated perimeter 749–755

Revue Roumaine Chim. **21**, *5*, 643–802 (1976) Bucarest

S. C. BENNUR, V. B. JIGAJINNI and V. V. BADIGER, Pyrimidines. VI. Synthesis of 2-methylthio-5-bromo-pyrimidine-4-carboxylic acid thiosemicarbazides, 3-pyrimidyl-1,2,4-(4*H*)-triazoles and 2-arylamino-1,3,4-thiadiazoles 757–762

M. DIMONIE, CR. OPRESCU and GH. HUBCA, Variation of molecular mass with time in polymerization by free radicals 763–768

I. MOŢOC, D. CIUBOTARIU, ŞT. HOLBAN, Zur Kopolymerisation. II. Die Simulierung der Bildung eines Makromoleküls. Das Programm MEMORY 1 769–773

I. MOŢOC, D. CIUBOTARIU, ŞT. HOLBAN, Zur Kopolymerisation. III. Die Simulierung der Bildung eines Makromoleküls. Das Programm MEMORY 2 775–780

R. M. ISSA, H. Z. YOUSSEF, F. M. ISSA and Y. M. ISSA, Spectrophotometric study of some arylidenemalononitriles in organic solvents and buffer solutions 781–788

CONSTANŢA MĂNTESCU, ANA GENUNCHE, DOINA CRISTU and T. COSTEA, Processes associated with the ^{6}Li(n, α)^{3}H nuclear reaction. III. Chemical evidence for the stabilization forms of recoil tritium in lithium halides 789–796

COMPTES RENDUS 797–802

Revue Roumaine de Chimie, 21, 5, 645–649 (1976)

MOLECULAR INTERACTIONS IN ANISIDINE ISOMERS. II[1]

ELECTRONIC SPECTRA

V. E. SAHINI and LILIANA TELEA
Centre of Physical Chemistry
Bucharest, Str. Galaţi 31, Romania

Received October 2, 1975

The electronic spectra of the anisidine isomers prove the existence of a weak intramolecular hydrogen bond in the *ortho*-anisidine molecule, as results from comparing the thermodynamic quantities characteristic of the intermolecular association with dioxane.

INTRODUCTION

The anisidine molecule represents an interesting case of disubstituted benzene with two electron-donor groups in which, in spite of the inductive and mesomeric effects, the *ortho* isomer is able to exhibit a superimposed weak intramolecular interaction as a hydrogen bond.

Both amino and methoxy radicals increase the energy levels, the excited ones to a lesser extent than those of the ground state, which leads to bathochromic shifts of both $A_{1g} \rightarrow B_{2u}$ and $A_{1g} \rightarrow B_{1u}$ benzene bands.[2] The aim of the present paper is to study the electronic structure and spectra of anisidine isomers, taking into account the intramolecular bond as well as the solvent effects.

EXPERIMENTAL

All compounds and solvents have been purified before the spectral measurements.[3] Solutions of anisidine in cyclohexane-dioxane mixtures have been prepared the anisidine concentration being constant ($\sim 2.10^{-4}$ mole. 1^{-1}). Corresponding binary mixtures of cyclohexane-dioxane have been used as references.

Spectra have been recorded at different temperatures with an UNICAM SP-800 spectrophotometer.

---

[1] V. E. Sahini and L. Telea, *Rev. Roumaine Chim.*, **21**, 321 (1976).

[2] A. E. Luţkii, A. C. Goliberkova and P. M. Bugai, *Zhur. obshchei Khim.*, **23**, 1625 (1963).

[3] A. Weissberger and A. Proskauer, "Technique of Organic Chemistry (Organic Solvents)", vol. 7, Interscience, London, 1965, p. 308–413.

Molecular orbital computations using Hückel and Pariser-Parr-Pople approximations were performed with the following set of parameters :

— for the Hückel method : $h_N = 1.5$; $k_{C-N} = 0.8$; $h_O = 2$; $k_{C-O} = 0.8$; $h_{CH_3} = 3$; $k_{O-CH_3} = 0.3$ — see.[4,5]

— for the Pariser-Parr-Pople method :

$I_O(2\,p) = 32.90$ eV $\gamma_{OO} = 21.53$ eV $\beta_{CO} = -2.30$ eV

$I_N(2\,p) = 25.8$ eV $\gamma_{NN} = 16.76$ eV $\beta_{CN} = -2.35$ eV

$I_C(2\,p) = 11.22$ eV $\gamma_{CC} = 10.53$ eV $\beta_{CC} = -2.39$ eV,

according to.[6,7]

The effects of hydrogen intramolecular bond were considered using an inductive perturbation.[4]

RESULTS AND DISCUSSIONS

Comparing the spectra of anisidine isomers in an inert solvent (*n*-hexane or cyclohexane), it can be noticed that the position of the longer-wavelength band is markedly different in the case of the ***para*** isomer. The transition energy values obtained by the PPP and HMO methods, the intramolecular hydrogen bond being taken into account for the *ortho* isomer, are in agreement with the experimental data, as shown in table 1.

Mentioning the fact that no appreciable change occurs in the energy levels when the hydrogen intramolecular bond is considered in the model, the anisidine isomers are ordered according to the maximum wavelength of both absorption bands as follows : *para* > *ortho* > *meta* > aniline.

Table 1

Transition energies (eV)

Compound	First absorption band			Second absorption band	
	Theoret.		Experim.	Theoret.	Experim.
	HMO	PPP		PPP	
Aniline	4.168	4.40[6]	4.30—4.40[2,7]	5.38[6]	5.28—5.35[2,7]
o-anisidine	4.065	4.66	4.29	5.08	5.21
m-anisidine	4.184	4.75	4.33	5.21	5.25
p-anisidine	3.89	4.17	4.10	5.10	5.22

For the $\pi \rightarrow \pi^*$ bands of aromatic systems, the most important change in the electron density takes place within the ring, and the hydrogen bond influences these transitions only through the participation of the electrons belonging to the X atom of the proton donor group X — H, i.e. of the amino nitrogen, in the conjugation with the aromatic π

---

[4] A. STREITWIESER JR., "Molecular Orbital Theory for Organic Chemists", Wiley, New York, 1962, p. 135.

[5] M. B. BAZILEVSKII, "Metod molekulearnykhorbit i reaktsionnaia sposobnosti organicheskikh soedinenii", Khimia, Moskva, 1969, p. 76.

[6] C. DECORET, *Thèse*, Fac. Sci. Univ. Lyon, Febr. (1968).

[7] D. L. BEVERIDGE and J. HINZE, *J. Amer. Chem. Soc.*, **93**, 3107 (1971).

system. Consequently, the intramolecular hydrogen bond formed between two groups with similar properties has not an important influence upon the position of the absorption maxima, the spectra of the *ortho* and *meta* isomers being quite similar.

The shift noticed in the case of solvent mixtures proves the existence of some weaker intramolecular hydrogen bonds as well, at the same time enabling the study of the stability of the chelate ring under the influence of various active solvents.[8]

The (partial or complete) break of the intramolecular bond by an active solvent, always shifts the maximum of the longwavelength electronic absorption band hypochromically and, depending on the solvent, hypochromically or bathochromically.[9]

The addition of dioxane to a diluted solution of *ortho*-anisidine in an inert solvent, cyclohexane, reduces the amount of internal hydrogen bonds and leads to the formation of some solvated (non-coplanar) species as we can see from the noticeable decrease in intensity of both $\pi \rightarrow \pi^*$ bands of *ortho* anisidine as compared to the spectra of the other two isomers (where the drop in intensity is less pronounced and sometimes the effect is hyperchromic. (Fig. 1).

The hydrogen bonded complex of the type 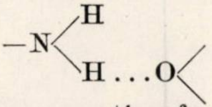
$-\mathrm{N}\begin{matrix}\diagup\mathrm{H}\\ \diagdown\mathrm{H}\ldots\mathrm{O}\langle\end{matrix}$
increases the amino group proton donor properties, thus accounting for the bathochromic shifts (more pronounced in *meta* and *para* compounds) shown by the spectra of the three isomers. Since both associated and non-associated (chelated in the ortho-anisidine case) species have fairly discrete spectra which cross each other, isosbestic points occur, thus proving the existence of an equilibrium in the solution between the two forms.

The method of estimating the equilibrium constant of anisidine-dioxane system by means of optical density measurements is the same with that described in Chandra's paper.[10] A linear relationship [B]/D against 1/[A] where [A] and $[B] = m[A]$ represents the anisidine and dioxane initial concentration respectively and D, the absorption of anisidine in dioxane, indicates the existence of an 1 : 1 complex in the above-mentioned system. From the intercept and the slope of the line, the equilibrium constant "K" of the hydrogen bonded complex has been calculated.

The optical density measurements have been made for several wavelengths on the right side of the band maximum. Table 2 gives the average values of k for the three isomeric anisidines, with an error of $\sim 0.03\ \mathrm{l \cdot mole^{-1}}$. Table 2 also includes the thermodynamic quantities ΔG and ΔH obtained from the temperature dependence of the equilibrium constant.

---

[8] L. Skulski and Z. Stolzarowa, *Bull. Acad. polon. Sci., Ser. Sci. chim.*, **21**, 359 (1973).

[9] L. Skulski and M. Kanabus, *Bull. Acad. polon. Sci., Ser. Sci. chim.*, **17**, 311 (1969).

[10] A. K. Chandra and S. Banerjee, *J. Phys. Chem.*, **66**, 953 (1962).

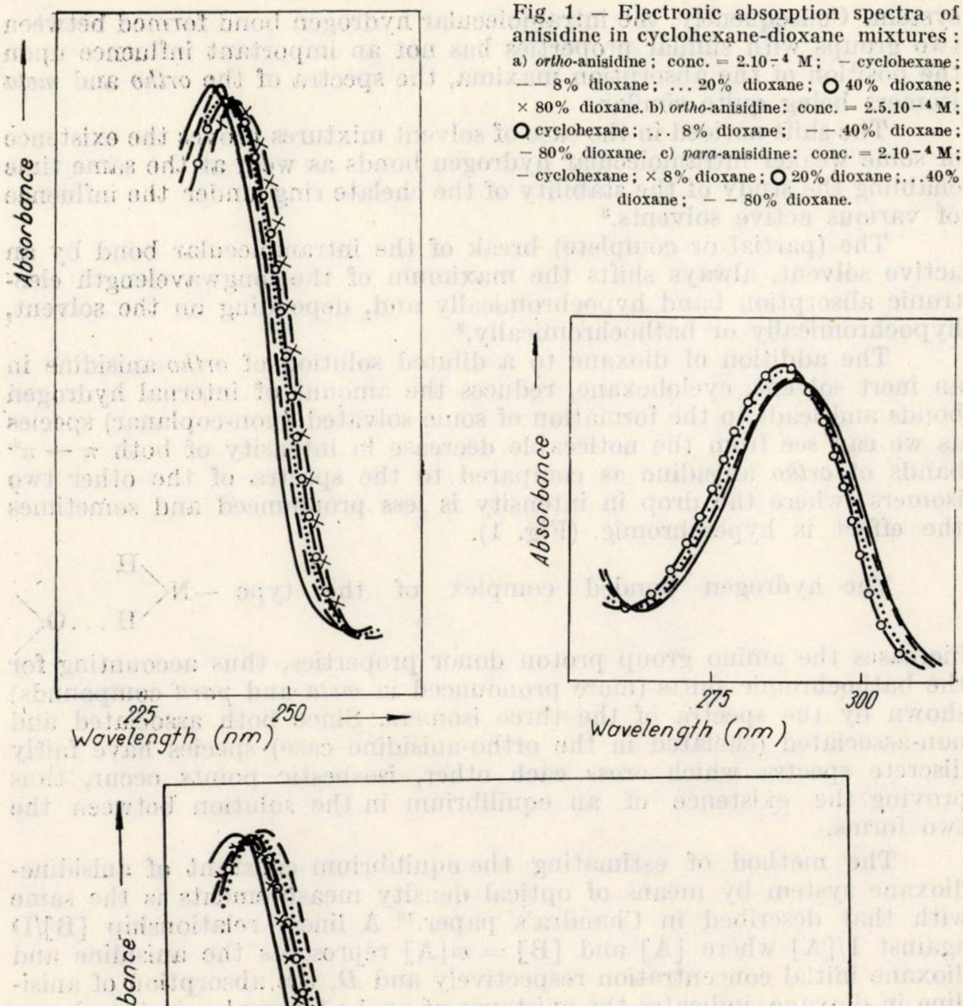

Fig. 1 — Electronic absorption spectra of anisidine in cyclohexane-dioxane mixtures : a) *ortho*-anisidine ; conc. = 2.10^{-4} M ; — cyclohexane ; — — 8% dioxane ; ... 20% dioxane ; O 40% dioxane ; × 80% dioxane. b) *ortho*-anisidine: conc. = $2.5.10^{-4}$ M ; O cyclohexane ; ... 8% dioxane ; — — 40% dioxane ; — 80% dioxane. c) *para*-anisidine: conc. = 2.10^{-4} M ; — cyclohexane ; × 8% dioxane ; O 20% dioxane ; ... 40% dioxane ; — 80% dioxane.

The association constant of *ortho*-anisidine with dioxane is a little smaller, but very close to that of the two other isomers, thus proving the reduced stability of the five-membered chelated ring to the action of this solvent, in agreement with the previously obtained dipole moment data.[1]

Table 2

The variation of association constant with temperature in anisidine isomers

Isomer	*o*-anisidine				*m*-anisidine			*p*-anisidine		
Temperature (°C)	22	25	30	38	25	30	35	25	30	38
$K (\mathrm{l \cdot mole^{-1}})$	0.39	0.33	0.23	0.19	0.49	0.39	0.32	0.40	0.34	0.24
$\Delta G (\mathrm{kcal \cdot mole^{-1}})$	0.565	0.657	0.835	1.017	0.422	0.567	0.698	0.543	0.640	0.883
$-\Delta H (\mathrm{kcal \cdot mole^{-1}})$	6.9±0.3				7.7±0.1			7.4±0.15		

As temperature increases, the intermolecular associations get partly broken, the equilibrium shifting towards the non-solvated (chelated in the *ortho*-anisidine case) species.

We can notice that our values are very close to those obtained by Meallier [11] through a similar method for a similar system, aniline-dioxane ($K = 0.38\ \mathrm{l \cdot mole^{-1}}$ and $\Delta G = 0.575\ \mathrm{kcal \cdot mole^{-1}}$).

As we can see, the UV spectral and dipole-moment studies do complement each other fairly well, giving thus information on the presence of the intramolecular hydrogen bond and its stability to the action of such active solvents like dioxane.

---

[11] P. Meallier, J. Randeau and B. Pouyet, *Spectrochim. Acta*, **27 A**, 2243 (1971).

Revue Roumaine de Chimie, **21**, 5 645–649 (1976)

Revue Roumaine de Chimie, **21**, 5, 651–653 (1976)

THE INFLUENCE OF Fe_2O_3 ON THE THERMAL STABILITY OF $BaCO_3$

MARINA BULZAN and E. SEGAL
Center of Physical Chemistry
Bucharest, Str. Dumbrava Roșie, 23

Received 29 April, 1975

In this paper the results concerning the influence of iron oxide on the decomposition temperature of the $BaCO_3$ are presented.

1. INTRODUCTION

The study of the thermal behaviour of $BaCO_3$ has shown that this compound, which exhibits two polymorphic transitions at 810 and 960°, respectively,[1] decomposes releasing carbon dioxide beginning from 1000°.

A nonisothermal kinetic study of $BaFe_{12}O_{19}$ (barium hexaferrite) formation in the system $BaO-Fe_2O_3$ has shown that $BaCO_3$ decomposes at a much lower temperature, because of the existence of Fe_2O_3, namely the evolution of CO_2 takes place in the temperature range 670–880°.[2] This was considered as due to the Hedvall effect [3] taking into account the phase transformation of $\alpha-Fe_2O_3$ at 675° and of $BaCO_3$ at 810°. The decomposition of $BaCO_3$ is accompanied by a solid state reaction between the newly formed BaO and Fe_2O_3 already present and the resulting $BaFe_{12}O_{19}$ was later identified by X-ray diffraction.

On these grounds, the thermal behaviour from room temperature up to 1500° of some mixtures in this system has been studied with Fe_2O_3 decreasing percentages.

2. EXPERIMENTAL

Fe_2O_3 (Reanal) and $BaCO_3$ (UCB) of analytical grade were used. The powdered mixtures were mechanically homogenized by the dry method.

The differential thermal analysis and thermogravimetric curves were obtained on a derivatograph MOM Budapest, Paulik-Paulik Erdey type, from room temperature up to 1500°, at various heating rates.

---

[1] E. K. Keler and A. K. Kuznetsov, *Zhur. priklad. Khim.*, **34**, 2146 (1961).

[2] S. Solacolu, M. Bulzan and E. Segal, *Rev. Roumaine Chim.*, **21**, 545 (1976).

[3] J. A. Hedvall and L. Leffter, *Z. anorg. Chem.*, **234**, 235 (1937).

3. RESULTS AND DISCUSSION

The mixtures studied in the system $BaO-Fe_2O_3$ have a continuously decreasing percentage of Fe_2O_3, from 86% Fe_2O_3 (corresponding to the mixture $BaFe_{12}O_{19}$) to 0.1% Fe_2O_3. For these values, see table 1, and the experimental data concerning each of the mixtures.

Table 1

Mixtures in the system $BaO-Fe_2O_3$

Composition of mixtures weight %	Heating rate °C/min	Ignition loss theoretical %	Ignition loss experiment %	Temperature of the beginning of CO_2 evolution °C
$BaCO_3$	7	22.3	20	1000
$86\ Fe_2O_3 + 14\ BaO$	10	3.8	3.7	670
$25\ Fe_2O_3 + 75\ BaO$	10	17.6	—	755
$15\ Fe_2O_3 + 85\ BaO$	7 10	19.6 19.6	19.4 —	735 740
$5\ Fe_2O_3 + 95\ BaO$	10	21.4	—	810
$1\ Fe_2O_3 + 99\ BaO$	7 10	22.1 22.1	20.4 —	870 880
$0.1\ Fe_2O_3 + 99.9\ BaO$	7	22.2	17	900

An analysis of the thermodifferential and thermogravimetric curves reveals an increase of the temperature at the beginning of the CO_2 evolution with the decrease of Fe_2O_3 concentration and namely from 670° for the mixture with 86% Fe_2O_3 until 900°, for the mixture with 0.1% Fe_2O_3. Weight losses up to 1500° are in good agreement with the theoretical values.

The occurrence of Fe_2O_3 in the mixture results in the decomposition of $BaCO_3$ at much lower temperatures; but this shifting effect decreases when the percentage of Fe_2O_3 decreases. In the case of the 0.1% Fe_2O_3 mixture, one may consider that the positive influence of the Fe_2O_8 on the temperature at the beginning of CO_2 evolution is minimal. This shifting might also be regarded as a consequence of a formation of $BaFe_{12}O_{19}$ and $Ba_8Fe_8O_{21}$,[4] which has been put into evidence in such systems in the used temperature range. The second compound which has a high probability of formation in the low amounts of Fe_2O_3 mixtures at temperatures above 800°, has an oxygen deficient elementary cell. This departure from stoichiometry and a possible stoichiometrization trend using the oxygen of $BaCO_3$ not yet decomposed might determine the decomposition of the latter at lower temperatures than the pure barium carbonate.

---

[4] P. P. Budnicov and A. M. Ghintsling, "Reaktsii v smesiakh tverdykh veshchestv", Gostroizdat, Moskva, 1961, p. 323.

4. CONCLUSIONS

The occurrence of Fe_2O_3 together with $BaCO_3$ in the mixture leads to its decomposition at temperatures much lower than of pure carbonate. There obviously exists a direct relationship between the amount of Fe_2O_3 in the mixture and the decrease of the temperature at which decomposition begins.

Revue Roumaine de Chimie, **21**, *5*, 655–660 (1976)

THERMODYNAMIC PROPERTIES OF AgI + NaI + KI FUSED SALT TERNARY SYSTEM BY FORMATION CELL METHOD

S. STERNBERG and LUCIA BEJAN
Institute of Physical Chemistry, Str. Galaţi 31, Bucharest, Romania

Received October 10, 1974

E.m.f. measurements on formation cells with $AgI + NaI + KI$ fused salt ternary system were carried out within 870–1020 K temperature range. The activity, activity coefficient and excess partial molar chemical potential of AgI were calculated.

INTRODUCTION

Thermodynamic properties of some fused salt ternary mixtures of the type $AX + BX + CX$ have been studied by e.m.f. measurements and interpreted by different authors, Hagemark [1–2] Guion and Blander,[2] Pelton and Flengas,[3] Markov [4–5] and Lantratov.[6] The values of thermodynamic functions of these systems have been approximated from the similar functions of binary subsystems which make up the ternary one.

This work reports the thermodynamic study of ternary system $AgI + NaI + KI$ as carried out on the basis of formation cells :

$$Ag(s)\ \|\ AgI(l,\ x_1) + NaI(l,\ x_2) + KI(l,\ x_3)\ \|\ I_2\ \ (g,\ 1\ atm)\ \text{graphite}.$$

Use has been made of iodine electrode. Details regarding the construction of the cell and the procedure of achieving the reversible iodine electrode have been given in previous papers. [7–8] The e.m.f.'s of the cells have been measured by a "Solartron" L.M. 1440.2 type, digital voltmeter, within ± 1–2 mV. Measurements of e.m.f. were carried out for various concentrations *versus* temperature within the range 870–1020 K ; the working temperatures were so chosen as to ensure the presence of homogeneous liquid phase in all compositions of the system.

---

[1] K. Hagemark, *J. Phys. Chem.*, **72**, 2316 (1968).

[2] J. Guion, M. Blander, D. Hengstenberg and K. Hagemark, *J. Phys. Chem.*, **72**, 2086 (1968).

[3] A. D. Pelton and S. N. Flengas, *J. Electrochem. Soc.*, **118**, 1307 (1971).

[4] B. F. Markov, *Rev. Roumaine Chim.*, **17**, 203 (1972).

[5] B. F. Markov and V. Horlbekk, *Ukrain. Khim. Zhur.*, **40**, 82 (1974).

[6] M. F. Lantratov, *Zhur. priklad. Khim.*, **46**, 2205 (1973).

[7] S. Sternberg, I. Adorian and I. Galasiu, *J. Chim. phys.*, **62**, 63 (1965).

[8] S. Sternberg and L. Bejan, *Rev. Roumaine Chim.*, **14**, 303 (1969).

Reagent grade salts have been used. AgI, NaI and KI have been predried, premelted then purified by bubbling through it dry pure gaseous HI.

RESULTS AND DISCUSSIONS

The e.m.f.'s measured at various compositions versus temperature in the ternary system under study are listed in Table 1. The equations $E = f(T)$ have been obtained from about 15–25 points by least square method.

Table 1

Experimental e.m.f.'s *versus* temperature in AgI + NaI + KI ternary system

x_{AgI}	$x' = \dfrac{x_2}{x_2 + x_3}$	$\dfrac{E}{V}$	Average standard deviation
1	0	$0.5510 - 0.272 \times 10^{-3}(T-873)$	± 0.0021
0.5	0.7	$0.6000 - 0.207 \times 10^{-3}(T-873)$	± 0.0027
0.3		$0.6361 - 0.175 \times 10^{-3}(T-873)$	±0.0023
0.15		0.6852 (at $T = 873$ K)	± 0.0028
0.7	0.5	$0.5803 - 0.246 \times 10^{-3}(T-873)$	± 0.0022
0.5		$0.6061 - 0.202 \times 10^{-3}(T-873)$	± 0.0019
0.3		$0.6447 - 0.153 \times 10^{-3}(T-873)$	± 0.0014
0.5	0.3	$0.6094 - 0.212 \times 10^{-3}(T-873)$	± 0.0014
0.3		$0.6528 - 0.161 \times 10^{-3}(T-873)$	± 0.0013
0.15		0.7010 (at $T = 873$ K)	± 0.0026

In Table 2 there are listed the experimental values of activity, activity coefficient and excess partial molar chemical potentials of AgI at 873 and 973 K.

The thermodynamic activity of silver iodide was calculated by the equation:

$$\ln a_1 = -\frac{n\mathcal{F}}{RT}\,[E(x_1) - E^0] \tag{1}$$

where E^0 refers to the cell with single AgI and $E(x_1)$ to cells with ternary mixture.

The activity coefficient is given by the equation:

$$\gamma_1 = \frac{a_1}{x_1} \tag{2}$$

Table 2

Experimental thermodynamic functions of AgI in AgI + NaI + KI ternary system at 873 K and 973 K; x_1 is the mole fraction of AgI

x_1	$x' = \frac{x_2}{x_2 + x_3}$	a_1		γ_1		$\Delta \mu_1$ cal·mol^{-1}		μ_1^Ecal · mol^{-1}	
		873 K	973 K	873 K	973 K	873 K	973 K	873 K	973 K
0.5	0.7	0.5213	0.5159	1.0426	1.0318	−1130	−1280	+ 73	+ 60
0.3		0.3227	0.3229	1.0757	1.0763	−1963	−2186	+126	+142
0.15		0.1680	0.1720	1.1200	1.1467	−3095	−3404	+197	+265
0.7	0.5	0.6774	0.6836	0.9677	0.9766	− 676	− 736	− 57	− 46
0.5		0.4808	0.4768	0.9616	0.9536	−1271	−1432	− 68	− 92
0.3		0.2878	0.2838	0.9593	0.9460	−2161	−2435	− 72	−107
0.5	0.3	0.4601	0.4639	0.9202	0.9278	−1347	−1485	−144	−145
0.3		0.2585	0.2602	0.8617	0.8673	−2348	−2604	−259	−276
0.15		0.1362	0.1301	0.9080	0.8673	−3459	−3944	−167	−275

where x_1 stands for mole fractions of AgI and a_1 for the thermodynamic activity of AgI in ternary mixture.

The partial molar chemical potential of AgI has been calculated according to the equation:

$$\Delta\mu_1 = \mu_1 - \mu_1^0 = - \mathcal{F}[E(x_1) - E^0] \tag{3}$$

and its excess value according to:

$$\mu_1^E = \Delta\mu_1 - \Delta\mu_1^{id} = - \mathcal{F}[E(x_1) - E^0] - RT \ln x_1 \tag{4}$$

As composition variables x_1 and x' were chosen where $x_1 = x_{AgI}$ and

$$x' = \frac{n_{NaI}}{n_{NaI} + n_{KI}} = \frac{x_2}{x_2 + x_3} \tag{5}$$

For constant x' the system may be treated as a quasi-binary one.

The experimental excess partial molar chemical potentials of AgI in AgI + NaI+KI ternary system are plotted against $(1 - x_1)$ on three quasi-binary curves ($x' = 0.7$; $x' = 0.5$; $x' = 0.3$ at 973 K) in Figure 1. On the same figure there are plotted the experimental partial molar chemical potentials of AgI in the two binary mixtures AgI + NaI[9] and AgI + KI[10].

---

[9] S. Sternberg and I. Adorian, *Electrochim. Acta.*, **13**, 1647 (1968).

[10] S. Sternberg, I. Adorian and I. Galasiu, *Electrochim. Acta*, **11**, 385 (1966).

The chemical potential is positive in the first system and negative in the second one. The curves of excess partial molar chemical potentials of ternary system lay between those of binary systems.

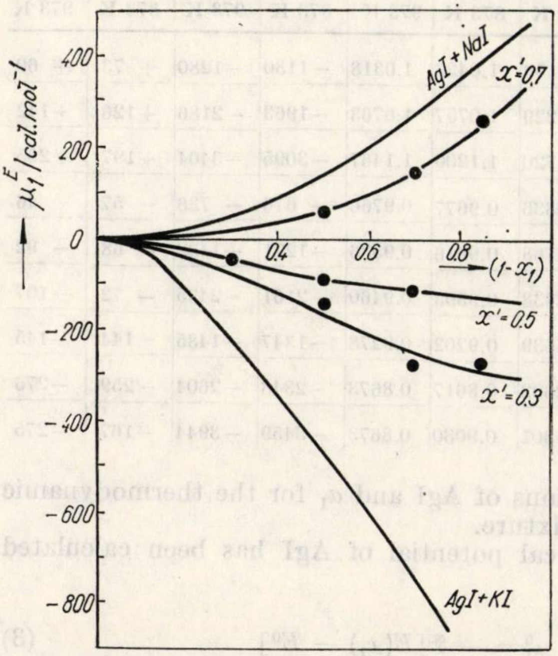

Fig. 1. — Experimental values of excess partial molar chemical potentials of AgI *versus* $(1-x_1)$ in AgI + NaI + KI ternary system at 973 K.

According to quasi-chemical theory as employed by Hagemark [1-2] in ternary systems, the excess partial molar chemical potential of AgI is given by:

$$\mu_1^E = x'\mu^E_{1\,(\mathrm{AgI+NaI})} + (1-x')\,\mu^E_{1\,(\mathrm{AgI+KI})} + x'(1-x')\,(1-x_1)^2\,g(x') \qquad (6)$$

where

$$x'(1-x')\,g(x') = -H^E_{(\mathrm{NaI+KI})} + f(x') \qquad (7)$$

and $f(x')$ is a term specific to ternary systems (calculated within quasi-chemical approximation).

Were $f(x')$ negligible, equation (6) would become:

$$\mu_1^E = x'\mu^E_{1\,(\mathrm{AgI+NaI})} + (1-x')\,\mu^E_{1\,(\mathrm{AgI+KI})} - (1-x_1)^2\,H^E_{(\mathrm{NaI+KI})} \qquad (8)$$

which leads to Alcock and Richardson's [11] equation when $x_1 \to 0$

$$\mu_1^E = x'\mu^E_{1(\mathrm{NaI})} + (1-x')\,\mu^E_{1(\mathrm{KI})} - H^E_{(\mathrm{NaI+KI})} \qquad (9)$$

---

[11] G. B. Alcock and F. D. Richardson, *Acta. Met.*, **6**, 385 (1958).

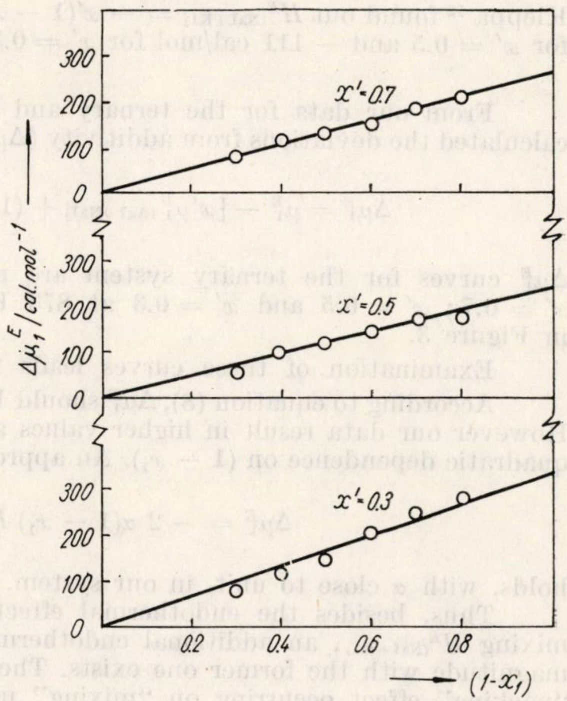

Fig. 2. — Deviations from additivity, $\Delta\mu_1^E$, *versus* $(1 - x_1)$ in AgI + NaI + + KI ternary system at 873 K.

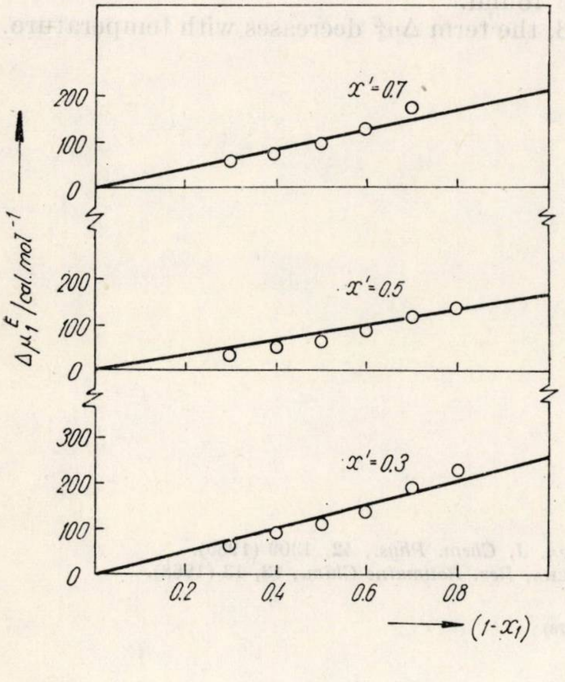

Fig. 3. — Deviations from additivity, $\Delta\mu_1^E$, *versus* $(1 - x_1)$ in AgI + NaI + + KI ternary system at 973 K.

Kleppa[12] found out $H^E_{(\mathrm{NaI+KI})} = -x'(1-x')\ 530$ cal/mol; -132 cal/mol for $x' = 0.5$ and -111 cal/mol for $x' = 0.3$ and $x' = 0.7$.

From our data for the ternary and two binary systems we have calculated the deviations from additivity ($\Delta\mu_1^E$) according to the equation :

$$\Delta\mu_1^E = \mu_1^E - [x'\mu^E_{1\,(\mathrm{AgI+NaI})} + (1-x')\,\mu^E_{1\,(\mathrm{AgI+KI})}]. \tag{10}$$

$\Delta\mu_1^E$ curves for the ternary system are plotted against $(1-x_1)$ with $x' = 0.7$; $x' = 0.5$ and $x' = 0.3$ at 873 K in Figure 2 and at 973 K in Figure 3.

Examination of these curves leads to the following conclusions.

According to equation (8), $\Delta\mu_1^E$ should be equal to $-(1-x_1)^2H^E_{(\mathrm{NaI+KI})}$. However our data result in higher values as well as in a linear and not quadratic dependence on $(1-x_1)$. An approximate equation of the type :

$$\Delta\mu_1^E = -2\,\alpha(1-x_1)\,H^E_{(\mathrm{NaI+KI})}$$

holds, with α close to unit, in our system.

Thus, besides the endothermal effect brought in by the heat of mixing $H^E_{(\mathrm{NaI+KI})}$, an additional endothermal term of the same order of magnitude with the former one exists. The existence of an endothermal "packing" effect occurring on "mixing" unevenly sized cations around a common anion has been considered in a previous work.[13] This effect may be stronger in ternary mixtures and may cause the additional positive deviation which we have found.

As seen in Figures 2 and 3, the term $\Delta\mu_1^E$ decreases with temperature.

---

[12] L. S. Hersh and O. J. Kleppa, *J. Chem. Phys.*, **42**, 1309 (1965).

[13] S. Sternberg and C. Herdlicka, *Rev. Roumaine Chim.*, **13**, 13 (1968).

Revue Roumaine de Chimie, 21, 5, 655−660 (1976)

Revue Roumaine de Chimie, **21**, 5, 661–666 (1976)

STUDY OF THE ISOMORPHIC TRANSITIONS OF SOME IRON OXIDES

D. I. MARCHIDAN and LIANA PANDELE
Centre of Physical Chemistry, Str. Galați 31, Bucharest, Romania

Received November 4, 1975

The isomorphic transitions of some iron oxides have been pointed out by the study of thermal properties *vs.* temperature. The heat content has been determined within the 400–965 K temperature range by means of the drop calorimetry method. The accuracy of the measurements is of ±0.4%.

Phase transitions are phenomena appearing with a state transformation of a heterogenous system in equilibrium, accompanied by the transition of the substance from one phase to another. Isomorphic transitions are phenomena occurring at a certain temperature and pressure. Actually, as a consequence of heterogenous fluctuations, an isomorphic transition is extented along a certain temperature range.[1]

The method of drop calorimetry has been used to investigate many substances and binary systems evincing phase transitions. In our laboratory the method has been used for the study of the high temperature crystalline transition of alumina T A_{600}.[2] The experimental technique and installation has been described in detail in a previous paper.[3]

EXPERIMENTAL

The main parts of the installation are the furnace, with an inoxitherm steel core, and the calorimeter proper made of electrolytic copper. The temperature variation of the furnace is kept constant with a ±0.5° accuracy by means of a proportional thermoregulating device.

The temperature variation of the calorimeter proper was measured by a thermistor (CICE—France), characterized by high sensitivity and reproductibility, which permitted the measurement of a small temperature variation of 0.001 K. The variation of the thermistor resistance in terms of temperature was measured by means of a Wheastone bridge. The platinum container containing 3 g iron oxide was suspended in the furnace and kept at constant temperature, for 1 hour, until a thermal equilibrium was reached. The container was then dropped into the calorimeter where the heat content of the substance and of container was determined by cooling up to 298 K.

In order to determine the quantity of the whole heat content, due to the empty container, as well as the amount of heat lost on dropping, blank measurements are carried out for the empty container in the same conditions of temperature.

---

[1] I. P. Bazarov, "Termodinamica", Ed. tehnică, Bucharest, 1962, p. 185.

[2] D. I. Marchidan, L. Pandele and A. Nicolescu, *Rev. Roumaine Chim.*, **17**, 1493 (1972).

[3] D. I. Marchidan and M. Ciopec, *Studii și cerc. chimie.*, **17**, 737 (1969).

RESULTS AND DISCUSSION

The heat content of iron oxides FTSB* and FTS has been determined in the 400 − 965 K temperature range. Iron oxides were prepared by a new method [4] termed mechanotopochemical and the obtained oxides were called FTSB and FTS. Iron oxides FTSB and FTS are of interest in view of their utilization for the preparation of specific catalysts.

The experimental results for FTSB iron oxide are listed in table 1 in comparison with calculated values obtained by the method of the least squares,[5] using an I.B.M. 360 computer.

Table 1

Experimental and calculated enthalpy increments for iron oxide FTSB *versus* temperature

T (K)	$H_T - H_{298.15}$ exp. (cal/mol)	$H_T - H_{298.15}$ calc. (cal/mol)	Deviation (cal/mol)	Deviation %
416.75	4403.4			
451.35	5510.3			
506.65	6320.1	6365	− 45.1	−0.7
510.75	6490.2	6438.6	51.6	0.8
560.75	7248	7260.9	− 12.9	−0.2
581.25	7542.5	7535.4	7.1	0.1
637.55	9480	9452.07	27.93	0.3
732.55	12753.79	12813.94	− 60.25	−0.5
799.20	14456.5	15021.2	−564.70	−3.9
829.3	16843.79	15984.12	859.67	5.1
926.4	18719.4	18974.2	−254.8	−1.4
965.2	19953.5	20126.05	−172.55	−0.9

The experimental results plotted in fig. 1 show that the variation of the heat content with temperature has some inflection points corresponding to the phase transitions of iron oxide FTSB.

The first transition has been pointed out around 453 K and it is attributed to the loss of adsorption water contained in the iron oxide. The second transition has been pointed out arround 578 K and is correlated with goethite dehydration and crystallization of the α iron oxide. The results obtained are in agreement with those supplied by D.T.A.[6]

Processing by the least squares method the experimental data for the temperatures between the first and the second transition points we obtained the following equation:

$$H_T - H_{298 \cdot 15} = -2424.18 + 38.2\,T - 0.0266\,T^2 - 1878562\,T^{-1}\ \text{cal/mol}.$$

---

* The iron oxides denoted by FTS and FTSB specify the origin of the products prepared and also their global composition.[4]

[4] I. V. Nicolescu, A. Spinzi, Z. Toma and G. Galațchi, *Rev. Roumaine Chim.*, **20**, 61 (1975).

[5] A. G. Worthing and J. Geffner, "Treatment of Experimental Data", Wiley, New York, 1955, p. 225.

[6] A. Spinzi and I. V. Nicolescu, *Rev. Roumaine Chim.*, **20**, 61 (1975).

Using the same method of processing experimental results we obtained for the temperature range 637–965 K an equation of the form:

$$H_T - H_{298 \cdot 15} = -686.5 + 28.37\,T - 0.002\,T^2 - 4552211\,T^{-1} \text{ cal/mol.}$$

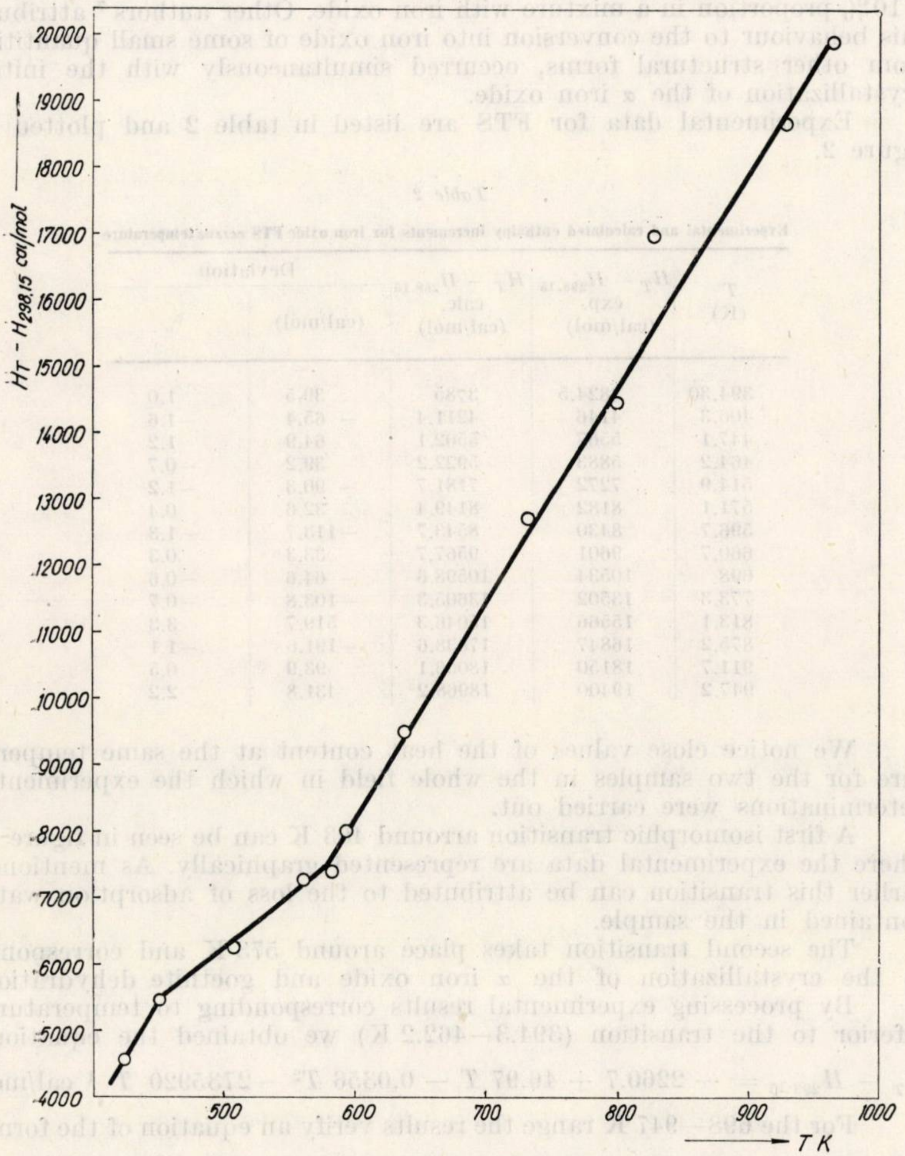

Fig. 1. — Heat content *vs.* temperature for FTSB iron oxide.

At temperatures around 800–820 K, an anomalous deviation of experimental data from the calculated curve can be noticed. This deviation, also perceptible in the plot of heat content variation with temperature, is to be found approximately in the same temperature range for the iron oxide FTS as well. This effect, also obtained by thermal analysis,[6] was attributed to the transition of the magnetite, existing in a 10% proportion in a mixture with iron oxide. Other authors [7] attribute this behaviour to the conversion into iron oxide of some small quantities from other structural forms, occurred simultaneously with the initial crystallization of the α iron oxide.

Experimental data for FTS are listed in table 2 and plotted in figure 2.

Table 2

Experimental and calculated enthalpy increments for iron oxide FTS *versus* temperature

T (K)	$H_T - H_{298.15}$ exp. (cal/mol)	$H_T - H_{298.15}$ calc. (cal/mol)	Deviation	
			(cal/mol)	%
394.30	3824.5	3785	39.5	1.0
406.3	4146	4211.4	− 65.4	−1.6
447.1	5567	5502.1	64.9	1.2
464.2	5883	5922.2	− 39.2	−0.7
514.9	7272	7181.7	− 90.3	−1.2
571.1	8182	8149.4	32.6	0.4
596.7	8430	8543.7	−113.7	−1.3
660.7	9601	9567.7	33.3	0.3
698	10534	10598.6	− 64.6	−0.6
773.3	13502	13605.3	−103.8	−0.7
813.1	15566	15046.3	519.7	3.3
875.2	16847	17038.6	−191.6	−1.1
911.7	18150	18056.1	93.9	0.5
947.2	19400	18968.2	431.8	2.2

We notice close values of the heat content at the same temperature for the two samples in the whole field in which the experimental determinations were carried out.

A first isomorphic transition arround 463 K can be seen in figure 2, where the experimental data are represented graphically. As mentioned earlier this transition can be attributed to the loss of adsorption water contained in the sample.

The second transition takes place around 573 K and corresponds to the crystallization of the α iron oxide and goethite dehydration.

By processing experimental results corresponding to temperatures inferior to the transition (394.3–462.2 K) we obtained the equation:

$$H_T - H_{298\cdot15} = -2260.7 + 46.97\,T - 0.0356\,T^2 - 2735920\,T^{-1}\ \text{cal/mol.}$$

For the 698–947 K range the results verify an equation of the form :

$$H_T - H_{298\cdot15} = 57843 + 120.3\,T - 0.0477\,T^2 + 5379526\,\mathrm{T}^{-1}\ \text{cal/mol.}$$

---

[7] C. S. Swamy, *Current Science*, **35**, 253 (1966).

Around 810 K a deviation from the calculated curve is to be found, whose nature has been discussed earlier.

Besides these transitions, also noticed with the first sample, the FTS iron oxide has also a transition around the 683 K temperature whose nature has not yet been studied.

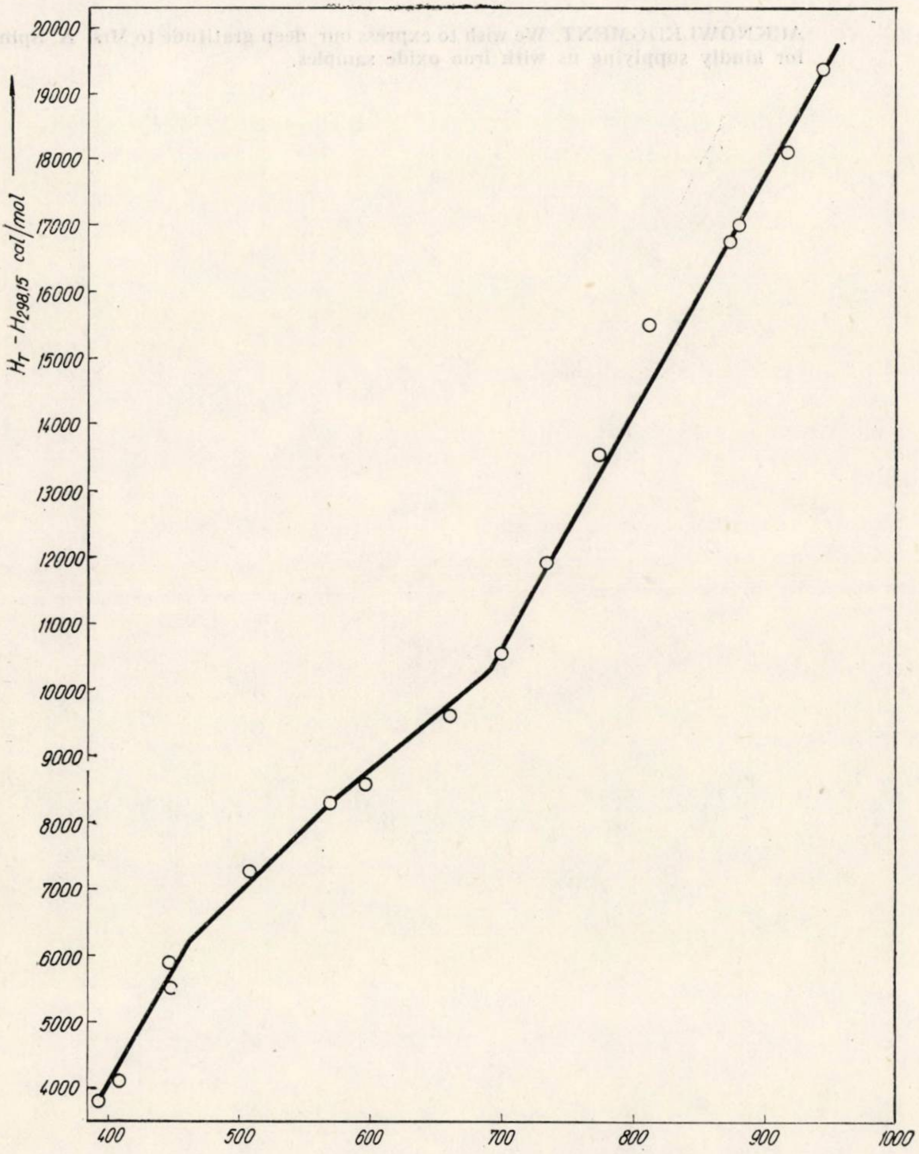

Fig. 2. — Heat content *vs.* temperature for F T S iron oxide.

As a general conclusion, we can say that the general aspect of the curve is alike, meaning that the thermochemical properties of the two iron oxides are related.

Along the whole temperature range the values of the heat content are close to one another and the phase transitions take place within approximately the same temperature range.

ACKNOWLEDGMENT. We wish to express our deep gratitude to Mrs. A. Spinzi for kindly supplying us with iron oxide samples.

Revue Roumaine de Chimie, 21, 5, 667–676 (1976)

ON THE STOCHASTIC ANALYSIS OF THE REACTION NETWORKS. I

MARCEL VLAD and EUGEN SEGAL
Bucharest Polytechnic Institute, Chemistry Institute, Department of Physical Chemistry and Electrochemical Technology, Bd. Republicii 13

Received May 22, 1975

A stochastic analysis of networks of the first order reactions is presented. From the basic postulate of the stochastic model, it is possible to derive the probability distribution, mean value and variance of composition vector. It is possible to derive the correlation coefficients between the molecule numbers and also the informational entropy.

A. GENERAL APPROACH

According to the literature informations, there are many attempts of applying the theory of stochastic processes to the study of the chemical reactions.[1-6] By using the stochastic models they rediscover the rate equations resulted from the classical representations for the kinetics of chemical reactions. Moreover by using the stochastic models it is possible, at least as a rule, to derive the probability of the concentration fluctuation, as well as the various characteristics of the system which are dependent on it. Such particular treatments of different types of reactions were more or less dealt with in literature. It is in our intention to derive a stochastic model for a first order reactions network. But before doing this we consider necessary to present the main results obtained in the study of the deterministic model of the first order reactions networks. These results will be further useful to us.

For the reactions:

$$A_i \underset{k_{ji}}{\overset{k_{ij}}{\rightleftarrows}} A_j \quad n \geqslant j > i = 1, \ldots, n-1 \tag{1}$$

---

[1] A. E. Bartholomay, *Bull. Math. Biophys.*, **20**, 97 (1958); *Biochemistry*, **1**, 223 (1962).
[2] L. M. Krieger and P. J. Gans, *J. Chem. Phys.*, **32**, 247 (1960).
I. G. Darvey and P. J. Staff, *J. Chem. Phys.*, **44**, 990 (1966).
[3] D. A. Mc Quarrie, *J. Appl. Prob.*, **4**, 413 (1967); *Adv. Chem. Phys.*, **15**, 149 (1969).
[4] G. Nicholis and A. Babloyantz, *J. Chem. Phys.*, **51**, 2632 (1969).
[5] M. Solc, *Z. phys. Chem. (Frankfurt)*, **83**, 65 (1973); **92**, 1 (1974).
[6] J. Keitzer, *J. Chem. Phys.*, **56**, 5775 (1972).

the classical chemical kinetics gives us the following system of differential equations :

$$\frac{\mathrm{d}N_j}{\mathrm{d}t} = \sum_{i=1}^{n} k_{ij} N_i \,;\; k_{jj} = -\sum_{i \neq j}^{n} k_{ij} \,;\; i = 1, \ldots, n \tag{2}$$

The system (2) was for the first time integrated by Zwolinsky and Eyring.[7] Pismen and Ioffe[8] integrated the same system by using the theory of matrix functions. They write this system in a matrix form as follows :

$$\frac{\mathrm{d}\boldsymbol{N}}{\mathrm{d}t} = \tilde{\boldsymbol{K}} \boldsymbol{N}^{*} \tag{2'}$$

where $\boldsymbol{N} = (N_i)$ is the n-dimensional vector of the composition and $\hat{K} = \|k_{ij}\|$ is the matrix of specific rates. Then, Pismen and Ioffe demonstrate that the solution of the matrix differential equation which fulfils the condition $\boldsymbol{N}(t = 0) = \boldsymbol{N}_0$ is the following :

$$\boldsymbol{N}\,(t) = \exp\,(\tilde{\boldsymbol{E}}(t))\,\boldsymbol{N}_0, \tag{3}$$

where the function :

$$\boldsymbol{E}(t) = \|\eta_{ij}(t)\| = \exp\,(\tilde{\boldsymbol{K}} t)$$

is called kinetic matrix and is defined by the expansion in series :

$$\exp\,(\tilde{\boldsymbol{K}} t) = \hat{I} + \sum_{n=1}^{\infty} \frac{\tilde{\boldsymbol{K}}^{n} t^{n}}{n\,!}$$

The kinetic matrix can be calculated by means of Sylvester's theorem.

Wei and Prater[9] offer another method of integrating equation (2′) based on the introduction of a set of orthogonal fictional molecule numbers, through a linear orthogonal transformation $\boldsymbol{N}' = \boldsymbol{\Phi N}$, transformation that leads to the breaking up of the differential matrix equation into n differential scalar independent equations. This method is suitable mainly for numerical calculations.

---

[7] B. Zvolinsky and H. Eyring, *J. Amer. Chem. Soc.*, **69**, 2702 (1947).

[8] L. M. Pismen and I. I. Joffe, *Kinetika i Kataliz*, 2, 606 (1961).

[9] J. Wei and C. D. Prater, *Adv. Catalysis*, **XIII**, 203 (1962).

* ~ is the sign for the act of matrix transposing

B. THE STUDY OF THE PROBLEM

Our aim is to find a formula for the probability distribution $P(\mathbf{N}, t)$ of the random vector $\mathbf{N}$. In order to achieve this we shall use the following differential – difference equation, found by Krieger and Gans [2]:

$$\frac{\partial P}{\partial t} = \sum_{i} \sum_{j \neq i} k_{ij}[(N_i + 1)\, P(N_i + 1, N_j - 1) - N_i P] \tag{4}$$

Introducing the generating function:

$$G(\mathbf{S}, t) = \sum_{\forall \mathbf{N} \geqslant 0} \prod_{i} s_i^{N_i}\, P(\mathbf{N}, t)^{\star} \quad \forall\, |s_i| \leqslant 1 \tag{5}$$

Equation (4) becomes:

$$\frac{\partial G}{\partial t} = \sum_{i} \sum_{j \neq i} k_{ij}(s_j - s_i) \frac{\partial G}{\partial s_i} \tag{6}$$

Taking into account that $P(\vec{\mathbf{N}}, 0) = \begin{cases} 1 \text{ if } \mathbf{N} = \mathbf{N}_0 \\ 0 \text{ if } \mathbf{N} \neq \mathbf{N}_0 \end{cases}$, we have:

$$G(t = 0) = \prod_{u} s_u^{N_{ou}} \tag{7}$$

The characteristic system attached to the equation with partial first order derivatives (6) is the following:

$$\frac{\mathrm{d}s_i}{\sum_{j} k_{ij} s_j} = -\mathrm{d}t\,; i = 1, \ldots, n\,;\ k_{ii} = -\sum_{j \neq i} k_{ij} \tag{8}$$

It can be written in a matrix way as follows:

$$-\frac{\mathrm{d}\mathbf{S}}{\mathrm{d}t} = \mathbf{K}\,\mathbf{S} \tag{8'}$$

---

[*] Because $P(\mathbf{N}, t)$ has a very sharp maximum, we are not too mistaken if while calculating the sum we do not take into consideration the law of conservation $\sum_{i} N_i = \sum_{i} N_{oi}$ and so we shall extend the upper bounds of the sum to ∞.

The solution of equation (8′) which fulfils the conditions $S(t=0)=S_0$ is :

$$S(t)=\exp(-Kt)\,S_0$$

As :

$$\exp(-Kt)=\left(\hat{I}+\sum_{n=1}^{\infty}\frac{\mathbf{K}^{n}t^{n}}{n!}\right)^{-1}=\overline{\left[\hat{I}+\sum_{n=1}^{\infty}\frac{\tilde{\mathbf{K}}^{n}t^{n}}{n!}\right]}^{-1}=\tilde{\mathbf{E}}^{-1}(t)$$

it follows that :

$$S=\tilde{E}^{-1}(t)\,S_0 \tag{9}$$

Eliminating the values of the independent variables from (7), (9), and $t=0$, we get :

$$G=\prod_i S_{0i}^{N0i}$$

Determining the value of S_0 from (9) we have

$$S_0=\tilde{E}(t)\,S \tag{9'}$$

and therefore :

$$G(S,t)=\prod_i\Big(\sum_j \eta_{ji}(t)\,s_j\Big)^{N_{o_i}} \tag{10}$$

From the normalization condition $\sum\limits_{\forall\ \geq\vec{o}} P(N,t)=1$ and from (10) we obtain:

$$G(1,t)=\prod_i\Big(\sum_j \eta_{ji}(t)\Big)^{N_{oi}}\equiv 1 \tag{11}$$

In order that the identity (11) may hold it is necessary that :

$$\forall i,\ \sum_j \eta_{ji}(t)=1 \tag{11'}$$

From (10), (11′) and from the relations [3] :

$$\bar{N}_i(t)=\left(\frac{\partial G}{\partial s}\right)_{S=1}\quad i=1,\ldots,n \tag{12}$$

we get:

$$\overline{N}_i(t) = \sum_j \eta_{ij}(t) N_{0j} \tag{13}$$

or in a matrix way:

$$\overline{\boldsymbol{N}}(t) = \boldsymbol{E}(t) \boldsymbol{N}_0 \tag{13'}$$

Comparing equations (3) and (15) we notice that the magnitude of the composition vector predicted by the deterministic theory is identical to the average value of the random vector $\boldsymbol{N}$ in the framework of the stochastic model. We refined so the conclusions of the deterministic theory of the first order reaction networks.

Formula (10) gives us the possibility of calculating the mean square deviation of the molecule numbers from the values obtained in the deterministic theory. It turns out that:

$$\overline{N_i^2}(t) = \left[\frac{\partial}{\partial s_i}\left(s_i \frac{\partial G}{\partial s}\right)\right]_{S=1} = \Big(\sum_j \eta_{ij}(t) N_{0j}\Big)^2 + \sum_j \eta_{ij}(t)\,(1 - \eta_{ij}(t))\, N_{0j} \tag{14}$$

and therefore:

$$\sigma_i(t) = \sqrt{\overline{(N_i - \overline{N}_i)^2}} = \sqrt{\sum_j \eta_{ij}(t)\,(1 - \eta_{ij}(t))\, N_{0j}} \tag{15}$$

As at the beginning of the reaction ($t = 0$) the concentrations of the subtances have a determined value it follows that $\sigma_i(0) = 0$. Further on, the average quadratic deviations increase. In certain conditions and at certain moments the existence of some maxima is possible, then the quantities $\sigma_i(t)$ decrease. The time values corresponding to these maxima can be calculated by solving the equations:

$$\frac{\mathrm{d}\overline{\Delta N_i^2}(t)}{\mathrm{d}t} = \sum_j N_{0j} \frac{\mathrm{d}\eta_{ij(t)}}{\mathrm{d}t}(1 - 2\,\eta_{ij}(t)) = 0$$

For instance, in the elementary case of the equilibrium $A \underset{k_2}{\overset{k_1}{\rightleftarrows}} B$ for which:

$$\boldsymbol{E}(t) = \begin{pmatrix} \dfrac{Ke^{-kt} + 1}{K + 1} & \dfrac{1 - e^{-kt}}{K + 1} \\ \dfrac{K(1 - \mathrm{e}^{-kt})}{K + 1} & \dfrac{K + e^{-kt}}{K + 1} \end{pmatrix}; \ \boldsymbol{N}_0 = \begin{pmatrix} a_0 \\ b_0 \end{pmatrix} \ \left(k = k_1 + k_2;\ K = \frac{k_1}{k_2}\right)$$

from equation (15) we get:

$$\sigma_A(t) = \sigma_B(t) = \frac{1}{k + 1}\sqrt{(1 - \mathrm{e}^{-kt})\,[\mathrm{e}^{-kt}(k^2 a_0 + b_0) + k(a_0 + b_0)]} \tag{16}$$

If $a_0 > b_0$ by analysing the sign of the derivative of expression (16) we get :

1) For $K < b_0/a_0$ or for $K > 1$, σ has a maximum point at the time value :

$$t_M = \frac{1}{k} \ln \frac{2(K^2 a_0 + b_0)}{(Ka_0 - b_0)(K-1)} \text{ for which } \sigma_M = \frac{Ka_0 + b_0}{2\sqrt{K^2 a_0 + b_0}}$$

2) For $b_0/a_0 \leqslant K \leqslant 1$, σ increases monotonically with the time.

The covariance and the coefficients of linear correlation between the quantities N_λ and N_μ ($\lambda \neq \mu$) are determined by the same method used in the case of the mean square deviation. So, we have :

$$\overline{N_\lambda\ N_\mu(t)} = \left(\frac{\partial^2 G}{\partial s_\lambda\ \partial s_\mu}\right)_{S=1} = -\sum_j \eta_{\lambda j}(t)\eta_{\mu}(t) N_{0j} + \Big(\sum_i \eta_{\lambda i}(t) N_{0i}\Big)\Big(\sum_j \eta_{\mu j}(t) N_{0j}\Big)$$

and therefore :

$$\operatorname{cov}(N_\lambda, N_\mu) = \overline{(N_\lambda - \overline{N}_\lambda)(N_\mu - \overline{N}_\mu)} = -\sum_j \eta_{\lambda j}(t)\ \eta_{\mu j}(t)\ N_{0j} \qquad (17)$$

and :

$$\rho_{\lambda\mu}(t) = \frac{\operatorname{cov}(N_\lambda, N_\mu)}{\sigma_\lambda(t)\ \sigma_\mu(t)} = \frac{-\sum\limits_j \eta_{\lambda j}(t)\eta_{0};\ (t) N_{0j}}{\sqrt{\sum\limits_i\sum\limits_j \eta_{\lambda i}(t)\eta_{\mu j}(t)\,(1 - \eta_{\lambda i}(t))\,(1 - \eta_{\mu j}(t))\, N_{0i}\, N_{0j}}} \qquad (17')$$

The coefficient of the linear correlation between the quantities N_λ and N_μ is the measure of the dependence of N_λ fluctuations on the N_μ fluctuations. If the fluctuations of the quantities N_λ and N_μ are independent, then $\rho_{\lambda\mu} = 0$. The maximum value is $\rho_{\lambda\mu} = \pm 1$. In the case of the equilibrium $A \underset{k_2}{\overset{k_1}{\rightleftarrows}} B$ it follows that $\rho_{AB} = -1$, an expectable result, as there is a relation $a + b = a_0 + b_0$ between the numbers of A and B molecules. In the case of reactions : $A \xrightarrow{k_1} B \xrightarrow{k_2} C$ for which :

$$E(t) = \begin{pmatrix} e^{-k_1 t} & 0 & 0 \\ \dfrac{k_1}{k_2 - k_1}(e^{-k_2 t} - e^{-k_1 t}) & 0 & e^{-k_2 t} \\ 1 + \dfrac{k_2 e^{-k_1 t} - k_1 e^{-k_2 t}}{k_1 - k_2} & 1 & 1 - e^{-k_2 t} \end{pmatrix}$$

considering that $N_0 = \begin{pmatrix} a_0 \\ 0 \\ 0 \end{pmatrix}$, we get :

$$\overline{\Delta a^2} = a_0 e^{-k_1 t}(1 - e^{-k_1 t}) \tag{18}$$

$$\overline{\Delta b^2} = a_0 \frac{k_1}{k_1 - k_2} (e^{-k_2 t} - e^{-k_1 t}) \left[1 - \frac{k_1}{k_1 - k_2} (e^{-k_2 t} - e^{-k_1 t}) \right] \tag{18'}$$

$$\overline{\Delta c^2} = a_0 \frac{k_1 e^{-k_2 t} - k_2 e^{-k_1 t}}{k_1 - k_2} \left(1 - \frac{k_1 e^{-k_2 t} - k_2 e^{-k_1 t}}{k_1 - k_2} \right) \tag{18''}$$

$$\rho_{AB} = -\sqrt{\frac{e^{-k_1 t}}{1 - e^{-k_1 t}} \cdot \frac{e^{-k_2 t} - e^{-k_1 t}}{1 - \dfrac{k_1}{k_2} + e^{-k_1 t} - e^{-k_2 t}}} \tag{19}$$

$$\rho_{AC} = -\sqrt{\frac{e^{-k_1 t}}{1 - e^{-k_1 t}} \cdot \frac{k_1 (1 - e^{-k_2 t}) - k_2 (1 - e^{-k_1 t})}{k_1 e^{-k_2 t} - k_2 e^{-k_1 t}}} \tag{19'}$$

$$\rho_{BC} = -\sqrt{\frac{e^{-k_2 t} - e^{-k_1 t}}{1 - \dfrac{k_2}{k_1} + e^{-k_1 t} - e^{-k_2 t}} \cdot \frac{k_1 (1 - e^{-k_2 t}) - k_2 (1 - e^{-k_2 t})}{k_1 e^{-k_2 t} - k_2 e^{-k_2 t}}} \tag{19''}$$

From the analysis of equations (19) – (19″) it follows that :

1) ρ_{AB} has initially the value -1 and then as time passes it increases taking finally the value o

2) ρ_{AC} has initially the value o, then decreases, passes through a minimum and then increases again, taking finally the value o (if $k_1 \geqslant k_2$) or $-\sqrt{1 - \dfrac{k_1}{k_2}}$ (if $k_1 \geqslant k_2$)

3) ρ_{BC} has initially the value o and then, as time passes it decreases taking finally the value -1 (if $k_1 \geqslant k_2$) or $-\sqrt{\dfrac{k_1}{k_2}}$ (if $k_1 < k_2$)

In order to determine the probability $P(\boldsymbol{N}, t)$ we shall develop the expression (10) according to the multinominal formula :

$$G = \sum_{\substack{\forall b_{\lambda i}\ \lambda,\ i=1,\ldots,n \\ \sum\limits_{\lambda} b_{\lambda i} = N_{0i}}} \left(\prod_i N_{0i}!\right) \left(\prod_{\lambda} s_{\lambda}^{\sum\limits_i b_{\lambda i}}\right) \prod_{i,\lambda} \frac{\eta_{\lambda i}^{b_{\lambda i}}}{b_{\lambda i}!} =$$

$$= \sum_{\forall \boldsymbol{N} \geqslant 0} \prod_{\lambda} s_{\lambda}^{N_{\lambda}} \left(\sum_{\substack{\forall b_{\lambda i}\ \lambda,\ i=1,\ldots,n \\ \sum\limits_{\lambda} b_{\lambda i} = N_{0i}\ \sum\limits_{i} b_{\lambda i} = N_{\lambda}}} \left(\prod_i N_{0i}!\right) \prod_{i,\lambda} \frac{\eta_{\lambda i}^{b_{\lambda i}}}{b_{\lambda i}!} \right) \tag{20}$$

Comparing equations (5) and (20) it follows that :

$$\mathrm{P}\,(\boldsymbol{N}, \mathrm{t}) = \sum_{\substack{\forall b_{\lambda i} \geqslant 0 \quad \lambda,\, i=1,\ldots,n \\ \sum_{\lambda} b_{\lambda i} = N_{0i};\ \sum_{i} b_{\lambda i} = N_{\lambda}}} \left(\prod_i N_{0i}\,!\right) \prod_{i,\lambda} \frac{\eta_{\lambda i}^{b_{\lambda i}}}{b_{\lambda i}\,!} \tag{20'}$$

For $P(\mathrm{N}, t)$ we can easily get an approximate convenient expression. As $\forall N_{0i} \gg 1$, we have :

$$G = \prod_i \left[1 + \sum_j \eta_{ji}\,(t)\,(s_j - 1)\right]^{N_{0i}} \cong \prod_i \exp\left[\sum_j \eta_{ji}\,(t)\,(s_j - 1)\right] =$$

$$= \exp\left[\sum_j \bar{N}_j\,(s_{.} - 1)\right] = \sum_{\forall N_u \geqslant 0} \left(\prod_u s_u^{N_u}\right) \prod_u \left(\frac{\bar{N}_u^{N_u}}{N_u\,!}\,\mathrm{e}^{-\bar{N}_u}\right)$$

and then

$$P(\boldsymbol{N},\ t) \cong \prod_u \left(\frac{N_u^{N_u}}{N_u\,!}\,\mathrm{e}^{-\bar{N}_u}\right) \tag{21}$$

For small fluctuations equation (21) becomes :

$$P(\boldsymbol{N},\ t) \cong \frac{1}{\prod_u \sqrt{2\pi N_u}} \exp\left[-\sum_u \frac{(N_u - \bar{N}_u)^2}{2\bar{N}_u}\right] \tag{21}$$

From (21′) we can notice that $P(\vec{\mathrm{N}}, t)$ follows approximately a normal n-dimensional law with :

$$\overline{N_u^2} = \bar{N}_u \ (14') \quad \overline{N_u\,N_v} = 0 \ (u \neq v) \ (17'').$$

Comparing equations (14) and (17′) with (14′) and (17″) we see that the use of equation (21′) involves the neglecting of the terms $\eta_{\lambda i} \times \eta_{\mu i}$ $\lambda, \mu = 1, \ldots, n$. Equation (21′) proves that the quantities $\bar{N}_u(t)$ are both the mean values and the most probable values of the molecule numbers N_u.

Expression (21′) allows us to find an approximate formula for the magnitude of the indetermination of the values of concentrations of all substances present in system, that is an approximate formula for the *informational entropy*. It follows that :

$$H(t) = -(\log_2 \mathrm{e}) \sum_{\forall \boldsymbol{N} \geqslant 0} P(\boldsymbol{N}\ t),\ \ln P(\boldsymbol{N}, t) \cong$$

$$\cong +\,(\log_2 \mathrm{e}) \int \cdots \int P(\mathbf{N}, t) \ln\left(P(\boldsymbol{N}, t) \prod_i \Delta N_i\right) \mathrm{d}N_1 \ldots \mathrm{d}N_n{}^{*)}$$

$$= \frac{1}{\ln 2} \sum_i \ln\left(\sqrt{\frac{2\pi \bar{N}_i\ \mathrm{e}}{\Delta N_i}}\right)$$

---

* For the integral calculus see the foot note from page 669.

For $\forall\ \Delta N_i = 1$ we have :

$$H(t) = \frac{n(1 + \ln 2\pi) + \sum_i \ln \bar{N}_i}{2 \ln 2} \tag{22}$$

From equation (22) it follows that if at least one of the quantities $\bar{N}_i$ vanishes (that can happen only at the beginning or at the end of the reaction, when $t = 0$ or $t = \infty$) then $H = -\infty$. This fact is contradictory to one of the fundamental features of the informational entropy which states that $H(t) \geqslant 0$. This non-concordance is given by the fact that in calculations we have made continuous the variables N_i. For values pretty remote from the extremities ($t = 0, \infty$), we can consider that formula (22) gives the correct value of the entropy. At the beginning of the reaction ($t = 0$) the indetermination is inexistent. The entropy increases further on. The existence of a maximum is also possible, after which the entropy decreases. At the moment t_M, corresponding to the maximum, the indetermination of the values of all concentrations on the whole is maximum. By solving the equation :

$$\frac{\mathrm{d}H(t)}{\mathrm{d}t} = \frac{1}{2 \ln 2} \sum_u \frac{1}{N_u(t)} \cdot \frac{\mathrm{d}N_u(t)}{\mathrm{d}t} = 0$$

it is possible to get the t_M value.

In order to establish the validity field of the equation (22) we consider the first order reaction. $A \xrightarrow{k} B$ with $\vec{N}_0 = \begin{pmatrix} \mathrm{a}_0 \\ 0 \end{pmatrix}$. From equation (22) we get :

$$H(t) = \frac{1 + \ln(2\pi) + \ln[\mathrm{a}_0\, x(1 - x)]}{\ln 2} \quad (x = \mathrm{e}^{-kt})$$

In order to determine the validity of this formula we shall look for the values of the time which cancel the expression of H. It follows that :

$$H(t) = 0 \Leftrightarrow = x^2 - x - 1/2\mathrm{e}a_0 = 0\,;\ x_{1.2} = \frac{1}{2}\left(1 \pm \sqrt{1 - \frac{2}{2\pi a_0}}\right)$$

As $\mathrm{a}_0 \gg 1$, $\frac{2}{2\pi a_0} \ll 1$ the square root can be approximately determined by the expansion in series and subsequent holding of the first term. Therefore :

$$\sqrt{1 - \frac{2}{2\pi a_0}} \cong 1 - 1/2\mathrm{e}\pi a_0$$

so that:

$$x_1 = 1 - 1/2e\pi a_0, \quad x_2 = 1/2e\pi a_0$$

Hence

$$(\mathrm{kt})_1 = -\ln(1 - 1/2e\pi a_0) \cong 1/2e\pi a_0, \quad (\mathrm{kt})_2 = \ln(2e\pi a_0)$$

Taking the half life period as a time unit and $a_0 \cong 10^{12}$ we get:

$$\frac{t_1}{T_{1/2}} = \frac{1}{2e\pi a_0 \ln 2} = 8.5\times10^{-12}, \quad \frac{t_2}{T_{1/2}} = \frac{\ln(2e\pi a_0)}{\ln 2} = 44$$

In the first case it is a matter of a value practically inaccessible to measurements and which can be considered 0. In the second case, after 44 half-life periods the reaction has almost completely taken place and therefore we can consider that $t_2 = \infty$. Generalizing this, it follows that equation (22) is practically valid throughout all the time values accessible to measurements.

In the above considered case, the entropy passes only through one maximum point at the time t_M given by the equation:

$$\frac{\mathrm{d}H}{\mathrm{d}t} = -k\,\frac{1-2x}{1-x} = 0$$

and therefore $t_M = T_{1/2}$

We can notice that t_M is the same, as the time to which the mean square deviation of the number of molecules A from the value included in the deterministic model has a maximum value.[1]

The value of the entropy, corresponding to the moment t_M is equal to

$$H(t = T_{1/2}) = 42 \text{ bits}$$

C. CONCLUSIONS

Throughout this paper, we have calculated (for a network of first order reactions) the probability that at a given moment, the system should be characterized by a certain vector of composition. We have shown that the value of the composition vector which resulted from the deterministic model is both the mean value of the random vector **N** and the most probable value. We have also calculated the mean square deviation from the most probable value of composition vector, the coefficients of the correlation between the constituents of the composition vector, and the informational entropy associated to the field of events. The obtained results can be applied to a great number of particular cases.

Revue Roumaine de Chimie, **21**, 5, 677–681 (1976)

ON THE FREQUENCY OF REACTION EVENTS IN A SYSTEM WITH FIRST ORDER REACTION NETWORK

MARCEL VLAD

Bucharest Polytechnic Institute, Chemistry Institute, Department of Physical Chemistry
and Electrochemical Technology, Bd. Republicii 13

Received May 22, 1975

This work presents a computation method of generating function of the reaction events probability in a system with first order reaction network. The mean values and variances of reaction events were also determined.

Recently, Šolc discussed the problem of determining the reaction events probability distribution and solved it in the case of the reaction $A \rightleftharpoons B$.[1] Our intention is to extend this analysis to the case of a certain first order reaction network.

Let us take the reactions:

$$A_i \underset{k_{ji}}{\overset{k_{ij}}{\rightleftharpoons}} A_j \quad n \geqslant j > i \geqslant 1 \tag{1}$$

For the reaction network (1) we want to determine the probability $P(\boldsymbol{N}, \boldsymbol{\beta}, t)$ $(\boldsymbol{N} = (N_i)\,;\ \boldsymbol{\beta} = \|\beta_{ij}\|\ i, j = 1, \ldots, n)$ as N_i molecules $A_i (i = 1, \ldots, n)$ should exist at a given moment in the system and as the number of reaction events $A_i \to A_j$ that have taken place up to that moment should be $\beta_{ij}(i, j = 1, \ldots, n (i \neq j))$. In order to achieve this, we shall make use of the standard method of the stochastic theory.[2] It follows that:

$$\frac{\partial P}{\partial t} = \sum_i \sum_{j \neq i} k_{ij}[(N_i + 1)\, P(N_i + 1, N_j - 1,\ \beta_{ij} - 1) - N_i P] \tag{2}$$

Introducing the generating function:

$$G_{(\boldsymbol{s}, \boldsymbol{h}, t)} = \sum_{\forall N_i\ \beta_{ij} \geqslant 0} \prod_i s_i^{N_i} \prod_{i,j} h_{ij}^{\beta_{ij}} P(\boldsymbol{N}, \boldsymbol{\beta}, t) \quad (\forall\, |s_i|,\ |h_{ij}| \leqslant 1) \tag{3}$$

---

[1] M. Šolc, *Z. phys. Chem. (Frankfurt)*, **83**, 64 (1973); **92**, 1 (1974).

[2] D. A. Mc. Quarrie, *J. Appl. Prob.*, **4**, 413 (1967); *Adv. Chem. Phys.*, **50**, 460 (1969).

the equation (2) becomes:

$$\frac{\partial G}{\partial t} = \sum_i \sum_{i \neq j} k_{ij}(h_{ij}\, s_j - s_i)\, \frac{\partial G}{\partial s_i} \cdot \tag{4}$$

The characteristic system attached to the equation with partial derivatives (4) is the following:

$$\frac{d\boldsymbol{S}}{dt} = \boldsymbol{R}(\boldsymbol{h})\, \boldsymbol{S} \tag{5}$$

where $\boldsymbol{R} = \| R_{ij} \|$ $R_{ij} = h_{ij}\, k_{ij}(i \neq j)$; $R_{ii} = -\sum_{j \neq i} k_{ji} = k_{ii}$

The solution of the matrix differential equation (5) which fulfils the initial condition $\boldsymbol{S}_{(t=0)} = \boldsymbol{S}_0$ is the following [3]:

$$\mathbf{S} = \overset{\times}{\widetilde{\boldsymbol{Z}}}(\hat{\boldsymbol{h}}, t)\, \mathbf{S}_0^{*)} \qquad \text{where } \overset{\times}{\boldsymbol{Z}}(\boldsymbol{h}, t) \overset{\Delta}{=} \| \overset{\times}{\eta}_{ij}(t) \| = \exp(\widetilde{\boldsymbol{R}} t) \tag{6}$$

As: $P(\boldsymbol{N}, \boldsymbol{\beta}, 0) = \begin{cases} 1 \text{ if } \boldsymbol{N} = \boldsymbol{N}_0 \text{ and } \boldsymbol{\beta} = \boldsymbol{0} \\ 0 \text{ if } \boldsymbol{N} \neq \boldsymbol{N}_0 \text{ or } \boldsymbol{\beta} \neq \boldsymbol{0} \end{cases}$ it turns out that:

$$G(t = 0) = \prod_i s_i^{N_{oi}} \tag{7}$$

From (6) and (7) it follows that the solution of the equation (4) which fulfils the condition (7) is:

$$G = \prod_i \Big(\sum_j \eta_{ji \times}(t)\, S_j \Big)^{N_{oi}} \tag{8}$$

The probability distribution $E(\boldsymbol{\beta}, t)$ of the reaction events is given by:

$$E(\boldsymbol{\beta}, t) = \sum_{\forall N_i \geqslant 0} P(\boldsymbol{N}, \boldsymbol{\beta}, t) \tag{9}$$

and then:

$$F(\boldsymbol{h}, t) = \boldsymbol{G}(\forall s_i = 1, \boldsymbol{h}, t) = \prod_i \Big(\sum_i \overset{\times}{\eta}_{ji(t)} \Big)^{N_{oi}} \tag{9'}$$

where $F(\boldsymbol{h}, t)$ is the generating function of the probability $E(\boldsymbol{\beta}, t)$.

---

* ~ is the sign for the act of a matrix transposing.

[3] R. Bellman, "Introduction to Matrix Analysis", Mc. Graw-Hill, New York, 1960

To determine the first and second order moments of reaction events with the help of the equation (9′) the derivatives $\left(\frac{\partial \eta_{ij}^{\times}}{\partial h_{uv}}\right)_{\forall h_{ij}=1}$ and $\left(\frac{\partial^2 \eta_{ij}^{\times}}{\partial h_{uv}\,\partial h_{\omega uv}}\right)_{\forall h_{ij}=1}$ have to be known. In order to calculate these derivatives we shall expand the matrix $\boldsymbol{Z}^{\times}$ with a perturbational method.[3] The matrix $\boldsymbol{Z}^{\times +}$ verifies the equation:

$$\frac{\mathrm{d}\boldsymbol{Z}^{\times}}{\mathrm{d}t} = \boldsymbol{KZ}^{\times} + \hat{B}\hat{Z}^{+} \quad \text{whith } \boldsymbol{Z}^{\times}(0) = \boldsymbol{I} \tag{10}$$

where $\boldsymbol{K} = \| k_{ji} \|$; $i, j = 1, \ldots, n$ and $\boldsymbol{B} = \widetilde{\boldsymbol{R}} - \boldsymbol{K}$

Supposing the term $\boldsymbol{BZ}^{\times}$ already known, from (10) we obtain:

$$\boldsymbol{Z}^{\times}(t) = \boldsymbol{Z}(t) + \int_0^t \boldsymbol{Z}(t-\lambda)\,\boldsymbol{BZ}(\lambda)\,\mathrm{d}\lambda \tag{11}$$

where $\boldsymbol{Z} = \| \eta_{ij} \| = \exp(\boldsymbol{K}t)$ is the kinetic matrix.[4] (11) is a Volterra matrix integral equation of the second kind. Its solution is:

$$\begin{aligned}\boldsymbol{Z}^{\times}(h, t) = \boldsymbol{Z}(t) &+ \int_0^t \boldsymbol{Z}(t-\lambda)\,\boldsymbol{BZ}(\lambda)\,\mathrm{d}\lambda + \\ &+ \int_0^t\!\!\int_0^\lambda \boldsymbol{Z}(t-\lambda)\,\boldsymbol{BZ}(\lambda-\mu)\,\boldsymbol{BZ}(\mu)\,\mathrm{d}\lambda\mathrm{d}\mu + \ldots\end{aligned} \tag{12}$$

Determining the derivative values from the equation (12) we have:

$$\left(\frac{\partial \eta_{ij}^{\times}}{\partial h_{uv}}\right)_{\forall h_{ij}=1} = k_{uv}\int_0^t \eta_{iu}(t-\eta)\,\eta_{vj}(\lambda)\,\mathrm{d}\lambda \tag{13}$$

$$\begin{aligned}\left(\frac{\partial^2 \eta_{ij}^{\times}}{\partial h_{uv}\,\partial h_{\omega u}}\right)_{\forall h_{ij}=1} &= k_{uv}\,k_{\omega u}\int_0^t\!\!\int_0^\lambda (\eta_{iu})\,t-\lambda)\,\eta_{v\omega}\,(\lambda-\mu)\,\eta_{wj}\,(\mu) + \\ &+ \eta_{i\omega}(t-\lambda)\,\eta_{wu}\,(\lambda-\mu)\,\eta_{vj}(\mu))\,\mathrm{d}\lambda\,\mathrm{d}\mu\end{aligned} \tag{13'}$$

With the help of the equation (9′), (13), (13′) and $\sum_j \eta_{ji} = 1$ we get:

$$\overline{\beta}_{uv}(t) = \left(\frac{\partial E}{\partial h_{uv}}\right)_{\forall h_{ij}=1} = k_{uv}\sum_i \int_0^t \eta_{ui}(\lambda)\,N_{0i}\,\mathrm{d}\lambda \tag{14}$$

---

[4] L. M. PISMEN and I. I. IOFFE, *Kinetika i Kataliz*, **2**, 606 (1961).

$$\overline{\beta_{uv}\,\beta_{\omega w}}\,(t)=\left(\frac{\partial^2 E}{\partial h_{uv}\,\partial h_{\omega w}}\right)_{\forall h_{ij}=1}+\delta_{u\omega}\,\delta_{wv}\left(\frac{\partial E}{\partial h_{uv}}\right)_{\forall h_{ij}=0}=\overline{\beta}_{uv}(t)\,\overline{\beta}_{\omega w}\,(t)+$$

$$+\,\delta_{u\omega}\,\overline{\delta}_{vw}\,\beta_{uv}\,(t)+k_{uv}\,k_{w\omega}\sum_i N_{0i}\left[\int_0^t\!\!\int_0^\lambda(\eta_{v\omega}(\lambda-\mu)\,\eta_{wi}(\mu)+\right. \qquad (14')$$

$$\left.+\,\eta_{wu}(\lambda-\mu)\,\eta_{vi}\,(\mu))\,\mathrm{d}\lambda\,\mathrm{d}\mu-\int_0^t\!\!\int_0^t\eta_{wi}(\lambda)\,\eta_{vi}(\mu)\,\mathrm{d}\lambda\,\mathrm{d}\mu\right]$$

Hence:

$$\overline{\Delta\beta_{uv}^2}(t)=\overline{\beta}_{uv}(t)+k_{uv}^2\sum_i N_{0i}\left[2\int_0^t\!\!\int_0^\lambda\eta_{vu}(\lambda-\mu)\,\eta_{vi}(\mu)\,\mathrm{d}\lambda\,\mathrm{d}\mu-\left(\int_0^t\eta_{vi}(\lambda)\,\mathrm{d}\lambda\right)^2\right] \qquad (15)$$

$$\mathrm{cov}(\beta_{uv},\,\beta_{\omega w})=k_{uv}\,k_{\omega w}\sum_i N_{0i}\left[\int_0^t\!\!\int_0^\lambda(\eta_{v\omega}(\lambda-\mu)\,\eta_{vi}\,(\mu)+\right. \qquad (15'),$$

$$\left.+\,\eta_{wu}\,(\lambda-\mu)\,\eta_{vi}\,(\mu))\,\mathrm{d}\lambda\mathrm{d}\mu-\int_0^t\!\!\int_0^t\eta_{vi}\,(\lambda)\,\eta_{wi}\,(\mu)\,\mathrm{d}\lambda\,\mathrm{d}\mu\right]$$

For $E(\boldsymbol{\beta}, t)$ we can easily find an approximate expression. As $N_{0i} \gg 1$, we can consider that:

$$F(\boldsymbol{h},t)\cong\prod_i\left[1+\sum_j\sum_{u,v\neq u}(h_{uv}-1)\left(\frac{\partial\eta_{ji}^{\times}}{\partial h_{uv}}\right)_{hij=1}\right]^{N_{0i}}\cong\exp\left[\sum_{i,j}\sum_{u,v\neq u}(h_{uv}-1)\cdot\right.$$

$$\left.\cdot\left(\frac{\partial\eta_{ji}^{\times}}{\partial h_{uv}}\right)_{h_{ij}=1}^{N_{0i}}\right]=\exp\left(\sum_{u,v\neq u}\overline{\beta}_{uv}\,(h_{uv}-1)\right)=\sum_{\forall\beta_{uv}\geqslant0}\prod_{u,v\neq u}h_u^{\beta_{uv}}\prod_{u,v\neq u}\left(\mathrm{e}^{-\overline{\beta}_{uv}}\,\frac{\overline{\beta}_{uv}^{\beta_{uv}}}{\beta_{uv}\,!}\right)$$

Hence:

$$E(\beta,t)\cong\prod_{u,v\neq u}\left(\mathrm{e}^{-\overline{\beta}_{uv}}\,\frac{\overline{\beta}_{uv}^{\beta_{uv}}}{\beta_{uv}\,!}\right) \qquad (16)$$

For small fluctuations the formula (16) becomes:

$$E(\beta,t)\cong\frac{1}{(2\pi)^{n'/2}\sqrt{\prod\limits_{u,v\neq u}\overline{\beta}_{uv}}}\exp\left[-\sum_{u,v\neq u}\frac{(\beta_{uv}-\overline{\beta}_{uv})^2}{2\overline{\beta}_{uv}}\right](n'=n(n-1)) \qquad (16')$$

The probability distribution, mean value and variance of the quantity $\beta=\sum\limits_{u,v\neq u}\beta_{uv}$ are given by:

$$E_1(\beta,t)=\sum_{\substack{\forall\beta_{uv}\geqslant0,\,\beta=\sum\beta_{uv}\\ u,v\neq u}}E(\boldsymbol{\beta},t) \qquad (17)$$

$$\beta(t)=\sum_{u,\,v\neq u}\beta_{uv}(t) \qquad (18)$$

$$\overline{\Delta\beta^2}(t) = \sum_{u,\, v\neq u} \overline{\Delta\beta^2_{uv}}(t) + \sum_{u, v\neq u} \; \sum_{\omega\neq u,\, w\neq\omega} \mathrm{cov}(\beta_{uv},\ \beta_{\omega w}) \tag{19}$$

and then

$$F_1(h, t) = \sum_{\forall\beta\geqslant 0} h^{\beta} E_1(\beta, t) = F(\forall h_{ij} = h, t) \tag{17'}$$

Using the same method as for $E(\boldsymbol{\beta}, t)$ we get :

$$E_1(\beta, t) \cong \mathrm{e}^{-\bar{\beta}} \frac{\bar{\beta}^{\beta}}{\beta!} \tag{20}$$

For small fluctuations, the equation (20) is equivalent to :

$$E_1(\beta, t) \cong \frac{1}{\sqrt{2\pi\bar{\beta}}} \exp\left[-\frac{(\beta-\bar{\beta})^2}{2\bar{\beta}}\right] \tag{20'}$$

In the particular case of the equilibrium $A \underset{k_2}{\overset{k_1}{\rightleftharpoons}} B$ for which :

$$\mathbf{Z}(t) = \begin{bmatrix} \dfrac{1+Ke^{-kt}}{K+1} & \dfrac{1-e^{-kt}}{K+1} \\ \\ \dfrac{K(1-e^{-kt})}{K+1} & \dfrac{K+e^{-kt}}{K+1} \end{bmatrix}; \ \mathbf{N_0} = \begin{bmatrix} N_0 \\ 0 \end{bmatrix}\left(k = k_1 + k_2\,;\ K = \frac{k_1}{k_2}\right)$$

by using the equations (17′), (18) and (19) we get :

$$F_1(h,t) = \exp\left(-\frac{kN_0 t}{2}\right)\left[\cos h\,(\alpha kt) + \frac{2Kh - K + 1}{2}\sin h\,(\alpha kt)\right]^{N_0} \tag{17''}$$

where $\alpha = \dfrac{\sqrt{(K-1)^2 + 4\,Kh^2}}{2(K+1)}$.

$$\bar{\beta}(t) = \frac{N_0\,!}{(K+1)^2}\left[2\,kt + \frac{(K-1)\,K}{K+1}(1 - e^{-kt})\right] \tag{18'}$$

$$\overline{\Delta\beta^2}(t) = \frac{N_0 K}{(K+1)^4}\,[4(K^2+1)\,kt - 4(K-1)\,(2K-1)\,(1-e^{-kt}) +$$
$$+ (K-1)^2\,(1+Ke^{-kt})\,(1-e^{-kt}) + 8\,K(K-1)\,kte^{-kt}] \tag{19''}$$

Similar results were found by M. Šolc by applying a different approach.[1]

ACKNOWLEDGEMENT : The author is grateful to professor Eugen Segal for his help in elaborating the present paper.

Revue Roumaine de Chimie, **21**, *5*, 683 – 694 (1976)

EXPERIMENTAL APPROACH TO THE CHARACTERIZATION OF PRETREATED ELECTRODE SURFACES. VI*

CHRONOPOTENTIOMETRIC STUDY OF DIFFERENTLY PRETREATED GOLD ELECTRODES

A. POPESCU** and L. KÉKEDY***
** Faculty of Chemistry, University of Craiova, Craiova, Romania
*** Department of Analytical Chemistry, "Babeş-Bolyai" University, Cluj-Napoca, Romania

Received October 4, 1974

Constant current cathodic and anodic chronopotentiograms of differently pretreated gold electrodes are given, recorded in different solutions as information for characterization of the surfaces obtained. Several pretreatment procedures have been investigated. Cathodization, soaking in $FeSO_4$, cc. HCl, H_2O_2 and KCN eliminate the oxide film (reducing effect). Anodization or soaking in cc. HNO_3, $K_2Cr_2O_7$ or $KMnO_4$ have oxidative effect. The corresponding total Q_c and Q_a values respectively have been calculated. The surface state of the electrodes are determined not only by the presence or absence of oxide film but also by their physical properties.

The role of surface state of solid electrodes in electrochemistry is well recognized now. The main attention has been directed to platinum, other solids being less investigated. Recently zero current bipotentiometric titration curves obtained with differently pretreated electrodes showed considerable pretreatment effects of gold,[1] with real possibilities of analytical exploration. The surface state of gold electrodes has been investigated mainly by charging curve techniques [2]; oxygen adsorption and Au_2O_3 formation being registered (at $E \simeq 1{,}36$ volts). Recently different forms of adsorbed oxygen on Au could be differentiated, depending on the duration of contact and on the anions present in solution.[3-7]

---

*Part V: L. Kékedy and S. Duşa, *Stud. Univ. Babeş-Bolyai, Chem.*, **18**, 65 (1973).

[1] L. Kékedy and A. Popescu, *Talanta*, **22**, 135 (1975).
[2] J. P. Hoare, "The Electrochemistry of Oxygen", Interscience, New York, 1968, p. 48.
[3] R. A. Bonewitz, *J. Electrochem. Soc.*, **116**, C, 78 (1969).
[4] R. A. Bonewitz and G. M. Schmid, J. Electrochem. Soc., **117**, 1367 (1970).
[5] S. Vasina and O. A. Petrii, *Elektrokhimiya*, **6**, 242 (1970).
[6] J. W. Schultze and K. J. Vetter, *Ber. Bunsengesellschaft Phys. Chem.*, **75**, 470 (1971).
[7] M. G. Goldstein, I. I. Zalkind and B. I. Veselovskii, *Elektrokhimiya*, **8**, 606 (1972) and **9**, 699 (1973).

In contrast to platinum, gold dissolves neither oxygen, nor hydrogen and the Au_2O_3 oxide film is better ionic than electronic conductor, capable of multilayer formation. The aim of this paper is to contribute to the characterization of gold surfaces subjected to pretreatments not mentioned in the literature, as well as to complete the existing data.

EXPERIMENTAL

Conventional constant current chronopotentiometry has been used as a means of characterization. Apparatus and experimental details were the same as previously described.[8] The working electrode consisted of a rectangular 0.5 mm thick gold plate with an apparent geometric area of 2 cm². The chronopotentiograms were run in oxygen-free acid (0.1 N $HClO_4$), neutral (0.1 N $NaClO_4$) and alkaline (0.1 N NaOH) solutions. The effect of the following pretreatment procedures has been investigated: A. Electrochemical; a) anodization till O_2 evolution, b) cathodization till H_2 evolution. B. Chemical. a) Treatment with oxidizing agents: conc. HNO_3, aqua regia, 1 N $KMnO_4$ (acidified with H_2SO_4), 1 N $K_2Cr_2O_7$ (acidified), 30% H_2O_2 (acidified); b) Treatment with reducing agents: 1 N $FeSO_4$ (acidified); c) Treatment with conc. HCl in order to eliminate the oxide film (to obtain so called bare electrode)[8]; d) Treatment with 1 N KCN in order to try to poison the electrode. The chemical treatment consisted in dipping the electrode in the respective solution for a minute, followed by a thorough washing with doubly distilled water. C. Thermal: heating of the electrode for 30 seconds in a colourless Teclu-flame (natural methane gas).

RESULTS AND DISCUSSIONS

A. Cathodic chronopotentiograms recorded in 0.1 N $HClO_4$ solution are given in Fig. 1. Previously cathodized (reduced) electrodes, or those treated with H_2O_2 exhibit cathodic chronopoten tiograms (Fig. 1,

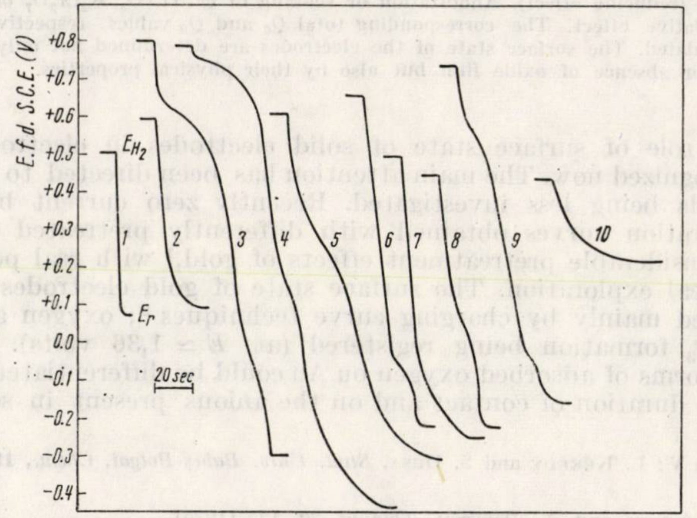

Fig. 1. — Cathodic chronopotentiograms of differently pretreated gold surfaces in 0.1 N $HClO_4$. Pretreatments:
1. cathodization (H_2 evolution); *2.* 30% H_2O_2 + H_2SO_4; *3.* $K_2Cr_2O_7$; *4.* $KMnO_4$; *5.* cc. HNO_3; *6.* cc. HCl; *7.* $FeSO_4$; *8.* KCN; *9.* aqua regia; *10.* heating. $i = 50\,\mu A$.

---

[8] L. Kékedy and F. Makkay, *Rev. Roumaine Chim.*, **13**, 739 (1968).

curves 1 and 2) characterized by the absence of any reduction process indicating that the surfaces investigated were reduced ones, i.e. free of oxide layers. Treatment with H_2O_2 in all cases yielded a reduced electrode having a rest potential somewhat higher than a cathodized one, indicating the presence of traces of oxygen on the electrode surface. The fact that the reduced electrodes obtained by cathodization were not identical with those obtained by treatment with H_2O_2 appeared when the chronopotentiograms were repeated after the first run, but without repeating the pretreatment (see Fig. 4). Pretreatment with cc. HCl, $FeSO_4$ or with KCN also yields reduced surfaces i.e. free of oxide film (curves 6,7 and 8, Fig. 1). The waves appearing at negative potentials probably are due to the adsorption of Cl^-, Fe^{2+} or CN^- ions repectively, and disappear on repeating the cathodic chronopotentiograms (Fig. 4, curves 6, 7 and 8). Oxidized surfaces are characterized by a reduction wave (curves 3, 4, 5 and 8, Fig. 1). The waves appear at different potentials depending on the oxidative pretreatment used. The corresponding values show that $KMnO_4$ produced the most oxidized surface and aqua regia the least, owing to the oxide film solving property of its HCl content. Generally chemical oxidation yielded poorly reproductible surfaces. The greatest H^+-ion discharge overpotential could be observed on these, initially oxidized surfaces. On standing, the oxidized surfaces gradually lose their oxide content, manifested in the decrease of the transition time of the corresponding reduction wave. This indicates the instability of the oxide layers in acid medium, observed by others too.[7] The reduction wave usually increases with the duration of the pretreatment and decreases with prolonged washing. Heated electrodes showed a charac-

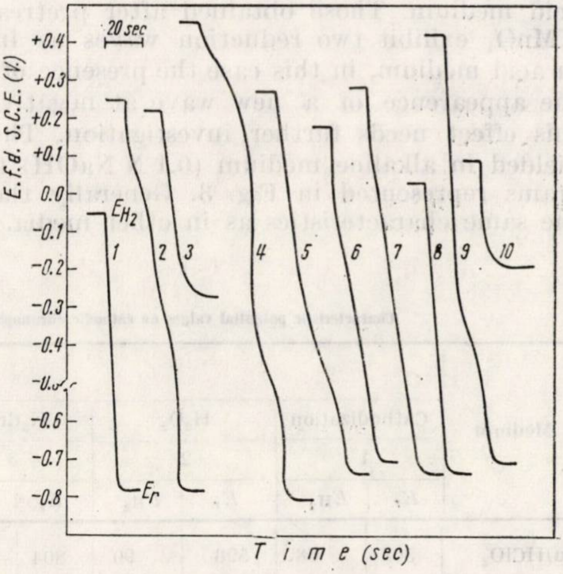

Fig. 2. — Cathodic chronopotentiograms of gold electrodes in 0.1 N $NaClO_4$. Pretreatments : *1.* cathodization (H_2 evolution) ; *2.* $K_2Cr_2O_7$; *3.* 30% $H_2O_2 + H_2SO_4$; *4.* $KMnO_4$; *5.* cc. HNO_3 ; *6.* $FeSO_4$; *7.* cc.HCl ; *8.* KCN ; *9.* anodization (O_2 evolution) ; *10.* heating $i = 50\,\mu A$.

teristic chronopotentiogram (Fig. 1, curve 10). Both the initial low rest potential value and the absence of an oxide reduction wave indicate a very active non-oxidized surface on which the H^+ discharge takes place with considerable undepotential. The cathodic chronopotentiograms of differently pretreated gold electrodes recorded in neutral solution are similar to those obtained in acid solution (Fig. 2). The reduction wave of the oxidized surfaces appears at more negative potentials than in acid medium. Those obtained after pretreatment with $K_2Cr_2O_7$ and/or $KMnO_4$ exhibit two reduction waves as in the previous case. Unlike in acid medium, in this case the presence of Cl^- ions does not determine the appearence of a new wave at negative potentials. The nature of this effect needs further investigation. The pretreated gold electrodes yielded in alkaline medium (0.1 N NaOH) the cathodic chronopotentiograms represented in Fig. 3. Generally the chronopotentiograms have the same characteristics as in other media. The appearence of a reduc-

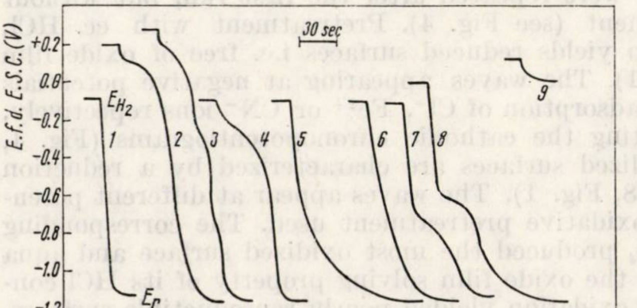

Fig. 3. — Cathodic chronopotentiograms of differently pretreated gold electrodes in 0.1 N NaOH. Pretreatments: *1.* cathodization (H_2 evolution); *2.* $K_2Cr_2O_7$; *3.* $KMnO_4$; *4.* $H_2O_2+H_2SO_4$; *5.* cc. HNO_3; *6.* aqua regia; *7.* cc. HCl; *8.* anodization(O_2 evolution); *9.* heating· $i = 50\,\mu A$.

Table

Characteristic potential values on cathodic chronopotentiograms in different media as a function of

Medium	Pretreatments									
	Cathodization		H_2O_2		$K_2Cr_2O_7$		$KMnO_4$		HNO_3 c.c.	
	1		2		3		4		5	
	E_r	E_{H_2}	E_r	E_{H_2}	E_r	E_{H_2}	E_r	E_{H_2}	E_r	E_{H_2}
$Au/HClO_4$	508	68	596	90	804	− 300	788	− 460	612	− 300
$Au/NaClO_4$	−50	− 780	220	− 270	250	− 780	450	− 810	270	− 740
Au/NaOH	−90	−1120	−100	−1160	190	−1180	230	−1180	−120	−1150

tion wave on curve 4, Fig. 3 (electrode pretreated with H_2O_2) is a new feature. Probably it is due to the reduction of adsorbed H_2O_2 which does not decompose rapidly in alkaline medium. Generally gold is known as a poor H_2O_2 decomposition catalyst. The presence of Cl^- ions determines the appearence of a characteristic wave encountered in acid medium too. Electrodes treated with $FeSO_4$ have a similar shape, due to strong Fe^{2+} adsorption (Fig. 7). — KCN yields also in this case a reduced surface. The heated electrode is a very active one (curve 9, Fig. 3).

Besides the differences in the behaviour of the pretreated electrodes in different media already mentioned, a shift of the initial rest potentials (E_r) and those of the final ones, corresponding to the H_2 evolution (E_{H_2}), (see Table 1) is also characteristic. The E_r and E_{H_2} potentials show considerable differences in function of the pretreatment applied shifting towards more negative values with the increase of the pH. Generally, in accordance with earlier observations more oxidized surfaces showed higher rest potentials. The theoretical potential shift corresponding to a variation of 12 pH units is round 700 mV practically exhibited by the electrode treated with H_2O_2. It is to be expected that this surface will be a good pH sensor. Similar behaviour was found at platinum too.[9] Other surfaces exhibited smaller potential variations except for those treated with cc. HNO_3 or aqua regia. The H_2 discharge potentials (E_{H_2}) also showed characteristic variations as a function of pretreatment and/or pH of the medium. The equilibrium values in our conditions were approximately -300 mV (pH $= 1$); -650 mV (pH $= 7$) and -1000 mV (pH $= 13$) (vs. SCE) respectively. Oxidized and bare surfaces (Table 1 columns 6, 7, 8) exhibited E_{H_2} potentials near these values, whereas on reduced surfaces the H_2 evolution in acid medium took place at more positive potentials (underpotential). Differences in E_{H_2} values as a function of pretreatment, observed in acid medium gradually disappear with the increase of pH, the E_{H_2} values at pH $= 13$ are the same regardless of the pretreatment applied. Considering the

1

pretreatment, E_r = rest potential; E_{H_2} = potential of hydrogen evolution

applied

HClc.c.		$FeSO_4$		KCN		Aqua regia		Heating		Anodization	
6		7		8		9		10		11	
E_r	E_{H_2}	E_r	E_{H_2}	E_r	E_{H_2}	E_r	E_{H_2}	E_r	E_{H_2}	E_r	E_{H_2}
660	− 220	500	− 252	450	− 220	740	− 156	440	220	—	—
280	− 740	180	− 710	30	− 740	—	—	90	190	420	− 710
−120	−1150	−120	−1110	−140	−1130	−120	−1150	120	30	−20	−1160

---

[9] L. Kékedy and L. Nemeș, *Studia Univ. Babeș-Bolyai Chem.*, **18**, 55 (1973).

poor reproducibility of the surfaces, the agreement of the observed potential values can be considered as acceptable. The heated electrodes proved to be the most active in this case too.

It is instructive to examine the characteristics of chronopotentiograms recorded immediately after those represented in Figs. 1—3, but without repeating the initial pretreatment. (Fig. 4). In these conditions all the curves in Fig. 4 represent the cathodic chronopotentiograms of electrochemically reduced surfaces (last pretreatment) having different last but one pretreatment. (indicated in Fig. 1.). The fact that different curves have been obtained reflect the effect of the last but one pretreatment observed at platinum too.[8] The curves do not reveal the existence of any significant oxide layer (being reduced during the first cathodization), the effect of last but one pretreatment manifesting in different initial rest potentials and mainly in the very striking differences in the hydrogen discharge potential (Table 2). This repeatead chronopotentiograms reveal e.g. that reduced electrodes obtained by cathodization are not identical with those treated with H_2O_2 (Fig. 4, curves 1,2). Never-

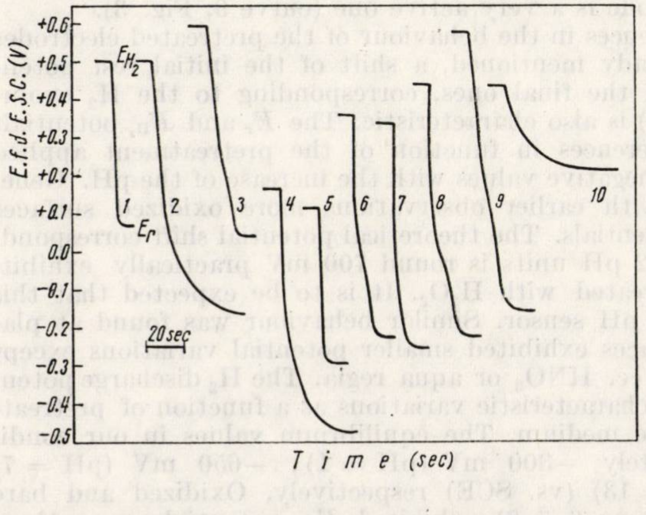

Fig. 4. — Cathodic chronopotentiograms of gold electrodes in 0.1 N $HClO_4$ taken immediately after those represented in Fig. 1, but without repeating the pretreatment. The initial pretreatments were the same as indicated in Fig. 1.

Table

Effect of the last but one pretreatment on cathodized gold electrodes

Medium	Pretreatments									
	Cathodization		H_2O_2		$K_2Cr_2O_7$		$KMnO_4$		HNO_3c.c.	
	1		2		3		4		5	
	E_r	E_{H_2}	E_r	E_{H_2}	E_r	E_{H_2}	E_r	E_{H_2}	E_r	E_{H_2}
Au/$HClO_4$	508	68	500	− 156	596	− 188	180	− 460	116	− 300
Au/$NaClO_4$	−50	− 780	− 40	− 750	− 20	− 780	− 10	− 770	10	− 720
Au/NaOH	−90	−1120	−100	−1160	−140	−1190	−180	−1100	−120	−1150

theless repetition of the cathodization several times, gradually reduces the differences which appear in Fig. 4, after a number of repetitions obtaining in all cases curves similar to curve 1, Fig. 1., characteristic to a reduced surface free of impurities. Like in the case of platinum, the initially heated electrode is an exception, it keeps its unusual properties even after several cathodizations indicating that heating has a long standing effect in the case of gold too.

B. The anodic chronopotentiograms of pretreated gold electrodes are also characteristic for the surfaces obtained. Differently pretreated electrodes in otherwise identical conditions as in the case of the cathodic ones gave in 0.1 N $HClO_4$ the chronopotentiograms represented in Fig. 5.

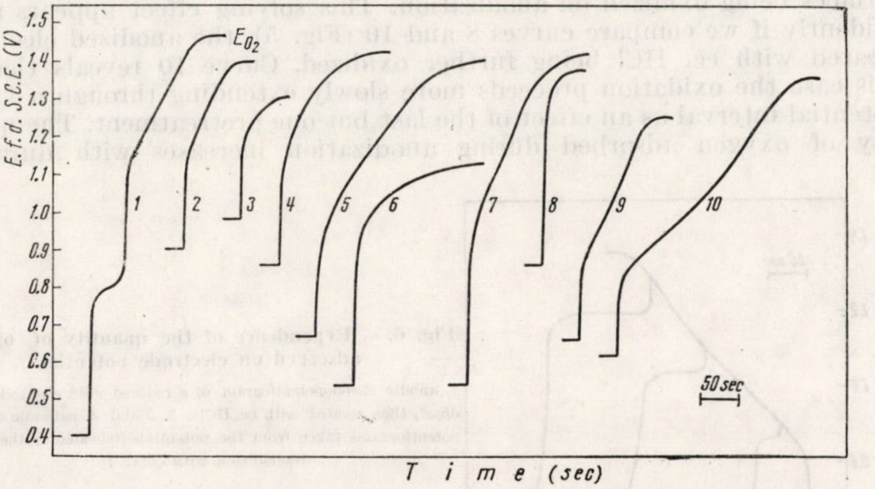

Fig. 5. — Anodic chronopotentiograms of differently pretreated gold surfaces in 0.1 N $HClO_4$. Pretreatments :

1. $FeSO_4$; *2.* $K_2Cr_2O_7$; *3.* $KMnO_4$; *4.* cc. HNO_3; *5.* H_2O_2 30% + H_2SO_4; *6.* cc. HCl; *7.* cathodization till H_2 evolution; *8.* anodization till O_2 evolution; *9.* KCN; *10.* anodization, then soaking in cc. HCl. $i = 50\,\mu A$.

If the electrode initially was anodized (oxidized electrochemically, curve 8, Fig. 5) its potential raised steeply up to the potential of oxygen evolu-

Characteristic cathodic chronopotentiograms as in Table 1

applied											
HClc.c.		$FeSO_4$		KCN		Aqua regia		Heating		Anodization	
6		7		8		9		10		11	
E_r	E_{H_2}	E_r	E_{H_2}	E_r	E_{H_2}	E_r	E_{H_2}	E_r	E_{H_2}	E_r	E_{H_2}
356	− 220	340	− 252	450	− 220	580	−156	440	220	—	—
30	− 740	30	− 740	30	740	—	—	90	190	70	− 710
−120	−1150	−120	−1100	−140	−1130	−120	−1150	120	30	−120	−1150

tion ($E_{O_2} \approx 1400$ mV vs. SCE). No oxidation wave appears. Ignited electrodes exhibit similar chronopotentiograms and approximately the same is true for chemically oxidized electrodes (curves 2, 3 and 4, Fig. 5). with the difference that on anodization a slight further oxidation can be noticed. This is more pronounced in the case of the electrodes previously oxidized with $K_2Cr_2O_7$ or cc. HNO_3 and less in the case of that pretreated with $KMnO_4$. This agrees with those stated in chapter A), namely that $KMnO_4$ produces the most oxidized surface. Initially reduced surfaces have lower rest potentials and on anodization they are oxidized, characteristic oxidation waves appearing on the corresponding chronopotentiograms (Fig. 5, curves 1, 5, 6, 7, 9, 10). It is evident that H_2O_2, cc. HCl and KCN have oxide film dissolving (reducing) effect, the respective surfaces being oxidized on anodization. This solving effect appears more evidently if we compare curves 8 and 10 (Fig. 5), the anodized electrode treated with cc. HCl being further oxidized. Curve 10 reveals that in this case the oxidation proceeds more slowly extending through a larger potential interval as an effect of the last but one pretreatment. The quantity of oxygen adsorbed during anodization increases with duration

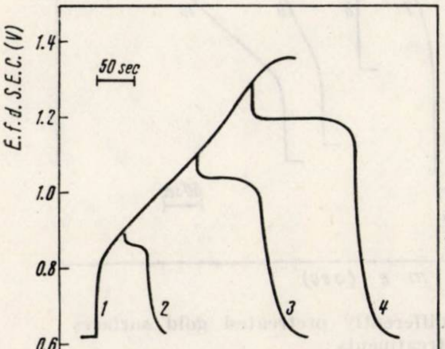

Fig. 6. — Dependence of the quantity of oxygen adsorbed on electrode potential.

1. anodic chronopotentiogram of a reduced gold electrode (anodized, then treated with cc. HCl); *2*, *3* and *4*. cathodic chronopotentiograms taken from the potentials indicated on the Figure (intersection with curve 1).

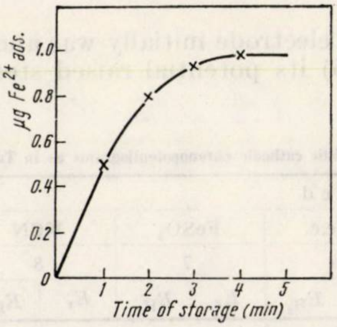

Fig. 7. — The quantitiy of Fe^{2+} ions adsorbed on gold during pretreatment with $FeSO_4$ as a function of the duration of the pretreatment. Calculated from subsequent anodic chonopotentiograms.

and/or electrode potential. Fig. 6. reveals that the higher the oxidation potential the greater is the quantity of oxygen found on subsequent cathodization. The electrode treated with $FeSO_4$ showed the lowest rest potential. Its anodic chronopotemtiogram showed a characteristic wave at +0.75 volts due to the oxidation of Fe^{2+} ions adsorbed on the surface during the pretreatment. The quantity of Fe^{2+} adsorbed depends on the time of contact, a Langmuir-type adsorption isotherm being obtained (Fig. 7). Considering that after each pretreatment the electrodes were throughly washed, it follows, that Fe^{2+} ions are strogly adsorbed

Table 3

Characteristic potential values on anodic chronopotentiograms in different media as a function of pretreatment, E_r = rest potential; E_i = potential of beginning oxygen adsorbtion; E_{O_2} = potential of oxygen evolution (see curve 1, Fig. 5)

Nº	Pretreatments applied	E(mV)	MEDIUM		
			Au/$HClO_4$	Au/$NaClO_4$	Au/NaOH
1	$FeSO_4$	E_r	400	208	−60
		E_i	900	740	300
		E_{O_2}	1460	1040	630
2	$K_2Cr_2O_7$	E_r	900	515	0
		E_i	1020	610	156
		E_{O_2}	1440	1006	366
3	$KMnO_4$	E_r	980	570	142
		E_i	1140	610	168
		E_{O_2}	1308	834	386
4	HNO_3cc.	E_r	852	268	−84
		E_i	900	490	220
		E_{O_2}	1428	958	630
5	H_2O_2	E_r	672	373	−48
		E_i	780	430	180
		E_{O_2}	1400	1000	624
6	HClcc.	E_r	536	178	−84
		E_i	780	478	200
		E_{O_2}	1128	1090	612
7	Catodization	E_r	536	250	−492
		E_i	780	514	88
		E_{O_2}	1410	1102	232
8	Anodization	E_r	864	616	204
		E_i	1080	922	250
		E_{O_2}	1380	958	618
9	KCN	E_r	660	250	−84
		E_i	780	430	200
		E_{O_2}	1260	1102	618
10	Anodization and HClcc.	E_r	624	—	—
		E_i	780	—	—
		E_{O_2}	1360	—	—
11	Heating	E_r	—	—	136
		E_i	—	—	270
		E_{O_2}	—	—	324

on gold. Chronopotentiograms taken in alcaline or neutral media are similar to those reported above, excepting the shift of potentials to negative values. The variation of some characteristic potential values with pretreatment can be observed from the anodic chronopotentiograms reported. The rest potentials (E_r), the beginning of oxygen adsorption (E_i) and the potentials of oxygen evolution (E_{O_2}) respectively are given in Table 3. The fact that the E_r values are not identical with those indicated in Table 1 reveals the poor reproductibility of the surfaces. It is evident that in acid medium oxygen adsorption is favoured by reduced surfaces, on oxidized ones appearing at more positive potentials with 250–350 millivolts. In neutral medium the differences are lesser, and in alcaline one even lesser. Fe^{2+} adsorption always increased the respective potential values.

Oxygen evolution potentials in acid medium show small differences as a function of pretreatment, evidently owing to the fact that it takes place on a surface already covered with adsorbed oxygen. The same is true in neutral medium too. In alcaline medium the ignited, cathodized electrodes and those treated with $K_2Cr_2O_7$ or $KMnO_4$ respectively manifested enhanced activity (small E_{O_2}) values. Some pretreatments have long standing effect. Repeating a cathodization-anodization procedure (cyclization) between H_2 evolution and O_2 evolution potentials respectively, the memory effects disappear obtaining perfect reproducible surfaces. The cyclic chronopotentiogram (anodic-cathodic) of a gold electrode in 0.1 N NaOH recorded after 10 cyclizations is represented in Fig. 8. The curve is perfectly reproducible and is identical with that

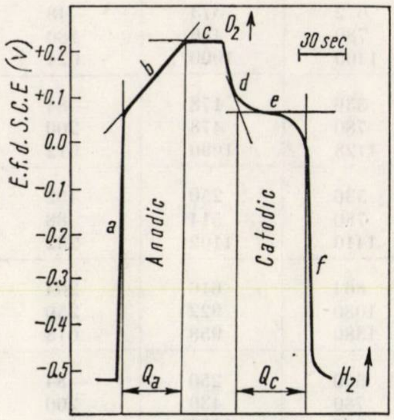

Fig. 8. — Anodic-cathodic cyclic chronopotentiogram of a gold electrode in 0.1 N NaOH, recorded after 10 cyclizations.

obtained by Laitinen and Chao, having the same characteristics.[10] We found that $Q_a = Q_c = 2100$ μC indicating the reproductibility and also the fact that unlike platinum, oxygen does not penetrate into gold.

As a rule, from the chronopotentiograms Q_a and Q_c values (the charge necessary for the oxidation and/or reduction of the electrode respectively) can be calculated, characterizing a given pretreatment procedure. Considering the known uncertainty of determinations, as well as the fact that in most cases poorly defined anodic and cathodic waves have been obtained, Q values have been calculated as necessary to bring the electrode from the initial rest potential (E_r) to the final constant potential (E_{H_2} or E_{O_2}) i.e. Q values involved in the whole chronopotentiogram (Table 4 and 5). Of course the Q values obtained in this way do not represent excusively the charge necessary for oxidation or reduction of the electrodes; but the possible other contributions (charge of the double layer, side reactions) also are influenced by the pretreatment, giving information on the surface state of the electrode. At the same time the values included in Tables 4 and 5 reflect again the poor reproducibility of a given pretreatment.

---

[10] H. A. Laitinen and M. S. Chao, *J. Electrochem. Soc.*, **108**, 726 (1961).

Table 4

Q_c values (charge necessary to reduce the electrode) from cathodic chronopotentiograms

Medium	Q_c(μC)										
	PRETREATMENTS APPLIED										
	Catodization	H_2O_2	$K_2Cr_2O_7$	$KMnO_4$	HNO_3 c.c.	HCl c.c.	$FeSO_4$	KCN	Aqua regia	Heating	Anodization
	1	2	3	4	5	6	7	8	9	10	11
Au/$HClO_4$	320	920	3200	4600	3600	1480	1800	1200	2400	1600	—
Au/$NaClO_4$	400	1120	1680	2400	1520	1400	1280	760	—	520	1400
Au/NaOH	800	3000	3400	3200	4800	2800	2500	800	2000	160	4800

Table 5

Q_a values (charge necessary to oxidize the electrode), from anodic chronopotentiograms

Medium	Q_a(μC)										
	PRETREATMENTS APPLIED										
	$FeSO_4$	$K_2Cr_2O_7$	$KMnO_4$	HNO_3c.c.	H_2O_2	HClc.c.	Cathodization	Anodization	KCN	Anodization and HCl c.c.	Heating
Au/$HClO_4$	7600	3200	2080	6720	10.000	7680	6800	1800	5200	12.000	—
Au/$NaClO_4$	4800	5700	2800	7200	17.650	9450	4920	280	5800	—	—
Au/NaOH	3200	2880	3360	4400	3620	4080	2320	2000	4120	—	800

CONCLUSIONS

1. Constat current chronopotentiometry gives valuable information on the surface state of pretreated gold electrodes, permetting to follow the effect of different pretreatment procedures.

2. It could be stated that oxidants like $K_2Cr_2O_7$, $KMnO_4$, cc. HNO_3, as well as anodization have an oxidative effect. The quantity of oxygen bonded with the gold surface increases with time of contact and stregth of the oxidant used. In spite of the fact that the electrodes were thoroughly washed after each pretreatment procedure, different oxidants gave surfaces with different properties owing to adsorption of the chemicals used.

3. Cathodization or reducing agents eliminate the oxide layer yielding reduced surfaces. The same effect is exhibited by substances capable to complex gold (cc. HCl, KCN, etc.).

4. H_2O_2 also has a strong reducing effect in accordance with its redox potential ($E^{\circ\prime} = 0.682$ volts) compared with that of the gold-oxygen system ($Au_2O_3 + 6\,H^+ + 6\,e = 2\,Au + 3\,H_2O^{1.36}$ volts (see [2], p. 47).

5. The electrodes treated with chemicals are contaminated with these, manifesting characteristic electrochemical properties. By several anodic-cathodic cyclizations pure and perfectly reproducible surfaces can be obtained.

6. Global Q_a and Q_c values have been calculated, necessary to oxidize or to reduce the respective surfaces, being partly characteristic of a given pretreatment.

7. Characterization of the surface state of the electrodes involves other parameters too, e. g. real surface area, adsorbed species, etc.

Revue Roumaine de Chimie, **21**, *5*, 695–702 (1976)

MATHEMATICAL MODEL IN THE RANGE 50–70° AND 5N–7N KOH FOR A HYDROGEN-OXYGEN FUEL CELL

MARIA MAVRODIN-TĂRĂBÎC, IOANA ONACA and I. SOLACOLU
Centre of Physical Chemistry, 31 Str. Galaţi, Bucharest, Romania

Received October 2, 1974

The effect of hydrogen overpressure (400–500 mm Hg), of temperature (60–80°) and electrolyte concentration (5 N–7 N) upon the performance of a cell of H_2-O_2 type with activated nickel anode and silver cathode (gas electrodes DSK type) has been studied. The dispersional analysis of data obtained from discharge curves on a variable resistor has been employed in testing the significance of the effect of working parameters variation. The optimal values of working parameters have been obtained by optimization through a factorial experiment program: 400–500 mm Hg, 79–82° and 6.5 N–6.7 N.

Generally, the efficiency of a fuel cell of hydrogen-oxygen type depends both on the thermodynamic yield of the reaction in working conditions [1] and on the electrical yield of the cell. Its value changes with the extent of irreversible losses (charge transfer, concentration and ohmic polarization). The performance reached depends both on the constructive solution chosen and on the stability of the working parameters.

In a previous paper, [2] the optimal working conditions for a $Zn/KOH/O_2$ cell with silver cathode have been established. At present work, we have aimed at establishing the optimal value, of the working parameters (hydrogen overpressure, temperature and electrolyte concentration) for a fuel cell with activated nickel anode and silver cathode (gas electrodes DSK type) worked out in our laboratory.

EXPERIMENTAL

A fuel cell of the type

$$(-)\,(Ni)\,H_2/KOH/O_2\,(Ag)\,(+)$$

with activated nickel anode and silver cathode in a concentrate KOH solution has been achieved.

The anode was obtained by pressing ($4.6 \times 10^8 N/m^2$) and sintering in hydrogen atmosphere (30 minutes at 700°). The composition of initial powder mixtures: 15% carbonyl nickel (less than 5 μ), 50% nickel carbonate (less than 5 μ), 25% oxalic acid (40–60 μ), 5% ammonium wolframate and 5% cobalt acetate (the last two serving as activationcompounds). The overall average porosity, determined by weighing before and after soaking with toluene, was 60.3%.

---

[1] M. Eiseberg, "Physical Chemistry", Vol. IXB, Academic Press, New York, 1970, p. 777.

[2] M. Mavrodin-Tărăbîc, I. Onaca and I. Solacolu, *Rev. Roumaine Chim.* (in press).

The cathode was obtained by pressing ($2.8 \times 10^8 N/m^2$) and sintering in hydrogen atmosphere (15 minute at 375°). The composition of the initial powder mixtures : 81.25% silver carbonate (less than 5 μ) and 18.75% ammonium dicarbonate (40–60 μ). The overall average porosity of electrodes was 30.5%.

The cell was discharged through a variable resistor in a wiring scheme which included : an electronic millivoltmeter type Radiometer 22 (precision ±1 mV), a milliampermeter type DU 20 (precision ±1%), a decade resistor box (precision ±0.1 Ω).

The basic parameters have been varied as follows : hydrogen overpressure within 400–500 mm Hg (in steps of 100 mm Hg, ±2 mm Hg precision), concentration between 5 N–7 N (in steps of 1 mequiv. cm^{-3}, ±0.005 mequiv. cm^{-3} precision), temperature between 60–80° (in 10° steps, ±0.1° precision). The optimal oxygen overpressure was previously established (400 mm Hg).[2]

RESULTS AND DISCUSSION

$E - i$ discharging curves have been interpreted according to the method advanced by Gilvarry and Slaughter [3] and described in a previous paper.[4] The chemical energy conversion yield as well as the electrical characteristics of the fuel cell, in various working conditions, have been calculated. The results are given in Table 1.

Examination of data in Table 1 shows that the effect of variation of hydrogen overpressure between 400–500 mm Hg is not significant. The optimal performances of the fuel cell are obtained at 70–80° and 6 N – 7 N.

The effect of the electrolyte concentration upon the performance of chemical source under study is accounted for by the influence of the concentration on the solubility of gases, on the electrolyte conductivity and is in good agreement with previous studies on the behaviour of silver gas electrodes in oxygen reduction.[5] The solubility of gases in KOH solutions decreases with increasing the concentration [6] but this effect is offset by the important increase of the electrolyte conductivity [7] which has a maximum at a concentration of about 6 N.[8]

The performance improvement of the studied cell as a result of the electrolyte temperature increase is explained by its favourable effect on the electrolyte conductivity [7] and on the development of anodic and cathodic processes which prevail over the unfavourable effect on gases solubility.[6] The electrolyte temperature increase favours the anodic and

---

[3] J. J. Gilvarry and J. Slaughter, *Electrochim. Acta*, **8** 711 (1963).

[4] O. Radovici, M. Mavrodin-Tărăbîc, I. Onacea and I. Solacolu, *Rev. Roumaine Chim.*, **18**, 767 (1973).

[5] I. Solacolu, M. Mavrodin-Tărăbîc and I. Onacea, *Rev. Roumaine Chim.* (in press).

[6] A. Seidell, "Solubilities of Inorganic and Metal Organic Compounds", Vol. I, Van Nostrand Co., New York, 1953, p. 1352.

[7] E. L. Simons, D. W. McKee and E. J. Cairns, "Comptes Rendus des Troisièmes Journées d'étude des piles à combustible", Presses Académiques Européennes, Bruxelles, 1969, p. 132.

[8] D. B. Lucesoli, *Thesis*, Univ. Paris, 1971, p. 89.

Table 1

Hydrogen-oxygen fuel cell performances in different working conditions

Working conditions			Electrical voltages			R	Electrical efficiency $\varepsilon = E_i - E_r)/E_i$	Average apparent c.d. $i_m = \frac{1}{2} E_i^2/E_t R$	Maxim power $P_{\max}=i_m^2 R$	Average conversion efficiency $\eta_m=(E_i-E_r)E_t-Ri_m/2$
Temp.	Conc.	ΔP_{H_2}	overall $E_t=-\Delta H/zF$	ideal $E_i=-\Delta G/zF$	real E_r					
°C	N	mmHg	mV	mV	mV	ohm	—	mV/cm²	mW/cm²	—
60	5	400	1200	960	690	2.4	0.7188	143.7	49.6	0.2875
		500	1200	950	695	2.45	0.7316	141.9	49.3	0.2895
	6	400	1200	950	675	2.15	0.7105	157.0	53.0	0.2812
		500	1200	935	660	2.2	0.7059	150.0	49.5	0.2750
	7	400	1200	920	700	2.15	0.7609	162.8	57.0	0.2917
		500	1200	925	720	2.3	0.7784	156.5	56.3	0.3000
70	5	400	1190	980	700	1.35	0.7143	259.3	90.7	0.2941
		500	1190	970	695	1.23	0.7165	282.5	98.2	0.2920
	6	400	1190	980	715	1.3	0.7296	275.0	98.3	0.3004
		500	1190	975	710	1.3	0.7282	273.1	96.9	0.2983
	7	400	1190	985	715	1.35	0.7259	264.8	94.7	0.3004
		500	1190	975	715	1.45	0.7333	246.5	88.1	0.3004
80	5	400	1180	985	735	1.25	0.7462	294.0	108.0	0.3114
		500	1180	985	730	1.3	0.7411	280.7	102.5	0.3093
	6	400	1180	985	765	1.15	0.7766	306.0	117.0	0.3241
		500	1180	985	750	1.25	0.7614	300.0	112.5	0.3187
	7	400	1180	975	740	1.1	0.7590	308.4	114.1	0.3136
		500	1180	970	750	1.2	0.7732	312.5	117.2	0.3178

cathodic reactions, the diffusion of reacting species and reaction products towards (from) the electrodes. The results agree with the previous work [9] and data available in the literature.[8,10,11]

The data discussed above prove the intricacy of the effect of working parameters variation. Establishing optimal values for these parameters requires exploration of the obtained results by a dispersional analysis. The values of average conversion efficiency (η_m), average apparent current density (i_m) and maximum power ($P_{\max}$) have been considered characteristic.

In order to carry out dispersional analysis,[12] a 3 factor model has been chosen (A = hydrogen overpressure, B = temperature, C = concentration) with two (400, 500 mm Hg), three (60°, 70°, 80°) and three (5 N, 6 N, 7 N), levels respectively. The results are shown in Table 2.

Examination of data listed in Table 2 shows that, for all electric characteristics (η_m, i_m, $P_{\max}$), the effect of variation of factor A (over-

Table 2

Dispersional analysis of the effect of parameter changes

Electric characteristics	Dispersion source	Square sum	Degrees of freedom	Dispersion	F	F_α	Obs.
i_m	A	41.4	1	41.4	0.44	7.71	
	B	72603.37	2	36301.68	384.22	6.94	⋆
	C	394.08	2	197.04	2.09	6.94	
	BC	840.13	4	210.03	2.22	6.94	
	AB AC s_r	$\left.\begin{matrix}36.61\\16.58\\702.6\end{matrix}\right\}755.79$	$\left.\begin{matrix}2\\2\\4\end{matrix}\right\}8$	$\left.\begin{matrix}\\\\\end{matrix}\right\}94.47$			
$P_{\max}$	A	7.87	1	7.87	0.47	7.71	
	B	11203.77	2	5601.88	335.2	6.94	⋆
	C	94.55	2	47.27	2.83	6.94	
	AB	3.44	2	1.72	0.1	6.94	
	AC	9.18	2	4.59	0.27	6.94	
	BC	132.86	4	33.21	1.98	6.94	
	s	66.87	4	16.71			
η_m	A	0.01	1	0.01	0.13	7.71	
	B	24.27	2	12.13	161.73	6.94	⋆
	C	1.4	2	0.7	9.33	6.94	⋆
	AB	0.07	2	0.04	0.53	6.94	
	AC	0.56	2	0.28	3.73	6.94	
	BC	4.52	4	2.26	30.13	6.94	
	s_r	0.3	4	0.08			⋆

⋆ significanjt effect

---

[9] M. Mavrodin-Tărăbîc, I. Onaca and I. Solacolu, *Rev. Roumaine Chim.* (in press).

[10] J. Jausta, *Coll. Czech. Chem. Comm.*, **33**, 160 (1968).

[11] M. Marinescu, S. Dobos and I. Minea, *Stud. Cerc. Energ. Electr.*, **19**, 427 (1969).

[12] G. E. P. Box and N. R. Draper, "Evolutionary Operation", Wiley New York, 1965, p. 63.

pressure) and of second order interactions AB (overpressure-temperature) and AC (overpressure-concentration) is not significant. However, the dispersional analysis has evidenced the significance of the effect of temperature (B) variation upon average apparent current density and maximal power, and of temperature (B), concentration (C) and temperature-concentration interaction (BC) upon average conversion efficiency. The relatively low dispersion induced by random factors (residual dispersion, s_r) indicates a satisfactory accuracy of experimental data and points out to the fact that the third order interaction (ABC) is not significant.

The values of reliability interval of experimental data are :

— average apparent current density, $i_m \pm 14.6$ mA/cm^2

— maximal power, $P_{\max} \pm 6.1$ mW/cm^2

— average conversion efficiency, $\eta_m \pm 0.4\,\%$.

According to the data presented above, the dispersional analysis has allowed the separation of parameters whose effect is significant (concentration and temperature), in view of carrying out the optimization study of chemical cells under study.

One considers the functions which describe the relations between significant independent variables — temperature (x_1) and concentration (x_2) — and dependent variables (y) — apparent current density, maximal power and conversion efficiency are as follows :

$$y = b_0 + b_1 x_1 + b_2 x_2 + b_{12} x_1 x_2 + b_{11} x_1^2 + b_{22} x_2^2.$$

The calculation of coefficients of regression functions ($b_0 \ldots b_{22}$) for each dependent variable has been effected [12] starting up with data obtained from a program of factorial experiments (an orthogonal system of $3^2 = 9$ experiments symmetrical against a central point whose coordinates are 70°, 6 N). It was considered that units of 10° and 1 mequiv·cm^{-3}, respectively, are characteristic of variations of working parameters. The coded values of independent variables correspond to :

$$-1 = 60°, \quad 0 = 70°, \quad 1 = 80° \qquad (\text{for } x_1)$$

$$-1 = 5\text{ N}, \quad 0 = 6\text{ N}, \quad 1 = 7\text{ N} \qquad (\text{for } x_2).$$

To check up the validity of regression functions, y_{calc} of each electric characteristic has been calculated for each temperature-concentration set and the deviation of values observed from those calculated has been verified (the linearity of regression functions has been verified).

By equating to zero the partial derivates of regression functions with respect to the two independent variables, a system of two linear equations has been obtained for each electric characteristic. Solving them has led to establishing optimal values of independent variables whose performances are maximum. The results are listed in Table 3.

Examination of data in Table 3 shows that for all electric characteristics under study the calculated F's are lower than critical F_α's corresponding to a significance limit $\alpha = 0.1$ which allows to accept the zero hypothesis and to draw the conclusion that regression functions established describe satisfactorily the relations between variables within the optimal working range.

Table 3

Regression functions for electric characteristics

	N	x_1	x_2	y_1	y_2	$\overline{y}$		y_{calc}	
i_m	1	−1	−1	143.7	141.9	142.8		147.6	$s_1^2 = 160.6$
	2	0	−1	259.3	282.5	270.9	$b_0 = 270.6$	270.9	$s_r^2 = 33.3$
	3	1	−1	294.0	280.7	287.3	$b_1 = 74.15$	292.6	$F = 4.82$
	4	−1	0	157.0	150.0	153.3	$b_2 = 4.1$	155.8	$F_\alpha = 6.99$
	5	0	0	275.0	273.1	274.0	$b_{12} = 1.6$	270.6	
	6	1	0	306.0	300.0	303.0	$b_{11} = -40.7$	304.0	
	7	−1	1	162.8	156.5	159.6	$b_{22} = -5.7$	152.6	
	8	0	1	264.8	246.5	255.6		259.0	
	9	1	1	308.4	312.5	310.5		304.2	
P_{max}	1	−1	−1	49.6	49.3	49.5		50.2	$s_1^2 = 27.4$
	2	0	−1	90.7	98.2	94.5	$b_0 = 96.17$	91.4	$s_r^2 = 5.59$
	3	1	−1	108.0	102.5	105.3	$b_1 = 29.7$	107.9	$F = 4.90$
	4	−1	0	53.0	49.5	51.3	$b_2 = 2.4$	54.1	$F_\alpha = 6.99$
	5	0	0	98.3	96.9	97.6	$b_{12} = 0.825$	96.2	
	6	1	0	117.0	112.5	114.8	$b_{11} = -12.5$	113.6	
	7	−1	1	57.0	56.3	56.6	$b_{22} = -2.4$	53.4	
	8	0	1	94.7	88.1	91.4		91.1	
	9	1	1	114.1	117.2	115.7		114.5	
η_m	1	−1	−1	28.8	29.0	28.9		28.9	$s_1^2 = 0.29$
	2	0	−1	29.4	29.2	29.3	$b_0 = 29.6$	29.1	$s_r^2 = 0.05$
	3	1	−1	31.1	30.9	31.0	$b_1 = 1.4$	31.0	$F = 5.96$
	4	−1	0	28.1	27.5	27.8	$b_2 = 0.667$	27.8	$F_\alpha = 6.99$
	5	0	0	30.0	29.8	29.9	$b_{12} = -0.02$	29.6	
	6	1	0	32.4	31.8	32.1	$b_{11} = 0.433$	31.9	
	7	−1	1	29.2	30.0	29.6	$b_{22} = 0.133$	29.5	
	8	0	1	30.0	30.0	30.0		30.5	
	9	1	1	31.4	31.8	31.6		32.0	

The regression functions have been employed in plotting the response curves in the plane of the two significant parameters for average conversion efficiency, average apparent current density and maximal power (Fig. 1).

Examination of curves in Fig. 1 shows that the centers of response curves P_{max} and i_m are close to each other (6.7 N—82° and, respectively, 6.5 N—79°). The shift of the maximum between these two points is not significant. For the coordinates of the center of response curves i_m, P_{max} is 113.9 mW/cm² and, since the reliability interval for P_{max} is ± 6.1 mW/cm², the shift toward its maximal value (115.2 mW/cm²) is not significant. The average apparent current density, for the coordinates of the center of response curves P_{max}, is 301.7 mA/cm^2 and, since the reliability interval for i_m is $\pm$ 14.6 mA/cm^2, the shift toward its maximal value (306.8 mA/cm^2) is also not significant.

For the coordinates maximum power and average apparent current density, the value of average conversion efficiency is higher than 31.5%, close to the maximum one (32.1%).

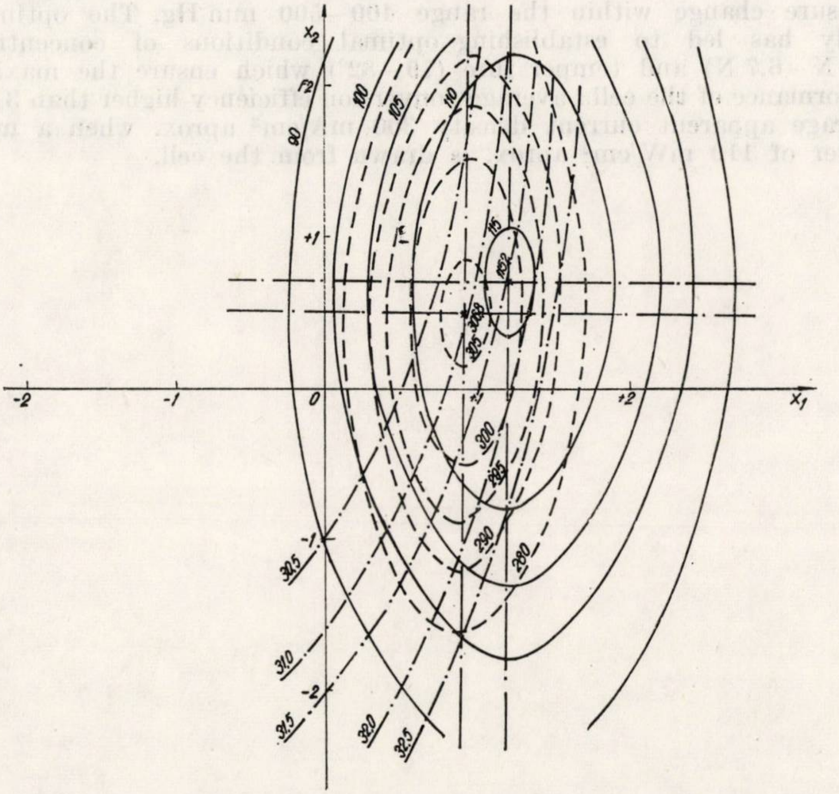

Fig. 1. — Response curves in the plane of the two parameters with significant effect ($\Delta P_{H_2} = 400-500$ mm Hg).

$-.-.-\eta_m-, --i_m, —— P_{max}$.

These data allow establishing the optimal working parameters of the fuel cell for the gases overpressure range 400—500 mm Hg : KOH concentration 6.5 N—6.7 N, temperature 79—82°. In these conditions the cell offers an average conversion efficiency of 31.5%. The average apparent current density is 300 mA/cm^2 aprox. while power is 110 mW/cm^2 aprox. under conditions of maximum power drawn by external circuit.

3. CONCLUSIONS

The study of the effect of changes in the working parameters upon the performance of chemical source of hydrogen-oxygen type with activated nickel anode and silver cathode (gas electrodes DSK type) has revealed the favourable effects of the concentration increase up to 6 N – 7 N, of temperature up to 70 – 80°. The dispersional analysis of experimental data has revealed the insignificant effect of hydrogen overpressure change within the range 400 – 500 mm Hg. The optimizing study has led to establishing optimal conditions of concentration (6.5 N – 6.7 N) and temperature (79 – 82°) which ensure the maximum performance of the cell : average conversion efficiency higher than 31.5 %, average apparent current density 300 mA/cm² aprox. when a maxim power of 110 mW/cm² aprox. is drawn from the cell.

Revue Roumaine de Chimie, **21**, *5*, 703–706 (1976)

ПОВЕДЕНИЕ ЦЕРИЯ (III) В ВОДНО-МЕТАНОЛЬНЫХ РАСТВОРАХ

А.А. ВОЛКОВ, З. Е. АКСЕНОВА, Э. С. ФИЛАТОВ, Ан. Н. НЕСМЕЯНОВ
Кафедра радиохимии МГУ, СССР

Получена 14 августа 1975 г.

Методом кондуктометрии, спектрофотометрии и растворимости показана возможность ассоциации солей церия (III) в водно-метанольных растворах с содержанием метанола свыше 85 % об.

Поведение ионов в растворе в значительной степени зависит от природы растворителя, от его свойств. В связи с этим представляет определенный интерес поведение представителя лантаноидовцерия — в неводных и смешанных растворителях.

В настоящей работе изучено поведение солей церия (III) в растворах содержащих метанол различными методами.

ЭКСПЕРИМЕНТАЛЬНАЯ ЧАСТЬ

Для методов спектрофотометрии и кондуктометрии использовали водно-метанольные растворы хлорида церия (III) с постоянной концентрацией 3.10^{-3}М. Растворы готовили на дважды перегнаной воде и метаноле.

Спектрофотометрирование производили в кварцевых тонкостенных 1,0 см кюветах в диапазоне 200—350 нм на EPS—3T. На рис. 1. представлены изменения спектров поглощения растворов. Рис. 2 отражает характер роста оптической плотности растворов при 300 нм с увеличением объемной доли метанола в системе.

Измерение электропроводности проводили в термостатированной при 25±0,1°С ячейке. Удельную электропроводность вычисляли по формуле: $\varkappa = К_{я} .I/R$ ом$^{-1}$ см$^{-1}$, где постоянный член $К_{я}$, определенный заранее, равен 0,4 см$^{-1}$. На рис. 3 показано изменение удельной электропроводности растворов хлорида церия (III).

Меченый радиоактивным изотопом церий-144 основной формат церия с удельной активностью 3,0 К/М использовали для определения растворимости по стандартной методике[1] с дополнениями.[2] Растворимость определяли в водно-метанольных смесях в той области где образуется кристаллический осадок, т.е. при содержании метанола более 85 %об. Растворимость также определяли в метаноле подкисленном HCOOH. Результаты представлены на рис. 4 и 5.

---

[1] Ан. Н. НЕСМЕЯНОВ, Применение радиоактивных элементов для определения растворимости, Сб. *Радиохимия*, изд. МГУ, 1952 г.

[2] С.С. БЕРДОНОСОВ, *Радиохимия*, **5**, 405 (1973).

ОБСУЖДЕНИЕ РЕЗУЛЬТАТОВ

Как видно из рис. 3 наблюдается падение электропроводности растворов хлорида церия(III) с увеличением содержания метанола. Подобное явление можно объяснить падением подвижности носителей заряда, уменьшением заряда или концентрации заряженных частиц за счет ассоциации и образования ионных пар.[3,4] Учитывая, что при переходе от воды к метанолу диэлектрическая постоянная уменьшается в 2,5 раза представляется несомненным, что с увеличением концентрации метанола происходит ассоциация частиц и уменьшение эффективного заряда.[5] Это, однако, не отрицает влкада первого фактора, т.е. подения подвижности обусловленного процессом пересольватации частиц.[6] Вероятно оба фактора действуют одновременно, причем более эффективный фактор-ассоциация—начинает действовать при значительной концентрации метанола. Действительно, при содержании метанола свыше 85%об. наблюдается более резкое падение электропроводности. Тот факт, что изменение хода кривой электропроводности вызвано процессом связанным с изменением состояния церия(III) в растворе подтверждается тем, что подобного эффекта не наблюдается при смешении чистых растворителей.

Спектры поглащения водных растворов разных солей церия(III) имеют много общего в ультрафиолетовой области.[6,7] Спектр водного раствора хлорида церия(III) показан на рис. 1. С увеличением в растворах содержания метанола имеет место изменение характерных полос поглощения. При этом увеличивается оптическая плотность раствора в интервале 290—310нм, наблюдается сдвиг всего спектра в длиноволновую область, причем отмечено наличие изобестической точки при 226 и 260нм. Второе изменение связанно с заменой растворителя на другой, менее полярный. Увеличение оптической плотности растворов солей церия(III) при 290—310нм ранее отмечено в литературе.[8] Было показано, что оно связано с процессом дегидратации. Наличие изобестических точек свидетельствует об образовании иной, отличной от исходной, формы, при переходе к метанолу. Концентрация вновь образующейся формы церия (III) поглощающей свет при 310 нм — рис, 2 — особенно интенсивно растет в растворах содержащих более 85%об. метанола. А так как, согласно данным кондуктометрии, в этой области происходит падение электропроводности, то, видимо, с уменьшением полярности среды идет процесс образования ассоциатов.

Абсорбционные спектры, полученные в результате проведенного исследования не содержат компонент характерных для четырехвалент-

---

[3] G. Brieri, N. Felici, *Compt. rend.*, **255**, 288(1962).

[4] Е. М. Рыжков, А. М. Сухотин, *Ж. Ф.Х.*, **36**, 2205 (1962).

[5] D. Roach, E. Amis, *Z. phys. Chem.*, **35**, 270 (1962).

[6] И. М. Батяев, В. В. Пальчевский, Л. П. Железнова, *Вестн. Ленингр. Унив.*, **4**, 91 (1966).

[7] В. М. Тараян, Л. И. Элиазян, *Изв. А. Н. Арм. ССР*, *Сер. хим. наук*, **13**, 245 (1960).

[8] В. В. Лапшин, А. И. Казаков, *Теор. и экспер. хим.*, **1**, 133 (1971).

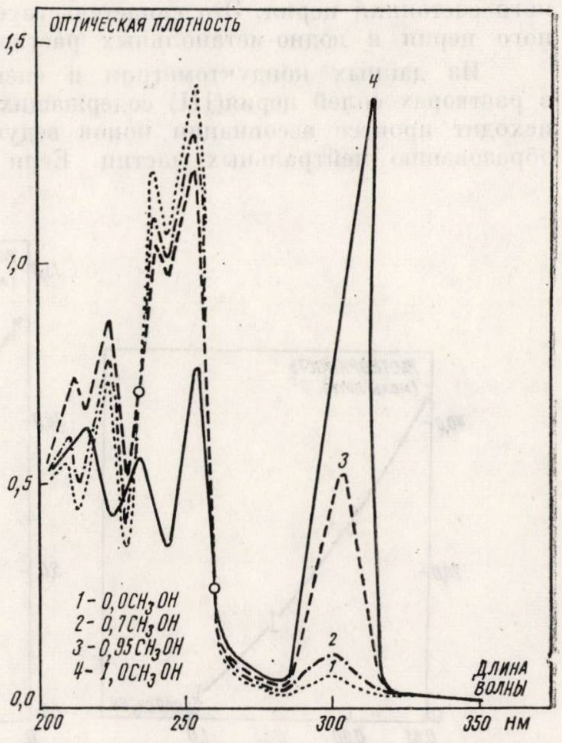

Рис. 1. — Влияние концентрации метанола на спектр поглощения 3.10^{-3} М раствор хлорида церия (III).

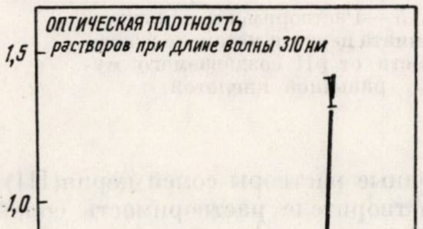

Рис. 2. — Изменение оптической плотности водно-метанольных растворов хлорида церия (III) в зависимости от содержания метанола.

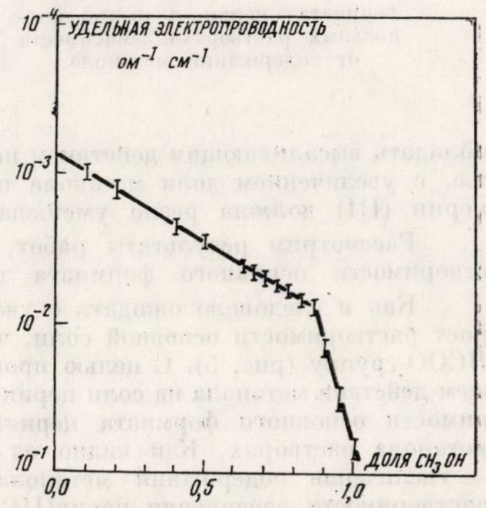

Рис. 3. — Изменение удельной электропроводности раствора хлорида церия в зависимости от содержания метанола в растворе.

ного состояния церия. Это свидетельствует об устойчивости трехвалентного церия в водно-метанольных растворах.

Из данных кондуктометрии и спектрофотометрии вытекает, что в растворах солей церия(III) содержащих более 85% об. метанола происходит процесс ассоциации ионов ведущий, в предельном случае, к образованию нейтральных частиц. Если это так, то метанол должен обладать высаливающим действием на водные растворы солей церия(III), т.е. с увеличением доли метанола в растворителе растворимость солей церия (III) должна резко уменьшаться.

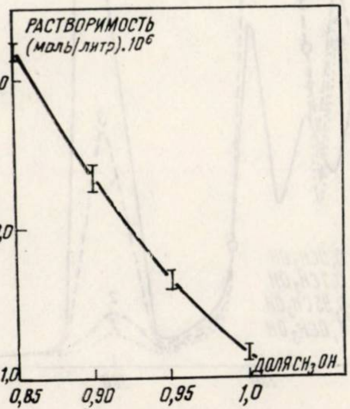

Рис. 4. — Растворимость основного формиата церия в водно-метанольных растворах в зависимости от содержания метанола.

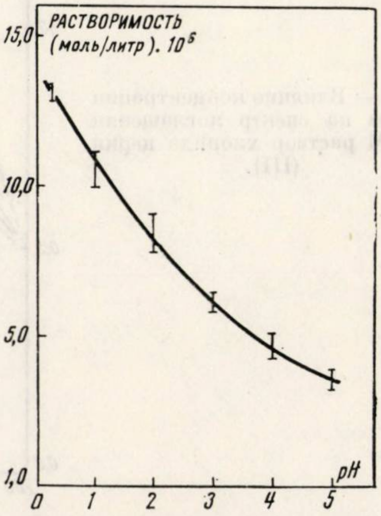

Рис. 5.—Растворимость основного формиата церия в метаноле в зависимости от pH создаваемого муравьиной кислотой.

Рассмотрим результаты работ, выполненных по определению растворимости основного формиата церия(III).

Как и следовало ожидать с увеличением кислотности наблюдается рост растворимости основной соли, что связано с заменой ООН-иона на НСОО-группу (рис. 5). С целью проверки предположения о высаливающем действии метанола на соли церия(III), проведено определении растворимости основного формиата церия(III) в различных по содержанию метанола растворах. Как видно из результатов определения — рис. 4 — увеличение содержания метанола на 15%об. вызывает изменение растворимости соединения церия(III) почти в 15 раз. т.е. наблюдается сильное высаливающее действие.

Следовательно, результаты работ не противоречат предположению об ассоциации ионсв в водно-метанольных растворах содержащих более 85%об. метанола.

Revue Roumaine de Chimie, 21, 5, 707–715 (1976)

CONTRIBUTION TO THE COORDINATION CHEMISTRY OF *s*-TRIAZINES. I

COORDINATION COMPOUNDS OF COPPER WITH THIOAMMELINE DERIVATIVES

CONSTANȚA GHEORGHIU * and CRISTINETA MĂRCULESCU **
* Faculty of Chemistry, Splaiul Independenței 89, Bucharest.
** Center of Physical Chemistry, str. Dumbrava Roșie 23, Bucharest.

Received October 10, 1974

The tendency of *s*-triazine derivatives to form copper coordination compounds was considered in this paper. Compounds of the type $CuTAX_2$ (X = Cl, Br, I, SCN, SeCN; TA = thioameline derivatives) were obtained, which undergo in certain conditions a reduction process in which compounds of the type Cu_2TAX_2 are formed. In order to establish the structure of these compounds and the oxidation state of the copper atom, chemical as well as physico-chemical methods were used including magnetic and conductivity measurements, electronic and i.r. spectra.

s-Triazines and their derivatives are seldom mentioned in the literature as ligands and the number of their coordination compounds is very restricted. No coordination compound formation was reported so far in the series of 1, 3, 5-triazines with exocyclic mercaptogroups (thioammelines). The first indication given in 1969,[1] in relation to a sulphur-containing *s*-triazine derivative, mentions the formation of a copper chelate, with 2,4-dichloro-6-ethoxymercapto-isocyano-*s*-triazine (DCT–$NCSOC_2H_5$) having the form $Cu(DCT-NCSOC_2H_5)_2$.

In 1971, we have shown [2] that 1,4-diphenyl-2-thioammeline (TA) reacts with copper halides, under various conditions, to yield copper (II) coordination compounds of the type $CuTAX_2$ (X = Cl, Br).

The present paper reports further contributions to the coordination chemistry of copper with this ligand (TA), aiming to establish the constitution and the nature of the bond by means of subtitution reaction and of physico-chemical methods.

EXPERIMENTAL

In order to obtain coordination compounds of copper with thioammeline derivatives, the following materials were used:

Solvents — Anhydrous methanol p.a. (MeOH), dimethylformamide (DMF) dried on molecular sieves, freshly distilled anhydrous ethanol (EtOH). Anhydrous ethyl ether (Et_2O), freshly distilled from metal sodium, was used for extractions.

---

[1] K. Kuwai, F. Mizukami and I. Kodama, *Bull. Chem. Soc. Japan*, **42**, 2396 (1969)
[2] P. Spacu and C. Mărculescu, *Rev. Roumaine Chim.*, **16**, 513 (1971).

The ligand 1,4-diphenyl-2-thioammeline (TA) was synthesized according to the method described in the literature.[2]

Reflectance spectra were recorded on a VSU-1 Zeiss-Jena spectrophotometer within a 260−1100 nm. range, using MgO as standard.

I.R. spectra were recorded in KBr pellets on a UR-20 Zeiss-Jena spectrophotometer.

Molar electric conductivities were determined in a DMF solution, at 25° by means of an OK 102/1 Radelkis conductometer with a 0.1 μ s−0.5 s measuring range. For the determination of the magnetic susceptibility the Gouy method was applied.

Preparation of the compounds of the type $CuTAX_2$, where $X = Cl, Br, I, SCN, SeCN$. The method of preparation for $CuTACl_2$ and $CuTACl_2 \cdot DMF$ was described in a previous paper.[2]

Coordination compounds (III−VI) were synthesized through an exchange reaction, starting from $CuTACl_2$ and potassium salts (KX), where X = Br, I, SCN, SeCN in a DMF concentrated solution and a 1 : 2 molar ratio. The formed potassium chloride was removed by filtration and the filtrate was treated on ice, with anhydrous ether, repeating the operation by decantation. The initially obtained viscous material changed over time into a microcrystalline product, which, in the case of bromide and iodide was filtered off and washed on the filter with CCl_4, EtOH and Et_2O.

In the case of thiocyanate and selenocyanate the viscous material formed changed into an amorphous product merely by treating with water. It was then filtered washed with ice-water and with ether.

Preparation of compounds of the type Cu_2TAX_2 where $X = Br, I$ (Compounds VII and VIII).

a. A $CuTACl_2$ suspension in EtOH, together with potassium bromide or iodide (1 : 2 molar ratio) was refluxed on a water bath until the product has turned deep yellow. After cooling, the resulted yellow precipitate was filtered, washed with ethanol and ether, then dried on P_4O_{10}.

b. By refluxing a suspension of $CuTaBr_2$ or $CuTAI_2$ for 2−4 hours, in ethanol, straw-yellow coloured products were obtained, which were filtered off, washed and dried under conditions similar to those reported for methanol(a).

c. Cu_2TABr_2 may also be obtained by direct synthesis from TA and $CuBr_2$ (1 : 1 molar ratio) in EtOH, under reflux for 4 hours, in a waterbath; the resulting yellow product is filtered off, washed with CCl_4, EtOH and Et_2O and then dried under reduced pressure.

RESULTS AND DISCUSSIONS

From experimental data, it follows that compounds of the form $CuTAX_2(X = Br, I, SCN, SeCN)$ are obtained in the reaction between $CuTACl_2$ and potassium, and ammonium halides and pseudohalides, in a 1 :2 molar ratio, in DMF concentrated solutions.

All these compounds appear as brick-red or greenish-khaky substances and are air-stable in solid state. They are readily soluble in DMF, sparingly soluble in MeOH and EtOH, insoluble in Et_2O and water. Solutions are stable only at room temperature.

Magnetical moments exhibit values ranging between 1.79−1.82 M.B. which indicate a paramagnetism, that corresponds to oxidation state two of copper (d^9) in these compounds.

The electric conductivities measured in DMF solution, at 25° display values between 30 and 58 $ohm^{-1}\ cm^2mol^{-1}$ (Table 1) thus indicating non-electrolyte type of compounds.

On heating, the solutions of these compounds in DMF as well as the suspensions in EtOH become less intensely coloured and deposit off microcrystalline yellow powders, over time.

These yellow products are air-stable in solid state, sparingly soluble in water, EtOH, Et_2O, partially soluble in DMF.

Table 1

Analytical data

Compounds			Colour	Found (Calculated) Cu %	N %	C %	Conductivity ohm^{-1} cm^2 mol^{-1}
I	CuTa Cl$_2$	$C_{15}H_{13}N_5SCl_2Cu$	greenish	14.14 (14.46)	15.93 (16.00)	40.95 (40.55)	44.72
II	CuTACl$_2$DMF	$C_{18}H_{20}N_6OSCl_2Cu$	yellow-green	12.47 (12.63)	16.50 (16.71)	42.88 (42.98)	48.53
III	CuTABr$_2$	$C_{15}H_{13}N_5SBr_2Cu$	red-brown	12.22 (12.00)	13.35 (13.50)	34.56 (34.72)	58.24
IV	CuTAI$_2$	$C_{15}H_{13}N_5SI_2Cu$	red-brown	10.23 (10.37)	11.23 (11.43)	29.01 (29.40)	49.92
V	CuTA(SCN)$_2$	$C_{17}H_{13}N_7S_3Cu$	brown-yellow	13.37 (13.38)	20.60 (20.65)	43.30 (42.99)	30.16
VI	CuTA(SeCN)$_2$	$C_{17}H_{13}N_7SSeCu$	orange-brown	11.37 (11.17)	16.93 (17.23)	35.50 (35.88)	46.80
VII	Cu$_2$TABr$_2$	$C_{15}H_{13}N_5SBr_2Cu_2$	yellow	22.08 (21.88)	11.95 (12.03)	30.41 (30.92)	57.20
VIII	Cu$_2$TAI$_2$	$C_{15}H_{13}N_5SI_2Cu_2$	yellow	18.64 (18.78)	10.33 (10.50)	26.57 (26.62)	53.56

TA = 2,4-diphenyl thioammeline.

The electric conductivities determined in DMF solution present values around 55 ohm^{-1} cm^2 mol^{-1}, proving that these products are also non-electrolytes.

The diamagnetism found in these two products suggests an oxidation state of copper (I), (d^{10}) respectively.

Based on analytical data, on electric conductivities and on magnetic data, the formulation Cu_2TAX_2(X = Br, I) may be assigned to the yellow products.

Electronic and i.r. spectra were performed, in order to confirm the formulation proposed for these two series of compounds.

ELECTRONIC SPECTRA

In the reflectance spectrum of the ligand used by us, 1,4-diphenyl-2-thioammeline (TA) show two bands at 270 nm (37,040 cm^{-1}) and 304 nm (32,890 cm^{-1}). The electronic spectra in a MeOH and DMF solution exhibit maxima slightly shifted towards lower frequencies at 276 nm (36,230 cm^{-1}) and 306 nm (32,680 cm^{-1}) and 276 nm and 314 nm (31,880 cm^{-1}) respectively.

Since the solvent shifts are insignificant and considering that literature data concerning different *s*-triazine derivatives refer only to spectra in solution, we decided to make a comparison between the spectrum of 1,4-diphenyl-2-thioammeline obtained by us and that mentioned by other authors in solution.

Table 2

Reflectance spectra

	Compound	$\pi \rightarrow \pi^*$		ΔE_{xz}		ΔE_{xy}	
		λ nm	ν cm^{-1}	λ nm	ν cm^{-1}	λ nm	ν cm^{-1}
	TA	270 304	37 040 32 890	—	—	—	—
I	$CuTACl_2$	296 310	33 780 32 260	415	24 100	775	12 900
II	$CuTACl_2 \cdot DMF$	320	31 250	420	23 810	780	12 820
III	$CuTABr_2$	290 328	34 480 30 490	410–420	24 390 23 810	765	13 070
IV	$CuTAI_2$	290 340	34 480 29 410	—	—	720–740	13 510 12 890
V	$CuTA(SCN)_2$	330	30 300	—	—	760–780	13 160 12 820
VI	$CuTA(SeCN)_2$	320	31 250	—	—	760–780	13 160 12 820
VII	Cu_2TABr_2	370	27 030	—	—	—	—
VIII	Cu_2TAI_2	370	27 030	—	—	—	—

The literature reports [3] that both spectra of 1, 3, 5-triazine and of all their derivatives show a sharp maximum at 272 nm (36,760 cm^{-1}).

The presence of amino- and mercapto-exocyclic groups (ammelines and thioammelines) change the aspect of these spectra. Thus, a large, highly intense absorption band can be seen in spectra of disubstituted ammelines between 265–270 nm (37,740–37,040 cm^{-1}) and the 1-substituted-2-thioammelines present a pronounced maximum in the 280–290 nm range (35,710–34,480 cm^{-1}), the absorption being exclusively a function of the nucleus of thioammeline.[4]

Spectra of 1,4-diaryl-2-thioammeline show, in solution, this band extremely flattened (272–284 nm ; 36,760–35,210 cm^{-1}) and also a maximum at 308 nm (32,470 cm^{-1}).[5]

The above mentioned data, obtained by us for TA (1.4-diphenyl-2-thioammeline), agree with results reported in the literature.

---

[3] C. Grundmann and A. Kreutzberger, *J. Amer. Chem. Soc.*, **76**, 5646 (1954).

[4] F. Kurzer and E. D. Pitchforck, *J. Chem. Soc.*, **1965**, 6296.

[5] F. Kurzer and E. D. Pitchforck, *J. Chem. Soc., C*, **1967**, 1878.

The spectra of the $CuTaCl_2$ compounds reveal in the u.v. range the same bands as the ligand, characteristic of aryl and mercapto-substituted *s*-triazine ring. However, they are slightly shifted towards longer wave-lengths, probably as a consequence of the coordination. Thus, the absorption band at 270 nm (37,040 cm^{-1}) in the TA ligand has shifted to 290—296 nm (34,480—33,780 cm^{-1}) in chloride, bromide and iodide, whereas in thio- and selenocyanate, it appears as a shoulder.

The absorption band at 304 nm (32,890cm^{-1}) is shifted in all these coordination compounds towards longer wavelengths and the shift gradually increases in the following order : $Cl < Br < SeCN < SCN < I$. These bands, appearing in the 290 and 310—340 nm range, can be assigned to a $\pi \rightarrow \pi^*$ transition.

The electronic spectra of these compounds show two visible bands around 400 nm (25,000 cm^{-1}) and at 720—780 nm (13,890—12,820 cm^{-1}) ; the former may be assigned to metal-ligand charge transfer, while the latter broad band at 750 nm (13,330 cm^{-1}) would correspond to a $d-d$ transition.[6]

The absorption band at 410—420 nm, due to a transition between the ${}^2B_{1g} \rightarrow {}^2E_g(\Delta E_{xz})$ levels, and the second at 720—780 nm, due to a transition between the ${}^2B_{1g} \rightarrow {}^2B_{2g}(\Delta E_{xy})$ levels suggest a distorded tetrahedron symmetry, to compounds obtained by us.

Reflectance spectra of the type Cu_2TAX_2 compounds ($X = Br, I$) show one single band at 370 nm (27,030 cm^{-1}). The aspect of the curve and the absence of an absorption band in visible range proves the existence of copper in a d^{10} configuration, for which the crystal field fails to report visible absorption bands.

I.R. SPECTRA

The i.r. spectrum of 1,4-diphenyl-2-thioammeline (TA) is shown in Table 3 and will be discussed by comparing it to spectra mentioned in the literature for 1, 3, 5-triazine,[3] 2, 4, 6-triamino-s-triazine [7] 1, 3, 5-triphenyl-hexahydrotriazine and 2, 4, 6-triphenylamino-*s*-triazine.[8,9]

Although these spectra are rather complex, assignments coresponding to vibration frequencies were made by analogy with literature data, taking into the account the presence of various substituents attached to the triazine ring.

The i.r. spectrum of TA exhibits 4 bands : at 701 and 735cm^{-1} and at 1350 cm^{-1} assigned to vibration frequencies of the *s*-triazine ring, as well as the 1585 cm^{-1} band ; they have also been found in the i.r. spectrum of 1,3,5-triazine (taken in CCl_4 and CS_2) at 673 and 735 cm^{-1} and at 1415 and 1560 cm^{-1} respectively [3].

---

[6] M. Tong and D. G. Brewer, *Canad. J. Chem.*, **49**, 102 (1971).

[7] W. M. Padgett and W. F. Hammer, *J. Amer. Chem. Soc.*, **80**, 803 (1958).

[8] R. Mecke and F. Langenbucher, "Infrared Spectra of Selected Chemical Compounds", Heyden, New York, 1962.

[9] H. Hershenson, "Ultraviolet and Visible Absorption Spectra", Academic Press, New York, 1954.

The shift of the 673 cm^{-1} band towards higher frequencies in the case of TA spectrum (701 cm^{-1}) and of the 1415 cm^{-1} band towards lower frequencies (1350 cm^{-1}) may be due to the overlapping with the vibration frequency of the S = C = N-group.[10] In the latter case the shift is also due to the N-ring substitution, a fact which has also been reported for the spectrum of 1.3.5-triphenyl-hexahydro-triazine (1337–1389 cm^{-1}).

The band at 1585 cm^{-1} in TA is shifted relative to the band at 1560 cm^{-1} from *s*-triazine spectrum, probably due to overlapping with the characteristic band for the aromatic structure (1600 cm^{-1}) [10] and the extended conjugation with the electron pair of the nitrogen atom from the exocyclic $-NH_2$ group.

Other absorption bands, appearing in the TA spectrum at 863, 953, 1033 and 1260 cm^{-1} as well as at 1490 cm^{-1} are assigned to the presence of nitrogen substituents in the *s*-triazine ring, which we also find in the spectrum of 1.3.5-triphenyl-hexahydrotriazine. Thus, the bands at 863 cm^{-1} and 1490 cm^{-1} are slightly shifted towards lower frequencies relative to the corresponding band in the spectrum of 1.3.5-triphenylhexahydrotriazine (883 and 1499 cm^{-1}).

Some of the bands found in the 900–1300 cm^{-1} range in the TA spectrum, comparatively, exhibit higher intensities than those corresponding to the triazine cycle substituted by phenylamino groups (2.4.6-triphenylamino-*s*-triazine), probably due to the overlapping of the vibration proper with the C = S group vibration (1140 ± 100 cm^{-1}).[11]

In fact, the presence of the C = S group in the molecule determines important changes in the spectrum of TA, by shifting or sharpening the bands characteristic of the sulphur-free *s*-triazine nucleus. But also the presence of other substituents (aminophenyl- and phenyl) in the thioammeline molecule influences the position of the bands specific for this compound.

This is why a band appears at 1655 cm^{-1} in the spectrum of 1.4-diphenyl-2-thioammeline (TA), which is largely shifted relative to the band at 1695 cm^{-1}, assigned by Bellamy [10] to unsubtituted thioammeline.

Due to the simple or substituted exocyclic $-NH_2$ groups, existing in TA, its spectrum is close to the spectrum of 2.4.6-triamino-*s*-triazine (melamine)[12] particularly in the 400–600 cm^{-1} range, where the literature fails to mention spectra of other *s*-triazines. Thus, the bands at 490 and 510 cm^{-1} are assigned to stretching vibration δ_{C-N}, the band at 572 cm^{-1} to the deformation vibration of melaminic cycle and that at 595 cm^{-1} to NH_2 groups attached to the *s*-triazine ring.

Table 3 presents, in addition to the i.r. spectrum of TA, spectra of coordination compounds formed by copper with TA.

The i.r. spectrum of compound $CuTACl_2$ shows bands characteristic of ligand TA, yet some of them are splitted, shifted or reduced in intensity, while others totally disappear.

Thus, the vibration modes of the *s*-triazine ring at 735 and 863 cm^{-1}, as well as those specific for the N-substituted heterocycle at 953, 1033

---

[10] J. Bellamy, "The Infrared Spectra of Complex Molecules", Methuen, London, 1962.

[11] C. N. Rao, "Chemical Applications of Infrared Spectroscopy", Academic Press, London, 1963.

[12] W. Sawodny, K. Niedenzu and J. W. Dawson, *J. Chem. Phys.*, **45**, 3155 (1966).

Table 3

Infrared spectra

TA	$CuTACl_2$	$CuTABr_2$	$CuTAI_2$	$CuTA(SCN)_2$	$CuTA(SeCN)_2$	Assignements
490	500	500	495	495	—	δ_{C-N} in melamine
510	513	510	515	515	512	δ_{C-N} in melamine
572	562	565	565	560	562	triazine ring
595	612	612	—	598	600	exocyclic NH_2
625	633	630	633	635	620−632	,, ,,
670	—	—	—	—	670	$>C = S$
701	692	695	705	702−710	705	triazine ring
735	—	—	—	—	—	,, ,,
—	—	—	—	755	755	$\nu_{C-S(Se)}$
772	770	768	775	785	775	
863	850	850	840	850−870	830−880	N-substituted triazine ring
925	910	910	920	—	920	,, ,, ,,
953	960	955	950	970	950−960	,, ,, ,,
1010	1015	1012	1015	1012	1000−1015	
1033	1036	1037	1035	1040	1040	C−N in ring
1050	1060	1060	—	—	—	triazine ring and C=S
1078	1080	1080	1090	1085	1085	triazine ring
1135	1110	1110	1115	1110	1105	N-substituted triazine ring and S = C−N
1170 1185	1160	1165	—	—	—	ρ_{NH_2}
1240	1240	1230	1240	1210	1240	$C-NH-C_6H_5$
1260	1260	1260	1280	1260	1280	,, ,,
1293	1293	1299	—	1300	—	
1316	1315	1320	—	—	—	
1350	1360	1355	1340	1360	1360	triazine ring
1410	—	—	—	1420	1420	
1460	1460	1460	1475	1470−1480	1480	$C = N-C_6H_5$ in non-conjugated system
1490	1490	1490	1505	1510	1515	,, ,, ,,
1585	1575	1570	1580	1595	1580−1600	unsubst. triazine ring
1637	1630	1620	1630	1635	1635	
1654	1666	1665	1680	1680	1690	Thioammeline
—	—	—	—	2098 ; 2190	2122	$\nu_{C\equiv N}$
3058	—	—	—	—	—	
—	3100	3100	3140	—	3140−65	
3185	3200	3200	—	3180	—	
3223	—	—	—	—	—	
—	3450	—	—	3450	—	

and 1260 cm^{-1} in the TA spectrum, disappear or are reduced in intensity in the i.r. spectrum of $CuTACl_2$.

The splitted band at 1460—1490 cm^{-1} in the $CuTACl_2$ spectrum is shifted relative to the very sharp and single band from the TA spectrum at 1495 cm^{-1}, attributed to the N-substituted *s*-triazine ring.

The bands assigned to vibration frequencies of the $S = C—N\langle$ group in TA, at 670 cm^{-1} and 1100—1200 cm^{-1}, vanish or present a reduced intensity in the $CuTACl_2$ spectrum. The band at 1654 cm^{-1} of TA, attributed to thioammeline, appears splitted (1630, 1670 cm^{-1}) probably due to the coordination effect.

Similar changes also appear in the spectra of $CuTABr_2$ and $CuTAI_2$ compounds, compared to that of TA.

From the i.r. spectrum of CuTA $(SCN)_2$, from the presence of $C \equiv N$ valence frequencies, it can be concluded about the coexistence of the SCN-bridged groups, with the specific band at 2190 cm^{-1} and the isothiocyanato group with the large band at 2098 cm^{-1}.

The single band present at 2122 cm^{-1} in the CuTA $(SeCN)_2$ spectrum, associated with the $C \equiv N$ vibration frequencies, suggests the bonding of these groups through Se.

The large shape of this band can be assigned to the "cis" configuration of the compound as a consequence of the broadening effect of this band.

The possibility of the SCN- and SeCN-groups to bond differently in these compounds can be considered as an effect of the electronic density shift from the copper ion towards the S-coordinated TA ligand. This fact determined an increased class "*a*" character of the metal and, consequently, the possibility of coordination by the N atom.

The SeCN-group less affected by the electronic factors coordinates in the normal mode, at the Se atom.

The possible dimerization of the $CuTA(SCN)_2$ compound may be a consequence of a spatial arrangement more favourable for stability.

In the i.r. spectrum of Cu_2TABr_2, the bands attributed to the $C = S$ and $S = C—N\langle$group vibrations in TA are largely reduced and shifted (670, 735, 1050 and 1135 cm^{-1}).

The TA splitted band (1170, 1185 cm^{-1}) and the Cu $TABr_2$ single band (1165 cm^{-1}), very reduced in the Cu_2TaBr_2 spectrum (1170 cm^{-1}), is assigned to the ρ_{NH_2} frequency (1178—1174 cm^{-1}) in the spectrum of 2.4.6-triamino-*s*-triazine.[13]

The band at 1420 cm^{-1}, very sharp in the Cu_2TaBr_2 spectrum, appears neither in TA nor in $CuTABr_2$ as it is characteristic for the melamine ring (1408 cm^{-1}).[8]

The overlapping of the vibration of $C = N$—group in a non-conjugated cyclic system [10] and of the stretching vibration of diamino-*s*-triazines (1610—1680 cm^{-1}) causes a considerable shift of the band at 1620 cm^{-1} in $CuTABr_2$ to 1635 cm^{-1} in Cu_2TABr_2 spectrum.

I.R. spectra of $CuTAX_2$ type coordination compounds ($X = Cl$, Br, I, SCN, SeCN), compared to the i.r. spectrum of the 1.4-diphenyl-2-

---

[13] R. Bacaloglu, F. Neamţu, I. Bacaloglu and G. Ostrogovich, *Rev. Roumaine Chim.*, **7**, 747 (1972).

thioammeline as ligand, reveal that the strongest perturbations appear at the vibration frequencies of exocyclic C = S and C = NH groups, reapectively; the vibration frequencies specific for the N-substituted *s*-triazine ring and for thioammeline, respectively, are equally disturbed.

The changes in the i.r. spectra discussed above and also the chemical and physico-chemical properties of the $CuTAX_2$ type compounds suggest a coordination of the copper atom with the participation of exocyclic S and N atoms.

As to the Cu(I) coordination compounds of Cu_2TAX_2 type, i.r. spectra point to significant perturbations of exocyclic C = NH groups (substituted and unsubstituted), while vibration frequencies specific to thioammeline are affected to a lesser degree.

These data, correlated with the physical and chemical properties of the compounds investigated lead us to conclude that copper atoms are bond to 1,4-diphenyl-2-thioammeline through the exocyclic nitrogen atoms.

Investigations in this field are in progress focussing on the tendency of other *s*-triazine derivatives to form coordination compounds with various transition metals.

Revue Roumaine de Chimie, **21**, *5*, 717–725 (1976)

PYRIDAZINIUM-YLURES. I

ADDITION DU 3-(*p*-CUMYL)-PYRIDAZINIUM-PHÉNACYLURE ET DU 3-(*p*-CUMYL)-PYRIDAZINIUM-(*p*-NITRO)-PHÉNACYLURE SUR LES ALCYNES ACTIVÉS

MAGDA PETROVANU, MAI VAN TRI et VIRGIL BĂRBOIU

Institut Polytechnique « Gh. Asachi », Laboratoire de Chimie organique,
Jassy, 11, str. 23 August, Roumanie

Reçu le 25 octobre 1974

L'addition du 3-(*p*-cumyl)-pyridazinium-phénacylure (VII) et du 3-(*p*-cumyl)-pyridazinium-(*p*-nitro)-phénacylure (VIII) à l'acétylène dicarboxylate de méthyle et aux esters des acides propioliques conduit aux structures pyrrolo-pyridaziniques du type (XI, XIII). Dans le cas de la réaction du 3-(*p*-cumyl)-pyridazinium-phénacylure avec l'ester acétylène dicarboxylique on obtient un cycloadduct dihydro-pyrrolo-pyridazinique (X).

La chimie des cycloimmonium-ylures présente beaucoup d'intérêt surtout par les réactions de cycloaddition qui aboutissent à une grande variété de structures hétérocycliques.

Dans ce sens, la réactivité des pyridazinium-ylures est encore peu étudiée. A notre connaissance, la littérature signale très peu d'exemples de cycloaddition de pyridazinium-ylures non stables aux dipolarophiles.

Ainsi Farnum et ses coll.[1] ont décrit la réaction entre le pyridazinium-carbéthoxyméthylure « in situ » et l'acétylènedicarboxylate de méthyle. L'addition du pyridazinium-dicyanméthylure et des 3-(*p*-tolyl)-pyridazinium-phénacylures au D.M.A.D. (l'acétylène dicarboxylate de méthyle = D.M.A.D.) a été également étudiée [2–4].

Tenant compte du nombre restreint de travaux concernant les pyridazinium-ylures, nous avons commencé une série de recherches visant l'obtention et l'étude de la réactivité de quelques nouveaux pyridazinium-ylures.

Comme dérivé pyridazinique nous avons choisi en premier lieu, la 3-(*p*-cumyl)-pyridazine, en considérant que la force nucléophyle de cette diazine est assez grande, grâce à l'effet inducteur + I exercé par le radical cumyle, fait qui favorise l'obtention et la stabilité des ylures[5].

La 3-*p*-cumyl-pyridazine (IV) a été obtenue à partir de la 3-*p*-cumyl-pyridazinone (I) [6] qui en présence du brome en milieu acétique conduit à la 3-*p*-cumyl-pyridazone (II) ; traité par l'oxychlorure de phosphore le produit (II) est transformé en dérivé chloruré (III) ; ce dernier, par réduction avec de l'acide iodhydrique conduit à la 3-*p*-cumyl-pyridazine, comme suit :

---

[1] D. G. Farnum, R. J. Alaimo et J. M. Dunston, *J. Org. Chem.*, **32**, 1130 (1967).

[2] T. Sasaki, K. Kanematsu, Y. Yukimoto et Sh. Ochiai, *J. Org. Chem.*, **36**, 813 (1971).

[3] E. Ştefănescu, I. Druţă et M. Petrovanu, *Anal. St. Univ. « Al. I. Cuza » Iaşi, Sect. I*, **19**, 175 (1973).

[4] M. Petrovanu, E. Ştefănescu et I. Druţă, *Rev. Roumaine Chim.*, **16**, 1107 (1971).

[5] I. Zugrăvescu et M. Petrovanu, « Chimia N-ilidelor », Ed. Academiei, Bucarest, 1974, p. 190, 243.

[6] L. I. Smith et C. P. Lo, *J. Amer Chem. Soc.*, **70**, 2209 (1948).

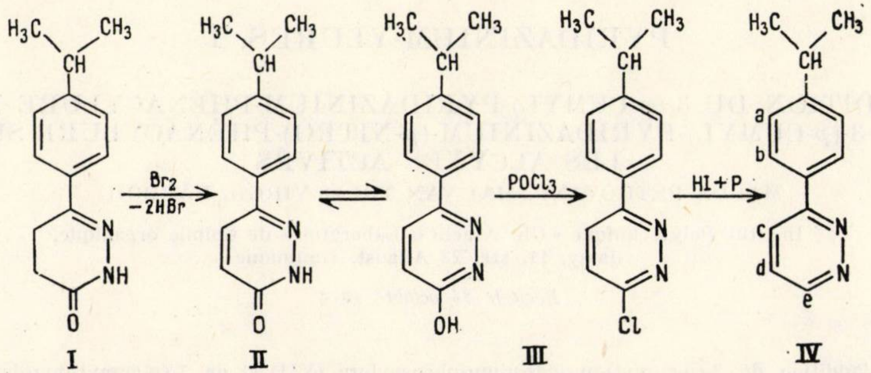

Pour l'obtention du 3-(*p*-cumyl)-pyridazinium-phénacylure (VII) on a utilisé la méthode du sel. Ainsi la 3-(*p*-cumyl)-pyridazine entre facilement en réaction avec le bromure de phénacyle pour former le bromure de N-phénacycle-3-(*p*-cumyl)-pyridazinium (V) : ce dernier conduit, par déhydrobromuration, au 3-(*p*-cumyl)-pyridazinium-phénacylure (VII) :

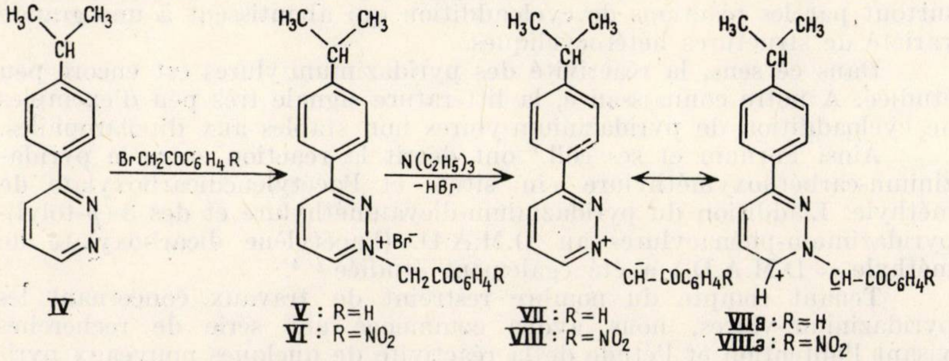

On constate que la formation du sel quaternaire a lieu sur l'atome d'azote en position 1, malgré le fait que selon les effets électroniques l'atome d'azote en position 2 aurait dû être plus électronégatif ; on peut expliquer la quaternisation sur l'azote n° 1 en considérant que les effets stériques sont prioritaires par rapport aux effets électroniques, la réaction ayant lieu sur l'atome d'azote le plus dégagé du point de vue stérique.

L'ylure (VII) est peu stable manifestant une forte tendance d'inactivation. Les spectres IR et RMN de cet ylure indiquent l'existence d'un mélange de l'ylure avec d'autres produits non identifiés jusqu'à présent.

La stabilité réduite du 3-(*p*-cumyl)-pyridazinium-phénacylure s'explique par la faible électronégativité du groupement benzoylique qui est insuffisante pour stabiliser la charge anionique.

Il était donc prévisible que par l'introduction d'un groupement qui exerce un effet d'attraction d'électrons tel que le groupement nitrique, la stabilité sera accrûe.

En effet, en traitant la 3-(*p*-cumyl)-pyridazine par bromure le de *p*-nitro-phénacyle, on obtient le bromure de N—[(*p*-nitro)-phénacyle]-3-

(p-cumyl)-pyridazinium (VI) qui en solution benzénique et en présence de triéthyl-amine conduit au 3-(p-cumyl)-pyridazinium-(p-nitro)-phénacylure (VIII, VIIIa), très stable.

La stabilité accrue de l'ylure (VIII), en comparaison de celle de l'ylure (VII), peut être expliquée par la délocalisation accentuée de la charge anionique due à l'effet d'attraction d'électrons exerçé par le groupement nitrique qui contribue également à l'élargissement des possibilités de résonance du système conformément aux structures (VIII, VIIIa, VIIIb...).

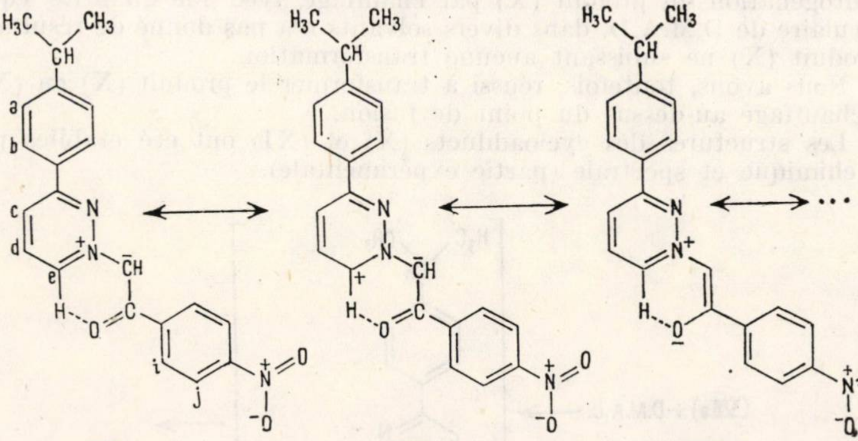

VIII VIIIa VIIIb

La structure de l'ylure (VIII) a été établie par voie chimique et spectrale (partie expérimentale).

La position du signal du proton ylurique $\rangle\overline{\mathrm{C}}\mathrm{H}$ dans le spectre RMN est à $\delta = 7,3$ p.p.m. ce qui peut être expliqué par les structures (VIII...). L'existence d'une liaison d'hydrogène comme dans les structures (VIII) est confirmée d'une part par la position du signal protonique H_e($\delta =$ $=11,17$ p.p.m.) à un champ très faible et d'autre part par le déplacement de ce signal vers des champs plus forts lorsqu'on emploie comme solvant le D.M.S.O. Il faut remarquer, en même temps, que dans le cas de la 3-(p-cumyl)-pyridazine le proton H_e correspond à un $\delta = 9,3$ p.p.m.

Le déplacement très accentué de l'absorption due au groupement carbonylique vers des fréquences assez faibles dans le spectre IR($\nu = 1540\ \mathrm{cm}^{-1}$) peut être aussi expliqué, dans les structures (VIII,...) par l'extension de la charge anionique, fait d'ailleurs observé aussi par d'autres auteurs[7].

Les cumyl-pyridazinium-phénacylures admettent à côté des structures (VII) et (VIII) stabilisées par un « octet » des structures (VIIa, VIIIa) dipolaires 1,3 («sextet sans double liaison ») (VIIa, VIIIa).[8]

Par l'intermédiaire de ces structures (VIIa, VIIIa) les ylures mentionnés peuvent participer à diverses réactions de cycloaddition 1,3 dipolaires.

Ainsi, si l'on traite le 3-(p-cumyl)-pyridazinium-phénacylure (VIIa « in situ » par le D.M.A.D. en solution benzénique anhydre on obtient un mélange de deux produits.

[7] C. A. Henrick, R. Ritchie et N. C. Taylor, *Austral. J. Chem.*, **20**, 2462 (1967).
[8] R. Huisgen, *Helv. Chim. Acta*, **50**, 2421 (1967).

Le produit principal de la réaction est représenté par l'ester diméthylique de l'acide 3-benzoyl-6-(*p*-cumyl)-8aH-pyrrolo-[1,2 b]-pyridazine-1,2-dicarboxylique (X), cycloadduct qui se forme par l'isomérisation de l'intermédiaire (IX) ; la force motrice de cette isomérisation réside dans la formation d'un système conjugué plus ample grâce aux électrons non participants de l'atome d'azote, fait qui ne peut se produire pour le composé (IX). Le second produit (XI), obtenu en très petite quantité, se forme par déhydrogénation du cycloadduct (X). La tentative de déhydrogénation du produit (X) par chauffage avec une quantité équimoléculaire de D.M.A.D. dans divers solvants n'a pas donné de résultats, le produit (X) ne subissant aucune transformation.

Nous avons, toutefois, réussi à transformer le produit (X) en (XI) par chauffage au-dessus du point de fusion.

Les structures des cycloadducts (X) et (XI) ont été établies par voie chimique et spectrale (partie expérimentale).

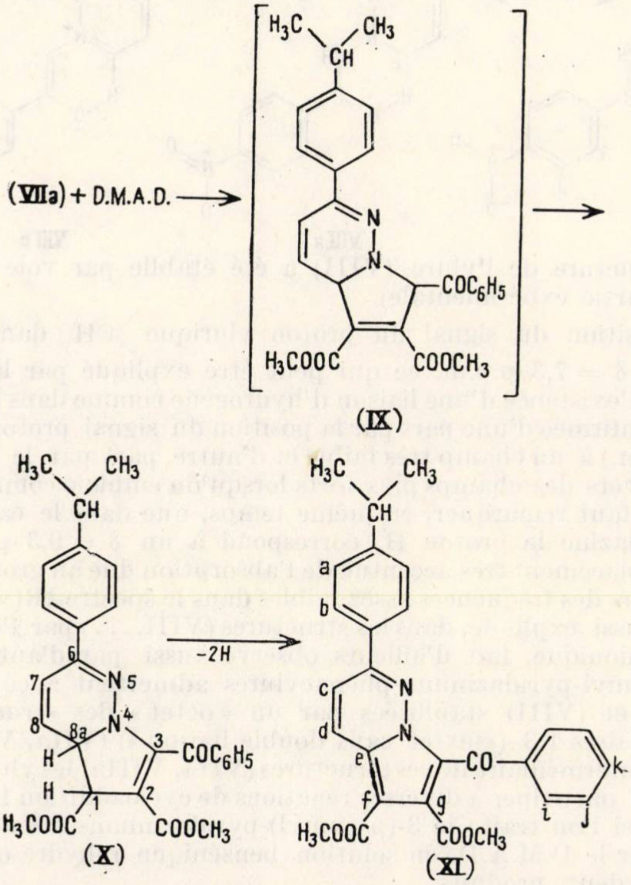

Dans le spectre IR du produit (X) on remarque une bande d'absorption à 1720 cm⁻¹ correspondant à un groupement estérique normal, une bande à 1675 cm^{-1} qui indique la présence d'un groupe estérique conjugué et une bande à 1660 cm^{-1} pour le groupement carbonylique.

L'existence des protons dans le cycle pyrrolique a été démontrée par le spectre RMN du produit (X).

Ainsi, les déplacements des protons H_c et H_d (6,60 p.p.m., respectivement 6,25 p.p.m.) vers des champs élevés en comparaison des valeurs 7,64 p.p.m., respectivement 7,45 p.p.m. dans le cas du produit (XI) est en concordance avec l'interruption de la conjugaison en position C_e. En même temps, la position des signaux des protons H_e et H_f, 4,7 p.p.m., respectivement 3,87 p.p.m., est en accord avec la structure (X). En plus, l'existence des couplages $J_{cd} = 9{,}8$; $J_{ce} = 2{,}0$; $J_{de} = 1{,}5$ et $J_{cf} = 14$ Hz confirme les positions des protons e et f du cycle pyrrolinique. La valeur basse du couplage J_{de} est une conséquence du fait que l'angle diédrique entre les liaisons C_d-H_d et C_e-H_e dans la structure (X) est d'approximativement 90°, valeur pour laquelle J vicinal est minimal.[9]

Dans le spectre IR du produit (XI) la bande carbonylique apparaît déplacée à 1640 cm^{-1} à cause d'une conjugaison avancée due à l'aromatisation, tandis que les bandes correspondant aux groupements estériques sont très rapprochées.

L'apparition d'une double liaison $C_e = C_f$ dans ce produit est en concordance avec le déplacemet des signaux des protons H_c et H_d 8,50 respectivement 7,50 p.p.m. en comparaison des valeurs 6,60 et 6,25 p.p.m. dans le spectre du produit (X).

Le 3-(*p*-cumyl)-pyridazinium-(*p*-nitro)-phénacylure est aussi capable de participer aux réactions de cycloadditions 3 + 2 dipolaires par l'intermédiaire de la structure (VIIIa).

Se comportant d'une manière différente du 3-(*p*-cumyl)-pyridazinium phénacylure, l'ylure (VIIIa) traité par le D.M.A.D. donne naissance à un seul cycloadduct complètement déhydrogéné. On obtient la même 1,2-dicarbométhoxy-3-[(*p*-nitro)-benzoyl]-6-(*p*-cumyl)-pyrrolo-[1,2 b]-pyridazine (XII) soit à partir de l'ylure « in situ » en milieu benzénique anhydre, soit à partir de l'ylure (VIII) préparé antérieurement et du D.M.A.D.

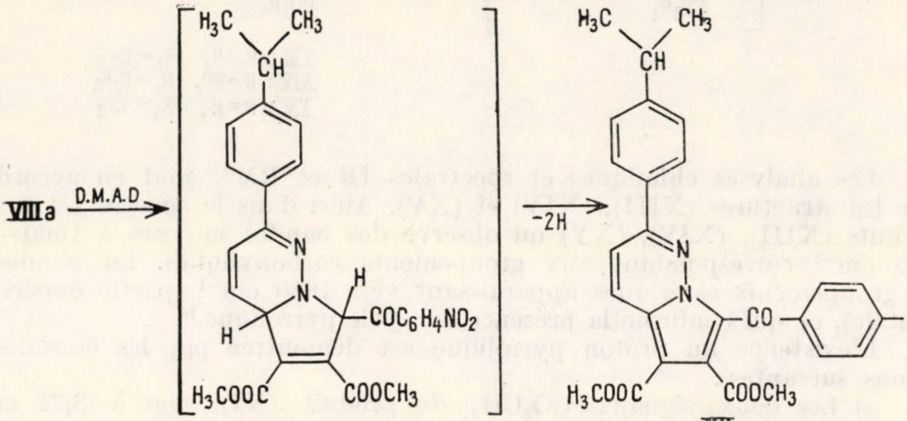

---

[9] M. Karplus, *J. Chem. Phys.*, **30**, 11 (1959).

La structure (XII) est basée sur les analyses chimiques et spectrales. Les spectres IR et RMN de ce produit ressemblent beaucoup à celui du produit (XI) la bande carbonylique apparaissant à 1620 cm^{-1} par suite de l'effet de conjuguaison avec le noyau phénylique d'une part et le système pyrrolo-pyridazinique, d'autre part.

La présence du groupement nitrique permet l'évaluation exacte des paramètres spectraux des protons *i* et *j* (partie expérimentale).

Un autre groupe d'alcynes activés étudié dans la réaction avec les 3-(*p*-cumyl)-pyridazinium-phénacylures (VII, VIII) est celui des esters de l'acide propiolique. Nous avons choisi ces alcynes asymétriques dans le but de pouvoir préciser le sens de l'addition des pyridazinium-phénacylures (VII, VIII) sur les dipolarophiles.

L'addition des ylures (VII) et (VIII) sur le propiolate d'éthyle conduit à la 1-carbéthoxy-3-benzoyl-6-(*p*-cumyl)-pyrrolo-[1,2 b]-pyridazine (XIII), respectivement à la 1-carbéthoxy-3-[(*p*-nitro)-benzoyl]-6-(*p*-cumyl)-pyrrolo-[1,2 b]-pyridazine (XIV) ; l'addition de l'ylure (VII) sur le propiolate de méthyle fournit la 1-carbométhoxy-3-benzoyl-6-(*p*-cumyl)-pyrrolo-[1,2 b]-pyridazine (XV).

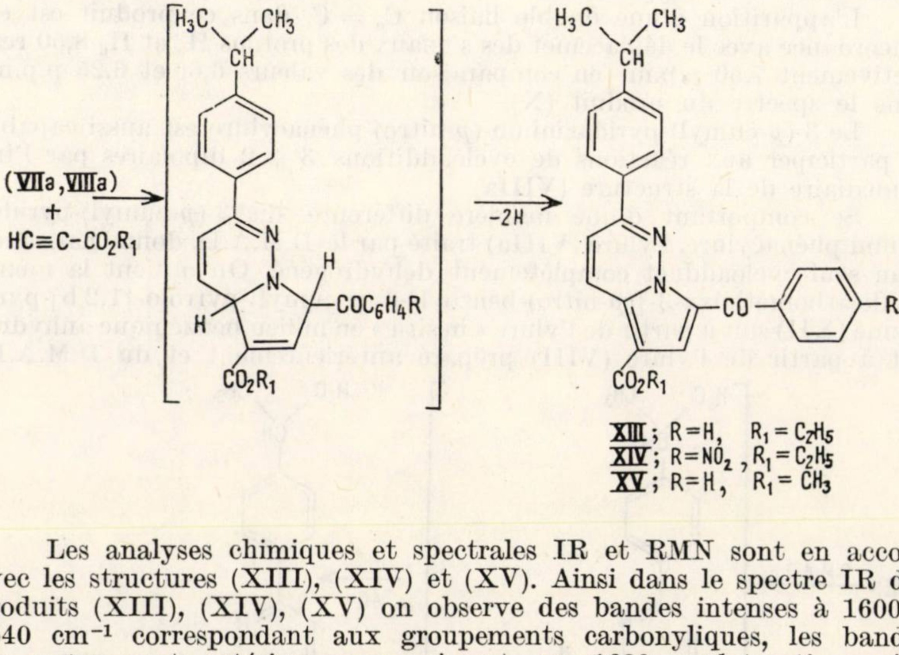

XIII ; R=H, $R_1 = C_2H_5$
XIV ; $R=NO_2$, $R_1 = C_2H_5$
XV ; R=H, $R_1 = CH_3$

Les analyses chimiques et spectrales IR et RMN sont en accord avec les structures (XIII), (XIV) et (XV). Ainsi dans le spectre IR des produits (XIII), (XIV), (XV) on observe des bandes intenses à 1600–1640 cm^{-1} correspondant aux groupements carbonyliques, les bandes des groupements estériques apparaissant vers 1680 cm^{-1} (partie expérimentale), ce qui confirme la présence du cycle pyrrolique.[10]

L'existence du proton pyrrolique est démontrée par les considérations suivantes :

a) Les deux signaux CO_2CH_3 du produit (XI) sont à 3,72 et 3,90 p.p.m. Il est fort probable que le groupement en *f* donne le signal de 3,90 p.p.m., les protons de ce groupe étant plus désécranés que ceux du groupement carbométhoxylique en *g*, du fait qu'ils se trouvent plus rapprochés des électrons π du bicycle pyrrolo-pyridazinique. Dans le produit (XI) il est très probable que l'influence des électrons π appartenant aux fragments COC_6H_5 soit pratiquement nulle à cause de la rotation libre autour de la liaison simple dans ce fragment moléculaire. Le groupement CO_2CH_3 dans le produit (XV) donne un singlet à 3,90 p.p.m., qui, en comparaison des signaux CO_2CH_3 du produit (XI), montre qu'il se trouve en position *f*. La position du signal du proton H_g à 7,70 p.p.m. est une conséquence de l'influence exercée par les deux groupements forts électronégatifs $-CO$ et CO_2CH_3 liés au noyau pyrrolique en *ortho* vis-à-vis du C_g.

---

[10] M. Avram et G. D. Mateescu, « Spectroscopia în infraroșu – Aplicații în Chimia organică », Ed. tehnică, Bucarest, 1966, p. 556.

b) Le spectre des protons appartenant au fragment $CO-C_6H_5$ dans le produit (XV) est identique à celui du produit (XIII), mais assez différent de celui du produit (XI). (Il faut toutefois mentionner que les autres protons des produits (XI), (XIII) et (XV) ont des spectres semblables.)

La différence peut être expliquée par le fait que le groupement carbométhoxylique lié au C_g dans (XI) perturbe la distribution des électrons du cycle benzénique.

Tenant compte des structures des cycloadducts (XIII), (XIV), (XV) on peut déduire que dans la réaction de cycloaddition le carbanion ylurique se lie à l'atome du dipolarophile ayant la densité électronique la plus faible.

PARTIE EXPÉRIMENTALE

Les spectres IR ont été enregistrés sur un spectromètre UNICAM SP-200. Les spectres RMN ont été enregistrés sur un spectromètre du type JEOL—AH 60. Les déplacements chimiques sont exprimés par rapport au TMS en p.p.m.

LA 3-(*p*-CUMYL)-PYRIDAZONE-(6) (II)

On dissout à chaud 10 g de 3-(*p*-cumyl)-pyridazinone-(6) (p. fus. 170° ; litt. :[6] 166—167°) dans 15 ml d'acide acétique glacial, on ajoute goutte à goutte 2,3 ml de brome à une température d'environ 90—100° et on chauffe au bain-marie pendant une heure. Après refroidissement du mélange de réaction on ajoute de l'éther éthylique et on filtre le précipité formé. Par recristallisation dans de l'alcool éthylique on obtient des cristaux blancs au p. fus. 202°. Rend. presque quantitatif. Analyse. $C_{13}H_{14}N_2O$ *calculé* : C 72,89 ; H 6,54 *trouvé* : C 73,06 ; H 6,62 %.

LA 6-CHLORO-3-(*p*-CUMYL)-PYRIDAZINE (III)

On suspend 10 g de cumyl-pyridazone-(6) en 30 ml de $POCl_3$ et on chauffe au bain-marie pendant 20—30 minutes jusqu'à dissolution complète de la cumyl-pyridazone. On verse le mélange réactionnel sur de la glace, on filtre le précipité formé et on le lave avec beaucoup d'eau. Par recristallisation dans de l'alcool on obtient des cristaux blanchâtres au p. fus. 142—143°. Rend. 13g (74 %). Analyse : $C_{13}H_{13}N_2Cl$, *calculé :* C 67,09 ; H 5,61 *trouvé :* C 67,42 ; H 5,58 %.

LA 3-(*p*-CUMYL)-PYRIDAZINE (IV)

On porte à reflux un mélange de 10 g de 6-chloro-3-(*p*-cumyl)-pyridazine, 5 g de phosphore rouge et 50 ml d'acide iodhydrique dilué pendant 6 heures ; on ajoute de l'eau chaude, on filtre et on traite le filtrat par de l'ammoniac ou par une solution de NaOH jusqu'au pH basique. On filtre la 3-(*p*-cumyl)-pyridazine formée ; par recristallisation dans un mélange d'alcool-eau ou D.M.F.A.-eau on obtient des cristaux blancs au p. fus. 99°. Rend. 3,5 g (40 %). Analyse : $C_{13}H_{14}N_2$ *calculé :* C 78,78 ; H 7,08 *trouvé :* C 78,74 ; H 7,32 %. RMN ($CDCl_3$) : doublet $\delta = 1{,}30$ (6 H, 2 CH_3) ; multiplet $\delta = 3{,}00$ (1 H, CH) ; multiplet $\delta = 7{,}3-8{,}1$ (6 H aromatiques) ; quartet $\delta = 9{,}30$ (1 H, H_e) ; $J_{CH.CH_3} = 6{,}8$ Hz.

LE BROMURE DE N-PHÉNACYL-3-(*p*-CUMYL)-PYRIDAZINIUM (V)

On dissout 10 mmole de 3-(*p*-cumyl)-pyridazine et 10 mmole de bromure de phénacyl dans 20 ml de benzène anhydre et on laisse le mélange au repos pendant 24 heures. On porte à reflux pendant 30 minutes, on filtre le sel formé et on lave le précipité avec du benzène. Produit blanc au p. fus. 195—197°. Rend. 3,20 g (82 %). Analyse : $C_{21}H_{21}N_2OBr$ *calculé :* C 63,47 ; H 5,29 *trouvé :* C 63,75 ; H 4,98 %.

LE BROMURE DE N-(*p*-NITRO)-PHÉNACYL-3-(*p*-CUMYL)-PYRIDAZINIUM (VI)

On l'obtient d'une façon analogue au produit (V) à partir de 10 mmole de 3-(*p*-cumyl)-pyridazine et 10 mmole de ω-brome-*p*-nitro-acétophénone ; on obtient 3,98 g (98 %). P. fus. 187°. Analyse : $C_{21}H_{20}N_3O_3Br$ *calculé :* C 57,01 ; H 4,52 *trouvé :* C 57,16 ; H 5,27 %.

Le 3-(*p*-CUMYL)-PYRIDAZINIUM-*p*-NITRO-PHÉNACYLURE (VIII)

2 mmole de bromure de N-(*p*-nitro)-phénacyl-3-(*p*-cumyl)-pyridazinium sont mis en suspension dans 30 ml de benzène anhydre et on ajoute 2 mmole de triéthyl-amine. On chauffe le mélange jusqu'à l'ébullition et on filtre immédiatement. Au refroidissement de la solution l'ylure (VIII) précipite sous forme de cristaux rouges. On filtre et on ajoute à la solution de l'éther de pétrole jusqu'à précipitation complète de l'ylure. Produit rouge, p. fus. 162—164° (dec.) Rend. 0,55 g (76 %). Analyse : $C_{21}H_{19}N_3O_3$ *calculé :* C 69,80 ; H 5,26 ; *trouvé :* C 70,10 ; H 5,44 % ; IR (KBr) : 1540 cm^{-1} $\nu_{C=O}$ cétonique ; 1530 cm^{-1}, 1340 cm^{-1} ν_{NO_2}. RMN ($CDCl_3$) : doublet $\delta = 7{,}32$ (2 H, H_a) ; doublet $\delta = 7{,}80$ (2 H, H_b) ; doublet $\delta = 7{,}64$ (1 H, H_c) ; multiplet $\delta = 7{,}45$ (1 H, H_d) ; doublet $\delta = 11{,}17$ (1 H, H_e) ; doublet $\delta = 7{,}95$ (2 H, H_i) ; singlet $\delta = 7{,}30$ (1 H, $\rangle C\overline{H}$) ; doublet $\delta = 8{,}20$ (2 H, H_j) ; doublet $\delta = 1{,}31$ (6 H, 2 CH_3) ; multiplet $\delta = 3{,}00$ (1 H, CH) ; $J_{a.b} = 9$ Hz ; $J_{c,d} = 8$ Hz ; $J_{d,e} = 4$ Hz ; $J_{i,j} = 8{,}5$ Hz ; $J_{CH.CH_3} = 6{,}8$ Hz.

MÉTHODE GÉNÉRALE D'OBTENTION DES PRODUITS (X), (XII), (XIII), (XIV), (XV)

On ajoute 10 mmole d'alcyne activé et 1,5 ml de triéthylamine à une suspension de 10 mmole sel de cycloimmonium dans 70 ml de benzène anhydre, on agite un peu et on laisse environ 2 heures à la température ambiante. On filtre le bromhydrate de triéthylamine formé et on chasse le solvant ; on recristallise le résidu dans de l'alcool éthylique.

1,2-DICARBOMÉTHOXY-3-BENZOYL-6-(*p*-CUMYL)-8 *a*H-PYRROLO-[1,2 b]-PYRIDAZINE (X)

On l'obtient selon la méthode générale à partir de 10 mmole de sel (V) et de 10 mmole d'acétylènedicarboxylate de méthyle, sous forme de cristaux jaunes au p. fus. 178°. Rend. 2,6 g (56 %). Analyse : $C_{27}H_{26}N_2O_5$ *calculé :* C 70,74 ; H 5,67, *trouvé* C 70,61 ; H 5,70 %. IR (KBr) : 1720 cm^{-1} $\nu_{C=O}$ $(COOR)_1$; 1675 cm^{-1} $\nu_{C=O}$ $(COOR)_2$; 1660 cm^{-1} $\nu_{C=O}$ cétonique. RMN ($CDCl_3$) : doublet $\delta = 7{,}07$ (2 H, H_a) ; doublet $\delta = 7{,}40$ (2 H, H_b) ; quartet $\delta = 6{,}60$ (1 H, H_c) ; quartet $\delta = 6{,}25$ (1 H, H_d) ; quartet $\delta = 8{,}00$ (2 H, H_i) ; multiplet $\delta = 7{,}4-7{,}6$ (3 H, $H_{j,k}$) ; quartet $\delta = 4{,}70$ (1 H, H_e) ; doublet $\delta = 3{,}87$ (1 H, H_f) ; singlet $\delta = 3{,}50$ (3 H, CH_3) estérique) ; singlet $\delta = 3{,}85$ (3 H, CH_3 estérique) ; doublet $\delta = 1{,}22$ (6 H, 2 CH_3) ; multiplet $\delta = 2{,}85$ (1 H, CH) ; $J_{a,b} = 9$ Hz ; $J_{c,d} = 9{,}8$ Hz ; $J_{d,e} = 1{,}5$ Hz ; $J_{c,e} = 2$ Hz ; $J_{CH.CH_3} = 6{,}8$ Hz.

1,2-DICARBOMÉTHOXY-3-BENZOYL-6-(*p*-CUMYL)-PYRROLO-[1,2 b]-PYRIDAZINE (XI)

On chauffe le cycloadduct (X) jusqu'à la fusion complète suivie de recristallisations répétées dans l'alcool. On obtient des cristaux aciculaires jaunes au p. fus. 125—126°. Analyse : $C_{27}H_{24}N_2O_5$ *calculé :* C 71,05 ; H 5,26 *trouvé :* C 71,18 ; H 4,90 % ; IR (KBr) : 1720 cm^{-1} $\nu_{C=O}(COOR)_1$; 1680 cm^{-1} $\nu_{C=O}(COOR)_2$; 1640 cm^{-1} $\nu_{C=O}$ cétonique. RMN ($CDCl_3$) : doublet $\delta = 7{,}15$ (2 H, H_a) ; doublet $\delta = 7{,}60$ (2 H, H_b) ; doublet $\delta = 8{,}50$ (1 H, H_c) ; doublet $\delta = 7{,}50$

(1 H, H_d) ; multiplet $\delta = 7{,}4-7{,}8$ (5 H, $H_{i,j,k}$) ; multiplet $\delta = 2{,}90$ (1 H, CH) ; doublet $\delta = 1{,}25$ (6 H, 2 CH_3) ; singlet $\delta = 3{,}72$ (3 H, CH_3 estérique) ; singlet $\delta = 3{,}90$ (3 H, CH_3 estérique) ; $J_{a,b} = 9$ Hz ; $J_{c,d} = 9{,}5$ Hz ; $J_{CH,CH_3} = 6{,}8$ Hz.

1,2-DICARBOMÉTHOXY-3-*p*-NITRO-BENZOYL-6-(*p*-CUMYL)-PYRROLO-[1,2 b]-PYRIDAZINE (XII)

On l'obtient d'après la méthode générale à partir de 10 mmole de sel (VI) et de 10 mmole de D.M.A.D. sous forme de cristaux jaunes claires. P. fus. 199°. Rend. 2 g (40%).

Ce même produit peut être obtenu avec un meilleur rendement dans la réaction de l'ylure (VIII) avec le D.M.A.D. en milieu chloroformique, comme suit :

On dissout des quantités équimoléculaires de produit (VI) et de D.M.A.D. dans du chloroforme, on agitte pendant 3 heures. On chasse le solvant et on recristallise le résidu dans de l'acétonitrile ; on obtient un mélange de cristaux jaunes et blancs qui ont le même point de fusion. On sépare le produit blanc grâce à son insolubilité dans le diméthyl-sulfoxyde qui est un bon solvant seulement pour le produit jaune. Le produit jaune sépare par précipitation avec de l'eau dans la solution dans le D.M.S.O.

Les analyses élémentaires, le point de fusion du mélange et la coïncidence des spectres démontrent l'identité des deux produits (jaune et blanc) ; il s'agit donc de deux formes différentes de cristallisation en fonction du solvant. Rend. 77%. Analyse : $C_{27}H_{23}N_3O_7$ *calculé* : C 64,67 ; H 4,59 ; *trouvé :* C 64,49 ; H 5,02% ; IR(KBr) : 1720 cm^{-1} $\nu_{C=O}$ $(COOR)_1$; 1685 cm^{-1} $\nu_{C=O}$ $(COOR)_2$; 1620cm^{-1} $\nu_{C=O}$ cétonique ; 1540cm^{-1}, 1340 cm^{-1} ν_{NO_2} ; R.M.N. ($CDCl_3$) : doublet $\delta = 7{,}13$ (2 H, H_a) ; doublet $\delta = 7{,}35$ (2 H, H_b) ; doublet $\delta = 8{,}50$ (1 H, H_c) ; doublet $\delta = 7{,}55$ (1 H, H_d) ; doublet $\delta = 7{,}82$ (2 H, H_i) ; doublet $\delta = 8{,}25$ (2 H, H_j) singlet $\delta = 3{,}82$ (3 H, CH_3 estérique) ; singlet $\delta = 3{,}90$ (3 H, CH_3 estérique) ; multiplet $\delta = 2{,}90$ (1 H, CH) ; doublet $\delta = 1{,}22$ (6H, 2 CH_3) ; $J_{a,b} = 9$Hz ; $J_{c,d} = 9{,}5$ Hz ; $J_{i,j} = 6{,}5$ Hz ; $J_{CH,CH_3} = 6{,}8$ Hz.

LE 1-CARBÉTHOXY-3-BENZOYL-6-(*p*-CUMYL)-PYRROLO-[1,2 b]-PYRIDAZINE (XIII)

On l'obtient d'après la méthode générale à partir de 10 mmole de sel (V) et 10 mmole de propiolate d'éthyle. Cristaux blancs au p. fus. 140°. Rend. 1,75 g (40%). Analyse $C_{26}H_{24}N_2O_3$ *calculé* : C 75,72 ; H 5,82 ; *trouvé :* C 75,69 ; H 5,37% ; IR (KBr) : 1680 cm^{-1} $\nu_{C=O}$ estérique ; 1640 cm^{-1} $\nu_{C=O}$ cétonique ; RMN ($CDCl_3$) : doublet $\delta = 7{,}35$ (2 H, H_a) ; doublet $\delta = 7{,}80$ (2 H, H_b) ; doublet $\delta = 8{,}52$ (1 H, H_c) ; doublet $\delta = 7{,}57$ (1 H, H_d) ; quartet $\delta = 7{,}82$ (2 H, H_i) ; multiplet $\delta = 7{,}4-7{,}6$ (3 H, $H_{j,k}$) ; singlet $\delta = 7{,}75$ (1 H, H_g) ; quartet $\delta = 4{,}45$ (2 H, CH_2) ; triplet $\delta = 1{,}45$ (3 H, CH_3) ; multiplet $\delta = 3{,}00$ (1 H, CH) ; doublet $\delta = 1{,}30$ (6 H, 2 CH_3) ; $J_{a,b} = 9$ Hz ; $J_{c,d} = 9{,}5$ Hz ; $J_{CH,CH_3} = 6{,}8$ Hz ; $J_{CH_2,CH_3} = 6{,}5$ Hz.

LE 1-CARBÉTHOXY-3-[(*p*-NITRO)-BENZOYL]-6-(*p*-CUMYL)-PYRROLO-[1,2 b]-PYRIDAZINE (XIV)

On l'obtient à partir de 10 mmole de sel (VII) et 10 mmole de propiolate d'éthyle Cristaux jaunes au p. fus. 177°. Rend. 2,2 g (48%). Analyse $C_{26}H_{23}N_3O_5$ *calculé* : C 68,27 ; H 5,03 ; *trouvé :* C 68,53 H 5,27% ; IR (KBr) : 1678 cm^{-1} $\nu_{C=O}$ estérique ; 1620 cm^{-1} $\nu_{C=O}$ cétonique ; 1520 cm^{-1}, 1320 cm^{-1} ν_{NO_2} ; RMN ($CDCl_3$) : doublet $\delta = 7{,}35$ (2 H, H_a) ; doublet $\delta = 7{,}80$ (2 H, H_b) ; doublet $\delta = 8{,}71$ (1 H, H_c) ; doublet $\delta = 7{,}65$ (1 H, H_d) ; doublet $\delta = 8{,}02$ (2 H, H_i) ; doublet $\delta = 8{,}40$ (2 H, H_j) ; singlet $\delta = 7{,}77$ (1 H, H_g) ; quartet $\delta = 4{,}45$ (2 H, CH_2) ; triplet $\delta = 1{,}45$ (3H, CH_3) ; multiplet $\delta = 2{,}95$ (1 H, CH) ; doublet $\delta = 1{,}30$ (6 H, 2 CH_3) ; $J_{a,b} = 9$ Hz ; $J_{c,d} = 9{,}5$ Hz ; $J_{CH\cdot CH_3} = 6{,}8$ Hz ; $J_{CH\cdot CH_3} = 6{,}5$ Hz ; $J_{i,j} = 8{,}5$ Hz.

LE 1-CARBOMÉTHOXY-3-BENZOYL-6-(*p*-CUMYL)-PYRROLO-[1, 2 b]-PYRIDAZINE (XV)

On l'obtient à partir de 10 mmole de sel (V) et 10 mmole de propiolate de méthyle, sous forme de cristaux aciculaires blancs. P. fus. 130°. Rend. 2,1 g (52%). Analyse : $C_{25}H_{22}N_2O_3$ *calculé* : C 75,37 ; H 5,52 ; *trouvé :* C 75,61 ; H 5,49% ; IR(KBr) : 1680 cm^{-1} $\nu_{C=O}$ estérique ; 1620 cm^{-1} $\nu_{C=O}$ cétonique ; RMN ($CDCl_3$) : doublet $\delta = 7{,}30$ (2 H, H_a) ; doublet $\delta = 7{,}80$ (2 H, H_b) ; doublet $\delta = 8{,}57$ (1 H, H_c) ; doublet $\delta = 7{,}52$ (1H, H_d) ; quartet $\delta = 7{,}85$ (2 H, H_i) ; multiplet $\delta = 7{,}4-7{,}6$ (3 H, $H_{j,k}$) ; singlet $\delta = 7{,}70$ (1 H, H_g) ; multiplet $\delta = 2{,}95$ (1 H, CH) ; doublet $\delta = 1{,}27$ (6 H, 2 CH_3) ; singlet $\delta = 3{,}90$ (1H, CH_3 estérique) ; $J_{a,b} = 9$ Hz ; $J_{CH\cdot CH_3} = 6{,}8$ Hz ; $J_{c,d} = 9{,}5$ Hz.

Revue Roumaine de Chimie, **21**, *5*, 727–731 (1976)

ALUMINIUM CHLORIDE CATALYZED REACTIONS OF UNSATURATED ACIDS WITH BENZENE. VIII[1]

PARTICIPATION OF CARBOXYL GROUP IN THE REACTION OF CYCLOPENTYLIDENEACETIC, 1- AND 2-CYCLOPENTENYLACETIC ACIDS WITH BENZENE

A. C. RĂZUŞ, ZS. ARVAY, ANA HANEŞ and ALICE MARIE GLATZ
Center of Organic Chemistry, Spl. Independenţei 202 B, Bucharest 15

Received May 8, 1975

In the reaction of cyclopentylideneacetic, 1- and 2-cyclopentenylacetic acids (**1**, **2** and **3**) with benzene, together with the normal condensation products, lactone **4** was isolated. The formation of this lactone and the behaviour of the esters of the acids **1**, **2** and **3** has been considered as a proof for the earlier proposed mechanism involving lactoid ions.

Although the nature of the products formed in the aluminium chloride catalyzed reaction of unsaturated acids with benzene is well explained by the inductively-directed hydride shifts followed by the reaction with the aromatic compound,[2] the interpretation of the product ratios led to numerous discussions.[3] Thus, in order to explain the stereoselective formation of the phenylated isomers in the case of alicyclic unsaturated acids, we recently proposed [4a,b] a reaction mechanism through lactoid ions.[5]

The present work, which deals with the condensation of unsaturated five-membered ring acids, namely cyclopentylideneacetic acid (**1**) and 1- and 2-cyclopentenylacetic acids (**2** and **3**) as well as their methyl esters with benzene, brings experimental proofs supporting the above mechanism.

In the reaction of these acids with benzene, after a reaction time lower than 5 minutes, we noticed the formation of the 2-hydroxycyclopentylacetic acid lactone (**4**) (yield about 3%), together with *cis*- and *trans*-2-phenylcyclopentylacetic acids (**5**), *cis*-3-phenylcyclopentylacetic acid (**6**), described earlier.[4a]

---

[1] Part VII. : A. C. Răzuş, F. Chiraleu and A. M. Glatz, *Rev. Roumaine Chim.* **20**, 781 (1975).

[2] C. D. Nenitzescu and A. M. Glatz, *Bull. Soc. chim. France*, **1961**, 218 ; A. M. Glatz, A. C. Răzuş and C. D. Nenitzescu, *Rev. Roumaine Chim.*, **11**, 555 (1966).

[3] Review for reactions of unsaturated acids with benzene in the presence of aluminium chloride : A. M. Glatz, *Rev. Roumaine Chim.*, **19**, 455 (1974).

[4] a) A. M. Glatz, A. C. Răzuş, F. Badea and C. D. Nenitzescu, *Rev. Roumaine Chim.*, **16**, 1567 (1971) ; b) A. M. Glatz, V. Wertheimer and F. Badea, *Rev. Roumaine Chim.*, **19**, 87 (1974).

[5] P. Four and D. Lefort, *Tetrahedron Letters*, **1968**, 6143.

The identification of lactone **4** (isolated by preparative v.p.c.) was made by elemental analysis, by IR and NMR spectra and by comparison with the retention time of an authentic sample.[6]

Although the acid-catalyzed formation of lactones from certain unsaturated acids [7] and the reaction of the lactones with benzene [8] are well known, lactones have never been noticed previously in Friedel-Crafts type condensations of unsaturated acids with aromatic hydrocarbons.

The mechanism through a lactoid intermediate is further supported by the difference between the phenylated products (regio-and stereospecifically formed) resulted in the condensation of acids **1**, **2** and **3** with respect to those obtained from their corresponding methyl esters. The results are given in Table 1 as molar ratios of the 1,2-disubstituted (**5**) and 1,3-disubstituted cyclopentanic products (**6**).

Table 1

Condensation of cyclopentylidene-, 1- and 2-cyclopentylacetic acids (1, 2 and 3) and their methyl esters with benzene in the presence of aluminium chloride [a, b]

Reactants		Ratio **6** (*cis*) : **5** (*trans*)[c] Reaction time (minutes)		
		1	5	10
Acid	**1**	—	4.9	—
	2	6.1	4.8	3.3
	3	10.1	6.8	3.6
Methyl esters	**1**	—	—	5.0
of the acids	**2**	—	—	8.0
	3	—	—	73.0

[a] Molar ratio of acid ester ; $AlCl_3 : C_6H_6 = 1 : 1.5 : 10$.

[b] The yields of phenylated products are about 75% ; the reaction mixture was analyzed by v.p.c.

[c] The product **5** is >95% *trans* and < 5% *cis*.

The regiospecificity is expressed as the ratio between compounds **6** and **5**. This ratio decreases at longer reaction times because, as evidenced by a separate experiment, **6** is converted into **5** under these conditions.

Since all the acids give comparable ratios of **6** : **5**, it is plausible that their reactions involve common intermediates, which we believe to be the lactone **4** or the stable lactoid carbocation **8a**.

Unlike the acids, their methyl esters afford higher ratios **6** : **5** (for the esters of acids **1** and **2**, about twice higher and for **3** much higher).

For the ester of the acid **3**, a ratio **6** : **5** of about 17 should be obtained if the inductive effect was the only factor determining the distribution of the products. Therefore, the exceedingly high value 73 suggests a pronounced polarization of the double bond, even though it is situated in the γ, δ position relatively to carboxyl.

---

[6] S. F. Birch, R. A. Dean and E. V. Whitehead, *J. Org. Chem.*, **23**, 785 (1958).

[7] M. F. Ansell and M. H. Palmer, *J. Chem. Soc.*, **1963**, 2640 ; M. F. Ansell, B. E. Grimwood and T. M. Kafka, *J. Chem. Soc.*, (*C*), **1967**, 1802.

[8] J. I. Brauman and A. J. Pandell, *J. Amer. Chem. Soc.*, **89**, 5421 (1967).

Assuming that the same effects determine the product distribution in the case of the acids **1**, **2** and **3**, the ratios should not differ essentially. Indeed, the experimental data show for the acids a levelling tendency of these ratios towards lower values. If we admit that acids may give rise to a more stable intermediate, beside carbocation **7** and perhaps **8 b**, the levelling effect becomes explainable.

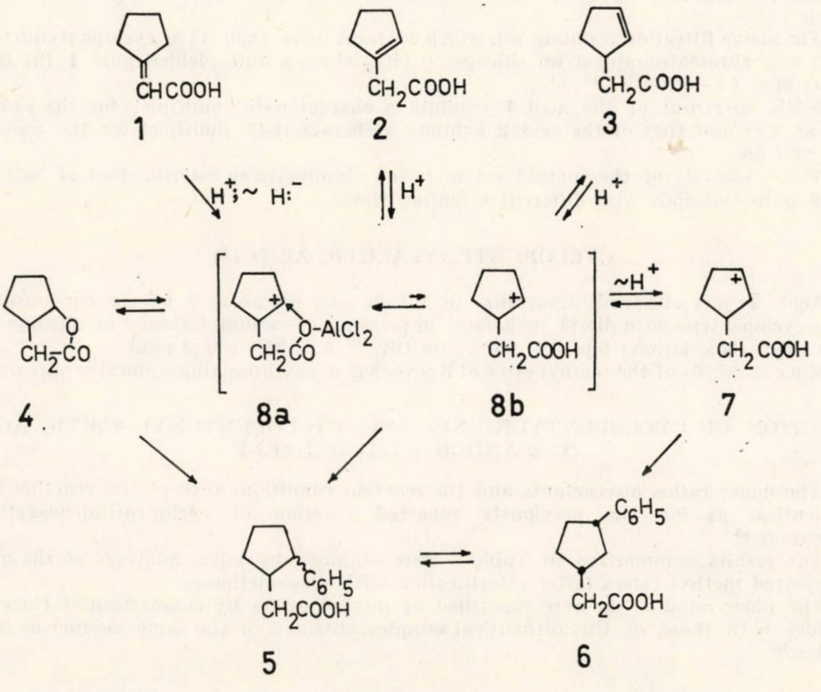

Schema 1

In the lactoid intermediates formed either directly from acids **2** or **3**, or from the above mentioned ions, the electrophilic center is stabilized by the carboxyl group in the γ-position. Thus the different behaviour of the acids and esters noted in Table 1 is well explained.

Running the reaction at longer times the resulted phenyl-cyclopentylacetic acids tend to equilibrate, their interconvertion having been already mentioned.[2a]

EXPERIMENTAL

All melting points are uncorrected. NMR spectra ($CDCl_3$, δ ppm) were recorded on a Varian A 60-A spectrometer, using TMS as internal standard. IR spectra (CCl_4, cm^{-1}) were recorded on a UR 20 Carl Zeiss Jena spectrophotometer. The v.p.c. analyses were carried out on a Carlo Erba gas chromatograph with FID using polyethylene-glycol, column temperature 160°.

CYCLOPENTYLIDENE- and CYCLOPENTENYLACETIC ACIDS (1 and 2)

Condensation of cyclopentanone with ethyl cyanoacetate,[9a] cyanoacetic acid [9b] or triethylphosphonoacetate [9c] yielded a mixture containing the exocyclic double bond ester or nitrile as major compound, however after saponification, the proportion of 1-cyclopentenylacetic acid (**2**) was always greater than that of cyclopentylideneacetic acid (**1**). 1-Cyclopentenylacetic acid was isolated from a mixture containing more than 70% of it, by filtration. The crystalline product gave by recrystallization from ethanol-water pure **2**, m.p. 50° (lit. [9c] m.p. 50–51°).

The above filtration resultant oil, which contains more than 45% cyclopentylideneacetic acid (**1**) was chromatographed on silicagel ($CHCl_3$ eluent) and yielded pure **1** (in the first fraction) m.p. 64–65° (lit. [9c] 63°).

NMR spectrum of the acid **1** exhibits a characteristic multiplet for the *exo*-alkene proton at 5.84 and that of the acid **2** exhibits a characteristic multiplet for the *endo*-alkene proton at 5.56.

V.p.c. analysis of the methyl esters (after diazomethane esterification of both acids) revealed pure materials with different retention times.

CYCLOPENTENYLACETIC ACID (3)

Acid **3** was obtained according to Mislow and Steinberg [10] by the condensation of 2-chloro-cyclopentene with dietyl malonate, in presence of sodium, followed by alcaline hydrolysis and decarboxylation; b.p. 98–99°/4 mm (lit. [10] b.p. 95–100°/4 mm).

V.p.c. analysis of the methyl ester of **3** revealed a gaschromatographically pure material.

REACTION OF CYCLOPENTYLIDENE- AND CYCLOPENTENYL-ACETIC ACIDS (1, 2 AND 3) WITH BENZENE

The molar ratios of reactants and the reaction conditions (except the reaction time *) were identical as for the previously reported reaction of cyclopentilideneacetic acid with benzene.[4a]

The results summarized in Table 2 were obtained by v.p.c. analyses of the mixture of phenylated methyl esters (after esterification with diazomethane).

The phenylated acids were identified as methyl esters by comparison of their retention times with those of the authentical samples obtained in the same manner as described earlier.[4a]

REACTION OF THE METHYL ESTERS OF THE ACIDS 1, 2 AND 3 WITH BENZENE

The molar ratios of the reactants and the reaction conditions (excepting the alcaline extraction) were identical as for the acids **1**, **2** and **3**. The results are summarized in Table 2.

2-HYDROXY-CYCLOPENTYLACETIC ACID LACTONE (4) AND ITS IDENTIFICATION FROM THE REACTION MIXTURE

From the mixture resulted by the reaction of the acids **1**, **2** and **3** with benzene, the lactone **4** was isolated by preparative v.p.c. as an oil.

---

* The reaction time was measured after the whole quantity of unsaturated acid was added to the suspension of aluminium chloride in benzene, this operation being made as quickly as possible.

[9] a) G. G. Ayerst and K. Schofield, *J. Chem. Soc.*, **1958**, 4097; b) L. A. Paquette, and R. J. Haluska, *J. Org. Chem.*, **35**, 132 (1970); c) J. Wolinsky and K. L. Erickson, *J. Org. Chem.*, **30**, 2208 (1965).

[10] K. Mislow and I. N. Steiberg, *J. Amer. Chem. Soc.*, **77**, 3807 (1955).

Table 2

Products of aluminium chloride catalyzed condensation of cyclopentylideneacetic and cyclopentenylacetic acids (1, 2 and 3) with benzene

Reactants	Time minutes	Products (% moles)		
		Lactone **4**	**5**[a]	**6**-*cis*
Acid **1**	5	—	16.7	81.9
2	1	2.7	13.8	83.9
	5	—	17.3	82.6
	10	—	23.1	76.9
	240	—	35.7	64.2
3	1	3.1	8.7	88.1
	5	1.0	12.5	85.4
	10	—	21.6	78.3
	240	—	36.5	63.2
Methyl esters of the acids				
1	10	—	15.2	75.9
2	10	—	11.2	88.7
3	10	—	1.3	95.0

[a] A mixture of *cis*- and *trans*-2-phenylcyclopentylacetic acids.

Preparative v.p.c. was carried out on a Carlo Erba model GV chromatograph, using a column with 104 PEG 20 M on sylanized chromosorb W 30–60 mesh, 1 = 2 m, Ø = 10 mm, temp. 158°; carrier gas H_2, 30 cm^3/min.

$C_7H_{10}O_2$ *Calc.* : C, 66.67 ; H, 7.99 ; *Found* : C, 66.74 ; H, 8.23 %.

IR : ν_{CO} 1782

NMR : 5.0 (m, 1 H, –CH–O–) ; 1.0–3.0 (m, 9 H, aliphatic).

The lactone **4** was identical with an authentic sample prepared[6] by catalytic reduction of 2-keto-cyclopentylacetic acid (identical IR and NMR spectra and the same retention time).

Revue Roumaine de Chimie, **21**, *5*, 733–738 (1976)

REACTION OF TELLURIUM TETRACHLORIDE WITH 4-FLUORO-4′-METHYL DIPHENYL ETHER

A. GIOABĂ, O. MAIOR and MARIA MITRAN
Institute of Chemistry, Bucharest — Department of Chemistry
and Organic Technology, Splaiul Independenţei, 89

Received 27 December, 1974

The paper describes the preparation of 2-fluoro-8-methylphenoxatellurine-10,10-dichloride (III) by the action of the tellurium tetrachloride on 4-fluoro-4′-methyldiphenyl ether (II). The ring closure, with formation of compound (III), was evidenced by chemical and physico-chemical methods.

This paper is an extension of investigations regarding the obtention of 2,8-disubstituted phenoxatellurines [1–4] and focusses on the cyclization reaction — under the action of tellurium tetrachloride — of some 4,4′-disubstituted diphenyl ethers with different substituents.

In the case of the tellurium tetrachloride reaction with 4-chloro-4’-bromodiphenyl ether, no unitary products may be isolated from the reaction mixture and 4-chloro-4′-nitrodiphenyl ether decomposes during the reaction, therefore the synthesis of phenoxatellurines with such substances presents no preparatory value.

Although the cyclization of 4-fluoro-4′-methyldiphenyl ether (II) occurs with a relatively small yield, it was possible to separate in this case the expected 2-fluoro-8-methylphenoxatellurine-10,10-dichloride (III) from the reaction mixture.

Substance II was obtained by a Schiemann reaction from 4-amino-4′-methyldiphenyl ether (I), a compound resulted by reduction with zinc and calcium chloride in a hydro-alcoholic medium, of 4-nitro-4′-methyldiphenyl ether.

The structure of 2-fluoro-8-methylphenoxatellurine-10,10-dichloride was evidenced as follows: by reduction with potassium bisulphite, substance III changes into 2-fluoro-8-methylphenoxatellurine (IV) with a good yield (Chart. 1). This substance was also characterized by its transformation into 2-fluoro-8-methylphenoxatellurine-10,10-dibromide (V) and 2-fluoro-8-methylphenoxatellurine-10,10-diiodide (VI).

---

[1] A. Gioabă and G. Vasiliu, *Anal. Univ. Bucureşti, Ser. Şt. Naturii, Chimie*, **15**, 89 (1966).

[2] G. Vasiliu and A. Gioabă, *Rev. Chim.* (*Bucureşti*), **19**, 253 (1968).

[3] G. Vasiliu and A. Gioabă, *Rev. Chim.* (*Bucureşti*), **20**, 357 (1969).

[4] A. Gioabă, Thesis, Univ. Bucureşti, 1972.

By melting with sulphur, 2-fluoro-8-methylphenoxatellurine changes into 2-fluoro-8-methylphenoxathiine (VII). This compound was also synthesized from 4-fluoro-4′-methyldiphenyl ether by a Ferrario reaction, respectively by treating with sulphur in the presence of aluminium chloride. The mixed melting point of compound VII prepared by procedures A and B fails to show depression, the IR spectrum is overlapping and the R_f value is identical. By oxidation of 2-fluoro-8-methylphenoxathiine with nitric acid in glacial acetic acid, it may oxidize selectively into 2-fluoro-8-methyl phenoxathiine-10-oxide (VIII) and with hydrogen peroxide in glacial acetic acid, it changes into 2-fluoro-8-methylphenoxathiine-10, 10-dioxide (IX).

A comparison of the IR spectrum of compound IV performed in a KBr pellet, with the spectrum of 2,8-difluoro-phenoxatellurine and 2,8-dimethyl phenoxatellurine (table 1) shows that the out-of-plane vibration γ_{2H} is not modified while the frequency of the ether bridge ν_{C-O-C} is situated at intermediate values to those corresponding to 2,8-dimethyl- respectively 2,8-difluorophenoxatellurine.

Table 1

Some characteristic properties of 2-fluoro-8-methyl-2,8-dimethyl and 2,8-difluorophenoxatellurine

Compound / Characteristic properties	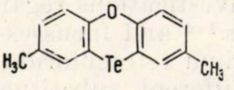	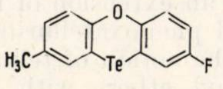	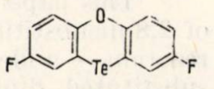
ν_{COC} cm^{-1}	1210 1238	1190 1205	1185 —
ν_{CH_3} cm^{-1}	2870 2925	2880 2930	— —
γ_{2H} cm^{-1}	830	830	830
m.p. °C	75–76	95–96	156–157
R_f	0.62	0.60	0.58

It has been found that the out-of-plane vibration γ_{2H} does not change in time while the frequency of the ether bridge ν_{C-O-C} is situated at intermediate values as against those corresponding to 2,8-dimethyl, respectively 2,8-difluoro-phenoxatellurine. The successive substitution of methyl radicals by fluorine results in a shift of this band towards lower frequencies. The symmetrical and asymmetrical absorption of the CH_3 group shifts towards higher frequencies by the substitution of a methyl by fluorine and totally disappears in 2,8-difluoro-phenoxatellurine. Similarly, the melting point and the R_f value of 2-fluoro-8-methylphenoxatellurine are intermediate relative to the other two comparable pheno-

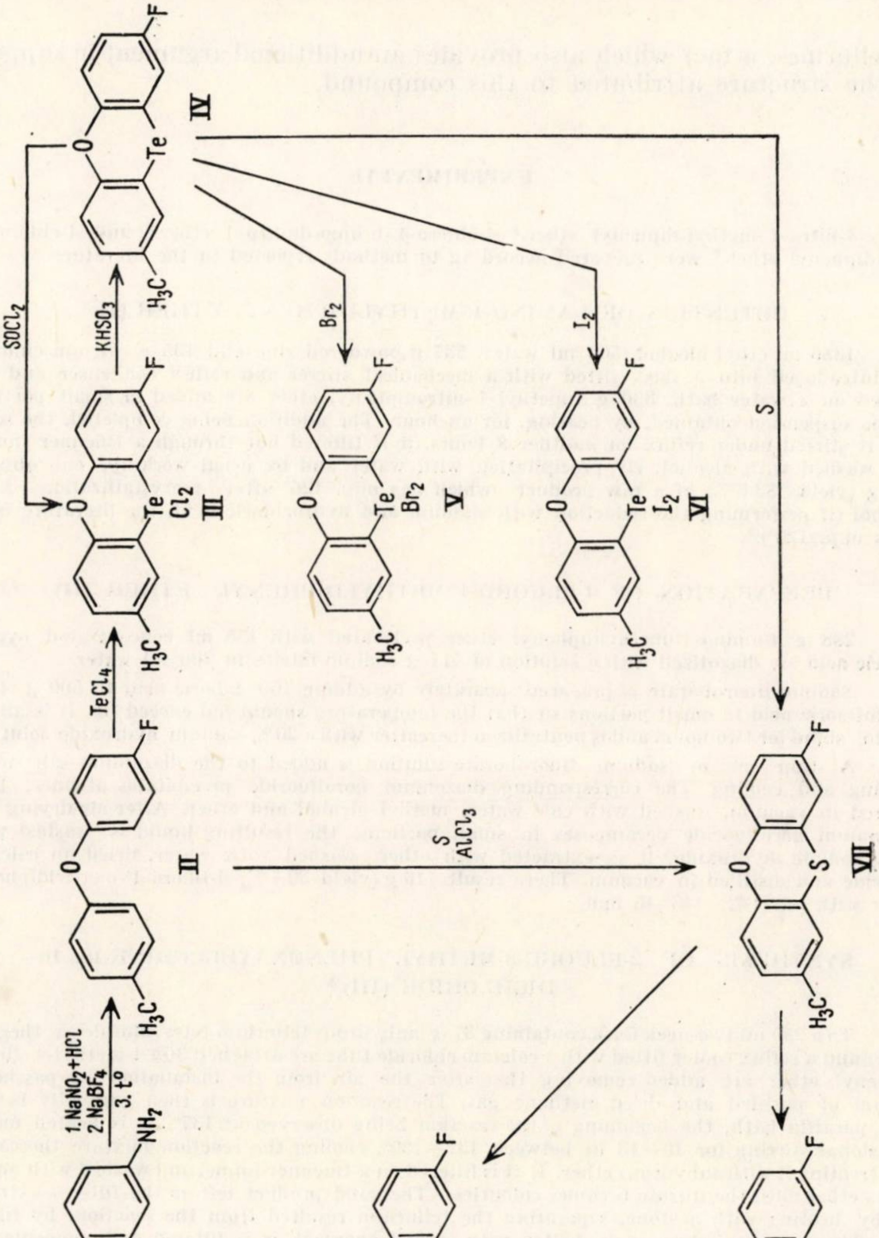
I
II
III
IV
V
VI
VII
VIII
IX
1.NaNO$_2$+HCl
2.NaBF$_4$
3.t°
TeCl$_4$
KHSO$_3$
SOCl$_2$
Br$_2$
I$_2$
S
AlCl$_3$
S

Schema 1

xatellurines, a fact which also provides an additional argument in support of the structure attributed to this compound.

EXPERIMENTAL

4-nitro-4′-methyl-diphenyl ether,[5] 4-chloro-4′-bromo-diphenyl ether[6] and 4-chloro-4′-nitrodiphenyl ether[7] were prepared according to methods reported in the literature.

OBTENTION OF 4-AMINO-4′-METHYLDIPHENYL ETHER (I)

1350 ml ethyl alcohol, 504 ml water, 537 g powdered zinc and 135 g calcium chloride are introduced into a flask fitted with a mechanical stirrer and reflux condenser and are heated on a water bath. 330 g 4-methyl-4′-nitrodiphenyl ether are added in small portions to the suspension obtained, by heating, for an hour. The addition being completed, the solution is stirred under reflux for another 8 hours, it is filtered hot through a Büchner funnel and washed with alcohol. By precipitation with water and by usual work-up, one obtains 240 g (yield 83.6%) of a raw product which has m.p. 126° after recrystallization from alcohol (if performing the reduction with stanium and hydrochloric acid, the literature indicates m.p. 126°).[5]

PREPARATION OF 4-FLUORO-4′-METHYLDIPHENYL ETHER (II)

288 g 4-amino-4′-methyldiphenyl ether pretreated with 455 ml concentrated hydrochloric acid are diazotized with a solution of 111 g sodium nitrite in 400 ml water.

Sodium fluoroborate is prepared separately by adding 150 g boric acid to 500 g 40% hydrofluoric acid in small portions so that the temperature should not exceed 10°. It is allowed to stand for two hours and is neutralized thereafter with a 20% sodium hydroxide solution.

A thin jet of sodium fluoroborate solution is added to the diazonium salt while stirring and cooling. The corresponding diazonium borofluoride precipitates at once. It is filtered in vacuum, washed with cold water, methyl alcohol and ether. After air-drying the diazonium borofluoride decomposes in small portions, the resulting liquid is washed with 20% sodium hydroxide, it is extracted with ether, washed with water, dried on calcium chloride and distilled in vacuum. There result 116 g (yield 39.7%) 4-fluoro-4′-methyldiphenyl ether with b.t. 142–143°/15 mm.

SYNTHESIS OF 2-FLUORO-8-METHYL PHENOXATELLURINE-10, 10-DICHLORIDE (III)[4]

To a 250 ml two-neck flask containing 37 g anhydrous tellurium tetrachloride a thermometer and a reflux cooler fitted with a calcium chloride tube are attached 30g 4-methyl-4′-fluoro diphenyl ether are added removing thereafter the air from the installation by passing a stream of purified and dried methane gas. The reaction mixture is then gradually heated on a paraffin bath, the beginning of the reaction being observed at 137°. It is heated under occasional stirring for 10–13 hr between 137–150°, cooling the reaction mixture thereafter and treating it with anhydrous ether. It it is filtered on a Buchner funnel and washed with anhydrous ether until the filtrate becomes colourless. The solid product left on the filter is extracted by heating with acetone, separating the tellurium resulted from the reaction, by filtration. The acetone solutions is boiled with animal charcoal, it is filtered and concentrated by distillation, depositing on cooling 13.3 g (yield 29.9%) of a pale yellow product with m.p. 270–275°. Twice recrystallized from acetone, 2-methyl-8-fluoro-phenoxatellurine-10,10-dichloride has m.p. 276–278°. Analysis for $C_{13}H_9OTeFCl_2$ Te% calculated : 32.00, found 32.36.

Working up in a similar manner 16 g 4-chloro-4′-bromodiphenyl ether with 9.5 g tellurium tetrachloride at 170–190° for 12 hr, no unitary compounds are obtained. Also, starting from 10 g 4-chloro-4′-nitrodiphenyl ether mixed with 5 g tellurium tetrachloride at 160–170° for 5 hr, the reaction occurs with decomposition.

---

[5] K. Fries, R. Böker and F. Wallbaum, *Liebigs Ann. Chem.*, **509** 83 (1934).

[6] R. Q. Brewster and G. Stevenson, *J. Amer. Chem. Soc.*, **62**, 3144 (1940).

[7] R. J. W. Le Fevre, S. L. M. Saunders and E. E. Turner, *J. Chem. Soc.*, **1927**, 1168.

SYNTHESIS OF 2-FLUORO-8-METHYLPHENOXATELLURINE (IV)[4]

20 ml water and 2.8 g 2-fluoro-8-methylphenoxatellurine-10,10-dichloride previously ground are introduced in a 100 ml flask. 5 g potassium metabisulphite are added in small portions for 30 minutes, cooling the exterior with ice. It is allowed to stand overnight, then it is filtered, washed with water and dried, obtaining 2.2 g (yield 95.6%) raw product which is recrystallized from extraction petrol appearing under the form of yellow crystals with m.p. 95–96°. With concentrated sulphuric acid it turns purple. The thin-layer chromatography on silicagel G in the extraction petrol-benzene system (1 : 1 V/V) shows one single spot with Rf 0.60, evidenced by means of iodine vapours.

Analysis for $C_{13}H_9OTeF$ Te% calculated : 38.92, found 39.17 IR (KBr) : ν_{COC} 1190, 1205 ; ν_{CH_3} 2880, 2930 ; γ_{2H} 830 cm^{-1}

SYNTHESIS OF 2-METHYL-8-FLUOROPHENOXATELLURINE-10,10-DIBROMIDE (V)

3.1 ml solution of 3.14% bromine in anhydrous carbon tetrachloride is added in small portions, with stirring, to 0.2 g solution of 2-fluoro-8-methyl-phenoxatellurine dissolved in 10 ml precooled anhydrous carbon tetrachloride. A citrine yellow product precipitates at once. It is filtered on a Büchner funnel, washed with anhydrous carbon tetrachloride and dried.

Yield, 0.27 g (93.1%). Recrystallized from acetone, its m.p. is 295–296° (with decomposition). Analysis for $C_{13}H_9OTeFBr_2$: Te% calculated 26.16, found 26.45.

SYNTHESIS OF 2-FLUORO-8-METHYL-PHENOXATELLURINE-10,10-DIIODIDE (VI)

To 0.2 g 2-fluoro-8-methylphenoxatelluurine dissolved in 4 ml chloroform a solution of 0.2 g iodine in 15 ml chloroform is added in small portions and under stirring at an ambient temperature. A reddish-brick product precipitates at once, which is filtered after 30 minutes on a Büchner funnel, it is washed with chloroform, then with extraction petrol until a colourless filtrate is obtained. 0.32 g (yield 81.4%) 2-fluoro-8-methylphenoxatellurine-10,10-diiodide result thereof, which, after recrystallization from acetone, take the form of reddish-ruby crystals with the m.p. 272–273° (with decomposition). Analysis for : $C_{13}H_9OTeFI_2$: Te % calculated 21.93, found 21.42.

SYNTHESIS OF 2-FLUORO-8-METHYLPHENOXATHIINE (VII)

Procedure A. 30 g 4-fluoro-4-methyldiphenyl ether, 3.4. g sulphur and 7.1 g anhydrous aluminium chloride are introduced into a reflux installation fitted with a calcium chloride tube. The mixture is heated on a water bath for 5 hr at a temperature of 90–95°. At the beginning, the reaction mixture turns purple, then blue and eventually brown. At the end of this interval, the reaction mixture becomes homogeneous and the hydrogen sulphide release is largely diminished.

The content of the flask is poured in small portions and under stirring into a diluted hydrochloric acid solution, an oily product settling on the bottom of the vessel. It is extracted with ether, washed with water and dried on calcium chloride thereafter. After removing the solvent, the unreacted 4-fluoro-4-methyldiphenyl ether is distilled in vacuum over an interval of 136–150°/12 mm and the residue (11.2 g) is poured into ethyl alcohol under stirring. 9.5 g (yield 77.2%) white solid amorphous product are obtained with m.p. 75–76°. Recrystallized from ethyl alcohol it takes the form of white crystals with m.p. 77–78°. With concentrated sulphuric acid it turns blue. Analysis for $C_{13}H_9OSF$ S % calculated : 13.80, found 13.52.

Procedure B. 0.5 g 2-fluoro-8-methylphenoxatellurine and 0.7 g sulphur are heated on a water bath in a stream of purified methane gas for about 30 minutes at 170–190°, in a 5 ml flask fitted with a reflux cooler. The reaction mixture darkens gradually and tellurium deposits on the wall of the flask. It is cooled and extracted with benzene. By adding a few drops of thionyl chloride to the benzene extract, unreacted 2-fluoro-8-methylphenoxatellurine precipitates under the form of 2-fluoro-8-methylphenoxatellurine-10, 10-dichloride which is eliminated by filtration. After benzene removal one obtains from the filtrate 0.2 g (yield 57.1%) raw product which, after repeated recrystallizations from ethyl alcohol takes the form of white films having an identical melting point and mixed melting point to the same substance synthesized by procedure A.

The thin-layer chromatography on silicagel G in the benzene-extraction petrol system (1 : 1 V/V) cf 2-fluoro-8-methylphenoxathiine prepared by the two procedures reveals unitary spots with identical Rf, both separately and in a mixture.

SYNTHESIS OF 2-FLUORO-8-METHYLPHENOXATHIINE-10-OXIDE (VIII)

2 g 2-fluoro-8-methyl phenoxathiine are introduced into a 50 ml round-bottomed flask fitted with a reflux condenser and a solution formed of 1.6 ml nitric acid (d 1.4) 9.7 ml acetic acid and 1.7 ml water is added under stirring. It is heated on a water bath at 30–40° for 15 minutes and allowed to stand overnight. The white crystalline product is then filtered on a Buchnner funnel, washed with water and dried, obtaining 1.95 g (yield 84.7%) raw 2-fluoro-8-methylphenoxathiine-10-oxide with m.p. 165–166°. Recrystallized twice from ethyl alcohol, its m.p. is 166–167°. Analysis for $C_{13}H_9O_2SF$: S% calculated 12.91, found 12.87.

SYNTHESIS OF 2-FLUORO-8-METHYLPHENOXATHIINE-10,10-DIOXIDE (IX)

a) 7.5 ml glacial acetic acid, 3 ml 30% hydrogen peroxide, 1 g 2-fluoro-8-methylphenoxathiine are introduced in a reflux installation and heated carefully on an air bath for 1.5 hr The reaction mixture is cooled and the white-pearly crystals formed are filtered on a Buchner. funnel, washed with water and dried. There results 1 g (90.9%). M.p. 170–171° (from acetic acid). Analysis for $C_{13}H_9O_3SF$: S% calculated 12.13, found 12.58.

b) Working like above (procedure a) on 0.5 g 2-fluoro-8-methylphenoxathiine-10-oxide, one obtains with a 95% yield, 2-fluoro-8-methylphenoxathiine-10,10-dioxide with a melting point 170–171°, without depression of the mixed melting point with the same substance obtained by procedure a.

Revue Roumaine de Chimie, **21**, 5, 739–744 (1976)

CHEMISTRY OF PHENOXATELLURINE. ACTION OF TELLURIUM TETRACHLORIDE ON 4-HALODIPHENYL ETHERS

A. GIOABĂ, MARILENA NEDEA and O. MAIOR
Institute of Chemistry, Department of Chemistry and Organic Technology, Bucharest
Splaiul Independenţei, 89

Received December 27, 1974

The paper describes the reaction of $TeCl_4$ with 4-halodiphenyl ethers. In the case of 4-fluoro, respectively 4-chlorodiphenyl ether, the presence of 2-fluoro, 2-chlorophenoxatellurine respectively, was revealed in the reaction mixture alongside with 2-fluoro-8-chlorophenoxatellurine, 2,8-dichlorophenoxatellurine, respectively, 4-bromodiphenyl ether decomposes partially, leading to a mixture of compounds in which 2-bromophenoxatellurine was evidenced alongside with elemental tellurium. The reaction of 4-iododiphenyl ether occurs with decomposition, elemental iodine resulting from the reaction mixture as well as other products of which no unitary compounds could be isolated.

Extending some investigations referring to the obtention of halophenoxatellurines,[1–3] this paper undertakes to study the cyclization reaction of 4-halodiphenyl ethers by means of tellurium tetrachloride, with a view to synthesizing the corresponding 2-halophenoxatellurines.

The nature of the halogen in position 4 of diphenyl ether was found to exert a decisive influence on the reaction development. Thus, cyclization normally occurs in the case of 4-fluoro- and 4-chlorodiphenyl ether while a partial decomposition is observed in the case of 4-bromodiphenyl ether. 4-iodo-diphenyl ether reacts with obvious decomposition, elemental iodine being released on heating. No unitary compound could be isolated from the reaction mixture.

The reaction has a reduced preparatory value even in the case of 4-fluoro, respectively 4-chlorodiphenyl ether since, apart from the expected 2-halo phenoxatellurines, the reaction mixture has always revealed the presence of some chlorinated phenoxatellurines in position 8 of the heterocycle :

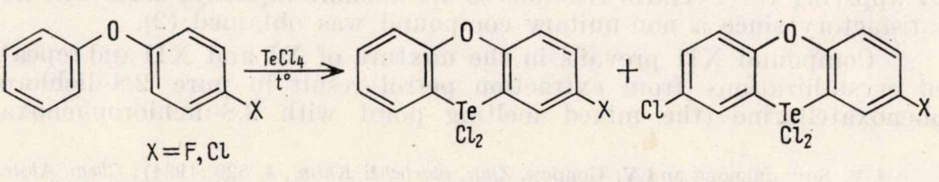

---

[1] G. Vasiliu and A. Gioabă, *Rev. Roumaine Chim.*, **20**, 357 (1969).
[2] G. Vasiliu and A. Gioabă, *Rev. Chim.*, **19**, 253 (1968).
[3] A. Gioabă and O. Maior, *Rev. Chim.*, **21**, 613 (1970).

In this cyclization reaction the tellurium tetrachloride certainly plays also the role of a chlorinating agent.

The literature reports some reactions in which $TeCl_4$ has catalyzed the chlorination of naphthalene[4] and phenol,[5] respectively.

Chlorination probably occurs after cyclization since in the reaction with phenetole $TeCl_4$ leads to a substituted product in paraposition with the $TeCl_3$ group rather than to 4-chloro-phenetole[6] and the diphenyl ether cyclization results in chlorine-unsubstituted phenoxatellurine.

Considering that in the case of 4-halodiphenyl ethers the ring closure occurs at a high temperature and tellurium also results from the reaction mixture, elemental chlorine may form under such conditions and, in the presence of $TeCl_4$ (which plays the role of an electrophilic catalyst) it may chlorinate 2-x-phenoxatellurine-10,10-dichloride resulted from the cyclization reaction.

The formation of 2-fluoro-8-chlorophenoxatellurine was proved as follows:

The reaction product of 4-fluorodiphenyl ether with $TeCl_4$—formed of a mixture of 2-fluoro phenoxatellurine-10,10-dichloride (I) and 2-fluoro-8-chlorophenoxatellurine-10,10-dichloride (II) — was reduced with a solution of potassium bisulphite, a mixture of 2-fluorophenoxatellurine (III) and 2-fluoro-8-chlorophenoxatellurine (IV) being obtained, in which compound IV prevails.

The thin-layer chromatography of this mixture reveals 2 spots. In order to define the spots corresponding to compound (III) and to compound (IV), the mixture was melted with sulphur to obtain a mixture containing 2-fluorophenoxathiine (V) and 2-fluoro-8-chlorophenoxathiine (VI). Both phenoxathiines were also synthesized by a different procedure which evidenced their constitution. Thus, substance (V) was prepared by Ferrario reaction from parafluorodiphenyl ether.

Starting from 4-chloro-4′-nitrodiphenyl ether, the reaction succession illustrated in chart A leads to (VI).

The action of tellurium tetrachloride on 4-chlorodiphenyl ether provides a mixture of 2-chlorophenoxatellurine-10,10-dichloride (IX) and 2-8-dichlorophenoxatellurine-10,10-dichloride (X).

The reduction of this mixture with $KHSO_3$ leads to: 2-chlorophenoxatellurine (XI) and 2,8-dichlorophenoxatellurine (XII). This mixture was revealed by thin-layer chromatography (see fig. 1).

The mixture of (XI) and (XII) heated in the presence of sulphur changes into the corresponding phenoxathiines (XIII) and (XIV) which were also prepared by a different procedure, as shown in chart B.

We mention that the attempt to prepare 2,8-dichlorophenoxathiine by applying the Ferrario reaction to 4,4-dichloro-diphenyl ether was not satisfactory since a non-unitary compound was obtained (2).

Compound XII prevails in the mixture of XI and XII and repeated crystallizations from extraction petrol result in pure 2,8-dichlorophenoxatellurine (the mixed melting point with 2,8-dichlorophenoxa-

---

[4] V. Shvemberger and V. Gordon, *Zhur. obschchei Khim.*, **4**, 529 (1934); *Chem. Abstr.*, **29**, 1804 (1935).

[5] W. Wojnowski, W. Rodiziewiez and J. Dobrowolski, *Przemysl. Chem.*, **37**, 645 (1958).

[6] G. Morgan and R. E. Kellett, *J. Chem. Soc.*, **1926**, 1080.

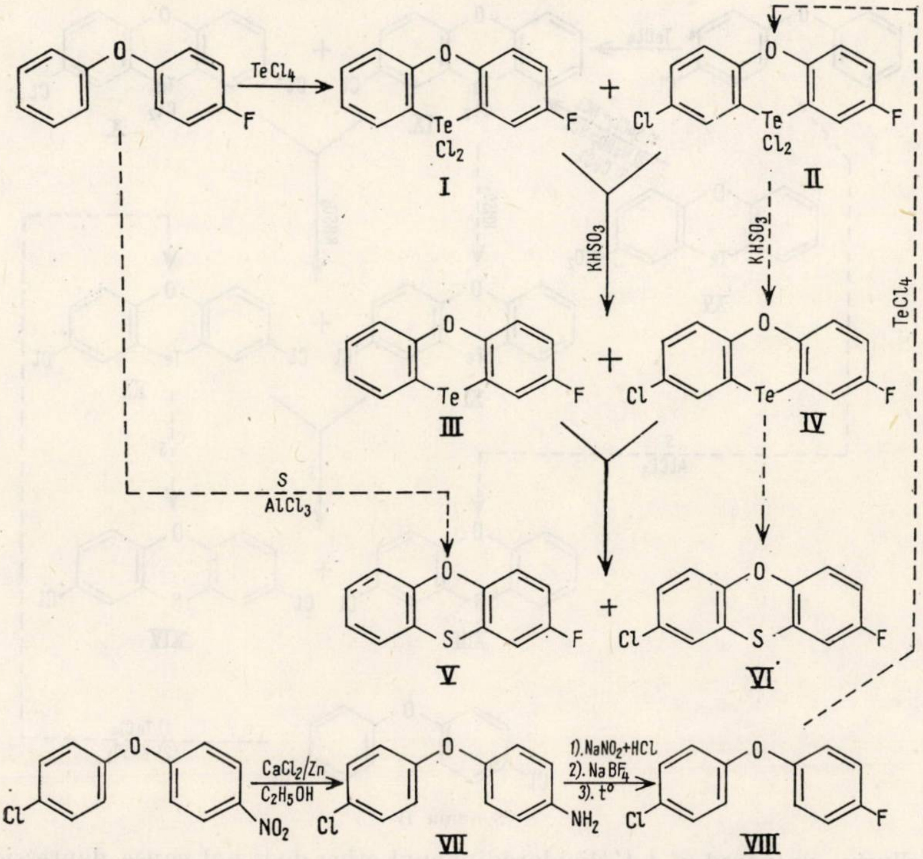
TeCl₄
I
II
KHSO₃
KHSO₃
TeCl₄
III
IV
S
AlCl₃
V
VI
CaCl₂/Zn
C₂H₅OH
1).NaNO₂+HCl
2).NaBF₄
3).t°
VII
VIII

Schema A

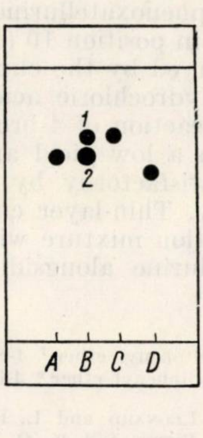

Fig. 1. Thin-layer chromatography of the reaction mixture: A – 2-chlorophenoxatellurine (prepared from 2-nitro-phenoxatellurine); B – mixture of XI and XII; C – 2,8-dichlorophenoxatellurine (prepared from 4,4′-dichlorodiphenylether); D – Phenoxatellurine.

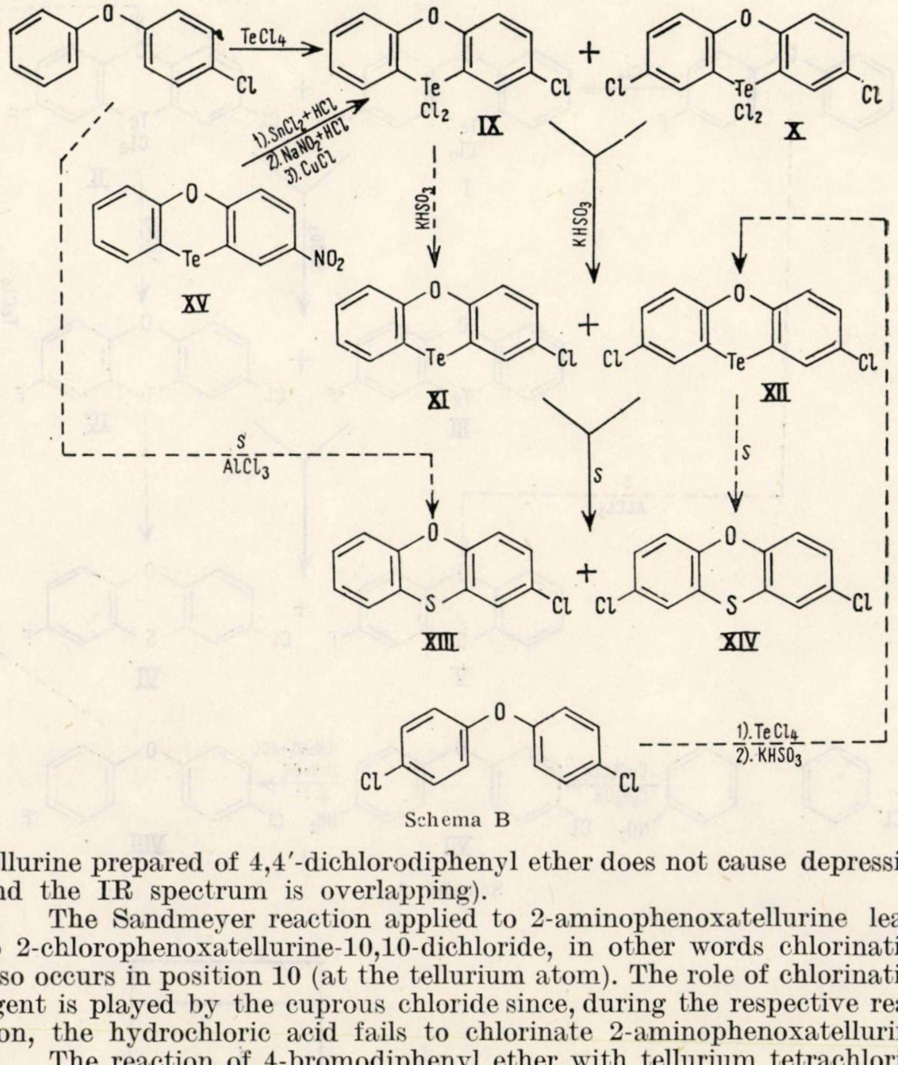

Schema B

tellurine prepared of 4,4′-dichlorodiphenyl ether does not cause depression and the IR spectrum is overlapping).

The Sandmeyer reaction applied to 2-aminophenoxatellurine leads to 2-chlorophenoxatellurine-10,10-dichloride, in other words chlorination also occurs in position 10 (at the tellurium atom). The role of chlorinating agent is played by the cuprous chloride since, during the respective reaction, the hydrochloric acid fails to chlorinate 2-aminophenoxatellurine.

The reaction of 4-bromodiphenyl ether with tellurium tetrachloride occurs with a low yield and gives a mixture of products which cannot separate satisfactorily by repeated crystallizations or by column chromatography. Thin-layer chromatography (performed after the reduction of the reaction mixture with KHSO$_3$) revealed the presence of 2-bromophenoxytellurine alongside with another unidentified spot.

EXPERIMENTAL

4-fluorodiphenyl ether,[7] 4-chlorodiphenyl ether,[8] 4-bromodiphenyl ether,[9] 4-iododiphenyl ether,[10]

---

[7] N. J. LEONARD and L. E. SUTTON, *J. Amer. Chem. Soc.*, **70**, 1564 (1948).

[8] C. M. SUTER and F. O. GREEN, *J. Amer. Chem. Soc.*, **59**, 2578 (1937).

[9] C. M. SUTER, *J. Amer. Chem. Soc.*, **51**, 2581 (1929).

[10] R. Q. BREWSTER and F. STRAIN, *J. Amer. Chem. Soc.*, **56**, 117 (1934).

4,4′-dichlorodiphenyl ether,[11] 4-chloro-4′-aminodiphenyl ether,[12]
4-nitro-4′-chlorodiphenyl ether,[12] 2-fluorophenoxathiine,[13]
2-chlorophenoxythiine,[8] 2-nitrophenoxatellurine[14],

2-aminophenoxatellurine,[15] 2,8-dichlorophenoxatellurine-10,10-dichloride, 2,8-dichlorophenoxatellurine and 2,8-dichloro-phenoxathiine [2] were prepared according to methods indicated in the literature.

p-fluoro-*p*′-chlorodiphenyl ether was prepared by the Schiemann reaction from *p*-amino-*p*′-chlorodiphenyl ether (b.t. 155–157°/14 Torr).

Synthesis of 2-chlorophenoxatellurine-10,10-dichloride (IX). A suspension of 2 g 2-aminophenoxatellurine in 5 ml concentrated hydrochloric acid is diazotized between 0–5° with a solution of 0.4 g sodium nitrite in 4 ml water. The diazonium salt obtained thereby is filtered and poured over a solution of 2 g cuprous chloride in 10.2 ml hydrochloric acid. After boiling for 30 minutes on a water bath, it is cooled, filtered, washed with water and dried. 1 g of a pale yellow product results (yield 41%) which is recrystallized from acetone. M.p. 310°.

Analysis for $C_{12}H_7OTeCl_3$: Te% *calculated* : 31.80 ; *found* : 31.46.

Synthesis of 2-chlorophenoxatellurine (XI). 2 g potassium metabisulphite are added under stirring for 30 minutes, to a suspension of 0.5 g 2-chlorophenoxatellurine-10,10-dichloride in 13 ml water cooled with ice. After completing this operation, the reaction mixture is allowed to stand in the cold for another 3 hours. It is filtered on Buchner, washed with water and dried. Yield 95%, m.p. 95–96°.

Analysis for $C_{12}H_7$ OTeCl : Te% *calculated* : 38.63 ; *found* 38.22.

Synthesis of 2-fluoro-8-chlorophenoxatellurine-10,10-dichloride (II). A thermometer and a reflux cooler fitted with a calcium chloride tube are attached to a 100 ml flask containing 19.8 g anhydrous tellurium tetrachloride. 17 g 4-fluoro-4′-chloro-diphenyl ether are introduced and after passing a stream of purified methane gas (or inert gas) the solution is heated for 5 hr at 180–225°, stirring intermittently. After cooling, the reaction mixture is treated with 30 ml anhydrous ether, it is filtered on Buchner and washed with ether until the filtrate becomes colourless. The crystals on the filter are extracted with acetone by heating, the solution is boiled with animal charcoal, then filtered and after concentration and cooling the filtrate provides 16.2 g (yield 50%) raw product. M.p. 311–312° (from acetone).

Analysis for $C_{12}H_6OTeCl_3F$: Te% *calculated* 30.44 ; *found* 30.68.

Synthesis of 2-fluoro-8-chlorophenoxatellurine (IV). By an analogous procedure to that applied to substance XI, 6.75 g (yield 98.5%) of a yellow product are obtained from 8.25 g 2-fluoro-8-chlorophenoxatellurine-10,10-dichloride, 13.5 g potassium metabisulphite and 100 ml water. M.p. 108–109° (from extraction petrol).

Analysis for $C_{12}H_6OTeCl_3F$: Te% calculated 36.64, found 36.39.

Synthesis of 2-fluoro-8-chlorophenoxatiine (VI). A mixture of 2 g 2-fluoro-8-chlorophenoxatellurine and 0.2 sulphur is heated at 260–265° for 1 hr in a stream of purified methane gas. The reaction mixture darkens gradually while heating and the tellurium resulting from the reaction deposits on the walls of the flask. It is extracted with benzene and, after removing the solvent, it is recrystallized from ethanol, obtaining 0.8 g (yield 51.7%) of a white product with m.p. 101–102°.

Analysis for $C_{12}H_6OSFCl$: S% *calculated* 12.68 ; *found* 12.39

---

[11] A. Peratoner and G. Ortoleva, *Gazz. chim. Ital.*, **28**, 197 (1898).

[12] R. J. W. Le Fevre, S. L. Saunders and E. E. Türner, *J. Chem. Soc.*, **1927**, 1168.

[13] G. Vasiliu and O. Maior, *Anal. Şti. Univ. Buc.*, **11**, 167 (1962).

[14] I. G. Campbell and E. E. Türner, *J. Chem. Soc.*, **1938**, 37.

[15] H. D. K. Drew and R. W. Thomason, *J. Chem. Soc.*, **1927**, 116.

Reaction of tellurium tetrachloride with p-fluorodiphenyl ether. Proceeding like in the synthesis of substance II, 35 g *p*-fluorodiphenyl ether and 51 g anhydrous tellurium tetrachloride are heated for 17 hr between 115–220° to obtain 20 g of a white product with the m.p. 291–293°.

This being reduced in similar conditions to the obtention of substance XI, a mixture of III and IV results which is evidenced by thin-layer chromatography performed on silicagel G in benzene : extraction petrol (1 : 1 V/V), using iodine vapours for developing. By repeated recrystallizations IV is obtained from extraction petrol.

Similar results are obtained by working with 66 g 4-chloro-diphenyl ether, 87 g tellurium tetrachloride at 150–240° for 9 hrs when 70 g raw product are obtained with m.p. 310–312°. By reducing as above, this has been chromatographically proved to be a mixture of XI and XII. Repeated recrystallizations from extraction petrol lead to substance XII (m.p. 111–112°).

By heating 50 g 4-bromodiphenyl ether and 53.5 g $TeCl_4$ at 120–210° for 9 hrs, one obtains, after the usual work-up 16 g of a pale yellow product with m.p. 319–324°. After reduction and chromatographic analysis the latter was found to be non-unitary, one of the spots representing 2-bromophenoxatellurine.

Proceeding as above, a decomposition takes place from 4.1 g iododiphenyl ether with 3.7 g $TeCl_4$ at 120–170° for 9 hrs, with release of elemental iodine and no unitary products were isolated by working up the reaction mixture.

Revue Roumaine de Chimie, 21, 5, 745–747, (1976)

SYNTHESES BASED ON THIENO[2,3-b]-BENZOTHIACHROMONE

O. MAIOR * and N. RĂŞANU **

* Institute of Chemistry, Department of Chemistry and Organic Technology, Bucharest
Splaiul Independenţei, 89
** Pedagogical Institute, Laboratory of Organic Chemistry, Constanţa

Received December 27, 1974

The paper presents the behaviour of the carbonyl group of this heterocycle in some specific reactions.

The carbonyl group of thieno [2,3-b]benzothiachromone is found in conjugation with π electrons from the benzene and the thiophene ring and also with *p* electrons of the sulphur atom in the central ring. For this reason, the specific reactions of the carbonyl group are expected to occur less readily, if at all, with such a heterocycle.

Thus it has been found that thieno [2,3-b]benzothiachromone fails to react with hydroxylamine, *p*-nitro-, 2,4-dinitrophenylhydrazine and semicarbazide under our working conditions. However, with P_2S_5 in anhydrous benzene it forms the respective thione (I).

The oxime of thieno [2,3-b]benzothiachromone (II) was obtained only from thione (I) with a 41.9% yield.

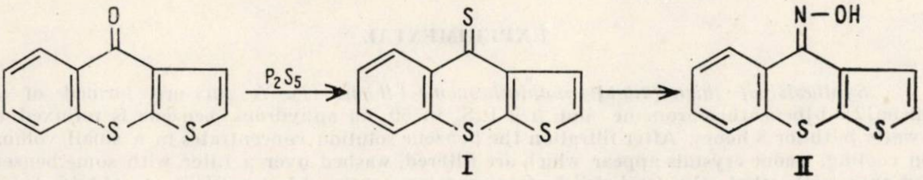

In the reaction with thionyl chloride, it behaves similarly to thioxanthone [1] and forms 4,4-dichloro-thieno [2,3-b]benzothiachromone (III) after refluxing for a few hours.

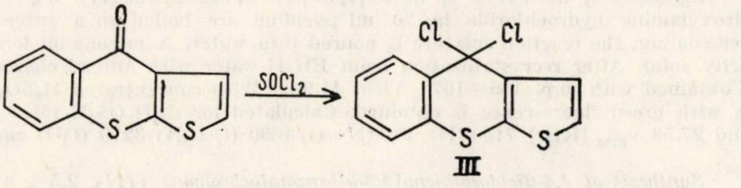

---

[1] M. M. Hafez, N. Latif and I. F. Zeid, *J. Org. Chem.*, **26**, 3988 (1961).

By oxidizing thieno [2,3-b]benzothiachromone with H_2O_2, the corresponding dioxide (IV) is formed in which the carbonyl group behaves similarly to that in thioxanthone-5,5-dioxide, in other words it becomes more reactive.

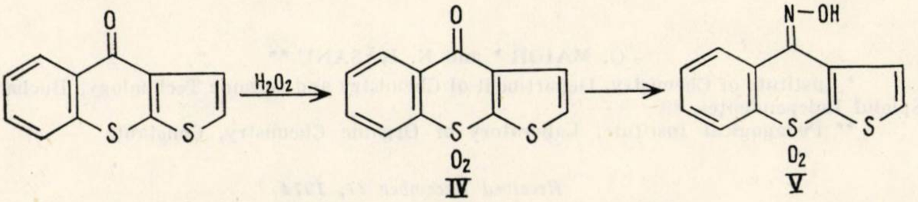

In this case, the reaction with hydroxylamine occurs with a 45% yield. A similar oxime has also been obtained from thione (VI), obtained, in turn, from its compound (IV) by treating with P_2S_5.

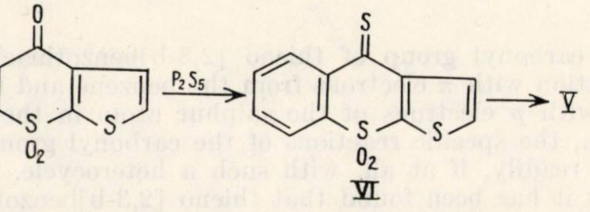

Thieno [2,3-b]benzothiachromone was obtained by cyclodehydration with polyphosphoric acid of 2-carboxyphenylthienylsulphide, this substance being prepared by Ullmann synthesis from thiosalicylic acid and 2-iodothiophene.

EXPERIMENTAL

Synthesis of thieno[2,3-b]benzothiachromone-4-thione (I). A mixture formed of 5g thieno[2,3-b]benzothiachromone and 5 g P_2S_5 in 50 ml anhydrous benzene is refluxed on a water bath for 3 hours. After filtration the benzene solution concentrates in a small volume. On cooling, thione crystals appear which are filtered, washed over a filter with some benzene and then with ethyl ether and dried at room temperature. 2.5 g product are obtained with m.p. 138−139°. The thin-layer chromatography on silicagel revealed one single spot in the substance with R_f (acetone, chloroform, methanol 1 : 1 : 1) = 0.83. Calculated for $C_{11}H_6S_3$(M = = 234.36) S % 41.04, found 40.64. ν_{max} (KBr) 720 (4H), 1219 ($c = s$), 3085 (= CH) cm^{-1}.

Synthesis of the oxime of thieno[2,3-b]benzothiachromone (II). 3 g thione (I) and 3g hydroxylamine hydrochloride in 20 ml pyridine are boiled on a water bath for 4 hours. After cooling, the reaction mixture is poured into water. A viscous oil forms which becomes shortly solid. After recrystallization from EtOH-water with animal charcoal, white crystals are obtained with m.p. 165−167°. Yield 41.9%. With concentrated H_2SO_4, a yellow coloration with green fluorescence is obtained. Calculated for $C_{11}H_7OS_2N$ (M = 233.31) S % 27.48, found 27.58 ν_{max} (KBr) 715 (4H), 940 (N−O) 1630 (C = N) 3270 (OH) cm^{-1}.

Synthesis of 4,4-dichlorothieno[2,3-b]benzothiachromone (III). 2.5 g thieno[2,3-b]benzothiachromone, 30 ml anhydrous benzene and 3 ml $SOCl_2$ are refluxed for 5 hours on a water bath. The solvent is removed and the residue left is dissolved in a reduced amount of dioxan.

Petroleum ether is added to the cooled solution. 0.7 g product are obtained with m.p. 102—104 Calculated for $C_{11}H_6S_2Cl_2$ (M = 273.20) S% 23.47 found 23.87.

Synthesis of thieno[2,3-b]benzothiachromone-9,9-dioxide (IV). 10 g thieno [2,3-b] benzothiachromone in 30 ml glacial acetic acid are oxidized with 15 ml 30% H_2O_2. 4.4 g product are obtained. After recrystallization from methanol its m.p. is 177—179°. Calculated for $C_{11}H_6O_3S_2$ (M = 250.30) S% 25.62, found 25.27. ν_{max} (KBr) 745 (4H), 540, 570, 1160, 1310 (SO_2) 1670 (c = 0), 3095 (= CH) cm^{-1}.

Synthesis of the oxime of thieno[2,3-b]benzothiachromone-9,9-dioxide (V). 3 g product IV, 3 g hydroxylamine hydrochloride and 20 ml pyridine are heated on a water bath for 4 hours. After cooling, the mixture is poured into water, the formed precipitate is filtered and recrystallized from methanol-water. M.p. 196—198°. Yield 45%. Calculated for $C_{11}H_7O_3S_2N$ (M = = 265.31) S% 24.21, found 23.73. ν_{max} (KBr) 730 (4H) 530, 560, 1140, 1160, 1300 (SO_2), 3110 (= CH), 3370 (OH) cm^{-1}.

Synthesis of thieno[2,3-b]benzothiachromone-9,9-dioxide-4-thione (VI). It was performed under similar conditions to thione (I) starting from product IV and P_2S_5. Yield 40%. M.p. 164—166°. The thin-layer chromatography on silicagel showed Rf (acetone, chloroform,methanol 1 : 1 : 1) = 0.70. Calculated for $C_{11}H_6O_2S_3$ (M = 266.36) S% 36.11, found 35.42.

Preparation of 2-carboxyphenylthienylsulphide. A mixture formed of 31 g thiosalicylic acid, 47 g 2-iodothiophene, 32 g anhydrous Na_2CO_3 0.1 g powdered Cu is refluxed for 4 hours in 150 ml dimethylformamide. The reaction mixture is poured into water, filtered and the filtrate is acidulated with concentrated HCl. The formed precipitate is filtered and dried at room temperature. 40 g raw product are obtained with m.p. 187—189°. After recrystallization from methanol with animal charcoal, white crystals are obtained with m.p. 195—196°.

Preparation of thieno[2,3-b]benzothiachromone. A mixture formed of 20 g of the above product and 100 g polyphosphoric acid is stirred for 2 hours at a temperature ranging betwen 110—120°. After cooling, water and ice are added to the reaction mixture with stirring. The formed precipitate is filtered in vacuo, it is washed on a filter with water then with a $KHSO_3$ solution and again with water. 13.2 g raw product are obtained (yield 71.7%) with m.p. 138—140°. After recrystallization from methanol with animal charcoal, white crystals are obtained with m.p. 156—158° Lit [2] m.p. 157—158°.

With concentrated H_2SO_4, a yellow coloration with green fluorescence is obtained.

ν_{max} (KBr) 720 (4H) 1640 (C = 0) cm^{-1}.

---

[2] J. Renz, P. Bourquin, G. Schwarb and L. Reusch, Brev. Elv. 405.354 iunie 1966; *Chem. Abstr.*, **66**, 2550 (1967).

Revue Roumaine de Chimie, **21**, 5, 749–755 (1976)

TOPOLOGICAL STUDIES OF FUSED TRICYCLIC AND TETRACYCLIC MOLECULES HAVING PLANAR CONJUGATED PERIMETER

J. V. KNOP *, N. TRINAJSTIĆ [1]*, and A. SABLJIĆ **
* Computing Center of the University, 4000 Düsseldorf, Universitätsstrasse 1,
F.R. Germany, and
** The Rugjer Bošković Institute, P.O.B. 1016, 41001 Zagreb, Croatia, Yugoslavia

Received December 3, 1974

The combinations of cycles leading to tricyclic and tetracyclic conjugated molecules having planar conjugated perimeter with different mode are discussed. In particular, π-electron perimeter with mode 2, i.e. polycyclic molecules containing $4m+2$ π-electrons, should exhibit aromatic stability (with a limitation that larger rings are weaker aromatics). Properties of some classes of polycyclic conjugated molecules (e.g. cyclazines) are discussed.

In the present work we wish to study the structural properties of tricyclic and tetracyclic molecules which consist of a conjugated perimeter held planar by central atom(s) bearing either two or zero π-electrons. Such molecules can be depicted by topological diagrams (I) and (II) given below.

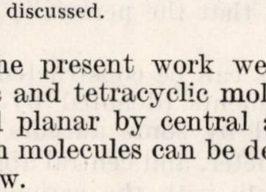

(I)

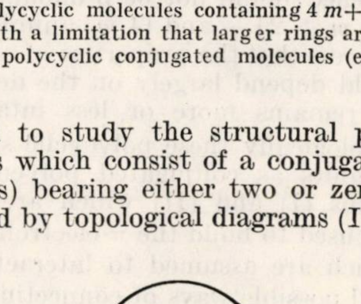

(II)

---

[1] Visiting Professor from the Rugjer Bošković Institute, P.O. Box 1016, 41001 Zagreb, Croatia, Yugoslavia.

Representative classes of molecules belonging to diagrams (I) and (II) are, for example, cyclazines [2] and hydrazine-bridged annulenes,[3] respectively.

Rings denoted by capital letters A, B and C may have either even or odd number of atoms starting from five because planar tri- or tetracyclic fused ring systems with lesser number of atoms (e.g. three or four) in an individual ring would be too strained to exist [4] (except as a short-lived species under the special experimental conditions).[5] Combination of rings of various sizes are possible. If the combination of rings is producing a perimeter with *an odd* number of atoms, i.e. with $4m+1$ or $4m+3$ topology (where m is an integer) and if each atom is bearing a single π-electron, then such a structure is expected to exhibit a radical reactivity.[6] However, if the combination of rings is leading to structures with *an even* number of atoms π-electron perimeter (and if each atom is bringing only one π-electron to the perimeter) then these structures could be classified in two groups depending whether the perimeter has $4m$ or $4m+2$ topology. [7] Polycyclic molecules belonging to these two classes should differ in their stabilities and reactivities. However, this difference should not be pronounced [2,3] to such an extent as it is in the case of $[4m+2]$ — and $[4m]$-annulenes.[6–8] An important point to emphasize here is that the properties of such planar tri- and tetracyclic molecules would depend largely on the demand that the pericyclic π-electron topology remains more or less intact.

Topologically these polycyclic systems can be constructed from the building units as conjugated polyene segments (denoted by solid line in diagrams (I) and (II) which are called by some authors [9] ribbons) which are used to build the π-electron perimeter, and central atoms (vertices [10]) which are assumed to interact weakly with the perimeter. There are several possible ways of connecting ribbons; here they will be connected directly: the end vertex of the first ribbon will be the starting vertex of the second ribbon. Thus, in our case three or four ribbons (depending whether a perimeter belongs to tricyclic or tetracyclic system) would produce the necessary π-electron perimeter. The weak interaction between the central atom(s) and the perimeter is denoted by a broken line and it is set in such a way that the interaction occurs between the central atom(s) and the starting (ending) vertices of ribbons making up the perimeter of a polycyclic molecule (see (I) and (II)).

---

[2] R. J. WINDGASSEN JR., W. H. SAUNDERS Jr., and V. BOEKELHEIDE, *J. Amer. Chem. Soc.*, **81**, 1459 (1959).

[3] W. FLITSCH and H. PEETERS, *Chem. Ber.*, **106**, 1731 (1973).

[4] L. J. SCHAAD and B. A. HESS JR., *J. Amer. Chem. Soc.*, **94**, 3068 (1972).

[5] O. CEDER and J. E. ANDERSSON, *Acta Chem. Scand.*, **26**, 611 (1972).

[6] A. T. BALABAN, *Rev. Roumaine Chim.*, **17**, 1531 (1972).

[7] A. T. BALABAN and Z. SIMON, *Rev. Roumaine Chim.*, **10**, 1057 (1965).

[8] F. SONDHEIMER, *Pure Appl. Chem.*, **7**, 363 (1963), *Proc. Roy. Soc.* **A 297**, 173 (1967), *Proc. Robert A. Welch Found. Conf. Chem. Res.*, **12**, 125 (1968), *Accounts Chem. Res.*, **5**, 81 (1972); R. C. HADDON, V. R. HADDON, and L. M. JACKMAN, *Topics Curr. Chem.*, **19**, 103 (1971); M.J.S. Dewar and G. J. Gleicher, *J. Amer. Chem. Soc.*, **87**, 685 (1965); H. F. FIGEYS, *Tetrahedron*, *26*, 4615 (1970); T. M. KRYGOWSKI. *Tetrahedron Letters*, **1970**, 1311; I. GUTMAN, M. MILUN, and N. TRINAJSTIĆ, *Croat. Chem. Acta*, **44**, 207 (1972); V. BUSS, *Chem. Phys. Lett.*, **22**, 191 (1974).

[9] M. J. GOLSTEIN and R. HOFFMANN, *J. Amer. Chem. Soc.*, **93**, 6193 (1971).

[10] I. GUTMAN and N. TRINAJSTIĆ, *Topics Curr. Chem.*, **42**, 49 (1973).

Algebraically each ribbon can be represented by its *mode* [9] (μ). The mode of a ribbon is given as one of the four integers 0, 1, 2, or 3 computed as $(m-Z)$ modulo 4, where m is the number of vertices in the ribbon and Z is a possible charge of the conjugated fragment represented by this particular ribbon. The list of modes of same selected ribbons is given in a paper by Goldstein and Hoffmann.[9] It is also convenient to introduce a mode of a monocyclic sequence of atoms (M), i.e. π-electron perimeter. A mode of a cycle could be defined [6,11] formally in a similar way as a mode of the ribbon, namely as $(m-Z)$ modulo 4. However m is now the size of a cycle (ring) and Z is the charge of a ring for homogeneous system. In the case of heterocyclics Z is the difference between the number of atoms and π-electrons (because some heteroatoms may bring two π-electrons each to the cyclic π-system, like it would $\ddot{S}$, $\ddot{N}$, $\ddot{S}e$, $\ddot{O}$, etc.) in the particular ring system with the sign + or − depending whether the number of π-electrons is greater (−) or smaller (+) than the number of atoms donating π-electrons to the cyclic system. For example, the modes of cyclopentadienyl cation and furan are given by: $[5-(+1)]$ modulo $4 = 0$ and $[5-(-1)]$ modulo $4 = 2$, respectively. Finally, $4m + 2$ rings are the mode 2 rings while $4m$ rings are the mode O rings. [6,11]

A perimeter of a polycyclic system is a composite cycle obtained from ribbons. Therefore, a mode of the perimeter is equal to the sum of modes of the individual ribbons making up the perimeter:

$$M = \sum_i \mu(i) \qquad (1)$$

The mode of a ribbon associated with a particular ring in a polycyclic system can be obtained by considering that fragment of a ring which is contributing to the perimeter of a polycyclic system. Thus, the mode of each individual ribbon making up the perimeter will vary depending whether it is associated with A, B, or C ring. This is, of course, a result of such a particular way of combining ribbons as descbribed earlier, i.e. direct attachment of one ribbon to the other, thus the second ribbon(s) would be shorter for one vertex and the third for two vertices, because these vertices are already counted in the previous ribbon. Note that we have arbitrarily denoted rings in topological diagrams (I) and (II). Hence, alternative ways of denoting rings in (I) and (II) are legitimate, but once the notation of rings is made it should be kept throughout the procedure. The mode of a ribbon associated with any one of A, B, or C rings could be estimated from the expression given below:

$$\mu(i) = (m - k_i) \text{ modulo } 4 \qquad (2)$$

---

[11] I. Gutman and N. Trinajstić, *Scientia Yug.*, *1*, 1 (1974).

where m is the size of the individual ring i (e.g., $m = 6$ for benzene, $m = 5$ for thiophene) while k_i is correction for that part of a particular ring which is not contributing to the outer π-electron perimeter plus the vertices counted twice in the second, third, and fourth ribbon.

The use of formulae (1) and (2) will be illustrated for cycl[3, 2, 2] azine (III), cycl[3, 3, 3] azine (IV), 8 b, 8c-diazapyracyclene (V) and 10 b,10 c-diazadicyclopentaheptalene (VI). Note that perimeter in all these molecules involves only carbon atoms.

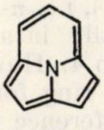
(III)

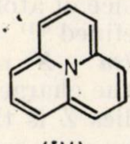
(IV)

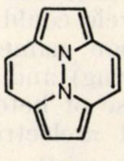
(V)

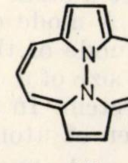
(VI).

Diagrams (I) and (II) represent these molecules. Assumptions about planarity and isolated perimeter conjugation appear to be experimentally verified. For example, an x-ray structural determination of III has shown this molecule to be completely planar.[12] Similarly, the N.M.R measurements carried out on IV indicated that this molecule possesses a single (perimeter) ring current.[13]

The evaluation of the perimeter modes is illustrated for (III) and (V):

$$\begin{aligned} M(\mathrm{III}) &= \mu(A) + \mu(B) + \mu(C) \\ &= (6-1) \text{ modulo } 4 + (5-2) \text{ modulo } 4 + (5-3) \text{ modulo } 4 \\ &= 10 \text{ modulo } 4 \\ &= 2 \\ M(\mathrm{IV}) &= 0 \\ M(\mathrm{V}) &= \mu(A) + \mu(B) + \mu(B) + \mu(C) \\ &= (5-1) \text{ modulo } 4 + (6-3) \text{ modulo } 4 + (6-3) \text{ modulo } 4 + \\ &\quad (5-3) \text{ modulo } 4 \\ &= 0 + 3 + 3 + 2 \\ &= 0 \\ M(\mathrm{VI}) &= 2 \end{aligned}$$

Therefore, cycl[3, 2, 2]azine ($M = 2$) and cycl[3, 3, 3]azine ($M = 0$) as well as 8b, 8c-diazapyracyclene ($M = 0$) and 10b, 10c-diazadicyclopentaheptalene ($M = 2$) should differ in their chemical properties. Cycl[3, 2, 2]azine (III) was prepared years ago (1959)[2] and today quite a few of its derivatives are known.[14] On the other hand, cycl[3, 3, 3]azine (IV) is made only recently (1969).[15] III is considered as an aromatic compound and theoretical indices of aromaticity Dewar resonance energy (DRE) and resonance energy per electron (REPE) have values characteristic of aromatic compounds (0.82 eV,[16] 0.040 β[17]). (For example, DRE and REPE values of benzene, which is considered as a prototype of an aromatic compound,[18] are 0.87 eV [19] and 0.065 β[20], respectively). However, DRE and REPE values (−0.024 eV,[16] 0.001 β[17]) indicate cycl[3, 3, 3]azine to be antiaromatic species. Cycl[3, 2, 2]azine is indeed, found to be a stable compound whereas cycl[3, 3, 3]azine is a rather reactive species decomposing rapidly on exposure to air. Similarly, V and VI differ in their stabilities and properties, VI being more stable [3,21] than V.

---

[12] A. W. Hanson, *Acta Cryst.*, **14**, 124 (1961).

[13] R. C. Haddon, *Tetrahedron*, **28**, 3613 (1972).

[14] A. Gailbraith, T. Small, and V. Boekelheide, J. Org. Chem., **24**, 582 (1959); A. Gailbraith, T. Small, R. A. Barnes, and V. Boekelheide, *J. Amer. Chem. Soc.*, **83**, 453 (1961); R. M. Acheson and D. A. Robinson, *J.C.S. Chem.* Comm., **1967**, 175; C. M. Gupta and A. Nitya, *Indian J. Chem.*, **11**, 427 (1973); E. Pohjala, *Acta Chem. Scand.*, **B 28**, 582 (1974).

[15] D. Farquhar and D. Leaver, *J.C.S. Chem. Comm.*, **1969**, 24.

Since the experience indicates that a perimeter with mode 2 belongs to stable aromatic polycyclic molecules and that a perimeter with mode 0 belongs to antiaromatic systems, it seems of interest to investigate the topological requirements leading to the mode 2 perimeter, i.e. structural conditions for a stable tricyclic and tetracyclic molecules with $4m + 2$ perimeter. The various combinations of rings donating ribbons of a specific mode and leading to the mode 2 perimeter for tricyclic and tetracyclic molecules are given in the table. Letters *A*, *B*, and *C* in Table denote as in diagrams (I) and (II) rings making up a particular polycyclic molecule. The numbers in columns indicate the mode of individual ribbons contributing to a molecular perimeter. It is clear that any Combination of ribbons is allowed for which $M = 2$.

Let us consider, as an example, two polycyclic systems (with nitrogens as central atoms), one (tricyclic) with the code (1 3 2) and the other

CODE (1 3 2)

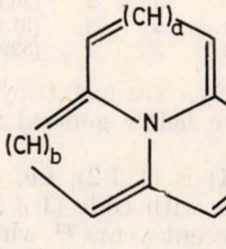

a,b,c = 1, 5, 9,........

CODE (2 3 0 1)

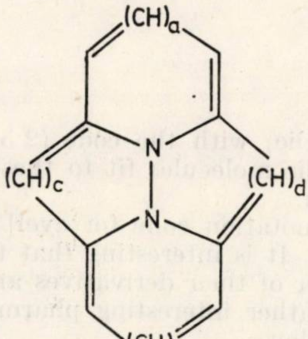

(i) a, b = 0
c, d = 1, 5, 9, ...

(ii) a, b, c, d = 1, 5, 9, ...

---

[6] M. J. S. Dewar and N. Trinajstić, *J. Chem. Soc.* (*A*), **1969**, 1754.

[17] B. A. Hess Jr., L. J. Schaad, and C. W. Holyoke Jr., *Tetrahedron*, **28**, 3657 (1972).

[18] G. M. Badger, "Aromatic Character and Aromaticity", University Press, Cambridge, 1969.

[19] M. J. S. Dewar and C. de Llano, *J. Amer. Chem. Soc.*, **91**, 780 (1969).

[20] B. A. Hess Jr., and L. J. Schaad, *J. Amer. Chem. Soc.* **93**, 305 (1971).

[21] W. W. Paudler, *J. Amer. Chem. Soc.*, **92**, 4468 (1970). J. L. Atwood, D. C. Hrncir, C. Wong, and W. W. Paudler, *ibid.*, **96**, 6132 (1974).

Table

Combinations of ribbons (each coded by its specific mode) which produce the perimeter with $M = 2$ (see text) in tricyclic and tetracyclic planar molecules with a conjugated perimeter

Polycyclic molecule / Individual ring	A	B	C	Code	A	B	B	C	Code
	0	0	2	(002)	0	0	0	2	(0002)
	0	1	1	(011)	0	0	1	1	(0011)
	0	2	0	(020)	0	0	2	0	(0020)
	0	3	3	(033)	0	0	3	3	(0033)
	1	0	1	(101)	0	1	1	0	(0110)
	1	2	3	(123)	0	1	2	3	(0123)
	1	3	2	(132)	0	1	3	2	(0132)
	2	1	3	(213)	0	2	2	2	(0222)
	2	2	2	(222)	0	2	3	1	(0231)
	3	0	3	(303)	0	3	3	0	(0330)
					1	0	0	1	(1001)
					1	0	2	3	(1023)
					1	0	3	2	(1032)
					1	1	1	3	(1113)
					1	1	2	2	(1122)
					1	1	3	1	(1131)
					1	2	2	1	(1221)
					1	3	3	3	(1333)
					2	0	1	3	(2013)
					2	0	2	2	(2022)
					2	1	1	2	(2112)
					2	2	3	3	(2233)
					2	3	3	2	(2332)
					3	0	0	3	(3003)
					3	1	3	3	(3133)
					3	2	2	3	(3223)

(tetracyclic) with the code (2 3 0 1), respectively. Various tricyclic and tetracyclic molecules fit to these codes. We give below general formulae for them.

In this notation code for cycl[3, 2, 2]azine (III) is (1 3 2), i.e. $a = b = c = 1$. It is interesting that the azacyclazines with code (1 3 2) [22] and a number of their derivatives are prepared in recent years [23] which have shown rather interesting pharmacological properties. Some of them are listed below.

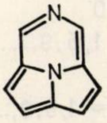

(VII)

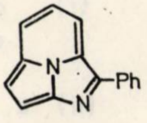

(VIII)

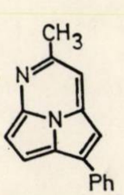

(IX)

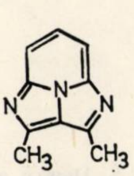

(X)

---

[22] V. Boekelheide and A. Miller, *J. Org. Chem.*, **26**, 431 (1961); V. Boekelheide and S. Kertely, *ibid.* **28**, 3212 (1963); K. Valentin and A. Taurins, *Tetrahedron Letters*, **1966**, 3621; M. A. Jessep and D. Leaver, *J.C.S. Chem. Comm.*, **1970**, 790.

[23] Azacyclines are formally obtained by substitution of a nitrogen on the periphery in a non-angular position for a carbon atom. Their syntheses were stimulated by possible pharmacological properties.

Some of ribbons in these compounds contain the heteroatom.

Polycyclic systems with rather large values of a, b, and c indices (i.e. with rings of a large size) even if $M = 2$, are expected to be of lesser interest. In these cases there is a little difference from polycyclic systems with a perimeter of $M = 0$, similarly as the difference between $4m + 2$ (mode 2) and $4m$ (mode 0) cyclic systems diminish rather rapidly [8,24] with m increasing. For example, the DRE and REPE values of [10]-annulene are 1.06 eV[19] and 0.026 β[20], respectively, whereas of [14]-annulene are already considerably smaller, i.e. 0.67 eV[19] and 0.016 eV[20], respectively. There appears to be an upper limit in the size of A, B and C rings considered. Experience shows that the higher monocyclic systems (e.g. 9-membered heterocyclics) behave as cyclic polyenes.[13,17,25] However, this is not a serious limitation of a topological approach because the largest number of tricyclic and tetracyclic molecules consist of various combinations of five-, six-, and/or seven-membered rings.

At the end of this note we wish to point out that the mode of a ring is related to the number of *even* (K^+, parity $= +1$) and *odd* (K^-, parity $= -1$) Kekulé structures [26] (the total number of Kekulé structures being $K = K^+ + K^-$). Characteristics of mode 2 rings is $K^+ = 2$ whereas of mode 0 rings $K^+ = K^- = 1$. Since the difference [27] between the K^+ and K^- ($K^+ - K^- = ASC$) is important for thermodynamic and chemical stability of conjugated molecules,[28] $ASC = 2$ for mode 2 rings and $ASC = 0$ for mode 0 rings.[29]

ACKNOWLEDGEMENTS. We thank Professor M. Randić (Medford, USA) for useful comments.

---

[24] H. C. LONGUET-HIGGINS and L. SALEM, *Proc. Roy. Soc.*, **A 251**, 172 (1959); *ibid.*, **A 257**, 445 (1960).

[25] A. G. ANASTASSIOU and R. P. CELLURA, *J.C.S. Chem. Comm.*, **1969**, 903, 1521; A. G. ANASTASSIOU and J. H. GEBRIAN, *J. Amer. Chem. Soc.*, **91**, 4011 (1969); *Tetrahedron Letters*, **1970**, 825; A. G. ANASTASSIOU, S. W. EACHUS, R. P. CELLURA, and J. H. GEBRIAN, *J.C.S. Chem. Comm.*, **1970**, 1133.

[26] M. J. S. DEWAR and H. C. LONGUET-HIGGINS, *Proc. Roy. Soc.*, **A 214**, 482 (1952).

[27] C. F. WILCOX JR., *Tetrahedron Letters*, **1968**, 795.

[28] I. GUTMAN, N. TRINAJSTIĆ, and C. F. WILCOX JR., *Tetrahedron*, 31, 143(1975).

[29] A. GRAOVAC, I. GUTMAN, N. TRINAJSTIĆ, and T. ŽIVKOVIĆ, *Theoret. Chim. Acta*, **26**, 67 (1972); I. Gutman and N. TRINAJSTIĆ, *Croat. Chem. Acta*, 45, 539 (1973); D. CVETKOVIĆ, I. GUTMAN, and N. TRINAJSTIĆ, *J. Chem. Phys.*, **61**, 2700 (1974).

Revue Roumaine de Chimie, **21**, *5*, 749–755 (1976)

8–c. 1096

Some of ribbons in these compounds contain the heteroatom.

Polycyclic systems with rather large values of a, b, and c indices (i.e., with rings of a large size) even if $M = 2$, are expected to be of lesser interest. In these cases there is a little difference from polycyclic systems with a perimeter of $M = 0$, similarly as the difference between $4n + 2$ (mode 2) and $4n$ (mode 0) cyclic systems diminish rather rapidly[illegible] with n increasing. For example, the DRE and REPE values of [10]annulene are 1.06 eV[illegible] and 0.026 [illegible], respectively, whereas of [14]annulene are already considerably smaller, i.e., 0.07 eV[illegible] and 0.013 eV[illegible], respectively. There appears to be an upper limit in the size of A, B and C rings considered. Experience shows that the higher monocyclic systems (e.g., 9-membered heterocycles) behave as cyclic polyenes.[illegible] However, this is not a serious limitation of a topological approach because the largest number of tricyclic and tetracyclic molecules consist of various combinations of five-, six-, and/or seven-membered rings.

At the end of this note we wish to point out that the mode of a ring is related to the number of even (K_e, parity = +1) and odd (K_o, parity = −1) Kekulé structures[illegible] (the total number of Kekulé structures being $K = K_e + K_o$). Characteristics of mode 2 rings is $K_o = 2$, whereas of mode 0 rings $K_e = K_o = 1$. Since the difference[illegible] between the K_e and K_o ($K_e - K_o = ASC$) is important for thermodynamic and chemical stability of conjugated molecules,[illegible] $ASC = 2$ for mode 2 rings and $ASC = 0$ for mode 0 rings.[illegible]

ACKNOWLEDGMENTS. We thank Professor M. Randić [illegible] for useful comments.

H. C. Longuet-Higgins and L. Salem, *Proc. Roy. Soc.*, A 251, 172 (1959); *ibid.*, A 257, 445 (1960).

A. G. Anastassiou and R. P. Cellura, *J.C.S. Chem. Comm.*, 1969, 903, 1521; A. G. Anastassiou and J. H. Gebrian, *J. Amer. Chem. Soc.*, 91, 4011 (1969); *Tetrahedron Letters*, 1970, 825; A. G. Anastassiou, S. W. Eachus, R. P. Cellura, and J. H. Gebrian, *J.C.S. Chem. Comm.*, 1970, 1133.

M. J. S. Dewar and H. C. Longuet-Higgins, *Proc. Roy. Soc.*, A 214, 482 (1952).

C. F. Wilcox Jr., *Tetrahedron Letters*, 1968, 795.

I. Gutman, N. Trinajstić, and C. F. Wilcox Jr., *Tetrahedron*, 31, 143 (1975).

A. Graovac, I. Gutman, N. Trinajstić, and T. Živković, *Theoret. Chim. Acta*, 26, 67 (1972); I. Gutman and N. Trinajstić, *Croat. Chem. Acta*, 45, 539 (1973); D. Cvetković, I. Gutman, and N. Trinajstić, *J. Chem. Phys.*, 61, 2700 (1974).

[illegible]

[illegible]

Revue Roumaine de Chimie, **21**, *5*, 757–762 (1976)

PYRIMIDINES * VI

SYNTHESIS OF 2-METHYLTHIO-5-BROMO-PYRIMIDINE-4-CARBOXYLIC ACID THIOSEMICARBAZIDES, 3-PYRIMIDYL-1,2,4-(4*H*)-TRIAZOLES AND 2-ARYLAMINO-1,3,4-THIADIAZOLES

S. C. BENNUR, V. B. JIGAJINNI and V. V. BADIGER
Department of Chemistry, Karnatak University, Dharwar-580003, India

Received 14 September, 1974

The preparation of six new thiosemicarbazides of 2-methylthio-5-bromopyrimidine-4-carboxylic acid and their cyclization to 1,2,4-(4 *H*)-triazoles and 1,3,4-thiadiazoles is described. These compounds are evaluated for antimicrobial and antitubercular activity.

Various 1-arylsulphonyl hydrazides [1] and 1-aryl-4-substituted thiosemicarbazides [2] have been reported as fungicides, antibacterials and antiviral agents, respectively. Budesinsky et al.[3–5] reported antitubercular activity in case of pyrimidine 4-carboxylic acid hydrazides. A large number of triazole derivatives have found application as diuretics,[6] blood pressure depressants [7] and potential fungicides.[8] Pianka [9] studied as many as twenty 2-substituted thio-5-(2,4-dinitrophenylthio)-1,3, 4-thiadiazoles and related compounds for their antifungal activity. Thiadiazole derivatives are being investigated for their antitumor potency by Endo et al.[10] Very recently nitrofuryl derivatives of 1, 2, 4-triazoles have been intensively investigated for antibacterial activity in urinary tract infections.[11]

---

[*] Part V : see [20]

[1] C. Sunkel and H. Gómez, *J. Med. Chem.*, **13**, 334 (1970).

[2] V. S. Mistra and N. S. Agarwal, *Indian J. Appl. Chem.*, **32**, 335 (1969).

[3] Z. Budesinsky and F. Roubinek, *Coll. Czech. Chem. Comm.*, **26**, 2871 (1961); *Chem. Abstr.*, **56**, 7315 (1962).

[4] Z. Budesinsky and V. Bydzovsky, *Pharmacotherap.*, **1950–59**, 129–42 (1963); *Chem. Abstr.*, **60**, 6095 (1964).

[5] Z. Budesinsky, F. Roubinek, and V. Bydzovsky, *Czech. Pat.*, 103, 545 (1962); *Chem. Abstr.*, **60**, 8043 (1964).

[6] H. L. Yale and J. J. Piala, *J. Med. Chem.*, **9**, 42 (1966).

[7] K. Shirakawa, T. Tsujikawa and T. Tsuda, *U.S.Pat.*, 3, 041, 339 (1962); *Chem. Abstr.*, **57**, 13774 (1962).

[8] A. K. Bhat, R. P. Bhamaria, R. A. Bellare and C. V. Deliwala, *Indian J. Chem.*, **5**, 397 (1967).

[9] M. Pianka, *J. Sci. Food Agric.*, **19 (a)**, 502 (1968).

[10] H. Endo, K. Sato, and T. Kawasaki, *Sci. Rept. Res. Inst., Tohoku Univ. Ser.*, **C11(2)**, 187 (1963); *Chem. Abstr.*, 60, 3385 (1964).

[11] E. B. Åkerblom and D. E. S. Campbell, *J. Med. Chem.*, **16**, 312 (1973).

Encouraged by these observations and as a part of our general search for pharmacologically active heterocyclic compounds, we wish to report the preparation of 1-(2-methylthio-5-bromo-pyrimidoyl)-4-(*p*-substituted-phenyl) thiosemicarbazides, 3-(2-methylthio-5-bromopyrimidyl)-4-(*p*-substituted phenyl)-1, 2, 4-(4 *H*)-triazoles and 2-(*p*-substituted phenylamino)-5-(2-methylthio-5-bromopyrimidyl)-1, 3, 4-thiadiazoles.

During the present work 2-methylthio-5-bromo-pyrimidine-4-carboxylic acid hydrazide (II) was obtained by the action of hydrazine hydrate on methyl 2-methylthio-5-bromopyrimidine-4-carboxylate (I). 1-(2-Methylthio-5-bromopyrimidoyl)-4-(*p*-substituted phenyl) thiosemicarbazides (III) were obtained by reacting II with isothiocyanates by the method of Silberg and Cosma.[12] These compounds are described in Table 1.

Table 1

Thiosemicarbazides (III a – f)

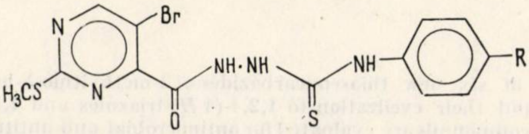

Thiosemi-carbazide *	M.P.°	Yield %	Formula	Calculated %			Found %		
				C	H	N	C	H	N
IIIa	194–95	58	$C_{13}H_{12}BrN_5OS_2$	39.19	3.79	17.58	39.31	3.52	17.33
IIIb	259–60	90	$C_{13}H_{11}BrN_5OS_2$	32.71	2.31	14.68	32.82	2.42	14.91
IIIc	196–97	85	$C_{13}H_{11}BrClN_5OS_2$	36.07	2.54	16.18	36.10	2.54	15.91
IIId	240–41	58	$C_{14}H_{14}BrN_5OS_2$	40.78	3.39	16.99	40.69	3.42	16.78
IIIe	161–62	91	$C_{14}H_{14}BrN_5O_2S_2$	39.25	3.27	15.36	39.39	3.33	15.98
IIIf	170–71	77	$C_{15}H_{11}BrN_5O_2S_2$	52.52	4.84	20.41	52.63	4.96	20.51

* All the compounds were recrystallized from a mixture of dioxane and ethanol.

The thiosemicarbazides (III) were cyclized according to the method of Hoggarth[13] to substituted 1, 2, 4-(4 *H*)-triazoles (IV) in presence of 5% alkali. These are described in Table 2.

The compounds (III) were cyclized with phosphoric acid at 120° to 1, 3, 4-thiadiazoles by the literature method.[13] These are described in Table 3.

The IR spectra were recorded in nujol mull on Beckmann IR–20 instrument.

Thiosemicarbazides showed absorption in the range 1395–3280, 1630–1750, and 1050–1210 cm^{-1} which were assigned to —NH—, C = 0 and C = S groups, respectively.

Triazoles and thiadiazoles showed distinct peaks at 3000–3200 cm^{-1} which were due to the overlapping of —NH— vibrations with —C—H

---

[12] Al. Silberg and N. Cosma, *Studii Cercetări Chim. Fil. Cluj.*, **10**, 151 (1959); *Chem. Abstr.*, **54**, 8794 (1960).

[13] E. Hoggarth, *J. Chem. Soc.*, **1949**, 1163.

Table 2

Triazoles (IV a−f)

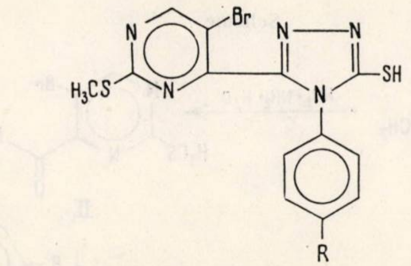

Trizole *	M.P.°	Yield %	Formula	Calculated %			Found %		
				C	H	N	C	H	N
IVa	177−78 d	31	$C_{13}H_{10}BrN_5S_2$	41.05	2.63	18.42	41.07	2.51	18.53
IVc	288−89 d	19	$C_{13}H_9Br_2N_5S_2$	33.98	1.36	15.25	34.01	1.51	15.01
IVd	196−97 d	30	$C_4H_{12}Br_2N_5S_2$	42.64	3.05	22.36	42.73	3.29	21.98
IVe.	199−200d	36	$C_1H_{12}BrN_5OS_2$	40.98	2.63	17.07	41.19	2.71	17.01
IVf	203−04 d	60	$C_{15}H_{14}BrN_5OS_2$	42.45	3.30	16.51	42.53	3.51	16.83

* Analytical samples of mercapto triazoles were obtained by reprecipitation from alkaline solution by dilute hydrochloric acid.

Table 3

Thiadiazoles (V a−e)

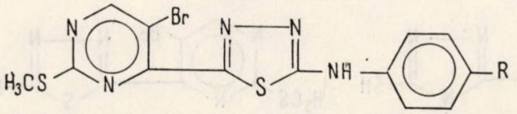

Thiadiazole*	M.P⁰.	Yield %	Formula	Calculated %			Found %		
				C	H	N	C	H	N
Va	283−84 d	63	$C_{13}H_{10}BrN_5S_2$	41.05	2.63	18.42	41.27	2.32	18.39
Vb	299−300d	60	$C_{13}H\ BrClN_5S_2$	37.63	2.16	16.98	37.71	2.00	16.75
Vc	255−56 d	35	$C_{13}H\ Br_2N_5S_2$	33.98	1.36	15.25	34.20	1.43	15.01
Vd	282−83 d	50	$C_{13}H_{12}BrN_5S_2$	42.64	3.04	17.60	42.78	3.31	17.86
Ve	275−76 d	78	$C_{14}H_{12}BrN_5OS_2$	40.98	2.63	17.07	40.87	2.51	17.22

* All compounds weve recryttallized from aqueous dimethylformamide.

stretching vibrations. −C−N stretching vibrations were observed at 1215−1250 cm^{-1}. Absorptions at 1030−1215 cm^{-1} were due to R−N vibrations.

Thiadiazoles showed —C—S and C—S—C, vibrations at 785—830 and 630—645 cm^{-1}.

Scheme

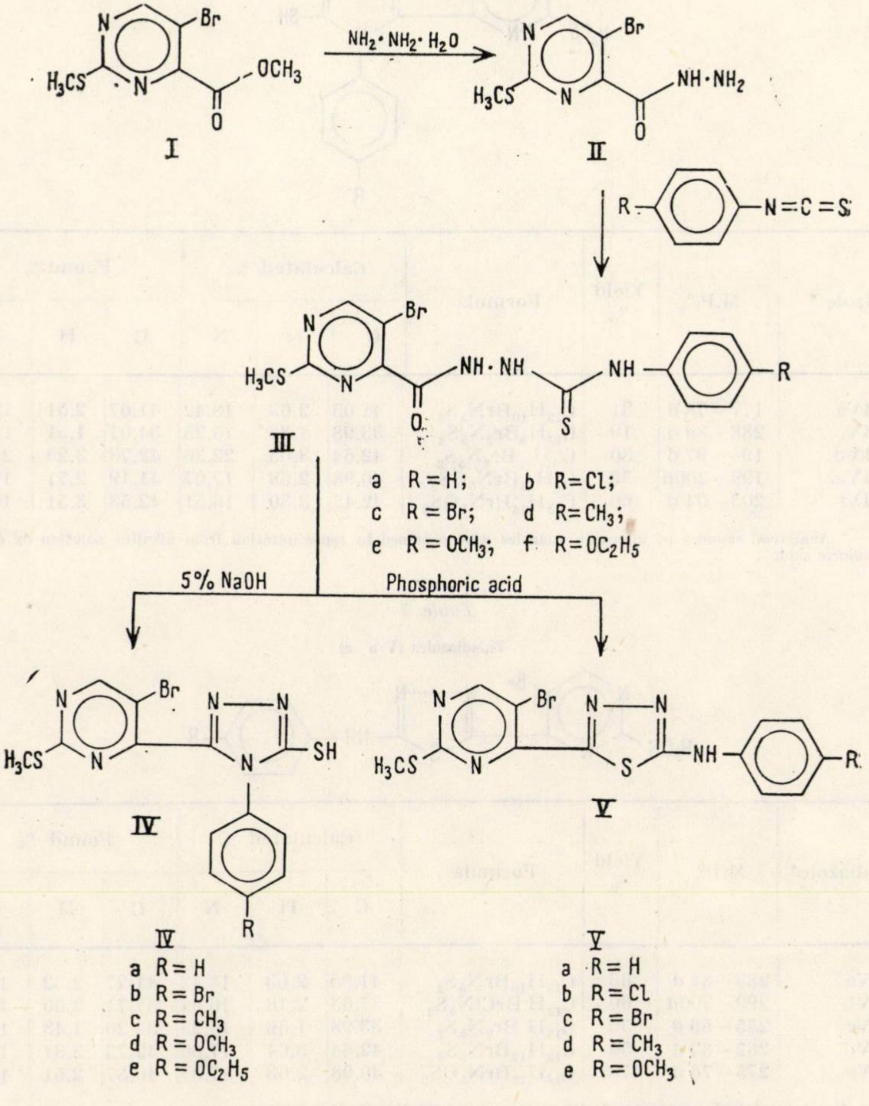

Br
N
H_3CS
N
OCH_3
O
I
$NH_2 \cdot NH_2 \cdot H_2O$
N
Br
H_3CS
N
$NH \cdot NH_2$
O
II
R
N=C=S
N
Br
H_3CS
N
NH · NH
NH
R
O
S
III
a R = H; b R = Cl;
c R = Br; d R = CH_3;
e R = OCH_3; f R = OC_2H_5
5% NaOH
Phosphoric acid
N
Br
N — N
N
H_3CS
N
SH
IV
R
N
Br
N — N
H_3CS
N
S
NH
R
V
IV
a R = H
b R = Br
c R = CH_3
d R = OCH_3
e R = OC_2H_5
V
a R = H
b R = Cl
c R = Br
d R = CH_3
e R = OCH_3

The compounds prepared in the present investigation were screened for antimicrobial activity against *S. aureus*, *E. coli*, *C. albicans* and *Cryptococcus neoformans* by Cupplate method. Dimethyl formamide was used as solvent control which did not show any bacterial inhibition. Phenol (5%) was used as positive control. Antitubercular activity of thiosemicarbazides was investigated against *M. tuberculosis* (H 37 Rv.

Strain) by serial dilution method using surface culture technique in aqueous dimethyl formamide. None of the thiosemicarbazides were active at dilution 10^{-4} and 10^{-5}.

Amongst thiosemicarbazides, compounds IIIb and IIIf showed marked activity against *S. aureus*. The compounds IIIa, IIId and IIIf showed activity against *E. coli*. Only compounds IIIa, IIIe and IIIf showed antifungal activity against both the fungal strains. The rest of the compounds were inactive.

The cyclized compounds IV and V were less potent antibacterial agents than the parent thiosemicarbazides (III), the maximum activity being observed in case of compound IVa. Compounds Va, Vb, Vc and Vf showed slight activity against *E. coli*. Highest activity against *E. coli* in this series was observed with Vc.

EXPERIMENTAL[14]

Phenylisothiocyanate,[15] *p*-bromophenylisothiocyanate, *p*-chlorophenylisothiocyanate,[16] *p*-methylphenylisothiocyanate,[17] *p*-methoxyphenylisothiocyanate,[18] *p*-ethoxyphenylisothiocyanate[19] were prepared by the literature methods. 2-Methylthio-5-bromopyrimidine-4-carboxylic acid hydrazide was prepared by the method described by Badiger and Bennur.[20]

GENERAL METHOD OF SYNTHESIS OF 1-(2-METHYLTHIO-5-BROMOPYRIMIDOYL)-4-(*p*-SUBSTITUTED PHENYL) THIOSEMICARBAZIDES (III a—b)

2-Methylthio-5-bromopyrimidine-4-carboxylic acid hydrazide (0.01 mole) in rectified spirit (50 ml.) was dissolved by heating *p*-substituted phenyli sothiocyanate (0.01 mole) was added to this solution under stirring. This mixture was refluxed on a steam-bath for three hours, cooled and the solid that separated was collected. It was dried and crystallized from suitable solvent.

GENERAL METHOD FOR THE SYNTHESIS OF *p*-SUBSTITUTED 3-(2-METHYLTHIO 5-BROMOPYRIMIDYL)-4-(PHENYL)-5-MERCAPTO-1, 2, 4-(4 *H*)-TRIAZOLES (IV a—f)

The appropriate thiosemicarbazide (III) (0.01 mole) was suspended in an aqueous solution of sodium hydroxide (5%, 33 ml.) and refluxed gently for an hour. The resulting solution was treated with decolorizing charcoal and filtered. The filtrate after cooling was acidified carefully with dilute hydrochloric acid. The precipitate so obtained was washed with water and further purified by repeated precipitation of the mercapto triazole from alkaline solution to get analytically pure samples.

---

[14] All melting points are uncorrected.

[15] F. B. Daine, "Organic Syntheses", Coll. Vol. I. J. Wiley, New York, 1947, p. 447.

[16] A. I. Vogel, "Practical Organic Chemistry", ELBS 3rd Edn., 1956, p. 644.

[17] A. W. Hofmann, *Ber.*, **1**, 173 (1868).

[18] E. Schmidt, E. Kammerl, D. Ross, and F. Zaller, *Liebigs Ann. Chem.*, **594**, 233 (1955).

[19] G. J. M. Van der Kerk, C. W. Pluygers and G. de Vries *Rec. trav. Chim.*, **74**, 1262 (1955); *Chem. Abstr.*, **50**, 8497 (1956).

[20] V. V. Badiger and S. C. Bennur, *J. Karnatak Univ.*, **18**, 1 (1973).

GENERAL PROCEDURE FOR THE PREPARATION OF 2-(p-SUBSTITUTED PHENYLAMINO)-5-(2-METHYLTHIO-5-BROMOPYRIMIDYL)-1, 3, 4-THIADIAZOLES (Va – f)

The appropriate thiosemicarbazide (III) (0.005 mole) was added gradually with stirring in twenty minutes to anhydrous phosphoric acid (10 ml) maintained at 120°. The temperature was maintained at 120°, for additional half an hour. The syrupy reactions mixture was poured over crushed ice and allowed to settle. The precipitated thiadiazole was collected, washed with water, dried and crystallized from suitable solvent.

***ACKNOWLEDGEMENT*. We thank Prof. S. Siddappa for his interest in our work. We thank Prof. M. Sirsi, Department of Pharmacology and Microbiology, I. I. Science, Bangalore, for providing facilities to carry out microbial testing and his guidance. One of us (S.C.B.), is grateful to U.G.C. New Delhi for awarding U.G.C. Scholarship and (V.B.J.), is grateful to C.S.I.R. for financial help. We thank Messrs. V. A. Desai and G. S. Gadaginmath for recording the analytical data.**

Revue Roumaine de Chimie, **21**, *5*, 763–768 (1976)

VARIATION OF MOLECULAR MASS WITH TIME IN POLYMERIZATION BY FREE RADICALS

M. DIMONIE, CR. OPRESCU and GH. HUBCA

Polytechnic Institute of Bucharest, Laboratory of Macromolecular Technology, Calea Victoriei nr. 149, București

Received October 8, 1974

Calculations based on Mayo's equation refering to the "instantaneous" polymerization degree in polymerization by free radicals resulted in the demonstration of a new relation providing the calculation of the polymerization degree of the polymer chain as a function of the conversion. Conditions for the applicability of the new calculation are discussed. Values resulted from calculation were compared to experimentally obtained values and a good agreement was generally observed.

The effect of molecular mass decrease in free radical polymerization in the presence of solvents has been known for a long time and explained by the existence of transfer reactions between the growing polymer and the solvent molecules.[1]

These processes have been first quantitatively expressed by Mayo [2] who demonstrates theoretically and verifies experimentally the well known relation :

$$\frac{1}{n} = \frac{1}{n_0} + C_s \frac{[S]}{[M]} + C_p \frac{[P]}{[M]}$$

in which :

n_0 – the average degree of polymerization in the absence of transfer reactions with the solvent

n – the average degree of polymerization in the presence of solvent

C_s – the transfer constant to solvent

C_p – the transfer constant to polymer

$[S]$ – the solvent concentration

$[M]$ – the monomer concentration

$[P]$ – the polymer concentration

In this form, Mayo's equation enables the determination of transfer constants to solvent; yet it can only be applied for maximum 5% conversion variations, due to the "instant" validity and this is insufficient for practical current cases.

---

[1] P. J. Flory, *J. Amer. Chem. Soc.*, **59**, 241 (1937).

[2] F. R. Mayo, *J. Amer. Chem. Soc.*, **65**, 2324 (1943).

The problem of finding a general method capable of correlating the variation of the polymerization degree with time or with comversion has frequently been approached.

Starting from kinetic considerations, Bamford [3] shows that for higher than 5% conversion variations, i.e. when the monomer concentration can no more be considered as constant, the simple expression of the instant polymerization degree must be replaced by relation :

$$n = \frac{\int (\mathrm{d}M_0/\mathrm{d}t)\,\mathrm{d}t}{\int \{k_M[M]\,[I/(k_t + k_t')]^{1/2} + I(k_t/2 + k_t')/(k_t + k_t')\}\,\mathrm{d}t}$$

in which :

k_M – rate constant of transfer to monomer

k_t and k_t' – rate constants for termination by combination and respectively disproportionation

I – initiation rate.

In this case it is obviously necessary to know the following dependences in order to calculate the polymerization degree :

$$[M] = f(t) \quad \text{and} \quad I = f(t)$$

Gee and Melwill [4] as well as Herington and Robertson [5] treat the problem of finding a calculation relation for the average degree of polymerization starting from the function of molecular mass distribution in radical polymerization.

The solution is possible without special difficulties only in some situations imposing certain restrictive conditions, i.e. – all reactants in the system are maintained at invariable concentrations

– the concentrations of the initiator and of the transfer agent are invariable and the constant of transfer to monomer is null.

In the general case, in which transfer constant to monomer is different from zero, and which actually is the only important case, the calculation becomes extremely complicated and the resulting expression for the average degree polymerization is very inconvenient for practical use.

Based on some similar considerations Shaginyan and Enicolopian [6] have tried to determine a series of reactions between the polymerization degree and conversion.

Calculation difficulties have caused the problem to be solved only in particular situations, a fact which greatly limits the use of the obtained relations.

---

[3] C. H. Bamford, W. G. Barb, A. D. Jenkins and P. F. Onyon, "The Kinetics of Vinyl Polymerization by Radical Mechanism", Academic Press, New York, 1958.

[4] G. Gee and H. W. Melvill, *Trans. Faraday, Soc.*, **40**, 240 (1944).

[5] E. F. G. Herington and A. Robertson, *Trans. Faraday Soc.*, **38**, 490 (1942).

[6] A. A. Shaginyan and N. S. Enicolopian, *Vysokomol Soedineniya*, **7**, 1866 (1965).

The present report introduces a new method for calculating the number-average degree of polymerization for polymers obtained by free-radical polymerization.

The method provides the advantage of a certain simpleness and the absence of restrictive conditions.

CALCULATION OF THE AVERAGE DEGREE OF POLYMERIZATION

In Mayo's equation:

$$\frac{1}{n} = \frac{1}{n_0} + C_s \frac{[S]}{[M]} + C_p \frac{[P]}{[M]} \tag{1}$$

magnitude $\frac{1}{n_0}$ represents the inverse of the polymerization degree in the absence of transfer reactions with the solvent and it can be expressed under the following form:

$$\frac{1}{n_0} = \frac{1/2(1+\lambda)\, k_t [R^\cdot]}{k_p [M]} + C_m \tag{2}$$

in which:

λ — fraction from polymer radicals which disappear by disproportionation reaction

k_t — the rate constant of the termination reaction

k_p — the rate constant of the propagation reaction

C_m — transfer constant with the monomer

$[R^\cdot]$ — free radical concentration.

Since the steady state and therefore the free radical concentration $R^\cdot$ is invariable in time[7] the magnitude:

$$\alpha = \frac{1/2(1+\lambda)\, k_t [R^\cdot]}{k_p} \text{ will also be constant.}$$

Under these conditions relation (2) becomes:

$$\frac{1}{n_0} = \frac{\alpha}{[M]} + C_m \tag{3}$$

Equation (3) which contains known or experimentally readily accessible magnitudes, enables to calculate constant α.

---

[7] H. S. Bagdazarian, "Teoria radikalnoi polimerizatsii", ed. Nauka, Moskva, 1966.

To this end for the sake of simplicity magnitudes n_{0i} and $[M_i]$, corresponding to the initial conditions of polymerization (index i refers always to the initial conditions), are introduced in relation (3):

$$\alpha = \frac{[M_i]}{n_{0i}} - C_m[M_i] \tag{4}$$

By substituting in equation (1) $1/n_0$ by its expression and taking into account (4) as well as the evident relations:

$$[M] = [M_i]\ (1 - \eta) \tag{5}$$

$$[P] = [M_i]\cdot\eta \tag{6}$$

in which η—conversion, we obtain:

$$\frac{1}{n} = \frac{\dfrac{1}{n_{0i}} + C_s\dfrac{[S]}{[M_i]} + (C_p - C_m)\cdot\eta}{1 - \eta} \tag{7}$$

Equation (7) is equivalent to Mayo's equation and consequently keeps its character of momentary validity.

The overall average polymerization degree n_g, for a more important conversion variation is given by:

$$n_g = \frac{1}{\eta}\int_0^{\eta} n(\eta)\,\mathrm{d}\eta \tag{8}$$

By simultaneously considering relations (7), (8) and after a convenient arrangement of terms and integration one obtains the following expression for the overall average polymerization degree:

$$n_g = -\frac{1}{C_p - C_m} + \frac{C_p - C_m + \dfrac{1}{n_{0i}} + C_s\dfrac{[S]}{[M_i]}}{(C_p - C_m)^2\,\eta}\cdot \ln\left(1 + \frac{C_p - C_m}{\dfrac{1}{n_{0i}} + C_s\dfrac{[S]}{[M_i]}}\cdot\eta\right) \tag{9}$$

By letting $\eta \to 0$ and after solving the type $\frac{0}{0}$ nondetermination which has appeared, one finds again Mayo's equation applied to the initial conditions of the polymerization:

$$\frac{1}{n} = \frac{1}{n_{0i}} + C_s\frac{[S]}{[M_i]} \tag{10}$$

For $[S] = 0$ we obtain the variation of the overall average polymerization degree as a function of conversion in bulk polymerization :

$$n_g = -\frac{1}{C_p - C_m} + \frac{C_p - C_m + \frac{1}{n_{0i}}}{(C_p - C_m)^2 \cdot \eta} \ln \left[1 + (C_p - C_m)\, n_{0i} \cdot \eta\right] \qquad (11)$$

The applicability of relation (9) is conditioned in the first place by the time-invariance of the termination constant.

In the case of polymerization developed in heterogeneous medium or in concentrated solutions, in which strongly branched polymers are formed due to some frequent polymer-transfer reactions there will obviously exist differences between experimental data and results obtained by calculation.

In such situations, dèviations from calculated values may be considered as an extent of the intensity of these processes.

DETERMINATION OF BRANCHING DEGREE

The branching degree has a marked influence on the average degree of polymerization, the disagreement between experimental n_g values and calculated ones resulting in the occurrence of branching.

This fact was clearly observed in the case of vinyl acetate polymerization.

The branching degree may be calculated starting from similar considerations to those leading to relation (9).

The probability for a monomer unit of the polymer chain to interact with a growing radical or in other words the probability of an elementary transfer act to polymer may be evidently expressed by relation :

$$\beta = \frac{k_{tp}[P]\,[R^\cdot]}{k_p[R^\cdot]\,[M] + k_s[S]\,[M] + k_{tp}[P]\,[R^\cdot] + k_m[M]\,[R^\cdot]^2} \qquad (12)$$

in which :

β — probability of an elementary transfer act to polymer

$[R^\cdot]$ — concentration of growing radicals

k_s, k_m, k_{tp} — rate constants of transfer reaction to solvent monomer and respectively polymer

Keeping into account the relation (5) and (6) and also the evident conditions $C_m,\ C_s\frac{S}{M},\ C_p\frac{P}{M} \ll 1$ and performing some transformations we obtain :

$$\beta = \frac{C_p \cdot \eta}{1 - \eta} \qquad (13)$$

The probability π for a polymer chain with n polymerization degree to interact with a growing radical is given by relation :

$$\pi = n \cdot \beta \qquad (14)$$

The average number of branches on a polymer chain may be expressed as:

$$\gamma = \frac{\text{number of branches}}{\text{number of macromolecules}}$$

i.e.

$$\gamma = \frac{\sum \beta \cdot n \cdot N_n}{\sum N_n} = \beta \frac{\sum n \cdot N_n}{\sum N_n} = \beta \cdot n_g \qquad (15)$$

in which

N_n – the number of macromolecules with n polymerization degree.

Replacing β and n_g from relations (13) and (9) into relation (15) we obtain the calculation relation for the average number of branches:

$$\gamma = -\frac{C_p \cdot \eta}{(C_p - C_m)(1-\eta)} + C_p \frac{C_p - C_m + \frac{1}{n_{0i}} + C_s \frac{[S]}{[M_i]}}{(C_p - C_m)^2 (1-\eta)} \ln\left(1 + \frac{C_p - C_m}{\frac{1}{n_{0i}} + C_s \frac{[S]}{[M_i]}} \cdot \eta\right) \qquad (16)$$

The applicability of equation (7) is illustrated by data concerning the solution polymerization of acrylonitrile in ethylene carbonate obtained by Peebles.[8]

Table 1

Calculation of global polymerization degree in acrylonitrile polymerization in ethylene carbonate at 50°C

Conv. %	n^* $x\,10^3$	$n^{**}_{g\,\text{calc.}}$ $x\,10^3$
6.9	3.11	3.10
14.81	2.89	2.98
27.13	2.76	2.90
46.78	2.72	2.40
71.53	2.29	2.01

* – Calculated by relation[9] $[\eta] = 3.92 \times 10^{-4} \cdot (53.06\,n)^{0.75}$

** – Calculated by relation (9) considering the following values; $n_0 = 10^4$ [10];
$k_p = 0.7 \times 10^{-4}$ [11]; $k_s = 5 \times 10^{-5}$ [12]

As results from table 1, $\bar{n}$ values experimentally obtained compare well with n_g values calculated according to relation (7).

Good agreement between experiment and calculation have been obtained in the case of other vinyl monomers like styrene and acrylates.[13]

Important deviations reaching up to 80% have been observed in the case of vinyl acetate polymerization in methanol and methyl acetate.[13] This behaviour is probably due to the branching reactions because of some frequent transfer processes with the polymer.[11]

---

[8] L. H. Peebles, *J. Polymer Sci.*, **3**, 341 (1965).

[9] P. F. Onyon, *J. Polymer Sci.*, **22**, 13 (1956).

[10] W. M. Thomas and J. J. Pellon, *J. Polymer Sci.*, **13**, 329 (1954).

[11] G. E. Ham, "Vinyl Polymerization", M. Dekker, New York, 1967.

[12] E. F. White and M. J. Zissel, *J. Polymer Sci.*, *A–1*, **2**, 189 (1963).

[13] M. Dimonie, Cr. Oprescu and Gh. Hubca, to be published.

Revue Roumaine de Chimie, 21, 5, 769–773 (1976)

ZUR KOPOLYMERISATION. II[1]

DIE SIMULIERUNG DER BILDUNG EINES MAKROMOLEKÜLS

DAS PROGRAMM MEMORY 1

IOAN MOŢOC, DAN CIUBOTARIU und ŞTEFAN HOLBAN
Chemiekatheder der Universität Timişoara
1900 — Timişoara, Rumänien

Eingegangen am 27. Juni 1974

Die Arbeit beschreibt den Algorithmus, das Ordinogramm und das Programm, welches die Simulierung der Bildung eines mischpolymerisierten Makromoleküls an einem Digitalrechner gestattet. Das Programm heißt MEMORY 1, ist in FORTRAN geschrieben und wurde an einem IRIS-50-Rechner getestet.

1. EINLEITUNG

MEMORY 1 ist das erste aus einer Reihe von Programmen die: Kopolymerisationsreaktionen (die Anzahl und die relative Lage der Blocks, die Dispersion der numerischen Molekülarmassen usw.), Terpolymerisationen modellieren.

Die theoretischen Grundlagen auf denen diese Programme beruhen, wurden in vorhergehenden Arbeiten erläutert.[1,2]

2. ÜBER DAS PROGRAMM

Der Name des Programms:	MEMORY 1
Sprache:	FORTRAN
Notwendiger Informationsspeicher:	80 K
Material des Programms:	100 Lochkarten
Ausführungsdauer:	3 Sekunden für ein Makromolekül mit dem Polymerisationsgrad 1000.

Hinweis:

Mit einer Konfiguration von 80 K kann man ein Makromolekül mit dem maximalen Polymerisationsgrad 15.000 simulieren.

---

[1] I. Moţoc und D. Ciubotariu, *Rev. Roumaine Chim.*, **21** (1976).

[2] I. Moţoc, Şt. Holban und D. Ciubotariu, *Rev. Roumaine Chim.*, **21** (1976).

2.1. EINGANGSDATEN

Für jedes simulierte Makromolekül sind der Reihe nach folgende Eingangsdaten auf einer Lochkarte notwendig:

a) Der Typ des ersten Mers, MER, der Polymerisationsgrad, N, FORMAT (I1, I6).

MER = 1, das erste Mer des Makromoleküls ist A,

MER = 2, das erste Mer des Makromoleküls ist B.

b) ALPHA, BETA (2, F14.10)

$$\text{ALPHA} = \frac{R1}{1+R1}, \quad \text{BETA} = \frac{R2}{1+R2}$$

wobei R_J, $J = 1, 2$, Mischpolymerisationskonstanten sind.

2.2. AUSGANGSDATEN

Die Ausgangsdaten sind folgende:

a) Die Eingangsdaten, um die Richtigkeit der ersteingeführten Daten zu prüfen.

b) Die höchstwahrscheinliche Form der makromolekulären Kette, in welcher die beiden Mers durch A und B symbolisiert sind.

2.3. MÖGLICHE ERWEITERUNGEN DES PROGRAMMS

Abhängig von der Kapazität des verfügbaren Informationsspeichers sind Änderungen des Programms möglich, die eine Simulierung der Bildung von Makromolekülen mit entsprechendem Polymerisationsgrad gestatten.

Im Bedarfsfalle kann das Programm erweitert werden, um die Anzahl und die Größe der homogenen Blocks von A und B in dem Makromolekül zu ermitteln, desgleichen kann die Natur und Größe der Stereoblocks ermittelt werden, die im simulierten Makromolekül auftreten können.

2.4. DIE BESCHREIBUNG DES PROGRAMMS

Die Abbildung 1 veranschaulicht die Struktur des Programms.

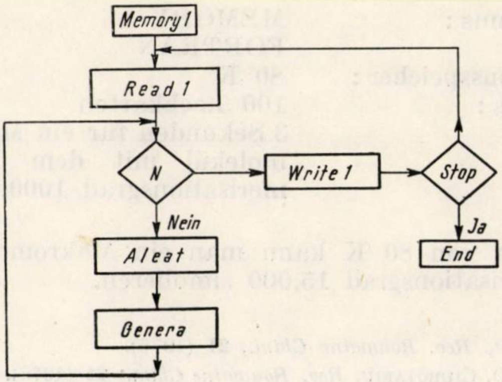

Abb. 1. — Die Struktur des Programms MEMORY 1.

Nachdem die Eingangsdaten gelesen werden, simuliert man das Anwachsen des Makromoleküls von Mer zu Mer, bis zu dem von den Eingangsdaten vorgeschriebenen Polymerisationsgrad. Danach werden die Ausgangsdaten, im Einklang mit Paragraph 2.2. gedruckt.

2.4.1. *READ 1.* Es werden die Eingangsmatrizen mit den Daten die den gewählten Mischpolymerisationsprozeß kennzeichnen, initialisiert (im Einklang mit Paragraph 2.1.).

2.4.2. *ALEAT.* ALEAT sichert die Generierung von pseudo-stochastischen Zahlen im Intervall (0,1). Es wird ein deterministisches Verfahren verwendet, das auf einer arithmetischen Methode zur Generierung jedes Gliedes der Reihe beruht.

Die verwendete Methode ist die Lehmer-Methode. Um die Überschreitung der Kapazität eines Wortes zu verhindern, verwendet man zwei Unterprogramme MAS, NMAS.

2.4.3. *GENERA.* Das Teilprogramm GENERA sichert die Simulierung der Bildung des Makromoleküls, unter Berücksichtigung des Umstandes, daß die Anlagerung eines Mischmers vom aktiven Ende des in Wachstum begriffenen Makroradikals bedingt wird.[3]

2.4.4. *WRITE 1.* WRITE 1 sichert das Drucken der Ausgangsdaten im Einklang mit Paragraph 2.2.

2.4.5. *Das Programm.* Das Programm ist folgendes:

```
C
C    MEMORY 1
C    DAS PROGRAMM SIMULIERT DIE BILDUNG EINES MAKROMOLE-
     KUELS DURCH
C    BINAERE KOPOLYMERISATION
C    ES WERDEN FOLGENDE EINGANGSGROESSEN GELESEN:
C    MER = 1 DAS ERSTE GLIED DES MAKROMOLEKUELS IST A
C    MER = 2 DAS ERSTE GLIED DES MAKROMOLEKUELS IST B
C    N POLYMERISATIONSGRAD                         FORMAT (I 1.I6)
C            ALPHA = R1/(1 + R1)
C            BETA = 1-R2/(1 + R2)                  FORMAT (2F. 14.10)
C    R1, R2 KOPOLYMERISATIONSKONSTANTEN            FORMAT (2F. 14.10)
C
*    DEFINE FILE *1 = 105, *2 = 108
             INTEGER SW
             DIMENSION POLYM (10000)
             DATA I/1/, PKT1, PKT2/2HA-, 2HB-/, K/1/
C
C    READ 1
C
          1  READ (105, 900, END = 90) MER, N
             READ (105, 910) ALPHA, BETA
             WRITE (108, 920) N, ALPHA, BETA
             IA = 65539
             IF (MER. EQ. 1) POLYM (I) = PKT1
             IF (MER. EQ. 2) POLYM (I) = PKT2
             IF (MER. LT. 1. OR. MER. GT. 2) GO TO 60
             SW = MER
         10  I = I + 1
```

---

[3] C. E. Ham, Copolymerization, Interscience, New York, London, Sydney (Übersetzung in russischer Sprache, Khimia, 1971).

```
      IF (I. GT. N) GO TO 80
      CALL MAS
      CALL ALEAT (IA, IB, X)
      CALL NMAS
      IA = IB
      IF (X. LT. O.. OR. X. GT. 1.) GO TO 70
C
C   GENERA
C
      GO TO (20,40), SW
   20 IF (X. LE. ALPHA) GO TO 30
      POLYM (I) = PKT2
      SW = 2
      GO TO 10
   30 POLYM (I) = PKT1
      GO TO 10
   40 IF (X. LE. BETA) GO TO 50
      POLYM (I) = PKT2
      GO TO 10
   50 POLYM (I) = PKT1
      SW = 1
      GO TO 10
   60 WRITE (108, 930)
      GO TO 1
   70 WRITE (108, 940)
      GO TO 90
C
C   WRITE1
C
   80 WRITE (108, 950) (POLYM (I), I = 1, N)
      I = 1
      GO TO 1
   90 STOP
  900 FORMAT (I1, I6)
  910 FORMAT (2F14.10)
  920 FORMAT ('1', 5X, 'POLYMERISATIONSGRAD =', I6, 5X, 'ALPHA=', F14.10,
      C 5X, 'BETA =', F14.10///)
  930 FORMAT ('  ', 5X, 'FALSCH EINGEFUENRTE EINGANSGROESSEN'/)
  940 FORMAT ('  ', 5X, 'FALSCHER GENERATOR FUER STOCHASTISCHE ZAHLEN'/)
  950 FORMAT (//5X, 'WAHRSCHEINLICHSTE FORM DES MAKROMOLEKUELS')
```

```
C
C
C
C   PROGRAMM ZUR GENERATION EINER PSEUDOSTOCHASTISCHEN ZAHLENREIHE
C
      SUBROUTINE ALEAT (IA, IB, Z)
C
C   IA : WENN ALEAT ZUM ERSTEN MAL GERUFEN WIRD, MUSS IA EINEN
C       GANZEN, UNPAARZAHLIGEN WERT BESITZEN,
C       DER HOCHSTENS ACHSTELLIG SEIN DARF.
C       NACHHER WIRD IA VON NEUEM GENERIERT, INDEM IA GLEICH IB GESETZT
C       WIRD.
C       NACHHER WIRD IA DIE WERTE VON IB, DIE IM PROGRAMM GENERIERT
```

```
C        WERDEN.
C  IB : DER PROGRAMMGENERIERTE WERT
C  Z : DER DURCH ALEAT GENERIERTE GLEICHFORMIGE WERT IM
         INTERVALL (0,1)
C
C        2** 16 + 3 = 65539
         IB = IA* 65539
         IF (IB, Ge. O) GOTO 1
         IB = IB + 2147483647 + 1
C        2** 31 = 2147483647 + 1
       1 Z = IB
         Z = Z* 0,4656613 E-9
C        2** (-31) = 0.4656613 E-9
         RETURN
         END
```

Revue Roumaine de Chimie, **21**, *5*, 769–773 (1976)

Revue Roumaine de Chimie, 21, 5, 775–780 (1976)

ZUR KOPOLYMERISATION. III[1,2]

DIE SIMULIERUNG DER BILDUNG EINES MAKROMOLEKÜLS DAS PROGRAMM MEMORY 2

I. MOŢOC, D. CIUBOTARIU, ŞT. HOLBAN
Hochschule für Industriechemie, Rechenzentrum, Timişoara

Eingegangen am 27. Juni, 1974

Vorliegende Arbeit beinhaltet ein Ordinogramm und Programm, die die Simulierung der Bildung eines Makromoleküls unter gegebenen Bedingungen, an einem Digitalrechner gestatten. Das Programm heißt MEMORY 2, wurde in FORTRAN formuliert und an einem Rechner der Klasse IRIS-50 getestet.

1. DAS PROGRAMM MEMORY 2

MEMORY 2 ist ein Programm, das die Bildung eines Makromoleküls aus zwei Monomeren A und B an einem Ziffernrechner simuliert. Die theoretischen Grundlagen auf denen dieses Programm beruht, wurden in vorhergehenden Arbeiten erläutert.[1,2]

1.1. ALLGEMEINES ÜBER DAS PROGRAMM

Name des Programms :	MEMORY 2
Sprache :	FORTRAN
Notwendiger Informationsspeicher :	80 K
Das Material des Programms :	160 Lochkarten
Durchführungsdauer :	20 Sekunden zur Simulierung der Bildung eines Makromoleküls mit dem Polymerisationsgrad 1000.

Hinweis :

Der maximale Polymerisationsgrad ist 15.000.

2. BESCHREIBUNG DES PROGRAMMS. EINGANGS- UND AUSGANGSDATEN

2.1. EINGANGSDATEN

Zur Initialisierung der Eingangsdaten werden von zwei Lochkarten in folgender Reihenfolge :

a) der Name des simulierten Makromoleküls, FORMAT (80 A2)

---

[1] I. Moţoc und D. Ciubotariu, *Rev. Roumaine Chim.*, **21** (1976).

[2] I. Moţoc, D. Ciubotariu und Şt. Holban, *Rev. Roumaine Chim.*, **21**, (1976).

b) der Typ des ersten Mers, A oder B, MER (= 1 oder 2), der Polymerisationsgrad, N, FORMAT (I1, I6)

c) die Konstanten der Mischpolymerisation, R1, R2, FORMAT (2 F14.10), gelesen.

2.2. AUSGANGSDATEN

Die Ausgangsdaten sind :

a) Die Eingangsdaten, um eine Kontrolle der primär eingesetzten Daten zu ermöglichen;

b) Den höchstwahrscheinlichen Aufbau der Kette des Makromoleküls, in welchen die beiden Mere durch A und B gekennzeichnet sind;

c) Die Anzahl der in der Kette des Makromoleküls enthaltenen homogenen Blocks von A bzw. B.

2.3. DIE BESCHREIBUNG DER HAUPTSEQUENZEN DES PROGRAMMS

Die logische Struktur ist in Abbildung 1 abgebildet.

Nach dem Lesen der Eingangsdaten wird das Wachsen der Makromoleküle von Mer zu Mer simuliert, im Einklang mit den von Anfang gestellten Bedingungen (gegeben durch RI, I = 1, 2). Danach werden die Ausgangsdaten im Einklang mit Paragraph 2.2. gedruckt.

2.3.1. *READ 2.* Das Unterprogramm gewährleistet das Lesen der Eingangsdaten, im Einklang mit Paragraph 2.1.

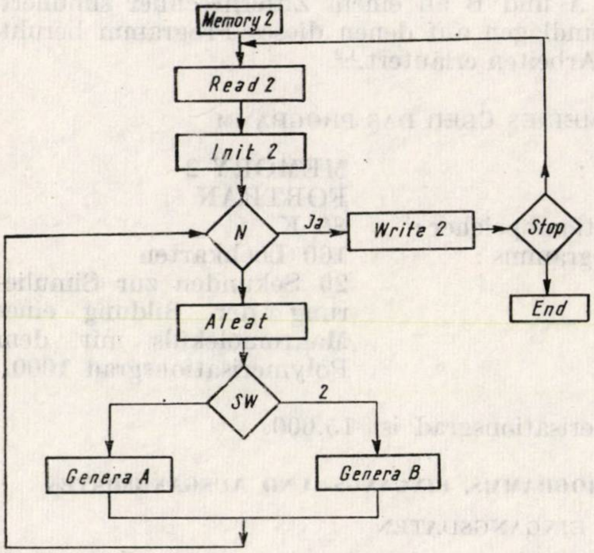

Abb. 1. — Die Struktur des Programms MEMORY 2.

2.3.2. *INIT 2.* Sichert die Konstruktion des Ereignisfeldes C, das das mathematische Modell des gewählten Mischpolymerisationsvorganges definiert.

2.3.3. *ALEAT.* ALEAT sichert die Generierung der pseudo-stochastischen Zahlen unter Verwendung der Lehmer-Methode, die den

Ablauf der Ereignisse des Feldes bestimmen. Zur Verhinderung der Überschreitung des Binärcodes werden die Unterprogramme MAS und NMAS verwendet.

2.3.4. *GENERA A und GENERA B*. GENERA A und GENERA B sichern die bedingte Zuordnung einer bestimmten chemischen Bedeutung zu jedem Ereignis aus $\mathcal{C}$, wodurch die Simulierung des Wachstums des Makromoleküls stattfindet.

2.3.5. *WRITE 2*. WRITE 2 sichert das Ausdrücken der initiellen Ausgangsdaten im Einklang mit Paragraph 2.2.

3. DAS PROGRAMM

Nachstehend ist das Programm im ursprünglichem Format gegeben :

```
C
C   MEMORY 2
C   DAS PROGRAMM SIMULIERT DIE BILDUNG EINES MAKROMOLE-
    KUELS DURCH
C   BINARE KOPOLIMERIZATION
C   ES WERDEN FOLGENDE EINGANGSGROSSEN GELESEN :
C   MER = 1 DAS ERSTE GLIED DES MAKROMOLEKUELS IST A
C   MER = 2 DAS ERSTE GLIED DES MAKROMOLEKUELS IST B
C   POLYMERISATIONSGRAD                    FORMAT (I1, I6)
C   R1, R2 KOPOLYMERISATIONSKONSTANTEN     FORMAT (2F14.10)
*   DEFINE FILE *1 = 105, *2 = 108
          COMMON GTAB (3,16)
          INTEGER SW
          DIMENSION POLYM (10000), NAME (40)
          DATA I/1/, PKT1, PKT2/2 HA-, 2 HB-/, K, J/2 *1/, NBA, NBB/2*0/
C   READ 2
        1 READ (105, 800, END = 110) (NAME (K), K = 1,40)
          WRITE (108, 890)
          WRITE (108, 800) (NAME (K), K = 1,40)
          READ (105, 800) (NAME (K), K = 1,40)
          WRITE (108, 800) (NAME (K), K = 1,40)
          READ (105, 900) MER, N
          READ (105, 910) R1, R2
          WRITE (108, 920) N, R1, R2
          IA = 65539
          NRA = 0
          NRB = 0
C
C   INIT 2
C
          ALPHA = R1/(1. +R1)
          BETA = 1. -R2/(1. +R2)
          IF (MER. EQ. 1) POLYM (I) = PKT1
          IF (MER. EQ. 1) NRA = 1
          IF (MER. EQ. 2) POLYM (I) = PKT2
          IF (MER. EQ. 2) NRB = 1
          IF (MER. LT. 1. OR. MER. GT. 2) GO TO 100
          SW = MER
       10 I = I + 1
          IF (I. GT. N) GO TO 80
          CALL MAS
        CALL ALEAT (IA, IB, X)
        CALL NMAS
        IA = IB
        IF (X. LE. O. OR. X. GE. 1.) GO TO 90
        GO TO (20,50), SW
C
C  GENERA 1
C
    20  IF (X. LE. ALPHA) GO TO 40
        IF (NRA. EQ. 1) GO TO 30
        IF (J. GT. 14) CALL GRTAB (J)
        NBA = NBA + 1
        GTAB (1, J) = PKT1
        GTAB (2, J) = NRA
        GTAB (3, J) = NBA
        J = J + 1
    30  NRB = NRB + 1
        POLYM (I) = PKT2
        NRA = 0
        SW = 2
        GO TO 10
    40  POLYM (I) = PKT 1
        NRA = NRA + 1
        GO TO 10
C
C  GENERA 2
C
    50  IF (X. GT. BETA) GO TO 70
        IF (NRB. EQ. 1) GO TO 60
        IF (J. GT. 14) CALL  GRTAB (J)
        NBB = NBB + 1
        GTAB (1, J) = PKT 2
        GTAB (2, J) = NRB
        GTAB (3, J) = NBB
        J = J + 1
    60  NRA = NRA + 1
        POLYM (I) = PKT 1
        NRB = 0
        SW = 1
        GO TO 10
    70  POLYM (I) = PKT 2
        NRB = NRB + 1
        GO TO 10
    80  IF (J. GT. 1) CALL  GRTAB (J)
        WRITE (108, 940) (POLYM (I), I = 1, N)
        WRITE (108, 950) NBA, NBB
        I = 1
        NBA = 0
        NBB = 0
        K = 1
        GO TO 1
    90  WRITE (108, 960)
   110  STOP
   100  WRITE (108, 970)
        GO TO 1
   800  FORMAT (40A2)
   890  FORMAT ('1'///)
   900  FORMAT (I1, I6)
   910  FORMAT (2F14.10)
   920  FORMAT ('1', 5X, 'POLYMERISATIONSGRAD = ', I6, 5X, 'R1 =',
        F14.10, 5X,
        C 'R2', F14.10)
    940 FORMAT (//5X, ‘WAHRSCHEINLICHSTE FORM DES MAKROMO-
        LEKELS’
        C/(12 X, 60A2))
    950 FORMAT (/5X, ‘ANZAHL DER GRUPPEN A = ’, I7
        C /5X, ‘ANZAHL DER GRUPPEN B = ’, I7)
    960 FORMAT (‘1’, 5X, ‘FALSCHER GENERATOR FUER STOCHASTI-
        SCHE ZAHLEN’/)
    970 FORMAT (‘1’, 5X, ‘FALSCHEINGEFUEHRTE EINGANSGROESSEN’/)
        END
```

```
          SUBROUTINE GRTAB (J)
C
C   WRITE 1
          DATA BLK/1 H/
          COMMON GTAB (3, 16)
          WRITE (108, 980) ((GTAB (II, JJ), JJ = 1,14), II = 1,3)
          DO 10 II = 1,3
          DO 10 JJ = 1,16
          GTAB (II, JJ) = BLK
       10 CONTINUE
          J = 1
          RETURN
      980 FORMAT (//2X, 130 (‘—’)/5X, ‘BESCHAFFENHEIT DER GRUPPEN !’,
          C          14 (‘ !’, A2, ‘  ’)
          C       /2X, 130 (‘—’)/5X,  ‘GROESSE DER GRUPPE      !’,
          C       /  14 (‘ !’, I4, ‘  ’)
          C       /2X, 130 (‘—’)/5X, ‘LAGE DER GRUPPE          !’,
          C          14 (‘ !’, I4, ‘  ’)
          C       /2X, 130 (‘—’))
          END
```

```
C
C
C
C   PROGRAMM ZUR GENERATION EINER PSEUDOSTOCHASTISCHEN
          ZAHLENREIHE
C
          SUBROUTINE ALEAT (IA, IB, Z)
C
C   IA : WENN ALEAT ZUM ERSTEN MAL GERUFEN WIRD, MUSS IA EINEN
C   GANZEN, UNPAARZAHLIGEN WERT BESITZEN, DER KLEINER ALS
C         NEUNSTELLIG IST (DER HOECHSTENS ACHTSTELLIG SEIN
          DARF).
C         NACHHER WIRD IA VON NEUEM GENERIERT, INDEM IA GLEICH
          IB GESETZT
C         WIRD.
C         NACHHER ERHAELT IA DIE WERTE VON IB, DIE IM PROGRAMM
          GENERIERT
C         WERDEN.
C   IB : DER PROGRAMMGENERIETE WERT
C   Z : DER DURCH ALEAT GENERIERTE GLEICHFORMIGE WERT IM
          INTERVALL (0,1)
C
C         2** 16 + 3 = 65539
          IB = IA* 65539
          IF (IB. GE. O) GOTO 1
          IB = IB + 2147483647 + 1
```

```
C       2** 31 = 2147483647 + 1
      1 Z = IB
        Z = Z* 0.4656613 E-9
C       2** (-31) = 0.4656613 E-9
        RETURN
        END
```

```
MASKEP    CSECT
          DEF          MAS
          DEF          NMAS
MASQUE    DATA, 4, 4   X' 50400000'
MAS       LDTM, 13     MASQUE
          BRU          *32
NMAS      LDTM, 13     MASQUE + 1
          BRU          *32
          END
```

Revue Roumaine de Chimie, **21**, *5*, 781–788 (1976)

SPECTROPHOTOMETRIC STUDY OF SOME ARYLIDENEMALONONITRILES IN ORGANIC SOLVENTS AND BUFFER SOLUTIONS

R. M. ISSA, H. Z. YOUSSEF, F. M. ISSA and Y. M. ISSA
Chemistry Department, Faculty of Science, Cairo University, A. R. Egypt

Received October 4, 1974

The electronic absorption spectra of some arylidenemalononitriles are recorded in organic solvents of varying polarities and buffer solutions of different pH. The spectra in organic solvents are discussed in the light of molecular structure and solvent effect. The spectra in buffer solutions are explained in terms of an acid-base equilibrium involving the dissociation of a proton from the alkene group. The pK_a of these equilibria are also determined and discussed in relation to molecular structure.

INTRODUCTION

Arylidenemalononitriles were the subject of many investigations concerning their preparation and properties. However, few spectrophotometric studies have been carried out on malononitrile and its arylidene derivatives.[1–4] The effect of temperature on the UV-spectra of salicylidenemalononitrile in alcoholic solutions was studied by Lauerer et al.[2] The results revealed a proton exchange between the solute and solvent molecules. Most of the spectral studies carried out on arylidenemalononitrile were not systematic and focussed on few compounds of this type. *o*-Chlorobenzylidenemalononitrile was studied in the UV-and IR-regions.[3]

The present article includes the results of a UV-spectrophotometric investigation of some arylidenemalononitriles in organics solvents of different polarities and buffer solutions of varying pH values.

EXPERIMENTAL

The arylidene derivatives used in the present investigation were prepared by condensation of aromatic aldehydes with malononitrile.[5] The compounds obtained have the following structure :

---

[1] D. G. I. Felto, and S. F. D. Drr, *J. Chem. Soc.*, **1955**, 2170.

[2] D. Lauerer, M. Goener, M. Pestemer and G. Scheibe, *Z. phys. Chem.* (*Frankfurt*), **10**, 236 (1957).

[3] S. Vasan, R. Velambur and R. A. Boese, *J. Forensic. Sci.*, **15**, 433 (1970).

[4] H. Kobler, B. Eichler and A. Kolbe, *Z. Chem.*, **10**, 154 (1970).

[5] B. B. Corson and R . W. Stoughton, *J. Amer. Chem. Soc.*, **50**, 2825 (1928).

(I)

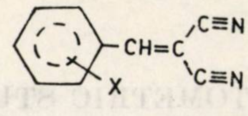

in which x = H (a), o-OCH_3(b), p-OCH_3 (c)
o-NO_2(d), p-NO_2(e), o-OH(f)
p-Cl (g), o-Cl (h)

(II)

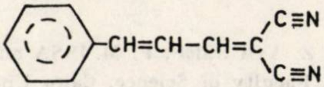

(III)

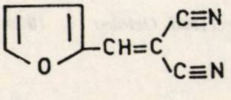

10^{-3} M stock solutions were prepared by dissolving the accurately weighed amount of the solid in the appropriate volume of ethanol or other solvent. The solutions used for spectral measurements were obtained by accurate dilutions. The buffer solutions used for pH control were the modified universal series of Britton and Robinson[6]. The pH of the final solutions was measured on a Prolabo pH-meter accurate to 0.05 unit. The spectra were recorded on a Unicam SP 800 quartz spectrophotometer within the 200−450 nm range using 1 cm matched silica cells.

RESULTS AND DISCUSSION

The spectra of the compounds under investigation are recorded in organic solvents of varying polarities and buffer solutions of different pH. The behaviour in each case shows some remarkable shifts which are considered separately.

(I) *Spectra in Organic Solvents*

(i) *Band assignment*. The spectra of the compounds under investigation (table 1) display two sets of bands. The first set, lying within the 220−300 nm range, comprises two bands which can be assigned to the $\pi-\pi^*$ transitions of the aromatic nucleus namely the $(1_{L_a} \leftarrow 1_A)$ and $(1_{L_b} \leftarrow 1_A)$ bands. The second set displays generally one band with high extinction and broad appearance within the 300−360 nm region. This band can be assigned to an intramolecular charge transfer from the aromatic nucleus to the neighbouring acceptor center. This interaction takes place under the strong acceptor character of the CN groups. The mesomeric shift representing such an intramolecular charge transfer may be represented as follows :

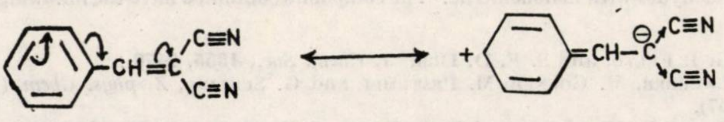

---

[6] H. T. S. Britton "Hydrogen Ions" vol. 1, 2nd edition, Chapman and Hall, London, 1955, p. 364.

Table 1

Results obtained in organic solvents λ = nm &ε = $1 \cdot \text{mole}^{-1} \cdot \text{cm}^{-1} \times 10^{-3}$

Compound N°	Solvent	$^1L_a \leftarrow {}^1A$		$^1L_b \leftarrow {}^1A$		CT	
		λ_{max}	ε_{max}	λ_{max}	ε_{max}	λ_{max}	ε_{max}
Ia	Ethanol	231	10.04			308	13.24
	Chloroform					312	21.80
H	Carbon tetra					305	18.93
	Cyclohexane	230	5.48			302	24.29
Ib	Ethanol	240	7.50	297	9.47	368	6.58
	Chloroform			300	13.90	372	10.21
o-OCH_3	CCl_4			300	17.04	362	14.04
	Cyclohexane	235	6.22	299	13.13	359	9.65
Ic	Ethanol	248	12.55	275	8.18	349	25.92
	Acetone					358	28.42
p-OCH_3	Chloroform					352	29.42
	CCl_4			280	11.47	345	25.50
	Cyclohexane	247	7.14	280	4.46	342	29.50
Ie	Ethanol	238	10.24	264	12.56	310	3.10
	Chloroform					307	22.07
p-NO_2	CCl_4					305	18.74
	Cyclohexane	238	3.75	257	3.98	300	1.28
If	Ethanol	265	9.87	278	8.10	360	3.00
	Chloroform			280	10.24	355	4.00
o-OH	CCl_4			279	9.41	353	3.25
	Cyclohexane	261	6.28	278	4.45	350	7.40
Ig	Ethanol	237	6.70	258	6.42	324	12.85
	Chloroform					324	25.31
p-Cl	CCl_4					320	23.26
	Cyclohexane	231	10.92	255	1.65	320	26.00
Ih	Ethanol	237	5.47	255	3.95	302	6.66
	Chloroform					306	13.50
o-Cl	CCl_4					301	17.72
	Cyclohexane	232	5.28	255	1.35	299	11.18
II	Ethanol	247	7.25	265	2.42	349	27.92
	Chloroform			265	2.47	353	29.53
	Acetone					347	28.06
	CCl_4					349	29.49
	Cyclohexane	246	5.85	265	1.60	345	16.16
III	Ethanol					341	17.94
	Acetone					340	17.86
	Chloroform					345	23.18
	CCl_4					340	17.77
	Cyclohexane					338	17.08

Accordingly, such an electronic transition would involve the whole molecule.

(ii) *Spectral structural correlation*. The spectra of the compounds under investigation indicate that the position of the C.T. band is influenced by the molecular structure. For compounds of series I, the plot of λ_{max} C T as a function of the σ-(Hammet) constant is a more or less linear relation for the *p*-substituted compounds (fig. 1). In figure 1 the position of the

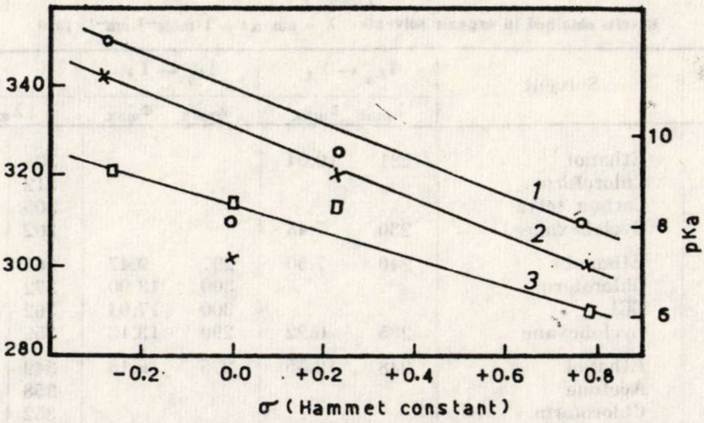

Fig. 1. — $\lambda_{max} - \sigma$ plots for *p*-derivatives in ethanol (*1*) and cyclohexane (*2*). $pK_a - \sigma$ plots for *p*-derivatives (*3*).

substituted compounds lies on the line representing the plot. The point deviating is that of the unsubstituted derivative. The deviation goes to shorter wavelength compared to the position of the plot. This can be explained by the probable existence of two types of intramolecular charge transfer in the unsubstituted compound :

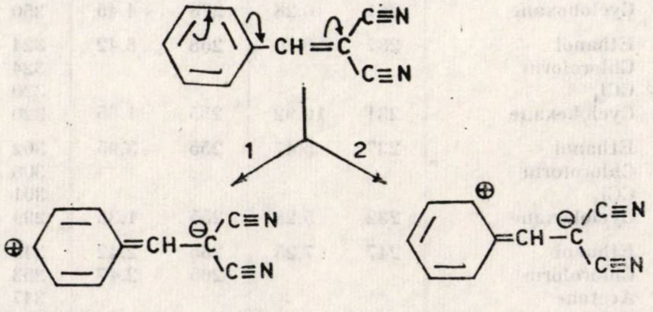

of which 1 is of lower energy than 2. The energy of the transition would be intermediate between both types.

For the *p*-substituted compounds the charge migration according to 1 is only possible, hence the transition in the substituted compounds would be of lower energy and the bands are red shifted compared to the nonsubstituted compound.

Comparing benzylidenemolononitrile (Ia) with (II) and (III) it becomes apparent that the band is red shifted in the order II > III > Ia. The highest red shift with (II) is probably due to increased conjugation in the molecule. The shift of (III) to red, compared to (Ia), is presumably related to the ease of charge transfer from the furfural rest compared to phenyl one as a result of the lower ionisation potential of furfuraldehyde compared to benzaldehyde.[7]

---

[7] R. C. Wheat, "Handbook of Chemistry and Physics", the Chemical Rubber Company, 50th edition, 1969–1970, Ohio, U.S.A.

(iii) *Solvent effect on band position.* The effect of solvent on the position of the bands (fig. 2) goes in a more or less regular manner with the $\pi-\pi^*$ of the aromatic system. The bands generally shift to red with increasing solvent polarity. For the charge transfer band, the shift goes to red with increasing polarity for cyclohexane, CCl_4 and $CHCl_3$. Acetone mostly shows a regular behaviour. On the contrary, with ethanol, though showing in general a red shift compared to cyclohexane, the shift is not in accordance with the high polarity of ethanol. The plot of λ_{max} as a function of the dielectric constant goes through a maximum, a behaviour which is common for merocyanines and can be explained on similar bases.[8] However, with the compounds under investigation the exchange of the alkene proton with polar solvents molecules should be considered.

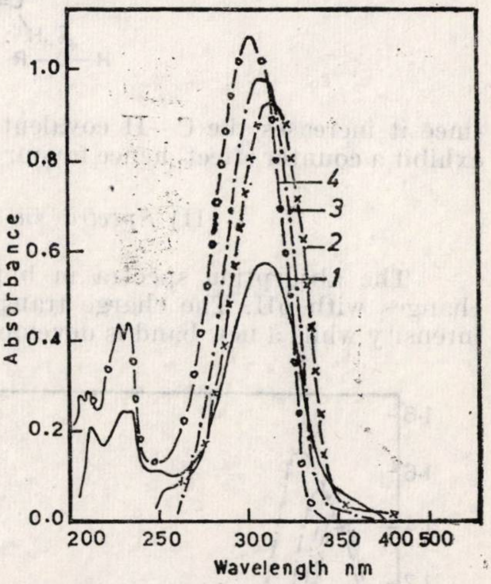

Fig. 2. — Absorption spectra of benzylidene malononitrile in organic solvents.
1. Ethanol 4.38×10^{-5}M; *2.* Chloroform 4.22×10^{-5} M; *3.* Carbontetrachloride 5.18×10^{-5} M; *4.* Cyclohexane 4.38×10^{-5} M.

The shift to red caused by increased solvent polarity in ethanol is most probably antagonised by another effect leading to a blue shift. Accordingly, the shift observed is the resultant of both red and blue shifts. The blue shift may be ascribed to a proton transfer from the active alkene group to ethanol. This increases the negative charge density on the alkene carbon which antagonises the intramolecular charge transfer as a result of its tendency to locate its charge on the phenyl ring.

Thus, the blue shift would be a measure for the acid character of the alkene group. This is substantiated by the fact that the shift to red on going from cyclohexane to ethanol is higher for molecules containing substituents with (+M) and lower for those with (−M). As a matter of fact, substituents with (+M) decrease the bonding of the proton to ethanol

---

[8] H. A. Staab "Einfuhrung in die theoretische organische Chemie" 4. Aufl., Verlag Chemie, 1970, p. 336.

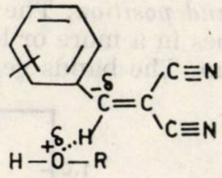

since it increases the C—H covalent character, while groups with (—M) exhibit a counter effect, hence favour the bonding of the proton to ethanol.

(II) *Spectra in buffer solutions*

The absorption spectra in buffer solutions, fig. 3, show regular changes with pH. The charge transfer band shows gradual decrease in intensity while a new band is developed at shorter wavelength. This behaviour is very different from previous observations [9] the new band observed with arylidenemalononitriles in solutions of high pH is located at shorter wavelength compared to that in acid solutions. The spectra show clearly an isosbestic point indicating the set of an acid-base equilibrium. The reaction involves probably the dissociation of a proton from the alkene group, namely :

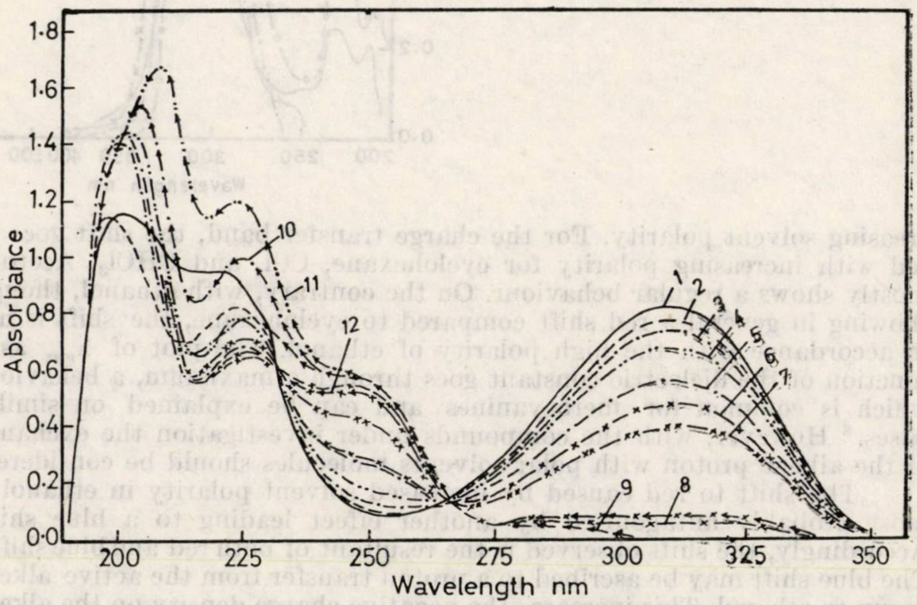

Fig. 3. — Absorption spectra of 4×10^{-5} M benzylidenemalononitrile in aqueous buffer solutions. pH = 2.0 (*1*), 4.0(*2*), 6.0(*3*), 8.0 (*4*), 8.5(*5*), 9.0(*6*), 9.5 (*7*), 10.0 (*8*), 10.5 (*9*), 11.0 (*10*), 11.5(*11*), 12.0(*12*).

---

[9] R. M. Issa, M. S. El-Ezaby and A. H. Zewail, *Z. phys. Chem.* (*Leipzig*), **242**, 1969, 196, *J. Chem. U.A.R.*, **14**, 1971, 113.

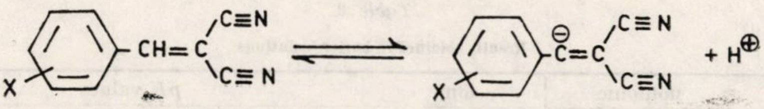

The plot of $A_{\max}$ as a function of pH, fig. 4, has typical dissociation and association curves denoting the existence of an acid-base reaction. The blue shift of the charge transfer band can be ascribed to the antagonising effect of the carbanion formed on the intramolecular CT; the carbanion favours an intramolecular charge transfer to the aromatic ring, hence leading to the blue shift of the charge transfer band involving the whole molecule.

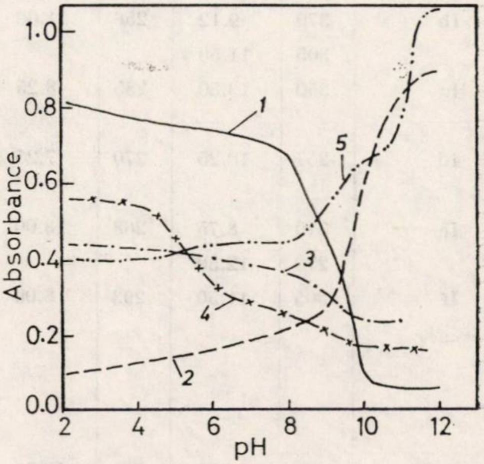

Fig. 4. — Absorbance — pH curves.
1. Benzylidenemalononitrile (λ = 320 nm) 2. o-OCH_3, (λ = 256 nm); 3. o-NO_2 (λ = 300 nm); 4. p-NO_2 (λ=325 nm) 5. o-OH (λ = 237 nm).

The acid dissociation constants of the compounds under investigation are determined applying the half-height [9] and modified limiting absorbance [10] methods. The values obtained are depicted in table 2.

For each compound, one pK_a value is determined, whereas for salicylidenemalononitrile two values are obtained. The lower value is the ionisation constant of the OH-group, while the higher one is that of the alkene hydrogen.

As a matter of fact, the pK_a values depend on the nature of the substituent on the aromatic ring, pK_a varies in a more or less linear manner with the σ-constant of the substituent (fig. 1). This fact supports the opinion that the polar character of the C—H group is related to the nature of the substituent. The ease of ionisation of the hydrogen from the alkene group is brought about by the strong acceptor character of the two nitryl groups in conjugation with it.

---

[10] N. A. Ibrahim, R. M. Issa, S. E. Zayan and G. B. El-Hefnawey, *J. prakt. Chem.*, **315**, 202 (1973).

Table 2

Results obtained in buffer solutions

Compound N°	nonionic		ionic		*pK* values			
	λ_{max}	$\varepsilon_{max} \times 10^{-3}$	λ_{max}	$\varepsilon_{max} \times 10^{-3}$	λ_{nm}	1st method	2nd method	mean *pK*
Ia	310	20.50	250sh	14.25	250	8.90	8.90	
					310	8.95	9.05	8.95
Ib	370	9.12	256	11.00	256	9.75	9.80	
	305	11.50			305	9.95	. . .	9.81
Ic	350	13.50	285	8.25	285	9.90	9.90	
					350	10.10	10.10	10.00
Id	257	10.25	270	7.25	275	8.40	8.50	
					300	8.50	8.60	8.50
Ie	310	8.75	268	13.00	310	6.00	5.90	
	270	12.50			325	5.90	6.20	6.00
If	305	11.50	293	8.00	232	8.60 ; 10.90	8.55 ; 10.95	
					305	8.50 ; 11.15	8.5 ; 11.1	
					325	8.50	8.40	
								8.50
								11.00
Ig	320	20.50	260	18.25	260	9.45	9.50	
					320	9.40	9.70	9.51
Ih	305	13.75	250	13.00	250	8.90	8.95	
					305	8.60	8.40	8.71
II	350	27.00	292	18.75	290	10.50	10.50	
					350	10.60	10.30	10.47
III	476	6.20	578	8.20	277	9.80	9.80	
	345	24.00	277	9.25	345	9.90	9.90	9.85

Revue Roumaine de Chimie, **21**, *5*, 789–796 (1976)

PROCESSES ASSOCIATED WITH THE ^{6}Li(n, α)^{3}H NUCLEAR REACTION. III*

CHEMICAL EVIDENCE FOR THE STABILIZATION FORMS OF RECOIL TRITIUM IN LITHIUM HALIDES

CONSTANȚA MĂNTESCU, ANA GENUNCHE, DOINA CRISTU and T. COSTEA
Institute of Atomic Physics, Bucharest, Romania

Received November 12, 1973
Completed June 26, 1975

Using some specific chemical reactions the species T was evidenced in the neutron irradiated LiF, LiCl, LiBr and LiI, besides the species TX (X = F, Cl, Br, I), LiT, TH, already established by the thermal treatment, as well as the role of water remaining in the crystalline lattice. It is interesting to emphasize that no difference was observed in the nature of reactions of recoil tritium whether it entered a chemical combination during the irradiation or after having trapped for a long period in the crystalline lattice.

INTRODUCTION

A method obtaining information on the chemical reactivity of the recoil tritium produced in crystalline lithium compounds consists in heating the irradiated compound and observing the activity of the gaseous fraction released as a consequence of the thermal treatment.[1,2]

It has been observed that the release of the volatile fractions has been associated with crystalline annealing [3] or with some modification of the state of aggregation (volatilization, melting, decomposition) of the target. By dissolving the samples in water after thermal treatment, the distribution of tritium could be established.[4] In the lithium halides a substantial quantity of volatile compound TX (X = F, Cl, Br, I) as well as LiT appeared in addition to tritium gas. TOH has been identified in compounds containing water.[4] It was not possible to use this method in measuring the ratio HT/T_2 in the uncondensable fraction or the atomic form in the crystalline lattice. Moreover, it was important to attempt at elucidating two problems : (i) — whether these various forms preexisted in the crystalline lattice before the thermal treatment or whether they resulted from it and (ii) — to find some chemical evidence to confirm these results and to discover other possible states unnoticed by the physical method employed.[5]

---

* Part II. C. MĂNTESCU, A. GENUNCHE, D. CRISTU and T. COSTEA, *Radiochim. Acta*, in press.

[1] C. MĂNTESCU and T. COSTEA, *Canad. J. Chem.*, **40**, 1232 (1962).

[2] C. MĂNTESCU and T. COSTEA, *Phys. Stat. Solidi*, **3**, K 290 (1963).

[3] C. MĂNTESCU and T. COSTEA, *J. Inorg. Nuclear Chem.*, **28**, 273 (1966).

[4] T. COSTEA and C. MĂNTESCU, *J. Inorg. Nuclear Chem.*, **28**, 2777 (1966).

The existence of the molecular and atomic form of tritium was taken into account in establishing the radiochemical yield of the tritiated compounds. The yield of tritiation in toluene was determined using crystals containing their normal water of crystallization and those from which the water had been pumped off as completely as possible. Toluene as model molecule was used in a series of studies on hot tritium reactions in the liquid phase.[6]

In order to prove the existence of the compound TX, we resorted to a chemical reaction in which a certain compound was able to fix the proton $H^+(T^+)$ irreversibly. Such a compound was the unsaturated diketone $Ph-CO-CH = C(Ph) - CH_2-CO-Ph$, the pseudo-base of the cation:

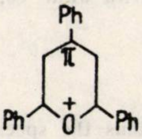

which in the presence of HX (TX)[7] gives rapidly and irreversibly the triphenyl pyrilium cation halides. The pseudo-base was separated from the triphenyl pyrilium cation in order to measure their radioactivities.

Additional evidence for LiT in LiF and LiCl was given by the result of the reduction reaction on acetone performed in the presence of $AlCl_3$ in diethyl ether during which the reductive entity $LiAlH_4$ (T) had to be formed.

EXPERIMENTAL PART

SAMPLE PREPARATION AND IRRADIATION

Twenty to twenty five mg of Merck Reagent LiF, LiCl, LiBr, LiI were heated in quartz tubes in high vacuum for almost 24 hr at 300°, after which the tubes were sealed in vacuo.[3] Another series of samples were sealed in vacuo without heating. The samples were irradiated at a thermal neutron flux of $1.2 \cdot 10^{11} cm^{-2} sec^{-1}$, and a gamma dose rate of about 10^6 rad. hr^{-1} or at a thermal neutron flux of 5.0. $10^{12} cm^{-2} sec^{-1}$ and a gamma dose rate of $1.2 \cdot 10^8$ rad hr^{-1}.

CHEMICAL REACTIONS

1. *Quantitative determination of water* contained in the crystalline lattice of LiF and LiCl before irradiation was carried out by dissolving 25 — 110 mg of the above-mentioned halides in 0.1 ml of HTO whose radioactivity was in the range 2.5 . 10^4—9.2 . 10^6 dps. The tritiated water was subsequently removed by heating the samples in vacuo at 300° for 24 hr.

---

[5] After the completion of this work, VAN URK (Ph. D. Thesis, University of Amsterdam (1970)), using other experimental techniques, has found the same type of compounds: LiT, molecular tritium and great quantities of labile tritium (much more than the sum of TX and TOH).

[6] A. SOKOLOWSKA, *Radiochim. Acta*, **10**, 44 (1968); including refs. 3—10 of this work.

[7] C. GEORGOULIS, J. LANDAIS, C. PREVOST and M. SIEMIATYCKI, *Compt. rend.*, **250**, 3168 (1960).

After heating, the samples were dissolved in water and the tritium radioactivity of the aqueous solution was measured.

2. *Reaction in toluene* was achieved by magnetic stirring of 20–25 mg irradiated lithium halides in 5 mMoles of pure toluene for 30 minutes in vacuo at room temperature. A GLC verification of purity and determination of the position of tritium in tritiated toluene followed.[8]

3. *Specific reaction for TX* made use of the irreversible fixation of $T^+(H^+)$ by an unsaturated diketone as mentioned above. The irradiated lithium salts were dispersed in a solution of 0.1 mMoles of diketone in 0.5 ml CCl_4 at room temperature. By dissolution of the reaction mixture in diethyl ether the pyrilium cation was separated with 0.025 mMoles perchlorate of triphenyl pyrilium as carrier, the pseudo-base remaining in the filtrate. The two compounds were purified by repeated recrystallization from appropriate solvents. It was found in most cases that two recrystallizations were sufficient to give a constant specific activity.

4. *Specific reaction for LiT* was performed for LiF and LiCl after thermal treatment. The sample was stirred in dry ether cooled to −20°, then a solution of $AlCl_3$ was added and the mixture stirred again until the evolution of gases ceased. An ethereal solution of acetone was added at the same temperature. The molar ratio of the reactants LiX : $AlCl_3$: Acetone was 4 : 1 : 4. The hydrolized mixture was separated and the components purified by GLC using: Celite — 22 as a support, carbowax 1500 as a stationary phase and hydrogen as a mobile phase on a 3 m long copper column of 0.6 cm id.

RADIOACTIVITY MEASUREMENTS

The tritium activities of the purified compound and of their derivatives were measured in a Packard Tri — Carb Liquid Scintillation Spectrometer Model 3375 in appropriate scintillating mixtures.

RESULTS AND DISCUSSION

1. *The role of water*

The results obtained for the determination of water contained in LiF and LiCl, are summarized in table 1.

Table 1

Quantitative determination of water in LiF and LiCl before irradiation

Compound	LiF	LiCl	LiCl
Weight mg	110*	25**	100***
Radioactivity of dps/0.1 ml TOH			
initial	2.5.10^4	9.2.10^6	2.5.10^4
final	1.5.10^2	8.0 .10^4	3.6.10^3
Number of T atoms (TOH molecules)			
initial	1.4.10^{13}	5.2.10^{15}	1.4.10^{13}
final	8.4.10^{10}	4.5.10^{13}	2.0.10^{12}
Molecular ratio H_2O/TOH	2.4.10^8	6.3.10^5	2.4.10^8
Water remaining mg in crystals	0.6	0.84	1.5
Water in crystal %	0.5	3.4	1.5

* Without heating

** and *** 5 and 24 hrs heating at 300° respectively.

---

[8] H. J. Ache, *J. Phys. Chem.*, **71**, 3388 (1967).

The existence of such quantities of water in the irradiated dried crystals is very important from two points of view :

a) Even at 300° in vacuo the complete dehydration of $LiCl.H_2O$ does not take place.

b) The remaining water must be considered as a possible reactant for recoil tritium.

The presence of water in irradiated crystals was also noted in a previous work[4] by measuring the radioactivity of HTO. This identification was made through noting the temperature of condensation of that fraction. Another fraction was considered by us to be T_2 since it was supposed that the concentration and mobility of water molecules was very small in comparison with those of the recoil tritium. Hence we drew the conclusion that the value of T_2/TH was $\gg 1$. It is now obvious that taking into account the results given in table 1 this conclusion is unjustified.

2. *Chemical evidence for atomic tritium*

Table 2 gives the results obtained from the dispersion of the lithium salts in toluene.

As it may be seen from Table 2 there is a difference in the tritiation yield between LiCl preheated before irradiation and LiCl containing the water of crystallization. We suppose, that a reaction between T and H_2O took place, diminishing the number of T atoms available and consequently the yield of tritiation in toluene. The fact that the tritiation yields for LiF (dried and nondried) show a less difference than for LiCl, tends to confirm our supposition concerning the role of water, since the content of water is small in both cases. Though LiBr and LiI underwent also a pretreatment before irradiation, the yield of tritiation is smaller than for

Table 2

Yield of tritiation of toluene *

Irradiated lithium compound	Pretreatment	Total activity of tritium in irradiated compound ; n° of atoms**	Tritium in toluene ; % n° of atoms
LiF	300° preheating for 24 hrs	$9.7 \cdot 10^{13}$	6.9
LiF	without preheating, 0.5 % H_2O	$14.0 \cdot 10^{13}$	1.8
LiCl	300° preheating for 24 hrs, 1.5 % remaining water	$32.0 \cdot 10^{13}$	9.4
LiCl	without preheating, water of crystallization	$35.0 \cdot 10^{13}$	0.4
LiBr	300° preheating for 24 hrs remaining water not measured	$10.4 \cdot 10^{13}$	1.4
LiI		$10.4 \cdot 10^{13}$	1.1

* The distribution of tritium in toluene molecule: 26% in chain, 74% in ring.

** No. of tritium atoms determined by measuring the radioactivity of sample (the radioactivity of gases after dissolution in water and the radioactivity of solution).

LiF and LiCl, the remaining quantity of water being greater. This remark is in agreement with the previous one.[4]

The radiolytic exchange of water and isotopic hydrogen gas using D_2 and TH is well known [9] as well as the recoil tritium reaction in aqueous solution of lithium halides,[10] but there is little knowledge on the reaction of a hot species trapped in an irradiated crystal containing the water of crystallization as in the experiments shown here.

The distribution of tritium in toluene molecule (see table 2 footnote) seems to be almost the same as in the "in situ" recoil tritium reactions [11] as if the same species were active in both cases.

Another evidence for the existence of T atoms in neutron irradiated lithium halides is the tritiation of pseudo-base of the pyrilium cation. Though the number of tritium atoms incorporated in the pseudo-base is small (see table 3 below) it could indicate the existence of atomic tritium. It was suspected that the activity in the pseudo-base might have been due to contamination. However, this possibility was excluded by a series of checked experiments and we concluded that the radioactivity in the pseudo-base could only arise from some reactions including atomic tritium.

3. *Chemical evidence for TX*

The results obtained in consequence of the specific reaction performed for TX are summarized in table 3.

Table 3

The distribution of tritium activity in the triphenyl pyrilium cation and unsaturated diketone $Ph-CO-CH_2-C(Ph)-CH_2-CO-PH$.

Irradiated lithium compound*	Total activity of tritium in irradiated compound; n°. of atoms**	Tritium in: Pseudo-base % of n° of atoms	Tritium in: Pyrilium cation
LiF	$4.8 \cdot 10^{14}$	1.2	4.0
LiCl	$16.0 \cdot 10^{14}$	1.5	7.9
LiBr	$5.2 \cdot 10^{14}$	0.5	20.4
LiI	$5.2 \cdot 10^{14}$	0.7	19.9

* All compounds were heated at 300° for 24 hr.

** Number of atoms determined by measuring the radioactivity of the sample (see table 2).

Among the lithium halides the number of tritium atoms incorporated into the triphenyl pyrilium cation decreased in the following order: $F < Cl < Br < I$, strengthening the conclusions derived from our studies involving the thermal treatment. These results showed that owing to its great reactivity, the recoil tritium atoms were stabilized by combining with halogens in the lattice giving TX partially during the irradiation. Another possibility to obtain TX (X = Cl) in CCl_4 solution would be the following reaction:

---

[9] M. ANBAR and D. MEYERSTEIN, "Radiation Chemistry of Aqueous Systems", Ed. G. Stein, 1967, p. 109.

[10] T. KAMBARA, R. M. WHITE and F. S. ROWLAND, *J. Inorg. Nuclear Chem.* **21**, 210 (1961).

[11] H. J. ACHE, W. HERR and A. THIEMANN, "Tritium in the Physical and Biological Sciences", vol. II, IAEA, Vienna, 1962, p. 21.

$$CCl_4 + T \rightarrow TCl + CCl_3$$

this compound being the carrier for the fixation of T^+ in the pyrilium cation in all cases studied. However, the differences among the lithium halides as shown in table 3 indicated the scavenger effect of the halogens and the possible preexistence of TX compounds before the thermal treatment.

4. *Chemical evidence for LiT*

The activity of 2- propanol -- 2T and the lack of activity in the acetone indicates that $LiAlH_4(T)$ was the reactive entity in the reduction reaction, having been formed as a consequence of tritium stabilization as LiT.

CONCLUSION

Taking into account the experimental data described above, the picture given previously[4] concerning the chemistry of recoil tritium in lithium halides may be amplified.

The distribution of recoil tritium could be a consequence of its interaction with partners in the damaged lattice, containing some quantity of water, the reactants being the species[4] resulted from the following reactions:

$$X^-_{X^-} \rightarrow X_{X^-} + e \tag{1}$$

$$X_{X^-} \rightarrow X_i + V_{X^-} \tag{2}$$

$$V_{X^-} + e \rightarrow V^-_{X^-} \quad \text{(F-center)} \tag{3}$$

$$X_i \rightarrow (X_2)_i \tag{4}$$

$$(X_2)_i + V^-_{X^-} \rightarrow (X_2)^-_{X^-} \quad \text{(V-center)} \tag{5}$$

$$X_i + X^-_{X^-} \rightarrow (X_2)^-_{X^-} \tag{6}$$

$$Li^+_{Li^+} \rightarrow Li_i + V^+_{Li^+} \tag{7}$$

$$Li^+_{Li^+} \rightarrow Li_i + V_{Li^+} + h \tag{8}$$

$$\mathrm{Li_i} \rightarrow \mathrm{Li_n} \ \text{(platelets)} \tag{9}$$

$$\mathrm{V^{+}_{Li^+}} + \mathrm{V^{-}_{X^-}} \rightarrow (\mathrm{V^{+}_{Li^+}}\,\mathrm{V_{X^-}})_n \ \text{(cavities)} \tag{10}$$

$$(\mathrm{V^{+}_{Li^+}}\,\mathrm{V^{-}_{X^-}})_n \rightarrow (\mathrm{V^{+}_{Li^+}}\,\mathrm{V^{-}_{X^-}}) \ \text{(divacancies)} \tag{11}$$

$$\mathrm{HOH} \rightarrow \mathrm{H} + \mathrm{OH} + \ldots \ \text{(radicals)} \tag{12}$$

As far as we are aware, there is no information about the position of water molecules and of its radiolytic products in the lattice. As regards the recoil tritium, it might be initially in an interstitial position.

The molecular tritium may appear by a process like

$$\mathrm{T} + \mathrm{HOH} \rightarrow \mathrm{TH} + \mathrm{OH} \tag{13}$$

or by a radical recombination

$$\mathrm{T} + \mathrm{H} \rightarrow \mathrm{TH}. \tag{14}$$

The tritiated water may result from an exchange or substitution reaction

$$\mathrm{T} + \mathrm{HOH} \rightarrow \mathrm{TOH} + \mathrm{H} \tag{15}$$

or from a reaction of type (14)

$$\mathrm{T} + \mathrm{OH} \rightarrow \mathrm{TOH}. \tag{16}$$

These reactions were also suggested by Rowland.[10]

The "protonic" form could result as a consequence of the following reactions :

$$\mathrm{T} + \mathrm{X_{x^-,i}} \rightarrow (\mathrm{TX})_{\mathrm{x^-,i}} \tag{17}$$

$$\mathrm{T} + (\mathrm{X_2})^{-}_{\mathrm{x^-}} + \mathrm{V_{x^-}} \rightarrow (\mathrm{TX})_{\mathrm{x^-}} + \mathrm{X^{-}_{x^-}} \tag{18}$$

For the formation of lithium tritide, we proposed earlier[4] a dissociation of a diatomic molecules by divacancies.

$$(\mathrm{TX})_{\mathrm{x^-}} + (\mathrm{V^{+}_{Li^+}}\,\mathrm{V^{-}_{x^-}}) \rightarrow \mathrm{T^{-}_{x^-}} + \mathrm{X^{-}_{x^-}} + \mathrm{V^{+}_{Li^+}} \tag{19}$$

since reaction

$$\mathrm{T} + \mathrm{Li} \rightarrow \mathrm{LiT} \tag{20}$$

is unlikely owing to the high temperature required.

Besides these already suggested species [4], the tritium atom must be considered as one of the chemical forms of stabilization of recoil tritium in neutron irradiated lithium halides. This species was also suggested by Rowland [12] in his work on the reactions of tritium trapped in inorganic crystals.

It is important to emphasize that the recoil tritium atoms are able to participate in some reactions which could have the same result whether they enter a chemical combination during the irradiation or afterwards. In the former case it was supposed that the translational energy of tritium atoms resulted from the nuclear recoil had been the "stimulus" of the reaction. In the latter case the interaction between the reagents (organic compound and tritium species) on the grain boundaries might seem to be an important factor.[13]

Acknowledgement. The authors thank Dr. G. Harbottle for valuable suggestions and Professor F. S. Rowland, Professor G. Stöcklin and Dr. L. Lindner for stimulative discussions.

---

[12] W. J. Hoff and F. S. Rowland, *J. Inorg. Nuclear Chem.*, **5**, 164 (58).

[13] A. Genunghe, D. Cristu, T. Costea and C. Măntescu, reprint IFA, CO-26 (1971).

Revue Roumaine de Chimie, **21**, *5*, 797–802 (1976)

COMPTES RENDUS

"Structure and bonding", Vol. 21 Springer Verlag, Berlin, Heidelberg, New York, 1975, 150 p.

Under the title "Recent impact of physics in inorganic chemistry" the 21th volume of the series contains two large chapters. The object of the first is a study of spin distributions and bonding in non-metallic solids by elastic magnetic neutron scattering. This type of study is analogous to the determination of the crystallographic space groups of crystals by X-ray or nuclear neutron scattering and depends in principle on the position in reciprocal space of diffraction peaks rather than on precise intensity measurements. A large variety of magnetic space groups is observed including helical structures as well as colinear ones. One and two-dimensional as well as three dimensional systems have been investigated.

The first discussion concerning the determination of covalency parameters from magnetic neutron scattering experiments is dated only in 1965. This latecoming was the result of the lack of general availability of neutron sources and their relative weakness. Since then, a considerable amount of information has been acquired, making another discussion timely. The author, Bruce C. Tofield, begins with the M.O. model, follows with the necessary elements of neutron scattering theory, and a brief description of experimental techniques, finally ending with a discussion of the data obtained. Compounds of the first row transition metals have been principally studied, but much application has also been made to rare earth and actinide materials, as well as to mixed materials like the rare earth iron garnets and the rare earth transition metal oxide perovskites. Most experiments performed up to now on salts have, however been principally concerned with the detailed determination of magnetic moments and spin distributions, essential in the study of bonding. Covalent interactions in solids, change inter alia, the charge distribution of the valence electrons of atoms relative to the isolated atoms or ions. For systems containing atoms with unpaired electrons, therefore, bonding effects should be reflected in the magnetic moment distribution and may be studied by magnetic scattering if a careful investigation of the intensity of the magnetic scattering is made. The experimental data may be compared either with *ab initio* calculations or interpreted via a bonding model. For many of the results obtained up to now by neutron scattering it has been convenient to make a simple interpretation using the molecular orbital model of transition metal complexes. This is useful both for relating trends observed from one ligand or metal to the next and for comparing neutron data with those obtained by magnetic resonance study of ligand hyperfine interactions. Nevertheless a number of experiments reveal the deficiencies of the simple model, and especially where fairly complete accurate spin density data are available, a more refined analysis is necessary. It must be noted that the M.O. model, a localized electron description, does not concern the spin distribution of the ferromagnetic metals iron, nickel and cobalt. Most compounds studied by neutrons with regard to bonding are concentrated (in respect to the metal ions with unpaired spins) magnetically ordered systems, generally antiferromagnetic. Except in few cases, where a fairly large set of data has been collected on single crystals and the magnetic moment in the unit cell, obtained by Fourier techniques, the derivation of covalency parameters has been achieved by comparison of the observed absolute intensities of magnetic reflections of polycrystalline samples with those calculated from a free model. In this situation it is assumed that the magnetisation density in the crystal is the sum of the magnetic moment densities associated with the individual ions. In paramagnetic systems the spin density on the ligands is not quenched and may be determined from the ligand hyperfine interactions measured by E.S.R. and N.M.R. Thus the neutron diffraction and the resonance techniques are complementary in the investigation of bonding effects.

In the second chapter of the volume concerning the superheavy elements, Burkhard Fricke lies the main emphasis on the prediction of their chemical properties, as this knowledge is expected to be very important for their detection.

Until 1940 the heaviest known element was uranium (Z = 92) and about 1944 the "actinide" concept of Seaborg was only a hypothesis. Since then, fourteen new elements have been added to the periodic table and much chemical and physical information has been obtained concerning this region of elements. The known elements heavier than uranium are unspecifically called "transuranium elements", the term overlapping in the upper range with the equally illdefined expression "superheavy elements". From a nuclear physics point of view the end of the transuranium elements and the beginning of the superheavy ones, may be defined as the element where the stability of the longest-lived isotope increases again with increasing Z. B. Fricke develops the theoretical predictions of the nuclear stability as a function of the number of protons and neutrons (their magic numbers). Like the closed shells in the atomic electron cloud for the structure of the periodic table, the closed nucleon shells and a large separation to the next unoccupied shell influence the nuclear stability. Regardless the approach followed, theoretical predictions of nuclear stability define a range of superheavy elements in the vicinity of the 114, with sufficiently long half-lives to allow their study, provided they can be synthesized. The prediction of the electronic configurations of the superheavy elements became much more reliable when *ab initio* atomic calculations became available and accurate enough to be used.

On the basis of the predicted electronic configuration and the trends obvious from the calculations as well as from the semi-empirical and empirical methods, detailed predictions of the properties of elements beyond lawrencium ($Z = 103$) are summarized. The stable oxidation states, the relative stabilities of these oxidation states, the heats of sublimation, ionization potentials, electronic energy levels, ionic and atomic radii are discussed regarding the 6 d transition elements ($Z = 104$ to 112), the 7 p and 8 s elements ($Z = 113$ to 120), the 5 g and 6 f elements ($Z = 121$ to 154), the $Z = 155$ to 172 elements and the $Z = 184$ element. The predictions of the physical properties and chemical behaviour of superheavy elements seem not too far away from reality, at least for the elements up to $Z = 120$, in this region close enough to the part of the periodic system with known elements. Beyond element $Z = 120$, the unknown chemical behaviour of five quite loosely bound and strongly mixed shells, together with the unknown behaviour of g electrons and in the region beyond that structure of the other electron shells, changed drastically, so that only conclusions drawn by analogy can give some idea of the chemical behaviour. Therefore, in constructing the continuation of the periodic table either more formal or more chemical arguments may be used.

The material included in the volume is presented in a clear and concise manner with tables and diagrams wherever necessary. The effort for assigning physical and chemical meaning to the theoretical and mathematical concepts is obvious and in important cases the calculated data are correlated with those determined experimentally. Each of both chapters ends with an up-to-data bibliography so that the whole work is valuable for the specialists in the matter.

Florica Popea

E. WYN-JONES, "Chemical and Biological Applications of Relaxation Spectrometry," NATO Advanced Study Institute Series, Series C, No. C18, D. Reidel Publ. Co., Dordrecht/Boston, 1975, 526 pp.

The relaxation spectrometry is in fact not a single technique, as its name would suggest, but a collection of techniques helping with the investigation of the kinetics and mechanism of fast chemical reactions. This collection encompasses a wide range of methods and has found many useful applications in studying micellar equilibria and micellization, ligand substitution mechanisms in metal complexes, complex formation in both aqueous and nonaqueous solvents, organic reaction mechanisms, protonation and deprotonation mechanisms, the kinetics of biochemical reactions, or the motion in polymer solutions or amorphous polymers. It is thus obvious that the relaxation spectrometry would interest several disciplines, including organic and inorganic chemistry, biochemistry, and molecular biology.

The state of the field had a good opportunity to be thoroughly and critically discussed at a symposium organized by the NATO Advanced Study Institute and held during the summer of 1974 at the University of Salford in Great Britain. The symposium's proceedings have been published recently under the editorship of a well-known personality in the field, Prof. Evan Wyn-Jones, of the University of Salford. The book includes 58 contributions from various researchers.

The ultrasonic relaxation spectrometry — selective absorption of acoustic frequencies in the range 100 kHz-1 GHz by the various reactions of a compound — allows determination of time constants in the range $10^{-5}-10^{-10}$ sec. Reactions as different as those occurring in acetic acid/acetone mixtures, or during hydrogen-bond polymerization of *N*-methyl acetamide can be efficiently studied, as well as some isomerization reactions; the organic chemist may benefit from this technique in stereochemical studies, whereas the biochemist in studying nucleotide or protein solutions. The dielectric relaxation is based on the measurement of the macroscopic electric polarization as a function of the strength of a variable electric field. The method is particularly suitable in studying solid and dissolved polymers. The stopped-flow method of investigating fast reactions, although introduced in the early '30 s, has only recently been adapted to the millisecond range. For rate constants less than 1 msec., extending down to 10—100 nsec., the temperature-jump technique, which is based on the "instantaneous" change in temperature and the subsequent slower readjustment of the chemical equilibrium to the new thermodynamic conditions, is very efficient. This method requires the heating of the system, which can be better made with a pulsed laser than by conventional methods. The temperature-jump technique thus modernized was successfully applied to the study of organic and biochemical reactions. By contrast, the pressure-jump technique has found fewer applications so far.

The chemical field which seems to have most benefited from the application of relaxation techniques is that of the micelle formation and micellar kinetics. More than 15 contributions were presented on this subject at the meeting, which seems explicable in view of the large extent to which the field has found important applications in the study of detergent and other surfactant solutions, as well as in studying dye-micelle interactions, micelle formation and dissociation, and other related problems.

The formation of weak metal complexes has also benefited from the improvement of the relaxation techniques, which provided, e.g. the much looked-for equilibrium constants for reactions proceeding in non-aqueous solvents. The proton transfer mechanism can also be satisfactorily studied in various systems — e.g. for elucidating the color change kinetics of phenolphtaleine in water or ethanol, or studying some laser dyes. Interactions of dyes with biopolymers — which are interesting in various fields of biology — can be studied not only by spectrophotometry, but by relaxation spectrometry as well, which can give kinetic information on aggregation and stacking.

The papers published in the book may be extremely useful to all those concerned with research or development in this field.

Al. Butucelea

ÉCOLE D'ÉTÉ

« THÉORIE DES MÉTAUX ET CATALYSE »

Les travaux de l'Ecole d'Eté « Théorie des Métaux et Catalyse », organisée par l'Institut de Recherches sur la Catalyse, ont eu lieu à Lyon-Villeurbanne, entre les 22—26 septembre 1975.

185 participants, spécialistes travaillant dans la recherche ou dans l'industrie, en France ou dans d'autres pays (Belgique, Pays-Bas, Suisse, Pologne, Roumanie, Mexique, Vénézuela, Brésil, Italie, Etats-Unis, etc.) ont suivi avec intérêt les travaux.

L'Ecole d'Eté a eu comme but d'apporter aux chercheurs concernés par la Catalyse par les métaux (spécialistes de la catalyse, physiciens et chimistes des surfaces, électrochimistes, etc.) les fondements théoriques nécessaires et de faire le point des connaissances actuelles dans ce domaine. En même temps, d'essayer de montrer l'application qui peut être faite des concepts modernes pour l'interprétation de l'acte catalytique.

Pendant l'Ecole d'Eté on a présenté des conférences suivies de nombreuses discussions. De même, on a organisé des tables rondes, sur des sujets dégagés des propositions exprimées par les participants eux-mêmes.

Les conférences ont été ainsi choisies pour essayer de mettre en discussion aussi les problèmes liés à l'aspect théorique des phénomènes de chimisorption et catalyse, que l'aspect pratique, applicatif.

La première conférence, « Physique des surfaces métalliques » a été présentée par le prof. Friedel, directeur du Laboratoire de Physique des Solides de l'Université Paris XI.

Le sujet traité s'est limité aux surfaces libres métalliques, essayant de mettre l'accent sur les problèmes en suspens. Il a envisagé successivement les problèmes au niveau atomique et électronique, tout en tenant compte que les deux sont liés et doivent idéalement être résolus ensemble.

Les rugosités de la surface et les petits grains ont été mentionnés, car ces structures superficielles jouent un rôle important dans les réactions superficielles.

M. le prof. F. Gault, du Laboratoire de Catalyse de l'Université de Strasbourg, a présenté la conférence « Mécanisme des réactions d'isomérisation sur métal », domaine dans lequel il possède une riche expérience.

Comme exemple d'étude des mécanismes de réaction en catalyse hétérogène sur métal et de leurs corrélations avec la structure superficielle, il a choisi les réactions de réarrangement de squelette. Ces réactions sont importantes, tant du point de vue pratique, puisque l'isomérisation représente une des deux grandes réactions qui interviennent dans le réforming, que du point de vue théorique car, bien que des controverses assez vives aient eu lieu sur le rôle du métal et de sa dispersion sur le support, un certain nombre de faits semble maintenant bien établi.

La troisième conférence, intitulée « Concept de coordinence en catalyse hétérogène appliquée » a été présentée par M. R. Montarnal, maître de recherches à l'Institut Français du Pétrole.

L'auteur examine successivement les réactions des paraffines et celles des oléfines, sur divers métaux. Il essaye d'interpréter l'intervention de la structure chimique des métaux dans leur activité catalytique et de mettre en évidence l'influence des ligands sur le caractère du site catalytique, pour en déduire les variations des forces de liaison de coordination et les conséquences qui en découlent sur les propriétés catalytiques. Il constate que les résultats expérimentaux s'interprètent assez bien à la lumière des notions de la chimie de coordination et affirme que la présentation faite, par son pouvoir de prévision, peut devenir un outil de travail susceptible de suggérer des voies concrètes de modification des catalyseurs dans le sens désiré.

Dans son exposé « Introduction à l'étude des métaux et alliages de transition », M. le prof. F. Gautier du Laboratoire de Structure Electronique des Solides de l'Université de Strasbourg a fait une introduction qualitative aux méthodes et aux concepts utilisés actuellement en physique des solides, pour comprendre les propriétés des métaux et de leurs alliages, à partir de leur structure électronique.

Après avoir rappelé les caractéristiques des structures de bandes des métaux de transition, il présente de façon détaillée les concepts nouveaux introduits pour l'étude des alliages, qu'ils soient dilués ou concentrés. Ensuite, il discute certains résultats qui ont été obtenus lors des études de surface et d'adsorption sur les métaux de transition.

Le problème de la « Chimisorption sur les métaux de transition » a été traitée dans la conférence de M. V. Mathieu, directeur de recherches dans l'Institut de Recherches sur la Catalyse, de Lyon – Villeurbanne.

Après avoir rappelé les particularités de la liaison métallique, en insistant sur les propriétés superficielles des cristaux métalliques, l'auteur a abordé les différentes théories permettant d'expliquer la chimisorption sur les métaux.

La partie finale de l'exposé présente la description de quelques systèmes de chimisorption des hydrocarbures (ethylène, benzène) sur des catalyseurs métalliques.

Le prof. R. Maurel du Laboratoire de Catalyse en Chimie Organique de l'Université de Poitiers a présenté son exposé sur l'« Hydrogénation catalytique par les métaux de transition ».

L'hydrogénation catalytique est une réaction des plus anciennement connues et largement pratiquée tant au laboratoire que dans l'industrie, sur différents composés. Abordant ce sujet vaste, l'auteur s'est limité à traiter l'hydrogénation des liaisons multiples C—C: éthyléniques, polyéniques, acétyléniques et aromatiques.

L'accent a été mis sur les problèmes du mécanisme des réactions.

Le prof. M. Boudart de l'Université Stanford des Etats-Unis, a été invité a présenter une conférence « Corrélations dans l'activité catalytique des métaux ».

Il a mis en évidence le comportement des différentes réactions, exigeantes et non exigeantes, sensibles à la structure ou insensibles, sur les catalyseurs métal sur support. L'exposé a été soutenu par de nombreux résultats expérimentaux des travaux de l'auteur ou de la littérature.

Un sujet directement lié aux problèmes de ceux qui travaillent dans l'industrie a été traité par M. M. Michel de Rhône-Poulenc Industries dans sa conférence « Préparation des catalyseurs métalliques ».

Après un aperçu du marché des catalyseurs, l'auteur a essayé de mettre en évidence les grandes possibilités de différenciation des propriétés des catalyseurs finis, apportées par le choix des supports et des méthodes de dépôt.

Toutes les phases importantes qui interviennent dans la préparation sont examinées et, on présente aussi quelques exemples de préparation industrielle des catalyseurs.

Un sujet de catalyse homogène a été présenté par le prof. R. Ugo de l'Institut de Chimie Générale de l'Université de Milan : « Contribution de la chimie organo-métallique et de la catalyse homogène à la compréhension des réactions de surface ».

Le prof. Ugo montre que l'influence de la chimie organo-métallique et de la catalyse homogène a joué un rôle déterminant en ce qui concerne l'introduction de concepts nouveaux dans le domaine de la catalyse hétérogène, particulièrement dans les quinze dernières années.

D'autre part, la chimie organo-métallique a fourni un moyen de contrôle et de critique vis-à-vis de quelques suggestions ou concepts qui furent développés dans les débuts de la catalyse hétérogène, contribution importante pour la théorie de la catalyse.

La dernière conférence a été présentée par M. G. A. Martin, maître de recherches à l'Institut de Recherches sur la Catalyse de Lyon-Villeurbanne, sur la « Caractérisation physico-chimique des catalyseurs métalliques ».

En soulignant que la caractérisation des catalyseurs, étape décisive dans l'étude de la catalyse, ne peut être envisagée qu'en relation avec l'acte catalytique et les méthodes de préparation, l'auteur essaye d'en définir les méthodes actuelles, les buts, les moyens, les tendances et les limites.

Il affirme que dans le domaine de la caractérisation, les tendances actuelles des méthodes d'étude des catalyseurs métalliques indiquent l'utilisation simultanée de plusieurs techniques, l'adaptation de la sensibilité des techniques en fonction des conditions et l'étude du catalyseur dans les conditions même de la réaction.

L'Ecole d'Eté « Théorie des Métaux et Catalyse », enseignement de niveau élevé, dispensé par des personnalités françaises et étrangères de la recherche et de l'industrie a constitué un excellent moyen d'actualisation des connaissances pour les chercheurs et ingénieurs.

En même temps, des efforts importants ont été faits par les physiciens, les chimistes et les industriels, pour partager leurs connaissances, pour accorder leurs points de vue, afin d'arriver à un progrès effectif dans la théorie et dans la pratique de la Catalyse.

Maria Gruia

THE FIFTH NATIONAL CONFERENCE OF PURE AND APPLIED PHYSICAL CHEMISTRY

The Centre of Physical Chemistry of the Central Institute for Chemical Research will be organizing The Fifth National Conference of Pure and Applied Physical Chemistry in Bucharest, 1—4 September 1976.

The principal objective of the Conference is to contribute to the mutual knowledge of the new original results obtained by people working in the research institutes, Universities and chemical industry.

The Conference aims at an exchange of experience between the Romanian and foreign scientists dealing with the various aspects of physical chemistry research.

The Conference will be organized in Sections covering the topics listed below :

1. Quantum chemistry ; theory of the chemical bond ; molecular structure ; reactivity.
2. States of the matter ; transport phenomena ; colloids ; chemical kinetics ; photochemistry ; radiochemistry.

3. Chemisorption; homogeneous and heterogeneous catalysis; catalytic reactions.
4. Chemical thermodynamics; thermochemistry; statistical thermodynamics; thermodynamics of metallurgical processes; thermodynamics of irreversible processes.
5. Electrochemistry; solutions of electrolytes; ionic liquids (molten salts); electrode processes; electrometallurgy; corrosion and anticorrosion protection.
6. Chemical engineering; mass and heat transfer: effect of surface phenomena; kinetics of unit processes; modelling, optimisation and automation of processes in chemical industry.
7. Physico-chemical analysis; automation of physico-chemical analysis and control.

Only unpublished original papers may be submitted. The time allowed for a lecture is 15 minutes, including discussions. The registration fee is 75 lei and it includes the Conference materials.

The official language of the Conference is Romanian; the foreign participants may deliver their papers in English, Russian, French, Spanish or German. No simultaneous translation will be provided, but all the papers will have their abstracts translated in one of the above mentioned languages.

In order to obtain supplementary details as well as for inquiries, please contact the Organizing Committee: *Centrul de Chimie Fizică, str. Galați 31, sector 2, 7000 București I. Cable: CHIMFIZ, București, ROMANIA.*

NOTE POUR LES AUTEURS

La *Revue Roumaine de Chimie* publie des articles en anglais, français, russe, allemand ou espagnol. Les auteurs sont priés d'envoyer des articles, notes, communications et comptes rendus inédits.

Les manuscrits seront dactylographiés à deux intervalles. Les tableaux seront dactylographiés sur des feuilles séparées, de même que la légende des figures. Les diagrammes seront tracés à l'encre de Chine sur papier calque. Les tableaux et les figures seront numérotés par des chiffres arabes, en nombre strictement nécessaire. Prière de ne pas inscrire les mêmes données dans les tableaux et les figures. Les formules chimiques seront incluses dans le texte ; en outre, elles seront transcrites sur des feuilles séparées. Les auteurs sont priés d'indiquer les caractères italiques (en soulignant les lettres au crayon), ainsi que tout autre caractère spécial. L'ordre des références bibliographiques sera celui de leur mention dans le texte ; le nom de l'auteur sera précédé de l'initiale du prénom ; les publications périodiques seront présentées suivant les prescriptions internationales. Les références seront ajoutées à la fin de l'article ; elles paraîtront comme des notes, au bas de la page. Le texte sera précédé d'un résumé comprenant 15 lignes au maximum.

L'entière responsabilité du contenu des articles appartient aux auteurs. On publie des articles dus aux collaborateurs roumains ou étrangers.

PRINTED IN ROMANIA

TRAVAUX PARUS AUX ÉDITIONS DE L'ACADÉMIE DE LA RÉPUBLIQUE SOCIALISTE DE ROUMANIE

I. GĂLĂŢEANU, **Radiochimia aplicată. Metode şi probleme** (La radiochimie appliquée. Méthodes et problèmes), 1976, 305 p., 19 lei.

FR. A. GOTHARD, **Echilibre lichid-vapori. I. Baze teoretice şi metode de calcul** (Equilibre liquide-vapeurs. I. Bases théoriques et méthodes de calcul), 1975, 262 p., 28 lei.

CONST. GH. MACAROVICI, DAN MACAROVICI, **Chimia oxizilor dubli şi utilizările lor** (La Chimie des oxydes doubles et leurs utilisations), 1975, 194 p., 13 lei.

ELENA CEAUŞESCU, **Research work on synthesis and caracterization of macromolecular compounds. Contributions**, 1974, 251 p., 20 lei.

I. ZUGRĂVESCU et MAGDA PETROVANU, **Chimia N-Ilidelor** (La chimie des N-Ylures), 1974, 347 p., 19 lei.

MARGARETA AVRAM, **Antidăunători** (Pesticides), 1974, 494 p., 41 lei.

CR. SIMIONESCU, VIORICA RUSAN et N. POPA, **Chimia algelor marine** (La Chimie des algues marines), 1974, 211 p., 18 lei.

TIBERIU NĂŞCUŢIU, **Metode radiochimice de analiză** (Méthodes radiochimiques d'analyse), 1973, 384 p., 23 lei.

MARIA FITI, **Dozimetria chimică a radiaţiilor ionizante** (La dosimétrie chimique des radiations ionisantes), 1973, 240 p., 13,50 lei.

MIHAI FLORESCU, **Eficienţa economică a cercetării ştiinţifice** (L'efficience économique de la recherche scientifique), 1972, 115 p., 15 lei.

GEORGETA LĂZĂRESCU, **Sistematizarea informaţiilor în Chimia organică** (La systématisation des informations dans la Chimie organique) ,1972, 252 p., 10,50 lei.

P. BALTĂ et E. BALTĂ, **Introducere în chimia fizică stării vitroase** (Introduction à la chimie physique de l'état vitreux), 1971, 240, 15,50 lei.

LYDIA-MARIA VAICUM, **Biodegrabilitatea detergenţilor** (La biodégrabilité des détergents), 1971, 254 p., 16 lei.

TIBERIU NĂŞCUŢIU, **Metode radiometrice de analiză** (Méthodes radiométriques d'analyse), 1971, 346 p., 19,50 lei.

I. ZUGRĂVESCU et L. STOICESCU-CRIVETZ, **Polimeri heterociclici** (Polymères hétérocycliques), 1971, 190 p., 9,50 lei.

I. MAXIM, **Materiale nucleare** (Matériaux nucléaires), 1969, 444 p., 30 lei.

1976 JUL 29

I. P. INFORMAŢIA c. 1096

43426

Lei 25. —

F 1103

ACADÉMIE DE LA RÉPUBLIQUE SOCIALISTE DE ROUMANIE

R

REFERÁLVA

REVUE ROUMAINE DE CHIMIE

TOME 21
N° 6
Juin 1976

RECHAX, **21**, *6*, 803–958 (1976)

EDITURA ACADEMIEI REPUBLICII SOCIALISTE ROMÂNIA

Rev. Roumaine Chim. **21**, *6*, p. 803–958 (1976), Bucarest

ACADÉMIE DE LA RÉPUBLIQUE SOCIALISTE DE ROUMANIE

COMITÉ DE RÉDACTION

Rédacteur en chef:

I. G. MURGULESCU, membre de l'Académie de la République Socialiste de Roumanie

Rédacteurs en chef adjoints:

A. T. BALABAN et V. EM. SAHINI, membres correspondants de l'Académie de la République Socialiste de Roumanie

Collège de rédaction:

EM. BRATU, ELENA CEAUŞESCU, ECATERINA CIORĂNESCU-NENITZESCU, C. DRĂGULESCU, CR. SIMIONESCU, membres de l'Académie de la République Socialiste de Roumanie ; P. SPACU, membre correspondant de l'Académie de la République Socialiste de Roumanie ; MARGARETA AVRAM, D. I. MARCHIDAN, I. MOLDOVAN, G. NIAC et D. SĂNDULESCU

La Revue Roumaine de Chimie paraît 10 fois par an. Toute commande de l'étranger pour les travaux parus aux Editions de l'Académie de la République Socialiste de Roumanie sera adressée à ILEXIM, Serviciul Export Import Carte (Livres)/Serviciul Export Import Presă (Revues), P.O.B. 2001, télex 011226, 64–66, Calea Griviţei, Bucarest 12 Roumanie

Les manuscrits, les livres et les revues proposés en échange, ainsi que toute correspondance seront envoyés à la rédaction :

REVUE ROUMAINE DE CHIMIE

23, str. Dumbrava Roşie, Bucarest, Roumanie, téléphone 124160

EDITURA ACADEMIEI REPUBLICII SOCIALISTE ROMÂNIA

125, Calea Victoriei, Bucarest, Roumanie, téléphone 507680

ORSZÁGOS MŰSZAKI KÖNYVTÁR ÉS DOKUMENTÁCIÓS KÖZPONT 1883

REVUE ROUMAINE DE CHIMIE

Tome 21, N° 6 Juin 1976

TATIANA ONCESCU and ECATERINA JURCONI, Solvent effect on the thermal decomposition of $[Mn(C_2O_4)_2(H_2O)_2]K.3H_2O$ in DMF$-H_2O$ mixtures 805–812
S. PETRESCU, S. STERNBERG and VALERIA PETRESCU, Galvanostatic study of the electrochemical adsorption process on a chlorine-activated carbon electrode in molten salts. IV. Cathodic polarization curve equation (discharge) 813–823
ANCA GHEORGHIU, D. FĂTU and E. SEGAL, Nonisothermal kinetic study of the transformations and nonstoichiometrization of cobalt and nickel oxides 825–830
ANA WECHSLER and E. SEGAL, Thermoelectric power variation during gas adsorption on thin semiconducting films. The zinc oxide-carbon monoxide system 831–833
И. П. АЛИМАРИН, Е. Н. ДОРОХОВА, С. А. МОРОСАНОВА, Е. Н. СЕМЕНОВСКАЯ, Изучение свойств и практическое использование гетерополисоединений с различными центральными атомами 835–852
C. DRĂGULESCU, ANA NIMARĂ and I. JULEAN, Bismuth(III)–ethylenediaminetetraacetic acid (EDTA) complexes. I. Polarographic study on formation and stability of the complexes in the solution 853–857
CONSTANȚA GHEORGHIU, M. CHIRCA, ELENA CRISTUREAN and FLORICA DINULESCU, Hexachlorocyclotriphosphazene derivatives . . . 859–867
FLORICA POPEA, ZAMFIRA TOMA and CRISTINETA MĂRCULESCU, Contributions to the coordination chemistry of phthalic acid derivatives. II. New copper compounds of phthalimide derivatives 869–877
V. M. BHATNAGAR, Preparation and unit cell dimensions of lead hydroxyapatite 879–880
RODICA MACAROVICI et MARIA IONESCU, Obtention et comportement des oxazoles. II. Bromuration des 2,5-diphényloxazoles 881–888
S. M. ABDEL RAHMAN, M. F. ISMAIL and Z. M. ISMAIL, Action of amines on 3-benzylidene phtalide and some allied compounds 889–895
M. VLASSA, Exo- and endohormones. II. Synthesis of peptidic juvenile hormone analogues. 897–902
B. C. KASHYAP, A. D. TANEJA and S. K. BANERJI, Ionization constants of some N-aryl, N′-2-(5-halo-pyridyl) thioureas 903–910

Rev. Roumaine Chim. **21**, *6*, p. 803–958 (1976), Bucarest

OANA PETREUŞ et M. DIMA, Sur les réactions des polymères vinyliques contenant des groupements aminiques avec les composés organiques du soufre. II. La réaction entre la poly(vinylamine) et le chlorure de thionyle . . . 911–925

CR. I. SIMIONESCU, D. FELDMAN and VIOLETA NUŢĂ, Contributions to the polymerization and copolymerization of the acrylonitrile in the presence of organo-metallic catalysts 927–931

C. LITEANU, ELENA HOPÎRTEAN and RODICA VLAD, Utilization of a Hg^{2+}-sensitive membrane–electrode in the determination of some α-amino–acids 933–936

STELIANA MAXIM and M. DIMA, Growth regulating polymers. III. Poly(4-vinylpyridine) salts with halogen (alkyl) aryloxyalkyl carboxylic acids . . . 937–947

I. MOŢOC und D. CIUBOTARIU, Zur Kopolymerisation. I. Mathematisches Modell der Bildung eines binären Kopolymerisationsproduktes 949–954

COMPTES RENDUS 955–958

Revue Roumaine de Chimie, **21**, *6*, 805–812 (1976)

SOLVENT EFFECT ON THE THERMAL DECOMPOSITION OF $[Mn(C_2O_4)_2(H_2O)_2]K.3H_2O$ IN DMF$-H_2O$ MIXTURES

TATIANA ONCESCU and ECATERINA JURCONI
Physical Chemistry Department, Bucharest University, Bd. Republicii 13, Romania

Received November 2, 1974

This paper deals with the kinetics of the thermal decomposition of $[Mn(C_2O_4)_2(H_2O)_2]K.3H_2O$ in N, N′-dimethylformamide-water mixtures, using a spectrophotometrical technique. Our experimental data permitted to calculate the kinetic and thermodynamic parameters ; on this ground a reaction mechanism has been elaborated which involves the solvent molecule as a reaction participant.

1. INTRODUCTION

Regarding the mechanism of the thermal decomposition of the oxalate complexes of the transitional metals there are two opinions : the spontaneous decomposition [1,2] and the decomposition by aquation mechanism.[3,4] Our results are in good agreement with the latter opinion.

2. EXPERIMENTAL

In order to study the variation of the complex concentration during the reaction, we measured the absorbance at $\lambda = 450$ nm in the absorption band of the complex, using a SP 800 Pye Unicam spectrophotometer. For the mixtures with a higher H_2O content, in which the reaction proceeds faster, we used the recording technique of the absorbance versus the reaction time. For the other mixtures in which the reaction runs slowly (higher DMF content), separated tests were carried out for each reaction time. These were stopped in a cooling mixture and centrifugated in order to deposit the precipitated MnC_2O_4 ; then the absorption spectra of the clear solution of the complex were recorded.

3. RESULTS AND DISCUSSION

Our experimental data on the decomposition of Mn(III) oxalate complex solutions verified satisfactorily a first order kinetic equation. Table 1 contains the rate constants, corresponding to one of the mixtures

---

[1] V. Vranek, *Z. Electrochem.*, **23**, 336 (1919).

[2] A. W. Adamson, H. Ogata, J. Grossman and R. Newbery, *J. Inorg. Nuclear Chem.*, **6**, 319 (1958).

[3] G. M. Harris and F. D. Graziano, *J. Phys. Chem.*, **63**, 330 (1959).

[4] T. B. Copstake and N. Uri, *Proc. Roy. Soc.*, **228**, 252 (1955).

studied (57% DMF). The absolute errors of these determinations were about 3%.

For each solvent mixtures we found the same behaviour and the values of the rate constants are listed in Table 2, for $T = 20.5°$.

Table 1

Rate constant of the thermal decomposition of $[Mn(C_2O_4)_2(H_2O)_2]K.3H_2O$ in 57% DMF

$a = 2\times10^{-3}$ mole l^{-1} $C_{H_2O} = 23.6$ mole l^{-1} $T = 20.5°$

Time (min)	Absorbance (A)	Rate constant $k_{exp}(sec^{-1})$
15	0.78	—
25	0.70	0.00016
40	0.61	0.00016
45	0.58	0.00014
60	0.51	0.00016
70	0.47	0.00011
95	0.40	0.00012
105	0.38	0.00013
120	0.35	0.00013
180	0.26	0.00013
	Average	0.00014 sec^{-1}

Table 2

Rate constants obtained in different DMF−H_2O mixtures

$a = 2\times10^{-3}$ mole l^{-1} $T = 20.5°$

C_{DMF} wt %	C_{H_2O} mole l^{-1}	k_{exp} sec^{-1}
0	54.4	0.00040
9	49.8	0.000764
19	44.8	0.000481
38	34.2	0.000326
48	28.6	0.000227
57	23.6	0.000136
78	11.9	0.000047
89	5.9	0.000011
100	14.7×10^{-3}	0.0000066

It is known that by dissolving this complex in water, the following equilibrium is established [5]:

$$[Mn(C_2O_4)_2(H_2O)_2]^- + H_2O \rightleftharpoons [Mn(C_2O_4)_2OHH_2O]^{--} + H_3O^+$$

In a previous paper, [6] we showed that in aqueous solution with a pH of about 7, this equilibrium is very much shifted to the left and $[Mn(C_2O_4)_2(H_2O)_2]^-$ is the predominant complex (> 90%).

On the other hand, in the solvent mixtures used, whose dielectric constants vary between 80.3 and 37.3, the equilibrium constant of this reaction decreases with the dielectric constant decrease, so that in these H_2O-DMF solutions only $[Mn(C_2O_4)_2(H_2O)_2]^-$ is practically present.

---

[5] G. H. Cartledge and W. P. Eriks, *J. Amer Chem. Soc.*, **58**, 2061 (1936).

[6] T. Oncescu and E. Jurconi — to be published.

Under these conditions we proposed the following mechanism :

$$[Mn(C_2O_4)_2(H_2O)_2]^- + H_2O \underset{k_1'}{\overset{k_1}{\rightleftharpoons}} [Mn(C_2O_4)OC_2O_3(H_2O)_3]^- \quad \text{(rapid)} \tag{1}$$

$$[Mn(C_2O_4)OC_2O_3(H_2O)_3]^- + H_2O \xrightarrow{k_2} MnC_2O_4 + C_2O_4^{\bullet -} + 4H_2O \text{(slow)} \tag{2}$$

$$Mn(C_2O_4)_2(H_2O)_2]^- + C_2O_4^{\bullet -} \xrightarrow{k_3} MnC_2O_4 + C_2O_4^{--} + 2CO_2 + 2H_2O \text{ (rapid)} \tag{3}$$

$$2[Mn(C_2O_4)_2(H_2O)_2]^- \rightarrow 2MnC_2O_4 + C_2O_4^{--} + 2CO_2 + 4H_2O$$

The rate-determining step is the slow aquation process, as in the case of the decomposition of $[Me(C_2O_4)_3]K_3$ complex, where Me = Cr, Rh. [7,8] This mechanism agrees with the main reaction product, MnC_2O_4, which was isolated, and with the formation of oxalyl radical ion, which was also revealed. [9,10]

The reaction mechanism leads to the following expression of reaction rate :

$$\frac{dx}{dt} = k_1(a - x)C_{H_2O} - k_1'C_A + k_3(a - x)C_{ox} \tag{4}$$

where C_A is the concentration of the aquated complex, and C_{ox} that of the oxalyl radical ion.

In the stationarity approximation :

$$k_1(a - x)C_{H_2O} - k_1'C_A - k_2C_AC_{H_2O} = 0 \tag{5}$$

$$C_A = \frac{k_1(a - x)C_{H_2O}}{k_1' + k_2C_{H_2O}}; \quad k_1' \gg k_2C_{H_2O}; \quad C_A = K_1(a - x)C_{H_2O} \tag{6}$$

$$k_2C_AC_{H_2O} - k_3(a - x)C_{ox} = 0 \tag{7}$$

$$C_{ox} = \frac{k_2C_AC_{H_2O}}{k_3(a - x)}; \quad C_{ox} = K_1\frac{k_2}{k_3}C_{H_2O}^2 \tag{8}$$

[7] K. V. Krishnamurty and G. M. Harris, *J. Phys. Chem.*, **64**, 346 (1960).

[8] D. Barton and G. M. Harris, *Inorg. Chem.*, **1**, 251 (1962).

[9] T. Oncescu, *Rev. Roumaine Chim.*, **15**, 209 (1970).

[10] I. G. Murgulescu, T. Oncescu and I. Vlagiu, *J. Chem. Phys.*, **10**, 1487 (1971).

In this case:

$$\frac{dx}{dt} = K_1 k_2 C^2_{H_2O}(a - x) = k_{exp}(a - x) \tag{9}$$

where:

$$k_{exp} = K_1 k_2 C^2_{H_2O} \tag{10}$$

characteristic of the first order reaction (pseudounimolecular). Consequently the obtained rate constants were calculated by using the integral relationship of the equation (9):

$$k_{exp} = \frac{2.303}{t_0 - t_1} \lg \frac{a}{a - x} = \frac{2.303}{t_0 - t_1} \lg \frac{A_0}{A_1} \tag{11}$$

where A is the solution absorbance measured experimentally.

Analysis of our experimental data shows that the rate values decrease with the decreasing of the water concentration of the solvent mixtures.

Figure 1 verified satisfactorily the kinetic equation (10). This behaviour supports the suggested mechanism in which the rate determining step is the pseudounimolecular slow process, confirmed in our experiments in H_2O-DMF mixtures. In a previous paper [11] we showed that $DMF-H_2O$ mixtures present a linear variation of the dielectric constant with the medium composition.

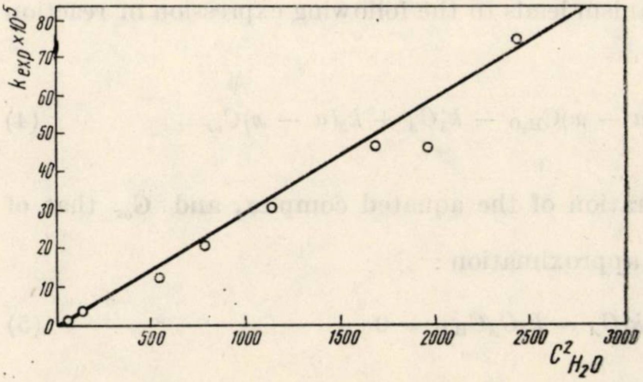

Fig. 1. — Plot of k_{exp} *vs* · $C^2_{H_2O}$.

In order to confirm such a behaviour of the rate constants, k_{exp} were correlated with the dielectric constant (D) of the solvent mixtures by means of the Amis [12] equation, typical of ion-dipole reactions:

$$\log k_{exp} = \log k_\infty + \frac{N Z e \mu}{2{,}303\, r_0^2\, RTD} \tag{12}$$

---

[11] T. Oncescu and E. Jurconi, *Rev. Roumaine Chim.*, **16**, 1033 (1971).

[12] E. S. Amis, *J. Chem. Educ.*, **30**, 351 (1953).

By plotting the rate constant logarithm against the reciprocal of the dielectric constant we obtained a linear dependence at each working temperature as illustrated in (Fig. 2), for 20.5°.

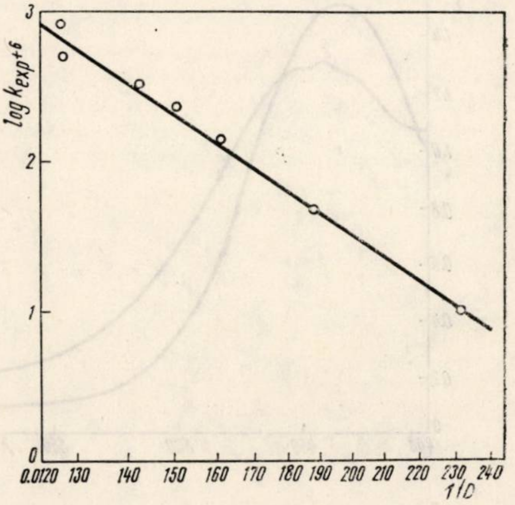

Fig. 2. — Plot of log $k_{\exp}$ vs. reciprocal dielectric constant, at $T = 20.5°$.

These results exclude the possibility of spontaneous decomposition of the complex.

Another interesting observation resulting from Table 2 is the inversion between the rate constant values as determined in 0% DMF and the two first mixtures; 9% and 19% DMF, characterized by very close macroscopic dielectric constant values in comparison to that in pure water.

This effect accounts for the structure modification of the Mn(III) complex in the solvent mixtures used, where a water molecule of the complex is replaced by DMF, leading to $[Mn(C_2O_4)_2(DMF)H_2O]^-$ ion. In this case the local dielectric constant decreases, so that the complex ion becomes more stable and the electron transfer from the ligand to the central ion is favoured.

In the mixtures with a higher DMF concentration or in pure DMF it is supposed to appear $[Mn(C_2O_4)_2(DMF)_2]^-$ ion. The formation of such complexes is supported by the absorption spectra presented in Fig. 3 in which the characteristic absorption bands in visible are slightly shifted of about 10 nm.

With the aid of the rate constant values $k_{\exp}$ determined at various temperature we calculated the Arrhenius activation energies given in Table 4. The error in the activation energy determination was about ± 0,5 kcal/mole^{-1}. Using the activation energy values we calculated the other kinetic and thermodynamic parameters given in Table 3.

One observes that the values of activation energy, frequency factor, activation entropy, activation enthalpy decrease in the series of investigated mixtures, passing through a minimum for the same composition of about 60% DMF.

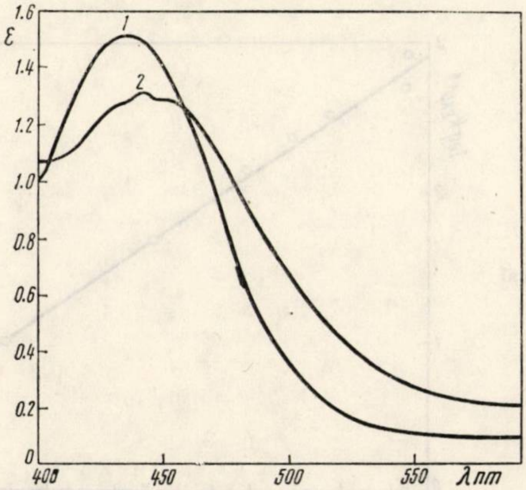

Fig. 3. — Absorbtion spectra of $[Mn(C_2O_4)_2(H_2O)_2]\ K \cdot 3H_2O$ in H_2O (1) and DMF (2).

Table 3

Kinetic and thermodynamic parameters of the thermal decomposition of $[Mn(C_2O_4)_2(H_2O)_2]K.3H_2O$ in H_2O – DMF mixtures

C_{DMF} wt %	C_{H_2O} (mole^{-1})	E (kcal mole^{-1})	log A (A sec^{-1})	$\Delta S^{\neq}$ e.u.	$\Delta H^{\neq}$ (kcal mole^{-1})	$\Delta G^{\neq}$ (kcal mole^{-1})
0	54.4	19.5	11.13	− 9.52	18.9	21.699
9	49.8	23.8	14.53	+ 6.01	23.2	21.322
19	44.8	19.7	11.36	− 8.37	19.1	21.591
38	34.2	18.3	10.15	−13.99	17.7	21.818
48	28.6	16.4	8.59	−21.12	15.8	22.029
57	23.6	12.9	5.75	−34.10	12.3	22.327
78	11.9	15.0	8.34	−22.27	16.4	22.946
89	5.9	25.1	13.75	+ 2.45	24.5	23.792
100	14.7×10^{-3}	28.0	14.42	+ 5.51	27.4	24.090

On the other hand the values of the activation free energy $\Delta G^{\neq}$, which is the determining factor of the reaction rate, show a monotonous variation with the medium composition.

The values of $\Delta G^{\neq}$ and k_{exp} verify the linear relationship of the free energy.

Figure 4, shows the presence of two isokinetic temperatures : — 2.4°, characteristic of the rate constant $k_{exp} = 0.0000178$ sec^{-1} as determined in the mixtures between 0%—57% DMF and 45.5° corresponding to the rate constant $k_{exp} = 0.000317$ sec^{-1} of the mixtures with a content of DMF higher than 57%.

This behaviour supports the linear relationship between $\Delta S^{\neq}$ and $\Delta H^{\neq}$, as indicated in Figure 5.

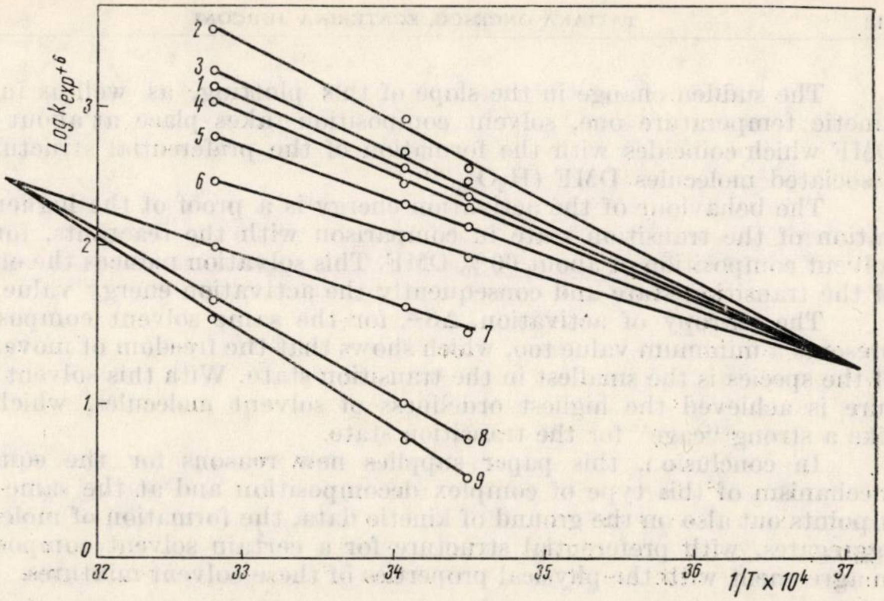

Fig. 4. — Arrhenius plot for determination of activation energy for the mixtures with the following composition in DMF; 1) 0 %, 2) 9 %, 3) 19 %, 4) 38 %, 5) 48 %, 6) 57 %, 7) 78 % 8) 89 %, 9) 100 %.

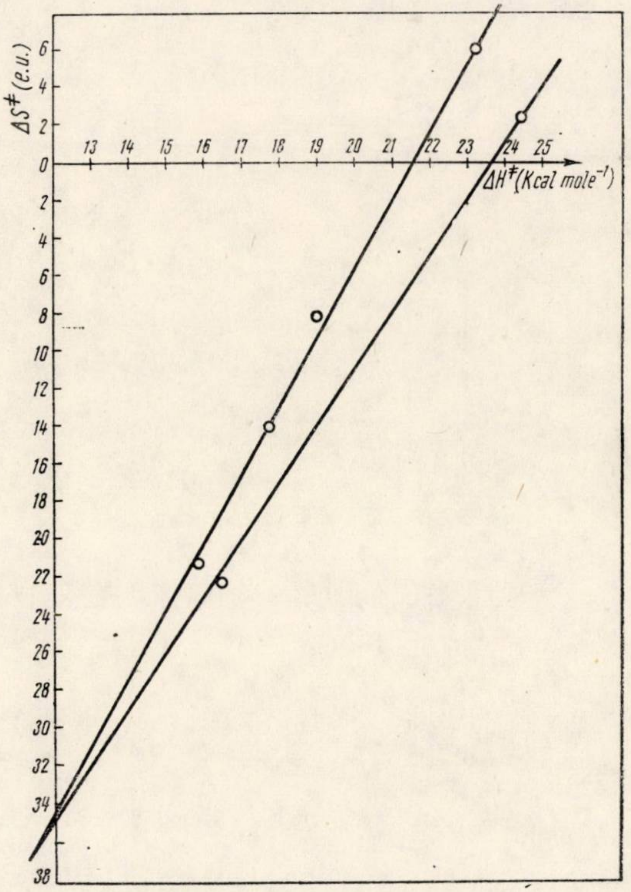

Fig. 5. — Plot of $\Delta S^{\neq}$ *vs.* $\Delta H^{\neq}$ for the thermal decomposition of $[Mn(C_2O_4)_2(H_2O)_2]^-$ in different H_2O-DMF mixtures.

The sudden change in the slope of this plotting, as well as in isokinetic temperature one, solvent composition takes place at about 60% DMF which coincides with the formation of the preferential structure of associated molecules DMF $(H_2O)_3$.[11]

The behaviour of the activation energy is a proof of the higher solvation of the transition state in comparison with the reactants, for the solvent composition of about 60% DMF. This solvation reduces the energy of the transition state and consequently the activation energy value.

The entropy of activation, $\Delta S^{\neq}$, for the same solvent composition presents a minimum value too, which shows that the freedom of movement of the species is the smallest in the transition state. With this solvent mixture is achieved the highest ordeliness of solvent molecules, which act like a strong "cage" for the transition state.

In conclusion, this paper supplies new reasons for the equation mechanism of this type of complex decomposition and at the same time it points out also on the ground of kinetic data, the formation of molecular aggregates, with preferential structure for a certain solvent composition in agreement with the physical properties of these solvent mixtures.

Revue Roumaine de Chimie, **21**, *6*, 813–823 (1976)

GALVANOSTATIC STUDY OF THE ELECTROCHEMICAL ADSORPTION PROCESS ON A CHLORINE-ACTIVATED CARBON ELECTRODE IN MOLTEN SALTS. IV[1]

CATHODIC POLARIZATION CURVE EQUATION (DISCHARGE)

S. PETRESCU, S. STERNBERG and VALERIA PETRESCU
Politechnic Institute of Bucharest, Str. Polizu No. 1

Received February 12, 1975

The paper presents a phenomenological model of the cathodic polarization process development of a chlorine-activated carbon electrode in molten salts. This model gives an equation which quantitatively describes such a process, expressing the φ potential as a function of time. The computer-processed equation agrees well with experimental data providing important information on the behaviour of the chlorine-activated carbon electrode in various systems and at various temperatures (400–800°).

The present paper undertakes to find an equation which should relate the φ activated carbon potential to the τ discharge time, in a cathodic polarization process in a molten salt, by analogy with the previously established equation for anodic polarization.[1]

The elementary cathodic polarization process is admitted to take place according to the phenomenological model of the partially filled pore[2] plotted in fig. 1, which leads to the equation

$$\mathrm{d}Q_d = -\,\mathrm{d}Q_{\mathrm{ads}} - \mathrm{d}Q_{\mathrm{p.d.t.}} \tag{1}$$

in which

$\mathrm{d}Q_d$ – the elementary chlorine amount removed from the activated carbon electrode during the elementary discharge time $\mathrm{d}\tau$ with I_d intensity, passing into solution as a ion

$$\mathrm{d}Q_d = I_d \mathrm{d}\tau \tag{2}$$

$\mathrm{d}Q_{\mathrm{ads}}$ – the variation of the chlorine amount absorbed on the activated carbon electrode during the elementary time involved in the electrochemical desorption process; since Q_{ads} decreases during the discharge, $\mathrm{d}Q_{\mathrm{ads}}$ sign in equation (1) is minus

---

[1] Part. III: S. Sternberg, S. Petrescu and V. Petrescu, *Rev. Roumaine Chim.*, **19**, 955 (1974).

[2] S. Petrescu, S. Sternberg and V. Petrescu, *Rev. Roumaine Chim.*, **18**. 1715 (1973).

$dQ_{p.d.t.}$ — the elementary chlorine amount removed from the electrode by thermal desorption in $d\tau$ time

$$dQ_{p.d.t.} = I_{p.d.t.}\ d\tau \tag{3}$$

Due to chlorine diffusion from inside outward during the cathodic polarization process, a concentration gradient appears in the δ_{dif} diffusion layer, shown in fig. 2.

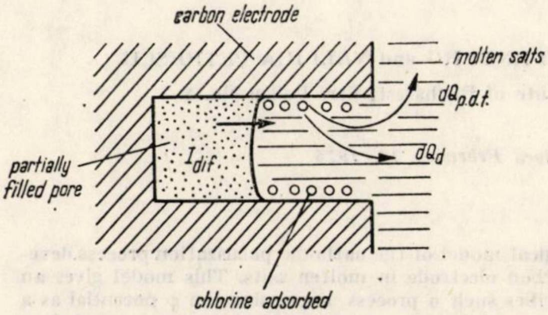

Fig. 1. — Phenomenological model representing the cathodic polarization process in a partially filled activated-carbon pore.

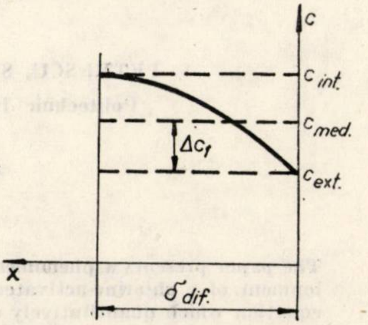

Fig. 2. — Influence of diffusion on the cathodic polarization process of the chlorine-activated carbon electrode

It has been hypothesized[1] that the thermal desorption loss in the time unit $I_{p.d.t.}$ (self-discharge current) is proportional to the concentration at the exterior of the pore C_{ext}:

$$I_{p.d.t.} = KC_{ext} \tag{4}$$

A similar hypothesis to that issued in an anodic polarization is admitted with regard to the proportionality between the φ electrode potential and the chlorine concentration at the exterior of the activated carbon C_{ext}

$$\varphi = K_1 \cdot C_{ext} \tag{5}$$

Replacing (5) and (4) in (3), the following expression results for $dQ_{p.d.t.}$

$$dQ_{p.d.t.} = \frac{K}{K_1} \cdot \varphi \cdot d\tau \tag{6}$$

Q_{ads} is expressed by means of the C_{med} mean concentration all over the S absorption surface of the activated carbon.

$$Q_{ads} = C_{med} \cdot S = \frac{C_{med}}{C_{ext}} \cdot C_{ext} \cdot S = \frac{1}{\alpha} \frac{\varphi}{K_1} S \tag{7}$$

where it was noted (according to fig. 2)

$$\alpha = \frac{C_{\mathrm{ext}}}{C_{\mathrm{med}}} = \frac{C_{\mathrm{med}} - \Delta C_1}{C_{\mathrm{med}}} = 1 - \frac{\Delta C_1}{C_{\mathrm{med}}} \leqslant 1 \tag{8}$$

The equal sign will hold if the discharge occurs very slowly, i.e. for a discharge current tending towards zero. Insofar as α is smaller than one, the system departs from the equilibrium state and accordingly the process is more irreversible. Hence, $\mathrm{d}Q_{\mathrm{ads}}$ will be given by (7) in a differentiated manner

$$\mathrm{d}Q_{\mathrm{ads}} = \frac{S}{\alpha K_1}\,\mathrm{d}\varphi \tag{9}$$

With (9) and (6) in (1) we obtain the differential equation of cathodic polarization in φ/τ coordinates

$$I_d\,\mathrm{d}\tau = -\frac{S}{\alpha K_1}\cdot\mathrm{d}\varphi - \frac{K}{K_1}\,\varphi\cdot\mathrm{d}\tau \tag{10}$$

Separating the variables

$$\alpha\mathrm{d}\tau = \frac{-\dfrac{S}{K_1}\mathrm{d}\varphi}{I_d + \dfrac{K}{K_1}\varphi} \tag{11}$$

and integrating, it results:

$$\alpha\tau = -\frac{S}{K}\ln\left(I_d + \frac{K}{K_1}\varphi\right) + \text{const.} \tag{12}$$

The integration constant can be found provided that the φ potential be equal to zero at time: $\tau = \tau_d$

$$\text{const} = \alpha\tau_d + \frac{S}{K}\ln I_d \tag{13}$$

With (13) in (12), we obtain

$$\varphi = \frac{K_1 I_d}{K}\left[\mathrm{e}^{-\frac{K}{S}\alpha(\tau - \tau_d)} - 1\right] \tag{14}$$

The ratio of K_1/K constants can be found by imposing the limit condition: for $\tau = 0$, the φ potential should be equal to the maximum attained potential during charging (the potential from which the discharge starts) $\varphi = \varphi_{\max}$

$$\varphi_{\max} = \frac{K_1 I_d}{K}\left[e^{-\frac{R}{K}\alpha(0-\tau_d)} - 1\right] \tag{15}$$

whence

$$K_1/K = \varphi_{\max}/I_d \cdot [\exp\,(K\,\alpha\,\tau_d/S) - 1] \tag{16}$$

We introduce (16) into (14) to obtain the equation of the cathodic polarization curve (charging):

$$\varphi = \varphi_{\max} \cdot [1 - e^{K\alpha(\tau_d - \tau)/S}]/(1 - e^{K\alpha\tau_d/S}) \tag{17}$$

The K/S ratio may be expressed in terms of two physical quantities, using for this purpose expression (4) applied at the discharge onset moment. Under such conditions $I_{\text{p.d.t.}}$ is maximum ($I_{\text{p.d.t.max}}$) while C_{ext} becomes the maximum concentration expressed as the ratio between the maximum adsorbed quantity $Q_{\text{ads.max}}$ and the active surface S

$$I_{\text{p.d.t.max}} = KC_{\max} = KQ_{\text{ads.max}}/S \tag{18}$$

whence

$$K/S = I_{\text{p.d.t.max}}/Q_{\text{ads.max}} \tag{19}$$

Introducing into (17) we obtain

$$\varphi = \varphi_{\max}\,\frac{1 - e^{\frac{I_{\text{p.d.t.max}}}{Q_{\text{ads.max}}}\alpha(\tau_d - \tau)}}{1 - e^{\frac{I_{\text{p.d.t.max}}}{Q_{\text{ads.max}}}\alpha\tau_d}} \tag{20}$$

By replacing (20) in (7) we find the variaton manner of the adsorbed chlorine amount as a function of time during discharge

$$Q_{\text{ads}} = \frac{S}{K_1} \cdot \frac{\varphi_{\max}[1 - e^{M(\tau_d - \tau)}]}{1 - e^{M\tau_d}} \tag{21}$$

in which we have noted

$$\frac{I_{\text{p.d.t.max}}}{Q_{\text{ads.max}}}\,\alpha = M \tag{22}$$

For $\tau = 0$, one obtains:

$$Q_{\text{ads.max}} = \frac{S}{\alpha K_1}\,\varphi_{\max} \tag{23}$$

Considering (23), relation (21) becomes

$$Q_{\text{ads}} = Q_{\text{ads.max}} \frac{[1 - e^{M(\tau_d - \tau)}]}{1 - e^{M\tau_d}} \tag{24}$$

With relations (4) and (5) we may write

$$I_{\text{p.d.t.}} = \frac{K}{K_1} \varphi \tag{25}$$

Relation (14) helps to obtain the expression of the chlorine thermal desorption loss current

$$I_{\text{p.d.t.}} = I_d[e^{M(\tau_d - \tau)} - 1] \tag{26}$$

The discharge equation can be verified by considering a known discharge curve experimentally resulted (fig. 3), having the characteristic elements $\varphi_{\max}$ and τ_d. Equation (20)

$$\varphi = \varphi_{\max} \frac{[1 - e^{M(\tau_d - \tau)}]}{[1 - e^{M\tau_d}]} \tag{27}$$

can be checked against an experimental curve after determining parameter M in equation (27), assigning to φ and τ a pair of values from the experimental curve: i.e. φ_1 and τ_1. A transcendental equation results thereby, with M as an unknown factor

$$\varphi_1 = \varphi_{\max} \frac{[1 - e^{M(\tau_d - \tau_1)}]}{[1 - e^{M.\tau_d}]} \tag{28}$$

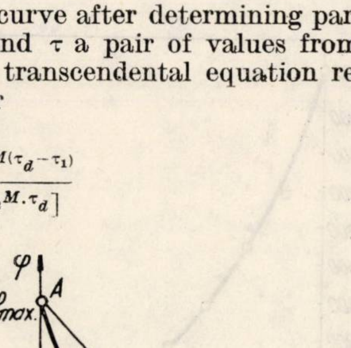

Fig. 3. – Necessary data for finding M in equation (28).

The M value is obtained for the case in question by solving this equation on a numerical computer. It is then introduced into equation (27). The same equation (27) assigns then τ values from 0 to τ_d providing the theoretical values of φ.

A program for solving equation (28) was first developed to find M and it applied only for upward-facing concave cathodic polarization curves (like in fig. 3). This program was applied for the following data:

$$\mathrm{TD} = \tau_d = 48.3 \text{ min}$$

$$\mathrm{F_{MAX}} = \varphi_{\max} = 1020 \text{ m}V$$

$$T_1 = \tau_1 = 20 \text{ min}$$

$$F_1 = \varphi_1 = 280 \text{ mV}$$

to system $PbCl_2 + KCl$ at a temperature of 700°. The program includes two stages; the first one solves equation (28) by successive attempts to find the value $M = 0.05679$. Introducing this value into (27), the computer gives values for τ (T — in the program) every minute, theoretical values resulting for φ(F — in the program). Using these values, the computer plotted curve φ/τ by a solid line and the experimentally determined points were identified by crosses. A good agreement was found between them (fig. 4).

Upward-facing concave cathodic polarization curves such as those seen in fig. 4 are characteristic of high temperatures when losses due to thermal desorption are significant. In parallel with the temperature drop the cathodic polarization curves were found to tend first towards linearity and next to change their concavity downwards.

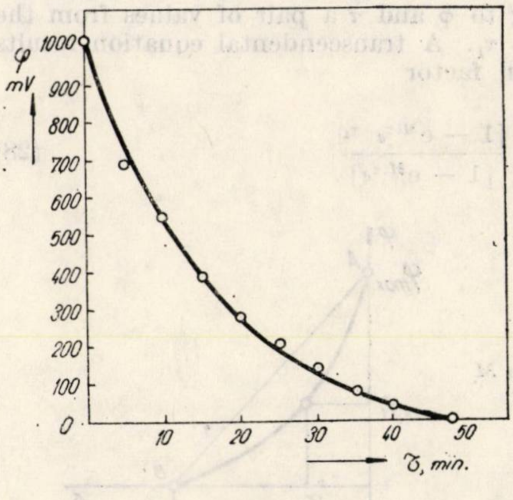

Fig. 4. — Cathodic polarization curve traced by computer (solid line) and the experimental points (crosses) in the $PbCl_2 + KCl$ system at a temperature of 700° with an $I_d = 0.1$ A discharge intensity.

Attempts were made to represent the downward-facing concave curves by the same equation (27) as in the case of upward-facing concave. The computer has failed to find a solution for M of the transcendental equation (28) for such a curve, since the successive values assigned to M tended towards zero by an infinite number of steps. The $M = 0$ solution would have corresponded to the AB straight line (of fig. 4). This result suggested that equation (27) may also represent the downward-facing concave provided that M take negative values in such curves.

The physical significance of negative M was found by the fact that the diffusion current in the partially filled pores rises with the temperature drop while the thermal desorption loss current diminishes (fig. 1,5).

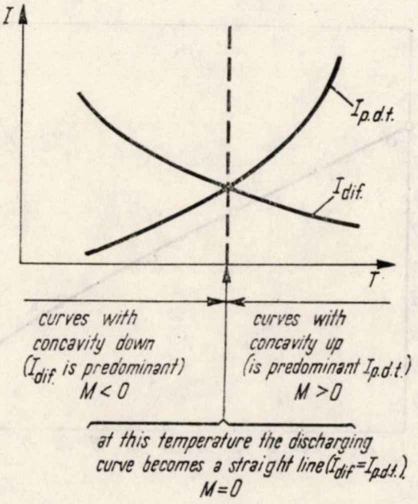
I
T
$I_{p.d.t.}$
$I_{dif.}$
curves with concavity down ($I_{dif.}$ is predominant) $M<0$
curves with concavity up (is predominant $I_{p.d.t.}$) $M>0$
at this temperature the discharging curve becomes a straight line ($I_{dif}=I_{p.d.t.}$) $M=0$

Fig. 5. — Influence of the variation manner of the diffusion current I_{dif} and of thermal desorption losses $I_{\text{p.d.t.}}$ on the aspect of cathodic polarization curves.

A computing program was developed for downward-facing concave curves. This program was applied to the case of a cathodic polarization curve 3—5 in the AgCl + KCl system at 400° with the following data:

$$\text{TD} = \tau_d = 30.5 \text{ min} \qquad T_1 = \tau_1 = 16 \text{ min}$$

$$\text{F}_{\text{MAX}} = \varphi_{\max} = 900 \text{ mV} \qquad F_1 = \varphi_1 = 490 \text{ mV}$$

The resulting value for M in this case is: $M = 0.01818$ (the sign results from the program editing). This M value was then used to calculate the theoretical values for φ(F — in the program) every minute. These values were used for plotting fig. 6

A generally valid computing program was next developed both for upward and for downward-facing concave cathodic polarization curves, intended to synthesize the two previous programs. The merit of this program is the ability to process any cathodic polarization curve so that any number of such curves can be fed into the computer to be processed without a prior selection of curves according to their concavity. Moreover, the computer specifies the concavity for each curve. This program provides information on the predominance of one of the two currents diffusion and thermal desorption loss, by *M* value and sign and in addition it may be extremely beneficial in processing experimental data as follows. It is no more necessary to record a large number of experimental data used for tracing the experimental curve, but instead, it is sufficient to note the maximum potential $\varphi_{\max}$, the total discharge time (when $\varphi = 0$) and one single pair of values $\varphi_1 = \tau_1$ somewhere along the discharge. These data help the

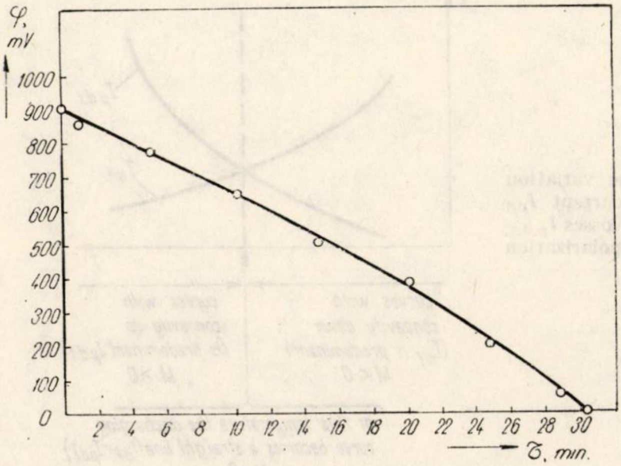

Fig. 6. — Cathodic polarization curve traced by computer (solid line) and the experimental points (crosses) in the AgCl + KCl system at the temperature of 400° with an I_d=0.1 A discharge intensity.

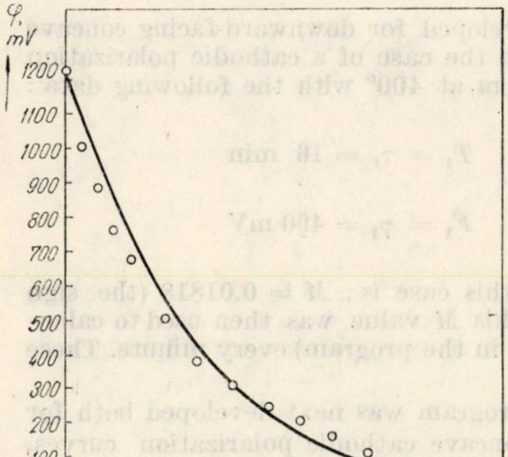

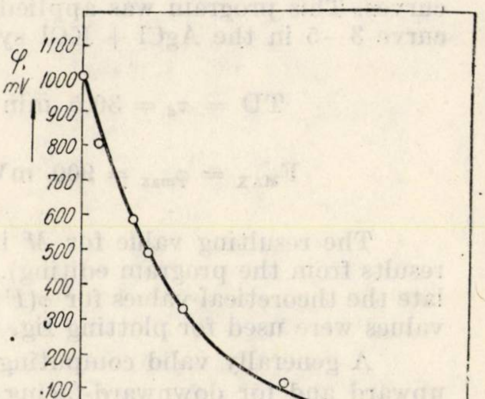

Fig. 7. — Cathodic polarization curve traced by computer (solid line) and the experimental points (crosses) in the KCl + $PbCl_2$ system at a temperature of 800° with an I_d = 0.1 A discharge intensity.

Fig. 8. — Cathodic polarization curve traced by computer (solid line) and the experimental points (crosses) in the KCl + $PbCl_2$ system at a temperature of 800° with an I_d = 0.1 A discharge intensity.

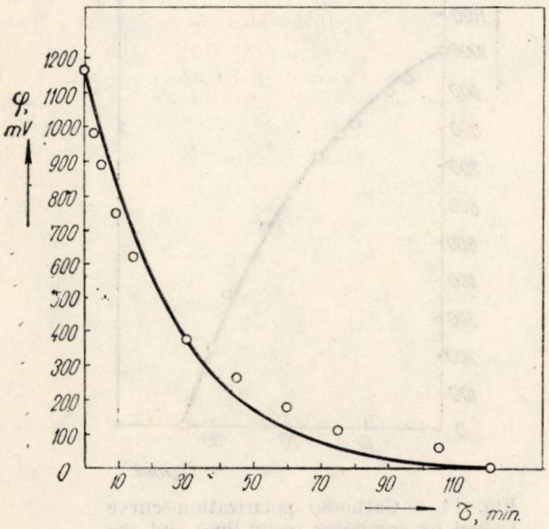

Fig. 9 — Cathodic polarization curve traced by computer (solid line) and the experimental points (crosses) in the KCl + $PbCl_2$ system at a temperature of 600° with an $I_d = 0.1$ A discharge intensity.

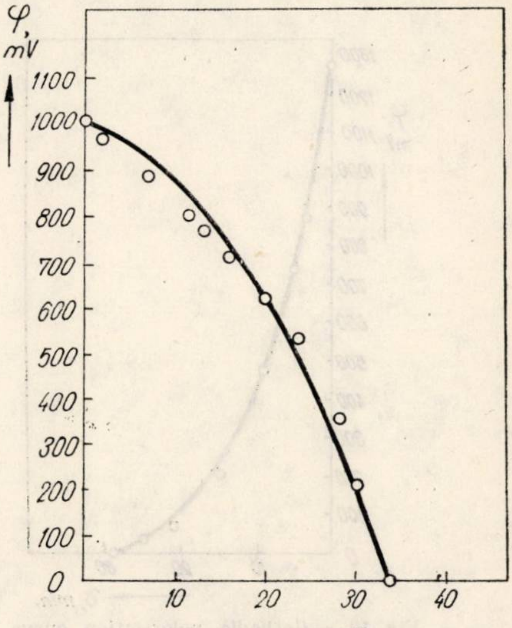

Fig. 10. — Cathodic polarization curve traced by computer (solid line) and the experimental points (crosses) in the LiCl + KCl system at a temperature of 400° with an $I_d = 0.1$ A discharge intensity

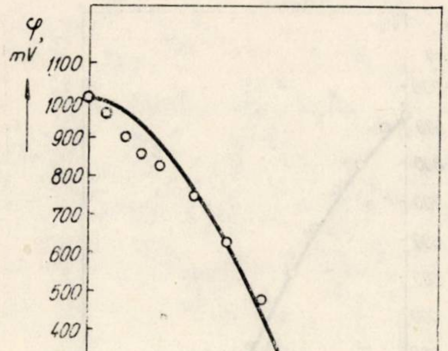

Fig. 11 — Cathodic polarization curve traced by computer (solid line) and the experimental points (crosses) in the LiCl + KCl system at a temperature of 400° with an $I_d = 0.1$ A discharge intensity.

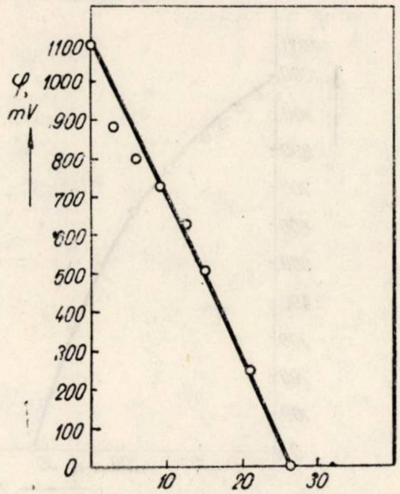

Fig. 12. — Cathodic polarization curve traced by computer (solid line) and the experimental points (crosses) in the LiCl + KCl system at a temperature of 600° with an $I_d = 0.1$ A discharge intensity.

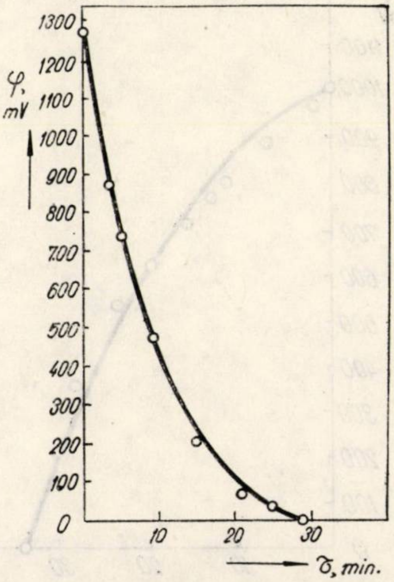

Fig. 13. — Cathodic polarization curve traced by computer (solid line) and the experimental points (crosses) in the NaCl + KCl + 2% AgCl system at a temperature of 700° with an $I_d = 0.1$ A discharge intensity.

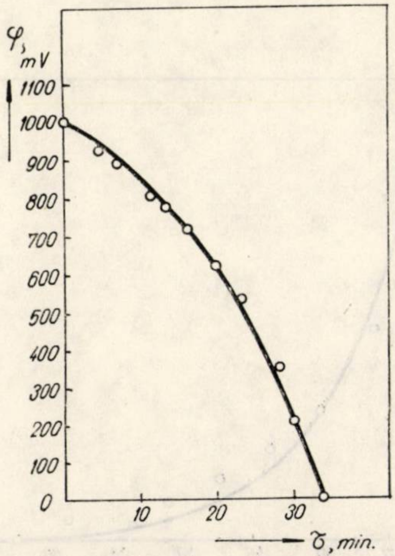

Fig. 14. — Cathodic polarization curve traced by computer (solid line) and the experimental points (crosses) in the LiCl + KCl system at a temperature of 400° with an $I_d = 0.1$ A discharge intensity.

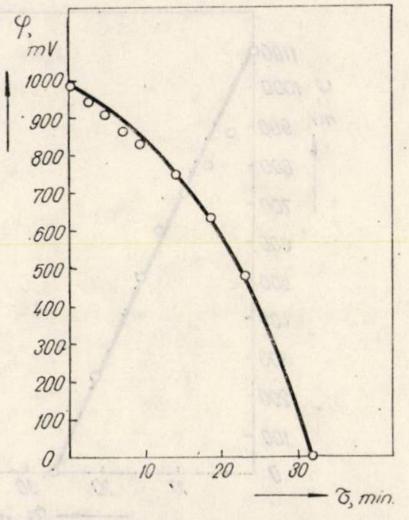

Fig. 15. — Cathodic polarization curve traced by computer (solid line) and the experimental points (crosses) in the LiCl + KCl system at a temperature of 400° with an $I_d = 0.1$ A discharge intensity.

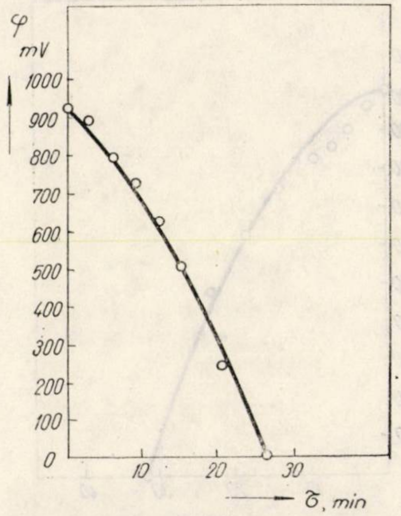

Fig. 16. — Cathodic polarization curve traced by computer (solid line) and the experimental points (crosses) in the LiCl + KCl system at a temperature of 600° with an $I_d = 0.1$ A discharge intensity.

computer to trace the theoretical curve which is in excellent agreement with experimental data, as has been seen.

This program was run to process a number of 15 cathodic polarization curves of various system[3–5] and at various temperatures. Table 1 exhibits their principal data. The processed results are plotted in figs. 7–17. the solid lines being the theoretical curves and the crosses the experimentally determined points. In most cases the results are in a perfect accord,

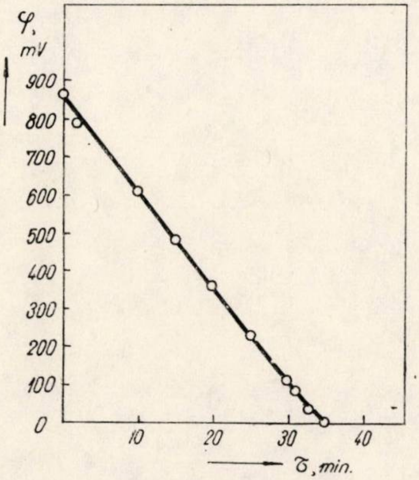

Fig. 17.—Cathodic polarization curve traced by computer (solid line) and the experimental points (crosses) in the AgCl +KCl system at a temperature of 500° with an $I_d = 0.1$ A discharge intensity.

Table 1

The principal data of the cathodic polarization curves

Curve N°	τ_d TD	φ_{max} F_{MAX}	τ_1 T_1	φ_1 F_1	systems	Temp. °C
1	2760	1017	1015	338	$KCl+PbCl_2$	700
2	7200	1220	3000	311	,,	800
3	3000	1026	900	333	,,	800
4	4870	1292	1800	392	,,	400
5	6075	1296	2700	266	,,	500
6	6380	1219	1305	540	,,	600
7	7250	1179	1800	378	,,	600
8	2040	1020	1200	625	$LiCl+KCl$	400
9	1900	1060	1120	630	,,	400
10	1600	1100	730	625	,,	600
11	1750	1285	540	480	$NaCl+KCl+$ $+2\%\ AgCl$	700
12	2040	1005	1200	625	$LiCl + KCl$	400
13	1900	990	1120	630	,,	400
14	1600	930	730	625	,,	600
15	2100	875	1200	360	$AgCl+KCl$	500

---

[3] V. Petrescu, Ph. D. Thesis, București 1974.

[4] S. Sternberg, V. Petrescu and I. Galasiu, *Rev. Roumaine Chim.*, **17**, 1689 (1972).

[5] S. Sternberg and V. Petrescu, *Rev. Roumaine Chim.*, **19**, 25 (1974).

Revue Roumaine de Chimie, 21, 6, 825–830 (1976)

NONISOTHERMAL KINETIC STUDY OF THE TRANSFORMATIONS AND NONSTOICHIOMETRIZATION OF COBALT AND NICKEL OXIDES

ANCA GHEORGHIU, D. FĂTU and E. SEGAL
Chair of Physical Chemistry and Electrochemical Technology, Polytechnic Institute of Bucharest Bd. Republicii 13, Bucharest, Romania

Received July 14, 1975

The results concerning the determination of the kinetic parameters values of the transformations, as well as of the nonstoichiometrization of cobalt and nickel oxides are presented.

INTRODUCTION

Following our research concerning the kinetics of oxide-oxygen system reactions, we present below the results obtained in the study of cobalt and nickel oxides.

These oxides are important for their applicability in metallurgy, electrotechnic material industry and heterogeneous catalysis.

EXPERIMENTAL

Cobalt oxides resulting from cobalt acetate tetrahydrate and cobalt carbonate decomposition, nickel oxide resulting from nickel acetate tetrahydrate, nickel carbonate and the complex combination $[\mathrm{Ni\ pald_2(OH_2)_2}](\mathrm{OH})_2$ [1] decomposition have been used.

The apparatus and the data processing methods have been described in a previous paper.[2]

RESULTS AND DISCUSSION

DECOMPOSITION AND NONSTOICHIOMETRIZATION OF COBALT OXIDES RESULTING FROM $Co(CH_3COO)_2.4H_2O$

The analysis of cobalt acetate tetrahydrate heating curves points out the following phenomena which take place after dehydration and decomposition (fig. 1):

– the formation of a Co_3O_4 oxide at 380°;

---

[1] P. Spacu, C. Gheorghiu and A. Nicolaescu, *Inorg. Chim. Acta*, **2**, 413 (1968).

[2] A. Gheorghiu, D. Fătu and E. Segal, *Rev. Roumaine Chim.*, (in print)

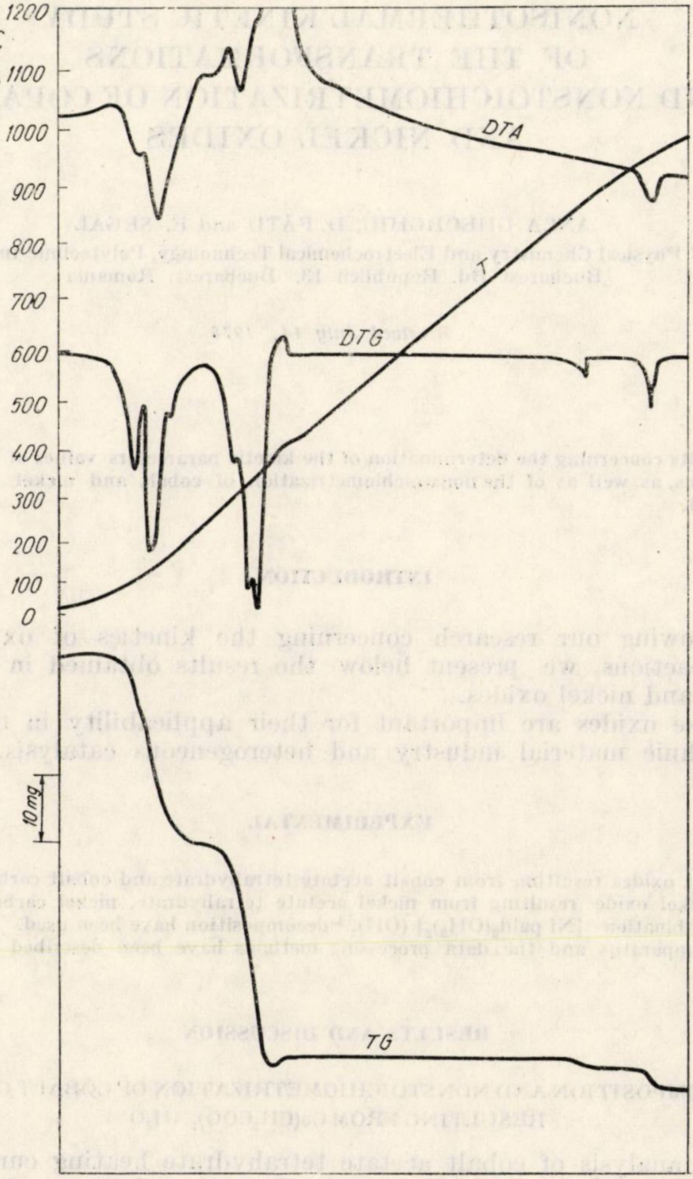

Fig. 1. — **ATD, DTG and TG curves of decomposition and nonstoichiometrization of cobalt oxides resulting from $Co(CH_3COO)_2\ 4H_2O$.**

— the oxidation of this compound to Co_2O_3, due to the removing of inert and partial reducing atmosphere at higher temperatures;

— the $Co_2O_3 \rightarrow Co_3O_4$ transition, taking place with maximum rate at 870°;

— the $Co_3O_4 \rightarrow CoO$ transition, taking place with maximum rate at 945°;

— CoO nonstoichiometrization which, at 1370°, leads to a nonstoichiometric $CoO_{0.95}$, still able to lose oxygen at a higher temperature.

Using Coats-Redfern[3] method, the kinetic analysis of the above mentioned phenomena, under proper conditions of sensibility, leads to the results given in Table 1:

Table 1

Kinetic parameters of cobalt oxide decomposition and nonstoichiometrization

The reaction	$n^{\neq}$	E (kcal/mole)	Z (s^{-1})
$3Co_2O_3(s) \rightarrow 2Co_3O_4(s) + 1/2O_2(g)$	3	606	$1.7\ 10^{108}$
$Co_3O_4(s) \rightarrow 3CoO(s) + 1/2O_2(g)$	3	715	$1.6\ 10^{126}$
$CoO(s) \rightarrow CoO_{0.95}(s) + 0.025O_2(g)$	1	12.7	$2.2\ 10^{-2}$

$\neq$*n*, *E* and *Z* stand for the reaction order, the activation energy and the preexponential factor, respectively.

The preexponential factor, *Z*, is expressed in (s^{-1}), regardless of the reaction order value, as the kinetics is described in terms of the conversion degree.

The value three of the reaction order, found for the first two processes, is quite surprising, though it checks best the experimental data.

The rate equation for the first reaction, Co_2O_3 decomposition, corresponds to the stoichiometric one.

As for the stoichiometric equation corresponding to Co_3O_4 decomposition, it has to be multiplied by three to agree with the kinetic data.

The high activation energy values must not be a surprise, as they are placed between a lower limit given by the dissociation heat and an upper limit corresponding to the lattice energy.

In the case of Co_2O_3 dissociation, the transformation heat is 38.4 kcal/ /mole[4] (the value has been calculated taking into account the tabulated values of the formation standard enthalpy for Co_3O_4 and CoO) and the lattice energy according to Kapustinsky's formula[5] is 3565 kcal/mole.

The preexponential factor values, excessively high, compensate the activation energy values, so that the processes characterized by these kinetic parameters take place with normal rates.

---

* In (fig. 1) is given only the beginning of CoO nonstoichiometrization

[3] A. W. Coats and J. P. Redfern, *Nature*, **21**, 68 (1964)

[4] "Selected values of chemical thermodynamic properties", part. I, Tables, NBS, 1961, p. 252.

[5] A. F. Kapustinsky, *Zhur. fiz. Khim.*, **5**, 59, (1934).

DECOMPOSITION AND NONSTOICHIOMETRIZATION OF COBALT OXIDES RESULTING FROM $CoCO_3$

Decomposing cobalt carbonate, Co_2O_3 is directly obtained. It also undergoes the first two transformations at the same temperatures, the decomposition curves being in fact identical.

The phenomenon of CoO nonstoichiometrization has been studied up to an unstable compound $CoO_{0.95}$, able to undergo further decomposition at higher temperatures.

The kinetic parameters values for the nonstoichiometrization are :

$$n = 1 ; E = 36.7 \text{ kcal/mole} ; Z = 10 \text{ s}^{-1}.$$

Comparing these values with those corresponding to the nonstoichiometrization of CoO resulting from cobalt acetate tetrahydrate, a compensation effect is noticed, so that the reaction rates have similar values.

NICKEL OXIDE NONSTOICHIOMETRIZATION

Nickel oxide nonstoichiometrization between 1020° — 1500° leads to a stable compound $NiO_{0.8}$, no matter what the generating substance is. The stabilization phenomenon around this composition is pointed out by the ATD curve (fig. 2).

The kinetic parameters values of the nonstoichiometrization are given in Table 2 :

According to these results, the kinetic parameters E and Z are dependent on the parent substance of nickel oxide.

In this case too, the compensation effect draws near the nonstoichiometrization rates.

The above mentioned experimental data raise the problem of correctly formulating the nonstoichiometric cobalt and nickel oxides.

Indeed, it is well known that under normal conditions, these materials present a nonstoichiometry through oxygen excess, having a p-type semiconducting character.

As it results from the thermogravimetric curves, at higher temperatures, between 1300 — 1500°, compounds with oxygen deficit are obtained.

It has been raised the problem both of disposing the interstitial cations in lattice and of their ionization capacity, that is the capacity of giving an n-type semiconductivity, through oxygen deficit, for the nonstoichiometric oxide.

As regards the position of the cations in the lattice, a comparison among zinc, cobalt and nickel ionic radia (according to Pauling) ($r_{Zn^{2+}} = 0.83\text{Å}$; $r_{Co^{2+}} = 0.72\text{Å}$; $r_{Ni^{2+}} = 0.69\text{Å}$) shows that Co^{2+} and Ni^{2+} can move in interstitial positions.

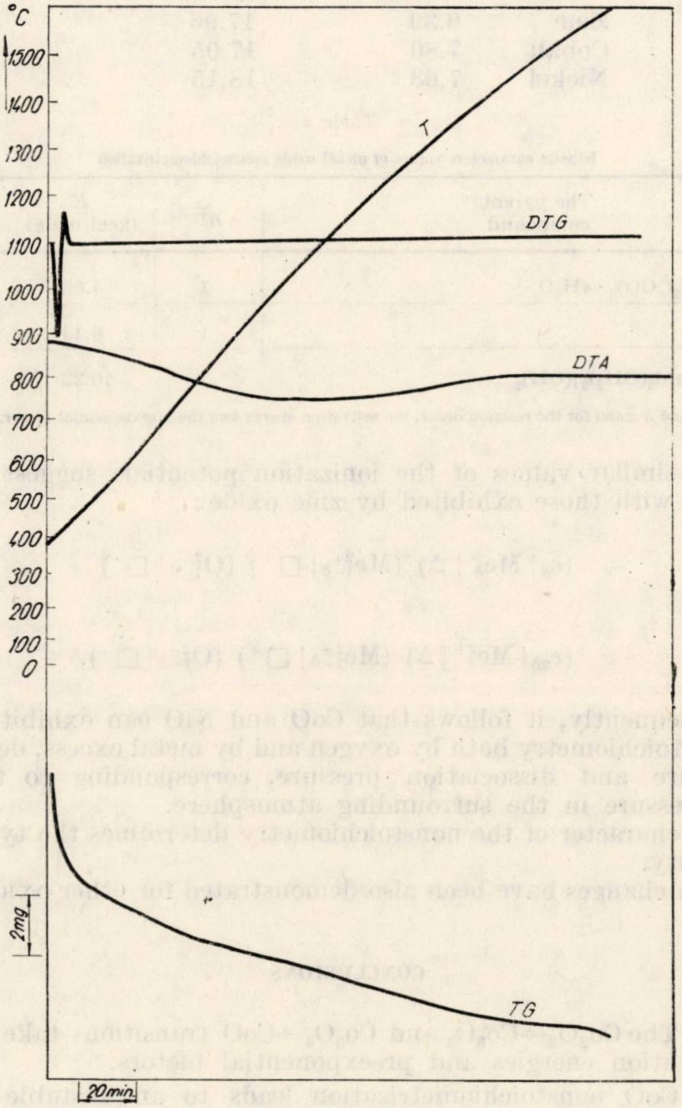

Fig. 2. ATD, DTG and TG curves of nonstoichiometrization of nickel oxide resulting from $NiCO_3$.

On the other hand, the ionization potentials of the first U_1 and second U_2 electron for Zn, Co and Ni have the values[6]:

	U_1(eV)	U_2(eV)
Zinc	9.39	17.96
Cobalt	7.80	17.05
Nickel	7.63	18.15

Table 2

Kinetic parameters values of nickel oxide nonstoichiometrization

The parent compound	$n^{\neq}$	E (kcal/mole)	Z (s^{-1})
$Ni(CH_3COO)_2 \cdot 4H_2O$	1	4.66	$6.7\ 10^{-4}$
$NiCO_3$	1	6.43	$1.68\ 10^{-3}$
$[Ni\ pald_2(OH_2)_2](OH)_2$	1	10.22	$1.04\ 10^{-2}$

$^{\neq}n$, E and Z stand for the reaction order, the activation energy and the preexponential factor, respectively.

The similar values of the ionization potentials suggest analogical structures with those exhibited by zinc oxide:

$$(e_{\delta} \mid Me^{+}_{\delta} \mid \Delta)\ (Me^{2+}_{1-\delta} \mid \square^{+})\ (O^{2-}_{1-\delta} \mid \square^{-}) \tag{I}$$

and

$$(e_{2\delta} \mid Me^{2+}_{\delta} \mid \Delta)\ (Me^{2+}_{1-\delta} \mid \square^{+})\ (O^{2-}_{1-\delta} \mid \square^{-}). \tag{II}$$

Consequently, it follows that CoO and NiO can exhibit deviations from the stoichiometry both by oxygen and by metal excess, depending on temperature and dissociation pressure, corresponding to the oxygen partial pressure in the surrounding atmosphere.

The character of the nonstoichiometry determines the type of semiconductivity.

Such changes have been also demonstrated for other oxides.

CONCLUSIONS

1 — The $Co_2O_3 \rightarrow Co_3O_4$ and $Co_3O_4 \rightarrow CoO$ transitions take place with high activation energies and preexponential factors.

2 — CoO nonstoichiometrization leads to an unstable compound $CoO'_{0.95}$.

3 — NiO nonstoichiometrization leads to a stable compound $NiO_{0.8}$.

4 — Cobalt and nickel oxides nonstoichiometrization processes are described by a kinetic law, corresponding to the unity value of the reaction order.

---

[6] "Spravochnik khimika", vol. I, G. Kh. I., Moskva, Leningrad, 1962, p. 325.

Revue Roumaine de Chimie, 21, 6, 831–833 (1976)

THERMOELECTRIC POWER VARIATION DURING GAS ADSORPTION ON THIN SEMICONDUCTING FILMS. THE ZINC OXIDE-CARBON MONOXIDE SYSTEM

ANA WECHSLER and E. SEGAL
Center of Physical Chemistry, str. Dumbrava Roşie 23, Bucharest, Romania

Received June 20, 1975

The experimental results concerning the surface interaction between carbon monoxide and zinc oxide thin films by the thermoelectric power variation method are presented.

INTRODUCTION

Following our research on the chemisorptive properties of zinc oxide thin films by thermoelectric power variation[1] method, the results concerning carbon monoxide chemisorption are presented. The choise of this gas was determined by its reducing properties, as well as by the fact that, according to our previous experiments, the surface interactions of both carbon monoxide and oxygen with zinc oxide thin films are accompanied by an increase of the electrical resistance.[2, 3]

EXPERIMENTAL

The experimental device used to obtain the thin films, the method of preparation, the way of performing the measurements and the procedure applied to obtain and introduce the carbon monoxide into the adsorption cell, were previously described.[2,3]

The measurements were performed at room temperature.

RESULTS AND DISCUSSIONS

In figure 1, the results concerning the thermoelectric force variations (absolute values) in time, after carbon monoxide introduction, for a zinc oxide thin film which at 8.10^{-7} torr pressure exhibits a 960 Ω initial resistence value and a -0.628 mV thermoelectric force, are shown.

The value of the thermoelectric force measured immediately after gas introduction is higher than the original one.

---

[1] M. Constantinescu, E. Segal and M. Vass, *Rev. Roumaine Chim.*, **20**, 911 (1975).

[2] E. Segal and M. Teodorescu, *Rev. Roumaine Chim.*, **12**, 75 (1967).

[3] E. Segal and M. Teodorescu, *Rev. Roumaine Chim.*, **13**, 1, 449 (1968).

The absolute value of the thermoelectric force decreases in time reaching finally a stationary value at 0.619 mV, value which is lower than the original one.

For a temperature difference of 43.4° between the warm and cold ends of the film, the thermoelectric power variation until saturation is 0.46 μV/°K with respect to the gas introduction moment and 0.20μV/°K with respect to the corresponding value in vacuum.

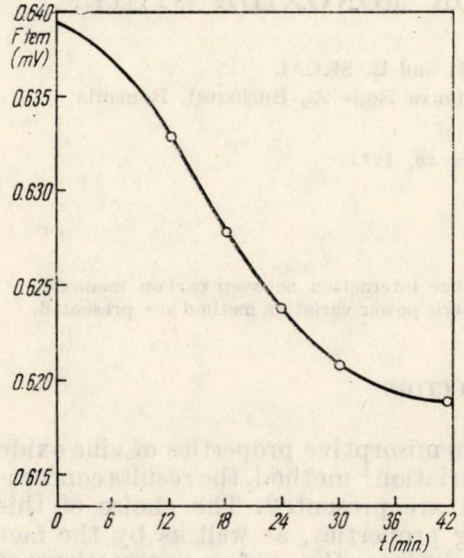

Fig. 1. — Thermoelectric force *versus* time for the ZnO thin film, after carbon monoxide introduction.

The increase of the thermoelectric force, measured immediately after the gas contact with the surface, may be due to the decrease of the thermal impedance of the thin film by carbon monoxide.

Chemisorption, in fact, induces an increase of the thermoelectric force, whose stationary value corresponding to saturation is lower with respect to the one measured in high vacuum.

In the oxygen chemisorption case, [1] an opposite effect was put into evidence, the phenomenon being accompanied by an increase of the thermoelectric power.

The decrease of the zinc oxide thin films thermoelectric power, consequence of surface interaction, can be qualitatively explained considering the one-band conduction mechanism [4] and taking into account the reducing properties of carbon monoxide. According to the above mentioned mechanism, the thermoelectric power of a n type semiconductor, Q, is expressed by the relationship:

$$Q = -\frac{k}{e}\left(\frac{E_C - E_F}{kT} + A_C\right) \qquad (1)$$

---

[4] H. Fritzche, *Solid State Comm.*, **9**, 1813 (1971).

where :

E_C — stands for the energy corresponding to the lower limit of the conduction band

E_F — is the Fermi level energy

T — the absolute temperature

k — Boltzmann's constant

e — the electron charge

A_c — a contribution characteristic to the conduction type.

Taking into account the reducing character of carbon monoxide, it is easy to understand its removing ability of some amounts of surface oxygen. The phenomenon is accompanied by a switch down of the conduction band lower limit, E_C, towards the Fermi level E_F, and a corresponding decrease of the thermoelectric power, in good agreement with the reported experimental data.

Taking into account these results and those obtained for oxygen chemisorption on zinc oxide thin films, [1] we consider that the thermoelectric power measurements are more sensitive to surface electronic interaction between gases and semiconducting thin films, as well as to the donor or acceptor character of the chemisorbed gases.

CONCLUSIONS

— The surface interaction of carbon monoxide with zinc oxide thin films is accompanied by a decrease of their thermoelectric power.

— The phenomenon is due to the partial removing of surface oxygen by the carbon monoxide.

Revue Roumaine de Chimie, **21**, *6*, 835–852 (1976)

ИЗУЧЕНИЕ СВОЙСТВ И ПРАКТИЧЕСКОЕ ИСПОЛЬЗОВАНИЕ ГЕТЕРОПОЛИСОЕДИНЕНИЙ С РАЗЛИЧНЫМИ ЦЕНТРАЛЬНЫМИ АТОМАМИ

И. П. АЛИМАРИН, Е. Н. ДОРОХОВА, С. А. МОРОСАНОВА,
Е. Н. СЕМЕНОВСКАЯ
Московский Государственный Университет им. М. В. Ломоносова

Получена 29 мая 1975 г.

Статья является обзором достижений последних лет по изучению свойств и практическому применению гетерополисоединений (ГПС), главным образом в лаборатории авторов. Рассмотрены образование и восстановление ГПС в водных растворах, поведение ГПС в неводных и смешанных средах, синтез новых ГПС и аналитическое применение ГПС.

Систематическое изучение свойств гетерополисоединений (ГПС) дает ценный материал для развития представлений о строении этого класса комплексов и расширяет возможность их практического применения. Исследование ГПС с типичными центральными атомами позволяет совершенствовать существующие методы анализа элементов, для которых ГПС является зачастую единственной аналитической формой. Накопление экспериментальных данных о ГПС с ,,нетипичными'' центральными атомами обогащает аналитическую химию этих элементов и способствует успешному развитию перспективного направления, химии тройных ГПС.

Благодаря исследованиям ученых всего мира, среди которых почетное место занимают работы академика Ралуки Рипан и ее школы,[1,2] решены многие кардинальные вопросы, касающиеся структуры и поведения ГПС.

На кафедре аналитической химии Московского Государственного Университета им. М. В. Ломоносова проводятся систематические исследования условий образования, восстановления и свойств молибденовых и вольфрамовых ГПС элементов основных IV, V и VI групп периодической системы, подгруппы титана и ГПС рения, т.е. с типичными атомами комплексообразователями ГПС (Si(IV), P(V), As(V)/ и ,,нетипичными'' (Hf)IV), Se(IV), Sn(IV), Re(IV)). Результаты исследований, проведенных до 1964 г., рассмотрены в статье Алимарина, Шаховой и Судакова в сборнике, посвященном 70-летию академика Рипан.[3]

В настоящем сообщении изложены результаты работ, полученные в нашей лаборатории в последнее десятилетие.

ОБРАЗОВАНИЕ И ВОССТАНОВЛЕНИЕ ГПС В ВОДНЫХ РАСТВОРАХ

Для образования ГПС с центральными атомами легкогидролизующихся ионов необходимо предварительное закомплексование иона в

---

[1] R. Ripan, A. Botar, *Rev. Roum. Chim.*, **15**, 1529 (1970).

[2] R. Ripan, A. Botar, *Rev. Roum. Chim.* **16**, 239 (1971).

[3] И. П. Алимарин, З. Ф. Шахова, Ф. П. Судаков в сб. ,,Omagiu acad. prof. Raluca Ripan'', Ed. Acad. R.S.R., Bucureşti, 1966, c. 45.

Таблица 1

Условия образования и спектралные характеристики ГПС в водных растворах

ГПС	Исходные соединения	Кислотность образования	Молярный избыток Mo(VI)	Температура °C	Состав Mo(VI) : Me	λ_{max} нм
Mo—Se—1	H_2SeO_3, Na_2MoO_4	0,5—0,6 Н, HNO_3 0,4—0,5Н, HCl H_2SO_4	>20	60—70	6 : 1	320
Mo—Se—2	H_2SeO_3, $(NH_4)_6Mo_7O_{24} \cdot 4H_2O$	pH—2	12	20	5 : 1	250—260
Mo—Hf—1	$(NH_4)_2[HfF_6]$,	0,1—0,5 Н HCl	12—16	20		360
	$Hf(SO_4)_2Na_2MoO_4$	pH 1,0—1,5	200—300	100	12 :1	
Mo—Sn	$(NH_4)_2[SnCl_6]$, $(NH_4)_6Mo_7O_{24} \cdot 4H_2O$	pH 3—4	14	20	12 : 1	250
Mo—Re	$K_2[ReCl_6]$, Na_2MoO_4	pH 1	30	100	12 : 1	

достаточно прочный комплекс. Это положение, впервые высказанное Шаховой с сотр.[4,5] подтвердилось при исследовании систем Sn(IV)-Mo(VI), Hf(IV)-Mo(VI), Se(IV)-Mo(VI), Re(IV)-Mo(VI). Селен (IV) и гафний (IV) образуют по два типа комплексов в зависимости от ионного состояния исходных компонентов, их концентрации, среды и т.д. (табл. 1). Природа кислоты, используемой для создания нужного значения pH, играет существенную роль. Так, бóльшая скорость образования молибденоселенистой кислоты — I (Mo-Se-1) в хлористоводородной среде, нежели в азотнокислой, связана с образованием промежуточных ,,активных'' хлоридных комплексов селена (IV).[6,7] Аналогичная закономерность проявляется и при образовании других ГПС: молибденографниевого комплекса — I (Mo-Hf-1) в присутствии фторид-иона, Mo—Hf—2 в присутствии сульфат-иона[8], молибденооловянного комплекса (Mo-Sn) из хлоридных комплексов олова (IV),[9] молибденорениевого комплекса (Mo-Re) из хлоридных комплексов рения (IV).[10] По-видимому при образовании ГПС в качестве центральной группы выступает первоначальный комплекс центрального иона, так как в отсутствие комплексующего реагента (F^-, Cl^-, SO_4^{2-} ионов) образования гетерополианиона (ГПА) не происходит.

Это предположение подтверждается анализом инфракрасного спектра молибденогафниевого комплекса -2, где удалось зафиксировать полосы, отнесенные к сульфат-группе.

---

[4] З. Ф. Шахова, Е. Н. Семеновская, *Ж. неорган. химии*, **7**, 1084 (1962).

[5] З. Ф. Шахова, Е. Н. Семеновская, Е. Н. Тимофеева, *Ж. неорган. химии*, **6**, 330 (1961).

[6] З. Ф. Шахова, В. Ф. Захарова, С. А. Моросанова, *Ж. неорган. химии*, **14**, 1895 (1969).

[7] З.Ф. Шахова, С.А. Гаврилова, В. Ф. Захарова, *Вестник МГУ*, *Химия*, **64** (1966).

[8] З. Ф. Шахова, Е. Н. Семеновская, Н. К. Соковикова, *Ж. аналит. химии*, **25**, 485 (1970).

[9] С.А. Моросанова, В. Н. Музыкантова, Л.А. Шкатова, И.П. Алимарин, *Изв. АН СССР*, *сер. Химия*, **8** (1975).

[10] Е. Н. Семеновская, В. А. Гордина, ВИНИТИ деп. № 6479-73 (1973).

Интересен механизм образования молибденорениевой кислоты: в избытке молибдена (VI) протекает окислительно-восстановительная реакция между рением (IV) и молибденом (VI) с образованием восстановленного изополимолибдата и рения (V), который стабилизируется в виде гетерополианиона.[10]

Наиболее существенное влияние на образование ГПА оказывает концентрация молибдена (VI) и природа и концентрация минеральной кислоты, используемой для поддержания необходимой кислотности среды. Совместное влияние концентрации молибдена (VI) и кислоты наглядно прослеживается при построении так называемых диаграмм устойчивости в координатах C_{Mo}—C_{H^+}.[11] Построены диаграммы устойчивости молибденокремневой (Mo—Si) и молибденофосфорной (Mo—P) кислот (рис. 1 и 2). Кривые, разделяющие зоны частичного и полного образования ГПС, описываются уравнениями, связывающими оба переменных параметра.[12] Важным практическим выводом при сопоставлении диаграмм устойчивости различных ГПС является заключение об избирательности условий определения элементов-комплексообразователей.

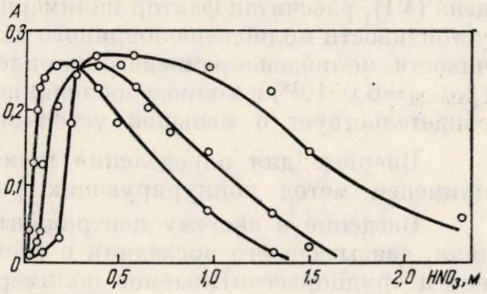

Рис. 1.— Зависимость оптической плотности молибденофосфорной кислоты от концентрации азотной кислоты при различной концентрации молибдена (VI).

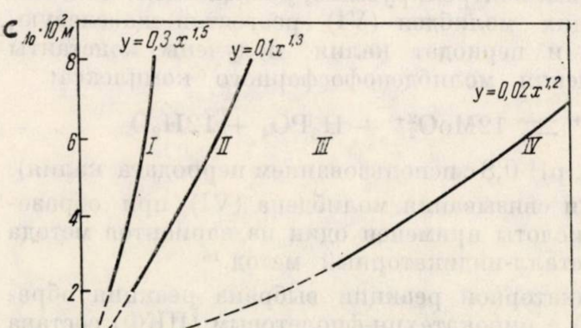

Рис. 2. — Диаграмма устойчивости молибденофосфорной кислоты в азотнокислой среде.

Определение состава и устойчивости ГПС сопровождается рядом трудностей. Высокая склонность лиганда к образованию изополиформ, находящихся в равновесии друг с другом и обладающих, по-видимому, близкой устойчивостью, делает затруднительной запись истинного уравнения диссоциации комплекса. Оценка прочности ГПС осложняется также отсутствием в литературе однозначности в представлении о формах изополимолибдата, вступающих в реакцию комплексообразования, а значит и о фактическом числе лигандных групп.

---

[11] L. Duval, *Chim. analyt.*, **45**, 237 (1963).

Для установления состава ГПС, полученных в растворах из компонентов, использованы метод изомолярных серий в классическом и видоизмененном вариантах (Mo—Se—1),[13] Mo—Hf—2 Mo—Sn[9] и Mo—Re[14], метод ослабления окраски молибденокремневой кислоты (Mo—Se—2),[6] метод молярных отношений (Mo—Se—2), метод Бьеррума (Mo—Sn[9]) и метод конкурирующих реакций (Mo—P[15] и Mo—Sn[16]) (табл. 1).

Методом сдвига равновесия определены степень связывания молибдена (VI), рассчитан фактор полимеризации и оценена условная константа устойчивости молибденооловянного комплекса.[9] Сравнение констант устойчивости молибденокремневого комплекса, определенной тем же методом ($\beta_{Mo-Si}=6{,}0\cdot10^{18}$) и молибденооловянного комплекса ($\beta_{Mo-Sn}=0{,}7$—$6{,}0\cdot10^{12}$) свидетельствует о меньшей устойчивости последнего.

Впервые для определения констант равновесий в растворах ГПС применен метод конкурирующих реакций. [15]

Введение в систему центральный ион — молибден (VI) маскирователя, связывающего последний в растворимый комплекс, заменяет сложное и труднорассчитываемое полимеризационное равновесие между изополиформами молибдена другим, контролируемым, равновесием. Используя в качестве комплексующих молибден (VI) реагентов щавелевую, винную, лимонную кислоты и периодат калия, получены константы реакции кислотного разложения молибденофосфорного комплекса:

$$[PMo_{12}O_{40}]^{3-} + 27H^+ \rightleftharpoons 12MoO_2^{2+} + H_3PO_4 + 12H_2O$$

($K=9{,}1\pm2{,}2.10^{-5}$ при $\tau=20°C$, рН 0,8 с использованием периодата калия).

Для определения степени связывания молибдена (VI) при образовании молибденооловянной кислоты применен один из вариантов метода конкурирующих реакций, металл-индикаторный метод.[16]

В качестве металл-индикаторной реакции выбрана реакция образования комплекса олова (IV) с пирокатехин-фиолетовым (ПКФ) состава $Sn(ПКФ)_2$. Проведение эксперимента в условиях, исключающих взаимодействие ПКФ с молибденом (VI) позволяет отнести ослабление оптической плотности комплекса $Sn(ПКФ)_2$ исключительно за счет связывания олова (IV) молибденом (VI) в бесцветный молибденооловянный комплекс:

$$Sn(ПКФ)_2 + nMo(VI) \rightleftharpoons SnMo_n + 2ПКФ \qquad (1)$$

$$K = \frac{[SnMo_n][ПКФ]^2}{[Sn(ПКФ)_2][Mo]^n} \qquad (2)$$

---

[12] Е. Н. ДОРОХОВА, Т. И. ТИХОМИРОВА, Г. В. ПРОХОРОВА, Proceedings of the XVth International Conference on Coordination Chemistry, Moscow, 1973, p. 656.

[13] В. Ф. ЗАХАРОВА. С. А. МОРОСАНОВА, *Ж. неорган. химии*, **17**, 184 (1972).

[14] Е. Н. СЕМЕНОВСКАЯ, Л. И. СМИРНОВА, В. А. ГОРДИНА, Тез. докл. XI Всес. совещ. по химии комплексных соединений (Алма-Ата, 1973), с. 183.

[15] Ф. П. СУДАКОВ, Н. В. АРСЛАНОВА, *Вестник МГУ*, *Химия*, **91** (1969).

[16] С. А. МОРОСАНОВА, В. Н. МУЗЫКАНТОВА, Л. А. ШКАТОВА, ВИНИТИ деп. № 2786-74.

Логарифмируя выражение 2 и построив графически зависимость $\lg \frac{[SnMo_n][ПКФ]^2}{[Sn(ПКФ)_2]_n}$ от $\lg$ [Mo], определили стехиометрический коэффициент в уравнении 1. Найденное значение $n=3$ совпадает со значением, полученным методом сдвига равновесия.

Исследования в области восстановления ГПС в водных растворах проводились в двух направлениях: получение и изучение восстановленных форм ряда новых ГПС и систематическое изучение процесса восстановления ГПС различными восстановителями с целью установления механизма реакции и разработки новых методов определения элементов. Восстановление проводилось хлоридом олова (II), оксалатом олова (II), хлоридом титана (III), гидразинсульфатом, аскорбиновой кислотой, 1—амино-2-нафтол-4-сульфокислотой („эйконоген''), ферроценом, молибденилхлоридом аммония (табл. 2).

Спектрофотометрическое исследование показало, что по действию на ГПС изученные восстановители можно разделить на два типа: соли олова (II), дающие синие продукты, характер спектров поглощения которых, устойчивость во времени и экстрагируемость, зависят от концентрации восстановителя и молибдена (VI) и остальные реагенты, продукты восстановления которыми характеризуются одинаковым спектром поглощения и сходным поведением независимо от концентрации восстановителя и других факторов. Спектры продуктов второго типа имеют один максимум поглощения, положение которого зависит от модификации ГПК. В спектрах продуктов восстановления солями олова (II) проявляется второй максимум (или „плечо'') в более коротковолновой части спектра. Отличительное поведение солей олова (II) можно, вероятно, объяснить с учетом образования молибденовых комплексов олова (IV). [17–27]

[17] Ф. П. Судаков, В. И. Клитина, Н. Т. Маслова, *Ж. аналит. химии*, **21**, 1089 (1966).

[18] Е. Н. Дорохова, Е. Д. Шигина, *Ж. неорган. химии*, **16**, 2554 (1971).

[19] З. Ф. Шахова, Е. Н. Дорохова, Н. К. Чуян, *Ж. аналит. химии*, **21**, 707 (1966).

[20] Ф. П. Судаков, В. И. Клитина, Н. Т. Маслова, *Вестник МГУ*, *Химия* **93** (1965).

[21] Е. Н. Семеновская, Н. К. Соковикова, Тез. докл. X Всес. совещ. по химии комплексных соединений, Киев, 1969, с. 133.

[22] З. Ф. Шахова, Е. Н. Семеновская, Н. К. Соковикова, Ogolnopolska, konferencja Analityczna komunikaty, Warszawa, 1968, c. 25.

[23] З.Ф. Шахова, Е.Н. Семеновская, Н.К. Соковикова, В. А. Ковальчук, *Ж. аналит. химии*, **25**, 490 (1970).

[24] З. Ф. Шахова, В. Ф. Захарова, С. А. Моросанова, *Ж. неорган. химии*, **15**, 2211 (1970).

[25] С. А. Моросанова, Г. А. Гришко, Л. А. Шкатова, *Ж. аналит. химии*, **29**, 529 (1974).

[26] С. А. Моросанова, Тез. докл. X Всес. совещ. по химии комплексных соединений, Киев, 1969, с. 132.

[27] Ф. П. Судаков, Н. Ф. Галанкина, Н. И. Хамракулова, *Ж. аналит. химии*, **25**, 548 (1970).

Таблица 2

Положение максимумов в спектрах поглощения (нм) и значения молярных коэффициентов погашения восстановленных ГПС ($\tilde{\varepsilon}$)

ГПС	Хлорид олова (II)		Оксалат олова (II)		Гидразинсульфат		Аскорбиновая кислота		« Эйконоген »	
	λ	$\tilde{\varepsilon}$	λ	$\tilde{\varepsilon}$	λ	$\tilde{\varepsilon}$	λ	$\tilde{\varepsilon}$	λ	$\tilde{\varepsilon}$
α-Mo—Si	740	$1{,}4\cdot10^4$	740	$1{,}4\cdot10^4$	790	$2{,}8\cdot10^3$	780	$5{,}0\cdot10^3$	720	$3{,}0\cdot10^3$
β-Mo—Si	800	$4{,}2\cdot10^4$	800	$4{,}0\cdot10^4$	825	$3{,}8\cdot10^4$	800	$3{,}8\cdot10^4$	805	$4{,}0\cdot10^4$
Mo—P	740	$1{,}7\cdot10^4$	830	$2{,}6\cdot10^4$	825	$2{,}9\cdot10^4$	825	$2{,}9\cdot10^4$	825	$2{,}8\cdot10^4$
Mo—As	830	$1{,}8\cdot10^4$	720—830	$1{,}8\cdot10^4$	830	$2{,}9\cdot10^4$	830	$2{,}8\cdot10^4$		
Mo—Hf—1	810	$6{,}7\cdot10^3$	—	—	—	—	825	$3{,}3\cdot10^3$		
Mo—Hf—2	730	$6{,}4\cdot10^3$	730	$6{,}8\cdot10^3$	—	—	730	$2{,}8\cdot10^3$		
Mo—Ti—1	800	$2{,}4\cdot10^3$	—	—	800	$1{,}9\cdot10^3$	800	$3{,}8\cdot10^3$		
Mo—Ti—2	755	$0{,}7\cdot10^3$	770	$0{,}7\cdot10^3$	—	$0{,}1\cdot10^3$	800	$3{,}5\cdot10^2$		
Mo—Zr—1	700	$1{,}4\cdot10^2$	—	—	750	—	780	$0{,}5\cdot10^3$		
Mo—Zr—2	750	$1{,}8\cdot10^3$	—	—	—	—	740	$1{,}1\cdot10^3$		
Mo—Se—1	—	разрушение	—	—	—	—	800—880	$1{,}0\cdot10^3$		
Mo—Sn	—	—	720	$6{,}2\cdot10^3$	—	—	—	—		
Mo—Th	—	—	—	—	—	$3{,}0\cdot10^4$	820	$4{,}0\cdot10^3$		
Mo—Ce	—	—	—	—	800		820*	$5{,}0\cdot10^4$		

*Mo-Ce восстанавливается аскорбиновой кислотой только в присутствии висмута или сурьмы.

Изучение восстановленных молибденовых ГПС циркония (IV), гафния (IV), титана (IV), селена (IV), олова (IV), церия (IV), тория (IV), рения (IV) подтвердило правильность положения о влиянии исходного состояния иона комплексообразователя на протекание реакции и характеристики конечных продуктов. ГПК, полученные из сульфатных комплексов металлов (Mo—Hf—2,Mo—Zr—2,Mo—Ti—2) при восстановлении дают продукты с полосой поглощения в более коротковолновой части спектра (720—780 нм), чем продукты восстановления ГПК тех же элементов, полученные из фторидных комплексов (Mo—Hf—1, Mo—Zr—1, Mo—Ti—1). Аналогично для молибденоселеновых комплексов: Mo—Se—1 восстанавливается в то время, как Mo—Se—2 не способен к восстановлению.

Положение максимумов спектрах поглощения зависит также и от природы центрального атома. Наблюдается смещение максимума в коротковолновую область в ряду ГПК с центральными атомами: Se(IV), As(V), P(V), Si(IV), Ti(IV), Zr(IV), Hf(IV), Th(IV), Ce(IV), что коррелируется с величинами их электроотрицательности.

Полнота восстановления гетерополианиона также, как и полнота его образования, определяется взаимно связанными величинами: концентрацией молибдена (VI) и кислотностью среды. Совместное влияние этих факторов путем построения диаграмм устойчивости восстановленной молибденофосфорной кислоты и молибденомышьяковой кислоты позволило выделить наиболее широкие зоны образования синего продукта, удобные для аналитического использования, и рекомендовать условия определения фосфора в присутствии мышьяка.[28]

ВЛИЯНИЕ ПОСТОРОННИХ ИОНОВ НА ОБРАЗОВАНИЕ И ВОССТАНОВЛЕНИЕ ГПС

Введение третьего компонента в систему центральный ион-молибден(VI) существенно сказывается на реакции комплексообразования.

Ионы хрома(III) и селена(IV) ослабляют окраску ГПС, что обусловлено большой устойчивостью молибденовых комплексов элементов VI группы периодической системы. Используя метод ослабления окраски ГПК, предложенный Шаховой и сотр., установлен состав комплексов хрома(III) и селена (IV) (табл. 3).[13]

Таблица 3

Состав соединений, образующихся при введении третьего компонента в раствор ГПС *

Ион	Mo—Si	Mo—Ge	Mo—P	Mo—As
Cr(III)	Mo : Cr = 6 : 1	Mo : Cr = 6 : 1	Mo : Cr = 6 : 1	
Se(IV)	Mo : Se = 5 : 1		Mo :Se = 5 :1	
Ti(IV)				Mo : Ti : As = 12 : 1 : 1
Bi(III)			Mo : Bi : P = 12 : 1 :1	Mo : Bi : As = = 18 : 1 : 1
Fe(III)		Mo : Fe : Ge = =12 : 1 : 1	Mo :Fe : P= = 12 : 1 : 1	

* приведены только результаты, полученные в нашей лаборатории

---

[28] И. П. Алимарин, С. А. Моросанова, Л. А. Шкатова, *Тез. докл.* II ВСЕС. совещ. по химии и технологии молибдена и вольфрама, Нальчик, 1974 с. 148.

Ряд ионов (Fe(III), Bi(III), Ti(IV), V(V)) усиливают интенсивность окраски ГПК, образуя смешанные комплексные соединения (табл. 3). Образование последних вызывает особый интерес как с точки зрения обогащения теоретических представлений о строении ГПС, так и в практическом аспекте. Обладая большей устойчивостью и светопоглощением, нежели двойные ГПС, смешанные комплексы очень перспективны в плане количественного определения многих элементов.

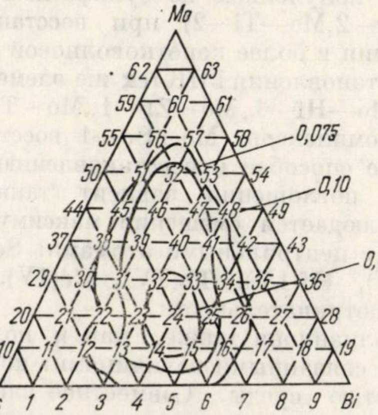
Mo
62
63
59
60
61
55
56
57
58
0,075
50
51
52
53
54
0,10
44
45
46
47
48
49
37
38
39
40
41
42
43
0,12
29
30
31
32
33
34
35
36
20
21
22
23
24
25
26
27
28
10
11
12
13
14
15
16
17
18
19
As
1
2
3
4
5
6
7
8
9
Bi

Рис. 3.—Тройная диаграмма системы As(V)—Bi(III)—Mo(VI).

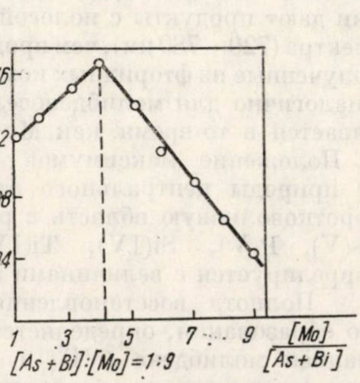

Рис. 4.— Центральные разрезы тройной диаграммы As(V)—Bi(III)—Mo(VI).

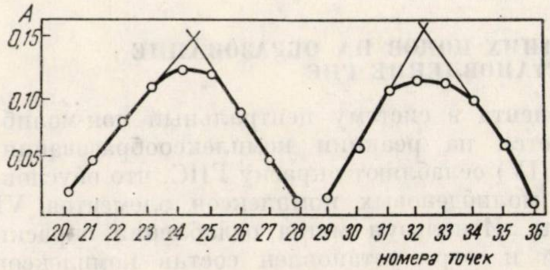

Рис. 5. — Дополнительный разрез тройной диаграммы As(V)—Bi(III)— Mo(VI).

Для доказательства образования тройных ГПС и определения их состава применен метод построения тройных диаграмм (рис. 3, 4, 5)[29,30] и другие методы.[31] Интересно отметить, что введение ионов титана (IV) и висмута(III) в систему мышьяк(V)-молибден(VI) приводит к образованию различных по составу, устойчивости и спектральным характеристикам смешанных соединений: в первом случае молибденотитаномышьяковой кислоты состава Mo:Ti:As=12:1:1 со спектром, аналогичным

---

[29] Е. Н. Дорохова, З. Ф. Шахова, Л. А. Сазанова, *Ж. аналит. химии*, **21**, 884 (1966).

[30] И. П. Алимарин, С. А. Моросанова, Л. В. Тумурова, *Изв. АН СССР, сер. химия* **2**, 428 (1971).

[31] З. Ф. Шахова, Е. Н. Дорохова, *Ж. неорган. химии*, **10**, 2060 (1965).

спектру поглощения молибденомышьяковой кислоты, и константой устойчивости $\beta=6,9.10^{13}$, во втором случае молибденовисмутомышьковой кислоты состава Mo:Bi:As$=18:1:1$ с максимумами поглощения при 260 нм и 310 нм и $\beta=3,1.10^{11}$.

Анализ диаграмм устойчивости смешанных ванадий-молибденовых ГПК кремния и фосфора подтвердил данные о повышении устойчивости комплексов при введении третьего компонента в координационную сферу.[12]

Особенно ценный материал получен при изучении восстановления ГПС в присутствии посторонних ионов, поскольку при этом удалось зафиксировать смешанные соединения, исследование которых обычными методами затруднено или невозможно. Влияние третьего компонента на восстановление молибденовых ГПК мышьяка (V), гафния (IV) и циркония (IV) прослежено при использовании одного восстановителя — аскорбиновой кислоты, дающей наиболее устойчивые синие продукты. В качестве третьих компонентов выбраны ионы элементов, либо сопутствующих элементам, которые выступают центральными атомами ГПК (Fe(III), Al(III), Bi(III), Sb(III), Cu(II)), либо ионы элементов, склонных к образованию ГПС (Si(IV), P(V), Zr(IV), Hf (IV), V(V)).

В присутствии всех изученных ионов интенсивность окраски ГПК возрастает. Увеличение интенсивности окраски обусловлено различными причинами. В присутствии ионов кремния (IV) и циркония(IV) при восстановлении молибденовых ГПК гафния(IV) и циркония (IV) наблюдается суммарный эффект образования двух восстановленных ГПК (Mo—Si и Mo—Hf, Mo—Si и Mo—Zr, Mo—Zr и Mo—Hf). Введение ионов меди (II) оказывает каталитическое действие на процесс восстановления.[32-36] В остальных случаях зафиксировано образование промежуточных смешанных комплексов состава: Mo:Hf:V$=12:1:1$, [33] Mo:Fe: Hf$=12:1:1$[34]; в случае ГПС мышьяка отношения As: Bi = и As: Sb1: =1. [32-35] Конечным продуктом восстановления во всех случаях является восстановленная двойная ГПК. Однако присутствие третьего компонента вносит существенные коррективы в условия и скорость протекания реакции. Так, восстановление молибденоарсената в присутствии ионов висмута (III), сурьмы(III), меди (II) позволяет избежать операции нагревания, которое необходимо при восстановлении двойного комплекса.[32]

С целью более детального изучения протекающих процессов и для трактовки полученных данных проведены некоторые исследования по кинетике и механизму восстановления ГПК в присутствии третьих компонентов.

---

[32] С. А. Моросанова, Л. В. Тумурова, Л. А. Лялюлина, *Вестник МГУ, Химия*, **88** (1972).

[33] Е. Н. Семеновская, Н. К. Соковикова, Л. И. Смирнова, *Вестник МГУ, Химия*, **358** (1973).

[34] И. П. Алимарин, Е. Н. Семеновская, Н. К. Соковикова, *Ж. аналит. химии*, **26**, 126 (1791).

[35] Л. В. Тумурова, Л. А. Лялюлина, С. А. Моросанова, И. П. Алимарин, *Ж. аналит, химии*, **26**, 2155 (1971).

[36] Н. К. Соковикова, Е. Н. Семеновская, И. П. Алимарин, Тез. докл. XI Всес. совещ. по химии комплексных соединений, Алма-Ата, 1973, с. 184.

Скорость реакции фиксировали фотометрически по изменению концентрации продуктов восстановления. Мерой скорости являлся тангенс угла наклона прямолинейного участка кривых зависимости $A - t_{\text{мин}}$. Исследование проведено в термостатированных условиях. Известными методами определены концентрационные и временные порядки реакций восстановления ГПС (табл. 4).

Таблица 4

Порядки реакций восстановления ГПС

ГПС	Третий компонент	Концентрационные порядки		Временные порядки
		По методу графического дифференцирования	По периоду полупревращения	
Mo—As	Bi(III)	1,2		1,2
Mo—As	Sb(III)	1,0		0,7
Mo—Zr		1,0	0,9	0,5
Mo—Zr	Fe(III)	0,8	0,9	0,5
Mo—Hf		1,0	1,2	0,5
Mo—Hf	Fe(III)	0,8	0,9	0,5
Mo—Zr	Cu(II)	0,7	1,1	0,5
Mo—Zr	Bi(III)	1,0	1,0	0,5
Mo—Hf	Cu(II)	0,9	1,0	0,5
Mo—Hf	Bi(III)	0,9	0,9	0,5

Процессы восстановления ГПК элементов-аналогов, циркония(IV) и гафния(IV), идут с различной скоростью, причем добавленные ионы в некоторых случаях избирательно ускоряют реакции.

Так, введение ионов железа(III) существенно дифференцировало скорость восстановления ГПК. Ряд специальных исследований (расчет энергий активации, определение порядков реакций, определение констант скорости) позволил предложить механизм восстановления молибденогафниевого комплекса в присутствии ионов железа(III):

$$\text{I Mo}-\text{Hf} + \text{аскорбиновая к-та} \xrightleftharpoons[K_2]{K_1} \text{Mo}-\text{Hf}_{\text{восст}} + \text{аскорбиновая к-та}_{\text{ок}}.$$

В присутствии ионов железа (III) в растворе образуются два комплекса: молибденогафниевый и молибденожелезогафниевый. При введении в систему аскорбиновой кислоты параллельно идут два процесса: первый по схеме I и второй в две стадии по схеме II.

$$\text{II Mo}-\text{Fe}-\text{Hf} + \text{аск. к-та} \xrightleftharpoons[K_4]{K_3\,(\text{быстро})} \text{Mo}-\text{Fe}-\text{Hf}_{\text{восст}} + \text{аск. к-та}_{\text{ок}}.$$

$$\text{Mo}-\text{Fe}-\text{Hf}_{\text{восст}} \xrightarrow{K_5\,(\text{медленно})} \text{Mo}-\text{Hf}_{\text{восст}} + \text{Mo}-\text{Fe}$$

Вторая стадия второго процесса является скорость-определяющей. Увеличение скорости восстановления молибденогафната в присутствии ионов железа (III) связано с изменением энергетического фактора.

Скорость восстановления молибденоцирконата не меняется в присутствии ионов железа(III), что хорошо согласуется с полученными значениями энергии активации (табл. 5).[37,36]

Таблица 5

Кинетические характеристики систем молибден (VI) – цирконий (IV) и молибден (VI) – гафний (IV)

Система	E, ккал/ моль		Начальная скорость м/л. сек·10^2				pK_5
	По методу трансформации	По уравнению Аррениуса	20°	25°	35°	45°	
Mo–Hf	14,5±0,5	15,2±1,0	0,25	0,60	0,90	1,70	1,56±0,02
Mo–Hf–Fe	9,5±0,5	9,3±0,9	0,50	0,86	1,40	3,30	1,45±0,03
Mo–Zr	13,0±0,5	13,9±0,8	0,30	0,60	0,52	1,70	1,90±0,03
Mo–Zr–Fe	13,0±0,6	13,8±0,5	0,32	0,65	1,00	1,80	1,87±0,03

Аналогичное исследование влияния ионов висмута(III) и сурьмы(III) на процесс восстановления молибденомышьяковой кислоты приводит к следующей схеме механизма реакции[32,35]

$$\mathrm{As(V) + Bi(III)\ (Sb(III)) + Mo(VI) \rightleftarrows Mo{-}Bi(Sb){-}As}$$

$$\begin{array}{l} \mathrm{Mo{-}Bi(Sb){-}As^{+}\ аскорб.\ к\text{-}та_{восст} \rightleftarrows Mo{-}Bi(Sb){-}As_{восст} + аск.\ к\text{-}та_{ок}.} \\ \qquad\qquad\qquad\qquad\qquad\qquad\quad \downarrow \\ \qquad\qquad\qquad\qquad\qquad\quad \mathrm{Mo{-}As_{восст} + Bi(III)} \end{array}$$

Результаты кинетического исследования ГПК циркония и гафния позволили предположить, что для элементов с аналитически близкими свойствами перспективны поиски кинетических различий. В этом плане определенный интерес представляет изучение поведения солей рения в присутствии молибдена(VI). Кинетические исследования системы рений(IV)-молибден(VI) (вывод кинетического уравнения, расчет констант скорости реакции и констант образования комплекса, равных соответственно $4{,}9.10^{-4}$ сек$^{-1}$, и $1{,}1.10^{2}$ м$^{-1}$ совпадение экспериментальных и рассчитанных кривых зависимости скорость реакции—концентрация молибдена (VI)) позволили предложить схему процесса:

$$\begin{array}{ll} \text{I стадия:} & \mathrm{Re(IV) + Mo(VI) \rightarrow Re(V) + Mo(V)} \\ & \mathrm{Re(V) + Mo(VI) + Mo(V) \rightarrow Re - Mc_{восст}} \\ \text{II стадия} & \\ & \mathrm{Re(V) + Mo(VI) \rightarrow Re{-}Mo} \end{array}$$

---

[37] Е. Н. Семеновская, В. А. Гордина, Докл. Всес. совещ. по проблеме рения, Москва, 1973.

[38] И. П. Алимарин, Ф. П. Судаков, В. И. Клитина, *Успехи химии*, **34**, 1368 (1965).

Моделирование процесса путем замены исходного препарата рения(IV) на препарат рения (V) подтвердило течение процесса по предложенной схеме.[37]

ПОВЕДЕНИЕ ГПС В НЕВОДНЫХ И СМЕШАННЫХ СРЕДАХ

Определенный вклад в представления о строении и механизме образования ГПС вносит исследования взаимодействия их с органическими растворителями. Аналитически важные эффекты, такие как увеличение светопоглощения и стабилизация во времени в смешанных водноорганических растворах и избирательная растворимость в неводных средах (экстракция) расширяет область применения ГПС. Большой экспериментальный материал, накопившийся в этой области к 1965 г., был систематизирован Алимариным, Судаковым и Клитиной.[38] Успехи в изучении экстракции кислородсодержащими растворителями в последние годы позволили отдать предпочтение гидратно-сольватному механизму взаимодействия ГПС с растворителем. Особенностью исследований последнего времени является привлечение разнообразных методов (инфракрасной спектроскопии, ядерного магнитного резонанса, радиохимических методов) и количественный подход к описанию процесса экстракции.

Систематическое изучение экстракции восстановленных молибденовых ГПС фосфора и кремния (α и β-модификаций), проведенное в нашей лаборатории, показало, что восстановление комплексов не меняет принципиально их экстракционного поведения: синие формы извлекаются кислородсодержащими и азотсодержащими экстрагентами и практически не экстрагируются бескислородными соединениями. Более высокозарядный гетерополианион молибденокремневой кислоты (в обоих модификациях) извлекается хуже молибденофосфорной кислоты, что укладывается в рамки гидратносольватного механизма взаимодействия ГПК с кислородсодержащими растворителями. Экстрагируемость ГПС ухудшается в ряду спирты→кетоны→эфиры [19,39] (табл. 6).

Таблица 6

Процент экстракции восстановленной молибденофосфорной кислоты

Растворитель	Хлорид олова (II)	Гидразин-сульфат	Аскорбиновая кислоты	метил-п-аминофенол («метол»)
Бутанол	97	93	100	90
Изобутанол	100	90	100	83
Пентанол	87	88	100	85
Изопентанол	91	99	100	81
Гексанол	91	90	98	83
Гептанол	93	83	90	77
Метилизобутилкетон	88	83	100	85
Этилацетат	85	98	90	68
Диэтиловый эфир	58	0	0	0
Хлороформ	0	0	0	0
Бензол	0	0	0	0

---

[39] В. И. КЛИТИНА, Ф. П. СУДАКОВ, И. П. АЛИМАРИН, *Ж. аналит. химии*, **20**, 1145 (1965).

Найденные закономерности сохраняются при экстракции невосстановленных форм ГПС кремния и фосфора,[40] а также молибденовых ГПК гафния и селена, что подтверждает идентичность строения желтых и синих форм ГПС и говорит в пользу одинакового механизма экстракции в обоих случаях.

Спектры поглощения экстрактов синих ГПС отличаются от спектров их водных растворов гипсохромным смещением максимумов поглощения. Величина смещения зависит от природы ГПК и восстановителя и не зависит от природы экстрагента (табл. 7).

Таким образом в экстракционном отношении продукты восстановления солями олова(II) отличаются от продуктов, полученных действием других восстановителей.

Введение в экстракционную систему высокомолекулярных аминов, триоктиламина и диоктиламина, улучшает экстрагируемость синих ГПС, при этом возможно даже извлечение комплекса в неполярные растворители. Диоктиламин как экстрагент более основного характера, обладает несколько большей экстракционной способностью, чем триоктиламин.[41] Характер спектров поглощения зависит от природы ГПК и разбавителя и не зависит от природы амина. Отсутствие гипсохромного смещения максимумов в спектрах поглощения экстрактов аминами, характерного для экстрактов кислородсодержащими растворителями, указывает на различный механизм экстракции ГПС в обоих случаях.

В качестве азотсодержащих реагентов использованы также сафранит Т (краситель группы эозина) и основные красители родамин С, родамин 6 Ж и метиловый фиолетовый.[42,43]

Таблица 7

Положение максимумов поглощения в спектрах экстрактов восстановленных ГПС

ГПС	Хлорид олова (II)	Оксалат олова (II)	Гидразин-сульфат	Аскорбиновая кислота	«Эйконоген»
α-Mo—Si	630 и 740	630 и 720	720	720	720
β-Mo—Si	630 и 740	630 и 720	805	780	800
Mo—P	625 и 725		780	780	780
Mo—Zr	—	—	—	700	—
Mo Hf	—	—	—	750	—

Невосстановленные формы ГПК количественно экстрагируются триоктиламином в различных разбавителях в широком интервале кислотности.[44,45] В органической фазе наблюдается небольшое увеличение светопоглощения ГПК, связанное с подавлением диссоциации комплексов. Характер инфракрасных спектров экстрактов свидетельствует об отсутствии донорно-акцепторного взаимодействия N→Mo и ионно-ассоциатной природе экстрагирующегося соединения. Состав последнего при экстракции как α, так и β-модификаций молибденокремневой кислоты отвечает отношению [Mo—Si]: $R_3H = 1:4$, где R_3N-триоктиламин. В органической фазе происходит диссоциация ионного ассоциата с отщеплением протонированных молекул триоктиламина.

---

[40] K. Murata, T. Kiba, *J. Inorg. nucl. chem*, **32**, 1667 (1970).

[41] В. И. Клитина, Ф. П. Судаков, И. П. Алимарин, *Ж. аналит. химии*, **21**, 338 (1966).

[42] Ф. П. Судаков, В. И. Клитина, Т. Я. Даньшова, *Ж. аналит. химии*, **21**, 1333 (1966).

[43] З. Ф. Шахова, Е. Н. Дорохова, Е. Н. Миронцева, *Ж. неорган. химии*, **13**, 2743 (1968).

[44] R. Kollan, V. Plichon, J. Saulnier, *J. Analyt. chim. acta*, **50**, 457 (1970).

[45] Т. И. Коровина, Е. Н. Дорохова, *Ж. неорган. химии*, **19**, 590 (1974).

Экстракционное равновесие описывается уравнением

$$[SiMo_{12}O_{40}]^{4-} + 4R_3NH^+ \rightleftharpoons [SiMo_{12}O_{40}](R_3NH)^{n-}_{4-n} + nR_2NH^+ \qquad (3)$$

Константа равновесия реакции выражается следующим образом:

$$K = \frac{C_{[Mo-Si]\,(R_3NH)^{n-}_{4-n}}\, C^{n}_{R_3NH^+}}{C_{[Mo-Si]_{вод.}} \cdot C^4_{R_3N}}$$

Поскольку $C_{R_3NH^+} = nC_{[Mo-Si]\,(R_3NH)^{n-}_{4-n}}$, то

$$K = n^n C^{n+1}_{[Mo-Si](R_3NH^+\,{}^{n-}_{4-n}} / C_{[Mo-Si]_{вод}} \cdot C^4_{R_3N}$$

Логарифмируя, получаем:

$$\lg C_{[Mo-Si]_{вод}} \cdot C^4_{R_3N} = K' + (n+1)\lg C_{[Mo-Si]\,(R_3NH)^{n-}_{4-n}}$$

По тангенсу угла наклона прямой зависимости $\lg C_{[Mo-Si]_{вод}} \cdot C^4_{R_3N}$ от $\lg C_{[Mo-Si]\,(R_3NH)^{n-}_{4-n}}$ находят стехиометрический коэффициент n в уравнении 3. Стехиометрия реакции и значения константы экстракции зависят от природы разбавителя (табл. 8).

Таблица 8

Экстракция молибденокремневой кислоты триоктиламином

Разбавитель	Диэлектрич. проницаемость, ε	n	lg Кэкстр.		Наличие присоединения дополнит. молекулы [Mo-Si]
			α—Mo—Si	β—Mo—Si	
Бензол	2,3	2	10,0± 0,3	—	есть
Толуол	2	2	10,0± 0,3	—	есть
Дихлорэтан	10,4	1	10,8± 0,2	9,7±0,1	нет
Дихлорэтан*	10,4	1			

* Приведены данные из работы [44]

При экстракции толуольным и бензольным раствором триоктиламина в избытке молибденокремневой кислоты наблюдается явление извлечения ГПК сверх стехиометрического, что можно объяснить присоединением избыточных молекул ГПК к ионному ассоциату с образованием водородных связей. Этот эффект отсутствует в дихлорэтановых растворах. Различия в поведении комплекса в различных растворителях удовлетворительно объясняется с точки зрения сольватирующей способности разбавителя, связанной с нуклеофильным характером толуола и электрофильным характером дихлорэтана.

Систематическое исследование образования молибденофосфорной и молибденокремневой кислот, проведенное в нашей лаборатории, в растворах вода-этанол, вода-ацетон, вода-диоксан, вода- диметилформамид, показало, что во всех случаях наблюдается увеличение светопоглощения ГПК, незначительное при образовании молибденокремневого комплекса (10—15%) и резкое при образовании молибденофосфорного комплекса; расширяется интервал pH оптимального образования, уменьшается избыточное количество молибдена(VI), повышается устойчивость комплексов во времени.[46]

При образовании молибденокремневой кислоты несмотря на небольшой выигрыш в чувствительности, улучшается воспроизводимость результатов за счет стабилизации β-модификации. В настоящее время нет убедительных данных по механизму стабилизирующего действия органического растворителя на ГПК. В связи с этим привлекает внимание гипотеза о способности всех молибденовых ГПС (Si, P, As, Ge) к существованию в двух модификациях и стабилизации β-модификаций в смешанных растворах.[47]

При обычных условиях компоненты водно-органической среды не проявляют восстановительной способности. Однако под действием ультрафиолетового света (УФ) некоторые из них восстанавливают ГПК. Исследование поведения молибденомышьяковой кислоты под действием УФ в присутствии ацетона, винной, аскорбиновой и муравьиной кислот, формальдегида и этанола показало, что восстановление ГПА происходит сравнительно быстро без нагревания, а в случае использования трех последних реагентов реакция характеризуется высокой чувствительностью $(\tilde{\varepsilon} = 19.10^3)$.[48]

В неводных средах исключается возможность гидролитического расщепления ГПА, что позволяет с большей достоверностью титровать ГПК, как многоосновные кислоты, различными основаниями. Потенциометрическое титрование молибденокремневой кислоты в различных неводных средах (ледяной уксусной кислоте, смеси изопропанола с бензолом, метилэтилкетоне) тетраэтиламином, триэтиламином и пиридином с использованием стеклянного и платиноокисного электрода показало принципиальную возможность использования метода для быстрого и надежного определения ГПК.[49]

---

[46] Ф. П. Судаков, Л. А. Обухова, Р. И. Ценская, *Ж. аналит. химии*, **25**, 765 (1970).

[47] R. A. Chalmer, A. Sinclair, *J. Analyt. Chim. acta*, **34**, 412 (1966).

[48] И. П. Алимарин, С. А. Моросанова, Л. В. Тумурова, Н. Я. Колли, *Ж. аналит. химии*, **28**, 1115 (1973).

[49] З. Ф. Шахова, Е. Н. Семеновская, А. А. Меркулова, *Ж. неорган. химии*, **13**, 1890 (1968).

СИНТЕЗ НОВЫХ ГЕТЕРОПОЛИСОЕДИНЕНИЙ

В нашей лаборатории продолжались работы по синтезу новых ГПК и их солей, а также по выделению в твердом виде ранее не выделенных восстановленных ГПС (табл. 9).

Таблица 9

Гетерополикислоты и их соли, выделенные в твердом виде

ГПК	Метод выделения кислот	Молярное отношение элемент: лиганд	Полученные соли
α—Mo—Si	Эфиратный	1 : 12	диазониевые [50]
,,	,,	1 : 12	родаминовая — 6Ж метилового фиолетового[43]
α—Mo—Si (восстановл.)	,,	1 : 12	хинолиновая
β—Mo—Si (восстановл.)	,,	1 : 12	хинолиновая
Mo—Sn	Ионообменный	1 : 12	аммониевая
Mo—Hf	,,	1 : 12	аммониевая, рубидиевая, цезиевая
Mo—Ce	,,	1 : 12	диазониевые [50]
Mo—Se	,,	1 : 6	аммониевая, гуанидиновая, этилендиаминовая[6]
Mo—Se	,,	1 : 5	аммониевая
W—Se	,,	1 : 6	натриевая и амониевая[51]
W—Ti	Эфиратный	1 : 12	хинолиновая
W—Zr	,,	1 : 12	хинолиновая
W—Se	,,	1 : 12	

Все полученные ГПК, кроме молибденоселенистой кислоты, являются предельными насыщенными ГПК.

В твердом виде с использованием различных восстановителей (оксалата олова и аскорбиновой кислоты) выделены восстановленные формы α и β-молибденокремневых кислот и их хинолиновые соли. Изучение состава и свойств полученных соединений показало, что в зависимости от используемого восстановителя получаются продукты различного состава. При применении более сильных восстановителей (оксалат олова(II)) образующиеся продукты имеют более высокую основность. Не ослаб интерес к выделению и изучению свойств продуктов взаимодействия органических азотсодержащих соединений с ГПК. Здесь впервые были выделены и изучены продукты (родамин 6Ж-[α—Mo—Si], метиловый фиолетовый — [α—Mo—Si]),[43] а также серия продуктов взаимодействия солей диазония с молибденокремневой и молибденоцериевой ГПК.[50]

---

[50] В. П. Сагалович, С. А. Гаврилова, В. В. Козлов, Ю. М. Куликов, З. Ф. Шахова, *Докл. АН СССР*, **168**, 832 (1968).

[51] З. Ф. Шахова, С. А. Моросанова, В. Ф. Захарова, О. Н. Куренкова, *Ж. неорган. химии*, **14**, 3053 (1969).

Термогравиметрически и элементным анализом показано повышение основности при восстановлении ГПК оксалатом олоба,[53] подтверждена высокая основность молибденоцериевой ГПК.[52] Исследование инфракрасных спектров диазониевых солей показало ионный характер исследуемых соединений, а также позволило сделать вывод о различном строении молибденокремневой и молибденоцериевой ГПК.[50]

АНАЛИТИЧЕСКОЕ ПРИМЕНЕНИЕ ГПК

Исследование свойств и поведения ГПК в водных, неводных и смешанных средах привели к разработке новых методов определения ряда элементов.

Спектрофотометрическое изучение новых ГПК с центральными атомами селена(IV) и гафния(IV), аналитическая химия которых весьма ограничена, позволили предложить методы анализа соединений этих элементов в фотометрическом и экстракционном вариантах.[7,54]

В результате систематического исследования условий восстановления ГПК разработаны методы фотометрического определения фосфора с применением ранее не используемых восстановителей (хлорид титана(III), ферроцен),[27,55] методы определения кремния и фосфора при совместном присутствии, метод потенциометрического восстановительного титрования для определения кремния в минералах,[56] метод определения кремния в чугунах и сталях, метод определения мышьяка и селена в растворах,[7,25,32] фотохимический метод определения мышьяка в латунях,[48] кинетический метод определения гафния на фоне циркония.[36]

Изучение экстракционного поведения ГПК дало возможность рекомендовать метод определения кремния и фосфора в пятиокиси ванадия без отделения основы,[57] а сочетание экстракции с восстановлением предложить высокочувствительные методы определения фосфора в растворах и кислотах,[41,39,42] кремния в конденсатах пара и растениях.[58] Выгодная стехиометрия ГПС позволила предложить чувствительный косвенный метод определения фосфора по молибдену (VI) (мультипликационный метод).[59]

Исследование условий образования ГПК в смешанных средах привело к рекомендации метода определения фосфора с чувствительностью, не уступающей методам с восстановлением молибденофосфорной кислоты.[46]

---

[52] З. Ф. Шахова, Е. Н. Дорохова, Н. К. Чуян, *Вестник МГУ*, *Химия*, **85** (1966).

[53] З. Ф. Шахова, Е. Н. Семеновская, Е. А. Моросанова, Е. Н. Дорохова, *Abstracts of Papers automation in analytical chemistry, XXI IPAK, Prague, A-96 (1967).*

[54] З. Ф. Шахова, Е. Н. Семеновская, Н. К. Соковикова, *Ж. аналит. химии*, **23**, 1164 (1968).

[55] Ф. П. Судаков, Н. А. Твердова, *Ж. аналит. химии*, **21**, 1089 (1966).

[56] Е. Н. Дорохова, Л. И. Опарина, *Ж. аналит. химии*, **25**, 544 (1970).

[57] Е. Н. Дорохова, Т. И. Тихомирова, О. Г. Черкасова. Г. В. Прохорова, *Ж. аналит. химии*, **29**, 2014 (1974).

[58] Е. Н. Дорохова, Л.Б. Жукова, А.П. Терещенко, В. В. Краснощеков, *Вестник МГУ*, *Химия*, **604** (1973).

Особенно ценным явилось изучение влияния третьего компонента в системе центральный ион — молибден(VI), которое привело к разработке методов определения хрома[60] и селена[13] по ослаблению окраски молибденокремневой кислоты и к многочисленным методам определения элементов в виде тройных ГПК: гафния в сплавах с ванадием в виде молибденованадийгафниевого комплекса,[33] фосфора в виде молибденожелезофосфорного комплекса,[29] мышьяка в растворах в виде молибденовисмутмышьякового комплекса[32] и в сурьме в виде молибденосурьмяномышьякового комплекса.[35]

---

[59] Н. В. Арсланова, А. С. Мясоедова, Ф. П. Судаков, *Ж. аналит. химии*, **26**, 947 (1971).

[60] З. Ф. Шахова, Е. Н. Дорохова, *Вестник МГУ, Химия*, **77** (1964).

Revue Roumaine de Chimie, **21**, *6*, 853−857 (1976)

BISMUTH(III)−ETHYLENEDIAMINETETRAACETIC ACID (EDTA) COMPLEXES. I

POLAROGRAPHIC STUDY ON FORMATION AND STABILITY OF THE COMPLEXES IN THE SOLUTION

C. DRĂGULESCU, ANA NIMARĂ and I. JULEAN
Chemical Research Centre, Bd. Mihai Viteazul, 24, Timişoara, Romania

Received July 25, 1975

The formation of the bismuth-EDTA complexes in the range of 0−3 pH was polarographically investigated. The formation of the complexes $[BiHY]$; $[BiY^-]$; $\{[Bi(OH)_2]_2H_2Y\}$ and respectively $[Bi(OH)_2H_3Y]$ as well as their stability constants were established. The two last complexes are probably only outer sphere complexes, which in a short period of time transform themselves into inner sphere complexes, $[BiY^-]$; $[BiHY]$.

The EDTA is one of the most widespread complexing agents, which is used for over thirty years for the determination of the majority of elements. [1]

The literature data shows that this chelation agent may form normal complexes, hydrogenous complexes, hydroxo-complexes and mixed complexes, the combination ratio being of 1 : 1. [2] The polarographical study of the metal complexes with EDTA shows that in the most cases, irreversible waves are obtained, probably due to their very stable chelatic structure.

Bismuth may be polarographically determined under the form of the $[Bi-Y]^-$ complex, over the whole pH range. Thus Faucherre and Souchay [3] indicated for pH 2 a half-wave potential of − 0.18 − 0.22 V; while Zabransky [4] points to − 0.6 V for pH 4. Brintzinger and Menkelt [5] evidenced the existence of the BiHY complex in an acid medium.

As concerns the value of the stability constants, there are in literature several attempts to determine them. [6,7] Beck and Gergely [8] have studied the formation of the Bi − Y complexes in 0.5−1 M potassium nitrate medium at different perchloric acid concentrations, thus obtaining different values of the stability constants function of pH.

---

[1] A. J. Barnard Jr., E. T. Joy, K. Little and J. D. Brooks, *Talanta*, **17**, 789 (1970).

[2] R. P. Pribil, "Complexonii în Chimia Analitică", Ed. tehnică, Bucharest, 1961, p. 60.

[3] J. Faucherre and P. Souchay, *Bull. Soc. chim. France*, **1949**, 222.

[4] Z. Zabransky, *Chem. Listy*, **48**, 617 (1948).

[5] H. Brintzinger and S. Menkelt, *Z. anorg. Chem.*, **256**, 65 (1948).

[6] I. Miklos and P. Szegedy, *Acta Chim. Acad. Sci. Hung.*, **26**, 365 (1961).

[7] N. Elenkova and L. Ilcheva, *Godishnik Khim. Tekhnol.*, **11**, 143 (1964).

[8] M. T. Beck and A. Gergely, *Magyar Kémiai Folyóirat*, **71**, 163 (1965).

Bhat and Krishna Iyer[9] have identified by means of spectrophotometry, the formation of a single complex 1 : 1 over the $2-7$ pH range, obtaining log K $= 26.47$ at an acidity of $0.1-0.6$ M.

Socevanov and Volkova[10] have determined polarographically the instability constants for a series of elements easily hydrolysable, obtaining for Bi — Y, the value of $10^{-27.94}$, in 1.78 M sodium nitrate medium.

In the present paper we studied polarographically the equilibria which appear between different hydrolysed species of bismuth and different protonated species of the EDTA both in a buffered and unbuffered medium in the $0-3$ pH range.

EXPERIMENTAL

REAGENTS AND APPARATUS

Bismuthyl perchlorate — $BiOClO_4 \cdot H_2O$ was prepared following the described procedure.[11] The concentration range was $5.6 \cdot 10^{-4} - 1.2 \cdot 10^{-3}$ M. The EDTA used was reagent grade.

The polarograms were recorded with a Radiometer PO4 polarograph. The capillary constants are : $t = 5.4$ s ; $m = 1.66$ mg s^{-1} in 0.1 M $NaClO_4$, at $h = 52$ cm, open circuit.

The pH was determined with a Radiometer PHM 25 pH-meter. The electrophoretic determinations were carried out using an electrophoresis apparatus of the type Zeiss, Jena. The gradient of potential was of 11 V/cm.

DISCUSSION AND RESULTS

1. THE DETERMINATION OF THE NATURE OF COMPLEXES

The Bi^{3+} ion, stable in aqueous medium at pH $= 0$, forms with EDTA a complex characterized by $E_{1/2} = -0.25$ V (SCE). As the pH increases $E_{1/2}$ shifts towards more negative values.[8] In order to determine the nature of the forming complex species, the influence of the pH and of the ligand concentration was followed both in buffered and in unbuffered medium.

The effect of the pH variation in buffered solution is manifested in a linear increase of the $E_{1/2}$ in the $1-5$ pH range.

The effect of the modification of the ligand concentration, illustrated in fig. 1, indicates the existence of an equilibrium between two complexes.

The curves obtained by means of the cyclic voltammetry (fig. 2) confirmed the irreversibility of the process and show the same shifting of E_p as $E_{1/2}$, function of the pH and of the ligand concentration. However, at a pH $= 1.61$ there are obtained concomitantly two peaks characterized by $E_{p1} = -0.25$ V (SCE) and $E_{p2} = -0.43$ V (SCE) thus confirming the existence of an equilibrium between two complexes.

---

[9] T. R. Bhat and R. K. Iyer, *Z. anorg. Chem.*, **335**, 331 (1965).

[10] B. G. Sochevanov and G. A. Volkova, *Zhur. neorg. Khim.*, **1**, 118 (1969).

[11] C. Drăgulescu, I. Julean and A. Nimară, *Rev. Roumaine Chim.*, **14**, 189 (1969).

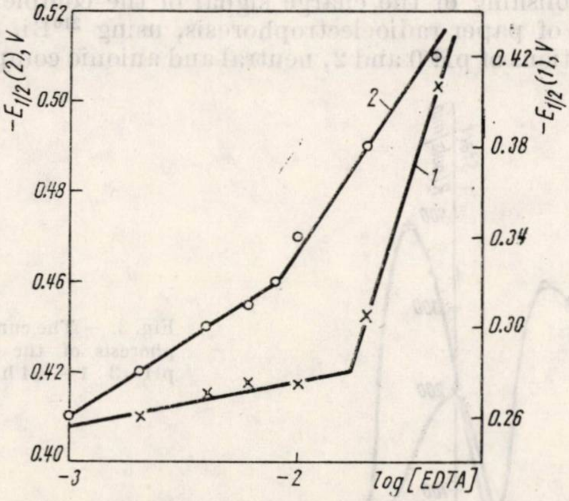

Fig. 1. — The influence of the EDTA concentration on $E_{1/2}$ in a $1 \cdot 10^{-3}$ M $BiOClO_4$ solution : 1 — pH = 1 ; 2 — pH = 3.

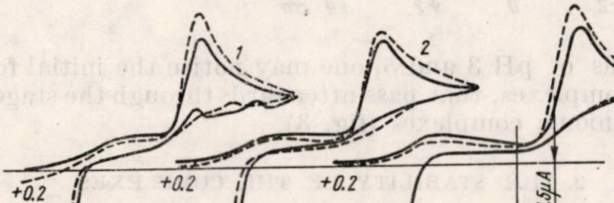

Fig. 2. — The curves of the cyclic voltammetry at different pH values : $1 \cdot 10^{-3}$ M $BiOClO_4$ $1 \cdot 10^{-2}$ M EDTA ; 1 M $NaClO_4$ *1* — pH = 0 ; *2* — pH = 1 ; *3* — pH = 2 ; *4* — pH = 1.61.

The establishing of the charge signal of the complexes was carried out by means of paper-radioelectrophoresis, using ^{210}Bi, at different pH values. In solutions of pH 0 and 2, neutral and anionic complexes are forming. In solutions of pH 3 and 5, one may notice the initial formation of some cationic complexes, that pass afterwards through the stage of neutral complexes in anionic complexes (fig. 3).

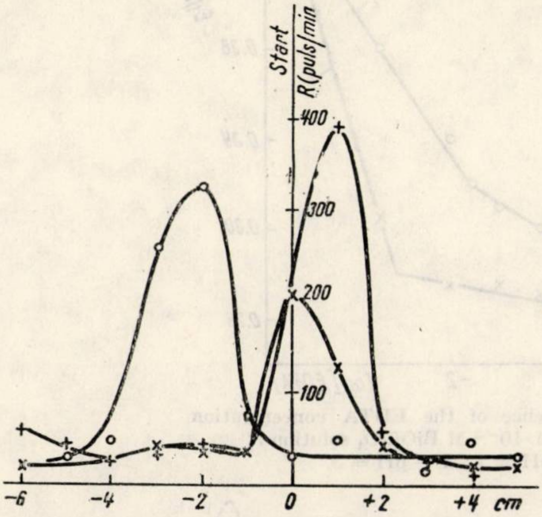

Fig. 3. — The curves of radioelectrophoresis of the Bi-EDTA complex, pH=3 : 1 —3/4 h ; 2—1 h ; 3 — 1.5 h.

2. THE STABILITY OF THE COMPLEXES

In the case of chelation agents with a great number of donor atoms, along with the normal chelates there may form also mixed or base chelates. [9] By the determination of the stability constants one must also take into account the side reactions that may appear both due to ligand protonation and to the hydrolysis reactions which the metal ion undergoes. [12]

The stability constants were evaluated by the graphical methods suggested by Tamamushi and Tanaka, [13] applicable in the case of irreversible reduction of the complexes.

$$\Delta E_{1/2} = (E_{1/2})_s - (E_{1/2})_c = \frac{2\cdot 3\,RT}{\alpha nF}\log K_n + \frac{2.3\,RT}{\alpha nF}\,n\log L$$

The value of the stability constants was obtained from the intercept and the number of the ligands, from the slope of a plot of $\Delta E_{1/2}/2.3\,RT/\alpha nF$ against log ligand concentration.

Such determinations were made at different pH values, and one of these is illustrated in fig. 4.

---

[12] A. Ringbom and L. Harju, *Analyt. Chim. Acta*, 59, 33 (1972).

[13] Tamamushi and Tanaka, "Proceedings of the 1st Intern. Polarography Congress" vol. I., Prague 1951.

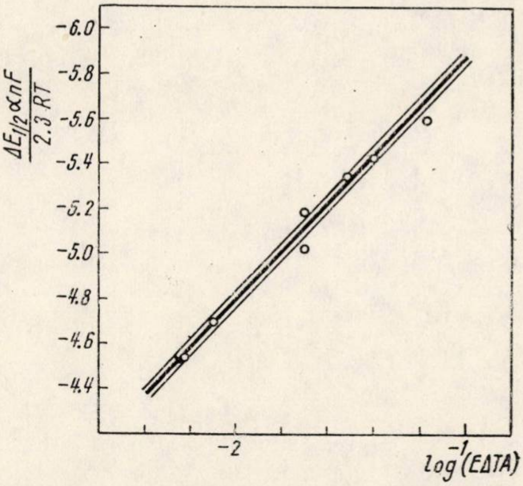

Fig. 4. — The calculation of the stability constants for the Bi-EDTA system, in a buffered solution of pH=2.

The conditional constants, calculated for different pH values, are listed in table 1.

Table 1

The value of the conditional stability constants function of pH

pH	$Bi(OH)_2^+$/EDTA	log K_{cond}
0	1 : 1	32.197
1	1 : 1	26.50
2	1 : 1	18.57
3	1 : 0.5	16.81
3	1 : 1	17.74

3. CONSIDERATION ON THE REACTION MECHANISM

In acid medium (pH 0 and 1), the neutral complexes of the type BiHY are forming.

At pH 2 and 3, the species $Bi_6(OH)_{12}^{6+}$, which is presented in the solution, is depolymerized in the presence of EDTA into the monomer species $Bi(OH)_2^+$. In the first moment probably, this reacts with the EDTA. The electrophoretic determinations evidenced the possibility of some other sphere complexes formation with the ratio of 1 $Bi(OH)_2^+$/1 H_3Y^-, respectively 2 Bi $(OH)_2^+$/1 H_2Y^{2-} which transforms in time into the inner sphere complexes with a ratio 1 : 1.

The formation of such outer sphere complexes was also ascertained in the case of Co(III) and Cr(III).[14] The formation rate of these complexes being slow enough, [15] it is possible to evidence these phases, either electrophoretically, electrochemically or by means of the isotopic exchange.

---

[14] L. Ilcheva and M. T. Beck, "Proceedings of the 3rd Symposium on Coordination Chemistry", Akadémiai Kiadó, Budapest, 1970, p. 89.

[15] S. S. Jones and F. A. Long, *J. Phys. Chem.*, **56**, 25 (1952).

Revue Roumaine de Chimie, **21**, *6*, 859–867 (1976)

HEXACHLOROCYCLOTRIPHOSPHAZENE DERIVATIVES

CONSTANȚA GHEORGHIU, M. CHIRCA, ELENA CRISTUREAN
and FLORICA DINULESCU
Department of Inorganic Chemistry, Polytechnic Institute of Bucharest, Spl. Independenței 89,
Bucharest, Romania

Received October 24, 1974

This paper reports the synthesis of hexachlorocyclotriphosphazene derivatives with *o*-tolyl-biguanide of the type $N_3P_3Cl_{6-n}(\text{tol-big})_n$, where $n = 1-4$. The influence of reaction parameters up on the substitution degree has been investigated. The new compounds have been characterized by chemical analyses, melting points and IR spectra ; some estimations have been made on the relationship between structure and properties. From the data collected, we assume that the geminal substituted isomers have been obtained.

The substitution reactions of chlorocyclophosphazene with amines provide an interesting field of research. The use of primary or secondary, aliphatic or aromatic amines has resulted in a large number of aminosubstituted derivatives. [1,2] The variety of products obtained is due both to different substitution degrees of chlorine and to the possibility to obtain, for the same substitution degree, positional and geometrical isomers ; some of these may exhibit optical antipodes, depending upon the arrangement of exocyclic groups at phosphorus atoms.

In addition to the mentioned structural aspects, aminosubstituted products of chlorocyclophosphazenes were reported to have several practical uses, such as : non-flammable and thermostable polymers, flame proofing agents, fertilizers, substances with anti-tumour effect [3-8].

Our investigation have focused on substitution products of hexachlorocyclotriphosphazene with biguanide derivatives of the type shown bellow. Owing to the possibility of binding biguanide derivatives by either primary or secondary aminic nitrogen or by the iminic nitrogen, and also owing to the possibility of obtaining spirocyclic derivatives by binding N^1 and N^5 atoms, these products may present interesting problems relating

---

[1] H. R. Allcock, *Chem. Rev.*, **72**, 315 (1972).

[2] D. B. Sowerby, *"M.T.P. – Int. Rev. Sci. Inorg. Chem"*, 2nd vol., ser. One, Ed. Addison, London, 1972, p. 117.

[3] P. H. Vallette, U.S.A. Pat. 2782133, 1957, *Chem. Abstr.*, **51**, 9 177 (1957).

[4] H. R. Allcock and R. L. Kugel, U.S.A. Pat. 3 364 189, 1968 ; *Chem. Abstr.*, **68**, 50558 (1968).

[5] B. Murray, U.S.A. Pat. 3412045, 1968 ; *Chem. Abstr* ; **70**, 29 723 (1969).

[6] S. Claude and B. Mourrut, Fr. Pat. 1 572 151, 1969 ; *Chem. Abstr.* ; **72**, 112702 (1970).

[7] W. Wanek, *Allg. prakt. Chem.*, **21**, 74 (1970).

[8] V. A. Chernov, V. B. Lytkina, S. I. Sergievskaya, A. A. Kropacheva, V. A. Pershin and L. E. Sventsitskaya, *Farmakol. i Toksikol*, **22**, 365 (1959) ; *Chem. Abstr.*, **54**, 7 900 (1960).

to structure and isomerism. Considering the antitumour properties of other aminophosphazene derivatives, and also the wide use of biguanide derivatives in pharmaceutical industry, hopefully some biguanide-substituted chlorocyclophosphazene may present therapeutical interest.

The present paper deals with the synthesis of substitution derivatives of hexachlorocyclotriphosphazene with *o*-tolyl-biguanide, leading to compounds $N_3P_3Cl_{6-n}(\text{tol-big})_n$, where $n=1-4$, which have been characterized by elemental chemical analysis, melting points and IR spectra.

EXPERIMENTAL

STARTING MATERIALS

Hexachlorocyclotriphosphazene, $N_3P_3Cl_6$. The product used was prepared in our laboratory by known procedures. The purity was checked by elemental analysis, melting point (114°) and IR spectrum.

o-Tolyl-biguanide, (tol-big), $C_9N_5H_{13}$, Dr. Theodor Schuchardt product, m.p. 141°.
Tetrahydrofuran, (THF), E. Merck A. G. Darmstadt product, b.p. 65.8°.
Triethylamine, (Et_3N), Carlo Erba product, b. p. 88–90°.
Anhydrous ethyl ether, (anh. Et_2O), E. Merck A. G. Darmstadt product, b.p. 34.6°.

SYNTHESIS METHODS

Preparation of hexachlorocyclotriphosphazene, $N_3P_3Cl_6$. It was obtained by ammonolysis of phosphorus pentachloride with ammonium chloride concomitently with PCl_5 formation in the reaction medium from PCl_3 and Cl_2, bubbled at the boiling temperature of the solvent (symmetrical tetrachlorethane, s-TCE, or chlorobenzene, PhCl). $POCl_3$ was used as a catalyst in a $POCl_3 : PCl_3 = 1 : 10$ molar ratio. The hydrochloric acid released from the reaction was used to produce NH_4Cl in an adjoining equipment by bubbling it together with gaseous ammonia through the inert solvent (s-TCE or PhCl) at 25°. The specific surface of the resulted NH_4Cl was higher than $1.2 \cdot 10^4$ cm^2/g. Hexachlorocyclotriphosphazene was separated by fractional crystallization from petroleum ether, vacuum fractional distillation and recrystallization from ethyl ether. Yields obtained in $N_3P_3Cl_6$ were 58% in s-TCE (reaction time 3 hr) and 50% in PhCl (reaction time 6hr) comparable to those mentioned in the literature [9–11].

Preparation of $N_3P_3Cl_5$(tol-big). The reaction was conducted at room temperature in a three-necked flask fitted with thermometer, dropping funnel and $CaCl_2$ tube, using magnetic stirring. To a solution of 1.16 g (3.3 mmoles) $N_3P_3Cl_6$ in 2 ml THF a solution of 0.64 g (3.3 mmoles) tol-big and 1 ml Et_3N in 8 ml THF was added during 0.5 hr. The reaction was carried out for 11 hr, at 25°. The precipitate formed was filtered and washed with cold THF. The filtrate was treated with anh. Et_2O, to give a white precipitate. This product was repeatedly washed by decantation with anh. Et_2O and then filtered dried and analysed.

Preparation of $N_3P_3Cl_4$ (tol-big)$_2$. The reaction was conducted in a three-necked flask fitted with thermometer, dropping funnel, reflux condenser, with magnetic stirring and heating on electric plate. A solution of 8.02 g (40 mmoles) tol-big and 6 ml Et_3N in 50 ml THF was added under reflux to a solution of 3.48 g (10 mmoles) $N_3P_3Cl_6$ in 20 ml THF. The reaction was carried out for another 4 hr. After cooling, the solution was filtered and the precipitate was washed. By adding anh. Et_2O to the filtrate, a white, crystalline product was separated, and identified as disubstituted product.

Preparation of $N_3P_3Cl_3$ (tol-big)$_3$. The reaction was achieved, by gradually adding to a solution of 3.48 g (10 mmoles) $N_3P_3Cl_6$, a solution of 16.04 g (80 mmoles) tol-big and 8.3 ml Et_3N in 90 ml THE. The total reaction time was 3.5 hr. at the solvent reflux temperature (65.5°). The white precipitate formed is a mixture of triethylamine hidrochloride and trisubstituted derivative, which was separated dissolving the hydrochloride in water.

---

[9] HOOKER Chemical Corp., Belg. Pat. 621 384, 1962; *Chem. Abstr.*, **58**, 12702 (1963).

[10] J. EMSLEY and P. B. UDY, *J. Chem. Soc. A.* **1971**, 786.

[11] D. T. JASKA and T. H. DEXTER, Fr. Pat. 1 382 954, 1964; *Chem. Abstr.*, **63**, 11 797 (1965).

Preparation of $N_3P_3Cl_2(tol\text{-}big)_4$. The reaction between 0.58 g (1.7 mmoles) $N_3P_3Cl_6$ and 2.67 g (14 mmoles) tol-big with 1.5 ml Et_3N in 30 ml THF was conducted in a similar fashion for 3.5 hr. at 65.5°, being then continued at room temperature for another 5 days without stirring. After filtering the white precipitate formed and treating the filtrate with anh. Et_2O the tetrasubstituted compound was obtained.

Melting points were determined on a Boetius apparatus and are listed in Table 1.

Methods of analysis. Phosphorus was determined after decomposition of the substance with HNO_3, by the gravimetric or volumetric method, using ammonium molybdate. Nitrogen was determined by Pregl microcombustion method. Carbon was determined by combustion in oxygen current. The results of elemental analysis are presented in Table 1.

IR spectra were recorded on a UR–10 Carl Zeiss–Jena spectrophotometer in the 400–1700 cm^{-1} range, in KBr pellets.

Table 1

Analytical data

Compound	m.p. °C	%P		%N		%C	
		found	calc.	found	calc.	found	calc.
$N_3P_3Cl_5(C_9N_5H_{12})$	262–4	18.26	18.51	21.82	22.28	21.13	21.49
$N_3P_3Cl_4(C_9N_5H_{12})_2$	275–7	14.05	14.15	28.11	27.70	32.08	32.86
$N_3P_3Cl_3(C_9N_5H_{12})_3$	294–6	11.63	11.46	30.70	31.05	39.35	39.92
$N_3P_3Cl_2(C_9N_5H_{12})_4$	182–4	9.45	9.63	33.60	33.33	44.08	44.72

DISCUSSION OF RESULTS

Substitution derivatives were obtained by the reaction between hexachlorocyclotriphosphazene and *o*-tolyl-biguanide in tetrahydrofuran in the presence of triethylamine:

$$N_3P_3Cl_6 + nR-NH_2 + n(C_2H_5)_3N \xrightarrow{THF} N_3P_3Cl_{6-n}(HN-R)_n + n(C_2H_5)_3N\cdot HCl$$

$$\text{where } n = 1-4$$

As shown in the experimental section, attention was focused on the factors which may influence the substitution degree: concentration and the initial molar ratio of reactants, temperature and the reaction time (Table 2).

Except for the monosubstituted derivative, the other derivatives were obtained in the presence of an excess of tolyl-biguanide, the initial molar ratio being undeterminative for the substitution degree. Even for the same initial molar ratio (8 : 1), the products obtained had different substitution degree, depending on the reaction time. The fact that penta- and hexasubstituted derivatives have not been obtained may be due ei-

Table 2

Reaction conditions for the preparation of compounds $N_3P_3Cl_{6-n}$ (tol-big)$_n$, n = 1−4

Compound	Molar ratio $N_3P_3Cl_6$: tol-big	Concentration (g $N_3P_3Cl_6$ at 100 ml THF)	Temperature (°C)	Reaction time (hr)	Yield (%)
$N_3P_3Cl_5$(tol-big)	1 : 1	12	25	11	32
$N_3P_3Cl_4$(tol-big)$_2$	4 : 1	5	65.5	4.5	46
$N_3P_3Cl_3$(tol-big)$_3$	8 : 1	3.5	65.5	3.5	26
$N_3P_3Cl_2$(tol-big)$_4$	8 : 1	2	65.5 25	3.5+ +5 days	30

ther to steric hindrances induced by very bulky substitutens or to the reaction conditions. The substitution degree is also influenced by concentration of $N_3P_3Cl_6$ in the reaction medium, meaning that dilution favours the formation of higher substituted derivatives.

The substituted derivatives of type $N_3P_3Cl_{6-n}$(tol-big)$_n$ are crystalline, white ($n = 1-3$) or light-brown ($n = 4$), air stable substances.

Except for the disubstituted product, which is water-soluble on heating, these derivatives are insoluble in water and in most organic solvents. They are only soluble in tetrahydrofuran and dimethylformamide.

All derivatives exhibit high melting points (Table 1) compared to $N_3P_3Cl_6$ (m. p. 114°) and to *o*-tolyl-biguanide (m. p. 141°). In view of the regular increase of the melting point from 262−4° to 294−6°, parallel with the increase of the substitution degree from $n = 1$ to $n = 3$, the tetrasubstituted compound presents an abnormally low melting point (182−4°).

The characterization of products obtained was made by IR spectra in the 400−1700 cm^{-1} range; the spectra were compared to those of hexachlorocyclotriphosphazene and of *o*-tolyl-biguanide (fig. 1).

The IR spectrum of $N_3P_3Cl_6$ prepared by us (fig. 1a) is identical to that reported in the literature. [12–18] The assignment of vibration frequencies corresponds to the D_{3h} symmetry species of the hexachlorocyclotriphosphazene molecule. In analyzing the spectrum we may refer to two regions: beyond 700 cm^{-1} where ring vibration frequencies occur, 600 cm^{-1}, where P—Cl vibration frequencies occur.

For all compounds $N_3P_3Cl_{6-n}$(tol-big)$_n$, $n = 1-4$, IR spectra (fig. 1c—f) are characterized by the occurrence of bands specific of N_3P_3 ring, indicating its maintenance subsequent to the reaction and also of tolyl-biguanide bands, with shifts which we shall further analyse.

[12] L. W. Daasch, *J. Amer. Chem. Soc.*, **76**, 3403 (1954).
[13] S. Califano, *J. Inorg. Nuclear Chem.*, **24**, 483 (1962).
[14] I. C. Hisatsune, *Spectrochim. Acta*, **21**, 1899 (1965).
[15] A. C. Chapman and N. L. Paddok, *J. Chem. Soc.*, **1962**, 635.
[16] E. Steger and R. Stahlberg, *Z. Naturforsch.*, **17b**, 780 (1962).
[17] E. Steger and R. Stahlberg, *Z. anorg. Chem.*, **326**, 243 (1964).
[18] R. Stahlberg and E. Steger, *Spectrochim. Acta*, **23A**, 627 (1967).

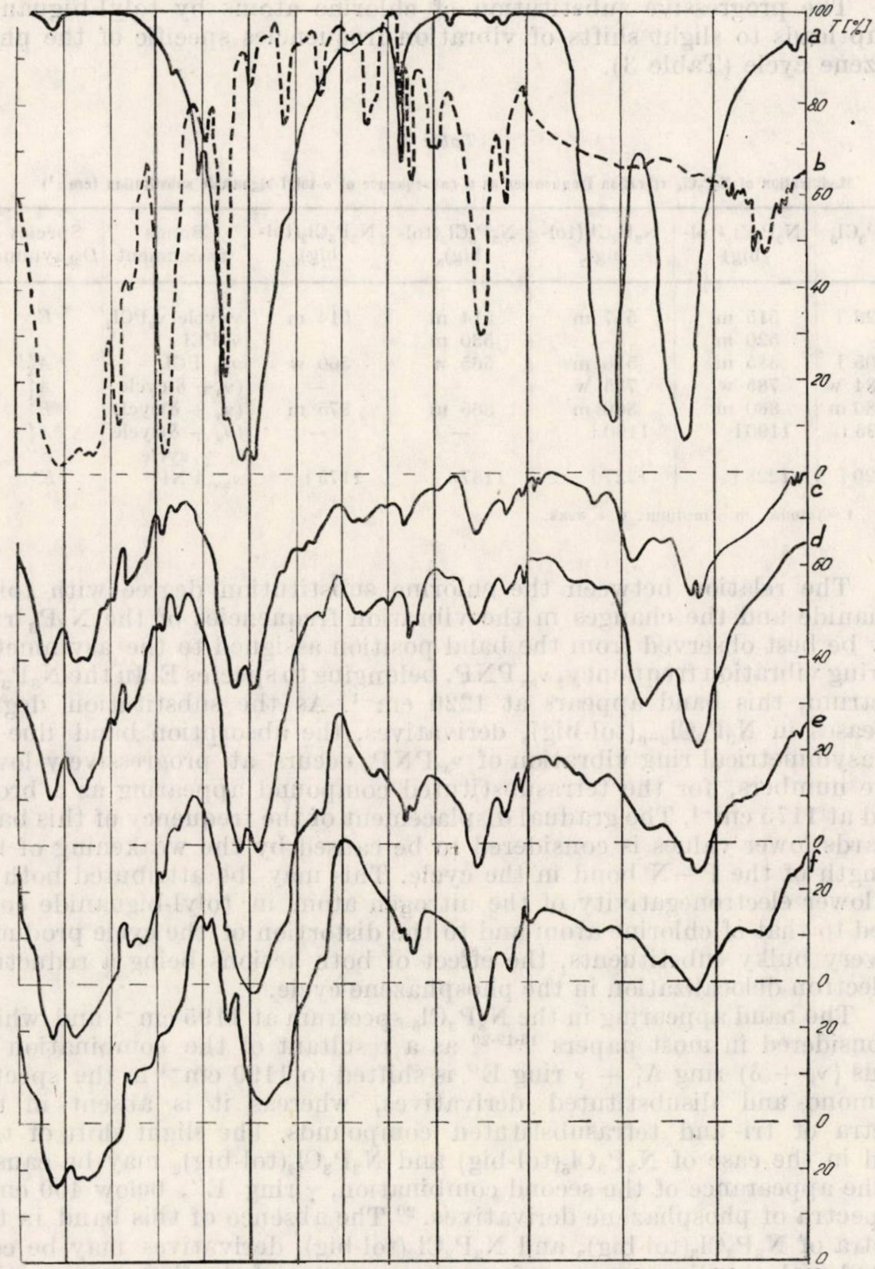

Fig. 1. — IR spectra of *a*) $N_3P_3Cl_6$; *b*) *o*-tolyl-biguanide ; *c*) $N_3P_3Cl_5$(tol-big) ; *d*) $N_3P_3Cl_4$(tol-big)$_2$; *e*) $N_3P_3Cl_3$ (tol-big)$_3$; *f*) $N_3P_3Cl_2$(tol-big)$_4$.

The progressive substitution of chlorine atoms by tolyl-biguanide group leads to slight shifts of vibration frequencies specific of the phosphazene cycle (Table 3).

Table 3

Modification of $N_3P_3Cl_6$ vibration frequencies as a consequence of *o*-tolyl-biguanide substitution (cm^{-1})

$N_3P_3Cl_6$	$N_3P_3Cl_5$(tol-big)	$N_3P_3Cl_4$(tol-big)$_2$	$N_3P_3Cl_3$(tol-big)$_3$	$N_3P_3Cl_2$(tol-big)$_4$	Bands assignment	Species of D_{3h} symmetry
528 i	515 m	517 m	514 m	514 m	γcycle, $\nu_s PCl_2$	E'
—	520 m	—	530 m	—	ν PCl	
605 i	585 m	576 m	565 w	560 w	ν_{as} PCl_2	A_2''
784 w	785 w	785 w	—	—	$(\nu_s + \delta)$cycle	A_1'
880 m	860 m	860 m	865 m	875 m	$(\nu_s + \delta)$cycle	E'
1195 i	1190 i	1190 i	—	—	$(\nu_s + \delta)$cycle $+ \gamma$ cycle	A_1' E''
1220 i	1228 i	1227 i	1187 i	1175 i	ν_{as} PNP	E'

i = intense; m = medium; w = weak.

The relation between the chlorine substitution degree with tolyl-biguanide and the changes in the vibration frequencies of the N_3P_3 ring may be best observed from the band position assigned to the asymmetrical ring vibration frequency, ν_{as} PNP, belonging to species E. In the $N_3P_3Cl_6$ spectrum, this band appears at 1220 cm^{-1}. As the substitution degree increases in $N_3P_3Cl_{6-n}$(tol-big)$_n$ derivatives, the absorption band due to the asymmetrical ring vibration of ν_{as}PNP, occurs at progressively lower wave numbers, for the tetrasubstituted compound appearing as a broad band at 1175 cm^{-1}. The gradual displacement of the frequency of this band towards lower values is considered to be caused by the weakening of the strength of the P—N bond in the cycle. This may be attributed both to the lower electronegativity of the nitrogen atom in tolyl-biguanide compared to that of chlorine atom and to the distortion of the cycle produced by very bulky substituents, the effect of both actions being a reduction of electron delocalization in the phosphazene cycle.

The band appearing in the $N_3P_3Cl_6$ spectrum at 1195 cm^{-1} and which is considered in most papers [15,19,20] as a resultant of the combination of bands $(\nu_s + \delta)$ ring $A_1' + \gamma$ ring E'' is shifted to 1190 cm^{-1} in the spectra of mono- and disubstituted derivatives, whereas it is absent in the spectra of tri- and tetrasubstituted compounds. The slight shift of this band in the case of $N_3P_3Cl_5$(tol-big) and $N_3P_3Cl_4$(tol-big)$_2$ may be caused by the appearance of the second combination, γ ring E'', below 400 cm^{-1} in spectra of phosphazene derivatives. [20] The absence of this band in the spectra of $N_3P_3Cl_3$(tol-big)$_3$ and $N_3P_3Cl_2$(tol-big)$_4$ derivatives may be correlated with the disappearance from these spectra of the first combination component appearing as a weak band at 785 cm^{-1} only in spectra of $N_3P_3Cl_5$ (tol-big) and $N_3P_3Cl_4$(tol-big)$_2$ derivatives.

---

[19] R. Stahlberg and E. Steger, *Spectrochim. Acta*, **23A**, 2057 (1967).

[20] J. Emsley, *J. Chem. Soc. A.*, **1970**, 109.

Since vibration bands of the N_3P_3 ring at 784 and 880 cm^{-1} appear with a weak intensity in the $N_3P_3Cl_6$ spectrum and overlap with some bands of tolyl-biguanide in the spectra of derivatives, no estimation can be made with regard to the influence of the substitution on these bands.

The increase in the number of tolyl-biguanide groups from $n = 1$ to $n = 4$ in $N_3P_3Cl_{6-n}(\text{tol-big})_n$ derivatives may be also observed in the 700 – 1700 cm^{-1} range by the decrease in the intensity of bands due to vibrations of the phosphazene ring, concomitently with an intensity increase of bands specific of tolyl-biguanide.

Thus, the band found at 750 cm^{-1}, assigned to out-of-plane deformation of the benzene ring in the tolyl group, γ CH, occurs in the spectra of $N_3P_3Cl_{6-n}(\text{tol-big})_n$ compounds at 757–755 cm^{-1} as a band whose intensity increases progressively for $n = 1-4$.

The band occurring in the spectrum of the free tolyl-biguanide at 1255 cm^{-1} is assigned to the stretching vibration C—N, ν CN. In the spectra of mono- and disubstituted derivatives it is covered by the broad band attributed to ν_{as} PNP, whereas in tri- and tetrasubstituted derivatives it appears partially resolved. The partial resolution of the band may be estimated as being an effect of its intensity growth together with the increase in the number of tolyl-biguanide groups and also of the displacement of the phosphazene ring band towards lower frequencies, parallel with the increase in the substituents number.

The bands appearing in the tolyl-biguanide spectrum, grouped in the 1530 – 1620 cm^{-1} interval and assigned to vibration frequencies of the $>C=NH$ group and of the C—C bond vibration in the *ortho*-tolyl ring, ν C—C, also show a gradual increase in intensity in the spectra of derivatives. By comparing the bands in the 1200 cm^{-1} region, specific of the phosphazene ring, to those found in the 1530–1620 cm^{-1} region, specific of tolyl-biguanide, it can be seen that the intensity ratio increases in favour of tolyl-biguanide bands, as the substitution degree increases.

The spectral field situated below 600 cm^{-1} may be better studied due to the absence of sharp bands in this region in the tolyl-biguanide spectrum. In the $N_3P_3Cl_6$ spectrum there are two intense bands in this domain at 528 and 605 cm^{-1}. Mention is made on the fact that some conflicting opinions have been found in the literature with regard to the origin of the band at 528 cm^{-1}, attributing it either to a symmetrical elongation frequency of the PCl_2 group, ν_s PCl_2,[15–17] or to a deformation vibration of the phosphazene ring, γ ring [12–14]. The fact that a band still appears around the value of 520 cm^{-1} in the IR spectrum of $N_3P_3(NCS)_6$ compound[24] or in the spectra of some substitution compounds of $N_3P_3Cl_6$ which fail to contain the PCl_2 group[19–22] shows that we must consider besides the symmetrical stretching vibration, ν_s PCl_2, also the deformation vibration of the phosphazene ring, γ ring, in order to explain the origin of this band. The band appearing at 605 cm^{-1} is assigned to the asymmetrical elongation frequency of the PCl_2 group, ν_{as} PCl_2.

---

[21] R. STAHLBERG and E. STEGER, *Spectrochim. Acta*, **23A**, 2185 (1967).

[22] R. STAHLBERG and E. STEGER, *Spectrochim. Acta*, **23A**, 2005 (1967).

In the spectra of $N_3P_3Cl_{6-n}$(tol-big)$_n$ derivatives, these two bands appear at values comprised between 515 cm^{-1} ($n = 1$) and 517 cm^{-1} ($n = 4$), respectively between 585 cm^{-1} ($n = 1$) and 560 cm^{-1} ($n = 4$). The continuous decrease in the wave number and in the intensity of the second band ($\nu_{as}PCl_2$) must be mentioned. The difference between the intensities of the two bands may be explained by the appearance at 515 cm^{-1} of the stretching frequencies characteristic of the phosphazene ring, which causes an increased intensity of this band. At the same time, the marked decrease in the intensity of the two bands for compounds $N_3P_3Cl_3$(tol-big)$_3$ and $N_3P_3Cl_2$(tol-big)$_4$ is due to one single PCl_2 group relative to two PCl_2 groups in mono- and disubstituted derivatives, which produce stronger absorptions.

The appearance of PCl_2 group bands in the spectra of tri- and tetrasubstituted derivatives is a proof in favour of a geminal substitution model for $N_3P_3Cl_3$(tol-big)$_3$ and $N_3P_3Cl_2$(tol-big)$_4$.

The appearance of a new band at 520 and 530 cm^{-1}, respectively only in the spectra of mono- and trisubstituted derivatives is a proof in favour of the same geminal substitution model. The characteristic band ν_sPCl_2 is maintained at the same wavelength (515, 514 cm^{-1}) like in di- and tetrasubstituted derivatives (517 cm^{-1}). The new band appearing at aprox. 525 cm^{-1} may be assigned to the valency vibration P—Cl, ν PCl, in agreement with the values at which this vibration appears in the spectra of other derivatives.[19,22,23] The absence of this band in the spectra of di- and tetrasubstituted derivatives confirms the geminal structure proposed for the obtained compounds :

(b) $N_3P_3Cl_5$(tol-big)
m.p. 262—4°

(c) *gem*-$N_3P_3Cl_4$(tol-big)$_2$
m.p. 275—7°

(d) *gem*-$N_3P_3Cl_3$(tol-big)$_3$
m.p. 294—6°

(e) *gem*-$N_3P_3Cl_2$(tol-big)$_4$
m.p. 182—4°

Similarly, because we have obtained unitary pure products, as revealed by the determination of melting points, we presume that they are geminal position isomers, owing to the fact that a mixture of *cis-trans* isomers will be more likely obtained in the non-geminal substitution.

To establish the nitrogen atom by which tolyl-biguanide is bound to the phosphazene cycle is a complex problem, taking into account the resonance and tautomeric possibilities presented by the molecule of the biguanide derivative.

Based on steric-type considerations, the N^5 atom may be estimated to have a favourable position for the formation of a new bond. The electronic factors, related to the high basicity of the nitrogen atom in the same position as compared to the remaining nitrogen atoms in the molecule of the substituent, act in the same sense.

---

[23] L. C. Thomas and R. A. Chittenclen, *Chem. and Ind.*, **1961**, 1913.

The absence of the band appearing in the spectrum of the free tolyl-biguanide at 800 cm^{-1} from IR spectra of all derivatives $N_3P_3Cl_{6-n}$(tol-big)$_n$ and which is attributed to the vibration frequency of the $>CH-NH_2$ group, shows that this group is severly affected by substitution, supporting the above statment.

The intense band at 1380 cm^{-1} in the spectrum of free tolyl-biguanide may be attributed to the $-NH_3^+$ group which appears in one of the tautomeric forms of tolyl-biguanide at N^5 atom. The pronounced decrease in the intensity of this band in the spectra of compounds $N_3P_3Cl_{6-n}$(tol-big)$_n$, $n = 1 - 4$, constitutes a proof of tolyl-biguanide binding by the nitrogen atom in position 5.

Despite the estimations made, it must be stressed that the high degree of complexity of these spectra fails however to allow the establishment of precise relationships between the modifications of spectra and the structure of the compounds formed.

In addition to the structural aspects revealed by the compounds obtained, the tests made so far have provided favourable answers to the therapeutical properties of partially substituted derivatives of hexachlorocyclotriphosphazene with *o*-tolyl-biguanide, a problem which will be also investigated in the case of other derivatives.

We shall further study problems related to the stereoisomerism of substitution products of hexachlorocyclotriphosphazene with biguanide derivatives.

Revue Roumaine de Chimie, **21**, *6*, 869–877 (1976)

CONTRIBUTIONS TO THE COORDINATION CHEMISTRY OF PHTHALIC ACID DERIVATIVES. II[1]

NEW COPPER COMPOUNDS OF PHTHALIMIDE DERIVATIVES*

FLORICA POPEA, ZAMFIRA TOMA and CRISTINETA MĂRCULESCU
Center of Physical Chemistry, Str. Dumbrava Roșie 23, Bucharest

Received October 28, 1974

In the condensation of phthalic anhydride (anh) with *m*-phenylenediamine (mfa) in the presence of copper ion, compounds of general formula $CuL(CH_3COO)_2$ ($L = L_1, L_2, L_3$)[1] were obtained. In the 1 : 1 : 1 reactant ratio a mixed salt of copper (II) with phthalamic and acetic acids was evidenced. Further, this intermediate led to Cu(mfa) $(CH_3COO)_2$ and Cu(mfa) (anh). The physical and chemical behaviour of all the new compounds is also described.

In a previous work, [1] the condensation of phthalic anhydride with *m*-phenylenediamine and the ability of the resulted compounds (L_1, L_2, L_3) to coordinate with copper acetate, were presented.

In this work, the condensation of phthalic anhydride with *m*-phenylenediamine (copper ion present) as well as the physical and chemical behaviour of the new compounds are reported.

The metal ions may be regarded to have the role of directing the course of the reaction, leading to some complex compounds of the respective metals (template effect).

It is also possible to observe the formation of some intermediate products in the process of condensation, leading to the elucidation of the reaction mechanism.

EXPERIMENTAL

Starting materials. The compounds were prepared using phthalic anhydride purified by crystallization from ethanol and *m*-phenylenediamine by crystallization from benzene solution.

Analyses. C, H, N were determined by microcombustion and Cu by G. Spacu analytical micromethod. [2]

---

* Presented at the IVth Conference in General and Applied Physical Chemistry, Bucharest — September 1974.

[1] F. Popea, C. Mărculescu and Z. Toma, *Rev. Roumaine Chim.*, **20**, 000 (1975).

[2] C. Gh. Macarovici, "Chimie Analitică Cantitativă", Ed. tehnică, Bucharest, 1959.

Measurements. The melting points were determined with a Boetius heating plate and were not corrected.

The X-ray diffraction data were obtained by the Debye-Scherrer powder technique using the X-ray source TURM—60 (GDR), the $CuK_{\alpha}(\lambda = 1.5418$ Å) radiation filtered on nickel (at 30 kV and 18 mA) and a 75.3 mm diameter camera.

The thermogravimetric analysis was performed using a Stanton HT—D type balance, for 10 mg samples with a 6° per minute rate of heating up to 800—900°.

The derivatograms were obtained by means of a MOME Budapest Paulik-Paulik-Erdey derivatograph, in inert atmosphere with Al_2O_3 as standard. The samples were heated in chamotte crucible up to 1200°.

The molar conductivity was measured using a OK—102/1 Model conductivity bridge, in DMF, in a cell with the 0.52 value of the constant.

The magnetic susceptibility was measured by the Faraday method. Diamagnetic corrections for ligands and ions were calculated from Pascal's constants.

The electronic spectra were drawn on a VSU—1C. Zeiss Jena spectrophotometer, using the standard reflectance attachment and magnesium oxide as reference, in the 260—1200 nm range.

The IR spectra were recorded as KBr pellets, by means of UR—10 C. Zeiss Jena spectrophotometer, in the 400—3500 cm^{-1} range.

PREPARATION OF THE COMPOUND $CuL_1(CH_3COO)_2$ (I)

To a solution of *m*-phenylenediamine in chloroform, heated to boiling, phthalic anhydride dissolved in a chloroform and ethanol mixture (5 : 1) is gradually added and finally treated dropwise with copper acetate solution in ethanol. The reaction mixture (phthalic anhydride/*m*-phenylene diamine/copper acetate in the ratio 2 : 1 : 1) is refluxed for 9 hours. An olive-green precipitate appears, grows abundant and ultimately agglomerates. After separating, the product purified by repeated boiling in chloroform, then in ethanol, finally filtered and dried *in vacuo* over P_4O_{10}.$CuL_1(CH_3COO)_2$.1/2$CHCl_3$: *Found*: C, 46.32, Cu, 13.25; N, 5.84%; $C_{18.5}H_{16.5}O_6N_2CuCl_{1.5}$.

Requires: C, 46.53; Cu, 13.32; N. 6.05%

PREPARATION OF THE COMPOUND $CuL_2(CH_3COO)_2$ (II)

To the refluxing solution of *m*-phenylenediamine in chloroform, a phthalic anhydride solution in a chloroform and ethanol mixture (5 : 1) and afterwards a copper acetate solution in ethanol, are dropwise added. The resulting solution (phthalic anhydride/ *m*-phenylenediamine/copper acetate in the ratio 4 :1 :1) is kept for 6 hours under reflux and the black (green upon grinding) granular precipitate is filtered. From the intense green mother liquor, an appreciable quantity of the same product is precipitated with diethylether, purified repeatedly with warm chloroform and ethanol, filtered and dried over P_4O_{10}. *Found*: C, 55.29; N, 5.10; Cu11.52. $C_{26}H_{18}O_8N_2Cu$. Requires: C, 55.49; N, 4.98; Cu, 11.30%

PREPARATION OF THE COMPOUND $CuL_3(CH_3COO)_2$ (III)

The solution obtained on mixing phthalic anhydride, *m*-phenylenediamine and copper acetate in $CHCl_3$ and anhydrous ethanol (ratio 2 :2 : 1), is allowed to boil under reflux for 16 hours. The resulting brown product is filtered, refluxed with ethanol and chloroform, filtered and dried *in vacuo* over P_4O_{10}. *Found*: C,54.35; N, 10.51; Cu, 12.17% $C_{24}H_{24}O_6N_4Cu$ Requires: C, 54.60; N, 10.62; Cu, 12.04%

PREPARATION OF THE COMPOUND $CuL_1(CH_3COO)$ (IV)

To the boiling solution of *m*-phenylenediamine in chloroform, a phthalic anhydride solution in chloroform-ethanol mixture (4 : 1) and afterwards a copper acetate solution in ethanol are stepwise added. The resulted solution is refluxed for 15 minutes, the green product formed filtered, refluxed several times in chloroform and then in ethanol, filtered and dried *in vacuo* over P_4O_{10}. $CuL_1(CH_3COO)$.$^1/_2CHCl_3$. *Found*: C, 51.25; N, 7.54; Cu,16.54% $C_{14.5}H_{12.5}O_2N_2CuCl_{1.5}$. Requires: C, 50.93; N, 7.42; Cu, 16.84%.

PREPARATION OF THE COMPOUNDS Cu(mfa) $(CH_3COO)_2$ (IV) and $Cu(mfa)_2(anh)$ (VI)

Keeping the same molar ratio of the reactants and the same medium of reaction like for the preparation of the $CuL_1(CH_3COO)$ compound and without isolating it from the solution, the refluxing is continued for 9 hours. Then, the precipitate formed is filtered, washed repeatedly in chloroform and ethanol. The black product separated by filtration is compound VI. $Cu(mfa)_2(anh)$. $CHCl_3$. Found : C, 48.20%, Cu, 12.38%, N, 10.38%. $C_{21}H_{17}N_4O_2CuCl_3$. Requires : C, 47.90%, Cu, 12.07%, N, 10.63%.

From the initial filtrate, a brown compound (V) separates, which is purified by the same operations like compound (VI). Cu(mfa) $(CH_3COO)_2$. *Found* : C, 41.78 ; N, 9.24 ; Cu, 21.73% $C_{10}H_{14}O_4N_2Cu$. Requires : C, 41.45 ; N, 9.60 ; Cu, 21.95%

RESULTS AND DISCUSSIONS

The experimental data reveal that in the same reaction medium a chloroform-ethanol mixture (5 : 1) for various ratios of the 3 components (phthalic anhydride, *m*-phenylenediamine and copper acetate) compounds of general formula $CuL(CH_3COO)_2$. $L = L_1, L_2, L_3$, are obtained.

The $CuL_1(CH_3COO)_2$ and $CuL_2(CH_3COO)_2$ compounds result for an excess of phthalic anhydride with respect to *m*-phenylenediamine (2 and 4 moles phthalic anhydride for 1 mole of *m*-phenylenediamine). For the 1 : 1 ratio (anhydride/amine) and only 0.5 mole metal, the $CuL_3(CH_3COO)_2$ compound is formed.

Considering L_1, L_2 and L_3 amine substituted derivatives of phthalimide or phthalamide, their compounds with metal ions could be discussed comparatively with those of the metal-phthalimides with amines, reported in the literature, of the general formula $M(ft)_2(am)_{1(2)}$.[3]

Although, as the syntheses performed in this work started from a copper salt instead of copper phthalimidate and the phthalimide as structural unit results only "in situ", the behaviour of the resulting compounds will probably be different.

All the new compounds are microcrystalline powders, intensely coloured olive-green to black, stable in air in solid state, soluble in DMF, DMSO and nitrobenzene but of very low solubility in water, diethyl ether, ethanol, chloroform. The high melting points (above 300°) can be assigned to the formation of compounds supposed to be dimeric, tetrameric or even macrocycles. These assumptions could not be confirmed by the molecular weights because of the very low solubility of the above compounds in the solvents required in these measurements.

The conductivity values of these compounds obtained in DMF (around 20 $ohm^{-1} \cdot cm^2 \cdot mol^{-1}$) suggest them to be nonelectrolytes. But as the conductivity of the $Cu(CH_3COO)_2$ in DMF solution is 15 $ohm^{-1} \cdot cm^2 \cdot mol^{-1}$, it appears that the low values concerning the compounds, I — VI may be due to the complexing ability of the solvent (DMF).

The presence as well as the number of the COOH groups supplied by the phthalamic or by the acetic acid are evidenced in the titration of the compound suspension in ethanol with a $n/200$ KOH solution in ethanol. These data provide a basis to distinguish the compounds including L_1, L_2, L_3 in imidic or carboxylic form.

---

[3] P. Shukla, M. D. Khare and L. N. Srivastava, *J. prakt. Chem.*, **28**, 21 (1965).

Thus in the $CuL(CH_3COO)_2$ compounds ($L = L_1, L_2$) two COOH groups were evidenced, both resulting by the alkaline hydrolysis of the copper acetate.

If the ratio of the reactants is 1 : 1 : 1 in the chloroform-ethanol 5 : 1 mixture, after 15 minutes reflux, a mixed salt of copper (II) with phthalamic and acetic acids, the compound IV, is formed. On further refluxing for 9 hours, in the same conditions as above, a compound of formula $Cu(mfa)(CH_3COO)_2$ (V) is obtained. In time, a slightly smaller quantity of the $Cu(mfa)_2$ (anh) (VI) is isolated from the filtrate.

As can be seen, two compounds result in this reaction, one (compound VI) includes the phthalic anhydride in the ratio 1 : 2, with respect to the diamine, the other does not include phthalic anhydride in the molecule (compound V). These data confirm once more that compounds of formula $CuL(CH_3COO)_2$ ($L = L_1$, L_2) are obtained only when using an excess of phthalic anhydride, otherwise solely the amine reacts with copper acetate, as in the case of compound V.

The stability and thermic decomposition of the compounds were also investigated. The thermal studies show that all the compounds reported in this note are stable up to 220—270°, afterwards the thermal decomposition starts. The changes appearing during the pyrolysis cannot be established, the thermic decomposition of the compounds proceeding through complicated phases, with superimposed exothermic effects in the 250—450° range, allowing to shape 4—7 maxima indicating complicated intermediate phases. However, it may be finally concluded that at 300° the system tends to become stable and the samples are at last converted to copper oxide.

The formation of the compounds is also confirmed by the X-ray diffraction spectra. At visual examination, the debyegrams are completely different for the starting components and for the resulting compounds. The diffraction effects, present as halos at small angles in the compounds, attest an amorphous and polymeric structure, like for the organic polymers.

The values obtained for the magnetic moments lie between 1.70 and 1.98 BM in the same range as for most of the copper (II) complexes. Only for the IV compound the value 1.40 BM, lower than that of the usual copper (II) compounds suggests the participation of the ligand. The magnetic moments of the Cu(II) ion have a reduced effect upon the stereochemistry of the coordination compounds of Cu(II).

In order to obtain more information about the nature of the compounds formed, in addition to that mentioned above, the electronic and IR spectra were also recorded.

The electronic and IR spectra will be discussed comparatively with those of phthalic anhydride, *m*-phenylenediamine, phthalimide and N-substituted phthalimide derivatives, as well as the spectra of the copper phthalimidate complexes with amines.

ELECTRONIC SPECTRA

The reflectance spectra of the I—VI compounds exhibit, in the UV range, a band centered around 280—290 nm (35710 — 34480 cm^{-1}), which may be assigned to the organic ligand of the molecule (table 1).

Table 1

Reflectance Spectra

Compounds	nm	cm^{-1}
I $CuL_1(CH_3COO)_2$	285–290	35090–34480
	390	25640
	670	14930
II $CuL_2(CH_3COO)_2$	280–285	35710–35090
	395–400	25320–25000
	750	13330
III $CuL_3(CH_3COO)_2$	280	35710
	420	23810
	620–670	16130–14930
IV $CuL_1(CH_3COO)$	285–290	35090–34480
	385	25970
	590–600	16950–16670
V Cu(mfa) $(CH_3COO)_2$	280	35710
	390	25640
	680	14710
VI $Cu(mfa)_2(anh)$	290	34480
	382	26180
	650	15380

In the literature [4] 3 absorption bands are reported at 216 nm (46300 cm^{-1}), 238 nm (12020 cm^{-1}) (inflexion) and 292 nm (34250 cm^{-1}) for phthalimide, 2 maxima at 218 nm (45670 cm^{-1}) and 279 nm (35840 cm^{-1}) for N-2(hydroxyphenyl) phthalimide, 3 absorption bands at 211 nm (47390 cm^{-1}), 238 nm (42020 cm^{-1}) and 289 nm (34600 cm^{-1}) for *m*-phenylenediamine.[5]

As can be seen, the maxima assigned to phthalimide and N-phenyl substituted phthalimide are superimposed upon those proper of *m*-phenylenediamine. Thus, the absorption band around 280–290 nm (35710–34480 cm^{-1}) in the spectra of the I–VI compounds may be ascribed to the phthalimide (292 nm–34250 cm^{-1}) as well as to the *m*-phenylenediamine (289 nm–34600 cm^{-1}) molecule. The remaining 2 bands at 216 nm (46300 cm^{-1}) and 238 nm (42020 cm^{-1}), proper to phthalimide and at 211 nm (7390 cm^{-1}) and 238 nm (42020 cm^{-1}), due to *m*-phenylenediamine, cannot be discussed, in relation to the respective bands in the new compounds, in view of the low sensitivity under 250 nm of the equipment used in these measurements.

In the visible range, the compounds under discussion exhibit absorption bands around 390 (25640 cm^{-1}) and 600 nm (16670 cm^{-1}). The first can be assigned to a metal-ligand charge-transfer and can be due to a $2B_{1g} \rightarrow 2E_{1g}$ transition. The second band is located in a region in which an absorption band for the copper phthalimide in DMF solution at 735 nm (13610 cm^{-1}) and an absorption band at 670 nm (14930 cm^{-1}) for the coordination compounds of copper phthalimide with aliphatic amines are referred.

---

[4] L. Lang, "Absorption Spectra in the UV and V Range", 11th vol. Akademiái Kiadó, Budapest, 1968.

[5] "DMS UV Atlas of Organic Compounds" 2nd vol. Butterworths London, 1966.

Indeed Srivastava [6] relates that in nitrobenzene, chloroform and DMF solutions, the electronic spectra of the copper phthalimide compounds exhibit in the 600—900 nm (16670—11110 cm^{-1}) region a well defined absorption band, shifting as a function of solvent polarity.

Besides, Narain [7] indicates for the $[Cu(H_2O)_4]^{2+}$ ion the presence of a band at 800 nm (12500 cm^{-1}), gradually shifting on the substitution of water with amines, up to 600 nm (16670 cm^{-1}) for $[Cu(am)_4]^{2+}$. This negative shift is deemed to be the result of a strong environment of the ligand field arisen around the metal. The presence of an absorption band at 670 nm (14930 cm^{-1}) in the spectrum of $Cu(ft)_2(am)$ in formamide solution, indicating $d_\gamma \rightarrow d_\varepsilon$ transitions, is also reported.

All these data support the assumption that in the 600—700 nm (16670 — 14290 cm^{-1}) region the bands exhibited by the new compounds, may be regarded as $d-d$ metal transition.

INFRARED SPECTRA

The IR spectra of the compounds I and II present 3 regions (table 2) rich in absorption bands, more frequently not very well shaped and differing from those of the *m*-phenylenediamine and phthalic anhydride. In the 500—800 cm^{-1} range, only some of the characteristic bands of phthalic anhydride but with lower intensity, at 660 (655), 690 and 795 cm^{-1}, are found. [8]

More significant is the 1200—1800 cm^{-1} region, with the bands at 1560(1550), 1625(1610), 1710—1720 cm^{-1} due to phthalimide coordination compounds, slightly displaced in respect to the bands of the pure phthalimide [3] and ascribed to the νCo vibration; the band at 1420 (1405) cm^{-1} is characteristic for the CO group symmetric vibration.

Further support for these assignments arises from the data available in the literature. [9] Thus, in the IR spectrum of the $AgNO_3L$ adduct (L = phthalimide) a series of weak bands or only shoulders are mentioned at 1540, 1620, 1710 cm^{-1}, slightly shifted with respect to those assigned to the CO vibration frequencies in the pure phthalimide. Besides, the band due to the frequency vibration of the carbonyl group, reported in the literature[3] at 1745 cm^{-1} for phthalimide is shifted to 1725 cm^{-1} in the copper phthalimidate and to 1655 cm^{-1} in the coordination compounds. This negative frequency shift is the result of an enhanced electron density on the nitrogen atom.

The 3rd range, around 3000 cm^{-1} is characteristic for the NH group. The band at 3070 (3065) cm^{-1} is slightly shifted and as weak as the splitted band present at 3020—3060 cm^{-1} in the *m*-phenylenediamine spectrum.

The band at 3300 cm^{-1} unique for the I compound in this spectral region is due to the valency vibrations of the imide group. The compound II exhibits also a second shoulder-shaped band, at 3410 cm^{-1}, probably due

---

[6] L. N. Srivastava, P. Shukla and M. P. Khare, *Z. phys. Chem.* (*Leipzig*), **234**, 159 (1967).

[7] G. Narain, *Indian J. Chem.*, **4**, 248 (1966).

[8] R. Mercke and F. Langenbucher, "Infrared Spectra of Selected Chemical Compounds", vol. VI, Hayden, London, 1961.

[9] R. C. Paul and S. L. Chandra, *Indian J. Chem.*, **9**, 175 (1971).

Table 2

Infrared Spectra
Max. cm^{-1}

Phthalic anhydride	*m*-phenylenediamine	Compound I	Compound II	Compound III	Compound IV	Compound VI
430	—	470	460–85	—	460	465
540	525	—	530	540	—	535
—	—	600	585	—	610	—
635	—	660	655	635	660	—
680	690	690	690	680	695	—
720	—	720	710	725	720	725
—	—	755	750	—	735	750
—	790	795	795	790	795	790
845	850	860	850	—	—	—
—	—	890	875–95	—	875–90	860–90
—	960	980	960–70	975	980	—
1015	1000	—	—	—	—	—
—	—	1050	1040	1050	1070–65	1070
1080	1080	1090	1080	1085	1090	1090
1120	—	—	1130	1120	—	1115
1180	1170–80	1175	1195	1170	1180	1160
1225	1210	1200	—	1220	1210	1210
1265	—	1280	1260	—	1270	1270
1345	1330	1330	1305	1310	1310	1310
1375	—	1420	1405	1385–95	1390–410	1370–405
480	—	1460	1440	—	1460	—
—	1515	1510	1490	1495–515	1515	—
—	—	1560	1550	1545–60	1550	1530–60
1620	1620	1625	1610	1600–20	1625–75	1610
1710	—	1715–20	1710–20	1705–40	—	1730
1780	—	—	—	1770–90	—	—
—	3020–60	3070	3065	—	3070	—
—	3345	3300	3300	3360	3260–340	3340–3210
—	3425	—	3410	—	—	—

to the presence of the free amine group and located at 3425 cm^{-1} in the *m*-phenylenediamine spectrum.

The IR spectrum of the compound III exhibits a series of bands at 635, 725 and at 1705–40 cm^{-1}, assigned to the vibrations of the secondary amides (frequency vibrations of the NH and CO groups) as well as amide bands of some combined vibrations. The first band at 620 cm^{-1} is thought to be a CO band, like the one at 635 cm^{-1} present in the phthalic anhydride spectrum.[8] The second well defined very strong band, at 725 cm^{-1} is slightly shifted with respect to the band corresponding to the deformation vibration of the NH group present only in the bonded secondary amides.[10]

The band at 1705–40 cm^{-1} is split and very sharp, due to the CO and NH combined vibration and is slightly shifted with respect to the "amide II band" characteristic of the N-aryl substituted amides, absorbing around 1700 cm^{-1}.[11]

---

[10] J. Bellamy, "The Infrared Spectra of Complex Molecules", Methuen, London, 1962.

[11] C.N.R. Rao, "Chemical Applications of Infrared Spectroscopy", Academic Press, New York, 1967.

The 3 additional bands at 1385—95, 1600—20 and 3360 cm^{-1}, are due to the frequency vibrations of the primary amines. The band at 1385—95 cm^{-1} enlarged and well marked is slightly shifted with respect to the band at 1365 cm^{-1} reported in the literature. [12] The appearance of the band at 1365 cm^{-1} involves the presence of the NH_2 group in the molecule.

The deformation vibration of the NH group in the primary amines at 1620 cm^{-1}, 1590 cm^{-1} in solution or at 1650—1620 cm^{-1} in solid state,[11] appears at 1620 cm^{-1} in the spectrum of the III compound.

The last band at 3360 cm^{-1} is slightly shifted with respect to the band present in the spectrum of *m*-phenylenediamine at 3345 cm^{-1}, assigned to the stretching vibration of the NH_2 group flattened by coordination. Besides, the literature [13] provides evidence for a band at 3300 cm^{-1} in the coordination compounds of $Cu(ft)_2$ with amines, attributed to the vibration of the coordinated NH group and for a negative shift on coordination of the band located at 3414 cm^{-1} in the free NH_3. Thus, a covalent bonding M—N is formed, which weakens the N—H bond.

A further support is supplied by the absence in the compound discussed of the band due to the free NH_2 group and present at 3425 cm^{-1} in the *m*-phenylenediamine spectrum. This indicates probably also a coordination effect.

Very important bands in the spectrum of compound III are those at 1035 cm^{-1}, assigned to the metal-acetate bond,[11] at 1120 cm^{-1} due to the C=O valency vibration in the phthalates and at 1495—1515 cm^{-1} presumably due to the valency vibrations of the C=C groups in the aromatic compounds.[11]

It may be concluded that secondary amide and primary amine groups are involved in coordination and are evidenced by modified or shifted characteristic bands in the IR spectra. The bands due to the copper-acetate bond and to the stretching vibrations of the C=C groups in the aromatic compounds are also present. [11]

The IR spectrum of the compound IV exhibits a series of bands more or less marked in the 700—600 cm^{-1} and 1675—1500 cm^{-1} ranges, due to the secondary amide groups. These bands involve the vibration frequencies of the CO group, as well as the vibration modes of the NH group, the location of the latter varying with the nature of the N—H bond. Thus, the bands at 1675 and 1625 cm^{-1} may be assigned to the absorption of the C=O group (amide I band), quoted at 1630—1680 cm^{-1} in the literature. [11]

The deformation vibration of the NH_2 group in the secondary amides, involving a mixed NH and CN vibration (amide II band) at 1550—1510 cm^{-1} is present at 1515 cm^{-1} in the IV compound. This is accompanied by a weak absorption at 1310 cm^{-1} (amide III band) also agreeing with the literature[11] data.

---

[12] N. A. Borisevich and N. N. Hovratovich, *Zhur. priklad. Spectrosk.*, **7**, 538 (1967).

[13] G. Narain, *Canad. J. Chem.*, *44*, 975 (1966).

The spectrum also includes a band at 610 cm^{-1} (amide IV band) characteristic of the secondary amides with a main contribution of the O=C—N and out-of-plane bonded C=O group, as well as the splitted amide V band at 720 cm^{-1}, assigned to the out-of-plane NH deformation vibration.

In the 3000—3400 cm^{-1} range a band is evidenced at 3070 cm^{-1} exhibited at 3100—3070 cm^{-1} by the secondary amides regardless of the NH bonding mode. A very enlarged band can also be seen at 3340—3260 cm^{-1}, assignable to the NH_2 valency vibrations, mentioned for the bonded primary amines at 3350—3180 cm^{-1} in the literature.[10,11]

Very important are the bands at 1210, 1090 and 1070—1065 cm^{-1}, characteristic of the acetates and the metal-acetate bond, as well as the phthalate group, evidenced at 1180 and 1090 cm^{-1} (quoted at 1100—1150 cm^{-1})[10,11] and only shoulder-shaped at 1310 cm^{-1} (quoted at 1250—1310 cm^{-1}).[10,11]

The out-of-plane deformation vibration of the C—H group in the 1,3-disubstituted aromatic compounds is represented by the 755 cm^{-1} band (reported at 810—750 cm^{-1}).[10,11]

All the bands of amide groups (amide I—VI bands) exhibited by compound IV disappear in the spectrum of the compound VI except the bonded primary amine bands at 3340—3210 cm^{-1}, much flattened as compared to those mentioned in the literature at 3180 and 3350 cm^{-1}. Also, the bands at 1530—60 and 1610 cm^{-1}, due to the NH group deformation vibration are weak bands probably as a coordination result. The well defined band appearing at 1390—1410 cm^{-1}, due to the primary amine group deformation vibration, is much shifted towards low frequencies (1370—1405) probably due to coordination. The metal-acetate bond arises in the 1080 cm^{-1} band located in the same domain like in the spectrum of the compound IV.

It may be concluded from the IR spectra that the carbonyl group, as well as simple and substituted imino or amino groups are present in the compounds under discussion. Thus, it seems likely that coordination, occurs via the oxygen of both carbonyl groups and through the imino or amino nitrogen. More likely appears the coordination via the imide-nitrogen as indicated by shifts in the vibration frequencies of the NH group.

If the CO groups were involved in coordination, the ligand would function as bidentate, the fixed spatial orientation of both groups, precluding the coordination at the same metal atom. If the ligand behaves as monodentate, the IR spectrum woul reveal shifted bands due to the coordinated CO groups and unshifted bands due to uncoordinated CO groups.[14]

Acknowledgements. The authors are grateful to Professor P. Spacu for valuable discussions and to Mrs. Marina Olteneanu for the registration of the IR spectra.

---

[14] E. M. Belousova and I. I. Seifulena, *Zhur. neorg. Khim.*, **16**, 151 (1971).

Revue Roumaine de Chimie, **21**, *6*, 879–880 (1976)

PREPARATION AND UNIT CELL DIMENSIONS OF LEAD HYDROXYAPATITE

VIJAY MOHAN BHATNAGAR
Alena Enterprises of Canada, P. O. Box 1779, Cornwall, Ontario, Canada

Received December 11, 1974

Lead hydroxyapatite, $Pb_{10}(PO_4)_6(OH)_2$, has been prepared by several reactions involving Na, K, NH_4, and Pb ions. The cell constants are dependent on the preparation process.

INTRODUCTION

The preparation and unit cell dimensions of lead hydroxyapatite were first reported by Klement.[1] Following this work, it seems that nothing was published on the subject till 1947 when Muller [2] described some mixed solutions between calcium and lead hydroxyapatites and reported the preparation of lead hydroxyapatite. Several papers on lead hydroxyapatite now exist in literature.[3-7]

RESULTS AND DISCUSSION

During our investigation on lead apatites, we have developed several methods for the preparation of lead hydroxyapatite. These processes are extremely simple and have proved quite effective. A number of preparations is reported here. The unit cell dimensions of each preparation are given at the end of the preparation. Preparation No. 1. A solution of $(NH_4)_2HPO_4$ (1.3 gm./50 ml.) was dropwise added to a continuously stirred solution of $Pb(CH_3COO_{/2}$ (4.8 gm./100 ml.) at about 100°. The mixture was stirred for 2 hours, filtered, washed with distilled water and dried at 100°. The cell constants are : $a = 9.88$ Å, $c = 7.43$ Å, and $c/a = 0.752$.

Preparation No. 2. The quantities of the chemical reagents and the experimental conditions were the same as prepartion number 1. However, this synthesis was carried out at room temperature (23°). The cell constants are : $a = 9.87$ Å, $c = 7.44$ Å, and $c/a = 0.753$.

---

[1] R. Klement, *Zeit. anorg. chem.*, **237**, 161 (1938).
[2] M. Muller, *Helv. Chim. Acta.*, **30**, 2069 (1947).
[3] A. S. Posner and A. Perloff, *J. Res. Natl. Bur. Std.*, **58**, 279 (1957).
[4] S. M. Krane and M. J. Glimcher, *J. Biol. Chem.*, **237**, 2991 (1962).
[5] F. H. Blood and W. H. Nebergall, *J. Inorg. Nuclear Chem.* **28**, 3060 (1966).
[6] T. Negas and R. S. Roth, *J. Res. Natl. Bur. Std.*, **72**, 783 (1968).
[7] V. M. Bhatnagar, *Arch. Oral Biol.*, **15**, 469 (1970).

Preparation No. 3. 2.56 gm. of $Pb(CH_3COO)_2$ was dissolved in 250 ml. of distilled water and added dropwise to $(NH_4)_2HPO_4$ (5.76 gm./250 ml) at 100°. The reacting solution was continuously stirred and heated for about 18 hours. The fine milky white precipitate was then filtered, washed with distilled water and dried at 100°. The cell constants are : $a = 9.87$ Å, $c = 7.42$ Å, and $c/a = 0.751$.

Preparation No. 4. The identical quantities and conditions as the preparation number 3 were employed. Only the reaction time was for about 5 hours. The cell constants were exactly the same.

Preparation No. 5. 5.76 gm. of $(NH_4)_2HPO_4$ and 2.56 gm. of $Pb(CH_3COO)_2$ were weighed and dropped in a 500 ml. flask. The reagents were dissolved in 400 ml. of distilled water and the flask thoroughly shaken for about 1 hour at room temperature (23°). The flask was tightly corked and placed aside for about 22 days. The white precipitate was filtered, washed with distilled water and dried at 100°. The cell constants are : $a = 9.87$ Å, $c = 7.41$ Å, and $c/a = 0.750$.

Preparation No. 6. A solution of 2.84 gm./300 ml. Na_2HPO_4 was slowly added to 9.76 gm./300 ml. of $Pb(CH_3COO)_2$ at 100°. The mixture was thoroughly stirred for about 2 hours, filtered, washed with distilled water, and dried at 100°. The cell constants are : $a = 9.88$ Å, $c = 7.41$ Å, and $c/a = 0.750$.

Preparation No. 7. The solutions of Na_2HPO_4 (4.25 gm./300 ml.) and NaOH (0.40 gm./100 ml.) were mixed and added dropwise to $Pb(CH_3COO)_2$ solution (16.24 gm./300 ml) with constant stirring at 100°. The reacting mixture was stirred for about 2 hours, filtered, washed with distilled water and dried at 100°. The cell constants are : $a = 9.88$ Å, $c = 7.41$ Å, and $c/a = 0.750$.

Preparation No. 8. Na_2HPO_4 solution (1.4 gm./50 ml.) was added dropwise to continuously stirred $Pb(CH_3COO)_2$ solution (4.8 gm./100 ml.) at 100°. The mixture was heated and stirred for about 4 hours, filtered, washed with distilled water and dried at 100°. The cell constants are : $a = 9.88$ Å, $c = 7.42$ Å, and $c/a = 0.751$.

Preparation No. 9. 0.96 gm./100 ml. K_2HPO_4 solution was added dropwise to continuously stirred solution of $Pb(CH_3COO)_2$ (2 gm./100 ml.) at 100°. The mixture was stirred for about 43 hours, filtered, washed with distilled water, and dried at 100°. The cell constants are : $a = 9.85$ Å, $c = 7.40$ Å, and $c/a = 0.751$.

Preparation No. 10. K_2HPO_4 solution (1.8 gm./50 ml.) was added dropwise to continuously stirred solution of $Pb(CH_3COO)_2$ (4.8 gm./100 ml.) at 100°. The system was stirred for about 4 hours, filtered, washed with distilled water and dried at 100°. The cell constants are : $a = 9.87$ Å, $c = 7.44$ Å, and $c/a = 0.753$.

The lead hydroxyapatite, $Pb_{10}(PO_4)_6(OH)_2$, is a milky white powder when freshly prepared or even kept for a long time. It is extremely insoluble in water and other known solvents but dissolves very slightly in HNO_3. The structure is very stable and the compound melts at 1000°. Depending upon the method of preparation, the unit cell dimensions in lead hydroxyapatite vary from 9.85 to 9.88 Å in case of a-axis and from 7.40 to 7.44 Å in case of c-axis. The c/a ratio varies from 0.750 to 0.753.

Revue Roumaine de Chimie, **21**, *6*, 881–888 (1976)

OBTENTION ET COMPORTEMENT DES OXAZOLES. II *

BROMURATION DES 2,5-DIPHÉNYLOXAZOLES

RODICA MACAROVICI et MARIA IONESCU
Institut de Chimie, 65—103, str. Donath Cluj-Napoca

Reçu le 2 décembre 1974

On décrit l'obtention d'une série de mono-, di- et tri-bromodérivés du 2,5-diphényloxazole au moyen de la bromuration directe par du brome élémentaire. Le nombre des atomes de brome et les positions dans la molécule d'oxazole dépendent des conditions de travail. La moins réactive s'avère être la position *para* du noyau phénylique du C_2 du cycle oxazolique. Lorsque le noyau phénylique du C_2 est substitué par un groupement nitro, on n'obtient que des mono- et dibromodérivés.

Dans le but d'obtenir des dérivés bromurés des phényloxazoles, qui ont une large utilisation,[1-4] on a essayé à plusieurs reprises la bromuration directe de ceux-ci.[5,6]

Gompper et Rühle [5] ont obtenu, par l'action du brome ou de la *N*-bromesuccinimide sur une série d'oxazoles, soit le dérivé bromuré sur le noyau oxazolique à C_4 ou C_5, soit la bromuration dans la chaîne latérale, quand celle-ci était aliphatique mais ils n'ont jamais isolé de produits bromurés sur le noyau phénylique.

En essayant la bromuration du 2,5-diphényloxazole, 4-méthyle-2,5-diphényloxazole et du 2-phénylbenzoxazole, les auteurs mentionnés n'ont isolé que les bromadducts de ces oxazoles, qu'ils ont formulé d'une manière analogue à celle connue pour d'autres combinaisons avec l'azote dans le cycle, telles que la pyridine et l'acridine :

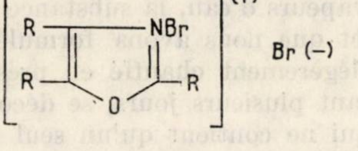

---

* Previous part : M. Ionescu, R. Macarovici et L. Beu, *Stud. Univ. Babeş-Bolyai, Chem.* (sous presse).

[1] I. Tsutmu et S. Shimao, Pat. Jap. 7015972, 3 juin 1970 ; *Chem. Abstr.*, **73**, 77226 (1970).

[2] D. O'Mant, Pat. Brit. 1139940, 15 janv. 1969 ; *Chem. Abstr.*, **70**, 106494 (1968).

[3] D. Ott, F. Hayes, E. Hansbury et V. Ker, *J. Amer. Chem. Soc.*, **79**, 5448 (1957).

[4] O. Süs, W. Neugebauer, E. Lind et K. Klüpfel, Pat. U. S. 3257203, 21 juin 1966 ; *Chem. Abstr.*, **65**, 16973 (1966).

[5] R. Gompper et H. Rühle, *Liebigs Ann. Chem.*, **626**, 83 (1959).

[6] T van Es, *J. Chem. Soc.*, **1963**, 1363.

En chauffant les bromadducts on a obtenu les bromhydrates.

Van Es[6] en essayant l'action du chlore et du brome sur le 4,5-diphényloxazole a obtenu les benzyles correspondants par la suite de l'ouverture du cycle. Le même auteur n'a obtenu de dérivés bromurés sur les noyaux phényliques ni en présence des catalyseurs, comme la limaille de fer, l'iode ou le chlorure ferrique.

De même, Svaika[7] n'a pas réussi à obtenir la bromuration des groupements phényliques des diphényloxazoles, mais seulement des bromadducts.

Dans le présent travail nous avons soumis à la bromuration le 2,5-diphényloxazole (I) et le 2,5-diphényloxazole avec le noyau phénylique de C_2, substitué par un groupement NO_2 dans les positions *o*, *m* et *p* (II, III et IV) qui ont été préparés conformément à la littérature[8,9] :

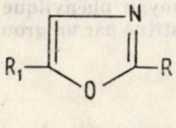

	R	R₁
I	C_6H_5	C_6H_5
II	$C_6H_4-NO_2$ (o)	C_6H_5
III	$C_6H_4-NO_2$ (m)	C_6H_5
IV	$C_6H_4-NO_2$ (p)	C_6H_5

Nous avons obtenu une série de mono-, di- et tribromodérivés du 2,5-diphényloxazole (I) et les mono- et dibromodérivés des oxazoles II, III et IV, le nombre des atomes de brome introduits dans la molécule, et parfois la formation de bromhydrates, dépendant des conditions de travail.

Le 2,5-diphényloxazole en solution d'acide acétique glacial, additionné d'une solution de brome en acide acétique glacial, forme une substance rouge-brique (V), qui est identique avec le perbromure (l'adduct) obtenu par Gompper et Rühle[5] en solution benzénique. Nous avons obtenu la même substance aussi en solution de CCl_4. L'analyse élémentaire a mis en évidence la présence de deux atomes de brome. Conservée, à l'abri du contact avec des vapeurs d'eau, la substance est stable pendant longtemps. Ce bromadduct que nous avons formulé comme un complexe à transfert de charge, légèrement chauffé en présence des vapeurs d'eau ou laissé à l'air pendant plusieurs jours, se décolore, jusqu'au blanc. La nouvelle substance, qui ne contient qu'un seul atome de brome — s'est avérée être le bromhydrate du 2,5-diphényloxazole (VI). On peut supposer que le brome lié assez faiblement à (V), réagit en présence de l'eau en formant l'acide bromhydrique et l'acide hypobromeux. A son tour l'acide bromhydrique agissant sur le 2,5-diphényloxazole forme un bromhydrate :

---

[7] O. Svaika et G. Klimova, *Khim. geterotsikl. Soedineniya*, **5**, 677 (1966).

[8] E. Fischer, *Ber. dtsch. Chem. Ges.*, **29**, 207 (1896).

[9] M. Ionescu et C. Makkay, *Stud. Univ. Babeş-Bolyai, Chem.*, **1963**, 283.

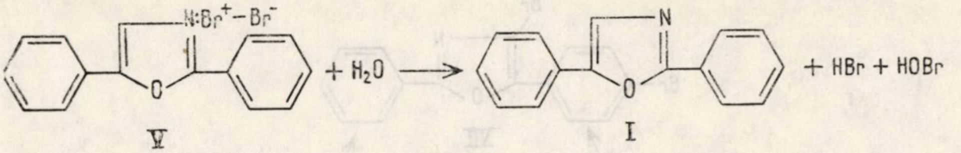

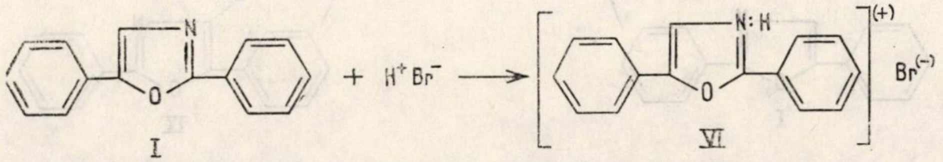

Afin de vérifier cette hypothèse, nous avons essayé l'action d'une solution d'acide bromhydrique en acide acétique sur le 2,5-diphényloxazole et nous avons obtenu une substance blanche cristalline identique à celle résultée à partir du bromadduct. L'atome de brome étant ionisable a pu être dosé par la méthode mercurimétrique. Le bromhydrate (VI) s'est aussi formé et a été isolé dans la réaction du 2,5-diphényloxazole avec du brome élémentaire en acide acétique à l'ébullition.

Par le traitement du 2,5-diphényloxazole (I) avec du brome élémentaire à la température ambiante et après l'élimination de l'excès de brome par évaporation, on obtient un dibromodérivé (VII) qui est totalement différent du bromadduct (V). Par recristallisation en alcool éthylique, on obtient une substance blanche aciculaire stable à l'air et à l'échauffement. Dans ce cas on peut supposer que la substitution a eu lieu soit sur chacun des groupements phényliques, soit sur l'un d'entre eux, à voir sur celui du C_5 où la densité électronique est plus grande, et sur le noyau oxazolique.

Par ébullition du 2,5-diphényloxazole (I) au bain-marie avec du brome élémentaire pendant plusieurs heures, on obtient un tribromodérivé (VIII). L'entrée du troisième atome de brome dans la molécule impose soit la présence d'un groupement phénylique doublement substitué, soit une substitution sur les deux groupements phényliques, à côté de la substitution sur le noyau oxazolique.

En vue d'établir la structure de ces nouvelles substances, nous avons eu recours à la bromuration, dans les mêmes conditions, de certains dérivés du 2,5-diphényloxazole qui contenaient dans leur molécule un ou plusieurs atomes de brome en positions connues et que nous avons préparés conformément aux indications de la littérature.[7,10]

Le dibromodérivé (VII) nous l'avons obtenu également par bromuration directe à la température de la chambre, du 2,5-diphényle-4-brome-oxazole (IX), [7] ce qui confirme la présence d'un atome de brome sur le

---

[10] M. Ionescu, R. Macarovici et L. Beu, *Stud. Univ. Babeş-Bolyai*, *Chem.* (sous presse).

noyau oxazolique, ce qui nous a permis de le formuler comme 2-phényle-4-brome-5(*p*-bromphényle)-oxazole (VII).

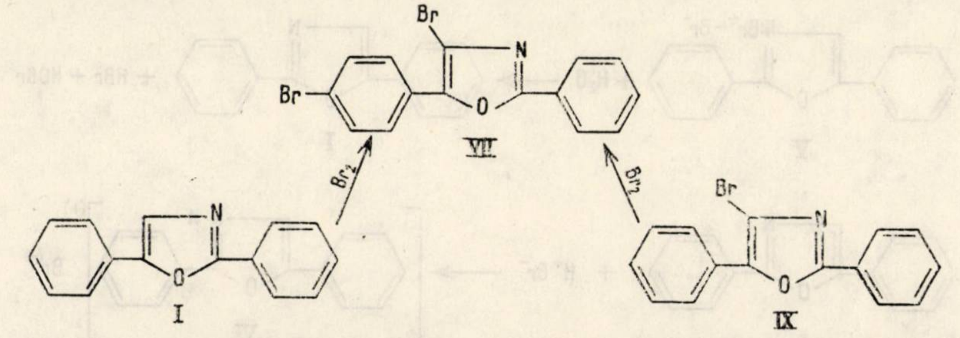
Br
Br
N
O
VII
Br_2
Br_2
N
O
I
Br
N
O
IX

Le tribromodérivé (VIII) s'est avéré être 2(*p*-bromphényle)-4-brome-5(*p*-bromphényle)-oxazole, parce que nous avons réussi à l'obtenir par une série de bromurations des dérivés bromurés en position connue, en vérifiant de cette manière chaque position séparement. Ainsi, en dehors de la bromuration au chaud du 2,5-diphényloxazole (I), le tribromodérivé (VIII) s'est formé dans les mêmes conditions à partir du 2,5-diphényle-4-brome-oxazole (IX) et du 2-phényle-4-brome-5(*p*-bromphényle)-oxazole (VII) et par bromuration à la température ambiante du 2(*p*-bromphényle)-5-phényle-oxazole (X) et du 2(*p*-bromphényle)-4-chlore-5(*p*-bromphényle)-oxazole (XI) dans lequel le chlore a été substitué par le brome.

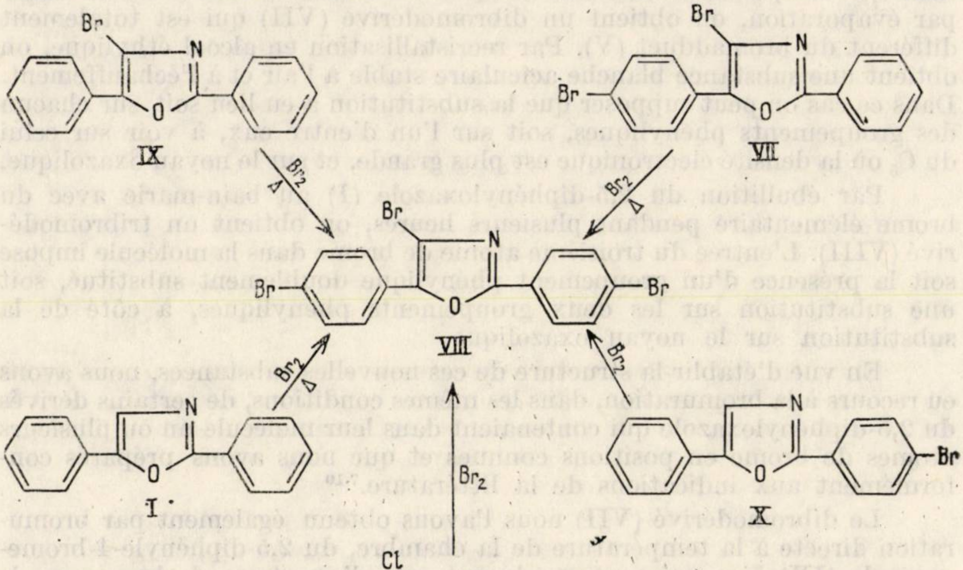
Br
N
O
IX
Br
N
Br
O
VII
Br_2 Δ
Br_2 Δ
Br
N
Br
Br
O
VIII
Br_2 Δ
Br_2
N
O
I
Br_2
N
Br
O
X
Cl
N
Br
Br
O
XI

En dehors des preuves de constitution fournies par cette voie pour le tribromodérivé (VIII) il est confirmé une fois de plus que le deuxième atome de brome du dibromodérivé (VII) se trouve dans la position *para* du groupement phénylique du C_5. Le noyau phénylique du C_2 — dû à la densité électronique réduite dans cette position — est celui qui est le plus difficile à bromurer et seulement dans des conditions énergiques. Toutes les fois que la position *para* du noyau phénylique de C_2 était bromuré au préalable, la bromuration directe des autres positions — respectivement C_4 et le groupement phénylique du C_5 — peut être faite au froid, sans difficultés.

Lorsque le radical phénylique du C_2 du 2,5-diphényle-oxazole est substitué par un groupement NO_2 — indifféremment de la position de celui-ci (II, III, IV) par bromurations directes, on n'obtient que les mono- et dibromodérivés, ce qui peut être expliqué par l'action désactivante du groupement nitro.

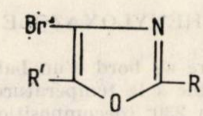

	R	R′
XII	$C_6H_4-NO_2$ (o)	C_6H_5
XIII	$C_6H_4-NO_2$ (m)	C_6H_5
XIV	$C_6H_4-NO_2$ (p)	C_6H_5

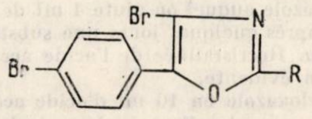

	R
XV	$C_6H_4-NO_2$ (o)
XVI	$C_6H_4-NO_2$ (m)
XVII	$C_6H_4-NO_2$ (p)

Le monobromodérivé (XII) qui avait été obtenu antérieurement par bromuration en acide acétique,[9] nous l'avons également retrouvé avec rendements quantitatifs au moyen de la bromuration en solution benzénique de l'oxazole (II) à la température ambiante. Par spectrométrie de masse on a établi que l'atome de brome se trouve à C_4.

Les monobromodérivés des oxazoles (III) et (IV), respectivement le 2(*m*-nitrophényle)-4-brome-5-phényloxazole (XIII) et le 2(*p*-nitrophényle)-4-brome-5-phényloxazole (XIV), ont été obtenus en solution d'acide acétique glacial, auquel on avait ajouté du brome en acide acétique.

Les dibromodérivés des oxazoles (II), (III) et (IV) nous les avons obtenus d'une manière analogue avec le dibromodérivé (VII) par le traitement des oxazoles par du brome élémentaire, à la température ambiante. Dans ce cas le noyau oxazolique est bromuré à C_4 et le groupement phénylique du C_5 dans la position *para*, en obtenant respectivement 2(*o*-nitrophényle)-4-brome-5(*p*-bromphényle)-oxazole (XV), 2(*m*-nitrophényle)-4-brome-5(*p*-bromphényle)-oxazole (XVI) et 2(*p*-nitrophényle)-4-brome-5-(*p*-bromphényle)-oxazole (XVII), structures qui ont été définies par des dégradations oxydatives et la spectrométrie de masse. Le groupement phénylique de C_2 n'est bromuré en aucun des cas, ni même après l'avoir fait chauffer à reflux pendant plusieurs heures avec du brome élémentaire.

L'étude des spectres de masse formera l'objet d'une autre communication.

PARTIE EXPÉRIMENTALE

1. LE BROMADDUCT DU 2,5-DIPHÉNYLOXAZOLE (V)

a) En 10 ml d'acide acétique glacial on dissout 0,5 g 2,5-diphényloxazole (I) et on ajoute 1 ml d'acide acétique glacial dans lequel ont été dissous 0,25 ml de Br_2. Au moment où est additionnée la solution de brome, est précipitée une substance rouge-brique. La substance est recristallisée de l'acide acétique glacial en chauffant légèrement. Le point de fusion ne peut en être exactement déterminé, parce que la substance se décompose lentement entre 160—220°.

$C_{15}H_{11}ONBr_2$ *Calculé :* C 47,23 ; Br 41,94 ; N 3,67%
Trouvé : C 46,98 ; Br 39,97 ; N 3,49%

b) On dissout 0,5 g de 2,5-diphényloxazole en 5 ml de CCl_4, auquel on ajoute 1 ml de CCl_4, qui contient 0,25 ml de Br_2. Pendant que l'on y ajoute la solution de brome, précipite une substance rouge-brique identique à celle trouvée au point *a*.

2. LE BROMHYDRATE DU 2,5-DIPHÉNYLOXAZOLE (VI)

a) Le bromadduct (V) laissé sur un verre de montre au bord d'un bain-marie, se décolore en 2—3 heures. Il en reste un substance blanche stable à la température ambiante. Recristallisée de l'acide acétique, elle a le point de fusion 230° (décomposition).

$C_{15}H_{12}ONBr$ *Calculé :* C 59,60 ; Br 26,45 ; N 4,63%
Trouvé : C 59,62 ; Br 25,98 ; N 4,56%

b) On prend 0,1 g de 2,5-diphényloxazole auquel on ajute 4 ml de HBr en acide acétique. Laissé dans un vase fermé, il dépose après quelques jours une substance blanche aciculaire, identique à celle obtenue au point *a*. Recristallisée de l'acide acétique, son point de fusion est à 228—230°, avec décomposition évidente.

c) On dissout 0,25 g de 2,5-diphényloxazole en 10 ml d'acide acétique, on y ajoute 0,025 ml de Br_2. On le fait bouillir à reflux en chauffant au bec pendant 20—30′, jusqu'à ce qu'il ne se dégage plus de brome dans le réfrigérant. Il se forme une huile jaune foncé de laquelle par refroidissement déposent des cristaux blancs. La substance recristallisée de l'acide acétique glacial a le point de fusion à 230° avec décomposition. La substance est identique à celle obtenue aux points *a* et *b*.

3. 2-PHÉNYLE-4-BROME-5(*p*-BROMPHÉNYLE)-OXAZOLE (VII)

a) A 0,5 g de 2,5-diphényloxazole on additionne 2,5 ml de Br_2. Une réaction énergique a lieu avec dégagement de chaleur, pendant laquelle toute la substance se dissout. Après l'élimination du brome en excès par évaporation, se dépose une substance cristalline. Par recristallisation de l'éthanol on obtient une substance blanche aciculaire ayant le point de fusion à 123°.

$C_{15}H_9ONBr_2$ *Calculé :* C 47,24 ; Br 41,99 ; N 3,67%
Trouvé : C 47,14 ; Br 41,11 ; N 3,74%

b) 0,5 g de 2,5-diphényle-4-brome-oxazole traité par 2 ml de brome élémentaire, à la température ambiante, forme après en avoir éliminé l'excès de brome par évaporation, une substance identique avec celle obtenue au point *a*. Recristallisée de l'alcool éthylique, elle a le point de fusion à 123°. Outre l'analyse élémentaire et l'épreuve du mélange, la substance a été identifiée aussi par comparaison des spectres en I.R.

4. 2(*p*-BROMPHÉNYLE)-4-BROME-5(*p*-BROMPHÉNYLE)OXAZOLE (VIII)

a) Par chauffage à reflux pendant 5 heures au bain-marie de 0,5 g de 2,5-diphényloxazole (I) avec 2,5 ml de Br on obtient — après élimination du brome en excès par évaporation — une substance blanche jaunâtre. Recristallisée deux fois de l'éthanol, la substance blanche, légèrement jaunâtre, a le point de fusion à 170—171°.

$C_{15}H_8ONBr_3$ *Calculé :* C 39,28 ; Br 52,40 ; N 3,05%
Trouvé : C 39,35 ; Br 51,86 ; N 2,94%

b) Par chauffage à reflux au bain-marie pendant 5 heures de 0,5 g de 2,5-diphényle-4--brome-oxazole (IX) avec 2 ml de brome élémentaire, après en avoir éliminé par évaporation l'excès de brome, se forme une substance identique à celle obtenue au point *a*, ayant le point de fusion à 170°. Le rendement est quantitatif.

c) Par l'ébullition de 0,5 g de 2-phényle-4-brome-5(*p*-bromphényle)oxazole (VII) avec 2 ml de brome élémentaire, se sépare par recristallisation de l'éthanol la même substance que celle décrite au point *a*. Point de fusion à 171°.

d) Par traitement à la température ambiante de 0,5 g de 2(*p*-bromphényle)-5-phényloxazole (X) par 2 ml de Br_2 on obtient aussi quantitativement le tribromodérivé mentionné au point *a*.

e) En traitant à la température ambiante 0,5 g de 2(*p*-bromphényle)-4Cl-5(*p*-bromphényl)oxazole (XI) avec 2 ml de Br_2 on obtient avec rendement quantitatif le 2(*p*-bromphényle)-4--brome-5(*p*-bromphényle)oxazole, ayant le point de fusion à 171°, identique avec celui obtenu au point *a*.

5. 2(*o*-NITROPHÉNYLE)-4-BROME-5-PHÉNYLOXAZOLE (XII)

On dissout 0,5 g de 2(*o*-nitrophényle)-5-phényloxazole en 4 ml de benzène additionné de 2 ml de benzène qui contiennent 0,5 ml de Br_2. Après l'élimination par évaporation de l'excès de benzène et de brome, la solution dépose une substance légèrement jaune, qui recristallise de l'acide acétique aqueux (2 :1) et a le point de fusion à 116—117°.

$C_{15}H_9O_3N_2Br$ *Calculé* : C 52,02 ; H 2,31 ; Br 23,12 ; N 8,09 %
Trouvé : C 51,65 ; H 2,26 ; Br 23,35 ; N 8,11 %

6. 2(*o*-NITROPHÉNYLE)-4-BROME-5(*p*-BROMPHÉNYLE)OXAZOLE (XV)

Par le traitement à la température ambiante de 0,5 g de 2(*o*-nitrophényle)-5-phényle--oxazole avec 2 ml de Br_2 se forme — après l'élimination du brome en excès — une substance cristalline jaune, qui a été recristallisée deux fois de l'éthanol. La substance purifiée, d'un jaune clair, a le point de fusion à 176°.

$C_{15}H_8O_3N_2Br_2$ *Calculé* : C 42,35 ; H 2,11 ; Br 37,73 ; N 6,58 %
Trouvé : C 42,64 ; H 2,18 ; Br 37,38 ; N 6,59 %

7. 2(*m*-NITROPHÉNYLE)-4-BROME-5-PHÉNYLE-OXAZOLE (XIII)

On dissout 0,5 g de 2(*m*-nitrophényle)-5-phényle-oxazole en 10 ml d'acide acétique glacial au chaud et on ajoute 0,25 ml de Br_2 en 2 ml d'acide acétique glacial. On verse la solution sur de la glace. Il se forme un précipité jaune clair. Recristallisée de l'éthanol la substance a la couleur jaune clair et le point de fusion à 150°.

$C_{15}H_9O_3N_2Br$ *Calculé* : C 52,02 ; Br 23,12 ; N 8,09 %
Trouvé : C 52,87 ; Br 22,68 ; N 8,26 %

8. 2(*m*-NITROPHÉNYLE)-4-BROME-5(*p*-BROMPHÉNYLE)OXAZOLE (XVI)

On traite 0,5 g de 2(*m*-nitrophényle)-5-phényle-oxazole par 2 ml de Br_2 à la température ambiante. Une réaction énergique a lieu, avec dégagement de chaleur. Après l'élimination de l'excès de brome, se dépose une substance jaune, très difficilement soluble dans les solvants usuels. La substance a été recristallisée en utilisant de grandes quantités d'acide acétique glacial. Le produit purifié est jaune clair et a le point de fusion à 240°.

$C_{15}H_8O_3N_2Br_2$ *Calculé* : C 42,35 ; Br 37,73 ; N 6,58 %
Trouvé : C 42,64 ; Br 37,12 ; N 6,96

9. 2(*p*-NITROPHÉNYLE)-4-BROME-5-PHÉNYLE-OXAZOLE (XIV)

On dissout 0,5 g de 2 (*p*-nitrophényle)-5-phényle-oxazole en 20 ml d'acide acétique glacial, à l'ébullition et on ajoute 0,25 ml de Br_2 en 2 ml d'acide acétique glacial. Par refroidissement se dépose une substance jaune, qui se recristallise de l'éthanol et a le point de fusion à 167°.

$C_{15}H_9O_3N_2Br$ *Calculé* : C 52,02 ; Br 23,12 ; N 8,09 %
Trouvé : C 51,64 ; Br 22,30 N 8,04 %

10. 2(*p*-NITROPHÉNYLE)-4-BROME-5(*p*-BROMPHÉNYLE)-OXAZOLE (XVII)

Le traitement de 0,5 g de 2(*p*-nitrophényle)-5-phényloxazole par 2,5 ml de Br_2 à la température ambiante, assure après l'élimination de l'excès de brome, l'obtention d'une substance jaune, qui peut être recristallisée de l'acide acétique et de l'éthanol. Le point de fusion est à 208—210°.

$C_{15}H_8O_3N_2Br_2$ *Calculé* : C 42,35 ; Br 37,73 ; N 6,58 %
Trouvé : C 42,30 ; Br 37,66 ; N 6,83 %

Revue Roumaine de Chimie, 21, 6, 889–895 (1976)

ACTION OF AMINES ON 3-BENZYLIDENE PHTHALIDE AND SOME ALLIED COMPOUNDS

S. M. ABDEL RAHMAN, M. F. ISMAIL and Z. M. ISMAIL
Chemistry Dept., Faculty of Science, Ain Shams University, Abbassia, Cairo, Egypt

Received December 2, 1974

3-Benzylidene phthalide (I) reacts with primary and secondary amines to give N-substituted desoxybenzoin-*o*-carboxamides (II & III). 3-Benzylidene phthalide 1-thione (V) reacts with primary amines to give N-substituted-3-benzylidene phthalimidine-1-thiones (VI), directly. The reaction of 3-α-bromobenzylidene phthalide with primary amines at room temperature proceeded yielding α-alkylamino- or α-arylamine-desoxybenzoin-*o*-carboxamides (VIII*a*−*c*) with the separation of the corresponding amine hydrobromide. (VIII*a*−*c*) were also obtained from the interaction of 3-bromo-3-α-bromobenzylphthalide with amines.

The present investigation deals with the reaction of 3-benzylidene phthalide, 3-benzylidene phthalide-1-thione, 3-α-bromobenzylidene phthalide and 3-bromo-3-α-bromobenzylphthalide with amines. Thus, when 3-benzylidene phthalide (I) is treated with some aliphatic and aromatic amines in benzene at room temperature, it undergoes ring opening to give N-substituted desoxybenzoin-*o*-carboxamides (II*a*−*f*) as the only crystallisable product in good yields.

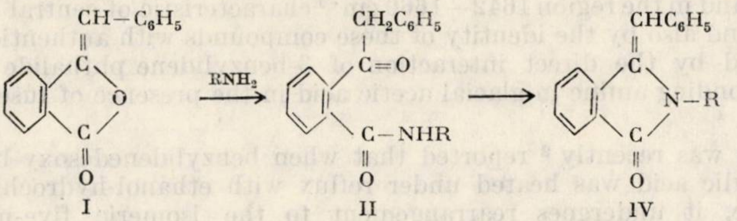

I

II

IV

a; R = $C_4H_9(n)$; *b*; R = $CH_2C_6H_5$; *c*; R = C_6H_5; *d*; R = $C_6H_4CH_3(p)$; *e*; R = $C_6H_4OCH_3(p)$; *f*; R = $C_6H_4Cl(p)$.

Similarly 3-benzylidene phthalide reacts with secondary amine, to give (III*a* and *b*).

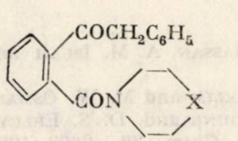

III

a; X = CH_2; *b*; X = O.

The structure of (II and III) is inferred from : — (i) Their analytical data, (ii) Their infrared spectra which show both aryl ketonic and secondary amides carbonyl stretching frequencies. That of (II) shows in addition a broad band in the 3190—3400 cm^{-1} region characteristic of both NH and OH stretching frequencies (cf. Table 1). The presence of the latter stretching frequency may be due to the partial presence of these compounds in the enol form. (iii) The electronic spectra of (II*a* and *b*) show narrow absorptions at λ_{max} 253 nm (ε_{max} 3825) and λ_{max} 252 nm(ε_{max} 4500), respectively characteristic of unconjugated benzoyl group. (iv) When desoxybenzoin-*o*-carboxamides (II*b*—*f*) are heated under reflux in glacial acetic acid containing fused sodium acetate, N-substituted-3-benzylidene phthalimidines (IV) are obtained in good yields.

Table 1

Infrared spectra of N-substituted desoxybenzoin-*o*-carboxamides (II and III)

Compound	ν NH,OH cm^{-1}	ν C=O cm^{-1}
II*a*	3300	1694, 1680, 1620
b	3240	1690, 1670, 1620
c	3190	1683, 1678, 1605
d	3280	1680, 1620
e	3400	1692, 1620
f	3320	1690, 1680, 1620
III*a*	—	1700, 1640, 1620
b	—	1700, 1640, 1620

The structure of (IV) is inferred from a study of their infrared spectra which show only the stretching frequencies of the carbonyl groups of γ-lactans in the (1715—1718 cm^{-1}) region. They show in addition another weak band in the region 1642—1660 cm^{-1} characteristic of central C=CH— bond, and also by the identity of these compounds with authentic samples obtained by the direct interaction of 3-benzylidene phthalide with the corresponding amine in glacial acetic acid in the presence of fused sodium acetate. [1]

It was recently [2] reported that when benzylidenedesoxy-benzoin-*o*-carboxylic acid was heated under reflux with ethanol-hydrochloric acid mixture, it undergoes rearrangement to the isomeric five-membered hydroxylactonic structure. It was also reported that *o*-acetylbenzoic acid and desoxybenzoin-*o*-carboxylic acid are present in the solid state in the open form, whereas in solution, the spectral data indicate the presence of both the open form as well as the hydroxy five-membered lactonic structure. [3-5]

[1] T. B. Hannout, E. A. Hassan, A. M. Islam and I. M. Ismail, *U. A.R. J. Chem.*, **13**, 199 (1970).

[2] A. Sammour, M. I. B. Selim and M. W. Osman, *U.A.R. J. Chem.*, **14**, 305 (1971).

[3] D. D. Weeler, D. C. Young and. D. S. Erley, *J. Org. Chem.*, **22**, 547 (1957).

[4] O. H. Weeler, *Canad. J. Chem.*, **39**, 2603 (1961).

[5] D. S. Erley. W. J. Potts, P. R. Jones and P. J. Desio, *Chem. Ind.*, 1915 (1964); *Chem. Abstr.*, **62**; 1618 (1965).

In the present investigation desoxybenzoin-*o*-carboxamides (II) were heated under reflux with ethanol-hydrochloric acid mixture in the hope to obtain the isomeric five-membered hydroxy lactams. However, in each case the only crystallisable product obtained was found to be N-substituted-3-benzylidene phthalimidines (IV) and not the desired product, even when the reaction was carried out by passing gaseous HCl into an ice-cooled solution of the amide in ethanol.

The investigation was extended to involve the interaction of 3-benzylidene phthalide-1-thione (V) [prepared by the action of phosphorous pentasulphide on 3-benzylidene phthalide [6]] and amines. Thus, when benzylamine or aniline was allowed to react with 3-benzylidene phthalide-1-thione in benzene at room temperature, N-substituted-3-benzylidene phthalimidine-1-thiones (VI*a* and *b*) were obtained as the only crystallisable product. The structure of (VI) is inferred by other means than by analytical data from a study of their infrared spectra which do not show the stretching frequencies characteristic of NH and OH or C=O group. They also show the presence of C=S stretching frequency at 1375 cm^{-1} and 1338 cm^{-1} respectively.

However, when piperidine or morpholine was allowed to react with the thione, no crystallisable products were isolated and, instead, untractable oily products were obtained.

The direct formation of (VI) as the sole product of the reaction between the thione and primary amines at room temperature might be explained according to the following scheme:

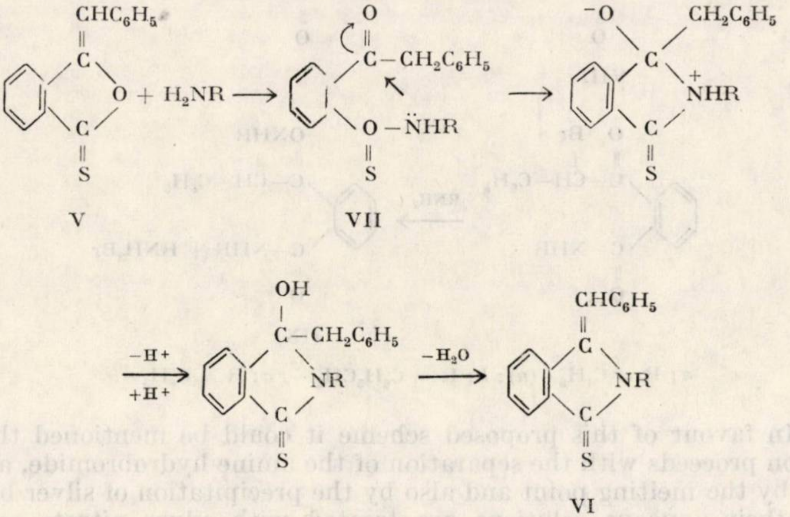

VI *a*; R = $C_6H_5CH_2-$ *b*; R = C_6H_5-

---

[6] A. El Maghraby, Ph. D. Thesis, Faculty od Science, El Azhar University (1974).

The failure to isolate the open-chain product analogous to II, namely VII, may be explained by the fact that the amidic-type conjugation strongly retains the non-participating electrons of nitrogen, making them inaccessible for cyclisation while in the thioamidic-type these electrons are available for cyclisation :

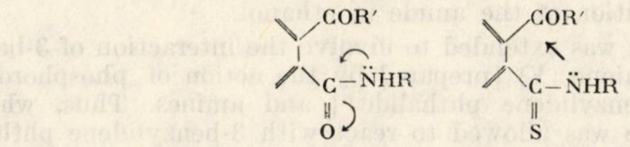

ACTION OF AMINES ON 3-α-BROMOBENZYLIDENE PHTHALIDE

When 3-α-bromobenzylidene phthalide (VIII) was allowed to react with *n*-butylamine, benzylamine and aniline at room temperature in benzene, α-alkylamino- or α-arylaminodesoxybenzoin-*o*-carboxamides (IX *a*–*c*) were obtained in moderate yields. The reaction seems to proceed according to the following scheme :

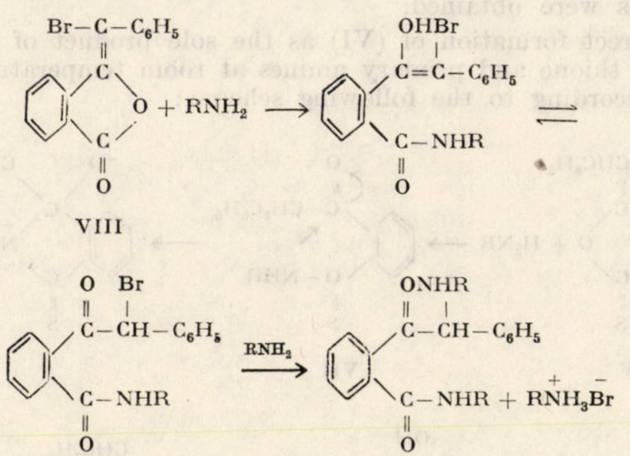

VIII

(IX)

a ; R = $C_4H_9-(n)$; *b* ; R = $C_6H_5CH_2-$; *c* ; R = C_6H_5-.

In favour of this proposed scheme it could be mentioned that the reaction proceeds with the separation of the amine hydrobromide, as identified by the melting point and also by the precipitation of silver bromide when their aqueous solutions are treated with silver nitrate solution. The structure of (IX) is inferred from :

(i) analytical data ;

(ii) their infrared spectra are similar to those of (II). Thus they show a broad band in the 3240–3380 cm^{-1} region characteristic of NH and OH stretching frequencies. The latter broad band suggests the partial existance of these compounds in the enol form. They also show both ketonic and secondary amide carbonyl stretching frequencies (cf. Table 2);

Table 2

Infrared spectra of α-alkylamino or α-arylaminodesoxybenzoin-o-carboxamides (IX)

Compound	ν NH,OH cm^{-1}	ν C=O cm^{-1}
IX*a*	3240–3260 (br.)	1660, 1670
b	3340–3370	1660, 1670
c	3365–3380	1600, 1680

(iii) the electronic spectrum of (IX *a*) is similar to those of (II) (λ_{max} 250 nm, ε_{max} 3530). It is to be noticed here that the reaction proceeds more easily and in good yields in the case of *n*-butylamine and benzylamine as compared with aromatic amine. Such observation can be explained on the basis of the relative basicity of these amines.

The reaction of 3-substituted phthalides with amines is extended to involve 3-bromo-3-α-bromobenzylphthalide (X). When this compound is treated with *n*-butylamine, benzylamine or aniline, (IX *a*–*c*) are obtained as the only crystallisable products, respectively with the liberation of the amine hydrobromide. Theoretically, the reaction might proceed either by removal of HBr from (X) to give (VIII) followed by reaction with a second molecule of the amine to give (IX), or a ring opening might take place at first under the influence of the amine followed by dehydrobromination and subsequent reaction of the α-bromoketone formed with the amine to give (IX).

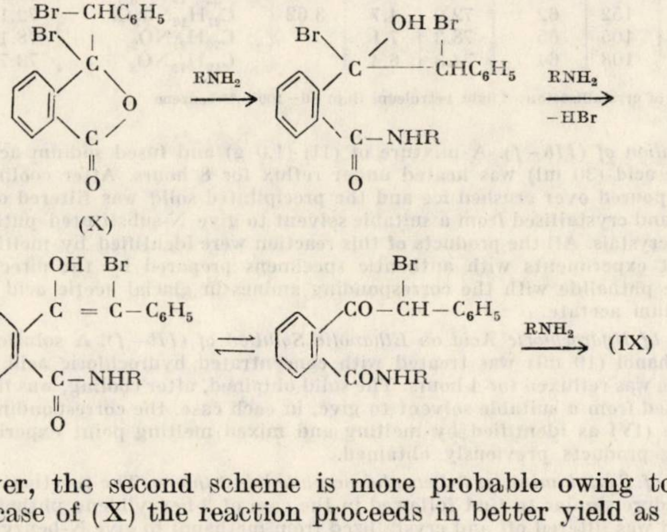

However, the second scheme is more probable owing to the fact that in the case of (X) the reaction proceeds in better yield as compared with that obtained with (VIII). Moreover, it was not possible to isolate 3-α-bromobenzylidene-phthalide when one mole of the amine was allowed to react with one mole of 3-bromo-3-α-bromobenzylphthalide.

EXPERIMENTAL

Melting points are not corrected. Analyses were carried out in the microanalytical laboratories in Cairo University and El-Nasr Company for pharmaceutical chemicals. Infrared spectra were carried out on PYE-UNICAM 1200 using KBr Wafer technique. Electronic spectra were carried out on Perkin Elmer spectracord. Model 4000 A spectrophotometer using ethanol as a solvent.

Action of Amines on 3-Benzylidene phthalide. A solution of 3-benzylidene phthalide (2.2 g; 0.01 mole) in benzene (25 ml) was treated dropwise with a solution of the amine (0.01 mole) in benzene (10 ml) and the reaction mixture was left overnight at room temperature and then after addition of light petroleum (b.p. 60—80°) the colourless solid obtained was filtered off, and crystallised from a suitable solvent to give N-substituted desoxybenzoin *o*-carboxamides (II and III) (cf. Table 3).

Table 3

N – Substituted desoxybenzoin-*o*-carboxamides (II)

Compd.	m.p.	Yield	Analyses Found C	H	N	Mol. Formula	Requires C	H	N
IIa *	153	67	76.6	7.2		$C_{19}H_{21}NO_2$	77.2	7.17	
IIb **	164	75	80.6	6.3	4.04	$C_{22}H_{19}NO_2$	80.2	5.8	4.2
IIc *	172	63	80.2	5.3		$C_{21}H_{17}NO_2$	79.98	5.43	
IId **	175	85	80.9	6.2		$C_{22}H_{19}NO_2$	80.2	5.8	
IIe **	178	86	76.6	5.9		$C_{22}H_{19}NO_3$	76.5	5.5	
IIf *	152	62	72.0	4.7	3.62	$C_{21}H_{16}NO_2Cl$	72.1	4.5	3.71
IIIa *	105	65	78.3	7.1		$C_{20}H_{21}NO_2$	78.1	6.9	
IIIb *	108	64	74.3	6.4		$C_{19}H_{19}NO_3$	73.78	6.11	

Solvent of crystallization: * light petroleum (b.p. 80—100°) ** benzene

Cyclization of (IIb—f). A mixture of (II) (1.0 g) and fused sodium acetate (0.3 g) in glacial acetic acid (30 ml) was heated under reflux for 8 hours. After cooling, the reaction mixture was poured over crushed ice and the precipitated solid was filtered off, washed with water, dried and crystallised from a suitable solvent to give N-substituted phthalimidines (IV) as colourless crystals. All the products of this reaction were identified by melting and mixture melting point experiments with authentic specimens prepared by the direct interaction of 3-benzylidene phthalide with the corresponding amines in glacial acetic acid in the presence of fused sodium acetate.

Action of Hydrochloric Acid on Ethanolic Solution of (IIb—f). A solution of the amide (1.0 g) in ethanol (10 ml) was treated with concentrated hydrochloric acid (5 ml) and the whole mixture was refluxed for 4 hours. The solid obtained, after cooling, was filtered off, dried and crystallised from a suitable solvent to give, in each case, the corresponding N-substituted phthalimidine (IV) as identified by melting and mixed melting point experiments with the corresponding products previously obtained.

Action of Benzylamine on 3-Benzylidene phthalide-1-thione. The reaction was carried out using a procedure similar to that followed in the case of 3-benzylidene phthalide. The yellow solid obtained was filtered off and crystallized from methanol to give N-benzyl-3-benzylidene-phthalimidine-1-thione (VI*a*) m.p. 168—170°, yield, 61%. *Found*: C, 80.9; H, 4.9; N, 3.9; S, 9.8; $C_{22}H_{17}NS$ requires: C, 81.04; H, 5.2; N, 4.28; S, 9.7.

Action of Aniline on (V). The reaction was carried out as shown in the previous experiment. The product was crystallized from methanol to give N-phenyl-3-benzylidene phthalimidine-1-thione (VI*b*) as yellow crystals, m.p. 153–5°, yield 51 %. *Found* : C, 80.2 ; H, 4.7 ; $C_{21}H_{15}NS$ requires : C, 80.5 ; H, 4.70 %.

Action of Amines on 3-α-bromobenzylidene phthalide. A solution of 3-α-bromobenzylidene phthalide (3.0 g, 0.01 mole) in benzene (25 ml) was treated dropwise with the amine (0.03 mole) in benzene (10 ml) at room temperature. The crystalline solid formed was filtered off, and dried. This solid was found to be the amine hydrobromide. The benzene solution was washed with water several times, dried over anhydrous sodium sulphate, concentrated and left overnight at room temperature. The colourless crystalline solid obtained was filtered off, and recrystallized from a suitable solvent to give (IX *a*–*c*) as colourless crystals (cf. Table 4).

Table 4

α-Alkylamino- or α-arylaminodesoxybenzoin-*o*-carboxamides (IX)

Compd.	m.p.	Yield	Analyses						
			Found			Requires			
			C	H	N	Mol. Formula	C	H	N
IXa *	110	66	75.3	8.5	7.9	$C_{23}H_{30}N_2O_2$	75.37	8.25	7.64
IXb **	185	60	80.33	6.22		$C_{29}H_{26}N_2O_2$	80.16	6.03	
IXc *	198	50	80.41	5.88	6.86	$C_{27}H_{22}N_2O_2$	79.78	5.46	6.89

Solvent of crystallization ; * Ethanol ** Methanol.

Action of Amines on 3-bromo-3-α-bromobenzylphthalide. The reaction was carried out as described in the previous experiment. The product obtained was crystallised from a suitable solvent to give (IX *a*–*c*) in 72, 65 and 58 % yields, respectively, as identified by melting point and mixed melting point experiments with the products obtained from the interaction of corresponding amine with (VII).

Revue Roumaine de Chimie, **21**, *6*, 897–902 (1976)

EXO- AND ENDOHORMONES. II*

SYNTHESIS OF PEPTIDIC JUVENILE HORMONE ANALOGUES

M. VLASSA
Laboratory of Natural Products, Institute of Chemistry Cluj-Napoca,
str. Donath 65–103

Received October 25, 1974

Peptidic juvenile hormone analogues containing ethyl L-alanyl-*p*-aminobenzoate or ethyl L-alanyl-γ-aminobutyrate were prepared.

A good deal of synthetic compounds exibit biological activity similar to that of natural juvenile hormone JH** (cecropia hormone) (**1**) which is essential for growth and development of young larval instars. These compounds, called juvenile hormone analogues (JHA), belong from the structural point of view to very different classes.[1] Slama, Zaoral et al.[2–5] have recently found that certain peptides containing an ethyl *p*-aminobenzoate moiety are potent JHA. Like the juvabione type compounds they are active only on Pyrrhocorid insects.[6]

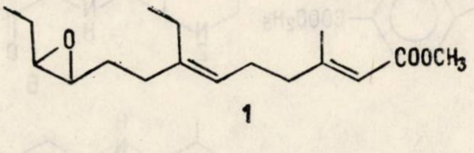

1

---

* Part I : M. Vlassa, *Rev. Roumaine Chim.*, **21**, 455 (1976).

** The abbreviations used for amino acids and their substituents are those recommended by the IUPAC–IUB Commission on Biochemical Nomenclature, published in *J. Biol. Chem.*, **247**, 977 (1972).

Other abbrevations used in this paper are AE = 1-etoxycarbonyl-propene-2-yl ; CP = = 2-etoxycarbonyl cyclopentene-1-yl ; DMF = dimethylformamide ; DCHA = dicyclohexylamine ; DCC = dicyclohexylcarbodiimide ; DCU = dicyclohexylurea ; AcOEt = ethyl acetate ; Et_2O = ethyl ether ; THF = tetrahydrofurane ; TEA = triethylamine ; EtOH = ethanol ; PE = petroleum ether.

[1] K. Slama, *Ann. Rev. Biochem.*, **40**, 1079 (1971).

[2] M. Zaoral, *Coll. Czech. Chem. Comm.*, **36**, 2080 (1971).

[3] K. Poduska, F. Sorm and K. Slama, *Z. Naturforsch.*, **266**, 719 (1971) ; K. Poduska, J. Hlavacek, F. Sorm and K. Slama, Czech., 151, 120 and 151, 121, 15 Nov. 1973 ; *Chem. Abstr.*, **80**, 146539 and 146538 (1974).

[4] M. Zaoral and K. Slama, *Science*, **170**, 92 (1970).

[5] T. H. Babu and K. Slama, *Science*, **175** (1972).

[6] a. K. Slama, M. Romanuk and F. Sorm, "Insect Hormones and Bioanalogues", Springer Verlag Wien, New York, 1974, p. 446 ; b. *idem* p. 190.

According to Slama[6a] the biological effectiveness of these peptidic JHA — fifty five compounds have been synthetized so far[6b] — consists in a specific interaction with a precisely optically-oriented tissue. This interaction depends on an alkyl group on the middle L-unit of the peptide chain, a terminal hydrophobic acyl group and an aromatic component.

On the other hand starting from the observation that there are JH active compounds having little or no structural resemblance to natural JH, Slade and Wilkinson [7] pointed out that the JHA activity arises from the ability of these compounds to interfere with the metabolic degradation of the natural hormone. In their opinion the activity of JHA is synergistic rather than intrinsically hormonal.

In connection with our permanent interest in the peptide chemistry and taking into account the above mentioned problems, we prepared the compounds **2**—**8**. All but two (**7** and **8**) contain the carbobenzoxy protecting group which can be, if necessary, easily removed to give the parent peptides. Two of these parent peptides, namely those deriving from compounds **4** and **6**, were already mentioned in the literature [6] however without detailed data concerning their preparation. The same is true for compound **8**, an enormously active JHA in Pyrrhocoridae, [4] whose method of preparation was not described so far.

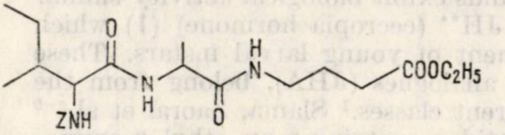

2

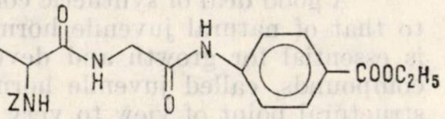

5

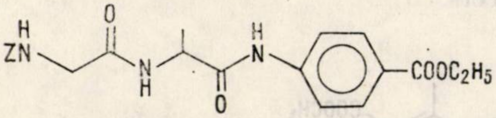

3

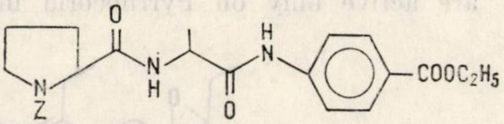

6

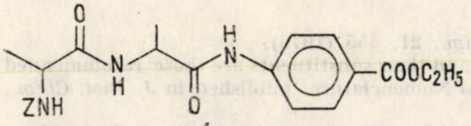

4

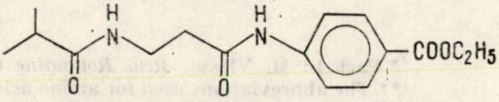

7

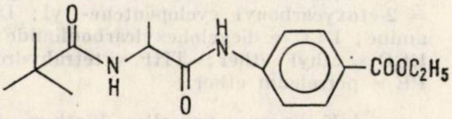

8

The first step in the synthesis of compounds **3**—**6** was the condensation of Phth-L-Ala with ethyl *p*-aminobenzoate using the acid chloride method. The dipeptide thus obtained could not be prepared by the mixed

---

M. SLADE and C. F. WILKINSON, Science, 181, 672 (1973).

anhydride method by way of the dicyclohexylamine salts of AE- or PA-L-Ala.[8] The second step was the condensation of the dipeptide with the appropriate aminoacid following the DCC method.

Compound **2** was obtained from ethyl γ-aminobutyrate and the N-protected L-Ala (protecting: Z, AE or CP) by the mixed anhydride method. The dipeptide thus prepared was condensed by the same method, after removal of the protecting group, with Z-L-Ile.

The synthesis of compound **7** and **8** was achieved following two routes:

a. condensation of ethyl *p*-aminobenzoate with pivaloyl-β (or L)-alanine,

b. acylation of ethyl β(or L)-alanyl-*p*-aminobenzoate with pivalic acid; both were performed using the DCC method. The second route gave unsatisfactory yields.

EXPERIMENTAL

All m.p.s. were taken on a "Mikroheiztztisch Boetius" and are uncorrected. The optical rotations were measured using a polarimeter Metra 400/a in a 1 dm cell. The ir spectra were recorded in KBr pellets with a Carl Zeiss Jena UR instrument. The pmr spectra were recorded by means of a BRUKER 90 MHz Proton Spectrum instrument, in $CDCl_3$ solutions, with TMS as internal reference. The mass spectra were recorded using a Varian MAT Model CH-7 instrument with single focusing, operated at an electron energy of 70 eV, the source temperature ranged from 100° to 180° and the electronbeam was held at 100 μA.

ETHYL γ-AMINOBUTYRATE HYDROCHLORIDE

To a suspension of γ-aminobutyric acid (10.1 g; 0.1 mole) in anh. EtOH (30 ml) thionyl chloride (7.9 ml; 0.11 moles) was added dropwise, the temperature being kept at −5° by external cooling. The solution was kept at 40° for 2 hrs., evaporated *in vacuo* and the residue distilled azeotropically, when a white substance was obtained. M.p. 67−72° (lit.[9] 65−72°). Y : quantitative.

ETHYL CARBOBENZOXY-L-ALANYL-γ-AMINOBUTYRATE

To a solution of Z-L-Ala (2.23 g; 0.01 mole) in THF (50 ml) TEA (1.4 ml; 0.01 mole), ethyl chloroformate (1 ml) and a few drops of N-methyl morpholine were added, at −10°. After 15 minutes the separated triethylamine hydrochloride was filtered. To the filtrate a solution of ethyl γ-aminobutyrate hydrochloride (1.7 g; 0.01 mole) and TEA (1.4 ml; 0.01 mole) in dichloromethane (30 ml) was added under stirring, at −10°. The mixture was stirred at this temperature for 1/2 hr., kept at room temperature for 24 hrs., treated with saturated $NaHCO_3$ solution (50 ml), and the organic layer evaporated *in vacuo*. The oily residue was extracted with AcOEt, dried over anh. Na_2SO_4, and evaporated *in vacuo*. The residue was triturated with PE when the oily substance became crystalline. White needles, from AcOEt−PE, m.p. 73−75°. Y :73%. Ir bands (cm^{-1}) : 3300, 1720, 1655, 1550. Anal. *Found* : C, 60.00; H, 7.00; N, 8.20

Calcd. for $C_{17}H_{24}N_2O_5$: C, 60.17; H, 7.14; N, 8.33

---

[8] A. Balogh, D. Breazu, E. Vargha, F. Gönczy and L. Beu, *Rev. Roumaine Chim.*, **15**, 1375 (1970).

[9] I. Fafel and M. Stern, *Ber. dtsch. chem. Ges.*, **33**, 2225 (1900).

ETHYL N-(1-ETOXYCARBONYL-PROPENE-2-YL)-L-ALANYL-γ-AMINOBUTYRATE

It was prepared from AE-L-AlaO$^-$ DCHA·H^{+}[8] (3.8 g; 0.01 mole) under the conditions described above. White crystals from benzene-PE, m.p. 88–89°. Y : 70%. Ir bands (cm^{-1}) : 3330, 1730, 1658, 1555. Anal. *Found* : C, 57.66 ; H, 8.17 ; N, 8.80

Calcd. for $C_{15}H_{26}N_2O_5$: C, 57.32 ; H, 8.23 ; N, 8.91

ETHYL N-(2-ETOXYCARBONYL-CYCLOPENTEN-1-YL)-L-ALANYL-γ-AMINOBUTYRATE

It was preparing from CP-L-AlaO$^-$ DCHA·H^{+}[8] (4.08 g; 0.01 mole) under the conditions described above. White crystals from benzene-PE, m.p. 99–101°. Y : 74%. Ir bands (cm^{-1}) : 3320, 1738, 1680, 1660, 1550. Anal. *Found* : C, 60.20 ; H, 8.23 ; N, 8.60

Calcd. for $C_{17}H_{28}N_2O_5$: C, 60.00 ; H, 8.23 ; N, 8.52

ETHYL L-ALANYL-γ-AMINOBUTYRATE

a. Ethyl Z-L-alanyl-γ-aminobutyrate (3.36 g ; 0.01 mole) was dissolved in a solution of 36% HBr in acetic acid (20 ml). After 1 hour's standing at room temperature anh. Et_2O was added. The oily precipitate was thoroughly washed with anh. Et_2O, dissolved in anh. EtOH and treated with an ethanolic solution of TEA (1.4 ml ; 0.01 mole). The precipitate (TEA·HCl) was filtered and the solvent removed in vacuo ; The dipeptide resulted as an oily product. Y : 60%.

b. To AE- or PA-L-alanyl-γ-aminobutyrate (0.01 mole) dissolved in anh. EtOH (20 ml). 1N HCl was added to achieve pH = 2.5–3 and the mixture kept overnight at room temperature. The reaction product was processed as above. Y : 70%.

ETHYL CARBOBENZOXY-L-ISOLEUCYL-L-ALANYL-γ-AMINOBUTYRATE (2)

To a mixed anhydride solution in THF (125 ml) prepared as usual from Z-L-Ile (2.65 g ; 0.01 mole) and ethyl chloroformate (1 ml ; 0.01 mole), a solution of ethyl L-alanyl-γ-aminobutyrate (2.06 g ; 0.01 mole) in THF (100 ml) was added. After 15 minutes the solution was processed as described for ethyl carbobenzoxy-L-alanyl-γ-aminobutyrate. White crystals from AcOEt, m.p. 186–187°, $/\alpha/_{D}^{22.5} -28^{\circ}$ (c. 1 ; $HCCl_3$). Y : 60%. Ir bands (cm^{-1}) : 3295, 1742, 1695, 1660, 1558, 1342, PMR (δ) : 7.32 (5H, s), 6.96 (1H, d, J = 3.5 Hz), 6.82 (1H, t, J = = 3.00 Hz), 5.65 (1H, d, J = 4.00 Hz), 5.08 (2H, s), 4.50 (1H, m, J = 3.50 Hz), 4.10 (3H, q, J = 3.80 Hz), 3.24 (2H, q, J = 3.50 Hz), 2.32 (3H, t, J = 3.50 Hz), 1.84 (4H, m), 1.33 (3H, t, J = 3.50 Hz), 1.23 (6H, t, J = 3.50 Hz), 0.91 (3H, d, J = 3.00 Hz). Mass spectrum peaks (m/e) : 449, 393, 342, 341, 319, 296, 292, 254, 248, 229, 220, 211, 210, 187, 185, 184, 183, 177, 176, 167, 158, 157, 156, 155, 154, 142, 141, 140, 139, 134, 131, 130, 129, 128, 127, 126, 115, 113, 112, 109, 108, 107, 100, 99, 98, 92, 91, 90, 89, 87, 86, 85, 84, 80, 79, 78, 77, 70, 69. Anal. *Found* : C, 61.64 ; H, 7.85 ; N, 9.56

Calcd. for $C_{23}H_{35}N_3O_6$: C, 61.49 ; H, 7.79 ; N, 9.35

ETHYL PHTHALOYL-L-ALANYL-*p*-AMINOBENZOATE

A solution of ethyl *p*-aminobenzoate (1.65 g ; 0.01 mole) and TEA (1.4 ml ; 0.01 mole) in chloroform (50 ml) was treated with Phth-L-Ala chloride (2.375 g; 0.01 mole) in chloroform (25 ml). The solvent was removed *in vacuo*, the residue triturated with 2N HCl, and washed with water. White crystals from aqueous EtOH, m.p. 160–162°, $/\alpha/_{D}^{22.5} -22.4^{\circ}$ (c. 1 ; $HCCl_3$). Ir bands (cm^{-1}) : 3300, 1710, 1658, 1566. Y : 80%. Anal. *Found* : C, 65.59 ; H, 4.63 ; N, 8.02

Calcd. for $C_{20}H_{18}N_2O_5$: C, 65.60 ; H, 4.90 ; N, 7.55

ETHYL L-ALANYL-*p*-AMINOBENZOATE HYDROCHLORIDE

To solution of ethyl phthaloyl-L-alanyl-*p*-aminobenzoate (3.66 g ; 0.01 mole) in EtOH (175 ml) a solution of 33.2% hydrazine hydrate (2.5 ml) was added and the mixture refluxed for 1 hour. The solvent was removed *in vacuo* and the residue treated with 2N HCl, kept at 0°

for 24 hors and evaporated to dryness *in vacuo* at a temperature not exceeding 45°. White crystals from isopropanol-PE, m.p. 232–234°, $/\alpha/^{24}_{D}-56°$ (c. 2 ; H_2O). Y : 70%; Ir bands (cm^{-1}) : 3270, 3200, 1710, 1695, 1665, 1560, 1340. Anal. *Found* : C, 52.71 ; H, 6.24 ; N, 10.16
Calcd, for $C_{17}H_{17}ClN_2O_3$: C, 52.71 ; H, 6.33 ; N, 10.31

ETHYL CARBOBENZOXY-GLYCYL-L-ALANYL-*p*-AMINOBENZOATE (3)

To a solution of Z-Gly (2.09 g; 0.01 mole) in AcOEt (10 ml) and DMF (15 ml) were added ethyl L-alanyl-*p*-aminobenzoate hydrochloride (2.73 g; 0.01 mole) and TEA (1.4 ml; 0.01 mole); the solution was stirred for 10 minutes. Thereafter DCC (2.01 g; 0.01 mole) was added at 0°, stirred at this temperature for 1 hr., kept at room temperature for 48 hrs., AcOEt removed *in vacuo*, and the DMF solution diluted with water. The precipitate was collected, extracted with AcOEt and filtered. The AcOEt solution was washed successively with 2N HCl, 5% $NaHCO_3$, water, dried over anh. Na_2SO_4, and evaporated *in vacuo*. White crystals from aqueous EtOH, m.p. 183.5–185°, $/\alpha/^{22}_{D}-21.7$ (c. 1.65 ; DMF). Y : 50%. Ir bands (cm^{-1}) : 3355, 3330, 3272, 1718, 1690, 1655, 1535, 1348. PMR (δ) : 8.68 (1H, s), 7.81 (4H, qAB, J = 4.8 Hz), 7.54 (1H, m), 7.32 (5H, s), 5.40 (1H, m), 5.13 (2H, s), 4.64 (1H, q, J = 3.50 Hz), 4.34 (2H, q, J = 3.50 Hz), 3.90 (2H, d, J = 3.00 Hz), 1.44 (3H, d, J = 3.50 Hz), 1.38 (3H, t, J = = 3.50 Hz). Mass spectrum peaks (m/e) : 427, 382, 275, 274, 263, 235, 217, 192, 165, 155, 146, 137, 134, 128, 127, 121, 120, 108, 107, 99, 92, 91, 90, 85, 80, 79, 78, 77. Anal. *Found* : C, 62.58 ; H, 6.08 ; N, 9.55
Calcd. for $C_{22}H_{25}N_3O_6$: C, 61.82 ; H, 6.08 ; N, 9.52

ETHYL CARBOBENZOXY-L-ALANYL-L-ALANYL-*p*-AMINOBENZOATE (4)

It was prepared starting with Z-L-Ala (2.23 g; 0.01 mole) as described for compound 3. White crystals from aqueous ethanol, m.p. 210–212°, $/\alpha/^{23}_{D}-4.6°$ (c. 2.1 ; DMF). Y : 60%. Ir bands (cm^{-1}) : 3295, 3270, 1716, 1695, 1655, 1550, 1350. PMR (δ) : 8.78 (1H, s), 7.82 (4H, qAB, J = 4.50 Hz), 7.13 (5H, s), 6.68 (1H, d, J = 3.50 Hz), 5.28 (1H, d, J = 3.00 Hz), 5.11 (2H, s), 4.69 (2H, q, J = 3.00 Hz), 4.35 (2H, q, J = 3.50 Hz), 1.42 (6H, d, J = 3.50 Hz), 1.38 (3H, t, J = 3.50 Hz). Mass spectrum peaks (m/e) : 441, 334, 333, 288, 206, 192, 169, 166, 165, 164, 146, 142, 141, 137, 134, 121, 120, 119, 114, 113, 109, 108, 107, 99, 93, 92, 91, 90, 89, 80, 79, 78, 77, 70. Anal. *Found* : C, 62.58 ; H, 6.08 ; N, 9.55
Calcd. for $C_{22}H_{25}N_3O_6$: C, 61.82 ; H, 6.08 ; N, 9.52

ETHYL CARBOBENZOXY-L-VALYL-L-ALANYL-*p*-AMINOBENZOATE (5)

To a solution of Z-L-Val (2.51 g; 0.01 mole) in acetonitrile (100 ml) were added ethyl L-alanyl-*p*-aminobenzoate hydrochloride (2.73 g; 0.01 mole) and TEA (1.4 ml; 0.01 mole); the solution was stirred for 10 minutes. Thereafter DCC (2.01 g; 0.01 mole) was added at 0°, the solution stirred at this temperature for 1 hr., and at room temperature for 5 hrs. The DCU formed was filtered, the residue dissolved in AcOEt, filtered, and the solution processed as described above for compound 3. The oily end product thus obtained was brought to crystallization by trituration with PE. White crystals from AcOEt-PE, m.p. 217–219°, $/\alpha/^{22}_{D}-61.7°$ (c. 1 ; $HCCl_3$). Y : 75%. Ir bands (cm^{-1}) : 3295, 1725, 1695, 1652, 1540, 1350. PMR (δ) : 9.05 (1H, s), 7.76 (4H, qAB, J = 4.30 Hz), 7.29 (6H, s), 5.67 (1H, 4, J = 4.00 Hz), 5.10 (2H, s), 4.75 (1H, m), 4.36 (2H, q, J = 3,50 Hz), 4.17 (1H, m), 2.08 (1H, m, J = 3.50 Hz), 1.41 (3H, d, J = 3.50), 1.37 (3H, t, J = 3.50 Hz), 0.94 (6H, d, J = 3.00 Hz). Mass spectrum peaks (m/e) : 424, 362, 361, 314, 305, 234, 206, 197, 192, 170, 169, 167, 166, 165, 164, 163, 162, 146, 142, 141, 137, 134, 128, 127, 126, 121, 120, 119, 109, 108, 107, 99, 98, 93, 92, 91, 90, 89, 80, 79, 78, 77, 72, 70. Anal. *Found* : C, 63.98 ; H, 6.98 ; N, 9.11
Calcd. for $C_{25}H_{31}N_3O_6$: C, 63.98 ; H, 6.61 ; N, 8.95

ETHYL CARBOBENZOXY-L-PROLYL-L-ALANYL-*p*-AMINOBENZOATE (6)

It was prepared started with Z-L-Pro (2.49 g; 0.01 mole) as described for compound 5. White crystals from aqueous EtOH, m.p. 150–152°, $/\alpha/^{21.5}_{D}-51°$ (c. 0.98 ; $HCCl_3$). Y : 86%.

Ir bands (cm^{-1}) : 3360, 3290, 1710, 1695, 1660, 1550, 1338. PMR (δ) : 9.10 (1H, s), 7.82 (4H, qAB, J = 4.80 Hz), 7.29 (6H, s), 6.84 (1H, d, J = 3.50 Hz), 5.14 (2H, s), 4.62 (1H, q, J = = 3.50 Hz), 4.33 (2H, q, J = 3.50 Hz), 3.55 (1H, t, J = 3.00 Hz), 2.70 (6H, m), 1.44 (3H, d, J = 3.50 Hz), 1.35 (3H, t, J = 3.50 Hz). Mass spectrum peaks : 467, 359, 330, 224, 205, 204, 202, 201, 200, 199, 198, 196, 195, 168, 167, 166, 165, 161, 160, 146, 143, 141, 140, 139, 137, 121, 120, 114, 108, 107, 100, 99, 98, 97, 92, 91, 83, 82, 91, 79, 77, 72, 71, 70, 69. Anal. *Found* : C, 64.24 ; H, 6.96 ; N, 9.12

Calcd. for $C_{25}H_{29}N_3O_6$: C, 64.24 ; H, 6.21 ; N, 8.94

PIVALOYL-β ALANINE

To a solution of β-alanine (8.9 g ; 0.1 mole) in 4N NaOH (53 ml) simultaneously were added dropwise and under stirring pivaloyl chloride (12.06 g ; 0.1 mole) in anh. toluene (15 ml) and 4N NaOH (29 ml). The mixture was stirred for 1 hr., the toluene layer separated, and the aqueous one extracted with Et_2O. The end product precipitated from the aqueous layer by acidulation with conc. HCl to pH 1.5—2, under external cooling. The precipitate was filtered and washed with water. White crystals from AcOEt, m.p. 130—132°, (lit.[10] 132—133°). Y : 85%.

ETHYL PIVALOYL-β-ALANYL-*p*-AMINOBENZOATE (7)

To a solution of ethyl *p*-aminobenzoate (16.5 g ; 0.1 mole) and pivaloyl-β-alanine (17.3 g ; 0.1 mole) in THF (75 ml) was added DCC (20.1 g; 0.1 mole) at 0°. The mixture was stirred at 0° for 1 hr. and kept at room temperature for 24 hrs. Thereafter a few drops of acetic acid were added, the DCU formed was filtered and the filtrate evaporated *in vacuo*. The end product was dissolved in AcOEt and processed as described for compounds **5**. White crystals were obtained by trituration with EtOH-water 1 :2 and recrystallization from aqueous EtOH, m.p. 168—169.5°. Y : 40%. Ir bands (cm^{-1}) : 3391, 3269, 1708, 1630, 1542. PMR (δ) : 8.80 (1H, s), 7.82 (4H, qAB, J = 4.80 Hz), 6.45 (1H, t, J = 3.00 Hz), 4.35 (2H, q, J = 3.50 Hz), 3.67 (2H, q, J = = 3.00 Hz), 2.65 (2H, t, J = 3.00 Hz), 1.38 (3H, t, J = 3.00 Hz), 1.18 (9H, s). Mass spectrum peaks : 320, 275, 224, 166, 165, 156, 143, 137, 129, 128, 120, 100, 99, 98, 87, 85, 70. Anal. *Found* : C, 64.00 ; H, 7.39 ; N, 9.00

Calcd. for $C_{17}H_{24}N_2O_4$: C, 63.74 ; H, 7.49 ; N, 9.15

ETHYL PIVALOYL-L-ALANYL-*p*-AMINOBENZOATE (8)

It was prepared starting with ethyl *p*-aminobenzoate (16.3 g ; 0.1 mole) and pivaloyl-L alanine[11] (17.3 g ; 0.1 mole) as described for compound **7**. White crystals from aqueous EtOH, m.p. 167—168°, $/\alpha/_{D}^{23.5}$ —60.6° (c. 0.165 ; $HCCl_3$). Y : 55%. Ir bands (cm^{-1}) : 3329, 3302, 3255, 1722, 1640, 1550. PMR (δ) : 8.50 (1H, s), 7.83 (4H, qAB, J = 4.20 Hz), 6.48 (1H, d, J = = 3.50 Hz), 4.80 (1H, q, J = 3.50 Hz), 4.35 (2H, q, J = 3.50 Hz), 1.45 (3H, t, J = 3.50 Hz), 1.25 (9H, s). Mass spectrum peaks : 320, 275, 235, 202, 200, 199, 166, 165, 157, 156, 140, 138, 137, 121, 120, 114, 93, 92, 91, 85, 72, 71, 70, 69. Anal. *Found* : C, 63.85 ; H, 7.77 ; N, 9.10

Calcd. for $C_{17}H_{24}N_2O_4$: C, 63.74 ; H, 7.49 ; N, 9.15

---

[10] J. S. MORELY and J. M. SMITH, *J. Chem. Soc.*, **1968**, 726.

[11] H. KREBS and W. SCHUMACHER, *Chem. Ber.*, **99**, 1341 (1966).

Revue Roumaine de Chimie, **21**, *6*, 903–910 (1976)

IONIZATION CONSTANTS OF SOME N-ARYL, N′-2-(5-HALO-PYRIDYL) THIOUREAS

B. C. KASHYAP, A. D. TANEJA and S. K. BANERJI
Birla Institute of Technology and Science
Pillani 333031, India

Received October 7, 1974

The ionization constants (pK_a) of N-phenyl, N′-2-(5-chloropyridyl)-, (PCTH) ; N-phenyl, N′-2-(5-bromo-pyridyl)-, (PBTH) ; N-phenyl, N′-2-(5-iodopyridyl)-, (PITH) ; N-*ortho*-tolyl, N′-2-(5-chloro-pyridyl)-, (TCTH) ; N-*ortho*-tolyl, N′-2-(5-bromo-pyridyl)-, (TBTH) and N-*ortho*-tolyl, N′-2-(5-iodo-pyridyl) — (TITH) thioureas have been determined in 75% acetonitrile at various ionic strengths. Thermodynamic dissociation constants (pK_a^T) were obtained by extrapolation to zero ionic strength. The dissociation constants of these compounds have also been determined at fixed ionic strength (0.1) over the temperature range 30—60°. From these results the thermodynamic parameters such as free energy change (ΔG), enthalpy change (ΔH) and entropy change (ΔS) have been calculated for the ionization process. The difference in dissociation constants of the studied compounds has been discussed on the basis of substituent effect. The values of pK_m (minimum pK_a values at temperature θ°) have also been calculated. ΔH values have also been calculated from the values of 'θ' and 'l' by using Harned's equation.

INTRODUCTION

Though the determination of ionization constants of thio-compounds has been the subject of various investigations, quantity correlations of these constants with substituents or medium effects are lacking. However, various studies are now being made in the direction of a better understanding of these effects on the ionization constants of thio-compounds. Edward and Chin[1] have studied the ionization of 2,4-dithiohydanations. The potentiometric determination of the acidity constants of 2,4-dithiobiuret and its derivatives was carried out by Usatenko and Sukhoruchkins. [2] The acid dissociation constants of various substituted thiocarbazone were determined spectrophotometrically in 50% dioxane-water mixture by Math and co-workers. [3] Recently ionization constants of some substituted pyridyl thioureas have been reported by Dutta Ahmad et al. [4] and Prasad.[5] The present paper reports the ionization constants of some N-aryl, N′-2-(5-halo-pyridyl) thioureas in 75% acetonitrile water mixture at various ionic strengths. The effect of temperature on ionization constants of these compounds has also been reported.

[1] J. T. Edward and O. J. Chin, *Canad. J. Chem.*, **41**, 1650 (1963).

[2] Yu. I. Usatanko and A. S. Sukhoruchkins, *Zhur. Analit. Khim.*, **18**, 1295 (1963).

[3] K. S. Math, Q. Fernando and H. Freiser, *Analyt. Chem.*, **36**, 1762 (1964).

[4] A. Dutta Ahmad and P. K. Mandal, *J. Inorg. Nuclear Chem.*, **29**, 2347 (1967).

[5] C. S. G. Prasad, Ph. D. Thesis, B.I.T.S., Pilani, India (1973).

EXPERIMENTAL

N-phenyl, N′-2-(5-chloro-pyridyl)-, (PCTH); N-phenyl, N′-2-(5-brome-pyridyl)-, (PBTH); N-phenyl, N′-2-(5-iodo-pyridyl)-, (PITH); N-*ortho*-tolyl, N′-2-(5-chloro-pyridyl)-, (TCTH); N-*ortho*-tolyl, N′-2-(5-brome-pyridyl)-, (TBTH) and N-*ortho*-tolyl, N′-2-(5-iodo-pyridyl)-, (TITH) thioureas were prepared as described elsewhere.[6] The pK_a values were determined by the direct pH titration techniques as described by Albert and Sarjeant.[7]

Instruments and chemicals : Most of the chemicals used were of Anala R BDH quality. For maintaining the ionic strength $NaClO_4 \cdot 2H_2O$ (Reidel) was used. Acetonitrile was dried over fused calcium chloride and distilled before use. Carbonate free KOH, which was used as the base in titrations was prepared following the method outlined by Albert and Sarjeant.[7] The pH measurements were made on a Beckman pH meter (Model H2) using a glass-calomel electrode assembly. The glass electrode had negligible salt error up to pH 12. All readings above pH 12 were neglected in subsequent calculations. Temperature was maintained using a thermostatic bath, Model 2095 of Forma Scientific U.S.A.

For finding the thermodynamic ionization constants of these compounds, studies were carried out at 25° and at the ionic strengths (μ) 0.05, 0.10, 0.15 and 0.20 and the results were extrapolated to zero ionic strength to obtain pK_a^T. For the determination of thermodynamic parameters, the studies were carried out at 30°, 45°, 50°, 55° and 60° at a fixed ionic strength of 0.10. The thermodynamic parameters, ΔG, ΔH and ΔS were then calculated using standard equation.

RESULTS AND DISCUSSION

The $p\mathrm{K}_a$ values at various ionic strengths and the $p\mathrm{K}_a^T$ values of these substituted thioureas are reported in Table 1 (Fig. 1). From this it can be observed that the $p\mathrm{K}_a$ values of these compounds increase with increase in ionic strength.

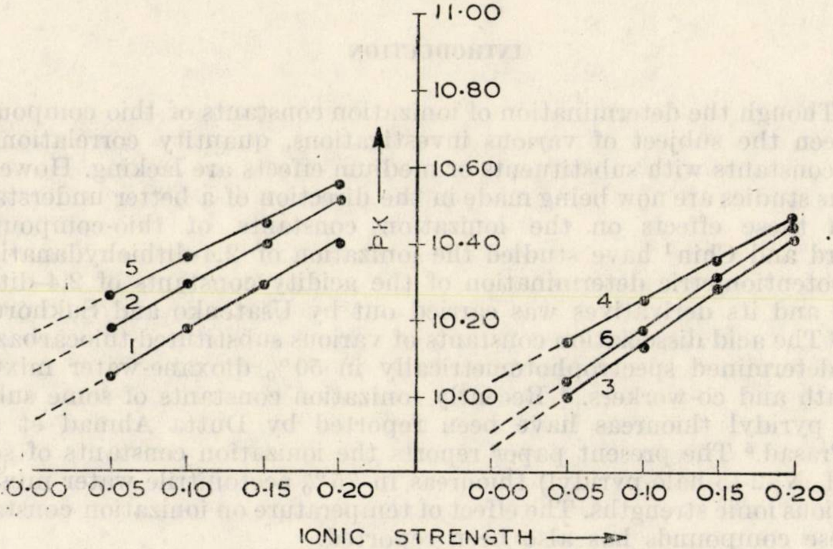

Fig. 1. — Variation of pK with ionic strength.

---

[6] B. C. Kashyap, Ph. D. Thesis, B.I.T.S., Pilani, India (1974).

[7] A. Albert and E. P. Sarjeant, "Ionization Constants of Acids and Bases", Methuen and Co., London, 1962.

Table 1

Effect of ionic strength on the pK values of some N-substituted, N′-2-(5-halo-pyridyl) thioureas

Temperature = 30°

Compound	Ionic strength	*pK*
PCT	0.00÷	9.94
	0.05	10.05
	0.10	10.18
	0.15	10.29
	0.20	10.40
PBT	0.00÷	10.06
	0.05	10.17
	0.10	10.29
	0.15	10.40
	0.20	10.51
PIT*	0.00÷	9.87
	0.05	10.00
	0.10	10.14
	0.15	10.29
	0.20	10.42
TCT	0.00÷	10.04
	0.05	10.15
	0.10	10.26
	0.15	10.36
	0.20	10.47
TBT	0.00÷	10.16
	0.05	10.26
	0.10	10.37
	0.15	10.46
	0.20	10.56
TIT*	0.00÷	9.91
	0.05	10.04
	0.10	10.18
	0.15	10.32
	0.20	10.45

* Temperature = 45°. ÷ Obtained by extrapolation

Tautomeric equilibrium exhibited by the substituted thioureas can be represented as

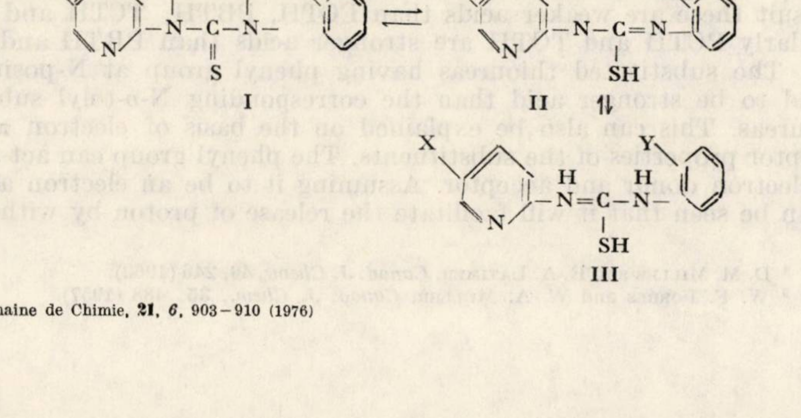

where X = – Cl, –Br or –I
and Y = –H or $-CH_3$
The enethiol form (II, III) is acidic and can donate a proton as shown below

II $\rightleftharpoons$

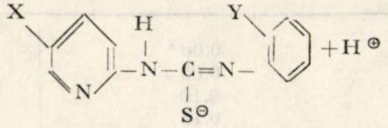

III $\rightleftharpoons$

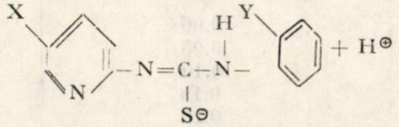

From the values of thermodynamic ionization constants of these substituted thioureas (Table 1), it can be observed that these are weak acids. Of all the compounds taken, PCT is found to be the strongest acid and TIT the weakest. The other compounds have the intermediate pK_a^T values. This can be explained on the basis of the electron donating power of the group with which the proton is attached. The ability of a compound to release a proton depends upon its electronegativity. If more electrons are available with the group to which the proton is attached, the proton would be bound to the group with a greater force and the donation of proton would be difficult. Thus the ionization constant of an acidic group will decrease with the increasing electron donating power of the group to which it is attached and vice-vera. Increasing size and electron donating group cause a drop in pK_T.[8] In the compounds studied, it is proposed that there is a delocalization of electron from the pyridine ring to the thiocarbonyl group. Due to this electronic charge transfer, the basic character of the substituted thioureas i.e. S-protonation is increased. Taking into consideration the mesomeric and inductive effects due to the halo-substituents in *p*-haloacetophenones, Forbes et al.[9] have shown that the halo group becomes increasingly electron donating in the order $I > Br > Cl$. In the present work also the halo-substituents are at para position to the thiourea unit. As more and more electrons are brought to sulfur-atom, its power to hold the proton increases. Therefore, the proton in the case of N-aryl, N′-2-(5-iodo-pyridyl) thioureas (PITH, TITH) is more firmly held and as a result these are weaker acids than PCTH, PBTH, TCTH and TBTH. Similarly PCTH and TCTH are stronger acids than PBTH and TBTH.

The substituted thioureas having phenyl group at N-position are found to be stronger acid than the corresponding N-*o*-tolyl substituted thioureas. This can also be explained on the basis of electron π donor-acceptor properties of the substituents. The phenyl group can act as both, an electron donor and acceptor. Assuming it to be an electron acceptor, it can be seen that it will facilitate the release of proton by withdrawing electrons from the system $-\underset{\underset{S^-}{|}}{C}=N-$ hence making the compounds stronger acids. The *o*-tolyl group acts basically as an electron donor making the donation of the proton more difficult and as a result the *o*-tolyl substituted thioureas are ionized to a lesser extent i.e. these are weaker acids as compared to the phenyl substituted thioureas.

---

[8] D. M. MILLER and R. A. LATIMER, *Canad. J. Chem.*, **40**, 246 (1962).

[9] W. F. FORBES and W. A. MULLER, *Canad. J. Chem.*, **35**, 488 (1957).

The variation in pK_a with temperature of all these compounds shows that an increase in temperature decreases the value of pK_a (cf. Table 2, Fig. 2). This is normally observed for most acids in the range studied (30–60°).[10] The ΔG and ΔH values are positive and ΔS values are negative.

Table 2

Effect of temperature on ionisation and thermodynamic functions of N-substituted, N′-2-(5-halo-pyridyl) thioureas

Compound	Temperature °K	pK	ΔG (kcal/mole)	ΔH_{av} (kcal/mole)	$-\Delta S$ (cal/mole)
PCT	303	10.18	14.10	8.54	18.63
	318	9.90	14.50		
	323	9.81	14.58		
	328	9.72	14.67		
PBT	303	10.29	14.29	7.93	20.89
	318	10.02	14.57		
	323	9.93	14.67		
	328	9.84	14.77		
PIT	318	10.14	14.74	7.65	22.27
	323	10.05	14.85		
	328	9.96	14.95		
	333	9.88	15.05		
TBT	303	10.37	14.37	7.93	21.33
	318	10.12	14.72		
	323	10.03	14.82		
	328	9.94	14.91		
TIT	318	10.18	14.80	8.54	19.63
	323	10.07	14.88		
	328	9.97	14.96		
	333	9.90	15.08		

In a series of papers [10–12] Harned and coworkers reported the results of their investigations on the ionization constants of several acids over a wide range of temperatures. They observed that the values of $\log K_a$ increased with increasing temperatures, passed through a maximum and

---

[10] H. S. Harned and L. K. Kazanjian, *J. Amer. Chem. Soc.*, **58**, 1912 (1936).

[11] H. S. Harned and R. W. Ehlers, *J. Amer. Chem. Soc.*, **55**, 652 (1933).

[12] H. S. Harned and N. D. Embree, *J. Amer. Chem. Soc.*, **56**, 1050 (1934).

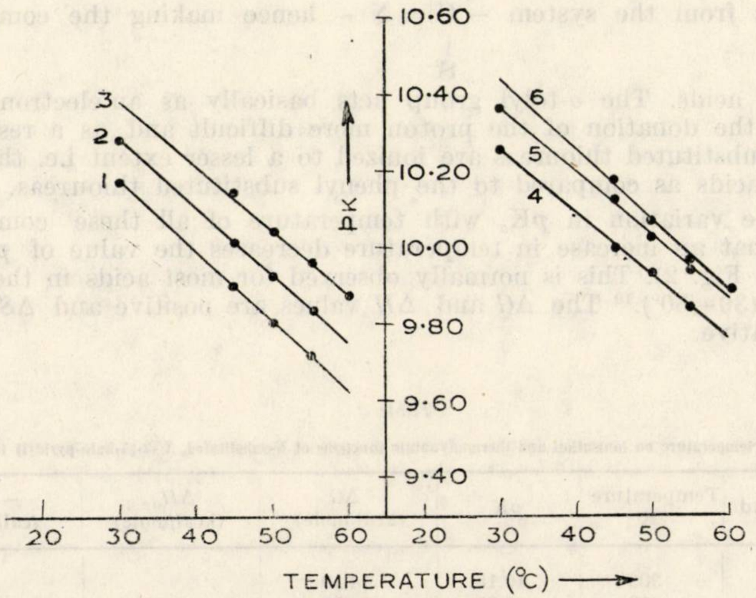

Fig. 2. — Variation of pK with temperature.

finally decreased with increasing temperature. The minimum pK_a termed as pK_m occurs at a definite temperature 'θ' which is different for different acids. A parabolic relationship between log K_a and 't' was found which could be expressed by an equation of the type

$$pK_a - pK_m = C(t - \theta)^2 \tag{1}$$

where $pK_a = -\log K_a$ at temperature 't'°

$pK_m =$ minimum pK_n value at temperature 'θ'°

$C =$ constant, 5.0×10^{-5} degree^{-2}

Rearranging equation (1)

$$pK_a - Ct^2 = pK_m + C\theta^2 - 2C\theta t \tag{2}$$

If $(pK_a - Ct^2)$ is plotted against 't' a straight line should be obtained, the slope of which is $-2C\theta$ and the intercept at $t = 0$ is $(pK_m + C\theta^2)$. The values of pK_m and 'θ' can be obtained from these plots. The values of $(pK_a - Ct^2)$ at various temperatures, for the substituted thioureas taken, were plotted versus 't' and it was observed that the plots were linear (Fig. 3). From these plots the values of 'θ' and pK_m for all these compounds were obtained and these are presented in Table 3. The 'θ' values increase in the order PIT < TCT < TBT < PBT < PCT < TIT where s pK_m values increase in the order PCT < TIT < PBT < TBT < < TIT < PIT. These trends cannot be explained easily because at the high energies of the molecules around the temperature 'θ'°, normal electronic and steric considerations may not be valid.

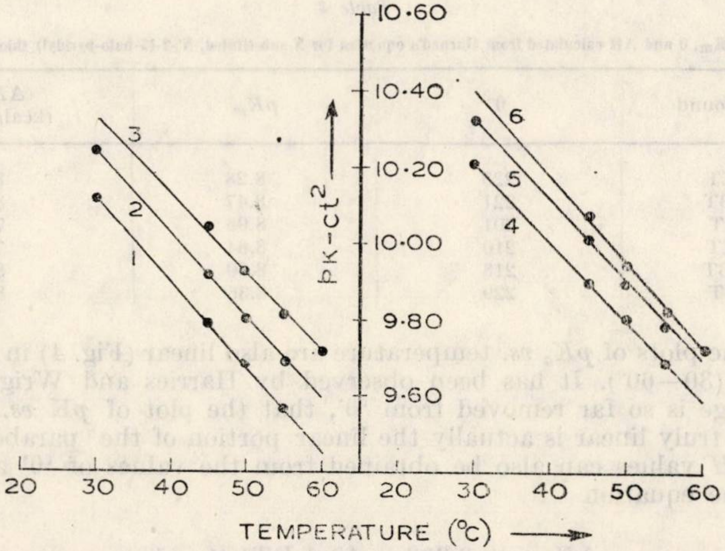

Fig. 3. — Harned's plot $pK - Ct^2$ *vs.* temperature (*t*).

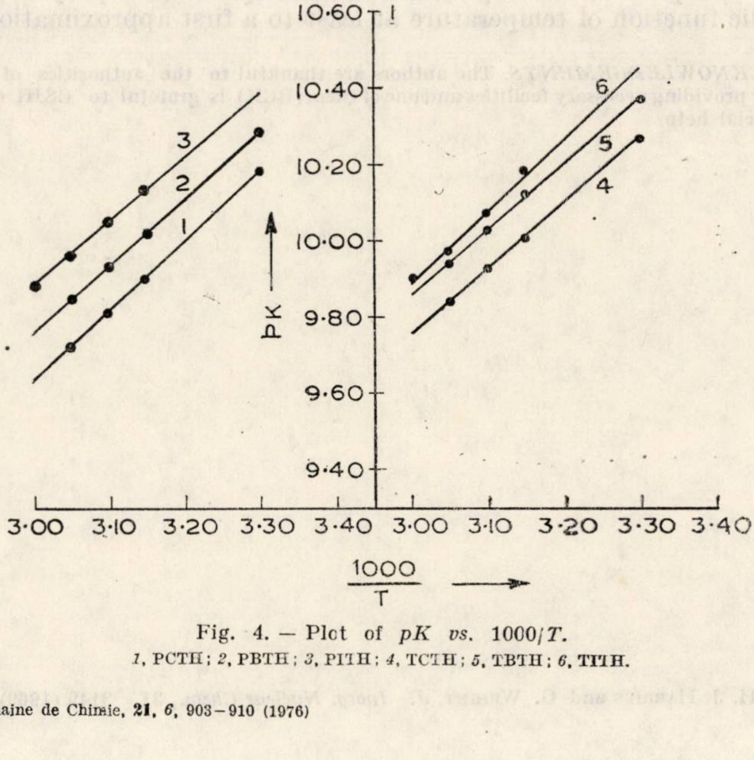

Fig. 4. — Plot of *pK vs.* 1000/*T*.
1, PCTH; *2*, PBTH; *3*, PITH; *4*, TCTH; *5*, TBTH; *6*, TITH.

Table 3

pK_m, θ and ΔH calculated from Harned's equation for N-substituted, N′-2-(5-halo-pyridyl) thioureas

Compound	θ°	pK_m	ΔH_{av} (kcal/mole)
PCT	225	8.28	8.33
PBT	221	8.47	8.14
PIT	201	8.96	7.21
TCT	210	8.64	7.632
TBT	218	8.60	8.00
TIT	229	8.36	8.51

The plots of pK_a *vs.* temperature are also linear (Fig. 4) in the range studied (30−60°). It has been observed by Harries and Wright[13] that this range is so far removed from 'θ', that the plot of pK *vs.* 't' which appears truly linear is actually the linear portion of the parabola.

ΔH values can also be obtained from the values of 'θ' and 't' by using the equation

$$\Delta H = -2.303 \times 10^{-4} RT^2 (t - \theta) \tag{3}$$

as suggested by Harned and coworkers.[10−12] The ΔH values at various temperatures were calculated for all compounds (cf. Table 3) and it was observed that they compare favourably with those obtained from the pK_a *vs* $1/T$ plot illustrating Harned's assumption that $pK_a - pK_m$ is a parabolic function of temperature at least to a first approximation.

ACKNOWLEDGEMENTS. The authors are thankful to the authorities of B.I.T.S., Pilani, for providing necessary facilities and one of them (BCK) is grateful to CSIR (India) for the financial help.

---

[13] H. J. Harries and G. Wright, *J. Inorg. Nuclear Chem.*, **31**, 3149 (1969).

Revue Roumaine de Chimie, **21**, *6*, 911–925 (1976)

SUR LES RÉACTIONS DES POLYMÈRES VINYLIQUES CONTENANT DES GROUPEMENTS AMINIQUES AVEC LES COMPOSÉS ORGANIQUES DU SOUFRE. II[1]

LA RÉACTION ENTRE LA POLY(VINYLAMINE) ET LE CHLORURE DE THIONYLE

OANA PETREUŞ et M. DIMA
Institut de Chimie macromoléculaire «P. Poni»,
41 A, Aleea Grigore Ghica Vodă, Jassy, Roumanie

Reçu le 18 novembre 1974

On a réalisé par un procédé relativement simple la synthèse du copolymère N-vinylthionylamine-vinylamine par la modification chimique de la poly(vinylamine) avec le chlorure de thionyle. Les produits obtenus ont été caractérisés par analyse élémentaire, spectrale en infrarouge et en ultraviolet et par analyse thermique différentielle. On a effectué une étude détaillée du comportement thermique de ces produits.

La réaction entre le chlorure de thionyle et les amines primaires est connue depuis longtemps.[2–5] Pourtant les études sur la structure du groupement thionyaminique des composés qui résultent ont paru beaucoup plus tard.[6–8] Hörhold [9] et ses collaborateurs ont effectué la synthèse de quelques monomères N-sulfinyl-uréthaniques et de leurs dérivés, qu'ils utilisent dans la synthèse des poly(kétaniles).[10]

La littérature ne signale pas de recherches concernant la réaction entre des polymères alcoylés qui contiennent des groupements aminiques primaires et le chlorure de thionyle.

Nous considérons important de connaître le mode de modification chimique du polymère ayant des groupements aminiques réactifs, l'influence de divers facteurs du milieu de réaction, de même que les différences qui apparaissent en comparaison de la structure obtenue aux composés à molécule petite et groupements similaires.

---

[1] Part I. A. Carpov, S. Maxim, O. Petreuş et M. Dima, *Bull. Inst. Polit. Iaşi*, **16**, 401 (1970).

[2] A. Michaelis et J. Herz, *Ber. dtsch. chem. Ges.*, **23**, 3481 (1890).

[3] A. Michaelis, *Ber. dtsch. chem. Ges.*, **24**, 745 (1891).

[4] A. Michaelis, *Liebigs Ann. Chem.*, **274**, 187 (1893).

[5] A. Michaelis, *Ber. dtsch. chem. Ges.*, **30**, 1013 (1897).

[6] W. K. Glass et D. E. Pullin, *Trans. Faraday Soc.*, **1961**, 546.

[7] A. J. Banister, L. F. Moore et J. S. Padley, *Spectrochim. Acta*, **23A**, 2710 (1967).

[8] G. Leandri et A. Mangini, *Spectrochim. Acta*, **6**, 421 (1959).

[9] H. H. Hörhold et H. Eibish, *Chem. Ber.*, **101**, 3567 (1968).

[10] H. H. Hörhold, R. Martin et H. Wolf, Germ. (East) Pat. 89.722, 5 mai 1972; *Chem. Abstr.*, **77**, 15283 (1973).

Vu que la poly(vinylamine) est fortement réactive et ne peut être synthétisée du monomère correspondant, on est parti dans le présent travail du chlorhydrate de la poly(vinylamine), qui est stable dans une atmosphère sans humidité. A partir du chlorhydrate on a préparé la poly(vinylamine)-base libre, au moment de la réaction avec le chlorure de thionyle.

MÉTHODE DE TRAVAIL

La synthèse du chlorhydrate de la poly(vinylamine) a été effectuée dans ce travail, indirectement, à partir de la poly(N-vinylphtalimide). Celle-ci, à son tour, a été synthétisée selon les méthodes de Reynolds[11] et de Nikolaev[12] à partir de l'anhydride phtalique et de la monoéthanolamine, produits techniques de « Petrochim Brazi » et de l'«Institut de produits organiques auxilières de Mediaş.

SYNTHÈSE DE LA POLY(VINYLAMINE)-BASE LIBRE

Le chlorhydrate de la poly(vinylamine), obtenu d'après les indications mentionnées, a été traité à l'hydroxyde de sodium non carbonaté, en atmosphère d'azote purifié, pour obtenir la poly(vinylamine)-base libre. Le chlorhydrate de la poly(vinylamine), de même que la poly(vinylamine)-base libre ont été caractérisés par analyse élémentaire et détermination de la viscosité intrinsèque (pour le chlorhydrate). Les résultats sont présentés dans le tableau 1.

Tableau 1

Analyse élémentaire du chlorhydrate de la poly(vinylamine) et de la base libre

Élément %	Chlorhydrate de la poly(vinylamine)		Poly(vinylamine)-base libre	
	Calculé	Déterminé	Calculé	Déterminé
Azote	17,60	17,63	32,50	30,50
Chlore	44,59	44,10	—	—
Carbone	30,10	30,60	55,80	56,42
Hydrogène	7,54	7,85	11,60	11,07

SYNTHÈSE DU COPOLYMÈRE N-VINYLTHIONYLAMINE-VINYLAMINE

On a utilisé le chlorure de thionyle puriss, la pyridine *p.a.* et comme solvant l'éther éthylique anhydre, le dioxanne *p.a.* et l'alcool éthylique absolu.

Dans un ballon à trois tubulures, muni d'un agitateur mécanique, un entonnoir à robinet et un réfrigérant à reflux, on a introduit 0,27 g (0,06 mole) de poly(vinylamine) récemment précipité dans de l'éther éthylique anhydre, et on a ajouté 0,77 g (0,47 ml) de chlorure de thionyle dilué avec 50 ml d'éther éthylique anhydre, la température de travail étant 25°. A la fin de la réaction on a ajouté 1,6 ml (0,018 mole) de pyridine, pour fixer l'acide chlorhydrique résultant de la réaction. Le copolymère se sépare de la solution éthérée par filtrage; il est séché in vacuo et dissous dans l'eau. La solution de polymère est soumise à la dialyse, jusqu'à la disparition des ions de chlore et ensuite est concentrée in vacuo. Finalement le polymère est précipité dans de l'acétone.

---

[11] D. D. Reynolds et V. O. Kenyon, *J. Amer. Chem. Soc.*, **69**, 911 (1947).

[12] A. F. Nikolaev et S. M. Uchakof, *Izvest. Akad. Nauk. S.S.S.R.*, *Otdel. khim. Nauk.*, **10**, 1235 (1957).

La synthèse du copolymère N-vinylthionylamine-vinylamine a été effectuée en tenant compte de la température, de la durée de la réaction, du rapport molaire, du dipôle-moment des milieux de réaction et du rapport solvant-non-solvant.

a. Influence de la température de réaction. La réaction a été conduite à −189°, −10°, 0°, 25° et 35°.

b. Influence de la durée de la réaction. Aux intervalles de 1, 2, 3, 10 et 24 heures après l'addition du chlorure de thionyle on arrête la réaction par l'introduction d'une quantité correspondante de pyridine.

c. Influence du rapport molaire des réactants. On a étudié la réaction correspondant aux divers rapports molaires poly(vinylamine)-chlorure de thionyle : 1 : 0,25 ; 1 : 0,5 ; 1 : 1 et 1 : 2.

d. Influence du dipôle-moment du milieu de réaction. On a utilisé comme milieu de réaction l'éther éthylique anhydre, le dioxanne anhydrisé, l'alcool éthylique absolu et l'eau.

e. Influence de l'ajout de l'eau sur la réaction. On a étudié l'évolution de la réaction lorsqu'on utilise comme milieu de réaction le mélange éther-eau dans les proportions 90 : 10 ; 80 : 20 ; 50 : 50, en volumes.

Le copolymère synthétisé dans les conditions de chaque cas mentionné a été caractérisé par l'analyse élémentaire et par la détermination de la viscosité intrinsèque de la solution dans l'eau à 25°.

Tableau 2

Analyses élémentaires pour les produits synthétisés à différentes conditions de travail

Variable introduite	Conditions de réaction	Valeur de la variable	S %	N %	Cl %
Température de la réaction	$t = 3$h	− 189°	5,07	14,07	16,23
	rapp. mol. 1 : 1	− 10°	7,50	14,88	1,72
	mil. réac. = éther	0°	7,93	13,34	0,93
		+ 25°	8,10	14,65	7,46
		+ 35°	9,54	13,78	0,91
Durée de réaction	$T = 25°$	1 h	7,02	14,07	5,23
	rapp. mol. 1 : 1	2 h	7,15	13,83	4,29
	mil. réac. éther	3 h	8,10	14,65	7,46
		10 h	13,51	12,23	0,57
		24 h	7,45	12,68	5,52
Rapport molaire P.V.A * − − $SOCl_2$	$T = 25°$	1 : 0,25	3,21	12,99	12,48
	$t = 3$ h	1 : 0,50	7,17	15,13	11,90
	mil. réac. éther	1 : 1	8,10	14,65	7,46
		1 : 2	6,48	11,71	9,67
Dipôle-moment des solvants	$T = 25°$	0 (éther)	8,10	14,65	7,46
	$t = 3$ h	0,5 (dioxanne)	2,36	15,55	18,35
	rapp. mol. 1 : 1	1,66 (alcool)	5,24	15,01	1,09
		1,88 (eau)	13,75	12,40	0,87
Rapport solvant-non-solvant	$T = 25°$	eau : éther			
	$t = 3$ h	0 % : 100 %	8,10	14,65	7,46
	rapp. mol. 1 : 1	10 % : 90 %	15,10	14,50	0,51
		20 % : 80 %	14,27	13,89	0,61
		50 % : 50 %	15,04	14,00	0,48
		100 % : 0 %	13,75	12,40	0,87

P.V.A.* = poly(vinylamine).

Si on compare le graphique de la détermination de la viscosité intrinsèque du chlorhydrate de la poly(vinylamine) avec celui du polymère transformé (fig. 1), apparaît évident le caractère de non-électrolyte de ce dernier (la viscosité intrinsèque du chlorhydrate de la poly(vinylamine) ne peut être déterminée qu'en solution de $NaNO_3$.

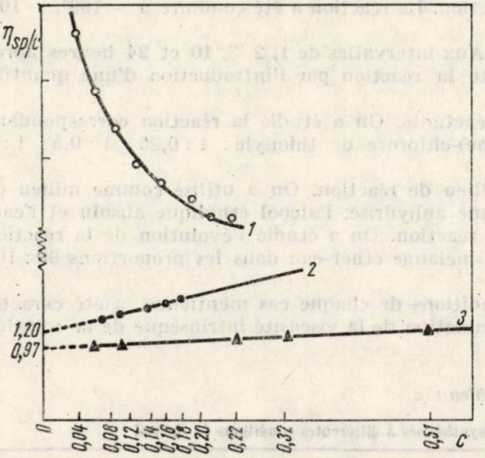

Fig. 1. Détermination de la viscosité intrinsèque de la poly(vinylamine) et du polymère chimiquement modifié.

1, chlorhydrate de la poly(vinylamine) en solution aqueuse; *2*, chlorhydrate de la poly(vinylamine) en solution 0,2M NaNo$_3$; *3*, copolymère N-vinylthionylamine-vinylamine en solution aqueuse.

La structure probable du copolymère synthétisé est de la forme :

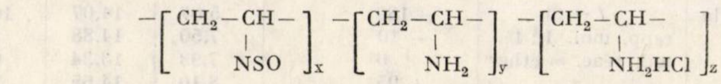

$$-\left[\begin{array}{c}CH_2-CH-\\ |\\ NSO\end{array}\right]_x -\left[\begin{array}{c}CH_2-CH-\\ |\\ NH_2\end{array}\right]_y -\left[\begin{array}{c}CH_2-CH-\\ |\\ NH_2HCl\end{array}\right]_z$$

Les spectres en infrarouge des polymères initiaux et de ceux transformés ont été enregistrés avec un spectrophotomètre UNICAM-SP-200, les produits étant mis en tablettes dans du bromure de potassium ; les spectres en ultraviolet ont été effectués sur des produits dissous dans de l'eau en concentration de 0,4 g/l et 0,8 g/l avec un spectrophotomètre UNICAM-SP-800 pour ultraviolet et en visible.

L'analyse thermique différentielle a été effectuée avec un dérivatographe Paulik-Erdey MOM-Budapest, à une vitesse de chauffage de 9°/mn.

La teneur en soufre a été déterminée par combustion Schöniger, suivie d'un titrage complexométrique.

L'analyse élémentaire a été déterminée par calcul d'après la méthode Scondac-Dima.[13]

RÉSULTATS ET DISCUSSIONS

En tenant compte du mode dont a lieu la réaction des amines à molécule petite avec le chlorure de thionyle, on peut admettre que dans le cas de la poly(vinylamine) la transformation a lieu suivant le schéma :

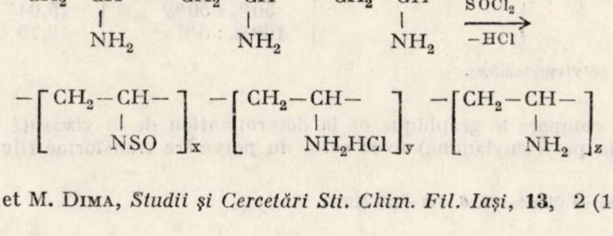

$$\begin{array}{ccc}-CH_2-CH- & -CH_2-CH- & -CH_2-CH-\\ | & | & |\\ NH_2 & NH_2 & NH_2\end{array} \xrightarrow[-HCl]{SOCl_2}$$

$$\longrightarrow -\left[\begin{array}{c}CH_2-CH-\\ |\\ NSO\end{array}\right]_x -\left[\begin{array}{c}CH_2-CH-\\ |\\ NH_2HCl\end{array}\right]_y -\left[\begin{array}{c}CH_2-CH-\\ |\\ NH_2\end{array}\right]_z$$

---

[13] I. Scondac et M. Dima, *Studii şi Cercetări Sti. Chim. Fil. Iaşi*, **13**, 2 (1962).

Les groupements aminiques non transformés du copolymère résulté absorbent en contact avec l'atmosphère de l'acide carbonique, en formant le sel de celui-ci.

Ce fait est connu dans la littérature,[12] la poly(vinylamine) présentant un pour cent plus bas d'azote à l'analyse élémentaire comparativement à la valeur théorique ce qui s'explique justement par la carbonatation de la poly(vinylamine), en présence du CO_2 et de l'humidité de l'atmosphère.

Le copolymère obtenu a l'aspect d'une substance amorphe poussièreuse, soluble dans l'eau si on utilise comme milieu de réaction l'éther, le dioxanne et l'alcool éthylique ; il est insoluble dans d'autres solvants. Le copolymère synthétisé dans un milieu aqueux ou dans un mélange d'éther éthylique et de l'eau, se gonfle dans l'eau, en donnant un matériaxu gluant qui ne se dissous plus. Il est fort probable que pendant la synthèse en milieu aqueux apparaissent, à cause de la réaction fortement exotherme, des ponts réticulaires de type iminique qui ont pour résultat l'insolubilisation du produit.

Si on poursuit, du point de vue analytique, la variation du contenu en soufre et respectivement à celui en chlore du copolymère, fonction des conditions de travail utilisées, on constate que dans la majorité des cas, la réaction effectuée dans un milieu d'éther éthylique, de dioxanne ou d'alcool éthylique conduit à l'accroissement du pourcentage de chlore dans le copolymère et à l'abaissement de celui de soufre. La baisse du degré de substitution du copolymère par rapport au soufre est attribuée à l'attaque de l'acide chlorhydrique qui résulte de la réaction sur les groupements aminiques du polymère.

Dans le cas où on utilise un milieu de réaction qui contient de l'eau, l'acide chlorhydrique se dissout et on ne constate plus la présence du chlore à l'analyse élémentaire. De même, si on réalise la réaction entre la poly(vinylamine) et le chlorure de thionyle en ajoutant la pyridine dès le début, on n'observe pas de modifications dans le degré de transformation du polymère par rapport au soufre. Nous pouvons donc retenir que la présence de la pyridine a comme effet le couplage de l'acide chlorhydrique qui résulte pendant la réaction du chlorure de thionyle avec les groupes aminiques de la poly(vinylamine).

La littérature [14] signale que les thionylamines, tant celles aliphatiques que celles aromatiques, réagisent avec l'eau et régénèrent l'amine

$$R{-}N{=}S{=}O + 2H_2O \longrightarrow R{-}NH_2 + H_2SO_3$$

D'autre part, le chlorure de thionyle est extrêmement sensible en présence de l'eau en formant l'acide chlorhydrique et le bioxyde de soufre.

Il résulterait que l'ajout de l'eau au milieu de réaction (l'éther) devrait produire d'une part le changement de l'équilibre de la réaction et d'autre part la formation préférentielle des groupements de chlorhydrate de la poly(vinylamine). En réalité, le degré de substitution du polymère par rapport au soufre, s'accroît à l'ajout de l'eau dans le milieu de réaction, tandis que le pourcentage de chlore reste au-dessous de 1 %.

---

[14] HOUBEN-WEIL, "Methoden der organishen Chemie" vol. 11/2,4, — ed, Georg Thime Verlag-Stuttgart, p. 740.

Nous constatons donc que dans le cas des macromolécules qui contiennent des groupements aminiques actives, la réaction avec le chlorure de thionyle présente quelques particularités.

On constate tout d'abord, une stabilité du groupement thionylaminique formé lorsque le polymère est dissous dans l'eau. S'il y avait eu une décomposition, situation constatée aux produits similaires à petite molécule, il aurait fallu que l'analyse élémentaire du polymère n'indique plus la présence du soufre après les processus de purification. Les analyses élémentaires et spectrales infirment ce mode de comportement du copolymère N-vinylthionylamine-vinylamine. Le comportement viscosimétrique du copolymère indique qu'il s'agit d'un produit macromoléculaire qui ne contient pas de groupes ionogènes sur la chaîne. Les groupements aminiques qui sont carbonatés ne sont pas dissociés, et les groupements aminiques sous forme de chlorhydrates sont en petit nombre et ont probablement une position qui ne leur permet pas d'influencer la conformation de la macromolécule.

De l'analyse du mode de comportement des réactions dans des solvants à polarité croissante (éther éthylique $\mu = 0$, dioxanne $\mu = 0,5$, alcool éthylique $\mu = 1,6$ et eau $\mu = 1,88$) on observe tout d'abord un abaissement du degré de substitution et ensuite un accroissement évident (fig. 2). En tenant compte du fait qu'un accroissement de la polarité du milieu devrait activer la réaction, on peut remarquer qu'au milieu polaire la règle est respectée.

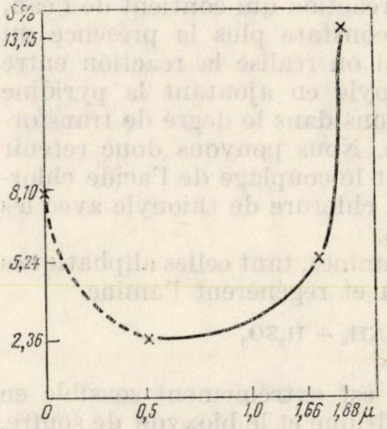

Fig. 2. — Variation du pourcentage en soufre dans le copolymère en fonction du dipôle-moment du milieu de réaction.

Si l'on poursuit l'influence de la durée de la réaction et du rapport molaire des réactants, on ne constate pas des déviations de la règle habituelle. Comme il résulte aussi du tableau 2 on constate un accroîssement évident du pourcentage du soufre dans le copolymère synthétisé à dix heures de réaction. Le degré de transformation indiqué par le contenu en soufre augmente tant que le rapport molaire des réactants ne dépasse pas le rapport stœchiométrique-poly(vinylamine)-chlorure de thionyle et diminue si l'on utilise un excès de chlorure de thionyle (fig. 3).

Si l'on poursuit aussi la variation du pourcentage en chlore du copolymère, on constate (tableau 1) qu'au rapport stœchiométrique des réactants le contenu en chlore est minimal. En conséquence, on peut mentionner qu'au rapport molaire des réactants on obtient le copolymère ayant le maximum d'unités thionylaminiques. A un excès de chlorure de thionyle c'est le nombre des groupements chlorhydratés qui augmente avec la diminution des groupements thionylaminiques.

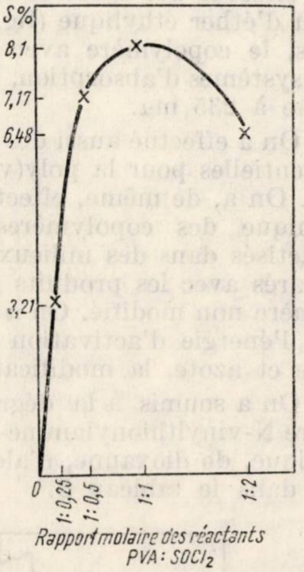

Fig. 3. — Variation du pourcentage en soufre dans le copolymère en fonction du rapport molaire des réactants.

Pour vérifier la structure du nouveau copolymère synthétisé on a tracé les spectres en IR et UV et on a aussi effectué des essais sur le comportement thermogravimétrique.

En comparant le spectre en IR de la poly(vinylamine) avec celui du copolymère préparé, on constate la présence d'une bande large à 1090 cm^{-1}, attribuée à la fonction thionylaminique (fig. 4). La bande pour la vibration du groupement aminique primaire à 3400 cm^{-1} est beaucoup diminuée par rapport à la vibration caractéristique pour le $-CH-$ située à 2998 cm^{-1}. On peut constater la même diminution pour la bande du groupement NH de déformation, située à 1600—1650 cm^{-1}. La bande de 1420 cm^{-1} caractéristique aux vibrations du groupement $-CH_2-CH-$ de la chaîne [évidente dans le spectre de la poly(vinylamine)] se transforme en deux bandes à 1440 et 1400 cm^{-1}. On remarque aussi un pic à 1540 cm^{-1}, inexistant dans le spectre de la poly(vinylamine) et qu'on peut attribuer à la carbonatation des groupements aminiques non transformés. Pour le spectre de la poly(vinylamine) complètement carbonatée, on constate un élargissement du pic à 1620 cm^{-1} et sa division en pics à 1560—1580 et 1720 cm^{-1}, caractéristique pour le groupe carboxyle.

Si la réaction entre la poly(vinylamine) et le chlorure de thionyle est réalisée dans un milieu d'azote purifié, on ne constate aucune modification dans le spectre du produit, ce qui nous fait admettre que la réaction de carbonatation des groupes non transformés est ultérieure à la formation des groupes thionylaminiques (fig. 4).

Vu que la bande de 1090 cm^{-1} caractéristique du groupement thionylaminique peut être soupçonnée d'interférence avec la bande de 1000 cm^{-1} correspondant au groupement $-C-N=$ du spectre de la poly(vinylamine), on a effectué des spectres en UV pour le copolymère synthétisé dans le milieu d'éther éthylique (fig. 5). De même que les thionylamines aliphatiques, le copolymère avec des groupements thionylaminiques présente deux systèmes d'absorption, l'un à 300–310 mμ et le deuxième d'intensité réduite à 235 mμ.

On a effectué aussi des analyses thermogravimétriques et thermiques différentielles pour la poly(vinylamine) et le polymère modifié chimiquement. On a, de même, effectué une étude comparative du comportement thermique des copolymères avec des groupements thionylaminiques synthétisés dans des milieux de réaction différents. Les produits ont été comparés avec les produits initiaux non dégradés et avec le support du polymère non modifié. On a ainsi obtenu des informations en ce qui concerne l'énergie d'activation de la réaction, la variation du contenu en soufre et azote, la modification des bandes d'absorption en IR.

On a soumis à la dégradation thermique des échantillons de copolymère N-vinylthionylamine-vinylamine synthétisés dans un milieu d'éther éthylique, de dioxanne, d'alcool éthylique et d'eau. Les résultats se trouvent dans le tableau 3.

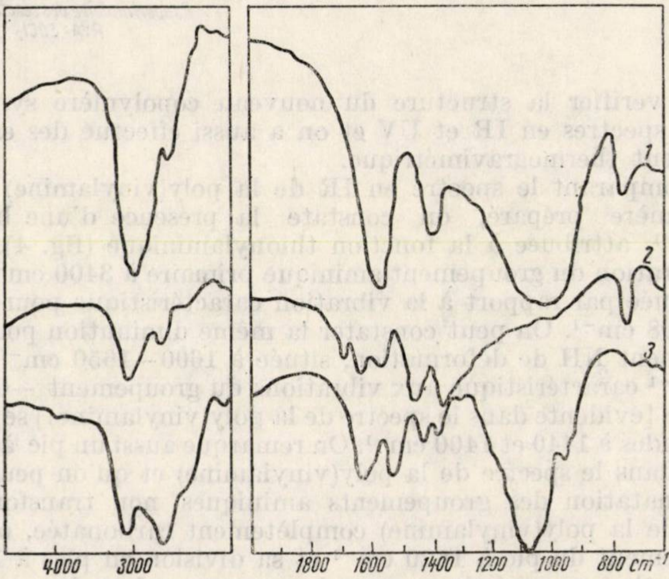

Fig. 4. — Spectres en IR de la poly(vinylamine)-base libre (1), de la poly(vinylamine)-carbonaté (2) et du copolymère (3).

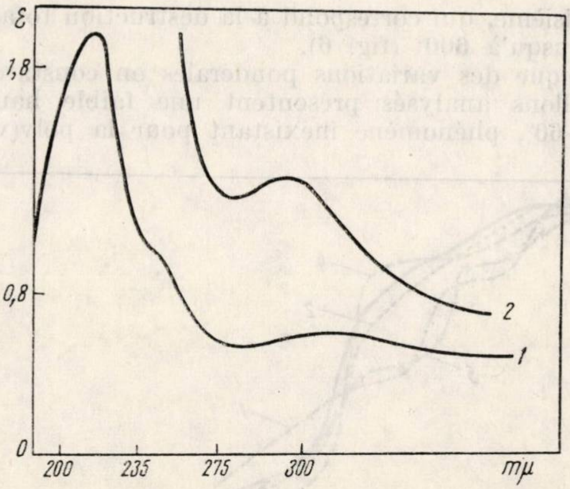

Fig. 5. — Spectres en UV du copolymère à la concentration de 0,4 g/l (1) et de 0,8 g/l (2).

On a chauffé dans l'air un échantillon dans un four à régime thermique contrôlé. Les domaines thermiques étudiés correspondent aux pics de la courbe DTA enregistrés en même temps au dérivatographe. L'échantillon est maintenu au régime thermique établi, pendant 15 mn, à l'aide d'un thermorégulateur monté dans le circuit. Pour chaque étape thermique on a effectué les analyses élémentaires du soufre et de l'azote, de même que le spectre IR des échantillons dégradés.

Tableau 3

Analyses élémentaires et degré de transformation pour les échantillons synthétisés dans des milieux de réaction différents

Échantillon	Solvant utilisé	Degré de transformation %	S %	N %	Cl %	C %	H %	O %
Poly(vinylamine)			—	30,60	—	56,42	11,07	—
Produit modifié chimiquement	Dioxanne (1)	6,49	2,36	15,55	18,35	39,09	8,13	16,52
,,	Alcool (2)	17,00	5,24	15,01	1,09	37,80	7,22	33,64
”	Ether (3)	27,4	8,10	14,60	7,83	34,88	6,40	28,34
,,	Eau (4)	32,00	13,75	12,40	0,87	30,38	4,20	38,40

En géneral, tous les échantillons présentent trois domaines de dégradation thermique : le premier entre 50—100°, le deuxième qui se termine à 300° et le troisième, qui correspond à la destruction totale de la chaîne du polymère, jusqu'à 600° (fig. 6).

Du graphique des variations pondérales on constate que tous les quatre échantillons analysés présentent une faible hausse pondérale autour de 50–60°, phénomène inexistant pour la poly(vinylamine) de départ. Nous considérons qu'en cette étape un phénomène d'oxydation du groupement thionylaminique et son transformation en sulfonamide ont lieu.

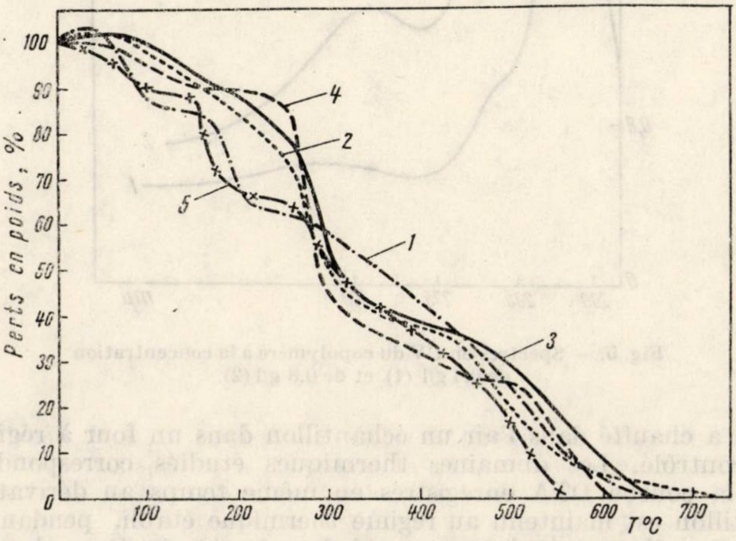

Fig. 6. — Courbes des pertes en pourcentage du poids en fonction de la température pour des échantillons synthétisés dans de l'alcool éthylique (1), du dioxanne (2), de l'éther éthylique (3) et dans de l'eau (4) et de la poly(vinylamine) — base libre (5).

Le milieu de réaction influence aussi le comportement du copolymère en cette étape. Dans le cas où l'on utilise un milieu de réaction aqueux, la hausse pondérale est insignifiante ; il est fort probable que la réaction d'oxydation a eu lieu partiellement au moment de la synthèse à cause de l'effet exothermique très énergique. En faisant la corrélation avec le dipôle-moment du milieu de la synthèse, on constate qu'à une hausse de celui-ci, le produit obtenu présente une capacité d'oxydabilité de plus en plus réduite. Le phénomène peut s'encadrer dans la règle générale de l'effet du milieu de réaction sur les composés résultés. Un milieu avec une polarité plus élevée stimulera la réaction dans le sens de la formation des groupements sulfonamidiques plus stables. Cette supposition est soutenue aussi par l'aspect du graphique des pertes en poids pour les échantillons synthétisés dans l'éther auquel on a ajouté des volumes calculés d'eau (fig. 7).

Pour l'échantillon synthétisé en milieu d'éther avec de petites quantités d'eau, la hausse du pourcentage en poids est la même que pour celui synthétisé en éther. Plus les échantillons sont synthétisés dans des conditions de réaction plus énergiques (l'ajout de quantités plus grandes d'eau), d'autant plus les pertes en poids sont moindres, respectivement l'activité d'oxydation des groupements est plus réduite.

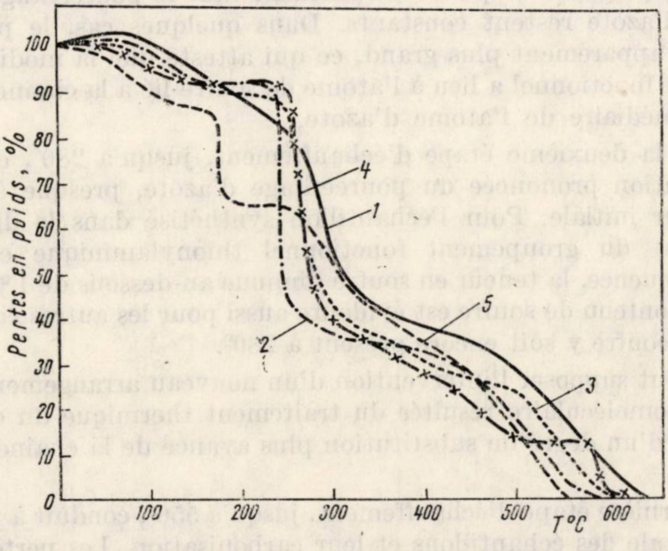

Fig. 7. — Courbes des pertes en pourcentage du poids en fonction de la température pour des échantillons synthétisés en milieu d'éther (1), éther : eau 90 : 10 (2), éther : eau 50 : 50 (3), eau (4) et de la poly(vinylamine)-base libre (5).

Pour l'étape suivante d'échauffement, l'échantillon de copolymère synthétisé dans l'eau présente un aspect stable jusqu'à 250°. Dans un court intervalle de température (30°), ce copolymère perd presque la moitié de son poids ; autour de 280—300° son aspect analytique et spectral est dégradé.

La dégradation thermique illustrée par les pertes en poids, peut être mise en correlation avec les résultats analytiques des échantillons chauffés. Les résultats sont présentés dans la tableau 4.

Tableau 4

Valeurs des pertes en poids pour des échantillons chauffés

Échantillon	Température 50 – 60°			Température 280 – 300°/Température 530 – 550°					
	Variation pondérale	S %	N %	Variation pondérale	S %	N %	Variation pondérale	S %	N %
1	+ 1,66	1,07	15,54	– 44,00	0,16	8,27	– 91,50	—	—
2	+ 1,40	4,99	16,09	– 41,50	3,77	8,24	– 93,00	—	—
3	+ 2,3	5,07	14,01	– 37,50	4,47	6,99	– 82,50	—	—
4	+ 0,64	14,39	13,47	– 49,00	9,21	6,23	– 91,50	—	—

Excepté l'échantillon synthétisé dans le dioxanne, où le degré de substitution est trop petit pour pouvoir tirer des conclusions sur l'influence du groupement fonctionnel concernant la stabilité thermique, on constate que dans la première étape d'échauffement tant le pourcentage de soufre que celui d'azote restent constants. Dans quelques cas, le pourcentage d'azote est apparément plus grand, ce qui atteste que la modification du groupement fonctionnel a lieu à l'atome de soufre lié à la chaîne principale par l'intermédiaire de l'atome d'azote.

Dans la deuxième étape d'échauffement, jusqu'à 280°, on constate une diminution prononcée du pourcentage d'azote, presque à la moitié de la valeur initiale. Pour l'échantillon synthétisé dans le dioxanne, le détachement du groupement fonctionnel thionylaminique est certain, et en conséquence, la teneur en soufre diminue au-dessous de 1 %. La diminution du contenu de soufre est évidente aussi pour les autres échantillons, quoique le soufre y soit encore présent à 280°.

On peut supposer l'intervention d'un nouveau arrangement des fragments micromoléculaire résultés du traitement thermique du copolymère dans le cas d'un degré de substitution plus avancé de la chaîne macromoléculaire.

La dernière étape d'échauffement, jusqu'à 550°, conduit à une décomposition totale des échantillons et leur carbonisation. Les pertes en poids sont maximales, variant entre 83–93 %. Il est intéressant que l'échantillon synthétisé dans de l'eau, qui pendant les deux premières étapes d'échauffement manifestait une stabilité plus grande, présente à la fin de la deuxième étape une perte brusque du poids et un aspect du spectre en IR qui indique une dégradation totale.

Pour compléter ces données concernant les pertes en poids, on a effectué des spectres en IR des produits résultés dans différentes étapes de dégradation thermique. Les résultats sont présentés dans le tableau 5. On constate que :

— Par le chauffage des échantillons synthétisés dans des milieux différents, à 50–60°, les bandes d'absorption en IR ne présentent pas de modifications essentielles, excepté l'apparition d'une nouvelle bande à 1340–1380 cm^{-1}. En tenant compte du fait que le bioxyde de soufre en solution de tétrachlorure de carbone [5] présente le même domaine d'absorption (1342 cm^{-1}), on peut attribuer cette fréquence aux groupements $-NSO$ oxydés à $=NSO_2$.

— Par le chauffage des échantillons à 280° on constate la disparition de certains pics, l'élargissement où l'unification des autres. Le fait que dans la majorité des cas il y a une fusion de la vibration fondamentale pour NH et pour CH avec déplacement et déformation de la vibration de 1620 cm^{-1}, on peut arriver à la conclusion qu'il y a des modifications principales à la liaison $C-N$. Le fait est confirmé par les déplacements subis par les vibrations $C-N$ situées à 820 et 1100 cm^{-1}.

Tableau 5

Valeurs des fréquences IR en cm^{-1} pour des échantillons chauffés dans chaque étape thermique

		$\nu NH_{fond.}$	$\nu CH_{fond.}$	$\nu NH_{def.}$	$\nu CH-CH_2$	νSO_2	νNSO	νCN
R—NSO aliphatiques (littérature)			2980		1380 ; 1468	1342	1252 ; 1135	1100 ; 830
Copolymère N-vinylthionylamine-vinylamine		3400	2950	1630	1540 ; 1440 ; 1400	—	1090	1090 ; 1100
Température de chauffage 50—60°	1	3440	2950	1630	1540 ; 1420 ; 1400	1340	1260 ; 1090	790
	2	3440	2950	1630	1540 ; 1440 ; 1400	1340	1260 ; 1100	1100 ; 800
	3	3440	2950	1630	1540 ; 1420 ; 1440	1380	1100	1100
	4	3440	2950	1630	1540 ; 1410 ; 1450	1380	1090 ; 1100	1100
Température de chauffage 280°	1	3400↔2900		1560	1420	—	—	820
	2	3400↔2900		1620	1410	—	1100	790
	3	3400↔2900		1620	1410	—	1120	1100
	4	3400	—	1620	—	—	1100	1100
Température de chauffage 550°	1	—	2900	—	—	—	—	—
	2	—	2900	—	—	—	—	—
	3	←3200→		1580	—	—	1200—1100	—
	4	—	—	—	—	—	—	—

— Les échantillons chauffés à 550° ne présentent plus de pics d'absorption que dans le cas des échantillons synthétisés dans de l'alcool et de l'éther, mais même dans ces cas ils sont peu distincts et étalés.

Les données sur l'énergie d'activation et sur l'ordre de réaction présentent des résultats intéressants. L'énergie d'activation calculée d'après la méthode de Freeman et Caroll [15] concernante le premier processus de décomposition confirme la supposition sur l'oxydation thermique du groupement thionylaminique (fig. 6).

Pour l'échantillon synthétisé dans l'eau, l'énergie d'activation est minimale — 8,2 kcal/mole — car le processus d'oxydation commence pendant la synthèse. L'ordre de réaction 2,3 correspond à un processus oxydatif.

Le deuxième processus de décomposition est caractérisé par une énergie d'activation du même ordre de grandeur pour tous les échantillons 53—55 kcal/mole.

---

[15] E. S. Freeman et B. Carrol, *J. Phys. Chem.*, **62**, 394 (1958).

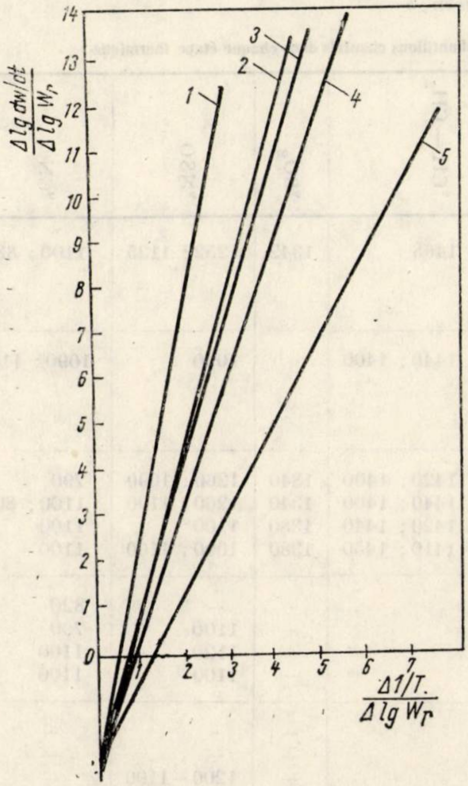

Fig. 8. — Energie d'activation et ordre de réaction pour les échantillons chauffés à 50—60° ; poly(vinylamine)-base libre (1), échantillon synthétisé en milieu d'alcool (2), d'éther (3), de dioxanne (4) et d'eau (5).

Tableau 6

Valeurs de l'énergie d'activation et l'ordre de réaction pour les produits non transformés et pour ceux modifiés chimiquement

Échantillon	Etape	Énergie d'activation (kcal/mole)	Ordre de réaction (n)
Poly(vinylamine)	1	23,33	2,8
	2	52,62	1,3
	3	55,36	1,0
	4	106,62	1,5
(1)	1	12,50	2,2
	2	55,00	2,0
	3	80,00	1,6
	4	50,33	1,9
(2)	1	15,10	2,3
	2	35,20	0,25
	3	69,60	0,35
	4	17,75	1,3
(3)	1	14,50	2,4
	2+3	45,76 + 46,3	1,7
	4	15,82	0,9
(4)	1	8,23	2,13
	2	53,18	1,8
	3	26,67	0,4

Le dernier processus de décomposition présente des valeurs énergétiques très petites par rapport aux échantillons antérieurs. On suppose que la décomposition en cette étape est un processus autocatalytique, rencontré aussi dans la décomposition des autres polymères qui contiennent de l'azote aminique dans le groupement fonctionnel lié à la chaîne principale.[16]

Le tableau 6 résume les données sur l'énergie d'activation et l'ordre de réaction dans les étapes de décomposition mentionnées.

En conclusion, nous pouvons signaler d'avoir réussi la synthèse d'un nouveau produit macromoléculaire qui contient des groupements thionylaminiques. Le copolymère obtenu par la modification chimique de la poly(vinylamine) est intéressant du point de vue structural et pourra constituer le point de départ d'une étude ultérieure des composés macromoléculaires qui contiennent des groupements sulfonyl-aliphatiques.

---

[16] F. Popescu, I. Petrariu et S. Percec, *Rev. Roumaine Chim.* (à paraître).

Revue Roumaine de Chimie, **21**, *6*, 927–931 (1976)

CONTRIBUTIONS TO THE POLYMERIZATION AND COPOLYMERIZATION OF THE ACRYLONITRILE IN THE PRESENCE OF ORGANO-METALLIC CATALYSTS

CR. I. SIMIONESCU, D. FELDMAN and VIOLETA NUŢĂ
Institute of Macromolecular Chemistry "P. Poni"
Iaşi, Aleea Grigore Ghica Vodă 41-A

Received December 14, 1974

The polymerization and copolymerization of the acrylonitrile with triisobutyl-aluminium in the presence of cocatalysts was studied. The influence of the catalytic system on the polymerization and copolymerization development and the nature of acrylonitrile-epichlorohydrin copolymer was investigated. After fractionation by successive extractions these copolymers have been characterized by elemental analysis, IR and NMR spectroscopy.

INTRODUCTION

Data about olefine and diolefine polymerization with catalysts containing organic derivatives of aluminium are known from the literature.[1–11]

Starting from the latest achievements in this domain, the present note tries to transfer the possible synthesis by means of these catalytic systems from the domain of olefines and diolefines polymerization to that of the polymerization of some polar vinylic monomers as acrylonitrile (AN) and its copolymerization with epichlorohydrin (ECH).

The extrapolation of Ziegler-Natta catalytic systems from the domain of olefines polymerization to that of polar monomers polymerization permits to increase the number of the monomers used in such syn-

---

[1] G. Natta, P. Pino, G. Mazzanti, U. Giannini, E. Mantica and M. Peraldo, *J. Polymer Sci.*, **26**, 120 (1957).

[2] G. Natta, P. Pino, G. Mazzanti and U. Giannini, *J. Inorg. Nuclear Chem.*, **8**, 612 (1958).

[3] F. Patat and H. Sinn, *Angew. Chem.*, **70**, 496 (1958).

[4] W. P. Long, *J. Amer. Chem. Soc.*, **81**, 5312 (1959).

[5] W. P. Long and D. S. Breslow, *J. Amer. Chem. Soc.*, **82**, 1953 (1960).

[6] G. L. Karapinka and W. L. Carrick, *J. Polymer Sci.*, **55**, 145 (1961).

[7] A. K. Zefirova and A. E. Shilov, *Proc. Akad. Sci. U.S.S.R. Chem. Sect.*, **136**, 77 (1961).

[8] G. Natta, I. Pasquon and A. Zambelli, *J. Amer. Chem. Soc.*, **84**, 1488 (1962).

[9] A. E. Shilov, A. K. Shilova and B. N. Babkov, *Vysokomol. Soedineniya*, **4**, 1688 (1962).

[10] F. S. Dyachovskii, *Vysokomol. Soedineniya*, **7**, 114 (1965).

[11] R. Reichert and J. Schubert, *Makromol. Chem.*, **123**, 59 (1969).

thesis and, at the same time, to obtain new polymers. By these means, one arrives to general conclusions correlating characteristics which arise from the structure and aggregation state of the catalyst, from the polymerization conditions in homogeneous or heterogeneous phases.

With this aim in view, various catalyst-cocatalyst systems have to be studied.

EXPERIMENTAL

$Al(i\text{-}C_4H_9)_3$ was used as toluene solution, and its concentration was determined by Crompton's method.[12]

As cocatalysts we used $Sn(C_6H_5)_4$, $TiCl_3$ (benzene solution), $VOCl_3$ (benzene solution). The polymerization was made in benzene and the methanol precipitated polymer was purified by successive reprecipitations from dimethylformamide (DMF) solutions and dried at 60° in vacuum.

RESULTS AND DISCUSSION

The polymerization and the copolymerization of AN with ECH in the presence of organo-aluminium compounds, with or without cocatalyst, provided the data presented in tables 1 and 2.

One can see from table 1 that aluminium-alkyl catalyst led to very low yields.

To increase conversion, we experimented some cocatalysts, complexing agents of aluminium-alkyl (organo-metals derivatives, protonic agents). The use of $VOCl_3$ and $Sn(C_6H_5)_4$ led to higher conversions.

Table 1

AN polymerization and copolymerization with various catalyst systems

Sample No	I/M mol/mol	I/(M + S) mol/mol	Catalyst system					Al/Cocatalyst ratio mol/mol	Conv. % gv.	Obs.
			$Al(i\text{-}Bu)_3$		Cocatalyst					
			ml	mol	Name	ml	mol			
1	0.180	0.0350	2.0	0.0080	—	—	—	—	1.43	a
2	0.043	0.0087	0.5	0.0019	$VOCl_3$	0.10	0.57×10^{-4}	33.33	17.41	b
3	0.178	0.0360	2.0	0.0080	$Sn(C_6H_5)_4$	0.01g	0.23×10^{-4}	347.00	22.45*	a
4	0.114	0.0320	2.0	0.0080	—	—	—	—	15.89*	c

I – catalyst; M – monomer; S – solvent; * After substraction of minerals; [a] Homopolymer; [b] Homopolymer (minerals as traces); [c] Copolymer with ECH ([ECH] = 0.025 mols)

In all polymer samples, the yield was not higher than 20–30%.

Experiments shown in table 1 were carried out at 40°, using a ratio monomer : solvent equal to 0.25. Triisobutyl-aluminium was used as toluenic solution with 60 g/l concentration. Benzene was used as solvent in all the samples.

---

[12] T. R. Crompton, *Analyst*, **91**, 374 (1966).

The duration of polymerization and copolymerization was in all samples 25 hours.

In contrast with the $VOCl_3$ system, in other cases the polymer presented a great minerals content, respectively 9.40% in copolymer and 20.50% in the sample obtained with Sn $(C_6H_5)_4$, amounts which result from the catalyst system.

The elemental analysis of the AN-ECH copolymer led to the following results :

%C – 42.65 ;
%H – 5.44 ;
%N – 2.84 ;
%Cl – 26.86.

These data prove that the end product of the reaction has AN units as well as ECH units, the latter being in predominant amount.

As we can see from the following, attempts to elucidate the nature of such a macromolecular compound show that in our experimental conditions, a synthesis of AN-ECH copolymer was possible.

One remarks in the case of the third run (table 1) that the I.R. spectrogram of the obtained polymer is markedly changed in comparison with that of radicalic or ionic PAN, a fact which can be explained by a high complexing action of the organo-tin compound with the polymer polar groups.

Table 2

AN polymerization and copolymerization with binary and ternary systems of catalyst

Run N°	I/M mol/mol	I/(M + S) mol/mol	Catalyst system						Al/Cocatalyst ratio mol/mol	Conv. % gv.	Obs.
			$Al(i-Bu)_3$		Cocatalysts						
					1		2				
			ml	mol	ml	mol	ml	mol			
					$TiCl_3$		$VOCl_3$				
1	0.045	0.0090	0.5	0.0019	0.20	0.64×10^{-4}	0.10	0.57×10^{-4}	15.70	10.95*	a
					$VOCl_3$		$Sn(C_6H_5)_4$				
2	0.044	0.0088	0.5	0.0019	0.10	0.57×10^{-4}	0.01g	0.23×10^{-4}	23.70	11.30*	a
					$Sn(C_6H_5)_4$						
3	0.115	0.0322	2.0	0.0080	0.01g	0.23×10^{-4}	–	–	352.00	32.50*	b

I – catalyst ; M – monomer ; S – solvent ; * After subtraction of minerals ; [a] Homopolymer ; [b] Copolymer with ECH ([ECH] = 0.025 mols)

The runs from table 2 were made under the same conditions, but using binary and ternary systems of catalyst.

Data from this table show that the system Al $(i-C_4H_9)_3-$ $Sn(C_6H_5)_4$ (run 3), leads to high conversions. Elemental analysis of the copolymer shows the following results :

%N — 3.30 ;

% Cl — 29.00.

Parts of polymers were separately extracted with hot DMF (PAN solvent), hot cyclohexanone (CH) and hot dioxan (solvents for PECH[13]), and we obtained every time soluble and insoluble fractions ; their elemental analysis is presented in table 3.

Fractions soluble in CH and dioxan are characterized by a high amount of chlorine and a low amount of nitrogen ; in the case of the DMF-soluble fraction, the situation is different. These data show that fractions are in fact copolymers in which ECH (the fractions soluble in CH and dioxan) or AN (DMF-soluble fractions) are predominant.

IR study of a CH-soluble fraction (Fig. 1) shows that the spectrogram evinces characteristic peaks for AN at 2250 cm^{-1}, the frequency range of the $-C{\equiv}N$ group, while for ECH at 1120 cm^{-1}, the range of the $-C-O-C-$ group. This proves the AN-ECH copolymer synthesis.

Table 3

Elemental analysis of fractions obtained with DMF, CH and dioxan

Solvent	Elemental analysis					Minerals* %
	C %	H %	N %	Cl %	O %	
DMF						
Soluble 30%	54.28	7.81	10.61	6.29	21.00	13.80
Insoluble 70%	43.56	6.60	3.30	30.20	16.34	43.50
CH						
Soluble 73%	43.91	5.54	4.31	30.85	15.39	8.07
Insoluble 27%	55.00	7.63	13.90	4.47	19.00	14.61
Dioxan						
Soluble 75%	51.37	6.54	2.46	27.59	12.04	—
Insoluble 25%	58.16	7.83	9.14	6.87	18.00	34.86

* Data were reported to the fraction without mineral compounds

NMR spectra (Jeol JNM—C) of the dioxan-soluble fraction is also characteristic of the AN-ECH copolymer. It seems that this is a block-copolymer which has long fragments with ECH and short fragments with

---

[13] M. Dimonie and I. Gavăt, *European Polymer J.*, 4, 541 (1968).

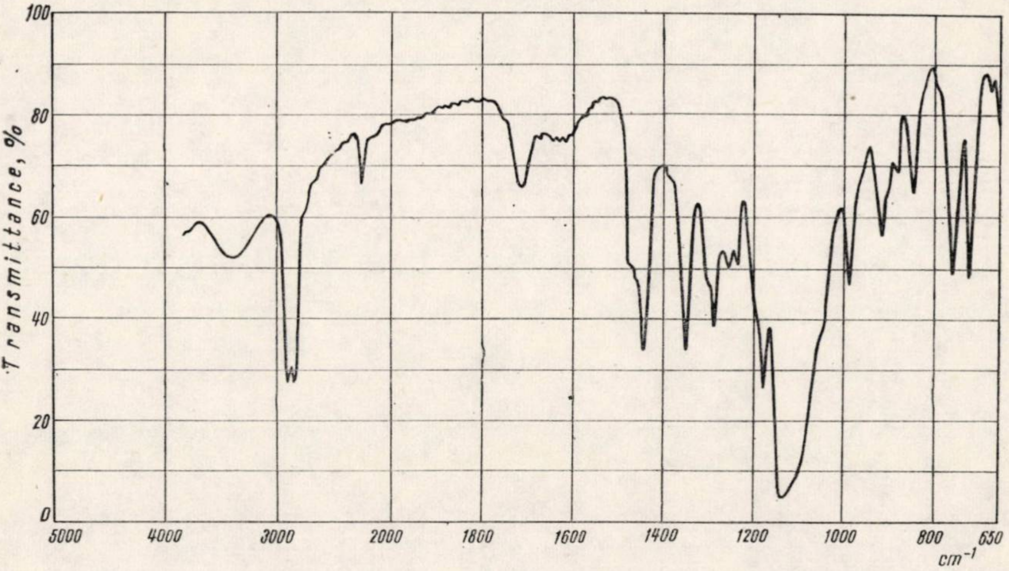

Fig. 1. — IR spectrogram of the fraction soluble in CH (table 2, run 3).

AN. At the ends of the chains there are also AN units :

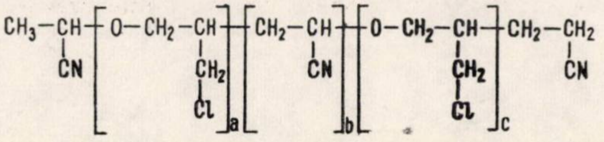

$$CH_3-\underset{\begin{array}{c}|\\CN\end{array}}{CH}-\left[O-CH_2-\underset{\begin{array}{c}|\\CH_2\\|\\Cl\end{array}}{CH}\right]_a\left[CH_2-\underset{\begin{array}{c}|\\CN\end{array}}{CH}\right]_b\left[O-CH_2-\underset{\begin{array}{c}|\\CH_2\\|\\Cl\end{array}}{CH}\right]_c CH_2-\underset{\begin{array}{c}|\\CN\end{array}}{CH_2}$$

Roentgen analysis shows that all fractions are amorphous.

CONCLUSIONS

1. AN polymerization with various catalyst systems including Al $(i-C_4H_9)_3$ is studied.
2. The binary systems used show that those with $VOCl_3$ or $Sn(C_6H_5)_4$ lead to conversions of about 20%.
3. An AN-ECH copolymer was synthesized.
4. With $Al(i-C_4H_9)_3 - Sn(C_6H_5)_4$, a copolymer with a higher conversion than 30% was obtained.

Revue Roumaine de Chimie, 21, 6, 927–931 (1976)

9 – c 1140

Revue Roumaine de Chimie, **21**, *6*, 933–936 (1976)

UTILIZATION OF A Hg^{2+}-SENSITIVE MEMBRANE-ELECTRODE IN THE DETERMINATION OF SOME α-AMINO ACIDS

C. LITEANU, ELENA HOPÎRTEAN and RODICA VLAD
Department of Analytical Chemistry, University of Cluj-Napoca,
Cluj-Napoca, Romania

Received July 3, 1974

The results obtained from the determination of some α-amino acids by potentiometric titration with Hg^{2+}-solution, using a Hg^{2+}-sensitive membrane-electrode as an indicating electrode, are presented. Special mention is made on the results obtained in the cysteine determination, which is possible even at a concentration of 0.13 μg cysteine/ml.

INTRODUCTION

The literature[1] reports that α-amino acids form 1 : 2 metal-ligand type complexes with Hg^{2+} ions. Evidently, in the case of all α-amino acids having in their molecule only the $-NH_2$ and $-COOH$ groups, as functional groups, chelate formation takes place by the same mechanism, i.e. release of the proton of the carboxyl group and formation of the donor-acceptor bond with the nitrogen of the amino group.[1] In the case of cysteine, Lenz and Martell[2] assumed that both groups $-SH$ and $-NH_2$ participate in the formation of the complex with Hg^{2+}. Subsequently, Van der Linden *et al.*[1] proved that only the $-SH$ group is involved in the formation of cysteine complex with Hg^{2+}.

Since the Hg^{2+}-sensitive electrode presented in a previous paper[3] was available, we undertook to extend its analytical utilization by employing it as indicating electrode for the determination of some α-amino acids by potentiometric titration with a Hg^{2+} solution.

EXPERIMENTAL RESULTS AND DISCUSSION

A Hg^{2+}-sensitive electrode was used, whose membrane has the composition 75% moles AgI + 25% moles Ag_2S. Potential measurements were performed on a MV-11 pH-meter (accuracy ± 2 mV), the membrane-electrode potential being assimilated to the e.m.f. of the following electrochemical cell :

$$\text{SCE} \left\| \begin{array}{l}\text{salt bridge}\\ KNO_3\ 10^{-1}M\ \text{agar-agar}\end{array} \right| \text{test solution} \left| \begin{array}{l}Hg^{2+}\text{-sensitive}\\ \text{membrane-electrode}\end{array}\right.$$

---

[1] W. E. Van der Linden and C. Beers, *Analyt. Chim. Acta*, **68**, 143 (1973).

[2] S. R. Lenz and A. E. Martell, *Biochemistry*, **3**, 745 (1964).

[3] I. C. Popescu, E. Hopîrtean, L. Savici and R. Vlad, *Rev. Roumaine Chim.*, **20**, 993 (1975).

Potential determinations were performed at room temperature under magnetic stirring.

Fig. 1 and Table 1 present the results obtained from cysteine determination in a concentration interval $10^{-2}-10^{-5}$M by titration with a Hg^{2+} solution of known concentration. The factor of the Hg^{2+} solution was established by titrating the solution with complexon III of a known factor in the presence of the Hg^{2+}-sensitive indicating electrode. The equivalence volumes were calculated by the Hahn-Weiler interpolation method.[4]

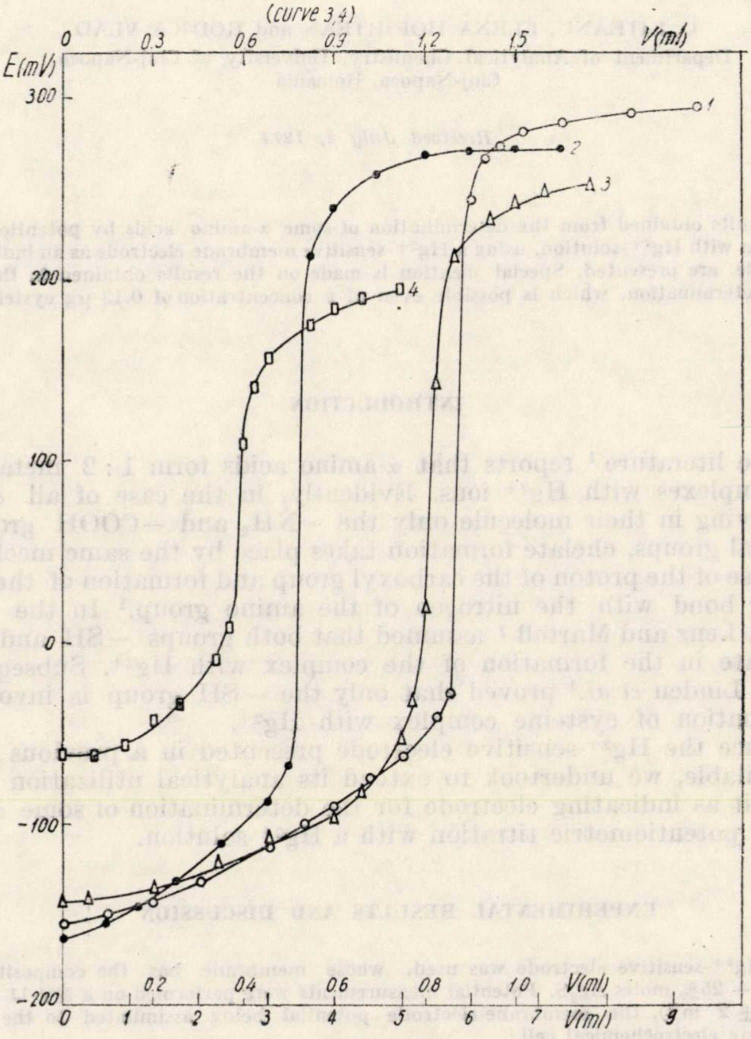

Fig. 1. — Titration curves of cysteine with Hg^{2+} solution.

1 — c = 10^{-2} M ; *2* — c = 10^{-3} M ; *3* — c = 10^{-4} M ; *4* — c = 10^{-5} M.

---

[4] F. L. Hahn and G. Weiler, *Z. analyt. Chem.*, **69**, 417 (1926).

Both titration curves in fig. 1 and data listed in table 1 point to the particularly high sensitivity of the electrode in cysteine determination by titration with Hg^{2+} solution. Even in the case of cysteine determination of a 0.13 μg cysteine/ml concentration, the potential jump around the equivalence point for a ±1% accuracy is 80 mV. The large potential variation around the equivalence point is due to the fact that up to the equivalence point, the electrode potential is established at negative values by cysteine relative to which electrode is sensitive, considering the presence of the Ag^+ ion in the membrane composition. After the equivalence point, the electrode is supposed to assume positive potential values due to the response relative to Hg^{2+} ions.

Table 1

Results of the cysteine determination by potentiometric titration with Hg^{2+} solution

Cysteine			$\Delta E_{\pm 1\%}$ (mV)
Concentration	Taken quantity (mg)	Found quantity (mg)	
10^{-2}M	14.0	14.1	240
10^{-3}M	1.3	1.27	180
10^{-4}M	0.13	0.12	115
10^{-5}M	0.013	0.013*	80

* The volume of the sample was 100 ml.

Further attempts were made to use Hg^{2+}-sensitive electrode as an indicating electrode for the determination by potentiometric titration of the following α-amino acids : arginine, leucine, histidine. Titration curves obtained at pH = 4.6, using 10^{-2}M Hg^{2+} solution as a titrating agent, are exhibited in Fig. 2 and the results are listed in Table 2.

Table 2

Results of the determination of some α-amino acids by potentiometric titration with Hg^{2+} solution

α-Amino acid	Quantity (mg)		$\Delta E_{\pm 1\%}$ (mV)
	Taken	Found	
Arginine	17.4	17.3	22
Leucine	13.2	13.4	35
Histidine	15.6	15.9	15

Samples of α-amino acids were weighed on an analytical balance. The potential jump around the equivalence point for the ±1% error in the case of the three α-amino acids, comprised between 15–35 mV (table 2), illustrates their practically identical behaviour relative to the Hg^{2+} ion and the clearly different behaviour from that of cysteine, where the potential variation around the equivalence point was 240 mV under similar conditions of concentration and of error. Of course, these results are closely related both to the mechanism underlying the formation of the

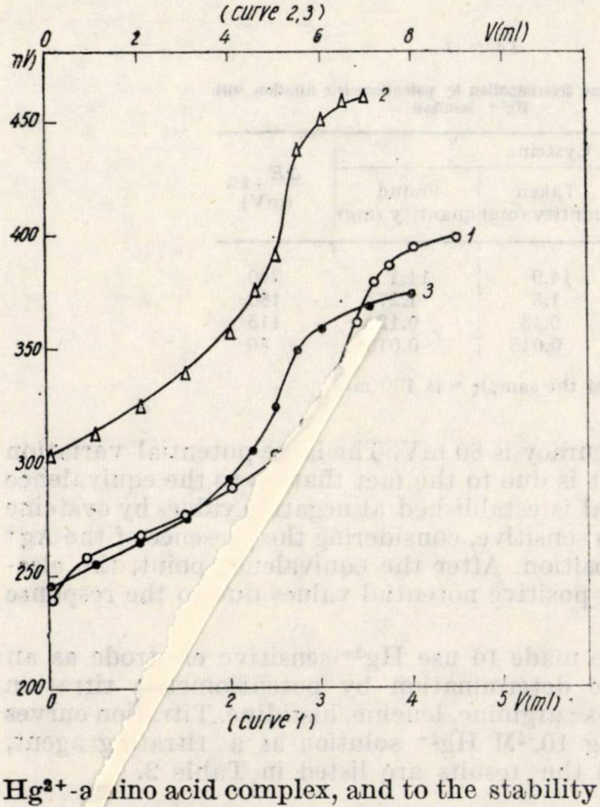

Fig. 2. — Titration curves of some α-amino acids with Hg^{2+} solution.
1, arginine; *2*, leucine; *3*, histidine.

Hg^{2+}-a ino acid complex, and to the stability constant value for the respectiv complexes.

In conclusion, the Hg^{2+}-sensitive membrane-electrode may be used for the determination of some α-amino acids by the potentiometric titration with Hg^{2+} solution. The possibility of determining cysteine traces (0.13 μg/ml) is particularly mentioned.

Revue Roumaine de Chimie, **21**, 6, 937–947 (1976)

GROWTH REGULATING POLYMERS. III[*]

POLY(4-VINYLPYRIDINE) SALTS WITH HALOGEN (ALKYL) ARYLOXYALKYLCARBOXYLIC ACIDS

STELIANA MAXIM and M. DIMA

Institute of Macromolecular Chemistry "P. Poni",
Aleea Grigore Ghica Vodă n⁰ 41-A, Jassy, Romania

Received February 16, 1974

The preparation of poly(4-vinylpyridine) salts with halogen (alkyl) aryloxyalkyl carboxylic acids, by means of the neutralization reaction of poly(4-vinylpyridine) with these acids, and also the double exchange reaction between poly(4-vinylpyridinium chloride) and the sodium salts of the above acids were studied. The preparation of these salts was corroborated by elementary analysis and by IR spectra.

Speciality studies have shown [1] that the efficiency of herbicide products depends on the nitrogen content of the soil. The efficiency of the herbicides is higher with a high nitrogen content.

It has also been proved [2–7] that certain nitrogen-containing substances with a small molecule, by simple mixture with the herbicides of the halogen(alkyl)aryloxyalkyl carboxylic acids, highly increase the activity of these.

The increase of the herbicide efficiency of the above mentioned class is obtained lowering their volatility by transforming them into the corresponding salts.[8–10]

---

[*] Part II. See ref.[14]

[1] "The Physiology and Biochemistry of Herbicides", Academic Press, London, 1964, p. 410.

[2] T. V. Lichoalt, *Okh. Birody. Tcentr. Chernozemnoi Plasty Voronezh. Sb.*, **205,** 4 (1962); *Chem. Abstr.*, **60,** 11303 (1964).

[3] V. I. Bozhukha, *Priemy Povysh. Urozheinosti Sel'sk Kul'z*, p. 239 (1969); *Chem. Abstr.*, **70,** 76651 (1969).

[4] E. D. Robison, *Tex. Agr. Exp. Sta. Progr. Rep.*, **2583–2609,** 21 (1968); *Chem. Abstr.*, **70,** 67025 (1969).

[5] R. H. Haas and R. L. Watson, *Tex. Agr. Exp. Sta. Progr. Rep.*, **2583–2609,** 47 (1968); *Chem. Abstr.*, **70,** 67631 (1969).

[6] K. Vorderberg, *Nachr. Bl. Dtsch. Pfl. Sch. Dienst.*, **15,** 68 (1961).

[7] Farbenfabriken Bayer A. G. Ger. Pat. 1 221 857 March 3, 1966; *Chem. Abstr.*, **64,** 16550 (1966).

[8] T. D. Evard and R. J. Morese, *Hyainth. Contrib. J.*, **1,** 9 (1962).

[9] Z. Stata and J. Dolezol, Czech. Pat. 119 166 July 15, 1966; *Chem. Abstr.*, **67,** 11336 (1967).

[10] W. K. Averitt, *Proc. S. Weed Conf.*, **342.** 20 (1967); *Chem. Abstr.*, **67,** 63204 (1967).

The mixtures of these herbicides with polymers or copolymers soluble in water [11,12] are also used to prevent the losses through volatilization.

In earlier papers,[13,14] Dima and co-workers have obtained macromolecular products containing the active physiological substance chemically bound to the polymer support.

In the present paper the authors have endeavoured to obtain the poly(4-vinylpyridinium) salts of the halogen(alkyl)aryloxyalkyl carboxylic acids.

MATERIALS AND METHODS

The following substances were used for this study :

- technical vinylpyridine
- poly(4-vinylpyridine) (PVP)
- poly(4-vinylpyridinium chloride) (PVP.HCl)
- *p*-chlorophenoxyacetic acid (CFA) *p.a.*
- 2,4-dichlorophenoxyacetic acid (2,4-D) *p.a.*
- sodium-2,4-dichlorophenoxyacetate (Na 2,4-D) *p.a.*
- 2,4,5-trichlorophenoxyacetic acid (2,4,5-T) *p.a.*
- sodium 2,4,5-trichlorophenoxyacetate (Na, 2,4,5-T) *p.a.*
- 2,4,5-trichloro-α-phenoxypropionic acid (2,4,5-T P) *p.a.*
- 2-methyl-4-chlorophenoxyacetic technical acid [15] (MCP)
- 2-methyl-4-chlorophenoxybutyric technical acid (MCPB) [15]

The technical acids were purified by recrystallization, and the vinyl pyridine by distillation in vacuum under nitrogen.

The poly(4-vinylpyridine) for use in this study was obtained by polymerization of the monomer under nitrogen, in methanol and in the presence of AIBN as catalyst.[16] During this study poly(4-vinylpyridinium chloride) has also been obtained processing PVP with concentrated hydrochloric acid.

The purity of the substances with which we started as well as that of the polymeric products obtained by the reaction was checked by elementary analysis.

The macromolecular salts of the halogen (alkyl)aryl-oxyalkyl carboxylic acids were obtained by means of the neutralization reaction of the PVP with the above mentioned acids, as well as by the double exchange reaction between the sodium salts of these acids and PVP·HCl.

The neutralization reaction was carried out in a three-necked flask provided with stirren, thermometer and refrigerator. The following solvents were used : dimethylformamide (DMF) formamide (FA) and dimethylsulphoxide (DMSO).

PVP 0.05714 moles solved in DMSO are introduced into the reaction flask over which a 0.08525 mole acid solution is added in the solvent. The polymer concentration is 3 g to 100 ml solvent. The reaction mixture is stirred for maximum 5 hours at a temperature of 25°.

After the end of the reaction, the viscous solution obtained is precipitated in water, when a rubbery white precipitate is obtained.

The purification is carried out by reprecipitations from the $DMSO-H_2O$ system. The purified polymer reaction product is a slightly yellow, translucid breakable mass.

The double exchange reaction was carried out in an outfit similar to the above one, using H_2O, DMSO and $H_2O/DMSO = 1/1$ (volumetric ratio) as reaction medium. When water is used as reaction medium, an instantaneous precipitation of the polymer reaction product takes place when mixing the reactants aqueous solutions. When the reaction is carried out in DMSO or $H_2O/DMSO = 1/1$, the polymer reaction product is recovered from the reac-

---

[11] Koho Co. Ltd. Jap. 7, 142, 218 ; *Chem. Abstr.*, 77, 115607 (1972).

[12] National Patent Develop. Corp. U.S. 3, 660, 071 ; *Chem. Abstr.*, **77,** 76065 (1972).

[13] M. Dima, A. Carpov and S. Maxim, *Rev. Roumaine Chim.*, **13,** 485 (1968).

[14] A. Carpov, S. Maxim and M. Dima, *Rev. Roumaine Chim.*, **20,** 707 (1975).

[15] VBE Synthesewerk Schwarzheide, DDR.

[16] A. Katchalsky and K. Rosenbek, *J. Polymer Sci.*, **23,** 955 (1967).

tion medium by precipitation in water. The purification of the polymer products obtained by the reaction was carried out by repeated dissolutions in DMSO and precipitations in water.

The chlorine analyses were carried out according to the known method.[17] The course of the reaction was controlled by the covalent chlorine content of the polymer reaction product, after which the transformation degree (α) into a macromolecular salt was calculated according to the calculation method.[18]

The IR spectra were recorded by means of a UNICAM SP 120 spectrophotometer, by pelleting with KBr.

The thermogravimetric analysis was carried out by means of a Paulik-Erdey derivatograph with a 9.8° per minute rate.

RESULTS AND DISCUSSIONS

The preparation of PVP salts with halogen(alkyl)aryloxyalkyl carboxylic acids, through the neutralization process, takes probably place according to the following pattern:

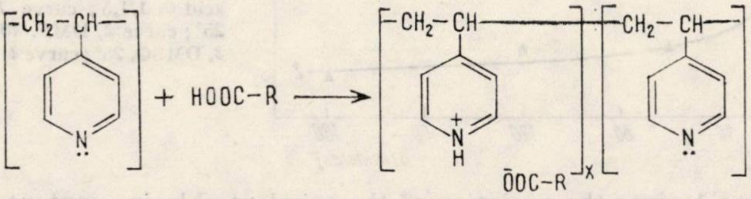

1

where : R = $ClC_6H_4OCH_2-$; $Cl(CH_3)C_6H_3OCH_2-$; $Cl_2C_6H_3OCH_2-$; $Cl_3C_6H_2OCH_2-$; $Cl_3C_6H_2OCH(CH_3)-$; $Cl(CH_3)C_6H_3O(CH_2)_3-$.

The double exchange reaction between PVP.HCl and the sodium salts of the above mentioned acids takes probably place according to the following pattern:

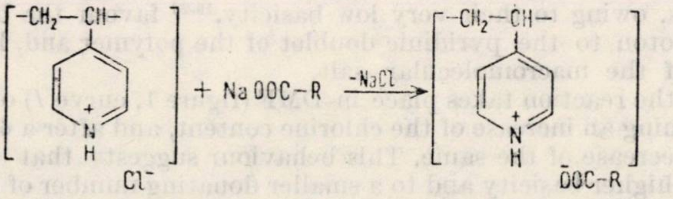

2

As may be seen in the reaction patterns 1 and 2, the polymer products obtained have the same electronic structure.

In both cases, one obtains in certain conditions a macromolecular salt with a transformation degree very near to the theoretical one (in our case 100%).

In the case of reaction pattern 1, this is easily understood as the pyridinic nitrogen is a stronger base than the carboxylate ion, and the reaction goes on normally towards the formation of the macromolecular salt.

In the second case (pattern 2), the shifting of the equilibrium towards the formation of the macromolecular salt is commanded by the formation of sodium chloride, which in reaction media such as DMSO or DMSO/ $H_2O = 1/1$ is precipitated or very slightly dissociated owing to the small dielectric constant. Also, if the reaction according to pattern 2 is carried out in water, it becomes practically irreversible, as in this case the polymeric reaction product precipitates at the mixture of the reactants.

---

[17] J. Haslam, J. B. Hamilton and C. D. M. Sowirell, *Analyst*, **85**, 556 (1960).

[18] I. Scondac and M. Dima, *St. şi Cerc. Şti. Chim. Fil. Iaşi*, **13**, 217 (1962).

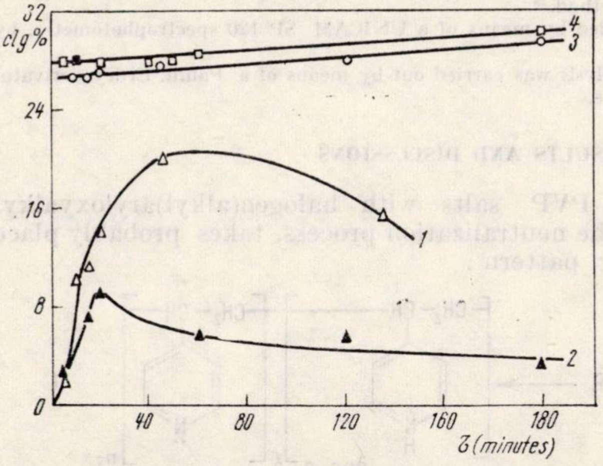

Fig. 1. Dependence of the covalent chlorine content of the poly(4-vinylpyridinium) salt of 2,4,5-T acid, *versus* time, nature of the solvent and temperature. Reaction conditions: molar ratio P V P/2,4,5-T acid = 1/1,5; curve *1*, DMF, 25°; curve *2*, DMF, 40°; curve *3*, DMSO, 25°; curve *4*, FA, 25°.

Figure 1 gives the variation of the covalent chlorine content of the polymer obtained according to reaction pattern 1, *versus* solvent and temperature.

From the data of curves *3* and *4* (figure 1) one notices that the reaction takes place rapidly, reaching a high chlorine content in FA as well as in DMSO. This rapid evolution of the reaction suggests that these two solvents, owing to their very low basicity,[19,20] favour the binding of the acid proton to the pyridinic doublet of the polymer and, hence, the formation of the macromolecular salt.

When the reaction takes place in DMF (figure 1, curve *1*) one notices at the beginning an increase of the chlorine content, and after a 60 minutes reaction a decrease of the same. This behaviour suggests that the DMF, owing to its higher basicity and to a smaller donating number of protons,[19] as compared to the other two solvents, can, in certain conditions, compete with the poly(4-vinylpyridine) in its protonation reaction.

The process determining the decrease of the chlorine content could be a solvolysis of the macromolecular salt assisted by a basic solvent.[21,22]

In the case of the reaction taking place in DMF at 40° (figure 1, curve *2*), one notices that the maximum of the curve is much displaced towards the ordinate, as compared to the maximum of curve *1*, and that its value is far lower. This may be assigned to the fact that the solvolysis rate increases with the temperature.

Figure 2 gives the dependence of the transformation degree (α) into macromolecular salt, *versus* time and nature of the acid.

---

[19] H. Liebig, *Sonderdruck*, **95**, 301 (1971).

[20] C. D. Nenițescu, "Chimie Organică", Vol. I, Ed. tehnică, Bucharest, p. 758.

[21] A. Hirosh and U. Michio, *Kogyo Kagaku Zasshy*, **71**, 3468 (1968); *Chem. Abstr.*, **69**, 279889 (1968).

[22] O. H. Myaykoi, T. G. Suslina and N. A. Bardina, *Tr. Voronezh. Gos. Univ.* **72**, 32 (1966).

From the data of curves in figure 2, one can infer the following series of reactivity of the halogen (alkyl)aryl-oxyalkyl carboxylic acids : 2,4,5–T acid > 2,4,5-TP acid > 2,4-D acid > MCP acid > MCPB acid.

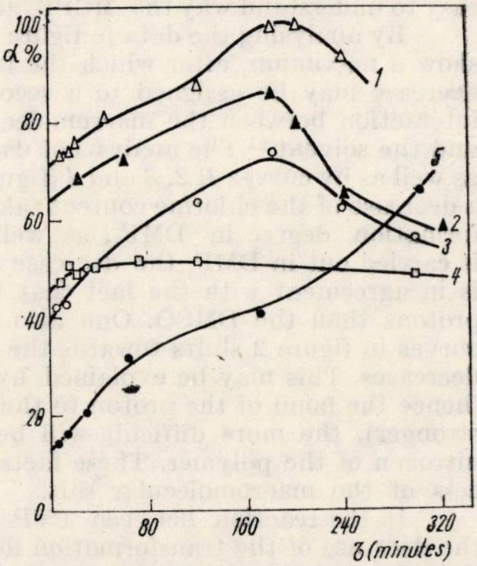

Fig. 2. Dependence of the transformation degree (α) of PVP into a macromolecular salt of the halogen(alkyl)aryloxyalkyl carboxylic acids, *versus* time and nature of the acid. Reaction conditions : molar ratio PVP/acid = 1/1,5, 25°, DMSO ; curve *1*, 2,4-D acid ; curve *2*, 2,4,5-T acid ; curve *3*, MCP acid ; curve *4*, 2,4,5-TP acid ; curve *5*, MCPB acid.

Taking into account the structural peculiarities of these acids, this order is a normal reactivity series.[23,24]

We know that halogens substituted in the benzenic cycle create, according to the alternating polarity, an electron deficiency in the *h*- and *p*-positions. The more the benzenic cycle is substituted by a higher number of halogen atoms, the more marked will be the electron deficiency in the mentioned positions. Owing to the *p*-π conjugation effect, the non-participating electrons of the phenoxide oxygen are displaced to compensate the electron deficiency in the *p*-position. This brings about a more labile carboxylic proton through the shifting of electrons of the O–H bond to compensate the electron deficiency of the carbonylic carbon (Pattern 3)

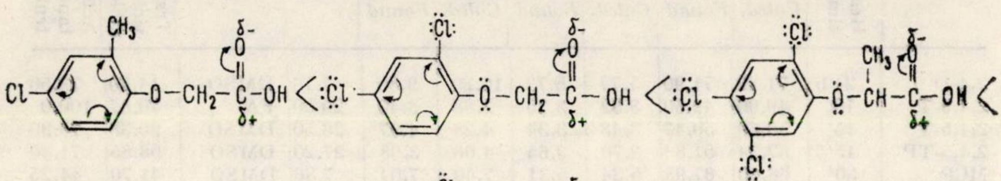

3

---

[23] W. Pritzkow, "Theoretische Gesichtspunkte in der Organischen Chemie", Verlag, Dresden, 1963, p. 64.

[24] "The Physiology and Biochemistry of Herbicides", Academic Press, London, 1964, p.56.

This effect of making the carboxylic proton more labile is so much the weaker, as the number of carbon atoms interposed between the halogen (alkyl)aryloxy radical and the carboxylic group is higher. It is therefore, easy to understand why the MCPB acid (figure 2, curve *5*) is less reactive.

By analysing the data in figure 2 one notices that most of the curves show a maximum, after which the transformation degree decreases. This decrease may be assigned to a secondary process, probably due to the interaction between the macromolecular salt formed during the reaction and the solvent.[21] The analysis of data given by curves *1* and *2* (figure 1) as well as by curves *1*, *2*, *3* and *4* (figure 2), shows that in certain conditions a decrease of the chlorine content takes place, and implicitely of the transformation degree in DMF., as well as in DMSO. When the reaction is carried out in DMF the decrease occurs faster than in DMSO. This is in agreement with the fact that the DMF has a smaller number of protons than the DMSO. One also notices that the maximum of the curves in figure 2 shifts towards the ordinate as the strength of the acids decreases. This may be explained by the fact that, the stronger the acid (hence the bond of the proton to the pyridinic nitrogen of the polymer is stronger), the more difficult will be its detachment from the pyridinic nitrogen of the polymer. These facts seem to confirm the solvolysis process of the macromolecular salt.

In the reaction between PVP and MCPB acid (figure 2, curve *5*) the decrease of the transformation degree is not observed, which suggests that the stability of the macromolecular salt is probably achieved owing to the formation of the hydrophobic bonds [25,26] between the macromolecular chain and the hydrocarbonate chain of the acid radical.

Table 1 gives the results of the elementary analyses of the products obtained in the reaction between PVP and the above mentioned acids.

Table 1

Elemental analysis data of the products obtained through the reaction between poly(4-vinylpyridine) and the halogen (alkyl) aryloxyalkyl carboxylic acids. Molar ratio: P.V.P./acid = 1/1.5; 25°

Acid	Reaction time	Carbon %		Hydrogen %		Nitrogen %		Cl g%	Solvent	Transformation degree mole %	Active substance content %
		Calcd.	*Found*	*Calcd.*	*Found*	*Calcd.*	*Found*				
2,4-D	24 h	71.42	71.90	5.77	5.73	10.20	9.80	7.76	DMSO	14.60	23.50
2,4,5-T	10′	49.90	49.60	3.32	3.35	3.88	3.40	29.50	FA	70.67	100.0
2,4,5-T	15′	50.69	50.47	3.48	3.34	4.28	4.97	26.50	DMSO	90.38	70.30
2,4,5-TP	15′	52.34	51.8	3.70	3.65	4.08	3.98	27.20	DMSO	98.85	71.40
MCP	30′	68.40	67.98	5.34	5.31	7.40	7.04	7.86	DMSO	41.70	44.25
MCP	20′	73.60	74.24	6.10	6.60	7.21	7.50	6.78	DMSO	35.70	44.20
MCP	120′	69.03	69.40	7.59	7.30	5.75	5.50	7.34	DMSO	37.80	50.20
MCP	205′	63.0	63.35	5.25	5.63	4.62	5.18	11.57	DMSO	98.70	65.30

The second approach used by us to obtain the macromolecular salts of PVP with halogenaryloxyalkyl carboxylic acids was the double exchange reaction according to pattern 2.

---

[25] D. O. Iordan, T. Kurucsev and R. L. Darskus, *Polymer*, **6**, 303 (1965).

[26] I. Sakurada, Yu. Sakaguki, T. Ono and S. T. Ueda, *Kobunshi Kagaku*, 22, 696 (1965); *Chem. Abstr.*, **64**, 12828 (1966).

As may be seen in table 2, when the reaction is carried out in a H_2O/DMSO = 1/1 (volumetric ratio) mixture for solvent, it is total and the transformation degrees obtained are in good enough agreement with the number of sodium 2,4-dichlorophenoxyacetate mole involved in the reaction.

When the reaction is carried out in an aqueous medium (table 2, line 5), the polymer reaction product gets instantaneously out of the system (precipitates), the reaction being practically total.

Table 2

Chlorine analysis data of the products resulting from the double exchange reaction between poly(4-vinylpyridinium chloride) and sodium 2,4-dichlorophenoxyacetate

Molar ratio PVP.HCl/Na 2,4-D	Time (hours)	Total chlorine g%	Ionic chlorine g%	Covalent chlorine g%	Transformation degree mol %	Solvent
1/0.25	24	20.8	18.87	1.97	25.5	DMSO/H_2O = 1/1
1/0.5	24	22.67	12.63	10.04	46	DMSO/H_2O = 1/1
1/0.75	24	23.7	6.1	17.6	75.9	DMSO/H_2O = 1/1
1/1	24	21.45	0	21.45	100	DMSO/H_2O = 1/1
1/1*	—	20.9	0	20.9	97.9	H_2O

* The polymer reaction product precipitates instantly at the mixing of the aqueous solutions of the reactants.

If DMSO is used as reaction medium (table 3), the reaction takes place in the heterogeneous phase, owing to the insolubility of the PVP. HCl as the reaction is in progress and the polymer reaction product is solved, the medium becomes homogeneous. In this case smaller transformation degrees are obtained, due precisely to the fact that the reaction rate is controlled by the solution process.

Table 3

Elemental analysis data of the products resulting from the double exchange reaction. Reaction conditions: molar ratio: PVP.HCl/salt = 1/1, DMSO, 25°, 4 hours

Carbon g%		Hydrogen g%		Nitrogen % g%		Chlorine g%		Transformation degree mol %	Small molecule reactant
Calcd.	*Found*	*Calcd.*	*Found*	*Calcd.*	*Found*	Tot.	Ionic		
57.00	57.53	4.25	4.35	4.71	5.00	18.78	1.02	80.03	Na-2,4-D
50.90	51.64	3.48	3.98	4.45	4.70	29.03	2.39	78.88	Na-2,4,5-T

The preparation of the macromolecular salts of the halogen (alkyl) aryloxyalkyl carboxylic acids was confirmed by spectral IR analysis.

By comparing the PVP, PVP. HCl spectra and those of the 2,4,5-TP acid (fig. 3) with those of the products obtained through the neutralizing reaction (fig. 4), we notice some significant changes. Thus, whenever the protonation of the pyridinic nitrogen with the proton of the respective acids takes place, there is a change of the absorption bands characteristic [27] of the valency vibrations of the pyridinic nitrogen at 2920 and 3450 cm^{-1}.

---

[27] H. W. Gibson and F. C. Bailey, *J. Polymer Sci.*, **10**, 3017 (1972).

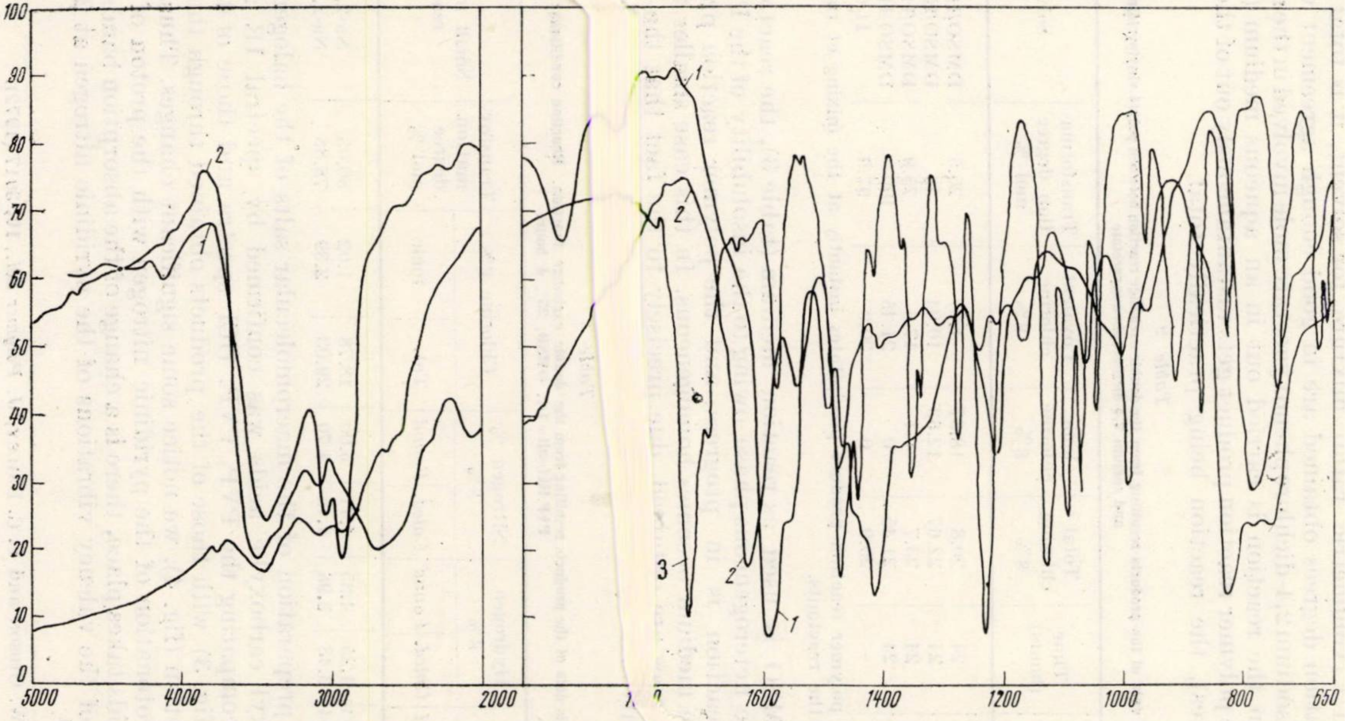

Fig. 3. IR spectra of PVP (1), PV HCl (2) and 2,4,5-TP acid (3).

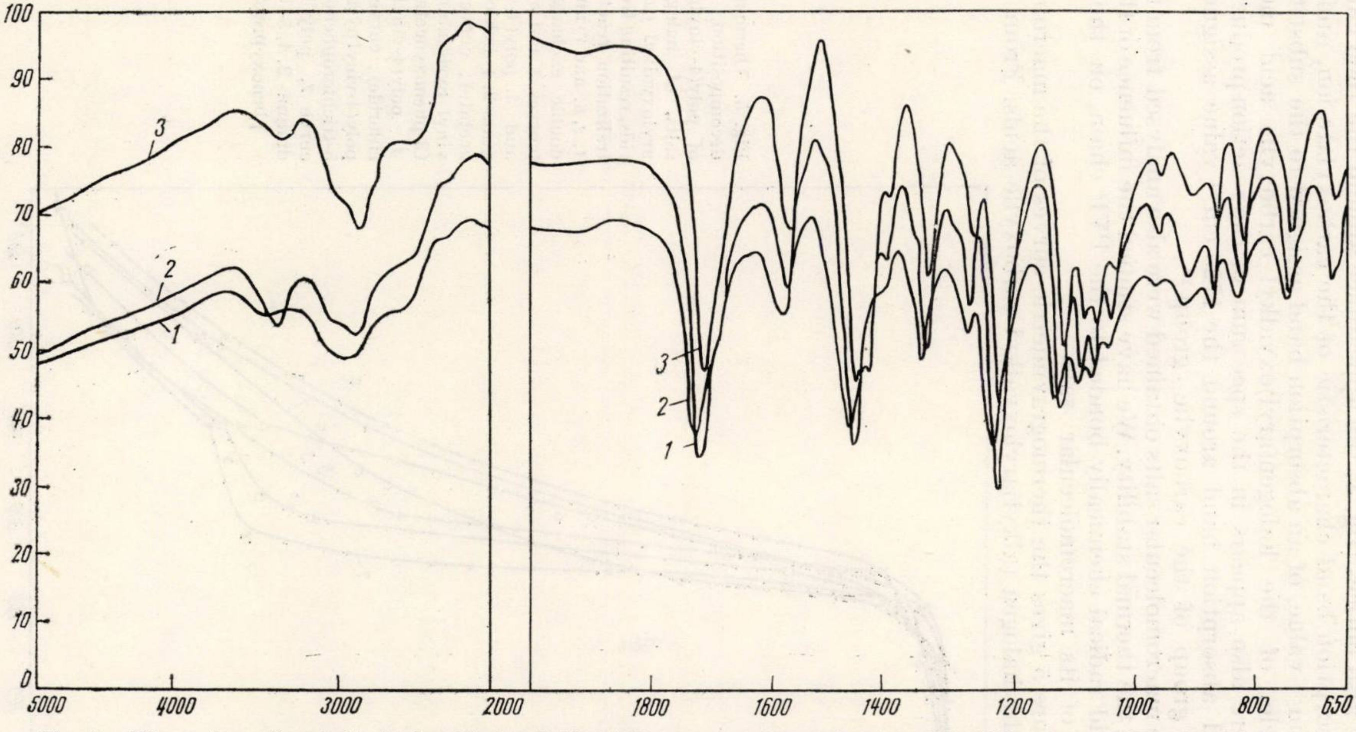

Fig. 4. IR spectra of poly(4-vinylpyridinium-2,4,5-trichloro-α-phenoxypropionate) with different transformation degrees (α) *1*, $\alpha = 57.8$; *2*, $\alpha = 65.5$; *3*, $\alpha = 72.4$.

One also notices (fig. 4) the appearance around the 1600 cm^{-1} value of an absorption band characteristic of the carboxylate ion, and around the 825 cm^{-1} value, of an absorption band assigned to the substitute benzenic cycle, of the halogen(aryl)oxyalkyl carboxylic acid molecule.[28]

There also appears in the spectrum of the reaction products (fig. 4) a marked absorption band around the 1725 cm^{-1} value assigned to the carbonyl group of the carboxylic group.[29]

The macromolecular salts obtained were also analysed from the point of view of the thermal stability. We have studied the influence of the nature of the acid radical chemically bonded to the PVP chain, on the thermal stability of its macromolecular salt.

Figure 5 gives the thermogravimetric curves of the macromolecular salts of the halogen (alkyl)aryloxyalkyl carboxylic acids. From the data

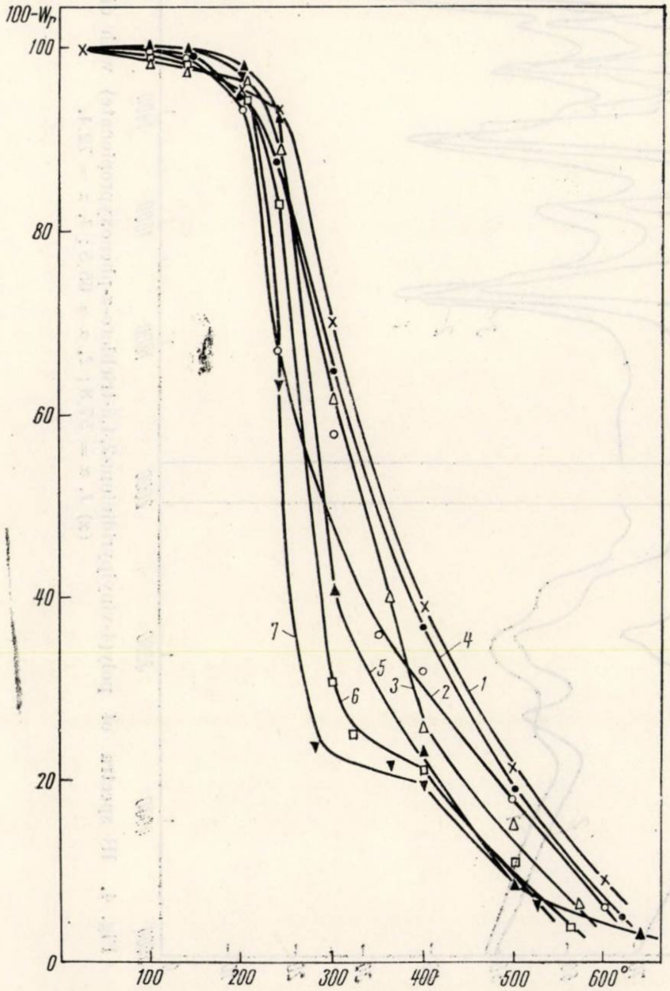

Fig. 5. Thermogravimetric decomposition curves of poly(4-vinylpyridinium) salts, of halogen (alkyl) aryloxyalkyl carboxylic acids, resulting from the neutralization reaction (curves *1*, *2*, *6*, and *7*) and from the double exchange reaction (curves *3* and *5*). Curves *1* and *3*, poly(4-vinylpyridinium-2, 4-dichlorophenoxyacetate); curve *2*, poly(4-vinyl pyridinium-2-Me-4-Cl-phenoxyacetate); curve *4*, poly(4-vinylpyridinium chloride); curves *5* and *6*, poly(4-vinyl pyridinium-2,4, 5-trichlorophenoxyacetate); curve *7*, poly(4-vinylpyridinium-2, 4, 5-trichloro-α-phenoxypropionate).

---

[28] J. F. Brown, *J. Amer. Chem. Soc.*, **77**, 6341 (1955).

[29] M. Avram and Gh. Mateescu "Spectroscopia în infraroșu și aplicațiile în chimia organică", Ed. tehnică, Bucharest, 1966.

of this figure one notices that up to a 100° temperature, the weight losses (expressed as $100-W_r\%$) are very small and have very near values for all samples. In the 100—200° interval, there probably takes place a breaking of the bond between the acid proton and the pyridinic nitrogen, this being influenced by the strength of the acid taking part in the bond. If we compare the weight losses at 200°, we notice that the products are set in the following series according to the acids bound to the pyridinic nitrogen of the polymer :

2,4,5-T acid < 2,4,5-TP acid < 2,4-D acid < MCP acid.

After the breaking of the bond between the pyridinic nitrogen of the polymer and the acid proton, the polymeric skeleton support being identical, it would seem normal to obtain in every case identical degradation curves in the temperature interval 200—600°. The differences in the thermal stability of the samples in this interval are assigned to the difference in the thermal stability of the acids which have formed the macromolecular salt as, after the first degradation process (around 200°), two processes take place simultaneously, namely : on the one hand, there begins a degradation of the PVP chain and, on the other hand, there takes place a degradation of the acid molecules freed in the first degradation stage.

CONCLUSIONS

1. The macromolecular salts of the halogen(alkyl)aryloxyalkyl acids with poly(4-vinylpyridine) were synthetized for the first time.

2. The existence of these salts was confirmed by elementary analysis as well as by IR spectroscopy.

3. The thermal stability of the macromolecular salts obtained was studied and the influence of the nature of the acid radical on their thermal stability was pointed out.

of this figure one notices that up to a 100° temperature, the weight losses (expressed as 100 − $R_{\%}$) are very small and have very near values for all samples. In the 100–200° interval, there probably takes place a breaking of the bond between the acid proton and the pyridinic nitrogen, this being influenced by the strength of the acid taking part in the bond. If we compare the weight losses at 200°, we notice that the products are set in the following series according to the acid bound to the pyridinic nitrogen of the polymer:

2,4,5-T acid < 2,4,5-TP acid < 2,4-D acid < MCP acid < [illegible]

After the breaking of the bond between the pyridinic nitrogen of the polymer and the acid proton, the polymeric skeleton support being identical, it would seem normal to obtain in every case identical degradation curves in the temperature interval 200–600°. The differences in the thermal stability of the samples in this interval are assigned to the difference in the thermal stability of the acids which have formed the macromolecular salts, after the first degradation process (around 200°), two processes take place simultaneously, namely: on the one hand, there begins a degradation of the PVP chain and, on the other hand, there takes place a degradation of the acid molecules freed in the first degradation stage.

CONCLUSIONS

1. The macromolecular salts of the halogen(alkyl)aryloxyalkyl acids with polyvinylpyridine were synthetized for the first time.

2. The existence of these salts was confirmed by elementary analyses as well as by IR spectroscopy.

3. The thermal stability of the macromolecular salts obtained was studied and the influence of the nature of the acid radical on their thermal stability was pointed out.

Revue Roumaine de Chimie, 21, 6, 949–954 (1976)

ZUR KOPOLYMERISATION. I

MATHEMATISCHES MODELL DER BILDUNG EINES BINÄREN KOPOLYMERISATIONSPRODUKTES

IOAN MOŢOC, DAN CIUBOTARIU

Chemiekatheder der Universität Timişoara, 1900—Timişoara, Rumänien

Eingegangen am 27. Juni 1974

Es wird das mathematische Modell der stufenweisen Bildung eines binären Kopolymeren beschrieben. Das vorgeschlagene mathematische Modell dient zur Ableitung eines Algorythmus, der die Simulation der Bildung eines Makromoleküls an einem Digitalrechner gestattet. Vorliegender Bericht leitet eine Reihe von Publikationen über die Simulation der Ko- und Homopolymerisation ein.

1. EINLEITUNG

Die Bildung eines Makromoleküls durch Kopolymerisation der Monomeren A und B kann mit folgenden Beziehungen beschrieben werden :[1–5]

$$\approx A. + A \xrightarrow{k_{11}} \approx A - A. \qquad (1)$$

$$\approx A. + B \xrightarrow{k_{12}} \approx A - B. \qquad (2)$$

$$\approx B. + B \xrightarrow{k_{22}} \approx B - B. \qquad (3)$$

$$\approx B. + A \xrightarrow{k_{21}} \approx B - A. \qquad (4)$$

k_{ij}, i, $j = 1, 2$ sind die Geschwindigkeitskonstanten der Reaktionen (1)–(4).

Die Verhältnisse :

$$k_{11}/k_{12} = r_1, \qquad k_{22}/k_{21} = r_2 \qquad (5)$$

[1] G. E. Ham, „Copolymerization", Interscience, New York, 1964 (Übersetzung in russischer Sprache, Khimia, 1971).

[2] Houben-Weyl, „Methoden der organischen Chemie", Band XIV/1, Makromolekulare Stoffe, Teil 1, Georg Thieme Verlag, Stuttgart, 1961.

[3] H. A. Stuart, „Physik der Hochpolymeren", Bd. II, Springer-Verlag, Berlin, 1953.

[4] P. J. Flory, „Principles of Polymer Chemistry", Cornell University Press, Ithaca, New York, 1953.

[5] W. J. Burlant und A. S. Hoffman, „Block and Graft Polymers", Reinhold, New York (Übersetzung in russischer Sprache, 1963).

stellen die Kopolymerisationskonstanten dar, r_1, r_2. k_{ij} kennzeichnet die Monomeren A und B hinreichend in bezug auf den Wachstumsprozeß des Makromoleküls. Darüberhinaus, kennzeichnen die Zahlenwerte für k_{ij} auch die Bildungsbedingungen des Makromoleküls.

2. DAS MATHEMATISCHE MODELL

Zur übersichtlicheren Darstellung des mathematischen Modells, wird dieses in zwei Etappen beschrieben.

2.1. PRÄMISSEN DES MODELLS

Wenn folgende Bedingungen erfüllt sind:

(a) niedriger Konversionsgrad, der zu keiner wesentlichen Änderung der Ausgangskonzentrationen von [A] und [B] führt, oder

(b) wird stationär in bezug auf die ursprünglichen Konzentrationen $[A_0]$ und $[B_0]$ gearbeitet. (D.h. wenn im Zeitpunkt

$$t = 0 \qquad [A_0] = [B_0] \qquad \text{ist,} \tag{6}$$

dann ist in jedem Augenblick $t \neq 0$ die Beziehung (6) gültig. Experimentell läßt sich das z.B. durch einen kontinuierlichen Zusatz jener Komponente erreichen, die rascher verbraucht wird.)

Dann gilt folgendes:

(i) k_{11} und k_{21} sind ein Maß für die Häufigkeit des Monomeres A im Makromolekül, durch die Reaktionen (1) bzw. (4).

(ii) k_{22} und k_{12} sind ein Maß für die Frequenz des Monomeren B im Makromolekül durch die Reaktionen (3) bzw. (2).

Es werden folgende Bezeichnungen eingeführt:

$$\alpha = \frac{k_{11}}{\sum_{i=1}^{2} k_{1i}}; \qquad \beta = \frac{k_{22}}{\sum_{j=1}^{1} k_{2j}} \tag{7}$$

Werden die Beziehungen (5) in Betracht gezogen, folgt daraus:

$$\alpha = \frac{r_1}{1 + r_1}; \qquad \beta = \frac{r_2}{1 + r_2} \tag{8}$$

Beachtet man weiterhin (i) und (ii), dann folgt auf Grund der Wahrscheinlichkeitstheorie unmittelbar:

(A1) $\alpha = r_1(1 + r_2)^{-1}$ ist die Wahrscheinlichkeit, in der Kette des Makromoleküls einen Meres A anzutreffen, der durch Reaktion (1) eingetreten ist.

(A2) $(1 - \alpha)$ ist die Wahrscheinlichkeit, in der Kette des Makromoleküls einen Meres B anzutreffen, der durch Reaktion (2) eingetreten ist.

(B1) $\beta = r_2/(1 + r_2)$ ist die Wahrscheinlichkeit, in der Kette des Makromoleküls einen Meres B anzutreffen, der durch Reaktion (3) eingetreten ist.

(B2) $(1 - \beta)$ ist die Wahrscheinlichkeit, in der Kette des Makromoleküls einen Meres A anzutreffen, der durch Reaktion (4) eingetreten ist.

Infolge der kinetischen Bedingungen (für die Reaktionen (1)—(4)) sind (A1) und (A2) unabhängig von (B1) und (B2). Diese Feststellung ist für das zu entwickelnde mathematische Modell von Bedeutung.

C1 und C2 seien zwei endliche Ereignisfelder. Im Falle der Bildung eines binären Kopolymeren, worin die Verteilung der Meren A und B von Interesse ist, bestehen C1 und C2 aus je zwei Ereignissen : A1 und A2, bzw. B1 und B2.

Nach genügend langer Zeit verhält sich die Anzahl der Meren A und B, die durch die Reaktionen (1)—(4) in das Makromolekül eingetreten sind, wie :

$$k_{11} : k_{12} : k_{21} : k_{22} \tag{9}$$

Das Stattfinden *eines* Ereignisses aus C1 (oder C2) ist *stochastisch*, aber nach Ablauf einer genügenden Anzahl von Einzelereignissen, wird (9) ihre relative Häufigkeit widerspiegeln.

Obige Behauptungen werden im Falle der Kopolymerisation als gültig angenommen[1].

Betrachten wir den Intervall (0,1) laut Abb. 1 alternativ durch die Punkte α und β geteilt :

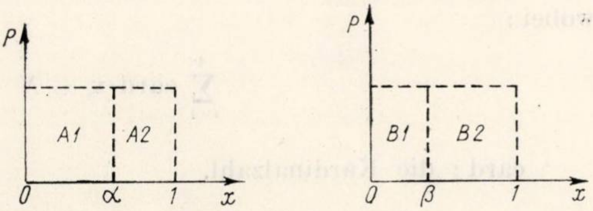

Abb. 1. — Die Partition des Intervalls (0,1).

Es werden die Zahlen $x \in (0, 1)$ stochastisch generiert. Diese Zahlen sind gleichförmig verteilt, und können vorteilhaft nach dem (auf Kongruenzen beruhenden) Verfahren von Lehner generiert werden.

Infolge der Gleichförmigkeit der Verteilung ist :

$$\forall x_1, \ x_2, \ldots \in (0,1) : \quad P(x_1) = P(x_2) = \ldots \tag{10}$$

$P(x)$ stellt die Wahrscheinlichkeit der Erscheinung von x bei einer Generation dar.

F sei eine folgendermaßen definierte Funktion :

$$F : (0, 1) \rightarrow (\text{A1, A2, B1, B2}) \tag{11}$$

die folgende Bedingungen erfüllt:

Wenn $x \in (0, \alpha)$ dann gilt A1 (mit $x \Leftrightarrow$ A1 bezeichnet), (12)

$\vdots$

wenn $x \in (\beta, 1)$ dann gilt B2 (mit $x \Leftrightarrow$ B2 bezeichnet).

Offensichtlich definiert F eine Äquivalenzbeziehung über (0, 1), indem

$$x_1 \Leftrightarrow \mathrm{A1},\ x_2 \Leftrightarrow \mathrm{A1} \Rightarrow x_1 \sim x_2 \tag{13}$$

$$x_7 \Leftrightarrow \mathrm{B2},\ x_8 \Leftrightarrow \mathrm{B2} \Rightarrow x_7 \sim x_8$$

wobei $x_1, \ldots x_8 \in (0,1)$, „$\sim$" : äquivalent.

Durch Beziehungen wie (12) und (13) kann jedwelche Äquivalenzbeziehung über (0,1) definiert werden. Daraus folgt die weitgehende Allgemeinheit eines Modells, das auf diesen Prämissen beruht.

Offensichtlich führt die Generation einer genügend großen Anzahl, N, von stochastischen Zahlen x, zu:

$$\mathbf{x}_1 = \{x / x \Leftrightarrow \mathrm{A1} \Rightarrow x_i \sim x_j\} \tag{14}$$

$$\vdots$$

$$\mathbf{x}_4 = \{x / x \Leftrightarrow \mathrm{B2} \Rightarrow x_p \sim x_q\}$$

und:

$$\text{card } \mathbf{x}_1 : \text{card } \mathbf{x}_2 : \text{card } \mathbf{x}_3 : \text{card } \mathbf{x}_4 = k_{11} : k_{12} : k_{22} : k_{21} \tag{15}$$

wobei:

$$\sum_{i=1}^{4} \text{card } \mathbf{x}_i = N$$

card: die Kardinalzahl.

2.2. DAS MODELL

Das mathematische Modell der Bildung des Makromoleküls besteht aus:

(a) der Generation von pseudo-stochastischen Zahlen gleichförmiger Verteilung, im Intervall (0,1).

(b) der Zuordnung einer bestimmten Bedeutung (in diesem Falle der Reaktionen (1)—(4)) zur über (0,1) definierten Äquivalenzbeziehung (13).

Obige Behauptungen beruhen auf der Beziehung (15).

Bemerkung: Dieses Modell zieht in jedem Augenblick das aktive Ende der Makromolekülkette in Betracht. Dieses wird durch den Übergang vom Feld C1 (wenn das Makromolekül auf $\sim$ A$\cdot$endet) in das Feld C2 (wenn das Makromolekül auf $\sim$ B$\cdot$endet) gewährleistet.

Das Modell ist mit dem Digitalrechner leicht erfaßbar. Unser Programm MEMORY 1 beruht auf dem oben Gesagten.

Das oben ausgeführte mathematische Modell kann die *wahrscheinlichste Verteilung* der beiden Monomeren in der Kette eines linearen binären Kopolymerisationsproduktes angeben.

3. TOPOLOGISCHE DARSTELLUNG DER BINÄREN KOPOLYMERISATION

Definition : folgendes Schema

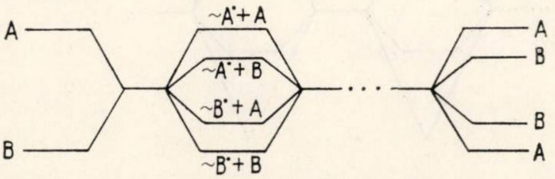

Abb. 2. – Die topologische Darstellung der binären Kopolymerisation.

nennen wir topologische Darstellung der binären Kopolymerisation.

Betrachten wir :

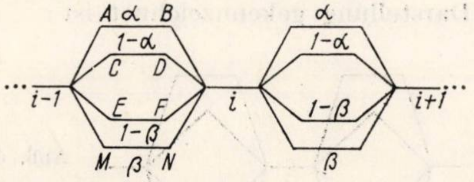

Abb. 3. – Die Bedeutung der topologischen Darstellung der binären Kopolymerisation.

Die Länge des Abschnittes AB ist mit α proportional; CD ist mit (1 – α) proportional; . . . ; MN ist mit (β) proportional.

Der Kopolymerisationsvorgang wird durch einen Durchgang durch die topologische Darstellung gekennzeichnet. Betrachten wir, z.B., folgenden Weg (mit – – – bezeichnet) :

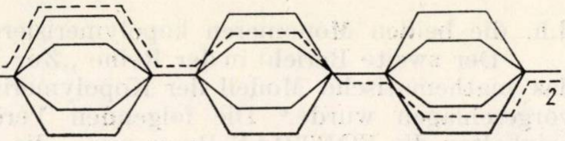

Abb. 4. – Die Darstellung eines willkürlichen Prozesses der binären Kopolymerisation.

Abbildung 4 zeigt folgendes :

– Der Makrorest endet im Punkte 1 mit A.

– Im Punkte 2, nach dem auf dem angezeigten Weg (– – –) erfolgten

Durchgang durch die topologische Darstellung ist der Makrorest :

$$\sim A - A - B - A.$$

Wenn eine Kopolymerisationsreaktion durch folgende topologische Darstellung gekennzeichnet ist :

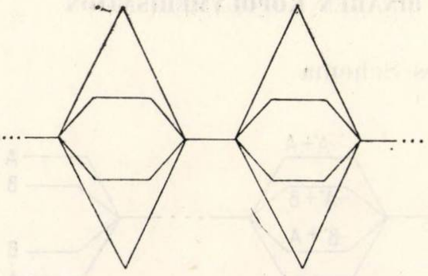

Abb. 5. – Die topologische Darstellung einer Wechselkopolymerisation.

dann entstehen Makromoleküle von folgendem Aufbau :

$$A - B - A - B - \ldots - A - B - \ldots - A - B.$$

Wenn eine Kopolymerisationsreaktion durch folgende topologische Darstellung gekennzeichnet ist :

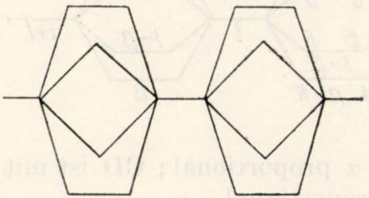

Abb. 6. – Die topologische Darstellung eines verbotenen Kopolymerisationsprozesses.

dann entstehen Makromoleküle von folgendem Aufbau :

$$A - A - A - \ldots - A \text{ und } B - B - \ldots - B - B.$$

d.h. die beiden Monomeren kopolymerisieren nicht.

Der zweite Bericht in der Reihe „Zur Kopolymerisation“ entwickelt das mathematische Modell der Kopolymerisation, das im vorliegenden vorgeschlagen wurde.[6] Die folgenden Veröffentlichungen dieser Reihe beinhalten die FORTRAN-Programme, die auf diesen Modellen beruhen.

---

[6] I. Moțoc, D. Ciubotariu und St. Holban, *Rev. Roumaine Chim.*, **00**, 000 (0000)

Revue Roumaine de Chimie, 21, 6, 955–958 (1976)

COMPTES RENDUS

"Topics in applied physics: Dye lasers", 1st. vol. Editor: F. P. Schäfer, Springer Verlag, Berlin–Heidelberg–New York, 1973, 285 p.

The book is the first volume of a new series of advanced monographs, "Topics in applied physics", edited by Springer Verlag. This series is devoted to critical reviews of subjects of current interest in applied physics and it is intended to provide theoretical and practical information on different topics for physicists, chemists, engineers and students.

The present volume deals with dye lasers, the hystory of their development and their potential applications.

The book is divided into five sections.

In chapter 1, "Principles of dye lasers operation", by F. P. Schäfer, the chemical, and spectroscopic properties of organic compounds are described and the general principles of dye laser operation are prezented. It provides the necessary background for the understanding of the physical and chemical principles involved and, in this way, a support for the development of the next four sections.

In chapter 2, "Continuous-wave dye lasers", B. B. Snavely discusses the factors affecting power output, efficiency tuning range, stability and linewidth of continuous-wave dye lasers. Special attention is given to the triplet problem and to the gain analysis.

Chapter 3, "Mode-locking of dye lasers", by C. V. Shank and E. P. Ippen, reviews at first the possibilities of measuring ultrashort pulses. Then the authors describe the experimental methods applicable to mode-locking, pulsed and continuous-wave dye lasers.

In chapter 4, "Structure and properties of laser dyes", by K. H. Drexhage, the chemical and physical properties of laser dyes are discussed. The principles outlined by the author proved to be efficient tools in the selection and synthesis of new useful laser dyes.

A list of laser dyes completes the chapter.

Chapter 5, "Applications of dye lasers" by T. W. Hänsch gives a number of recently reported dye laser applications and suggests perspectives for future developments.

A comprehensive bibliography and additional references with titles are given at the end of the book.

Moreover, a systematized subject index facilitates the choice of particular subjects.

Florian Urseanu

F. MÁRTA and D. KALLÓ, editors; "MECHANISMS OF HYDROCARBON REACTIONS", Akademiai Kiadó Budapest, 1975, 812 p.

"Mechanisms of Hydrocarbon Reactions" includes the papers submitted to the Symposium held in Siofok (Hungary) on June 5–7, 1973. The participants in this event had come from 12 European countries and from the U.S.A. The most numerous delegation was from the host country, as expected, and an adequate number of papers were forwarded. The editors have logically grouped the whole material into two distinct parts, their classification criterion being the nature of the processes involved in hydrocarbon conversion (exclusively functional derivatives).

The first part deals with heterogeneous catalysis reactions and covers topics treating: catalysis with (by) metals (13 papers), catalysis with metal oxides (7 papers), catalysis on insulators (4 papers) and catalysis with zeolites (9 papers). The second part of the book includes homogeneous reactions such as catalysis by coordinative compounds (6 papers) pyrolysis (6 papers), radiolysis (7 papers) and oxidation (5 papers). Each contribution brings proper new elements and a review of all the studied reactions is not possible. Their comparative study provides the reader with a better insight into the phenomena occurring in the conversion of hydrocarbons as such. In addition to original contributions, plenary lectures are also included in the appropriate chapters, with more extended subjects which appeal to a broader circle of specialists:

Kazanskii, B. A. On the mechanism of hydrocarbon conversions in the presence of some heterogeneous catalysts;

Bond G. C. An extension of the "active centre" concept in hydrocarbon reactions on metal catalysts;

Ausloos, P. Pulse radiolysis of alkanes in the gas phase ion molecule reactions and neutralization mechanism of hydrocarbon ions;

Goldstein, M. J., Benzon M. S., Haiby W. A., Judson J. A.: The linear analysis of labeling experiments (LALE).

Each contribution or plenary lecture is accompanied by abstracts of the discussion carried on the papers in question and this enables the reader to get a better picture on the atmosphere of the symposium. The volume also contains a list of participants and an index of authors which facilitates the retrieval of the papers of choice. In general, the papers devoted to the chemistry of hydrocarbons are disseminated in almost all the periodicals in the field of specialty so that it is almost impossible to consult all of them. Undoubtedly, the presentation of the proceedings of this symposium in a special volume is of a real help for researchers studying the chemical reactions of hydrocarbons. The volume is also intended for researchers and teaching staff in higher education institutes, who work in the chemistry of hydrocarbons, since it discusses numerous subjects and modern methods in one of the most important domains of science and production.

F. Cuiban

F. BESSANI and G. PASTORI PARRAVICINI, "Electronic States and Optical Transition, in Solids", Pergamon Press, Oxford-New York—Toronto—Sydney—Braunschweig 1975, XI + 300 p.

There are now so many textbooks on the electronic structure of solids that one may ask reasonably enough what a new one can offer. Unless it brings to the reader new facts or a new point of view, or an entirely novel manner of explaining old-known phenomena, it scarcely justifies itself.

As a matter of fact, many of the well-known textbooks on the subject were written before the scientists began to understand properly the relationship between the energy band properties of crystals and the number of valence electrons per unit cell. This understanding came from recent sophisticated band structure calculations in a large variety of materials. It turned out that the full symmetry of the crystal space group is the essential feature in determining the structure and sequence of the electronic levels. Adequately enough, this new book starts with a detailed account of the use of space group symmetry in quantum mechanical calculations. In subsequent chapters, wide use is made of the group theoretical arguments.

The book, intended to postgraduate students of the field, does justify itself by many other qualities as well. It is self-contained and thus qualifies itself as a textbook. It gives a thorough theoretical background of the electronic energy levels and wave functions in solids, as well as the basic facts. Including a well-presented chapter on the interaction of electrons with the electromagnetic field, the authors — original contributors themselves to the field — offer a good understanding of the optical properties of crystals. Chapters are dedicated to the exciton spectra, interband transitions-optical properties relationships, and impurity states of solids, whereas the effects of external perturbations — significant for testing theoretical results and understanding optical properties — are thoroughfully treated, though briefly, in another chapter. Finally, the references quoted, without being exhaustive, give the reader a safe orientation in the field and indicate to the researcher the main modern trends in the study of the optical properties of crystals.

Alex. Butucelea

J. P. MATHIEU, "Optics", Pergamon Press, Oxford-New York—Toronto—Sydney, 1975, X + 550 p.

Professor Jean-Paul Mathieu's well-known book *Optique* has now been published for the first time in English. Developed over several years as a university course and revised periodically, the textbook succeeded in keeping its structure and contents as close as possible to the latest developments in optics. In the present form, the treatment of this branch is divided into two sections — the electromagnetic optics and the quantum optics.

In each section, the new developments have forced out some topics of the traditional optics, or have led to abbreviating their coverage. One of the greatest assets of Mathieu's book in comparison to other books on optics is the thoroughful use of the electromagnetic theory from the outset. This allows for a logical and consistent treatment of optical phenomena all along.

The quantum optics section, although brief if we take account of the subject's diversity, manages at the same time to introduce the optics from a modern angle, and to serve as an excellent initiation in relativity and quantum mechanics. The ratio between historical not-so-significant facts and genuine physical facts was skillfully shifted by the author towards the latter.

Now it is time that a good and modern book of optics is published also in Romanian, since the otherwise excellent book of Landsberg is quite old (it was translated about twenty years ago). Professor Mathieu's book, long tested in French universities, looks like the right choice.

Alex. Butucelea

C. L. KHETRAPAL, A. C. KUNWAR, A. S. TRACEY şi P. DIEHL "NMR Basic Principles and Progress. 9. Lyotropic liquid crystals", Editors : P. Diehl, E. Fluk and R. Kosfeld Springer-Verlag Berlin, 1975, 85 pag.

The monograph belongs to a series of publications referring to the nuclear magnetic resonance (NMR) and its application in the various fields of activity. There are presented the researches performed with NMR on the lyotropic liquid crystals. *)

These substances are particularly met in nature in living organisms. They have large prospects in future both in the structural research as matrixes creating an anisotropic medium — where the molecules of a compound under investigation can be better structurally examined, and for the syntheses of some components with long-term utilization; an example for this class is the possibility of obtaining polypeptides $(NH-CHR-CO)_n$ which in the α-helical form develop liquid crystals at a certain concentration.

At present many properties of the liquid lyotropic crystals are not well known and the performed investigations have a disparate character, they being not compared, discussed and presented concisely and methodically.

This monograph including 85 pages and 18 pictures, the 9th in the series, has the merit of trying and succeeding in drawing us a comprehensive, unitary and systematic presentation of the situation existing in this field at present.

The content of the book is divided into three parts :

— Introduction (I)

— Study of the liquid lyotropic crystals (II)

— Structural examination of some substances dissolved in the nematic phase of the lyotropic liquid crystals (III).

---

*) The lyotropic liquid crystals belong to the class of thermotropic crystals extensively investigated and used in technics in the last years. These crystals get their anisotropic characteristics when blending two or more components; one of the components contains a polar group connected by one or more long-chain hydrocarbons and the second one is usually water (H_2O or D_2O).

Part I of the monograph concisely presents a structural description of the main types of lyotropic phases; there are presented representative images of the molecules, both in space and on the interfaces surface. There are then presented the basic principles regarding the NMR of the lyotropic liquid crystals, namely the basic experimental or calculated spectra of a lyotropic substance, both for nuclei with the spin $I = \frac{1}{2}$ and for those with $I > \frac{1}{2}$ as well as the principles regarding the calculation methods for the theoretical spectra of the molecules dissolved in the nematic, lyotropic phases. At the end of the first part there are specified the NMR experimental methods, sample dressing working methods.

Part II of the monograph presents the study, by NMR methods, of the liquid crystal systems as such, strictly individualized, micellar and vesicular (isotropic) and lamellar or hexagonal (anisotropic), occurring function of the relative concentration of the component elements and the temperature of the environment.

There are presented and interpreted the following aspects:

— critical micellar concentration,
— phase transition and afferent spectral changes,
— protonic and deuteric resonance in lyotropic liquid fibrous, hydrated crystals,
— self-diffusion in lyotropic liquid crystals,
— NMR study of the lamellar systems dispersed with ultrasonics.

In the table at the end of the second part, there are indicated the systems investigated till 1975; they are systematized as presented in the text, according to the type of the substances and the examined nuclei (^{1}H, ^{2}H, ^{13}C, ^{14}N, ^{17}O, ^{19}F, ^{23}Na, ^{35}Cl, ^{79}Br, ^{81}Br, and ^{85}Rb).

In Part III of the publication there are presented the investigations performed with NMR on the molecules and ions belonging to different species dissolved in the nematic phase of the lyotropic liquid crystals. There are structural indications as regards the substances belonging to the class of alcohols, ketones, halogenated derivatives, amides, amines, nitro-compounds aromatic hydrocarbons, the organo-metalic compounds, ammonium ions and its compounds and the fluoroboric ion.

The investigations are grouped in the following chapters:

— spectral analysis of the solvent and dissolvant;
— study of the systems with ^{14}N, rapidly coming into equilibrium;
— analysis of some systems by which the bond angle can be determined (e.g. of CN^- group in amides);
— structure of some ionic groups.

In this part there are also presented the investigations establishing the orientation degree (arrangement) in lyotropic phases.

The third part of the monograph has also a table, included at the end, in which the systems of the examined compounds (solute and solvent) are presented and there are given structural indications.

The bibliographical studies on which the monograph is based are extensive, 461 works being mentioned, and other 32 were examined after submitting the manuscript to the publishing house. The period till mid 1975 was thus exhaustively covered.

It is finally appreciated that the monograph presented by the authors is a scientific success having in view both its documentary value, as such, and the systematic and critical estimation of the works performed by now, all over the world, in this very new field of research and application, which has developed only after 1963.

The monograph succeeds in demonstrating the fact that NMR is a working technique adequate for a precise determination of the nuclei relative arrangement in the liquid crystal phases as well as of the substances dissolved in them.

NMR is consequently a new method of determining molecular structure in the range of the present current methods of structural investigation as: X-rays, electron diffraction, neutron diffraction and spectroscopy in the microwaves field.

Mihai Cerchez

NOTE POUR LES AUTEURS

La *Revue Roumaine de Chimie* publie des articles en anglais, français, russe, allemand ou espagnol. Les auteurs sont priés d'envoyer des articles, notes, communications et comptes rendus inédits.

Les manuscrits seront dactylographiés à deux intervalles. Les tableaux seront dactylographiés sur des feuilles séparées, de même que la légende des figures. Les diagrammes seront tracés à l'encre de Chine sur papier calque. Les tableaux et les figures seront numérotés par des chiffres arabes, en nombre strictement nécessaire. Prière de ne pas inscrire les mêmes données dans les tableaux et les figures. Les formules chimiques seront incluses dans le texte ; en outre, elles seront transcrites sur des feuilles séparées. Les auteurs sont priés d'indiquer les caractères italiques (en soulignant les lettres au crayon), ainsi que tout autre caractère spécial. L'ordre des références bibliographiques sera celui de leur mention dans le texte ; le nom de l'auteur sera précédé de l'initiale du prénom ; les publications périodiques seront présentées suivant les prescriptions internationales. Les références seront ajoutées à la fin de l'article ; elles paraîtront comme des notes, au bas de la page. Le texte sera précédé d'un résumé comprenant 15 lignes au maximum.

L'entière responsabilité du contenu des articles appartient aux auteurs. On publie des articles dus aux collaborateurs roumains ou étrangers.

PRINTED IN ROMANIA

TRAVAUX PARUS AUX ÉDITIONS DE L'ACADÉMIE DE LA RÉPUBLIQUE SOCIALISTE DE ROUMANIE

CONST. V. UGLEA, **Cromatografia pe gel permeabil. Noi domenii de aplicare** (La chromatographie sur gel perméable. Nouveaux domaines d'application), 1976, 122 p., 6,75 lei.

FRANCISC A. GOTHARD, **Echilibre lichid-vapori, I, Baze teoretice și metode de calcul** (Equilibres liquide-vapeurs. I. Bases théoriques et méthodes de calcul), 1975, 263 p., 2 pl., 28 lei.

CONST. GH. MACAROVICI, D. MACAROVICI, **Chimia oxizilor dubli și utilizările lor** (La chimie des oxydes doubles et leur utilisation), 1975, 195 p., 13 lei.

M. AVRAM, **Antidăunători** (Pesticides), 1974, 496 p., 41 lei.

ELENA CEAUȘESCU, **Research work on synthesis and characterization of macromolecular compounds. Contributions**, 1974, 251 p., 20 lei.

DUMITRU COSTACHE, **Analiza chimică prin metoda cinetică** (L'Analyse chimique par la méthode cinétique), 1974, 276 p., 15,50 lei.

G. A. RĂDULESCU, **Proprietățile țițeiurilor românești** (Les propriétés des pétroles roumains), 1974, 267 p., 2 pl. 18 lei.

CR. SIMIONESCU, VIORICA RUSAN, V. POPA, **Chimia algelor marine** (La chimie des algues marines), 1974, 212 p., 1 pl., 18 lei.

I. ZUGRĂVESCU, MAGDA PETROVANU, **Chimia n-ilidelor** (La chimie des n-Ilures), 1974, 348 p., 19 lei.

MARIA FITI, **Dozimetria chimică a radiațiilor ionizante** (La dosimétrie chimique des radiations ionisantes), 1973, 240 p., 13,50 lei.

TIBERIU NĂSCUȚIU, **Metode radiochimice de analiză** (Méthodes radiochimiques d'analyse), 1973, 384 p., 23 lei.

CRISTOFOR SIMIONESCU, MARGARETA GRIGORAȘ, Agata Cernătescu-Asanei, Rozmarin Gheorghe, **Chimia lemnului în România. Plopul și salcia** (La Chimie du bois en Roumanie. Le peuplier et le saule), 1973, 299 p., 13 pl., 26 lei.

MIHAI FLORESCU, **Eficiența economică a cercetării științifice** (L'efficience économique de la recherche scientifique), 1972, 115 p., 15 lei.

GEORGETA LĂZĂRESCU, **Sistematizarea informațiilor în chimia organică** (Systématisation des informations en Chimie organique), 1972, 243 p., 1 pl., 10,50 lei.

1976 IUL 16

I. P. I. – c. 1140

43 426

Lei 25. –

F 1103

ACADÉMIE DE LA RÉPUBLIQUE SOCIALISTE DE ROUMANIE

R

REFERÁLVA

REVUE ROUMAINE DE CHIMIE

TOME 21
N° 7
Juillet 1976

RECHAX, **21**, 7, 959–1112 (1976)

EDITURA ACADEMIEI REPUBLICII SOCIALISTE ROMÂNIA

Rev. Roumaine Chim. **21**, 7, p. 959–1112 (1976), Bucarest

ACADÉMIE DE LA RÉPUBLIQUE SOCIALISTE DE ROUMANIE

COMITÉ DE RÉDACTION

Rédacteur en chef:

I. G. MURGULESCU, membre de l'Académie de la République Socialiste de Roumanie

Rédacteurs en chef adjoints:

A. T. BALABAN et V. EM. SAHINI, membres correspondants de l'Académie de la République Socialiste de Roumanie

Collège de rédaction:

EM. BRATU, ELENA CEAUŞESCU, ECATERINA CIORĂNESCU-NENITZESCU, C. DRĂGULESCU, CR. SIMIONESCU, membres de l'Académie de la République Socialiste de Roumanie; P. SPACU, membre correspondant de l'Académie de la République Socialiste de Roumanie; MARGARETA AVRAM, I. HAIDUC, D. I. MARCHIDAN, I. MOLDOVAN, G. NIAC et D. SĂNDULESCU

La Revue Roumaine de Chimie paraît 10 fois par an. Toute commande de l'étranger (fascicules ou abonnements) sera adressée à ILEXIM — Serviciul Export-Import Carte (Livres)/Serviciul Export Import Presă (Revues), P.O.B. 2001, télex 011226, 64—66, Calea Griviţei, Bucarest 12, Roumanie

Les manuscrits, les livres et les revues proposés en échange, ainsi que toute correspondance seront envoyés à la rédaction :

REVUE ROUMAINE DE CHIMIE

23, str. Dumbrava Roşie, Bucarest, Roumanie, téléphone 12 41 60

EDITURA ACADEMIEI REPUBLICII SOCIALISTE ROMÂNIA

125, Calea Victoriei, Bucarest, Roumanie, téléphone 50 76 80

ORSZÁGOS MŰSZAKI KÖNYVTÁR ÉS DOKUMENTÁCIÓS KÖZPONT 1983

REVUE ROUMAINE DE CHIMIE

Tome 21, Nº 7 Juillet 1976

I. G. MURGULESCU, EUGENIA IVANA and E. POPA, Absorption spectra of solid and molten PbI_2 . . . . 961— 964

RODICA GRIGOROVICI, A. BUTUCELEA, V. E. SAHINI and M. K. DeARMOND, Normal coordinate analysis of hexahaloethanes 965— 976

V. POPA and E. SEGAL, Adsorption of gaseous mixtures within the framework of Jovanović model . . . . 977— 983

TATIANA ONCESCU and ECATERINA JURCONI, Solvent effect on the kinetics of the thermal decomposition of dioxalatodiaquomanganate (III) in dimethylsulphoxide-water mixtures . . . . 985— 990

A O. RADOVICI, MARIA MAVRODIN-TĂRĂBÎC, IOANA ONACA and I. SOLACOLU, Hydrogen oxidation on porous nickel electrodes. IV. The improvement of the electrode performances by addition of different electrocatalysts . . . . 991— 996

M. CIOPEC and D. I. MARCHIDAN, The influence of non-stoichiometry upon heat capacity of uranium oxides. A model of quantitative approach . . . 997—1005

MARIANA CIUREANU, A theoretical study of azaindoles . . . . 1007—1011

MARIA ENCULESCU, Influence of some oxides of transitional metals on the formation of calcium orthosilicate . . . . 1013—1022

MARIA PREDA and R. DINESCU, Thermal equilibria in the binary systems $MgO-CeO_2$, $CaO-CeO_2$, $SrO-CeO_2$, $BaO-CeO_2$ . . . . 1023—1030

MARGARETA TEODORESCU, The structure of dark-red compound $[Fe(II)phen_2(NCS)_2].H_2O$ . . . . 1031—1036

ELENA CATRINA, Z. SIMON, Z. SZABADAY and GH. CATRINA, Electronic spectra of Co^{III} thiazolidine chelates . . . . 1037—1043

A. T. BALABAN, Chemical graphs. XXVI. Codes for configurations of conjugated polyenes . . . . 1045—1047

A. T. BALABAN, Chemical graphs. XXVII. Enumeration and codification of staggered conformations of alkanes . . . . 1049—1071

Rev. Roumaine Chim., 21, 7, p. 959–1112 (1976), Bucarest

I. SIMITI and ANA MUREȘAN, Contributions to the study of heterocycles. XXXVIII. Application of the Sommelet reaction in the series of 2-aryl-4-methyl-5-chloromethyl-thiazole . . . . 1073—1081

M. BANCIU, On the pyrolysis of Nenitzescu's hydrocarbons . . . . 1083—1095

R A. CARPOV, STELIANA MAXIM and M. DIMA, Growth regulating polymers. II. The poly(N,N-dimethylaminoethyl methacrylate salts) of 2,4-dichlorophenoxyacetic and 2,4,5-trichlorophenoxyacetic acids . . . . 1097—1102

JACEK SZYMURA and BOGDAN DIRSKA, Electron microscopic investigations of silica gels structure and dispersion of synthetic aluminosilicates . . 1103—1107

COMPTES RENDUS . . . . 1109—1112

Revue Roumaine de Chimie, **21**, 7, 961–964 (1976)

ABSORPTION SPECTRA OF SOLID AND MOLTEN PbI_2

I. G. MURGULESCU, EUGENIA IVANA and E. POPA

Centre of Physical Chemistry
31, Galaţi Street, Bucharest, Romania

Received September 11, 1975

Temperature influence on the absorption band edge of solid and molten PbI_2 was investigated. A sharp decrease of transmittance and an energy jump of 0.359eV were noted at the melting point.

Studies on optical properties of molten lead halides have rarely been reported.[1-6] There are some studies concerning PbX_2-MX (X=Cl, Br and M = Na, K) binary mixtures, in which the existence of PbX_n^{2-n} complex ion has also been proved by other different methods.[7-9]

The Raman spectra study[4,6,10] of molten $PbCl_2$ and $PbBr_2$ indicate that no complexes of PbX_3^- type were present. Still, the electronic absorption spectra have not clearly revealed the existence of PbX_n^{2-n}-type complexes in these molten halides.[5] It is supposed that the continuous absorption observed is a result of absorption band overlapping of Pb^{+2} and PbX^+ ions.

In the present study the absorption spectrum of both solid and molten PbI_2 has been investigated. The interest for PbI_2 was determined by the fact that, according to the absorption spectrum and the theory of coulombian interactions in crystal, PbI_2 can be taken for an

---

[1] T. Retschinsky, *Ann. Physik*, **27**, 100 (1908).

[2] B. R. Sundheim and J. Greenberg, *J. Chem. Phys.*, **28**, 439 (1958).

[3] J. Greenberg, *J. Chem. Phys.*, **40**, 3128 (1964).

[4] K. Balasubrahmanyan and L. Nenis, *J. Chem. Phys.*, **40**, 2657 (1964).

[5] I. G. Murgulescu, E. Popa and E. Ivana, *Rev. Roumaine Chim.*, **15**, 669 (1970).

[6] R. Oganoda, *J. Phys. Soc. Japan*, **36**, 903 (1974).

[7] J. L. Barton and H. Bloom, *Trans. Faraday Soc.*, **55**, 1792 (1959).

[8] I. G. Murgulescu and St. Zuca, *Rev. Roumanie Chim.*, **10**, 129 (1965).

[9] S. Sternberg and V. Vasilescu, *Rev. Roumanie Chim.*, **12**, 1187 (1967).

[10] V. A. Maroni, *J. Chem. Phys.*, **54**, 4126 (1971).

intermediate case between typically ionic alkali halides and covalent semiconductors.[11-17]

EXPERIMENTAL

Lead iodide was obtained from very diluted solutions of recrystallized $Pb(NO_3)_2$ and HI. In order to have a better purification PbI_2 so obtained was vaporized in vacuum.

The spectra were carried out with a Specord UV-VIS spectrophotometer.

The experimental set up and the cell designs, as well as the method of their loading and handling were similar to those previously employed.[5] The cells employed have layer thicknesses between 8 and 10 μ.

RESULTS AND DISCUSSIONS

The absorption spectrum of solid and molten PbI_2 is presented in fig. 1. In fig. 2 the temperature variation of the absorption band edge is shown.

At the melting point there is an energy jump of about 2,900 cm^{-1}.

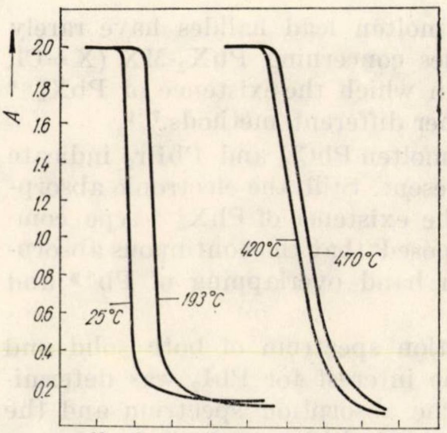

Fig. 1. — Absorption spectrum of PbI_2.

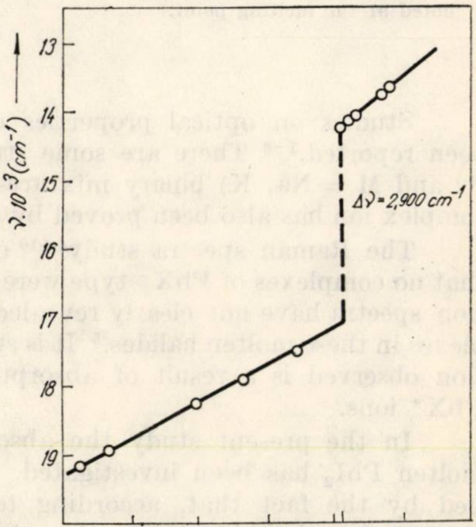

Fig. 2. — Temperature variation of the absorption band edge at $T = 40\%$.

---

[11] S. Nikitine, "Exciton spectra in semiconductors and ionic compounds. II. Experimental", Coopérative universitaire, Strasbourg 1960, p. 271.

[12] R. I. Darwood, A. J. Forty and M. R. Tubbs, *Proc. Roy. Soc.*, **284**, 272 (1965).

[13] M. R. Tubbs, *Proc. Roy. Soc.*, **280**, 566 (1964).

[14] M. R. Tubbs and A. J. Forty, *J. Phys. Chem. Solids*, **26**, 711 (1965).

[15] M. R. Tubbs, *J. Phys. Chem. Solids*, **29**, 1191 (1968).

[16] E. Doni, G. Grosso and G. Spavieri, *Solid State Comm.*, **11**, 493 (1972).

[17] I. Ch. Schlüter and M. Schlüter, *Phys. Review*, **9**, 1652 (1974).

The variation of transmittance with temperature at $\nu=13{,}000$ cm^{-1} on both heating and cooling has been also studied.

As shown in fig. 3, transmittance varies slowly with temperature. At the melting point, during both heating and cooling (the temperature varies with 4°/min.) a sharp variation of transmittance can be noticed.

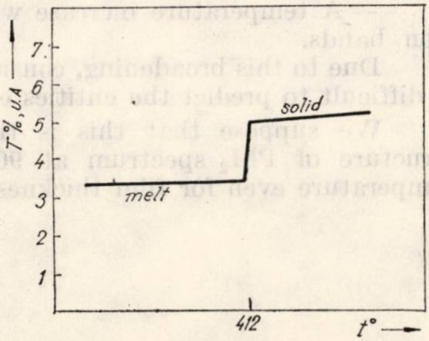

Fig. 3. — Temperature variation of the transmittance at $\nu = 13{,}000$ cm^{-1}.

The absorption spectra are characterized by a continuous absorption which then suddenly decreases down to under 0.2. The sharp decrease of the absorption band for both the solid and molten PbI_2 ranges within $\nu = 19{,}500 - 18{,}700$ cm^{-1} and $\nu = 15{,}800 - 15{,}200$ cm^{-1}, respectively.

As one can see in fig. 1 the absorption band edge is shifted by temperature towards low energy values.

The study of the absorption spectrum of solid and molten PbI_2 as a function of temperature pointed out a shift of the absorption band edge of 6×10^{-4} eV/° and 9.6×10^{-4} eV/°, respectively.

Tubbs found a shift of 2×10^{-4} eV/K for the maximum located at $\nu=20{,}360$ cm^{-1} over the temperature range 90—298 K. Tubbs attributed this maximum to the doublet component of the (6s + 6p) excited state of the I^- ion.[15]

If we suppose that the absorption band edge of molten PbI_2 spectrum is due to the excitation of the I^- ion, then, it results from the above that higher shifts, of the same order of magnitude, are to be expected at higher temperatures.

The shift values (eV/degr.) increase with temperature. This can be a result of the structural transformations that alter the powerful electric field (characteristic for layered iodides), to which the I^- ion is subjected. The energy jump and the sharp decrease of transmittance indicate the deep structural transformation occurring at the melting point. As a result of thermal expansion a new structure is formed at this temperature. Both the monotonous variation of absorption and shift of absorption band edge towards low energy indicate that the new structure formed at the melting point remains the same within the whole studied temperature range. Thus, the I^- ion excitation takes place in an electric field undergoing continuous changes with temperature, before and after melting.

This conclusion appears also to be supported by the temperature variation of specific conductivity (0.0022 Ω^{-1} cm^{-1}/degr.).[18]

Within the temperature range of 25–350° no absorption maxima have been noted. We consider the continuous absorption as a result of the following two factors:

— Thickness of solid and molten films which is of about 10μ;

— A temperature increase which leads to a broadening of absorption bands.

Due to this broadening, considerable overlapping occurs that makes it difficult to predict the entities existing in molten state.

We suppose that this is the reason for which the well-defined structure of PbI_2 spectrum at 90 K becomes hardly visible at room temperature even for film thicknesses of 0.1–0.2 μ.

---

[18] W. Karl and A. Klem, *Z. Naturforsch.*, **19a**, 1619 (1964).

Revue Roumaine de Chimie, **21**, 7, 965–976 (1976)

NORMAL COORDINATE ANALYSIS OF HEXAHALOETHANES

RODICA GRIGOROVICI, A. BUTUCELEA and V. E. SAHINI

Center of Physical Chemistry, 31 Galaţi Str., Bucharest-9, Romania

and

M. KEITH DeARMOND

Department of Chemistry, North Carolina State University,
Raleigh, N. C. 27607, U.S.A.

Received November 27, 1975

A normal coordinate analysis of C_2F_6, C_2Cl_6 and C_2Br_6 was carried out, using an unmodified Urey-Bradley force field. On the basis of the fairly good agreement between calculated and observed frequencies reached for all compounds, the UBFF seems to be a satisfactory compromise within the approximation used. Correct band assignments were given based on the potential energy distribution and the optimum calculated set of force constants. The modes of A_{2u} and E_g species change entirely their character in passing from C_2F_6 to C_2Br_6. The stretching (K) and repulsive (F) force constants are discussed in terms of some molecular parameters.

Although ethane and various ethyl halides have been individually considered from the point of view of normal coordinate analysis, no systematic study of the whole series of existing hexahaloethanes (C_2F_6, C_2Cl_6, C_2Br_6) has been, to our knowledge, undertaken so far. Such a study would nevertheless be interesting for following the change in mode assignments, value of force constants and atoms' displacements in passing from one molecule to the other along the series. The conclusions drawn from such a study would also be useful for understanding the nature of the metal-metal bond and the normal vibration modes in X_2Y_6-type compounds such as the halosubstituted disilanes or digermanes.

A wealth of vibrational data is now available on the hexahaloethanes. The infrared and Raman spectra of C_2F_6 were reported recently for the gaseous, liquid and α- and β-crystalline phases,[1] confirming or correcting earlier data[2] existing for the gaseous state, especially with respect to the C—C stretching vibration. The complete solid-phase vibrational spectra of C_2Cl_6 and C_2Br_6 were reported earlier,[2] whereas for C_2Br_6 alone single crystal spectra were published recently.[3] Most of the earlier data were systematically entered in Shimanouchi's *Tables*.[4] Since normal coordinate analyses were already carried out[5,6] for ethane and ethane-d_6, an extension of the analysis to hexahalo-substituted ethanes seems interesting.

---

[1] A. Lewis and E. L. Pace, *J. Chem. Phys.*, **58**, 3661 (1973).

[2] R. A. Carney, Y. A. Piotrowski, A. G. Meister, J. H. Braun and F. F. Cleveland, *J. Mol. Spectroscopy*, **7**, 209 (1961).

[3] R. D. McLachlan and V. B. Carter, *Spectrochim. Acta*, **26A**, 2247 (1970).

[4] T. Shimanouchi, "Tables of Molecular Vibrational Frequencies", Consolidated Volume 1, NSRDS-NBS 39, Washington D.C., 1972, and references therein.

In this paper, we attempt to prove the validity of a simple Urey-Bradley force field (UBFF) for all hexahaloethanes, to estimate the extent to which the concept of group frequency, as defined for ethane, remains correct upon complete hydrogen substitution with halides, and to obtain the optimum sets of force constants which give the best fit between calculated and observed frequencies (in solid state) under the approximation used in this calculation. By using frequencies measured in solid state only, possible lattice interactions were taken automatically into account, although the specific modification of the low energy molecular modes through coupling with appropriate intermolecular modes was not worked out explicitly, by a detailed factor group analysis, in this work. For reasons of comparison, the calculations for C_2H_6 and C_2D_6 were repeated in the same approximation (though in gaseous phase).

METHOD OF CALCULATION

The hexahaloethanes, C_2X_6 (X = F, Cl, Br), have in their staggered configuration a D_{3d} symmetry. Therefore, the 18 normal vibrations are grouped into 5 species, $3A_{1g} + A_{1u} + 2A_{2u} + 3E_g + 3E_u$. The symmetry coordinates used to factorize the secular equation, written in terms of the internal coordinates indicated in Figure 1, are given in Table 1. They

Table 1

Symmetry coordinates of $C_2X_6(D_{3d})$ molecules

Species	Coordinate	Mode description [a]
A_{1g}	$S_1 = R$	C−C stretching
	$S_2 = 1/\sqrt{6}(r_1 + r_2 + r_3 + r_4 + r_5 + r_6)$	CX_3 sym. str.
	$S_3 = 1/\sqrt{6}(\alpha_1 + \alpha_2 + \alpha_3 + \alpha_4 + \alpha_5 + \alpha_6)$	CX_3 sym. def.
	$S_3' = 1/\sqrt{6}(\beta_{12} + \beta_{23} + \beta_{13} + \beta_{45} + \beta_{56} + \beta_{46})$	CX_3 sym. def. (redundant)
A_{1u}	$S_4 = \tau$	$CX_3 - CX_3$ torsion
A_{2u}	$S_5 = 1/\sqrt{6}(r_1 + r_2 + r_3 - r_4 - r_5 - r_6)$	CX_3 sym. str.
	$S_6 = 1/\sqrt{6}(\alpha_1 + \alpha_2 + \alpha_3 - \alpha_4 - \alpha_5 - \alpha_6)$	CX_3 sym. def.
	$S_6' = 1/\sqrt{6}(\beta_{12} + \beta_{23} + \beta_{13} - \beta_{45} - \beta_{56} - \beta_{46})$	CX_3 sym. def. (redundant)
E_g	$S_7 = 1/2\sqrt{3}(r_1 + r_2 - 2r_3 + r_4 + r_5 - 2r_6)$	CX_3 asym. str.
	$S_8 = 1/2\sqrt{3}(2\beta_{12} - \beta_{23} - \beta_{13} + 2\beta_{45} - \beta_{56} - \beta_{46})$	CX_3 asym. def.
	$S_9 = 1/2\sqrt{3}(\alpha_1 + \alpha_2 - 2\alpha_3 + \alpha_4 + \alpha_5 - 2\alpha_6)$	$C-CX_3$ rocking
E_u	$S_{10} = 1/2\sqrt{3}(r_1 + r_2 - 2r_3 - r_4 - r_5 + 2r_6)$	CX_3 asym. str.
	$S_{11} = 1/2\sqrt{3}(2\beta_{12} - \beta_{23} - \beta_{13} - 2\beta_{45} + \beta_{56} + \beta_{46})$	CX_3 asym. def.
	$S_{12} = 1/2\sqrt{3}(\alpha_1 + \alpha_2 - 2\alpha_3 - \alpha_4 - \alpha_5 + 2\alpha_6)$	$C - CX_3$ rock.

[a]. The selection of these vibrational motions is based on the assignments given for ethane, cf. Ref.[7].

---

[5] J. L. Duncan, *Spectrochim. Acta*, **20**, 1197 (1964).

[6] I. Nakagawa and T. Shimanouchi, *J. Mol. Spectroscopy*, **39**, 255 (1971).

[7] K. Nakamoto, "Infrared Spectra of Inorganic and Coordination Compounds", Wiley, New York, 1963, p. 122.

involve one redundant coordinate in each of the A_{1g} and A_{2u} species, which gives two zero frequencies in the final results. The torsion internal coordinate τ was chosen as the dihedral angle between the planes formed by the atoms 3—1—2—6 and 5—1—2—8.

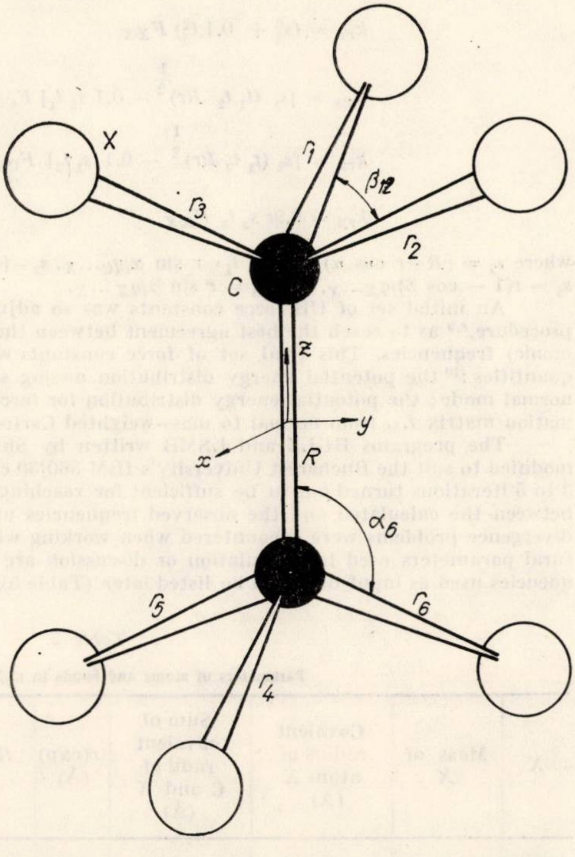

Fig. 1.—Valence internal coordinates of staggered C_2X_6 molecules.

In the first step of our calculation, reported in this paper, a simple Urey-Bradley force field, involving 7 force constants (K_{CC}, K_{CX}, H_{CCX}, H_{XCX}, F_{CX}, F_{XX} and K_τ), was used to build up the potential energy. The constants F' were assumed to be equal to $-(1/10)F$. Written in terms of the internal coordinates R, the potential energy in our case involves general valence force field (GVFF) force constants, which are related to the UB force constants through the Z_R matrix as follows: [8,9]

Diagonal force constants k_{ii}:

$$k_R = K_{CC} + 6\,(s_1^2 - 0.1\,t_1^2)\,F_{CX}$$

$$k_r = K_{CX} + (s_2^2 - 0.1\,t_2^2)\,F_{CX} + 2\,(s_3^2 - 0.1\,t_3^2)\,F_{XX}$$

$$k_\alpha = Rr\,[H_{CCX} + (t_1\,t_2 + 0.1\,s_1\,s_2)\,F_{CX}] \qquad (1)$$

$$k_\beta = r^2\,[H_{XCX} + (t_3^2 + 0.1\,s_3^2)\,F_{XX}]$$

$$k_\tau = r^2\,K_\tau$$

---

[8] J. Overend and J. R. Scherer, *J. Chem. Phys.*, **32**, 1289 (1960).

[9] J. H. Schachtschneider and R. G. Snyder, *Spectrochim. Acta*, **19**, 117 (1963).

Off-diagonal force constants k_{ij} :

$$\begin{aligned}
k_{Rr} &= (s_1 s_2 + 0.1\, t_1 t_2)\, F_{CX} \\
k_{rr} &= (s_3^2 + 0.1\, t_3^2)\, F_{XX} \\
k_{R\alpha} &= [s_1\, (t_1 t_2\, Rr)^{\frac{1}{2}} - 0.1\, s_2 t_1]\, F_{CX} \\
k_{r\alpha} &= [s_2\, (t_1 t_2\, Rr)^{\frac{1}{2}} - 0.1\, s_1 t_2]\, F_{CX} \\
k_{r\beta} &= 0.9 r\, s_3 t_3\, F_{XX}
\end{aligned} \tag{2}$$

where $s_1 = (R - r\cos\alpha)/q_{C\cdots X}$, $t_1 = r\sin\alpha/q_{C\cdots X}$, $s_2 = (r - R\cos\alpha)/q_{C\cdots X}$, $t_2 = R\sin\alpha/q_{C\cdots X}$, $s_3 = r(1-\cos\beta)/q_{X\cdots X}$, and $t_3 = r\sin\beta/q_{X\cdots X}$.

An initial set of UB force constants was so adjusted, using a well-known least-square procedure,[8,9] as to reach the best agreement between the calculated and the observed (anharmonic) frequencies. This final set of force constants was used for calculating the following quantities :[10] the potential energy distribution among symmetry coordinates (PES) for each normal mode ; the potential energy distribution for force constants (PEF) ; and the transformation matrix L_M from normal to mass-weighted Cartesian coordinates.

The programs BGLZ and LSMB written by Shimanouchi *et al.*[10] were used, slightly modified to suit the Bucharest University's IBM 360/30 computer's operating system. Usually, 3 to 5 iterations turned out to be sufficient for reaching the best obtainable degree of fitness between the calculated and the observed frequencies under the assumed approximation. No divergence problems were encountered when working with the unmodified UBFF. The structural parameters used for calculation or discussion are listed in Table 2. The measured frequencies used as input data will be listed later (Table 5), together with the calculated values.

Table 2

Parameters of atoms and bonds in C_2X_6 molecules

X	Mass of X	Covalent radius of atom X (Å)	Sum of covalent radii of C and X (Å)	r(exp) (Å)	R (exp) (Å)	α (deg)	Electro-negativity of X	Ionic character of C−X bond (%)[a]
H	1.008	0.30	1.07	1.07[b]	1.54[b]	108	2.1	3
D	2.014	0.30	1.07	1.07	1.54	108	2.1	3
F	18.998	0.64	1.41	1.30[c]	1.54[c]	108	4.0	43
Cl	35.45	0.99	1.76	1.76[b]	1.54[b]	108	3.0	7
Br	79.91	1.11	1.88	1.93[d]	1.52[d]	108	2.8	3

a. According to Pauling ; *b*. Ref. [11] ; *c*. Ref. [11] ; *d*. Refs.[11,12].

RESULTS AND DISCUSSION

The optimum sets of UB force constants obtained after 6 iterations for the hexahaloethanes are given in Table 3 (see also Table 4). They

---

[10] T. Shimanouchi, "Normal Coordinate Treatment of Polyatomic Molecules", Tokyo University, Tokyo, 1968.

[11] R.W.G. Wyckoff, "Crystal Structures", Interscience, New York, 1966, Vol. 5, pp. 225−232.

[12] G. Mandel and J. Donohue, *Acta Cryst.*, **28B**, 1313 (1972).

Table 3

Estimated Urey-Bradley force constants for C_2X_6 (mdyne/Å) and their dispersions

X	K_{CC}	K_{CX}	H_{CCX}	H_{XCX}	F_{CX}	F_{XX}	K_τ
H, D	2.72 ± 0.44	4.52 ± 0.17	0.23 ± 0.03	0.41 ± 0.04	0.41 ± 0.09	0.08 ± 0.10	0.068 ± 0.01
F	4.39 ± 0.59	4.13 ± 0.32	0.01 ± 0.13	0.48 ± 0.15	1.19 ± 0.34	1.16 ± 0.24	0.07 ± 0.02
Cl	2.08 ± 0.17	1.91 ± 0.12	0.09 ± 0.04	0.17 ± 0.05	0.63 ± 0.09	0.63 ± 0.07	0.11 ± 0.02
Br	1.96 ± 0.40	1.19 ± 0.29	0.12 ± 0.07	0.13 ± 0.11	0.69 ± 0.24	0.54 ± 0.16	0.17 ± 0.08

Table 4

Valence force constants for C_2X_6[a]

X	k_R	k_r	k_α	k_β	k_{Rr}	k_{rr}	$k_{R\alpha}$	$k_{r\alpha}$	$k_{r\beta}$	k_τ
H, D	4.56	4.82	0.65	0.50	0.27	0.06	0.25	0.18	0.04	0.08
F	9.27	6.48	0.98	1.58	0.81	0.82	0.76	0.65	0.64	0.12
Cl	4.23	3.14	0.94	1.29	0.43	0.45	0.42	0.47	0.47	0.34
Br	4.15	2.37	1.16	1.27	0.47	0.38	0.44	0.55	0.44	0.63

a. In mdyne/Å for k_R, k_r, k_{Rr} and k_{rr}; in mdyne·Å for k_α, k_β and k_τ; and in mdyne for $k_{R\alpha}$, $k_{r\alpha}$ and $k_{r\beta}$.

will be discussed later on. Table 5 gives the normal vibration frequencies, calculated on the basis of the optimum set of force constants. The agreement between these and the experimental frequencies can be regarded as satisfactory under the assumed approximation of a simple UBFF and if we take into account that the calculated frequencies, obtained in the harmonic approximation, should be compared in fact to experimental frequencies corrected for anharmonicity.

Table 5

Observed and calculated frequencies of hexahaloethanes[a] (cm^{-1})

Species	Mode	C_2H_6 (gas)		C_2D_6 (gas)		C_2F_6 (solid)		C_2Cl_6 (solid)		C_2Br_6 (solid)	
		obs.[b]	calc.	obs.[b]	calc.	obs.[c]	calc.	obs.[d]	calc.	obs.[e]	calc.
A_{1g}	ν_1	995	1003	1155	1161	1417	1417	975	975	938	938
	ν_2	2954	2906	2083	2083	807	840	431	440	256	258
	ν_3	1388	1359	843	825	348	352	170	176	143	113
A_{1u}[f]	ν_4	289	291	208	206	68	68	61	61	51	51
A_{2u}	ν_5	2896	2927	2087	2110	1099	1077	675	675	558	597
	ν_6	1379	1399	1077	1071	715	661	372	363	223	225
E_g	ν_7	2969	2975	2226	2218	1220	1220	859	854	760	783
	ν_8	1468	1455	1041	1054	621	597	340	326	206	204
	ν_9	1190	1103	970	870	382	384	223	211	137	135
E_u	ν_{10}	2985	2987	2235	2227	1222	1220	778	781	656	630
	ν_{11}	1468	1476	1081	1071	522	561	271	282	169	172
	ν_{12}	822	920	594	666	216	230	114	121	108	82

a. For solid-state spectra, some observed frequencies were taken as average values for various components resulting from factor group splitting in the crystalline field; *b.* Ref.[4]; *c.* α-phase, cf. Ref.[1]; *d.* Ref.[2]; *e.* Ref.[3]; *f.* Inactive mode; values obtained from combination bands.

Table 6

Potential energy distribution among symmetry coordinates (PES) and for force constants (PEF), and assignment of modes for C_2X_6 molecules

Species	Mode	X	Frequency (cm^{-1})	PES				PEF (%)							Assignment[a]
								K_{CC}	K_{CX}	H_{CCX}	H_{XCX}	F_{CX}	F_{XX}	K_τ	
				S_1	S_2	S_3	S_3'								
A_{1g}	ν_1	H	995	1.00	0.01	0.01	0.01	54	1	1	1	42			νCC
		D	1155	1.00	0.00	0.51	0.36	44		22	24	8	2		
		F	1417	1.00	0.15	0.08	0.12	62	10	1	8	17	3		
		Cl	975	1.00	0.15	0.10	0.12	62	9	3	6	17	3		
		Br	938	1.00	0.10	0.10	0.10	63	5	4	5	20	3		
	ν_2	H	2954	0.00	1.00	0.00	0.00		92			3	4		ν_sCX_3
		D	2083	0.01	1.00	0.00	0.00		92			2	4		
		F	807	0.01	1.00	0.00	0.00	1	48			11	41		
		Cl	431	0.00	1.00	0.00	0.00		44			11	44		
		Br	256	0.00	1.00	0.00	0.00		39			13	48		
	ν_3	H	1388	0.31	0.00	1.00	0.71	11		36	40	8	3		δ_sCX_3[b]
		D	843	1.00	0.02	0.72	0.51	21	1	15	17	44	2		
		F	348	0.00	0.03	0.71	1.00		1	1	30	47	21		
		Cl	170	0.00	0.04	0.81	1.00		1	10	21	44	23		
		Br	143	0.00	0.00	1.00	0.98			14	18	44	23		
					S_4										
A_{1u}	ν_4	H	289		1.00									100	τCX_3-CX_3
		D	208		1.00									100	
		F	68		1.00									100	
		Cl	61		1.00									100	
		Br	51		1.00									100	
				S_5	S_6	S_6'									
A_{2u}	ν_5	H	2896	1.00	0.00	0.00			91		5	4			ν_sCX_3
		D	2087	1.00	0.00	0.00			90		6	4			
		F	1099	1.00	0.16	0.22			42		9	35	13		
		Cl	675	1.00	0.30	0.38			33	5	11	42	10		
		Br	558	1.00	0.71	0.70			18	10	12	52	8		$\nu_sCX_3+\delta_sCX_3$
	ν_6	H	1379	0.02	1.00	0.71			1	34	38	22	4		δ_sCX_3
		D	1077	0.03	1.00	0.71			2	34	38	22	4		
		F	715	0.49	0.71	1.00			11		21	19	49		
		Cl	372	1.00	0.74	0.91			16	6	12	8	58		$\nu_sCX_3+\delta_sCX_3$
		Br	223	1.00	0.33	0.32			21	5	7	3	63		ν_sCX_3
				S_7	S_8	S_9									
E_g	ν_7	H	2969	1.00	0.00	0.00			96			3	1		ν_aCX_3
		D	2226	1.00	0.00	0.01			95	1	1	2	1		
		F	1220	1.00	0.24	0.27			75		12	9	3		
		Cl	859	1.00	0.26	0.66			59	14	9	15	3		$\nu_aCX_3+\rho CCX_3$
		Br	760	0.74	0.26	1.00			39	26	9	23	3		$\rho CCX_3+\nu_aCX_3$
	ν_8	H	1468	0.00	1.00	0.04				2	89	1	7		δ_aCX_3
		D	1041	0.00	1.00	0.00					92		8		
		F	621	0.25	1.00	0.20			11		29	19	41		
		Cl	340	1.00	0.83	0.57			22	4	10	31	33		$\nu_aCX_3+\delta_aCX_3$
		Br	206	1.00	0.15	0.14			34	2	3	34	26		ν_aCX_3
	ν_9	H	1190	0.00	0.04	1.00				57	4	39			ρCCX_3
		D	970	0.00	0.00	1.00				59		41			
		F	382	0.00	0.36	1.00				1	13	74	10		
		Cl	223	0.05	1.00	0.63			2	9	24	35	29		$\delta_aCX_3+\rho CCX_3$
		Br	137	0.05	1.00	0.27			3	6	30	23	38		δ_aCX_3

(cont'd)

Table 6 (continued)

Species	Mode	X	Frequency (cm^{-1})	PES			PEF (%)							Assignment[a]
				S_{10}	S_{11}	S_{12}	K_{CC}	K_{CX}	H_{CCX}	H_{XCX}	F_{CX}	F_{XX}	K_τ	
E_u	ν_{10}	H	2985	1.00	0.00	0.00		95		1	4	1		ν_aCX_3
		D	2235	1.00	0.01	0.00		94		11	4	1		
		F	1222	1.00	0.22	0.00		77		10	9	3		
		Cl	778	1.00	0.24	0.00		74		13	12	3		
		Br	656	1.00	0.30	0.01		63			18	5		
	ν_{11}	H	1469	0.00	1.00	0.08			4	85	3	7		δ_aCX_3
		D	1081	0.01	1.00	0.06		1	3	86	2	7		
		F	522	0.09	1.00	0.00		5		43		51		
		Cl	271	0.07	1.00	0.00		5		33	1	61		
		Br	169	0.14	1.00	0.00		6		29	2	62		
	ν_{12}	H	822	0.01	0.08	1.00		1	55	7	36			$\rho\,CCX_3$
		D	594	0.00	0.06	1.00			56	5	38			
		F	216	0.05	0.00	1.00		4	2		93			
		Cl	114	0.05	0.00	1.00		4	27		68			
		Br	108	0.09	0.00	1.00		6	34		59			

---

a. Abbreviations; νCC = C$-$C stretching; $\nu_{s(a)}CX_3$ = symmetric (asymmetric) CX_3 str.; $\delta_{s(a)}CX_3$ = CX_3 symmetric (asymmetric) deformation; τCX_3-CX_3 = torsion; ρCCX_3=C$-CX_3$ rocking; *b*· Except for C_2D_6, where ν_3 is predominantly a C$-$C stretching mode.

Taking the frequency fit as a criterium for the validity of the chosen force field, it results that for C_2H_6 and C_2D_6, where the fit is generally within about 2%, the UBFF is a good approximation for the actual field, although a rather poor fit ($\sim$10%) was obtained for both rocking mode frequencies (ν_9 and ν_{12}). For the hexahaloethanes, non-agreement as high as about 5% between calculated and observed frequencies occurs for several modes, not necessarily the same for C_2F_6, C_2Cl_6 and C_2Br_6, but the simple UBFF still remains a fairly good approximation.

Frequency assignments. These are based on the potential energy distribution (PES) listed in Table 6. It can be seen that the modes of A_{1g}, A_{1u} and E_u species remain pure along the whole series of compounds. The only exception is C_2D_6, for which both the 843 and 1155 cm^{-1} frequencies are described as a coupling of the C$-$C stretching motion with a CD_3 symmetric deformation. Since from Table 6 it results that the band at 1155 cm^{-1} has more C$-$C stretching and less deformational character than the former, and also that the contribution of the stretching force constant K_{CC} is greater for this frequency, we placed this value among the ν_1 modes, although, strictly speaking, neither a proper C$-$C stretching, nor a CD_3 symmetric deformation vibration mode exists for hexadeuteroethane. In passing from C_2H_6 to the hexahaloethanes, the frequency ν_1 — which for ethane is smaller than ν_3 — becomes larger than ν_3 from C_2F_6 on in the series. We believe this to be an effect of increasing mass of the three atoms X relative to the mass of carbon; details of this change of assignment of the A_{1g} frequencies are reported elsewhere [13].

For all the other compounds, the A_{1g}-, A_{1u}- and E_u-spoecies frequencies can be assigned unambiguously to certain pure normal modes of vibration. Therefore, the frequency assignments given previously by various authors[1–4] by analogy alone with ethane remain valid.

On the other hand, the A_{2u}- and E_g-species frequencies are far from remaining pure for all the compounds studied. The mode coupling occurs always after substitution of H or D with halides, increases through the series, and leads for nearly all A_{2u} and E_g frequencies of C_2Br_6 to a complete change of assignment. The actual assignment of the observed bands is given for each compound in Table 6 and proves that an assignment based on analogy with ethane is no longer justified for bands of A_{2u} and E_g symmetry.

Form of normal vibrations. In order to visualize various couplings between modes, mentioned above, in particular the contrast between the mixing behaviour of the E_g and E_u modes, we used the L_M matrix. Figures 2 and 3, based on the L_M matrix elements, represent the relative nuclear motions in each of the 12 normal vibration modes, in mass-weighted Cartesian displacement coordinates.

The form of the normal modes illustrates the previously given assignments. It is seen that in passing from C_2H_6 to C_2Br_6 through the series of hexahaloethanes, some of the $C-X$ stretching motions no longer take place independently, but only with the simultaneous deformation of the $C-C-X$ and/or $X-C-X$ angles.

Force constants. The optimum set of UB force constants, which gave the best attainable fit between calculated and observed (anharmonic) frequencies within the assumed approximation, is listed, for each molecule, in Table 3. Table 4 contains the GVFF force constants k_{ij}, calculated from the former ones on the basis of Eqs. (1) and (2). For ethane, these force constants, as well as the symmetry force constants calculated from the set in Table 3, are in good agreement with the values found by other authors.[5,6,9]

For all bond stretching force constants in the series of C_2X_6 compounds, correct values, in good agreement with those resulting from the normal coordinate treatment (Tab. 4) are obtained by applying the classical relation $k' = 4\pi^2c^2\nu^2\mu$ to a properly chosen diatomic molecular model for the corresponding bond (μ being the reduced mass of the system). For each stretching normal mode, the model was chosen on the basis of the form of normal modes (Figs. 2 and 3), taking into account for the calculation of the reduced mass μ only those terminal atoms which actually move (the atoms at rest being considered as having an infinite mass).

Thus, for the frequency ν_1 of the $C-C$ stretching mode, a good fit between the k'_R and k_R values was obtained for C_2H_6 (4.4 mdyne/Å) with a model considering the relative motion of the two CH_3-group point masses, while for C_2X_6 ($X =$ F, Cl, Br), where the X atoms are practically at rest, only the mass of the carbon atom had to be considered.

[13] R. Beldie, A. Butucelea and V. E. Sahini, *Rev. Roumaine Chim.*, **21**, 327 (1976).

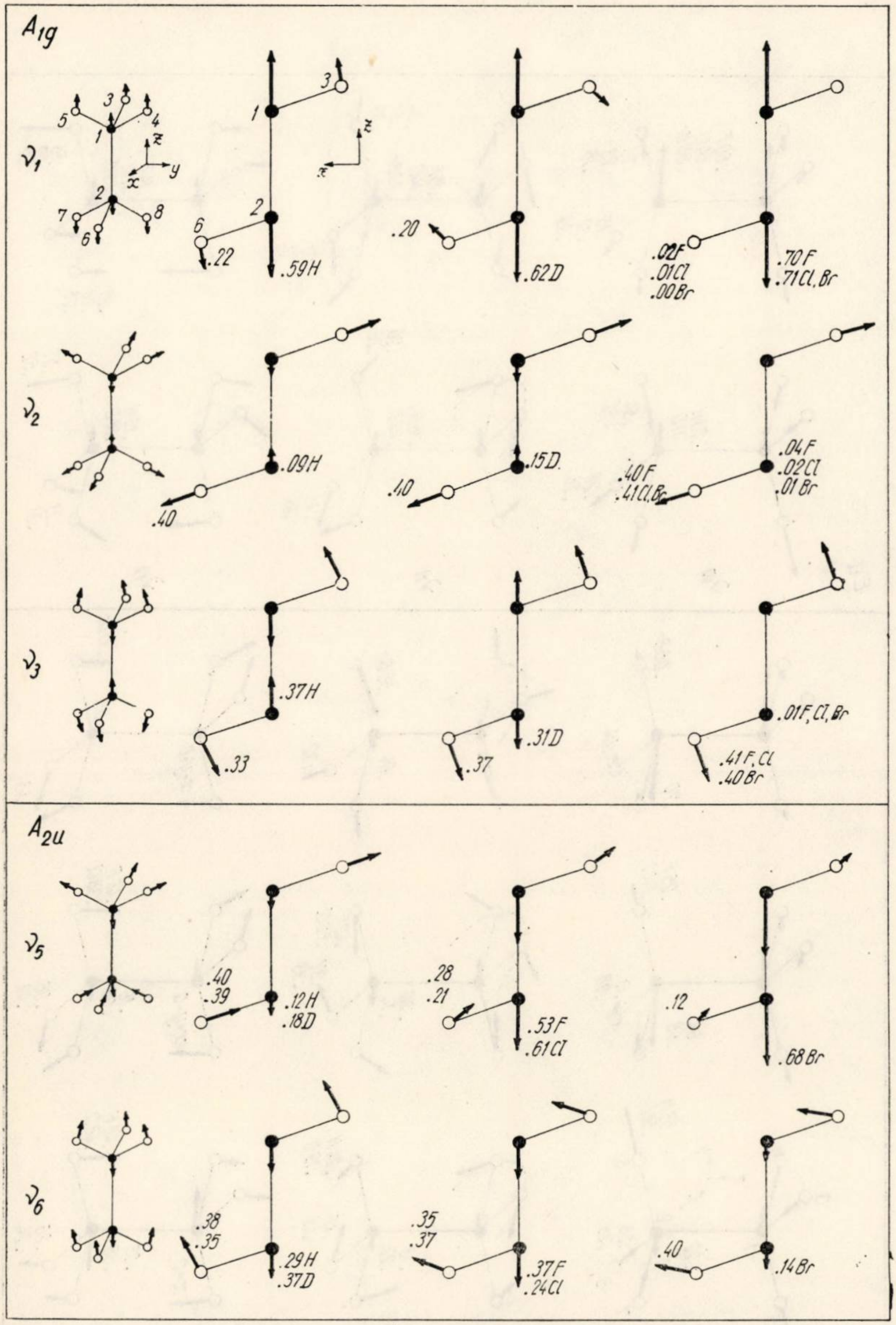
A_{1g}
ν_1
3
5
4
1
z
y
x
2
7
8
6
3
1
z
x
2
6
.22
.59H
.20
.62D
.02F
.01Cl
.00Br
.70F
.71Cl, Br
ν_2
.09H
.40
.15D
.40
.40F
.41Cl,Br
.04F
.02Cl
.01Br
ν_3
.37H
.33
.31D
.37
.01F, Cl, Br
.41F, Cl
.40Br
A_{2u}
ν_5
.40
.39
.12H
.18D
.28
.21
.53F
.61Cl
.12
.68Br
ν_6
.38
.35
.29H
.37D
.35
.37
.37F
.24Cl
.40
.14Br

Fig. 2. — Form of the A_{1g} and A_{2u} modes of ethane and hexahaloethanes. The arrows represent the relative nuclear displacements, proportional to the values of the L_M matrix elements, written alongside for each compound (X stands for C_2X_6). The interatomic distances and atomic sizes are not drawn to scale. For the sake of simplicity, a single plane, containing the atoms 3—1—2—6 is represented.

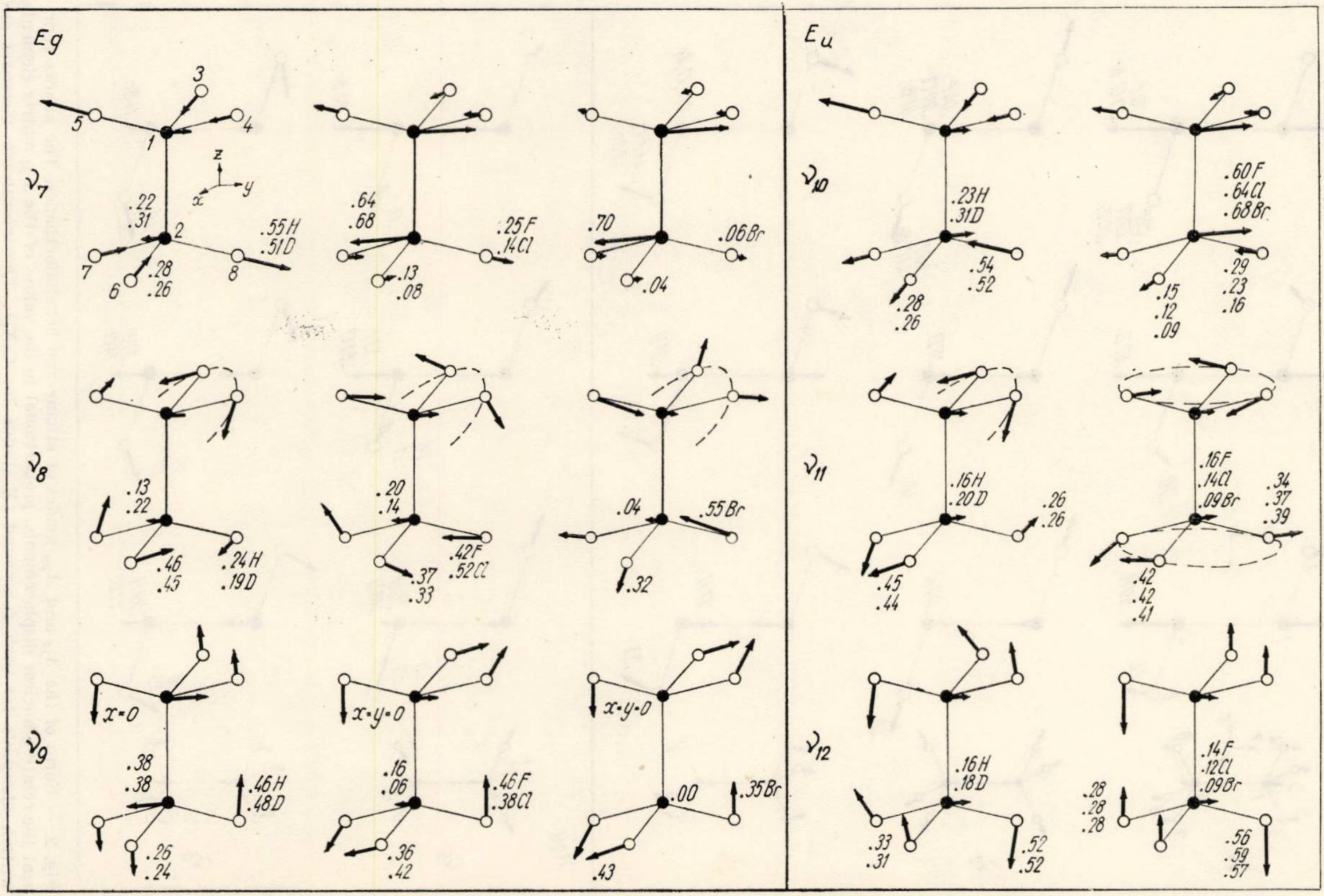
Eg
Eu
ν7
ν8
ν9
ν10
ν11
ν12
1
2
3
4
5
6
7
8
z
y
x
.22
.31
.55H
.51D
.28
.26
.64
.68
.25F
.14Cl
.13
.08
.70
.06Br
.04
.13
.22
.46
.45
.24H
.19D
.20
.14
.42F
.52Cl
.37
.33
.04
.55Br
.32
x=0
.38
.38
.46H
.48D
.26
.24
x-y=0
.16
.06
.46F
.38Cl
.36
.42
x-y=0
.00
.35Br
.43
.23H
.31D
.54
.52
.28
.26
.60F
.64Cl
.68Br
.29
.23
.16
.15
.12
.09
.16H
.20D
.26
.26
.45
.44
.16F
.14Cl
.09Br
.34
.37
.39
.42
.42
.41
.16H
.18D
.33
.31
.52
.52
.14F
.12Cl
.09Br
.28
.28
.28
.56
.59
.57

Fig. 3. — Form of the E_g and E_u modes of ethane and hexahaloethanes. For explanations see Fig. 2.

For the C$-X$ stretching modes ν_5, ν_7 and ν_{10}, the agreement between k_r' and k_r was obtained by taking into account both C and X atomic masses for all compounds (Figs. 2 and 3), while for the C$-X$ stretching mode ν_2 the mass of atom X alone had to be considered, since the carbon atom is at rest in this case (Fig. 2).

Both GVFF force constants k_R and k_r (Tab. 4) have, in comparison with K_{CC} and K_{CX}, respectively (Tab. 3), a pronounced maximum value for C_2F_6, which is in agreement with the great stability of this compound. This is due to the contribution of the repulsive UB force constants F_{CX} and F_{XX}, according to the expressions (1) of k_R and k_r. The F_{CX} and F_{XX} force constants are large only for this compound, reflecting the high electronegativity of fluorine and the corresponding increase of the ionic character of the C$-X$ bond in C_2F_6 (Tab. 2). For such relationships between stretching force constants and electronegativity (or bond length), the empirical relations of Gordy [14] and Badger [15] are known. The values of the force constant k_r'' calculated on the basis of these relations are represented as a function of the electronegativity [14] of atom X in Figure 4, and as a function of C$-X$ bond length[14,15] in Figure 5, together with the results of our normal coordinate treatment. The UB force constant K_{CX} shows a behaviour roughly similar to that of k_r'', but only after

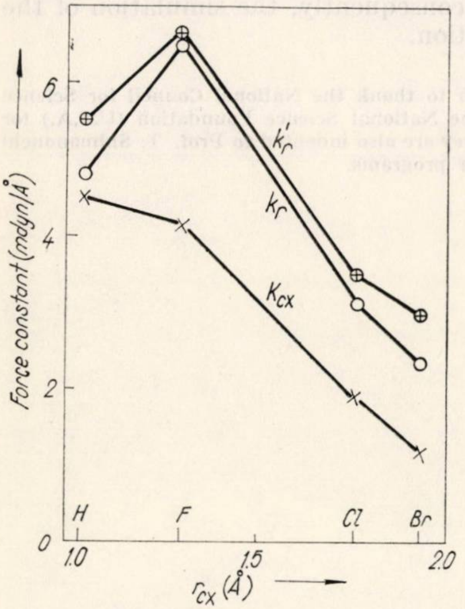

Fig. 4. — Dependence of the C$-X$ stretching force constants of C_2X_6 compounds on the C$-X$ bond length.

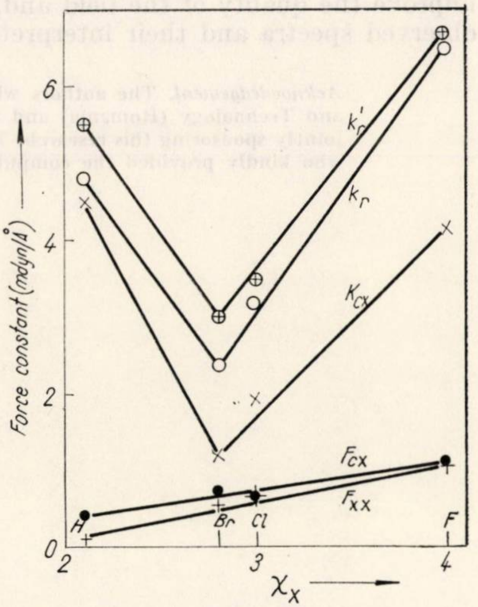

Fig. 5. — Dependence of the C$-X$ stretching force constants of C_2X_6 compounds on the electronegativity of X.

---

[14] W. Gordy, *J. Chem. Phys.*, **14**, 305 (1946).

[15] R. M. Badger, *J. Chem. Phys.*, **3**, 710 (1935).

taking account of all interactions between non-bonded X atoms – whether they belong or not to the same CX_3 group – does the resulting k_r ($= K_{CX} + aF_{CX} + bF_{XX}$) agree very well with the empirical value k_r''.

The values of the force constants F_{XX}, representing the repulsion between non-bonded X atoms within the same CX_3 group, obtained for C_2F_6, C_2Cl_6 and C_2Br_6, are listed in Table 3. They are in good agreement with the force constants calculated by Shimanouchi *et al.* [16] from non-bonded Ne-Ne, Ar-Ar and Kr-Kr interactions, respectively, for interatomic distances equal to those separating the X atoms in tetrahalomethanes and hexahaloethanes.

In conclusion, the simple UBFF has led to reliable assignments for all bands of the hexahaloethanes, the calculated frequencies being always (except for the rocking modes) within 5% of the observed values. Though only a crude approximation for the real field, the unmodified UBFF may be used further for investigating bonding in series of similar molecules, such as the series of ethanes substituted in identical positions with various halides. In fact, the force constant values obtained in this work have proved to be transferable, with only slight modifications, to 1,1,1-trihaloethanes[17] and, we hope, to other haloethanes as well.

A modified UBFF, which would take account of the most significant interactions specific for each member of the series, would certainly improve the quality of the field and, consequently, the simulation of the observed spectra and their interpretation.

Acknowledgement. The authors wish to thank the National Council for Science and Technology (Romania) and the National Science Foundation (U.S.A.) for jointly sponsoring this research. They are also indebted to Prof. T. Shimanouchi who kindly provided the computer programs.

---

[16] T. SHIMANOUCHI, I. NAKAGAWA, J. HIRAISHI and M. ISHII, *J. Mol. Spectroscopy*, **19**, 78 (1966).

[17] A. BUTUCELEA and R. GRIGOROVICI, unpublished results.

Revue Roumaine de Chimie, **21**, 7, 977–983 (1976)

ADSORPTION OF GASEOUS MIXTURES WITHIN THE FRAMEWORK OF JOVANOVIĆ MODEL

V. POPA and E. SEGAL
Chair of Physical Chemistry and Electrochemical
Technology, Polytechnic Institute of Bucharest,
Bd. Republicii 13, Bucharest, Romania.

Received July 24, 1975

In the kinetic — molecular terms of Jovanović model, an isotherm equation is established which describes the monolayer adsorption of gaseous mixtures on uniform surfaces without lateral interaction between the adsorbed molecules. The result of this investigation confirms the higher generality of the model (in comparison with the Langmuir model) first proved by Jovanović for one-component adsorption.

The critical analysis of Langmuir model of adsorption[1] stimulated a large amount of research, most of which is concerned with the influence of surface heterogeneity on adsorbtive and catalytic properties. Moreover, this in-depth analysis revealed the necessity of a new adsorption model on homogeneous surfaces; this one was elaborated by Jovanović [2] in 1969. It first led to a new isotherm equation for monolayer adsorption, then being easily extended to multilayer adsorption: the previous kinetic-molecular models for this kind of adsorption (B.E.T.,[3] Hüttig[4]) were thus critically examined, their failure in describing experimental data being assigned to the fact that they are merely an extention of the Langmuir model.

The derivation of the Langmuir isotherm was possible by assuming the following conditions: adsorption takes place on surface sites having the same adsorption potential; each site can be occupied by maximum one molecule, that is adsorption is restricted to a monolayer; there is no lateral interaction between the adsorbed molecules; finally, the adsorbed molecules are confined to their sites not being allowed to move freely on the surface, that is adsorption is immobile.

From the kinetic-molecular point of view, the adsorption-desorption equilibrium involves the equality between the adsorption and desorption rates. On these rates, within the framework of the Langmuir model, the following assumptions are made:

a) the adsorption rate depends only on the gas pressure and the surface fraction available (uncovered with adsorbed molecules);

---

[1] I. Langmuir, *J. Amer. Chem. Soc.*, **40**, 1361 (1918).

[2] D. S. Jovanović, *Kolloid Z.*, **235**, 1203 (1969); **235**, 1241 (1969).

[3] S. Brunauer, P. H. Emmett and E. Teller, *J. Amer. Chem. Soc.*, **60**, 309 (1938).

[4] G. F. Hüttig, *Monatsh.*, **78**, 177 (1948).

b) the desorption rate depends only on the covered surface fraction and does not depend on the gas pressure.

Considering the adsorbent surface area as unity, under the circumstances described above, the Langmuir adsorption isotherm is readily obtained in a well-known way :

— the adsorption rate v_a is given by

$$v_a = \alpha p(1 - \theta)/\sqrt{2\pi mkT} = (1 - \theta)p/\sqrt{2\pi mkT}, \tag{1}$$

where α is the sticking probability (taken as unity in most cases), θ is the coverage (the surface fraction covered by adsorbed molecules), p and m the pressure and the mass of gas molecules, respectively ;

— the desorption rate is given by

$$v_d = b\theta, \tag{2}$$

where b is a kinetic constant. Then the isotherm equation we are looking for is given by

$$\theta = \frac{ap}{1 + ap}, \tag{3}$$

where

$$a = 1/b\sqrt{2\pi mkT}. \tag{4}$$

Within the framework of Jovanović model, one takes into account the mechanical contact between the adsorbed and the bulk (gaseous) phase, i.e. the collisions that can take place between impinging molecules (moving from the bulk phase to the surface) and desorbing ones (moving, after the desorption, from the surface to the bulk phase). Considering that the assumptions a) and b) mentioned above are no longer valid, they change as follows :

a′) due to the collisions, in sufficiently short periods of time the number of adsorbed molecules fluctuates considerably and the available surface fraction too ; it follows thus the possibility of having different momentary adsorption rates ;

b′) due to the collisions, the *desorbing* molecules (which in terms of the Langmuir model are considered as *desorbed* ones) are partially readsorbed : the desorption rate cannot any longer be considered as independent of the gas pressure (which is proportional to the number of impinging molecules).

The Langmuir model would be correct only in the case of an instantaneous substitution of desorbing molecules by adsorbing those situated on the same level, but this is equivalent to the absurd situation of not having the possibility to distinguish between adsorbing and desorbing molecules.

In view of the dynamical equilibrium adsorption-desorption and taking into account the multitude of collisions that can take place, the assumption of rapid fluctuations is straightforward : the number of settled molecules on the surface varies round an equilibrium value and deviations from this value, being of both signs, cancel each other within a sufficiently long period of time.

The problem that now arises is the choice of the time period within which the chancelling of these fluctuations takes place. Jovanović introduces the *average settling time* of a molecule on the surface, τ, and takes this time as the reference period mentioned above, demonstrating the utility of this choice. In terms of the model, local fluctuations of the settling times of molecules can take place even on homogeneous surfaces, making thus necessary the definition of an *average* settling time.

By means of a rather complicated argument, Jovanović got the following expressions for the numbers of desorbed, N^*, and absorbed, N^{**}, molecules during the reference time τ, respectively :

$$N^* = N \exp(-a'p); \tag{5}$$

$$N^{**} = \frac{1-\theta}{\sigma}[1 - \exp(-a'p)]; \tag{6}$$

$$a' = \tau\sigma/\sqrt{2\pi mkT}, \tag{7}$$

where N is the total (equilibrium) number of adsorbed molecules, σ is the effective cross-section of collision between two molecules and is expressed by the following formula :

$$\sigma = \frac{\pi D^2}{2} \tag{8}$$

where D is the molecular diameter.
The whole argument is refered to unit surface area so that

$$\sigma N = \theta \tag{9}$$

and from the equilibrium condition $N^* = N^{**}$, we get

$$\theta = 1 - \exp(-a'p), \tag{10}$$

which is the expression of the Jovanović isotherm for monolayer adsorption of one component. We notice that by substituting in (10) $\exp(a'p)$ by $1 + a'p$, the expression reduces to Langmuir isotherm

$$\theta = 1 - \frac{1}{\exp(a'p)} \rightarrow 1 - \frac{1}{1 + a'p} = \frac{a'p}{1 + a'p}, \tag{11}$$

which proves the higher generality of the Jovanović model in comparison with the Langmuir one.

The problem of mixtures adsorption generally presents an interest for catalytical kinetics studies; in this case, the problem presents a special interest as it provides a means for further confirming of the Jovanović model generality. Indeed by means of a similar operation with that described above (exponential expansion and taking the first two terms), the Jovanović isotherm for mixtures adsorption, which is the aim of the present paper, has to reduce to the well-known Langmuir one.

Considering the competitive adsorption of a gaseous mixture A, $B, \ldots I, J, \ldots$ on the same surface, the partial coverage θ_I referred to a representative component I, in terms of the Langmuir model, is given by

$$\theta_I = \frac{a_I p_I}{1 + \sum_I a_I p_I}, \tag{12}$$

where

$$a_I = \frac{1}{b_I \sqrt{2\pi m_I k T}} \tag{13}$$

and p_I is the partial pressure of the component I; all the constants in (13) correspond to the same component and the summation is extended over all mixture components.

In the following, we shall derive a similar expression in terms of the Jovanović model. Considering the same mixture $A, B, \ldots I, J, \ldots$ we define the average settling times for different species $\tau_A, \tau_B \ldots \tau_I, \tau_J \ldots$ We must take into account the mechanical contact between the adsorbed and bulk phases which in the case of mixture adsorption entails the conclusion that the desorption rate for a certain component depends on the respective partial pressure, but also on the partial pressures of the other components. For each species, the time periods within which the fluctuations of the dynamical equilibrium adsorption-desorption cancel each other are taken equal to the respective average settling times. The equilibrium condition entails the equality between the adsorption and desorption rates of different species; for a certain component, say I, this reduces to the equality between the numbers of adsorbed and desorbed molecules during the corresponding time period, τ_I.

Let us examine the desorption rates: for one component, say A, the period of time we are referring to is τ_A. N_A^A, the number of A molecules that would desorb within this period if the other components were absent, is calculated taking into account only the collisions with A molecules. The situation is analogous with the simple Jovanović model: this number depends on the Knudsen factor for A molecules, $\xi_A = p_A/\sqrt{2\pi m_A kT}$, that is the number of A molecules which strike the surface of unit area per second; it depends also on the effective cross-section of collision between two A molecules, σ_{AA}. The expression we are looking for is similar with that given in (5)

$$N_A^A = N_A \exp\left(-a'_{AA}\, p_A\right), \tag{14}$$

$$a'_{AA} = \sigma_{AA}\, \tau_A / \sqrt{2\pi m_A kT}, \tag{15}$$

where N_A is the equilibrium number of adsorbed A molecules. In order to take into account the collisions with the molecules of other types, we proceed as follows: we calculate first the number of desorbing A

molecules that "escape" the collisions with both A and B molecules within the period τ_A. Let this number be N_A^{AB}. In order to calculate it, we suppose that the number of adsorbed A molecules is N_A^A, i.e. those that "escape" collisions with gaseous A molecules. Then we repeat the above argument, this time taking into account the collisions with B molecules only : we must consider the Knudsen factor for B molecules $\xi_B = p_B/\sqrt{2\pi\, m_B kT}$ and the effective cross-section of collision between one A molecule and one B molecule, σ_{AB}. It is easy to notice that the whole argument can be carried out in probabilistic terms. The number of molecules we are looking for is given by the following expression :

$$N_A^{AB} = N_A^A \exp(-a'_{AB}\, p_B) \tag{16}$$

$$a'_{AB} = \sigma_{AB}\, \tau_A/\sqrt{2\pi\, m_B kT}, \tag{17}$$

or, using (14)

$$N_A^{AB} = N_A \exp(-a'_{AA} p_A - a'_{AB}\, p_B). \tag{18}$$

In general, the number of A molecules that effectively desorb within the time period τ_A, i.e. that "escape" collisions with the molecules of all types present in the mixture, $N_A^{AB\ldots IJ\ldots}$, can be obtained by repeating the argument for all the components.

$$N_A^{AB\ldots IJ\ldots} = N_A \exp[-(a'_{AA}\, p_A + a'_{AB}\, p_B + \ldots + a_{AI} p_I + a_{AJ}\, p_J + \ldots)] \tag{19}$$

In the same way we calculate the number of B molecules that effectively evaporate within the characteristic time period (τ_B) of the species, $N_B^{AB\ldots IJ\ldots}$, and so on. Taking the I component as the representative one and using the more convenient notation $N_I^* = N_I^{AB\ldots IJ\ldots}$ for the number of I molecules effectively desorbing within the time period τ_I, we can write

$$N_I^* = N_I \exp(-\sum_J a'_{IJ}\, p_J) = N_I \exp\left(-\sum_J \frac{\sigma_{IJ}\tau_I}{\sqrt{2\pi\, m_J kT}}\, p_J\right). \tag{20}$$

It remains to calculate the number of adsorbed I molecules within the same period τ_I, let it be N_I^{**}. In the case of adsorption, there is a competition between the various components, but for each one the conditions of the simple Jovanović model are fulfilled : the molecules number of a certain type which are adsorbed within the characteristic period of the species depends on the corresponding partial pressure and on the available surface fraction. The dependence we are looking for is similar to that given in (6) ; the available surface fraction is given in this case by $1 - \sum_I \theta_I$ where θ_I is the partial coverage corresponding to the component I.

As before, the whole argument is referred to the unit surface area so that (9) still holds, and in this case it becomes

$$\theta_I = N_I \, \sigma_{II} \tag{21}$$

where σ_{II} is the effective cross-section of collision between two I molecules and N_I is the equilibrium number of adsorbed I molecules. Similarly, the expression we are looking for is obtained by the generalization of that given in (6)

$$N_I^{**} = \frac{1 - \sum\limits_I \theta_I}{\sigma_{II}} \left[1 - \exp(-a'_{II}\, p_I)\right]. \tag{22}$$

From the equilibrium condition $N_I^* = N_I^{**}$ and making use of (20), (21) and (22) we get

$$\theta_I \exp(-\sum_J a'_{IJ}\, p_J) = (1 - \sum_I \theta_I)\left[1 - \exp(-a'_{II}\, p_I)\right], \tag{23}$$

which can also be written as follows:

$$\theta_I = (1 - \sum_I \theta_I)\left[1 - \exp(-a'_{II}\, p_I)\right] \exp(\sum_J a'_{IJ}\, p_J). \tag{24}$$

In (24), summing over I, we get

$$\sum_I \theta_I = (1 - \sum_I \theta_I) \sum_I \{[1 - \exp(-a'_{II}\, p_I)] \exp(\sum_J a'_{IJ}\, p_J)\}, \tag{25}$$

where, from

$$\sum_I \theta_I = \frac{\sum\limits_I \{[1 - \exp(-a'_{II}\, p_I)] \exp(\sum\limits_J a'_{IJ}\, p_J)\}}{1 + \sum\limits_I \{[1 - \exp(-a'_{II} p_I)] \exp(\sum\limits_J a'_{IJ}\, p_J)\}} \tag{26}$$

and combining (26) and (22), we get the expression we are looking for

$$\theta_I = \frac{[1 - \exp(-a'_{II}\, p)] \exp(\sum\limits_J a'_{IJ}\, p_J)}{1 + \sum\limits_I \{[1 - \exp(-a'_{II} p_I)] \exp(\sum\limits_J a'_{IJ}\, p_J)\}}, \tag{27}$$

where

$$a_{IJ} = \sigma_{IJ}\, \tau_I / \sqrt{2\pi\, m_J kT}. \tag{28}$$

The relationship (27) which is the Jovanović isotherm for mixtures adsorption, may also be written as:

$$\theta_I = \frac{\exp(\sum\limits_J a'_{IJ}\, p_J) - \exp(\sum\limits_{J \neq I} a'_{IJ}\, p_J)}{1 + \sum\limits_I [\exp(\sum\limits_J a'_{IJ}\, p_J) - \exp(\sum\limits_{J \neq I} a'_{IJ}\, p_J)]}. \tag{29}$$

Expanding the exponentials in power series and taking the first two terms we get

$$\theta_I = \frac{a'_{II}\, p_I}{1 + \sum_I a'_{II}\, p_I}, \qquad (30)$$

which is identical with (12). The constants depending on two subscripts accounting for the mechanichal contact between different components vanish, as if the adsorption of each component became independent of the other components presence. Hence Langmuir isotherm for mixtures adsorption is a special case of the Jovanović one.

Obviously, it is difficult to distinguish between the two by means of direct experiment. From purely theoretical reasons eq. (29) can be used with a higher degree of confidence for the kinetic description of heterogeneous catalytic reactions.

Revue Roumaine de Chimie, **21**, 7, 985–990 (1976)

SOLVENT EFFECT ON THE KINETICS OF THE THERMAL DECOMPOSITION OF DIOXALATODIAQUOMANGANATE (III) IN DIMETHYLSULPHOXIDE-WATER MIXTURES

TATIANA ONCESCU and ECATERINA JURCONI
Physical Chemistry Department, Polytechnic Institute
Faculty of Chemistry, Bd. Republicii 13, Romania

Received December 16, 1974

The decomposition reaction of dioxalatodiaquomanganate (III) in dimethylsulphoxide-water mixtures has been investigated at various temperatures and the activation parameters were reported. The presence of molecular aggregates with preferential structure for a certain solvent composition was revealed from kinetic data. The dependence of the rate constants upon dielectric constants of the solvent mixtures pleads for a ion-dipole reaction.

1. INTRODUCTION

The present investigations of the decomposition reaction of dioxalatodiaquomanganate (III) in dimethylsulphoxide-water solutions represent a sequel of our previous study[1] on the kinetic of the same complex decomposition in *N*,*N'*-dimethylformamide-water mixtures. The kinetic data obtained in the latter case showed that at a certain solvent composition of about 0.27 mole fraction DMF characterized by the formation of the molecular aggregates with preferential structure,[2] the activation parameters passed through a minimum. It is known that similar molecular aggregates have been supposed to form also in the dimethylsulphoxide-water mixtures at 0.33 mole fraction DMSO composition.[3] The purpose of the present study was to verify if also in the case of these mixtures, this preferential composition can be connected with the kinetic behaviour.

2. EXPERIMENTAL

Kinetic runs were made in a SP 800 Pye Unicam Spectrophotometer, using a thermostated cell compartment capable of temperature control ± 0.3°. A detailed description of the experiments was presented in our previous paper.[1]

---

[1] T. ONCESCU and E. JURCONI, *Rev. Roumaine Chim.* (in press).

[2] T. ONCESCU and E. JURCONI, *Rev. Roumaine Chim.*, **16**, 1033 (1971).

[3] R. K. WOLFORD, *J. Phys. Chem.*, **68**, 3392 (1964).

3. RESULTS AND DISCUSSION

In our research the order of reaction with respect to Mn(III) complex was first investigated in series of runs. For individual run, plot of log A_0/A_t against time gives a good straight line, as seen in Fig. 1.

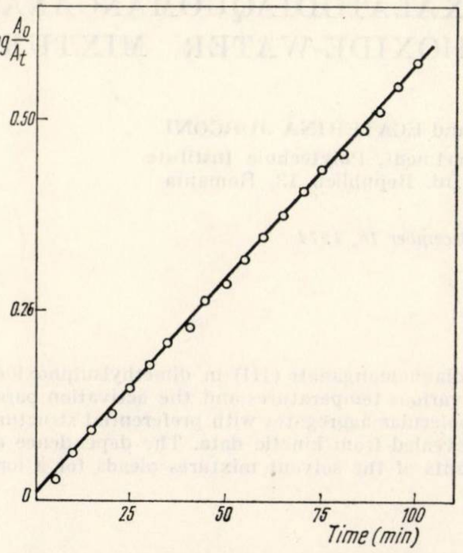

Fig. 1. — Plot of log A_0/A_t against time.

Table 1

Rate constants obtained in different H_2O – DMSO mixtures

$a = 2 \times 10^{-3}$ mole l^{-1} $T = 20°$

DMSO mole fraction	$k_{\exp}$, sec^{-1}
0.017	0.000411
0.065	0.000322
0.097	0.000271
0.143	0.000224
0.274	0.000132
0.371	0.000055
0.504	0.000031
0.607	0.000026

This seeming first order dependence on Mn(III), complex concentration was confirmed by a series of runs; therefore we calculated the rate constant values by applying the least square method.

These values at $T = 20°$ are summarized in Table 1 for all working mixtures. The error of this determinations is about 3%.

The rate data can be interpreted as in the case of DMF-H_2O mixtures,[1] by the following reaction mechanism:

$$[Mn(C_2O_4)_2(H_2O)_2]^- + H_2O \underset{k_1}{\overset{k_1}{\rightleftharpoons}} [Mn(C_2O_4)OC_2O_3(H_2O)_3]^- \quad (1)\ \text{(rapid)}$$

$$[Mn(C_2O_4)OC_2O_3(H_2O)_3]^- + H_2O \xrightarrow{k_2} MnC_2O_4 + C_2O_4^{\cdot -} + 4H_2O \quad (2)\ \text{(slow)}$$

$$[Mn(C_2O_4)_2(H_2O)_2]^- + C_2O_4^{\cdot -} \xrightarrow{k_3} MnC_2O_4 + 2CO_2 + C_2O_4^{2-} + 2H_2O \quad (3)\ \text{(rapid)}$$

$$2[Mn(C_2O_4)_2(H_2O)_2]^- \rightarrow 2MnC_2O_4 + 2CO_2 + C_2O_4^{\cdot -} + 4H_2O$$

As we previously pointed out, the rate determining step is the aquation slow process (2). The main reaction product, MnC_2O_4, was isolated and the oxalyl radical ion was revealed [4,5].

---

[4] T. ONCESCU, *Rev. Roumaine Chim.*, **15**, 209 (1970).

[5] I. G. MURGULESCU, T. ONCESCU and I. VLAGIU, *J. Chem. Phys.*, **10**, 1487 (1971).

This reaction mechanism leads to the following differential kinetic equation :

$$\frac{dx}{dt} = k_1(a - x)C_{H_2O} - k'_1 C_A + k_3(a - x)C_{ox} \tag{4}$$

where C_A is the concentration of the aquated complex and C_{ox} that of the oxalyl radical ion. By applying the stationary-state approximation to C_A and C_{ox}, we found finally :

$$\frac{dx}{dt} = k_{exp}(a - x) \tag{5}$$

where

$$k_{exp} = K_1 k_2 C^2_{H_2O} \tag{6}$$

characteristic of the first order reaction (pseudounimolecular). From the equation (6) it appears that k_{exp} decreases with the decrease in the water concentration. Our data confirm this behaviour, as shown in figure 2.

A principal aim of our experiments was to study the influence of the dielectric properties of the medium on the reaction rate. Hence we correlated the rate constants with the dielectric constants of the solvent mixtures by means of Laidler-Eyring[6] equation :

$$\log k_D = \log k' + \frac{N(Z\varepsilon)^2}{2RTD}\left(\frac{1}{r_A} - \frac{1}{r^{\neq}_x}\right) \tag{7}$$

Plotting $\log k_{exp}$ against $\frac{1}{D}$ there results a straight line with negative slope at each working temperature, as shown in Fig. 3, for 20°.

As in the case of DMF-H_2O solvents, it is probably the formation of the following complexes : $[Mn(C_2O_4)_2(DMSO)H_2O]^-$ and $[Mn(C_2O_4)_2(DMSO)_2]^-$, similar to Cr(III) complexes put into evidence from studies[7] of the exchange of DMSO for water in DMSO solution of $[Cr(C_2O_4)(H_2O)_2]^-$ and of water for DMSO in aqueous $[Cr(C_2O_4)_2(DMSO)_2]^-$. Our study confirms also such a behaviour which is presented in Fig. 4.

The shift of the absorption band during the reaction pleads for the formation $[Mn(C_2O_4)_2(DMSO)_2]^-$ in which water was substituted completly by DMSO.

The rate constant data were also used to calculate the kinetic and thermodynamic parameters for the investigated reaction, given in Table 2.

---

[6] K. J. Laidler, "Chemical Kinetics", McGraw-Hill, London, 1965, p. 227.

[7] K. R. Ashley and R. E. Hamm, *Inorg. Chem.*, **5**, 1645 (1966).

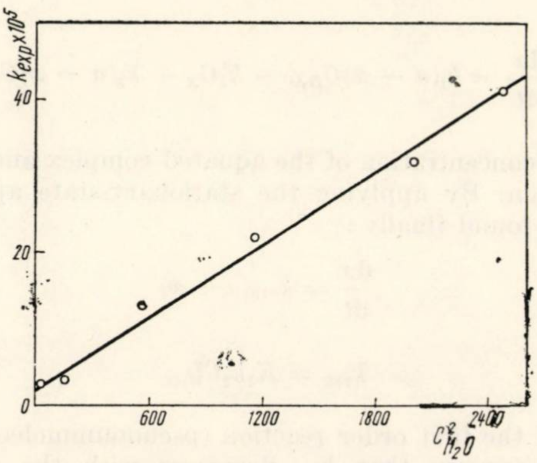

Fig. 2. — Plot of k_{exp} *vs.* $C^2_{H_2O}$ at $T = 20°$.

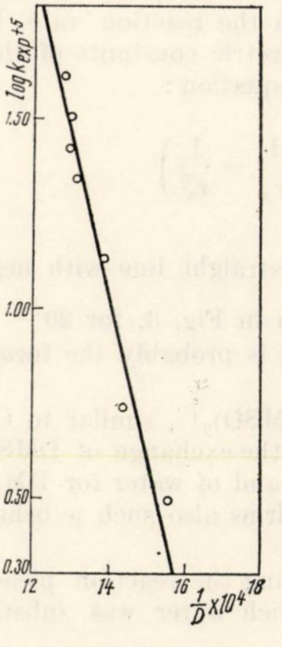

Fig. 3. — Plot of log k_{exp} *vs.* reciprocal dielectric constant at $T = 20°$.

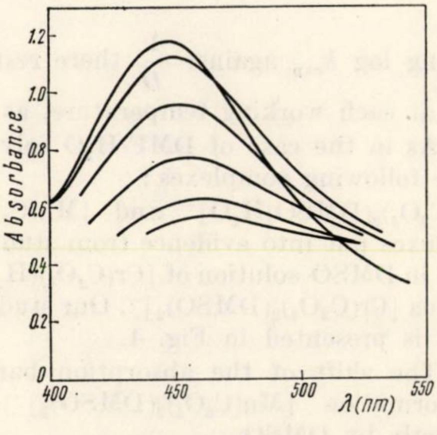

Fig. 4. — Shifting of the absorption spectra during the course of the reaction.

Table 2

Activation parameters of the thermal decomposition of $[Mn(C_2O_4)_2(H_2O)_2]K \cdot 3H_2O$ in DMSO – H_2O mixtures

DMSO mole fraction	$E_{Arrh.}$ (Kcal/mole)	log A (A, sec)	$\Delta H^{\neq}$ (Kcal/mole)	$\Delta S^{\neq}$ (u.e.)	$\Delta G^{\neq}$ (Kcal mole^{-1})
0.017	14.6	7.54	14.0	−25.97	21.776
0.065	16.5	8.90	15.9	−19.76	21.867
0.097	17.0	9.15	16.4	−18.59	21.975
0.143	20.4	11.61	19.8	− 7.38	22.075
0.274	24.8	13.78	24.2	+ 2.55	22.286
0.371	21.9	12.11	21.3	− 5.09	22.865
0.504	16.0	7.43	15.4	−26.46	23.294
0.607	14.2	4.80	13.6	−38.47	23.409

The values of the Arrhenius activation energies were determined by plotting log k_{exp} against $\frac{1}{T}$ (fig. 5). The error in the activation energy determinations was about ± 0.5 Kcal/mole^{-1}.

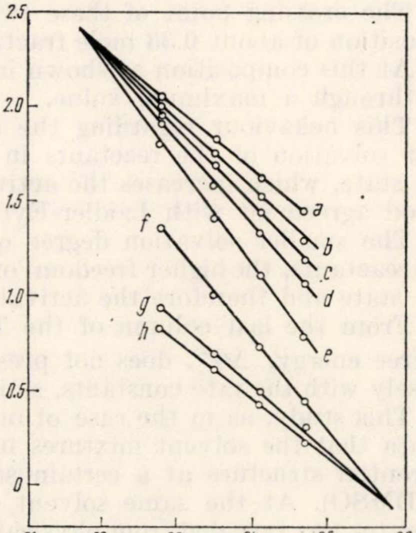

Fig. 5. — Arrhenius plot for the mixtures with the following mole fractions in DMSO :

a) 0.0.17, b) 0.065, c) 0.097, d) 0.143, e) 0.274, f) 0.371, g) 0.504 and h) 0.607.

This figure shows the presence of two isokinetic temperatures : 40°, characteristic of the rate constants as determined in the mixtures between 0.017 – 0.274 mole fraction DMSO, and 6°, corresponding to the rate constants of the mixtures with a content in DMSO higher than 0.37 mole fraction.

The sudden change of the slope of this plotting takes place at about 0.33 mole fraction DMSO, which coincides with the formation of the preferential structure of associated molecules. [3]

The presence of the isokinetic temperatures supposes the linear relationship between $\Delta S^{\neq}$ and $\Delta H^{\neq}$, as indicated in figure 6.

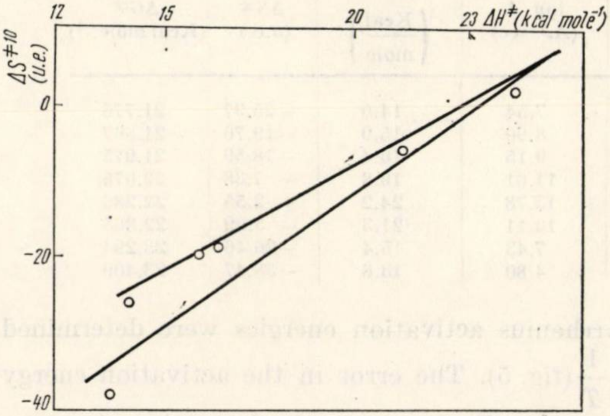

Fig. 6. — Plot of $\Delta S^{\neq}$ *vs.* $\Delta H^{\neq}$ for the thermal decomposition of $[Mn(C_2O_4)_2(H_2O)_2]^-$ in different $H_2O-DMSO$ mixtures.

The crossing point of these two lines occurs at the same solvent, composition of about 0.33 mole fraction DMSO.

At this composition as shown in table 2, the activation parameters pass through a maximum value.

This behaviour regarding the activation energy is a proof of the higher solvation of the reactants in comparison with that of the transition state, which increases the activation energy of the system. This is in good agreement with Laidler-Eyring equation (7).

The smaller solvation degree of the transition state towards that of the reactants, the higher freedom of movement of species in the transition state and therefore the activation entropy has a maximum value.

From the last column of the Table 2 it can be seen that activation free energy, $\Delta G^{\neq}$, does not present such a behaviour and it varies inversely with the rate constants, as it was to be expected.

This study, as in the case of our previous paper, shows from kinetic data that the solvent mixtures used form molecular aggregates with preferential structure at a certain solvent composition (0.33 mole fraction DMSO). At the same solvent composition the formation of such aggregates was revealed from physical properties measurements. [3]

Revue Roumaine de Chimie, **21**, 7, 991–996 (1976)

HYDROGEN OXIDATION ON POROUS NICKEL ELECTRODES. IV.[1]

THE IMPROVEMENT OF THE ELECTRODE PERFORMANCES BY ADDITION OF DIFFERENT ELECTROCATALYSTS

O. RADOVICI, MARIA MAVRODIN-TĂRĂBÎC, IOANA ONACA and I. SOLACOLU
Centre of Physical Chemistry, str. Galaţi 31, Bucharest, Romania

Received December 30, 1974

The possibility of nickel gas electrode activation with oxides or transitional metal salts (Ti, Mn, Zr, V, Cr, W, Co, Cu) has been studied. Activation was carried out either by mixing the powders before sinterization or by soaking the sintered nickel gas electrodes with the catalytic active salt. In order to establish the efficiency of the activated electrodes, polarization curves (obtained by potentiostatic method) and electrical performances of the hydrogen-oxygen fuel cells with nickel activated anode and silver cathode have been compared. The best results were obtained by the ammonium wolframate and cobalt acetate activation.

The improvement of the gas electrode performances depends both on the achievement of suitable microgeometrical structures and on the improvement of the electrode activity by using electrocatalysts. For the activation of the hydrogen oxidation in alkaline solution, the platinic metals are very efficient,[2-5] but the high cost of these metals is still quite prohibitive, in spite of all the attempts which have been made in order to reduce the consumption of the catalytic substance.[6] Consequently, there is a new line of research aiming towards the discovery of less expensive catalysts (transitional metals).

Besides the geometrical parameters (crystalline structure, reticular distance, distance between active centers, as well as the presence of active centers), the catalytic activity is characterized by the electronic parameters (extraction work, and *d* character).[7] Thus, many properties should be considered in order to choose a catalytic substance. If one considers the influence of the electronic extraction work upon the exchange current, in the case of the reaction under study here, metals can be classified in to three classes, according to their overvoltage : high overvoltage metals (Cd, Tl, Pb, In, Ge, Sn, Hg), average overvoltage metals (Ti, Zr, Al, Bi, Nb, Ta, Mo, Cu, W, Co, V, Fe, Ni, Au, Mn) and low overvoltage metals (Rh, Pd, Pt, Ir). This is also a classification according to the type of the slowest process, which is the discharging process in the first class, desorption in the second, and recombination in the third.[8,9] From the viewpoint of the strength of the metal-hydrogen bond, it is known that the hydrogen adsorption enthalpy decreases with the percentage of *d*-vacancies. Further, from studies of hydrogen overvoltage at constant current density as a function of the adsorption enthalpy,[10] there is the following classification of the transitional metals : high overvoltage metals (Pb, Hg, Tl), and average or low overvoltage metals (Be, Al, Ta, Ga, Nb, Mo, Cu, Co, Cd, Fe, Ni, W, Au, Pt, Rh, Pd).

---

[1] Part III: I. Onaca, M. Mavrodin-Tărăbîc and I. Solacolu, *Rev. Roumaine Chim.*, **20**, 611 (1975)

[2] R. Bihan, "Les piles à combustible", Ed. Technip, Paris, 1965, p. 245.

[3] M. Clark, *Electrochem. Technol.*, **3**, 166 (1965).

[4] D. M. Drazic, *Electrochim. Acta*, **14**, 405 (1969).

[5] J. Mrha, *Coll. Czech. Chem. Comm.*, **32**, 708 (1967).

[6] M. Litzsik and K. V. Kordesch, *Adv. Chem. Ser.*, **47**, 166 (1965).

[7] J.O'M. Bockris, M.A.V. Devanathan and K. Müller, *Proc. Roy. Soc.*, **A274**, 55 (1963).

These considerations have led us to choose, as catalysts, transitional metals with an average overvoltage and a relatively weak metal-hydrogen bond (Ti, Mn, Zr, V, Cr, Co, W, Cu).

1. EXPERIMENTAL

1.1. PREPARATION OF THE ELECTRODES

Optimal conditions for preparation of the nickel gas DSK type electrodes (i.e. compressing pressure, and sintering temperature) were established in a previous paper[1] : compression at $4.6.10^8$ N/m^2 and sinterization, in hydrogen atmosphere, 30 minutes at 700° (initial powder mixture : 25% carbonyl nickel, 50% nickel carbonate, and 25% oxalic acide). The electrodes obtained in these conditions are considered as standard electrodes (M).

In order to obtain the electrode activation, two methods were used :

— *Method 1* — introduction of the catalyst (10%) in the initial powder mixtures (before compression). Initial powder compositions were : 15% carbonyl nickel, 50% nickel carbonate, 25% oxalic acid, and 10% activation substances (TiO_2, MnO_2, ZrO_2, V_2O_5, Cr_2O_3, $(NH_4)_2WO_4$, $Co(CH_3COO)_2$, $(NH_4)_4WO_4 + Co(CH_3COO)_2$, NH_4VO_3) — Al...A9 electrodes. Among these electrodes only A8, activated with 5% $(NH_4)_2WO_4$ + 5% $Co(CH_3COO)_2$, had a mechanical strength suitable for the electrochemical study. Powder mixtures containing 25% carbonyl nickel, 40% nickel carbonate,25% oxalic acid, and 10% activation compounds ($2CuCO_3 . Cu(OH)_2$, $(NH_4)_2WO_4$, $Co(CH_3COO)_2$, NH_4VO_3, TiO_2, MnO_2, ZrO_2, V_2O_5, Cr_2O_3) were also prepared — B1 ...B9 electrodes. Among these electrodes only B1, B2, B3, and B4 had a suitable mechanical strength.

— *Method 2* — activation by soaking the sintered electrodes (M) with 0,3M NH_4VO_3, 1M $Co(CH_3COO)_2$, and 0.3M $2CuCO_3 . Cu(OH)_2$ solutions — C1...C3 electrodes. In order to decompose the catalytic compounds, the C1...C3 electrodes were heated again in a hydrogen atmosphere (1 hour at 400°).

Microscopic examination of the electrodes was carried out using a metallographic microscope type MIM-7 (500×). The total porosity was determined by weighing the electrodes before and after soaking in toluene.

---

[8] A. KALBERLACH and A. WINSEL, *Ber. Bunsengesellschaft Phys. Chem.*, **68**, 250 (1964).

[9] R. A. MUNSON, *J. Phys. Chem.*, **66**, 727 (1962).

[10] R. H. BURSHTEIN, A. G. PSHENICHNIKOV, F. Z. SHABIROV and V. N. JURAVLEVA, *Elektrokhimiya*, **4**, 13 (1968).

1.2. ELECTROCHEMICAL MEASUREMENTS

The electrode activation efficiency was determined by polarization measurements and by comparing performances of hydrogen-oxygen fuel cells with activated nickel anode and silver cathode. The working conditions were : room temperature, KOH concentration 6N, hydrogen/oxygen overpressure 400 mm Hg.

1.2.1. Polarization measurements

The electrode polarization study (for the hydrogen oxidation) was carried out by potentiostatic method in the wiring scheme elsewhere described.[11]

The potentiostat was a Tacussel device type PRT 500 LC (± 1 mV precision), the voltage was measured by means of an electronic millivoltmeter Radiometer type 22 (± 1 mV precision), and the current by a milliampermeter type DU 20 (± 1% precision). The polarization curves were obtained by applying potential steps of 10 mV at 1 minute intervals. The working cell (120 × 70 × 56 mm) was made of polystyrene. The auxiliary electrode was a 99.9% nickel tape. The reference electrode was a saturated calomel electrode.

The electrodes were supplied with hydrogen at constant overpressure by a device described in a previous paper.[11]

1.2.2. Determination of the hydrogen-oxygen fuel cell performances

Fuel cells with activated nickel anode and silver cathode[11] have been achieved.

The electrodes were supplied with hydrogen/oxygen at constant overpressure (400 mmHg).

The $E-i$ curves were determined by discharging the cells through a variable resistor in a wiring scheme [12] including an electronic millivoltmeter type Radiometer 22 (precision ± 1 mV), a milliampermeter type DU 20 (precision ± 1%), and a decade resistor box (precision ± 0.1Ω).

2. RESULTS AND DISCUSSIONS

2.1. STRUCTURAL CHARACTERISTICS

Microscopic examination showed an advanced degree of sinterization and a uniform repartition of pores.

The porosity determinations lead to the following average values: 58% – M electrodes, 60.5% – *A* type electrodes, 57.3% – *B* type electrodes, and 57.9% – *C* type electrodes.

The low mechanical strength of the *A* electrodes may be explained by the fact that the active catalytic compound was inserted into the initial mixture by removing 10% of the carbonyl nickel which, after sinterization, gives the resistance body of the gas electrodes.

The *B* electrodes, activated by removing 10% of the nickel carbonate, have porous structures characterized by a good mechanical strength, especially when transition metal salts are used.

The activation with oxides is not suitable, the B5...B9 electrodes having no good mechanical strength.

---

[11] O. Radovici, M. Mavrodin-Tărăbîc, I. Onaca and I. Solacolu, *Rev. Roumaine Chim.*, **17**, 1153 (1972).

[12] O. Radovici, M. Mavrodin-Tărăbîc, I. Onaca and I. Solacolu, *Rev. Roumaine Chim.*, **18**, 767 (1973).

2.2. POLARIZATION CHARACTERISTICS

The potential values applied in order to obtain current densities of 50, 75, and 100 mA/cm² (reported at the external electrode surface) are listed in Table 1. (One considers that these current densities characterize the behaviour of the gas eletrodes under study in the hydrogen-oxygen fuel cells.)

Table 1

Applied potential values for different current densities

Electrode type	Potential values for		
	50 mA/cm²	75 mA/cm²	100 mA/cm²
	mV	mV	mV
M	315	375	430
A8	305	330	375
B1	295	315	350
B2	295	315	340
B3	295	310	335
B4	310	345	400
C1	315	350	420
C2	300	315	350
C3	305	325	380

Comparative examination of data listed in Table 1 shows that in all the cases the activated nickel electrodes have lower polarization than the standard electrode (*M*).

The lowest polarizations were found for the ammonium wolframate (B2), cobalt acetate (B3 and C2), and copper carbonate (B1) activated electrodes. Thus, in order to obtain current densities of 50 mA/cm² the applied potentials are by 20 mV (B1, B2, B3) or 15 mV (C2) lower than the applied potential corresponding to the M electrode. For a current densities of 75 mA/cm² the differences are of 60 mV (B1, B2, C2), and of 65 mV (B3).

Examination of data listed in Table 1 shows that at current densities of 100 mA/cm² the applied potentials are considerably lower for the activated electrodes than for the M electrodes. Copper carbonate activation (B1) produces a decrease of the applied potential of about 80 mV, ammonium wolframate activation (B2) of about 90 mV, cobalt acetate activation (B3) of about 95 mV. Cobalt acetate activation by method 2 produces a decrease of the applied potential of about 80 mV.

Among the transition metals used for the nickel gas electrode activation vanadium has the lowest effect. Thus, at current densities of 100 mA/cm², the applied potentials were 400 mV (B4), 420 mV (C1), and 430 mV for the unactivated electrodes (M).

From the examination of data listed in Table 1 it comes out that, in all cases, for the same catalyst the best results were obtained by method 1. Thus, in order to obtain current densities of 100 mA/cm² the applied potentials are 400 mV, and 420 mV, for the electrodes activated with vanadium by method 1 (B4), and by method 2 (C1), respectively. For the cobalt activated electrodes (B3 and C2) the applied potentials are 335 mV and 350 mV, respectively. For the copper activated electrodes (B1 and C3) the applied potentials are 350 mV and 380 mV, respectively.

2.3. BEHAVIOUR OF THE ACTIVATED NICKEL ELECTRODES IN FUEL CELLS

Electrical performances of hydrogen-oxygen fuel cells with nickel activated anodes and silver cathodes (Table 2) are calculated from $E-i$ discharging curves by a method previously described .[12]

Table 2

Electrical characteristics of hydrogen-oxygen fuel cell with nickel anode and silver cathode

Anode type	Electrical voltages			R	Electrical efficiency $\varepsilon = (E_i - E_r)/E_i$	Average apparent current density $i_m = \frac{1}{2} E_i^2/E_t . R$	Maxim power $P_{\max} = i_m^2 \cdot R$	Average electrical voltage $E_m = E_r - i_m \cdot R$	Average conversion efficiency $\eta_m = (E_i - E_r)/2E_t$
	overall $E_t = -\Delta H/zF$	ideal $E_i = -\Delta G/zF$	real E_r						
	mV	mV	mV	ohm	%	mA/cm²	mW/cm²	mV	%
M	1230	970	735	5.35	75.77	68.7	25.2	367.5	29.87
A8	1230	965	670	3.5	69.42	95.7	32.0	335.0	27.23
B1	1230	1100	885	5.8	80.45	76.3	38.4	503.0	35.96
B2	1230	1025	920	5.2	89.76	88.4	40.7	460.0	37.40
B3	1230	1055	895	5.3	85.31	84.4	37.7	447.5	36.58
B4	1230	975	745	5.3	76.42	70.3	26.2	372.5	30.28
C1	1230	1000	750	5.9	75.00	63.5	23.8	375.0	30.49
C2	1230	1080	935	6.7	86.58	69.8	32.6	467.5	38.00
C3	1230	980	820	6.4	83.68	64.0	26.2	410.0	33.33

Examination of data listed in Table 2 are in good agreement with the study of the polarization curves. Method 1 leads to better results than method 2. Thus, the performances of the fuel cell with copper carbonate activated nickel anode are : $i_m = 76.3$ mA/cm², $E_m = 503$ mV, $P_{\max} = 38.4$ mW/cm², and $\eta_m = 35.96$ % (for the method 1 activated anode), and 64 mA/cm², 410 mV, 26.2 mW/cm². and 33.33%, respectively (for the method 2 activated anode).

The best performances were realised by the fuel cells with ammonium wolframate (B2) and cobalt acetate (B3) activated nickel anodes. The average current densities (i_m) increase from 68.7 mA/cm² (M) to 88.4 mA/cm² (B2), and to 84.4 mA/cm² (B3). The maximal power ($P_{\max}$) increases from 25.2 mW/cm² (M) to 40.7 mW/cm² (B2), and 37.7 mW/cm². The average voltage (E_m) increase from 365.7 mV (M) to 460 mV (B2), and 447.5 mV (B3). From these data it comes out that the increase of the hydrogen-oxygen fuel cell performances is of about 25% for the ammonium wolframate activated nickel anode, and 25% for cobalt acetate activated nickel anode.

The efficiency of the catalytic active substances (fig. 1) decreases as follows : ammonium wolframate > cobalt acetate > copper carbonate > ammonium vanadate.

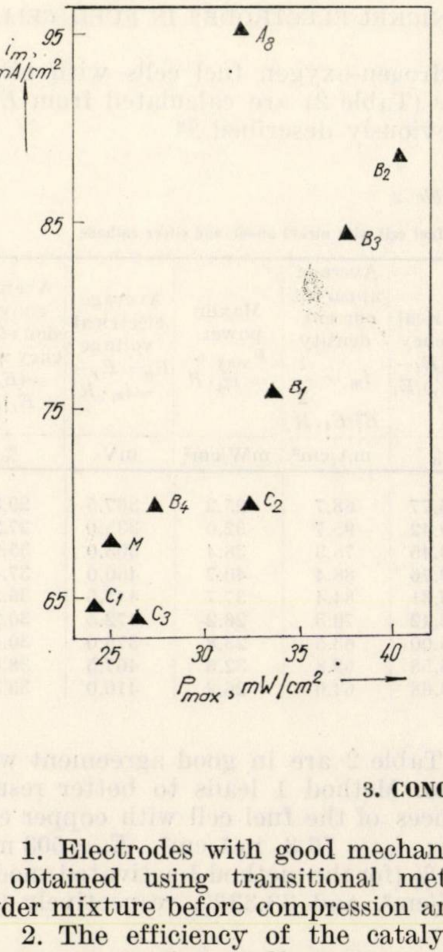

Fig. 1. — Performances of hydrogen-oxygen fuel cell with different anodes.

3. CONCLUSIONS

1. Electrodes with good mechanical strength and high performances are obtained using transitional metal salts introduced in the initial powder mixture before compression and sinterization.

2. The efficiency of the catalytic active substances decreases as follows : ammonium wolframate > cobalt acetate > copper carbonate > ammonium vanadate.

3. The performances of the hydrogen-oxygen fuel cells with anodes activated using ammonium wolframate or cobalt acetate are about 25% greater than those realised by the fuel cell with unactivated nickel anode.

Revue Roumaine de Chimie, **21**, 7, 997–1005 (1976)

THE INFLUENCE OF NON-STOICHIOMETRY UPON HEAT CAPACITY OF URANIUM OXIDES. A MODEL OF QUANTITATIVE APPROACH

M. CIOPEC and D. I. MARCHIDAN

Center of Physical Chemistry, 31 Galaţi street,
P.O.Box 2103, Bucharest, Romania

Received November 21, 1975

A calculation model is advanced for quantitative evaluation of the influence of non-stoichiometry upon heat capacity of uranium oxides; use has been made of experimental data supplied by e.m.f. measurements at high temperatures in cells with solid electrolyte whose working electrode was made of uranium oxide. The model has been tested on uranium oxides of various stoichiometries within the range of O/U ratio = 0.125 — 0.63; for such oxides data are available on variation of heat capacity with temperature as supplied by drop calorimetry measurements of enthalpy. Two equations have been established: for deviation from uranium dioxide stoichiometry within 0.01—0.20 and 0.20—0.63 ranges respectively.

1. INTRODUCTION

Three stable uranium oxides (UO_2, U_3O_8 and UO_3) have been known for over a century; four decades ago another one was discovered, the uranium monoxide UO; only recently the last one was found, U_4O_9. The nuclear technology is very interested in oxides whose stoichiometry is characterized by a O/U 2.00 ratio, that is by the UO_2 phase, which are at the basis of preparation of all nuclear fuels.

Uranium dioxide has a crystal structure of fluorite type; in this lattice (figure 1) the metal is surrounded by 8 oxygen atoms located at the corners of a coordination cube (figure 2). Thus the coordination of metal atoms is eight. Six cubes of MeO_8 have 12 edges in common and enclose a void cube. In the ordered phases, the oxygen atoms located at cube diagonals are replaced by vacancies (along all [111] axes) so that the coordination number is six. X-ray studies have shown that by bringing together six coordination cubes, empty spaces are left which can accomodate excess oxygen atoms.

The phase diagram of uranium-oxygen system evidences that above 300° (figure 3) the solid uranium dioxide may dissolve oxygen forming the hyperstoichiometric oxide UO_{2+x}; the amount oxygen included is fairly important.

This process which may be present in many intermediate stage of UO_2 preparation technology entails the diluting of fissionable material that is the decreasing of fuel performance. That is why it is outstandingly important to know the amount of non-stoichiometric oxygen included into UO_2 lattice, as well as its influence upon the thermal properties of fuel.[1]

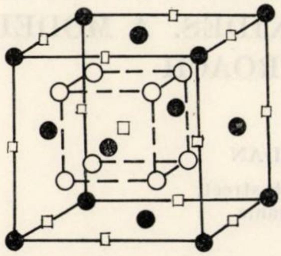

Fig. 1. — Unit cell of fluorite type crystal of uranium dioxide:

O — oxygen; ● — uranium; □ — vacancy in fluorite lattice. Broken lines pass through oxygen atoms which form a cubic arrangement around central vacancy.

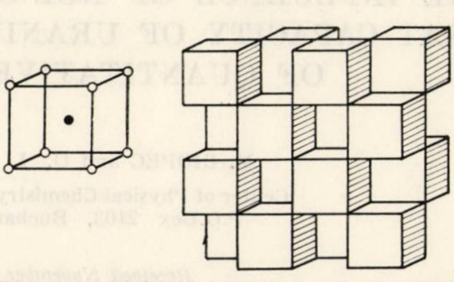

Fig. 2. — MeO_8 coordination cube in MeO_2 oxide of fluorite type and the structure formed by coordination cubes.

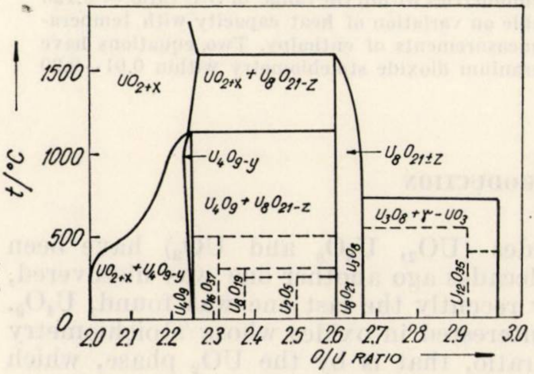

Fig. 3. — Uranium — oxygen phase diagram for stoichiometries characterized by O/U ratios between 2.00 and 2.66.

2. UTILIZATION OF FREE ENERGY IN THERMODYNAMIC CHARACTERIZATION OF NON-STOICHIOMETRIC URANIUM OXIDES

The formation of non-stoichiometric uranium oxides take place according to the reaction :

$$UO_2 + \frac{x}{2} O_2 \rightarrow UO_{2+x}.$$

---

[1] "Thermodynamic and Transport Properties of Uranium Dioxide and Related Phases", Technical Reports Series No. 39, I.A.E.A. Vienna, 1965, p. 3.

The main criterion of establishing the conditions of obtaining stable phases is the minimizing of free energy in a (G, T, x) equilibrium diagram where G is the free energy per atom and x the composition expressed through atomic ratio. In a (G, T, x) type plot, each phase is represented by a parabolic surface of free energy. An isothermal section of such a surface would be a parabola whose apex indicates the condition of stable phase [2] (figure 4).

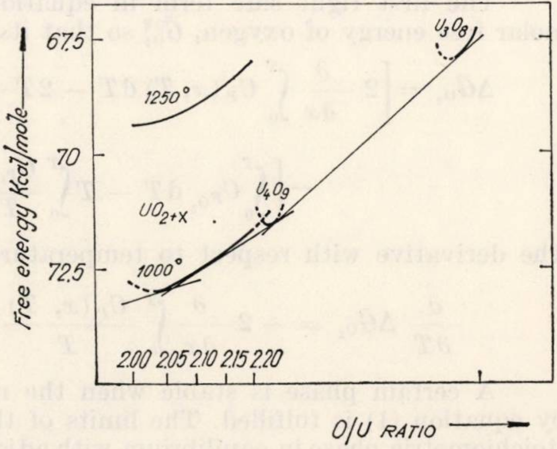

Fig. 4. — Free energy per atom in uranium-oxygen system (UO_{2+x}; U_4O_9; U_3O_8).

The minimizing of free energy for the reaction of formation of non-stoichiometric uranium oxides requires equating to zero the first derivative, with respect to temperature, of partial molar free energy change of the oxygen involved into the reaction

$$\frac{\partial}{\partial T}\,\Delta \bar{G}_{O_2} = 0. \tag{1}$$

According to classical definition, the partial molar free energy of oxygen is :

$$\bar{G}^{T}_{O_2} = \bar{H}^{T}_{O_2} - T\,\bar{S}^{T}_{O_2}, \tag{2}$$

where free partial molar quantities that characterize the oxygen in the non-stoichiometric oxide may be written as :

$$\bar{H}^{T}_{O_2} = \bar{H}^{0}_{O_2} + 2\,\frac{\partial}{\partial x}\int_0^T C_P\,(x,\ T)\,\mathrm{d}T - \int_0^T C_{P_{O_2}}\,\mathrm{d}T, \tag{3}$$

$$\bar{S}^{T}_{O_2} = \bar{S}^{0}_{O_2} + 2\,\frac{\partial}{\partial x}\int_0^T \frac{C_P\,(x,\ T)}{T}\,\mathrm{d}T - \int_0^T \frac{C_{P_{O_2}}}{T}\,\mathrm{d}T. \tag{4}$$

---

[2] J. S. Anderson, "Non-Stoichiometric and Ordered Phases : Thermodynamic Considerations", in "Chemistry of Extended Defects in Non-Metalic Solids", North-Holland Publishing Company, Amsterdam, 1970, p. 1.

Substitution of equations (3, 4) into (2) yields:

$$\bar{G}^{T}_{O_2} = (\bar{H}^{0}_{O_2} - T\,\bar{S}^{0}_{O_2}) + \left[2\,\frac{\partial}{\partial x}\int_0^T C_P\,(x,\,T)\,\mathrm{d}T - 2T\,\frac{\partial}{\partial x}\int_0^T \frac{C_P(x,\,T)}{T}\,\mathrm{d}T\right] - \left[\int_0^T C_{P_{O_2}}\,\mathrm{d}T - T\int_0^T \frac{C_{P_{O_2}}}{T}\,\mathrm{d}T\right]. \tag{5}$$

The first right side term in equation (5) is the standard partial molar free energy of oxygen, $\bar{G}^{0}_{O_2}$, so that its variation is:

$$\Delta\bar{G}_{O_2} = \left[2\,\frac{\partial}{\partial x}\int_0^T C_P\,(x,\,T)\,\mathrm{d}T - 2T\,\frac{\partial}{\partial x}\int_0^T \frac{C_P\,(x,\,T)}{T}\,\mathrm{d}T\right] - \left[\int_0^T C_{P_{O_2}}\,\mathrm{d}T - T\int_0^T \frac{C_{P_{O_2}}}{T}\,\mathrm{d}T\right]. \tag{6}$$

The derivative with respect to temperature is:

$$\frac{\partial}{\partial T}\,\Delta\bar{G}_{O_2} = -\,2\,\frac{\partial}{\partial x}\int_0^T \frac{C_P\,(x,\,T)}{T}\,\mathrm{d}T + \int_0^T \frac{C_{P_{O_2}}}{T}\,\mathrm{d}T. \tag{7}$$

A certain phase is stable when the minimum condition expressed by equation (1) is fulfilled. The limits of the composition range of non-stoichiometric phase in equilibrium with adjacent phases may be established through the condition of tangency at the same chemical potential. The calculation of the second derivative with respect to temperature of the variation of partial molar free energy is thus required. The derivative of equation (7) with respect to temperature gives:

$$\frac{\partial^2}{\partial T^2}\,\Delta\bar{G}_{O_2} = -\,\frac{2}{T}\,\frac{\partial}{\partial x}\,C_P\,(x,\,T) + \frac{C_{P_{O_2}}}{T}. \tag{8}$$

Equation (8) is very important since it allows to correlate the experimental heat capacities with partial molar free energy determined by other methods. One can make use of experimental data supplied by measurements on cells with solid electrolyte.[3,4] With equation (8) rewritten as:

$$\Delta C_P\,(x,\;T) = -\,\frac{T}{2}\int_0^x \frac{\partial_2}{\partial T^2}\,\Delta\bar{G}_{O_2}\,\mathrm{d}x + \frac{1}{2}\int_0^x C_{P_{O_2}}\,\mathrm{d}x, \tag{9}$$

one can correlate heat capacity with atomic ratio x, that is with the deviation from the stoichiometry of uranium dioxide.

One can consider that second derivative of partial molar free energy with respect to temperature is approximately independent of x for small intervals of its variation so that equation (9) becomes:

$$\Delta C_P\,(x,\;T) = \frac{x}{2}\left[C_{P_{O_2}} - T\,\frac{\partial^2}{\partial T^2}\,\Delta\bar{G}_{O_2}\right], \tag{10}$$

---

[3] K. Kiukkola, *Acta Chem. Scand.*, **16**, 327 (1962).

[4] D. I. Marchidan and S. Tănăsescu, *Rev. Roumaine Chim.*, **15**, 1491 (1970); **16**, 1053 (1971); **17**, 195 (1972); **18**, 1487 (1973); **19**, 1435 (1974).

which connects the variation of experimental heat capacity with the non-stoichiometry of uranium oxides.

In the following the correlation of calorimetric data with the non-stoichiometry of uranium oxides is attempted by applying the model described above.

3. THE VARIATION OF HEAT CAPACITY OF URANIUM OXIDES DUE TO DEVIATIONS FROM STOICHIOMETRY

To establish the equations which describe the change of heat capacity of uranium oxides versus non-stoichiometry (according to the model represented by equation (10)), one has to impose the conditions of stability of non-stoichiometric phase in equilibrium with adjacent phases. Use has been made of data on emf's of cells with solid electrolyte[4] i.e. the variation of partial molar free energy of oxygen in equilibrium with the non-stoichiometric oxide, $\Delta\bar{G}_{O_2}$; to avoid getting a zero value of second derivative with respect to temperature, $\Delta\bar{G}_{O_2}$ was assumed to have the expression :[5]

$$-\Delta\bar{G}_{O_2} = a + bT + cT^2. \qquad (11)$$

The processing of data for various non-stoichiometric uranium oxides by the least square method has led to imposing the above stability condition, the following results being obtained :

$$UO_{2.125} \; \frac{\partial^2 \Delta\bar{G}_{O_2}}{\partial T^2} = -17.508\ (10^{-3})\ \text{J/mol K}^2 \qquad (12)$$

$$\text{within } 1073 - 1373 \text{ K range;}$$

$$UO_{2.19} \begin{cases} \dfrac{\partial^2 \Delta\bar{G}_{O_2}}{\partial T^2} = -38.266\ (10^{-3})\ \text{J/mol K}^2 & (13) \\ \qquad \text{within } 1073 - 1233 \text{ K range;} & \\ \dfrac{\partial^2 \Delta\bar{G}_{O_2}}{\partial T^2} = -35.638\ (10^{-3})\ \text{J/mol K}^2 & (14) \\ \qquad \text{within } 1233 - 1373 \text{ K range;} & \end{cases}$$

$$UO_{2.21} \begin{cases} \dfrac{\partial^2 \Delta\bar{G}_{O_2}}{\partial T^2} = 201.703\ (10^{-3})\ \text{J/mol K}^2 & (15) \\ \qquad \text{within } 1073 - 1283 \text{ K range;} & \\ \dfrac{\partial^2 \Delta\bar{G}_{O_2}}{\partial T^2} = 196.660\ (10^{-3})\ \text{J/mol K}^2 & (16) \\ \qquad \text{within } 1283 - 1373 \text{ K range;} & \end{cases}$$

$$UO_{2.5} \; \frac{\partial^2 \Delta\bar{G}_{O_2}}{\partial T^2} = 40.918\ \text{J/mol K}^2 \qquad (17)$$

$$\text{within } 1073 - 1373 \text{ K range;}$$

$$UO_{2.63} \; \frac{\partial^2 \Delta\bar{G}_{O_2}}{\partial T^2} = 0.126\ \text{J/mol K}^2 \qquad (18)$$

$$\text{within } 1073 - 1373 \text{ K range.}$$

---

[5] C. Affortit and J. Marcon, *Rev. Int. Hautes Tempér. et Réfract.*, **7**, 236 (1970).

If one makes use of the following equation for the variation of heat capacity of oxygen with temperature :[6]

$$C_P = 29.957 + 4.184\ (10^{-3})\ T - 1.673\ (10^5)\ T^{-2}\ \text{J/g atom K} \qquad (19)$$

the temperature dependence of $\Delta\, C_P\,(x,\, T)$ can be deduced ; it mirrors the change of heat capacity due to deviations x of any oxide from the uranium dioxide stoichiometry.

Replacement of values given by equations (12—18) and (19) into equation (10) yields :

— for $x = 0.125$

$$\Delta C_P = 1.872 + 1.355\ (10^{-3})\ T - 0.104\ (10^5)\ T^2 \qquad (20)$$

— for $x = 0.19$

$$\Delta C_P = 2.846 + 4.033\ (10^{-3})\ T - 0.159\ (10^5)\ T^{-2} \qquad (21)$$

up to 1233 K

$$\Delta C_P = 2.846 + 3.783\ (10^{-3})\ T - 0.159\ (10^5)\ T^{-2} \qquad (22)$$

above 1233 K

— for $x = 0.21$

$$\Delta C_P = 3.145 - 20.739\ (10^{-3})\ T - 0.175\ (10^5)\ T^{-2} \qquad (23)$$

up to 1283 K

$$\Delta C_P = 3.145 - 20.209\ (10^{-3})\ T - 0.175\ (10^5)\ T^{-2} \qquad (24)$$

above 1283 K

— for $x = 0.50$

$$\Delta C_P = 7.489 - 9.183\ (10^{-3})\ T - 0.418\ (10^5)\ T^{-2} \qquad (25)$$

— for $x = 0.63$

$$\Delta C_P = 9.436 + 1.278\ (10^{-3})\ T - 0.527\ (10^5)\ T^{-2}. \qquad (26)$$

To obtain such equations for non-stoichiometric oxides whose e.m.f.'s in solid electrolyte cells are not available, finding out the dependence of $(\partial^2 \Delta \bar{G}_{O_2} / \partial T^2)$ on x has been attempted. The data were precessed by least square method and there has been obtained :

$$\frac{\partial^2 \Delta \bar{G}_{O_2}}{\partial T^2} = 1.263\ (10^{-3}) - 0.052x - 0.783\ x^2 \qquad (27)$$

which holds for x within 0.01 and 0.20 and

$$\frac{\partial^2 \Delta \bar{G}_{O_2}}{\partial T^2} = 0.372 - 0.937\ x + 0.552\ x^2 \qquad (28)$$

for $0.20 < x \leqslant 0.63$.

---

[6] D. R. Stull (Editor), "JANAF thermochemical tables", Dow Chemical Co., Midland, Mich., 1965, N° PB 168—370.

Substitution of equation (27) and equation (28) together with (19) into equation (10) yields the general equations of heat capacity change of uranium oxides due to nonstoichiometric oxygen:

— for $0.01 \leqslant x < 0.20$

$$\Delta C_P(x,\ T) = 14.978\ x + 1.460\ (10^{-3})\ Tx + 0.026\ T\,x^2 + \\ + 0.392\ Tx^3 - 0.836\ (10^5)\ T^{-2}\,x\ \text{J/mol K}; \qquad (29)$$

— for $0.20 < x \leqslant 0.63$

$$\Delta C_P(x,\ T) = 14.978\,x - 0.184\ Tx + 0.469\ Tx^2 - 0.276\ Tx^3 - \\ - 0.836\,(10^5)\ T^{-2}\ x\ \text{J/mol K}. \qquad (30)$$

4. DISCUSSION

The temperature dependence of $\Delta C_p(x,\ T)$ for various x in those oxides for which calorimetric data are available[7] has been plotted (figure 5); use was made of equations (20—26) and (29—30).

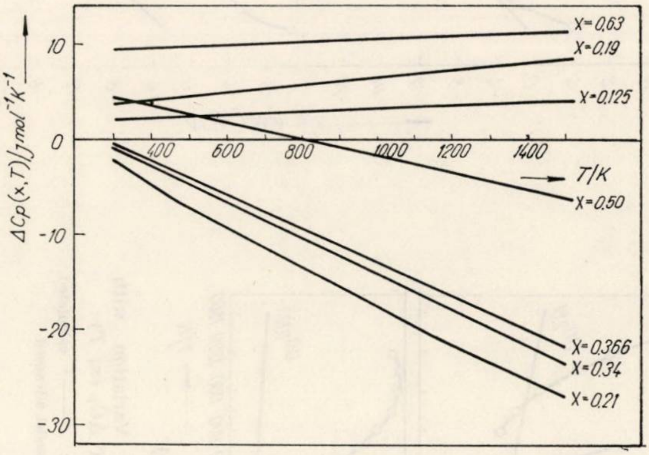

Fig. 5. — Variation with temperature of $\Delta C_P(x,\ T)$ due to deviation x of stoichiometry of every oxide studied from that of uranium dioxide (O/U = 2).

---

[7] D. I. Marchidan and M. Ciopec, *Rev. Roumaine Chim.*, **15**, 1287 (1970); **16**, 1145 (1971); **17**, 1657 (1972); **20**, 143 (1975).

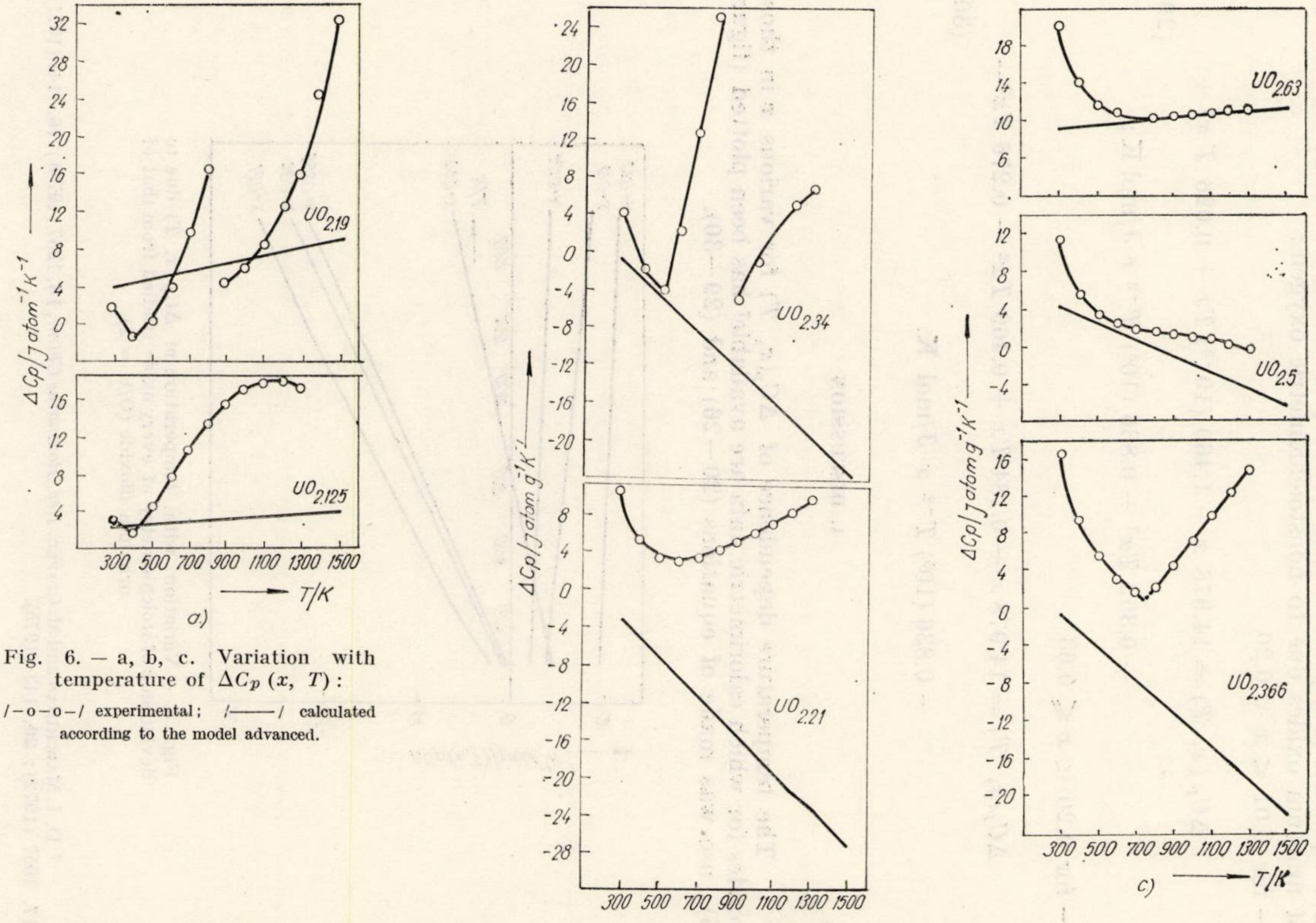

Fig. 6. — a, b, c. Variation with temperature of $\Delta C_p\ (x,\ T)$:
/–o–o–/ experimental; /——/ calculated according to the model advanced.

Establishing the validity domain of equations that have been advanced was carried out by graphically comparing the calculated curves with experimental values of $\Delta C_P(x, T)$; thus the difference between the heat capacity of every nonstoichiometric oxide and the heat capacity of uranium dioxide has been plotted versus temperature (figure 6). Figure 6 shows that experimental and calculated curves have the same kind of variation in $UO_{2.125}$; $UO_{2.19}$; $UO_{2.5}$; $UO_{26.3}$ and opposite variations in $UO_{2.21}$; $UO_{2.34}$; $UO_{2.366}$.

In conclusion, one may state that the model for the evaluation of heat capacity change due to deviations from stoichiometry applies successfully above 700 K for an oxygen excess ranging between 0.125 -- − 0.19 and 0.5 − 0.63 as against one atom at uranium.

Revue Roumaine de Chimie, **21**, 7, 1007–1011 (1976)

A THEORETICAL STUDY OF AZAINDOLES

MARIANA CIUREANU
Physical Chemistry Department, Polytechnic
Institute of Bucharest, Bd. Republicii, 13

Received December 19, 1974

A simple SCF-CI π-electron method is used to predict the first electronic transitions of azaindoles. The theoretical results are found to be in a good agreement with the available experimental data. The π and σ electron densities are calculated and discussed; on the basis of the results it is concluded that the overall atomic charges can be used to predict the reactivity toward electrophilic and nucleophilic agents, as well as the basicity of these compounds.

1. INTRODUCTION

The electronic structure of the condensed benzoderivatives of five-membered heterocycles has been the object of numerous studies [1–4] which aimed at giving an explanation of their chemical and spectral behaviour and at establishing how far the π electrons of the five-membered ring interact with the six-membered ring. Mason [5] interpreted the UV spectra of indole and azaindoles in terms of a carbocyclic model, the indenyl anion, that is, he considered the π electrons of the pyrrolic nitrogen to be completely delocalized; however, he noted that the differences between the absorptions of 4- and 7-azaindole cations, as well as those of the neutral and cationic species of 5- and 6-azaindoles, could arise from an incomplete delocalization. Bochvar, [6] Minkin [7] et al. used the simple LCAO method to calculate the π electron density and delocalization energies of 7-azaidole, benzopyrazole and benzimidazole; the results were found to be in a satisfactory agreement with the reactivity of these compounds toward electrophilic and nucleophilic agents. Momichiolli and Rastelly [3] carried out SCF MO calculations followed by limited configuration interaction, in order to demonstrate the correspondence between the electronic spectra of indole, benzofurane, thionaphthene,

---

[1] R. E. Villette, *Adv. Heterocyclic Chem.*, **9**, 27 (1968).

[2] E. M. Evleth, *Theor. Chim. Acta*, **16**, 22 (1970).

[3] F. Momicchioli and A. Rastelli, *J. Mol. Spectroscopy*, **22**, 310 (1967).

[4] P. J. Black, R. D. Brown and M. L. Heffernan, *Austral. J. Chem.*, **20**, 7 (1967).

[5] S. F. Mason, *Phys. Meth. Heterocycl. Chem.*, **2**, 1 (1963).

[6] D. A. Bochvar, A. A. Bogaturyants, A. V. Tutkevich, L. N. Yakhontov, M. Ya Uritskaya, D. N. Krasnokutskaya and V. M. Rubsov, *Izvest. Akad. Nauk S.S.S.R. Ser. Khim.*, **1966**, 354.

[7] V. I. Minkin, A. F. Pozharski and J. A. Ostroumov, *Khim. Heterocycl. Soedineniya*, **4**, 550 (1966).

and those of naphtalene and benzoderivatives. Their results show that in benzofuran the delocalization of the two π electrons of oxygen is very small, and the properties of the molecule are quite similar tot hose of styrene ; in indole, the delocalization is increased and the spectral properties of the molecule can be described by analogy with naphtalene.

In connection with the latter point of view, we consider that an interesting problem to solve is to establish how and how far the azasubstitution in indole changes the electronic structure and influences the chemical and spectral properties of the basic molecule. Thus, we have carried out SCF CI calculations for a number of seven aza-derivatives of indole : benzimidazole, indazole, benzotriazole, 4-azaindole, 5-azaindole 6-azaindole and 7-azaindole.

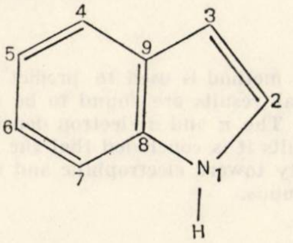

2. METHOD OF CALCULATION

In order to calculate the first three electronic transitions and the π electron density the PPP SCF MO method was used, followed by limited CI among the first nine configurations. The σ electronic charges were calculated using Del Re's method.[8]

Table 1

Choice of parameters

X	β_{c-x}(eV)	γ_{xx}(eV)	I_x(eV)
C	−2.39	11.14	11.16
$\ddot{N}$	−1.45	16.57	28.53
$\dot{N}$	−1.76	11.98	14.12

The bond lenghts and angles in azaindoles were considered to be the same as in indole.[9] The parameters used in the SCF calculation were taken as shown in table 1.

The bielectronic integrals were calculated using Klopman's formula.[10]

The valence state ionization potentials are those recommended by Dewar and Gleicher.[11] The resonance integrals β_{cx} where not available, were calculated by the formula :

$$\beta_{cx} = \frac{S_{cx}}{S_{cc}} \beta_{cc} \tag{1}$$

where S_{cx} were evaluated using Mulliken's tables.

---

[8] G. Del Re, *J. Chem.*, **1958**, 4031; G. Del Re and B. Pullman, *J. Chem. Phys.*, **2**. 942 (1965).

[9] Z. Yoshida and T. Kobayashi, *Theor. Chim. Acta*, **20**, 216 (1971).

[10] G. Klopman, *J. Amer. Chem. Soc.*, **86**, 4550 (1964).

[11] M. J. S. Dewar and G. J. Gleicher, *J. Chem. Phys.*, **44**, 759 (1966).

3. RESULTS AND DISCUSSIONS

3.1. ELECTRONIC TRANSITIONS

The calculated wavelenghts for the first transitions, as well as the available spectral data,[1,5,12–14] are presented in table 2. As seen from this table, the ultraviolet absorption spectra show three bands, which are all $\pi \rightarrow \pi^*$ transitions; these bands were related to the α, p and β bands of benzene by Mason[5]. The first two bands lie generally under the same envelope, but move independently with hydrogen bonding

Table 2

Calculated and experimental spectra of azaindoles

Compound	λ_{calc}(nm)	λ_{exp} (nm)*		
		Water	95 % ethanol	other solvents
Indole	270	288	278	
	258	261	270	
	211	219	219	
Indazole	292	296		
	276	250		
	230	—		
Benzimidazole	289	277		
	262	244		
	229	—		
4-Azaindole	296	292		
	276	—		
	224	d		
5-Azaindole	294	273	—	
	274	265	265	
	215	d	216	
6-Azaindole	293	291	296	
	282	260	263	
	217	d	218	
7-Azaindole	288	290	290	294(h)
	279	—	—	280 (h)
	222	d	219	d (h)
Benzotriazole	299			278 (i)
	286			248 (i)
	235			220 (i)

* Experimental spectra in different solvents [1,5,13,14]

h = heptane, i = isooctane

d = bands at or bellow 220 nm

---

[12] T. K. ADLER and A. ALBERT, *J. Chem. Soc.*, **1960**, 1974.

[13] S. OKUDA and M. M. ROBINSON, *J. org. Chem.*, **24**, 1008 (1959).

[14] F. MASON, *J. Chem. Soc.*, **1954**, 2071.

Table 3

Overall effective atomic charges*

Indole		Indazole		Benzimidazole		Benzotriazole		4-Azaindole		5-azaindole		6-azaindole		7-azaindole	
Atom	Q_t	Atom	Q_t	Atom	Q_t	Atom	Q_t	Atom	Q_t	Atom	Q_t	Atom	Q_t	Atom	Q_t
N_1	−0.3102	N_1	−0.1163	N_1	−0.2560	N_1	−0.0750	N_1	−0.3101	N_1	−0.3045	N_1	−0.3082	N_1	−0.2784
C_2	0.0216	N_2	−0.6769	C_2	0.4350	N_2	−0.2463	C_2	0.0620	C_2	−0.0011	C_2	0.0679	C_2	−0.0044
C_3	−0.0700	C_3	0.3602	N_3	−0.7029	N_3	−0.2522	C_3	−0.0520	C_3	−0.0529	C_3	−0.0926	C_3	−0.0577
C_4	−0.0356	C_4	0.0026	C_4	−0.0386	C_4	−0.0073	N_4	−0.7171	C_4	0.3456	C_4	−0.1155	C_4	0.0891
C_5	−0.0356	C_5	−0.0157	C_5	−0.0309	C_5	−0.0571	C_5	0.3185	N_5	−0.7333	C_5	0.2889	C_5	−0.1320
C_6	−0.0469	C_6	−0.0028	C_6	−0.0683	C_6	−0.0295	C_6	−0.1250	C_6	0.3015	N_6	−0.7264	C_6	0.3294
C_7	−0.0535	C_7	−0.0771	C_7	−0.0398	C_7	−0.0598	C_7	0.0691	C_7	−0.1271	C_7	0.3229	N_5	−0.7169
C_8	0.0495	C_8	0.1502	C_8	0.0071	C_8	0.1032	C_8	−0.0183	C_8	0.1527	C_8	−0.0245	C_8	0.3641
C_9	−0.0192	C_9	0.0923	C_9	0.2155	C_9	0.1762	C_9	0.2846	C_9	−0.0823	C_9	−0.0861	C_9	−0.0816
H_1	0.2265	H_1	0.2258	H_1	0.2258	H_1	0.2567	H_1	0.2265	H_1	0.2265	H_1	0.2265	H_1	0.2265
H_2	0.0570	H_3	0.0610	H_2	0.0700	H_4	0.0480	H_2	0.0570	H_2	0.0570	H_2	0.0570	H_2	0.0570
H_3	0.0480	H_4	0.0480	H_4	0.0480	H_5	0.0480	H_3	0.0480	H_3	0.0480	H_3	0.0480	H_3	0.0480
H_4	0.0480	H_5	0.0480	H_5	0.0480	H_6	0.0480	H_5	0.0610	H_4	0.0610	H_4	0.0480	H_4	0.0480
H_5	0.0480	H_6	0.0480	H_6	0.0480	H_7	0.0480	H_6	0.0480	H_6	0.0610	H_5	0.0610	H_5	0.0480
H_6	0.0480	H_7	0.0480	H_7	0.0480			H_7	0.0480	H_7	0.0480	H_7	0.0610	H_6	0.0610
H_7	0.0480														

* The numbering of the atoms in the azaderivatives of indole was made according to figure 1.

and conjugative effects. The third band could be obtained only in ethanol; in other solvents it shifts to shorter wavelengths, inaccessible to quartz spectrometers.[1]

The agreement between the calculated results and the experimental data is very good in all cases. The theory predicts the existence of three bands in the near ultraviolet region, which corresspond to the electronic bands of indole; among these, there are two electronic bands at longer wavelenghts, very close to each other, and a band placed at shorter at wavelengths; as seen from table 2, both experimental and theoretical results have shown that azasubstitution in indole does not seem to change to a significant extent the spectral behaviour of the basic molecule.

3.2. CHARGE DENSITIES

The overall effective atomic charges (calculated as the sum of π and σ charges) are shown in table 3 for the seven compounds studied here and for indole. Our calculations show that the pyrrolic nitrogen acts as a π donor and a σ acceptor whereas the pyridine nitrogen is both π and σ acceptor; therefore the negative charge on the former is, in all cases, considerably smaller than on the latter.

Unfortunately a complete study on the effect of the azanitrogen position on the chemical reactivity in this series is lacking, which makes impossible a detailed comparison between theory and experiment. However, the few existing experimental data are in a satisfactory agreement with our results.

Thus, evidence for electrophilic substitution at the 3 position in case of 4-, 6- and 7-azaindole is provided by Clayton,[1,15a] Yakhontov.[15b] et al.

On the basis of our calculations, the most reactive positions toward electrophilic reagents should be 3,6 for 4-azaindole 3,4 for 6 azaindole and 3,5 for 7-azaindole.

The predicted reactivity towards nucleophiles is $6 > 4$ for 7-azazaindole, which is in a good agreement with the existing experimental data.[1]

On the basis of the calculated electron density of the pyridine nitrogen, the following order of basicity is to be expected:
benzotriazole < indazole < benzimidazole < 7-azaindole ≈ 4-azaindole < < 5-azaindole.

The experimental order, given by the *pKa* values of these compounds,[16] is:
benzotriazole < indazole < 7-azaindole < benzimidazole ≈ 4-azaindole < < 5-azaindole.

Thus, except for the inversion between benzimidazole and 7-azaindole a satisfactory agreement is found between calculated charge densities and the experimental data.

[15a)] J. C. Clayton and J. Kenyon, *J. Chem. Soc.*, **1950**, 2952; b) L. N. Yakhontov, M. Ya, Uritskaia and M. V. Rubstov, *Zhur org. Khim.*, **1**, 2032 (1965).

[16a)] L. N. Yakhontov, M. A. Portnov, V. A. Azimov and E. J. Lapan, *Zhur. Org. Khim.*, **5**, 956 (1969); b) W. C. Aten and K. Buechel, *Z. Naturforsch. B.* **25**, 961 (1970).

Revue Roumaine de Chimie, 21, 7, 1013–1022 (1976)

INFLUENCE OF SOME OXIDES OF TRANSITIONAL METALS ON THE FORMATION OF CALCIUM ORTHOSILICATE

MARIA ENCULESCU
FOREXIM, Bucharest, Calea Victoriei, 111

Received February 12, 1975

The paper discusses the influence exerted by some oxides of transitional elements on the formation and stabilization of calcium orthosilicate and also the calcium orthosilicate polymorphism relations with them. Solubilization limits, formulas of solid solutions of calcium orthosilicate with iron, manganese, chromium, cobalt, nickel and copper oxides are briefly discussed as well as the structural modifications of calcium orthosilicate by exceeding the limit of solid solution and the possible occurrence of new mineralogical compounds with the oxides of transitional elements.

1. SOME CONSIDERATIONS ON THE STRUCTURE AND POLYMORPHISM OF CALCIUM ORTHOSILICATE

Calcium orthosilicate represents one of the important crystalline phases in white and coloured Portland cement clinkers and it is of a particular interest to know its various polymorphic forms and its solid solutions with various oxides.

1.1. STRUCTURE OF CALCIUM ORTHOSILICATE

Dicalcium orthosilicate has several polymorphic forms which have formed the subject of several studies. [1-14] We shall briefly examine below the structure of forms α, α', β and γ.

---

[1] A. Guinier and M. Regourd, "Congress of Cements Chemistry", Tokyo, 1968.

[2] G. Yamaguchi, Y. Ono, S. Kawamura and Y. Soda, *J. Ceram. Assoc. Japan*, **71**, 9 (1963).

[3] M. A. Bredig, *J. Amer. Ceram. Soc.*, **33**, 6, 188 (1950).

[4] V. Valkenburg and H. F. McMurdie, *J. Res. Nat. Bur. Stand.*, **38**, 415 (1947).

[5] A. M. S. Douglas, *Mineral Mag.*, **29**, 875 (1952).

[6] C. M. Midgley, *Britt. J. Appl. Phys.*, **3**, 10 (1951).

[7] G. Yamaguchi, H. Miyabe, K. Amano and S. Komatsu, *J. Ceram. Assoc. Japan.*, **65**, 99 (1957).

[8] N. Niesel and P. Thormann, *Tonindustrie Ztg. Dtsch.*, **91**, 405 (1961).

[9] D. K. Smith, A. Y. Majundar and F. Ordway, *J. Amer. Ceram. Soc.*, **44**, 405 (1961).

[10] I. Trömhel, *Naturwiss*, **36**, 88 (1949).

[11] H. O'Daniel and L. Tscheischwili, *Z. Kryst.*, **104**, 124 (1942).

[12] K. Thilo and F. Lieban, *Z. Physik*, **199**, 125 (1952).

[13] A. Dietzel and L. Tscheischwili, *Ber. Deutsch, Keram. Ges.*, **30**, 151 (1953).

[14] M. Enculescu, Thesis, Polytechnical Institute Bucharest, 1972.

$\alpha - 2CaO.SiO_2$. Of all the polymorphic forms of calcium orthosilicate, the α variety, which exists only in the interval 1425° – 2130°, has been less studied due to difficulties encountered in runs performed at high temperature.

The most accurate result has been provided by Yamaguchi, Ono, Kawamura and Soda,[1,2] who determined at 1500° a trigonal lattice with hexagonal parameters : $a = 5.527$; $c = 7.311$ Å. These results agree with those reported by Bredig,[3] Van Valkenburg and McMurdie.[4] Other researchers[5-8] have studied the existence of two forms of α'_{C_2S} : α'_H and α'_L having their stability domains at 1420 – 1160° and 1160 – 675°.

$\beta 2CaO.SiO_2$. Yannaquis,[1] Yamaguchi, Ono, Kawamura and Soda[2] have analyzed the pure β C_2S phase defined by the parameters of the monoclinic lattice : $a = 5.48$; $b = 6.76$; $c = 9.28$; $\beta = 94°33'$.

The structure of β C_2S microcrystals stabilized with 0.5 % B_2O_3 is monoclinic,[6] it is constructed starting from independent $[SiO_4]^{4-}$ tetrahedra and from two sorts of calcium atoms. Four of the eight Ca (Ca_I) atoms are alternatively placed above and beneath the $[SiO_4]^{4-}$ tetrahedra along the direction of axis *b*.

The structure may be defined by alternative columns of tetrahedra and Ca atoms bonded by 4 Ca(Ca_{II}) atoms placed in the cavities between tetrahedra. The pseudotrigonal arrangement of tetrahedra around Ca (Ca_{II}) atoms is illustrated in fig. 1.

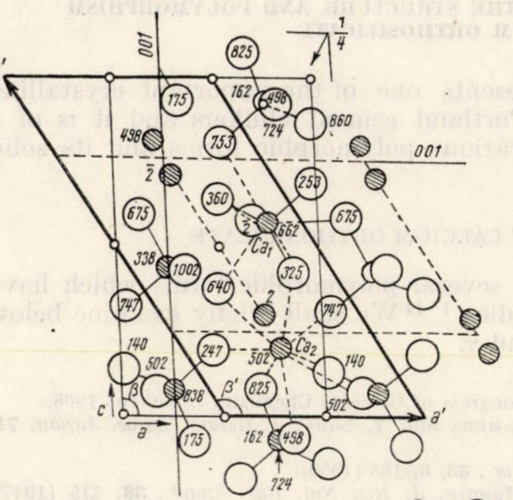

Fig. 1. — Projection of $\beta - 2CaO.SiO_2$ structure on a perpendicular plane to axis *b* (Midglei[6]). The pseudo-hexagonal lattice corresponds to axes *a′* and *b′* (Yamaguchi, Ono, Kawamura and Soda[2]).

γ C_2S. Its elementary lattice was calculated by several authors. Results correspond to :

$$a = 5.076 \; ; \; b = 6.756 \; ; \; c = 11.230 \text{ Å}.$$

Smidth, Majumdar and Ordway[9] prepared γ C_2S and found that its structure is of olivin type, $2MgO.SiO_2$ (fig. 2).

The bigger Ca^{2+} ions which replaced Mg^{2+} ions dilated the $2MgO.SiO_2$ lattice without, however, altering the general arrangement.[1-13]

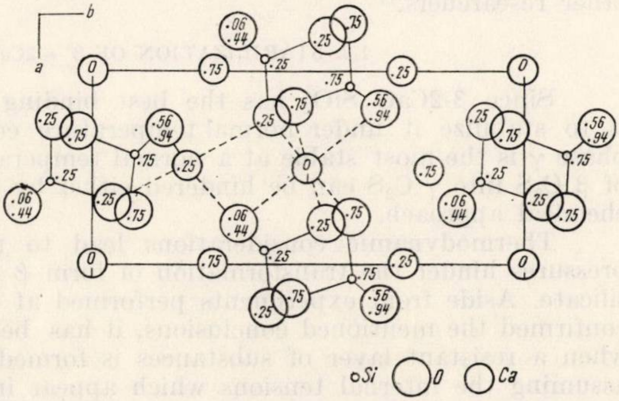

Fig. 2. — Projection of structure $\gamma-2CaO.SiO_2$ on a perpendicular plane to axis *c* (Smith, Majumdar, Ordway[11,12]).

1.2. POLYMORPHISM OF CALCIUM ORTHOSILICATE

Calcium orthosilicate polymorphic transformations may be schematically represented in fig. 3.

As schematically suggested, transformations from one polymorphic form into another of calcium orthosilicate must be studied at both increasing and decreasing temperatures. Starting from temperatures beyond 1420°, when α form is stable, $\alpha \rightleftharpoons \alpha_H$ transformation occurs on cooling to 1400° ± 50. It is reversible from $\alpha_H \rightleftharpoons \alpha'_L$. By further cooling to temperatures of 680° — 630°, α'_L changes into β. This process is rever-

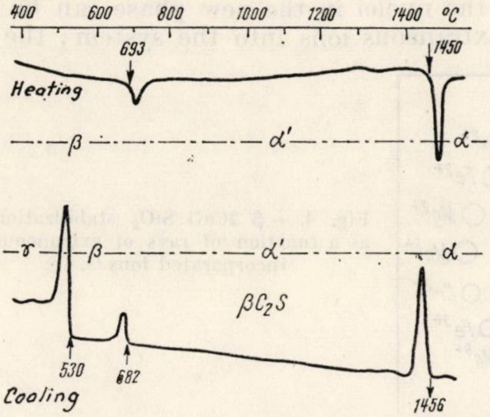

Fig. 3. — DTA diagram of forms γ and β $2CaO.SiO_2$ (Coustault[1]).

sible. Vasenin and Budnikov[15] have also reported phase β. Likewise Kurdowski[14] refers to obtaining at 600° a β-stabilized calcium orthosilicate phase with SiO_2 excess, very similar to form β. However this phase seems certain, as a silica excess fails to stabilize form β C_2S, favouring in turn the $\beta \rightarrow \gamma$ change. Such a phase has not been identified by other researchers.[14]

1.3. STABILIZATION OF $\beta - 2CaO.SiO_2$

Since β-$2CaO.SiO_2$ has the best binding properties, the problem is to stabilize it under normal temperature conditions. As was shown, phase γ is the most stable at a normal temperature. The transformation of β C_2S into γ C_2S can be hindered either by physical or by crystallochemical approach.

Thermodynamic considerations lead to the conclusion that high pressures hinder the transformation of form β into form γ of dicalcium silicate. Aside from experiments performed at high pressure and which confirmed the mentioned conclusions, it has been practically found that when a resistant layer of substances is formed around β-C_2S particles, assuming the internal tensions which appear in the system and at the same time creating an overpressure state, β modification is stabilized (as for instance in the case of calcium orthosilicate in slag or obtained in the presence of molybdenum and zirconium oxides). [13-15]

The assumption relative to β C_2S crystallochemical stability starts from the considerations made by Volmer and Stranski et al.[15] They show that a polymorphic transformation can occur only if the crystalline nuclei of the new phase exceed a certain limit dimension which decreases with the undercooling increase. This means that the change into the new phase, stable at low temperatures, occurs at a higher rate at lower temperatures.

However the growth of the nuclei in the new phase can be interrupted by introducing some extraneous ions into the system; the high-temperature polymorphic form is thus stabilized. According to Dietzel and Tscheischwili's [13] hypothesis (figure 4) substances introducing into the lattice either ions with larger sizes than Ca^{2+} or ions forming smaller

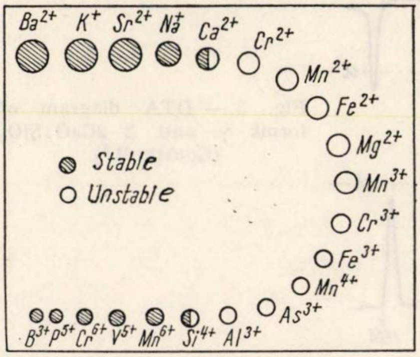

Fig. 4. — β $2CaO.SiO_2$ stabilization as a function of rays of extraneous incorporated ions [13].

---

[15] I. Teoreanu, M. Enculescu and I. Gheorghe, *Rev. Matériaux de Construction*, **655**, 103 (1971).

anionic complexes than $[SiO_4]^{4-}$ group may stabilize the β C_2S form lattice special results are obtained when $[SiO_4]^{4-}$ radical is substituted by anionic groups with a higher charge (simultaneously having also smaller sizes) for instance $[BO_4]^{5-}$. The amount of the stabilizing substance to be added in order to manifest its action, depends on its nature.

2. SOLID SOLUTIONS OF CALCIUM ORTHOSILICATE

Calcium orthosilicate possesses to a large extent the property to form solid solutions with various oxides.

Extraneous cations introduced into the system may replace both Si^{4+} and Ca^{2+}. As a result, the solid solutions of calcium orthosilicate may be described by the general formula : $(Ca_{2-x}.M_x)(Si_{1-x}.M_x)O_{4-z}$ in which : M — metallic cation and $z = x(3 - n)$, n being the valence of metallic cation.

By introducing some polyvalent cations with a relatively small ionic ray, such as Fe^{3+}, Al^{3+}, Cr^{3+}, they may more likely substitute the Si^{4+} ion. Consequently, in this case the following exchange is involved :

$$2Si^{4+} + O^{2-} \rightarrow 2M^{3+}$$

$$(2Si^{4+} + 2e \rightarrow 2M^{3+}).$$

For divalent ions with a larger ionic ray, an exchange is more likely in which Ca^{2+} is involved :

$$Ca^{2+} \rightarrow M^{2+}.$$

2.1. β $2CaO.SiO_2$-Fe_2O_3 SOLID SOLUTIONS

Iron oxide introduced to 1—2 % together with boric anhydride is solubilized in the β $2CaO.SiO_2$ lattice. Free calcium oxide determinations indicate values below 0.14 % which shows the practically total CaO bonding.

Ferric oxide introduced in a proportion of 4 and 8% leads to a probable physical stabilization of β C_2S; in fact, Dietzel and Tscheischwili [13] claim that Fe^{3+} fails to crystallochemically stabilize β-$2CaO.SiO_2$.

The diffractogram in table 1 for the sample with 8% Fe_2O_3 reveals highly intense lines characteristic of β—$2CaO.SiO_2$; however line $d = 2.6961$ Å also appears characteristic of Fe_2O_3 which proves that the solubilization limit of Fe_2O_3 in calcium orthosilicate is exceeded.

The formation of calcium ferrites is also possible.

According to Regourd et al.,[16] iron introduced alone in the lattice of dicalcium silicate substitutes Si^{4+} as previously shown; the same substitution is likely when it is introduced together with Al^{3+}.

---

[16] M. Regourd, "Congress of Cements Chemistry", Tokyo, 1968.

Table 1

Diffractograms of calcium orthosilicate with oxides of transitional metals

− 2 CaO . SiO$_2$	x 3.0153	x 2.9005	y 1.9163	y 3.8306	z 4.3497	z 2.4661	z 2.3305	z 1.8091	z 1.7591	z 1.6353	z 1.5266
− 2 CaO . SiO$_2$ + 0.5 % B$_2$O$_3$	x 2.7719	x 2.7460	y 2.1910	y 3.0192	y 2.6143	z 1.9201	z 1.9837	z 1.8054	z 1.6267	z 1.6007	
− 2CaO . SiO$_2$ + 2 %Fe$_2$O$_3$	x 2.7776	x 2.7444	y 2.6196	y 2.1892	y 2.4274	z 2.4264	z 3.0354	z 1.1892	z 1.7697		
− 2CaO . SiO$_2$+8 %Fe$_2$O$_3$	x 2.7776	x 2.7444	y 2.6961 } Fe$_2$O$_3$	y 2.6196	y 2.1493	z 3.0354	z 2.4148	z 2.2962	z 2.2962	z 1.9877	z 1.8790 1.7697
− 2CaO . SiO$_2$+2 %M$_n$ O$_2$	x 3.03	x 2.76	x 1.92	y 3.84	y 1.809	z 4.37	z 4.11	z 2.91	z 2.66	z 2.47	
− 2CaO . SiO$_2$+2 %M$_n$ O$_2$ + 0.5% B$_2$O$_3$	x 2.79	x 2.73	y 2.61	y 2.19	z 2.45	z 2.41	z 2.29	z 2.02	z 1.987	z 1.809	
− 2CaO . SiO$_2$+4 %MnO$_2$ +0.5 % B$_2$O$_5$.	x 2.79	x 2.75	y 2.61	y 2.19	z 2.41	z 2.29	z 2.02	z 1.987	z 1.901	z 1.809	
− 2CaO . SiO$_2$+0.6% Co$_3$O$_4$.	x 2.79	x 2.75	y 2.61	y 2.19	z 2.41	z 2.29	z 2.14	z 1.987	z 1.901	z 1.809	Co304 } 1.809
− 2CaO . SiO$_2$+0,4 % Co$_3$O$_4$ + 0.5 %B$_2$O$_3$.	x 2.79	x 2.75	y 2.61	y 2.19	z 2.41	z 2.29	z 1.987	z 1.809	z 1.76	z 1.63	z 1.57
− 2CaO . SiO$_2$+0.6 % Co$_3$O$_4$+0.5 %B$_2$O$_3$	x 2.79	x 2.75	y 2.61	y 2.19	z 2.41	z 2.29	z 1.987	z 1.901	z 1.809	z 1.635	0.40 %Co304 +0.5 %B$_2$O$_3$
− 2CaO . SiO$_2$+1.2 %NiO	x 2.8079	x 2.7719	y 3.0293	y 2.6143	y 2.4419	z 2.2804	z 2.1899	z 2.0836 } NiO	z 2.0388	z 1.9124	z 1.8084 z 1.9878
− 2CaO . SiO$_2$+0.6 % NiO + 0.5 % B$_2$O$_3$.	x 2.7553	y 2.1909	y 2.0293	z 2.4443	z 2.2882	NiO 2.0891	z 1.9787	z 1.8890	z 1.8054	z 1.7049	z 1.6294
− 2CaO . SiO$_2$+1.2 %NiO +0.5 % B$_2$O$_3$.	x 2.7719	x 2.7454	y 2.6143	y 2.2421	y 2.5422	y 2.4417	y 2.2859	z 2.2412	z 2.0321	z 1.9837	NiO } 1.4268
− 2CaO . SiO$_2$+1.2 % CuO + 0.5 %B$_2$O$_3$.	x 2.7827	x 2.7354	y 2.6113	y 2.1910	z 2.5422	z 2.4453	z 2.2804	z 2.0258	z 1.9837	z 1.8445	z 1.7045

x = parameter "d" in Å, with large intensity.

y = parameter "d" in Å, with middle intensity.

z = parameter "d" in Å, with small intensity.

However the presence of some ions of transitional metals may determine the substitution of Ca^{2+} ion by Fe^{3+} too; thus in the presence of Ti, V or Cr, which possess a higher oxygen bonding energy than Fe, it may have an octahedral coordination and in the presence of Mn, Co, Ni, Cu which possess a lower oxygen bonding energy than Fe, it may have a tetrahedral coordination. It must be noted that the simultaneous presence of other transitional metals changes the Fe solubility limit in calcium orthosilicate; thus Ti, V, Cr may favour Fe solubility in the calcium orthosilicate lattice while Co, Ni, Cu may diminish it.[17]

Keeping the above into account and also our own data,[14] the dicalcium silicate solid solutions with iron may be described by formula:

$$Ca_2[Fe_x . Si_{1-x}]\, O_{4-\frac{x}{2}} \quad \text{where}: 0 \leqslant x \leqslant 0.05.$$

2.2. β $2CaO . SiO_2-MnO_2$ SOLID SOLUTIONS

Studies made by Maslyi[18] suggest the possibility of substituting Ca^{2+} ions by manganese in the case of β-$2CaO . SiO_2$ and also the partial Si^{4+} substitution in larger MnO_2 amounts.

He claims that (over 1 % MnO_2) some lines specific of pure β-$2C_2S$ are observed to be displaced and a new line is found to appear, attributed to orthosilicate solid solutions (2.675 Å). Likewise, over 1.1 % MnO_2 (which seems to be the solid solution limit) produces no longer colour intensification.

Hornain,[17] as well as Maslîi,[18] showed that intermediate Mn^{4+} between Ti, V, Cr, and Ni, Cu, Zr groups may substitute both Si and Ca. Yet the author stresses that considering ionic rays, its valence and polarization power, Ca substitution is easier. Our own studies[14] have shown that MnO_2 introduced to 2% fails to stabilize the β-$2CaO . SiO_2$ form (figure 6a) lines at $d = 3.03$ Å; $d = 2.76$ Å and $d = 1.92$ Å. being characteristic of γ−$2CaO . SiO_2$; this confirms Dietzel and Tscheischwili's hypothesis [13] according to which Mn^{4+}, or with a lower valence, fails to stabilize the β $2CaO . SiO_2$ form. By introducing a 0.5% B_2O_3 addition we obtain a stabilization of form β C_2S which has characteristic lines at $d = 2.79$ Å, $d = 2.73$ Å, 2.6Å and 2.19 Å as resulted from table 1.

By increasing the MnO_2 amount to 4% and introducing 0.5% B_2O_3 we observe an intensification of the principal lines characteristic of β $2CaO . SiO_2$, table 1.

Free CaO determinations show values included between 0.16 and 0.26 %. Thus it seems that MnO_2 is introduced into the solid solution C_2S lattice. Solid solutions of $2CaO . SiO_2$ may be described by the general formula[14]:

$$(Ca_{2-x} . Mn_x)(Si_{1-x} . Mn_x)O_{4-z}, \text{ in which } z = x(3 - n)$$

---

[17] H. Hornain, Service Physique du CERILH, ILD/2080, Paris 1971.

[18] E. N. Maslyi, *Politech. Inst. im. S. M. Kirova*, Tomsk, 1971.

2.3. β 2CaO.SiO$_2$–Cr$_2$O$_3$ SOLID SOLUTIONS

Hornain[17] specifies in his work that Cr^{6+} is one of the elements which are most readily included into β C_2S lattice. Being ions with a small ray Cr^{6+} ions possess a great bonding energy and a great polarization power and may substitute Si^{4+}.

On the other hand, Glasser and Osborn[14] propose valence 5 for chromium in β C_2S and Kondo[14] mentions β C_2S stabilization by substitution of SiO_2 at small CrO_2 and Cr_2O_5 additions.

Studying the roentgenogram of pure β C_2S and of β C_2S with Cr_2S_3 addition, Maslyi[18] shows that it is difficult to draw conclusions on Cr_2O_3 influence on C_2S synthesis. Only with 10% Cr_2O_3 does line 2.65 Å appear on the roentgenogram and it may be attributed to free, unbound Cr_2O_3 as solid solution in the β C_2S lattice; using data from IR spectra, the Cr_2O_3 presence is identified even with 1.6%.

Our own studies[14] have indicated that chromium introduced both as Cr^{6+} and as Cr^{3+} in a 2CaO.SiO$_2$ raw mixture and burned at 1500° fails to lead to β C_2S stabilization.

Chemical and ESR analyses[14] have revealed that chromium exists only as Cr^{3+} at the respective working temperature; based on Dietzel and Tscheischwili's hypothesis,[13] Cr^{3+} ion fails to stabilize β C_2S. Sîcev, Newman and Wells[19] however, found that over 1% Cr_2O_3 produces a stabilizing effect of β 2CaO.SiO$_2$ form. Such an effect may be achieved only if chromium is eventually found as Cr^{6+} in the product obtained. In syntheses performed with 0.5 to 8.0% Cr_2O_3 additions, β C_2S stabilization takes place only with the simultaneous introduction of a 0.5 % B_2O_3 amount into the sample subject to burning.

The free calcium oxide in all synthesized samples varied between 0.1 and 0.4%. Considering the results obtained by Maslyi [13] by spectroscopic studies, the existence of such reduced amount of free calcium oxide must be explained not only by the solubilization of chromium oxide in the C_2S lattice but also by the chromate formation; likewise, the decomposition effect of β C_2S by chromium oxide with the increasing proportion of addition beyond the solubilization limit may be less important so that chromium oxide in excess may not be detected as chromate or chromite but as unbound chromium oxide. Besides, neither has Maslyi[18] revealed the unbound chromium oxide by roentgenographic approach.

By studying Cr_2O_3 effect on Portland clinker, Butt, Timaşev and Malojon[19] showed that a 0.5 % Cr_2O_3 addition contributes to the formation of a large number of β C_2S polygonal crystals with rounded ends and also to the occurrence of green striated crystals, which is explained by the solubilization of chromium oxide in the calcium orthosilicate lattice. The green colour of βC_2S crystals becomes more intense, refraction indices increase, the crystals size increases and microdensity decreases with the concentration rise.

---

[19] M. BUTT, V. V. TIMAŞEV and L. I. MALOJON, "Processes 9th Conference Silicate Industry" — Budapesta, 1968.

Considering that chromium oxide substitutes more likely Si^{4+} ion in the β C_2S lattice, the formed solid solutions may be described by formula[14]:

$$Ca_2[Cr^{3+}_x . Si_{1-x}]O_{4-\frac{x}{2}} .$$

2.4. β $2CaO.SiO_2-Co_2O_3$ SOLID SOLUTIONS

In case of introducing cobalt oxides into the lattice of dicalcium silicate, Maslîi[18] claims that an isomorphic substitution of Ca^{2+} by Co^{2+} is possible ($r_i = 0.72$ Å). The same author shows that additions over 1.1% Co_2O_3 produce no longer colour intensification.

Hornain[17] suggests that Co^{2+} ion may substitute in β C_2S lattice both Si^{4+} and Ca^{2+} ions but that Ca^{2+} substitution is easier, considering the ionic ray, the valence and the polarization power.

According to Dietzel and Tscheischwili's hypothesis,[13] keeping into account the sizes of Co^{2+} ions ($r_i = 0.72$ Å), Co^{3+} ($r_i = 0.63$ Å) (table 1) the cobalt oxide fails to stabilize β $2CaO.SiO_2$ crystallochemically.

Results obtained by our own previous investigations[14] have shown that β C_2S stability by 0.4% and 0.6% Co_3O_4 addition may be explained by its possible physical action, similar to that remarked in the case of molybdenum and zirconium oxides. A fact supporting this assumption is that β C_2S stabilization with Co_3O_4 is found only when cobalt oxides addition exceeds the solubilization limit in dicalcium silicate, therefore only when a part of the cobalt oxide is included in the dicalcium silicate lattice.

Microphotographs of thin sections of stabilized β C_2S evidence a growth of round, striated calcium orthosilicate twin crystals, proportional with the content in cobalt oxides and also a textural improvement.

For solid solutions of β $2CaO.SiO_2$, the following formula may be written[14] : $(Ca_{2-x}.Co_x)(Si_{1-x}.Co_x)O_{4-z}$, in which : $z = x(3-n)$ n being the valence of metallic cation and $0 \leqslant x \leqslant 0.06$.

2.5. β C_2S-NiO SOLID SOLUTIONS

Some researchers, among whom also Maslyi[18], show that in the synthesis of $2CaO.SiO_2$ with NiO in percentages over 2.4%, a part of NiO remains in a free state, unbound, a fact revealed by intense lines at 2.080 and 2.394 which have a small intensity in the case of 0.3...2.4 % NiO percentages, the diffractogram being not different from that of pure calcium orthosilicate.

Hornain[17] suggests that Ni^{2+} belongs to ions introduced less readily into the calcium orthosilicate lattice, Ni^{2+} ions with a significant ray and reduced polarization power replace Ca^{2+}.

Our own investigations[14] have evidenced that nickel oxide below 1.2% fails to stabilize β $-2CaO.SiO_2$; however, a partial β $-2CaO.SiO_2$ stabilization occurs with 1.2% NiO ; diffractometric analyses evidence, aside from characteristic β $CaO.SiO_2$ lines (at $d = 2.781$ Å, $d = 2.61$ Å, $d = 2.19$ Å), also characteristic lines of the γ $-2CaO.SiO_2$ form (at $d = 2.01$ Å and $d = 1.91$ Å) (table 1).

The same diffractogram also reflects the small intensity line of nickel oxide at $d = 2.08$ Å.

When 0.6% NiO and 1.2% NiO are introduced together with boric anhydride, we obtain β $2CaO.SiO_2$ stable form (characteristic lines at $d = 2.78$ Å; 2.73 Å; 2.60 Å and 2.19 Å).

Microphotographies indicate a homogeneous β C_2S texture, the appearance of evenly distributed crystals having a polygonal shape, small sizes and also larger striated, polysynthetic twin crystals (100μ m) and having a green colour in parallel light and yellowish-red with crossed nicols.

According to data reported by various authors [13-19] and according to our own data,[14] solid solutions of nickel oxide with calcium orthosilicate may be described by the general formula:

$$(Ca_{2-x}.Ni_x)SiO_4$$

2.6. β C_2S–CuO SOLID SOLUTIONS

In his paper, Hornain[17] shows that copper oxide forms less readily solid solutions with calcium orthosilicate. The introduction of Cu^{2+} ions into its lattice is more difficult since, having a relatively large ray and small polarization power, they may possibly replace Ca^{2+}.

Our own investigations[14] have revealed that copper oxide as well as other oxides of transitional elements fail to stabilize β $2CaO.SiO_2$. Only adding it to 0.5 % B_2O_3 it is possible to obtain the stabilization of β $2CaO.SiO_2$ form (table 1 characteristic lines of β C_2S at $d = 2.78$Å; $d = 2.73$ Å; $d = 2.61$ Å and $d = 2.19$ Å). Microphotographs of stabilized β $2CaO.SiO_2$ sample indicate large β C_2S crystals which are polygonal, striated, polysynthetic, having a faint grey colour (in natural light) and yellowish-orange (in polarized light).

The formula of the solid solution formed by β $-2CaO.SiO_2$ with CuO may be written as follows:[14]

$$Ca_{2-x}.Cu_x.SiO_4.$$

Revue Roumaine de Chimie, **21**, 7, 1023–1030 (1976)

THERMAL EQUILIBRIA IN THE BINARY SYSTEMS $MgO-CeO_2$, $CaO-CeO_2$, $SrO-CeO_2$, $BaO-CeO_2$

MARIA PREDA and RADU DINESCU
Polytechnical Institute, Bucharest, Polizu 1

Received July 5, 1974

Phase thermal equilibrium relations have been studied in the binary systems $MgO-CeO_2$, $CaO-CeO_2$, $SrO-CeO_2$ and $BaO-CeO_2$. It has been established that the binary $MgO-CeO_2$ is a simple system without a defined chemical compound. $CaO-CeO_2$ system presents calcium metacerate, a solid phase incongruent compound. The existence of strontium and barium metacerate, respectively, is confirmed in the systems $SrO-CeO_2$ and $BaO-CeO_2$, being compounds with congruent melting in the presence of the liquid phase.

1. INTRODUCTION

Ceramic masses obtained from ceric oxide are of interest for the present technology due to their high refractarity. They also present a particular stability to molten metals and for this reason they are used for obtaining high-purity metals.

The ceric oxide presents a fluorite-type cubic structure, which explains its high melting temperature assumed to be 2725[1-2], 2750[3-5] or 2810°.[6-7]

The $MgO-CeO_2$ binary system was partially studied and the liquidus curve[8] as well as the presence of solid solutions of magnesium oxide in ceric oxide were established.[9-11]

[1] E. G. Ivanov and A. F. Filipov, *Ogneupory*, **1966**, 27.

[2] G. V. Samsonov, G. A. Yasinscaya and E. F. Lapteva, *Ogneupory*, **1961**, 41.

[3] F. A. Acopov and D. N. Poluboyarinov, *Ogneupory*, **1965**, 37.

[4] P. P. Budnicov, "Novaia Keramika", Izdatelstvo literatury po stroitelstvu, Moscow, 1969, p. 187.

[5] A. M. Cherepanov and A. G. Trestviatski, "Vysokoogneupornye materialy i ijhdelia ijh okislov", Izdatelstvo Metallurgia, Moscow, 1964, p. 357.

[6] A. M. Anthony Barbier, *Ind. Ceram.*, **1961**, 298.

[7] A. T. Green and G. N. Stewart, "Ceramics", A Symposion, London, 1953, referred to in the paper 5.

[8] H. Wartenberg, *Z. anorg. Chem.*, **207**, 1 (1932).

[9] V. N. Strecalovski, "Trudy Instituta Electrokhimii" EFAN, vol. 3, 1959, p. 165, referred to in the paper[10].

[10] P. P. Budnicov, Redactor, "Silicaty i okisly v khimii vysokikh temperatur", Academia Nauk S.S.S.R., Institut khimia Silicatov imeni I. V. Grebeschicova, Moscow, 1963, p. 215.

[11] A. Cocco and L. Podda, *Ann. Chim.* (*Ital*), **59**, 488 (1969).

The liquidus curve of the $CaO-CeO_2$ binary system was determined by Wartenberg[12] and calcium oxide solid solutions were also identified in ceric oxide[10-11,13-14].

Two defined chemical compounds were found in the $SrO-CeO_2$ binary system; strontium metacerate[10-11,15-17] and strontium orthocerate[18] as well as the existence of strontium oxide solid solutions in ceric oxide.[10,11,13,17,19]

The $BaO-CeO_2$ binary system was studied by Guha and Kolar[20]. One single defined chemical compound was reported in this system, namely $BaO.CeO_2$.[15,20-21]

Since data referring to these systems are scarce and unsystematic, we initiated a more detailed study of these systems.

2. WORKING PROCEDURE

Synthesis of samples. The raw materials used for experimental determinations were chemically pure ceric oxide, magnesium carbonate, calcium carbonate, strontium carbonate and barium carbonate. The homogeneity of the prepared masses was achieved through a wet procedure in a ball mill for 1 h. Samples underwent a thermal treatment at temperatures ranging between 1200–1600°.

Phase and structural analysis. The crystalline phases in samples were roentgenographically-identified by the Debye-Scherrer method with CuK_α radiation using a TUR-60 apparatus. The debyegrams were analytically indexed by the Hesse and Nilson method[22-25] in view of investigating the structure of the initial products and of the reaction products as well. The amount of alkaline-earth oxides solubilized in ceric oxide or in metacerate was determined by measuring the variation in the parameter of the elemental cell of ceric oxide and of metacerates, respectively.

Determination of liquidus temperatures. It was performed by melting in an argon plasma jet. The temperature was measured by an optical pyrometer with the disappearance of the filament. The determined melting temperature represents an average of 15 samples, with deviations of temperature values of maximum ± 50°.

---

[12] H. Wartenberg and E. Prophet, *Z. anorg. Chem.*, **208**, 369 (1932).

[13] L. S. Zueva, N. A. Godina and E. K. Keler, *Ogneupory*, **1960**, 368.

[14] A. D. Nenimin and S. F. Palguev, "Tr. Inst. Electrohim. Acad. Nauk S.S.S.R. Uralsk Filial", vol. 3, 1962, p. 141.

[15] R. S. Roth. *Res. Nat. Bur. Stand*, **58**, 75 (1957) referred to in the paper 16.

[16] N. A. Toropov, V. P. Barjhzacovski, V. V. Lapin and N. N. Curseva, "Diagramy sostoyania silicatnykh sistem", Izdatelstvo Nauka, Leningrad, 1965, p. 320.

[17] E. K. Keler and N. A. Godina, *Zhur. neorg. Khim.*, **2**, 210 (1957).

[18] M. Danelon, I. Barbirol and A. Cocco, *Ann. Chim.* (*Ital.*), **59**, 465 (1969), refered to in the paper 11.

[19] E. K. Keler, *Zhur. neorg. Khim.*, **1**, 2556 (1956).

[20] J. Guha and D. Kolar, *Mat. Sci.*, **6**, 1174 (1971)

[21] A. J. Smith and A. Welch, *Acta Cryst.*, **13**, 653 (1960).

[22] N. F. M. Henry, H. Lipson and W. A. Wooster, "The Interpretation of X-ray Diffraction Photographs", St. Martin Press, New York, 1960, p. 177.

[23] A. Guinier, "Théorie et technique de la radiocristallographie", Dunod, Paris, 1956, p. 215.

[24] L. Azaroff and M. Buerger, "The Powder Method in X-ray Crystallography", McGraw Hill Book Company, New York, 1958, p. 56.

[25] L. I. Mirkin, "Spravochinik po roentgenomustructurnomu analizu polikristalov", Gosudarstvenoe Izdatelstvo Fiziko-Matematicheskoi Literatury, Moscow, 1961, p. 223.

3. EXPERIMENTAL RESULTS

Ceric oxide. Ceric oxide has been proved to crystallize in a fluorite-type cubic system having the parameter of the elemental cell $a = 5.420$ Å. The melting temperature of the ceric oxide was found to be 2750° in agreement with data from the literature [3-5]. Ceric oxide molten in plasma presents a structural type which is similar to the initial one, yet the parameter of the elemental cell changes from 5.420 Å to 5.304 Å. It may be considered that ceric oxide loses a certain amount of oxygen at high temperatures, leading to the reduction of tetravalent cerium to trivalent cerium

$$2Ce^{4+} + 2e \rightarrow 2Ce^{3+}$$

Since the structural type of the partially reduced ceric oxide remains the same as in the case of the non-reduced one, we have considered that Ce^{3+} ions are statistically distributed in the ceric oxide system. A quantitative evaluation of the cerium trioxide formed during the melting process in plasma may be made starting from the reduction of the parameter of the ceric oxide elemental cell. Keeping into account that cerium trioxide presents a hexagonal structure with the parameters of the elemental cell $a = 3.89$ Å and $c = 6.07$ Å, we started from the premise that parameter $a = 5.304$ Å of ceric oxide molten in plasma may be interpolated between the value $a = 5.420$ Å of the initial ceric oxide and $a = 3.89$ Å of cerium trioxide. The presence of 8% Ce_2O_3 is thus deduced in the system of ceric oxide molten in plasma.

The ATD curve of pure ceric oxide presents no thermal effect which shows that it fails to hydrate and presents no polymorphic changes, a fact which was also confirmed by its dilatogram within 20–900° (fig. 1).

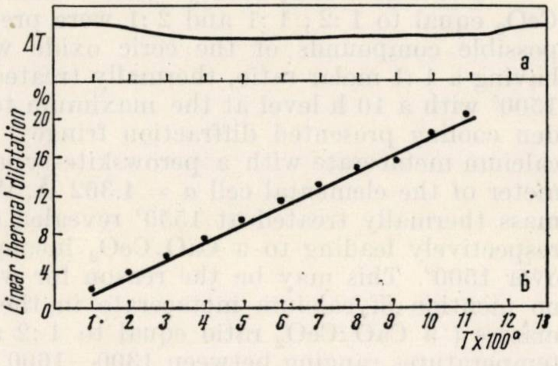

Fig. 1.—a. Differential thermal analysis curve of pure ceric oxide. b. Liniar thermal dilatation of ceric oxide.

The MgO—CeO₂ binary system. The possible existence of binary compounds with molar ratios MgO :CeO_2 equal to 1 :1 ; 1 :2 and 2 :1 was studied. The masses corresponding to these compositions, thermally treated at temperature ranging between 1200–1600° and rapidly cooled thereafter presented in DS diagrams only the diffraction lines characteristic of ceric and magnesium oxide, respectively, which shows that neither the compounds suggested nor others will form under these conditions.

The existence of magnesium oxide solid solutions was revealed in ceric oxide by measuring the variation in the parameter of the elemental cell of ceric oxide. This was found to vary from 5.42 Å for ceric oxide to 5.32 Å for the solid solution at a temperature of 2100°. By interpolation we deduce the solubilization of 8% molar MgO in the ceric oxide.

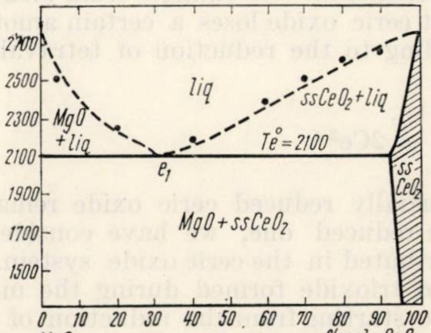

Fig. 2. — Phase thermal equilibrium diagram of the $MgO - CeO_2$ binary system.

The experimentally determined liquidus curve of the $MgO-CeO_2$ system is similar to that given by Wartenberg[8]. The existence of a binary eutectic e_1 with a composition of 70% mol MgO and 30% mol CeO_2 and the melting temperature of 2100° have been identified.

The phase thermal equilibrium diagram is presented in fig. 2.

The $CaO-CeO_2$ binary system. Masses having a molar ratio CaO : CeO_2 equal to 1 :2 ; 1 :1 and 2 :1 were prepared in order to reveal some possible compounds of the ceric oxide with calcium oxide. The mass having a 1 :1 molar ratio, thermally treated at temperatures of 1400 and 1500° with a 10 h level at the maximum temperature followed by a sudden cooling presented diffraction fringes, showing only the presence of calcium metacerate with a perowskite-type cubic structure and the parameter of the elemental cell $a = 4.302$ Å. A sample taken from the same mass thermally treated at 1550° revealed ceric oxide and calcium oxide respectively leading to a $CaO . CeO_2$ incongruence in a temperature area over 1500°. This may be the reason for which Cocco and Podda[11] made no mention of calcium metacerate in their work. As to the other two masses (a CaO :CeO_2 ratio equal to 1 :2 and 2 :1) thermally treated at temperatures ranging between 1300—1600°, only calcium metacerate and the initial components were found.

DS diagrams illustrate that the parameter of the elemental cell of CeO_2 changes from 5.42 for ceric oxide, to 5.35 Å for the limiting solid solution with calcium oxide at an eutectic temperature of 1800° in the $CaO-CeO_2$ binary system. It results that 15% mol CaO is solubilized in ceric oxide a fact which supports the existing data [11,13-14].

The shape of the liquidus curve is similar to that given by Wartenberg[12]. The binary eutectic e_2 has a melting temperature of 1800° and a composition of CaO 53% mol and CeO_2 47% mol.

An inspection of the thermal equilibrium diagram shows that the system appears as a binary system without defined compounds, in the subsolidus domain between the eutectic temperature of 1800° and the solid phase incongruence temperature of calcium metacerate. Below the incongruence temperature of calcium metacerate, it is divided into two subsystems

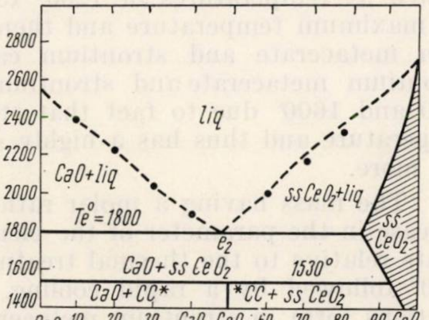

Fig. 3. – Phase thermal equilibrium diagram of the CaO – CeO_2 binary system.

$$\text{I. } CaO - CaO.CeO_2$$

and

$$\text{II. } CaO.CeO_2 - CeO_2$$

The SrO–CeO_2 binary system. Masses were synthesized having molar ratios SrO :CeO_2 equal to 1 :1 ; 2 :1 and 1 :2. Theoretical data report the existence of two crystalline forms of strontium metacerate : a perowskite-type cubic form with the parameter of the elemental cell $a = 4.29$ Å[25] and a rhombic one with the parameters of the elemental cell $a = 5.986$ Å, $b = 8.531$ Å and $c = 6.125$ Å[15]. The results of syntheses conducted on a mass having the composition of strontium metacerate led to new conclusions, as follows : this mass, thermally treated at 1250, 1300, 1400 and 1500° for 6 h, followed by a sudden cooling presented in all the cases a perowskite-type cubic system with the parameter of the elemental cell $a = 4.236$ Å. By subjecting the same mass to a thermal treatment at the above mentioned temperatures and then to a slow cooling process it presented in all the cases a tetragonal system with the parameters of the elemental cell $a = 4.29$ Å and $c = 3.50$ Å. The fact was thus revealed that strontium metacerate presents two polymorphic changes : a high-temperature stable form having a perowskite-type cubic structure and a low-temperature one having a tetragonal structure. This fact may be correlated to the change of perowskite-type structures. Hence, it results that the cubic type of the crystalline system reported in the literature is the high-temperature form. Determinations of the melting point of strontium metacerate showed a congruent melting process at 1900°.

The mass having a molar ratio SrO :CeO_2 equal to 1 :2, thermally treated at temperatures of 1250, 1300, 1400 and 1500° and then subjected to a rapid cooling process presented only strontium metacerate, the cubic form, and ceric oxide.

The mass having a molar ratio SrO :CeO_2 equal to 2 :1, thermally treated at temperatures of 1250, 1300 and 1400° with a 10 h level at the maximum temperature and then rapidly cooled presents only strontium metacerate and strontium carbonate, under a hexagonal form. Strontium metacerate and strontium oxide appear at temperatures of 1500 and 1600° due to fact that strontium oxide was burnt at a high temperature and thus has a highly stable structure without carbonating any more.

The mass having a molar ratio SrO : CeO_2 equal to 2 :1 shows an increase in the parameter of the elemental cell of cubic strontium metacerate relative to the thermal treatment temperatures of 1300, 1400 and 1500° followed by a rapid cooling. As a result, strontium oxide solid solutions form in strontium metacerate. The maximum solubility represents 17% mol SrO dissolved in strontium metacerate at an eutectic temperature of 1650°. It has been found that a maximum amount of 14% mol strontium oxide is dissolved in ceric oxide at an eutectic temperature, which is in agreement with data from the literature.[10–11,13,17,19]

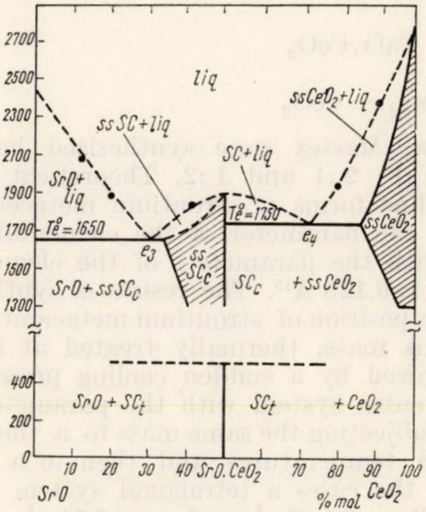

Fig. 4. — Phase thermal equilibrium diagram of the SrO — CeO_2 binary system.

Based on the facts mentioned above, it was possible to trace the phase thermal equilibrium diagram of the binary system SrO—CeO_2 (fig. 4). The presence of strontium metacerate causes the binary system SrO—CeO_2 to be divided into two subsystems :

I. SrO — SrO.CeO_2 subsystem which presents an eutectic e_3 with a melting temperature of 1650° corresponding to a composition of 70% mol SrO and 30% mol CeO_2.

II. $SrO.CeO_2-CeO_2$ subsystem which presents an eutectic e_4 with the melting temperature 1760° corresponding to a composition of SrO 28% mol and CeO_2 72%.

The $BaO-CeO_2$ *binary system.* The mass having a molar ratio BaO : CeO_2 equal to 1 :1, thermally treated at temperatures of 1250, 1350, 1450 and 1550° and rapidly cooled, thereafter, presents in all cases a compound with a perowskite-type cubic structure with the parameter of the elemental cell $a = 4.431$ Å, which confirms the data from the literature[15,20-21]. The same mass, if thermally treated and then slowly cooled, presents a tetragonal structure with the parameters of the elemental cell $a = 4.30$ Å and $c = 3.46$ Å. The existence of two polymorphic changes of barium metacerate was thus revealed : a high-temperature form having a cubic structure, and which has been mentioned in the literature, and a low-temperature form with a tetragonal structure.

Masses having the molar ratios BaO :CeO_2 equal to 1 :2 and 2 :1 comprise only barium metacerate and the free oxides, meaning that other compounds defined in the system are absent.

The mass having a molar ratio BaO : CeO_2 equal to 2 :1 thermally treated at 1300 and 1400° and then rapidly cooled presents a partial solubilization of barium oxide in barium metacerate. The solubility of barium oxide in barium metacerate is 5% mol at an eutectic temperature of 1480°.

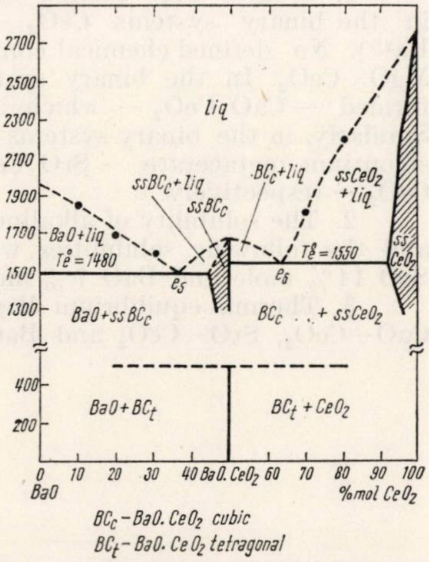

Fig. 5. — Phase thermal equilibrium diagram of the $BaO-CeO_2$ binary system.

Masses of CeO_2 with 5 and 10% BaO, respectively, thermally treated at 1300, 1400 and 1500° and rapidly cooled thereafter present a change in the parameter of the elemental cell from 5.420 Å for pure ceric oxide to 5.427 Å for solid solution. This change corresponds to a limiting solid solution of 7% mol BaO in ceric oxide. Since the difference between the parameters of the elemental cells of ceric oxide and of barium oxide is small, the proportion of solubilized oxide may be determined with a reduced accuracy.

In the thermal equilibrium diagram of the $BaO-CeO_2$ binary system (fig. 5), the presence of barium metacerate divides the phase thermal equilibrium diagram into two subsystems :

I. $BaO-BaO.CeO_2$ subsystem presenting an eutectic e_5 with a melting temperature of 1480° corresponding to a composition of 63% mol BaO and 37% mol CeO_2.

II. $BaO.CeO_2 - CeO_2$ subsystem, presenting an eutectic e_6 with a melting temperature of 1550°, corresponding to a composition of 35% mol BaO and 65% mol CeO_2.

CONCLUSIONS

1. Studies were carried out on compound formation possibilities in the binary systems $CeO_2 - RO$ (where R is Mg^{2+}, Ca^{2+}, Sr^{2+} and Ba^{2+}). No defined chemical compound was found to form in the system $MgO - CeO_2$. In the binary system $CeO_2 - CaO$, calcium metacerate is formed — $CaO.CeO_2$ — which is a solid phase incongruent compound. Similarly, in the binary systems $SrO - CeO_2$ and $BaO - CeO_2$ there exists strontium metacerate — $SrO.CeO_2$ — and barium metacerate — $BaO.CeO_2$ — respectively.

2. The solubility of alkaline-earth oxides in ceric oxide was studied and the following solubilities were found: MgO 8%; CaO 15% mole; SrO 14% mole and BaO 7% mole in ceric oxide.

3. Thermal equilibrium diagrams of the binary systems $MgO - CeO_2$, $CaO - CeO_2$, $SrO - CeO_2$ and $BaO - CeO_2$ were traced.

Revue Roumaine de Chimie, **21**, 7, 1031–1036 (1976)

THE STRUCTURE OF DARK-RED COMPOUND $[Fe(II)phen_2(NCS)_2].H_2O$

MARGARETA TEODORESCU

Laboratory of Inorganic Chemistry of the University of Bucharest,
Str. Splaiul Independenței, 89

Received September 21, 1974

The structure of the mixed ammine $[Fe(II)phen_2(NCS)_2].H_2O$ is studied using different physical methods. It was established that this compound is not the simple hydrate of the paramagnetic $[Fe(II)phen_2(NCS)_2]$ compound, but its diamagnetic isomer.

INTRODUCTION

In the coordination chemistry of Fe(II), the compounds of the type $[Fe(II)\ phen_2X_2]$ are very interesting from the point of view of their magnetic and optical properties.[1–5] If one starts from the dried compound $[Fe(II)\ phen_3]X_2$, heated in the presence of inert solvents, one easily obtains dichelates $[Fe(II)phen_2X_2]$ which are usually paramagnetic at room temperature, when $X=Cl^-$, Br^-, I^-, NCS^-, or diamagnetic at room temperature when $X=CN^-$, CNO^- or NO_2^-. Since 1931, Klemm[6] has obtained compounds of the type $[Fe(II)phen_2X_2]$ where $X = Br^-$ and I^-, dark-red and diamagnetic. Between 1954–1964 the above syntheses have been reproduced, but the final products were paramagnetic dichelates.

A previous work reported the substitution of pyridine by the hydrated phenanthroline in the compound $[Fe(II)py_4(NCS)_2]$, the violet species[7], the final product being a diamagnetic complex[8] of dark-red colour containing the thiocyanate group, corresponding, according to the chemical analysis, to the formula $[Fe(II)phen_2(NCS)_2].H_2O$. Driver and Walker[9] have later tried to prepare the thiocyanate derivative of the binuclear compounds of Iron(II) containing hydroxo bridges, $[phen_2FeOH_2X_4]$, by adding KSCN to a solution of $[phen_2FeOH_2]Cl_4$, from which a dark-red compound $[Fe(II)phen_2(NCS)_2].H_2O$ is obtained, con-

---

[1] W. A. Baker and H. M. Bobonich, *Inorg. Chem.*, **2**, 1071 (1963).

[2] A. T. Casey and F. Isaacs, *Austral. J. Chem.*, **20**, 2765 (1967).

[3] E. König and K. Madeja, *Inorg. Chem.*, **6**, 48 (1967).

[4] R. L. Collins and R. L. Pettit, *J. Chem. Phys.*, **39**, 3433 (1963).

[5] E. König, *Coord. Chem. Rev.*, **3**, 471 (1968).

[6] W. Klemm, H. Jacodi and W. Tilk, *Z. anorg. Chem.*, **201**, 1 (1931).

[7] P. Spacu, M. Teodorescu and C. Lepădatu, *Rev. Roumaine Chim.*, **9**, 1 (1964).

[8] P. Spacu, M. Teodorescu and D, Ciomârtan, *Rev. Roumaine Chim.*, **12**, 145 (1967).

[9] R. Driver and W. R. Walker, *J. Austral. Chem,*, **20**, 1376 (1967).

sidered as a pentacoordinated Iron(II) compound. This complex loses the water molecule and passes into a violet paramagnetic compound.

It should be therefore interesting to elucidate the structure of the dark-red diamagnetic species which were obtained by us and by Driver and Walker, and to see the structural differences existing between the diamagnetic $[Fe(II)phen_2(NCS)_2].H_2O$ and the violet paramagnetic $[Fe(II)phen_2(NCS)_2]$ species.

EXPERIMENTAL

The synthesis of the dark-red compound $[Fe(II)phen_2\ (NCS)].H_2O$ has been made according to the method previously reported[8] the chemical analysis calc. for $[Fe(II)phen_2(NCS)_2].H_2O$ gives: C, 56.70; H, 3.30; N, 15.30; Fe, 10.10. Found: C, 56.20; H, 3.80; N, 15.26; Fe, 10.19.

The IR spectra were determined on the solid state using a UR 10 C. Zeiss Jena spectrophotometer and KBr pellets.

The magnetic moment was measured by means of Faraday method, according to the formula $\mu = 2.8(\chi_m' \cdot T)^{1/2}$ where $\chi_m' = \chi_m - \chi_{dia}$.

The electronic spectra were recorded on the solid state using a Zeiss VSU_1 spectrophotometer equipped with a reflectance device 0/*r* and using MgO as a standard. For measurements in the IR range the Cs photocell has been used. The diffraction spectra of powders have been obtained with a diffractometer HZG 1 joined to TUR-M-61 equipment, using the radiation = 1.93597 Å of $FeK\alpha_1$ passed through a Mn-filter. The Moessbauer spectra were obtained by means of a spectrometer with a linear velocity, using a Co^{57} source deposit on Cu.

RESULTS AND DISCUSSIONS

To elucidate the structural changes between the two species, dark-red and violet, of the complex $[Fe(II)phen_2(NCS)_2]$, we have used different physical methods, as described below.

IR SPECTRA

The IR spectra for $[Fe(II)phen_2(NCS)_2].H_2O$ and $[Fe(II)phen_2(NCS)_2]$ were recorded under the same conditions, the same concentrations in the KBr pellets. They are presented in fig. 1.

The following conclusions may be drawn from the IR spectra:

— the absorption maxima at 475.808 and 2060 cm^{-1} show the existence of the coordinated thocyanate group, the chemical bonding being made via nitrogen atom. The first two absorption maxima have the same positions, both in hydrated and unhydrated $[Fe(II)phen_2(NCS)_2]$ compounds. The stretching frequence ν_{C-N} in the dark-red species is shifted toward lower wavenumbers compared with that in the violet compound (but it assumes a higher value than that in $[Fe(II)phen_3](NCS)_2$). This shift shows a lowering in the strength of C—N chemical bond, and hence an increasing in the covalency degree of the Fe-NCS. bond. The position of this band excludes the formulation of the dark-red species as a polymer.

— referring to the absorption maxima characteristic of the phenanthroline, it may be seen that in $[Fe(II)phen_2(NCS)_2].H_2O$ two absorption maxima occur at 535 and 560 cm^{-1} (ν_{CCC}). The band at 640 cm^{-1} intense in the high-spin complex [Fe(II)phen$_2$(NCS)$_2$] becomes a very weak absorption band in the dark-red compound as in the trichelate [Fe(II)phen$_3$](NCS)$_2$. The intense absorption band at 850 cm^{-1} has no more the shoulder at 870 cm^{-1}. The maximum at 1505 cm^{-1}, assigned to the vibration frequence ν_{C-C}, which is intense in the high-spin complex [Fe(II)phen$_2$(NCS)$_2$], has in the hydrated compound a medium intensity, as in the trichelate [Fe(II)phen$_3$](NCS)$_2$. The absorption maxima of medium intensity at 1600 cm^{-1}, of the characteristic triplet of the phenanthroline, change their position and intensity, the change being similar to those observed by König[10] for the IR spectrum of [Fe(II)phen$_2$(NCS)$_2$] measured at 232 K (Fe(II) ground state $^5T_2$) and at 105 K (ground state $^1A_1$). The IR spectrum of [Fe(II)phen$_2$(NCS)$_2$].H$_2$O recorded at room temperature is similar with that determined by König for [Fe(II)phen$_2$(NCS)$_2$] at 105 K.

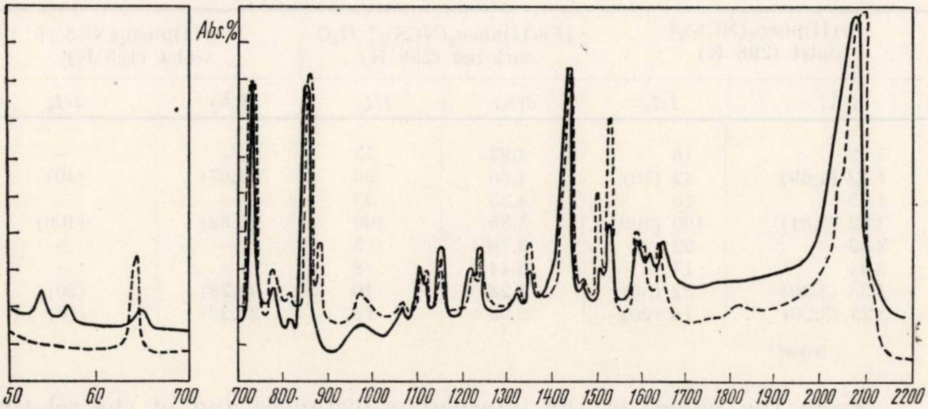

Fig. 1. — Infrared spectra at room temperature of :
——— [Fe(II)phen$_2$(NCS)$_2$].H$_2$O (dark-red) and
– – – [Fe(II)phen$_2$(NCS)$_2$[(violet).

MAGNETIC MEASUREMENTS

The dark-red compound [Fe(II)phen$_2$(NCS)$_2$].H$_2$O presents at room temperature a weak paramagnetism corresponding to ~ 0.60 BM, similar to the low-spin compounds of the type Fe(II)(AA)$_2$.X$_2$, where AA — phenanthroline or dipyridil and X=CN$^-$, NO$_2^-$, CNO$^-$, the weak paramagnetism being most likely due to a TIP contribution.

X-RAY SPECTRA

The powder Debyegrams of the two compounds [Fe(II)phen$_2$(NCS)$_2$].H$_2$O (dark-red) and [Fe(II)phen$_2$(NCS)$_2$] (violet) have been determined under the same conditions. The interplanar distances (*d*) and the relative intensities (I/I_0) are given in table 1.

---

[10] E. König and K. Madeja, *Spectrochim. Acta*, **23**, 45 (1967).

Table 1

X-ray data at room temperature

$[Fe(II)phen_2(NCS)_2]$ violet (298 K)		$[Fe(II)phen_2(NCS)_2] \cdot H_2O$ dark-red (298 K)		$[Fe(II)phen_2(NCS)_2]$ violet (158 K)	
d(Å)	I/I_0	*d*(Å)	I/I_0	*d*(Å)	I/I_0
5.09	16	4.92	13	—	—
4.72 (4.69)	42 (50)	4.66	50	(4.67)	(40)
4.05	10	4.25	33	—	—
3.82 (3.81)	100 (100)	3.85	100	(3.82)	(100)
3.62	22	3.70	5	—	—
3.44	17	3.44	8	—	—
3.33 (3.30)	32 (30)	3.28	10	(3.28)	(20)
3.23 (3.20)	16 (20)	3.08	16	(3.20)	(10)

( ) Baker[11]

From the values of the interplanar distances and of the relative intensities, one may observe that there are no striking differences between the two complexes, except for the broadening of the diffraction lines which may be caused by the presence of the interstitial water molecules. The X-ray data for $[Fe(II)phen_2(NCS)_2] \cdot H_2O$ (at room temperature) are very similar to those obtained by Baker,[11] for violet $[Fe(II)phen_2(NCS)_2]$ at 158 K, when the low-spin state is stable.

ELECTRONIC SPECTRUM

The reflectance spectrum of the complex $[Fe(II)phen_2(NCS)_2] \cdot H_2O$ has been recorded in the UN, visible and near infrared range. The electronic spectrum is similar to those of the diamagnetic compounds[11] $[Fe(II)phen_2X_2]$, having in the near IR range a weak absorption band assigned to the spin forbidden transition $^1A_1 \to {}^3T_1$, the spin allowed *d*–*d* transition being masked by the intense charge transfer bands occuring in the visible range. The absorption maxima and their assignments (according to their relative intensities) for the compound $[Fe(II)phen_2(NCS)_2] \cdot H_2O$ are given in table 2.

Table 2

The experimental absorption maxima

Maxima		Band assignments
λ(mμ)	$\bar{\nu}$(cm^{-1})	
960	10400	$^1A_1 \to {}^3T_1$
530	18860	
450	22200	$\pi^2 t_2^6 \to \pi^2 t_2^5 \pi^{**}$

---

[11] W. A. Baker and H. M. Bobonich, *Inorg. Chem.*, **3**, 1184 (1964).

The assignments made according to the relative intensity may be theoretically checked, using the rule of average environment[12] for the low-spin complex $[Fe(II)phen_2(NCS)_2]$:

$$\Delta^{l.s.}_{av.}[Fe(II)phen_2(NCS)_2] = 2/3\,\Delta^{l.s.}_{phen} + 1/3\,\Delta^{l.s.}_{NCS} =$$

$$= 2/3(18{,}000) + 1/3\,(12{,}900) = 16{,}300\ \text{cm}^{-1}$$

For the low-spin Fe(II) ion, the values of the frequencies corresponding to the spin forbidden and spin-allowed transitions are estimated according to the following expressions[13].

$$^1A_{1g} \rightarrow {}^1T_{1g} \qquad \nu_1 = \Delta - C + 86\,B^2/\Delta$$

$$^1A_{1g} \rightarrow {}^1T_{2g} \qquad \nu_2 = \Delta + 16B - C + 2\,B^2/\Delta$$

$$^1A_{1g} \rightarrow {}^3T_{1g} \qquad \nu_3 = \Delta - 3C + 50\,B^2/\Delta$$

$$^1A_{1g} \rightarrow {}^3T_{2g} \qquad \nu_4 = \Delta + 8B - 3C + 14B^2/\Delta$$

For $B = 580$ cm^{-1}, $C \approx 4B$ and $B^2/\Delta = 20$ cm^{-1}, the calculated transitions are collected in table 3.

If we compare the experimental values (table 2) with those theoretically estimated (table 3), one may observe that the assignments are correct. The important conclusion drawn from the electronic spectra is that Fe(II) ion in the compound $[Fe(II)\,phen_2(NCS)_2]\cdot H_2O$ is hexacoordinated, with the ground state $^1A_1$.

MOESSBAUER SPECTRA

The Moessbauer parameters were determined at room temperature for $[Fe(II)phen_2(NCS)_2]\cdot H_2O$ (table 4).

Table 4 shows comparatively the Moessbauer parameters determined under the same experimental conditions for the other two low-spin Fe(II) hexacoordinate compounds. The values assumed by the isomer shift (δ) and by the quadrupole splitting (ΔE_Q) show that the dark-red compound $[Fe(II)\,phen_2(NCS)_2]\cdot H_2O$ has the ground state $^1A_1$. The covalency degree of Fe-N bonds is fairly noticeable, close to that of the octahedral complex $[Fe(II)phen_3](NCS)_2$, the molecular asymmetry for the ground state being close to that found for the low-spin $[Fe(II)\,phen_2(NCS)_2]$.

Table 3

The theoretical absorption maxima

Transition	$\overline{\nu}$ calculated (cm^{-1})
$^1A_1 \rightarrow {}^3T_1$	10340
$^1A_1 \rightarrow {}^3T_2$	14260
$^1A_1 \rightarrow {}^1T_1$	15700
$^1A_1 \rightarrow {}^1T_2$	23300

---

[12] C. K. Jörgensen, "Absorption Spectra and Chemical Bonding in Complexes", Pergamon Press, Oxford, 1962.

[13] A. B. Lever, "Inorganic Electronic Spectroscopy", Elsevier Amsterdam, 1968,

One may therefore conclude that the physical methods used to elucidate the structure of the dark-red $[Fe(II)phen_2(NCS)_2].H_2O$ compound give the following results:

i) the new Fe(II) compound is not pentacoordinated, but hexacoordinated, having the ground state ${}^1A_1$.

Table 4

Moessbauer effect measurements

Compound	T K	δ (mm/sec)	ΔE_Q (mm/sec)
$[Fe(II)phen_2(NCS)_2]. H_2O$ (dark-red)	298	0.08	0.32
$[Fe(II)phen_3](NCS)_2$	298	0.07	0.16
$[Fe(II)phen_2(NCS)_2]$ violet (${}^1A_1$)	T_N	0.40 (0.37)*	0.32 (0.34)*

* König[5]

ii) the dark-red compound is not a simple hydrated species of the violet form $[Fe(II)phen_2(NCS)_2]$, striking differences being observed with the electron distribution on the antibonding MO's, E_g^* and T_{2g}^*, having in view that $[Fe(II)phen_2(NCS)_2].H_2O$ is low-spin at room temperature.

iii) one may state that the two Fe(II) compounds are magnetical isomers, the coupling of the electrons being probably produced in this critical case when $\Delta \approx \pi$, by the existence of water molecules which may lead to small changes in the crystal packing. There are similar magnetic isomers reported[14,15] for Ni(II) complexes, which occur as a consequence of the presence of water molecules in the crystal.

---

[14] G. A. Mellson and D. H. Buch, *J. Amer. Chem. Soc.*, **86**, 4830 (1964).

[15] D.M.L. Goodgame and M. L. Venanzi, *J. Chem. Soc.*, **1963**, 1125.

Revue Roumaine de Chimie, **21**, 7, 1037–1043 (1976)

ELECTRONIC SPECTRA OF CO^{III} THIAZOLIDINE CHELATES

ELENA CATRINA*, Z. SIMON**, Z. SZABADAY*** and GH. CATRINA*

* Agricultural Institute, Department of Chemistry, Spl. T. Vladimirescu 14-a, Timişoara, Romania

** University of Timişoara, Department of Chemistry, Bd. V. Pârvan 4, Timişoara, Romania

*** Chemical Research Center, Bd. Mihai Viteazu 24, Timişoara, Romania

Received November 6, 1973
Completed November 18, 1975

The electronic spectra of Co^{III}-L$_3$-chelates with 2-methyl-2,2′-dimethyl-, 2,2′, 5,5′ tetramethyl-, and 2-phenyl-thiazolidine-4-carboxylic acid, respectively, are recorded. The transition frequencies are calculated with the monoelectronic approximations with the *d*-orbitals split by the crystal field potential of the three O and N atoms arranged according to a C_{3v} or C_{2v} symmetry. The C_{3v}-symmetry calculations predict only two transitions, while for C_{2v}-ligand symmetry all four observed transitions are predicted, as well as the approximative relation $\nu_1 + \nu_4 \cong \nu_2 + \nu_3$ between the frequencies of the successive transitions.

The chelates of trivalent cobalt with thiazolidine-4-carboxylic acid contain, according to the elemental analysis data, three bidentated ligands in their coordination spheres,[1] but one has to discern between two possible structures for this coordination sphere, either of C_{3v} or C_{2v} symmetry (fig. 1, formulae II and III). These substances present well-defined elec-

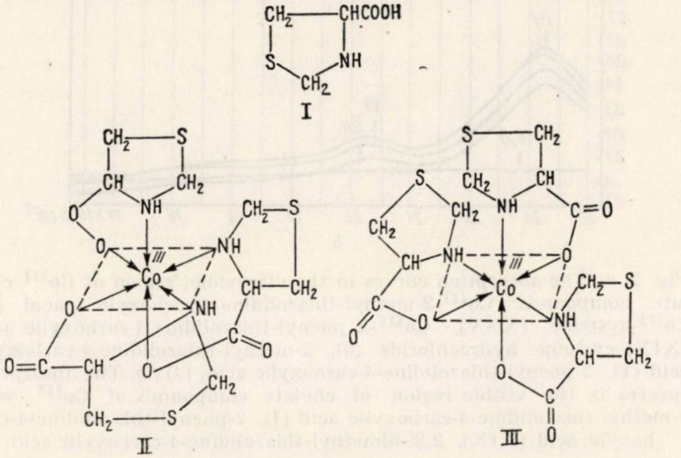

Fig. 1. — Structural formulae for thiazolidine-4-carboxylic acid (I) and the two possible isomers of its Co^{III}-chelate, C_{3v} symmetry (II) and C_{2v} symmetry (III).

---

[1] E. Catrina, Z. Simon and G. Catrina, *Rev. Roum. Chim.*, **20**, 65 (1975).

tronic spectra in the visible and near ultraviolet region, whose interpretation may allow one to make distinctions between the two possible structures.

ELECTRONIC SPECTRA AND MAGNETIC PROPERTIES

The electronic absorption spectra (water solution $\sim 10^{-4}$ M concentration) were recorded on a SPECORD U.V. and VIS spectrophotometer. The recorded spectra are given in fig. 2 *a* and *b* for the 50.000 – 28.000 cm^{-1} and 30.000 – 12.000 cm^{-1} regions, respectively. A peak in the ultraviolet region at 35.600 cm^{-1} and three in the visible at 28.500 cm^{-1}, 22.600 cm^{-1} and 18.450 cm^{-1} are observed for both compounds,

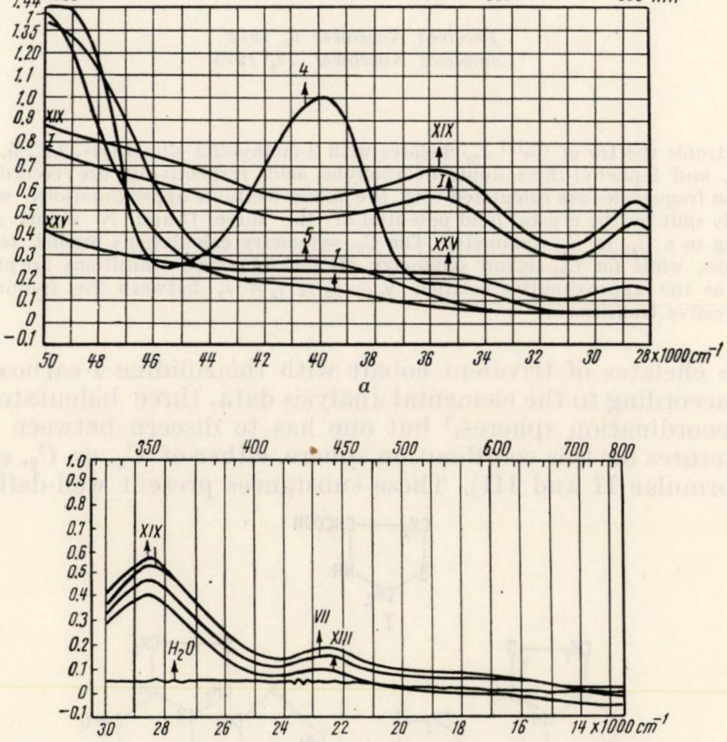

Fig. 2. *a*, The absorption curves in the ultraviolet region of Co^{III} chelate compounds. Co^{III}-2-methyl-thiazolidine-4-carboxylic acid (I), Co^{III}-cysteine (XXV), Co^{III}-2 phenyl-thiazolidine-4-carboxylic acid (XIX) cysteine hydrochloride (5), 2-methyl-thiazolidine-4-carboxylic acid (1), 2 phenyl-thiazolidine-4-carboxylic acid. (4) ; *b*, The absorption spectra in the visible region of chelate compounds of Co^{III} with 2-methyl-thiazolidine-4-carboxylic acid (I), 2-phenyl-thiazolidine-4-carboxylic acid (XIX), 2,2′-dimethyl-thiazolidine-4-carboxylic acid.

with maximal extinction coefficients (ε cm^{-1} l^{-1}) of 3.5×10^3; 1.3×10^4; 1.3×10^4 and 1.6×10^4, respectively. Thus, probably all absorption bands correspond to the same type, $d - d^*$ transitions. The magnetic moment of a solid sample of Co^{III}-thiazolidine-4-carboxylic acid chelate was measured at 20 − 25°, with a Guy-balance. With a diamagnetic correction of $+ 330 \cdot 10^{-6}$, a figure of $\mu = 3.97 \pm 0.005$ MB was obtained for this compound.[2]

SPLITTING OF *d*-ORBITALS. CRYSTAL FIELD POTENTIAL CALCULATIONS

The existence of four, instead of two, *dd**-transitions, was well as the paramagnetic character demonstrate a sensibly different splitting of the central ion "*d*"-orbitals, as compared to the stable hexacoordinated Co^{III}-complexes of octahedral (Oh) symmetry. The splitting of *d*-orbitals in crystal field potentials of C_{2v} and C_{3v} symmetry is given in figs. 3 and 4, respectively, while the coordination between the pertinent T_{2g} and E_g representations of the Oh group with these of C_{3v} and C_{2v} groups are listed in table 1 according to the rules of the group theory.[3,4]

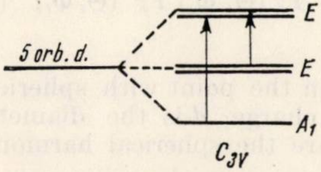

Fig. 3. — Splitting of "*d*" orbitals in a crystalline field of C_{3v} symmetry.

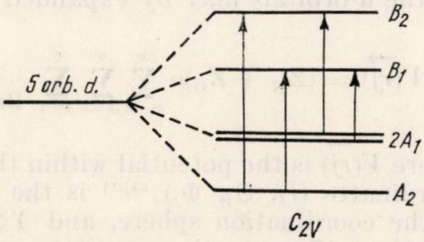

Fig. 4. — Splitting of "*d*" orbitals in a crystalline field of C_{2v} symmetry.

Table 1

The correlations of the T_{2g} and E_g Oh group representations with those of C_{3v} and C_{2v} groups

Oh	C_{3v}	C_{2v}
T_{2g}	$A_1 + E$	$A_1 + B_1 + B_2$
E_g	E	$A_1 + A_2$
	$A_1 + 2E$	$2A_1 + A_2 + B_1 + B_2$

---

[2] V. Mincu, unpublished results.

[3] I. B. Bersucher and A. B. Ablov "Khimicheskaya sviaz v. komplexnikh soedinenii", Kishinev Izdat. Ştiinţa, 1959, annex I.

[4] T. M. Dunn "The Visible and Ultraviolet Spectra of Complex Compounds", in J. Lewis, R. G. Wilkinson "Modern Coordination Chemistry. Principles and Methods". Inter. Publ. Inc., New York, 1960.

Revue Roumaine de Chimie, 21, 7, 1037−1043 (1976)

As a first observation from Fig. 3, the C_{3v} symmetry with one and two degenerate *E-d* levels could hardly explain the four *dd** transitions, especially if one takes into account the accidental degeneracy between the A_1 and one E level, which results from the crystal field calculations below. The C_{2v} symmetry splits completely the *d*-orbital degeneracy (fig.4).

We shall analyze the electronic spectrum in the framework of the unielectronic approximation, the transitions being given simply by the energy difference between the split *d*-orbitals. The crystal field potential is calculated according to the method described by Figgis,[5] taking into account the positions corresponding to the three oxygen and three nitrogen atoms for coordination spheres of C_{3v} and respectively C_{2v} symmetry.

If we note by Z_N and Z_O the electric charge localized on the N and O atoms respectively, it may be shown that the potential acting on the *d*-orbitals may by expanded in a power series of r;

$$V(\overrightarrow{rj}) = (Z_{\mathrm{N}} + Z_{\mathrm{O}})\mathrm{e} \sum_{n=0}^{\infty} \sum_{m=n}^{n} \sum_{i=1}^{6} \frac{4\pi}{2n+1} \frac{r^n}{d^{n+1}} Y_n^m (\Theta_j\, \Phi_j)\, Y_n^{m*} (\Theta_i\, \Phi_i) \quad (1)$$

where $V(\overrightarrow{rj})$ is the potential within the sphere, in the point with spherical coordinates $(r_j,\ \Theta_j,\ \Phi_j)$ "*e*" is the electronic charge, *d*-is the diameter of the coordination sphere, and $Y_n^m(\Theta_i,\ \Phi_j)$ are the spherical harmonic functions (*means the complex conjugate).

The splitting of the central ion energy levels is obtained with the aid of the perturbation theory, the perturbational operator being the potential given by (1).

The expression of the perturbation potentials in the form of (1) is convenient, since the *d*-orbitals are expressible (in the approximation of independent electrons) in terms of spherical functions. The evaluation of the perturbation matrix elements requires the calculation of some integrals of the form.

$$H_{kl} = \int \Psi_k^* V(\overrightarrow{rj})\, \Psi_l \, \mathrm{d}\tau \quad (2)$$

where Ψ means the *d* orbital wave functions of the central ion; *d* is the elementary volume expressed in spherical coordinates. The integral (2) contains, of course, also the following function

$$\Theta_n^m = \left[\frac{(2n+1)\,(n-1-m)\,!}{2(n+1+m)\,!} \right]^{1/2} \cdot P_n^m (\cos\Theta) \quad (3)$$

where P_n^m are the normalized Legendre polynomials, and thus, the calculation of integral (2) depends on the calculation of other integrals with the form :

$$\int \Theta_1^m\, \Theta_n^m\, \Theta_1^m \sin\Theta \, \mathrm{d}\Theta \quad (4)$$

which vanish for odd n values.

Therefore, in expanding the potential $V(\overrightarrow{rj})$ of eq. (1) only the terms, $Y_n^m(\Theta_j, \Phi_j), Y_n^{m*}(\Theta_i, \Phi_i)$ with n even appear. One may show, also, that in the expansion (1) the terms $n > 4$ have a negligible contribution to the perturbational potential.[5]

Performing the expansion (1) for the C_{3v} and C_{2v} symmetry, one gets, for C_{3v}:

$$V_{C_{3v}}(\overrightarrow{rj}) = \frac{3e}{d}(Z_O + Z_N) + \frac{4\pi}{9\sqrt{2}}\frac{er^4}{d^5}\Bigg[Y_4^0(\theta_i, \theta_j) + \\ + \sqrt{\frac{5}{14}}(Y_4^4(\theta_i, \theta_j) + Y_4^{-4}(\theta_i, \theta_j))\Bigg] \tag{5}$$

The first term represents an equal perturbation of the five d orbitals and, hence, does not split them; the second term leads to a splitting similar with that of an octahedral ligand configuration. Thus, the potential (C_{3v}) does not agree, even qualitatively, with the experimental spectrum.

For the case C_{2v}, the expansion (1) differs from (5) in the sense that the contribution of the term:

$$K\,[Y_2^2(\theta_j, \Phi_j) + Y_2^{-2}(\theta_j, \Phi_j)]\frac{r^2}{d^3} \tag{6}$$

appears, where K is a constant that comprises all constant coefficients. Thus, the C_{2v} potential may be written as:

$$V_{C_{2v}}(\overrightarrow{rj}) = V_{O_h}(\overrightarrow{rj}) + K\,(Y_2^2 + Y_2^{-2})\frac{r^2}{d^3} \tag{7}$$

The perturbation matrix for the C_{2v} case will be different from that for the Oh case as some new finite elements appear leading to a more advanced splitting of the energy levels. The d-orbitals may be expressed by the spherical functions:

$$\Psi_l^m = R_l^{(r)} \cdot Y_l^m(\theta, \Phi) = R_l^{(r)}\Theta_l^m (2\pi)^{-\frac{1}{2}} \cdot e^{im\Phi} \tag{8}$$

Let be

$$r^{-2} = \int_0^\infty R_l(r)\, r^2 \cdot R_l(r)\, r^2 \cdot dr \tag{9}$$

the quadratic average of the d-orbital radius; including it in the constant K, the calculation of the perturbation matrix elements is reduced to the integration of the functions Y.

---

[5] B. N. Figgis, " Introduction to Ligand Fields", Inter. Publ. Inc., New York, 1966.

For:

$$\int_0^{2\pi} Y^{m_{n_1}}_{n_1} \cdot Y^{m_{n_2}}_{n_2} \cdot Y^{m_{n_3}}_{n_3} \cdot d\Phi = 0 \tag{10}$$

the following relation is valid:

$$m_{n_1} + m_{n_2} + m_{n_3} = 0 \tag{11}$$

Taking into account eq. (11), the matrix elements (2) are reduced to the following two expressions:

$$\begin{gathered}\Delta^1 = \int_0^{\pi} \Theta_2^1 \, \Theta_2^2 \, \Theta_2^1 \sin\theta \, d\theta = \frac{15}{8\pi}\left(\frac{15}{32\pi}\right)^{\frac{1}{2}} \frac{2^3 \cdot 2!}{3.5.7.} K \\ \Delta^2 = \int_0^{\pi} \Theta_2^2 \, \Theta_2^2 \, \Theta_2^0 \sin\theta \, d\theta = \frac{15}{32\pi}\left(\frac{5}{16\pi}\right)^{\frac{1}{2}} \frac{2^3 \cdot 2!}{3!\,5!\,7!}\end{gathered} \tag{12}$$

Putting $\Delta^2 = B$, $\Delta^1 = 4\sqrt{\frac{3}{2}}\,B$ results.

Denoting by A the parameter D_q which occurs in the perturbation matrix for the octahedral symmetry, (table 2) for the perturbation matrix is obtained for the C_{2v} case expressed in terms of the semiempirical parameters A and B.

Table 2

The perturbation matrix for the C_{2v} case in terms of the semiempirical parametres A and B

m	2	1	0	-1	-2
2	A	0	B	0	$5A$
1	0	$4\left(\frac{3}{2}\right)^{\frac{1}{2}} B-4A$	0	0	0
0	B	0	$6A$	0	B
-1	0	0	0	$4\left(\frac{3}{2}\right)^{\frac{1}{2}} B-4A$	0
-2	$5A$	0	B	0	A

The "p" eigen values of this matrix give the splitting energies. From the four experimental transitions, two (35.600 cm^{-1} and 18.450 cm^{-1}) are used for the calibration of the parameters A and B. Once calibrated and replaced in the matrix of table 2, they have to give the frequencies for all the four transitions. Their values are

$$A = 2026 \cdot 5 \ \text{cm}^{-1}$$

$$B = 2251 \cdot 7 \ \text{cm}^{-1}$$

Figure 5 shows the positions of the energy levels for the isomer III, their values in cm^{-1}, the electronic transitions and also the calculated frequencies. The experimental values of the frequencies are also given in the brackets. It may be seen that the agreement is good, the maximum relative error being not more than 8%.

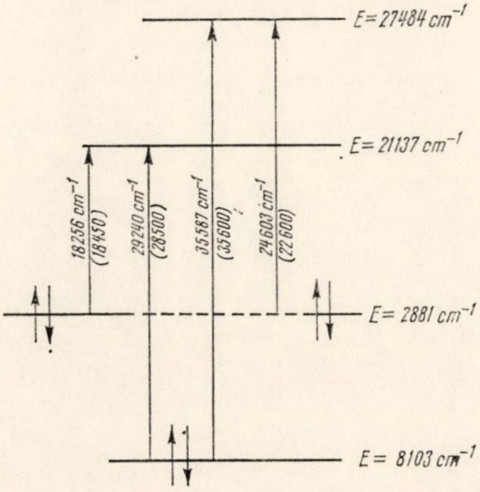

Fig. 5. —The positions of the energy levels for the C_{2v}-isomer III, their values in cm^{-1}, the electronic transition calculated frequencies.

RESULTS AND CONCLUSIONS

The analysis of the electronic spectra indicate that the coordination sphere in these complexes has a C_{2v} symmetry (III, fig. 1). The approximative relation :

$$\nu_1 + \nu_4 \cong \nu_2 + \nu_3$$

between the calculated transition frequencies (53.843 $\cong$ 54.827) is satisfied as well as the sums of observed frequencies (54050 and 51100) respectively.

The paramagnetism observed for the Co^{III} thiazolidine-4-carboxylic acid chelate suggests the existence of electrons also on the B_1 and B_2 levels. Two further transitions should thus be possible, at about 11.000 cm^{-1} and 600 cm^{-1}, i.e. beyond the reach of the spectrophotometer used in the work.

Revue Roumaine de Chimie, 21, 7, 1037–1043 (1976)

Revue Roumaine de Chimie, **21**, 7, 1045–1047 (1976)

CHEMICAL GRAPHS. XXVI.[1]

CODES FOR CONFIGURATIONS OF CONJUGATED POLYENES

ALEXANDRU T. BALABAN
Org. Chem. Dept., Institute of Chemistry, The Polytechnic, Bucharest, Roumania

Received January 30, 1976

A coding system for describing non-branched acyclic or cyclic paths on a graphite lattice is described. The code is a degenerate triplet code, where the *transoid* configuration IV is coded by 0 and the *cisoid* one V by 1; the result is a two-digit code, each triplet of which is in a one-to-one correspondence with one digit of the three-digit code described previously; this two-digit code can be read as binary number and converted into decimal notation.

It was shown earlier[2] that by assigning digits 1–3 to the three possible orientations of bonds (I) on a graphite lattice,[3] configurations of conjugated cyclopolyenes (of annulenes) could be coded by a string of these digits. This three-digit code (3DC) was made unique by finding a non-arbitrary starting point and direction, through the convention that from all strings of digits for one configuration, the 3DC had to be the smallest number. A simple rule for ring-closure resulted: for each type of digit, the number of times this digit appears in the code in odd positions must be equal to the number of times it appears in even positions.

The first codification of annulene configurations[4,5] had used a different system, namely the assignment of digit 0 to *cis* configurations of double bonds and digit 1 to *trans*; the sequence of configurations of double bonds was then codified with the minimal-number convention. It was shown by counter-examples[2] that this system was ambiguous e.g. the two resonance structures II and III of [14]annulene gave different codes, presented beneath each configuration.

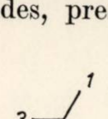

I

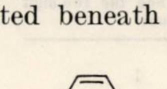

0101011[4,5]

II

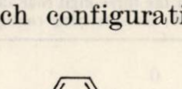

0000011[4,5]

III

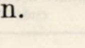

3DC:121
2DC:0

IV

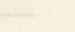

3DC:123
2DC: 1

V

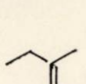

VI

---

[1] A. T. Balaban, Part XXV, *Rev. Roumaine Chim.*, **20**, 239 (1975).
[2] A. T. Balaban, *Tetrahedron*, **27**, 6115 (1971).
[3] M. Gordon and W. H. T. Davison, *J. Chem. Phys.*, **20**, 428 (1952).

A third possible system, coding for sequences of two bonds by two digits, one for "left bend", the second for "right bend", was mentioned earlier[2] but not used because it did not lead to a simple condition for ring closure.

In the present paper, a fourth system is applied. It can be easily derived from the 3DC, and codes paths on a graphite lattice (which will be named configurations) by assigning two digits, 0 and 1, to the two possible sequences of three bonds : 0 to the *transoid* configuration IV, and 1 to the *cisoid* one V. This system will be called two-digit code, and abbreviated 2DC. Unlike the previously mentioned system proposed by Oth, [4,5] (whose *cisoid* and *transoid* bonds were coded by subsequent triplets having in common only one digit, namely the last digit of one triplet was the first digit of the next triplet) the present one consists of degenerate (overlapping) triplets, where two subsequent triplets have two digits in common, namely the last two digits of one triplet are the first two digits of the next triplet.

The minimal-number convention is adopted to ensure a one-to-one correspondence between each configuration and each code. Configurations may be open paths or ring-closed ones (cyclopolyenes, or circuits) ; one bond may be used only once (single-edge configurations) or several times (multiple-edge configurations). Formula VI presents an open multiple-edge configuration as an example. The number of edges may be even or odd in open paths, but it is always even in circuits.

The following rules apply to 2DC's of configurations on a graphite lattice :

— (i) For open paths, the code starts from one free end ; for circuits, from any point; in both cases the minimal-number convention eliminates ambiguities. Therefore, whenever in a circuit there exist *transoid* sequences, one of these is the starting point.

— (ii) The dictionary for converting 3DC into 2DC is very simple : in the 2DC, 0 corresponds to any triplet formed from two digits only, i.e. any combination $\binom{3}{2} = C_3^2$ of two out of three digits, and 1 corresponds to any permutation of 123, as shown in table 1.

Table 1

Correspondence between the three-digit code (3DC) and the two-digit code (2DC) for specifying configurations

2DC	0			1		
3DC	121	212	313	123	213	312
	131	232	323	132	231	321

— (iii) For the conversion of a 3DC into a 2DC for a circuit, the first two digits are repeated once more at the end in brackets. For

---

[4] J. F. M. Oth and J.-M. Gilles, *Tetrahedron Letters*, **1968**, 6259.

[5] J. F. M. Oth, G. Anthoine and J.-M. Gilles, *Tetrahedron Letters*, **1968**, 6265.

instance, 12123121312313 is the 3DC of configurations II and III. The conversion into 2DC is illustrated below in formula VII.

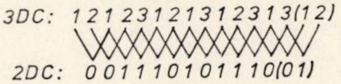

VII

— (iv) Branched acyclic paths, or rings possessing side-chains can also be coded using brackets (these brackets, however, cannot appear at the end of the code as above), but such systems will not be examined in detail.

— (v) Following Oth et al.,[4,5] the resulted unique 2DC, which is a binary number (B), may be converted into decimal notation (D). For conjugated cyclopolyenes the brackets are disregarded in this conversion.

The 3DC of an open polyene with n vertices contains $n-1$ digits coding for the $n-1$ edges; its 2DC only contains $n-3$ digits. However, for cyclopolyenes, owing to (iii), both the 3DC and the 2DC have the same number of digits which equals the number of vertices and edges of the cyclopolyene.

Some examples follow. An open-chain *all-trans* polyene has a 3DC 121212... and a 2DC formed only from zeroes. For benzene, the 3DC is[2] 123123; the 2DC (B) is 1111(11), and the 2DC (D) is 63. For the naphthalene perimeter, the 3DC is[2] 1212312123, the 2DC (B) is 00111001(11), and the 2DC (D) is 231.

One possible application of this coding system may be for configurations of carotenoids where correlations between UV spectral data and the code may be found.

The correspondence between 3DC and 2DC is completely analogous to the correspondence between three-digit codes used for the enumeration and codification of catafusenes,[6-8] and four-digit codes used for staggered alkane C-rotamers[9,10] and for diamondoid hydrocarbons.[8,10,11]

---

[6] A. T. Balaban and F. Harary, *Tetrahedron*, **24**, 2505 (1968).

[7] A. T. Balaban, *Tetrahedron*, **25**, 2949 (1969).

[8] A. T. Balaban, *MatCh*, No. 1, 33 (1975).

[9] A. T. Balaban, following paper.

[10] A. T. Balaban, *MatCh* (1976, in press).

[11] Manuscript in preparation, in collaboration with P.v.R. Schleyer.

Revue Roumaine de Chimie, **21**, 7, 1049–1071 (1976)

CHEMICAL GRAPHS. XXVII[1]

ENUMERATION AND CODIFICATION OF STAGGERED CONFORMATIONS OF ALKANES

ALEXANDRU T. BALABAN *
Department of Organic Chemistry, Polytechnic, Bucharest, Romania

Received January 30, 1976

Staggered conformations of alkanes may be coded in terms of four digits (1, 2, 3, 4) symbolizing the four bond directions on a diamond lattice. A one-to-one correspondence exists between these C-rotamers of an n-alkane C_kH_{2k+2} and non-branched catafusenes with $k - 1$ condensed benzenoid rings. The four-digit code may be thus translated into the three-digit (0, 1, 2) code used previously for catafusenes, allowing the enumeration of n-alkane C-rotamers. This correspondence originates in the helicities of the carbon chain, coded by overlapping triplets from four digits. Each four-digit triplet can be translated into a single symbol of the three-digit code, namely 0 for *trans*, 1 or 2 for the two *gauche* conformations giving rise to different helicities. The three-digit code is a topological one and gives information about the chirality of the C-rotamer. Conformers involving both C—C and C—H bonds (CH-rotamers) were examined previously. A similar approach is used for C-rotamers of branched alkanes C_kH_{2k+2} with t tertiary carbon atoms and no quaternary carbons, whose three-digit codes are identical to those of catafusenes with the same type of branching but with $k + t - 1$ benzenoid rings. Alkanes with quaternary carbon atoms and cycloalkanes are also examined.

STAGGERED CARBON ATOM ROTAMERS (C-ROTAMERS) OF n-ALKANES

The carbon atom skeleton of staggered conformations of alkanes is always a portion of the diamond lattice. In a recent paper,[1] graph theory was applied to the enumeration and nomenclature of diamondoid hydrocarbons (DH) : the DH is symbolized by its dualist graph,** which is itself a portion of the diamond lattice.

By analogy with the corresponding bidimensional problem of enumerating condensed benzenoid polycyclic systems (polyhexes), whose dualist graphs are portions of the graphite lattice,[2] two kinds of condensation were defined : *cata*, leading to catafusenes (2-dimensions) and catamantanes (3-dim.), when the dualist graph is a tree, leading to isomeric systems and being amenable to an exact mathematical treatment, and *peri*, leading to perifusenes (2-dim.) or perimantanes (3-dim.) when systems with the same number of condensed rings are no longer isomeric and when no simple mathematical solution was found.

---

* Correspondence address : Institute of Atomic Physics, P.O.B. 5206, Bucharest

** The points or vertices of the dualist graph are the centres of adamantane units (or benzenoid rings for catafusenes), and its lines or edges join points corresponding to condensed units. Unlike dual graphs, angles of dualist graphs are fixed (109.5° in the tridimensional case, 120, 180 or 240° in the planar case).

[1] A. T. Balaban *MatCh*, No. 1, 33 (1975) ; part XXVI, preceding paper.

[2] A. T. Balaban and F. Harary, *Tetrahedron*, **24**, 2505 (1968).

It was established [2] that the number F_n of isomeric nonbranched n-catafusenes consisting of n benzenoid rings is : *

$$(1) \qquad F_{2m-1} = \frac{1}{4}(3^{2m-3} + 3^{m-1} + 3^{m-2} + 1) \text{ for odd } n = 2m - 1$$

$$(2) \qquad F_{2m} = \left(\frac{3^{m-1} + 1}{2}\right)^2 \qquad \text{for even } n = 2m$$

For branched catafusenes, a complicated formula results .[3] A notation and codification system was proposed[2-4] for dualist (characteristic) graphs of catafusenes making use of three digits 0, 1 and 2 : linear annelation (i.e. angle 180°) is indicated by 0, angular annelation in one direction (e.g. angle 120°) by 1, and in the other direction (i.e. angle 240°) by digit 2, starting from one end of the dualist graph. Among all possible numbers resulted from the digits which specify the annelation of a catafusene by coding the topology of its dualist graph, the minimal number is selected as the adopted code for that catafusene .[2] The code of an n-catafusene consists of $n - 2$ digits 0, 1, and/or 2. Branching is indicated in the code by brackets.[4] If the branch of a catafusene dualist graph has only one vertex, then this is symbolized by a period (dot) in the brackets.

Four possible types of dualist graph of a non-branched n-catafusene were distinguished by their symmetry elements (in addition to the molecular plane) :

— acene (the number of acenes with n benzenoid rings is denoted by a_n) with point group $\mathbf{D}_{2h}$, coded by a string of $n - 2$ digits 0 ;

— catafusenes with a symmetry plane perpendicular to the molecular plane, with point group $\mathbf{C}_{2v}$ (their number is denoted by s_n) whose code has the same digits disposed symmetrically relatively to the middle of the code ;

— catafusenes with a centre of inversion, point group $\mathbf{C}_{2h}$ (their number is denoted by c_n) : the digits of the code disposed symmetrically relatively to the middle of the code differ by the permutation (0) (1,2) ;

---

* To avoid confusions between c_n and the symbol used previously [2] for the number of catafusenes, C_n, we replace here the previous notation C_n by F_n.

[3] F. Harary and R. C. Read, *Proc. Edinburgh Math. Soc.* **17**, 1 (1970).

[4] A. T. Balaban, *Tetrahedron*, **25**, 2949 (1969).

— unsymmetric catafusenes (their number is u_n) with no symmetry element except the plane of the molecule.

The following formulas were found [2] for these numbers of isomers of an n-catafusene :

$$a_n = 1 \qquad \text{for any } n \tag{3}$$

$$s_{2m-1} = \frac{1}{2}(3^{m-1} - 1) \qquad \text{for odd } n = 2m - 1 \tag{4}$$

$$s_{2m} = \frac{1}{2}(3^{m-1} - 1) \qquad \text{for even } n = 2m \tag{5}$$

$$c_{2m-1} = \frac{1}{2}(3^{m-2} - 1) \qquad \text{for odd } n \tag{6}$$

$$c_{2m} = \frac{1}{2}(3^{m-1} - 1) \qquad \text{for even } n \tag{7}$$

$$u_{2m-1} = \frac{1}{4}(3^{2m-3} - 3^{m-1} - 3^{m-2} + 1) \qquad \text{for odd } n \tag{8}$$

$$u_{2m} = \left(\frac{3^{m-1} - 1}{2}\right)^2 \qquad \text{for even } n \tag{9}$$

$$F_n = a_n + s_n + c_n + u_n \qquad \text{for any } n \tag{10}$$

By analogy, a four-digit code for specifying the geometry of a portion of the diamond lattice was devised,[1,5] consisting of strings of digits 1, 2, 3, and/or 4 (corresponding to the four orientation of edges in the diamond lattice) and adopting as code the sequence of digits forming the smallest number, when all possibilities of starting point (endpoint) and of assignment of digits to the four orientations are considered. The code for an alkane C_kH_{2k+2} * consists of $k - 1$ digits, but only $k - 3$ digits convey information because the first two digits are always 12. Therefore, 4-digit codes for alkane rotamers and 3-digit codes for catafusenes contain the same number of information-carrying digits, when referred to the same number of units (carbon atoms, and benzenoid rings, respectively). References[1,2,4,5] should be consulted for further details con-

---

* To avoid confusion in notations, letters n and m are used for catafusenes, while corresponding letters k and j are used for rotamers. Note that n-alkane means normal (non-branched) alkane, and that n-catafusene indicates the presence of n condensed benzenoid rings.

[5] a) M. Gordon and W.H.T. Davison, *J. Chem. Phys.* **20**, 428 (1952) ; b) M. Saunders, *Tetrahedron*, **23**, 2105 (1967).

Table 1

One-to-one correspondence between staggered C-rotamers of n-alkanes and non-branched catafusenes

n-Alkane C-rotamers			Catafusenes							Total No.
n-Alkane	4DC	Permutations	Point group	Achiral	Chiral	*D*	Catafusene	3DC	Symm.	
n-Butane	121	(1) (2)	C_{2h}	1		0	Tri	0	*a*	2
	123	(2) (1,3)	C_2		1	1		1	*s*	
n-Pentane	1212	(1,2)	C_{2v}	2		0	Tetra	00	*a*	4
	1231	(1) (2,3)	C_s			0		12	*c*	
	1234	(1,4) (2,3)	C_2		2	2		11	*s*	
	1213	—	C_1			1		01	*u*	
n-Hexane	12121	(1) (2)	C_{2h}	2		0	Penta	000	*a*	10
	12321	(1) (2) (3)	C_i			0		102	*c*	
	12131	(1) (2,3)	C_2		8	1		010	*s*	
	12312	(3) (1,2)	C_2			1		121	*s*	
	12324	(2) (3) (1,4)	C_2			2		101	*s*	
	12341	(1) (3) (2,4)	C_2			3		111	*s*	
	12123	—	C_1			1		001	*u*	
	12132	—	C_1			0		012	*u*	
	12134	—	C_1			2		011	*u*	
	12314	—	C_1			1		112^a	*u*	
n-Heptane	121212	(1,2)	C_{2v}	5		0	Hexa	0000	*a*	25
	121323	(2) (1,3)	C_s			0		0120	*c*	
	123123	(2) (1,3)	C_s			0		1212	*c*	
	123231	(1) (2,3)	C_s			0		1002	*c*	
	123421	(1) (2) (3) (4)	C_s			0		1122	*c*	
	121343	(1,3) (2,4)	C_2		20	2		0110	*s*	
	123143	(1,3) (2,4)	C_2			0		1221	*s*	
	123234	(1,4) (2,3)	C_2			2		1001	*s*	
	123412	(1,2) (3,4)	C_2			4		1111	*s*	
	121213	—	C_1			1		0001	*u*	
	121231	—	C_1			0		0012	*u*	
	121232	—	C_1			1		0010	*u*	
	121234	—	C_1			2		0011	*u*	
	121312	—	C_1			0		0102	*u*	
	121314	—	C_1			2		0101	*u*	
	121321	—	C_1			1		0121	*u*	
	121324	—	C_1			−1		0122	*u*	
	121341	—	C_1			1		0112	*u*	
	121342	—	C_1			3		0111	*u*	
	123124	—	C_1			2		1121^a	*u*	
	123132	—	C_1			1		1021^a	*u*	
	123134	—	C_1			1		1012^a	*u*	
	123142	—	C_1			2		1112^a	*u*	
	123214	—	C_1			−1		1022	*u*	
	123241	—	C_1			3		1011	*u*	
n-Octane	1212121	(1) (2)	C_{2h}	5		0	Hepta	00000	*a*	70
	1213121	(1) (2) (3)	C_i			0		01020	*c*	
	1231321	(1) (2) (3)	C_i			0		12012	*c*	
	1232321	(1) (2) (3)	C_i			0		10002	*c*	
	1234321	(1) (2) (3) (4)	C_i			0		11022	*c*	
	1212323	(2) (1,3)	C_2		65	1		00100	*s*	
	etc.	etc.						etc.		

[a] The catafusene 3DC does not result directly by translation of the 4DC starting 1231..., but by reading the translated notation from the right to the left and converting it into the minimal number.

cerning the codes. For convenience, the four-digit code will be abbreviated as 4DC, and the three-digit code as 3DC.

Thus we are able to code all conformations of the carbon skeleton of an alkane C_kH_{2k+2} which are superimposable on the diamond lattice, i.e. all staggered C-rotamers of alkanes.

The number of staggered C-rotamers of a normal alkane is found to be identical to the number of non-branched catafusenes : if the former number is denoted by R_k, we find $R_k = F_{n-1}$ when $k = n$. Indeed, a one-to-one correspondence may be established between each C-rotamer and one isomer of a non-branched catafusene, as presented in table 1. In this table, achiral C-rotamers are listed first for each k in the increasing numerical order of their code (these have at least one symmetry element, as will be discussed in detail below), then chiral rotamers : the point groups of chiral n-alkane C-rotamers are either $\mathbf{C}_2$ (dissymmetric conformations with a binary axis) listed next in the same order, or $\mathbf{C}_1$ (asymmetric conformations with no symmetry element) listed last in the same order.

The four-digit code of a C-rotamer can be used for determining whether this rotamer does or does not possess symmetry elements : if it does, then on reading the code from right to left and on converting the digits by an appropriate permutation so that again in this case the minimal number results from all possible permutations, the resulted code is identical to the initial one, as shown by some examples for n-heptane rotamers in table 2.

Table 2

Examples for determining the presence of symmetry elements in n-alkane C-rotamers from their four-digit code

Initial code	123231	121343	123143	123123	121213	123124
Permutations	(1) (2,3)	(1,3) (2,4)	(1,3) (2,4)	(2) (1,3)	(1,2,3)	(2) (1,3,4)
Converted code	132321	343121	341321	321321	232321	324321
Code reverted	123231	121343	123143	123123	123232	123423
Symmetric ?	Yes	Yes	Yes	Yes	No	No

From table 1 it is apparent that the *trans* achiral rotamer[*] of each alkane C_kH_{2k+2} corresponds to the acene : for even k, this rotamer has point group $\mathbf{C}_{2h}$ and its 4DC has the identity permutation (1) (2), while for odd k, the point group is $\mathbf{C}_{2v}$ and the code has the transposition (1,2). The remaining achiral rotamers have point group $\mathbf{C}_i$ for even k (their code has the identity permutation involving three of four digits, and their symmetry element is an inversion centre), whereas for odd k they have point group $\mathbf{C}_s$ with a plane of symmetry, and their code has one transposition, e.g. (3,4) ; all these remaining achiral rotamers correspond to

---

[*] We shall use the terms *trans* and *gauche* for staggered conformers, because *anti* and *skew* indicate intermediates between staggered and eclipsed conformations.

Revue Roumaine de Chimie, 21, 7, 1049–1071 (1976)

c-type catafusenes with an inversion centre. Chiral rotamers with point group $\mathbf{C}_2$, i.e. one binary axis, correspond to *s*-type catafusenes; for even *k*, their code has a permutation containing one transposition, whereas for odd *k* it is a product of two transpositions. The remaining chiral C-rotamers with point group $\mathbf{C}_1$ correspond to *u*-type catafusenes.

Table 3

Numbers of C-rotamers of n-alkanes C_kH_{2k+2} according to formulas (11) – (24)

n-Alkane	k	Achiral rotamers			Chiral rotamers			Grand total
		$\mathbf{C}_{2v/h}$	$\mathbf{C}_{i/s}$	Total	$\mathbf{C}_2$	$\mathbf{C}_1$	Total	
		Z	P	A	S	U	K	R
Propane	3	1	0	1	0	0	0	1
Butane	4	1	0	1	1	0	1	2[a]
Pentane	5	1	1	2	1	1	2	4[a]
Hexane	6	1	1	2	4	4	8	10[a]
Heptane	7	1	4	5	4	16	20	25[a]
Octane	8	1	4	5[a]	13	52	65	70
Nonane	9	1	13	14	13	169	182	196
Decane	10	1	13	14	40	520	560	574

[a] These C-rotamers are presented individually in table 1.

This one-to-one correspondence exemplified in table 1 gives the possibility to enumerate staggered C-rotamers of normal alkanes C_kH_{2k+2} by adapting formulas (1)—(10). The total number of rotamers R_k, formula (11), results from formulas (15) and (16). The number A_k of achiral rotamers, formula (12), is composed of the $Z_k=1$ *trans* conformer with point groups $\mathbf{C}_{2h}$ or $\mathbf{C}_{2v}$, formula (14), and of P_k conformers with a centre or plane of symmetry (point groups $\mathbf{C}_i$ or $\mathbf{C}_s$), formula (18). The number K_k of chiral rotamers, formulas (19) and (20), is composed of S_k dissymmetric conformers with a C_2 axis, formulas (21) and (22), and from U_k asymmetric conformers, formulas (23) and (24). All these formulas yield numerical results which are presented in table 3 for staggered C-rotamers of n-alkanes propane through decane (and which apply also to non-branched *k*-catamantanes, with the exception of those whose rotamer codes contain sequences like *axya* . . . with the same digit *a* repeated in the third place : these correspond to perimantanes,[1] while the n-heptane rotamer 123123 and similar rotamers cannot correspond even to a perimantane owing to overlap).

$$R_k = A_k + K_k \qquad \text{for any } k \tag{11}$$

$$A_k = Z_k + P_k \qquad \text{for any } k \tag{12}$$

$$K_k = S_k + U_k \qquad \text{for any } k \tag{13}$$

$$Z_k = 1 \qquad \text{for any } k \tag{14}$$

$$R_{2j} = \frac{1}{4}(3^{2j-3} + 3^{j-1} + 3^{j-2} + 1) \qquad \text{for even } k = 2j \tag{15}$$

$$R_{2j-1} = \left(\frac{3^{j-2}+1}{2}\right)^2 \qquad \text{for odd } k = 2j-1 \tag{16}$$

$$A_{2j} = A_{2j-1} = \frac{1}{2}(3^{j-2}+1) \qquad \text{for even/odd } k \tag{17}$$

$$P_{2j} = P_{2j-1} = \frac{1}{2}(3^{j-2}+1) \qquad \text{for even/odd } k \tag{18}$$

$$K_{2j} = \frac{1}{4}(3^{2j-3} + 3^{j-1} - 3^{j-2} - 1) \qquad \text{for even } k = 2j \tag{19}$$

$$K_{2j-1} = \frac{1}{4}(3^{2j-4} - 1) \qquad \text{for odd } k = 2j-1 \tag{20}$$

$$S_{2j} = \frac{1}{2}(3^{j-1} - 1) \qquad \text{for even } k = 2j \tag{21}$$

$$S_{2j-1} = \frac{1}{2}(3^{j-2} - 1) \qquad \text{for odd } k = 2j-1 \tag{22}$$

$$U_{2j} = \frac{1}{4}(3^{2j-3} - 3^{j-1} - 3^{j-2} + 1) \qquad \text{for even } k = 2j \tag{23}$$

$$U_{2j-1} = \left(\frac{3^{j-2}-1}{2}\right)^2 \qquad \text{for odd } k = 2j-1 \tag{24}$$

The one-to-one correspondence originates in the fact that the n-alkane C-rotamer four-digit code is composed of overlapping triplets (triads) specifying helicities; this reduces the number of information-carrying digits by two, i.e. the first digit of the first triplet, and the last digit of the last triplet do not carry information by themselves. A triplet of the form *aba** indicates absence of helicity (i.e. *trans* conformation) corresponding to digit 0 in the 3DC code which indicated absence of bending in the annelation of catafusenes. A triplet of the form *abc* indicates one or the other of the two possible *gauche* orientations of the helix, corresponding to notations 1 or 2 in the 3-digit catafusene code.

In order to establish the dictionary between the two codes, 3DC and 4DC, the following observations are important:

(i) The 4DC consists of overlapping triplets, while the 3DC consists of single digits, having in both cases the same object: absence of, or presence of, alternatively oriented bending or helicity along a path in the graph. Therefore, each triplet of the 4DC corresponds to one digit of the 3DC.

(ii) Triplets *aba* in the 4DC correspond to digit 0 in the 3DC.

(iii) If a triplet *abc* in an even position of the 4DC is translated by 1 in the 3DC, then the same triplet *abc* in an odd position will be translated by 2. This can be proved by examining the helicities of models* for the n-heptane C-rotamer 123123 whose C—C bonds coincide with the chair conformation of cyclohexane: the helicities of the two halves 123 are mutually opposite because one is in an odd, and the other in an even position of the 4DC.

---

* In this and subsequent triplet notations, letters *a*, *b*, *c*, and *d* stand each for one of the digits 1, 2, 3, or 4, in the 4DC, while *x* and *y* stand for any of the same digits; *v* and *w* stand each for one of the digits 1 or 2 in the 3DC.

On each of the four orientations of bonds in the diamond lattice, two opposite senses (directions) are possible.[5b] Since these two senses are opposite in even and odd positions of the four-digit code, their specification (presence or absence of a bar above the digit indicating the orientation) as in fig. 1 is not necessary. However, this explains why a triplet in an odd position of the 4DC has a different helicity from the same triplet in an even position: as seen from fig. 1, the senses are opposite on each orientation.

(iv) A permutation of the first two or last two digits of a triplet *abc* reverts the helicity. Also, reverting a triplet *abc* into *cba* reverts the helicity, as seen by inspection of a model of the n-hexane rotamer 12321, where triplets 123 and 321 have different helicities, though they are both in an odd position.

(v) As a consequence of observations (iii) and (iv), the triplets corresponding to circular permutations *abc*, *cab* and *bca* correspond to the same helicity: indeed, inspection of a model of the n-pentane rotamer 1231 (see also fig. 1) shows that the helicities of the triplets 123 and 231 are different, hence they must be translated by the same digit in the catafusene code, since the former triplet is in an odd position, and the latter in an even one.

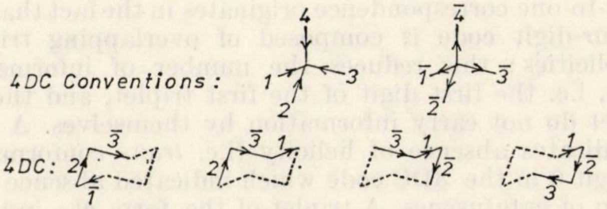

Fig. 1. — Alternating helicities for 4-digit triplets in even and odd positions of the 4DC.

The resulting dictionary between the two codes** is presented in table 4. The correspondence between the n-alkane rotamers and catafusenes contained in table 1 agrees with the dictionary from table 4. Thus, the tridimensional problem of the n-alkane rotamers can be apparently reduced to a bidimensional one. Actually, the single digit notation as for catafusenes in the 3DC is just another convention for denoting helicities. The translation operates both ways, i.e. a given catafusene-type code (3DC) can be translated into a n-alkane C-rotamer code (4DC) by starting with the digits 12 and then adding digit 1 if the 3DC starts with 0, or digit 3 if the 3DC starts with 1. The next digit is then unambiguously found from table 4, namely 2 if the second 3DC digit is 0 (to yield 1212 or 1232, respectively) ; if it is 1, we obtain with the help of table 4, 1213 or 1234 ; if it is 2, we obtain 1214* or 1231, and so on for the next digits.

---

* Framework Molecular Models (Prentice-Hall Inc.) are convenient, and the four orientations may be additionally distinguished by black, white, red and blue plastic tubings.

** For simplicity, in the preceding discussion the four-digit code (4DC) was called the alkane C-rotamer code, and the three-digit code (3DC) was called the catafusene code, although it is evident that both codes may be used for n-alkane C-rotamers.

Table 4

Dictionary relating the triplets (triads) of digits written in the four-digit code to the single digits of the three-digit code

Three-digit code :	0	1	2
	121	123	124
Triplets	131	134	143
	141	142	132
written	212	214	213
	232	243	234
	242	231	241
in the	313	312	314
	323	324	342
	343	341	321
four-digit	414	413	412
	424	432	423
code :	434	421	431

The correspondence between triplets *abc* (four-digit code) and single digits in the three-digit code may be expressed as follows : the 3-digit code is 1 when the sum of the digits in the *abc* triplet has the same parity as the number of inversions in the triplet (i.e. the number of necessary transpositions or (1,2) permutations to restore the natural order), and is 2 if the parities are opposite.

The description of alkane C-rotamers in terms of three- or four-digit codes is analogous to the alternative descriptions of configurations of annulenes : either by enumerating *cis* and *trans* configurations of double bonds (symbolized by 0 and 1, respectively, and converting the resulted smallest binary number into decimal notation),[6] or by the smallest number formed from the three digits coding the three orientations of bonds in the graphite lattice.[7]

Examination of models for n-alkane C-rotamers, and of the dualist graphs of catafusenes, reveals that the 1–1 correspondence from table 1 does not involve similarity of shape, but rather of symmetry elements, as shown by fig. 2 : the achirality of C-rotamers with point groups $\mathbf{C}_i$ or $\mathbf{C}_s$, which correspond to catafusenes with a symmetry centre, is due to the mutual compensation of helicities symbolized by digits 1 and 2 in the three-digit code.

---

* This situation never happens actually, since no catafusene code starts 02..., but all codes starting with 0 have the form 01...

[6] J.F.M. Oth and J.-M. Giles, *Tetrahedron Letters*, **1968**, 6259 ; J. F. M. Oth, G. Anthoine and J.-M. Giles, *ibid.*, **1968**, 6265.

[7] A. T. Balaban, *Tetrahedron*, **27**, 6115 (1971).

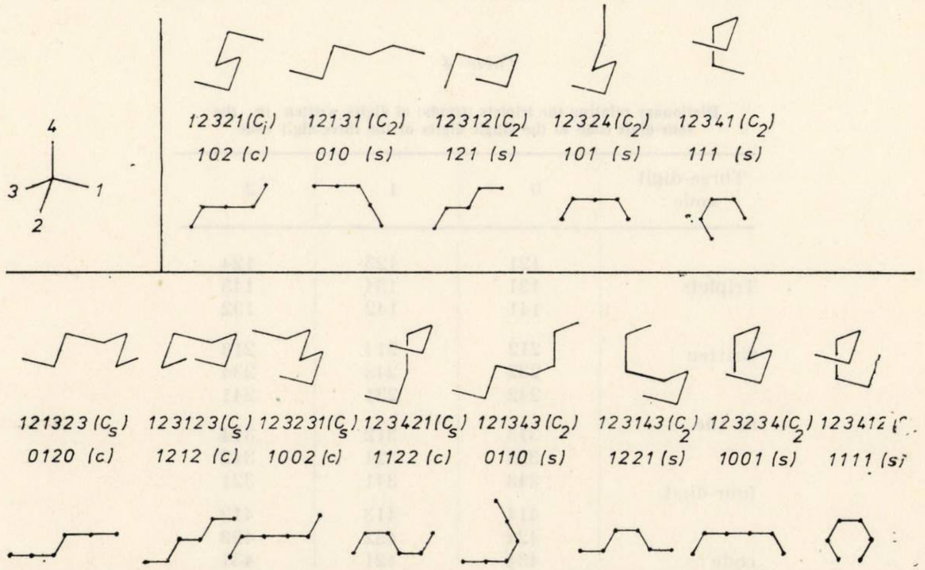

Fig. 2. — Symmetrical C-rotamers of n-hexane and n-heptane with their 4- and 3-digit codes, and the catafusenes corresponding to the 3-digit code. Symmetries of C-rotamers and of catafusenes are indicated above and below, respectively.

The three-digit catafusene code expresses in condensed form the topology of the catafusene molecule, and this was used for estimating resonance energies of catafusenes without finding eigenvalues of the secular determinant or of the adjacency matrix of the molecular graph.[8] If the same three-digit code is regarded as expressing the helicity of an alkane C-rotamer, it gives the possibility of a rough quantitative estimation of the optical rotating power of this rotamer. Assuming that each helical triad (triplet) of bond orientations contributes a fixed amount to the total chirality of the rotamer, and that chiralities symbolized by 1 and 2 are equal and of opposite signs, then the difference D between the number of digits 1 and the number of digits 2 in the three-digit code gives a semi-quantitative measure of the optical activity of the rotamer. With the help of table 4, this difference may be calculated directly on the formula, as exemplified by two C-rotamers of n-heptane I and II, presented in fig. 3.

This difference D may be seen in table 1 : all achiral rotamers have $D = 0$, and a few chiral rotamers also, hence $D = 0$ is a necessary but insufficient condition for chirality of C-rotamers ; the initial postulate, that all triplets (triads) contribute equally to the chirality, is only an approximation : only in achiral rotamers, where the opposite helicities are equidistant from the centre of the molecule, is exact compensation possible; in chiral rotamers with $D = 0$, the mutual compensation of helicities will not be total, but only partial, because they are not exactly matched. As indicated elsewhere,[9] it may be possible to evidence chirality in branched alkanes with undetectably small optical activity by indirect methods. In the present case, even if the interconversion of individual rotamers would be slowed down by lowering the temperature, racemic mixtures of several rotamers would be obtained, unless a chiral matrix would be present. Comparing D values from table 1, it can be seen that the highest D value for each k is always associated with one helical rotamer whose 3DC is composed only of the digit 1 (e.g. I in fig. 3). A negative sign for D only indicates an excess of digits 2 over 1 in the 3DC.

---

[8] A. T. BALABAN, *Rev. Roumaine Chim.*, **15**, 1243 (1970).

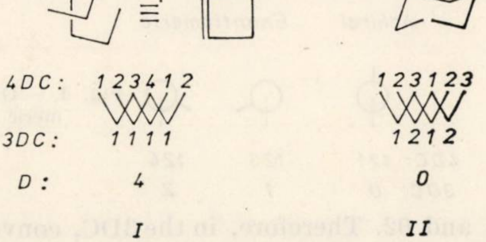

Fig. 3. — Correspondence between the 4- and 3-digit codes, and calculation of the D value from the latter code, for two n-heptane C-rotamers.

The topological 3DC for n-alkane C-rotamers may also give an estimation of the potential energy of the rotamers : since the zig-zag (*trans*) conformation of each triplet of bond orientations in an n-alkane C-rotamer is energetically favoured by *ca.* 0.8 kcal/mole over the *gauche* conformation,[10] the most stable conformation is that one which possesses the largest number of 0 digits in the three-digit code[*] (for catafusenes, the resonance energy was the lowest for acenes, possessing the largest number of 0 digits in the code).

Both the 3DC and the 4DC discussed so far do not discriminate among enantiomers, which possess the same codes. However, if such a discrimination is necessary, it may be achieved in the 4DC by abandoning the request for the minimal number and by converting the notation of one enantiomer into that of the opposite one through the permutation (1)(2)(3,4); thus the two pairs of enantiomeric n-pentane C-rotamers are coded by: 1234 and 1243; 1213 and 1214. Similarly, in the three-digit code, the same pairs of enantiomers will be coded by: 11 and 22; 01 and 02. Therefore, in the 3DC, conversion of one enantiomer into its opposite is effected by the permutation (0)(1,2). The single pair of chiral n-butane C-rotamers is shown in fig. 4 in Newman projection with the two codes 3DC and 4DC. It is necessary, however, to specify if the notation does or does not discriminate among enantiomers, i.e. whether the request for the minimal number is, or is not, disregarded.

---

[*] This is strictly valid only for hydrocarbons. When more electronegative heteroatoms with non-participating electron pairs are present, however, *gauche* conformations have lower energies (the *gauche* effect[11]) : such is the long-known situation in hydrazine, hydrogen peroxide, disulphane, fluoromethanol, etc ; [11] in the case of carbon-chains containing heteroatoms, the most conspicuous examples are those of 1,2-dicarbalkoxy-[12-15] or 1,2-difluoro-derivatives.[16]

[9] R. W. Robinson, F. Harary and A. T. Balaban, *Tetrahedron*, **32**, 355 (1976).

[10] M. Kobelt, P. Barman, V. Prelog and L. Ruzicka, *Helv. Chim. Acta*, **32**, 256 (1949).

[11] S. Wolfe, *Acc. Chem. Res.*, **5**, 102 (1972) and further references therein.

[12] A. A. Bothner-By and C. Naar-Colin, *J. Amer. Chem. Soc.*, **84**, 743 (1962).

[13] G. H. Schmid, *Canad.J. Chem.*, **46**, 3415 (1968).

[14] L. Phillips and V. Wray, *Chem. Commun.* **90** (1973); *J. Chem. Soc. Perkin II*, **1972**, 536.

[15] C. A. Kingsbury and C. R. Cowles, *J. Org. Chem.*, **40**, 1302 (1975).

[16] R. J. Abraham and R. H. Kemp, *J. Chem. Soc. B*, **1971**, 1240; R. J. Abraham and P. Loftus, *Chem. Commun.*, **1974**, 180; R. J. Abraham and K.G.R. Pachler, *Mol. Phys.*, **1963**, 165.

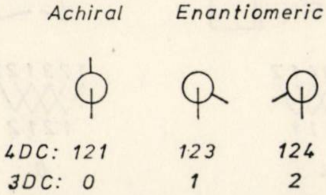

Fig. 4. — Discrimination among enantiomeric rotamers of n-butane.

If enantiomerism of C-rotamers is no longer disregarded, the total number E_k of geometrically distinct n-alkane C-rotamers is given by formulas (25) — (27), with the values of A_k and K_k from (17) — (20).

$$E_k = A_k + 2K_k \quad \text{for any } k \tag{25}$$

$$E_{2j} = \frac{1}{2}(3^{2j-3} + 3^{j-1}) \quad \text{for even } k \tag{26}$$

$$E_{2j-1} = \frac{1}{2}(3^{2j-4} + 3^{j-2}) \quad \text{for odd } k \tag{27}$$

STAGGERED HYDROGEN AND CARBON ATOM ROTAMERS (CH-ROTAMERS) OF n-ALKANES

If rotamers involving not only C—C bonds but also C—H bonds are considered (CH-rotamers) their number increases considerably over C-rotamers. For ethane there are three staggered CH-rotamers, for propane there are nine, and for an n-alkane C_kH_{2k+2} there are 3^{k-1} CH-rotamers.[17,18] "Reaction graphs" depicting the interconversions of such CH-rotamers were called power graphs $G(3^s)$ in a previous paper.[18] Since this case is already analyzed, we will no longer discuss CH-rotamers.

STAGGERED CARBON ATOM ROTAMERS (C-ROTAMERS) OF BRANCHED ALKANES WITHOUT QUATERNARY CARBON ATOMS

Staggered C-rotamers of branched alkanes are found by a method similar to that employed for n-alkanes. The symbolization of any kind of branched alkane staggered C-rotamers using the four digits 1, 2, 3 and 4 according to refs.[2,4,5] takes into account the following additional rules.

---

[17] J. Dugundji, P. Gillespie, I. Ugi and D. Marquarding, in "Chemical Applications of Graph Theory" (A. T. Balaban, editor), Academic Press, London, 1976, p. 167.

[18] A. T. Balaban and F. Kerek, *Rev. Roumaine Chim.*, **19**, 631 (1974).

The longest chain is coded by the four digits, and the branches are indicated by brackets following the digits where branching occurs. Two branches at the same quaternary vertex are separated by a comma inside the brackets.

Again, from several longest paths and from several starting points of the path, the minimal number is selected as the code, ignoring brackets or commas, but taking into account only the digits.

When two or more minimal codes differ only by the position of the bracket(s), the code with the bracket(s) further to the right has precedence over those with the brackets closer to the left side of the symbol, e.g. for the achiral rotamer of 2-methylbutane, 12(3)4 is preferred over 1(2)34.

On studying the C-rotamers of branched alkanes C_kH_{2k+2} with t tertiary and no quaternary carbon atoms it appeared that there is a one-to-one correspondence between the number of these C-rotamers and the branched catafusenes possessing the same type of branching in the dualist graph but with $k + t - 1$ condensed rings: C-rotamers of n-alkanes C_kH_{2k+2} with $t = 0$ correspond to non-branched catafusenes with $k-1$ rings; an additional linear branch introduces into the dualist graph of the corresponding catafusene not only as many vertices of degree two as the number of carbon atoms in the branch, but also a vertex of degree three (cf. fig. 5). Thus, even though the alkane may have two adjacent tertiary carbon atoms (V in fig. 5), the dualist graph of the corresponding catafusene never has two adjacent vertices of degree three.

Table 5 presents the smallest branched alkanes devoid of quaternary carbon atoms, and their codes (4DC and 3DC). In the case of higher branched alkanes, which are not included in table 5, more than one C-rotamer with *a*-type 3DC may exist, for instance 3,4-diethylhexane has 3 *a*-type ($\mathbf{C}_{2k}$) and 3 *c*-type ($\mathbf{C}_i$) achiral rotamers, as well as 15 *s*-type ($\mathbf{C}_2$) and 44 *u*-type ($\mathbf{C}_1$) chiral rotamers. In the case of a symmetrically branched decane with four adjacent tertiary carbons, 2,4-dimethyl-3-isopropylpentane (VI), the corresponding catafusene graph (e.g. VII for one particular rotamer) has 13 vertices; there exist a total of

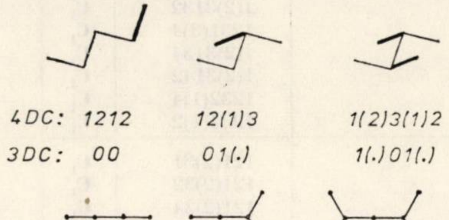

Fig. 5. — Alkanes and corresponding catafusenes: each branching (heavy line) increases by one the number of vertices of the corresponding catafusene.

seven C-rotamers, which have the same point groups as those for 3-ethylpentane (table 5) or 3-ethyl-3-methylpentane which will be mentioned in table 7.

Table 5

Branched alkane C-rotamers without quaternary carbon atoms

Alkane	4-Digit code	Point group	Achiral	Chiral	3-Digit code	Symm.	Total no.
2-Methylpropane	1(2)3	C_{3v}	1		1(·)	★	1
2-Methylbutane	1(2)34	C_s	1		01(·)	*s*	2
	12(1)3	C_1		1	11(·)	*u*	
2-Methylpentane	121(3)4	C_s	1		001(·)	*s*	5
	121(2)3	C_1		4	011(·)	*u*	
	123(1)2	C_1			1(·)12	*u*	
	123(1)4	C_1			101(·)	*u*	
	1(2)314	C_1			111(·)	*u*	
3-Methylpentane	12(1)31	C_s	3		11(·)1	*s*	6
	12(3)12	C_s			12(·)1	*s*	
	12(3)41	C_s			01(·)0	*s*	
	12(1)32	C_1		3	11(·)2	*u*	
	12(1)34	C_1			01(·)1	*u*	
	12(3)14	C_1			01(·)2	*u*	
2,3-Dimethylbutane	1(2)3(1)2	C_{2h}	1		1(·)01(·)	*a*	2
	1(2)3(1)4	C_2		1	1(·)11(·)	*u*	
2-Methylhexane	1212(3)4	C_s	1		0001(·)	*s*	14
	1212(1)3	C_1		13	0011(·)	*u*	
	1213(1)2	C_1			0121(·)	*u*	
	1213(1)4	C_1			0111(·)	*u*	
	1213(2)4	C_1			0101(·)	*u*	
	1231(2)3	C_1			1(·)121	*u*	
	1231(2)4	C_1			1(·)012	*u*	
	1(2)3124	C_1			1121(·)	*u*	
	1(2)3132	C_1			1021(·)	*u*	
	1231(3)4	C_1			1(·)112	*u*	
	1(2)3134	C_1			1011(·)	*u*	
	1(2)3142	C_1			1111(·)	*u*	
	1232(1)4	C_1			1001(·)	*u*	
	1234(1)2	C_1			1(·)011	*u*	
3-Methylhexane	121(2)31	C_1		27	011(·)2	*u*	27
	121(2)32	C_1			011(·)1	*u*	
	121(2)34	C_1			011(·)0	*u*	
	12(1)312	C_1			11(·)12	*u*	
	12(1)314	C_1			112(·)2	*u*	
	121(3)21	C_1			012(·)1	*u*	
	12(1)321	C_1			121(·)1	*u*	
	121(3)23	C_1			012(·)2	*u*	
	121(3)24	C_1			012(·)0	*u*	
	12(1)324	C_1			111(·)1	*u*	
	121(3)41	C_1			001(·)2	*u*	
	12(1)341	C_1			101(·)1	*u*	

(continues on next page)

Table 5 (continued)

Alkane	4-Digit code	Point group	Achiral	Chiral	3-Digit code	Symm.	Total no.
	121(3)42	C_1		27	001(·)0	*u*	27
	12(1)342	C_1			102(·)2	*u*	
	121(3)43	C_1			001(·)1	*u*	
	123(1)23	C_1			121(·)2	*u*	
	123(1)24	C_1			01(·)21	*u*	
	12(3)124	C_1			111(·)2	*u*	
	12(3)132	C_1			122(·)1	*u*	
	12(3)134	C_1			112(·)1	*u*	
	123(1)42	C_1			01(·)01	*u*	
	12(3)142	C_1			101(·)2	*u*	
	123(1)43	C_1			102(·)1	*u*	
	123(2)14	C_1			01(·)12	*u*	
	123(2)41	C_1			01(·)11	*u*	
	123(4)12	C_1			01(·)02	*u*	
	123(4)21	C_1			01(·)22	*u*	
3-Ethylpentane	12(31)41	C_{3v}	3		01(0)0	*	7
	12(12)34	C_s			01(2)1	*s*	
	12(13)41	C_s			01(1)2	*s*	
	12(13)32	C_3		4	11(2)2	*	
	12(12)31	C_1			11(1)1	*u*	
	12(13)34	C_1			01(1)1	*u*	
	12(13)43	C_1			01(0)1	*u*	
2,3-Dimethylpentane	12(1)3(1)2	C_1		9	1(·)01(·)1	*u*	9
	12(1)3(1)4	C_1			1(·)12(·)2	*u*	
	12(1)3(2)4	C_1			11(·)11(·)	*u*	
	12(3)1(2)3	C_1			1(·)01(·)2	*u*	
	12(3)1(2)4	C_1			1(·)12(·)1	*u*	
	1(2)3(1)24	C_1			01(·)01(·)	*u*	
	12(3)1(3)4	C_1			1(·)11(·)2	*u*	
	1(2)3(1)42	C_1			01(·)11(·)	*u*	
	12(3)4(1)2	C_1			01(·)21(·)	*u*	
2,4-Dimethylpentane	1(2)34(1)2	C_{2v}	2		1(·)001(.)	*a*	4
	1(2)31(2)3	C_s			1(·)121(·)	*c*	
	1(2)31(3)4	C_2		2	1(·)111(·)	*s*	
	1(2)31(2)4	C_1			1(·)011(·)	*u*	
3,4-Dimethylhexane	12(1)3(1)21	C_i	3		11(·)02(·)2	*c*	33
	12(3)1(3)21	C_i			12(·)01(·)2	*c*	
	12(3)4(3)21	C_i			01(·)02(·)0	*c*	
	12(1)3(1)41	C_2		30	11(·)11(·)1	*s*	
	12(1)3(2)12	C_2			11(·)01(·)1	*s*	
	12(1)3(4)24	C_2			11(·)21(·)1	*s*	
	12(3)1(2)31	C_2			12(·)02(·)1	*s*	
	12(3)1(3)41	C_2			12(·)22(·)1	*s*	
	12(3)1(4)21	C_2			12(·)12(·)1	*s*	
	12(3)4(1)23	C_2			01(·)21(·)0	*s*	
	12(3)4(2)31	C_2			01(·)01(·)0	*s*	
	12(3)4(3)12	C_2			01(·)11(·)0	*s*	
	12(1)3(1)23 etc.	C_1			11(·)01(·)1	*u*	

* Unlike 3DC for C-rotamers of *n*-alkanes, branched alkanes and their 3DC may also have ternary axes.

Those branched alkanes which are constitutionally chiral,[9] e.g. 3-methylhexane and 2,3-dimethylpentane in table 5, have no achiral C-rotamers, and all their rotamers have point group $\mathbf{C}_1$. The other branched alkanes have C-rotamers which are either chiral or achiral, as shown in table 5.

By analogy with table 4, one could discuss chirality around branching points (tertiary carbon atoms of the alkane), i.e. in the 4DC a quadruplet or tetrad, $a(b)cx$ or $xa(b)c$, and a quintuplet or pentad of digits, $a(b)c(x)y$.

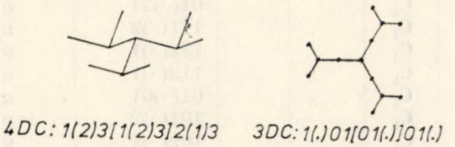

VI VII

Fig. 6. — A branched decane C-rotamer and the corresponding catafusene.

The following rules for such multiplets result by inspection of models :

(i) Quadruplets using all four digits in the 4DC, of the form $ab(c)d$ or $a(b)cd$, are achiral (VIII in fig. 7).

(ii) Quadruplets using only three of the four digits, of the form $a(b)cb$, $a(b)ca$, $ab(c)a$ or $ab(a)c$, are chiral, i.e. possess helicity (IX and X in fig. 7). We assign 3DC to IX and X so that the shape of the catafusene is reminiscent of the alkane rotamer (fig. 7).

(iii) Change of one digit in the preceding type of quadruplet changes the helicity, i.e. $ab(a)c$ and $ab(a)d$ have opposite helicities, and so have : $a(b)cb$ and $a(b)db$; or $a(b)cb$ and $a(b)ca$.

(iv) The order of branches does not affect the helicity, hence $ab(a)c\ldots$ and $ab(c)a\ldots$ have the same helicity, and likewise... $a(b)cb\ldots$ and $\ldots b(a)cb\ldots$, or $a(b)c(a)b\ldots$ and $a(b)c(b)a\ldots$

(v) When the alkane C-rotamer has two adjacent tertiary carbons, the four-digit code contains a quintuplet of the form $a(b)c(x)y$. Examination of models shows that quintuplets $a(b)c(a)b$ or $a(b)c(b)a$ are achiral (XI, fig. 8).

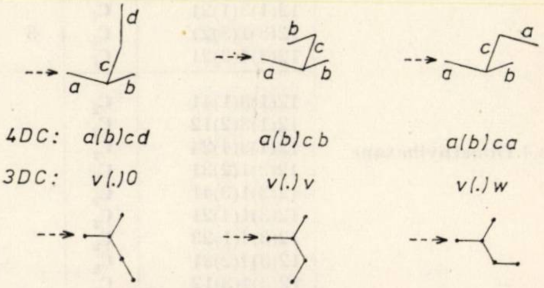

VIII IX X

Fig. 7. — Quadruplets (4DC) and the corresponding catafusenes (3DC).

(vi) Quintets (4DC) shown in fig. 8 for XII and XIII indicate chiral rotamers. The assignments of 3DC take into account that *trans* branches (denoted by *a* in XII) appear as the marginal branches of the wide **M** in fig. 8 for the corresponding catafusene.

It is tedious to devise dictionaries analogous to table 4 for quadruplets and quintuplets because the numbers of possible combinations increases rapidly: there are 48 chiral quadruplets $a(b)cx$ or $xc(b)a$ (where $x = a$ or b) and 24 achiral quadruplets $a(b)cd$ or $ab(c)d$ and there are still more quintuplets. However, a few of the underlying principles were presented in fig. 7 for quadruplets and in fig. 8 for quintuplets; these lie at the basis of the correspondences contained in table 5. Figure 9 presents examples with one branching point, and fig. 10 with two branching points.

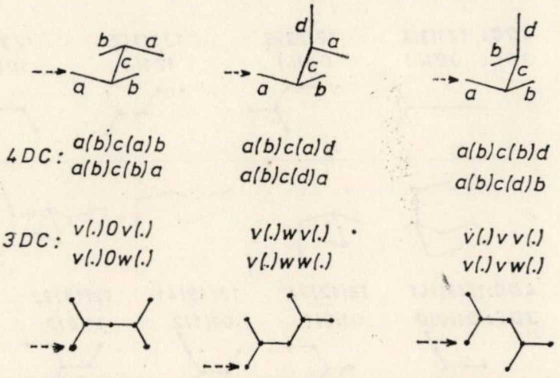

XI XII XIII

Fig. 8. — Quintuplets (4DC) and the corresponding catafusenes (3DC).

It should be borne in mind that in the four-digit code for branched alkanes, the digits before the bracket indicate orientations *towards* the next branching point, whereas digits within or after the bracket indicate orientations of the bonds in carbon chains *after* the preceding branching point. This is also true for the three-digit code. Therefore, the chirality for branched alkanes can no longer be directly inferred from their three-digit codes; however, when only one tertiary branching point is present, the 3-digit codes of the three branches considered *from* the branching point do give a *D* value which correctly represents the chirality of the C-rotamer. This is exemplified in fig. 9 for the 3-ethylpentane C-rotamers where, under each catafusene, the 3DC for the three branches are given starting from the branching point, and the *D* value correctly correlates with the chirality. In fig. 9, *D* is the difference between the number of digits 1 and 2 in the two branches given in and after the brackets in the 3DC, whereas digits of the branch before the brackets (excluding the digit immediately preceding the brackets) undergo the permutation (0)(1,2).

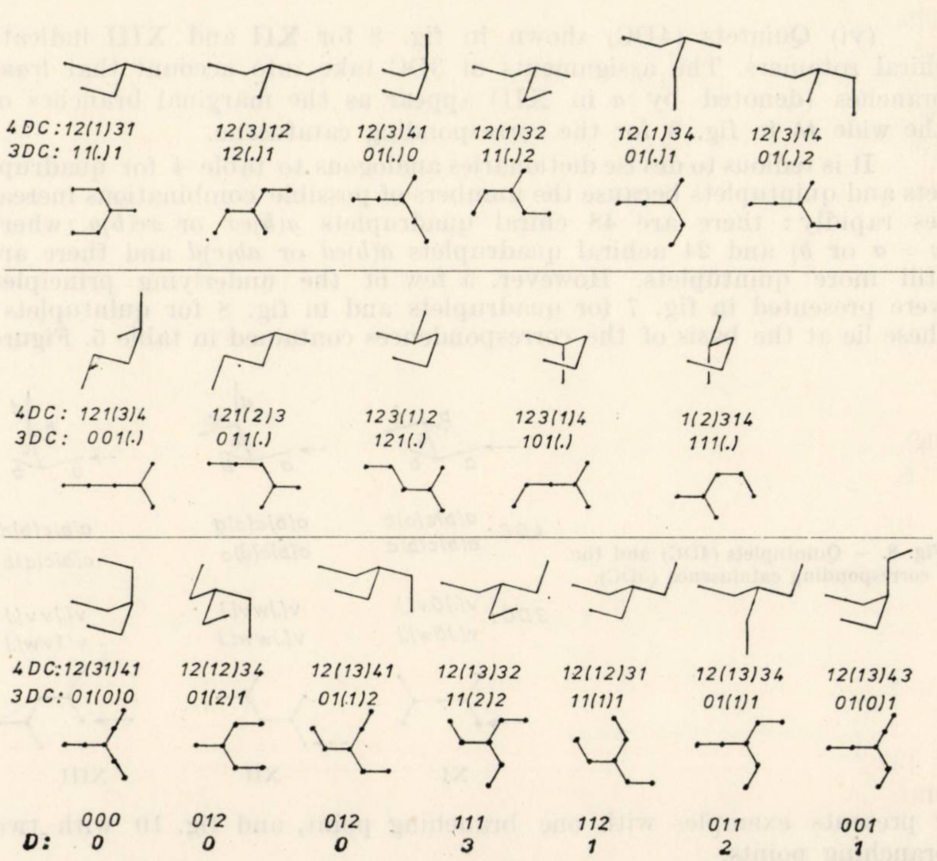
4DC:12(1)31
3DC: 11(.)1
12(3)12
12(.)1
12(3)41
01(.)0
12(1)32
11(.)2
12(1)34
01(.)1
12(3)14
01(.)2
4DC: 121(3)4
3DC: 001(.)
121(2)3
011(.)
123(1)2
121(.)
123(1)4
101(.)
1(2)314
111(.)
4DC:12(31)41
3DC: 01(0)0
12(12)34
01(2)1
12(13)41
01(1)2
12(13)32
11(2)2
12(12)31
11(1)1
12(13)34
01(1)1
12(13)43
01(0)1
000
D: 0
012
0
012
0
111
3
112
1
011
2
001
1

Fig. 9. — 3-Ethyl-, 2- and 3-methylpentane C-rotamers with their corresponding catafusenes.

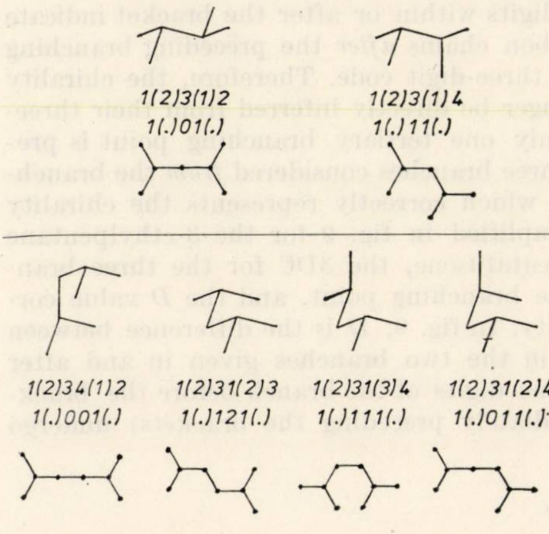
1(2)3(1)2
1(.)01(.)
1(2)3(1)4
1(.)11(.)
1(2)34(1)2
1(.)001(.)
1(2)31(2)3
1(.)121(.)
1(2)31(3)4
1(.)111(.)
1(2)31(2)4
1(.)011(.)

Fig. 10. — 2,3-Dimethylbutane and 2,4-dimethylpentane C-rotamers with their corresponding catafusenes.

All achiral and enantiomeric C-rotamers will give rise to an achiral mixture of C-rotamers on starting from an achiral alkane. However, in the case of constitutionally chiral branched alkanes, this chirality will influence the populations of enantiomeric C-rotamers, so that the result will be a combination of constitutional and conformational chirality. A similar influence may be manifested on C-rotamers of achiral alkanes by a chiral solvent which will induce unequal populations of enantiomeric C-rotamers.

STAGGERED C-ROTAMERS OF ALKANES WITH QUATERNARY CARBON ATOMS

When quaternary carbon atoms are present in the branched alkane, it is no longer possible in principle to find a correspondence with catafusenes, whose dualist graphs have points of degree 1, 2, or 3, but not 4. Alkanes C_kH_{2k+2} with one quaternary carbon may be found as partitions of the integer $k-1$ into four smaller non-zero integers corresponding to the branches b_i:

$$\sum_{i=1}^{4} b_i = k - 1$$

The numbers of such alkanes are presented in table 6. When the four branches b_i corresponding to the partition numbers are unequal

Table 6

Staggered C-rotamers of alkanes with one quaternary carbon

k	Alkane $C_k\ H_{2k+2}$	Partition	Achiral				Chiral				Total no.
			T	C_{3v}	C_{2v}	C_s	S_4	C_3	C_2	C_1	
5	2,2-Dimethylpropane	1+1+1+1	1	—	—	—	—	-	—	—	1
6	2,2-Dimethylbutane	1+1+1+2	—	—	—	1	—	—	—	—	1
7	2,2-Dimethylpentane	1+1+1+3	—	—	—	1	—	—	—	1	2
	3,3-Dimethylpentane	1+1+2+2	—	—	1	1	—	—	1	1	4
8	2,2-Dimethylhexane	1+1+1+4	—	—	—	1	—	—	—	4	5
	3,3-Dimethylhexane	1+1+2+3	—	—	—	1	—	—	—	13	14
	3-Ethyl-3-methylpentane	1+2+2+2	—	1	—	2	—	1	—	3	7
9	2,2-Dimethylheptane	1+1+1+5	—	—	—	1	—	—	—	13	14
	3,3-Dimethylheptane	1+1+2+4	—	—	—	1	—	—	—	40	41
	4,4-Dimethylheptane	1+1+3+3	—	—	1	4	—	—	4	16	25
	3,3-Diethylpentane	2+2+2+2	—	—	1	1	1	1	1	2	6
	3-Ethyl-3-methylhexane	1+2+2+3	—	—	—	3	—	—	—	39	42
10	2,2-Dimethyloctane	1+1+1+6	—	—	—	1	—	—	—	40	41
	3,3-Dimethyloctane	1+1+2+5	—	—	—	1	—	—	—	121	122
	4,4-Dimethyloctane	1+1+3+4	—	—	—	1	—	—	—	121	122
	3-Ethyl-3-methylheptane	1+2+2+4	—	—	—	3	—	—	—	120	123
	4-Ethyl-4-methylheptane	1+2+3+3	—	—	—	9	—	—	—	117	126
	3,3-Diethylhexane	2+2+2+3	—	—	—	3	—	—	—	39	42
11	4,4-Diethylheptane	2+2+3+3	—	—	1	5	—	—	13	176	195
	2,2-Dimethylnonane etc.	1+1+1+7	—	—	—	1	—	—	—	121	122

(methyl groups being disregarded), the number of C-rotamers is:

$$\frac{1}{2}\cdot 3^{\sum_i (b_i-1)}+1$$

where only those branches with $b_i > 1$ are considered. However, 2,2-dimethylalkanes C_kH_{2k+2} yield only $(3^{k-6}+1)/2$ staggered C-rotamers because they have actually only one branch longer than methyl. The number of C-rotamers of *gem*-dimethyl alkanes with the other two branches equal, e.g. 3,3-dimethylpentane, 4,4-dimethylheptane, etc. is equal to that of the respective n-alkane without the *gem*-dimethyl branches, i.e. n-pentane and n-heptane, respectively.

Table 7

Four-digit codes of staggered C-rotamers of alkanes with quaternary carbon atoms

Alkane	Code	Permutation	Point group
2,2-Dimethylpentane	121(2,3)4	(1)(2)(3,4)	C_s
	123(1,2)4	—	C_1
3,3-Dimethylpentane	12(3,4)12	(1,2)(3,4)	C_{2v}
	12(1,3)41	(1)(3)(2,4)	C_s
	12(1,3)43	(1,3)(2,4)	C_2
	12(1,3)42	—	C_1
2,2,3-Trimethylbutane	1(2)3(1,2)4	—	C_1
3-Ethyl-3-methylpentane	12(1,31)41	(1)(2,3,4)	C_{3v}
	12(1,32)42	(1)(2)(3,4)	C_s
	12(1,34)43	(1)(2)(3,4)	C_s
	12(14,3)42	(3)(1,2,4)	C_3
	12(1,31)42	—	C_1
	12(1,32)43	—	C_1
	12(12,3)42	—	C_1
3,3-Diethylpentane	12(12,34)43	(1,2)(3,4)	C_{2v}
	12(12,31)41	(1)(2)(3,4)	C_s
	12(13,34)42	(1,2,4,3)	S_4
	12(12,31)42	(1,2)(3,4)	C_2
	12(12,31)43	—	C_1
	12(13,32)41	—	C_1
4,4-Dimethylheptane	121(3,4)212	(3)(4)(1,2)	C_{2v}
	121(2,3)424	(2)(3)(1,4)	C_s
	123(1,2)421	(1)(2)(3,4)	C_s
	123(1,4)231	(1)(4)(2,3)	C_s
	123(2,4)123	(2)(4)(1,3)	C_s
	121(2,3)434	(1,4)(2,3)	C_2
	123(1,2)412	(1,2)(3,4)	C_2
	123(1,4)234	(1,4)(2,3)	C_2
	123(2,4)143	(1,3)(2,4)	C_2
	121(2,3)412	—	C_1
	etc.		

No simple general formula was found for the case of alkanes with quaternary carbons having equal longer branches, or having more than one quaternary carbon. Examples of C-rotamers of some alkanes with quaternary carbons are presented in table 7 and in fig. 11.

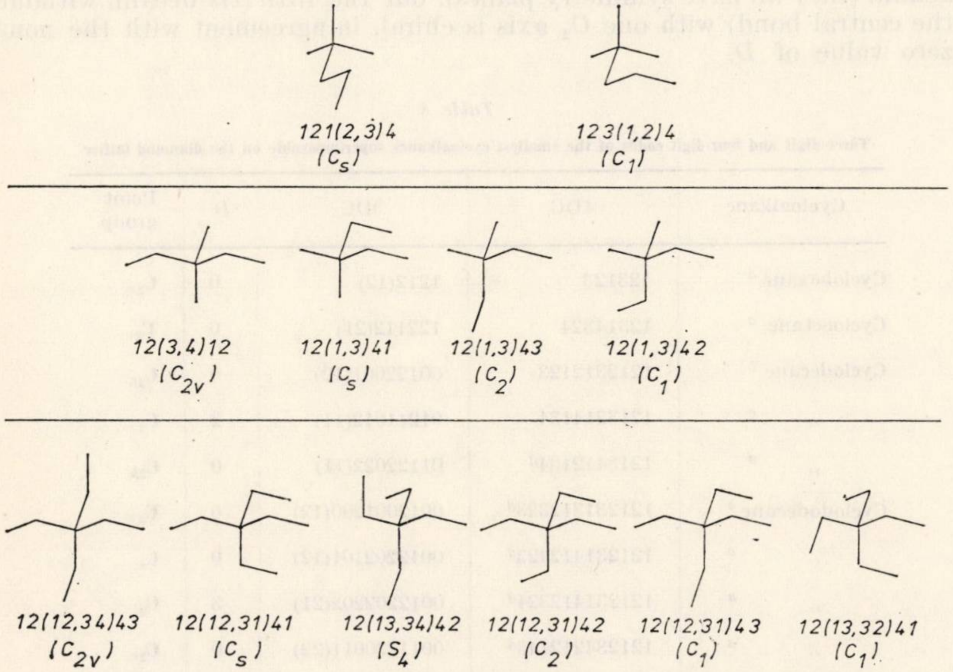

Fig. 11. — Rotamers of 2,2- and 3,3-dimethylpentane and of 3,3-diethylpentane.

CYCLOALKANES SUPERIMPOSABLE ON THE DIAMOND LATTICE

This problem was examined by Saunders[5b] using the four-digit code and a computer program; overcrowded conformations like the *cis* or *trans* decalin frameworks for cyclodecane were disregarded.

Conversion of the four-digit code into the three-digit code is straightforward by means of table 4. The four-digit code of cycloalkanes ends where the ends meet; with the three-digit code, an overlap of the last two digits is useful, i.e. for a cycloalkane C_kH_{2k} both codes will have k digits. For obtaining the last two overlapping digits in the 3-digit code, the 4-digit code being cyclic, its initial digits are repeated at the end prior to the translation. We will adopt the convention that the overlapping last two digits of the three-digit code will be included in brackets. There is no possibility of confusion since long branches are not indicated by brackets at the end of the code. The 3-digit code affords as before an indication D of the chirality of the cycloalkane. Some examples for the smallest cycloalkanes superimposable on the diamond lattice are given in table 8. Four of the first five cycloalkanes from table 8 are achiral (they all have symmetry planes), but the fifth (*cis*-decalin without the central bond) with one C_2 axis is chiral, in agreement with the non-zero value of D.

Table 8

Three-digit and four-digit codes of the smallest cycloalkanes superimposable on the diamond lattice

Cycloalkane	4DC	3DC	D	Point group
Cyclohexane [a]	123123	1212(12)	0	C_{3v}
Cyclooctane [a]	12314324	122112(21)	0	C_{2v}
Cyclodecane [b]	1212312123	00122001(12)	0	C_{2h}
,, [c]	1213214134	01211012(11)	2	C_2
,, [a]	1213412134[d]	01122022(11)	0	C_{2h}
Cyclododecane [a]	121231312323[d]	0012001200(12)	0	C_{3v}
,, [a]	121231412423[d]	0012202101(12)	0	C_s
,, [a]	121231412324[d]	0012202202(21)	3	C_2
,, [a]	121234212143[d]	0011220011(22)	0	C_{2v}
,, [e]	121321423124	0121122211(21)	1	C_2
,,	121231214324	0012101112(21)	3	C_1

[a] Included in Saunders's paper.[5b]

[b] Envelope of *trans*-decalin.

[c] Envelope of *cis*-decalin.

[d] The 4DC[5b] was rearranged to yield the smallest number.

[e] Envelope of *cis*-bicyclo[6.4.0]dodecane (staggered conformer).

[f] Envelope of *trans*-bicyclo[6.4.0]dodecane (staggered conformer).

CONCLUSIONS

1. The number R_k of C-rotamers of n-alkanes C_kH_{2k+2} is equal to that of non-branched catafusenes with $k-1$ benzenoid rings. Explicit formulas were found for this number and for its partitions into various classes with different symmetries, considering or disregarding enantiomerism.

2. Two coding systems (four- and three-digit codes) can be employed for specifying one particular C-rotamer. The 3DC can be correlated with the optical activity of the alkane rotamer and with its energy.

3. The number of branched alkane C-rotamers with t tertiary, and no quaternary, carbon atoms is equal to that of branched catafusenes with $k+t-1$ benzenoid rings. No explicit formula for this number has yet been found. Codings (4DC and 3DC) were devised for these rotamers. When only one tertiary carbon is present, the 3DC again gives a D value which can be correlated with optical activity.

4. Branched alkane C-rotamers with quaternary carbons can only be coded with the 4DC, therefore explicit enumeration formulas or correlations are no longer possible.

5. Cycloalkane rotamers can be coded by 4DC and 3DC, the latter code giving the possibility to correlate the conformation with its optical activity.

6. Though it is not yet possible to investigate individual alkane C-rotamers at room temperature (see, however ref.[19] for an overcrowded hydrocarbon which gives stable rotamers at room temperature), ideas are presented which may prove useful for interpreting low-temperature NMR spectra.

Previous reports in the literature dealing with the enumeration and codification of rotamers [20–22] contained some of the above ideas, in different formulation.

---

[19] M. Minabe and K. Suzuki, *J. Org. Chem.*, **40**, 1298 (1975) and previous papers.

[20] J. Shimanouchi and S. Mizushima, *Sci. Papers Inst. Phys. Chem. Res.* (Tokyo), **40**, 467 (1943); "The Structure of Molecules and Internal Rotation", Academic Press, New York, 1954, p. 162.

[21] F. Becker, *Z. Naturforsch.*, **14a**, 547 (1959).

[22] M. Hanack, "Conformation Theory", Academic Press, New York, 1965, pp. 36, 69.

Revue Roumaine de Chimie, **21**, 7, 1073–1081 (1976)

CONTRIBUTIONS TO THE STUDY OF HETEROCYCLES. XXXVIII *

APPLICATION OF THE SOMMELET REACTION IN THE SERIES OF 2-ARYL-4-METHYL-5-CHLOROMETHYL-THIAZOLE

I. SIMITI and ANA MUREŞAN
Institute of Medicine and Pharmacy, Cluj-Napoca,
Laboratory of Organic Chemistry, Str. V. Babeş 41, Romania

Received March 9, 1974
Completed January 7, 1976

There are indicated the obtention of 2-aryl-4-methyl-5-chloromethyl-thiazole and the use of the Sommelet reaction in this series.

The Sommelet reaction is one of the convenient methods of introducing the formyl group by the intermediate of halomethyl derivatives[1]. After attempts of applying this reaction, Angyal and his co-workers concluded that in the hetero-aromatic series the Sommelet reaction cannot be applied in order to introduce the formyl group "in α position relative to the nitrogen atom", the only exception being that of obtaining the 2-phenyl-4-formyl thiazole.[2,3]

In a series of previous papers, we proved, however, that this reaction can be successfully applied for obtaining 2-R-4-formyl thiazoles[4–11] and 2-aryl-4-formyl oxazoles.[12]

The fact that we were not successful in applying this reaction to the 1,3,4-thiadiazole series,[13] along with the good results obtained in the above mentioned series, determined us to consider that the Sommelet reaction depends on the density of electrons at the carbon atom on which the chloromethyl group is bound.[7,14]

---

* Part XXXVII. I. Simiti, I. Schwartz, M. Farkaş and E. Chindriş. *Rev Roumaine Biochim.*, **11,** 145 (1974).

[1] M. M. Sommelet, *C. R. hebd. Séances Acad. Sci.* **157**, 852 (1913).

[2] S. J. Angyal, G. B. Barlin and P. C. Wailes, *J. Chem. Soc.* **1953**, 1740.

[3] S. J. Angyal, *Organicheschie Reactsii*, **8**, 267 (1956) Moscva.

[4] Al. Silberg, Z. Frenkel and L. Cormoş, *Studia Univ. "Babeş-Bolyai", ser. Chem.* **7**, 23 (1962).

[5] Al. Silberg, I. Simiti and H. Mantsch, *Chem. Ber.*, **94**, 11, 2887 (1961).

[6] I. Simiti, M. Farkas and S. Silberg, *Chem. Ber.* **95**, 2672 (1962).

[7] I. Simiti and M. Farkas, *Bull. Soc. chim. France*, **1968**, 3862.

[8] I. Simiti and G. Hintz, *Pharmazie*, **3**, 146 (1972).

[9] I. Simiti and M. Farkas, *Arch. Pharm.*, **307**, 81 (1974).

[10] I. Simiti and G. Hintz, *Pharmazie*, **29**, 443 (1974).

[11] I. Simiti and H. Demian, *Ann. Chim.* (in press).

[12] I. Simiti and E. Chindris, *Arch. Pharm.*, **308**, 688 (1975).

[13] I. Simiti and L. Proinov, *Rev. Roumaine Chim.* **11**, 429 (1966).

[14] I. Simiti and L. Proinov, *Arch. Pharm.* **303**, 134 (1970).

Our supposition is based on the fact that the electron densities of the heterocycle positions, where the Sommelet reaction was not possible to be used, are lower than those of a C atom in the benzene ring, in contrast to the position 4 of thiazole and oxazole, where the density is closer to that of the latter.

In order to prove again the importance of the electron density of the C atom as bearer of the chloromethyl group, we tried to use the Sommelet reaction in position 5 of the thiazole being well known that the 2-aryl-thiazole has the highest electron density in position 5 of the heterocycle.[15,16]

As it was not possible to obtain the 2-aryl-4-methyl-5-chloro-methyl thiazoles in a convenient way directly by a Hantzsch condensation, we had to introduce the chloromethyl group in the position 5 by transforming other groups. For this purpose we tried to obtain the 2-aryl-4-methyl-5-carbetoxy thiazoles IIa-e by condensation of the corresponding thioamides with α-bromo-aceto-acetic ester, when we found that the Hubacher's method,[17] which used α-chloro-aceto-acetic ester, does not give good results. Therefore, we had to modify the reaction conditions for the preparation of these compounds in order to obtain better yields. We mention that in our experimental conditions the intermediate compounds in the synthesis of the thiazoles can be isolated, i.e. the 2-*p*-(X-phenyl)-4-hydroxy-4-methyl-5-carbethoxy-Δ_2-thiazolines, (Ia, b) in the case of compounds IIa, b.

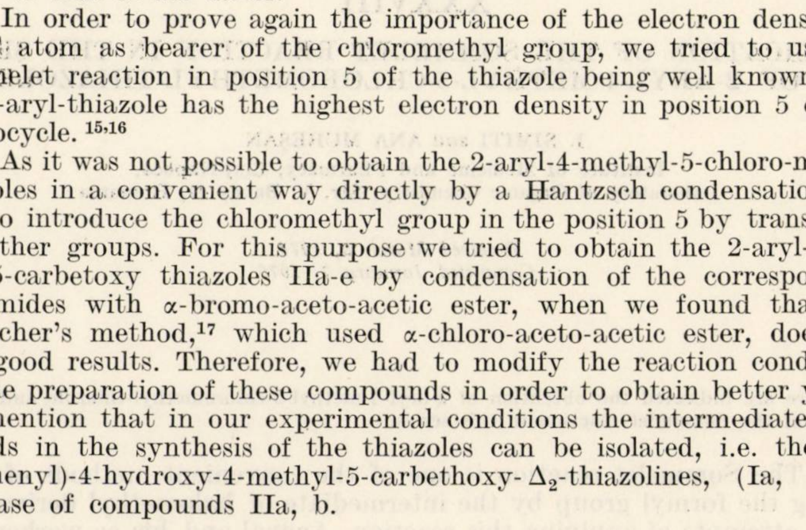

We have to point out that the stability of these hydroxy-thiazolines is lower than that of intermediates in analogous series,[18,19] a fact that can be explained by their increased tendency for aromatisation which is, probably, due to the influence of the carbetoxy group in position 5. The UV spectra of these intermediates, show a single absorption band at 244 nm, contrary to the corresponding thiazoles which give two bands.

The compounds IIa-e were transformed by reduction with lithium aluminium hydride, at room temperature,[20] in the corresponding alco-

---

[15] I. Schwartz, Thesis, Babeș Bolyai University, Cluj, 1970.

[16] N. Bodor, M. Farkas and N. Trinajstic, *Croat. Chem. Acta*, **43**, 107 (1971).

[17] K. Hubacher, *Liebigs Ann. Chem.*, **259**, 237 (1890).

[18] I. Simiti, M. Coman and I. Schwartz, *Rev. Roumaine Chim.*, **18**, 685 (1973).

[19] K. Brown and R. A. Newberry, *Quart. Rephs., Sulphur. Chem.*, **3**, 4 (1969).

[20] B. A. Jansen and M. Szelke, *J. Chem. Soc.* **1961**, 405.

hols IIIa-e. The reduction of the esters to alcohols has been carried out also at temperatures below zero degree[21] but there were not great differences in the yields. By adding thionyl chloride to the alcohols these have been transformed into the chloromethyl derivatives IVa-e. We proposed to investigate the behaviour of these chloromethyl derivates in the Sommelet reaction.

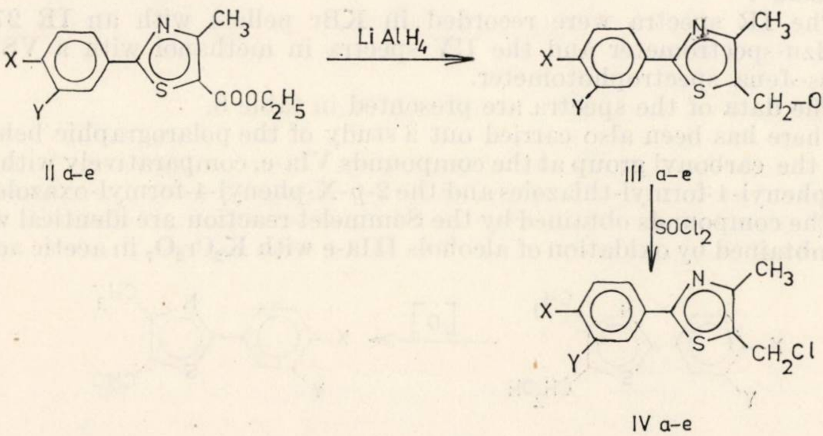

By boiling compounds IVa-e with urotropine in chloroform, they were transformed into the corresponding urotropine salts Va-e.

On hydrolysis with 50% acetic acid these salts lead to the aldehydes VIa-e. We also tried to effect the Sommelet reaction directly, without separating the urotropine salts, but the results were unsatisfactory.

The aldehydes VIa-e gave the characteristic reactions for the carbonyl function.

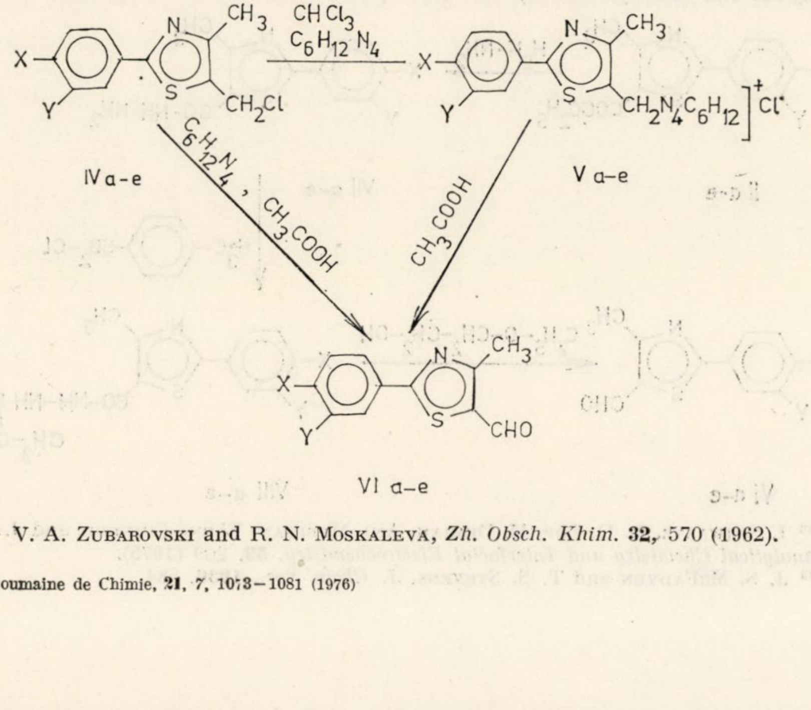

---

[21] V. A. Zubarovski and R. N. Moskaleva, *Zh. Obsch. Khim.* **32**, 570 (1962).

The IR spectra of these compounds show an absorption band characteristic of the carbonyl group at about 1660 cm^{-1}, at a frequency lower than that of similar compounds with the CHO group in position 4 which presumes a stronger conjugation in this case.

The UV spectra of these compounds show two maxima at 322—346nm and 234—248 nm, very similar to the 2,4,5-trisubstituted derivatives of thiazole[18].

The IR spectra were recorded in KBr pellets with an IR 27 G Shimadzu-spectrometer and the UV spectra in methanol with a VSU-2 C. Zeiss-Jena spectrophotometer.

The data of the spectra are presented in table 8.

There has been also carried out a study of the polarographic behaviour of the carbonyl group at the compounds VIa-e, comparatively with the 2-*p*-X-phenyl-4-formyl-thiazoles and the 2-*p*-X-phenyl-4-formyl-oxazoles.[22]

The compounds obtained by the Sommelet reaction are identical with those obtained by oxidation of alcohols IIIa-e with $K_2Cr_2O_7$ in acetic acid :

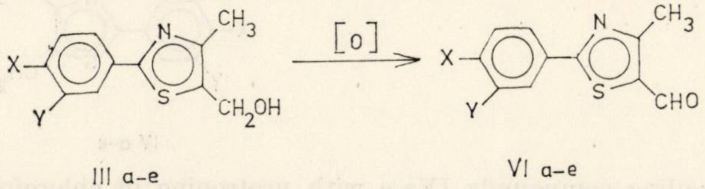

and with those prepared by the reaction of McFadyen and Stevens [23] starting from the esters II a-e.

In order to obtain the compounds VIa-e by this last method, the esters IIa-e have been transformed into the corresponding hydrazides VIIa-e which were then acylated with the chloride of *p*-tolyl-sulphonic acid. By boiling the compounds VIIIa-e obtained by this method in ethylene glycol monoethyl ether, the aldehydes VIa-e were obtained.

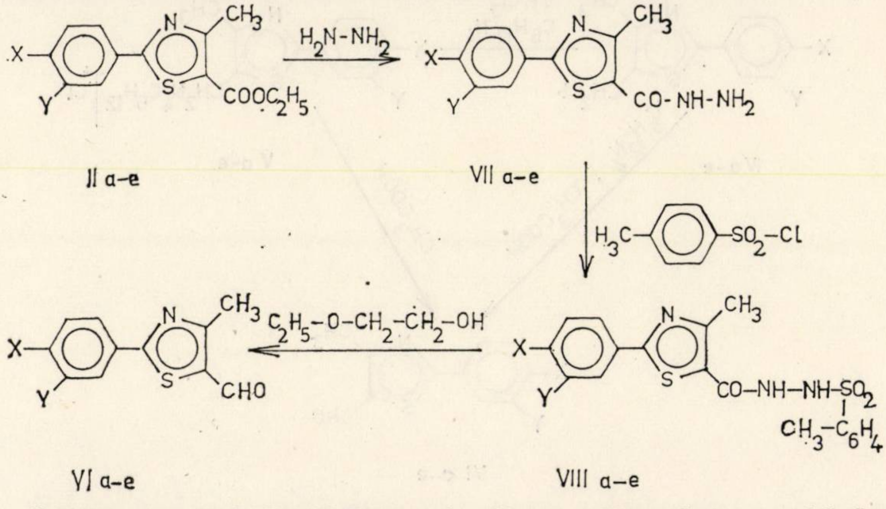

---

[22] I. Schwartz, R. D. Pop, H. Demian, Ana Mureşan, Elena Chindris and I. Simiti. *Electroanalytical Chemistry and Interfacial Electrochemistry*, **59**, 209 (1975).

[23] J. S. McFadyen and T. S. Stevens, *J. Chem. Soc.*, **1936**, 584.

We mention that if the reaction is carried out in ethylene glycol, which is the usual solvent for this reaction, the results are poorer.

Our results show the applicability of the Sommelet reaction also for position 5 of the thiazole ring, even when in *para* position of the benzene ring there are several substituents (CH_3, Br, OC_2H_5). This seems to confirm our early assumption on the importance of the electron density of the carbon atoms on which the halomethyl group is bound, concerning the application of the Sommelet reaction.

EXPERIMENTAL

2-Phenyl-4-methyl-4-hydroxy-5-carbetoxy-Δ_2-thiazoline Ia

a) 1.37 g (0.01 moles) thiobenzamide were dissolved in 20 ml acetone. This solution was added in portions to a solution of 1.5 ml (0.01 moles) α-bromo-aceto-acetic ester in 20 ml acetone in which a few pieces of ice were previously introduced. It is shaken for an hour then poured out on water and after filtering substance Ia is obtained which after repeated recrystallizations melts at 109–10°. M.W. 265.117
N% *Calcd.* = 5.28
N% *Found* = 5.39

b) 1.37 g (0.01 moles) of thiobenzamide are dissolved in 20 ml acetone and the obtained solution is added in portions to 1.5 ml (0.01 moles) α-bromoaceto-acetic ester. The mixture is left at room temperature for 6 hours. The deposited substance is filtered, washed with water until it is freed from Br^-. After recrystallization it melts at 107–9°.

The compound Ib was prepared in a similar way.
M.p. 123–5°. M.W. 279.361
N% *Calcd.* = 5.01
N% *Found* = 5.21

2-Phenyl-4-methyl-5-carbetoxy-thiazole IIa

1.37 g (0.01 moles) thiobenzamide were dissolved in 20 ml acetone. This solution was added in portions to a solution of 1.5 ml (0.01 moles) α-bromo-aceto-acetic ester in 20 ml acetone in which a few pieces of ice were previously introduced. After shaking for 4 hours the mixture was allowed to stand for 20 hours at room temperature. After filtration, the solution was poured on ice, and the compound IIa was filtered and recrystallized from alcohol; m.p. 43°. Yield: 75%.

The compounds IIb-e in table 1 were similarly prepared.

Table 1

2-Aryl-4-methyl-5-carbetoxy thiazoles *)

Derivatives	X	Y	Formula	M.p.°	N%	
					Calcd.	*Found.*
IIa	H	H	$C_{13}H_{13}NO_2S$	43[17)]	5.66	5.71
IIb	CH_3	H	$C_{14}H_{15}NO_2S$	120–1	5.36	5.40
IIc	Br	H	$C_{13}H_{12}BrNO_2S$	89–91	4.29	4.60
IId	H	CH_3	$C_{14}H_{15}NO_2S$	45–7	5.36	5.65
IIe	OC_2H_5	H	$C_{15}H_{17}NO_3S$	98–9	4.80	4.46

* All derivatives were recrystallized from alcohol.

2-Phenyl-4-methyl-5-hydroxymethyl thiazole IIIa

2.47 g (0.01 moles) of Ia were dissolved in 20 ml of anhydrous ethylic ether and to this solution 0.30 g lithium aluminium hydride were added. The mixture was stirred, left for an hour at room temperature, then were added 50 ml water and HCl until the pH became acid. After filtration the solution was extracted with ether. Evaporation of the ether gave compound IIIa which melted after recrystallization from water, at 100—1°. Yield 65%. Compounds IIIb-e shown in table 2 were similarly obtained.

Table 2

2-Aryl-4-methyl-5-hydroxymethyl thiazoles*

Derivatives	X	Y	Formula	M.p.°	N%	
					Calcd.	*Found.*
IIIa	H	H	$C_{11}H_{11}NOS$	100—1	6.82	6.55
IIIb	CH_3	H	$C_{12}H_{13}NOS$	107—9	6.38	6.12
IIIc	Br	H	$C_{11}H_{10}BrNOS$	145—7	4.93	5.03
IIId	H	CH_3	$C_{12}H_{13}NOS$	105—7	6.38	6.17
IIIe	OC_2H_5	H	$C_{13}H_{15}NO_2S$	139—40	5.61	5.24

* IIIa, IIIb, IIId — recrystallization from water.
IIIc, IIIe — recrystallization from alcohol.

2-Phenyl-4-methyl-5-chloromethyl thiazole IVa

5 ml of thionyl chloride were dropwise added to 1 g of IIIa, maintaining after this the vessel in a refrigerating mixture for 30 minutes.

After keeping the reaction mixture for 3 hours at room temperature, it was boiled on a steambath for 1 hour. The excess of thionyl chloride was removed and a solution of $NaHCO_3$ was added. After filtration and recrystallization from cyclohexane the compound melted at 85—7°. Yield 45 %. The compounds IVb-e shown in table 3 were similarly prepared.

Table 3

2-Aryl-4-methyl-5-chloromethyl thiazoles *

Derivatives	X	Y	Formula	M.p.°	N%	
					Calcd.	*Found*
IVa	H	H	$C_{11}H_{10}NSCl$	85—7	6.25	6.64
IVb	CH_3	H	$C_{12}H_{12}NSCl$	92—3	5.88	5.93
IVc	Br	H	$C_{11}H_9NSBrCl$	118—20	4.61	4.94
IVd	H	CH_3	$C_{12}H_{12}NSCl$	oil	5.88	6.03
IVe	OC_2H_5	H	$C_{13}H_{14}NOClS$	88—90	5.23	4.90

* All derivatives were recrystallized from cyclohexane.

The urotropine salt of 2-phenyl-4-methyl-5-chloromethyl thiazole Va

1 g (0.005 moles) of IVa was dissolved in chloroform together with an excess of urotropine and the solution boiled until an abundent precipitate appeared. Compound Va was then filtered and dried. Yield 85%. Compounds Vb-e were similarly obtained.

2-Phenyl-4-methyl-5-formyl thiazole VIa

a) 1 g Va and 0.2 g of urotropine were dissolved in a mixture of 10 ml conc. acetic acid and 10 ml water. The solution was boiled for 40 minutes, then poured into a glass, cooled and precipitated with water. Compound VIa filtered and recrystallized from water melted at 111–12°. Yield 65%. Compounds VIb-e were similarly obtained.

b) 0.20 g (0.001 moles) compound IIIa were dissolved in 5 ml of warm glacial acetic acid. The solution was mixed with a warm solution of 0.10 g kalium bichromate in 10 ml glacial acetic acid. The mixture was heated on a steam bath for 60 minutes. Then it was cooled, poured on water and after recrystallization from water VIa was obtained. Yield 70 %.

The method is also used for the preparation of the aldehydes VIb-e.

c) 0.9 g (0.025 moles) VIIa were dissolved by boiling in 15 ml ethylene glycol monoethyl ether; 0.9 g anhydrous sodium carbonate were added and then boiled for 15 minutes. The mixture was then poured in cold water, when VIa precipitated. Yield 50 %. Compounds VIb-e shown in table 4 were similarly prepared.

Table 4

2-Aryl-4-methyl-5-formyl thiazoles *

Derivatives	X	Y	Formula	M.p.°	N %		C %		H %	
					Calcd.	*Found*	*Calcd.*	*Found*	*Calcd.*	*Found*
VIa	H	H	$C_{11}H_9NOS$	111–2	6.88	6.94	65.0	65.33	4.46	4.12
VIb	CH_3	H	$C_{12}H_{11}NOS$	119–20	6.44	6.62	66.33	66.73	5.10	4.94
VIc	Br	H	$C_{11}H_8BrNOS$	164–5	4.96	5.16	46.82	47.24	2.85	2.44
VId	H	CH_3	$C_{12}H_{11}NOS$	108–9	6.44	6.64	66.33	66.80	5.10	4.77
VIe	OC_2H_5	H	$C_{13}H_{13}NO_2S$	160–2	5.66	5.63	63.13	63.55	5.29	4.83

* Va, Vb, Vd – recrystallization from water ;
Vc – recrystallization from acetic acid ;
Ve – recrystallization from alcohol.

The 2,4-dinitro-phenylhydrazones of VIa-e are presented in table 5.

Table 5

2,4-Dinitro-phenylhydrazones of VIa-e *

Derivatives	X	Y	Formula	M.p.°	N %	
					Calcd.	*Found.*
VIa′	H	H	$C_{17}H_{13}N_5O_4S$	275–6	18.21	18.48
VIb′	CH_3	H	$C_{18}H_{15}N_5O_4S$	270–1	17.59	17.45
VIc′	Br	H	$C_{17}H_{12}BrN_5O_4S$	282–3	15.14	15.25
VId′	H	CH_3	$C_{18}H_{15}N_5O_4S$	263–5	17.59	17.98
VIe′	OC_2H_5	H	$C_{19}H_{17}N_5O_5S$	278–9	16.38	16.60

* All derivatives were recrystallized from acetic acid.

The hydrazide of the 2-phenyl-4-methyl-5-thiazolyl carboxylic acid VIIa

2.47 g (0.01 moles) IIa were dissolved in 25 ml alcohol and 2 ml of hydrazine hydrate were added. The mixture was boiled on a steam bath for 10 hours. After cooling, compound VIIa precipitated. Recrystallization from alcohol gave the m.p. 168–9°. Yield 60 %. Compounds VIIb-e shown in table 6 were similarly prepared.

Table 6

The hydrazides of the 2-aryl-4-methyl-5-thiazolyl-carboxylic acids *

Derivatives	X	Y	Formula	M.p.°	N % Calcd.	N % Found.
VIIa	H	H	$C_{11}H_{11}N_3OS$	168–9	18.01	18.07
VIIb	CH_3	H	$C_{12}H_{13}N_3OS$	182–3	16.99	16.78
VIIc	Br	H	$C_{11}H_{10}BrN_3OS$	215–16	13.46	13.71
VIId	H	CH_3	$C_{12}H_{13}N_3OS$	165–6	16.99	16.76
VIIe	OC_2H_5	H	$C_{13}H_{15}N_3O_2S$	175–7	15.15	14.83

* All derivatives were recrystallized from alcohol.

N′-Tosylhydrazide of 2-phenyl-4-methylthiazole-5-carboxylic acid VIIIa

1.16 g (0.005 moles) compound VIIa were dissolved in 40 ml pyridine and 1.9 g (0.01 moles) of toluene sulphochloride were added. The mixtures was cooled, left at room temperature for 12 hours, and poured in cold water. After filtration and recrystallization from alcohol, compound VIIIa was obtained; m.p. 185–6°. Yield 70 %.

Compounds VIIIb-e shown in table 7 have been similarly prepared.

Table 7

N′-Tosylhydrazides of 2-aryl-4-methylthiazole-5-carboxylic acid *

Derivatives	X	Y	Formula	M.p.°	N % Calcd.	N % Found.
VIIIa	H	H	$C_{18}H_{17}N_3O_3S_2$	185–6	10.84	10.65
VIIIb	CH_3	H	$C_{19}H_{19}N_3O_3S_2$	195	10.46	10.33
VIIIc	Br	H	$C_{18}H_{16}BrN_3S_2O_3$	209–11	9.01	9.41
VIIId	H	CH_3	$C_{19}H_{19}N_3O_3S_2$	207–8	10.46	10.57
VIIIe	OC_2H_5	H	$C_{20}H_{21}N_3O_4S_2$	188–9	9.96	9.68

* All derivatives were recrystallized from alcohol.

Table 8

I. R. and UV spectra of 5-formyl thiazoles

Derivatives	IR $\nu C = O(cm^{-1})$	UV	
		λ max(nm)	ε
VIa	1660	322 236	19030 10000
VIb	1655	330 238	21070 8660
VIc	1640	326 240	13700 7070
VId	1660	324 236	17300 6070
VIe	1650	346 248	25300 8090

Revue Roumaine de Chimie, **21**, 7, 1083–1095 (1976)

ON THE PYROLYSIS OF NENITZESCU'S HYDROCARBONS*

M. BANCIU
Laboratory of Organic Chemistry, Polytechnic Institute, Bucharest, str. Polizu 1, Romania

Received December 22, 1975

The mechanism of pyrolysis of Nenitzescu's hydrocarbons are reviewed. The importance of recent investigations on the benzoannelated hydrocarbons **2**, **3** and **4** for the elucidation of the mechanism involving the parent compound **1** is underlined.

INTRODUCTION

The rapid development of the $(CH)_n$ hydrocarbons field, especially due to various possibilities of thermal and photochemical interconversions, continues after the appearance of the Woodward-Hoffmann selection rules[1] which control many of these isomerisations. Among $(CH)_n$ hydrocarbons, the $(CH)_{10}$ valence isomers have received special attention. The first $(CH)_{10}$ hydrocarbon, tricyclo$[4.2.2.0^{2,5}]$deca-3,7,9-triene (**1**), was synthesized by Nenitzescu, Avram and Sliam in 1960.[2] After Doering's proposal,[3] this compound was named Nenitzescu's hydrocarbon.

The papers of Balaban, in which all the possible valence isomers of $(CH)_n$[4] and benzo$(CH)_n$[5] are tabulated, have greatly contributed to the development of the syntheses and to the understanding of the interconversions of these compounds.

From the 93 possible[4] $(CH)_{10}$ isomers, 23 are known at present. Recently, the area of research was extended to the benzo$(CH)_{10}$ series by

---

* By an extension of accepted nomenclature, throughout this paper, benzo- and dibenzo-derivatives of **1** will also be considered as "Nenitzescu hydrocarbons".

[1] R. B. Woodward and R. Hoffmann, "The Conservation of Orbital Symmetry", Academic Press, New-York, 1970.

[2] M. Avram, E. Sliam and C. D. Nenitzescu, *Liebigs Ann. Chem.*, **636**, 184 (1960).

[3] W. v. E. Doering and J. W. Rosenthal, *J. Amer. Chem. Soc.*, **88**, 2078 (1966).

[4] A. T. Balaban, *Rev. Roumaine Chim.*, **11**, 1097 (1966).

[5] A. T. Balaban, *Rev. Roumaine Chim.*, **19**, 1185 (1974).

Vedejs,[6–16] Paquette[17–19] and Murata[20–21] (who realised syntheses and interconversions of 15 isomers from the 113 possible[5] ones) and to the dibenzo$(CH)_{10}$ series by Nenitzescu and his coworkers[22–27], Stiles[28] and Friedman[29] (who described 7 from the 102 possible[5] isomers).

From the three possible benzo-Nenitzescu's hydrocarbons, the *anti*-benzo (**2**) was synthesized in 1970 by Vedejs[7] and the *syn*-benzo (**3**). in 1973 by Murata.[21] From the three possible dibenzo derivatives of **1**, the isomers **4**[22] and **5**[25] were described by Nenitzescu and coworkers in 1966 and 1974, respectively. The unique tribenzo derivative of **1** is not yet known.

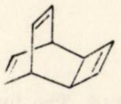
1

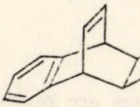
2

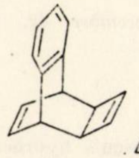
3

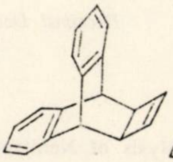
4

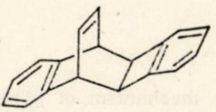
5

[6] E. Vedejs, *Tetrahedron Letters*, **1968**, 2633.

[7] E. Vedejs and R. A. Shepherd, *Tetrahedron Letters*, **1970**, 1863.

[8] E. Vedejs, R. A. Shepherd and R. P. Steiner, *J. Amer. Chem. Soc.*, **92**, 2158 (1970).

[9] E. Vedejs, *Tetrahedron Letters*, **1970**, 4963.

[10] E. Vedejs, M. F. Salomon and P. D. Weeks, *J. Amer. Chem. Soc.*, **95**, 6770 (1973).

[11] E. Vedejs and R. P. Steiner, *Chem. Comm.*, **1973**, 599.

[12] E. Vedejs and E. S. C. Wu, *Tetrahedron Letters*, **1973**, 3793.

[13] E. Vedejs, *Chem. Comm.*, **1971**, 536.

[14] E. Vedejs, M. F. Salomon and P. D. Weeks, *J. Amer. Chem. Soc.*, **95**, 6770 (1973).

[15] E. Vedejs, R. P. Steiner and E. S. C. Wu, *J. Amer. Chem. Soc.*, **96**, 4040 (1974).

[16] E. Vedejs and E. S. C. Wu, *J. Amer. Chem. Soc.*, **97**, 4706 (1975).

[17] L. A. Paquette and J. C. Stowell, *Tetrahedron Letters*, **1970**, 2259.

[18] L. A. Paquette and J. C. Stowell, *J. Amer. Chem. Soc.*, **92**, 2584 (1970).

[19] L. A. Paquette, M. J. Kukla and J. C. Stowell, *J. Amer. Chem. Soc.*, **94**, 4920 (1972).

[20] I. Murata and Y. Sugihava, *Tetrahedron Letters*, **1972**, 3785.

[21] I. Murata, Y. Sugihava and N. Ueda, *Tetrahedron Letters*, **1973**, 1183.

[22] M. Avram, I. G. Dinulescu and C. D. Nenitzescu, *Liebigs Ann. Chem.*, **691**, 9 (1966).

[23] M. Banciu, M. Elian, E. Ciorănescu and C. D. Nenitzescu, *Tetrahedron Letters*, **1972**, 2573.

[24] M. Banciu, M. Elian, C. Drăghici and E. Ciorănescu, *Rev. Roumaine Chim.*, **19**, 1179 (1974).

[25] I. G. Dinulescu, M. Pop, F. Chiraleu, M. Avram and C. D. Nenitzescu, *Rev. Roumaine Chim.*, **19**, 1197 (1974).

[26] I. G. Dinulescu, M. S. Pop, F Chiraleu and M. Avram, *Chem. Ber.*, **108**, 283 (1975).

[27] M. Elian, M. Banciu, L. Stănescu and E. Ciorănescu, *Rev. Roumaine Chim.*, **21**, 90 (1976).

[28] M. Stiles, U. Burckhardt and G. Freund, *J. Org. Chem.*, **32**, 3718 (1967).

[29] L. Friedmann, *J. Amer. Chem. Soc.*, **89**, 3071 (1967).

A number of reviews [30–35] are available, dealing with $(CH)_{10}$ hydrocarbons.

The present paper discusses the data concerning the pyrolysis of Nenitzescu's hydrocarbons, which was the object of numerous investigations and controversial proposals. It could be mentioned that recent works in the benzo$(CH)_{10}$ and dibenzo$(CH)_{10}$ series have brought important elucidations compared with the situation presented in reviews 2–3 years back. Attempts were also made to remedy some omissions from the literature in this domain. It is interesting that Nenitzescu's hydrocarbon seems to become a very useful compound, due to anticancerous properties exhibited by its $PdCl_2$-complex.[36]

PYROLYSIS OF NENITZESCU'S HYDROCARBON

The first pyrolyses of **1**, achieved by Nenitzescu and his coworkers,[37] were performed in a sealed tube and afforded as reaction products naphthalene (**6**), 1,2-dihydronaphthalene (**7**) and tetraline (**8**) in variable ratios depending on the heating time:

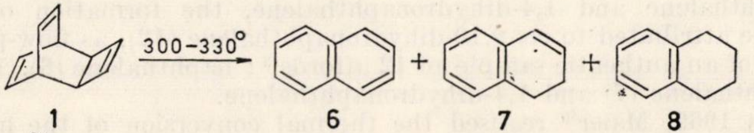

1 **6** **7** **8**

	6	7	8
(2 hrs) →	48%	27%	25% (+ traces of benzene)
(12 hrs) →	76.3%	—	17.2% (+ traces of benzene + 6.5%unknw.

The suggested mechanism [37] comprised the conversion to the tricyclic derivative **9** which affords then 9,10-dihydronaphthalene (**11**)* *via* cyclodecapentaene (**10**), the products **6**—**8** being formed through disproportionation, (and isomerisation) * :

---

* of unspecified configuration.

[30] L. T. Scott and M. Jones jr., *Chem. Rev.*, **72**, 181 (1972).

[31] S. Masamune and N. Darby, *Acc. Chem. Res.*, **5**, 272 (1972).

[32] T. L. Burkoth and E. E. van Tamelen, in "Nonbenzenoid Aromatics", J. P. Snyder (editor), Academic Press, New-York, 1969, Chapter 3.

[33] F. Sondheimer, I. C. Calder, J. E. Elix, U. Gaoni, P. J. Garrat, K. Grohmann, G. di Maio, M. V. Sargent and R. Wolovsky, *Chem. Soc. Spec. Publ.* No **21**, 75 (1967).

[34] M. Banciu, *Stud. Cerc. Chim., Acad. R.S.R.*, **18**, 347, 657 (1970).

[35] A. T. Balaban, *Rev. Roumaine Chim.*, **17**, 865 (1972).

[36] T. W. Wickersham, J. P. Li and E. J. Warawa, *Synthesis*, 399 (1975).

[37] C. D. Nenitzescu, M. Avram, I. Pogany, G. Mateescu and M. Fărcaşiu, *Stud. Cerc. Chim., Acad. R.P.R.*, **11**, 7 (1963).

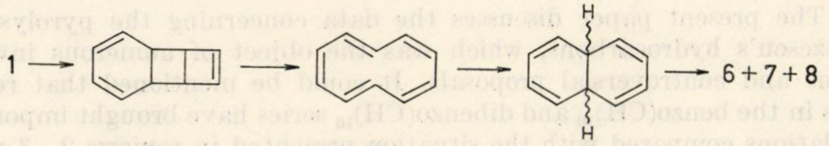

9 **10** **11**

Re-investigation, by Doering,[3] of the pyrolysis of **1** in a flow-system permitted the isolation of 9,10-dihydronaphthalene and the attribution of the configuration *cis* (**12**). Beside **12**, 1,2-dihydronaphthalene (**7**) and *cis*-1-phenylbutadiene (**13**) were obtained. The product distribution depends on temperature :

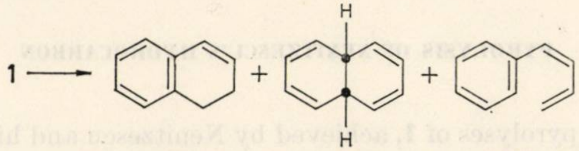

	7	**12**	**13**
(301°) →	66.7 %	20 %	13.3 %
(354°) →	53.8 %	30.8 %	15.4 %

At temperatures above 400° the pyrolysis product was composed[3] of naphthalene and 1,4-dihydronaphthalene, the formation of which could be attributed to *cis*-9,10-dihydronaphthalene (**12**), as flow-pyrolysis at 396° of an authentic sample of **12** affords[3] : naphthalene (**6**), 1,2-dihydronaphthalene (**7**) and 1,4-dihydronaphthalene.

In 1969, Maier[40] realised the thermal conversion of the heterocyclic compound **14** (structurally related to Nenitzescu's hydrocarbon) into the isomer **15**, suggesting **16**, **17** and **18** as intermediates :

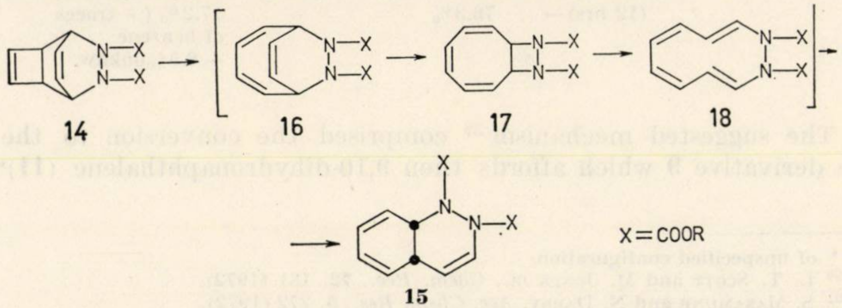

14 **16** **17** **18**

15

---

* A similar mechanism, proposed by Nenitzescu in 1957[38] for the thermolysis of some substituted derivatives of **1** (adducts of cyclooctatetraene) will not be discussed here because as later works[39] showed, the configuration ascribed to the adducts as well as the structures of the products were not correct.

[38] M. Avram, C. D. Nenitzescu and E. Marica, *Chem. Ber.*, **90**, 1857 (1957).

[39] a) M. Avram, G. Mateescu and C. D. Nenitzescu, *Liebigs Ann. Chem.*, **636**, 174 (1960) ; b) R. C. Cookson, J. Hudec and M. Marsden, *Chem. and Ind.* (*London*), **1961**, 21 ; c) B.C.T. Pappas, *Thesys*, Univ. of Wisconsin, USA, 1963 ; d) E. E. van Tamelen and B.C.T. Pappas, *J. Amer. Chem. Soc.*, **93**, 6111 (1971).

[40] G. Maier, *Chem. Ber.*, **102**, 3310 (1969).

By analogy, Maier[40] suggested that in the pyrolyses of **1** the intermediates **19**, **20** and **10** are involved.

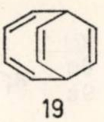

19

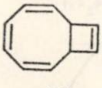

20

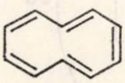

10

The absence of an intermediate **19*** in the pyrolysis of **1** was proved by Vedejs[9] who carried out the comparative flow-pyrolysis of **1** and **19** (the latter compound was synthesized independently, in 1967, by Jones[41] and Doering[42]). The very different product distributions indicated clearly that the majority of pyrolysis products of **1** (84% **7**−2% **7** + 8% **13** = = 90%) did not arise from **19**:

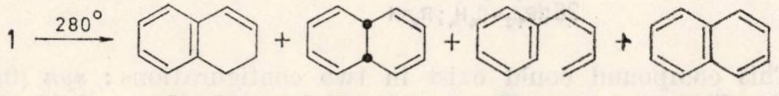

7 (84%) + 12 (7%) + 13 (8%) + 6 (1%)

$$19 \xrightarrow{280^\circ} 7\ (2\%) + 12\ (86\%) + 13\ \text{(traces)} + 6\ (6\%)$$

A general mechanism which explains well the pyrolyses of **1** was proposed in 1970, on the basis of the above data, by Vedejs[9] (Scheme 1) and completed in 1975 by the same author,[16] using stirred-flow kinetic determinations.

The key intermediate is the tricyclic derivative **9**, which was proposed as early as 1963 by Nenitzescu[37]. **

---

* We mention here that intermediate **19** was suggested by Maier[40] and not by Nenitzescu[37], as erroneously cited. [9]

** This proposal seems to have been overlooked by different authors,[30,31,13] but was recognized recently in a paper of Vedejs.[16]

[41] M. Jones and L. T. Scott, *J. Amer. Chem. Soc.*, **89**, 150 (1967).

[42] W.v.E. Doering and J. W. Rosenthal, *Tetrahedron Letters*, **1967**, 349.

Scheme 1

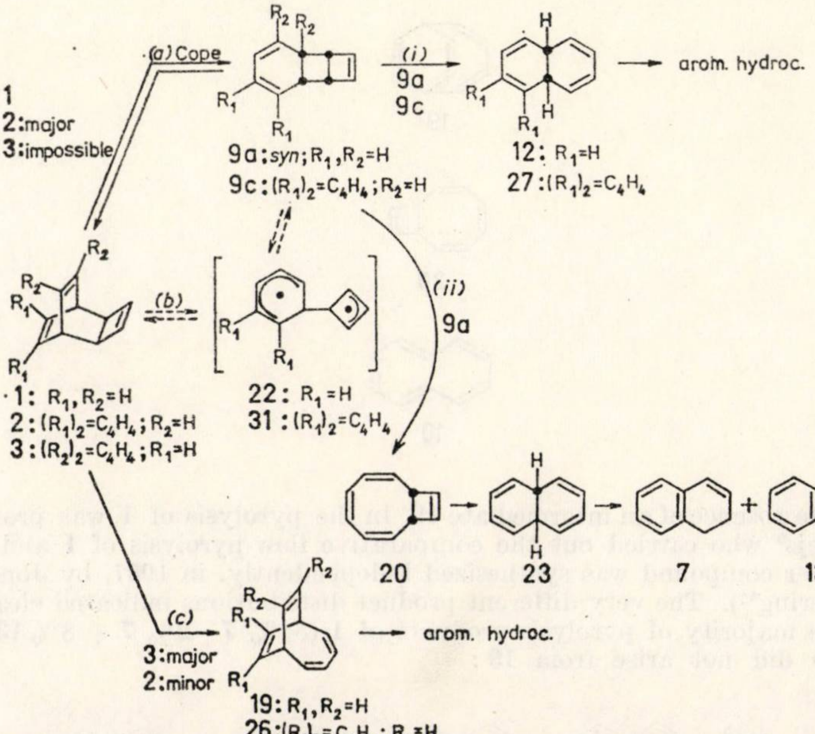
(a) Cope
1
2: major
3: impossible
9a: syn; R1, R2=H
9c: (R1)2=C4H4; R2=H
(i)
9a
9c
12: R1=H
27: (R1)2=C4H4
arom. hydroc.
(b)
22: R1=H
31: (R1)2=C4H4
(ii)
9a
1: R1, R2=H
2: (R1)2=C4H4; R2=H
3: (R2)2=C4H4; R1=H
20
23
7
13
(c)
3: major
2: minor
19: R1, R2=H
26: (R1)2=C4H4; R2=H
arom. hydroc.

This compound could exist in two configurations: *syn* (**9a**) and *anti* (**9b**). The *syn*-isomer (**9a**) was trapped by Masamune [43] (during the pyrolysis of another $(CH)_{10}$ isomer, basketene (**21**); (see Scheme 2) as an adduct with tetracyanoethylene, then it was synthesized by Vedejs.[13] The isomer **9a** and Nenitzescu's hydrocarbon **1** are interconvertible through a Cope rearrangement. The easy conversion of an authentic sample of **9a** (half-life at 70°, 28 min. [13]) into **1**, as well as the complete equilibration between **1** and **9a** [43] * (after 23 hrs at 180°) support this proposal. The above data [43,13] indicate clearly that a diradical intermediate such as **22** is not required to interconvert **1** and **9** (Scheme 1).

The formation of *cis*-9,10-dihydronaphthalene (**12**) is accounted for by a symmetry-forbidden cyclobutene ring opening of **9a** [9,16] (path *i*, Scheme 1). For the other reaction products, **7** and **13**, another reaction path involving **9a** was considered. The proposed sequence[9] involves bicyclo [6.2.0]deca-2,4,6,9-tetraene (**20**) (suggested previously by Maier[40] as intermediate), then *trans*-9,10-dihydronaphthalene (**23**), as precursors of **7** and **13** (path *ii*, Scheme 1).

---

* demonstrated by means of deuterium labelling.

[43] H. H. Westberg, E. N. Cain and S. Masamune, *J. Amer. Chem. Soc.*, **91**, 7512 (1969).

Details concerning the conversion **9a** → **20** were recently provided by Vedejs[16] who showed that the stable tub conformation of **20** (**20a**) could arise by facile disrotatory opening of the *anti* isomer **9b** (Scheme 2). The latter could result from **9a** through the freely rotating diradical intermediate **22**.[16] The Arrhenius parameters ($Ea = 46.4$ kcal/mol; log $A = 15.5$ at 289–330°) characterising the formation of 1,2-dihydronaphthalene (**7**) from **1** are consistent with this diradical process as rate determining step in the pyrolysis.[16] It must be added that the *anti* isomer **9b** possesses no suitable geometry for a Cope rearrangement leading to **1**. On the other hand, the conversion **9b** → **12** (suggested by Scott[30]) as part of the sequence **1** → **9a** → **22** → **9b** → **12**, including radical steps, can be discarded since the Arrhenius parameters ($E_a = 40.4$ kcal/mol; log $A = 12.2$ at 309–331°) are not consistent with a radical process.[16] It follows that the actual steps of this pyrolysis are: **1**→**9a**→**12** and **9a**→**22** → → **9b** → **20a** (Scheme 2).

Scheme 2

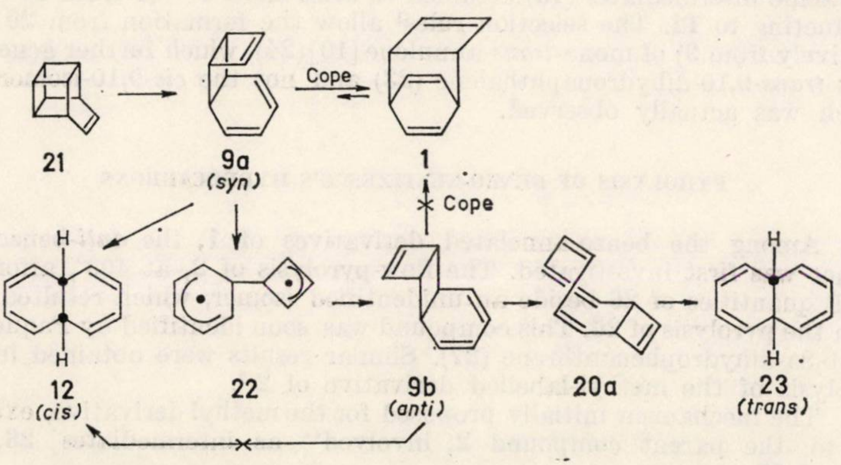

The further conversions of **20** are well documented on the basis of the known evidence: the authentic compound **20**, synthesized by Masamune,[44] isomerises quantitatively and rapidly ($k_{70°} = 1.72 \times 10^{-3}\ s^{-1}$)[44] into *trans*-9,10-dihydronaphthalene (**23**). The thermally allowed mechanism suggested for this conversion comprises[44] a $C_1 - C_8$ conrotatory ring opening of **20** to *cis*, *cis*, *cis*, *trans*-cyclodecapentaene (**24**) followed by $C_1 - C_6$ disrotatory ring closure affording **23** (Scheme 3). The thermal conversion of **23** into *cis*-1-phenylbutadiene (**13**) is also known[45,9] and it was explained[45,46] through a [1.5] suprafacial H migration (thermally allowed) followed by Cope rearrangement. The formation of 1,2-dihydronaphthalene (**7**) was explained [9,16] through a new [1.5] H migration in the same intermediate **25** (Scheme 3).

---

[44] S. Masamune, C. G. Chin, K. Hojo and R. T. Seidner, *J. Amer. Chem. Soc.*, **89**, 4804 (1967).

[45] a) E. E. van Tamelen, T. L. Burkoth and R. H. Greeley, *J. Amer. Chem. Soc.* **93**, 6120 (1971); b) E. E. van Tamelen and R. H. Greeley, *Chem. Comm.*, **1971**, 601.

[46] M. Jones, S. D. Reich and L. T. Scott, *J. Amer. Chem. Soc.*, **92**, 3118 (1970).

Scheme 3

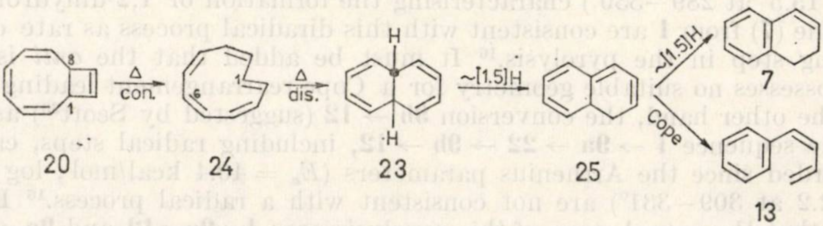

The Woodward-Hoffmann rules * permit to rule out cyclodecapentaenic intermediates (**10**) assumed to arise from **9**[37] or from **20**[40] and conducting to **12**. The selection rules[1] allow the formation from **20** (respectively from **9**) of mono-*trans*-annulene [10] (**24**), which further generates only *trans*-9,10-dihydronaphthalene (**23**) and not the *cis*-9,10-isomer (**12**) which was actually observed.

PYROLYSIS OF BENZO-NENITZESCU'S HYDROCARBONS

Among the benzo-annelated derivatives of **1**, the *anti*-benzo (**2**) isomer was first investigated. The flow-pyrolysis of **2**, at 400°, afforded[7] small quantities of **26** beside an unidentified isomer, which resulted also from the pyrolysis of **26**. This compound was soon identified by Paquette[17] as 4b,8a-dihydrophenanthrene (**27**). Similar results were obtained in the pyrolysis of the methyl-labelled derivative of **2**[17].

The mechanism initially proposed for the methyl derivative, extended to the parent compound **2**, involved** as intermediates **26**, **28**, **29** and **30**:

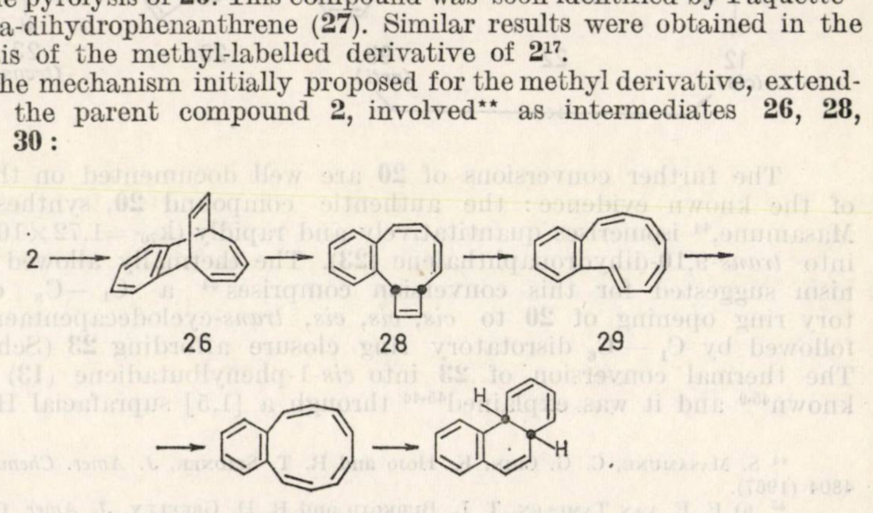

* which were not known when the first data on the pyrolyses of 1 were reported.
** by some analogy with the first proposed mechanisms in the (CH)$_{10}$ series.[37,40]

This mechanism was soon rejected by Vedejs[9] who pyrolysed **2** and **26** under the same conditions (see Table 1, entries 1 and 7).

Table 1

Pyrolyses of hydrocarbons 2, 3 and 26

Nr.	Starting material	Temp. of flow-pyrolysis (°C)	Conversion (%)	Products					Ref.
				Phenanthrene	+ Dihydrophenanthrenes	**26**	**5**	Other products	
1	**2**	280	?	2 + 85		13	—	—	9
2	**2**	330	8.5	91.6[a]		8.4[a]	—	—[c]	12
3	**2**	370	98.0	5 + 72		11	1	11[c]	9
4	**2**	380	99.9	97.7[a]		2.3[a]	—	—[c]	12
5	**3**	330	0.8	4.8[a]		95.2[a]	—	—	12
6	**3**	380	56.0	66.7[a]		33.3[a]	—	—	12
7	**26**	280	0	—		—	—	—	9
8	**26**	330	1−1.5	not indicated					12
9	**26**	370	15.0[b]	4 + 86		—	1	9	9
10	**26**	380	98.4[b]	not indicated					12

a) Figures calculated after the data from ref. 12) ignoring other secundary products; *b*) the discrepancy between the two values could be due to different contact times or to a higher accuracy in the recent work[12]; *c*) traces or small quantities of **3** were also formed.

The hydrocarbon **26** could be isolated, beside **27**, in the pyrolysis of **2** at 280° (Table 1, entry 1), under which conditions it is perfectly stable. This hydrocarbon is converted into **27**, with the same contact time, only above 350° (Table 1, entry 9). It follows[9] that the hydrocarbon **26** with butadiene bridge is not an intermediate in the conversion of *anti*-benzo hydrocarbon **2** into dihydrophenanthrene (**27**).

The mechanism proposed[9] for the pyrolysis of **2** (Scheme 1) resembles that of the pyrolysis of **1**. Actually, the mechanism for **2** has been used, by extension, as a model in explaining the pyrolysis of **1**.[9] This mechanism was later adopted also by Paquette.[19]

The key intermediate **9c**, was initially supposed[9] to arise from **2** either through a Cope rearrangement (path *a*) or through a diradical **31** (path *b*). The recent synthesis of **9c**[16] and its easy (50−80°) and clean conversion into **2**,[16] with the activation parameters identical to those of the Cope rearrangement **9a** → **1**, $E_a = 24.2$ kcal/mol and log $A = 12.3$, rules out the radical pathway (*b*) at these lower temperatures.

Since the radical pathway *b* can be discarded at higher temperatures (as shown further), the Cope rearrangement (path *a*) remains the single alternative for the formation of **9c** from **2**. The intermediate **9c** could not react further after path *ii* due to the fact that the concerted cyclohexadiene ring opening would destroy the aromatic stability of the condensed ring. It follows that the intermediate **9c** reacts only after path *i*, giving rise to dihydrophenanthrene **27**.

The formation of some quantities of **26** (8.4 – 13%) in the pyrolyses of **2** must be regarded[9] as a result of an independent reaction path (path *c*), namely a symmetry forbidden cyclobutene ring opening*.

The formation of minor quantities of *syn*-benzo isomer (**3**) in the pyrolyses of **2** could be explained through a diradical intermediate [12] of the type **31** occurring *subsequent* to the Cope rearrangement (Scheme 4).

Scheme 4

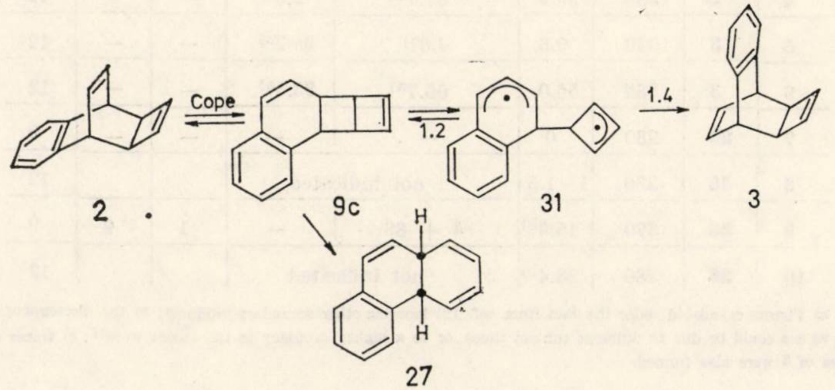

This diradical (**31**) could suffer minor reclosure in 1,4 positions affording **3** or in 1,2-positions regenerating **9c**. In the case of hydrocarbons **2** labelled with a methyl group[19] the above Scheme 4 explains[16] the majority of the observed reaction products.

The small quantities of phenanthrene observed in the pyrolyses of **2** could be explained by a thermal aromatisation of **27**, since an authentic sample of **27** afforded 50% phenanthrene in flow-pyrolysis at 600°.[19]

When discussing the pyrolysis mechanism of **2** we should mention that a phenanthrene derivative **34** was obtained as early as 1957 by Nenitzescu and his coworkers [38] by the pyrolysis (in a sealed tube) of **32** (substituted *anti*-benzo-Nenitzescu's hydrocarbon), and dihydrophenanthrene **33** was proposed as one of the intermediates.

---

* In principle, such a reaction path is possible also for Nenitzescu's hydrocarbon **1**, but the compound **19** cannot be isolated, being more reactive than **1**.

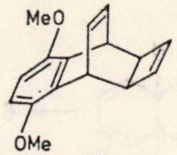

32

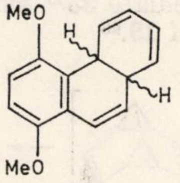

33

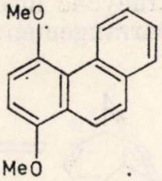

34

The pyrolysis of *syn*-benzo hydrocarbon (**3**) was described in 1973 by Vedejs[12] (Table 1). In striking difference from **2**, the *syn*-isomer **3** is less reactive (0.8% conversion at 330° in comparison with 8.5% for **2**) and affords at 330°*, the hydrocarbon **26** with butadiene bridge as major product beside *cis*-dihydrophenanthrene (**27**) and products formed from **27** (phenanthrene and other dihydrophenanthrenes).

These results rule out the importance of the radical path *b* (Scheme 1) in the pyrolyses of **2** and **3**, on the basis of the following arguments. The formation of diradicals **31** should occur with comparable rates either from **2** or from **3**. In the case of a radical pathway, there is no reason for the *syn* and *anti*-isomers to react differently. In other words, if the reaction passes through diradicals **31**, the latter should give rise to the same type of products starting either from **2** or from **3**; if that is not the case, none of the isomers **2** and **3** would react through path *b* (Scheme 1). The different product distributions observed in the pyrolyses of **2** and **3** (Table 1, entries 2, 5) and the higher reactivity of the *anti*-isomer **2** (at least 180 times greater than that of **3**[12]) confirm the last hypothesis. It follows that for compound **2** the Cope rearrangement (path *a*) remains the single pathway in formation of **9c** and then of **27**.

In the case of the *syn* isomer (**3**) even the Cope mechanism is not operative due to the fact that the fused benzene ring hinders the intervention of a concerted process and on the other hand the 1,5-hexadiene system including the ethylene double bonds of **3** has a geometry unfavourable to a Cope rearrangement. The single available pathway for **3** remains the symmetry forbidden cyclobutene ring opening leading to **26**. The above data support the reaction mechanism shown in Scheme 1; the reaction **2** → **9c**, being a thermally allowed Cope rearrangement, proceeds fast, whereas the reactions **2** → **26** and **3** → **26** proceed slower (practically at the same rate[12]), being thermally forbidden processes.

The formation of dihydrophenanthrene from **26** is more difficult to explain. After Vedejs[9], the comparable product distributions in the pyrolysis of **2** and **26** (Table 1, entries 3, 9) indicate probably a common intermediate. It should be mentioned in this respect that the analogous conversion **19** → **12** + **6** observed in the $(CH)_{10}$ series by Doering[42] involves a tetracyclic intermediate **35**[47] which is also encountered in the degenerate rearrangements of **19**.[48]

---

* The correct comparative analysis of reaction products should be made at the lowest temperature (here 330°, Table 1, entries 2, 5) where, in spite of low conversions, further reactions of primary products are not significant.

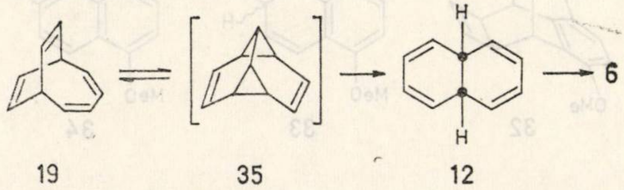

Benzoannelated derivatives of **35** do not seem to form during analogous transformations in the benzo$(CH)_{10}$ series, since the aromaticity of the benzene ring would be destroyed.

PYROLYSIS OF DIBENZO-NENITZESCU'S HYDROCARBON

Some interesting comments concerning the pyrolysis of dibenzo Nenitzescu's hydrocarbon **4** could be made on the basis of the general Scheme 1. The Cope pathway (*a*) (Scheme 5) is forbidden since two double bonds are included in aromatic rings. The route *b* seems very improbable due to the fact that diradical intermediates **36**, even formed, would further react in their benzylic form, **36a**, regenerating **4**; mesomeric forms **36b** and **36c**, due to their structures, should have little contribution and the covalent compound **37** (analogous to intermediates **9**) would have a very unusual fused structure.

Scheme 5

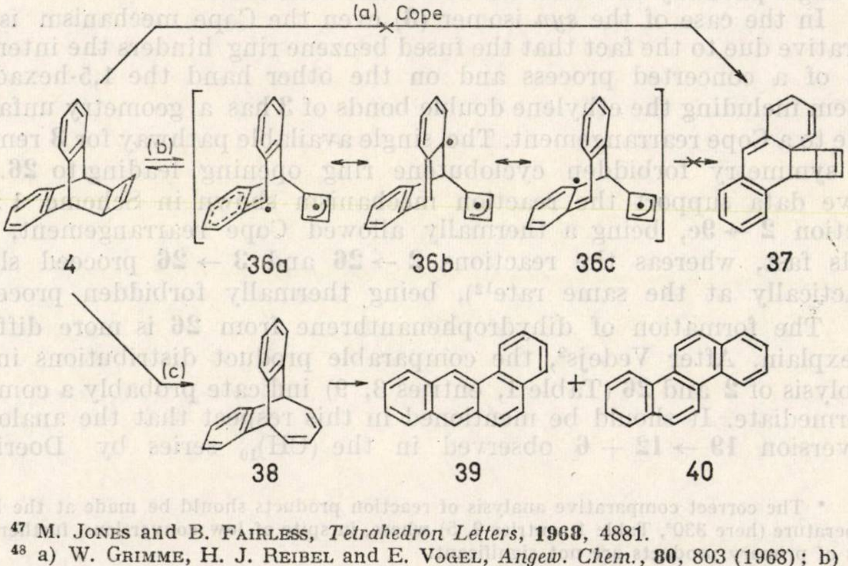

---

[47] M. Jones and B. Fairless, *Tetrahedron Letters*, **1968**, 4881.

[48] a) W. Grimme, H. J. Reibel and E. Vogel, *Angew. Chem.*, **80**, 803 (1968); b) J. S. McConaghy and J. J. Bloomfield, *Tetrahedron Letters*, **1969**, 1121; c) J. Altman, E. Babad, M. B. Rubin and D. Ghinsburg, *Tetrahedron Letters*, **1969**, 1125.

The single available pathway for **4** remains the symmetry forbidden cyclobutene ring opening (path *c*).

The pyrolysis in sealed tube of **4**[22] does not permit the isolation of the products. The flow-pyrolysis of **4** at 425°[23,27] affords practically quantitatively the hydrocarbon **38**, in agreement with the above suppositions. At higher temperatures benzo[*a*]anthracene (**39**) and chrysene (**40**) (resulted probably through aromatisation of dihydroderivatives) were isolated in increasing quantities from the pyrolysis mixtures. The exclusive formation of **38** in the pyrolyses of **4** at lower temperatures, as well as the closely similar product distribution found in the pyrolyses of **4** and **38** at temperatures above 650°,[27] prove that the aromatic compounds **39** and **40** are formed from **38** and not from **4**. Thus, for the dibenzo-hydrocarbon **4**, unlike for **1** and **2**, the compound with butadiene bridge, **38**, is the single intermediate of conversion into aromatic derivatives. The same conclusion could be drawn also for hydrocarbon **3** on the basis of a recent report of Vedejs.[16]

Concerning the mechanism of the conversion **38** → **39** + **40** (respectively into dihydroderivatives), only suppositions could be made, e.g. successive [1.3] migrations of an aromatic ring. [27]

CONCLUSIONS

Considerable work on the pyrolyses of Nenitzescu's hydrocarbons (which is only a small area of the field of $(CH)_{10}$ hydrocarbons) allowed the elucidation of the mechanism. From the data commented above it may be seen that the mechanism for the parent compound **1** was completely understood only after the investigation of the benzoannelated derivatives. The mechanism of the pyrolysis of **1** resulted as an extension of the mechanism proposed for *anti*-benzo(**2**) hydrocarbon, for which the simpler product distribution could be more easily explained. Pyrolysis of the *syn*-benzo(**3**) hydrocarbon clarified further the picture by ruling out one of radical pathway in the reactions of **2** and **3**. Pyrolyses of **3** and **4** indicated in these series the butadiene bridged isomers as unique intermediates in the formation of aromatic compounds. The recent stirred-flow kinetic determinations permitted the localisation of the radical steps in the pyrolyses of **1** and **2**.

It is also worth mentioning that of the many different intermediates proposed, sometimes without any solid evidence, the compound **9**, intuited by Nenitzescu [37], and **20**, suggested by Maier,[40] in the first papers about the pyrolysis of **1**, are now generally accepted as the intermediates of this reaction.

Revue Roumaine de Chimie, 21, 7. 1097–1102 (1976)

GROWTH REGULATING POLYMERS. II*

THE POLY(N,N-DIMETHYLAMINOETHYL METHACRYLATE SALTS) OF 2,4-DICHLOROPHENOXYACETIC AND 2,4,5-TRICHLOROPHENOXYACETIC ACIDS

A. CARPOV, STELIANA MAXIM and M. DIMA
"P Poni" Institute of Macromolecular Chemistry Jassy, Aleea Gr. Ghica Vodă 41 A.

Received December 1, 1972

The macromolecular salts of the polyelectrolyte poly(N,N-dimethylaminoethyl methacrylate) with 2,4-dichlorophenoxyacetic and 2,4,5-trichlorophenoxyacetic acids, were synthetized. The confirmation of these salts was achieved through elementary analysis and IR spectra.

It is a common practice in the application of herbicides to use different kinds of formulation ingredients to improve their persistance in the soil. Another way to improve the persistence properties of herbicides, is to obtain their insoluble and low volatile salts. For example to improve the formulations and the applicability of halogenphenoxy acids, it is necessary to use their salts with amines.[1] For the same purposes it is recommended to use different mixture of polymers with herbicides.[2,3]

In a previous paper,* we have synthetized a polymeric herbicide by reacting the poly(vinylalcohol) with the halogenphenoxyacetic acids chlorides.

In the present work we intend to obtain the macromolecular salts of halogenphenoxyacetic acids by their simple neutralization with polymers containing tertiary amino groups. It may be expected that these herbicide macromolecular salts will have lower volatility compared to the salts of lower alkyl amines and therefore a prolonged remanence.

The results of biological experiments will be presented in a future paper.

EXPERIMENTAL

The synthesis of poly(N,N-dimethylaminoethylmethacrylate) was achieved in the presence of potassium persulphate.[4] The polymer obtained, poly(N,N-dimethylaminoethylmethacrylate) (PDAM), was purified by precipitation from acetone between −45 and −50°, and characterised by viscosimetric determinations using an Ubbelhode viscosimeter (O_a capillary).

---

* Part I. M. Dima, A, Carpov and Steliana Maxim, *Rev. Roumaine Chim.*, **13**, 485 (1968).

[1] C. Popa and R. Drimuş ,,Chimia produselor fitofarmaceutice", Edit. Tehnică Bucureşti, 1965, p. 332.

[2] Koho Co. Ltd. Jap. 71,42,218 ; *Chem. Abstr.*, **77**, 115607 (1972).

[3] National Patent Develop. Corp. U.S., 3, 660, 071 ; *Chem. Abstr.*, **77**, 76065 (1972).

[4] A. Alfrey and S. H. Pinner, *J. Polymer Sci.*, **23**, 533 (1957).

The macromolecular salts of this polymer were obtained by making use of the specific representatives of chloroaryloxyalkyl-carboxylic acids, the 2,4-dichlorophenoxyacetic p.a. (2,4-D) acid and the 2,4,5-trichlorophenoxyacetic p.a. (2,4,5-T) acid. The neutralization reaction for obtaining the salts has been carried out at room temperature (20°) in the following solvents : dioxane (DO), dimethylformamide (DMF), pyridine (PY) and tetraline (Te).

The PDAM (0.0127 moles) was dissolved, at a convenient concentration in an appropriate solvent for the final product, in a flask fitted with a stirrer, and a solution of 2,4-D (0.0189 moles) or 2,4,5 T (0.0189 moles) acid was gradually introduced in the same solvent. In general, the molar ratio PDAM/acid of 1 : 1.5 was used. The reaction product was purified by repeated precipitations in ethyl ether. The chemical composition and the purity of the obtained copolymer were verified using the known calculating procedure.[4,5]

The neutralization reaction was followed by pH-metric titration, a n/10 and n/100 polymer and acid solution being used. The pH variation during the neutralization reaction, was observed on a pH-meter Radiometer type PHM-22 ; a glass electrode and a calomel reference electrode with porous pin (to limit salts diffusion) were used.

It was observed that the neutralization reaction is practically accomplished in about 8 hrs. One must wait some 15 minutes before adding a new quantity of acid solution, to allow the pH to stabilize. The neutralization reaction was followed by the degree of transformation into macromolecular salt (α), which was calculated from the chlorine content of the polymer salt (determined according to Schöniger). Also, the composition of the polymer salt was determined by elementary analysis, computations being made according to a method described in one of our former papers.[5]

THE POLY(N,N-DIMETHYLAMINOETHYL METHACRYLATE SALT) OF 2,4 DICHLOROPHENOXYACETIC ACID OBTAINED IN DO AS SOLVENT

An almost colourless glassy polymer soluble in DMF, DO and PY, was obtained.
Elementary analysis for $\alpha = 65.70$
Found : C, 53.00 ; H, 6.50 ; O, 21.06 ; N, 4,80 ; Cl, 15.44
Calcd. : (52.70) ; (6.20) ; (21.06) ; (4.60) ; (15.44)

THE POLY(N,N-DIMETHYLAMINOETHYLMETHACRYLATE SALT) OF 2,4,5-TRICHLOROPHENOXYACETIC ACID

The salt was obtained under the same conditions as in the case of the 2,4 D acid. A faintly yellow-coloured polymer with a glassy aspect, soluble in the above mentioned solvents, resulted.
Elementary analysis for $\alpha = 66.49$
Found : C, 49.40 ; H,5.01 ; O, 19.50 ; N, 4.10 ; Cl. 21.70
Calcd. : (49.10) ; (5.40) ; (19.50) ; (4.30) ; (21.70)

Controls of the polymer salts obtained were made by IR spectra recorded on a S.P. 200 Unicam Spectrophotomer.

RESULTS AND DISCUSSION

The viscosity curves of PDAM are given in figure 1. The aspect of the curves is characteristic of a polyelectrolyte in the absence of a simple electrolyte (curve 1, fig. 1) and in the presence of a simple electrolyte (curve 2, fig. 1).

In figure 2, one can observe the shape of potentiometric titration curves for PDAM, showing a typical behaviour for medium strength organic bases. The size of pH-slope increases as a function of the strength of the utilised acid.

---

[5] I. Scondac and M. Dima, *Studii şi Cercetări Şti. Chim. Acad. R.P.R. Fil. Iaşi,* **13**, 217 (1962).

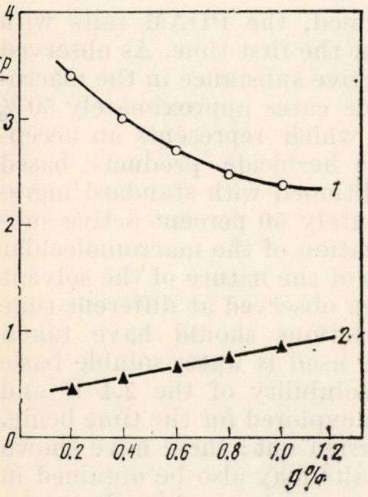

Fig. 1. — Variation of the ratio η_{sp}/c, versus concentration ;1 —free of simple electrolytes ; 2 — in 0.01 M KNO_3 solution.

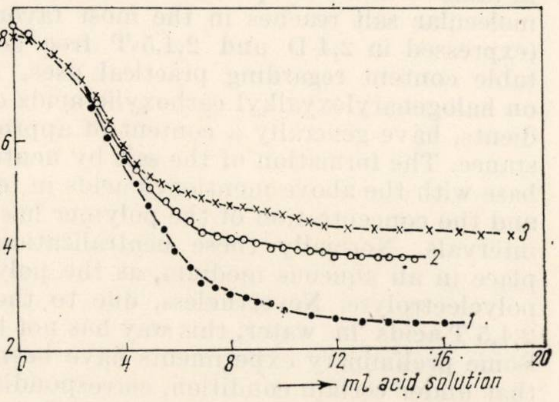

Fig. 2. — pH variation during neutralization reaction of PDAM (M/100, solution) ; 1—hydrochloric acid ; 2—acetic acid ; 3 — 2,4,5-trichlorophenoxyacetic acid.

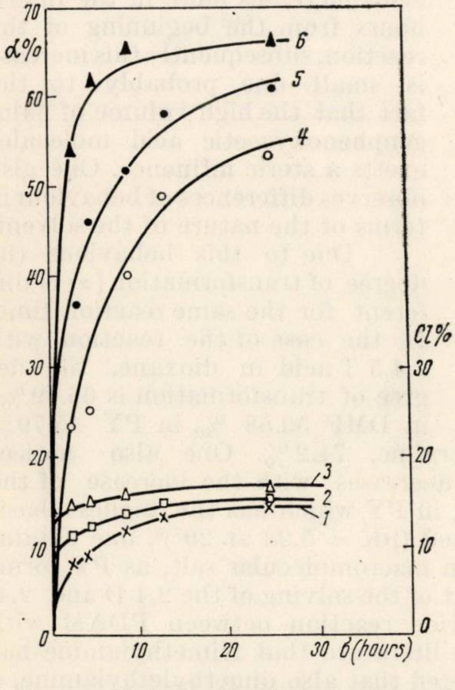

Fig. 3. — Variation of chlorine content of the macromolecular salt of 2,4-D acid, versus reaction time, with different solvents (1—PY, 2 — DMF, 3 — DO). Variation of transformation degree (α) versus time for different solvents (4 — PY, 5 — DMF, 6 — DO).

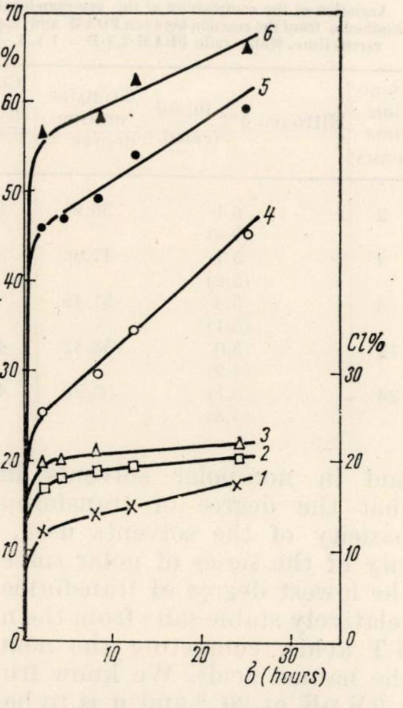

Fig. 4.—Variation of chlorine content in the macromolecular salt of 2,4,5-T acid, versus reaction time, with different solvents (1 — PY, 2 — DMF, 3 — DO). Variation of the transformation degree (α) versus time in different solvents (4—PY, 5 — DMF, 6 — DO).

As a result of the experiments performed, the PDAM salts with the 2,4-D and 2,4,5-T acids were obtained for the first time. As observed in tables 1 and 2 the percent content of the active substance in the macromolecular salt reaches in the most favourable cases approximately 50 % (expressed in 2,4-D and 2,4,5-T free acid) which represents an acceptable content regarding practical uses, since herbicide products based on halogenaryloxyalkyl carboxylic acids conditioned with standard ingredients, have generally a content of approximately 50 percent active substance. The formation of the salt by neutralization of the macromolecular base with the above-mentioned acids in terms of the nature of the solvent and the concentration of the polymer has been observed at different time intervals. Normally these neutralization reactions should have taken place in an aqueous medium, as the polymer used is water-soluble basic polyelectrolyte. Nevertheless, due to the insolubility of the 2,4 D and 2,4,5 T acids in water, this way has not been explored for the time being. Some preliminary experiments have been carried out; these have shown that under certain condition, corresponding salts may also be obtained in an aqueous medium. In the choice of the solvent we observed by the necessity for both components being soluble in the same solvent.

Table 1

Variation of the composition of the macromolecular salt obtained a from the reaction between PDAM and 2,4-D acid, versus time. Molar ratio PDAM/2,4-D = 1/1.5, DMF

Reaction time hours	Nitrogen g % found (calcd.)	Transformation degree %	Content in active substance %.
2	6.1 (5.9)	36,98	34,23
4	5.7 (5.6)	47.06	39.85
8	5.4 (5.1)	51.48	42.03
12	5.0 (4.9)	58.42	46.67
24	5.1) (4.8)	63.26	47.21

From figures 3 and 4 and tables 1 and 2, one notices that the degree of transformation for both acids increases more in the first 8 hours from the beginning of the reaction, subsequently this increase is small due probably to the fact that the high volume of halogenphenoxyacetic acid molecules exerts a steric influence. One also observes differences of behaviour in terms of the nature of the solvent.

Due to this behaviour the degree of transformation (α) is different for the same reaction time. In the case of the reaction with 2,4,5 T acid in dioxane, the degree of transformation is 66.49 %; in DMF 59.58 %, in PY 45.79 % and in non-polar solvents like tetraline, 74.2 %. One also notices that the degree of transformation decreases with the increase of the basicity of the solvents used. Thus, in PY which has the highest basicity of the series of polar solvents used (pK = 5.23 at 20°)[6], one obtains the lowest degree of transformation in macromolecular salt, as PY forms relatively stable salts from the moment of the solving of the 2,4 D and 2,4,5-T acids, competing the neutralisation reaction between PDAM with the named acids. We know from the literature that trimethylamine has a 9.9 pK at 20°,[6] and it is to be expected that also dimethylethylamine, a characteristic functional group of the utilised polymer, has a pK of the

---

[6] D. D. PERRIN Dissociation Constants of Organic Bases in Aqueous Solutions, Butterworths, London, 1965, p. 141.

Table 2

Variation of the composition of the macromolecular salt obtained from the reaction between PDAM and 2,4,5-T acid, versus time and solvent. Molar ratio PDAM/2,4,5-T : 1/1.5

Solvent	Reaction time hours	Nitrogen g% found (calcd.)	Transformation degree %	Content in active substance %
DO	2	4.90 (4.70)	56.20	47.85
DO	8	4.90 (4.60)	58.50	48.86
DO	12	4.29 (4.40)	62.61	50.56
DMF	2	5.30 (5.05)	46.06	43.07
DMF	4	5.05 (5.00)	47.43	43.63
DMF	8	5.20 (4.90)	49.76	44.82
DMF	12	4.74 (4.70)	54.54	47.12
DMF	24	4.16 (4.50)	59.18	49.15
PY	2	6.10 (6.40)	25.50	29.36
PY	8	6.16 (6.00)	31.95	34.25
PY	12	(5.20 (5.60)	34.71	36.14
PY	24	(5.21 (5.00)	45.71	42.75

same order of magnitude and, as a consequence, with all the above mentioned screening, the equilibrium diseplacement towards the formation of macromolecular salts, should be favoured. In DMF and DO, which have much lower basicity constants compared to PY, the formation of the macromolecular salts with halogenphenoxyacetic acids is highly favoured and the degrees of transformation are much higher.

It is known that the aliphatic substituents of the tertiary aminic groups of the polymer screen the electron doublet of the nitrogen hindering the protonation, and as a consequence, the neutralization reaction is lowered and the polarity of the solvents cannot exert its influence, taking into account also the low dissociation constants of the 2,4 D and 2,4,5 T acids.

One observes, however, that in non-polar solvents such as tetralin, one obtains much higher transformation degrees in macromolecular salts, due probably to the absence of any secondary effects of the solvents on the neutralization reaction. The IR spectra of the macromolecular salt, compared to the spectra of the 2,4-D and 2,4,5 T free acids and of the PDAM, show, in the range of 2400 cm^{-1}, a broad band made of two supperposed bands. It is not impossible that this composed band might be due to the existence of a tertiary amine salt with an acid.[7] Other spectral modifications are also observed, as for instance the appearance of a broad band around the value of 640 cm^{-1}, which can be connected to a CO vibration hindered because of some hydrogen bonds. Added to the other proofs, these data confirm the formation of the macromolecular salts of the polymethacrylate of N,N-dimethylaminoethyl with the 2,4 D and 2,4,5 T acids.

CONCLUSIONS

The macromolecular salts of poly(N,N-dimethylaminoethylmethacrylate) with 2,4-D and 2,4,5-T acids have been synthetised for the first time, and new, practically non-volatile, herbicide polymers have been obtained.

The formation of the macromolecular salts in different organic solvents was studied, reaction conditions were established and the existence of the macromolecular salts obtained was confirmed by elementary analysis and IR spectra.

---

[7] L. J. Bellamy "Ultrarot Spektren and chemische Konstitution" Steinkopff, Darmstdat, 1953, p. 193 (translated from English).

Revue Roumaine de Chimie, **21**, 7, 1103–1107 (1976)

ELECTRON MICROSCOPIC INVESTIGATIONS OF SILICA GELS STRUCTURE AND DISPERSION OF SYNTHETIC ALUMINOSILICATES

JACEK SZYMURA and BOGDAN DIRSKA
Department of Chemical Technology, College of Engineering
Str. Seminaryjna 3,85326 Bydgoszcz, Poland

Received December 11, 1974

The silica adsorbents were investigated by means of the electron microscopy with the help of elaborated effective specimen preparation method. Information concerning the differences between two types of silica gels and synthetic zeolites was obtained.

The electron microscopy has the important role of imparting new impulses to the present views on the structure of silica adsorbents. With the help of electron microscope the theory of globular gel structure formulated by Kisielew has been confirmed.[1,2]

The investigation of finely pored silica gels and the high dispersed aluminosilicates can be applied to determine the structure of the different types of this silica adsorbents and catalyst supports.

The earlier investigations of aluminosilicates and silica gels were realized by using the direct method in transmission electron microscopy.[3,4] Therefore with the help of the direct method it is only possible to observe the general shape of particles without obtaining any information on the morphology of their surfaces.

The raster and scanning electron microscopes used to silica gel examination[5] have too low range of optimum magnifications and low resolving power (in most of popular serial instruments it reaches 250 Å).

Dorling and Moss[6] applied the ultrathin sections of silica gel samples for electron microscopic investigations but the prepared specimens gave poor contrast on the micrographs.

Application of replicating methods (indirect methods) enlarges the possibilities of observation of gel structure with the electron microscope and measuring various details on gel surface. But in this case some diffi-

---

[1] V.M.Lukjanovic, "Elektronnaya mikroskopiya v fiziko-khimicheskikh issledovaniyakh", Izd. Akademii Nauk SSSR, Moscov 1960.

[2] T. Sugar and F. Cuba, *Acta Chim. Acad. Sci. Hung.*, **7**, 233 (1955).

[3] W. J. Nicolina, L. I. Knish, A. E. Wojciechowsky and L. I. Oboznaia, "Adsorbienty ikh sintez, svoistva i primenenie", Nauka, Leningrad, 1971, p. 59.

[4] E. N. Jegorova and S. P. Zdanov, "Khimia tseolitov", Nauka, Leningrad, 1968.

[5] F. Eisenbeiss, *Kontakte Merck*, **3**, 35 (1973).

[6] T. A. Dorling and R. L. Moss, *J. Catalysis*, **7**, 378 (1967).

culties are encountered. The difficulties are connected with the need of special preparation of samples for observation.

The literature gives a few data concerning the investigations of aluminosilicates and silica gels by replicating method[7,8] but none of them describes the preparation procedure and they cannot be applied in laboratory practice. Leontjev and Lukjanovic[9] described the preparation of preshadowing single-stage collodion replica and two-stage replica from polystyrene matrix to silica gels. Both of them have poor replicating resolution (> 100 Å).

In this paper an effective method of specimen preparation of aluminosilicates and silica gels for transmission electron microscopy is described. It was elaborated during the investigations of the carriers of metal catalysts, produced on a silica base.

The method depends on preparing the single-stage carbon replicas : unshadowed with respect to aluminosilicates and shadowed with platinum to silica gels. The initial results of observation of the silica specimens prepared by means of elaborated method are presented.

EXPERIMENTAL

As materials were used the samples of synthetic aluminosilicates (molecular sieves ZK-4A and ZK-5A) before the granulation and the samples of silica gels : modified wide pored SKM-3 and finely pored SMG, all produced by Inowrocław Soda Factory.

The specimens were examined by the BS-613 Electron Microscope manufactured by "Tesla". This microscope is a high-resolution instrument with a resolving power better than 5 Å and was operated at accelerating voltages 50—80—100 kV.

PREPARATION OF ALUMINOSILICATES

Particles of aluminosilicate samples suspended in ethanol have been disintegrated in MSE Ultrasonic Disintegrator (100 Watt, 25 kHz), for one minute. Then the suspensions were placed on a fresh support mica plate and after being air-dried, they were evaporated with thick layer (about 200 Å) of carbon in Zeiss Jena Evaporator. The evaporations were carried out using the simple electrode system[10] with the rotary shadower for 20 seconds. The rotations of rotary shadower were 200 cycles per minute, the current tension was changed in the range between 0—60 A. The distance between the contact of electrodes and the sample was 11 cm. The aluminosilicate particles were dissolved in 20% aqueous HF solution. The aluminosilicate specimen with replica is placed on a surface of HF solution. Aluminosilicate particles are dissolved during a few minutes and replica is left on the surface of HF solution. Next the replica is carefully washed first with two changes of the acid solution and then with water, using a mica plate for transferring the replica. The replicas obtained in this manner were placed on support nets using a method described by Reimer [10].

PREPARATION OF SILICA GELS

The samples of silica gels were grained to powder first in an agate mortar and then suspended in ethanol. The drops of suspension were placed on a fresh support mica plate and next shadowed by the angle 45° with the mixture of platinum and carbon.[11] After shadow-

---

[7] Z. L. Butsco and P. M. Statnic, *Kolloid Zhur.*, **35**, 339 (1973).

[8] B. A. Lipkind, "Adsorbienty ikh sintez, svoistva i primenenie,", Nauka, Leningrad, 1971, p. 51.

[9] E. A. Leontjev and V. M. Lukjanovic, *Doklady Akad. Nauk S.S.S.R.*, **103**, 1039 (1955).

[10] L. Reimer, "Elektronenmikroskopische Untersuchungs-und Präparationsmethoden", Springer Verlag, Berlin, 1967, p. 312, p. 322.

[11] E. Balcerzyk and G. Włodarski, *Cellulose Chem. Technol.*, **4**, 666 (1970).

ing the thick layer (about 200 Å) of carbon was evaporated. The evaporation of platinum and carbon was carried out using the Zeiss Jena Evaporator. The next operations of preparing the replicas are according to the method used in the case of aluminosilicates.

RESULTS AND CONCLUSIONS

The elaborated method is sure and effective. It gave perfect results in electron microscopic investigation of silica gel structure and dispersion of synthetic aluminosilicates. On the base of prepared micrographs (fig. 1a, 1b) the granulometric analysis of molecular sieves ZK-4A and ZK-5A was done.[12] It was shown that the diameter of predominant morphological form is 3–5 μm. Electron microscopic investigations of silica gels confirmed their porous structure and showed the clear difference between the surfaces of finely pored and wide pored gels (fig. 2a, 2b). The observed difference depends on various diameters of the gel globules. The obtained data can be applied to the qualitative and quantitative estimation of silica gels formed under various conditions of pH and temperature. With the method of transmission electron microscopy it is possible to identify the types of gels and control the structures of their surfaces during forming and modifying processes.

In all cases the prepared replicas had a good contrast and the resolution better than 50 Å. The described method of specimen preparation can be successfully applied to other silica materials as : silicates, aluminosilicates, pored glasses, etc. The presented procedure, in comparison with the methods known in literature, eliminates the use of the expensive platinum support nets and prepares teflon holders [13] or the necessity of application of the two-stage replica[9] with poor replicating resolutions (> 100 Å), thus reducing the possibility of contaminating the replica.

---

[12] B. Dirska and J. A. Szymura, to be published.

[13] J. M. Kandykin and L. N. Kozlenkov, *Zavodskaya Lab.*, **32**, 190 (1966).

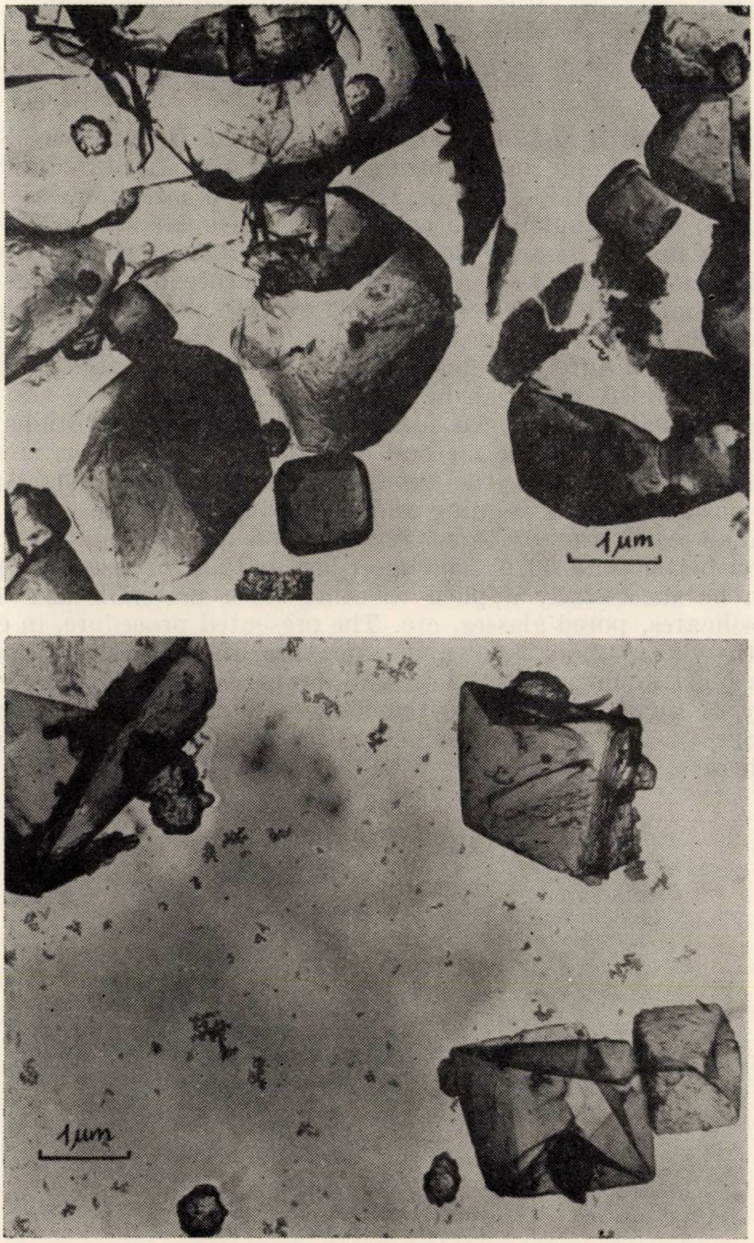

Fig. 1. – Electron micrographs of synthetic zeolite crystals (molecular sieves)

a) type 4A, b) type 5 A.

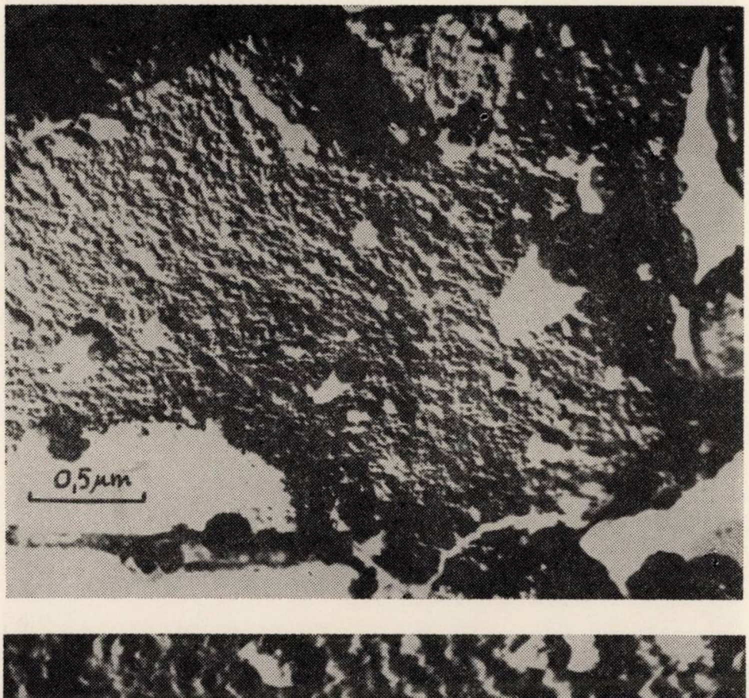

Fig. 2. — Electron micrographs of fracture of silica gels

a) finely pored type SMG, b) wide pored type SKM–3.

Revue Roumaine de Chimie, 21, 7, 1109–1112 (1976)

COMPTES RENDUS

BELA A. NEMETH, Chemical Tables, Akademiai Kiadó-Budapest, 477 p., 256 tabl.

La révolution de la technique et de la science contemporaines a permis de perfectionner continûment les procédés expérimentaux utilisés pour la caractérisation quantitative de la matière et des propriétés des substances. Il en résulte la nécessité de tables de constantes de précision élevée, en accord avec les résultats des plus récents mesurages.

L'ouvrage de Bela A. Nemeth met à la disposition des chimistes les plus nouvelles données quantitatives Ainsi que l'explique l'auteur, le but de cet ouvrage est d'assurer aux travailleurs des laboratoires d'usines ou de recherches un instrument d'applications multiples et variées, facilement déplaçable. Les données présentées ont été calculées à partir des poids atomiques établis par la Commission Atomique de l'UPAC en 1969.

Des nombreuses et utiles données que contient cet ouvrage, nous mentionnons les tables pour le calcul rapide des analyses (facteurs analytiques), les poids équivalents pour les analyses volumétriques, les équivalents électrochimiques des ions, etc.

Nous signalons surtout à l'attention des lecteurs les tables concernant la densité des solutions aqueuses, les solutions tampon, le degré de dissociation et la constante de dissociation de certains électrolytes.

L'ouvrage est d'autant plus utile qu'il parcourt des domaines plus variés, parmi lesquels nous citons le mesurage correct des propriétés des systèmes gazeux, les tables de lignes spectrales des éléments, les tables de chaleurs spécifiques des éléments et des composés inorganiques, etc.

E. Segal

FRANCISC A. GOTHARD, "Echilibre lichid-vapori. I. Baze teoretice şi metode de calcul" (Liquid-vapor equilibria. I. Theoretical backgrounds and computational methods), Ed. Academiei, Bucharest, 1975, 260 p.

Liquid-vapor equilibria is a monograph (3 volumes) intended to researchers, students, designers and technologists, which gives not only an up-to-date information in the field but also many selected numerical data. It is also a handbook for those who have to solve various problems concerning the separation processes by distillation and rectification.

The first volume of the monograph (Theoretical backgrounds and computational methods) represents a synthesis of the essential theoretical elements necessary for obtaining fundamental data in the design of distillation and rectification plants, in a form adapted to the use on computers. The second volume, which is to appear, will include the description of all experimental methods and the means for measuring all variables and constants. The third volume will include a series of constants for pure components and experimental data for binary and multicomponent systems selected and processed by means of unified criteria.

The present volume discusses a series of problems which so far have not been included in other similar synthesis works, such as prediction of the parameters of various equations by multiproperty analysis, use of scaling parameters instead of critical constants in the equations of state, use of measurable excess properties for predicting equilibria and several correlation methods, which preserves the information included in the experimental data (spline-fit, Mixon—Gumowski — Carpenter methods). Results obtained by the author and his co-workers are also included, concerning for example improvements in the prediction of molar volumes, prediction of the parameters of the Wilson equations for hydrocarbon systems proceeding from pure component properties and the prediction of vapor-liquid equilibrium data on the basis of the mixture "synthesis' 'effects which avoid analytical work.

Chapter 2 gives synthetically the fundamental principles for deducing the relations necessary in the other chapters and closes by obtaining the fundamental equations of vapor-liquid equilibria. In the following chapters the exposition is systematized according to the elements of the basic relations. The third chapter is concerned with fugacity coefficients computed for the vapor phase, using the improved forms of the virial coefficients, Redlich—Kwong and BWR equations of state. The fourth and fifth chapters deal with prediction of liquid molar volumes, and critical constants (pseudocritical) data of mixtures. Analysis of recently published data are used in the discussion of the performances of the best methods.

Chapter 6 examines the equations for the activity coefficients, systematized according to the complexity of the models of the solutions used, the forms which allow the generalized prediction of data in multicomponent systems being underlined. Chapter 7 begins with a classification of the correlation methods of the experimental data and gives extensive information on the correlating procedures.

The last two chapters treat methods for analysing the consistency of the experimental data and finally discuss indirect prediction methods based on new principles which imply the use of measurable excess properties for the calculation of the boiling and due points in hydrocarbon multicomponent mixtures are given.

The monograph is thought of as a means of information for research workers and specialist in the field and as a handbook for designers and technologists.

D. Marchidan

C. GH. MACAROVICI et D. MACAROVICI, "Chimia oxizilor dubli și utilizările lor" (La chimie des oxydes doubles et leur utilisation), Ed. Academiei, Bucarest 1975, 186 p.

Le livre se propose de faire une synthèse des connaissances actuelles dans le domaine des oxydes simples et doubles et de donner les notions nécessaires pour l'étude des oxydes, qui présentent une grande importance théorique et pratique. On donne la classification des oxydes selon le nombre des composants et le type de structure cristalline, ainsi que les règles qui régissent l'arrangement des oxydes dans les cristaux. On présente des méthodes d'obtention des oxydes doubles et les méthodes utilisées à l'étude des réactions de synthèse, ainsi que le mode d'interprétation des résultats. Sommairement sont présentées les méthodes de détermination des propriétés physico-chimiques des oxydes doubles. Les données pratiques ont été prises, dans la plupart, des travaux des auteurs. Le livre est divisé en six chapitres.

Dans le premier chapitre sont présentés les critériums actuels de classification des oxydes simples et doubles, la formule chimique et la structure cristalline. Une partie assez importante de ce chapitre est réservée aux notions concernant la structure cristalline de la matière à l'état solide et particulièrement des oxydes métalliques. On discute les forces de réseau, le rôle de l'électronégativité, les règles de Pauling pour la détermination de la structure des cristaux ioniques, les réseaux stratifiés, les phénomènes d'isomorphisme et de polymorphisme, les solutions solides, etc.

Le second chapitre se réfère aux structures cristallines types, d'après lesquelles cristallisent les oxydes simples et doubles et selon lesquelles a été faite la classification. On donne la classification des oxydes simples d'après la formule chimique, les structures caractéristiques des oxydes doubles, la structure spinelle, ilmenitique et perowskitique. On décrit les représentants et les règles selon lesquelles les oxydes doubles prennent l'une ou l'autre des structures caractéristiques. Dans le cadre de chaque structure chimique, une classification à part a été faite pour les oxydes doubles possédant des propriétés spéciales comme sont les bronzes et les ferrites.

Le troisième chapitre se réfère aux méthodes de synthèse classiques des oxydes simples et doubles, ainsi qu'aux méthodes spéciales.

Les méthodes analytiques utilisées à l'étude des réactions de synthèse et à l'établissement de la structure des oxydes doubles sont décrites dans le quatrième chapitre.

Le cinquième chapitre comprend la description des propriétés des oxydes : chimiques, optiques, électriques, magnétiques, catalytiques et quelques considérations théoriques concernant l'interprétation des propriétés des oxydes doubles.

Le dernier chapitre donne les utilisations les plus importantes des oxydes simples et doubles, comme masses céramiques, couleurs minérales, émaux, pierres précieuses, divers matériaux utilisés en électrotechnique et électronique, catalyseurs, luminophores, etc.

Le livre s'adresse aux spécialistes, ainsi qu'aux chercheurs, ingénieurs et aux technologues.

D. I. Marchidan

Thermal Analysis. Proceedings of the fourth International Conference on Thermal Analysis, Budapest, July 8–13 1974, edited by I. Buzás. Akadémiai Kiadó, Budapest joint edition with Heyden & Son Ltd., London

The fourth International Conference on Thermal Analysis under the auspices of the International Confederation for Thermal Analysis took place in Budapest in July 1974 and was organized by the Analytical Section of the Hungarian Chemical Society. The Conference was characterized by the presence of more than 600 participants from 30 countries and 277 papers were delivered in six sections. This proceedings contains the full text of the papers. Besides numerous contributions on thermal analytical theory, methodics and instrumentation, and the usual high number of papers falling into the fields of inorganic and organic chemistry, the Conference was particularly rich in work rooted in applied and earth sciences.

The first volume (1040 pp) comprises 100 papers, delivered in sections : theory and inorganic chemistry.

The second volume (760 pp) comprises 72 papers included in sections : organic and macromolecular chemistry and earth sciences.

The third volume (1120 pp) reports in 105 papers recent trends of developement in applied sciences (section 5) and methodics and instrumentation (section 6).

The purpose of these proceedings has been to establish an up-to-date account of the results obtained in studies of the matter by thermal analysis.

The high theoretical and experimental level of the papers presented at the Conference have proved that this field is still the subject of active research, owing to the refinement of DTA methods, etc.

The three volumes give to physical chemists a general view of the problems concerning the thermal analysis and stimulates the interest for further research in this field.

D. I. Marchidan

MAURICE WILLIAM RANNEY, "Fire Resistant and Flame Retardant Polymers", Noyes Data Corporation Park Ridge, New Jersey, London, England, 1974, 394 p.

A detailed descriptive information concerning different synthesis and applications of the fire and flame retardant polymers is given in the book "Fire Resistant and Flame Retardant Polymers", by M. W. Ranney. This book also presents an advanced and technically oriented review and can be used as a guide to the U.S. patent literature in this field. Many of these patents are being utilized commercially. The author gives details of over 275 processes relating to flame resistant polymers and plastics and brings together in a single source over twenty years of flame retardant research (since 1952– to 1974 years).

New polymers, which are not able to burn, or are self-extinguishing after the ignition source is removed have been developed in the last time. Reactive intermediates and flame retardant additives now generally available for most polymer systems, are included in 394 pages. A large quantity of easy assimilable information is presented in this space. It is evident from the patent references that the development of nonburning, self-extinguishing and flame retardant polymers is based, to a large extent, on the incorporation into the resin of organohalides, organophosphorus compounds or additives which contain halogen and phosphorus atoms at the same molecule. In this book the application of metal oxide, particularly antimony oxide, titanium dioxide and copper oxide is also described. These products are not active themselves but have a synergistic effect upon halide and phosphorus additives or silicones.

The first chapter presents polyurethane systems containing organo-phosphorus reactants as follows : phosphorus containing sugar polyols, phosphorylamides, phosphorus containing polyolsynergysts, phosphorus-epychlorohydrin based polyol, phosphorus polyhydroxil compounds, mixtures of hydroxylated ureas and phosphorus containing polyols, nitrogen containing phosphonates, phosphonic acid derivatives and phosphoryl isocyanates. It also describes phosphorus containing additives for polyurethanes : condensation products of halogen substituted phosphites, organic phosphate amine salts, tertiary esters of phosphorus and phosphorus polymers. Halogen containing reactants, halogen containing additives and other reactives and intermediates for polyurethanes are showed in 42 pages of the first chapter.

The second chapter describes polyesters, epoxies, silicones, phenolics, urea-formaldehyde resins and other thermosets with flame retarding properties. It specifies the bromo and phosphorus containing reactive intermediates, phosphorus containing polymers, chlorinated resins, use of copper, copper oxide and many other additives.

The third chapter presents the major techniques for making fire retarding polypropylene and polyethylene : compounds with antimony oxide, halogen compounds and other additives (modified olefins, wire and cable compounds).

The fourth and fifth chapters refer to advanced composition and production methods for polystyrene, ABS, polyamides, acrylics and other non flammable thermoplastics : by incorporation of certain organic bromides or saturated polychlorinated aliphatic hydrocarbons, preparation of terpolymers from halogenated monomers, ABS-PVC blends, lactam polymerization with alumina trihydrate filler and other methods.

The sixth chapter shows additives of general utility as halogenated compounds, phosphorus compounds and halogenated phosphorus compounds.

Finally, the book contains three bibliographical lists : Company index (92 Company names), Inventor index (378 author names), US patent number index (236 patents).

This book is a valuable working instrument and offers the possibility to know new profitable areas of the research and development, in this field.

Florin Popescu

NOTE POUR LES AUTEURS

La *Revue Roumaine de Chimie* publie des articles en anglais, français, russe, allemand ou espagnol. Les auteurs sont priés d'envoyer des articles, notes, communications et comptes rendus inédits.

Les manuscrits seront dactylographiés à deux intervalles. Les tableaux seront dactylographiés sur des feuilles séparées, de même que la légende des figures. Les diagrammes seront tracés à l'encre de Chine sur papier calque. Les tableaux et les figures seront numérotés par des chiffres arabes, en nombre strictement nécessaire. Prière de ne pas inscriere les mêmes données dans les tableaux et les figures. Les formules chimiques seront incluses dans le texte ; en outre, elles seront transcrites sur des feuilles séparées. Les auteurs sont priés d'indiquer les caractères italiques (en soulignant les lettres au crayon), ainsi que tout autre caractère spécial. L'ordre des références bibliographiques sera celui de leur mention dans le texte ; le nom de l'auteur sera précédé de l'initiale du prénom ; les publications périodiques seront présentées suivant les prescriptions internationales. Les références seront ajoutées à la fin de l'article ; elles paraîtront comme des notes, au bas de la page. Le texte sera précédé d'un résumé comprenant 15 lignes au maximum.

L'entière responsabilité du contenu des articles appartient aux auteurs. On publie des articles dus aux collaborateurs roumains ou étrangers.

PRINTED IN ROMANIA

TRAVAUX PARUS AUX ÉDITIONS DE L'ACADÉMIE DE LA RÉPUBLIQUE SOCIALISTE DE ROUMANIE

I. GĂLĂŢEANU, **Radiochimia aplicată. Metode şi probleme** (La radiochimie appliquée. Méthodes et problèmes), 1976, 305 p., 19 lei.

FRANCISC A. GOTHARD, **Echilibre lichid-vapori. I. Baze teoretice şi metode de calcul** (Equilibres liquide-vapeurs. I. Bases théoriques et méthodes de calcul). 1975, 263 p., 2 pl,. 28 lei.

CONST. GH. MACAROVICI, D. MACAROVICI, **Chimia oxizilor dubli şi utilizările lor** (La chimie des oxydes doubles et leur utilisation), 1975, 195 p., 13 lei.

ELENA CEAUŞESCU, Research work on synthesis and characterization of macromolecular compounds. Contributions, 1974, 251 p., 20 lei.

M. AVRAM, **Antidăunători** (Pesticides), 1974, 496 p., 41 lei.

DUMITRU COSTACHE, **Analiza chimică prin metoda cinetică** (L'Analyse chimique par la méthode cinétique), 1974, 276 p., 15,50 lei.

G. A. RĂDULESCU, **Proprietăţile ţiţeiurilor româneşti** (Les propriétés des pétroles roumains), 1974, 267 p., 2 pl. 18 lei.

CR. SIMIONESCU, VIORICA RUSAN, V. POPA, **Chimia algelor marine** (La chimie des algues marines), 1974, 212 p., 1 pl., 18 lei.

I. ZUGRĂVESCU, MAGDA PETROVANU, **Chimia n-ilidelor** (La chimie des n-Ilures), 1974, 348 p., 19 lei.

MARIA FITI, **Dozimetria chimică a radiaţiilor ionizante** (La dosimétrie chimique des radiations ionisantes), 1973, 240 p., 13,50 lei.

TIBERIU NĂSCUŢIU, **Metode radiochimice de analiză** (Méthodes radiochimiques d'analyse), 1973, 384 p., 23 lei.

CRISTOFOR SIMIONESCU, MARGARETA GRIGORAŞ, AGATA CERNĂTESCU-ASANEI, ROZMARIN GHEORGHE, **Chimia lemnului în România. Plopul şi salcia,** (La Chimie du bois en Roumanie. Le peuplier et le saule), 1973, 299 p., 13 pl., 26 lei.

MIHAI FLORESCU, **Eficienţa economică a cercetării ştiinţifice** (L'efficience économique de la recherche scientifique), 1972, 115 p., 15 lei.

GEORGETA LĂZĂRESCU, **Sistematizarea informaţiilor în chimia organică** (Systématisation des informations en Chimie Organique), 1972, 243 p., 1 pl., 10,50 lei.

I.P.I.—c. 1233

43 426

Lei 25.—

1977 JAN 18

F 1103

R

ACADÉMIE DE LA RÉPUBLIQUE SOCIALISTE DE ROUMANIE

REVUE ROUMAINE DE CHIMIE

REFERÁLVA

TOME 21
Nº 8
Août, 1976

RECHAX, **21**, *8*, 1113–1272 (1976)

EDITURA ACADEMIEI REPUBLICII SOCIALISTE ROMÂNIA

Rev. Roumaine Chim. **21**, *8*, p. 1113–1272 (1976), Bucarest

ACADÉMIE DE LA RÉPUBLIQUE SOCIALISTE DE ROUMANIE

COMITÉ DE RÉDACTION

Rédacteur en chef:

I. G. MURGULESCU, membre de l'Académie de la République Socialiste de Roumanie

Rédacteurs en chef adjoints:

A. T. BALABAN et V. EM. SAHINI, membres correspondants de l'Académie de la République Socialiste de Roumanie

Collège de rédaction:

EM. BRATU, ELENA CEAUŞESCU, ECATERINA CIORĂNESCU-NENITZESCU, C. DRĂGULESCU, CR. SIMIONESCU, membres de l'Académie de la République Socialiste de Roumanie; P. SPACU, membre correspondant de l'Académie de la République Socialiste de Roumanie; MARGARETA AVRAM, I. HAIDUC, D. I. MARCHIDAN, I. MOLDOVAN, G. NIAC et D. SĂNDULESCU

La Revue Roumaine de Chimie paraît 10 fois par an. Toute commande de l'étranger (fascicules ou abonnements) sera adressée à ILEXIM — Serviciul Export-Import Presă (Revues), P.O.B. 2001, télex 011226 64—66, Calea Griviţei, Bucarest 12, Roumanie

Les manuscrits, les livres et les revues proposés en échange ainsi que toute correspondance seront envoyés à la rédaction :

REVUE ROUMAINE DE CHIMIE

23, str. Dumbrava Roşie, Bucarest, Roumanie, téléphone 124160

EDITURA ACADEMIEI REPUBLICII SOCIALISTE ROMÂNIA

125, Calea Victoriei, Bucarest, téléphone 507680

ORSZÁGOS MŰSZAKI KÖNYVTÁR ÉS DOKUMENTÁCIÓS KÖZPONT 1883

REVUE ROUMAINE DE CHIMIE

Tome 21, N° 8/1976 Août 1976

I. G. MURGULESCU, EUGENIA IVANA, E. POPA and IULIA CONTINEANU, Absorption spectra of molten $SnCl_2$ and SnI_4 1115–1119

V. E. SAHINI, JOSETTE WEINBERG and MARILENA VASILESCU, Xylidine isomers. IV. Dipole moments in the first excited singlet state . . . 1121–1125

LUCIA CIOHODARU and AURELIA MEGHEA, Electronic structure of some stilbene derivatives. I. Electronic spectra and transmission of the substituent effects in molecules of some nitro-containing *trans*-stilbene derivatives 1127–1135

V. MACOVEI, Spectral solvent effects in aromatic compounds solutions. III. The solvent effects on the position and intensity of nitrobenzene band at 2500 Å 1137–1147

R S. CINCA, MIHAELA CONSTANTINESCU and E. SEGAL, Chemisorptive properties of zinc oxide thin films 1149–1152

T. VIȘAN, D. P. GEANĂ and S. STERNBERG, Voltammetric and chronopotentiometric study of silver ion in molten potassium nitrate 1153–1160

N. DUȘOIU, Temperature dependence of the dielectric permittivity of ionic crystals with cubic structure. I. Potassium bromide, iodide and chloride 1161–1169

C. DRĂGULESCU, ANA NIMARĂ, ELISABETA PRINCZ, AGNETA BALINT and I. JULEAN, Bismuth(III)-Ethylenediaminetetraacetic acid (EDTA) complexes. II. Kinetic studies on the isotopic exchange reaction between the hydrolysed bismuth ion and its EDTA complex 1171–1175

N. B. SINGH, Interaction between acenaphthene and picric acid 1177–1182

A. T. BALABAN, ANISIA BOTA and ILEANA I. STĂNOIU, Pyrylium salts formed by diacylation of olefins. XXII. Triacylation of 2,3-dimethyl-2-butene 1183–1187

M. D. GHEORGHIU and P. FILIP, Electronic structure of cyclobutadiene fused with heterocyclic ring. II. Cyclobutadienes condensed with five-membered heterocyclic rings 1189–1201

EUGENIA CARP, MARIA DORNEANU and I. ZUGRĂVESCU, Bicyclic bridgehead nitrogen systems. V. Pyrazolo- and tetrazolo-benzocinnolines by 1,3-dipolar cycloaddition reactions 1203–1206

L. V. FEYNS, I. I. DRAGOTĂ and I. NICULESCU-DUVĂZ, Infrared spectra of some new chromanone and coumarine derivatives 1207–1219

R V. B. JIGAJINNI, S. C. BENNUR, R. S. BENNUR and V. V. BADIGER, Hydrazones of piperidino-N-acetohydrazide and morpholino-N-acetohydrazide of pharmacological interest 1221–1225

Revue Roumaine de Chimie **21,** *8,* **p.** 1113–1272 (1976), Bucarest

F. URSEANU, New syntheses of dyes with naphth[2,3-c]xanthene-5,8,14-trione and naphth[2,3-c]thioxanthene-5,8,14-trione structure 1227–1235

CR. I. SIMIONESCU et AMALIA CRUSOS, Greffage mécano-chimique des polyoxyméthylènes. V. Aspects cinétiques au broyage vibratoire 1237–1245

I. MOŢOC, D. CIUBOTARIU und Ş. HOLBAN, Zur Kopolymerisation. IV. Das mathematische Modell der Bildung eines binären Kopolymers: die verbesserte Version 1247–1251

D. CIUBOTARIU, I. MOŢOC, und Ş. HOLBAN, Zur Kopolymerisation. V. Die Simulierung der Bildung eines Makromoleküls durch binäre Kopolymerisation. Das Programm MEMORY 3 1253–1261

R. CIUPE und MARIA GĂVAN, Der gaschromatographische Nachweis und die quantitative Bestimmung einer Mischung von 1-Chlor-3-thia-pentan und 3,6-Dithia-octan aus den bei der Synthese dieser Stoffe sich ergebenden Abflußwässern 1263–1264

A. D. MAGRÌ, G. D'ASCENZO, U. BIADER CEIPIDOR et A. MARINO, Analyse thermique des composés du cobalt (III) tétrammine avec des acides organiques dicarboxyliques 1265–1272

Revue Roumaine de Chimie, **21**, *8*, 1115–1119 (1976)

ABSORPTION SPECTRA OF MOLTEN $SnCl_2$ AND SnI_4

I. G. MURGULESCU, EUGENIA IVANA, E. POPA and IULIA CONTINEANU
Centre of Physical Chemistry, str. Galaţi 31, Bucharest Romania

Received January 30, 1976

The absorption spectra of both solid and molten $SnCl_2$ and SnI_4 have been determined over the temperature range of 25–300°.

Studies of spectral characteristics of tin halides have rarely been reported in literature; the existing data deal mainly with their thermodynamic properties.[1-5]

It is known that tin chloride is a compound with a predominantly covalent character.[6] The X-ray analysis[6,7] established that solid $SnCl_2$ consists of $(SnCl_2)_n$ chains in which three Cl atoms are coordinated around the Sn atom.

The study of the Raman spectra[1,2] of both solid and molten $SnCl_2$ indicated that these chains tended to breake down when the temperature was increased.

Solid SnI_4 consists of discrete tetrahedral molecules.[8] The presence of SnI_4 individual molecules in the fused state was also confirmed by the Raman spectroscopy.[9]

EXPERIMENTAL

The measurements were carried out with anhydrous $SnCl_2$ obtained by dehydration of $SnCl_2 \cdot 2H_2O$ with acetic anhydride.

The $SnCl_2$ was then purified by vacuum vaporization and a product with a 250° melting point was obtained.

SnI_4 was prepared according to the method indicated by Brauer.[10]

After having been purified by vacuum vaporization the product thus obtained had the melting point at 143.5°.

---

[1] J. H. R. Clarke and C. Solomons, *J. Chem. Phys.*, **47**, 1823 (1967).
[2] E. J. Hatway and V. A. Maroni, *J. Phys. Chem.*, **76**, 2796 (1971).
[3] L. Andews and D. Tredorick, *J. Amer. Chem. Soc.*, **92**, 775 (1970).
[4] B. Mishra and V. Ramakdrishna, *Indian J. Chem.*, **11**, 790 (1969).
[5] R. J. Zolweg and L. S. Frost, *J. Chem. Phys.*, **50**, 3281 (1969).
[6] R. E. Rundle and D. H. Olson, *Inorg. Chem.*, **3**, 596 (1964).
[7] J. M. Van den Berg, *Acta Cryst.*, **14**, 1002 (1961).
[8] R. E. Wood and H. L. Ritter, *J. Amer. Chem. Soc.*, **74**, 1763 (1952).
[9] U. Trolle and A. Kvist, *Z. Naturforsch.*, *B*, **25**, 1374 (1970).
[10] G. Brauer, "Handbook of Preparative Inorganic Chemistry", vol. 1 Academic Press, New York, 1963, p. 735.

The cell designs, as well as the method of their loading and handling were similar to those previously employed.[11]

The spectra were recorded on a Specord UV-VIS spectrophotometer (Carl Zeiss Jena). The cells employed in the present work had layer thicknesses between 8 and 10 μm. Due to the deterioration of the film contained in the cells, it was not possible to extend our investigations over a larger temperature range.

RESULTS AND DISCUSSIONS

Figures 1 and 2 show the absorption spectra of both solid and molten $SnCl_2$ and SnI_4, respectively.

The spectra are characterized by a continuous absorption which exhibits a sharp decrease from high values of A, down to values of A less than 0.2.

In figures 3 and 4, the temperature variation of the absorption edge of the two halides is presented. Energy jumps of $\sim$2000 cm^{-1} for $SnCl_2$ and $\sim$ 130 cm^{-1} for SnI_4 have been observed at the melting temperatures of these two salts.

The temperature variation of transmittance is presented in figures 5 and 6. Sharp changes can be noticed at the two melting points (for a temperature variation of 6 — 7 degrees per minute).

The study of the absorption spectra of solid and molten $SnCl_2$ and SnI_4 as a function of the temperature revealed a displacement of the absorption edge towards low energy values.

The magnitude of these displacements, expressed in eV/degrees, together with the transmittances for which the displacements have been measured, are listed in table 1.

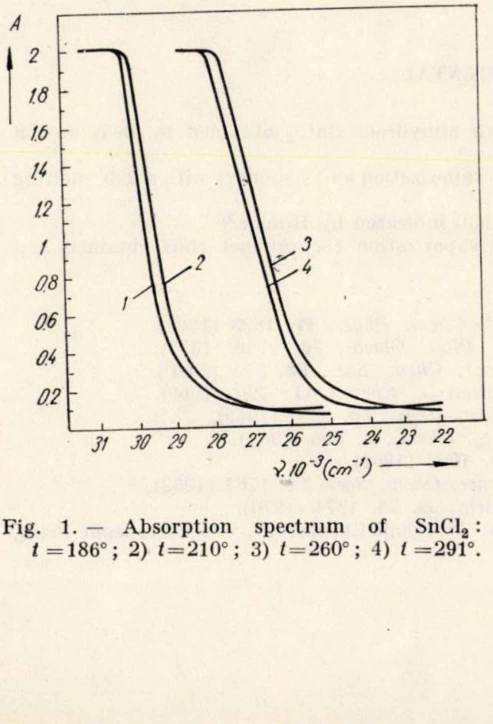

Fig. 1. — Absorption spectrum of $SnCl_2$: $t = 186°$; 2) $t = 210°$; 3) $t = 260°$; 4) $t = 291°$.

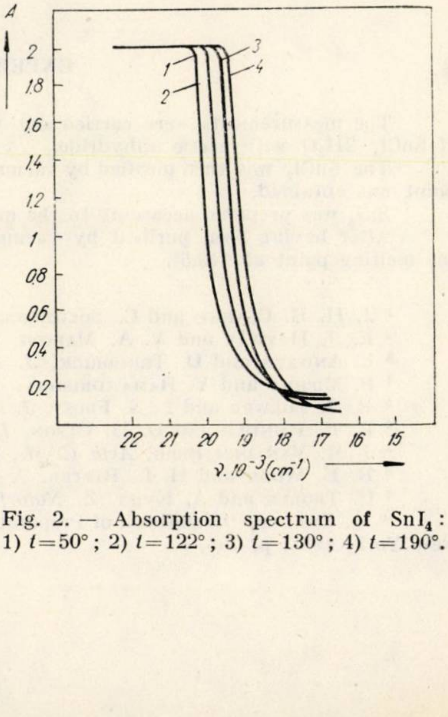

Fig. 2. — Absorption spectrum of SnI_4: 1) $t = 50°$; 2) $t = 122°$; 3) $t = 130°$; 4) $t = 190°$.

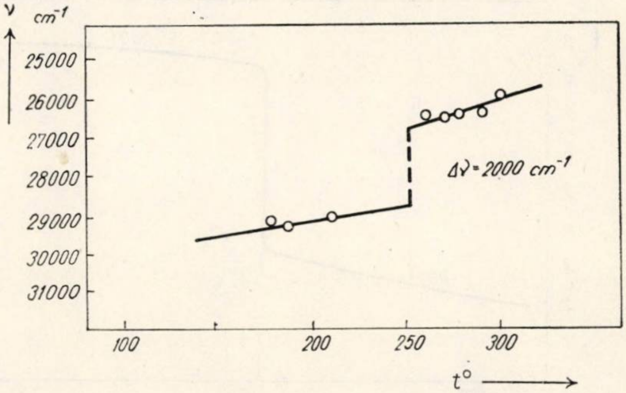

Fig. 3. — Temperature variation of the absorption band edge of $SnCl_2$ at $T = 30\%$.

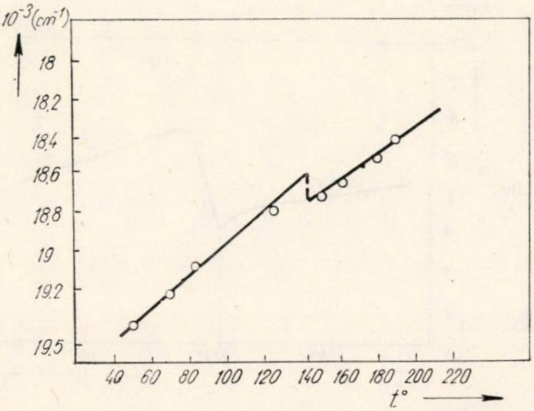

Fig. 4. — Temperature variation of the absorption band edge of SnI_4 at $T = 40\%$.

Table 1

$$\frac{\Delta\lambda}{\Delta t}\left(\frac{\text{eV}}{\text{degree}}\right)$$

	Solid	Melt	$T\%$
SnI_4	$1.04.10^{-3}$	$0.8.10^{-3}$	40
$SnCl_2$	$1.55.10^{-3}$	$1.98.10^{-3}$	30

Both the sharp variation of transmittance and the energy jump at the melting point indicated that some transformations such as structural changes, dissociations, auto-ionizations, etc., occur on melting. SnI_4 is the exception among the pure molten halides which have been investigated in our laboratory. [11-13]

[11] I. G. Murgulescu, E. Popa and E. Ivana, *Rev. Roumaine Chim.*, **18**, 189 (1973).

[12] E. Popa, E. Ivana and S. V. Volkov, *Rev. Roumaine Chim.*, **15**, 1707 (1970).

[13] I. G. Murgulescu, E. Ivana and E. Popa, *Rev. Roumaine Chim.*, **21**, 000 (1976).

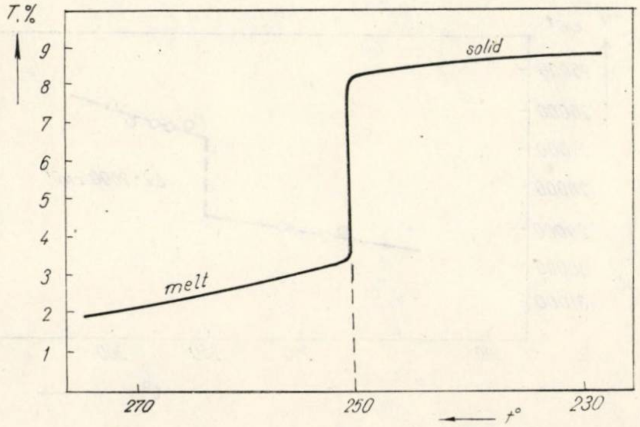

Fig. 5. — Temperature variation of the transmission of the $SnCl_2$ at $\nu = 27.000\ cm^{-1}$.

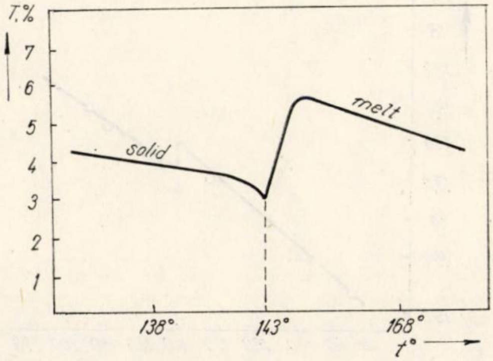

Fig. 6. — Temperature variation of the transmission of the SnI_4 at $\nu=18.400\ cm^{-1}$.

In contrast to the other halides, the edge of the SnI_4 absorption band is displaced towards high energy values.

The higher value of the displacements of solid SnI_4 absorption edges indicates that structural changes due to the temperature increase occurring in the solid are more important than those occurring in the molten salt.

The moderate energy jump noted at the melting point and the displacements of the absorption edge for the solid and molten SnI_4 (Table 1) suggest that the predominant effect of temperature increase is thermal expansion. This conclusion is in agreement with the results obtained by X-ray studies concerning the structure of molten SnI_4 and its density change on melting. [8]

The values of $\frac{\Delta\lambda}{\Delta t}\left(\frac{eV}{degree}\right)$ for molten $SnCl_2$ are somewhat higher, but are of the same order of magnitude, as those obtained for the solid over the investigated temperature range.

If the displacements of the absorption edges are the result of the structural changes, it appears that these changes will be more accentuated in the molten state as compared with those in the solid state. This observation agrees with the results obtained by studies of the Raman spectra[1,2] in the molten $SnCl_2$ that have envinced the presence of $(SnCl_2)_n$ polymer aggregates as a result of degradation of the polymer chains which constitute the solid.

As we have already established, the absorption spectrum at the melting point of $SnCl_2$ shows an energy jump of 2000 cm^{-1}.

The high value of this jump supports the assumption that aside from the process of fragmentation of the polymer chains occurring on melting, processes leading to the formation of $SnCl_3^-$ and $SnCl^+$ species also occur. Such species may appear either by dissociation, or by autoionization.

The hypothesis of the presence of $SnCl^+$ and $SnCl_3^-$ ions together with $(SnCl_2)_n$ aggregates is also supported by the electrical conductivity measurements. [14,15] The specific conductivity of molten $SnCl_2$ at 300° is 1.107 ohm^{-1} cm^{-1}, which is only half the value for KCl at 787°. [16]

The fact that the ionic species could not be identified in the molten $SnCl_2$ absorption spectrum might be attributed to overlapping of the absorption bands, a phenomenon which is common in molten halide spectra. [11-13]

---

[14] V. V. Rafalski, *Ukrain. khim. Zhur.*, **26**, 585 (1960).
[15] W. Blitz and W. Kemm, *Z. anorg. Chem.*, **152**, 225 (1926).
[16] K. W. Fung and K. E. Johnson, *Canad. J. Chem.*, **48**, 3635 (1970).

Revue Roumaine de Chimie, **21**, *8*, 1121–1125 (1976)

XYLIDINE ISOMERS. IV[1]

DIPOLE MOMENTS IN THE FIRST EXCITED SINGLET STATE

V. E. SAHINI, JOSETTE WEINBERG and MARILENA VASILESCU
Centre of Physical Chemistry, Str. Galați 31, Bucharest, Romania

Received December 12, 1975

The dipole moments of xylidine isomers in the first excited singlet state were determined; the experimental values have been compared with the theoretical ones obtained by a SCF-MO calculation.
The steric and the substituents effects of CH_3-group are discussed in terms of H-bond formation between the isomers and two specific solvents, dioxane and isopropanol.

The determination of dipole moments has been of considerable value in understanding the physical-chemical properties of molecules in the ground and excited electronic states.

From the study of the difference between the solvent effects upon the absorption spectra and those upon the fluorescence spectra one may derive experimental information on the electronic structure of the excited molecule.

The dipole moment can be obtained by measuring the solvent induced shift of 0–0 transition and by using some equations which relate these shifts to the solute polarity and to the moment change on excitation.[2,3]

The aim of the present paper is to study, by comparison with the ground state, the change of the dipole moment of xylidines in their first excited singlet state and to discuss the substituent and steric effects, depending on the position of CH_3-group in molecule, in terms of H bonding effects in spectral solvent shifts.

We have used a method based on Kawski's relations [4] as modified by Chamma. [5]

These relations allow the direct determination of the dipole moment μ_{S_1} without referring to the angle between μ_{S_0} and μ_{S_1} and make use of absorption and emission spectra observed in solvents of different polarity.

---

[1] Previous paper: V. E. Sahini, J. Weinberg, C. Bendic and M. Milescu, *Rev. Roumaine Chim.*, **19**, 1685 (1974).

[2] E. Lippert, *Z. Naturforsch.* (*A*), **10**, 541 (1955).

[3] N. Mataga, *Bull. Chem. Soc. Japan*, **36**, 654 (1963).

[4] I. Janic and A. Kawaski, *Bull. Acad. Polon. Sci., Ser. Sci. Math., Astron. et Phys.*, **20**, 519 (1972).

[5] A. Chamma et P. Viallet, *Compt. rend., Sér. Sci. Chim.*, **270**. 1901 (1970).

The second experimental method used here originates in Varma and Groenen's work [6] and makes use of either absorption or emission spectra observed in different solvents.

Use has been made of least square method to process the data.

1. EXPERIMENTAL

Spectral grade solvents of dielectric constant between 1.95 and 26.00 (*n*-heptane, cyclohexane, dioxane, isooctane, chlorobenzene, dichloromethane, *n*-butanol, isopropanol) have been used without further purification, since no interfering emission was observed from these solvents. The xylidines (Schuchardt) were purified by fractional distillation under low pressure.

The concentration was of about 10^{-5} M.

All measurements were carried out at room temperature.

Ultraviolet and fluorescence spectra were recorded by means of an UNICAM SP-800 spectrophotometer and a Perkin-Elmer 204 fluorescence spectrophotometer.

2. THEORETICAL

The π net charge distribution on xylidine atoms in S_1 state was determined by an SCF–MO–PPP–CI formalism.

The theoretical values of dipole moment μ_{S_1} have been obtained by considering, like in case of the μ_{S_0} dipole moment, [7] the vectorial summation of unchanged aniline dipole moment σ, with π dipole moment of each isomer in the S_1 state.

The parameter values used here were the same as in case of μ_{S_0},[7] yet optimized by the above mentioned formalism.

The presence of the methyl group is taken into account by an inductive effect upon π net charge of the adjacent carbon atom. [7]

3. RESULTS AND DISCUSSION

The experimental and theoretical values of dipole moments in the first excited singlet state μ_{S_1}, as well as in the ground state μ_{S_0} of xylidine isomers are presented in Table 1.

Table 1

Experimental and theoretical dipole moments in S_1 state

Isomer	$\mu_{S_0}(D)^7$	$\mu_{S_1}(D)$		
		Experimental		Theoretical
		(Abs. + Fl.)	(Abs.)	
2,6-xylidine	1.67	3.11	2.67	3.85
2,3-xylidine	1.58	3.56	2.91	4.52
2,5-xylidine	1.53	3.14	1.85	3.66
2,4-xylidine	1.41	2.79	1.97	3.42
3,4-xylidine	1.28	2.84	2.66	3.60
3,5-xylidine	1.40	3.35	3.20	4.09

---

[6] C. A. G. O. Varma and E. J. J. Groenen, *Rec. Trav. chim.*, **91**, 296 (1972).

[7] V. E. Sahini and J. Weinberg, *Rev. Roumaine Chim.*, **18**, 1493 (1973).

The increase in the dipole moment values of all xylidine isomers in the S_1 state is evident from the experimental and theoretical values μ_{S_1}.

The agreement between experimental data obtained by both absorption and fluorescence data and the theoretical ones is satisfactory and the increase sequence of the two sets of determination is identical.

The agreement is poorer in the case of absorption data probably due to the simplified approximation of the angle between $\vec{\Delta\mu}$ and $\vec{\mu}_{S_0}$ as zero.

Table 2 shows the π-net charge on the nitrogen atom in both the ground ($\rho_N^{S_0}$) and first excited singlet ($\rho_N^{S_1}$) states, the π — electron bond orders between the nitrogen atom and the adjacent carbon atom P_{CN} in S_0 and S_1 states, and the corresponding interatomic distances r_{CN}.

One can notice the increase in the π-electron bond orders in S_1 state and consequently the decrease in interatomic distances; a minor but identifiable geometry change in S_1 state is also noticeable.

Absorption spectra were used to calculate the difference of interaction energies of ground and excited states ΔE_d[6]; this originates in the dispersion interaction between substance and surrounding solvent molecules.

This difference of interaction energies is negative i.e. a red shift is caused by dispersion interactions. The dispersion interaction in solutions leads to a red shift compared to the vapor state, at least if one of the participating states of the transition considered is the electronic ground state and if the transition energy is smaller than the energy of the electronic transitions of the solvent molecule.[8]

Fig. 1 plots this difference ΔE_d versus dipole moment μ_{S_1} in cyclohexane.

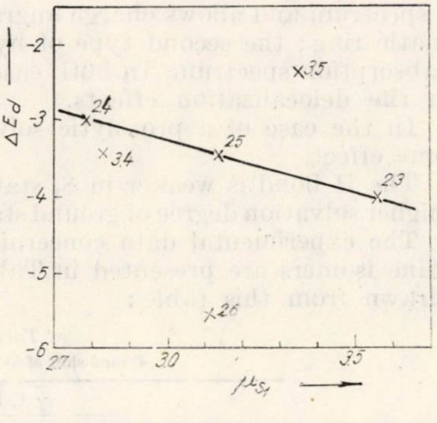

Fig. 1. — Dipole moments in the first excited singlet state.

One can observe the linear correlation of 2,4-; 2,5- and 2,3-isomers which have all an *ortho* methyl group. The position of 2,6- as well as of 3,5-isomers will be discussed below.

---

[8] W. Liptay "Modern Quantum Chemistry, Istanbul Lectures" vol. II, Interactions, ed. O. Sinanoglu, Academic Press. New York, 1965, p. 173.

The dipole moment change during the electronic transition is generated by the electron migration from the nitrogen atom to the aromatic ring which is seen in Table 2. At the same time an electronic redistribution occurs within the aromatic ring and it entails an increase in dipole moment value μ_{S_1}.

Table 2

π-net charge, π-electron bond orders and interatomic distances between the nitrogen atom and the adjacent carbon atom

Isomer	$\rho_N^{S_0}$	$\rho_N^{S_1}$	$P_{CN}^{S_0}$	$P_{CN}^{S_1}$	$r_{CN}^{S_0}$ (Å)	$r_{CN}^{S_1}$ (Å)	δr_{CN}
2,6-xylidine	0.1646	0.3272	0.3525	0.5582	1.447	1.416	−0.031
2,3-xylidine	0.2048	0.3302	0.3805	0.5637	1.443	1.416	−0.027
2,5-xylidine	0.2067	0.2998	0.3803	0.5034	1.443	1.424	−0.018
2,4-xylidine	0.2020	0.3176	0.3618	0.5498	1.446	1.418	−0.028
3,4-xylidine	0.2037	0.3214	0.3889	0.5599	1.442	1.416	−0.026
3,5-xylidine	0.2082	0.3358	0.4065	0.5784	1.439	1.413	−0.016

The decrease in π electron density on nitrogen atom in excited state is responsible for the deviations of $\Delta\tilde{\gamma}$ values corresponding to the solvent induced shift of xylidine-C band in the following two solvents characterized by formation of an H bond : dioxane and isopropanol.

With xylidines, these solvents can form hydrogen bonds of the types[3] :

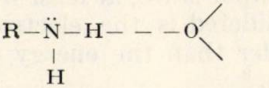

(1)

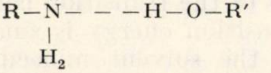

$$\mathrm{R{-}\ddot{N}(H_2){-}\,-\,-H{-}O{-}R'}$$

(2)

The hydrogen bond of the first type causes a red shift of the absorption spectrum and allows charge migration from the nitrogen atom to the aromatic ring; the second type of hydrogen bond causes a blue shift of the absorption spectrum. In both cases the H bond energy comes mainly from the delocalization effects.

In the case of a protolytic solvent, isopropanol, it gives a hypsochrome effect.

The H bond is weaker in S_1 state than in dioxane, probably due to the higher solvation degree of ground state, which tends to hinder excitation.

The experimental data concerning the C-band shifts in dioxane for xylidine isomers are presented in Table 3; the following conclusions can be drawn from this table :

Table 3

C-band shift of xylidines in dioxane

Isomer	$\tilde{\gamma}$ C-band in cyclohexane (cm^{-1})	$\tilde{\gamma}$ C-band in dioxane (cm^{-1})	$\Delta\tilde{\gamma}$
2,6-xylidine	35.149	34.934	−215
2,3-xylidine	34.965	34.602	−363
2,5-xylidine	34.722	34.335	−387
2,4-xylidine	34.153	33.870	−283
3,4-xylidine	34.101	33.613	−488
3,5-xylidine	34.542	34.130	−412

Xylidine isomers form with dioxane H bond of the first type, which entails a red shift of C band.

The shift is larger or smaller, depending on the position of methyl groups in molecule.

The *ortho*-CH_3 group has a small $(+I)$ substituent effect and a larger $(-S)$ steric strain.[9]

In case only one *ortho*-methyl group exists, some π-overlap can apparently occur between the lone-pair electrons of nitrogen atom and the ring; thus a charge migration to the ring is possible resulting the red shift of C-band in dioxane, of about the same order, for 2,3 and 2,5 xylidines; this is confirmed in Table 3.

For 2,6-xylidine the two ortho-methyl groups bring about a larger steric strain which prevents the H bond from forming; we have found the lowest red shift of C band and a special location of this isomer in Fig. 1.

The 3,5-xylidine does not undergo any steric (and mesomeric) effect so that it exhibits the largest red shift of C band among all isomers listed above as well as another special location in the same figure. A particular case is provided by 2,4- and 3,4-xylidine isomers, whose substituent effect $(+I)$ of one *para* methyl group is sensibly larger.

For the 2,4-xylidine, the steric strain of *ortho* methyl group is higher than the substituent $(+I)$ effect of *para* methyl group and the result is a red shift of C-band of only 283 cm^{-1}; a larger shift (488 cm^{-1}) of C band is obtained for 3,4-xylidine whose $(+I)$ effect of *para* methyl group is not offset by any steric effect.

Isopropanol probably favours formation of the second type of H-bond which entails a blue shift of C band. One can see in Table 4 that the largest blue shift is displayed by 2,6-xylidine (+124 cm^{-1}), which favours the formation of this kind of bridge through the two *ortho* methyl groups.

Table 4

C-Band shift of xylidine in isopropanol

Isomer	$\tilde{\gamma}$ C-Band in cyclohexane (cm^{-1})	$\tilde{\gamma}$ C-Band in isopropanol (cm^{-1})	$\Delta\tilde{\gamma}$
2,6-xylidine	35.149	35.273	+124
2,3-xylidine	34.965	35.026	+ 61
2,4-xylidine	34.153	34.247	+ 94
3,5-xylidine	34.542	34.483	− 59

However, as already mentioned, this H bridge is weaker in excited state. The other isomers whose steric effect decreases show a lower blue shift ending up with 3,5-xylidine which already has a 59 cm^{-1} red C band shift.

ACKNOWLEDGEMENT. We are very grateful to Mrs. Mihaela Hillebrand and Mr. C. Bendic for kindly supplying us with their SCF-MO-PPP-CI program.

---

[9] L. N. Ferguson "The Modern Structural Theory of Organic Chemistry" Prentice-Hall, Englewood Cliffs, New Jersey, 1964, p. 353.

Revue Roumaine de Chimie, **21**, *8*, 1127–1135 (1976)

ELECTRONIC STRUCTURE OF SOME STILBENE DERIVATIVES. I

ELECTRONIC SPECTRA AND TRANSMISSION OF THE SUBSTITUENT EFFECTS IN MOLECULES OF SOME NITRO-CONTAINING *TRANS*-STILBENE DERIVATIVES

LUCIA CIOHODARU and AURELIA MEGHEA
Department of Physical Chemistry, Polytechnic Institute, str. Polizu 1,
Bucharest, Romania

Received September 15, 1975

◆

Electronic spectra of 24 *trans*-stilbene derivatives are reported. The transmission of the substituent effects was evidenced in both qualitative and semiquantitative treatment, taking into account the contribution of both steric and conjugative effect. The bathochromic shift was used as a measure of the overall electronic and steric effect, in order to obtain correlations between the spectral parameters and the molecular structure of the stilbene derivatives.

Stilbene and its derivatives are well-known due to their various applications in most fields of science and engineering, from medicine and biochemistry to the dyes' industry and the semiconductors' technique. Especially, their interesting physiological properties, connected with carcinogenicity, growth-inhibition and oestrogenic activity[1–3] are of great importance.

The correlations between the physiological properties and the molecular structure represent an unsolved problem until now.

That is why we begin a systematic study of a great number of stilbene derivatives, using a series of methods of investigation, namely the ultraviolet-visible, infrared and electron spin resonance spectra, molecular orbitals calculations, determination of dipole moments, etc.

The aim of the present paper is to give the spectral parameters of the ultraviolet and visible spectra of some nitro-containing *trans*-stilbene derivatives, as well as their correlations with the molecular structure. There are no data in the literature referring to these spectra until now. The correlations are of use not only to check and complete the literature data referring to similar compounds, but, also, to identify other stilbene derivatives having unknown structure.

---

[1] J. Arcos and M. Arcos, *Progr. Drug Res.*, **4**, 407 (1962).

[2] R. A. Andersen, M. Enomato, E. C. Miller and J. A. Miller, *Cancer Res.*, **24**, 128 (1964).

[3] E. Ciorănescu, "Medicamente de sinteză", 2nd ed., Edit. tehnică, Bucharest, 1966, p. 531–536.

The assignment of the three absorption bands (*A*, *B*, *C*) in the electronic spectrum of the unsubstituted *trans*-stilbene was long time disputed, and elucideted only in 1966, as a result of a LCAO–MO–SCF–CI–PPP calculation.[4]

These bands appear, also, in the spectra of the substituted stilbene derivatives having different chromophores, but they undergo great bathochromic shifts, as well as modifications of absorption intensity.

The *C* band is very little influenced by the nature of the substituents, but the shifts of both *B* and *A* band are well correlated with the molecular strucuture of the corresponding derivatives.

EXPERIMENTAL PART

The ultraviolet and visible absorption spectra of 24 nitro-containing *trans*-stilbene derivatives are given; the substituents for the investigated derivatives, given in Table 1, agree with the following general formula:

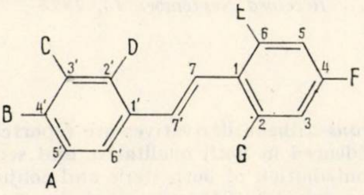

Table 1

The nitro-containing *trans*-stilbene derivatives

No.	*A*	*B*	*C*	*D*	*E*	*F*	*G*	M.p. (°)	Ref.	Comments
1	H	H	H	H	H	NO_2	CN	141	6	
2	H	H	H	H	H	NO_2	$CONH_2$	262	7	2-cyano-
3	H	OH	H	H	H	NO_2	CN	219	8	4-nitro-
4	H	OCH_3	H	H	H	NO_2	CN	197	9	*trans*-stilbene
5	H	NMe_2	H	H	H	NO_2	CN	209	9	derivatives
6	H	NMe_2	H	H	H	NO_2	COOH	206	10	
7	H	H	H	H	H	CN	NO_2	168	6	
8	H	H	H	H	H	$CONH_2$	NO_2	180	6	
9	H	OH	H	H	H	CN	NO_2	230	11	
10	H	OCH_3	H	H	H	CN	NO_2	153	9	
11	H	NMe_2	H	H	H	CN	NO_2	180	9	2-nitro-
12	H	NMe_2	H	H	H	$CONH_2$	NO_2	228	8	4-cyano-
13	H	$NHCOCH_3$	H	H	H	CN	NO_2	244	12	*trans*-
14	$O-CH_2-O$		H	H	H	CN	NO_2	191	9	stilbene
15	OCH_3	OH	H	H	H	CN	NO_2	210	11	derivatives
16	H	H	H	H	H	NO_2	NO_2	140	13	2,4-dinitro-
17	H	H	H	NO_2	H	NO_2	NO_2	190	14	*trans*-
18	H	H	NO_2	H	H	NO_2	NO_2	179	14	stilbene
19	H	NO_2	H	H	H	NO_2	NO_2	238	14	derivatives
20	H	NMe_2	H	H	H	NO_2	NO_2	174	14	
21	H	H	H	H	NO_2	NO_2	NO_2	155	15	2, 4, 6-tri-
22	H	OCH_3	H	H	NO_2	NO_2	NO_2	165	9	nitro-*trans*-
23	H	Cl	H	H	NO_2	NO_2	NO_2	154	9	stilbene
24	H	NO_2	H	H	NO_2	NO_2	NO_2	190	6	derivatives

---

[4] D. L. Beveridge, *Diss. Abstr.*, **26**, 3644 (1966).

The derivatives were synthetised by means of the Bishop and Brady's method,[5] based on the Ullmann [11] and Pfeiffer's [6] works, through the direct condensation of some substituted benzaldehydes with the corresponding substituted toluenes, having the methyl group activated by the presence of one or more nitro groups.

In order to obtain pure *trans*-stilbene derivatives, assuming that the reaction product contains a little amount of *cis* isomer, the Syz and Zollinger's method [16] was employed.

The verification of the *trans*-stilbene isomers' purity was made through : the elemental analysis (C, H, N), the determination of the melting points, the pursuit of the constancy for a certain time of the ultraviolet spectra, the record of the infrared spectra and the verification of the absence of the band corresponding to the *cis* isomer.

The electronic spectra were recorded by means of a VSU-1 Carl Zeiss Jena spectrophotometer, in the range of wavelengths between 220 and 750 nm. The same temperature and solvent were used for all studied stilbene derivatives. The solutions ($10^{-4} - 10^{-5}$M) were prepared in absolute ethanol, at cold and dark or red light, little before use.

RESULTS AND DISCUSSION

For the presented stilbene derivatives (table 1), on the basis of the electronic spectra' analysis, we studied the transmission of the substituent effects in qualitative and semiquantitative manner.

1. QUALITATIVE CORRELATIONS BETWEEN COLOUR AND MOLECULAR STRUCTURE OF SOME NITRO-CONTAINING *trans*-STILBENE DERIVATIVES

The unsubstituted *trans*-stilbene is colourless, but its nitro-containing derivatives are coloured, due to the extension of the conjugated system. The followings may be stated in connection with the correlation between colour and molecular strucuture :

— the presence of one or more nitro groups in molecule of the stilbene derivative determines a yellow colour, regardless of the number and the position of nitro groups ;

— the presence of CN, $CONH_2$ or COOH groups in molecule, beside nitro group, does not modify the yellow colour ;

— the presence of one or more nitro groups in one ring and of some OH or OCH_3 groups in another ring shifts the colour to orange ;

— the presence of at least one nitro group and of some other substituents (CN, $CONH_2$, COOH) in one ring and of one NMe_2 group in another ring shifts the colour to dark red and black.

---

[5] G. Bishop and O. L. Brady, *J. Chem. Soc.*, **1922**, 2366.

[6] F. Ullmann and M. Gschwind, *Ber. dtsch. chem. Ges.*, **41**, 2291 (1908).

[7] E. Macovschi, I. I. Georgescu and C. Bachmeyer, *Ber. dtsch. chem. Ges.*, **74**, 1279 (1941).

[8] P. Pfeiffer, L. Klinkert and A. Politzer, *Ber. dtsch. chem. Ges.*, **49**, 2426 (1916).

[9] P. Pfeiffer, S. Braude, L. Kléber, G. Marconet and P. Wittkop, *Ber. dtsch. chem. Ges.*, **48**, 1797 (1915).

[10] P. Pfeiffer, J. Engelhardt and M. Allfuss, *Liebigs Ann. Chem.*, **467**, 158 (1928).

[11] P. Pfeiffer, *Ber. dtsch. chem. Ges.*, **51**, 564 (1918).

[12] P. Pfeiffer, *J. prakt. Chem.*, **109**, 225 (1927).

[13] J. Thiele and O. Dimroth, *Ber. dtsch. chem. Ges.*, **28**, 1412 (1895).

[14] J. Thiele and R. Escales, *Ber. dtsch. chem. Ges.*, **34**, 2850 (1901).

[15] P. Pfeiffer and P. Monath, *Ber. dtsch. chem. Ges.*, **39**, 1306 (1906).

[16] M. Syz and H. Zollinger, *Helv. Chim. Acta*, **48**, 517 (1965).

Table 2

The spectral parameters for the B band

No.	λ_{max} (nm)	Intensity of absorption			Line-width	
		ε_{max} [a] ($l.mol^{-1}\cdot cm^{-1}$)	$A \times 10^{-8}$ [b] ($l.mol^{-1}\cdot cm^{-2}$)	f_{exp} [c]	$\frac{f_{exp} \times 10^7}{\varepsilon_{max}}$	$\Delta\nu_{\frac{1}{2}} \times 10^{-1}$ [d] (cm^{-1})
1	250	15 820	1.063	0.522	274	324
3	265	14 360	1.133	0.556	387	396
4	265	16 880	1.272	0.549	325	326
5	300	8 940	0.658	0.284	318	339
6	295	12 220	0.890	0.384	314	360
8	274	14 400	0.794	0.343	238	202
10[e]	240	31 400				
11	260	28 000	2.844	1.228	439	398
12	240	21 300	3.097	1.297	609	719
13	260	12 000	1.236	0.533	444	490
14	255	15 600	1.327	0.572	367	425
15	250	15 200	1.591	0.686	451	622
16	230	22 000	2.268	0.979	445	617
17[e]	240	21 600				
18	245	27 800	3.083	1.331	469	561
20	300	15 300	1.058	0.457	299	321
22	280	15 600	1.707	0.736	472	513
23	250	18 000	1.603	0.692	384	466

[a] the molar extinction coefficient; [b] the molar integrated extinction coefficient or the integrated absorption intensity[17]; [c] the oscillator strength[17]; [d] the frequency difference between the absorption maximum and the point corresponding to $\varepsilon_{max}/2$ towards the greater wavelengths[18]; [e] the *B* band does not wholly appear.

2. SEMIQUANTITATIVE CORRELATIONS REFERRING TO THE SHIFTS OF THE B AND A ABSORPTION BANDS

There are no available literature data referring to the position or to the displacement of the *B* band of the corresponding mono-substituted stilbene derivatives. Also, there are available data only for the *A* band of the mono-substituted and the *p, p'*-disubstituted derivatives; data for the polysubstituted derivatives are missing.

In connection with the studied stilbene derivatives, *o, p*-dinitrostilbene (no. 16), placed in the middle of table 4 (the XIIth position), may be considered as a *reference compound* for the appreciation of the contributions of the electronic effects. The comparatively great value of its bathochromic shift ($\Delta\lambda_A$) among *o, p*-disubstituted stilbene derivatives points out a considerable conjugative effect of the nitro groups; this effect cancels the contribution of the steric effect of the nitro group in *ortho*-position (the steric effect is proved by the great width of the absorption band). As a consequence, *o, p*-dinitro-stilbene has a certain planarity.

The two *B* and *A* absorption bands undergo bathochromic shifts in comparison with the corresponding bands of the unsubstituted *trans*-stilbene, regardless of number, nature and position of the substituents.

---

[17] H. Suzuki, "Electronic Absorption Spectra and Geometry of Organic Molecules. An Application of Molecular Orbital Theory", Academic Press, New York, 1967, p. 9.

[18] H. Suzuki, *Bull. Chem. Soc. Japan*, **35**, 1715 (1962).

Table 3

The spectral parameters for the A band

No.	λ_{max} (nm)	Intensity of absorption		f_{exp} [c]	Line-width	
		ε_{max} [a] $(l.mol^{-1}.cm^{-1})$	$A \times 10^{-8}$ [b] $(l \cdot mol^{-1} \cdot cm^{-2})$		$\frac{f_{exp} \times 10^7}{\varepsilon_{max}}$	$\Delta\nu_{\frac{1}{2}} \times 10^{-1}$ [d] (cm^{-1})
1	340	20 400	0.677	0.292	143	148
2	336	18 800	0.609	0.263	140	135
3	395	29 500	1.561	0.674	229	238
4	390	33 100	1.631	0.704	212	183
5	464	24 200	1.183	0.511	211	217
6	444	21 300	1.171	0.505	236	211
7	314	21 800	1.242	0.536	246	209
8	310	20 800	1.658	0.716	344	267
9	345	28 400	1.485	0.473	166	296
10	340	30 880	2.436	1.052	345	441
11	430	39 000	2.928	1.264	325	268
12	400	23 400	2.351	1.015	435	340
13	370	20 360	1.154	0.498	245	203
14	375	21 200	1.970	0.850	401	385
15	366	21 400	1.403	0.605	283	204
16	356	23 200	1.633	0.695	299	245
17	340	27 600	1.515	0.654	237	179
18	340	28 600	1.538	0.664	232	179
19	352	29 760	1.913	0.825	278	195
20	476	26 000	1.521	1.656	252	235
21	350	14 400	1.168	0.504	349	225
22	400	14 800	1.406	0.607	410	217
23	350	16 300	1.114	0.481	295	154
24	310	20 000	2.074	1.018	225	417

[a] the molar extinction coefficient; [b] the molar integrated extinction coefficient or the integrated absorption intensity[17]; [c] the oscillator strength[17]; [d] the frequency difference between the absorption maximum and the point corresponding to the $\varepsilon_{max}/2$ towards the greater wavelengths.[18]

The highest bathochromic shifts belong to the derivatives no 20, 5 and 6; these three compounds have at the extremities of the conjugated system, in the direction of the long axis of the molecule, the substituents with the strongest opposite electronic effects (NMe_2 and NO_2). It may be presumed that in the electronically ground state of these molecules is probable the existence of some ionic structure, for ex.:

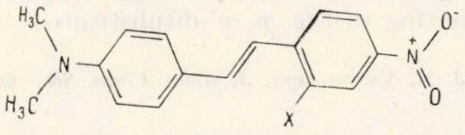

Table

The influence of the substituents on the bathochromic shifts of the

Order	I	II	III	IV	V	VI	VII	VIII	IX	X	XI
$\Delta\lambda_A$	182	170	150	136	106	106	101	96	81	76	72
No	20	5	6	11	12	22	3	4	14	13	15
p'	NMe_2	NMe_2	NMe_2	NMe_2	NMe_2	OCH_3	OH	OCH_3	O $\vert$ CH_2 $\vert$	$NHCOCH_3$	OH
m'									O		OCH_3
o'											
p	NO_2	NO_2	NO_2	CN	$CONH_2$	NO_2	NO_2	NO_2	CN	CN	CN
o	NO_2	CN	COOH	NO_2	NO_2	$2NO_2$	CN	CN	NO_2	NO_2	NO_2
$\Delta\lambda_B$	80	80	75	60	54	45	45	40	40	35	30
No.	20	5	6	22	8*	3	4	11**	13	14	15

* the *B* band undergoes a bathochromic shift greater than the *A* band; ** the *B* bands undergo bathochromic

But, in the first electronically excited state, the following high-polar intramolecular structure is more probable:

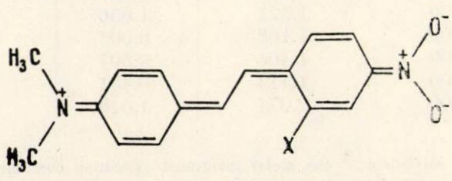

These structures explain the stabilization of the excited state to a greater extent than that of the ground state, the decrease of the transition energy between them and, therefore, the strong bathochromic shifts of the absorption bands.

In comparison with the *p*, *p'*-derivative studied in literature (NO_2, NMe_2; $\Delta\lambda_A = 135$ nm*), the introduction of the third substituent in *o*-position having electron-withdrawing effect (NO_2) determines a great difference of the shift; in this case, the polarity of the molecule increases additionally. According to that, there is a supplemental bathochromic shift.

The increasing polarity brings about the extension of the conjugation, which is in good agreeement with one of the empiric Doub and Vandelbelt's rules,[19] referring to the *p*, *p'*-disubstituted benzene derivatives.

---

[19] L. Doub and J. M. Vandelbelt, *J. Amer. Chem. Soc.*, **69**, 2714 (1947); *ibid.*, **77**, 4535 (1955).

* in its turn, this bathochromic shift exceeds the value which was obtained based on the additivity of the bathochromic shifts of the corresponding monò-substituted derivatives: $\Delta\lambda_A = 55$ nm (NO_2), $\Delta\lambda_A = 50$ nm (NMe_2).

4

B and A bands of the investigated *trans*-stilbene derivatives

XII	XIII	XIV	XV	XVI	XVII	XVIII	XIX	XX	XXI	XXII	XXIII	XXIV
62	58	56	56	51	46	46	46	46	42	20	16	16
16	19	21	23	9	1	10	17	18	2	7	8	24
—	NO_2	—	Cl	OH	—	OCH_3	—	—	—	—	—	NO_2
NO_2 NO_2	NO_2 NO_2	NO_2 $2NO_2$	NO_2 $2NO_2$	CN NO_2	NO_2 CN	CN NO_2	NO_2 NO_2 NO_2	NO_2 NO_2 NO_2	NO_2 $CONH_2$	CN NO_2	$CONH_2$ NO_2	NO_2 $2NO_2$
—	—	—	30	30	25	20	20	20	—	—	10	—
9	19	21	23	1	18	10	17	12**	2	7	16**	24

shifts much smaller than were expected in comparison with the bathochromic shifts of the *A* bands.

The two substituents in *p*, *p'*-positions force the molecule to adopt a planar conformation; therefore, the contribution of the steric effect of nitro group in *o*-position to the ethylenic bridge is small enough.

The bathochromic shift becomes smaller when :

1. The nitro group in *o*-position is replaced by the substituents having a weaker conjugative effect (CN, COOH), preserving the NMe_2 and NO_2 substituents in *p*, *p'*-positions (no 5, 6).

2. One or both substituents (NMe_2, NO_2) in *p*, *p'*-positions, together with the substituent in *o*-position, are replaced by the substituents having a weaker conjugative effect.

3. One of the two nitro groups in *o*, *p*-dinitro-stilbene is replaced by one group having a weaker electron-withdrawing effect (CN, $CONH_2$) (the positional isomers no 1,7 and 2, 8). The considerable decrease of the

Table 5

***o*-*p*-Positional isomers**

No	Substituents		$\Delta\lambda_A$	No	Substituents		$\Delta\lambda_A$	$\Delta(\Delta\lambda_A)'^a$
	p	*o*			*p*	*o*		
1	NO_2	CN	46	7	CN	NO_2	20	26
2	NO_2	$CONH_2$	42	8	$CONH_2$	NO_2	16	26
$\Delta(\Delta\lambda_A)''^b$			4				4	

[a] $\Delta(\Delta\lambda_A)'$ represents the changes of the bathochromic shift due to the presence of *o*-nitro group; [b] $\Delta(\Delta\lambda A)''$ represents the changes of the bathochromic shift due to the replacement of CN group by $CONH_2$ group.

bathochromic shift for *o*-nitro-stilbene derivatives proves that the molecule has a nonplanar conformation and the steric effect becomes preponderant if the *p*, *p'*-substituents with opposite electronic effects are missing. The same conclusion may be drawn if we take into account the twofold variation in band-width for the *o*-nitro-substituted derivatives (no 7, 8) by comparison with their positional isomers (no 1, 2).

Table 6

o, *p*-**Positional isomers additionally substituted in *p'*-position**

No	Subst.		$\Delta\lambda_A$	No	Subst. *p'*	$\Delta\lambda_A$	$\Delta(\Delta\lambda_A)'^{a}$	No	Subst. *p'*	$\Delta\lambda_A$	$\Delta(\Delta\lambda_A)'^{a}$	No	Subst. *p'*	$\Delta\lambda_A$	$\Delta(\Delta\lambda_A)'^{a}$
	p	*o*													
1	NO_2	CN	46	5	NMe_2	170	124	3	OH	101	55	4	OCH_3	96	50
7	CN	NO_2	20	11	NMe_2	136	116	9	OH	51	31	10	OCH_3	46	20
$\Delta(\Delta\lambda_A)''^{b}$			26			34				50				50	

[a] $\Delta(\Delta\lambda_A)'$ points out the effect of the substitution in *p'*-position on the conjugation through the ethylenic bridge; [b] $\Delta(\Delta\lambda_A)''$ is a measure of the isomerism effect on the conjugation through the ethylenic bridge.

4. The substituents in *p'*-position are changed; they have an opposite electronic effect in comparison with the preserved substituents in *o*, *p*-positions (CN and NO_2, respectively NO_2 and CN) (the positional isomers no 5, 3, 4, 1 and 11, 9, 10, 7). In the latter series of the positional isomers, the bathochromic shifts are smaller, because, along the main direction of the transmission of the electronic effect, the conjugative effect of the CN group is much weaker than that of the NO_2 group. When the intensity of the opposite electronic effects in *p*, *p'*-positions decreases, the polarity and the planarity of the molecule decrease; therefore, the steric effect increases. This fact is proved, also, by the line-width corresponding to the *o*-nitro-stilbene derivatives (table 3).

5. In the molecule of *o*, *p*-dinitro-stilbene the third nitro substituent is introduced, regardless of its position (no. 19, 21, 17, 18). Other empiric Doub and Vandelbelt's rule [19] is verified here, namely that the shift of the symmetric disubstituted benzene derivative, having the same groups, is about the same or little smaller than the shift of the mono-substituted compound. We can mention that there is a greater steric hindrance in *o*, *o*, *p*-trinitro-stilbene (no. 21), which has the smallest absorption intensity and the greatest line-width among the trinitro-stilbene derivatives (table 3).

The bathochromic shift of the A band becomes smallest when the molecule has 4 nitro groups (no. 24); in this case, the line-width is very great. These observations point out a small stabilization of the excited state in comparison with the ground state, due to the high degree of molecular symmetry (*p'*, *p*, *o*, *o*), and, simultaneously, a great contribution of the steric effect, which leads to the nonplanar conformation of the molecule.

Furthermore, we can mention that:

— the substitution with OH in *p'* — position and OCH_3 in *m'* — position brings about the same shift as the substitution with the methylendioxy group in the same positions (no. 15 and 14);

— the nitro group in o' or m' — position has the same steric effect (no. 17 and 18);

— the inductive effect of the halogeno group is of no importance in connection with the transmission of the electronic effects along the conjugated stilbene system.

From table 4 it is possible to remark a parallelism between the relative values of the bathochromic shifts of both B and A bands; $\Delta\lambda_B < \Delta\lambda_A$ with some exceptions, namely the o-nitro-stilbene derivatives no. 8, 11, 12 and 16.

For the compound no. 8, $\Delta\lambda_B \gg \Delta\lambda_A$ and the bathochromic shift of the A band is smallest. In this case, the steric effect is preponderant and the two bulky substituents (o, p) will participate in little measure to the extension of the conjugation through the ethylenic bridge; their electronic effect operates only in one benzene ring.

For the compounds no 11, 12 and 16, the inverse phenomenon is observed: they have the great bathochromic shifts of the A bands, but $\Delta\lambda_B \ll \Delta\lambda_A$ than were expected; therefore, they have a great degree of planarity in the excited state; the o-nitro group participates to a greater extent in the conjugation with the ethylenic bridge than with the benzene ring.

These two kinds of "anomalies" in the sequence of the shifts of the B and A bands represent arguments which confirm the hypothesis that the A band — due to the whole extensive conjugated system of the stilbene derivatives — could be attributed, essentially, to the excitation of the double ethylenic bond; also, the B band could be attributed to the excitation of the benzene rings.

In conclusion, the followings may be stated:

— for the p, p' — substituted derivatives having the substituents with opposite electronic effects, the excited state of the molecule allows a high degree of planarity, the conjugative effect is preponderant and the corresponding bathochromic shifts are great;

— for derivatives substituted in one ring or for polynitro-derivatives, the steric effect is preponderant and, therefore, the corresponding bathochromic shifts are comparatively small;

— for the positional isomers new semiquantitative correlations are reported; these correlations prove the dialectics of the transmission of the electronic effects of the substituents (through the ethylenic bridge, from one benzene ring to the other), as a result of the competition between the increasing conjugation (due to the substituents having opposite electronic effects) and the decreasing conjugation (caused by the steric effect);

— the "anomalies" in the order of the bathochromic shifts of both B and A band strenghten, in fact, the stated regularities connected with the transmission of the electronic effects in the stilbene derivatives molecules.

Revue Roumaine de Chimie, **21**, *8*, 1137–1147 (1976)

SPECTRAL SOLVENT EFFECTS IN AROMATIC COMPOUNDS SOLUTIONS. III [*]

THE SOLVENT EFFECTS ON THE POSITION AND INTENSITY OF NITROBENZENE BAND AT 2500 Å

VASILE MACOVEI
Physical Chemistry Laboratory, University of Jassy, Calea 23 August, 11, Romania

Received May 28, 1974

The present paper follows the change of the spectral band position and the variation of the band intensity, as well as the dipole moment in the excited state of the nitrobenzene molecule. The aim is to contribute to the elucidation of the interactions of the solute and the surrounding solvent medium.

I. INTRODUCTION

The electronic absorption spectrum of nitrobenzene is complex and consists of several transitions,[1–5] but the easiest to investigate is the band in the near ultraviolet, appearing at 2400 Å in the gas phase spectrum.[4,6] Without having a fine structure, the band is isolated from the other bands and is symmetrical around the absorption peak. [4,6,7] There are different opinions regarding the nature of this band : thus, one considers that it is the displaced benzenoide band [3,8] from 2000 Å, having approximately the same intensity ; it is alleged that the band originates in the local electrons optically excited. [9–14] We believe the correct assignment as a transition with intramolecular charge transfer [15] by the electron migration from the benzene ring to the nitro group. Thus, it is a supplemental band characterizing the conjugation interaction between the benzene ring and the substituent. [16,17] From X-ray analysis [18,19] the resonance (conjugation) between benzene ring and nitro group is doubtful, but the calculation of the π-electronic charge distribution indicates that the conjugation effect exists even in the ground state of the nitrobenzene molecule. [5] The following arguments [5] convince on the charge transfer character of the band : the contribution of the charge transfer configuration to the excited state ; the augmentation of the spectral shifts in solution with the polarity increase of the solvent ; the behaviour of the nitrobenzene spectrum as compared with the spectrum of nitromesitylene, [20] indicating the sensitivity of the charge transfer band to the conjugation interaction, [21-22] and the appearance of the band corresponding to the $A_{1g} \to B_{1u}$ benzene transition as a shoulder of the band at 1930Å. From the behaviour of the band under the solvent influence conclusions may be drawn in connection with some of the nitrobenzene properties and, therefore, the solvent effects on the charge transfer band are investigated.

---

[*] Previous parts : see [31] and [32].

[1] H. E. Ungnade, *J. Amer. Chem. Soc.*, **75**, 432 (1953).

[2] A. I. Kiss and G. Horvath, *Acta Chim. Acad. Sci. Hung.*, **39**, 39 (1963).

[3] L. Doub and J. M. Vandenbelt, *J. Amer. Chem. Soc.*, **69**, 2714 (1947).

[4] G. S. Hammond and F. Modic, *J. Amer. Chem. Soc.*, **75**, 1385 (1953).

[5] S. Nagakura, M. Kojima, and Y. Maruyama, *J. Mol. Spectroscopy*, **13**, 174 (1964).

[6] W. M. Schubert, J. Robins, and J. L. Haun, *J. Amer. Chem. Soc.*, **79**, 910 (1957).

[7] W. M. Schubert, J. M. Craven, and H. Steadly, *J. Amer. Chem. Soc.* **81**, 2695 (1959).

[8] A. Wenzel, *J. Chem. Phys.*, **22**, 1623 (1954).

[9] A. E. Lutskii, *Zhur. obshchei Kim.*, **29**, 2998 (1959).

[10] A. E. Lutskii, *Zhur. obshchei Khim.*, **29**, 3248 (1959).

[11] A. E. Lutskii, *Zhur. obshchei Khim.*, **30**, 3737 (1960).

[12] A. E. Lutskii, *Zhur. obshchei Khim.*, **30**, 3773 (1960).

[13] A. E. Lutskii, *Zhur. obshchei Khim.*, **30**, 3782 (1960).

[14] A. E. Lutskii, *Zhur. obshchei Khim.*, **30**, 3789 (1960).

[15] S. Nagakura and J. Tanaka, *J. Chem. Phys.*, **22**, 236 (1954).

II. RESULTS AND DISCUSSION

Nitrobenzene is a strong polar compound, with a dipole moment of 4.28 D in the gas phase,[23] and its spectral behaviour under the solvents action must be associated with this property. The characteristic band of the nitro-aromatic compounds in solution,[4] at 2600Å, exhibits a red shift which increases in the order : ethanol, water and sulphuric acid. Even in nitro-olefins the $\pi \to \pi^*$ transition is displaced on the red, in ethanol, as compared with hexane, [24] indicating an increased dipole moment in the upper state, that is :

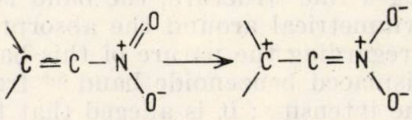

and we must admit [25, 26] a similar behaviour for nitrobenzene. Some of our results in solution confirm the preceding data, [4,24] as it is seen in figure 1. To establish the band displacement in solution we considered as the position in the vapour spectrum of nitrobenzene [6] the value of 41,680 cm^{-1}, with an error of ± 20 cm^{-1}. The band positions in some solvents are listed in table 1,

---

[16] K. Bowden and E. A. Braude, *J. Chem. Soc.*, **1952**, 1068.

[17] A. Mangini, A. Trombetti, and C. Zauli, *J. Chem. Soc.*, **B(2) 1967**, 153.

[18] J. Trotter, *Acta Cryst.*, **12**, 884 (1959).

[19] J. Trotter, *Tetrahedron*, **8**, 13 (1960).

[20] J. Trotter, *Acta Cryst.*, **12**, 605 (1959).

[21] W. G. Brown and H. Reagan, *J. Amer. Chem. Soc.*, **69**, 1032 (1947).

[22] J. N. Murrell, *Quart. Rev.*, **15**, 191 (1961).

[23] A. L. McClellan, "Tables of Experimental Dipole Moments", W. H. Freeman, San-Francisco, 1963.

[24] E. A. Braude, E. R. H. Jones, and G. G. Rose, *J. Chem. Soc.*, **1947**, 1104.

[25] N. S. Bayliss and E. G. McRae, *J. Chem. Phys.*, **18**, 292 (1950).

[26] N. S. Bayliss and E. G. McRae, *J. Phys. Chem.*, **58**, 1006 (1964).

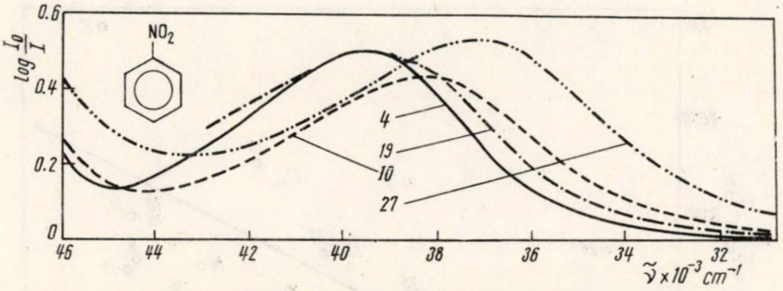

Fig. 1. – The nitrobenzene spectrum in the solvents: 4. Hexane; 10. Ethanol; 19. Carbon tetrachloride; 27. Water.

Table 1

The nitrobenzene electronic band at 2500 Å in some of the solvents used. The $\tilde{\nu}_{max.}$ (cm^{-1}) values compared with reference results

Solvent	Present work	Literature data	
		7	26
Cyclohexane	39,499	39,540	39,540
Heptane	39,717	39,700	39,740
Ethanol	38,242	—	38,580
Chloroform	38,026	—	38,150
Carbon tetrachloride	39,174	—	39,170
Acetonitrile	38,216	38,280	—
Water	37,208	37,440	37,370

together with the data from the literature,[7,26] for comparison. The numbers in figures correspond to the solvents in table 2. The nitrobenzene spectrum shows very great displacements [1] even in non-polar solvents. Being a strong polar compound, the dipolar forces are expected to determine, to a great extent, the spectral shift of nitrobenzene, and the displacement must correlate with the $f(D) = (D - 1)/(D + 2)$ function of the solvents,[27] where D is the dielectric constant of the solvent. This correlation is given in figure 2; the general orientation of the representative points is along a straight line, with a pronounced dispersion, which may be ascribed to the complexity of the solute-solvent interactions. The subtraction of the displacement part due to the dispersion forces, that is the $f(n^2)$ function, n being the refractive index of the solvent, from the function $f(D)$ of the solvent, means the correlation of the spectral shift with the complex function $[f(D)-f(n^2)]$ of the solvent, and is shown in figure 3, where the representative points for non-polar or weak polar solvents are placed on the ordinate and in its very proximity, but the representative points for the polar solvents are somewhat more assembled around the straight line. The consideration of the square Stark effect, [28,29] i.e. the displacement correlation with the function $[f(D) -$

---

[27] P. Suppan, *J. Chem. Soc.*, **(A) 1968**, 3125.

[28] M. Baur and M. Nicol, *J. Chem. Phys.*, **44**, 3337 (1966).

[29] M. Nicol, J. Swain, Yin-Yau Shum, R. Merin, and R. H. H. Chen, *J. Chem. Phys.*, **48**, 3587 (1968).

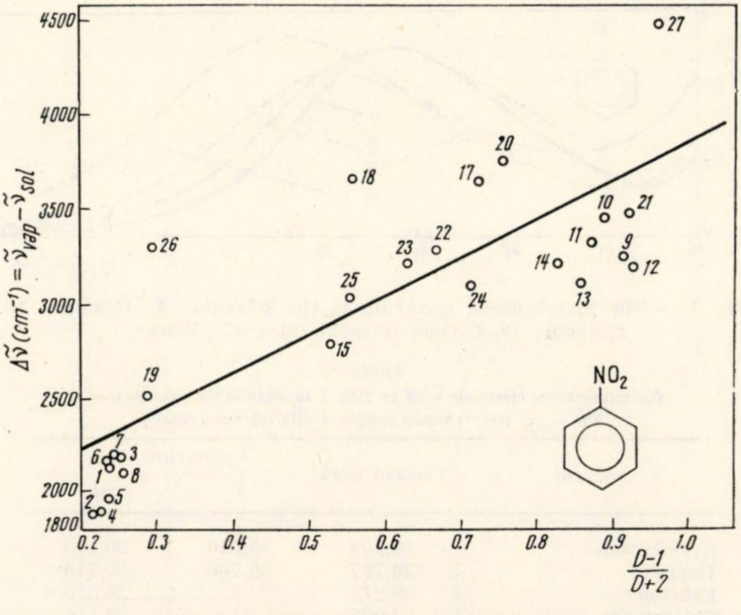

Fig. 2. — The shift dependence of the nitrobenzene band ($\tilde{\nu}_{max}$) on the $(D-1)/(D+2)$ function of the solvent.

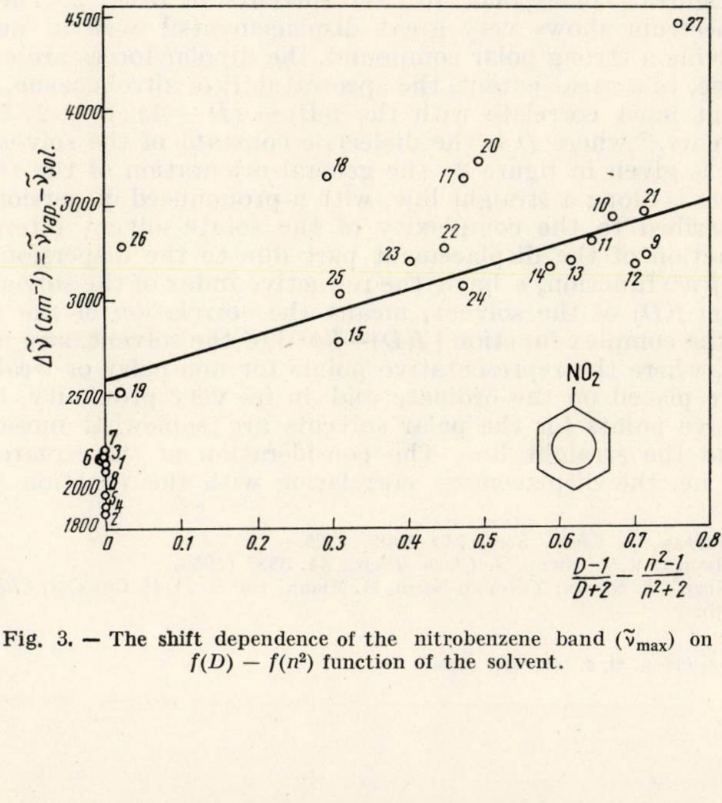

Fig. 3. — The shift dependence of the nitrobenzene band ($\tilde{\nu}_{max}$) on the $f(D) - f(n^2)$ function of the solvent.

$- f(n^2)]^2$ does not improve the situation. All these show the intervention in the spectral displacement of some more complex factors. The first which must be taken into account is the substituent group, $-NO_2$, which is strongly polar. [30] This fact is striking if a comparison is made between the spectral shifts in solution of the nitrobenzene and those of the chlorobenzene, [31] a less polar molecule, and of benzene, [32] a non-polar molecule, as it is seen in table 2. The comparison shows that the presence of the nitro group on the benzene ring causes very large displacements of the spectrum, and this effect must be connected with the structure of the nitro group. The dipole moment measurements showed that the nitro group is symmetrical in relation to its resultant dipole moment acting in the direction of the valence bond of the group. [33] In ordinary conditions, the symmetry

Table 2

Experimental shifts of nitrobenzene band at 2500 Å, as compared with the chlorobenzene and benzene shifts, under the solvent influence

No	Solvent	$\Delta\tilde{\nu}_{exp.}$ (cm^{-1}) $C_6H_5NO_2$	$\Delta\tilde{\nu}_{exp.}$ (cm^{-1}) C_6H_5Cl	$\Delta\tilde{\nu}_{exp.}$ (cm^{-1}) C_6H_6
1	Cyclopentane	2 137	272	279
2	Pentane	1 889	242	259
3	Cyclohexane	2 181	262	259
4	Hexane	1 901	227	259
5	Heptane	1 963	252	279
6	Octane	2 159	247	259
7	Decane	2 194	282	259
8	Dodecane	2 108	312	279
9	Methanol	3 241	187	219
10	Ethanol	3 438	212	259
11	1-Propanol	3 317	232	259
12	2-Propanol	3 199	232	259
13	1-Butanol	3 207	242	259
14	3-Methyl-1-butanol	3 183	257	259
15	Ethyl ether	2 789	232	239
16	Isoamyl ether	—	282	299
17	Methylene chloride	3 639	292	359
18	Chloroform	3 654	352	399
19	Carbon tetrachloride	2 506	452	459
20	1,2-Dichloroethane	3 746	307	359
21	Acetonitrile	3 464	192	239
22	Methyl acetate	3 278	187	259
23	Ethyl acetate	3 203	207	239
24	Butyl acetate	3 077	222	239
25	Amyl acetate	3 027	347	259
26	1,4-Dioxane	3 298	252	299
27	Water	4 472	132	179

---

[30] C. P. Smith, "Dielectric Behaviour and Structure", McGraw-Hill, New York, 1955.

[31] V. Macovei, *Rev. Roumaine Chim.*, **21**, 193 (1976).

[32] V. Macovei, *Rev. Roumaine Chim.*, **20**, 1413 (1975).

[33] C. P. Smith, "Dielectric Constant and Molecular Structure", Chemical Catalog, New York, 1941.

of the group was confirmed by electron diffraction measurements.[34-36] The group may be represented by two resonance structures equally stable[37] as :

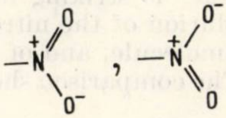

and a small contribution from the structure :

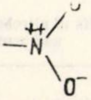

the group being coplanar with the remainder phenyl.[18,38] The resultant great dipole lies on the axis of the group bond, bisecting the ONO angle. For the nitrobenzene one may write two Kékulé structures, with a negative oxygen, and two structures with the other negative oxygen of the nitro group. Then, structures with double bond between benzene ring and nitro group may be written, the second electron pair coming from the ring. The dipole moment of the structure with double bond acts in the same direction as the Kékulé structure moments, the mesomeric component being added to the original moment.[30] The calculation on the planar model of the nitrobenzene molecule shows that the substituent withdraws the electrons from the ring, especially from the *ortho* and *para* positions, in the ground state,[39] and the structures contributing to the dipole moment of the ground state are of the type :

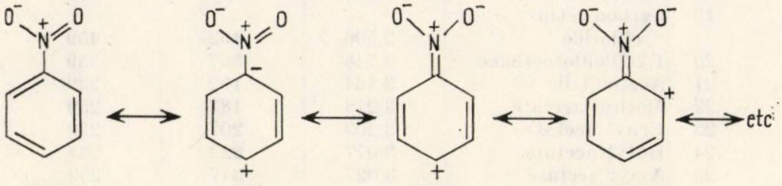

(I) (II) (III) (IV)

The theoretical value[39] of the dipole moment of the ground state of the nitrobenzene molecule is 4.26 D, being very close to the experimental value[23] in the gas phase, of 4.28 D. The strong polarity of the nitrobenzene causes powerful dipolar interactions with the solvent and, consequently, a great red shift of the spectrum in solution. But the dipole moment

---

[34] L. O. Brockway, J. Y. Beach, and L. Pauling, *J. Amer. Chem. Soc.*, **57**, 2693 (1935).

[35] F. Rogowski, *Ber. dtsch. chem. Ges.*, **75 B**, 244 (1942).

[36] P. W. Alen and L. E. Sutton, *Acta Cryst.*, **3**, 46 (1950).

[37] L. Pauling, "The Nature of the Chemical Bond", Cornel Univ. Press, Ithaca, New York, 1960.

[38] Y. Hanyu and J. E. Boggs, *J. Chem. Phys.*, **43**, 3454 (1965).

[39] W. J. Hehre, L. Radom, and J. A. Pople, *J. Amer. Chem. Soc.*, **94**, 1496 (1972).

is substantially concentrated in the nitro group, and we must conclude that either of the two dipoles of the N–O bonds interacts independently with the solvent ; this way of interpreting agrees with the point of view[40] of considering the solvation of the nitro group oxygens, that is the local solute-solvent interactions. The theoretical quantitative check of the experimental displacements, $\Delta\tilde{\nu}$, is realized in applying equation (1) from the preceding paper,[31] established by McRae.[41] This equation comprises the displacement parts due to the polarization and dipolar forces. The parameter values[*] in the quoted equation[41] were calculated by the least-squares method,[42] and are : $(A + B + C) = 11{,}351.82\ \text{cm}^{-1}$; $E = 3{,}093.53\ \text{cm}^{-1}$, and $F = 1{,}417.82\ \text{cm}^{-1}$. The agreement between the experimental and theoretical values of the spectral shifts in solution is given in figure 4, and is satisfactory, with the exceptions of water and 1,4-dioxane, where the experimental values are greater. Similar results were found previously.[43] The great red shifts indicate an increased dipole moment in the excited state.[24] This increased dipole moment may be evaluated using the above calculated value of the parameter E and its explicit form given in equation (2) of the preceding paper[31] from the McRae's[41] equation. The solvent cavity radius was evaluated as previously described,[31] assuming to be equal with the average radius of the molecule in

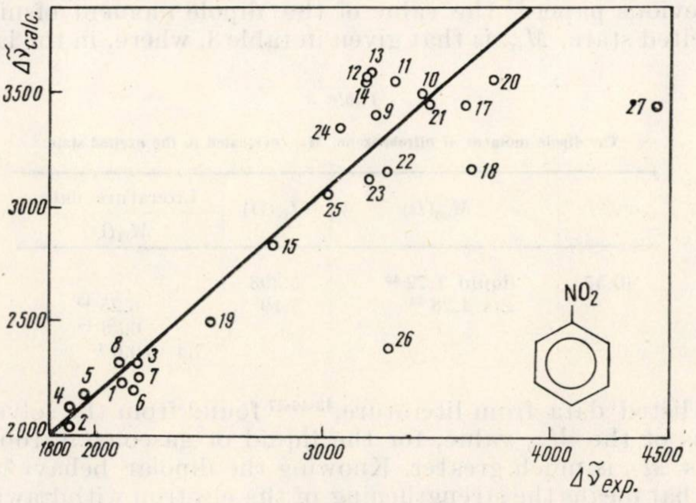

Fig. 4. — The agreement of the experimental and calculated shifts of the nitrobenzene band under solvents influence.

---

[*] The calculation program was established at the Territorial Center of Electronic Calculus, Jassy.

[40] K. Semba, *Bull. Chem. Soc. Japan*, **34**, 722 (1961).

[41] E. G. McRae, *J. Phys. Chem.*, **61**, 562 (1957).

[42] D. York, *Canad. J. Phys.*, **44**, 1079 (1966).

[43] M. Lamotte, G. A. Gerhold, and J. Joussot-Dubien, *J. Chim. phys.*, **67**, 2006 (1970).

the liquid state or in the pure crystal. [43] Using the known values [44] of the molecular weight, and of the density (at 20°), according to equation (3) in the preceding paper, [31] the value of the cavity radius is $a^3(\text{Å}^3) = 40.57$. The dipole moment of the ground state, M_{00}, for the liquid nitrobenzene [45] is 1.72 D, and for the gas phase [23] is 4.28 D. From the expression (2) given in the previous paper [31] the value of the dipole moment of nitrobenzene in the excited state, M_{ii}, is that given in table 3, where, in the last column, there are listed data from literature,[43,46,47] found from the solvent effects. Regardless of the M_{00} value, for the liquid or gaseous nitrobenzene, in both cases M_{ii} is much greater. Knowing the dipolar behaviour of nitrobenzene, that means the strengthening of the electron withdrawing process from the ring [39] in the excited state, one may easily interpret the spectral shift in the Bayliss and McRae's theory, [25] according to the Franck-Condon principle. [32] Thus, since the dipole moment of the excited state increases in non-polar solvents, the solvation energy due to dipol-polarization interactions will be greater in the excited state, as compared with the solvation energy of the ground state and the spectral shift, coming from the difference of the solvation energies, will be on the red, depending on the refractive index of the solvent. The polarization shift is also present [32] and increases the red shift. This behaviour corresponds well to the case IIIa in the theory mentioned. [25] In polar solvents, the dipolar forces are greater in the excited state than in the ground state. The Franck-Condon excited state [32] is formed in a partly oriented cavity and will act the orientation strain. The solvation energy of the excited state is greater than that of the ground state, and the spectrum is red shifted. The polarization shift on the red increases the total effect. This behaviour agrees with the case IVa in the theory of Bayliss and McRae. [25] The enhancement of the electron withdrawing process from the ring in the excited state is confirmed by the spectrum vibrational structure obliteration in non-polar and polar solvents, the conjugation effect existing even in the ground state, because the conditions for it are fulfilled. [48] Thus, the qualitative

Table 3

The dipole moment of nitrobenzene, $\mathbf{M}_{ii}$, evaluated in the excited state

a^3(Å)	$M_{00}(D)$	M_{ii}(D)	Literature data
			M_{ii}(D)
40.57	liquid 1.72 [45]	5.398	
	gas 4.28 [23]	7.19	6.25 [43]
			6.78 [46]
			7.4−10.6 [47]

---

[44] A. Weissberger, E. S. Proskauer, J. A. Riddick, and E. E. Toops, "Technique of Organic Chemistry, Vol. VII, Organic Solvents", 2nd Edition, Interscience, New York, 1955.

[45] O. A. Osipov, V. J. Minkin, and A. D. Garnovskii, "Spravochink po Dipolnym Momentam", Izd. Vysshaya Shkola, Moskva, 1971.

[46] T. Abe, *Bull. Chem. Soc. Japan*, **40**, 1571 (1967).

[47] M. Masamichi, *Rika Gaku Kenkyusho Hokoku*, **43**, 195 (1967), *Chem. Abstr.*, **69**, 71658 f (1968).

[48] C. A. Coulson, "Valence", 2nd Edition, Oxford Univ. Press, 1961.

interpretations explain the great displacements obtained experimentally, and lead to the idea that the two component parts of the nitrobenzene molecule, the aromatic ring and the substituent, interact, to a certain extent, independently with the solvent. However, the representative points, in figure 4, for the agreement between theoretical and experimental spectral shifts exhibit some dispersion around the straight line; this disagreement may be originated even in the model adopted in McRae's theory, [41] that of point dipole [49] for the dissolved molecule. The solute molecule has defined sizes and the number of the solvent molecules which surround it varies from one solvent to another, according to the molecular dimensions of the solvent; the geometrical form of the solute molecule is planar and will determine a certain orientation of the solvent molecules on the two faces of the dissolved molecule; the different polarities of the remainder phenyl and of the nitro group cause unlike local interactions with the solvent molecules; the distance, as far as the solvent molecules may approach the solute molecule, and the hydrogen bond formation are also factors which are not explicitly given in the theory used. [41] All these last factors answer each, partly, for the disagreement between the theoretical and experimental results.

The second parameter of a spectral band which changes under the solvent influence is the band intensity, [50,51] which increases in solution[31,32] and is redistributed among the vibrational components of the electronic band. [52,53] The intensity values of a spectral band in solution and vapour phase are compared as molar extinction coefficients, [54] ε_ν, or as oscillator strengths, [55] f, involving the integrated (absolute) intensity. The quantities ε_{max}, for the band without structure of the nitrobenzene in various solvents, were evaluated according to equation (2) from a preceding paper, [32] and the values of the oscillator strengths, f, in each solvent, were calculated by means of relation (4) in the quoted paper. [32] Both, the ε and f values are listed in table 4, together with the data from literature. [7,26] The examination of table 4 shows that for the band without vibrational structure in solution the quantities ε and f behave similarly. However, the spectral band intensities in vapour and in solution are compared by using the oscillator strengths measuring the total probability of the transition. In this respect, Chacko[56] and Bakhshiev *et al.* [51,57,58] have established, on classical bases, the β factor for the intensity increase in solution given in relation (5) of the previous paper. [32] On the other hand, Abe has formulated, [59] on quantum bases, the increase factor of the spectral

---

[49] L. Onsager, *J. Amer. Chem. Soc.*, **58**, 1486 (1936).

[50] S. E. Sheppard, *Rev. Mod. Phys.*, **14**, 303 (1942).

[51] O. P. Girin, and N. G. Bakhshiev, *Uspekhi Fiz. Nauk*, **79**, 235 (1963).

[52] V. Macovei and C. Ghirvu, *Anal. Sti., Univ. "Al. I. Cuza", Iași. Sect. I, c*, **15**, 1 (1969).

[53] V. Macovei and C. Ghirvu, *Anal. Sti., Univ. "Al. I. Cuza", Iași. Sect. I, c*, **15**, 7 (1969).

[54] H. H. Willard, L. L. Merritt, Jr., and J. A. Dean, "Instrumental Methods of Analysis", 3rd edition, D. Van Nostrand, Princeton, 1960.

[55] R. S. Mulliken, *J. Chem. Phys.*, **7**, 14 (1939).

[56] N. Q. Chako, *J. Chem. Phys.*, **2**, 644 (1934).

[57] N. S. Libov, N. G. Bakhshiev, and O. P. Girin, *Opt. i Spektrosk.*, **16**, 1016 (1964).

[58] N. G. Bakhshiev, *Opt. i Spektrosk.*, **24**, 896 (1968).

[59] T. Abe, *Bull. Chem. Soc. Japan*, **43**, 625 (1970).

Table 4

Position and intensity of nitrobenzene band at 2560 Å in various solvents, compared with reference results

Nº	Solvent	$\tilde{\nu}_{\max}$ (cm^{-1})	$\lambda_{\max}$ (Å)	$\varepsilon_{\max}$ (1.mol^{-1}.cm^{-1})	$f \cdot 10^3$
1	Cyclopentane	39,543	—	12,060	3.27
2	Pentane	39,791	—	12,320	3.31
3	Cyclohexane	39,499	2532	11,800	3.16
		—	2529[26]	9,900[26]	2.60[26]
4	Hexane	39,778	—	11,280	3.13
5	Heptane	39,717	2518	10,900	2.99
		—	2518[7]	8,700[7]	—
		—	2516[26]	8,530[26]	2.30[26]
6	Octane	39,521	—	6,980	1.89
7	Decane	39,486	—	9,360	2.50
8	Dodecane	39,572	—	8,780	2.33
9	Methanol	38,439	—	8,020	2.33
10	Ethanol	38,242	2615	8,500	2.55
		—	2592[26]	8,240[26]	2.60[26]
11	1-Propanol	38,363	—	8,740	2.54
12	2-Propanol	38,481	—	8,680	2.56
13	1-Butanol	38,473	—	10,620	3.05
14	3-Methyl-1-butanol	38,497	—	8,280	2.38
15	Ethyl ether	38,891	—	9,320	2.70
16	Isoamyl ether	—	—	—	—
17	Methylene chloride	38,014	—	9,780	2.86
18	Chloroform	38,026	2630	8,820	2.33
		—	2621[26]	8,330[26]	2.50[26]
19	Carbon tetrachloride	39,174	2553	10,060	—
		—	2553[26]	9,790	—
20	1,2-Dichloroethane	39,734	—	8,620	2.25
21	Acetonitrile	38,216	—	9,260	2.75
22	Methyl acetate	38,402	—	7,600	—
23	Ethyl acetate	38,477	—	8,340	—
24	Butyl acetate	38,603	—	8,480	—
25	Amyl acetate	38,653	—	8,820	—
26	1,4-Dioxane	38,382	—	8,920	2.74
27	Water	37,208	—	5,210	1.76

band intensity in solution as β', also given in the preceding paper,[32] in equation (6). The meanings of β and β' are explained there.[32] Having the magnitude $f_{\text{exp.vap.}} = 1.7$ for the nitrobenzene[5] and using our values $f_{\text{exp. sol.}}$ from table 4, we listed in table 5 the ratio values $f_{\text{exp. sol.}}/f_{\text{exp.vap.}}$ together with theoretical evaluated quantities β and β', for comparison. A check of table 5 shows that the increase factors of the band intensities in solution, β and β', are smaller as compared with the ratio $f_{\text{exp. sol.}}/f_{\text{exp.vap.}}$, except for octane and water where the theoretical values are greater than the experimental ones. This fact proves that, besides the solute-solvent interactions due to the dispersion forces and contributing to the intensity increase,[31,32] one must take into account the interactions due to the dipolar forces, which are not included in the theories used.[51,56–59] Also, the geometrical factors of the solute and the solvent molecules, as well as the hydrogen bond formation in the solvents which have this ability may contribute to the intensity increase. All of these indicate the need

Table 5

Comparison of experimental and theoretical intensities of the 2500 Å nitrobenzene band

Solvent	$\frac{f_{exp.sol.}}{f_{exp.vap.}}$	β	β'
Cyclopentane	1.923	1.248	1.358
Pentane	1.947	1.208	1.329
Cyclohexane	1.859	1.267	1.374
Hexane	1.481	1.223	1.340
Heptane	1.759	1.233	1.350
Octane	1.112	1.242	1.350
Decane	1.470	1.225	1.322
Dodecane	1.370	1.264	1.371
Methanol	1.370	1.186	1.289
Ethanol	1.500	1.211	1.278
1-Propanol	1.494	1.231	1.302
2-Propanol	1.506	1.223	1.298
1-Butanol	1.794	1.243	1.317
3-Methyl-1-butanol	1.400	1.251	1.326
Ethyl ether	1.588	1.205	1.294
Methylene chloride	1.682	1.267	1.322
Chloroform	1.312	1.285	1.334
1,2-Dichloroethane	1.482	1.286	1.334
Acetonitrile	1.619	1.198	1.266
1,4-Dioxane	1.612	1.264	1.330
Water	1.035	1.189	1.222

of a new and more comprehensive theory for the interpretation of the spectral shift and for the explanation of the spectral band intensity increase in solution.

III. EXPERIMENTAL

The nitrobenzene and solvent purification is done as previously described,[32] the criteria of purity being the same. The refractive indices, *n*, the dielectric constants, *D*, and the boiling points, b.p., were given in the preceding paper.[32] The solutions were prepared in the same conditions, the concentrations being $0.5 \cdot 10^{-3}$M. The spectra were recorded with the previously described apparatus, in the same conditions.[32] Each of the results is the average of at least three spectral recordings. The integrated intensities were determined as previously shown.[31,32]

Revue Roumaine de Chimie, **21**, *8*, 1149 – 1152 (1976)

CHEMISORPTIVE PROPERTIES OF ZINC OXIDE THIN FILMS

S. CINCA *, MIHAELA CONSTANTINESCU ** and E. SEGAL *

*) Politechnical Institute of Bucharest, Chair of Physical Chemistry and Electrochemical Technology, Boul. Republicii 13, Bucharest

**) Institute of Physical Chemistry, Bucharest, Str. Galați 31, Bucharest

Received July 29, 1975

The results obtained in a chemisorption study of cyclohexane and methanol vapours on zinc oxide thin film by the electric resistance variation method are presented. The observed electric resistance diminution indicates a donor type adsorption. A mechanism which explains this resistance variation is proposed.

Following our researches on the chemisorptive properties of semiconducting zinc oxide thin films,[1] we present the results concerning the adsorption of cyclohexane and methanol vapours on zinc oxide, by the electric resistance variation method.

EXPERIMENTAL

Cyclohexane, BDH reagent, spectroscopically pure, and methanol, Romanian product, whose purity was checked chromatographically, were used. Both substances were distilled in vacuum. Zinc, Merck reagent, spectroscopically pure, was also used.

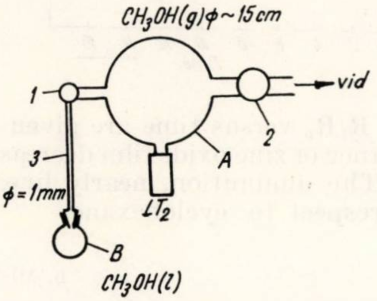

Fig. 1. — Methanol introductor : *1, 2*- stopcocks ; *3*- capillary ; *A*-bulb for vapours of methanol ; *B*-bulb for liquid methanol ; LT_2- manometric lamp.

The experimental device was described in another paper.[1] A Phillips recorder, connected with a Wheastone bridge, allowed to record the variation of the electric resistance. For cyclohexane studies, we used a Murgulescu-Vass [2] type gas-introductor, and for methanol an original one (fig. 1), which allowed us to introduce higher amounts of gas.

---

[1] E. Segal and M. Teodorescu, *Rev. Roumaine Chim.*, **11**, 75 (1967) ; **13**, 1449 (1968) ; M. Constantinescu and E. Segal, *Rev. Roumaine Chim.*, **16**, 801, 1701 (1971) ; M. Constantinescu and E. Segal, *Intern. Chem. Eng.*, **12**, 581 (1971).

[2] I. G. Murgulescu and M. Vass, *Rev. Roumaine Chim.*, **11**, 299 (1966).

The procedure was already described.[1] Cyclohexane adsorption was carried out in the 25–300° temperature range. In order to avoid the cocking, every measurement was carried out on a new film and to avoid the reduction of zinc oxide by hydrogen, the maximum working temperature was 300°. For methanol introduction, the stopcock 1 was opened, the stopcock 2 being closed. A gas dose was introduced into bulb A. Then the stopcock 1 was closed and the second one opened, being kept so until the pressure reached $10^{-3} - 10^{-2}$ torr. When the electric resistance of the semiconducting film became nearly constant (fig. 3), the gas was again introduced, until saturation. Temperatures were relatively low, namely liquid nitrogen temperature (−197°) and room temperature (25°).

RESULTS

a. CYCLOHEXANE

At lower temperatures (until 250°), we observed very little and reversible variations of the electric resistance. Reproducible results were obtained in the 250 – 300° range. The relative variations of the electric resistance R/R_0 versus time are given in fig. 2. In all the cases, the electric resistance of zinc oxide film decreases, indicating thus a donor type adsorption. The diminution, nearly linear, may suggest a zero order kinetics, with respect to cyclohexane.

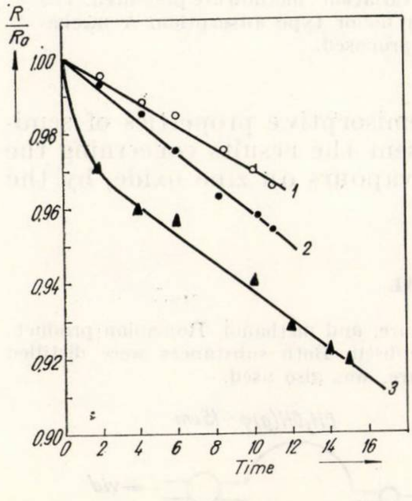

Fig. 2. — Relative electrical resistance variation in time, for cyclohexane adsorption : *1* — for temperature of 280° ; *2*—for temperature of 290° ; *3* — for temperature of 300°.

b. METHANOL

The relative electric resistance variations, versus time, are given in fig. 3. The A points indicate the moment of the second methanol introduction. As the first time high enough amounts of methanol were introduced, the second introduction influenced less the surface, most of the active centers being already covered. As one can see from these graphs, even at a low temperature, the electric resistance decreases, in other words the adsorption of methanol is of a donor type too. It may be also observed

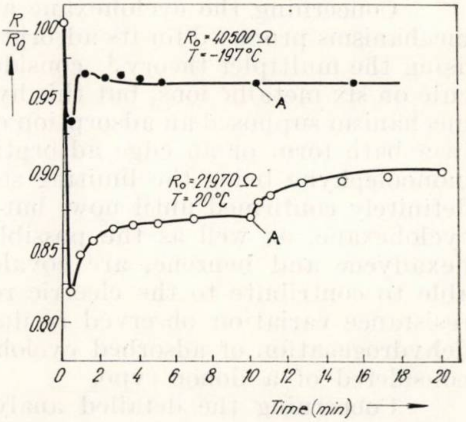

Fig. 3. — Relative electrical resistance variation in time, for methanol adsorption.

that the adsorption increases as temperature increases. The ratio R/R_0 has lower values than in the cyclohexane case; the adsorption being therefore stronger.

DISCUSSION

a. CYCLOHEXANE

The electric resistance diminution, observed for cyclohexane adsorption, may be explained by the donor chemisorption of this compound on zinc oxide. There are very few previous studies on this system, in the literature. [3] Most of the studies were made on oxides of the same period, with $d^1 - d^4$ and $d^6 - d^9$ structures, with a higher activity. In the zinc oxide case, zinc has a stable d^{10} structure, so it seems that its activity is due to the defects generated during the degasing period. Literature data indicate that the desorption products are always benzene and hydrogen. [3] Therefore, the probable reaction mechanism would be the following: the adsorbed cyclohexane partially dehydrogenates to benzene, possible intermediates being unstable. During adsorption, the resulted hydrogen transfers electrons to the surface, this phenomenon being expressed in the diminution of the electric resistance:

$$C_6H_{12} \rightarrow C_6H_{12_{ads}} \quad (1)$$

$$C_6H_{12_{ads}} \rightarrow C_6H_{6_{ads}} + 6H_{ads} \quad (2)$$

$$6H_{ads} \rightarrow 6H^+ + 6\,e \quad (3)$$

---

[3] P. C. Richardson and D. R. Rossington, *J. Catalysis*, **14**, 175 (1969).

Concerning the cyclohexane adsorption it is usefull to discuss the mechanisms proposed for its adsorption on this kind of oxides. Balandin, using the multiplet theory,[4] considered a planar adsorption of the molecule on six metallic ions, but this hypothesis was not confirmed. Another mechanism supposed an adsorption of cyclohexane on four metallic ions,[5] in a bath form or an edge adsorption, [6] the intermediate generation of monoolephyne being the limiting step. None of these mechanisms was definitely confirmed until now, but on this basis we may suppose that cyclohexane, as well as the possible intermediates, cyclohexene, cyclohexadyene and benzene, are covalently adsorbed, being therefore not able to contribute to the electric resistance changes. Thus, the electric resistance variation observed is due to hydrogen resulted from the dehydrogenation of adsorbed cyclohexane, whose adsorption is generally considered of a donor type.

Concerning the detailed analysis of the interaction of hydrogen with zinc oxide surface, several mechanisms were proposed.[7,8]

b. METHANOL

In order to explain the electric resistance diminution observed, we partialy used some previous results obtained by Ueno [9] who applied the ir method to study the methanol-zinc oxide system, as well as the results obtained by McArthur,[8] who studied a similar system, ethanol-zinc oxide, by the method of the electric resistance variation.

The ir studies allowed to put into evidence the metoxide and formiate adsorbed ions and the desorption of the following products : CO, CO_2 and H_2.

Taking into account these papers, our results could be explained in terms of a competition between fast donor and slow acceptor interaction of methanol with zinc oxide surface.

CONCLUSIONS

The results obtained in a chemisorption study of cyclohexane and methanol on zinc oxide are presented. In both cases, an electric resistance diminution, which indicates a donor mechanism, was put into evidence. Besides donor interaction, methanol adsorption exhibits an acceptor interaction.

[4] A. A. Balandin, *Adv. Catalysis*, **10**, 96 (1958).

[5] P. W. Selwood, *J. Amer. Chem. Soc.*, **79**, 4637 (1957).

[6] E. F. Harington and E. K. Rideal, *Proc. Roy. Soc. A.*, **190**, 309 (1947).

[7] F. B. Verduraz, B. Arghiropoulos and S. J. Teichner, *Bull. Soc. Chim. France*, **1967**, 2857.

[8] D. P. Mc Arthur, H. Bliss and J. P. Butt, *J. Catalysis*, **28**, 183 (1973).

[9] A. Ueno, T. Onishi and K. Tamaru, *Trans. Faraday Soc.*, **67**, 3585 (1971).

Revue Roumaine de Chimie, **21**, *8*, 1153–1160 (1976)

VOLTAMMETRIC AND CHRONOPOTENTIOMETRIC STUDY OF SILVER ION IN MOLTEN POTASSIUM NITRATE

T. VIŞAN, D. P. GEANĂ and S. STERNBERG
Department of Physical Chemistry and Electrochemical Technology,
Politechnical Institute, Bucharest

Received May 28, 1975

The electrochemical behaviour of silver ion on platinum electrodes in the molten KNO_3 has been studied using cyclic voltammetry and chronopotentiometry. The interdiffusion coefficient of silver ion and the activation energy of diffusion have been evaluated.

1. INTRODUCTION

The electrochemical process $Ag^+ + e \rightleftharpoons Ag$ in the molten systems $AgNO_3-KNO_3$ (with very small concentrations of silver ion) has been studied previously by different authors using the chronopotentiometric method. [1-4]

In this work the study of the same system by cyclic voltammetry is presented. Some chronopotentiometric measurements (single chronopotentiometry, reversal chronopotentiometry and cyclic chronopotentiometry) have also been carried out in order to compare both methods.

2. EXPERIMENTAL

The voltammetric determinations were performed in the molten systems $AgNO_3-KNO_3$, with $AgNO_3$ concentrations range $0.5-2.0 \times 10^{-2}$ mole·l^{-1}.

A platinum plate of 1 cm^2 surface area was used as working electrode.

The counterelectrode was also a platinum plate of relatively large area (3–4 cm^2) and the reference electrode was a platinum wire immersed in the same solution.

The electrolysis cell of Rasotherm glass was described in the previous publication.[2] The electrolyte was prepared from A.R. chemicals, dried and melted in the usual way.

For cyclic voltammetry measurements a Wenking potentiostat and a low frequency waveform generator, Orion TR-0403 type, were used. The voltammograms were recorded on a X–Y recorder Philips (type PM-8120) at sweep rates between 0.01–1.00 V.s^{-1}.

The pseudo-ohmic drop compensation was not performed, in molten electrolytes the resistance between the reference and working electrode being very small.

---

[1] C. E. Thalmayer, S. Bruckenstein and D. M. Gruen, *J. Inorg. Nuclear Chem.*, **26**, 347 (1964).

[2] S. Sternberg and C. Herdlicka, *Rev. Roumaine Chim.*, **14**, 991 (1969).

[3] G. A. Mazzochin and G. Schiavon, *J. Electroanalyt. Chem.*, **38**, 229 (1972).

[4] S. Sternberg and T. Vişan, *Rev. Roumaine Chim.*, **18**, 221 (1973).

For the chronopotentiometric determinations a constant current source (ca. 100 V) in conjunction with a variable high resistance was used. The working electrode is a platinum plate of 0.3—0.6 cm^2 surface area. The cell current was obtained by measuring the voltage developed across a standard resistor (with electronic voltmeter Philips PM-2440) in series with the variable resistance.

Potential-time curves were recorded on the same X—Y recorder Philips with time base type PM-8120.

In the reversal chronopotentiometry the current was reversed after the complete chronopotentiometric deposition of Ag. Each chronopotentiometric measurement was started at the stationary electrode potential attained after a sufficient waiting time.

Cyclic chronopotentiometric measurements were performed with equal rectangular pulses (0.5—1.5 s) supplied from the low frequency waveform generator.

3. RESULTS AND DISSCUSION

3.1. CYCLIC VOLTAMMETRY

Typical cyclic voltammograms are shown in Fig. 1 (a, b) which illustrates the electrochemical deposition and dissolution of silver on platinum. The anodic peak current exceeded that for the cathodic process.

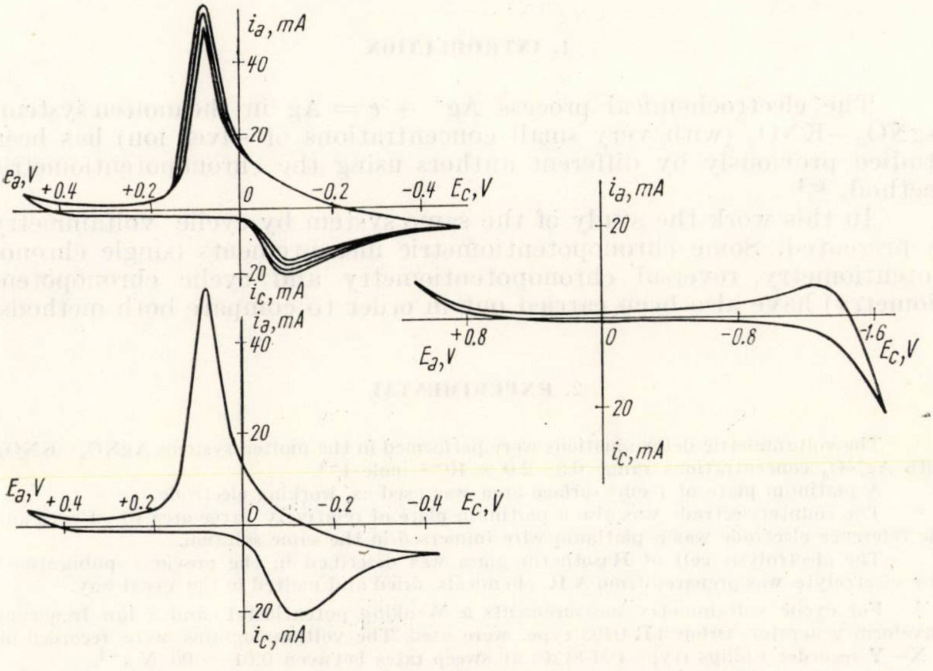

Fig. 1. — Cyclic voltammograms of AgNO$_3$ dissolved in molten KNO$_3$ (a, b) and of KNO$_3$ solvent (c). Platinum electrode 1 cm^2; $t = 370°$; Potentials were measured *vs.* the Pt/solution reference electrode. a) $c° = 5.10^{-5}$ mole.cm^{-3}; $v = 0.07$ V.s^{-1}; b) $c° = 4.10^{-5}$ mole. cm^{-3}; $v = 0.24$ V.s^{-1}; c) $v = 0.1$ V.s^{-1}.

At low sweep rates (lower than 0.25 V.s^{-1}) a stationary shape is reached after all 3 — 5 cycles.

At higher sweep rates no appreciable change of the voltammogram area is noticed even in the initial sweep, as shown in Fig. 1b. The shape of voltammograms and the peak potentials are similar to those for the reduction of Ag^+ at a platinum electrode in $NaNO_3-KNO_3$ [5].

Figure 1c shows a cyclic voltammogram for the molten KNO_3 (solvent). As it can be seen from Fig. 1c, the faradaic current is not observed in the solvent within the potential range corresponding to the electrochemical processes of silver ion[6] ($-0.3V + 0.3V$).

Figures 2 — 5 show the cathodic peak current density (i_p) *vs.* square root of potential sweep rate dependence for different concentrations of silver ion at constant temperature. The plots seem to be linear, passing through the origin.

The current-potential relationships in cyclic voltammetry (voltammetry with linearly varying potential) for reversible deposition of metals at solid microelectrodes under diffusion—controlled conditions was derived by Berzins and Delahay [7].

When the applied electrode potential is linearly changed with time (t):

$$E = E_i - vt \tag{1}$$

the voltammogram equation is:

$$i = \frac{2(nF)^{3/2}\, c^\circ D^{1/2}\, v^{1/2}}{(\pi\, R\, T)^{1/2}}\, \Phi\left[\left(\frac{nF}{R\,T}\, v\, t\right)^{1/2}\right] \tag{2}$$

where:

E_i — initial electrode potential, V;

v — rate of potential sweep (voltage scan), $V.s^{-1}$;

n — number of electrons which particípe in the cathodic process;

c° and D — concentration ($mole.cm^{-3}$) and interdiffusion coefficient ($cm^2.s^{-1}$) of the electrodepositing species;

Φ — a function the different values of which have been tabulated. The other terms have their usual meaning.

Equation (2) leads to a peak current density expression of

$$i_p = \frac{1.082(nF)^{3/2}}{(\pi\, R\, T)^{1/2}}\, c^\circ D^{1/2}\, v^{1/2} \tag{3}$$

at the peak potential value, which is simply obtained from,

$$\left[\frac{nF}{RT}(E_i - E_p)\right]^{1/2} = 0.9241 \tag{4}$$

---

[5] G. J. Hills, D. J. Schiffrin and J. Thompson, *Electrochim. Acta*, **19**, 657 (1974).

[6] S. Sternberg and T. Vişan, *Rev. Roumaine Chim.*, (to be published).

[7] T. Berzins and P. Delahay, *J. Amer. Chem. Soc.*, **75**, 555 (1953).

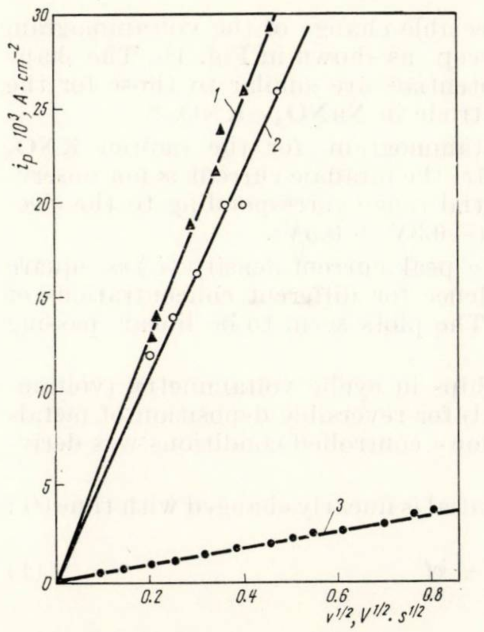

Fig. 2. — Dependence of the cathodic peak current (i_p) on the square root of the sweep rate (v) for $AgNO_3$ in KNO_3; $t = 350°$. Ag^+ concentrations (mole. cm^{-3}): $1 - 5.10^{-5}$; $2 - 3.8 \cdot 10^{-5}$; $3 - 0.43 \cdot 10^{-5}$.

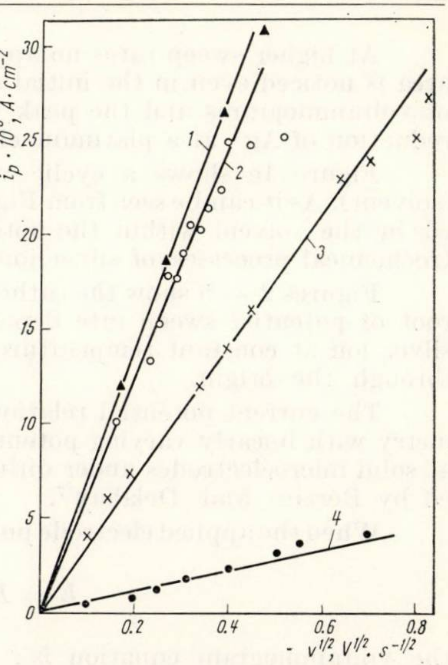

Fig. 3. — i_p dependence *vs.* $v^{1/2}$ for $AgNO_3$ in KNO_3 at $t = 370°$. Ag^+ concentrations (mole. cm^{-3}): $1 - 5.10^{-5}$; $2 - 4.10^{-5}$; $3 - 1.95.10^{-5}$; $4 - 0.44.10^{-5}$.

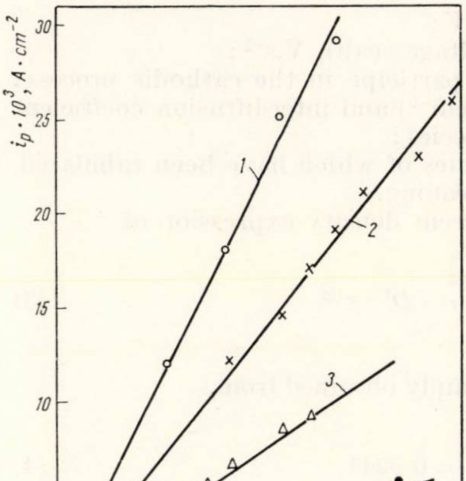

Fig. 4. — i_p dependence *vs.* $v^{1/2}$ for $AgNO_3$ in KNO_3 at $t = 400°$. Ag^+ concentrations (mole. cm^{-3}): $1 - 4.10^{-5}$; $2 - 2.10^{-5}$; $3 - 10^{-5}$; $4 - 0.45.10^{-5}$.

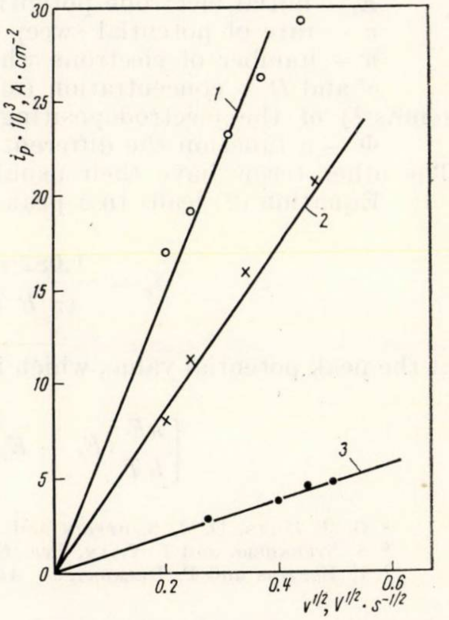

Fig. 5. — i_p dependence *vs.* $v^{1/2}$ for $AgNO_3$ in KNO_3 at $t = 420°$. Ag^+ concentrations (mole. cm^{-3}): $1 - 4.10^{-5}$; $2 - 2.10^{-5}$; $3 - 0.45.10^{-5}$.

An usual procedure in voltammetry, similar to polarography, is to determine the half-peak potential value ($E_{p/2}$). In this case, the corresponding equation is

$$\left[\frac{nF}{RT}(E_i - E_{p/2})\right]^{1/2} = 0.2855 \qquad (5)$$

By combining equations (4) and (5) a relationship for $\Delta E = E_p - E_{p/2}$ in reversible deposition of an insoluble substance is obtained (the sole mode of mass transport for ion to the electrode surface is semiinfinite linear diffusion),

$$\Delta E = E_p - E_{p/2} = -\frac{RT}{nF}(0.9241^2 - 0.2855^2). = -0.77\frac{RT}{nF} \qquad (6)$$

The n-values calculated from eqn. (6) from the majority of current-voltage curves are found to be 0.9 – 1.

Mamantov and coworkers[8] have shown that the plot of log $(i_p - i)$ *vs.* E is linear in the approximate current range $0.5\ i_p - 0.9\ i_p$, having the slope $2.2\ \frac{nF}{RT}$.

The application of this procedure for the deposition of silver ion is shown in Fig. 6, confirming the theoretical slope of $2.2\ \frac{nF}{RT}$ in a large potential range.

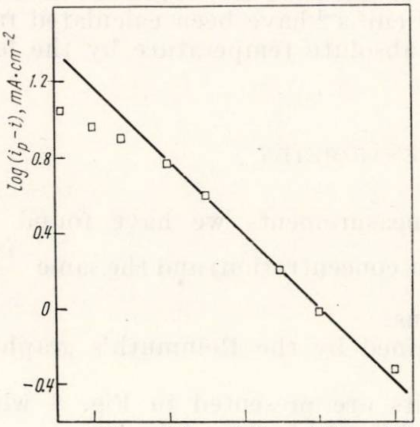

Fig. 6. — Plot of log $(i_p - i)$ *vs.* E for cathodic deposition of Ag^+ dissolved in KNO_3; $t = 350°$; $c° = 3.8 \cdot 10^{-5}$ mole. cm^{-3}; $v = 0.1$ *V.* s^{-1}. Potentials were measured *vs.* the *Pt*/solution reference electrode.

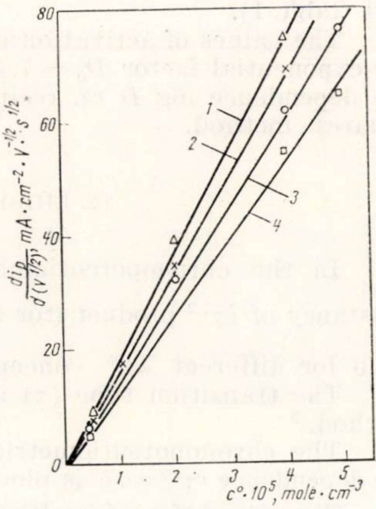

Fig. 7. — Plot of $d\ i_p / d(v^{1/2})$ against Ag^+ concentration (c°) at different temperatures: 1 – 420°; 2 – 400°; 3 – 370°; 4 – 350°.

---

[8] G. Mamantov, D. L. Manning and J. M. Dale, *J. Electroanalyt. Chem.*, **9**, 253 (1965)

The comparison of three different results of voltammetry (the plot i_p *vs.* $v^{1/2}$, n-value calculated from equation 6 and the plot log $(i_p - i)$ *vs.* E) indicate that the cathodic process is reversible and diffusion —controlled, at relatively low sweep rates as used in this work. At greater sweep rates it is possible that both faradaic and capacitive currents be involved.

Equation (3) is suitable for the evaluation of interdiffusion coefficient of silver ion.

Table 1

The interdiffusion coefficients of silver ion in molten KNO_3 at different temperatures from voltammetric and chronopotentiometric measurements

Temperature °C	Mean values $D_{Ag^+} \cdot 10^5\ cm^2 \cdot s^{-1}$	
	Cyclic voltammetry	Chronopotentiometry
350	3.38	1.93
370	3.98	2.19
400	4.87	—
420	5.93	2.87

In Fig. 7 the slopes of straight lines of Fig. 2 — 5 *vs.* Ag^+ concentration are plotted at different temperatures. Inserting the slopes of these new straight lines in equation (3) one obtains the interdiffusion coefficients (table 1).

The values of activation energy of diffusion $E = 6740$ cal and the pre-exponential factor $D_0 = 7.72.10^{-3}$ $cm^2.s^{-1}$ have been calculated from the dependence log D *vs.* reciprocal absolute temperature by the least squares method.

3.2. CHRONOPOTENTIOMETRY

In the chronopotentiometric measurements we have found the constancy of $i\tau^{1/2}$ product (for a given concentration) and the same $\frac{i\tau^{1/2}}{c^\circ}$ ratio for different Ag^+ concentrations.

The transition time (τ) is obtained by the Reinmuth's graphical method. [9]

The chronopotentiometric results are presented in Fig. 8 where the dependence $i\tau^{1/2}$ *vs.* c° is plotted at different temperatures.

The interdiffusion coefficients of silver ion calculated on the basis of Sand's equation from the slopes of the straight lines $i\tau^{1/2}$ *vs.* c° are presented in table 1.

The numerical value of activation energy of diffusion and preexponential factor determined by the least squares method are $E = 5060$ cal and $D_0 = 1.21.10^{-3}$ $cm^2.s^{-1}$. The results are very close to the values previously reported and a good agrement with another results of different workers is obtained, too.[3]

---

[9] W. H. Reinmuth, *Analyt. Chem.*, **33**, 485 (1961).

In order to prove the reversibility of the system by other methods, some measurements using reversal as well as cyclic chronopotentiometry have been performed.

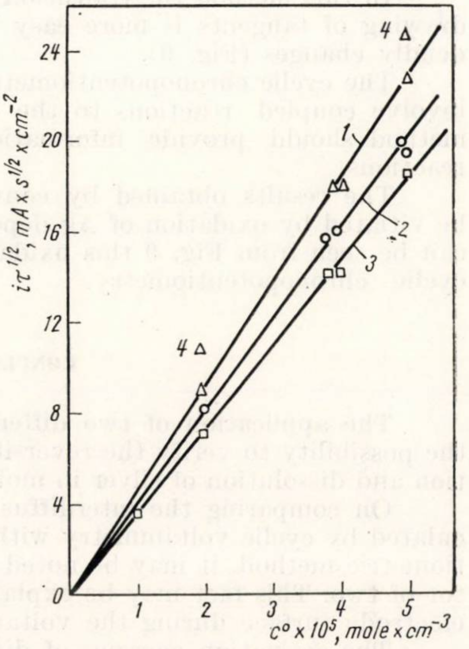

Fig. 8. — Dependence chronopotentiometric $i\tau^{1/2}$ product *vs.* Ag^+ concentration (c°) at different temperatures: 1 — 420°; 2 — 370°; 3 — 350°; 4 — 420° (cyclic chronopotentiometry).

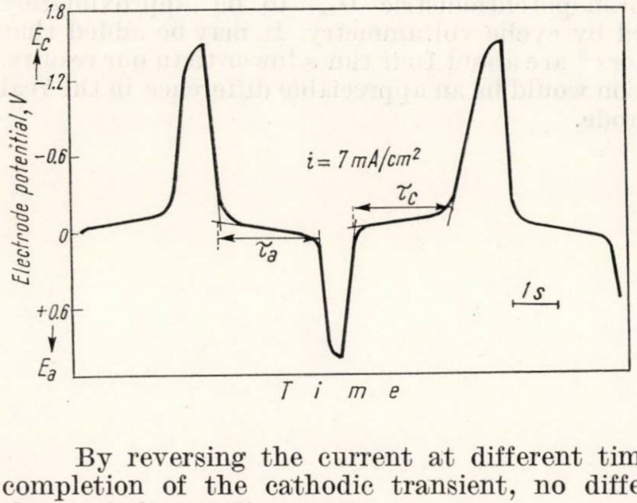

Fig. 9. — Cyclic chronopotentiogramms of $AgNO_3 - KNO_3$ at 420°; $c^{\circ} = 2.10^{-5}$ mole. cm^{-3}

By reversing the current at different times before and after the completion of the cathodic transient, no differences appeared in the shape of the anodic curves.

An analysis of reversal and cyclic chronopotentiograms evidences that τ_{cathodic} is approximately equal to τ_{anodic} and $E_{\tau/4}$ potentials for reduction and oxidation are very close, as expected for a reversible electrochemical process. Figure 8 shows a satisfactory approached value for $i\tau^{1/2}$ product obtained by cyclic chronopotentiometry.

In this method the transition time determination by the graphical drawing of tangents is more easy because the electrode potential suddendly changes (Fig. 9).

The cyclic chronopotentiometry is very suitable for systems which involve coupled reactions to the eloctrode process. In such cases the method should provide information on the kinetics of these coupled reactions.

The results obtained by conventional chronopotentiometry could be vitiated by oxidation of Ag deposited on the electrode surface. As it can be seen from Fig. 9 this oxidation process was not observed using cyclic chronopotentiometry.

CONCLUSIONS

The application of two different electrochemical techniques gives the possibility to verify the reversibility and diffusion-control of deposition and dissolution of silver in molten KNO_3.

On comparing the interdiffusion coefficients of the silver ion calculated by cyclic voltammetry with those obtained by the chronopotentiometric method, it may be noted that the D – values differ by a factor of two. This fact may be explained by the activation process of the eloctrode surface during the voltammetric measurements.

The activation energies of diffusion are also different.

Similar results were obtained in $NaNO_3-KNO_3$ by Hills et al. [5] They also found the chronopotentiometric D_{Ag^+} to be approximately the half of that obtained by cyclic voltammetry. It may be added that D_{Ag^+} values of these authors [5] are about four times lower than our results.

A possible explanation would be an appreciable difference in the real surface of working electrode.

Revue Roumaine de Chimie, **21**, 8, 1161–1169 (1976)

TEMPERATURE DEPENDENCE OF THE DIELECTRIC PERMITTIVITY OF IONIC CRYSTALS WITH CUBIC STRUCTURE. I

POTASSIUM BROMIDE, IODIDE AND CHLORIDE

N. DUŞOIU
Center of Physical Chemistry
Str. Galaţi 31, Bucharest 9, Romania

Received November 19, 1974

The temperature dependence of the dielectric permittivity of KI, KBr, KCl (single crystals) within the 0–500° range, was studied by applying a microwave technique in the X band frequency. The polarizability temperature coefficients were calculated from experimental data at a constant volume. These coefficients are positive. The optical and infrared polarizability contributions to the total dependence of macroscopic polarizability on temperature were also calculated.

1. INTRODUCTION

The measurements of complex dielectric permittivity $\varepsilon^* = \varepsilon' - j\varepsilon''$ provide information on the inherent properties of the crystal lattice and on the behaviour of the lattice imperfections.

The value of the dielectric permittivity is also useful for the study of the dynamics of ionic crystals lattice. [1,2] A good knowledge of the dielectric permittivity value is absolutely necessary in order to evaluate the effects of electrostatic interactions on the charge transfer in ionic crystals. [3]

The ionic conductivity studies reported in[4] have shown that the experimental values for KI are usually higher by 20 – 30% than the theoretical ones in the vicinity of the melting point. Lidiard [5] and Suptitz and Teltow [6] have suggested that this discrepancy is due to Debye-Hückel interactions. Debye-Hückel interactions can be included in calculations only if the dielectric permittivity is thoroughly known in the investigated zone. The dielectric permittivity value at high temperatures cannot be deduced directly by extrapolation of the known data at room temperature or at low temperatures, since the increase rate at high temperatures

---

[1] B. Sziqti, *Trans. Faraday Soc.*, **45**, 155 (1949).

[2] R. P. Lowndes, *Phys. Lett.*, **21**, 26 (1966).

[3] S. Chandra and J. Rolfe, *Canad. J. Phys.*, **4**, 412 (1970).

[4] S. Chandra and J. Rolfe, *Canad. J. Phys.*, **4**, 397 (1970).

[5] A. B. Lidiard, "Handbuch der Physik – Ionic Conductivity", vol. 20, Springer Verlag, Berlin, 1957, p. 246–349.

[6] P. Süptitz and J. Teltow, *Phys. Status Solidi*, **23**, 9 (1967).

is different (the observation was made by Narasimhan [7] and Panchenko [8]). These considerations have prompted Chandra [9] to perform measurements on KI single crystals.

Dielectric permittivity measurements of alkaline halides at high temperatures set a series of special problems. At low frequencies, ionic conductors exhibit a large capacitance increase due to the blocking of ions at the electrodes. At high frequencies, electrodes polarization effects are eliminated or diminished. Chandra [9] has developed an experimental method for measuring KI dielectric permittivity at high temperatures in the microwaves domain (K frequency band). This paper reports the permittivity determinations within the 0 — 500° range, using a microwaves technique (X frequency band) on KI, KBr and KCl single crystals.

2. EXPERIMENTAL

The dielectric permittivity $\varepsilon^* = \varepsilon' - j\varepsilon''$ can be determined if the intrinsic impedance of the studied medium is known. The intrinsic impedance of the studied medium may be deduced by means of a standing wave detector which measures the amplitude and the phase of the reflected wave in the presence and in the absence of the medium in question.

The block diagram is shown in Fig. 1 and consists of: microwave generator, ferrite isolator, directional coupler, wavemeter, crystal detector, microampermeter, variable attenuator, standing wave detector and the actual sample holder.

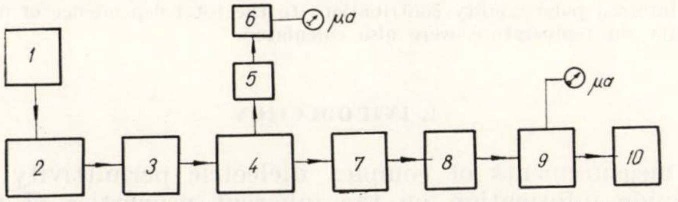

Fig. 1.— The block diagram of the measurement installation.

1. power supply; 2. klystron K-19; 3. ferrite isolator; 4. directional coupler; 5. wavemeter; 6. cristal detector; 7. ferrite isolator; 8. variable attenuator; 9. standing wave detector; 10. shorted sample holder.

The sample holder is shown in Fig. 2 and consists of a waveguide segment for X band (22.86 × 10.16 × 200) short-circuited at the end. The waveguide is introduced into a glass tube stoppered by metallic contacts. The tube is deaerated and inert gases are passed into it to reduce the sample evaporation. The temperature is measured by a Pt-Pt.Rh thermocouple. The sample holder is separated from the unit by mica foils and is cooled by circulating water through a spiral.

The propagation constant of the electromagnetic wave $\gamma = \alpha + i\beta$ for a dielectric medium found inside the guide [10] is:

$$\frac{\tanh \gamma d}{\gamma d} = -\, i \frac{\lambda_g}{2\pi d} \cdot \frac{1 + ir \tan\, [2\pi(\mathrm{D} + d)/\lambda_g]}{r + i \tan\, [2\pi(\mathrm{D} + d)/\lambda_g]} \tag{1}$$

where:

$$\gamma d = id \left(\frac{\omega}{c} \right) \left[\varepsilon' - i\varepsilon'' - \left(\frac{\lambda_0}{\lambda_c} \right)^2 \right]^{1/2} = T(\cos\tau + i \sin\tau) \tag{2}$$

---

[7] P. T. Narashimhan, *Proc. Nat. Inst. India.* Pt. A., **21**, 133 (1955).

[8] V. V. Panchenko, *Acad. Sci. USSR (Phys. Ser.)*, **24**, 141 (1960).

[9] S. Chandra, *Canad. J. Phys.*, **9**, 969 (1969).

where :

λ_g = wavelength inside the air-filled waveguide ;
λ_0 = free space wavelength ;
λ_c = the cutoff wavelength ;
λ_d = the wavelength inside the dielectric medium.

$$\lambda_d = 2\,\pi d/\beta d \tag{3}$$

where :

D = the standing wave minimum shift when introducing the sample into the waveguide ;
d = the sample thickness ;
r = the standing wave amplitudes ratio in the presence of the sample $= \lambda g/\pi\Delta X_s$
ΔX_g = the wave width at half distance from the minimum height
T and τ = values are given in tables.[10,11]

In the case of samples with small losses (within the range of low temperatures), $\alpha \approx 0$, equation (1) is simplified to :

$$\frac{\tan\beta d}{\beta d} = \frac{\lambda_d}{2\pi d}\tan\frac{2\pi(D+d)}{\lambda_g}, \tag{4}$$

and

$$\varepsilon' = \left(\frac{\lambda_0}{\lambda_c}\right)^2 + \left(\frac{\lambda_0}{\lambda_d}\right)^2, \tag{5}$$

and for samples with high losses[12] :

$$\varepsilon' = \left(\frac{\lambda_0}{\lambda_c}\right)^2 - \left(\frac{\lambda_0}{2\pi d}\right)^2 T^2 \cos 2\tau \tag{6}$$

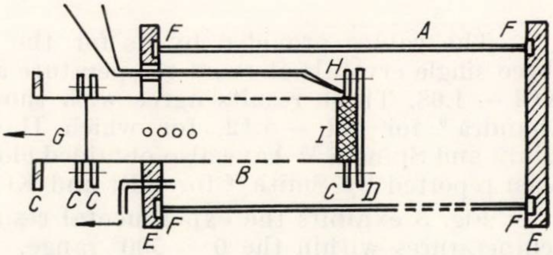

Fig. 2. — Waveguide sample holder.
A. glass tube; B. X-band waveguide; C. waveguide flanges; D. short-circuite plate; E. end seals; F. gasket; G. mica window; H. Pt-Pt.Rh thermocouple; I. sample.

3. WORKING PROCEDURE

The investigated samples were cut from single crystals supplied by the Institute of Physics, Bucharest.* Their inner dimensions were similar to the waveguide used and their thicknesses ranged within 3 and 6 mm. Equation (6) was used to calculate ε' permittivity at

---

[10] A. VON HIPPEL, "Dielectric Materials and Applications", John Wiley Inc., New York, 1954, p. 67.

[11] A. LEBRUN, "Methodes de mesure de la permitivité complexe des diélectriques du continu à l'infrarouge", Univ. Lille, Fac. Sciences, Inst. de Radiotechnique, France, 1967.

[12] M. SUCHER and J. FOX, "Handbook of Microwave Measurements", $3_{\rm rd}$ edition, Polyt. Press of the Polyt. Inst. of Brooklyn, USA, vol. II, 1963, p. 496.

* Lab. Dr. Liviu Matei

high temperatures and equation (5), to calculate permittivity at low temperatures. Samples were wrapped in a thin paper foil to avoid waveguide corrosion.

The value and the position of the minimum are determined by readings with the standing wave detector, in the case of a short-circuited waveguide. The sample under study with "d" thickness is then introduced into the sample holder and the measurement is repeated to obtain the values "D" and "r". Determinations are repeated for 2–3 samples with various thicknesses. The frequency was measured on a resonant cavity wavemeter.

X-band frequency measurements present an advantage over those performed in K-band, since the number of the measured minimum is 3 times smaller than in the case of the K band. A source of errors appearing in these measurements is due to the thermal expansion of the wave guide and to the decrease of its conductivity at high temperatures. In our case, the length of the measurement line is 50 cm.

To obtain the position and the thickness of the wave minimum at various temperatures in the presence of the sample, the data obtained are corrected by relation :

$$\Delta X_s = \Delta X_s' - \Delta X_c \frac{d_e - d}{d_e} \tag{7}$$

where : $\Delta X_s'$ = the measured width of the minimum in the presence of the sample, ΔX_0 = the measured width of the minimum without the sample at the same temperature and d_e is the position of the sample at the end of the measurement line $d_e \sim 50$ cm.

The determination errors of ε' are : ± 2% at low temperatures and ± 5% at high temperatures. We employed a TESLA (Czechoslovakia) measurement line and a K-19 klystron.

4. EXPERIMENTAL RESULTS

The values provided by us for the dielectric permittivity of the three single crystals at room temperature are : KI – 5.10 ; KBr – 4.76 ; KCl – 4.68. These results agree with those reported in the literature : Chandra [9] for KI – 5.12, for which Haussühl, [13] Lowndes [14] and Di Giura and Spinola [15] have also obtained close values. Similar results have been reported by Smith [16] for KBr and KCl.

Fig. 3 exhibits the experimental results obtained for ε' at various temperatures within the 0 – 500° range.

The curves plotted in fig. 3 show a much more rapid increase of ε at high temperatures as compared to the variations within the range of lower temperatures. This fact is more evident for KI.

Fig. 4 shows the temperature coefficient of the dielectric permittivity $1/\varepsilon' \, (d\varepsilon'/dT)_p$, for the investigated samples.

The experimental data reveal a linear variation of the temperature coefficient of the dielectric permittivity with temperature. For KBr and KCl crystals, the experimental points are positioned on the same straight line whose slope is milder than in the KI case.

---

[13] S. von Haussühl, *Z. Naturforsch.*, **12a**, 445 (1957).

[14] H. J. Wintle and J. Rolfe, *Canad. J. Phys.*, **44**, 965 (1966).

[15] V. Di Giura and G. Spinola, *Nuovo Cimento*, **56 B**, 192 (1968).

[16] G. C. Smith, "Materials Science Center", Cornell University, Ithaca, New York, 1962, Rept. No. 51.

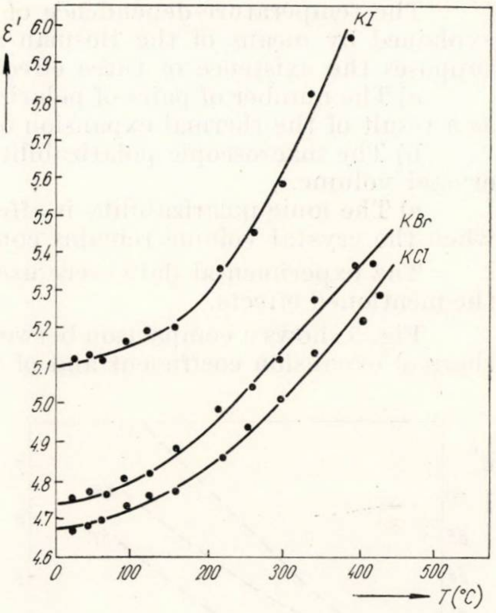

Fig. 3. — The temperature dependence of the dielectric permittivity of the KI, KBr and KCl (single crystals).

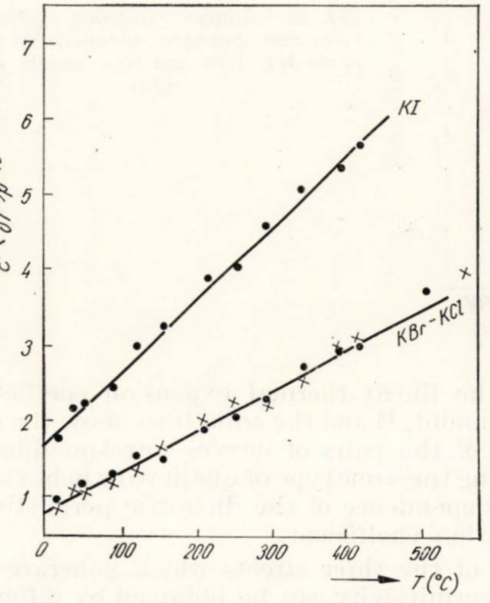

Fig. 4. — Temperature coefficient of dielectric permittivity of KI, KBr and KCl (single crystals).

5. DISCUSSION OF THE EXPERIMENTAL RESULTS

The temperature-dependence of the dielectric permittivity may be explained by means of the Bosman and Havinga model.[17] This model supposes the existence of three effects of the temperature:

a) The number of pairs of polarizable ions per unit volume decreases as a result of the thermal expansion of the crystal.

b) The macroscopic polarizability rises due to the expansion of the crystal volume.

c) The ionic polarizability is affected by the temperature variations when the crystal volume remains constant.

The experimental data were used to calculate the contributions of the mentioned effects.

Fig. 5 shows a comparison between the variation curves of the linear thermal expansion coefficient and of the dielectric permittivity.

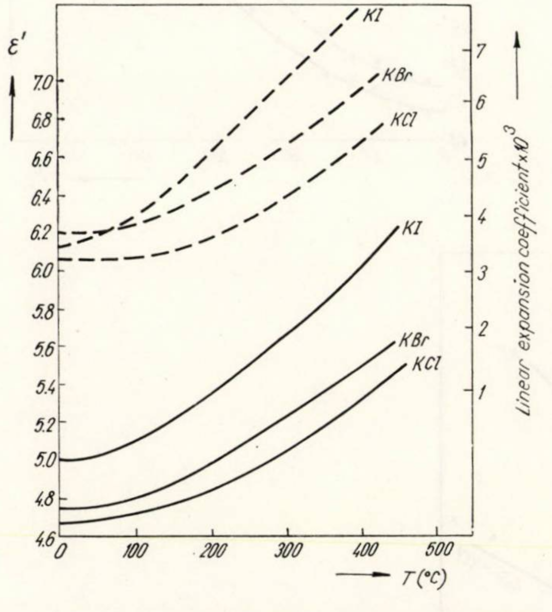

Fig. 5. — Linear expansion coefficient (---) and dielectric permittivity (——) of the KI, KBr and KCl (single crystals.)

The dotted curves show the linear thermal expansion coefficient reproduced after Eücken and Dannöhl,[18] and the solid lines show the dielectric permittivity. The aspect of the pairs of curves corresponding to the three crystals is similar, showing the same type of qualitative behaviour. It results that the temperature-dependence of the dielectric permittivity is related to the thermal expansion coefficient.

A complete representation of the three effects which generate the temperature-dependence of the permittivity can be obtained by differentiating the Clausius-Mosotti relation :

---

[17] R. J. Bosman and E. E. Havinga, *Phys. Rev.*, **129**, 1593 (1963).

[18] A. von Eücken and W. Dannöhl, *Z. Electrochem.*, **40**, 814 (1934).

$$\frac{\varepsilon-1}{\varepsilon+2}=\left(\frac{4}{3}\right)\left(\frac{\alpha_m}{V}\right) \tag{8}$$

where α_m is the macroscopic polarizability of a small sphere having a V volume.

By deriving relation (8) as a function of temperature at a constant pressure one obtains :

$$\frac{1}{(\varepsilon-1)(\varepsilon+2)}\left(\frac{\partial\varepsilon}{\partial T}\right)_P=\overset{(a)}{-\frac{1}{3V}\left(\frac{\partial V}{\partial T}\right)_P}+\overset{(b)}{\frac{V}{\alpha_m}\left(\frac{\partial\alpha_m}{\partial V}\right)\left(\frac{\partial V}{\partial T}\right)_P}+\overset{(c)}{\frac{1}{3\alpha_m}\left(\frac{\partial\alpha_m}{\partial T}\right)_V} \tag{9}$$

The first two terms of the second member [(a) + (b)] show the total effect of the volume thermal expansion and may be written under the form :

$$\begin{aligned}[(a)+(b)]&=\frac{1}{(\varepsilon-1)(\varepsilon+2)}\left(\frac{\partial\varepsilon}{\partial V}\right)_T\left(\frac{\partial V}{\partial T}\right)_P=\\&=\frac{1}{(\varepsilon-1)(\varepsilon+2)}\left(\frac{\partial\varepsilon}{\partial P}\right)_P\frac{(1/V)\,(\partial V/\partial T)_P}{(1/V)(\partial V/\partial P)_T}\end{aligned} \tag{10}$$

which results from permittivity differentiation in relation to the pressure at a constant temperature.

Equations (9) and (10) can be used to separately determine the three terms if the following are known : the dependence of the dielectric permittivity on temperature $(\partial\varepsilon/\partial T)_p$, the dependence of the dielectric permittivity on the pressure $(\partial\varepsilon/\partial p)_T$, the thermal expansion coefficient $(1/V)(\partial V/\partial T)_p$ and the compressibility $(1/V)(\partial V/\partial p)_T$. The term (c) may be determined from the difference [(a) + (b) + (c)] − [(a) + (b)]. In the main this term could also be determined directly if eqn. (8) were differentiated in relation to the temperature at a constant volume :

$$(c)=\frac{1}{(\varepsilon-1)(\varepsilon+2)}\left(\frac{\partial\varepsilon}{\partial T}\right)_V \tag{11}$$

This approach is not convenient due to the experimental difficulties.

Bosman and Havinga [17] report in their study values ranging within 1.8 and 2, for factor $(V/\alpha_m)\,(\partial\alpha_m/\partial V)_T$ in the case of ionic crystals with a NaCl type structure. Thus, for KI, the value is 1.9 and hence :

$$\frac{1}{(\varepsilon-1)(\varepsilon+2)}\left(\frac{\partial\varepsilon}{\partial T}\right)_P=0.9\,\frac{1}{3V}\left(\frac{\partial V}{\partial T}\right)_P+\frac{1}{3\alpha_m}\left(\frac{\partial\alpha_m}{\partial T}\right)_V \tag{12}$$

Equation (12) was used to calculate the temperature coefficient of the polarizability at a constant volume (term (c)). The results obtained for the three crystals are given in fig. 6.

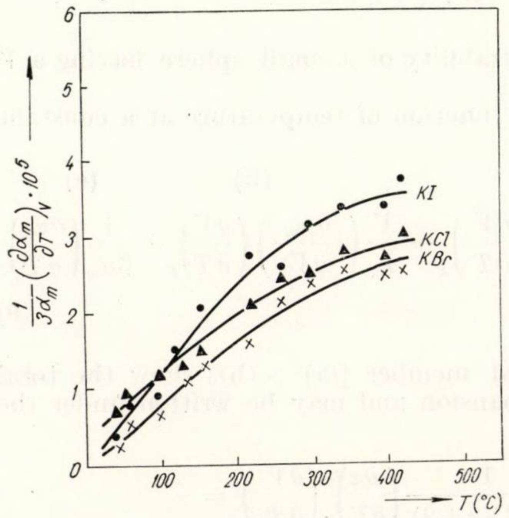

Fig. 6. — The temperature dependence of the KI, KBr and KCl polarizability (single crystals).

The values plotted in fig. 6 indicate that the temperature coefficients of polarizability $(1/3\ \alpha_m)\ (\partial\ \alpha_m/\partial\ T_T)$ are positive. This remark must apply to all ionic crystals with a NaCl type structure and with $\varepsilon < 10$.

The experimental data show that, in the case of the temperature-dependence of the dielectric permittivity, the contribution of the direct polarizability variation with temperature (term (c)) is much smaller than half of the total variation of the permittivity expressed by the sum of terms [(a) + (b) + (c)] for all the three single crystals. We also mention the fact that the direct volume-dependence of the dielectric constant, terms [(a) + (b)], is positive for these crystals. Although the number of ion pairs polarizable per unit volume decreases with the volume expansion, this effect is compensated by the substantial polarizability growth and the sum of these two terms [(a) + (b)] remains positive, completing the contribution of term (c) to the dependence of ε' on temperature. A detailed analysis of the microscopic phenomena conditioning the temperature-dependence of the dielectric permittivity will be made in a subsequent article.

6. CONTRIBUTION OF THE OPTICAL AND INFRARED POLARIZABILITY

The macroscopic polarizability α_m of the studied crystals contains two terms : α_m^{op} (optical polarizability) and α_m^{ir} (ionic or infrared polarizability). The α_m^{op} component determines the optical part of the dielectric permittivity $\varepsilon^{\mathrm{op}} = n^2$, where n is the refraction index in the visible domain.

The Clausius-Mosotti relation for the optical component of the dielectric permittivity is :

$$\frac{(\varepsilon^{\mathrm{op}} - 1)}{(\varepsilon^{\mathrm{op}} + 2)} = \left(\frac{4\pi}{3}\right)\left(\frac{\alpha_m^{\mathrm{op}}}{V}\right) \tag{13}$$

The infrared polarizability, α_m^{ir}, may be obtained from the difference between macroscopic polarizability α_m and the optical one α_m^{op} if the two components of the macroscopic polarizability are assumed to be additive $\alpha_m = \alpha_m^{\mathrm{op}} + \alpha_m^{\mathrm{ir}}$. The temperature-dependence terms (b) and (c) assume the following form :

$$(\mathrm{b}) = (\alpha_m^{\mathrm{op}}/\alpha_m)\cdot(\mathrm{b})^{\mathrm{op}} + (\alpha_m^{\mathrm{ir}}/\alpha_m)\cdot(\mathrm{b})^{\mathrm{ir}} \tag{14}$$

$$(\mathrm{c}) = (\alpha_m^{\mathrm{op}}/\alpha_m)\cdot(\mathrm{c})^{\mathrm{op}} + (\alpha_m^{\mathrm{ir}}/\alpha_m)\cdot(\mathrm{c})^{\mathrm{ir}} \tag{15}$$

where $(\mathrm{b})^{\mathrm{op}}$, $(\mathrm{c})^{\mathrm{op}}$, $(\mathrm{b})^{\mathrm{ir}}$ and $(\mathrm{c})^{\mathrm{ir}}$ are obtained by substituting α_m in (b) and (c) by α_m^{op} and α_m^{ir}, respectively $(\mathrm{b})^{\mathrm{op}}$ and $(\mathrm{c})^{\mathrm{op}}$. These terms may be determined from temperature and pressure-dependence measurements of the dielectric permittivity ε' and of the refraction index.

Burnstein and Smith [19] reported measurements referring to the pressure and temperature-dependence of the refraction indices for the crystals under study. Using the data from [19] and those obtained in the present study, it was possible to calculate the terms for a temperature of 200°. The results are listed in table 1.

Table 1

The temperature dependence coefficients of the polarizability

Sample	ε	α_m^{op}/α_m	α_m^{ir}/α_m	(a) × 10^5 $(^\circ\mathrm{K})^{-1}$	(b) × 10^5 $(^\circ\mathrm{K})^{-1}$	(c) × 10^5 $(^\circ\mathrm{K})^{-1}$
KCl	4.68	0.50	0.50	−3.8	$7.4 = 1.1 + 6.3$	$1.8 = -0.3 + 2.2$
KBr	4.75	0.55	0.45	−4.0	$7.2 = 1.1 + 6.1$	$2.6 = 0.0 + 2.6$
KI	5.10	0.49	0.51	−4.0	$8.0 = 1.3 + 6.7$	$1.2 = -0.2 + 1.4$

ACKNOWLEDGMENT. The author is much indebted to Acad. Prof. I. G. Murgulescu for having suggested this problem and for his constant encouragement. Also he wants to thank Dr. Liviu Matei for having kindly supplied some of the samples studied in this paper.

---

[19] E. Burnstein and P. L. Smith, *Phys. Rev.*, **74**, 229 (1948).

Revue Roumaine de Chimie, **21**, *8*, 1161–1169 (1976)

Revue Roumaine de Chimie, **21**, *8*, 1171–1175 (1976)

BISMUTH(III)-ETHYLENEDIAMINETETRAACETIC ACID (EDTA) COMPLEXES. II[1]

KINETIC STUDIES ON THE ISOTOPIC EXCHANGE REACTION BETWEEN THE HYDROLYSED BISMUTH ION AND ITS EDTA COMPLEX

C. DRĂGULESCU, ANA NIMARĂ, ELISABETA PRINCZ, AGNETA BALINT and I. JULEAN

Chemical Research Centre, Bd. Mihai Viteazul, N⁰ 24, Timişoara, Romania

Received July 25, 1975

The rate of the isotopic exchange between the hydrolysed bismuth ion and its EDTA complex is measurable at pH = 2 and 3 and for the concentrations of the order of 10^{-3} – 10^{-4}M of each reactant. Under these conditions the exchange rate was of the first order to the complex concentration and of partial order to the concentration of Bi(III). The exchange rates are expressed within the experimental precision by :

$$\text{pH} = 2 \qquad \underset{(\text{Mole/l sec})}{R} = k_1[\text{BiHY}]\,[\text{Bi}^{3+}] + k_2[\text{BiHY}]\,[\text{H}^+] + k_3[\text{BiHY}]\,[\text{H}^+]^2$$

$$\text{pH} = 3 \qquad \underset{(\text{Mole/l sec})}{R} = k_1[\text{Bi(OH)}_2\text{H}_2\text{Y}]\,[\text{Bi(OH)}_2^+] + k_2[\text{Bi(OH)}_2\text{H}_2\text{Y}]\,[\text{H}^+]$$

where at pH = 2 $k_1 = 0.5$ l/mole per sec ; $k_2 = 0.0144$ l/mole per sec ; $k_3 = 0.866$ l/mole per sec and at pH = 3 $k_1 = 0.85$/l mole per sec ; $k_2 = 0.0515$ l/mole per sec. In the acid solutions the exchange reaction takes place by protonation and bimolecular collision process. With decreasing acidity the bimolecular collision process is predominant.

Ethylenediaminetetraacetic acid (EDTA) forms with the bismuth ion in an acid medium neutral and anionic very stable chelates.[2-6] As the acidity of the solution decreases, the bismuth ion hydrolyses and the complexation reaction occurs with the initial formation of some outer sphere complexes, which gradually transform, with different rates, into inner sphere complexes.[1]

The literature data [7] show that the formation rate of the chelatic EDTA complexes with different metals is slow enough, so that the acquirement of some data referring to the metal ion exchange may give direct information concerning the mechanism of the substitution reaction in the transition state.

---

[1] Previous part : C. Drăgulescu, A. Nimară and I. Julean, *Rev. Roumaine Chim.*, **21**, 853 (1976).

[2] I. Miklos and P. Szegedy, *Acta Chim. Acad. Sci. Hung.*, **26**, 365 (1961).

[3] N. Elenkova and L. Ilcheva, *Godishnik Khim. Tekhnol.*, **11**, 143 (1964).

[4] M. T. Beck and A. Gergely, *Magyar Kémiai Folyóirat*, **71**, 163 (1965).

[5] T. R. Bhat and R. K. Iyer, *Z. anorg. Chem.*, **335**, 331 (1965).

[6] B. G. Socevanov and G. A. Volkova, *Zhur. neorg. Khim.*, **1**, 118 (1969).

[7] S. S. Jones and F. A. Long, *J. Phys. Chem.*, **56**, 25 (1952).

The aim of the present paper is to elucidate the mechanism of the formation of the Bi-EDTA chelate at pH 2 and 3, by means of the isotopic exchange reaction.

EXPERIMENTAL

MATERIALS

The bismuthyl perchlorate was obtained by the described procedure.[8] The marked bismuthyl perchlorate was prepared starting from Bi_2O_3, marked with ^{210}Bi. The di-sodium salt of EDTA was reagent grade.

PROCEDURE

A bismuthyl perchlorate solution containing ^{210}Bi was mixed with the solution of the Bi-EDTA complex in 0.1 M $NaClO_4$ and distilled water added to a volum of 50 ml and adjusted to the desired pH value. The reaction mixture was thermostated at $25° \pm 0.1$. At the proper time the unbounded bismuth from the complex was precipitated with NaOH. Eighteen ml of the filtration were used to measure the activity, using an electronical counter "Vakutronik VAM – 16D" with VAZ 410 G.M. tubes.

DISCUSSION AND RESULTS

The exchange reaction between the hydrolysed bismuth ion and its EDTA complex was studied at different concentrations of reactants, at constant pH values.

The isotopic exchange rate, R (mole/l per sec) and, hence, the rate of the substitution of bismuth ion in the EDTA chelate at equilibrium between the species, could be related to the variables of the system by McKay's formula: [9]

$$\ln(1 - F) = -\frac{Rt(a + b)}{ab}$$

where F is the fractional exchange obtained at time t, and a and b represent the molar concentrations of the total radioactive and non-radioactive species of Bi(III) ion and of its EDTA complex respectively.

The rate R was calculated from the half-exchange time.

The exchange reaction was observed to be of first order with respect to the chelate concentration and of partial order to the concentration of Bi(III) ion at pH 2 and 3 (Fig. 1 ; 2). The order with respect to the concentration of BI(III) ion increases as the pH increases.

The experimental data were found to fit a rate law of the form :

$$\mathrm{pH} = 2\, R\ \mathrm{Msec}^{-1} = k_1[\mathrm{BiHY}][\mathrm{Bi}] + k_2[\mathrm{BiHY}][\mathrm{H}^+] + k_3[\mathrm{BiHY}][\mathrm{H}^+]^2 \qquad (1)$$

$$\mathrm{pH} = 3\, R\ \mathrm{Msec}^{-1} = k_1[\mathrm{Bi(OH)_2H_2Y}]^-[\mathrm{Bi(OH)}_2^+] + k_2[\mathrm{Bi(OH)_2H_2Y}]^-[\mathrm{H}^+] \qquad (2)$$

---

[8] C. Drăgulescu, A. Nimară and I. Julean, *Rev. Roumaine Chim.*, **18**, 583 (1973).
[9] H. A. McKay, *Nature*, **142**, 997 (1938).

The rate constants were evaluated by graphical methods, plotting $R/[\text{complex}]$ against $[\text{Bi}]$, and their values at 25°, $\mu = 0.1$, are as follows :

$\text{pH} = 2$ $k_1 = 0.5$ 1/mole per sec ; $\text{pH} = 3$ $k_1 = 0.85$ 1/mole per sec
$k_2 = 0.0144$ 1/mole per sec ; $k_2 = 0.0515$ 1/mole per sec
$k_3 = 0.866$ 1/mole per sec ;

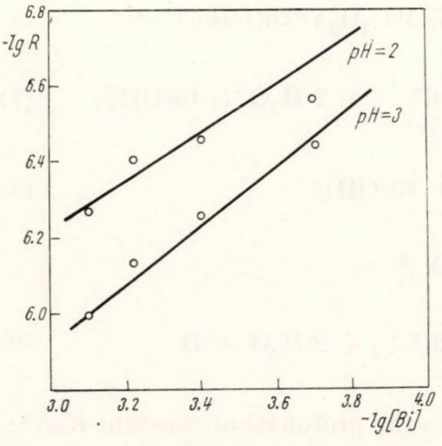

Fig. 1. — Dependence of rate on bismuth ion concentration : $[\text{Bi-EDTA}] = 4 \cdot 10^{-3}$ M (Plots represent experimental results and lines represent results calculated using the rate equation).

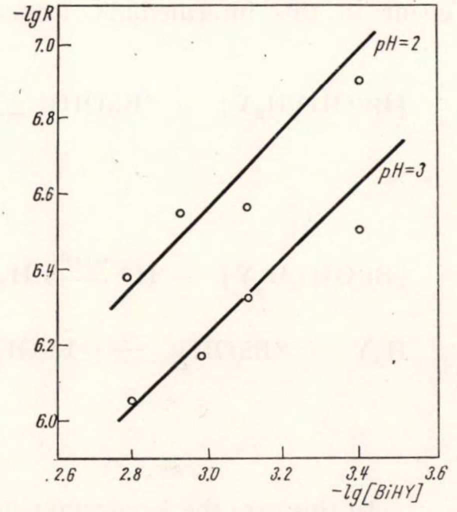

Fig. 2.— Dependence of rate on Bi-EDTA complex : $[\text{Bi}^{3+}] = 4 \cdot 10^{-4}$ M (Plots represent experimental results and lines represent results calculated using the rate equation).

A comparison between the experimentally measured rate and the rate calculated from equations (1) and (2) using the above rate constants shows a good agreement. In fig. 1 and 2 the solid lines have been calculated from equations (1) and (2).

The several terms of the rate equation (1) are consistent with the following postulated, parallel reaction pathes :

$$\text{BiHY} + {}^*\text{Bi(OH)}_2^+ \overset{k_1}{\rightleftharpoons} [{}^*\text{BiHY}] + \text{Bi(OH)}_2^+ \qquad (3)$$

$$\text{BiHY} + \text{H}^+ \overset{k_2}{\rightleftharpoons} \text{BiH}_2\text{Y} \rightarrow \text{Bi}^{3+} + \text{H}_2\text{Y}^{2-} \qquad (4)$$

$$\text{BiH}_2\text{Y} + \text{Y}^+ \overset{k_3}{\rightleftharpoons} \text{BiH}_3\text{Y} \rightarrow \text{Bi}^{3+} + \text{H}_3\text{Y}^- \qquad (5)$$

$$\text{and } \text{H}_n\text{Y}^{(4-n)-} + {}^*\text{Bi(OH)}_2^+ \xrightarrow{\text{rapidly}} {}^*\text{BiHY} + (n-1)\text{H}^+ \qquad (6)$$

The rate constant k_3 includes K_{eq} (4).

Reaction (3) would involve a direct bimolecular reaction between bismuth ion and the chelate species, and reactions (4) and (5) a protonation process in stepwise followed by the decomposition of the protonated complexes and, finally, the exchange.

At pH = 3, the previous determinations evidenced the possibility of an outer sphere complex formation and the exchange mechanism could occur in this intermediary transition state according to the pathes:

$$[\mathrm{Bi(OH)_2H_2Y}]^- + {}^*\mathrm{Bi(OH)}_2^+ \underset{}{\overset{k_1}{\rightleftharpoons}} [\mathrm{Bi(OH)_2H_2Y{}^*Bi(OH)_2}]^0 \rightarrow$$

$$[{}^*\mathrm{BiY}^-] + 2\,\mathrm{H_2O} + \mathrm{Bi(OH}_2^+) \qquad (7)$$

$$[\mathrm{Bi(OH)_2H_2Y}]^- + \mathrm{H}^+ \xrightarrow{\text{rapidly}} \mathrm{H_3Y}^- + \mathrm{Bi(OH)}_2^+ \qquad (8)$$

$$\mathrm{H_3Y}^- + {}^*\mathrm{Bi(OH)}_2^+ \overset{k_2}{\rightleftharpoons} [{}^*\mathrm{Bi(OH)_2H_3Y}]^0 \rightarrow$$

$$[{}^*\mathrm{BiY}^-] + 2\,\mathrm{H_2O} + \mathrm{H}^+ \qquad (9)$$

In this case the k_2 constant includes the protonation constant K_{eq} (8).

The first path (7) could be the stepwise dissociation as uncoiling of the metal chelate followed by progressive simultaneous bounding of the free ligand with the marked hydrolysed metal ion.

The second path (8) could be the protonation of the complex which decomposed afterwards, creating the possibility of the ligand to form a complex with the marked hydrolysed bismuth ion.

The relative contribution of these parallel reaction pathes for a given set of representative experimental conditions are listed in tables 1 and 2.

Table 1

Bi-BiEDTA at 25°. The contribution of each exchange reaction path. $[\mathrm{Bi}^{+3}] = 8.10^{-4}$M ; $[\mathrm{Bi-Y}] = 1.10^{-3}$ M; pH=2; μ = 0.1 M

Total reaction rate mole/l per sec	Simple bimolecular path (term 1) mole/l per sec	Double protonated chelate (term 2) mole/l per sec	Triple-protonated chelate (term 3) mole/l per sec
$5.2 \cdot 10^{-7}$ (R_{calc})	$4.0 \cdot 10^{-7}$ 77 %	$0.878 \cdot 10^{-7}$ 17 %	$0.322 \cdot 10^{-7}$ 6 %

From these tables it follows that at pH = 3 the bimolecular displacement mechanism is predominant and as the pH decreases the protonated complexes contribute to a large extent to the total exchange process.

Table 2

Bi-BiEDTA exchange at 25°. The contribution of each exchange reaction path. [Bi] = [Bi-EDTA] = 1.10^{-3}M; pH = 2; μ = 0.1 M

Total reaction rate (mole/l per sec	Bimolecular path (term 1) mole/ lper sec	Protonated chelate (term 2) mole/l per sec
$8.69 \cdot 10^{-7}$ (R_{calc})	$8.5 \cdot 10^{-7}$ 98 %	$0.194 \cdot 10^{-7}$ 2 %

The bimolecular displacement mechanism could take place in this case by the dissociation of the complex, which might be only an outer sphere complex in this case; that is the reason why the almost total contribution is due to this term as the pH increases.

Revue Roumaine de Chimie, **21**, *8*, 1177–1182 (1976)

INTERACTION BETWEEN ACENAPHTHENE AND PICRIC ACID

N. B. SINGH
Department of Chemistry
University of Gorakhpur,
Gorakhpur (UP), INDIA

Received January 6, 1975

The nature of chemical interaction between picric acid and acenaphthene has been studied with the help of phase – diagram, absorption spectra in solution, I.R. Spectra and reflectance spectra in solid state. Heat of formation by partition method has also been determined. Probabily charge – transfer interaction is involved in the formation of acenaphthene picrate. X-ray diffraction studies show that the crystal of acenaphthene picrate belongs to orthorhombic system.

INTRODUCTION

Picric acid forms intensely coloured addition complexes with aromatic hydrocarbons, amines and phenols. It is expected that charge – transfer interaction is involved in the formation of picrates. In order to understand the nature of interaction in acenaphthene and picric acid system, the present study is undertaken.

EXPERIMENTAL

Purification of materials : Picric acid (BDH) was purified several times by fractional crystallization from ethyl alcohol. The melting point of the purified sample is 122.5°. Acenaphthene (BDH) was first distilled twice under vacuum and recrystallized from alcohol. The m.p. of the purified sample is 94.2°. Chloroform (AR BDH) was washed several times with cold distilled water to remove any ethanol present as an impurity. It was then fractionally distilled twice.

Phase diagram study : Solid liquid equilibria data were obtained by using thaw melt method.[1]

STUDY OF SPECTRA

Absorption spectra in solution : The absorption spectra of acenaphthene, picric acid and acenaphthene picrate in chloroform were studied with Carl-Zeiss spectrophotometer.

Reflectance spectra : The reflectance spectra of acenaphthene, picric acid and acenaphthene picrate in the solid state were studied with the help of Beckmann DU spectrophotometer using $MgCO_3$ reference.

---

[1] R. P. Rastogi and K. T. Rama Verma, *J. Chem. Soc.*, **1964**, 2097.

I. R. Spectra: I.R. Spectra of acenaphthene, picric acid and acenaphthene picrate were taken with perkin Elmer 137 spectrophotometer using KBr optics.

Partition studies: The association constant of acenaphthene picrate in chloroform — water system was determined at 25° and 35° by the method used earlier.[2]

X-ray diffraction studies: The X-ray diffraction pattern of acenaphthene picrate (powdered sample) was taken with the help of diffractometer using CuKα radiation. The observed and the calculated $\sin^2\theta(hkl)$ values are given in table 1.

Table 1

Numerical values of the parameters of eq. (2).

Temperature (°)	Y (g mole/l)	P (g mole/l)	Z (g mole/l)	K	ΔH (kcals/mole)
25	0.0344	0.0309	0.0500	3.0±0.1	
35	0.0321	0.0294	0.0500	2.5±0.1	−3.0

RESULTS AND DISCUSSIONS

The phase diagram studies suggest that 1 : 1 complex is formed between acenaphthene and picric acid (Fig. 1). The phase diagram studies do not give any idea about the nature of interaction. The electronic spectra of acenaphthene, picric acid and 1 : 1 complex in chloroform suggestr that the absorption for the complex in the region 380-500 mμ is greate than the sum of the absorption of acenaphthene and picric acid. This suggests that probabily charge-transfer interaction is involved in the formation of acenaphthene picrate and the molecule of acenaphthene will act as donor and picric acid as acceptor. According to Mulliken the wave function of the complex in the ground state and the excited state would be

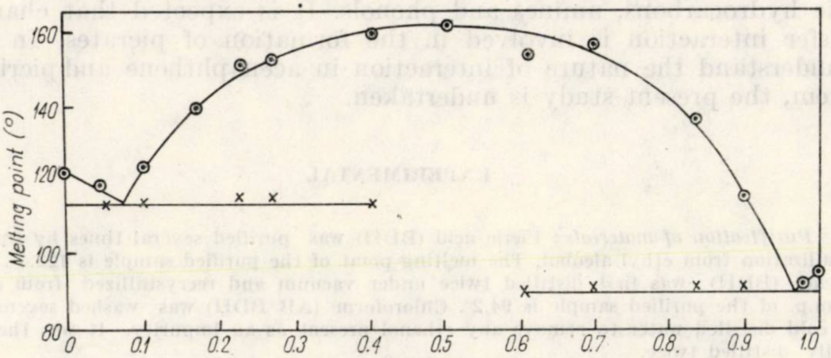

Fig. 1. — Phase diagram of acenaphthene-picric acid system.

$$\Psi_N = a\Psi_{(A.P)} + b\Psi(A^+ - P^-)$$

$$\Psi_E = a\Psi_{(A.P)} - b\Psi(A^+ - P^-)$$

where Ψ_N and Ψ_E are the wave functions in the ground state and the excited states a and b are constants, A and P represent acenaphthene and picric acid molecules, respectively.

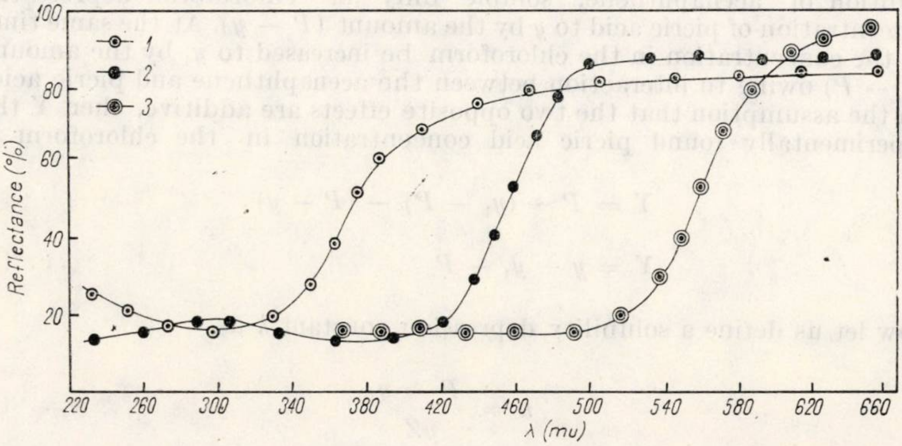

Fig. 2. — Reflectance spectra of 1 acenaphthene, 2 picric acid, 3 acenaphthene picrate.

The reflectance spectra of the components and the complex have also been taken in the solid state (Fig. 2). The reflectance spectra of the complex do not show any *CT* band but a sharp cut off, in the case of picrate, is obtained at longer wavenength than that of picric acid and acenaphthene. This suggests that some sort of weak interaction is involved in the formation of picrate.

The broad features of I.R. Spectra of acenaphthene picrate are given below.

(1) The C—H out of plane bending frequency of picric acid (785 cm^{-1}) comes at higher frequency in picrate (790 cm^{-1}).

(2) The NO_2 assymetric stretching frequency (1528 cm^{-1}) comes at higher frequency (1535 cm^{-1}) in picrate.

This suggests the existence of localized intermolecular interaction in addition to the general charge-transfer between delocalized π-orbitals of component molecules.

In order to understand more about the nature of interaction, the heat of formation of the complex, by partition study, was determined. In order to determine the heat of formation of the complex, the association constants at two different temperatures were determined. The association constant of various picrates were determined by various workers,[2-5] — using partition method in water-chloroform system. The equations

---

[2] H. D. Anderson and D. L. Hammick, *J. Chem. Soc.*, **1950**, 1089.

[3] Moore, Shephered and Goodall, *J. Chem. Soc.*, **1931**, 1447.

[4] R. Foster, D. L. Hammick and S. K. Pearce, *J. Chem. Soc.*, **1959**, 244.

[5] P. D. Gardener and W. E. Stump, *J. Amer. Chem. Soc.*, **79**, 2759 (1957).

used by previous workers were approximate. A more rigorous derivation for the equation is given below.

Let us consider the distribution of picric acid between water and chloroform and the concentration in the latter is P (in gm/l). Let the addition of acenaphthene, soluble only in chloroform, depress the concentration of picric acid to y by the amount $(P - y)$. At the same time let the concentration in the chloroform be increased to y_1 by the amount $(y_1 - P)$ owing to interaction between the acenaphthene and picric acid. On the assumption that the two opposite effects are additive, then Y the experimentally found picric acid concentration in the chloroform is

$$Y = P + (y_1 - P) - (P - y)$$

$$Y = y + y_1 - P \qquad \ldots (1)$$

Now let us define a solubility depression constant k as

$$k = \frac{P - y}{yZ} \qquad \ldots (2)$$

where Z is the number of gram moles of acenaphthene in a litre of the chloroform layer.

$$\text{From eq (1)} \quad Y - y = y_1 - P \qquad \ldots (3)$$

$$\text{From eq (2)} \quad ykZ = P - y \qquad \ldots (4)$$

$$\text{or} \quad y(1 + kZ) = P \qquad \ldots (5)$$

$$\text{or} \quad y = \frac{P}{1 + kZ} \qquad \ldots (6)$$

$$Y - y = y_1 - P = Y - P/1 + kZ \qquad \ldots (7)$$

$$\text{Stability constant } K = \frac{C_{\text{complex}}}{C_{\text{picric acid}} \quad X \, C_{\text{acenaphthene}}} \qquad \ldots (8)$$

$$= \frac{y_1 - P}{P(z - (y_1 - P))}$$

or

$$K = \frac{Y + Y\,kZ - P}{P(Z + kZ^2 - Y - YkZ + P)} \qquad (9)$$

The solubility depression constant k is mainly a molecular volume effect and it is written as $k = k_1 V/1000$, where V is the molecular volume in 1000 cc of solvent and k_1 is a proportionality constant generally written as 3.8. For acenaphthene V is 142 and hence k becomes equal to 0.54.

The values of various parameters of eq (9) is given in table 1. The heat of formation of picrate is also given in the same table. The value of heat of formation simply suggests that partition study measures the number of interactions in addition to charge-transfer interaction.[6-8] The total interaction may be written as :

Total interaction = Charge-transfer interaction + Van der Waals interaction + Dipole-dipole interaction + Dipole-induced dipole interaction + Intermolecular hydrogen bonding.

In the present case the possibility of hydrogen bonding is very small. The other interactions may exist.

The values of dipole moment of acenaphthene, picric acid and acenaphthene picrate are 0.79 D, 2.04 D and 2.25 D respectively. The magnitude of the dipole moment of the picrate suggests the possibility of dipolar interaction in addition to charge-transfer interaction.

In order to understand the arrangement of picric acid and acenaphthene molecules in the crystal lattice of acenaphthene picrate, X-ray studies were made. The crystal data of acenaphthene picrate fitted the orthorhombic type. The agreement between the calculated and observed $\sin^2\theta$ (*hkl*) values is satisfactory (table 2). The unit cell dimensions are

Table 2

Comparison of observed and calculated $\sin^2\theta$ (*hkl*) values

h k l	$\sin^2 \theta_{obs}$	$\sin^2 \theta_{cal}$
1 2 0	0.0084	0.0085
0 2 1	0.0105	0.0106
2 1 0	0.0120	0.0115
1 2 1	0.0130	0.0131
1 4 0	0.0264	0.0265
2 0 2	0.0281	0.0284
2 1 2	0.0302	0.0299
2 2 2	0.0348	0.0344
4 0 0	0.0397	0.0400
0 5 1	0.0422	0.0421
0 1 3	0.0432	0.0429
3 4 0	0.0465	0.0465
1 2 3	0.0499	0.0499
4 3 0	0.0535	0.0535
4 3 1	0.0581	0.0581
0 5 3	0.0788	0.0789
2 7 0	0.0835	0.0835
6 1 2	0.1103	0.1099
0 2 5	0.1204	0.1210
5 0 4	0.1362	0.1362

---

[6] R. Eienchitz and F. London, *Z. Physik*, **60**, 491 (1930).

[7] F. London, *J. Amer. Chem. Soc.*, **63**, 245 (1930).

[8] F. London, *Z. Physik Chem. Bull.*, **1930**, 222.

$a = 15.42$ A°, $b = 19.91$ A°, $c = 11.37$ A° and $Z = 8$. The density of the picrate was found to be 1.39 g/ml and density using *X*-ray data was found to be 1.37 g/ml.

A study of the *hkl* values shows that the crystal of acenaphthene picrate is neither body-nor face-centered. More structural information is needed in order to understand the arrangement of acenaphthene and picric acid molecules in the crystal lattice of acenaphthene picrate.

ACKNOWLEDGMENT. The author is grateful to Prof. R. P. Rastogi, Head of Chemistry Department, University of Gorakhpur for useful discussions.

Revue Roumaine de Chimie, 21, 8, 1183–1187 (1976)

PYRYLIUM SALTS FORMED BY DIACYLATION OF OLEFINS. XXII[1]

TRIACYLATION OF 2,3-DIMETHYL-2-BUTENE

ALEXANDRU T. BALABAN,[a,b] ANISIA BOTA[a] and ILEANA I. STĂNOIU[b]

[a] Chemistry Institute, Department of Organic Chemistry,
The Polytechnic, str. Polizu 1, Bucharest
[b] Institute of Atomic Physics, P.O.B. 5206, Bucharest

Received February 17, 1976

Isobutyryl chloride, anhydrous aluminium chloride and 2,3-dimethyl-2-butene afford the triacylation product V instead of the diacylation product III which had been expected by analogy with the result of acetylating the same olefin with acetyl chloride in the presence of the same catalyst. The structure of V results from ^{1}H–NMR, ^{13}C–NMR and infrared data. An explanation of this different reaction course is provided.

INTRODUCTION

For a comparative study of the deuteration rate of α- *versus* γ-isopropyl groups in the same molecule (intermolecular comparisons for such groups were recently made),[2] we attempted the preparation of 2,4,6-triisopropylpyrylium (III, R = iPr) by reacting 2,3-dimethyl-2-butene (tetramethylethylene, I) with isobutyryl chloride in the presence of aluminium chloride; similar diacetylation of the same olefin I with acetyl chloride had afforded indeed 2,6-dimethyl-4-isopropylpyrylium (III, R = Me).[3] When the reaction was effected, a crystalline pyrylium perchlorate was

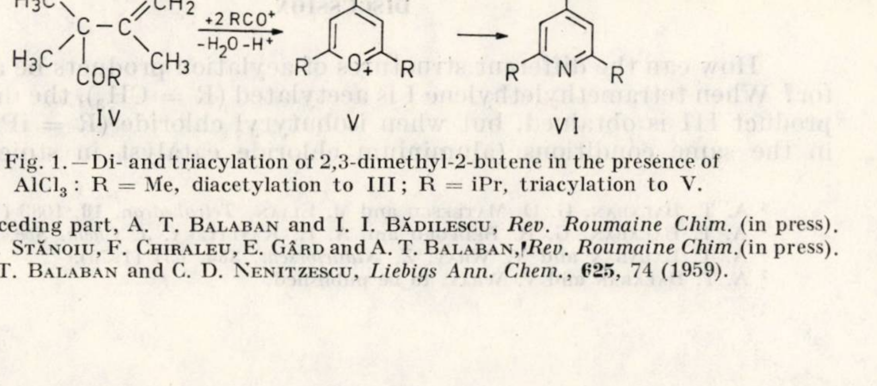

Fig. 1.—Di- and triacylation of 2,3-dimethyl-2-butene in the presence of $AlCl_3$: R = Me, diacetylation to III ; R = iPr, triacylation to V.

---

[1] Preceding part, A. T. Balaban and I. I. Bădilescu, *Rev. Roumaine Chim.* (in press).

[2] I. I. Stănoiu, F. Chiraleu, E. Gârd and A. T. Balaban, *Rev. Roumaine Chim.* (in press).

[3] A. T. Balaban and C. D. Nenitzescu, *Liebigs Ann. Chem.*, **625**, 74 (1959).

obtained, which on reaction with ammonia was converted into a pyridine. However, elemental analyses, IR and NMR spectra indicated that the products were not derived from III, R = iPr, but had a different structure. On the basis of evidence which will be discussed below, the pyrylium cation is the triacylation product, 2,6-diisopropyl-4-(1′,1′,3′-trimethylbutan-2′-on-1′-yl)-pyrylium, V (R = iPr) and the pyridine has structure VI (R = iPr).

SPECTRA

In the infrared spectrum of the pyrylium perchlorate, besides the normal[4] bands (1635, 1535 cm^{-1} due to ring vibration modes, 1100 and 625 cm^{-1} due to the perchlorate anion), a strong band at 1723 cm^{-1} proves the existence of a carbonyl group.

In the ^1H-NMR spectrum (cf.[5]) the same salt presents in CF_3COOH two aromatic protons (s) at τ 2.15, two kinds of isopropyl groups (septets centered at τ 6.41 and 6.45, doublets at τ 8.42 and 8.70; there are two equivalent isopropyl groups at lower field and one isopropyl at higher field) and one singlet for 6H at τ 8.18. On refluxing in CH_3COOD only the lower-field isopropyl methine proton exchanges, as seen from the disappearance of the low-field septet and from the coalescence of the 12H peaks to a broad singlet. Exactly the same types of protons appear in the corresponding pyridine (τ 3.20, 2H, singlet; τ 7.03, 2H, septet; τ 7.43, 1H, septet; τ 8.57, 6H, singlet; τ 8.76, 12H, doublet; τ 9.13, 6H, doublet). The coupling constant in both types of isopropyl groups, in both pyrylium salt and pyridine, is 7 Hz.

The ^{13}C-NMR spectrum (noise-decoupled, and off-resonance for establishing the number of protons bonded to each carbon) gives the signals indicated under formula VII, with relative intensities presented on the bottom level. Assignments were made by comparison with the CMR spectra of pyrylium salts of known structure,[6] in particular of the isopropyl-substituted ones, VIII[6] and IX.[7]

On the basis of this evidence, and of elemental analyses for the pyrylium salt and of the picrate, picrolonate and chloroplatinate of the pyridine, the only structure which fits these data and the starting materials, is V for the perchlorate and VI for the corresponding pyridine (R = iPr in both formulas).

DISCUSSION

How can the different structures of acylation products be accounted for? When tetramethylethylene I is acetylated (R = CH_3), the diacylation product III is obtained, but when isobutyryl chloride (R = iPr) is used in the same conditions (aluminium chloride catalyst in stoichiometric amount to the olefin, without solvent, in excess acyl chloride), the triacylation product V (R = iPr) is formed instead.

---

[4] A. T. Balaban, G. D. Mateescu and M. Elian, *Tetrahedron*, **18**, 1083 (1962).
[5] A. T. Balaban, G. R. Bedford and A. R. Katritzky, *J. Chem. Soc.* **1964**, 1646.
[6] A. T. Balaban and V. Wray, *Z. Naturforsch.*, **30b**, 654 (1975).
[7] A. T. Balaban and V. Wray, to be published.

Triacetylation of olefins (e.g. isobutene, 2-methyl-2-butene) was shown [8] to afford products with structures analogous to V, but always diacetylation products were also present in major amounts.

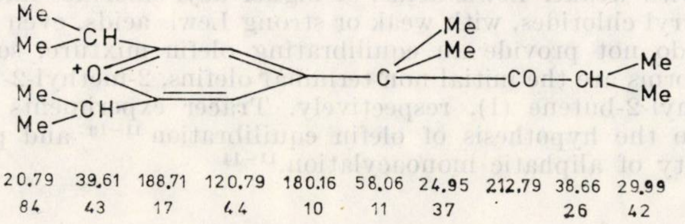
Me
Me
CH
+O
Me
Me
CH
C
Me
Me
CO
CH
Me
Me
20.79 39.61 188.71 120.79 180.16 58.06 24.95 212.79 38.66 29.99
84 43 17 44 10 11 37 26 42

VII

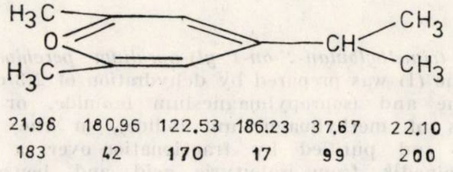
H3C
O
H3C
CH
CH3
CH3
21.96 180.96 122.53 186.23 37.67 22.10
183 42 170 17 99 200

VIII

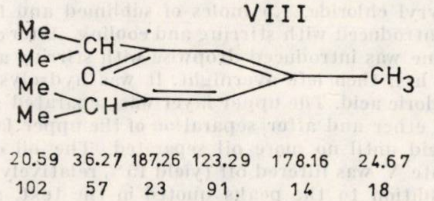
Me
Me
CH
O
Me
Me
CH
CH3
20.59 36.27 187.26 123.29 178.16 24.67
102 57 23 91 14 18

IX

Fig. 2. — ^{13}C−NMR spectra of pyrylium salts in CD_2Cl_2 (20%) — CF_3COOH (80%); upper row, chemical shifts of the above carbons (in ppm from internal TMS); lower row, relative intensities.

The explanation of the influence exerted by the nature of the acyl chloride on the course of the reaction relies on studies of 2-methyl-2-butene diacylation. It had been found that diacetylation of 2-methyl-2-butene by acetyl chloride afforded 2,6-dimethyl-4-ethylpyrylium in the presence of strong Lewis acid catalysts like aluminium chloride or antimony pentachloride,[9] but mainly 2,3,4,6-tetramethylpyrylium with weaker catalysts like tin tetrachloride,[9] zinc chloride[7] or beryllium chloride.[10] However, with propionyl chloride instead of acetyl chloride, the product was the tetrasubstituted pyrylium salt, 2,6-diethyl-3,4-dimethylpyrylium, even in the presence of strong Lewis acids like aluminium chloride.[9]

---

[8] A. T. Balaban, P. T. Frangopol, A. R. Katritzky and C. D. Nenitzescu, *J. Chem. Soc.*, **1962**, 3889.

[9] A. T. Balaban and C. D. Nenitzescu, *J. Chem. Soc.*, **1961**, 3553.

[10] A. T. Balaban, E. Barabas and M. Fărcașiu, *Chem. and Ind.*, **1962**, 781.

It is therefore suggested that a similar mechanism operates in both reactions under discussion. Aluminium chloride and acetyl chloride afford a medium which allows the fast equilibration of olefins, so that the product is derived only from the more reactive isomer with marginal double bond (2-methyl-1-butene, and 2,3-dimethyl-1-butene II), whereas acetyl chloride with weaker Lewis acids, or higher acyl chlorides like propionyl or isobutyryl chlorides, with weak or strong Lewis acids, even aluminium chloride, do not provide an equilibrating olefin mixture, so that the reacting forms are the initial non-terminal olefins, 2-methyl-2-butene and 2,3-dimethyl-2-butene (I), respectively. Tracer experiments had given support to the hypothesis of olefin equilibration [11-13] and proved the reversibility of aliphatic monoacylation.[11-14]

EXPERIMENTAL PART

2,6-Diisopropyl-4-(1′,1′,3′-trimethylbutan-2′-on-1′-yl)-pyrylium perchlorate (VII, or V, R = iPr). 2,3-Dimethyl-2-butene (I) was prepared by dehydration of 2,3-dimethylbutan-2-ol (obtained either from acetone and isopropylmagnesium bromide, or from ethyl isobutyrate and two equivalents of methylmagnesium iodide), in the presence of iodine or of anhydrous oxalic acid and purified by fractionation over a packed column. Isobutyryl chloride was obtained[15] from isobutyric acid and benzoyl chloride and was redistilled. Into 5 moles isobutyryl chloride, 1.5 moles of sublimed and freshly ground anhydrous aluminium chloride were introduced with stirring and cooling. After complete dissolution, 1 mole of 2,3-dimethyl-2-butene was introduced dropwise with stirring at room temperature. The mixture was stirred for 3 hrs, then left overnight. It was hydrolysed by pouring on crushed ice acidified with hydrochloric acid. The upper layer was separated and discarded, the aqueous layer was extracted with ether and after separation of the upper layer, the lower layer was treated with perchloric acid until no more oil separated. The oil crystallized on cooling with ice. The crude perchlorate V was filtered off (yield 15 % relatively to the olefin); its NMR spectrum presented, in addition to the peaks quoted in the text, small impurity peaks at τ 2.20 and 8.62 which may be due to 2,4,6-triisopropylpyrylium, and which disappeared on purification. After recrystallization from 1 % perchloric acid with charcoal, white crystals of V, R = iPr were obtained, m.p. 98°. *Found* : C, 57.46 ; H, 8.01 ; Cl, 9.61 % ; $C_{18}H_{29}O_2^+ \; ClO_4^-$ requires : C, 57.34 ; H, 7.76 ; Cl, 9.40 %.

Deuteration of the perchlorate was effected by refluxation in CH_3COOD (obtained from equimolar amounts of fractionated acetic anhydride and deuterium oxide by refluxation for two hours) for one hour, followed by precipitation with ether.

2,6-Diisopropyl-4-(1′,1′,3′-trimethylbutan-2′-on-1′-yl)-pyridine (VI, R = iPr). The above perchlorate was refluxed for 5 minutes with an excess of aqueous ammonia. The upper layer was separated, the lower layer was extracted with ether. The combined organic layers were extracted with 15 % aqueous hydrochloric acid. The aqueous layer was extracted with ether, the upper layer was discarded, and the lower layer was treated with an excess of sodium hydroxide solution. The purified pyridine was extracted with ether, dried over sodium hydroxide and distilled in vacuum.

[11] M. Frangopol, A. Genunche, P. T. Frangopol and A. T. Balaban, *Tetrahedron*, **20**, 1881 (1964).

[12] D. Fărcașiu, M. Fărcașiu and A. T. Balaban, *Rev. Roumaine Chim.*, **9**, 137 (1964) ; *Studii și Cercetări Chim. Acad. RPR*, **12**, 131 (1964).

[13] A. T. Balaban, D. Fărcașiu and M. Gutman, *Rev. Roumaine Chim.*, **9**, 727 (1964).

[14] M. Frangopol, A. Genunche, N. Negoiță, P. T. Frangopol and A. T. Balaban, *Tetrahedron*, **23**, 841 (1967).

[15] H. C. Brown, *J. Amer. Chem. Soc.*, **60**, 1325 (1938).

Picrate, m.p. 150° (from ethanol), *found* : C, 56.51 ; H, 6.67 ; N, 11.17 % ;

$C_{24}H_{32}N_4O_8$ requires : C, 57.03 ; H, 6.39 ; N, 11.30 %

Picrolonate, m.p. 168° (from ethanol), *found* : C, 62.73 ; H, 7.05 ; N, 12.53 % ;

$C_{28}H_{37}N_5O_6$ requires : C, 62.30 ; H, 6.91 ; N, 12.92 %

Chloroplatinate, m.p. 250° dec. (from water), *found* : C, 45.04 ; H, 6.38 ; N, 2.50 ; Cl, 21.26 ; Pt, 19.57 % ;

$C_{36}H_{60}N_2O_2$ $PtCl_6$ requires : C, 44.98 ; H, 6.25 ; N, 2.92 ; Cl, 22.15 ; Pt, 20.33 %

Infrared spectra were determined in KBr pellet with a Jena-UR10 instrument, PMR spectra with a Varian A—60A instrument and CMR spectra with a CFT-20 instrument in $CD_2Cl_2-CF_3COOH$ (1 : 5) with natural abundance samples.

ACKNOWLEDGEMENTS. Thanks are expressed to Mr. F. Chiraleu for PMR spectra, to Miss E. Sliam and Mrs. V. Daniel for elemental analyses, and to Dr. V. Wray (Stöckheim, W. Germany) for the CMR spectrum.

Revue Roumaine de Chimie **21**, *8*, 1189 – 1201 (1976)

ELECTRONIC STRUCTURE OF CYCLOBUTADIENE FUSED WITH HETEROCYCLIC RING. II[1]

CYCLOBUTADIENES CONDENSED WITH FIVE-MEMBERED HETEROCYCLIC RINGS

M. D. GHEORGHIU and P. FILIP
Center of Organic Chemistry, Spl. Independenței 202-B, Bucharest 15, Romania

Received October 2, 1975

The electronic structure of eight cyclobutadienes fused with five-membered heterocyclic rings is discussed with the aid of a procedure which decomposes the mo's of the molecule into orbitals of some chosen fragments. The investigated compounds are very reactive, owing to the presence of a destabilized ethylenic bond in the four-membered ring.

The chemistry of transient species is a research field in which theory and experiment are interwoven more than in the chemistry of stable shelf-compounds. It is quite difficult to assess the actual weight of quantum chemistry contribution, and of course such an evaluation is beyond the aim of this paper. However, it appears that numerical experiments for elusive compounds are of vital importance, in most cases the numerical information precedes the experimental achievements, while for shelf-compound chemistry, their importance is only optional. Theoretical works regarding, for example, arynes,[2] hetarynes,[3] cyclobutadiene [4] and tetrahedrane [4] are essential to design strategies for, and understand the experimental chemistry of, these elusive compounds. One of the basic questions to be answered regarding the chemical behaviour of elusive compounds is related to their kinetic and thermodynamic stability. Less ambitiously, one may compare their stability with that of a standard, for which we possess experimental information. This is the reason why we think that in the area of presumably elusive compounds even preliminary numerical explorations, as it is done in the present paper, are welcome. Our interest was focused on the class of benzocyclobutadiene, which as far as experiments have shown, belongs to the area of elusive compounds. The formal substitution of the benzo-ring in benzocyclobutadiene with heteroaromatic six-membered rings, leads to an unknown class of compounds and to a decrease in stability relatively to benzocyclobutadiene itself, as we have shown in our previous paper.[1]

---

[1] M. D. GHEORGHIU and P. FILIP, *Rev. Roumaine Chim.*, **19**, 859 (1974), part I.

[2] D. L. WILHITE and J. L. WHITTEN, *J. Amer. Chem. Soc.*, **93**, 2858 (1971).

[3] W. ADAM, A. GRIMISON and R. HOFFMANN, *J. Amer. Chem. Soc.*, **91**, 2590 (1969).

[4] R. J. BUENKER and S. D. PEYERIMHOFF, *J. Amer. Chem. Soc.*, **91**, 4342 (1969).

We think that one of the chief reason of the instability stems primarily from the existence in these compounds of a very reactive double bond, in the cyclobutadiene part of the molecules.

We would like to present in this paper some of our results regarding the electronic structure of cyclobutadienes condensed with five-membered heteroaromatics (Five-membered Heterocyclo Cyclobutadienes, FHC) of structural types **2** and **3**, where X for both representations is one of the isoelectronic groups **a** to **d**.

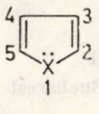

1

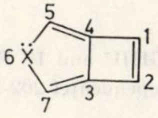

2 (TA)

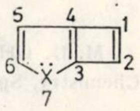

3 (SA)

2 (TA)	3 (SA)
a. $X = -\ddot{\bar{C}}H-$	a. $X = -\ddot{\bar{C}}H-$
b. $X = -\ddot{O}-$	b. $X = -\ddot{O}-$
c. $X = -\ddot{N}H-$	c. $X = -\ddot{N}H-$
d. $X = -\ddot{\underset{\cdot\cdot}{S}}-$	d. $X = -\ddot{\underset{\cdot\cdot}{S}}-$

Both structural types could conceptually be regarded as deriving from the annelation of a double bond at the 2,3 and respectively at 3,4 positions of the heterocyclic molecule **1**. Let us call for convenience the first mode **3** a side attachement (SA) of the double bond, and respectively **2** a top attachement (TA) for the second one. The two structural types are very different with respect to the π-topology. Compounds of structural type **3** preserve the main structural resemblance with benzocyclobutadiene and its six-membered heteroaromatic congeners, since one could represent them by canonical structures possessing the cyclobutadiene moiety as **3A** and **3B**.

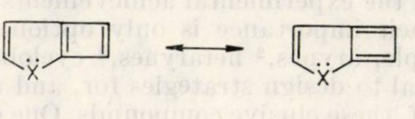

3A 3B

Compounds of type **2** are formally not cyclobutadiene derivative since neither of the canonical structures display for the four-membered part of the molecule a genuine cyclobutadiene. Therefore, compounds with TA structure, avoiding one of the most unstable π-structures from organic chemistry, the antiaromatic 4 π-system, invite to more optimistic experimental attempts for synthesis than SA structural compounds. However one should keep in mind that the stability increase of **2** over **3** is rather small, therefore compounds **2** should be still quite reactive. In the FHC field, synthesis and chemical properties were reported only for some representatives of the TA class.

Thus the compound **2b** ($X = -O-$) [5] does foreshadow the expected properties for a FHC system : it dimerizes, polymerizes easily in the presence of oxygen and reacts very readily with cyclopentadiene; in the ^{1}H$-$NMR spectrum, the resonance signal of α-furanic protons is shifted from 7.40 ppm in furan to 6.28 ppm in **2b**. In the class of thiophenocyclobutadiene (**2d**), so far both the parent compound [6] and the 1,2-diphenyl derivative **5**[7] are known. Compound **5** dimerizes at higher temperature than **2b**, but reacts with tetracyanoethylene at room temperature. In the NMR spectrum the two α-standing protons resonate at higher field that the corresponding thiophene protons, and this fact was interpreted as being due to the paramagnetic ring current occuring in the four-membered ring of compound **5**.

---

[5] K. P. C. Vollhardt and R. G. Bergman, *J. Amer. Chem. Soc.*, **94**, 8950 (1972) ; R. G. Bergman and K. P. C. Vollhardt, *J.C.S. Chem. Comm.* 214 (1973).

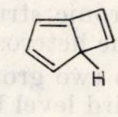

4

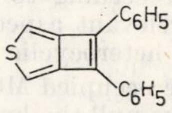

5

Breslow *et al.*[8] have reported that the pK_a of **4** is 1.5 times higher than for cyclopentadiene. Although both compounds have a cyclopentadiene system, which in principle by losing the proton would give the same 6 π-electron pattern, in the case of *4*, the presence of the double bond attached to this system destabilizes the anion by 15 kcal/mole in comparison with the cyclopentadiene anion.

We would like to present here some of our conclusions regarding the π-electronic structure of **2a**$-$**2d** and **3a**$-$**3d**. These comments result from SCF$-$PPP calculations, based on a procedure presented in Appendix A.

Essentially we suspect that FHC's should have similar behaviour to benzocyclobutadiene, in other words they should be chemically unstable. This is the consequence of the destabilization of the highest occupied molecular orbital (HOMO) of the FHC, as the result of the overall repulsion of the two closed-shell π-systems from the five-membered heterocyclic moiety and the ethylene moiety.

Are there in the composite molecule, i.e. the FHC, the two fragments mentioned above, substantially altered; in which part of the molecule are most located the predicted chemical properties? How could one visualize the build-up of the MO wave functions from the MO's of fragments, and how could one formulate probable chemical properties of the FHC's?

The aim of the present paper is to discuss these topics with the help of a procedure which transforms the MO's from a linear combination of atomic orbitals into linear combinations of MO's of the fragments. By this procedure, the practising organic chemist, will "perceive" for example, that in the frontier orbitals, the cyclobutadiene contribution of the π-system of the molecule is prevailing, so one could expect at least partially similar properties.

---

[6] P. J. Garratt and D. N. Nicolaïdes, *J.C.S. Chem. Comm.* 1014 (1972); K. P. C. Vollhardt and R. G. Bergman, *J. Amer. Chem. Soc.*, **95**, 7538 (1973).

[7] P. J. Garratt and K. P. C. Vollhardt, *J. Amer. Chem. Soc.*, **94**, 1022 (1972).

[8] R. Breslow, W. Washburn and R. C. Bergman, *J. Amer. Chem. Soc.*, **91**, 196 (1969); R. Breslow and W. Washburn, *J. Amer. Chem. Soc.*, **92**, 427 (1970).

The decomposition of a molecule in fragments was used extensively in Hoffmann's group, as for example in their elegant paper concerning bonding capabilities of transition metal carbonyl fragments.[9]

DISCUSSION OF THE RESULTS

Before proceeding to discuss details of our results, let us briefly resume some relevant aspects regarding the electronic structures of the five-membered heterocyclic molecule (**1**), having one heteroatom.

The three occupied MO's can be divided into two groups. The first two levels "take up" the heteroatom, while the third level has no heteroatom. Essentially the wave functions are resulted from the MO's of butadiene. Thus, the first MO is the in-phase combination of the lowest occupied MO of butadiene with the p_z orbital of the heteroatom, while the second one is the out-phase combination of the same orbitals. The third occupied MO of the heterocyclic system is the butadiene highest occupied MO. The visualization of this recapitulation is presented in fig. 1. The radii of circles are proportional with the magnitude of the respective atom coefficient. Here they represent the MO's of furan, those of pyrrole follow the same pattern, while in thiophene the sulphur has a greater coefficient in $\varphi_2(0.91)$ than in $\varphi_1(0.38)$.

The analysis of electronic structure is aided substantially if the structure has symmetry elements, since in these situations one could

Fig5

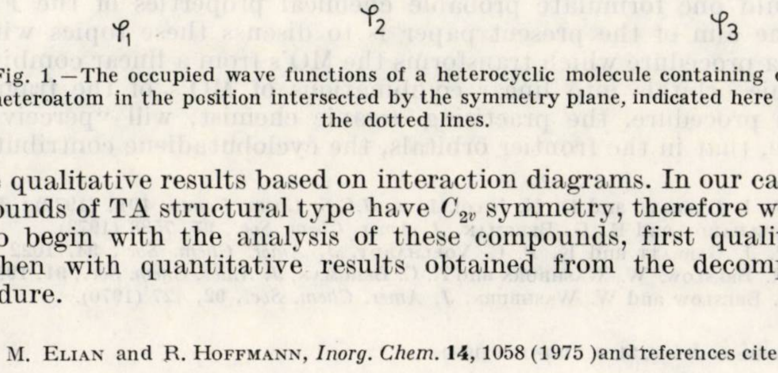

Fig. 1.—The occupied wave functions of a heterocyclic molecule containing one heteroatom in the position intersected by the symmetry plane, indicated here by the dotted lines.

derive qualitative results based on interaction diagrams. In our case, only compounds of TA structural type have C_{2v} symmetry, therefore we would like to begin with the analysis of these compounds, first qualitatively and then with quantitative results obtained from the decomposition procedure.

---

[9] M. Elian and R. Hoffmann, *Inorg. Chem.* **14**, 1058 (1975)and references cited therein.

FHC OF STRUCTURAL TYPE 2

We would like to trace the origin of the four occupied MO's of FHC in terms of two alternative partition's : (*a*) one ethylene fragment and a five-membered heterocyclic ring or (*b*) a dimethylenecyclobutene and the heteroatom. More precisely such a treatment could be viewed as a perturbation between the two fragments, giving rise to the molecular orbital of the FHC.

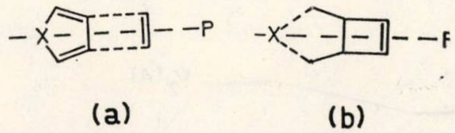

Fig. 2.—Specific partition for a FHC of structural type **2**.

Let us illustrate this discussion for the oxygen heteroatom, **X = O.**

The MO's of the fragments are classified according to their symmetry in respect to the plane *P* (see fig. 2) in both partitions.

For partition *a*, the interaction diagram only for the occupied MO's is presented in Fig. 3.

It is considered, and the numerical results confirm, that the φ_1 MO of FHC is essentially the φ_1 MO of furan. The symmetric φ_2 MO interacts with the bonding orbital of ethylene giving rise to the HOMO of FHC, which therefore has an *S* symmetry, while the subjacent MO is antisymmetric, by virtue of the antibonding φ_E^* MO mixing in the φ_3. While the φ_E contribution will strengthen the respective double bond, the φ_E^* mixing will weaken the same bond. Thus the double bond from the cyclobutadiene part of the molecule, which is not involved in the condensation, has a reduced bond order (relative to the same bond in the SA isomer or benzocyclobutadiene), and therefore is longer than a normal double bond

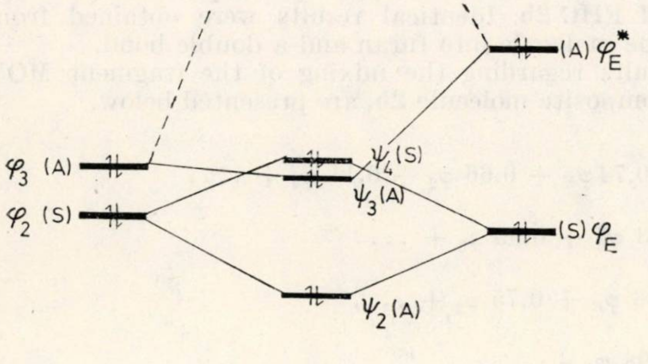

Fig. 3.— Interaction diagram to build up occupied MO's of the molecule **2b**, ψ_i, from MO's of furane, φ_i, and ethylene φ_E.

This effect of bond relaxation will probably reduce partly the strain of the four-membered ring, stabilizing the system.

A qualitative inspection of the second partition *b* (dimethylenecyclobutene and oxygen) shows that the HOMO and subjacent MO's derived from the corresponding orbitals of dimethylenecyclobutene do not contain the heteroatom, while the oxygen participates only in the innermost two MO's of FHC-**2b**. Identical results were obtained from the first partition of the molecule into furan and a double bond.

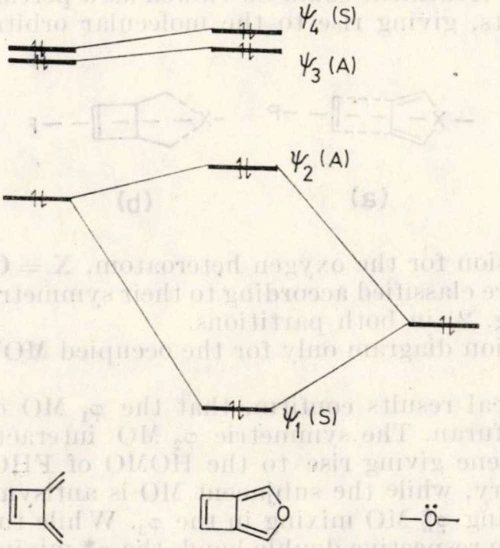

Fig. 4. — Interaction diagram to build up occupied MO's of molecule **2b** from dimethylenecyclobutene and oxygen.

Quantitative results regarding the mixing of the fragment MO's into the MO's of the composite molecule **2b**, are presented below.

Partition (*a*):

$$\Psi_4 = -0.74\varphi_E + 0.66\ \varphi_2 + 0.11\ \varphi_4 + \ldots$$

$$\Psi_3 = 0.13\ \varphi_E^* + 0.99\ \varphi_3 + \ldots$$

$$\Psi_2 = 0.66\ \varphi_E + 0.75\ \varphi_2 + \ldots$$

$$\Psi_1 = 0.998\ \varphi_1 + \ldots$$

Partition (*b*):

$$\Psi_4 = 0.95\ \pi_3 - 0.25\ p_{\ddot{O}} - 0.13\ \pi_5^*$$

$$\Psi_3 = 0.999\ \pi_2 + \ldots$$

$$\Psi_2 = 0.92\ \pi_1 - 0.18\ \pi_3 + 0.33\ p_{\ddot{O}} + \ldots$$

$$\Psi_1 = 0.88\ p_{\ddot{O}} + 0.38\ \pi_1 + 0.23\ \pi_3 + 0.19\ \pi_5^* + \ldots$$

For partition (*a*), the HOMO consists mainly of the ethylene HOMO and the subjacent MO of furan. This is the reason why we believe that the frontier orbitals act like destabilized double bonds. The same conclusion is reached from the second partition (*b*), where in the HOMO, the decisive participation is that of π_3 from dimethylenecyclobutene, in which (cf. fig. 4), the coefficients belonging to the ring double bond are the greatest (0.57). A computer-generated cross-section in the frontier MO's of **2b** at 2.5 A above the molecular plane is presented in fig. 5.

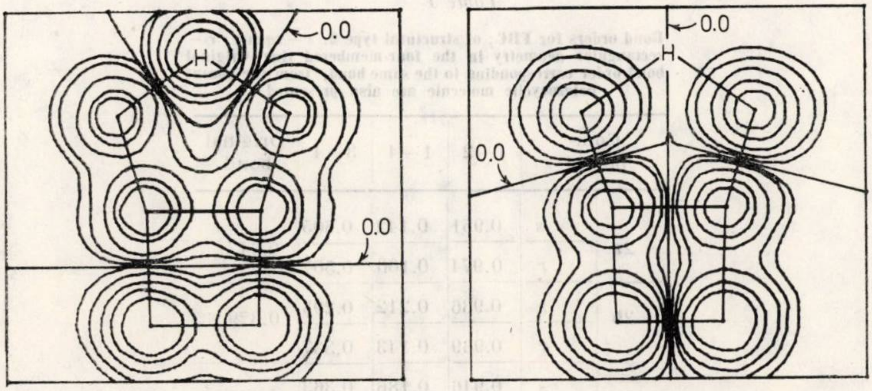

(a) HOMO (b) LUMO

Fig. 5. — Cross-section at 2.5Å above the molecular plane, in the frontier orbitals of **2b**. The heteroatom position is marked by "H". Contour lines, from outside to inside correspond to the following wave functions value : 0.13, 0.07, 0.02, 0.012, 0.006. Missing contour lines correspond to 0.006 and 0.012. The plott was generated with a Hewlett Packard 9862A Calculator Plotter.

As it is seen from both partitions, the HOMO is again (as for six-membered ring heterocyclic cyclobutadienes) mainly located on the double bond not involved in the condensation of the four membered ring. Therefore for HOMO-controlled reactions, this part of the molecule will be involved. Indeed, this conclusion is supported by experimental findings such as the dimerization and the Diels-Alder reaction.

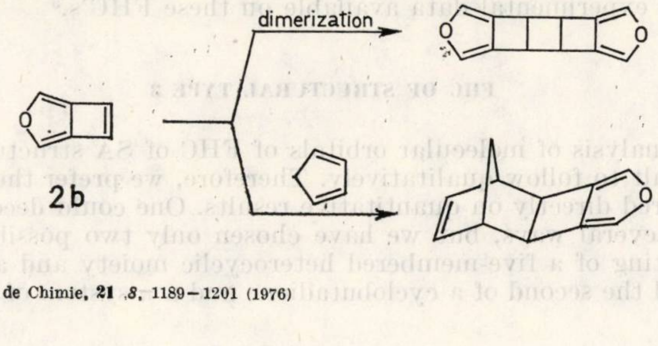

The 2 + 2 dimerization is probably a nonconcerted process, since it violates the $2a + 2s$ condition, the HOMO possessing a suprafacial symmetry.

Table 1 presents the bond orders for the four-membered ring of the molecule, considering two geometries. The square geometry for the FHC was obtained attaching a double bond at 1.35 A to a heterocyclic molecule; the rectangular geometry was considered at 1.53 A between the double bond and the side of the heterocyclic compound.

Table 1

Bond orders for FHC: of structural type 2. ***s*** **– square;** ***r*** **– rectangular geometry in the four-membered ring. Original bond order corresponding to the same bond, from the parent heterocyclic molecule are also presented**

Compound		1−2	1−4	3−4	Original bond
2a	*s*	0.951	0.142	0.605	0.647
	r	0.974	0.100	0.507	
2b	*s*	0.936	0.212	0.298	0.379
	r	0.969	0.143	0.337	
2c	*s*	0.946	0.186	0.363	0.447
	r	0.974	0.124	0.405	
2d	*s*	0.916	0.260	0.194	0.269
	r	0.959	0.177	0.230	

As a general trend one should note (*i*) a low bond order for the 1−4 and 2−3 bonds meaning a lack in the tendency of delocalization, (*ii*) the 3−4 bond order is lower than the corresponding bond from the heterocyclic molecule meaning an "avoiding" of a cyclobutadiene π-structure, at the expense of the π-system of the heterocycle.

Next, we would like to define an energetic stabilization index as the difference between the total energy of FHC (E_{tot}) and the energies of the two isolated fragments ($E_{hetero} + E_{ethylene}$). The result is that the most stable system is obtained for X = S(**2d**), while the FHC with X = = NR (**2c**) represents the least stable system. This point of view is supported by the experimental data available on these FHC's.[5]

FHC OF STRUCTURAL TYPE 3

The analysis of molecular orbitals of FHC of SA structural type is more difficult to follow qualitatively. Therefore, we prefer the discussion to be centered directly on quantitative results. One could decompose the system in several ways, but we have chosen only two possibilities, the first consisting of a five-membered heterocyclic moiety and an ethylene moiety, and the second of a cyclobutadiene and a π-system of vinyl derivative (ether, thioether, enamine). In all cases the fragments are suposed to have the same geometry as they have in the parent FHC.

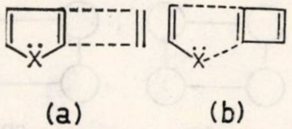

As for the previous discussion the conclusions are convergent, both partitions lead to the same qualitative result, but some features are better visualized in partition **a**, while partition **b** serves to evidence other facets.

It seems that the FHC is better expressed by the **a** type partitions, therefore we shall begin our discussion with this partition. The result of the decomposition is:

$$\Psi_4 = 0.549\ \varphi_E + 0.803\ \varphi_3 \ - 0.226\ \varphi_2\ + \ldots .$$

$$\Psi_3 = 0.457\ \varphi_E - 0.517\ \varphi_3 \ - 0.721\ \varphi_2\ + \ldots .$$

$$\Psi_2 = 0.695\ \varphi_E - 0.297\ \varphi_3 \ + 0.653\ \varphi_2\ + \ldots .$$

$$\Psi_1 = 0.997\ \varphi_1 + \ldots .$$

Our main concern is the frontier occupied orbital, φ_4, which is composed mainly from an in-phase interaction among φ_E and the furan HOMO φ_3. As it seen from fig. 6 which represents a computer-generated diagram, obtained by sectioning the Ψ_4 at the height of 2.5 A, this MO is reminding of the highest occupied MO of cyclobutadiene (φ_2^{CB}).

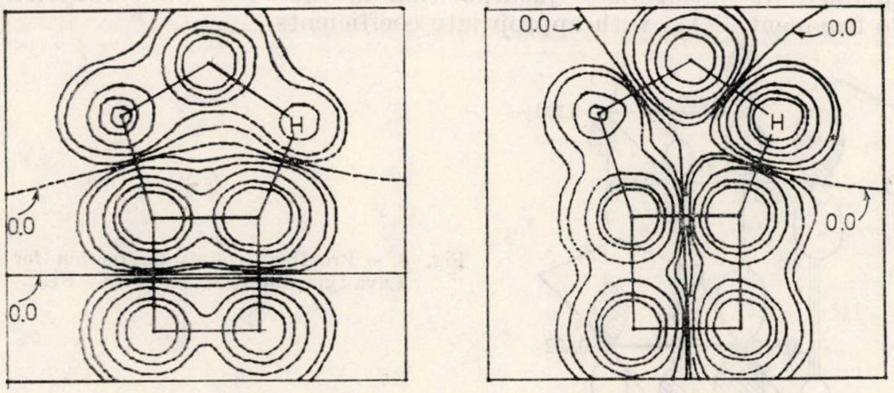

(a) HOMO (b) LUMO

Fig. 6. — Cross-section at 2.5Å above the molecular plane, in the frontier orbitals of **3b**. The plot was generated with a Hewlett Packard 9862A Calculator Plotter.

Therefore we expect again a high reactivity to be located in the four-membered ring, in which the most accessible is the double bond not involved in the condensation, the second one being more or less part of an aromatic system.

Also it is easy to recognize the first occupied MO of cyclobutadiene (φ_1^{CB}) in the Ψ_2 MO of FHC. It is thus interesting to note that the two cyclobutadienic occupied MO's are intercalated between two other orbitals, the latter belonging essentially to the furan fragment.

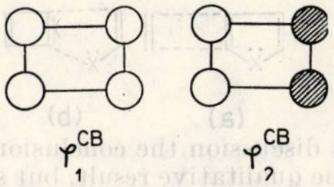

Fig. 7. — π-Molecular orbitals of cyclobutadiene.

Such a view is better expressed in the second partition :

$$\Psi_4 = 0.887\ \varphi_2^{CB} + 0.339\ \varphi_2 + 0.211\ \varphi_1 + \dots\dots$$

$$\Psi_3 = 0.259\ \varphi_1^{CB} + 0.387\ \varphi_2^{CB} + 0.855\ \varphi_2 + \dots\dots$$

$$\Psi_2 = 0.908\ \varphi_1^{CB} - 0.260\ \varphi_1 + 0.283\ \varphi_2 + \dots\dots$$

$$\Psi_1 = 0.933\ \varphi_1 + \dots\dots$$

in which is seen that in Ψ_4 and Ψ_2 participate heavily φ_2^{CB} and φ_1^{CB} respectively.

The decomposition in fragments of **a**-type serves also to explain a minor aspect, but quite puzzling, namely the very small value of coefficients in Ψ_4 for oxygen, for C_3 in Ψ_3 and for C_6 in Ψ_2. Essentially this fact is explained by out-of-phase justaposition in the total wave function of two fragment MO's, with appropriate coefficients.

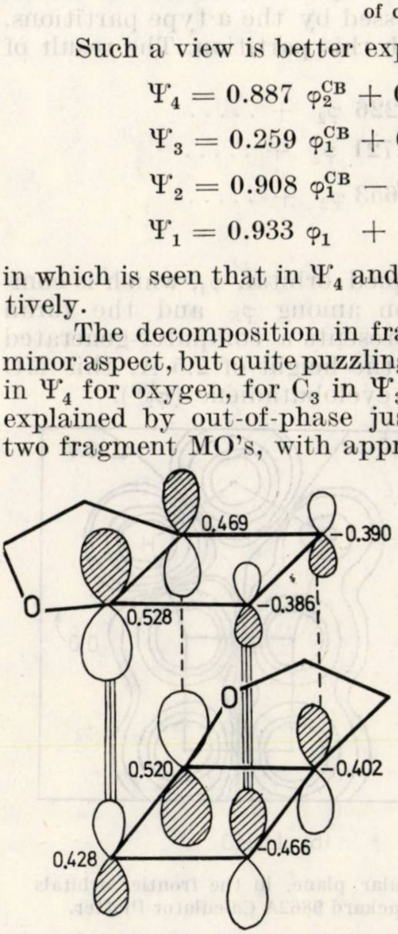

Fig. 8. — Frontier orbitals interaction for the Cava-type dimerization of SA—FHC.

Since it is expected that FHC's of type **3** are very reactive, it would be interesting to speculate some presumable reactions. We think that a Cava-type dimerization is still an allowed process of $4\pi + 2\pi$ mode, as it was shown for benzocyclobutadiene.[10] This dimerization is visualized in fig. 8, where by full lines are represented the newly developed bonds while the dotted lines represent secondary interactions, responsible for the *endo* approach of the molecules.

---

[10] M. D. Gheorghiu and M. Avram, *Rev. Roumaine Chim.*, **12**, 1063 (1967).

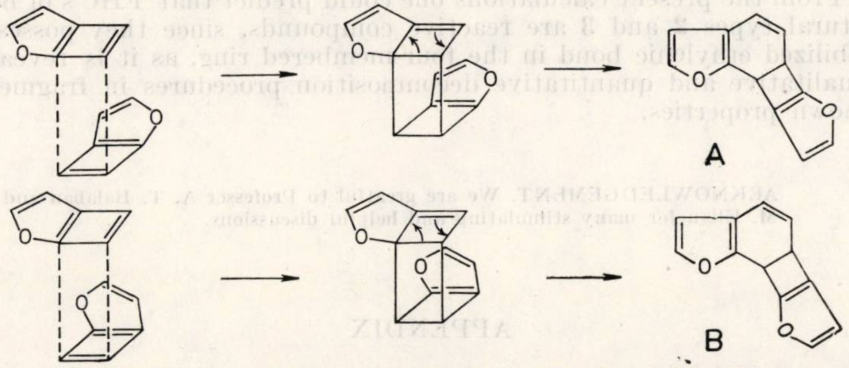

Fig. 9.—Cycloaddition modes for the dimerization of SA-FHC.

There are two possibilities in the orientation of the furan rings in the Cava-type dimerization (see fig. 9). Based on the Houk's rule[11] for regiospecificity in four-center cycloadditions, the most favourable approach is that in which interacting atoms possess both the highest coefficient in their fragment MO's. In our case, one predicts the predominant formation of dimer **A**.

Table 2

Bond orders for FHC of structural type 3*

Compound		1 – 2	3 – 4	Original bond	1 – 4	2 – 3
3a	*r*	0.974	0.507	0.647	0.507	0.100
	s	0.951	0.605		0.605	0.142
3b	*r*	0.995	0.839	0.854	0.025	0.029
	s	0.988	0.823		0.045	0.038
3c	*r*	0.997	0.892	0.901	0.025	0.010
	s	0.993	0.882		0.037	0.015
3d	*r*	0.997	0.955	0.959	0.020	0.025
	s	0.997	0.957		0.029	0.017

* *r* – rectangular geometry; *s* – square geometry; the original bond order means the bond order of the same bond in the parent heterocycle.

The bond orders, presented in Table 2, for both rectangular and square geometry for the cyclobutadiene, reveal a strong localization of the π electrons on bonds 1–2 and 3–4.

---

[11] K. N. Houk, J. Sims, C. R. Watts and L. J. Luskus, *J. Amer. Chem. Soc.*, 95 7301 (1973).

CONCLUDING REMARKS

From the present calculations one could predict that FHC's of both structural types **2** and **3** are reactive compounds, since they possess a destabilized ethylenic bond in the four-membered ring, as it is revealed by qualitative and quantitative decomposition procedures in fragments of known properties.

ACKNOWLEDGEMENT. We are greatful to Professor A. T. Balaban and Dr. M. Elian for many stimulating and helpful discussions.

APPENDIX

The π-electron SCF secular equation 1 was solved in the assumption of zero differential overlap.[12]

$$|F_{ij} - E \cdot \delta_{ij}| = 0 \tag{1}$$

F_{ij} is the matrix element of Fock operator, given by

$$F_{ii} = W_i + 0.5\ P_{ii}\ \langle ii|ii\rangle + \sum_{j\neq i}(P_{jj} - Z_j)\ \langle ii|jj\rangle \tag{2}$$

$$F_{ij} = \beta_{ij} - 0.5\ P_{ij}\ \langle ii|jj\rangle \tag{3}$$

where

W_i	is the valence state ionization potential
P_{ij}	the elements of the charge and bond order matrix
$\langle ii\mid jj\rangle$	the repulsion integrals
Z_j	the effective nuclear charge
β_{ij}	the resonance integrals

The valence state ionization potentials[13,14] were taken as equal with −11.16 eV for C, −28.58 eV for $\ddot{\mathrm{N}}$, −33.9 eV for $\ddot{\mathrm{O}}$, −23.74 eV for $\ddot{\mathrm{S}}$.

The monocentric repulsion integrals $\langle ii|ii\rangle$ were considered[13,14] as follows: 10.88 eV for $\dot{\mathrm{C}}$, 14.47 eV for $\ddot{\mathrm{N}}$, 16.20 eV for $\ddot{\mathrm{O}}$ and 12.05 eV for $\ddot{\mathrm{S}}$.

The two-center electronic repulsion integrals $\langle ii|jj\rangle$ were determined for $r \geqslant 2.80$ A from the uniformly charged sphere model formula[12]:

$$\langle ii|jj\rangle = (7.1975/\mathrm{r})\ ((1 + (1/2\mathrm{r})^2\ (R_i - R_j)^2)^{0.5} +$$

$$(1+(1/2r)^2\ (R_i + R_j)^2)^{-0.5})\ \mathrm{eV} \tag{4}$$

---

[12] J. A. Pople, *Trans. Faraday Soc.*, **49**, 1375 (1953); R. Pariser and R. G. Parr, *J. Chem. Phys.*, **21**, 466, 767 (1953).

[13] M. Bossa, *J. Chem. Soc. D*, **1969**, 1182; M. Bossa, A. Sgamallotti, F. A. G. Gianturco, *J. Chem. Soc. D*, **1969**, 743.

[14] M. J. Dewar, ''The Molecular Orbital Theory of Organic Chemistry'', McGeaw-Hill, New York, 1969, p. 380.

in which $R_i = (4.597/Z_i)$ Å; for $r < 2.80$ Å, the integrals $\langle ii|jj\rangle$ were determined by extrapolation down to $r = 0$ by use of an equation of the form

$$ar + br^2 = 0.5\,(\langle ii|ii\rangle + \langle jj|jj\rangle) - \langle ii|jj\rangle \tag{5}$$

in which the constants a and b were obtained by fitting values calculated from eq. 4 for $r = 2.80$ and 3.70 Å.

The resonance integrals were calculated according to Flurry[15]

$$\beta_{ij} = ((2 - S_{ij})\,S_{ij}/(2 - S_{ij}))\,(W_i \cdot W_j)^{0.5} \tag{6}$$

where the overlap integral is approximated by

$$S_{ij} = A \cdot (0.5\,Z_{eff}R_{ij})^B \cdot \exp(C \cdot Z_{eff} \cdot R_{ij}) \tag{7}$$

taking $A = 3.503$; $B = 1.1526$ and $C = -0.7946$; R_{ij} is the distance between atoms "i" and "j", while Z_{eff} was considered as $0.5\,(Z_i + Z_j)$. The following Z_i were used[16]; 3.25 for $\dot{\mathrm{C}}$, 3.90 for $\ddot{\mathrm{N}}$, 4.55 for $\ddot{\mathrm{O}}$ and 5.45 for $\ddot{\mathrm{S}}$.

Calculations were carried out in double precision using programs written in BASIC for HP 9830 A computer.

---

[15] R. L. Flurry, Jr. and J. J. Bell, *J. Amer. Chem. Soc.*, **89**, 525 (1967).

[16] F. Momicchioli and G. DelRe, *J. Chem. Soc. B*, **1969**, 674.

Revue Roumaine de Chimie, **21**, *8*, 1203–1206 (1976)

BICYCLIC BRIDGEHEAD NITROGEN SYSTEMS. V
PYRAZOLO- AND TETRAZOLO- BENZOCINNOLINES BY 1,3-DIPOLAR CYCLOADDITION REACTIONS

EUGENIA CARP, MARIA DORNEANU and ION ZUGRĂVESCU
Department of Organic Chemistry, Polytechnic Institute, Iassy

Received February 6, 1975

The synthesis of benzo[c]pyrazolo [1.2a] cinnolines and benzo[c]tetrazolo [1.2a]cinnolines by 1,3-dipolar cycloaddition reactions between diethyl acetylenedicarboxylate and diethyl azodicarboxylate as dipolarophiles and the ylides generated *in situ* from N-(carbethoxymethyl)-benzo-cinnolinium bromides, as 1,3-dipoles, are reported.

1,3-Dipolar cycloadditions have proved extremely useful in the synthesis of bicyclic bridgehead systems.[1-2] In order to illustrate the potential of the benzo[c]cinnoline system as a starting product for obtaining such structures, we reported in our previous paper [3-5] the formation of benzocinnolinium ylides and we have investigated their cycloaddition reactions with dipolarophiles.

The present study is concerned with the synthesis of benzo[c]pyrazolo[1.2a]cinnoline (IVa, b) and benzo[c] tetrazolo [1.2a] cinnoline (Va, Vb) systems and describes the course of the reaction between N-(carbethoxymethyl)-benzo[c]cinnolinium bromide (IIa, IIb), via related ylides, with diethyl acetylenedicarboxylate and diethyl azodicarboxylate. In order to make these [3 + 2] cycloaddition reactions, the corresponding ylides were prepared from benzo[c]cinnoline by the "salt method". Thus, the quaternization of benzocinnoline and 3,8-dimethylbenzocinnoline was carried out with ethyl bromoacetate in dimethylformamide (DMFA) as solvent, resulting the quaternary salts (IIa, IIb) in moderate yields.

The conversion of IIa and IIb into related ylides (III ; R = H and CH_3, respectively) has produced by treatment of the salts with triethylamine in methylene chloride, when the ylides were generated *in situ* (the change of the colour of the solution) ; these ylides, in anhydrous solvent, can be trapped by dipolarophiles. In the benzocinnoline series the carbethoxymethylides III (R = H ; R = CH_3) are very unstable and could not be isolated, in contrast with dicyanomethylides which are quite stable compounds.[5]

---

[1] R. Huisgen, *Angew. Chem. Internat. Edn.*, **2**, 565, 633 (1963).

[2] D. G. Farnum, R. J. Alaimo and J. M. Dunston, *J. Org. Chem.*, **32**, 1130 (1967).

[3] E. Carp, M. Dorneanu and I. Zugrăvescu, *Anal. Sti. Univ. "Al. I. Cuza" Iași, Sect I*, **14**, 169 (1968).

[4] M. Dorneanu, E. Carp and I. Zugrăvescu, *Anal. Sti. Univ. "Al. I. Cuza" Iași, Sect I*, **19**, 223 (1973) ; sect I, **20**, 35 (1974).

[5] E. Carp, M. Dorneanu and I. Zugrăvescu, *Rev. Roumaine Chim.*, **19**, 9, 1507 (1974).

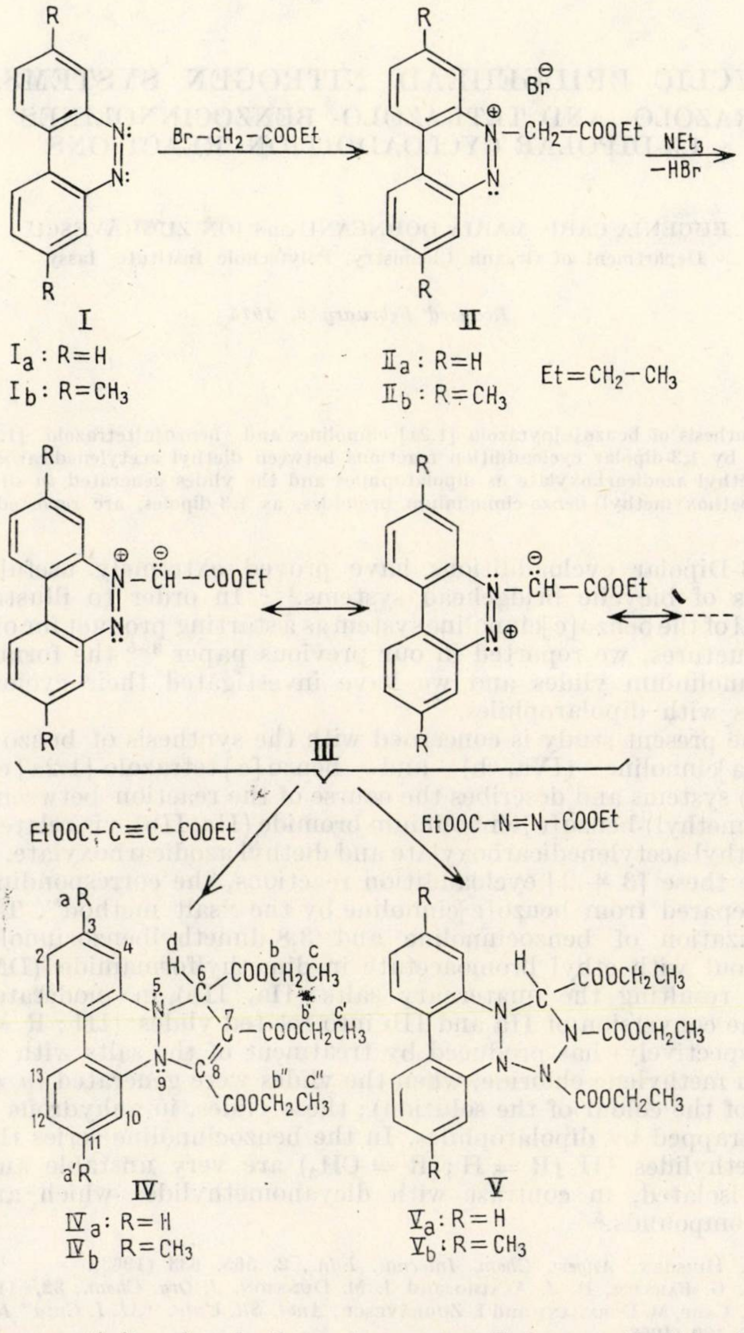
R
N:
N:
R
Br−CH₂−COOEt
R
Br⊖
N⊕−CH₂−COOEt
N
R
NEt₃
−HBr
I
Ia : R=H
Ib : R=CH₃
II
IIa : R=H
IIb : R=CH₃
Et=CH₂−CH₃
R
N⊕−CH⊖−COOEt
N
R
R
N
CH⊖−COOEt
N⊕
R
III
EtOOC−C≡C−COOEt
EtOOC−N=N−COOEt
aR
3
4
2
1
d
H
6
C
b c
COOCH₂CH₃
5
N
7
C−COOCH₂CH₃
b' c'
N
C 8
9
b" c"
COOCH₂CH₃
13
12
10
11
aR
IV
IVa : R=H
IVb : R=CH₃
R
H
C
COOCH₂CH₃
N
N−COOCH₂CH₃
N
N
COOCH₂CH₃
R
V
Va : R=H
Vb : R=CH₃

The reactivity of carbethoxy-benzocinnolinium-methylides has been investigated by the reaction with diethyl acetylenedicarboxylate and diethyl azodicarboxylate, which proceeds with spontaneous cyclic adducts formation (IVa, IVb, Va and Vb). In basic medium (triethylamine), the salts II underwent dehydrohalogenation and the possible 1,3-dipole structure of the ylides III is responsible for the further cycloaddition reaction. Thus, the reaction with dipolarophiles occurs normally with the formation of the required bridgehead N—N systems. When equimolecular amounts of the salt II and diethyl acetylenedicarboxylate were treated with triethylamine, in anhydrous methylene chloride the benzo[c]pyrazolo [1.2a] cinnoline (IVa and IVb) were obtained; we have also synthetically established that the reaction of salts II with diethyl azodicarboxylate occurs in the same manner, leading to the benzo[c]tetrazolo[1.2a]cinnoline structures (Va and Vb, respectively), in spite of the fact that the nitogen bridge would be strongly disfavoured because of the low N—N bond energy. The formation of the expected [3 + 2] adducts from the above ylides may be regarded as a result of the generally accepted concerted 1,3-dipolar cycloaddition mechanism.

The IR and NMR spectra for these compounds provide confirmatory proof of structures; the evidence of spectral data will be described in experimental section.

EXPERIMENTAL

N-(Carbethoxymethyl)-benzo[c]cinnolinium bromide (I). A mixture of 1.8 g (0,01 mole) of benzocinnoline and 1.7 g (0.01 mole) of ethyl alfa-bromacetate in a minimum volume of DMFA (5ml) was kept at room temperature for four days. Then ethyl acetate was added to the reaction mixture when yellow needles was precipitated, filtered and recristalized from ethanol-ether. Light-yellow needles with m.p. 171°

Analysis : $C_{16}H_{15}N_2O_2Br$ *Calcd.* : C% 55.34; H% 4.35; N% 8.07
Found: C% 54.96; H% 4.58; N% 8.21
IR : $\nu_{C=O} = 1730\ \text{cm}^{-1}$; $\nu_{C-O-C} = 1220\ \text{cm}^{-1}$.

N-(Carbethoxymethyl)-3, 8-dimethylbenzo[c]cinnolinium bromide (II_b). 3, 8-Dimethylbenzocinnoline was prepared from 4,4′-dimethyl-2,2′-dinitrobiphenyl, which was reduced with lithium aluminium hydride in refluxing anhydrous ether-benzene, similarly Badger's procedure[6] (product I_b).

A 1 :1 mixture (0.01 mole) of I_b (2.08 g) and ethyl bromoacetate (1.7 g) was treated with 5 ml DMFA. The resulting suspension was allowed to stand at room temperature for three days, and then was precipitated with ethyl acetate. The collected product was recrystallized from ethanol-ether; yellow crystals, m.p. 181°.

Analysis : $C_{18}H_{19}O_2N_2Br$ *Calcd* : C% 57.60; H% 5.13; N% 7.46
Found : C% 57.24; H% 5.10; N% 7.52
IR(KBr) : $\nu_{C=O} = 1720\ \text{cm}^{-1}$; $\nu_{C-O-C} = 1210\ \text{cm}^{-1}$.

6, 7, 8-Tricarbethoxy-6H-benzo[c]pyrazolo[1.2a]cinnoline (IVa). To a solution of 2.30 g (0.006 mole) of the salt IIa and 1.20 g (0.006 mole) of diethyl acetylenedicarboxylate in 50 ml of methylene chloride was added dropwise 0.8 ml of triethylamine. The mixture reaction was boiled under reflux for two hr. and then kept at room temperature for two days. The solution was washed with water, dried over anhydrous natrium sulphate and the solvent was removed *in vacuo*. The residue was recrystallized twice from absolute ethanol affording the orange crystalline adduct, m.p. 117°.

Analysis : $C_{24}H_{24}N_2O_6$ *Calcd.* : C% 66.04; H% 5.54; N% 6.42
Found : C% 65.97; H% 5.74; N% 6.32
IR(KBr) : $\nu_{C=O} = 1670,\ 1730\ \text{cm}^{-1}$; $\nu_{C-O-C} = 1205,\ 1245\ \text{cm}^{-1}$;
$\nu_{CH(6)} = 1365\ \text{cm}^{-1}$.

---

[6] G. M. Badger, J. H. Seidler and B. Thompson, *J. Chem. Soc.*, **1951**, 3211.

NMR($CDCl_3$) : $\delta = 1.27$ ppm (3Hc, triplet), $\delta = 1.32$ ppm (3Hc′, triplet), $\delta = 1.38$ ppm (3Hc″, triplet) ; $\delta = 4.19$ ppm (2Hb, quartet), $\delta = 4.31$ ppm (2Hb′, quartet), $\delta = 4.43$ ppm (2Hb″, quartet) ; $\delta = 5.47$ ppm (1Hd, singlet) ; $\delta = 6.80 - 7.60$ ppm (aromatic multiplet).

6, 7, 8-Tricarbethoxy-6H-3,11-dimethylbenzo[c]pyrazolo[1.2a]cinnoline(IV b). The 1, 3-dipolar addition was carried out in the same way as for the cycloadduct IVa, using 1.25 g of the salt IIb and 0.6 g of diethyl acetylenedicarboxylate in 30 ml of methylene chloride, by addition dropwise 0.4 ml of triethylamine. The crude product was recrystallized from absolute ethanol to give a crystalline yellow compound with m.p. 103°.

Analysis : $C_{26}H_{28}N_2O_6$ *Calcd* : C% 67.22 ; H% 6.07 ; N% 6.03
Found : C% 67.40 ; H% 5.67 ; N% 5.91

IR(KBr) : $\nu_{C=O} = 1730$ cm^{-1}; $\nu_{C-O-C} = 1220$, 1270 cm^{-1};
$\nu_{CH(6)} = 1380$ cm^{-1}.

NMR ($CDCl_3$) : $\delta = 2.27$ ppm (3Ha, singlet), $\delta = 2.35$ ppm (3Ha′, singlet).
$\delta = 1.28$ ppm (3Hc, triplet), $\delta = 1.35$ ppm (3Hc′, triplet),
$\delta = 1.42$ ppm (3Hc″, triplet) ; $\delta = 5.50$ ppm (1Hd, singlet) ;
$\delta = 6.70 - 7.50$ ppm (6H aromatic multiplet).

6, 7, 8- Tricarbethoxy-6H- benzo[c]tetrazolo[1.2a]cinnoline (Va). The adduct with diethyl azodicarboxylate was prepared from 1.16 g salt II a, 0.58 g diethyl azodicarboxylate and 0,4 ml triethylamine in 50 ml methylene chloride, in the same manner as for the above cycloadducts. Recrystallization from ethanol gave white needles, m.p. 120°.

Analysis : $C_{22}H_{24}N_4O_6$ *Calcd.* : C% 59.99 ; H% 5.49 ; N% 12.72
Found : C% 60.07 ; H% 5.45 ; N% 12.83

IR(KBr) : $\nu_{C=O}$ 1710, 1735 cm^{-1}; $\nu_{C-O-C} = 1160$, 1225 cm^{-1};
$\nu_{CH(6)} = 1300$ cm^{-1}.

NMR ($CDCl_3$) : $\delta = 1.17$ ppm (3Hc, triplet), $\delta = 1,25$ ppm (3Hc′, triplet).
$\delta = 1.35$ ppm (3Hc″, triplet) ; $\delta = 4.07$ ppm (2Hb, quartet), $\delta = 4.21$ ppm (2Hb′, quartet), $\delta = 4.32$ ppm (2Hb″, quartet) ; $\delta = 7.0 - 7.7$ ppm (6H aromatic multiplet).

6, 7, 8-Tricarbethoxy-6H-3,11-dimethylbenzo[c]tetrazolo[1.2a] cinnoline (Vb). Similarly with the above procedure was obtained this cycloadduct from 1.25 g of the salt IIb, ethyl azodicarboxylate (0.58 g) and triethylamine (0.4 ml) in methylene chloride. The crude product was recrystallized from ethanol ; white crystals, m.p. 123°.

Analysis : $C_{24}H_{28}N_4O_6$ *Calcd.* : C% 61.52 ; H% 6.02 ; N% 11.95
Found : C% 61.74 ; H% 6.22 ; N% 11.74

IR(KBr) : $\nu_{C=O} = 1700$ cm^{-1}; $\nu_{C-O-C} = 1150$, 1240 cm^{-1};
$\nu_{CH(6)} = 1300$ cm^{-1}.

NMR ($CDCl_3$) : $\delta = 2.35$ ppm (3Ha, a′, singlet) ; $\delta = 1.17$ ppm (3Hc, triplet), $\delta = 1.25$ ppm (3Hc′, triplet), $\delta = 1.32$ ppm (3Hc″, triplet) ; $\delta = 4.05$ ppm (2Hb, quartet) $\delta = 4.17$ ppm (2Hb′, quartet), $\delta = 4.26$ ppm (2Hb″, q) ; $\delta = 6.28$ ppm (1Hd, singlet) ; $\delta = 6.90 - 7.70$ ppm (aromatic multiplet).

ACKNOWLEDGMENTS. We express our thanks to dr. V. Bărboi and dr. I. Druţă for determinations and interpretation of the NMR spectra.

Revue Roumaine de Chimie, 21, 8, 1207–1219 (1976)

INFRARED SPECTRA OF SOME NEW CHROMANONE AND COUMARINE DERIVATIVES

LIVIU VALENTIN FEYNS, ION ILIE DRAGOTĂ and ION NICULESCU-DUVĂZ
Oncological Institute, Bd. 1 Mai 11, Bucharest, Romania

Received December 16, 1974

The infrared spectra of some new chromanone and coumarine derivatives were examined and characteristic absorption bands were assigned to ketone and lactone carbonyl vibrations, aromatic and heterocyclic rings and to the hydroxy- and *gem*-dimethyl-substituents.

In an attempt to find new carrier structures for the cytotoxic functions, a series of chromanone and coumarine urethane-type nitrogen mustards has been synthesized (I–IV, VII, IX).[1]

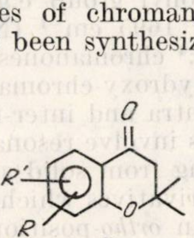
I

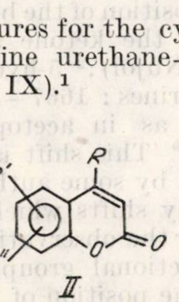
II

$R,R' = OH, OCON(CH_2CH_2Cl)_2$

$R = H, CH_3$

$R',R'' = CH_3, OH, OCON(CH_2CH_2Cl)_2$

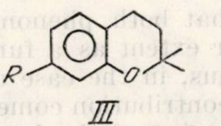
III

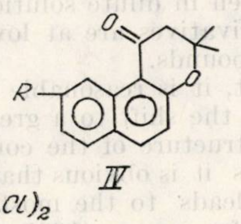
IV

$R = OH, OCON(CH_2CH_2Cl)_2$

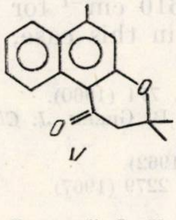
V

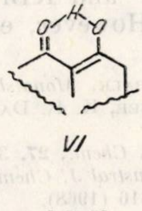
VI

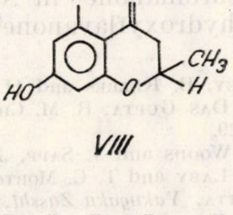
VIII

---

[1] I. I. Dragotă, L. V. Feyns and I. Niculescu-Duvăz, *Rev. Roumaine Chim.*, **20**, 665 (1975).

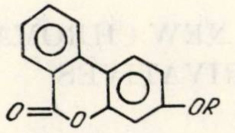

VII

R=OH, OCON (CH$_2$CH$_2$Cl)

R=H, CH$_3$

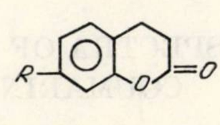

IX

In the present paper, some characteristic infrared absorption bands of these new compounds and of their intermediates are examined. The spectra of the related compounds V and VIII were also included.

The basic work on the characteristic infrared frequencies of benzopyranes was carried out on flavones, whose ir spectra were widely used for structural assignments.

The most carefully examined region was that of the $\nu_{C=O}$ frequency, particular attention being given to the influence of substituents on the position of this band. Methoxy- and hydroxy-substitution, especially in 5- and/or 7-position of the benzene ring lowers up to 70 cm^{-1} the absorption frequency of the ketone and lactone carbonyl group e.g. coumarine: 1730 cm^{-1} (Nujol);[2] 5-hydroxy-coumarine: 1695 cm^{-1} (Nujol);[3] 7-hydroxy-coumarines: 1667–1686 cm^{-1} (KBr);[4] chromanones: 1680–1690 cm^{-1} (same as in acetophenones)[5-9]; 5-hydroxy-chromanones: under 1640 cm^{-1}.[5-9] This shift is accounted for intra and inter-molecular hydrogen bonds by some authors,[3] while others involve resonance effects.[8,9] The frequency shifts which occur on passing from solid state to dilute solutions and the observation that in the derivatives which have H-bond acceptor functional groups (acetyl, nitro) in *ortho*-position against the OH-group, the position of the $\nu_{C=O}$ band lies close to that of the unsubstituted compound,[5] support the first hypothesis. The conjugation contribution is supported by the effects of the methoxy-substitution and by the fact that even in dilute solutions, the maxima of the $\nu_{C=O}$ bands in the hydroxy-derivatives are at lower frequencies than in the unsubstituted parent compounds.

In fact, it is reasonable to assume that both phenomena are responsible for the shift to a greater or lesser extent as a function of the particular structure of the compounds. Thus, in the case of 5-hydroxychromanones it is obvious that the major contribution comes from chelation which leads to the most marked lowering of the ketone carbonyl absorption frequency (1635 and 1637 cm^{-1} for 2,2-di-methyl-5,7-dihydroxy-4-chromanone in Nujol[6] and KBr;[7] 1610 cm^{-1} for 3′,4′,7-trimethoxy-5-hydroxyflavanone[8]). However, even in this case, both phe-

[2] V. Prey, B. Kerres and H. Berbalk, *Monatsh.*, **91**, 774 (1960).

[3] A. K. Das Gupta, R. M. Chaterjee, K. R. Das and B. Green, *J. Chem. Soc. (C)*, **1969**, 29.

[4] L. L. Woods and J. Sapp, *J. Org. Chem.*, **27**, 3703 (1962).

[5] R. H. Laby and T. C. Morton, *Austral J. Chem.*, **20**, 2279 (1967).

[6] A. Nitta, *Yakugaku Zasshi*, **88**, 816 (1968).

[7] H. B. Bhat and K. Venkataraman, *Tetrahedron*, **19**, 77 (1963).

[8] H. L. Hergert and E. F. Kurth, *J. Amer. Chem. Soc.*, **75**, 1622 (1953).

nomena can be brought together in a formula (VI) (conjugate chelation), first suggested in this class for 5-hydroxy-flavanone.[8,9]

Another effect of the conjugate chelation is that sometimes the position of the OH stretching frequency is difficult to define, the maxima being shifted to the C—H absorption range.

EXPERIMENTAL

The structure and purity of the compounds[1] were checked by tlc, uv and nmr spectroscopy and by elemental analysis.

The ir spectra were recorded on an UR-10 Carl Zeiss Jena spectrophotometer in KBr disks and in CCl_4, $CHCl_3$ and CS_2 solutions.

RESULTS AND DISCUSSION

CHROMANONE DERIVATIVES (I)

The main absorption bands are shown in Table 1.

The characteristic bands of the N,N-di(2-chlorethyl) carbamoyl moiety will be discussed in a further paper.

$\nu_{C=O}$ FREQUENCY

The effect of chelation could be pointed out (for the 5,7-dihydroxy-derivative, the band has the same position in KBr and in $CHCl_3$), as well as the marked contribution of the intermolecular hydrogen bonds (important shifts could be observed on passing from solid state to dilute solutions).

Carbamoylation of the hydroxyl group had the expected effect on the $\nu_{C=O}$ band, which returned to the usual range for alkyl-aryl-ketones (1674—1697 cm^{-1}).

ν_{O-H} FREQUENCY

In accordance with the previously mentioned data, these bands were found at unusually low frequency values (3130—3170 cm^{-1}). In solution, both free (about 3585 cm^{-1}) and hydrogen bonded (about 3250 cm^{-1}) absorptions could be pointed out. The relative intensities of these bands are a function of the solution concentration.

The following *aromatic characteristics bands*, were tabulated:

a) those occurring within the ranges 1600—1620 cm^{-1} and 1570—1580 cm^{-1}. As expected, due to the conjugation with the carbonyl group, one of these two bands (usually that of higher frequency) is one of the strongest bands in the spectrum (more intense than the carbonyl band in the hydroxy derivatives).

---

[9] B. L. Shaw and T. H. Simpson, *J. Chem. Soc.*, **1955**, 655.

Table

Infrared Spectra of Some

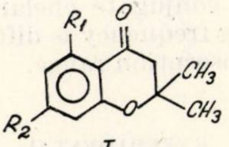

I

R_1	R_2		$\nu_{C=O}$		ν_{O-}	Aromatic		
			ketone	carbam.		I	II	Subst.
1	2	3	4	5	6	7	8	9
H	OH	KBr	1 630 1 643	—	3 133	1 613	1 577*	855s 876 m
		$CHCl_3$	1 675	—	3 274 3 586	1 617*	1 589	853 m 876 m
H	OCONM	KBr	1 696	1 710	—	1 614	1 582	868 m 884 s
		$CHCl_3$	1 691	1 729	—	1 616	1 583	852 w 879 m
		CCl_4	1 697	1 733	—	1 616	1 583	?
CH_3	OH	KBr	1 626 sh 1 636 sh	—	3 140	1 606	1 567*	886 m
		$CHCl_3$	1 672	—	3 270 3 589	1 612*	1 586	886 m
CH_3	OCONM	KBr	1 694	1 713	—	1 608	1 582	886 m
		$CHCl_3$	1 686	1 729	—	1 611	1 585	884 mw
OH	OH	KBr	1 644*[1]	—	3 154[1]	1 602[1]	1 582[1]	877 m
		$CHCl_3$	1 643	—	3 248 3 580	1 603 sh	1 595	?
OCONM	OCONM	CCl_4	1 695	1 742	—	1 623	1 583	884 m
		$CHCl_3$	1 691	1 731	—	1 622	1 582	883 mw
H	OCH_3	KBr	1 675	—	—	1 607*	1 575	841 s 871 mw
		$CHCl_3$	1 678	—	—	1 611	1 581	843 s 871 mw
		CCl_4	1 689	—	—	1 614*	1 582	859 mw 873 mw
		CS_2	1 691	—	—	1 620		845 s 861 m 878 mw
Compound R = OH	III	$CHCl_3$	—	—	3 439	1 606		850 mw 884 m
Compound R=OCONM	III	$CHCl_3$	—	1 727	—	1 619	1 592	857 m 879 m
Compound R=OH	IV	KBr	1 644	—	3 170	1 622*	1 604	866 m 889 s

1
New Chromanone Derivatives

$-OCONM= -OCON(CH_2CH_2Cl)_2$

Gem-dimethyl		Phenolic group		X-sens.	Ether		?
10	11	12	13	14	15	16	17
1 361	1 377	1 315s	1 173vs	825 m	1 258vs	1 138s 1 112s	1 391
?	1 376	1 324s	1 168s	825mw	1297vs 1 260s 1 233s	1 129s	1 391
1 368	1 378	—	—	—	1 266s 1 246vs 1 231s	1 142vs 1 119m	1 391
1 365sh	1 376	—	—	—	?	1 126s	1 392
1 365	1 375	—	—	—	1 233s	1 123s	1 390
1 355	1 377	1 333s	1 171vs	820mw	1 278vs	1 128mw	1 392
1 354	1 377	1 325vs	1 176vs	?	1 296vs	1 121ms 1 075ms	1 392
1 359	1 379	—	—	—	1 246s 1 283ms	1 142vs 1 087m 1 069m	1 392
1 369sh	1 376	—	—	—	1 285s	1 145vs 1 086m 1 071m	1 392
?	1 374^1	1 303vs	1 173vs	829ms	1 256ms	1 087^1	1 386
?	1 372	1 330s	1 165vs 1 150s	?	1 246s 1 280ms	1 089s	1 391
1 367sh	1 374	—	—	—	1 241ms	1 095s	1 394sh
1 366sh	1 374	—	—	—	?	1 099s	1 393sh
1 357	1 371	—	—	822m	1 301s 1 275s^2 1 259vs	1 161vs^2 1 124s 1 259vs	1 385
1 359	1 375	—	—	824m	1 291s 1 276vs^2 1 264ms	1 136ms^2 1 124s 1 163vs^2	1 390
1 358	1 377	—	—	826mw	1 290s 1 274vs^2 1 262s	1 138s^2 1 162vs^2 1 123s	1 389
1 362	1 378	—	—	829m	1 293vs 1 270vs^2	1 168vs^2 1 140s 1 128s	1 392
1 352	?	1 315s	1 152	846sh ?	1 245s	1 122vs	1 392
1 359	1 378	—	—	—	1 244s	1 122s	1 389
?	1 374	1 335s	1 171s	839s	1 251s	1 139s 1 102m	1 394

Table

R_1	R_2		$\nu_{C=O}$		ν_{O-H}	Aromatic		
			ketone	carbam.		I	II	Subst.
1	2	3	4	5	6	7	8	9
Compound R=OCONM	IV	$CHCl_3$	1 644 1 660sh^3	—	3 225 3 590	1 624*	1 605	868 m 888 ms
		KBr	1 674	1 722	—	1 626	1 602	874 m 891 m
		CCl_4	1 680	1 738	—	1 627	1 603	874 mw 893 m
Compound	V	KBr	1 635	—	3 120	1 611	1 570*	
Compound R=H	VIII	$CHCl_3$	1 658	—	3 230 3 594	1 620	1 593*	
		KBr	1 653	—	3 050	1 608sh	1 583*	862 ms 902w
		$CHCl_3$	1 679	—	3 260 3 585	1 617*	1 592	860 m ?
Compound $R=CH_3$	VIII	KBr	1 642	—	3 050	1 608	1 570	870 m 899 w
		$CHCl_3$	1 672	—	3 275 3 590	1 614	1 588	869 m ?

[1] lit[7] : 3115, 1637, 1595, 1575, 1376, 1083 cm^{-1}; [2] probably the methoxy group; $^{-1}$ the intensity of the shoulder increases with the dilution.

vs = very strong; s = strong; m = medium; w = weak; * = the most intense band in the spectrum

b) the out-of-plane C—H deformation vibrations.

Characteristic absorption for 1,2,4-trisubstituted derivatives (7-substituted I) and for 1,2,3,5-tetrasubstituted derivatives (5,7-disubstituted I) were found in the following ranges :

— 841—868 cm^{-1}, two adjacent ring hydrogen atoms (lit.[10] 800—860 cm^{-1}),

— 869—899 cm^{-1}, one isolated ring hydrogen atom (lit.[10] 860—900 cm^{-1}).

For 7-substituted chromanes, these bands were reported at 800—827 cm^{-1}'[11] and for substituted flavones at 808—834 cm^{-1} (2H) and at 868—912 cm^{-1} (1H).[12] The frequency range assigned to the 2H band seems to be too low. There is a possibility of confusion, since the X-sensitive ring bands fall in the same range (see "Phenolic group").

The gem-dimethyl group was characterized by the doublet arising from the splitting of the symmetrical deformation band of the methyl group (1366—1372 cm^{-1} and 1380—1385 cm^{-1},[10]). This doublet has already been reported for 2,2-dimethyl-chromanes ;[7,13] In our compounds, it occurred within the ranges 1352—1369 cm^{-1} and 1371—1379 cm^{-1}, the intensity of the latter being usually somewhat higher.

The 1000—1400 cm^{-1} region covers the characteristic absorption of the phenolic group and of the etheric function of the pyrane ring.

---

[10] M. Avram and Gh. D. Mateescu "Spectroscopia în infraroșu. Aplicații în chimia organică", Editura Tehnică, București, 1966.

[11] L. W. Deady, R. D. Tomson and J. Vaughan, *J. Chem. Soc.*, **1963**, 5718.

[12] J. H. Looker and W. W. Hanneman, *J. Org. Chem.*, **27**, 381 (1962).

[13] J. Bourgidou and H. Christol, *Bull. Soc. chim. France*, **1966**, 1974.

1 (cont.)

Gem-dimethyl		Phenolic group			Ether		?
				X-sens.			
10	11	12	13	14	15	16	17
1 362	1 376	1 333ms	1 172s	842s	1 250s	1 141s 1 100m	1 394
1 364	1 377	—	—	—	1 247s	1 143s 1 095m	1 389
1 365sh	1 376	—	—	—	1 247s	1 142s 1 093ms	1 392sh
?	1 372	1 352vs 1 330ms	1 174s	835s	1 260vs	1 152s 1 122ms	1 390sh
?	1 375	1 351vs 1 325m	1 173s	?	?	1 148s 1 115ms	1 392sh
—	—	1 349s	1 171s	852ms	1 290s 1 249vs	1 123	
—	—	1 356s	1 164s	?	1 292vs 1 250s	1 134s	1 392
—	—	1 336s	1 169s	844s	1 268vs	1 109m 1 066ms	1 390
—	—	?	?	?	?	? 1 072ms	

As the region is very crowded and the carbamoylation introduces additional absorption bands, the assignments in Table 1 (based on literature data for similar compounds and on the comparison between the two series of derivatives) must be considered as tentative.

THE PHENOLIC GROUP

Besides the O—H stretching frequency, the phenolic derivatives are characterized by two strong bands in the ranges 1140—1230 and 1310—1410 cm^{-1}, respectively. For the derivatives in Table 1, these bands occurred at 1150—1176 and 1404—1335 cm^{-1}.

An absorption band to which little attention is paid in the literature, from the analytical point of view, is the X-sensitive ring vibration. In our hydroxy-chromanones this band lies between 820 and 852 cm^{-1} and it disappeared from this region on carbamoylation, so it can be easily differentiated from the bands characteristic of the aromatic ring substitution.

THE ETHERIC FUNCTION

In six-membered unsaturated cyclic ethers, the bands associated with the stretching vibrations of the C—O—C bonds (rather modes of the whole ring) can be found at about the same frequency as in open chain compounds (1200—1270 cm^{-1} and 1050—1100 cm^{-1}).[10] Multiple band structures were reported for the chromane derivatives in the 1210–1295 cm^{-1} and 1020–1155 cm^{-1} regions.[8,12-16]

In our compounds, we assigned to these vibrations, two or more medium and strong bands in the overall ranges 1231–1300 cm^{-1} and 1066–1152 cm^{-1}.

In 2,2-dimethyl-5,7-dihydroxy-chromanone, the strong band near 1300 cm^{-1} was assigned to the ether function.[7] We assigned this band to the phenolic group, since it disappears on carbamoylation.

COUMARINE DERIVATIVES (II)

$\nu_{C=O}$ STRETCHING VIBRATIONS

A Fermi resonance band accompanies the lactone C=O stretching mode in coumarine.[17] The phenomenon is reported for solutions, the relative intensity of the doublet components changing with the polarity of the solvent and being independent of the concentration. In the solid state spectra of some hydroxy [17] and methoxy [18] derivatives, the bands near 1700 cm^{-1} were also reported.

The hydroxy-derivatives studied by us show the $\nu_{C=O}$ band in the 1659–1697 cm^{-1} range in solid state and in the 1710–1723 cm^{-1} range in solution. The lowering of the frequency (as against unsubstituted coumarine, halo- and alkyl-derivatives : 1725–1730 cm^{-1}) in this case is also determined by an overlapping of conjugation effects and of intermolecular hydrogen bonds. The electronic effects of the substituents were illustrated by the uv spectra^{-1} and the influence of the H bonds is indicated by the significant frequency shifts from solid state to solution (see Table 2).

It should be mentioned that in all cases, the $\nu_{C=O}$ bands are broad and accompanied by a sequence of shoulders (only the most prominent were tabulated).

The lowest frequencies both for the $\nu_{C=O}$ and ν_{O-H} bands were found in compound X_A, R = CH_3, the only coumarine derivative in our series having a 5-hydroxy substituent. In the synthesis of this derivative, there are two possibilities for the closure of the pyrane ring.

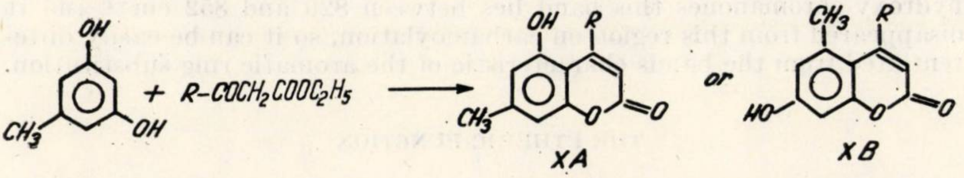

---

[14] T. R. Kasturi, and T. Arunachalam, *Indian J. Appl. Chem.*, **8**, 203 (1970).

[15] R. Merten and G. Müller, *Chem. Ber.*, **97**, 682 (1964).

[16] G. E. Inglett, *J. Org. Chem.* **23**, 93 (1958).

[17] R. N. Jones, C. L. Angell, T. Ito and R. J. D. Smith, *Canad. J. Chem.*, **37**, 2007 (1959).

[18] M. E. Perelson and I. N. Seinker, *Zhur. priklad. Spektrosc.*, **5**, 104 (1966).

Table 2

Infrared Spectra of Some New Coumarine Derivatives

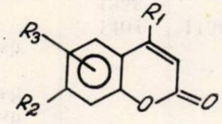

II

$-OCONM = -OCON(CH_2CH_2Cl)_2$

N°	R_1	R_2	R_3		$\nu_{C=O}$	Phenolic group				Aromatic			Lactone	
								ν_{O-H}	X-sens	I	II	Subst.		
1	2	3	4	5	6	7	8	9	10	11	12	13	14	15
1.	H	OH	H	KBr	1687* 1729sh	1321	1136 ?	3164	854	1626 1608	1569	834 903	1238	1136 ?
				$CHCl_3$	1710 1730	1318	1125 ?	3240	?	1614	1571	?	?	1125 ?
2.	H	OCONM	H	KBr	1729 1714sh 1706sh	—	—	—	—	1625	1570	839 898	1237	1133
				$CHCl_3$	1733 1706sh	—	—	—	—	1624	1569	842 897	1230	1124
3.	CH_3	OH	H	KBr	1680^1 1698sh	1389^2 1369	1161	3150	847	1600 1615sh	?	866 878 ? 899 ?	1273	1132 1068
				$CHCl_3$	1715 1694sh	1393 1371	1155	3262	?	1621	1576	857 ?	1274	1139
4.	CH_3	OCONM	H	KBr	1728 1718sh 1695sh	—	—	—	—	1618	1572	860 890	1266	1138 1081
				$CHCl_3$	1727 1721sh 1713sh	—	—	—	—	1619	1573	859 888	1265	1135 1080
5.	CH_3	H	6−OH	KBr	1694 1679sh	1400	1176	3359	821	1624 1615sh	1576	832 ? 856 ? 878	1233 1210	1119 1065
				$CHCL_3{}^3$	1713 1694sh					? 1605	1575			

Table 2 (cont.)

N°	R_1	R_2	R_3		$\nu_{C=H}$	Phenolic group				Aromatic			Lactone	
								ν_{O-H}	X-sens	I	II	Subst.		
1	2	3	4	5	6	7	8	9	10	11	12	13	14	15
6.	CH_3	H	6–OCONM	KBr	1727 1715sh	—	—	—	—	1628	1578	839 ? 856 ? ?	1227 1207	1126 1068
				CCL_4	1737	—	—	—	—	1636	1588	865 882	1227 1206	1125 1065
7.	H	OH	5–CH_3	KBr	1697	1336	1148	3251	822	1626sh 1613	1570	903	1246	1126
				$CHCl_3$	1721	?	1155	3415	?	1628sh 1615	1585	?	?	1123
8.	H	OCONM	5–CH_3	KBr	1726 1711sh	—	—	—	—	1618	1570	898	1243	1123
				$CHCl_3$	1727 1712sh	—	—	—	—	1615	1573	?	1238	1120
9.	CH_3	CH_3	5–OH	KBr	1659	1340	1151	3056	829	1616h	?	?	1252	1099
				$CHCl_3$	1712	1337	1156	3275	839	1621s 1610sh	1565	900	?	1093
10.	CH_3	CH_3	5–OCONM	KBr	1729 1714sh	—	—	—	—	1626 1614	?	898	1236	1095
				$CHCl_3$	1727 1712sh	—	—	—	—	1626	1560	900	1233	1097
11.	CH_3	OH	5–OH	KBr	1675	1302 1367 1388	1162	3180	833	1624 1592	1559	?	1239	1099 1079
				$CHCl_3^3$	1723 1712sh					1622 1604				? 1078
12.	CH_3	OCONM	5–OCONM	KBr	1728 1740sh 1711sh	—	—	—	—	1621	1570	896	1242	1141 1095
				$CHCl_3$	1734 1711sh	—	—	—	—	1623	1570	902	1240	1140 1095
13.	CH_3	OH	6–OH	KBr	1662	1404 1358	1158	3260	847	1623sh 1616	1570	865	1222	1065
				$CHCl_3^3$	1718					? 1602				1071

14.	CH_3	OCONM	6−OCONM	KBr	1734 1713sh	—	—	—	—	1627	1574	868	1230	1077
				$CHCl_3$	1731 1712sh					1631	1573			
15.	Compound VII,		R=OH	KBr	1705 1693	1330 1364	1170	3295	836	1627	1609	819 873	1275	1105
				$CHCL_3$	1735 1719	?	1169	3265 3580	?	1621	1612	?	1270	1111sh
16.	Compound VII, R = OCONM			KBr	1733 1720sh 1711sh	—	—	—	—	1622	1609	820 873sh	1273	1111 1100
				$CHCl_3$	1732 1719sh 1713sh	—	—	—	—	1624	?	? 875	1271	1111 1101
17.	Compound IX,		R=OH	KBr	1751 1721	1353	1144 1153	3285	816	1622	1590	837? 851 901	1251	1111
				$CHCl_3$	1767 1749sh	1343	?	3360 3591	816	1628	1598	858 878	1248	1110
18.	Compound IX R=OCONM			KBr	1763 1714	—	—	—	—	1620	1600	829 848 892	1246	1113
				$CHCl_3$	1768 1723	—	—	—	—	1624	1599	842 875	1241	1112

* sh = shoulder; [1]) lit. [4]: 1667, 3077, 1267, 1130 and 1066 cm^{-1}; [2]) these two bands were tabulated, although they were found also in the carbamate spectrum; no other bands were found in this region; [3]) very springly soluble

The most convenient way to distinguish between the X_A and X_B structures is the examination of their uv spectra. The monohydroxy derivatives with the OH group in the 5-position have an absorption band at about 300 nm, while the 7-OH-isomers present the same band at about 330 nm (λ max for X_A, $R = CH_3$: 303 nm; for X_B, $R = H$: 337 nm).[1] This rule holds also for other similar derivatives reported in the literature.

As expected, in 3,4-dihydrocoumarines, the $\nu_{C=O}$ band of the lactone group is shifted to higher frequencies.

In the carbamoyl-derivatives, the absorption bands due to the urethane and lactone carbonyl groups are overlapped. The bands (both in solution and in solid state) show the same pattern — a broad peak at 1727—1740 cm^{-1}, accompanied by a sequence of medium and weak shoulders and inflexions, especially in the ranges 1710—1724, 1705—1710 and 1690—1696 cm^{-1} (the latter being weak but very constant). Only in a few cases, additional weak absorptions at a frequency higher than that of the main peak could be observed.

O—H STRETCHING VIBRATION

In accordance with the literature data,[19-21] this band is shifted to very low frequencies. The lowest position of this band (4,7-dimethyl-5-hydroxy-coumarine: 3056 cm^{-1}) is correlated with the lowest position of the $\nu_{C=O}$ band.

THE AROMATIC SYSTEM

The two highest frequency vibrations of the system were tabulated It is noteworthy that in the case of the 6-OH derivative where conjugation of the hydroxy and lactone functions cannot take place, the intensity of the bands is much lower (the strong absorption at 1574 cm^{-1} in 7-hydroxy-coumarine was assigned to a C_7-O δ-asymmetric stretching vibration.[18] The bands characteristic of the substitution pattern were also tabulated.

There is an analogy between the coumarine and chromanone derivatives concerning the complex absorption pattern in the 1000—1400 cm^{-1} region. The phenol and lactone absorptions fall in this region and no band can be unequivocally assigned.

THE PHENOL GROUP

Two series of bands, in the ranges 1300—1400 cm^{-1} and 1300—1176 cm^{-1}, respectively, were assigned to this function (it is very difficult to distinguish between the latter and a characteristic band of the lactone group occurring in the same region).

The X-ring sensitive band, which appears in the 820—850 cm^{-1} range and disappears on carbamoylation, was also tabulated.

---

[19] J. Polonsky, *Bull. Soc. chim. France*, **1956**, 914.

[20] J. Polonsky, *Bull. Soc. chim. France*, **1955**, 541.

[21] A. K. Das Gupta, K. R. Das and A. Das Gupta, *Indian J. Appl. Chem.*, **10**, 32 (1972).

LACTONE ABSORPTIONS

One of the three weak bands occurring at 1120, 1140 and 1200 cm^{-1} was assigned to the C—O stretching mode in 2-pyrones.[22] In the tetrahydro-derivatives, the band was found in the 1220—1240 cm^{-1} (much stronger). In the coumarine derivatives, two or more characteristic absorption bands were reported without assignment in the range 1040—1120 cm^{-1}·[3,4,21,23,24]

In our compounds the bands which were the most likely ascribed to the lactone function fall in the 1210—1274 cm^{-1} and 1065—1145 cm^{-1} ranges. For some of the compounds, two bands were tabulated for one or both regions, when they changed neither the position nor the intensity on carbamoylation.

ACKNOWLEDGEMENT. The authors wish to thank Mr. Tiberiu Răzvan for the highly qualified technical assistance.

---

[22] R. H. WILEY and J. G. ESTERLE, *J. Org. Chem.*, **22**, 1257 (1957).

[23] F. EYDEN and P. MEINS, *Arch. Pharm.*, **305**, 124 (1972).

[24] J. A. VIDA and M. GUT, *J. Org. Chem.*, **23**, 1202 (1968).

C–O–C ABSORPTIONS

One of the three weak bands observed at 1120, 1140 and 1290 cm⁻¹ was assigned to the C–O stretching mode in γ-pyrones.[illegible] In the tetrahydro derivatives the band was found in the 1236–1250 cm⁻¹ region[illegible]. In the coumarine derivatives, two or more characteristic absorption bands were reported without assignment in the range 1010–1130 cm⁻¹.[12-14]

In our compounds the bands which were the most likely ascribed to the ketone function fall in the 1270–1274 cm⁻¹ and 1062–1145 cm⁻¹ ranges. For some of the compounds, two bands were tabulated for one or both regions, when they obscured neither the position nor the intensity of carbonyl stretching.

ACKNOWLEDGEMENT. The authors wish to thank Mr. [illegible] for the highly qualified technical assistance.

---

[12] H. H. [illegible] and [illegible], J. Org. Chem. 23, [illegible] (1958).
[13] [illegible] and [illegible], Appl. Spectry. 66, [illegible] (1962).
[14] [illegible] A. [illegible] and M. [illegible], J. [illegible] 21, 1560 (1962).

Revue Roumaine de Chimie, **21**, *8*, 1221-1225, (1976)

HYDRAZONES OF PIPERIDINO-N-ACETOHYDRAZIDE AND MORPHOLINO-N-ACETOHYDRAZIDE OF PHARMACOLOGICAL INTEREST

V. B. JIGAJINNI, S. C. BENNUR, RAJANI S. BENNUR & V. V. BADIGER
Department of Chemistry, Karnatak University, Dharwar-580003, India

Received January 8, 1975

Seventeen new acetohydrazones of piperidino-N-acetohydrazide and morpholino-N-acetohydrazide have been prepared and screened for antimicrobial and anticholinesterase activity. Some of them showed antimicrobial activity. Compounds 2, 5, 9, 16, 20 and 21 exhibited remarkable anticholinesterase activity in the preliminary investigation. The compounds are characterized by elemental analysis and IR spectroscopy.

A large number of aliphatic, aromatic and heterocyclic carboxylic acid hydrazides, their derivatives and related compounds were tested for antimicrobial and antitubercular activity. The derivatives of isonicotinic acid hydrazide and other heterocyclic substituted hydrazones were studied to establish the structural requirements for antimicrobial and antitubercular activity.[1-3] With a view to decrease the toxicity of free amino group in isoniazid, various benzaldehydes were condensed with isoniazid to yield Schiff's bases which were reported to possess antitubercular activity.[4] Bavin et al.,[5,6] claimed that 1-isonicotinyl-2-(*o*-hydroxy) benzylidene hydrazine was better than isoniazid as antitubercular compound because it was almost as active as the latter and much less toxic.

Carrara et al.,[7] discovered that the above activities did not depend either on the isonicotinic structure or even on the pyridine ring, hence they prepared a series of hydrazides and hydrazones of pyrimidine, pyridine, oxazole carboxylic acids. The activities were increased by the presence of azin, phenyl hydrazone or nitrophenyl hydrazone groups.[8]

---

[1] S. Kakimoto, E. K. Thiemer and E. Wempe, *Arzneimittel-Forsch.*, **10**, 963 (1960); *Chem. Abstr.*, **55**, 8659 (1961).

[2] J. Supniewski, T. Bany and J. Krupinska, *Bull. acad. polon. Sci.*, *Classe II*, **3**, 55 (1955); *Chem. Abstr.*, **50**, 7801 (1955).

[3] K. M. Miyatake, S. Ichimura, S. Nagasaki and K. Hoji, *J. Pharm. Soc.*, *Japan*, **75**, 1066 (1955); *Chem. Abstr.*, **50**, 5616 (1956).

[4] J. R. Merchant and D. S. Chothia, *J. Med. Chem.*, **13**, 335 (1970).

[5] E. M. Bavin, B. James, E. Kay, R. Lazare and D. E. Seymour, *J. Pharm. and Pharmacol.*, **7**, 1032 (1955).

[6] E. M. Bavin, E. Kay and D. E. Seymour, *Lancet*, **2**, 337 (1954).

[7] G. Carrara, F. M. Chiancone, V. D'Amato, E. Ginoulhiac, C. Martinuzzi, U. M. Teotino and N. Visconti, *Gazz. Chim. Ital.*, **82**, 652 (1952); *Chem. Abstr.*, **48**, 6423 (1954).

[8] E. Jeney, T. Zsolnai and J. Lazar, *Zentr. Bakteriol. Parasitenk. Abt. I Orig.*, **160**, 670 (1954); *Chem. Abstr.*, **48**, 10836 (1954).

Yale and Bernstein[9] showed that the carbohydrate heterocyclic acylhydrazones were useful as environmental antimycobacterial and antitubercular agents. Schiff's bases and hydrazone derivatives of pyrimidine-4-carboxaldehydes as potential anticancer agents were reported by Hall et al.[10]

Tajana and Pozzi [11] synthesized a series of disubstituted acetohydrazones and screened them for hypotensive activity. 5-Nitrofuran-2-aldehyde diethylamino acetohydrazone ;-N-pyrrolidino acetohydrazone and -N-piperidino acetohydrazones were investigated for hypertensive activity.[12]

The present investigation was prompted by the possibility that examination of a wider spectrum of substituted hydrazones might lead to more potent antimicrobial compounds. Consequently, a series of Schiff's bases of piperidino-N-acetohydrazide and morpholino-N-acetohydrazide which were required as intermediates for the synthesis of triazoles, thiadiazoles and oxadiazoles were prepared and tested for their pharmacological activities.

CHEMISTRY

Acetohydrazides were obtained by the action of hydrazine hydrate on ethyl piperidino-N-acetate and ethyl morpholino-N-acetate. A series of hydrazones, described in this paper have been prepared by condensing acetohydrazides with various aldehydes in equimolar quantities in ethanol. The hydrazones so prepared are described in tables 1 and 2.

Scheme

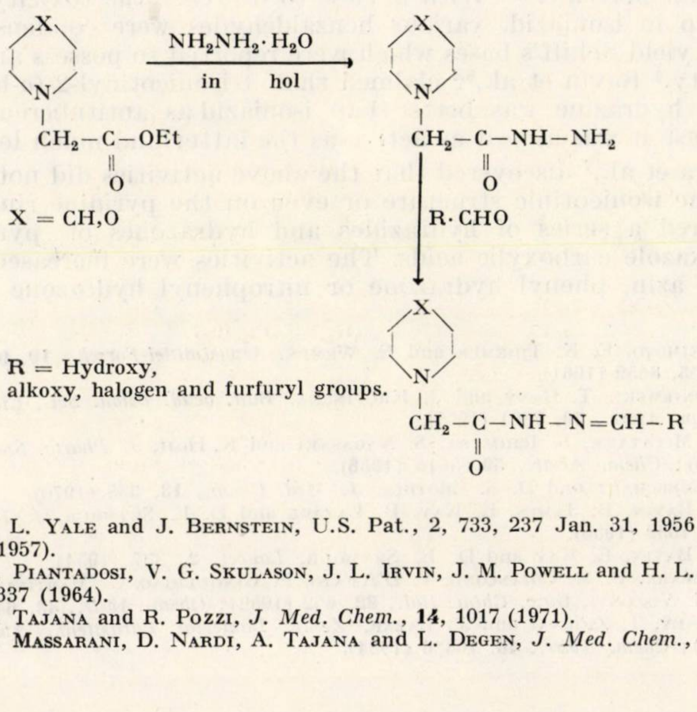

---

[9] H. L. YALE and J. BERNSTEIN, U.S. Pat., 2, 733, 237 Jan. 31, 1956 ; *Chem. Abstr.*, **51**, 1283 (1957).

[10] C. PIANTADOSI, V. G. SKULASON, J. L. IRVIN, J. M. POWELL and H. L. HALL, *J. Med. Chem.*, **7**, 337 (1964).

[11] A. TAJANA and R. POZZI, *J. Med. Chem.*, **14**, 1017 (1971).

[12] E. MASSARANI, D. NARDI, A. TAJANA and L. DEGEN, *J. Med. Chem.*, **14**, 633 (1971).

Table 1

Piperidino-N-acetohydrazones

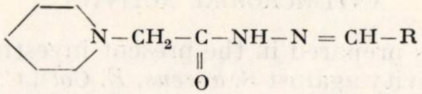

N°	R	M.P. °C	Yield %	Formula	Analysis					
					Calculated %			*Found* %		
					C	H	N	C	H	N
1	2-Hydroxy-5-methyl-phenyl[b]	221–222	63	$C_{15}H_{21}N_3O_2$	65.46	7.69	15.27	65.76	7.50	15.45
2	2,4-Dichlorophenyl[c]	210–211	79	$C_{14}H_{17}N_3OCl_2$	53.51	5.42	13.38	53.33	5.36	13.48
3	3,4-Dichlorophenyl[c]	171–172	53	$C_{14}H_{17}N_3OCl_2$	53.51	5.42	13.38	53.11	5.39	13.65
4	4-Methoxyphenyl[d]	170–171	59	$C_{15}H_{21}N_3O_2$	65.46	7.64	15.27	65.70	7.49	15.34
5	3,4-Dimethoxyphenyl[b]	195–196	75	$C_{16}H_{23}N_3O_3$	62.95	7.54	13.78	63.07	7.63	13.54
6	2,5-Dimethoxyphenyl[b]	152–153	67	$C_{16}H_{23}N_3O_3$	62.95	7.54	13.78	62.59	7.32	13.84

Crystallization solvent: *a*, EtOH–H_2O; *b*, EtOH; *c*, EtOH-dioxane; *d*, MeOH.

Table 2

Morpholino-N-acetohydrazones

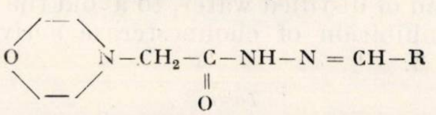

N°	R	M.P. °C	Yield %	Formula	Analysis					
					Calculated %			*Found* %		
					C	H	N	C	H	N
7	Phenyl[a]	95–96	83	$C_{13}H_{17}N_3O_2$	63.16	6.88	17.00	62.83	6.70	16.87
8	2-Hydroxyphenyl[a]	201–202	84	$C_{13}H_{17}N_3O_3$	59.30	6.46	15.97	58.93	6.59	16.15
9	4-Hydroxyphenyl[d]	266–267	71	$C_{13}H_{17}N_3O_3$	59.30	6.46	15.97	58.98	6.26	15.77
10	2-Hydroxy-5-methyl-phenyl[c]	210–211	77	$C_{14}H_{19}N_3O_3$	60.64	6.68	15.16	60.39	6.91	15.41
11	2-Chlorophenyl[d]	148–149	79	$C_{13}H_{16}N_3O_2Cl$	55.42	5.68	14.91	55.71	5.50	15.16
12	2,4-Dichlorophenyl[a]	212–213	61	$C_{13}H_{15}N_3O_2Cl_2$	49.37	4.76	13.29	49.14	4.60	12.91
13	3,4-Dichlorophenyl[a]	172–173	81	$C_{13}H_{15}N_3O_2Cl_2$	49.37	4.76	13.29	49.53	4.81	13.51
14	4-Methoxyphenyl[d]	172–173	55	$C_{14}H_{19}N_3O_3$	60.54	6.86	15.16	60.15	6.67	14.81
15	3,4-Dimethoxyphenyl[b]	193–194	63	$C_{15}H_{21}N_3O_4$	58.64	6.84	13.68	54.01	6.70	13.93
16	2,5-Dimethoxyphenyl[c]	154–155	65	$C_{15}H_{21}N_3O_4$	58.64	6.84	13.68	58.35	6.91	13.91
17	2-Furyl[c]	112–113	76	$C_{11}H_{15}N_3O_3$	55.71	6.33	17.72	55.39	6.12	17.45

Crystallization solvent: *a*, EtOH–H_2O; *b*, EtOH; *c*, EtOH – dioxane; *d*, MeOH.

The characteristic IR absorptions were observed in the range 3200–3460, 1650–1700 and 1490–1550 cm^{-1}. These were assigned to –NH, –C=O, –C=C– and –C=N– vibrations respectively.

SCREENING RESULTS

ANTIMICROBIAL ACTIVITY

The compounds prepared in the present investigation were screened for antimicrobial activity against *S. aureus*, *E. Coli*, *C. albicans* and *Cryptococcus neoformans*, by cupplate method. Ethylene glycol was used as solvent control which did not show any bacterial inhibition. Phenol (5%) was used as positive control.

Of the different hydrazones investigated for antibacterial activity, compounds 5, 8, 18 and 21 showed marked activity against both Gram-positive and Gram-negative micro-organisms. The compounds 2, 4, 6, 7, 8, 9, 10 were less potent against *S. aureus* and 8, 9 were active against *E. coli*. The remaining compounds were inactive against both the micro-organisms.

Only compounds 1, 3 and 4 showed activity against *C. albicans*. The rest of the compounds were inactive against both the fungal strains.

ANTICHOLINESTERASE ACTIVITY

The preliminary investigation of anticholinesterase activity was evaluated in human serum by the method described in SIGMA technical bulletin [13] with a slight modification. The drug concentration was 1 mg. per ml. This was diluted with ethylene glycol to make a total volume equal to 10 ml. instead of distilled water, to avoid the formation of turbidity. The percent inhibition of cholinesterase activity by hydrazones is recorded in table 3.

Table 3

Results of cholinesterase activity of acetohydrazones

N°	Name of the compound	Per cent inhibition
1	1-(Benzylidene)-2-(piperidino-N-acetyl)hydrazine [11]	14.29
2	1-(2-Hydroxybenzylidene)-2-(piperidino-N-acetyl)hydrazine [11]	100
3	1-(4-Hydroxybenzylidene)-2-(piperidino-N-acetyl)hydrazine [11]	90
4	1-(2-Hydroxy-5-methylbenzylidene)-2-(piperidino-N-acetyl)hydrazine	85.72
5	1-(2-Chlorobenzylidene)-2-(piperidino-N-acetyl)hydrazine [11]	100
6	1-(2,4-Dichlorobenzylidene)-2-(piperidino-N-acetyl)hydrazine	91.47
7	1-(3,4-Dichlorobenzylidene)-2-(piperidino-N-acetyl)hydrazine	86.98
8	1-(4-Methoxybenzylidene)-2-(piperidino-N-acetyl)hydrazine	75.48
9	1-(3,4-Dimethoxybenzylidene)-2-(piperidino-N-acetyl)hydrazine	100
10	1-(2,5-Dimethoxybenzylidene)-2-(piperidino-N-acetyl)hydrazine	75.03
11	1-(Benzylidene)-2-(morpholino-N-acetyl)hydrazine	60.01
12	1-(2-Hydroxybenzylidene)-2-(morpholino-N-acetyl)hydrazine	85.72
13	1-(4-Hydroxybenzylidene)-2-(morpholino-N-acetyl)hydrazine	81.23
14	1-(2-Hydroxy-5-methylbenzylidene)-2-(morpholino-N-acetyl)hydrazine	90.69
15	1-(2-Chlorobenzylidene)-2-(morpholino-N-acetyl)hydrazine	81.49
16	1-(2,4-Dichlorobenzylidene)-2-(morpholino-N-acetyl)hydrazine	100
17	1-(3,4-Dichlorobenzylidene)-2-(morpholino-N-acetyl)hydrazine	80
18	1-(4-Methoxybenzylidene)-2-(morpholino-N-acetyl)hydrazine	66.60
19	1-(3,4-Dimethoxybenzylidene)-2-(morpholino-N-acetyl)hydrazine	91.03
20	1-(2,5-Dimethoxybenzylidene)-2-(morpholino-N-acetyl)hydrazine	100
21	1-(2-Furfurylidene)-2-(morpholino-N-acetyl)hydrazine	100

---

[13] SIGMA Chemical Co., Tentative Technical Bulletin No. 420, Revised July, 1967.

Amongst the compounds investigated, 2, 5, 9, 16, 20 and 21 showed 100 per cent inhibition whereas compounds 3, 6, 14 and 19 showed 90 per cent inhibition of cholinesterase activity.

EXPERIMENTAL

All melting points are taken in capillary and are uncorrected. The IR spectra were recorded in nujol mull on Beckmann IR–20 instrument.

Anisaldehyde, furfuraldehyde, benzaldehyde, and veratraldehyde were B.D.H. samples. Salicylaldehyde was Riedel sample. 2,4-Dichlorobenzaldehyde, 3,4-dichlorobenzaldehyde, 4-hydroxybenzaldehyde and 2,5-dimethoxy-benzaldehyde were L. Light samples. Substituted 2-hydroxybenzaldehydes[14] were prepared according to the literature methods. Acetohydrazides[15] were obtained by the reaction of the corresponding esters with hydrazine hydrate.

GENERAL METHOD OF SYNTHESIS OF HYDRAZONES

To a solution of acetohydrazide (0.025 mole) in absolute ethanol (30 ml.) aldehyde (0.025 mole) was added.

The mixture was heated under reflux for about three hours, cooled and the separated hydrazone was collected. The product was purified by crystallisation from appropriate solvent.

ACKNOWLEDGEMENT. We thank Dr. E. S. Jayadevappa, Professor and Head Department of Chemistry, Karnatak University, Dharwar for providing facilities. One of us (V.B.J.) is grateful to C.S.I.R. for financial assistance. We thank Messers V. A. Desai and G.S. Gadaginamath for the analytical data recorded. We also thank Dr. P. B. Sattur, Assistant Director, R.R.L. Hyderabad for providing the facilities to record the spectral data.

---

[14] J. C. Duff, *J. Chem. Soc.*, **1941**, 547.

[15] M. Pesson and S. Dupin, *Bull. Soc. chim. France*, **1962**, 252 *Chem. Abstr.*, **57**, 808 (1962).

Revue Roumaine de Chimie, **21**, *8*, 1227–1235 (1976)

NEW SYNTHESES OF DYES WITH NAPHTH[2,3-c] XANTHENE-5,8,14-TRIONE AND NAPHTH[2,3-c] THIOXANTHENE-5,8,14-TRIONE STRUCTURE

F. URSEANU

Laboratory of Chemistry and Technology of Aromatic Intermediates and Dyes: Chemistry Institute, Calea Victoriei 149, Bucharest, Romania

Received October 11, 1975

The work describes new syntheses and experimental procedures for the preparation of naphth [2,3-c]xanthene-5, 8, 14-trione and naphth [2,3-c]thioxanthene-5,8,14-trione dyes, analyses and dyeings with newly obtained compounds.

1. INTRODUCTION

The first dyes with naphth[2,3-c]xanthene-5,8,14-trione and naphth[2,3-c]thioxanthene-5,8,14-trione structure* were synthesized in 1909–1912 by Ullmann and his co-workers [1–9] and were utilized as vat dyes for dyeing cotton.

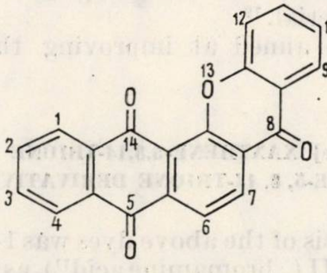

naphth[2,3-c]xanthene-5,8,14-trione

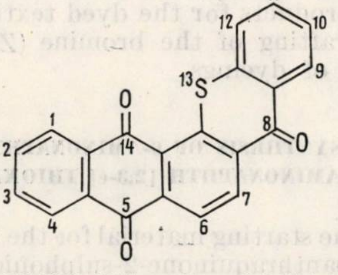

naphth[2,3-c]thioxanthene-5,8,14-trione

---

* According to the older nomenclature: anthraquinonexanthonic and anthraquinonethioxanthonic dyes.

[1] Badische Anilin und Sodafabrik, Ger. Pat. 251 696, April 6, 1911; Frd., **11**, 682.

[2] F. Ullmann and D. Urményi, *Ber. dtsch. chem. Ges.*, **45**, 2259 (1912).

[3] F. Ullmann and I. Ch. Dasgupta, *Ber. dtsch. chem. Ges.*, **47**, 566 (1914).

[4] Farbenfabriken vorm Friedrich Bayer Co. in Elberfeld, Ger. Pat. 216 480, Nov. 1, 1909; *Frd.*, **9**, 746.

[5] F. Ullmann, Ger. Pat. 238 983, July 1, 1910; *Frd.*, **10**, 723.

[6] Badische Anilin und Sodafabrik, Ger. Pat. 243 750, Jan. 20, 1911; *Frd.*, **10**, 726.

[7] F. Ullmann and E. Knecht, *Ger. dtsch. chem. Ges.*, **44**, 3125 (1911).

[8] I. M. Kogan, "Khimiia Krasitelei" Goshimizdat, Moskva, 1956, p. 590.

[9] J. Reichel, „Tehnologia coloranţilor antrachinonici", Ed. Academiei, Bucharest, 1961, p. 243.

These dyes have a weak affinity for cotton, especially those with napht [2,3-c]xanthene-5,8,14-trione structure, [8,9] and moderate fastness to light and wet treatments (washing, perspiration a.s.o.), that in why their number is relatively reduced ; some of them have been used later as starting materials for synthesizing polyheterocycles vat dyes : thioxanthonecarbazoles,[10,11] thioxanthoneanthraquinoneacridines [12] e.g.o.

An important problem nowadays for the dye industry is to manufacture a varied series of disperse dyes, necessary to synthetic fibre dyeing.

Thus, the present work describes the synthesis of new dyes, derivatives of 6-aminonaphth[2,3-c]xanthene-5,8,14-trione [13–15] and 6-aminonaphth[2, 3-c]thioxanthene-5,8,14-trione, [16–18] with the following general formula :

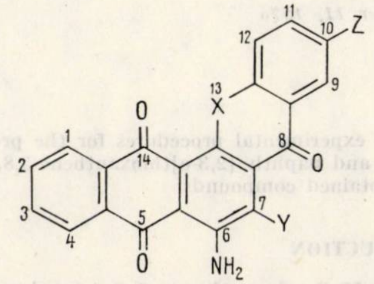

$X=O$ $Y=H$ $Z=H$ (VIII)
$X=O$ $Y=OCH_3$ $Z=H$ (IX)
$X=O$ $Y=H$ $Z=Br$ (X)
$X=O$ $Y=OCH_3$ $Z=Br$ (XI)
$X=S$ $Y=H$ $Z=H$ (XVI)
$X=S$ $Y=OCH_3$ $Z=H$ (XVII)
$X=S$ $Y=H$ $Z=Br$ (XVIII)
$X=S$ $Y=OCH_3$ $Z=Br$ (XIX)

The products obtained were tested as disperse dyes for polyester fibres. Grafting of the substituent $Y = OCH_3$ aimed at changing the colour from that of the corresponding unsubstituted structure ($Y = H$), favouring the dyes dispersability in water and increasing the affinity of the products for the dyed textile material. [19]

Grafting of the bromine ($Z = Br$) aimed at improving the light fastness of dyeings.

2. SYNTHESIS OF 6-AMINONAPHTH [2,3-c] XANTHENE-5,8,14-TRIONE AND 6-AMINONAPHTH [2,3-c] THIOXANTHENE-5, 8, 14-TRIONE DERIVATIVES

The starting material for the synthesis of the above dyes was 1-amino-4-bromoanthraquinone-2-sulphonic acid III („bromamine acid''), as sodium

---

[10] F. Max and D. I. Randall, U.S. Pat. 2 533 170, Dec. 5, 1950 ; *J. Soc. Dyers and Colourists*, **67**, 467 (1951).

[11] F. Max and D. I. Randall, Brit. Pat. 652 386, April 25, 1951 ; *J. Soc. Dyers and Colourists*, **67**, 389 (1951).

[12] W. B. Hardy and R. E. Herd, U.S. Pat. 3 027 375, June 8, 1953 ; *Chem. Abstr.*, **57**, 3594 (1962).

[13] F. Urseanu and L. Floru, R.S.R. Pat. 59 949, July 25, 1973.

[14] F. Urseanu, M. Olteanu, M. Ianăș and S. Degeratu, Rom. Pat. 59 952, July 25, 1973.

[15] F. Urseanu and R. Vintilă, Rom. Pat. 59 953, July 25, 1973.

[16] F. Urseanu, Rom. Pat. 59 950, July 25, 1973.

[17] F. Urseanu, Rom. Pat. 59 951, July 25, 1973.

[18] F. Urseanu and R. Vintilă, Rom. Pat. 59 954, July 25, 1973.

[19] C. Călin, *Bul. Inform. Laborat. Centr. Coloristic*, **7**, 23 (1967).

salt, which represents a very good anthraquinonic intermediate for the preparation of many dyes. [20]

From the bromamine acid III, 6-aminonaphth[2,3-c]xanthene-5, 8, 14-trione and 6-aminonaphth [2, 3 -c] thioxanthene-5 8, 14-trione derivatives were obtained based on the reaction schemes given below, according to literature procedures [21] for the synthesis of some 6-aminonaphth[2,3-c]acridan-5,8,14-trione dyes.

2.1. CONDENSATION OF BROMAMINE ACID WITH SALICYLIC ACID AND THIOSALICYLIC ACID, AS ALKALINE SALTS

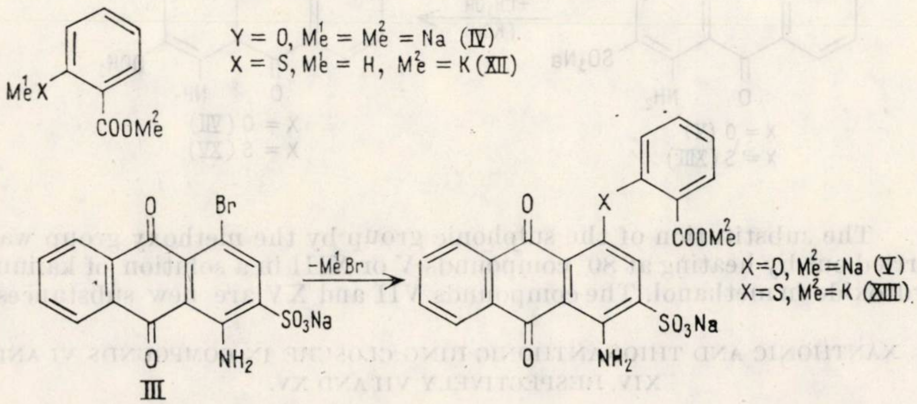
Me^1X
$COOMe^2$
$Y = O, Me^1 = Me^2 = Na$ (IV)
$X = S, Me^1 = H, Me^2 = K$ (XII)
O
Br
SO_3Na
O
NH_2
III
$-Me^1Br$
O
X
$COOMe^2$
$X=O, Me^2=Na$ (V)
$X=S, Me^2=K$ (XIII)
SO_3Na
O
NH_2

The condensation was achieved by heating at 95 – 98° the reagents III and IV or III and XII in aqueous alkaline solution (sodium hydroxide, kalium carbonate), in the presence of copper sulphate, respectively copper powder, as catalysts. The compounds V and XII which are thus obtained represent new substances.

2.2. REPLACEMENT OF THE SULPHONIC GROUP FROM COMPOUNDS V and XIII

2.2.1. Replacement of the sulphonic group by hydrogen.

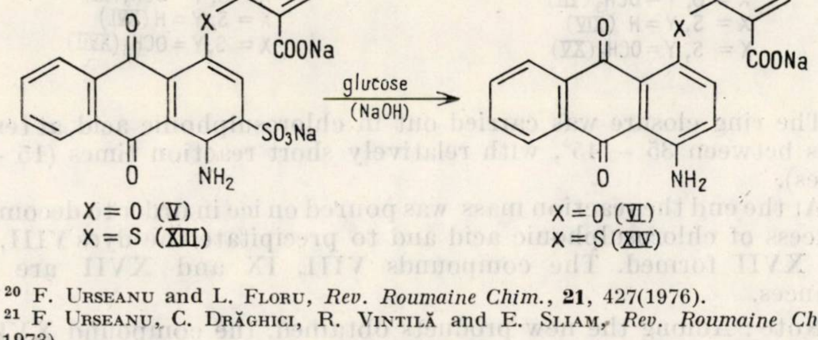
O
X
COONa
SO_3Na
O
NH_2
X = O (V)
X = S (XIII)
glucose
(NaOH)
O
X
COONa
O
NH_2
X = O (VI)
X = S (XIV)

---

[20] F. Urseanu and L. Floru, *Rev. Roumaine Chim.*, **21**, 427(1976).

[21] F. Urseanu, C. Drăghici, R. Vintilă and E. Sliam, *Rev. Roumaine Chim.*, **18**, 1019 (1973).

The sulphonic group of compounds V and XIII was eliminated by heating them at 95° in aqueous solution with glucose and sodium hydroxide. The compound VI is a new substance.

2.2.2. Replacement of the sulphonic group by the methoxy group.

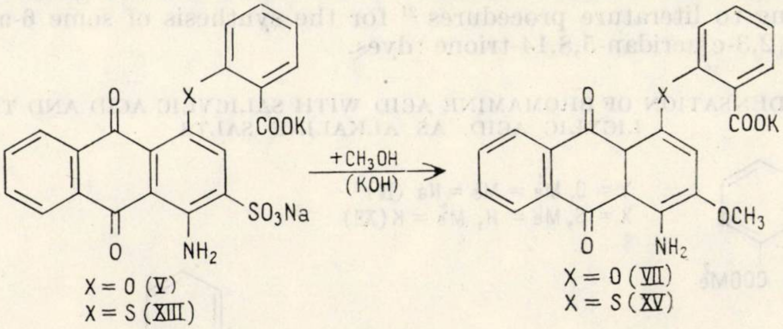
O
X
COOK
SO₃Na
O
NH₂
X = O (V)
X = S (XIII)
+CH₃OH
(KOH)
O
X
COOK
OCH₃
O
NH₂
X = O (VII)
X = S (XV)

The substitution of the sulphonic group by the methoxy group was carried out by heating at 80° compounds V or XIII in a solution of kalium hydroxide in methanol. The compounds VII and XV are new substances.

2.3. XANTHONIC AND THIOXANTHONIC RING CLOSURE IN COMPOUNDS VI AND XIV, RESPECTIVELY VII AND XV.

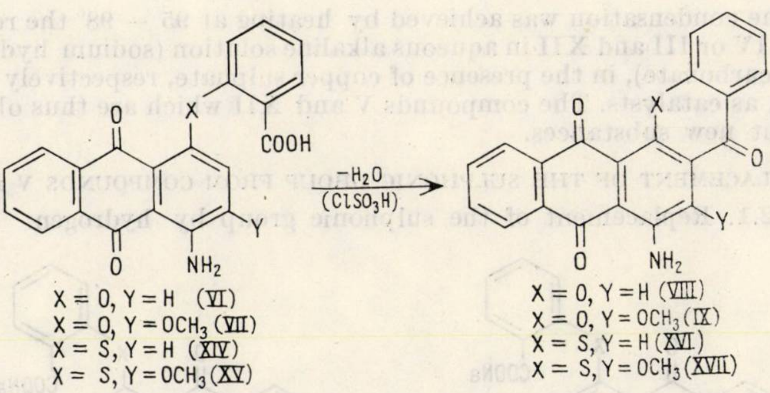
O
X
COOH
Y
O
NH₂
X = O, Y = H (VI)
X = O, Y = OCH₃ (VII)
X = S, Y = H (XIV)
X = S, Y = OCH₃ (XV)
−H₂O
(ClSO₃H)
O
X
O
Y
O
NH₂
X = O, Y = H (VIII)
X = O, Y = OCH₃ (IX)
X = S, Y = H (XVI)
X = S, Y = OCH₃ (XVII)

The ring closure was carried out in chlorosulphonic acid, at temperatures between 35 — 45°, with relatively short reaction times (15 — 20 minutes).

At the end the reaction mass was poured on ice in order to decompose the excess of chlorosulphonic acid and to precipitate the dyes VIII, IX, XVI, XVII formed. The compounds VIII, IX and XVII are new substances.

Note : Among the new products obtained, the compound XVI has been described in literature ;[12] it is prepared by refluxing the 1-amino-4-chloroanthraquinone with methylthiosalicylate in amylic alcohol as solvent, in the presence of sodium carbonate and cupreous chloride. In the present work, compound XVI was synthesized in a new way: condensation of bromamine acid III with thiosalycilic acid (XII), replacement of the sulphonic group of product XIII by hydrogen followed by thioxanthonic ring closure of intermediate XIV.

2.4. SYNTHESIS OF BROMINATED DERIVATIVES

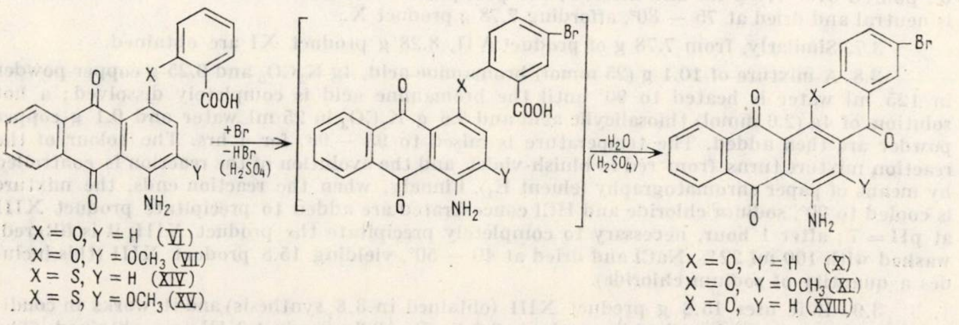

X = O, Y = H (VI)
X = O, Y = OCH_3 (VII)
X = S, Y = H (XIV)
X = S, Y = OCH_3 (XV)

X = O, Y = H (X)
X = O, Y = OCH_3 (XI)
X = O, Y = H (XVIII)

The brominated derivatives were prepared by bromination of the compounds VI, VII, XIV and XV at 0 − 10° with the theoretical amount of bromine in 100% H_2SO_4, followed by heating the reaction mass at 98° in order to close the xanthonic, respectively thioxanthonic ring.

3. EXPERIMENTAL

3.1. A mixture of 10.1 g (25 mmol) bromamine acid (III), 1g NaOH and 0.6 g $CuSO_4 \cdot 5H_2O$ in 120 ml water is heated to 85 − 90° until the bromamine acid is completely dissolved; a hot solution of 3.59 g (26 mmol) salicylic acid IV and 2.1 g NaOH in 40 ml water is then added and the temperature is raised to 98° for 10 hrs. The colour of the reaction mixture turns from red to bluish-violet.

Note: The conversion of bromamine acid to product V is followed by means of paper chromatography, in ascendent system, using an eluent (E_1) made up 5 vol. CH_3COOH + + 5 vol. water + 4 vol. butanol.

Finally, when the reaction ends, the temperature is reduced to 80°, 10 ml 36% HCl are added and filtered; sodium chloride is added in filtrate until the formed compound V is completely precipitated, then it is filtered, washed with 150 ml 22% NaCl solution and dried at 60−70°, yielding 14 g product V (This includes a quantity of sodium chloride).

3.2. 14 g product V (obtained in 3.1 synthesis) are dissolved in a solution of 3.9 g NaOH in 125 ml water at 85 − 90°, then a warm solution of 8.2 g glucose in 16.5ml water is added dropwise to the solution resulted; the reaction is completed by heating at 95° for 20 minutes. The mixture is then cooled to 20°, neutralized with concentrated HCl to pH = 6 − 6,5 and filtered; the precipitate is washed with 150 ml water and dried at 70 − 80°, yielding 7.35 g product VI.

3.3. 7.35 g product VI are dissolved in 90 ml $ClSO_3H$ and the resulted solution is heated at 40 − 45°, for 20 minutes. The mixture is cooled at 10 − 15°, poured over 150 g crushed ice and filtered; the precipitate is washed with water until the filtrate is neutral and dried at 70 − 80°, yielding 6.29 g product VIII.

3.4. To a solution of 13.8 g KOH in 40 ml CH_3OH, 4.61 g compound V (obtained in 3.1 synthesis) are added, for 0.5 hour, at 40 − 50°. The mixture is refluxed (≈ 80°) for 3 hrs, when the compound V is converted into product VII, as checked by means of paper chromatography (eluent E_2 = HCOOH). 50 ml water are added, the alcohol is distilled, then the mixture is poured over 100 ml water, neutralized with concentrated HCl to pH 6 — 6.5 and filtered; the precipitate is washed with 250 ml water and dried at 70 — 80°. 3.27 g product VII are obtained.

3.5. Using analogous conditions to those described of synthesis 3.3, from 3.27 g product VIII and 40 ml $ClSO_3H$, 2.8 g product IX are obtained.

3.6. To a solution of 1.12 ml (3.52 g; 0.022 mol) Br_2 in 45 ml 100 % H_2SO_4de 7.18g compound VI are added, for 0.5 hour, at 0 — 10°. The solution is stirred for 6 hrs raising slowly the temperature up to 25°, then is heated for 3 hrs at 96 — 100°. The mixture is cooled to 0°, poured over 170 g ice and filtered; the precipitate is washed with water until the filtrate is neutral and dried at 75 — 80°, affording 7.78 g product X.

3.7. Similarly, from 7.78 g of product VII, 8.28 g product XI are obtained.

3.8. A mixture of 10.1 g (25 mmol) bromamine acid, 4g K_2CO_3 and 0.25 g copper powder in 125 ml water is heated to 90° until the bromamine acid is completely dissolved; a hot solution of 4g (2.6 mmol) thiosalicylic acid and 3.6 g K_2CO_3 in 25 ml water and 0.1 g copper powder are then added. The temperature is raised to 95 — 98° for 4 hrs. The colour of the reaction mixture turns from red to bluish-violet, and the evolution of the reaction is controlled by means of paper chromatography (eluent E_1). Finnaly, when the reaction ends, the mixture is cooled to 20°, sodium chloride and HCl concentrated are added to precipitate product XIII at pH= 7; after 1 hour, necessary to completely precipitate the product XIII, it is filtered, washed with 100 ml 22 % NaCl and dried at 40 — 50°, yielding 15.8 product XIII (this includes a quantity of sodium chloride).

3.9. If it uses 15.8 g product XIII (obtained in 3.8 synthesis) and it works in conditions similar to those described in synthesis 3.2 finally, 8.8g product XIV are obtained. (The drying was carried out, finally, at 60 — 70°).

3.10. Using analogous conditions to those described of synthesis 3.3, from 8.8 g product XIV and 100 ml $ClSO_3H$, 8.2 g product XVI are obtained. (The drying was carried out, finally, at 60—70^3.)

3.11. Using analogous conditions to those described of synthesis 3.4, from 9.54 g product XIII (obtained in 3.8 synthesis), 27.6 g KOH and 75 ml CH_3OH, 7.05 g product XV are obtained. (The drying was carried out, finally, at 60 — 70°).

3.12. Using analogous conditions to those described of synthesis 3.3, from 7.05 g product XV and 85 ml $ClSO_3H$, 6.13 g product XVII are obtained. (The drying was carried out, finally, at 60 — 70°).

3.13. Using analogous conditions to those described of synthesis 3.6, from 3.75 g product XIV, 0.56 ml (1.76 g; 0.011 mol) Br_2 and 25 ml 100 % H_2SO_4, 3.97 g product XVIII are obtained.

3.14. Similarly, from 4.05 g of product XV, 4.33 g product XIX are obtained.

4. ANALYSES

The analyzed compounds were previously purified by recrystallization from glacial acetic acid. The melting points of the compounds and N % (by microcombustions) were determined. The results are presented in table 1. The purified compounds were subjected to chromatographic, spectral and tinctorial analyses.

4.1. CHROMATOGRAPHY

Chromatographic elutions were carried out on Whatman paper No. 1, in ascendent system, at 25°, in order to follow the reaction and to chek the purity of recrystallized compounds. The results are presented in table 1.

Table 1

Melting points of compounds, N% analyses and paper chromatography

Compounds	Empirical formula	MP °C	N% Calc. Found	Eluent	Elution time [min.]	R_f
V	$C_{21}H_{11}O_3NSNa_2$	—	—	E_1	20	0.661
VI	$C_{21}H_{13}O_5N$	210	—	E_2	30	0.643
VII	$C_{22}H_{15}O_6N$	183	—	E_2	60	0.302
VIII	$C_{21}H_{11}O_4N$	215	4.10 3.87	E_2	30	0.627
IX	$C_{22}H_{13}O_5N$	196	3.77 3.58	E_2	60	0.282
X	$C_{21}H_{10}O_4NBr$	157	3.33 3.65	E_1	20	0.660
XI	$C_{22}H_{12}O_5NBr$	187	3.11 3.41	E_1	20	0.434
XIII	$C_{21}H_{11}O_7NS_2Na_2$	—	—	E_1	30	0.747
XIV	$C_{21}H_{13}O_4NS$	115	—	E_1	30	0.808
XV	$C_{22}H_{15}O_5NS$	197−9	—	E_1	30	0.828
XVI	$C_{21}H_{11}O_3NS$	172−4	3.92 3.66	E_1	30	0.722
XVII	$C_{22}H_{13}O_4NS$	175	3.61 3.34	E_1	30	0.683
XVIII	$C_{21}H_{10}O_3NSBr$	180	3.21 3.52	E_1	20	0.680
XIX	$C_{22}H_{12}O_4NSBr$	250	3.00 3.31	E_1	20	0.385

$E_1 = CH_3COOH : H_2O : n - C_4H_9OH = 5 : 5 : 4$ (in volumes).
$E_2 = HCOOH$

In all the cases, N.N-dimethylformamide was used as solvent; the chromatography papers were impregnated with a 10% solution of 1-bromonaphthalene in ethanol.

4.2. SPECTRAL ANALYSIS

Infrared and visible absorption spectra of products were recorded. *IR spectra* were recorded using a UR−10 spectrophotometer, in pellet KBr.

Characteristic vibration frequencies ν (cm^{-1}):

Compound VIII : 710 s; 740 m; 800 m; 832 m; 1170 m; 1287 v.s; 1459 m; 1545s; 1595 v.s; 1616 v.s; 1642 s 1670 m; 3315 m; 3432 m.

Compound IX : 721 m; 751 m; 1159 m; 1285 v.s; 1460 s;

1480 s ; 1539 s ; 1570 m ; 1590 s ; 1611 m ; 1625 m ; 1660 m ; 2930 m ; 3290 m ; 3450 m.

Compound X : 712 s ; 740 m ; 1170 m ; 1285 v.s ; 1535 s ; 1598 v.s ; 1641 m ; 1672 m ; 3315 m ; 3435 m.

Compound XI : 722 m ; 742 m ; 1170 m ; 1215 m ; 1287 v.s ; 1442 s ; 1460 s ; 1480 s ; 1538 s ; 1580 s ; 1592 s ; 1622 m ; 1661 m ; 2930 m ; 3295 m ; 3432 m.

Compound XVI : 719 m ; 800 w ; 1169 m ; 1291 s ; 1440 m ; 1591 s ; 1665 m ; 3340 m ; 3425 m.

Compound XVII : 725 m ; 800 w ; 840 w ; 1160 m ; 1215 m ; 1285 s ; 1470 m ; 1540 s ; 1590 s ; 1645 s ; 2920 m ; 3322 m ; 3440 m.

Compound XVIII : 725 m ; 800 w ; 828 w ; 1165 m ; 1250 s ; 1280 s ; 1410 s ; 1460 m ; 1595 s ; 1662 s ; 3330 m ; 3420 w.

Compound XIX : 718 m ; 810 m ; 830 m ; 1165 m ; 1270 m ; 1290 m ; 1460 m ; 1605 s ; 1645m ; 1690 m ; 2925 m ; 3290 m ; 3422 m.

(w = weak ; m = medium ; s = strong ; v.s. = very strong).

Visible spectra were determined with a "CF–4 Optica Milano" apparatus. The determinations were carried out in N.N.-dimethyl-formamide and the extinction coefficients ε_{max} were calculated. The characteristic absorption maxima λ_{max} and lg ε_{max} are presented in table 2.

Table 2

Maxima absorption in the visible range

Compound	DMF $\lambda_{max.}$ [nm]	lg $\varepsilon_{max.}$	Compound	DMF $\lambda_{max.}$ [nm]	lg $\varepsilon_{max.}$
VI	495 524 568	3.82 3.76 3.60	XIV	457.5 481	3.41 3.48
VII	490 551	3.75 3.74	XV	490 517 550	3.83 3.98 3.88
VIII	494 530 568.5	3.66 3.54 3.37	XVI	473 519	3.41 3.31
IX	495 545	3.92 3.87	XVII	482 518 551 590	3.35 3.45 3.44 3.31
X	498 532 568.5	3.80 3.68 3.53	XVIII	479.5	3.47
XI	496 516 549	4.00 4.02 3.93	XIX	487 515 547.5 589	3.21 3.27 3.24 3.04

4.3. TINCTORIAL ANALYSIS

The synthesized compounds with 6-aminonaphth [2, 3-c] xanthene-5,8,14-trione and 6-aminonaphth[2,3-c]thioxanthene-5,8,14-trione structure were used as disperse dyes for "Terom" polyester fibres.

The results of the determinations with dyed fibres are presented in table 3 ; the colours were defined according to C.I. Hue Chart .[22]

Generally, the dyeings obtained are distinguished by very good affinity of the dyes for polyester fibres, good fastness to light and moderate fastness to wet treatments.

A good agreement is observed between the colours seen on the dyed samples and the values of the determined absorption maxima. [23]

The tinctorial analysis shows that synthesized products have suited qualities for applying to polyester fibres dyeing.

Table 3

Determinations with dyed fibres

Compound	Colour	Fastness				
		Light	Washing 40°	Alkaline perspiration pH = 8.4	Thermofixation	Rubbing
VIII	reddish-brown 26	5	4–5/5/4–5	4–5/4/4–5	4/3/3–4	4
IX	red 9	5–6	4–5/4–5/4–5	4–5/4/4–5	4/3–4/4	4
X	reddish-brown 26–32	5	4–5/5/4–5	4–5/5/4	4/3–4/4	4
XI	bluish-red 9–10	5–6	4–5/4–5/4–5	4–5/4/4–5	4–5/4/4	4
XVI	brown 24–25	4–5	4–5/5/4–5	4–5/4–5/4–5	4/3–4/4	3–4
XVII	reddish-violet 35–36	4–5	4–5/4–5/4–5	4–5/4/4–5	3–4/3–4/4	4
XVIII	brown 24–23	4–5	4–5/4–5/4	4–5/4–5/4	4/4–5/4–5	4
XIX	pink 50–49	4–5	4–5/4–5/4–5	4–5/4–5/4–5	4/4/4	4

---

[22] C. I. Hue Indication Chart, American Association of Textile Chemists and Colourists, Lowell Institute. Lowell. Massachusetts, USA.

[23] E. N. ABRAHART, "Deyes and their Intermediates", Pergamon Press, London, 1966, p. 3.

Revue Roumaine de Chimie, **21**, *8*, 1237–1245 (1976)

GREFFAGE MÉCANO-CHIMIQUE DES POLYOXYMÉTHYLÈNES. V[1]

ASPECTS CINÉTIQUES AU BROYAGE VIBRATOIRE

CR. I. SIMIONESCU et AMALIA CRUSOS
Institut de Chimie Macromoléculaire « P. Poni », Jassy, 41 A, Aleea Gr. Ghica Vodă

Reçu le 15 juillet 1975

Les auteurs étudient l'influence du milieu de la destruction par broyage vibratoire des polyoxyméthylènes. On détermine les modifications de la constante de vitesse de destruction, de la masse moléculaire limite et du nombre des macroradicaux formés dans le processus.

I. INTRODUCTION

Au commencement, quelques données sur le sujet abordé. En 1940 Löbering et Hilber montrent que la solubilité des polyoxyméthylènes augmente par broyage vibratoire.[2] Plus tard, Butiaghin et collab. [3,4] présentent les spectres R.P.E. obtenus à la destruction mécano-chimique des polymères à base de formaldéhyde, établissant que le processus de la scission des chaines se déroule d'après le mécanisme radicalaire.

Pazonyi et ses collab. [5] étudient la corrélation entre le degré de destruction et les dimensions des granules du polymère dans le processus de broyage vibratoire. Pour les démonstrations, à côté des polyméthylmétacrylate, polychlorure de vinyle et polystyrène ils utilisent aussi le polyformaldéhyde.

En suivant l'élucidation des nouveaux aspects et pour compléter les données concernant la destruction par broyage vibratoire des polyoxyméthylènes, dans des travaux antérieurs [1,6–8] nous avons présenté et commenté une série de résultats.

En ce qui suit nous nous occuperons de quelques aspects de la cinétique du processus de broyage vibratoire en fonction de la nature du milieu de destruction.

[1] IVème partie : A. Crusos et Cr. Simionescu, *Rev. Roumaine Chim.*, **20**, 929 (1975).
[2] J. Löbering et Hilber, *Ber. dtsch. chem. Gess.*, **73**, 1382 (1940).
[3] V. Radzig et P. Butiaghin, *Vysokomol. Soedineniya*, **7**, 922 (1965).
[4] M. Kisliuk et P. Butiaghin, *Vysokomol. Soedineniya*, **9**, 612 (1967).
[5] T. Pazonyi, F. Tudos et M. Miklos, *Műanyag Gumi*, **6**, 462 (1969).
[6] Cr. Simionescu, D. Feldman et A. Crusos, *Bull. Soc. chim. France*, **1968**, 1525.
[7] A. Crusos, D. Feldman et Cr. Simionescu, *Rev. Roumaine Chim.*, **13**, 1489 (1968).
[8] Cr. Simionescu, A. Crusos et D. Feldman, *Rev. Roumaine Chim.*, **16**, 4 (1971).

II. RÉSULTATS ET DISCUSSIONS

En maintenant les conditions expérimentales données dans un travail antérieur,[8] on a étudié l'influence du milieu gazeux sur le processus mécanochimique. Ainsi on a travaillé tant en milieu inerte (azote), qu'en milieu actif en présence d'accepteurs de radicaux (oxygène, monoxyde d'azote).

Conformément aux données de la figure 1, la plus puissante destruction a lieu en présence du monoxyde d'azote, accepteur des radicaux bien connu. Le comportement résulte de son paramagnétisme plus prononcé.

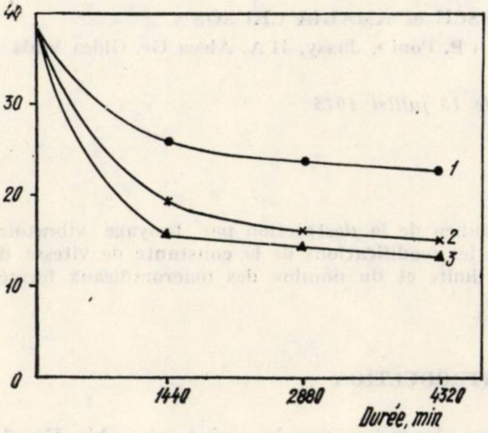

Fig. 1. — Variation de la masse moléculaire en fonction de la durée et du milieu de broyage : (1) Delrin-500 dégradé en milieu d'azote ; (2) Delrin-500 dégradé en milieu d'oxygène ; (3) Delrin-500 dégradé en milieu de monoxyde d'azote.

Dans ces conditions dans lesquelles le processus de destruction se déroule différemment nous avons calculé la constante de la vitesse de destruction, (K_d), la masse moléculaire limite, (M_∞) et le nombre des macroradicaux, (R), formés dans le processus.

L'étude de la scission des chaînes macromoléculaire soumises à l'action des différentes sollicitations mécaniques a permis d'établir des expressions qui définissent la cinétique du processus de la destruction. Ainsi Baramboim propose l'équation [9] :

$$\frac{\mathrm{d}\left(\dfrac{P_t - P_\infty}{P_\infty}\right)}{\dfrac{P_t - P_\infty}{P_\infty}} = -K_d \, \mathrm{d}t$$

D'après l'intégration il résulte :

$$P_t = (P_0 - P_\infty)\, \mathrm{e}^{-K_d t} + P_\infty \qquad (1)$$

où P_0 est le degré de polymérisation initial, P_t est le degré de polymérisation au moment t, et K_d représente la constante de la vitesse de destruction.

---

[9] N. Baramboim, « Mekhanokhimia polimerov », Izd. nauchino-tekhnicheskoi literatury, RSFSR, Moskva, 1961, p. 42.

Pour le même processus, Goto-Fujiwara ont établi la relation[10] :

$$-\frac{\mathrm{d}P_t}{\mathrm{d}t} = K_d(P_t - P_\infty)^2$$

ou sous forme intégrée :

$$\frac{1}{(P_t - P_\infty)} = \frac{1}{(P_0 - P_\infty)} + K_d\, t \tag{2}$$

Pour vérifier la validité de ces deux équations et pour préciser laquelle exprime plus fidèlement le processus de destruction par broyage vibratoire on a effectué les calculs correspondants.

Ainsi, partant de l'équation de Baramboim de la forme :

$$M_t = (M_0 - M_\infty)\, \mathrm{e}^{-Kd\, t} + M_\infty$$

pour augmenter la précision des déterminations on a appliqué la méthode des moindres carrés, de laquelle on retient les parties principales du raisonnement de calcul. Comme il est connu, si on note avec M_0 ; $M_1, M_2, \ldots M_4$ les masses moléculaires respectives au moment $t = 0$, $t_1 = 24\ h, \ldots t_4 = 96\ h$ et $Z = \mathrm{e}^{-24K_d}$ de l'équation (1) nous conduit au système linéaire ;

$$\begin{cases} Z(M_1 - M_0) + M_1 - M_2 = 0 \\ Z(M_2 - M_1) + M_2 - M_3 = 0 \\ Z(M_3 - M_2) + M_3 - M_4 = 0 \end{cases} \tag{3}$$

On applique à ce système linéaire la méthode des moindres carrés, et il résulte :

$$Z = \sum_{K=0}^{3} (M_{k+1} + M_k)\,(M_{k+2} - M_{k+1}) / \sum_{K=0}^{3} (M_{k+1} - M_k)^2 \tag{4}$$

Une fois Z déterminé la valeur de K_d se calcule à l'aide de la relation :

$$K_d = -1/24 \ln Z, \tag{5}$$

On peut déterminer la valeur de M_∞ soit par voie graphique, soit par la méthode des moindres carrés. Dans ce dernier cas, en remplaçant dans le système d'équation : $M_k = (M_0 - M_\infty)Z^k + M_\infty$, où $k = 1, 2, 3, 4$, la valeur du Z déterminée antérieurement, on obtiendra un système d'équations linéaires pour M_∞. En appliquant la méthode des moindres carrés pour ce système linéaire, il résulte :

---

[10] K. Goto et H. Fujiwara, *Chem. High. Polymers* (*Japan*), **258**, 827 (1966).

$$M_\infty = \sum_{K=1}^{4} (1 - Z^k)(M_k - M_0 Z^k) / \sum_{K=1}^{4} (1 - Z^k)^2 \qquad (6)$$

Les valeurs obtenues pour K_d et M_∞ sont présentées dans le tableau 1.

Tableau 1

La masse moléculaire limite (M_∞) et la constante de la vitesse de destruction, (K_d) calculées à base d'équation de Baramboim

Milieu de destruction	Masse moléculaire limite (M_∞)	Constante de la vitesse de destruction (K_d) min^{-1}
Azote	$20{,}83 \cdot 10^3$	$1{,}128 \cdot 10^{-3}$
Oxygène	$14{,}42 \cdot 10^3$	$1{,}499 \cdot 10^{-3}$
Monoxyde d'azote	$13{,}58 \cdot 10^3$	$2{,}342 \cdot 10^{-3}$

Pour l'équation Goto-Fujiwara, en appliquant le principe des moindres carrés nous arrivons à un système d'équations non linéaires pour K_d et M_∞, dont la résolution est plus compliquée et non compensée par une précision plus avancée. C'est la raison pour laquelle on a fait appel à la méthode graphique (figure 2 et tableau 2).

Tableau 2

Données pour le calcul de la constante de la vitesse de destruction, (K_d), par la méthode graphique (équation Goto-Fujiwara), au broyage vibratoire du Delrin-500 en différents milieux

Milieu de broyage	Durée (min)	M_t	Degré de polymérisation (P_t)	$\left(\frac{1}{P_t - P_\infty}\right) \cdot 10^2$
Azote	0	$47 \cdot 10^3$	1 566	0,11
”	1 440	$26 \cdot 10^3$	866	0,50
”	2 880	$24 \cdot 10^3$	733	1,49
”	4 320	$21{,}7 \cdot 10^3$	723	1,75
		$K_d = \text{tg}\alpha$ $K_d = 0{,}395 \cdot 10^{-3} \text{min}^{-1}$		
Oxygène	0	$47 \cdot 10^3$	1 566	0,10
”	1 440	$19 \cdot 10^3$	633	0,30
”	2 880	$16 \cdot 10^3$	533	0,59
”	4 320	$14{,}3 \cdot 10^3$	476	0,90
		$K_d = 0{,}194 \cdot 10^{-3} \text{min}^{-1}$		
Monoxyde d'azote	0	$47 \cdot 10^3$	1 566	0,10
”	1 440	$16 \cdot 10^3$	533	0,59
”	2 880	$15 \cdot 10^3$	500	0,74
”	4 320	$14 \cdot 10^3$	466	1
		$K_d = 0{,}232 \cdot 10^{=3}\ \text{min}^{-1}$		

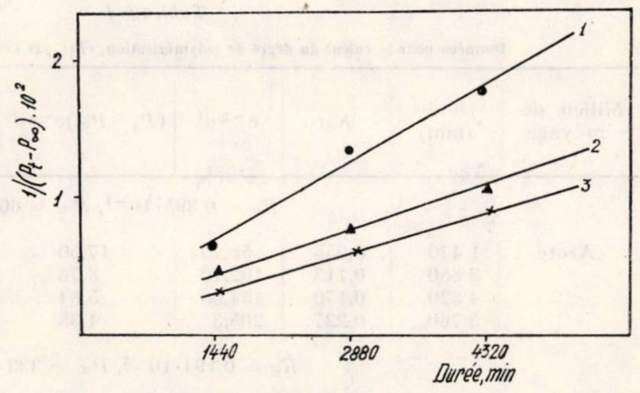

Fig. 2. – Relation $1/(P_t-P_\infty)$ en fonction de la durée du processus de destruction : (1) en milieu d'azote ; (2) en milieu de monoxyde d'azote ; (3) en milieu d'oxygène.

Une fois déterminées les constantes de destruction, on a pu passer au calcul pour le degré de polymérisation (tableaux 3 et 4).

À la fin, conformément aux données centralisées dans le tableau 5 et les graphiques des figures 3 – 5, il résulte que l'équation de Baramboim satisfait mieux le processus de destruction par mouture vibratoire.

Un autre aspect cinétique qui a été étudié concerne le nombre des macroradicaux libres, formés dans différents milieux de réaction.

Tableau 3

Données pour le calcul du degré de polymérisation, (P_t), par l'équation de Baramboim

Milieu de broyage	Durée (min)	$K_d t$	$e^{-K_d t}$	$(P_0-P_\infty)e^{-K_d t}$	$P_t=(P_0-P_\infty)e^{-K_d t}+P_\infty$	
					Valeurs calculées	Valeurs expérimentales
		$K_d = 1{,}128\cdot 10^{-3}$,		$P_\infty = 694$		
Azote	1 440	1,6263	0,2019	176,144	870,1	867
”	2 880	3,2486	0,0407	35,750	729	733
”	4 320	4,8720	0,0082	6,970	701	723
”	5 760	6,4971	0,0015	1,308	695	666
		$K_d = 1{,}499\cdot 10^{-3}$,		$P_\infty = 481$		
Oxygène	1 440	2,158	0,122	132,37	613	633
”	2 880	4,317	0,013	14,105	495	533
”	4 320	6,470	0,0015	1,620	483	467
”	5 760	8,630	0,00017	0,184	481	433
		$K_d = 2{,}342\cdot 10^{-3}$,		$P_\infty = 452$		
Monoxyde d'azote	1 440	3,372	0,036	40,104	492	533
”	2 880	6,744	0,0011	1,225	453	500
”	4 320	10,117	0,00004	0,045	452	466
”	5 760	13,489	$0{,}14.10^{-5}$	0,001	452	367

Tableau 4

Données pour le calcul du degré de polymérisation, (P_t), par l'équation de Goto-Fujiwara

Milieu de broyage	Durée (min)	$K_d t$	$e^{-K_d t}$	$(P_0 - P_\infty)e^{-K_d t}$	$P_t = (P_0 - P_\infty)e^{K_d t} + P_\infty$ Valeurs calculées	 Valeurs expérimentales
$K_d = 0{,}395 \cdot 10^{-1}$, $P_\infty = 666$						
Azote	1 440	0,056	51,40	17,50	684	867
,,	2 880	0,113	102,70	8,76	675	733
,,	4 320	0,170	154,00	5,84	672	723
,,	5 760	0,227	205,3	4,38	670	666
$K_d = 0{,}194 \cdot 10^{-3}$, $P_\infty = 433$						
Oxygène	1 440	0,027	27,03	34,51	468	633
,,	2 880	0,055	53,06	17,58	451	533
,,	4 320	0,083	79,18	11,78	445	467
	5 760	0,117	110,16	8,46	441	433
$K_d = 0{,}232 \cdot 10^{-3}$, $P_\infty = 366$						
Monoxyde d'azote	1 440	0,033	40,60	29,55	396	533
	3 880	0,066	81,66	14,78	381	500
	4 320	0,100	121,24	9,89	376	466
	5 760	0,133	160,60	7,47	373	367

Tableau 5

Degré de polymérisation en fonction de la durée du processus de destruction

Milieu de broyage	Durée (min)	Degré de polymérisation Valeurs calculées avec l'équation (1)	 Valeurs calculées avec l'équation (2)	 Valeurs expérimentales
		$K_d = 1{,}128 \cdot 10^{-3}$	$K_d = 0{,}395.10^{-3}$	
Azote	1 440	870	684	867
,,	2 880	729	675	733
,,	4 320	701	672	723
,,	5 760	695	670	666
		$K_d = 1{,}499 \cdot 10^{-3}$	$K_d = 0{,}194 \cdot 10^{-3}$	
Oxygène	1 440	613	468	633
,,	2 880	495	451	533
,,	4 320	483	445	467
,,	5 760	481	441	433
		$K_d = 2{,}342 \cdot 10^{-3}$	$K_d = 0{,}232 \cdot 10^{-3}$	
Monoxyde d'azote	1 440	492	396	533
,,	2 880	453	381	500
,,	4 320	452	376	466
,,	5 760	452	373	367

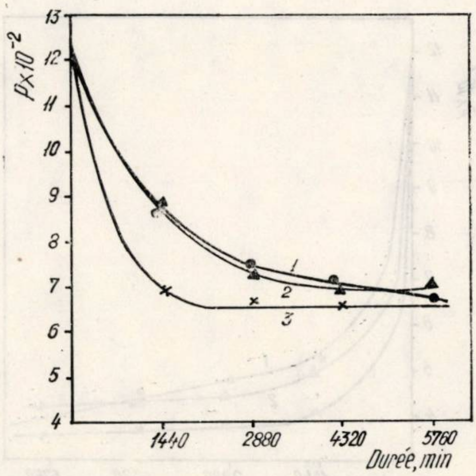

Fig. 3. — Comparaison entre les données expérimentales et les valeurs calculées, à la destruction en milieu d'azote : (1) valeurs expérimentales ; (2) valeurs calculées avec l'équation (1) ; (3) valeurs calculées avec l'équation (2).

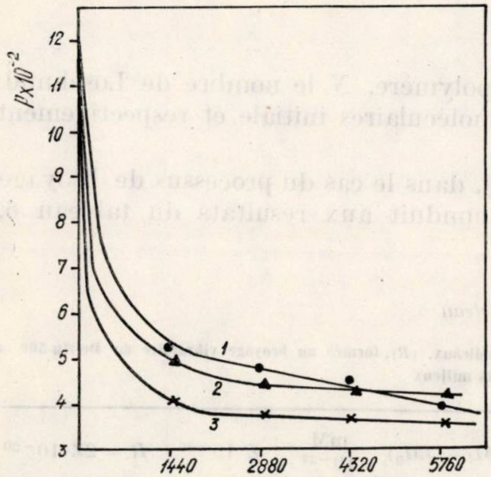

Fig. 4. — Comparaison entre les données expérimentales et les valeurs calculées, à la destruction en milieu d'oxygène : (1) valeurs expérimentales ; (2) valeurs calculées avec l'équation (1) ; (3) valeurs calculées avec l'équation (2).

Si on admet que pendant le processus de destruction, à la scission d'une liaison Z, il se forme deux fragments radicalaires, (R), le nombre de ceux-ci est donné par la relation :

$$R = 2Z \tag{7}$$

Pour les conditions limites de destruction, quand le polymère atteint la masse moléculaire limite, Baramboim propose l'expression [9] :

$$R = 2Z = 2\mathrm{m}N(I/M_{\infty} - 1/M_0) \tag{8}$$

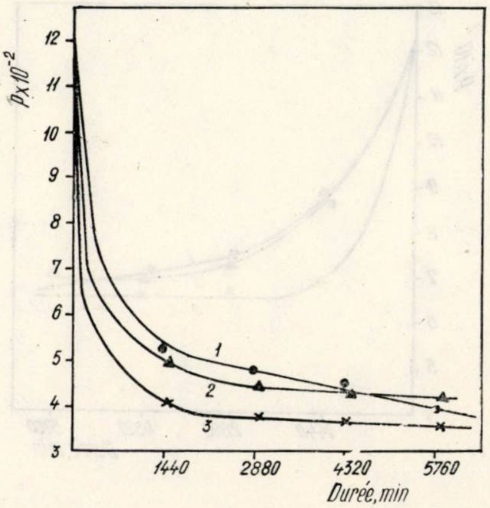

Fig. 5. — Comparaison entre les données expérimentales et les valeurs calculées, à la destruction en milieu de monoxyde d'azote : (1) valeurs expérimentales ; (2) valeurs calculées avec l'équation (1) ; (3) valeurs calculées avec l'équation (2).

dans laquelle *m* sont grammes de polymère, *N* le nombre de Loschmid, M_0 et M_∞ représentent les masses moléculaires initiale et respectivement limite.

L'application de la relation (8), dans le cas du processus de broyage vibratoire des polyoxyméthylènes conduit aux résultats du tableau 6,

Tableau 6

Nombre des liaisons rompues, (Z), et nombre des macroradicaux, (*R*), formés au broyage vibratoire du Delrin-500 en différents milieux

Milieu de broyage	Durée (h)	$M_t \cdot 10^{-3}$	$(1/M_t - 1/M_0)$	$\frac{\text{mM}}{10^{-23}}$	$Z \cdot 10^{-20}$	$R = 2Z \cdot 10^{-20}$
Azote	0	47,64	—	—	—	—
,,	24	26,13	$0{,}017 \cdot 10^3$	120,46	2,047	4,094
,,	48	21,95	$0{,}024 \cdot 10^3$	120,46	2,891	5,782
,,	72	21,67	$0{,}025 \cdot 10^3$	120,46	3,011	6,022
,,	96	20,36	$0{,}028 \cdot 10^3$	120,46	3,373	6,746
Oxygène	0	47,64	—	—	—	—
,,	24	19,54	$0{,}030 \cdot 10^3$	120,46	3,614	7,228
,,	48	16,20	$0{,}041 \cdot 10^3$	120,46	4,939	9,878
,,	72	14,52	$0{,}048 \cdot 10^3$	120,46	5,782	11,564
,,	96	13,39	$0{,}054 \cdot 10^3$	120,46	6,505	13,010
Monoxyde	0	47,64	—	—	—	—
d'azote	24	15,40	$0{,}044 \cdot 10^3$	120,46	5,300	10,600
,,	48	15,07	$0{,}045 \cdot 10^3$	120,46	5,421	10,142
,,	72	14,94	$0{,}046 \cdot 10^3$	120,46	5,541	11,082
,,	96	10,92	$0{,}070 \cdot 10^3$	120,46	8,432	16,864

qui montre le nombre des liaisons rompues en fonction des conditions de broyage et de la durée de destruction.

III. CONCLUSIONS

Dans le processus de broyage vibratoire des polyoxyméthylènes, la nature du milieu de destruction exerce une influence puissante, déterminant les modifications de la constante de vitesse de destruction, de la masse moléculaire limite et le nombre des radicaux formés.

Pour le calcul des constantes de la vitesse de destruction on a appliqué avec de bons résultats la méthode des moindres carrés.

Les résultats obtenus mettent en évidence que l'équation proposée par Baramboim satisfait mieux le processus de destruction par broyage vibratoire.

Revue Roumaine de Chimie, **21**, *8*, 1247–1251 (1976)

ZUR KOPOLYMERISATION. IV[1–3]

DAS MATHEMATISCHE MODELL DER BILDUNG EINES BINÄREN KOPOLYMERS : DIE VERBESSERTE VERSION

IOAN MOȚOC, DAN CIUBOTARIU und ȘTEFAN HOLBAN
Chemiekatheder der Universität Timişoara, 1900 – Timişoara, Rumänien

Eingegangen am 8. November 1974

In einer vorhergehenden Arbeit wurde ein mathematisches Modell der Bildung eines binären Kopolymers unter folgenden Bedingungen mitgeteilt : die Konzentrationen der Monomere sind einheitlich und es wird mit geringen Umsätzen gearbeitet, und/oder die Konzentrationen sind einheitlich und stationär. Vorliegender Bericht bringt die verbesserte Variante dieses Modells, in der sich die weiter oben erwähnten Einschränkungen erübrigen. Das hier vorgeschlagene Modell liegt unserem Programm MEMORY 3 zugrunde.

1. EINLEITUNG

Wie schon bekannt[4–6] wird die binäre Kopolymerisation von den Reaktionen :

$$\sim A_I^\bullet + A_J \xrightarrow{k_{ij}} \sim A_I A_J^\bullet,\ J = 1, 2\,;\ I = 1, 2 \tag{1}$$

in denen A_I und A_J, $I = 1, 2$, $J = 1, 2$ Monomere sind und
$\sim A_I^\bullet$ ein mit einem aktiven Ende $A_I^\bullet$ versehenem Makroradikal ist, beschrieben.

Die Verhältnisse :

$$\frac{k_{ii}}{k_{ij}} = r_I,\ I = 1, 2\,;\quad J = 1, 2\,;\quad I \neq J$$

bestimmen die Kopolymerisationskonstanten.

---

[1] I. Moțoc und D. Ciubotariu, *Rev. Roumaine Chim.*, **21**, 949 (1976).
[2] I. Moțoc, D. Ciubotariu und Șt. Holban, *Rev. Roumaine Chim.*, **21**, 769 (1976).
[3] I. Moțoc, D. Ciubotariu und Șt. Holban, *Rev. Roumaine Chim.*, **21**, 775 (1976).
[4] G. E. Ham, ,,Copolymerization'', Interscience, New York, 1964.
[5] Houben-Weyl, ,,Methoden der organischen Chemie'', Band XIV/1, Makromolekuläre Stoffe, Teil 1, Georg Thieme Verlag, Suttgart, 1961.
[6] P. T. Flory, ,,Principles of Polymer Chemistry'', Cornell University Press, Ithaca, New York, 1953.

2. DAS MATHEMATISCHE MODELL

In einer vorhergehenden Arbeit[1] wurde ein mathematisches Modell unter den Bedingungen:

$$[A_1] = [A_2] = 1 \tag{2}$$

oder

$$[A_1] \simeq [A_2] \simeq 1 \tag{3}$$

vorgeschlagen, mit der Spezifikation, daß im Falle (3) die Differenz bis zu eins sehr klein ist. [ ] : Konzentration.*

Unter diesen Bedingungen sind folgende Formeln gültig:

$$\frac{r_1}{1 + r_1} = P_{11}; \quad 1 - P_{11} = P_{12} \tag{4}$$

$$\frac{r_2}{1 + r_2} = P_{22}; \quad 1 - P_{22} = P_{21} \tag{5}$$

in denen,

P_{11} die Wahrscheinlichkeit der Addition eines Monomers A_1 an das Makroradikal$-A_1^\bullet$, und

P_{21} die Wahrscheinlichkeit der Addition eines Monomers A_1 an das Makroradikal$-A_2^\bullet$ darstellen.

Die Gleichungen (4) und (5) werden durch folgende Formeln:

$$P_{11} = \frac{r_1[A_1]}{[A_2] + r_1[A_1]} = \frac{r_1}{[A_2]/[A_1] + r_1} = \frac{r_1}{C + r_1} \tag{4a}$$

$$\mathrm{C} = \frac{[A_2]}{[A_1]}$$

$$P_{22} = \frac{r_2}{C^{-1} + r_2} \tag{4b}$$

ersetzt (und, wie ersichtlich, $P_{12} = 1 - P_{11}$; $P_{21} = 1 - P_{22}$); außerdem bleiben die Gleichungen (10) bis (13) aus der vorhergehenden Arbeit[1] erhalten.

Unter diesen Bedingungen wurde ein mathematisches Modell geschaffen, durch welches die Einschränkungen (2) und (3) vermieden werden konnten.

Auf Grund der oben besprochenen Bedingungen wurde das Programm, FORTRAN, MEMORY 3 ausgearbeitet.

---

* Die Hasseinheit der Konzentrationen ist indifferent, wenn diese einheitlich ausgedrückt werden.

Was das Programm betrifft, ist es vorteilhaft, $C = [A_2]/[A_1]$ in folgende Form zu bringen:

$$C = \frac{N(A_2)}{N(A_1) + N(A_2) + S} \bigg/ \frac{N(A_1)}{N(A_1) + N(A_2) + S}$$

$$C = N(A_2)/N(A_1)$$

Mit N(   ) wurde die Anzahl der Monomermoleküle (   ), mit S aber die Anzahl der Moleküle des Lösungsmittels oder des Verdünnungsmittels bezeichnet.

Die Hypothese einer gleichmäßigen Verteilung des Initiators im Reagenzgemisch ist notwendig. Wir nehmen an, daß diese Bedingung hier erfüllt ist. Wenn die Hypothese für gewisse Zonen des Reagenzgemisches wahr ist, so wird eine jede Zone einzeln behandelt, indem wir N (   ) nach Belieben wählen.

Das Programm MEMORY 3 beinhaltet den Zähler FRMOL der der Anzahl der die Polymerkette bildenden A_1 und A_2 Rechnung trägt, und die Umwertung der P_{IJ}, $I = 1{,}2$; $J = 1{,}2$ bestimmt, wenn:

$N(A_1) + N(A_2) = \text{FRMOL}$ und

$\text{FRMOL} \geqslant 1$

N(   )-Anzahl von (   )-Mol.

Betrachten wir den Anfangsmoment gekennzeichnet durch des Auslösen der Reaktion und durch den Start des Zählens der das Makromolekül bildenden Meren A_1 und A_2. Nach einiger Zeit erhält man:

die Anzahl der A_1-Meren: FRMOL 1

die Anzahl der A_2-Meren: FRMOL 2,

die die Bedingung:

FRMOL = FRMOL 1 + FRMOL 2

prüfen.

In diesem Falle wird:

$$P_{11} = r_1 \Big/ \left(r_1 + \frac{N(A_2)_0 - \text{FRMOL 2}}{N(A_1)_0 - \text{FRMOL 1}} \right), \tag{6}$$

und

$$P_{22} = r_2 \Big/ \left(r_2 + \frac{N(A_1)_0 - \text{FRMOL 1}}{N(A_2)_0 - \text{FRMOL 2}} \right) \tag{7}$$

Mit $N($ $)_0$ wurde die (   )-Molekülanzahl im Anfangsmoment notiert.

Ersichtlich ist FRMOL $\geqslant 1$ und eine ganze Zahl. Durch FRMOL wird die Umwertung der Wahrscheinlichkeiten P_{IJ}, $I = 1, 2$; $J = 1, 2$, mit der erwünschten Genauigkeit bestellt.

Die Gleichungen (6) und (7) verbessern wesentlich die erste Version[1] des mathematischen Modells der binären Kopolymerisation.

3. DIE TOPOLOGISCHE DARSTELLUNG

Auch hier bewahren wir die im Paragraph 3 der vorhergehenden Arbeit [1] angegebene Definition der topologischen Darstellung der Kopolymerisation.

Unter den von den Gleichungen (4a), (4b), (6) und (7) abgeleiteten Bedingungen wird sich die Länge der horizontalen Strecke dem „Graphen" entlang ändern. Die Änderung dieser Längen kann mittels der weiter oben erwähnten Gleichungen berechnet werden.

Durch den Verbrauch eines der Monomere können folgende Grenzfälle entstehen.

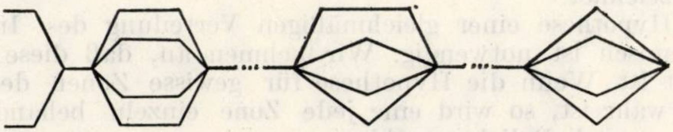

Abb.1. — Der Fall in welchem die Konzentration des Monomers *B* Null wird.

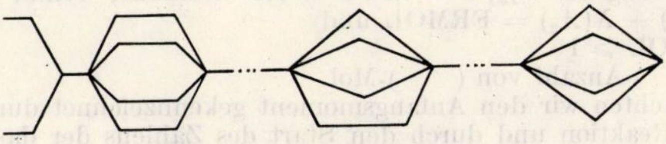

Abb.2. — Der Fall in welchem die Konzentration des Monomers A Null wird.

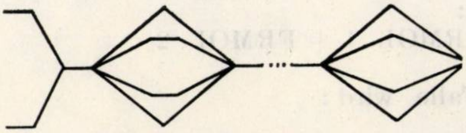

Abb.3. — Der Fall in welchem $r_1 = r_2 = 0$.

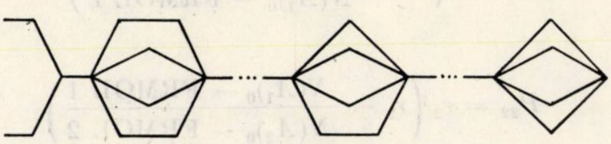

Abb. 4. — Der Fall in welchem $r_1 = \infty$ und $r_2 = \infty$.

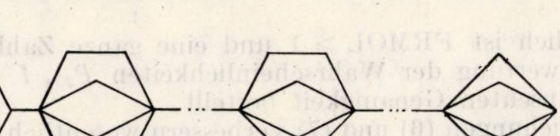

Abb. 5. — Der Fall in welchem $r_1 = \infty$, $r_2 = \infty$ und die Konzentration des Monomers A Nu l wird.

Abb. 1. weist jenen Fall auf, in welchem das Monomer A_2 während des Wachsens des Makroradikals verbraucht wird; in Abb. 2 wurde das Monomer A_1 verbraucht; in Abb. 3 homopolymerisieren A_1 und A_2 nicht, aber sie kopolymerisieren. Im Augenblick des Verbrauchs eines Monomers hört das Wachsen des Makroradikals auf. In Abb. 4 kopolymerisieren A_1 und A_2 nicht, aber ein jedes von ihnen homopolymerisiert und das Monomer A_2 wurde verbraucht; in Abb. 5 wurde das Monomer A_1 verbraucht.

SCHLUSSFOLGERUNGEN

i) Es wird ein verbessertes mathematisches Modell der binären Kopolymerisation vorgeführt;

ii) Die in vorhergehender Arbeit vorgeschlagene topologische Darstellung ist mit dem verbesserten Modell vereinbar und ist außerdem auch sehr anschaulich;

iii) Das vorgeschlagene mathematische Modell ist auf dem Digitalrechner darstellbar und liegt unserem Programm MEMORY 3 zugrunde.

Abb. 1 weist jenen Fall auf, in welchem das Monomer A_1 während des Wachsens des Makroradikals verbraucht wird; in Abb. 2 wurde das Monomer A_2 verbraucht; in Abb. 3 homopolymerisieren A_1 und A_2 nicht, aber sie kopolymerisieren. Im Augenblick des Verbrauchs eines Monomers hört das Wachsen des Makroradikals auf. In Abb. 4 kopolymerisieren A_1 und A_2 nicht, aber ein jedes von ihnen homopolymerisiert und das Monomer A_2 wurde verbraucht; in Abb. 5 wurde das Monomer A_1 verbraucht.

SCHLUSSFOLGERUNGEN

i) Es wird ein verbessertes mathematisches Modell der binären Kopolymerisation vorgeführt;

ii) Die in vorhergehender Arbeit vorgeschlagene topologische Darstellung ist mit dem verbesserten Modell vereinbar und ist außerdem auch sehr anschaulich;

iii) Das vorgeschlagene mathematische Modell ist auf dem Digitalrechner darstellbar und liegt unserem Programm MEMORY 3 zugrunde.

Revue Roumaine de Chimie, **21**, *8*, 1253–1261 (1976)

ZUR KOPOLYMERISATION. V[1-4]

DIE SIMULIERUNG DER BILDUNG EINES MAKROMOLEKÜLS DURCH BINÄRE KOPOLYMERISATION DAS PROGRAMM MEMORY 3

DAN CIUBOTARIU, IOAN MOŢOC, ŞTEFAN HOLBAN
Chemiekatheder der Universität Timişoara, 1900 – Timişoara, Rumänien

Eingegangen am 8. November 1974

Die Arbeit bringt das Programm in FORTRAN-Sprache, welches die Simulierung der Bildung eines Makromoleküls durch binäre Kopolymerisation, sichert. Es wird die wahrscheinlichste Verteilung der beiden Mere im Makromolekül geliefert. Es werden die kinetischen Bedingungen, in denen die Reaktion stattfindet (r_1, r_2), d.h. die Konversion, in Betracht gezogen.

ALLGEMEINES ÜBER DAS PROGRAMM

Name des Programms :	MEMORY 3
Sprache :	FORTRAN
Hardware :	IRIS 50
Notwendiger Informationsspeicher :	60 K
Das Material des Programms :	254 Lochkarten
Durchführungsdauer :	7 Sekunden je Makromolekül mit dem Polymerisationsgrad 1000.

HINWEIS

Mit einem Informationsspeicher von 60 K kann der maximale Polymerisationsgrad 10000 betragen.

1. EINLEITUNG

In vorhergehenden Arbeiten[1-3] wurde ein mathematisches Modell zur Bildung eines Makromoleküls durch binäre Kopolymerisation, in gegebenen Bedingungen, gebaut.

---

[1] I. Moţoc und D. Ciubotariu, *Rev. Roumaine Chim.*, **21**, 949 (1976).
[2] I. Moţoc, D. Ciubotariu und Şt. Holban, *Rev. Roumaine Chim.*, **21**, 769 (1976).
[3] I. Moţoc, D. Ciubotariu und Şt. Holban, *Rev. Roumaine, Chim.*, **21**, 775 (1976).
[4] I. Moţoc, D. Ciubotariu und Şt. Holban, *Rev. Roumaine Chim.*, **21**, 1247 (1976).

Das Programm, das in einer vorhergehenden Arbeit gebracht wurde und das das mathematische Modell als Basis hat, beseitigt die Beschränkungen, die in vorhergehenden Programmen aus der Serie MEMORY[1-3], gestellt wurden.

2. DIE BESCHREIBUNG DES PROGRAMMS

Die Struktur des Programms ist in Abbildung 1 dargestellt. Im Programm sind folgende funktionelle Einheiten enthalten:

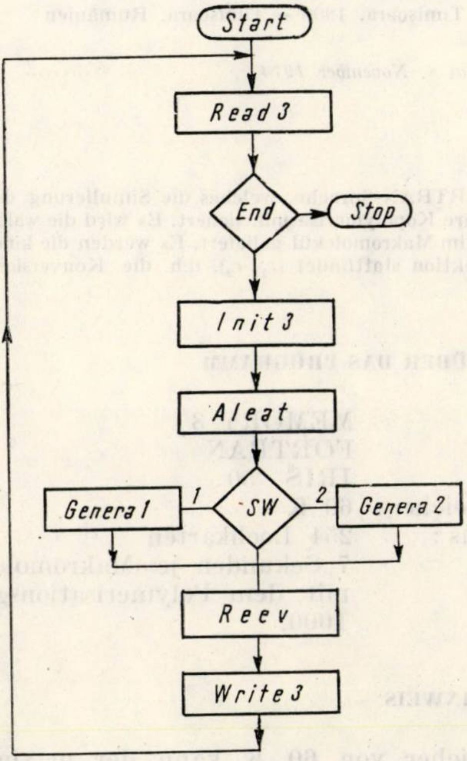

Abb. 1. — Die Struktur des Programms MEMORY 3.

2.1. READ 3

READ 3 sichert das Ablesen der Daten und das Ausfüllen der Matrixen mit den initiellen Daten. Es werden folgende Daten gelesen:

Lochkarte 1: Daten in bezug auf den simulierten Prozeß, NAME, FORMAT (40 A2);
Lochkarte 2: MER, *N*, FORMAT (I1, I6)
MER = 1, das erste Mer des Makromoleküls ist *A*,
= 2, das erste Mer des Makromoleküls ist *B*.
N, der Polymerisationsgrad.
Lochkarte 3: *R1*, *R2*, FORMAT (2F 14.10)
R1, *R2* — Kopolymerisationskonstanten.

Lochkarte 4 : *NA*, *NB*, FRMOL, FORMAT (3 I6),
NA — die Anzahl der Monomere *A*, die im Anfangsmoment im System vorhanden sind,
NB — die Anzahl der Monomere *B*, die im Anfangsmoment im System vorhanden sind,
FRMOL — die Anzahl der Monomere *A* plus *B*, notwendig zur Wieder-Bewertung der kinetischen Bedingungen des Prozeßablaufes ($1 \leqslant \text{FRMOL} \leqslant N$).

2.2. INIT 3

INIT 3 ist aus mehreren Teilen gebildet und hat folgende Rolle :

— sichert die Generierung des Makromoleküls mit der Bedingung, daß A das erste Mer sei, (INIT 1) ;

— sichert das Entstehen des Makromoleküls mit der Bedingung, daß B das erste Mer sei (INIT 2) ;

— sichert das Modellieren der kinetischen Bedingungen in denen der Prozeß stattfindet ;

— sichert die Bildung des Makromoleküls, mit der Bedingung, daß ein Monomer verbraucht wird (ENDA, ENDB).

2.3. ALEAT

ALEAT ist jener Teil durch welchen man eine Reihe von pseudoalleatoren Zahlen mit einer gleichförmigen Verteilung im Intervall (0,1) generiert. Es wird die Lehner-Methode verwendet. Der Teil verwendet ein Unterprogramm, in Assembler geschrieben, der nur für den Rechner IRIS 50 unbedingt notwendig ist. Man umgeht damit die binäre Überschreitung.

2.4. GENERA 1, GENERA 2

Das sind die Teile, durch welche man das Wachsen des Makromoleküls von Mer zu Mer simuliert, indem man die Natur des aktiven Endes des Makroradikals berücksichtigt, sowie die Reaktivität der Monomere diesem gegenüber [4,5].

2.5. REEW

Durch REEW sichert man :

— die Wieder-Bewertung der kinetischen Bedingungen, in denen sich der Prozeß des Wachsens des Makromoleküls abgewickelt hat, so daß :

— für FRMOL = 1 eine Wieder-Bewertung für jedes zusätzliche Monomermolekül stattfindet (höchster Feinheitsgrad) ;

---

[5] G. E. Ham, ,,Copolymerisation'', Interscience, New York, (Übersetzung in russischer Sprache, Khimia, 1971).

— für FRMOL $= K (K < N)$ die Bedingungen neu eingestellt werden, nachdem K Monomermoleküle reagiert haben;

— für FRMOL $= N$ man die in den Programmen MEMORY 1 und 2 beschriebene Lage erhält;

— die Bestellung ist in INIT 3 durchgeführt.

2.6. WRITE 3

WRITE 3 ist der Ausgangsteil, durch welchen folgende Daten geliefert werden:

— die Eingangsdaten,

— die wahrscheinlichste Form des Makromoleküls,

— die Natur der Blocks, ihre Größe und Lage durch Hinweis auf die Blocks derselben Natur, in Tabellenform.

3. DAS PROGRAMM

Das Programm ist folgendes:

```
C    1   C
C    2   C   MEMORY 3
C    3   C   DAS PROGRAM SIMULIERT DIE BILDUNG EINES MAKROMO-
             LEKUELS DURCH
C    4   C   BINARE KOPOLIMERIZATION
C    5   C   ES WERDEN FOLGENDE EINGANGSGROSSEN GELESEN :
C    6   C   MER = 1 DAS ERSTE GLIED DES MACROMOLEKUELS IST A
C    7   C   MER = 2 DAS ERSTE GLIED DES MACROMOLEKUELS IST B
C    8   C   N POLYMERISATIONSGRAD                 FORMAT (I1, I6)
C    9   C   R1, R2 KOPOLYMERISATIONSKONSTANTEN FORMAT (2F14.10)
C   10   C   NA, NB : URSPRUENGLICHE ANZAHL DER MONOMEREN VOM
             TYP A BZW. B.
C   11   C   FRMOL : DER WERT, DER DIE FREQUENZ DER NEUORDNUNG
             DER VERTEILUNG
C   12   C   DER MENGE PI BEDINGT (1 < FRMOL < N)    FORMAT (3I6)
C   13   C
    14   *   DEFINE FILE *1= 105, *2 = 108
    15       COMMON POLYM (10000), GTAB (5, 16)
    16       INTEGER SW, FRMOL, MER, NA, NB, NTBS, NTAS, NRA, NRB,
             NBA, NBB, RA, RB
    17       DIMENSION NAME (40)
    18       DATA I, J/2*1/, NBA, NBB/2*0/, PKT1, PKT2/2HA−, 2HB−/, KK/1/
    19       1 READ (105, 900, END = 170) (NAME (K), K = 1, 40)
    20       READ (105, 910) MER, N
    21       READ (105,  920)R1,  R2
    22       READ (105, 930) NA, NB, FRMOL
    23       WRITE (108, 940)
    24       WRITE (108, 900) (NAME (K), K = 1,40)
    25       WRITE (108, 950), N, R1, R2, FRMOL, NA, NB
    26       IA = 65539
    27       NRA = 0
    28       NRB = 0
    29       NTAS = 0
    30       NTBS = 0
    31       I = 1
C   32   C
C   33   C   INIT3
C   34   C
```

```
         IF((NB. LE.0). OR.(NA. LEXO)) GO TO 160
         IF(FRMOLXLEXO) GO TO 150
         C = FLOAT  (NA)/FLOAT  (NB)
         IF(MERXEQX1) CALL INIT 1 (SW, NRA, NTAS)
         IF(MERXEQ. 2) CALL INIT2 (SW, NRB, NTBS)
         IF(MERXLT. 1. OR. MERXGT.2) GO TO 150
    10   ALPHA = R1/(1./C + R1)
         BETA = 1.-R2/(C + R2)
         IF((ALPHA. LT. O.). OR. (ALPHA. GT. 1.) OR.
    C    (BETA. LT. O.).OR. (BETA. GT. 1.)) GO TO 150
    20   CONTINUE
         CALL MAS
         CALL ALEAT (IA, IB, X)
         CALL NMAS
         IA = IB
         IF(X.LE.O..OR. X GE.1.)GO  TO  140
         I = I + 1
         IF(I.GT.N)  GO  TO  130
         GO  TO  (30,  80),  SW
C   C
C   C    GENERA 1
C   C
         30 IF(NA. GT. NTAS) GO TO 40
         CALL ENDA (ALPHA, BETA, NTAS ,FRMOL, N. NA)
         GO  TO  50
         40 IF(X. LE. ALPHA) GO TO 70
    50   CONTINUE
         IF(NRA.EQ.1.OR. NRA. EQ. O) GO TO 60
         RA = NA - NTAS
         RB = NB-NTBS
         NBA = NBA + 1
         GTAB(1, J) = PKT1
         GTAB(2, J) = NRA
         GTAB(3,  J) = NBA
         GTAB (4,J) = RA
         GTAB (5,  J) = RB
         J = J + 1
         IF(J. GT. 14) CALL GRTAB(J)
    60   CONTINUE
         POLYM (I) = PKT2
         SW = 2
         NRA = 0
         NRB = NRB + 1
         NTBS = NTBS + 1
         CO  TO  120
      70 CONTINUE
         POLYM (I) = PKT1
         NRA = NRA + 1
         NTAS = NTAS + 1
         GO  TO  120
C   C
C   C    GENERA 2
C   C
    80   CONTINUE
         IF(NB. GT. NTBS)GO TO 90
         CALL ENDB(ALPHA, BETA, NTBS, FRMOL, N, NB)
         GO TO 100
    90   CONTINUE
         IF(X. LE. BETA) GO TO 100
         POLYM (I) = PKT2
```

```
             NRB = NRB + 1
             NTBS = DTBS + 1
             GO TO 120
       100   CONTINUE
             IF(NRB. EQ. 1. OR. NRB. EQ.0) GO TO 110
             RA = NA - NTAS
             RB = NB - NTBS
             NBB = NBB + 1
             GTAB(1, J) = PKT2
             GTAB(2, J) = NRB
             GTAB(3,  J) = NBB
             GTAB(4, J) = RA
             GTAB (5, J) = RB
             J = J + 1
             IF(J. GT. 14) CALL GRTAB (J)
       110   CONTINUE
             POLYM(I) = PKT1
             SW = 1
             NRB = 0
             NRA = NRA + 1
             NTAS = NTAS + 1
             GO  TO  120
C      C
C      C     REEW
C      C
       120   CONTINUE
             IF((ALPHA. EQ. O.). AND. (BETA. EQ. O.) OR.
             C ((ALPHA, EQ. 1.). AND. (BETA, EQ. 1))) GO TO 20
             IF ((NTAS + NTBS). LT. FRMOL) GO TO 20
             NA = NA-NTAS
             NB = NB - NTBS
             NTAS = 0
             NTBS = 0
             IF((NB.LT.O). OR. (NA. LT. O)) GO TO 160
             IF(NA, EQ. O) GO TO 123
             IF(NB. EQ. O) GO TO 126
             C = FLOAT  (NA)/FLOAT  (NB)
             GO  TO  10
C    C       ENDA
        123  CALL ENDA (ALPHA, BETA, NTAS, FRMOL, N. NA)
             GO  TO  50
C      C     ENDB
        126 CALL ENDB (ALPHA, BETA, NTBS, FRMOL, N, NB)
             GO  TO  100
          130 CONTINUE
C      C
C      C     WRITE 3
C      C
             IF(J. GT. 1) CALL GRTAB (J)
             WRITE (108, 1000) (POLYM) (I), I = 1, N)
             WRITE (108, 1000) NBA, NBB
             I = 1
             NBA = 0
             NBB = 0
             GO  TO  1
       140   WRITE (108, 1020)
             STOP 333
       150   WRITE  (108,  1030)
             GO TO 1
       160   CONTINUE
             WRITE  (108,  1040), NA, NB
             I = 1
             NBA = 0
             NBB = 0
             GO TO 1
       170   STOP 170
       900   FORMAT (40A2)
       910   FORMAT(I 1,16)
       920   FORMAT (2F14.10)
       930   FORMAT (316)
       940   FORMAT (1HO/////)
       950   FORMAT ('1', 5X, 'POLYMERISATIONSGRAD = 'I6, 5X, 'R1 =
             = ', F14.10,5X, 'R2 = '.
             CF14.10/5X, 'WERT, DER DIE NEUORDNUNG BEDINGT = ', I6,
             15.5X, 'NA = 'I 14.
             C5X, 'NB = 'I14)
     1 000   FORMAT (//5X, 'WAHRSCHEINLICHSTE FORM DES MAKROMO-
             LEKUELS'
             C/(12X.60A2))
     1 010   FORMAT (/5X, 'ANZAHL DER GRUPPEN A = ',I7
         C   /5X, 'ANZAHL DER GRUPPEN B = ', I7)
     1 020   FORMAT ('', 5X, 'FALSCHER GENERATOR FUER STOCHASTISCHE
             ZAHLEN'/)
     1 030   FORMAT (' ', 5X,' FALSCH EINGEFUEHRTE EINGANGSROSSEN'/)
     1 040   FORMAT (5X, 'SIMULARE IMPOSIBILA :',5X, 'NA = 'I5,5X, 'NB =
             = 'I5)
               END

             SUBROUTINE INIT 1 (S, NR, NT)
             COMMON POLYM (10 000)
             INTEGER S
C        C   INIT1
C        C   BEDINGT DIE GENERATION DES ERSTEN GLIEDES DES
             MAKROMOLEKUELS (A)
C        C
             DATA PK1/2HA-/
             I = 1
             POLYM (I) = PK1
             S = I
             NR = I
             NT = I
             RETURN
             END

             SUBROUTINE INIT 2 (S, NR, NT)
             COMMON POLYM (10000)
             DATA PK2/2HB-/
             INTEGER S
C        C
C        C   BEDINGT DIE GENERATION DES ERSTEN GLIEDES DES
             MAKROMOLEKUELS (B)
C        C
             I = 1
             POLYM (I) = PK2
             S = 2
             NR = 1
             NT = I
             RETURN
             END
14.05    9                                 MEMORY 3 19/06/74 16.50.20
```

```
              SUBROUTINE ENDA (AL, BE, NTA, FRM, N, NA)
C       C
C       C     ENDA
C       C     DIE PARAMETER WERDEN BEI VERBRAUCH DES MONOMERESA
C       C     WIEDER ANGEGLICHEN.
C       C
              INTEGER FRM
              AL = 0.0
              BE = 0.0
              NTA = 0
              FRM = 2*N
              NA = 0
              WRITE (108, 970)
        970   FORMAT ('', 5X'*** VERBRAUCHTER MONOMERES A ***')
              RETURN
              END
```

```
              SUBROUTINE GRTAB (J)
C       C
C       C     WRITE1
C       C
              COMMON POLYM (10000), GTAB (5, 16)
              DATA BLK/1H/
              WRITE (108, 980) ((GTAB (II, JJ), JJ = 1, 14), II = 1,5)
              DO 10 II = 1,5
              DO 10  JJ = 1,16
              GTAB  (II,  JJ) = BLK
        10    CONTINUE
              J = 1
              RETURN
              980 FORMAT (//2X, 130('-')/5X, 'BESCHAFFENHEIT DER GRUP-
                  PEN'',
        C         14('!  ,A2,'')
        C         /2X, 130('-'(/5X,' GROSSE DER GRUPPE    !',
        C         14('I', I4.'')
        C         /2X, 130('-')X/5, LAGE DER GRUPPE !
        C                 14('!   ',I4,  '')
        C         /2X, 130('-')/5X, 'UBRIGGEBLIEBENE MERES A  !,
        C                 14('I  'I4,  '')
        C         /2X, 130('-')/5X, 'UBRIGGEBLIEBENE MERES B  !'
        C                 14('I ',  I1,  '')
        C                 /2X,  130)  '-'))
              END
```

```
              SUBROUTINE ENDB (AL, BE, NTB, FRM, N, NB)
C       C
C       C     ENDB
C       C     DIE PARAMETER WERDEN BEI VERBRAUCH DES MONOMERES B
C       C     WIEDER ANGEGLICHEN.
C       C
              INTEGR FRM
              AL = 1.0
              BE = 1.0
              NTB = 0
              FRM = 2 * N
              NB = 0
              WRITE  (108,  990)
        990   FORMAT  ('',   5X,'*** VERBRAUCHTER   MONOMERES   B   ***')
              RETURN
              END
```

```
C    C
C    C
C    C
C    C   PROGRAMM ZUR GENERATION  EINER  PSEUDOSTOCHASTI-
         SCHEN ZAHLENREIHE
C    C
         SUBROUTINE ALEAT (IA, IB, Z)
C    C
C    C   IA : WENN ALEAT ZUM ERSTEN MAL  GERUFEN WIRD, MUSS
         IA EINEN
C    C   GANZEN, UNPAARZAHLIGEN WERT BESITZEN, DER KLEINER
         ALS
C    C   NEUNSTELLIG  IST  (DER  HOECHSTENS  ACHTSTELLIG  SEIN
         DARF).
C    C   NACHHER WIRD IA VON NEUEM GENERIERT, INDEM IA GLEICH
         IB GESETZT
C    C   WIRD.
C    C   NACHHER ERHAELT IA DIE WERTE VON IB, DIE IM PROGRAMM
         GENERIERT
C    C   WERDEN.
C    C   IB :DER  PROGRAMMGENERIERTE  WERT
C    C   Z: DER  DURCH  ALEAT  GENERIERTE  GLEICHFORMIGE  WERT
         IM INTERVALL (0.1)
C    C
C    C   2**16 + 3 = 65539
         IB = IA*65539
         IF(IB.GE.O)  GOTO  1
         IB = IB + 2147483647 + 1
C    C   2**31 = 2147483647 + 1
       1 Z = IB
         Z = Z*0.4656613E-9
C    C   2**(-31) = 0.4656613E-9
         RETURN
         END
```

```
MASKEP              CSECT
          DEF               NMAS
          DEF               MAS
MASQUE    DATA,4,4          X'50400000'
MAS       LDTM,13           MASQUE
          BRU               *32
NMAS      LDTM,13           MASQUE+
          BRU               *32
          END
```

Revue Roumaine de Chimie, **21**, *8*, 1263–1264 (1976)

DER GASCHROMATOGRAPHISCHE NACHWEIS UND DIE QUANTITATIVE BESTIMMUNG EINER MISCHUNG VON 1-CHLOR-3-THIA-PENTAN UND 3,6-DITHIA-OCTAN AUS DEN BEI DER SYNTHESE DIESER STOFFE SICH ERGEBENDEN ABFLUSSWÄSSERN

ROMANO CIUPE und MARIA GĂVAN

Institut für Hygiene und Gesundheitswesen, Cluj-Napoca, Pasteur Str. Nr. 6

Eingegangen am 18. November 1974

Die Arbeit stellt eine gaschromatographische Methode für die Bestimmung von 1-Chlor-3-thia-pentan und 3,6-Dithiaoctan in Mischungen, sowohl aus Abwässern, als auch aus Reinsubstanzen vor.

In der Synthese[1] des 0, 0-Diäthyl-S (2-äthylthio)-äthyl-esters der Dithiophosphorsäure (Disulfoton), ein wichtiges Bodeninsektizid, benützt man als Reaktionspartner 1-Chlor-3-thiapentan[2] und das Natrium-Salz des 0,0-Diäthyl-dithiophosphorsäureesters.

Eine der einfachsten Methoden[2] zur Gewinnung von 1-Chlor-3-thiapentan (I) beruht auf der folgenden Reaktion:

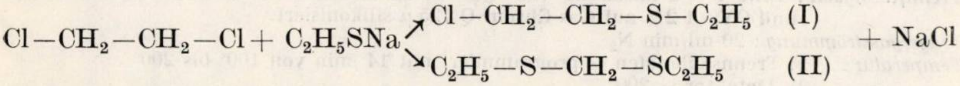

$$Cl-CH_2-CH_2-Cl + C_2H_5SNa \begin{array}{l} \nearrow Cl-CH_2-CH_2-S-C_2H_5 \quad (I) \\ \searrow C_2H_5-S-CH_2-SC_2H_5 \quad (II) \end{array} + NaCl$$

Produkt (I) ist der Vermittler aus der Disulfotonsynthese.

Nebenprodukt (II) ist als Nematozid in der Literatur[3] patentiert.

Auf Grund der großen Toxizität* der Produkte (I) und (II) gegenüber Warmblütern ist ihr Nachweis und ihre quantitative Bestimmung im Abflußwasser ihrer technologischen Synthese von besonderem Interesse.

Wenn man in Betracht zieht, daß die chemischen analytischen Bestimmungsverfahren im Wasser für die Substanzen (I) und (II) sehr schwierig und relativ wenig genau sind, ergibt sich die Notwendigkeit eine physisch-chemische Methode zu diesem Zweck zu finden.

Die gaschromatographische Analyse eignet sich gut auch zur Bestimmung sehr kleiner Konzentrationen dieser Gemische im Wasser (so wie aus Folgendem hervorgeht).

---

* DL_{50} = 19μl/kg, bzw. 123 μl/kg, bestimmt im Institutul de Igienă şi Sănătate Publică Cluj-Napoca (Dr. D. Coloşi).

[1] K. Lutz, M. Schuller und O. Jucher, Swiss Pat. 319. 579, 15. April 1957; *Chem. Abstr.*, **51**, 17979 (1957).

[2] V. S. Tsinumin, G. Kh. Kamai und V. V. Kornmachev, „Problemî Organiceskovo Sinteza", Akademia Nauk S.S.S.R., Moscova, 1965, S. 40–2.

[3] C. B. Scott, U.S. Pat. 2.998 346, 1952; *Chem. Abstr.*, **56**, 3851 (1962).

Die Produkte (I) und (II) als Reinsubstanzen (kontrollierte Reinheit durch physikalische Konstante, molekulare Refraktion und Dünnschichtchromatographie) waren uns vom Forschungskollektiv für phosphoorganische Verbindungen des Institutes für Chemie aus Cluj-Napoca, Dr. Almasi zur Verfügung gestellt.

Die gaschromatographische Bestimmung beider Komponenten des Abflußwassers erlaubte eine Abschätzung der Ergebnisse die von dem obengenannten Kollektiv in den Untersuchungen zur Reinigung dieser Abflußwässer erhalten wurden.

GASCHROMATOGRAPHISCHE BEDINGUNGEN

Es wurden zwei Parameter-Serien benützt, in Abhängigkeit von dem Medium aus welchem die zu analysierenden Substanten zu trennen sind.

A) Im wäßrigen Medium befanden sich die Substanzen in sehr kleinen Mengen. In diesem Fall waren die optimalen Parameter die folgenden;

Gerät: Carlo-Erba Typ GD—ACI mit Doppelflammenionisationsdetektor (FID) und Doppelsäulen.
Säulen: zwei gepackte Stahl-Säulen
Länge: 2 m; Durchmesser: 6 ×4 mm
Trännflüssigkeit: Carbowax 20 M auf Chromosorb W 100—120 mesh. A.W.
Trägergasströmmung: 30 ml/min N_2
Temperatur: 1) Trennsäulenofen — programmiert mit 15°/min, von 55° bis 140°
2) Detektor — 200°
3) Injektor — 200°
FID-Abschwächung: 10 × 8
Probenmenge: 1μl

B) Gaschromatographische Bedingungen der Analyse reiner Mischungen, entstanden durch die Synthese:

Dasselbe Gerät:
Säulen: zwei gefüllte Stahl-Säulen
Länge: 2m: Durchmesser: 4×2mm
Trennflüssigkeit: Eine 1 × 8 Mischung von QF—1; 1,6% auf Gas. Chrom. P; 200 — 250μ und OV—1 2% auf Gas-Chrom Q 125 μ silikonisiert.
Trägergasströmmung: 20 ml/min N_2
Temperatur: 1) Trennsäulenofen — programmiert mit 14°/min von 100° bis 200°
2) Detektor — 200°
3) Injektor — 200°
FID-Abschwächung: 10 × 128
Probenmenge: 0,4 μl

Tabelle 1

Relative Retentionszeiten der Komponenten. (**3,6-Dithiaoctan** = 1)

Lfd. Nr.	Komponente	Tr(A)	Tr(B)
1	3,6-Dithiaoctan	1,00	1,00
2	Disiston	1,87	3,55

SCHLUSSFOLGERUNGEN

Die Arbeit löst, ohne Hilfe der vorgängigen Arbeitsgänge, die kurzdauernde quantitative Bestimmung einer Mischung der erwähnten Substanzen, die für die industrielle Herstellung der Insektiziden von Bedeutung ist.

Diese Technik zeichnet sich durch die direkte Bestimmung der Substanzen auch aus der wäßrigen Mischung aus.

Revue Roumaine de Chimie, **21**, *8*, 1265–1272 (1976)

ANALYSE THERMIQUE DES COMPOSÉS DU COBALT (III) TÉTRAMMINE AVEC DES ACIDES ORGANIQUES DICARBOXYLIQUES*

A. D. MAGRÌ, G. D'ASCENZO, U. BIADER CEIPIDOR et A. MARINO
Institut de Chimie Analytique de l'Université de Rome, Italie

Reçu le 13 janvier 1975

On a examiné du point de vue thermoanalytique deux séries de composés solides du type $[Co(NH_3)_4X]NO_3.nH_2O$ où X = oxalate, malonate, succinate dans la première série et X = succinate, maléate, phatalate dans la deuxième.

Les résultats expérimentaux permettent de mettre en évidence quelques corrélations entre les propriétés thermiques et la longueur de la chaîne paraffinique (première série) et entre les propriétés thermiques et le type de liaison (deuxième série) entre les deux groupements carboxyliques du coordinat.

Deux séquences ont été déterminées pour chaque série en fonction du démarrage de la décomposition des composés anhydres et en fonction de la réaction violente qui aboutit à l'oxyde de cobalt.

INTRODUCTION

Dans ce mémoire nous avons étudié les décompositions thermiques des composés du cobalt (III) tétrammine dont la formule peut être exprimée par $[Co(NH_3)_4X]NO_3.nH_2O$ où n = 1,2 et X = oxalate, malonate, succinate, maléate, phtalate.

Le choix de ces composés particuliers a permis d'établir deux groupes, à trois termes chacun, dont le premier avec X = oxalate, malonate, succinate, et le deuxième avec X = succinate, maléate, phtalate.

De cette façon l'influence sur les processus thermiques peut être suivie en ce qui concerne la chaîne paraffinique aussi bien que en ce qui concerne la présence d'une liaison simple, double ou aromatique dans l'anion coordinné.

Quelques données thermochimiques peuvent être tirées de la littérature [1] au sujet des composés du type $[Co(NH_3)_4C_2O_4]Y$ où $Y = Cl^-, Br^-$.

Cependant, dans notre étude nous avons préféré l'utilisation du nitrate, en tant qu' ion de balancement, car il a un faible pouvoir de coordination. [2] De cette façon il est possible, en principe, de réduire les réactions d'anation qui pourraient masquer les effets des coordinats sur la décomposition thermique. Le perchlorate n'a pas été utilisé afin de ne pas avoir d'explosions pendant le réchauffage des composés examinés.

---

* Travail présenté à la « 30 Conférence Nationale de Chimie Physique pure et appliquée », Bucarest les 4–7 septembre 1972, Roumanie Travail effectué avec la contribution du C.N.R.

[1] M. Matsui et T. Nakanishi, *J. Scient. Res. Inst.*, **51**, 159 (1957).

[2] U. Mayer et V. Gutmann, *Structure and Bonding*, **12**, 113 (1972).

APPAREILLAGE

Thermobalance Du Pont 951 ;
Analyseur thermique différentiel Du Pont 990 ;
pH-mètre PHM 22r.

PRÉPARATION DES COMPOSÉS

Les complexes avec le malonate et l'oxalate ont été préparés à partir de $[Co(NH_3)_4CO_3]NO_3.O,5H_2O$ [3] en utilisant la méthode proposée par Schramm.[4]

Cette méthode, au contraire, n'a pas donné des résultats à la préparation des autres composés de la série.

Pour cela nous avons mis au point une technique différente : à température ambiante, l'on a ajouté à une solution, contenant 0,016 moles de $[Co(NH_3)_4CO_3]NO_3.O.5H_2O$ dans 100 ml d'eau, un nombre égal de moles d'anhydride succinique ou bien d'acide maléique ou phtalique.

Après avoir laissé reposer pour une heure environ, la solution a été concentrée 10 fois à peu près dans un turboévaporateur sous vide et à une température au-dessous de 40°. Un mélange gélatineux a été obtenu. Celui-là a été traité d'abord à 50 ml d'éthanol absolu-éther éthylique (1/1, v/v) et ensuite à de faibles quantités d'éthanol absolu jusqu'à l'obtention d'un précipitat violet poussiéreux.

ANALYSE DES COMPOSÉS

Après fusion de chaque composé avec bisulfate de potassium, le cobalt a été déterminé par titrage complexométrique avec EDTA.

Les résultats, par rapport à ceux obtenus par thermogravimétrie, sont montrés au tableau 1.

Tableau 1

Fraction de cobalt dans les complexes $[Co(NH_3)_4X]NO_3 . nH_2O$

Composé	Cobalt %		
	Trouvé		Calculé
	Complexométrie	Thermogravimétrie	
$[Co(NH_3)_4oxalate]NO_3.2H_2O$	18.7	18.6	18.82
$[Co(NH_3)_4$ malonate$]NO_3.H_2O$	19.1	19.1	19.06
$[Co(NH_3)_4$ succinate$]NO_3.H_2O$	18.2	18.2	18.23
$[Co(NH_3)_4maléate]NO_3.H_2O$	18.3	18.3	18.34
$[Co(NH_3)_4phtalate]$ $NO_3.H_2O$	15.6	15.8	15.87

Les composés ont résultés purs à l'analyse conduite sur papier chromatographique cationique (Mache Rey, Nagel and Co. M. N.) sous forme de Na^+ en utilisant une solution de $NaNO_3$ 1 M pour l'élution.

---

[3] G. SCHLESSINGER, « Inorganic Syntheses », VIe vol. Mc Graw-Hill, New York, 1960, p. 173.

[4] W. SCHRAMM, *Z. anorg. Chem.*, **180**, 178 (1929).

RÉSULTATS EXPÉRIMENTAUX

$[Co(NH_3)_4$*oxalate*$]\ NO_3 2H_2O$

Les courbes TG, DTG et DTA (fig. 1) montrent la présence de deux molécules d'eau par atome de cobalt : la perte de masse jusqu'au premier palier est de 11,3 % par rapport à une valeur calculée de 11,50 % pour deux molécules d'eau.

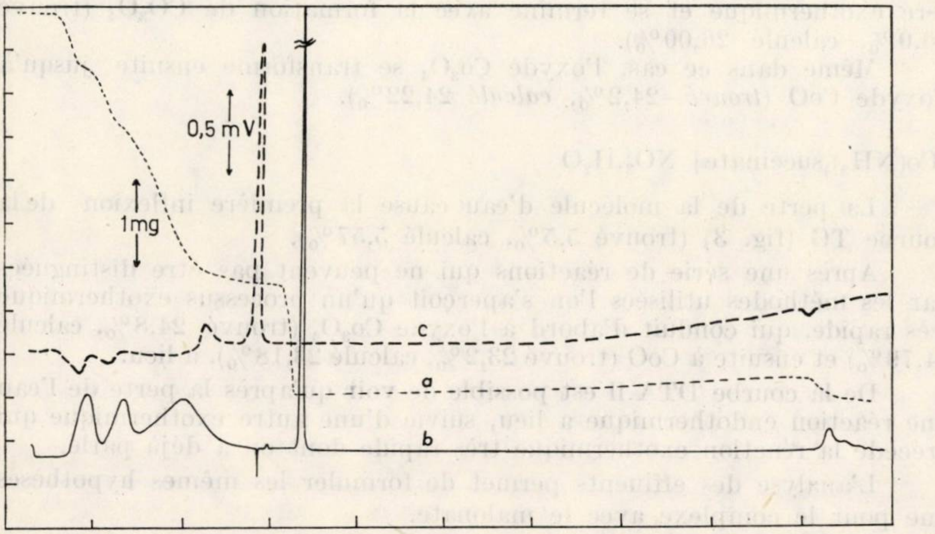

FIG. 1

Fig. 1. — Analyse thermique de $[Co(NH_3)_4\ oxalate]NO_3.2H_2O$
a, thermogravimétrie (TG) ; *b*, thermogravimétrie différentielle (DTG) ; *c*, analyse thermique différentielle (DTA), vitesse de réchauffage 10°C min^{-1}, atmosphère : air statique.

Le processus suivant peut être assigné à la perte de deux molécules de NH_3 (trouvé 10,7 %, calculé 10,88 %) ; de plus, l'analyse des effluents a permis d'établir que seulement le NH_3 est éliminé à ce point.

Le composé obtenu après ces deux premières réactions décomposé à travers deux processus dont le dernier, très rapide, conduit à l'oxyde CO_3O_4 (trouvé 25,4 %, calculé 25,35 %).

Cet oxyde se transforme ensuite en CO_2O_3 (trouvé 26,6 %, calculé 26,48 %) et en CoO (trouvé 24,0 %, calculé 23,92 %).

La courbe DTA montre un caractère endothermique pour les deux premiers processus identifiés par TG. Au contraire la formation de l'oxyde du métal a lieu à travers une réaction endothermique suivie de deux autres exothermiques dont la dernière très rapide.

$[Co(NH_3)_4malonate]NO_3.H_2O$

Ce composé livre sa molécule d'eau au-dessous de 140° (trouvé 5,9%, calculé 5,82%) (fig. 2). Lorsque la température monte au-dessous de cette valeur une série d'au-moins trois réactions, non pas bien séparées même en DTG, a lieu.

De toute façon les données tirées des courbes TG, DTG, DTA (fig. 2) et de l'analyse des effluents permettent de supposer que les deux premiers processus sont dus à la perte du nitrate avec réduction du composé et à l'élimination de NH_3. La dernière réaction, très rapide, montre un caractère exothermique et se termine avec la formation de CO_3O_4 (trouvé 26,0%, calculé 26,00%).

Même dans ce cas, l'oxyde Co_3O_4 se transforme ensuite jusqu'à l'oxyde CoO (*trouvé*—24,2%, *calculé* 24,22%).

$[Co(NH_3)_4succinate]\ NO_3.H_2O$

La perte de la molécule d'eau cause la première inflexion de la courbe TG (fig. 3) (trouvé 5,5%, calculé 5,57%).

Après une série de réactions qui ne peuvent pas être distinguées par les méthodes utilisées l'on s'aperçoit qu'un processus exothermique très rapide, qui conduit d'abord à l'oxyde Co_3O_4 (trouvé 24,8%, calculé 24,79%) et ensuite à CoO (trouvé 23,2%, calculé 23,18%), a lieu.

De la courbe DTA il est possible de voir qu'après la perte de l'eau une réaction endothermique a lieu, suivie d'une autre exothermique qui précède la réaction exothermique très rapide dont on a déjà parlé.

L'analyse des effluents permet de formuler les mêmes hypothèses que pour le complexe avec le malonate.

$[CO(NH_3)_4maléate]\ NO_3.H_2O$

A travers l'analyse de la courbe DTG (fig. 4) il est possible de distinguer la perte de l'eau même sur la courbe TG (trouvé 5,5%, calculé 5,61%). Par effet de la température croissante d'autres réactions mélangées se développent jusqu'à une dernière, presque explosive, qui conduit à l'oxyde Co_3O_4 (trouvé 24,9%, calculé 25,00%).

La courbe DTA (fig. 4) montre des processus assez différents par rapport à ceux des composés précédents, exclusion faite pour la perte de l'eau.

$[CO(NH_3)_4phtalate]\ NO_3.H_2O$

La perte de la molécule d'eau peut être relevée sur la courbe TG (fig. 5) (trouvé 4,9%, calculé 4,85%).

Même pour ce composé une série de réactions, qui ne peuvent pas être séparées, se termine avec la formation de Co_3O_4 (trouvé 21,5%, calculé 21,62%) qui se transforme ensuite de la même façon que dans les autres cas.

Après la perte de l'eau la courbe DTA montre une réaction endothermique qui précède d'autres exothermiques.

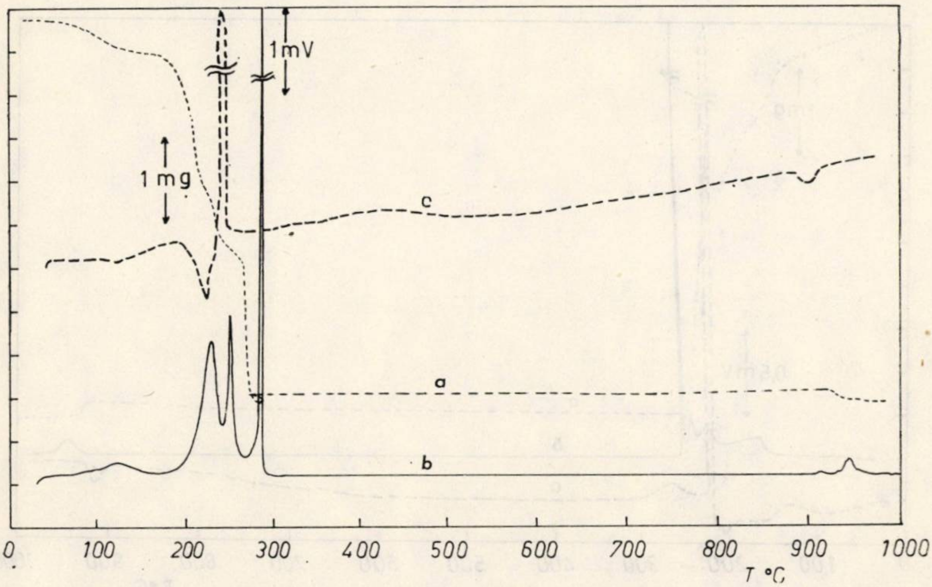

Fig. 2. — Analyse thermique de $[Co(NH_3)_4$ malonate$]$ $NO_3.H_2O$
a, thermogravimétrie (TG) ; *b*, thermogravimétrie différentielle (DTG) ; *c*, analyse thermique différentielle (DTA) vitesse de réchauffage 10°C min^{-1}, atmosphère : air statique.

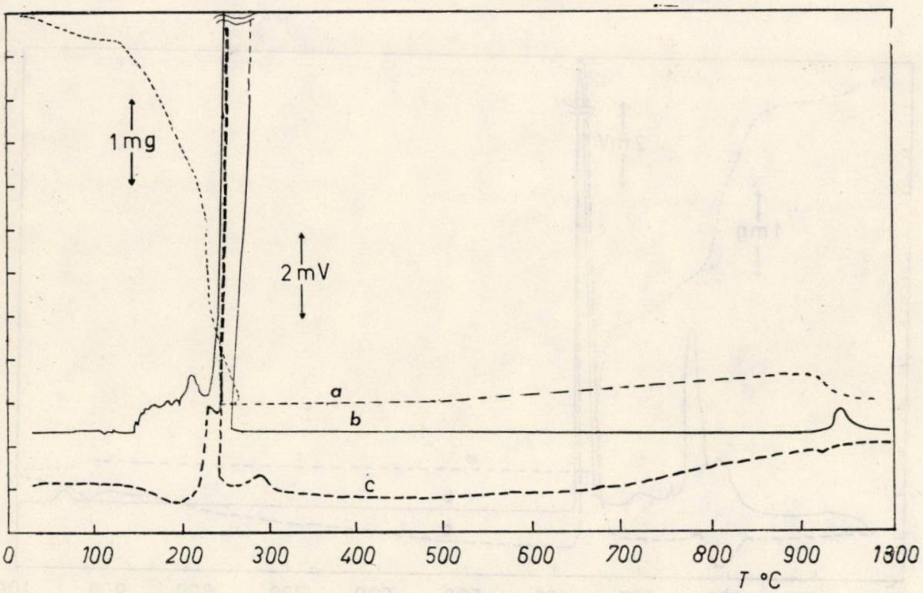

Fig. 3. — Analyse thermique de $[Co(NH_3)_4$ succinate$]$ $NO_3.H_2O$
a, thermogravimétrie (TG) ; *b*, thermogravimétrie différentielle (DTG) ; *c*, analyse thermique différentielle (DTA), vitesse de réchauffage 10°C min^{-1}, atmosphère : air statique.

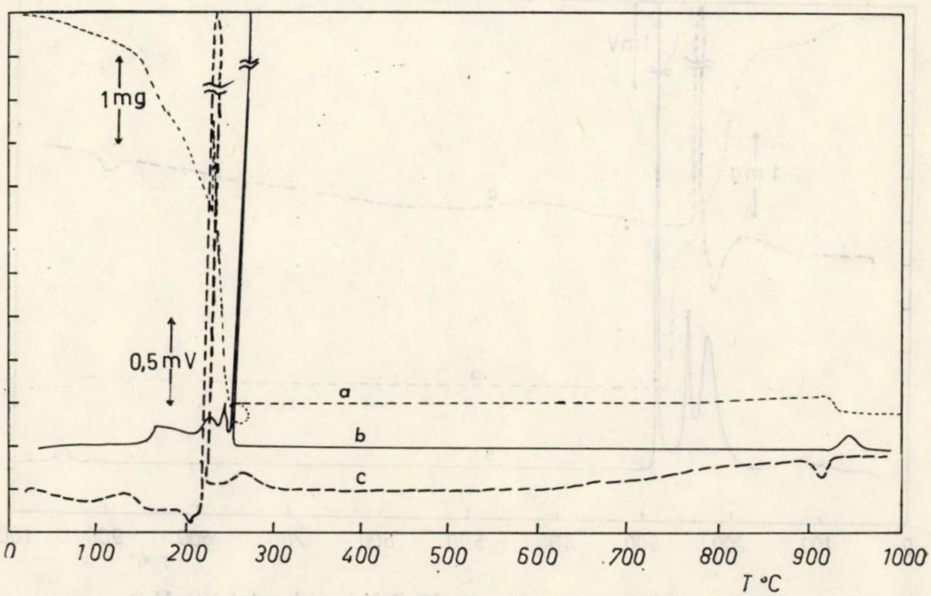

Fig. 4. — Analyse thermique de [Co(NH$_3$)$_4$ maléate]NO$_3$.H$_2$O

a, thermogravimétrie (TG) ; *b*, thermogravimétrie différentielle (DTG) ; *c*, analyse thermique différentielle (DTA). vitesse de réchauffage 10°C min^{-1}, atmosphère : air statique.

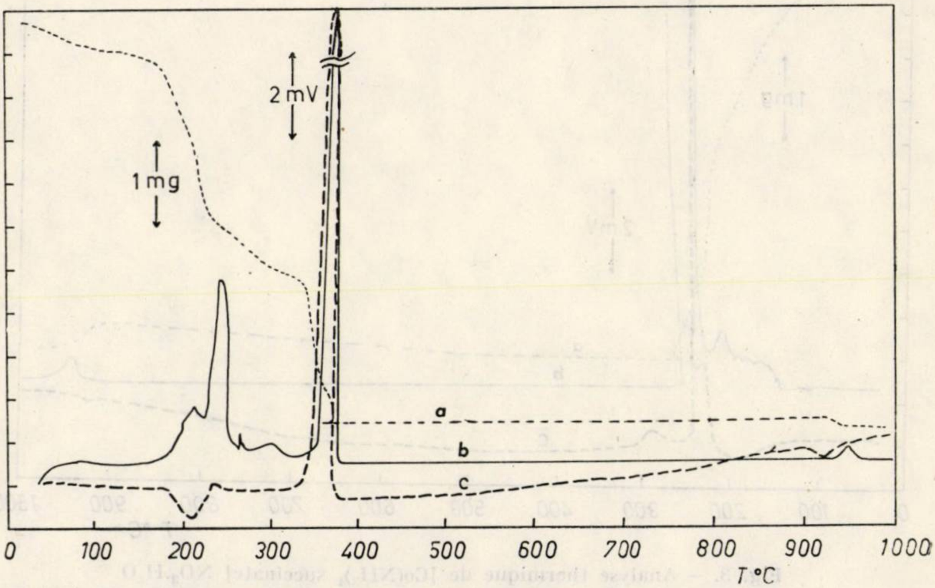

Fig. 5. — Analyse thermique de [Co(NH$_3$)$_4$ phtalate] NO$_3$.H$_2$O

a, thermogravimétrie (TG) ; *b*, thermogravimétrie différentielle (DTG) ; *c*, analyse thermique différentielle (DTA), vitesse de réchauffage 10°C min^{-1}, atmosphère : air statique.

DISCUSSION

Il vaut la peine, d'abord, de mettre en évidence quelques propriétés des composés examinés qui peuvent être tirées des résultats expérimentaux.

i) Dans tous les cas la perte de l'eau de cristallisation a lieu autour de 100°. Le processus de déshydratation montre en TG une pente qui n'est pas trop marquée et qui se termine au-dessus de 100°, sauf le cas où l'oxalate joue le rôle d'agent de coordination.

Cette exception peut être reliée à la présence de deux molécules d'eau par atome de cobalt (il y en a une seulement dans les autres composés) mais probablement encore plus, aux positions qui peuvent être occupées par l'eau dans la maille solide. A ce propos-là l'on peut souligner que tous les acides dicarboxyliques utilisés à la préparation des composés examinés, lorsqu'ils sont précipités purs ne donnent que des solides à l'état anhydre, sauf l'acide oxalique qui retient deux molécules d'eau. [5]

Malheureusement même les courbes DTA ne permettent point de confirmer cette hypothèse car toute une série de processus doit être cachée sous l'effet endothermique remarquable dû à l'évaporation de l'eau.

ii) Lorsque la température monte au-dessus des valeurs demandées par la perte de l'eau l'on a trouvé une série de réactions qui n'ont pas été séparées par milieu des techniques thermoanalytiques. A travers l'élimination de molécules NH_3, NO_2 et CO_2 (retrouvés dans les effluents) l'oxyde Co_3O_4 se forme après une réaction très rapide qui présente en quelques cas un caractère explosif. Selon nous il ne devrait pas être possible de supposer que le père de cette dernière réaction soit le même dans tous le cas, par exemple le carbonate et/ou l'acétate, de cobalt, même si la formation d'un mélange de tous les deux peut être acceptée en principe. En effet, les proportions des poids demandées par l'hypothèse de formation d'une espèce bien identifiée ne sont pas respectées en TG où les températures couvertes par ce processus varient de 230 à 350°.

Cet intervalle aussi semble trop large pour être assigné au même processus, même lorsqu'on considère les différentes conditions de réchauffage local et d'atmosphère de fonctionnement qui se présentent pendant l'analyse thermique des différents composés. [6]

Par rapport aux températures où les réactions de décomposition commencent, on peut observer les successions.

Oxal. $<$ malon. $\simeq$ succ.

maléate $<$ succ. $<$ phtal.

En observant la première série, la diminution de stabilité thermique peut être reliée à l'approchement des deux groupements carboxylate avec réduction de la longueur de la chaîne paraffinique.

Cela, probablement, puisque la réaction de décarboxylation devient plus facile, due aux effets inductifs entre les deux groupes $-COO^-$. Cependant, lorsque la chaîne croît, l'effect de stabilisation doit être balancé par des tensions moléculaires : le composé avec le succinate présente une température de décomposition qui ne s'éloigne pas tellement de celle du composé avec le malonate.

---

[5] J. R. A. Pollock et R. Stevens éditeurs « Dictionary of Organic Compounds », Eyre & Spottiswoode Publishers—LTD, Londres, 1965.

[6] P. D. Garn, « Thermoanalytical Methods of Investigation », Academic Press, New York, 1965.

La deuxième série, où la chaîne entre le deux groupements carboxylate ne varie pas sa longueur, peut être justifiée en termes de réactivité de la liaison double qui est plus grande par rapport à celle de la liaison simple, favorisant même la décarboxylation par conjugation de deux carboxylates. Avec le phtalate on a un composé qui montre la température de décomposition la plus haute probablement car il y a une stabilisation de la maille solide due à la présence du cycle aromatique.

iii) Le processus de démolition thermique se termine dans tous les cas par une réaction très rapide qui finit, à son tour, avec la formation de Co_3O_4 et, après, de Co_2O_3 et de CoO.

L'ordre de stabilité thermique tiré de cette réaction est :

oxal. > mal. $\simeq$ succ.

maléate $\simeq$ succ. < phtal.

Ces séquences ne s'accordent pas aux précédentes, exception faite pour le phtalate qui présente la température la plus haute même dans ce cas.

Cela peut être attribué à des espèces assez résistantes aux sollicitations thermiques qui se forment à partir de la démolition du cycle aromatique.

Un processus semblable doit arriver pour l'oxalate aussi, qui montre une température de réaction bien élevée et, de la même façon que le phtalate, un palier plutôt marqué en TG qui précède cette dernière réaction.

1977 FEB 21

NOTE POUR LES AUTEURS

La *Revue Roumaine de Chimie* publie des articles en anglais, français, russe, allemand ou espagnol. Les auteurs sont priés d'envoyer des articles, notes, communications et comptes rendus inédits.

Les manuscrits seront dactylographiés à deux intervalles. Les tableaux seront dactylographiés sur feuilles séparées, de même que la légende des figures. Les diagrammes seront tracés à l'encre de Chine sur papier calque. Les tableaux et les figures seront numérotés par des chiffres arabes, en nombre strictement nécessaire. Prière de ne pas inscrire les mêmes données dans les tableaux et les figures. Les formules chimiques seront incluses dans le texte ; en outre, elles seront transcrites sur des feuilles séparées. Les auteurs sont priés d'indiquer les caractères italiques (en soulignant les lettres au crayon), ainsi que tout antre caractère spécial. L'ordre des références bibliographiques sera celui de leur mention dans le texte ; le nom de l'auteur sera précédé de l'initiale du prènom ; les publications périodiques seront présentées suivant les prescriptions internationales. Les références seront ajoutées à la fin de l'article ; elles paraîtront comme des notes, au bas de la page. Le texte sera précédé d'un résumé comprenant 15 lignes au maximum.

L'entière responsabilité du contenu des articles appartient aux auteurs. On public des articles dus aux collaborateurs roumains ou étrangers.

PRINTED IN ROMANIA

1977 FEB 21

TRAVAUX PARUS AUX ÉDITIONS DE L'ACADÉMIE DE LA RÉPUBLIQUE SOCIALISTE DE ROUMANIE

I. GĂLĂŢEANU, **Radiochimia Aplicată. Metode şi probleme** (Laradiochimie appliquée. Méthodes et problèmes), 1976, 305 p., 19 lei.

FRANCISC A. GOTHARD, **Echilibre lichid-vapori. I. Baze teoretice şi metode de calcul** (Equilibres liquide-vapeurs. I. Bases théoriques et méthodes de calcul), 1975, 263 p., 2 pl., 28 lei.

CONST. GH. MACAROVICI, D. Macarovici, **Chimia oxizilor dubli şi utilizările lor** (La chimie des oxydes doubles et leur utilisation), 1975, 195 p., 13 lei.

ELENA CEAUŞESCU, **Research work on synthesis and characterization of macromolecular compounds. Contributions**, 1974, 251 p., 20 lei.

M. AVRAM, **Antidăunători** (Pesticides), 1974, 496 p., 41 lei.

DUMITRU COSTACHE, **Analiza chimică prin metoda cinetică** (L'Analyse chimique par la méthode cinétique), 1974, 276 p., 15,50 lei.

G. A. RĂDULESCU, **Proprietăţile ţiţeiurilor româneşti**, (Les propriétés des pétroles roumains), 1974, 267 p., 2 pl. 18 lei.

CR. SIMIONESCU, VIORICA RUSAN, V. POPA, **Chimia algelor marine**, (La chimie des algues marines), 1974, 212 p., 1 pl., 18 lei.

I. ZUGRĂVESCU, MAGDA PETROVANU, **Chimia n-ilidelor**, (La chimie des n-Ilures), 1974, 348 p., 19 lei.

MARIA FITI, **Dozimetria chimică a radiaţiilor ionizante**, (La dosimétrie chimique des radiations ionisantes), 1973, 240 p., 13,50 lei.

TIBERIU NĂSCUŢIU, **Metode radiochimice de analiză** (Methodes radiochimiques d'analyse), 1973, 384 p., 23 lei.

CRISTOFOR SIMIONESCU, Margareta Grigoraş, Agata Cernătescu-Asandei, Rozmarin Gheorghe, **Chimia lemnului în România. Plopul şi salcia**, (La Chimie du bois en Roumanie. Le peuplier et le saule), 1973, 299 p., 13 pl., 26 lei.

MIHAI FLORESCU, **Eficienţa economică a cercetării ştiinţifice**, (L'efficience économique de la recherche scientifique), 1972, 115 p., 15 lei.

GEORGETA LĂZĂRESCU, **Sistematizarea informaţiilor în chimia organică** (Systématisation des informations en chimie organique), 1972, 243 p., 1 pl., 10,50 lei.

I.P.I. – c. 1296

43426

Lei 25.–

F 1103

ACADÉMIE DE LA RÉPUBLIQUE SOCIALISTE DE ROUMANIE

R REFERALVA

66

REVUE ROUMAINE DE CHIMIE

TOME 21
N°s 9—10
Septembre—Octobre 1976

RECHAX, 21, *9—10*, 1273—1432 (1976)

EDITURA ACADEMIEI REPUBLICII SOCIALISTE ROMÂNIA

Rev. Roumaine Chim. 21, *9—10*, p. 1273—1432 (1976), Bucarest

ACADÉMIE DE LA RÉPUBLIQUE SOCIALISTE DE ROUMANIE

COMITÉ DE RÉDACTION

Rédacteur en chef :

I. G. MURGULESCU, membre de l'Académie de la République Socialiste de Roumanie

Rédacteurs en chef adjoints :

A. T. BALABAN et V. EM. SAHINI, membres correspondants de l'Académie de la République Socialiste de Roumanie

Collège de rédaction :

EM. BRATU, ELENA CEAUŞESCU, ECATERINA CIORĂNESCU-NENITZESCU, C. DRĂGULESCU, CR. SIMIONESCU, membres de l'Académie de la République Socialiste de Roumanie ; P. SPACU, membre correspondant de l'Académie de la République Socialiste de Roumanie ; MARGARETA AVRAM, I. HAIDUC, D. I. MARCHIDAN, I. MOLDOVAN, G. NIAC et D. SĂNDULESCU

La Revue Roumaine de Chimie paraît 10 fois par an. Toute commande de l'étranger pour les travaux parus aux Editions de l'Académie de la République Socialiste de Roumanie sera adressée à ILEXIM, Serviciul Export Import Carte (Livres)/Serviciul Export Import Presă (Revues), P.O.B. 2001, telex 011226, 64—66, Calea Griviţei, Bucarest 12 Roumanie
Les manuscrits, les livres et les revues proposés en échange, ainsi que toute correspondance seront envoyés à la redaction :

REVUE ROUMAINE DE CHIMIE
23, str. Dumbrava Roşie, Bucarest, Roumanie, téléphone 12 41 60

EDITURA ACADEMIEI REPUBLICII SOCIALISTE ROMÂNIA
125, Calea Victoriei, 71021, Bucarest, Roumanie, téléphone 50 76 80

ORSZÁGOS MŰSZAKI KÖNYVTÁR ÉS DOKUMENTÁCIÓS KÖZPONT 1883

REVUE ROUMAINE DE CHIMIE

Tome 21, Nos 9–10 Septembre–Octobre 1976

I. G. MURGULESCU und MAIA WEISSMANN, Der Einfluss des Methans auf den thermischen Zerfall des Chloroforms. I. Die ersten drei Reaktionsschritte 1275–1286

L. ONICIU, I. MITRACHE, V. A. TOPAN and FLORENTINA DAMALAN, Contributions to the study of the superficial phenomena in porous media 1287–1292

N. PETRESCU and LUCIA GANOVICI, Self-diffusion in liquid thallium . . 1293–1303

P. BUDRUGEAC and M. I. VASS, On the surface stress and surface tension of gas-solid interface 1305–1309

MARCEL VLAD and E. SEGAL, On the stochastic analysis of the reaction networks. II. The principle of detailed balance for reaction networks . . . 1311–1317

MARCEL VLAD and E. SEGAL, On the stochastic analysis of the reaction networks. III. Langevin approaches 1319–1326

VIORICA CIMPU et D. CAMBOLI, Des combinaisons complexes du Pd(II) avec le Romergan et les ions Cl^- et CNS^- 1327–1330

A. C. BANCIU and P. SPACU, Cu(II) chelates synthesized with ligands containing donor nitrogen atoms 1331–1338

A. T. BALABAN and I. I. BĂDILESCU, Pyrylium salts formed by diacylation of olefins. XXI. Diacetylation of cyclodecene to 9,11-dimethyl-[7](2,6)-pyrylophanium perchlorate 1339–1343

R AURELIA BOLDEA, C. DRUGĂRIN, M. MRACEC and Z. SIMON, New urea and thiourea derivatives. I. Syntheses, IR and UV spectra of some new disubstituted urea and thiourea derivatives with possible physiological effects 1345–1353

R I. PARCHAMAZAD, M. KHOSROVI and N. SADEGHI, Selectivity in the alkylation of benzene by cyclopropane. 1355–1357

SUDARSHAN LAL, Polarographic maximum of cobalt (II) 1359–1366

D. DONESCU, Kinetic studies on the copolymerization of β-propiolactone with epichlorohydrin and 1,3-dioxepane 1367–1372

DIANA GIURGIU and I. POPESCU, Reactivity of organo-aluminum compounds towards Lewis bases. II. Diaryl- and dialkylaluminum ketiminphosphines 1373–1379

Revue. Roumaine Chim. 21, *9–10*, 1273–1432 (1976), Bucarest

GH. DRĂGAN, Amorphous-crystalline coupling in polyethylene. III. Interlamellar orderings in polyethylene with chemical etched defects 1381–1394

C. LITEANU, ELENA HOPÎRTEAN, I. C. POPESCU, N. L. KÉKEDY, ELISABETA VERESS and V. LITEANU, On a new procedure for obtaining sulphur dioxide starting from calcium sulphate. II. Utilization of phosphogypsum and of natural gypsum with impurities of $CaCO_3$ 1395–1404

R G. BOURCEANU, V. ABABI, GH. POPA and M. SANDULOVICIU, Phenol obtention from benzene in oxygen plasma generated by high frequency discharges. I. Dispersional analysis of the data and the multiple regression equation of the process 1405–1415

R CR. SIMIONESCU, C. UNGUREANU et AMALIA CRUSOS, Electropolymérisation des monomères vinyliques en solvants aprotiques polaires. III. Electropolymérisation de l'acrylonitrile en carbonate de propylène et d'éthylène. 1417–1427

L. BADEA, An equation for the thermal conductivity of water 1429–1431

Revue Roumaine de Chimie, **21**, *9–10*, 1275–1286 (1976)

DER EINFLUSS DES METHANS AUF DEN THERMISCHEN ZERFALL DES CHLOROFORMS. I

DIE ERSTEN DREI REAKTIONSSCHRITTE

I. G. MURGULESCU und MAIA WEISSMANN
Zentrum fur physikalische Chemie,
Str. Galaţi Nr. 31, Bukarest, Romania

Eingegangen am 3. November 1973
Ergänzt am 1. März 1976

Es wurde festgestellt, daß bei dem thermischen Zerfall des Chloroforms in Gegenwart von Methan neben den üblichen Zerfallsprodukten auch Vinylchlorid entsteht. Beim Ansteigen des Verhältnisses der Ausgangsreaktantenkonzentrationen, $(CH_4)_i/(CHCl_3)_i$, wächst die Ausbeute von Vinylchlorid bis zu ~100 % an, während die Ausbeute an Chlor- und Dichlormethan bis unter die Empfindlichkeitsgrenze des Chromatographen abfällt. Die Geschwindigkeitskonstanten erster Ordnung fallen mit Anwachsen der Kontaktzeit und der anfänglichen Chloroformkonzentration ab. Dieses Verhalten ist im Einklang mit einem Reaktionsmechanismus der den Primärakt $CHCl_3 \rightleftarrows \ddot{C}Cl_2 + HCl$, gefolgt von zwei parallelen Reaktionen des Dichlorkarbens: $\ddot{C}Cl_2 + CH_4 \rightarrow CHCl_2 - CH_3$; $CCl_2 + CHCl_3$; $CHCl_2 - CCl_3$ und nachherigen Reaktionen des Pentachloräthans und 1,1-Dichloräthans, voraussetzt.

EINLEITUNG

Die ersten Untersuchungen [1–4] über den thermischen Zerfall des Chloroforms zeigten, daß der Zerfall eine merkliche Geschwindigkeit erst von 450° aufwärts erreicht, der Druck unregelmäßig schwankt und sich Salzsäure, Hexachloräthan und andere kristalline Substanzen bilden.

In den eingehenden von Semeluk und Bernstein [5] sowie Schilow und Sabirewa,[6] in den Jahren 1954–1960 ausgeführten Studien, wurden zwei Reaktionsmechanismen vorgeschlagen. Der erste Mechanismus [5] sieht als Primärakt das Austreten eines Chloratoms vor:

$$CHCl_3 \rightarrow \dot{C}HCl_2 + \dot{C}l \qquad (1)$$

---

[1] A. Besson, *Compt. rend.*, **116**, 108 (1893).
[2] W. Lob, *Z. Electrochem.*, **7**, 903 (1901).
[3] E. T. Lessing, *J. Phys. Chem.*, **34**, 23 (1932).
[4] F. H. Verhoek, *Trans. Faraday Soc.*, **91**, 1525 (1935).
[5] G. P. Semeluk und R. B. Bernstein, *J. Amer. Chem. Soc.*, **76**, 3793 (1954); **79**, 16 (1957).
[6] A. E. Schilow und P. O. Sabirewa, *Doklady Akad. Nauk S.S.S.R.*, **114**, 1058 (1957); **4**, 860 (1960); **6**, 1365 (1959).

Durch die folgenden Reaktionsschritte des Chloratoms und des Radikals $\cdot CHCl_2$ wurde das Auftreten der vielfachen Reaktionsprodukte (CH_3Cl, CH_2Cl_2, CCl_4, C_2Cl_4, C_6Cl_6, C_2Cl_6, C_2HCl_5, $4\ Cl_2H_3Cl_4$, HCl, Cl_2) erklärt.

$$\dot{C}l + CHCl_3 \rightleftarrows HCl + \dot{C}Cl_3$$

$$\dot{C}l + \dot{C}Cl_3 \rightarrow CCl_4 \qquad (2)$$

$$\dot{C}Cl_3 \rightarrow \ddot{C}Cl_2 + \dot{C}l$$

$$\ddot{C}Cl_2 + CHCl_3 \rightarrow C_2Cl_4 + HCl$$

Schilow und Sabirewa[6] schlugen als Primärakt die Spaltung des Chloroformmoleküls in Salzsäure und Dichlorokarben vor:

$$CHCl_3 \rightleftarrows \ddot{C}Cl_2 + HCl \qquad (3, \ -3)$$

Die folgenden Ergebnisse dienten zur Stütze ihrer Hypothese: a) Wurde der Zerfall im Toluolstrom durchgeführt, so konnte man feststellen, daß Dibenzyl nur in Spuren auftrat. Es ist bekannt, daß in Gegenwart von Chloratomen ein Wasserstoffatom abgespalten wird wobei Salzsäure und das Benzylradikal gebildet wird, das nachträglich durch Dimerisierung zu Dibenzyl führt:

$$\dot{C}l + C_6H_5 - CH_3 \rightarrow C_6H_5 - \dot{C}H_2 + HCl \qquad (4)$$

$$2C_6H_5 - \dot{C}H_2 \rightarrow C_6H_5 - CH_2 - CH_2 - C_6H_5 \qquad (5)$$

Da aber Dibenzyl in den Reaktionsprodukten nur in Spuren angetroffen wird, ist die Hypothese von Semeluk und Bernstein nach der im Primärakt Chloratome gebildet werden nicht haltbar. b) Werden Chloroform und Tetrachlormethan zusammen thermisch zersetzt, so änderten sich die individuellen Reaktionsgeschwindigkeitskonstanten nicht. Dieses ist nur dann möglich, wenn die Reaktionen nicht ein gemeinsames Zwischenprodukt – in diesem Fall das Chloratom – haben. c) Die Größe des Isotopeneffekts ist genügend um eine Teilnahme der Wasserstoffatome am Primärakt zu rechtfertigen, d) Die an dem, von Semeluk und Bernstein vorgeschlagenen Mechanismus durchgeführten thermodynamischen Berechnungen führten zu unwahrscheinlichen Werten einiger Bindungsenergien.

In ihren Arbeiten, haben Le Moan,[7] Vacherot und Paraut[8] (1962–1965) weitere Ergebnisse hinsichtlich der Zerfallprodukte und deren zeitlicher Entwicklung erhalten. Was ihre Bildungsweise anbetrifft wird lediglich angeführt, daß ,,die Reaktion sehr komplex ist und sich wahrscheinlich die Radikale $\dot{C}Cl_3$, $\dot{C}HCl_2$, $\ddot{C}Cl_2$ bilden, die durch Zusammensetzung, Umlagerung, Disproportionierung, Dehydrochlorierung, u.s.w., zu den nachgewiesenen Produkten führen". Die Arbeiten den thermischen Zerfall der Chloroformdämpfe in Gegenwart ungesättigter Kohlenwasserstoffe betreffend,[9-13] haben bewiesen, daß sich Additionsprodukte des Dichlorkarbens an die Doppelbindung bilden, was eine charakteristische Reaktion der Karbene darstellt. Die Ergebnisse der Reaktion von Wasserstoffatomen und Tetrachlormethandämpfen [14] sowie auch die Pyrolyse bei sehr niederem Druck (Very Low Pressure Pyrolysis) des Chloroforms [15] stützen den von Schilow und Sabirewa vorgeschlagenen Mechanismus.[6] Durch Steudel [16] wurden 1967 direkte Beweise für die Teilnahme des Dichlorkarbens beim thermischen Zerfall des Chloroforms durch Massenspektrometrie und Ultrarotspektrophotometrie erbracht.

---

[7] G. Le Moan, *Compt. rend.*, **254**, 2602 (1962); **1260**, 5588 (1965).

[8] M. Vacherot und N. Peraut, *Compt. rend.*, **257**, 3938 (1963).

Wird der Schilow-Sabirewa-Mechanismus als richtig angesehen, dann muß die Vielzahl der aufgefundenen Produkte den nachträglichen Reaktionen des Dichlorkarbens zugeschrieben werden. Nach Schilow und Sabirewa ist die Dimerisierung des Dichlorkarbens zu Tetrachloräthylen bei kleinen Drucken wenig wahrscheinlich. Sie nehmen ohne theoretische oder experimentelle Argumente einen Sekundärakt der Form (6) an:

$$\ddot{C}Cl_2 + CHCl_3 \rightarrow C_2Cl_4 + HCl \qquad (6)$$

Wenn die bisherigen Ergebnisse hinsichtlich der Reaktivität der Karbene herangezogen werden, kann, wie aus der ,,Disskussion" hervorgeht, der Sekundärakt als ein Einschub des Dichlorkarbens in die C—H Bindung des Chloroforms angesehen werden.

In der vorliegenden Arbeit sind die experimentellen Ergebnisse über den thermischen Zerfall des Chloroforms in Gegenwart von Methan, die mit einem Primärakt (3) und einem Sekundärakt als Einschub in die C—H Bindung im Einklang sind, angeführt.

EXPERIMENTELLER TEIL

Die Versuche wurden in einer Vakuuminstallation mittels der Fließmethode bei verschiedenem Unterdruck durchgeführt. Die Installation ist in der Abbildung 1 dargestellt. Die Spezifikationen der Abbildung sind für den gesamten Abschnitt gültig.

Das Methangas mit einer Reinheit von 99,9% (ohne Sauerstoff, mit Verunreinigungen von Stickstoff, Wasserstoff, Äthylen) wurde beim Durchströmen durch mit Molekularsieben 5 Å und B.T.S.-Katalysator gefüllten Röhren gereinigt, wonach es durch das Nadelventil (b) in einen 2 l Glaskolben (c) eingeführt wurde und von dort in eine thermostatierte mit Chloroform gefüllte Phiole strömt (f).

---

[9] J. W. Engelsma und R. V. Helden, Shell Intern. Research Chaatschappy Neth., 104 879, mai 1963; *Chem. Abstr.*, **60**, 5333 (1964).

[10] F. E. Young und W. E. Bissinger, *J. Org. Chem.*, **29**, 2739 (1964).

[11] F. Strain und P. D. Barrett, Brit. 986 060 (to Pittsburgh Plate-Glass Co.); *Chem. Abstr.*, **62**, 16 116 (1965).

[12] J. W. Engelsma, *Rec. Trav. chim.*, **84**, 2, 187 (1965).

[13] P. Wescott und K. Skell, *J. Amer. Chem. Soc.*, **87**, 1721 (1965).

[14] D. T. Clarck und M. Tedder, *Trans. Faraday Soc.*, **62**, 518, 393 (1966).

[15] S. W. Benson und N. Spokes, *J. Amer. Chem. Soc.*, **11**, 2529 (1967).

[16] R. Steudel, *Tetrahedron letters*, **19**, 1845 (1967).

Das Chloroform (Carlo Erba per chromatographia) wurde von Alkohol und Wasser gereinigt. Durch eine Vakuumdestillation von Kühlfalle (e) zu Kühlfalle (f) konnte die restliche Luft entfernt werden, so daß Chloroform chromatographisch rein war. Das Gemisch von Chloroformdämpfen und Methan wurde durch eine Vakuumpumpe angesogen und trat nach dem Passieren einer Glasspirale (g), die die Elastizität der Installation vergrößert, in den Reaktor (i) ein. Beim Austritt aus dem Reaktor befand sich eine mit Glaswolle gefüllte Falle (1) um die bei der Reaktion entstehenden Verkohlungsprodukte abzufangen, wonach durch ein Kapillarrohr (n) die Produkte in zwei in flüssigen Stickstoff getauchten Kühlfallen (s, t) aufgehalten werden konnten und eine Absorbtionsröhre mit Natriumbikarbonat (u) die Salzsäure abfing.

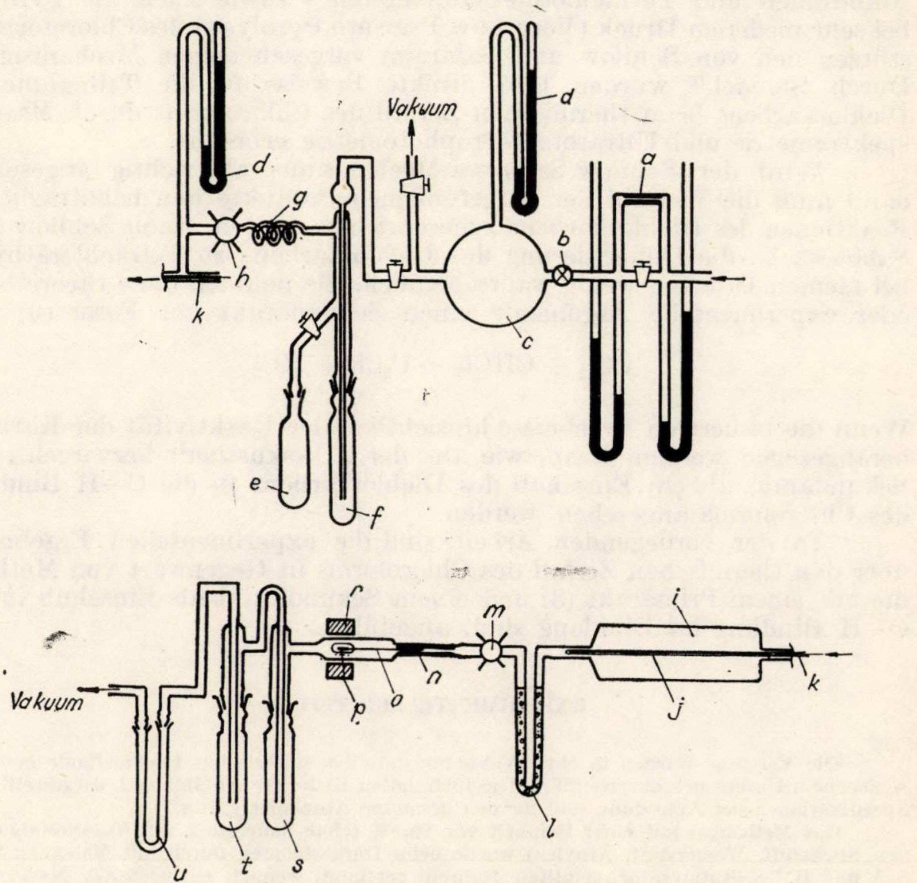

Abb. 1. — Schema der Installation.

a — Kapilarflowmeter ; b — Nadelventil ; c — Glaskolben ; d — Quecksilbermanometer ; e — Kühlhalle ; f — Phiole ; g — Glasspirale ; h — Gasdosierventil ; i — Reaktor ; j — Glasrohr ; k — Thermokouple ; l — Falle mit Glaswolle ; m — Gasdosierventil ; n — Kapillarrohr ; o — Wolframnadel ; p — Eisenkern ; r — Induktionsspule ; s — Kühlfalle ; t — Kühlfalle ; u — Absorbtionsrohre mit Natriumbikarbonat.

Der aus Quarz hergestellte röhrenförmige Reaktor (i) enthielt im Inneren eine konzentrisch angebrachte Hülse in der sich ein Chromel-Alumel-Thermoelement befand, mit dessen Hilfe das Temperaturprofil bestimmt wurde. Reaktoren mit drei verschiedenen Volumen (58, 65 und 80 cm^3) kamen zur Verwendung. Vor und nach dem Reaktor (i) waren zwei chromatographische Gasdosierventile (h, m) angebracht. Die chromatographische Anordnung gestattete die gleichzeitige Probeentnahme mittels beider Ventile (h, m) am Ein- und Ausgang des Reaktors.

Es wurde ein isothermer, mit Katharometer vorgesehener Chromatograph der Firma Pye (Modell 34) und zwei Säulen benutzt. Eine, 1 m lang, mit 5% Squalane auf 30/60 mesh gefüllt, zur Analyse der Reaktanten und die zweite, 5 m lang, mit 20% Squalane auf 80/100 mesh Chromosorb gefüllt, für die Analyse der Produkte. Die Fließgeschwindigkeit des Trägergases, H_2, betrug 22 ml/min.; die Temperatur der Säulen und des Katharometers waren 100°; der Strom im Katharometer betrug 300 mA. Die Eichungen wurden mittels Mischungen bekannter Zusammensetzung durchgeführt.

Der Druck des Methans wurde mit Hilfe des Nadelventils (b) eingestellt während die Fließgeschwindigkeit durch eine sich im Kapilarrohr (n) bewegende Wolframnadel (o) regliert wurde. Die Wolframnadel (o) war an einen in Glas eingeschlossenen Eisenkern (p) befestigt. Der Eisenkern (p) konnte mittels einer Induktionsspule (r) bewegt werden. Der Methandruck und der Druck im Reaktor wurden mittels Quecksilbermanometers bestimmt (c) während die Fließgeschwindigkeit mit einem Kapilarflowmeter (a) gemessen wurde. Durch Veränderung der Temperatur der mit Chloroform gefüllten Phiole (f), wurden verschiedene Konzentrationen desselben erhalten.

ERGEBNISSE UND DISKUSSION

Die bisherigen Ergebnisse hinsichtlich der Reaktivität der Karbene[17-20] haben gezeigt, daß diese mit einer C—Y gesättigten Bindung reagieren und dabei entweder das Y-Atom abspalten und zwei Radikale bilden:

$$\ddot{C}X_2 + \begin{array}{c}\diagdown\\ \diagup\end{array}\!C - Y \rightarrow \dot{C}X_2Y + \begin{array}{c}\diagdown\\ \diagup\end{array}\!\dot{C} \qquad (7)$$

oder durch Einschub in diese Bindung ein neues Molekül durch C—C Bindung bilden:

$$\ddot{C}X_2 + \begin{array}{c}\diagdown\\ \diagup\end{array}\!C - Y \rightarrow \begin{array}{c}\diagdown\\ \diagup\end{array}\!C - CX_2Y \qquad (8)$$

Wenn Dichlorokarben mit der C—H Bindung des Chloroforms reagiert und ein Wasserstoffatom abspaltet:

$$\ddot{C}Cl_2 + Cl_3C - H \rightarrow \dot{C}Cl_2H + \dot{C}Cl_3 \qquad (9)$$

dann würde in Gegenwart von Toluol, das eine schwächere C—H Bindung besitzt, insbesondere diese Bindung gespalten werden:

$$\ddot{C}Cl_2 + C_6H_5 - CH_3 \rightarrow C_6H_5\dot{C}H_2 + \dot{C}HCl_2 \qquad (10)$$

---

[17] V. B. De More und S. W. Benson, *Adv. Photochem.*, **2**, 219 (1967).

[18] M. L. Halberstadt und J. R. McNesby, *J. Amer. Chem. Soc.*, **14**, 7 (1967).

[19] B. M. Herzog und R. W. Karr, *J. Phys. Chem.*, **7**, 2688 (1967).

[20] A. J. Bell und G. B. Kistiakovsky, *J. Amer. Chem. Soc.*, **84**, 3417 (1962).

In diesen Versuchen wurde kein Dibenzyl festgestellt,[6] woraus ersichtlich ist, daß Dichlorkarben mit dem Toluol durch Einschub in die C—H Bindung reagiert :

$$\ddot{C}Cl_2 + C_6H_5 - CH_3 \rightarrow C_6H_5 - CH_2 - CHCl_2 \qquad (11)$$

In den Versuchsbedingungen spaltet 1,1-Dichlor, 2-Phenyläthan HCl ab und es bildet sich 1-Chlor, 2-Phenyläthylen welches identifiziert wurde :

$$C_6H_5 - CH_2 - CHCl_2 \rightarrow C_6H_5 - CH = CHCl + HCl \qquad (12)$$

Wenn Dichlorkarben durch Einschub mit der C—H Bindung des Toluols reagiert, kann man annehmen, daß es mit der C—H Bindung des Chloroforms, in welchem Wasserstoff stärker gebunden ist, umsomehr durch Einschub und nicht durch Abspaltung desselben reagieren wird. Die Beziehung zwischen der Abspaltungsmöglichkeit des Wasserstoffatoms und der C—H Bindungsenergie scheint eine plausible Hypothese zu sein. Infolgedessen würde der Sekundärakt des thermischen Zerfalls des Chloroforms im Einschub des Dichlorkarbens in die C—H Bindung des Chloroforms bestehen, wobei sich Pentachloräthan bildet :

$$\ddot{C}Cl_2 + Cl_3C - H \rightarrow Cl_3C - CCl_2H \qquad (13)$$

Es ist bekant, daß Pentachloräthan in den Arbeitsbedingungen folgendermaßen zerfällt :[21]

$$C_2HCl_5 \rightarrow \dot{C}l + \dot{C}_2HCl_4 \qquad (14)$$

Die Geschwindigkeit dieser Reaktion ist ungefähr 50 mal größer als die des thermischen Zerfalls des Chloroforms. Die Radikale $\dot{C}_2HCl_4$ und die Cl-Atome die in der Reaktion (14) gebildet werden, können das Auftreten der zahlreichen Produkte erklären.

Es besteht die Möglichkeit, daß Dichlorkarben auch mit der C—Cl Bindung des Chloroforms durch Abspaltung oder Einschub reagiert. Da die C—Cl Bindung im CCl_4 schwächer ist, könnte man in einer gleichzeitigen Pyrolyse von $CHCl_3$ und CCl_4 eine Wechselwirkung der zwei Zerfallksreaktionen festellen. Dieses ist aber nicht der Fall, woraus hervorgeht das Dichlorkarben mit der C—Cl Bindung des Chloroforms höchstens eine unbedeutende Reaktion eingeht.

Wenn der thermische Zerfall des Chloroforms in Gegenwart von Methan ausgeführt wird, dann könnte neben Reaktion (13) auch die Reaktion des Dichlorkarbens mit der C—H Bindung des Methans stattfinden, wobei aus denselben oben angeführten Gründen ein Einschub stattfinden würde :

$$\ddot{C}Cl_2 + H_3C - H \rightarrow H_3C - CCl_2H \qquad (15)$$

---

[21] T. J. Houser und R. B. Bernstein, *J. Amer. Chem. Soc.*, **80**, 4439 (1958).

1,1-Dichloräthan zerfällt in den Arbeitsbedingungen molekular und homogen zu Vinylchlorid[22]:

$$H_3C - CCl_2H \rightarrow HCl + H_2C = CHCl \qquad (16)$$

Also, müßte, beim Zusatz von Methan zum Chloroform, unter den Reaktionsprodukten, vor allem, Vinylchlorid auftreten. Wenn der Einfluß der Bindungsenergie des C—H auf die Reaktion mit Dichlorkarben eine richtige Hypothese ist, dann müßte Reaktion (15) eine kleinere Geschwindigkeitskonstante als Reaktion (13) haben, weil die C—H Bindung des Methans fester ist als die des Chloroforms. Um vergleichbare Geschwindigkeiten zu erhalten, müßte die Methankonzentration, die des Chloroforms übersteigen. Gleichzeitig ist auch auf Grund der Tatsache, daß (13) und (15) Konkurenzreaktionen sind, vorauszusehen, daß bei Anwachsen des Verhältnisses der Anfangskonzentrationen, $(CH_4)_i/(CHCl_3)_i$, die Konzentration des Reaktionproduktes zwischen Dichlorkarben und Methan — Vinylchlorid — anwächst, während die aus der Reaktion des Dichlorkarbens mit Chloroform (13) hervorgegangenen Produkte — Chlormethan, Dichlormethan, u.s.w. — kleinere Ausbeuten aufweisen. Bei sehr hohen Verhältnissen der Anfangskonzentrationen müßte die Reaktion (13) praktisch unterdrückt werden, so daß Vinylchlorid das einzige Reaktionsprodukt wäre.

Für eine Korrelation der experimentellen Ergebnisse mit den Literaturangaben wurde zuerst der thermische Zerfall des Chloroforms in einem trägen Gas (Ar) untersucht.

Bei der Analyse der Reaktionsprodukte, welche in den Kühlfallen kondensierten, identifizierten wir die in der Literatur angegebenen Produkte (C_2Cl_4, C_2HCl_6, C_2HCl_3, C_2Cl_6, CCl_4, CH_2Cl_2, C_4Cl_6, C_6Cl_6, HCl). Vinylchlorid wurde nicht aufgefunden und ist auch in der Literatur nicht angeführt.

Wie in der Literatur haben wir die Reaktion homogen und erster Ordnung befunden: die Reaktionsgeschwindigkeitskonstanten erster Ordnung wurden nach der Gleichung $k_1 = 1/t \ln (CHCl_3)_i/(CHCl_3)_f$ berechnet, wo $(CHCl_3)_i$ die Anfangskonzentrationen des Chloroforms und $(CHCl_3)_f$ die Konzentrationen desselben im Produktgemisch bedeuten. Man erhielt keine Änderung der Reaktionsgeschwindigkeitskonstanten wenn die Anfangskonzentration des Chloroforms um 400% vergrößert wurde. Die Geschwindigkeitskonstanten erster Ordnung fallen aber mit der Kontaktzeit ab (Abb. 2) was auch aus den von Schilow und Sabirewa erhaltenen Werte[6] hervorgeht. Dieses Verhalten kann auf das Vorhandensein einer durch ein Reaktionsprodukt hervorgerufenen Inhibitionsreaktion zurückgeführt werden. Der Inhibitionseffekt wurde auch von Semeluk und Bernstein[5] aufgefunden und der Salzsäure zugeschrieben. Versuche mit Zugabe von Salzsäure führten zu einem Ausdruck der Geschwindigkeitskonstanten welcher von der Salzsäurekonzentration abhängt.

---

[22] D. H. R. Barton und K. E. Howlett, *J. Chem. Soc.*, **1949**, 165; H. Hartman, H. Heydtmann und G. Rinck, *Z. Phys. Chem. (Frankfurt)*, **28**, 711 (1961).

$$-\frac{d(CHCl_3)}{dt} = k(CHCl_3) \,/\, [1 + b(HCl)]^{1/2} \qquad (17)$$

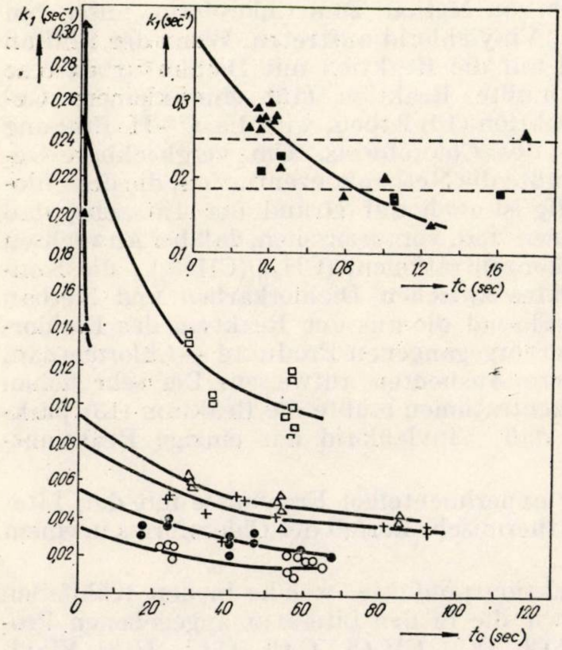

Abb. 2. — Thermischer Zerfall des Chloroforms in einem Argonstrom. Abhängigkeit der Geschwindigkeitskonstante erster Ordnung von der Kontaktzeit.

○ 522° ● 536° + 553° △ 561° □ 584°
▲ Schilow und Sabirewa[6], 584° ■ Idem, 510°
– – –Idem, aus der gegebenen Arrhenius-Formel berechnete Werte.

Schilow und Sabirewa[6] formulieren den Primärakt als eine reversible Reaktion (3, —3), was den Inhibitionseffekt der Salzsäure erklärt. Vacherot und Peraut[8] haben denselben Effekt der Salzsäure festgestellt. Auch bei anderen ähnlichen Substanzen (CHF_2Cl,[23] CHF_2Br[24]) wurde festgestellt, daß die Reaktion monomolekular ist und von Salzsäure inhibiert wird.

Um die Geschwindigkeitskonstante erster Ordnung bei $t = 0$ zu erhalten, wurden die Kurven x/a in Abhängigkeit von t_c aufgetragen, wo x die Konzentrationsverminderung des Chloroforms, a, seine Anfangskonzentration und t_c, die Kontaktzeit bedeuten (Abb. 3). Aus der Tangente im Nullpunkt des Achsensystems an diese Kurven wurden die anfänglichen Geschwindigkeitskonstanten berechnet. Gleichzeitig wurden durch die experimentellen Punkte im Koordonatensystem $k/(x/a)$ Geraden gezogen die bei Extrapolierung auf $x/a = 0$ Werte für k_1^0 ergaben, die mit den obigen im Rahmen der experimentellen Fehler im Einklang stehen (Abb. 4).

Aus der Temperaturabhängigkeit der wie oben erhaltenen Geschwindigkeitskonstanten erster Ordnung für die Temperaturen 522, 536,

---

[23] R. A. Cox und R. F. Simmons, *J. Chem. Soc.*, *B*, **1971**, 1625.
[24] G. R. Barnes, R. A. Cox und R. F. Simmons, *J. Chem. Soc.*, *B*, **1971**, 1176.

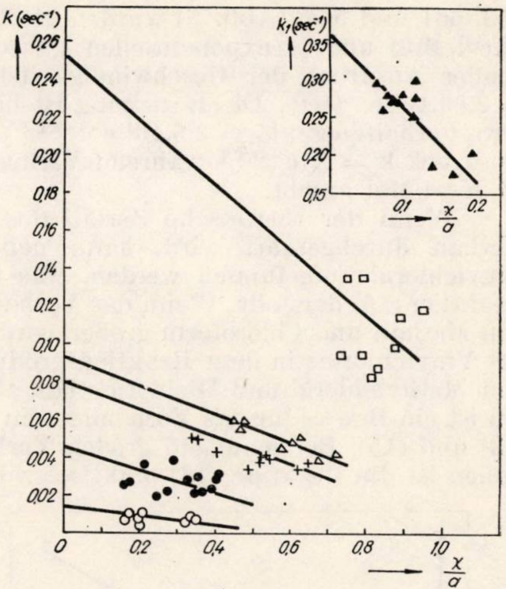

Abb. 3. – Thermischer Zerfall des Chloroforms im Argonstrom. Abhängigkeit der Geschwindigkeitskonstante erster Ordnung vom Konversionsgrad.

○ 522° ● 536° + 553° △ 561° □ 584°
▲Schilow und Sabirewa[6], 584°.

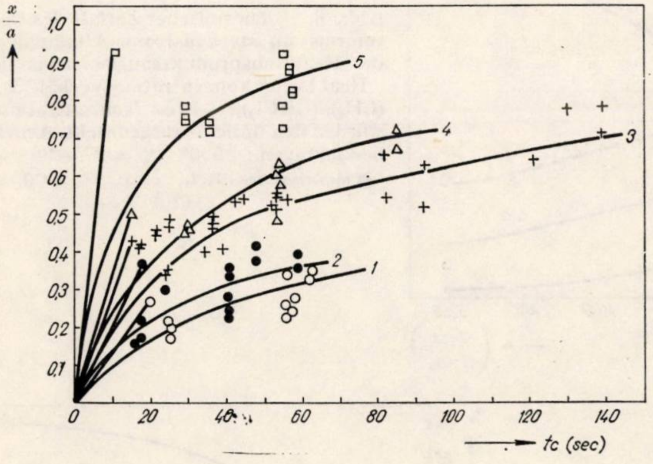

Abb. 4. – Thermischer Zerfall des Chloroforms im Argonstrom. Abhängigkeit des Konversionsgrads von der Kontaktzeit

○522° ●536° +553° △561° □584°

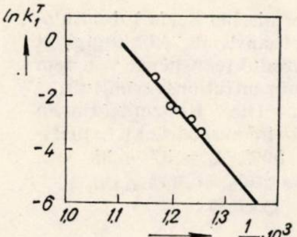

Abb. 5. – Thermischer Zerfall des Chloroforms im Argonstrom. Abhängigkeit der Geschwindigkeitskonstante erster Ordnung von der Temperatur.

553, 561 und 584° (Abb. 5) wurden die Werte für die Aktivierungsenergie (Kcal/Mol) und preexponentiellen Faktor (sek^{-1}) berechnet, so daß folgender Ausdruck der Geschwindigkeitskonstante erhalten wurde: $k_1 = 2{,}89.10^{11}e^{-47{,}5/RT}$. Die Beziehung ist näher der von Schilow und Sabirewa[6] erhaltenen: $k_1 = 2{,}6.10^{11}e^{-47/RT}$. Vacherot und Peraut[8] geben den Ausdruck $k = A\ e^{-57/RT}$ während Verhoek[4] eine Aktivierungsenergie von 49 Kcal/Mol angibt.

Wenn der thermische Zerfall des Chloroforms in Gegenwart von Methan durchgeführt wird, kann neben den Zerfallsprodukten auch Vinylchlorid aufgefunden werden, was ein Beweis für die Existenz der Reaktion (15) darstellt. Wenn das Verhältnis der Anfangskonzentrationen von Methan und Chloroform größer wird, wächst auch die Konzentration des Vinylchlorids in dem Reaktionsprodukt während die Konzentrationen von Methylchlorid und Dichlormethan abfallen (Abb. 6,7). Dieses Verhalten ist ein Beweis für das Vorhandensein der beiden Konkurenzreaktionen (13) und (15). Bei genügend großen Verhältnissen der Anfangskonzentrationen ist die Reaktion (13) praktisch von der Reaktion (15) des Dichlor-

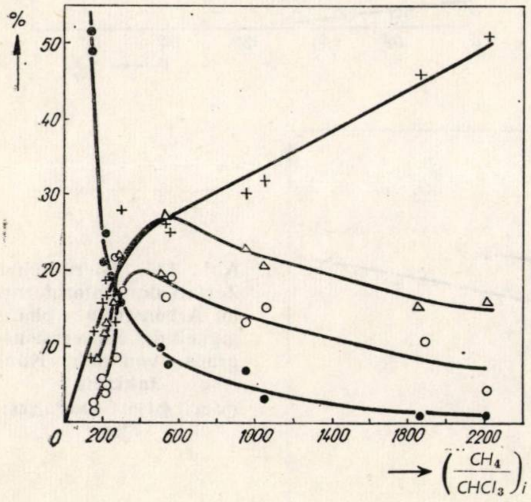

Abb. 6. — Thermischer Zerfall des Chloroforms im Methanstrom. Abhängigkeit der Reaktionsprodukteausbeute von dem Reaktantenkonzentrationsverhältnis, $(CH_4)_i/(CHCl_3)_i$. Die Konzentrationen wurden in μMol/cm³ ausgedrückt. Arbeitsbedingungen: 590°, $t_c = 27 - 30$ sek.
● nichtreagiertes $CHCl_3$ + C_2H_3Cl △ CH_2Cl_2 ○ CH_3Cl.

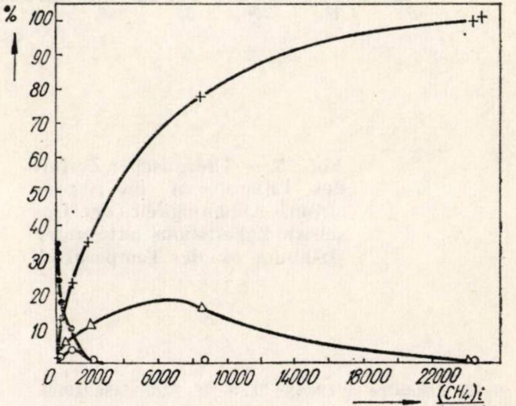

Abb. 7. — Thermischer Zerfall des Chloroforms im Methanstrom. Abhängigkeit der Reaktionsprodukteausbeute von dem Reaktantenkonzentrationsverhältnis, $(CH_4)_i/(CHCl_3)_i$. Die Konzentrationen wurden in μMol/cm³ ausgedrückt. Arbeitsbedingungen: 599°, $t_c = 37 - 38$ sek.
● nichtreagiertes $CHCl_3$ + C_2H_3Cl △ CH_2Cl_2 ○ CH_3Cl.

karbens mit Methan unterdrückt. Das Reaktionsprodukt dieser Reaktion – Vinylchlorid – wird mit einer Ausbeute von ~100 % erhalten, während die Reaktionsprodukte der Reaktion mit Chloroform (13) unter die Empfindlichkeitsgrenze des Chromatotraphen absinken.

Die Geschwindigkeitskonstanten erster Ordnung wurden nach der Formel $k_1 = 2{,}303/tc \log (CHCl_3)_i/(CHCl_3)_r$ berechnet und fallen mit der Kontaktzeit ab, was auf eine Inhibitionsreaktion durch ein Reaktionsprodukt zurückzuführen ist sowie es auch bei der Abwesenheit des Methans festgestellt wurde.

Zum Unterschied von dem Zerfall in Abwesenheit von Methan sind diese Geschwindigkeitskonstanten von der anfänglichen Konzentration des Chloroforms nicht mehr unabhängig : es wird ein bedeutender Abfall mit dem Anwachsen der Anfangskonzentrationen des Chloroforms festgestellt (Tab. 1, Abb. 8). Die Verkleinerung der Reaktionsordnung kann

Tabelle 1

Abhängigkeit der Geschwindigkeitskonstanten erster Ordnung von der Kontaktzeit und der anfänglichen Chloroformkonzentration

$t = 541°C$; $(CH_4)_i = 41{,}8 \frac{\mu Mol}{cm^3}$				$t = 599°C$; $(CH_4)_i = 43{,}0 \frac{\mu Mol}{cm^3}$			
t_c sek.	$(CHCl_3)_i$ $\frac{\mu Mol}{cm^3}$	k_1 sek^{-1}	k_1^0 sek^{-1}	t_c sek.	$(CHCl_3)_i$ $\frac{\mu Mol}{cm^3}$	k_1 sek^{-1}	k_1^0 sek^{-1}
25,8	0,026	0,118		37,4	0,020	0,348	
,,	0,026	0,113		,,	0,024	0,348	
,,	0,030	0,091		,,	0,042	0,268	
,,	0,121	0,072		,,	0,047	0,295	
,,	0,235	0,058		,,	0,084	0,201	
,,	0,248	0,058		,,	0,084	0,179	
17,9	0,295	0,101	0,045	,,	0,149	0,138	0,326
,,	0,334	0,080		,,	0,169	0,116	
12,9	0,035	0,133		19,4	0,206	0,204	
,,	0,096	0,111		,,	0,223	0,147	
,,	0,099	0,097		,,	0,197	0,255	
7,9	0,126	0,127		8,5	0,250	0,281	
,,	0,131	0,120		,,	0,259	0,249	

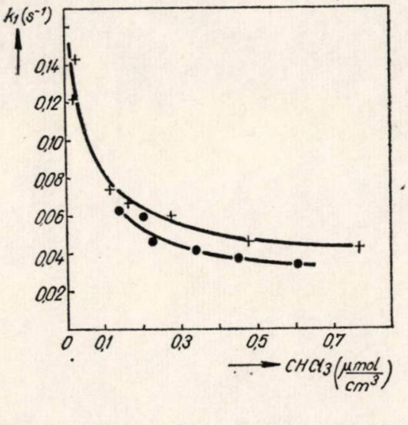

Abb. 8. – Thermischer Zerfall des Chloroforms im Methanstrom. Abhängigkeit der Geschwindigkeitskonstante erster Ordnung von der Anfangskonzentration des Chloroforms und von der Kontaktzeit.

Arbeitsbedingungen: 590°.

Konzentration des Methans: 43,2 μMol/cm³.

+ Kontaktzeit: 15 sek.

○ Kontaktzeit: 28 – 29 sek.

durch das Auftreten der Reaktion (15) erklärt werden, umsomehr als durch Ansteigen derselben die Verkleinerung der Reaktionsordnung bedeutender ist.

SCHLUSSFOLGERUNGEN

1. Methanzusatz beim thermischen Zerfall des Chloroforms führt zum Auftreten von Vinylchlorid.

2. Mit dem Anwachsen des Verhältnisses der Anfangskonzentrationen, $(CH_4)_i/(CHCl_3)_i$, wächst die Ausbeute an Vinylchlorid bis zu $\sim 100\%$ während die des Chlor- und Dichlormethans unter die Empfindlichkeitsgrenze des Chromatographen sinkt.

3. Die Geschwindigkeitskonstanten erster Ordnung wurden nach der Formel $k_1 = 2{,}303/tc \log (CHCl_3)_i/(CHCl_3)_i$ berechnet und fallen mit dem Anwachsen der Kontaktzeit und der anfänglichen Chloroformkonzentration ab.

4. Das Verhalten ist im Einklang mit einem Reaktionsmechanismus, dessen Primärakt von Schilow und Sabirewa[6] vorgeschlagen wurde und welcher, in Folge, mit den Erkenntnissen im Bereich der Karbenreaktionen in Übereinstimmung, zwei Konkurrenzreaktionen des Dichlorkarbens (Einschub in die C—H Bindung des Methans und des Chloroforms. Reaktionen (15) und (13) bzw.) aufweisen kann.

Revue Roumaine de Chimie, 21, 9–10, 1287–1292 (1976)

CONTRIBUTIONS TO THE STUDY OF THE SUPERFICIAL PHENOMENA IN POROUS MEDIA

L. ONICIU, I. MITRACHE, V. A. TOPAN and FLORENTINA DAMALAN
University "Babeş-Bolyai", Faculty of Chemistry, Str. Arany Janos, Cluj-Napoca, 11, Romania

Received December 20, 1974; Completed February 7, 1976

The Darcy equation, was used to develop a method of calculating the contact angle for porous electrodes by measuring the flowing rate through the porous sample. The investigations carried out by us were so far directed towards finding the best PTFE * concentration in our electrodes, so we have not yet calculated the contact angle value. The results obtained were used for this purpose.

INTRODUCTION

One of the most important problems which should be solved in the highly complex technology of gas-diffusive electrodes for fuel cells, is to award a partial hydrophobic character to the active layer and to obtain a porous hydrophobic layer through which the gas diffuses to the active centers located in the pores of the catalytic layer. This problem is closely connected with the superficial phenomena occurring in the considered porous medium, characterized by the interfacial tensions.

Let us consider, e.g., a liquid drop on a smooth solid surface; in this case there are three phases in contact: the liquid, its saturated vapours and the solid phase. They are separated, two by two, by an interfacial tension and the final shape of the drop will be determined by the equilibrium of the three interfacial tensions (fig. 1).

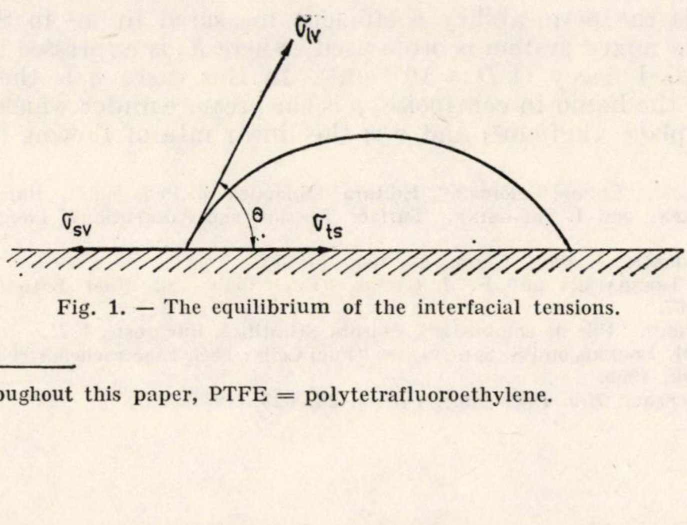

Fig. 1. — The equilibrium of the interfacial tensions.

---

* Throughout this paper, PTFE = polytetrafluoroethylene.

In a preliminary approximation, the equilibrium condition is given by the Young-Laplace equation :

$$\sigma_{sv} = \sigma_{sl} + \sigma_{lv} \cos\theta \tag{1}$$

where σ_{sv}, σ_{sl} and σ_{lv} are the interfacial tensions between solid and vapours, solid and liquid and liquid and vapours respectively ; θ is the contact angle. This angle (or its cosine) characterizes quantitatively the wetting degree ; when the contact angle is between 0° and 90°, the solid is wetted by the liquid, and when it is over 90°, the solid is not wetted.

The presence of interfacial tensions involves the capillar ascension under the influence of the capillary pressure p_c, whose value inside a capillary tube having the radius r, is :

$$p_c = \frac{2\sigma\cos\theta}{r} \tag{2}$$

It can be immediately seen that the capillary pressure may have positive or negative values, as a function of the behaviour of the liquid, as far as the wetting of the solid is concerned.[1–3]

The capillary pressure, which depends on the nature, or more exactly on the porous material composition of the gas-diffusive electrode, has a decisive influence on the performances of the fuel cell.[4–7]

The most usual methods for wetting determinations are not applicable for the porous medium of the gas-diffusive electrode, because of the hysteresis of wetting, which is a characteristic feature of the rugged surfaces.[1] That is why we decided to work out a method for the determination of the contact angle, which can be used for porous media. For this reason, the Darcy equation, which expresses the flowing rate of a liquid through a porous medium of a given porosity, was taken into consideration :

$$\vec{v} = -\frac{K_v}{\eta}\,\mathrm{grad}\,p \tag{3}$$

where K_v is the permeability coefficient measured in m^2 in SI system. In practice a mixed system is often used, where K_v is expressed by an unit measure called darcy ($1\,D = 10^{-8}\,\mathrm{cm}^2$). In this case, η is the dynamic viscosity of the liquid in centipoise, p is the pressure under which the flowing takes place (kgf/cm^2) and v is the linear rate of flowing (cm/s). In transient state, in which the determination of the contact angle was performed, when to the hydrostatic pressure of the liquid flowing through the porous medium is added the capillary pressure in pores, the relationship is true again (fig. 2).

---

[1] E. Chifu, "Chimie Coloidală", Editura Didactică şi Pedagogică, Bucureşti, 1969.

[2] R. Defay and I. Prigogine, "Surface Tension and Adsorbtion", Longmans-Green, London, 1966.

[3] R. Johnson, *J. Phys. Chem.*, **63**, 1655, (1959).

[4] H. A. Liebhafsky and E. J. Cairns, "Fuel Cells and Fuel Batteries", Wiley New York, 1967.

[5] L. Oniciu, "Pile de combustie", Editura Ştiinţifică, Bucureşti, 1971.

[6] J. O'M. Bockris and S. Srinivasan, "Fuel Cells : Their Electrochemistry", Mc. Graw-Hill, New York, 1969.

[7] D. Lucesoli, *Rev. Inst. franç. Pétrole*, **25**, 623, (1970).

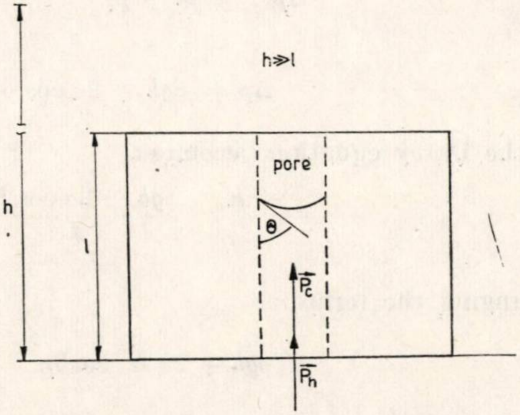

Fig. 2. — Determination of the flowing rate through a porous pellet.

EXPERIMENTAL

The determinations were carried out on samples obtained by pressing a mixture of carbon powder and PTFE, containing 15%, 20%, 30%, 40%, 45% and 50% PTFE. The mixtures were similar to those obtained for methanol-air and amalgam-air fuel cells.[8,9] The flowing rate of certain solutions of 3N, 4N, 5N and 6N KOH through each sample was measured. The samples were held by a fixing system which allowed the application of variable hydrostatic pressures. A disk of indicator paper was held above the sample; the time when the liquid enters the sample was detected with an electric sensor and the time when the sample was crossed by the liquid was shown by the indicator paper. The bending resistance was determined on the same samples.

RESULTS AND DISCUSSION

Knowing the thickness of the sample and measuring the time necessary for the liquid to cross the sample, we can calculate the flowing rate. In the considered case, the Darcy equation takes the form :

$$v = \frac{K_v \cdot \Delta p}{\eta \cdot \Delta z} \tag{4}$$

Since the actually measured flow rate is the one corresponding to the least sinuous pore oriented in the direction of the flow, the Oz axis was taken parallel to the axis of the sample and the gradient was calculat-

---

[8] L. Oniciu, A. Soó, E. Schmidt, E. M. Suciu and V. A. Topan, "A Methanol-Air Fuel Cell", Paper presented at the 4th National Conference of Physical Chemistry, Bucharest, 1974.

[9] L. Oniciu and M. Olaru, "An Application of the Sodium Amalgam-Oxygen Fuel Cell", Paper presented at the Student Scientific National Symposium, Bucharest, 1974.

ed only along this Oz axis. In this situation:

$$\Delta z = l = \text{sample thickness}$$

$$\Delta p = \rho gh + p_c$$

or

$$\Delta p = \rho gh + 2\sigma \cos \theta / r \tag{5}$$

Then the Darcy equation becomes:

$$v = \frac{K_v}{\eta} \, \frac{\rho gh + 2\sigma \cos \theta / r}{l} \tag{6}$$

Rearranging the terms:

$$K_v \, \rho gh + 2\sigma \, K_v \cos\theta / r = \eta \cdot l_v \tag{7}$$

Then:

$$\cos \theta = \frac{r}{2\sigma \, K_v} (\eta lv - K_v \, \rho \, gh) \tag{8}$$

and:

$$\theta = \arccos \frac{r}{2\sigma \, K_v} (\eta lv - K_v \, \rho gh) \tag{9}$$

The only parameter which requires a previous determination is the permeability coefficient K_v, whose value is the same in both the transient regime and the steady one. The final expression for the permeability coefficient is:

$$K_v = \frac{Q_v \, \eta l}{S \cdot \Delta p} \tag{10}$$

where Q_v is the volumetric flow rate through the sample (cm^3/s), η is the liquid viscosity (centipoise), l is the thickness of the sample (cm) Δp is the pressure drop (kgf/cm^2) and S is the surface of the sample (cm^2). In this case the permeability coefficient is expressed in darcy.

On fig. 3 we plotted the flowing rate of the solutions vs. concentration of PTFE and the bending resistance of the same samples on fig. 4.

A study of the curves presented in fig. 3 leads to some interesting conclusions:

— at PTFE concentrations lower than 20%, the flowing rate decreases suddenly as the PTFE concentration increases. This can be explained by the binding of carbon particles by the PTFE, without entering the pores.

– up to 20% PTFE concentration, once the binding finished, the PTFE enters massively the pores, which leads to a nearly constant hydrophobic character, so the curves show a horizontal portion.

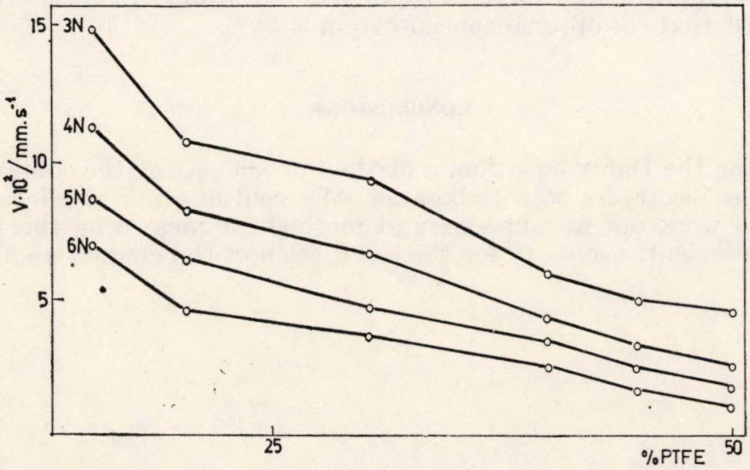

Fig. 3. – Flowing rate value vs. PTFE concentration in the sample.

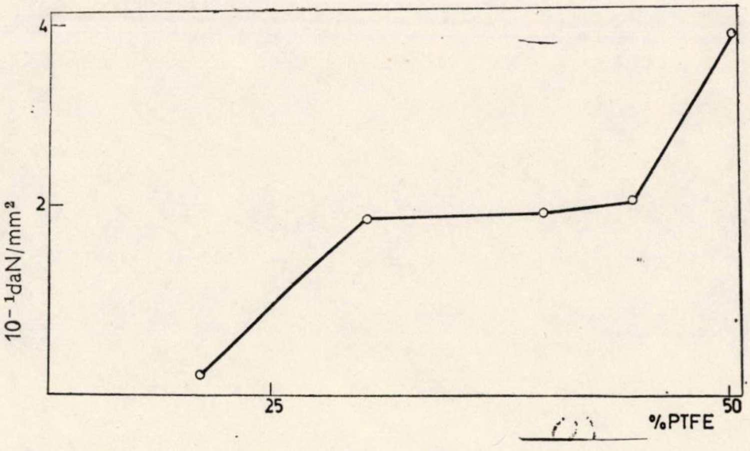

Fig. 4. – Bending resistance value vs. PTFE concentration in the sample.

The process of filling up the pores ends close to 30% PTFE concentration. Up to this value, PTFE agglomerates appear and the carbon particles are screened. Therefore the best PTFE concentration is between

20 and 30%; this value is in a good agreement with those found in other reports.[10–12]

Comparing the bending resistances from fig. 4 with the results in fig. 3, it is obvious that for a content of PTFE close to 30%, a constant resistance appears on a large range of concentrations. In this way it can be proved that the optimal concentration is 30%.

CONCLUSIONS

Using the Darcy equation, a method of calculating the contact angle for porous electrodes was elaborated. We continue our studies and we intend to work out an experimental method for measuring the permeability coefficient, necessary for the calculation of the contact angle value.

---

[10] D. Lucesoli and P. Degobert, *Rev. Inst. franc. Pétrole*, **25**, 1037, (1970).

[11] K. Berger, "Handbook of Fuel Cell Technology", Prentince-Hall, Englewood, Cliffs, New Jersey, 1968.

[12] T. Katan, Paper presented at Roth Meeting of CITCE, 15–20 Sept. 1969, 436, Strasbourg, France.

Revue Roumaine de Chimie, **21**, *9–10*, 1293–1303 (1976)

SELF-DIFFUSION IN LIQUID THALLIUM

N. PETRESCU and LUCIA GANOVICI
Centre of Physical Chemistry, Str. Galaţi 31, Bucharest 9, Romania

Received October 20, 1975

The self-diffusion in liquid thallium was studied in a temperature range from 350 to 800°, by the semi-infinite capillary method, using isotope Tl^{204} as radioactive tracer. A statistical treatment of experimental data according to the activated mechanism of diffusion, leads to the exponential dependence of the self-diffusion coefficients :

$$D = (3.17 \pm 0.27).10^{-4}.\exp.[(-3620 \pm 130)/RT]$$

Assuming that diffusion is a result of cooperative atomic motions based on the density fluctuations in liquid, the largest distance of diffusion displacement, the atomic radius of the diffusing particle and the force constante of inter-atomic bonds were calculated from experimental diffusion data. The results were compared with the structural characteristics of liquid thallium obtained by diffraction techniques. The experimental self-diffusion coefficients were confronted with those derived theoretically on a hard sphere model approach of the liquid and good agreement was obtained.

The progress of the knowledges about the metallic melts, about their structure and the mechanism of the processes involving liquid metals imperatively required more numerous data on the properties of metallic melts ; such experimental determinations will serve for a better substantiation of the theoretical assumptions in this field.

The diffusion coefficients may be listed among the experimental information best suited to be used in the substantiation of the theories of metallic melts.

There is not plenty of data on diffusion in metallic melts ; there are few pure metals for which diffusion coefficients in liquid state are known.

This scarceness of diffusion data in melts is partially understandable in view of the severe conditions imposed in order to maintain during the experiment one of the less characteristic properties of the melt, i.e. the stability of its macrostructure or the absence of any macroscopic mass transport.

Carrying on our previous works on the determination of self-diffusion coefficients in liquid metals,[1–6] the present paper aims at increasing the number of liquid metals for which the diffusion coefficients are available.

---

[1] N. Petrescu and L. Ganovici, *Rev. Roumaine Chim.*, **19**, 187 (1974).

[2] N. Petrescu and M. Petrescu, *Rev. Roumaine Chim.*, **15**, 189 (1970).

[3] I. Ganovici and L. Ganovici, *Rev. Roumaine Chim.*, **15**, 23, (1970).

[4] E. Nicoloiu, L. Ganovici and I. Ganovici, *Rev. Roumaine Chim.*, **15**, 1713 (1970).

[5] N. Petrescu, St. Zămârcă, L. Ganovici and I. Ganovici, *Rev. Roumaine Chim.* **13**, 865, (1968).

[6] M. Petrescu, *Z. Metallkde*, **61**, 14 (1970).

EXPERIMENTAL

The self-diffusion coefficients in liquid thallium were determined by the semi-infinite capillary method, based on the diffusional isothermal exchange between a little amount of radioactive thallium placed at the bottom of a long cylinder and the nonradioactive metal which fills up the cylinder. For diffusion the cylinder is kept at the wanted temperature for a length of time chosen such that no alteration of the initial concentration occurs at the opposite end of the cylinder. After rapidly cooling the sample, the radioactive concentration profile is measured along the cappillary and the self-diffusion coefficient is derived.

If the thickness of the radioactive thallium source is far less than the diffusion penetration length, the solution of the second Finck's law for the appropriate initial and limit conditions is given by the following equation :

$$c(x, t) = \frac{M}{\sqrt{\pi D t}} \cdot \exp \cdot \left(- \frac{x^2}{4\,Dt} \right) \qquad (1)$$

where t is the diffusion time and M is the whole amount of material which diffused in time t through the unit cross area of the cylinder (at the initial moment $t = 0$, this amount M is supposed to be concentrated in the plane $x = 0$).

By measuring the penetration of the radioactive substance one can derive the diffusion coefficient with good accuracy from the slope of the line representing $\lg[c(x, t)] = f(x^2)$.

The diffusion runs were performed in an apparatus similar to that we used in our previous works [1-6] on diffusion in metallic melts by the capillary — reservoir method. Some slight modifications were imposed by the characteristic of the method we chose for studying the diffusivity in liquid thallium.

The diffusion samples were contained in capillary containers 1 mm in diameter and 40 mm length drilled in spectrally pure graphite rods of 5 mm out diameter. The capillary graphite recipients closed at the bottom and equiped with a cup at the top were filled with inert liquid thallium by vacuum melting and argon admission under pression. After solidification each capillary was controlled radiographically in order to discard the defective samples which contained voids or interruptions of the metallic capillary column. The selected samples were cut at both ends and polished on metallographic paper and finally the metal was bored out at one end on a length of 1 mm by using a fine boring-bit fixed in a micrometric device. In this extremity hole a little bit of radioactive thallium was introduced and pressed by means of a graphite part so as to ensure a perfect surface contact with the inert thallium column within the capillary.

The outline in figure 1 represents a diffusion sample and the pieces used for pressing the radioactive thallium into the capillary. The graphite muff at the capillary top, acts as a thermal sink which ensures the solidification of the metallic column taking place from bottom to top, thus preventing the appearance of shrinkage voids in the active end of diffusion sample.

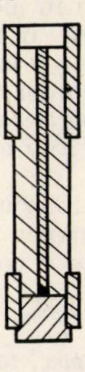

Fig. 1. — Graphite capillary for diffusion-runs.

In order to avoid the oxidation of the contact interface between the thin radioactive source and the capillary column, all manipulations of the radioactive source were performed quickly, and the oxide was dissolved with distilled water just before putting it into the graphite capillary. A plane and clean contact interface is of chief importance to have a succesful diffusion run at the chosen temperature. Any kind of imperfection at the contact interface results in modifications in the concentration profile and consequently will lead to errors in the determination of the diffusion coefficients.

The diffusion runs were performed in purified argon atmosphere and lasted 2—4 hours, according to the sample length and the temperature. For each run 2 or 3 capillary samples were rapidly put into the diffusion room heated at the desired temperature.

The radioactive thallium was obtained by irradiation of high purity metallic thallium (99.999%) in a nuclear reactor in conditions resulting in a specific activity of about 0.3 mCi/g.

The natural thallium comprises two isotopes: Tl^{203} with neutron cross section of 8.0 barns and Tl^{205} with neutron cross section of 0.7 barns. By (n, γ) reaction these natural stable isotopes give rise to the radioactive isotopes: Tl^{204} (decay time = 3.9 years), and Tl^{206} (decay time = 4.19 min). After a storage of about 10 days, the remaining activity is accounted for only by the long life isotope Tl^{204}, which decays in proportion of 98% by β^- emission (0.766 MeV) and by electron capture in proportion of 2%.

In order to check the radioactive purity of the irradiated thallium sources, a spectral analysis in the range from 0 to 1 MeV was performed by means of a multichannel analyser. The results of the measurements made on one of the thallium radioactive sources are given in fig. 2 and they point to the existence of an energy peak at 766 KeV corresponding to the β^- radiation of Tl^{204}; three additional peaks in the low energy range (75; 85 and 12 KeV) can be ascribed to the characteristic X rays K_α, K_β and L_α emitted by Tl^{204} consequent to its decay by electron capture. The calculated values of the characteristic X ray energy were 72 KeV, 83 KeV and 11 KeV, in good agreement with the observed ones.

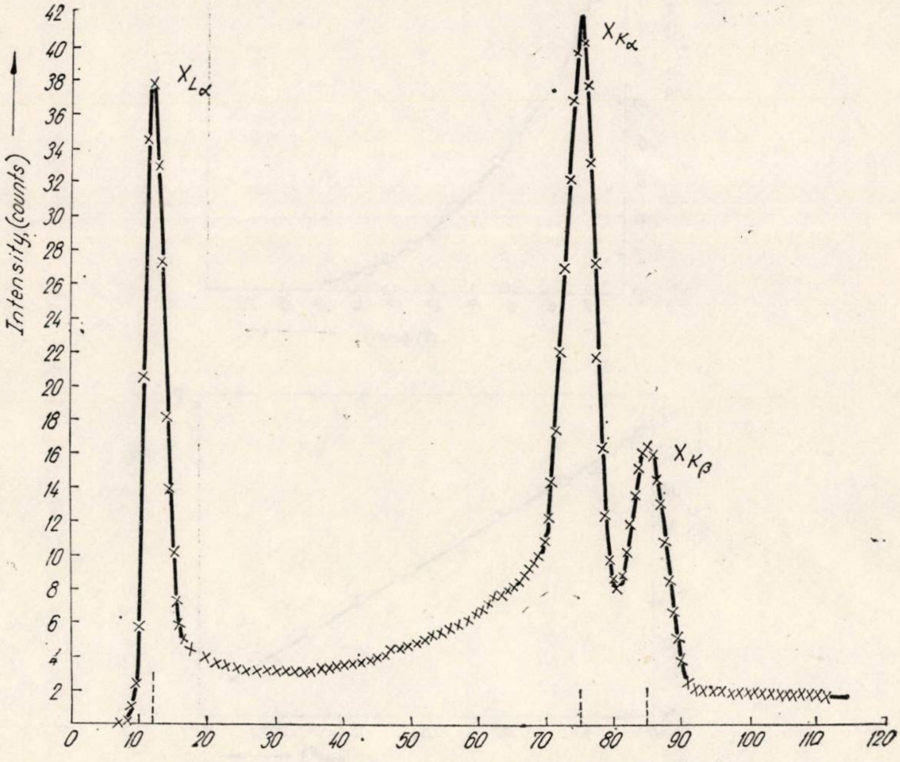

Fig. 2. — Spectral analysis of the radioactive thallium.

The concentration profile of the radioactive thallium along the capillary length after diffusion was determined by the following method : succesive layers of 1 mm thickness of the capillary were ground on a little bit of metallographic paper, the exact thickness of each layer being infered from two measurements of the capillary length, before and after the grinding of the layer. The radioactivity of each layer was measured directly on the metallographic paper on which it was ground ; the metallographic paper was put into the counting device of a scintillation counter mounted on a special holder.

RESULTS AND DISCUSSIONS

A typical radioactivity penetration curve in a diffusion sample is given in fig. 3.a. The x values on the abscisa represent the distance from the diffusion interface ($x = 0$) to the middle point of the thickness of the

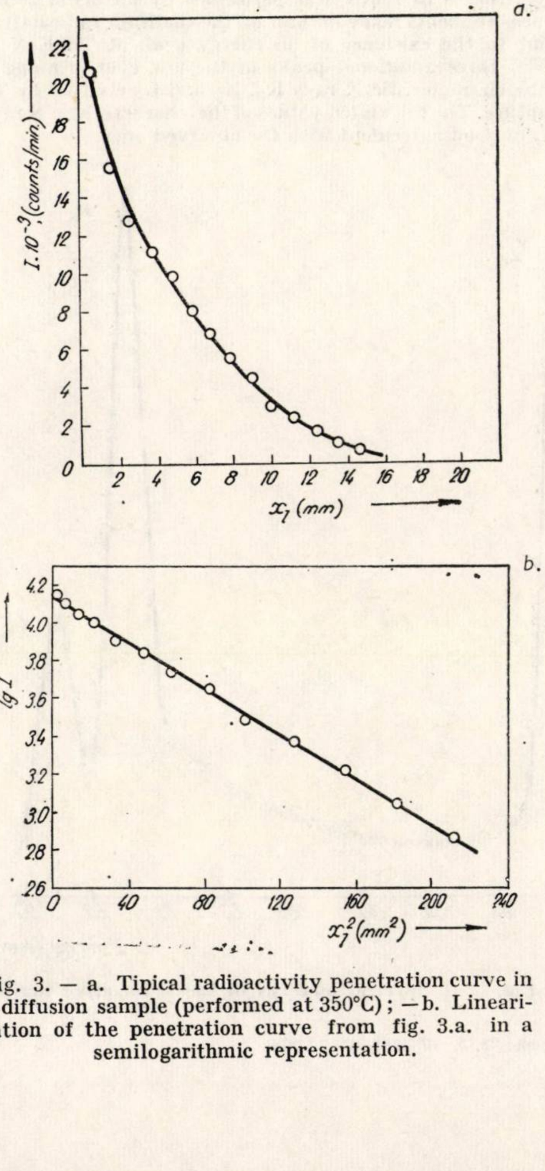

Fig. 3. — a. Tipical radioactivity penetration curve in a diffusion sample (performed at 350°C) ; —b. Linearisation of the penetration curve from fig. 3.a. in a semilogarithmic representation.

bouring holes, and the small fluctuation model which assumes that diffusion is achieved by movements of atoms on small and variable distances arising from density fluctuations in the liquid.

The temperature dependence of the diffusion coefficients derived from these two models is expressed either by an Arrhenius type equation :

$$\ln D = AT^{-1} + B \tag{3}$$

or by a polynomial type equation

$$D = AT^{n} + B \tag{4}$$

where *n* can take the values 1 or 2, while *A* and *B* are constants which can be corroborated with the physical properties or with the structural parameters of the melt.

Most of the existing diffusion data in metallic melts are discussed in the literature in terms of the Arrhenius type temperature dependence expressed by eq. (3). A statistical treatment of the self-diffusion experimental data in liquid thallium leads to the following Arrhenius type equation, whose plot is given in figure 4.

$$D = (3.17 \pm 0.27)\cdot 10^{-4} \exp\left[\left(-\frac{3620 \pm 130}{\mathrm{RT}}\right)\right] \tag{5}$$

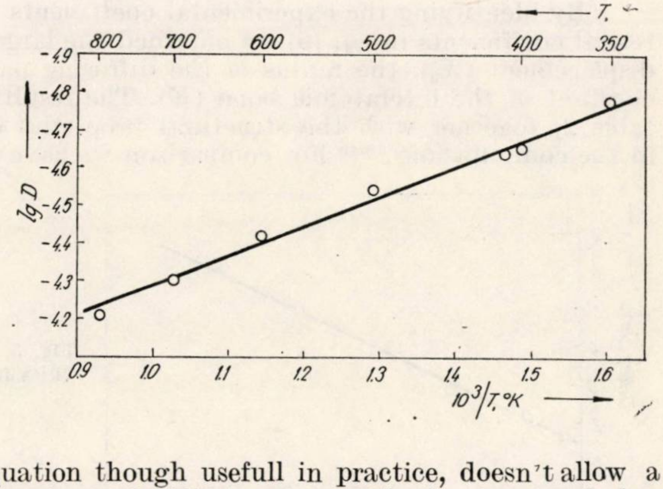

Fig. 4. — Arrhenius temperature dependence of the self-diffusion coefficients in liqud thallium.

The Arrhenius equation though usefull in practice, doesn't allow a confrontation of the experimental diffusion data with the structural characteristics of the melt directly obtained by X-Ray or neutron diffraction techniques.

We judged usefull to discuss the experimental data on self-diffusion in liquid thallium in terms of a mechanism different from the classic one presumed in the Arrhenius dependence, because this would have given us the possibility to corroborate our diffusion data with the information on the structure of the melt derived from diffraction data. The small density fluctuations theory takes into account the dynamical character of the structure of the melt and states that diffusion is a result of the cooperative motion of a large number of atoms on small and variable distances. In its initial form [12] the small fluctuations theory resulted in a temperature dependence of the diffusion coefficient of the form $D = AT^2$.

A modified form of the small fluctuation theory proposed by Reynik [13] and experimentally [6] checked results in a liniar dependence of the self-diffusion coefficients upon the absolute temperature:

$$D = -1.72 \cdot 10^{24}\, Z X_0^4 K + 2.08 \cdot 10^9 Z X_0^2\; T \tag{6}$$

where Z is the coordination number in the melt, K is the force constant of the interatomic bond (dyne/cm) and X_0 is the largest distance for the diffusive jumps (A°).

Our experimental data on the self-diffusion in liquid thallium fits well such a liniar temperature dependence, at least in the temperature range we investigated (fig. 5).

A statistical treatment of the experimental data on diffusion in liquid thallium results in the following liniar equation:

$$D = -4.25 \cdot 10^{-5} + 0.009 \cdot 10^{-5}\; T \tag{7}$$

By identifying the experimental coefficients in eq. (7) and the theoretical coefficients in eq. (6) we obtained the largest distance of diffusive displacement (X_0), the radius of the diffusing particle (r) and the force constant of the interatomic bond (K). The resulting values are given in table 2, together with the structural properties of liquid thallium used in the computations.[19,20] For comparison we have included in table 2 the

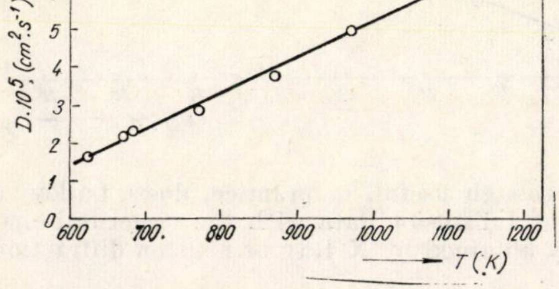

Fig. 5. — Dependence of the diffusivities in liquid thallium on the absolute temperature.

---

[19] L. Pauling, "The Nature of the Chemical Bond and the Structure of Molecules and Crystals", New York, Cornell University Press, 1962, p. 410, 420, 516.

[20] R. M. Waghornee, V. G. Rivlin and G. I. Williams, *Adv. in Physics*, **16**, 215 (1967).

same information derived from our previous works[1–3] on self-diffusion in Sb, Bi and Cd.

The largest distance of atomic displacement in table 2 is of the order of some tens of angströms, which represents 0.08 of the interatomic distance in thallium. This results is consistent with the diffusion mechanism based on microscopic density fluctuations which allow the cooperative movement of an atom and of his Z nearest neighbours to be done on variable distances far less than the interatomic distance.

Table 2

Physical properties and structural characteristics of liquid Tl, Sb, Bi and Cd

Element	Z coordination number in the melt	$\bar{d}$, Å Interatomic distance in the first coordination sphere	X_0, Å Largest jump distance (from diffusion data)	r, Å			$\frac{X_0}{2r}$	$K \cdot 10^{-4}$ dyne·cm^{-1}	
	From X-ray diffraction data			Radius of the diffusing particle (from diffusion data) $r = \frac{\bar{d} - X_0}{2}$	Metallic radius	Ionic radius		from diffusion data	from other physical measurements (20)
Tl	8	3.30	0.237	1.53	1.44 – 1.59	1.15	0.08	9.67	1.28
Sb	6.1	3.12	0.386	1.37	1.39 – 1.66	0.89	0.14	5.12	—
Bi	7.5	3.32	0.326	1.50	1.55 – 1.74	0.98	0.11	3.62	—
Cd	8.3	3.06	0.298	1.38	1.38 – 1.51	1.14	0.11	6.71	0.64

The radius of the diffusing particle derived from our experimental diffusion data compares well with the value of the single bond metallic radius of thallium.

The agreement between the value of the force constant of the interatomic bond derived from experimental diffusion data and the value of the force constant derived from other physical measurements [21] lays in the limits of the same order of magnitude.

In the last years several theoretical models were devised on the basis of Enskog's theory of dense spheres.[17] By succesive refinements these models succeed to allow the self-diffusion coefficients to be derived with good accuracy. For instance the theoretical relation proposed by Ascarelli and Paskin in its last form [22] leads to calculated self-diffusion coefficients in good agreement with the experimental data on the self-diffusion in liquid thallium obtained in the present paper.

---

[21] J. Wasser and L. Pauling, *J. Chem. Phys.*, **18**, 747 (1950).

Another theoretical relation recently proposed by Protopapas, Andersen and Parlee,[23] considers also the liquid metal similar to a fluid of dense spheres where the transport is accurately described by the Enskog theory plus corrections obtained from molecular dynamics calculations using the approach of Dymond and Alder. [24] Based on the expression of the self-diffusion coefficient given by Enskog's theory of dense spheres fluid and using the Carnahan-Starling [25] state equation, Protopapas et al. derived the following temperature dependence of the self-diffusion coefficient in liquid metals:

$$D = \frac{\sigma(\pi RT/M)^{1/2}C(\eta)(1-\eta)^3}{8\eta(2-\eta)} \tag{8}$$

where M is the atomic weight of the metal, $C(\eta)$ is a correction factor depending on the packing fraction (η) which is calculated and tabulated by Alder and Wainwright.[26] The correction factor lays between 1.0 and 0.4 for fluids whith packing fraction $0 \leqslant \eta \leqslant 0.49$. The diameter of the rigid spheres (σ) was considered equal to the mean interatomic distance for the repulsive collisions in the fluid. Taking into account that the higher the temperature the stronger the collisions, Protopapas et al., considered the diameter of the rigid spheres in liquid metals to decrease with temperature according to:

$$\sigma = \sigma_m[1 - B(T/T_m)^{1/2}] \tag{9}$$

where T_m is the melting point of the given metal and B is a dimenssionless positive number connected to the curvature of the interatomic potential at its minimum. It was shown [27] that for all liquid metals B can be taken to have the same value namely $B = 0.112$. The diameter of the rigid spheres at the melting point was evaluated from the expression:

$$\sigma_m = [6\eta_m M/\pi \rho_m N_0]^{1/3} \tag{10}$$

where ρ_m is the density of the metal at its melting point and N_0 is Avogadro's number. The packing fraction at the melting point η_m is also a dimensionless constant which equals 0.472 for all liquid metals.[27]

---

[22] P. Ascarelli and A. Paskin, *Phys. Rev.*, **165**, 222 (1968).

[23] D. Protopapas, H. C. Andersen and N. A. D. Parlee, *J. Chem. Phys.*, **59**, 15 (1973)

[24] J. H. Dymond and B. J. Alder, *J. Chem. Phys.*, **45**, 2061 (1966); **48**, 343 (1968); **52**, 923 (1970).

[25] N. F. Carnahan and K. E. Starling, *J. Chem. Phys.*, **51**, 635 (1969).

[26] B. J. Alder, D. M. Gass and T. E. Wainwright, *J. Chem. Phys.*, **53**, 3813 (1970).

[27] K. Furukawa, *Sci. Rep. Res. Inst. Tohoku Univ., Ser. A.* **12**, 368 (1968).

The last parameter needed in eq. (8) is the packing fraction η at the given temperature which can be evaluated [23] from :

$$\eta = \eta_m(\rho\sigma^3/\rho_m\sigma_m^3) \tag{11}$$

where all values are known.

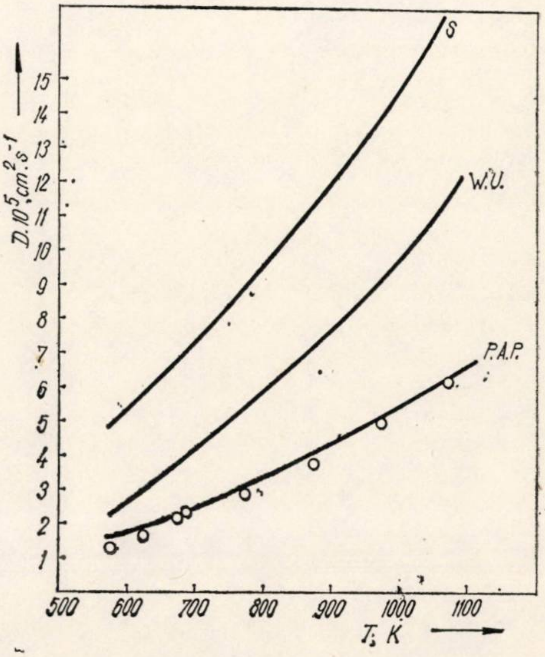

Fig. 6. — Comparison of experimental (O) and theoretical self-diffusion coefficients for liquid thallium, after Swalin (S) Walls and Upthegrove (W–U) and Protopapas et al. (PAP).

In fig. 6 the temperature dependence of the self-diffusion coefficient in liquid thallium is plotted both for theoretical values calculated through eq. 8 (curve PAP) and for experimental values obtained in the present paper. Fig. 6 shows that the agreement between the experimental data and the theoretical ones derived from PAP expression is particulary good. For comparison other theoretical curves for the self-diffusion temperature dependence are also plotted in fig. 6 i.e. theoretical values derived on the small density fluctuation diffusion mechanism (Swalin's theory — curve S) and Walls and Upthegrove's theory (curve $W - U$).

The best theoretical model to suit the experimental diffusion data is still an open problem, which can be solved only by gathering up more experimental results on the properties of the melts.

[illegible]

[illegible]

$$[illegible]$$

[illegible]

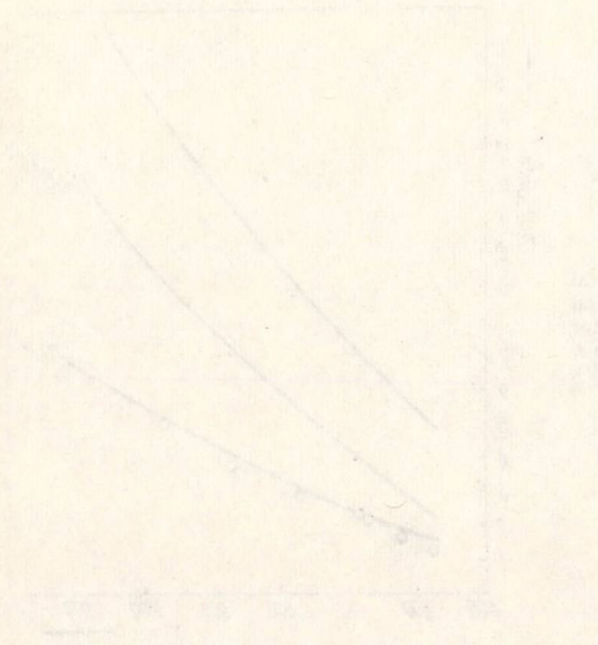

[illegible]

In Fig. 6 [illegible]

[illegible]

[illegible]

Revue Roumaine de Chimie, **21**, *9–10*, 1305–1309 (1976)

ON THE SURFACE STRESS AND SURFACE TENSION OF GAS-SOLID INTERFACE

P. BUDRUGEAC and M. I. VASS
Institute of Physical Chemistry, Str. Dumbrava Roşie 23,
Bucharest, Romania

Received August 7, 1975

We point out that the hypothesis of the plastic increase of the area of the gas-solid interface in the case of localized adsorption leads to a disagreement between the value of surface stress which results from the definition of this quantity and the statistical calculated value. A relation for calculating the surface tension in the case of adsorption without lateral interactions on homogeneous surfaces is given. The phenomenological results are checked for the Langmuir model, the BET model and the model of ideal two-dimensional gas.

In the thermodynamic treatments of physical adsorption of gases on solid surfaces, which are usually used in the interpretation of the experimental data,[1,2] it is considered that both in the case of localized adsorption and in the case of mobile adsorption, the change of surface area is made plastically, like the change of the area of a liquid surface. The aim of this paper is to show that the hypothesis of plastic change of interface area leads, in the case of localized adsorption, to a disagreement between the value of surface stress which results from the definition of this quantity and its statistical calculated value. We will show that this disagreement can be overcame by using Eriksson's treatment of adsorption thermodynamics.[3]

Let us assume that the thermodynamic system consists of: the adsorbent with a homogeneous surface, the gas-solid interface and the gas. We also make the assumptions that the adsorption is reversible and the chemical nature of the adsorbent is not changed by adsorption.

The expression of infinitesimal change of the internal energy of the gas-solid interface is given by the relation.[1]

$$dE^s = TdS^s - Pdv^s - \gamma^s dA + \mu^s dn^s \tag{1}$$

where the upper index s refers to the gas-solid interface; γ^s is the surface stress; A is the surface area and E, S, V, n, T, P, μ are the usual symbols of thermodynamics.

---

[1] T. L. Hill, *Adv. Catalysis*, **4**, 212 (1952).
[2] D. H. Everett, *Trans. Faraday Soc.*, **46**, 453 (1950).
[3] J. C. Eriksson, *Surface Sci.*, **14**, 221 (1969).

Since $(-\gamma^s dA)$ is the work of stretching the surface, it results that γ^s is the force per unit length of the exposed edge which must be applied to the boundary of the interface in order to keep it in equilibrium. This definition is an extension of the definition of surface stress given in surface thermodynamics [4-8] for gas-solid interface.

From the above-mentioned meaning of the surface stress, it results that in the case of localized adsorption without lateral interactions we have the following relation :

$$\gamma^s = 0 \tag{2}$$

On the other hand, in order to calculate the surface stress in the case of localized adsorption without lateral interactions, Hill [9] and Clark[10] make the assumption that $dA = \frac{A}{B}\, dB$, B denoting the number of adsorption sites on the adsorbent surface. Using this assumption, at $dT = 0$ and $V^s \simeq 0$, the relation (1) could be written :

$$dF^s = d(E^s - TS^s) = -\gamma^s \frac{A}{B}\, dB + \mu^s dn^s \tag{3}$$

Because between the Helmholtz free energy and partition function, Q^s, there is the well-known relation :

$$F^s = -kT\, lnQ^s \tag{4}$$

it results that :

$$\gamma^s = \frac{kTB}{A}\left(\frac{\partial lnQ^s}{\partial B}\right)_{T,\, n^s} \tag{5}$$

Because Q^s is function of B,[10] it results that the surface stress given by the relation (5) is not zero.

This disagreement between the relations (2) and (5) appears because we supposed that $dA = \frac{A}{B}\, dB$. To solve this disagreement we introduce the surface tension which appears in the integral form of equation (1) :

$$E^s = TS^s - \pi^s A + \mu^s n^s \tag{6}$$

---

[4] J. W. Gibbs, "Collected Works", New York, Longmans, Green & Co., 1928, p. 315.

[5] C. Hering, "The Structure and Properties of Solid Surface", Eds. R. Gomer and C. S. Smith, Univ. Chicago Press., Chicago, 1952, p. 5.

[6] J. S. Vermaak, C. W. Mays and D. Kuhlmann-Wilsdorf, *Surface Sci.*, **12**, 128 (1968).

[7] P. R. Couchman, W. A. Jesser, D. Kuhlmann-Wilsdorf and J. P. Hirth, *Surface Sci.*, **33**, 429 (1972).

[8] P. R. Couchman and W. A. Jesser, *Surface Sci.*, **34**, 212 (1973).

[9] T. L. Hill, "An Introduction to Statistical Thermodynamics", Ch. 7, Addison-Wesley, Reading, Mass., 1960.

[10] A. Clark, "The Theory of Adsorption and Catalysis", Ch. 2, Academic Press, New York, 1970.

π^s is the surface tension or the reversible cleavage work.[3] Eriksson [3] showed that, generally, $\pi^s \neq \gamma^s$ and $\pi^s = \gamma^s$ only in the case of mobile adsorption when the change of interface area is plastic like the change of the area of a liquid surface.

We return to equation (5) from which it results that:

$$\gamma^s \frac{A}{B} dB = d(L - L_0) \tag{7}$$

where: dL is the necessary work to increase a surface having B_0 adsorption sites and n^s localized adsorbed molecules, with dB adsorption sites; dL_0 is the work to increase the surface of the clean adsorbent which has B_0 adsorption sites, with dB adsorption sites.

Because the adsorption is localized and the state of the adsorbent is not changed by adsorption, it follows that $d(L - L_0)$ is zero and so we find, once again, that, in the case of localized adsorption, $\gamma^s = 0$.

γ^s will be different from zero only if we consider that after the increase of the number of adsorption sites with dB, the n^s adsorbed molecules would redistribute on the $(B_0 + dB)$ adsorption sites. But, supposing this redistribution, we suppose in fact that the adsorption is mobile (when $\pi^s = \gamma^s$ [3]) and, therefore, the equation (5) is correct for π^s and not for γ^s.

Also, it results that, both in the case of localized adsorption and in the case of mobile adsorption on homogeneous surfaces and without lateral interactions, an increase of the interface area with dA, at $dT = 0$ and $dn^s = 0$, requires a work to redistribute n^s adsorbed molecules on the surface with an area $(A_0 + dA)$, work which is necessary for increasing the entropy of the adsorbed layer:

$$\pi^s dA = T dS^s \tag{8}$$

from which results:

$$\pi^s = T \left(\frac{\partial S^s}{\partial A} \right)_{T, n^s} \tag{9}$$

The above results will be clarified below by means of a discussion based on the statistical-mechanical treatments of adsorption. We will consider the following models of physical adsorption: the Langmuir model, the BET model and the model of ideal two-dimensional gas.

In order to calculate the surface tension we will use the following relation which results from equations (4) and (6):

$$\pi^s = \frac{kT}{A} \left[\ln Q^s - n^s \left(\frac{\partial \ln Q^s}{\partial n^s} \right)_{T,A} \right] \tag{10}$$

In the case of Langmuir model, the partition function of the adsorbed layer is given by relation:[9,10]

$$Q^s = \frac{B\,!}{(B-n^s)\,!n^s\,!}\,(q^s)^{n^s}\,\exp\left(-\frac{n^s U_0}{kT}\right) \tag{11}$$

where $q^s \exp\left(-\frac{U_0}{kT}\right)$ is the partition function of an adsorbed molecule and U_0 is the adsorption potential.

By using this partition function, it results that γ^s given by relation (5) is equal with π^s given by relation (10) and this shows that the assumption $\mathrm{d}A = \frac{A}{B}\,dB$ leads to the calculation of the surface tension instead of the surface stress. Also, the same value of surface tension results from the equation (5), where S^s is calculated from the well-known relation: $S^s = kT\left(\frac{\partial \ln Q^s}{\partial T}\right)_{n^s,A} + k\,lnQ^s$.

In the case of BET model, the statistical treatment is made by using the grand partition function:[9,10]

$$\Xi^s = \left[1 + q_1\lambda^s\,\frac{1-(q_L\lambda^s)^m}{1-q_L\lambda^s}\right]^B = F^B \tag{12}$$

where: q_1 is the partition function for a molecule adsorbed in the first layer; q_L is the partition function of a molecule in the liquid state; $\lambda^s = \exp\left(\frac{\mu^s}{kT}\right)$; m is the maximum number of molecules on an adsorption site.

In this case, from the definition of Ξ^s, it results that the relation:

$$\pi^s = \frac{kT}{A}\ln \Xi^s \tag{13}$$

is correct and the relation:[9,10]

$$\gamma^s = \frac{kT}{A}\ln \Xi^s \tag{14}$$

which would leads to the incorrect results $\gamma^s \neq 0$, is not correct.

Let us prove that relation (9) holds in this case. S^s is given by the well-known relation:

$$S^s = k\,ln\,\Xi^s + kT\left(\frac{\partial ln \Xi^s}{\partial T}\right)_{\mu^s,B} \tag{15}$$

From relations (12) and (15) it results :

$$S^s = kB\, lnF + kTB\left(\frac{\partial lnF}{\partial T}\right)_{\mu^s, B} \qquad (16)$$

where F is function of $\bar{n}^s$ and $\frac{q_1}{q_L}$. We consider that $\bar{n}^s = \text{const.}$ and, because $\frac{q_1}{q_L}$ depends very little on the temperature, it results :

$$\pi^s = \frac{kTB}{A}\, lnF = \frac{kT}{A}\, ln\, \Xi^s \qquad (17)$$

equation which is identical with relation (13).

In the case of ideal two-dimensional gas, Q^s is given by the relation :[9,10]

$$Q^s = \frac{1}{n^s\,!}\left(\frac{2\pi\, mkTA}{h^2}\right)^{n^s} \exp\left(-\frac{n^s U_0}{kT}\right) \qquad (18)$$

In this case also it results that the value of π^s calculated by using relation (9) is identical with the value of π^s calculated by using relation (10).

To conclude, it was shown that the substitution of dA with $\frac{A}{B}\, dB$ is not correct for locallized adsorption. To avoid the disagreement shown above, the introduction of the surface stress and the surface tension as two distinct quantities appears once again necessary.

Also, starting with the fact that the increase of the interface in the case of adsorption without lateral interactions on homogeneous surfaces is accompanied only by an increase of entropy, a relation for calculating the surface tension was given. This relation was checked for three models : the Langmuir model, the BET model and the model of ideal two dimensional gas.

Revue Roumaine de Chimie, 21, *9–10*, 1311–1317, (1976)

ON THE STOCHASTIC ANALYSIS OF THE REACTION NETWORKS. II[1]

THE PRINCIPLE OF DETAILED BALANCE FOR REACTION NETWORKS

M. VLAD and E. SEGAL
Polytechnical Institute of Bucharest, Institute of Chemistry, Department of Physical Chemistry and Electrochemical Technology, Bd. Republicii 13

Received September 30, 1975

Starting from the stochastic theory of reaction rates, the validity of detailed balance principle for the unimolecular reactions $A_i \rightleftarrows A_j \; n \geqslant i > j \geqslant 1$ is discussed. In the case of a large (macroscopic) system the discussion can be extended to the elementary reactions

$$\sum_i \nu_{ij} A_i \rightleftarrows \sum_i \nu'_{ij} A_i \; n \geqslant i \geqslant 1 ; \; j = 1, \ldots, R ; \; 2 \geqslant \sum_i \nu_{ij}, \; \sum_i \nu'_{ij} \geqslant 1.$$

In this paper we shall continue the stochastic analysis of the reaction networks.[1] Using the stochastic theory, we shall show that the detailed balance principle [2] is a consequence of the microreversibility principle.[3] We shall refine thus the conclusions of the non-equilibrium thermodynamics.[4]

A. UNIMOLECULAR REACTIONS

For the system :

$$A_i \rightleftarrows A_j \; n \geqslant i > j \geqslant 1$$

we can define the probability $P(\mathbf{N}_1, t_1 ; \mathbf{N}_2, t_2 ; \ldots ; \mathbf{N}_m, t_m)$ as at the moment t_i the composition vector of the system should have the value $\mathbf{N}_i (i = 1, \ldots, m)$. According to the theory of Markov processes,[5] $P(\mathbf{N}_1, t_1 ; \ldots ; \mathbf{N}_m, t_m)$ is equal to :

$$P(\mathbf{N}_1, t_1 ; \ldots ; \mathbf{N}_m, t_m) = \prod_\alpha P(\mathbf{N}_{u_\alpha}, t_{u_\alpha} / \mathbf{N}_{u_{\alpha-1}}, t_{u_{\alpha-1}}) \, P(\mathbf{N}_{u_1}, t_{u_1}) \qquad (1)$$

---

[1] Part I: M. VLAD and E. SEGAL, *Rev. Roumaine Chim.* **21**, 667 (1976).

[2] G. N. LEWIS, *Proc. Nat. Acad. Sci. U.S.A.*, **11**, 179 (1925).

[3] R. C. TOLMAN, *Phys. Rev.*, **23**, 699 (1926).

[4] R. S. de GROOT and P. MAZUR, "Non-Equilibrium Thermodynamics" North Holland Publ. Comp., Amsterdam, 1962.

[5] A. T. BHARUCHA-REID, "Elements of the Theory of Markov Processes and their Applications", Mc. Graw-Hill, New-York, 1960.

where $t_{u_\alpha} = \min[\{t_1, \ldots, t_m\} \setminus \{t_1, \ldots, t_{u_{\alpha-1}}\}]$; $t_{u_1} = \min\{t_1, \ldots, t_m\}$.
As[1,6]

$$P(\boldsymbol{N}, t/\boldsymbol{N}_0, 0) = \sum_{\substack{\forall b_{\lambda i} \geqslant 0 \quad \lambda, i = 1, \ldots, n \\ \sum_\lambda b_{\lambda i} = N_{0i};\ \sum_i b_{\lambda i} = N_\lambda}} \prod_i N_{0i}! \prod_{i,\lambda} \frac{\eta_{\lambda i}^{b_{\lambda i}}(t)}{b_{\lambda i}!}, \tag{2}$$

$$G(\boldsymbol{S}, t/\boldsymbol{N}_0, 0) = \sum_{\forall N_i \geqslant 0} \prod_i s_i^{N_i} P(\boldsymbol{N}, t/\boldsymbol{N}_0, 0) = \prod_i \Big(\sum_j \eta_{ij}(t) s_j\Big)^{N_{0i}} \tag{2'}$$

the conditional probabilities $P(\boldsymbol{N}_{u_\alpha}, t_{u_\alpha}/\boldsymbol{N}_{u_{\alpha-1}}, t_{u_{\alpha-1}})$ and their generating functions $G(\boldsymbol{S}_{u_\alpha}, t_{u_\alpha}/\boldsymbol{N}_{u_{\alpha-1}}, t_{u_{\alpha-1}})$ are given by :

$$P(\boldsymbol{N}_{u_\alpha}, t_{u_\alpha}/\boldsymbol{N}_{u_{\alpha-1}}, t_{u_{\alpha-1}}) = \sum_{\substack{\forall b_{\lambda i} \geqslant 0 \quad \lambda, i = 1, \ldots, n \\ \sum_\lambda b_{\lambda i} = N_{iu_{\alpha-1}};\ \sum_i b_{\lambda i} = N_{\lambda u_\alpha}}} \prod_i N_{iu_{\alpha-1}}! \prod_{\lambda, i} \frac{\eta_{\lambda i}^{b_{\lambda i}}(t_{u_\alpha} - t_{u_{\alpha-1}})}{b_{\lambda i}!}, \tag{3}$$

$$G(\boldsymbol{S}_{u_\alpha}, t_{u_\alpha}/\boldsymbol{N}_{u_{\alpha-1}}, t_{u_{\alpha-1}}) = \prod_i \Big[\sum_j \eta_{ji}(t_{u_\alpha} - t_{u_{\alpha-1}})\, s_{j u_\alpha}\Big]^{N_{iu_{\alpha-1}}}. \tag{3'}$$

Inserting (2) and (3) into (1), we obtain :

$$P(\boldsymbol{N}_1, t_1; \ldots; \boldsymbol{N}_m, t_m) = \prod_{\omega=1}^{m} \Bigg[\sum_{\substack{\forall b_{\lambda i}^{(\omega)} \geqslant 0 \quad \lambda, i = 1, \ldots, n \\ \sum_\lambda b_{\lambda i}^{(\omega)} = N_{iu_{\omega-1}};\ \sum_i b_{\lambda i}^{(\omega)} = N_{\lambda u_\omega}}} \prod_i N_{iu_{\omega-1}}! \prod_{\lambda, i} \frac{\eta_{\lambda i}^{b_{\lambda i}^{(\omega)}}(t_{u_\omega} - t_{u_{\omega-1}})}{b_{\lambda i}^{(\omega)}!} \Bigg]. \qquad (4$$

$(t_{u_0} = 0\,;\ N_{iu_0} = N_{0i})$
From (1), (2′) and (3′), it follows that :

$$G(\boldsymbol{S}_1, t_1; \ldots; \boldsymbol{S}_m, t_m) = \sum_{\forall N_{iu_\alpha} \geqslant 0} \prod_{i,\alpha} s_{iu_\alpha}^{N_{iu_\alpha}} P(\boldsymbol{N}_1, t_1; \ldots; \boldsymbol{N}_m, t_m) =$$

$$= \sum \prod_{i_{m-1}} s_{i_{m-1}u_1}^{N_{i_{m-1}u_1}} P(\boldsymbol{N}_{u_1}, t_{u_1}) \Big\{ \sum_{\forall N_{i_{m-2}u_2} \geqslant 0} \prod_{i_{m-2}} s_{i_{m-2}u_2}^{N_{i_{m-2}u_2}} P(\boldsymbol{N}_{u_2}, t_{u_2}/\boldsymbol{N}_{u_1}, t_{u_1}) \Big[\ldots .$$

$$\ldots . \sum_{\forall N_{i_0 u_m} \geqslant 0} \prod_{i_0} s_{i_0 u_m}^{N_{i_0 u_m}} P(\boldsymbol{N}_{u_m}, t_{u_m}/\boldsymbol{N}_{u_{m-1}}, t_{u_{m-1}})) \ldots \Big]\Big\} =$$

$$= \sum_{\forall N_{i_{m-1}u_1} \geqslant 0} \prod_{i_{m-1}} s_{i_{m-1}u_1}^{N_{i_{m-1}u_1}}$$

---

[6] L. M. Krieger and P. J. Gans, *J. Chem. Phys.*, **32**, 247 (1960).
I. G. Darvey and P. J. Staff, *J. Chem. Phys.*, **44**, 990 (1966).

$$P(\mathbf{N}_{u_1}, t_{u_1}/\mathbf{N}_0, 0)\{\ldots \sum_{\forall N_{i_1 u_{m-1}} \geqslant 0} \prod_{i_1} s_{i_1}^{\prime N_{i_1 u_m}} P(\mathbf{N}_{u_{m-1}}, t_{u_{m-1}}/\mathbf{N}_{u_{m-2}}, t_{u_{m-2}})) \ldots\} = \tag{5}$$

$$= \ldots = \sum_{\forall N_{i_{m-1} u_1} \geqslant 0} \prod_{i_{m-1}} s_{i_{m-1} u_1}^{\prime N_{i_{m-1} u_1}} P(\mathbf{N}_{u_1}, t_{u_1}/\mathbf{N}_0, 0) = G(\mathbf{S}'_1, t_{u_1}/\mathbf{N}_0, 0)$$

where

$$s'_{i_1 u_{m-1}} = s_{i_1 u_{m-1}} \sum_{i_0} \eta_{i_0 i_1}(t_{u_m} - t_{u_{m-1}}) s_{i_0 u_m}$$

$$s'_{i_\omega u_{m-\omega}} = s_{i_\omega u_{m-\omega}} \sum_{i_{\omega-1}} \eta_{i_{\omega-1} i_\omega}(t_{u_{m-\omega+1}} - t_{u_{m-\omega}}) s'_{i_{\omega-1} u_{m-\omega+1}} \quad \omega = 2, \ldots, m$$

and then:

$$G(\mathbf{S}_1, t_1; \ldots; \mathbf{S}_m, t_m) =$$

$$= \prod_{i_m} \Big[\sum_{i_0} \sum_{i_1} \ldots \sum_{i_m} \prod_{\omega=1}^{m} (\eta_{i_{\omega-1} i_\omega}(t_{u_{m-\omega+1}} - t_{u_{m-\omega}})\, s_{i_{\omega-1} u_{m-\omega+1}}) \Big]^{N_{0 i_m}}. \tag{6}$$

Using the relationships:

$$\overline{\prod_\alpha [N_{j_\alpha}(t_{v_\alpha}) - \bar{N}_{j_\alpha}(t_{v_\alpha})]} = \left(\frac{\partial^m \ln G(\mathbf{S}_1, t_1; \ldots; \mathbf{S}_m, t_m)}{\partial \ln s_{i_1 v_1} \ldots \partial \ln s_{i_m v_m}} \right)_{\forall \vec{\mathrm{S}}_i = \vec{1}} \tag{7}$$

we can find the temporal correlation functions of the variables $N_{j_\alpha}(t_{v_\alpha})$ $(n \geqslant j_\alpha \geqslant 1; m \geqslant v_\alpha \geqslant 1)$.

For $m = 1$, as $t_{u_1} - t_{u_2} = |t_2 - t_1| = |\tau|$, the equations (6) and (7) yield:

$$G(\mathbf{S}_1, t_1; \mathbf{S}_2, t_2) = \prod_i \Big(\sum_\alpha \sum_\beta \eta_{\alpha\beta}(|\tau|)\, \eta_{\beta i}(t)\, s_{\alpha u_1} s_{\beta u_2} \Big)^{N_{0i}}, \tag{6'}$$

$$\overline{(N_{j_1}(t_{v_1}) - \bar{N}_{j_1}(t_{v_1}))\,(N_{j_2}(t_{v_2}) - \bar{N}_{j_2}(t_{v_2}))} =$$

$$= \sum_i N_{0_i}[(\eta_{j_1 j_2}(|\tau|) - \eta_{j_1 i}(t + |\tau|))\, \eta_{j_2 i}(t)\, \delta_{u_1 v_2} \delta_{u_2 v_1} +$$

$$+ (\eta_{j_2 j_1}(|\tau|) - \eta_{j_2 i}(t + |\tau|))\, \eta_{j_1 i}(t)\, \delta_{u_1 v_1} \delta_{u_2 v_2}]. \tag{7'}$$

($t = \min(t_1, t_2)$ and δ_{ij} is Kronecker delta).

Taking into account that[7] $\lim\limits_{t\to\infty} \eta_{ij}(t) = p_i = \dfrac{\bar{N}_i(\infty)}{\sum\limits_i N_{0_i}}$, at the equilibrium state ($t \to \infty$) (6′) and (7′) become:

$$G(S_1, S_2, \tau) = \left(\sum_\alpha \sum_\beta \eta_{\alpha\beta}(|\tau|)\, p_\beta\, s_{\alpha u_1} s_{\beta u_2} \right)^{\sum\limits_i N_{0_i}}, \tag{6''}$$

$$\lim_{t\to\infty} \operatorname{cov}(N_{j_1}(t_{v_1}), N_{j_2}(t_{v_2})) = [p_{j_2}(\eta_{j_1 j_2}(|\tau|) - p_{j_1})\, \delta_{u_1 v_2} \delta_{u_2 v_1} +$$

$$+ p_{j_1}(\eta_{j_2 j_1}(|\tau|) - p_{j_2})\, \delta_{u_1 v_1} \delta_{u_2 v_2}] \sum_i N_{0_i}. \tag{7''}$$

The principle of microscopic reversibility [3, 4] states that:

$$G(S_1, S_2, \tau) = G(S_1, S_2, -\tau). \tag{8}$$

As $u_1(\tau) = u_2(-\tau)$; $u_2(\tau) = u_1(-\tau)$, the equality (8) may hold only if:

$$\eta_{\alpha\beta}(|\tau|)\, p_\beta = \eta_{\beta\alpha}(|\tau|)\, p_\alpha. \tag{9}$$

From (9), through a differentiation we get:

$$\frac{d\eta_{\alpha\beta}(0)}{d\tau} \bar{N}_\beta(\infty) = \frac{d\eta_{\beta\alpha}(0)}{d\tau} \bar{N}_\alpha(\infty). \tag{9'}$$

But

$$\left(\frac{d\,\|\eta_{\alpha\beta}\|}{d\tau} \right)_{\tau=0} = \left(\frac{d}{d\tau} \exp\, [\|k_{\beta\alpha}\|\tau] \right)_{\tau=0} = \|k_{\beta\alpha}\| \tag{9''}$$

and then

$$k_{\alpha\beta} \bar{N}_\alpha(\infty) = k_{\beta\alpha} \bar{N}_\beta(\infty).$$

These equations are the expression of detailed balance principle.

B. UNI-BIMOLECULAR REACTIONS

Let us consider the elementary reactions:

$$\sum \nu_{ij} A_i \rightleftarrows \sum v'_{ij} A_i \quad i = 1, \ldots, n; \quad j = 1, \ldots, R; \quad 2 \geqslant \sum_i \nu_{ij}, \quad \sum v'_{ij} \geqslant 1.$$

---

[7] J. Wei and C. D. Prater, *Adv. Catalysis*, **13**, 203 (1962).

It is easy to show that the conditional probability $P(\boldsymbol{N}_{u_2} t_{u_2}/\boldsymbol{N}_{u_1}, t_{u_1})$ verifies the equation

$$\frac{\partial P}{\partial t_{u_2}} = \sum_j \left\{ k_j \left[\prod_i \binom{N_{iu_2}+f_{ij}}{\nu_{ij}} P(N_{1u_2}+f_{1j}, \ldots, N_{nu_2}+f_{nj}) - \prod_i \binom{N_{iu_2}}{\nu_{ij}} P \right] + \right.$$

$$\left. + k'_j \left[\prod_i \binom{N_{iu_2}-f_{ij}}{\nu'_{ij}} P(N_{1u_2}-f_{1j}, \ldots, N_{nu_2}-f_{nj}) - \prod_i \binom{N_{iu_2}}{\nu'_{ij}} P \right] \right\} \tag{10}$$

with $f_{ij} = \upsilon'_{ij} - \upsilon_{ij}$ and $P(\boldsymbol{N}_{u_2}, t_{u_1}/\boldsymbol{N}_{u_1}, t_{u_1}) = \begin{cases} 1 & \text{if } \boldsymbol{N}_{u_2} = \boldsymbol{N}_{u_1} \\ 0 & \text{if } \boldsymbol{N}_{u_2} \neq \boldsymbol{N}_{u_1} \end{cases}.$

From (10) it is obvious that:

$$P(\boldsymbol{N}_{u_2}, t_{u_2}/\boldsymbol{N}_{u_1}, t_{u_1}) = P(\boldsymbol{N}_{u_2}, t_{u_2} - t_{u_1}/\boldsymbol{N}_{u_1}, 0) = P(\boldsymbol{N}_{u_2}, |\tau|/\boldsymbol{N}_{u_1}, 0). \tag{11}$$

Hence:

$$\lim_{t_{u_1}\to\infty} P(\boldsymbol{N}_{u_2}, t_{u_2}; \boldsymbol{N}_{u_1}, t_{u_1}) = P(\boldsymbol{N}_{u_2}, |\tau|/\boldsymbol{N}_{u_1}, 0)\, P(\boldsymbol{N}_{u_1}, \infty). \tag{11'}$$

In the case of a large (macroscopic) system, the fluctuations are small $(N_{iu_2} - \bar{N}_i(\infty) \ll N_{iu_2}, \bar{N}_i(\infty))$ and then:

$$\binom{N_{iu_2}}{\nu_{ij}} = \binom{\bar{N}_i(\infty)}{\nu_{ij}} \prod_{\varepsilon=0}^{\nu_{ij}-1} \left(1 + \frac{N_{iu_2} - \bar{N}_i(\infty)}{\bar{N}_i(\infty) - \varepsilon}\right) \cong \binom{\bar{N}_i(\infty)}{\nu_{ij}} \left[1 + \right.$$

$$\left. + \sum_{\varepsilon=0}^{\nu_{ij}-1} \frac{N_{iu_2} - \bar{N}_i(\infty)}{\bar{N}_i(\infty) - \varepsilon} \right] \cong \binom{\bar{N}_i(\infty)}{\nu_{ij}} \left(1 + \nu_{ij} \frac{N_{iu_2} - \bar{N}_i(\infty)}{\bar{N}_i(\infty)}\right), \tag{12}$$

$$\prod_i \binom{N_{iu_2}}{\nu_{ij}} \cong \prod_i \binom{\bar{N}_i(\infty)}{\nu_{ij}} \left(1 + \sum_i \nu_{ij} \frac{N_{iu_2} - \bar{N}_i(\infty)}{\bar{N}_i(\infty)}\right). \tag{12'}$$

Inserting (11′) and (12′) into (10) and introducing the generating function:

$$G(\boldsymbol{S}_{u_2}, |\tau|; \boldsymbol{S}_{u_1}, 0) = \sum_{\forall N_{iu_1}, x_i} \prod_i (s_{iu_1}^{N_{iu_1}} s_{iu_2}^{x_i})\, P(\boldsymbol{N}_{u_2}, |\tau|; \boldsymbol{N}_{u_1}, 0)$$

$$(x_i = N_{iu_2} - \bar{N}_i(\infty)) \tag{13}$$

we obtain:

$$\frac{\partial \ln G}{\partial|\tau|}=\sum_j\left[\bar{r}_j\left(\prod_\alpha s_{\alpha u_2}^{-\nu_{\alpha j}+\nu'_{\alpha j}}-1\right)+\bar{r}'_j\left(\prod_\alpha s_{\alpha u_2}^{-\nu'_{\alpha j}+\nu_{\alpha j}}-1\right)\right]+$$

$$+\sum_i\frac{\partial \ln G}{\partial \ln s_{iu_2}}\sum_j\left[g_{ij}\left(\prod_\alpha s_{\alpha u_2}^{-\nu_{\alpha j}+\nu'_{\alpha j}}-1\right)+g'_{ij}\left(\prod_\alpha s_{\alpha u_2}^{-\nu'_{\alpha j}+\nu_{\alpha j}}-1\right)\right]. \quad (14)$$

$$\left(\bar{r}_j=k_j\prod_i\binom{\bar{N}_i(\infty)}{\nu_{ij}};\quad g_{ij}=\frac{\nu_{ij}\bar{r}_j}{\bar{N}_i(\infty)}\right)$$

The differentiation of equation yields:

$$\frac{\partial}{\partial|\tau|}\left(\frac{\partial^2 \ln G}{\partial \ln s_{\mu u_2}\,\partial \ln s_{\xi u_1}}\right)_{||s_{ij}||=||1||}=$$

$$=\sum_i\left(\frac{\partial^2 \ln G}{\partial \ln s_{iu_2}\,\partial \ln s_{\xi u_1}}\right)_{||s_{ij}||=||1||}\sum_j(\nu'_{\mu j}-\nu_{\mu j})(g_{ij}-g'_{ij}). \quad (15)$$

As:

$$\overline{\Delta N_{\mu u_2}\,\Delta N_{\xi u_1}(\tau)}=\left(\frac{\partial^2 \ln G}{\partial \ln s_{\mu u_2}\,\partial \ln s_{\xi u_1}}\right)_{||s_{ij}||=||1||}$$

the solutions of differential equations (15) are:

$$\overline{\Delta N_{\mu u_2}\Delta N_{\xi u_1}(\tau)}=\sum_i a_{\mu i}(|\tau|)\,\overline{\Delta N_{iu_1}\Delta N_{\xi u_1}(0)} \quad (16)$$

where

$$||a_{\mu i}||=\exp\left[||\sum_j(\nu'_{\mu j}-\nu_{\mu j})(g_{ij}-g'_{ij})||\;|\tau|\right].$$

For small fluctuations, we can use the thermodynamic formula:[8]

$$P(\bar{N}_{u_1},\infty)=\frac{1}{\prod_i\sqrt{2\pi\bar{N}_{iu_1}}}\exp\left[-\sum_i\frac{(N_{iu_1}-\bar{N}_{iu_1})^2}{2\bar{N}_{iu_1}}\right] \quad (17)$$

to which correspond the mean values

$$\overline{\Delta N_{iu_1}\Delta N_{\xi u_1}}=\bar{N}_{iu_1}\delta_{\xi i} \quad (17')$$

and then:

$$\overline{\Delta N_{\mu u_2}\Delta N_{\xi u_1}(\tau)}=a_{\mu\xi}(|\tau|)\bar{N}_{\xi u_1}. \quad (16')$$

Taking into account that

$$\lim_{t\to\infty}\overline{\Delta N_{\mu u_2}(t+\tau)\,\Delta N_{\xi u_1}(t)}=\lim_{t\to\infty}\overline{\Delta N_{\mu u_2}(t)\,\Delta N_{\xi u_1}(t-\tau)},$$

---

[8] P. Glensdorf and I. Prigojin, "Termodinamicheskaia teoria structuryi ustoichivosti i fluctuatsii", Izd. Mir, Moskva, 1973.

the principle of microscopic reversibility leads to:

$$\overline{\Delta N_{\xi u_2} \Delta N_{\mu u_1}}(-\tau) = \overline{\Delta N_{\mu u_2} \Delta N_{\xi u_1}}(\tau)$$

or:

$$a_{\mu\xi}(|\tau|)\bar{N}_{\xi}(\infty) = a_{\xi\mu}(|\tau|)\bar{N}_{\mu}(\infty), \tag{18}$$

$$\frac{\partial a_{\mu\xi}(0)}{\partial\tau}\bar{N}_{\xi}(\infty) = \frac{\partial a_{\xi\mu}(0)}{\partial\tau}\bar{N}_{\mu}(\infty), \tag{18'}$$

$$\sum_{j=1}^{R}(\nu'_{\mu j}\nu_{\xi j} - \nu'_{\xi j}\nu_{\mu j})(\bar{r}_j - \bar{r}'_j) = 0 \quad \mu, \xi = 1, \ldots, n; \mu \geqslant \xi. \tag{19}$$

The equations (19) express the principle of detailed balance. They may be written in the form:

$$\sum_{j=1}^{R}\varepsilon_{ij}(\bar{r}_j - \bar{r}'_j) = 0, \quad i=1, \ldots, \frac{n(n-1)}{2}\cdot \tag{19'}$$

If $\frac{n(n-1)}{2} \geqslant rank\|\varepsilon_{ij}\| \geqslant R$,(19′) are equivalent to:

$$\bar{r}_j = \bar{r}'_j \qquad j = 1, \ldots, R. \tag{19''}$$

An example for which $\bar{r}_j = \bar{r}'_j$ is the reaction network:

$$\nu_{ij}A_i \rightleftarrows \nu_{ji}A_j \;\; n \geqslant i > j \geqslant 1;\; 2 \geqslant \nu_{ij} \geqslant 1 \left(R = \frac{n(n-1)}{2}\right).$$

Indeed, the equations (19) become:

$$\nu_{\alpha\beta}\nu_{\beta\alpha}(\bar{r}_{\alpha\beta} - \bar{r}_{\beta\alpha}) = 0 \quad n \geqslant \alpha > \beta \geqslant 1$$

and then

$$\bar{r}_{\alpha\beta} = \bar{r}_{\beta\alpha}.$$

C. CONCLUSIONS

In this paper we have presented a computation method (for the reaction system $A_i \rightleftarrows A_j$) of the temporal correlation functions between the molecule numbers A_i and A_j $i, j = 1, \ldots, n$. At the equilibrium state the obtained results lead to the detailed balance principle. In agreement with the non equilibrium thermodynamics, the principle of detailed balance is a consequence of the microreversibility principle. Unlike the thermodynamic theory, in the framework of the stochastic theory the principle of detailed balance remains valid even for small systems. In the case of a large (macroscopic) system, the discussion can be easily extended to an arbitrary sequence of elementary reactions.

he principle of microscopic reversibility leads to:

$$[illegible]$$

or

$$[illegible] \quad (15)$$

$$[illegible] \quad (16)$$

he equations (16) express the principle of detailed balance. They can be written in the form:

$$[illegible] \quad (17)$$

[illegible] equations (16) are equivalent to:

$$[illegible] \quad (18)$$

n example for which [illegible] is the [illegible] network:

$$[illegible]$$

Thus, the equations (16) become:

$$[illegible]$$

and then

$$[illegible]$$

[illegible] CONCLUSIONS

In this paper we have presented a computational method for the [illegible] of the [illegible] stochastic [illegible] [illegible] in a [illegible] [illegible] the principle of detailed balance [illegible] principle. [illegible] is a consequence of the [illegible] principle [illegible] the [illegible] theory [illegible] of detailed [illegible] small systems. In the case of a large [illegible] systems, the discussion can be easily extended to an arbitrary [illegible] of elementary reactions.

Revue Roumaine de Chimie, **21**, *9–10*, 1319–1326 (1976)

ON THE STOCHASTIC ANALYSIS OF THE REACTION NETWORKS. III[1,2]

LANGEVIN APPROACHES

M. VLAD and E. SEGAL

Polytechnical Institute of Bucharest, Institute of Chemistry, Department of Physical Chemistry and Electrochemical Technology, Bd. Republicii 13

Received January 21, 1976

A Langevin theory for the kinetics of chemical reactions $A_i \underset{k_{ji}}{\overset{k_{ij}}{\rightleftarrows}} A_j$ $n \geqslant i > j \geqslant 1$ is elaborated. For a system not far from equilibrium, the theory can be extended to the reactions

$$\sum_i \nu_{ij} A_i \underset{k'_j}{\overset{k_j}{\rightleftarrows}} \sum_i \nu'_{ij} A_i \quad n \geqslant i \geqslant 1;\ R \geqslant j \geqslant 1;\ 2 \geqslant \sum_i \nu_{ij},\ \sum_i \nu'_{ij} \geqslant 1.$$

In our previous papers [1,2] we dealt with some aspects of the stochastic theory of reaction rates from a Markovian standpoint, i.e. using the master equation technique. The purpose of the present paper is to discuss the same problems from a Langevin (noise — source) point of view.

A. UNIMOLECULAR REACTIONS

Let us consider the reactions

$$A_i \underset{k_{ji}}{\overset{k_{ij}}{\rightleftarrows}} A_j \quad n \geqslant i > j \geqslant 1 \tag{1}$$

The classical chemical kinetics gives us the following rate equation [1]

$$\vec{r} = d\vec{N}/dt = \hat{K}^{+}\vec{N} \qquad \hat{K} = \| k_{ij} \|;\ k_{ii} = -\sum_{j \neq i} k_{ij}. \tag{2}$$

---

[1] Part I: M. Vlad and E. Segal, *Rev. Roumaine Chim.*, **21**, 667 (1976).

[2] Part II: M. Vlad and E. Segal, *Rev. Roumaine Chim.*, **21**, 9 (1976).

In the framework of the Langevin theory[3,4] Eq. (2) becomes

$$\vec{r} = d\vec{N}/dt = \hat{K}^{+}\,\vec{N} + \vec{F} \tag{3}$$

or

$$\Delta\vec{r} = d\,\Delta\vec{N}/dt = \hat{K}^{+}\,\Delta\vec{N} + \vec{F} \tag{3'}$$

where

$\Delta\vec{N} = \vec{N} - \overline{\vec{N}}$ and $\vec{F} = (f_i)\; i = 1,\dots,n$ is the n – dimensional vector of noise sources.
Obviously

$$\vec{F}\,(t) = \langle\vec{F}\,(t)\rangle = \vec{0}. \tag{4}$$

To determine the correlation matrix of the noise sources $\hat{C}\,(t_1, t_2) = \overline{\vec{F}\,(t_1)\,\vec{F}^{+}\,(t_2)}$, we shall apply Lax's method.[3] Eq. (3) gives

$$C\,(t_1,\; t_2) = (\hat{I}d/dt_1 \rightarrow -\,K^{+})\;\overline{\Delta\vec{N}\,(t_1)\,\Delta\vec{N}^{+}\,(t_2)}\,(\leftarrow \hat{I}d/dt_2 - \hat{K}) \tag{5}$$

But[2]

$$\begin{aligned}\overline{\Delta N_{j_1}(t_1)\,\Delta N_{j_2}(t_2)} = \sum_i N_{0i}\,[(\eta_{j_1 j_2}\,(|\tau|) - \eta_{j_1 i}\,(t + |\tau|))\,\eta_{j_2 i}\,(t)\,h\,(-\tau) +\\ + (\eta_{j_2 j_1}\,(|\tau|) - \eta_{j_2 i}\,(t + |\tau|))\,\eta_{j_1 i}\,(t)\,h\,(\tau)]\end{aligned} \tag{6}$$

or

$$\overline{\Delta\vec{N}\,(t_1)\,\Delta\vec{N}^{+}\,(t_2)} = h\,(-\,\tau)\,\hat{E}\,(\,|\,\tau\,|)\,\hat{M}\,(t) + h\,(\tau)\,\hat{M}\,(t)\,\hat{E}^{+}\,(\,|\tau|) \tag{6'}$$

where

$$\tau = t_2 - t_1\,;\; t = \min\,(t_1,\, t_2)\,;$$

$$\hat{E}\,(t) = \exp\,(\hat{K}^{+}\,t) = \|\,\eta_{ij}\,(t)\,\|\,;\;\; \hat{M}\,(t) = \overline{\Delta\vec{N}\,(t)\,\Delta\vec{N}^{+}(t)} =$$

$$= \|\sum_{\alpha}\,(\,\delta_{ij} - \eta_{j\alpha}\,(t))\;\eta_{i\alpha}\,(t)\,N_{0\alpha}\,\|.$$

and $h(t)$ is Heaviside's function.
Noticing that:

$$(\hat{I}d/\mathrm{d}t\; - \;\hat{K}^{+})\,h\;(t)\,\hat{E}\,(t) = \delta(t),$$

---

[3] M. LAX, *Rev. Mod. Phys.*, **32**, 25 (1960).

[4] M. LAX, *Rev. Mod. Phys.*, **38**, 541 (1966).

Eqs. (5) and (6′) yield

$$\hat{C}(t_1, t_2) = \delta(-\tau)\,\hat{M}(t_2)\,(\leftarrow \hat{I}d/dt_2 - \hat{K}) + (\hat{I}d/dt_1 \rightarrow - \hat{K}^{+})\,\hat{M}(t_1)\,\delta(\tau) =$$

$$= \delta(t_1 - t_2)\,[d\hat{M}(t_2)/dt_2 + d\hat{M}(t_1)/dt_1 - \hat{M}(t_2)\,\hat{K} - \hat{K}^{+}\,\hat{M}(t_1)] \qquad (7)$$

As

$$d\hat{M}(t)/dt - \hat{K}^{+}\,\hat{M}(t) - \hat{M}(t)\,\hat{K} = \|\,\delta_{ij}\sum_{\alpha}\sum_{\lambda} k_{\lambda i}\,\eta_{\lambda\alpha}\,N_{0\alpha} -$$

$$- \sum_{\alpha}(k_{ij}\,\eta_{i\alpha} + k_{ji}\,\eta_{j\alpha})\,N_{0\alpha}\,\| = \|\,\delta_{ij}\sum_{\lambda\neq i}(k_{\lambda i}\,\bar{N}_{\lambda} + k_{i\lambda}\,\bar{N}_{i}) -$$

$$- (1 - \delta_{ij})\,(k_{ij}\,\bar{N}_{i} + k_{ji}\,\bar{N}_{j})\,\| \overset{\Delta}{=} 2\hat{D}$$

Eq. (7) receives the following form :

$$\hat{C}(t_1, t_2) = \delta(t_1 - t_2)\,[2\hat{D}(t_1) + 2\hat{D}(t_2) + \hat{M}(t_1)\,\hat{K} + \hat{K}^{+}\,\hat{M}(t_2)] =$$

$$= \delta(\tau)\,[4\hat{D}(t) + \hat{K}^{+}\,\hat{M}(t) + \hat{M}(t)\,\hat{K}] \qquad (7')$$

Similarly :

$$\overline{\Delta\vec{N}(t_1)\,\vec{F}^{+}(t_2)} = \overline{\Delta\vec{N}(t_1)\,\Delta\vec{N}^{+}(t_2)}\,(\leftarrow \hat{I}\,d/dt_2 - \hat{K}) =$$

$$= \delta(\tau)\,[\hat{M}(t_1) - \hat{E}(|\tau|)\,\hat{M}(t_2)] + 2h(-\tau)\,\hat{E}(|\tau|)\,\hat{D}(t_2) =$$

$$= 2h(-\tau)\,\hat{E}(|\tau|)\,\hat{D}(t); \qquad (8)$$

$$\overline{\vec{F}(t_1)\,\Delta\vec{N}^{+}(t_2)} = 2h(\tau)\,\hat{D}(t)\,\hat{E}^{+}(|\tau|); \qquad (9)$$

$$\overline{\Delta\vec{r}(t_1)\,\Delta\vec{r}^{+}(t_2)} = \hat{K}^{+}\,\overline{\Delta\vec{N}(t_1)\,\Delta\vec{N}^{+}(t_2)}\,\hat{K} + \hat{K}^{+}\,\overline{\Delta\vec{N}(t_1)\vec{F}^{+}(t_2)} +$$

$$+ \overline{\vec{F}(t_1)\,\Delta\vec{N}^{+}(t_2)}\,\hat{K} + \overline{\vec{F}(t_1)\,\vec{F}^{+}(t_2)} = \delta(\tau)\,[4\hat{D}(t) + \hat{K}^{+}\,\hat{M}(t) + \hat{M}(t)\hat{K}] +$$

$$+ h(-\tau)\,\hat{K}^{+}\,\hat{E}(|\tau|)\,[\hat{M}(t)\,\hat{K} + 2\hat{D}(t)] + h(\tau)\,[\hat{K}^{+}\hat{M}(t) + 2\hat{D}(t)]\hat{E}^{+}(|\tau|)\,\hat{K} \qquad (10)$$

Revue Roumaine de Chimie, 21, *9–10*, 1319–1326 (1976)

Introducing the noise spectrum[5]

$$\hat{\Phi}(\vec{\alpha}, \omega, t) = \frac{1}{2\pi} \cdot \lim_{T \to \infty} \frac{\partial}{\partial t} \left\langle \left\| \int_{-T/2}^{t} \int_{-T/2}^{t} \alpha_i(t_1)\, \alpha_j(t_2)\, \mathrm{e}^{-i\omega(t_1 - t_2)}\, \mathrm{d}t_1\, dt_2 \right\| \right\rangle =$$

$$= \frac{1}{2\pi} \int_0^{\infty} \overline{\vec{\alpha}(t)\, \vec{\alpha}^{+}(t - \tau')}\, \mathrm{e}^{-i\omega\tau'}\, d\tau' + \frac{1}{2\pi} \int_{-\infty}^{0} \overline{\vec{\alpha}(t + \tau')\, \vec{\alpha}^{+}(t)}\, \mathrm{e}^{-i\omega\tau'}\, \mathrm{d}\tau' \quad (11)$$

$(\tau' = t_1 - t_2)$

Eqs. (6′), (7′) and (10) lead to

$$\hat{\Phi}(\Delta\vec{N}, \omega, t) = \frac{1}{2\pi} \int_0^{\infty} \hat{E}(\tau')\, \hat{M}(t - \tau')\, \mathrm{e}^{-i\omega\tau'}\, \mathrm{d}\tau' +$$

$$+ \frac{1}{2\pi} \int_{-\infty}^{0} \hat{M}(t + \tau')\, \hat{E}^{+}(-\tau')\, \mathrm{e}^{-i\omega\tau'} d\tau' = \quad (12)$$

$$= \frac{1}{2\pi} \sum_{k=0}^{\infty} (-1)^k [(\hat{I} i\omega - \hat{K}^{+})^{-k-1}\, d^k\, \hat{M}(t)/dt^k + d^k \hat{M}(t)/dt^k\, (-\hat{I} i\omega - \hat{K})^{-k-1}];$$

$$\hat{\Phi}(\vec{F}, \omega, t) = \frac{1}{2\pi} (4\hat{D}(t) + \hat{K}^{+} \hat{M}(t) + \hat{M}(t)\, \hat{K}); \quad (13)$$

$$\hat{\Phi}(\Delta\vec{r}, \omega, t) = \frac{1}{2\pi} (4\hat{D}(t) + \hat{K}^{+}\, \hat{M}(t) + \hat{M}(t)\hat{K}) +$$

$$+ \frac{1}{2\pi} \sum_{k=0}^{\infty} (-1)^k [d^k/dt^k\, (d\hat{M}(t)/dt - \hat{M}(t)\, \hat{K})(-\hat{I} i\omega - \hat{K})^{-k-1}\, \hat{K} +$$

$$+ \hat{K}^{+}\, (\hat{I} i\omega - \hat{K}^{+})^{-k-1}\, d^k/dt^k (d\hat{M}(t)/dt - \hat{K}^{+}\, \hat{M}(t))] \quad (14)$$

Eq. (14) is a generalization of the Nyquist formula.[3]

---

[5] B. Levine, "Fondements théoriques de la radiotechnique statistique", Tome I, Ed. Mir, Moscou, 1973, p. 187.

At equilibrium ($t = \infty$), we have

$$\overline{\Delta\vec{N}(t_1)\,\Delta\vec{N}^{+}(t_2)} = h(-\tau)\hat{E}(|\tau|)\,\hat{M}_e + h(\tau)\,\hat{M}_e\,\hat{E}^{+}(|\tau|); \tag{6''}$$

$$\hat{C}(t_1, t_2) = 2\delta(\tau)\hat{D}_e; \tag{7''}$$

$$\overline{\Delta\vec{N}(t_1)\,\vec{F}^{+}(t_2)} = 2h(-\tau)\,\hat{E}(|\tau|)\,\hat{D}_e; \tag{8'}$$

$$\overline{\vec{F}(t_1)\,\Delta\vec{N}^{+}(t_2)} = 2h(\tau)\hat{D}_e\,\hat{E}^{+}(|\tau|); \tag{9'}$$

$$\overline{\Delta\vec{r}(t_1)\,\Delta\vec{r}^{+}(t_2)} = 2\delta(\tau)\,\hat{D}_e - h(-\tau)\,\hat{K}^{+}\,\hat{E}(|\tau|)\,\hat{K}^{+}\hat{M}_e - h(\tau)\hat{M}_e\,\hat{K}\,\hat{E}^{+}(|\tau|)\,\hat{K}; \tag{10'}$$

$$\hat{\Phi}(\Delta\vec{N}, \omega) = \frac{1}{2\pi}\left[(\hat{I}i\omega - \hat{K}^{+})^{-1}\,\hat{M}_e - \hat{M}_e(\hat{I}i\omega + \hat{K})^{-1}\right]; \tag{12'}$$

$$\hat{\Phi}(\vec{F}, \omega) = \frac{\hat{D}_e}{\pi}; \tag{13'}$$

$$\hat{\Phi}(\Delta\vec{r}, \omega) = \frac{\hat{D}_e}{\pi} - \frac{1}{2\pi}\left[\hat{K}^{+}(\hat{I}i\omega - \hat{K}^{+})^{-1}\,\hat{K}^{+}\,\hat{M}_e - \hat{M}_e\hat{K}(\hat{I}i\omega + \hat{K})^{-1}\,\hat{K}\right] \tag{14'}$$

with :

$$p_i = \lim_{t\to\infty} \eta_{ij}(t) = \bar{N}_i(\infty)/N_0,\ N_0 = \sum_i N_{0i} = \sum_i \bar{N}_i(\infty)$$

$$\hat{M}_e = \| \delta_{ij}\, p_i - p_i\, p_j \| N_0$$

$$\hat{D}_e = \| \delta_{ij} \sum_{\lambda \neq i} (k_{\lambda i}\, p_\lambda + k_{i\lambda}\, p_i) - (1 - \delta_{ij})(k_{ij}\, p_i + k_{ji}\, p_j) \| N_0$$

Taking the Fourier transforms of Eqs. (6″), (7″) and (8′) – (10′), we obtain

$$\overline{\Delta\vec{N}(\omega_1)\,\Delta\vec{N}^{+}(\omega_2)} = \frac{1}{(2\pi)^2}\iint_{-\infty}^{+\infty} \overline{\Delta\vec{N}(t_1)\,\Delta\vec{N}^{+}(t_2)}\,\mathrm{e}^{-i\omega_1 t_1 - i\omega_2 t_2}\,dt_1\,dt_2 =$$

$$= \delta(\omega_1 + \omega_2)\Phi(\Delta\vec{N}, \omega_1); \tag{15}$$

$$\overline{\vec{F}(\omega_1)\vec{F}^{+}(\omega_2)} = \delta(\omega_1 + \omega_2)\,\hat{\Phi}(\vec{F}, \omega_1); \tag{16}$$

$$\overline{\Delta\vec{N}(\omega_1)\vec{F}^{+}(\omega_2)} = \frac{1}{\pi}\,\delta(\omega_1 + \omega_2)[\hat{I}i\omega_1 - \hat{K}^{+}]^{-1}\hat{D}_e; \tag{17}$$

$$\overline{\vec{F}(\omega_1)\,\Delta\vec{N}^{+}\omega_2)} = -\frac{1}{\pi}\,\delta(\omega_1 + \omega_2)\,\hat{D}_e[\hat{I}i\omega_1 + \hat{K}]^{-1}; \tag{18}$$

$$\overline{\Delta\vec{r}(\omega_1)\,\Delta\vec{r}^{+}(\omega_2)} = \delta\,(\omega_1 + \omega_2)\,\hat{\Phi}(\Delta\vec{r}, \omega_1) \tag{19}$$

B. UNI-BIMOLECULAR REACTIONS

For the reaction network

$$\sum_i \nu_{ij} A_i \underset{k'_j}{\overset{k_j}{\rightleftarrows}} \sum_i \nu'_{ij} A_i,\ n \geqslant i \geqslant 1;\ R \geqslant j \geqslant 1;\ 2 \geqslant \sum_i \nu_{ij},\ \sum_i \nu'_{ij} \geqslant 1 \tag{20}$$

the generalized kinetics [6] gives the rate equations

$$\frac{dN_i}{dt} = \sum_j (\nu'_{ij} - \nu_{ij}) \left[k_j \prod_i \binom{N_i}{\nu_{ij}} - k'_j \prod_i \binom{N_i}{\nu'_{ij}} \right] \quad i = 1, \ldots, \eta \tag{21}$$

If the system is not far from equilibrium, we can consider that [2]

$$\prod_i \binom{N_i}{\nu_{ij}} \cong \prod_i \binom{\bar{N}_i(\infty)}{\nu_{ij}} \left(1 + \sum_i \nu_{ij} \frac{N_i - \bar{N}_i(\infty)}{\bar{N}_i(\infty)} \right) \tag{22}$$

and then

$$\frac{\mathrm{d}x_i}{\mathrm{d}t} = \sum_j k'_{ji}\, x_j \quad i = 1, \ldots, n \tag{23}$$

with

$$x_i = N_i - \bar{N}_i(\infty),$$

$$\bar{r}_j = k_j \prod_i \binom{\bar{N}_i(\infty)}{\nu_{ij}}, \quad g_{ij} = \frac{\nu_{ij}\, \bar{r}_j}{\bar{N}_i(\infty)}$$

$$k'_{ji} = \sum_\alpha (\nu'_{j\alpha} - \nu_{j\alpha})(g_{i\alpha} - g'_{i\alpha})$$

Using the stochastic theory, we can show that the probability

$$P(\vec{N}_{u_2},\ t_{u_2} - t_{u_1} / \vec{N}_{u_1}, 0) = P(\vec{N}_{u_2}, |\tau| / \vec{N}_{u_1}, 0)\ (t_u = \min(t_1, t_2),$$

$t_{u_2} = \max(t_1, t_2)$, $|\tau| = t_{u_2} - t_{u_1} = |t_2 - t_1|$) is the solution of equation [2]

$$\frac{\partial P}{\partial |\tau|} = \sum_j \Bigg\{ k_j \Bigg[\prod_i \binom{N_{iu_2} + f_{ij}}{\nu_{ij}} P(N_{1u_2} + f_{1j}, \ldots, N_{nu_2} + f_{nj}) -$$

$$- \prod_i \binom{N_{iu_2}}{\nu_{ij}} P \Bigg] + k'_j \Bigg[\prod_i \binom{N_{iu_2} - f_{ij}}{\nu'_{ij}} P(N_{1u} - f_{1j}, \ldots, N_{nu_2} - f_{nj}) -$$

$$- \prod_i \binom{N_{iu_2}}{\nu'_{ij}} P \Bigg] (f_{ij} = \nu'_{ij} - \nu_{ij}) \tag{24}$$

---

[6] D. A. Mc Quarrie, C. J. Jachimowski and M. E. Russell, *J. Chem. Phys.*, **40**. 2194 (1964).

or

$$\frac{\partial P}{\partial|\tau|} \cong \sum_j \{[\bar{r}_j + \sum_i g_{ij}(x_{iu_2} + f_{ij})]\, P(N_{1u_2} + f_{1j}, \ldots, N_{nu_2} + f_{nj}) +$$

$$+ [\bar{r}'_j + \sum_i g'_{ij}(x_{iu_2} - f'_{ij})]'\, P(N_{1u_2} - f'_{1j}, \ldots, N_{nu_2} - f'_{nj}) -$$

$$- [\bar{r}_j + \bar{r}'_j + \sum_i (g_{ij} + g'_{ij})\, x_{iu_2}]\, P\} \tag{24'}$$

Taking into account that

$$P(\vec{N}_{u_2}, t_{u_2};\ \vec{N}_{u_1}, t_{u_1}) = P(\vec{N}_{u_2}, |\tau|/\vec{N}_{u_1}, 0)\, P(\vec{N}_{u_1}, t_{u_1}) \tag{25}$$

and introducing the generating function

$$G(\vec{S}_{u_2}, t_{u_2};\ \vec{S}_{u_1}, t_{u_1}) = \sum_{\forall N_{iu_1}, x_{iu_2}} \prod_i (s_{iu_1}^{N_{iu_1}} s_{iu_2}^{x_{iu_2}})\, P(\vec{N}_{u_2}, t_{u_2};\ \vec{N}_{u_1}, t_{u_1}), \tag{26}$$

Eq. (24′) becomes :

$$\begin{aligned} \frac{\partial \ln G}{\partial\,|\tau|} &= \sum_j\ [\bar{r}_j(\prod_\alpha s_{\alpha u_2}^{-\nu_{\alpha j}+\nu'_{\alpha j}} - 1) + \bar{r}'_j(\prod_\alpha s_{\alpha u_2}^{-\nu'_{\alpha j}+\nu_{\alpha j}} - 1)] + \\ &+ \sum_i \frac{\partial \ln G}{\partial \ln s_{iu_2}} \sum_j\ [g_{ij}(\prod_\alpha s_{\alpha u_2}^{-\nu_{\alpha j}+\nu'_{\alpha j}} - 1) + g'_{ij}(\prod_\alpha s_{\alpha u_2}^{-\nu'_{\alpha j}+\nu_{\alpha j}} - 1)] \end{aligned} \tag{27}$$

As

$$\overline{\Delta x_\mu(t_{u_1})\, \Delta x_\lambda(t_{u_2})} = \left(\frac{\partial^2 \ln G}{\partial \ln s_{\mu u_1}\, \partial \ln s_{\lambda u_2}}\right)_{||s_{ij}|| = ||1||}$$

and

$$\overline{\Delta x_\mu(t_{u_2})\, \Delta x_\lambda(t_{u_2})} = \left(\frac{\partial^2 \ln G}{\partial \ln s_{\mu u_2}\, \partial \ln s_{\lambda u_2}}\right)_{||s_{ij}|| = ||1||}$$

the differentiation of Eq. (27) yields

$$\frac{\partial}{\partial\,|\tau|}\ \overline{\Delta x_\mu(t_{u_1})\, \Delta x_\lambda(t_{u_2})} = \sum_i k'_{i\mu}\ \overline{\Delta x_i(t_{u_2})\ \Delta x_\lambda(t_{u_1})} \tag{28}$$

and

$$\frac{\partial}{\partial t_{u_2}}\ M'_{\mu\lambda}(t_{u_2}) = 2D'_{\mu\lambda} + \sum_i M'_{\mu i}(t_{u_2})\, k'_{i\lambda} + \sum_i k'_{i\mu}\, M'_{i\lambda}(t_{u_2}) \tag{29}$$

where

$$2D'_{\mu\lambda} = \sum_j (\bar{r}_j + \bar{r}'_j)(\nu'_{\mu j} - \nu_{\mu j})(\nu'_{\lambda j} - \nu_{\lambda j})$$

$$M'_{\mu\lambda}(t) = \overline{\Delta x_\mu(t)\, \Delta x_\lambda(t)}$$

Writing Eqs. (28) and (29) in the form :

$$\frac{\partial}{\partial|\tau|}\, \overline{\Delta\vec{X}(t_1)\, \Delta\vec{X}^+(t_2)} = \hat{K}'^+\, \overline{\Delta\vec{X}(t_1)\, \Delta\vec{X}^+(t_2)} \quad \text{for } \tau = t_2 - t_1 \leqslant 0, \qquad (28')$$

$$\frac{\partial}{\partial|\tau|}\, \overline{\Delta\vec{X}(t_1)\, \Delta\vec{X}^+(t_2)} = \overline{\Delta\vec{X}(t_1)\, \Delta\vec{X}^+(t_2)}\,\hat{K}' \quad \text{for } \tau = t_2 - t_1 \geqslant 0 \qquad (28'')$$

and

$$\frac{\mathrm{d}\hat{M}'(t)}{\mathrm{d}t} = 2\hat{D}' + \hat{K}'^+\, \hat{M}'(t) + \hat{M}'(t)\, \hat{K}' \qquad (29')$$

we get

$$\overline{\Delta\vec{X}(t_1)\, \Delta\vec{X}^+(t_2)} = h(-\tau)\, \hat{E}'(|\tau|)\, \hat{M}'(t_2) + h(\tau)\, \hat{M}'(t_1)\, \hat{E}'^+(|\tau|) \qquad (30)$$

and

$$\hat{M}'(t) = \hat{E}'(t)\, \hat{M}'(0)\, \hat{E}'^+(t) + \int_0^t \hat{E}'(t-u) 2\hat{D}'\, \hat{E}'^+(t-u)\, \mathrm{d}u \qquad (31)$$

with

$$\hat{E}'(t) = \exp(\hat{K}'^+ t)$$

Comparing Eqs. (23) (30) and (31) with Eqs. (2), (30) and (31), we can see that the method of the master equation leads approximately to the same results for both systems. It follows that operating the substitutions: $\vec{N} \to \vec{X}$, $\hat{K} \to \hat{K}'$, $\hat{E} \to \hat{E}'$, $\hat{M} \to \hat{M}'$, $\hat{D} \to \hat{D}'$, $\hat{D}_e \to \hat{D}'$, $\hat{M}_e \to \int_0^\infty \hat{E}'(u)\, 2\hat{D}'\hat{E}'^+(u)\, \mathrm{d}u$ Eqs. (7′), (8) – (10), (12) – (19), (6″) – (7″), (9′) and (10′) become valid for a system near to equilibrium in which the reactions (20) occur (i.e., for a complex relaxation process).[7]

C. CONCLUSIONS

A Langevin theory for the networks of first order reactions was presented. The theory was extended to the processes of chemical relaxation.

[7] M. Eigen and D. L. Mayer, "Technique of Organic Chemistry", vol. VIIIb, ed A. Weissberger, Interscience, New York, 1963 p. 896.

Revue Roumaine de Chimie, **21**, *9–10*, 1327–1330 (1976)

DES COMBINAISONS COMPLEXES DU Pd(II) AVEC LE ROMERGAN ET LES IONS Cl^- ET CNS^-

VIORICA CIMPU et D. CAMBOLI
Institut Polytechnique, Faculté de Chimie Industrielle 1, str. Polizu,
Bucarest, Roumanie

Reçu le 18 janvier 1975

On a synthétisé six complexes du Pd(II) avec le Romergan et les ions Cl^- et CNS^-. En partant des données analytiques, ainsi que d'autres paramètres, on a attribué aux complexes obtenus les formules : [Pd. romerg. X_2], [Pd. $romerg_2$] [PdX_4] et [Pd. $romerg_4$]X_2. On a étudié les spectres en infrarouge entre 400 et 4 000 cm^{-1}.

Le nombre des travaux publiés sur les dérivés de la phénothiazine est très grand, compte tenu des applications pharmacologiques de ces dérivés.[1-14]

Dans les notes [10] et[12] on mentionne la formation d'un complexe défini, ayant la formule $Pd(C_{12}H_9NS)_2Cl_2$, ce qui correspond au rapport stœchiométrique Pd : phénotiaz. = 1 : 1, tandis que dans [13] on affirme qu'avec les ions Ni^{2+} et Co^{2+} on obtient de même des complexes dans des rapports phénothiaz. : Me^{n+} = 1 : 1. Dans les travaux cités,[4-6] ainsi que dans [14] on mentionne la formation des complexes thiocyaniques des phénotiazines avec les ions Fe^{3+}, Co^{2+}, Ni^{2+} ; Analguidis [15] montre que la prométhazine est précipitée par le HSCN, le produit obtenu est stable et permet une détermination gravimétrique. Spacu et collab., [16,17] proposent l'utilisation du sel de Reinecke pour doser des dérivés phénothiaziniques.

---

[1] J. Blazek, *Die Pharmazie*, **22**, 129 (1967).
[2] J. Blazek, V. Spinkova et E. Stejkal, *An. Farm. Hosp.*, **10**, 7 (1967).
[3] J. Blazek et E. Stejkal, *Die Pharmazie*, **27**, 506 (1972).
[4] J. Barbe et J. Hurwic, *Compte rend.*, **273**, 1481 (1971).
[5] J. Barbe, J. P. Gaby et J. Hurwic, *Ann. Pharm. Fr.*, **30**, 665 (1972).
[6] J. Lagubeau et P. Mesnard, *Bull. Soc. chim. France*, **1965**, 2815.
[7] F. Gutmann et H. Kayzer, *Agressologie*, **9**, 27 (1968).
[8] F. Gutmann et H. Kayzer, *J. Chem. Phys.*, **46**, 1969 (1967).
[9] L. G. Overholser et J. H. Yoe, *Ind. Eng. Chem. Analyt. Ed.*, **14**, 646 (1942).
[10] T. I. Bulencov et G. A. Starcova, *Med. Prom. S.S.S.R.*, **16**, 31 (1962).
[11] P. Majlat et I. Bayer, *Acta Pharm. Hung.*, **32**, 116 (1962).
[12] J. A. Ryan, *J. Amer. Pharm. Assoc. Sci. Ed.*, **48**, 240 (1959).
[13] J. Hojman et A. Milosevic, *Arhch. Pharm*, **18**, 81 (1968).
[14] M. Tarasiewicz, *Acta Pol. Pharm.*, **29**, 583 (1972).
[15] C. Analguidis, *Prakt. Akad. Athenon*, **31**, 276 (1956).
[16] P. Spacu et E. Antonescu, *Studii şi Cercetări Chim. Acad. R.P.R.*, **2**, 247 (1959).
[17] P. Spacu, E. Antonescu et C. Gheorghiu, *Rev. Chim. Acad. R.P.R.*, **2**, 243 (1959).

Nous avons élaboré [18] une méthode spectrophotométrique pour déterminer le Romergan.

En continuant nos préoccupations d'obtenir des complexes du palladium avec des ligands azotés et sulphurés,[19-21] nous avons étudié les réactions entre les ions Pd^{2+} et le Romergan, en présence des anions Cl^- et SCN^-. Nous présentons ici les six complexes obtenus.

SYNTHÈSES ET ANALYSES

A. COMPLEXES HALOGÉNÉS

Substance I. Dans une solution aqueuse de $PdCl_2$, contenant environ 0,2 g de sel dans 100 ml, on ajoute des cristaux de Romergan dans le rapport stœchiométrique Pd^{2+} : Romerg. = =1 :1. En chauffant légèrement au bain-marie, on obtient un précipité couleur brique. On filtre sur un creuset G3, on lave plusieurs fois avec de l'eau, de l'alcool éthylique et de l'éther. La substance se dissout aisément dans l'acétone ; elle est insoluble dans le benzène et l'éther.

Substance II. On prend les réactifs dans le même rapport que pour la substance I, mais on chauffe à 80—85° et on maintient au bain-marie jusqu'à la transformation du précipité brique formé initialement en une substance de couleur rouge cerise, aisément filtrable sur un creuset G3. On lave plusieurs fois avec de l'eau, de l'alcool et de l'éther. Cette substance est soluble dans l'acétone et insoluble dans le benzène et l'éther.

Substance III. On ajoute le Romergan cristallisé dans la solution du sel du palladium dans le rapport molaire 4 : 1. A la température ambiante se forme un précipité de couleur violette, qui se dissout partiellement dans le milieu de la réaction. Le rendement de la synthèse s'accroît en maintenant au bain-marie environ une heure. En refroidissant, on obtient un précipité violet abondant. On le lave avec de l'eau, de l'alcool et de l'éther.

B. COMPLEXES THIOCYANIQUES

La substance IV. Dans une solution de $PdCl_2$ on ajoute des cristaux de Romergan dans le rapport Pd^{2+} : Romerg = 1 : 1. En chauffant légèrement au bain-marie, on obtient un précipité brique. On introduit des cristaux de KSCN (deux moles pour un mole de Romergan), on agite en maintenant sur le bain-marie environ 30 minutes. On obtient un précipité beige filtrable sur un creuset G3, on le lave avec de l'eau, de l'alcool et de l'éther. La substance est aisément soluble dans l'acétone, peu soluble dans l'alcool et insoluble dans l'éther.

La substance V. Les quantités des réactifs sont les mêmes que pour la substance IV, mais on chauffe au bain-marie à 80—85°. On constate que le précipité brique formé initialement devient rouge-cerise. Ensuite on ajoute du KSCN cristallisé, on agite et on continue de chauffer. La couleur du précipité devient brune, avec une teinte rougeâtre. On filtre sur un creuset G3, on lave avec de l'eau, de l'alcool et de l'éther. La substance est insoluble dans l'éther, partiellement soluble dans l'alcool, soluble dans l'acétone.

La substance VI. Dans la solution de $PdCl_2$ on introduit des cristaux de KSCN, la couleur vire vers le rouge, on ajoute en agitant le Romergan solide dans le rapport romerg : Pd^{2+} = =4 : 1. On obtient un précipité orange foncé. On peut réaliser la synthèse en suivant une autre voie : on ajoute le Romergan solide dans la solution du chlorure de palladium dans le rapport stœchiométrique Romerg : Pd^{2+} = 4 : 1. Il se forme un précipité de couleur violette, lequel, en présence des cristaux de KSCN, se transforme en une substance de couleur orange foncée, identique avec celle obtenue dans la première variante de la méthode.

Le palladium a été déterminé par calcination jusqu'à l'état métallique, l'azote — par microcombustion. Les résultats des analyses sont les suivants : [Pd. romerg. Cl_2] : Pd% calculé 23,09 ; déterminé 22,77 ; N% calculé 6,08 ; déterminé 5,28. [Pd. $romerg_2$][$PdCl_4$] : Pd% calculé 23,09; déterminé 22,45; N% calculé 6,08; déterminé 5,63. [Pd. $romerg_4$]Cl_2 : Pd% calculé

---

[18] F. M. Albert, D. Camboli et V. Cîmpu, *Bul. Inst. Polit. Buc.*, **32**, 41 (1971).

[19] P. Spacu et D. Camboli, *Anal. Univ. Buc.*, **13**, 117 (1964).

[20] P. Spacu et. D. Camboli, *Anal. Univ. Buc.*, **14**, 101 (1965).

[21] D. Camboli, M. Stoia, L. Papahagi et D. Braşoveanu, *Bul. Inst. Polit. Buc.*, **32**, 27 (1970).

8,11 ; déterminé 8,02 ; N % calculé 8,55 ; déterminé 7,73. [Pd. romerg$(SCN)_2$] : Pd % calculé 20,99 ; déterminé 21,32. N % calculé 11,05 ; déterminé 10,43. [Pd. $romerg_2$][Pd$(SCN)_4$] : Pd % calculé 20,99 ; déterminé 20,10 ; N % calculé 11,05 ; déterminé 10,20. [Pd. $romerg_4$] $(SCN)_2$: Pd % calculé 7,82 ; déterminé 7,67 ; N % calculé 10,30 ; déterminé 10,65.

Ci-dessous sont donnés les points de fusion des complexes synthétisés :

Substance	*p.f.*
I [Pd. romerg Cl_2]	225–226°
II [Pd. $romerg_2$] [Pd.Cl_4]	254–255°
III [Pd. $romerg_4$]Cl_2	200–201°
IV [Pd. romerg$(SCN)_2$]	208–210°
V [Pd. $romerg_2$] [Pd$(SCN)_4$]	236–238°
VI [Pd. $romerg_4$] $(SCN)_2$	180–182°

On peut avancer certains arguments en faveur des formules proposées. Quoique les substances I et II et IV et V respectivement aient la même teneur en azote et en palladium, les couleurs et les points de fusion différents indiquent qu'il s'agit de paires de composés, dont le second peut être le dimère du premier. La possibilité d'obtenir un monomère et un dimère en partant du même rapport stœchiométrique des réactifs est connue pour les ammines du Pd(II). Nous avons obtenu [19] [Pd. $pip_2(SCN)_2$] et son dimère [Pd.pip_4] [Pd$(SCN)_4$] ainsi que [Pd.$thio_2(SCN)_2$] et [Pd.$thio_4$] [Pd$(SCN)_4$]. Nous avons constaté que les dimères ont des couleurs plus foncées, ce qui concorde avec d'autres travaux sur les complexes du Pd(II), par exemple,[22,23] ainsi qu'avec les résultats de la présente note. Les substances I, II, IV et V sont très peu solubles dans l'eau, tandis que les complexes III et VI présentent une meilleure solubilité, ce qui est en concordance avec les formules proposées, selon lesquelles ces composés contiennent des ions Cl^- et SCN^-. Ceux-ci donnent les réactions caractéristiques avec $AgNO_3$ et $FeCl_3$; pour les substances I, II, IV, V ces réaction sont négatives.

LES SPECTRES EN INFRAROUGE

On a effectué les déterminations spectrales sur des pastilles avec un spectrophotomètre UR.20 Karl-Zeiss Jéna, dans le domaine 400–4000 cm^{-1} ; entre 400–700 cm^{-1} on a utilisé des prismes de KBr, entre 700–1800 cm^{-1} – de NaCl et entre 1800–4000 cm^{-1} – de LiF.

Dans les spectres obtenus on constate la présence des bandes caractéristiques du Romergan qui est une phénothiazine N-substituée, mais ces bandes sont souvent déplacées en comparaison du spectre du ligand libre.

On sait que les bandes caractéristiques pour le chlore se trouvent dans le domaine des longueurs d'onde plus élevées, donc elles manquent sur nos spectrogrammes.

Dans la note [5] sont présentés les maxima pour les phénothiazines substituées, comparés à ceux des complexes de ces amines avec un sel du Co(II). Dans le spectre du Romergan que nous avons déterminé, on retrouve les bandes des phénothiazines. Du tableau 1 il résulte que les spectres des complexes I et II, et IV et V respectivement se ressemblent beaucoup. Ceci est en concordance avec les résultats de nos études antérieures,[19,20] sur des complexes similaires du Pd(II) avec la pipéridine et la thio-urée. Pour ces dérivés, les spectres en infrarouge des diammines présentent une ressemblance accentuée avec ceux des dérivés du type Vauquelin – les dimères des premières. Les spectres des substances III et VI, qui sont des tétrammines, diffèrent de ceux des complexes I, II, IV, V.

---

[22] H. Drew, F. Pinkard, G. Preston et W. Wardlaw, *J. Chem. Soc.*, **1932**, 1895.

[23] F. Mann, D. Crowfoot, D. Gattiker et N. Wooster, *J. Chem. Soc.*, **1935**, 1642.

De l'examen des spectres on constate que le déplacement des maxima d'absorption comme conséquence de la formation des complexes est de l'ordre de $\pm 15\ \text{cm}^{-1}$, en concordance avec les données de Barbe et collab.[5]

La présence des maxima dans le domaine $2000-2200\ \text{cm}^{-1}$ est due à ce que dans les combinaisons synthétisées existent des groupes CNS. On sait que ces maxima correspondent aux vibrations du groupe $C{=}N$ et que s'ils se trouvent dans le domaine des nombres d'onde supérieurs à $2100\ \text{cm}^{-1}$, la liaison entre l'ion métallique central et les groupes CNS se réalise par l'atome de soufre, tandis que la présence des mêmes pics dans le domaine situé à moins de $2100\ \text{cm}^{-1}$ est une preuve que les groupes CNS se lient avec l'ion métallique par l'atome d'azote. Dans les spectres des combinaisons décrites dans la présente note on trouve des pics dans le domaine supérieur à $2100\ \text{cm}^{-1}$; on peut donc conclure que ces combinaisons sont thiocyaniques et non pas isothiocyaniques. Ce résultat confirme ceux des notes,[24,25] ainsi que les constatations de nos travaux antérieurs.[26] Le fait que dans les spectres présentés dans cette note on constate dans le domaine $2000-2200\ \text{cm}^{-1}$ l'existence de deux pics pour chacune des combinaisons complexes est aussi en concordance avec les études spectrales des combinaisons complexes thiocyaniques du cuivre.[27]

Tableau 1

Certaines bandes d'adsorption (cm^{-1})

Le Romergan	Les complexes					
	I	II	III	IV	V	VI
436 m	436 f	436 f	428 f	440 f	440 f	432 m
749 i	759 i	761 i	754 m	762 i	752 i	758 i
1053 m	1051 f	1053 f	1056 m	1059 m	1060 m	1059 m
1125 m	1131 f	1129 m		1136 m	1138 m	1138 m
1287 m	1293 m	1294 m	1289 m	1294 m	1293 m	1296 m
1396 i	1399 m	1381 m	1381 m	1397 m	1397 m	1402 i
				2118 i	2114 i	2113 i
				2161 i	2160 m	2162 m
2738 f	2733 m	2731 i	2742 m	2716 m	2720 m	2745 f

f = faible ; m = moyenne ; i = intense.

CONCLUSIONS

1. On a synthétisé six complexes du Pd(II) avec le Romergan, appartenant aux classes des diammines, tétrammines et des combinaisons de type Vauquelin.

2. Des données analytiques, des points de fusion et des couleurs des complexes I et II et IV et V respectivement on a conclu que les seconds de chaque paire sont les dimères des premiers.

3. On a déterminé les spectres en infrarouge dans le domaine de 400 à $4000\ \text{cm}^{-1}$. Les spectrogrammes viennent confirmer les conclusions sur la formulation des complexes synthétisés.

---

[24] R. C. H. Mitchell et R. J. P. Williams, *J. Chem. Soc.*, **1960**, 1912.

[25] A. Sabatini et I. Bertini, *Inorg. Chem.*, **4**, 1665 (1965).

[26] P. Spacu et D. Camboli, *Rev. Roumaine Chim.*, **11**, 157 (1966).

[27] R. H. Toeniskoetter, et S. Solomon, *Inorg. Chem.*, **7**, 617 (1968).

Revue Roumaine de Chimie, **21**, *9–10*, 1331–1338 (1976)

Cu(II) CHELATES SYNTHESIZED WITH LIGANDS CONTAINING DONOR NITROGEN ATOMS

A. C. BANCIU and P. SPACU

Center of Physical Chemistry, Bucharest, Str. Dumbrava Roşie 23, Romania

Received January 30, 1975

This paper studies the synthesis and the physico-chemical properties (IR and electronic spectra, molar electric conductivities and magnetic moments) of four new Cu(II) tetra-coordinated chelate complexes, formed with organic ligands from the class of aryl-substituted 1-methyl-2-carbethoxy-glyoxalanil-(1)-arylhydrazones-(2). The electronic spectra of all complexes reveal an intermediate structure between a distorted square-planar and a flattened tetrahedral configuration, but much closer to the latter.

Our previous papers [1–5] have reported the synthesis and the physio-chemical properties of Co(II) and Ni(II) chelate complexes obtained with the chelate ligands of formula I, belonging to the class of 1-methyl-2-car-bethoxy-glyoxalanil-(1)-arylhydrazones-(2), differently substituted on the benzene ring of the hydrazone group.

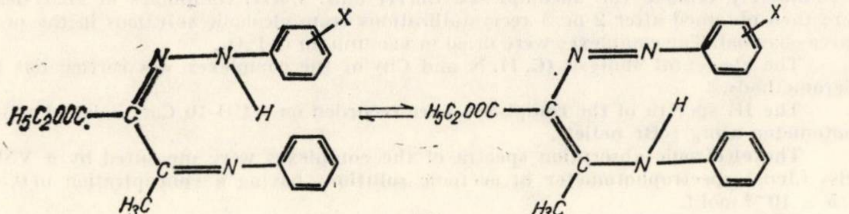

I

$X = H$; $p-$, $m-$, $o-CH_3$; $p-$, $m-$, $o-O-CH_3$; $p-$, $m-$, $o-NO_2$

---

[1] P. Spacu, A. C. Banciu and C. I. Lepădatu, *Rev. Roumaine Chim.*, **18**, 7, 1143 (1973).

[2] A. C. Banciu and P. Spacu, *Rev. Roumaine Chim.*, **19**, 5, 817 (1974).

[3] A. C. Banciu and P. Spacu, *Rev. Roumaine Chim.*, **19**, 6, 1019 (1974).

[4] A. C. Banciu and P. Spacu, *Rev. Roumaine Chim.*, **19**, 7, 1177 (1974).

[5] A. C. Banciu and P. Spacu, *Rev. Roumaine Chim.*, **19**, 8, 1307 (1974).

The present paper is concerned with the study of the four Cu(II) complexes, of formula II, which have been synthesized by attempts performed with the above mentioned ligands.

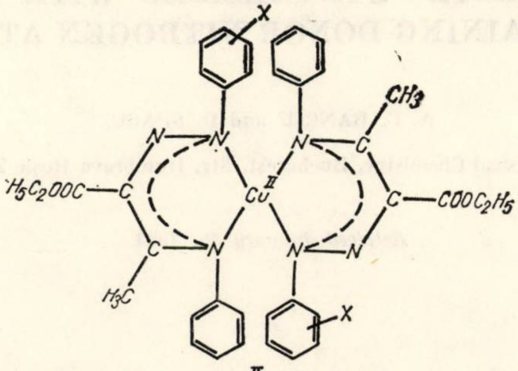

II

a : X = H ; b : X = $p-CH_3$; c : X = $p-NO_2$; d : X = $m-NO_2$

EXPERIMENTAL

The synthesis of the organic ligands of formula I was described in our previous papers.[1-5]

Cu(II) complexes were synthesized by a similar method to the synthesis of the corresponding Co(II) and Ni(II) complexes.[1-5] A concentrated alcoholic solution of the respective ligand (1/100 moles) and $CuCl_2.2H_2O$ (1.15/200 moles) were refluxed (for about 30 minutes) in the presence of (approx. 0.8 ml) triethylamine. During complexation the reaction mass turns dark and becomes almost black. The separation and purification of the Cu(II) complexes are much more difficult than for the analogous Co(II) and Ni(II) complexes. Only the very sparingly-soluble complex IId, with X = $m-NO_2$, has readily precipitated on cooling the reaction mass. In general, the solvent must be almost totally evaporated and the dark greenish-blue precipitate is the Cu(II) complex with impurities of the ligand and its degradation products. The color of the latter is light yellow, positively differing from the bright yellow, orange or red color of the initial ligands. The precipitate was repeatedly washed with 3% acetic acid heated to 40° in order to completely remove the uncomplexed Cu(II) ions. Cu(II) complexes of analytical purity were then obtained after 2 or 3 recrystallizations from alcoholic solutions in the presence of active charcoal. The complexes were dried in vacuum on di-P_2O_5.

The elemental analysis (C, H, N and Cu) of the complexes was carried out by usual micromethods.

The IR spectra of the complexes were recorded on a UR-10 Carl Zeiss (Jena) spectrophotometer using KBr pellets.

The electronic absorption spectra of the complexes were measured by a VSU-2 Carl Zeiss (Jena) spectrophotometer in acetonic solutions having a concentration of 0.5×10^{-4} to 5×10^{-4} mol/l.

The electric conductivity of the complexes was determined at 25° in solution of absolute ethanol with a concentration of 2.5×10^{-4} mol/l, using a Radelkis OK 102 conductometer.

The magnetic susceptibilities were determined in solid compounds, at room temperature, according to the Faraday methods, using $Hg[Co(NCS)_4]$ as standard.

RESULTS AND DISCUSSIONS

The synthesis of the complexes with Cu(II) ions and the type I organic compounds *ortho*-substituted at the benzene ring of the hydrazone group (I : X = $o-CH_3$; $o-O-CH_3$ and $o-NO_2$) were not successful, as was the case with the Co(II) and Ni(II) ions. The color of the refluxed solution of the Cu(II) ions and *ortho*-substituted type I compounds indicates that complexation did not occur. The impossibility of Co(II), Ni(II) and Cu(II) ions to complex with the *ortho*-substituted organic compounds of formula I is explained by the major steric hindrances caused by any of the mentioned substituents whenever they are situated in an *ortho* position of the benzene ring of the hydrazone group. In this position the substituents are in the vicinity of a nitrogen atom which most play a donor-atom role in complexation.

None of the other type I organic compounds display a steric hindrance caused by the respective substituents (CH_3, OCH_3, NO_2) situated in *meta*- or *para*-positions at the benzene ring of the hydrazone group. These compounds also proved to be real chelate ligands with Co(II) and Ni(II) ions. The fact that only the four Cu(II) complexes systematized in table 1 were obtained in analytical purity is explained by the extremly high solubility of the initial formed Cu(II) complexes. In all the synthesis performed with these *para* and *meta* substituted ligands, the reaction mass darkened drastically, indicating that the complexation had occurred. But when the formed complexes were readily soluble, their separation and purification were not possible, at least under the experimental working conditions (with 1/100 mole organic ligand).

All the four Cu(II) complexes synthesized and systematized in table 1 are formed with the more sparingly soluble type I ligands. The complexes themselves are sparingly soluble and they are always less soluble than the secondary organic reaction products. Nevertheless, their solubility in ethy alcohol and acetone is higher than of the analogous Co(II) and Ni(II) complexes.

Table 1

Analytical data of the Cu(II) chelates

Chelate of formula II	Cu %		C %		H %		N %	
	Calc.	Found	Calc.	Found	Calc.	Found	Calc.	Found
II-a	9.34	9.10	63.56	63.36	5.33	5.82	12.35	12.70
II-b	8.97	8.60	64.44	64.80	5.69	6.00	11.86	12.27
II-c	8.25	8.00	56.14	55.72	4.45	4.83	14.55	15.02
II-d	8.25	7.92	56.14	56.40	4.45	5.10	14.55	15.12

The analytical data of the Cu(II) complexes agree well with their formula II. Their chelatic structure is supported by the non-electrolyte character of the complexes (the molar electric conductivity is smaller than 4 ohm^{-1} cm^2mol^{-1}, in absolute ethanol) and also by the data provided by their IR spectra. The complexes positively adopt a *trans* configuration (according to formula II) in which the steric hindrances are minimized, compared to the corresponding *cis* configuration.

Table 2

IR spectra (cm^{-1}) of 1-methyl-2-carbethoxy-glyoxalanil-(1)-p-NO$_2$-phenylhydrazone-(2) (ligand I: X = p-NO$_2$) and of the Cu(II) chelate formed with this ligand (chelate II: X = p-NO$_2$)

Ligand I X = p—NO$_2$	Chelate II X = p—NO$_2$	Assignments
695 m	705 m	Deformation vibration of the benzene ring
740 m	740 m	Out-of-plane deformation vibration of the C—H bond (γC—H) for the mono-substituted benzene
755 m-s	755 m	
765 m	785 m	
815 m		γ-C-H vibration for the 1,4-disubstituted benzene
845 m	855 s	
870 w		
925 w	915 w	Symmetrical stretching vibration of the C—O—C bond
	1000 m-s	Ring vibration of the benzene ring
1025 w		
1035 w	1035 w-m	
1080 s-vs	1080 vs	Asymmetrical stretching vibration of the C—O—C bond from the —COOC$_2$H$_5$ group
1125 s-vs	1115 vs	
1170 s-vs	1160 vs	Different vibrations of the C—O and O—C$_2$H$_5$ bonds from the —COOC$_2$H$_5$ group
	1190 s	
1215 m	1220 vs	
1235 m		
1280 s		C—N stretching vibration for the C$_6$H$_5$-NH-group
	1310 vs	C—N stretching vibration for the C$_6$H$_5$—N < group
1305 m		
1330 s	1330 ...	Symmetrical NO$_2$ stretching vibration
1345 vs	..1350 vs	
1380 m	1380 m	CH$_3$—C stretching vibration
	1415 vs	
1470 m		C—C skeletal vibration of benzene ring
1500 vs	1500 w-m	Vibrations of the conjugated C=N bonds and N=N bond vibrations
1525 vs	1525 s	
	1570 m	
1610 vs	1605 vs	
1730 vs	1725 vs	Stretching vibration of the C=O bond (νCO) from the —COOC$_2$H$_5$ group
2940 w	2940 w	Asymmetrical C—H stretching vibration from CH$_2$ group
2965 w	2965 w	Asymmetrical C—H stretching vibration from CH$_3$ group
2985 w	2985 w	
3060 w	3070 w	C—H stretching vibrations of the substituted benzene ring

vs = very strong; s = strong; m = medium; w = weak

IR SPECTRA

Table 2 gives a comparative systematization of the IR spectra for the Cu(II) complex which is p-NO_2-substituted at the benzene ring of the hydrazone group (complex IIc : X $= p-NO_2$) and of the free ligand (I :X$=$ $=p-NO_2$) corresponding to it. The same table also exhibits the more likely assignments of the vibration bands.

The most stringent difference between the two compounds in their IR spectra is reflected within the range 1270$-$1320 cm^{-1}. An intense band is outlined here in the case of the free ligand, with a maximum situated at 1280 cm^{-1}. As a result of the perturbations induced by coordination, this band appears only slightly shifted, with the maximum situated at 1310 cm^{-1}, but strongly intensified, in the spectrum of the corresponding Cu(II) complex. In the latter case, the mentioned band represents one of the most intense bands of the whole IR spectrum. In the case of the free ligand this band (1280 cm^{-1}) was assigned to the C$-$N stretching vibration of the secondary aromatic amine group (Aryl$-$NH$-$), which is known[6] to appear within the range of 1280$-$1350 cm^{-1}. The band found in the case of the Cu(II) complex (1310 cm^{-1}) was equally assigned to the C$-$N stretching vibration but yet of the tertiary aromatic amino group (Aryl$-$ $-$N$=$), which is known[6] to appear almost within the same range (1310$-$1360 cm^{-1}) as the former but strongly intensified comparison to it.

These data together with the others from the IR spectrum suggest for the ligand the open I type structure instead of the closed form, where the hydrogen bridges the nitrogen atoms of the hydrazone group and of the aryl group.

The IR data of the Cu(II) complex show that the coordination of the metallic ion occurs by the nitrogen atom of the hydrazone group which becomes a tertiary nitrogen subsequent to coordination.

The absence of any modification after coordination in the 1710$-$1740 cm^{-1} range for the C$=$O stretching vibration (νCO) from the esteric group $COOC_2H_5$ indicates that this group does not participate in coordination, a possibility which could not be a priori excluded.

If the carbonyl group had been coordinated the mentioned band would have been expected to appear markedly shifted to approx. 1635$-$1665 cm^{-1}, which is not, obviously, the case.

ELECTRONIC SPECTRA AND MAGNETIC MOMENTS

The electronic spectra of all the new Cu(II) complexes of type II are very similar to each other, although they present some detectable differences in certain cases. The best resolved is the spectrum of the complex with the $p-NO_2$ substituent at the benzene ring of the hydrazone group (IIc : X $= p-NO_2$). Its spectrum as well as the spectrum of the complex IId ($m-NO_2$ substituted) is illustrated in fig. 1.

---

[6] L. J. Bellamy, "The Infrared Spectra of Complex Molecules", Methuen, London, 1962.

The absorption spectra of the other two complexes IIa (X = H) and IIb (X = $p-CH_3$) are very similar to that of the complex IId (X = $=m-NO_2$). All these three complexes exhibit in the near UV region a highly intense and broad band (its maximum extends over a 50 nm domain, between 350—400 nm). The broadness and the non-gaussian aspect of this band indicate that it actually represents two transitions.

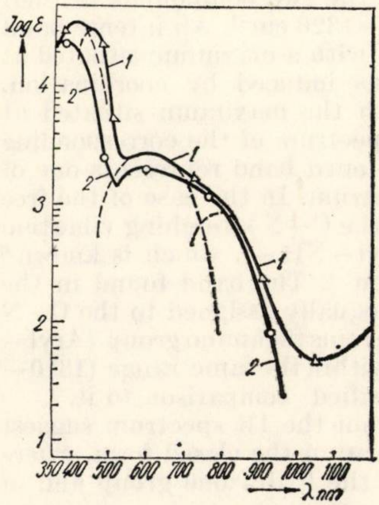

Fig. 1. — Absorption spectra of Cu(II) chelates.
1. Chelate IIc($X=p-NO_2$); 2. Chelate II d($X=m-NO_2$).

The $p-NO_2$ substituted complex IIc exhibits, in turn, two bands in this domain: a very intense one ($\varepsilon_{max} = 3.6 \times 10^4$) with a well-shaped maximum at 405 nm and an equally intense shoulder ($\varepsilon_{max} \sim 3.2 \times 10^4$) of this band. The shoulder represents a band whose maximum may be located at approx. 455 nm. The first band represents only a weak bathochromic shift of 20 nm, for the band corresponding to the allowed $\pi \rightarrow \pi^*$ transition of the organic ligand in question. For this reason it may be certainly assigned to this transition specific of the organic ligand. The band at approx. 455 nm is so intense that it may be reasonably assigned onyl to a charge transfer (CT) transition, as it is not specific of the organic ligand.

Considering these two assignments and also the aspect of spectra, it may be concluded that in the case of the other three complexes whose spectra are not so well resolved, the very broad band in the near UV region represents the summation of two transitions. The energies for these two transitions are very close (for the $p-NO_2$ substituted complex 24,700 cm^{-1} and 22,000 cm^{-1}) and their intensities are almost identical, but they are of different nature. One is an allowed $\pi \rightarrow \pi^*$ transition proper for the organic ligand and the other is a charge transfer (CT) transition. Only in the case of the $p-NO_2$ substituted complex IIc does the CT band differ significantly from the $\pi \rightarrow \pi^*$ band (by 2,700 cm^{-1}), so that it can be experimentally detected in the spectrum in the form of a shoulder.

All the complexes exhibit an unusually broad band in the region of 500 to 900 nm (fig. 1). This supports the fact that at least two transitions are present. In this domain the spectrum of the $p-NO_2$-substituted complex is again better resolved than the spectrum of the other complexes. The spectrum indicates a maximum exactly located at 600 nm in acetonic solutions and at 585 nm in DMF solutions, of $\varepsilon_{max} \sim 2.8 \times 10^3$, and a more well defined shoulder appears between 700–900 nm (fig. 1). This shoulder was determined to be from an absorption band at approx. 775 nm ($\varepsilon_{max} \sim 800$). This band positively represents a $d-d$ transition. In turn, the assignment of the band with a maximum situated at 600 nm is rather ambigous. Its large absorbance may indicate the CT nature of this band. In the case of the Cu(II) tetracoordinated complexes the bands plausibly assigned to a CT transition are close to the UV region (approx. 20,000 cm^{-1}) rather than at 16,600 cm^{-1} as in this case. Therefore it appears more likely to assign this band to a $d-d$ transition. In this last case, the high intensity of the band may be explained by the closeness and overlapping of the absorption bands at 405 and 455 nm, which are more intense by over one order of magnitude.

As it is known [7] the Cu(II) tetracoordinated complexes will never possess one of the two possible limiting geometrical structures : square-planar or tetrahedral configurations. They always adopt an intermediate structure between the (distorted) square-planar and the (distorted) tetrahedral configurations. In the case of the complex IIc ($X = p-NO_2$) the electronic spectrum indicate the dominant configuration, that is to say a more marked tendency to assume one of the two mentioned limiting structures.

Thus a comparison between the spectrum of this complex and that of the Cu(II) complex formed with the N-t-butyl derivative of salicylaldimine [7,8] (375 nm : $\varepsilon = 5400$; shoulder 435 nm : $\varepsilon = 1100$; 500 nm : $\varepsilon = 1100$; 745 nm : $\varepsilon = 180$) reveals a close similyrity. Based on the accurate X-ray determination, we positively know that the latter complex is closer to a flattened tetrahedral structure than to a distorted square planar one. There is no question of finding such a close similarity between the spectrum of the $p-NO_2$ substituted complex IIc and the spectra of other Cu(II) tetracoordinated complexes with known [9] *cis* or *trans* square planar structures. Since the electronic spectra of all the new type II Cu(II) complexes are similar, this fact seems to indicate that all the new Cu(II) complexes have flattened tetrahedron structures rather than square planar structure.

The magnetic susceptibilities were experimentally determined at room temperature for the complexes IIa ($X = H$) and IIc ($X = p-NO_2$). Their magnetic moments were calculated from :

$$\mu = 2.828\ [\chi'_M \cdot T]^{1/2}$$

---

[7] T. P. Cheeseman, D. Hall and T. N. Waters, *J. Chem. Soc.*, **A 1966**, 685.

[8] L. Sacconi and M. Ciampolini, *J. Chem. Soc.*, **1964**, 276.

[9] D. Hall, S. V. Sheat and T. N. Waters, *Chem. Comm.*, **1966**, 436.

where $\chi'_M = \chi_M - \chi_{dia}$ is the corrected molar susceptibility. The following corrections were made for the diamagnetism

$$\chi_{dia} = -339 \times 10^{-6} \text{ c.g.s.u. for chelate IIa}$$

$$\chi_{dia} = -360 \times 10^{-6} \text{ c.g.s.u. for chelate IIc.}$$

For the calculation of these corrections and also of the χ_M values both complexes were assumed to be monomers, according to their formula II.

For both complexes was calculated

$$\mu = 1.8 \pm 0.1 \text{ B.M.}$$

a value close to the spin only value for the d^9 electronic configuration of the Cu(II) ion with one unapired electron (1.73 B.M.).

ACKNOWLEGEMENT. We wish to thank lecturer V. Mincu from the Polytehnic Institute of Bucharest for the magnetic susceptibility measurements.

Revue Roumaine de Chimie, **21**, *9–10*, 1339–1343 (1976)

PYRYLIUM SALTS FORMED BY DIACYLATION OF OLEFINS. XXI[1]

DIACETYLATION OF CYCLODECENE TO 9,11-DIMETHYL-[7](2,6)-PYRYLOPHANIUM PERCHLORATE

ALEXANDRU T. BALABAN[a,b] and ILIE I. BĂDILESCU[c]

[a] Chair of Organic Chemistry, The Polytechnic, Bucharest, Roumania

[b] Correspondence address : Institute of Atomic Physics, P.O.B. 5206, Bucharest, Roumania

[c] Pedagogical Institute, Chemistry Department, Piteşti, Roumania

Received March 31, 1976

Diacetylation of cyclodecene affords the title compound (I), whose IR, UV, ^{1}H- and ^{13}C-NMR spectra confirm the structure. In the ^{1}H-NMR spectrum, one strongly shielded methylene group appears. The corresponding pyridine, 9,11-dimethyl-[7](2,6)-pyridinophane (II), has its central methylene protons at even higher field than the corresponding peak of I, namely at τ 10.08. The bathochromically shifted UV absorption maximum of I relatively to the analogous diacetylation product of cyclododecene, III, indicates some steric strain in I.

Previous papers [2,3] described the diacetylation of cyclododecene to a 3,5-bridged pyrylium salt (III) with a nonamethylene bridge. We report now the preparation of a similar pyrylium salt, I, with a smaller bridge joining positions 3 and 5, which consists of only a heptamethylene chain.

cis-Cyclodecene [4] was mostly resinified on treatment with acetic anhydride and perchloric acid, a procedure which did afford III from cyclododecene in 24 % yield. However, on treating a mixture of *cis*-cyclodecene and acetic anhydride with Schneider's "sulphoacetic acid",[5] a pyrylium salt was formed. It was isolated as the perchlorate in 2–3 % yield. Its name, according to a recent nomenclature proposal,[6] is 9,11-dimethyl-[7](2,6)-pyrylophanium perchlorate, and the numbering is apparent from formula I.

---

[1] Part XX, A. Bota, A. T. Balaban* and F. Chiraleu, *Rev. Roumaine Chim.* **21**, 101 (1976).

[2] A. T. Balaban, *Tetrahedron Letters*, **1968**, 4643.

[3] A. T. Balaban, *Rev. Roumaine Chim.*, **18**, 1609 (1973).

[4] Kindly provided by prof. G. Wilke, Max-Planck-Institut für Kohlenforschung, Mülheim an der Ruhr, W. Germany.

[5] W. Schneider and D. Seebach, *Ber. dtsch. chem. Ges.*, **54**, 2285 (1921).

[6] a. E. Vögtle and P. Neumann, *Tetrahedron*, **26**, 5847 (1970).
b. B. H. Smith, "Bridged Aromatic Compounds", Academic Press, New York, 1964

In its infrared absorption spectrum (KBr pellet) the usual[7] bands appear at 3035 (ν CH arom.), 1612, 1500 (pyrylium ring deformation modes), 1100 and 624 cm^{-1} (perchlorate anion bands).

An interesting difference is manifested in the ultraviolet absorption spectra of perchlorates I and III (in ethanol acidified with perchloric acid) : 307 nm for III, and 316 nm for the absorption maximum of I. This bathochromic effect of reducing the bridge length indicates a distortion of the pyrylium π-electron system, which is probably caused by a slight puckering of the aromatic ring in order to accomodate the steric strain. 2,3,5,6-Tetramethylpyrylium perchlorate,[8] with a similar substitution pattern, presents in the same solvent an absorption maximum at 304 nm (2,4,6-trialkyl-substituted pyrylium salts have maxima at lower wavelengths, about 285 nm).[9]

The ^1H-NMR spectrum of perchlorate I is presented in Table 1 together with that of III, in trifluoroacetic acid. The chemical shifts agree with those of other pyrylium salts,[10] and with one another, excepting the broad signal of one (hence the central) methylene group in I, which appears at an exceptionally high field, τ 9.51. Models show that, unlike the flexible bridge of III, in I the bridge is rather rigid with its central methylene group above the ring ; the protons of this methylene group are therefore shielded by the ring current of the pyrylium nucleus. The small value of the coupling constant (ca. 3 Hz) indicates a *skew* or *gauche* conformation of the heptamethylene chain, in agreement with the Karplus-Conroy equation. By contrast, the corresponding coupling constant of III was ca. 6 Hz.

Proton-decoupled Fourier transform $^{13}C-NMR$ spectra (in natural abundance) were recorded for I and III perchlorates in CD_2Cl_2 — F_3CCOOH 20 : 80% with TMS as internal standard. The results are presented in Table 2 for the methyl-deuterated and non-deuterated analogs. Assignments are based on the disappearance of the ^{13}C peaks due to carbons bonded to deuterium and of their neighbouring carbon peaks, on off-resonance experiments, and on analogy with CMR spectra of other alkyl-substituted pyrylium salts.[11] In the CMR spectra of I, all corresponding methylene carbons appear at lower fields with 3—5 ppm relatively to those in III, probably due to a ring strain effect. This obscures any additional shielding of the central methylene carbon (which, anyway, would be less pronounced than for the PMR spectrum).

Conversion of the pyrylium salt I into the corresponding pyridine (II) by reaction with aqueous-ethanolic ammonia revealed a similar upfield shift of its central methylene protons in the PMR spectrum: in CS_2 it appears at τ 10.08 ; other peaks at 2.70 (1H, s, ArH), 7.60 (6H, s, CH_3), 7.40 (4H, t, 1-CH_2, J = ca. 3 Hz) and 8.62 τ (8H, quintet, J = ca. 3 Hz, 2- and 3-CH_2) confirm the structure, as do also the elemental analyses of I and of the picrate, picrolonate and hexachloroplatinate of II. The difference of 0.4—0.6 ppm between all but one corresponding peaks in the

---

[7] A. T. Balaban, G. D. Mateescu and M. Elian, *Tetrahedron*, **18**, 1083 (1962).

[8] P. F. G. Praill and A. L. Whitear, *J. Chem. Soc.*, **1961**, 3573 ; E. Gârd, I. Stănoiu, A. T. Balaban and F. Chiraleu, *Rev. Roumaine Chim.* **14**, 247 (1969).

[9] A. T. Balaban, V. E. Sahini and E. Keplinger, *Tetrahedron*, **9**, 163 (1960).

[10] A. T. Balaban, G. R. Bedford and A. R. Katritzky, *J. Chem. Soc.*, **1964**, 1646.

[11] A. T. Balaban and V. Wray, *Z. Naturforsch.* **30b**, 654 (1975).

PMR spectra of II and I is due to the change in solvent and to electrostatic effects caused by the positive charge of I; these effects manifest themselves most strongly for the aromatic proton, the only one which gives a difference of 1.5 ppm between II and I, and of 1.6 ppm between the pyridine V, X = N and the pyrylium salt III.

Table 1

Proton NMR spectra (τ-values from internal tetramethylsilane)[a]

Comp. Position	Cyclodecene diacetylation products				Cyclododecene diacetylation products			
	I	IV, R = = Me	IV, R=H	II	III	V, X = = NMe$^+$	V,X = = NH$^+$	V, X = N
Solvent	F_3CCO_2H	F_3CCO_2H	F_3CCO_2H	CS_2	F_3CCO_2H	F_3CCO_2H	F_3CCO_2H	CS_2
γ−H	1.15 s	1.46 s	1.45 s	2.70 s	1.20 s	1.80 s	1.71 s	2.88 s
α−CH[b]	7.08 s	7.15 s	7.25 s	7.60 s	7.04 s	7.12 s	7.27 s	7.67 s
$1-CH_2$	7.00 t^c	6.94 t^c	7.05 t^c	7.40 t^c	6.97 t^d	6.88 t^d	7.03 t^d	7.39 t^d
$2-CH_2$	8.22 q^c	8.33 q^c	8.34 q^c	8.62 q^c	8.02 q^d	8.07 q^d	8.11 q^d	8.39 q^d
$3-CH_2$	8.22 q	8.33 q	8.34 q	8.62 q	8.65 q	8.75 b	8.80 b	9.00 b
$4-CH_2$	9.51 b	9.73 b	9.80 b	10.08 b	8.65 q	8.75 b	8.80 b	9.00 b
$5-CH_2$	—	—	—	—	8.73 b	8.75 b	8.80 b	9.00 b
$N-CH_3$	—	5.78 s	—	—	—	5.73 s	—	—

[a] Abbreviations: s = singlet; t = triplet; q = quintet; b = broad peak.

[b] Peaks disappear on deuteration.

[c] Coupling constant ca. 3 Hz.

[d] Coupling constant ca. 6 Hz.

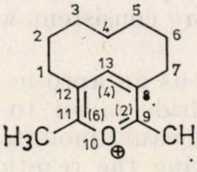

I

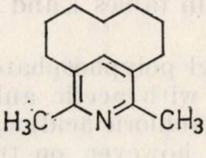

II

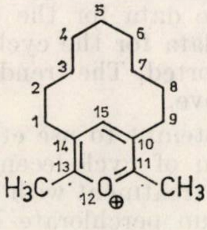

III

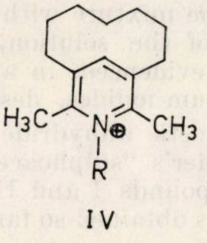

IV

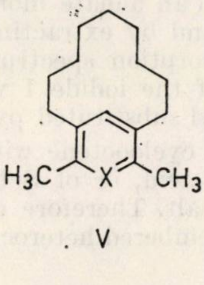

. V

Reaction of the pyrylium salt I with methylamine affords the N-methylpyridinium perchlorate of II, i.e. IV, R = Me.

Tables 1 and 2 present the PMR and CMR spectra of pyrylium salts obtained by the diacetylation of cyclodecene and cyclododecene, as well as of the corresponding pyridines (in carbon disulphide as such, in trifluoroacetic acid as NH$^+$-pyridinium salts) and N-methylpyridinium salts. Most of the data for the cyclododecene diacetylation products, and of course all data for the cyclodecene diacetylation products, were not previously reported. The trends in tables 1 and 2 are consistent with the discussion above.

Table 2

Carbon – 13 NMR spectra (δ-values from internal TMS) in F_3CCOOH (80% v/v) – CD_2Cl_2 (20% v/v) solvent mixture

Comp.	Cyclodecene diacylation		Cyclododecene diacylation	
Position	I	IV, R=Me	III	V, X=NMe$^+$
$\alpha-C^a$	176.67	?	178.03	153.99
$\beta-C$	138.81	141.25	137.53	139.81
$\gamma-C$	161.83	149.56	158.14	148.59
$\alpha-CH_3{}^a$	19.34	17.53	19.59	18.16
1–C	33.13	35.59	30.62	33.65
2–C	29.75	29.82	26.56^b	26.27^b
3–C	29.23	29.82	24.18	25.73
4–C	30.28	29.58	26.48^b	26.79^b
5–C	—	—	26.26	27.58
$N-CH_3$	—	42.46	—	42.34

[a] Peaks disappear on deuteration.

[b] Assignments may be interchanged between carbons 2 and 4.

An attempt to use ethyl polyphosphate[12] as an aprotic catalyst in the reaction of cyclodecene with acetic anhydride failed to afford (on subsequent treatment with perchloric acid) significant amounts of crystalline pyrylium perchlorate I; however, on treating the reaction mixture with ammonia, a 2.2% yield of pyridine III was obtained.

By grinding in an achate mortar a mixture of perchlorate I and of potassium iodide, and by extracting the mixture with CH_2Cl_2 and recording the visible absorption spectrum of the solution, a charge-transfer band at 422 nm of the iodide I was evidenced, in agreement with CT bands of other alkyl-substituted pyrylium iodides, described previously.[13]

Treatment of cyclooctene with acetic anhydride either in the presence of perchloric acid, or of Schneider's "sulphoacetic acid", failed to yield a pyrylium salt. Therefore compounds I and II are the samllest *meta*-bridged six-membered heterocycles obtained so far [6b] by diacetylation of cyclic olefins.

---

[12] L. F. Fieser and M. Fieser, "Reagents for Organic Synthesis", Wiley, New York, 1967, vol. 1, p. 892.

[13] A. T. Balaban, M. Mocanu and Z. Simon, *Tetrahedron*, **20**, 119 (1964); S. Bădilescu and A. T. Balaban, *Spectrochimica Acta*, **32 A**, 1311 (1976).

EXPERIMENTAL PART

Diacetylation of cyclodecene to 9,11-dimethyl-[7](2,6)-pyrylophanium perchlorate (I). Into a mixture of 13.8 g (0.1 mol) *cis*-cyclodecene[4] (purity 94.7%) and 30 ml (0.32 mol) acetic anhydride, 40 ml (ca. 0.18 mol) of Schneider's "sulphoacetic acid"[5] was added under vigorous stirring for 10 minutes. The mixture was heated to 60° when, owing to the exothermal reaction, the temperature rose to 70°. Stirring was continued for two hours with external heating at 75°, and the mixture was left overnight. Then 5 ml of 70% perchloric acid were added and the mixture was stirred vigorously at room temperature for one hour; 600 ml of anhydrous ether was added with stirring, and the heavy black oil was separated by decantation, washed with several portions of ether, and extracted with two 100 ml portions of 1% perchloric acid at 100° in the presence of charcoal. On cooling, the filtered solutions separated white crystals of perchlorate I, m. p. 210° (dec.), 0.85 g, 2.8% yield. One more recrystallization raised the m. p. to 218°, white needles. *Found*: C, 55.04; H, 7.20; Cl, 11.68%. $C_{14}H_{21}O^+ClO_4^-$ requires: C, 55.17; H, 6.95; Cl, 11.63%. Methyl-deuteration was effected[14] by refluxing the perchlorate I in CH_3COOD (prepared from equimolar $D_2O + Ac_2O$) for two hours and reprecipitating the methyl-deuterated perchlorate with anhydrous ether.

9,11-Dimethyl-[7](2,6)-pyridinophane (II). The perchlorate I was dissolved in a small amount of warm ethanol which had been acidified with a drop of perchloric acid, then the solution was treated with an excess of aqueous ammonia and refluxed for five minutes. The pyridine was extracted with ether, purified from non-basic side-products by extraction into dilute hydrochloric acid, and after alkalinization extracted with ether, dried over NaOH and distilled under reduced pressure.

Picrate of II, m. p. 171–2° (from ethanol), *Found*: C, 55.72; H, 5.82; N, 12.78%. $C_{20}H_{24}N_4O_7$ requires: C, 55.55; H, 5.59; N, 12.96%.

Piroclonate of II, m. p. 259°(dec.), from ethanol; *Found*: C, 61.63; H, 6.40; N, 14.91%. $C_{24}H_{29}N_5O_5$ requires: C, 61.65; H, 6.25; N, 14.98%.

Chloroplatinate of II, m. p. (dec.) 265° in a preheated bath (from dilute hydrochloric acid); *Found*: C, 41.11; H, 5.45; Cl, 25.95; Pt, 23.85; N, 3.25%. $C_{28}H_{44}N_2PtCl_6$ requires: C, 41.18; H, 5.43; Cl, 26.05; Pt, 23.91; N, 3.43%.

9,10,11-Trimethyl-[7](2,6)-pyridinophanium perchlorate, IV, R = Me (N-methylpyridinium salt of II) was obtained from I with excess of methylamine in aqueous ethanol, m. p. 200° (from ethanol.). *Found*: C, 57.52; H, 7.99; Cl, 10.36; N, 4.43%. $C_{15}H_{24}N^+ClO_4^-$ requires: C, 56.58; H, 7.61; Cl, 11.16; N, 4.41%.

Spectra were recorded with the following instruments: infrared spectra with a Zeiss-Jena UR-10 spectrophotometer; PMR spectra with a Varian A-60A instrument; CMR spectra with XL-100 and CFT-20 Varian instruments; ultraviolet spectra with a CF–4 Optica (Milano) spectrophotometer; visible spectra with a Unicam SP–700 instrument.

ACKNOWLEDGEMENTS. Thanks are expressed to prof. dr. G. Wilke for a generous sample of cyclodecene, to dr. V. Wray for recording the CMR spectra, to Mr. F. Chiraleu for the PMR spectra, to Mrs. M. Paraschiv for the UV spectra, to Miss E. Sliam and Mrs. V. Daniel for elemental analyses, and to dr. Simona Bădilescu for recording the visible charge-transfer spectrum of the iodide.

---

[14] E. Gârd, A. Vasilescu, G. D. Mateescu and A. T. Balaban, *J. Labelled Comp.*, **3**, 196 (1967).

Revue Roumaine de Chimie, **21**, *9–10*, 1345–1353 (1976)

NEW UREA AND THIOUREA DERIVATIVES. I

SYNTHESES, IR AND UV SPECTRA OF SOME NEW DISUBSTITUTED UREA AND THIOUREA DERIVATIVES WITH POSSIBLE PHYSIOLOGICAL EFFECTS

AURELIA BOLDEA, C. DRUGĂRIN, M. MRACEC and Z. SIMON
University of Timişoara, Bv. V. Pârvan, nr. 4.

Received January 13, 1975

Nine new urea and thiourea derivatives have been synthesized by the process of condensation of the isocyanates and isothiocyanates with primary aromatic amines, in the presence of characteristic anhidrous solvents. Experimental data are given concerning the procedure, properties of the new derivatives and the IR and UV spectra which confirm the structures attributed of the new compounds.

Urea and thiourea exhibit diuretic and antileukemic effects but their mono and disubstituted derivatives are drugs with action on the central nervous system.[1]

The new phenyl-urea and phenyl-thiourea compounds anticipate a synergism of action by means of the association of hypnosedative effect with the effects of the substituents introduced at the second nitrogen atom (i.e. anesthetic, hypoglycemic effect).

Three classes A, B, C of new compounds have been synthesized which formulae are:

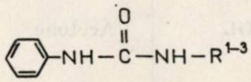

A.

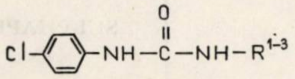

B.

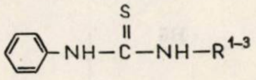

C.

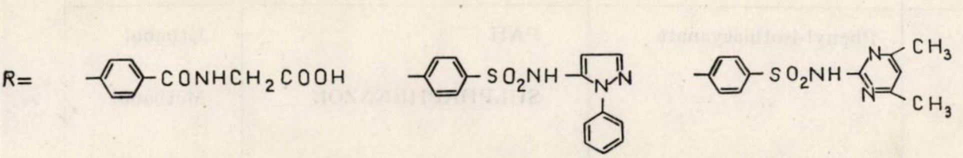

The general method of preparing these compounds consists in the condensation of isocyanates (for **1–6**) or isothiocyanates (for **7–9**) with primary aromatic amines in equimolecular quantities; the reaction temperature, time and yield are dependent on the basicity of the amines.[2,3] The synthesized products are generally crystalline colourless, insoluble in water and nonpolar solvents, but more soluble in polar organic solvents.

---

[1] S. Chaque, *J. Pharmacol.*, **138**, 224 (1962).

EXPERIMENTAL

To a solution of 0.01 m of amine in characteristic anhidrous solvent, 0.011 m of phenyl-isocyanate (for compounds A), *p*-chlorophenyl isocyanate (for compounds B) or phenyl-isothiocyanate (for compounds C) was added dropwise under continuous stirring. The time and temperature at which the reaction mixture was maintained under stirring and the separation and purification conditions are given in table 1.

The test data concerning the properties and analytical data of the new derivatives are presented in table 2.

The IR spectra have been realized in KBr pellets with Unicam SP 2006 and Perkin Elmer 417–5001 spectrophotometers.

The electronic spectra have been recorded in ethanolic solutions with a Unicam SP 800 spectrometer.

Table

Reaction and

Class Nº	Reaction parteners		Anhydrous solvent
	Iso(thio)cyanate 0.011 m	Aromatic amines 0.01 m	
A1	Phenyl-isocyanate	*p*-aminohippuric acid (PAH)	Acetone
A2	,,	5-sulphanilamido-1-phenyl-pyrazole (SULPHAPHENAZOL, ORISUL)	Acetone
A3	,,	2-sulphanilamido-4,6-dimethyl-pyrimidine (SULPHAMETHAZIN, SULPHAMIDIN)	Acetone
B4	*p*-chloro-phenylisocyanate	PAH	Acetone
B5	,,	SULPHAPHENAZOL	Acetone
B6	,,	SULPHAMETHAZIN	Acetone
C7	Phenyl-isothiocyanate	PAH	Ethanol
C8	,,	SULPHAPHENAZOL	Methanol
C9	,,	SULPHAMETHAZIN	Methanol

---

[2] W. Gerhardt, *J. prakt. Chem.*, **38**, 77 (1968).

[3] J. Dick and C. Drugarin, *Studii şi Cercetări Ştiinţifice., Chim., Baza Cercetări Şti., Timişoara*, **8**, 225 (1960).

THE STUDY OF THE IR SPECTRA

The IR spectra study of the new derivatives confirms the experimental data concerning their structure by the appearance of vibrations corresponding to urea groups and the disappearance of primary amine group vibrations. As the syntheses of the new classes of compounds presented above have been achieved by the reaction of isocyanates and isothiocyanate with physiological active aromatic amines (the amines corresponding to R_1, R_2 and R_3; see also table 1), we considered as adequate to performe a comparative study of the IR vibrations of these amines with those of the final products obtained (**1**–**9**), in the domains of characteristic frequencies: 1): 3500–3200 cm^{-1}; 2): 1750–1450 cm^{-1}; **3**): 1360–1200 cm^{-1}.

The values of the IR characteristic vibrations are given in table 3.

1

purification conditions

Reaction time (hrs)	Temperature (°C)	Products separation	Washing[a] and recrystallisation solvent[b]	Yield (%)
5	50	Precipitate	Acetone+ether (WM); E 60	75
3	Reflux	Distil. solv., dissolv. Na_2CO_3 20%, reprecip. HCl pH=6	Ethanol+ether (WM); E 100	70
3	Reflux	ibid.	Ethanol+ether (WM); E 100	75
5	50	Precipitate	Acetone+ether (WM); E 100	85
3	Reflux	Distil. solv., dissolv. Na_2CO_3 20%, reprecip. HCl pH=6	Ethanol+ether (CM); E 100	70
3	Reflux	ibid.	Ethanol+ether (CM); E 100	75
12(48 at room temp.)	10	Precipitate	Consecutive ether(W) and water(W); E 100	80
12(60 at room temp.)	10	Distil. solv., dissolv. Na_2CO_3 20%, reprecip. HCl pH=6	ibid.	70
12(60 at room temp.)	10	ibid.	ibid.	75

[a] WM – Warm mixture; CM – Cold mixture; W – Warm; C – Cold.

[b] Ethanol 60%; E 60; Ethanol 100%; E 100.

Table 2

N, N′–disubstituted urea derivatives

Class N°	Name	Formula	M.p.(°C) (solvent)	Aspect	Cryst. system	Elemental anal. calc. found.			Solubility[a)]					
						C	H (%)	N	H_2O	EtOH	Me_2CO	Et_2O	$CHCl_3$	C_6H_6
A1	N-phenyl-N′(*p*-benzoylglycin) urea	$C_{16}H_{15}N_3O_4$	220 dec. (Me_2CO)	Scaly white-beige crystals	Pseudohexagonal	61.33 61.09	4.82 4.93	13.41 13.48	ls	s	lsw	i	i	i
A2	N-phenyl-N′[*p*-phenylen(5-sulphonamido-1-phenyl-pyrazole)] urea	$C_{22}H_{19}N_5O_3S$	194 (EtOH)	Nacreous scaly crystals	Pseudohexagonal	60.95 61.43	4.41 4.56	16.14 16.30	i	ls	s	i	ls	i
A3	N-phenyl-N′[*p*-phenylen(2-sulphonamido-4,6-dimethyl-pyrimidin)] urea	$C_{19}H_{19}N_5O_3S$	219.5 (EtOH)	Microcrystl.	Rhombic pseudocubic	57.41 57.56	4.81 4.90	17.62 17.48	i	ls	s	i	ls	i
B4	N-*p*-chlorophenyl-*N′* (*p*-benzoylglycin)urea	$C_{16}H_{14}ClN_3O_4$	242 dec. (Me_2CO)	Beige microcrystl. powder	Rhombic pseudocubic	55.26 55.32	4.05 4.22	12.08 12.25	i	sw	i	i	i	i
B5	*N*-*p*-chlorophenyl-N′ [*p*-phenylen(5-sulphonamido-1-phenyl-pyrazole)] urea	$C_{22}H_{18}ClN_5O_3S$	209 (EtOH)	White crystals	Hexagonal prisms	56.47 56.30	3.88 3.95	14.96 14.78	i	sw	s	i	ls	i
B6	N-*p*-chlorophenyl-N′ [*p*-phenylen(2-sulphonamido-4,6-dimethyl-pyrimidin)] urea	$C_{19}H_{18}ClN_5O_3S$	216 (EtOH)	Microcrystl. powder	Rhombic pseudocubic	52.84 52.71	4.20 4.34	16.20 16.15	i	sw	s	i	ls	i
C7	N-phenyl-N′(*p*-benzoylglycin) thiourea	$C_{16}H_{15}N_3O_3S$	210 dec. (Me_2CO)	Scaly crystals	Pseudohexagonal	58.34 58.23	4.59 4.65	12.75 12.56	lsw	sw	lsw	i	i	i
C8	N-phenyl-N′[*p*-phenylen(5-sulphonamido-1-phenyl-pyrazole)] thiourea	$C_{22}H_{19}N_5O_2S_2$	168 (EtOH)	White crystals	Hexagonal prisms	58.78 58.80	4.26 4.32	15.57 15.45	i	s	s	i	i	i
C9	N-phenyl-N′[*p*-phenylen(2-sulphonamido-4,6-dimethyl-pyrimidin)] thiourea	$C_{19}H_{19}N_5O_2S_2$	172 (EtOH)	Milky white crystaline powder	Rhombic	55.19 55.10	4.62 4.72	16.92 16.80	i	s	s	i	i	i

a) s-soluble ; i-insoluble ; sw-soluble on heating ; ls-little soluble ; lsw-little soluble on heating.

Table 3

Comparative analytical values of characteristic vibrations in IR

The derivatives of physiological active amines used in the synthese					Class A				Class B				Class C			
R	Name	Domain (cm^{-1})			Nº prod.	Domain (cm^{-1})			Nº prod.	Domain (cm^{-1})			Nº prod.	Domain (cm^{-1})		
		1 3500 3200	2 1750 1450	3 1360 1200		1	2	3		1	2	3		1	2	3
R_1	*p*-Aminohippuric acid	3480s 3390m —	1742s 1642s 1560s	— 1320 1300 — —	1	3320s — 3220sh	1725s 1650s 1550s	— 1320s — 1245s —	4	3330s — 3220sh	1710s 1650s 1545s	— 1310s — 1238s —	7	3330 — —	1742 1650 1550	— 1320 — 1250 —
R_2	Sulphaphenazol	3480 3450 3360	— 1630s 1544m —	1315s — — —	2	3480s — 3170s	1710s — 1150s 1535	1320s — 1240s —	5	3480s — 3220s	1715s — 1545s 1538s	1310s — 1240s —	8	3370s — 3170	— — 1545s	1320m 1267m — —
R_3	Sulphamethazin	3440s 3350s 3250s	— 1649s 1545w —	1325m 1305s — —	3	3360s — 3310sh	1711s — 1550 1535	1315s — 1240m —	6	3360s — 3310sh	1711s — 1545 1540	1312s 1270s 1240s —	9	3350s — 3310sh	— — — 1534s	1315s — 1255s —

s-strong intensity; m-medium intensity; w-weak intensity; sh-shoulder.

1. ANALYTICAL STUDY IN THE FREQUENCY DOMAIN: 3500–3200 cm^{-1}

The bands which occur in the 3500–3200 cm^{-1} domain are generally due to the N–H amine and amide stretching vibrations.[4]

The starting primary aromatic amines (see table 1 and 3) exhibit two bands within this domain which are attributed to symmetrical and asymmetrical stretching vibrations. The band corresponding to asymmetrical N–H aminic vibration from *p*-aminohippuric acid (PAH) appears coupled with the N–H amide band from the molecule of the same compound.

For 2-sulphanylamido-4,6-dimethyl-pyrimidine and 5-sulphanylamido-1-phenyl-pyrazole the bands at 3360 and respectively 3350 cm^{-1} belong to N–H vibration from sulphonamide groups.

The substituted (*1–9*) NN′-urea derivatives have only one more intense and extended absorption band placed in the region of N–H stretching vibrations which is attributed to free N–H bonds.

The formation of N–H...O=C hydrogen bonds, at the substituted urea derivatives in solid state, causes the displacement of the N–H band to lower frequencies.

The urea derivatives which contain the SO_2NH group (**2, 3, 5, 6, 8, 9**) present absorbtions around 3370 cm^{-1} corresponding to the coupling of N–H sulphonamide and N–H urea vibrations.

In general, the ureas have weak absorptions at about 3200 cm^{-1} which probably occur also due to the hydrogen bonds of the urea group.[4]

The conclusion of the study of IR vibrations in this domain is the disappearance of the N–H stretching vibrations corresponding to the primary aromatic amines and the appearance of N–H stretching vibraons of the secondary amides.

2. THE ANALYTICAL STUDY IN THE 1750–1450 cm^{-1} FREQUENCY DOMAIN

The bands characteristic of amine (N–H deformation) and amidic (amide I band, amide II band) groups appear in this region together with the other bands, characteristic of the groups of the molecules of the initial products (COOH, C=N from heterocycles).

In order to estimate the absorption with greater precision we can subdivide this region into three parts: 2.1): 1750–1650 cm^{-1}; 2.2): 1650–1580 cm^{-1}; 2.3): 1580–1450 cm^{-1}. We shall refer below to each part separately.

2.1. In general, the vibrations of C=O group of amides, urea and carboxyl acids appear in this domain.[5]

The ureic C=O stretching vibration appears in our case at unusually high frequencies because the amidic conjugation is changed by the double substitution with electron attracting group on the ureic nitrogen.

The frequency of 1725 cm^{-1} at which the C=O band from the urea derivatives of *p*-aminohippuric acid appears is due to the coupling of the

---

[4] M. Avram and Gh. D. Mateescu, "Spectroscopia în Infraroşu", Editura tehnică Bucureşti, 1966, p. 524.

[5] A. D. Gross, "Introduction to Practical Infra-red Spectroscopy", Butterworths, London, 1960, p. 60.

C=O vibration of urea with the C=O vibration of carboxyl. The C=O band from the carboxyl group appears for PAH at the frequency of 1742 cm^{-1}.

2.2. This frequency domain is characteristic of the N—H deformation vibration, all primary amines exhibiting bands in this region.

Thiourea compounds of 5-sulphanylamido-1-phenyl-pyrazole and 2-sulphanylamido-4,6-dimethyl-pyrimidine, do not present absorptions in this domain. In addition, the *p*-aminohippuric acid posses in its molecule an amide group and its C=O stretching vibration appears coupled with the N—H deformation vibration from the NH_2 group.

By the disappearance of the NH_2 group, the band of the *p*-aminohippuric acid urea derivatives is displaced with $+8\ cm^{-1}$ as compared to the amine one. In this domain there appear some additional intense vibrations (such as C=C stretching vibrations from the aromatic ring) which have not been listed in table 3.

2.3. The interval 1575—1480 cm^{-1} corresponds to the amide II band and is attributed to the deformation vibration of the secondary amide N—H bond.

Such bands occur at *p*-aminohippuric acid, 5-sulphanylamido-1-phenyl-pyrazole and 2-sulphanylamido-4,6-dimethyl-pyrimidine (at average intensity for the last two products). They are caused by the CONH group, and respectively C=N group of heterocycles. In this interval the intramolecular —NH...O=C— hydrogen bonds and the coupling of the amide II band with the C=N band from heterocycles determines the occurrence of a doublet for all urea derivatives. The vibrations corresponding to the aromatic ring and those of C—H deformation from $-CH_2-$ occur here too.

In conclusion the presence of the vibrations corresponding to amide I and amide II bands at the derivatives **1—9** as well as the disappearance of the N—H deformation vibration, confirm the urea structure of the new products.

3. THE ANALYTICAL STUDY IN THE 1360—1200 cm^{-1} FREQUENCY DOMAIN

This frequency domain corresponds to stretching vibration (C—N of amine, C—O of acids), amide III bands and to the sulphonamide band of 2-sulphanylamido-4,6-dimethyl-pyrimidine and 5-sulphanylamido-1-phenyl-pyrazole and their derivatives.[4] At *p*-aminohippuric acid 2-sulphanylamido-4,6-dimethyl-pyrimidine and 5-sulphanylamido-1-phenyl-pyrazole the C—N vibration appears coupled with the C—O (carboxyl), respectively with the $-SO_2NH-$ group vibration at about 1300 cm^{-1}.

All urea derivatives exhibit at about 1240 cm^{-1} the amide III band attributed to some vibrations which involve the O—C—N and N—H bonds.

At the thiourea compounds, the C=S and C=N vibrations from the NH—CS—NH group appear associated with frequencies of about 1260 cm^{-1}.

We can conclude that the comparative study of the IR spectra confirms the attributed structure of the new synthesized derivatives.

THE STUDY OF ELECTRONIC SPECTRA

In order to clear up the nature of bands which occur in the electronic spectra, the spectra of the synthesized substances are compared with those of known derivatives, with similar groups, given in the literature (table 4).

Table 4

The position of absorption maxima (λ) and the molar extinction coefficients (lgε) in electronic spectra

Substance[a)]	lit.	Solvent	λ_1 nm	lgε	λ_2 nm	lgε	λ_3 nm	lgε
Benzaldehyde	6	heptane	339	1.43	288	2.86	240	4.09
		alcohol	—	—	281	3.08	246	4.01
p-amino acetophenone	7	heptane	330	—	284	4.29	223	4.02
		alcohol	—	—	319	4.33	—	—
Diphenylurea	8	alcohol	—	—	256	4.57	—	—
Phenylurea	9	alcohol	—	—	273	3.0	237	4.2
Thiourea	8	alcohol	280	1.8	—	—	240	1.2
A_1		alcohol	—	—	280	5.89	209	5.64
A_2		alcohol	—	—	263	5.00	204	4.93
A_3		alcohol	—	—	275	4.99	207.5 (222)	4.85 (4.70)
B_4		alcohol	—	—	280	5.02	212	4.59
B_5		alcohol	—	—	264	5.08	208	4.91
B_6		alcohol	—	—	273	5.31	218	5.06
C_7		alcohol	—	—	275	5.22	221.5	5.34
C_8		alcohol	—	—	278	3.77	214 (250)	3.69 (3.68)
C_9		alcohol	—	—	275	5.22	221.5	5.34
			$n-\pi^*$ transition		$\pi-\pi^*$benzene transition		Charge transfer	

a) Nomenclature of compounds **1** to **9**, see table 2.

It should be noticed that the recorded spectra exhibit generally 2 bands : 260—290 nm and 200—240 nm.

---

[6] L. Lang, "Absorption Spectra in the Ultraviolet and Visible Region", Vol. IV, Akadémiai Kiadò, Budapest, 1963, p. 63.

[7] J. Tanaka, S. Nagakura and M. Kobayasi, *J. Chem. Phys.*, **24**, 311 (1956).

[8] "Organic Electronic Spectral data", Vol. II, Interscience, New York, 1957, p. 151.

[9] "Organic Electronic Spectral data", Vol. V, Interscience, New York 1957, p. 15.

[10] A. Gillem and E. Stern, "Electronyc Spectry Pogloshchenia Organicheskich Soedinenii" Izdatelstvo Inostrannoi Literatury, Moskva, 1957, p. 93.

The first band coresponds probably to $\pi-\pi^*$ transitions, and orriginates in the displacement of the first band (at 260 nm) of benzene.

The second band may be attributed to a transition characteristic to the substituent of the aromatic ring. This conclusion is strengthened in comparison with the bands from the spectra of ureic and thioureic derivatives given in literature.

Comparing the values of λ at which the bands of the recorded spectra occur one can notice that the derivatives which contain the same substituents at the nitrogen atom present a bathochrome displacement for thioureic derivatives. This particular displacement is generated by the influence of C=S group which is a stronger chromophore than the C=O group.[10]

The influence of the chlorine in para position at the substances from class B seems to be relatively small. This results from the fact that the corresponding displacements in spectra are negligible.

In conclusion the comparative study of IR and UV spectra, as well as the analytical results, confirm the structure and purity of the new synthesized derivatives.

Revue Roumaine de Chimie, **21**, *9–10*, 1345–1353 (1976)

6 – c 1339

Revue Roumaine de Chimie, **21**, *9–10*, 1355–1357 (1976)

SELECTIVITY IN THE ALKYLATION OF BENZENE BY CYCLOPROPANE*

I. PARCHAMAZAD, M. KHOSROVI and N. SADEGHI
Department of Chemistry, Faculty of Science, Tehran University,
Tehran, Iran

Received January 14, 1975

Under the conditions described in this paper it is possible to prepare *n*-propylbenzene selectively by the alkylation of benzene by cyclopropane. The effect of the amount and the kind of the catalyst, the effect of the duration of the reaction upon the distribution of monoalkylbenzenes, the effect of the change of the temperature and the mutual effects of these parameters were investigated.

Alkylation of benzene by olefines is well known.[1] Cyclopropane is also capable of alkylating benzene, to produce *n*-propylbenzene and isopropylbenzene.[2,3,4] Some efforts have been previously carried out to ellucidate the mechanism of this alkylation.[5,6,7,8]. The present work pertains to the study of the selectivity in alkylation of benzene by cyclopropane.

Under various experimental conditions, alkylation of benzene by chemically pure cyclopropane in the presence of different catalysts, such as sulphuric acid and anhydrous aluminium chloride, has been investigated by the authors. Using sulphuric acid — under the same conditions as described by IPATIEFF[2] — a mixture containing *n*-propylbenzene (I), isopropylbenzene (II), *n*-propylsulphate and some unidentified polyalkylated compounds was obtained, which was not in accordance with the results previously obtained.[2]

[1] V. N. Ipatieff, B. B. Corson and H. Pines, *J. Amer. Chem. Soc.*, **58**, 919 (1936).
[2] V. N. Ipatieff, H. Pines and B. B. Corson, *J. Amer. Chem. Soc.*, **60**, 577 (1938).
[3] I. Parchamazad, M. Khosrovi and N. Sadeghi, Abstracts of papers, Vol. 23, IUPAC, o-c-7, 114, Boston, 1971.
[4] V. A. Siderov, B. V. Ioffe and B. V. Stolyarov, *Chem. Abstr.*, **77**, 139111 (1972) and *Doklady Akad. Nauk S.S.S.R.*, **205** (3), 585 (1972) (Chem.) (Russ.).
[5] E. S. Corner and R. N. Pease, *J. Amer. Chem. Soc.*, **67**, 2067 (1945).
[6] H. Pines, D. Huntsman and V. N. Ipatieff, *J. Amer. Chem. Soc.*, **75**, 2315 (1953).
[7] N. C. Deno, D. Lavietes, J. Mockus and P. C. Scholl, *J. Amer. Chem. Soc.*, **90** (23), 6457 (1968).
[8] R. L. Baird and A. Aboderin, *J. Amer. Chem. Soc.*, **86**, 252 (1964).

---

[*] The abstract of an approach to this research[3] was presented at the XIIIth International Congress of Pure and Applied Chemistry, Boston, 1971.

The increase in the duration of the reaction - at least up to 30 min. —did not seem to affect the ratio of (I) to (II), but evidently raised the yields of monoand polyalkyl benzenes.

Under the best selective conditions (experiment No 1), we prepared selectively *n*-propylbenzene "99% (I) and 1% (II)". By analyzing the data in table 1, it was found that in the presence of sulphuric acid the ratio of (I) to (II) decreased with the increase of the temperature of the reaction mixture and also with augmentation of the relative amounts of the catalyst to benzene. These results did not agree with those recently described by Stolyarov.[9] However, in the presence of aluminum chloride catalyst, the effect of the change of temperature and the amount of catalyst seemed to be negligible on the distribution of the two isomers. The experimental results are summarized in table 1.

Table 1

Alkylation of benzene by gaseous cyclopropane under different experimental conditions

Experiment	Benzene in ml	Type of Catalyst	Amount of Catalyst	Temperature °C	$\frac{n\text{-propylbenzene}}{\text{isopropylbenzene}}$
1	100	H_2SO_4	2 ml	~2	≥99/1
2	—		—	~30	89/2
3	—	—	—	Reflux	90/10
4	—	—	10 ml	~2	96/4
5	—	—	25 ml	5–8	93/7
6	—	—	—	~30	88/12
7	—	—	—	Reflux	23/77
8*	50	—	12.5–50 ml	~2	96/4 to 90/10
9*	—	—	25 ml	40–45	59.5/40.5
10	100	$AlCl_3$	4 gr	~2	60/40
11	—	—	—	~40	58.5/41.5
12	—	—	—	Reflux	59.5/40.5
13	—	—	10 gr	~30	61/39
14	—	—	20 gr	~30	61.5/38.5
15	—	—	—	Reflux	59.5/40.5
16*	25	—	1–2 gr	~2	67/33 to 64/36

I.C.I. cyclopropane and Edison cyclopropane (Anesthesia grade) were both used. Merck sulphuric acid and Riedel anhydrous aluminium chloride were utilized.

---

[9] B. V. Stolyarov, V. A. Siderov and B. V. Ioff, *Chem. Abstr.*, **73**, 25020 (1970) and *Doklady Akad. Nauk S.S.S.R.*, **191** (2), 369 (1970), (Chem.) (Russ.).

In all cases except in experiments No 8, 9, 16 cyclopropane was introduced into the aromatic. The latter was placed in a reactor equipped with a reflux condenser, a mixing system, and a gas inlet tube passing through the condenser into the reaction mixture. The reactor was placed in a suitable thermostatic bath. In experiments No 8, 9, 16 cyclopropane was first dissolved in benzene at the given temperature and the catalyst was then added to the mixture.

After the end of each run, bubbling of cyclopropane was stopped and then the mixture was stirred for another ten minutes. The catalyst was separated either by filtration or decantation. The non-aqueous layer was then washed several times with water until no acidity or alkalinity was observed. The organic layer was carefully collected and dried over anhydrous magnesium sulphate.

The products were analyzed qualitatively and quantitatively by the comparison of their chromatograms with those of authentic mixtures and the interpretation of their N.M.R. spectra. The experimental apparatus used in this work included a Varian Aerograph gas chromatograph (series 1800) and a T-60 Varian N.M.R. spectrometer.

ACKNOWLEDGEMENTS. A. Guillemonat, Professor of Organic and Applied Chemistry, Aix-Marseille University, and Director of Marseille College of Chemistry, for his scientific cooperation.

Miss M. Fakhrai for her help on preparation of the chromatograms.

Revue Roumaine de Chimie, **21**, *9–10*, 1359–1366 (1976)

POLAROGRAPHIC MAXIMUM OF COBALT (II)

SUDARSHAN LAL
The Thomas Hunt Morgan Institute of Genetics
628 North Broadway
Lexington, Kentucky 40508, U.S.A.

Received January 28, 1975

The dependence of first kind negative maximum (Cobalt (II) in KCl) on capillary characteristics and depolarizer concentration has been studied. The current was found to vary as $m^{0.71}t^{0.68}$, close to the previously reported and theoretically predicted dependence on $m^{2/3}t^{2/3}$. At high flow rates (mixed maximum of first and second kind present), intermediate values for these exponents were obtained. It is noteworthy that by inspection of the exponents of m and t, maximum can be characterized. The depencence on concentration of the current seems to be potential variant and varies between 0.8 to 1.50. Current-time behaviour in impure and purified solutions is discussed.

INTRODUCTION

Polarographic electro-reduction of cobalt (II) has been studied earlier by several workers.[1–3] Suppression of cobalt maximum by aliphatic alcohols and inorganic ions was reported by Lal and Srivastava.[4–5] A recent study on cobalt (II) maximum in KCl based on classical trends has been published by Gaur and coworkers [6]. Several of the earlier classical reports on maxima lacked control of precise conditions e.g. flow rate (useful in maximum characterization), solution purity, three electrode circuitry with a positive feed back to ensure that currents are not limited by solution resistance, conductivity of solution and capillary geometry. Thus, it seems difficult to compare and generalize the results of some earlier workers where experimental conditions were poorly controlled and this has resulted sometimes in experimental artefacts which may not be the true behavior of a given system. A survey of the previous literature shows that most of the work with maxima of the first kind was carried without IR compensation in two electrode mode and shapes of maxima obtained in the absence of resistance control (failing the use of positive feed back) were quite different.[7] Sparse data are available concerning the dependence of strea-

---

[1] R. Brdicka, *Coll. Czech. Chem. Comm.*, **2**, 489, 545 (1930); **3**, 596 (1931).

[2] J. Prazler, *Coll. Czech. Chem. Comm.*, **3**, 406 (1931).

[3] K. Zutshi, and D. S. Jain, *J. Electroanalyt. Chem.*, **5**, 389, 392 (1963).

[4] S. Lal and S. N. Srivastava, *Indian J. Chem.*, **6**, 382 (1968).

[5] S. Lal and S. N. Srivastava, *Indian J. Appl. Chem.*, **32**, 287 (1969).

[6] J. N. Gaur, D. S. Jain and A. K. Maheshwari, *Indian J. Chem.*, **12**, 390 (1974).

[7] F. M. Hawkridge, T. W. Holt and H. H. Bauer, *Analyt. Chim. Acta*, **58**, 203 (1972).

ming polarographic maxima on the rate of mercury flow, *m* and drop time, *t*. For maxima of the first kind, it has been reported[8] that the current varies as $m^{2/3}t^{2/3}$ and current with a given capillary remained unaltered with change in the mercury head.[9] On the other hand, several reports have mentioned the decrease in current with increase in head of mercury.[10-12] Similarly, different values have been reported for the dependence of current on concentration of electroactive species : 1.4 (Heyrovsky and Vavricka)[13] 1.5 (von Stackelberg and Doppelfeld)[14] or 1.6–1.8 (Kryukova).[15] A recent study on positive maximum of first kind (Cu(II) in Na_2SO_4) and second kind maximum (Cd in Satd. KCl) has shown the dependence on capillary characteristics and depolarizer concentration under carefully controlled conditions.[16] In the present communication, results on negative maximum of cobalt in potassium chloride on several aspects e.g. dependence of maximum current on capillary characteristics, depolarizer concentration, effect of mercury pressure, IR compensation, solution purity, current-vs.-time behaviour are presented. It is shown that exponents of *m* and *t* can be used for characterization of a maximum provided the experiments are done under carefully controlled conditions.

EXPERIMENTAL

Polarograms were recorded with a Princeton Applied Research Corporation Electrochemistry System Model 170 in the three electrode mode in conjunction with a mechanical droptimer Model 172. The drop-time was controlled in the range of 0.5 to 5 secs ; *m* values were between 1.10–3.38 mg. sec.$^{-1}$Higher flow rates were achieved with a short capillary. A saturated calomel electrode (S.C.E.), isolated from the polarographic cell with a salt bridge containing the same solution as in the cell, served as reference whereas a mercury pool acted as a counter electrode. Current-vs.-time behaviour was monitored with a Tektronix Model 502 A oscilloscope fitted with a C–12 camera. Streaming of the solution was observed with a small stereo-microscope (Anchor Optical Co. magnification 4X–10X) in the presence of suspended particles of charcoal. The relative distances between the mercury pool, capillary tip and reference electrode bridge were kept identical (extent of streaming seemed to vary with change in shielding of capillary).[17]

The mercury was triple distilled (Bethlehem Instrument Co). Double distilled water (final distillation in alkaline $KMnO_4$) and A. R. grade cobalt chloride and potassium chloride were used for preparation of solutions.

Purification of solutions was done as described earlier.[18] All studies were done at 25±0.1°C in a thermostated water-jacketed cell with a window used for streaming observations.

[8] J. Dvorak, "Proceedings 1st. Congress Polarographie", vol. 3, Prague, 1951, p. 418.

[9] J. Heyrovsky and J. Kuta, "Principles of Polarography" Czechoslovak Academy of Sciences, 1965, Prague, Ch. XIX.

[10] L. Meites, "Polarographic Techniques", 2nd edn. Interscience, New York, 1965, Ch. VI.

[11] I. M. Kolthoff and J. J. Lingane, "Polarography", 2nd edn. Interscience, New York, 1952, Ch. X.

[12] L. Holleck, S. Vavricka and M. Heyrovsky, *Z. Naturforsch.*, **226**, 1226 (1967).

[13] M. Heyrovsky and S. Vavricka, *Coll. Czech. Chem. Comm.*, **34**, 1204 (1969).

[14] M. von Stackelberg and R. Doppelfeld, "Advances in Polarography", vol. 1, Pergamon Press, Oxford, 1960, p. 68.

[15] T. A. Kryukova, *Z. phys. Chem. (Leipzig)*, **212**, 247 (1959).

[16] A. Kumar and H. H. Bauer, *J. Electroanalyt. Chem.*, **45**, 187 (1973).

[17] S. Lal, Unpublished Results.

[18] S. Lal and H. H. Bauer, *J. Electroanalyt. Chem.*, **51**, 319 (1974).

The current in general depends on $^{x}m^{y}t^{z}C$ where C is the concentration of the electroactive species. The exponents x, y and z were determined by plotting the logarithm of the current against the logarithm of the relevant parameter ; in all cases, a linear relationship was found. The current-time curves were also analyzed similarly by log plots.

RESULTS AND DISCUSSION

Cobalt (II) in KCl shows a typical negative maximum of the first kind in the potential range −1.35 to −1.45 V vs. S.C.E. The maximum occurs over a limited potential range with an upward motion starting from bulk of solution to the bottom of drop, towards its neck and then away from it.

RESISTANCE EFFECTS

In most of the solutions used, polarograms in a three electrode mode prevented satisfactorily control of the current magnitude by the resistance of the circuit as described earlier.[18] However, at concentration of cobalt greater than 5 mM in supporting electrolyte 0.1 M KCl and in more dilute electrolytes, resistance seemed to play an important role and positive feed back to accomplish compensation was required. Figure 1 shows the effect of IR compensation both at high and low mercury flow rate. The i_{max} is increased and E_{max} shifts to more anodic potentials which is due to elimination of resistance effects.

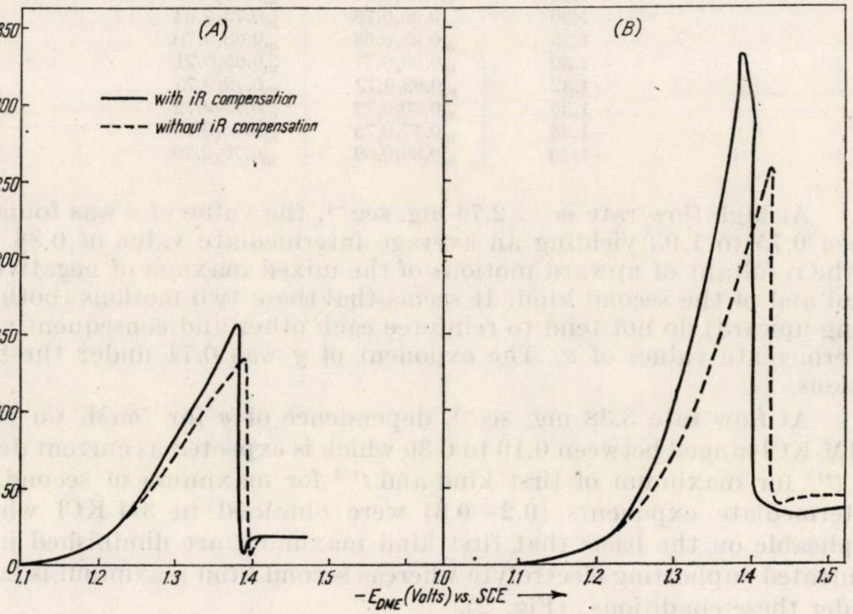

Fig. 1. — Polarograms of 5mM Co (II) ; in 0.1M KCl with three electrode circuitry with and without iR compensation at flow rates

(A) 1.10 mg. sec^{-1}. (B) 2.74 mg. sec^{-1}.

DEPENDENCE ON CAPILLARY CHARACTERISTICS

Current measurements were carried out at various potentials in the range −1.15 V to −1.40 V for *m* values between 1.10 to 2.74 mg. sec^{-1}, *t* varying from 0.5 sec to 5 sec. Studies were done with a long and short capillary in order to cover a wide range of flow rates. The value of x was almost independent on each of the parameters varied within these ranges. At low flow rates, the value of x ranged 0.63−0.75 mean value = 0.71 which is found to be slightly higher than cited value of 0.66. The value of y was found to be 0.68, average deviation of 0.04 for 30 determinations. (Table 1). An upward streaming was clearly observed under these conditions.

Table 1

Dependence of current on capillary characteristics as a function of potential with negative maximum : 5 *m* M Co (II) in 0.1 M KCl

Potential Volts vs. S.C.E.	Current varies as	
	at m values (1.90−2.74 mg. Sec^{-1}.)	at m values (1.10−1.34mg. Sec^{-1}.)
−1.15	$m^{1.05}t^{0.94}$	$m^{0.75}t^{0.65}$
−1.20	$m^{0.95}t^{0.78}$	$m^{0.73}t^{0.64}$
−1.25	$m^{0.95}t^{0.68}$	$m^{0.63}t^{0.70}$
−1.30	$m^{0.90}t^{0.71}$	$m^{0.66}t^{0.71}$
−1.32	$m^{0.83}t^{0.72}$	$m^{0.72}t^{0.73}$
−1.35	$m^{0.80}t^{0.72}$	$m^{0.73}t^{0.72}$
−1.38	$m^{0.77}t^{0.73}$	$m^{0.75}t^{0.70}$
−1.40	$m^{0.80}t^{0.69}$	$m^{0.70}t^{0.70}$

At high flow rate $m = 2.74$ mg. sec^{-1}, the value of x was found between 0.75 to 1.05 yielding an average intermediate value of 0.88 which is the resultant of upward motions of the mixed maxima of negative first kind and of the second kind. It seems that these two motions (both streaming upward) do not tend to reinforce each other and consequently yield intermediate values of x. The exponent of y was 0.71 under these conditions.

At flow rate 3.38 mg. sec^{-1}, dependence of y for 5mM Co (II) in 0.1M KCl ranged between 0.10 to 0.30 which is expected as current depends as $t^{2/3}$ for maximum of first kind and $t^{1/6}$ for maximum of second kind. Intermediate exponents (0.2−0.3) were obtained in 3M KCl which is explicable on the basis that first kind maximum are diminished in concentrated supporting electrolyte whereas second kind maximum is favored under these conditions. (Fig. 2).

At low value of m(1.17 mg.sec.$^{-1}$), y varied in the range of 0.67−0.75 which is in close agreement to the accepted value of 0.67 in 0.1 M KCl whereas in 3M KCl, y values ranged between 0.29−0.88 (potential variant) which are intermediate values due to mixed motion of streaming for maximum of first and second kinds. This is but natural as high flow rate and concentrated supporting electrolyte favor maximum of second kind and retard the first kind maximum. This is supported by a typical polarogram (*C*) in figure 2 where the maximum height is rendered low due to the two counteracting effects.

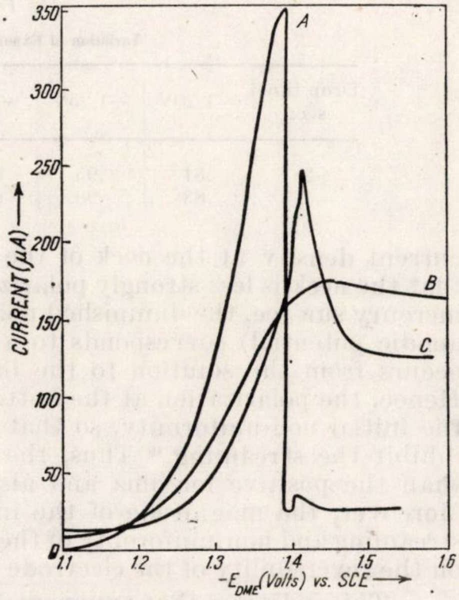

Fig. 2. — Polarograms of 5mM Co (II) in
(A) 0.1M KCl; m = 1.10 mg sec.$^{-1}$
(B) 3.0M KCl; m = 3.38 mg. sec.$^{-1}$
(C) 0.1M KCl; m = 3.38 mg sec.$^{-1}$

DEPENDENCE ON CONCENTRATION OF DEPOLARIZER

With IR compensation and increasing concentration of cobalt in 0.1M KCl, maximum increased non-linearly and this behavior is due to the non-diffusion process accompanied by upward streaming motion in the immediate vicinity of mercury drop. $E_{\max}$ is shifted to more cathodic potentials (Table 2).

Table 2

Co (II) maximum at varying concentration of depolarizer t**=2 Sec.** m **= 1.10 mg. Sec.**$^{-1}$

Conc. Co (II) mM	$-E_{\max}$ V vs. S. C. E.	$i_{\max}$, μa
1	1.340	7
2	1.370	29
3	1.395	62
5	1.440	166

Experiments at controlled m and t reveal that z seems to be potential dependent and lower values are met with at the beginning of the step. (Table 3). The values of z are lower than those reported for the positive maximum of the first kind. This can be explained on the basis of gradients in current density, surface tension and induced depolarizer effect. The current density at the neck of the drop is lower than at the bottom, so that the neck is less strongly polarized (more anodic) at negatively charged mercury surface, the diminished polarization at the neck of the drop (more anodic potential) corresponds to a higher surface tension and streaming occurs from the solution to the bottom of the drop then to the neck. Hence, the polarization at the bottom is decreased and this acts to lessen the initial non-uniformity, so that the induced depolarizer effect acts to inhibit the streaming.[19] Thus, the negative maxima tend to be smaller than the positive maxima and also cover a smaller range of potential. Moreover, the magnitude of the induced depolarizer effect, intensity of streaming and non-uniformity of the interfacial current-distribution depend on the reversibility of the electrode reaction.

Table 3

Variation of Exponent 'Z' with Potential

Drop time sec.	−1.20V	−1.25V	−1.30V	−1.33V	−1.35V	−1.40V
2	.81	.95	1.08	1.12	1.20	1.54
1	.83	.90	1.08	1.15	1.29	1.57

This indicates that exponent Z is potential dependent and is suggestive of the conclusion that maximum begins at a definite potential on the rising step[20,21] and it increases to the highest value at $E_{\max}$. It shall be interesting to study the potential dependence of maxima of other systems on depolarizer concentration.

EFFECT OF VARYING HEIGHTS OF MERCURY COLUMN

In purified solutions with 5mM Co(II) in 0.1M KCl, mercury height was varied and polarograms recorded with iR compensation. The results are summarized in table 4.

The percentage deviation from average value of maximum current varied in the range of ±3.0%, which is the limit of reproductibility. This shows that negative maximum of first kind is independent of mercury pressure. Earlier reports by Dvorak,[8] Kumar and Bauer [16] and others[22] have also shown that current is invariant as the height of the mercury column is altered with a given capillary. However, a recent report on cobalt maximum by Gaur and co-workers [6] shows that the maximum is decreased with the decrease in mercury height which is misleading and is caused presumably by lack of iR compensation, solution purity, and control of mercury flow rate. Normally, with pure solutions (absence of surfactants), three electrode circuitry and a positive feed back to counteract the uncompensated resistance, no effective change in the height of maximum is encountered under these conditions.

---

[19] V. G. Levich, "Physicochemical Hydrodynamics" Prentice-Hall, 1962, New York, pp. 561–590.

[20] M. Heyrovsky, *Rev. Chim. Mineral*, **5**, 403 (1968).

[21] F. M. Hawkridge and H. H. Bauer, *Analyt. Chem.*, **43**, 768 (1971).

[22] H. Hasselbach and D. K. Schwabe, *Z. phys. Chem. (Leipzig)*; Sonderheft, **209**, 17 (1958).

Table 4

5mM Co (II) Maximum at Varying Mercury Heights

Height, Cms.	m, mgs sec. $^{-1}$	i_{max}, μ_a	%Deviation from average (320 μ_a)
110.7	2.74	323	+0,93
90.7	2.25	325	+1.56
76.0	1.90	318	−0.62
62.4	1.78	312	−2.50
54.2	1.53	330	+3.12
47.0	1.34	310	−3.12
38.6	1.10	322	−0.62

CURRENT-TIME BEHAVIOUR

Typical current-time ($i-t$) curves of cobalt (II) maximum in impure and purified solutions are presented in figure 3. Log plot analysis indicated that exponents of t in early drop life vary from 0.42 to 0.52 and as the

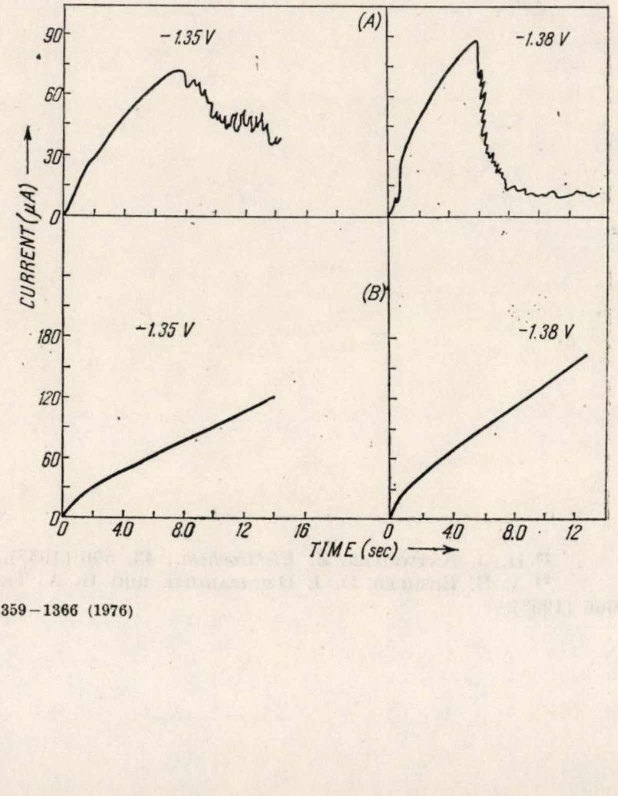

Fig. 3. — Current vs. time behaviour in
(A) Unpurified (B) Purified solutions. 5mM Co (II) in 0.1M KCl at potentials indicated.

drop grows in greater size, the exponent increases which is due to increased surface area accentuating upward streaming till the exponent reaches values ranging from 0.67—0.73 in purified solutions whereas in impure solutions, exponents in the later part of drop life varied between 0.52—0.60. Thus, surfactant impurities tend to diminish the exponent which increases in purified solutions. Current-time patterns are especially distorted, kinky with irregular fluctuations at high concentration of depolarizer in impure solutions and then irregularities arise from adsorption or/turbulence in the streaming of the solution and or mercury. Current-time curves with irregular oscillations indicative of irregular pulsation of mercury surface have been also observed by Antweiler [23] and Ershler et al.[24] on other systems. At longer drop times, in impure solutions, the decrease in current at the end of drop life is ascribed to adsorption of surfactants which is favored with longer drop life (figure 3B).

ACKNOWLEDGEMENT. The author is grateful to Prof. H. H. Bauer for laboratory facilities and guidance. The author also expresses thanks to Mr. V. B Dixit for this technical assistance.

---

[23] H. J. Antweiler, *Z. Elektrochem.*, **43**, 596 (1937)., **44**, 719, 831, 888 (1938).

[24] A. B. Ershler, D. I. Dzhaparidze and G. A. Tedoradze, *Zhur. fiz. Khim*; **37**, 666 (1963).

Revue Roumaine de Chimie, **21**, *9–10*, 1367–1372 (1976)

KINETIC STUDIES ON THE COPOLYMERIZATION OF β-PROPIOLACTONE WITH EPICHLOROHYDRIN AND 1,3-DIOXEPANE

DAN DONESCU

Institute of Macromolecular Chemistry "P. Poni", Polymerization Process Departament,
Bucharest, Str. Dumbrava Roşie 18, Romania

Received January 14, 1975

The paper studies the kinetics of the copolymerization of β-propiolactone(PL) with epichlorohydrin(ECH) and 1,3-dioxepane(DH) in the presence of the catalyst BF_3OEt_2. The initial consumption rates of ECH and DH decrease in the presence of PL due to its complexing ability with cationic active sites. Owing to the smaller basicity of PL relative to that of ECH and DH, lactone reactivity is smaller than that of the studied cyclic ether and cyclic formal.

1. INTRODUCTION

The cationic copolymerization of β-propiolactone with cyclic ethers and cyclic formals has been studied extensively.[1-10] The existing literature reports that the formed copolymers do not have a statistical structure,[2-4,8,9] and PL has a different behaviour in copolymerization due to its complexing ability with cationic active sites.[8-10]

This paper studies the kinetics of the copolymerization of PL with epichlorohydrin and with 1,3-dioxepane using as catalyst BF_3OEt_2 in order to establish the manner in which the presence of the complexing comonomer, PL, influences the consumption rates of monomers.

[1] K. Frisch and S. Reegen, "Ring-Opening Polymerization", M. Dekker, New York, 1969.

[2] K. Tada, T. Saegusa and J. Furukawa, *Kogyo Kagaku Zasshi*, **66**, 1561 (1963); *Chem. Abstr.*, **61**, 727 (1964).

[3] K. Tada, T. Saegusa and J. Furukawa, *Makromol. Chem.*, **71**, 71 (1964).

[4] K. Tada, T. Saegusa and J. Furukawa, *Makromol. Chem.*, **102**, 47 (1966).

[5] H. Cherdron and H. Ohse, *Makromol. Chem.*, **92**, 213 (1966).

[6] T. Tsuda, T. Shimizu and Y. Yamashita, *Kogyo Kagaku Zasshi*, **67**, 1661 (1964); *Chem. Abstr.*, **62**, 10519 (1965).

[7] T. Tsuda and Y. Yamashita, *Makromol. Chem.*, **86**, 301 (1965).

[8] Y. Yamashita, T. Asakura, M. Okada and K. Ito, *Macromolecules*, **2**, 613 (1969).

[9] K. Ito, T. Inoue and Y. Yamashita, *Makromol. Chem.*, **139**, 153 (1970).

[10] Y. Yamashita, S. Kozawa, M. Hirota, K. Chiba, H. Matsui, A. Hirao and K. Ito, *Makromol. Chem.*, **142**, 171 (1971).

2. EXPERIMENTAL

The working procedure and the purification of reagents were similar to those mentioned in earlier works.[11,12] The reaction temperature was 30° and the concentration of BF_3OEt_2 was $1.5 \cdot 10^{-2}$ mol/l for the PL + ECH comonomer system and $3.0 \cdot 10^{-2}$ mol/l for the PL+DH system.

The chromatographic analysis of unreacted monomers was performed by means of a column of 25% LB polypropyleneglycol on Chromosorb P 30/60 mesh. The temperature of the column was 85° for PL+ECH and 100° for PL+DHD.

3. RESULTS AND DISCUSSION

3.1. COPOLYMERIZATION OF β-PROPIOLACTONE WITH EPICHLOROHYDRIN

The comonomer system studied in this section consists of a more basic monomer, ECH($pK_b = 8.84^{13}$) and a less basic monomer, PL($pK_b = 10.06^{13}$). For this reason the PL consumption rate in the presence of ECH is much smaller than that established for homopolymerization (Fig. 1).

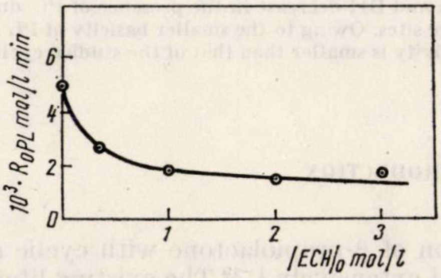

Fig. 1. — Dependence of initial consumption rate of PL on the initial concentration of ECH($|ECH|_0$). ($|PL|_0$ = 2 mol/l, $|PL|_0$ = initial concentration of PL).

The initial consumption rate of ECH is also affected by the presence of the other comonomer (Fig. 2).

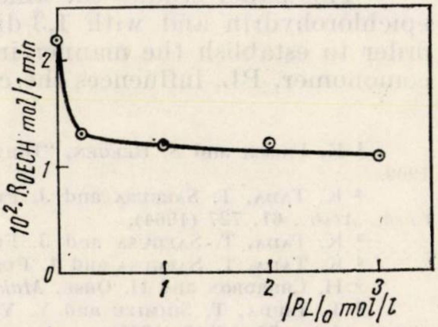

Fig. 2. — Dependence of the initial consumption rate of ECH on $|PL|_0$($|ECH|_0$ = 1mol/l).

The decrease of this rate in the presence of the less basic monomer is certainly due to the interaction ability of the C=O group of lactone ring, interaction which has as result a decrease in the activity of the active site.[8-10,14] The decrease of the reaction rate of more basic cyclic ethers in the presence of less basic lactones was also observed and attributed to coordination in the case of tetrahydrofuran(THF) copolymerization with ε-caprolactone [14] or with diketene.[15] A decrease of the polymerization rate of cyclic ethers such as THF[16] and even PL[17] also appears in the presence of polyesters or of low-molecular weight linear esters. Since the ring-opening of PL results in structural units similar to linear esters, this means that the growing active sites may complex at the beginning of the polymerization process with lactone and, at high conversions, also with the ester group of the polymer.

The initial consumption rates of each monomer will be directly proportional with the initial concentration of the proper monomer if the concentration of the other monomer is constant (Fig. 3, 4).

The dependence of the initial consumption rate of ECH on the first power of its concentration shows that, in the case of the studied comonomer system, its consumption in the initiation reaction is not so important as in the case of the copolymerization with DH.[12] Hence it results that the appearance of the catalyst complexing with the carbonyl from lactone modifies even the initial processes of formation of active sites.

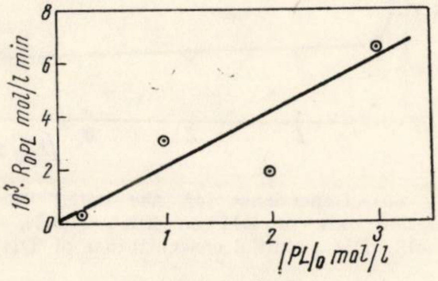

Fig. 3. — Variation of the initial consumption rate of PL depending on $|PL|_0$ ($|ECH|_0 = 1$ mol/l).

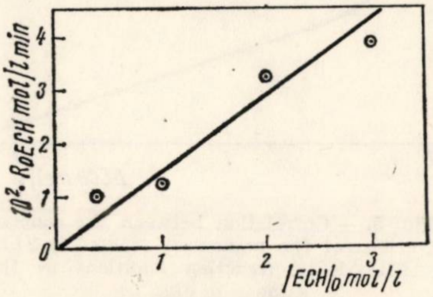

Fig. 4. — Variation of the initial consumption rate of ECH depending on $|ECH|_0$ ($|PL|_0 = 2$ mol/l).

The results presented in figures 1—4 point to the fact that the consumption rate of the more basic monomer, ECH, is higher than that of the less basic monomer, PL, a behavior which is characteristic of cationic copolymerization.[13] Differences between the reactivities of the two monomers are found throughout the process. The concentration of PL reacted

---

[11] V. Dimonie, D. Donescu and I. Gavăt, *Rev. Roumaine Chim.*, **19**, 125 (1974).

[12] D. Donescu, *Rev. Roumaine Chim.*, **19**, 277 (1976).

[13] Y. Yamashita, T. Tsuda, M. Okada and S. Iwatsuki, *J. Polymer Sci. A— 1*, **4**, 2121 (1966).

[14] E. A. Djavadian, B. A. Rosemberg, N. S. Enicolopian, *Vysokomol. Soedineniya A*, **15**, 1982 (1973).

[15] M. Okada, Y. Yokoyama and H. Sumitomo, *Makromol. Chem.*, **170**, 131 (1973).

[16] E. A. Djavadian, B. A. Rosemberg and N. S. Enikolopian, *Vysokomol. Soedineniya A*, **11**, 2330 (1969).

[17] E. B. Lyudvig and A. K. Homiakov, *Vysokomol. Soedineniya B*, **9**, 698 (1973).

after 24 hr, for instance, is smaller than that of ECH (see Fig. 5) and also depends on the initial ratio between comonomers : at a constant initial concentration of PL, the larger the concentration of the reacted monomer, the smaller is the concentration of ECH, which is the more basic monomer.

The differences between the reactivities of PL and ECH and the complexing ability of PL with the growing active centers account for the non-statistical behaviour of these two monomers in the cationic copolymerization.[1,2]

3.2 COPOLYMERIZATION OF β-PROPIOLACTONE WITH 1,3-DIOXEPANE

In this monomer system too, PL is less basic than DH ($pK_b = 6{,}12$[13]). By studying the dependence of the initial rate of DH on the initial concentration of comonomer, the latter is again found to decrease with the increase in the concentration of the complexing monomer (Fig. 6).

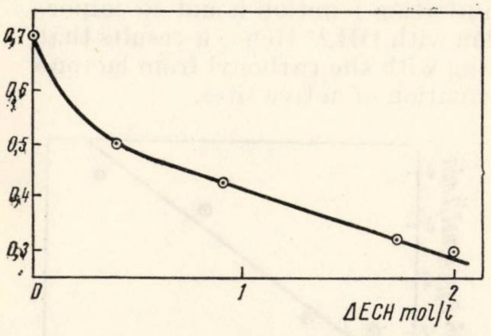

Fig. 5. — Correlation between the concentrations of the monomers reacted in 24 hr (ΔPL, ΔECH) (reaction conditions are the same as in Fig. 1.)

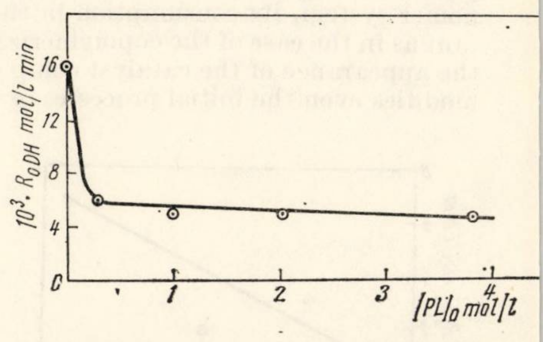

Fig. 6. — Dependence of the initial consumption rate of DH on $|PL|_0$ ($|DH|_0 = $ $=$mol/l, $|DH|_0 =$ initial concentration of DH).

The marked decrease of the consumption rate of DH in the range of small concentration of PL is explained by the fact that since the formation of the complex lactone-active site requires a small monomer concentration (of the order of magnitude of the catalyst concentration[9]) its excess will influence no longer significantly the rate of the cyclic formal.

The decrease in the polymerization rate of cyclic formals due to the coordination of active sites with C=O groups was also observed in the polymerization of 1,3-dioxolane in the presence of low-molecular weight linear esters.[18]

Figure 7 shows the influence of the initial concentration of DH on its consumption rate. It can be observed that by neglecting the variation of equilibrium concentration of DH as a function of the composition of the initial mixture, the influence is similar to that established for homopolymerization.[19]

The difference found also in this case relative to copolymerization of DH with ECH[12] illustrates that, since lactone is no longer a promoter in the copolymerization of DH with PL, the consumption of formal in the initiation can no more be neglected, hence the secondary reactions observed in the initiation of the homopolymerization also occur.

---

[18] A O. Tonoian, S. P. Davtian, B. A. Rosemberg and N. S. Enicolopian, *Vysokomol. Soedineniya A*, **16** , 1042 (1974).

[19] D. Donescu, *Rev. Roumaine Chim.*, **21**, 139 (1976)

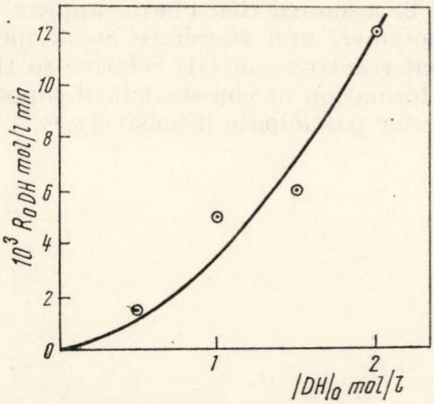

Fig. 7.—Influence of $|DH|_0$ on the initial consumption rate of DH($|PL|_0 = 2$ mol/l).

The consumption rate of PL is markedly smaller than that of DH. Similar to the copolymerization of PL with ECH, the amount of PL consumed in time depends on the concentration of the more basic monomer. The relationship between the concentrations of monomers consumed after 48 hr presents the same characteristic as mentioned in Fig. 5 : the concentration of reacted PL decreases with the increase in the concentration of the more basic monomer (Fig. 8).

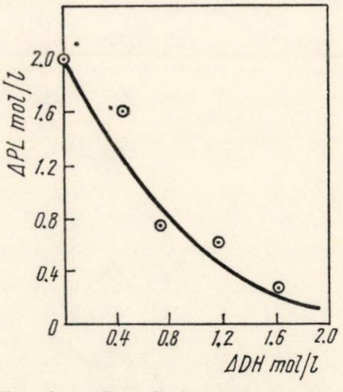

Fig. 8. — Correlation between the concentrations of monomers reacted in 48 hr (ΔPL, ΔDH) (reaction conditions are the same as in Fig.7).

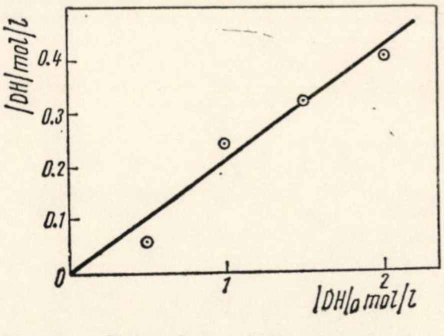

Fig. 9. — Dependence of the concentrations of unreacted DH after 48 hr on $|DH|_0$ ($|PL|_0 = 2$ mol/l).

Like in the copolymerization of DH with ECH,[12] the concentration of DH in the polymerization medium decreases below the equilibrium concentration found in homopolymerization.[20] (Fig. 9)

---

[20] Y. Yamashita, M. Okada and K. Suyama, *Makromol. Chem.*, **114**, 146 (1968).

Since the concentration of the unreacted formal is not minimum when the concentration of the reacted proper monomer is maximum,[21] but only when the concentration of the reacted lactone is maximum, it may be assumed that chains appear which differ from those of the DH homopolymer, and therefore copolymers may possibly be formed. The different reactivity of DH relative to that of PL indicates the possibility of the formation of non-statistical copolymers, unless secondary reactions of transfer participate intensively.[22]

---

[21] J. Leonard and D. Maheux, *J. Macromol. Sci.-Chem A*, **7**, 1421 (1973).

[22] Y. Yamashita, T. Asakura, M. Okada and K. Ito, *Makromol. Chem.*, **129**, 1 (1969).

Revue Roumaine de Chimie, **21**, *9–10*, 1373–1379 (1976)

REACTIVITY OF ORGANO-ALUMINUM COMPOUNDS TOWARDS LEWIS BASES. II[1]

DIARYL- AND DIALKYLALUMINUM KETIMINPHOSPHINES

DIANA GIURGIU and I. POPESCU
Institute of Macromolecular Chemistry "P. Poni"
Aleea Gr. Ghica Vodă 41-A, Iassy

Received January 28, 1975

Studies were made on the reactivity of diaryl- and dialkylaluminum diphenylphosphide compounds to alkyl and aryl nitriles. Diorgano-aluminum ketiminphosphine compounds were obtained which were characterized by IR spectra, molecular weights and elemental analyses. The structures of newly obtained compounds and their reaction mechanisms were proposed. Protolysis reactions of diorgano-aluminum ketiminphosphine derivatives were investigated.

Compounds of $(R_2Al-XR_n)_2$[2,3] type were considered to be of interest, mainly due to the structural particularities of substituted heteroelement organo-aluminum derivatives and to their reactivity to organic compounds with functional groups, comparable to the reactivity of organo-aluminum hydrides.[4,5]

The action of organo-aluminum derivatives of type $(R_2Al-XR_n)_2$ on organic compounds with functional groups which contain a carbon-nitrogen multiple bond is conditioned by the nature of groups bound to the aluminum atom (alkyl, aryl, alkenyl) and by the electronegativity of the X heteroatom, respectively by the polarity of the Al–X bond.[6]

The behaviour of $(R_2Al-XR_n)_2$ compounds to nitriles is analogous to that of organo-aluminum hydrides,[5] leading to the formation of some addition products at the triple bond, as a result of the Al–X bond selective splitting.

---

[1] Part I: D. Giurgiu and I. Popescu, *Rev. Roumaine Chim.*, **18**, 1961 (1973).

[2] H. Hoberg and T. Tkatchenko, *Liebigs Ann. Chem.*, **751**, 77 (1971); H. Hoberg and J. B. Mur, *Liebigs Ann. Chem.*, **733**, 141 (1970).

[3] K. Ziegler, K. Schneider and J. Schneider, *Liebigs Ann. Chem.*, **623**, 9 (1959); J. E. Lloyd and K. Wade, *J. Chem. Soc.*, **1965**, 2662. L. I. Zakharkin and I. M. Khrolina, *Proc. Acad. Sci. URSS. Engl. Trans.*, **116**, 879 (1957).

[4] K. Issleib, *Z. Chem.*, **2**, 163 (1964); H. Lehmkuhl and K. Ziegler, "Houben-Weyl Methoden der Organischen Chemie", 4_{th} edn., 13/4, 1970, p. 215: H. Reinheckel, K. Haage and D. Jahnke, *Organometal. Chem.*, *A.* **4**, 47 (1969).

[5] T. Hirabayashi, K. Itoh, S. Sakai, Y. Ishii, *J. Organometal. Chem.*, **21**, 273 (1970).

[6] H. Hoberg and J. B. Mur, *J. Organometal. Chem.*, **17**, P 30 (1969).

$(R'_2Al-PR_2)_2$ compounds[7] react with nitriles in a 1 : 1 combination ratio leading to the formation of some organo-aluminum ketiminphosphine derivatives, generally dimer combinations. Their structure with heteroatomic bridges achieved by donor-acceptor bond types was proposed, based on results of elemental analysis, on molecular weight determinations and on IR spectral analysis as shown below :

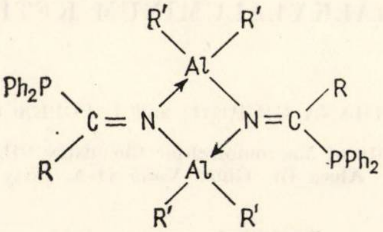

Analogous structures were attributed to dimer combinations $(R'_2N-C(R)=NAlR_2)_2$ obtained by the reaction of trialkylaluminum derivatives with dimethylcyanamide.[3,8]

EXPERIMENTAL

Diorgano-aluminum diphenylphosphide compounds $(R_2Al-PPh_2)_2$ $R = i-Bu$, Ph, *p*-Tolyl were prepared by the diphenylphosphine action on the corresponding organo-aluminum derivative.[7]

Nitriles used were anhydrized by depositing on Na_2SO_4 and distillation on a Vigreux column.

Acetylacetone previously dried on $CaCl_2$, distilled on a fractionation column (b.p. 137°) was immediately used.

Triphenylaluminum and tri-*p*-tolylaluminum were prepared according to the Krause Dittmar method.[9] Triisobutylaluminum was supplied from the market and diluted with anhydrous benzene.

Diphenylphosphine was obtained by the Issleib method.[10]

Solvents were purified and anhydrized.

All synthesis operations were performed in an inert and dry atmosphere.

Molecular weights were cryoscopically determined in anhydrous benzene solution. The phial for measurements was adapted to perform determinations in inert atmosphere.

IR spectra were recorded on a Unicam Sp 200 spectrophotometer for the 3,500–600 cm^{-1} domain and on a 621 Perkin Elmer spectrophotometer for the 800–300 cm^{-1} domain on KBr pelletted samples. Samples were withdrawn in a box under nitrogen stream.

OBTENTION OF DONOR-ACCEPTOR COMPLEXES WITH NITRILES

For the formation of donor-acceptor complexes we shall refer to the method of obtaining the diphenylaluminum diphenylphosphide complex with benzonitrile.

$(C_6H_5)_2Al-P(C_6H_5)_2\cdot N\equiv C-C_6H_5$ 1g (2.75 mmole) diphenylaluminum diphenylphosphide was dissolved in 10 ml benzene adding 0.2 g (2.75 mmole) benzonitrile in 5 ml benzene with stirring, and cooling the reaction mixture at 10°. The reaction mixture was stirred at room temperature for 3 hr. A white product crystallizes by benzene concentration under vacuum. It was repeatedly washed with a 1 : 1 benzene/*n*-hexane mixture and also vacuum-dried. The results of the elemental analysis and the physical characteristics are given in table 1.

---

[7] D. GIURGIU, I. POPESCU, A. CIOBANU, M. BOSTAN, N. VOICULESCU and L. ROMAN, *Rev. Roumaine Chim.*, **15**, 1581 (1970).

[8] G. K. GIBSON and D. W. HUGHES, *Chem. Ind.* (London), **1964**, 544.

[9] E. KRAUSE and P. DITTMAR, *Chem. Ber.*, **63**, 2401 (1930).

[10] K. ISSLEIB and A. TZSCHACH, *Chem. Ber.*, **92**, 1118 (1959).

OBTENTION OF DIORGANO-ALUMINUM KETIMINPHOSPHINE COMPOUNDS

a) $(C_6H_5)_2Al-N=C(C_6H_5)P(C_6H_5)_2$. 0.85 g (8.2 mmole) benzonitrile in 5 ml benzene was added to a solution of 3 g (8.2 mmole) diphenylaluminum diphenylphosphide in 10 ml benzene, with magnetic stirring. It was stirred for a while at room temperature and then the reaction mixture was heated for 16 hr at 180° under a weak nitrogen stream. After cooling, *n*-heptane was added with vigorous stirring. A white product was formed which readily deposited. The product was repeatedly washed with *n*-heptane and vacuum-dried. It is a white powder, soluble in benzene, insoluble in petroleum ether and in *n*-heptane.

The compound is more stable at air and humidity than the phosphine aluminum derivative of which it results.

b) By isolating complex $(C_6H_5)_2Al-P(C_6H_5)_2 \cdot N \equiv C-C_6H_5$ prepared according to the above-described procedure and heating it at 150—200°, in a sealed tube, colourless drops will be seen on the cold tube walls, which crystallize after a while. Elemental analyses and the IR spectrum indicates the formation of the same compound. X-ray diffraction images show an ordered structure.

$(i-C_4H_9)_2Al-N=C(C_6H_5)P(C_6H_5)_2$ · 2.5 g diisobutylaluminum diphenylphosphide in benzene were treated with 1.2 g benzonitrile at 10°, while stirring vigorously. The reaction mixture was gradually heated at 80° and refluxed for 5 hr. After solvent removal, a white product crystallizes. It is repeatedly washed with benzene, cooled and vacuum-dried. The compound is very soluble in benzene and toluene and is sensitive to air and humidity.

An intensive isobutane release will be observed if the reaction mixture is heated at 150°. After solvent removal, *n*-heptane was added and the product was washed several times and then vacuum-dried elemental analyses fail to indicate the formation of a unitary product.

REACTION OF DIPHENYLALUMINUM PHENYLKETIMIN DIPHENYLPHOSPHINE WITH ACETYLACETONE

0.6 g freshly distilled acetylacetone were gradually added to a benzene solution of 1.5 g diphenylaluminum phenylketimindiphenylphosphine cooled at −20°. The reaction mixture was vigorously stirred to render it homogeneous and was brought to room temperature and treated with *n*-heptane. The white pulverous product was filtered on a G_4 frit and vacuum-dried (m.p. 180°). The compound was identified as being diphenylaluminum acetylacetonate. A crystalline product (m.p. 217—220°) characterized as benzylidine aminodiphenylphosphine was isolated from the benzene solution by precipitation with anhydrous ethyl alcohol.

DISCUSSION OF RESULTS

Due to their character of strong bases, nitriles rapidly and totally displace other weaker bases coordinated at the organo-aluminum derivative or, in the case of some dimer associated derivatives, they act upon the dimer dissociating it and forming the donor-acceptor complex between the monomer activated form and nitrile.

R'_1Al-PR_2 dimer compounds react with aromatic and aliphatic nitriles at room temperature in 1 : 1 combination ratio, forming donor-acceptor complexes by an irreversible exothermal reaction :

$$(R'_2Al-PR_2)_2 + 2N \equiv CR'' \rightarrow 2R'_2Al-PR_2 \cdot N \equiv CR''$$

$$R = -C_6H_5$$

$$R' = -C_6H_5,\ -p-C_6H_4CH_3,\ -i-C_4H_9$$

$$R'' = -C_6H_5,\ -CH_3$$

The reaction may be stopped at this first stage and the isolated complexes are stable until they reach temperatures varying between 90° and 150°. Their hydrolysis affects only the phosphide aluminum derivative which decomposes, whereas nitrile is recuperated unchanged. Complexes of this type $R'_2Al-PR_2N \equiv CR''$ are probably achieved by a "σ" type coordinative bond using the nitrogen non-participating electron doublet. A linear structure corresponding to the "*sp*" hybridization of the nitrogen atom was assigned to similar known compounds.[11, 12]

If the reaction is continued, the intramolecular reorganization with selective splitting of the Al—P bond and nucleophilic attack of the remaining $-PR_2$ at the carbon atom of the nitrile group will occur by heating the mixture or the complex as such in a sealed tube at 150—200°. The mechanism involved in the formation reaction of diorgano-aluminum ketiminphosphine compounds may be thus formulated in two stages:

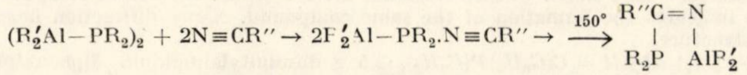

$$(R'_2Al-PR_2)_2 + 2N\equiv CR'' \rightarrow 2R'_2Al-PR_2.N\equiv CR'' \rightarrow \xrightarrow{150°} \begin{array}{cc} R''C & =N \\ | & | \\ R_2P & AlR'_2 \end{array}$$

Thus, the addition reaction of organo-aluminum phosphide derivatives to nitriles may be considered to occur by "insertion" of the nitrile group as a result of the selective splitting of the Al—P bond which is more polar and more reactive than the Al—C bond.

The compounds obtained were characterized as dimer diorgano-aluminum ketimindiphenylphosphine compounds, and a structure with heteroatomic bridges achieved by donor-acceptor bonds was suggested.

Diisobutylaluminum diphenylphosphide reacts with benzonitrile and acetonitrile according to the same mechanisms. The particularity of this reaction consists in the reactants stoichiometry. In the 1 : 1 combination ratio, the addition reaction and the formation of the ketiminphosphine derivative will not occur, in the 1 : 2 nitrile/organo-aluminum derivative ratio the reaction eventually leads to the formation of diisobutylaluminum ketimindiphenylphosphine. A reaction mechanism was proposed, which admits the formation of a transition intermediate complex:

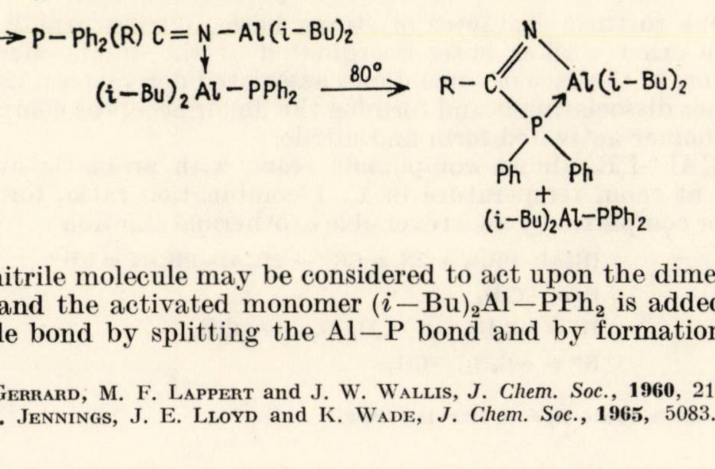

The nitrile molecule may be considered to act upon the dimer dissociating it, and the activated monomer $(i-Bu)_2Al-PPh_2$ is added to the nitrile triple bond by splitting the Al—P bond and by formation of the

---

[11] W. Gerrard, M. F. Lappert and J. W. Wallis, *J. Chem. Soc.*, **1960**, 2182.

[12] J. R. Jennings, J. E. Lloyd and K. Wade, *J. Chem. Soc.*, **1965**, 5083.

ketiminphosphine derivative which may coordinate another monomer molecule $i-Bu_2Al-PPh_2$ by the non-participating electron doublet of the imine nitrogen. The formed complex is not stable and it loses $i-Bu_2Al-PPh_2$ up to 80°. The product obtained, diisobutylaluminum ketimindiphenylphosphine, is monomer and a structure was proposed in which the aluminum atom is tetracoordinated by a four-atom ring closure :

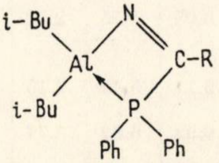

Acetylacetone reacts in equimolecular quantities and at low temperatures (−20°) with diorganoaluminum ketiminsphosphine derivatives leading to the formation of a diorgano-aluminum acetylacetonate compound and of diphenylphosphine benzylideneymide.

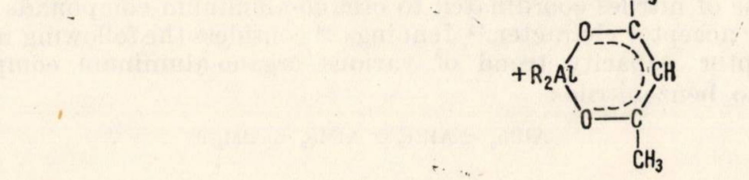
$$\frac{1}{2}\left[R_2Al-N=\underset{P(C_6H_5)_2}{C}-C_6H_5\right]_2 + CH_3COCH_2COCH_3 \longrightarrow HN=C(C_6H_5)P(C_6H_5)_2 +$$

The formation of the same compound diphenylphosphinbenzylideneymide in the acetylacetonolysis reaction in all the investigated cases in which different groups ($i-$Bu or Ph) are bound to the Al atom may be looked upon as a proof of the selective protolytic splitting of the $Al-N$ bond in diorgano-aluminum ketiminphosphine compounds.

Table 1

Analytical results of donor-acceptor complexes

Compound	Elemental analysis							
	Al %		N %		P %		*M* %	
	found	calcd.	found	calcd.	found	calcd.	found	calcd.
$(C_6H_5)_2Al-P(C_6H_5)_2.N\equiv C-C_6H_5$	6.05	5.75	2.52	2.98	6.69	6.60	475	569
$(CH_3C_6)_2Al-P(C_6H_5)_2.N\equiv C-C_6H_5$	5.11	5.43	2.63	2.82	5.97	6.25	—	—
$(C_6H_5)_2Al-P(C_6H_5)_2.N\equiv C-CH_3$	6.92	6.70	5.30	5.79	7.25	7.81	400	387
$(CH_3C_6H_4)_2Al-P(C_6H_5)_2.N\equiv C-CH_3$	6.03	6.20	2.98	3.22	5.57	7.12	—	—

Table 2

Analytical results of diorgano-aluminum ketiminphosphide compounds

Compound	m.p. °C	Elemental analyses							
		Al%		N%		P%		M	
		found	calcd.	found	calcd.	found	calcd.	found	calcd.
$[(C_6H_5)_2Al-N=C(C_6H_5)P(C_6H_5)_2]_2$	210–216	6.05	5.75	2.52	2.98	6.25	6.60	867	938
$[(CH_3C_6H_4)_2Al-N==C(C_6H_5)P(C_6H_5)_2]_2$	220	5.11	5.43	2.15	2.82	5.87	6.22	838	994
$[(C_6H_5)_2Al-N=C(CH_3)P(C_6H_5)_2]_2$	186	6.92	6.62	3.74	3.44	7.25	7.62	794	814
$[(C_6H_5)_2Al-N=C=C=CH_2]$ insoluble polymer	—	11.11	11.57	5.13	6.00	—	—	—	233
$(C_4H_9)_2Al-N=C(C_6H_5)P(C_6H_5)_2$	139	6.43	6.29	2.93	3.27	7.61	7.20	476	429

IR spectra of diorgano-aluminum diphenylphosphide complexes with nitriles indicate characteristic absorptions of group $C \equiv N$ in the 2,230 cm^{-1} region,[13] shifted towards greater wavenumbers $+30\ cm^{-1}$, due to the coordination effect. The shift of the position of the absorption maximum characteristic of group $C \equiv N$ towards greater wavenumbers in the case of nitriles coordinated to organo-aluminum compounds varies with their acceptor character.[14] Jennings [12] considers the following increasing acceptor capacity trend of various organo-aluminum compounds relative to benzonitrile:

$$AlPh_3 < AlEt_3 < AlMe_3 \leqslant AlM_2Cl$$

Table 3

Principal IR absorptions of R_2Al-PR_2 complexes with nitrile

Compound	C = N cm^{-1}	cm^{-1}	P − C$_6$H$_5$ cm^{-1}	P − C cm^{-1}	P − Al cm^{-1}
$C_6H_5-C\equiv N$	2230	—			
$CH_3C\equiv N$	2253	—			
$(C_6H_5)_2Al-P(C_6H_5)_2.N\equiv C-C_6H_5$	2260	+30	1460	1290	760
$(CH_3C_6H_5)_2Al-P(C_6H_5)_2.N\equiv C-C_6H_5$	2260	+30	1435	1290	760
$(C_6H_5)_2Al-P(C_6H_5)_2.N\equiv C-CH_3$	2290	+37	1430	1230	760
$(CH_3C_6H_4)_2Al-P(C_6H_5)_2.N\equiv C-CH_3$	2285	+32	1435	1290	760
$(C_6H_5)_3Al.N\equiv CH_3$	2780	+27	—	—	—
$(C_6H_5)_3Al.N\equiv C-C_6H_5$	2265	+35	—	—	—

The formation of diorgano-aluminum ketiminphosphine addition compounds as a result of thermal rearrangement reaction of the corresponding complexes was revealed by IR spectra.

---

[13] H. J. Corever and C. Curran, *J. Amer. Chem. Soc.*, **80**, 3522 (1958).

[14] J. Cook, *Canad. J. Chem.*, **40**, 480 (1962).

Table 4

Principal IR absorptions of compounds $R_2Al-N=C(R)PR_2$

Compound	N=C cm^{-1}	P–C cm^{-1}		Al–C_6H_5 cm^{-1}			Al–N cm^{-1}
$[(C_6H_5)_2Al-N=C(C_6H_5)P(C_6H_5)_2]_2$	1590	1435	1160	680	442	330	484
$[(C_6H_5)_2Al-N=C(CH_3)P(C_6H_5)_2]_2$	1585	1440	1160	680	440	330	480
$[(CH_3C_6H_4)_2Al-N=C(C_6H_5)P(C_6H_5)_2]_2$	1593	1440	1145	680	440	320	485
$[(CH_3C_6H_4)_2Al-N=C(CH_3)P(C_6H_5)_2]_2$	1585	1435	1140	680	440	220	485
$[(C_6H_5)_2Al-N=C=C=CH_2]_2$	1625	—	—	680	570	440	480
$(C_4H_9)_2Al-N=C(C_6H_5)P(C_6H_5)_2$	1575	1440	1160	680	560	440	470
$[(C_6H_5)_2Al-N=C(C_6H_5)_2]_2$	1613	—	—	729	700	620 560 440	480

Important differences are found in the vibrational spectra of $C\equiv N$ group by comparing the effect of the coordination reaction of the aluminum phosphine derivative to nitriles with that of triple bond addition. The disappearance of the absorption maximum from the 2,260 cm^{-1} region and the appearance of an intense maximum at 1,625 – 1,575cm^{-1} corresponding to the vibration of the N = C bond is a proof of changes occurred during thermal treatment of donor-acceptor complexes with nitriles.

Results obtained agree with those reported in the literature for similar compounds.[15,16]

A common feature of the studied compounds is the presence in the IR spectrum of an intense absorption in the 1,450 cm^{-1} region characteristic of the P–C bond vibration and of two maxima in the 1,290 – 1,260 and 1,140 cm^{-1} regions attributed to the tetracoordinated phosphorus atom in dimer compounds of $(R_2M-PR_2)_2$ type, where M = Al, Ga, In.[17-19]

The absorption maximum attributed to the Al–P bond in type $(R_2Al-PR_2)_2$ compounds in 760 cm^{-1} and 430 cm^{-1} domains[8] is not evident in the diorgano-aluminum ketiminiphosphine compounds, a maximum being observed only in the 480–470 cm^{-1} region, frequently attributed to Al–N bond vibrations.[17-19]

---

[15] G. Costa and A. Puxeddu, *Univ. Studi Trieste Fac. Sci. Ist. Chim.*, **27**, 13 (1958); *Chem. Abstr.*, **53**, 14689 (1959).

[16] G. Costa and R. Calcinari, *Gazz. Chim. Ital.*, **89**, 1415 (1959).

[17] O. T. Beachley and G. E. Coates, *J. Chem. Soc.*, **1965**, 3241.

[18] D. F. Clements, and H. H. Sisler, *Inorg. Chem.*, **5**, 527 (1966).

[19] W. A. Hart and H. H. Sisler, *Inorg. Chem.*, **3**, 617 (1964).

Revue Roumaine de Chimie, **21**, *9–10*, 1373–1379 (1976)

Revue Roumaine de Chimie, **21**, *9–10*, 1381–1394 (1976)

AMORPHOUS-CRYSTALLINE COUPLING IN POLYETHYLENE. III[1]

INTERLAMELLAR ORDERINGS IN POLYETHYLENE WITH CHEMICAL ETCHED DEFECTS

GH. DRĂGAN
Institute of Chemical Research, ICECHIM,
Spl. Independenţei 202, Bucharest

Received April 11, 1975

The DTA study of the amorphous-crystalline coupling is continued on three sorts of polyethylene essentially linear with different concentrations of conformation defects. After annealing, an interlamellar ordering is obtained through chemical etching. The migration of the resulting defects resembles the process of precipitation recently studied in silicon and germanium. The interlamellar ordering resulting from annealing is interpreted as the formation of a nematic structure with twist disclinations between the lamellar fragments and amorphous domains. The activation energies associated to the process of interlamellar ordering under observation of the order 24–53 kcal/mole are obtained from the Arrhenius dependences of some parameters deduced from the melting endotherm (according to Baughman and Turnbull's reasoning).

INTRODUCTION

As the majority of crystalline polymers, polyethylene (PE) has a morphology made up of crystalline domains and amorphous (intercrystalline) domains. In the first [2] and second [1] part of this series it was concluded that the thermal, mechanical and chemical treatments result in a more distinct separation of these two components so that when in equilibrium the morphology is characterized by an intercrystalline orientation higher than that of the initial polymer.[3] The rearranging in a temperature field, mechanical stresses or concentration field is essentially due to crystalline defects that tend to migrate to equilibrium in the intercrystalline domains. For PE these defects come out from the chain configuration (ramifications)[2] and/or chain conformation, defects that appear incidentally in the crystalline domains. For the case of a higher density PE where the absence of groups adjacent to the chain is spectroscopically established, the only possible defects are those due to the planar deviation by kinks or jogs,[4] that is by GG, GTG and GTTG, sequences have a certain mobility along the chain and their concentration in the morphology can be spectroscopically established.[1,5] Based on the concentration and on the mobility mechanism of the defects, containing in principal the isomers G and G′, one can generally explain the phase transitions which occur in PE.[6] Pechhold and Blasenbrey [4] forsaw theoretical in the pair interactions approximation a first order transition connected to a jump

---

[1] Part II: Gh. Drăgan, *Rev. Roumaine Chim.*, **20**, 687 (1975).

[2] Gh. Drăgan, *Materiale Plastice*, **10**, 87 (1973).

[3] The term of "lamellar" crystalline domain does not always correspond to the morphological data. There is data, especially at PE, that correspond to a habit crystallization with extended chains that have habit faces (001) that are no good delimited.

[4] W. Pechhold, *J. Polymer Sci.*, **C 32**, 123 (1971).

[5] G. Zerbi, L. Piseri and F. Cabassi, *Mol. Phys.*, **22**, 241 (1971).

[6] T. Ishinabe, *J. Phys. Soc. Japan*, **4**, 1022, 1029 (1971).

in the defect concentration in the solid state. In terms of morphology, this occurs in equilibrium, or close to equilibrium, supposing that these defects divide the molecular bundles in segment layers by the mechanism of formation of *kinkblock structure*. In this context, the calorimetric methods have the advantage of giving the possibility to perform the energetic balance-sheet by heat and mass transfer dun while reaching the equilibrium morphology and during the phase transitions.

The behaviour of the response functions [7] used for testing the morphological modifications appeared during the migration processes of these defects emphasizes their activated character. The glass transition [8] and the interlamellar rearrangement in the equilibrium morphology are explained by mechanisms in Eyring's signification.

This paper uses the chemical etching (decoration) technique of the conformation defects, knowing that reactivity of the solid is a function of their concentration. [1,9] On the other hand it has been previously observed that the interlamellar order degree to equilibrium is much easier to reach in this case than in that of the original polymer.[1] This has been explained by the existence of the induced stresses during the chemical treatment and pointed out spectroscopically. The annealing effect in the 115—130° range for a period of the order of 10^2 minutes is actually visible on the thermograms only in the case of chemically treated samples. For PE with lamellar crystalline morphology and essentially linear configuration, the activation energy of the process of interlamellar arrangement (through equilibrium by annealing) after mechanical treatments has been established to be about 30 Kcal/mole. [1,10,11] The values obtained in this paper for the chemical etched samples using the judgement of Baughman and Turnbull[12] give the possibility to better separate the morphological specific features of the initial polymer. These specific features were correlated with the results obtained from IR spectrum and wide angle X-ray diffraction diagrams (WAXRDD). [11,13] The values of the activation energies obtained are to be found in the interval 24—53 Kcal/mole.

EXPERIMENTAL

Studies have been made on the behaviour during annealing of the three sorts of linear PE considered previously [1] called LPE and, respectively, of three samples of photochlorinated PE in suspension that result from those three LPE, respectively. These latter are noted by CPE 1, CPE 2 and CPE 3, respectively, and are chlorinated under identical conditions up to a content of 40 ± 1% chlorine by weight.

The majority of the results in the paper were provided by the DTA thermograms on the LPE and CPE samples, annealed at the temperatures of 115, 120, 125 and 130° for almost 10^2 minutes. The samples were used as such (dry) and also annealed in a mixture with silicon oil as an annealing medium. The dry annealed samples were DTA analyzed as such (dry) and also in a mixture with silicon oil as a transfer medium. High purity silicon oil has been used (type Schuchardt 702) in a proportion of 45—50% in weight.

---

[7] Gh. Drăgan, "Morphology of Polymers. Principles of Characterization and Processing", ICECHIM, Lectures, June 1974, Bucharest.

[8] B. Wunderlich, *J. Chem. Phys.*, **37**, 2429 (1962).

[9] J. M. Thomas and J. O. Williams in "Progress in Solid State Chemistry", vol. 6, edited by H. Reiss and J. O. McCaldin, Pergamon Press, 1971, pp. 119.

[10] N. G. McCrum and D. L. Pearce, *Nature*, **243**, 52 (1973).

[11] R. Hoseman, J. Loboda-Cackovic and H. Cackovic, *J. Polymer Sci.*, **42**, 563 (1973).

[12] R. H. Baughman and D. Turnbull, *J. Phys. Chem. Solids*, **32**, 1375 (1971).

[13] Gh. Drăgan and N. Radovici, to be published.

The annealing was performed using a cylindrical metallic block having vertical, cylindrical and parallel orifices with a diameter equal to the inner diameters of the two containers of the DTA device. The samples were encapsulated in aluminium foil cells. In every orifice, two, and respectively three such cells of the same sample were placed, corresponding to the dry annealing case, relative to the medium. The two methods of annealing were carried out separately but both included simultaneously all the samples LPE and CPE. In all cases the same relative position of the samples was kept in the metallic block. The samples prepared in this way were annealed plunging the metallic block in the bath of an ultrathermostate with paraffine oil, the temperature of which has been previously established with an accuracy of ±0.05°.

The DTA apparatus used is of the same type with the one previously used,[1] but with metallic containers and the joints of the differential thermocouple are also welded to them. The reproducibility and the accuracy of the apparatus were tested for three heating rates $K1 = 3.5$, $K2 = 6.5$ and $K3 = 10.0$°/minute, using the melting enthalpies for high purity indium and benzoic acid. The mass of the samples was established with good accuracy (±0.0002 g) by weighting the aluminium capsules and knowing the concentration of the polymer in the medium for the samples in the mixture. The capsules with samples have a mass whose value ranges between 150–200 mg as a function of the heating rate (round speed) in order to maintain as long as possible the baseline horizontally.

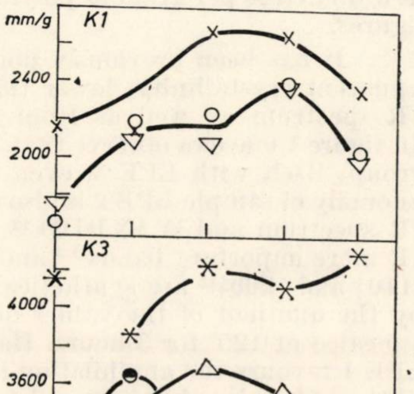

Fig. 1. — Dependence of parameter h_1 on T_a in LPE samples in set III. The symbols of the points correspond to those used in Table 1 for CPE samples respectively.

Table 1

Symbols used in the figures of the present work

	$K1$	$K2$	$K3$
CPE 1	×	+	✳
CPE 2	○	●	◓
CPE 3	▽	▼	△

Table 2

Variation on dry annealing of some IR bands and halfwidth of WAXRDD maxima in samples LPE (see the text) *

	δI_{1350}	δI_{2853}	δI_{2926}	$\frac{\delta I_{2926}}{\delta I_{2853}}$	$\beta_{\|110\|}$	$\beta_{\|200\|}$
LPE 1	0.45	2.07	2.27	1.10	0.78	0.83
LPE 2	1.06	2.73	2.74	1.00	0.68	0.61
LPE 3	1.22	1.70	1.87	1.10	0.86	0.80

* The variation δ is defined as $\delta x = x_{\text{ann}}/x_{\text{unann}}$.

Revue Roumaine de Chimie, **21**, *9–10*, 1381–1394 (1976)

RESULTS AND DISCUSSIONS

The results are grouped in three sets, as follows :

I – the dry annealed samples and DTA analyzed as such ;

II – the dry annealed samples and DTA analyzed with medium, and

III – the samples annealed with medium and DTA analyzed with medium.

The following important parameters are established from the DTA thermograms : the total melting enthalpy ΔH_m, the heights of peak-baseline of effect T_m^0 and T_m^1,[1] noted by h_1 and h_2, respectively ; the splitting coefficient $\alpha = h_2/(h_1 + h_2)$ and the melting enthalpy of the lamellar phase $\Delta H_m^1 = \Delta H_m - \alpha\Delta H_m$. The melting enthalpies are given in calories per gram of polymer (in the CPE samples it has been reported to the whole mass of polymer including also chlorine) and the heights h_1 and h_2 in millimeters per gram of polymer. Table 1 gives the symbols used in the figures.

It has been previously pointed out that the sample LPE 2 has an apparent crystallinity, lower than the other ones. This results from the IR spectrum as well as from the melting enthalpy and WAXRDD.[1] In figure 1 one can observe that in the mixture with silicon oil this sample groups itself with LPE 3, even for the case of unannealed samples. This anomaly of sample LPE 2 is also explained by the results obtained from the IR spectrum and WAXRDD.[13] In Table 2 the relative variations of the IR more important bands [1,5] and of the WAXRDD maxima on directions |110| and |200|[13] are synthetically given. These variations are expressed by the quotient of the values obtained on initial samples and those dry annealed at 125° for 3 hours. Having a smaller molecular weight, sample LPE 1 favours the annihilation of the conformation defects by annealing, so that δI_{1350} is subunitary, whereas especially in sample LPE 3 annealing reveals a bigger quantity of defects.[1] The anomaly that repeats itself with sample CPE 2 (set II, figures 3, 4) can thus be due to a segmentation of the lamellae subsequent to the chemical treatment of the polymer. This division superposes itself as a thermal effect in the global melting endotherm by diffusion of silicon oil during the DTA round.

This segmentation process is actually a cleavage process on faces (001). In general terms of morphology,[14] the annealing process, by which one can generally observe the thickening of the lamellar habit on direction |001|,[15] is explained by the superficial crystallization on habit face (001) up to a minimum value of the superficial free energy [15] or adhesion energy [14] proper to this habit face. The model suggested by Hiray [15] for crystallization by dimensional nucleation during annealing starts from the premise that face (001) is of class F,[14] hence it is responsible for the lamellar habit. The samples LPE and CPE keep this habit and, even more, it results from the strange behaviour of sample CPE 2 in the set II that face (001) is not attacked during the chemical treatment. On the other hand one can observe (Table 2) a differentiated increase of the valence bands intensities

---

[14] P. Hartma, *Redinconti della Societa Italiana di Mineralogia e Petrologia*, **29**, 153 (1973).

[15] I. C. Sanchez, J. P. Colson and R. K. Eby, *J. Appl. Phys.*, **44**, 4332 (1973).

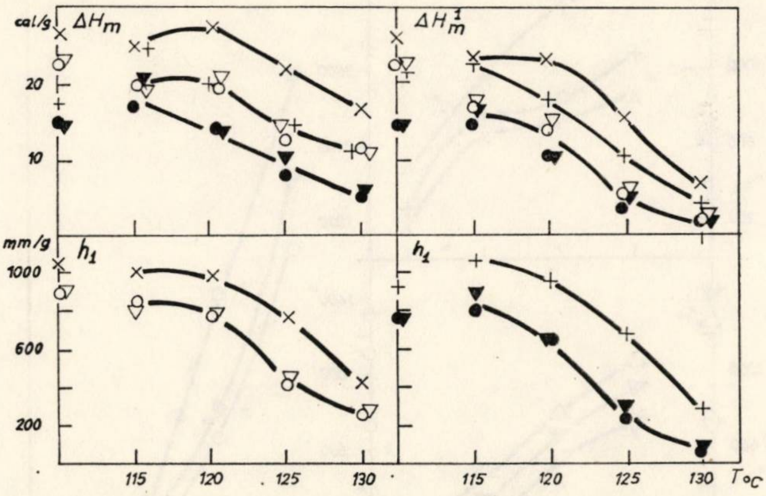

Fig. 2. — Dependence of parameters ΔH_m, ΔH_m^1 and h_1 on T_a for samples in set I.

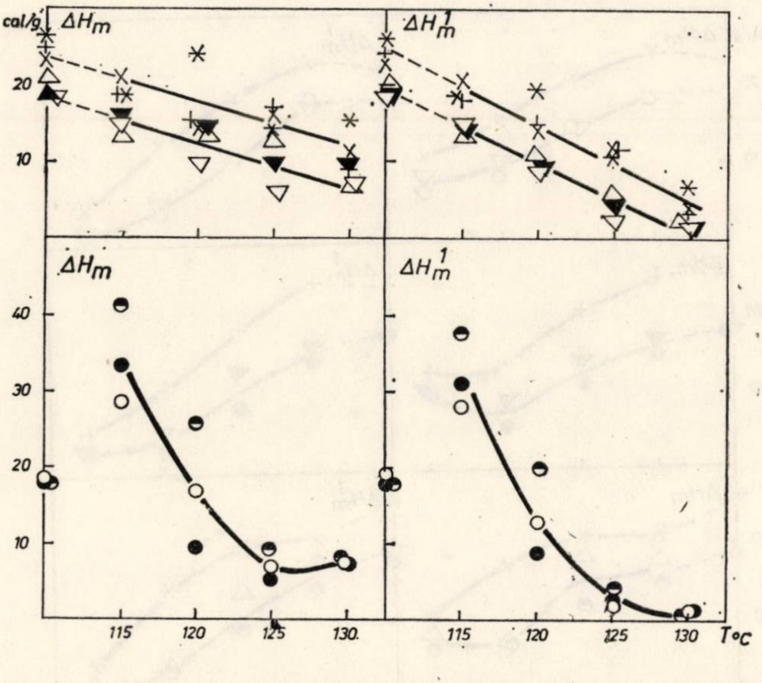

Fig. 3. — Dependence of parameters ΔH_m, and ΔH_m^1 on T_a for CPE samples in set II.

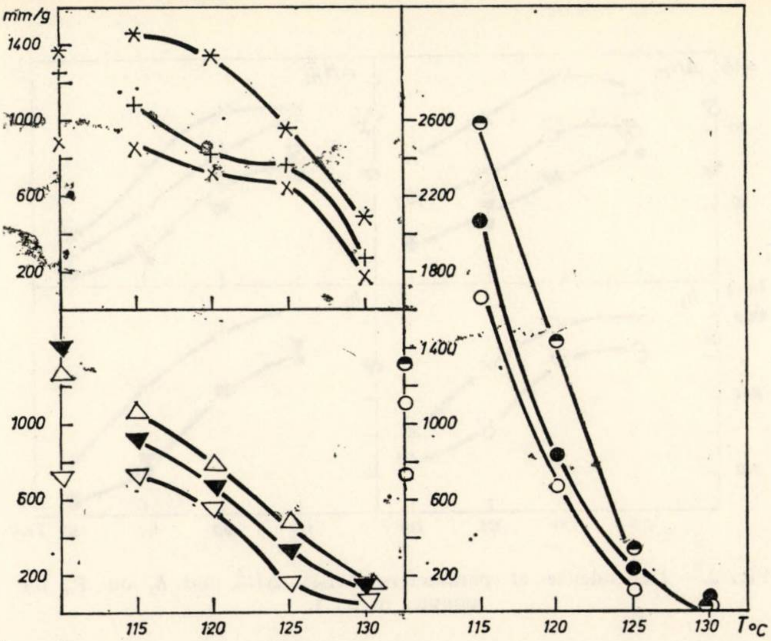

Fig. 4. — Dependence of parameters h_1 on T_a for CPE samples in set II.

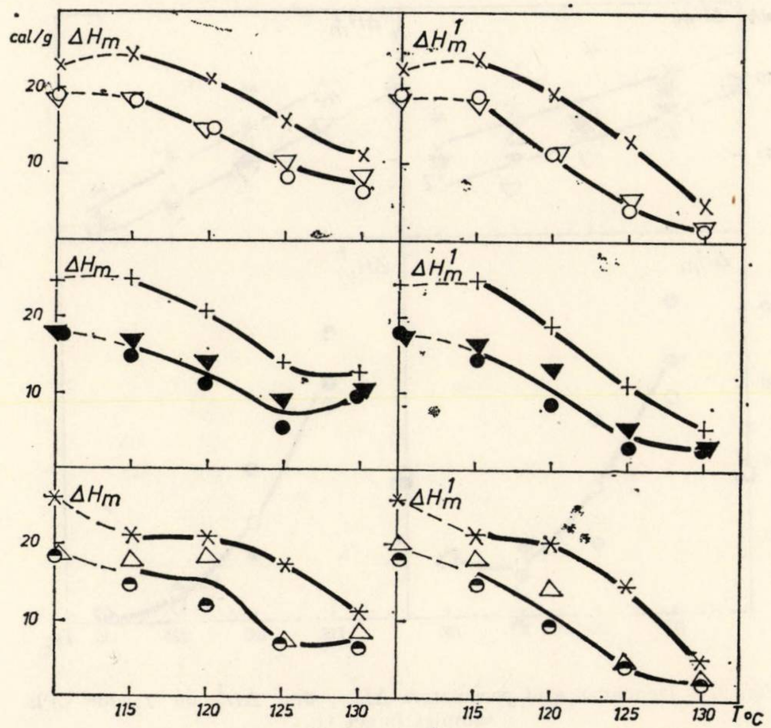

Fig. 5. — Dependence of parameters ΔH_m and ΔH_m^1 on T_a for CPE samples in set III.

νCH_2sym ($2853\ cm^{-1}$) and νCH_2asym($2926\ cm^{-1}$)[1] after annealing. The fact that the increases of these bands are proportional ($\delta I_{2926}/\delta I_{2853} \sim 1$) indicates that the contributions come out principally from the CH_2 groups from the interlamellar phase. It is also remarked that there is no connexion between the variation of the active defect concentration in $1350\ cm^{-1}$ band and the variation of νCH_2 bands. For the latter, the anomaly for LPE 2 sample is also observed. These facts lead to the conclusion that the increase of the νCH_2 band intensities is not due to the groups that migrate at the same time with the lamellar defects, but to the folded portions of the habit faces (001). This is in good agreement with the variation of the halfwidth of the WAXRDD maxima on directions |110| and |200| (Table 2). It is known that the halfwidth of these diffraction maxima is a function of the dimensions of the crystals, of the defects and/or the crystalline distortions,[16] therefore it results that in those three LPE samples the perfecting of the lamellar habit faces on annealing comes principally to perfecting habit faces (001). This process has no connexion with the precipitation process of the chemically etched defects for CPE samples, because of the fact that face (001) is not affected by the chemical treatment. Thus, for a lamellar morphology, annealing implies two generally independent processes : (i) perfecting of the lamellar habit on face (001), and (ii) precipitation of lamellar defects towards amorphous domains. From the results obtained on set II, it is possible to observe that the first process is affected by the existence of a transfer medium. This fact was remarked in the early studies on PE annealing.[17] As the second process is an interlamellar process, it is not affected by the annealing medium. From the results on set I and III one can observe that the presence of the silicon oil as an annealing medium does not influence the precipitation process, but leads to a dispersion of the values of the considered parameters because of their dependence on the DTA round speed.

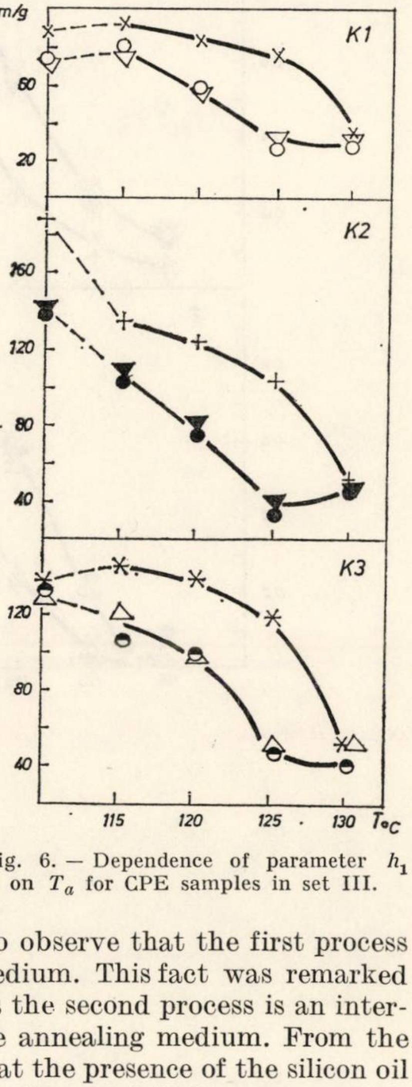

Fig. 6. — Dependence of parameter h_1 on T_a for CPE samples in set III.

---

[16] T. Nagasawa and K. Kobayashi, *J. Appl. Phys.*, **41**, 4276 (1970).

[17] P. H. Geil, "Polymer Single Crystals", Interscience Publishers, New York, 1963.

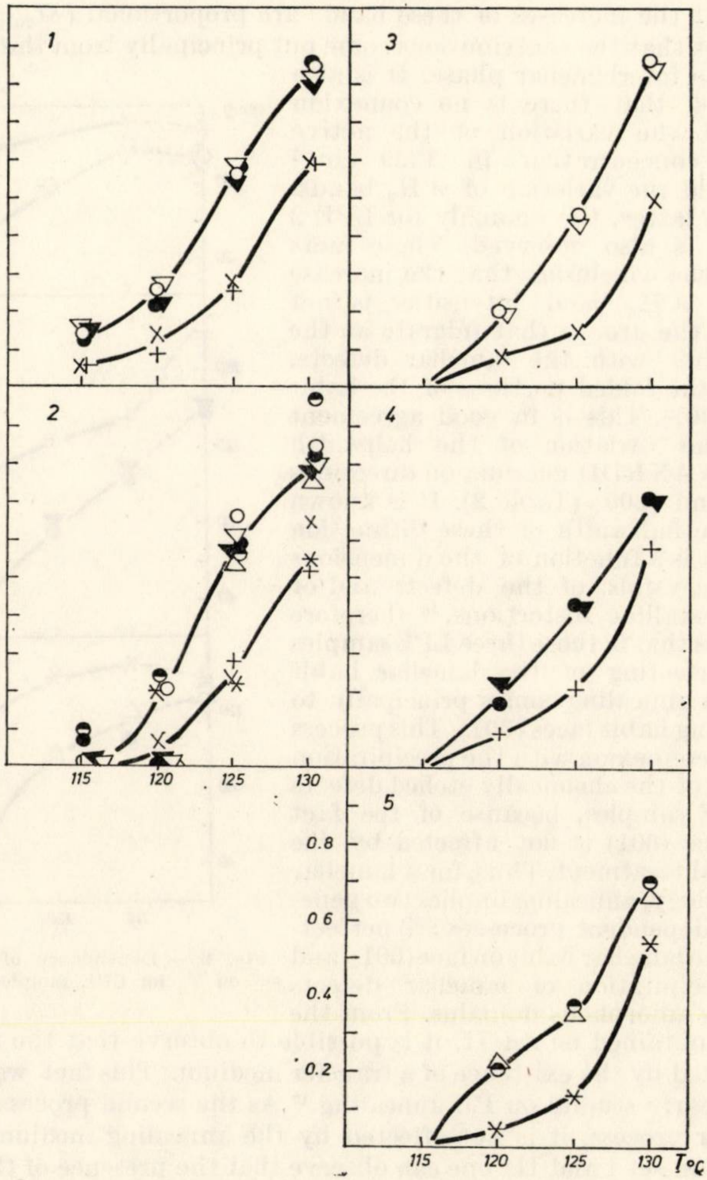

Fig. 7. — Dependence of the splitting coefficient α on T_a for samples from set I(1), II(2) and III(3–5).

The effect T_m^1 was considered [1,2] to be associated to the order-disorder transition due to the interlamellar order induced by the precipitation of lamellar defects. This process is vaguely observed in the LPE samples annealed in the mentioned conditions, while the CPE samples in the same conditions present a more advanced splitting. Figure 7 represents the variation of the relative amplitude of the T_m^1 process relative to T_m^0 by the splitting coefficient α, for the CPE samples with the annealing conditions. It is also observed that the existence of the annealing medium does not influence these dependences, therefore the precipitation process is not affected for the samples in the three sets. The amplitude of effects T_m^1 and T_m^0 is characterized by ΔH_m, h_2 and ΔH_m^1, h_1, respectively. From the results of CPE samples in sets I and III (Figures 2,5 and 6) it is observed that ΔH_m, ΔH_m^1 and h_1 have variations with similar aspect, namely they decrease monotonously while α increases. This means that the precipitation process diminishes the crystalline lamellae so that the interlamellar order appears between the resulted lamellar fragments.

It has been previously mentioned [1] that the chemical etching of conformation defects for the study of crystalline morphology in a linear PE with lamellar habit was extended by other chemical treatments. Recently, Nagasawa and Kobayashi [16] have studied the migration process of induced reticles at γ-irradiation in the PE single crystals. It has been established that for such a habit (see for example the Table from reference 9) the principal gliding plane is (001), the one with directions |110|, |100| and |010|. Based on the elastic anisotropy of the lamellae theoretically and experimentally determined, it has been established that the modulus on direction |020| is greater than on direction |200|.[16] This agrees with the observation that the preferential gliding direction is |100| with an experimental factor 2.52 in comparison with |010| direction. A similar judgement has been used in the study of the precipitation mechanism in semiconductors decorated with atoms having a high diffusion coefficient in their crystalline habit,[18] that is precipitation was observed on the direction with a minimum elastic modulus.

The crystallization conditions for a linear polymer in solution or melt with lamellar habit influence the relative position and the interactions between lamellae.[7] The habit is principally established by the nature of the chain. Recently Lindenmeyer [19] has explained the manner of crystallization based on the free energy of the chain. During the annealing process the lamellar modifications by precipitation of the defects after |100|(001) and |010|(001) are independent of the process of growth by thickening of the (001) face explained by the mechanism of transverse screw dislocations.[20] The first process induces shear forces between the lamellar fragments by means of precipitation domains. In this way, there is a similarity between coherent interlamellar shear forces induced by crystallization from the solution or the melt subjected to shearings,[7] and the shear forces induced on annealing by coherent precipitation.

[18] S. M. Hu and M. R. Poponiak, *J. Appl. Phys.*, **43**, 2067 (1972).

[19] P. H. Lindenmeyer, *Polymer Eng. Sci.*, **14**, 456 (1974).

[20] J. M. Schultz and D. R. Kinloch, *Polymer* (*London*), **10**, 271 (1969).

For a linear PE whose lamellar structure contains a small quantity of conformation defects, not enough to form coherent precipitation, one can observe on annealing only the thickening process.[21] The interlamellar rearrangement observed in the plastic uniaxial deformations is due to interlamellar shearings resulted partially from deformation (mechanical treatment) and partially from defect annealing.[11] From the X-ray diffraction study of the combined effect of the two contributions on elongated and separately annealed samples,[11] the activation energy of the global rearrangement process has been estimated at almost 35 Kcal/mole.[1] Recently a similar PE was studied by stretching and simultaneous annealing (creep)[10] and the value of 30 Kcal/mole was determined for the same process.

Based on the values determined by the DTA thermograms and represented in figures 2—7, attempts were made to estimate the values of

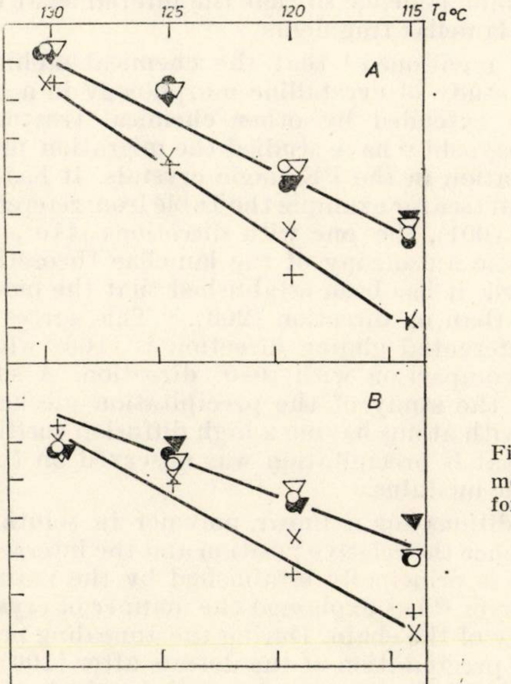

Fig. 8. — Arrhenius dependence of parameters $A=\alpha T_a^2$, $B=h_2 T_a^2$ and $C=\alpha \Delta H_m$ for CPE samples in set I (T_a in Kelvin degrees).

[21] W. Wilke, W. Vogel and R. Hoseman, *Kolloid Z. Z. Polymere*, **237**, 317 (1970).

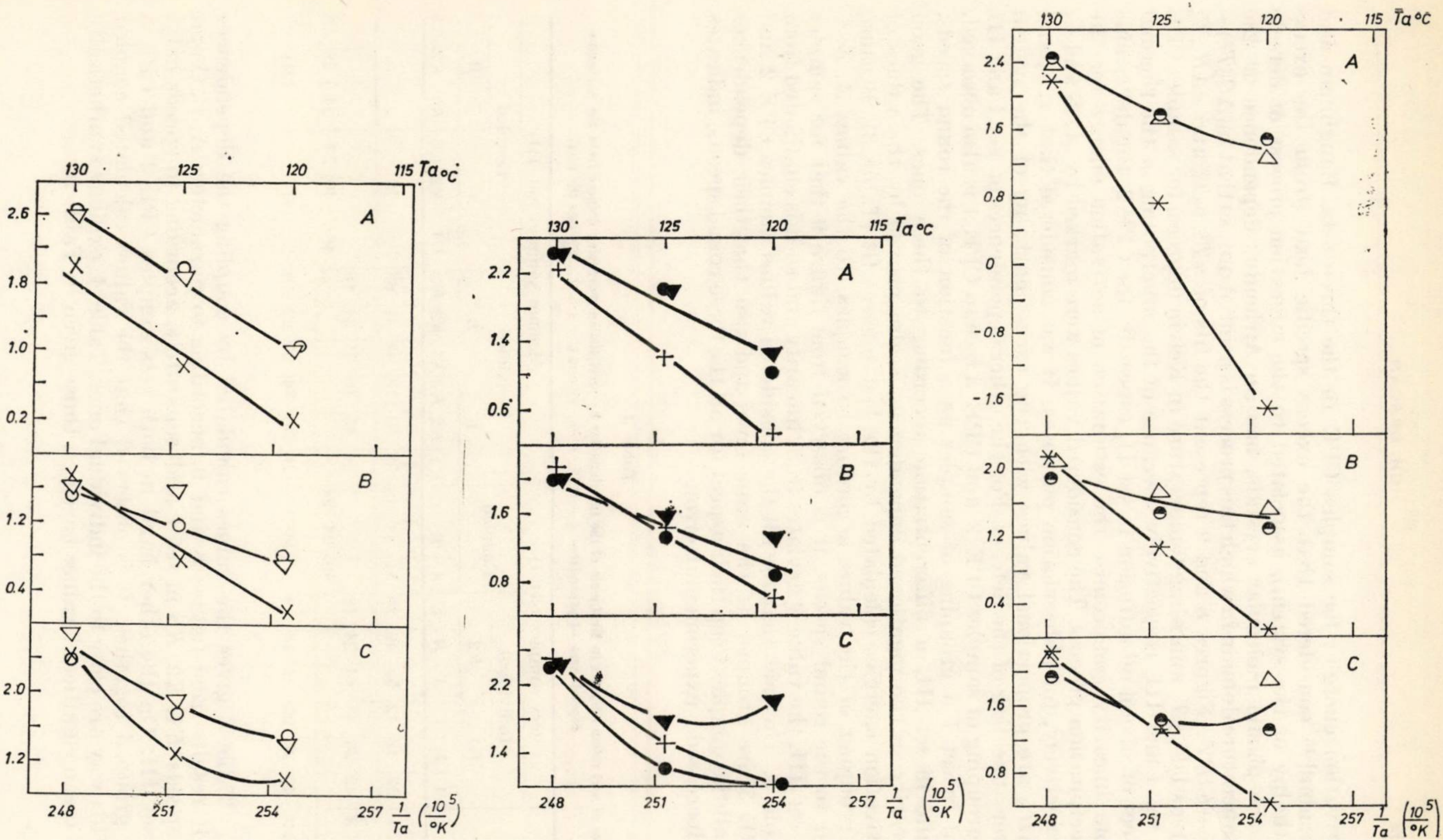

Fig. 9. — Arrhenius dependence of *A*, *B*, *C* parameters (see the text) for CPE samples in set III grouped according to the DTA round speeds.

activation energies for samples CPE in the three sets. Baughman and Turnbull[12] considered that the excess specific heat (from the excess enthalpy of the system), associated to the migration process of defects in the plastic molecular crystals, has an Arrhenius dependence on the temperature domain in which this process is pointed out, so that $\ln(\Delta C_p T^2) \sim$ $\sim -E/RT$. Figures 8 and 9 represent the fits of αT_a^2, $h_2 T_a^2$ and $\sigma \Delta H_m T_a^2$ versus $1/T_a$ (T_a annealing temperature in Kelvin degrees) for samples CPE in set I and III, respectively. Because of the superposing of the thermal effect of silicon oil diffusion in set II, especially for CPE 2, the deviations from linearity compromise the estimation of activation energy for the precipitation process. The considered values were marked by A, B and C, respectively, for abbreviation purposes. It was considered that α, h_2 and $\alpha \Delta H_m$ are proportional values with the excess enthalpy of the system after annealing of the defects. For the other dependences of set I and III a grouping of samples CPE 2 and CPE 3 face to CPE 1 is also observed, and in set I a grouping of samples as a function of the round speeds, while in set III, a differentiation according to these ones. The good linearity in the mentioned dependences is also proved by the values of activation energies calculated by the last squares fit (Table 3). Because of grouping of the values according to samples, to the values A, B, C and to the round speeds, it is observed from figure 9 that for samples in set III, the value C deviates from linearity and so it is eliminated from Table 3. The fact that for all the considered values samples CPE 2 and CPE 3 are grouped at the same level and also that their dependences in all the samples keep their aspect for all the three round speeds, indicates a decreased experimental error.

Table 3

Values of activation energies in Kcal/mole of the interlamellar by precipitation reordering deduced from the Arrhenius dependences of parameters $A = \alpha T_a^2$, $B = h_2 T_a^2$ and $C = \alpha \Delta H_m T_a^2$ (see the text)

	Dry samples (set I)									Medium samples (set III)											
	Individual						Coupled			Individual						Coupled					
	$K1$			$K2$						A			B			A			B		
	A	B	C	A	B	C	A	B	C	$K1$	$K2$	$K3$	$K1$	$K2$	$K3$	$K1$	$K2$	$K3$	$K1$	$K2$	$K3$
CPE 1	53	42	42	55	46	36	51	44	43	57	59	118	49	47	63		78			—	
CPE 2	42	26	45	44	24	18	40	24	24	46	45	40	21	34	18	46	40	37	24	28	18
CPE 3	40	25	25	38	18	9		(28)		46	36	34	27	22	19		(41)			(21)	

Table 3 gives the values calculated by coupling the dependences as it results from figures 8 and 9, according to parameters A, B, C and to speeds $K1$, $K2$, $K3$ in set I and separately, according to speeds only, in set III. On the other hand in both sets samples CPE 2 and CPE 3 are grouped together. It is observed that the values calculated coupled in this way are close to the individual ones. Table 4 exhibits synthetically the mean significant values based on those given in Table 3.

Before discussing the obtained results, a morphological model will be imagined for samples CPE resulted after annealing, using the facts known up to now. The observed interlamellar order after the coherent precipitation in CPE samples is visualized by an order-disorder transition.[1,2]

Table 4

Mean values of activation energies in Kcal/mole deduced from Table 3

	A		*B*		*C*	
	dry	medium	dry	medium	dry	medium
CPE 1	53	78	44	53	44	—
CPE 2 CPE 3	40	41	24	24	24	—

In the calorimetric measurements, particularly in the dynamic ones used, an important role in the response function [7] is played by the contribution of the dissipation modes. In this paper, this problem was stressed so that by using a precise sample geometry, homogeneous and with good thermal contact with the walls of the containers, the experimental errors were reduced. Because of the shear forces existing between the lamellar fragments in annealed CPE samples, the principal dissipation mode associated to T_m^1 transition is a viscous one. The precipitation process was established to be an interlamellar process. The activation energy of this process is assessed by the T_m^1 transformation process which is an interlamellar one. From the parameters A, B, C used in this assession the most adequate to Baughman and Turnbull judgement are B and C. Deviations from linearity for C parameter in set III reveal that the shape of the endotherm T_m^1 modifies because of the silicon oil as a parasite transfer medium. From Tables 3 and 4 one can observe that the two parameters give identical values. Parameter α indicates the relative variation of the amplitude of this effect face to T_m^0. During the precipitation process, the T_m^0 effect decreases, so that the dependence $\ln A$ versus $1/T_a$ will give an activation energy different from the other two.

The reorientation process by precipitation explained the reduction of the lamellar volume. Thus the T_m^1 effect is influenced in principle by the annealing medium. It is observed in sample CPE 1 that the activation energy in set III is higher than the one for set I. In turn, the presence of the silicon oil as annealing medium in the other samples, and as thermal transfer in DTA round, does not influence the T_m^1 process. This differentiation can be explained by the different contribution of the viscous dissipation mode in phase transition to sample CPE 1 in the dry case and with a transfer medium.

CONCLUSIONS

As a conclusion of the presented results, figure 10 suggests a reordination model of the lamellar fragments by twist disclination.[22]

The conformation defects (kinks and jogs)[4] chemically etched migrate coherently to local interlamellar amorphous domains on a gliding direction $\vec{T}$ in plane (001). Because of the fact that the cathenary portions separated by such defects are translated along the chain direction (see figure 2 from reference [4]), the lamellar fragments will be sheared along the |001| direction as figure 10a indicates. The disclination state that appears at the interaction local amorphous layer-lamellar fragment (on the habit face with normal $\vec{T}$), stores in this way an elastic energy expressed principally by the tangent stress components $\sigma_{00}\vec{n}$ (where $\vec{n}$ is the director of the chains like in the nematic structure). Thus the study of annealing in DTA apparatus under isothermal conditions (similar to conduction calorimetry),[23] has shown that this is an endothermal process. The higher the precipitation process, in other words, the tensions $\sigma_{00}\vec{n}$, the higher this energy gets. By T_m^1 transition this disclination can be relaxed in a viscous mode, so that the lamellar fragments will twist one another under an angle $\omega \sim \sigma_{00}$ around an axis parallel with $\vec{T}$ (figure 10 b).[22] The suggested model is consistent with the observation that the more advanced the annealing, the higher the T_m^1 effect is. The fact that the process is endotherm and not exotherm is however not explained by this model. It is stipulated that the study of energy transfer topology during annealing and during phase transition T_m^1 will explain this paradox too.

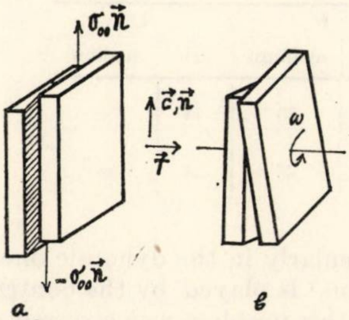

Fig. 10.a. — The model of lamellar fragments ordering after defect precipitation. b. — Lamellar reorientation after the viscous relaxation for the interaction of twist disclination.

---

[22] T. W. Chou, *J. Appl. Phys.*, **42**, 4931 (1971).

[23] The metallic block of the DTA apparatus that contains the containers, was plunged in the bath of an ultrathermostate regulated at annealing temperature.

Revue Roumaine de Chimie, **21**, *9–10*, 1395–1404 (1976)

ON A NEW PROCEDURE FOR OBTAINING SULPHUR DIOXIDE STARTING FROM CALCIUM SULPHATE. II[1]

UTILIZATION OF PHOSPHOGYPSUM AND OF NATURAL GYPSUM WITH IMPURITIES OF $CaCO_3$

C. LITEANU, ELENA HOPÎRTEAN, I. C. POPESCU, N. L. KÉKEDY, ELISABETA VERESS and V. LITEANU

Department of Chemistry, University "Babeş-Bolyai" Cluj-Napoca

Received January 18, 1975

This paper presents a study on the conditions for obtaining SO_2 by electrolysis of a melt of NaCl-phosphogypsum and NaCl-natural gypsum with impurities of $CaCO_3$, respectively. Applying the method of current-tension curves coupled with the analytical control of the electrolysis process the possible use of the starting materials studied, as sources of $CaSO_4$ in the above mentioned process, was confirmed. The electrolysis was established to occur under optimal conditions at a temperature of 750°—850°, the electrolysis tension ranging between 2 and 12 V for a current density of $1.2 A/cm^2$ (when using baked coal electrodes of Ø = 20 mm). The current efficiency is in this case of 40%.

The procedure for obtaining SO_2 starting from pure $CaSO_4$ by electrolysis of a $NaCl-CaSO_4$ melt was reported earlier. [1,2]

Since the procedure cannot be applied on industrial scale by using pure $CaSO_4$ as starting material, electrolysis conditions have been studied, when natural gypsum, or phosphogypsum, is the source of $CaSO_4$. The present paper presents the results of a detailed study on this procedure.

I. EXPERIMENTAL SECTION

Starting materials: The following materials have been used in the experiments: $CaSO_4$ p.a, commercial NaCl (extra fine iodinated salt), phosphogypsum (table 1), natural gypsum (table 1).

Electrolytic cell and electrodes used. The electrolytic cell consists of a porcelain crucible with a 100 mm outer diameter and 150 mm high. The quantity of the electrolyte has been chosen so as to have a 50 mm (approximately 400 g) mean level of the melt. Coppered baked coal electrodes of Ø = 4.6.8 and 20 mm have been used for the electrolysis. Before use, the copper layer was removed from the portion in contact with the melt.

In order to collect the anodic gases, the anode was covered with a porcelain bell fitted with a copper pipe for the removal and cleaning of gases.

Continuous current source. The electrolysis tension was obtained from a selenium rectifier capable to deliver 15A.

---

[1] Part I: C. Liteanu and E. Cordoş, *Rev. Roumaine Chim.*, **12**, 985 (1967).

[2] C. Liteanu and E. Cordoş, Patent R. S. Romania nr. 43174, 2 March, 1964.

The tension and current intensity control in the electrolysis circuit was carried out by two universal instruments having a class of precision 1.5. An ammeter fitted on the rectifier (class of accuracy 2.5) was used for intensities of electrolysis current higher than 6 A.

Table 1

Chemical composition of the starting materials used

Substance determined	Content (%) in	
	phosphogypsum	natural gypsum
H_3PO_4	0.62	—
$Ca(H_2PO_4)_2$	0.59	—
$CaSO_4$	52.58	74.15
$CaCO_3$	—	4.61
H_2O	41.60	14.13
insoluble residue	4.61	7.11

Heating installation and temperature control. The working temperature was accomplished by introducing the electrolytic cell in a vertical, cylindrical electric furnace with a crucible of Ø = 105 mm and a depth of 150 mm fed by an autotransformer of 1.6 kW maximum power.

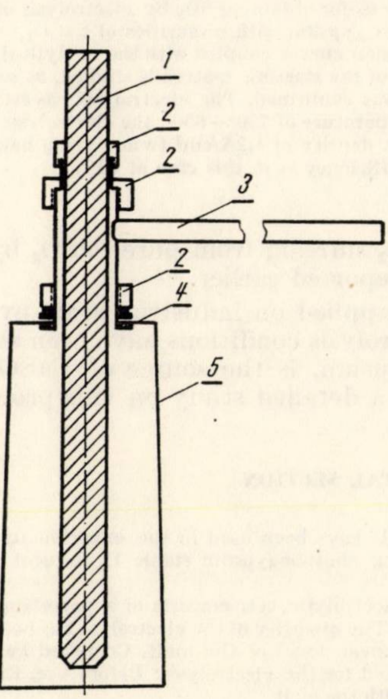

Fig. 1. — Gas collector. *1.* coal anode; *2.* packing nut; *3.* copper tube; *4.* asbestos packing; *5.* porcelain bell.

The temperature was controlled by a contact thermometer using a Pt-PtRh thermocouple plunged into the melt. This device allowed a constant working-temperature to be maintained with an error of ±10°. Fig. 2 exhibits the block diagram of the heating and temperature control device.

II. RESULTS

1. *Working temperature.* Since at temperatures above 250° the $CaSO_4$ content is 90.07 % in the phosphogypsum and 86.48 % in the natural gypsum used attempts were made to work with phosphogypsum—NaCl, and gypsum—NaCl mixtures, respectively, of a composition corresponding to the eutectic used for the electrolysis of pure $CaSO_4$.[1] This eutectic had the composition : 37 % $CaSO_4$ and 63 % NaCl melts at 726°.[3]

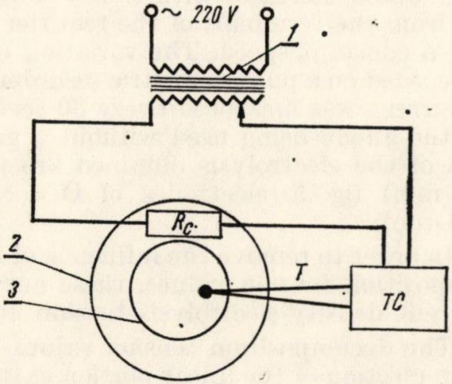

Fig. 2. — Block diagram of the furnace with the temperature control assembly and the electrical energy feed system. *1*. autotransformer ; *2*. furnace crucible ; *3*. electrolytic cell ; thermocouple (*T*) ; contact thermometer (*TC*) ; furnace resistance (R_c).

It was established after several trials that the presence of $Ca(H_2PO_4)_2$ in phosphogypsum and also $CaCO_3$ in gypsum ores does not change either the solubility of $CaSO_4$ in NaCl or the melting temperature of the mixtures whose composition corresponded to this eutectic.

Based on these results, the working temperature chosen was 750° (minimum).

2. *Study of the electrolysis process.* The previous study [1] has established that the electrolytic decomposition of $CaSO_4$ in the melt, using iron cathode and graphite anode, begins within the 2—3 V tension range at 740°. Under these conditions the electrode processes are the following :

$$\text{— at the cathode}: Ca^{2+} + 2e \rightarrow Ca$$

$$4Ca + CaSO_4 \rightarrow 4CaO + CaS$$

$$\text{— at the anode}: \quad SO_4^{2-} - 2e \rightarrow SO_2 + O_2$$

On the basis of these data, a detailed study was developed on the influence of various factors upon the electrolytic process. For this purpose, the method of electrolysis current-tension curves was used coupled with an analytical study of the electrolysis products.

2.1. *The method of current-tension curves.* The method of $I = f(U)$ curves was used to investigate the following problems : a) to establish the value of the decomposition tension ($U_{dec.}$) of the pure NaCl and of $CaSO_4$, when different eutectics are used; b) the influence of the composition of the melt upon the decomposition tension value of $CaSO_4$; c) the influence of the quality and of the size of the electrode surface upon U_{dec} of $CaSO_4$.

---

[3] J. Bye and J. G. Kiehl, *Bull. Soc. chim. France*, **1948**, 847.

2.1.1. *Decomposition tension* ($U_{dec.}$) *of NaCl and* $CaSO_4$ *in different meltings used.* The $I-U$ curves have been recorded for the different starting materials used by means of the connection given in fig. 3. The electrolysis tension which increases with time was obtained by applying the tension taken from the terminals of the rectifier on a polarographic tambour (T) run at a constant speed. The variation in time of the electrolysis tension was recorded on a potentiometric recorder (P). The intensity of the electrolysis current was measured every 30 seconds. Baked coal electrodes were used, the anode being used without a gas collector. The current tension curves of the electrolysis obtained are presented in fig. 4 (electrodes of Ø = 4 mm) fig. 5 (electrodes of Ø = 8 mm) and fig. 6 (electrodes of Ø = 6 mm).

In order to remove the influence of the surface of electrodes upon the decomposition tension values, these curves (fig. 4—6) were recalculated in current density-electrolysis tension coordinates.

The decomposition tension values from table 2 were obtained from the intersection of the linear portion extrapolated with the abscissa.

Table 2

Decomposition tension of the different $CaSO_4$ sources used

	$U_{dec.}$ (V)		
	Eutectic pure $CaSO_4$	Eutectic phosphogypsum	Eutectic natural gypsum
	2.34	2.35	2.20
	2.45	2.00	1.90
Working temperature (°C)	840	840	860

2.1.2. *Influence of the melt composition upon* $U_{dec.}$ *of* $CaSO_4$. In order to establish the influence of the melt composition (the $CaSO_4$ content by %) upon the electrolysis process, the I—V curve were recorded for pure $CaSO_4$—NaCl melting (electrodes of Ø = 4 mm), phosphogypsum — NaCl melting (electrodes of Ø = 8 mm) and natural gypsum — NaCl (electrodes of Ø = 6 mm) of different composition. The working temperature was constant during the electrolysis of the mixture of the same type. No gas collector was used.

Although the shape of the I—V curves changes with the increase of the $CaSO_4$ content in the meltings under study (the slope of the ascending branch decreases), the decomposition tension values have not been found to change significantly. Table 3 presents the external decomposition-tension values corresponding to the $CaSO_4$ concentration ranges used in the meltings.

2.1.3. *Influence of the temperature upon* $V_{\text{dec.}}$ *of* $CaSO_4$. $I = f(V)$ curves were recorded, corresponding to the electrolysis of the NaCl-pure $CaSO_4$ eutectic melt, with baked coal electrodes of Ø = 8 mm without gas collector at the anode, at several working temperature values, situated within an interval of 100°. Also in this case, the decomposition tension values do not differ significantly within the limits of experimental error, being placed in the interval 2.20–2.60 V for a temperature variation from 770° to 840°.

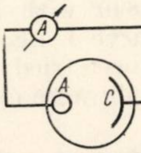

Fig. 3. — Block diagram of the connection used for recording the current (*I*)-electrolysis tension (*U*) curves. *A*-anode; *C*-cathode; *P*-recording potentiometer; *T*-potentiometrical tambour; *S*-source of continuous current.

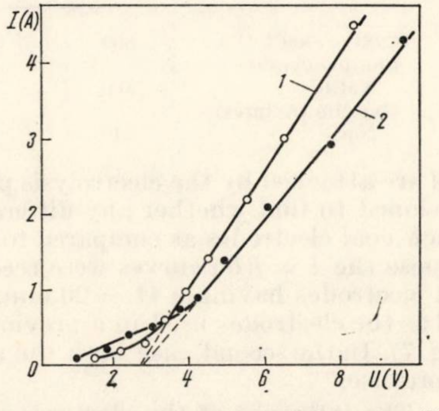

Fig. 4. — Current (*I*)-electrolysis tension (*U*) curves for NaCl (1) and for the eutectic chemically pure $CaSO_4$—NaCl (2); *T*=840°.

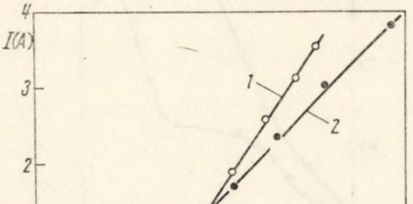

Fig. 5. — Current (*I*)-electrolysis tension (*U*) curves for NaCl(1) and for the eutectic phosphogypsum-NaCl (2); *T*=840°.

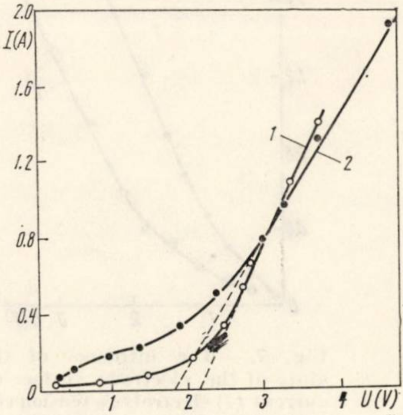

Fig. 6. — Current (*I*)-electrolysis tension (*U*) curves for NaCl (1) and for the eutectic natural gypsum (Aghireș)-NaCl (2); *T*=860°.

2.1.4. *Influence of the quality and surface area of the electrodes upon the decomposition tension of $CaSO_4$*. During the electrolysis the electrodes used are attacked by the electrolysis products. For this reason a study was developed to find whether any difference appears between the behaviour of new coal electrodes as compared to the electrodes already used. To this purpose the $I = f(U)$ curves were recorded for a melt of 840° with baked coal electrodes having a Ø $= 20$ mm. New electrodes (curve 1 fig. 7) as well as the electrodes used in a previous electrolysis have been tried (curve 2 fig. 7). In the second case both the anode and the cathode were cleaned before use.

Table 3

Influence of the composition of the melt upon $U_{dec.}$ of $CaSO_4$

Mixture used	T (°C)	Concentration range (% $CaSO_4$)	Extremal values of $U_{dec.}$ (V)
$CaSO_4$–NaCl	860	10.9–42.3	2.35–2.45
Phosphogypsum NaCl	800	10.9–48.1	1.80–2.20
Gypsum (Aghireş)–NaCl	840	10.9–48.1	1.75–1.90

The influence of the electrode surface area in the case of a couple of baked coal electrodes of Ø $= 8$ mm and Ø $= 20$ mm, respectively, has been also investigated. The electrolysis of the melted pure $CaSO_4$–NaCl eutectic was performed obtaining the $I-U$ curves presented in fig. 8.

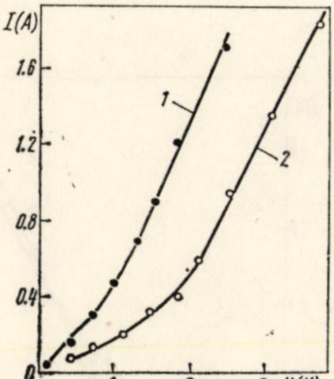

Fig. 7. — The influence of the state of the electrode surface on current (I) electrolysis tension (U) curves for NaCl-pure $CaSO_4$ (eutectic). *1.* new electrodes of Ø = =20 mm ; *2.* used electrodes of Ø = 20 mm.

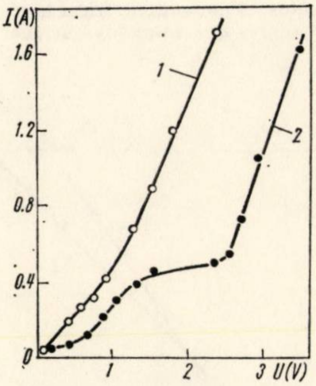

Fig. 8. — Influence of the electrode surface on the current (I)-electrolysis tension (U) curves (coal cathode). *1.* anode of Ø=20 mm ; *2.* anode of Ø = 8 mm.

2.1.5. *Study of the electrode processes*. In order to establish whether a succession of processes takes place or not in the course of the electrolysis, some current(I) electrode potential (E) measurements were made using a silver electrode immersed into the melt as a reference electrode. Using the connection shown in fig. 9 points $I = f(E)$ were recorded for melted NaCl and for the eutectics pure $CaSO_4$-melted NaCl (fig. 10 and 11) as well as for melted NaCl and the eutectic NaCl-melted phosphogypsum (fig. 12), respectively.

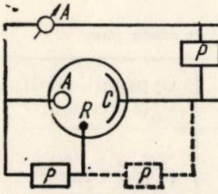

Fig. 9. — Block diagram of the connection used for recording the current (I)-electrode potential (E_a, E_c) curves. A-anode ; C-cathode ; R-reference electrode ; P-recording potentiometer ; T-potentiometrical tambour ; S-source of continuous current.

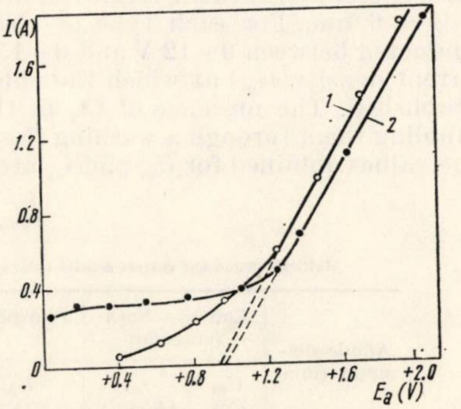

Fig. 10. — Current (I)-anodic potential (E_a) curves against the Ag reference electrode. *1.* NaCl$-CaSO_4$ (eutectic) ; *2.* pure NaCl ; $T = 820°$.

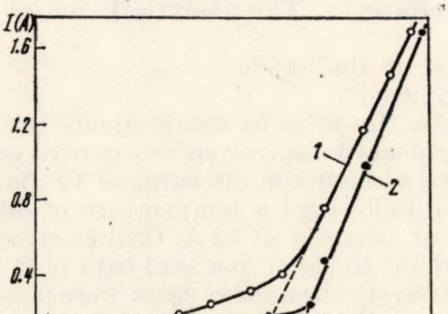

Fig. 11. — Current (I)-cathodic potential (E_c) curves against the Ag reference electrode. *1.* NaCl$-CaSO_4$ (eutectic) ; *2.* pure NaCl ; $T = 820°$.

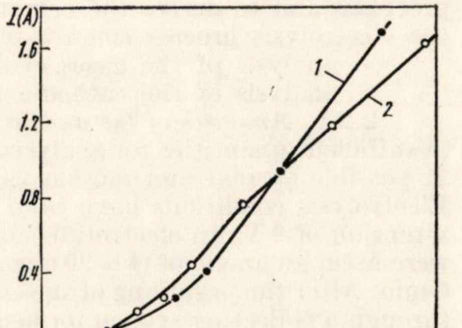

Fig. 12. — Current (I)-electrode potential curves against the Ag reference electrode, corresponding to NaCl-phosphogypsum (eutectic). *1.* Ag-cathode (E_c) ; *2*, Ag-anode (E_a).

2.1.6. *Determination of the tension* (U_{cr}) *and of the anodic current density* (I_{cr}) *at which the discharge of the* Cl^- *ions begins.* A prolonged electrolysis of the three electrolytes already used (eutectic melting of pure $CaSO_4$–NaCl, phosphogypsum–NaCl and natural gypsum–NaCl) has been accomplished with baked coal anodes having different diameters provided with gas collector and cathode formed of four serially-connected baked coal bars of Ø = 6 mm. For each type of electrode (anode) the electrolysis was conducted between 0–12 V and 0–15 A at 800°. In each case, the critical current density (i_{cr}) at which the chlorine appears in the anodic gas was established. The presence of Cl_2 in the anodic gases was established by bubbling them through a washing flask with a 0.1 N $AgNO_3$ acid solution. The values obtained for U_{cr} and i_{cr} are included in table 4.

Table 4

Critical tension and current density values for the appearence of Cl_2 in anodic gases

Anode diameter (mm)	$CaSO_4$ – NaCl (eutectic)		Phosphogypsum – NaCl (eutectic)		Gypsum–NaCl (eutectic)	
	U_{cr} (V)	i_{cr} (A/cm^2)	U_{cr} (V)	i_{cr} (A/cm^2)	U_{cr} (V)	i_{cr} (A/cm^2)
20	12	1.2	12	1.2	12	1.2
8	—	—	7.90	0.840	7.80	0.750
6	5.85	0.419	6.40	0.476	—	—

2.2. *Analytical control of the electrolytic process.* The electrolysis products were analyzed in order to determine the nature of the electrode processes and to derive the current efficiency. The analytical control of the electrolysis process consists of:

- analysis of the gases evolved at the anode
- analysis of the cathodic products.

2.2.1. *Analysis of the anodic gases.* In order to obtain anodic gases in sufficient quantities for analysis, prolonged electrolysis was carried out, at possible current and tension values without the discharge of Cl^- ions. Electrolysis conditions have been the following: a temperature of 800°, a tension of 9 V, an electrolysis current intensity of 13 A. Coal electrodes were used, an anode of Ø = 20 mm and a cathode of four coal bars of Ø = 6 mm. After the beginning of the electrolysis, the anodic gases were passed through a collecting system formed of a collecting bell, a gas exhaust and cooling tube and a rheometer (used for keeping the pressure of the collected gases at a constant value, till the complete evacuation of the air). The gases evolved at the anode were then collected in a gasometer. 100 ml gas samples were removed from the gasometer for analysis.

The preliminary studies showed that the anodic gas mixture contains SO_2 CO_2, CO, O_2 and traces of SO_3. The sulphur dioxide and sulphur trioxide were absorbed in a 10% solution of H_2O_2. The CO_2 determination was made by absorption in a 30% KOH solution. The absorbent used in the O_2 determination was an alkaline solution of pirogallol and, in the case of CO determination, an ammoniacal cuprous chloride solution. The composition of the anodic gases is given in table 5.

2.2.2. *Current efficiency*. By measuring the evolution time of 10 ml anodic gas, at 730 mm Hg atmospheric pressure, at a temperature of 25°, and knowing its composition as well as the current intensity of the electrolysis : $I = 13.2$ A, the anodic gas yield was calculated : $R(SO_2) = 40.5\%$.

Table 5

Chemical composition of the anodic gases

Compound determined	% Volume		
	$CaSO_4$-NaCl (eutectic)	Phosphogypsum-NaCl (eutectic)	Gypsum-NaCl (eutectic)
$SO_2 + SO_3$	48.5	48.5	48.5
CO_2	18.9	18.8	19.5
O_2	15.1	14.8	14.0
CO	17.5	17.9	18.0

III. DISCUSSIONS AND CONCLUSIONS

From the shape of the current-electrolysis tension curves obtained for the following melts : NaCl (curve 1, fig. 4), NaCl-pure $CaSO_4$ (curve 2, fig. 4) NaCl-phosphogypsum (curve 2, fig. 5) and NaCl-natural gypsum (curve 2, fig. 6) as well as from data given in table 2, it results that the electrolysis of $CaSO_4$ begins in the electrolysis tension interval between 2–3 V, irrespective of the nature of the starting material used.

The decomposition tension of the $CaSO_4$ melt (irrespective of the source from which it is obtained), dissolved in a melted NaCl, does not depend on the quantity of $CaSO_4$ present in the melting (table 3). However the melts with higher $CaSO_4$ content have been observed to have an ever lower conductibility (the slope of the linear portions of the current-electrolysis tension curves decreases). Presumably, this is explained by the decrease of the $CaSO_4$ dissociation degree, due to the increase of the $CaSO_4$ concentration in the solution.

Based on the results of the measurements made, it can be concluded that the influence of the temperature upon the decomposition tension of the $CaSO_4$ melt in eutectic with NaCl is minor. The increased conductibility of the melt materialized by a vertical shift of the V curves does not modify the U_{dec} values.

The baked coal electrodes used are constructed by agglomerating the coal grains under pressure using a binder (bitumineous earth), and by baking them at 1000–1100° thereafter. Therefore, at the working temperature (750–850°) under the action of the electrolysis products (O_2, CO, i.e.) the superficial grains may be detached increasing in this way the porosity of the electrode and consequently increasing its active surface. The shift on the abscissa of the $I-U$ curves in fig. 7 can be explained in this manner. The shape of $I-U$ curves in fig. 8 pleads for the same thing. That is why exact values of the decomposition tension of $CaSO_4$ in the NaCl–$CaSO_4$ eutectic melt may be obtained by means of the method of

$I = f(U)$ curves only if experimental data are presented in current density (i)-electrolysis tension coordinates (see data tabulated in table 2).

The current-electrode potential measurements (the cathode and the anode potential, respectively, against an Ag electrode) prove the existence of a single electrode process, both at the anode and at the cathode during the electrolysis of the $CaSO_4$ used (figs 10–12). The analysis of the anodic gases supports this statement (table 5). The analysis of the cathodic products has not been repeated, because both the analysis of the starting materials and the shape of $I = f(E_c)$ curves have revealed that there is no difference between the behaviour of the three melts under such conditions.

In conclusion, as long as the electrolysis tension corresponding to a current density of 1.2 A/cm² does not exceed 12 V, the electrolysis of a $CaSO_4$ (37%)–NaCl (63%) melt at 750°–850° will provide an anodic gas mixture with 48–50% SO_2 while a mixture of $CaS \cdot 4CaO$ results at the cathode irrespective of the source of $CaSO_4$ used.

Revue Roumaine de Chimie, **21**, *9–10*, 1405–1415 (1976)

PHENOL OBTENTION FROM BENZENE IN OXYGEN PLASMA GENERATED BY HIGH FREQUENCY DISCHARGES. I

DISPERSIONAL ANALYSIS OF THE DATA AND THE MULTIPLE REGRESSION EQUATION OF THE PROCESS

G. BOURCEANU [*], V. ABABI[*], GH. POPA[**] and M. SANDULOVICIU[**]

[*] Faculty of Chemistry and Chemical Engineering, Polytechnic Institute of Jassy, Splai Bahlui 71 ;

[**] Faculty of Physics, "Al. I. Cuza" University, Jassy, Calea 23 August 11, Romania.

Received January 28, 1975

The conditions for obtaining phenol from benzene, in oxygen plasma, have been found. The dispersional analysis of a great number of experimental data has been made in order to establish the influence of each macroscopic parameter over the phenol yield, as well as the interaction between parameters.

Phenol obtention by other ways than the classical ones constitutes a permanent concern of many investigations. Thus, the radiolytic oxidation of benzene in aqueous solution was much studied being of both theoretical and practical interest to obtain phenol by direct oxidation of benzene.[1–4] The main products which occur after irradiation of aqueous benzene solution are : phenol, diphenyl, hydrogen and hydrogen peroxide.[2] Phenol was also obtained in the plasma of luminescence discharges in an atmosphere of benzene and water,[5] and recently attempts have been made to obtain phenol from toluene and water in the high frequency discharges plasma.[6]

EXPERIMENTAL

The oxygen plasma was generated in a high frequency electromagnetic field under impulse regime, using a Jena glass tube with a section of 5.30 cm^2 and the volume of the discharge zone of about 212 cm^3. The experiments were carried out at different values of the

---

[1] K. M. Dorfman, R. E. Bühler and I. A. Taub, *J. Chem. Phys.*, **36**, 309, (1962).

[2] P. V. Phung and M. Burton, *Radiation Res.*, **7**, 199 (1957).

[3] M. A. Proscurnin, F. V. Barelko and L. I. Kartosheva, *Doklady Akad. Nauk S.S.S.R.*, **121**, 671 (1958).

[4] B. Claire and L. Ordinaire, in "Solid State and Chemical Radiation Dosimetry in Medicine and Biology", IAEA, Vienna, 1967, p. 287.

[5] H. Schuler, E. Lutz and G. Arnold, *Naturwiss.*, **48**, 426 (1961).

[6] G. Bourceanu, Gh. Popa, M. Sandulovicu and V. Ababi, *Rev. Roumaine de Chimie*, **19**, 207 (1974).

generator power, and the field frequency was 30 MHz. The initial mixture, benzene-oxygen, in different molar ratios, was fed in a continuous flow. The flow rates of reactants were measured by means of two flowmeters with silicone oil. The pressure of gaseous mixture in the discharge zone was measured using a differential manometer with silicone oil too. The condensable products under the operating conditions of temperature and pressure were captured in traps cooled with liquid nitrogen.

The reaction products. The reactions which took place in the discharge plasma resulted in a liquid mixture, made up of an organic layer and an aqueous layer. Also, a gaseous mixture was obtained. The analysis of both organic liquid mixture and gaseous mixture was performed by means of gas chromatography. Only one new component dissolved in unreacted benzene was identified in the organic mixture. Its detection was made on the basis of the retaining parameters in the chromatographic column. The components in the gaseous mixture were identified in the same way. For this reason, a chromatograph with hot wire detector was used. Carbowax 20 M (C.W. – 20 M) was used as stationary phase and hydrogen was employed as carrying gas. The analyses were carried out in the programmed temperature regime. On the basis of the analysis, only phenol dissolved in the unreacted benzene was identified in the organic liquid mixture. Acetylene, ethylene and propylene were found in the gaseous mixture. Hydrogen peroxide was detected in the aqueous layer by means of an acid solution of potassium permanganate. A polymer, deposited on the discharge tube, was also obtained.

DISPERSIONAL ANALYSIS OF THE DATA

In experiments carried out with the oxygen-benzene reactant mixture having the oxygen to benzene molar ratio ranged between 1.0 and 10.0, phenol was not obtained; only diphenyl dissolved in unreacted benzene was found. Further on by increasing the oxygen content and having an oxygen to benzene molar ratio from 10.0 to 25.0, both diphenyl and phenol were formed. Using an oxygen to benzene molar ratio, larger than 25.0, only phenol is obtained. Furthermore, the benzene conversion to phenol increases with the increase of the oxygen to benzene molar ratio, up to a certain value, after which it starts decreasing. Also, the phenol yield increases with the increase of the generator power.

Taking into account these experimental observations, we wanted to establish the influence of each parameter, namely, generator power P, flow rate of oxygen O and flow rate of benzene B, as well as the interaction effect between these parameters on the phenol yield. For this reason we made the factorial experiments for several levels of each parameter. The phenol yields obtained at each levels combination are summarized in table 1.

The data listed in table 1 show that the phenol yield increases with the increase of the oxygen flow rate up to a certain value after which it decreases.

Since in the case in which there are several parameters at several levels, the computing procedure and the interpretation method of the experimental data is a complicated operation, table 1 including an analysis with several parameters is divided into several tables with two parameters, through successive elimination of one parameter in turn from the initial table[7]. Thus three tables were obtained 2, 3 and 4, from the initial table 1 having each two parameters.

Table 1

The phenol yield obtained at benzene transformation to various powers, and flow rates of oxygen and benzene

	P_1 215.5 W				P_2 265.5 W				P_3 305.5 W				P_4 364.5 W				Total
	B_1 0.05 (mol/h)	B_2 0.07 (mol/h)	B_3 0.09 (mol/h)	B_4 0.12 (mol/h)	B_1	B_2	B_3	B_4	B_1	B_2	B_3	B_4	B_1	B_2	B_3	B_4	
O_1 4.01 (mol/h)					7.92	6.32	4.28	2.88	7.76	7.56	7.52	5.78	10.36	11.94	9.36	7.54	89.22
O_2 4.95 (mol/h)		9.02	5.52		9.62	8.54	8.62	6.06	16.54	15.82	11.76	8.66	16.80	19.60	14.26	10.60	146.84
O_3 5.80 (mol/h)		7.76	5.44		18.90	17.34	9.70	8.40	22.72	20.02	21.30	12.56	21.32	21.08	21.08	15.39	210.07
O_4 6.69 (mol/h)		5.30	2.80		21.42	11.44	12.62	8.40	26.28	22.04	22.04	15.52	25.06	25.46	22.30	17.76	230.34
O_5 7.58 (mol/h)					16.48	9.04	8.54	7.50	20.90	18.54	16.20	13.52	22.36	20.98	19.23	16.27	189.36
TOTAL					74.34	52.68	43.56	33.20	94.20	83.98	78.82	56.04	95.94	99.06	86.49	67.56	865.87

Table 2

The partial table *PB* with two factors

	B_1	B_2	B_3	B_4	Total
P_1	—	—	—	—	—
P_2	74.34	52.68	43.56	33.20	203.78
P_3	94.20	83.98	78.82	56.04	313.04
P_4	94.94	99.06	86.49	67.56	349.05
TOTAL	264.48	235.72	208.87	156.80	865.87

Table 3

The partial table *PO* with two factors

	O_1	O_2	O_3	O_4	O_5	Total
P_1	—	—	—	—	—	—
P_2	21.40	32.84	54.34	53.88	41.36	203.78
P_3	28.62	52.78	76.70	85.88	69.16	131.04
P_4	39.20	61.26	79.13	90.58	78.84	349.05
TOTAL	89.22	146.88	210.07	230.34	189.36	865.87

Table 4

The partial table *BO* with two factors

	O_1	O_2	O_3	O_4	O_5	Total
B_1	26.04	42.96	62.94	72.76	59.74	264.44
B_2	25.82	43.96	58.44	58.84	48.56	235.77
B_3	21.16	34.64	52.34	56.96	43.77	208.87
B_4	16.20	25.28	36.35	41.68	37.29	156.80
TOTAL	89.22	146.84	210.07	230.34	189.36	865.87

Having computed the partial tables, the sums of squares for principal effects and the sums squares for the interaction effects may be calculated from each of these table.

The table required for the dispersional analysis will be made up using the results obtained, and then dispersions will be tested by comparing Fisher-Snedecor's test F with the value of F_α written in table 5, where, α is the chosen significance threshold.[7-9]

Comparing the calculated value F to the value $F_{0.05}$, it can be seen that $F \gg F_{0.05}$ so that the zero hypothesis cannot be admitted, conse-

---

[7] A. Glück, "Metode matematice în industria chimică", Ed. Tehnică, București, 1971, p. 45, 84, 348.

[8] D. Ceaușescu, "Tratarea statistică a datelor chimico-analitice", Ed. tehnică, București, **1973**, p. 134.

[9] I. Văduva, "Analiza dispersională", Ed. tehnică, București, 1970, p. 182.

Table 5

The results of dispersional analysis

Source of dispersion	Sum of squares	Degrees of freedom	Dispersion S^2	$F = \frac{S^2}{S_r^2}$	$F_{0.05}$
P	572.30	$m - 1 = 2$	$\frac{S_P}{m-1} = 286.15$	63.73	3.88
B	419.58	$n - 1 = 3$	$\frac{S_B}{n-1} = 139.86$	31.14	3.49
O	1052.57	$l - 1 = 4$	$\frac{S_O}{l-1} = 263.14$	58.60	3.26
PB	41.19	$(m-1)(n-1) = 6$	$\frac{S_{PB}}{(m-1)(n-1)} = 6.86$	1.52	3.00
PO	55.27	$(m-1)(l-1) = 8$	$\frac{S_{PO}}{(m-1)(l-1)} = 6.90$	1.53	2.85
BO	63.10	$(n-1)(l-1) = 12$	$\frac{S_{BO}}{(n-1)(l-1)} = 5.25$	1.16	2.69
S_r	53.91	$(n-1)(l-1) = 12$	$\frac{S_r}{(n-1)(l-1)} = 4.49$		

quently the three parameters (P, B and O) influence directly the phenol yield.

Since for the interaction effects between parameters there is $F < F_{0.05}$, the zero hypothesis can be admitted, namely the hypothesis according to which the interaction effects PB, PO and BO do not influence the phenol yield.

THE CONFIDENCE INTERVAL CALCULATION

For a better interpretation of findings relating to the significance of the effects caused by parameters variation, the confidence interval including the difference of values observed at the passage of parameters P, B and O from one level to another was calculated. Its calculation utilizes the relation[7]:

$$d \pm t_\alpha \cdot s_r \sqrt{\frac{1}{K_1} + \frac{1}{K_2}} \tag{1}$$

in which K_1 and K_2 is the number of experiments at the two levels of the investigated parameters; t is the t-test, which, for the significance threshold, $\alpha = 0.05$, and number of degrees of freedom, $\nu = 12$, $t\ 0.05\ (12)$, is 2.179; s_r is the residual dispersion which in our case is $\sqrt{4.49}$ and d is the difference between the yields obtained for each combination of parameters P, B and O. Table 6 presents the confidence interval when passing from a power to another and from an oxygen flow rate to another.

Table 6

The values of the confidence intervals

Passing between levels	Difference between levels, d	Nr. of runs	The confidence interval $d \pm t_\alpha s_r \sqrt{\frac{1}{K_1} + \frac{1}{K_2}}$
$P_3 \rightarrow P_2$	15.46	20	5.46 ± 1.42
$P_4 \rightarrow P_3$	1.80	20	1.80 ± 1.42
$O_2 \rightarrow O_1$	4.80	12	4.80 ± 1.83
$O_3 \rightarrow O_2$	5.26	12	5.26 ± 1.83
$O_4 \rightarrow O_3$	1.85	12	1.85 ± 1.83
$O_4 \rightarrow O_5$	3.41	12	3.41 ± 1.83

The results listed in table 6 could be interpreted as follows: for example, in the case of power changing from P_2 to P_3, the phenol yield will increase with a probability of 95%, namely with 5.46 ± 1.42, a value ranging between 4.04 and 6.88%.

THE EQUATION OF MULTIPLE REGRESSION

A second degree multiple regression equation has been proposed in order to describe the process of phenol obtention from benzene and oxygen, taking into account the variation range of parameters as well as their influence on the yield[8]:

$$y = b_0 + b_1x_1 + b_2x_2 + b_3x_3 + b_{12}x_1x_2 + b_{13}x_1x_3 + b_{23}x_2x_3 + \\ + b_{11}x_1^2 + b_{22}x_2^2 + b_{33}x_3^2 \tag{2}$$

where y is the dependent variable, namely in our case the phenol yield; x_1, x_2 and x_3 are the independent variables, namely power P, benzene flow rate B and oxygen flow rate 0; and b_0, b_1, ... b_{33} are the regression coefficients whose value must be determined by computing.

The first four terms in eq. 2 express the linear dependence between the dependent variable y and the independent variables x_1, x_2 and x_3. The following three terms show whether there are interaction effects between the independent variables. Finally, the last three terms indicate a nonlinear dependence between the dependent variable y and the independent variables x_1, x_2 and x_3.

The regression coefficients $b_0, b_1, \ldots, b_{33}$ are usually computed by means of the least squares method. Therefore, the following expression:

$$\begin{aligned}\sum_{i=1}^{60}(y-Y)^2 &= \sum_{i=1}^{60}[y_i-(b_0+b_1x_1+b_2x_2+b_3x_3+\cdots+b_{33}x_3^2)]^2 = \\ &= \text{minimum}\end{aligned} \qquad (3)$$

must be minimized.

Making equal to zero the partial derivatives as against the regression coefficients, $b_0, b_1, b_2, \ldots, b_{33}$, after rearrangement of terms, a system of 10 equations results with 10 unknown quantities (4).

$$\left.\begin{aligned}
& mb_0 + b_1\sum x_1 + b_2\sum x_2 + b_3\sum x_3 + b_{12}\sum x_1x_2 + b_{13}\sum x_1x_3 + \\
& \quad + b_{23}\sum x_2x_3 + b_{11}\sum x_1^2 + b_{22}\sum x_2^2 + b_{33}\sum x_3^2 = \sum y \\
& b_0\sum x_1 + b_1\sum x_1^2 + b_2\sum x_1x_2 + b_3\sum x_1x_3 + b_{12}\sum x_1^2x_2 + b_{13}\sum x_1^2x_3 + \\
& \quad + b_{23}\sum x_1x_2x_3 + b_{11}\sum x_1^3 + b_{22}\sum x_1x_2^2 + b_{33}\sum x_1x_3^2 = \sum x_1y \\
& b_0\sum x_2 + b_1\sum x_1x_2 + b_2\sum x_2^2 + b_3\sum x_2x_3 + b_{12}\sum x_1x_2^2 + b_{13}\sum x_1x_2x_3 + \\
& \quad + b_{23}\sum x_2^2x_3 + b_{11}\sum x_1^2x_2 + b_{22}\sum x_2^3 + b_{33}\sum x_2x_3^2 = \sum x_2y \\
& b_0\sum x_3 + b_1\sum x_1x_3 + b_2\sum x_2x_3 + b_3\sum x_3^2 + b_{12}\sum x_1x_2x_3 + b_{13}\sum x_1x_3^2 + \\
& \quad + b_{23}\sum x_2x_3^2 + b_{11}\sum x_1^2x_3 + b_{22}\sum x_2^2x_3 + b_{33}\sum x_3^3 = \sum x_3y \\
& b_0\sum x_1x_2 + b_1\sum x_1^2x_2 + b_2\sum x_1x_2^2 + b_3\sum x_1x_2x_3 + b_{12}\sum x_1^2x_2^2 + \\
& \quad + b_{13}\sum x_1^2x_2x_3 + b_{23}\sum x_1x_2^2x_3 + b_{11}\sum x_1^3x_2 + b_{22}\sum x_1x_2^3 + \\
& \quad + b_{33}\sum x_1x_2x_3^2 = \sum x_1x_2y \\
& b_0\sum x_1x_3 + b_1\sum x_1^2x_3 + b_2\sum x_1x_2x_3 + b_3\sum x_1x_3^2 + b_{12}\sum x_1^2x_2x_3 + \\
& \quad + b_{13}\sum x_1^2x_3^2 + b_{23}\sum x_1x_2x_3^2 + b_{11}\sum x_1^3x_3 + b_{22}\sum x_1x_2^2x_3 + \\
& \quad + b_{33}\sum x_1x_3^3 = \sum x_1x_3y \\
& b_0\sum x_2x_3 + b_1\sum x_1x_2x_3 + b_2\sum x_2^2x_3 + b_3\sum x_2x_3^2 + b_{12}\sum x_1x_2^2x_3 + \\
& \quad + b_{13}\sum x_1x_2x_3^2 + b_{23}\sum x_2^2x_3^2 + b_{11}\sum x_1^2x_2x_3 + b_{22}\sum x_2^3x_3 + \\
& \quad + b_{33}\sum x_2x_3^3 = \sum x_2x_3y \\
& b_0\sum x_1^2 + b_1\sum x_1^3 + b_2\sum x_1^2x_2 + b_3\sum x_1^2x_3 + b_{12}\sum x_1^3x_2 + b_{13}\sum x_1^3x_3 + \\
& \quad + b_{23}\sum x_1^2x_2x_3 + b_{11}\sum x_1^4 + b_{22}\sum x_1^2x_2^2 + b_{33}\sum x_1^2x_3^2 = \Sigma x_1^2y \\
& b_0\sum x_2^2 + b_1\sum x_1x_2^2 + b_2\sum x_2^3 + b_3\sum x_2^2x_3 + b_{12}\sum x_1x_2^2 + b_{13}\sum x_1x_2^2x_3 + \\
& \quad + b_{23}\sum x_2^3x_3 + b_{11}\sum x_1^2x_2^2 + b_{22}\sum x_2^4 + b_{33}\sum x_2^2x_3^2 = \sum x_2^2y \\
& b_0\sum x_3^2 + b_1\sum x_1x_3^2 + b_2\sum x_2x_3^2 + b_3\sum x_3^3 + b_{12}\sum x_1x_2x_3^2 + b_{13}\sum x_1x_3^3 + \\
& \quad + b_{23}\sum x_2x_3^3 + b_{11}\sum x_1^2x_3^2 + b_{22}\sum x_2^2x_3^2 + b_{33}\sum x_3^4 = \sum x_3^2y
\end{aligned}\right\} \quad (4)$$

Table 7

Numerical value of sums in system

```
                 60.00         18710.00            4.95          348.36            1542.45
      108630.08           28.50        5933615.00             .43            2117.04
       18710.00      5933615.00           1542.45       108630.08          489453.05
    34450512.55         8886.86     1913102277.20          139.60          660218.96
           4.95         1542.45               .43           28.50             139.60
        9886.86            2.28         489453.05             .04             172.95
         348.36       108630.08             28.50         2117.04            8886.86
      660218.96          172.95       34450512.55            2.28           13389.47
        1542.45       489453.05            139.60         8886.86           44353.45
     2473001.75          805.82      157808679.26           13.61           54033.68
      108630.08     34450512.55           8886.86       660218.96         2473001.75
   209379005.48        54033.68    11107454013.35          805.82         4175385.87
          28.50         8886.86              2.28          172.95             805.82
       54033.68           15.36        2473001.75     34450512.06            1039.23
     5933615.00   1913102277.20         489453.05             .06       157808679.26
  1106454013.35      2473001.75           * * * *        44353.45       209379005.48
            .43          139.60               .04            2.28              13.61
         805.82             .60          44353.45             .00              15.36
        2117.04       660218.96            172.95        13389.47           54033.68
     4175385.87         1093.23      209379005.48           15.36           87532.79
                865.87         276966.03           67.32         5289.83           21585.75
     1688601.75          404.07       89955474.86            3.13           33285.42
                                          THE SYSTEM    SOLUTIONS
       −33.3354           .0171         −104.9481         12.8100             −.0057
         −.0019           .3578             .0001        −53.1998             −.8482
```

The system was solved through Gauss-Jordan's method using the FORTRAN language on a FELIX C–256 computer. Both sums from system and solutions of the system are given below.
The computer reading of the system data was vertical. After replacing the values of regression coefficients in eq. 2, it results :

$$y = -33.3354 + 0.0171x_1 - 104.9481x_2 + 12.8100x_3 - \\ - 0.0057x_1x_2 - 0.0019x_1x_3 + 0.3578x_2x_3 + 0.0001x_1^2 - \\ - 53.1998x_2^2 - 0.8482x_3^2 \qquad (5)$$

In order to find out the optimum parameters, namely the values of power, benzene flow rate and oxygen flow rate, as operating values for obtaining the maximum phenol yield, the partial derivatives as against x_1, x_2 and x_3 of eq. 5 must be calculated :

$$\left.\begin{aligned} \frac{\partial y}{\partial x_1} &= 0.0171 - 0.0057x_2 - 0.0019x_3 + 0.0002x_1 = 0 \\ \frac{\partial y}{\partial x_2} &= -104.9481 - 0.0057x_1 + 0.3578x_3 - 106.3996x_2 = 0 \\ \frac{\partial y}{\partial x_3} &= 12.8100 + 0.3578x_2 - 0.0019x_1 - 1.6964x_3 = 0 \end{aligned}\right\} \qquad (6)$$

By solving the system it gets the displacing unities : $\Delta x_1 = -4.8060$, $\Delta x_2 = -0.9629$ and $\Delta x_3 = 7.3504$. As it can be seen, negative values have been obtained for the first two parameters. On the one hand, these values do not have physical sense, and on the other hand, if the product between them and displacing distances utilized is performed, and taking into account the initial values of parameters, it gets, for example, the power : $x_1 = 365.6 - 45 \times 4.3060 = 171.73$ W. Or, at this power with the oxygen and benzene flow rates utilized in experiments, not even the discharge setting in can be achieved.

The condition expressed by eq. 6 is only necessary not also sufficient. The sufficient condition is that matrix A, made up by the partial derivatives of the IInd order

$$\left.\begin{aligned} &\frac{\partial^2 y}{\partial x_1^2} = 0.0002\,; \frac{\partial^2 y}{\partial x_1 \partial x_2} = -0.0057\,; \frac{\partial^2 y}{\partial x_1 \partial x_3} = -0.0019 \\ &\frac{\partial^2 y}{\partial x_2^2} = -106.3996\,; \frac{\partial^2 y}{\partial x_2 \partial x_3} = 0.3578\,; \frac{\partial^2 y}{\partial x_3^2} = -1.6964 \end{aligned}\right\} \qquad (7)$$

$$A = \begin{pmatrix} \dfrac{\partial^2 y}{\partial x_1^2} & \dfrac{\partial^2 y}{\partial x_1 \partial x_2} & \dfrac{\partial^2 y}{\partial x_1 \partial x_3} \\ \dfrac{\partial^2 y}{\partial x_2 \partial x_1} & \dfrac{\partial^2 y}{\partial x_2^2} & \dfrac{\partial^2 y}{\partial x_2 \partial x_3} \\ \dfrac{\partial^2 y}{\partial x_1 \partial x_3} & \dfrac{\partial^2 y}{\partial x_2 \partial x_3} & \dfrac{\partial^2 y}{\partial x_3^2} \end{pmatrix} = \begin{pmatrix} 0.0002 & -0.0057 & -0.0019 \\ -0.0057 & -106.3996 & 0.3578 \\ -0.0019 & 0.3578 & -1.6964 \end{pmatrix} \qquad (8)$$

should be defined either positively or negatively.[10] If it is defined positively it admits a minimum, and if it is defined negatively, it admis a maximum. Therefore, the scalar product between Au and an uncertain vector $\vec{u}$, must fulfil the condition :

$$(\mathrm{Au}, \mathrm{u}) \leqslant 0, = 0 \Leftrightarrow \mathrm{u} = 0 \qquad (9)$$

$$(Au, u) = \begin{pmatrix} 0.0002u_1 & -0.0057u_2 & -0.0019u_3 \\ -0.0057u_1 & -106.3996u_2 & +0.3578u_3 \\ -0.0019u_1 & +0.3578u_2 & -1.6964u_3 \end{pmatrix}^T \begin{pmatrix} u_1 \\ u_2 \\ u_3 \end{pmatrix} =$$

$$= 0.0002u_1^2 - 0.0114u_1u_2 - 0.0038u_1u_3 - 106.3996u_2^2 + \qquad (10)$$

$$+ 0.7156u_2u_3 - 1.6964u_3^2$$

A quadratic form was obtained. The matrix A is defined positively if and only if the quadratic form is defined positively too. In order to prove this, we must find a transformation of coordinates through which the quadratic form would be converted into a sum of squares. After a series of calculus tricks, we got the final formula :

$$(Au, u) = 0.0002(u_1^2 - \frac{57}{2}u_2 - \frac{19}{2}u_3)^2 - 0.0002\left(\frac{57}{2}\right)^2 u_2^2 -$$

$$- 0.0002\left(\frac{19}{2}\right)^2 u_3^2 - 0.0002\,\frac{57\cdot 19}{2}\,u_2u_3 - 106.3996u_2^2 + \qquad (11)$$

$$+ 0.7156u_2u_3 - 1.6964u_3^2$$

It can be easily observed that the quadratic form is defined neither positively nor negatively, therefore we can say nothing about the optimal points. Indeed, as it was also observed in the dispersional analysis, the phenol yield increases with the increase of the generator power. The kinetic study of the reaction will show that the formation rate of phenol also increases with the increase of the generator power. It results that the values of the power are far from the optimum value at which the maximum phenol yield could be obtained. Consequently, it can be said that eq. 5 obtained from eq. 2, with its regression coefficients computed from the experimental data, can describe the process only in a domain in which the values of parameters P, B and O are ranged or in their neighbourhood. Of course, if some values of parameters, close to those used in experiments, are taken, for example : $P = 380$ W ; $B = 0.04$ mol.h^{-1} and $O = 6.70$ mol.h^{-1}, one gets : $y = 27.01\%$.

---

[10] M. Nicolescu, N. Dinculeanu and S. Marcus, "Analiza matematică", Ed. didactică şi pedagogică, Bucureşti, 1971, p. 645–652.

Consequently, it can be said that the equation of multiple regression describes the process correctly, if the parameters take values close to those utilized in the real experiments.

Revue Roumaine de Chimie, **21**, *9–10* 1417–1427 (1976)

ÉLECTROPOLYMÉRISATION DES MONOMÈRES VINYLIQUES EN SOLVANTS APROTIQUES POLAIRES. III[1]

ÉLECTROPOLYMÉRISATION DE L'ACRYLONITRILE EN CARBONATE DE PROPYLÈNE ET D'ÉTHYLÈNE

CR. SIMIONESCU, C. UNGUREANU et AMALIA CRUSOS
Institut de Chimie Macromoléculaire « P. Poni », Jassy
41 A, Aleea Gr. Ghica Vodă

Reçu le 4 novembre 1975

On a étudié l'électropolymérisation de l'acrylonitrile en carbonate de propylène (CP) et carbonate d'étylène (CE), en présence de l'iodure de tétraéthylammonium. La cinétique de la réaction a été poursuivie par détermination de l'influence de l'intensité du courant électrique, la concentration du monomère, la durée de réaction et la température. L'analyse des résultats a permis d'établir que la polymérisation de l'acrylonitrile a lieu par un mécanisme anionique. Dans le processus il y a une dépendance du premier ordre en fonction de la concentration du monomère et du courant. Le rapport des constantes de la vitesse, k_p/k_t, a été commenté et l'effet des solvants sur la réaction a été établi.

I. INTRODUCTION

Des recherches récentes concernant l'électropolymérisation des monomères vinyliques dans des solvants organiques attestent le fait que le processus de polymérisation est influencé par les conditions où ont lieu les réactions électrochimiques. Ainsi Chapiro et Henrychowski,[2] en étudiant la polymérisation électrochimique de l'acrylonitrile en diméthylformamide, en présence de l'azotate de sodium comme électrolyte, établissent qu'au cathode la réaction a lieu par un mécanisme anionique, tandis qu'à l'anode la formation du polymère est de type radicalaire.

Un autre aspect relativement à l'effet du solvant a été mis en évidence par Tidswell et Dougthy [3] dans le cas de l'électropolymérisation du styrène. En utilisant le même électrolyte les auteurs mentionnent que dans le cas du sulfolan, comme milieu de réaction, la polymérisation est de type cationique et dans celui de diméthylacétamide elle est de type anionique.

Sans trouver l'explication, Funt et Bhadani [4] constatent, dans le cas de la polymérisation électrochimique du méthacrylate de méthyle un effet important des solvants (diméthylacétamide, diméthylformamide, diméthylsulfoxyde et acétonitrile) sur la vitesse de formation du polymère. La quantité de polymère formée au cathode diminue dans l'ordre mentionné des solvants ; dans l'acétonitrile la polymérisation du monomère n'a pas lieu.

---

[1] C. Ungureanu et Cr. Simionescu, *Rev. Roumaine Chim.*, **16**, 709 (1971).

[2] A. Chapiro et E. Henrychowski, *J. Chem. Phys.*, **65**, 616 (1968).

[3] B. M. Tidswell et A. G. Doughty, *Polymer*, **12**, 431, 760 (1971).

[4] B. L. Funt et S. N. Bhadani, *J. Polymer Sci.*, **A3**, 4191 (1965).

Le choix des solvants organiques convenables aux processus d'électropolymérisation des monomères vinyliques présente quelques difficultés. On sait que certains solvants avec une grande constante diélectrique quoique bons dissolvants pour le monomère, le polymère et l'électrolyte ne peuvent pas être utilisés dans ce but à cause de leur interaction avec les ions qui se forment dans le processus électrolytique. D'autre part, ceux à constante diélectrique petite, sont de faibles dissolvants pour les électrolytes ayant pour effet la formation de certaines solutions avec une conductibilité très réduite.[5] Le nombre réduit des solvants employés à la polymérisation électrochimique des monomères vinyliques plaide en faveur de ces constatations. Un petit nombre de ces solvants a été étudié comme milieu de réaction pour l'électropolymérisation de l'acrylonitrile : diméthylformamide,[6,8] diméthylsulfoxyde [9] et diméthoxyétane.[10]

L'utilisation du carbonate de propylène (CP) et du carbonate d'éthylène(CE) qui font l'objet de la présente étude est peu connue. On a comme seules indications dans la littérature les recherches effectuées par Pistoia[11,12] sur l'électropolymérisation du styrène dans les solutions de CP—$LiClO_4$. La formation à l'anode de $HClO_4$ dans le système étudié mène à la polymérisation cationique du monomère ayant certaines ressemblances avec la polymérisation classique catalysée de $HClO_4$ en $C_2H_4Cl_2$[13] et CH_2Cl_2.[14] D'autres auteurs présentent l'utilisation du CP comme solvant pour des déterminations conductométriques.[15,16]

II. PARTIE EXPÉRIMENTALE

Les solvants, du carbonate de propylène, (BDH), et du carbonate d'éthylène, (CIFFCh — Săvinești), ont été purifiés par distillation à pression réduite.

L'électrolyte, l'iodure de tétraéthylammonium, (BDH) de pureté analytique, a été utilisé sans purification préalable. Les monomères, l'acrylonitrile, AN, (UCB) et le styrène, St. (Borzești) ont été purifiés par la méthode habituelle.

L'électropolymérisation a été effectuée en deux types de cellules. L'une de forme cylindrique, ayant un seul compartiment et une autre double avec les compartiments, cathodique et anodique séparées par une plaque en verre fritté, G_4.

Les électrodes qui forment le cathode et l'anode ont été confectionnées en plaque de platine, chacune ayant la surface de 1,2 cm². Le courant électrique continuel a été fourni par un stabilisateur automatique de courant (MICM — CCPAS) construit d'après un schéma indiqué par Breitenbach,[6] à l'aide duquel on obtient un courant de 1—100 mA.

---

[5] N. Yamazaki, *Adv. Polymer Sci.*, **6**, 377 (1969).

[6] J. W. Breitenbach et Ch. Srna, *Pure Appl. Chem.*, **4**, 245 (1962).

[7] B. L. Funt et F. D. Williams, *J. Polymer Sci.*, **A2**, 865 (1964).

[8] K. Sato, M. Ogaswara et K. Hayashy, *J. Polymer Sci.*, **B 11,5** (1973).

[9] C. Ungureanu, D. A. Ungureanu et Cr. Simionescu, *Rev. Roumanie Chim.*, **13**, 913 (1968).

[10] N. Yamazaki, I. Tanaka et N. Nakahama, *J. Macromol. Sci. Chem.*, **A2**, 1121 (1968).

[11] G. Pistoia, *J. Polymer Sci.*, **B 10**, 787 (1972).

[12] G. Pistoia, *European Polymer J.*, **10**, 279, 285 (1974).

[13] D. Pepper et P. Reilly, *Proc. Roy. Chem. Soc.*, **A 291**, 41 (1966).

[14] A. Gandini et P. Plesch, *J. Chem. Soc.*, **1965**, 4826.

[15] R. M. Fuoss et E. Hirsch, *J. Amer. Chem. Soc.*, **82**, 1013 (1960).

[16] R. E. Meredith et C. W. Tobias, *J. Electrochem. Soc.*, **108**, 286 (1961).

La technique expérimentale consiste en l'introduction dans les cellules de réaction de certaines quantités convenables de solvant, monomère et électrolyte en prenant, en même temps, les mesures nécessaires pour éviter le contact des composantes de réaction avec l'atmosphère. Après avoir effectué l'électrolyse, les produits de réaction ont été précipités dans l'alcool méthylique acidulé avec de l'acide chlorhydrique, filtrés, lavés et séchés. Durant le processus électrolytique les cellules ont été thermostatées et la solution a été agitée continuellement avec un agitateur magnétique. En ce qui concerne la cellule compartimentée l'agitation a été effectuée seulement dans l'espace cathodique. Les déterminations viscosimétriques du polymère ont été faites en diméthylformamide, à 25° avec un viscosimètre Ubelhode.

III. LA CINÉTIQUE DU PROCESSUS DE POLYMÉRISATION ÉLECTROCHIMIQUE

Les réactions de polymérisation initiées par voie électrochimique sont influencées par l'ensemble complexe des phénomènes physiques et chimiques qui accompagnent les processus d'électrode et par les conditions dans lesquelles ont lieu ces réactions. On sait qu'à l'électrolyse d'une solution qui contient différentes espèces d'ions ou molécules, la réduction de ceux-ci est fonction du potentiel de réduction, $E^{1/2}$, les réactions d'électrode ayant lieu premièrement pour les espèces avec les potentiels les plus positifs. On a prouvé par des études polarographiques en diméthylformamide que l'acrylonitrile est réduit directement sur l'électrode compte-goutte de mercure à un potentiel plus positif que celui de l'électrolyte (sel de tétraalchilammonium[7,17,18]).

Les composantes du système étudié, conformément aux données de la littérature, présentent les caractéristiques électrochimiques convenables au but proposé. Ainsi l'acrylonitrile se réduit sur l'électrode de mercure en acétonitrile à un potentiel $E^{1/2} = -1{,}86$[19], tandis que l'ion de tétraéthylammonium et le carbonate de propylène analysés dans des conditions similaires mènent aux tensions des décomposition, respectivement $-2{,}67$ V[19] et $-2{,}50$ V.[20] Les résultats expérimentaux concernant la polymérisation électrochimique de l'acrylonitrile en carbonate d'éthylène et carbonate de propylène attestent une réaction d'initiation au cathode, le processus ayant lieu par transfert d'électrons partant de l'électrode à la double liaison du monomère. Dans ce cas conformément à un mécanisme décrit par Szwarc,[21] l'anion-radical formé va dimériser à un dianion :

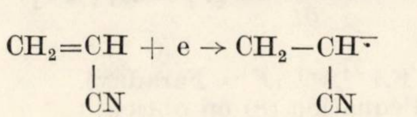

$$CH_2=\underset{\displaystyle CN}{\underset{|}{CH}} + e \rightarrow CH_2-\underset{\displaystyle CN}{\underset{|}{CH^{\dot{-}}}} \tag{1}$$

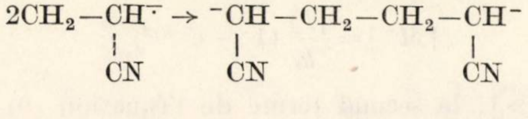

$$2CH_2-\underset{\displaystyle CN}{\underset{|}{CH^{\dot{-}}}} \rightarrow {}^{-}\underset{\displaystyle CN}{\underset{|}{CH}}-CH_2-CH_2-\underset{\displaystyle CN}{\underset{|}{CH^{-}}} \tag{2}$$

---

[17] M. Murphy, M. G. Carangelo, M. B. Ginaine et M. C. Markham, *J. Polymer Sci.*, **54**, 107 (1961).

[18] S. Lazarov, A. Trifinova et T. Vitanov, *Z. phys. Chem. (Leipzig)*, **226**, 221 (1964).

[19] F. Sommer, J. W. Breitenbach et O. F. Olay, *Monatsh. Chem.*, **99**, 2422 (1968).

[20] R. F. Nelson et R. N. Adams, *J. Electroanalyt. Chem.*, **13**, 184 (1967).

[21] M. Szwarc, M. Levy et R. Milkovitch, *J. Amer. Chem. Soc.*, **78**, 2656 (1956).

La polymérisation du monomère, dans ces conditions étant de type anionique, les processus de réaction ont à la base le schéma cinétique suivant :

Électroinitiation

$$\mathrm{M} + \mathrm{I} \longrightarrow \mathrm{M}^{\bar{\cdot}} \underset{\longrightarrow}{\text{diméris.}}\ {}^{-}\mathrm{M}{-}\mathrm{M}^{-} \tag{3}$$

Propagation

$$-M^{-} + M \xrightarrow{k_p} -M^{-} \tag{4}$$

Transfert au monomère

$$-M^{-} + M \xrightarrow{k_{tr}M} P + M^{-} \tag{5}$$

La désactivation déterminée par les produits secondaires de l'électrolyse ou bien la désactivation spontanée de la chaîne :[22]

$$-M^{-} \xrightarrow{k_t} P \tag{6}$$

où M, est le monomère ; I, la charge électrique ; M^{-}, anion-radical ; $-M^{-}$, le macroanion ; P, le polymère et k_p, $k_{tr}\ M$, k_t les constantes de propagation, transfert au monomère et la désactivation.

Pour des processus de type anionique, la vitesse de polymérisation donnée par Zilkha [23] a la forme :

$$-\frac{\mathrm{d}[M]}{\mathrm{d}t} = K_p\,[M]\,[M^{-}] \tag{7}$$

Dans le cas des processus de polymérisation électro-initiée, la vitesse apparente de formation des chaînes ioniques est donnée par la relation :

$$-\frac{\mathrm{d}[M]}{\mathrm{d}t} = [I] - K_t\,[M^{-}] \tag{8}$$

I, étant exprimé en $\mathrm{F.1^{-1}.s^{-1}}$ (F = Faraday).

En intégrant l'équation (8) on obtient :

$$[M^{-}] = \frac{[I]}{k_t}\left(1 - \mathrm{e}^{-K_t \cdot t}\right) \tag{9}$$

Puisque $k_t \cdot t \gg 1$, le second terme de l'équation (9) est négligé et alors :

$$[M^{-}] = \frac{[I]}{k_t} \tag{10}$$

---

[22] M. Szwarc, *Adv. Polymer. Sci.*, **9**, 275 (1960).

[23] F. C. Foster, *J. Amer. Chem. Soc.*, **74**, 2299 (1952).

Dans ce cas l'équation (7) a la forme :

$$-\frac{\mathrm{d}[M]}{\mathrm{d}t}=\frac{k_p}{k_t}[M][I] \tag{11}$$

ou :

$$\log\frac{[M_0]}{[M]}=\frac{k_p}{k_t}[I]\log \mathrm{e}.t \tag{12}$$

IV. RÉSULTATS ET DISCUSSIONS

Le mécanisme du processus de polymérisation électrochimique peut être établi principalement par deux méthodes expérimentales. L'une se rapporte à l'effet des inhibiteurs sur la réaction, indiqué par Breitenbach[6] et l'autre au processus de copolymérisation. Le résultat de nos recherches concernant l'influence des inhibiteurs radicalaires et anioniques est présenté dans le tableau 1. On remarque une réduction importante de la conversion avec l'augmentation de la concentration des substances donneuses de protons dans le milieu de réaction, tandis que DPPH (diphényl-picryle hydrazine), connu comme inhibiteur des processus radicalaires, n'a aucun effet.

Tableau 1

L'effet des inhibiteurs du type radicalaire et anionique sur l'électropolymérisation de l'acrylonitrile en CP et CE

Solvant : CP				Solvant : CE		
DPPH mole/l	H_2O mole/l	CH_3OH mole/l	Polymère g	DPPH mole/l	H_2O mole/l	Polymère g
—	—	—	0,714	—	—	0,270
$2{,}1.10^{-3}$	—	—	0,701	$2{,}4.10^{-3}$	—	0,298
—	$3{,}1.10^{-2}$	—	0,380	—	$3{,}2.10^{-2}$	0,106
—	$9{,}3.10^{-2}$	—	0,186	—	$9{,}0.10^{-2}$	0,011
—	$18{,}5.10^{-2}$	—	0,007	—	—	—
—	—	$6{,}0.10^{-2}$	0,466	—	—	—
—	—	$8{,}8.10^{-2}$	0,255	—	—	—

On sait que par copolymérisation anionique d'un mélange équimoléculaire d'acrylonitrile et de styrène, dans la composition du copolymère obtenu, l'acrylonitrile se trouve en proportion prédominante. L'aspect mentionné a été étudié par nous dans ce travail en effectuant la copolymérisation électrochimique des deux comonomères en solution de carbonate de propylène et d'iodure de tétraéthylammonium comme électrolyte. Les résultats obtenus confirment la formation dans l'espace cathodique d'un polymère dans la composition duquel prédomine l'acrylonitrile (fig. 1), indifféremment du rapport AN/St.

On a effectué également l'analyse du produit séparé de l'espace anodique de la cellule de réaction. Les données analytiques (spectres IR et l'analyse élémentaire) attestent la formation exclusivement du polystyrène. La polymérisation du styrène dans l'espace anodique, quand on utilise CP comme milieu de réaction, a lieu, probablement, par un mécanisme cationique.[3,24] Les constantes de réactivités des deux comonomères étudiés, déterminées par la méthode proposée par Finemann et Ross,[25] (fig. 2), concordent avec les réactivités indiquées dans la littérature [3,26] pour des processus anioniques de polymérisation (tableau 2).

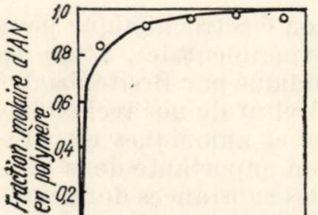

Fig. 1. — Composition du copolymère AN — St, obtenu par voie électrochimique en carbonate de propylène.

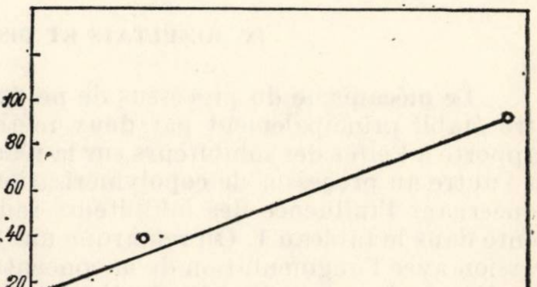

Fig. 2. — Détermination des constantes de réactivité de l'acrylonitrile (M_1) et du styrène (M_2).

Tableau 2

Constantes de réactivité obtenues par copolymérisation anionique du système, $AN_{(r_1)} - ST_{(r_2)}$.

Mode d'initiation	Solvant	Const. diél. du solv.	Électrolyte ou catalys.	Const. de réactivité	
				r_1	r_2
Catalytique[26]	i-octane	2	n-Butyl-lithium	14	0,2
Électrochimique	DMA		$NaBF_4$	14,2	0,4
Nos résultats	CP	69	$(C_2H_5)_4NI$	16	0,12

Les recherches effectuées pour établir le mécanisme de réaction par lequel a lieu la polymérisation électrochimique de l'acrylonitrile, dans nos conditions expérimentales, prouvent le caractère anionique du processus. L'endroit où se produit l'initiation et la croissance de la chaîne, comme il en a résulté des études effectuées, est l'espace cathodique. Dans l'espace anodique à de petites durées de réaction on n'a pas mis en évidence le polymère. Celui-ci apparaît seulement à de grandes durées à cause de la diffusion à travers la plaque poreuse qui sépare les deux compartiments.

[24] B. L. Funt et T. J. Blain, *J. Polymer Sci.*, **A1**, 3339 (1970).
[25] M. Finemann et S. D. Ross, *J. Polymer Sci.*, **5**, 259 (1950).
[26] N. L. Zutty et F. T. Welch, *J. Polymer Sci.*, **43**, 445 (1960).

Pour caractériser la cinétique de réaction de polymérisation électrochimique de l'acrylonitrile dans les deux solvants, CP et CE, on a étudié l'influence de la concentration du monomère, de l'intensité du courant électrique, de la température et de la durée de réaction sur le processus de formation du polymère. L'effet de la concentration initiale de l'acrylonitrile a été étudié dans les deux types de cellules. En comparant les résultats de l'expérience, présentés dans le tableau 3, on constate que la vitesse de réaction pour la même quantité de monomère du système présente des valeurs plus élevées dans le cas des cellules compartimentées par rapport à l'autre type. Ces données attestent le fait que les produits de l'électrolyse à l'anode inhibent les réactions de formation du polymère.

Tableau 3

Électropolymérisation de l'acrylonitrile en solution de CP et CE*

AN mole.l^{-1}.s^{-1}	Vitesse de polymérisation ; mol.l^{-1}.s^{-1}		
	Carbonate de propylène		Carbonate d'éthylène
	Cellule compartimentée	Cellule non compartimentée	Cellule compartimentée
0,8	—	$1,6.10^{-5}$	—
1,4	$7,2.10^{-5}$	—	—
1,5	—	$3,3.10^{-5}$	—
2,0	$11,5.10^{-5}$	—	$4,3.10^{-5}$
2,2	—	$5,2.10^{-5}$	—
2,8	—	$6,3.10^{-5}$	—
3,3	$17,0.10^{-5}$	$7,2.10^{-5}$	$6,5.10^{-5}$
4,3	—	$11,1.10^{-5}$	—
4,7	$23,8.10^{-5}$	$11,3.10^{-5}$	$9,2.10^{-5}$
5,1	—	$12,5.10^{-5}$	—
6,0	—	—	$11,8.10^{-5}$
6,1	$30,7.10^{-5}$	—	—

* $I = 20$ mA ; $t = 38°$ C.

En ce qui concerne l'effet des deux solvants sur la conversion on remarque une meilleure efficience de CP utilisé comme milieu de réaction, que pour CE (tableau 3). Le même aspect résulte plus clairement des calculs effectués pour déterminer le rapport des constantes absolues de polymérisation, k_p/k_t, conformément à l'équation (12). Les résultats expérimentaux présentés dans le tableau 4, pour les solutions de CP et CE ont été obtenus en variant la concentration d'acrylonitrile et en maintenant constantes l'intensité du courant, la concentration de l'électrolyte et la température, la quantité de courant utilisé à l'électrolyse étant $7,5.10^{-4}$ Faraday pour CP et $11,2.10^{-4}$ Faraday pour CE, à $I = 20$ mA.

Les valeurs calculées des rapports k_p/k_t prouvent que la désactivation des ions, dans le processus d'électropolymérisation de l'acrylonitrile est plus grande en solution de CE que dans CP. Des valeurs proches ont été établies, de même, dans les conditions expérimentales ou l'on a varié

Tableau 4

Détermination du rapport des constantes absolues de réaction k_p/k_t, à l'électropolymérisation de l'acrylonitrile en fonction de la concentration de monomère, en solution de CP et CE

Solvant	AN mole/l	Polymère mole/l	$\log \frac{M_0}{M}$	$F.l^{-1}.s^{-1}$	k_p/k_t
CP	1,35	0,260	0,09290	$9{,}4.10^{-6}$	6,2
	2,02	0,413	0,09933	,,	6,6
	3,37	0,612	0,08704	,,	5,8
	4,72	0,857	0,08702	,,	5,8
	6,07	1,105	0,08727	,,	5,8
CE	2,01	0,228	0,0523	$9{,}4.10^{-6}$	2,4
	3,35	0,350	0,0479	,,	2,1
	4,66	0,500	0,0493	,,	2,2
	5,96	0,637	0,0491	,,	2,2

l'intensité du courant électrique, 10—60 mA (tableau 5), en gardant constantes les concentrations du monomère, de l'électrolyte et la température. La quantité de polymère formée dans l'espace cathodique par polymérisation électrochimique de l'acrylonitrile dans les deux solvants croît proportionnellement à la durée d'électrolyse (fig. 3).

Tableau 5

Détermination du rapport des constantes absolues de réaction k_p/k_t, à l'électropolymérisation de l'acrylonitrile en fonction de l'intensité du courant en solution de CP et CE

Solvant	AN mole/l	Polymère mole/l	$\log \frac{M_0}{M}$	I $F.l^{-1}.s^{-1}$	k_p/k_t
CP	3,37	0,360	0,04906	$4{,}64.10^{-6}$	5,5
	3,37	0,612	0,08704	$9{,}47.10^{-6}$	5,8
	3,37	0,645	0,09226	$18{,}62.10^{-6}$	5,8
	3,37	0,552	0,07769	$28{,}41.10^{-6}$	5,3
CE	3,35	0,190	0,02534	$4{,}8.10^{-6}$	2,2
	3,35	0,232	0,03116	$9{,}6.10^{-6}$	2,7
	3,35	0,939	0,14284	$18{,}8\cdot10^{-6}$	3,2
	3,35	0,730	0,10674	$28{,}3.10^{-6}$	3,2

En conséquence, on a étudié l'influence de la concentration du monomère et de l'intensité du courant sur la vitesse de polymérisation pour déterminer l'ordre de réaction (éq. 11). Les recherches ont été effectuées dans différentes conditions de température, solvant, type de cellule. Une partie des résultats expérimentaux sont représentés sur les figures 4 et 5. Dans toutes les conditions étudiées on a constaté une relation linéaire entre la vitesse et les deux facteurs d'influence qu'on a analysés. Ainsi les pentes des courbes indiquent une dépendance du premier ordre de la concentration du monomère et du courant électrique, par rapport à la vitesse de polymérisation. Ces résultats attestent la validité de l'équation (11) prise en considération pour le processus d'électropolymérisation de l'acrylonitrile dans ces deux solvants aprotiques CP et CE.

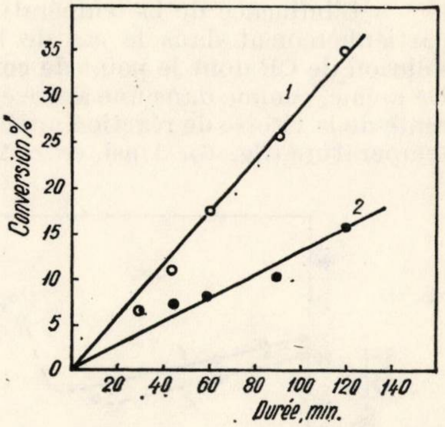

Fig. 3. — Variation de la conversion avec la durée d'électrolyse, à la polymérisation de l'acrylonitrile en solution de CP et CE.

1, solvant = CP ; *2*, solvant = CE ; I = 20 mA ; AN = 4 mole/l ; $T = 38°$.

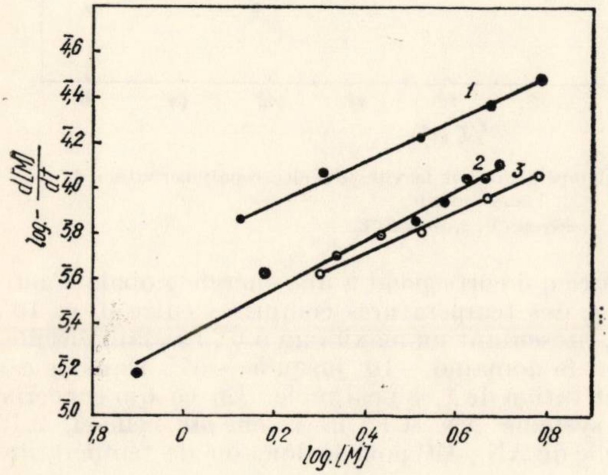

Fig. 4. — Dépendance de la vitesse de polymérisation vers la concentration d'acrylonitrile.

1, Solution de CP ; cellule compartimentée ; $T = 38°$. *2*, Solution de CP ; cellule non compartimentée ; $T = 25°$. *3*, Solution de CE ; cellule compartimentée ; $T = 38°$.

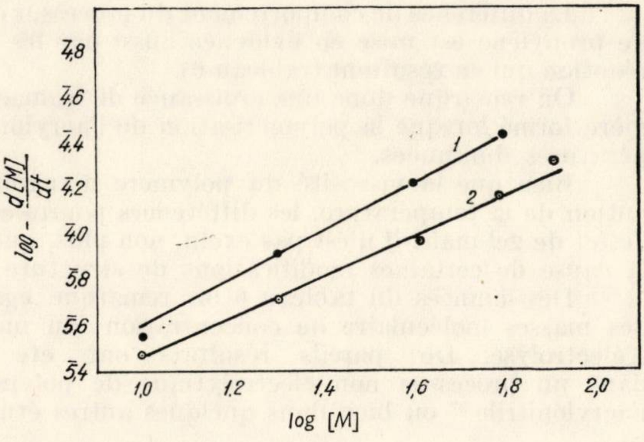

Fig. 5. — Dépendance de la vitesse de polymérisation vers l'intensité du courant.

1, Solution de CE ; cellule compartimentée ; $T = 38°$. *2*, Solution de CP ; cellule compartimentée ; $T = -30°$.

L'influence de la température a été examinée entre +58 et −57°, particulièrement dans le cas de la polymérisation de l'acrylonitrile en solution de CP dont le point de congélation est plus bas que celui du CE. De même, comme dans une autre étude,[2] on remarque une variation différente de la vitesse de réaction qui correspond à deux domaines distincts de température (fig. 6). Ainsi, entre 20° et 58° on obtient pour la vitesse un diagramme Arrhenius linéaire qui correspond à une énergie globale d'activation de 2,17 kcal/mole. A des températures comprises entre 0° et 10°, la vitesse croît rapidement, présentant un maximum à 0°, baissant ensuite, presque uniformément dans le domaine −10° jusqu'à −57°. Dans ce cas on obtient une énergie d'activation de 1,88 kcal/mole. En ce qui concerne l'énergie d'activation du système AN−CE, la valeur de celle-ci, 2,40 kcal/mole, est proche de celle de AN−CP pour le domaine de température de 38° à 58°.

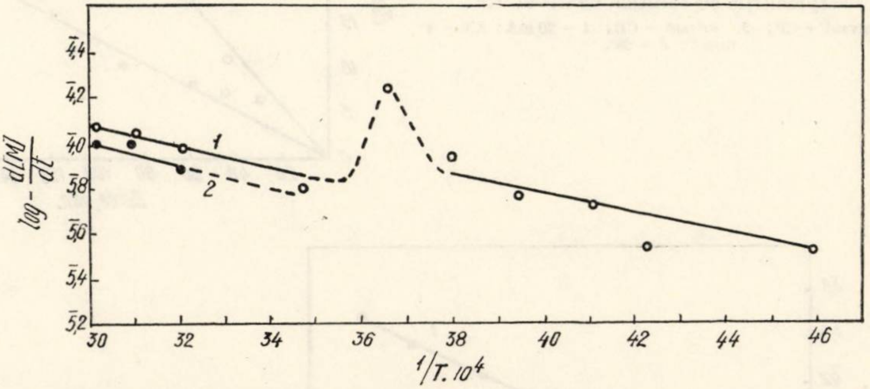

Fig. 6. — Influence de la température sur la vitesse d'électropolymérisation de l'acrylonitrile.

1, Solvant CP ; *2*, Solvant CE.

La différence de comportement du processus en solution de carbonate de propylène est mise en évidence aussi par les valeurs des produits de réaction qui en résultent (tableau 6).

On remarque donc une croissance de la masse moléculaire du polymère formé lorsque la polymérisation de l'acrylonitrile a lieu à des températures diminuées.

Bien que la viscosité du polymère n'augmente pas avec la diminution de la température, les différences pourraient être déterminées par l'effet de gel mais, il n'est pas exclu, non plus, que ces phénomènes soient la cause de certaines modifications de structure du milieu de réaction.

Des données du tableau 6 on remarque également l'indépendance des masses moléculaire de concentration du monomère et du courant d'électrolyse. De pareils résultats ont été obtenus par Zilkha dans un processus non électrolytique de polymérisation anionique de l'acrylonitrile [27] ou bien dans quelques autres études concernant la poly-

---

[27] A. Zilkha, B. A. Flit et M. Frankel, *J. Polymer Sci.*, **49**, 231 (1961).

Tableau 6

Influence des conditions de réaction sur la viscosité du polymère formé en solution de CP

[AN] mole/l	I mA	T °C	η dl/g
1,5	20	25	0,072*
3,8	20	25	0,058*
4,7	20	25	0,063*
1,4	20	38	0,069
3,4	20	38	0,063
6,1	20	38	0,061
3,4	40	38	0,071
3,4	60	38	0,067
2,0	20	−10	0,151
3,4	20	−10	0,146
4,7	20	−10	0,155
3,4	20	−20	0,144
3,4	20	−30	0,150
3,4	20	−37	0,142
3,4	20	−57	0,157
3,4	60	−30	0,147
3,4	80	−30	0,158
4,7	20	−30	0,161
6,1	20	−30	0,155

* polymère obtenu dans la cellule noncompartimentée.

mérisation électrochimique du même monomère.[7,9] On a démontré par comparaison des résultats obtenus à la polymerisation du métacrylonitrile catalytique [27] et électrochimique [1] que le transfert de la chaîne qui mène à ce nivellement des masses moléculaires est dû à l'hydrogène tertiaire de l'acrylonitrile. Cet aspect n'apparaît pas dans le cas de la polymérisation du métacrylonitrile.

V. CONCLUSIONS

L'électropolymérisation d'acrylonitrile en solvants aprotiques polaires, carbonate de propylène et carbonate d'éthylène se produit à la cathode par un processus de réaction anionique établi par voie cinétique et copolymérisation d'acrylonitrile avec du styrène et à l'aide des inhibiteurs.

Quoique la vitesse de réaction dans les deux solvants soit exprimée par une dépendance du premier ordre par rapport au monomère et au courant, le processus de formation du polymère a lieu avec une vitesse plus grande en carbonate de propylène qu'en carbonate d'éthylène. Les valeurs du rapport des constantes de réaction, k_p/k_t, indiquent le même ordre, CP > CE, ce qui atteste un effet de désactivation plus grand dans le cas de carbonate d'éthylène. A la suite des études, concernant l'influence de la température sur le processus de polymérisation électrochimique de l'acrylonitrile en carbonate de propylène, on a obtenu deux valeurs de l'énergie d'activation : l'une pour le domaine positif de température et l'autre pour le domaine au-dessous de 0°. Les températures diminuées (au-dessous de 0°) ont conduit de même à des produits de réaction avec des masses moléculaires plus élevées que celles obtenues dans des conditions ordinaires pour de pareils processus.

Revue Roumaine de Chimie, **21**, *9–10*, 1417–1427 (1976)

Tableau [illegible]

[illegible]

[illegible]

[illegible]

[illegible]

[illegible]

[illegible]

Revue Roumaine de Chimie, **21**, *9–10*, 1429–1431 (1976)

AN EQUATION FOR THE THERMAL CONDUCTIVITY OF WATER

L. BADEA

Ministry of Chemical Industry, Technical Department,
Splaiul Independenţei, 202, Bucharest, Romania

Received February 22, 1975

An equation for the calculation of water thermal conductivity as a function of specific heat at constant pressure, of density and temperature is presented. The equation was established by including a correction constant, representing the mean deviation from the cubical arrangement of molecules, in a general equation for the thermal conductivity of liquids.

In a previous paper [1] the following equation for the thermal conductivity of liquids was suggested:

$$\lambda = R_0^{1/2} N^{-1/3} c_p^{3/2} d^{2/3} T^{1/2} M^{1/3} (M c_p - R^+)^{-1/2} \tag{1}$$

where λ is the coefficient of thermal conductivity of liquid (cal cm^{-1}s^{-1}°C^{-1}), c_p the specific heat at constant pressure (cal g^{-1}°C^{-1}), d the density (g cm^{-3}), T the absolute temperature (K), M the molecular mass (g mol^{-1}), R_0, R^+ the gas constant ($R_0 = 8.3153.10^7$ erg mol^{-1} °C^{-1} or g cm^{2}s^{-2}mol^{-1}°C^{-1}, $R^+ = 1.9867$ cal mol^{-1} °C^{-1}) and $\mathcal{N}$ the Avogadro number ($\mathcal{N} = 6.0228.10^{23}$ mol^{-1}).

Equation (1) was established by developing Kardos' physical model. It was considered that in the intermolecular space of the liquid medium the ideal gas thermodynamic and kinetic equations are valid.

Taking into account the large applicability of water as heat transfer agent, on the one hand, and the systematic errors (always positive) between the calculated and experimental values of thermal conductivity, on the other hand, a modification of equation (1), in order to satisfy the accuracy requirements necessary in the designing of heat transfer equipment, was suggested.

Based on the consideration that the errors of the calculated thermal conductivity of water are due to the deviation between the real arrangement of molecules in the liquid medium and the cubical arrangement assumed by establishing equation (1), the right term of this equation was multiplied by a constant $a = \Delta'/\Delta$, where Δ', Δ is the mean distance of separation of molecule centers corresponding to their real arrangement, and the same distance assuming a cubical arrangement on the average, respectively.

The mean value of a, determined on the basis of experimental values of thermal conductivity, was found to be 1.200.

---

[1] L. Badea, *Rev. Chim. (Bucureşti)*, **26**, 209 (1975).

Substituting into equation (1) the values for the constants a, R_0, R^+, N and $M = 18.016$, we finally get:

$$\lambda = 0.00033968\ c_p^{3/2} d^{2/3} T^{1/2} (18.016\ c_p - 1.9867)^{-1/2} \tag{2}$$

Equation (2) was tested for 33 experimental values of thermal conductivity of water, at various temperatures (t, °C), published by different authors. The concordance between the calculated and experimental values is presented in table 1.

The data of table 1 indicate that the maximum error (calculated as (λ calcd/λ exp) 100−100) is 7 % and the average error is +0.5 %.

Table 1

Check of equation (2)

Nr	t	c_p	d	$\lambda \cdot 10^6$ calcd.	$\lambda \cdot 10^6$ exp.	Error %
1	0	1.0080	0.99987	1413	1320[2]	+7.0
2					1450[2]	−2.5
3					1390[2]	+1.6
4	5	1.0043	0.99999	1421	1372[2]	+3.6
5	8.8	1.0024	0.99982	1428	1370[3]	+4.2
6	15	1.0004	0.99913	1440	1400[2]	+2.9
7					1380[2]	+4.3
8					1440[2]	0.0
9	18	0.99978	0.99862	1446	1418[3]	+2.0
10	20	0.99947	0.99823	1450	1400[2]	+3.6
11					1490[2]	−2.7
12					1422[4]	+2.0
13					1410[5]	+2.8
14	27.8	0.99874	0.99632	1466	1484[6]	−1.2
15	30	0.99866	0.99568	1471	1440[2]	+2.1
16					1440[7]	+2.1
17					1485[8]	−0.9
18	38.4	0.99865	0.99285	1488	1509[6]	−1.4
19	40	0.99869	0.99224	1492	1470[2]	+1.5
20					1530[2]	−2.5
21					1549[8]	−3.7
22	40.4	0.99870	0.99209	1493	1512[3]	−1.3
23	41.2	0.99872	0.99178	1494	1515[6]	−1.4
24	47.8	0.99906	0.98905	1507	1548[6]	−2.6
25	50	0.99919	0.98807	1512	1500[2]	+0.8
26	60	1.0001	0.98324	1531	1560[2]	−1.9
27					1560[2]	−1.9
28					1590[2]	−3.7
29	75	1.0021	0.97489	1559	1540[2]	+1.2
30					1480[7]	+5.3
31	80	1.0029	0.97183	1568	1600[2]	−2.0
32					1575[2]	−0.4
33					1586[4]	−1.1

---

[2] J. F. D. Smith, *Trans. Am. Soc. Mech. Engrs.*, **58**, 719 (1936).

[3] E. Schmidt and W. Sellschopp, *Forsch. Ing.-Wes.*, 3, 277 (1932).

[4] L. Riedel, *Chem. Ing.-Tech.*, **23**, 321 (1951).

[5] O. K. Bates, G. Hazzard and G. Palmer, *Ind. Eng. Chem.*, **10**, 314 (1938).

[6] D. L. Timrot and N. B. Vargaftik, *Zhur. tech. Fiz.*, **10**, 106 (1940).

[7] J. F. D. Smith, *Ind. Eng. Chem.*, **22**, 1246 (1930).

[8] L. Badea, Thesis, Polytechnical Institute of Bucharest, 1953.

Since the errors between the experimental values of thermal conductivity at the same temperature are sometimes greater (for example $(1450/1320)100-100 = 9.8\%$), equation (2) can be considered to satisfy the most severe requirements of the heat transfer equipment designing.

Equation (2) was also tested for seven experimental values of thermal conductivity of water at various pressures (p, ata), without considering the influence of liquid compressibility (Table 2).

Table 2

Check of equation (2) at various pressures

Nr	t	p	c_p	d	$\lambda \cdot 10^6$ calcd.	$\lambda \cdot 10^6$ exp.	Error %
1	29.3	400	0.99868	0.99688	1470	1560[6]	−5.8
2	39.6	300	0.99868	0.99240	1491	1551[6]	−3.9
3	75.0	29.6	1.0021	0.97489	1559	1593[3]	−2.1
4	85.5	28.5	1.0040	0.96832	1578	1610[3]	−2.0
5	90.0	7.5	1.0050	0.96534	1587	1629[3]	−2.6
6	90.8	19.5	1.0052	0.96480	1588	1626[3]	−2.3
7	95.8	27.8	1.0065	0.96136	1597	1618[3]	−1.3

The data in table 2 indicate a maximum error of 5.8% and an average error of −2.9%, allowing to conclude that equation (2) can also be used for the calculation of thermal conductivity of water at high pressures, in the limits of very severe accuracy requirements.

In connection with equation (2) the following comments can be made :

The value of Δ, which was necessary to the establishment of equation (1), was calculated from relation

$$\Delta = (\Delta^3)^{1/3} = \left(\frac{m}{d}\right)^{1/3}$$

where Δ^3 is the volume occupied by four nearest molecules forming a cube with the side Δ (cm^3) and m the mass of a molecule (g).

Since the volume of octahedron with the side Δ is $0.4714\ \Delta^3$, the value of Δ, assuming a mean octahedral arrangement of molecules, is

$$\Delta = \left(\frac{1}{0.4714}\right)^{1/3} \left(\frac{m}{d}\right)^{1/3} = 1.285 \left(\frac{m}{d}\right)^{1/3}$$

By comparing the values 1.285 and $a = 1.200$, we get

$$\frac{1.200}{1.285}\,100 - 100 = 93\%$$

indicating that equation (2) corresponds to a mean octahedral arrangement of molecules, rather than to a cubical one.

Equation (2) is very convenient for the calculation of thermal conductivity of water because the necessary parameters c_p and d were determined experimentally with a very high degree of accuracy and the respective data can be found in the common literature for chemical and physical constants.

Revue Roumaine de Chimie, **21**, *9–10*, 1429–1431 (1976)

Since the errors between the experimental values of thermal conductivity in the same temperature are sometimes greater (for example [illegible] 1952 [illegible] 1953 = 3.5 %), equation (2) can be considered to satisfy the most severe requirements of the heat transfer equipment designing.

Moreover, it was also tested for experimental values of thermal conductivity of water at various pressures [illegible] without considering the influence of liquid compressibility (Table 2).

Table 2

[illegible]

[illegible]	[illegible]	[illegible]	[illegible]	[illegible]	[illegible]	[illegible]	[illegible]
1	[illegible]	[illegible]	[illegible]	[illegible]	[illegible]	[illegible]	[illegible]
2	[illegible]	[illegible]	[illegible]	[illegible]	[illegible]	[illegible]	[illegible]
3	[illegible]	[illegible]	[illegible]	[illegible]	[illegible]	[illegible]	[illegible]
4	[illegible]	[illegible]	[illegible]	[illegible]	[illegible]	[illegible]	[illegible]
5	[illegible]	[illegible]	[illegible]	[illegible]	[illegible]	[illegible]	[illegible]
6	[illegible]	[illegible]	[illegible]	[illegible]	[illegible]	[illegible]	[illegible]
7	[illegible]	[illegible]	[illegible]	[illegible]	[illegible]	[illegible]	[illegible]

The data in table 2 indicates maximum error of [illegible] and an average error of −2.0 %, allowing to conclude that equation (2) can also be used for the calculation of thermal conductivity of water at high pressures in the limits of very severe accuracy requirements.

In connection with equation (2) the following comments can be made:

The value of [illegible] which was necessary to the establishment of equation [illegible] was calculated from relation

$$[illegible]$$

where Δ is the volume occupied by [illegible] molecule [illegible] forming a cube with the side [illegible] and m is the mass of a molecule (kg).

Since the volume of [illegible] with the side Δ is [illegible] the value of Δ, assuming a mean [illegible] arrangement of molecules, is

$$[illegible]$$

By [illegible] the values [illegible] and [illegible] 1200, we get

$$[illegible]$$

indicating that equation (2) corresponds to a [illegible] arrangement of molecules, rather than to a cubical one.

Equation (2) [illegible] for the calculation of thermal conductivity of water because the necessary parameters [illegible] with a very high degree of accuracy and [illegible] data can be found in the [illegible] for chemical and physical constants.

[illegible]

NOTE POUR LES AUTEURS

La *Revue Roumaine de Chimie* publie des articles en anglais, français, russe, allemand ou espagnol. Les auteurs sont priés d'envoyer des articles, notes, communications et comptes rendus inédits.

Les manuscrits seront dactylographiés à deux intervalles. Les tableaux seront dactylographiés sur des feuilles séparées, de même que la légende des figures. Les diagrammes seront tracés à l'encre de Chine sur papier calque. Les tableaux et les figures seront numérotés par des chiffres arabes, en nombre strictement nécessaire. Prière de ne pas inscrire les mêmes données dans les tableaux et les figures. Les formules chimiques seront incluses dans le texte ; en outre, elles seront transcrites sur des feuilles séparées. Les auteurs sont priés d'indiquer les caractères italiques (en soulignant les lettres au crayon), ainsi que tout autre caractère spécial. L'ordre des références bibliographiques sera celui de leur mention dans le texte ; le nom de l'auteur sera précédé de l'initiale du prénom ; les publications périodiques seront présentées suivant les prescriptions internationales. Les références seront ajoutées à la fin de l'article ; elles paraîtront comme des notes, au bas de la page. Le texte sera précédé d'un résumé comprenant 15 lignes au maximum.

L'entière responsabilite du contenu des articles appartient aux auteurs. On publie des articles dus aux collaborateurs roumains ou étrangers.

PRINTED IN ROMANIA

TRAVAUX PARUS AUX ÉDITIONS DE L'ACADÉMIE DE LA RÉPUBLIQUE SOCIALISTE DE ROUMANIE

CONSTANTIN V. UGLEA, **Cromatografia pe gel permeabil. Noi domenii de aplicare** (La chromatographie sur gel perméable. Nouveaux domaines d'application), 1976, 122 p., 6,75 lei.

I. GĂLĂŢEANU, **Radiochimia aplicată. Metode și probleme** (La radiochimie appliquée. Méthodes et problèmes), 1976, 305 p., 19 lei.

FRANCISC A. GOTHARD, **Echilibre lichid-vapori. I. Baze teoretice şi metode de calcul** (Equilibres liquide-vapeurs. I. Bases théoriques et méthodes de calcul), 1975, 263 p., 2 pl., 28 lei.

CONST. GH. MACAROVICI, D. MACAROVICI, **Chimia oxizilor dubli şi utilizările lor** (La chimie des oxydes doubles et leur utilisation), 1975, 195 p., 13 lei.

M. AVRAM, **Antidăunători** (Pesticides), 1974, 496 p., 41 lei.

ELENA CEAUŞESCU, **Research work on synthesis and characterization of macromolecular compounds. Contributions**, 1974, 251 p., 20 lei.

DUMITRU COSTACHE, **Analiza chimică prin metoda cinetică** (L'Analyse chimique par la méthode cinétique), 1974, 276 p., 15,50 lei.

G. A. RĂDULESCU, **Proprietăţile ţiţeiurilor româneşti** (Les propriétés des pétroles roumains), 1974, 267 p., 2 pl. 18 lei.

CR. SIMIONESCU, VIORICA RUSAN, V. POPA, **Chimia algelor marine** (La chimie des algues marines), 1974, 212 p., 1 pl., 18 lei.

I. ZUGRĂVESCU, MAGDA PETROVEANU, **Chimia n-ilidelor** (La chimie des n-Ilures), 1974, 348 p., 19 lei.

MARIA FITI, **Dozimetria chimică a radiaţiilor ionizante** (La dosimétrie chimique des radiations ionisantes), 1973, 240 p., 13,50 lei.

TIBERIU NĂSCUŢIU, **Metode radiochimice de analiză** (Méthodes radiochimiques d'analyse), 1973, 384 p., 23 lei.

CRISTOFOR SIMIONESCU, MARGARETA GRIGORAŞ, AGATA CERNĂTESCU-ASADEI, ROZMARIN GHEORGHE, **Chimia lemnului în România. Plopul şi salcia** (La chimie du bois en Roumanie. Le peuplier et le saule), 1973, 299 p., 13 pl., 26 lei.

MIHAIL FLORESCU, **Eficienţa economică a cercetării ştiinţifice** (L'efficience économique de la recherche scientifique) 1972, 115 p. 15 lei.

GEORGETA LĂZĂRESCU, **Sistematizarea informaţiilor în chimia organică** (Systématisation des informations en Chimie organique), 1972, 243 p., 1 pl. 10,50 lei.

1977 FEB 21

I.P.I. — c. 1339

43 426

Lei 25.—

1103

R

REFERÁLVA

ACADÉMIE DE LA RÉPUBLIQUE SOCIALISTE DE ROUMANIE

REVUE ROUMAINE DE CHIMIE

70

TOME 21
N°s 11–12
Novembre–Décembre 1976

RECHAX, **21**, *11–12* 1433–1598 (1976)

EDITURA ACADEMIEI REPUBLICII SOCIALISTE ROMÂNIA

Rev. Roumaine Chim. **21**, *11–12*, p. 1433–1598 (1976), Bucarest

ACADÉMIE DE LA RÉPUBLIQUE SOCIALISTE DE ROUMANIE

COMITÉ DE RÉDACTION

Rédacteur en chef:

I. G. MURGULESCU, membre de l'Académie de la République Socialiste de Roumanie

Rédacteurs en chef adjoints:

A. T. BALABAN et V. EM. SAHINI, membres correspondants de l'Académie de la République Socialiste de Roumanie

Collège de rédaction:

EM. BRATU, ELENA CEAUŞESCU, ECATERINA CIORĂNESCU-NENITZESCU, C. DRĂGULESCU, CR. SIMIONESCU, membres de l'Académie de la République Socialiste de Roumanie; P SPACU, membre correspondant de l'Académie de la République Socialiste de Roumanie; MARGARETA AVRAM, I. HAIDUC, D. I. MARCHIDAN, I. MOLDOVAN, G. NIAC et D. SĂNDULESCU

La Revue Roumaine de Chimie paraît 10 fois par an. Toute commande de l'étranger (fascicules ou abonnements) sera adressée à ILEXIM Departamentul Export-Import Presă (Revues), P.O. B. 136–137, télex 11226, Bucarest, 3, str. 13 Decembrie, Roumanie

Les manuscrits, les livres et les revues proposés en échange, ainsi que toute correspondance seront envoyés à la rédaction :

REVUE ROUMAINE DE CHIMIE

23, str. Dumbrava Roşie, Bucarest, Roumanie, téléphone 124160

EDITURA ACADEMIEI REPUBLICII SOCIALISTE ROMÂNIA

125, Calea Victoriei, 71021, Bucarest, Roumanie, téléphone 507680

REVUE ROUMAINE DE CHIMIE

ORSZÁGOS MŰSZAKI KÖNYVTÁR ÉS DOKUMENTÁCIÓS KÖZPONT 1883

Tome 21, N°s 11–12 Novembre-Décembre 1976

I. G. MURGULESCU und MAIA WEISSMANN, Der Einfluss des Methans auf den thermischen Zerfall des Chloroforms. II. Die vierte Reaktionsstufe 1435–1444

LILIANA CIUREA, V. EM. SAHINI and A. MATEESCU, Spectral study of 4,7-phenanthroline-5,6-dione radical anion 1445–1449

D. I. MARCHIDAN and SPERANŢA TĂNĂSESCU, Thermodynamic study of some uranium oxides by solid electrolyte EMF measurements. Solid state coulometric titration technique 1451–1455

S. STERNBERG and V. VASILESCU, Ultrasonic velocity and compressibility in fused AgCl-AgBr, AgCl-KCl and AgI 1457–1461

H. FREYDANK und MARGIT T. RÄTZSCH, Zur Berechnung von Parametern des zwischenmolekularen Potentials aus 2. Druckvirialkoeffizienten . . . 1463–1471

LUCIA CIOHODARU and AURELIA MEGHEA, The electronic structure of some stilbene derivatives. II. Quantitative correlations referring to the substituent effects on the electronic spectra of some stilbene derivatives 1473–1477

D. CAMBOLI, D. FĂTU et VIORICA CIMPU, La décomposition thermique des combinaisons complexes thiocyaniques du Pd(II) avec la pyridine et les pyridines substituées 1479–1485

A. C. BANCIU, Tetracoordinated Co(II) chelates with $Co(d^7)-N(sp^2)$ bonds 1487–1495

ECATERINA DRAGU, M. BANCIU, C. DRĂGHICI, M. ELIAN and ECATERINA CIORĂNESCU, Carbenium ion reactions. XIII. Acetolysis of 5-tosyloxymethyl-5H-6,7-dihydrodibenzo[a, c]cyclopropa[e]cycloheptene . . 1497–1512

M. D. GHEORGHIU and A. T. BALABAN, Ground and excited state SCF-PPP-CI calculations for pyrylium salts 1513–1525

N. S. BĂRBULESCU and MINODORA LECA, Elimination reactions in the 8-substituted tricyclo [$7.3.1.0^{2,7}$] tridecane series. VII. Pyrolytic elimination of 8-methyl-tricyclo [$7.3.1.0^{2,7}$] tridecen-13-acetates 1527–1535

R GH. DRĂGAN, Amorphous-crystalline coupling in polyethylene. IV. Earth gravity effect on defect precipitation during annealing 1537–1541

R I. DRAGOTĂ, D. IONESCU, EUSTANŢA TĂRNĂUCEANU, V. DOBRE and I. NICULESCU-DUVĂZ, Potential anticancer agents. XII. Synthesis of new methanesulphonate derivatives from benzo- and naphtopyrans 1543–1554

CR. I. SIMIONESCU and ADELAIDA LIGA, Researches in the terpolymerization field. VII. Theoretical structural characterization of the low conversion acrylonitrile—methacrylic acid—methyl methacrylate terpolymer 1555–1561

R A. M. QURESHI, A. A. USMANI, ABDUL MALIK and J. AHMAD, Quantitative determination of cadmium as cadmium oxalate 1563–1565

COMPTES RENDUS 1567–1569

INDEX DES AUTEURS 1571–1586

INDEX DES SUJETS 1587–1597

Rev. Roumaine Chim. **21**, *11–12*, **p.** 1433–1598 **(1976), Bucarest**

Revue Roumaine de Chimie, **21**, *11–12*, 1435–1444 (1976)

DER EINFLUSS DES METHANS AUF DEN THERMISCHEN ZERFALL DES CHLOROFORMS. II[1]

DIE VIERTE REAKTIONSSTUFE

I. G. MURGULESCU und MAIA WEISSMANN

Zentrum für Physikalische Chemie, Str. Galaţi N°. 31, Sector 2, Bukarest, Rumänien

Eingegangen am 1. März 1976

Der thermische Zerfall des Chloroforms in Überschuß von Methan wurde mittels der Fließmethode bei Normal- und Unterdruck untersucht. Außer der gaschromatographischen Bestimmung der organischen Reaktionsprodukte wurde auch die Konzentration der erhaltenen Salzsäure bestimmt. Die Chlor- und Wasserstoffbilanz erlaubte die Formulierung einer vierten Reaktionsstufe in welcher die radikalischen Zerfallsprodukte des Pentachloräthans das in Reaktion 2′ gebildet wird, ($\ddot{C}Cl_2 + CHCl_3 \xrightarrow{2'} (C_2HCl_5)^*$) mit Methan reagieren. Die Bildung großer Mengen HCl durch diese Reaktionsstufe, die von den relativen Reaktantenkonzentrationen abhängen, erklärt, auf Grund des Anwachsens der Abbruchreaktion 1′ ($\ddot{C}Cl_2 + HCl \xrightarrow{1'} CHCl_3$), den Abfall der Reaktionsgeschwindigkeitskonstanten erster Ordnung der Gesamtreaktion in Abhängigkeit von der Reaktantenkonzentration.

EINFÜHRUNG

In einer vorangegangenen Mitteilung wurden die Erwägungen angezeigt, die zu der Formulierung der zweiten Reaktionsstufe des thermischen Chloroformzerfalls und der Reaktion des Dichlorkarbens mit Methan als Einschubreaktionen in die C—H Bindungen des Chloroforms bzw. Methans führen. Gleichfalls wurden auch experimentelle Ergebnisse angeführt, die diese Hypothese belegen und einige Kennzeichen der Kinetik des thermischen Zerfalls des Chloroforms in Gegenwart des Methans anzeigen.

In der vorliegenden Arbeit wurde eine weitere Untersuchung der Reaktion angestrebt um die vierte Reaktionsstufe zu formulieren und die Änderung der Reaktionsordnung in Abhängigkeit der relativen Reaktantenkonzentration zu erklären.

EXPERIMENTELLES

Es wurde die Versuchsanordnung (Abbildung 1) und die in der vorangegangenen Mitteilung [1] beschriebene Arbeitsweise verwendet. In einigen Versuchen wurde bei Normaldruck gearbeitet, so daß die Reaktionsprodukte vor der variablen Kapillare, n, aufgefangen wurden (Abb. 1). Die Reaktionsprodukte und die unverbrauchten Reaktanten die in diesem Punkt aus der Versuchsvorrichtung ausströmten, wurden durch einen Dreiweghahn (Abb. 1 a) geleitet, entweder direkt in die Atmosphäre oder in ein Absorptionsrohr (Abb. 1 c) das mit destilliertem Wasser gefüllt war und anschließend in die Atmosphäre.

---

[1] Part. I: I. G. Murgulescu und M. Weissmann, *Rev. Roumaine Chim.*, **21**, 1275 (1976).

Die Fließgeschwindigkeit wurde mit einem Flowmeter gemessen (Abb. 1 d) das vor dem Ausgang in die Atmosphäre angebracht war.

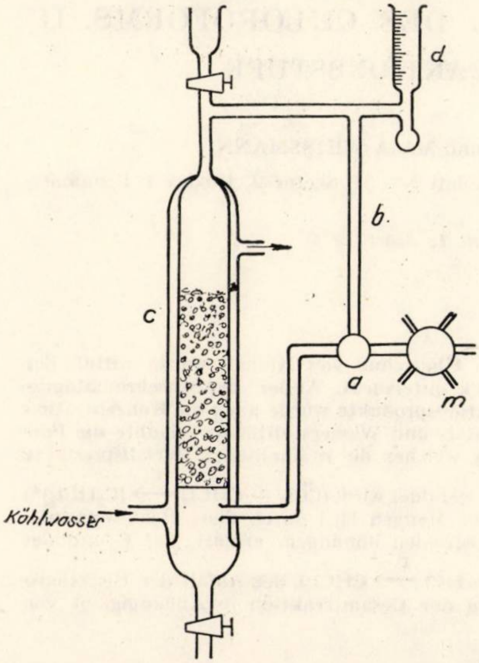

Abb. 1. — Schema der Vorrichtung für die Absorption der in der Reaktion gebildeten Salzsäure.

m — Chromatographisches Gasdosierventil, *a* — Dreiwegbahn, *b* — By-pass, *c* — Absorptionsgefäß, *d* — Flowmeter

In verschiedenen stationären Bedingungen wurde der Gasstrom der Reaktionsprodukte und unverbrauchten Reaktanten genau bemessene Zeitspannen durch das Absorptionsrohr geleitet (Abb. 1 c). Die gebildete Salzsäure konnte so im destillierten Wasser absorbiert werden. Nach dem Ablauf der entsprechenden Zeit wurde der Gasstrom mittels des Dreiweghahns direkt in die Atmosphäre geleitet (Abb. 1 b) und die Salzsäure im Absorptionsrohr mit Natriumhidroxid titriert.

Da die Fließgeschwindigkeit, der atmosphärische Druck und der Druck im Reaktor sowie die Durchflußzeit des Gases durch das Absorptionsrohr bekannt waren, konnte die HCl-Konzentration beim Austritt aus dem Reaktor bestimmt werden.

Während der Versuche wurden durch Probeneinführung mittels der 6 Wegehähne (h) und (m) (Abb. 1[1]) die Anfang- und Endkonzentrationen der Reaktanten und Reaktionsprodukte gaschromatographisch bestimmt. Die Salzsäure wurde auch chromatographisch bestimmt indem vor der chromatographischen Trennsäule ein Rohr mit $NaHCO_3$ angebracht wurde, wodurch HCl durch eine äquivalente Menge H_2O aufgrund der Reaktion $HCl + NaHCO_3 = H_2O + CO_2 + NaCl$ ersetzt wurde. Die chromatographische Säule war mit Porapak Q gefüllt. Das Eichen wurde durch den thermischen Zerfall des 1,1-Dichloräthans ausgeführt, wobei HCl und C_2H_3Cl in stoechiometrischen Mengen gebildet werden. Die Oberfläche der chromatographischen Peaks der Salzsäure wurde auf die des Vinylchlorids bezogen und unter Verwendung des Eichfaktors der letzten, der durch Einspritzen von reiner Substanz bestimmt war, wurde die Eichkurve für Salzsäure (Oberfläche des chromatographischen Peaks/Konzentration) bestimmt.

ERGEBNISSE UND DISKUSSIONEN

1. *Die Chlorbilanz* wurde aufgrund der Beziehungen (A) und (B) durchgeführt.

$$\sum Cl_i = 3\,(CHCl_3)_i \qquad (A)$$

$$\sum Cl_f = (C_2H_3Cl)_f + (CH_3Cl)_f + 2\,(CH_2Cl_2)_f + 3\,(CHCl_3)_f + (HCl)_f \qquad (B)$$

wo mit i die anfänglichen Konzentrationen und mit f die Endkonzentrationen, in Mol/cm^3, im Reaktionsgemisch angegeben sind.

Wie in Abb. 2 angegeben ist, ergibt sich eine lineare Beziehung mit einer Neigung von ≈ 1 für die Abhängigkeit von $\sum Cl_f$ von $\sum Cl_i$.

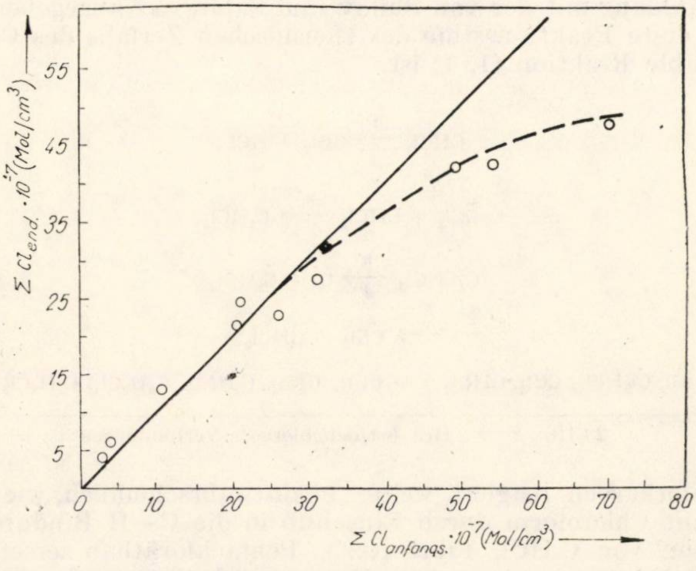

Abb. 2. – Chlorbilanz. Arbeitsbedingungen : 603°, $(CH_4)_i = 46{,}2 \cdot 10^{-5}$ Mol/cm^3.

Bei großen Anfangskonzentrationen von Chloroform (also bei kleinen $(CH_4)/(CHCl_3)$ Verhältnissen) treten Abweichungen von der Linearität im Sinne einer Neigungsverringerung auf. Diese Abweichungen werden durch Anwachsen der anfänglichen Konzentration betonter.

Diese Ergebnisse zeigen an, daß bei kleineren Anfangskonzentrationen als $8 \cdot 10^{-7}$ Mol/cm^3 des Chloroforms, also bei $(CH_4)/(CHCl_3)$ Verhältnissen die größer als 450 sind, wenn die C_2H_3Cl Ausbeuten größer als 8% sind, da $\sum Cl_f/Cl_1$ ist, die Cl_f sämtliche Chlorverbindungen der Reaktion enthält.

Bei größeren Anfangskonzentrationen des Chloroforms als $8 \cdot 10^{-7}$ Mol/cm^3, also bei $(CH_{4i})/(CHCl_3)_i$ kleiner als 450 und Vinylchloridausbeute kleiner als 8%, wird die Cl_f, die nach Beziehung (B) berechnet wurde, kleiner als Cl_i.

Diese deutet darauf hin, daß in diesen Versuchsbedingungen außer den in Gleichung (B) angegebenen Chlorverbindungen auch andere nicht zur Bilanz herangezogene Chlorverbindungen auftreten. Die Analyse der flüssigen Phase die in den Kühlfallen eingefroren wurden (Ab. 1[1]), ergab, daß in diesen Arbeitsbedingungen außer der in Gleichung (B) aufgeführten Verbindungen auch noch CCl_4, C_2Cl_4, C_2Cl_6, C_2HCl_5, $C_2H_2Cl_4$ auftreten.

Diese Ergebnisse deuten auf die Existenz einer vierten Reaktionsstufe hin in der die radikalischen Reaktionsprodukte der Reaktion (C3) mit dem Methan reagieren.

Die bisher angeführten Argumente erlauben die Formulierung der ersten, zweiten und dritten Reaktionsstufen.[1] Es wurde gezeigt, daß im Einklang mit der von Shilov und Sabireva[2] angegebenen Hypothese die erste Reaktionsstufe des thermischen Zerfalls des Chloroforms die reversible Reaktion (1, 1) ist.

$$\begin{array}{rl}
\mathrm{CHCl_3} \underset{1}{\overset{1}{\rightleftarrows}} \mathrm{\ddot{C}Cl_2} + \mathrm{HCl} & \\
\mathrm{\ddot{C}Cl_2} + \mathrm{CHCl_3} \xrightarrow{2'} \mathrm{C_2HCl_5} & \\
\mathrm{C_2CHCl_5} \underset{3''}{\overset{3'}{\longrightarrow}} \mathrm{\dot{C}l} + \mathrm{\dot{C}_2HCl_4} & \\
\longrightarrow \mathrm{\dot{C}Cl_3} + \mathrm{\dot{C}HCl_2} & \qquad (C) \\
\mathrm{\dot{C}l, \dot{C}l_2HCl_4, \dot{C}Cl_3, \dot{C}HCl_2} \longrightarrow \mathrm{CCl_4, C_2Cl_4, C_2HCl_5, C_2H_2Cl_4, C_2H_3Cl_3} & \\
\hline
2\,\mathrm{CHCl_3} \longrightarrow 2\,\mathrm{HCl} + \text{Hochchlorierte Verbindungen} &
\end{array}$$

Dichlorkarben reagiert weiter, höchstwahrscheinlich, wie angezeigt wurde[1], mit Chloroform durch Einschub in die C—H Bindung, was zu der Bildung von C_2HCl_5 führt (C2′), Pentachloräthan zersetzt sich in den Versuchsbedingungen, nach Houser und Cuczano[3] wie Reaktion C3′ angibt und in kleinem Maße nach Reaktion C3″. Da das aus Reaktion C2′ erhaltene Pentachloräthan bis zu dem ersten entaktivierenden Zusammenstoß, die ganze Aktivierungsenergie sowie auch die C—C Bindungsenergie enthält, könnte der Zerfall nach C3″ in größerem Maße als bei dem thermisch aktivierten Pentachloräthan stattfinden.

Weiterhin führen die in C3′, C3″ erhaltenen Radikale, durch Vereinigung, Substitution, Atomabriß usw. zur Bildung von höheren Chlorverbindungen die experimentell beim thermischen Zerfall des Chloroforms aufgefunden werden.

Beim thermischen Zerfall des Chloroforms in Gegenwart von Methan wird die Reaktion C2′ von der Einschubreaktion des : CCl_2 in die C—H Methanbindung (D2) konkurriert, was zu 1, $1C_2H_4Cl_2$ führt, welches durch Dehydrochlorierung, in den angegebenen Versuchsbedingungen[4] zu Vinylchlorid führt (Reaktion D3).

Wie angezeigt, ist die Reaktion C2′ von der Reaktion D2 bei hohen $(CH_4)_i/(CHCl_3)_i$ Verhältnissen verdrängt und die einzigen Reaktionsprodukte sind C_2H_3Cl und HCl wobei Molarproportionalität gewahrt ist(E):

---

[2] A. E. Shilov und P. O. Sabireva, *Doklady Akad. Nauk S.S.S.R.*, **114**, 1058 (1957); *Zhur. fiz. Khim.*, **4**, 860 (1960); **6**, 1365 (1959).

[3] T. S. Houser und R. B. Bernstein, *J. Amer. Chem. Soc.*, **79**, 2429 (1957); T. S. Houser und T. Cuczano, *Intern. J. Chem. Kim.*, **7**, 331 (1975).

[4] K. E. Howlett, *J. Chem. Soc.*, **1952**, 3695; *J. Chem. Soc.*, **1952**, 4487 (1952); P. H. Barton und K. E. Howlett, *J. Chem. Soc.*, **1949**, 155; H. Hardtmann, *Z. phys. Chem. (Frankfurt)*, **28**, 71 (1961); **42**, 329 (1964).

$$CHCl_3 \underset{1'}{\overset{1}{\rightleftarrows}} \ddot{C}Cl_2 + HCl$$

$$\ddot{C}Cl_2 + CH_4 \xrightarrow{2} 1,1\ C_2H_4Cl_2$$

$$1,1\ C_2H_4Cl_2 \xrightarrow{3} HCl + C_2H_3Cl \qquad \text{(D)}$$

$$CHCl_3 + CH_4 \longrightarrow C_2H_3Cl + 2\,HCl$$

$$(CHCl_3)_{\text{verbraucht}} = (CH_4)_{\text{verbraucht}} = (C_2H_3Cl)_{\text{gebildet}} = 2\,(HCl)_{\text{gebildet}} \qquad \text{(E)}$$

Bei kleineren $(CH_4)_i/(CHCl_3)_i$ Verhältnissen fällt das Anmaß der Reaktion D2 zu Gunsten von C2′ ab, wobei die Ausbeute an C_2H_3Cl gleichfalls abfällt und die der Reaktionsprodukte von C2′ anwächst.

Da bis $(CH_4)_i/(CHCl_3)_i \approx 450$, wo die Ausbeute an C_2H_3Cl auf etwa 8% abfällt, festgestellt wurde, daß außer C_2H_3Cl als einzige Reaktionsprodukte CH_3Cl, CH_2Cl_2 und HCl erhalten werden, geht hervor, daß die radikalischen Produkte der Reaktionen C3′ und C3″ nicht die Reaktionen eingehen, die bei dem thermischen Zerfall des Chloroforms (C4′) auftreten, und wodurch sich höhere Chlorverbindungen bilden, sondern Reaktionen eingehen, aus denen nur CH_3Cl und CH_2Cl_2 hervorgeht. Es muß bemerkt werden, daß die Darstellung der Produktausbeuten in Abhängigkeit des Verhältnisses der Reaktantenkonzen-

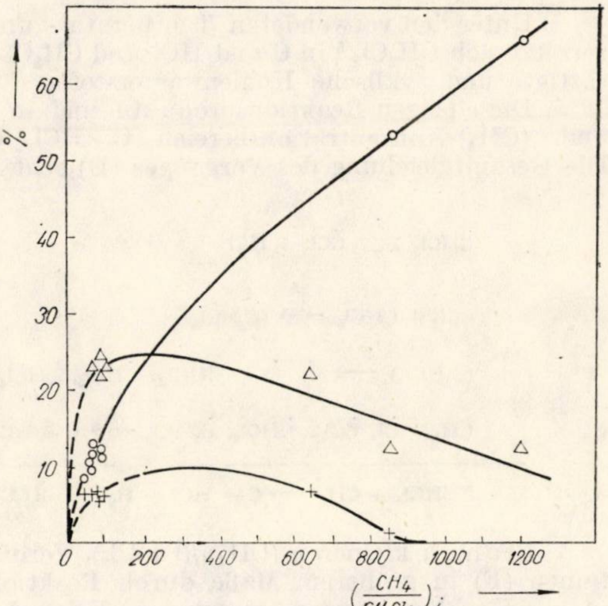

Abb. 3. – Abhängigkeit der Reaktionsprodukteausbeute von dem Reaktantenkonzentrationsverhältnis. ○ C_2H_3Cl, △ CH_2Cl_2, + CH_3Cl.

trationen nicht wesentlich, im Rahmen der Fehlergrenzen, bei unterschiedlichen Temperaturen und Fließgeschwindigkeiten verschieden sind.

Als vierter Reaktionsschritt können die Reaktionen dieser Radikale mit Methan, das im großen Überschuß im Reaktionsmedium vorliegt, angesehen werden. Solche Reaktionen können, zum Beispiel, die Reaktionen (F) sein :

$$\begin{array}{ll}
\dot{C}Cl_3 + CH_4 \xrightarrow{4a} CHCl_3 + \dot{C}H_3 & \\
\dot{C}HCl_2 + CH_4 \xrightarrow{4b} CH_2Cl_2 + \dot{C}H_3 & \\
\dot{C}H_3 + \cdot Cl \xrightarrow{5a} CH_3Cl & \\
\dot{C}l + CH_4 \xrightarrow{4c} \dot{C}H_3 + HCl & \text{(F)} \\
\dot{C}H_3 + CHCl_3 \xrightarrow{5b} CH_3Cl + \dot{C}Cl_3 & \\
\dot{C}l + CH_3Cl \xrightarrow{5c} \dot{C}H_2Cl + HCl & \\
\dot{C}H_2Cl + .Cl \xrightarrow{6c} CH_2Cl_2 &
\end{array}$$

Unter den verwendeten Temperatur- und Verweilzeitbedingungen, zersetzt sich CH_2Cl_2 [5] in C und HCl und CH_3Cl [6] in C, HCl, H_2 und ungesättigte und zyklische Kohlenwasserstoffe.

Die einzigen Reaktionsprodukte sind in diesem relativen ($CHCl_3$)- und (CH_4)-Konzentrationsbereich C, HCl, CH_2Cl_2, CH_3, Cl, C_2H_3Cl. Die Gesamtgleichung des Vorganges (D) geht in (D′) über

$$\begin{array}{ll}
CHCl_3 \underset{1'}{\overset{1}{\rightleftarrows}} \ddot{C}Cl_2 + HCl & \\
\ddot{C}Cl_2 + CHCl_3 \xrightarrow{2'} (C_2HCl_5) & \\
(C_2HCl_5) \xrightarrow{3'} \dot{C}l,\ \dot{C}Cl_3,\ \dot{C}HCl_2,\ \dot{C}HCl_2, \dot{C}_2HCl_4 & \text{(D′)} \\
CH_4 + \dot{C}l,\ \dot{C}Cl_3,\ \dot{C}HCl_2,\ \dot{C}_2HCl_4 \xrightarrow{4} C + HCl + CH_3Cl + CH_2Cl & \\
\hline
2\,CHCl_3 + CH_4 \longrightarrow C + HCl + H_3Cl + CH_2Cl_2 \longrightarrow C + 5\,HCl &
\end{array}$$

Bei noch kleineren $(CH_4)_i/(CHCl_3)_i$ Verhältnissen werden die Reaktionen (F) in größerem Maße durch Reaktionen (C4) konkurriert und so kann erklärt werden, warum als Folge der Bildung höherer Chlorverbindungen durch die Reaktionen (C4) und die nachfolgenden Reaktionen, die Chlorbilanz nicht ausschließlich mit den in (B) angegebenen Verbindungen gemacht werden kann.

---

[5] M. R. Hoare, R.G.W. Norrish und G. W. Hingham, *Proc Roy. Soc. A.* **250**, 180 (1959) ; M. Vacherot, *Compt. rend.*, **252**, 1945 (1961) ; M. Chaigneau, *Compt.rend.* **232**, 719, 1.111 (1951) ; G. Le Moan, *Compt. rend.*, **257**, 179 (1963).

[6] R. E. Kinney, Brevet U. S., 2 488 996 (1949) ; A. E. Silov und P. K. Sabireva, *Zhur. fiz. Khim.*, **6**, 1365 (1959) ; J. Halbrook, *Trans. Faraday Soc.*, **57**, 2, 151 (1961) ; M. Vacherot, *Compt. rend.*, **252**, 1945 (1961) ; G. Le Moan, *Compt. rend.*, **258**, 1535 (1964) ; **260**, 5 588 (1965).

2. *Wasserstoffbilanz*. Die Hypothese der vierten Reaktionsstufe (F) kann auf Grund der Wasserstoffbilanz geprüft werden. Ist die Anzahl der Wasserstoffatome in den Produkten des Reaktionsweges (C) größer als in den $CHCl_3$ Molekülen die durch (C) reagieren, so konnte die Beteiligung des Methans im Reaktionsweg (C) bewiesen werden, da Methan die einzige Wasserstoffquelle außer $CHCl_3$ sein kann.

Die durch Reaktionsweg (C) reagierte Chloroformmenge, $(CHCl_3)_C$ wurde aus der Differenz zwischen der Gesamtmenge des verbrauchten Chloroforms, $(CHCl_3)_i-(CHCL_3)_f$, und des durch Reaktionsweg (D) verbrauchten Chloroforms, $(CHCl_3)_D$, berechnet (G) :

$$(CHCl_3)_i - (CHCl_3)_f = (CHCl_3)_D + (CHCl_3)_C \qquad (G)$$

da aus (D) hervorgeht, daß :

$$(CHCl_3)_D = (C_2H_3Cl)_f \qquad (H)$$

(G) verwandelt sich in (I) :

$$(CHCl_3)_C = (CHCl_3)_i - (CHCl_3)_f - (C_2H_3Cl)_f \qquad (I)$$

Die Gesamtmenge der Wasserstoffatome, in Atomgramm/cm³, die im Reaktionsprodukt enthalten sind, $\sum H_f$, ist gleich der Summe der in den Reaktionswegen (D) und (C), $\sum H_D$, bzw. $\sum H_C$, entstandenen Produkte (J) :

$$\Sigma H_C = \Sigma H_f - \Sigma H_D \qquad (J)$$

Wenn CH_4 nur in Reaktion (D2) teilnimmt und die einzige Wasserstoffquelle des Reaktionssweges (C) $(CHCl_3)_C$ ist, ergibt sich (K)

$$\Sigma H_C = (CHCl_3)_C \qquad (K)$$

Wenn $\sum H_C > (CHCl_3)_C$ dann wird bei der Produktbildung des Reaktionsweges (C) noch ein wassestoffhaltiger Reaktant außer $CHCl_3$ verbraucht. Dieser, wie gesagt, kann nur CH_4 sein. Die Differenz (M) gibt die Wasserstoffmenge, in Atomgramm/cm³ ausgedrückt, die in den Produkten des Reaktionsweges (C) vorhanden sind und von einer anderen Wasserstoffquelle als $(CHCl_3)_C$ stammen :

$$\Sigma H_C - (CHCl_3)_C \qquad (M)$$

Ein Viertel dieser Menge, (0), stellt die Methanmenge (Mol/cm³) dar die in der Reaktion (C) verbraucht wird, $(CH_4)_C$:

$$(CH_4)_C = \frac{1}{4}\left[\Sigma H_C - (CHCl_3)_C\right] \qquad (O)$$

Mit Beziehung (L) erhält man (P):

$$(CH_4)_C = \frac{1}{4}\,[\sum H_f - \sum H_D - (CHCl_3)_C] \qquad (P)$$

$$\text{Da}: \sum H_f = HCl + 3\,(CH_3Cl) + 2\,(CH_2Cl_2) + 3(C_2H_3Cl) \qquad (R)$$

$$\sum H_D = 3\,(C_2H_3Cl) + (HCl)_D \qquad (S)$$

$$(HCl)_D = 2\,(C_2H_5Cl) \qquad (T)$$

$$\sum H_D = 3(C_2H_3Cl) + (C_2H_3Cl) = 5(C_2H_3Cl) \qquad (U)$$

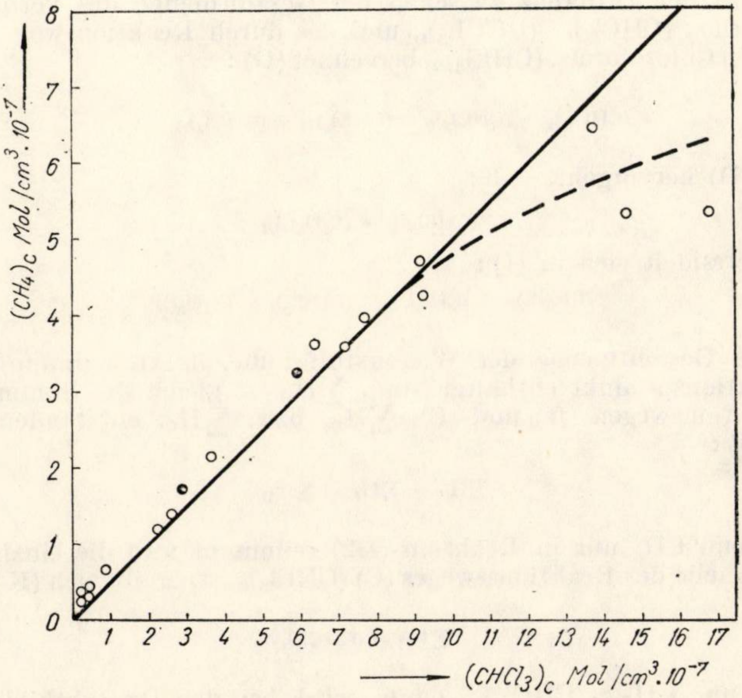

Abb. 4. — Wasserstoffbilanz. Abhängigkeit der Methanmenge die durch Reaktionsweg (C) reagiert hat, $(CH_4)_C$, von der Chloroformmenge die durch Reaktionsweg (C) reaktioniert hat, $(CHCl_3)_C$.

folgt daß:

$$(CH_4)_C = \frac{1}{4}\,[(HCl) + 3(CH_3Cl) + 2(CH_2Cl_2) + 3(C_2H_3Cl) - 5(C_2H_3Cl) - (CHCl_3)_C] \qquad (V)$$

$$(CH_4)_C = \frac{1}{4}\,[HCl + 3(CH_3Cl) + 2(CH_2Cl_2) - (2C_2H_3Cl) - (CHCl_3)_C] \qquad (X)$$

In Abb. 3 wurde $(CH_4)_C$ in Abhängigkeit von $(CHCl_3)_C$ dargestellt. Es ist ersichtlich, daß $(CH_4)_C > 0$ die Methanbeteiligung an der Reaktion (C) anzeigt. Die Neigung der Geraden ist ≈ 0,5 im Einklang mit den Bedingungen des vierten Reaktionsschrittes (F).

3. *Änderung der Reaktionsgeschwindigkeitskonstanten erster Ordnung mit der relativen Reaktantenkonzentration.* Die Geschwindigkeitskonstanten erster Ordnung die aufgrund der Beziehung $k_i = \frac{2,303}{tc} \log \frac{(CHCL_3)_i}{(CHCl_3)_f}$ berechnet wurden, fallen mit der Verweilzeit ab (Abb. 5) wodurch eine Inhibitionsreaktion durch ein Reaktionsprodukt angezeigt wird so wie es auch bei dem thermischen Zerfall des Chloroforms in Abwesenheit von Methan festgestellt wurde. Eine solche Reaktion ist (1′), die beim thermischen Zerfall des Chloroforms sowohl in Gegenwart als auch in Abwesenheit des Methans abläuft.

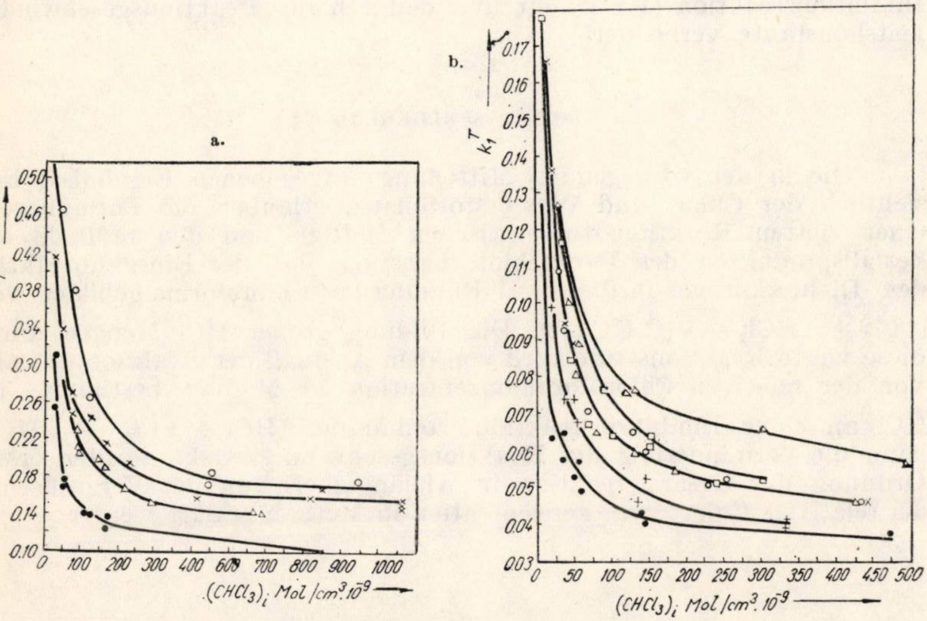

Abb. 5. a.b. – Abhängigkeit der Geschwindigkeitskonstanten erster Ordnung von der Temperatur, der Kontaktzeit und der relativen Konzentration des Chloroforms.

Zum Unterschied des thermischen Chloroformzerfalls, fallen die Geschwindingkeitskonstanten erster Ordung mit dem Anwachsen des $(CH_4)_i/(CHCl_3)_i$ Verhältnisses ab.

Bei kleinen Verhältnissen der Anfangskonzentration des Chloroforms, wenn die Zerfallsreaktion des Chloroforms mit Unterbildung von Vinylchlorid (Reaktionen 2,3) vorherrscht, sind die Geschwindigkeitskonstanten erster Ordnung viel größer als die entsprechenden bei dem thermischen zerfall des Chloroforms in Abwesenheit des Methans. Mit Anwachsen der relativen Chloroformkonzentration fällt das Ausmaß der Vinylchloridbildung (2,3) ab und gleichzeitig damit fällt auch die Geschwindigkeitskonstante erster Ordhung ab, so daß bei anfänglich hohen Chloroformkonzentrationen bei denen die Ausbeute an Vinylchlorid sehr klein ist die Reaktionsgeschwindigkeitskonstanten erster Ordnung kleiner werden als die in Abwesenheit des Methans bei gleichen Temperaturen und Fließgeschwindigkeiten.

Dieses kann durch das Vorhandensein der vierten Reaktionsstufe (F), durch welche viel größere HCl Mengen gebildet werden als in Abwesenheit dieser, erklärt werden. Solchermaßen ist das Ausmaß der Inhibitionsreaktion (1′) erhöht und dadurch die Reaktionsgeschwindigkeitskonstante verkleinert.

SCHLUSSFOLGERUNG

Die in der vorliegenden Mitteilung angegebenen Ergebnisse hinsichtlich der Chlor- und Wasserstoffbilanz, erlauben die Formulierung einer vierten Reaktionsstufe zwischen Methan und den radikalischen Zerfallsprodukten des Pentachloräthans das bei der Einschubreaktion des Dichlorkarbens in die C—H Bindung des Chloroforms gebildet wird ($\ddot{C}Cl_2 + CHCl_3 \xrightarrow{2'} (C_2HCl_5)^*$). Die Bildung großer HCl Mengen durch diese vierte Reaktionsstufe wird von dem Ausmaß der Reaktion (2′) also von der relativen Chloroformkonzentration in Methan bestimmt. Da HCl an einer Inhibitionsreaktion teilnimmt ($HCl + \ddot{C}Cl_2 \xrightarrow{1'} CHCl_3$) kann die Verminderung der Reaktionsgeschwindigkeitskonstanten erster Ordnung der Gesamt-reaktion in Abhängigkeit von der Vergrößerung der relativen Chloroform-konzentration in Methan erklärt werden.

Revue Roumaine de Chimie, **21**, *11–12*, 1445–1449 (1976)

SPECTRAL STUDY OF 4,7-PHENANTHROLINE-5,6-DIONE RADICAL ANION

LILIANA CIUREA, V. EM. SAHINI and A. MATEESCU

Polytechnic Institute of Bucharest, Department of Physical Chemistry and Electrochemical Technology
Bd. Republicii, 13

Received March 1, 1975

ESR and optical spectra of the radical anion obtained by the chemical and the electrochemical reduction of 4,7-phenanthroline-5,6-dione in dimethylformamide, dimethylsulphoxide and acetonitrile were studied. Its spectral behaviour was compared with that of the radical anion from 9,10-phenanthrenequinone. MO calculations in the frame of Hückel and McLachlan approximations were performed, and the results account for the observed hyperfine splittings.

4,7-Phenanthroline-5,6-dione is known for its antibacterial properties, but its electronic structure and spectral behaviour was less studied. There is only one paper [1] about the radical anion from the above mentioned compound concerning the effect of solvent, namely DMSO in mixture with dioxane, methyl cyanide and ethanol on its ESR spectrum.

In this paper the ESR data of the radical anion of 4,7-phenanthroline-5,6-dione (Entobex) were correlated with its optical spectra in order to provide information about the nature of the radicalic species present in solution.

EXPERIMENTAL PART

4,7-Phenanthroline-5,6-dione was recrystallized from ethanol. The solvents, dimethylformamide (DMF), dimethylsuphoxide (DMSO) and acetonitrile (AN) were purified by refluxing and fractional distillation from calcium hydride. The chemical reduction was made in a nitrogen atmosphere with the alkali and alkali-earth metals in a cell connected to the ESR tube or to the optical cell. The electrochemical reduction was performed on a 10^{-3}M solution of the parent compound, using two Pt electrodes and 0.1 M tetrabutylammonium iodide as supporting electrolyte. The potential was controlled by means of an Ag wire passed through a glass capillary and dipped into the solution till above the catode. For the ESR study the anions were generated directly within the microwave cavity. The platinum cathode passed through a glass capillary was dipped into the ESR tube of the electrochemical-ESR cell, till reaching the center of the microwave cavity. For the optical study an electrolytic cell with two separated compartments was used, in order to prevent the diffusion of the anodic products to the cathode.

The ESR spectra were recorded on a JES-3B Spectrometer in the X-band frequency and the optical ones on a Unicam SP-800 and a Unicam SP-100 Spectrometer. The MO calculations were carried out at the Computer Center of the Polytechnic Institute.

---

[1] A. G. Evans, J. C. Evans and E. H. Godden, *J. Chem. Soc.*, **1970 B**, 149.

RESULTS AND DISCUSSION

The ESR spectra of the radical anion from Entobex obtained by electrochemical reduction in DMF and by reduction with Na in the same solvent are given in Fig. 1 and 2, respectively.

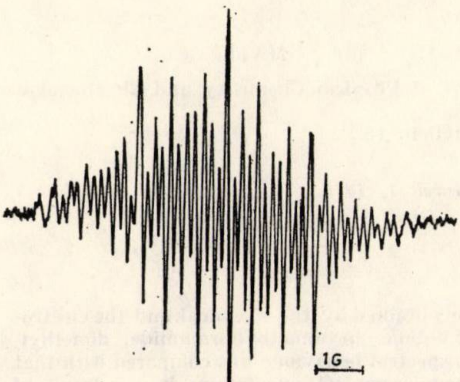

Fig. 1. — ESR spectrum of the electrochemically generated Entobex radical anion in DMF.

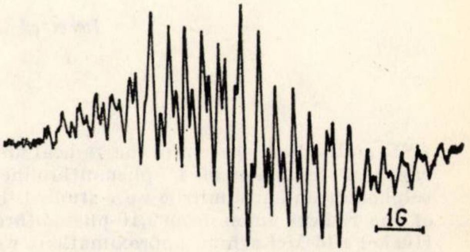

Fig. 2. — ESR spectrum of Entobex — Na in DMF.

The ESR spectrum of the electrochemically generated radical is very well resolved in 47 lines on a total length of 7.90 G and evidences all the hyperfine splitting constants. The values of the experimental hyperfine splitting constants are in the solvents DMF and AN are close with those reported by Evans. [1]

The assignments of the experimental hyperfine splittings were based on the MO calculations. The experimental and calculated spin densities in the frame of Hückel and McLachlan approximations and the used parameters are given in Table 1.

Table 1

Experimental and calculated spin densities *

Radical	Position	a_{exp} (G)**	ρ_{exp}	ρ_{calc}	
				Hückel	McLachlan ($\lambda = 1.2$)
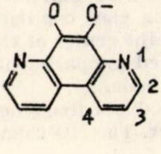	1	0.69 (1.35)	0.033	0.037	0.038
	2	0.28 (0.20)	0.012	0.009	−0.008
	3	1.80 (1.67)	0.076	0.046	0.055
	4	0.47 (0.42)	0.020	0.002	−0.020

* The used parameters are ; $h_0 = 1.2$; $k_{CO} = 1.65$; $h_N = 0.5$; $k_{CN} = 1$.

** For comparison the splitting constants of phenanthrenequinone radical anion [5] are given in the brackets.

The experimental spin densities ρ_{exp} were obtained from the splitting constants of the electrochemically generated radical anion using the McConnell relationship[2] with the following $\sigma - \pi$ interaction parameters : $|Q^{H}_{CH}| = 23.7$ G and $|Q^{N}_{N}| = 21$ G. From the Table 1 one can see a good agreement between the experimental and calculated spin densities after the McLachlan method. The protons from *para* position to the carbonyl group are responsible for the greatest splitting constants. The proton hyperfine splittings of Entobex radical anion are close to those of the corresponding splitting constants of the phenanthrenequinone radical anion. The substitution of the carbon atom from the position 1 with nitrogen in the case of Entobex leads to a considerable decrease of the spin density on this position in the corresponding radical anion (from 1.35 G to 0.69 G).

The visible spectrum of the radical anion provided by Entobex shows comparatively to the neutral molecules the additional maxima in the range 380–700 nm. Fig. 3. presents the spectrum in AN of Entobex radical anion generated by electrochemical reduction which shows an intense band in the region of 386–400 nm and one weak band at about 575 nm. Curve 2 from Fig. 3 represents the spectrum of the decomposed radical.

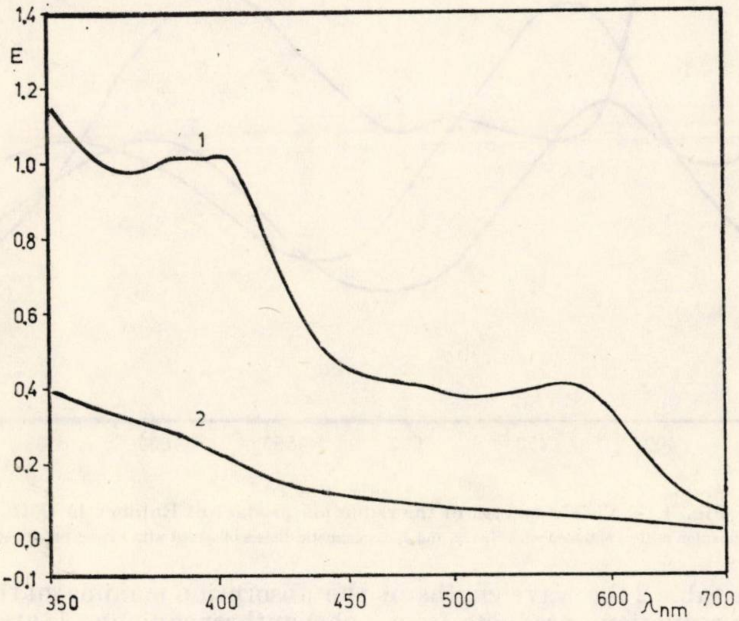

Fig. 3. – Visible spectrum of Entobex radical anion in AN obtained by electrochemical reduction (1) and that of decomposed sample (2).

---

[2] H. M. McConnell, *J. Chem. Phys.*, **24**, 764 (1956).

The study of Entobex radical anion obtained by chemical reduction evidences the existence of two species depending on the concentration and the used reduction agent. One of the species which is present at small concentration of $10^{-4} - 10^{-5}$ M/l was assigned to the paramagnetic monoanion, because its optical and ESR spectra are identical to those of the corresponding radical anion obtained by electrochemical reduction. The second species, which was obtained at high concentration or by using alkali-earth metals as reduction agents, has no ESR signal, being thus assigned to the diamagnetic dimer.

In Fig. 4 the spectrum of the paramagnetic monoanion generated by the reduction with Na in DMF are comparatively given with those of the diamagnetic dimers obtained by reduction with Li and Sr.

The optical spectral data of the paramagnetic monoanion and diamagnetic dimer provided by Entobex in different solvents and reduction agents are contained in Table 2.

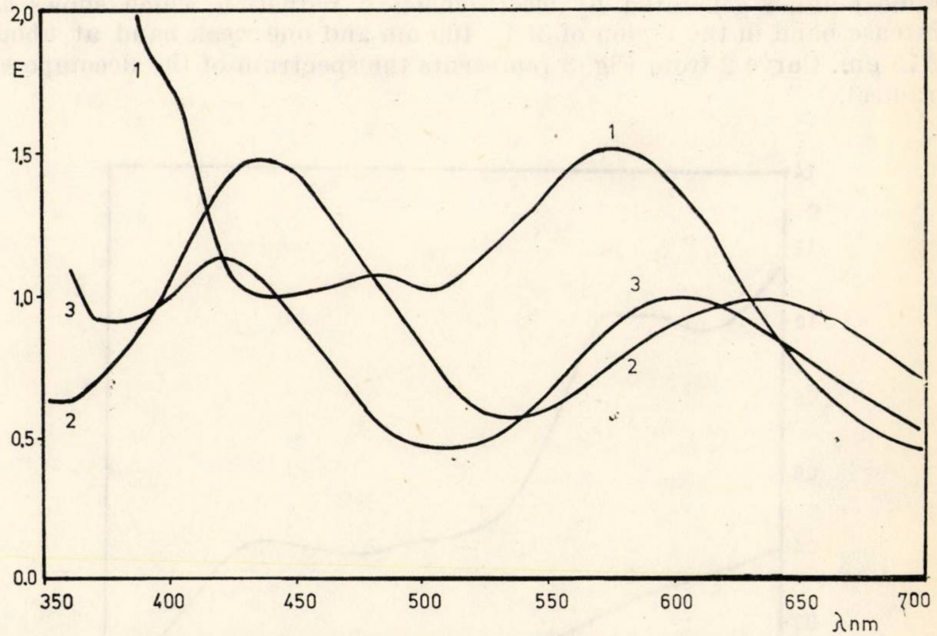

Fig. 4. — Visible spectra of the reduction product of Entobex in DMF :
1, monoanion radical obtained with Na ; *2*, and *3*, diamagnetic dimers obtained with Li and Sr, respectively.

In table 2 the wavelengths of the absorption maxima of the corresponding reduction products from phenanthrenequinone [3] are given in the brackets. It may be seen from Table 2, that in comparison with phenanthrenequinone, Entobex radical anion exhibits a batochromic shift of its absorption maxima, in concordance with the values of the transition energies calculated by HMO method.

---

[3] T. L. Staples and M. Szwarc, *J. Amer. Chem. Soc.*, **92**, 5022 (1970).

Table 2

Wavelengths of the absorption maxima of the reduction products of Entobex

Method of the reduction and solvent	λ_{nm}	
	Monoanion	Dimer
Electrochemical reduction in AN	386 – 400 568	—
Electrochemical reduction in DMSO	380 – 400 575	—
Na + DMSO	380 – 405 570	—
Na + DMF	380 (335) 585 (510)	425 (440) 670 (675)
Sr + DMF	—	422 602
Li + t-butyl alcohol	—	408 630

A similar spectral behaviour of Entobex radical anion to that of phenanthrenequinone radical was observed in the infrared region. In the IR spectra of the reduction product of Entobex with Na in DMSO a shift of the carbonyl band from 1665 cm^{-1} to 1564 cm^{-1} was observed. The carbonyl frequency differences passing from the neutral molecule to its anion is reflected in the decrease of the bond orders from 0.893 to 0.707 and of the carbonyl force constants from 11.13×10^5 to 9.37×10^5 dyne/cm. The carbonyl force constants were obtained from MO calculations with the parameters given in Table 1 using Coulson and Longuet-Higgins formula,[4] which had been adjusted to the systems with unpaired electrons.

---

[4] C. A. Coulson and H. C. Longuet-Higgins, *Proc. Roy. Soc.*, **191 A**, 39 (1947).

[5] R. Dehl and G. K. Fraenkel, *J. Chem. Phys.*, **39**, 1793 (1963).

Revue Roumaine de Chimie, 21, *11–12*, 1451–1455 (1976)

THERMODYNAMIC STUDY OF SOME URANIUM OXIDES BY SOLID ELECTROLYTE EMF MEASUREMENTS. SOLID STATE COULOMETRIC TITRATION TECHNIQUE

D. I. MARCHIDAN and SPERANŢA TĂNĂSESCU
Center of Physical Chemistry
Str. Galaţi 31, Bucharest, Romania

Received March 31, 1976

A high-temperature galvanic cell containing solid electrolyte, reversible to oxygen ions (o^{2-}) only, has been used to measure thermodynamic data for some nonstoichiometric uranium oxides. A titration technique for oxygen ions from the standard metal/metal oxide to uranium oxide has been used to change the oxygen-to-metal ratio of the uranium oxide electrode.

In order to obtain thermodynamic data for some nonstoichiometric uranium oxides with predetermined oxygen-to-uranium ratios, in our laboratory, galvanic cells of the type :

$$\mathrm{Fe,\ Fe_xO} \mid (0.85\ \mathrm{ZrO_2} + 0.15\ \mathrm{CaO}) \mid \mathrm{UO_{2+x}}$$

have been previously investigated. [1,2] The cells involve on the left side an iron-wüstite reference electrode with a known relative partial molar free energy of oxygen. The electrolyte is a solid solution of 85 mole% zirconium oxide and 15 mole % calcium oxide. Due to its defect structure containing oxygen ion vacancies, this electrolyte is a purely anionic conductor over wide variations in the ambient oxygen partial pressure as shown by Kiukkola and Wagner [3-5] and verified by Kingery et al. [6] and Carter. [7] The right-hand electrode is made of uranium oxide with a predetermined oxygen-to-uranium ratio.

This kind of measurements is limited by the possibility of accurately obtaining some compounds having a predetermined and slightly changed O/U ratio, especially because with O/U ratios that are close to the stoichiometry, the changes of the composition are accompanied by very rapid changes of the oxygen potential.

[1] D. I. Marchidan and S. Matei, *Rev. Roumaine Chim.*, *15*, 1491 (1970).
[2] D. I. Marchidan and S. Matei, *Rev. Roumaine Chim.*, *17*, 195 (1972).
[3] K. Kiukkola and C. Wagner, *J. Electrochem. Soc.*, *104*, 308 (1957).
[4] K. Kiukkola and C. Wagner, *J. Electrochem. Soc.*, *104*, 379 (1957).
[5] J. B. Wagner and C. Wagner, *J. Electrochem. Soc.*, *104*, 509 (1957).
[6] W. D. Kingery, J. Pappis, M. E. M. Doty and D. C. Hill, *J. Amer. Ceram. Soc.*, *42*, 393 (1959).
[7] W. H. Rhodes and R. E. Carter, *Bull. Amer. Ceram. Soc.*, *41*, 283 (1962).

By using EMF measurements with the coulometric titration method developed by Wagner, [8] we get the possibility of enlarging the determination range, the electrode composition being able to be changed at the temperature set for the determination. In this method, since the electrolyte is a purely anionic conductor, the passing of current i across the cell during an interval t causes a corresponding transport of oxygen from one electrode to the other and thus, it is possible to change the O/U ratio of a given electrode by known amounts and measure the corresponding oxygen potential of the electrode.

EXPERIMENTAL

The cell assembly consisting of an electrolyte tablet between the two electrode tablets was inserted into a quartz cell, the form and construction of which have been minutely described in previous papers. [1,2]

The technique of preparing the tablets has been also previously shown. [2]

Electromotive force measurements were made by a high inner resistance digital voltmeter (Solartron, type LM 1440.2, 10^{10} ohms, made in England).

The measuring circuit was also provided by instruments for measuring the amount of current passed and the potential applied during coulometric titration. The method consisted of imposing an EMF onto the cell through a resistance and of accurately measuring the current as well as the duration of the titration.

The titrations were done at 1073, 1173 and 1273 K to ensure an ionic mobility, high enough for the homogeneization of the electrodes to occur within a reasonable time. For the same reason, it was essential that only small samples of oxide were used. Thus, a current of 5 μA that passed for 117 minutes increased the O/U ratio of a 40 mg sample by 0.001. After the titration, sufficient time is allowed for the electrode to equilibrate internally and then the EMF of the cell at equilibrium was measured.

In titration experiments the current density should not be exceed 100 μA/cm^2. This is necessary in order to avoid the possible precipitation of blocking layers in the reference electrode or on the specimen. [9] To obtain valid experiments it is absolutely necessary to prevent both mixed electrode reactions and extraneous electrode-gas interactions.

RESULTS AND DISCUSSION

Electromotive force measurements combined with coulometric titrations were used by us for studying some oxides that are part of the series of nonstoichiometric oxides UO_{2+x}, comprised between UO_2 and U_4O_9

---

[8] C. Wagner, *J. Chem. Phys.*, *21*, 1819 (1953).

[9] K. S. Goto and W. Pluschkell, in "Physics of Electrolytes", vol. 2, Editor J. Hladik, Academic Press, 1972, p. 589.

which make up a single phase at high temperatures, with the fluorite-type structure.

In previous papers[1,2] thermodynamic data for uranium oxides with atomic ratio of 2.11 and 2.125 were related. Thus, using the EMF solid electrolyte technique, the partial molar free energies, enthalpies and entropies of solution of oxygen in uranium oxides and the corresponding relative integral quantities as a function of the temperature, as well as equilibrium pressures of oxygen over the two oxides have been calculated.[1,2]

Taking into account the difficulties that are usually encountered when obtaining as accurately as possible some oxides having a predetermined composition with very small O/U ratio differences between them (for instance, a 0.001 difference), we proposed ourselves to change the electrode composition at the determination temperature, by starting from a cell with an oxide having a predetermined composition, and using solid state coulometric titration. By following one of these titrations, the O/U atomic ratio, initially $2 + x$, changes to $2 + x + y$, where y is :

$$y = \mathrm{it}/2\, n_U\, \mathcal{F} \tag{1}$$

In this equation, i represents the current passed through the cell for a time t, n_U is the number of gramatoms of the initially uranium and $\mathcal{F}$ is the Faraday constant.

The EMF of the cell as a function of temperature was measured after each small increase in O/U ratio. After equilibration, the cell voltage allowed to calculate the partial molar free energy of the oxygen in equilibrium with the uranium oxide corresponding to the changed composition of the electrode, from the equation :

$$\Delta G_{\mathrm{cell}} = 2\ \Delta G^0_{\text{wüstite}} - \overline{\Delta G_{O_2}} \tag{2}$$

where the measured free energy of the cell is :

$$\Delta G_{\mathrm{cell}} = -\ 4\mathcal{F}E \tag{3}$$

and the $\Delta G^0_{\text{wüstite}}$ is the standard free energy of wüstite, known from equilibrium measurements in gas.[4]

In our experiments we started from $UO_{2.11}$ oxide, the composition of which was previously checked by gravimetric analysis.

In Fig. 1 we show the points of three titrations at the temperatures of 1073, 1173, 1273 K, along with a diagram obtained by the conventional method using an electrode with a predetermined $UO_{2.11}$ composition.

Fig. 2 shows the $\overline{\Delta G_{O_2}}$ isotherm *vs.* O/U ratio that includes the points measured at 1150 K with cells having predetermined composition of uranium oxide, and the experimental points from the coulometric titrations. On the same diagram, we also inscribed the values obtained by Aronson and Belle[10] at the same temperature and Kiukkola[11] at 1173 K from usual measurements with nonstoichiometric oxides having predetermined atomic ratio O/U close to 2.11, as well as the values calculated for some oxides from the equations related by Rand and Kubaschewski.[12]

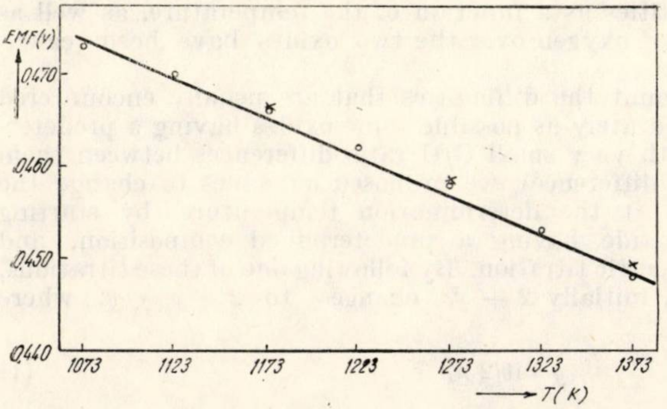

Fig. 1. — E.M.F. versus temperature plot for $UO_{2.11}$ and three points obtained from coulometric titration results corresponding to $UO_{2.111}$

Fig. 2. — $\overline{\Delta G}_{O_2}$ versus O/U ratio: *1.* Obtained by authors[1,2] for $UO_{2.11}$ and $UO_{2.125}$ at 1150*K*. *2.* Obtained by Aronson and Belle at 1150K.[10] *3.* Obtained by Kiukkola at 1773 K.[11] *4.* Calculated from the equations related by Rand and Kubaschewski.[12] *5.* Obtained from coulometric titration results for the $UO_{2.111}$ and $UO_{2.113}$ oxides.

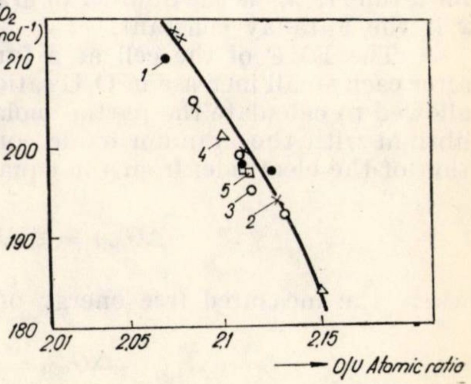

One can observe that the values of the partial molar free energies fo $UO_{2.111}$ and $UO_{2.113}$ obtained by us using coulometric titration inscribe themselves in the series of the molar partial free energies values of the oxides existing in this single phase region.

Coulometric titration experiences connected with EMF measurements have been retaken also for oxides with higher O/U ratios, namely for oxides comprised between $UO_{2.19}$ and $UO_{2.20}$. Fig. 3 represents an isotherm of $\Delta\overline{G}_{O_2}$ as a function of O/U ratio. Some difficulty was experienced

[10] S. Aronson and J. Belle, *J. Chem. Phys.*, *29*, 151 (1958).

[11] K. Kiukkola, *Acta. Chem. Scand.*, *16*, 327 (1962).

[12] M. H. Rand and O. Kubaschewski, "The Thermochemical Properties of Uranium Compounds", Oliver and Boyd, Edinburgh, 1963, p. 26.

with these atomic ratios was found to be due to depletion of oxygen at the Fe, Fe_xO/electrolyte interface. Cleaning the surface of the Fe, Fe_xO pellet between titration of oxygen ions and equilibrium EMF measurements overcame the trouble. Nevertheless at higher O/U ratios, the titrations were not satisfactory, presumably due to the escape from the uranium oxide electrode of a part of the transported oxygen. As Kiukkola also showed, the flow of current, despite its low density, polarized the cell to a potential over 0.9 V which caused oxygen to develop at atmospheric pressure.[11] In addition, the phase change of UO_{2+x} to $UO_{2.25}$ may be slow and cause overshooting since the mobility of uranium is very low.[11] Therefore, one can conclude that the titrations may prove useful at small values of O/U atomic ratio (O/U $\leqslant$ 2.2).

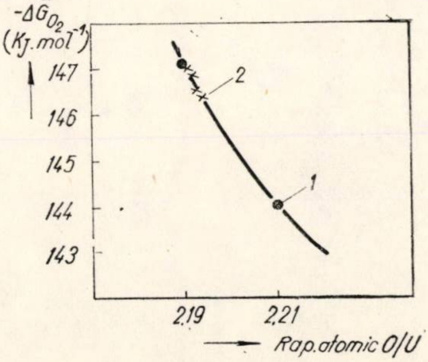

Fig. 3.— Variation $\Delta\bar{G}_{O_2}$ with uranium oxide composition at 1273 K, for some oxides comprised between $UO_{2.19}$ and $UO_{2.21}$.
1. Measured with cells having predetermined constant composition of uranium oxide. *2.* Experimental points from coulometric titrations.

Revue Roumaine de Chimie, **21**, *11–12*, 1457–1461 (1976)

ULTRASONIC VELOCITY AND COMPRESSIBILITY IN FUSED AgCl–AgBr, AgCl–KCl and AgI

S. STERNBERG and V. VASILESCU

Centre of Physical Chemistry, ICCCHIM 31, Str. Galaţi
Bucharest 9, Romania

Received February 4, 1975

The velocity of sonic waves of 1 MHz were measured in fused AgCl–AgBr, AgCl–KCl and AgI. From velocity data in single salts and mixtures some thermodynamic functions were calculated. In mixtures, the excess compressibility variation with composition parallels that of excess volume; the hole theory was used to correlate the two excess quantities. A classification of the mixtures studied so far from the compressibility standpoint is advanced.

I. INTRODUCTION

Silver halides are salts characterized by low volume increase on melting (around 10% compared to 15–20% for corresponding alkali halides) that is, these fused salts have a low hole content. This was explained by the existence of stronger interionic forces than in alkali halides or the existence of a certain degree of covalence.

Thus, extending the sonic velocity measurements to these salts could confirm the findings of other measurements of physical properties.

II. EXPERIMENTAL

The equipment and procedure were described elsewhere.[1] AgCl, AgBr and AgI were prepared from $AgNO_3$ and the respective hydrogen halide. The precipitate was dried and melted. In case the salt contained traces of silver, purification by electrolysis was made. Salts were handled only in artificial light.

III. RESULTS

The sound velocity in single salts and mixtures varies linearly with temperature according to eq :

$$u = u_0 - at \tag{1}$$

where u_0 and a are the velocity at 0°C and temperature coefficient respectively. Velocities were determined to ± 0,4% (standard deviation of a run (40 measurements) was less than 0,5 m/s); u_0 and a values are given in Table 1 together with the temperature range over which measurements were carried out.

---

[1] S. Sternberg and V. Vasilescu, *Rev. Roumaine Chim.*, **12**, 1187 (1967).

Table 1

Temperature dependence of sonic velocity in simple salts and mixtures

AgCl – AgBr

X_{AgCl}	u_0 $m.s^{-1}$	a $m.s^{-1} K^{-1}$	Temperature range
0.0	1658	0.510	450–630
0.342	1712	0.498	480–670
0.597	1797	0.546	450–620
0.733	1829	0.536	460–660
1.0	1928	0.608	530–700
1.0*	1945	0.604	475–550

* Reference [2]

AgCl – KCl

0.0	2273	0.865	830–970
0.478	1911	0.765	590–760
0.680	1860	0.732	450–650
0.806	1835	0.649	500–670
1.0	1928	0.608	530–700

AgI

	1333	0.353	590–800

No comparison values are given for AgBr and AgI as no other ultrasonic measurements were carried out on them so far.

IV. DISCUSSION

A. To start with, in Table 2 are given the values of thermodynamic functions for silver salts as calculated from sonic velocity ;[1,3-10] use has been made of density [11,12] and specific heat data [13] available in the literature.

---

[2] J. G. Marchessault and T. A. Litovitz, *J. Acoust. Soc. America*, **34**, 616 (1962).

[3] S. Sternberg and V. Vasilescu, *Rev. Roumaine Chim.*, **13**, 265 (1968).

[4] S. Sternberg and V. Vasilescu, *J. Chem. Thermodynamics*, **1**, 595 (1969).

[5] S. Sternberg and V. Vasilescu, *Rev. Roumaine Chim.*, **15**, 1665 (1970).

[6] V. Vasilescu, S. Volkov and S. Sternberg, *Rev. Roumaine* Chim., **15**, 1819 (1970).

[7] V. Prissiajnyi, V. Vasilescu and S. Sternberg, *J. Chem. Thermodynamics*, **3**,867 (1971).

[8] S. Sternberg and V. Vasilescu, *J. Chem. Thermodynamics*, **3**, 877 (1971).

[9] V. Prissiajnyi and V. Vasilescu, *Rev. Roumaine Chim.*, **17**, 455 (1972).

[10] V. Vasilescu and V. Prissiajnyi, *Zhur fiz. Khim.*, **47**, 874 (1973).

[11] N. K. Boardman, F. H. Dorman and E. Heyman, *J. Phys. Chem.*, **53**, 375 (1949).

[12] G. J. Janz, F. W. Dampier, G. R. Lakshminarayanan, P. K. Lorenz and R. P.T. Tomkins, "Molten Salts, Vol. 1, Electrical Conductance, Density and Viscosity Data", NSRDS-NBS 15, U.S. Government Printing Office, Washington 1968.

[13] O. Kubashewski, E. L. Evans and C. B. Alcock, "Metallurgical Thermo-Chemistry", Pergamon Press, New York, 1967.

Bockris et al.[14] have shown that isothermal compressibility (β) increases linearly with the square of average ionic radii; in a series of alkali halides M^+X^- for given M^+, β increases with the radius of X^- which is so in case of silver halides. However the lower compressibility of silver halides (compared to similar values in alkali halides) has been assigned to their lower content of holes.

Table 2

Values of expansion coefficient (α), $\gamma = C_p/C_V$, adiabatic (β_S), and isothermal (β) compressibility, $C_p \cdot C_V$, interval pressure (p_i) and free volume (V_f) for silver salts at 873 K

Salt	$10^4 \cdot \alpha$ K^{-1}	γ	$10^{11} \cdot \beta_s$ $m^2 \cdot N^{-1}$	$10^{11} \cdot \beta$ $m^2 \cdot N^{-1}$	C_p $J \cdot mol^{-1} K^{-1}$	C_V $J.mol^{-1} \cdot K^{-1}$	$10^9 \cdot p_i$ $m^{-2} \cdot N$	$10^6 \cdot V_f$ $m^3 \cdot mol^{-1}$
AgCl	2.001	1.18	8.7	10.3	66.94	56.73	1.6960	0.01
AgBr	1.925	1.18	10.1	11.9	62.34	52.83	1.4122	0.11
AgI	1.825	1.18	14.4	17.0	62.13	52.65	1.1065	0.17

The two mixtures investigated here, that is AgCl—AgBr and AgCl—KCl, are characterized by values of exces thermodynamic functions listed in Tables 3 and 4 respectively; γ was calculated additively from values for single salts while the β^E/β_0 ratio was calculated according to the equation

Table 3

Excess quantities for AgCl – AgBr; 873 K

X_{AgCl}	0.0	0.342	0.597	0.773	1.000
$10^{11} \cdot \beta_s/m^2 \cdot N^{-1}$	10.1	9.7	9.3	9.0	8.7
	1.18	1.18	1.18	1.18	1.18
$10^{11} \cdot \beta/m^2 \cdot N^{-1}$	11.9	11.4	11.0	10.6	10.3
$10^{11} \cdot \beta^E/m^2 \cdot N^{-1}$	0.0	0.0	0.0	−0.1	0.0
$10^6 \cdot V^E/m^3 \cdot mol^{-1}$	0.0	−0.05	−0.01	0.0	0.0
$10^4 \cdot \alpha/K^{-1}$	1.925	2.062	2.237	2.215	2.001
$100 \cdot \beta^E/\beta_0$	0.0	0.0	0.0	−0.9	0.0
$100 \cdot \beta^E/\beta_0$ calc *	0.0	0.2	0.0	0.0	0.0

* eq. (2).

$$\frac{\beta^E}{\beta_c} = \frac{V_0}{V} \frac{\Delta V + V^E}{\Delta V} - 1 \tag{2}$$

where V_0 and β_0 are the ideal values of V and β and ΔV the volume change on melting „expanded'' to the working temperature. Equation (2) was deduced on the basis of hole theory.[4]

---

[14] J. O'M Bockris and N. E. Richards, *Proc. Roy. Soc.*, **241 A**, 44 (1957).

The common cation mixtures are characterized by values of physical properties close to the ideal ones ; mixing is random and no complex ions turn up. In these mixtures packing of ions in liquid does not change when Br^- is replaed for Cl^-, given the small difference between their ionic radii.

Although formed of two "peculiar" constituents $AgCl + AgBr$ behaves ideally : the isotherms of sonic velocity and compressibility are straight lines, β^E and V^E close to zero, the agreement between the two sets of β^E/β_0 values is not significant since they are very small. Additive behaviour has also been reported for viscosity ,[15] surface tension[16] and electric conductivity. [17]

The $AgCl + KCl$ mixture is characterized by small β^E and V^E; however these quantities are correlated which turns out of the two sets of β^E/β_0 values (Table 4).

Table 4

Excess quantities for AgCl – KCl; 873 K

X_{AgCl}	0.0	0.478	0.678	0.806	1.000
$10^{11}\cdot\beta_{\gamma s}/m^2\cdot N^{-1}$	20.0	17.2	14.5	12.3	8.7
γ	1.41	1.30	1.25	1.22	1.18
$10^{11}\cdot\beta/m^2\cdot N^{-1}$	28.2	22.4	18.1	15.0	10.3
$10^{11}\cdot\beta^E/m^2\cdot N^{-1}$	0.0	1.0	0.4	−0.1	0.0
$10^6\cdot V^E/m^3\cdot mol^{-1}$	0.0	0.46	0.01	−0.09	0.0
$10^4\cdot\alpha/K^{-1}$	3.686	3.191	2.803	2.440	2.001
$100\cdot\beta^E/\beta_0$	0	5	2	−1	0
$100\cdot\beta^E/\beta_0$ calc*	0	8	0	−2	0

* eq. (2)

B. Since this paper concludes the investigations carried out by us on compressibility of some 44 fused salt mixtures,[1,3-10] drawing some conclusions is recommanded. [18]

1. In all studied mixtures β increases with temperature.

2. The compressibility conforms to a model which considers the following possible contributions :

— simple mixing ; $\beta^E > 0$ and small, explained by geometric packing of differently sized ions. The behaviour was met with in the mixtures ; $KCl-KBr$;[1] $LiBr-LiCl$; [7] $AgCl-AgBr$; $LiCl-(Na, K, Rb, Cs)\ Cl$;[8] $NaCl-(K, Rb, Cs)\ Cl$; [5] $KCl-(Rb, Cs)\ Cl$;[8] $RbCl-CsCl$;[8] $LiBr-KBr$[8] ; $RbBr-(Li, Na)\ Br$; [8] $NaI-RbI$;[8] $AgCl-KCl$; $PbBr_2-PbCl_2$;[9] $CdCl_2-CdBr_2$;[7] $ZnBr_2-ZnCl_2$;[10] of all these systems the ones with common cation are quasiideal ;

— formation of complex ions ; $\beta^E > 0$ and the larger, the more stable the complex ions : $PbCl_2-(Li, Na, K, Rb, Cs)\ Cl$ [1, 3]

---

[15] B. S. Harrap and E. Heymann, *Trans. Faraday Soc.*, **51**, 259 (1955).

[16] N. K. Boardman, A. R. Palmer and E. Heymann, *Trans. Faraday Soc.*, **51**, 277 (1955).

[17] H. Bloom "The Chemistry of Molten Salts", W. A. Benjamin, New-York, 1967, p. 15.

[18] V. Vasilescu, Doctoral Dissertation, Univ. of Bucharest, 1971.

— polymer breaking in Mg, Cd and Zn — containing salts [4,6] $\beta^E < 0$. The explanation is roughly supplied by better packing of smaller size ions into which polymers decompose. The effect may emerge by itself like in $PbCl_2 - CdCl_2$; [9] $PbBr_2 - CdBr_2$; [9] $PbCl_2 - ZnCl_2$; [10] $PbBr_2 - ZnBr_2$; [10] $MgCl - BaCl_2$; [4] $ZnCl_2 - NaCl$; [6] or in conjunction with complex forming as in $CdCl_2 - KCl$; [7] $CdBr_2 - KBr$; [7] $ZnCl_2 - KCl$; [6] $MgCl_2 - Kl$ [4] (it is worth mentioning that in the latter mixture a spectacular *S* shaped curve was obtained for the isotherms of β^E);

— deviation from random mixing due to exchange reactions in reciprocal salt mixtures; $PbBr_2 - CdCl_2$; [9] $PbCl_2 - CdBr_2$; [9] $LiBr - KCl$; [7] $LiCl - KBr$; [7] $ZnCl_2 - PbBr_2$; [10] $ZnBr_2 - PbCl_2$; [10] $CdBr_2 - KCl$; $CdCl_2 - KBr$. [7]

The overall effect of these contributions may be $\beta^E > 0$ (most mixtures), $\beta^E < 0$, and S shape curves with both positive and negative β^E.

3. Methods of calculating compressibilities from those of constituents or from those of common anion-binary mixtures have given a good agreement with experimental data; this agreement has emphasized the relative importance of contributions to compressibility of binary and order terms.

4. Equation (2) which correlated β^E and V^E was successfully applied to alkali halide mixtures as well as to nearly all others; in the former mixtures this was an indication that the hole model holds while in the latter equation (2) was considered a semiempirical relation expressing β^E in terms of V^E. One can conclude that mixing entails an increase or decrease of total hole volume which is sensed by β^E. Equation (2) fails in predicting correctly effects of ordering which takes places in reciprocal salt mixtures.

5. Another equation which relates β^E and V^E was deduced [4] on the basis of Hildelerand's regular solution theory. [19,20] It is merely a thermodynamic relation in whose deduction several approximations were made; however it gives a fairly good agreement and always sign agreement, which is not so with the original Hildelerand's relation applied to molten salts.

---

[19] J. H. HILDEBRAND and R. L. SCOTT, "Regular Solutions", Prentice Hall Inc., Englewood, 1962, p. 14.

[20] J. H. HILDEBRAND and R. L. SCOTT, "The Solubility of Nonelectrolytes", Reinhold, New York, 1950, p. 136.

Revue Roumaine de Chimie, **21**, *11–12*, 1463–1471 (1976)

ZUR BERECHNUNG VON PARAMETERN DES ZWISCHENMOLEKULAREN POTENTIALS AUS 2. DRUCKVIRIALKOEFFIZIENTEN

HARRI FREYDANK und MARGIT T. RÄTZSCH

Technische Hochschule ,,Carl Schorlemmer" Leuna-Merseburg, Sektion Verfahrenschemie, WB Thermodynamik, DDR-42 Merseburg, Geusaer Straße

Eingegangen am 12. Februar 1975

Aus der Temperaturfunktion der 2. Virialkoeffizienten der Edelgase Argon, Krypton und Xenon sowie der *n*-Alkane C_1 bis C_8 wurden nach verschiedenen Methoden die Lennard-Jones-(12–6)-Potentialparameter berechnet. Aus den Untersuchungen folgt, daß die Methode der Minimierung der Temperaturfunktion des Energieparameters ε durch Variation des Stoßdurchmessers σ beim Vorhandensein experimenteller Daten bis zur Boyle-Temperatur ein eindeutiges und realistisches Wertepaar liefert.

EINLEITUNG

In der Literatur findet man eine Reihe von Versuchen zur Gewinnung realistischer Potentialparameter. So verschieden die untersuchten Eigenschaften und die Methoden zur Parametergewinnung sind, so verschieden sind auch die erhaltenen Werte für den Stoßdurchmesser σ und das Potentialminimum ε. Tabelle 1 zeigt die Breite am Beispiel von *n*-Pentan und *n*-Hexan für das Lennard-Jones-(12–6)-Potential. Bei der Überprüfung des bei Hirschfelder u. a. [5] aufgeführten Verfahrens zur

Tabelle 1

Lennard-Jones-(12–6)-Potentialparameter

Substanz	$\frac{\sigma}{\text{Å}}$	$\frac{\varepsilon/k}{\text{K}}$	Lit.
n-Pentan	2,7	900	1
	8,5	219	2
n-Hexan	5,9	413	3
	2,7	985	4

---

[1] J. M. Prausnitz und R. N. Keeler, *A.I.Ch.E.J.*, **7**, 399 (1961).

[2] A. L. Sherwood und J. M. Prausnitz, *J. Chem. Phys.*, **41**, 429 (1964).

[3] J. O. Hirschfelder, R. B. Bird und L. E. Spotz, *Chem. Rev.*, **44**, 205 (1949).

[4] J. F. Connolly und G. A. Kandalic, *Phys. Fluids*, **3**, 463 (1960).

[5] J. O. Hirschfelder, C. F. Curtiss und R. B. Bird, ,,The Molecular Theory of Gases and Liquids", John Wiley Inc., New York, 1954.

Bestimmung der Parameter zeigte es sich, daß auch dort zwei stark voneinander abweichende Werte erhalten werden. Bei früheren Berechnungen von Potentialparametern[6] nach einem Computerverfahren:

1. Für ein vorgegebenes σ wird aus dem 2. Virialkoeffizienten bei der höchsten gemessenen Temperatur $B(T_{\max})$ ein ε bestimmt und mit diesem Parameterpaar die gesamte $B(T)$-Funktion berechnet. Durch Variation des σ wird das Minimum in der Fehlerquadratsumme gesucht

$$\sum_{n=1}^{\infty} (B_{\text{exp.}} - B_{\text{ber.}}) \overset{!}{=} \text{Min.}$$

Es wurden auch zwei Minima gefunden, von denen das tiefere für weitere Berechnungen verwendet wurde. Die durchgezogene Kurve der Abb. 1 zeigt am Beispiel von Methan den Verlauf der Fehlerquadratsumme. Wir bestimmten ε aus $B(T_{\max})$, da im allgemeinen die experimentellen Werte bei höheren Temperaturen genauer sind. Lin und Robinson[7] untersuchten den Einfluß des Temperaturbereiches und der Fehler der 2. Virialkoeffizienten auf die Potentialparameter. Sie zeigten, daß der Energieparameter ε sehr unsicher wird, wenn er auf Hochtemperaturdaten basiert, da der Einfluß der Potentialtiefe abnimmt, während der Stoßdurchmesser σ unsicher wird, wenn er aus Tieftemperaturdaten berechnet wurde. Aus Hochtemperaturdaten läßt sich zwar ein Energieparameter mit geringem Fehler bzw. geringer Temperaturabhängigkeit berechnen, der aber kein Maß für die wirkliche Tiefe der Potentialmulde ist. Für den Stoßdurchmesser gilt das gleiche für Tieftemperaturdaten. Hanley und Klein[8] stellten bei Untersuchungen zur Auswahl von Potentialmodellen fest, daß nur experimentelle Daten bei niedrigen Temperaturen $T^* < 2{,}0$ und bei hohen $T^* > 10{,}0$ empfindlich in bezug auf die Potentialfunktion sind, wobei für 2. Virialkoeffizienten der letztere Bereich außerhalb der experimentellen Möglichkeiten liegt. Weiterhin sind Potentialparameter, die aus Tieftemperaturdaten bestimmt wurden, in der Lage, die Temperaturfunktion des 2. Virialkoeffizienten im mittleren Temperaturbereich zu beschreiben. Erst bei höheren Temperaturen treten größere Abweichungen auf. Wir untersuchten deshalb anhand der Edelgase Argon, Krypton, Xenon und der n-Alkane C_1 bis C_8 den Einfluß des Temperaturbereiches auf die Gewinnung der Parameter für das Lennard-Jones-(12–6)-Potential. Für die Berechnung der Parameter wird einerseits das oben genannte Verfahren 1, wobei ε aus dem 2. Virialkoeffizienten bei der minimalen Temperatur $B(T_{\min})$ bestimmt wird und andererseits eine Methode, die auf Buckingham und Pople[9] zurückgeht, verwendet:

2. Für vorgegebene σ wird aus jedem B-T-Wertepaar ein ε bestimmt. Es wird das σ gesucht, bei dem ε am wenigsten temperaturabhängig ist. Die Parameter für die nach der Funktion

$$B = \frac{D}{T^S} + H \tag{1}$$

---

[6] H. Freydank und M. Rätzsch, *Z. phys. Chem.* (*Leipzig*), **248**, 83 (1971); **249**, 33 (1972).

[7] H.-M. Lin und R. L. Robinson jr., *J. Chem. Phys.*, **52**, 3727 (1970).

[8] H. J. M. Hanley und M. Klein, NBS Technical Note 360, 1967.

[9] A. D. Buckingham und J. A. Pople, *Trans. Faraday Soc.*, **51**, 1173 (1955).

ausgeglichenen 2. Virialkoeffizienten sind in Tabelle 2 oder in[6] enthalten, wobei für Ar, Kr, Xe und CH_4 auch Daten oberhalb der Boyle-Temperatur zur Verfügung stehen. Für die Berechnungen dienten USASI FORTRAN-MASTER-Programme.

Tabelle 2

Ausgleichsparameter für die Temperaturfunktion des 2. Virialkoeffizienten

Substanz	Temp.-Bereich K	$-D$	S	H
Argon	78,15 – 1108,15	3,91142109E5	1,63566194	21,0650057
Krypton	108,15 – 1008,15	5,72383312E5	1,55462454	30,7333333
Xenon	273,15 – 903,15	1,08412967E6	1,53653338	39,6
Methan	108,15 – 603,15	5,19528065E5	1,54985108	33,166667

B in cm^3/Mol^{-1}, E5 $\equiv 10^5$.

ERGEBNISSE UND DISKUSSION

Für die Berechnung der Potentialparameter nach Verfahren 1 wird für die Bestimmung des ε der 2. Virialkoeffizient bei der niedrigsten Temperatur $B(T_{\min})$ verwendet. Die unterbrochene Linie in Abb. 1 zeigt für Methan den Verlauf der Fehlerquadratsumme, die ihr Minimum jetzt deutlich beim kleineren σ hat. Es werden aber in allen Fällen zwei Parametersätze erhalten, wobei im Vergleich zu den Daten aus $B(T_{\max})$ (siehe Tab. 4) die σ etwas größer und die ε etwas kleiner sind.

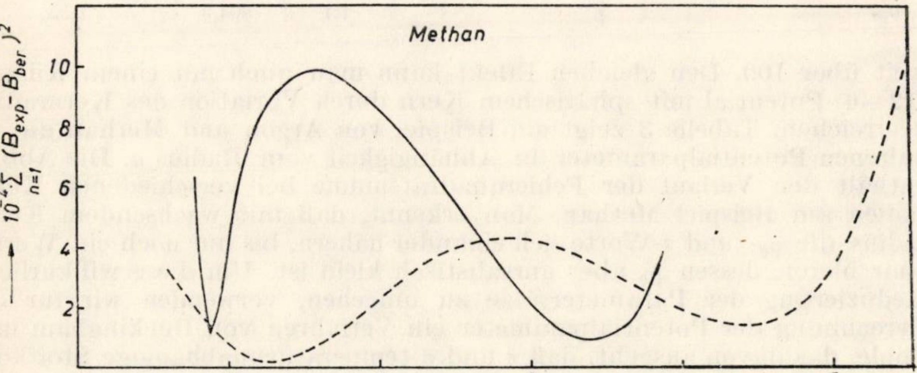

Abb. 1. – Änderung der Fehlerquadratsumme mit dem Stoßdurchmesser σ.
durchgezogene Linie ; ε aus $B(T_{\max})$;
gestrichelte Linie ; ε aus $B(T_{\min})$.

Opel[10] versucht nun, durch Variation der Exponenten des Lennard-Jones-Potentials eindeutige Parameter zu gewinnen, da mit steigenden Exponenten die zunächst erhaltenen zwei Parametersätze bis auf ein Wertepaar zusammenrücken. Der Abstoßungsexponent liegt dabei aber weit über 100. Den gleichen Effekt kann man auch mit einem Kihara-(12−6)-Potential mit sphärischem Kern durch Variation des Kernradius a erreichen. Tabelle 3 zeigt am Beispiel von Argon und Methan die erhaltenen Potentialparameter in Abhängigkeit vom Radius a. Die Abb. 2 enthält den Verlauf der Fehlerquadratsumme bei verschiedenen Kernradien am Beispiel Methan. Man erkennt, daß mit wachsendem Kernradius die ρ_0- und ε-Werte sich einander nähern, bis nur noch ein Wertepaar bleibt, dessen ρ_0 aber unrealistisch klein ist. Um diese willkürliche Reduzierung der Parametersätze zu umgehen, verwenden wir für die Berechnung der Potentialparameter ein Verfahren von Buckingham und Pople, das davon ausgeht, daß ε und σ temperaturunabhängige Stoffkonstanten sind. Tabelle 4 enthält die Potentialparameter, die bei Berücksichtigung des gesamten Temperaturbereiches berechnet wurden. Bei den Edelgasen und Methan werden nur je ein Parameterpaar erhalten. Abb. 3 zeigt die Temperaturfunktion des ε bei verschiedenen σ-Werten für Argon und man erkennt, daß es nur einen Stoßdurchmesser gibt, für den diese Temperaturfunktion minimal ist. Bei sehr kleinen σ gehen die berechneten ε mit steigender Temperatur schnell gegen Null, während bei großen σ die Kurven immer steiler werden.

Tabelle 3

Stoßdurchmesser ρ_0 und Potentialminimum ε für das Kihara-(12−6)-Potential bei verschiedenem Kernradius a

	Argon			Methan		
$\frac{a}{\text{Å}}$	$\frac{\rho_0}{\text{Å}}$	$\frac{\varepsilon/k}{\text{K}}$	$10^{-3}\Sigma(B_{\text{ber}}-B_{\text{exp}})^2$	$\frac{\rho_0}{\text{Å}}$	$\frac{\varepsilon/k}{\text{K}}$	$10^{-3}\Sigma(B_{\text{ber}}-B_{\text{exp}})^2$
0	1,7	347,9	6,25	1,3	710,8	0,5
	4,5	93,1	44,1	4,4	129,6	1,5
0,1	1,7	330,5	5,2	1,2	703,2	1,52
	4,3	98,0	42	4,1	142,3	12,7
0,2	1,6	330,3	4,26	1,1	708,9	1,34
	4,0	107,4	3,76	3,8	158,2	12,4
0,3	1,6	314,3	3,5	1,1	667,8	1,05
	3,5	128,4	32,7	3,5	175,9	11,4
0,4	1,6	300,5	2,55	1,1	632,6	0,85
				3,2	196,5	10,4
0,5	1,6	287,7	1,74	1,0	638,4	0,51
				2,9	220,2	9,13
0,6	1,6	276,3	1,29	1,0	607,9	0,29
				2,4	273,4	7,5
0,7	1,5	279,4	1,68	1,1	546,3	0,19
0,8				1,1	523,9	0,41
0,9				1,1	504,3	1,55

Für die n-Alkane C_2 bis C_8 folgen je zwei Parameterpaare. Wir berechneten deshalb für Argon nochmals die Temperaturfunktion von ε für kleinere Temperaturintervalle. Tab. 5 enthält die Potentialparameter, während in den Abbn. 4 und 5 die Temperaturfunktionen von ε dargestellt sind. Man erkennt, daß bei Temperaturbereichen weit unterhalb der Boyle-Temperatur zwei Parametersätze folgen, während Temperaturbereiche, die in die Nähe der Boyle-Temperatur oder darüber hinaus führen, nur ein Wertepaar liefern. Der Boyle-Punkt, bei Argon 411,52 K, bildet gewissermaßen als Schnittpunkt der ε (*T*)-Kurven bei verschiedenen σ einen Indikator für die Eindeutigkeit des Ergebnisses. So bestimmen auch Straub und Waibel [11] die ε-Werte direkt aus der Boyle-Temperatur. Die Daten zeigen weiterhin, daß mit steigender Temperatur der große σ-Wert langsam abnimmt mit gleichzeitig steigendem ε, während das kleinere σ schnell geringer wird und im Bereich des

---

[10] G. Opel, *Wiss. Z. TH Leuna-Merseburg,* **17**, 339 (1975).

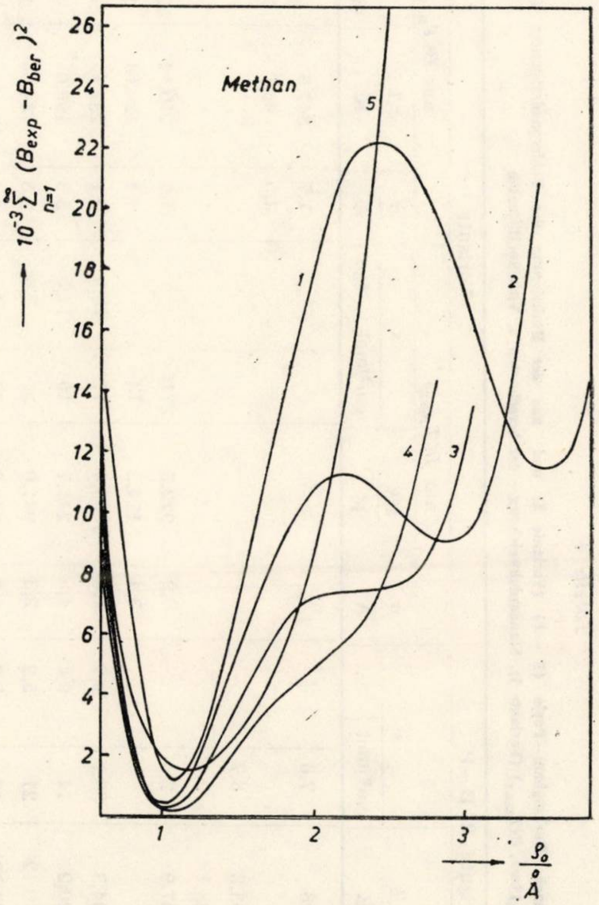

Abb. 2. – Änderung der Fehlerquadratsumme mit dem Stoßdurchmesser ρ_0 bei verschiedenen Kernradien *a*.

Kurve;	1	2	3	4	5;
a/Å;	0,3	0,5	0,6	0,7	0,9.

---

[11] D. Straub und R. Waibel, *Chem. Eng. Sci.*, **28**, 439 (1973).

Tabelle 4

Berechnete Potentialparameter reiner Stoffe nach Buckingham–Pople ($B - P$) (Variante 2) und aus der Minimierung der Fehlerquadratsumme (FQS) mit ε aus $B(T_{\min})$ bzw. $B(T_{\max})$ (Variante 1), Standardabweichung s der berechneten 2. Virialkoeffizienten

Substanz	Variante 2 B–P				Variante 1							
					aus $B(T_{\max})$				aus $B(T_{\min})$			
	σ	ε/k	s		σ	ε/k	s		σ	ε/k	s	
	Å	K	cm³/mol	%	Å	K	cm³/mol	%	Å	K	cm³/mol	%
Argon	3,2	128	7,6						1,7	347,9	20	
									4,5	93,1	34	
Krypton	3,6	193,3	8,7									
Xenon	4,0	228,1	2,1									
Methan	3,9	147,9	2,5		0,9	922,2	271		1,3	710,84	125	
					3,4	174,2	13		4,4	129,64	13,3	
Äthan	1,6	1094,3	30,1	9,7	1,6	1055,4	17	10,5	2,1	784,13	8,7	15
	4,7	220,2	14	9,6	4,5	241,7	15	14,5	5,3	196,0	18	20
Propan	2,3	970,12	27	5,2	2,3	941,0	21	7,6	2,8	784,06	33	17
	5,8	232,59	17	5,3	5,6	249,6	19	8	6,4	208,07	22	11,6
n-Butan	2,7	1019,17	43	5,1	2,6	1041,0	42	7,9	3,2	821,23	24,5	9,3
	7,3	223,79	34	6,8	7,0	242,1	39	9,1	7,8	212,8	50	12
n-Pentan	2,8	1182,4	60	4,9	2,8	1145,2	58	8,5	3,3	970,8	33	8,3
	8,7	217,0	47	6,8	8,4	231,7	56	9,2	9,7	193,31	63	15,4
n-Hexan	3,5	1070,02	29	1,8	3,4	1094,9	45,5	3,1	3,7	1002,98	34	2,6
	12,4	164,05	44	3,4	11,9	173,0	55	3,6	13,0	156,83	65	5,7
n-Heptan	3,0	1467,08	42	3,1	2,9	1507,8	46	4,5	3,4	1269,3	31	5,3
	10,0	243,69	40	4,5	9,7	256,3	50	6,1	10,8	225,3	55,5	8,9
n-Oktan	3,2	1534,43	37	2,1	3,2	1517,3	42	3,5	3,5	1386,19	28,6	3,8
	11,7	227,22	40	3,4	11,3	238,2	49,4	4,0	12,4	214,71	59	6,2

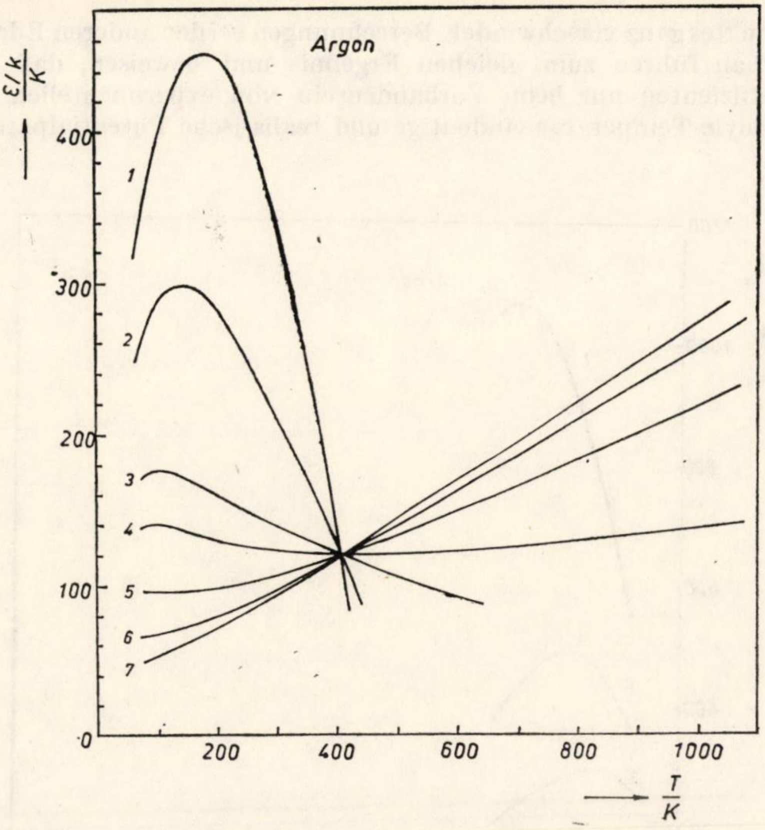

Abb. 3.— Temperaturfunktion des Energieparameters ε bei verschiedenen Stoßdurchmessern σ [ε(T) = Min bei 4].

Kurve;	1	2	3	4	5	6	7;
σ/Å;	1,5	2,0	2,8	3,2	4,0	5,0	5,9.

Tabelle 5

Argon-Potentialparameter nach Buckingham-Pople für Teiltemperaturintervalle

Temp.-Bereich K	σ Å	ε/k K
78– 308	3,7	108,2
	1,4	449,8
308– 608	3,2	120,5
608–1108	3,1	116,3
78– 208	3,9	99,5
	2,1	267,6
208– 308	3,4	117,3
	0,8	923,5
308– 408	3,3	119,6
408– 508	3,2	119,7
508–1108	3,1	116,0

Boyle-Punktes ganz verschwindet. Berechnungen bei den anderen Edelgasen und Methan führen zum gleichen Ergebnis und beweisen, daß aus 2. Virialkoeffizienten nur beim Vorhandensein von experimentellen Daten bis zur Boyle-Temperatur eindeutige und realistische Potentialparameter

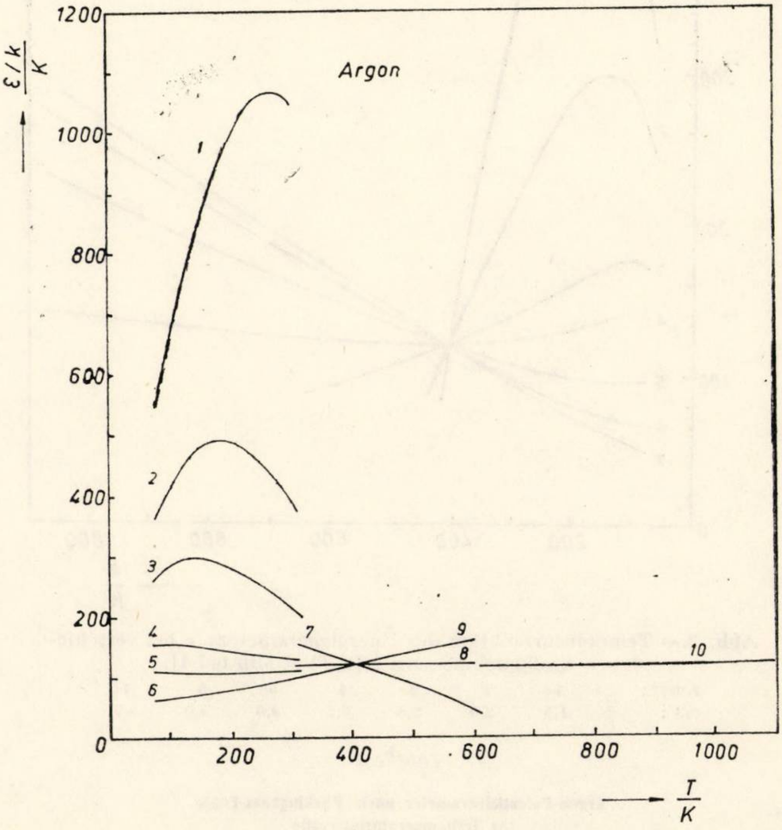

Abb. 4. – Temperaturfunktion von ε für 300 K-Intervalle bei verschiedenen $\sigma[\varepsilon(T) = \mathrm{Min}$ bei 2, 5, 8 und 10].

Kurve:	1	2	3	4	5	6	7	8	9	10;
σ/Å:	0,7	1,4	2,0	3,0	3,7	5,0	2,5	3,2	5,0	3,1.

erhalten werden. Aus der Entwicklung der σ-Werte mit steigender Temperatur beim Argon folgt, daß für die *n*-Alkane nur das Parameterpaar mit dem großen σ für Folgerechnungen verwendet werden sollte. Dabei ist klar, daß das σ etwas zu hoch und das ε entsprechend zu klein ist.

Dem VEB Leuna-Werke „Walter Ulbricht" sei für finanzielle Unterstützung gedankt.

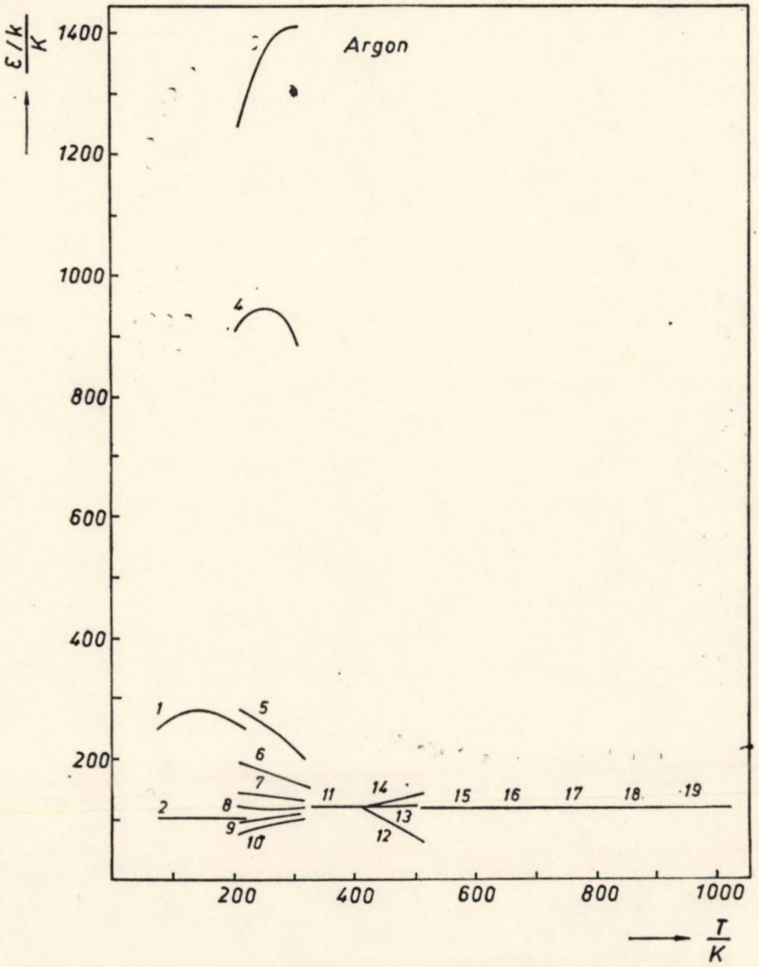

Abb. 5. — Temperaturfunktion von ε für 100 K-Intervalle bei verschiedenen σ[ε (*T*) = Min bei 1, 2, 4, 8, 11, 13, 15—19].

Kurve:	1	2	3	4	5	6	7	8	9	10;	11	12	13	14	15—19;
σ/Å:	2,1	3,9	0,5	0,8	2,0	2,5	3,0	3,4	4,0	5,0.	3,3	2,3	3,2	5,0	3,1.

SYMBOLIK

ε — potentielle Energie am Minimum der Potentialmulde
σ — Stoßdurchmesser — Lennard-Jones-Potential
ρ_0 — Stoßdurchmesser — Kihara-Potential
k — Boltzmann-Konstante
T^* — reduzierte Temperatur kT/ε

Revue Roumaine de Chimie, **21**, *11—12*, 1463—1471 (1976)

Revue Roumaine de Chimie, **21**, *11–12*, 1473–1477 (1976)

THE ELECTRONIC STRUCTURE OF SOME STILBENE DERIVATIVES. II[1]

QUANTITATIVE CORRELATIONS REFERRING TO THE SUBSTITUENT EFFECTS ON THE ELECTRONIC SPECTRA OF SOME STILBENE DERIVATIVES

LUCIA CIOHODARU and AURELIA MEGHEA

Department for Physical Chemistry, Polytechnic Institute, st. Polizu 1, Bucharest, Romania

Received September 15, 1975

New quantitative correlations between both experimental and calculated bathochromic shifts of the *A* bands of some polysubstituted *trans*-stilbene derivatives are obtained. The difference of these shifts represents, in fact, a measure of the steric factor. Also, new Hammett-type correlations are reported.

In a previous paper[1] the electronic absorption spectra of 24 nitro-containing *trans*-stilbene derivatives, as well as the qualitative and semi-quantitative correlations between the shifts of both *A* and *B* absorption bands and the molecular structure were reported.

In this work we continue with new quantitative correlations between the characteristics of the electronic spectra of same derivatives and the substituent effects on these extensive conjugated systems.

For convenience, the following general formula will be used for the compounds dealt with in this work (the significance of the letters is given in Table 1 for every compound):

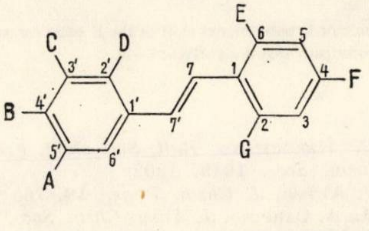

The syntheses of the derivatives (according to the literature data), as well as the electronic spectra were previously reported.[1]

---

[1] Part I : L. Ciohodaru and A. Meghea, *Rev. Roumaine Chim.*, 1473–1477 (1976).

1. CORRELATIONS BETWEEN THE EXPERIMENTAL AND CALCULATED WAVELENGTHS CORRESPONDING TO THE *A* BAND

With regard to the stilbene derivatives, there is only one relation [2] with reference to the absorption bands shifts in the electronic spectra of the *p*, *p*′-disubstituted derivatives :

$$\Delta\lambda_{1(\mathrm{exp})} = 2.12\times10^{-1}\Delta\lambda'\times\Delta\lambda''$$

$$\Delta\lambda_{2(\mathrm{calc})} = 2.08\times10^{-2}\Delta\lambda'\times\Delta\lambda'' + 50$$

Table 1

The substituents for the studied stilbene derivatives and the shifts corresponding to the *A* band

No.	A	B	C	D	E	F	G	$\Delta\lambda_{A_{\mathrm{exp}}}$[a]	$\Delta\lambda_{A_{\mathrm{calc}}}$[b]	$\Delta(\Delta\lambda_A)$[c]
1	H	H	H	H	H	NO_2	CN	46	73	−27
2	H	H	H	H	H	NO_2	$CONH_2$	42	—	—
3	H	OH	H	H	H	NO_2	CN	101	79	22
4	H	OCH_3	H	H	H	NO_2	CN	96	86	10
5	H	NMe_2	H	H	H	NO_2	CN	170	123	47
6	H	NMe_2	H	H	H	NO_2	COOH	150	—	—
7	H	H	H	H	H	CN	NO_2	20	−55	75
8	H	H	H	H	H	$CONH_2$	NO_2	16	−59	75
9	H	OH	H	H	H	CN	NO_2	51	−49	100
10	H	OCH_3	H	H	H	CN	NO_2	46	−42	88
11	H	NMe_2	H	H	H	CN	NO_2	136	− 5	141
12	H	NMe_2	H	H	H	$CONH_2$	NO_2	106	− 9	115
13	H	$NHCOCH_3$	H	H	H	CN	NO_2	76	−26	102
14	$O-CH_2-O$		H	H	H	CN	NO_2	81	—	—
15	OCH_3	OH	H	H	H	CN	NO_2	72	−47	119
16	H	H	H	H	H	NO_2	NO_2	62	− 24	86
17	H	H	H	NO_2	H	NO_2	NO_2	46	−103	149
18	H	H	NO_2	H	H	NO_2	NO_2	46	− 23	69
19	H	NO_2	H	H	H	NO_2	NO_2	58	31	27
20	H	NMe_2	H	H	H	NO_2	NO_2	182	26	156
21	H	H	H	H	NO_2	NO_2	NO_2	56	−106	159
22	H	OCH_3	H	H	NO_2	NO_2	NO_2	106	−90	196
23	H	Cl	H	H	NO_2	NO_2	NO_2	56	−99	155
24	H	NO_2	H	H	NO_2	NO_2	NO_2	16	−48	64

[a] – the experimental bathochromic shift of the *A* band, regardless of the number and the position of substituents in every stilbene derivative ;

[b] – the calculated (bathochromic or hypsochromic) shift of the *A* band for same derivative, assuming, the additivity of shifts of the corresponding monosubstituted derivatives ; [2–15]

[c] $= \Delta\lambda_{A_{\mathrm{exp}}} - \Delta\lambda_{A_{\mathrm{calc}}}$

---

[2] H. Veschambre and A. Kergomard, *Bull. Soc. chim. France*, **1**, 336 (1966).

[3] E. A. Braude, *J. Chem. Soc.*, **1949**, 1902.

[4] M. Calvin and H. W. Alter, *J. Chem. Phys.*, **19**, 765 (1951).

[5] DeLos F. DeTar and L. A. Carpino, *J. Amer. Chem. Soc.*, **78**, 476 (1956).

[6] E. M. F. Roe, *Spectrochim. Acta*, suppl. **1957**, 515.

[7] H. H. Jaffé and M. Orchin, *J. Chem. Soc.*, **1960**, 1078.

[8] A. R. Katritzky, A. J. Boulton and D. J. Short, *J. Chem. Soc.*, **1960**, 2954.

[9] O. H. Wheeler and H. N. Battle de Pabon, *J. Org. Chem.*, **30**, 1473 (1965).

[10] A. E. Luţki , A. S. Golberkova, Z. M. Kanevskaia, L. Ia. Malkes, L. V. Subina,

where : $\Delta\lambda'$, $\Delta\lambda''$ are the shifts of the *A* band corresponding to the two monosubstituted derivatives ;

$\Delta\lambda_1$ is the experimental shift of the *A* band corresponding to the disubstituted derivative ;

$\Delta\lambda_2$ is the calculated shift of the *A* band for the disubstituted derivative, if we take into account the additivity of the shifts of the corresponding monosubstituted derivatives.

There are no available literature data referring to tri- or tetrasubstituted derivatives, taking into account all posible permutations of substituents ; these are required by a successive correlation, i.e. the shifts of the disubstituted derivatives depending on the shifts of the monosubstituted derivatives, the shifts of the trisubstituted derivatives depending on the shifts of the disubstituted derivatives and so on.

Therefore, we attempted to obtain a new relation, taking into account the overall effects (electronic and steric) of 2, 3 and 4 substituents in molecule.

It seems interesting to notice the fact that the values $\Delta(\Delta\lambda_A)$, which represent the deviations of experimental shifts from the additivity of individual substituent effects, are laid in a very large region of wavelengths ($-27 \div 196$ nm). These different and very great "exaltations" are thought to be due to strong interactions in the polysubstituted stilbene derivatives molecules.

It may be seen from Table 2 that the stilbene derivatives could be divided into three main classes :

I. In the first one, the *ortho*-cyano-*para*-nitro-stilbene derivatives are found ; in this case, the contribution of the steric effect is small. We can notice the best agreement between the experimental and calculated bathochromic shifts.

II. In the second class, the *ortho*-nitro-*para*-cyano-stilbene derivatives are found ; these compounds show great deviations from the additivity, $\Delta(\Delta\lambda_A)$ being between 75 and 141 nm. This fact is explainable if we take into account the presence, in every compound, of the bulky nitro group in *ortho* position to the ethylenic bridge, which brings about a considerable steric effect. Especially for the disubstituted derivatives no. 7 and 8, the steric effect is preponderant. But, for the trisubstituted derivatives, the deviations from the additivity increase due to the superposition of both steric and conjugative effect, the latter one appearing by the introduction in the *p'*-position of some substituents, with increasing electron-donating effect (OCH_3, OH, $NHCOCH_3$, NMe_2).

III. In the third class, the stilbene derivatives having the greatest values $\Delta(\Delta\lambda_A)$ (between 149 and 196 nm) are found. We can notice the

---

V. E. Bondarenko and A. N. Timcenko, *Teor. eksper. Khimiia, Akad. Nauk Ukr. S.S.R.*, **2**, 117 (1966).

[11] H. Güsten and M. Salzwedel, *Tetrahedron*, **23**, 173 (1967).

[12] G. Riezebos and E. Havinga, *Rec. Trav. chim.*, **80**, 447 (1961).

[13] W. E. Hillis and N. Ishikura, *J. Chromatog*, **32**, 323 (1968).

[14] M. Metzler and H. G. Neumann, *Tetrahedron*, **27**, 2225 (1971).

[15] J. E. Bloor, B. R. Gilson and N. Brearley, *Theor. Chim. Acta*, **8**, 35 (1967).

presence of the compounds with the greatest steric hindrance to planarity (di-*ortho*- and *o,o'*-dinitro-, i.e. no. 17, 21, 22 and 23), as well as the presence of *o,p*-dinitro-*p'*-dimethylamino-stilbene (no. 20) with the greatest conjugative effect in *p,p'* direction.

Table 2

The increasing steric effect in the studied stilbene derivative [a]

$\Delta(\Delta\lambda_A)$[b]	No.	Substituents					Class
		o	*p*	*p'*	*o'*	*m'*	
−27	1	CN	NO_2				I
10	4	CN	NO_2	OCH_3			
22	3	CN	NO_2	OH			
27	19	NO_2	NO_2	NO_2			
47	5	CN	NO_2	NMe_2			
64	24	$2NO_2$	NO_2	NO_2			II
69	18	NO_2	NO_2			NO_2	
75	7	NO_2	CN				
75	8	NO_2	$CONH_2$				
86	16	NO_2	NO_2				
88	10	NO_2	CN	OCH_3			
100	9	NO_2	CN	OH			
102	13	NO_2	$CONH_2$	$NHCOCH_3$			
115	12	NO_2	$CONH_2$	NMe_2			
119	15	NO_2	CN	OH		OCH_3	
141	11	NO_2	CN	NMe_2			
149	17	NO_2	NO_2		NO_2		III
155	23	$2NO_2$	NO_2	Cl			
156	20	NO_2	NO_2	NMe_2			
159	21	$2NO_2$	NO_2				
196	22	$2NO_2$	NO_2	OCH_3			

[a] for the compounds no. 2, 6, 14 we cannot indicate the values $\Delta(\Delta\lambda_A)$, because there are no shifts referring to the corresponding monosubstituted derivatives in the literature data;

[b] $\Delta\lambda_{A_{exp}} - \Delta\lambda_{A_{calc}}$

As it was shown in the previous paper, [1] the increasing steric effect due to phenyl groups in the stilbene derivatives brings about a strong interaction between the nitro groups and the ethylenic bridge, therefore a great bathochromic shift of the *A* band.

The tetranitro-stilbene derivative (no. 24) has, again, a different behaviour, owing to its high symmetry.

We can conclude that, while the experimental bathochromic shift of the *A* band ($\Delta\lambda_{A_{exp}}$), taken as a classifying criterion in the series of investigated stilbene derivatives in the previous paper, [1] represented the resultant of the superposition of both conjugative and steric effect, the "exaltation" $\Delta(\Delta\lambda_A)$, reported in this paper, represents, in essence, a criterion for the contribution of the steric factor. The existence of the steric factor is, also, confirmed by the negative values of $\Delta\lambda_{A_{calc}}$.

For the three classes of compounds, we established new correlations between the experimental shifts and the exaltations of the *A* band;

they agree with the general form:

$$\Delta\lambda_{A_{\mathrm{exp}}} = f(\Delta\lambda_{A_{\mathrm{exp}}} - \Delta\lambda_{A_{\mathrm{calc}}}).$$

Therefore, for the first class of stilbene derivatives, the equation of regression line is:

$\Delta\lambda_{A_{\mathrm{exp}}} = 80.89 + 1.72\ (\Delta\lambda_{A_{\mathrm{exp}}} - \Delta\lambda_{A_{\mathrm{calc}}})$, having the correlation coefficient $r = 1.006$ [16].

For the second class of stilbene derivatives:

$$\Delta\lambda_{A_{\mathrm{exp}}} = -\ 95.70 + 1.56\ (\Delta\lambda_{A_{\mathrm{exp}}} - \Delta\lambda_{A_{\mathrm{calc}}}),\ r = 0.989.$$

For the trinitro-derivatives in the third class:

$$\Delta\lambda_{A_{\mathrm{exp}}} = -\ 143.23 + 1.27\ (\Delta\lambda_{A_{\mathrm{exp}}} - \Delta\lambda_{A_{\mathrm{calc}}}),\ r = 0.996.$$

2. HAMMETT-TYPE CORRELATIONS

Further on, we attempt to correlate the experimental values $\Delta\lambda_A$ and/or $1/\lambda_{A_{\mathrm{max}}}$ and the sum of σ-Hammett constants of substituents, in order to obtain new Hammett-type relations. The σ-values correspond to the literature data. [17-19]

Therefore:

— for the *o*-nitro-*p*-cyano stilbene derivatives, the equation of regression line is:

$$10^3/\lambda_{A_{\mathrm{max}}} = 2.78 - 2.28 \sum\sigma,\ r = -\ 0.670;$$

— for the trinitro-stilbene derivatives, two relations are reported:

$$10^3/\lambda_{A_{\mathrm{max}}} = 2.82 + 0.41 \sum\sigma,\ r = 0.968;$$

$$\Delta\lambda_A = 54.65 - 49.62\ \Sigma\sigma,\ r = -\ 0.790.$$

In conclusion, the following may be stated:

— for the three classes of stilbene derivatives new quantitative correlations between the experimental bathochromic shifts of the |*A* bands and their exaltations are reported;

— for two classes of stilbene derivatives new Hammett-type correlations are established.

---

[16] D. CEAUŞESCU, "Tratarea statistică a datelor chimico-analitice", Editura Tehnică, Bucureşti, 1973, p. 225.

[17] L. P. HAMMETT, "Physical Organic Chemistry", McGraw-Hill Book Company, Inc., NewYork, 1940, p. 188.

[18] H. BEKKUM, P. E. VERKADE and B. M. WEPSTER, *Rec. Trav. chim.*, **78**, 815 (1959).

[19] D. FĂRCAŞIU, *Studii şi Cercetări Chim. Acad. R.S.R.*, **14**, 37 (1966).

they agree with the [illegible] form

$$\Delta\lambda_{\exp} \approx \Delta\lambda_{[illegible]} - \Delta\lambda_{[illegible]}$$

Therefore, for the first class of stilbene derivatives, the equation of regression line is:

$\Delta\lambda_{\exp} = [illegible] + 1.28 (\Delta\lambda_{[illegible]} - \Delta\lambda_{[illegible]})$, having the correlation coefficient $r = 1.000$.

For the second class of stilbene derivatives:

$$\Delta\lambda_{\exp} = -36.76 + 1.56 (\Delta\lambda_{[illegible]} - \Delta\lambda_{[illegible]}), r = 0.993.$$

For the trinitro derivatives in the third class:

$$\Delta\lambda_{\exp} = -144.32 + 1.37 (\Delta\lambda_{[illegible]} - \Delta\lambda_{[illegible]}), r = 0.996.$$

4. HAMMETT-TYPE CORRELATIONS

Further on, we attempt to correlate the experimental values $\Delta\lambda_1$ and/or $1/\lambda_{\exp}$ and the sum of σ-Hammett constants of substituents, in order to obtain new Hammett-type relations. The σ-values correspond to the literature data.[17-19]

Therefore:

— for the o-nitro-p-cyano stilbene derivatives, the equation of regression line is:

$$10^3/\lambda_{\exp} = 2.16 + 2.28 \sum\sigma, r = -0.770;$$

— for the trinitro-stilbene derivatives, two relations are reported:

$$10^3/\lambda_{\exp} = 2.82 + 0.41 \sum\sigma, r = 0.993;$$

$$\Delta\lambda_1 = 64.65 - 49.02 \sum\sigma, r = -0.790.$$

In conclusion, the following may be stated:

— for the three classes of stilbene derivatives new quantitative correlations between the experimental bathochromic shifts of the [illegible] bands and their evaluations are reported;

— for two classes of stilbene derivatives new Hammett-type correlations are established.

---

[17] [illegible], "Tabele statistice [illegible]", Editura [illegible], Bucureşti, 1973, p. 225.

[18] L. P. Hammett, "Physical Organic Chemistry", McGraw-Hill Book Company, Inc., New York, 1940, p. 188.

[19] [illegible], [illegible] and [illegible], Rec. Trav. chim., 78, 815 (1959).

[20] [illegible], Acad. R.S.R., 14, [illegible] (1963).

Revue Roumaine de Chimie, **21**, *11–12*, 1479–1485 (1976)

LA DÉCOMPOSITION THERMIQUE DES COMBINAISONS COMPLEXES THIOCYANIQUES DU Pd(II) AVEC LA PYRIDINE ET LES PYRIDINES SUBSTITUÉES

D. CAMBOLI, D. FĂTU et VIORICA CIMPU

Institut Polytechnique, Faculté de Chimie Industrielle 1, str. Polizu, Bucarest, Roumanie

Reçu le 18 janvier 1975

On a entrepris une étude du processus de la décomposition thermique des combinaisons complexes thiocyaniques du Pd (II) avec la pyridine et les pyridines substituées, en utilisant comme moyen d'investigation l'analyse thermogravimétrique (ATG), l'analyse thermogravimétrique dérivée (ATGD) et l'analyse thermique différentielle (ATD). Les résultats obtenus permettent de formuler certaines conclusions en ce qui concerne les étapes de la décomposition et la stabilité thermique de ces combinaisons complexes.

Dans les notes [1,2] publiées antérieurement on a décrit la synthèse de quelques combinaisons thiocyaniques que forme l'ion Pd^{2+} avec des amines, ainsi que certaines de leurs propriétés physico-chimiques. La note présente s'inscrit dans le contexte de ces préoccupations. On a entrepris une étude du comportement thermique des combinaisons complexes du Pd(II) avec la pyridine et les pyridines substituées, obtenues selon les procédés décrits dans les notes.[1,2]

Les courbes thermogravimétriques (TG), thermogravimétriques dérivées (TGD), celles d'analyse thermique différentielle (ATD) et celles de la variation de la température (T) ont été tracées simultanément avec un Dérivatographe MOM Budapest type Paulik-Paulik-Erdey.

RÉSULTATS ET DISCUSSIONS

Dans les figures 1 et 2 sont représentées les courbes ATG, ATGD et ATD qui indiquent, dans des unités arbitraires, la variation de la masse de l'échantillon Δm durant la décomposition, la vitesse de la variation de la masse dm/dt, ainsi que la différence des températures de l'échantillon et du matériel inerte de référence ($\alpha - Al_2O_3$ calciné à 1000° pendant quelques heures).

On a tracé les courbes pour une vitesse de chauffage dans une atmosphère statique (air) $\beta = 10°/min$.

---

[1] P. Spacu et D. Camboli, *Rev. Chim. Acad. R.P.R.*, **7**, 1311 (1962).

[2] P. Spacu et D. Camboli, *Anal. Şti. Univ. Bucureşti*, **13**, 117 (1964).

En examinant les courbes, on conclut que la décomposition présente plusieurs étapes intermédiaires. Pour chaque étape, on a noté sur les courbes les températures correspondant au moment initial à la vitesse maximale et au moment final du processus.

L'élimination du composant volatil est très énergique, surtout pour les complexes contenant la pyridine et les α et β-picolines, c'est pourquoi la différentiation des étapes intermédiaires sur les courbes ATG,

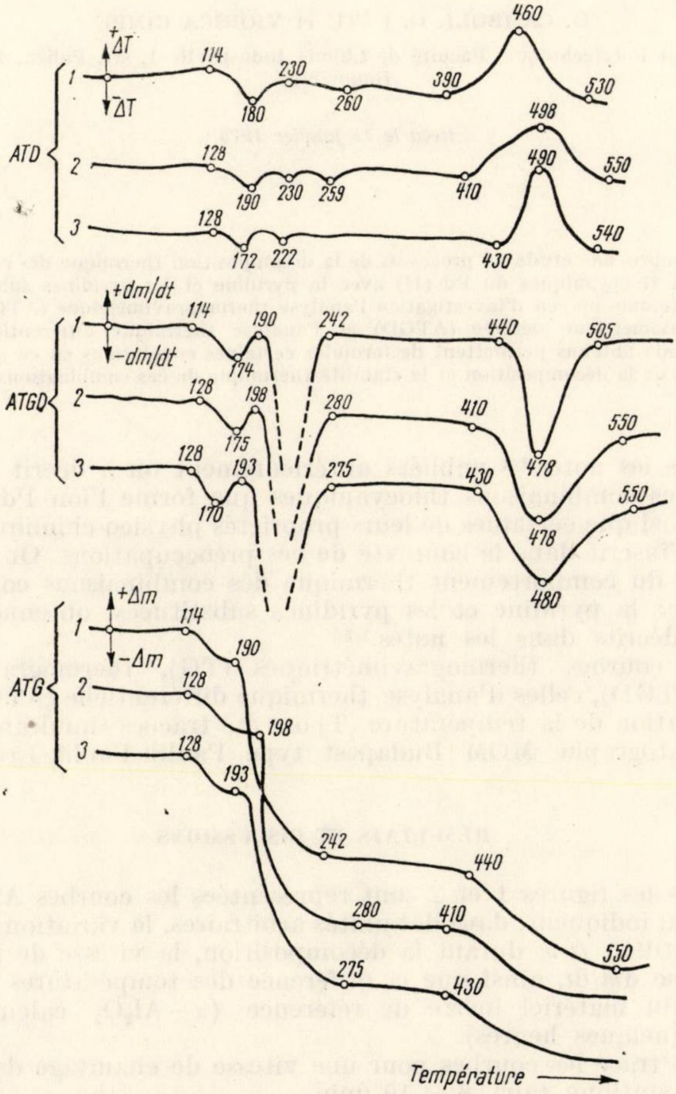

Fig. 1. — Courbes ATG, ATGD et ATD des combinaisons complexes thiocyaniques du Pd(II) : *1* — [Pd.py$_2$ (SCN)$_2$] ; *2* — [Pd(α-pic)$_2$ (SCN)$_2$] ; *3* — [Pd(β−pic)$_2$ (SCN)$_2$].

ATGD et ATD est moins satisfaisante pour les combinaisons mentionnées (fig. 1), que pour celles qui contiennent les lutidines et la γ-picoline (fig. 2).

La réduction de la vitesse de chauffage jusqu'à 2°/min ne conduit à aucune amélioration sensible en ce qui concerne la séparation des étapes de la décomposition thermique. Néanmoins, des vitesses de chauffage

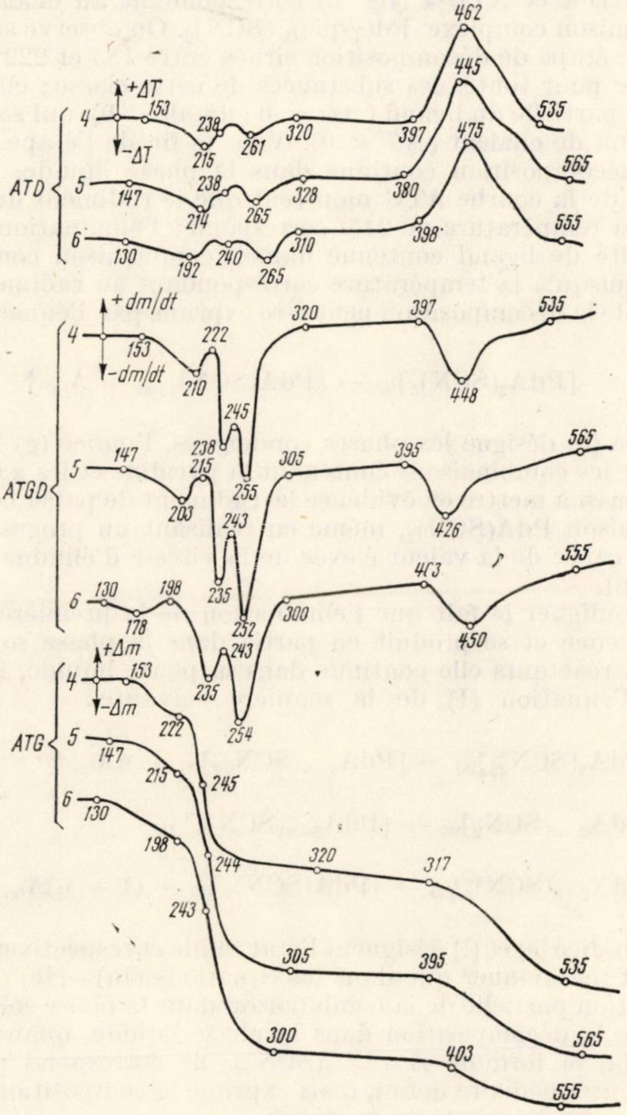

Fig. 2. — Courbes ATG, ATGD et ATD des combinaisons complexes thiocyaniques du Pd(II) : *4* — [Pd(γ-pic)$_2$ (SCN)$_2$] ; *5* — [Pd. 2,4-lutid$_2$ (SCN)$_2$] ; *6* — [Pd. 2,6-lutid$_2$ (SCN)$_2$].

élevées ne sont pas indiquées, car la séparation violente du composant volatil entraîne des particules condensées, ce qui donne sur les courbes ATG et ATGD des effets secondaires.

Pour élucider les processus intermédiaires qui ont lieu au cours de la décomposition de cette classe de substances, on va examiner les courbes ATG-4, ATGD-4 et ATD-4 (fig. 2) correspondant au chauffage linéaire de la combinaison complexe $Pd(\gamma\text{-pic})_2(SCN)_2$. On observe sur les courbes une première étape de décomposition située entre 153 et 222°. Cette étape est commune pour toutes les substances de cette classe ; elle consiste en l'élimination partielle du ligand ($\Delta m < 0$; $dm/dt < 0$), qui se produit avec une absorption de chaleur ($\Delta T < 0$). Vers la fin de l'étape, l'échantillon fond et la décomposition continue dans la phase liquide, jusqu'à 245°. Les données de la courbe ATG montrent que le rudiment du palier enregistré pour la température de 245° correspond à l'élimination de la moitié de la quantité de ligand contenue dans la combinaison complexe. Il en résulte que, jusqu'à la température correspondant au rudiment du palier, le processus de la décomposition peut être exprimé par l'équation stœchiométrique :

$$[PdA_2(SCN)_2]_{(c)} \rightarrow [PdA(SCN)_2]_{(c)} + A_{(g)}\uparrow \qquad (I)$$

L'indice (c) désigne les phases condensées, l'indice (g) le composant gazeux. Pour les combinaisons contenant la pyridine et les α et β-picolines on n'a pas réussi à mettre en évidence le rudiment de palier correspondant à la combinaison $PdA(SCN)_2$, même en réalisant un programme lent de chauffage, à cause de la valeur élevée de la vitesse d'élimination du composant volatil.

Pour souligner le fait que l'élimination de la première molécule de ligand commence et se produit en partie dans la phase solide et après la fusion des réactants elle continue dans la phase liquide, il est indiqué d'exprimer l'équation (I) de la manière suivante :

$$[PdA_2(SCN)_2]_{(s)} \rightarrow [PdA_{2-n}(SCN)_2]_{(s)} + nA_{(g)}\uparrow \qquad (Ia)$$

$$[PdA_{2-n}(SCN_2]_{(s)} \rightarrow [PdA_{2-n}(SCN)_2]_{(1)} \qquad (Ib)$$

$$[PdA_{2-n}(SCN)_2]_{(1)} \rightarrow [PdA(SCN)_2]_{(1)} + (1-n)A_{(g)}\uparrow \qquad (Ic)$$

Ici, les indice (s) et (l) désignent l'état solide et respectivement liquide.

On doit mentionner que dans les équations (Ia)—(Ic) qui décrivent la décomposition partielle de la combinaison dans la phase solide, la fusion et la suite de la décomposition dans la phase liquide, quand il se forme $[PdA(SCN)_2]_{(1)}$ la formule $[PdA_{2-n}(SCN)_2]$ ne correspond pas à la formation d'un intermédiaire défini, mais exprime la composition du mélange des réactants au moment de la fusion.

En effet, la valeur du paramètre *n* a varié pour cette classe de combinaisons complexes entre 0,3 et 0,42 — en fonction de leurs températures de fusion. Pour chaque combinaison, la valeur du paramètre *n* varie avec la vitesse de chauffage. Ainsi, par exemple, si on règle la vitesse de chauffage à 10°/min, la première molécule de γ-picoline de la combinaison $[Pd(\gamma\text{-pic})_2(SCN)_2]$ est éliminée en phase solide dans une proportion de 33,3% (n = 1/3) ; si on réduit la vitesse à 2°/min, cette proportion s'accroît jusqu'à 72% (n = 0,72).

L'accroissement des valeurs du paramètre n en cas de chauffage lent est dû au fait que dans ces conditions le système est maintenu pendant un plus long intervalle de temps aux températures situées au-dessous du point de fusion de la combinaison complexe et en conséquence l'élimination de la première molécule de ligand a lieu surtout en présence de la phase solide.

L'élimination de la seconde molécule de ligand se produit intégralement en phase liquide, selon l'équation :

$$[PdA(SCN)_2]_{(l)} \rightarrow Pd(SCN)_{2(s)} + A_{(g)}\uparrow \qquad (II)$$

Sur la courbe ATG-4 l'étape de la décomposition endotermique (II) est localisée dans l'intervalle de température situé entre 245° et 320°. L'étape finale (397 – 535°) consiste dans la décomposition du thiocyanure de palladium et l'élimination d'une quantité appréciable de chaleur ($\Delta T > 0$), comme conséquence des processus d'oxydation.

Le résidu final de la décomposition est le palladium métallique spongieux.

Le dernier processus est décrit par l'équation :

$$Pd(SCN)_{2(s)} + 4O_{2(g)} \rightarrow Pd_{(s)} + 2SO_{2(g)}\ (+\ 2CO_{2(g)} + N_{2(g)}) \qquad (III)$$

Les variations de masse déterminées en utilisant les courbes ATG concordent d'une manière satisfaisante avec celles calculées des équations stœchiométriques (I), (II) et (III).

Les étapes de la décomposition de toutes les combinaisons complexes appartenant à cette classe sont les mêmes, les seules différences, d'ailleurs assez peu importantes, consistent dans les valeurs des températures auxquelles commencent et s'achevent les étapes intermédiaires. Le ligand pour lequel l'élimination commence à la plus basse température (114°) est la pyridine (courbe 1, fig. 1).

La première étape de la décomposition a lieu en phase solide ; il en résulte que le développement du processus implique la diffusion du composant volatil dans le réseau cristallin et « l'évaporation » de celui-ci au niveau de l'interface solide-gaz. La pyridine a pour le poids moléculaire et pour le point d'ébullition des valeurs moindres que les autres ligands, ce qui favorise le processus de diffusion à travers la phase solide et « l'évaporation » sur l'interface solide-gaz.

La stabilité thermique des combinaisons complexes est aussi conditionnée en grande mesure par l'énergie de la liaison entre l'ion Pd^{2+} et la molécule du ligand. A la température ambiante, ces combinaisons peuvent être maintenues pendant des années sans constater ni une décomposition, ni une modification des courbes d'analyse thermique.

Outre des informations concernant la stabilité thermique et le nombre et la nature des étapes intermédiaires du processus de décomposition les courbes ATG, ATGD et ATD offrent en général la possibilité de calculer les paramètres cinétiques. [3] Dans notre cas, un calcul de ce genre rencontre certaines difficultés, dues au fait que d'une part les processus (Ia) et (Ic) et d'autre part les processus (Ic) et (IIa) se superposent partiellement. C'est pourquoi, pour calculer l'énergie d'activation de ces étapes on a eu recours à la méthode proposée par Kissinger [4] qui n'analyse pas les courbes ATD et ATDG sur toute leur étendue, mais seulement le point correspondant à leurs pics. On a proposé initialement cette méthode pour calculer les paramètres cinétiques en partant des données ATD, mais elle se prête — et même avec de meilleurs résultats — à l'analyse de la courbe ATGD.

La méthode est basée sur la relation suivante :

$$\frac{\mathrm{dlg}(\beta/T^2_{\max})}{\mathrm{d}\cdot T^{-1}_{\max}} \approx -E/(2{,}303\ \mathrm{R}) \tag{1}$$

dans laquelle E représente l'énergie d'activation, R — la constante des gaz, $T_{\max}$ — la température absolue de l'échantillon au moment pour lequel la vitesse de l'évolution de l'étape considérée est maximale.

L'application de la relation (1) pour les courbes tracées pour les vitesses de chauffage $\beta = 10$, 5, 3 et 2,5°/min conduit aux valeurs des énergies d'activations : $E_{(\mathrm{Ia})} = 33{,}9$ kcal/mole ; $E_{(\mathrm{Ic})} = 22{,}6$ kcal/mole et $E_{(\mathrm{II})} = 18{,}2$ kcal/mole.

On constate que l'énergie d'activation de l'étape (Ia) qui a lieu en phase solide est supérieure à celle de l'étape (II) qui se produit en phase liquide. Ce résultat est en concordance avec l'observation que la mobilité des molécules en état liquide, et en conséquence la réactivité de cet état, est supérieure à celui solide. La différence entre les valeurs des énergies d'activation pour les deux états est de 11,3 kcal/mole, donc elle a le même ordre de grandeur que la chaleur latente de fusion Q des cristaux moléculaires :

$$E_{(\mathrm{Ia})} - E_{(\mathrm{Ic})} \approx Q_{(\mathrm{Ib})}$$

Le même procédé de calcul conduit, pour les processus de décomposition des complexes avec les 2,4— et 2,6 — lutidines, aux résultats suivants :

$E_{(\mathrm{Ia})} = 43{,}3$ kcal/mole ; $E_{(\mathrm{Ic})} = 34{,}0$ kcal/mole ; $E_{(\mathrm{II})} = 24{,}7$ kcal/mole

et

$E_{(\mathrm{Ia})} = 46{,}2$ kcal/mole ; $E_{(\mathrm{Ic})} = 37{,}6$ kcal/mole ; $E_{(\mathrm{II})} = 26{,}4$ kcal/mole

ce qui est en concordance avec la relation précédente.

Il est intéressant de mentionner qu'on a fait une observation similaire [5] pour le cas des substances organiques dont la décomposition peut

[3] D. FĂTU, *Studii şi Cercetări Chim. Acad. Bucureşti*, **19**, 849 (1971) ; **20**, 141 (1972).

[4] H. KISSINGER, *Analyt. Chem.*, **29**, 1702 (1957).

[5] S. BON, « Razlozhjenie tverdykh organichesckhikh soedinenii » dans le recueil « Khimia tviordogo sostoyania », édité par W. E. Garner éd. lit. Moscou, 1961, p. 535.

avoir lieu — selon les conditions expérimentales — tant en phase solide qu'en celle liquide. Les données de Hinshelwood par exemple [6] indiquent pour la décomposition de l'acide malonique des valeurs de l'énergie d'activation de 32,4 et 60,4 kcal/mole, pour le processus en phase liquide ou solide.

CONCLUSIONS

1. Les combinaisons complexes de type $[PdA_2(SCN)_2]$ dans lesquelles A = py ; α, β, γ-pic ; 2,4- et 2,6-lutid présentent des courbes ATG, ATGD et ATD similaires.

2. Le complexe avec la pyridine $[Pdpy_2(SCN)_2]$ a la plus faible stabilité thermique. On a expliqué cette particularité par le fait que cette amine a des valeurs du poids moléculaire et du point d'ébullition moindres que les picolines et les lutidines.

3. Au cours de l'élimination de la première molécule de ligand survient la fusion de la combinaison. Après la fusion, la vitesse de décomposition s'accroît brusquement.

4. Pour les complexes contenant la γ-picoline et les lutidines on a mis en évidence le fait que pendant la décomposition thermique il se forme un composant intermédiaire de type $[PdA(SCN)_2]$.

5. Du calcul des énergies d'activation pour les processus de décomposition des combinaisons complexes avec la γ-picoline et les lutidines il résulte que les valeurs de ce paramètre sont plus élevées pour l'étape en phase solide que pour celle en phase liquide. La différence entre ces valeurs a le même ordre de grandeur que la chaleur latente de fusion des cristaux moléculaires. La diminution de la valeur de l'énergie d'activation après la fusion peut être interprétée par une réactivité accrue de la phase liquide en comparaison de la phase solide.

---

[6] C. N. Hinshelwood, *J. Chem. Soc.*, **1920**, 156.

Revue Roumaine de Chimie, **21**, *11–12*, 1487–1495 (1976)

TETRACOORDINATED Co(II) CHELATES WITH $Co(d^7)-N(sp^2)$ BONDS

A. C. BANCIU

Center of Physical Chemistry Bucharest, Str. Dumbrava Roşie, 23 — Romania

Received February 24, 1975

The paper discusses the electronic spectra and the magnetic moments of two new Co(II) chelate complexes. The chelate ligands are from the class of 1-methyl-2-carbethoxy-glyoxalanil-(1)-phenylhydrazones-(2) with NO_2 *para*- or *meta*- substituted at the benzene ring of the hydrazone group. The electronic spectra show that in solution both complexes exhibit a tetrahedral structure with Co(II)-N chemical bonds. As a result of the strong electronic effects of the NO_2 substituent the covalence degree of the Co(II)-N bonds is lower ($\beta \approx 0.82 \pm 0.04$) than in the unsubstituted analog complex ($\beta = 0.76 \pm 0.02$). A good, semiquantitative agreement for the series of Co(II) analog complexes is found between the variations of the β nephelauxetic ratio of complexes and the values of σ^+-Brown substituent constants for the different substituents at the benzene ring of the hydrazone group.

Our previous papers[1–3] have presented the synthesis of 1-methyl-2-carbethoxy-glyoxalanil-(1)-arylhydrazones-(2) with different substituents at the benzene ring of the hydrazone group (I : Y = H; *o*-, *m*-, *p*-CH_3; *o*-, *m*-, *p*-O-CH_3) and also the synthesis and the physico-chemical properties of the Co(II) complexes obtained with such ligands. The five complexes are tetracoordinated chelates of type II (Y = H; *p*-, *m*-CH_3; *p*-, *m*-O-CH_3). The electronic spectra and the magnetic moments indicate for these complexes a tetrahedral geometrical structure for the Co(II)-N chemical bonds and an appreciable, yet often differing, covalence degree for these bonds (β nephelauxetic ratio = 0.71 ... 0.76).

The present paper is concerned with the electronic spectra and the magnetic moments of the two new, type II, chelate complexes IIa (Y = = *p*-NO_2) and IIb (Y = *m*-NO_2). The complexes include a set of 4 identical donor nitrogen atoms in sp^2-hybridization. The complexes were synthesized by means of the new organic ligands Ia and Ib. In contrast to these the compound Ic (Y = *o*-NO_2) has failed to complex Co(II)

---

[1] P. Spacu, A. C. Banciu and C. I. Lepădatu, *Rev. Roumaine Chim.*, **18**, 7, 1143 (1973).

[2] A. C. Banciu and P. Spacu, *Rev. Roumaine Chim.*, **19**, 6, 1019 (1974).

[3] A. C. Banciu and P. Spacu, *Rev. Roumaine Chim.*, **19**, 7, 1169 (1974).

ions as a result of major steric hindrances caused by the NO_2 group found in the *ortho* position.

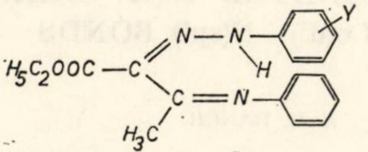

I

a: Y=p–NO_2 b: Y=m–NO_2 ; c: Y=o–NO_2

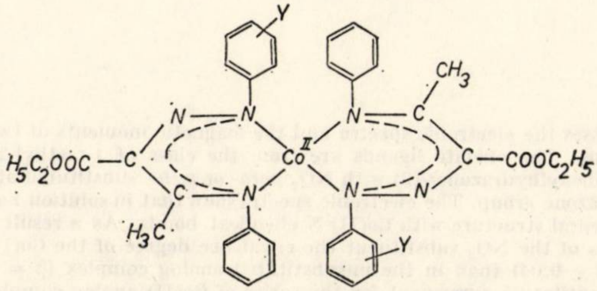

II a: Y=p–NO_2 b: Y=m–NO_2

EXPERIMENTAL

The synthesis of the new ligand Ia has already been described in our previous paper.[1] The new compounds Ib and Ic were synthesized according to the same method indicated in our earlier works.[1–3] Their analytical data are listed in table 1.

Table 1

1-Methyl-2-carbethoxy-glyoxalanil-(1)-nitro-phenyl-hydrazones-(2)

Compound of type I	Y	C % calc. found	H % calc. found	N % calc. found	m.p. °C
Ib	m-NO_2-	61.01 60.82	5.12 5.70	15.81 15.99	95–99
Ic	o-NO_2-	61.01 61.34	5.12 5.72	15.81 16.25	146–149

The new complexes IIa and IIb were synthesized according to the method reported in our earlier papers,[1–3] by means of compounds Ia and Ib which proved to be real bidentate chelate ligands. The analytical data of the new complexes are listed in table 2.

The elemental analysis of Co, C, H and N was conducted by usual micromethods.

The absorption spectra of chelates were determined on a VSU-2 Carl Zeiss (Jena) spectrophotometer for $0.5\times10^{-4} - 5\times10^{-4}$ mol/l solutions in acetone.

Table 2

Co(II) chelates. Analytical data

Chelate of type II	Y	Co %	C %	H %	N %	m.p. °C
		calc. found	calc. found.	calc. found.	calc. found	
IIa	p-NO_2-	7.70 7.59	56.47 56.30	4.48 5.00	14.64 14.89	208−9
IIb	*m*-NO_2-	7.70 7.19	56.47 56.36	4.48 5.07	14.64 14.97	179−80

The reflectance spectra of chelates were determined on a VSU-1 Carl Zeiss (Jena) spectrophotometer using MgO as a standard substance.

The magnetic susceptibilities were determined in solid complexes according to Faraday's method, at room temperature, using $Hg[Co(NCS)_4]$ as a standard. The magnetic moments were calculated by the formula

$$\mu = 2.828\ [\chi'_M \cdot T]^{1/2}$$

where $\chi'_M = \chi_M - \chi_{\mathrm{dia}}$ is the corrected molar susceptibility. The correction for diamagnetism $\chi_{\mathrm{dia}} = -361 \times 10^{-6}$ c.g.s.u. was applied in the case of both isomeric chelates. For this calculation, as well as for χ_M, the molecular weight of the complexes were formulated as monomer, according to formula II.

RESULTS AND DISCUSSIONS

ELECTRONIC SPECTRA

The electronic absorption spectra of both chelates are given in fig. 1.

Both chelates have three bands in the 350−1200 nm range, only differing from each other in intensity. The first, very intense band ($\varepsilon_{\max} > 1 \times 10^4$), with its maximum situated at about 400 nm definitely represents a $\pi \rightarrow \pi^*$ transition characteristic of the organic ligand. Although the other two, with maxima situated at approx. 550 nm ($\varepsilon_{\max} > 1 \times 10^3$) and approx. 1050 nm ($\varepsilon_{\max} \sim 1 \times 10^2$), differ greatly in intensity, they are both attributed to spin-allowed *d-d* transitions for the d^7 electronic configuration of the central Co(II) ion with a tetrahedral surrounding.

In contrast to the previously studied spectra of the other Co(II) chelates synthesized with ligands from the class of substituted glyoxal-anil-(1)-arylhydrazones-(2), the central band at approx. 550 nm in the spectrum of both chelates in question, IIa and IIb, fails to exhibit a well-defined maximum. The band appears as a very large shoulder of the more intense $\pi \rightarrow \pi^*$ transition of the organic ligand. For this reason, the evaluation of the band position at approx. 550 nm is not accurate. However, the peak position for well shaped shoulders, which are broad and flattened, can be determined satisfactorily from previous analogies.

In the case of chelate IIa, the band maximum at approx. 550 nm cannot be situated at a wavelength below 535 nm, because a single *d-d* transition could not represent a shoulder from 530 to 620 nm, neither could the ε values sensibly decrease only at 620 nm, as in the present case. Similarly, the band maximum at approx. 550 nm cannot be situated at longer wavelengths than 570 nm. Despite the mentioned difference, the spectrum of chelate IIa is very similar to the spectra of the other previously studied tetrahedral Co(II) chelates [1-3] and thus it allows for a comparison with the latter. If the maximum values in question were situated at $\lambda > 570$ nm the absorption due to the $\pi \rightarrow \pi^*$ band would become practically equal to that of the band in question. The band at approx. 550 nm will always be well-shaped if it is separated by more than 35 nm ($= 1150\ \mathrm{cm}^{-1}$) from the $\pi \rightarrow \pi^*$ band. If the separation exceeds the 35 nm ($= 1150\ \mathrm{cm}^{-1}$) value, then the spectrum of the chelate IIa would also be well-shaped, rather than displaying it somewhere on the almost horizontal plateau of the shoulder corresponding to the band, as in the present case. Although the band would be mostly overlapped by the $\pi \rightarrow \pi^*$ band, as in the case of analog Co(II) complexes, [1-3] over one half of the band in question would be well-shaped, accurately indicating the position of the maximum.

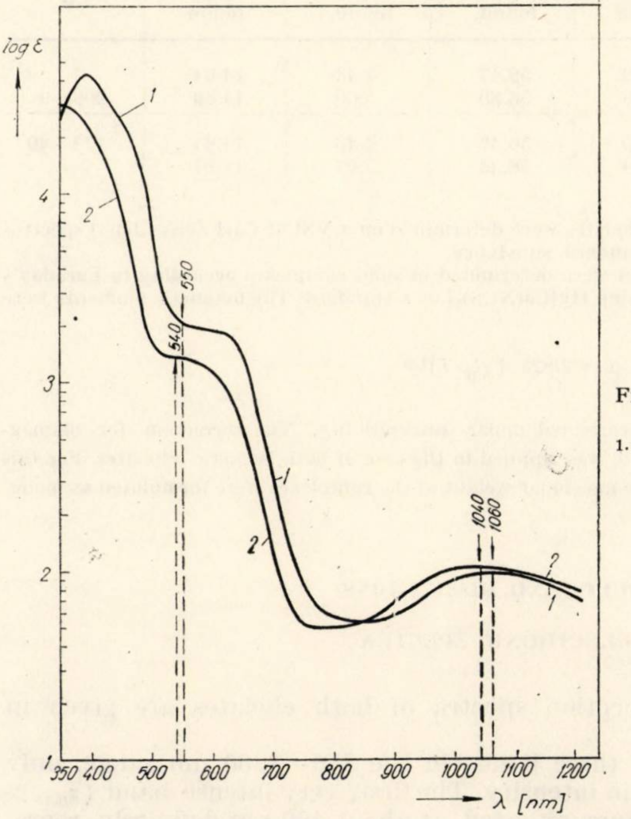

Fig. 1. — Absorption spectra of the Co(II) chelates.
1. Chelate IIa (Y = $p-NO_2$); 2. Chelate IIb (Y = $m-NO_2$).

It results from the above that in the case of chelate IIa the band maximum at approx. 550 nm must be situated between 535 and 565 nm. The most plausible value for the maximum position appears to be the median, 550 nm, with a $\pm$ 15 nm ($= \pm$ 500 cm^{-1}) error.

The same considerations applied to the spectrum of chelate IIb (fig. 1). show that the band maximum at approx. 550 nm must be situated within the horizontal portion of the shoulder between 525 nm ($\varepsilon = 1.37 \times 10^3$) and 560 nm ($\varepsilon = 1.35 \times 10^3$). The most plausible assignment of the maximum position seems to be the median, 540 nm, likewise with a $\pm$ 15 nm ($= \pm$ 500 cm^{-1}) error. With this spectrum , the existence of a perfectly horizontal portion of almost gaussian shaped shoulder readily permits a graphic verification of the above conclusion.

The energetic expressions of spin-allowed transitions for the $d^7(T_d)$ electronic configuration obtained in a weak field coupling are as follows [4-6] :

$${}^4A_2(e^4\,t_2^3) \rightarrow {}^4T_2\,(e^3\,t_2^4) \qquad \Delta$$

$${}^4\mathrm{A}_2(e^4\,t_2^3) \rightarrow {}^4T_1^a\,(e^3\,t_2^4) \qquad 1.5\ \Delta + 7.5\ B - Q$$

$${}^4A_2(e^4\,t_2^3) \rightarrow {}^4T_1^b\,(e^3\,t_2^4) \qquad 1.5\ \Delta + 7.5\,B + Q$$

where

$$Q = \frac{1}{2}\,[(0.6\,\Delta - 15\,B)^2 + 0.64\,\Delta^2]^{1/2},$$

Δ is the orbital splitting parameter (the energetic difference between the t_2 and e subshells) and B is the Racah parameter for the interelectronic repulsion energies ($B_{\mathrm{Co(II)}} = 980$ cm^{-1}).

Since the energy of the first spin allowed transition is actually equal to parameter Δ, as $\Delta_{T_d} = 4/9\ \Delta_{O_h}$, and $\Delta_{O_h} = 10{,}000 - 15{,}000$cm^{-1} (a relationship also valid in the framework of the LCAO-MO theory[7]) it results that this transition must appear in the IR domain, beyond the measuring capabilities of the used instrumentation.

The two bands at longer wavenlengths in the spectra may be attributed to the last two spin allowed *d-d* transitions as follows :

$$\nu_3({}^4A_2 \rightarrow {}^4T_1^b) = 18{,}200 \pm 500\ \mathrm{cm}^{-1}$$

(550 $\pm$ 15 nm) for chelate IIa

$$= 18{,}350 \pm 500\ \mathrm{cm}^{-1}$$

(540 $\pm$ 15 nm) for chelate IIb.

---

[4] A. B. P. Lever, "Inorganic Electronic Spectroscopy", Elsevier, Amsterdam, 1968, Ch. 8–9.

[5] Y. Tanabe and S. Sugano, *J. Phys. Soc. Japan*, **9**, 753 (1954).

[6] E. König, *Struct. and Bonding*, **9**, 175 (1971).

[7] H. H. Schmidtke, *Z. Naturforsch.*, **19a**, 1502 (1964).

$$\nu_2({}^4A_2 \rightarrow {}^4T_1^a) = 9{,}430 \pm 130\ \text{cm}^{-1}$$

$$(1{,}060 \pm 15\ \text{nm})\ \text{for chelate IIa}$$

$$= 9{,}620 \pm 130\ \text{cm}^{-1}$$

$$(1{,}040 \pm 15\ \text{nm})\ \text{for chelate IIb.}$$

Solving the energetic expressions of these transitions we obtain the values below :

$$\Delta = \frac{0.9(\nu_2 + \nu_3) - \sqrt{0.81(\nu_2 + \nu_3)^2 - 3.4\ \nu_2\nu_3}}{3.6}\ [\text{cm}^{-1}]$$

and thence the values

$$B = \frac{(\nu_2 + \nu_3)/2 - 1.5\ \Delta}{7.5}\ [\text{cm}^{-1}]$$

and $\beta = \dfrac{B}{B_0} = \dfrac{B}{980}$.

The determination error of the parameters Δ, B and β is observed to depend on the error of ν_3 and ν_2 for the bands at approx. 550 nm and approx. 1050 nm. The error in evaluating ν_2 for the broad shoulder is 15 nm, which corresponds to a $\pm$ 130 cm^{-1} error in the band in the 1000 nm region. This is negligible when evaluating parameters Δ, B and β, compared to the $\pm$500 cm^{-1} error with which the ν_3 values were determined in the case of the complexes under study. Thus, we have shown in earlier works [2,3] that even considering the highest possible determination error of the ν_2 band maximum, i.e. $\pm$ 20 nm = $\pm$200 cm^{-1}, it will only induce a modification in the calculated value of β of one unit situated in the second decimal place. The large, 500 cm^{-1} error in the determination of the ν_3 values in the case of the complexes under study has a more sensible influence on the calculated values of the nephelauxetic ratio β.

Table 3 systematizes the Δ, B and β values calculated for the median and extreme ν_3 values of both Co(II) complexes in question.

It is observed that the values of the nephelauxetic ratio, β, have been determined for both complexes with an error of $\pm$ 0.04. The error is sensibly larger than for the analogous Co(II) complexes previously studied [2,3] which had at most a $\pm$ 0.02 error.

Despite the large $\pm$ 0.04 calculation error of β for both complexes in question, the β values are however certainly higher than 0.77–0.78.

In the analog Co(II) complex which was not substituted at the benzene ring of the hydrazone group, the value of β was[2] 0.76 $\pm$ 0.02. Since β is 0.81 $\pm$ 0.04 for the complex IIa and 0.82 $\pm$ 0.04 for the complex IIb, both complexes have a lower degree of covalence for the Co(II)-N chemical bonds than for the unsubstituted complex. The difference in the degree of covalency is explained by the electronic effects of the substituent NO_2 on the electronic densities of the benzene ring and the coor-

Table 3

The Δ, B and β values of the Co(II) chelates

Chelate	ν_3		Δ	B	β
	[nm]	[cm^{-1}]	[cm^{-1}]	[cm^{-1}]	
IIa	535	18,690	5,245	825	0.84
	550	18,180	5,260	790	0.81
	565	17,700	5,295	750	0.77
					$\beta = 0.81 \pm 0.04$
IIb	525	19,050	5,350	845	0.86
	540	18,520	5,375	800	0.82
	555	18,020	5,400	765	0.78
					$\beta = 0.82 \pm 0.04$

dinated nitrogen atom. It is known [8,9] that the NO_2 substituent always reduces the electronic densities of the benzene ring (in the *ortho* and *para* positions by an inductive (-I) and an conjugation (-*M*) effect, both of equal sign, and only by an inductive effect in the *meta* position). The degree of covalence for the Co(II)-N bonds is lowered because of the decrease in the electronic density of the donor nitrogen atom.

The opposite effect occurs for the Co(II) complex with a *para*-methoxy substituent (p-OCH_3)[3]. In this case the electronic density of the donor nitrogen atom was increased by the strong conjugation effect (+$M > -I$) of the substituent and the complex exhibited a higher degree of covalence for the Co(II)-N bonds than for the unsubstituted complex.

Table 4

The values of the nephelauxetic ratio, β, of the Co(II) chelates of type II, different substituted at the benzene ring of the hydrazonic group

Type II chelate Y	β	References
H-	0.76 ± 0.02	1,2
p-CH_3	0.75 ± 0.02	2
m-CH_3	0.75 ± 0.02	2
p-CH_3-O-	0.71 ± 0.02	3
m-CH_3-O-	0.76 ± 0.02	3
p-NO_2-	0.81 ± 0.04	this paper
m-NO_2-	0.82 ± 0.04	this paper

Table 4 systematizes the values for the Co(II) complexes formed with ligands of the class of glyoxalanil-(1)-arylhidrazones-(2), differently substituted at the benzene ring of the hydrazone group.

---

[8] H. Beker, "Einführung in die Elektronen-theorie organisch-chemischer Reaktionen", Deutscher Verlag der Wissenschaften, Berlin, 1965, p. 362.

[9] F. Badea, "Mecanisme de reacţie în chimia organică", Editura Ştiinţifică, Bucureşti, 1971.

The difference in the degree of covalency for the Co(II)-N bonds for the unsubstituted and the *p*-OCH_3 and *p*-NO_2 and *m*-NO_2 substituted case is greater than the experimental error, because the substituents exhibit strong electronic effects. In the case of the Co(II)-N bonds in the complexes it has been found that only the *p*-O-CH_3 substituted complex, on the one hand (indicating a higher covalence degree), and the *p*- and *m*-NO_2-substituted complexes, on the other hand (indicating a lower covalence degree) really differ from the unsubstituted complex, exceeding the experimental error in the evaluation of the β ratio. The substituents existing in these complexes are those which induce the strongest electronic effects.

The quantitative measure of these electronic effects is often made [8,9] using the σ-Hammett and σ^+-Brown substituent constants (table 5).

Only a tentative correlation can be made between the β values of the complexes and the σ-Hammett constants for the different substituted complexes. Thus, there is no satisfactory explanation for the fact that the substituent *p*-OCH_3 ($\sigma = 0.286$) increases the covalence degree ($\beta = 0.71 \pm 0.02$) of the Co(II)-N bonds, whereas the substituent *p*-CH_3, with the σ constant of equal sign and with a close numerical value ($\sigma = 0.170$), leaves it practically unchanged ($\beta = 0.75 \pm 0.02$).

However, a good, semiquantitative correlation is found to exist between the σ^+- Brown values of all substituents in question and the values of β, the nephelauxetic ratio of the complexes. Thus, when the σ^+-Brown constants are below 0.400, in absolute value, the substituents fail to influence the covalence degree of the Co(II)-N bonds. However, when the σ^+-Brown constants are larger than 0.650, in absolute value, the substituents greatly influence the covalence degree of the Co(II)-N bonds, which exceeds the determination error of β, either increasing it (*p*-O-CH_3) or reducing it (*p*- and *m*-NO_2).

Table 5

The values of the σ -Hammett and $\sigma+$ -Brown substituent constants

Substituent	σ-Hammett		σ^+-Brown	
	σ-para	*σ-meta*	*$\sigma^+ - para$*	*$\sigma^+ - meta$*
CH_3-	−0.170	−0.069	−0.306	−0.065
CH_3-O-	−0.268	+0.115	−0.764	+0.046
NO_2-	+0.778	+0.710	+0.777	+0.662

This successful correlation between the values of β, the nephelauxetic ratio of complexes, and the values of the σ^+-Brown constants is possible because the σ^+-Brown constants are sensitive to conjugation electronic effects, whereas the σ-Hammett constants are not. This indicates the large role of the conjugation electronic effect of certain substituents, such as the *p*-O-CH_3 substituent, in modifying the covalent degree of the Co(II)-N bonds in the complexes.

MAGNETIC MOMENTS

The electronic reflectance spectrum of the chelate IIb as a solid agrees well with the electronic absorption spectrum of the chelate in solution. This proves that even in the solid state the chelate has the same tetrahedral structure for the Co(II)-N bonds. For this reason, the values of the parameter Δ, calculated from the electronic spectrum measured in chelate solutions, may be correctly correlated with the results obtained from magnetic susceptibility measurements performed in the solid state chelate.

For a d^7 high-spin tetrahedral configuration the magnetic moment can be calculated by formula[10,11]:

$$\mu = \left(\mu_s - 15.59 \frac{\lambda}{\Delta}\right) \text{B.M.}$$

where $\lambda = -178 \text{ cm}^{-1}$ is the spin-orbit coupling constant, Δ is the orbital splitting parameter, and $\mu_s = 3.89$ B.M. is the spin-only magnetic moment. Using the value $\Delta = 5375 \text{ cm}^{-1}$ (table 3), the magnitude ($-15.59\ \lambda/\Delta$), i.e. the orbital contribution to the magnetic moment value, is ound to be 0.51 B.M. so that:

$$\mu = (3.89 + 0.51) \text{ B.M.} = 4.40 \text{ B.M.}$$

The value

$$\mu = (4.35 \pm 0.05) \text{ B.M.}$$

was experimentally determined for the chelate IIb, in very good agreement with the theoretical value.

Similarly, the value $\Delta = 5260 \text{ cm}^{-1}$, obtained from the electronic spectrum of the chelate IIa in solution, helps to calculate with the above formula a magnetic moment of:

$$\mu = (3.89 + 0.53) \text{ B.M.} = 4.42 \text{ B.M.}$$

The experimental value of μ is

$$\mu = (4.41 \pm 0.05) \text{ B.M.}$$

Although the agreement is excellent it is only incidental in the case of this complex and may easily lead to erroneous conclusions if applied indiscriminately. In reality, the electronic reflectance spectrum measured in the solid state complex positively shows that the latter is not tetrahedral, like in solution, and hence the experimental determined value of its magnetic moment requires a different explanation. We shall provide it in a future paper.

Acknowledgement. I wish to thank lecturer V. Mincu from the Polytehnic Institute Bucharest for the magnetic measurements.

---

[10] R. Stahl-Broda and W. Low, *Phys. Rev.*, **113**, 775 (1959).
[11] F. A. Cotton and M. Goodgame, *J. Amer. Chem. Soc.*, **83**, 1777 (1961).

MAGNETIC MOMENTS

The electronic reflectance spectrum of the chelate IIb as a solid agrees well with the electronic absorption spectrum of the chelate in solution. This proves that even in the solid state the chelate has the same tetrahedral structure for the Co(II)-N bonds. For this reason, the values of the parameter Δ calculated from the electronic spectrum measured in chelate solutions, may be correctly correlated with the results obtained from magnetic susceptibility measurements performed in the solid state chelate.

For a d^7 high-spin tetrahedral configuration the magnetic moment can be calculated by formula[28,29]:

$$\mu = \left(\mu_s - 15.59\,\frac{\lambda}{\Delta}\right)\ \text{B.M.}$$

where $\lambda = -178\ \text{cm}^{-1}$ is the spin-orbit coupling constant, Δ is the orbital splitting parameter, and $\mu_s = 3.89$ B.M. is the spin-only magnetic moment. Using the value $\Delta = 5475\ \text{cm}^{-1}$ of Table 3, the magnitude $(-15.59\,\lambda/\Delta)$, i.e. the orbital contribution to the magnetic moment value, is found to be 0.51 B.M. so that:

$$\mu = (3.89 + 0.51)\ \text{B.M.} = 4.40\ \text{B.M.}$$

The value

$$\mu = (4.35 \pm 0.05)\ \text{B.M.}$$

was experimentally determined for the chelate IIb, in very good agreement with the theoretical value.

Similarly, the value $\Delta = 5290\ \text{cm}^{-1}$, obtained from the electronic spectrum of the chelate IIa in solution, helps to calculate with the above formula a magnetic moment of:

$$\mu = (3.89 + 0.53)\ \text{B.M.} = 4.42\ \text{B.M.}$$

The experimental value of μ is:

$$\mu = (4.41 \pm 0.03)\ \text{B.M.}$$

Although the agreement is excellent it is only incidental in the case of this complex, and may easily lead to erroneous conclusions if applied indiscriminately. [illegible] the electronic reflectance spectrum measured in the solid state complex positively shows that the latter is not tetrahedral like in solution and hence the experimentally determined value of its magnetic moment requires a different explanation. We shall develop this in a future paper.

Acknowledgements. — I wish to thank [illegible] from the Polytechnic Institute [illegible] for the magnetic measurements.

[28] [illegible] Figgis and [illegible] Lewis, Phys. [illegible], 118, 775 (1960).

[29] [illegible] Chem. Soc., 83, [illegible]

[illegible]

Revue Roumaine de Chimie, **21**, *11–12*, 1497–1512 (1976)

CARBENIUM ION REACTIONS. XIII.*

ACETOLYSIS OF 5-TOSYLOXYMETHYL-5H-6,7-DIHYDRODIBENZO[a, c]CYCLOPROPA [e] CYCLOHEPTENE

ECATERINA DRAGU, M. BANCIU, C. DRĂGHICI, M. ELIAN
and ECATERINA CIORĂNESCU

Center of Organic Chemistry, Spl. Independenţei 202B, 7000 Bucharest 15, Romania

Received April 15, 1976

The unbuffered acetolysis of **2-OTs**, which proceeds very rapidly ($k_{25}{}^{\circ} = 2.4 \cdot 10^{-4} s^{-1}$), gives rise, after $LiAlH_4$-reduction, to a mixture of the rearranged alcohols **11-OH** and **12-OH** along with small quantities of unrearranged **2-OH**. In buffered acetolysis the alcohol **11-OH** is the single major product (after $LiAlH_4$-reduction). In strongly acidic medium, the alcohols **11-OH** and **12-OH** are rapidly equilibrated. The acetolysis of **2-OTs** as well as the reaction of **11-OH** or **12-OH** with *p*-toluenesulphonic acid in acetic acid give rise, at longer reaction times, to the homoallylic tosylate **14-OTs**, beside the corresponding acetate **14-OAc**. A reaction mechanism for the solvolyses of **2-OTs** including cyclopropylmethyl rearrangements and internal return is proposed, and the absence of a phenonium route is noted.

In the course of our investigations on dibenzocycloalkane systems it was shown[1] that the acetolysis of tosylate **1** proceeds with ring expansion involving phenyl participation in the ionization step.

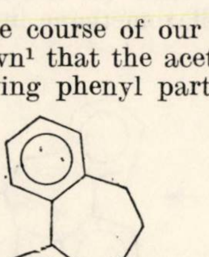

1: X=OTs

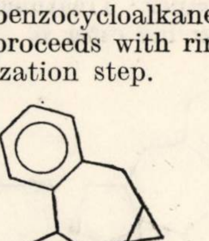

2-OTs : X=OTs
2-OH : X=OH
2-OAc: X=OAc

The present paper deals with the synthesis and solvolysis of the related compound **2-OTs**, possessing a cyclopropyl and a phenyl group favourably located to provide anchimeric assistance.

---

* Part XII : M. Banciu, F. Badea, R. Jelescu and E. Ciorănescu, *Rev. Roumaine Chim.*, **20**, 121 (1975).

[1] E. Ciorănescu, M. Banciu, M. Elian, A. Bucur and C. D. Nenitzescu, *Liebigs Ann. Chem.*, **739**, 121 (1970).

A few compounds possessing a carbinyl group attached to the angular position of an [*n*.1.0] bicyclic fused system, **3**, have been investigated in connection with the solvolytic ring closure of homoallylic systems of the type **4**.[2–5] The solvolysis of both systems affords similarly rearranged products (at least when $n = 2,3$ for which comparative data exist).

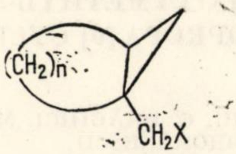

3

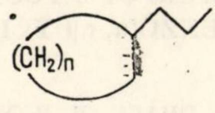

4

The structures of the intermediate carbenium ions involved in the interconversion reactions of cyclopropylcarbinyl, cyclobutyl and allylcarbinyl derivatives are the object of a considerable number of experimental and theoretical studies.[6] Bicyclic compounds of different geometries possessing a cyclopropylcarbinyl group were thoroughly investigated affording new information as compared with the parent cyclopropylcarbinyl system.[7] In this connection the investigation of tosylate **2-OTs**, which is the dibenzo-analog of **3**($n = 5$), looks promising.

RESULTS

Synthesis

The synthesis of the tosylate **2-OTs** was achieved starting with the 5*H*-dibenzo[*a, c*]cycloheptene-7-carboxylic acid (**5**) described in a previous paper.[1] Treatment of this acid with diazomethane in excess led to a pyrazoline ester **6**.

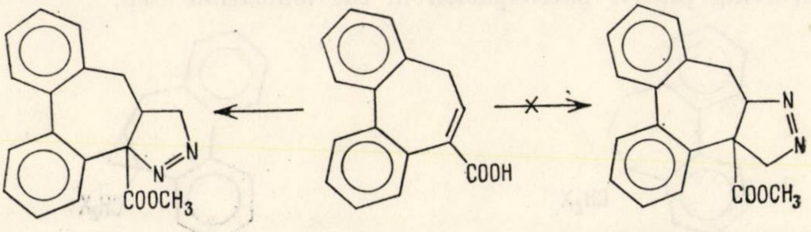

6 **5** **7**

---

[2] W. D. Closson and G. Kwiatkowski, *Tetrahedron*, **21**, 2779 (1965).

[3] a) M. Hanack and H. J. Schneider, *Liebigs. Ann. Chem.*, **686**, 8 (1965) ; b) M. Hanack, H. Schneider-Bernlöhr, H. J. Schneider, R. Huttinger and G. Wentrup, *ibid.*, **717**, 41 (1968).

[4] W. G. Dauben and J. R. Wiseman, *J. Amer. Chem. Soc.*, **89**, 3545 (1967).

[5] a) K. B. Wiberg and J. Hiatt, *J. Amer. Chem. Soc.*, **90**, 6495 (1968) ; b) K. B. Wiberg, J. E. Hiatt and K. Hseih, *ibid.*, **92**, 544 (1970).

[6] a) H. G. Richey in "Carbonium Ions", vol. 3, G. A. Olah and P.v.R. Schleyer, J. Wiley-Interscience, New York, 1972, p. 1201 ; b) M. Hanack and H. J. Schneider, *Angew, Chem.*, **69**, 709 (1967).

[7] K. B. Wiberg, B. A. Hess jr. and A. J. Ashe, in "Carbonium Ions", vol. 3, G. A. Olah and P.v.R. Schleyer, J. Wiley-Interscience, New York, 1972, p. 1295.

The formation of a 3-substituted Δ^1-pyrazoline, **6**, and not of the isomeric 4-substituted Δ^1-pyrazoline, **7**, is in agreement with the observed[8] regioselectivity in 1,3-dipolar cycloadditions, explained by the frontier orbitals method.[9]

Irradiation of the ethereal solution of **6** caused the elimination of nitrogen, affording the cyclopropanic ester **8** (m.p. 84–85°). The ester **8** was converted into the alcohol **2-OH** (m.p. 92–93°) by $LiAlH_4$ reduction and subsequently into the tosylate **2-OTs** (m.p. 72–73°) by reaction with tosyl chloride and powdered KOH in ether.

The structure of the tosylate **2-OTs** as well as of the intermediates, the pyrazoline **6**, the ester **8**, the alcohol **2-OH** (and also of the acetate **2-OAc**) was confirmed by NMR spectroscopy. The first compound in this series possessing a 1-substituted bicyclo [5.1.0] octane skeleton is the ester **8**. The NMR spectrum of ester **8** (Fig. 1) which is very complex in the usual solvents, was simplified by using tris(dipivaloylmethanato) europium[10] as shift reagent; the spectrum obtained with an $Eu(DPM)_3$/substrate molar ratio of 0.22 is presented in Fig. 1b.

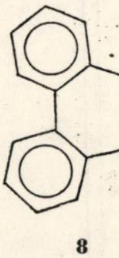

8

All the compounds mentioned above correspond to the general formula **9**. They show the signals of the benzylic protons (H_1 and H_2) at $\delta = 2-3$ ppm; the geminal coupling constant is about 13 Hz (Table 1).

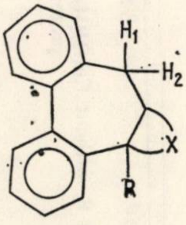

9

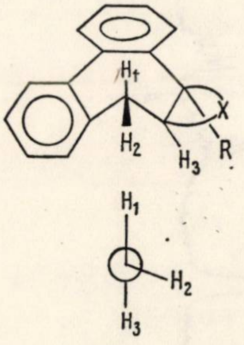

9a

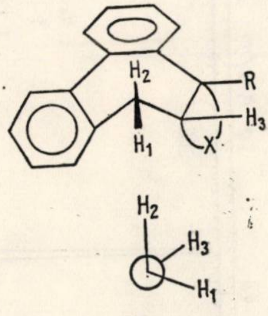

9b

The signal of the proton H_3 is at $\delta = 1.4$ ppm in cyclopropane-containing compounds and at $\delta = 3.5$ ppm in pyrazoline **6**. The cyclopropanic CH_2 group is at $\delta = 0.7-1$ ppm; the coupling constants of the three cyclopropanic protons are in agreement with the substitution pattern.

---

[8] a) R. Huisgen, *Angew. Chem.* (*Internat. Ed.*), **2**, 633 (1963); b) G. W. Cowell and A. Ledwith, *Quart. Rev.*, **24**, 119 (1970).

[9] a) K. N. Houk, *J. Amer. Chem. Soc.*, **94**, 8953 (1972); b) K. N. Houk, J. Sims, R. E. Duke, R. E. Strozier and J. K. George, *ibid.*, **95**, 7287 (1973); c) K. N. Houk, J. Sims, C. R. Watts and L. J. Luscus, *ibid.*, **95**, 7301 (1973).

[10] J. K. M. Sanders and D. H. Williams, *J. Amer. Chem. Soc.*, **93**, 641 (1971).

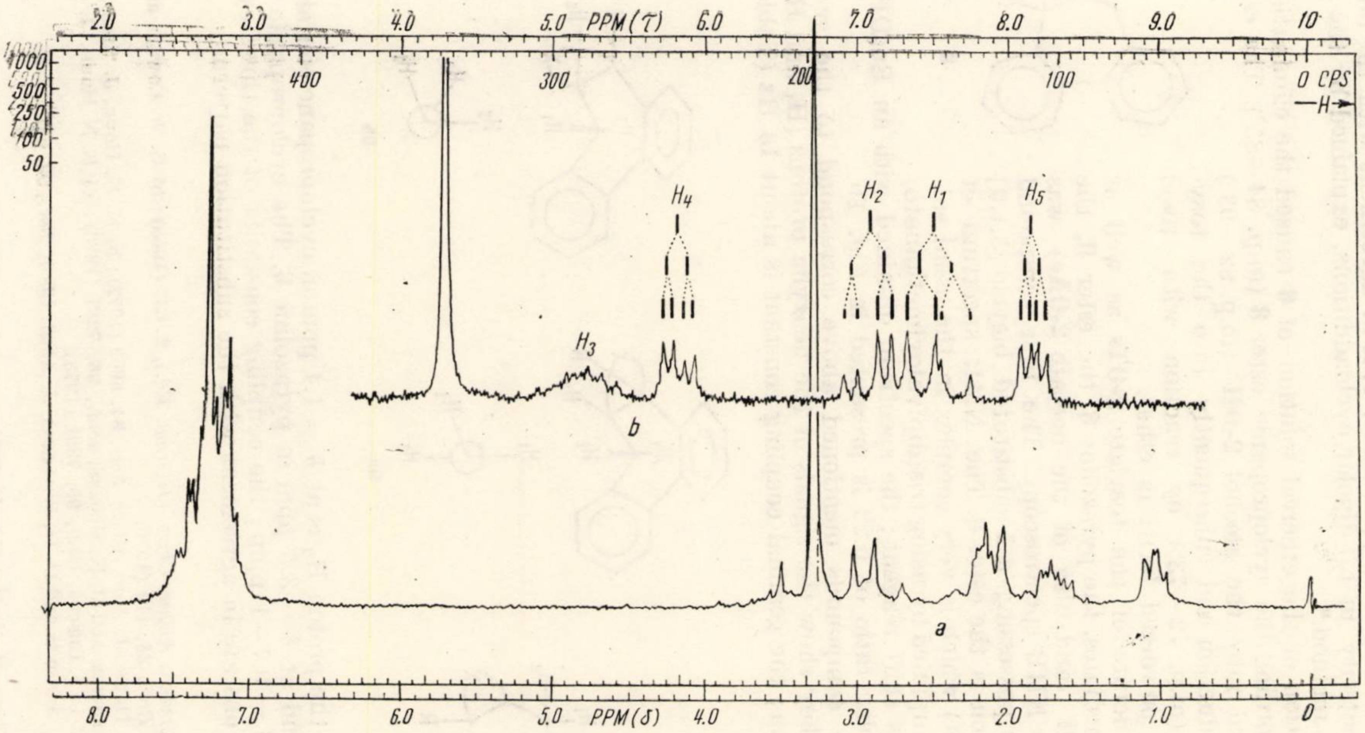

Fig. 1. — NMR spectrum of the ester **8**, without $Eu(DPM)_3$ (*a*) and with an $Eu(DPM)_3$/ester **8** = 0.22 molar ratio (*b*) (only aliphatic protons are shown in *b*).

Table 1

NMR spectra of compounds 9 *

	9 : X =	R =	δ_1	δ_2	δ_3	J_{12}	J_{13}	J_{23}	Other signals, δ
6	-N=N-CH_2-	$COOCH_3$	2.20	2.70	3.4–3.7	13	12.5	4.5	$COOCH_3$: 3.37
8	-CH_2-	$COOCH_3$				13.5	11	5	$COOCH_3$: 3.30
2-OH	-CH_2-	CH_2OH	2.15	2.97	1.42	13	11	5	CH_2OH : 3.30
2-OAc	-CH_2-	CH_2OAc	2.15	2.90	1.40	13	11	5	CH_2OAc : 3.80 ; OAc : 1.65
2-OTs	-CH_2-	CH_2OTs	2.10	2.95	1.40	13	11	5	CH_3 : 2.40 ; CH_2 : 3.8
10 conf. **9a**	-NH-N=CH-	$COOCH_3$	2.50	2.85	4.50	13	13	5.5	$COOCH_3$: 3.29
10 conf. **9b**			2.55	2.90	4.25	14	4	4	$COOCH_3$: 3.90

* chemical shifts in ppm ; coupling constants in Hz ; $CDCl_3$ or CCl_4 as solvents and TMS as internal standard.

Some knowledge about the conformation of the tosylate **2-OTs** is important since the formation of a phenonium ion during the solvolyses involves a severe steric interference between the $-CH_2OTs$ group and the neighbouring aromatic ring. There are two possible conformations, **9a** and **9b**, for the compounds **9**. The $-CH_2OTs$ group of **2-OTs** is in the plane of the adjacent aromatic nucleus in the conformer **9b**; by contrast in the conformer **9a** it has an almost ideal orientation for the formation of a phenonium ion.

As the Newman projections under the formulas **9a** and **9b** show, the position of the proton H_3 relative to H_1 and H_2 is very different in the two conformers. The expected magnitudes of the coupling constants are $J_{13} \gg J_{23}$ in **9a**, while both J_{13} and J_{23} are small and approximately equal in **9b**. The observed coupling constants in **6**, **8**, **2-OH**, **2-OAc** and **2-OTs** (Table 1) are $J_{13} = 11-12.5$ Hz and $J_{23} = 4.5-5$ Hz, indicating a preference for the conformation **9a**. Another hint in the same direction is the unusual chemical shift of the CH_3 signals of the carbomethoxy group (3.37 ppm in **6**, 3.30 ppm in **8**) and acetoxy group (1.65 ppm in **2-OAc**) due to the upfield shift induced by one of the aromatic rings which is possible only in the conformer **9a**.

Further information about the conformers **9a** and **9b** was found in the NMR spectrum of the isomeric Δ^2-pyrazoline **10** obtained from **6** in acidic medium. The spectrum shows that the signals of both conformers **9a** and **9b** are in the approximate molar ratio 2 : 1. The chemical shift of $COOCH_3$ protons is at $\delta = 3.29$ ppm for one of the conformers (**9a**) — exactly the same as for the compounds discussed previously — and at the more usual value of $\delta = 3.90$ ppm for the second one whose coupling constants J_{13} and J_{23} are equal, as expected for the conformer **9b**.

In all compounds presented in Table 1, except **10**, the conformer **9a** is free from steric constraints, while in the conformer **9b** one of the protons in the CH_2 group of the cyclopropanic or pyrazolinic nucleus is very close (about 2 Å) to a carbon or a hydrogen atom of the aromatic rings. As the examination of Dreiding models shows, both conformers of **10** seem to be free of steric interactions, which explains the complex NMR spectrum of this compound.

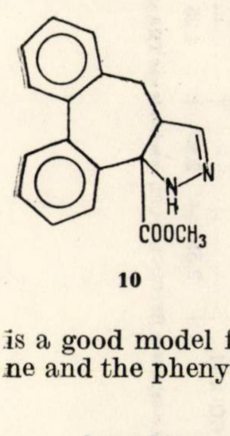

10

The tosylate **2-OTs**, constrained to the conformation **9a**, where the $-CH_2OTs$ group has an almost ideal location for the formation of a phenonium ion, is a good model for the study of the competition between the cyclopropane and the phenyl ring in assisting the ionization during solvolyses.

Acetolyses of tosylate 2-OTs

The acetolyses of **2-OTs** were performed at 30° for 3 hrs with and without added sodium acetate. The composition of the reaction product (92% and 94% respectively) was determined, after $LiAlH_4$ reduction, by means of v.p.c.-analysis (Table 2).

Two alcohols, **11-OH** and **12-OH**, were separated by column chromatography on alumina, beside small amounts of the parent alcohol **2-OH**. The alcohol **11-OH** was identified as 5H*—6,7-dihydrodibenzo* [a, c] *cyclobuta*[e]*cyclohepten-5-ol*, and the alcohol **12-OH** as *spiro* [5H — *6,7-dihydro-dibenzo*[a, c]*cyclohepten-6-ol-5,1′-cyclopropane*], as will be shown later.

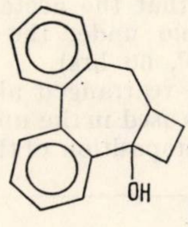

11-OH

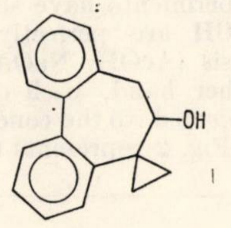

12-OH

From the acetolysis product of **2-OTs** (in the absence of NaOAc) for 200 hrs at 30°, followed by $LiAlH_4$ reduction, two new components beside the alcohols **11-OH, 12-OH** and **2-OH** were found (Table 2, entry 3). Separation of these components, achieved by column chromatography on alumina, permitted their identification by means of NMR spectroscopy. The new components were the alkene **13** and the unsaturated alcohol **14-OH** (37% and 15% respectively).

Table 2

Acetolysis products of 2-OTs at 30° (v.p.c. analysis after $LiAlH_4$ reduction)

	Tosylate **2-OTs** [*M*]	NaOAc [*M*]	Time (hrs)	Products (%)					
				13	**11-OH**	**12-OH**	**2-OH**	**14-OH**	Unidentified
1	0.043	—	3	—	60	29	4.5	—	6.5 (5 components)
2	0.043	0.061	3	—	91	1.5	6.0	—	1.5
3	0.043	—	200	37	12	15	10	15	11 (10 components)

When the mixture obtained in this solvolysis was chromatographed before $LiAlH_4$ reduction, the acetate **14-OAc** and the tosylate **14-OTs** were the new products.

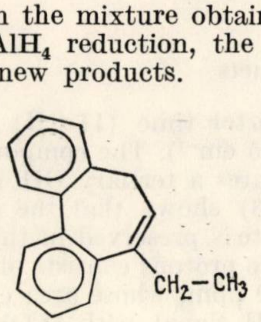

13

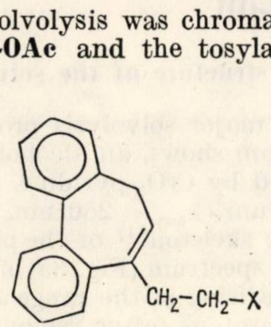

14-OH : X=OH
14-OAc: X=OAc
14-OTs : X=OTs

Thus, the alkene **13** is not a solvolysis product, but is formed from the tosylate **14-OTs** during $LiAlH_4$ reduction (the alkene **13** was obtained in more than 90% purity by $LiAlH_4$ reduction of a sample of tosylate **14-OTs**).

Control experiments have shown that the acetates of the alcohols **11-OH** and **12-OH** are perfectly stable under the conditions of the buffered acetolysis (AcOH, NaOAc, 30°, 60 hrs).

On the other hand, each of the rearranged alcohols **11-OH** and **12-OH** were subjected to the conditions used in the unbuffered acetolysis (AcOH, TsOH). Fig. 2 represents the composition of the reaction mixture in the acidolyses of **11-OH** at 30° and 50°. The data indicate an interconversion of **11-OH** and **12-OH** accompanied by ring opening to an allylcarbinyl system, which generates the tosylate **14-OTs** and the acetate **14-OAc***, i.e. the same products as in the unbuffered acetolysis of **2-OTs** with a longer reaction time. A similar behaviour was observed with the alcohol **12-OH**.

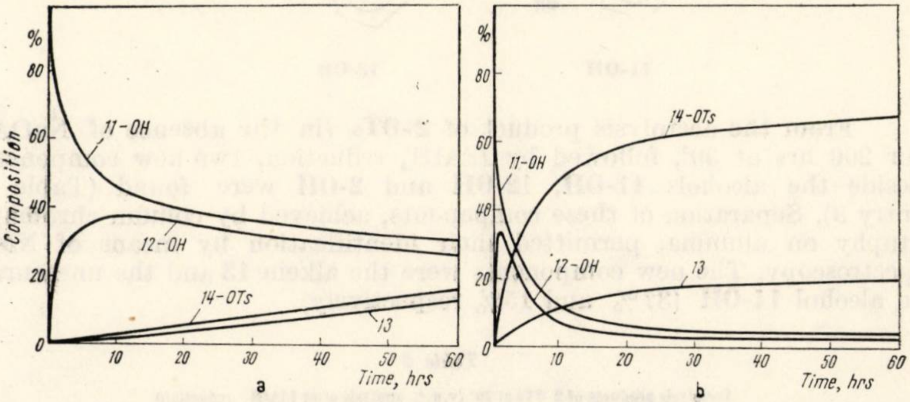

Fig. 2. — The composition of the reaction mixtures in the acidolyses of **11-OH** at 30° (*a*) and 50° (*b*), after $LiAlH_4$ reduction.

The structure of the solvolysis products

The major solvolysis product at shorter time (**11-OH**) is, as the IR spectrum shows, an alcohol ($\nu_{OH} = 3585$ cm^{-1}). The compound cannot be oxidized by CrO_3-pyridine, which indicates a tertiary OH group. The UV spectrum ($\lambda_{max} = 250$ nm, $\log \varepsilon = 4.13$) shows that the dibenzocycloheptene skeleton[1,11] of the parent tosylate is preserved in this product. The NMR spectrum (Fig. 3a) of the aliphatic protons consists of a complex multiplet arising in the range $\delta = 1.2-3.0$ ppm, whose area corresponds to seven protons (after removal of the OH signal with D_2O).

There are no signals corresponding to olefinic or cyclopropanic CH_2 protons. The addition of tris(dipivaloylmethanato)europium allows the separation of all aliphatic protons. The spectrum recorded at an $Eu(DPM)_3$:

---

* represented in Fig. 2 as **13** and **14-OH**, respectively, resulted after the treatment with $LiAlH_4$.

[11] a) G. H. Beaven, G. R. Bird, D. Muriel-Hall, E. A. Johnson, J. E. Ladbury, M. S. Leslie and E. E. Turner, *J. Chem. Soc.*, **1955**, 2708 ; b) G. H. Beaven, D. Muriel-Hall, M. S. Leslie and E. E. Turner, *ibid.*, **1952**, 854.

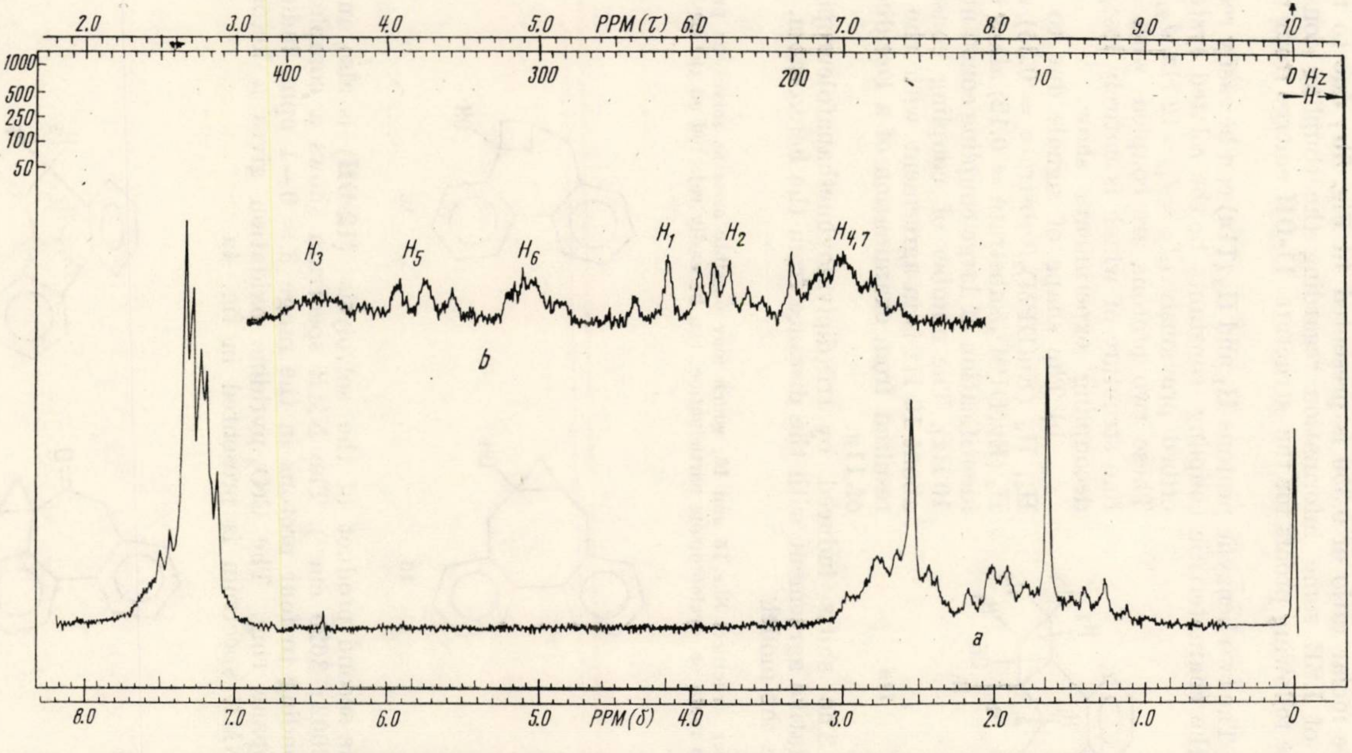

Fig. 3. — NMR spectrum of the alcohol **11-OH**, without $Eu(DPM)_3$ (*a*) and with an $Eu(DPM)_3$/alcohol **11-OH** = 0.35 molar ratio (*b*).

substrate molar ratio of 0.350 is presented in Fig. 3b; due to the large amount of LSR some information regarding the coupling constants is lost. The following proofs for the structure **11-OH** emerge from the spectrum:

a) The two benzylic protons H_1 and H_2 (**11a**) can be easily recognized due to the characteristic coupling constants in the related systems described previously ($J_{12}=J_{13}=12$ Hz, $J_{23}=5$ Hz). These two protons are coupled with H_3 (the fine structure of which is entirely lost) as the decoupling experiments show.

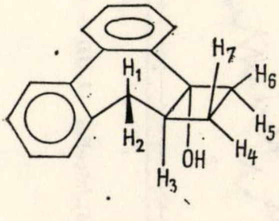

11a

b) The shape of signals due to protons H_5, H_6 ($Eu(DPM)_3$/substrate = 0.35) and H_4, H_7 ($Eu(DPM)_3$/substrate = 0.12) allow only the identification of large coupling constants (about 10 Hz). The number of coupling constants of about 10 Hz is in agreement with the number resulted from examination of a Dreiding model of **11a**.

c) The shifts induced by tris(dipivaloylmethanato)europium are in qualitative agreement with the distance from the heteroatom, as measured on the model.

Other structures like **15** and **16**, which may possibly arise as solvolytic products by phenonium route or cyclopropane participation, can be easily rejected on the basis of spectral data.

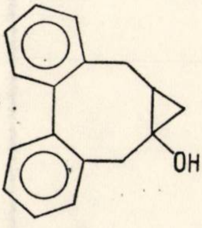

15

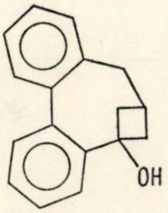

16

The second product of the solvolysis (**12-OH**) is also an alcohol ($\nu_{OH} = 3602$; 3620 cm^{-1}). The NMR spectrum shows a complex signal corresponding to four protons in the range $\delta = 0-1$ ppm, indicating a cyclopropane ring. The CrO_3-pyridine oxidation gives a ketone (**17**), whose NMR spectrum is presented in fig. 4a.

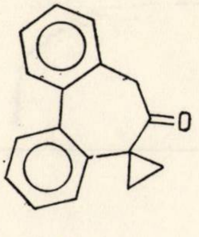

17

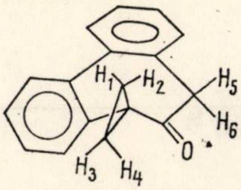

17a

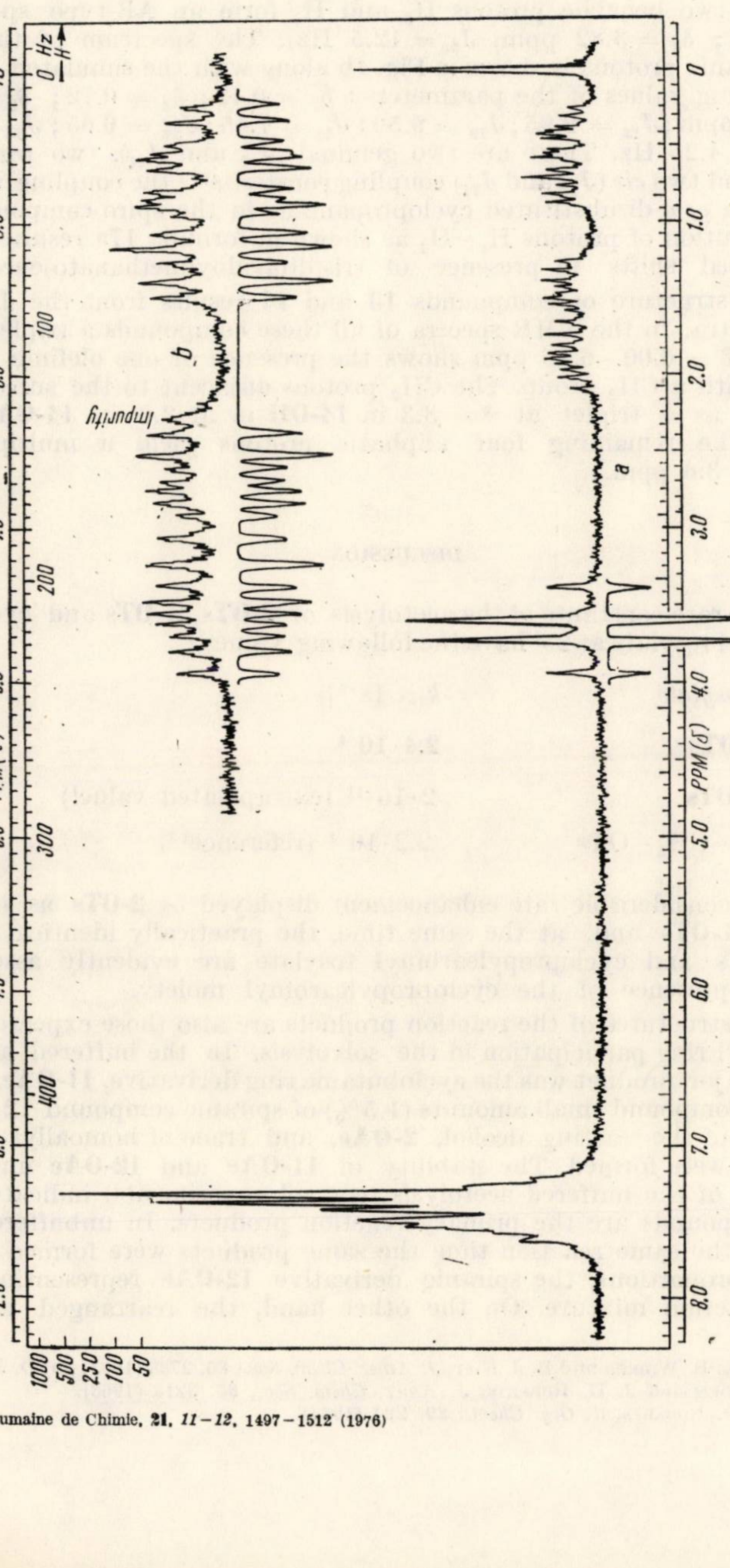

Fig. 4. — NMR spectrum of the ketone **17**: experimental (*a*) and calculated spectrum of cyclopropanic protons (*b*).

The two benzylic protons H_5 and H_6 form an AB-type spectrum ($\delta_5 = 3.53$; $\delta_6 = 3.82$ ppm, $J_{56} = 12.5$ Hz). The spectrum of the four cyclopropanic protons is shown in Fig. 4b along with the simulated one for the following values of the parameters: $\delta_1 = 0.42$; $\delta_2 = 0.72$; $\delta_3 = 1.48$; $\delta_4 = 1.91$ ppm; $J_{12} = 2.95$; $J_{13} = 9.50$; $J_{14} = 7.45$; $J_{23} = 6.65$; $J_{24} = 9.65$ and $J_{34} = 4.25$ Hz. There are two geminal (J_{12} and J_{34}), two *trans* (J_{14} and J_{23}) and two *cis* (J_{13} and J_{24}) coupling constants[12]; the coupling scheme indicates a *gem*-disubstituted cyclopropane as in the spiro compound **17.** The attribution of protons $H_1 - H_4$ as shown in formula **17a** resulted from the induced shifts in presence of tris(dipivaloylmethanato)europium.

The structure of compounds **13** and **14** results from the IR and NMR spectra. In the NMR spectra of all these compounds a triplet ($J = 7$ Hz) at $\delta = 6.00 - 6.15$ ppm shows the presence of one olefinic proton coupled with a CH_2 group. The CH_2 protons adjacent to the substituent X appear as a triplet at $\delta = 3.3$ in **14-OH** or at 3.9 in **14-OAc** and **14-OTs**. The remaining four aliphatic protons yield a multiplet at $\delta = 2.2 - 3.6$ ppm.

DISCUSSION

The rate constants of the acetolysis of **2-OTs**, **1-OTs** and cyclopropylcarbinyl tosylate at 25° have the following values:

Tosylate	k_{25° [s^{-1}])
2-OTs	$2.4 \cdot 10^{-4}$
1-OTs	$2 \cdot 10^{-11}$ (extrapolated value[1])
$\triangleright - CH_2 - OTs$	$2.2 \cdot 10^{-4}$ (reference[13])

The considerable rate enhancement displayed by **2-OTs** as compared with **1-OTs** and, at the same time, the practically identical values for **2—OTs** and cyclopropylcarbinyl tosylate are evidently associated with the presence of the cyclopropylcarbinyl moiety.

The structures of the reaction products are also those expected from cyclopropyl ring participation in the solvolysis. In the buffered acetolysis the major product was the cyclobutanic ring derivative, **11-OAc**. Along with this compound small amounts (1.5%) of spiranic compound **12—OAc,** of acetate of the starting alcohol, **2-OAc**, and trace of homoallyl derivatives, **14**, were formed. The stability of **11-OAc** and **12-OAc** under the conditions of the buffered acetolysis (control experiments) indicates that these compounds are the primary reaction products. In unbuffered acetolysis at the same reaction time the same products were formed but in different proportions, the spiranic derivative **12-OAc** representing 29% of the reaction mixture. On the other hand, the rearranged acetates

[12] a) K. B. Wiberg and B. J. Nist, *J. Amer. Chem. Soc.*, **85**, 2788 (1963); b) D. J. Patel M.E.H. Howden and J. D. Roberts, *J. Amer. Chem. Soc.*, **85**, 3218 (1963).

[13] D. D. Roberts, *J. Org. Chem.*, **29**, 294 (1964).

11-OAc and **12-OAc** underwent acid-catalysed rearrangements under mild conditions (30°); beside the interconversion **11-OAc** $\rightleftarrows$ **12-OAc**, a slow ring opening occurred, leading to the homoallylic derivatives **14-OAc** and **14-OTs**. A similar behaviour was observed in unbuffered acetolysis at a longer reaction time.

The results suggest that a common cationic intermediate is involved in all these reactions. This could be a bicyclobutonium ion of the type suggested by Roberts and coworkers[14] to account for the characteristic rearrangements of cyclopropylcarbinyl-cyclobutyl-and homoallyl derivatives.

The cation **18**, which could arise by ionisation of **2-OTs** assisted by cyclopropanic ring, undergoes a rapid equilibration with **19**. These cations may either react with the solvent to give **11-OAc**, **12-OAc** and **14-OAc**, or may form, by internal return, the covalent tosylate **14-OTs**. The same intermediates could also arise when **11-OAc** and **12-OAc** are treated with strong acid (TsOH).

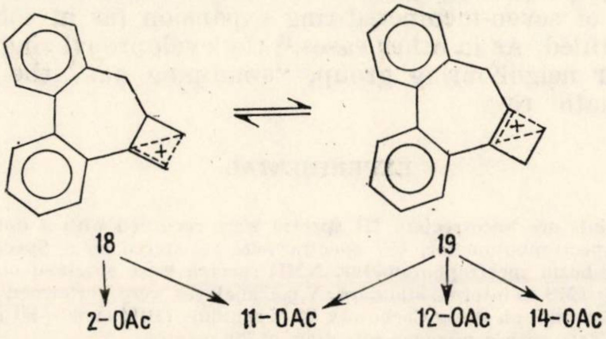

The homoallylic tosylate **14-OTs** displays, under the conditions used (30°), a very low rate (even at 118°, after 30 hrs, only about 60% conversion was observed). It seems therefore that **14-OTs** is not the main precursor of **14-OAc**, both homoallylic derivatives being probably formed from a common intermediate.

The significant amounts of **14-OAc** formed in the solvolysis of **2-OTs** (much larger than expected from the solvolysis of **14-OTs**) support the proposed scheme. The low rates of certain homoallylic derivatives as well as the internal return are well-known phenomena in such rearrangements.[6,7] The very low rate of **14-OTs** could be the result of the thermodynamic stability of this compound due to the conjugation of the phenyl ring with the double bond.

The secondary tosylate **12-OTs** which could be also formed through internal return is much more reactive than **14-OTs** (and than **2-OTs** also) and could not be isolated; even much less stable should be the tertiary benzylic tosylate **11-OTs**.

---

[14] a) M. C. Caserio, W. H. Graham and J. D. Roberts, *Tetrahedron*, **11**, 171 (1960); b) R. H. Mazur, W. N. White, D. A. Semenov, C. C. Lee, M. S. Silver and J. D. Roberts, *J. Amer. Chem. Soc.*, **81**, 4390 (1959).

As might be expected, the positive charge in cations **18** and **19** could be localized mainly on the benzylic position which becomes thus the preferred reaction site with the nucleophilic agent. The cyclobutanic derivative **11-OAc** which predominates can be regarded as the product of kinetic control; its formation is favoured also by the fact that it could arise from both structures of the cationic intermediate.

Under equilibrating conditions (in the presence of acids) the thermodynamically favoured homoallylic system accumulates and becomes the main component as the proportion of the two initially formed products (**11-OAc** and **12-OAc**) decreases.

The compounds with structure **3**, described in literature ($n = 2,3$), give on solvolysis ring-enlarged products (five- and six-membered rings, respectively), the driving force of the reaction being attributed to a relief of strain.[2] In the present case this factor should not operate due to the annelation with a seven-membered ring.

Although the $-CH_2OTs$ group in the tosylate **2-OTs** is ideally oriented for β-aryl participation, an assistance was actually not observed and products of seven-membered-ring expansion (as in solvolyses of **1**) were not identified. As in other cases,[15] the cyclopropyl ring is certainly a much stronger neighbouring group, "swamping out" the participation of the β-aromatic ring.

EXPERIMENTAL

Melting points are uncorrected. IR spectra were recorded with a double-beam UR-20 Carl Zeiss Jena spectrophotometer. UV spectra were registered on a Specord UV-VIS Carl Zeiss Jena double-beam spectrophotometer. NMR spectra were obtained on a Varian A-60A spectrometer using TMS as internal standard. V.p.c. analyses were performed on a Carlo Erba model D gas chromatograph using Carbowax 20 M columns (10% on 60—80 mesh Chromosorb W), 1 m long, at 200°, with a nitrogen-rate flow of 30 ml/min.

*5-Carboxymethyl-5*H*-6,7-dihydro-dibenzo* [a,c] *Δ^1-pyrazolino* [e]*cycloheptene* (**6**). Over an ice-cooled solution of *5*H*-dibenzo* [a, c] *cycloheptene-7-carboxylic acid* (**5**)[1](10 g; 42.5 mmoles), in 500 ml anhydrous ether, 150 ml ethereal solution of diazomethane* (prepared from 15.5 g nitrosomethyl-urea) was dropped with stirring during 1 hr. The reaction mixture was left overnight at room temperature, then evaporated *in vacuo*, affording the crude pyrazoline **6**, 11.5 g (93%) which could be used in the next step without purification. *The pyrazoline* **6**, m.p. 109—110° (methanol). Found: C, 74.13; H, 5.81; N, 9.55. $C_{18}H_{16}O_2N_2$ requires: C, 73.94; H, 5.52; N, 9.59%. *IR spectrum* (KBr; cm^{-1}): 761 s, 770 (shoulder), 786 m, 1253 s, 1732 s, 2856 vw, 2901 w, 2947 w, 2991 vw, 3016 vw and 3070 vw.

Acid-catalysed tautomerization of pyrazoline **6**. Over a solution of pyrazoline **6** (0.25 g; 0.86 mmole) in 150 ml acetone, 1 ml $HClO_4$ (70%) was added and the mixture was maintained for 2 hrs at room temperature. The reaction mixture was neutralized with 10% $NaHCO_3$ solution, then extracted with chloroform. The organic extracts were washed, dried and evaporated *in vacuo*, affording the *pyrazoline isomer* **10** which, after two recrystallizations from methanol, melted at 165—168°. *IR spectrum* (KBr; cm^{-1}): 715 m, 750 m, 760 m, 1230 s, 1249 s, 1600 w, 1744 s, 2951 w, 3062 w and 3332 s.

*5-Carboxymethyl-5*H*-6,7-dihydro-dibenzo* [a, c] *cyclopropa* [e] *cycloheptene* (**8**). A solution of pyrazoline **6** (10 g; 34 mmoles) in 200 ml anhydrous ether was irradiated for 4 hrs with a medium pressure Hg immersion UV lamp (150 W; quartz). The yellow solution was then evaporated *in vacuo* and the oily residue was triturated with 40 ml methanol at room temperature, affording the solid ester **8**, 5.5 g (60.5%). Evaporation of the methanolic solution afforded 3.5 g of a thick oil which was not further investigated. *The ester* **8**, m.p. 84–85° (methanol). Found : C, 81.49 ; H, 6.32. $C_{18}H_{16}O_2$ requires : C, 81.78 ; H, 6.10 %. *IR spectrum* (CS_2 ; CCl_4 ; cm^{-1}) : 740 s, 751 vs, 1263 vs, 1275 vs, 1431 s, 1731 vs, 2851 w, 2944 m, 2951 m, 3020 m and 3064 m.

---

* 1 ml solution contained 0.0189 g CH_2N_2 as indicated by benzoic acid titration.

[15] a) D. Lenoir, J. Ipatzky and P.v.R. Schleyer, *Liebigs Ann. Chem.*, **750**, 28 (1971); b) J. W. Wilt and D. D. Roberts, *J. Org. Chem.*, **27**, 3430 (1962); c) D. D. Roberts, *ibid.*, **30**, 23 (1965).

*5-Hydroxymethyl-5*H-*6,7,dihydro-dibenzo*[a, c]*cyclopropa*[e]*cycloheptene* (**2-OH**). A solution of ester **8** (6 g ; 22.7 mmoles) in 40 ml anhydrous ether was dropped with stirring over a suspension of $LiAlH_4$ (1 g ; 26.3 mmoles) in 50 ml anhydrous ether. The reaction mixture was then refluxed 12 hrs and worked-up in the usual manner, affording *the alcohol* **2-OH** (5 g, 94 %), m.p. 92–93° (cyclohexane). Found ; C, 86.15 ; H, 7.02. $C_{17}H_{16}O$ requires : C, 86.40 ; H, 6.83. *IR spectrum* (CS_2 ; CCl_4 ; cm^{-1}) : 747 vs, 762 vs, 1019 s, 1036 vs, 1065 vs, 1376 s, 1432 vs, 1442 vs, 1483 vs, 2860 s, 2934 vs, 3066 s and 3609 m. *UV spectrum* (EtOH) : $\lambda = 252$ nm, log $\varepsilon = 4.14$.

Acetate **2-OAc** (from the alcohol **2-OH** with acetic anhydride in presence of pyridine) m.p. 82–84° (methanol). Found : C, 81.67 ; H, 6.62. $C_{19}H_{18}O_2$ requires : C, 81.97 ; H, 6.52 %. *IR spectrum* (CS_2 ; CCl_4 ; cm^{-1}) : 746 vs, 761 s, 1034 s, 1228 vs, 1238 vs, 1742 vs, 2856 w, 2881 w, 2941 m, 3020 m and 3068 m.

*5-Tosyloxymethyl-5*H-*6,7-dihydro-dibenzo*[a, c]*cyclopropa*[e]*cycloheptene* (**2-OTs**). Over an ice-cooled solution of alcohol **2-OH** (3 g, 12.7 mmoles) in 150 ml anhydrous ether, *p*-toluenesulphonylchloride (2.4 g, 12.8 mmoles) and finely powdered KOH (3 g ; 53.5 mmoles) were added with stirring. The mixture was maintained for 70 hrs at –5°–0° with continuous stirring, then decomposed with water. The organic layer was washed with water, dried and evaporated in vacuo at room temperature, affording 2.5 g (50.5 %) **2-OTs**, m.p. 72–73°. Found : C, 73.54 ; H, 5.99 ; S, 7.49. $C_{24}H_{22}O_3S$ requires : C, 73.81 ; H, 5.68 ; S, 8.21 %. *IR spectrum* (KBr ; cm^{-1}) : 661 s, 744 m, 810 m, 854 s, 943 m, 1174 s, 1350 s, 1596 w, 2849 vw, 2919 w, 2949 w, 3018 w and 3070 vw.

Acetolysis of tosylate **2-OTs** *in unbuffered acetic acid.* A solution of tosylate **2-OTs** (2 g, 5.1 mmoles) in 60 ml anhydrous acetic acid was heated in a thermostate at 30° for 3 hrs, then poured in 200 ml cold water and neutralized with solid Na_2CO_3. The organic components were ether-extracted (4 × 50 ml) and the combined ethereal layers were washed with water, dried and evaporated. The solid residue of acetates (1.35 g ; 94 %) was dissolved in 40 ml anhydrous ether and reduced (8 hrs at reflux) with $LiAlH_4$ (0.2 g ; 5.25 mmoles) in 10 ml ether. After the usual work-up the oily residue of alcohols (1.05 g ; 94 %) whose composition was determined by v.p.c. (see Table 2) was subjected to column-chromatography on neutral alumina. On elution with petroleum ether (b.p. 30–40°) – ethyl ether mixtures (8 : 2 vol) an oily product **11-OH** (see later) was first separated (450 mg ; 43 %), then, after some mixed fractions, the second major product **12-OH** (see later) was obtained, as white crystals (270 mg ; 25.5 %). In the last eluates small quantities of starting alcohol **2-OH** were identified.

5H-*6,7-Dihydro-dibenzo*[a, c]*cyclobuta*[e]*cyclohepten-5-ol* (**11-OH**) uncrystallizable colourless oil. Found : C, 85.79 ; H, 7.27. $C_{17}H_{16}O$ requires : C, 86.40 ; H, 6.83 %. *IR spectrum* CS_2 ; CCl_4 ; cm^{-1}) : 733 m, 750 vs, 762 vs, 778 m, 1060 m, 1129 m, 1163 m, 1446 m, 1485 m, 2845 m, 2859 m, 2833 s, 2972 s, 2983 s, 3027 m, 3063 m and 3585 m. *UV spectrum* (EtOH) $\lambda = 250$ nm, log $\varepsilon = 4.13$.

Acetate **11-OAc** (from the alcohol **11-OH** with acetic anhydride in presence of pyridine), m.p. 145.5° (methanol). Found ; C, 82.04 ; H, 6.55, $C_{19}H_{18}O_2$ requires : C, 81.97 ; H, 6.52 %. *IR spectrum* (CS_2 ; CCl_4 ; cm^{-1}) : 744 s, 761 s, 784 s, 1028 m, 1241 vs, 1740 s, 2861 w, 2942 m, 2976 m, 3016 w and 3066 w. *NMR spectrum* (CCl_4 ; δ ppm) : 1.5 (s, 3H, $COCH_3$) ; 1.4–3.5 (m, 7H) ; 7.1–7.9(m, $8H_{arom}$).

Spiro[*5*H-*6,7-dihydro-dibenzo*[a, c]*cyclohepten-6-ol-5,1′-cyclopropane*] (**12-OH**) m.p. 81–83° (cyclohexane). Found ; C, 86.23 ; H, 6.90. $C_{17}H_{16}O$ requires : C, 86.40 ; H, 6.83 %. *IR spectrum* (CS_2 ; CCl_4 ; cm^{-1}) : 750 s, 759 (shoulder), 1033 vs, 1448 s, 2865 m, 2920 m, 2946 m, 3021 m, 3064 m, 3602 m and 3620 m. *UV spectrum* (EtOH) $\lambda = 249$ nm, log $\varepsilon = 4.16$.

Acetate **12-OAc** (from the alcohol **12-OH** with acetic anhydride in presence of pyridine) m.p. 102–4° (methanol). Found ; C, 81.93 ; H, 6.71. $C_{19}H_{18}O_2$ requires : C, 81.97 ; H, 6.52 %. *IR spectrum* (CS_2 ; CCl_4 ; cm^{-1}) : 731 w, 748 s, 752 s, 1240 vs, 1740 vs, 2861 w, 2946 m, 3024 m and 3069 m. *NMR spectrum* (CCl_4 ; δ ppm) ; 0–1.2 (m, 4H) ; 1.98 (s. 3H, $COCH_3$) ; 2.51 (q, 1H, J= 13 ; 10 Hz) ; 2.98 (q, 1H, J=13 ; 6.5 Hz) ; 4.67 (m, 1H) ; 7.2–7.5 (m, $8H_{arom}$).

Acetolysis of tosylate **2-OTs** *in buffered acetic acid.* A solution of tosylate **2-OTs** (1 g ; 2.55 mmoles) and freshly fused NaOAc (0.3 g ; 3.7 mmoles) in 60 ml anhydrous acetic acid was heated in a thermostate at 30° for 3 hrs. The reaction mixture was then worked-up and the acetates (0.66 g ; 92 %) reduced with $LiAlH_4$ as described above for the unbuffered acetolysis. The composition of the alcoholic reaction mixture (0.55 g ; 95 %), determined by v.p.c., is presented in Table 2. The alcohol **11-OH**, which represents 91 % of the reaction products, was further purified to about 97% by column chromatography on neutral alumina (elution with mixtures of petroleum ether and ethyl ether, 8 : 2 vol).

Acetolysis of tosylate **2-OTs** *at longer reaction time*. A solution of tosylate **2-OTs** (0.5 g; 1.27 mmoles) in 30 ml anhydrous acetic acid was maintained at 30° for 200 hrs, then worked-up and $LiAlH_4$ reduced as described above. The results of the v.p.c. analysis of the reaction mixture (0.25 g) are shown in Table 2. The elution chromatography on neutral alumina column affords as the first component the alkene **13** (about 35%) (elution with petroleum ether). *7-Ethyl-5*H*-dibenzo* [a, c] *cycloheptene* (**13**) colourless oil, *IR spectrum* (CCl_4 ; cm^{-1}) ; 901 m, 941 m, 1436 s, 1443 s (shoulder), 1485 s, 2851 m, 2879 m, 2934 s, 2969 vs, 3022 s, 3063 s and 3096 w. *NMR spectrum* (CCl_4 ; δppm) : 0.92 (t, 3H) ; 2.3—3.2 (m, 4H) ; 6.0 (t, 1H) ; 7.1—7.8 (m, $8H_{arom}$).

By continuing the elution with petroleum ether : ethyl ether mixtures (9 : 1 vol), after some mixed fractions (containing **11-OH**, **12-OH** and **2-OH**) 7(*2′-hydroxyethyl*)*-5*H*-dibenzo-*[a, c]*cycloheptene* (**14-OH**) was obtained (about 15%) as a viscous colourless oil. *IR spectrum* (CCl_4 ; cm^{-1}) : 1041 s, 1434 m, 1482 m, 2847 m, 2951 s, 2978 m, 3020 m, 3059 m, 3582 w and 3628 w. *NMR spectrum* (CCl_4 ; δ ppm) : 1.84 (s, 1H, OH) ; 2.2—3.6 (m, 6H) ; 6.08 (t,1H) ; 7.0—7.8 ($8H_{arom}$).

In a preparative run the reaction mixture was chromatographed on neutral alumina column before $LiAlH_4$ reduction. On elution with petroleum ether : ethyl ether (9 : 1 vol) *the acetate of 7*(*2′-hydroxyethyl*)*-5*H*-dibenzo*[a, c]*cycloheptene* (**14-OAc**) was obtained. *IR spectrum* (CCl_4 ; cm^{-1}) : 1041 vs, 1238 vs, 1369 s, 1437 s, 1483 s, 1739 vs, 2846 m, 2901 m, 2957 s, 3020 s and 3059 s. *NMR spectrum* (CCl_4 ; δ ppm) : 1.6 (s, 3H, $COCH_3$) ; 2.6-3.2 (m, 4H) ; 3.9 (m, 2H) ; 6.15 (t, 1H) ; 7.1—7.7(m, $8H_{arom}$). On further elution of the column with ethyl ether *the tosylate of 7-*(*2′-hydroxyethyl*)*-5*H*-dibenzo*[a, c]*cycloheptene* (**14-OTs**) was separated as a pale yellow oil. *IR spectrum* (CCl_4 ; cm^{-1}) : 971 vs, 1179 vs, 1188 vs, 1371 vs, 1599 m, 2845 m, 2899 m, 2957 m, 3021 m and 3059 m. *NMR spectrum* (CCl_4 ; δ ppm) : 2.35 (s, 3H, CH_3) ; 2.70 (m, 4H) ; 3.90 (m, 2H) ; 6.07 (t, 1H) ; 7.1—7.7 (m, $12H_{arom}$).

Acid-catalysed reactions of alcohols **11-OH** and **12-OH**. A solution of the alcohol **11-OH** (or **12-OH**) (0.5 g ; 2.1 mmoles) and *p*-toluenesulphonic acid (0.4 g ; 2.1 mmoles) in 50 ml anhydrous acetic acid was maintained at 30°. From time to time samples (5 ml) were taken off, then worked-up and $LiAlH_4$ reduced as described above for acetolyses of **2-OTs**. The composition of the reaction mixtures (after $LiAlH_4$ reduction) was determined by v.p.c. analysis (see Fig. 2 for **11-OH**). The product of such an acidolysis of **11-OH** at 50° was worked up (after 60 hrs reaction time) and chromatographied on alumina column affording the acetate **14-OAc** and the tosylate **14-OTs**, as in the acetolysis of **2-OTs** at longer reaction time.

Spiro [5H*-6,7,dihydro-dibenzo* [a, c] *cyclohepten-6-one-5,1′-cyclopropane*] (**17**). A solution of the alcohol **12-OH** (0.3 g ; 1.27 mmoles) in 20 ml anhydrous pyridine was dropped over an ice-cooled preformed complex from CrO_3 (0.35 g ; 3.5 mmoles) in 10 ml pyridine. The reaction mixture was stirred for 12 hrs, left overnight, then decomposed with cold water and ether-extracted (5 × 30 ml). The combined organic layers were washed with water, dilute HCl, again with water, dried and evaporated *in vacuo*, affording *the ketone* **17** (0.25 g ; 83.5%), m.p. 74—75° (90% ethanol). Found : C, 86.74 ; H, 6.36. $C_{17}H_{14}O$ requires : C, 87.14 ; H, 6.03%. *IR spectrum* (CS_2 ; CCl_4 ; cm^{-1}) : 741 s, 752 vs, 1297 s, 1712 vs, 2853 vw, 2925 w, 2980 w, 3024 m and 3070 m.

Kinetic procedure. The *p*-toluenesulphonic acid formed in solvolysis was determined, after adding a known excess of 0.05 M NaOAc/AcOH solution, by titration with an 0.05 M $HClO_4$/AcOH solution in the presence of crystal-violet.

Acknowledgement : We wish to thank Miss Doina Georgescu for v.p.c. analyses and Ms. Elvira Sliam and Mrs. Violeta Daniel for elemental analyses.

Revue Roumaine de Chimie, **21**, *11–12*, 1513–1525 (1976)

GROUND AND EXCITED STATE SCF-PPP-CI CALCULATIONS FOR PYRYLIUM SALTS

MIRCEA D. GHEORGHIU and ALEXANDRU T. BALABAN

Department of Organic Chemistry, Polytechnic, Str. Polizu 1, Bucharest, Romania

Received october 11, 1975

The ground and excited states for pyrylium, 2,4,6,-trimethylpyrylium, 4-phenylpyrylium, 2,4-dimethyl-6-phenyl-pyrylium, 2,6-dimethyl-4-phenylpyrylium and 2,4,6-triphenylpyrylium cations are discussed as a result of SCF-PPP-CI calculations, which considered for phenyl-substituted pyrylium the possibility of non-planar geometries. Theoretical results are correlated with experimental data for electronic absorption spectra, fluorescence and phosphorescence spectra, ^{13}C-NMR spectra.

Pyrylium salts, one of the fundamental heterocyclic systems and a congener of benzene, have received a widespread attention by experimental chemists,[1] complemented in the last ten years by theoretical work concerning their electronic structure.[2–18] The increasing number of experimental findings as for example ^{13}C-NMR,[19,20] X-ray structure determinations[21,22] and UV-spectroscopy[17,23-26] of pyrylium salts offers a new set of observables which could serve to check the correctness of theoretical conclusions.

---

[1] A. T. Balaban, W. Schroth and G. Fischer, in "Advances in Heterocyclic Chemistry" A. R. Katritzky and A. J. Boulton (Eds.), Academic Press, New York, **10**, 241 (1969).

[2] Z. Simon and C. Volanski, *Studii Cercetări Chim. Acad. R. P. România*, **8**, 641 (1960).

[3] Z. Simon, *Optika i Spektroskopiya*, **12**, 22 (1962).

[4] A. T. Balaban, M. Mocanu and Z. Simon, *Tetrahedron*, **20**, 119 (1964).

[5] Z. Simon and A. T. Balaban, *Rev. Roumaine Chim.*, **9**, 339 (1964).

[6] G. V. Boyd and N. Singer, *Tetrahedron*, **21**, 1263 (1965).

[7] C. C. Renţia, A. T. Balaban and Z. Simon, *Rev. Roumaine Chim.*, **11**, 1193 (1966).

[8] M. J. S. Dewar and G. J. Gleicher, *J. Chem. Phys.*, **44**, 768 (1966).

[9] G. V. Boyd, *Rev. Roumaine Chim.*, **12**, 1133 (1967).

[10] G. V. Boyd and A. T. Balaban, *Rev. Roumaine Chim.*, **14**, 1575 (1969).

[11] G. Karlsson and O. Martensson, *Theoret. Chim. Acta*, **13**, 195 (1969).

[12] O. Martensson, *Acta Chem. Scand.*, **24**, 3417 (1970).

[13] O. Martensson and C. H. Warren, *Acta Chem. Scand.*, **24**, 2745 (1970).

[14] Z. Yoshida, H. Sugimoto and S. Yoneda, *Tetrahedron*, **28**, 5873 (1972).

[15] O. Chalvet, C. Decoret, J. Dreux, A. Safiedinne and J. Royer, *Bull. Soc. Chim. France*, **1972**, 716.

[16] C. Decoret, J. Royer and B. Tinland, *Bull. Soc. Chim. France*, **1972**, 2235.

[17] S. K. Chakrabarti, P. T. Frangopol and M. Frangopol, *Rev. Roumaine Phys.*, **17**, 1053 (1972).

[18] M. H. Palmer, R. H. Findlay, W. Maydes and A. J. Gaskell, *J. Chem. Soc. Perkin II*, **1975**, 841.

[19] A. T. Balaban and V. Wray, to be published in *Org. Magn. Resonance*.

[20] A. T. Balaban and V. Wray, *Z. Naturfsch.*, **30b**, 654 (1975).

In this paper we present results obtained with SCF-PPP-CI calculations, carried out on the parent compound **1** and on several substituted derivatives: 2,4,6-trimethylpyrylium (**2**), 4-phenyl-pyrylium (**3**), 2,6-dimethyl-4-phenylpyrylium (**4**), 2,4-dimethyl-6-phenylpyrylium (**5**) and 2,4,6-triphenylpyrylium (**6**).

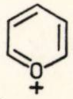

1

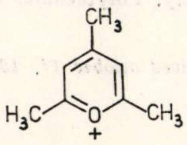

2

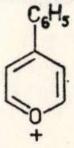

3

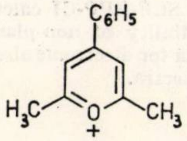

4

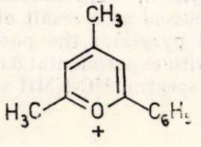

5

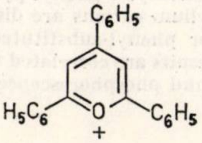

6

Although the theoretical discussions reported so far are based on a wide range of techniques such as Hückel,[2-7] ω-Hückel,[9,10] PPP of various levels of approximations,[13,14] *all-valence* procedures such as EH and CNDO-2,[8,11-13,15-17] and recently non-empirical procedures,[18] they refer mainly to planar π-systems, conformational aspects being neglected. In the present paper we focus our attention on (i) the distribution of π-electrons both in the ground state and in excited states; (ii) for compounds **3**–**5**, possessing a phenyl substituent in positions α or γ, we considered various conformations as the result of phenyl rotation. All calculations were carried out using extensive configuration interactions (CI) including singly and doubly excited configurations. The algorithm of the computation method is based on the formalism developed and implemented on the computer by Hoffmann and Imamura.[27] For details of calculations the reader should consult their original paper. Parametrizations of the present calculations are presented in the Appendix.

---

[21] G. B. Drey, G. W. A. Fowles, D. A. Rice, K. J. Shanton, *J.C.S., Chem. Comm.*, **1974**, 614.

[22] T. Tamamura, T. Yamane, N. Yosuoka, N. Kasai, *Bull. Chem. Soc. Japan*, **47**, 832 (1974).

[23] Y. Maroni-Barnaud, P. Maroni, M. Simalty and Y. Madaule, *Bull. Soc. Chim. France*, **1970**, 1398.

[24] M. Simalty, J. Carretto and S. Sib, *Bull. Soc. Chim. France*, **1970**, 3920.

[25] H. Khedija, H. Strzelecka and M. Simalty, *Bull. Soc. Chim.* France, **1972**, 3178.

[26] J. R. Wilt, G. A. Reynolds and J. A. Van Allan, *Tetrahedron*, **29**, 795 (1973).

[27] R. Hoffmann, A. Imamura and G. D. Zeiss, *J. Amer. Chem. Soc.*, **89**, 5215 (1967); see also ref. 30.

RESULTS AND DISCUSSIONS

A. ELECTRON DENSITIES

The introduction into a benzene ring of a highly electronegative atom $-\overset{+}{O}=$ as in pyrylium, **7**, in the place of $-CH=$ group, will determine a marked charge redistribution, which results from the composite polarization of the σ-skeleton and of the π-system.

Two aspects regarding charge distribution are worth mentioning. The first is related to the electron density of the pyrylium oxygen heteroatom which appears to be dependent of parametrization. According to Martensson and Warren,[13] or Decoret *et al.*,[16] within the CNDO-2 approximations, and to Palmer *et al.*[18] using non-empirical calculations, there is a slightly negative charge on oxygen, while CNDO-S results [16] predict a slightly positive charge on the oxygen. In all π-procedures published so far, the oxygen atom, however, carries a positive charge. Our results (see Table 1) yield the same conclusion, namely that the oxygen has a positive charge.

Secondly, although it is generally agreed that the charges of C_α and C_γ are positive, while the charge on C_β is either slightly positive or slightly negative, two features are generating conflicting views. One of these concerns the actual magnitude of charges on the carbon atoms, a question which still requires a careful study of the system, while the second, probably more easily soluble, regards the relative charge of C_α and C_γ.

Our calculations (see Table 1), suggest a higher positive charge on C_α (and $C_{\alpha'}$) than on C_γ, contrary to some reports which according to charge-iterative [11] or noniteratve [16] PPP calculations suggest a reverse order. The charge on C_β according to the present calculations is negative.

The present results, namely a higher positive charge on C_α than on C_γ and a higher electron density on C_β than on C_α and C_γ, are very nicely supported by the ^{13}C-NMR spectra of pyrylium salts.[19,20] Thus, the present

Table 1

Electron density distribution in the heterocyclic part from 2, 4, 6-trisubstituted pyrylium cation (7)*

Comp.	Rα	Rγ	Rα′	Observation	O^+	C_α	C_β	C_γ	$C_{\beta'}$	$C_{\alpha'}$
1	H	H	H	—	1.699	0.624	1.133	0.788	1.133	0.624
				methyl as heteroatom	1.782	0.623	1.262	0.769	1.262	0.623
2	CH_3	CH_3	CH_3	methyl hyperconjugative	1.738	0.611	1.186	0.769	1.186	0.611
3	H	C_6H_5	H	coplanar	1.709	0.629	1.150	0.776	1.150	0.629
4	CH_3	C_6H_5	CH_3	coplanar	1.774	0.627	1.225	0.795	1.225	0.627
5	CH_3	CH_3	C_6H_5	coplanar	1.767	0.646	1.208	0.771	1.247	0.616
6	C_6H_5	C_6H_5	C_6H_5	coplanar	1.740	0.643	1.159	0.795	1.159	0.643

* For compounds **4** and **5**, the methyl was considered as a heteroatom.

calculations predict the ordering of the chemical shifts of ^{13}C : $\delta_\alpha > \delta_\gamma > \delta_\beta$ identical with the observed order from experimental spectra (see Table 2) Moreover, the same order for charge distribution was observed for ^{1}H-NMR chemical shifts [28] of the parent system. The charge densities of the carbon atoms belonging to the phenyl ring attached to C_α and C_γ, partly do not correlate with the observed ^{13}C chemical shifts, for example from 2,4,6-triphenylpyrylium cation. Our simplified model regarding both the mechanism of the ^{13}C chemical shift, as resulted only from the charge distribution, and some particularities proper to the NMR spectroscopy, are responsible for the lack of correlation charge — ^{13}C NMR chemical shifts of the carbon atoms from the phenyl ring.

Table 2

^{13}C-chemical shifts [19,20] of some pyrylium derivatives 7 (ppm relative to internal TMS)

Comp.	R_α	R_γ	$R_{\alpha'}$	C_α	C_β	C_γ
1	H	H	H	169.32	127.24	161.21
2	CH_3	CH_3	CH_3	180.15	124.88	177.20
4	CH_3	C_6H_5	CH_3	181.15	120.62	171.08
6	C_6H_5	C_6H_5	C_6H_5	173.41	115.88	169.13

The calculations of charge densities were performed assuming static conformations which perforce lead to non-equivalence of *ortho* and *meta* positions of phenyl rings bonded to pyrylium α-sites. However, the time scale of ^{13}C-NMR spectra is long enough for the phenyl groups to behave as if they rotate freely determining an "effective" equivalence of *ortho* and *meta* positions. Therefore the ^{13}C-NMR chemical shifts will reflect a charge distribution in the phenyl rings which will probably be approximated better* by an average of nearly planar conformations than by the orthogonal conformation (which, as expected, gives automatically equivalent charges in *o*- and *m*-positions).

B. BOND ORDERS

The ground state bond orders of the pyrylium ring for compounds **1**—**6** are presented in Table 3. Though we have carried out the calculations on an idealized geometry (hexagonal) for the pyrylium ring, the bond orders could be correlated qualitatively with the geometry obtained for 3-acetoxy-2,4,6-trimethylpyrylium[21] and 2,4,6-triphenylpyrylium.[22] An inspection of bond orders reveals that the shortest bond in the parent compound is the bond C_2-C_3, while in the substituted compounds **2**—**6**, it seems that the shortest bond is the bond C_3-C_4. For the parent compound, there is no experimental evidence regarding its geometry, therefore we compare our results only with the two reported geometries for the compounds mentioned above. One may note that the relative bond lengths in the two known geometries of the pyrylium rings are different. In the case of triphenylpyrylium cation [22] the longest bond is C_3-C_4, while in 3-acetoxy-2,4,6-trimethylpyrylium [21] the longest bond is C_2-C_3. Our results are related qualitatively with the former experimental evidence.

---

* This is justified by a simplified model which assumes lower energies for those nearly planar conformations which have maximal conjugative interactions and tolerable steric repulsions of *ortho* hydrogens; under this assumption, residence times in the extremes of the oscillating phenyl groups will be large enough to prevail over all other conformations.

[28] A. T. Balaban, G. R. Bedford and A. R. Katritzky, *J. Chem. Soc.*, **1964**, 1646.

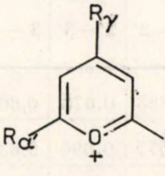

7

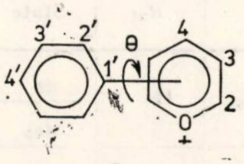

8

For phenyl-substituted pyrylium **8**, Table 3 presents the bond orders of two extreme conformations: the coplanar and the orthogonal conformations. Note that the trend in the geometry of the heterocyclic ring as discussed above seems to be independent of the inter-ring rotational angle θ.

An interesting feature in the bond order diagram of a pyrylium system is the existence of a relatively high C_2-C_4 bond order, which for example in the parent compound is 0.214. The same bond order becomes antibonding in the first excited state, and has magnitude −0.079.

Table 3

Ground-state bond orders in the pyrylium ring 8

Comp.	*Rα*	*Rγ′*	*Rα*	Observations	1−2	2−3	3−4	4−5	5−6	1−6
1	H	H	H	—	0.469	0.632	0.706	0.706	0.632	0.468
				methyl as heteroatom	0.393	0.671	0.600	0.600	0.671	0.393
2	CH_3	CH_3	CH_3	methyl-hyper conjugative	0.431	0.684	0.612	0.612	0.684	0.431
				θ = 0°	0.458	0.720	0.599	0.599	0.720	0.458
3	H	C_6H_5	H	θ = 90°	0.468	0.707	0.631	0.631	0.707	0.468
				θ = 0°	0.400	0.661	0.613	0.613	0.661	0.400
4	CH_3	C_6H_5	CH_3	θ = 90°	0.405	0.651	0.642	0.642	0.651	0.405
				θ = 0°	0.398	0.709	0.574	0.620	0.654	0.409
5	CH_3	CH_3	C_6H_5							
				θ = 90°	0.418	0.756	0.552	0.634	0.646	0.416
6	C_6H_5	C_6H_5	C_6H_5	coplanar	0.423	0.681	0.607	0.607	0.681	0.423

Concerning the bond orders in the phenly groups, they have in all conformations virtually the same values, all equal with one another, indicating that the hexagonal geometry is still valid. In the first excited state of **8**, however, $C'_2 - C'_3$ bonds are strengthened while $C'_1 - C'_2$ and $C'_3 - C'_4$ bonds are weakened.

In the ground state of α- or γ-phenylpyrylium, the inter-ring bond order is smaller than in the first excited state (see Table 5).

Table 4

Bond order diagram for the phenyl group in the ground state (gs) and first excited state (fes)

Comp.	R_α	R_γ	$R_{\alpha'}$	State	1′−2′	2′−3′	3′−4′	4′−5′	5′−6′	6′−1′
3	H	C_6H_5	H	gs	0.638	0.673	0.662	0.662	0.673	0.638
				fes	0.577	0.696	0.635	0.635	0.696	0.577
4	CH_3	C_6H_5	CH_3	gs	0.641	0.672	0.661	0.661	0.672	0.641
				fes	0.558	0.705	0.621	0.621	0.705	0.558
5	CH_3	CH_3	C_6H_5	gs	0.637	0.671	0.664	0.662	0.674	0.634
				fes	0.522	0.720	0.599	0.607	0.718	0.515
6	C_6H_5	C_6H_5	C_6H_5	α: gs	0.636	0.675	0.662	0.663	0.662	0.671
				α: fes	0.572	0.698	0.633	0.636	0.633	0.693
				γ: gs	0.639	0.673	0.662	0.662	0.673	0.639
				γ: fes	0.599	0.688	0.643	0.643	0.688	0.599

Table 5

Inter-ring bond order of phenyl-substituted pyrylium derivatives in the ground state and in the first excited state

Comp.	R_α	R_γ	$R_{\alpha'}$	ground state	first excited state
3	H	C_6H_5	H	0.280	0.404
4	CH_3	C_6H_5	CH_3	0.271	0.417
5	CH_3	CH_3	C_6H_5	0.295	0.489
6	C_6H_5	C_6H_5	C_6H_5	α : 0.300	0.403
				γ : 0.276	0.362

A relatively small inter-ring bond order in the ground state makes possible a rotation around the inter-ring bond, allowing phenylpyrylium cations **8** to take that conformation which represents a balance between electronic energies and pertinent steric repulsions. For biphenyl-like systems [22,29] (biphenyl, 4-phenyl-pyridine, 4-phenylpyridinium and 2,4,6-triphenylpyrylium) such an energetic balance, in which normally the electronic factor would impose a coplanar geometry, the steric factor is usually dominant and Van der Waals repulsions among the hydrogen atoms from *o*-, *o'*-positions [30] will determine a slight tilting of the two rings. The high inter-ring bond order, however, leads to a firm conclusion, that the conformation of phenylpyrylium **8** in the first excited state is planar (see also the discussion below on energetic aspects).

C. TRANSITION ENERGIES

The ground state of the parent pyrylium is $(b_2)^2(b_2)^2(a_2)^2$. The transition $a_2 \rightarrow b_2$ gives rise to state B_1, corresponding to the lowest energy transition, the next is a transition $a_2 \rightarrow a_2$ giving state A_1, followed by transitions $b_2 \rightarrow a_2$, and $a_2 \rightarrow b_2$ resulting in states B_1 and A_1, respectively (fig. 1).

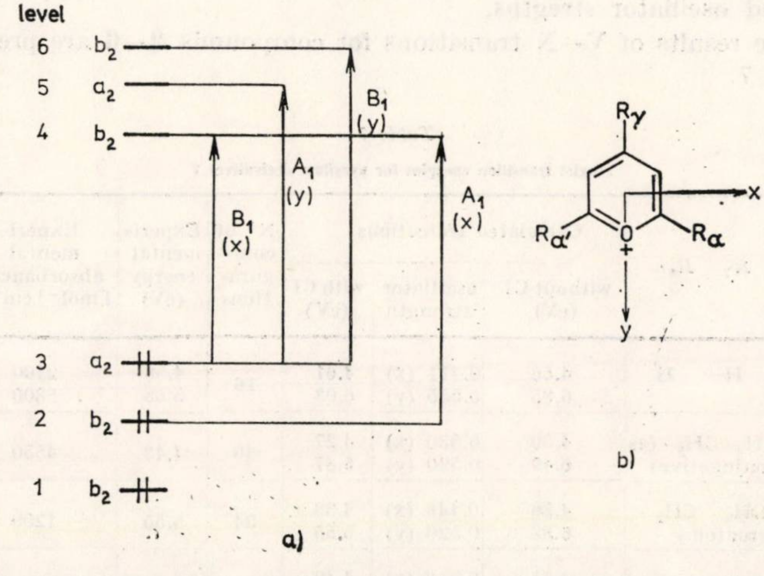

Fig. 1. a) Energy levels, electronic transitions and polarizations ; b) System of coordinates.

The UV spectrum of the parent pyrylium cation was reported [31] as possessing two bands, one at 4.5883 eV ($\varepsilon = 2100$ l mol^{-1} cm^{-1}) and a second at 5.651 eV ($\varepsilon = 8800$ l mol^{-1}cm^{-1}). The first calculated transition energy (seee Table 6) agrees quite well with the experimental value;

---

[29] A. Camerman, L. H. Jensen and A. T. Balaban, *Acta Cryst.* **B25**, 2623 (1969) ; see also R. Knorr, A. Weiss, H. Polzer and E. Bischler, *J. Amer. Chem. Soc.*, **97**, 644 (1975) and references cited therein.

[30] See for example the discussion in : A. Imamura and R. Hoffmann, *J. Amer. Chem. Soc.*, **90**, 5379 (1968).

[31] A. T. Balaban and C. D. Nenitzescu, *Izvest. Akad. Nauk S.S.S.R.*, *Otdel Khim. Nauk*, **1960**, 2064.

Table 6

Calculated UV spectrum of the unsubstituted pyrylium cation 1 (see fig. 1)

State	transition between levels	V←N (eV)	oscillator strength	polarization	*T←N* (eV)
B_1	3→4	4.565	0.411	x	3.048
A_1	3→5	6.853	0.555	y	4.862
B_1	2→4	7.022	0.585	y	5.116
A_1	3→6	7.882	0.050	x	6.650

the second transition was improved by using CI calculations (see also Table 7). Note the qualitative agreement of the experimental and the calculated oscillator stregths.

The results of V←N transitions for compounds **2**–**6** are presented in Table 7.

Table 7

Singlet transition energies for pyrylium derivatives 7

Comp.	R_α R_γ $R_{\alpha'}$	Calculated transitions			N° of configurations	Experimental energy (eV)	Experimental absorbance $\mathrm{l\,mol^{-1}\,cm^{-1}}$	Ref.
		without CI (eV)	oscillator strength	with CI (eV)				
1	H H H	4.56 6.85	0.411 (x) 0.555 (y)	4.61 6.03	16	4.58 5.68	2100 8800	4, 29
2	CH_3 CH_3 CH_3 (as hyperconjugative)	4.39 6.49	0.530 (x) 0.590 (y)	4.27 5.87	40	4.43	4550	4, 32
	CH_3 CH_3 CH_3 (as heteroatom)	4.36 6.33	0.448 (x) 0.520 (y)	4.33 5.55	34	5.55	1200	
3	H C_6H_5 H (coplanar)	4.75 5.50 6.31	0.310 (x) 1.036 (y) 0.230 (x)	4.49 5.12 5.230	40	3.67 4.46	23000 20000	4, 24
4	CH_3 C_6H_5 CH_3 (coplanar)	4.36 5.60	0.369 (x) 1.046 (y)	4.12 5.24	60	3.78 4.07	23100 20000	4
5	CH_3 CH_3 C_6H_5	4.38 6.27 6.30	0.767 (–) 0.011 (–) 0.416 (–)	4.18 5.21 5.52	60	3.59 5.07 5.45	24000 10220 11260	4, 24
6	C_6H_5 C_6H_5 C_6H_5	4.06 5.60 5.84	0.731 (x) 1.040 (y) 0.43 (y)	— — —	—	3.30 3.42 4.45	18000 30000 24500	4, 32

In the case of 2,4,6-trimethylpyrylium we have considered two models for the methyl group, one as a hyperconjugative group and the second as a heteroatom. Although both models gave reasonable agreement

---

[32] A. T. Balaban, V. E. Sahini and E. Keplinger, *Tetrahedron*, **9**, 163 (1960).

between the calculated transition energies and the experimental values, the heteroatom model seems to be, however, a better representation of the methyl group. The calculated oscillator direction agrees with the observed relative polarization.[17]

Table 8

Triplet transition energies (in eV) for pyrylium derivatives 7

Comp.	R_α R_γ $R_{\alpha'}$	Calculated transitions		Observed	Ref.
		without CI	with CI		
1	H H H	3.05 4.86 5.11	3.25 4.62 4.73	—	
2	CH_3 CH_3 CH_3 (hyperconjugative)	3.27 5.18 5.40	3.10 4.26 5.09	3.06 — —	17
2	CH_3 CH_3 CH_3 (as heteroatom)	3.22 4.78 5.27	3.23 4.33 4.54	3.06 —	17
3	H C_6H_5 H (coplanar)	3.61 4.55 4.56	3.27 3.98 4.73	—	—
4	CH_3 C_6H_5 CH_3 (coplanar)	3.40 4.53 4.67	—	—	—
5	CH_3 CH_3 C_6H_5 (coplanar)	3.53 5.32 5.40	—	—	—
6	C_6H_5 C_6H_5 C_6H_5 (coplanar)	3.36 4.96 5.11	—	4.50	21

Table 8 presents the results obtained for triplet transition energies Unfortunately, experimental values to serve as a test for our calculations are scarce. Note the good coincidence between the calculated and observed first band of 2,4,6,-trimethylpyrylium cation.[17]

D. GROUND AND EXCITED STATE CONFORMATION OF α- AND γ-PHENYLPYRYLIUM CATIONS

The conformation of biphenyl and heteroaromatic congeners is a subject of great interest.[29] While the experimental and theoretical data for biphenyl and its substituted derivatives are numerous, heteroaromatic analogues of biphenyl (with one or both rings heteroaromatic) are less ilustrated by experimental or theoretical observations. Thus the only information so far for the conformation of a phenylpyrylium is the X-ray structure determination of 2,4,6-triphenylpyrylium cation.[22]

The actual conformations of a biphenyl-like derivative is a delicate balance of electronic factors, steric requirements of the substituents from *o*- and *o'*-positions, and the pyhysical state of the compound under consideration (e.g. packing interactions in the crystal).

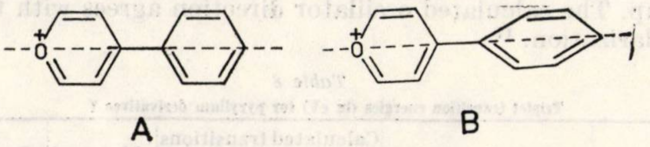

Here, we have considered only the electronic factors as determining the conformation of 4-phenylpyrylium **3**, 2,6-dimethyl-4-phenylpyrylium **4** and 2,4-dimethyl-6-phenylpyrylium **5**.

The ground state total energy in **8** has a minimum at the coplanar conformation of the two rings. As it is observed from our figures (Table 9) distorsion to angles up to 30–40 degrees leads to quite small energy increases, allowing presumably those states to be still populated (fig. 2).

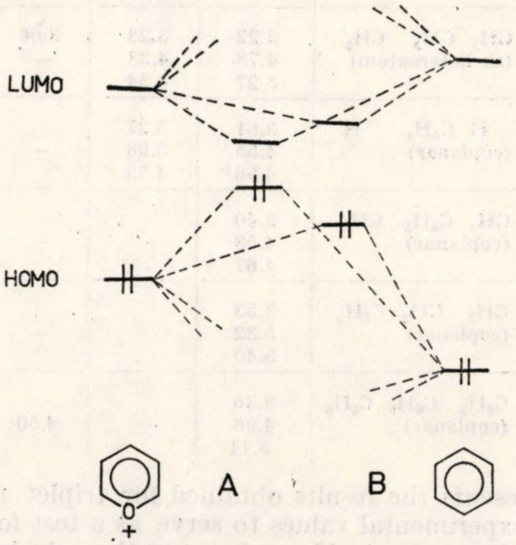

Fig. 2. — The dependence of ground state, first singlet and first triplet states *versus* the dihedral angle θ betwen the two rings in the case of 4-phenylpyrylium cation.

The only experimental evidence which supports our conclusions is the X-ray structure determination of the 2,4,6-triphenylpyrylium cation, in which the phenyl rings are found to be tilted with 2–18 degrees[22] (the γ phenyl having the highest angle).

For the first singlet and tripled states, according to our calculations, a coplanar conformation is predicted for compounds **3**, **4** and **5**. This conclusion resulted from both total energy considerations as well as from a comparison of transition energies with experimental values.

The total first singlet and triplet energies has a quite deep minimum for $\theta = 0°$. The best fit between experimental and theoretical transition energies is accomplished only for the coplanar conformations (see also Tables 8 and 9).

Table 9

The dependence of singlet-transition energies (in eV) in α- and γ-phenylsubstituted pyrylium cations *versus* the dihedral angle θ between the two rings

Comp.	R_α	R_γ	$R_{\alpha'}$	No of congfigurations	Dihedral angle θ between pyrylium and phenyl rings				
					0°	30°	45°	60°	90°
3	H	C_6H_5	H	1	4.75 5.50 6.31	4.76 5.74 6.44	4.74 6.01 6.58	4.69 6.35 6.76	4.59 6.80 6.97
				40	4.49 5.12 5.23	4.52 5.28 5.29	4.54 5.34 5.48	4.56 5.40 5.70	4.58 5.46 5.93
4	CH_3	C_6H_5	CH_3	1	4.37 5.60 6.27	4.41 5.87 6.25	4.43 6.18 6.24	4.40 6.60 6.24	4.20 6.23 7.37
				60	4.02 5.24 5.27	4.17 5.32 5.43	4.21 5.38 5.62	4.26 5.46 5.82	5.31 6.00 7.29
5	CH_3	CH_3	C_6H_5	1	4.38 6.27 6.30	4.48 6.47 6.49	4.56 6.70 6.75	4.62 7.20 6.94	4.54 7.85 7.78
				60	4.08 5.51 5.41	4.18 5.22 5.53	4.29 5.29 5.65	4.42 5.39 5.79	4.62 5.56 5.87

E. FRONTIER ORBITALS OF PHENYL-SUBSTITUTED PYRYLIUM

Rotation around the inter-ring bond lowers the energy of the highest occupied molecular orbital (HOMO) on going from the coplanar towards the orthogonal conformation of the rings. The lowest unoccupied molecular orbital (LUMO) in the same range of rotation is destabilized. The understanding of the results follows the same line of reasoning as discussed by Hoffmann and Imamura [22] for their interpretation of conjugation and spiroconjugation for biphenyl and related systems. Consider the two extreme conformations of a 4-phenylpyrylium **3** : *A*, coplanar, and *B*, orthogonal.

The frontier orbitals of the pyrylium cation are both of S symmetry with respect to the symmetry plane of the pyrylium nucleus, and have a higher energy than the corresponding orbitals of benzene for HOMO, and lower energy for LUMO, respectively. Thus the frontier π-orbitals of 4-phenylpyrylium are esentially of pyrylium provenience. A strong interaction between the two rings will destabilize HOMO and stabilize LUMO. A weaker interaction between the two rings will bring the frontier orbitals of 4-phenylpyrylium towards the frontier orbitals of a pyrylium cation. Some typical figures are presented in Table 10.

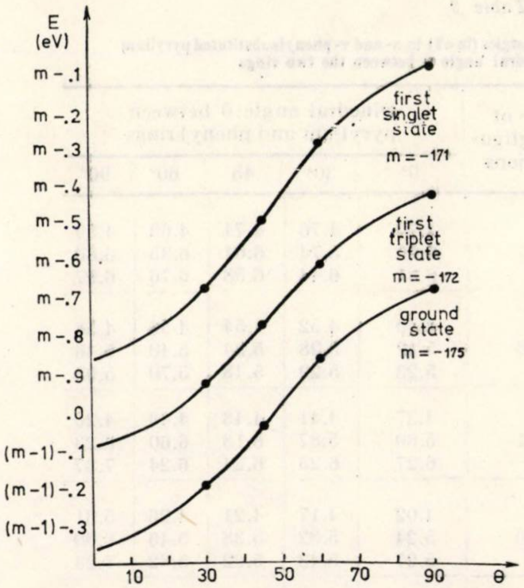

Fig. 3. — Interaction diagram between π-HOMO and LUMO energy levels of pyrylium and phenyl rings: A, strong interaction (coplanar system); B, weak interaction (orthogonal conformation).

Table 10

Frontier orbitals, total energy (or relative energy in respect to coplanar geometry) and electronic energy (in eV)

Comp.	R_α	R_γ	$R_{\alpha'}$	rotation angle θ	HOMO	LUMO	electron energy (relative electron energy)	total energy (relative total energy)
1	H	H	H	—	− 10.96	− 1.00	− 487.36 (0)	− 175.36 (0)
2	Me as hyperconj.	Me	Me		− 9.118	0.142	− 494.60 (0)	− 194.85 (0)
2	Me as heteroatom	Me	Me	—	− 9.282	0.292	− 512.67 (0)	− 208.51 (0)
3	H	Ph	H	0	− 10.816	− 1.290	(0)	(0)
				30	− 10.844	− 1.207	(0.029)	(0.154)
				45	− 10.869	− 1.126	(0.367)	(0.318)
				60	− 10.894	− 1.024	(0.716)	(0.492)
				90	− 10.919	− 0.958	(1.074)	(0.572)
4	Me	Ph	Me	0	− 9.320	− 0.620	(0)	(0)
				30	− 9.335	− 0.511	(0.363)	(0.149)
				45	− 9.349	− 0.393	(0.744)	(0.309)
				60	− 9.363	− 0.260	(0.972)	(0.457)
				90	− 9.377	− 0.092	(1.536)	(0.650)
5	Me	Me	Ph	0	− 9.357	− 0.435	(0)	(0)
				30	− 9.485	− 0.362	(0.403)	(0.174)
				45	− 9.626	− 0.293	(0.822)	(0.363)
				60	− 9.793	− 0.229	(1.079)	(0.531)
				90	− 10.017	− 0.171	(1.675)	(0.749)
6	Ph	Ph	Ph	0	− 9.411	− 1.318	—	− 342.26

CONCLUDING REMARKS

The charge distribution in the pyrylium ring, with decreasing positive charges $C_\alpha > C_\gamma > C_\beta$, found by SCF-PPP-CI calculations, is supported by ^{13}C-NMR spectroscopy observations. The transition energies giving rise to singlet states, obtained in our calculation, correlate satisfactorily with the experimentally observed transition bands. The values of transitions to triplet states (for those compounds for which they were reported up till now in the literature), are virtually identical with the calculated values. Based on π-electronic energies only, we conclude that the coplanar or slightly distorted conformation of phenylpyrylium represents the conformation of the ground state, while the excited states must have strictly coplanar conformations.

Acknowledgement. M. G. expresses his gratitude to Prof. R. Hoffmann (Cornell University Ithaca, New York) for providing a stimnlating environment and for a generous offer of computation time enabling this work to be started.

APPENDIX

The geometries of pyrylium ring and benzene were assumed as being regular hexagonal with all bond lengths equal to 1.397 Å. The inter-ring distance was considered as equal to 1.484, while the methyl-to--pyrylium distance was taken as equal to 1.484 Å.

The following valence state ionization potentials (in eV), one-center integrals (in eV) and Slater exponents were used : C : −11.16, 11.13, 1.625 ; $\overset{+}{O}$: −20.17, 15.23, 2.45 ; CH_3 (heteroatom) : −13.12, 11.67, 1.625 ; CH_3 (hyperconjugative, for the corresponding C and H_3 of a pseudovinyl group) : −14.61, −8.80, 11.67, 8.43, 1.625, 1.28.

Revue Roumaine de Chimie, **21**, *11–12*, 1527–1535 (1976)

ELIMINATION REACTIONS IN THE 8-SUBSTITUTED TRICYCLO[7.3.1.$0^{2,7}$]TRIDECANE SERIES. VII[1]

PYROLYTIC ELIMINATION OF 8-METHYL-TRICYCLO-[7.3.1.$0^{2,7}$]TRIDECEN-13-ACETATES

N. S. BĂRBULESCU* and MINODORA LECA **

* Polytechnic Institute of Bucharest, Institute of Chemistry, Chemistry Department, Organic Chemistry Laboratory, Splaiul Independenţei 89

** Polytechnic Institute of Bucharest, Institute of Chemistry, Chemistry Department, Macromolecular Chemistry Laboratory, Bulevardul Republicii 13.

Received December 20, 1974

The pyrolytic elimination of 8-methyl-tricyclo [7.3.1.$0^{2,7}$] tridecen-13-acetates (IIa, b) at 490° has been studied and found to follow the ion-pair mechanism given for tricyclo-[7.3.1.$0^{2,7}$]-tridec-2-en-13-acetate (I). The structure of pyrolytic elimination products has been established on the basis of NMR and IR spectra and retention times on carbowax 20M chromatographic column.

INTRODUCTION

Organic esters undergo elimination on heating at elevated temperature (300–500°), with no other reagent present. Since rearrangement and other side reactions are few, the reaction is synthetically very useful and is often carried out as an indirect method of accomplishing the dehydration of alcohols. The yields are excellent, and the work-up is easy. Many olefins have been prepared in this manner. [2,3] For higher olefins (above C_{10}) a better method is to pyrolyse the alcohol in the presence of acetic anhydride. [4]

The mechanism of such reactions is obviously different from those of the elimination reactions in solution.

Three mechanisms have been suggested for the pyrolytic eliminations of acetates [3,5]: the six-membered ring concerted mechanism *Ei*[6] – observed for most acetates,[7] the ion-pair mechanism[8] —demonstrated for 1-arylethyl and 1,2-diarylethyl acetates,[9-11] and the free radical mechanism — proved for allylic acetates and their derivatives.[5,12]

---

[1] Part. VI: N. S. BĂRBULESCU and M. LECA, *Rev. Roumaine Chim.*, in press.

[2] S. PATAI, "The Chemistry of Alkenes", Interscience Publishers, Inc., New York 1964, p. 149.

[3] J. MARCH, "Advanced Organic Chemistry: Reactions, Mechanisms, and Structure", McGraw-Hill Book Company, 1968, p. 747.

[4] D. W. AUBREY, A. BARNATT and W. GERRARD, *Chem. Ind. (London)*, **1965**, 681.

[5] F. H. RUMMENS, *Rec. Trav. chim.*, **83**, 901 (1964).

[6] C. D. HURD and F. H. BLUNCK, *J. Amer. Chem. Soc.*, **60**, 2419 (1938.)

The existence of isomers and orientation according to the Zaitsev rule[13] are indications of an ion-pair mechanism.

As the products formed in pyropytic eliminations often differ appreciably in composition from those formed in other types of eliminations, 8-methyl-tricyclo[7.3.1.$0^{2,7}$]tridecen-13-acetates have been subjected to pyrolytic elimination reaction. The present work deals with the structure of pyrolytic elimination products and the reaction mechanism.

RESULTS AND DISCUSSION

The pyrolytic eliminations of bicyclic [n.m.1] acetates with the acetate group in one-membered bridge were not studied. Their eliminations are of particular interest in relation to both reaction mechanism — which must be different from *Ei* — and the structure of the resulted products — different from those formed in eliminations in solution.

The pyrolytic elimination of tricyclo[7.3.1.$0^{2,7}$]tridec-2-en-13-acetate (I) has been studied in an earlier work,[14] such kind of eliminaton reactions presenting theoretical and — maybe — practical interest, and an ion-pair mechanism was suggested. To verify this mechanism, the pyrolytic elimination of 8-methyl-tricyclo[7.3.1.$0^{2,7}$]tridecen-13-acetates (IIa, b) has been studied in the present work.

The unsaturated acetates IIa, b were obtained by dehydration of 8-methyl-tricyclo[7.3.1.$0^{2,7}$]tridecan-2,13-diol (III) using zinc chloride and acetic anhydride.[15] They can be separated on a carbowax 2OM analytical chromatographic column, the ratio IIb : IIa being 5,5 : 1.[16] The preparative separation could not be performed due to the poor resolution of the preparative column.

Bredt's rule[17] applies in pyrolytic eliminations of bridged bicyclic compounds as in the *E1—E2—E1cB* mechanistic spectrum. Bredt's rule, reformulated by Wiseman[18] predicts isolable bicyclic bridgehead alkenes when the larger of the two rings containing the double bond has at least eight atoms. The elimination of the acetate group from C_{13} carbon atom of I and IIa, b would lead to the introduction of a trans-double bond in a six-membered ring. Thus, the elimination of this group cannot occur without the isomerization of the bridged bicyclic system.

[7] C. H. DePuy and R. W. King, *Chem. Rev.*, **60**, 431 (1960).

[8] A. Maccol, *J. Chem. Soc.*, **1958**, 3398.

[9] G. G . Smith, F. D. Bagley and R. Taylor, *J. Amer. Chem. Soc.*, **83**, 3647 (1961).

[10] R. Taylor, G. G. Smith and W. H. Wetzel, *J. Amer. Chem. Soc.*, **84**, 4817 (1962).

[11] G. G. Smith, K. A. K. Jones and D. F. Brown, *J. Org. Chem.*, **28**, 403 (1963).

[12] R. Low and E. C. Kooyman, *Rec. Trav. chim.*, **84**, 1511 (1965).

[13] K. G. Rutherford and D. P. C. Fung, *Canad. J. Chem.*, **42**, 2657 (1964).

[14] N. Bărbulescu and M. Leca, *Rev. Roumaine Chim.*, **19**, 443 (1974).

[15] N. Bărbulescu and M. Leca, *Rev. Roumaine Chim.*, **19**, 233 (1974).

[16] M. Leca, "Reacţii de eliminare în clasa 8-R-tricyclo[7.3.1.$0^{2,7}$]tridecanului", Thesis, Bucharest, 1973.

[17] J. Bredt, *Liebigs Ann. Chem.*, **437**, 1 (1924).

[18] J. P. Wiseman, *J. Amer. Chem. Soc.*, **89**, 5966 (1967).

Dehydration and acetylation of diol III can be explained by the mechanism given above [15] :

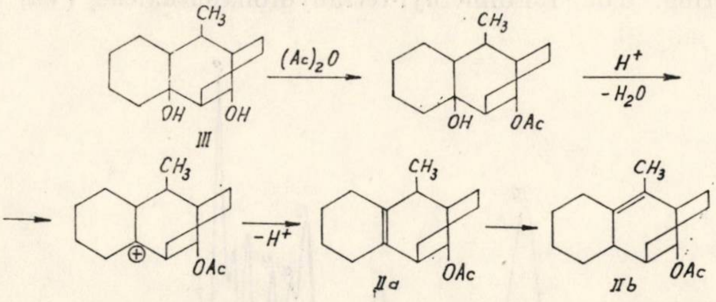

The larger quantity of acetate IIb is due to the hyperconjugation effect, which makes acetate IIb more stable than IIa.

The NMR spectrum of the acetates IIa, b mixture allows to establish the position of the double bond [15] but does not permit to determine the position of the acetate group.

The coupling constant magnitude of the proton geminal to acetate group[19–21] cannot be used to assign the configuration, the dihedral angles being almost equal, as Dreiding models show. Neither is the half width of this signal [22] of use because of the conformational modifications generated by the introduction of the double bond. Since the alkaline hydrolysis of the acetates I and IIa, b results only in *endo*-alcohols [23] one may conclude that they are *endo*.

8-Methyl-tricyclo $[7.3.1.0^{2,7}]$ tridecen-13-acetates IIa, b have been subjected to pyrolytic elimination in flow system at 490°, giving a very complex mixture of products. This mixture is difficult to separate even on analytical chromatographic columns. The best resolution was obtained using a 5m long and 6 mm o.d. chromatographic column, having 12% carbowax 2OM on celite C_{22} 60–80 mesh as packing material (Figure 1). The chromatogram shows 19 peaks. It is impossible to establish the base line, therefore their concentrations cannot be calculated from the chromatogram.

The resolution was poorer on preparative columns. The following peaks were collected : 9, 11, 14 and 15, 17 and 18 and finally 19, but only some of them were pure enough to allow the determination of the structure on the basis of NMR and IR spectra and retention times.

The peak 9 gave a NMR spectrum very similar to that of β-methyltetrahydronaphthalene (IV) [14] (Figure 2), but the ratio between the aromatic and aliphatic protons was 1 : 7. The IR spectrum of the peak 9

---

[19] D. W. Mathieson, "NMR for Organic Chemists", Academic Press, London 1967, p. 138.

[10] L. M. Jackman and S. Sternhell, "Application of NMR Spectroscopy in Organic Chemistry", Pergamon Press, London, 1969, p. 280.

[21] F. A. Bovey, "NMR Spectroscopy", Academic Press, New York 1969, p. 132.

[22] A. Hassner and C. Heathcock, *J. Org. Chem.*, **29**, 1350 (1964).

[23] N. Bărbulescu and M. Leca, *Rev. Roumaine Chim.*, **19**, 1381 (1974).

did not exhibit the 829 cm^{-1} band of the hydrocarbon IV, but there were bands at 883, 864 and 860 cm^{-1} indicating isolated hydrogen atoms in benzene ring. The 1,3-dimethyl-tetrahydronaphthalene (Va) structure was assigned to peak 9 on the basis of the ratio between aromatic and aliphatic protons, the NMR signals and IR bands.

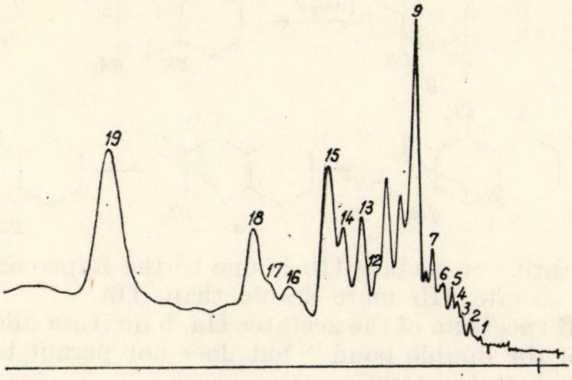

Fig. 1. — Chromatogram of pyrolytic elimination products of the acetates IIa, b, at 490° on carbowax 20M.

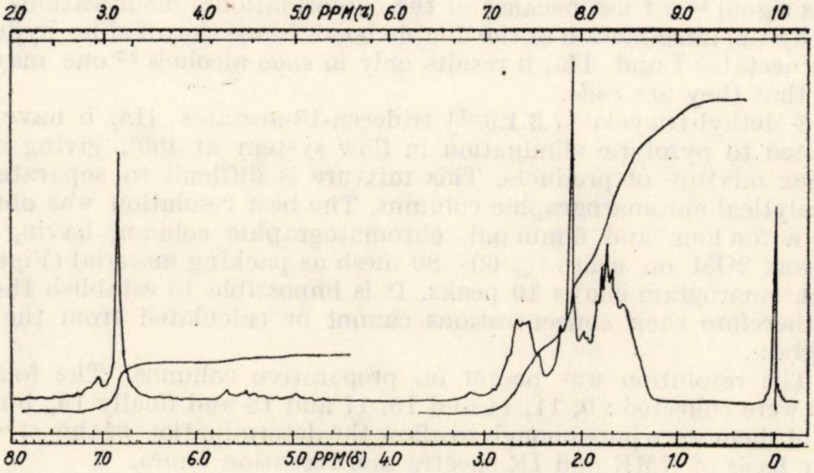

Fig. 2. — NMR spectrum of the peak 9.

The peak 11 was not pure enough even after refractionation. The NMR spectrum shows the presence of the tetrahydronaphthalene skeleton and a doublet (or possibly two singlets) centered at $\delta = 2.16$ ppm, assigned to CH_3-Ar system. The ratio between aromatic and aliphatic protons was again : 1 : 7. The IR spectrum exhibited a band at 852 cm^{-1}, indicating some vicinal hydrogen atoms in the aromatic ring. This compound might be 1,2- or 1,4-dimethyl-tetrahydronaphthalene (Vb, 2c).

The peak 15 was not collected alone, being accompanied by peak 14. The NMR spectrum of this mixture looks like that of β-propyl-tetrahydronaphthalene (VI) [14] (Figure 3), but there was an extra singlet at $\delta = 2.12$ ppm assigned to a methyl group attached to aromatic ring. The IR spectrum exhibited a weak band at 829 cm^{-1}, showing neighbouring aromatic hydrogen atoms. This structure corresponds to the two isomers of tetrahydronaphthalene substituted 1,2 or 1,4 in aromatic ring with methyl and propyl (VIIa, b).

The peaks 17 and 18 were collected together, and the NMR spectrum is similar with that of the 3,4-tetrahydrobenzindane (VIII) and 2,3-tetrahydrobenzindane (IX) mixture [14,15] (Figure 4).

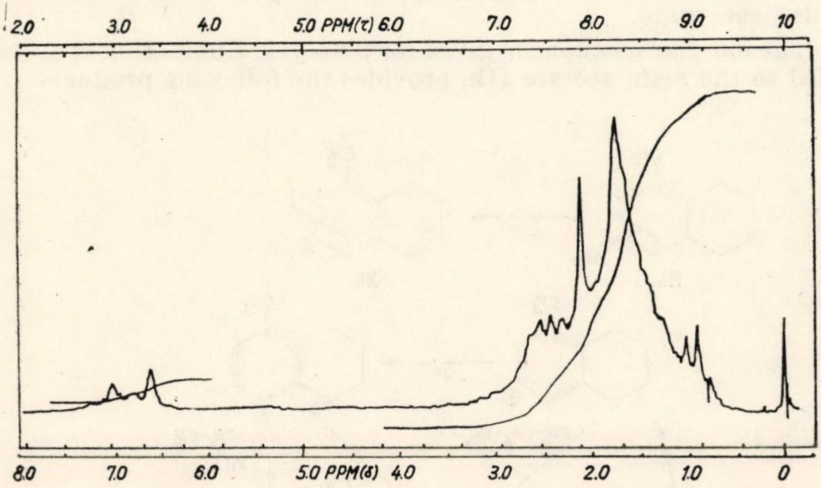

Fig. 3. — NMR spectrum of the peaks 14 + 15.

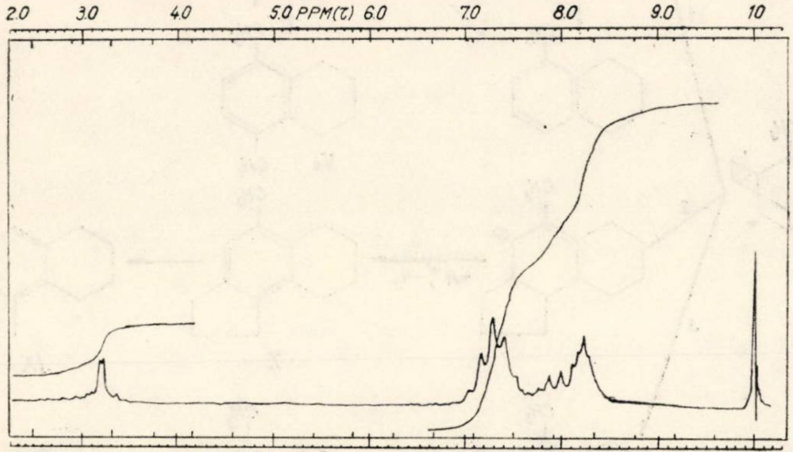

Fig. 4. — NMR spectrum of the peaks 17 + 18.

The concentration of 2,3-tetrahydrobenzindane (peak 18) prevailing, the signals of aromatic protons were distinct. A strong band at 833 cm^{-1} appeared in the IR spectrum of the mixture for the two neighbouring aromatic hydrogen atoms of IX and two weak bands at 882 and 865 cm^{-1} for the isolated aromatic hydrogen atoms of VIII. The retention times of the peaks 17 and 18 on columns having different length and stationary phase concentration were identical with those of the hydrocarbon VIII and IX, respectively.

The NMR spectrum of the peak 19 is identical with that of the 4-methyl-tetrahydro-2,3-benzindane (X) and 5-methyl-tetrahydro-3,4-benzindane (XI) mixture[14,15] (Figure 5); the IR spectra and retention times are also the same.

The ion-pair mechanism given for pyrolytic elimination of acetate I,[14] applied to the main acetate IIb, provides the following products :

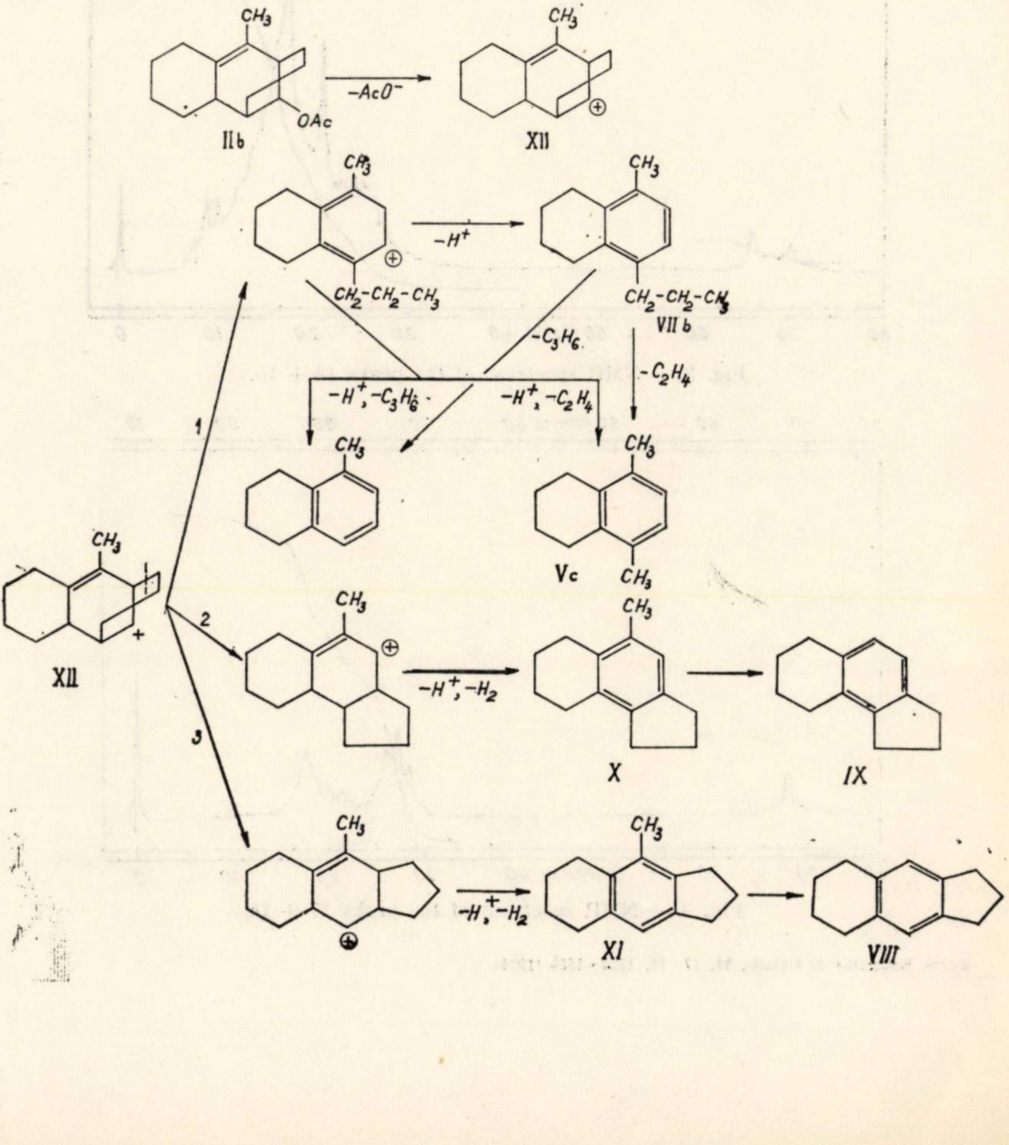
CH3
OAc
IIb
-AcO⁻
CH3
XII
CH3
CH2-CH2-CH3
-H+
CH3
CH2-CH2-CH3
VII b
-C3H6
-H+, -C3H6
-H+, -C2H4
-C2H4
CH3
CH3
Vc
CH3
1
CH3
XII
2
3
CH3
-H+, -H2
CH3
X
IX
CH3
-H+, -H2
CH3
XI
VIII

The mechanism explains the formation of hydrocarbons : Vc, VIIb, X and XI. Following the same scheme, the acetate IIa gives on pyrolytic elimination the hydrocarbons Vb, VIIa, X and XI. The thermal cracking of hydrocarbons X and XI accounts for the hydrocarbons VIII and IX.

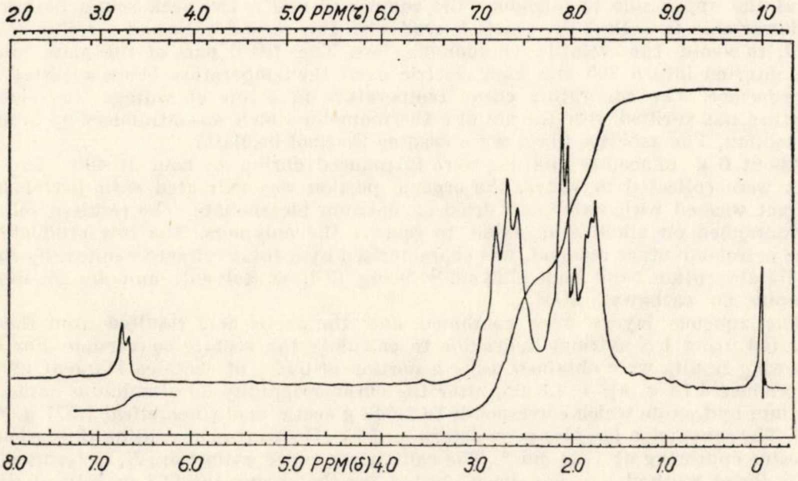

Fig. 5. — NMR spectrum of the peak 19.

The given reaction mechanism is therefore verified for the pyrolytic elimination of acetates IIa, b.

The chromatogram superposition with that of tetrahydronaphthalene — recorded in the same conditions — and the introduction of tetrahydronaphthalene in the elimination products demonstrate that peak 5 is tetrahydronaphthalene.

The large number of peaks having low concentrations, observed on chromatogram, arise from heterogenous decomposition which could not be eliminated completely in the reaction conditions used, even with acclimatized vessel.

CONCLUSIONS

The pyrolytic elimination of 8-methyl-tricyclo[7.3.1.$0^{2,7}$]tridecen-13-acetates (IIa, b) supports the ion-pair mechanisms suggested for pyrolytic elimination of tricyclo[7.3.1.$0^{2,7}$]tridec-2-en-13-acetate (I), supplemented with the thermal cracking of the alkyl-aromatic intermediates. This mechanism is also supported by the reaction products common with those resulted from alcohol III dehydration using zinc chloride, which follows an ionic mechanism too.

EXPERIMENTAL PART

The preparation of 8-methyl-tricyclo[$7.3.1.0^{2,7}$]*tridecen-13-acetates* (IIa, b) has been described in an earlier paper. [15]

Pyrolytic elimination of 8-methyl-tricyclo[$7.3.1.0^{2,7}$]*tridecen-13-acetates* (IIa, b). The equipment for pyrolytic elimination of acetates IIa, b consisted of a 245 mm vertical Rasotherm tube, 28 mm in diameter, filled with 205 mm high porcelain bits, equipped with a separating funnel at the upper side to introduce the compound and a two-neck round bottomed flask at the lower side to collect the reaction products. The second neck had a reflux refrigerator attached, to avoid the volatile compounds loss. The filled part of the glass column was entirely inserted into a 205 mm high electric oven, the temperature being adjusted using an autotransformer. The calibrating curve temperature in terms of voltage was plotted. The temperature was verified with the aid of a thermometer which was introduced up to the middle of the column. The asbestos fibres were used as thermal insulator.

About 6 g of acetate mixture were introduced during an hour at 490°. The reaction products were collected in water, the organic portion was extracted with petroleum ether, the extract washed with water and dried on natrium bicarbonate. The resulted solution was chromatographed on aluminium oxide to remove the polymers. The row product, resulted after the petroleum ether removal, was characterized by a total refractive index, by the height of the IR absorption band from 1723 cm^{-1} using CCl_4 as solvent, and by gas-liquid chromatography on carbowax 2OM.

The aqueous layers were combined and the acetic acid resulted from the reaction was titrated using 1 N natrium hydroxide to calculate the acetate conversion. For example, the following results were obtained using a portion of 6.52 g of acetates IIa, b at 490° : elimination product 4.15 g, $n_D^{20} = 1.5495$, after the chromatography on aluminium oxide, 25.8 ml 1 N natrium hydroxide which corresponds to 1.548 g acetic acid (theoretical 1.577 g, 88% conversion). The conversion has also been determined by IR spectroscopy, using the carbonyl band of the ester appearing at 1723 cm^{-1}. The calibrating curve extinction, E, in terms of concentration — Pirlot method [24] — has been plotted for that, using the CCl_4 as solvent (Figure 6).

The results are in good agreement with those obtained from acetic acid titration (Table 1).

The unsaturated acetates can be removed by careful elution with petroleum ether on aluminium oxide column.

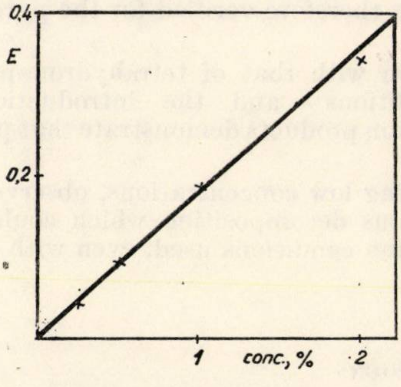

Fig. 6. — Calibrating curve extinction, E, in terms of concentration.

Analytical chromatography has been performed by employing a Becker 401 type gas-liquid chromatograph, using a 6 mm o.d. cooper column, 5 m in length. Packing material was 12% Carbowax 2OM on 60—80 mesh celite C_{22}. The flame ionization detector was used, with nitrogen as carrier gas. The conditions were as follows :

injection temperature	260°
column temperature	210°
detector temperature	280°
gas flow rate	45 ml/min
injected quantity	1—1.5 μl.

---

[24] D. Bîrcă-Gălăţeanu, M. Giurgea, I. Iova, V. Sahini, A. Truţia and R. Ţiţeica, "Introducere în spectroscopia experimentală", Editura Tehnică, Bucureşti, 1966, p. 224.

The pyrolytic elimination products chromatogram of the above example, after the acetates removal, consists of 19 peaks (Figure 1).

Preparative chromatography was carried out on a Carlo Erba GT type chromatograph by employing a 10 mm o.d. stainless steel column, 2 m in length and 20% carbowax 2OM on 30–60 mesh chromosorb W as packing material. The thermal conductivity detector was used with hydrogen as carrier gas. The conditions were:

Table 1

The degree of conversion obtained for pyrolytic elimination of acetates IIa, b by acetic acid titration and IR spectroscopy

n_D^{20} of the elimination products	Conversion, %	
	AcOH titration	$E = f(c)$
1.5381	64.00	63.72
1.5495	90.20	94.77
1.5515	92.10	95.77
1.5535	92.40	96.45

injection temperature	290°
column temperature	195°
detector temperature	280°
hydrogen flow rate	640 ml/min
auxiliary gas flow rate	60 ml/min
injected quantity	160 μl.

The purity of the collected samples was checked using a 4 mm o.d. stainless steel column, 2 m in length and 20% Carbowax 2OM on 60–80 mesh chromosorb W as packing material, on an analytical Carlo Erba GT chromatograph in the following conditions:

injection temperature	260°
column temperature	115–190°, 3°/min programing
detector temperature	270°
nitrogen flow rate	25 ml/min
injected quantity	0.2–0.3 μl.

The main characteristics of the collected samples, for which structural assignements were made, are given in Table 2.

Table 2

The main characteristics of the collected samples and the structural assignements

Peak	9	14 + 11	17 + 18	19
NMR signals δ (ppm)	1.75 (c) J=3; 2.13 (s); 2.40–3.00; 6.80	1.75 (m); 2.12 (s); 2.20 (s); 2.39–2.98; 6.62–6.80	1.75 (m); 2.69 (c) J=7.3 Hz; 6.75 (s); 6.78(s)	1.75 (m); 2.04 (s); 2.10(s); 2.67(c) J=7.5 Hz; 6.66 (s); 6.72 (s)
IR bands, cm^{-1}	883, 864, 860	829	882, 865, 833	887, 867
Structure	Va	VIIa, b	VIII + IX	X + XI

Revue Roumaine de Chimie, **21**, *11–12*, 1537–1541 (1976)

AMORPHOUS-CRYSTALLINE COUPLING IN POLYETHYLENE. IV[1]

EARTH GRAVITY EFFECT ON DEFECT PRECIPITATION DURING ANNEALING

GH. DRĂGAN

Institute of Chemical Research, ICECHIM, Spl. Independenţei 202, Bucharest

Received April, 11, 1975

The process of coherent precipitation of crystalline defects was found in previous studies to be responsible for the interlamellar order observed in various types of polyethylene with lamellar habit. The study of defect annealing for linear polyethylene with conformation defects and chemically etched is resumed. For various orientations of the thermal transfer direction during annealing in the gravitational terrestrial field, the amplitude of this process is different. The present study is a part of the recent observations on the influence of terrestrial gravitational field on the liquid-gas critical region. It is considered that the momentum-energy tensor associated to the transfer process in the two cases explains this effect.

In the present series [1–3] the modifications occurred in the crystalline morphology of polyethylene (PE) after the mechanical, thermal and/or chemical treatments were studied. For the PE types that crystallize in a lamellar habit, the conditions of crystallization or the treatments imposed to the material in solid state influence the habit but not so much as the relative position of the lamellae [1]. Subjecting the melt or the polymer solution to shearings during the crystallization, the nuclei of crystallization orientate themselves on the shearing lines and this finally results in an uniform distribution of the lamellae on these lines [4]. The relative position of the lamellae in this *row crystallized* morphology depends on the intensity of the shearing stresses [4]. For the polymer in a solid state, it was established that the mentioned treatments lead to a clearer separation of the lamellae from the amorphous regions (by decreasing the superficial free energy) due to migration of defects to interlamellar regions. [1–3]

The dynamic calorimetric methods approached in this series, point out the conformation and configuration defects annealing by a first order transition of an order-disorder type. This effect, T_m^1, was associated to the interlamellar order resulted after the coherent precipitation of defects. It has been previously established [1] that for essentially linear PE types, where the conformation defects are predominant, the precipitation process of chemically etched defects (by photochlorination) has an activation energy which ranges between 24 — 53 Kcal/mole relative to 30 — 35 kcal/mole deduced by other ways for the initial polymer.

---

[1] Part III: Gh. Drăgan, *Rev. Roumaine Chim.*, **21**, 1381 (1976)

[2] Gh. Drăgan, *Materiale Plastice*, **10**, 87 (1973).

[3] Gh. Drăgan, *Rev. Roumaine Chim.* **20**, 687, (1975).

[4] Gh. Drăgan, "Morphology of Polymers. Principles of Characterization and Processing", Lectures, ICECHIM, June 1974, Bucharest.

This precipitation process is basically an activated process of energy and mass transfer extended over a characteristic temperature range of $110° - T_m°$. [1,3,5] To this, one can associate a momentum-energy tensor on the base of which one should asses its gravitational coupling within the framework of the generalized theory of relativity. Recent calorimetric studies [6,7] have shown that the apparent thermodynamic properties of a fluid are negligibly influenced by the effects of terrestrial gravity while in the critical point region, this influence becames dominant. The theoretical models of the first order phase transitions, especially for the liquid-gas case, are based on the coupling of dissipation modes [8] that contributes to the response function of the system.[4] Thus the problem of phase transition becames a problem of nonequilibrium thermodynamics, the formalism of which can be expressed in hydrodynamic approximation by the laws of conservation of densities and current densities for mass, momentum and energy.[8] For static (drop) adiabatic calorimetry one can establish the dependence of the response function (C_p, C_v) with temperature by a critical exponent. In the case of dynamic calorimetry [6,7] for the same response function, the exponent is modified,[7] and this indicates the different contribution of the dissipation modes based on the mentioned model. Buckingham [7] verified on a dynamic calorimetric system the influence of its orientation in the terrestrial gravity field on the response function in a liquid-gas critical region. It is observed that although the energetic amplitude of the transition $\left(\int C_p(T(t))\mathrm{d}t\right)$ is retained, the shape of the response function dependence ($C_p(T(t))$) differs clearly. Similarly by the precipitation process and the energy and mass transfer process associated to the phase transition can be characterized by an momentum-energy tensor on the base of which one can asses the coupling of the system response function in the terrestrial gravity field.

The present paper reports the results on the influence of the orientation of one dominant transfer direction in the annealing process for a PE sample with chemically etched defects in the terrestrial gravitational field. It also gives the influence of simultaneous annealing of samples with different mutual orientations of dominant direction. The checking of this influence is determined with the aid of the splitting coefficient [1,3] from the thermograms of the samples after annealing. This parameter indicates

---

[5] J. Loboda-Cackovic, R. Hoseman and H. Cackovic, *Kolloid Z. Z. Polymere*, **247**, 824 (1971).

[6] J. A. Lipa, C. Edwards and M. J. Buckingham, *Phys. Rev. Lett.*, **25**, 1086 (1970).

[7] J. Buckingham, *Ber. Bunsengesellschaft Phys. Chem.*, **76**, 287 (1972).

[8] L. P. Kadanoff and J. Swift, *Phys. Rev.*, **166**, 89 (1968).

that for chosen orientations the amplitude of the precipitation process is different.

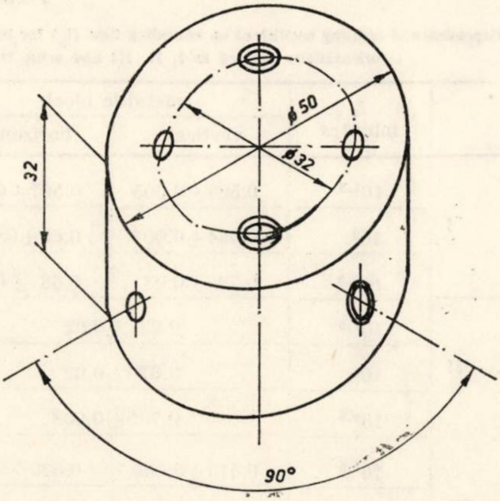

Fig. 1.—Disposition of the cylindrical holes in matallic block for annealing in the three reciprocal orientations.

EXPERIMENTAL

The behaviour on annealing of sample CPE 1 from the series previously considered[1] was studied. To keep the form of the annealed sample in order to analyze it by DTA scan, the sample was annealed in a mixture with silicon oil (set III)[1] in the same proportions as before. The sample was placed in a metallic block, directly or in a Pyrex tube. The brass block with a cylindrical shape (figure 1) has four orifices, also cylindrical and vertical, having the same distance between them and in relation to the center of the block, and two others horizontal ones with the centers at half the height of the metallic block whose axes form an angle of 90 degrees. Two of the vertical orifices and one of the horizontal ones have the inner diameter equal to the inner diameter of the used DTA containers (almost 6 mm)[1]. The other orifices have a 10 mm diameter so that the Pyrex cylindrical tubes with the inner diameter equal to that of the containers are placed therein. In this way, the annealing can be effected using as a transfer medium[3,9] the direct metallic block or the Pyrex glass. The samples and the Pyrex tubes are fixed using an aluminium foil for a good thermal contact. These have the length permitted by the metallic orifices from the block. After fixing the samples, the metallic block is put into the metallic cylinder which is plunged into the bath of an ultrathermostate. For all the cases in the present paper, the annealings take place at the initially fixed temperature of 131.3 ± 0.05°. The metallic cylinder and the annealing block is maintained permanently in vertical position.

The influence of annealing conditions was checked by DTA round on equal fragments cut from the sample that was taken from the block. Because the orifices are equal in length and diameter, the quantities of material subjected to annealing are equal, as the four fragments

---

[9] We refer to the transfer function $R(t)$ defined for similar case in conduction calorimetry. So, the response function $\theta(t)$) the direct measurable function) for a process characterized by the heat flux $w(t)$, can be expressed by the relation $\widetilde{\theta} = \widetilde{R}\widetilde{W}$, where $\widetilde{\theta}$, $\widetilde{R}$, $\widetilde{W}$ are the Laplace transforms of the respective functions. (See for example M. Hattori, S. Tanaka and K. Amaya, *Bull. Chem. Soc. Japan*, **43**, 1027 (1970)).

used in DTA rounds. This is how the error of the determined values from the thermograms can be established, using the same DTA round speed K2 = 6.5°/minute.[1]

Table 1

Dependence of splitting coefficient on annealing time (t_a) for medium samples CPE 1 [3] at 131,3° in the three different orientations denoted as I, II, III and using two external transfer media (see the text)

	t_a minutes	metallic block		PYREX	
		vertical	horizontal	vertical	horizontal
I	$10^{1.5}$	0.599±0.005	0.597±0.006	0.620±0.008	0.601±0.003
	10^2	0.654±0.007	0.65±0.01	0.66±0.01	0.65±0.02
	$10^{2.5}$	0.73 ±0.03	0.68 ±0.01	0.71 ±0.01	0.71 ±0.02
II	$10^{1.5}$	0.63 ±0.02		0.625±0.006	
	10^2	0.67 ±0.02		0.682±0.007	
	$10^{2.5}$	0.705±0.008		0.72 ±0.01	
III	$10^{1.5}$	0.513±0.006	0.510±0.009	0.601±0.006	0.607±0.004
	10^2	0.587±0.002	0.602±0.002	0.62 ±0.01	0.618±0.005
	$10^{2.5}$	0.68 ±0.01	0.688±0.007	0.68 ±0.02	0.69± 0.01

RESULTS AND DISCUSSIONS

Because of the cyllindrical form of the sample in which length is dominant (length/diameter ~ 5) the heat transfer during annealing is effected preferentially on a radial direction. The presented results are obtained by separated annealing of one sample with the axis in vertical and horizontal position, respectively (I), simultaneously of two samples in vertical position (II) and simultaneously of one sample in vertical position and one in horizontal position (III). These conditions are used for annealing directly in the metallic block and separately for annealing by Pyrex. Table 1 lists the values of the splitting coefficient α of the precipitation process of the defects during annealing[1] at three periods of annealing time ($t_a = 10^{1.5}$, 10^2 and $10^{2.5}$ minutes) for the six distinct cases.

A clear difference is observed for the first three annealing conditions in metallic block where the amplitude of the precipitation process (α) is grouped as follows: $\alpha_{II} > \alpha_I > \alpha_{III}$. Therefore the process of precipitation is affected by the terrestrial gravitational field as well as by the mutual gravitational perturbations of the samples annealed in couples. Thus two samples annealed simultaneuously with axes parallel in vertical position influence each other so that the precipitation process of the defects is accelerated. For two simultaneous annealed samples, one in horizontal and one in vertical position (III), this process is slowed down. Generally, for conditions I and III no significant differences are observed between the vertical samples and the horizontal ones, which means that the terrestrial gravitational interaction as well as the mutual interaction of the simultaneous annealed samples, dominate the precipitation process. For the samples in conditions II the mean value and the error is established out of the eight DTA rounds.

For the Pyrex annealed samples the results group themselves as the above mentioned ones. The α values for annealing in Pyrex are systematically higher than for annealing in direct metallic block. This is somewhat unexpected keeping in mind the fact that the equilibrium thermoconductivity coefficient is higher in brass than in glass.

In conclusion we see that the process of precipitation of chemically etched defects is influenced by the transfer medium but the gravity influence that dominates this process is practically independent of the orientation of the transfer direction in the gravitational field of the earth. It seems that the interaction of the pairs of samples simultaneously annealed at the chosen distances between their axes is more powerful than the interaction of samples annealed one by one in the terrestrial gravitational field. Based on a more complete model of the precipitation process, the momentum-energy tensor associated to this transfer process can be established. By continuing these studies, important completions can be brought to the theory of gravitational interaction found for the moment in a deadlock.

simultaneous annealing samples, dominate the precipitation process. For the samples in conditions 1) the [illegible] value and the error is established out of the eight [illegible] rounds.

For the [illegible] annealed samples the results [illegible] themselves as the ones mentioned above. The [illegible] values for annealing in [illegible] are [illegible] higher than for annealing in direct magnetic field. This is [illegible] expected keeping in mind the fact that the [illegible] coefficient [illegible] is higher in [illegible] than in glass.

In conclusion we see that the process of precipitation of [illegible] effect is influenced by the transfer moment by the gravity [illegible] and it appears this process is practically independent of the orientation of the [illegible] as well as the gravitational field of the earth. It seems that the interaction of the [illegible] simultaneously moving at the chosen distances between their axes is more powerful than the interaction of samples annealed one by one in the terrestrial gravitational field. Based on a more complete model of the precipitation process the momentum-energy transfer [illegible] to the transfer process can be established. By continuing these studies, important conclusions can be brought to the theory of gravitational interaction found for the moment in a deadlock.

Revue Roumaine de Chimie, **21**, *11–12*, 1543–1554 (1976)

POTENTIAL ANTICANCER AGENTS. XII*

SYNTHESIS OF NEW METHANESULPHONATE DERIVATIVES FROM BENZO- AND NAPHTOPYRANS

I. DRAGOTĂ, D. IONESCU, EUSTANȚA TĂRNĂUCEANU, V. DOBRE and
I. NICULESCU-DUVĂZ

Oncological Institute, Bd. 1 Mai 11, Bucharest
Romania

Received December 16, 1974

Revised September 15, 1976

Eighteen new methanesulphonate derivatives from chromanes, benzochromanes and coumarins were synthesized and studied. The assigned structures were in good agreement with the n.m.r., i.r. and u.v. data. 4-N-Mesyloxy-coumarin (*15*), proved to be moderately active against W256 carcinosarcoma. No activity was found against L1210.

* * *

Only sporadic attempts $^{1-7}$ were made in order to utilize the pyranic structure for the design and synthesis of effective compounds against experimental and human tumors. However some pyranic derivatives i.e. : hydroxylated 3,4-diaryl-coumarins, 2(2-furyl)-, 2(2-thienyl)- and 2(3-pyridyl)-chromones ; [4] Δ^2-α-chromano-malono-nitriles, [7] etc. demonstrated moderate activity against experimental tumor and the naturally occurring

---

[*] Part. XI — D. C. Suster, G. Botez, L. V. Feyns, V. Dobre and I. Niculescu-Duvaz, *Rev. Roumaine Chim.*, (in press).

[1] Ng. Ph. Buu-Hoi and B. Ekert, *J. Org. Chem.*, **19**, 1390 (1954).

[2] Ng. Ph. Buu-Hoi, B. Ekert and R. Royer, *J. Org. Chem.*, **19**, 1584 (1954).

[3] Ng. Ph. Buu-Hoi and D. Lavit, *J. Org. Chem.*, **21**, 1022 (1956).

[4] P. F. Devitt, A. Timoney and M. A. Vikars, *J. Org. Chem,*. **26**, 4941 (1961).

[5] K. A. Takao and N. R. Manjaramkar, *Indian J. Appl. Chem,*. **9**, 892 (1971).

[6] D. Donnelly, R. Geoghegan, C. O. Brien, E. Philbin, T. S. Wheeler, *J. Med. Pharmaceut. Chem,*. **8**, 872 (1965).

[7] N. Latif, I. Zeid, F. Askad, *Chem. & Ind.*, **1970**, 1539.

compound mammein (I) proved to be significantly effective against sarcoma 180.[8]

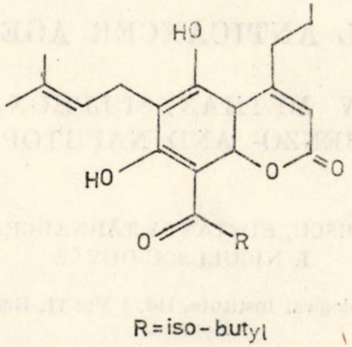

The few attempts to use the pyran structure as the carrier moiety of alkylating functions proved to be unsuccessful (i.e. in nitrogen mustards[9-11] and urethane type nitrogen mustards[12] from benzo- and naphtopyrans).

However the number of pyranic compounds investigated from this point of view was too small in order to allow final conclusions.

It seemed therefore to be of interest to continue the exploration of the capabilities of pyranic structures to function as effective carriers of alkylating moieties.

In this report we present the results of incorporation of one or two methanesulphonate functions into both aromatic and pyranic ring of such derivatives.

Very few such coumarinic or chromanonic methanesulphonates[13] were mentioned in the literature and from them only the 4-methyl-7-mesyloxy coumarin was reported to be tested against L1210 ·- (OD = = 13 mg/kg, I.L.S. = 113%).[14]

1. SYNTHESIS

Mono and dimethanesulphonates were prepared starting from the following hydroxylated precursors :

— 2,2-dimethyl-7-hydroxy-chroman-4-one, 2,2,5,-trimethyl-7-hydroxy-chroman-4-one,[15,16] and some of the corresponding N-oximes[17-19]

---

[8] R. A. Finnegan, K. E. Merkel and N. Back, *J. Pharm. Sci.*, **61**, 1599 (1972).

[9] R. C. Elderfield and A. C. Mehta, *J. Medicin Pharmaceut. Chem.*, **10**, 921 (1967).

[10] R. C. Elderfield and J. Roy, *J. Medicin Pharmaceut. Chem.*, **10**, 918 (1967).

[11] F. D. Popp, *J. Medicin Pharmaceut. Chem.*, **5**, 627 (1962).

[12] I. Dragota, L. V. Feyns and I. Niculescu-Duvaz, *Rev. Roumaine Chim.*, **20**, 665 (1975).

[13] R. Desai and P. Desai, *J. Indian Chem. Soc.*, **40**, 456 (1963).

[14] J. Sandberg, H. B. Wood, R. Engle, J. Venditti and A. Goldin, *Cancer Chemoth. Repts.*, Part. 2, **3**, 137 (1972).

[15] P. R. Iyer and G. D. Shah, *Indian J. Appl. Chem.*, **6**, 227 (1968).

[16] A. S. Mujumdar and R. N. Usgaonkar, *Indian J. Appl. Chem.*, **9**, 249 (1971).

[17] S. G. Powell, *J. Amer. Chem. Soc.*, **45**, 2708 (1923).

[18] S. G. Powell, N. G. Johnson, *J. Amer. Chem. Soc.*, **46**, 2861 (1924).

[19] J. Colonge and A. Guyot, *Bull. Soc. chim. France*, **1958**, 325.

— 2,2-dimethyl-6′-hydroxy-benzo-[f]-chroman-4-one and 2,2-dimethyl-9-hydroxy-benzo-[h]-chroman-4-one previously obtained by condensation of 1,3 or 2,7-dihydroxynaphtalene with dimethylacrylic acid [8,12]

— 2-methyl-7-hydroxy-chroman-4-one [16]

— 7-hydroxy-4-methyl- and 7-hydroxy-coumarin [20−23]

— 7-hydroxy-, 5-hydroxy-7-methyl-, 5,7-dihydroxy-, 6,7-dihydroxy-, 7,8-dihydroxy-coumarins [24,25] and 7-hydroxy-8-nitro-coumarins [26]

— lactone of 2′, 4′-dihydroxyphenyl-2-carboxylic acid [27,28]

Treatment of the precursors (including oximes) with mesyl chloride in dry pyridine and in the cold [29−33] afforded in good yields the corresponding mono- or dimethanesulphonate derivatives :

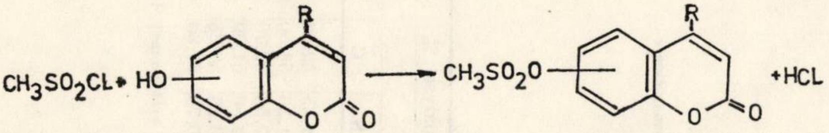

The new methanesulphonates thus obtained were summarized in tables 1, 2, 3.

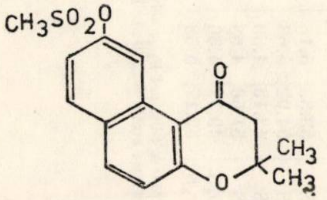

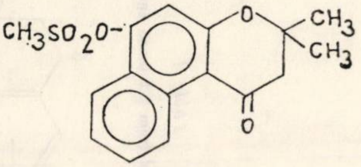

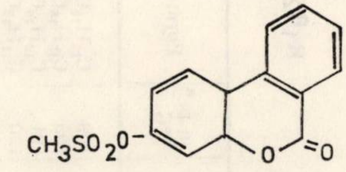

[20] J. L. Bose, R. C. Shah and V. R. Shah, *Chem. & Ind.*, **1960**, 623.

[21] S. Sethna and R. Phadke, "Organic Reactions" vol. 7, John Wiley & Sons Inc., New York, 1953, p. 1.

[22] W. Bridge, A. J. Crocker, T. Cubin and A. Robertson, *J. Chem. Soc.*, **1937**, 1536.

[23] W. D. Langley and R. Adams, *J. Amer. Chem. Soc.*, **44**, 2320 (1922).

[24] L. Beichel and N. Hampel, *Liebigs Ann. Chem.*, **733**, 1 (1953).

[25] H. Appel, *J. Chem. Soc.*, **1935**, 1031.

[26] K. D. Kaufmann, W. E. Russey and L. R. Worden, *J. Org. Chem.*, **27**, 875 (1962).

[27] R. Adams, D. C. Pearse, J. A. Clarck and B. R. Baker, *J. Amer. Chem. Soc.*, **62**, 2197 (1940).

[28] W. R. H. Hurtley, *J. Chem. Soc.*, **1929**, 1870.

[29] A. Furst and F. Koller, *Helv. Chim. Acta.*, **30**, 1454 (1947).

[30] J. Tadanier, R. Hallas and J. R. Martin, *J. Org. Chem.*, **34**, 3837 (1969).

[31] J. H. Sooker, J. A. Mc. Mechan and Yen-Lung-Hung, *J. Org. Chem.*, **27**, 1080 (1962).

[32] J. H. Sooker, *J. Org. Chem.*, **24**, 1039 (1959).

[33] F. R. Stermitz, J. P. Gillespie, L. G. Amoros, R. Romero, T. A. Stermitz, K. A. Larsen, S. Earl and L. E. Ogg, *J. Medicin Pharmaceut. Chem.*, **18**, 708 (1975).

Table 1

New methanesulphonates derived from 2,2 mono and dihydroxy-chroman-4-ones

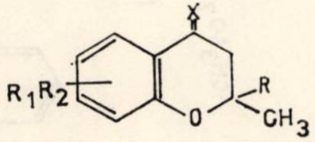

N°	R_1	R_2	R_3	X	m.p. [a] °C	Formula	Analysis % Calculated C	H	N	S	Found C	H	N	S	Yield %	Rf[b]
1	7−OMeS	H	CH_3	O	109	$C_{12}H_{14}O_5S$	53.33	5.18	—	11.85	52.49	5.14	—	10.50	68	0.79
2	5−CH_3	7−OMeS	CH_3	O	105	$C_{13}H_{16}O_5S$	54.92	5.63	—	11.30	54.50	6.00	—	11.30	73	0.82
3	5−OMeS	7−OMeS	CH_3	O	91	$C_{13}H_{16}O_8S_2$	43.13	4.39	—	17.58	42.70	4.35	—	17.41	90	0.71
4	7−OMeS	H	H	O	120	$C_{11}H_{12}O_5S$	51.56	4.68	—	12.50	51.09	4.86	—	12.40	70	0.78
5[c]	H	H	H	NOMeS	124−5	$C_{10}H_{11}NO_4S$	49.79	4.56	5.72	13.26	50.28	4.90	5.72	—	50	0.81[d]
6	7−OCH_3	H	CH_3	NOMeS	134	$C_{13}H_{17}NO_5S$	52.17	5.68	4.67	10.70	51.80	6.05	4.32	—	56	0.73[e]

[a] Recryst. from $CHCl_3$-petroleum ether (b.p. 30−60°C); [b] TLC on Merck Silicagel $F_{2\cdot4}$; solvent system: cyclohexane: tetrahydrofuran: benzene: methanol (2:1:1:1) − [c] 7-hydroxy-chroman-4-one oxime; [d] solvent system: benzen: acetone: acetic acid (9:1:1).

Table 2

New methanesulphonates derived from coumarins

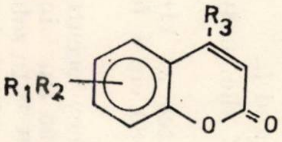

Nº	R_1	R_2	R_3	m.p. [a] °C	Formule	Analysis % Calculated C	H	N	S	Found C	H	N	S	Yield %	Rf[b]
7	H	H	OMeS	112	$C_{10}H_8O_5S$	50.00	3.33	—	13.33	50.20	3.34	—	13.38	81	0.59
8	6—OMeS	H	CH_3	198	$C_{11}H_{10}O_5S$	51.96	3.93	—	12.59	52.16	4.37	—	11.91	69	0.58[c]
9	7—OMeS	H	CH_3	165	$C_{11}H_{10}O_5S$	51.96	3.93	—	12.59	51.46	3.80	—	12.78	72	0.71
10[d]	7—OMeS	H	H	141—2	$C_{10}H_8O_5S$	50.00	3.33	—	13.33	49.59	3.34	—	13.59	65	0.52[c]
11	7—OMeS	H	H	180	$C_{10}H_{10}O_5S$	49.58	4.13	—	13.22	49.81	3.98	—	13.07	70	0.50[e]
12	5—CH_3	7—OMeS	H	102—5	$C_{11}H_{10}O_5S$	51.96	3.93	—	12.59	51.80	3.37	—	12.41	70	0.57[c]
13	7—OMeS	8—NO_2	CH_3	157—9	$C_{11}H_9NO_7S$	44.14	3.01	4.68	—	44.00	2.98	4.86	—	39	0.58[e]
14	5—OMeS	7—OMeS	CH_3	156	$C_{12}H_{12}O_8S_2$	41.37	3.44	—	18.36	40.93	3.73	—	18.18	71	0.64
15	7—OMeS	8—OMeS	CH_3	219	$C_{12}H_{12}O_8S_2$	41.37	3.44	—	18.36	40.99	3.40	—	18.05	78	0.73

[a] Recryst. from $CHCl_3$-petroleum ether (b.p. 30—60°C); [b] TLC on Merck Silicagel F_{254}; solvent system (when not otherwise noted): cyclohexane: tetrahydrofurane: benzen: methanol (2 : 1 : 1 : 1)$_7$ [c] solvent system ethyl acetate: cyclohexane (2 : 1); [d] by hydrogenation *11* (the double bond of the pyranic ring); [e] solvent system: benzene; acetone; acetic acid (9 ; 1 ; 1).

Table 3

New methanesulphonates derived from benzo-chromanes and coumarin

N°	m.p.[a] °C	Formula	Analysis %						Yield %	Rf[b]
			Calculated			Found				
			C	H	S	C	H	S		
16	180	$C_{16}H_{16}O_5S$	60.00	5.00	10.00	59.58	5.28	10.20	62	0.79
17	135–7	$C_{16}H_{16}O_5S$	60.00	5.00	10.00	59.89	5.03	9.80	70	0.74
18	165	$C_{14}H_{10}O_5S$	57.99	3.45	11.03	57.30	3.73	10.50	71	0.72[c]

[a] Recryst. from $CHCl_3$ – petroleum ether (b.p. 30–60°C); [b] TLC on Merck Silicagel F_{254}; solvent system; petroleum ether: ethylacetate (1:1) [c] idem: ethylacetate: cyclohexane (2:1).

2 SPECTRAL DATA

The structural assignments for the new derivatives by respect to the precursor ones are based on i.r., u.v. and n.m.r. spectra.

Infrared spectra. The i.r. spectral data of mono- and dimethanesulphonate derivatives were listed in tables 4 and 5.

The following characteristic bands of the mesyloxy moiety were examined and discussed :

— ν *$-SO_2$ (sim.) frequency* was located at 1168–1195 cm^{-1} for chromanonic derivatives and at 1177 – 1189 cm^{-1} for the coumarinic ones. [34–39]

— ν $-SO_2$ (*asim*) stretching frequency occurred as one or two strong bands [39] within the ranges 1355–1396 cm^{-1} in chromanones and 1355–1394 cm^{-1} in coumarins respectively.[34–39] In solution the SO_2 band was usually split into a doublet (relative intensity 1 :1) probably in accordance with the existence of *gauche* and *trans* conformations in the C–S–O–C– chain. In some cases this band was only broadened in solution ($CHCl_3$).

— ν *S–O–C stretching frequency* was found as a strong absorption maxima in 792–833 cm^{-1} (for chromanones) and 806–818 cm^{-1} (for coumarins) regions. [35,40,41]

— *the deformation frequency* δ CH_3-S was assigned to the bands located in the following ranges : 963–988 cm^{-1} for chromanonic derivatives and 969–988 cm^{-1} for coumarinic ones.[40]

For the coumarinic methanesulphonates, also the 2800–3100 cm^{-1} region was investigated in respect with the deuterated precursors. We

---

[34] K. C. Sehreiber, *Analyt. Chem.*, **21**, 1168 (1949).

[35] A. K. Katritzky, R. G. Schephard, A. J. Waring, *Rec. Trav. chim.*, **81**, 443 (1962).

[36] E. A. Robinson, *Canad. J. Chem.*, **39**, 247 (1961).

[37] E. M. Philbin, R. E. Stuart, R. F. Timoney, T. S. Wheeler, *J. Chem. Soc.*, **1965**, 4414.

[38] R. S. Tipson, *J. Amer. Chem. Soc.*, **74**, 1354 (1952).

[39] M. Avram, G. D. Mateescu, "Spectroscopia în infraroşu. Aplicaţii în Chimia organică", Ed. Tehnică, Bucureşti, 1966, p. 361.

[40] A. Simon, H. Kriegsmann and H. Duts, *Chem. Ber.*, **89**, 2378 (1965).

[41] D. E. Freeman and A. N. Hanbly, *Austral. J. Chem.*, **10**, 239 (1957).

Table 4

Spectral data * (U.V. and I.R.) of new chromanonic derivatives

N^{o}[a]	U.V. Spectra [b,c]				Solvent	I.R. Spectra cm^{-1}				
	Band II		Band I			$\nu C=O$	νSO_2		$\nu S-O-C$	δCH_3-S
	λ(nm)	logε	λ(nm)	logε			sim	asim		
1	258	4.09	322	3.66	KBr	1683 vs	1181 vs	1396 vs	816 s	975 s
					$CHCl_3$	1695 vs	1183 vs	1364 s; 1381 vs	818 s	971 vs
2	261	3.96	323	3.60	KBr	1687 vs	1185 vs	1363 vs; 1377 s	811 m	983 sm
					$CHCl_3$	1686 vs	1183 vs	1364 s; 1378 vs	816 s	970 vs
3	258	3.97	323	3.70	KBr	1701 vs	1183 vs	1361 vs; 1371 vs	807 vs	973 vs
					$CHCl_3$	1709 sm	1193 vs	1366 s; 1380 vs	816 s	972 vs
4	256	3.99	318	3.61	KBr	1691 vs	1184 vs	1376 vs; 1394 vs	812 s	971 vs
					$CHCl_3$	1692 vs	1185 vs	1360 shs; 1381 vs	815 s	970 s
5	257	4.13	315	3.83	KBr	1624 m	1184 vs	1359 vs	810 vs	981 sm
					$CHCl_3$	1624 mw	1184 vs	1373 vs	812 vs	973 m
6	276	4.16	314	4.01	KBr	1625 m	1174 vs	1373 vs	806 sm	969 m
					$CHCl_3$	1635 s	1168 s; 1190 vs	1382 vs	?	970 m
16	265 (sh)	4.08	316	3.91	KBr	1631 m; 1671 vs	1181 vs	1370 vs	811 vs	988 s
			360	3.79	$CHCl_3$	1632 vs; 1682 vs	1183 vs	1385 vs	?	991 m
17	240 (sh)	4.40	315	3.78	KBr	1668 s	1186 vs	1365 vs; 1396 s	811 w	976 sm
	263 (sh)	3.87	344	3.62	$CHCl_3$	1637 s	1189 vs	1355 vs; 1376 vs	?	973 sm
			354 (sh)	3.61						

[a] The number is the same as in Table 1, 2, 3; [b] the spectra of precursors were reported elsewhere [8], with the following exceptions: λ (nm), log γ in EtOH; *4* (OH) 277 (4.13), 315 (3.98) and *6* (OH) 265 (4.18) 306 (3.95); [c] $\nu c \equiv N$ stretching frequency.

* The following abbreviations were used: vs = very strong; s = strong; sm = strong medium; m = medium; mw = medium weak; w = weak; sh = shoulder.

Table 5

Spectral data * (U.V. and I.R.) of new coumarinic derivatives

N°[a]	u.v. Spectra [b]				Sol-vent	i.r. Spectra cm^{-1}						
	band K		band B			$\nu C=O$	νSO_2		$\nu S-O-C$	δCH_3-S	νCH_3-S	
	λmax(nm)	logε	max (nm)	log ε			sim	asim			sim	asim
7	280	4.00	310	3.86	KBr	1735 vs	1178 s	1375 vs	798 s	988 sm	2933	3011
	271	3.96			$CHCl_3$	1733 vs	1179 s	1377 vs	797 s	970 sm	2930	3009
8	278 (sh)	3.90	319	3.70	KBr	1720 s; 1731 s	1189 s	1361 vs	803 sm	983 m	2963	3017
	270	4.09			$CHCl_3$	1725 s; 1735 s	1184 vs	1360 vs; 1379 vs	805 sm	969 mw	?	?
9	278 (sh)	4.08	310	3.99	KBr	1710 shs; 1724 vs	1177 s	1360 vs; 1380 vs	827 m	975 vs	2965	3015
					$CHCl_3$	1734 vs	1182 s	1368 vs; 1394 m	833 shm	970 vs	2960	3031
10	280	4.05	313	3.77	KBr	1743 vs	1189 s	1385 vs	800 s	988 vs	2940	3017
	271 (sh)	3.15			$CHCl_3$	1741 vs	1183 sm	1370 sm; 1386 vs	?	972 vs	2940	3033
11	276	3.18			KBr	1774 vs	1184 vs	1364 vs	803 s	982 s	2336	3016
					$CHCl_3$	1775 vs	1179 vs	1355 s; 1373 vs	803 sm	965 s	2937	3030
12	292	4.03	315	3.85	KBr	1720 s; 1743 vs	1185 vs	1374 vs	792 m	976 s	2960	3038
					$CHCl_3$	1750 vs	1188 vs	1370 s; 1376 vs	?	971 vs	2951	3044
13	272	4.14	314	4.01	KBr	1756 vs	1189 vs	1380 vs; 1394 vs	822 s	963 s	2921	3023
			360 (sh)	3.61	$CHCl_3$	1758 vs	1184 vs	1378 vs; 1389 vs	832 s	972 s	?	3035
14	282	3.98	310	3.81	KBr	1754 vs; 1737 vs	1184 vs	1375 vs; 1389 vs	801 s	975 s	2962	3016
					$CHCl_3$	1737 vs	1185 vs	1365 vs; 1380 s	802 m	965 m	2966	3035
15	280	4.00	317	3.80	KBr	1745 vs	1185 vs	1363 vs; 1378 vs	830 s	980 m	2990	3031
					$CHCl_3$	1746 vs	1181 s	1376 vs	833 s	972 m	2995	3035
18	264	3.99			KBr	1738 vs	1180 vs	1367 vs	808 m	971 m	2933	3012
	273	4.06	316.5	3.74	$CHCl_3$	1744 vs	1188 vs	1365 vs; 1381 vs	810 m	968 s	2940	3034
	299	3.81										

[a] The numbers were the same as in table 1, 2 and 3; [b] The spectra of precursors were reported elsewhere, [12] with the following exceptions; ($\lambda_{(nm)}$, log ε in EtOH); *11* (OH): 280 (3.47); *13* (OH): 258 (sh), 283 (sh), 344 (3.94) 418

* The same abbreviations as in Table 4 were used

found that the stretching frequencies $\nu-S-CH_3$ (both sym. and asym.) were shifted to shorter wavelengths.[40,42]

These details on bands belonging to coumarinic and chromanonic structures were reported elsewhere.[43]

Ultraviolet spectra. Conversion of the hydroxy-chromanones and coumarins into methanesulphonates with the subsequent interruption of the conjugation, results – as in the case of carbamoylation[12] – in a return to the "chromanonic" or "coumarinic" aspect of the spectra (of the unsubstituted compounds) (see table 4 and 5).

N.m.r. spectra were used for structural assignments in the new compounds.[12,44] The results were given in Table 6.

a) *Chromane-4-ones.* The signals arising from pyran ring, namely the C_2-gem-CH_3 groups ($\delta = 1.55$; 6H) and those belonging to C_3-protons ($\delta = 2.68-2.78$; 2H) were indicated for these structures and in good agreement with previously reported data.[12,45,46]

b) *Coumarins.* Characteristic of these compounds were the signals arising from C_3 and C_4 protons. When the C_4 position is substituted (with a methyl group) the signal belonging to C_3-proton was located at $\delta = 6.40-6.78$ (1H).

In the unsubstituted derivatives an AB spectra was obtained ($J_{3,4} = 9.5$ cps), the signal arising from C_4-proton being located at $\delta = 7.70-7.92$ (1H).

Assignments for aromatic protons in tricyclic derivatives were uncertain.

c) *Methanesulphonate function.* The signals arising from these protons were located in the range $\delta = 3.13-3.77$ (3H) (depending on the substituent position in the aromatic nucleus) as follows :

$C_4-OSO_2CH_3$	$\delta = 3.39$ (1 compound)
$C_5-OSO_2CH_3$	$\delta = 3.30$ (2 compounds)
$C_6-OSO_2CH_3$	$\delta = 3.18$ (1 compound)
$C_7-OSO_2CH_3$	$\delta = 3.13-3.62$; $\delta = 3.13-3.18$ in CF_3COOH $\delta = 3.25-3.39$ in $CDCl_3$, CCl_4 (12 compounds)
$C_8-OSO_2CH_3$	$\delta = 3.77$ (for compound *15* in which the $C_7OSO_2CH_3$ signal arises at $\delta = 3.62$)

The $N-OSO_2CH_3$ signal was found in $\delta = 3.22-3.23$ (2 compounds) region.

3. BIOLOGICAL DATA

The new compounds were tested against L1210 leukemia and W256 carcinosarcoma. The results were given in Table 7.

---

[42] A. Simon, H. Kriegsmann and H. Dutz, *Chem. Ber.*, **89**, 2390 (1956).

[43] V. Feyns, I. Dragota and I. Niculescu-Duvaz, *Rev. Roumaine Chim.*, in press.

[44] A. K. Katritzky and B. Ternay, *J. Heterocycl. Chem.*, **5**, 745 (1968).

[45] W. E. Parham and L. D. Hestio, *J. Amer. Chem. Soc.*, **84**, 813 (1962).

[46] A. C. Waiss and J. Corse, *J. Amer. Chem. Soc.*, **87**, 2068 (1965).

Table 6

NMR spectral data for the new benzo- and naphto pyrans methanesulphonates

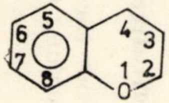

N°[a]	Solvent	Chemical shift δ(ppm) ; J(cps)[b]						
		C_2	C_3	C_4	C_5	C_6	C_7	C_8
0	1	2	3	4	5	6	7	8
1	CF_3CO_2H	1.32 s[c] (6H)	2.71 s (2H)	—	7.84 m (1H) $J_{5,6}$ = 9.45	6.76 m (1H)	3.16 s[d] (3H)	6.81 m (1H) $J_{6,8}$ = 2.5
2	CF_3CO_2H	1.29 s[c] (6H)	2.74 s (2H)	—	2.48 s (3H)	6.50 m (1H) $J_{6,8}$ = 2.4	3.13 s[d] (3H)	6.65 m (1H) $J_{6,8}$ = 2.4
3	CF_3CO_2H	1.36 s[c] (6H)	2.72 s (2H)	—	3.30 s (3H)	6.85 m (1H) $J_{6,8}$ = 2.0	3.16 s[d] (3H)	6.80 m (1H) $J_{6,8}$ = 2.0
4	$CDCl_3$	1.54 d (3H) $J_{2,2}$ = 6.0	2.67 d (2H)	—	7.97 d (1H) $J_{5,6}$ = 9.0	6.93 m (1H)	3.19 s[d] (3H)	6.97 m (1H) $J_{6,8}$ = .25
5	$CDCl_3$	4.25 t (2H) $J_{2,3}$ = 6.5	3.07 t(2H)	3.23 s[d] (3H)	8.14 m (1H)	6.95−7.45 m (3H)		
6	$CDCl_3$	1.43 s[c] (6H)	2.94 s (2H)	3.22 s[d] (3H)	7.82 d (1H) $J_{5,6}$ = 9.0	6.52 m (1H)	3.92 s[g] (3H)	6.35 m (1H) $J_{6,8}$ = 3.0
7	CCl_4+ $CDCl_3$	—	6.56 s (1H)	3.39 s[c] (3H)		7.40−7.90 m (4H)		
8	CF_3CO_2H	—	6.48 d (1H) $J_{3,4}(CH_3)$ = 1.5	2.42 d (3H)[f]		3.18 s[d] (3H)	7.40−7.60 m (3H)	
9	$CDCl_3$	—	6.23 d (1H) $J_{3,4}(CH_3)$ = 1.5	2.48 d (3H)	7.74 d (1H) $J_{4,5}$ = 9.5	Arom. reg. 7.15−7.85 (3H) m	3.23 s[d] (3H)	—

10	$CCl_4 + CDCl_3$	—	6.45 d (1H) $J_{3,4} = 9.5$	7.70 d (1H)	7.15–7.60 m (3H)		3.25 s [d] (3H)	
11	$CDCl_3$ + DMSO	—	2.89 m (4H)		6.96–7.36 m (3H)		3.26 s [d] (3H)	
12	$CCl_4 + CDCl_3$	—	6.40 d (1H) $J_{3,4} = 9.5$	7.92 d (1H)	2.54 s [f] (3H)	7.10 s (2H)	3.25 s [d] (3H)	7.10 s (2H)
13	$CDCl_3+(CD_3)_2CO$	—	6.46 d (1H) $J_{3,4}(CH_3) = 1.5$	2.56 d (3H) [f]	7.60 d (1H)	8.00 d (1H) $J_{5,6} = 8.5$	3.39 s [d] (3H)	—
14	CF_3CO_2H	—	6.42 s (1H)	2.64 s [f] (3H)	3,30 s [f] (3H)	7.42 d (1H) $J_{6,8} = 2.0$	3.17 s [d] (3H)	7.33 d (1H) $J_{6,8} = 2.0$
15	$CDCl_3+CF_3CO_2H$	—	6.78 s (1H)	2.78 s [f] (3H)	8.00 d (1H)	7.78 d (1H) $J_{5,6} = 9.8$	3.62 s [d] (3H)	3.77 s [d] (3H)
16	$CDCl_3$	1.55 s [c] (6H)	2.78 s (2H)	—	3.30 s [f] (3H)	Arom. reg. 7.40–8.20 (m) (5H)		
17	$CDCl_3$	1.55 s [c] (6H)	2.78 s (2H)	—	Arom. reg.: 7.08–8.10 m (5H)			3.28 s [h] (3H)
18	CF_3CO_2H	Arom. reg.: 7.18–8.25 m (6H)					3.18 s [d] (3H)	

[a] The number is the same as in Table 1, 2, 3.

[b] Internal standard TMS; [c] $C_2-(CH_3)_2$ (6H); [d] $Cn-OSO_2CH_3$ (3H); [e] $N-OSO_2CH_3$ (3H); [f] Cn(arom)$-CH_3$(3H); [g] C_7-OCH_3(3H); [h] probably $C_6-OSO_2CH_3$ (3H).

Table 7

Biological evaluation of new-compounds

N°	Compound	DL$_{50}$ [a] mg/kg	L 1210[b] no admin. × dose (mg/kg b.w.)	W 256[d] ILS%[c]	no. admin.	× doses	TWI%[e]
1	IOB 311	>1000	8×200	0	—	—	
2	IOB 310	>1000	8×150	0	—	—	
3	IOB 264[f] NCI 250−824	—	9× 12.5	0	—	—	
4	IOB 309	>1000	10×150	0	14×150	27	
5	IOB 307	>1000	10×200	0	—	—	
6	IOB 306	>1000	10×200	0	14×150	57	
7	IOB 272[f]	> 500	9×100	9	14×150	25	
8	NCI 250−825 IOB 290[f] NCI 250 828	—	9×100	1	—	—	
9	IOB 274	> 500	8×100	0	14×100	23	
10	IOB 298	>1000	—	—	5×200	43	
11	IOB 299	>1000	—	—	5×200	28	
12	IOB 273[f] NCI 250 826	> 500	8×100	19	14×100	49	
13	IOB 312	>1000	3×200	0	—	—	
14	IOB 309	>1000	10×200	0	—	—	

[a] Single doses, on Wistar rats (according to J. Cornfield and N. Nantal, *J. Amer. Statist. Ass.*, **45**, 181 (1950) [b] on BDF$_1$ bearing mice the treatment began 24 hrs. after i.p. inoculation of 10^6 leukemic cells; [c] ILS = increase of life span (T/C. 100−100); [d] W256 = Walker 256 carcinosarcoma. The treatment began 7 days after tumour transplantation; [e] TWI = tumour weight inhibition; these compounds were screened under the auspice of NCI (Bethesda) against L1210 (values ⩾ 25% are positive, denoting activity).

The new methanesulphonates were non toxic but also ineffective against L1210. 4-N-(mesiloxy)-7-methoxy-chroman-4-one-oxime (*6*) and 7,8-dimesyloxy-coumarin (*15*) proved to be moderately active against W256.

The results were in good agreements with previous Sandberg's findings.[14]

EXPERIMENTAL PART

The m.p. were taken on a Franz Küster-Dresden apparatus and are uncorrected. The purity of the hydroxychromanes and coumarins was checked by elemental analysis and melting points (which agreed with literature data).

1) *Mono- and dimethanesulphonate derivatives.* To a solution of 0.010 moles hydroxybenzo-(or naphto-)pyran in 5 ml. dry pyridine (cooled at − 10°), 0.012 moles of mesyl chloride were added slowly under stirring. After standing over night at room temperature, it was poured into 50 ml HCl 5%, and the precipitated solid filtered and dried in vacuo. Usually the methanesulphonates thus obtained were purified by recrystallyzation from appropriates solvents (usually: ethanol, CH_2Cl_2-petroleum ether or $CHCl_3$-petroleum ether (30−60°).

The u.v. spectra were determined with a CF_4 Optica Milano spectrophotometer in ethanol solutions.

The i.r. spectra were run on a U.R.10 Carl Zeiss Jena spectrophotometer.

The n.m.r. spectra were run on a Tesla B487 B 80 MHz spectrometer (in CF_3CO_2H solution) or on a VARIAN A 60−A spectrometer (in $CDCl_3$ or CCl_4 solutions).

Acknowledgement. We are indebted to Dr. A. Goldin and Dr. H. B. Wood (NCI) who facilitated the screening of our compunds. We thank Dr. M. Elian (Organic Chemistry Center) and Dr. A. Vasilescu (IFA) for the n.m.r. data and Mrs. V. Zamfir for technical assistance.

Revue Roumaine de Chimie, **21**, *11–12*, 1555–1561 (1976)

RESEARCHES IN THE TERPOLYMERIZATION FIELD. VII*

THEORETICAL STRUCTURAL CHARACTERIZATION OF THE LOW CONVERSION ACRYLONITRILE – METHACRYLIC ACID – METHYL METHACRYLATE TERPOLYMER

CR. I. SIMIONESCU and ADELAIDA LIGA
Institute of Macromolecular Chemistry "Petru Poni"
Aleea Gr. Ghica Vodă 41 A, Jassy, Romania

Received December 30, 1974

The possibilities of theoretical structural characterization of low conversion terpolymers are presented, using both the relationships known from the literature and that proposed by the authors ; the examined copolymer was based on acrylonitrile, methacrylic acid and methyl methacrylate in different molar ratios.

For binary copolymers the problem of sequences distribution is widely treated in literature, being substantiated from theoretical point of view and lacking only a sufficient experimental check. The application of this study to terpolymers has received a much smaller attention from both points of view.

As it has been pointed out by a recent paper,[1] a theoretical treatment of sequences distribution in terpolymers cannot be obtained by generalizing that employed for copolymers owing to mathematical difficulties and some differences between the two cases, as follows :

— the mean sequence length of the major monomer in copolymers is always bigger than that of the other monomer, whereas in terpolymers this is not mandatory ;

— the number of sequences of the constituent monomers which is always the same in copolymers, is generally different in terpolymers.

Tosi [1] has pointed out that the knowledge of the feed composition is essential to describe the sequences distribution in terpolymers and he has proposed some mathematical relationships for the quantitative treatment of this distribution. These relationships, together with the previously known expressions [2,3] and some deduced by us in a recent paper[4]

* Part VI : see ref. [4]

---

[1] C. Tosi, *European Polymer J.*, **6**, 161 (1970).
[2] T. Alfrey and G. Goldfinger, *J. Chem. Phys.*, **12**, 205 (1944).
[3] J. Seiner, *Polymer Lett.*, **2**, 985 (1964).
[4] Cr. I. Simionescu, A. Liga and I. Negulescu, Paper presented at the Vth ACS Meeting, Rochester, USA, oct. 1973.

have been used to characterize the low conversion acrylonitrile-methacrylic acid-methyl methacrylate terpolymer, synthetised as in paper.[5] The results of these calculations refer to the following parameters :

1. NUMERICAL FRACTION OF SEQUENCES CONTAINING "N" MONOMERIC UNITS

In the case of three monomers M_1, M_2 and M_3, considering only the effect of the terminal units, the propagation step is characterized by nine growing reactions and nine addition types, respectively ; the corresponding conditional probabilities $P_{ij}(i, j = 1, 2, 3)$ which take into account that every monomer unit M_j adds to a growing chain ending in $m_i^{\cdot}$ in presence of the other two comonomers, have the general form : [2]

$$P_{ij} = \frac{k_{ij}[M_j]}{\sum\limits_{i,j=1}^{3} k_{ij}[M_j]} \tag{1}$$

where k represent the rate constants and M are the monomer concentration in the feed.

The distribution law of different length sequences for multicomponent polymers deduced by Alfrey and Goldfinger [6] has a similar form as that proposed by them for binary copolymerization :

$$P(m_i)_n = \left(\frac{M_i}{\frac{M_1}{r_{i1}} + \frac{M_2}{r_{i2}} + \ldots M_i + \ldots + \frac{M_n}{r_{in}}}\right)^{n-1} \times$$

$$\times \left(1 - \frac{M_i}{\frac{M_1}{r_{i1}} + \frac{M_2}{r_{i2}} + \ldots + M_i + \ldots + \frac{M_n}{r_{in}}}\right) \tag{2}$$

where $P(m_i)_n$ is the ratio between the number of sequences of the monomer M_i containing n units and the total number of M_i sequences and r_{ij} represents the comonomer reactivity ratios.

The application of these calculations to the acrylonitrile-methacrylic acid-methyl methacrylate terpolymer for different feed compositions leads to the conclusion that, as for binary copolymers, [7,8], in the case of multicomponent systems an increase of the monomer content is followed by the increase of the existence probability of long sequences constituted from the considered monomer (tab. 1).

---

[5] CR. I. SIMIONESCU, N. ASANDEI and A. LIGA, *Makromol. Chem.*, **110**, 278 (1967).

[6] T. ALFREY and G. GOLDFINGER, *J. Chem. Phys.*, **12**, 322 (1944).

[7] A. LIGA, I. NEGULESCU and CR. I. SIMIONESCU, *Rev. Roumaine Chim.*, **19**, 911 (1974).

[8] CR. I. SIMIONESCU, A. LIGA and I. NEGULESCU, Paper presented at IUPAC Symposium on Macromolecules, Aberdeen, sept. 1973.

Table 1

Numerical fraction of sequences containing "n" monomeric units in acrylonitrile (M_1) – methacrylic acid (M_2) – methyl methacrylate (M_3) terpolymer

Seq. length -n-	Terpolymer I *			Terpolymer II *			Terpolymer III *		
	$m_1=0.309$ $m_2=0.596$ $m_3=0.095$			$m_1=0.134$ $m_2=0.800$ $m_3=0.059$			$m_1=0.189$ $m_2=0.275$ $m_3=0.536$		
	$P(m_1)_n$	$P(m_2)_n$	$P(m_3)_n$	$P(m_1)_n$	$P(m_2)_n$	$P(m_3)_n$	$P(m_1)_n$	$P(m_2)_n$	$P(m_3)_n$
$n=1$	86.5	53.0	91.0	96.0	27.0	93.0	94.4	89.0	42.0
$n=2$	11.7	25.0	8.2	3.8	19.7	6.5	5.3	9.8	24.4
$n=3$	1.5	14.4	0.7	0.15	14.4	0.5	0.2	1.0	14.2
$n=4$	0.2	5.5	—	—	10.5	—	—	0.2	8.2
$n=5$	—	3.5	—	—	7.5	—	—	—	3.4
$n=6$	—	1.4	—	—	5.5	—	—	—	1.9
$n=7$	—	—	—	—	3.8	—	—	—	1.1
$n=8$	—	—	—	—	7.9	—	—	—	4.4

* Terpolymer composition was determined by applying Alfrey-Goldfinger's equations in differential form. [6]

2. CLUSTERING TENDENCY

In a multicomponent system, the sum of self-addition probabilities represents the clustering tendency in the given system. This amount was estimated by Seiner [3] as :

$$C_T = \sum_{i=1}^{n} \frac{k_{ii}[M]_i^2}{\sum_{j=1}^{n} k_{ij}[M]_j} \tag{3}$$

Introducing the expressions deduced by Alfrey and Price [9]

$$k_{ij} = P_i Q_j \exp\ (-e_i e_j) \tag{4}$$

where P_i is characteristic of radical i, Q_j is the mean reactivity of monomer j, and e_i and e_j are measures of the polarity of the radical and monomer, respectively, equation (3) becomes :

$$C_T = \sum_{i=1}^{n} \frac{M_i^2 Q_i\ \exp\ (-e_i^2)}{\sum_{j=1}^{n} M_j Q_j\ \exp\ (-e_i e_j)} \tag{5}$$

The value zero of C_T shows the total absence of clustering in given system ; $C_T = 1$ represents the maximum value for the less probable case when every radical adds only the own monomer, obtaining a physical mixture of homopolymers. Table 2 presents the results obtained for the three compositions of examined terpolymer.

---

[9] T. Alfrey, and C. C. Price, *J. Polymer Sci.*, **2**, 101 (1947).

Table 2

Clustering tendencies in acrylonitrile (M_1) – methacrylic acid (M_2) – methy lmethacrylate (M_3) system

Terpolymer	Feed composition %mol.			Terpolymer composition % mol.			C_T
	M_1	M_2	M_3	m_1	m_2	m_3	
I	0.6	0.3	0.1	0.309	0.596	0.095	0.211
II	0.3	0.6	0.1	0.134	0.800	0.059	0.531
III	0.3	0.1	0.6	0.186	0.275	0.534	0.386

In general, C_T values of these terpolymers lie within normal limits $(O < C_T < 1)$; for the product with predominant content of methacrylic acid (monomer with self-addition preference), a more pronounced value of the clustering tendency is registered.

3. MEAN SEQUENCE LENGTH

The average number of the monomer units corresponding to one sequence of each monomer may be obtained from eqn. (6) : [1]

$$\bar{n}_i = \frac{\sum_{n=1}^{\infty} n\, P(m_i)_n}{\sum_{n=1}^{\infty} P(m_i)_n} \tag{6}$$

In table 3 are presented the mean length of the sequences in the studied terpolymers.

Table 3

Mean sequences length of acrylonitrile (M_1) – methacrylic acid (M_2) – methyl methacrylate (M_3) terpolymer

Terpolymer	$\bar{n}_1$	$\bar{n}_2$	$\bar{n}_3$
I	1.15	2	1
II	1.04	4	1.08
III	1.06	1.1	2.4

Considering that the number of sequences constituted from a single monomer unit is $s_i = 1/\bar{n}_i$, the data from table 4 attest the tendency of acrylonitrile to form unitary predominant sequences (at the considered feed compositions). In this way, the values obtained in table 3 are confirmed.

Table 4

Number of unitary sequences in terpolymers

Terpolymer	$m_1 s_1$	$m_2 s_2$	$m_3 s_3$
I	0.25	0.30	0.048
II	0.134	0.20	0.059
III	0.189	0.25	0.224

4. F_{ij} FRACTIONS OF THE NINE POSSIBLE BONDS IN TERPOLYMERS (THE RATIO BETWEEN THE NUMBER OF m_i-m_i BONDS AND THE TOTAL NUMBER OF BONDS PRESENT IN THE TERPOLYMER).

This problem refers to the determination of both homo- $(i = j)$ and hetero-bonds $(i \neq j)$ in the terpolymer. A first mathematical approach for F_{ij} expressions belongs to Tosi [1] and the second was proposed by Simionescu and coworkers,[4] based on general equation (1). According to the last contribution, the following general relationships are obtained :

$$1/F_{ii} = 1 + 2(M_{ji}/r_{ij} + M_{ki}/r_{ik}) + M_{ji}^2 r_{ji}/r_{ij} + M_{ki}^2 r_{ki}/r_{ik} + + 2M_{ji}\, M_{ki}\, r_{ki}/r_{ik}\, r_{kj} \tag{7}$$

$$1/F_{ij} = 2 + M_{ij}\, r_{ij} + M_{ji}\, r_{ji} + r_{ij}\, (2M_{kj} + M_{ki}\, r_{ki}/r_{kj})/r_{ik} + + M_{ki}\, r_{ki}/r_{ik} \cdot (r_{ij}/r_{kj} + M_{kj}\, r_{ij}) \tag{8}$$

where

$$M_{ji} = M_j/M_i\, ;\; M_{ki} = M_k/M_i\, ;\; M_{ij} = M_i/M_j$$

and i, j and k have the values 1,2 and 3, respectively.

Table 5 presents the results of F_{ij} calculations for the above mentioned terpolymers, using eqns. (7)–(8).

Table 5

Bond fractions F_{ij} in acrylonitrile (M_1) – methacrylic acid (M_2) – methyl methacrylate (M_3) terpolymer

F_{ij}	Terpolymer I	Terpolymer II	Terpolymer III
F_{11}	0.0116	0.0066	0.0103
F_{22}	0.2580	0.5460	0.0216
F_{33}	0.0117	0.0075	0.2699
F_{12}*	0.235	0.1243	0.0431
F_{23}*	0.0934	0.0930	0.1259
F_{13}*	0.187	0.186	0.1325

* $F_{12} = F_{21}$; $F_{13} = F_{31}$; $F_{23} = F_{32}$.

5. ALTERNATION DEGREE

As a measure of this parameter in terpolymers, the expression (9) is considered :

$$\sum F_{ij} = F_{12} + F_{23} + F_{31} \tag{9}$$

which leads to the determination of M_1, M_2 and M_3 values corresponding to a maximum alternation degree.

Using a FORTRAN program based on eqs. (8)—(9) the initial M_1, M_2 and M_3 values were determined for a maximum alternation of monomeric units in acrylonitrile-methacrylic acid-methyl methacrylate terpolymer (table 6).

Table 6

Feed and copolymer composition corresponding to a maximum degree of alternation

F	F_{mx}	Feed composition			Polymer composition			Seq. length		
		M_1	M_2	M_3	m_1	m_2	m_3	$\bar{n}_1$	$\bar{n}_2$	$\bar{n}_3$
$F_{12}^{a)}$	0.329	0.829	0.171	—	0.500	0.500	—	1	1	—
$F_{23}^{a)}$	0.287	—	0.447	0.553	—	0.500	0.500	—	2	2
$F_{13}^{a)}$	0.356	0.730	—	0.270	0.500	—	0.500	1	—	1
$\sum F_{ij}^{b)}$	0.414	0.687	0.124	0.189	0.405	0.394	0.201	1	1	1

a Binary copolymers; b terpolymer.

It can be seen that at maximum alternation of monomeric units, in binary copolymers both components coexist in equimolar amounts whereas in terpolymer the three comonomers are present in different proportions. Table 6 illustrates as a common feature the fact that at maximum degree of alternation, the sequences constituted from the corresponding monomers have the same mean length, both in terpolymer and in binary copolymers.

6. AVERAGE NUMBER OF MONOMERIC UNITS OF THE TWO MONOMERS m_j AND m_k COMPRISED BETWEEN TWO SUCCESSIVE UNITS OF MONOMER m_i

This parameter can be evaluated by eqn. [1]:

$$\bar{N}_i = \frac{m_j + m_k}{m_i\, S_i} \tag{10}$$

where all the terms are known. The values of $\bar{N}_i$ parameter for the studied terpolymers are presented in table 7.

Table 7

Average values $\bar{N}_i$ for acrylonitrile (M_1)-methacrylic acid (M_2)-methyl methacrylate (M_3) terpolymer

Terpolymer	$\bar{N}_1$	$\bar{N}_2$	$\bar{N}_3$
I	2.7	1.3	18.0
II	3.5	1.0	8.0
III	4.0	6.0	1.5
IV *	1.4	1.5	4.0

* Feed composition corresponding to maximum degree of alternation.

These data provide some supplementary information on monomeric units distribution in the macromolecular chain.

7. MOLAR FRACTION OF THE MONOMER UNITS IN THE CENTER OF COMPOSITIONAL TRIADS

Depending on the feed composition and the reactivity values, each of the three comonomers can be the center of triads of type :

$$M_1:\ M_1M_1M_1;\ M_1M_1M_2\ (M_2M_1M_1);\ M_1M_1M_3(M_3M_1M_1);$$
$$M_3M_1M_3;\ M_2M_1M_3\ (M_3M_1M_2);\ M_2M_1M_2.$$
$$M_2:\ M_2M_2M_2;\ M_2M_2M_1\ (M_1M_2M_2);\ M_2M_2M_3(M_3M_2M_2);$$
$$M_1M_2M_1;\ M_3M_2M_3;\ M_1M_2M_3\ (M_3M_2M_1).$$
$$M_3:\ M_3M_3M_3;\ M_3M_3M_1(M_1M_3M_3);\ M_3M_3M_2\ (M_2M_3M_3);$$
$$M_2M_3M_2;\ M_1M_3M_1;\ M_1M_3M_2(M_2M_3M_1).$$

The molar fraction of central monomer units is determined by applying the same expressions as in binary copolymers[7,8]. The conditional probabilities P_{ij} are calculated by general equation (1), valid for multicomponent systems. The results of these calculations are presented in table 8.

Table 8

Distribution of monomeric units in the center of compositional triads, calculated for acrylonitrile (M_1)-methacrylic acid (M_2)-methyl methacrylate (M_3) terpolymer

Terpolymer	Molar fraction of central M_1 monomer units					
	F_{111}	F_{112}	F_{113}	F_{212}	F_{313}	F_{213}
I	0.004	0.19	0.05	0.58	0.04	0.12
II	0.001	0.07	0.017	0.76	0.08	0.14
III	0.003	0.022	0.08	0.04	0.55	0.29

Terpolymer	Molar fraction of central M_2 monomer units					
	F_{222}	F_{221}	F_{223}	F_{121}	F_{323}	F_{123}
I	0.22	0.36	0.14	0.13	0.029	0.12
II	0.54	0.21	0.18	0.019	0.016	0.03
III	0.012	0.028	0.17	0.016	0.58	0.19

Terpolymer	Molar fraction of central M_3 monomer units					
	F_{333}	F_{331}	F_{332}	F_{132}	F_{232}	F_{131}
I	0.008	0.08	0.07	0.400	0.21	0.23
II	0.004	0.028	0.14	0.29	0.49	0.05
III	0.33	0.31	0.19	0.08	0.02	0.06

In conclusion, the calculation of these parameters gives a general picture of the chemical structure characteristic of any polymer constituted from more than two components, synthetised at low conversion.

Two subsequent papers will elaborate on the variation with conversion of these parameters and the possible correlation between the chemical structure and some properties emphasized, in the case of high conversion terpolymers.

Revue Roumaine de Chimie, **21**, *11–12*, 1555–1561 (1976)

Revue Roumaine de Chimie, 21, *11–12,* 1563–1565 (1976)

QUANTITATIVE DETERMINATION OF CADMIUM AS CADMIUM OXALATE

A. M. QURESHI, A. A. USMANI, ABDUL MALIK and J. AHMAD
University of Karachi, Pakistan
and
Makerere University, Kampala, Uganda

Received July 1974
Revised August 12, 1976

A method is described for the quantitative separation of cadmium (II) as cadmium oxalate from solution in which a number of other metalions is present. The method successfully allows a separation of Cd from Al(III), Cr(III), Fe(II), Fe(III), Ni(II), Cu(II), Zn(II) and Hg(II), but not from Co(II) and Ag(I) which interfere.

The oxalate ion, $C_2O_4^{2-}$, is a bidendate ligand and is widely used in analytical chemistry because many metals form not only simple oxalates but also oxalato complexes.[1] One of the methods of determination of calcium, for example, involves its precipitation as insoluble calcium oxalate monohydrate,[2] which however cannot be weighed directly due to its hygroscopic nature and its decomposition on drying.[3]

A corresponding method for the quantitative determination of cadmium as cadmium oxalate does not appear to have been reported, although oxalic acid has been recommended as a specific and selective precipitant for cadmium.[4] The precipitation of Zn and Cd as insoluble oxalates has been reported,[5–7] only to study the phenomenon of coprecipitation. We describe below a method for the quantitative separation of Cd from a number of cations as cadmium oxalate trilydrate, $CdC_2O_4 \cdot 3H_2O$, and its determination as CdC_2O_4.

EXPERIMENTAL

About 500 ml of each of 0.1M aqueous solutions of $CdCl_2 \cdot 2H_2O$, $Cd(CH_3COO)_2 \cdot 2H_2O$ and $3CdSO_4 \cdot 8H_2O$ were prepared. Twenty five ml portions of these solutions were taken in turn, and about 50 ml water added to each. The resulting solution was warmed and 25 ml of 2.5% hot ammonium oxalate was added to it, with constant slow stirring. The precipitate was allowed to settle and the supernatant liquid was checked for complete precipitation. The precipitate was filtered off through a weighed sintered glass crucible (porosity 4) and washed with water until the test with a $CaCl_2$ solution showed that the washings were free from oxalate ions. The precipitate was dried at 105° to a constant weight to convert it to CdC_2O_4 and the weight noted.

---

[1] K. V. Krishnamurty and G. M. Harris, *Chem. Rev.*, **61**, 213 (1961).

[2] A. I. Vogel, "A Text Book of Quantitative Inorganic Analysis", Longman, London, 1962, p. 473.

[3] E. B. Sandell and I. M. Kolthoff, *J. Phys. Chem.*, **37**, 153 (1933).

[4] F. J. Welcher, "Standard Methods of Chemical Analysis", Vol. 2, D. Van Nostrand Co. Ltd., 1963, p. 103.

[5] T. Osawa, *J. Chem. Soc., Japan*, **71**, 68 (1950).

[6] T. Osawa, *J. Chem. Soc., Japan*, **72**, 463 (1951).

[7] T. Osawa, *Bull. Chem. Soc. Japan*, **23**, 244 (1950).

Ten ml of 0.1M solution of Al(III), Cr(III), Fe(II), Fe(III), Ni(II), Cu(II), Zn(II), Hg(II), Co(II) and Ag(I) were then added to separate 25 ml portions of the Cd (II) solutions. The experiment was repeated with each of these solutions using a large excess of 2.5% hot ammonium oxalate solution. As before, the precipitate was dried at 105° in each case and the final constant weight noted. Guaranteed reagent grade chemicals from E. Merck were used for the study.

RESULTS

The results of the determinations are shown in Table I along with the known amounts of Cd for comparison. It is evident from the table that within the range of concentration of Cd(II) studied (100 mg to 300 mg) the accuracy is within 0.5%. A similar accuracy was found for the samples mixed with other cations (except Co(II) and Ag(I)). The method yielded satisfactory result only when the solution if free from mineral acids.

Table 1

Comparison between known wt. of Cd and the weight determined by the reported method

Compound	Known wt. of Cd(g)	Wt. of Cd determined (g)
1. $CdCl_2 \cdot 2H_2O$	a. 0.2687	0.2684
	b. 0.1344	0.1341
2. $Cd(CH_3COO)_2 \cdot 2H_2O$	a. 0.2804	0.2800
	b. 0.1406	0.1404
3. $3CdSO_4 \cdot 8H_2O$	a. 0.2867	0.2864
	b. 0.1165	0.1163

DISCUSSION

The results show that this is a reliable method of determining Cd from solutions which may also be containing other cations mentioned above with the exception of the interfering cations Co(II) and Ag(I).

The white crystalline precipitate obtained above corresponds to the formula Cd $C_2O_4 \cdot 3H_2O$ which turns to Cd C_2O_4 after drying at 105° for two hours. The band in the infra red spectrum due to water disappears in the dried product. Cadmium oxalate dissolves in mineral acids but not in excess of 2.5% hot ammonium oxalate. However it dissolves easier in hot ammonium oxalate when the concentration exceeds 3% and instantaneously in hot saturated solution of ammonium oxalate. This observation is in agreement with the reported preparation of $Cd(C_2O_4)_2^{2-}$.

The other cations of this study except Co(II) and Ag(I) either do not give a precipitate with hot 2.5% ammonium oxalate or dissolve readily in excess of ammonium oxalate solution. The simple oxalates of Co(II) and Ag(I) unlike cadmium oxalate do dissolve but only partially in excess of 2.5% hot ammonium oxalate without prolonged heating.

The general reaction between the metal ion, M^{n+} and $C_2O_4^{2-}$ can be represented by the equation :

$$2M^{n+} + nC_2O_4^{2-} \rightleftharpoons M_2(C_2O_4)_n \tag{1}$$

denoting the formation of an insoluble oxalate. This is followed by the complex formation reaction.

$$M_2(C_2O_4)_n + (2x - n)C_2O_4^{2-} \rightleftharpoons 2[M(C_2O_4)_x]^{(n-2x)} \tag{2}$$

The metal oxalates are generally insoluble and equilibrium I lies far to the right. The Handbook value of the solubility product of cadmium oxalate is 1.5×10^{-8} at 18°.

It has been found in this work that cadmium oxalate dissolves only in excess of concentrated ammonium oxalate to form $Cd(C_2O_4)_2^{2-}$, [8] but not in the hot 2.5% ammonium oxalate. Therefore even if a large excess of 2.5% ammonium oxalate is present, the equilibrium.

$$CdC_2O_4 + C_2O_4^{2-} \rightleftharpoons Cd(C_2O_4)_2^{2-}$$

lies towards the left. This concentration is, however, sufficient to convert Al(III), Cr(III), Fe(II), Fe(III), Ni(II), Cu(II), Zn(II) and Hg(II) cations into the corresponding oxalato complexes and thus makes possible the quantitative separation of Cd from these cations.

The foregoing observation is consistent with the reported [9] values of the stability constants of the complexes $[M(C_2O_4)_x]^{n-2x}$, some of which are listed in Table II. The values of stability constant (Table II) are mostly at 25° and were determined by different methods under non uniform conditions. In the case of some of the ions, different workers have reported widely different values. A caution has thus to be exercised in interpreting the above experimental observation in the light of the reported values of stability constants. Moreover in the separation described above we used a hot ammonium oxalate solution making the reported K values at 25° not quite relevant.

The fact that Ag(I) interferes is substantiated by the low formation constant of its complex. In the case of Co(II), however it seems to be the kinetic factor, i.e. the slow rate of complex formation, that is of over riding importance — although there are no kinetic data to substantiate this view.

Table 2

Stability constants of the metal oxalato-complexes

Cation	log K
Cd^{2+}	5.77
Al^{3+}	16.3
Fe^{2+}	9.57
Fe^{3+}	21.6
Zn^{2+}	8.51
Hg_2^{2+}	13.04
Ag^{+}	0
Co^{2+}	9.7

K is the gross stability constant of $M^{n+} + nL \rightleftharpoons ML_n$

$$K = \frac{[ML_n]}{[M^{n+}][L]^n}$$

---

[8] D. P. GRADDON, *J. Inorg. Nuclear Chem.*, **3**, 308 (1956).

[9] L. G. SILLEN and A. E. MARTELL "Stability Constants of Metal-Ion Complexes", Chemical Society, London, 1964.

Revue Roumaine de Chimie, 21, 11 – 12 1567 – 1569 (1976)

COMPTES RENDUS

« RADIONUCLIDES IN PHARMACOLOGY » (International Encyclopaedia of Pharmacology and Therapeutics, Section 78) edited by Y. Cohen, Pergamon Press, Oxford, 1971, 2 vol., 962 p. ; Author and Subject Indexes.

L'ouvrage « Radionuclides in Pharmacology » paru en deux volumes sous la direction du professeur Yves Cohen (Centre d'Etudes Nucléaires de Sacley, France) un des plus remarquables spécialistes dans le domaine des produits radiopharmaceutiques, constitue vraiment une révélation scientifique pour les spécialistes qui travaillent dans la production et l'utilisation des radiopharmaceutiques. Par le contenu et la manière d'aborder les problèmes on peut considérer l'ouvrage comme le premier et le plus important publié jusqu'à présent dans ce domaine.

Elaboré par un groupe de spécialistes dont la riche expérience accumulée au cours des années a fait de chacun un lieder en sa spécialité, cet ouvrage a un caractère scientifique fondamental et en même temps didactique. Les 13 chapitres du premier volume avec les dix autres du second volume couvrent tout le domaine en commençant par la production et jusqu'à l'utilisation des radiopharmaceutiques. Un trait caractéristiques de cet ouvrage est l'unité et la cohérence des problèmes traités, la théorie étant étroitement liée à la pratique. En dehors de leurs hautes connaissances, accumulées au cours des années, les auteurs font part aux lecteurs de leur expérience. Outre les problèmes fondamentaux, des problèmes de perspective sont traités aussi, ce qui constitue une autre caractéristique essentielle de cet ouvrage.

Après une introduction dans le premier chapitre sur la place et l'importance des radionuclides en pharmacologie, on traite sous une forme élégante et accessible aux non-spécialistes, les problèmes fondamentaux de physique et de chimie de la production des radioisotopes, la détection et la mesure de dose des radiations ionisantes. De cette façon les chapitres 2—6 décrivent la physique de la radioactivation et la production des radioisotopes, la préparation des traceurs radioactifs inorganiques, la préparation des traceurs organiques par synthèse, traceurs organiques d'origine biologique, la détection et la mesure des radiations ionisantes. Les chapitres 7—13 contiennent les sous-sections : méthodes pharmacologiques polyvalentes et analyses radioisotopiques compartimentales en pharmacologie. Les auteurs traitent avec beaucoup de compétence les problèmes spécifiques d'application des radiopharmaceutiques : l'autoradiographie en pharmacologie, la liaison (chimique) des radiopharmaceutiques avec les protéines de plasma et dans le tissu biologique (un problème de grande actualité et complexité), méthodes isotopiques quantitatives pour la détermination de l'activité des enzymes et le niveau des substrats endogènes. Les méthodes d'analyse radioisotopique sont traitées d'une manière supérieure dans la dernière sous-section du premier volume ayant les sujets : aspects théoriques d'analyse compartimentale, méthodes d'analyse compartimentale d'organisme appliquées en pharmacologie, l'utilisation des traceurs radio-actifs dans l'étude de la circulation de nutrition, analyse compartimentale radioisotopique de l'échange au niveau cellulaire, et isotopes utilisés en pharmacologie et médecine nucléaire. A mesure que le lecteur avance dans la profondeur du livre, d'autant plus les problèmes deviennent plus complexes et de stricte spécialité. De cette façon dans le second volume et les chapitres 14—18 on traite les problèmes concernant les radioisotopes utilisés dans les expériences pharmacodynamiques sur animaux : l'étude de la perméabilité de membranes et hématoencéphalique, l'étude de perméabilité cutanée à l'aide des radioisotopes, le transfert placentaire des composés marqués, l'utilisation des radioisotopes pour la détermination du métabolisme des médicaments ou en chimiothérapie et microbiologie. L'avant-dernière sous-section du second volume est consacrée aux problèmes d'utilisation en médecine des radionuclides ayant les chapitres : les radionuclides administrés aux hommes et en pharmacologie clinique, les produits radiopharmaceutiques utilisés pour diagnostique et thérapie. Les problèmes de radioprotection constituent le contenu de la dernière sous-section du second volume et ils sont consacrés tant à la dosimétrie des radiations ionisantes qu'à l'organisation des laboratoires de radiopharmacie dans les unités médicales.

L'ouvrage « Radionuclides in Pharmacology », événement remarquable dans la littérature, sera une aide précieuse à tous ceux qui travaillent dans le domaine d'application de l'énergie atomique pour l'amélioration de la santé de la population.

Ioan Gălățeanu

TOPICS IN CURRENT CHEMISTRY, 60, Springer Verlag Berlin, 1975, 205 p.

The volume contains two general critical papers dedicated to a fascinating field, namely "Structure of liquids".

The first one, entitled "Molecular Models for the Solvation of Small Ions and Polar Molecules", dedicated to Prof. Dr. H. Hartmann on the occasion of his 60th. birthday, is signed by Prof. Dr. Peter Schuster, Dr. Werner Jakubetz and Dr. Wolfgang Marius from "Institut für Theoretische Chemie der Universität Wien", and has the following contents :

I. Introduction
II. Theoretical Concepts of Molecular Interactions
  A. Electrostatic Models for Molecular Interactions
  B. Quantum Mechanical Calculations on Intermolecular Interactions
    1. Perturbation Theory
    2. Molecular Orbital Theory
III. Experimental Background
  A. Gas-Phase Solvation
  B. Ions in Solution
IV. Electrostatic Models and Further Developments
  A. Electrostatic Models
  B. Further Developments for the Treatment of Ion-Solvent Interactions
V. Results from Quantum Chemical Calculations
  A. Cation-Solvent Interactions
    1. One to One Complexes
    2. Interaction of Cations with Two or More Solvent Molecules
    3. Results obtained with Semiempirical Procedures
  B. Anion-Solvent Interactions
    1. Anion Hydration Studies
    2. Results obtained with Semiempirical Procedures
VI. The Solvation of Polar Molecules
  A. The Solute Molecules
  B. Solute-Solvent Interactions
VII. Conclusion and Further Developments
VIII. References.

The second paper, entitled "Conjectures on the Structure of Amorphous Solid and Liquid Water", signed by Dr. Stuart A. Rice from "Department of Chemistry and James Franck Institute, University of Chicago", proposes to the reader the following chapters :

I. Introduction
II. Preparation of Amorphous Solid Water
III. X-Ray and Neutron Diffraction Studies
  A. Liquid Water
  B. Amorphous Solid Water
  C. Polycrystalline Ice Ih at 77 K
  D. H_2O(as) 77 K/77 K
  E. H_2O(as) 10 K/10 K
  F. Comparison with Neutron Diffraction Data
IV. Vibrational Spectroscopy
  A. Liquid Water
  B. Amorphous Solid Water
V. Some Features of Models of Liquid Water
  A. Lattice and Cell Models
  B. A Phenomenological Synthesis
  C. The Cluster Model
  D. Molecular Dynamics and Monte Carlo Computer Simulations
VI. Conjectures concerning the Structures of Amorphous Solid and Liquid Water
VII. Some Tests
VIII. References

Both papers are written at a very high level, with a rich literature up to date (276 references and 94 references respectively). They are adressed to all research and industrial chemists who wish to keep abreast of advances in their subject.

Eugen Segal

J. INCZEDY "Analytical Applications of Complex Equilibria", Akadémiai Kiadó, Budapest 1976, 415 p.

In writing this book, the author's aim has been to guide and aid the analytical chemist working in industrial and research laboratories in solving everyday problems, and by working through typical problems to show how rapid exploratory calculations may be performed with a slide rule (or other simple means).

The development of coordination chemistry has brought considerable changes in chemical analysis, in that empirical relationships are being replaced more and more by fundamental relationships. Now, the solution of various analytical problems can be predicted and the optimum conditions (solution composition, pH etc) can be simply calculated before the experimental work. The appropriate choice of analytical method and the proper planning of the experimental conditions are of great importance, particularly in connection with the application of instrumental method of analysis.

The introductory part of the book reviews the chemistry of complexes : complex-formation equilibria both for mononuclear complexes and for polynuclear complexes, equilibria of acid-base reactions and redox reactions ; practical instructions for equilibrium calculations and worked examples have been presented. There are discussed conditional equilibrium constants, factors affecting complex formation, kinetics of the reactions of complexes, energy changes involved in complex formation reactions and dependence of equilibrium constants on the solvent.

Methods of determining the protonation constants (potentiometric, spectrophotometric) and determination of the stability constants both for mononuclear complexes (potentiometric, spectrophotometric, polarographic, extraction, ion-exchange methods) and for polynuclear complexes, are described together with worked examples.

In its main chapters the book discusses all those analytical methods (gravimetric, potentiometric and polarographic methods ; spectrophotometry, ion-exchange and other methods) in which complexes are utilized. Acid-base, complexation, precipitation and redox reactions are all treated in similar terms. By using equilibrium correlations and work examples it is demonstrated how the most suitable parameters of analytical determination can be designed in a given case.

The reliability of the calculations depends on the reliability of the fundamental relationships, on the accuracy of the data used and also on the knowledge and the critical sense of the person doing calculations, who has to consider various factors according to their importance. Calculations done with appropriate circumspection will yield results which can be verified experimentally.

The book contains a tabulated collection of equilibrium constants necessary for analytical calculations. Thus, there are the tables with the logarithms of the successive protonation and complex formation constants for room temperature. The following table contains the precipitate formation constants of metal salts and complexes which are only slightly soluble in water, for room temperature. The redox extraction and ion-exchange equilibrium constants are also presented.

A useful bibliography is given (880 references) and an index to complete the book.

Mihaela Constantinescu

REVUE ROUMAINE DE CHIMIE

INDEX DU TOME 21, 1976

INDEX DES AUTEURS

Page

A

ABABI V., voir BÎLBĂ N. 285

— , voir BOURCEANU G. 1405

ABDEL L. RAHMAN S. M. and M. F. ISMAIL, Z. M. ISMAIL, Action of amines on 3-benzylidene phtalide and some allied compounds 889

ABDOU I. K., voir YOUSSEF M. H. 263

AKSENOVA Z. E., voir VOLKOV A. A. 703

ALIMARIN I. P. i E. N. DOROHOVA, S. A., MOROSANOVA, E. N. SEMENOVSKAYA, Izuchenie svoistv i practichescoe ispolzovanie gheteropolisoedinenii s razlichinymi ţsentralnymi atomani 835

ANTONESCU E. and E. VASILESCU, The corrosion of some steels in synthetic river waters, in heat transfer conditions 461

ARVAY ZS., voir RĂZUŞ A. C. 727

ASCENZO G. D', voir MAGRI A. D. 1265

AVRAM M., voir ŞTEFAN N 107

AZZARO M., voir L. FERRERO 49

B

BACIU I. and M. HILLEBRAND, V. EM. SAHINI, E. VOLANSCHI, ESR spectra of nitrodibenzo-*p*-dioxin radicalic species 485

BADEA L., An equation for the thermal conductivity of water 1429

BADIGER V. V., voir BENNUR S. C. 757

— , voir JIGAJINNI V. B. 1221

BĂDILESCU I. I., voir BALABAN A. T. 1339

BALABAN A. T., Chemical graphs. XXVI. Codes for configurations of conjugated polyenes 1045

— , Chemical graphs. XXVII. Enumeration and codification of staggered conformations of alkanes 1049

— , Mass spectrum of 3,7-di-t-butyl-5-methyl-4H-1,2-diazepine : possible steric inhibition of dinitrogen expulsion 241

— , and I. I. BĂDILESCU, Pyrylium salts formed by diacylation of olefins. XXI. Diacetylation of cyclodecene to 9,11-dimethyl-[7](2,6)

Rev. Roumaine de Chimie | 21, *11–12*, p. 1571–1586 (1976), Bucarest

pyrylophanium perchlorate 1339

— , voir BOTA A. 101

— , and A. BOTA, I. I. STĂNOIU, Pyrylium salts formed by diacylation of olefins. XXII. Triacylation of 2,3-dimethyl-2-butene . . 1183

— , voir GHEORGHIU M. D. 1513

— , voir UNCUȚA C. 251

BALINT A., voir DRĂGULESCU C. 1171

BALTĂ P. and C. SPURCACIU, Study of the formation and homogenization processes of the melts by means of EMF measurements 469

BANCIU A. C., Tetracoordinated Co(II) chelates with Co(d^7)-N(sp^2) bonds 1487

— and P. SPACU, Cu(II) chelates synthesized with ligands containing donor nitrogen atoms 1331

BANCIU M., On the pyrolysis of Nenitzescu's hydrocarbons 1083

— , voir DRAGU E. 1497

— , voir ELIAN M. 89

BANERJI S. K., voir KASHYAP B. C. 903

BĂRBOIU V., voir PETROVANU M. 717

— , voir WEXLER M. 127

BĂRBULESCU N. S. and M. LECA, Elimination reactions in the 8-substituted tricyclo[7.3.1.$0^{2,7}$]tridecane series. VII. Pyrolytic elimination of 8-methyl-tricyclo [7.3.1.$0^{2,7}$]tridecen-13-acetates 1527

BEJAN L., voir STERNBERG S. 655

BELDIE R. and A. BUTUCELEA, V. E. SAHINI, The carbon-carbon stretching frequency in ethane, ethane-d_6 and ethane-t_6 327

BENEDEK I., voir IOAN S. 145

BENNUR S. C., voir JIGAJINNI V. B. 1221

— and V. B. JIGAJINNI, V. V. BADIGER, Pyrimidines. VI. Synthesis of 2-methylthio-5-bromo-pyrimidine-4-carboxylic acid thiosemicarbazides, 3-pyrimidyl-1,2,4-(4H)-triazoles and 2-arylamino-1,3,4-thiadiazoles 757

BENNUR R. S., voir JIGAJINNI V. B. 1221

BHATNAGAR V. M., Preparation and unit cell dimensions of lead hydroxyapatite 879

BIADER CEIPIDOR U., voir MAGRI A. D. 1265

BÎLBĂ N. et V. ABABI, La synthèse des zéolithes du système $Na_2O-Al_2O_3-SiO_2-H_2O$, de type A et faujasitique 285

BOLDEA A. and C. DRUGĂRIN, M. MRACEC, Z. SIMON, New urea and thiourea derivatives. I. Syntheses, IR and UV spectra of some new disubstituted urea and thiourea derivatives with possible physiological effects 1345

BOTA A., voir BALABAN A. T. 1183

— and A. T. BALABAN, F. CHIRALEU, Pyrylium salts formed by diacylation of olefins. XX. PMR spectra of 2,4,6-trimethyl-3-phenylpyrylium and -pyridinium salts 101

BOURCEANU G. and V. ABABI, GH. POPA, M. SANDULOVICIU, Phenol obtention from benzene in oxygen plasma generated by a high frequency discharges. I. Dispersional analysis of the data and the multiple regression equation of the process 1405

BRĂUTIGAM G., voir EMONS H. H. 223

BREZEANU M. and I. JITARU, Coordination compounds with iron-tin bonds 407

BUDRUGEAC P. and M. I. VASS, On the surface stress and surface tension of gas-solid interface 1305

BULZAN M. and E. SEGAL, The influence of Fe_2O_3 on the thermal stability of $BaCO_3$ 651

— , voir SOLACOLU Ș. 545

BUTUCELEA A., voir BELDIE R. 327

— , voir GRIGOROVICI R. 965

C

CAMBOLI D., voir CIMPU V. 1327

— et D. FĂTU, V. CIMPU, La décomposition thermique des combinaisons complexes thiocyaniques du Pd(II) avec la pyridine 1479

CARP E. and M. DORNEANU, I. ZUGRĂVESCU, Bicyclic bridgehead nitrogen systems. V. Pyrazolo- and tetrazolobenzocinnolines by 1,3-dipolar cycloaddition reactions 1203

CARPOV A. and S. MAXIM, M. DIMA, Growth-regulating polymers. II. The poly(N,N-dimethylaminoethyl methacrylate salts) of 2,4-dichlorophenoxyacetic and 2,4,5-trichlorophenoxyacetic acids 1097

CATRINA E., IR spectra of some chelates of thiazolidinic acids 81

— and Z. SIMON, Z. SZABADAY, GH. CATRINA, Electronic spectra of Co^{III} thiazolidine chelates 1037

CATRINA GH., voir CATRINA E. 1037

CENUȘE Z., voir VÎLCU R. 343

CHIRALEU F., voir BOTA A. 101

CHIRCA M., voir GHEORGHIU C. 859

CIMPU V., voir CAMBOLI D. 1479

— et D. CAMBOLI, Des combinaisons complexes du Pd(II) avec le Romergan et les ions Cl^- et CNS^- 1327

CINCA S. and M. CONSTANTINESCU, E. SEGAL, Chemisorptive properties of zinc oxide thin films 1149

CIOHODARU L. and A. MEGHEA, The electronic structure of some stilbene derivatives. I. The electronic spectra and transmission of the substituent effects in molecules of some nitro-containing *trans*-stilbene derivatives 1127

— and A. MEGHEA, The electronic structure of some stilbene derivatives. II. Quantitative correlations referring to the substituent effects on the electronic spectra of some stilbene derivatives 1473

CIOMÂRTAN D., voir NICOLESCU I. V. 73

CIOPEC M. and D. I. MARCHIDAN, The influence of non-stoichiometry upon heat capacity of uranium oxides. A model of quantitative approach 997

CIORĂNESCU E., voir DRAGU E. 1497

— , voir ELIAN M. 89

CIUBOTARIU D., voir MOȚOC I. 769, 775, 949, 1247

— und I. MOȚOC, S. HOLBAN, Zur Kopolymerisation. V. Die Simulierung der Bildung eines Makromoleküls durch binäre Mischpolymerisation. Das Programm MEMORY 3 1253

CIUBOTARIU M., voir FELDMAN D. 269

CIUGUREANU M., voir FELDMAN D. . . . 269

CIUPE R. und M. GĂVAN, Der gaschromatographische Nachweis und die quantitative Bestimmung einer Mischung von 1-Chlor-3-thia-pentan und 3,6-Dithia-octan aus den bei der Synthese dieser Stoffe sich ergebenen Abflusswässern . . . 1263

CIUREA L. and V. EM. SAHINI, A. MATEESCU, Spectral study of 4,7-phenanthroline-5,6-dione radical anion . . . 1445

CIUREANU M., A theoretical study of azaindoles . . . 1007

Comptes rendus, 161, 162, 163, 313, 314, 315, 317, 481, 481, 637, 638, 639, 640, 640, 797, 798, 799, 955, 955, 956, 957, 957, 1109, 1109, 1110, 1111, 1111, 1567, 1568, 1569 . . . 1479

CONSTANTINESCU C. und GH. C. CONSTANTINESCU, Einfluss der Substituenten auf die analytischen Eigenschaften von organischen Reagenzien in der Reaktion mit [TlBr$_4$] . . . 571

— und GH. C. CONSTANTINESCU, Einfluss von Methoxy-Substituent auf die Reaktion zwischen [TlBr$_4$] und Malachitgrün . . . 391

CONSTANTINESCU GH. C., voir CONSTANTINESCU C. . . . 571, 391

CONSTANTINESCU M., voir CINCA S. . . . 1149

— and E. SEGAL, M. VASS, Field effect investigation of adsorption on semiconductor films . . . 503

CONTINEANU I., voir MURGULESCU I. G. . . . 1115

CORNEA I. and V. ICHIM, The efficiency of organic corrosion inhibitors in oilfield waters . . . 59

COSTEA T., voir MĂNTESCU C. . . . 789

CRISTU D., voir MĂNTESCU C. . . . 789

CRISTUREAN E., voir GHEORGHIU C. . . . 859

CRUSOS A., voir SIMIONESCU CR. I. . . . 1237, 1417

CSÁVÁSSY G., voir SUCIU D. . . . 113

D

DAMALAN F., voir ONICIU L. . . . 1287

DeARMOND M. K., voir GRIGOROVICI R. . . . 965

DIACONESCU M., voir GAVRILĂ D. . . . 155

DIMA M., voir CARPOV A. . . . 1097

— , voir MAXIM S. . . . 631, 937

— , voir PETREUŞ O. . . . 911

DIMONIE M. and CR. OPRESCU, GH. HUBCA, Variation of molecular mass with time in polymerization by free radicals . . . 763

DINESCU R., voir PREDA M. . . . 1023

DINULESCU F., voir GHEORGHIU C. . . . 859

DINULESCU I. G., voir ŞTEFAN N. . . . 107

DIRSKA B., voir SZYMURA J. . . . 1103

DONESCU D., Kinetics of polymerization of 1,3-dioxepane with BF$_3$OEt$_2$ . . . 139

— , Kinetic studies on the copolymerization of 1,3-dioxepane with epichlorophydrin initiated with BF$_3$OEt$_2$ . . . 277

— , Kinetic studies on the copolymerization of β-propiolactone with epichlorohydrin and 1,3-dioxepane . . . 1367

DORNEANU M., voir CARP E. . . . 1203

DOROHOVA E. N., voir ALIMARIN I. P. . . . 835

DRĂGAN GH., Amorphous-crystalline coupling in polyethylene. III. Interlamellar orderings in polyethylene with chemical etched defects . . . 1381
— , Amorphous-crystalline coupling in polyethylene. IV. Earth gravity effect on defect precipitation during annealing 1537

DRĂGHICI C., voir DRAGU E. 1497
DRAGOTĂ I., IONESCU D., TARNĂUCEANU EUSTANŢA, DOBRE V. and NICULESCU-DUVĂZ I., Potential anticancer agents. XII. Synthesis of new methanesulfonate derivatives from benzo and naphtopyrans 1543

DRAGOTĂ I. I., voir FEYNS L. V. 1207
DRAGU E. and M. BANCIU, C. DRĂGHICI, M. ELIAN, E. CIORĂNESCU, Carbenium ion reactions. XIII. Acetolysis of 5-tosyloxymethyl-5H-6,7-dihydro-dibenzo[a, c] cyclopropa[e]cycloheptene. 1497

DRĂGULESCU C. and A. NIMARĂ, I. JULEAN, Bismuth(III)-ethylenediaminetetraacetic acid (EDTA) complexes. I. Polarographic study on formation and stability of the complexes in the solution 853
— and A. NIMARĂ, E. PRINCZ, A. BALINT, I. JULEAN, Bismuth (III)-ethylenediaminetetraacetic acid (EDTA) complexes. II. Kinetic studies on the isotopic exchange reaction between the hydrolysed bismuth ion and its EDTA complex 1171

DRUGĂRIN C., voir BOLDEA A. 1345
— , voir NUŢIU R. 355

DUŞOIU N. Anisotropie diélectrique de certains blocs en carton et en papier dans le domaine de micro-ondes. 563
— , The temperature dependence of the dielectric permittivity of ionic crystals with cubic structure. I. Potassium bromide, iodide and chloride 1161

E

EL-KASSAS A. G., voir YOUSSEF M. H. 263
ELIAN M. and M. BANCIU, L. STĂNESCU, E. CIORĂNESCU, Thermal and photochemical rearrangements of dibenzo-bullvalene and related dibenzo-$(CH)_{10}$ hydrocarbons 89
— , voir DRAGU E. 1497

EMONS H. H. und G. BRÄUTIGAM, Physikalisch-chemische Eigenschaften von Schmelzgemischen aus Calciumchlorid und Cäsiumchlorid . . 223

ENCULESCU M., Influence of some oxides of transitional metals on the formation of calcium orthosilicate. 1013
— , Influence of titanium dioxide on the structure and on the properties of mineralogical compounds in white Portland cements 549

F

FĂRCĂŞAN V. and S. FLOREA, Benzofuro-benzothiazoles. V. 2-Amino- and 2-mercapto-benzofuro-benzothiazoles 621

FĂTU D., voir CAMBOLI D. 1479
— , voir GHEORGHIU A. 367, 825
— , and E. SEGAL, Decomposition kinetics of copper tetra-ammine sulphate monohydrate 187

FELDMAN D. and M. CIUGUREANU, M. CIUBOTARIU, Some data on the compatibility of polyacrylonitrile with other polymers 269
— , voir SIMIONESCU CR. I. 927

FERRERO L. et S. GERIBALDI, M. AZZARO, Essai de généralisation du phénomène de régiosélectivité dans la réduction des oximes par des agents aluminiques. 49

FEYNS L. V. and I. I. DRAGOTĂ, I. NICULESCU-DUVĂZ, Infrared spectra of some new chromanone and coumarine derivatives 1207

FIGUERA J. M., voir MARTÍN M. 31

FILATOV E. S., voir VOLKOV A. A. 703

FILIP P., voir GHEORGHIU M. D. 1189

FLOREA S., voir FĂRCĂŞAN V. 621

FLORU L., voir URSEANU F. 257, 427

FREYDANK H. und M. T. RÄTZSCH, Zur Berechnung von Parametern des zwischenmolekularen Potentials aus 2. Druckvirialkoeffizienten . . 1463

G

GALASIU I., voir PETRESCU S. 517

GALINOS A. G. et P. B. ISSOPOULOS, Préparation d'antimoine colloïdal de haute pureté 229

GANOVICI L., voir PETRESCU N. 1293

GĂVAN M., voir CIUPE R. 1263

GAVRILĂ D. and M. DIACONESCU, D. IORDACHE, Mechanical and electrical properties of irradiated polypropylene 155

GEANĂ D. P., voir VIŞAN T. 1153

GENUNCHE A., voir MĂNTESCU C. 789

GERIBALDI S., voir L. FERRERO 49

GHEORGHE P., voir SPILIADIS A.. 595

GHEORGHIU A., and D. FĂTU, E. SEGAL, Critical considerations on the nonisothermal methods for the evaluation of the kinetic parameters of endothermal decompositions in solid-gas systems. Nickel acetate tetrahydrate dehydration 367
— and D. FĂTU, E. SEGAL, Nonisothermal kinetic study of the transformations and nonstoichimetrization of cobalt and nickel oxides 825

GHEORGHIU C. and M. CHIRCA, E. CRISTUREAN, F. DINULESCU, Hexachlorocyclotriphosphazene derivatives 859
— and C. MĂRCULESCU, Contribution to the coordination chemistry of s-triazines. I. Coordination compounds of copper with thioammeline derivatives 707

GHEORGHIU M. D. and A. T. BALABAN, Ground and excited state SCF—PPP—CI calculations for pyrylium salts 1513
— and P. FILIP, Electronic structure of cyclobutadiene fused with heterocyclic ring. II. Cyclobutadienes condensed with five-membered heterocyclic rings 1189

GHIZDAVU L., voir MARCU GH. 589

GIOABĂ A. and O. MAIOR, M. MITRAN, Reaction of tellurium tetrachloride with 4-fluoro-4′-methyldiphenyl ether 733
— and M. NEDEA, O. MAIOR, Chemistry of phenoxatellurine. Action of tellurium tetrachloride on 4-halodiphenyl ethers 739

GIURGIU D. and I. POPESCU, Reactivity of organo-aluminium compounds towards Lewis bases. II. Diaryl- and dialkylaluminium ketiminphosphines 1373

GLATZ A. M., voir RĂZUŞ A. C. 727

GOCAN A. and F. HODOŞAN, Exo- and endohormones. III. New derivatives of synthetic ecdysone analogous and related compounds 627

GRIGOROVICI R. and A. BUTUCELEA, V. E. SAHINI, M. K. DeARMOND, Normal coordinate analysis of hexahaloethanes 965

GROZA I. et D. I. MARCHIDAN, L'énergie accumulée par la déformation plastique à froid des laitons binaires et alliés 509

H

HAJJAR R. F., Correlation between energy of vaporization, molecular parameters and critical temperatures and pressures 217

HALGERI A. B., voir WALVEKAR S. P. 237

HANEŞ A., voir RĂZUŞ A. C.. 727

HILLEBRAND M., voir BACIU I. 485

HODOŞAN F., voir GOCAN A. 627

HOLBAN ŞT., voir MOŢOC I. 769, 775, 1247

— , voir CIUBOTARIU D. 1253

HOPÎRTEAN E., voir LITEANU C. 933, 1395

— and E. ŞTEFĂNIGĂ, Membrane-electrodes of the metallic wire-plastic membrane type. III. Membrane-electrodes for organic cations 305

HUBCA GH., voir DIMONIE M. 763

I

ICHIM V., voir CORNEA I. 59

IOAN S. and I. BENEDEK, Study of N-vinylcarbazole ethyl methacrylate statistical copolymer by light scattering 145

IONESCU C., voir MIHAIL R. 293

IONESCU M., voir MACAROVICI R. 881

IORDACHE D., voir GAVRILĂ D. 155

IOVU M. and E. VOINA, Mixed aromatic esters of phosphoric acid 447

IRINEI F., voir VÎLCU R. 333, 491

ISMAIL M. F., voir ABDEL RAHMAN S. M. 889

ISMAIL Z. M., voir ABDEL RAHMAN S. M.. 889

ISSA F. M., voir R. M. ISSA 781

ISSA R. M. and H. Z. YOUSSEF, F. M. ISSA. Y. M. ISSA, Spectrophotometric study of some arylidenemalononitriles in organic solvents and butter solutions 781

ISSA Y. M., voir ISSA R. M. 781

ISSOPOULOS P. B., Complex chelate compounds of iso- and heteropolyanions of Mo(VI) and W(VI) with Chrome Azurol S. II. Complex chelate compounds of heteropolyanions of Mo(VI) and W(VI) 585

— , Complex chelate compounds of Mo(VI) and W(VI) iso- and heteropolyanions with Chrome Azurol S. I. Complex chelate compounds of Mo(VI) and W(VI) isopolyanions 401

— , voir GALINOS A. G. 229

IVANA E., voir MURGULESCU I. G. 169, 961, 1115

J

JIGAJINNI V. B., voir BENNUR S. C. 757

— , and S. C. BENNUR, R. S. BENNUR, V. V. BADIGER, Hydrazones of piperidino-N-acetohydrazide and morpholino-N-acetohydrazide of pharmacological interest 1221

JITARU I., voir BREZEANU M. 407

JOVANOVIĆ N. N., voir JOVANOVIĆ Ž. D.. 65

JOVANOVIĆ Ž. D. et N. N. JOVANOVIĆ, Texture des catalyseurs à base d'oxyde de zinc, cuivre et chrome pour la conversion de l'oxyde de carbone 65

JULEAN I., voir DRĂGULESCU C. 853, 1171

JURCONI E., voir ONCESCU T.. . . . . 805, 985

K

KASHYAP B. C. and A. D. TANEJA, S. K. BANERJI, Ionization constants of some N-aryl, N′-2-(5-halo-pyridyl)thioureas 903

KÉKEDY L. and I. KOVÁCS, Polarographic investigation of the decomposition of xanthates in acid medium 121

— , voir POPESCU A. 683

KÉKEDY N. L., voir LITEANU C. 1395

KHOSROVI M., voir PARCHAMAZAD I.. 1355

KNOP J. V. and N. TRINAJSTIĆ, A. SABLJIĆ, Topological studies of fused tricyclic and tetracyclic molecules having planar conjugated perimeter 749

KOVÁCS I., voir KÉKEDY L. 121

L

LAL S., Polarographic maximum of cobalt (II) 1359

LAURENT P. A. et M. J. LAURENT-DUHAMEL, Sur une transformée simple de certains isothermes de démixtion ternaire 11

LAURENT-DUHAMEL M. J., voir LAURENT P. A. 11

LECA M., voir BĂRBULESCU N. S. 1527

LEONTE C. and I. ZUGRĂVESCU, The reaction of pyridinium-cyano-carbalkoxy-methylids with α-nitroso-β-naphtol, a route to naphthoxazinones 423

LITEANU C. and H. HOPÎRTEAN, R. VLAD, Utilization of a Hg^{2+} — sensitive membrane-electrode in the determination of some α-aminoacids 933

— and E. HOPÎRTEAN, I. C. POPESCU, N. L. KÉKEDY, E. VERESS, V. LITEANU, On a new procedure for obtaining sulphur dioxide starting from calcium sulphate. II. Utilization of phosphogypsum and of natural gypsum with impurities of $CaCO_3$ 1395

LITEANU V., voir LITEANU C. 1395

LUCA C. and A. POPA, Utilization of the urea-polyvinyl chloride adducts in the polyvinyl chloride fractionation 231

M

MACAROVICI R. et M. IONESCU, Obtention et comportement des oxazoles. II. Bromuration des 2,5-diphényloxyzoles 881

MACOVEI V., Spectral solvent effects in aromatic compounds solutions. II. The solvent effects on the position and intensity of chlorobenzene band, at 2600 Å 193
— , Spectral solvent effects in aromatic compounds solutions. III. The solvent effects on the position and intensity of zinc oxide thin films 1137

MADRIÑAN E. C. DE, voir VÎLCU R.. 333

MAGRI A. D. et G. D'ASCENZO, V. BIADER CEIPIDOR, A. MARINO, Analyse thermique des composés du cobalt (III) tétrammine avec des acides organiques dicarboxyliques 1265

MAI VAN TRI, voir PETROVANU M. 717

MAIOR O., voir GIOABĂ A. 733, 739
— , and N. RĂȘANU, Syntheses based on thieno [2,3-b] benzothiachromone 745

MĂNTESCU C. and A. GENUNCHE, D. CRISTU, T. COSTEA, Processes associated with ^{6}Li(n, α)^{3}H nuclear reaction. III. Chemical evidence for the stabilization forms of recoil tritium in lithium halides 789

MARCHIDAN D. I., voir CIOPEC M. 997
— , voir GROZA I. 509
— and L. PANDELE, Study of the isomorphic transitions of some iron oxides 661
— and S. TĂNĂSESCU, Thermodynamic study of some uranium oxides by solid efectrolyte EMF measurements. Solid state coulometric titration technique 1451
— and L. VASU, Melting heats of alkali halide solid solutions 25

MARCU GH. and L. GHIZDAVU, New mixed heteropolycompounds : tungstoniobiosilicates 589
— and M. RUSU, Heteropolytungstates with U(IV) as central atom. I. Photocolorimetrical study of the formation of heteropolycombinations UL_2, where $L = PW_{11}O_{39}^{7-}$ and $P_2W_{21}O_{71}^{6-}$ 385

MĂRCULESCU C., voir GHEORGHIU C. 707, 413, 869

MARINO A., voir MAGRI A. D. 1265

MARTÍN M. and V. MENÉNDEZ, J. M. FIGUERA, Equilibrium geometry and heat of formation of aliphatic diazocompounds diazirines and related singlet carbenes. AMINDO/2 calculations 31

MATEESCU A., voir CIUREA L. 1445

MAVRODIN-TĂRĂBÎC M., voir ONACA I. 207
— et I. ONACA, I. SOLACOLU, Contribution à l'étude de la réduction de l'oxygène sur les électrodes poreuses en argent. II. L'influence de la concentration de l'électrolyte sur les performances des électrodes 41
— et I. ONACA, I. SOLACOLU, Contribution à l'étude de la source chimique de courant Zn(MeOH)O_2. III. La détermination des paramètres optimaux de fonctionnement pour une pile à cathode en argent 373

— and I. ONACA, I. SOLACOLU, Mathematical model in the range 50—70° and 5N—7N KOH for a hydrogen-oxygen fuel cell . . . 695

— , voir RADOVICI O. 991

— , voir SOLACOLU I. 531

MAXIM S., voir CARPOV A. 1097

— and M. DIMA, Growth regulating (adjusting) polymers. III. Poly(4-vinylpyridine) salts with halogen (alkyl) aryloxyalkylcarboxylic acids 937

— and M. DIMA, Viscosimetric study of the poly(4-vinylpyridine) salts with the halogen(alkyl)aryloxyalkyl carboxylic acids . . . 631

MEGHEA A., voir CIOHODARU L. 1127

MENÉNDEZ V., voir MARTÍN M. 31

MIHAIL R. und C. SINGER, C. IONESCU, Ein Modell für die Verweilzeitverteilung der dispersen Phase in einem Gas-Flüssig oder Flüssig System 293

MITRACHE I., voir ONICIU L. 1287

MITRAN M., voir GIOABĂ A. 733

MOLDOVEANU I., voir TOPOR L. 495

MOROSANOVA S. A., voir ALIMARIN I. P 835

MOŢOC I., voir CIUBOTARIU D 1253

— und D. CIUBOTARIU, Zur Kopolymerisation. I. Mathematisches Modell der Bildung eines binären Kopolymerisationsproduktes 949

— und D. CIUBOTARIU, ŞT. HOLBAN, Zur Kopolimerization. II. Die Simulierung der Bildung eines Makromoleküls. Das Programm MEMORY 1 769

— und D. CIUBOTARIU, ŞT. HOLBAN, Zur Kopolymerisation. III. Die Simulierung der Bildung eines Makromoleküle. Das Programm MEMORY 2 775

— und D. CIUBOTARIU, ŞT. HOLBAN, Zur Kopolymerization. IV. Das mathematische Modell der Bildung eines binären Kopolymers: die verbesserte Version. 1247

MRACEC M., voir BOLDEA A 1345

MUREŞAN A., voir SIMITI I 1073

MURGULESCU I. G. and E. IVANA, The absorption spectrum of PbI_2 in vapour phase 169

— and E. IVANA, E. POPA, absorption spectra of solid and molten PbI_2 961

— and E. IVANA, E. POPA, I. CONTINEANU, Absorption spectra of molten SnCf_2 and SnI_4 1115

— und M. WEISSMANN, Der Einfluss des Methans auf den thermischen Zerfall des Chloroforms. I. Die ersten drei Reaktionsschritte. . . . 1275

— und M. WEISSMANN, Der Einfluss des Methans auf der thermischen Zerfall des Chloroforms. II. Die vierte Reaktionsstufe 1435

N

NEDEA M., voir GIOABĂ A 739

NESMEIANOV AN. N., voir VOLKOV A. A 703

NICOLESCU I. V. and M. SPINZI, D. CIOMÂRTAN, Relationship between properties and activity of alumo-chromia catalysts. I. Role of precursors in obtaining aluminium oxides 73

NICULESCU-DUVĂZ I., voir FEYNS L. V 1207

NIMARĂ A., voir DRĂGULESCU C 853, 1171

NUŢĂ V., voir SIMIONESCU CR. I 927

NUŢIU R. and Z. SIMON, C. DRUGĂRIN, Molecular orbital study of 2-thio-5-nitro-barbituric acid 355

O

ONACA I., voir MAVRODIN-TĂRĂBÎC M 41, 373, 695

— et M. MAVRODIN-TĂRĂBÎC, I. SOLACOLU, L'étude de la réduction de l'oxygène sur les électrodes. Energies apparentes d'activation 207

— , voir RADOVICI O 991

— , voir SOLACOLU I 531

ONCESCU T. and E. JURCONI, Solvent effect on the kinetics of the thermal decomposition of dioxalato-diaquomanganate(III) in dimethyl sulphoxide-water mixtures 985

— and E. JURCONI, Solvent effect on the thermal decomposition of $[Mn(C_2O_4)_2(H_2O)_2]K \cdot 3H_2O$ in DMF$-H_2O$ mixtures 805

ONICIU L. and I. MITRACHE, V. A. TOPAN, F. DAMALAN, Contributions to the study of the superficial phenomena in porous media 1287

OPRESCU CR., voir DIMONIE M. 763

OSCHERIN B. N., Vzaismosviaz poverkhnostnogo natiyazheniya, szhimaemosti i blizhnego poriadka rasplavov vblizy tochiki plavleniya. I. Schelochino-galoidnye soli i poluprovodniki 351

P

PANDELE L., voir MARCHIDAN D. I. 661

PARCHAMAZAD I. and M. KHOSROVI, N. SADEGHI, Selectivity in the alkylation of benzene by cyclopropane 1355

PETRESCU N. and L. GANOVICI, Self-diffusion in liquid thallium 1293

PETRESCU S. et S. STERNBERG, I. GALASIU, V. PETRESCU, Application du modèle du pore partiellement rempli dans le processus d'adsorption électrochimique sur les électrodes halogène-charbon actif dans les sels fondus 517

— and S. STERNBERG, V. PETRESCU, Galvanostatic study of the efectrochemical adsorption process on a chlorine-activated carbon electrode in molten salts. IV. Cathodic polarization curve equation (discharge) 813

PETRESCU V., voir PETRESCU S. 517, 813

PETREUŞ O. et M. DIMA, Sur les réactions des polymères vinyliques contenant des groupements aminiques avec les composés organiques du soufre. II. La réaction entre la poly(vinylamine) et le chlorure de thionyle 911

PETROVANU M. et MAI VAN TRI, V. BĂRBOIU, Pyridazinium-ylures. I. Addition du 3-(*p*-cumyl)-pyridazinium-phénacylure et du 3-(*p*-cumyl)-pyridazinium-(*p*-nitro)-phénacylure sur les alcynes activés 717

POPA A., voir LUCA C. 231

POPA E., voir MURGULESCU I. G. 961, 1115

POPA GH., voir BOURCEANU G. 1405

POPA V. and E. SEGAL, Adsorption of gaseous mixtures within the framework of Jovanović model 977

POPEA F. and C. MĂRCULESCU, Z. TOMA, Contributions to the coordination chemistry of phtalic acid derivatives. I. Condensation products of phthalic anhydride with *m*-phenylenediamine as coordination ligands for cooper 413

— and Z. TOMA, C. MĂRCULESCU, Contributions to the coordination chemistry of phthalic acid derivatives. II. New copper compounds of phthalimide derivatives 869

POPESCU A. and L. KÉKEDY, Experimental approach to the characterization of penetrated electrode surfaces. VI. Chronopotentiometric study of differently pretreated gold efectrodes 683

POPESCU I., voir GIURGIU D. 1373

POPESCU I. C., voir LITEANU C. 1395

POPESCU L., Influence of the cell diaphragm on the efectromotive force of concentration cells with transport in molten salts 359

PREDA M. and R. DINESCU, Thermal equilibria in the binary systems $MgO-CeO_2$, $CaO-CeO_2$, $SrO-CeO_2$, $BaO-CeO_2$ 1023

PRINCZ E., voir DRĂGULESCU C 1171

Q

QURESHI A. M., USMANI A. A., MALIK ABDUL and AHMAD J., Quantitative determination of cadmium as cadmium oxalate 1563

R

RADOVICI O. and M. MAVRODIN-TĂRĂBÎC, I. ONACA, I. SOLACOLU, Hydrogen oxidation on porous nickel electrodes. IV. The improvement of the electrode performances by addition of different electrocatalysts 991

RAMANNA S., voir WALVEKAR S. P. 237

RĂŞANU N., voir MAIOR O. 745

RĂTZSCH M. T., voir FREYDANK H. 1463

RĂZUŞ A. C. and ZS. ARVAY, A. HANEŞ, A. M. GLATZ, Aluminium chloride catalyzed reactions of unsaturated acids with benzene. VIII. Participation of carboxyl group in the reaction of cyclopentylideneacetic, 1- and 2-cyclopentenylacetic acids with benzene 727

RUSHDY M. I., voir YOUSSEF M. H 263

RUSU M., voir MARCU GH. 385

S

SABLJIĆ A., voir KNOP J. V. 749

SADEGHI N., voir PARCHAMAZAD I. 1355

SAHINI V. E., voir BACIU I. 485

— , voir BELDIE R. 327

— , voir CIUREA I. 1445

— , voir GRIGOROVICI R. 965

— and L. TELEA, Molecular interactions in anisidine isomers. I. Dipole moments 321

— and L. TELEA, Molecular interactions in anisidine isomers. II. Electronic spectra 645

— and J. WEINBERG, M. VASILESCU, Xylidine isomers. IV. Dipole moments in the first excited singlet state 1121

SANDULOVICIU M., voir BOURCEANU G. 1405

SĂVULESCU A., voir SPILIADIS A 595

SEMENOVSKAIA E. N., voir ALIMARIN I. P. 835

SEGAL E., voir BULZAN M. 651

— , voir CINCA S. 1149

— , voir CONSTANTINESCU M. 503

— , voir FĂTU D 187

— , voir GHEORGHIU A. 367, 825

— , voir POPA V 977

— , voir SOLACOLU Ş. 545

— , voir VLAD M. 667, 1311, 1319

— , voir WECHSLER A 831

SIMION A., voir VÎLCU R 3, 177

SIMIONESCU CR. I. et A. CRUSOS, Greffage mécano-chimique des polyoxyméthylènes. V. Aspects cinétiques au broyage vibratoire 1237

— and D. FELDMAN, V. NUŢĂ, Contributions to the polymerization and copolymerization of the acrylonitrile in the presence of organometallic catalysts 927

SIMIONESCU CR. I. and LIGA ADELAIDA, Researches in the terpolymerization field. VII. Theoretical structural characterization of the low conversion acrylonitrile-methacrylic acid-methyl methacrylate terpolymer 1555

— et C. UNGUREANU, A. CRUSOS, Electropolymérisation des monomères vinyliques en solvants aprotiques polaires. III. Électropolymérisation de l'acrylonitrile en carbonate de propylène et d'éthylène 1417

SIMITI I. and A. MUREŞAN, Contributions to the study of heterocycles. XXXVIII. Application of the Sommelet reaction in the series of 2-aryl-4-methyl-5-chloromethyl-thiazole 1073

SIMON Z., voir BOLDEA A 1345

— , voir CATRINA E 1037

— , voir NUŢIU R 355

SINGER C., voir MIHAIL R 293

SINGH N. B., Interaction between acenaphtene and picric acid 1177

SOLACOLU I., voir MAVRODIN-TĂRĂBÎC M 41, 373, 695

— et M. MAVRODIN-TĂRĂBÎC, I. ONACA, L'étude de la réduction de l'oxygène sur les électrodes poreuses en argent. IV. L'effet de la variation des paramètres de fonctionnement sur la polarisation des électrodes à de différentes densités de courant 531

— , voir ONACA I. 207

— , voir RADOVICI O. 991

SOLACOLU Ş. and M. BULZAN, E. SEGAL, Studies on the formation kinetics of barium hexaferrite $BaO \cdot 6Fe_2O_3$ in the binary system $BaO-Fe_2O_3$ 545

SPACU P., voir BANCIU A. C. 1331

SPILIADIS A. and P. GHEORGHE, H. SZÖGY, A. SĂVULESCU, Dyes for synthetic fibers. IX. Disperse azo-dyes for polyester fibers 595

SPINZI M., voir NICOLESCU I. V. 73

SPURCACIU C., voir BALTĂ P 469

SRINIVA SAN T. N., voir WALVEKAR S. P. 237

STĂNESCU L., voir ELIAN M 89

STĂNOIU I. I., voir BALABAN A. T. 1183

ŞTEFAN N. and I. G. DINULESCU, M. AVRAM, Investigations in the cyclobutane series. XXXVIII. Rearrangement of the dibenzo[*b*, *g*]bicyclo[4·2·0]octa-2,7-diene system 107

ŞTEFĂNIGĂ E., voir HOPÎRTEAN E 305

STERNBERG S. and L. BEJAN, Thermodynamic properties of AgI + NAI + KI fused salt ternary system by formation cell method 655

— , voir PETRESCU S 517, 813

— and V. VASILESCU, Ultrasonic velocity and compressibility in fused AgCl—AgBr, AgCl—KCl and AgI 1457

— , voir VIŞAN T. 1153

SUCIU D. and G. CSÁVÁSSY, Thiazole compounds. III. Kinetics of hydrolysis of some 2-aryl-4 and 5-diazo ketone derivatives 113

SZABADAY Z., voir CATRINA E 1037

SZÖGY H., voir SPILIADIS A. 595

SZYMURA J. and B. DIRSKA, The electron microscopic investigations of silica gels structure and dispersion of synthetic aluminosilicates 1103

T

TĂNĂSESCU S., voir MARCHIDAN D. I. 145

TANEJA A. D., voir KASHYAP B. C. 903

TĂRĂBĂŞANU-MIHĂILĂ C., voir URSEANU F. 257

TATU E., voir VÎLCU R 491

TELEA L., voir SAHINI V. E. 321, 645

TEODORESCU M., The structure of dark-red compound [Fe(II)Phen$_2$(NCS)$_2$]·H$_2$O 1031

TOMA Z., voir POPEA F 413, 869

TOPAN V. A., voir ONICIU L. 1287

TOPOR L. and I. MOLDOVEANU, Thermodynamic properties of NaCl—CaCl$_2$ and KCl—CaCl$_2$ molten systems 495

TRINAJSTIĆ N., voir KNOP J. V. 749

U

UNCUŢA C. and A. T. BALABAN, Reaction of pyrylium salts with nucleophiles. XI. Chemical shift non-equivalence of isopropyl in atropisomeric 1-aryl-2-isopropyl-4,6-dimethylpyridinium salts 251

UNGUREANU C., voir SIMIONESCU CR. 1417

URSEANU F., New syntheses of dyes with napht[2,3-c] xanthene-5,8,14-trione and naphth[2,3-c]thioxanthene-5,8,14-trione structure. 1227

— and L. FLORU, Bromamine acid-anthraquinonic intermediate used in dyes syntheses 427

— and C. TĂRĂBĂŞANU-MIHĂILĂ, L. FLORU, New disperse dyes with naphth[2,3-c]acridan[5,6-de]pyrimidin-5,11-dione structure 257

V

VASILESCU E., voir ANTONESCU E. 461
VASILESCU M., voir SAHINI V. E. 1121
VASILESCU V., voir STERNBERG S. 1457
VASS M. I., voir BUDRUGEAC P. 1305
— , voir CONSTANTINESCU M. 503
VASU L., voir MARCHIDAN D. I. 25
VERESS E., voir LITEANU C. 1395
VÎLCU R. and Z. CENUȘE, Activity coefficients and hydrogen bond energy from calorimetric measurements 343
— and F. IRINEI, E. TATU, Extension of some regularities of ternary electrolytic aqueous solutions in ionic liquids 491
— and E. C. DE MADRIÑAN, F. IRINEI, Thermodynamic properties of electrolyte solutions. V. Differential cryoscopy in $NaCl + CuCl_2 + H_2O$ and $KCl + CuCl_2 + H_2O$ ternary systems and in associated binaries 333
— and A. SIMION, Acoustic and volumetric properties of aqueous salt solutions 3
— et SIMION A., Grandeurs d'excès par des mesures acoustiques, dans les systèmes binaires de liquides 177
VIȘAN T., and D. P. GEANĂ, S. STERNBERG, Voltammetric and chronopotentiometric study of silver ion in molten potassium nitrate 1153
VLAD M., On the frecvency of reaction events in a system with first order reaction network 677
— and E. SEGAL, On the stochastic analysis of the reactions networks. I 667
— and E. SEGAL, On the stochastic analysis of the reaction networks. II. The principle of detailed balance for reaction networks 1311
— and E. SEGAL, On the stochastic analysis of the reaction networks. III. Langevin approaches 1319
VLAD R., voir LITEANU C. 933
VLASSA M., Exo- and endohormones. I. Application of the ketoxime activation to the synthesis of the melanocyte inhibiting factor 455
— , Exo- and endohormones. II. Synthesis of peptidic juvenile hormone analogues 897
VOINA E., voir IOVU M. 447
VOLANSCHI E., voir BACIU I 485
VOLKOV A. A. i Z. E. AKSENOVA, E. S. FILATOV, AN. N. NESMEYANOV, Povedenie seria (III) v vodno-metanolnykh rastvorakh 703

W

WALVEKAR S. P. and A. B. HALGERI, S. RAMANNA, T. N. SRINIVASAN, Thermal effect on surface acidity and catalytic activity of $ZrO_2-Al_2O_3$ and ZrO_2-SiO_2 catalysts 237
WECHSLER A. and E. SEGAL, Thermoelectric power variation during gas adsorption on thin semiconducting films. The zinc oxide-carbon monoxide system 831
WEINBERG J., voir SAHINI V. E. 1121

WEISSMANN M., voir MURGULESCU I. G 1275, 1435

WEXLER H. and V. BĂRBOIU, Contributions to the study of condensation reactions between cresols and isatin and its derivatives. I. A new molecular transposition 127

Y

YOUSSEF H. Z., voir R. M. ISSA 781

YOUSSEF M. H. and A. G. EL-KASSAS, M. I. RUSHDY and I. K. ABDOU, Aromatic hydrocarbons from high boiling petroleum distillates 263

Z

ZUGRĂVESCU I., voir CARP E 1203

—, voir LEONTE C 423

REVUE ROUMAINE DE CHIMIE

INDEX DES SUJETS

Page

A

Absorption spectra of molten $SnCl_2$ and SnI_4, I. G. MURGULESCU, E. IVANA, E. POPA and I. CONTINEANU 1115

Absorption spectra of solid and molten PbI_2, The –, I. G. MURGULESCU, E. IVANA and E. POPA 961

Absorption spectrum of PbI_2 in vapour phase, The –, I. G. MURGULESCU and E. IVANA 167

Acenaphtene and picric acid, Interaction between –, N. B. SINGH 1177

Acoustic and volumetric properties of aqueous salt solutions, R. VÎLCU and A. SIMION 3

Activity coefficients and hydrogen bond energy from calorimetric measurements, R. VÎLCU and Z. CENUȘE 343

Adsorption électrochimique sur les électrodes halogène-charbon actif dans les sels fondus. Application du modèle du pore partiellement rempli dans le processus d' –, S. PETRESCU, S. STERNBERG, I. GALASIU et V. PETRESCU 517

Adsorption of gaseous mixtures within the framework of Jovanović model, V. POPA and E. SEGAL 977

Adsorption on semiconductor films, Field effect investigation of –, M. CONSTANTINESCU, E. SEGAL and M. VASS 503

Alkylation of benzene by cyclopropane, Selectivity in the –, I. PARCHAMAZAD, M. KHOSROVI and N. SADEGHI 1355

Aluminium chloride catalyzed reactions of unsaturated acids with benzene. VIII. Participation of carboxyl group in the reaction of cyclopentylideneacetic, 1- and 2-cyclopentenylacetic acids with benzene, A. C. RĂZUȘ, ZS. ARVAY, A. HANEȘ and A. M. GLATZ 727

Alumo-chromia catalysts. I. Role of precursors in obtaining aluminium oxides. Relationships between properties and activity of –, I. V. NICOLESCU, M. SPINZI and D. CIOMÂRTAN 73

Amines on 3-benzylidene phtalide and some allied compounds, Action of –, S. M. ABDEL RAHMAN, M. F. ISMAIL and Z. M. ISMAIL . . . 889

Anizotropie diélectrique de certains blocs en carton et en papier dans le domaine des micro-ondes, N. DUȘOIU. 563

Antimoine colloïdal de haute pureté, Préparation d' –, A. G. GALINOS et P. B. ISSOPOULOS. 229

Rev. Roumaine de Chimie | 21, *11–12*, p. 1587–1597 (1976), Bucarest

Aromatic compounds solutions. III. The solvent effects on the position and intensity of nitrobenzene band at 2500 Å, Spectral solvent effects in —, V. MACOVEI 1137

Aromatic hydrocarbons from high boiling petroleum distillates, M. H. YOUSSEF, A. G. EL-KASSAS, M. I. RUSHDY and I. K. ABDOU 263

Arylidenemalononitriles in organic solvents and buffer solutions, Spectrophotometric study of some —, R. M. ISSA, M. Z. YOUSSEF, F. M. ISSA and Y. M. ISSA 781

Azaindoles, A theoretical study of —, M. CIUREANU 1007

B

Barium hexaferrite $BaO \cdot 6Fe_2O_3$ in the binary system $BaO-Fe_2O_3$, Studies on the formation kinetics of —, Ș. SOLACOLU, M. BULZAN and E. SEGAL 545

Benzofuro-benzothiazoles. V. 2-Amino- and 2-mercapto-benzofuro-benzothiazoles, V. FĂRCĂȘAN and S. FLOREA 621

Bicyclic bridgehead nitrogen systems. V. Pyrazolo- and tetrazolo-benzocinnolines by 1,3-dipolar cycloaddition reactions, E. CARP, M. DORNEANU and I. ZUGRĂVESCU. 1203

Bismuth(III)-ethylenediamine-tetraacetic acid (EDTA) complexes. I. Polarographic study on formation and stability of the complexes in the solution. C. DRĂGULESCU, A. NIMARĂ and I. JULEAN . . . 853

Bismuth(III)-ethylenediaminetetraacetic acid (EDTA) complexes. II. Kinetic studies on the isotopic exchange reaction between the hydrolysed bismuth ion and its EDTA complex, C. DRĂGULESCU, A. NIMARĂ, E. PRINCZ, A. BALINT and I. JULEAN 1171

C

Cadmium quantitative determination, of —, A. M. QURESHI, A. A. USMANI, ABDUL MALIK and J. AHMAD 1563

Calcium orthosilicate, Influence of some oxides of transitional metals on the formation of —, M. ENCULESCU 1013

Carbenium ion reactions. XIII. Acetolysis of 5-tosyloxy-methyl-5H-6,7-dihydrodibenzo[a, c]cyclopropa[e] cycloheptene, E. DRAGU, M. BANCIU, C. DRĂGHICI, M. ELIAN and E. CIORĂNESCU . . . 1497

Carbon-carbon stretching frequency in ethane, ethane-d_6 and ethane-t_6, The —, R. BELDIE, A. BUTUCELEA and V. E. SAHINI 327

Catalyseurs à base d'oxyde de zinc, cuivre et chrome pour la conversion de l'oxyde de carbone, Texture des —, Ž. D. JOVANOVIĆ et N. N. JOVANOVIĆ 65

Chelates of thiazolidinic acids, IR spectra of some —, E. CATRINA 81

Chemical graphs. XVI. Codes for configurations of conjugated polyenes, A. T. BALABAN 1045

Chemical graphs. XXVII. Enumeration and codification of staggered conformations of alkanes, A. T. BALABAN 1049

Chemisorptive properties of zinc oxide thin films, S. CINCA, M. CONSTANTINESCU and E. SEGAL 1149

Chloroforms. I. Die ersten drei Reaktionschritte, Der Einfluss des Methans auf den thermischen Zerfall des —, I. G. MURGULESCU und M.WEISSMANN 1275

Chloroforms. II. Die vierte Reaktionsstufe, Der Einfluss des Methans auf den termischen Zerfall des —, I. G. MURGULESCU und M. WEISSMANN 1435

Chromanone and coumarine derivatives, Infrared spectra of some new —, L. V. FEYNS, I. I. DRAGOTĂ and I. NICULESCU-DUVĂZ 1207

Cobalt(II), Polarographic maximum of —, S. LAL 1359

Cobalt(III) tétrammine avec des acides organiques dicarboxyliques, Analyse thermique des composés du —, A. D. MAGRI, G. D'ASCENZO, U. BIADER CEIPIDOR et A. MARINO 1265

Complex chelate compounds of iso- and heteropolyanions of Mo(VI) and W(VI) with Chrome Azurol S. II. Complex chelate compounds of heteropolyanions of Mo(VI) and W(VI), P. B. ISSOPOULOS 585

Complex chelate compounds of Mo(VI) and W(VI) iso- and heteropolyanions with Chrome Azurol S. I. Complex chelate compounds of Mo(VI) and W(VI) isopolyanions, P. B. ISSOPOULOS 401

Complexes du Pd(II) avec le Romergan et les ions Cl^- et CNS^-, Des combinaisons —, V. CIMPU et D. CAMBOLI 1327

Comptes rendus, 161, 162, 163, 313, 314, 315, 317, 481, 481, 637, 638, 639, 640, 640, 797, 798, 799, 955, 955, 956, 957, 957, 1109, 1109, 1110, 1111, 1111, 1567, 1568, 1569 . . . .

Condensation reactions between cresols and isatin and its derivatives. I. A new molecular transposition, Contributions to the study of —, H. WEXLER and V. BĂRBOIU 127

Coordination chemistry of phthalic acid derivatives. II. New copper compounds of phthalimide derivatives, Contributions to the —, F. POPEA, Z. TOMA and C. MĂRCULESCU. 869

Coordination chemistry of s-triazines. I. Coordination compounds of copper with thioammeline derivatives, Contribution to the —, C. GHEORGHIU and C. MĂRCULESCU 707

Coordination compounds with iron-tin bonds, M. BREZEANU and I. JITARU 407

Copolymerization of 1,3-dioxepane with epichlorohydrin initiated with BF_3OEt_2, Kinetic studies on the —, D. DONESCU 277

Copolymerization of β-propiolactone with epichlorohydrin and 1,3-dioxepane, Kinetic studies on the —, D. DONESCU 1367

Copper tetra-ammine sulphate monohydrate, Decomposition kinetics of —, D. FĂTU and E. SEGAL 187

Corrosion inhibitors in oil-field waters, The efficiency of organic —, I. CORNEA and V. ICHIM 59

Corrosion of some steels in synthetic river waters, in heat transfer conditions, The —, E. ANTONESCU and E. VASILESCU 461

Cu(II) chelates synthesized with ligands containing donor nitrogen atoms, A. C. BANCIU and P. SPACU. 1331

Cyclobutadiene fused with heterocyclic ring. II. Cyclobutadienes condensed with five-membered heterocyclic rings, Electronic structure of —, M. P. GHEORGHIU and P. FILIP 1189

Cyclobutane series. XXXVIII. Rearrangement of the dibenzo [*b*, *g*]bicyclo[4·2·0] octa-2,7-diene system, Investigations in the —, N. ŞTEFAN, I. G. DINULESCU and M. AVRAM 107

D

Décomposition thermique des combinaisons complexes thiocyaniques du Pd(II) avec la pyridine et les pyridines substituées, La —, D. CAMBOLI, D. FĂTU et V. CIMPU 1479

Démixtion ternaire, Sur une transformée simple de certains isothermes de —, P. A. LAURENT et M. J. LAURENT-DUHAMEL 11

Dibenzobullvalene and related dibenzo-$(CH)_{10}$ hydrocarbons, Thermal and photochemical rearrangements of —, M. ELIAN, M. BANCIU, L. STĂNESCU and E. CIORĂNESCU 89

Disperse dyes with naphth[2,3-c]acridan[5,6-de]pyrimidin-5,11-dione structure, New —, F. URSEANU, C. TĂRĂBĂŞANU MIHĂILĂ and L. FLORU 257

Dyes for synthetic fibers. IX. Disperse azo-dyes for polyester fibers, A. SPILIADIS, P. GHEORGHE, M. SZÖGY and A. SĂVULESCU. 595

Dyes syntheses, Bromamine acid-anthraquinonic intermediate used in —, F. URSEANU and L. FLORU 427

Dyes with napth[2,3-c]xanthene-5,8,14-trione and naphth [2,3-c]thioxanthene-5,8,14-trione structure, New syntheses of —, F. URSEANU . . . 1227

E

Electrodes poreuses en argent. II. L'influence de la concentration de l'électrolyte sur les performances des électrodes. Contribution à l'étude de la réduction de l'oxygène sur les —, M. MAVRODIN-TĂRĂBÎC, IOANA ONACA et I. SOLACOLU 41

Electrodes poreuses en argent. III. L'effet de la température de l'électrolyte sur les performances des électrodes. Energies apparentes d'activation, L'étude de la réduction de l'oxygène sur les —, I. ONACA, M. MAVRODIN-TĂRĂBÎC et I. SOLACOLU. 207

Electrodes poreuses en argent. IV. L'effet de la variation des paramètres de fonctionnement sur la polarisation des électrodes à de différentes densités de courant, L'étude de la réduction de l'oxygène sur les —, I. SOLACOLU, M. MAVRODIN-TĂRĂBÎC et I. ONACA 531

Electronic spectra of Co^{III} thiazolidine chelates, E. CATRINA, Z. SIMON, Z. SZABADAY and GH. CATRINA 1037

Electropolymérisation des monomères vinylique en solvants aprotiques polaires. III. Electropolymérisation de l'acrylonitrile en carbonate de propylène et d'éthylène, CR. SIMIONESCU, C. UNGUREANU et A, CRUSOS 1417

Endothermal decompositions in solid-gas systems. Nickel acetate tetrahydrate dehydration, Critical considerations on the nonisothermal methods for the evaluation of the kinetic parameters of —, A. GHEORGHIU, D. FĂTU and E. SEGAL 367

Energies of vaporization, molecular parameters and critical temperatures and pressures, Correlation between —, R. F. HAJJAR. 217

Equilibrium geometry and heat of formation of aliphatic diazocompounds, diazirines and related singlet carbenes. AMINDO/2 calculation, M. MARTIN, V. MENÉNDEZ and J. M. FIGUERA 31

ESR spectra of nitrodibenzo-*p*-dioxin radicalic species, I. BACIU, M. HILLEBRAND, V. EM. SAHINI and E. VOLANSCHI . . . 485

Exo- and endohormones. I. Application of the ketoxime activation to the synthesis of the melanocyte inhibiting factor, M. VLASSA . . . 455

Exo- and endohormones. II. Synthesis of peptidic juvenile hormone analogues, M. VLASSA 897

Exo- and endohormones. III. New derivatives of synthetic ecdysone analogues and related compounds, A. GOCAN and F. HODOŞAN 627

F

First order reaction network, On the frequency of reaction events in a system with —, M. VLAD. 677

Fused salt ternary system by formation cell method, Thermodynamic properties of $AgI + NaI + KI$ —, S. STERNBERG and L. BEJAN 655

Fused tricyclic and tetracyclic molecules having planar conjugated perimeter, Topological studies, of —, J. V. KNOP, N. TRINAJSTIĆ and A. SABLJIĆ 749

G

Galvanostatic study of the electrochemical adsorption process on a chlorine-activated carbon electrode in molten salts. IV. Cathodic polarization curve equation (discharge), S. PETRESCU, S. STERNBERG and V. PETRESCU 813

Gas adsorption on thin semiconducting films. The zinc oxide-carbon monoxide system, Thermoelectric power variation during —, A. WECHSLER and E. SEGAL 831

Gaschromatographische Nachweis und die quantitative Bestimmung einer Mischung von 1-Chlor-3-thia-pentan und 3,6-Dithia-octan aus den bei der Synthese dieser Stoffe sich ergebenen Abflusswässern, Der —, R. CIUPE und M. GĂVAN 1263

Geteropolisoedinenie s razrazlichinymi sentralnymi atomami, Izuchenie svoistv i prakticheskoe ispolzovanie —, I. P. ALIMARIN, E. N. DOROHOVA, S. A. MOROSANOVA i E. N. SEMENOVSKAIA 835

H

Heterocycles. XXXVIII. Application of the Sommelet reaction in the series of 2-aryl-4-methyl-5-chloromethyl-thiazole, Contributions to the study of —, I. SIMITI and A. MUREŞAN 1073

Heteropolycompounds: tungstoniobiosilicates, New mixed —, GH. MARCU and L. GHIZDAVU 589

Heteropolytungstates with U(IV) as central atom. I. Photocolorimetrical study of the formation of heteropolycombination UL_2 where $L = PW_{11}O_{39}^{7-}$ and $P_2W_{21}O_{71}^{6-}$, GH. MARCU and M. RUSU 385

Hexachlorocyclotriphosphazene derivatives, C. GHEORGHIU, M. CHIRCA, E. CRISTUREAN and F. DINULESCU 859

Hexahaloethanes, Normal coordinate analysis of —, R. GRIGOROVICI, A. BUTUCELEA, V. E. SAHINI and M. K. DeARMOND 965

Hydrazones of piperidino-N-acetohydrazide and morpholino-N-acetohydrazide of pharmacological interest, V. B. JIGAJINNI, S. C. BENNUR, R. S. BENNUR and V. V. BADIGER 1221

Hydrogen-oxygen fuel cell, Mathematical model in the range 50—70° and 5N—7N KOH for a —, M. MAVRODIN-TĂRĂBÎC, I. ONACA and I. SOLACOLU 695

I

Ionic crystals with cubic structure. I. Potassium bromide, iodide and chloride, The temperature dependence of the dielectric permittivity of —, N. DUŞOIU 1161

Ionic liquids, Extension of some regularities of ternary electrolytic aqueous solutions in —, R. VÎLCU, F. IRINEI and E. TATU 491

Ionization constants of some N-aryl, N′-2-(5-halo-pyridyl) thioureas, B. C. KASHYAP, A. D. TANEJA and S. K. BANERJI 903

Iron oxides, Study of the isomorphic transitions of some —, D. I. MARCHIDAN and L. PANDELE 661

Irradiated polypropylene, Mechanical and electrical properties of—, D. GAVRILĂ, M. DIACONESCU and D. IORDACHE 155

K

Kopolymerisation. I. Mathematisches Modell der Bildung eines binären Kopolymerisationsproduktes, Zur —, I. MOŢOC und D. CIUBOTARIU 949

Kopolymerisation. II. Die Simulierung der Bildung eines Makromoleküls. Das Programm MEMORY 1, Zur —, I. MOŢOC, D. CIUBOTARIU und ŞT. HOLBAN 769

Kopolymerisation. III. Die Simulierung der Bildung eines Makromoleküls. Das Programm MEMORY 2, Zur —, I. MOŢOC, D. CIUBOTARIU und ŞT. HOLBAN 775

Kopolymerisation. IV. Das mathematische Modell der Bildung eines binären Kopolymers: die verbesserte Version, Zur —, I. MOŢOC, D. CIUBOTARIU und ŞT. HOLBAN 1247

Kopolymerisation. V. Die Simulierung der Bildung eines Makromoleküls durch binäre Mischpolymerisation. Das Programm MEMORY 3, Zur —, D. CIUBOTARIU, I. MOŢOC und ŞT. HOLBAN 1253

L

Laitons binaires et alliés, L'énergie accumulée par la déformation plastique à froid des —, I. GROZA et D. I. MARCHIDAN 509

Lead hydroxyapatite, Preparation and unit cell dimensions of —, W. M. BHATNAGAR 879

M

Mass spectrum of 3,7-di-t-butyl-5-methyl-4H-1,2-diazepine: possible steric inhibition of dinitrogen expulsion, A. T. BALABAN 241

Melting heats of alkali halide solid solutions, D. I. MARCHIDAN and L. VASU 25

Melts by means of EMF measurements, Study of the formation and homogenization processes of the —, P. BALTĂ and C. SPURCACIU 469

Membrane-electrode in the determination of some α-amino-acids, Utilization of a Hg^{2+}-sensitive, C. LITEANU, E. HOPÎRTEAN and R. VLAD 933

Membrane-electrodes of the metallic wire-plastic membrane type. III. Membrane-electrodes for organic cations, E. HOPÎRTEAN and E. ŞTEFANIGĂ 305

Methoxyl-Substituent auf die Reaktion zwischen $[TlBr_4]^-$ und Malachitgrün, Einfluss von —, C. CONSTANTINESCU und GH. C. CONSTANTINESCU 391

Molecular interactions in anisidine isomers. I. Dipole moments, V. E. SAHINI and L. TELEA 321

Molecular interactions in anisidine isomers. II. Electronic spectra, V. E. SAHINI and L. TELEA 645

Molecular orbital study of 2-thio-5-nitro-barbituric acid, R. NUŢIU, Z. SIMON and C. DRUGĂRIN 355

Molten potassium nitrate, Voltammetric and chronopotentiometric study of silver ion in —, T. VIŞAN, D. P. GEANĂ and S. STERNBERG 1153

Molten salts, Influence of the cell diaphragm on the electromotive force to concentration cells with transport in —, L. POPESCU 359

N

Napththoxazinones, The reaction of pyridinium-cyano-carbalkoxy-methylids with α-nitroso-β-naphtol, a route to —, C. LEONTE and I. ZUGRĂVESCU 423

Nickel electrodes. IV. The improvement of the electrode performances by addition of different efectrocatalysts, Hydrogen oxidation on porous —, O. RADOVICI, M. MAVRODIN-TĂRĂBÎC, I. ONACA and I. SOLACOLU 991

Nonisothermal kinetic study of the transformations and nonstoichiometrization of cobalt and nickel oxides, A. GHEORGHIU, D. FĂTU and E. SEGAL 825

O

Organischen Reagenzien in der Reaktion mit $[TlBr_4]^-$, Einfluss der Substituenten auf die analytischen Eigenschaften von —, C. CONSTANTINESCU und GH. CONSTANTINESCU 571

Organo-aluminium compounds towards Lewis bases. II. Diaryl- and dialkylaluminum ketiminphosphines, Reactivity of —, D. GIURGIU and I. POPESCU 1373

Oxazoles. II. Bromuration des 2,5-diphenyloxazoles, Obtention et comportement des —, R. MACAROVICI et M. IONESCU 881

P

Phenol obtention from benzenes in oxygen plasma generated by a high frequency discharges. I. Dispersional analysis of the data and the multiple regression equation of the process, G. BOURCEANU, V. ABABI, GH. POPA and M. SANDULOVICIU 1405

Phenoxatellurine. Action of tellurium tetrachloride on 4-halodiphenyl ethers, Chemistry of —, A. GIOABĂ, M. NEDEA and O. MAIOR 739

Phosphoric acid, Mixed aromatic esters of —, M. IOVU and E. VOINA 447

Phthalic acid derivatives. I. Condensation products of phthalic anhydride with *m*-phenylenediamine as coordination ligands for copper, Contributions to the coordination chemistry of —, F. POPEA, C. MĂRCULESCU, and Z. TOMA 413

Pile à cathode en argent, Contribution à l'étude de la source chimique de courant $Zn(MeOH)O_2$. III. La détermination des paramètres optimaux de fonctionnement pour une —, M. MAVRODIN-TĂRĂBÎC, I. ONACA et I. SOLACOLU 373

Polarographic investigation of the decomposition of xanthates in acid medium, L. KÉKEDY and I. KOVÁCS 121

Polyacrylonitrile with other polymers, Some data on the compatibility of —, D. FELDMAN, M. CIUGUREANU and M. CIUBOTARIU 269

Polyethylene. III. Interlamellar orderings in polyethylene with chemical etched defects, Amorphous-crystalline coupling in —, GH. DRĂGAN 1381

Polyethylene. IV. Earth gravity effect on defect precipitation during annealing, Amorphous-crystalline coupling in —, GH. DRĂGAN 1537

Polymères vinyliques contenant des groupements aminiques avec les composés organiques du soufre. II. La réaction entre la poly(vinylamine) et le chlorure de thionyle, O. PETREUŞ et M. DIMA 911

Polymerization and copolymerization of the acrylonitrile in the presence of organometallic catalysts, Contributions to the —, CR. I. SIMIONESCU, D. FELDMAN and V. NUŢĂ 927

Polymerization by free radicals, Variation of molecular mass with time in —, M. DIMONIE, CR. OPRESCU and GH. HUBCA 763

Polymerization of 1,3-dioxepane with BF_3OEt_2, Kinetics of —, D. DONESCU 139

Polymers. II. The poly(N,N-dimethylaminoethyl methacrylate salts) of 2,4-dichlorophenoxyacetic and 2,4,5-trichlorophenoxyacetic acids, Groth regulating —, A. CARPOV, S. MAXIM and M. DIMA 1097

Polymers. III. Poly(4-vinylpyridine) salts with halogen (alkyl) aryloxyalkyl carboxylic acids, Growth regulating —, S. MAXIM and M. DIMA 937

Polyoxyméthylène. V. Aspects cinétiques au broyage vibratoire, Greffage mécanochimique des —, CR. I. SIMIONESCU et A. CRUSOS 1237

Polyvinyl chloride fractionation, Utilization of the ureapolyvinyl chloride adducts in the —, C. LUCA and A. POPA 231

Porous media, Contributions to the study of the superficial phenomena in —, L. ONICIU, I. MITRACHE, V. A. TOPAN and F. DAMALAN 1287

Portland cements, Influence of titanium dioxide on the structure and on the properties of mineralogical compounds in white —, M. ENCULESCU 549

Potential anticancer agents. XII. Synthesis of new methanesulfonate derivatives from benzo and naphtopyrans, I. DRAGOTĂ, D. IONESCU, EUSTANTA TĂRNAUCEANU, V. DOBRE and I. NICULESCU-DUVĂZ 1543

Potentials aus 2. Druckvirialkoeffizienten, Zur Berechnung von Parametern des zwischenmolekularen —, H. FREYDANK und M. T. RÄTZSCH 1463

Pretreated electrode surfaces. VI. Chronopotentiometric study of differently pretreated gold electrodes, Experimental approach to the characterization of —, A. POPESCU and L. KÉKEDY 683

Pyridazinium-ylures. I. Addition du 3-(*p*-cumyl)-pyridazinium-phénacylure et du 3-(*p*-cumyl)-pyridazinium-(*p*-nitro)-phénacylure sur les alcynes activés, M. PETROVANU, MAI VAN TRI et V. BĂRBOIU . . . 717

Pyrimidines. VI. Synthesis of 2-methylthio-5-bromo-pyrimidine-4-carboxylic acid thiosemicarbazides, 3-pyrimidyl-1,2,4-(4H)-triazoles and 2-arylamino-1,3,4-thiodiazoles, S. C. BENNUR, V. B. JIGAJINNI and V. V. BADIGER 757

Pyrolysis of Nenitzescu's hydrocarbons, On the —, M. BANCIU 1083

Pyrylium salts formed by diacylation of olefins. XX. PMR spectra of 2,4,6-trimethyl-3-phenylpyrilium and -pyridinium salts, A. BOTA, A. T. BALABAN and F. CHIRALEU 101

Pyrylium salts formed by diacylation of olefins. XXI. Diacetylation of cyclodecene to 9,10-dimethyl-[7](2,6)-pyrylophanium perchlorate, A. T. BALABAN and I. I. BĂDILESCU 1339

Pyrylium salts formed by diacylation of olefins. XXII. Triacylation of 2,3-dimethyl-2-butene, A. T. BALABAN, A. BOTA and I. I. STĂNOIU 1183

Pyrylium salts, Ground and excited state SCF—PPP—CI calculations for —, M. D. GHEORGHIU and A. T. BALABAN 1513

Pyrylium salts with nucleophiles. XI. Chemical shift non-equivalence of isopropyl in atropisomeric 1-aryl-2-isopropy-4,6-dimethylpyridinium salts, Reaction of —, C. UNCUŢA and A. T. BALABAN 251

R

Régiosélectivité dans la réduction des oximes par les agents aluminiques, Essai de généralisation du —, L. FERRERO, S. GERIBALDI et M. AZZARO 49

S

Schmelzgemischen aus Calciumchlorid und Cäsiumchlorid, Physikalisch-chemische Eigenschaften von —, M. M. EMONS und G. BRÄUTIGAM . . . 223

Silica gel structure and dispersion of synthetic aluminosilicates, The electron microscopic investigations of —, J. SZYMURA and B. DIRSKA 1103

Spectral solvent effects in aromatic compounds solutions. II. The solvent effects on the position and intensity of chlorobenzene band, at 2600 Å, V. MACOVEI 193

Spectral study of 4,7-phenathroline 5,6-dione radical anion, L. CIUREA, V. EM. SAHINI und A. MATEESCU 1445

Statistical copolymer by light scattering, Study of N-vinylcarbazole ethyl methacrylate —, S. IOAN and I. BENEDEK 145

Stilbene derivatives. I. The electronic spectra and transmission of the substituent effects in molecules of some nitro-containing *trans*-stilbene derivatives, The electronic structure of some —, L. CIOHODARU and A. MEGHEA 1127

Stilbene derivatives. II. Quantitative correlations referring to the substituent effects on the electronic spectra of some stilbene derivatives, The electronic structure of some —, L. CIOHODARU and A. MEGHEA 1473

Stochastic analysis of the reaction networks. I. On the —, M. VLAD and E. SEGAL. 667

Stochastic analysis of the reaction networks. II. The principle of detailed balance for reaction networks, On the —, M. VLAD and E. SEGAL . . . 1311

Stochastic analysis of the reaction networks. III. Langevin approaches, On the —, M. VLAD and E. SEGAL 1319

Structure of dark-red compound $[Fe(II)phen_2(NCS)_2].H_2O$, The —, M. TEODORESCU 1031

Sulphur dioxide starting from calcium sulphate. II. Utilization of phosphogypsum and of natural gypsum with impurities of $CaCO_3$, On a new procedure for obtaining —, C. LITEANU, E. HOPÎRTEAN, I. C. POPESCU, N. L. KÉKEDY, E. VERESS and V. LITEANU 1395

Surface tension of gas-solid interface, On the surface stress and —, P. BUDRUGEAC and M. I. VASS 1305

Systèmes binaires de liquides, Grandeurs d'excès par des mesures acoustiques, dans les —, R. VÎLCU et A. SIMION 177

T

Tellurium tetrachloride with 4-fluoro-4′-methyldiphenyl ether, Reaction of —, A. GIOABĂ, O. MAIOR and M. MITRAN 733

Tseria (III) v vodno-metanolnykh rastvorakh, Povedenie —, A. A. VOLKOV, Z. E. AKSENOVA, E. S. FILATOV, AN. N. NESMEIANOV 703

Terpolymerization field. VII. Theoretical structural characterization of the low conversion acrylonitrile-methacrylic acid-methyl methacrylate terpolymer, Researches in the —, CR. I. SIMIONESCU and ADELAIDA LIGA 1555

Tetracoordinated Co(II) chelates with Co(d^7)-N(sp^2) bonds, A. C. BANCIU 1487

Thallium, Self-diffusion in liquid —, N. PETRESCU and L. GANOVICI 1293

Thermal conductivity of water, An equation for the —, L. BADEA 1429

Thermal decomposition of dioxalato-diaquomanganate(III) in dimethyl sulphoxide-water mixtures, Solvent effect on the kinetics of the —, T. ONCESCU and E. JURCONI 985

Thermal decomposition of $[Mn(C_2O_4)_2(H_2O)_2]K.3H_2O$ in $DMF-H_2O$ mixtures, Solvent effect on the —, T. ONCESCU and E. JURCONI 805

Thermal effect on surface acidity and catalytic activity of $ZrO_2-Al_2O_3$ and ZrO_2-SiO_2 catalysts, S. P. WALVEKAR, A. B. HALGERI, S. RAMANNA and T. N. SRINIVA SAN 237

Thermal equilibria in the binary systems $MgO-CeO_2$, $CaO-CeO_2$, $SrO-CeO_2$, $BaO-CeO_2$, M. PREDA and R. DINESCU 1023

Thermal stability of $BaCO_3$, The influence of Fe_2O_3 on the —, M. BULZAN and E. SEGAL 651

Thermodynamic properties of electrolyte solutions. V. Differential cryoscopy in $NaCl+CuCl_2+H_2O$ and $KCl+CuCl_2+H_2O$ ternary systems and in associated binaries, R. VÎLCU, E. C. DE MADRIÑAN and F. IRINEI 333

Thermodynamic properties of $NaCl-CaCl_2$ and $KCl-CaCl_2$ molten systems, L. TOPOR and I. MOLDOVEANU 495

Thiazole compounds. III. Kinetic of hydrolysis of some 2-aryl-4- and 5-diazo ketone derivatives, D. SUCIU and G. CSÁVÁSSY 113

Thieno[2,3-b]-benzothiachromone, Syntheses based on —, O. MAIOR and N. RĂȘANU 745

Tricyclo[7.3.1.$0^{2,7}$]tridecane series. VII. Pyrolytic elimination of 8-methyltricyclo[7.3.1.$0^{2,7}$]tridecen-13-acetates, Elimination reactions in the 8-substituted —, N. S. BĂRBULESCU and M. LECA 1527

Tritium in lithium halides, Processes associated with the ^{6}Li(n, α)^{3}H nuclear reaction. III. Chemical evidence for the stabilization forms of recoil —, C. MĂNTESCU, A. GENUNCHE, D. CRISTU and T. COSTEA 789

U

Ultrasonic velocity and compressibility in fused AgCl—AgBr, AgCl—KCl and AgI, S. STERNBERG and V. VASILESCU 1457

Uranium oxides. A model of quantitative approach, The influence of non-stoichiometry upon heat capacity of —, M. CIOPEC and D. I. MARCHIDAN 997

Uranium oxides by solid electrolyte EMF measurements. Solid state coulometric titration technique, Thermodynamic study of some —, D. I. MARCHIDAN and S. TĂNĂSESCU. 1451

Urea and thiourea derivatives. I. Syntheses, IR and UV spectra of some new disubstituted urea and thiourea derivatives with possible physiological effects, New —, A. BOLDEA, C. DRUGĂRIN, M. MRACEC and Z. SIMON 1345

V

Verweilzeitverteilung der dispersen Phase in einem Gas-Flüssig oder Flüssig-Flüssig System, Ein Modell für die —, R. MIHAIL, C. SINGER und C. IONESCU 293

Viscosimetric study of the poly(4-vinylpyridine) salts with the halogen (alkyl) aryloxyalkyl carboxylic acids, S. MAXIM and M. DIMA 631

Vzaimosviaz poverkhnostnogo natiyazheniya, szhimaemosti i blizhnego poriadka rasplavov vblizy tochiki plavleniya. I. Schelochino-galoidnye soli i poluprovodniki, B. N. OSCHERIN 351

Z

Zéolithes du système $Na_2O—Al_2O_3—SiO_2—H_2O$, de type A et faujasitique, La synthèse des —, N. BÎLBĂ et V. ABABI 285

X

Xylidine isomers. IV. Dipole moments in the first excited singlet state, V. E. SAHINI, J. WEINBERG and M. VASILESCU 1121

NOTE POUR LES AUTEURS

La *Revue Roumaine de Chimie* publie des articles en anglais, français, russe, allemand ou espagnol. Les auteurs sont priés d'envoyer des articles, notes, communications et comptes rendus inédits.

Les manuscrits seront dactylographiés à deux intervalles. Les tableaux seront dactylographiés sur des feuilles séparées, de même que la légende des figures. Les diagrammes seront tracés à l'encre de Chine sur papier calque. Les tableaux et les figures seront numérotés par des chiffres arabes, en nombre strictement nécessaire. Prière de ne pas inscrire les mêmes données dans les tableaux et les figures. Les formules chimiques seront incluses dans le texte ; en outre, elles seront transcrites sur des feuilles séparées. Les auteurs sont priés d'indiquer les caractères italiques (en soulignant les lettres au crayon), ainsi que tout autre caractère spécial. L'ordre des références bibliographiques sera celui de leur mention dans le texte ; le nom de l'auteur sera précédé de l'initiale du prénom ; les publications périodiques seront présentées suivant les prescriptions internationales. Les références seront ajoutées à fin de l'article ; elles paraîtront comme des notes, au bas de la page. Le texte sera précédé d'un résumé comprenant 15 lignes au maximum.

L'entière responsabilité du contenu des articles appartient aux auteurs. On publie des articles dus aux collaborateurs roumains ou étrangers.

PRINTED IN ROMANIA

TRAVAUX PARUS AUX ÉDITIONS DE L'ACADÉMIE DE LA RÉPUBLIQUE SOCIALISTE DE ROUMANIE

CONST. V. UGLEA, **Cromatografia pe gel permeabil. Noi domenii de aplicare** (La chromatographie sur gel perméable. Nouveaux domaines d'application), 1976, 122 p., 6,75 lei.

FRANCISC A. GOTHARD, **Echilibre lichid-vapori. I. Baze teoretice şi metode de calcul** (Equilibres liquide-vapeurs. I. Bases théoriques et méthodes de calcul), 1975, 263 p., 2 pl. 28 lei.

CONST. GH. MACAROVICI, D. MACAROVICI, **Chimia oxizilor dubli şi utilizările lor** (La chimie des oxydes doubles et leur utilisation), 1975, 195 p., 13 lei.

M. AVRAM, **Antidăunători** (Pesticides), 1974, 496 p., 41 lei.

ELENA CEAUŞESCU, **Research work on synthesis and characterization of macromolecular compounds. Contributions**, 1974, 251 p., 20 lei.

DUMITRU COSTACHE, **Analiza chimică prin metoda cinetică** (L'Analyse chimique par la méthode cinétique), 1974, 276 p., 15,50 lei.

G. A. RĂDULESCU, **Proprietăţile ţiţeiurilor româneşti** (Les propriétés des pétroles roumains), 1974, 267 p., 2 pl. 18 lei.

CR. SIMIONESCU, VIORICA RUSAN, V. POPA, **Chimia algelor marine** (La chimie des algues marines), 1974, 212 p., 1 pl., 18 lei.

I. ZUGRĂVESCU, MAGDA PETROVANU, **Chimia n-ilidelor** (La chimie des n-Ilures), 1974, 348 p., 19 lei.

MARIA FITI, **Dozimetria chimică a radiaţiilor ionizante** (La dosimétrie chimique des radiations ionisantes), 1973, 240 p., 13,50 lei.

TIBERIU NĂŞCUŢIU, **Metode radiochimice de analiză** (Méthodes radiochimique d'analyse), 1973, 384 p., 23 lei.

CRISTOFOR SIMIONESCU, MARGARETA GRIGORAŞ, AGATA CERNĂTESCU-ASANEI, ROZMARIN GHEORGHE, **Chimia lemnului în România. Plopul şi salcia** (La Chimie du bois en Roumanie. Le peuplier et le saule), 1973, 299 p. 13 pl. 26 lei.

MIHAI FLORESCU, **Eficienţa economică a cercetării ştiinţifice** (L'efficience économique de la recherche scientifique), 1972, 115 p., 15 lei.

GEORGETA LĂZĂRESCU, **Sistematizarea informaţiilor în chimia organică** (Systématisation des informations en Chimie organique), 1972, 243 p., 1 pl., 10,50 lei.

I.P.I. c. 1457

43426

Lei 25.—